Scientific and Technical Aerospace Reports

STAR

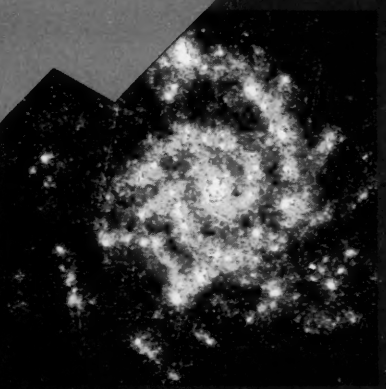

An Abstract Journal

NASA Publication

Volume 31, Number 3
March 1993
N93-12544 to N93-14101

Scientific and Technical Aerospace Reports (STAR) is an abstract journal that provides comprehensive coverage of worldwide aerospace-related reports. It is a major product of the International Aerospace Database managed by the NASA Scientific and Technical Information (STI) Program. The coverage includes reports on aeronautics, space, and supporting disciplines. *STAR* lists current, publicly available reports entered into the NASA STI Database during the 4-week period preceding publication. A typical citation and abstract appear on page viii. They explain how to read the items that are announced in this journal.

NASA sponsors a companion journal, *International Aerospace Abstracts (IAA) (NOVA* for internal NASA use) that lists abstracts of the open literature on aerospace subjects available worldwide. *IAA* is available for sale through the AIAA.

Entries found in *STAR* and *IAA* are available through NASA's online service, RECON, as the International Aerospace Database and through DIALOG as the Aerospace Database.

Information on aerospace and related subjects is gathered by the NASA STI Program through national and international agreements and exchanges and is made available to the NASA community as well as to the public in many forms through various outlets. The section on NASA STI Program Products and Services contains additional information.

For further information please contact:
NASA Center for AeroSpace Information (CASI)
800 Elkridge Landing Road
Linthicum Heights, MD 21090-2934
(301) 621-0390

US ISSN 0036-8741

Volume 31 Number 3 / March 1993

TABLE OF CONTENTS

AERONAUTICS For related information see also *Astronautics.*

01 AERONAUTICS (GENERAL) **491**

02 AERODYNAMICS **491**
Includes aerodynamics of bodies, combinations, wings, rotors, and control surfaces; and internal flow in ducts and turbomachinery. For related information see also *34 Fluid Mechanics and Heat Transfer.*

03 AIR TRANSPORTATION AND SAFETY **497**
Includes passenger and cargo air transport operations; and aircraft accidents. For related information see also *16 Space Transportation* and *85 Urban Technology and Transportation.*

04 AIRCRAFT COMMUNICATIONS AND NAVIGATION **499**
Includes digital and voice communication with aircraft; air navigation systems (satellite and ground based); and air traffic control. For related information see also *17 Space Communications, Spacecraft Communications, Command and Tracking* and *32 Communications and Radar.*

05 AIRCRAFT DESIGN, TESTING AND PERFORMANCE **499**
Includes aircraft simulation technology. For related information see also *18 Spacecraft Design, Testing and Performance* and *39 Structural Mechanics.* For land transportation vehicles see *85 Urban Technology and Transportation.*

06 AIRCRAFT INSTRUMENTATION ..... **N.A.**
Includes cockpit and cabin display devices; and flight instruments. For related information see also *19 Space craft Instrumentation* and *35 Instrumentation and Photography.*

07 AIRCRAFT PROPULSION AND POWER **502**
Includes prime propulsion systems and systems components, e.g., gas turbine engines and compressors; and onboard auxiliary power plants for aircraft. For related information see also *20 Spacecraft Propulsion and Power, 28 Propellants and Fuels,* and *44 Energy Production and Conversion.*

08 AIRCRAFT STABILITY AND CONTROL **503**
Includes aircraft handling qualities; piloting; flight controls; and autopilots. For related information see also *05 Aircraft Design, Testing and Performance.*

09 RESEARCH AND SUPPORT FACILITIES (AIR) **506**
Includes airports, hangars and runways; aircraft repair and overhaul facilities; wind tunnels; shock tubes; and aircraft engine test stands. For related information see also *14 Ground Support Systems and Facilities (Space).*

ASTRONAUTICS For related information see also *Aeronautics.*

12 ASTRONAUTICS (GENERAL) **508**
For extraterrestrial exploration see *91 Lunar and Planetary Exploration.*

13 ASTRODYNAMICS **517**
Includes powered and free-flight trajectories; and orbital and launching dynamics.

14 GROUND SUPPORT SYSTEMS AND FACILITIES (SPACE) **518**
Includes launch complexes, research and production facilities; ground support equipment, e.g., mobile transporters; and simulators. For related information see also *09 Research and Support Facilities (Air).*

15 LAUNCH VEHICLES AND SPACE VEHICLES **519**
Includes boosters; operating problems of launch/space vehicle systems; and reusable vehicles. For related information see also *20 Spacecraft Propulsion and Power.*

16 SPACE TRANSPORTATION **520**
Includes passenger and cargo space transportation, e.g., shuttle operations; and space rescue techniques. For related information see also *03 Air Transportation and Safety* and *18 Spacecraft Design, Testing and Performance.* For space suits see *54 Man/System Technology and Life Support.*

17 SPACE COMMUNICATIONS, SPACECRAFT COMMUNICATIONS, COMMAND AND TRACKING . **N.A.**
Includes telemetry; space communications networks; astronavigation and guidance; and radio blackout. For related information see also *04 Aircraft Communications and Navigation* and *32 Communications and Radar.*

N.A.—no abstracts were assigned to this category for this issue.

18 SPACECRAFT DESIGN, TESTING AND PERFORMANCE **521**
Includes satellites; space platforms; space stations; spacecraft systems and components such as thermal and environmental controls; and attitude controls. For life support systems see *54 Man/System Technology and Life Support.* For related information see also *05 Aircraft Design, Testing and Performance, 39 Structural Mechanics,* and *16 Space Transportation.*

19 SPACECRAFT INSTRUMENTATION **524**
For related information see also *06 Aircraft Instrumentation* and *35 Instrumentation and Photography.*

20 SPACECRAFT PROPULSION AND POWER **525**
Includes main propulsion systems and components, e.g., rocket engines; and spacecraft auxiliary power sources. For related information see also *07 Aircraft Propulsion and Power, 28 Propellants and Fuels, 44 Energy Production and Conversion,* and *15 Launch Vehicles and Space Vehicles.*

CHEMISTRY AND MATERIALS

23 CHEMISTRY AND MATERIALS (GENERAL) **527**

24 COMPOSITE MATERIALS **528**
Includes physical, chemical, and mechanical properties of laminates and other composite materials. For ceramic materials see *27 Nonmetallic Materials.*

25 INORGANIC AND PHYSICAL CHEMISTRY **536**
Includes chemical analysis, e.g., chromatography; combustion theory; electrochemistry; and photochemistry. For related information see also *77 Thermodynamics and Statistical Physics.*

26 METALLIC MATERIALS **540**
Includes physical, chemical, and mechanical properties of metals, e.g., corrosion; and metallurgy.

27 NONMETALLIC MATERIALS **544**
Includes physical, chemical, and mechanical properties of plastics, elastomers, lubricants, polymers, textiles, adhesives, and ceramic materials. For composite materials see *24 Composite Materials.*

28 PROPELLANTS AND FUELS **555**
Includes rocket propellants, igniters and oxidizers; their storage and handling procedures; and aircraft fuels. For related information see also *07 Aircraft Propulsion and Power, 20 Spacecraft Propulsion and Power,* and *44 Energy Production and Conversion.*

29 MATERIALS PROCESSING **556**
Includes space-based development of products and processes for commercial application. For biological materials see *55 Space Biology.*

ENGINEERING For related information see also *Physics.*

31 ENGINEERING (GENERAL) **557**
Includes vacuum technology; control engineering; display engineering; cryogenics; and fire prevention.

32 COMMUNICATIONS AND RADAR **560**
Includes radar; land and global communications; communications theory; and optical communications. For related information see also *04 Aircraft Communications and Navigation* and *17 Space Communications, Spacecraft Communications, Command and Tracking.* For search and rescue see *03 Air Transportation and Safety,* and *16 Space Transportation.*

33 ELECTRONICS AND ELECTRICAL ENGINEERING **569**
Includes test equipment and maintainability; components, e.g., tunnel diodes and transistors; microminiaturization; and integrated circuitry. For related information see also *60 Computer Operations and Hardware* and *76 Solid-State Physics.*

34 FLUID MECHANICS AND HEAT TRANSFER **574**
Includes boundary layers; hydrodynamics; fluidics; mass transfer and ablation cooling. For related information see also *02 Aerodynamics* and *77 Thermodynamics and Statistical Physics.*

35 INSTRUMENTATION AND PHOTOGRAPHY **595**
Includes remote sensors; measuring instruments and gauges; detectors; cameras and photographic supplies; and holography. For aerial photography see *43 Earth Resources and Remote Sensing.* For related information see also *06 Aircraft Instrumentation* and *19 Spacecraft Instrumentation.*

36 LASERS AND MASERS **603**
Includes parametric amplifiers. For related information see also *76 Solid-State Physics.*

37 MECHANICAL ENGINEERING **609**
Includes auxiliary systems (nonpower); machine elements and processes; and mechanical equipment.

38 QUALITY ASSURANCE AND RELIABILITY **619**
Includes product sampling procedures and techniques; and quality control.

39 STRUCTURAL MECHANICS **620**
Includes structural element design and weight analysis; fatigue; and thermal stress. For applications see *05 Aircraft Design, Testing and Performance* and *18 Spacecraft Design, Testing and Performance.*

GEOSCIENCES For related information see also *Space Sciences.*

42 GEOSCIENCES (GENERAL) **632**

43 EARTH RESOURCES AND REMOTE SENSING **632**
Includes remote sensing of earth resources by aircraft and spacecraft; photogrammetry; and aerial photography. For instrumentation see *35 Instrumentation and Photography.*

44 ENERGY PRODUCTION AND CONVERSION **636**
Includes specific energy conversion systems, e.g., fuel cells; global sources of energy; geophysical conversion; and windpower. For related information see also *07 Aircraft Propulsion and Power, 20 Spacecraft Propulsion and Power,* and *28 Propellants and Fuels.*

45 ENVIRONMENT POLLUTION **641**
Includes atmospheric, noise, thermal, and water pollution.

46 GEOPHYSICS **648**
Includes aeronomy; upper and lower atmosphere studies; ionospheric and magnetospheric physics; and geomagnetism. For space radiation see *93 Space Radiation.*

47 METEOROLOGY AND CLIMATOLOGY **660**
Includes weather forecasting and modification.

48 OCEANOGRAPHY **668**
Includes biological, dynamic, and physical oceanography; and marine resources. For related information see also *43 Earth Resources and Remote Sensing.*

LIFE SCIENCES

51 LIFE SCIENCES (GENERAL) **671**

52 AEROSPACE MEDICINE **674**
Includes physiological factors; biological effects of radiation; and effects of weightlessness on man and animals.

53 BEHAVIORAL SCIENCES **676**
Includes psychological factors; individual and group behavior; crew training and evaluation; and psychiatric research.

54 MAN/SYSTEM TECHNOLOGY AND LIFE SUPPORT **676**
Includes human engineering; biotechnology; and space suits and protective clothing. For related information see also *16 Space Transportation.*

55 SPACE BIOLOGY ..... **N.A.**
Includes exobiology; planetary biology; and extraterrestrial life.

MATHEMATICAL AND COMPUTER SCIENCES

59 MATHEMATICAL AND COMPUTER SCIENCES (GENERAL) **681**

60 COMPUTER OPERATIONS AND HARDWARE **681**
Includes hardware for computer graphics, firmware, and data processing. For components see *33 Electronics and Electrical Engineering.*

61 COMPUTER PROGRAMMING AND SOFTWARE **682**
Includes computer programs, routines, algorithms, and specific applications, e.g., CAD/CAM.

62 COMPUTER SYSTEMS **688**
Includes computer networks and special application computer systems.

63 CYBERNETICS **690**
Includes feedback and control theory, artificial intelligence, robotics and expert systems. For related information see also *54 Man/System Technology and Life Support.*

64 NUMERICAL ANALYSIS **695**
Includes iteration, difference equations, and numerical approximation.

65 STATISTICS AND PROBABILITY **697**
Includes data sampling and smoothing; Monte Carlo method; and stochastic processes.

66 SYSTEMS ANALYSIS ..... **N.A.**
Includes mathematical modeling; network analysis; and operations research.

67 THEORETICAL MATHEMATICS ..... **N.A.**
Includes topology and number theory.

PHYSICS For related information see also *Engineering.*

70 PHYSICS (GENERAL) **698**
For precision time and time interval (PTTI) see *35 Instrumentation and Photography;* for geophysics, astrophysics or solar physics see *46 Geophysics, 90 Astrophysics,* or *92 Solar Physics.*

71 ACOUSTICS **699**
Includes sound generation, transmission, and attenuation. For noise pollution see *45 Environment Pollution.*

72 ATOMIC AND MOLECULAR PHYSICS **701**
Includes atomic structure, electron properties, and molecular spectra.

73 NUCLEAR AND HIGH-ENERGY PHYSICS **705**
Includes elementary and nuclear particles; and reactor theory. For space radiation see *93 Space Radiation.*

74 OPTICS **708**
Includes light phenomena and optical devices. For lasers see *36 Lasers and Masers.*

75 PLASMA PHYSICS **712**
Includes magnetohydrodynamics and plasma fusion. For ionospheric plasmas see *46 Geophysics.* For space plasmas see *90 Astrophysics.*

76 SOLID-STATE PHYSICS **719**
Includes superconductivity. For related information see also *33 Electronics and Electrical Engineering* and *36 Lasers and Masers.*

77 THERMODYNAMICS AND STATISTICAL PHYSICS **727**
Includes quantum mechanics; theoretical physics; and Bose and Fermi statistics. For related information see also *25 Inorganic and Physical Chemistry* and *34 Fluid Mechanics and Heat Transfer.*

SOCIAL SCIENCES

80 SOCIAL SCIENCES (GENERAL) **729**
Includes educational matters.

81 ADMINISTRATION AND MANAGEMENT **731**
Includes management planning and research.

82 DOCUMENTATION AND INFORMATION SCIENCE **732**
Includes information management; information storage and retrieval technology; technical writing; graphic arts; and micrography. For computer documentation see *61 Computer Programming and Software.*

83 ECONOMICS AND COST ANALYSIS **740**
Includes cost effectiveness studies.

84 LAW, POLITICAL SCIENCE AND SPACE POLICY **741**
Includes NASA appropriation hearings; aviation law; space law and policy; international law; international cooperation; and patent policy.

85 URBAN TECHNOLOGY AND TRANSPORTATION **742**
Includes applications of space technology to urban problems; technology transfer; technology assessment; and surface and mass transportation. For related information see *03 Air Transportation and Safety, 16 Space Transportation,* and *44 Energy Production and Conversion.*

SPACE SCIENCES For related information see also *Geosciences.*

88 SPACE SCIENCES (GENERAL) ..... **N.A.**

89 ASTRONOMY **742**
Includes radio, gamma-ray, and infrared astronomy; and astrometry.

90 ASTROPHYSICS **749**
Includes cosmology; celestial mechanics; space plasmas; and interstellar and interplanetary gases and dust. For related information see also *75 Plasma Physics.*

91 LUNAR AND PLANETARY EXPLORATION **758**
Includes planetology; and manned and unmanned flights. For spacecraft design or space stations see *18 Spacecraft Design, Testing and Performance.*

92 SOLAR PHYSICS **769**
Includes solar activity, solar flares, solar radiation and sunspots. For related information see *93 Space Radiation.*

93 SPACE RADIATION **771**
Includes cosmic radiation; and inner and outer earth's radiation belts. For biological effects of radiation see *52 Aerospace Medicine.* For theory see *73 Nuclear and High-Energy Physics.*

GENERAL

Includes aeronautical, astronautical, and space science related histories, biographies, and pertinent reports too broad for categorization; histories or broad overviews of NASA programs.

99 GENERAL **773**

SUBJECT INDEX **I-1**

PERSONAL AUTHOR INDEX **I-109**

CORPORATE SOURCE INDEX **I-121**

CONTRACT NUMBER INDEX **I-139**

REPORT NUMBER INDEX **I-143**

APPENDIX **A-1**

TYPICAL CITATION AND ABSTRACT

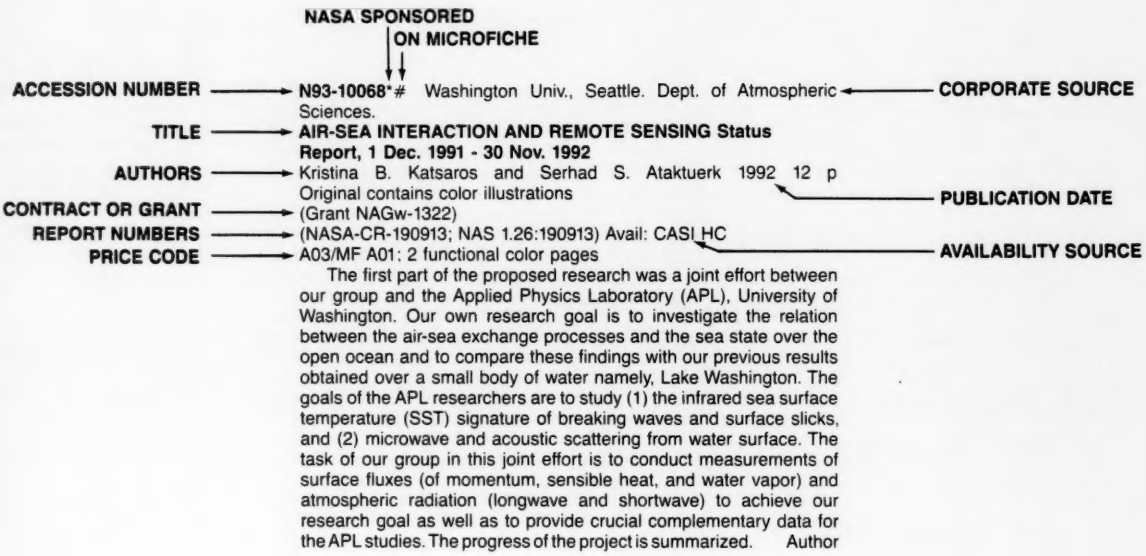
NASA SPONSORED
ON MICROFICHE
ACCESSION NUMBER
N93-10068*# Washington Univ., Seattle. Dept. of Atmospheric Sciences.
CORPORATE SOURCE
TITLE
AIR-SEA INTERACTION AND REMOTE SENSING Status Report, 1 Dec. 1991 - 30 Nov. 1992
AUTHORS
Kristina B. Katsaros and Serhad S. Ataktuerk 1992 12 p
Original contains color illustrations
PUBLICATION DATE
CONTRACT OR GRANT
(Grant NAGw-1322)
REPORT NUMBERS
(NASA-CR-190913; NAS 1.26:190913) Avail: CASI HC
AVAILABILITY SOURCE
PRICE CODE
A03/MF A01: 2 functional color pages
The first part of the proposed research was a joint effort between our group and the Applied Physics Laboratory (APL), University of Washington. Our own research goal is to investigate the relation between the air-sea exchange processes and the sea state over the open ocean and to compare these findings with our previous results obtained over a small body of water namely, Lake Washington. The goals of the APL researchers are to study (1) the infrared sea surface temperature (SST) signature of breaking waves and surface slicks, and (2) microwave and acoustic scattering from water surface. The task of our group in this joint effort is to conduct measurements of surface fluxes (of momentum, sensible heat, and water vapor) and atmospheric radiation (longwave and shortwave) to achieve our research goal as well as to provide crucial complementary data for the APL studies. The progress of the project is summarized. Author

VOLUME 31 NUMBER 3 / MARCH 1993

Scientific and Technical Aerospace Reports

A Monthly Publication of the National Aeronautics and Space Administration

01 AERONAUTICS (GENERAL)

N93-13025*# National Aeronautics and Space Administration. Langley Research Center, Hampton, VA.

FUTURE REGIONAL TRANSPORT AIRCRAFT MARKET, CONSTRAINTS, AND TECHNOLOGY STIMULI

W. Don Harvey and Brent Foreman (Auburn Univ., AL.) Oct. 1992 89 p

(RTOP 505-69-20-01)

(NASA-TM-107669; NAS 1.15:107669) Avail: CASI HC A05/MF A01

This report provides updated information on the current market and operating environment and identifies interlinking technical possibilities for competitive future commuter-type transport aircraft. The conclusions on the market and operating environment indicate that the regional airlines are moving toward more modern and effective fleets with greater passenger capacity and comfort, reduced noise levels, increased speed, and longer range. This direction leads to a nearly 'seamless' service and continued code-sharing agreements with the major carriers. Whereas the benefits from individual technologies may be small, the overall integration in existing and new aircraft designs can produce improvements in direct operating cost and competitiveness. Production costs are identified as being equally important as pure technical advances. Author

N93-13110*# National Aeronautics and Space Administration, Washington, DC.

NASA AERONAUTICS: RESEARCH AND TECHNOLOGY PROGRAM HIGHLIGHTS

[1990] 77 p LIMITED REPRODUCIBILITY: More than 20 percent of this document may be affected by color photographs Original contains color illustrations

(NASA-NP-159; NAS 1.83:159) Avail: CASI HC A05/MF A01; 44 functional color pages

This report contains numerous color illustrations to describe the NASA programs in aeronautics. The basic ideas involved are explained in brief paragraphs. The seven chapters deal with Subsonic aircraft, High-speed transport, High-performance military aircraft, Hypersonic/Transatmospheric vehicles, Critical disciplines, National facilities and Organizations & installations. Some individual aircraft discussed are : the SR-71 aircraft, aerospace planes, the high-speed civil transport (HSCT), the X-29 forward-swept wing research aircraft, and the X-31 aircraft. Critical disciplines discussed are numerical aerodynamic simulation, computational fluid dynamics, computational structural dynamics and new experimental testing techniques. R.L.B.

N93-13946# Air Force Inst. of Tech., Wright-Patterson AFB, OH. Foreign Aerospace Science and Technology Center.

ACTA AERONAUTICA ET ASTRONAUTICA SINICA (SELECTED ARTICLES)

7 Apr. 1992 36 p Transl. into ENGLISH from Hangong Xuebao (China), v. 12, no. 3, 1991 p 167-172 and 173-179

(AD-A255070; FASTC-ID(RS)T-0608-91) Avail: CASI HC A03/MF A01

This article introduces the use of a compensation type of non-coherent model sidelobe suppression filter (SSF) and actually develops the theoretical calculations and experimental results associated with 13 place Barker code pulse compression sidelobe suppression. Compensation type non-coherent models of SSF opt for the use of least square approximate inverse filtering techniques for designs if the subpulse width is 0.7 microsec and the peak sidelobe values do not exceed -30dB. This type of SSF Doppler tolerance is capable of reaching -40 kHz to +40 kHz. Theoretical calculations and experimental results both clearly show that compensation type non-coherent model SSF which have been designed have associated with them Doppler tolerances which, as compared to R-G-1 SSF series which possess the same type of length impact excitation effects, are a clear improvement. GRA

02 AERODYNAMICS

Includes aerodynamics of bodies, combinations, wings, rotors, and control surfaces; and internal flow in ducts and turbomachinery.

For related information see also *34 Fluid Mechanics and Heat Transfer.*

N93-12716# Tokyo Univ. (Japan). Inst. of Space and Astronautical Science.

EFFECT OF THE FLOW NON-UNIFORMITY ON THE MIXING LAYER AT THE INTERFACE OF PARALLEL SUPERSONIC FLOWS

Takashi Abe (Tokyo Univ., Sagamihara, Japan), Katsushi Funabiki, Hironobu Ariga (Musashi Inst. of Tech., Tokyo, Japan), and Katsumi Hiraoka (Tokai Univ., Tokyo, Japan) Jun. 1992 20 p

(ISAS-RN-646) Avail: CASI HC A03/MF A01

The effect of flow non-uniformity on the supersonic mixing layer was investigated. The mixing layer is formed at the interface between the parallel supersonic flows of air and helium. The mixing layer was directly investigated by measuring the concentration ratio of helium. As for the flow non-uniformity, the stream-wise pressure gradient and the shock wave penetrating the mixing layer were considered. The effect of the stream-wise pressure gradient enhances the mixing rate by around 2 times in comparison with the one of the mixing layer without the effect. The shock impingement further enhances the mixing rate in comparison with the one of the mixing layer with the stream-wise pressure gradient but without the shock impingement. The enhancement of the mixing layer growth rate caused by the flow non-uniformities is attributed to the vorticity enhancement at the mixing layer, for which the baroclinic torque is a strong candidate. Author

N93-12721*# National Aeronautics and Space Administration. Ames Research Center, Moffett Field, CA.

NAVIER-STOKES SIMULATIONS OF UNSTEADY TRANSONIC FLOW PHENOMENA

C. A. Atwood Aug. 1992 131 p

(Contracts NCC2-540; NCC2-677; RTOP 505-59-00)

(NASA-TM-103962; A-92159; NAS 1.15:103962) Avail: CASI HC A07/MF A02

Numerical simulations of two classes of unsteady flows are obtained via the Navier-Stokes equations: a blast-wave/target interaction problem class and a transonic cavity flow problem class. The method developed for the viscous blast-wave/target interaction problem assumes a laminar, perfect gas implemented in a structured finite-volume framework. The approximately factored implicit scheme uses Newton subiterations to obtain the spatially and temporally second-order accurate time history of the blast-waves with stationary targets. The inviscid flux is evaluated using either of two upwind techniques, while the full viscous terms are computed by central differencing. Comparisons of unsteady numerical, analytical, and experimental results are made in two- and three-dimensions for Couette flows, a starting shock-tunnel, and a shock-tube blockage study. The results

show accurate wave speed resolution and nonoscillatory discontinuity capturing of the predominantly inviscid flows. Viscous effects were increasingly significant at large post-interaction times. While the blast-wave/target interaction problem benefits from high-resolution methods applied to the Euler terms, the transonic cavity flow problem requires the use of an efficient scheme implemented in a geometrically flexible overset mesh environment. Hence, the Reynolds averaged Navier-Stokes equations implemented in a diagonal form are applied to the cavity flow class of problems. Comparisons between numerical and experimental results are made in two-dimensions for free shear layers and both rectangular and quieted cavities, and in three-dimensions for Stratospheric Observatory For Infrared Astronomy (SOFIA) geometries. The acoustic behavior of the rectangular and three-dimensional cavity flows compare well with experiment in terms of frequency, magnitude, and quieting trends. However, there is a more rapid decrease in computed acoustic energy with frequency than observed experimentally owing to numerical dissipation. In addition, optical phase distortion due to the time-varying density field is modelled using geometrical constructs. The computed optical distortion trends compare with the experimentally inferred result, but underpredicts the fluctuating phase difference magnitude. Author

N93-12741# Naval Surface Weapons Center, Dahlgren, VA.
NEW METHODS FOR PREDICTING NONLINEAR LIFT, CENTER OF PRESSURE, AND PITCHING MOMENT ON MISSILE CONFIGURATIONS Final Report
Frank G. Moore, Tom Hymer, and Leroy Devan Jul. 1992 183 p
(AD-A255078; NSWCDD/TR-92/217) Avail: CASI HC A09/MF A02

A new semiempirical method has been developed to predict normal force, pitching moment, and center of pressure on missile configurations up to angles of attack of 30 deg. The new method is based on linear theory and slender body techniques at low angle of attack and uses wind tunnel data to derive nonlinear angle-of-attack corrections as angle of attack increases. The new improved theories include body alone, wing alone, and body-wing and wing-body interference. While the new theory is databased, simple analytical formulas are derived that allow general use of the techniques. Comparison of the new theory to the linearized approaches used in the former NSWCDD aeroprediction code shows significant reductions in errors of aerodynamics dynamics above about 5 deg to 10 deg angle of attack. Limited comparisons of the new theory to other state-of-the-art engineering codes show the new theory to be as good as or better than anything known to be available computing planar aerodynamics up to 30 deg angle of attack. GRA

N93-13010 Florida Atlantic Univ., Boca Raton.
DYNAMIC STALL EFFECTS ON HINGELESS ROTOR STABILITY WITH EXPERIMENTAL CORRELATION Ph.D. Thesis
Dinesh Barwey 1992 283 p
Avail: Univ. Microfilms Order No. DA9213129

The effects of dynamic stall, lift, drag and pitching moment on the aeroelastic stability of hingeless rotors are predicted. The emphasis is on correlating the predictions with the measured lag-damping levels of a three-bladed model rotor operated in an untrimmed mode. The correlation covers a wide range of test conditions for several values of rotor speed, collective pitch angle, shaft-tilt angle and advance ratio. The database includes cases that vary from near zero-thrust conditions in hover to highly stalled forward-flight conditions with dimensionless speed or advance ratios as high as 0.55 and shaft angles as high as 20 degrees. The aerodynamic representation is based on the ONERA dynamic stall models comprising virtually independent unified lift, drag and pitching-moment models. The nonlinear equations of blade motion and stall dynamics are perturbed about a periodic forced response, and the damping is evaluated by Floquet analysis. The extensive correlation study, based on a rigid-blade flap-lag analysis, demonstrates the viability of Floquet analysis in predicting lagmode damping under dynamically stalled forward-flight conditions. It also demonstrates the limitations of the linear and quasisteady stall aerodynamic theories. In comparison to these theories, the theory with dynamic stall lift and quasisteady stall drag qualitatively improves the correlation and is viable over the entire range of the database. Addition of dynamic stall drag provides further quantitative improvement. Also presented is a comparative study of two dynamic stall drag models: circulation-like drag variables incorporating unsteady air-velocity variations and conventional drag-coefficient variables. While the formulation with drag coefficients exhibits computational sensitivity to convergence with respect to blade discretization for some isolated cases, the formulation with circulation-like drag variables removes this sensitivity and is computationally robust. The investigation concludes with an elastic blade analysis that includes blade flexibility in lag bending, flap bending and torsion as well as root-flexure elasticity. This analysis shows increasing sensitivity to structural refinements in blade and root-flexure modeling, and this sensitivity increases with increasing pitch setting. Correlation and parametric studies show that the root-flexure elasticity introduces significant bending-torsion couplings that have considerable impact on the stability of a rotor for which the root-flexure is soft, and the blade is stiffer in comparison with the root. This research is expected to serve as a reference comparison with other correlations based on different approaches of modeling dynamic stall and the elasticity of hingeless rotor blades and root-flexure. Dissert. Abstr.

N93-13128 Michigan Univ., Ann Arbor.
A NUMERICAL STUDY OF HYPERSONIC FLOW WITH STRONG SURFACE BLOWING Ph.D. Thesis
Nelson David Carter 1992 153 p
Avail: Univ. Microfilms Order No. DA9226861

A possible means of controlling hypervelocity vehicles within the atmosphere is the use of boundary-layer blowing (blowing a gas from the vehicle surface) to introduce desired modifications in the pressure distribution along the surface, and thus provide the required control forces for the vehicle. This study considers the effects of massive blowing on the simple geometries of a flat plate and a wedge in a hypersonic flow. A computer code has been developed which can calculate the resulting flow field for a variety of different blowing distributions. A higher-order Godunov-type finite-volume approach is used to discretize the Euler and Navier-Stokes equations. Interface values of the state variable are reconstructed using a monotone interpolation technique based on Van Leer's kappa scheme. The inviscid fluxes are computed using Roe's upwind-biased flux-difference splitting technique. The viscous fluxes are calculated using central differencing. The time-differencing algorithms used are a line-implicit Gauss-Seidel iteration scheme and an explicit multi-stage scheme with optimized short-wave damping. Ideal and non-ideal gas flows are considered. For non-ideal gas flows, curve fit equations of state are used. The injection of gases other than air is also considered. The resulting numerical solutions compare well with analytical solutions which are known for certain blowing distributions and free-stream conditions. Favorable comparisons between the numerical solutions and experimental results are also found for several cases. The computer code is also used to investigate the time evolution of the flow for both slot and continuous gas injection. Dissert. Abstr.

N93-13141 Purdue Univ., West Lafayette, IN.
APPLICATION OF A SOLUTION ADAPTIVE GRID TO FLOW OVER AN EMBEDDED CAVITY Ph.D. Thesis
Anthony Linn Thornton 1992 124 p
Avail: Univ. Microfilms Order No. DA9229199

The effect of a surface discontinuity (e.g. gaps, notches, cavities, etc.) on the local flowfield over flight vehicles has been an area of interest to researchers in fluid mechanics for many years. The most relevant problems relating to cavity flow include determining the effect the surface defect has on the local pressure and drag. A multivariable adaptive grid technique was developed to resolve the essential viscous and inviscid flow features in a compressible flow problem. The adaptive methodology, although one-dimensional in nature, assists in equally distributing the solution error throughout the flowfield. The adaptive scheme was applied to the steady 'open' cavity configuration in which the dividing streamline spans the length of the cavity. The analysis involves the numerical solution of the 2-D, compressible Navier-Stokes equations using the method of Beam and Warming. The goal of this investigation was to develop an understanding, both qualitative and quantitative, of the dominant flow features in the neighborhood of small gaps and notches embedded in a laminar supersonic boundary layer. The results of this research provide a clearer understanding of the effects of Reynolds number on the wall shear stress and pressure distribution within an open cavity in laminar, supersonic flow.

Dissert. Abstr.

N93-13292*# National Aeronautics and Space Administration. Lewis Research Center, Cleveland, OH.
RADIAL TURBINE COOLING

Richard J. Roelke Apr. 1992 42 p Presented at the Lecture Series on Radial Turbines at the von Karman Inst. for Fluid Dynamics, Brussels, Belgium, 6-10 Apr. 1992 Original contains color illustrations
(RTOP 535-05-10)
(NASA-TM-105658; E-7022; NAS 1.15:105658) Avail: CASI HC A03/MF A01; 2 functional color pages

Radial turbines have been used extensively in many applications including small ground based electrical power generators, automotive engine turbochargers and aircraft auxiliary power units. In all of these applications the turbine inlet temperature is limited to a value commensurate with the material strength limitations and life requirements of uncooled metal rotors. To take advantage of all the benefits that higher temperatures offer, such as increased turbine specific power output or higher cycle thermal efficiency, requires improved high temperature materials and/or blade cooling. Extensive research is on-going to advance the material properties of high temperature superalloys as well as composite materials including ceramics. The use of ceramics with their high temperature potential and low cost is particularly appealing for radial turbines. However until these programs reach fruition the only way to make significant step increases beyond the present material temperature barriers is to cool the radial blading. Author

N93-13322*# National Aeronautics and Space Administration. Hugh L. Dryden Flight Research Facility, Edwards, CA.
IN-FLIGHT FLOW VISUALIZATION RESULTS FROM THE X-29A AIRCRAFT AT HIGH ANGLES OF ATTACK
John H. DelFrate and John A. Saltzman (PRC Kentron, Inc., Edwards, CA.) Nov. 1992 17 p Presented at the 6th Biennial Flight Test Conference, Hilton Head, SC, 24-26 Aug. 1992 Previously announced in IAA as A93-11272
(RTOP 533-02-38)
(NASA-TM-4430; H-1825; NAS 1.15:4430; AIAA Paper 92-4102)
Copyright Avail: CASI HC A03/MF A01

Flow visualization techniques were used on the X-29A aircraft at high angles of attack to study the vortical flow off the forebody and the surface flow on the wing and tail. The forebody vortex system was studied because asymmetries in the vortex system were suspected of inducing uncommanded yawing moments at zero sideslip. Smoke enabled visualization of the vortex system and correlation of its orientation with flight yawing moment data. Good agreement was found between vortex system asymmetries and the occurrence of yawing moments. Surface flow on the forward-swept wing of the X-29A was studied using tufts and flow cones. As angle of attack increased, separated flow initiated at the root and spread outboard encompassing the full wing by 30 deg angle of attack. In general, the progression of the separated flow correlated well with subscale model lift data. Surface flow on the vertical tail was also studied using tufts and flow cones. As angle of attack increased, separated flow initiated at the root and spread upward. The area of separated flow on the vertical tail at angles of attack greater than 20 deg correlated well with the marked decrease in aircraft directional stability. Author

N93-13353*# National Aeronautics and Space Administration. Langley Research Center, Hampton, VA.
EFFECTS OF FOREBODY STRAKES AND MACH NUMBER ON OVERALL AERODYNAMIC CHARACTERISTICS OF CONFIGURATION WITH 55 DEG CROPPED DELTA WING
Gary E. Erickson and Lawrence W. Rogers (Wright Lab., Wright-Patterson AFB, OH.) Nov. 1992 171 p
(RTOP 505-68-30-03)
(NASA-TP-3253; L-17060; NAS 1.60:3253) Avail: CASI HC A08/MF A02

A wind tunnel data base was established for the effects of chine-like forebody strakes and Mach number on the longitudinal and lateral-directional characteristics of a generalized 55 degree cropped delta wing-fuselage-centerline vertical tail configuration. The testing was conducted in the 7- by 10-Foot Transonic Tunnel at the David Taylor Research Center at free-stream Mach numbers of 0.40 to 1.10 and Reynolds numbers based on the wing mean aerodynamic chord of 1.60 x 10(exp 6) to 2.59 x 10(exp 6). The best matrix included angles of attack from 0 degree to a maximum of 28 degree, angles of sidesip of 0, +5, and -5 degrees, and wing leading-edge flat deflection angles of 0 and 30 degrees. Key flow phenomena at subsonic and transonic conditions were identified by measuring off-body flow visualization with a laser screen technique. These phenomena included coexisting and interacting vortex flows and shock waves, vortex breakdown, vortex flow interactions with the vertical tail, and vortices induced by flow separation from the hinge line of the deflected wing flap. The flow mechanisms were correlated with the longitudinal and lateral-directional aerodynamic data trends. Author

N93-13451 Oxford Univ. (England).
MATHEMATICAL PROBLEMS IN INVISCID HYPERSONIC FLOW Ph.D. Thesis
Ken Louie 1991 156 p
Avail: Univ. Microfilms Order No. BRD-95126

Some simple models for inviscid gas flows are studied in the hypersonic limit. Initially, the treatment will be restricted to perfect gases but a major part of the thesis will be concerned with the effects when simple chemical reactions also occur. Unsteady 1-D flows are studied first and the piston problem is examined in detail. When the piston is given a power-law path with time, solutions do not always exist when the exponent in the power-law is less than a critical value. This is shown to be the case whether or not reactions are included. Hence the question of regularization of the piston problem arises and is addressed in a later chapter. Steady 2-D and axisymmetric flow past thin and slender bodies is then studied and its equivalence to unsteady 1-D flow demonstrated. This equivalence is shown to also apply to some reacting flows. For the general piston problem and the steady flow past thick and non-slender bodies, the Newtonian limit enables simple results to be obtained. The usual perfect gas analysis is extended to include the effects of a simple reaction. For steady flow, this does not seem to greatly modify the singularities manifest in this limit, the most important of which is the vanishing of the surface pressure at some point downstream. The resolution of this difficulty is to allow the shock layer to separate at the point where the surface pressure vanishes. This idea is shown to be useful also for the piston problem in the case where the solution breaks down. A novel regularization is presented for the piston problem which enables a scenario to be put forward for those piston motions previously untreatable. The solution is not completely independent of the regularization in the limit as the regularizing parameter tends to zero. Dissert. Abstr.

N93-13463*# Pennsylvania State Univ., University Park. Dept. of Aerospace Engineering.
ANALYSIS AND DESIGN OF PLANAR AND NON-PLANAR WINGS FOR INDUCED DRAG MINIMIZATION Final Progress Report
Karl W. Mortara, Dennis M. Straussfogel, and Mark D. Maughmer Nov. 1992 60 p
(Grant NAG1-1198)
(NASA-CR-191274; NAS 1.26:191274) Avail: CASI HC A04/MF A01

The goal of the work reported herein is to develop and validate computational tools to be used for the design of planar and non-planar wing geometries for minimum induced drag. Because of the iterative nature of the design problem, it is important that, in addition to being sufficiently accurate for the problem at hand, these tools need to be reasonably fast and computationally efficient. Toward this end, a method of predicting induced drag in the presence of a free wake has been coupled with a panel method. The induced drag prediction technique is based on the application of the Kutta-Joukowski law at the trailing edge. Until now, the use of this method has not been fully explored and pressure integration and Trefftz-plane calculations favored. As is shown in this report, however, the Kutta-Joukowski method is able to give better results for a given amount of effort than the more commonly used techniques, particularly when relaxed wakes and non-planar wing geometries are considered. Using these methods, it is demonstrated that a reduction in induced drag can be achieved through non-planar wing geometries. It remains to determine what overall drag reductions are possible when the induced drag reduction is traded-off against increased wetted area. With the design methodology that is described herein, such trade studies can be performed in which the non-linear effects of the free wake are taken into account. Author

N93-13493 Oklahoma State Univ., Stillwater.
CHAOTIC VORTICAL MOTION IN THE NEAR REGION OF A PLANE JET Ph.D. Thesis
James W. Cutbirth 1991 157 p
Avail: Univ. Microfilms Order No. DA9220551

The primary objective of this thesis is to understand on a quantitative

basis the detailed nonlinear interactions between vortical structures in the near region of a planar jet. For the purpose of this investigation, lowlevel acoustic excitation near the most unstable natural jet shear layer frequency and at three times the jet column mode were introduced in order to organize the initial instability and isolate specific pairing mechanisms. Flow visualization and power spectra were the primary tools used for the investigation. The quantitative analysis based on flow visualization data indicates that the coherent structure formation near the nozzle exit is not exactly periodic. Shortly after the first pairing, the vortex motion becomes chaotic. Thus no long term, continuously repeating pattern of vortex roll-up, motion and pairing exists. The coherent structures remain strongly two-dimensional until the end of the potential core where the structures breakdown into three-dimensional motion. This is substantially further downstream as compared to the location where chaotic motion was identified. Dissert. Abstr.

N93-13521 Washington Univ., Seattle.
NUMERICAL SIMULATION OF THE ACOUSTIC INSTABILITY IN THE SPATIALLY DEVELOPING, CONFINED, SUPERSONIC MIXING LAYER Ph.D. Thesis
Linda Sigalla Hedges 1991 147 p
Avail: Univ. Microfilms Order No. DA9216120

The spatially developing, confined, two-dimensional, supersonic mixing layer is investigated using both linear stability theory and numerical simulation. The purpose of this work is to further the understanding of the physical instability mechanisms responsible for transition from laminar to turbulent flow (and hence for mixing) in the supersonic mixing layer. Though the type of instability initially responsible for transition to turbulent flow is unknown, a prime candidate is the acoustic instability. The acoustic instability, present in confined, supersonic mixing layers, results from the interaction of the shear layer interface with compression and expansion waves reflecting off of the channel walls. Numerical simulations are used to investigate the supersonic acoustic instability modes and their nonlinear interactions. The subsonic mixing layer is also simulated to provide a basis for comparison and validation. In the simulations, the two-dimensional, nonsteady Euler equations are solved using a total variation diminishing (TVD) finite difference technique. Numerical simulations include simulations of isolated modes, simple modal interactions, and the instability generated with a broadbanded white noise perturbation. Results show that the acoustic instability is robust in the two-dimensional supersonic mixing layer and that the physical instability mechanism responsible for mixing and instability growth is engulfment. The behavior of the acoustic instability seen in the supersonic mixing layer is significantly different from the behavior of the Kelvin-Helmholtz instability seen in the subsonic mixing layer. In the supersonic mixing layer, many acoustic modes grow simultaneously. In the subsonic mixing layer, generally one primary Kelvin-Helmholtz mode grows, followed by its subharmonics as the downstream distance increases. Numerical simulations of interacting pairs of acoustic modes show that the modes interact destructively and suppress each other's growth. At the same time, new modes are excited and grow. The supersonic mixing layer does not exhibit pairing by the subharmonic, as seen in subsonic mixing layers. However, evidence of accretion of vortices is seen in the broadbanded mixing layer. Finally, a one-to-one relationship between the temporally and spatially developing mixing layers is shown. Dissert. Abstr.

N93-13578 Stanford Univ., CA.
DEVELOPMENT AND COMPUTATION OF CONTINUUM HIGHER ORDER CONSTITUTIVE RELATIONS FOR HIGH-ALTITUDE HYPERSONIC FLOW Ph.D. Thesis
Xiaolin Zhong 1991 147 p
Avail: Univ. Microfilms Order No. DA9206895

The use of computational fluid dynamics (CFD) to study the aerodynamics of compressible viscous flow in the continuum transitional regime at high altitudes is discussed. The CFD codes are based on continuum higher order constitutive relations, i.e. the Burnett equations, which are more accurate than the conventional Navier-Stokes equations at high altitudes. Until 1988, the Burnett equations were rejected for high-altitude flow computations primarily because no solution could be obtained for hypersonic flow. Recent solutions were possible for low altitudes, but not for high altitudes, because the conventional Burnett equations are unstable to disturbances of short wavelengths. This fundamental instability precludes Burnett flow-field computations above a certain maximum altitude for any given vehicle. Therefore, it is necessary to overcome this Burnett instability. The objective is to develop a set of higher order and nonlinear constitutive equations representing a generalization of the Burnett equations, which would be stable to numerical computations at all altitudes. A new set of equations termed the 'augmented Burnett equations' was developed in order to stabilize and to maintain the accuracy of the conventional Burnett equations. Subsequently, an implicit numerical method was developed to solve the augmented Burnett equations. The first Burnett solutions for 2-D hypersonic flow past blunt bodies were obtained and compared with the corresponding Navier-Stokes and Direct Simulation Monte Carlo solutions. The comparison showed that the Burnett equations provide the same results as the Navier-Stokes equations do at low altitudes, but provide more accurate results at high altitudes. In conclusion, the Burnett equations seem to be able to progress into regions of strong nonequilibrium flow at high altitudes where the Navier-Stokes equations are inaccurate. Further research is needed to resolve some remaining technical issues concerning the Burnett equations, including the issues of the most appropriate surface boundary conditions for their higher derivative terms and their frame dependence. Dissert. Abstr.

N93-13632 Georgia Inst. of Tech., Atlanta.
VELOCITY AND TEMPERATURE MEASUREMENTS IN A NON-PREMIXED REACTING FLOW BEHIND A BACKWARD FACING STEP Ph.D. Thesis
Men-Zan Bill Wu 1992 150 p
Avail: Univ. Microfilms Order No. DA9223802

A basic design requirement for aerospace propulsion systems is the inclusion of a flame anchoring region in the combustor. This region must be characterized by highly turbulent flow for enhancing extensive mixing of fuel and air for combustion and by flow velocities lower than the flame propagation speed of the mixture. One such configuration, applicable to ramjet type combustion problems, is that of a backward facing step. The application takes advantage of the flow recirculation region for flameholding, and of the high mixing rates in the free shear layer for enhanced combustion efficiency. The specific effort of this research was to investigate experimentally the temperature and velocity distributions in a flow field, generated by the non-premixed hydrogen combustion behind a backward facing step. The region of interest includes turbulent reacting flow with recirculation. The diagnostics used include laser Doppler velocimetry (LDV), Rayleigh scattering and laser Raman spectroscopy (LRS), which permit in-situ measurements with good spatial and temporal resolution. The velocity measurements were carried out using a two component LDV system. Time averaged measurements were used to acquire mean velocities and turbulence intensities. LRS has been utilized to investigate the temperature or species concentration in high temperature reacting flows. The intensity of the Stokes line of nitrogen was used to infer the temperature of the flow in this study. The temperature distribution obtained using LRS measurement is consistent with those using Rayleigh scattering and thermocouple. The following results were obtained in this study: (1) a comparison of velocity fields for the non-reacting and reacting flows has shown that chemical reaction lengthens the reattachment length of the flowfield; (2) combustion occurs primarily in the free shear layer with the flame sheet, as indicated by the location of maximum temperature coinciding with the region of maximum turbulence intensity; (3) the location of maximum temperature fluctuation coincides with the area of steepest mean temperature gradient near the upper edge of the flame; and (4) the presence of chemical reaction in the flow appears to reduce the turbulence intensities inside the free shear layer, resulting in a lower mixing rate for the reacting flow. Dissert. Abstr.

N93-13729 Georgia Inst. of Tech., Atlanta.
HIGH-SPEED AERODYNAMICS OF UPPER SURFACE BLOWING AIRCRAFT CONFIGURATIONS Ph.D. Thesis
Larry Dean Birckelbaw 1992 209 p
Avail: Univ. Microfilms Order No. DA9223767

Excellent Short Take-Off and Landing (STOL) performance is achieved by Upper Surface Blowing (USB) aircraft as a result of mounting high by-pass turbofan engines over the forward part of the wing. High lift levels are generated by directing the engine exhaust over the wing upper surface to entrain additional airflow and by using the Coanda effect to turn the exhaust flow downward over a large radius 'Coanda' flap. Commercial application of USB technology could reduce airport congestion and

community noise if future configurations can be designed with economically acceptable cruise drag levels. An experimental investigation of the high speed aerodynamics of USB aircraft configurations has been conducted to accurately define the magnitude and causes of the powered configuration cruise drag. A highly instrumented wind tunnel model of a realistic USB configuration has been used which permitted parametric variations in the number and spanwise location of the nacelles and accurately modeled the engine power effects with turbofan propulsion simulators. The measured force data provides an accurate definition of the cruise drag penalty associated with each configuration and the constructed pressure contour plots provide detailed insight into their causes. It was found that the high speed aerodynamics of USB configurations is a complex interaction of jet induced and wing transonic flowfields. The presence of the nacelles on the wing upper surface created a severe drag penalty which increased with freestream Mach number, power setting and angle of attack. The more widely spaced two nacelle configurations exhibited improved flowfields at moderate Mach numbers but suffered from drag levels comparable to the baseline configuration for high speed cruise conditions. At high Mach numbers and power settings, all of the tested configurations displayed strong shocks and separated zones in the wing/nacelle junction regions. Detailed discussions of the causes of the cruise drag penalty and recommended future design improvements are presented. Dissert. Abstr.

N93-13745 Maryland Univ., College Park.
PERFORMANCE AND CONTROL OF ASCENDING TRAJECTORIES TO MINIMIZE HEAT LOAD FOR TRANSATMOSPHERIC AERO-SPACE PLANES Ph.D. Thesis
Ahmed Zafer Al-Garni 1991 373 p
Avail: Univ. Microfilms Order No. DA9205023

This is a study of the performance and control of ascending trajectories for Transatmospheric Vehicles (TAV), that use air-breathing propulsion. The minimization of heat load per unit area near the stagnation point is addressed. The vehicle is modelled as a variable point mass with parabolic drag polar, and variable lift and thrust. The earth is assumed to be spherical, with an exponential atmosphere. The research is structured in two parts. The first part is analytical, and seeks closed form solutions for the non-linear feedback controls (aerodynamic and thrust), which are necessary to transfer the TAV from one specified state (e.g., altitude, h(sub 1) is approximately 20 km; Mach number M is approximately 5; and heat load, Q(sub 1) is approximately 5 kJ/sq cm, etc.), to a second specific state (e.g., altitude h(sub 2) is approximately 65 km; Mach number M(sub 2) is approximately 25; and heat load, Q(sub 2) is less than or equal to 500 kJ/sq cm, etc.), while satisfying given equality constraints such as constant dynamic pressure with constant rate of climb. Certain algebraic relationships among the state variable and controls have been derived, and the heat load, along with most of the state variable, were integrated analytically. The achieved heat load can be less than 300 kJ/sq cm for most of the cases and situations discussed, which is less than that obtained in previous literature. The analytical results were a useful guide to the numerical studies in the second part. The second part is an extensive numerical optimization study. A feedback law was selected with parameters chosen by computational methods. A heat load Q less than or equal to 300 kJ/sq cm and controls in the reachable domain were achieved in most cases and situations. The trajectories of the aerospace planes or (TAV) were found to be within a reasonable flight corridor given current research and technology. The effect of certain vehicle design parameters were studied. The research has revealed no fundamental barriers in the performance and control of the TAV although improvement is necessary in all of the propulsion, aerodynamic, and cooling systems. Dissert. Abstr.

N93-13746 Stanford Univ., CA.
APPLICATION OF A VECTORIZED PARTICLE SIMULATION TO THE STUDY OF PLATES AND WEDGES IN HIGH-SPEED RAREFIED FLOW Ph.D. Thesis
Michael Stanley Woronowicz 1991 255 p
Avail: Univ. Microfilms Order No. DA9205745

The scientific community has placed a great deal of emphasis on understanding the unique phenomena associated with hypersonic, rarefied flowfields in order to successfully design future high-speed, high-altitude flight vehicles. Scientists are interested in using particle simulation methods to recreate the combinations of speeds and rarefaction associated with flight through the upper atmosphere. Particle methods build up a macroscopic flowfield based on the interactions of thousands or millions of particles that behave as molecules on the microscopic level. Unfortunately, most particle methods employ basic algorithms that are incompatible with the architecture and resources of most high-speed computers. The Stanford Particle Simulation Method (SPSM) overcomes these disadvantages by paying strict attention to details incorporating the advantages of these machines while retaining correct macroscopic physical behavior. Since this method is still quite new, it must be adequately tested in order to gain acceptance in the scientific and engineering communities. The purpose of the current investigation is to use the advantages afforded by the SPSM to help establish the method's legitimacy by thoroughly studying a relatively simple two-dimensional flowfield: high-speed, low-density, viscous flow over a flat plate at zero incidence. The freestream Knudsen number is varied such that the simulation's solutions range from continuum flow all the way to the free-molecule limit. Issues concerning proper implementation of boundary conditions for simulation wind tunnels and geometry models are discussed, and novel approaches are used to develop a diffuse adiabatic boundary condition and make necessary alterations for highly-rarefied and free-molecule conditions. A review of experimental data is present, and a new parameter is developed using aspects of kinetic theory and demonstrated to correlate hypersonic, rarefied drag and heat transfer data better than commonly-used alternatives. Surface-flux quantities, such as drag and heat transfer, obtained by the simulation are compared to experimental data whenever possible. Aspects of the simulation's surface-flux and flowfield results are compared to theories, where available. In addition, a more complicated hypersonic, rarefied, two-dimensional flow over a wedge was studied and compared to experimental results. Dissert. Abstr.

N93-13801 Virginia Univ., Charlottesville.
PLANAR MEASUREMENT OF FLOW FIELD PARAMETERS IN NONREACTING SUPERSONIC FLOWS WITH LASER-INDUCED IODINE FLUORESCENCE Ph.D. Thesis
Roy James Hartfield, Jr. 1991 187 p
Avail: Univ. Microfilms Order No. DA9219294

Planar measurements of temperature, pressure, velocity, and injectant mole fraction were conducted in cold supersonic milling flow fields using laser-induced iodine fluorescence. The measurements were conducted by seeding the flow fields with iodine, inducing fluorescence with an argon ion laser sheet, and imaging the fluorescence with a liquid nitrogen cooled charge coupled device (CCD) camera. To conduct these measurements, it was necessary to develop and verify new measurement techniques for temperature and pressure suitable for use with planar imaging. Injectant mole fraction and temperature were measured using fluorescence induced by broad band excitation. Pressure and velocity were determined from the profile and position of an absorption transition. The shape and position of the transition were measured using fluorescence resulting from narrow band excitation. The flow fields investigated are configured geometrically as SCRAMJET combustors. Both tangential and transverse injection flow fields were investigated. These measurements provide extensive maps of the thermodynamic parameters and are suitable for the validation of computational fluid dynamic codes. The measurements of injectant mole fraction are spatially complete and provide a measure of milling efficiency. Dissert. Abstr.

N93-13803 Virginia Polytechnic Inst. and State Univ., Blacksburg.
AIRFOIL-VORTEX INTERACTION AND THE WAKE OF AN OSCILLATING AIRFOIL Ph.D. Thesis
Michael Curtis Wilder 1992 223 p
Avail: Univ. Microfilms Order No. DA9218519

Laser Doppler velocimetry, a non-intrusive flow measurement technique, was employed to experimentally investigate two-dimensional airfoil-vortex interaction. Vortices were generated by sinusoidally oscillating a NACA 0012 airfoil about its quarter-chord at a reduced frequency of k = 2.05 and an amplitude of +/- 10 deg angle of attack. The target airfoil, a NACA 632A015, was immersed in the wake, two chord lengths downstream of the vortex generator's trailing edge. Phase-averaged velocity measurements of the flow around the target airfoil were made with the airfoil at angles of attack of alpha = 0 deg and alpha = 10 deg. A close encounter with a counterclockwise rotating vortex was observed for both angles of attack, and a head-on collision, which split the counterclockwise rotating vortex in two, was observed for alpha = 10 deg. Vorticity fields were constructed from the velocity measurements and the circulation of

the vortex was evaluated throughout the interaction. The surface pressure fluctuations on the airfoil were determined by substituting the measured velocities into the Navier-Stokes equations and numerically integrating the resulting pressure gradients. Furthermore, an extensive investigation of the undisturbed wake of the oscillating airfoil was performed in order to determine the effect of oscillation frequency and amplitude on the wake development. Dissert. Abstr.

N93-13822 Georgetown Univ., Washington, DC.
ASSESSMENT OF POTENTIAL AERODYNAMIC BENEFITS FROM SPANWISE BLOWING AT THE WING TIP Ph.D. Thesis
Raymond Edward Mineck 1992 359 p
Avail: Univ. Microfilms Order No. DA9222636

A comprehensive set of experimental and analytical investigations have been conducted to assess the potential aerodynamic benefits from spanwise blowing at the tip of a moderate aspect ratio, swept wing. An analytical model has been developed to simulate a jet exhausting from the wing tip. The model demonstrated that vorticity added to the flowfield by the jet near the wing tip tends to diffuse the tip vortex and displace it outwards. The diffused and displaced vortex should induce a smaller downwash at the wing and, consequently, the wind should have increased lift and decreased induced drag. An experimental study of a subsonic jet exhausting from the wing tip was conducted to investigate the effect of spanwise blowing from the tip on the aerodynamic characteristics of a moderate aspect ratio, swept wing. Special attention was given to obtaining accurate balance measurements in the presence of the air supply lines. Wing force and moment data and surface pressure data were measured at Mach numbers up to 0.72. Results indicated that small amounts of blowing from small jets increase the lift curve slope a small amount but have little effect on drag. Larger amounts of blowing from longer jet blowing increase lift near the tip and reduce drag at low Mach numbers. These benefits become smaller and vanish as the Mach number increased to 0.5. A Navier-Stokes solver with modified boundary conditions at the tip was used to extrapolate the results to a Mach number of 0.72. Calculations indicated that lift increases with increasing jet momentum coefficient and that a separate flow region develops near the tip which is consistent with the experimental trend that the drag benefit vanishes. With current technology and conventional wing shapes, spanwise blowing at the tip does not appear to be a practical means of reducing drag moderate aspect ratio wings at high subsonic Mach numbers. Dissert. Abstr.

N93-13917 Tennessee Univ., Knoxville.
DYNAMICS OF VORTEX RINGS IN CROSS-FLOW Ph.D. Thesis
Young Keun Chang 1991 211 p
Avail: Univ. Microfilms Order No. DA9221743

Vortex rings formed in a cross-flow by continuous and/or single pulsations of a jet were studied. The pulsations were provided by the periodic closing and opening of a jet flow and/or by the sudden movement of a circular piston inside a cylinder, respectively. Single pulsations were selected to investigate the effects of different jet exit geometries on the generation, dynamics and penetration of vortex rings: one geometry was a straight walled tube, and the other was a sharp-edged orifice with the same exit diameter. Continuous pulsation was used to study its effects on the development of vortex rings and their penetration in a cross-flow. Pulsation frequency and the ratio of piston velocity to cross-flow velocity were selected as key parameters for each experiment. Detailed measurements were made using flow visualization techniques, including laser induced fluorescence, and hot-film anemometry. Characteristic parameters investigated consisted of the translational velocity, circulation, diameter and core of the ring. To theoretically simulate the dynamics of vortex rings in cross-flow, a numerical simulation for three-dimensional vortex rings was performed based on a Lagrangian, grid-free, three-dimensional vortex method. For continuous pulsations, it was found that, at low frequencies, the fluid in the vortex rings penetrated into the cross-flow to a height much greater than that for high frequency pulsation or for a steady jet injection (up to five times). Dynamically, the downstream segment of the vortex rings moved upward (tilted) by about 3 degrees to 4 degrees under the effect of interaction between the vortex ring and the cross-flow. This type of motion was also qualitatively predicted by the numerical simulation of three-dimensional vortex rings in cross-flows. The detailed velocity field within a vortex ring generated by pulses at 1 Hz was measured using a hot-film probe. From the study of the velocity field along the exit centerlines it was observed that the vortex rings were fully-formed at Z = 3.0 d(sub j). This is in agreement with other experiments in air as well as computational results. Single pulsations showed that the vortex ring penetration height was much greater for a sharp-edged orifice than for a straight walled tube, for the same piston and cross-flow velocities. Hence, it was seen that the jet exit boundary condition is a key parameter which determines the formation process of a vortex ring, its penetration and characteristic parameters mentioned above. Dissert. Abstr.

N93-13929 Notre Dame Univ., IN.
THE UNSTEADY AERODYNAMICS OF A DELTA WING UNDERGOING LARGE-AMPLITUDE PITCHING MOTIONS Ph.D. Thesis
Scott Andrew Thompson 1992 241 p
Avail: Univ. Microfilms Order No. DA9222020

An experimental wind tunnel investigation was performed using a series of 70 deg sweep delta wings. The goal was to examine the relationship between the aerodynamic loads and the vortex flow characteristics of a highly swept wing undergoing both steady and unsteady pitching motions. Extensive testing was conducted consisting primarily of the measurement of surface pressure and vortex breakdown locations as functions of angle of attack. The effects of several parameters were examined, including motion amplitude, pitching frequency, Reynolds number, and leading edge geometry. The data obtained was then correlated to data from the literature on the aerodynamic loads and the surface flow characteristics for similar wings. The effects of wing size and blockage were also examined. The steady and unsteady flow visualization data indicated that the trailing edge of the wing significantly influences the smooth forward or aft motion of breakdown when breakdown is near the trailing edge. The data indicated that this may be caused by the pressure gradient downstream of the wing. The unsteady surface pressure data could be separated into two regimes, dependent on the angle of attack range: a regime where quasisteady behavior occurred, and a regime where significant unsteady effects occurred. The first regime included angle of attack ranges which precluded the occurrence of vortex breakdown, and ranges for which breakdown existed on the wing throughout the motion. The second regime included angle of attack ranges where breakdown moved onto or off of the wing, and ranges which included very high angles of attack involving full scale leeward flow separation. For the second regime, the unsteady effects occurred in the form of a hysteresis in the surface pressures relative to the steady case. Lags in the unsteady breakdown location relative to the steady location were also measured. It appeared that either the onset of breakdown or the reformation of the vortex system (at very high incidences) was responsible for the unsteady effects. The size of the model relative to the wind was seen to affect the magnitude of the surface pressure coefficients. However, the qualitative trends were not changed significantly.
Dissert. Abstr.

N93-13930 McGill Univ., Montreal (Quebec).
OVERALL EFFECTS OF SEPARATION ON THIN AEROFOILS Ph.D. Thesis
Man-Chun Tse 1991 211 p
(ISBN-0-315-67464-4) Avail: Univ. Microfilms Order No. DANN67464

The separation bubble at the leading edge of a thin sharp-edged aerofoil in steady, incompressible and two-dimensional flow was studied. A simple method, using irrotational flow and source singularities, has been developed for predicting bubble reattachment length, drag and lift. For a flat-plate aerofoil, predictions compare favorably with new experiments. The non-dimensional reattachment length x(sub r)/c is proportional to the square of the incidence (alpha) and the slope x(sub r)/c(alpha)(exp 2) depends on the growth of the outer part of the separated shear layer. The value of the term x(sub r)/c(alpha)(exp 2) was determined experimentally as pi/0.08. At incidences above 2 deg, the bubble drag becomes increasingly dominant when compared with the skin friction drag. Although the details of the bubble geometry are not simulated, the lift and stall are predicted fairly well. The theory is extended to a circular-arc aerofoil. This part of the study is much less satisfactory. New experimental measurements do not appear to be sufficiently accurate to provide the empiricism to support the extended theory which must now account for regions of separated flow near the trailing edge. Dissert. Abstr.

N93-13970 Houston Univ., TX.
WAKE CHARACTERIZATION: FULL FLOW SIMULATION OF SPACE STRUCTURES IN LOW EARTH ORBIT Ph.D. Thesis
Charles Richard Justiz 1991 250 p
Avail: Univ. Microfilms Order No. DA9220669

The problem of wake effects, particularly the near wake, from spacecraft in Low Earth Orbit is of increasing interest. The flow simulation reported herein combines the fully coupled effects of neutral particle flow, plasma flow, electromagnetic field effects and spacecraft charging. The simulation necessarily allows for chemically reacting flows (associative ionization, dissociation, and chain exchange). The simulation also allows for thermal accommodation at a spacecraft surface. Due to the highly coupled nature of the flow physics, a full solution simultaneous approach is used. This is required due to the need for extremely high resolution data of the near wake region. In this approach, the neutral flow is modeled using a Direct Simulation Monte Carlo technique. The charged particles are modeled using a particle approach to solve the Poisson equation. A technique of having a separate neutral particle grid and charged particle grid is used. Neutral and charged particles are allowed collisional interaction. During one time step, the neutral-particle-move process is done separately from the charged-particle-move process which is accomplished in the presence of the electromagnetic field. A major advantage of the technique is that results may be obtained with the dominant effects of orbital flows simultaneously modeled. A major disadvantage is that the technique is computationally expensive. Flow calculations for the neutral and charged particle cases are compared to independent computational simulations to confirm the accuracy. The solution procedure and technique are presented for several types of flows with orbital altitudes ranging from 250 km to 500 km. Excellent agreement with previously verified computational algorithms has been obtained for the case of neutral particle flow and charged particle flow. Results for the full flow simulation are presented for 250 km and 500 km. Dissert. Abstr.

N93-14035 Stanford Univ., CA.
NAVIER-STOKES FLOWFIELD COMPUTATION OF WING/ROTOR INTERACTION FOR A TILT ROTOR AIRCRAFT IN HOVER Ph.D. Thesis
Ian George Fejtek 1992 159 p
Avail: Univ. Microfilms Order No. DA9217819

The download on the wing produced by the rotor-induced downwash of a tilt rotor aircraft in hover is of major concern because of its severe impact on payload-carrying capability. A method has been developed to help gain a better understanding of the fundamental fluid dynamics that causes this download, and to help find ways to reduce it. In particular, the method is employed in this work to analyze the effect of a tangential leading edge circulation-control jet on download reduction. Because of the complexities associated with modeling the complete configuration, this work focuses specifically on the wing/rotor interaction of a tilt rotor aircraft in hover. The three-dimensional, unsteady, thin-layer compressible Navier-Stokes equations are solved using a time-accurate, implicit, finite difference scheme that employs LU-ADI factorization. The rotor is modeled as an actuator disk which imparts both a radial and an azimuthal distribution of pressure rise and swirl to the flowfield. A momentum theory/blade element analysis of the rotor is incorporated into the Navier-Stokes solution method. Solution blanking at interior points of the mesh has been shown here to be an effective technique in introducing the effects of the rotor and tangential leading edge jet. Results are presented both for a rotor alone and for wing/rotor interaction. The overall mean characteristics of the rotor flowfield are computed including the flow acceleration through the rotor disk, the axial and swirl velocities in the rotor downwash, and the slipstream contraction. Many of the complex tilt rotor flow features are captured including the highly three-dimensional flow over the wing, the recirculation fountain at the plane of symmetry, wing leading and trailing edge separation, and the large region of separated flow beneath the wing. Mean wing surface pressures compare fairly well with available experimental data, but the time-averaged download/thrust ratio is twenty to thirty percent higher than the measured value. This discrepancy is due to a combination of factors that are discussed. Leading edge tangential blowing is shown to be effective in reducing download. Dissert. Abstr.

N93-13205# National Aerospace Lab., Amsterdam (Netherlands).
AERODYNAMIC ANALYSIS OF SLIPSTREAM/WING/NACELLE INTERFERENCE FOR PRELIMINARY DESIGN OF AIRCRAFT CONFIGURATIONS
C. M. vanBeek, W. J. Piers, and B. Oskam *In* AGARD, Aerodynamic Engine/Airframe Integration for High Performance Aircraft and Missiles Sep. 1992 20 p Sponsored by Netherlands Agency for Aerospace Programs (For primary document see N93-13199 03-34)
Copyright Avail: CASI HC A03/MF A04

N93-13214# Alenia Aeronautica, Torino (Italy). Defence Aircraft Div.
MASS FLOW EFFECTS ON THE LOW SPEED CHARACTERISTICS OF AN ADVANCED COMBAT AIRCRAFT
E. Barbantini, A. Ferretti, and A. Gatti *In* AGARD, Aerodynamic Engine/Airframe Integration for High Performance Aircraft and Missiles Sep. 1992 7 p (For primary document see N93-13199 03-34)
Copyright Avail: CASI HC A02/MF A04

N93-13221# Deutsche Forschungs- und Versuchsanstalt fuer Luft- und Raumfahrt, Goettingen (Germany).
COMPARATIVE PERFORMANCE TESTS OF A PITOT-INLET IN SEVERAL EUROPEAN WIND-TUNNELS AT SUBSONIC AND SUPERSONIC SPEEDS
P.-A. Mackrodt, E. L. Goldsmith (Aircraft Research Association Ltd., Bedford, England), I. McGregor (Royal Aircraft Establishment, Bedford, England), J. Leynaert (Office National d'Etudes et de Recherches Aerospatiales, Paris, France), F. Garcon (Office National d'Etudes et de Recherches Aerospatiales, Modane, France), and J. Brill (Messerschmitt-Boelkow-Blohm G.m.b.H., Munich, Germany) *In* AGARD, Aerodynamic Engine/Airframe Integration for High Performance Aircraft and Missiles Sep. 1992 14 p (For primary document see N93-13199 03-34)
Copyright Avail: CASI HC A03/MF A04

N93-13222# Aerospatiale, Verrieres-L-Buisson (France). Div. Engins Tactiques.
AERODYNAMIC STUDIES OF SUPERSONIC AIR INTAKES [ETUDES AERODYNAMIQUES DE PRISES D'AIR SUPERSONIQUES]
P. Garnero and R. G. Lacau *In* AGARD, Aerodynamic Engine/Airframe Integration for High Performance Aircraft and Missiles Sep. 1992 16 p In FRENCH (For primary document see N93-13199 03-34)
Copyright Avail: CASI HC A03/MF A04

N93-13223# Nangia Associates, Bristol (England).
APPLICATION OF SUBSONIC FIRST-ORDER PANEL METHODS FOR PREDICTION OF INLET AND NOZZLE AERODYNAMIC INTERACTIONS WITH AIRFRAME
R. K. Nangia and M. E. Palmer *In* AGARD, Aerodynamic Engine/Airframe Integration for High Performance Aircraft and Missiles Sep. 1992 16 p (For primary document see N93-13199 03-34)
Copyright Avail: CASI HC A03/MF A04

03 AIR TRANSPORTATION AND SAFETY

Includes passenger and cargo air transport operations; and aircraft accidents.

For related information see also *16 Space Transportation* and *85 Urban Technology and Transportation.*

N93-12816# Aerodyne Research, Inc., Billerica, MA.
ICING PREVENTION BY ULTRASONIC NUCLEATION OF SUPERCOOLED WATER DROPLETS IN FRONT OF SUBSONIC AIRCRAFT
Douglas R. Worsnop, Richard Miake-Lye, and Zeev Hed Oct. 1992 58 p
(Contract DTFA03-91-C-00038)
(DOT/FAA/CT-TN92/38) Avail: CASI HC A04/MF A01

Experiments were performed in the NASA Lewis Research Center (LeRC) Icing Research Tunnel (IRT) to explore the possible application of an icing prevention technique. This technique is based on nucleation ice crystallization in supercooled cloud droplets upstream of the impingement surface and relying on evaporative cooling to remove the latent heat of

fusion from the droplet so that it can completely freeze before striking the solid surface. Ice accretion on the impingement surface was measured to quantify the changes due to induced nucleation. A flow duct was designed to provide a uniform, parallel flow from the nucleation excitation volume to the test surface, a simple symmetric airfoil. The distance between the excitation volume and the airfoil in the flow duct could be varied, but the maximum length of over 2 m was chosen to maximize the time for freezing. Ice accretion was measured over a range of tunnel parameters, including tunnel velocities of 50-100 mph and temperatures from 0 to -36 F. At colder temperatures, spontaneous freezing of supercooled droplets led to reductions in observed ice accretion. However, the range of active nucleation parameters explored in this set of experiments had no measurable effect on ice accretion on the subject airfoil. Suggested future work includes expanding the measurement parameter space and obtaining static measurements in a cloud chamber. Author

N93-13364 Toledo Univ., OH.
SIMULATION OF TWO-DIMENSIONAL ICING, DE-ICING AND ANTI-ICING PHENOMENA Ph.D. Thesis
William Benjamin Wright 1991 134 p
Avail: Univ. Microfilms Order No. DA9216671

An algorithm has been developed to numerically model the concurrent phenomena of two-dimensional transient heat transfer, ice accretion and ice shedding which occur in the operation of an electrothermal pad. The Alternating Direction Implicit method is used to simultaneously solve the heat transfer and accretion equations for a multilayered body covered with ice. In order to model the phase change between ice and water, a technique was used which assumes a phase for each node. This allows the governing equations to be linearized such that a direct solution is possible. This technique requires an iterative procedure to find the correct phase at each node. Numerical solutions illustrating deicer performance for various conditions are presented. Comparisons are made with previous numerical models and with experimental data. The computer program developed to determine this solution has been integrated with the NASA-Lewis flow/trajectory code LEWICE to provide a more complete analysis of de-icing and anti-icing phenomena. Dissert. Abstr.

N93-13426# National Transportation Safety Board, Washington, DC.
AIRCRAFT ACCIDENT REPORT: BRITT AIRWAYS, INC., D/B/A, CONTINENTAL EXPRESS FLIGHT 2574, IN-FLIGHT STRUCTURAL BREAKUP, EMB-120RT, N33701, EAGLE LAKE, TEXAS, SEPTEMBER 11, 1991
21 Jul. 1992 91 p
(PB92-910405; NTSB/AAR-92/04) Avail: CASI HC A05/MF A01

The structural breakup is examined in flight and crash of Continental Express Flight 2574, an Embraer 120, in a cornfield near Eagle Lake, Texas. The safety issues discussed include the feasibility of developing a means to advise flightcrews of recent maintenance work on aircraft and the need for reviewing regulations, policies and practices for establishing required inspection items (RIIs) with a view toward developing more specific identification of RIIs. Safety recommendations concerning these issues were made to the Federal Aviation Administration. GRA

N93-13470# National Transportation Safety Board, Washington, DC.
AIRCRAFT ACCIDENT/INCIDENT SUMMARY REPORT: CONTROLLED FLIGHT INTO TERRAIN, BRUNO'S INC., BEECHJET, N25BR, ROME, GEORGIA, DECEMBER 11, 1991
8 Jul. 1992 34 p
(PB92-910404; NTSB/AAR-92/01/Sum) Avail: CASI HC A03/MF A01

The report explains the crash of N25BR into mountainous terrain near Rome, Georgia. The safety issues discussed include the policies and procedures in corporate flight operations, the role of the first officer in corporate flight operations, and the use of ground proximity warning systems in FAR Part 91 operations of turbojet-powered airplanes. GRA

N93-13787# Transportation Research Board, Washington, DC.
PUBLIC-SECTOR AVIATION ISSUES: GRADUATE RESEARCH AWARD PAPERS, 1990 - 1991
Robert S. Dodd, Michael T. Drollinger, Julie Anne Yates Hegwood, Susan J. Heidner, and Virginia Stouffer 1992 56 p
(PB92-222629; TRB/TRR-1332; LC-92-15610; ISBN-0-309-05171-1) Avail: CASI HC A04/MF A01

Factors Involved in Emergency Medical Service Helicopter Occupant Crash Survival; Land Use Planning Approaches to Mitigating General Aviation Accidents; Trends at United States International Gateway Airports to Europe; Commercial Aviation Safety and Risk. GRA

N93-14024# Massachusetts Inst. of Tech., Lexington.
BIRDS MIMICKING MICROBURSTS ON 2 JUNE 1990 IN ORLANDO, FLORIDA
M. A. Isaminger 10 Jul. 1992 74 p
(Contract DTFA01-89-Z-02033)
(AD-A255703; ATC-184) Avail: CASI HC A04/MF A01

During 1990 and 1991, the Terminal Doppler Weather Radar (TDWR) testbed collected Doppler radar measurements in Orlando, Florida in support of the TDWR Project. The main focus of the project is to develop algorithms that automatically detect wind shears such as microbursts anti gust fronts. While the primary goal of the TDWR is to detect scattering from raindrops, the sensitivity of the system allows for the detection of biological echoes as well. Previous research has shown that under certain conditions the scattering from birds and insects will lead to divergent signatures that mimic microbursts. This type of pattern has been documented in Alabama (Rinehart, 1986), Illinois (Larkin and Quine, 1989), and Missouri (Evans, 1990). In the Alabama and Illinois events, a divergent pattern similar to a microburst was produced when a large number of birds departed in the early morning hours from an overnight roosting site. On 2 June 1990 in Orlando, Florida, there were 11 surface divergent signatures similar to microbursts detected by the TDWR testbed radar. The maximum differential velocity of these events ranged from 11 to 36 m/s, while the maximum reflectivity varied from 0 to 44 dBz. There was light rain in the area and low-reflectivity returns aloft; however, the reflectivity was more like low-reflectivity microbursts in Denver than high-reflectivity microbursts that generally are observed in Orlando. These divergences were not detected by the microburst algorithm since the TDWR site adaptation parameters have been adjusted to avoid issuing alarms for signatures such as those on 2 June. Detailed investigation was conducted of two events to verify that these were not actual microbursts. GRA

N93-14026# Federal Aviation Administration, Oklahoma City, OK. Civil Aeromedical Inst.
POSTMORTEM ALCOHOL PRODUCTION IN FATAL AIRCRAFT ACCIDENTS Final Report
Dennis V. Canfield, Thomas C. Kupiec, and Edwin F. Huffine Jul. 1992 5 p
(AD-A255766; DOT/FAA/AM-92/24) Avail: CASI HC A01/MF A01

During 1989 and 1990, the Civil Aeromedical Institute (CAMI) received specimens from 975 victims of fatal aircraft accidents. The maximum concentration of ethanol allowed Linder FAA regulations (0.04 percent, 40mg/dL) was exceeded in 79 of these cases (8 percent). It was determined based on the distribution of ethanol in urine, vitreous, blood, and tissue that 21 of the positive cases (27 percent) were from postmortem alcohol production. Twenty-two of the positive cases (28 percent) were found to be from the ingestion of ethanol. In 36 cases (45 percent) no determination could be made in regards to the origin of the ethanol. In two cases, postmortem alcohol production exceeded 0.15 percent (150mg/dL). The opinion held by some toxicologists that postmortem alcohol production can be inferred from the presence of acetaldehyde, acetone, butanol, and other volatiles was found to be incorrect. Several cases with postmortem ethanol had no other volatiles. Volatile compounds were found in several cases where no ethanol was present. In addition, a case was found where the relative ethanol concentrations in blood, bile, and vitreous humor were solely consistent with the ingestion of ethanol, but acetaldehyde, acetone, and 2-butanol were also found in blood. This clearly indicates that the presence or absence of other volatiles does not establish postmortem ethanol production. GRA

04 AIRCRAFT COMMUNICATIONS AND NAVIGATION

Includes digital and voice communication with aircraft; air navigation systems (satellite and ground based); and air traffic control.

For related information see also *17 Space Communications, Spacecraft Communications, Command and Tracking* and *Communications and Radar.*

N93-12557# Massachusetts Inst. of Tech., Cambridge. Dept. of Earth, Atmospheric and Planetary Sciences.
GPS MEASUREMENTS AT VANDENBERG AFB Annual Report, 15 Jan. 1991 - 14 Jan. 1992
Robert W. King 14 Jan. 1992 5 p
(Grant AF-AFOSR-0339-90)
(AD-A254978; AFOSR-92-0822TR) Avail: CASI HC A01/MF A01

The objective was to measure directly the tectonic deformation in the Santa Maria Fold and Thrust Belt (SMFTB), northwest of Santa Barbara California. The principal measurement technique was space geodesy, using microwave signals transmitted by Block 2 satellites of the Global Positioning System (GPS), from March to August 1990. Geodetic observations were analyzed to resolve tectonic deformation across the SMFTB. The geodetic network forms a braced quadrilateral with 40 km sides whose southwest corner is the Vandenberg Very Long Baseline Interferometry (VLBI) Station. Three different types of data were combined to estimate two-dimensional station position and strain rate parameters simultaneously. Significant strain rates were discovered using a model which constrains the relative velocity field to be linear in space and constant in time. The maximum compressive strain is oriented N17e+/-5E, and the compressive strain rate in that direction is 0.13 +/- 0.03 strain/yr. Under the assumption that the unresolved rotational component of the velocity field is zero, the integrated rate of deformation across the basin was estimated at 7 +/- 1 mm/yr oriented at N3E +/- 13. This vector can be decomposed into 6 +/- 2 mm/yr of crustal shortening on the general structural trend of N30E and 3 +/- 1 mm/yr of right-lateral shear across the axis. GRA

N93-13348# Army Topographic Engineering Center, Fort Belvoir, VA.
GPS AZIMUTH DETERMINATION
Richard B. Marth 24 Mar. 1992 6 p
(AD-A254687; TEC-R-161) Avail: CASI HC A02/MF A01

The NAVSTAR Global Positioning System (GPS) is a tool which will support military needs for positioning, navigation and precise timing. The U.S. Army Topographic Engineering Center (TEC) is studying tactical applications of GPS to Army system orientation requirements. The work is being sponsored by the Army Space Technology and Research Office (ASTRO). Three brassboard Azimuth Determining System (ADS) were built under contracts to Adroit, Magnovox and Texas Instruments. All three contractors used the principles of microwave interferometry to determine azimuth. The ADS were successfully demonstrated at the U.S. Army Field Artillery School, Fort Sill, OK in Sep 1990. The demonstration proved the concept of using GPS and a short (1 meter) baseline to determine azimuth. The accuracy achieved by the brassboard ADS is 5 - 8 mils (6400 mils = 360 degrees). GRA

N93-13351# Army Topographic Engineering Center, Fort Belvoir, VA.
TOPOGRAPHIC SURVEYOR: TRANSITIONING TO THE 90'S
Richard B. Marth 16 Dec. 1991 7 p
(AD-A254688; TEC-R-156) Avail: CASI HC A02/MF A01

As we transition to the 90s, the tasks of the Army Topographic Surveyor will remain the same--provide control, layout construction, etc. His tools will change. The Automated Integrated Survey Instrument (AISI) will be a total station survey instrument replacing some of the old survey tools. AISI will speed up the tedious task of data logging. Global Positioning System (GPS) will be added to the Army Topographic Surveyors tool box. GPS will not replace existing instruments but will supplement those already used by the surveyor. If not limited by natural surroundings or man-made surroundings's GPS will be used to perform the long legs of control extension. The Army Topographic Battalions have invested their own money in the future by purchasing commercial total stations and GPS receivers. Informal training to support this move in the future has been conducted by USAETL. A training base needs to be established. GRA

N93-13377# Federal Aviation Administration, Atlantic City, NJ.
TERMINAL DOPPLER WEATHER RADAR (TDWR) OPERATIONAL TEST AND EVALUATION (OT/E) INTEGRATION TEST PLAN
Eric Hess and Peter Guthlein Nov. 1992 67 p
(Contract DTFA01-89-C-00002)
(DOT/FAA/CT-TN92/6) Avail: CASI HC A04/MF A01

The Terminal Doppler Weather Radar (TDWR) Operational Test and Evaluation (OT&E) Integration Test Plan provides the overall philosophy and approach to the TDWR OT&E Integration portion of Technical Field Test and Evaluation (TFT&E) to be conducted at the Federal Aviation Administration Aeronautical Center (FAAAC) in Oklahoma City, OK. This plan identifies the necessary support that is required to accomplish OT&E Integration; test roles and responsibilities of personnel requirements, and overall schedule of activities. This plan identifies the National Airspace System (NAS) operational and integration requirements of the TDWR. These requirements are contained in a Test Verification Requirements Traceability Matrix (TVRTM). Author

05 AIRCRAFT DESIGN, TESTING AND PERFORMANCE

Includes aircraft simulation technology.

For related information see also *18 Spacecraft Design, Testing and Performance* and *39 Structural Mechanics.*For land transportation vehicles see *85 Urban Technology and Transportation.*

N93-12602# Search Technology, Inc., Norcross, GA.
SPECIFICATION OF ADAPTIVE AIDING SYSTEMS Final Report
Robert C. Andes and William B. Rouse 1 Mar. 1992 32 p
(Contract F33615-88-C-3612)
(AD-A254537; NAWCADWAR-92034-60) Avail: CASI HC A03/MF A01

Designers' decision making in specifying adaptive aiding systems is considered. A study of design decision in specifying aiding for a fighter aircraft mission scenario is discussed. Results indicate a high degree of consistency on the part of individual designers. However, there was substantial variations among designers in terms of both decisions made and information used to make the decisions. The implications of these results for development of design tools, as well as the type of research studies whose results would be valued by designers, are considered. GRA

N93-12605# Air Force Environmental Technical Applications Center, Scott AFB, IL.
SAC CONTRAIL FORMATION STUDY
Brian M. Bjornson May 1992 55 p
(AD-A254410; USAFETAC/PR-92/003) Avail: CASI HC A04/MF A01

This report documents the results of a study that compares the Appleman contrail forecasting method used at the Air Force Global Weather Central (AFGWC) with the SAC method using pilot report (PIREP) data collected by SAC/DOW between March 1990 and July 1991. The study resulted in development of two other contrail forecasting techniques. The first (ETACFCST) was developed using discriminant analysis schemes to obtain best fit curves of contrail formation as a function of altitude and temperature, or altitude, temperature, and vertical motion. Statistics showed ETACFCST to be better than either the Appleman or SAC contrail prediction curves. But another technique developed near the end of the study incorporated aircraft engine type as a factor for the first time. The new engine-specific contrail forecasting technique is recommended as a replacement for the Appleman method used at AFGWC. GRA

N93-12613# Catholic Univ. of America, Washington, DC. Cognitive Science Lab.
THEORY AND DESIGN OF ADAPTIVE AUTOMATION IN AVIATION SYSTEMS Progress Report
Raja Parasuraman, Toufik Bahri, John E. Deaton, Jeffrey G. Morrison, and Michael Barnes 17 Jul. 1992 48 p
(Contract N62269-90-0022-5931)
(AD-A254595; NAWCADWAR-92033-60) Avail: CASI HC A03/MF A01

Recent technological advances have made viable the implementation of intelligent automation in advanced tactical aircraft. The use of this

technology has given rise to new human factors issues and concerns. Errors in highly automated aircraft have been linked to the adverse effects of automation on the pilot's system awareness, monitoring workload, and ability to revert to manual control. However adaptive automation, or automation that is implemented dynamically in response to changing task demands on the pilot, has been proposed to be superior to systems with fixed, or static automation. This report examines several issues concerning the theory and design of adaptive automation in aviation systems, particularly as applied to advanced tactical aircraft. An analysis of the relative costs and benefits of conventional (static) aviation automation provides the starting point for the development of a theory of adaptive automation. This analysis includes a review of the empirical studies investigating effects of automation on pilot performance. The main concepts of adaptive automation are then introduced, and four major methods for implementing adaptive automation in the advanced cockpit are described and discussed. GRA

N93-12752# Wright Lab., Wright-Patterson AFB, OH.
X-29 LINEAR AERODYNAMIC PERTURBATION MODEL
Thomas A. Gentry Jul. 1992 152 p
(AD-A254810; WL-TM-92-338-FIGC) Avail: CASI HC A08/MF A02

This memo documents the linear aerodynamic and thrust perturbation model of the X-29 simulation model resident in the Control Integration and Assessment Branch of Wright Laboratory (WL/FIGD) at Wright-Patterson Air Force Base, Ohio. This model was used to perform flying qualities evaluations of the X-29 aircraft at Wright Laboratory during the airplane's development in the early to mid-1980s. This work was conducted in order to document the X-29 longitudinal and lateral-directional linear aero model at numerous trim flight conditions for use in future research work in flying qualities. The X-29 is representative of typical fighter aircraft, even with its forward-swept wing, although the airframe is very unstable longitudinally. This memo is divided into four sections: Introduction, Definition of Terms, Explanation of Computer Printouts, and Computer Printouts sections. Definitions of all terms associated with the linear model are given in the Definition of Terms section. Explanation of all of the data in the computer printouts is given in the Explanation of Computer Printouts section. The Computer Printouts section contains the actual computer printouts for each trim flight condition. GRA

N93-13140 Michigan Univ., Ann Arbor.
MINIMUM-TIME FLIGHT PATHS OF SUPERSONIC AIRCRAFT Ph.D. Thesis
Donglong Sheu 1992 169 p
Avail: Univ. Microfilms Order No. DA9227000

In this dissertation, the methods of analysis for the minimum-time flight of supersonic aircraft are presented. There are at least two substantial contributions in this study. First, a method called 'increment algorithm' is exploited. Second, the conditions for a reduced-space subarc are explicitly derived. With the first development, the starting procedure for the second-order gradient method becomes easy. This method needs to satisfy three conditions: the convexity condition, the normality condition, and the no-conjugate-point condition. In addition, the concept of this development is very helpful in dealing with a problem which involves many parameters. With the second development, a theoretical basis is provided for artificially imposing a reduced-space subarc in the analysis when a sensitivity problem is encountered. With both significant developments, the computational technique is successfully applied to solve problems of minimum-time maneuvers of supersonic aircraft in both two-dimensional and three-dimensional formulations. The various problems differ in the final conditions imposed. From the analysis in each problem, the optimal aerodynamic and thrust controls are obtained and the piloting technique to achieve the minimum time is explained. Dissert. Abstr.

N93-13253# General Accounting Office, Washington, DC.
NATIONAL AERO-SPACE PLANE: KEY ISSUES FACING THE PROGRAM. TESTIMONY BEFORE THE SUBCOMMITTEE ON TECHNOLOGY AND COMPETITIVENESS, COMMITTEE ON SCIENCE, SPACE, AND TECHNOLOGY, HOUSE OF REPRESENTATIVES
31 Mar. 1992 17 p
(GAO/T-NSIAD-92-26) Avail: CASI HC A03/MF A01; GAO, PO Box 6015, Gaithersburg, MD 20877 HC

Since its inception in December 1985, the NASP (National Aero-Space Plane) Program has undergone significant evolutionary changes. Its cost estimates have increased dramatically and some key schedule milestones may be delayed up to 11 years. While the program has achieved technical progress, it has also encountered problems with its weight and propulsion system. These problems, in conjunction with budget constraints and increasing costs, have resulted in various options being explored to reduce program costs and technical risks. As a part of this assessment, the primary goal of the program--to conduct single-stage-to-orbit flight testing of the X-30--is being reconsidered. Even without additional technical problems, potential cost increases and budget constraints are likely to be significant contributors to future schedule delays in the NASP Program. Furthermore, determining how much funding is needed and when, focusing development activities on needed technologies, and developing achievable long-range plans are complicated by the lack of a determination of whether the X-30 will conduct single-stage-to-orbit flight testing. For these reasons, we believe that a timely decision on this issue is critical. The Joint Program Office's recent proposal to concentrate on the X-30's propulsion system in the near term and defer a decision to build the X-30 until 1996 would likely reduce the program's near-term technical risk. Nevertheless, testing of several critical components and an analysis of the test results are not expected to occur until after the scheduled Phase 3 go-ahead decision in September 1993. Author

N93-13256 Aeronautical Research Labs., Melbourne (Australia). Dept. of Defence.
STRUCTURAL FATIGUE ASPECTS OF THE P-3 ORION
J. M. Grandage May 1992 28 p
(ARL-STRUC-TM-558; AR-007-068) Copyright Avail: Issuing Activity

Material relevant to continuing Aeronautical Research Laboratory/Headquarter Logistics Command (ARL/HQLC) work on structural fatigue of the Royal Australian Air Force (RAAF) P-3 fleet is presented. In 1991 the RAAF developed a proposal to refurbish the avionics of the P-3 fleet and to extend its life to year 2015. As part of the project definition study for the refurbishment, ARL/HQLC investigated the fatigue implications of the proposal. This investigation produced a project report which drew conclusions on cost and operational implications arising from fatigue considerations and recommended a structural fatigue work program aimed at justifying the life extension on airworthiness grounds. The investigation has generated extensive information on the P-3 fatigue status, and this information is presented here. The discussion focusses mainly on the Lockheed service life evaluation program (SLEP) and the US Navy service life assessment program (SLAP). Author

N93-13305*# Iowa State Univ. of Science and Technology, Ames. Dept. of Aerospace Engineering and Engineering Mechanics.
AN INVERSE DYNAMICS APPROACH TO TRAJECTORY OPTIMIZATION FOR AN AEROSPACE PLANE
Ping Lu 1992 25 p
(Grant NAG1-1255)
(NASA-CR-191277; NAS 1.26:191277) Avail: CASI HC A03/MF A01

An inverse dynamics approach for trajectory optimization is proposed. This technique can be useful in many difficult trajectory optimization and control problems. The application of the approach is exemplified by ascent trajectory optimization for an aerospace plane. Both minimum-fuel and minimax types of performance indices are considered. When rocket augmentation is available for ascent, it is shown that accurate orbital insertion can be achieved through the inverse control of the rocket in the presence of disturbances. Author

N93-13565*# National Aeronautics and Space Administration. Langley Research Center, Hampton, VA.
MULTIPLE-FUNCTION MULTI-INPUT/MULTI-OUTPUT DIGITAL CONTROL AND ON-LINE ANALYSIS
Sherwood T. Hoadley, Carol D. Wieseman, and Sandra M. McGraw (Lockheed Engineering and Sciences Co., Hampton, VA.) Oct. 1992 16 p Presented at the DSP(sup x) Exposition and Symposium, San Jose, CA, 14-16 Oct. 1992
(RTOP 505-63-50-15)
(NASA-TM-107697; NAS 1.15:107697) Avail: CASI HC A03/MF A01

The design and capabilities of two digital controller systems for aeroelastic wind-tunnel models are described. The first allowed control of flutter while performing roll maneuvers with wing load control as well as coordinating the acquisition, storage, and transfer of data for on-line analysis. This

system, which employs several digital signal multi-processor (DSP) boards programmed in high-level software languages, is housed in a SUN Workstation environment. A second DCS provides a measure of wind-tunnel safety by functioning as a trip system during testing in the case of high model dynamic response or in case the first DCS fails. The second DCS uses National Instruments LabVIEW Software and Hardware within a Macintosh environment. Author

N93-13807 Missouri Univ., Rolla.
AN INVESTIGATION OF THE DYNAMIC RESPONSE OF LIFTING SURFACES WITH CONCENTRATED STRUCTURAL NONLINEARITIES Ph.D. Thesis
Iyad Khalil Qumei 1992 244 p
Avail: Univ. Microfilms Order No. DA9224680

The dynamic response of rigid and flexible lifting surfaces with elastic root restraint is studied both experimentally and analytically. Testing is performed on two straight wings with symmetrical cross sections elastically supported at the root with a rigid structure. The root support motion is constrained by two springs which involve an adjustable freeplay mechanism. The active degrees of freedom considered are the rigid body plunge and pitch and the flexural motion of the lifting surface relative to the root support. Testing is carried out at relatively low speeds in a subsonic wind tunnel. The analytical model is developed using the finite element method for the structural part, and recently-developed transient unsteady aerodynamics to represent the air force in the time domain, instead of the usual representation in the frequency domain. The dynamic responses of the linear and nonlinear system configurations are obtained by directly integrating the equations of motion. Predicting the response of the lifting surface close to the nonlinear flutter speed from a linearized form of the equations of motion which utilizes the harmonic balance method proved to be possible and effective. But modeling the system without resorting to approximate forms for the freeplay nonlinearity has the advantage of predicting all possible responses the nonlinear system may experience at all airspeeds within the sustained oscillation region, such as nonperiodic. A satisfactory correlation between experimentally and analytically-obtained responses on both a qualitative and a quantitative basis has been achieved. Dissert. Abstr.

N93-13815 Texas Univ., Arlington.
OPTIMUM DESIGN OF AIRCRAFT STRUCTURES WITH MANUFACTURING AND BUCKLING CONSTRAINTS Ph.D. Thesis
Daniel Patrick Costin 1991 172 p
Avail: Univ. Microfilms Order No. DA9217626

Aircraft design incorporates a large number of structural and aerodynamic disciplines. Each discipline must be considered in order to obtain a feasible and optimum design. All too often, however, some constraints are left out of the optimization problem, leading to an 'optimum' design that is not feasible. In practical terms the design looks good on paper, but does not perform well when tested, or can not be built as designed. The constraints developed in this dissertation are two that are commonly left out of aircraft design optimization problems. The first group of constraints ensures that the structure will be manufacturable. The constraints are especially useful for composite wing skins, because the flexibility allowed in the optimization of composites will often lead to unorthodox laminates. Composite laminates designed with optimization programs often have large variations in both the ply orientation percentage and the total laminate thickness across the plane of the laminate. Also, the ply orientation percentage is often outside the range that is recommended. The second constraint type is a panel buckling constraint. The loads from the finite element model are used in a closed-form buckling solution. The constraint prevents the wing skin from local buckling in the unsupported regions bounded by the ribs and spars. These constraints were used in a number of design studies that evaluated the relative impact of the constraints of the design weight. Also, a design and manufacturing case study was done. In this study an optimum design obtained by using the manufacturing constraints of this dissertation was compared with a conventional design of the same structure. The two designs were built and tested to determine the accuracy of the design and modelling techniques. Dissert. Abstr.

N93-13821 Maryland Univ., College Park.
FORMULATION AND VALIDATION OF HIGH-ORDER MATHEMATICAL MODELS OF HELICOPTER FLIGHT DYNAMICS Ph.D. Thesis
Frederick Dong Kim 1991 304 p
Avail: Univ. Microfilms Order No. DA9222710

A high-order mathematical model of a helicopter that models the complete dynamics of the aircraft, including the rotor, inflow, and propulsion dynamics is descibed. The model is formulated so that time invariant linear models can be extracted rigorously to include the high-order dynamics of the aircraft in addition to the dynamics associated with the six fuselage degrees of freedom. Such models are essential to examine compliance with new handling qualities specifications, and to design advanced flight control systems capable of high-bandwidth and low cross couplings. A trim procedure is developed to provide an equilibrium position about which the nonlinear model can be linearized. The procedure is capable of providing the steady state periodic response of the rotor blades and the equilibrium states of the propulsion system, in addition to the trim states of the fuselage for both straight and level, and turning flight. A refinement technique that gives the correct periodicity of all the states is also described. The mathematical model is validated by comparing model responses against flight test data measured on an articulated rotor helicopter. Static trim cases compared include pilot controls, fuselage attitudes, and power required curves against flight test data for hover and up to a forward speed of 170 knots. The frequency domain validation for the bare-airframe configuration is conducted for both hover and forward speeds of 80 knots and 120 knots. The accuracy in modeling the cross coupling are examined by validating both the on-axis and off-axis frequency response to control inputs in hover. The importance of high-order dynamics on the dynamic response of the aircraft is examined by comparing frequency responses of reduced order models against the full-order model. Reduced order models with the main rotor lag, the propulsion system, and inflow degrees of freedom removal are examined. The dynamic response of a helicopter in a maneuvering flight condition, deemed important for modern military applications, is studied by comparing poles and frequency responses from a helicopter in a 2-g turn against those from a helicopter in straight and steady level flight. Dissert. Abstr.

N93-13914 Florida Atlantic Univ., Boca Raton.
TRIM ANALYSIS BY SHOOTING AND FINITE ELEMENTS AND FLOQUET EIGENANALYSIS BY QR AND SUBSPACE ITERATIONS IN HELICOPTER DYNAMICS Ph.D. Thesis
Nagari Shriranga Achar 1992 161 p
Avail: Univ. Microfilms Order No. DA9220990

The trim analysis for the initial state and control inputs that satisfy response periodicity and flight conditions, and the Floquet eigenanalysis for a few largest eigenvalues of the Floquet transition matrix (FTM) are investigated. In the trim analysis, the convergence of Newton iteration is investigated in computing the periodic initial state and control inputs sequentially and in parallel. The trim analysis uses the shooting method and two h-versions of temporal finite element methods, one based on displacement formulation and the other on mixes formulation of displacements and momenta. In each method, both the sequential and in-parallel schemes are used, and the resulting nonlinear equations are solved by damped Newton iteration with an optimally selected damping parameter. The reliability of damped Newton iteration, including earlier-observed divergence problems, is quantified by the maximum condition number of the Jacobian matrices of the iterative scheme. For illustrative purposes, rigid flap-lag and flap-lag-torsion models based on quasisteady aerodynamics are selected. Demanding trim analysis conditions are included by considering advance ratios or dimensionless flight speeds twice as high as those of current helicopters. Concerning the Floquet eigenanalysis, the feasibility of using the Arnoldi-Saad method, one of the emerging subspace iteration methods, is explored as an alternative to the currently used QR method, which is not economical for partial eigenanalysis. The reliability of the Arnoldi-Saad method is quantified by the eigenvalue condition numbers and the residual errors of the eigenpairs. In the three trim analysis methods, while the optimally selected damping parameter provides almost global convergence, the in-parallel scheme requires much less machine time than the conventional sequential scheme; both schemes have comparable reliability of the Newton iteration without and with damping. The Arnoldi-Saad method takes much less machine time than the QR method with comparable reliability. Dissert. Abstr.

N93-13207# Deutsche Airbus G.m.b.H., Bremen (Germany).
RECENT DEVELOPMENTS IN LOW-SPEED TPS-TESTING FOR ENGINE INTEGRATION DRAG AND INSTALLED THRUST REVERSR SIMULATION
W. Burgsmueller, C. Castan (Aerospatiale, Toulouse, France), J. W. Kooi (Duits-Nederlandse Windtunnel, North East Polder.), and J. P. Becle (Office National d'Etudes et de Recherches Aerospatiales, Paris, France) *In* AGARD, Aerodynamic Engine/Airframe Integration for High Performance Aircraft and Missiles Sep. 1992 15 p (For primary document see N93-13199 03-34)
Copyright Avail: CASI HC A03/MF A04

N93-13208# Fokker B.V., Schipol-Oost (Netherlands). Aerodynamics and Aeroelasticity Dept.
AERODYNAMIC INTEGRATION OF THRUST REVERSERS ON THE FOKKER 100
J. vanHengst *In* AGARD, Aerodynamic Engine/Airframe Integration for High Performance Aircraft and Missiles Sep. 1992 9 p (For primary document see N93-13199 03-34)
Copyright Avail: CASI HC A02/MF A04

N93-13212# Societe Nationale d'Etudes et de Construction de Moteurs Aeronautiques, Moissy-Cramayel (France).
FLIGHT ANALYSIS OF AIR INTAKE/ENGINE COMPATIBILITY [ANALYSE EN VOL DE LA COMPATIBILITE ENTREE D'AIR-MOTEUR]
H. Joubert and J. L. Eyraud *In* AGARD, Aerodynamic Engine/Airframe Integration for High Performance Aircraft and Missiles Sep. 1992 12 p In FRENCH (For primary document see N93-13199 03-34)
Copyright Avail: CASI HC A03/MF A04

N93-13219# Aircraft Research Association Ltd., Bedford (England).
SOME ASPECTS OF INTAKE DESIGN, PERFORMANCE AND INTEGRATION WITH THE AIRFRAME
E. L. Goldsmith *In* AGARD, Aerodynamic Engine/Airframe Integration for High Performance Aircraft and Missiles Sep. 1992 19 p (For primary document see N93-13199 03-34)
Copyright Avail: CASI HC A03/MF A04

N93-13224# Wright Lab., Wright-Patterson AFB, OH.
SURVEY ON TECHNIQUES USED IN AERODYNAMIC NOZZLE/AIRFRAME INTEGRATION
Douglas L. Bowers and James A. Laughrey *In* AGARD, Aerodynamic Engine/Airframe Integration for High Performance Aircraft and Missiles Sep. 1992 11 p (For primary document see N93-13199 03-34)
Copyright Avail: CASI HC A03/MF A04

N93-13228# Wright Lab., Wright-Patterson AFB, OH.
PROPULSION INTEGRATION RESULTS OF THE STOL AND MANEUVER TECHNOLOGY DEMONSTRATOR
J. A. Laughrey and D. J. Moorhouse *In* AGARD, Aerodynamic Engine/Airframe Integration for High Performance Aircraft and Missiles Sep. 1992 12 p (For primary document see N93-13199 03-34)
Copyright Avail: CASI HC A03/MF A04

06 AIRCRAFT INSTRUMENTATION

Includes cockpit and cabin display devices; and flight instruments.

For related information see also *19 Spacecraft Instrumentation* and *35 Instrumentation and Photography*.

No abstracts in this category.

07 AIRCRAFT PROPULSION AND POWER

Includes prime propulsion systems and systems components, e.g., gas turbine engines and compressors; and onboard auxilliary power plants for aircraft.

For related information see also *20 Spacecraft Propulsion and Power*, *28 Propellants and Fuels*, and *44 Energy Production and Conversion*.

N93-12695*# General Motors Corp., Indianapolis, IN. Gas Turbine Div.
INVESTIGATION OF ADVANCED COUNTERROTATION BLADE CONFIGURATION CONCEPTS FOR HIGH SPEED TURBOPROP SYSTEMS. TASK 4: ADVANCED FAN SECTION AERODYNAMIC ANALYSIS Final Report, Jul. 1991 - Jul. 1992
Andrew J. Crook and Robert A. Delaney Nov. 1992 74 p Original contains color illustrations
(Contract NAS3-25270; RTOP 535-03-10)
(NASA-CR-187128; NAS 1.26:187128) Avail: CASI HC A04/MF A01; 3 functional color pages

The purpose of this study is the development of a three-dimensional Euler/Navier-Stokes flow analysis for fan section/engine geometries containing multiple blade rows and multiple spanwise flow splitters. An existing procedure developed by Dr. J. J. Adamczyk and associates and the NASA Lewis Research Center was modified to accept multiple spanwise splitter geometries and simulate engine core conditions. The procedure was also modified to allow coarse parallelization of the solution algorithm. This document is a final report outlining the development and techniques used in the procedure. The numerical solution is based upon a finite volume technique with a four stage Runge-Kutta time marching procedure. Numerical dissipation is used to gain solution stability but is reduced in viscous dominated flow regions. Local time stepping and implicit residual smoothing are used to increase the rate of convergence. Multiple blade row solutions are based upon the average-passage system of equations. The numerical solutions are performed on an H-type grid system, with meshes being generated by the system (TIGG3D) developed earlier under this contract. The grid generation scheme meets the average-passage requirement of maintaining a common axisymmetric mesh for each blade row grid. The analysis was run on several geometry configurations ranging from one to five blade rows and from one to four radial flow splitters. Pure internal flow solutions were obtained as well as solutions with flow about the cowl/nacelle and various engine core flow conditions. The efficiency of the solution procedure was shown to be the same as the original analysis. Author

N93-13155*# National Aeronautics and Space Administration. Hugh L. Dryden Flight Research Facility, Edwards, CA.
SUBSONIC FLIGHT TEST EVALUATION OF A PROPULSION SYSTEM PARAMETER ESTIMATION PROCESS FOR THE F100 ENGINE
John S. Orme and Glenn B. Gilyard Nov. 1992 27 p Presented at the 28th AIAA/SAE/ASME/ASEE Joint Propulsion Conference, Nashville, TN, 6-8 Jul. 1992
(RTOP 533-02-36)
(NASA-TM-4426; H-1809; NAS 1.15:4426; AIAA Paper 92-3745)
Copyright Avail: CASI HC A03/MF A01

Integrated engine-airframe optimal control technology may significantly improve aircraft performance. This technology requires a reliable and accurate parameter estimator to predict unmeasured variables. To develop this technology base, NASA Dryden Flight Research Facility (Edwards, CA), McDonnell Aircraft Company (St. Louis, MO), and Pratt & Whitney (West Palm Beach, FL) have developed and flight-tested an adaptive performance seeking control system which optimizes the quasi-steady-state performance of the F-15 propulsion system. This paper presents flight and ground test evaluations of the propulsion system parameter estimation process used by the performance seeking control system. The estimator consists of a compact propulsion system model and an extended Kalman filter. The extended Laman filter estimates five engine component deviation parameters from measured inputs. The compact model uses measurements and Kalman-filter estimates as inputs to predict unmeasured propulsion parameters such as net propulsive force and fan stall margin. The ability to track trends and estimate absolute values of propulsion system parameters was demonstrated. For example, thrust stand results show a good correlation,

especially in trends, between the performance seeking control estimated and measured thrust. Author

N93-13697*# Illinois Univ., Urbana. Coordinated Science Lab.
SUMMARY: EXPERIMENTAL VALIDATION OF REAL-TIME FAULT-TOLERANT SYSTEMS Final Report
R. K. Iyer and G. S. Choi Oct. 1992 5 p
(Grant NAG1-602)
(NASA-CR-190985; NAS 1.26:190985) Avail: CASI HC A01/MF A01

Testing and validation of real-time systems is always difficult to perform since neither the error generation process nor the fault propagation problem is easy to comprehend. There is no better substitute to results based on actual measurements and experimentation. Such results are essential for developing a rational basis for evaluation and validation of real-time systems. However, with physical experimentation, controllability and observability are limited to external instrumentation that can be hooked-up to the system under test. And this process is quite a difficult, if not impossible, task for a complex system. Also, to set up such experiments for measurements, physical hardware must exist. On the other hand, a simulation approach allows flexibility that is unequaled by any other existing method for system evaluation. A simulation methodology for system evaluation was successfully developed and implemented and the environment was demonstrated using existing real-time avionic systems. The research was oriented toward evaluating the impact of permanent and transient faults in aircraft control computers. Results were obtained for the Bendix BDX 930 system and Hamilton Standard EEC131 jet engine controller. The studies showed that simulated fault injection is valuable, in the design stage, to evaluate the susceptibility of computing sytems to different types of failures. L.R.R.

N93-13218# Deutsche Forschungsanstalt fuer Luft- und Raumfahrt, Brunswick (Germany). Inst. fuer Entwurfsaerodynamik.
THE JET BEHAVIOUR OF AN ACTUAL HIGH-BYPASS ENGINE AS DETERMINED BY LDA-MEASUREMENTS IN GROUND TESTS
H. Hoheisel, K. A. Buetefisch (Deutsche Forschungs- und Versuchsanstalt fuer Luft- und Raumfahrt, Goettingen, Germany), B. Lehmann (Deutsche Forschungs- und Versuchsanstalt fuer Luft- und Raumfahrt, Berlin, Germany), R. Henke (Deutsche Airbus G.m.b.H., Bremen, Germany), H. J. Roscher, and U. Seelhorst (Deutsche Forschungs- und Versuchsanstalt fuer Luft- und Raumfahrt, Goettingen, Germany) *In* AGARD, Aerodynamic Engine/Airframe Integration for High Performance Aircraft and Missiles Sep. 1992 14 p (For primary document see N93-13199 03-34)
Copyright Avail: CASI HC A03/MF A04

N93-13229# Wright Lab., Wright-Patterson AFB, OH.
HYPERSONIC PROPULSION SYSTEM FORCE ACCOUNTING
K. Numbers *In* AGARD, Aerodynamic Engine/Airframe Integration for High Performance Aircraft and Missiles Sep. 1992 p 15 (For primary document see N93-13199 03-34)
Copyright Avail: CASI HC A03/MF A04

N93-13230# Messerschmitt-Boelkow-Blohm G.m.b.H., Munich (Germany).
INTEGRATION OF TURBO-RAMJET ENGINES FOR HYPERSONIC AIRCRAFT
O. Herrmann *In* AGARD, Aerodynamic Engine/Airframe Integration for High Performance Aircraft and Missiles Sep. 1992 7 p (For primary document see N93-13199 03-34)
Copyright Avail: CASI HC A02/MF A04

08 AIRCRAFT STABILITY AND CONTROL

Includes aircraft handling qualities; piloting; flight controls; and autopilots.

For related information see also *05 Aircraft Design, Testing and Performance.*

N93-12578# Catholic Univ. of America, Washington, DC. Cognitive Science Lab.
ADAPTIVE AUTOMATION AND HUMAN PERFORMANCE: MULTI-TASK PERFORMANCE CHARACTERISTICS Final Report
Raja Parasuraman, Toufik Bahri, and Robert Molloy Mar. 1992 40 p
(AD-A254596; CSL-N91-1; NAWCADWAR-92035-60) Avail: CASI HC A03/MF A01

The present investigation had three major objectives: (1) develop software that provides a robust and sensitive set of flight-relevant tasks; (2) provide operator performance data for each flight task under normal (manual), single-task conditions; and (3) evaluate the sensitivity of operator performance on each task to changes in task difficulty and in the number and type of concurrent tasks performed. The overall goal was to provide an empirical 'baseline' from which the results of future adaptive-automation studies (in which task difficulty and operator workload would vary) could be successfully interpreted. Overall, the three studies were successful in meeting the first major goal of the adaptive automation research program: to establish a baseline of empirical performance data in a multi-task flight-simulation environment. These results will help in the design and interpretation of results of future adaptive-automation studies that will be carried out as part of this research program. GRA

N93-12815*# National Aeronautics and Space Administration. Ames Research Center, Moffett Field, CA.
EQUATIONS OF MOTION OF SLUNG-LOAD SYSTEMS, INCLUDING MULTILIFT SYSTEMS
Luigi S. Cicolani and Gerd Kanning Nov. 1992 126 p
(RTOP 505-66-01)
(NASA-TP-3280; A-91099; NAS 1.60:3280) Avail: CASI HC A07/MF A02

General simulation equations are derived for the rigid body motion of slung-load systems. This work is motivated by an interest in trajectory control for slung loads carried by two or more helicopters. An approximation of these systems consists of several rigid bodies connected by straight-line cables or links. The suspension can be assumed elastic or inelastic. Equations for the general system are obtained from the Newton-Euler rigid-body equations with the introduction of generalized velocity coordinates. Three forms are obtained: two generalize previous case-specific results for single-helicopter systems with elastic and inelastic suspensions, respectively; and the third is a new formulation for inelastic suspensions. The latter is derived from the elastic suspension equations by choosing the generalized coordinates so that motion induced by cable stretching is separated from motion with invariant cable lengths, and by then nulling the stretching coordinates to get a relation for the suspension forces. The result is computationally more efficient than the conventional formulation, is readily integrated with the elastic suspension formulation, and is easily applied to the complex dual-lift and multilift systems. Results are given for two-helicopter systems; three configurations are included and these can be integrated in a single simulation. Equations are also given for some single-helicopter systems, for comparison with the previous literature, and for a multilift system. Equations for degenerate-body approximations (point masses, rigid rods) are also formulated and results are given for dual-lift and multilift systems. Finally, linearlized equations of motion are given for general slung-load systems are presented along with results for the two-helicopter system with a spreader bar. Author

N93-12903*# West Virginia Univ., Morgantown. Dept. of Mechanical and Aerospace Engineering.
DETERMINATION OF THE STABILITY AND CONTROL DERIVATIVES OF THE F/A-18 HARV FROM FLIGHT DATA USING THE MAXIMUM LIKELIHOOD METHOD Semianr.ual Status Report, May - Nov. 1992
Marcello R. Napolitano and Joelle M. Spagnuolo 12 Nov. 1992 12 p
(Contract NCC2-759)
(NASA-CR-191216; NAS 1.26:191216) Avail: CASI HC A03/MF A01

The research being conducted pertains to the determination of the stability and control derivatives of the F/A-18 High Alpha Research Vehicle (HARV) from flight data using the Maximum Likelihood Method. The document outlines the approach used in the parameter estimation (PID) process and briefly describes the mathematical modeling of the F/A-18 HARV and the maneuvers designed to generate a sufficient data base for the PID research. Author

N93-12959# Massachusetts Inst. of Tech., Cambridge. Lab. for Advanced Composites.
NONLINEAR STALL FLUTTER OF WINGS WITH BENDING-TORSION COUPLING Final Technical Report, 1 Feb. - 31 Oct. 1991
Peter E. Dunn and John Dugundji 31 Dec. 1991 277 p

(Grant AF-AFOSR-0159-91)
(AD-A254323; TELAC-91-16A; AFOSR-92-0783TR) Avail: CASI HC A13/MF A03

The nonlinear, stalled, aeroelastic behavior of rectangular, graphite/epoxy, cantilevered plates with varying amounts of bending-torsion stiffness coupling and with NACA 0012 Styrofoam airfoil shapes is investigated for low Reynolds number flow (less than 200,000). A general Rayleigh-Ritz formulation is used to calculate point load static deflections, and nonlinear static vibration frequencies and mode shapes for varying tip deflections. Nonlinear lift and moment aerodynamics are used in the context of the Rayleigh-Ritz formulation to calculate static airload deflections. The nonlinear, stalled ONERA model using non-constant coefficients - initially developed by Tran and Petot - is reformulated into a harmonic balance form and compared against a time-marching Runge-Kutta scheme. Low angle-of-attack, linear flutter calculations are done by applying Fourier analysis to extract the harmonic balance method and a Newton-Raphson solver to the resulting nonlinear. GRA

N93-13068*# National Aeronautics and Space Administration. Langley Research Center, Hampton, VA.
HYPERSONIC VEHICLE CONTROL LAW DEVELOPMENT USING H INFINITY AND MU-SYNTHESIS
Irene M. Gregory, Rajiv S. Chowdhry (Lockheed Engineering and Sciences Co., Hampton, VA.), John D. McMinn, and John D. Shaughnessy Oct. 1992 13 p Presented at the AIAA Fourth International Aerospace Planes Conference, Orlando, FL, 1-4 Dec. 1992
(RTOP 505-64-40-01)
(NASA-TM-107689; NAS 1.15:107689) Avail: CASI HC A03/MF A01

Applicability and effectiveness of robust control techniques to a single-stage-to-orbit (SSTO) airbreathing hypersonic vehicle on an ascent accelerating path and their effectiveness are explored in this paper. An SSTO control system design problem, requiring high accuracy tracking of velocity and altitude commands while limiting angle of attack oscillations, minimizing control power usage and stabilizing the vehicle all in the presence of atmospheric turbulence and uncertainty in the system, was formulated to compare results of the control designs using H infinity and mu-synthesis procedures. The math model, an integrated flight/propulsion dynamic model of a conical accelerator class vehicle, was linearized as the vehicle accelerated through Mach 8. Controller analysis was conducted using the singular value technique and the mu-analysis approach. Analysis results were obtained in both the frequency and the time domains. The results clearly demonstrate the inherent advantages of the structured singular value framework for this class of problems. Since payload performance margins are so critical for the SSTO mission, it is crucial that adequate stability margins be provided without sacrificing any payload mass. Author

N93-13367*# National Aeronautics and Space Administration. Langley Research Center, Hampton, VA.
ACTIVE FLUTTER SUPPRESSION USING DIPOLE FILTERS
S. Srinathkumar (National Aeronautical Lab., Bangalore, India) and Martin R. Waszak Sep. 1992 40 p
(RTOP 505-64-52-03)
(NASA-TM-107594; NAS 1.15:107594) Avail: CASI HC A03/MF A01

By using traditional control concepts of gain root locus, the active suppression of a flutter mode of a flexible wing is examined. It is shown that the attraction of the unstable mode towards a critical system zero determines the degree to which the flutter mode can be stabilized. For control situations where the critical zero is adversely placed in the complex plane, a novel compensation scheme called a 'Dipole' filter is proposed. This filter ensures that the flutter mode is stabilized with acceptable control energy. The control strategy is illustrated by designing flutter suppression laws for an active flexible wing (AFW) wind-tunnel model, where minimal control effort solutions are mandated by control rate saturation problems caused by wind-tunnel turbulence. Author

N93-13566# National Aeronautical Lab., Bangalore (India). Flight Mechanics and Control Div.
IDEAL AIRCRAFT HANDLING QUALITY MODELS: LONGITUDINAL AXIS
Shaik Ismail and Shyam Chetty Jun. 1992 18 p
(NAL Proj. FC-8-121)
(NAL-PD-FC-9203) Avail: CASI HC A03/MF A01

This document deals with an algorithm for generating Ideal Handling Quality Models for the Longitudinal Axes of modern high performance aircraft when a flight condition is specified. The technique solves a set of non-linear equations which express the performance requirements in terms of the unknown equivalent aircraft stability and control derivatives of the ideal models. The software package is developed using PC-MATLAB and the ideal HQ models are analyzed using the HQ package already developed. The designer can directly incorporate the ideal HQ models as reference models for his feedback synthesis. Author

N93-13735*# McDonnell Aircraft Co., Saint Louis, MO.
MULTIPLEXING ELECTRO-OPTIC ARCHITECTURES FOR ADVANCED AIRCRAFT INTEGRATED FLIGHT CONTROL SYSTEMS Final Report
D. W. Seal Jun. 1989 90 p
(Contract NAS3-25345)
(NASA-CR-182268; NAS 1.26:182268) Avail: CASI HC A05/MF A01

This report describes the results of a 10 month program sponsored by NASA. The objective of this program was to evaluate various optical sensor modulation technologies and to design an optimal Electro-Optic Architecture (EOA) for servicing remote clusters of sensors and actuators in advanced aircraft flight control systems. The EOA's supply optical power to remote sensors and actuators, process the modulated optical signals returned from the sensors, and produce conditioned electrical signals acceptable for use by a digital flight control computer or Vehicle Management System (VMS) computer. This study was part of a multi-year initiative under the Fiber Optic Control System Integration (FOCSI) program to design, develop, and test a totally integrated fiber optic flight/propulsion control system for application to advanced aircraft. Unlike earlier FOCSI studies, this program concentrated on the design of the EOA interface rather than the optical transducer technology itself. Author

N93-13820 California Univ., Los Angeles.
NUTATIONAL STABILITY AND PASSIVE CONTROL OF SYMMETRIC SPINNING BODIES WITH AXIAL FORCING AND INTERNAL MASS MOTION Ph.D. Thesis
Dominic Michael Halsmer 1992 136 p
Avail: Univ. Microfilms Order No. DA9224113

Necessary and sufficient conditions for asymptotic stability are developed for symmetric spinning bodies with axial forcing and dissipative internal mass motion of various types. Results show that spin about the minor axis is asymptotically stable provided that three conditions are satisfied: (1) the axial force magnitude is sufficiently large; (2) the mass motion is sufficiently stiff; and (3) the mass motion occurs aft of the system mass center. Under these same conditions, spin about the major device with such characteristics can be designed to attenuate and/or suppress the coning of prolate spinners such as those transfer orbit boost vehicles which have recently been plagued by unexpectedly pronounced coning instabilities. Dissert. Abstr.

N93-13827 Texas Univ., Austin.
A DOMAIN DECOMPOSITION METHOD FOR PARALLEL TRANSIENT RESPONSE CALCULATIONS Ph.D. Thesis
Jiann-Yuarn Wu 1992 134 p
Avail: Univ. Microfilms Order No. DA9225768

The objective of this research is to develop parallel algorithms for transient response calculations of large-scale structures. The algorithms are based on a domain decomposition method. The essential idea is to divide a problem domain into a number of smaller subdomains so that the computation can be carried out in parallel. In the algorithms, transient responses of subdomains due to excitation within subdomains are computed independently. Then, these subdomain responses are corrected to give the solution of the global problem by taking into account the interaction between subdomains. In contrast to the approach of most domain decomposition methods, the correction is done directly rather than iteratively. In the first algorithm, piecewise linear interpolation in time is used to approximate the interaction between subdomains and subdomain responses computed independently are corrected at every time step. In the second algorithm, interface responses are sampled less frequently with the use of quintic interpolation functions between samples, which results in less computational effort for the correction of subdomain solutions. Although good accuracy of these methods has been shown on several numerical examples, they are only conditionally stable and their stability behavior is very complicated

compared to global time-stepping algorithms. Motivated by this fact, an unconditionally stable parallel algorithm permitting multi-step independent subdomain computation is developed. Numerical experiments and implementation considerations are presented. Speedup factors obtained from benchmark problems are given. Dissert. Abstr.

N93-13872# Wright Lab., Wright-Patterson AFB, OH.
SYMPOSIUM PROCEEDINGS ON QUANTITATIVE FEEDBACK THEORY Final Report
Constantine H. Houpis and Phillip R. Chandler Aug. 1992 628 p Symposium held in Fairborn, OH, 2-4 Aug. 1992
(AF Proj. 2403)
(AD-A255527; WL-TR-92-3063) Avail: CASI HC A99/MF A06

This document contains the proceedings of Qualitative Feedback Theory (QFT) Symposium at Hope Hotel, WPAFB, OH on 2-4 August 1992. Included are QFT tutorials, and session papers on application to a wide variety of physical systems. The sessions include (1) Theory and Design, (2) Aerospace, and (3) Industrial applications. QFT is a Multiple-Input Multiple Output (MIMO) frequency based synthesis technique that explicitly employs quantitative performance standards and plant uncertainty during controller design. GRA

N93-13915 Notre Dame Univ., IN.
AN EXPERIMENTAL AND COMPUTATIONAL INVESTIGATION OF SLENDER WINGS UNDERGOING WING ROCK Ph.D. Thesis
Andrew Salvatore Arena, Jr. 1992 376 p
Avail: Univ. Microfilms Order No. DA9222008

The problem of self-induced roll oscillations of slender delta wings has been studied in order to identify physical mechanisms responsible for the limit cycle oscillations. The investigation is a combination of both experimental and computational methodologies. The experimental and computational investigations focussed on the wing rock characteristics of a slender flat plate delta wing with 80 degree leading edge sweep. Two unique experimental apparatus have been developed for the investigation. A free to roll system was developed using an air bearing spindle which allows the isolation of applied torques due to the flow field. An unsteady pressure acquisition system was also developed in order to measure the unsteady surface pressure distributions acting on the wing during wing rock time histories. The system consists of a motion control system which accurately matches the time dependent boundary conditions of wing rock, and is synchronized with a pressure acquisition system. The computational model is a discrete vortex potential flow method. The time dependent positions and strengths of the leading edge vortices are solved by coupling the flowfield equations to the rigid body equation of motion in roll for the wing. The computational model has captured all the qualitative characteristics of the wing motion and flowfield behavior observed in experiment with the exception of the secondary vortices which are not modelled. Based on the results of the experiment and computational investigations a theory has been developed for the cause of wing rock of slender wings. The theory is broad enough to account for variations in sweep angle and angle of attack. Wing rock is initiated by some initial perturbation or wing imperfection. The motion builds in time due to an instability caused by a time lag in the position of the vortices normal to the wing surface. A steady state is reached when damping contributions from the top and bottom surfaces are in equilibrium with the instability. Damping is provided by conventional roll damping on the bottom surface of the wing, and by the unsteady behavior of vortex strength on the top surface. Dissert. Abstr.

N93-13916 Rensselaer Polytechnic Inst., Troy, NY.
AN INVESTIGATION OF DYNAMIC STRESS REDUCTION OF MULTI-BODY AIRCRAFT USING ACTIVE GUST CONTROL Ph.D. Thesis
John Chang 1991 125 p
Avail:. Univ. Microfilms Order No. DA9220881

In the future there will be aircraft which are much larger than current aircraft now in service. It is important that their efficiency also be increased. One way to increase their efficiency is to reduce the percentage of gross weight devoted to structural weight. These savings can then be translated into payload weight increases. Structural weight savings can be achieved by reducing those bending moments and/or torsion moments which design major parts of the structure. One way to attain this is to redistribute the load so as to be closer to where the lift is. A multibody aircraft can provide such advantages. Another means which is becoming increasingly acceptable is through active control alleviation of dynamic loads. Gusts usually define the structural design through fatigue allowables. By active control of control surfaces such as ailerons and elevators, it may be possible to reduce the bending moments resulting from gust encounters. This thesis will compare structural weight among three large aircraft designs: single-body, two-body and three-body on the basis of equal structural margins of safety. In addition it examines how a multibody aircraft with active control can further reduce the moments associated with response to gusts. This will then allow a further assessment of the extent to which structural weight can be reduced. Dissert. Abstr.

N93-13926 Iowa State Univ. of Science and Technology, Ames.
SEQUENTIAL QUADRATIC PROGRAMMING SOLUTIONS TO RELATED AIRCRAFT TRAJECTORY OPTIMIZATION PROBLEMS Ph.D. Thesis
Shaw Yang Ong 1992 153 p
Avail: Univ. Microfilms Order No. DA9223956

Aircraft performance optimization continues to play an important role in the aerospace sciences. These studies explore the performance of high speed aircraft with regard to missile evasion, 'minimum time to climb', 'minimum time to turn', and the unorthodox approach of obtaining a robust optimality-based control law for real-time aircraft control. Four papers are included which were presented at major conferences. The similarity in each paper, in addition to the focus on optimal aircraft trajectories, is that an existing nonlinear programming method, sequential quadratic programming (SQP), is used to treat each trajectory optimization problem. This approach is suitable since the emphasis is on applications and problem solving, and the method is accurate and computationally inexpensive. Also, the flexibility of SQP allows for performance index, mathematical model, and constraint changes with relatively little reprogramming. This enables a wide range of trajectory optimization problems to be formulated and studied. In the study of the aircraft missile-evasion problem in horizontal planar flight, unlike earlier studies, the full original equations of motion are used. Also, no linearization about a nominal pursuit triangle is done. The velocity ratio, that is, the velocity of the aircraft to the velocity of the missile for the duration of the confrontation, becomes a major factor in deciding optimal evasive strategies. Evasion against a surface-to-air missile involves a large nonlinear optimal control problem of dynamic order of at least thirteen. Evasive maneuvers are investigated. The results show that the missile enters the 'hit region' of the aircraft for constrained vertical plane flight, but not for constrained horizontal flight. The optimal throttle setting for constrained horizontal plane flight is of 'bang-bang' type. For the minimum-time turn problems, having free final velocity provides the biggest impact on turn times, which can be reduced by as much as fifty percent. For a wide range of final energies studied in the 3-D turns, it was found that the aircraft tends to initially lose altitude in the optimal turn even though the nominal control from which the optimization process started corresponds to an initial climbing turn. This tendency of favoring kinetic energy over potential energy had not been featured in earlier papers. Finally, the study of optimality-based control laws for real-time aircraft control is a significant departure from the usual open-loop solutions to trajectory optimization problems. It was found that the robustness of the optimal control obtained from the 'optimality-condition' is not guaranteed, but by introducing a certain 'correction' term, it can be enhanced significantly. It appears that this technique of enhancing robustness has not been used until now. Dissert. Abstr.

N93-13928 Stanford Univ., CA.
HYPERSONIC PANEL FLUTTER IN A RAREFIED ATMOSPHERE Ph.D. Thesis
Hugo B. Resende 1992 118 p
Avail: Univ. Microfilms Order No. DA9221657

Panel flutter is a form of dynamic aeroelastic instability resulting from the interaction between motion of an aircraft structural panel and the aerodynamic loads exerted on that panel by air flowing past one of the faces. It is not usually catastrophic, the panel's motion being limited by nonlinear membrane stresses produced by the transverse displacement. Above some critical airflow condition, the linear instability grows to a limit cycle. The present investigation studies panel flutter in an aerodynamic regime known as 'free molecule flow', wherein intermolecular collisions can be neglected and loads are caused by interactions between individual molecules and the bounding surface. After collision with the panel, molecules may be reflected specularly or reemitted in diffuse fashion. Two parameters

characterize this process: the 'momentum accommodation coefficient', which is the fraction of the specularly reflected molecules; and the ratio between the panel temperature and that of the free airstream. This model is relevant to the case of hypersonic flight vehicles traveling at very high altitudes and especially for panels oriented parallel to the airstream or in the vehicle's lee. Under these conditions the aerodynamic shear stress turns out to be considerably larger than the surface pressures, and shear effects must be included in the model. This is accomplished by means of distributed longitudinal and bending loads. The former can cause the panel to buckle. In the example of a simply-supported panel, it turns out that the second mode of free vibration tends to dominate the flutter solution, which is carried out by a Galerkin analysis. Several parametric studies are presented. They include the effects of (1) temperature ratio; (2) momentum accommodation coefficient; (3) spring parameters, which are associated with how the panel is connected to adjacent structures; (4) a parameter which relates compressive end load to its value which would cause classical column buckling; (5) a parameter proportional to the pressure differential between the front and back faces; and (6) initial curvature. The research is completed by an investigation into the possibility of accounting for molecular collisions, which proves to be infeasible given the speeds of current mainframe supercomputers. Dissert. Abstr.

09 RESEARCH AND SUPPORT FACILITIES (AIR)

Includes airports, hangars and runways; aircraft repair and overhaul facilities; wind tunnels; shock tubes; and aircraft engine test stands.

For related information see also *14 Ground Support Systems and Facilities (Space).*

N93-12552# Calspan Field Services, Inc., Arnold AFS, TN. Engineering Development Center Div.

DESIGN PHILOSOPHY FOR WIND TUNNEL MODEL POSITIONING SYSTEMS

H. D. Hagar and R. G. Butler Apr. 1992 15 p

(Contract F40600-90-C-0002)

(AD-A254958) Avail: CASI HC A03/MF A01

Wind tunnel testing usually requires positioning of the aircraft model in the airstream. This paper presents the design philosophy for a typical generic automatic control system for use in the wind tunnel facilities at Arnold Engineering Development Center in Tullahoma, Tennessee, and is presently used to accurately control the position and/or velocity of an aircraft in one to six degrees of freedom while taking into account the effects of outside influences. Selection of feedback devices, controller design concepts, safeguard implementation, operator status and display capabilities, and mechanism movement simulation are topics that are addressed.

GRA

N93-12668# Federal Aviation Administration, Atlantic City, NJ.

ILS MATHEMATICAL MODELING STUDY OF THE EFFECTS OF AN ASR-9 STRUCTURE AT THE LONG ISLAND MACARTHUR AIRPORT, ISLIP, NY Technical Report, Jun. 1992

James D. Rambone Sep. 1992 24 p

(Contract FAA-T0603-S)

(DOT/FAA/CT-TN92/25) Avail: CASI HC A03/MF A01

This Technical Note describes the instrument landing system (ILS) math modeling performed by the Federal Aviation Administration (FAA) Technical Center at the request of the Eastern Region. Computed localizer data are presented showing the effects of an ASR-9 antenna structure proposed for construction on the performance of an ILS localizer serving runway 24 at the Long Island MacArthur Airport. The ASR-9 antenna structure was modeled at four proposed sites. The Eastern Region is concerned that radio frequency signal reflections from the ASR-9 structure may degrade the localizer course. Modeled course structure results indicate that category 1 localizer performance should be maintained with the Wilcox 8-element log periodic dipole antenna with the ASR-9 structure constructed at any of the proposed locations. The ASR-9 structure provided minimal signal interference at each site modeled. Computed clearance orbit results indicate satisfactory linearity, course crossover, and signal clearance levels.

Author

N93-12899# Federal Aviation Administration, Atlantic City, NJ.

LIMITED PRODUCTION PRECISION RUNWAY MONITOR (PRM) MASTER TEST PLAN

Thomas Bratton Nov. 1992 36 p

(DOT/FAA/CT-TN92/23) Avail: CASI HC A03/MF A01

This Master Test Plan (MTP) establishes the basic framework to guide and direct the Limited Production (LP) Precision Runway Monitor (PRM) test program. This MTP explains the relationship between all test phases. It concerns the LP PRM system's readiness to be integrated into the National Airspace System (NAS). Sufficient detail is provided to define and direct the development of the next lower level of documentation. The MTP addresses the responsibilities of the LP PRM contractor and the Federal Aviation Administrator (FAA). Author

N93-12902# Federal Aviation Administration, Atlantic City, NJ.

PROTOTYPE STOP BAR SYSTEM EVALUATION AT JOHN F. KENNEDY INTERNATIONAL AIRPORT Final Report

Eric S. Katz and Earl S. Stein Sep. 1992 47 p Original contains color illustrations

(DOT/FAA/CT-92/24) Avail: CASI HC A03/MF A01

A prototype stop bar system was installed and evaluated at John F. Kennedy International Airport. The purpose of the year-long evaluation was to gain operational experience on the use of a stop bar system and how it could possibly impact the air traffic system. To determine the effectiveness of the stop bar system, data were collected from both user pilots and air traffic controllers. Results of the pilot data indicate that the system is somewhat effective in preventing inadvertent runway incursions, but not as effective as stop bar systems operating at European airports. Results of the air traffic controller data indicate that although the majority of the controllers felt that stop bars are conceptually a good idea, almost all of them agreed that the system was not acceptable, especially when combined with the local control position at moderate to high traffic load. Author

N93-13013*# Alabama Univ., Huntsville.

TEST EQUIPMENT DATA PACKAGE FOR THE KC-135 FIBER PULLING APPARATUS Final Report

Sue Kosten, Guy A. Smith, Gary Workman, and Dennis Tucker Jul. 1991 34 p Sponsored by NASA. Lyndon B. Johnson Space Center

(Contract NAS8-36955)

(NASA-CR-184446; NAS 1.26:184446) Avail: CASI HC A03/MF A01

The Fiber Pulling Apparatus (FPA) is a device designed to produce continuous glass fibers from simulated lunar soil, and to determine the effects of reduced gravity, specifically 1/6 g on fiber formation and resultant properties. Briefly, pre-melt simulated lunar soil will be placed in a pint crucible and heated to 1200 C or higher, up to a maximum temperature of 1400 C. At a given temperature, a quartz fiber will be immersed into the melt and then pulled through a chill block and wound onto a cylindrical bobbin using a servo motor control. A high resolution video camera will record the fiber as it is being pulled. This assembly wil be enclosed in Plexiglas. Before fiber pulling commences, the apparatus will be backfilled with dry nitrogen. A separate data acquisition system will support this apparatus. This system will contain a personal computer, video recorder, and monitor. Temperature, acceleration, winding speed, and video images will be controlled and recorded using the data acquisition system. Thus, the FPA will consist of two hardware packages, the fiber production assembly and the data acquisition rack. The primary objective of this test is to determine the effects of 1/6 g on the formation of continuous glass fiber made from simulated lunar soil. Baseline studies using the FPA on the ground will provide a reference for the 1/6 g studies. Of particular interest will be the effect of 1/6 g on the free fluid zone where the fiber exits the crucible. In the fiber spinning parlance this zone is known as the upper jet region, where the boundary slope is greater than one tenth. The properties of the resulting glass fiber will depend on the jet shape as well as distributions of velocity, temperature and tension within the jet. It is unknown at this time how 1/6 g will effect these parameters. Author

N93-13407# National Science Foundation, Washington, DC.

SCIENTIFIC AND ENGINEERING RESEARCH FACILITIES AT UNIVERSITIES AND COLLEGES: 1992

Sep. 1992 138 p

(NSF-92-325) Avail: CASI HC A07/MF A02

The highlights of this survey are outlined in the introduction. Research

facility refers to the physical plant in which research activities take place. Research space includes the net assigned square feet (NASF) of space in which organized research activities take place. Research space at universities and colleges contained in early 1992 an estimated 122 million NASF, based on 525 of the largest research-performing U.S. universities and colleges. Suitable research space increase 22 per cent from 1988-1992. Spending for research facility construction and repair renovation increased nearly $1 billion in expected spending between 1986 and 1991 (3.80 billion for 1990+91). Other highlights reported on results for different topics related to research facilities including research facilities at historically black colleges and universities. R.L.B.

N93-13447# Federal Aviation Administration, Atlantic City, NJ.
A NASPAC-BASED ANALYSIS OF THE DELAY AND COST EFFECTS OF THE DALLAS/FORT WORTH METROPLEX PLAN Technical Report, Sep. 1991 - Jul. 1992
Joseph M. Richie, Douglas Baart, and Arthur Pomerantz Dec. 1992 81 p
(Contract FAA-F2006-E)
(DOT/FAA/CT-TN92/21; DOT/FAA/AOR-100-93/007) Avail: CASI HC A05/MF A01

This technical note contains the findings and analysis of the effects of the Dallas/Fort Worth (DFW) Metroplex Plan on local and system-wide traffic delays. The National Airspace System Performance Analysis Capability (NASPAC) was used to perform this task, and calculates the local (DFW) and system-wide delays with and without the Metroplex Plan. Cost savings were derived using the cost of delay module based on these delays, on passenger cost, and on airline and aircraft specific cost. The results indicate that the plan will reduce delay in the years 1995, 2000, and 2005 at DFW and system-wide for all scenarios modeled. The Southwest Region will be using these results in its planning efforts to execute the Metroplex Plan. Author

N93-13542 Toronto Univ. (Ontario).
THE MODELLING OF TURBULENCE AND DOWNBURSTS FOR FLIGHT SIMULATORS Ph.D. Thesis
Paul Aaron Robinson 1990 394 p
Avail. Univ. Microfilms Order No. DANN59945

With their increasing complexity and sophistication, modern flight simulators have formed the core of commercial airline pilot training curricula. The fidelity of the simulation will have an effect on the quality of training provided, and in order to ensure its realism, all elements of a flight simulation must be modelled in such a way as to represent the actual system in as complete a manner as possible, including the presence of external disturbances due to the atmosphere. This study investigates the degree of complexity required in the simulation of turbulence and thunderstorm downburst wind shear for flight simulation. A turbulence model is presented which contains all the correlations found in homogeneous isotropic turbulence. As part of the development of this turbulence model a method is introduced by which a time series may be modulated to alter its statistical properties while not affecting its spectral properties. Several simplifications and alternate models are considered. This report also presents further developments in the simulation of thunderstorm downbursts. A single ring vortex system, a triple ring vortex system, and Joint Airport Weather Studies (JAWS) data are implemented on the UTIAS B-747 Flight Simulator. By means of pilot evaluations on this simulator, it was found that the inclusion of the isotropic turbulence correlations did not seem to affect the pilots' performance on aircraft response. Overall, spectral methods were favored as a means of generating turbulence for flight simulation. Pilot evaluations of the downburst models showed that both single and triple ring vortex systems produced similar pilot reactions to the actual downbursts (JAWS data). It is suggested that the ring vortex models be expanded upon to include more than one downburst cell. Dissert. Abstr.

N93-13712# National Science Foundation, Washington, DC.
NSF SCIENCE AND TECHNOLOGY CENTERS
Aug. 1992 70 p
(NSF-92-104; OMB-3145-0058) Avail: CASI HC A04/MF A01

The National Science Foundation (NSF) established the Science and Technology Centers (STC) Program in 1987 to fund important basic research and education activities and to encourage technology transfer and innovative approaches to interdisciplinary problems. The centers have the opportunity to explore new areas and build bridges among disciplines, institutions, and other sectors. They offer the basic research community a significant mechanism to take a longer term view of science and explore better and more effective ways to educate students. The distribution of these centers by scientific field is six in the biological sciences, three in computer and information science and engineering, one that spans both the behavioral science and computer and information science; five in the geosciences, and ten in the mathematical and physical sciences. A brief summary of administrative, scientific, and educational information on each Center is included. L.R.R.

N93-13882# Federal Aviation Administration, Washington, DC. Office of Airport Planning and Programming.
REPORT TO CONGRESS: STATE BLOCK GRANT PROGRAM
May 1992 189 p
(AD-A254569; DOT/FAA/PP-92-1) Avail: CASI HC A09/MF A02

The State Block Grant Pilot Program was authorized initially for two years by the Airport and Airway Safety and Capacity Expansion Act of 1987, which reauthorized the Airport Improvement Program (AIP). The pilot program was extended an additional year to a total of three years by the Aviation Safety and Capacity Expansion Act of 1990. The purpose of the State Block Grant Pilot Program is to identify administrative functions which might successfully be shifted to or shared with states in carrying out the AIP. The pilot program potentially allows greater state discretion in selecting and managing projects within several categories of AIP funding. The legislation directs the FAA to conduct a review and report to Congress recommendations for further action relating to state administration of the AIP. Detailed information about the pilot program, state-by-state findings, conclusions, as well as recommendations resulting from FAA review and evaluation are reported. L.R.R.

N93-14060 Ohio State Univ., Columbus.
AN INVESTIGATION OF JET ENGINE TEST CELL AERODYNAMICS BY MEANS OF SCALE MODEL TEST STUDIES WITH COMPARISONS TO FULL-SCALE TEST RESULTS Ph.D. Thesis
Richard Jeffrey Freuler 1991 180 p
Avail: Univ. Microfilms Order No. DA9211127

Using a methodology developed for modeling of engine test facilities and simulating turbofan engines, an investigation of large turbofan engine test cell aerodynamics was conducted by means of several scale model studies with comparisons to full-scale test results. The results of the scale model studies were used to determine recommended modifications to existing airline owned and operated test cell facilities which would improve the engine test environment and permit stable, reliable, and repeatable testing capability for the GE CF6-80C2 engine. In all cases, the full-scale test cells after modification met or exceeded the aerodynamic performance goals necessary to achieve the required stable and repeatable engine testing environment. Comparisons were made between the results of the model tests and the results obtained from the full-scale facilities after the modifications to each test cell were completed. Test cell performance parameters compared included front cell velocity, cell airflow, cell bypass ratio, inlet system total loss, cell depression, and bellmouth pressure distortion. Particular emphasis was focused on the ability of the model tests to correctly predict the amount of front cell airflow, and subsequently the cell bypass ratio, for the full-scale test cells. The model studies conducted as part of this work have helped bring needed changes to the considerations made in process of test cell design and have provided a solid basis for improved engine test facilities now in use by several airlines. The full-scale results and operational experiences included in this work have served to validate the model test methodology by successfully demonstrating that the implementation in full-scale of recommended modifications based on the model studies resulted in the achievement of specific test cell aerodynamic performance goals and engine parameter variation guidelines. A much improved understanding and heightened awareness of the fundamental importance of the aerodynamics of the large turbofan engine indoor testing environment have resulted in significantly improved engine test facilities now in use world-wide. Dissert. Abstr.

N93-13213# Aircraft Research Association Ltd., Bedford (England).
ASTOVL MODEL ENGINE SIMULATORS FOR WIND TUNNEL RESEARCH
A. E. Harris, G. L. Wilde (TKD Ltd., England), V. J. Smith (TKD Ltd.,

England), A. R. G. Mundell (Defence Research Agency, Farnborough, England), and D. P. Davidson (Rotadata Ltd., Derby, England) *In* AGARD, Aerodynamic Engine/Airframe Integration for High Performance Aircraft and Missiles Sep. 1992 10 p (For primary document see N93-13199 03-34)
Copyright Avail: CASI HC A02/MF A04

12 ASTRONAUTICS (GENERAL)

For extraterrestrial exploration see *91 Lunar and Planetary Exploration.*

N93-12891* National Aeronautics and Space Administration, Washington, DC.
NASA MISSION: THE UNIVERSE
[1990] 27 p LIMITED REPRODUCIBILITY: More than 20% of this document may be affected by color photographs Original contains color illustrations
(NASA-NP-141; NAS 1.83:141) Avail: CASI HC A03/MF A01; 26 functional color pages

This booklet is mainly a recruitment tool for the various NASA Centers. This well illustrated booklet briefly describes NASA's mission and career opportunities on the NASA team. NASA field installations and their missions are briefly noted. NASA's four chief program offices are briefly described. They are: (1) Aeronautics, Exploration, and Space Technology; (2) Space Flight; (3) Space Operations; and (4) Space Science and Applications.
R.L.B.

N93-12892# European Space Agency. European Space Research and Technology Center, ESTEC, Noordwijk (Netherlands).
EUROPE QUALIFIES FOR SPACE
Valerie David, comp. May 1992 46 p Prepared in cooperation with Industrieanlagen-Betriebsgesellschaft m.b.H., Munich, Germany, Centre National d'Eudes Spatiales, Toulouse, France and Liege Univ., Belgium LIMITED REPRODUCIBILITY: More than 20% of this document may be affected by color photographs Original contains color illustrations
(ESA-BR-64; ISBN-92-9092-035-1) Copyright Avail: CASI HC A03/MF A01

This study of national aerospace test centers was undertaken with a view to ensure that optimal use was made of the existing facilities and expertise in Europe. Three centers were identified: The CNES/INTERSPACE (Centre National d'Etudes Spatiales) center in Toulouse (France) the IABG (Industrieanlagen-Betriebsgesellschaft mbH) center in Munich (Germany), and the IAL Space Centre - now known as the CSL (Centre Spatial de'Universite de Liege) Test Centre at the University of Liege in Belgium. These three, together with the ESTEC (European Space Research and Technology Centre) at Noordwijk in the Netherlands, make up the European coordinated facilities available for use by the European Space Agency and its member states. ESTEC operates the Large Space Simulator (LSS) and the Large European Acoustic Facility. At ESTEC space simulation, dynamic testing, and electromagnetic testing are carried out. Similar tests are conducted at IABG and CNES/INTERSPACE. At CSL similar activities take place, but there is also a clean room. R.L.B.

N93-13151# Joint Publications Research Service, Arlington, VA.
JPRS REPORT: SCIENCE AND TECHNOLOGY. CENTRAL EURASIA: SPACE
17 Nov. 1992 48 p Transl. into ENGLISH from various Russian articles (JPRS-USP-92-006) Avail: CASI HC A03/MF A01

Papers on the following topics are presented: manned missions, space sciences, interplanetary sciences, space engineering, space applications, and space policy and administration. L.R.R.

N93-13158*# National Aeronautics and Space Administration. Goddard Space Flight Center, Greenbelt, MD.
THE 1992 SHUTTLE SMALL PAYLOADS SYMPOSIUM
Lawrence R. Thomas, ed. and Frances L. Mosier, ed. (Interstel, Inc., Beltsville, MD.) Washington Oct. 1992 284 p Symposium held in Lanham, MD, 20-23 Oct. 1992
(RTOP 740-00-00)
(NASA-CP-3171; Rept-92B00110; NAS 1.55:3171) Avail: CASI HC A13/MF A03

The 1992 Shuttle Small Payloads Symposium is a continuation of the Get Away Special Symposium convened from 1984 through 1988, and is proposed to continue as an annual conference. The focus of this conference is to educate potential Space Shuttle Payload Bay users as to the types of carrier systems provided and for current users to share experiment concepts. For individual titles, see N93-13159 through N93-13186.

N93-13159*# National Aeronautics and Space Administration. Goddard Space Flight Center, Greenbelt, MD.
THE ORBITER STABILITY EXPERIMENT ON STS-40 **c16**
Werner M. Neupert, Gabriel L. Epstein, James Houston, Kenneth J. Meese, William S. Muney, Thomas B. Plummer, and Frank P. Russo *In its* The 1992 Shuttle Small Payloads Symposium Oct. 1992 p 1-8 (For primary document see N93-13158 03-12)
Avail: CASI HC A02/MF A03

The Orbiter Stability Experiment (OSE) was developed to evaluate the steadiness of the STS Orbiter as a potential platform for instrumentation that would image the Sun in its extreme ultraviolet and soft X-ray radiations. We were interested in any high frequency motions of the Orbiter's orientation due to normal operations and manned activities. Preliminary results are presented of the observations. Other than the expected slow motion of the Orbiter within the specified angular deadband of 0.1 degrees during the observations, it was found that high frequency (above 1 Hz) angular motions (jitter) were not detectable at the 0.25 arc sec detection limit of the most sensitive detector, for most of the period of observation. No high frequency motions were recorded during intervals that were identified with vernier thruster firings. However, one short interval with detectable spectral power to a frequency of 10 Hz has been found to date. It has not yet been correlated with a particular activity going on at the time. The results of the observations may also be of value in assessing perturbations to the Orbiter's micro-gravity environment produced by normal operations.
Author

N93-13160*# Worcester Polytechnic Inst., MA.
SPACEFLIGHT PAYLOAD DESIGN FLIGHT EXPERIENCE G-408 **c18**
William W. Durgin, Fred J. Looft, Albert Sacco, Jr., Robert Thompson, Anthony G. Dixon, Dino Roberti (Raytheon Co., Portsmouth, RI.), Robert Labonte (Mitre Corp., Bedford, MA.), and Larry Moschini (Mitre Corp., Bedford, MA.) *In* NASA. Goddard Space Flight Center, The 1992 Shuttle Small Payloads Symposium Oct. 1992 p 9-19 (For primary document see N93-13158 03-12)
Avail: CASI HC A03/MF A03

Worcester Polytechnic Institute's first payload of spaceflight experiments flew aboard Columbia, STS-40, during June of 1991 and culminated eight years of work by students and faculty. The Get Away Special (GAS) payload was installed on the GAS bridge assembly at the aft end of the cargo bay behind the Spacelab Life Sciences (SLS-1) laboratory. The Experiments were turned on by astronaut signal after reaching orbit and then functioned for 72 hours. Environmental and experimental measurements were recorded on three cassette tapes which, together with zeolite crystals grown on orbit, formed the basis of subsequent analyses. The experiments were developed over a number of years by undergraduate students meeting their project requirements for graduation. The experiments included zeolite crystal growth, fluid behavior, and microgravity acceleration measurement in addition to environmental data acquisition. Preparation also included structural design, thermal design, payload integration, and experiment control. All of the experiments functioned on orbit and the payload system performed within design estimates. Author

N93-13161*# Saint Mary's Hospital, Milwaukee, WI. Laser Lab.
POST FLIGHT OPERATION OF A HIGH PEAK POWER NEODYMIUM YAG LASER ABOARD THE G-449 PAYLOAD FLOWN ON SPACE SHUTTLE COLUMBIA MISSION 61-C **c36**
M. C. Muckerheide *In* NASA. Goddard Space Flight Center, The 1992 Shuttle Small Payloads Symposium Oct. 1992 p 21-27 (For primary document see N93-13158 03-12)
Avail: CASI HC A02/MF A03

The Nd Yag laser flown on board the G-449 payload completed its postflight testing successfully. There was no indication that the laser had undergone any electronic or optical component failure. A postflight video

was taken immediately following the return of the payload to the laboratory. Early anticipation of vibration and temperature changes contributed to the successful operation of the laser. Photographic material resulting from post flight videotape are presented. NASA safety reviews and recommendations supplied the insights which helped contribute to the successful operation of the Nd Yag laser. The safety review data is part of the technical presentation and gives some insight into why the system survived the severe environment of temperature and vibration during the flight of Space Shuttle 61-C. Author

N93-13162*# Booker T. Washington's High School for Engineering Professions, Houston, TX.

A DECADE OF DISCOVERY: EXPERIMENTS WITH THE GET AWAY SPECIAL (GAS) CANISTER

Robert Brienzo *In* NASA. Goddard Space Flight Center, The 1992 Shuttle Small Payloads Symposium Oct. 1992 p 29-37 (For primary document see N93-13158 03-12)

Avail: CASI HC A02/MF A03

The experiments from Booker T. Washington's High School for Engineering Profession designed an experiment for a Shuttle flight. The experiments which was flown on STS-42, were contained in three layers of a Get Away Special canister. The first layer housed the Heterogeneous Flow Experiment, to test the commercial application of space exploration; layer two housed an Artemia Salinas Growth Experiment, a test to determine the success and range of food production in microgravity for longer future missions; and layer three, reserved for the computer and monitoring equipment. What was learned from these experiments; and more importantly, what impact they had on education on a broader scale is the subject of this article. E.R.

N93-13163*# Morgan State Univ., Baltimore, MD.

IIaO ULTRAVIOLET AND NUCLEAR EMULSION FILMS RESPONSES TO ORBITAL FLIGHTS ON STS-3, STS-7, STS-8, AND STS-40 c27

E. C. Hammond, Jr., K. A. Peters, S. M. Blake, Y. Bailey, D. Johnson, S. Robancho, and A. Stober *In* NASA. Goddard Space Flight Center, The 1992 Shuttle Small Payloads Symposium Oct. 1992 p 39-45 (For primary document see N93-13158 03-12)

Avail: CASI HC A02/MF A03

Two types of film were flown on STS-40 space shuttle mission in June 1991. The IIaO special purpose ultraviolet film showed continued desensitization because of various thermal and cosmic ray interactions. The films were exposed to the space orbital environment for 9 days. There were several built-in launch pad delays of the shuttle mission. However, there was adequate monitoring of the temperature variations on board the shuttle that allowed for adequate knowledge of the thermal film history. This IIaO film was flown on the ASTRO I mission and is currently slated for use with the ASTRO II mission. A 50 micron thick Illford Nuclear emulsion film was also placed on a 175 micron polyester base. The exposure to space produced several cosmic ray interactions that were analyzed and measured using Digital Image Processing techniques. This same nuclear emulsion film was flown on STS-8 and produced a similar number of cosmic ray and thermal interactions. From previous experiments of film using various laboratory electromagnetic radiation sources (e.g., alpha, beta, and neutron particles), we have been able to infer the possible oribtal interactions of both IIaO and nuclear emulsion films. The characteristic responses of IIaO on STS-40 compared favorably to the results obtained from previous STS-7 and STS-8 gas can experiments. The results indicate sufficient evidence correlating increased density on the film with possible cosmic ray, thermal and shuttle out gassing interactions. Author

N93-13164*# Medical Univ. of South Carolina, Charleston.

EARTH OBSERVATION PHOTOGRAPHY: LOOKING BACK 20 YEARS AFTER SKYLAB c43

James H. Nicholson *In* NASA. Goddard Space Flight Center, The 1992 Shuttle Small Payloads Symposium Oct. 1992 p 47-56 (For primary document see N93-13158 03-12)

Avail: CASI HC A02/MF A03

A committee of trained classroom teachers, backed by a volunteer team of technical experts and academic advisors has developed a program for earth science based on photographs obtained from low earth orbit. In selecting targeting objectives, immediate note was made of the fact nearly one generation (20 years) has passed since the United States' ambitious SKYLAB program was conducted. A critical part of those missions was the acquisition of earth photography using a six camera, multi-spectral camera system. This objective was systematically furthered through the term of three separate crew visits to the Space Station. Not merely an exercise in randomly photographing the Earth below, the purpose of the Earth Resource Experiment Package (EREP) was to determine what kind, and how much, photographic data could be acquired of the broad variety of Earth features witnessed on the mission's ground track. The collection of 35,000 photos produced by EREP represents the most complete coverage of Earth. However, it remains under used. GAS 324 intends to revisit, and to add a tier of relevancy to this inventory. The photography of GAS 324 should allow a direct examination and comparison of the changes in the globe in the last 20 years. format in both coverage and quality. The photogra phy acquired by CAN DO should allow a direct examination and comparison of the changes that have occured to the Globe in the last twenty years. E.R.

N93-13165*# Rockwell International Corp., Cocoa Beach, FL. Space Systems Div.

A PATH TO IN-SPACE WELDING AND TO OTHER IN-SPACE METAL PROCESSING TECHNOLOGIES USING SPACE SHUTTLE SMALL PAYLOADS c37

David Tamir *In* NASA. Goddard Space Flight Center, The 1992 Shuttle Small Payloads Symposium Oct. 1992 p 57-76 (For primary document see N93-13158 03-12)

Avail: CASI HC A03/MF A03

As we venture into space, it becomes necessary to assemble, expand, and repair space-based structures for our housing, research, and manufacturing. The zero gravity-vacuum of space challenges us to employ construction options which are commonplace on Earth. Rockwell International (RI) has begun to undertake the challenge of space-based construction via numerous options, of which one is welding. As of today, RI divisions have developed appropriate resources and technologies to bring space-based welding within our grasp. Further work, specifically in the area of developing space experiments to test RI technology, is required. RI Space Welding Project's achievements to date, from research and development (R&E) efforts in the areas of microgravity, vacuum, intra- / extra- vehicular activity and spinoff technologies, are reviewed. Special emphasis is given to results for G-169's (Get Away Special) microgravity flights aboard a NASA KC-135. Based on these achievements, a path to actual development of a space welding system is proposed with options to explore spinoff in-space metal processing technologies. This path is constructed by following a series of milestone experiments, of which several are to utilize NASA's Shuttle Small Payload Programs. Conceptual designs of the proposed shuttle payload experiments are discussed with application of lessons learned from G-169's design, development, integration, testing, safety approval process, and KC-135 flights. Author

N93-13166*# National Aeronautics and Space Administration. Goddard Space Flight Center, Greenbelt, MD.

A PAYLOAD TO EVALUATE PHOTODIODES FOR THE DETECTION OF SOFT AND HARD X RAYS IN A SPACE ENVIRONMENT USING A GET AWAY SPECIAL c19

Upendra D. Desai and AmyElizabeth C. Stewart (Maryland Univ., College Park.) *In its* The 1992 Shuttle Small Payloads Symposium Oct. 1992 p 77-84 (For primary document see N93-13158 03-12)

Avail: CASI HC A02/MF A03

We propose to use the Get Away Special (GAS) facility to evaluate P-intrinsic-N (PIN) detectors and avalanche photodiodes (APD's) for the detection of both solar and nonsolar soft and hard x rays. We would like to fly both types of silicon detectors for the direct detection of the x ray photons in the energy range from 1 to 30 keV with an energy resolution of about 1 keV. We would also like to use both types of photodiodes viewing CsI(Tl) scintillators to extend the energy range up to 1 MeV with -6 percent resolution at 660 keV. Solar flares would be detected with this instrumentation during periods of solar pointing providing high energy resolution spectra with high time resolution. Similar data would be obtained in the scanning mode on nonsolar transient and steady x ray sources with the same instrumentation. A commandable door over the detectors would be required to allow measurements to be made as low as 1 keV. Author

N93-13167*# National Aeronautics and Space Administration. Marshall Space Flight Center, Huntsville, AL.

A STUDY OF THE EFFECTS OF MICRO-GRAVITY ON SEED GERMINATION **c51**

Lynn Suzanne Klein (Washington Univ., Seattle.), Mark McKibben (Ohio Univ., Athens.), David A. Brain (Rice Univ., Houston, TX.), Theodore C. Johnson (Stanford Univ., CA.), and Konrad K. Dannenberg *In* NASA. Goddard Space Flight Center, The 1992 Shuttle Small Payloads Symposium Oct. 1992 p 85-94 (For primary document see N93-13158 03-12)

Avail: CASI HC A02/MF A03

This study will identify characteristics of seed germination dependent upon gravity. To accomplish this objective, four different seed types will be germinated in space and then be compared to a control group germinated on Earth. Both the experimental and control groups will be analyzed on the cellular level for the size of cells, structural anomalies, and gravitational effects. The experiment will be conducted in a Get Away Special Canister (GAS Can no. 608) owned by the U.S. Space and Rocket Center and designed for students. The GAS Can will remain in the cargo bay of the Space Shuttle with minimal astronaut interaction. Author

N93-13168*# Science Applications International Corp., Glendora, CA.

INVESTIGATION OF MICROGRAVITY EFFECTS ON SOLIDIFICATION PHENOMENA OF SELECTED MATERIALS **c29**

Carl R. Maag and Patricia A. Hansen (Engineering and Economics Research, Inc., Seabrook, MD.) *In* NASA. Goddard Space Flight Center, The 1992 Shuttle Small Payloads Symposium Oct. 1992 p 95-101 (For primary document see N93-13158 03-12)

Avail: CASI HC A02/MF A03

A Get Away Special (GAS) experiment payload to investigate microgravity effects on solidification phenomena of selected experimental samples has been designed for flight. It is intended that the first flight of the assembly will (1) study the p-n junction characteristics for advancing semiconductor device applications, (2) study the effects of gravity-driven convection on the growth of HgCd crystals, (3) compare the textures of the sample which crystallizes in microgravity with those found in chondrite meteorites, and (4) modify glass optical characteristics through divalent oxygen exchange. The space flight experiment consists of many small furnaces. While the experiment payload is in the low gravity environment of orbital flight, the payload controller will sequentially activate the furnaces to heat samples to their melt state and then allow cooling to resolidification in a controlled fashion. The materials processed in the microgravity environment of space will be compared to the same materials processed on earth in a one-gravity environment. This paper discusses the design of all subassemblies (furnance, electronics, and power systems) in the experiment. A complete description of the experimental materials is also presented. Author

N93-13169*# Sverdrup Technology, Inc., Brook Park, OH.

ENVIRONMENTAL QUALIFICATION TESTING OF PAYLOAD G-534, THE POOL BOILING EXPERIMENT **c29**

J. Andrew Sexton *In* NASA. Goddard Space Flight Center, The 1992 Shuttle Small Payloads Symposium Oct. 1992 p 103-113 (For primary document see N93-13158 03-12)

(Contract NAS3-25266)

Avail: CASI HC A03/MF A03

Payload G-534, the prototype Pool Boiling Experiment (PBE), is scheduled to fly on the STS-47 mission in September 1992. This paper describes the purpose of the experiment and the environmental qualification testing program that was used to prove the integrity of the hardware. Component and box level vibration and thermal cycling tests were performed to give an early level of confidence in the hardware designs. At the system level, vibration, thermal extreme soaks, and thermal vacuum cycling tests were performed to qualify the complete design for the expected shuttle environment. The system level vibration testing included three axis sine sweeps and random inputs. The system level hot and cold soak tests demonstrated the hardware's capability to operate over a wide range of temperatures and gave wider latitude in determining which shuttle thermal attitudes were compatible with the experiment. The system level thermal vacuum cycling tests demonstrated the hardware's capability to operate in a convection free environment. A unique environmental chamber was designed and fabricated by the PBE team and allowed most of the environmental testing to be performed within the hardware build laboratory. The completion of the test program gave the project team high confidence in the hardware's ability to function as designed during flight. Author

N93-13170*# National Aeronautics and Space Administration. Lewis Research Center, Cleveland, OH.

ELECTRICAL DESIGN OF PAYLOAD G-534: THE POOL BOILING EXPERIMENT **c29**

David R. Francisco *In* NASA. Goddard Space Flight Center, The 1992 Shuttle Small Payloads Symposium Oct. 1992 p 115-124 (For primary document see N93-13158 03-12)

Avail: CASI HC A02/MF A03

Payload G-534, the Pool Boiling Experiment (PBE), is a Get Away Special that is scheduled to fly on the shuttle in 1992. This paper will give a brief overall description of the experiment with the main discussion being the electrical design with a detailed description of the power system and interface to the GAS electronics. The batteries used and their interface to the experiment Power Control Unit (PCU) and GAS electronics will be examined. The design philosophy for the PCU will be discussed in detail. The criteria for selection of fuses, relays, power semiconductors and other electrical components along with grounding and shielding policy for the entire experiment will be presented. The intent of this paper is to discuss the use of military tested parts and basic design guidelines to build a quality experiment for minimal additional cost. Author

N93-13171*# Brigham Young Univ., Provo, UT. Dept. of Physics and Astronomy.

G-133: A SOFT X RAY SOLAR TELESCOPE **c89**

Memorie K. Williams, Branton Campbell, Peter W. A. Roming, Mark K. Spute, and J. Ward Moody *In* NASA. Goddard Space Flight Center, The 1992 Shuttle Small Payloads Symposium Oct. 1992 p 125-131 (For primary document see N93-13158 03-12)

(Grant NAGw-2612)

Avail: CASI HC A02/MF A03

The GOLDHELOX Project, NASA payload number G-133, is a robotic soft x ray solar telescope designed and built by an organization of undergraduate students. The telescope is designed to observe the sun at a wavelength of 171 to 181 A. Since we require observations free from atmospheric interference, the telescope will be launched in a NASA Get-Away-Special (GAS) canister with a Motorized Door Assembly (MDA). In this paper we primarily discuss the most important elements of the telescope itself. We also elaborate on some of the technical difficulties associated with doing good science in space on a small budget (about $100,000) and mention ways in which controlling the instrument environment has reduced the complexity of the system and thus saved us money. Author

N93-13172*# Sierra Coll., Sacramento, CA. Dept. of Computer Science.

TAGGING INSULIN IN MICROGRAVITY **c29**

Michael Dobeck and Ronald S. Nelson (Nelson, Ronald S., Fresno, CA) *In* NASA. Goddard Space Flight Center, The 1992 Shuttle Small Payloads Symposium Oct. 1992 p 133-141 (For primary document see N93-13158 03-12)

Avail: CASI HC A02/MF A03

Knowing the exact subcellular sites of action of insulin in the body has the potential to give basic science investigators a basis from which a cause and cure for this disease can be approached. The goal of this project is to create a test reagent that can be used to visualize these subcellular sites. The unique microgravity environment of the Shuttle will allow the creation of a reagent that has the possibility of elucidating the subcellular sites of action of insulin. Several techniques have been used in an attempt to isolate the sites of action of items such as insulin. One of these is autoradiography in which the test item is obtained from animals fed radioactive materials. What is clearly needed is to visualize individual insulin molecules at their sites of action. The insulin tagging process to be used on G-399 involves the conjugation of insulin molecules with ferritin molecules to create a reagent that will be used back on Earth in an attempt to elucidate the sites of action of insulin. Author

N93-13173*# California Inst. of Tech., Pasadena. Dept. of Physics, Mathematics, and Astronomy.

GAMCIT: A GAMMA RAY BURST DETECTOR **c93**

Derek M. Surka, John M. Grunsfeld, and Brett A. Warneke *In* NASA. Goddard Space Flight Center, The 1992 Shuttle Small Payloads Symposium Oct. 1992 p 143-149 (For primary document see N93-13158 03-12)
Avail: CASI HC A02/MF A03

The origin of celestial gamma ray bursts remains one of the great mysteries of modern astrophysics. The GAMCIT Get-Away-Special payload is designed to provide new and unique data in the search for the sources of gamma ray bursts. GAMCIT consists of three gamma ray detectors, an optical CCD camera, and an intelligent electronics system. This paper describes the major components of the system, including the electronics and structural designs. Author

N93-13174*# Utah State Univ., Logan.
G254 UNDERGRADUATE EXPERIMENT **c29**
Doran Barton, Karilyn Bogh, Brett Evans, Steve Folkman, Marc Hammond, Casey Hatch, Neva Herr, Tina Hubble, Jeff Humpherys, and Steve Johnson et al *In* NASA. Goddard Space Flight Center, The 1992 Shuttle Small Payloads Symposium Oct. 1992 p 151-163 Prepared in cooperation with Kinkaid High School, UT (For primary document see N93-13158 03-12)
Avail: CASI HC A03/MF A03

This paper describes the experiments on payload G254. Each experiment is accommodated in a spacepak and six experiments fly in a full canister. One of the experiments will be housed in a new Isospacepak structure, which will be described briefly. Five of the six experiments have dedicated controllers. The objective of each experiment is discussed. In addition, the operational scenario is provided. Author

N93-13175*# Hernandez Engineering, Inc., Greenbelt, MD.
STRUCTURAL VERIFICATION FOR GAS EXPERIMENTS **c39**
Mark Daniel Peden *In* NASA. Goddard Space Flight Center, The 1992 Shuttle Small Payloads Symposium Oct. 1992 p 165-174 (For primary document see N93-13158 03-12)
Avail: CASI HC A02/MF A03

The purpose of this paper is to assist the Get Away Special (GAS) experimenter in conducting a thorough structural verification of its experiment structural configuration, thus expediting the structural review/approval process and the safety process in general. Material selection for structural subsystems will be covered with an emphasis on fasteners (GSFC fastener integrity requirements) and primary support structures (Stress Corrosion Cracking requirements and National Space Transportation System (NSTS) requirements). Different approaches to structural verifications (tests and analyses) will be outlined especially those stemming from lessons learned on load and fundamental frequency verification. In addition, fracture control will be covered for those payloads that utilize a door assembly or modify the containment provided by the standard GAS Experiment Mounting Plate (EMP). Structural hazard assessment and the preparation of structural hazard reports will be reviewed to form a summation of structural safety issues for inclusion in the safety data package. Author

N93-13176*# Hernandez Engineering, Inc., Greenbelt, MD.
PROPER BATTERY SYSTEM DESIGN FOR GAS EXPERIMENTS **c33**
Stephen A. Calogero *In* NASA. Goddard Space Flight Center, The 1992 Shuttle Small Payloads Symposium Oct. 1992 p 175-184 (For primary document see N93-13158 03-12)
Avail: CASI HC A02/MF A03

The purpose of this paper is to help the GAS experimenter to design a battery system that meets mission success requirements while at the same time reducing the hazards associated with the battery system. Lead-acid, silver-zinc and alkaline chemistry batteries will be discussed. Lithium batteries will be briefly discussed with emphasis on back-up power supply capabilities. The hazards associated with different battery configurations will be discussed along with the controls necessary to make the battery system two-fault tolerant. Author

N93-13177*# Pennsylvania State Univ., University Park. Dept. of Engineering and Science.
A PENNSYLVANIA STATE UNIVERSITY/GENERAL ELECTRIC GET AWAY SPECIAL (GAS) EXPERIMENT **c76**
George Evanisko, Theodore Grosch, Milad Youssef, and Jim Yurack *In* NASA. Goddard Space Flight Center, The 1992 Shuttle Small Payloads Symposium Oct. 1992 p 185-193 Sponsored in part by GE (For primary document see N93-13158 03-12)
Avail: CASI HC A02/MF A03

We describe four student-designed experiments by the Pennsylvania State University, which are planned for a GAS canister. The four experiments will measure: the effects of radiation on semiconductors; orbital debris impacts; the Space Shuttle's magnetic field; and the photoelectric yield of several different materials. These experiments are the result of the efforts of more than one hundred students. Author

N93-13178*# Alabama Univ., Huntsville. Consortium for Materials Development.
CONCAP 4: A COMPLEX AUTONOMOUS PAYLOAD (CAP) FOR GROWING ORGANIC THIN FILMS IN MICROGRAVITY **c29**
W. E. Carswell and F. C. Wessling *In* NASA. Goddard Space Flight Center, The 1992 Shuttle Small Payloads Symposium Oct. 1992 p 195-204 (For primary document see N93-13158 03-12)
Avail: CASI HC A02/MF A03

A GAS facility has been developed for carrying out low temperature experiments. The arrangement being used on CONCAP IV-01 is designed for thin film growth in microgravity and can process up to twelve samples per mission. The nonlinear optical oven hardware can also be made suitable for other low temperature applications, such as gradient freeze and solution growth of crystals. Author

N93-13179*# National Aeronautics and Space Administration. Goddard Space Flight Center, Greenbelt, MD.
THE ROMPS ROBOT IN HITCHHIKER **c37**
George Voellmer *In its* The 1992 Shuttle Small Payloads Symposium Oct. 1992 p 205-219 (For primary document see N93-13158 03-12)
Avail: CASI HC A03/MF A03

The Robotics Branch of the Goddard Space Flight Center has under development a robot that fits inside a Get Away Special can. In the RObotic Materials Processing System (ROMPS) HitchHiker experiment, this robot is used to transport pallets containing wafers of different materials from their storage rack to a halogen lamp furnace for rapid thermal processing in a microgravity environment. It then returns them to their storage rack. A large part of the mechanical design of the robot deait with the potential misalignment between the various components that are repeatedly mated and demated. A system of tapered guides and compliant springs was designed to work within the robot's force and accuracy capabilities. This paper discusses the above and other robot design issues in detail, and presents examples of ROMPS robot analyses that are applicable to other HitcherHiker materials handling missions. Author

N93-13180*# Defense Systems, Inc., McLean, VA.
THE DSI SMALL SATELLITE LAUNCHER **c18**
S. Nichols, D. Gibbons, J. Wise, and D. Nguyen *In* NASA. Goddard Space Flight Center, The 1992 Shuttle Small Payloads Symposium Oct. 1992 p 221-231 (For primary document see N93-13158 03-12)
Avail: CASI HC A03/MF A03

A new launcher has been developed by DSI, that is compatible with the GAS canisters. It has the proven capability to deploy a satellite from an orbiting Shuttle that is 18 inches in diameter, 31 inches long, and weighing 190 pounds. These DSI Launchers were used aboard the Discovery (STS-39) in May 1991 as part of the Infrared Background Signature Survey (IBSS) to deploy three small satellites known as Chemical Release Observation (CRO) satellites A, B, and C. Because the satellites contained hazardous liquids (MMH, UDMH, and MON-10) and were launched from GAS Cylinders without motorized doors, the launchers were required to pass NASA Shuttle Payload safety and verification requirements. Some of the more interesting components of the design were the V-band retention and separation mechanism, the separation springs, and the launcher electronics which provided a properly inhibited release sequence operated through the Small Payload Accommodations Switch Panel (SPASP) on board the Orbiter. The original plan for this launcher was to use a motorized door. The launcher electronics, therefore has the capability to be modified to accommodate the door, if desired. Author

N93-13181*# National Aeronautics and Space Administration. Goddard Space Flight Center, Greenbelt, MD.

THE CAPILLARY PUMPED LOOP FLIGHT EXPERIMENT (CAPL): A PATHFINDER FOR EOS **c34**

D. Butler and T. Hoang (NSI Technology Services Corp., Greenbelt, MD.) *In its* The 1992 Shuttle Small Payloads Symposium Oct. 1992 p 233-245 (For primary document see N93-13158 03-12)

Avail: CASI HC A03/MF A03

The CAPL shuttle flight experiment will provide microgravity verification of the prototype capillary pumped loop (CPL) thermal control system for EOS. The design of the experiment is discussed with particular emphasis on the new technology areas in ammonia two-phase reservior design and heat pipe heat exchanger development. The thermal and hydrodynamic analysis techniques and results are also presented, including pressure losses, fluid flow, and non-orbit heat rejection capability. CAPL experiment results will be presented after the flight, presently planned for 1993. Author

N93-13182*# Martin Marietta Corp., Denver, CO.

THE VTRE PROGRAM: AN OVERVIEW **c34**

William J. Bailey and John P. Gille *In* NASA. Goddard Space Flight Center, The 1992 Shuttle Small Payloads Symposium Oct. 1992 p 247-256 (For primary document see N93-13158 03-12)

(Contract NAS3-25977)

Avail: CASI HC A02/MF A03

The Vented Tank Resupply Experiment (VTRE) Program is a NASA In-Space Technology Experiments Program (IN-STEP) that will develop, and fly a small, low cost space experiment to investigate, develop, and acquire needed data to extend and advance the technology of capillary vane fluid management devices to applications requiring direct venting of gas from tanks in low-gravity. GAS venting may be required for control of pressure, or to allow low-g fill of a tank with liquid while holding a constant tank back pressure by gas venting. Future space applications requiring these fluid management capabilities include both cryogenic and Earth storable fluid systems. The experiment is planned as a Shuttle Hitchhiker payload, and will be developed around two transparent tanks equipped with capillary vane devices between which a test liquid can be transferred. Experiments will be conducted for vented transfer, direct venting, stability of liquid positioning to accelerations within and significantly above the design values, and fluid reorientation by capillary wicking of liquid into the vane device following intentional liquid upset. Author

N93-13183*# Science Applications International Corp., Glendora, CA.

THE LDCE PARTICLE IMPACT EXPERIMENT AS FLOWN ON STS-46 **c25**

Carl R. Maag, William G. Tanner (Baylor Univ., Waco, TX.), Janet Borg (Centre National de la Recherche Scientifique, Orsay, France), Jean-Pierre Bibring (Centre National de la Recherche Scientifique, Orsay, France), W. Merle Alexander (Baylor Univ., Waco, TX.), and Andrew J. Maag (Stanford Univ., Palo Alto, CA.) *In* NASA. Goddard Space Flight Center, The 1992 Shuttle Small Payloads Symposium Oct. 1992 p 257-266 (For primary document see N93-13158 03-12)

Avail: CASI HC A02/MF A03

Many materials and techniques have been developed by the authors to sample the flux of particles in Low Earth Orbit (LEO). Though regular in-site sampling of the flux in LEO the materials and techniques have produced data which compliment the data now being amassed by the Long Duration Exposure Facility (LDEF) research activities. Orbital debris models have not been able to describe the flux of particles with d sub p less than or = 0.05 cm, because of the lack of data. Even though LDEF will provide a much needed baseline flux measurement, the continuous monitoring of micron and sub-micron size particles must be carried out. A flight experiment was conducted on the Space Shuttle as part of the LDCE payload to develop an understanding of the Spatial Density (concentration) as a function of size (mass) for particle sizes 1 x 10(exp 6) cm and larger. In addition to the enumeration of particle impacts, it is the intent of the experiment that hypervelocity particles be captured and returned intact. Measurements will be performed post flight to determine the flux density, diameters, and subsequent effects on various optical, thermal control and structural materials. In addition to these principal measurements, the Particle Impact Experiment (PIE) also provides a structure and sample holders for the exposure of passive material samples to the space environment, e.g., thermal cycling, and atomic oxygen, etc. The experiment will measure the optical property changes of mirrors and will provide the fluence of the ambient atomic oxygen environment to other payload experimenters. In order to augment the amount of material returned in a form which can be analyzed, the survivability of the experiment as well as the captured particles will be assessed. Using Sandia National Laboratory's hydrodynamic computer code CTH, hypervelocity impacts on the materials which comprise the experiments have been investigated and the progress of these studies are reported. Author

N93-13184*# National Aeronautics and Space Administration. Lewis Research Center, Cleveland, OH.

BATTERY SELECTION FOR SPACE EXPERIMENTS **c33**

David R. Francisco *In* NASA. Goddard Space Flight Center, The 1992 Shuttle Small Payloads Symposium Oct. 1992 p 267-276 (For primary document see N93-13158 03-12)

Avail: CASI HC A02/MF A03

This paper will delineate the criteria required for the selection of batteries as a power source for space experiments. Four basic types of batteries will be explored, lead acid, silver zinc, alkaline manganese and nickel cadmium. A detailed description of the lead acid and silver zinc cells while a brief exploration of the alkaline manganese and nickel cadmium will be given. The factors involved in battery selection such as packaging, energy density, discharge voltage regulation, and cost will be thoroughly examined. The pros and cons of each battery type will be explored. Actual laboratory test data acquired for the lead acid and silver zinc cell will be discussed. This data will include discharging under various temperature conditions, after three months of storage and with different types of loads. A description of the required maintenance for each type of battery will be investigated. The lifetime and number of charge/discharge cycles will be discussed. Author

N93-13185*# Brigham Young Univ., Provo, UT. Dept. of Physics and Astronomy.

THE UNIQUE CHALLENGE OF MANAGING AN UNDERGRADUATE GET-AWAY-SPECIAL EXPERIMENT **c81**

Peter W. A. Roming, Mark K. Spute, and Memorie K. Williams *In* NASA. Goddard Space Flight Center, The 1992 Shuttle Small Payloads Symposium Oct. 1992 p 277-284 (For primary document see N93-13158 03-12)

(Grant NAGw-2612)

Avail: CASI HC A02/MF A03

A group of Bringham Young University (BYU) undergraduate students has undertaken an experiment to design and build a normal incidence soft x ray robotics telescope for solar observations. The design phase of this, GOLDHELOX project, has now been completed and final construction and modifications are in progress. The design and manufacture of the payload is under the direction of team leaders and a system's integrator. A goal of this project is educating and furnishing experiences in space engineering and physics for undergraduate students. Our main source of funding is NASA and the BYU Colleges of Physical and Mathematical Sciences and Engineering and Technology. This project is possible because of the NASA Get-Away Special (GAS) program. The only feasible alternative is using an expensive sounding rocket. We estimate the sun tracking and guidance package alone would cost upwards of a million dollars -- at least ten times our entire budget. Because of the GAS program, we simplified the construction, operation, and programming of the instruments with resulting savings in weight, cost, and time spent. Author

N93-13186*# National Aeronautics and Space Administration. Goddard Space Flight Center, Greenbelt, MD.

PREPARING SAFETY DATA PACKAGES FOR EXPERIMENTERS USING THE GET AWAY SPECIAL (GAS) CARRIER SYSTEM **c81**

Jerome Kosko *In its* The 1992 Shuttle Small Payloads Symposium Oct. 1992 p 285-292 (For primary document see N93-13158 03-12)

Avail: CASI HC A02/MF A03

The implementation of NSTS 1700.7B and more forceful scruntiny of data packages by the Johnson Space Flight Center (JSC) lead to the development of a classification policy for GAS/CAP payloads. The purpose of this policy is to classify experiments using the carrier system so that they receive an appropriate level of JSC review (i.e., one or multiphase reviews). This policy is based on energy containment to show inherent payload safety. It impacts the approach to performing hazard analyses and

the nature of the data package. This paper endeavors to explain the impact of this policy as well as the impact of recent JSC as well as Kennedy Space Flight Center (KSC) 'interpretations' of existing requirements. The GAS canister does adequately contain most experiments when flown in the sealed configuration (however this must be shown, not merely stated). This paper also includes data package preparation guidelines for those experiments that require an opening door which often present unique safety issues. Author

N93-13265*# National Aeronautics and Space Administration, Washington, DC.

SOLAR SYSTEM EXPLORATION DIVISION STRATEGIC PLAN, VOLUME 1. EXECUTIVE SUMMARY AND OVERVIEW

Jul. 1991 32 p

(NASA-TM-107843; NAS 1.15:107843) Avail: CASI HC A03/MF A01

This first document is the first of a six-volume series presenting the Solar System Exploration Division's Strategic Plan for the 10-year period FY 1994 to FY 2003. The overall strategy is characterized by five fundamental precepts: (1) execute the current program; (2) improve the vitality of the program and the planetary science community; (3) initiate innovative, small, low-cost planetary missions; (4) initiate new major and moderate missions; and (5) prepare for the next generation of missions. This Strategic Plan describes in detail our proposed approach to accomplish these goals. Volume 1 provides first an Executive Summary of highlights of each of the six volumes, and then goes on to present an overview of the plan, including a discussion of the planning context and strategic approach. Volumes 2, 3, 4, and 5 describe in detail the initiatives proposed. An integral part of each of these volumes is a set of responses to the mission selection criteria questions developed by the Space and Earth Science Advisory Committee. Volume 2, Mission From Planet Earth, describes a strategy for exploring the Moon and Mars and sets forth proposed moderate missions--Lunar Observer and a Mars lander network. Volume 3, Pluto Flyby/Neptune Orbiter, discusses our proposed major new start candidate for the FY 1994 to FY 1998 time frame. Volume 4, Discovery, describes the Near-Earth Asteroid Rendezvous, as well as other candidates for this program of low-cost planetary missions. Volume 5, Toward Other Planetary Systems, describes a major research and analysis augmentation that focuses on extrasolar planet detection and the study of planetary system processes. Finally, Volume 6 summarizes the technology program that the division has structured around these four initiatives. Author

N93-13266*# National Aeronautics and Space Administration, Washington, DC.

SMALL PLANETARY MISSION PLAN: REPORT TO CONGRESS

Apr. 1992 11 p

(NASA-TM-107809; NAS 1.15:107809) Avail: CASI HC A03/MF A01

This document outlines NASA's small planetary projects plan within the context of overall agency planning. In particular, this plan is consistent with Vision 21: The NASA Strategic Plan, and the Office of Space Science and Applications (OSSA) Strategic Plan. Small planetary projects address focused scientific objectives using a limited number of mature instruments, and are designed to require little or no new technology development. Small missions can be implemented by university and industry partnerships in coordination with a NASA Center to use the unique services the agency provides. The timeframe for small missions is consistent with academic degree programs, which makes them an excellent training ground for graduate students and post-doctoral candidates. Because small missions can be conducted relatively quickly and inexpensively, they provide greater opportunity for increased access to space. In addition, small missions contribute to sustaining a vital scientific community by increasing the available opportunities for direct investigator involvement from just a few projects in a career to many. Author

N93-13282# Joint Publications Research Service, Arlington, VA.

JPRS REPORT: SCIENCE AND TECHNOLOGY. CENTRAL EURASIA: SPACE

10 Jun. 1992 111 p Transl. into ENGLISH from various Russian articles

(JPRS-USP-92-004) Avail: CASI HC A06/MF A02

Translations are presented of articles from Russian publications. The areas of study are: Manned mission highlights; Space sciences; Interplanetary sciences; Life sciences; Space engineering; Space applications; and Space policy and administration. Some representative titles are as follows: Russian-German mission to MIR; Scientific rules from gamma astronomy satellite; Martian composition, structure, and gravity field; Measurement of radiation dose on Mir station during solar proton events; Transport system for lunar base; Simulation of spectral brightnesses of natural features at upper boundary of atmosphere; and Report of ESA contracts with Russian Institutes. E.R.

N93-13304# Joint Publications Research Service, Arlington, VA.

JPRS REPORT: SCIENCE AND TECHNOLOGY. CENTRAL EURASIA: SPACE

21 Aug. 1992 80 p Transl. into ENGLISH from various Russian articles

(JPRS-USP-92-005) Avail: CASI HC A05/MF A01

Translations are presented of articles from Russian publications. The areas of study are: Manned mission highlights; Space sciences; Interplanetary sciences; Space engineering; Space applications; and Space policy and administration. Some representative titles are as follows: MIR cosmonauts complete two hour EVA; Subauroral ionosphere in SUNDIAL period, June 1987, from data of Kosmos-1809; Possibility of the Existence of two transplutonian planets; Institute developing remote manipulator arm for Buran; Determination of economic efficiency of using space derived information in agriculture; and Russian-U.S. Space cooperation agreement. E.R.

N93-13308* National Aeronautics and Space Administration, Washington, DC.

ADVANCED TECHNOLOGY FOR AMERICA'S FUTURE IN SPACE. EXECUTIVE SUMMARY

Dec. 1990 19 p Original contains color illustrations

(NASA-TM-107969; NAS 1.15:107969) Avail: Issuing Activity; 6 functional color pages

This report summarizes the results of a review by a select external technology advisory committee of NASA's recently developed Integrated Technology Plan for the Civil Space Program. This document is the Summary Report from the review by the Space Systems and Technology Advisory Committee (SSTAC), a subcommittee of the NASA Advisory Committee with the assistance of the Space Science and Applications Advisory Committee and the Aerospace Medicine Advisory Committee, and the Aeronautics and Space Engineering Board and Space Studies Board of the National Research Council. The report asks the question 'Why should space technology be a national priority?' The report describes the benefits to the nation as Improving National Competitiveness, Stimulating Quality Science and Engineering Education, Developing Broadly Applicable New Technologies. Specific Benefits for future space endeavors include Improving the Quality for Future U.S. Flight Programs, Reducing the Cost of Access to Space, Increasing Safety and Reliability, Enabling New Space Missions, and Sustaining NASA Expertise. Other improvements and the value of the Integrated Technology Plan are emphasized. Almost uniformly, the review team found that the quality of individual research projects was very high and well integrated with other national efforts. R.L.B.

N93-13548 International Space Univ., Inc., Toronto (Ontario).

INTERNATIONAL ASTEROID MISSION Final Report

1990 449 p Project held in Toronto, Ontario, 1990; sponsored by NASA and York Univ. Original contains color illustrations

Copyright Avail: Issuing Activity

The International Asteroid Mission (IAM) is a large-scale space exploration project in which all nations of the world have the opportunity to participate, grow, and learn from the experience of operating on the frontier of science and technology. A driving theme of this mission is to participate in the expansion of sustained human presence beyond Earth orbit. This mission will achieve this theme through a manned mission to mine a near-Earth asteroid, and return asteroid-derived hydrogen and oxygen for cryogenic propulsion fuel in the Earth-Moon system. This could eliminate the high cost of launching fuel from the surface of the Earth. This fuel can be used for future space mission, including voyages to Mars, and Earth-Moon excursions. Asteroids can be used as sources of other raw-materials commonplace on Earth, but difficult or expensive to deliver to the Earth-Moon System. This report contains the results of the IAM project. For individual titles, see N93-13549 through N93-13562.

N93-13549 International Space Univ., Inc., Toronto (Ontario).

[INTRODUCTION TO THE INTERNATIONAL ASTEROID MISSION]

In its International Asteroid Mission 1990 p 1-10 (For primary document see N93-13548 03-12)
Copyright Avail: Issuing Activity

A driving theme of this mission is to participate in the expansion of sustained human presence beyond Earth orbit. This mission will achieve this theme through a manned mission to mine a near-Earth asteroid, and return asteroid-derived hydrogen and oxygen for cryogenic propulsion fuel in the Earth-Moon system. In the long run, this could eliminate the high cost of launching fuel from the surface of the Earth. This fuel can be used for future space missions, including voyages to Mars, and Earth-Moon excursions. Asteroids can be used as sources of other raw-materials commonplace on Earth, but difficult or expensive to deliver to the Earth-Moon system. These include water, metals, hydrocarbons, and building materials. The International Asteroid Mission design project has four main goals: (1) define the possible uses of asteroids through a survey of existing literature to determine what materials, processes, and applications are most profitable for an asteroid mission; (2) review the current methods and instrumentation used in searches of asteroids, (3) review the current proposals for unmanned, robotic probes to asteroids in the context of an international manned mission, and (4) develop one scenario for an economically viable manned mission to extract and return asteroid resources from a near-Earth asteroid to the Earth-Moon system. L.R.R.

N93-13550 International Space Univ., Inc., Toronto (Ontario).
ASTEROID SEARCH PROGRAM
In its International Asteroid Mission 1990 p 11-33 (For primary document see N93-13548 03-12)
Copyright Avail: Issuing Activity

This document is dedicated first to the criteria used to select a candidate asteroid. It contains the known characteristics of this asteroid as well as the assumptions made about it. It ends with a preliminary study of other possible more favorable candidates which might be found in the near future. Special attention is paid to the possible existence of Earth-Sun Trojan asteroids. Second, there is a description of the current state of our limited knowledge about the asteroids, and of the instruments and techniques being used to improve this knowledge. The contribution to asteroid research which can be expected from the new instruments already in space or due to be launched in this decade is then discussed. The last part of this document gives a description of different ways of improving our knowledge about the asteroids, both quantitatively and qualitatively. A proposal requiring reasonable financing and manpower to improve asteroid research is presented. It is believed that the implementation of such a program would have a dramatic effect on asteroid research. For example, a significant increase in both the rate of discovery of asteroids and their corresponding orbital parameters would be obtained. This program could be fully operational 3 years after its implementation. L.R.R.

N93-13551 International Space Univ., Inc., Toronto (Ontario).
SUMMARY OF LITERATURE ON UNMANNED PROBES TO ASTEROIDS AND PRECURSOR DATA REQUIREMENTS FOR IAM
In its International Asteroid Mission 1990 p 34-50 (For primary document see N93-13548 03-12)
Copyright Avail: Issuing Activity

The objectives linked to the different steps of the exploration process with automatic probes are described. Special attention is given to specific objectives linked to asteroids. Missions proposed or under development, where asteroids are the main or partial goal, are described. Also described are missions to comets which are the most comparable bodies to asteroids. The typical sequence of exploration of a space object with automatic probes is the following: (1) the fly-by which allows preliminary investigations of the object, (2) the orbiting or rendezvous mission which furnishes geological and geophysical informations, and (3) performing automatic sampling with either in-situ analyses or samples return. L.R.R.

N93-13552 International Space Univ., Inc., Toronto (Ontario).
CONCEPTUAL DESIGN OF A HUMAN PILOTED MINING MISSION
In its International Asteroid Mission 1990 p 51-76 (For primary document see N93-13548 03-12)
Copyright Avail: Issuing Activity

An international mission to mine an asteroid, and return some useful product to the vicinity of planet Earth, is a complex undertaking from both the technical and political points of view. Furthermore, attempting to make such a mission profitable, in the true economic sense, in essence doubles the challenge. This report proposes a mission to return liquid water, obtained from a near Earth asteroid, for processing in Low Lunar Orbit (LLO). The sellable products will be liquid hydrogen and liquid oxygen for use as cryogenic propulsion fuel to support activities based on the Moon (liquid oxygen and liquid water are also available). The equipment and operations for mining a hydrous carbonaceous chondrite asteroid were considered in several stages: site selection, development, exploitation, and beneficiation stages. Due to the limitation on the amount of manpower available at the mine, an automated mining process was designed. Author

N93-13553 International Space Univ., Inc., Toronto (Ontario).
[THE PROGRAM PLAN: AN OVERVIEW OF THE DEVELOPMENT AND IMPLEMENTATION OF THE INTERNATIONAL ASTEROID MISSION]
In its International Asteroid Mission 1990 p 77-88 (For primary document see N93-13548 03-12)
Copyright Avail: Issuing Activity

The program plan presents an overview of the development and implementation of the International Asteroid Mission. The final mission scenario was determined following an examination of over 20 different possibilities. Criteria, including delta V costs, round-trip mission opportunities, mass requirements, and cargo delivery requirements were compared. The candidate asteroid is 3361 Orpheus (1982 HR). Orpheus is believed to be carbonaceous and hydrous, and is 800 meters in diameter. The asteroid lies in an orbit inclined 2.69 degrees to the ecliptic with a semi-major axis of 1.21 astronomical units. The synodic period of the orbit is four years, assuming constant orbital elements. However, reasonable round-trip mission opportunities occur every 3.4 years, on the average. This feature of the orbit permits the crew and cargo vehicles to be cycled, thus extending the economic return time for the deliverable products. The time-table for the nominal first mission is shown and the delta V costs associated with the trips to and from Orpheus are presented. Author

N93-13554 International Space Univ., Inc., Toronto (Ontario).
[BUSINESS ANALYSIS: THE COMMERCIAL MISSION OF THE INTERNATIONAL ASTEROID MISSION]
In its International Asteroid Mission 1990 p 89-110 (For primary document see N93-13548 03-12)
Copyright Avail: Issuing Activity

The mission of the International Asteroid Mission (IAM) is providing asteroidal resources to support activities in space. The short term goal is to initiate IAM by mining a near-Earth, hydrous carbonaceous chondrite asteroid to service the nearer-term market of providing cryogenic rocket fuel in low lunar orbit (LLO). The IAM will develop and contract for the building of the transportation vehicles and equipment necessary for this undertaking. The long-term goal is to expand operations by exploiting asteroids in other manners, as these options become commercially viable. The primary business issues are what revenue can be generated from the baseline mission, how much will the mission cost, and how funding for this mission can be raised. These issues are addressed. Author

N93-13555 International Space Univ., Inc., Toronto (Ontario).
[LEGAL AND POLITICAL ISSUES RAISED BY THE INTERNATIONAL ASTEROID MISSION]
In its International Asteroid Mission 1990 p 111-130 (For primary document see N93-13548 03-12)
Copyright Avail: Issuing Activity

The legal and political environment in which the International Asteroid Mission (IAM) will occur is discussed. The following description examines first existing international space law together with the legal issues that are raised directly by IAM, such as liability, contamination, and the use of nuclear power sources. An IAM institutional model and operational policies are developed which are appropriate to creating a commercially-oriented international enterprise. Potential participants and their interests in IAM are then identified. Throughout the paper, an effort is made to examine the political elements critical to the success of this international activity, with particular attention paid to technology transfer problems. Author

N93-13556 International Space Univ., Inc., Toronto (Ontario).
[ENGINEERING AND ARCHITECTURAL ISSUES ASSOCIATED WITH THE ASTEROID MISSION]

In its International Asteroid Mission 1990 p 131-190 (For primary document see N93-13548 03-12)
Copyright Avail: Issuing Activity

Engineering and architectural issues associated with the asteroid mission are discussed. The overall designs of the crew vehicle and cargo vehicle are presented. Consideration is given to the design of power and propulsion systems for the vehicles to meet the specified mission requirements. The power plant for the mining and processing equipment and the crew vehicle at the asteroid is also presented. Guidance, navigation, and control of the vehicles is discussed in terms of sensors, reaction control systems, computer interfaces, and docking procedures. The life support system for the crew vehicle is also addressed. Finally, materials issues relating to durability, degradation in the space environment and thermal control are presented.
Author

N93-13557 International Space Univ., Inc., Toronto (Ontario).
[MINING EQUIPMENT AND OPERATIONS FOR MINING THE 1982HR (ORPHEUS) ASTEROID]
In its International Asteroid Mission 1990 p 191-244 (For primary document see N93-13548 03-12)
Copyright Avail: Issuing Activity

The equipment and operations for mining the 1982HR (Orpheus) asteroid is described. First, an introduction is given to mining methods and automation to update the reader on current technology. Details are given into those mining methods which are most suitable for asteroid mining, with emphasis given on the drill and blast method selected for this project. The equipment used both for mining, and for maintaining and repairing the mining and processing equipment is described as well as the control operations for the mining and processing, including communications, the telerobotics human interface, and telemetry and control are summarized.
Author

N93-13558 International Space Univ., Inc., Toronto (Ontario).
[A MICROGRAVITY PROCESSING PLANT FOR THE MANUFACTURING OF PROPELLANT AND WATER FROM ASTEROID ORE]
In its International Asteroid Mission 1990 p 245-256 (For primary document see N93-13548 03-12)
Copyright Avail: Issuing Activity

A microgravity processing plant for the manufacturing of propellant and water from asteroid ore is described. Although several studies of lunar-soil processing have been conducted in the past, this study is one of the first focusing on materials processing in a true microgravity environment. The relative size of the processing plant is also quite large - handling 15.5 tons ore per hour. This large scale has implied power and mass requirements far beyond the limits of currently planned space projects. The processing technique proposed - mainly electrolysis with subsystems - is a well known and energy intensive process. Terrestrial materials processing equipment, however, is not generally mass-optimized, for the simple reason that there is no justification for minimizing the weight of, for example, a chemical or metallurgical plant. Until some years ago, this was true not only for the mass but also for the energy consumption. Thus, a space-based processing system must be optimized with respect to two factors which traditionally have not been considered in the terrestrial design of similar equipment. These and other critical design issues are listed.
Author

N93-13559 International Space Univ., Inc., Toronto (Ontario).
[HUMAN FACTORS DEALING WITH THE INTERNATIONAL ASTEROID MISSION]
In its International Asteroid Mission 1990 p 257-314 (For primary document see N93-13548 03-12)
Copyright Avail: Issuing Activity

Human factors encompass many concerns in the 2.83 year International Asteroid Mission ¿IAM) mission from the initial crew selection to the final readaptation to Earth environment. These factors include radiation, physical deconditioning, crew selection and interaction, psychosocial issues, and health maintenance. The main theme that runs throughout the group's work is the lack of current available research into the problem areas. This stems from the relatively short mission durations in the last 30 years of spaceflight and thus no heavy emphasis in the human factors area. In short, no one has been in space for 3 years and thus we do not know what the effects of a three year flight are. It will be one of the goals in the IAM mission to do some research that may contribute to the fundamental knowledge of preparing for how humans can live in space.
L.R.R.

N93-13560 International Space Univ., Inc., Toronto (Ontario).
[GROUND OPERATIONS AND LOGISTICS IN THE CONTEXT OF THE INTERNATIONAL ASTEROID MISSION]
In its International Asteroid Mission 1990 p 315-328 (For primary document see N93-13548 03-12)
Copyright Avail: Issuing Activity

The role of Ground Operations and Logistics, in the context of the International Asteroid Mission (IAM), is to define the mission of Ground Operations; to identify the components of a manned space infrastructure; to discuss the functions and responsibilities of these components; to provide cost estimates for delivery of the spacecraft to LEO from Earth; to identify significant ground operations and logistics issues. The purpose of this dissertation is to bring a degree of reality to the project. 'One cannot dissociate development and set up of a manned infrastructure from its operational phase since it is this last one which is the most costly due to transportation costs which plague space station use' (Eymar, 1990). While this reference is to space stations, the construction and assembly of the proposed crew vehicle and cargo vehicles will face similar cost difficulties, and logistics complexities. The uniqueness of long duration space flight is complicated further by the lack of experience with human habitated, and non-refurbishable life support systems. These problems are addressed.
L.R.R.

N93-13561 International Space Univ., Inc., Toronto (Ontario).
[SCIENTIFIC EXPERIMENTATION AFFORDED BY THE INTERNATIONAL ASTEROID MISSION]
In its International Asteroid Mission 1990 p 329-354 (For primary document see N93-13548 03-12)
Copyright Avail: Issuing Activity

The International Asteroid Mission (IAM) affords scientists the opportunity to perform interesting and important experimentations. This opportunity is not sufficient in its own right to mandate inclusion of science into the mission. Certain scientific experimentations are essential to the success of the mission, and are the driving force behind the inclusion of science. Instrument designs incorporate the need for direct contribution to the success of the mining mission. Examples of these applications include the search for additional candidate asteroids, especially at the Earth-Sun Trojan points, with an infrared telescope facility; a gamma ray burst detector provides the crew with real-time notification of potentially harmful solar-flare activity; and a materials processing laboratory provides information on the porosity, composition, and crystalline structure of samples to optimize the mining operations in addition to yielding great insight into the history and formation of the solar-system. Instrument designs have emphasized the use of off-the-shelf hardware, demonstrated technologies. Their scientific value is derived from the location on an interplanetary platform, not necessarily advancements in technology or detection methods. Instrumentation will be delivered to the IAM project after completion of a thorough certification program. The program will include qualification, acceptance, performance, thermal balance, thermal vacuum, vibration, electromagnetic susceptibility and compatibility, and calibration testing. After delivery to the assembly-site in low-Earth orbit, an additional series of functional and compatibility tests will be required prior to initiation of the mission. The scientific instrumentation proposed for the IAM consists of experiments using a Gamma Ray Burst Detector, a Infrared Observatory, a Materials Processing Facility, Long-Wavelength Radar, Seismic Measurement Devices, Cosmic Ray Detectors, Interplanetary Plasma Measurements, a Solar Observatory, and Magnetic Field Measurements. The details of each of these experiments are included.
L.R.R.

N93-13562 International Space Univ., Inc., Toronto (Ontario).
RESEARCH AND TECHNOLOGY IN SUPPORT OF IAM
In its International Asteroid Mission 1990 p 355-364 (For primary document see N93-13548 03-12)
Copyright Avail: Issuing Activity

Some research and technology needs of the International Asteroid Mission (IAM) are examined. Critical technology development and implementation are addressed. The first section tries to spot which technologies have to be developed before the project can be realized. Technologies may be developed from already existing technology, or they may have to be developed from scratch. The section includes essential research projects. Types of institutions that can take on these technology

developments and research projects are suggested. Also discussed are business and management issues. L.R.R.

N93-13564*# Essex Corp., Huntsville, AL.
SPACELAB J: MICROGRAVITY AND LIFE SCIENCES
[1992] 61 p Sponsored by NASA. Marshall Space Flight Center Prepared for Teledyne Brown Engineering, Huntsville, AL Original contains color illustrations
(NASA-CR-191353; NAS 1.26:191353) Avail: CASI HC A04/MF A01; 26 functional color pages

Spacelab J is a joint venture between NASA and the National Space Development Agency of Japan (NASDA). Using a Spacelab pressurized long module, 43 experiments will be performed in the areas of microgravity and life sciences. These experiments benefit from the microgravity environment available on an orbiting Shuttle. Removed from the effects of gravity, scientists will seek to observe processes and phenomena impossible to study on Earth, to develop new and more uniform mixtures, to study the effects of microgravity and the space environment on living organisms, and to explore the suitability of microgravity for certain types of research. Mission planning and an overview of the experiments to be performed are presented. Orbital research appears to hold many advantages for microgravity science investigations, which on this mission include electronic materials, metals and alloys, glasses and ceramics, fluid dynamics and transport phenomena, and biotechnology. Gravity-induced effects are eliminated in microgravity. This allows the investigations on Spacelab J to help scientists develop a better understanding of how these gravity-induced phenomena affect both processing and products on Earth and to observe subtle phenomena that are masked in gravity. The data and samples from these investigations will not only allow scientists to better understand the materials but also will lead to improvements in the methods used in future experiments. Life sciences research will collect data on human adaptation to the microgravity environment, investigate ways of assisting astronauts to readapt to normal gravity, explore the effects of microgravity and radiation on living organisms, and gather data on the fertilization and development of organisms in the absence of gravity. This research will improve crew comfort and safety on future missions while helping scientists to further understand the human body. L.R.R.

N93-13691# European Space Agency, Paris (France).
EURECA: A FIRST FOR EUROPE
Wolfgang Nellessen, Luisa Innocenti, Dicky A. M. Mesland, Egidio Suppa, Kurt Aubeck, and Norman Longdon, ed. Jun. 1992 33 p LIMITED REPRODUCIBILITY: More than 20 percent of this document may be affected by color photographs Original contains color illustrations
(ESA-BR-85; ISBN-92-9092-119-6) Copyright Avail: CASI HC A03/MF A01; 20 functional color pages

The background and potential of Eureca, which stands for EUropean REtrievable CArrier, is illustrated and explained in this brief pamphlet. Eureca is a unique, re-usable, user-oriented space facility that has been developed to meet the needs of both scientific and applications-oriented users. Its primary use is in the field of microgravity. The first mission of Eureca will consist of the following multi-user facilities: Automatic Mirror Furnace (AMF), Solution Growth Facility (SGF), Multi-Furnace Assembly (MFA), and Protein Crystallization Facility (PCF). In addition, there are ten single-user instruments. Overall, 80 percent of the Eureca-1 payload will be dedicated to microgravity experiments. R.L.B.

N93-13756# Joint Publications Research Service, Arlington, VA.
JPRS REPORT: SCIENCE AND TECHNOLOGY. USSR: SPACE
20 Sep. 1991 94 p Transl. into ENGLISH from various Russian articles (JPRS-USP-91-004) Avail: CASI HC A05/MF A01

Soviet articles are presented that cover the following areas: manned mission highlights; space sciences; space engineering; space applications; and space policy administration. Author

N93-13855# European Space Agency. European Space Research and Technology Center, ESTEC, Noordwijk (Netherlands).
HORIZON 2000: SEVEN YEARS ON [HORIZON 2000: SEPT ANS APRES]
Norman Longdon, ed. 1 Oct. 1991 11 p In ENGLISH and FRENCH LIMITED REPRODUCIBILITY: More than 20 percent of this document may be affected by color photographs Original contains color illustrations
(ESA-BR-37-B; ISBN-92-9092-159-5) Copyright Avail: CASI HC A03/MF A01; 10 functional color pages

The objectives of the future ESA's science program for Horizon 2000 described are: (1) to contribute to the advancement of fundamental scientific knowledge; (2) to establish Europe as a major participant in the world-wide development of space science; (3) to offer a balanced distribution of opportunities for frontline research to the European scientific community; and (4) to provide major technological challenges for innovative industrial developments. The main elements of the program consists of four cornerstones, which are: (1) the Solar-Terrestrial Science Programme (STSP); (2) X-ray Multi-Mirror mission (XMM); (3) FIRST - the Far InfraRed and submillimetre Space Telescope mission; and (4) Rosetta, Comet Nucleus Sample Return Mission. I.I.C.

N93-13856# European Space Agency. European Space Research and Technology Center, ESTEC, Noordwijk (Netherlands).
TAKING A GLOBAL VIEW [UNE VUE D'ENSEMBLE]
Norman Longdon, ed. 1991 9 p In ENGLISH and FRENCH LIMITED REPRODUCIBILITY: More than 20 percent of this document may be affected by color photographs Original contains color illustrations
(ESA-BR-37-C; ISBN-92-9092-159-5) Copyright Avail: CASI HC A02/MF A01; 5 functional color pages

The strategy for future ESA's Earth Observation Programs described focuses on the following themes: (1) studying the Earth's environment on various scales, from local or regional to global; (2) management and monitoring of the Earth's resources, both renewable and non-renewable; (3) continuation and improvement of the service provided to the worldwide operational meteorological community; and (4) contributing to the understanding of the structure and dynamics to the Earth's crust and interior. I.I.C.

N93-13857# European Space Agency. European Space Research and Technology Center, ESTEC, Noordwijk (Netherlands).
MESSENGERS IN SPACE [DES MESSAGERS DANS L'ESPACE]
Norman Longdon, ed. 1991 10 p In ENGLISH and FRENCH LIMITED REPRODUCIBILITY: More than 20 percent of this document may be affected by color photographs Original contains color illustrations
(ESA-BR-37-D; ISBN-92-9092-159-5) Copyright Avail: CASI HC A02/MF A01; 7 functional color pages

The ESA Telecommunications Programme described consists of satellite development programs aimed at the development and launch of spacecraft, either as technology and demonstration missions or, in the case of Data Relay, as an operational service to users. The satellite development programs consist of: (1) Artemis (Advanced Geostationary Communications development); (2) Minisat (Small Platform Technology development); (3) Archimedes (Advanced Non-Geostationary Communications development); and (4) AOTS (Orbital Test Systems after 2000). I.I.C.

N93-13858# European Space Agency. European Space Research and Technology Center, ESTEC, Noordwijk (Netherlands).
A HOME PORT IN SPACE [UN PORT D'ATTACHE DANS L'ESPACE]
Norman Longdon, ed. 1991 8 p In ENGLISH and FRENCH LIMITED REPRODUCIBILITY: More than 20 percent of this document may be affected by color photographs Original contains color illustrations
(ESA-BR-37-E; ISBN-92-9092-159-5) Copyright Avail: CASI HC A01/MF A01; 7 functional color pages

The Columbus Programme described is a part of the ESA International Space Station Freedom for Earth observation from a Polar Platform. The Columbus Programme involves the following elements: (1) the Columbus Attached Laboratory, a pressurized module which will be permanently connected to Space Station Freedom; (2) the Columbus Free-Flying Laboratory, which will orbit higher than the Space Station Freedom in order to benefit from better microgravity conditions, operates automatically for periods of six months or more at a time, and will be serviced by the Hermes spaceplane; and (3) the Columbus Polar Platform, which will operate automatically and mainly carry Earth observation instruments. I.I.C.

N93-13859# European Space Agency. European Space Research and Technology Center, ESTEC, Noordwijk (Netherlands).
REACHING FOR THE SKIES: THE NEXT GENERATION [A L'ASSAUT DU CIEL: LA PROCHAINE GENERATION]

Norman Longdon, ed. 1991 8 p In ENGLISH and FRENCH LIMITED REPRODUCIBILITY: More than 20 percent of this document may be affected by color photographs Original contains color illustrations
(ESA-BR-37-G; ISBN-92-9092-159-5) Copyright Avail: CASI HC A02/MF A01; 6 functional color pages

The ESA Space Transportation Systems described consist of: (1) Ariane 4, which is Europe's current operational launcher assuring Europe independent access to space through the launch of automatic satellites and enabling Europe's space industry to compete successfully with the United States launch service suppliers, and Ariane 5, which is under development for low launch cost, very high level of reliability and safety, and high payload capability; and (2) Hermes, which is a space vehicle launched atop Ariane 5. I.I.C.

N93-13860# European Space Agency. European Space Research and Technology Center, ESTEC, Noordwijk (Netherlands).
PREPARING FOR THE FUTURE [PREPARER L'AVENIR]
Norman Longdon, ed. 1991 10 p In ENGLISH and FRENCH LIMITED REPRODUCIBILITY: More than 20 percent of this document may be affected by color photographs Original contains color illustrations
(ESA-BR-37-H; ISBN-92-9092-159-5) Copyright Avail: CASI HC A02/MF A01; 9 functional color pages

The ESA programs described consist of: (1) the Basic Technological Research Programme, which takes care of all the common domains of technology applicable to medium and far-term missions, and advances technological research to the point of demonstrated feasibility; (2) Harmonisation, which is for both economic and resource reasons; (3) the In-Orbit Technology Demonstration Programme, which is for designing and testing technological performance of future spacecraft equipment and examining space environmental effects; (4) the General Support Technology Programme, which is to enhance the cost effectiveness of various technological development; and (5) Technology Transfer Programme. I.I.C.

N93-13861# European Space Agency. European Space Research and Technology Center, ESTEC, Noordwijk (Netherlands).
THE NEXT STEP FORWARD [LA PROCHAINE ETAPE]
Norman Longdon, ed. 1991 12 p In ENGLISH and FRENCH LIMITED REPRODUCIBILITY: More than 20 percent of this document may be affected by color photographs Original contains color illustrations
(ESA-BR-37-A; ISBN-92-9092-159-5) Copyright Avail: CASI HC A03/MF A01; 10 functional color pages

The ESA supporting medium-sized mission for the International Space Station Freedom described consists of the following programs: (1) the Earth Observation Programme; (2) the Microgravity Programme; (3) the Telecommunication Programme; (4) the Space Station and Platforms Programme; (5) the Space Transportation Programme; (6) Hermes; (7) the Echnological Research Programme; and (8) the In-Orbit Infrastructure. I.I.C.

N93-13902# European Space Agency. European Space Research and Technology Center, ESTEC, Noordwijk (Netherlands).
A GROWING DIMENSION IN SPACE [UN NOUVEAU DOMAINE DE CROISSANCE]
Norman Longdon, ed. 1991 9 p In ENGLISH and FRENCH LIMITED REPRODUCIBILITY: More than 20 percent of this document may be affected by color photographs Original contains color illustrations
(ESA-BR-37-F; ISBN-92-9092-159-5) Copyright Avail: CASI HC A03/MF A01; 7 functional color pages

The ESA Microgravity Programme described is built around materials sciences, fluid sciences, and life sciences. The ultimate goal of the program is to make sure that when the Columbus laboratories are operational, sufficient experience has been gathered to make the most effective, and cost-effective use of the laboratories. I.I.C.

N93-13903# European Space Agency. European Space Research and Technology Center, ESTEC, Noordwijk (Netherlands).
EVER WATCHFUL [TOUJOURS EN EVEIL]
Norman Longdon, ed. 1991 11 p In ENGLISH and FRENCH LIMITED REPRODUCIBILITY: More than 20 percent of this document may be affected by color photographs Original contains color illustrations
(ESA-BR-37-I; ISBN-92-9092-159-5) Copyright Avail: CASI HC A03/MF A01; 8 functional color pages

The ESA Ground Infrastructure described is generally classified under: (1) facilities for the development phases; (2) launch and landing facilities; (3) ground operations facilities; (4) the European Astronauts Centre; and (5) data handling and data arching facilities. The Ground Infrastructure encompasses support during all stages of the projects from their conception and operational control during the launch and in-orbit phases. I.I.C.

13 ASTRODYNAMICS

Includes powered and free-flight trajectories; and orbital and launching dynamics.

N93-12690*# Draper (Charles Stark) Lab., Inc., Cambridge, MA.
ROBUST RENDEZVOUS MANEUVER POINT CONDITIONS M.S. Thesis - Massachusetts Inst. of Tech.
Debra Ann Fogle Jun. 1992 91 p
(Contract NAS9-18426)
(NASA-CR-190996; NAS 1.26:190996; CSDL-T-1134) Copyright Avail: CASI HC A05/MF A01

This study develops rendezvous maneuver point conditions that are robust to one dimensional errors in state estimation and burn execution. Allowing small deviations in the time of intercept provides a degree of freedom that can be used to compensate for these errors. The direction of allowable burn deviation is developed for errors in state estimation and burn execution. The maneuver points for which the error is aligned with the insensitive direction provide excellent rendezvous initiation points. The method is applied to sample rendezvous for vehicles in circular and elliptic orbits. Robust maneuver points are selected and the vehicles' relative motion plotted, demonstrating the validity of the maneuver points. Finally, a graphical illustration of the error focusing effect is demonstrated by means of a Monte Carlo simulation. Dissert. Abstr.

N93-13766 Texas Univ., Austin.
A GUIDANCE METHODOLOGY FOR THE CISLUNAR TRANSFER OF LOW-THRUST SPACECRAFT Ph.D. Thesis
David Jerome Korsmeyer 1991 151 p
Avail: Univ. Microfilms Order No. DA9128272

The research focuses on the development of a guidance methodology for cislunar low-thrust spacecraft and the resulting computer model to generate the trajectories between the Earth and Moon. Rather than developing an optimal trajectory and finding the guidance required to match it, the guidance scheme developed here for the cislunar problem was allowed to generate the trajectory. The cislunar trajectory guidance and generation problem is broken into three distinct phases, all of which are equally important. These phases are the Orbital Plane Alignment, the Midcourse cislunar transfer, and the Capture and Circularization to the target orbit. The restricted three-body formulation is used to model the dynamical system and perturbations on the trajectory in the Earth-Moon system. A cislunar trajectory generation computer model, LOWTHRST, was developed to evaluate this low-thrust cislunar guidance methodology. The model allows the determination of some of the low-thrust orbital transfer vehicle's operational characteristics. These operation characteristics include the following: time-of-flight, propellant mass, payload mass, and thrusting history. Transfers from both Earth orbit to lunar orbit and from lunar orbit back to Earth orbit are considered. Several example cases were run using only the Orbital Plane Alignment segment of LOWTHRST to establish that this phase was working properly and to focus on the performance of the plane alignment algorithms. In order to evaluate the whole program, four complete cislunar case studies were made with the LOWTHRST model. Two Earth to Moon, and two Moon to Earth trajectories were generated, each with different spacecraft mass and propulsion system characteristics. The principal goal of this research was to develop a prototype guidance methodology for cislunar low-thrust spacecraft. The performance of the guidance algorithms in the computer model has indicated the fulfillment of this goal. The LOWTHRST trajectory model developed in this research also provides a mission analyst and planner with the capability to easily develop cislunar trajectories and evaluate EOTV characteristics that can satisfy NASA mission architectures. This capability could help show the

relative worth of low-thrust nuclear electric spacecraft for cislunar operations and provide the ability for quick mission analysis. Dissert. Abstr.

N93-13768 Texas Univ., Austin.
THE USE OF CONSIDER COVARIANCE ANALYSIS IN CHOOSING DATA WEIGHTS TO REDUCE THE EFFECT OF ERRORS IN MODEL PARAMETERS ON SATELLITE ORBIT DETERMINATION ACCURACY Ph.D. Thesis
Steven Ross Poole 1991 293 p
Avail: Univ. Microfilms Order No. DA9128331

Choosing data weights to reduce the effect of errors in model parameters on satellite orbit determination accuracy is studied. The effect of these errors is evaluated using consider covariance analysis. A derivation of consider covariance analysis is given. In consider covariance analysis, errors are modeled as random variables. Three weighted least squares (WLS) filters are investigated. The first filter uses a scalar weight for each batch of data. Values of the weights are found that reduce the trace of the consider covariance, tr(P(sub c)). This filter is the Reduced Consider Covariance (RCC) filter. The weights are determined in a numerical minimization. The RCC filter is able to minimize tr(P(sub c)) with respect to the scalar data weights at the batch epoch. When the accuracy of the mapped estimate is examined, it is found that, for some cases, the RCC filter is among the poorest performers. In general, the RCC filter is not useful for mapping problems because it is not possible to predict how suitable a weight is for a mapping interval based on epoch results. The next filter investigated is the SRCC filter. This filter is similar to the RCC filter, except that each scalar data point is assigned a scalar weight. The data are processed one scalar data point at a time, and the weights are solved for analytically. The SRCC filter is found to be unpredictable and unreliable. The final filter investigated is the minimum consider covariance (MCC) filter. The MCC filter uses a weight matrix that is a full matrix in order to obtain the absolute minimum tr(P(sub c)) at epoch. In mapping, the MCC filter performs poorly. This is due to the MCC filter being equivalent to estimating the consider parameters. The MCC filter should not be used to obtain mapped estimates. The MCC filter could be used in nonmapping problems. However, this would be equivalent to estimating all of the consider parameters. There could be two unwanted effects. First, the covariance could be optimistic. Second, information that should go to the estimate could be absorbed by the estimation of the consider parameters.
Dissert. Abstr.

N93-13922 Stanford Univ., CA.
AERONOMY COEXPERIMENTS ON DRAG-FREE SATELLITES WITH PROPORTIONAL THRUSTERS: GP-B AND STEP Ph.D. Thesis
Yusuf R. Jafry 1992 369 p
Avail: Univ. Microfilms Order No. DA9221629

GP-B and STEP are two proposed experiments in basic physics which will utilize drag-free spacecraft in 600 km polar orbits around the earth. By monitoring the activity of the drag-free compensators, it will be possible to obtain in situ drag measurements from which variations in atmospheric density and winds can be observed with unprecedented resolution. With the inclusion of neutral mass spectrometers, it will be possible to distinguish the effects of the various species; thus significantly enhancing the aeronomic contribution of the drag data. The drag information will be contained in both the motion of the spacecraft about the drag-free proof-mass, and the thruster activity. A new smoother has been developed to deconvolve the net forces from the proof-mass sensor measurements. The smoother is an adaptation of an existing algorithm, which has been tailored to cater for completely unknown inputs. After the deconvolution process, the thrust force must be subtracted from the net force to yield the estimate of the drag. Hence, the accuracy of the drag measurements will ultimately depend on the accuracy of the thruster calibration. Perhaps the largest source of uncertainty will be associated with impingement of the thruster plumes on the spacecraft surfaces. It is thus desirable to model these effects. Owing to the low thrust levels, the flow through the GP-B nozzles will be highly rarefied, rendering the conventional continuum model invalid. An experimental procedure was thus devised to characterize the plume structure. A mass spectrometer, modified from a helium leak detector, was used to measure the mass flux distribution. The observed plume shapes were found to be essentially unchanged with mass flow. The experimental results were compared with Boyd's DSMC solutions pertaining to the nozzle geometries and flow conditions used in the experiments. For the assumption of diffuse interaction with the nozzle walls, the numerical results were found to be in excellent agreement with the experimental results. From the results of the plume study, it is concluded that the impingement effects will not be significantly detrimental to the aeronomy coexperiments. Dissert. Abstr.

N93-14038 Purdue Univ., West Lafayette, IN.
ORBIT DETERMINATION ERROR ANALYSIS AND STATION-KEEPING FOR LIBERATION POINT TRAJECTORIES Ph.D. Thesis
Steven Craig Gordon 1991 222 p
Avail: Univ. Microfilms Order No. DA9215555

In the elliptic restricted three-body problem (ER3BP), the two primary masses are assumed to be in known elliptic orbits about their common center of mass. The third (infinitesimal) mass may be positioned near one of the five known Lagrange points located in the coordinate system rotating with the primaries. The bounded motion of the infinitesimal mass relative to a Lagrange point can then be computed. In particular, for the Sun-Earth plus Moon three-body system (where the Earth plus Moon barycenter is treated as one primary mass), orbits in the vicinity of the Lagrange point L1 between the Sun and the Earth are ideal for the study of solar-terrestrial interactions. A quasi-periodic 'Lissajous' trajectory and a much larger, nearly periodic 'halo-type' orbit are used in this effort as nominal paths near L1 in the Sun-Earth plus Moon ER3BP. Trajectory determination for a spacecraft that moves under the influence of the two-body system of forces will be affected by many error sources, including tracking errors and modeling uncertainty. Orbit determination error analysis seeks to quantify the impact of these errors. Covariance analysis is a method of error analysis used in this effort to predict state vector error levels. After a predetermined tracking period, using a selected range and range-rate tracking schedule, specific covariance matrix entries are used to compute standard deviations for each of the six states. The results of error analysis using the Kalman and batch weighted least squares filters are compared, and covariance analysis is used to incorporate additional error sources, such as solar radiation pressure uncertainty. The means and the probability distributions of these state errors are tested using statistical hypothesis tests and goodness of fit tests, respectively. The state error levels are then used in Monte Carlo simulations of three station-keeping methods - two delta velocity controllers and an on/off controller developed from a state feedback algorithm. The total control cost from a single station-keeping simulation is a random variable, and a group of 30 such simulations is used as a random sample. Station-keeping costs for a spacecraft near Lissajous and halo-type nominal paths are then compared using statistical hypothesis tests. Dissert. Abstr.

14 GROUND SUPPORT SYSTEMS AND FACILITIES (SPACE)

Includes launch complexes, research and production facilities; ground support equipment, e.g., mobile transporters; and simulators.

For related information see also *09 Research and Support Facilities (Air).*

N93-13113*# National Aeronautics and Space Administration. Marshall Space Flight Center, Huntsville, AL.
FIRST INTERNATIONAL MICROGRAVITY LABORATORY
Tracy McMahan (Essex Corp., Huntsville, AL.), Charlotte Shea (Essex Corp., Huntsville, AL.), Margaret Wiginton (Essex Corp., Huntsville, AL.), Valerie Neal (Essex Corp., Huntsville, AL.), Michele Gately (Essex Corp., Huntsville, AL.), Lila Hunt (Essex Corp., Huntsville, AL.), Jean Graben (Essex Corp., Huntsville, AL.), Julie Tiderman (Essex Corp., Huntsville, AL.), and Denise Accardi (Essex Corp., Huntsville, AL.) 1990 69 p Original contains color illustrations
(NASA-TM-108007; NAS 1.15:108007) Avail: CASI HC A04/MF A01; 38 functional color pages

This colorful booklet presents capsule information on every aspect of the International Microgravity Laboratory (IML). As part of Spacelab, IML is divided into Life Science Experiments and Materials Science Experiments. Because the life and materials sciences use different Spacelab resources, they are logically paired on the IML missions. Life science investigations generally require significant crew involvement, and crew members often participate as test subjects or operators. Materials missions capitalize on

these complementary experiments. International cooperation consists in participation by the European Space Agency, Canada, France, Germany, and Japan who are all partners in developing hardware and experiments of IML missions. IML experiments are crucial to future space ventures, like the development of Space Station Freedom, the establishment of lunar colonies, and the exploration of other planets. Principal investigators are identified for each experiment. R.L.B.

N93-13372*# National Aeronautics and Space Administration. Goddard Space Flight Center, Greenbelt, MD.
NONCONSERVATIVE FORCE MODEL PARAMETER ESTIMATION STRATEGY FOR TOPEX/POSEIDON PRECISION ORBIT DETERMINATION
S. B. Luthcke (Hughes STX, Inc., Lanham, MD.) and J. A. Marshall Nov. 1992 42 p
(NASA-TM-104575; NAS 1.15:104575; Rept-93B00013) Avail: CASI HC A03/MF A01

The TOPEX/Poseidon spacecraft was launched on August 10, 1992 to study the Earth's oceans. To achieve maximum benefit from the altimetric data it is to collect, mission requirements dictate that TOPEX/Poseidon's orbit must be computed at an unprecedented level of accuracy. To reach our pre-launch radial orbit accuracy goals, the mismodeling of the radiative nonconservative forces of solar radiation, Earth albedo an infrared re-radiation, and spacecraft thermal imbalances cannot produce in combination more than a 6 cm rms error over a 10 day period. Similarly, the 10-day drag modeling error cannot exceed 3 cm rms. In order to satisfy these requirements, a 'box-wing' representation of the satellite has been developed in which, the satellite is modelled as the combination of flat plates arranged in the shape of a box and a connected solar array. The radiative/thermal nonconservative forces acting on each of the eight surfaces are computed independently, yielding vector accelerations which are summed to compute the total aggregate effect on the satellite center-of-mass. Select parameters associated with the flat plates are adjusted to obtain a better representation of the satellite acceleration history. This study analyzes the estimation of these parameters from simulated TOPEX/Poseidon laser data in the presence of both nonconservative and gravity model errors. A 'best choice' of estimated parameters is derived and the ability to meet mission requirements with the 'box-wing' model evaluated. Author

N93-14015*# Tokyo Univ., Sagamihara (Japan). Inst. of Space and Astronautical Science.
MOON PARK: A RESEARCH AND EDUCATIONAL FACILITY
Kyoichi Kuriki, Takao Saito (Obayashi Corp., Tokyo, Japan), and Yukimasa Ogawa (Obayashi Corp., Tokyo, Japan) *In* NASA. Johnson Space Center, The Second Conference on Lunar Bases and Space Activities of the 21st Century, Volume 2 Sep. 1992 p 673-676 (For primary document see N93-13972 03-91)
Avail: CASI HC A01/MF A03

15 LAUNCH VEHICLES AND SPACE VEHICLES

Includes boosters; operating problems of launch/space vehicle systems; and reusable vehicles.

For related information see also *20 Spacecraft Propulsion and Power.*

N93-12611# Wright Lab., Wright-Patterson AFB, OH.
DATA ACQUISITION APPLICATIONS FOR LONG DURATION ELECTROMAGNETIC LAUNCHER EXPERIMENTS Final Report, Mar. 1991 - Apr. 1992
Mark W. Heyse and James B. Cornette Jul. 1992 13 p
(AD-A254546; WL-TP-92-007) Avail: CASI HC A03/MF A01

Investigation of the basic physics associated with Electromagnetic Launcher (EML) operation requires accurate measurement of a number of diverse phenomena. Monitoring and recording EML phenomena during operation over relatively long time frames places unusual demands on a Data Acquisition System (DAS). While the sampling rate requirement is modest by DAS standards of today, the combination of the sampling rate and the number of events to be monitored presents challenges. This paper describes the evolution of a data acquisition approach in use for basic research in the EML area, discusses data acquisition capabilities and requirements, and presents examples of the data that has been obtained using this approach. GRA

N93-13379*# National Aeronautics and Space Administration. Langley Research Center, Hampton, VA.
WEIGHT OPTIMIZATION OF AN AEROBRAKE STRUCTURAL CONCEPT FOR A LUNAR TRANSFER VEHICLE
Lance B. Bush, Resit Unal (Old Dominion Univ., Norfolk, VA.), Lawrence F. Rowell, and John J. Rehder Dec. 1992 20 p
(RTOP 593-11-11-01)
(NASA-TP-3262; L-17120; NAS 1.60:3262) Avail: CASI HC A03/MF A01

An aerobrake structural concept for a lunar transfer vehicle was weight optimized through the use of the Taguchi design method, finite element analyses, and element sizing routines. Six design parameters were chosen to represent the aerobrake structural configuration. The design parameters included honeycomb core thickness, diameter-depth ratio, shape, material, number of concentric ring frames, and number of radial frames. Each parameter was assigned three levels. The aerobrake structural configuration with the minimum weight was 44 percent less than the average weight of all the remaining satisfactory experimental configurations. In addition, the results of this study have served to bolster the advocacy of the Taguchi method for aerospace vehicle design. Both reduced analysis time and an optimized design demonstrated the applicability of the Taguchi method to aerospace vehicle design. Author

N93-13462*# ARC Professional Service Group, Inc., Rome, NY.
PHASED ARRAY FEED DESIGN TECHNOLOGY FOR LARGE APERTURE MICROWAVE RADIOMETER (LAMR) EARTH OBSERVATIONS Final Report
H. K. Schuman Dec. 1992 69 p Prepared for Research Triangle Inst., Research Triangle Park, NC
(Contract NAS1-18925; RTOP 506-49-64-01)
(NASA-CR-189727; NAS 1.26:189727; RTI/4500/017-01F) Avail: CASI HC A04/MF A01

An assessment of the potential and limitations of phased array antennas in space-based geophysical precision radiometry is described. Mathematical models exhibiting the dependence of system and scene temperatures and system sensitivity on phased array antenna parameters and components such as phase shifters and low noise amplifiers (LNA) are developed. Emphasis is given to minimum noise temperature designs wherein the LNA's are located at the array level, one per element or subarray. Two types of combiners are considered: array lenses (space feeds) and corporate networks. The result of a survey of suitable components and devices is described. The data obtained from that survey are used in conjunction with the mathematical models to yield an assessment of effective array antenna noise temperature for representative geostationary and low Earth orbit systems. Practical methods of calibrating a space-based, phased array radiometer are briefly addressed as well. Author

N93-13819 Texas Univ., Austin.
APPROXIMATE OPTIMAL GUIDANCE FOR THE ADVANCED LAUNCH SYSTEM Ph.D. Thesis
Timothy Scott Feeley 1992 166 p
Avail: Univ. Microfilms Order No. DA9225574

A real-time guidance scheme for the problem of maximizing the payload into orbit subject to the equations of motion for a rocket over a spherical, nonrotating Earth is presented. An approximate optimal launch guidance law is developed based upon an asymptotic expansion of the Hamilton-Jacobi-Bellman or dynamic programming equation. The expansion is performed in terms of a small parameter, which is used to separate the dynamics of the problem into primary and perturbation dynamics. For the zeroth-order problem the small parameter is set to zero and a closed-form solution to the zeroth-order expansion term of the Hamilton-Jacobi-Bellman equation is obtained. Higher-order terms of the expansion include the effects of the neglected perturbation dynamics. These higher-order terms are determined from the solution of first-order linear partial differential equations requiring only the evaluation of quadratures. This technique is preferred as a real-time on-line guidance scheme to alternative numerical iterative optimization schemes because of the unreliable convergence properties of these iterative guidance schemes and because the quadratures needed for

the approximate optimal guidance law can be performed rapidly and by parallel processing. Even if the approximate solution is not nearly optimal, when using this technique the zeroth-order solution always provides a path which satisfies the terminal constraints. Results for two-degree-of-freedom simulations are presented for the simplified problem of flight in the equatorial plane and compared to the guidance scheme generated by the shooting method which is an iterative second-order technique. Dissert. Abstr.

16 SPACE TRANSPORTATION

Includes passenger and cargo space transportation, e.g., shuttle operations; and space rescue techniques.

For related information see also *03 Air Transportation and Safety* and *18 Spacecraft Design, Testing and Performance*. For space suits see *54 Man/System Technology and Life Support*.

N93-12876*# National Aeronautics and Space Administration. Langley Research Center, Hampton, VA.

RADIATION DOSE TO CRITICAL BODY ORGANS FOR OCTOBER 1989 PROTON EVENT

Lisa C. Simonsen, William Atwell (Rockwell International Corp., Houston, TX.), John E. Nealy, and Francis A. Cucinotta Sep. 1992 35 p

(RTOP 593-42-31-01)

(NASA-TP-3237; L-17078; NAS 1.60:3237) Avail: CASI HC A03/MF A01

The Geostationary Operational Environmental Satellite (GOES-7) provides high-quality environmental data about the temporal development and energy characteristics of the protons emitted during a solar particle event. The GOES-7 time history of the hourly averaged integral proton flux for various particle kinetic energies are analyzed for the solar proton event occurring October 19-29, 1989. This event is similar to the August 1972 event that has been widely studied to estimate free-space and planetary radiation-protection requirements. By analyzing the time-history data, the dose rates, which can vary over many orders of magnitude in the early phases of the flare, can be estimated as well as the cumulative dose as a function of time. When basic transport results are coupled with detailed body organ thickness distributions calculated with the Computerized Anatomical Man and Computerized Anatomical Female models, the dose rates and cumulative doses to specific organs can be predicted. With these results, the risks of cancer incidence and mortality are estimated for astronauts in free space protected by various water shield thicknesses. Author

N93-12910*# University of Central Florida, Orlando. Mechanical and Aerospace Engineering.

ASSURED CREW RETURN VEHICLE POST LANDING CONFIGURATION DESIGN AND TEST Final Report

1992 363 p

(Grant NAG10-0103)

(NASA-CR-191253; NAS 1.26:191253) Avail: CASI HC A16/MF A03

The 1991-1992 senior Mechanical and Aerospace Engineering Design class continued work on the post landing configurations for the Assured Crew Return Vehicle (ACRV) and the Emergency Egress Couch (EEC). The ACRV will be permanently docked to Space Station Freedom fulfilling NASA's commitment of Assured Crew Return Capability in the event of an accident or illness aboard Space Station Freedom. The EEC provides medical support and a transportation surface for an incapacitated crew member. The objective of the projects was to give the ACRV Project Office data to feed into their feasibility studies. Four design teams were given the task of developing models with dynamically and geometrically scaled characteristics. Groups one and two combined efforts to design a one-fifth scale model for the Apollo Command Module derivative, an on-board flotation system, and a lift attachment point system. This model was designed to test the feasibility of a rigid flotation and stabilization system and to determine the dynamics associated with lifting the vehicle during retrieval. However, due to priorities, it was not built. Group three designed a one-fifth scale model of the Johnson Space Center (JSC) benchmark configuration, the Station Crew Return Alternative Module (SCRAM) with a lift attachment point system. This model helped to determine the flotation and lifting characteristics of the SCRAM configuration. Group four designed a full scale EEC with changeable geometric and geometric and dynamic characteristics. This model provided data on the geometric characteristics of the EEC and on the placement of the CG and moment of inertia. It also gave the helicopter rescue personnel direct input to the feasibility study. Section 1 describes in detail the design of a one-fifth scale model of the Apollo Command Module Derivative (ACMD) ACRV. The objective of the ACMD Configuration Model Team was to use geometric and dynamic constraints to design a one-fifth scale working model of the Apollo Command Module Derivative (ACMD) configuration with a Lift Attachment Point (LAP) System. This model was required to incorporate a rigidly mounted flotation system and the egress system designed the previous academic year. The LAP system was to be used to determine the dynamic effects of locating the lifting points at different locations on the vehicle. The team was then to build and test the model; however, due to priorities, this did not occur. To better simulate the ACMD after a water landing, the nose cone section was removed and the deck area exposed. The areas researched during the design process were construction, center of gravity and moment of inertia, and lift attachment points. Author

N93-13032*# National Aeronautics and Space Administration. John F. Kennedy Space Center, Cocoa Beach, FL.

DEBRIS/ICE/TPS ASSESSMENT AND INTEGRATED PHOTOGRAPHIC ANALYSIS FOR SHUTTLE MISSION STS-47 Final Report, 11-21 Sep. 1992

Gregory N. Katnik, Scott A. Higginbotham, and J. Bradley Davis Nov. 1992 140 p Original contains color illustrations

(NASA-TM-107553; NAS 1.15:107553) Avail: CASI HC A07/MF A02; 65 functional color pages

A debris/ice/TPS assessment and integrated photographic analysis was conducted for Shuttle Mission STS-47. Debris inspections of the flight elements and launch pad were performed before and after launch. Ice/frost conditions on the External Tank were assessed by the use of computer programs, nomographs, and infrared scanner data during cryogenic loading of the vehicle followed by on-pad visual inspection. High speed photography was analyzed after launch to identify ice/debris sources and evaluate potential vehicle damage and/or in-flight anomalies. This report documents the debris/ice/TPS conditions and integrated photographic analysis of Shuttle Mission STS-47, and the resulting effect on the Space Shuttle Program. Author

N93-13455*# National Aeronautics and Space Administration, Washington, DC.

SPACE SHUTTLE ORBITER MODIFICATIONS TO SUPPORT SPACE STATION FREEDOM

Randall Segert and Allyson Lichtenfels (McDonnell-Douglas Space Systems Co., Houston, TX.) 1992 8 p Presented at the 43rd Congress of the International Astronautical Federation, Washington, DC, 28 Aug. - 5 Sep. 1992 Previously announced in IAA as A92-57120

(NASA-TM-108050; NAS 1.15:108050; IAF-92-0689) Avail: CASI HC A02/MF A01

The Space Shuttle will be the primary vehicle to support the launch, assembly, and maintenance of the Space Station Freedom (SSF). In order to accommodate this function, the Space Shuttle orbiter will require significant modifications. These modifications are currently in development in the Space Shuttle Program. The requirements for the planned modifications to the Space Shuttle orbiter are dependent on the design of the SSF. Therefore, extensive coordination is required with the Space Station Freedom Program (SSFP) in order to identify requirements and resolve integration issues. This paper describes the modifications to the Space Shuttle orbiter required to support SSF assembly and operations. Author

N93-13613*# National Aeronautics and Space Administration, Washington, DC.

SLS-1 FLIGHT EXPERIMENTS PRELIMINARY SIGNIFICANT RESULTS

Jan. 1992 39 p Original contains color illustrations

(NASA-TM-108033; NAS 1.15:108033) Avail: CASI HC A03/MF A01; 22 functional color pages

Spacelab Life Sciences-1 (SLS-1) is the first of a series of dedicated life sciences Spacelab missions designed to investigate the mechanisms involved in the physiological adaptation to weightlessness and the subsequent readaptation to 1 gravity (1 G). Hypotheses generated from the physiological effects observed during earlier missions led to the formulation of several integrated experiments to determine the underlying

mechanisms responsible for the observed phenomena. The 18 experiments selected for flight on SLS-1 investigated the cardiovascular, cardiopulmonary, regulatory physiology, musculoskeletal, and neuroscience disciplines in both human and rodent subjects. The SLS-1 preliminary results gave insight to the mechanisms involved in the adaptation to the microgravity environment and readaptation when returning to Earth. The experimental results will be used to promote health and safety for future long duration space flights and, as in the past, will be applied to many biomedical problems encountered here on Earth. Author

N93-13854 Utah State Univ., Logan.
INFRARED EMISSION FROM THE WATER OUTGAS CLOUD OF AN ORBITING VEHICLE INDUCED BY COLLISIONS WITH ATMOSPHERIC GASES Ph.D. Thesis
Kezheng Zhou 1992 114 p
Avail: Univ. Microfilms Order No. DA9222299

The visible and infrared environment at surface of an outgassing spacecraft in low earth orbit was noted as 'space vehicle glow' as early as the 1980's. Studies of the interaction of the large-scale outgas cloud from an orbiter platform with the ambient upper atmospheric environment led to predictions of the possibility of sufficient energy transfer to IR action molecules to produce the possibility of volume IR emission around the platform. An infrared radiation model (IR model) has been developed to study the excitation of water molecules, a major constituent of the vapor cloud surrounding manned spacecraft, by collisions with atmospheric atomic oxygen and molecular nitrogen. In this work, the cylindrical symmetry about a spacecraft's velocity vector is assumed, and the effects of gravity are neglected. Chemical reactions and effects of the vehicle's surfaces are also neglected, and solar and Earth-shine excitation are not considered. The excitation energy (average internal energy approximately 0.5 eV for H2O 6.3-micron band) with respect to the relative collision energy (approximately 2.7 eV) is neglected. The collision energy and momentum are assumed to be conserved in the collision process. The collisional cross section dependent on the collision energy and the scattering angle is used, and the velocity-distribution functions of the interacting neutral gases obtained from the neutral gases interaction model are used to calculate the productions of water excitation states. The excited water molecules are allowed to traverse a distance determined by their velocities after collision and their lifetime until they spontaneously emit an infrared photon. Using the Maxwellian average approximation for water molecule velocity-distribution, the production of the excitation and subsequent emission of IR photons from the large-scale gas cloud as a function of position and their azimuth angle from the orbital platform are presented. The results from various sets of atmospheric and outgassing conditions are presented, and the dependence of the structure and brightness of the emission on outgassing rates and altitudes is discussed. Also, a comparison of these results with some other related works and with the measured radiance levels from the space shuttle flight 51-F has been made. Dissert. Abstr.

N93-13159*# National Aeronautics and Space Administration. Goddard Space Flight Center, Greenbelt, MD.
THE ORBITER STABILITY EXPERIMENT ON STS-40
Werner M. Neupert, Gabriel L. Epstein, James Houston, Kenneth J. Meese, William S. Muney, Thomas B. Plummer, and Frank P. Russo *In its* The 1992 Shuttle Small Payloads Symposium Oct. 1992 p 1-8 (For primary document see N93-13158 03-12)
Avail: CASI HC A02/MF A03

17 SPACE COMM., SPACECRAFT COMM., COMMAND & TRACKING

Includes telemetry; space communications networks; astronavigation and guidance; and radio blackout.

For related information see also *04 Aircraft Communications and Navigation* and *32 Communications and Radar.*

No abstracts in this category.

18 SPACECRAFT DESIGN, TESTING AND PERFORMANCE

Includes satellites; space platforms; space stations; spacecraft systems and components such as thermal and environmental controls; and attitude controls.

For life support systems see *54 Man/System Technology and Life Support.* For related information see also *05 Aircraft Design, Testing and Performance, 39 Structural Mechanics,* and *16 Space Transportation.*

N93-12579# Georgia Inst. of Tech., Atlanta. Computational Mechanics Center.
INNOVATIVE METHODS IN THE DYNAMICS OF LARGE SPACE STRUCTURES Final Report, 15 Jul. 1987 - 14 Sep. 1991
Satya N. Atluri Jul. 1992 10 p
(Contract F49620-87-C-0064)
(AD-A254630; CMC-GIT-92-3; AFOSR-92-0808TR) Avail: CASI HC A02/MF A01

This report presents a summary of 14 papers published in archival literature. The papers deal with the following issues: nonlinear dynamics of finitely deformed space structures; mixed-time, finite element methods for large space structures; rotational motions of constrained multibody systems; and wave propagation in lattice structures. GRA

N93-12720*# National Aeronautics and Space Administration. Ames Research Center, Moffett Field, CA.
PHYSIOLOGICALLY CONSTRAINED AEROCAPTURE FOR MANNED MARS MISSIONS
James Evans Lyne Aug. 1992 151 p
(Grant NAGw-1331; RTOP 505-40-61)
(NASA-TM-103954; A-92149; NAS 1.15:103954) Avail: CASI HC A08/MF A02

Aerobraking has been proposed as a critical technology for manned missions to Mars. The variety of mission architectures currently under consideration presents aerobrake designers with an enormous range of potential entry scenarios. Two of the most important considerations in the design of an aerobrake are the required control authority (lift-to-drag ratio) and the aerothermal environment which the vehicle will encounter. Therefore, this study examined the entry corridor width and stagnation-point heating rate and load for the entire range of probable entry velocities, lift-to-drag ratios, and ballistic coefficients for capture at both Earth and Mars. To accomplish this, a peak deceleration limit for the aerocapture maneuvers had to be established. Previous studies had used a variety of load limits without adequate proof of their validity. Existing physiological and space flight data were examined, and it was concluded that a deceleration limit of 5 G was appropriate. When this load limit was applied, numerical studies showed that an aerobrake with an L/D of 0.3 could provide an entry corridor width of at least 1 degree for all Mars aerocaptures considered with entry velocities up to 9 km/s. If 10 km/s entries are required, an L/D of 0.4 to 0.5 would be necessary to maintain a corridor width of at least 1 degree. For Earth return aerocapture, a vehicle with an L/D of 0.4 to 0.5 was found to provide a corridor width of 0.7 degree or more for all entry velocities up to 14.5 km/s. Aerodynamic convective heating calculations were performed assuming a fully catalytic, 'cold' wall; radiative heating was calculated assuming that the shock layer was in thermochemical equilibrium. Heating rates were low enough for selected entries at Mars that a radiatively cooled thermal protection system might be feasible, although an ablative material would be required for most scenarios. Earth return heating rates were generally more severe than those encountered by the Apollo vehicles, and would require ablative heat shields in all cases. Author

N93-12834 Stanford Univ., CA.
STUDIES OF RADIATIVE EMISSION FROM THE SIMULATED SHOCK LAYER OF THE HUYGENS PROBE Ph.D. Thesis
Chung Sik Park 1992 136 p
Avail: Univ. Microfilms Order No. DA9217864

The presence of methane in the atmosphere of titan leads to substantial radiation and radiative heat transfer in the shock layer of the Huygens probe which will penetrate the Titanian atmosphere in the year of 2003.

Study of the hypervelocity aerophysics of Titan entry is challenging due to the presence of methane which affects the gas radiation significantly and provided motivation for the present study. There are two aspects to the present work, one dealing with a numerical analysis, the other with a shock tube experiment to generate an equivalent radiative environment downstream of a shock entering a simulated Titan atmosphere. In this problem, the flow field is strongly influenced by the lack of thermochemical equilibrium. Thus, the chemical rate equations play an important role as does the choice of a fluid model characterized by three temperatures, namely, a heavy particle translational temperature, a vibrational temperature and an electron temperature. The set of governing equations was solved numerically, which gave results for the distribution of the various major species behind the shock. The radiative emission has been calculated by use of these results. The shock tube experiments made use of a simulated Titan atmosphere energized by a shock wave traveling at 5.75 km/sec; the shock was generated by hydrogen-oxygen combustion in the Stanford High Pressure Shock Tube. Numerical and experimental results were compared. An important result of this study is the estimation of the stagnation point heat transfer, which can be used in the design process, allowing for a more rational heat shield design in the regions of the flight envelope where aerothermodynamic nonequilibrium phenomena are likely to occur.

Dissert. Abstr.

N93-12893*# Alabama Univ., Huntsville. Dept. of Electrical and Computer Engineering.

A MULTIPLE POINTING-MOUNT CONTROL STRATEGY FOR SPACE PLATFORMS Final Report, 11 Apr. 1991 - 10 Apr. 1992

C. D. Johnson Jun. 1992 100 p

(Contract NAS8-36955)

(NASA-CR-184448; NAS 1.26:184448; UAH-5-32639) Avail: CASI HC A05/MF A02

A new disturbance-adaptive control strategy for multiple pointing-mount space platforms is proposed and illustrated by consideration of a simplified 3-link dynamic model of a multiple pointing-mount space platform. Simulation results demonstrate the effectiveness of the new platform control strategy. The simulation results also reveal a system 'destabilization phenomena' that can occur if the set of individual platform-mounted experiment controllers are 'too responsive.' Author

N93-12962# DYNACS Engineering Co., Inc., Clearwater, FL.

ON-ORBIT SUPERVISOR FOR CONTROLLING SPACECRAFT Final Report

Richard J. Vandervoort Jul. 1992 32 p

(Contract F29601-91-C-0033)

(AD-A254342; PL-TR-92-3024; AD-E201165) Avail: CASI HC A03/MF A01

Spacecraft systems of the 1990's and beyond will be substantially more complex than their predecessors. They will have demanding performance requirements and will be expected to operate more autonomously. This underscores the need for innovative approaches to Fault Detection, Isolation and Recovery (FDIR). A hierarchical expert system is presented that provides on-orbit supervision using intelligent FDIR techniques. Each expert system in the hierarchy supervises the operation of a local set of spacecraft functions. Spacecraft operational goals flow top down while responses flow bottom up. The expert system supervisors have a fairly high degree of autonomy. Bureaucratic responsibilities are minimized to conserve bandwidth and maximize response time. Data for FDIR can be acquired local to an expert and from other experts. By using a blackboard architecture for each supervisor, the system provides a great degree of flexibility in implementing the problem solvers for each problem domain. In addition, it provides for a clear separation between facts and knowledge, leading to an efficient system capable of real time response.

GRA

N93-12964# European Space Agency. European Space Research and Technology Center, ESTEC, Noordwijk (Netherlands). Publications Div.

EURECA

Valerie David, ed. 1991 77 p LIMITED REPRODUCIBILITY: More than 20% of this document may be affected by color photographs Original contains color illustrations

(ESA-F-26) Copyright Avail: CASI HC A05/MF A01

The European Space Agency's Eureca space platform is described in pictures and text using colorful folders. This Space Shuttle launched unmanned space platform is unique in that it can be launched, recovered, returned to earth, and possibly be relaunched with a different payload. In fact, Eureca has been designed to carry out five missions over a ten year period. A mission duration of six months at low earth orbit (515 km) offers opportunities to conduct valuable experiments. Introductory folders deal with the spacecraft itself, flight operations, and a user-friendly program. Eureca has 15 components that are each described in a separate folder. Some components included are an Automatic Mirror Furnace, a Solution Growth Facility, Protein Crystallization Facility, and a Multi-Furnace Assembly. Other components included are Exobiology and Radiation Assembly, High Precision Thermostat Instrument, Surface Forces Adhesion Instrument, Solar Spectrum Instrument, and Solar Constant and Variability Instrument. In addition, components such as the Occultation Radiometer Instrument, the Wide Angle Telescope, the Timeband Capture Cell Experiment, the Radio Frequency Ionisation Thruster Assembly, the Inter-Orbit Communication Instrument, and the Advance Solar Gallium Arsenide Array are included.

R.L.B.

N93-13119 Texas Univ., Austin.

DYNAMICS AND CONTROL OF A TUMBLING SATELLITE RETRIEVAL DEVICE Ph.D. Thesis

Jon Mark Neff 1991 116 p

Avail: Univ. Microfilms Order No. DA9128315

The problem of capturing and despinning a satellite in an uncontrolled three-axis tumble is addressed. The proposed solution is a device which resembles a hollow cage. Thin cylindrical elements are arranged in a regular octahedron, forming a three-dimensional space truss with masses mounted at each corner of the octahedron. The device, which is larger than the tumbling satellite, opens at one end and engulfs the satellite. The device maneuvers such that its center of mass is coincident with the satellite's center of mass. By adjusting the corner masses, the device can match the satellite's moment of inertia ratios. Torques are then applied to the device to cause it to match the tumble rates of the satellite. Once this occurs, the torques can be neutralized and the device will follow the satellite's motion in a torque-free tumble. The target (i.e., the satellite) is then motionless in the reference frame of the retrieval device and the satellite can be grappled without fear of damaging solar panels, antennas, or other equipment. Equations are derived which show how the device can vary the mass distribution to match any set of inertia moment ratios. The physical system is shown to be controllable. An optimal control algorithm for tumble matching is then derived and a computer simulation is developed. The results of the computer simulation show that the control algorithm is stable for four test cases involving different satellites in different tumbles.

Dissert. Abstr.

N93-13152*# Alabama Univ., Huntsville. Dept. of Electrical and Computer Engineering.

STUDY OF PLASMA ENVIRONMENTS FOR THE INTEGRATED SPACE STATION ELECTROMAGNETIC ANALYSIS SYSTEM Final Report, 27 Jul. 1991 - 26 Aug. 1992

Nagendra Singh 26 Aug. 1992 64 p

(Contract NAS8-36955)

(NASA-CR-191263; NAS 1.26:191263) Avail: CASI HC A04/MF A01

The final report includes an analysis of various plasma effects on the electromagnetic environment of the Space Station Freedom. Effects of arcing are presented. Concerns of control of arcing by a plasma contactor are highlighted. Generation of waves by contaminant ions are studied and amplitude levels of the waves are estimated. Generation of electromagnetic waves by currents in the structure of the space station, driven by motional EMF, is analyzed and the radiation level is estimated. Author

N93-13425*# Anco Engineers, Inc., Culver City, CA.

TETHER DEPLOYMENT MONITORING SYSTEM, PHASE 2 Final Report

Aug. 1989 183 p

(Contract NAS8-37336; SBIR-09.02-5050)

(NASA-CR-184098; NAS 1.26:184098) Avail: CASI HC A09/MF A02

An operational Tether Deployment Monitoring System (TEDEMS) was constructed that would show system functionality in a terrestrial environment. The principle function of the TEDEMS system is the launching and attachment of reflective targets onto the tether during its deployment. These targets would be tracked with a radar antenna that was pointed

towards the targets by a positioning system. A spring powered launcher for the targets was designed and fabricated. An instrumentation platform and launcher were also developed. These modules are relatively heavy and will influence tether deployment scenarios, unless they are released with a velocity and trajectory closely matching that of the tether. Owing to the tracking range limitations encountered during field trails of the Radar system, final TEDEMS system integration was not completed. The major module not finished was the system control computer. The lack of this device prevented any subsystem testing or field trials to be conducted. Other items only partially complete were the instrumentation platform launcher and modules and the radar target launcher. The work completed and the tests performed suggest that the proposed system continues to be a feasible approach to tether monitoring, although additional effort is still necessary to increase the range at which modules can be detected. The equipment completed and tested, to the extent stated, is available to NASA for use on any future program that requires tether tracking capability. Author

N93-13715*# California Univ., Los Angeles. Dept. of Mechanical, Aerospace and Nuclear Engineering.

FINDINGS OF A REVIEW OF SPACECRAFT FIRE SAFETY NEEDS Final Report

G. E. Apostolakis, I. Catton, T. Paulos, K. Paxton, and S. Jones Jul. 1992 203 p

(Contract NAS3-25975; RTOP 506-48-4C)

(NASA-CR-189181; NAS 1.26:189181; UCLA-ENG-92-19) Avail: CASI HC A10/MF A03

Discussions from a workshop to guide UCLA and NASA investigators on the state of knowledge and perceived needs in spacecraft fire safety and its risk management are reviewed, for an introduction to an analytical and experimental project in this field. The report summarizes the workshop discussions and includes the visual aids used in the presentations. Probabilistic Safety Assessment (PSA) methods, which are currently not used, would be of great value to the designs and operation of future human-crew spacecraft. Key points in the discussions were the importance of understanding and testing smoldering as a likely fire scenario in space and the need for smoke damage modeling, since many fire-risk models ignore this mechanism and consider only heat damage. Author

N93-13919 Southampton Univ. (England).

STUDIES OF SURFACE-INDUCED LUMINESCENCE RELEVANT TO SPACECRAFT GLOW, USING A SEEDED ARC-JET Ph.D. Thesis

William Andrew Derek Greer 1991 253 p

Avail: Univ. Microfilms Order No. BRDX96162

An experimental investigation has been undertaken of surface-induced luminescence under conditions of energetic rarefied flow. A two chamber differentially pumped vacuum system and a dc arc-jet source were used to produce beams seeded with oxygen, nitrogen or nitrous oxide. The beams have been characterized using a combined cylindrical mirror analyzer and quadrupole mass spectrometer instrument. Typically, beams of 0.2 eV (1.55kms exp -1) atomic oxygen seeded in argon, and 0.9eV (3.29kms exp -1) atomic oxygen seeded in helium were obtained, with absolute fluxes of 1.1 x 10(exp 15)/sq cm/s on entry into the test chamber. Analysis of the observations indicates that the process is surface-mediated and that the emissions result from excited particles leaving the surface with a radiative lifetime in the range 15-150 micro-s. The average reaction probability to form an excited particle has been calculated to be approx. 4 x 10(exp -5) per oxygen atom and approx. 1 x 10(exp -4) per nitric oxide molecule. These results are consistent with the formation, desorption and subsequent radiative relaxation of excited nitrogen dioxide. An extensive review of the spacecraft glow phenomenon has been carried out. It has been found that much of the anomalous behavior, including that between different spacecraft and altitudes, can be reconciled by a single hypothesis based on emissions from excited NO2*, via a mechanism similar to the laboratory luminescence. The additional critical process which must be included, under orbital conditions, is the mechanism for provision of sufficient NO flux on the surface. The combination of ambient NO, atom exchange O1 + N2 yields NO + N1, and surface recombination N1 + O1 yields NO can provide such a flux. With certain realistic assumptions the majority of spacecraft glow observations can be explained using the new model. Dissert. Abstr.

N93-14037 Aston Univ., Birmingham (England).

RESONANCE STUDIES OF ARTIFICIAL EARTH SATELLITES Ph.D. Thesis

Mark Steven Gilthorpe 1991 142 p

Avail: Univ. Microfilms Order No. BRDX95558

Orbit determination from artificial satellite observations is a key process in obtaining information about the Earth and its environment. A study of the perturbations experienced by these satellites enables knowledge to be gained of the upper atmosphere, the gravity field, ocean tides, solid-Earth tides, and solar radiation. The gravity field is expressed as a double infinite series of associated Legendre functions (tesseral harmonics). In contemporary global gravity field models, the overall geoid is well determined. An independent check on these gravity field harmonics of a particular order may be made by analysis of satellites that pass through resonance of that order. For such satellites the perturbations of the orbital elements close to resonance are analyzed to derive lumped harmonic coefficients. The orbital parameters of 1984-106A were determined at 43 epochs, during which time the satellite was close to 14th order resonance. Analysis of the inclination and eccentricity yielded six lumped harmonic coefficients of order 14 while analysis of the mean motion yielded additional pairs of lumped harmonics of orders 14, 28, and 42, with the 14th order harmonics superseding those obtained from analysis of the inclination. This thesis concentrates in detail on the theoretical changes of a near-circular satellite orbit perturbed by the Earth's gravity field under the influence of minimal air-drag while in resonance with the Earth. The satellite 1984-106A experienced the interesting property of being temporarily trapped with respect to a secondary resonance parameter due to the low air-drag in 1987. This prompted the theoretical investigation of such a phenomenon. Expressions obtained for the resonance parameter lead to the determination of 8 lumped harmonic coefficients, coincidental to those already obtained. All the derived lumped harmonic values are used to test the accuracy of contemporary gravity field models and the underlying theory in this thesis.

Dissert. Abstr.

N93-14040 Purdue Univ., West Lafayette, IN.

MODEL REDUCTION, SENSOR/ACTUATOR SELECTION AND CONTROL SYSTEM REDESIGN FOR LARGE FLEXIBLE STRUCTURES Ph.D. Thesis

Jae Hoon Kim 1991 139 p

Avail: Univ. Microfilms Order No. DA9215581

The purpose is to study some practical methods for designing a control system for large flexible structures, and to pave a way to integrate all the established ingredients. Three methods are examined: (1) model reduction in both the system and component level; (2) selection of actuators and sensors; and (3) optimal redesign of both the structure and the controller. For system model-reduction, we consider the dynamics of finite bandwidth inputs. When the input dynamics are added to the plant to be reduced by the component cost analysis, the method is called Weighted Component Cost Analysis (WCCA). Analytical expressions of component costs will be drived for both continuous and discrete time cases when a mechanical system is described by modal data. For component model reduction, the component cost analysis and the canonical correlation analysis are combined into a new method, which reduces the model of each component in a large scale multibody system, while taking into account the interactions with the rest of the system. A specified number of actuators are selected from a given set of admissible actuators. The selected set of actuators is likely to use minimum control energy while the required output variance constraints are guaranteed to be satisfied. The actuator selection procedure is an iterative algorithm composed of an output variance constrained control and an input variance constrained control algorithm. In the covariance control theory, there are two conditions for a specified covariance to be assignable to the closed loop system by some stabilizing controller. Sensors and actuators are selected so as to reduce the two assignability conditions to standard Lyapunov and Riccati equations. By solving the Lyapunov and Riccati equations, we may get an assignable closed-loop covariance. The minimum numbers of actuators and sensors needed to assign a covariance to the closed-loop system will be given. For a class of mechanical systems with a given initial controller, the best combination of structure redesign and active dynamic controller will be derived by minimizing active control power. Dissert. Abstr.

N93-14046 Texas A&M Univ., College Station.
CONTROL ALGORITHMS FOR AEROBRAKING IN THE MARTIAN ATMOSPHERE Ph.D. Thesis
Buford Wiley Shipley, Jr. 1991 186 p
Avail: Univ. Microfilms Order No. DA9217023

The Analytic Predictor Corrector (APC) and Energy Controller (EC) atmospheric guidance concepts have been adapted to control an interplanetary vehicle aerobraking in the Martian atmosphere. Changes are made to the APC to improve its robustness to density variations. These modifications include adaptation of a new exit phase algorithm, an adaptive transition velocity to initiate the exit phase, refinement of the reference dynamic pressure calculation and two improved density estimation techniques. The modified controller with the hybrid density estimation technique is called the Mars Hybrid Predictor Corrector (MHPC), while the modified controller with a polynomial density estimator is called the Mars Predictor Corrector (MPC). A Lyapunov Steepest Descent Controller (LSDC) is adapted to control the vehicle. The LSDC lacked robustness, so a Lyapunov tracking exit phase algorithm is developed to guide the vehicle along a reference trajectory. The equilibrium glide entry phase is used for the first part of the trajectory. This algorithm, when using the hybrid density estimation technique to define the reference path, is called the Lyapunov Hybrid Tracking Controller (LHTC). With the polynomial density estimator used to define the reference trajectory, the algorithm is called the Lyapunov Tracking Controller (LTC). These four new controllers are tested using a six degree of freedom computer simulation to evaluate their robustness. MARS-GRAM is used to develop realistic atmospheres for the study. The atmospheres are then perturbed using square wave density pulses. The MHPC, MPC, LHTC and LRC show dramatic improvements in robustness over the APC and EC. The MHPC, MPC, LHTC and LTC all complete the initial phase of testing (using square wave density pulses) with no failures. The second phase tests the MHPC, MPC, LHTC and LTC against atmospheres where the inbound and outbound density functions are different. Square wave density pulses are again used, but only for the outbound leg of the trajectory. All four controllers are able to compensate for the outbound leg density pulses with no hard failures, but the algorithms are sensitive to large amplitude density pulses. Dissert. Abstr.

N93-14087# Aerospace Corp., El Segundo, CA. Engineering and Technology Group.
ON THE SUITABILITY OF NON-HARDENED HIGH DENSITY SRAMs FOR SPACE APPLICATIONS
R. Koga, W. R. Crain, D. D. Lau, S. D. Pinkerton, and B. K. Yi 16 Jul. 1992 27 p
(Contract F04701-88-C-0089)
(AD-A255898; TR-0091(6940-05)-3; SMC-TR-92-36) Avail: CASI HC A03/MF A01

Several non-radiation-hardened high density static RAM's (SRAM's) were tested for susceptibility to single-event upset (SEU) and latchup. Test results indicated that at present only a few such device types are suitable for use in space applications. Several additional factors such as susceptibility to multiple-bit upsets and to radiation-induced permanent damage need to be taken into consideration before these device types can be recommended. One non-hardened SRAM device type has recently been used on a low-Earth orbit satellite, enabling the upset rate measured in space to be compared to that predicted from ground-based testing. GRA

N93-12772*# National Aeronautics and Space Administration. Lewis Research Center, Cleveland, OH.
LDEF YAW AND PITCH ANGLE ESTIMATES
Bruce A. Banks and Linda Gebauer (Cleveland State Univ., OH.) *In* NASA. Langley Research Center, LDEF Materials Workshop 1991, Part 1 Sep. 1992 p 71-92 (For primary document see N93-12769 03-27)
Avail: CASI HC A03/MF A04

N93-13160*# Worcester Polytechnic Inst., MA.
SPACEFLIGHT PAYLOAD DESIGN FLIGHT EXPERIENCE G-408
William W. Durgin, Fred J. Looft, Albert Sacco, Jr., Robert Thompson, Anthony G. Dixon, Dino Roberti (Raytheon Co., Portsmouth, RI.), Robert Labonte (Mitre Corp., Bedford, MA.), and Larry Moschini (Mitre Corp., Bedford, MA.) *In* NASA. Goddard Space Flight Center, The 1992 Shuttle Small Payloads Symposium Oct. 1992 p 9-19 (For primary document see N93-13158 03-12)
Avail: CASI HC A03/MF A03

N93-13180*# Defense Systems, Inc., McLean, VA.
THE DSI SMALL SATELLITE LAUNCHER
S. Nichols, D. Gibbons, J. Wise, and D. Nguyen *In* NASA. Goddard Space Flight Center, The 1992 Shuttle Small Payloads Symposium Oct. 1992 p 221-231 (For primary document see N93-13158 03-12)
Avail: CASI HC A03/MF A03

19 SPACECRAFT INSTRUMENTATION

For related information see also *06 Aircraft Instrumentation* and *35 Instrumentation and Photography.*

N93-13516# Los Alamos National Lab., NM.
THE ALEXIS EXPERIMENT: CURRENT STATUS AND PERFORMANCE
J. J. Bloch, W. C. Priedhorsky, D. Roussel-Dupre, B. C. Edwards, and B. W. Smith 1992 11 p Presented at the SPIE International Symposium on Optical Applied Science and Engineering, San Diego, CA, 19-24 Jul. 1992
(Contract W-7405-eng-36)
(DE92-018601; LA-UR-92-2431; CONF-920792-18) Avail: CASI HC A03/MF A01

The Array of Low Energy X-ray Imaging Sensors (ALEXIS) experiment consists of a mini-satellite containing six wide angle EUV/ultrasoft X-ray telescopes. Its purpose is to map out the sky in three narrow (approximately 5 percent) bandpasses around 66, 71, and 93 eV. The mission will be launched on the Pegasus Air Launched Vehicle in 1992 into a 400 nautical mile, high inclination orbit. The project is a collaborative effort between Los Alamos National Laboratory, Sandia National Laboratory, and the University of California-Berkeley Space Sciences Laboratory. The six telescopes are arranged in three pairs in such a manner that as the satellite spins twice a minute they scan the entire antisolar hemisphere. Each f/1 telescope consists of a spherical multilayer coated mirror with a spherical microchannel plate detector located at the prime focus and a thin aluminum or lexan/boron filter in front of the detector. The multilayer coatings determine the bandpasses of the telescopes. Each telescope has a field of view of 33 degrees. Unlike grazing incidence x-ray telescopes, the point spread function is uniform over the entire field of view with a FWHM of approximately 0.5 degrees determined by spherical aberration. In this paper we present the status of the project as of July 1992 as well as summary results from the pre-flight telescope calibration procedures.
DOE

N93-13870# Naval Research Lab., Washington, DC.
COMPUTER SIMULATION OF A SPACE-BASED INFRARED SURVEILLANCE SENSOR Final Report
R. Lucke, W. Shaffer, and R. Rhodes 7 Sep. 1992 23 p
(AD-A255521; NRL/FR/6521-92-9508) Avail: CASI HC A03/MF A01

Simulation of a Naval Research Laboratory space-based infrared surveillance sensor must include such basic effects as the time-varying geometry of the satellite-to-earth line of sight (LOS), atmospheric emission and attenuation, the optical blur of the sensor's telescope, and the noise and nonuniform response characteristics of the solid-state detectors. A user-oriented, menu-driven software, package called the End-to-End Simulation Package (EESP) has been developed to perform the necessary calculations. In addition to generating accurately simulated imagery, it includes a set of signal processing algorithms for finding moving targets. The EESP computation begins with real IR data (TIMS 1 and Hi-Camp 2 are the primary sources), accepts user inputs for many parameters (e.g., orbital altitude and position of satellite, pixel size, ground and observation point), and ends with target declarations. In between, all effects must be taken into account with sufficient accuracy to give valid results. The simulated sensor is a satellite-borne, scanning, IR radiometer. The satellite is placed in a circular orbit, unrestricted in altitude. The linear focal plane array is mounted in a telescope which, at the user's option can either be placed on a gimbal or use an external steering mirror to achieve LOS pointing control. The linear focal plane array consists of 512 detectors arranged vertically and scans horizontally across the scene through 512 pixels (pixel = resolution element) by means of a scan mirror. GRA

N93-13166*# National Aeronautics and Space Administration. Goddard Space Flight Center, Greenbelt, MD.
A PAYLOAD TO EVALUATE PHOTODIODES FOR THE DETECTION OF SOFT AND HARD X RAYS IN A SPACE ENVIRONMENT USING A GET AWAY SPECIAL
Upendra D. Desai and AmyElizabeth C. Stewart (Maryland Univ., College Park.) *In its* The 1992 Shuttle Small Payloads Symposium Oct. 1992 p 77-84 (For primary document see N93-13158 03-12)
Avail: CASI HC A02/MF A03

20 SPACECRAFT PROPULSION AND POWER

Includes main propulsion systems and components, e.g., rocket engines; and spacecraft auxilliary power sources.

For related information see also *07 Aircraft Propulsion and Power, 28 Propellants and Fuels, 44 Energy Production and Conversion,* and *15 Launch Vehicles and Space Vehicles.*

N93-12575# California Univ., San Diego, La Jolla. Dept. of Applied Mechanics and Engineering Sciences.
AFOSR CONTRACTORS MEETING IN PROPULSION
M. A. Birkan and J. M. Tishkoff 7 Jul. 1992 299 p Meeting held in La Jolla, CA, 15-19 Jun. 1992
(AF Proj. 2308)
(AD-A254484; AFOSR-92-0740TR) Avail: CASI HC A13/MF A03

Abstracts are given for research in airbreathing combustion, rocket propulsion, and diagnostics in reacting media. The research was supported by the Air Force Office of Scientific Research. GRA

N93-12638*# Sverdrup Technology, Inc., Brook Park, OH.
SCALING OF 100 kW CLASS APPLIED-FIELD MPD THRUSTERS Final Report
Roger M. Myers Jul. 1992 30 p Presented at the 28th Joint Propulsion Conference and Exhibit, Nashville, TN, 6-9 Jul. 1992; cosponsored by AIAA, SAE, ASME, and ASEE Previously announced in IAA as A92-54033 Sponsored by NASA. Lewis Research Center
(RTOP 506-42-31)
(NASA-CR-190791; E-7405; NAS 1.26:190791; AIAA Paper 92-3462)
Avail: CASI HC A03/MF A01

Three cylindrical applied-field magnetoplasmadynamic thrusters were tested with argon propellant over a broad range of operating conditions to establish empirical scaling laws for thruster performance. Argon flow rates, discharge currents, and applied-field strengths were varied between 0.025 and 0.14 g/s, 750 to 2000 A, and 0.034 to 0.20T, respectively. The results showed that the thrust reached over five times the self-field value, and that thrust increased linearly with the product of discharge current and applied-field strength and quadratically with the anode radius. While increasing the propellant flow rate increased the thrust, it did not affect the rate of thrust increase with applied-field strength, and at low propellant flow rates the self-field thrust approached 30 percent of the measured thrust. The voltage increased linearly with applied-field strength but was insensitive to the discharge current. The rate of voltage increase with applied-field strength dependent on anode radius. Thruster efficiency increased monotonically with applied-field strength and propellant flow rate. Peak thruster efficiencies were insensitive to changes in anode radius. Electrode power loss and thruster efficiency measurements showed that while the electrode losses decreased with increasing anode radius the plasma losses increased. The opposite behaviors of electrode and plasma losses demonstrates the need to identify ways of independently controlling the thruster loss mechanisms. Author

N93-12659*# Alabama Univ., Huntsville.
STABILITY CODES FOR A LIQUID ROCKET IMPLEMENTED FOR USE ON A PC Final Report, FY 1992
Wilbur Armstrong, George C. Doane, III, and Garvin Dean Jun. 1992 65 p
(Contract NAS8-36955)
(NASA-CR-184453; NAS 1.26:184453) Avail: CASI HC A04/MF A01

The high frequency code has been made an interactive code using FORTRAN 5.0. The option to plot n-tau curves was added using the graphics routines of FORTRAN 5.0 and GRAFMATIC. The user is now able to run with input values non-dimensional (as in the original code) or dimensional. Input data may be modified from the keyboard. The low and intermediate frequency codes have been run through a set of variations. This will help the user to understand how the stability of a configuration will change if any of the input data changes. Author

N93-12840# Lawrence Livermore National Lab., CA.
DEMAND THRUST PUMPED PROPULSION WITH AUTOMATIC WARM GAS VALVING
J. C. Whitehead Jun. 1992 8 p Presented at the 28th Joint Propulsion Conference, Nashville, TN, 6-8 Jul. 1992
(Contract W-7405-eng-48)
(DE92-017435; UCRL-JC-110828; CONF-920747-4) Avail: CASI HC A02/MF A01

Operation of a thrust-on-demand, monopropellant rocket propulsion system which uses lightweight low-pressure tankage, free-piston pumps, and a small high-pressure thrust chamber, is explained. The pump intake-exhaust valves use warm gas pneumatic signals to ensure that two reciprocating pumps are alternately pressurized, with overlap during switchover to permit uninterrupted propellant flow. Experiments demonstrate that the miniature pumps operate at any speed depending on downstream demand, and can deliver nearly their own mass in hydrazine per second, at 7 MPa (1000 psi). The valves, which use the alternating layers of metal and graphite to mitigate the effects of differential thermal expansion, have been warm-gas tested for thousands of cycles. For biopropellant operation, a pair of reciprocating oxidizer pumps would be slaved to the fuel pumps' pneumatic oscillator, to provide for pulsed or continuous demand-driven flow of both liquids. Mass ratios and thrust-to-weight ratios of demand-thrust pumped propulsion systems compare quite favorably to those of pressure-fed and turbo-pumped systems. Due to the relatively high densities of storable propellants, liquid mass fractions greater than 0.95 are attainable with these novel pumps, with thrust/weight ratios above 10. The high performance potential of small propulsion systems which use reciprocating pumps suggests that this technology can significantly increase the capability of many types of small spacecraft. DOE

N93-12874*# Alabama Univ., Huntsville.
BRIEFING NOTES ON PROPULSION STABILITY CODES ADMIT, NYQUIST, AND SSFREQ Final Report
W. C. Armstrong Mar. 1992 28 p
(Contract NAS8-36955)
(NASA-CR-184449; NAS 1.26:184449) Avail: CASI HC A03/MF A01

The piping in a liquid rocket can assume complex configurations due to multiple tanks, multiple engines, and structures that piping must go around. The capability to handle some of these complex configurations have been incorporated into the Low Frequency Code (ADMIT), the Nyquist Code (NYQUIST), and the Intermediate Frequency code (SSFREQ). The capability to modify the input on line has been implemented. The configurations allowed include multiple tanks, multiple engines, and the splitting of a pipe into unequal segments going to different (or the same) engines. Straight pipes, bends, inline accumulators, tuned stubs, Helmholtz resonators, parallel resonators, and pumps are the types of piping that may be used. The three codes require the computation of admittance looking toward the tank. Therefore, they all have a number of similar routines for reading in the tank, piping, and engine descriptions. They also have similar routines for computing the admittance looking toward the tank. ADMIT uses only one type of feedline, either a LOX or FUEL line. NYQUIST can use no feedlines, one feedline (either LOX or FUEL), or two feedlines (both LOX and FUEL). SSFREQ requires both feedlines to be present (LOX and FUEL). The common features of the three codes are discussed first, with two sample runs described. Then each of the three codes are discussed along with the sample runs. Several on-line variations are suggested for the second sample run. Input descriptions and the input for the sample runs are given in the appendices. L.R.R.

N93-12963# Phillips Lab., Edwards AFB, CA.
HIGH ENERGY PROPULSION SYSTEM (HEPS) ANALYSIS Final Report, Jul. 1989 - Jun. 1992
Robert T. Nachtrieb Jul. 1992 117 p
(AD-A254343; AD-E201154; PL-TR-92-3025) Avail: CASI HC A06/MF A02

Deep space missions will require high specific impulse (I(sub sp)) and

large changes in velocity (delta v). The compact energy storage of nuclear fission systems and advanced fusion reactor concepts make them ideal power source candidates for future space applications. Fusion is particularly attractive because it produces more energy than fission, and does not produce long-lived radioactive waste. The purpose of this study was to produce a FORTRAN computer code to analyze the performance of fusion reactors as propulsion concepts. The code simplifies the task of comparing thruster performance while varying individual or multiple reactor parameters. Two potential candidate fusion reactor concepts were modeled and inserted into the reactor system model: (1) the Dense Plasma Focus (DPF); and (2) the Field-Reversed Configuration (FRC). For a fusion thermal rocket, the propulsion relations were established between fusion output and rocket performance, system mass, and mission capability. By varying fusion plasma temperature, fuel mixture ratio, and mission delta v, performance values for comparison are generated, including thrust, I(sub sp), jet power, jet specific power (alpha), thrust-to-weight ratio, and payload-to-system initial mass ratio. GRA

N93-12968*# GenCorp Aerojet, Sacramento, CA. Propulsion Div.
PRESSURE FED THRUST CHAMBER TECHNOLOGY PROGRAM Final Report
Glenn M. Dunn 20 Aug. 1992 126 p
(Contract NAS8-37365)
(NASA-CR-184461; NAS 1.26:184461; KGG-29) Avail: CASI HC A07/MF A02

This is the final report for the Pressure Fed Technology Program. It details the design, fabrication and testing of subscale hardware which successfully characterized LOX/RP combustion for a low cost pressure fed design. The innovative modular injector design is described in detail as well as hot-fire test results which showed excellent performance. The program summary identifies critical LOX/RP design issues that have been resolved by this testing, and details the low risk development requirements for a low cost engine for future Expendable Launch Vehicles (ELVi). Author

N93-13283*# Sverdrup Technology, Inc., Brook Park, OH.
ANODE POWER DEPOSITION IN APPLIED-FIELD MPD THRUSTERS Final Report
Roger M. Myers and George C. Soulas (Ohio State Univ., Columbus.) Jul. 1992 25 p Presented at the 28th Joint Propulsion Conference and Exhibit, Nashville, TN, 6-8 Jul. 1992; sponsored by AIAA, SAE, ASME, and ASEE Previously announced in IAA as A92-54034 Sponsored by NASA. Lewis Research Center
(RTOP 506-32-31)
(NASA-CR-190790; E-7404; NAS 1.26:190790; AIAA Paper 92-3463)
Avail: CASI HC A03/MF A01

Anode power deposition is the principal performance limiter of magnetoplasmadynamic (MPD) thrusters. Current thrusters lose between 50 and 70 percent of the input power to the anode. In this work, anode power deposition was studied for three cylindrical applied magnetic field thrusters for a range of argon propellant flow rates, discharge currents, and applied-field strengths. Between 60 and 95 percent of the anode power depositions resulted from electron current conduction into the anode, with cathode radiation depositing between 5 and 35 percent of the anode power, and convective heat transfer from the hot plasma accounting for less than 5 percent. While the fractional anode power loss decreased with increasing applied-field strength and anode size, the magnitude of the anode power increased. The rise in anode power resulted from a linear rise in the anode fall voltage with applied-field strength and anode radius. The anode fall voltage also rose with decreasing propellant flow rate. The trends indicate that the anode fall region is magnetized, and suggest techniques for reducing the anode power loss in MPD thrusters. Author

N93-13299# Sandia National Labs., Albuquerque, NM.
A COMPUTER PROGRAM FOR ENGINEERING SIMULATIONS OF SPACE REACTOR SYSTEM PERFORMANCE
D. Dobranich 1992 4 p Presented at the Joint American Nuclear Society/European Nuclear Society International Meeting, Chicago, IL, 15-20 Nov. 1992
(Contract DE-AC04-76DP-00789)
(DE92-016400; SAND-92-1200C; CONF-921102-8) Avail: CASI HC A01/MF A01

Nuclear thermal propulsion systems are envisioned as a fast and efficient form of transportation for the exploration of space. Several nuclear reactor concepts have been proposed. This document discusses SAFSIM (System Analysis Flow SIMulator) which is an engineering computer program that allows the fluid mechanic, heat transfer, and reactor dynamic simulation of the entire propulsion system. SAFSIM currently contains three basic physics modules: (1) fluid mechanics, (2) heat transfer, and (3) reactor dynamics. All three modules are coupled to allow the prediction of system performance. The analyst can employ any or all of the physics modules as the problem dictates. DOE

N93-13429*# National Aeronautics and Space Administration. Marshall Space Flight Center, Huntsville, AL.
PROCESS COMPARISON STUDY. MSFC CENTER DIRECTOR'S DISCRETIONARY FUND (CDDF) Final Report
T. Golden and J. Krawiec (Thiokol Corp., Huntsville, AL.) Nov. 1992 12 p
(Proj. 89-03)
(NASA-TM-108382; NAS 1.15:108382) Avail: CASI HC A03/MF A01

A process comparison study was conducted using four different advanced manufacturing techniques to fabricate a composite solid rocket booster systems tunnel cover. Costs and labor hours were tracked to provide the comparison between the processes. A relative structural comparison of the components is also included. The processes utilized included filament winding, pultrusion, automated tape laying, and thermoplastic thermoforming. The hand layup technique is also compared. Of the four advanced processes evaluated, the thermoformed thermoplastic component resulted in the least total cost. The automated tape laying and filament winding techniques closely followed the thermoplastic component in terms of total cost; and, these techniques show the most promise for high quality components and lower production costs. The pultruded component, with its expensive tooling and material requirements, was by far the most expensive process evaluated, although the results obtained would not be representative of large production runs. Author

N93-13818 Auburn Univ., AL.
NUMERICAL INVESTIGATION OF THE FLOW FIELD IN THE HEAD-END, STAR GRAIN SECTION OF A SOLID ROCKET MOTOR DURING IGNITION TRANSIENTS Ph.D. Thesis
Alessandro Ciucci 1991 126 p
Avail: Univ. Microfilms Order No. DA9224036

A model to analyze the unsteady, multi-dimensional, turbulent flows in the head-end, star slot section of a solid rocket motor during ignition transients is developed. This investigation examines the fluid dynamic aspects of the starting transient, and attempts to simulate the time dependent interactions between the igniter plume flow, convective heat transfer to the propellant, mass injection from the surface of the burning propellant grain, and flame spreading. A finite-difference solution of the unsteady, compressible, full Navier-Stokes equations, along with a two-equation k-epsilon turbulence model, is performed utilizing the MacCormack explicit, predictor-corrector technique. The model is validated by comparing computed results with known experimental data. The prediction of the ignition transient sequence from the onset of igniter flow to complete ignition of the head-end, star slot section of a solid rocket motor is performed for three different cases: a single-port igniter and two multi-port igniters, with angles of inclination of the port axis of symmetry to the motor centerline of 22.5 and 45 degs, respectively. The solution shows the temporal development of the flame front and the associated velocity field, and indicates that the multi-port igniters provide a faster ignition transient of the head-end section than the single-port igniter, with shorter ignition lags and higher flame spreading rates. Dissert. Abstr.

N93-13824 Arizona Univ., Tucson.
SCIENTIFIC PREDICTABILITY OF SOLID ROCKET PERFORMANCE: ANALYSES OF THE PROCESSING PARAMETERS Ph.D. Thesis
Daniel Lizarraga Perez 1992 223 p
Avail: Univ. Microfilms Order No. DA9225178

The objective is to present a computational model of the suspensions composing uncured composite solid propellant. Highly concentrated suspensions of more than 50 pct. solid volume were examined with attendence to bimodal mixtures. Study of propellant processing was conducted to determine how this model can be applied to processing.

Experimental work was conducted to supply data for comparison to the computational results. This involved data gathered from an orifice viscometer on viscosity and flow behavior. This model is a tool to study goodness of mixing throughout the processing stages of the propellant. The study into processing focused both on mixing and casting of the suspension. By studying this model for concentration, velocity and thermal behaviors, a better understanding of how well the propellant composition progresses in processing was obtained. A multiple mixture approach was taken. This involved a continuum description for the mixture and each constituent. A Fortran program was written to construct this routine. It was run on both a VAXstation 3100, Model 40 using VMS Digital operating system, and a SUN IPX, using SUN UNIX operating system. The code examined two-dimensional monomodal and bimodal mixture flows through a pipe. It examined concentration between 65 and 75 pcts. Due to the high concentration, it was necessary to apply all inertial and viscous terms within each constituent and the entire mixture. Proper boundary conditions and initial conditions to produce stable runs were found. Both monomodal and biomodal computational results showed good correlations with the experimental data, although a slight dilatation was produced by the program. No dilatation appeared in the experimental work. No concentration drop was detected in either the computational results or experimental work. Dissert. Abstr.

N93-13927 Tennessee Univ., Knoxville.
PARTICLE SIMULATION OF GRID EROSION IN AN ION THRUSTER Ph.D. Thesis
Xiaohang Peng 1991 106 p
Avail: Univ. Microfilms Order No. DA9221797

A particle simulation computational code has been developed to study the effect of charge-exchange-induced grid erosion in electron bombardment ion thrusters. The code is based on the particle-in-cell (PIC) method to simulate the ion flow and a Monte Carlo method to calculate the charge exchange collisions. Both two- and three-dimensional versions of this code have been developed. The two-dimensional model provides a qualitative description of the details of the ion flow and the charge exchange collisions. The three-dimensional version has successfully predicted the experimentally observed erosion pattern in which the maximum erosion occurs at the geometric centers of accelerator grid apertures. Dissert. Abstr.

N93-13971 Carnegie-Mellon Univ., Pittsburgh, PA.
PUBLIC PERCEPTIONS OF THE RISKS OF AN UNFAMILIAR TECHNOLOGY: THE CASE OF USING NUCLEAR ENERGY SOURCES FOR SPACE MISSIONS Ph.D. Thesis
Michael Maharik 1992 449 p
Avail: Univ. Microfilms Order No. DA9220220

This thesis addresses the public perception of the risk of a technology not widely known to laypeople. Its aims were (1) to characterize public perceptions of the risk of using nuclear energy in space and decisions related to this risk, and (2) to extend the 'mental model' methodology to studying public perception of unfamiliar, risky technologies. A model of the physical processes capable of creating risks from using nuclear energy sources in space was first constructed. Then, knowledge and beliefs related to this topic were elicited from three different groups of people. The generality of the findings was examined in a constructive replication with environmentally-oriented people. The possibility of involving the public in decision-making processes related to engineering macro-design was then investigated. Finally, a communication regarding these risk processes was developed and evaluated in an experiment comparing it with communications produced by NASA. Although they included large portions of the expert model, people's beliefs also had gaps and misconceptions. Respondents often used scientific terms without a clear understanding of what they meant. Respondents' mental models sometimes contained scattered and inconsistent entries. The impact of pre-existing mental models was clearly seen. Different groups of people had different patterns of knowledge and beliefs. Nevertheless, respondents expressed reasonable and coherent opinions on choices among engineering options. The CMU brochure, derived from the study of readers' existing mental models, provided a better risk communication tool than NASA's material, reflecting primarily experts' perspective. The better performance of subjects reading either brochure generally reflected adding knowledge on issues that they had not previously known, rather than correcting wrong beliefs. The communication study confirmed a hypothesis that improving knowledge on risk processes related to the use of a technology causes a more favorable attitude towards that technology. Recommendations related to the design and targeting of risk communication, and to public participation in decision-making on using new and risky technologies, are derived. Additional studies that will elicit laypeople's definitions of risk related to specific technologies, and link their detailed understanding of risk-development processes to the perceived dimensions of risk, are suggested. Dissert. Abstr.

N93-14079*# National Aeronautics and Space Administration. Lewis Research Center, Cleveland, OH.
VALIDATION TEST OF 125 Ah ADVANCED DESIGN IPV NICKEL-HYDROGEN FLIGHT CELLS
John J. Smithrick and Stephen W. Hall (Naval Weapons Support Center, Crane, IN.) Jan. 1993 12 p Proposed for presentation at the Eighth Annual Battery Conference on Applications and Advances, Long Beach, CA, 12-14 Jan. 1993; sponsored by California State Univ.
(RTOP 506-41-21)
(NASA-TM-105912; E-7393; NAS 1.15:105912) Avail: CASI HC A03/MF A01

An update of validation test results confirming the advanced design nickel-hydrogen cell is presented. An advanced 125 Ah individual pressure vessel (IPV) nickel-hydrogen cell was designed. The primary function of the advanced cell is to store and deliver energy for long-term, Low-Earth-Orbit (LEO) spacecraft missions. The new features of this design, which are not incorporated in state-of-the-art design cells, are: (1) use of 26 percent rather than 31 percent potassium hydroxide (KOH) electrolyte; (2) use of a patented catalyzed wall wick; (3) use of serrated-edge separators to facilitate gaseous oxygen and hydrogen flow within the cell, while still maintaining physical contact with the wall wick for electrolyte management; and (4) use of a floating rather than a fixed stack (state-of-the-art) to accommodate nickel electrode expansion due to charge/discharge cycling. The significant improvements resulting from these innovations are extended cycle life; enhanced thermal, electrolyte, and oxygen management; and accommodation of nickel electrode expansion. Six 125 Ah flight cells based on this design were fabricated by Eagle-Picher. Three of the cells contain all of the advanced features (test cells) and three are the same as the test cells except they do not have catalyst on the wall wick (control cells). All six cells are in the process of being evaluated in a LEO cycle life test at the Naval Weapons Support Center, Crane, IN, under a NASA Lewis Research Center contract. The catalyzed wall wick cells have been cycled for over 19000 cycles with no cell failures in the continuing test. Two of the noncatalyzed wall wick cells failed (cycles 9588 and 13,900). Author

23 CHEMISTRY AND MATERIALS (GENERAL)

N93-12895*# National Aeronautics and Space Administration. Ames Research Center, Moffett Field, CA.
SOL-GEL SYNTHESIS AND DENSIFICATION OF ALUMINOBOROSILICATE POWDERS. PART 1: SYNTHESIS
Jeffrey Bull, Guna Selvaduray (San Jose State Univ., CA.), and Daniel Leiser Sep. 1992 16 p
(RTOP 506-43-31)
(NASA-TM-103964; A-92107; NAS 1.15:103964) Avail: CASI HC A03/MF A01

Aluminoborosilicate powders high in alumina content were synthesized by the sol-gel process utilizing various methods of preparation. Properties and microstructural effects related to these syntheses were examined. After heating to 600 C for 2 h in flowing air, the powders were amorphous with the metal oxides comprising 87 percent of the weight and uncombusted organics the remainder. DTA of dried powders revealed a T(sub g) at approximately 835 C and an exotherm near 900 C due to crystallization. Powders derived from aluminum secbutoxide consisted of particles with a mean diameter 5 microns less than those from aluminum isopropoxide. Powders synthesized with aluminum isopropoxide produced agglomerates comprised of rod shaped particulates while powders made with the secbutoxide precursor produced irregular glassy shards. Compacts formed from these powders required different loadings for equivalent densities according to the method of synthesis. Author

N93-12896*# National Aeronautics and Space Administration. Ames Research Center, Moffett Field, CA.
SOL-GEL SYNTHESIS AND DENSIFICATION OF ALUMINOBOROSILICATE POWDERS. PART 2: DENSIFICATION
Jeffrey Bull, Guna Selvaduray (San Jose State Univ., CA.), and Daniel Leiser Sep. 1992 25 p
(RTOP 506-43-31)
(NASA-TM-103969; A-92174; NAS 1.15:103969) Avail: CASI HC A03/MF A01

Aluminoborosilicate (ABS) powders, high in alumina content, were synthesized by the sol-gel process utilizing four different methods of synthesis. The effect of these methods on the densification behavior of ABS powder compacts was studied. Five regions of shrinkage in the temperature range 25-1184 C were identified. In these regions, the greatest shrinkage occurred between the gel-to-glass transition temperature (T sub g approximately equal to 835 C) and the crystallization transformation temperature (T sub t approximately equal 900 C). The dominant mechanism of densification in this range was found to be viscous sintering. ABS powders were amorphous to x-rays up to T sub t at which a multiphasic structure crystallized. No 2Al2O3.B2O3 was found in these powders as predicted in the phase diagram. Above T sub t, densification was the result of competing mechanisms including grain growth and boria fluxed viscous sintering. Apparent activation energies for densification in each region varied according to the method of synthesis. Author

24 COMPOSITE MATERIALS

Includes physical, chemical, and mechanical properties of laminates and other composite materials.

For ceramic materials see *27 Nonmetallic Materials.*

N93-12583# Army Materials Technology Lab., Watertown, MA.
COMPRESSION TEST SIMULATION OF THICK-SECTION COMPOSITE MATERIALS Final Report
Tzi-Kang Chen Apr. 1992 24 p
(DA Proj. 1L1-61101-AH-42)
(AD-A255021; MTL-TR-92-25) Avail: CASI HC A03/MF A01

An improved compression test concept for thick-section composite materials based on a stress analysis simulation study is presented. An end loading method involving specimen support by a locked hemispherical seat was identified as the most desirable. The results showed that this method could substantially reduce the stress variation due to specimen imperfection and loading eccentricity. Compression test methods are analyzed using a finite element methodology. Limitations of the test methods are identified with respect to their ability to obtain the desired uniform stress field. The end loading method proved to be superior to the side loading method for the thick-section composite material. The frictional forces introduced by the end loading method can reduce local failure at the specimen end. The zone of end effects on the stress distribution was obtained for the composite material. GRA

N93-12584# Naval Surface Warfare Center, Bethesda, MD. Ship Materials Engineering Dept.
THE 3-D NONLINEAR CONSTITUTIVE MODELING APPROACH FOR COMPOSITE MATERIALS Research and Development Report, Sep. 1990 - May 1992
Karin L. Gipple May 1992 53 p
(NR Proj. R36-25)
(AD-A255022; CDNSWC-SME-92/25) Avail: CASI HC A04/MF A01

This program outlines a three step process to develop nonlinear composite material models, and incorporates those models in a general, large scale structural finite element analysis code. The steps include detailed finite element analyses at the micromechanical (fiber-matrix) level to study material response and nonlinear mechanisms, development of a simplified material model that is representative of the behavior observed in the micromechanical analyses, and the inclusion of the simplified model in the large scale finite element analysis. Only the first two steps are addressed in this paper. Micromechanical finite element analyses of AS4/3501-6 and S2/3501-6 determined stress-strain responses for in-plane and transverse shear, transverse tension, and transverse compression. Variation of the predicted behavior with failure criteria and comparisons to experimental data were also shown. The performance of a simplified material model based on a unit cell analogy was compared to the behavior observed in the micromechanical analyses. GRA

N93-12590*# National Aeronautics and Space Administration. Langley Research Center, Hampton, VA.
PROPERTIES OF FIVE TOUGHENED MATRIX COMPOSITE MATERIALS
Roberto J. Cano and Marvin B. Dow Oct. 1992 60 p
(RTOP 505-63-50)
(NASA-TP-3254; L-17083; NAS 1.60:3254) Avail: CASI HC A04/MF A01

The use of toughened matrix composite materials offers an attractive solution to the problem of poor damage tolerance associated with advanced composite materials. In this study, the unidirectional laminate strengths and moduli, notched (open-hole) and unnotched tension and compression properties of quasi-isotropic laminates, and compression-after-impact strengths of five carbon fiber/toughened matrix composites, IM7/E7T1-2, IM7/X1845, G40-800X/5255-3, IM7/5255-3, and IM7/5260 have been evaluated. The compression-after-impact (CAI) strengths were determined primarily by impacting quasi-isotropic laminates with the NASA Langley air gun. A few CAI tests were also made with a drop-weight impactor. For a given impact energy, compression after impact strengths were determined to be dependent on impactor velocity. Properties and strengths for the five materials tested are compared with NASA data on other toughened matrix materials (IM7/8551-7, IM6/1808I, IM7/F655, and T800/F3900). This investigation found that all five materials were stronger and more impact damage tolerant than more brittle carbon/epoxy composite materials currently used in aircraft structures. Author

N93-12629 Washington Univ., Saint Louis, MO.
HIERARCHIC MODELS FOR LAMINATED PLATES Ph.D. Thesis
Ricardo Luis Actis 1991 232 p
Avail: Univ. Microfilms Order No. DA9223569

Structural plates and shells are three-dimensional bodies, one dimension of which happens to be much smaller than the other two. Thus the quality of a plate or shell model must be judged on the basis of how well its exact solution approximates the corresponding three-dimensional problem. Of course, the exact solution depends not only on the choice of the model but also on the topology, material properties, loading and constraints. The desired degree of approximation depends on the analyst's goals in performing the analysis. For these reasons models have to be chosen adaptively. Hierarchic sequences of models make adaptive selection of the model which is best suited for the purposes of a particular analysis possible. The principles governing the formulation of hierarchic models for laminated plates are presented. The essential features of the hierarchic models described herein are: (1) The exact solutions corresponding to the hierarchic sequence of models converge to the exact solution of the corresponding problem of elasticity for a fixed laminate thickness, and (2) the exact solution of each model converges to the same limit as the exact solution of the corresponding problem of elasticity with respect to the laminate thickness approaching zero. The formulation is based on one parameter (beta) which characterizes the hierarchic sequence of models, and a set of constants whose influence has been assessed by a numerical sensitivity study. The recommended selection of these constants results in the number of fields increasing by three for each increment in the power of beta. Numerical examples analyzed with the proposed sequence of models are included and good correlation with the reference solutions was found. Results were obtained for laminated strips (plates in cylindrical bending) and for square and rectangular plates with uniform loading and with homogeneous boundary conditions. Cross-ply and angle-ply laminates were evaluated and the results compared with those of MSC/PROBE. Hierarchic models make the computation of any engineering data possible to an arbitrary level of precision within the framework of the theory of elasticity. Dissert. Abstr.

N93-12630 State Univ. of New York at Buffalo, Amherst.
FRACTURE TOUGHNESS OF SHORT FIBER/BRITTLE MATRIX COMPOSITES Ph.D. Thesis
Lalit Kumar Jain 1992 148 p
Avail: Univ. Microfilms Order No. DA9222064

The effective fracture toughness of brittle materials can be increased through the addition of short, poorly bonded fibers which bridge the growing

crack. In this research, a micromechanics model is proposed for the post-cracking behavior using the force-crack opening displacement relation for an arbitrarily oriented fiber bridging a matrix crack, the fiber orientation density function, and the fiber location density function. Analytical expressions are obtained for the bridging stress-crack opening displacement relationship and for the steady state fracture energy increment due to bridging fibers. The orientation distribution is likely to be biased depending on the manufacturing process. The model allows the orientation distribution to be prescribed. The location distribution of the fiber centroids is assumed uniform. The model incorporates the snubbing effect observed during fiber withdrawal at an angle to the matrix crack. First, short, inextensible fibers which do not break are analyzed. The results are found to be in the form of a product of the aligned fiber results times a modifying orientation factor. The effect of slip-softening or slip-hardening of the interfacial shear stress caused due to fiber surface smoothing or abrasion, or due to matrix breakdown is also studied. The model is then extended to include fiber breakage, which is observed during pull-out of fibers at large angles. The snubbing effect causes an improvement in bridging stress and energy at smaller fiber lengths (L(f) is less than L(c)), and a reduction in these quantities at large fiber lengths due to an increase in fiber breakage. The effect of fiber length, orientation distribution, and other physical and material parameters is also studied. The extensibility of fibers is then taken into consideration. The comparison with the inextensible case showed that the effect of extensibility on bridging energy is negligible for common material systems. However, it may have a significant effect on bridging stress. The results are expressed as the sum of results for inextensible fibers and an additional term due to extensibility. Dissert. Abstr.

N93-12678*# National Aeronautics and Space Administration. Marshall Space Flight Center, Huntsville, AL.

THE EFFECTS OF COMPRESSIVE PRELOADS ON THE COMPRESSION-AFTER-IMPACT STRENGTH OF CARBON/EPOXY Final Report

A. T. Nettles and D. G. Lance Nov. 1992 21 p

(NASA-TP-3303; M-701; NAS 1.60:3303) Avail: CASI HC A03/MF A01

A preloading device was used to examine the effects of compressive prestress on the compression-after-impact (CAI) strength of 16-ply, quasi-isotropic carbon epoxy test coupons. T300/934 material was evaluated at preloads from 200 to 4000 lb at impact energies from 1 to 9 joules. IM7/8551-7 material was evaluated at preloads from 4000 to 10,000 lb at impact energies from 4 to 16 joules. Advanced design of experiments methodology was used to design and evaluate the test matrices. The results showed that no statistically significant change in CAI strength could be contributed to the amount of compressive preload applied to the specimen. Author

N93-12737*# National Aeronautics and Space Administration. Lewis Research Center, Cleveland, OH.

TRANSVERSE FLEXURAL TESTS AS A TOOL FOR ASSESSING DAMAGE TO PMR-15 COMPOSITES FROM ISOTHERMAL AGING IN AIR AT ELEVATED TEMPERATURES

Kenneth J. Bowles Oct. 1992 15 p

(RTOP 510-01-50)

(NASA-TM-105848; E-7293; NAS 1.15:105848) Avail: CASI HC A03/MF A01

To date, the effect of thermo-oxidative aging on unidirectional composite mechanical properties has been monitored by the measurement of interlaminar shear strength (ILSS) and either three or four point longitudinal flexural strength (LFS) of the composites being tested. Both results are affected by the fiber-to-matrix bonding, the former being dependent on the shear resistance of the interface and the latter on the degree of load sharing by the fibers through the fiber/matrix interface. Recently, fiber/matrix interfacial bond strengths have been monitored using a transverse flexural strength (TFS) test method. This test method was used to evaluate the effect of fiber surface treatment on the fiber/matrix bond. The interface bonding was varied in these tests using Hercules A-fibers with three-types of surfaces that produce bonds of poor, better, and good quality. The TFS was found not only to be sensitive to the bonding, but also to the aging time of unidirectional A-fiber/PMR-15 composites. This relationship reflects the mechanism by which the PMR-15 degrades during thermal aging. Author

N93-12757# Naval Air Development Center, Warminster, PA. Air Vehicle and Crew Systems Technology Dept.

CONSOLIDATION OF POWDER COATED THERMOPLASTIC PREFORM PROCESS MODELING Final Report, Jun. 1989 - Jun. 1991

Roland Cochran 30 Sep. 1992 46 p

(AD-A255094; NADC-91116-60) Avail: CASI HC A03/MF A01

The purpose of this report was to characterize the consolidation of thermoplastic powder coated material. The process of consolidation was studied using several techniques. These included the wedge laminate, direct consolidation measurements and mechanical testing of laminates. The wedge laminate was used to visually characterize the steps of consolidation. The process of particle melting, resin flow, void removal and fiber deformation were determined from this experiment. The consolidation measurements were performed in order to determine the rate of consolidation and the effect of temperature and pressure on the consolidation process. The results of the consolidation experiments were compared to predictions made by a computer model. GRA

N93-12835 Purdue Univ., West Lafayette, IN.

PREDICTIVE FORMING OF ADVANCED THERMOPLASTIC COMPOSITE STRUCTURES Ph.D. Thesis

Cong Wang 1991 184 p

Avail: Univ. Microfilms Order No. DA9215686

The objective of this research is to provide an analytical methodology to model the solid-phase forming of the advanced thermoplastic composite structures. This is achieved through the modelling of the material behavior of the APC-2 thermoplastic composite under forming conditions and the development of a numerical scheme to simulate the forming process. Material responses were observed during the entire forming process. An elastic/viscoplastic constitutive model is used to describe the inelastic and rate-dependent behavior of the advanced thermoplastic composites in the forming and relaxation stages. The strong anisotropy exhibited in the plastic flow is accounted for by a one-parameter plastic potential. Because of a rapid crystallization process in the thermoplastic resin, the thermal stresses developed during the cooling are not sensitive to the cooling rate and can be predicted by a thermo/elastic relationship. The increased mismatch in fiber and matrix properties at elevated temperatures may induce a significant dependence of the composite laminate properties on the change in fiber orientation during forming. The case of a strong scissoring effect on the thermal expansion behavior of (plus or minus 45)ns laminate is shown. A finite element code was developed to numerically simulate the solid-phase forming process. An isoparametric four-node Mindlin plate element with assumed transverse shear strain distribution was implemented in the program. The program was implemented in an updated Lagrange scheme to model the forming of initially preconsolidated and flat composite laminates into general shell structures. Simple contact condition at the part-tool interface is assumed. In the integration of the elastic/viscoplastic constitutive equation, an implicit return-mapping algorithm was developed. This numerical integration scheme is efficient and unconditionally stable. Even though the forming of advanced thermoplastic composites appears to resemble the sheet metal forming process, the underlying deformation mechanisms involved are fundamentally different. Deformation in the former case is mainly contributed by the intraply and interply shear, instead of membrane stretch and local bending. In the finite element implementation, all the inelastic transverse shear deformation at the forming temperature is attributed to the slip in the soft resin-rich layer at the interface of adjacent plies. This assumption reflects the dominance role of interply shear and also facilitates the entire simulation process by keeping the analysis to the first order plate/shell model. The cases of forming (90/0)ns and (plus or minus 45)ns composite laminates over cylindrical and doulbe-curvature tools are included as illustrations. Dissert. Abstr.

N93-12842# Ballistic Research Labs., Aberdeen Proving Ground, MD.

INFLUENCE OF CURE SHRINKAGE ON PROCESS-INDUCED STRESS AND DEFORMATION IN THICK THERMOSETTING COMPOSITES Final Report, Jun. 1989 - Jul. 1991

Travis A. Bogetti and John W. Gillespie, Jr. Jul. 1992 30 p

(AD-A254325; BRL-TR-3380) Avail: CASI HC A03/MF A01

The development of residual sum is strongly influenced by processing history. Residual stress can have a significant effect on the mechanics and performance of composite structures by inducing warpage or initiating matrix cracks and delaminations. A fundamental study of the complex

relationship between processing of thermosetting composites and residual sum has ban conducted by the authors (Bogetti and Gillespie 1989, 1990a, 1990b). A cure simulation analysis coupled to a laminated plate theory model was used to study the development of processing-included sum and deformation in thick-section thermosetting composite laminates. Constitutive models were proposed to describe material behavior chemical hardening and shrinkage) during cure. Thermal expansion and chemical cure shrinkage contribute to changes in material specific volume and represent important sources of internal loading included in the analysis. In this work we focus on the effects cure shrinkage has on residual sum and deformation development in thick section glass/polyester and graphite/epoxy composite laminates. Additionally, model predictions of cure dependent modulus and dimensionless laminate curvature of graphite epoxy cross-ply are presented and found to be in good agreement with previously published experimental data. GRA

N93-12929*# Washington Univ., Seattle. Dept. of Mechanical Engineering.

AN INVESTIGATION OF THE THERMOVISCOPLASTIC BEHAVIOR OF A METAL MATRIX COMPOSITE AT ELEVATED TEMPERATURES

John R. Rogacki and Mark E. Tuttle Oct. 1992 160 p

(Grant NAG1-974; RTOP 505-63-50-04)

(NASA-CR-189706; NAS 1.26:189706) Avail: CASI HC A08/MF A02

This research investigates the response of a fiberless 13 layer hot isostatically pressed Ti-15-3 laminate to creep, constant strain rate, and cyclic constant strain rate loading at temperatures ranging from 482C to 649C. Creep stresses from 48 to 260 MPa and strain rates of .0001 to .01 m/m/sec were used. Material parameters for three unified constitutive models (Bodner-Partom, Miller, and Walker models) were determined for Ti-15-3 from the experimental data. Each of the three models was subsequently incorporated into a rule of mixtures and evaluated for accuracy and ease of use in predicting the thermoviscoplastic response of unidirectional metal matrix composite laminates (both 0 and 90). The laminates were comprised of a Ti-15-3 matrix with 29 volume percent SCS6 fibers. The predicted values were compared to experimentally determined creep and constant strain rate data. It was found that all three models predicted the viscoplastic response of the 0 specimens reasonably well, but seriously underestimated the viscoplastic response of the 90 specimens. It is believed that this discrepancy is due to compliant and/or weak fiber-matrix interphase. In general, it was found that of the three models studied, the Bodner-Partom model was easiest to implement, primarily because this model does not require the use of cyclic constant strain rate tests to determine the material parameters involved. However, the version of the Bodner-Partom model used in this study does not include back stress as an internal state variable, and hence may not be suitable for use with materials which exhibit a pronounced Baushinger effect. The back stress is accounted for in both the Walker and Miller models; determination of the material parameters associated with the Walker model was somewhat easier than in the Miller model. Author

N93-13007 Illinois Univ. at Urbana-Champaign, Savoy.

FINITE ELEMENT ANALYSIS OF ANISOTROPIC VISCOELASTIC COMPOSITE STRUCTURES AND ANALYTICAL DETERMINATION OF OPTIMUM VISCOELASTIC MATERIAL PROPERTIES Ph.D. Thesis

Sung Yi 1992 129 p

Avail: Univ. Microfilms Order No. DA9215915

Quasi-static linear anisotropic viscoelastic responses of composite structures subjected to mechanical and hygrothermal loads are formulated in terms of finite element algorithms. Laplace and/or Fourier transforms rather than direct time integrations are used in this formulation in order to improve accuracy and to save extensive computational time and storage. The present quasi-static viscoelastic analyses require the same computer memory as is needed for corresponding elastic eigenvalue problems. Bending and stretching of composite plates for which analytical solutions exist are examined in order to evaluate the accuracy and effectiveness of the present approach. The time dependent displacement fields in the transverse direction for the cross ply and angle ply laminates are calculated and the stacking sequence effects of the laminates are discussed in detail. Creep responses for GY70/339 composite laminates with or without a circular hole are also studied. The numerical results compare favorably with analytical solutions, i.e., with 1.8 percent for bending and 10(exp -3) percent for tension. Numerical procedures for analyzing dynamic responses of composite structures with time, temperature and moisture dependent linear viscoelastic damping also have been developed in the time domain using variational principles and the Newmark average acceleration method. Recursion formulas have been formulated in order to reduce computer storage and only the previous time solution is required to compute the next time solution. Verification studies were conducted to evaluate the accuracy and convergence of the present numerical algorithm and they show that the numerical solutions agree well with the analytical ones. As examples, the dynamic transient responses of long cantilevered T300/934 composite Euler beams subjected to unit step and impulse loads were calculated using the presently developed procedures. By using generalized Maxwell models, expressions for stored and dissipated energies in anisotropic viscoelastic bodies are derived. The relaxation modulus curves are analytically generated for parameters such as the initial modulus, the fully relaxed equilibrium modulus, the slope of the transition region and the time span of the relaxation. The influences of relaxation modulus shapes and parameters on stored and dissipated energies under specific loads are then analyzed. By using the present finite element methods, the dynamic transient response of cantilever beams with free damping layers on both sides is calculated in order to evaluate performance of free layer damping treatments.

Dissert. Abstr.

N93-13008 Illinois Univ. at Urbana-Champaign, Savoy.

LARGE-DEFLECTION ANALYSIS OF CORD COMPOSITE PLATES Ph.D. Thesis

Ching-Chang Charles Lin 1992 127 p

Avail: Univ. Microfilms Order No. DA9215850

Cord composites, which are constructed by embedding cords in a rubber matrix, have been used in industry for many years. This type of composite is strong in extension in the cord direction but very flexible with regard to bending. Previous studies in predicting the elastic constants of wire cord composites treated the cords as solid cylindrical wires and neglected the mechanical properties of wire strand. Wire strand usually consists of a center wire surrounded by six helical outer wires. It extends and twists when it is loaded by an axial load and twists and extends when it is subjected to a twisting moment. It is also more flexible than the solid cylindrical cord with the same cross sectional area. This coupling and flexibility should be apparent in the response of a cord composite. In the present work, the mechanical properties of wire strand are taken into account in determining the stiffnesses of the cord composite. Kirchhoff plate theory with large deflections is used to study a loaded thin cord composite plate by means of both the energy method and matched asymptotic method. Both the symmetric and antisymmetric part of the displacements are considered for simply supported and clamped boundaries under various loadings and orientations of the cord. The results indicate that when the cord is nearly parallel to the edge of a rectangular plate, the extensional stiffness in the cord direction is much larger than any other stiffnesses of the plate and the membrane effect of the plate is much more important than the bending effect. Since the stiffness transverse to the cord direction is much less than that of the cord direction, distinct transverse boundary layers are found when the displacements become large. Antisymmetry in the displacements becomes apparent when the cord angle is large or when the helix angle of outer wires in the cord is not close to 90 degrees. Dissert. Abstr.

N93-13012 Maryland Univ., College Park.

STRUCTURAL INTEGRITY OF COMPOSITES UNDER LOAD AND THERMAL INSULT Ph.D. Thesis

James Albert Milke 1991 280 p

Avail: Univ. Microfilms Order No. DA9222733

The failure of loaded composite structures exposed to moderate heating conditions for short durations is examined experimentally and analytically using a first-order thermomechanical model. Observations pertaining to the heat flux, load, and time-to-failure are summarized in a three-dimensional failure surface. The experimental and analytical efforts complement each other to develop a broad-based understanding of the conditions leading to failure. Two sets of small-scale tests are performed, one to acquire elevated temperature material property data of a glass-reinforced, thermoplastic composite. The other set of tests are used to provide insight into the failure mechanisms as well as to formulate the failure surface of composite laminates exposed to asymmetric heating conditions. The analytical model includes three-dimensional thermal and structural response analyses. A

progressive failure analysis is conducted to account for the sequence of ply failures leading to laminate failure. Reasonable agreement is obtained between the predictions from the thermal and structural response models and the experimental data. Both experimental and analytical results indicate that char depth and temperature are inadequate predictors of failure. The char depth varies with the level of damage in addition to the severity of the thermal insult. The time-to-failure increases with decreasing flux for all laminates. Differences in the time-to-failure for the three layups increase with decreasing heat flux or load. Thus, at low flux or load levels, the phenomenon is multi-dimensional; whereas at high flux or load levels, failure is one-dimensional. Dissert. Abstr.

N93-13144 Pennsylvania State Univ., University Park.
ACOUSTIC RADIATION FROM A POINT EXCITED INFINITE BILAMINAR PLATE Ph.D. Thesis
Si-Hwan Yum 1992 209 p
Avail: Univ. Microfilms Order No. DA9226810

Presented in this thesis is a refined model for plate deformation which allows for new types of thickness and extensional displacements not currently feasible in the classical or Timoshenko-Mindlin plate theories. An infinite bilaminar plate is fabricated in such a way that the two plates, made of different, isotropic, homogeneous materials, are perfectly bonded. A new mathematical model of the vibration of an infinite bilaminar plate has been obtained by using energy methods. The displacement field is based on symmetric and anti-symmetric displacement functions in both the thickness stretch and the thickness shear of each layer. From this model, the Timoshenko-Mindlin thick plate theory and the Bernoulli-Euler classic plate theory for a single plate can be recovered as special limiting cases. For this model, six-branched frequency-wavenumber spectrums of the single and the bilaminar plates are computed. This allows the introduction of suitable correction coefficients to correct the resulting frequency spectra so that they correspond to those of the exact elasticity theory. In addition, the relationship between frequency and critical angle spectra has been examined. The acoustic pressure directivity of a point force excited plate has been obtained, and the influence of structural damping on the directivity function of the plate is investigated. Dissert. Abstr.

N93-13264# Ames Lab., IA.
DUCTILE FRACTURE PROCESS OF DISCONTINUOUS FIBER REINFORCED COMPOSITES
S. B. Biner 1992 17 p Presented at the Composites 2, Anaheim, CA, 8 Nov. 1992
(Contract W-7405-eng-82)
(DE92-016298; IS-M-714; CONF-921172-1) Avail: CASI HC A03/MF A01

In this study the role of fiber morphology, interface failure and void nucleation mechanisms within the matrix on the deformation and fracture behavior of discontinuous fiber reinforced composites was numerically investigated. The matrix was modeled using a constitutive relationship that accounts for strength degradation resulting from the nucleation and growth of voids, and fibers are assumed to be elastic. The debonding behavior at the fiber interfaces was simulated in terms of a cohesive zone model which describes the decohesion by both normal and tangential separation. The results indicate that in the absence of interface failure, for a given matrix failure mechanism the fiber morphology strongly affects the strength and ductility of discontinuous fiber reinforced composites. The weak interfacial behavior can significantly increase the ductility without sacrificing the strength for certain fiber morphology and for certain void nucleation mechanisms. DOE

N93-13309*# Connecticut Univ., Storrs. Dept. of Mechanical Engineering.
NONLINEAR MECHANICS OF COMPOSITE MATERIALS WITH PERIODIC MICROSTRUCTURE
E. H. Jordan and K. P. Walker (Engineering Science Software, Inc., Smithfield, RI.) 8 Mar. 1991 117 p
(Grant NAG3-882)
(NASA-CR-190750; NAS 1.26:190750) Avail: CASI HC A06/MF A02

This report summarizes the result of research done under NASA NAG3-882 Nonlinear Mechanics of Composites with Periodic Microstructure. The effort involved the development of non-finite element methods to calculate local stresses around fibers in composite materials. The theory was developed and some promising numerical results were obtained. It is expected that when this approach is fully developed, it will provide an important tool for calculating local stresses and averaged constitutive behavior in composites. NASA currently has a major contractual effort (NAS3-24691) to bring the approach developed under this grant to application readiness. The report has three sections. One, the general theory that appeared as a NASA TM, a second section that gives greater details about the theory connecting Greens functions and Fourier series approaches, and a final section shows numerical results. Author

N93-13311*# Alabama Univ., Huntsville. Materials Processing Lab.
FNAS MODIFY MATRIC AND TRANSPARENT EXPERIMENTS Final Report, period ending Nov. 1991
Guy A. Smith, Sue E. Kosten, and Gary L. Workman Apr. 1992 50 p
(Contract NAS8-36955)
(NASA-CR-184442; NAS 1.26:184442) Avail: CASI HC A03/MF A01

Monotectic alloy materials are created by rapid melt/rapid solidification processing on the NASA KC-135. Separation of the uniform liquid into two liquids may occur by either of two processes; spinodal decomposition or nucleation followed by growth. In the first case, the liquid is unstable to composition waves, which form and grow, giving liquids of two different compositions. In the latter process discrete particles of the second liquid phase form via thermal fluctuations and then grow by diffusion. The two processes are very different, with the determining process being dictated by temperature, composition, and thermodynamic characteristics of the alloy. The first two quantities are process variables, while the third is determined by electronic interactions between the atoms in the alloy. In either case the initial alloy decomposition is followed by coarsening, resulting in growth of the particle size at nearly constant volume fraction. In particular, reduced gravity experiments on monotectic solutions have shown a number of interesting results in the KC-135. Monotectic solutions exhibit a miscibility gap in the liquid state, and consequently, gravity driven forces can dominate the solidification parameters at 1 g. In reduced gravity however, the distribution of the phases is different, resulting in new and interesting microstructures. The Rapid Melt/Rapid Quench Furnace allows one to melt a sample and resolidify it in one parabola of the KC-135's flight path, thus eliminating any accumulative influence of multiple parabolas to affect the microstructure of the material. Author

N93-13324# Stanford Univ., CA.
ENABLING TECHNOLOGIES FOR ECONOMICAL MANUFACTURING OF COMPOSITES Final Report, 10 Apr. 1989 - 9 Apr. 1992
Alan K. Miller and George S. Springer 24 Jul. 1992 13 p
(Contract DAAL03-89-K-0083)
(AD-A253615; ARO-26882.3-MS-A) Avail: CASI HC A02/MF A01

Two separate contributions to the state-of-the-art in on-line (out-of-autoclave) consolidation of thermoplastic matrix composites have been developed under this program. First, an induction consolidation sensor has been developed which appears capable of detecting differences in consolidation state without physical contact. The consolidation defects detected are in the category of kissing unbonds (KUB's). Second, in collaboration with Lockheed and the Air Force Phillips Lab, in-situ consolidation of thermoplastic composites by means of direct electrical heating has been demonstrated at realistically high winding speeds. A version of the top-of-component electrode which is capable of off-axis laydown and fabrication of crossplied tubular laminates has been constructed and tested. Reasonably good consolidation has been obtained, though quality assessment is still in progress. GRA

N93-13416* National Aeronautics and Space Administration. Langley Research Center, Hampton, VA.
A TOUGH HIGH PERFORMANCE COMPOSITE MATRIX Patent
Ruth H. Pater, inventor (to NASA) and Norman J. Johnston, inventor (to NASA) 27 Oct. 1992 13 p Filed 31 Oct. 1989 Supersedes N90-26881 (28 - 21, p 2970)
(NASA-Case-LAR-14338-1; US-Patent-5,159,029;
US-Patent-Appl-SN-429514; US-Patent-Class-525-421;
US-Patent-Class-525-426; US-Patent-Class-525-432;
US-Patent-Class-525-436; US-Patent-Class-525-903;
Int-Patent-Class-C08L-49/08; Int-Patent-Class-C08J-5/08) Avail: US Patent and Trademark Office

This invention is a semi-interpenetrating polymer network which includes

a high performance thermosetting polyimide having a nadic end group acting as a crosslinking site and a high performance linear thermoplastic polyimide. An improved high temperature matrix resin is provided which is capable of performing in the 200 to 300 C range. This resin has significantly improved toughness and microcracking resistance, excellent processability, mechanical performance and moisture and solvent resistances.

Official Gazette of the U.S. Patent and Trademark Office

N93-13428*# National Aeronautics and Space Administration. Langley Research Center, Hampton, VA.

RESULTS OF ASTM ROUND ROBIN TESTING FOR MODE 1 INTERLAMINAR FRACTURE TOUGHNESS OF COMPOSITE MATERIALS

T. Kevin OBrien and Roderick H. Martin (Analytical Services and Materials, Inc., Hampton, VA.) Nov. 1992 122 p Prepared in cooperation with Army Aerostructures Directorate, Hampton, VA

(RTOP 505-63-50)

(NASA-TM-104222; NAS 1.15:104222; AVSCOM-TR-92-B-013) Avail: CASI HC A06/MF A02

The results are summarized of several interlaboratory 'round robin' test programs for measuring the mode 1 interlaminar fracture toughness of advanced fiber reinforced composite materials. Double Cantilever Beam (DCB) tests were conducted by participants in ASTM committee D30 on High Modulus Fibers and their Composites and by representatives of the European Group on Fracture (EGF) and the Japanese Industrial Standards Group (JIS). DCB tests were performed on three AS4 carbon fiber reinforced composite materials: AS4/3501-6 with a brittle epoxy matrix; AS4/BP907 with a tough epoxy matrix; and AS4/PEEK with a tough thermoplastic matrix. Difficulties encountered in manufacturing panels, as well as conducting the tests are discussed. Critical issues that developed during the course of the testing are highlighted. Results of the round robin testing used to determine the precision of the ASTM DCB test standard are summarized. Author

N93-13490 Virginia Polytechnic Inst. and State Univ., Blacksburg.

MICROMECHANICS OF FINITE LENGTH FIBERS IN COMPOSITE MATERIALS Ph.D. Thesis

Gregory Paul Carman 1991 210 p

Avail: Univ. Microfilms Order No. DA9204632

A theoretical model is derived to study the point-wise stress variations which occur in the constituents of a hybrid three dimensional short fiber composite subjected to arbitrary homogeneous loading conditions. Validation of the model is accomplished by comparing predicted stiffness properties to experimental data and other accepted models presently available in the literature for polymer matrix composites (PMC's), metal matrix composites (MMC's), and brittle matrix composites (BMC's). A derivation of a theoretical model describing the resulting point-wise stress redistribution which occurs in the matrix and the fibrous regions caused by fiber-fiber interaction at the ends of finite length fibers or fractured fibers is also presented. This theoretical development includes the significant dependence of stress redistribution of fiber volume fraction, constituent properties, and crack size. Therefore, its use is not limited to polymeric composites but is also applicable to metal matrix and ceramic matrix systems. A fiber discount method is proposed to study multiple fiber fractures. A test methodology employing a macro-model composite with embedded strain gauges is presented which can be used to validate (or invalidate) micro-mechanical models. Results obtained with the embedded resistance gauges and the embedded fiber optic strain sensors (FP-FOSS) are validated with classical test and analytical techniques. The ability to vary specific physical parameters in the experimental model, such as fiber aspect ratio, fiber volume fraction, interphase/interface, and constituent properties (i.e., model PMC's and MMC's), in a systematic fashion enables this technique to study various physical aspects present in actual composite systems. The capability to initiate a fiber fracture at a specific location and load level is demonstrated. It is revealed that significantly different strain concentration exists in PMC composites which contain different fiber volume fractions and crack sizes. By varying fiber spacing between neighbors, a study is initiated on composites containing eccentrically located fibers. These results demonstrate that an asymmetric stress state exists in composites containing variable fiber spacing and fiber fractures. The fact that multiple fiber fracture is achieved in a methodical fashion demonstrates the versatility of the model.

Dissert. Abstr.

N93-13527 Michigan Univ., Ann Arbor.

MECHANICAL BEHAVIOUR OF FIBER-REINFORCED CERAMIC MATRIX COMPOSITES Ph.D. Thesis

Chongdu Cho 1991 155 p

Avail: Univ. Microfilms Order No. DA9208515

A detailed investigation of the matrix crack distribution and frictional heating phenomena in fiber-reinforced ceramic composites was undertaken. The distribution of matrix cracks in a uniaxial ceramic composite was examined to determine how the matrix strength distribution influences the distribution in matrix cracks. The analysis shows that matrix strength statistics have a significant effect on the distribution of matrix cracks in a uniaxial composite loaded in tension and that a large variance is to be expected in the crack spacing distribution even when the matrix strength is relatively homogeneous. In the limiting case of a completely homogeneous material, the crack spacing distribution tends to an inverse square distribution between l(sub max) and l(sub max)/2. Experimental measurements of crack spacing distribution for a (0)16 SiC(sub f)/CAS composite show good agreement with the theoretical predictions and suggest that the standard deviation of the matrix strength is of the order of 40 percent of the mean strength. With this magnitude of strength variation, the material exhibits a significant size effect. Frictional heating in a unidirectionally fiber-reinforced ceramic composite is strongly dependent upon loading frequency and mean crack spacing. A mechanism of internal heating which involves the frictional slip of fibers within debonded slip-zones was proposed. Internal heating begins at a peak fatigue stress which was approximately 50 percent below the monotonic proportional limit strength of the composite. For a constant loading frequency and matrix crack spacing, the maximum temperature rise exhibits an approximately linear dependence on stress range or strain range. The dynamic interfacial shear stress remained approximately constant for cyclic loading frequencies from 5 to 25 Hz. During long duration cyclic loading at a frequency of 25 Hz and peak stress of 180 Mpa, the dynamic interfacial showed an initially rapid decrease, followed by a partial recovery. A potential advantage of the frictional heating technique for determining interfacial shear stress is that an average value of frictional shear stress is obtained, rather than a value based upon discrete measurements made on individual fiber/matrix interfaces. The technique can also be readily extended to allow determining the temperature dependence of interfacial shear stress.

Dissert. Abstr.

N93-13724 Virginia Polytechnic Inst. and State Univ., Blacksburg.

EFFECTS OF LAYER WAVINESS ON COMPRESSION-LOADED THERMOPLASTIC COMPOSITE LAMINATES Ph.D. Thesis

Daniel OHare Adams 1991 291 p

Avail: Univ. Microfilms Order No. DA9214567

The effects of layer waviness on the compression response of T300/P1700 carbon/polysulfone composite laminates were investigated both experimentally and analytically. A three-step procedure was used to fabricate isolated layer waves into the central 0 deg layer of laminates. The influence of various layer wave geometries on the static compression strength and compression fatigue life were determined experimentally. Moire interferometry was used to investigate the disturbance in the displacement fields and the modes of deformation associated with layer waviness under compression loading. The state of stress in the vicinity of the layer waves and the influence of the layer waves on static compression strength were predicted using a plane-strain finite element analysis which included material nonlinearity. Layer wave geometries up to 1.5 layer thicknesses in amplitude and 22 layer thicknesses in length were tested. These levels of layer waviness are shown to produce reductions in static strength as high as 36 percent, although the wavy 0 deg accounts for only 20 percent of the load carry capacity of the laminate. Moderate layer wave geometries produce a one and a half decade loss of compression fatigue life as compared to specimens without layer waviness. Specimen failures in both static compression and compression fatigue tests were sudden and catastrophic. Brooming failure, characterized by through-the-thickness splaying of the layers and by numerous delaminations, was the common failure mode. Finite element predictions are shown to correlate with Moire interferometry results in regions of accurate in-plane 0 deg fiber alignment. Interlaminar tension failure is predicted for a more moderate layer wave geometry whereas fiber compression failure is predicted for a more severe layer wave.

Dissert. Abstr.

N93-13748 Delaware Univ., Newark.
VIBRATION DAMPING RESPONSE OF COMPOSITE MATERIALS Ph.D. Thesis
Roger Michael Crane 1991 295 p
Avail: Univ. Microfilms Order No. DA9206320

The investigation of the mechanical vibration damping characteristics of glass/epoxy and graphite/epoxy composite materials are discussed. The objective was to develop an analytical model that incorporates the frequency dependence of the vibration damping loss factor and to experimentally determine the loss factor for frequencies up to 1000 Hz. Numerous analytical models were proposed to determine the loss factor of composites, including micromechanical, macromechanical, and structural models. Of these generic types, the macromechanical models incorporate important material characteristics that can affect the loss factor. The most widely accepted model utilizes the elastic-viscoelastic correspondence principle. Although investigators acknowledge the viscoelastic characteristic of composites, they fail to incorporate the frequency dependence in their analyses. In this effect, the elastic viscoelastic correspondence principle is extended to incorporate the frequency dependence of the composite material. The analytical model requires as input the inplane material loss factors as functions of frequency. An experimental apparatus was designed and fabricated to determine these loss factors. Cantilever beam specimens were excited using an impulse from an instrumented force hammer. The loss factor was calculated using the half power band width technique. The apparatus was calibrated using a well characterized low damping material. The effect of clamping pressure and of the clamp block to specimen interface material was also investigated. While testing the composites, it became evident that the amplitude of vibration had a pronounced effect on the calculated loss factor. Calculated loss factors were significantly reduced if the tip displacement amplitudes vs. time were lower than 0.001 in. for more than 25 percent of the data set. To alleviate this problem, a robust testing methodology was proposed and tested. This methodology was then utilized to determine the composite inplane loss factors. The analytical model was validated using two generic laminated configurations. The model predictions fell within the scatter of the experimental data. Parametric studies were also performed using the model. Trends shown by other investigators as well as inconsistencies between them were accounted for by this model. Dissert. Abstr.

N93-13752 Georgia Inst. of Tech., Atlanta.
STUDIES ON NUMERICAL AND EXPERIMENTAL DETERMINATION OF ENERGY RELEASE RATE FOR COMPOSITE LAMINATES Ph.D. Thesis
Kyong Yop Rhee 1991 133 p
Avail: Univ. Microfilms Order No. DA9206105

Current methods were examined and new alternatives are provided for calculating the energy release rate. First, a simple approach using near-tip stress and displacement distributions was introduced for the computation of the energy release rate component. A cracked lap shear (CLS) specimen with a zero degree stacking sequence was employed. The mode II strain energy release rate, calculated by this approach, was compared with that determined by using the crack closure method. The approach is effective to calculate the energy release rate components and does not require exact information of the stress and displacement distributions at the crack tip. Second, the elastic work factor, eta sub el, concept was applied to calculate the total energy release rate. This was done to examine the applicability of the work factor approach, used in traditional fracture mechanics to calculate the J-integral from a single specimen, for computing energy release rates of composite structures. Four different unidirectional fiber orientations were used to examine the dependence of eta sub el on the material properties, and three different thickness ratios (lap/strap) were used to study how geometric conditions affect eta sub el. Two different calculations of eta sub el were made: compliance method and crack closure method. The two methods produce very comparable eta sub el. Also, while eta sub el is affected significantly by geometric conditions, it is almost independent of fiber orientation once the specimen geometry is defined. Third, experimental study was directed to verify the effectiveness of the eta sub el concept developed previously for calculating total energy release rate from a single specimen. Also, a theoretical elastic work factor, (eta sub el) sub th was developed from a beam analysis. The experimentally determined elastic work factor, (eta sub el) sub exp was compared both with (eta sub el) sub th and with that calculated from finite element analysis, (eta sub el) sub fem. The elastic work factors determined from these three ways are comparable to each other. In addition, the elastic work factor was applied to determine the critical energy release rate, and it was found that the total energy release rate can be determined from a single specimen. Dissert. Abstr.

N93-13775 Wisconsin Univ., Madison.
EXPERIMENTAL CHARACTERIZATION OF CONTINUOUS ALUMINA FIBER/EPOXY Ph.D. Thesis
Yijun Gu 1991 210 p
Avail: Univ. Microfilms Order No. DA9120045

A study of the experimental characteristics of continuous alumina-fiber (FP) reinforced epoxy is presented. The mechanical properties are investigated at ambient and cryogenic temperatures. The experimental research includes compressive strength tests of lamina and laminate, and laminate compressive fatigue. The composites investigated include 0 deg lamina, 90 deg lamina, (0 deg (sub 2)/90 deg (sub 2))(sub s) laminate, and (0 deg/90 deg)(sub 7) laminate; the experimental results are analyzed statistically. The surfaces of the damaged specimens are examined with scanning electron microscopy to reveal failure mechanisms. It is found that under a static load the compressive behavior of FP/Epoxy depends on fiber orientations, stacking sequences, and temperatures. Fibers parallel to the loading direction possess the highest Young's modulus and the lowest ultimate strain, and fibers transverse to the loading direction have the lowest modulus and the highest ultimate strain; crossply laminates are intermediate. The compressive strengths at 77 K are higher than at 295 K, and Young's moduli are about the same at 77 K and at 295 K. Two statistical modeling methods, the linearized stress-life method and the equivalent strength method, are applied to describe the S-N curves from the fatigue data for FP/Epoxy. The fatigue lives of the symmetric laminates and of the 0 deg cylinders of FP/Epoxy become longer if the stress levels are lower. The S-N curves depend on fiber directions, shapes, and testing environments, such as the temperature. Visual observations and an SEM examination of fractured specimens reveal that the loading methods, fiber orientations, testing temperatures, and reinforcing materials influence the failure modes and failure mechanisms of FP/Epoxy composites.
Dissert. Abstr.

N93-13778 Virginia Polytechnic Inst. and State Univ., Blacksburg.
CONTACT OF ORTHOTROPIC LAMINATES WITH A RIGID SPHERICAL INDENTOR Ph.D. Thesis
Chun-Fu Chen 1991 157 p
Avail: Univ. Microfilms Order No. DA9126868

Three dimensional contact problems of square orthotropic laminates indented by a rigid spherical indentor are solved. Simplified problems of indentations of beams and isotropic square plates are studied first to develop an efficient numerical technique and to gather the knowledge of the shape of the contact area in order to solve for the three dimensional orthotropic cases. The approach combines an exact solution method in conjunction with a simple discretization numerical scheme. Numerical sensitivity due to the ill-posed nature of the problem was experienced but was cured by enhancing the numerical approach with a least square spirit. For isotropic plates, the contact area is found to be either a circle or a hypotrocoid of four lobes featured with a shorter length of contact along the through-the-corner directions of the plate. Hertz's theory fails earlier than assuming the contact area to be a circle. In-plane dependence of the contact stress is presented to illustrate the difference of contact behavior between a square plate and a circular plate. Load indentation relation reveals indenting a square plate is harder than indenting a circular plate of a diameter equal to the side length of the square plate. Solutions of multi-layered orthotropic cases are achieved by employing a modified analytical approach with the same numerical method. Three different configurations of plate are implemented for the orthotropic case, namely, a single layered magnesium (Mg) plate, which is slightly orthotropic, and single and double layered plates of graphite-epoxy (G-E), which are highly orthotropic. The concept of modifying the previous hypotrocoids is introduced to investigate the contact stresses for comparatively large indentation conditions. A single-layered G-E plate was implemented for small indentations. The result supports the validity of Hertz's theory for small indentations and shows a relatively longer contact length in the direction of less stiffness. The two-layered G-E plate illustrates similar distributions for the contact stresses along both of the in-plane directions with a smaller

range of validity of Hertzian type behavior than the previous cases. The boundary effect prevails at the initial stage of indentation but is overcome by the effect of material orthotropy as the indentation proceeds. Thus, the contact area for small indentation appears to be the same kind of hypotrocoids as located in the isotropic case but changes to be the other type of hypotrocoids as the indentation advances. Dissert. Abstr.

N93-13779 Brunel Univ., Uxbridge (England).
A NEW ROUTE FOR FIBRE MANAGEMENT IN METAL MATRIX COMPOSITES Ph.D. Thesis
Faiz Ahmad 1990 318 p
Avail: Univ. Microfilms Order No. BRDX93603

Control over the orientation of short fibers in metal matrix composites results in the enhancement of mechanical properties. A systematic approach was adopted for the development of a method for the production of metal matrix composites containing short fibers oriented in preferred directions. The method involves the preparation of polymer binder based compounds containing higher volume loadings of aluminum powder and ceramic fibers. A range of compounds were prepared for conversion into moulded bars using the Multiple Live-Feed Moulding (MLFM) process. Rheological measurements showed that a volume loading of aluminum powder greater than 75 percent can be achieved using a wide particle size distribution in the range 8-45 micron diameter. The flow properties of the metal matrix compounds were measured in the shear rate range required for injection moulding. The concentration with one exception exhibited an increase in viscosity with increase in volume fraction of fibers. The MLFM process was used for the purpose of controlling fiber orientation in a preferred direction in metal matrix compounds. Defect free mouldings of thickness in the range 6 mm to 10 mm were produced; this thickness range was selected for the purpose of binder removal and sintering operations. Fiber degradation analysis was carried out for all compounds and the results showed that volume fraction of fibers had little effect on fiber breakage and an increase in viscosity of the compounds results in an increase in fiber degradation. Moulded bars were produced by conventional and multiple live-feed moulding processes using a range of eight compounds. The fiber orientation distributions were measured and showed that high levels of alignment are possible in thick section moulding. For example, a compound containing 9.75 percent vol. glass fibers and 55.25 percent vol. aluminum powder in a polymer binder and processed using MLFM resulted in more than 70 percent of the fibers aligned parallel to the process direction.
Dissert. Abstr.

N93-13810 Illinois Univ. at Urbana-Champaign, Savoy.
AN INVESTIGATION INTO THERMOMECHANICAL FATIGUE OF METAL MATRIX COMPOSITES Ph.D. Thesis
Metin Karayaka 1992 191 p
Avail: Univ. Microfilms Order No. DA9215835

Experimental and theoretical approaches are used to characterize the thermomechanical deformation behavior of metal matrix composites. Experiments on unreinforced and SiC particulate reinforced Al 2xxx-T4 have been conducted under several mechanical strain-temperature phasing conditions. Based on stress range, substantial improvements in fatigue life have been observed. However, based on strain range, the effect of reinforcement on fatigue lives differs depending on the mechanical strain-temperature phasing, temperature, and strain rate. Several deformation mechanisms of unreinforced and reinforced Al 2xxx-T4 have been identified, including void formation, crack initiation, inter-granular/transgranular crack growth, oxide penetration at the crack tips, crack deflection due to particle interference, and mean stress effects. Theoretical approaches include the development of a general micromechanistic constitutive equation, based on Eshelby's equivalent inclusion theory, and a life prediction methodology for metal matrix composites. Synergistic effects of particulate reinforcement on high temperature thermomechanical behavior are studied. The constitutive model provides insight into the internal stress-strain behavior, including effective and hydrostatic stresses, of both the matrix and the reinforcement developed during cyclic loading conditions. The deformation behavior of the constituents is used to develop an experimentally based micromechanistic life prediction model. The damage caused by internal stresses, oxidation, creep, and fatigue mechanisms as a function of reinforcement volume fraction is quantified for wide range of loading conditions. Dissert. Abstr.

N93-13908 Tennessee Univ., Knoxville.
INVESTIGATIONS OF THE MECHANICAL BEHAVIOR OF GRAPHITE/PEEK (APC-2) COMPOSITES Ph.D. Thesis
Kyun Lee 1991 204 p
Avail: Univ. Microfilms Order No. DA9221780

The effects of two phenomena that are specific to thermoplastic resin composites are investigated. These phenomena are: (1) the significant non-linear creep, that occurs especially at high temperatures, which affects the residual thermal stresses in a geometrically constrained structure, and (2) the spatially non-uniform transverse crystallinity which develops in some fiber-reinforced thermoplastic composites, which introduces spatial variability and non-linearity in the stiffness of the composite. The first part of the thesis is related to the former phenomenon. It presents a computational scheme for the optimal temperature path for APC-2 composite laminate, modeled as non-linear, thermorheologically complex, viscoelastic material. The laminate is assumed to be sufficiently thin to obviate the accounting for temperature non-uniformities across the thickness. An iterative, computational scheme is developed for the particular case of a cross-ply lay-ups laminate, which can be generalized to other symmetric lay-up with minor modifications. As prototype cases, which can provide the guidance, as well as verification checks, for the iterative numerical scheme, analytic solutions are developed for two idealized relaxation models. The second part of the thesis, which concerns the latter phenomenon, presents analytical/computational results for the in-plane stresses in a moderately thick, cross-ply, graphite/PEEK (APC-2) laminate accounting for effects of non-uniform PEEK crystallinity across the plate's thickness. These effects are incorporated as crystallinity-induced variations in the longitudinal modulus E(sub L), including its non-linear dependence on strain. Dissert. Abstr.

N93-13940# Battelle Memorial Inst., Columbus, OH.
NUMERICAL ANALYSIS OF PERMITTIVITY WITH LOSS IN ISOTROPIC BINARY COMPOSITES Technical Report, May - Aug. 1991
Stephen R. Wallin, Marta J. Wallin, John Kosinski, and Arthur Ballato Jun. 1992 124 p
(Contract DAAL03-86-D-0001)
(AD-A255203; SLCET-TR-92-8) Avail: CASI HC A06/MF A02

The use of composite materials and structures to provide characteristics unattainable directly from the constituent materials is well known. Work has been undertaken to apply this principle to the development of new dielectric materials for use in capacitors with greater energy density, lower loss, and higher breakdown resistance. This report describes the numerical analysis of permittivity in isotropic binary composite dielectrics through three-dimensional computer simulation. GRA

N93-13950 Council for National Academic Awards (England).
MECHANICAL PROPERTIES OF EPOXY/ALUMINA TRIHYDRATE-FILLED COMPOSITIONS Ph.D. Thesis
Robin Wainwright 1991 247 p
Avail: Univ. Microfilms Order No. BRDX96142

The mechanical properties of alumina trihydrate (ATH)-filled epoxy resin at loadings of up to 100 parts by weight ATH per hundred of resin (epoxy and hardener) (pphr) have been investigated. A low peak exotherm, increased Young's modulus and increased critical strain energy release rate (G(sub IC)) and critical stress intensity factor (K(sub IC)) can be achieved by incorporating a dispersion of ATH into an epoxy resin. However, the high filler loadings required for effective fire resistance reduce tensile strength and elongation. Tensile modulus increases with filler loading in line with previous studies and theoretical equations. However, the tensile strength is higher and the ultimate elongation lower than current theories predict. The tensile and fracture process in ATH-filled epoxy follows linear elastic fracture mechanics, but can be considered in two parts. The initiation of a crack occurs from a large critical flaw, either as a large particle or agglomerations of particles. A flaw can also be formed on the application of a tensile load, when large stress concentrations cause localized microcracking of the matrix. The propagation of a flaw requires more energy and is dependent on several possible mechanisms. Shear yielding and associated crack blunting are shown to be the most important mechanisms, whilst minor contributions from matrix microcracking and debonding of ATH particles are possible. The absence of crack pinning in this study is believed to be due to the inherently weak nature of ATH particles. The presence of a 10 ppr rubber dispersion in ATH-filled epoxy only increases the values of G(sub IC) and K(sub IC) at low filler loadings.

Amine-terminated butadiene-acrylonitrile rubber (ATBN)-modified epoxy matrix exhibits little adhesion to ATH and therefore the efficiency of stress transfer between particle and matrix is reduced, diminishing shear yielding.
Dissert. Abstr.

N93-13954 Rensselaer Polytechnic Inst., Troy, NY.
THERMOVISCOPLASTIC ANALYSIS OF METAL MATRIX COMPOSITES Ph.D. Thesis
Nan-Ming Yeh 1991 210 p
Avail: Univ. Microfilms Order No. DA9220917

Micromechanics-based thermoviscoplasticity theories based on overstress are developed for metal matrix composites. Three micromechanics models, the vanishing fiber diameter model, the Mori-Tanaka method, and the bimodal model, are used in conjunction with the orthotropic thermoviscoplasticity theory based on overstress to study the thermomechanical behavior of metal matrix composites. Orthotropic thermoviscoplasticity theory based on overstress is a unified theory and does not use yield surfaces and loading/unloading conditions. All material constants can depend on current temperature. It is capable of modeling creep, relaxation, rate sensitivity, and cyclic loading. Numerical experiments using the vanishing fiber diameter model and the orthotropic thermoviscoplasticity theory based on overstress are performed to study the effects of residual stresses, volume fraction, creep, thermal cycling, and ratchetting on the behavior of metal matrix composites. Numerical results for uniaxial and biaxial proportional loading cases of the rate-dependent and the rate-independent vanishing fiber diameter composite model are compared. In addition path-dependent phenomenon is shown for the rate-dependent vanishing fiber diameter composite model under biaxial nonproportional loading cases. To characterize fiber-dominated and matrix-dominated behavior of the metal matrix composite systems numerical experiments using thermoviscoplastic composite models (the vanishing fiber diameter model and the Mori-Tanaka method) are performed for boron/aluminum and graphite/aluminum under thermomechanical loading in different directions. The results for both models are compared and the biomodal assumptions (fiber-dominated and matrix-dominated modes) is found to be appropriate for boron/aluminum. For matrix-dominated stress state the bimodal viscoplasticity theory based on overstress is proposed based on the local orthotropic invariant approach. Numerical simulations of uniaxial (transverse or longitudinal shear direction) and biaxial (transverse and longitudinal shear direction) cases are performed and are compared with the experimental data. The results are discussed. For the purpose of modeling the matrix-dominated low-cycle fatigue damage of metal matrix composites under multiaxial creep-fatigue interaction, an incremental multiaxial life prediction law for metal matrix is proposed. This model consists of the three-dimensional, cyclic neutral thermoviscoplasticity theory based on overstress combined with a multiaxial damage accumulation law to compute the life-time or cycles to crack initiation. The method is intended for application to high temperature low-cycle fatigue with and without hold times and for triangular and trapezoidal waveforms when creep-fatigue interaction takes place. The damage accumulation law correlates fatigue life of 304 stainless steel at 1000 deg F under biaxial tension-torsion cycling with and without hold times. Application to metal matrix composites is possible for matrix low-cycle fatigue failure. At the present time sufficient metal matrix composite low-cycle fatigue data do not appear to be available.
Dissert. Abstr.

N93-13967 Florida Univ., Gainesville.
FINITE ELEMENTS FOR FREE EDGE DELAMINATIONS AND DELAMINATED ANISOTROPIC BEAMS Ph.D. Thesis
Marco Antonio Santos Pinheiro 1991 143 p
Avail: Univ. Microfilms Order No. DA9219229

The major objective of this study is to develop a technique to analyze delaminations in composite beams by using the finite element method. A method is proposed to obtain the strain energy release rate and the stresses ahead of the crack for the specific case of free edge delaminations. A shear deformable beam finite element with nodes offset to either top or bottom side has been developed. The thermal effects originating from the curing process are included in the formulation of the problem. Three different expressions to calculate the strain energy release rate are derived, one in terms of the force and moment resultants in the elements surrounding the crack-tip, and the two others in terms of the forces transmitted by a rigid element placed at the tip of the crack. The stresses ahead of the crack are obtained by using discrete spring elements in the uncracked portion of the beam. The results calculated are in good agreement with results obtained from other studies of the same problem. The advantage of using the present method is that it requires less computational effort, and is capable of modeling any type of geometry, loading, and boundary conditions. An efficient beam finite element has been developed based on a generalized beam theory for anisotropic beams, in which the equilibrium equations are assumed to be satisfied in an average sense over the width of the beam. This introduces a new set of force and moment resultants for the beam. The displacements in the beam are expressed in terms of three deflections, three rotations and one warping term. The effectiveness of the method is illustrated by solving problems where the beam theory solutions are known. The strain energy release rate is determined for the cases of delaminated cantilever beam under torsion and simply supported delaminated beam under transverse loading. Studies are performed to understand the influence of the position of the delamination on the strain energy release rate.
Dissert. Abstr.

N93-13968 Virginia Polytechnic Inst. and State Univ., Blacksburg.
THE ROLE OF THE FIBER/MATRIX INTERPHASE IN THE STATIC AND FATIGUE BEHAVIOR OF POLYMERIC MATRIX COMPOSITE LAMINATES Ph.D. Thesis
Robert Edward Swain, III 1992 290 p
Avail: Univ. Microfilms Order No. DA9220649

Two formidable challenges await those who wish to correlate the strength of the interphase to the mechanical performance of polymeric matrix composite materials. First, one seeks to systematically alter the interphase in order to exploit this variable. Herein, 14 materials systems representing permutations of four carbon fibers, three matrix systems, percentages of fiber surface treatment, and three sizing conditions were examined. Secondly, one needs to quantitatively characterize the properties of the resultant interphase in order to correlate the bond condition to the composite's mechanical behavior. This study uses two techniques, the Continuous Ball Indentation Test and transverse flexure testing, as a means of interrogating the strength of the interphase. The influence of the interphase on the tensile and compressive strength and modulus of cross plied laminates possessing a center hole is studied. Unnotched angle ply laminates are also tested in order to assess the role of the interphase in the strength of a matrix dominated laminate. Fully reversed, axial fatigue of notched cross plied laminates from each of the 14 materials systems is performed. During fatigue testing, several data are monitored, including cycles to failure, dynamic modulus, and notch temperature. The tension-tension fatigue response of the unnotched angle-ply laminates is also studied. Results from x ray radiography of fatigue damaged specimens help to explain the relationship between the interphase and the initiation and propagation of life critical damaged mechanisms. An attempt was made to introduce variables representing the interphase into micromechanical models of composite behavior.
Dissert. Abstr.

N93-14030 Virginia Polytechnic Inst. and State Univ., Blacksburg.
DELAMINATION INITIATION IN POSTBUCKLED DROPPED-PLY LAMINATES Ph.D. Thesis
Carlos Guido Davila 1991 203 p
Avail: Univ. Microfilmes Order No. DA9218021

The compression strength of dropped-ply, graphite-epoxy laminated plates for the delamination mode of failure is studied by analysis and corroborated with experiments. The nonlinear response of the test specimens is modeled by a geometrically nonlinear finite element analysis. The methodology for predicting delamination is based on a quadratic interlaminar stress criterion evaluated at a characteristic distance from the ply drop-off. The details of the complex state of stress in the region of the thickness discontinuity are studied using three-dimensional solid elements, while the uniform sections of the plate are modeled with quadrilateral shell elements. A geometrically nonlinear transition element was developed to couple the shell elements to the solid elements. The analysis was performed using the COmputational MEchanics Testbed (COMET), an advanced structural analysis software environment developed at the NASA Langley Research Center to provide a framework for research in structural analysis methods. Uniaxial compression testing of dropped-ply, graphite-epoxy laminated plates has confirmed that delamination along the interfaces above and/or below the dropped plies is a common mode of failure initiation. The compression strength of specimens exhibiting a linear response is greater than the

compression strength of specimens with the same layup exhibiting geometrically nonlinear response. Experimental and analytical results also show a decrease in laminate strength with increasing number of dropped plies. For linear response there is a large decrease in compression strength with increasing number of dropped plies. For nonlinear response there is less of a reduction in compression strength with increasing number of dropped plies because the nonlinear response causes a redistribution and concentration of interlaminar stresses toward the unloaded edges of the laminate. Dissert. Abstr.

N93-14056 State Univ. of New York at Buffalo, Amherst.
IMPROVING THE TEMPERATURE RESISTANCE OF ALUMINUM-MATRIX COMPOSITES BY USING AN ACID PHOSPHATE BINDER Ph.D. Thesis
Jeng-Maw Chiou 1991 250 p
Avail: Univ. Microfilms Order No. DA9210595

The fabrication of metal-matrix composites by vacuum infiltration of a liquid metal (close to the liquidus temperature) into a SiC whisker preform under an inert gas pressure was shown to produce SiC whisker reinforced aluminum (12 to 37 vol. pct.) which was comparable in quality to those produced by powder metallurgy or squeeze casting. The alpha-SiC whisker preform (22 vol. pct.) was made by wet forming using water and a binder. The use of phosphate binders (with Al(OH)3 and H3PO4 as precursors) instead of the widely used silica (SiO2) binder resulted in increased tensile strength and temperature resistance of the SiC whisker composites. The excess H3PO4 from the acid phosphate binder reacted with SiC to form SiP2O7, which strengthened the preform by acting as an in-situ binder. The excess H3PO4 also reacted with Al to form AlP, which strengthened the Al/binder interface. The combination of SiP2O7 and AlP caused the tensile strength of the SiC whisker composite to increase. The phases Al(PO3)3, SiP2O7 and AlP all contributed to the strenthening of the composites. Upon heating the SiC whisker composites at 400 or 600 C for 240 h, the tensile strength decreased for composites made with the silica binders, but increased for composites made with the phosphate binders. The latter effect increased with increasing P/Al ration in the phosphate binder. This is attributed mainly to the increased amount of SiP2O7, which was present in greater quantity than Al(PO3)3 or AlP. Al-matrix composites containing short (0.1 mm) pitch-based carbon fibers (55 vol. pct.) were similarly prepared, except that the carbon fiber preforms were heated at 200 C prior to metal infiltration. Upon heating the composites at 600 C for 2 to 240 h, the tensile strength decreased for composites made with phosphate or silica binders. This is attributed to the absence of a binder/carbon reaction for both binders. The improvement of the fiber/matrix bonding due to the binder/Al reaction for the case of the phosphate binder was insufficient to overshadow the negative effect related to the absence of a binder/carbon reaction. Nevertheless, the strength decreases after heating at 600 C for 14 h was less for composites made with the phosphate binder than those made with the silica binder. Moreover, the strength decreased less as the phosphate binder amount was increased. Dissert. Abstr.

N93-12780*# National Aeronautics and Space Administration. Marshall Space Flight Center, Huntsville, AL.
PERFORMANCE OF THERMAL CONTROL TAPE IN THE PROTECTION OF COMPOSITE MATERIALS
Rachel R. Kamenetzky and Ann F. Whitaker *In* NASA. Langley Research Center, LDEF Materials Workshop 1991, Part 1 Sep. 1992 p 223-232
(For primary document see N93-12769 03-27)
Avail: CASI HC A02/MF A04

25 INORGANIC AND PHYSICAL CHEMISTRY

Includes chemical analysis, e.g., chromatography; combustion theory; electrochemistry; and photochemistry.

For related information see also *77 Thermodynamics and Statistical Physics.*.

N93-12618# Pittsburgh Univ., PA. Dept. of Chemistry.
HALOGEN SURFACE CHEMISTRY ON Si(100)-(2X1)
John T. Yates, Jr., C. C. Cheng, Q. Gao, and W. J. Choyke 2 Jul. 1992 24 p
(Contract N00014-82-C-0280)
(AD-A254643; TR-50) Avail: CASI HC A03/MF A01

The surface chemistry of adsorbed halogen atoms on Si(100) has been studied using several surface science methods. It has been found using electron-stimulated desorption ion angular distribution (ESDIAD) that Cl atoms bond to dangling bonds on symmetric Si2 dimer sites, and that the Si-Cl bond angle is tilted (25 deg +/- 4 deg) from the normal in the vertical plane containing the symmetric Si2 dimer bond. The covalently-bonded halogens Cl, Br, and I have been studied on Si(100) using atomic hydrogen bombardment at low substrate temperatures (300 - 630 K). In all cases, facile elimination of the hydrogen halide occurs, and the coverage of halogen may be driven to zero by moderate exposure to atomic hydrogen. The halogen extraction process is almost non-activated, suggesting that the chemical reaction to produce hydrogen halide species is driven by the potential energy carried by the atomic hydrogen species. This is an example of an Eley-Rideal reaction process and provides a potentially useful new approach for controlling atomic layer chemistry on semiconductors. GRA

N93-12743# Chemical Research and Development Center, Aberdeen Proving Ground, MD.
VAPOR PRESSURE DATA ANALYSIS METHODOLOGY, STATISTICS, AND APPLICATIONS Final Report, Mar. 1969 - May 1992
Elwin C. Penski Jul. 1992 72 p
(DA Proj. 1L1-62706-A-553)
(AD-A255090; CRDEC-TR-386) Avail: CASI HC A04/MF A01

A method of fitting vapor pressure temperature data to the Antoine equation is described along with a detailed statistical analysis of the fits and calculations of vapor pressures, enthalpies of vaporization, volatilities (concentration of saturated vapors), and boiling points with the Antoine constants. It is shown that the number of digits required to accurately perform vapor pressure calculations is greater than previously believed. The system permits calculation of the limits of error for any level of confidence. A program is used to analyze and plot the available vapor pressure data for diethyl malonate. GRA

N93-12836 Stanford Univ., CA.
COMPUTATION OF STEADY AND UNSTEADY SHOCK-INDUCED COMBUSTION OVER HYPERVELOCITY BLUNT BODIES Ph.D. Thesis
Gregory Jon Wilson 1992 181 p
Avail: Univ. Microfilms Order No. DA9217897

Ballistic-range experiments performed in the 1960s and early 1970s provide excellent data for studying the coupling between supersonic fluid dynamics and nonequilibrium chemical kinetics and for evaluating combustion flow codes. In these experiments, small projectiles were fired at supersonic speeds into a variety of premixed combustible mixtures. Depending on the conditions of the experiment, one will observe either steady or unsteady phenomenon in these complex flows. The unsteady flows are notable for remarkable periodic, high-frequency oscillations (often over 1 MHz) which are still not fully understood. In this dissertation, previous difficulties in numerically simulating ballistic-range exothermic flows are investigated and solutions to both the steady and unsteady cases are presented. A detailed hydrogen-air chemical reaction mechanism with thirteen species and thirty-three reactions is coupled to the Navier-Stokes equations for this purpose. The resulting differential equations are solved using a finite-volume formulation with flux-vector splitting for the spatial differencing and a two-step predictor-corrector scheme to advance the solution in time. A fully-implicit scheme is utilized for the steady cases and a time-accurate point-implicit scheme is used for the unsteady cases. Solutions for the steady ballistic-range flows are used to establish the physical and numerical modeling requirements for accurate computations. The computations of the unsteady ballistic-range cases, believed to be the first such calculations to include a detailed chemical reaction mechanism, help explain the physical mechanism responsible for the observed periodic oscillations. Shadowgraphs made from the numerical solutions are able to reproduce intricate features observed in the experimental shadowgraphs. Further validation is obtained by comparing calculated oscillation frequencies to measured values. In the present work, grid requirements are significantly reduced by the application of a recently proposed logarithmic transformation of the species conservation equations for chemically reacting flow. The choice of the transformation is

motivated by the exponential growth of species concentrations seen in combustion flows and the assumption that a more accurate numerical discretization can be made in a logarithmic space. Dissert. Abstr.

N93-12897# Federal Aviation Administration, Atlantic City, NJ.
VAPOR TO LIQUID RATIO TEST AS AN INDICATOR OF VOLATILITY
Marc Zemel Oct. 1992 11 p
(DOT/FAA/CT-TN92/40) Avail: CASI HC A03/MF A01

A laboratory study on the effects of adding ethanol to motor fuel was performed. This technical note presents the results of Reid vapor pressure and vapor to liquid ratio tests performed on the blended fuels. Increased volatility problems with ethanol blends were uncovered, particularly at 10 to 15 percent ethanol. The investigation also showed how vapor to liquid ratio tests can be useful in areas where Reid vapor pressure data are inconclusive. Author

N93-12935*# Wake Forest Univ., Winston-Salem, NC. Dept. of Chemistry.
THE VIBRATIONAL SPECTRUM OF H2O3: AN AB INITIO INVESTIGATION
Charles F. Jackels [1991] 50 p
(Contract NCC1-55; NSF CHE-89-13800)
(NASA-CR-190968; NAS 1.26:190968) Avail: CASI HC A03/MF A01

Theoretically determined frequencies and absorption intensities are reported for the vibrational spectrum of the covalent HOOOH and hydrogen bonded HO---HOO intermediates that may form in the reaction of the hydroxyl and hydroperoxyl radicals. Basis sets of DZP quality, augmented by diffuse and second sets of polarization functions have been used with CASSCF wave functions. The calculated harmonic vibrational frequencies of HOOOH have been corrected with empirical factors and presented in the form of a 'stick' spectrum. The oxygen backbone vibrations, predicted to occur at 519, 760, and 870 cm(exp -1), are well separated from most interferences, and may be the most useful for the species' identification. In the case of the hydrogen bonded isomer, emphasis has been placed upon prediction of the shifts in the intramolecular vibrational frequencies that take place upon formation of the complex. In particular, the HO stretch and HOO bend of HO2 are predicted to have shifts of -59 and 53 cm(exp -1), respectively, which should facilitate their identification. It is also noted that the antisymmetric stretching frequency of the oxygen backbone in HOOOH exhibits a strong sensitivity to the degree of electron correlation, such as has been previously observed for the same mode in ozone. Author

N93-12995# Massachusetts Univ., Amherst. Dept. of Chemical Engineering.
KINETICS AND DYNAMICS OF OXIDATION REACTIONS INVOLVING AN ADSORBED CO SPECIES
Michael P. Harold and W. Curtis Conner Jul. 1992 8 p
(Contract DE-FG02-87ER-13772)
(DE92-019745; DOE/ER-13772/5) Avail: CASI HC A02/MF A01

Objectives were to formulate kinetic models/mechanistic sequences and to develop bifunctional catalysts for selective oxidation of hydrocarbons. Efforts are reported this year on 3 items: development of Fourier transform infrared emission spectroscopy to monitor near infrared (IR) under reaction conditions (ethylene oxidation on V2O5); kinetics study of methanol oxidation on supported Pt catalysts (methanol-rich feed the CO2 yield exhibits a maximum at an intermediate temperature); and comparative kinetics study of CO oxidation on Pt, Pd, and Rh. The IR spectra of V2O5 show a correlation between the IR features and the degree of surface oxidation. DOE

N93-13096# Polytechnic Univ., Farmingdale, NY.
MICROWAVE AND INFRARED DIELECTRIC RELAXATION OF ALKYLCARBONATES, CHLOROFORM AND THEIR MIXTURES AT 25 C
R. Chandra, Meizhen Xu, Paul Firman, Edward M. Eyring, and Sergio Petrucci 15 Jun. 1992 46 p
(Contract DAAL03-89-K-0148)
(AD-A253606; ARO-26636.3-CH) Avail: CASI HC A03/MF A01

Microwave data yielding the complex permittivity, infrared and visible refractive indices, and infrared attenuation coefficients for liquid dimethyl-carbonate ((CH3O)2CO; abbrev: DMC), chloroform, and their mixtures have been recorded at 25 C. For pure DMC the real part of the complex permittivity versus frequency shows two relaxation domains: the microwave frequency range interpreted as the rotational relaxation of the methoxy groups, -OCH3, around the carbonyl moiety, C=O, and a newly discovered relaxation domain at infrared frequencies. The profile of n(exp 2)(sub IR), (the squared refractive index) versus frequency for pure CHCl3 reveals a new dielectric phenomenon hinted at by literature data obtained at far-IR frequencies. Mixtures of DMC and CHCl3 have a microwave dielectric spectrum that differs markedly from that which would be expected for mole fraction X(sub DMC) = 0.50, if the two components did not interact strongly with each other. The dielectric relaxation frequencies of pure DMC and pure CHCl3 are f(sub r) = 22 GHz and 27 GHz respectively. When mixed at a composition X(sub DMC) = 0.50, a dielectric relaxation spectrum is produced that can be interpreted by a Cole-Cole distribution with an average relaxation frequency f(sub r) = 17 GHz and a distribution relaxation parameter alpha = 0.08 (0 less than alpha less than 1 with alpha = 0 for a singe Debye relaxation process). This dielectric relaxation is ascribed to the formation of H-bonded complexes arising from interactions of the proton of CHCl3 and the carbonyl moiety of DMC. GRA

N93-13188# Lehigh Univ., Bethlehem, PA.
HIGH OCTANE ETHERS FROM SYNTHESIS GAS-DERIVED ALCOHOLS
K. Klier, R. G. Herman, M. A. Johansson, and O. C. Feeley Apr. 1992 23 p
(Contract DE-AC22-90PC-90044)
(DE92-015467; DOE/PC-90044/6) Avail: CASI HC A03/MF A01

The objective of the proposal research is to synthesize high octane ethers, primarily methyl isobutyl ether (MIBE) and methyl tertiary butyl ether (MTBE), directly from H2/CO/CO2 coal-derived synthesis gas via alcohol mixtures that are rich in methanol and 2-methyl-1-propanol (isobutanol). The overall scheme involves gasification of coal, purification and shifting of the synthesis gas, higher alcohol synthesis, and direct synthesis of ethers. DOE

N93-13232# Sandia National Labs., Livermore, CA.
HIGH-RESOLUTION INVESTIGATION OF DEGENERATE FOUR-WAVE MIXING IN THE (GAMMA)(0,0) BAND OF NITRIC OXIDE
R. L. VanderWal, R. L. Farrow, and D. J. Rakestraw 1991 20 p Presented at the 24th International Symposium on Combustion, Sydney (Australia), 5-10 Jul. 1992
(Contract DE-AC04-76DR-00789)
(DE92-005312; SAND-91-8711; CONF-920707-3) Avail: CASI HC A03/MF A01

We report investigations of degenerate four-wave mixing (DFWM) in the NO A 2 Sigma + (left arrow) X 2 Pi (upsilon' = 0 (left arrow) upsilon'' = 0) band for combustion-diagnostic applications. Our objectives were to test the predictions of simple DFWM models concerning the dependence of line shapes and intensities on foreign-gas pressure, to investigate the ability to detect flame-generated NO using DFWM, and to test predictive capabilities of the models by comparing flame spectra to model spectra. Measurements were performed using a single-frequency laser (0.004 cm(sup -1) bandwidth) and a widely tunable multi-mode laser operating near 226 nm. DFWM spectra from thermally generated NO in an H2/O2N2 diffusion flame were obtained with high signal-to-noise ratio and with relatively low saturation. A comparison of a flame spectrum with a model simulation exhibited excellent agreement for the dominant (Q-branch) transitions. The model used the moving-absorber line-shape model and NO spectral data from the literature with no adjusted parameters. The comparison also indicated that the DFWM intensities were well described by a quartic line-strength dependence and that intensities of overlapped transitions were consistent with coherent addition of amplitudes. DOE

N93-13233# Sandia National Labs., Livermore, CA.
THE REACTIONS OF IMIDOGEN WITH NITRIC OXIDE AND MOLECULAR OXYGEN
J. A. Miller and C. F. Melius 1991 18 p Presented at the 24th International Symposium on Combustion, Sydney (Australia), 5-10 Jul. 1992
(Contract DE-AC04-76DR-00789)
(DE92-006697; SAND-91-8732; CONF-920707-13) Avail: CASI HC A03/MF A01

Using potential energy surface information from BAC-MP4 calculations and statistical-dynamical methods, we have calculated the branching fraction for the NH + NO reaction, NH + NO yields N2 + H (1); NH + NO

yields N2O + H (2). We find that reaction (2) dominates over the entire temperature range considered, 300 K less than T less than 3500 K, with f = k(sub 1)/(k(sub 1) + k(sub 2)) varying from about 0.07 at room temperature to about 0.20 at 3500 K. In addition, we have calculated rate coefficients for the two-channel process, NH + O2 yields HNO + O (3); NH + O2 yields NO + OH (4). In this case we find that reaction (4) dominates at low temperature, reaction (3) at high temperature. All these results are discussed in terms of the experimental results available and compared with previous theoretical investigations where appropriate. DOE

N93-13234# Sandia National Labs., Livermore, CA.
HIGH-RESOLUTION RESONANT DEGENERATE 4-WAVE MIXING SPECTROSCOPY
R. L. Farrow, R. L. VanderWahl, and D. J. Rakestraw 1992 2 p Presented at the 13th International Conference on Raman Spectroscopy, Wuerzburg, Fed. Republic of Germany, 31 Aug. - 4 Sep. 1992
(Contract DE-AC04-76DR-00789)
(DE92-012146; SAND-92-8463C; CONF-920872-1) Avail: CASI HC A01/MF A01

In this paper we report high-resolution investigations of degenerate four-wave mixing (DFWM) line shapes in the A 2 Sigma + (left arrow) X 2 Pi (upsilon' = 0 (left arrow) upsilon'' = 0) electronic band of NO. We have quantitatively evaluated a two-level line shape model that accounts for the effects of absorber motion. To our knowledge, this is the first such investigation for a wide range of foreign-gas pressures. Experiments were performed using a single-frequency pulsed laser operating near 226 nm with a bandwidth of 0.0035 cm(sup -1) and pulse energies of less than 2 mJ. A small cell contained NO at pressure typically below 70 mTorr with foreign-gas (He) pressures ranging up to 1100 Torr. We used a (nearly) phase-conjugate geometry in which the pump beams were colinear and counterpropagating and where the probe beam had a small (2.5 degrees) angle in the horizontal plane relative to the pumps. DOE

N93-13314# Institute of Gas Technology, Chicago, IL.
THE MAGSORB PROCESS FOR BULK SEPARATION OF CARBON DIOXIDE
R. A. Knight, R. H. Carty, R. G. Duthie (Bechtel Corp., San Francisco, CA.), and P. A. Pechtl (Bechtel Corp., San Francisco, CA.) Apr. 1992 93 p
(Contract DE-AC21-90MC-26364)
(DE92-001296; DOE/MC-26364/3101) Avail: CASI HC A05/MF A01

The experimental work performed in this program has revealed the impact of formulation procedure on MAGSORB properties, and has shown that the sorbent has adequate potential as a CO2 sorbent for synthesis gas production. MAGSORB is a highly selective CO2 sorbent that does not react with other synthesis gas components (H2, CO, H2O, H2S, or NH3), nor is its performance adversely affected by these components. A technoeconomic analysis has shown that the integration of MAGSORB into a syngas conditioning train can result in significant capital and operating cost benefits when compared with conventional technology. Several areas of further development are still needed. The laboratory preparation method used in this program may not be optimal in terms of sorbent properties and practicality on a commercial scale. Alternative methods involving co-precipitation or co-crystallization of MgCO3 and K2CO3 should be investigated. The life-cycle tests have shown that the sorbent as made in this study loses reactivity after absorption/desorption cycling. A fundamental study of surface properties should be made to determine the cause of deactivation. Specific recommendations for future MAGSORB development activities are given. DOE

N93-13316# Midwest Research Inst., Golden, CO.
HYDROGEN PROGRAM PLAN, FY 1993 - 1997
Jun. 1992 90 p Prepared in cooperation with Energetics, Inc., Columbia, MD
(Contract DE-AC02-83CH-10093)
(DE92-010556; DOE/CH-10093/147) Avail: CASI HC A05/MF A01

This multiyear plan has been developed by the US Department of Energy (DOE) to provide overall guidance and leadership for federal investment in hydrogen research and development (R&D). It suggests critical research programs that can make significant contributions to the development of competitive hydrogen energy systems. It identifies areas where federal research is not timely because even successful results would not sufficiently improve hydrogen's attractiveness in large, national end-use markets. The plan's principal evaluation tool for addressing hydrogen applications is energy pathway analysis. Pathway analysis involves the consideration of all elements of an energy delivery system: required energy input, conversion, transmission, storage, and utilization. Energy losses occur in each of these steps, and inefficiencies are compounded as the energy flow progresses. The final pathway efficiency is the ratio of end-use energy consumed to the input of primary energy. The pathway efficiencies are important because they may affect the required quantity of energy (or fuel), the total delivery system cost, and the level of environmental impact. The analysis shows that some hydrogen pathways are clearly preferable to others when the combined factors of energy efficiency, capital cost, emissions, and domestic resource ownership are considered. Attractive pathways include photoconversion, coal gasification, and bioconversion for both utility and transportation applications. Although they may be preferred approaches, these energy paths involve numerous processes or steps that require technical advancement. The critical technologies that need to be developed, if practical hydrogen pathways are to emerge in the mid and long term, are listed. DOE

N93-13317# Oak Ridge National Lab., TN.
CHEMICAL POTENTIALS IN DILUTE, MULTICOMPONENT SOLUTIONS
D. A. Jonah (Tennessee Univ., Knoxville.) and H. D. Cochran (Tennessee Univ., Knoxville.) Mar. 1992 42 p Presented at the American Institute of Chemical Engineers Annual Meeting, Miami, FL, 1-6 Nov. 1992
(Contract DE-AC05-84OR-21400)
(DE92-011041; CONF-921104-1) Avail: CASI HC A03/MF A01

A new theory of dilute, multicomponent solutions has been derived by expansion about the infinite dilution limit. For dilute, binary mixtures to first order, the theory reduces to that of Debenedetti and Kumar. It is shown that models can be derived within the theory by application of conformal solution theory, fluctuation theory, or their combination. These models have been shown to be useful and accurate in test applications to solutions two solid solutes in a supercritical solvent, quantitatively reproducing the cosolute effect for which correlation with the Peng-Robinson equation of state was only partially successful. Other potential applications include solubility of gases in liquids and solid solubilities in entrained supercritical solvents. DOE

N93-13341# Los Alamos National Lab., NM.
RESONANCE IONIZATION MASS SPECTROMETRY IN BIOCHEMICAL ANALYSIS
J. E. Anderson, B. L. Perez-Lopez, N. S. Nogar, R. C. Estler, and J. E. Conia 1992 5 p Presented at the 6th International Symposium on Resonance Ionization Spectroscopy and its Applications, Santa Fe, NM, 24-29 May 1992
(Contract W-7405-eng-36)
(DE92-017407; LA-UR-92-1813; CONF-920574-12) Avail: CASI HC A01/MF A01

Resonance Ionization Mass Spectrometry (RIMS) is a form of laser-based mass that is finding increasing applications in elemental and isotopic analysis, particular in biochemical systems. Significant attributes include: (1) excellent sensitivity--sub-fg, absolute; sub-ppb, relative; (2) information on isotopic distributions; (3) reduction of background (relative to conventional mass spectrometry) due to the sample matrix. The high sensitivity allows the use of very small sample sizes; this is potentially important in trace element analysis for infants, neonates, or other hard-to-obtain samples. Isotopic measurements can provide direct absolute signal calibration, as well as being applicable to kinetic analysis, such as trace metal uptake studies. The selectivity of RIMS provides for accurate measurements with little or no sample preparation. This, in turn, improves the speed and accuracy of the analysis. Furthermore, resonance ionization can be adapted for use with many pre-existing mass spectrometric systems. We report here on three applications of RIMS: the detection of trace levels of chromium; the quantification of trace chromium in urine; and, the uptake of copper by single cells. DOE

N93-13456*# Old Dominion Univ., Norfolk, VA. Dept. of Mechanical Engineering and Mechanics.
INVESTIGATION OF HYPERSONIC SHOCK-INDUCED COMBUSTION IN A HYDROGEN-AIR SYSTEM Progress Report, period ending 30 Jun. 1992

J. K. Ahuja, S. N. Tiwari, and D. J. Singh (Analytical Services and Materials, Inc., Hampton, VA.) Nov. 1992 64 p Presented at the 30th AIAA Aerospace Sciences Meeting, Reno, NV, 6-9 Jan. 1992 Previously announced in IAA as A92-25785
(Grants NAG1-423; NAG1-363)
(NASA-CR-191239; NAS 1.26:191239; AIAA Paper 92-0339) Avail: CASI HC A04/MF A01

A numerical study is conducted to simulate the ballistic range experiments at Mach 5.11 and 6.46. The flow field is found to be unsteady with periodic instabilities originating in the stagnation zone. The unsteadiness of the flow field decreased with increase in the Mach number, thus indicating that it is possible to stabilize such flow fields with a high degree of overdrive. The frequency of periodic instability is determined using Fourier power spectrum and is found to be in good agreement with the experimental data. The physics of the instability is explained by the wave interaction models available in the literature. Author

N93-13530# Westinghouse Idaho Nuclear Co., Inc., Idaho Falls.
SYSTEMATIC CHEMICAL EQUATION BALANCING
E. E. Filby 20 Mar. 1992 11 p Presented at the 34th Annual Meeting on Systematic Chemical Equation Balancing, Caldwell, ID, 26-28 Mar. 1992
(Contract DE-AC07-84ID-12435)
(DE92-017234; WINCO-11795; CONF-9203182-1) Avail: CASI HC A03/MF A01

Many technical studies have a fundamental need for balanced chemical equations. Yet students in chemistry courses are often given only minimal guidance on how to obtain these profoundly important expressions. All of the beginning chemistry texts the author has reviewed show 'balancing by inspection' as the initial method of choice, and offer systematic methods only when oxidation-reduction systems are examined. Balancing ordinary equations basically becomes a 'black art' and redox equations are treated as being, fundamentally different from all other systems. This paper will present a systematic equation-balancing method based on very simple algebraic manipulations. The method is foolproof (if one can do simple algebra), strongly rooted in chemical fundamentals, and can handle all types of chemical systems. The author has successfully taught this method to groups at many different educational levels (high school through working professionals); they only needed to be willing and able to use simple algebra. DOE

N93-13573# Virginia Polytechnic Inst. and State Univ., Blacksburg. Dept. of Chemical Engineering.
INFLUENCE OF SURFACE DEFECTS AND LOCAL STRUCTURE ON OXYGENATE REACTION PATHWAYS OVER METAL OXIDE SURFACES
D. F. Cox Jul. 1992 4 p
(Contract DE-FG05-90ER-14129)
(DE92-040013; DOE/ER-14129/2) Avail: CASI HC A01/MF A01

Work during the last year (August 1991 to July 1992) has concentrated on completing the previously initiated studies of the surface chemistry of C(sub 1) oxygenates on particularly methanol SnO2 (110) and beginning studies of C(sub 2) oxygenate surface chemistry. During the remaining six months of the second budget period, the C(sub 2) studies will be continued. DOE

N93-13616# Edgerton, Germeshausen and Grier, Inc., Idaho Falls, ID.
VERIFICATION AND VALIDATION OF TMAP4
G. R. Longhurst, S. L. Harms, E. S. Marwil, and B. G. Miller Jul. 1992 94 p
(Contract DE-AC07-76ID-01570)
(DE92-019684; EGG-FSP-10347) Avail: CASI HC A05/MF A01

The Tritium Migration Analysis Program MODI/CY04 (TMAP4) was written to be used in analyzing experiments and for safety calculations that involve the injection, solution, diffusion, trapping, release, and other related processes experienced by hydrogen isotopes in materials. Because of the desire to make it suitable for analyzing safety issues, it is important that TMAP4 be certified (verified and validated) at Quality Assurance Level A. This report documents the work done to achieve that certification. The process includes assuring that the developed code meets the software requirements specified in the Software Quality Assurance Plan, verifying that the code functions in accordance with the written description and that it is self-consistent and internally correct, and validating that its computed results are in agreement with experimental data and/or known analytical solutions. Quality Level A certification for TMAP4 is specifically for implementation on an IBM PS/2 Model 70 operating under DOS 5.0. Certification for any other environment will require demonstration that all of the verification and validation tests documented here give the same results in the new environment. DOE

N93-13617# Pittsburgh Univ., PA. Dept. of Chemical and Petroleum Engineering.
A NOVEL PROCESS FOR METHANOL SYNTHESIS
J. W. Tierney and I. Wender 1992 12 p
(Contract DE-FG22-89PC-89786)
(DE92-019719; DOE/PC-89786/T13) Avail: CASI HC A03/MF A01

A bench-scale reactor is being used to conduct studies of the conversion of synthesis gas to methanol (MeOH) by a novel process. In previous reports, we provided evidence for a two-step reaction in series, the carbonylation reaction taking place mainly in a non-equilibrium region in the vicinity of the copper chromite surface, and the hydrogenolysis reaction taking place on the surface of the copper chromite. Interaction between the two catalysts enhances the rate of methanol formation. In this quarter, we investigated the effect of pore diffusion on reaction rate and obtained an expression for the rate of reaction for the methanol/methyl formate concurrent synthesis. DOE

N93-13641# National Inst. of Standards and Technology, Gaithersburg, MD. Building and Fire Research Lab.
SEMI-QUANTITATIVE MODEL FOR THE BURNING RATE OF SOLID MATERIALS
James G. Quintiere Jun. 1992 43 p
(PB92-213362; NISTIR-4840) Avail: CASI HC A03/MF A01

An analytical model was developed to describe the processes involved in the burning and extinction of solid materials and is described in the report. Included are flame heat transfer, charring, transient conduction, and water application. The model qualitatively describes the burning rate of both charring and thermoplastic-like solids. It illustrates how the steady-state heat of gasification can be derived from peak burning rate test data taken as a function of irradiance. Experimental data are shown to support this derivation. The model, in conjunction with a critical flame temperature, is used to describe suppression and extinction by water. GRA

N93-13763*# Northwestern Univ., Evanston, IL. Dept. of Chemistry.
STUDIES OF THE KINETICS AND MECHANISMS OF PERFLUOROETHER REACTIONS ON IRON AND OXIDIZED IRON SURFACES Final Technical Report
Mary E. Napier and Peter C. Stair 25 Nov. 1992 180 p
(Grant NAG3-869)
(NASA-CR-191363; NAS 1.26:191363) Avail: CASI HC A09/MF A02

Polymeric perfluoroalkylethers are being considered for use as lubricants in high temperature applications, but have been observed to catalytically decompose in the presence of metals. X-ray photoelectron spectroscopy (XPS) and temperature programmed desorption (TPD) were used to explore the decomposition of three model fluorinated ethers on clean polycrystalline iron surfaces and iron surfaces chemically modified with oxygen. Low temperature adsorption of the model fluorinated ethers on the clean, oxygen modified and oxidized iron surfaces was molecular. Thermally activated defluorination of the three model compounds was observed on the clean iron surface at remarkably low temperatures, 155 K and below, with formation of iron fluoride. Preferential C-F bond scission occurred at the terminal fluoromethoxy, CF3O, of perfluoro-1-methoxy-2-ethoxy ethane and perfluoro-1-methoxy-2-ethoxy propane and at CF3/CF2O of perfluoro-1,3-diethoxy propane. The reactivity of the clean iron toward perfluoroalkylether decomposition when compared to other metals is due to the strength of the iron fluoride bond and the strong electron donating ability of the metallic iron. Chemisorption of an oxygen overlayer lowered the reactivity of the iron surface to the adsorption and decomposition of the three model fluorinated ethers by blocking active sites on the metal surface. Incomplete coverage of the iron surface with chemisorbed oxygen results in a reaction which resembles the defluorination reaction observed on the clean iron surface. Perfluoro-1-methoxy-2-ethoxy ethane reacts on the oxidized iron surface at 138 K, through a Lewis acid assisted cleavage of the carbon oxygen bond, with preferential attack at the terminal fluoromethoxy, CF3O. The oxidized iron surface did not passivate, but

became more reactive with time. Perfluoro-1-methoxy-2-ethoxy propane and perfluoro-1,3-diethoxy propane desorbed prior to the observation of decomposition on the oxidized iron surface. Author

N93-13802 Oxford Univ. (England).
MODELLING COMBUSTION ZONES IN POROUS MEDIA Ph.D. Thesis
Helen M. Byrne 1991 194 p
Avail: Univ. Microfilms Order No. BRD-95100

In this thesis two simple models of porous medium combustion are studied. Where existing work has concentrated on processes for which solid fuel consumption is significant and gas conversion negligible, here attention is centered on applications for which the relative importance of solid and gas consumption is either reversed or equally balanced. Thus the work on catalytic converters in chapters 2, 3 and 4 does not involve change of the solid and focuses on gaseous conversion, enhanced by the presence of the solid catalyst. Chapters 5, 6 and 7, however, treat conversion of both media. Indeed, solutions for which the solid and gaseous fuels are simultaneously exhausted are obtained. The unifying theme is the notion of reaction processes terminated by gaseous exhaustion which is made possible by the adoption of modified reaction rates. This idea has not appeared in connection with porous medium combustion studies before, and follows from a new type of two or three stage reaction rate adopted to model the detailed porous medium combustion chemistry. Various types of combustion solutions are described and analyzed: steady-state solutions and their stability, similarity solutions and (forward and reverse) travelling combustion waves. An inequality relating the system's parameters is derived as a necessary condition for the existence of the steady-state solutions. In addition, for a particular choice of the reaction rate, the stability of steady solutions characterized by gaseous exhaustion is demonstrated. Asymptotic power series expansions for the different types of travelling wave solutions are constructed and local expressions for the surfaces which partition the parameter space into separate solution regimes are presented. Numerical results in support of this analysis are also included. Dissert. Abstr.

N93-14033# Georgia Tech Research Inst., Atlanta.
INFORMAL CONFERENCE ON PHOTOCHEMISTRY Final Report, 1 Apr. - 31 Jul. 1992
Paul H. Wins 1 May 1992 236 p Conference held in Atlanta, GA, 26 Apr. - 1 May 1992
(Contract F49620-92-J-0180)
(AD-A255824; AFOSR-92-0880TR) Avail: CASI HC A11/MF A03

The 20th Informal Conference on Photochemistry was held at the Colony Square Hotel in Atlanta, Georgia during the period April 26 - May 1, 1992. A total of 74 oral papers and 105 poster papers were presented. Most participants agreed that the scientific level of the conference was very high. One of the goals of this conference was to bring together leading researchers in a variety of basic and applied sub-areas of physical photochemistry. In this regard, discussion was stimulated which hopefully will lead to new interdisciplinary research initiatives. GRA

N93-13183*# Science Applications International Corp., Glendora, CA.
THE LDCE PARTICLE IMPACT EXPERIMENT AS FLOWN ON STS-46
Carl R. Maag, William G. Tanner (Baylor Univ., Waco, TX.), Janet Borg (Centre National de la Recherche Scientifique, Orsay, France), Jean-Pierre Bibring (Centre National de la Recherche Scientifique, Orsay, France), W. Merle Alexander (Baylor Univ., Waco, TX.), and Andrew J. Maag (Stanford Univ., Palo Alto, CA.) *In* NASA. Goddard Space Flight Center, The 1992 Shuttle Small Payloads Symposium Oct. 1992 p 257-266 (For primary document see N93-13158 03-12)
Avail: CASI HC A02/MF A03

N93-13984*# Spectra Research Systems, Inc., Huntsville, AL.
IMPACT OF LUNAR OXYGEN PRODUCTION ON DIRECT MANNED MARS MISSIONS
Roy M. Young, Jr. and William B. Tucker (Nichols Research Corp., Huntsville, AL.) *In* NASA. Johnson Space Center, The Second Conference on Lunar Bases and Space Activities of the 21st Century, Volume 2 Sep. 1992 p 453-458 (For primary document see N93-13972 03-91)
Avail: CASI HC A02/MF A03

N93-13986*# Orbital Technologies Corp., Madison, WI.
SYNERGISM OF He-3 ACQUISITION WITH LUNAR BASE EVOLUTION
T. M. Crabb and M. K. Jacobs (Science Applications International Corp., Schaumburg, IL.) *In* NASA. Johnson Space Center, The Second Conference on Lunar Bases and Space Activities of the 21st Century, Volume 2 Sep. 1992 p 475-482 Previously announced as N89-14852 (For primary document see N93-13972 03-91)
Avail: CASI HC A02/MF A03

26 METALLIC MATERIALS

Includes physical, chemical, and mechanical properties of metals, e.g., corrosion; and metallurgy.

N93-12573# Argonne National Lab., IL.
EXPERIMENTAL STUDIES OF CASCADE PHENOMENA IN METALS
M. L. Jenkins (Oxford Univ., England), M. A. Kirk, and W. J. Phythian (United Kingdom Atomic Energy Authority, Harwell, England) Jun. 1992 29 p Presented at the 3rd Conference on Evolution of Microstructure in Metals During Irradiation, Minett, Canada, 29 Sep. - 2 Oct. 1992
(Contract W-31-109-eng-38)
(DE92-019586; ANL/CP-76480; CONF-920970-1) Avail: CASI HC A03/MF A01

We review recent ion-irradiation experiments which have been performed to investigate the collapse of displacement cascades to dislocation loops in a range of metals and alloys. Many of the results including the dependencies of the collapse probabilities on irradiation temperature, and ion dose, energy and mass, can be explained within the framework of a thermal spike/cascade melting model which has been suggested by computer molecular dynamics simulations. Other aspects, such as the dependence of collapse probabilities on the crystal structure and the effects of alloying and impurities, are less well understood. DOE

N93-12595# Pennsylvania State Univ., University Park. Dept. of Materials Science and Engineering.
HIGH TEMPERATURE OXIDATION AND ELECTROCHEMICAL STUDIES RELATED TO HOT CORROSION Final Report, Nov. 1985 - May 1992
R. Reidy, D.-H. Kim, J. Patton, and G. Simkovich 24 Jul. 1992 99 p
(Contract N00014-91-J-1528)
(AD-A254435) Avail: CASI HC A05/MF A02

This research has examined the transport mechanisms relevant to hot corrosion. Three different approaches were used to elucidate this problem: an examination of the corrosion of the base metal, an exploration of the transport properties in Na2SO4, and an investigation in the role of defects in the transport behavior of a protective coating. The transport properties of molten Na2SO4 have been investigated to aid further understanding of hot corrosion processes at 1173 K. Tests were conducted to determine the following: the effect of height of Na2SO4 melts, the effect of electronic short circuiting the Na2SO4 melts with gold wires, and the effect of presaturating the salt melt with corrosion products in the hot corrosion process. Basically, these tests showed that neither ionic nor electronic transport in the bulk melt controls the hot corrosion process. However, the amount of Na2SO4 present, which is directly proportional to the height of the melt, does affect the rate of corrosion. This was demonstrated by the decrease in rate observed when the melt was presaturated with the corrosion products. An A.C. impedance technique for the total electrical conductivity, the potentiostatic polarization method for ionic transport numbers, and the steady state polarization method of Wagner and Hebb for the electronic conductivity were employed as a function of Na2O activity in the melt by controlling the gas atmosphere. These results showed that the conductivities of the pure Na2SO4 were on the order of 0.232 (ohm-cm)(sub -1) and varied only slightly with Na2O, activity changes. From the polarization measurements, on the pure Na2SO4, it was found that electron conductivity was much higher than electron hole conductivity. The transport numbers were T(sub e) = 7.0(10)(exp -3) and t(sub e) = 5.7(10)(exp -5). GRA

N93-12603# United Technologies Research Center, East Hartford, CT.
FATIGUE AND FRACTURE OF INTERMETALLIC ALLOYS Final Report, 1 Apr. 1989 - 31 Mar. 1992
C. V. Cooper, H. R. Inoue, A. F. Giamei, and L. H. Favrow 25 Jul. 1992 71 p
(Contract F49620-89-C-0047)

(AD-A254543; R92-917992-3; AFOSR-92-0798TR) Avail: CASI HC A04/MF A01

The compound, Al3Ti, was alloyed with 7.5 at. percent Fe to produce a cubic L1(sub 2) structure. This material was arc cast and either directly homogenization heat treated (HHT) or comminuted into powder and consolidated by hot isostatic pressing (HIP). Microstructures were carefully evaluated by optical and electron microscopy. Mechanical properties were measured as a function of temperature using compression and flexure. Utilizing a novel test fixture, both monotonic and cyclic tensile properties were determined as a function of temperature for specimens which had been sequentially cast, HIPed, and HHTed. Despite quasi-brittle behavior below 1000 C, failure was within the gauge section in most cases. The fracture surfaces showed increasing evidence of ductile tearing as the temperature was increased, and pores were determined to play an important role in the fracture process. The yield strength vs. temperature response was relatively flat up to intermediate temperature, possibly attributable to competing slip systems. The compressive yield strength and strain to failure were typically greater than those measured in tension, particularly at the lower temperatures. The fatigue data were reasonably well behaved, with fatigue specimens showing clear evidence of striations. Attempts to alloy the binary D0(sub 22) compound with Nb did not produce the desired cubic structure. GRA

N93-12616# Army Armament Research, Development and Engineering Center, Watervliet, NY.

TEMPERING EFFECTS FOR LOWER BAINITE, MARTENSITE, AND MIXED MICROSTRUCTURES ON IMPACT, FRACTURE, AND RELATED MECHANICAL PROPERTIES OF ASTM A723 STEEL Final Report

J. M. Barranco, P. J. Cote, and J. A. Kapp Jun. 1992 54 p

(AD-A254617; ARCCB-TR-92024) Avail: CASI HC A04/MF A01

Mixed microstructures were produced by cooling ASTM A723 steel from 830 C (1526 F) to lower temperatures, notably at 210 and 250 C (410 and 482 F), which are below the start of the martensite transformation (M(sub s)) temperature of 286 C (547 F), and held for 2-1/4 hours. This resulted in the isothermal formation of 25 or 66 percent lower bainite as one part of the mixed microstructure with martensite. Tempering studies were conducted from 260 to 704 C (500 to 1300 F). Optimum tempering occurred at 593 C (1100 F), where differences between strength and hardness levels were minimized and the yield strength-to-ultimate tensile strength ratio was maximized. This allowed impact and toughness tests to be performed on an equal basis. Impact tests, conducted from -100 to 88 C (-148 to 190 F), revealed that mixed microstructures could produce higher impact energy values compared to all-martensite. When the mixed microstructure containing 25 percent lower bainite was tested at -40 F), the impact energy was increased by about 18 ft-lbs, compared to quenched and tempered martensite, and had the lowest ductile-brittle transition temperature of -73.3 C (-100 F) versus -68.3 C (-91 F) for martensite. Fracture toughness tests at -40 C revealed only a slight improvement in toughness for mixed microstructures at 188 Ksi the square root of in., compared to all-martensite at 183.8 Ksi the square root of in. GRA

N93-12746# Pratt and Whitney Aircraft, West Palm Beach, FL. Government Engines and Space Propulsion.

FATIGUE IN SINGLE CRYSTAL NICKEL SUPERALLOYS Technical Progress Report, 16 Jun. - 15 Jul. 1992

Daniel P. DeLuca 15 Jul. 1992 7 p

(Contract N00014-91-C-0124)

(AD-A254704; PW/GESP-FR-21998-09) Avail: CASI HC A02/MF A01

This program investigates the seemingly unusual behavior of single crystal airfoil materials. The fatigue initiation processes in single crystal (SC) materials are significantly more complicated and involved than fatigue initiation and subsequent behavior of a (single) macrocrack in conventional, isotropic, materials. To understand these differences is the major goal of this project. GRA

N93-12790# Lawrence Livermore National Lab., CA.

WASTAGE-RESISTANT FBC EVAPORATOR TUBING THROUGH MICROALLOYING

C. E. Witherell Oct. 1991 75 p

(Contract W-7405-eng-48)

(DE92-001256; DOE/NBM-92001256; UCRL-CR-109002) Avail: CASI HC A04/MF A01

This phase of the LLNL study of wastage of carbon steel evaporator tubing in fluidized-bed coal combustors (FBC) of the bubbling-bed type focused upon leads uncovered during the previous phase suggesting that trace-element residuals in the tubing steel influenced wastage response. Experimental steels of controlled compositions, but simulating commercial steelmaking practices, were prepared within several elements indicated to be important in these respects were varied independently. This initial series showed that additions of some of these elements, principally aluminum, nickel, and copper -- when present singly -- improved scale adhesion in room temperature bend tests. In a second series of experimental steels, aluminum additions significantly decreased elevated temperature indentation hardness, even with co-present residuals of chromium, nickel, and copper. Steels of the same series having combined residuals of aluminum, chromium, nickel, and copper had improved resistance to scale exfoliation in room temperature bend tests over steels without these trace-elements. DOE

N93-12798# Argonne National Lab., IL.

WEAK-BEAM IMAGING OF DISSOCIATED DISLOCATIONS IN HVEM-IRRADIATED Fe-Ni-Cr ALLOYS

S. L. King (Oxford Univ., England), M. L. Jenkins (Oxford Univ., England), M. A. Kirk (Oxford Univ., England), and C. A. English (United Kingdom Atomic Energy Authority, Harwell, England) Jun. 1992 14 p Presented at the 3rd Conference on Evolution of Microstructure in Metals During Irradiation, Minett, Canada, 29 Sep. - 2 Oct. 1992

(Contract W-31-109-eng-38)

(DE92-019587; ANL/CP-74687; CONF-920970-2) Avail: CASI HC A03/MF A01

We report here on studies by weak-beam electron microscopy of the evolution of microstructures at and near preexisting line dislocations in a number of Fe-Ni-Cr alloys under electron irradiation in a high-voltage electron microscope (HVEM). The detailed observations are discussed in terms of dislocation climb mechanisms in these materials and a model based on interstitial pipe diffusion. DOE

N93-12820# Pacific Northwest Lab., Richland, WA.

INFLUENCE OF COLD WORK LEVEL ON THE IRRADIATION CREEP AND CREEP RUPTURE OF TITANIUM-MODIFIED AUSTENITIC STAINLESS STEELS

F. A. Garner, M. L. Hamilton, C. R. Eiholzer (Westinghouse Hanford Co., Richland, WA.), M. B. Toloczko (California Univ., Berkeley.), and A. S. Kumar (Missouri Univ., Rolla.) Jun. 1992 20 p Presented at the 16th Annual Symposium of American Society of Testing and Materials (ASTM), Denver, CO, 21-22 Jun. 1992

(Contract DE-AC06-76RL-01830)

(DE92-019078; PNL-SA-19946; CONF-920673-8) Avail: CASI HC A03/MF A01

A titanium-modified austenitic type stainless steel was tested at three cold work levels to determine its creep and creep rupture properties under both thermal aging and neutron irradiation conditions. Both the thermal and irradiation creep behavior exhibit a complex non-monotonic relationship with cold work level that reflects the competition between a number of stress-sensitive and temperature-dependent microstructural processes. Increasing the degree of cold work to 30 percent from the conventional 20 percent level was detrimental to its performance, especially for applications above 550 C. The 20 percent cold work level is preferable to the 10 percent level, in terms of both in-reactor creep rapture response and initial strength. DOE

N93-12879# Argonne National Lab., IL.

A STUDY OF THE VACANCY LOOP FORMATION PROBABILITY IN Ni-Cu AND Ag-Pd ALLOYS

K. Smalinskas, Gengsheng Chen, J. Haworth, I. M. Robertson, and M. A. Kirk Apr. 1992 14 p Presented at the 3rd Conference on Evolution of Microstructure in Metals During Irradiation, Minett, Ontario, 29 Sep. - 2 Oct. 1992

(Contract W-31-109-eng-38)

(DE92-019584; ANL/CP-74791; CONF-920970-3) Avail: CASI HC A03/MF A01

The molten-zone model of vacancy loop formation from a displacement cascade predicts that the loop formation probability should scale with the melting temperature. To investigate this possibility, the vacancy loop formation probability has been determined in a series of Cu-Ni and Ag-Pd

alloys. The irradiations were performed at room temperature with 50 keV Kr(+) ions and the resulting damage structure was examined by using transmission electron microscopy. In the Cu-Ni alloy series, the change in loop formation probability with increasing Ni concentration was complex, and at low- and high-nickel concentrations, the defect yield did not change in the predicted manner. The defect yield was higher in the Cu-rich alloys than in the Ni-rich alloys. In the Ag-Pd alloy, the change in the loop formation probability followed more closely the change in melting temperature, but no simple relationship was determined. DOE

N93-12973# Argonne National Lab., IL.
INFLUENCE OF DILUTE IMPURITIES ON THE EVOLUTION OF DEFECT CASCADES IN NICKEL
J. S. Vetrano (Pacific Northwest Lab., Richland, WA.), I. M. Robertson (Illinois Univ., Urbana.), and M. A. Kirk Apr. 1992 13 p Presented at the 3rd Conference on Evolution of Microstructure in Metals During Irradiation, Minett, Canada, 29 Sep. - 2 Oct. 1992
(Contracts W-31-109-eng-38; DE-FG02-91ER-45439)
(DE92-019585; ANL/CP-74789; CONF-920970-4) Avail: CASI HC A03/MF A01

We have employed transmission electron microscopy to study the formation of vacancy dislocation loops from defect cascades produced by a 50 key Kr(+) ion irradiation of Ni and its dilute alloys with Si and Al. An unusual and reproducible dependence of the loop collapse probabilities and loop size distributions on solute content was found. The results are explained by impurity caused changes in both the collisional and thermal spike (molten zone) phase of the defect cascade. Specific mechanisms include disruption of focussons by impurities to change the energy density profile within the collision cascade, interruption of replacement collision sequences, and interstitial trapping to reduce recombination during the thermal spike phase. Applying these mechanisms to a statistical distribution of the spatial extent of cascades and to the melt-zones, all the experimental observations can be explained. DOE

N93-12998# Connecticut Univ., Storrs.
STRUCTURE SENSITIVE REACTIONS OVER Co, Fe AND MIXED METAL CLUSTERS IN ZEOLITES
S. L. Suib 1 Aug. 1992 12 p
(Contract DE-FG02-86ER-13622)
(DE92-040359; DOE/ER-13622/T2) Avail: CASI HC A03/MF A01

Transient and steady state kinetic studies of structure sensitive reactions of cyclopropane (c-C3H6) and hydrogen over zeolites is the first area of this studied. Low level impurity Fe(+++) ions in zeolites complicate interpretation of spectroscopic and catalytic studies of these systems. We focused our efforts on selectively substituting Fe(+++) ions in the frameworks of various zeolites to understand their role in catalytic reactions such as with c-C3H6 and H2. These studies led to isomorphous substitution of other ions like B(+++) and their use in isomerization of n-butenes to isobutylene. The third area of research involves the synthesis, characterization and catalysis of a new class of molecular sieve manganese oxide tunnel structure materials. DOE

N93-13043# Oak Ridge National Lab., TN.
ORDERING ENERGIES AND MECHANISMS IN BETA-PHASE NiAl
G. M. Stocks, D. M. Nicholson, W. A. Shelton, G. A. Geist, F. J. Pinski (Cincinnati Univ., OH.), B. Ginatempo (Messina Univ., Italy), A. Barbieri (Bristol Univ., England), and B. L. Gyoerffy (Bristol Univ., England) 1992 19 p Presented at the Minerals, Metals, and Materials Society (TMS) Annual Meeting and Exhibition, San Diego, CA, 1-5 Mar. 1992
(Contract DE-AC05-84OR-21400)
(DE92-040031; CONF-920305-14) Avail: CASI HC A03/MF A01

We review calculations of the ordering energies of Ni(c)Al(l-c) alloys based on the generalized perturbation method and the KKR-CPA. First principles KKR-CPA calculations of ordering energies of beta phase Ni(c)Al(l-c) alloys as a function of the long range order parameter are presented. We also show alloy Fermi surfaces in beta-phase Ni(0.625)Al(0.375) that support a recent suggestion that the phonon anomalies observed in neutron scattering experiments are driven by Fermi surface nesting. DOE

N93-13080# Oak Ridge National Lab., TN.
THE NATURE OF SCALES GROWN ON BINARY Cr-Nb ALLOYS
P. F. Tortorelli and J. H. DeVan 1992 8 p Presented at the 182nd Meeting of the Electrochemical Society, Toronto, Ontario, 11-16 Oct. 1992
(Contract DE-AC05-84OR-21400)
(DE92-019283; CONF-921036-5) Avail: CASI HC A02/MF A01

The nature of the scales formed on Cr-Cr2Nb alloys was studied for exposures to air at 900 and 950 C. The kinetics, scale composition, and spallation tendencies of Cr-6 and -12 at. percent Nb alloys were characterized. Multilayer scales with a pure chromia outer layer were formed, and the alloy with the higher niobium content performed significantly better in terms of overall weight gain and resistance to spallation. This behavior was ascribed to an increased volume fraction of the Cr2Nb-Cr eutectic mixture at the expense of the Cr-rich phase. DOE

N93-13190# Oak Ridge National Lab., TN.
DEVELOPMENT OF WELDABLE HIGH-STRENGTH IRON ALUMINIDES
C. G. McKamey, T. Zacharia, and P. J. Maziasz 1992 10 p Presented at the 6th Annual Fossil Energy Materials Conference, Oak Ridge, TN, 12-14 May 1992
(Contract DE-AC05-84OR-21400)
(DE92-016018; CONF-9205123-6) Avail: CASI HC A02/MF A01

Using alloy development and thermomechanical processing techniques, Fe3Al-based alloys with room temperature tensile ductilities of 10-20 percent and tensile yield strengths of 500 MPa at temperatures to 600 C have been developed at the Oak Ridge National Laboratory (ORNL). However, the high-temperature (above 500 C) creep-rupture properties of these alloys are not adequate for many applications. Studies at ORNL and at other laboratories have shown that binary Fe3Al, which has very poor creep resistance (approximately 2 h at 593 C and 207 MPa), can be strengthened by alloy additions. Recently, small additions of molybdenum, zirconium, and niobium were shown to produce strengthening through a combination of effects, including grain boundary strengthening, precipitation strengthening, increased recrystallization temperature, and control of dislocation nucleation and mobility. This paper describes our current efforts to develop an Fe3Al-based alloy with improved high-temperature creep-rupture strength, while maintaining weldability and an acceptable room temperature tensile ductility of approximately 10 percent. DOE

N93-13237# Oak Ridge National Lab., TN.
ENVIRONMENTAL EFFECTS ON IRON ALUMINIDES
J. H. DeVan and P. F. Tortorelli 1992 10 p Presented at the 6th Annual Fossil Energy Materials Conference, Oak Ridge, TN, 12-14 May 1992
(Contract DE-AC05-84OR-21400)
(DE92-016341; CONF-9205123-9) Avail: CASI HC A02/MF A01

Iron aluminide alloys containing aluminum concentrations in the range of 16 to 28 at. percent and 0 to 5 at. percent chromium were fabricated into corrosion coupons and tested in H2S-H2H2O gas mixtures at 800 C and in air at 900 to 1000 C. Similar tests were conducted on developmental Fe-Cr-Al alloys supplied by Harwell Laboratory (UK). Effects of zirconium additions on scaling resistance in air were also evaluated based on the comparative performance of alloys containing 28 percent Al, 0 to 5 percent Cr, and 0 to 0.5 percent Zr. The critical aluminum content required to sustain sulfidation resistance in H2S-H2-H2O was found to be on the order of 18 at. percent. However, all of the Fe-Al alloys were much more resistant to the H2S-H2-H2O gas mixture than the Fe-Cr-Al alloys under equivalent conditions. A 20 percent Al level was found to be critical for sustained oxidation resistance of binary Fe-Al alloys in air at 900 C or above. Air tests of the Fe-Cr-Al class of alloys at 800 and 900 C gave oxidation rates comparable to Fe3Al-based alloys. In the case of alloys containing 28 percent Al, additions of zirconium significantly improved the spalling resistance in air above 900 C. DOE

N93-13302# Sandia National Labs., Albuquerque, NM.
ELEVATED TEMPERATURE TENSILE PROPERTIES OF BORATED 304 STAINLESS STEEL: EFFECT OF BORIDE DISPERSION ON STRENGTH AND DUCTILITY
J. J. Stephens, K. B. Sorenson, and P. McConnell 1991 8 p Presented at the 10th International Symposium on the Packaging and Transportation of Radioactive Materials: PATRAM 1992, Yokohama, Japan, 13-18 Sep. 1992
(Contract DE-AC04-76DP-00789)

(DE92-040096; SAND-91-2774C; CONF-920905-5) Avail: CASI HC A02/MF A01

This paper has documented the increase in strain to fracture and yield strength obtained with Grade A versions of types 304B5 and 304B7 relative to their respective Grade B, counterparts. The apparent microstructural reason for these property increases is the finer dispersion of boride in the Grade A material, obtained by means of a powder metallurgy process, relative to the conventional Grade B material which is produced using an ingot metallurgy process. The area size distribution of borides can be well approximated using a log-normal distribution, with the largest boride particles in the Grade B material having areas in the range of 450-600 sq. microns. By comparison, the largest boride particles in the Grade A material have areas nearly an order of magnitude smaller than the largest particles in their Grade B counterparts. A Section 3 ASME B&PV code case inquiry has been initiated for non-welded versions of 304B4A, 3045A, and 3046A material. DOE

N93-13346# North Carolina Univ., Charlotte. Dept. of Chemistry.
OLIGOMER AND MIXED-METAL COMPOUNDS POTENTIAL MULTIELECTRON TRANSFER CATALYSTS
D. P. Rillema 30 Mar. 1992 10 p
(Contract DE-FG05-84ER-13263)
(DE92-011347; DOE/ER-13263/8) Avail: CASI HC A02/MF A01

Projects related to the design and characterization of multimetallic complexes has proceeded forward with a number of achievements. First, photoprocesses in hydrogel matrices lead to the conclusion that cationic metallochromophores could be ion exchanged into a hydrogel matrix (kappa-carageenan) and substantial photocurrents could be generated. Second, x-ray structures of (Ru(bpy)3)(2+), (Ru(bpm)3)(2+), and (Ru(bpz)3)(2+), where bpy is 2,2(prime)-bipyridine, bpm is 2,2(prime)-bipyrimidine, and bpz is 2,2(prime)-bipyrizine, were obtained and revealed similar Ru-N bond distances in each complex even though their sigma-donor and pi-acceptor character differ markedly. The structure parameters are expected to provide theoreticians with the information needed to probe the electronic character of the molecular systems and provide us with direction in our synthetic strategies. Third, a copper(I) complex was synthesized with a dimeric-ethane-bridged, 1,10-phenanthroline ligand that resulted in isolation of a bimetallic species. The copper(I) complex did luminesce weakly, suggesting that the dimer possesses potential electron transfer capability. Fourth, the photophysical properties of (Re(CO)4)(L-L)(+), where L-L = heterocyclic diimine ligands, and Pt(bph)X2, where bph = the dianion of biphenyl and X = CH3CN, py, or ethylendiamine, displayed luminescence at high energy and underwent excited-state electron transfer. Such high energy emitters provide high driving forces for undergoing excited-state electron transfer. Fifth, both energy and electron transfer were observed in mixed-metal complexes bridged by 1,2-bis(2,2(prime)-bipyridyl-4(prime)-yl) ethane. DOE

N93-13378*# National Aeronautics and Space Administration. Marshall Space Flight Center, Huntsville, AL.
A COMPARISON OF CHROMIC ACID AND SULFURIC ACID ANODIZING
M. D. Danford Nov. 1992 18 p
(NASA-TM-108383; NAS 1.15:108383) Avail: CASI HC A03/MF A01

Because of federal and state mandates restricting the use of hexavalent chromium, it was deemed worthwhile to compare the corrosion protection afforded 2219-T87 aluminum alloy by both Type I chromic acid and Type II sulfuric acid anodizing per MIL-A-8625. Corrosion measurements were made on large, flat 2219-T87 aluminum alloy sheet material with an area of 1 cm(exp 2) exposed to a corrosive medium of 3.5-percent sodium chloride at pH 5.5. Both ac electrochemical impedance spectroscopy and the dc polarization resistance techniques were employed. The results clearly indicate that the corrosion protection obtained by Type II sulfuric acid anodizing is superior, and no problems should result by substituting Type II sulfuric acid anodizing for Type I chromic acid anodizing. Author

N93-13545# Los Alamos National Lab., NM.
IS THERE A UNIQUE EFFECTIVE INTERACTION PROFILE FOR DISLOCATIONS?
U. F. Kocks, Shuh Rong Chen, and H. Mecking (Technische Univ., Hamburg, Germany) 1992 33 p Presented at the Z.S. Basinski International Symposium on Crystal Plasticity, Kingston, Ontario, 16 Jun. 1992
(Contract W-7405-eng-36)
(DE92-018615; LA-UR-92-2400; CONF-9206241-1) Avail: CASI HC A03/MF A01

Thermal activation affects plastic flow in two ways: it lowers the stress for dislocations to cross each other; and it helps them to break loose from the high-energy configurations in which they are initially stored during strain hardening, which manifests itself in the phenomenon of dynamic recovery. It is shown that both effects may be described by a single effective dislocation interaction profile, the main difference being an additional strong internal driving force for recovery. The dependence of the effective activation energy on stress may be described by a surprisingly simple form. A single adjustable parameter, which scales with the normalized stacking-fault energy, may allow for this interaction profile to be universal, at least for fcc metals. DOE

N93-13690 Open Univ., Milton (England).
FATIGUE STUDIES IN Al-Mg-Si ALLOYS Ph.D. Thesis
Salih Guengoer 1990 157 p
Avail: Univ. Microfilms Order No. BRDX92975

This work presents an investigation into the effect of microstructure and forming process on both fatigue life and small crack growth behavior of Al-Mg-Si alloys. The influence of slip distribution on initiation and propagation of small fatigue cracks was examined in a series of wrought Al-Mg-Si alloys which contain differing volume fraction of dispersoids. The lip homogenization caused by manganese bearing dispersoids profoundly increases the alloy's resistance to the propagation of long fatigue cracks due to the decrease in intergranular failure. But, the extent of this effect on the propagation of small cracks was found to be less pronounced because of the frequent interruption of the growth of small cracks at the microstructural features and the decrease in effective driving force for crack growth by crack deflection, so that the increase in growth rates due to intergranular failure will be less in small cracks. Thus, the increase in fatigue life seen with increasing homogenization of slip is shown to be due to the relative ease of fatigue crack initiation in alloys exhibiting inhomogeneous slip. The fatigue crack initiation and small crack growth behavior of wrought, forged and squeeze-cast Al-Mg-Si alloys were examined to explain the effect of manufacturing process on fatigue life. The squeeze-cast alloy shows the lowest fatigue limit because of its lower tensile strength compared to the wrought and forged alloys. It has also the worst ratio of crack initiation life to the total fatigue life due to the presence of microporosity which eases the formation of cracks. However, the difference in their small crack growth rates controls the low-life high-stress region of the S-N curve, where the wrought alloy shows the lowest lives whereas the forged alloy the highest. Fatigue tests on the as-formed surface specimens of the forged and squeeze-cast alloys showed that surface texture has little effect on small fatigue crack growth rates. However, coarse particles and large defects introduced into the surface during the forming process of the forged and squeeze-cast alloys eased the formation of cracks and consequently reduced their fatigue limits by 20 and 25 percent, respectively. The low-cycle high stress region of the S-N curves of the alloys was successfully predicted using the small crack growth data. However, at stress levels near the fatigue limit, calculations from the small crack growth data underestimate the fatigue lives because a significant fraction of the life is spent in temporary crack arrests.
Dissert. Abstr.

N93-13733# SRI International Corp., Menlo Park, CA.
THERMOCHEMISTRY OF ATMOSPHERIC METAL REACTIONS Final Report, 10 May 1990 - 31 Dec. 1991
K. H. Lau and D. L. Hildenbrand Nov. 1991 48 p
(Contract F19628-90-K-0030)
(AD-A248651; SRI-1165; PL-TR-91-2280) Avail: CASI HC A03/MF A01

As part of a research program carried out during the period May, 1990 through September 1991, we have used effusion-beam mass spectrometry to study the thermochemistry and related aspects of several chemical systems pertinent to the understanding of some atmospheric metal reactions. First, the Na2O-CO2-H2O system was examined for evidence of gaseous NaHCO3 or other carbonates that may be important as sinks for sodium in the atmosphere. Second, the mass spectrum and ionization efficiency curves of Na2O vapor were studied to obtain information about the thermodynamic stability of the superoxide NaO2. And thirdly, the

thermochemical properties of the gaseous oxides OsO2 and OsO-were determined to supplement earlier work on OsO3. The results are summarized in three journal preprints. GRA

N93-13945# Naval Postgraduate School, Monterey, CA.
AN INVESTIGATION OF THE INTERATOMIC BONDING CHARACTERISTICS OF A Ti - 51 ATOMIC PERCENT Al ALLOY BY X RAY DIFFRACTION M.S. Thesis
Steven C. Cade Jun. 1991 71 p
(AD-A245362) Avail: CASI HC A04/MF A01

The lattice parameters and atomic structure factors of an homogenized, binary, Ti-51 at. percent Al intermetallic alloy were investigated using powder X-ray diffraction (XRD) procedures. Powder samples were prepared by pulverizing in a mortar and pestle lathe turnings taken from a sample ingot. The powder was then annealed to relieve the induced stress and passed through a U.S. Standard no. 400 sieve mesh (38 microns). Lattice parameters of the face-centered tetragonal structure determined from XRD peak positioned indicated a c/a ratio of 1.020; values of 4.077A and 3.997A were obtained for C(sub 0) and a(sub 0) respectively. These results are in agreement with previous research into gamma phase TiAl. Measurement of diffracted intensities was accomplished to determine the Debye-Waller temperatures factor with a value of B = 0.58A(exp 2) obtained by the Wilson Method. A reduction in expected measured intensities was noted, particularly at lower Bragg angles. This was attributed to extinction based on the results of a powder particle size average of 24.3 microns. Despite the problems of extinction, the observed Debye-Waller factor was judged to be reasonably accurate upon comparison to characteristic temperature and melting point data of the Ti-Al system. GRA

N93-14047 Manitoba Univ., Winnipeg.
ON GRAIN BOUNDARY TRANSPORT OF HYDROGEN AND MECHANISM OF HYDROGEN-INDUCED INTERGRANULAR FRACTURE Ph.D. Thesis
Jing Yao 1990 188 p
Avail: Univ. Microfilms Order No. DANN63273

The mechanism of hydrogen induced intergranular cracking in Ni has been investigated in this study. Two fundamental aspects are addressed: (1) the role of grain boundaries in the mass transport of hydrogen in materials contacted with hydrogen atmosphere, and (2) the effect of grain boundary pre-segregated hydrogen on the fracture mode and its mechanism. To accomplish these goals, three major investigations have been undertaken which can be summarized as follows. (1) A new grain boundary diffusion model is presented. The model can be utilized to calculate the contribution of grain boundary diffusion to total mass transport in metals where lattice diffusion occurs interstitially. (2) A dynamic technique to obtain qualitative information regarding hydrogen transport along grain boundaries in metallic materials has been proposed by reinterpreting and modifying the silver decoration technique proposed by Schober and Dieker. The results of decoration tests in polycrystalline nickel and palladium with and without hydrogen charging show that there is not a one-to-one correspondence between escaped hydrogen atoms and deposited silver atoms during the decoration process as reported previously. It is the oxidation film formed during electropolishing that prevents silver deposition. (3) Electrochemical permeation tests, silver decoration tests and penetration tests were performed in polycrystalline nickel with different grain sizes. Comparison of experimental results with theoretical predictions of the new grain boundary diffusion model indicated that grain boundaries are not high diffusivity paths for hydrogen. The dominant role played by grain boundaries during mass transport of hydrogen is retardation due to the trapping effect. A new mechanism of hydrogen induced intergranular cracking is proposed as follows. Hydrogen enters the material and diffuses into the interior through the lattice. The hydrogen concentration in grain boundaries develops at almost the same rate as the lattice but is much higher because of the segregation factor. The segregated hydrogen at grain boundaries increases the driving force for intergranular cracking by increasing the resistance to the leading dislocations in pileups in entering grain boundaries. If the local stress applied by dislocation pileups reaches the critical stress for grain boundary fracture before large scale cross slip takes place, intergranular cracking occurs. Dissert. Abstr.

N93-14098# Aerospace Corp., El Segundo, CA. Technology Operations.
THE CHEMISTRY OF THE EXTREME PRESSURE LUBRICANT ADDITIVE LEAD NAPHTHENATE ON STEEL SURFACES
S. V. Didziulis and P. D. Fleischauer 1 Sep. 1992 48 p
(Contract F04701-88-C-0089)
(AD-A255828; TR-0091(6945-03)-3; SMC-TR-92-39) Avail: CASI HC A03/MF A01

The adsorption and chemical reactivity of the extreme pressure (EP) oil additive lead naphthenate (Pbnp) on steel surfaces is examined with X-ray photoelectron spectroscopy. In addition, the chemical compositions of AISI 440C and 52100 steel surfaces are studied as a function of sample cleaning treatment, including solvent cleaning, and treatments with acidic and basic solutions. At room temperature, Pbnp is shown to physisorb on the iron oxide overlayer present on both steel surfaces following solvent cleaning. A chemisorbed form of Pbnp is characterized by Pb 4f peaks chemically shifted by 0.3 to 0.4 eV to lower binding energy and significantly lower intensity of the C 1s feature associated with the Pbnp carboxylate group. This form of Pbnp is observed on acid- and base-pretreated surfaces that lose their iron oxide overlayers. The chemisorbed Pbnp surface species is also observed when the steel surfaces are scratched while being immersed in the Pbnp solution. When the Pbnp-treated steel surfaces are heated to simulate the EP conditions for which Pbnp is used, most of the Pbnp on the oxide-covered surfaces desorbs. In addition, metallic Pb is readily formed on the scratched surfaces and whenever significant amounts of metallic Fe are present. These results point to two possible modes of boundary protection: chemisorbed Pbnp under mild wear conditions and a layer of metallic Pb under severe wear conditions. GRA

N93-12779*# Boeing Co., Seattle, WA. Defense and Space Group.
ANODIZED ALUMINUM ON LDEF: A CURRENT STATUS OF MEASUREMENTS ON CHROMIC ACID ANODIZED ALUMINUM
Johnny L. Golden *In* NASA. Langley Research Center, LDEF Materials Workshop 1991, Part 1 Sep. 1992 p 211-221 (For primary document see N93-12769 03-27)
Avail: CASI HC A03/MF A04

27 NONMETALLIC MATERIALS

Includes physical, chemical, and mechanical properties of plastics, elastomers, lubricants, polymers, textiles, adhesives, and ceramic materials.

For composite materials see *24 Composite Materials.*

N93-12589*# Pratt and Whitney Aircraft, East Hartford, CT. Development Operations and Materials Engineering.
THERMAL BARRIER COATING LIFE PREDICTION MODEL DEVELOPMENT, PHASE 2 Final Report
Susan Manning Meier, Keith D. Sheffler, and David M. Nissley Jul. 1991 198 p
(Contract NAS3-23944)
(NASA-CR-189111; NAS 1.26:189111) Avail: CASI HC A09/MF A03

The objective of this program was to generate a life prediction model for electron-beam-physical vapor deposited (EB-PVD) zirconia thermal barrier coating (TBC) on gas turbine engine components. Specific activities involved in development of the EB-PVD life prediction model included measurement of EB-PVD ceramic physical and mechanical properties and adherence strength, measurement of the thermally grown oxide (TGO) growth kinetics, generation of quantitative cyclic thermal spallation life data, and development of a spallation life prediction model. Life data useful for model development was obtained by exposing instrumented, EB-PVD ceramic coated cylindrical specimens in a jet fueled burner rig. Monotonic compression and tensile mechanical tests and physical property tests were conducted to obtain the EB-PVD ceramic behavior required for burner rig specimen analysis. As part of that effort, a nonlinear constitutive model was developed for the EB-PVD ceramic. Spallation failure of the EB-PVD TBC system consistently occurred at the TGO-metal interface. Calculated out-of-plane stresses were a small fraction of that required to statically fail the TGO. Thus, EB-PVD spallation was attributed to the interfacial cracking caused by in-plane TGO strains. Since TGO mechanical properties were not measured in this program, calculation of the burner rig specimen TGO in-plane strains was performed by using alumina properties. A life model based on maximum

in-plane TGO tensile mechanical strain and TGO thickness correlated the burner rig specimen EB-PVD ceramic spallation lives within a factor of about plus or minus 2X. Author

N93-12651# Pennsylvania Univ., Philadelphia. Dept. of Chemistry.
ELECTROCHEMICAL AND CHEMICAL CHARACTERISTICS OF A NEW AMBIENT TEMPERATURE Li(I) POLYMER ELECTROLYTE
R. Huq, R. Koksbang, and G. C. Farrington 12 Jun. 1992 17 p
(Contract N00014-90-J-1559)
(AD-A254918; TR-1992-17) Avail: CASI HC A03/MF A01

A new type of highly conductive Li(+) polymer electrolyte, referred to as the Innovision polymer electrolyte, is completely amorphous at room temperature and has an ionic conductivity in the range of 10-3 S/cm. This paper discusses the electrochemical characteristics (lithium oxidation and reduction), conductivity, and physical properties of Innovision electrolytes containing different dissolved salts. These electrolytes are particularly interesting since they appear to have some of the highest room temperature lithium ion conductivities yet observed among polymer electrolytes. GRA

N93-12697# Cornell Univ., Ithaca, NY. Dept. of Chemistry.
SYNTHESIS AND PROPERTIES OF NOVEL CLUSTER PHASES
F. DiSalvo 15 May 1992 9 p
(Contract DE-FG02-87ER-45298)
(DE92-017388; DOE/ER-45298/8) Avail: CASI HC A02/MF A01

Research on cluster compounds this period (past periods covered such compounds such as NbMTe2 TaFe(1.25)Te3, Nb3SiTe6, etc.) was concentrated on LiMo3Se3. A LiMo3Se3 bundle approximately 70 nm wide was grown on a holey carbon substrate; STEM was used to resolve individual 6 A wires, and the Mo3Se3 flat 'monomer' units is resolved at 2.3 A (Mo atoms wrapped in Se atoms). Inorganic-organic polymer composites are being studied; conducting films have been prepared. The sheet structure of Nb3SiTe6 is shown. DOE

N93-12729# Cornell Univ., Ithaca, NY. Dept. of Theoretical and Applied Mechanics.
EXPERIMENTS, THEORY, AND SIMULATION ON THE EVOLUTION OF FABRIC IN GRANULAR MATERIALS Final Report, 1 Aug. 1988 - 31 Dec. 1991
J. T. Jenkins, P. A. Cundall, and I. Ishibashi 27 Jul. 1992 119 p
(Contract F49620-88-C-0090)
(AD-A254820; AFOSR-92-0811TR) Avail: CASI HC A06/MF A02

In this research, we have attempted to characterize the anisotropy in particle arrangement and particle interactions that develop when a granular material is deformed and to determine the influence of this anisotropy on the subsequent behavior of the material. The research has dealt with the behavior of an idealized granular material consisting of glass spheres and has involved the close interaction between physical experiments, numerical simulations, and the development of theory. We have focused on: (1) Understanding the relationship between the developing anisotropy of the material and the changes in volume observed in deformations in which the mean stress is held constant. In particular, we have considered the volume change of a hollow cylindrical sample in triaxial compression and extension; (2) Using elastic waves to probe the evolution of the internal structure of the granular material as it is being deformed; and (3) Developing constitutive relations for general stress paths in the triaxial/torsional device through the combined efforts of theoretical modeling and numerical simulation. GRA

N93-12749# Pennsylvania Univ., Philadelphia. Dept. of Chemistry.
ELECTRONIC PHENOMENA IN POLYANILINES Technical Report, 31 May 1991 - 30 Jun. 1992
A. J. Epstein and A. G. MacDiarmid 5 Jun. 1992 14 p
(Contract N00014-90-J-1559)
(AD-A254803; TR-1992-9) Avail: CASI HC A03/MF A01

Polyanilines have been known for over one hundred years. Recent studies of this chemically flexible polymer have demonstrated unusual chemical, electrical, and optical phenomena, both in insulating forms and conducting forms. Polyaniline has three stable insulating forms, leucoemeraldine base (LEB), emeraldine base (EB), and pernigraniline base (PNB). These three forms exhibit differing phenomena ranging from intramonomer luminescing excitons and ring rotation polarons in LEB, to nonluminescing charge transfer excitons and also ring rotational polarons in EB, to a degenerate ground state with bond order parameter solitons and ring order parameter polarons in PNB. The LEB form can be p-doped (oxidatively doped), the EB form can be protonic acid doped and the PNB form can be n-doped (reductively doped) to form conducting systems. Charge conduction studies of oriented films and fibers demonstrate that three-dimensional order between chains is critical for high conductivities. The ability to derivatize polyaniline at ring and nitrogen positions allows one to test concepts for the control of conductivity as well as improved processing. GRA

N93-12753# Pennsylvania Univ., Philadelphia. Dept. of Chemistry.
SOLVATION OF COBALT SALTS BY OLIGOMERIC POLYETHERS Technical Report, 31 May 1991 - 30 Jun. 1992
M. S. Mendolia and G. C. Farrington 12 Jun. 1992 12 p
(Contract N00014-90-J-1559)
(AD-A254815; Rept-1992-19) Avail: CASI HC A03/MF A01

Polyether-salt systems involving CoBr2 dissolved in oligomeric polyethylene glycol (PEG) and polytetra-methylene glycol (PTMG) have been investigated. Both systems demonstrated conductivity maxima as a function of salt concentration. PTMG electrolytes had dramatically lower conductivities (max. sigma approx. 3.6 x 10(exp -7) Scm for PTMG, max. sigma approx. 1.45 x 10(exp -5) Scm for PEG at room temperature) which can be explained on the basis of spectral data which indicate the existence of predominantly neutral species in PTMG. The reason for the difference in the types of species present in PEG and PTMG can be rationalized on the basis of the chelate effect. GRA

N93-12754# Pennsylvania Univ., Philadelphia. Dept. of Chemistry.
EFFECT OF PLASTICIZERS ON THE PROPERTIES OF NEW AMBIENT TEMPERATURE SOLID POLYMER ELECTROLYTES Technical Report, 31 May 1991 - 30 Jun. 1992
R. Huq, R. Koksbang, P. E. Tonder, and G. C. Farrington 12 Jun. 1992 11 p
(Contract N00014-90-J-1559)
(AD-A254817; TR-1992-20) Avail: CASI HC A03/MF A01

The effect of different plasticizers on the conductivities and physical/chemical properties of radiation polymerized polyethers formed by cross-linking mixtures of acrylate oligomers and dissolved salts have been studied. The plasticizers used were propylene carbonate, ethylene carbonate and a mixture of ethylene carbonate and propylene carbonate. The conductivities of all the compositions studied were in the range of 10(exp -3) to 10(exp -4) S/cm. In this paper, the relationship of the conductivities to the physical, chemical, and electrochemical properties of these materials is discussed. GRA

N93-12755# Pennsylvania Univ., Philadelphia. Dept. of Chemistry.
STUDIES OF PLASTICIZED-POLYMER ELECTROLYTES CONTAINING MIXED Zn(2) AND Li(1) Technical Report, 31 May 1991 - 30 Jun. 1992
B. V. Chowdari, R. Hug, and G. C. Farrington 12 Jun. 1992 11 p
(Contract N00014-90-J-1559)
(AD-A254818; TR-1992-21) Avail: CASI HC A03/MF A01

Thin solid films of mixtures of PEGDME and PEO containing various ratios of ZnBr2 and LiBr have been prepared. Equal parts of PEGDME and PEO were used, and the ether oxygen to total metal ratio was kept constant at 16. TG data have shown that the thermal stability of the polymer electrolytes is affected more so by the zinc salt than the lithium salt DSC data show that these electrolytes are inhomogeneous mixtures of amorphous regions and crystalline PEO and PEO/salt complexes. Conductivity data did not show a mixed-cation effect. GRA

N93-12769*# National Aeronautics and Space Administration. Langley Research Center, Hampton, VA.
LDEF MATERIALS WORKSHOP 1991, PART 1
Bland A. Stein, comp. and Philip R. Young, comp. Washington Sep. 1992 461 p Workshop held in Hampton, VA, 19-22 Nov. 1991
(RTOP 506-48-91-08)
(NASA-CP-3162-Pt-1; L-17135-Pt-1; NAS 1.55:3162-Pt-1) Avail: CASI HC A20/MF A04

The workshop comprised a series of technical sessions on materials themes, followed by theme panel meetings. Themes included materials, environmental parameters, and data bases; contamination; thermal control and protective coatings and surface treatments; polymers and films; polymer

matrix composites; metals, ceramics, and optical materials; lubricants adhesives, seals, fasteners, solar cells, and batteries. This report contains most of the papers presented at the technical sessions. It also contains theme panel reports and visual aids. This document continues the LDEF Space Environmental Effects on Materials Special Investigation Group (MSIG) pursuit of its charter to investigate the effects of LEO exposure on materials which where not originally planned to be test specimens and to integrate this information with data generated by principal investigators into an LDEF materials data base. For individual titles, see N93-12770 through N93-12789.

N93-12770*# National Aeronautics and Space Administration. Langley Research Center, Hampton, VA.

LDEF MATERIALS: AN OVERVIEW OF THE INTERIM FINDINGS

Bland A. Stein *In its* LDEF Materials Workshop 1991, Part 1 Sep. 1992 p 1-5 (For primary document see N93-12769 03-27)

Avail: CASI HC A04/MF A04

The flight and retrieval of the National Aeronautics and Space Administration's Long Duration Exposure Facility (LDEF) provided an opportunity for the study of the low-Earth orbit (LEO) environment and long-duration space environmental effect (SEE) on materials that are unparalleled in the history of the U.S. space program. The 5.8-year flight of LDEF greatly enhanced the potential value of materials data from LDEF to the international SEE community, compared to that of the original 1-year flight plan. The remarkable flight attitude stability of LDEF enables specific analyses of various individual and combined effects of LEO environmental parameters on identical materials of the same space vehicle. NASA recognized the potential by forming the LDEF Space Environmental Effects on Materials Special Investigation Group (MSIG) to address the greatly expanded materials and LEO space environment parameter analysis opportunities available in the LDEF structure, experiment trays, and corollary measurements, so that the combined value of all LDEF materials data to current and future space missions will be assessed and documented. This paper provides an overview of the interim LDEF materials findings of the Principal Investigators and the Materials Special Investigation Group. These revelations are based on observations of LEO environmental effects on materials made in-space during LDEF retrieval and during LDEF tray deintegration at the Kennedy Space Center, and on findings of approximately 1.5 years of laboratory analyses of LDEF materials by the LDEF materials scientists. These findings were extensively reviewed and discussed at the MSIG-sponsored LDEF Materials Workshop '91. The results are presented in a format which categorizes the revelations as 'clear findings' or 'confusing/unexplained findings' and resultant needs for new space materials developments and ground simulation testing/analytical modeling in seven categories: environmental parameters and data bases; LDEF contamination; thermal control coatings and protective treatments; polymers and films; polymer-matrix composites; metals, ceramics, and optical materials; and systems-related materials. General outlines of findings of the other LDEF Special Investigation Groups (Ionizing Radiation, Meteoroid and Debris, and Systems) are also included. The utilization of LDEF materials data for future low-earth orbit missions is also discussed, concentrating on Space Station Freedom. Some directions for continuing studies of LDEF materials are outlined. In general, the LDEF data is remarkable consistent; LDEF will provide a 'benchmark' for materials design data bases for satellites in low-Earth orbit. Some materials were identified to be encouragingly resistant to LEO SEE for 5.8-years; other 'space qualified' materials displayed significant environmental degradation. Molecular contamination was widespread; LDEF offers an unprecedented opportunity to provide a unified perspective of unmanned LEO spacecraft contamination mechanisms. New material development requirements for long-term LEO missions have been identified and current ground simulation testing methods/data for new, durable materials concepts can be validated with LDEF results. LDEF findings are already being integrated into the design of Space Station Freedom. Author

N93-12771*# Boeing Co., Seattle, WA. Defense and Space Group.

LDEF ATOMIC OXYGEN FLUENCE UPDATE

Roger J. Bourassa and J. R. Gillis *In* NASA. Langley Research Center, LDEF Materials Workshop 1991, Part 1 Sep. 1992 p 59-69 (For primary document see N93-12769 03-27)

(Contract NAS1-18224)

Avail: CASI HC A03/MF A04

The definition of LDEF atomic oxygen exposure involves theoretical prediction of fluxes, modeling of shielding and scattering effects, and comparison of predicted with observed atomic oxygen effects on LDEF experiments. Work is proceeding as follows: atomic oxygen fluxes and fluences have been recalculated using a more detailed orbit prediction program; a micro-environments program is being developed to account for the effects of experiment geometry on atomic oxygen flux; and chemical and physical measurements are being made on copper grounding straps to verify correspondence between predicted exposures and observed surface property variations. These three areas of work are reported briefly.

Author

N93-12772*# National Aeronautics and Space Administration. Lewis Research Center, Cleveland, OH.

LDEF YAW AND PITCH ANGLE ESTIMATES **c18**

Bruce A. Banks and Linda Gebauer (Cleveland State Univ., OH.) *In* NASA. Langley Research Center, LDEF Materials Workshop 1991, Part 1 Sep. 1992 p 71-92 (For primary document see N93-12769 03-27)

Avail: CASI HC A03/MF A04

Quantification of the LDEF yaw and pitch misorientations is crucial to the knowledge of atomic oxygen exposure of samples placed on LDEF. Video camera documentation of the LDEF spacecraft prior to grapple attachment, atomic oxygen shadows on experiment trays and longerons, and a pinhole atomic oxygen camera placed on LDEF provided sources of documentation of the yaw and pitch misorientation. Based on uncertainty-weighted averaging of data, the LDEF yaw offset was found to be 8.1 plus or minus 0.6 degrees, allowing higher atomic oxygen exposure of row 12 than initially anticipated. The LDEF pitch angle offset was found to be 0.8 plus or minus 0.4 degrees, such that the space end was tipped forward toward the direction of travel. The resulting consequences of the yaw and pitch misorientation of LDEF on the atomic oxygen fluence is a factor of 2.16 increase for samples located on row 12, and a factor of 1.18 increase for samples located on the space end compared to that which would be expected for perfect orientation. Author

N93-12773*# Boeing Co., Kent, WA. Defense and Space Group.

MATERIALS SIG QUANTIFICATION AND CHARACTERIZATION OF SURFACE CONTAMINANTS

E. Russ Crutcher *In* NASA. Langley Research Center, LDEF Materials Workshop 1991, Part 1 Sep. 1992 p 95-114 (For primary document see N93-12769 03-27)

Avail: CASI HC A03/MF A04

When LDEF entered orbit its cleanliness was approximately a MIL-STD-1246B Level 2000C. Its burden of contaminants included particles from every part of its history including a relatively small contribution from the shuttle bay itself. Although this satellite was far from what is normally considered clean in the aerospace industry, contaminating events in orbit and from processing after recovery were easily detected. The molecular contaminants carried into orbit were dwarfed by the heavy deposition of UV polymerized films from outgassing urethane paints and silicone based materials. Impacts by relatively small objects in orbit could create particulate contaminants that easily dominated the particle counts within a centimeter of the impact site. During the recovery activities LDEF was 'sprayed' with a liquid high in organics and water soluble salts. With reentry turbulence, vibration, and gravitational loading particulate contaminants were redistributed about LDEF and the shuttle bay. Author

N93-12774*# Boeing Co., Seattle, WA. Defense and Space Group.

Z306 MOLECULAR CONTAMINATION AD HOC COMMITTEE RESULTS

Johnny L. Golden *In* NASA. Langley Research Center, LDEF Materials Workshop 1991, Part 1 Sep. 1992 p 115-140 (For primary document see N93-12769 03-27)

Avail: CASI HC A03/MF A04

LDEF external surfaces which did not receive significant amounts of atomic oxygen were observed to be coated with a brown contamination, apparently the result of a condensed organic residue darkened due to UV radiation exposure. During the initial Materials Special Investigation Group (MSIG) Meeting after LDEF deintegration, held in Seattle - July 1990, this organic contamination was the subject of much discussion. The amount of contamination was thought to be significant and its source was immediately believed to be the Z306 black thermal control coating used to coat the entire inner surface of LDEF. Due to the size of the structure, it was not

feasible to bake-out the coating. However, initial data on the contamination film was confusing in that significant amounts of silicon was observed by several different researchers. Silicon (from silicone) was not expected to be a potential outgassing product of the Z306 polyurethane coating. To investigate the connection between external contamination and the interior paint, a MSIG ad hoc committee was formed. Author

N93-12775*# Applied Science Technology, Inc., Littleton, CO.
LONG DURATION EXPOSURE FACILITY (LDEF) CONTAMINATION MODELING
Tim Gordon and Ray Rantanen (ROR Enterprises, Castle Rock, CO.) *In* NASA. Langley Research Center, LDEF Materials Workshop 1991, Part 1 Sep. 1992 p 141-157 Sponsored by NASA. Marshall Space Flight Center (For primary document see N93-12769 03-27)
Avail: CASI HC A03/MF A04

The Integrated Spacecraft Environments Model (ISEM) was used to model the LDEF induced neutral molecular environment at several different times and altitudes during the mission. The purpose of this effort was to provide the community with an estimate of the neutral molecular environment to assist in phenomenology studies. Author

N93-12776*# Aerospace Corp., El Segundo, CA.
SURFACE CONTAMINATION ON LDEF EXPOSED MATERIALS
Carol S. Hemminger *In* NASA. Langley Research Center, LDEF Materials Workshop 1991, Part 1 Sep. 1992 p 159-174 (For primary document see N93-12769 03-27)
(Contract F04701-88-C-0089)
Avail: CASI HC A03/MF A04

X-ray photoelectron spectroscopy (XPS) has been used to study the surface composition and chemistry of Long Duration Exposure Facility (LDEF) exposed materials including silvered Teflon (Ag/FEP), Kapton, S13GLO paint, quartz crystal monitors (QCM's), carbon fiber/organic matrix composites, and carbon fiber/Al Alloy composites. In each set of samples, silicones were the major contributors to the molecular film accumulated on the LDEF exposed surfaces. All surfaces analyzed have been contaminated with Si, O, and C; most have low levels (less than 1 atom percent) of N, S, and F. Occasionally observed contaminants included Cl, Na, K, P, and various metals. Orange/brown discoloration observed near vent slots in some Ag/FEP blankets were higher in carbon, sulfur, and nitrogen relative to other contamination types. The source of contamination has not been identified, but amine/amide functionalities were detected. It is probable that this same source of contamination account for the low levels of sulfur and nitrogen observed on most LDEF exposed surfaces. XPS, which probes 50 to 100 A in depth, detected the major sample components underneath the contaminant film in every analysis. This probably indicates that the contaminant overlayer is patchy, with significant areas covered by less that 100 A of molecular film. Energy dispersive x-ray spectroscopy (EDS) of LDEF exposed surfaces during secondary electron microscopy (SEM) of the samples confirmed contamination of the surfaces with Si and O. In general, particulates were not observed to develop from the contaminant overlayer on the exposed LDEF material surfaces. However, many SiO2 submicron particles were seen on a masked edge of an Ag/FEP blanket. In some cases such as the carbon fiber/organic matrix composites, interpretation of the contamination data was hindered by the lack of good laboratory controls. Examination of laboratory controls for the carbon fiber/Al alloy composites showed that preflight contamination was the most significant factor for all the contaminants generally detected at less than 1 atom percent, or detected only occasionally (i.e., all but Si, O, and C). Flight control surfaces, including sample backsides not exposed to space radiation or atomic oxygen flux, have accumulated some contamination on flight (compared to laboratory controls), but experimentally, the LDEF exposed surface contamination levels are generally higher for the contaminants Si and O. For most materials analyzed, Si contamination levels were higher on the leading edge surfaces than on the trailing edge surfaces. This was true even for the composite samples where considerable atomic oxygen erosion of the leading edge surfaces was observed by SEM. It is probable that the return flux associated with atmospheric backscatter resulted in enhanced deposition of silicones and other contaminants on the leading edge flight surfaces relative to the trailing edge. Although the Si concentration data suggested greater on-flight deposition of contaminants on the leading edge surfaces, the XPS analyses did not conclusively show different relative total thicknesses of flight deposited contamination for leading and trailing edge surfaces. It is possible that atomic oxygen reactions on the leading edge resulted in greater volatilization of the carbon component of the deposited silicones, effectively 'thinning' the leading edge deposited overlayer. Unlike other materials, exposed polymers such as Kapton and FEP-type Teflon had very low contamination on the leading edge surfaces. SEM evidence showed that undercutting of the contaminant overlayer and damaged polymer layers occurred during atomic oxygen erosion, which would enhance loss of material from the exposed surface. Author

N93-12777*# National Aeronautics and Space Administration. Langley Research Center, Hampton, VA.
SOURCES AND TRANSPORT OF SILICONE NVR
Gale A. Harvey *In its* LDEF Materials Workshop 1991, Part 1 Sep. 1992 p 175-185 (For primary document see N93-12769 03-27)
Avail: CASI HC A03/MF A04

The retrieved LDEF had varying amounts of visible contamination films (brown stains) at many locations. FTIR spectra of heavy film deposits at vents and of optical windows from tray E5 indicated methyl silicone and silica in the contaminant films. Two possible sources of the methyl silicone are DC-710 phenyl methyl silicone in the shuttle-bay-liner beta cloth, and the shuttle tile waterproofing silane. It is concluded that much of the silicon and silica contamination came from ground operations and the orbiter. Author

N93-12778*# National Aeronautics and Space Administration. Marshall Space Flight Center, Huntsville, AL.
THERMAL CONTROL SURFACES ON THE MSFC LDEF EXPERIMENTS
Donald R. Wilkes (AZ Technology, Huntsville, AL.), Ann F. Whitaker, James M. Zwiener, Roger C. Linton, David Shular, Palmer N. Peters, and John C. Gregory (Alabama Univ., Huntsville.) *In* NASA. Langley Research Center, LDEF Materials Workshop 1991, Part 1 Sep. 1992 p 187-209 (For primary document see N93-12769 03-27)
Avail: CASI HC A03/MF A04

There were five Marshall Space Flight Center (MSFC) experiments on the LDEF. Each of those experiments carried thermal control surfaces either as test samples or as operational surfaces. These materials experienced varying degrees of mechanical and optical damage. Some materials were virtually unchanged by the extended exposure while others suffered extensive degradation. The synergistic effects due to the constituents of the space environment are evident in the diversity of these material changes. The sample complement for the MSFC experiments is described along with results of the continuing analyses efforts. Author

N93-12779*# Boeing Co., Seattle, WA. Defense and Space Group.
ANODIZED ALUMINUM ON LDEF: A CURRENT STATUS OF MEASUREMENTS ON CHROMIC ACID ANODIZED ALUMINUM **c26**
Johnny L. Golden *In* NASA. Langley Research Center, LDEF Materials Workshop 1991, Part 1 Sep. 1992 p 211-221 (For primary document see N93-12769 03-27)
Avail: CASI HC A03/MF A04

Chromic acid anodize was used as the exterior coating for aluminum surfaces on LDEF to provide passive thermal control. Chromic acid anodized aluminum was also used as test specimens in thermal control coatings experiments. The following is a compilation and analysis of the data obtained thus far. Author

N93-12780*# National Aeronautics and Space Administration. Marshall Space Flight Center, Huntsville, AL.
PERFORMANCE OF THERMAL CONTROL TAPE IN THE PROTECTION OF COMPOSITE MATERIALS **c24**
Rachel R. Kamenetzky and Ann F. Whitaker *In* NASA. Langley Research Center, LDEF Materials Workshop 1991, Part 1 Sep. 1992 p 223-232 (For primary document see N93-12769 03-27)
Avail: CASI HC A02/MF A04

The selection of materials for construction of long duration mission spacecraft has presented many challenges to the aerospace design community. After nearly six years in low earth orbit, NASA's Long duration Exposure Facility (LDEF), retrieved in January of 1990, has provided valuable information on both the nature of the space environment as well as the effects of the space environment on potential spacecraft materials. Composites, long a favorite of the design community because of a high strength-to-weight ratio, were flown in various configurations on LDEF in

order to evaluate the effects of radiation, atomic oxygen, vacuum, micrometeoroid debris, and thermal variation on their performance. Fiberglass composite samples covered with an aluminum thermal control tape were flown as part of the flight experiment A0171, the Solar Array Materials Passive LDEF Experiment (SAMPLE). Visual observations and test results indicate that the thermal control tape suffered little degradation from the space exposure and proved to be a reliable source of protection from atomic oxygen erosion and UV radiation for the underlying composite material. Author

N93-12781*# National Aeronautics and Space Administration. Marshall Space Flight Center, Huntsville, AL.

FLUORESCENCE OF THERMAL CONTROL COATINGS ON S0069 AND A0114

James M. Zwiener, Richard J. Mell, Palmer N. Peters, Donald R. Wilkes (AZ Technology, Huntsville, AL.), Edgar R. Miller (AZ Technology, Huntsville, AL.), and John C. Gregory (Alabama Univ., Huntsville.) *In* NASA. Langley Research Center, LDEF Materials Workshop 1991, Part 1 Sep. 1992 p 233-244 (For primary document see N93-12769 03-27)

Avail: CASI HC A03/MF A04

Many of the thermal control surfaces exposed to the space environment during the 5.8 year LDEF mission experienced changes in fluorescence. All of the thermal control coatings flown on LDEF experiments S0069 and A0114 were characterized for fluorescence under ambient conditions. Some of the black coatings, having protective overcoats, appear bright yellow under ultraviolet exposure. Urethane based coatings exhibited emission spectra shifts toward longer wavelengths in the visible range. Zinc oxide pigment based coatings experienced a quenching of fluorescence, while zinc orthotitanate pigment based and other ceramic type coatings had no measurable fluorescence. Author

N93-12782*# Dayton Univ. Research Inst., OH.

LONG DURATION EXPOSURE FACILITY M0003-5 THERMAL CONTROL COATINGS ON DOD FLIGHT EXPERIMENT

Charles J. Hurley and William L. Lehn (Nichols Research Corp., Dayton, OH.) *In* NASA. Langley Research Center, LDEF Materials Workshop 1991, Part 1 Sep. 1992 p 245-282 (For primary document see N93-12769 03-27)

Avail: CASI HC A03/MF A04

The M0003-5 thermal control coatings and materials orbited on the LDEF M0003 Space Environment Effects on Spacecraft Materials were a part of a Wright Laboratories Materials Directorate larger experiment. They were selected from new materials which emerged from development programs during the 1978-1982 time frame. Included were materials described in the technical literature which were being considered or had been applied to satellites. Materials that had been exposed on previous satellite materials experiments were also included to provide data correlation with earlier space flight experiments. The objective was to determine the effect of the LDEF environment on the physical and optical properties of thermal control coatings and materials. One hundred and two specimens of various pigmented organic and inorganic coatings, metallized polymer thin films, optical solar reflectors, and mirrors were orbited on LDEF. The materials were exposed in four separate locations on the vehicle. The first set was exposed on the direct leading edge of the satellite. The second set was exposed on the direct trailing edge of the vehicle. The third and fourth sets were exposed in environmental exposure control canisters (EECC) located 30 degrees off normal to the leading and trailing edges. The purpose of the experiment was to understand the changes in the properties of materials before and after exposure to the space environment and to compare the changes with predictions based on laboratory experiments. The basic approach was to measure the optical and physical properties of materials before and after long-term exposure to a low earth orbital environment comprised of UV, VUV, electrons, protons, atomic oxygen, thermal cycling, vacuum, debris, and micrometeoroids. Due to the unanticipated extended orbital flight of LDEF, the thermal control coatings and materials in the direct leading and trailing edge were exposed for a full five years and ten months to the space environment and the canister materials were exposed for approximately one year to the full environment. Author

N93-12783*# Ishikawajima-Harima Heavy Industries Co. Ltd., Tokyo (Japan). Thermal Control and Structure Group.

ELEMENT MATERIAL EXPOSURE EXPERIMENT BY EFFU

Yoshihiro Hashimoto, Masaaki Ito, and Masahiro Ishii *In* NASA. Langley Research Center, LDEF Materials Workshop 1991, Part 1 Sep. 1992 p 283-291 (For primary document see N93-12769 03-27)

Avail: CASI HC A02/MF A04

The National Space Development Agency of Japan (NASDA) is planning to perform an 'Element Material Exposure Experiment' using the Exposed Facility Flyer Unit (EFFU). This paper presents an initial design of experiments proposed for this project by our company. The EFFU is installed on the Space Flyer Unit (SFU) as a partial model of the Space Station JEM exposed facility. The SFU is scheduled to be launched by H-2 rocket in January or February of 1994, then various tests will be performed for three months, on orbit of 500 km altitude, and it will be retrieved by the U.S. Space Shuttle and returned to the ground. The mission sequence is shown. Author

N93-12784*# Nichols Research Corp., Dayton, OH.

SKYLAB D024 THERMAL CONTROL COATINGS AND POLYMERIC FILMS EXPERIMENT

William L. Lehn and Charles J. Hurley (Dayton Univ. Research Inst., OH.) *In* NASA. Langley Research Center, LDEF Materials Workshop 1991, Part 1 Sep. 1992 p 293-308 (For primary document see N93-12769 03-27)

Avail: CASI HC A03/MF A04

The Skylab D024 Thermal Control Coatings and Polymeric Films Experiment was designed to determine the effects of the external Skylab space environment on the performance and properties of a wide variety of selected thermal control coatings and polymeric films. Three duplicate sets of thermal control coatings and polymeric films were exposed to the Skylab space environment for varying periods of time during the mission. The specimens were retrieved by the astronauts during extravehicular activities (EVA) and placed in hermetically sealed return containers, recovered, and returned to the Wright Laboratory/Materials Laboratory/WPAFB, Ohio for analysis and evaluation. Postflight analysis of the three sets of recovered thermal control coatings indicated that measured changes in specimen thermo-optical properties were due to a combination of excessive contamination and solar degradation of the contaminant layer. The degree of degradation experienced over-rode, obscured, and compromised the measurement of the degradation of the substrate coatings themselves. Results of the analysis of the effects of exposure on the polymeric films and the contamination observed are also presented. The D024 results were used in the design of the LDEF M0003-5 Thermal Control Materials Experiment. The results are presented here to call to the attention of the many other LDEF experimenters the wealth of directly related, low earth orbit, space environmental exposure data that is available from the ten or more separate experiments that were conducted during the Skylab mission. Results of these experiments offer data on the results of low altitude space exposure on materials recovered from space with exposure longer than typical STS experiments for comparison with the LDEF results. Author

N93-12785*# European Space Agency. European Space Research and Technology Center, ESTEC, Noordwijk (Netherlands).

EFFECTS OF THE LDEF ENVIRONMENT ON THE Ag/FEP THERMAL BLANKETS

Francois Levadou and H. Gary Pippin (Boeing Co., Seattle, WA.) *In* NASA. Langley Research Center, LDEF Materials Workshop 1991, Part 1 Sep. 1992 p 311-344 (For primary document see N93-12769 03-27)

Avail: CASI HC A03/MF A04

This presentation was made by Francois Levadou at the NASA Langley Research Center LDEF materials workshop, November 19-22, 1991. It represents the results to date on the examination of silvered teflon thermal blankets primarily from the Ultra-heavy Cosmic Ray Experiment and also from the blanket from the Park Seed Company experiment. ESA/ESTEC and Boeing conducted a number of independent measurements on the blankets and in particular on the exposed fluorinated ethylene-propylene (FEP) layer of the blankets. Mass loss, thickness, and thickness profile measurements have been used by ESA, Boeing, and NASA LeRC to determine recession and average erosion yield under atomic oxygen exposure. Tensile strength and percent elongation to failure data, surface

characterization by ESCA, and SEM images are presented. The Jet Propulsion Laboratory analysis of vacuum radiation effects is also presented. The results obtained by the laboratories mentioned and additional results from the Aerospace Corporation on samples provided by Boeing are quite similar and give confidence in the validity of the data. Author

N93-12786*# Boeing Co., Seattle, WA. Defense and Space Group.
RECESSION OF FEP SPECIMENS FROM TRAYS D11 AND B7
H. Gary Pippin *In* NASA. Langley Research Center, LDEF Materials Workshop 1991, Part 1 Sep. 1992 p 345-356 (For primary document see N93-12769 03-27)
Avail: CASI HC A03/MF A04

We report work done at Boeing Defense and Space Group on analysis of silvered teflon specimens taken from selected locations of the Long Duration Exposure Facility under support from a contract provided by NASA LaRC. The samples discussed in this presentation were taken from the unexposed side of D11 and extended through the folded area of this blanket into the exposed area. Two similar areas were cut from blanket B7, one from the edge of the blanket near row six and one from the edge of the blanket near row eight and within a few centimeters of the copper grounding strap for B7. The specimens were each divided into three sections by cutting with a scapel. Two of the sections were mounted in a potting compound, which was cut and polished such that the cross-sectional thickness of each was exposed. One piece was mounted straight and the other was mounted in an attempt to configure the specimens such that it was bent with a radius of curvature similar to the on-orbit configuration. The third portion of each specimen was used for SEM images to help define the angle of exposure with respect to the ram at each location on the specimen. Photomicrographs were taken in cross section from the edge of the blanket through the curved transition region into the exposed area of the blanket. The thickness of the Fluorinated Ethylene Propylene (FEP) layer was determined at known distances from the edge of the blanket. SEM images were obtained at known distances to help define the angle with respect to ram and therefore establish the atomic oxygen fluence on each location and correlate this exposure with thickness. Thickness measurements made with a two to three centimeter distance minimized the uncertainty arising from variations in the as-manufactured thickness of each blanket. The nominal angle from ram of the exposed portion of each blanket, and the fact that the unexposed edge portions are approximately at right angles to the exposed portion were also used to help define the angles. Thickness measurements were taken at specified locations. An average thickness for the unexposed portion of the blanket was determined. Changes in thickness were then determined by difference. Author

N93-12787*# National Aeronautics and Space Administration. Langley Research Center, Hampton, VA.
CHARACTERIZATION OF SELECTED LDEF: EXPOSED POLYMER FILMS AND RESINS
Philip R. Young and Wayne S. Slemp *In its* LDEF Materials Workshop 1991, Part 1 Sep. 1992 p 357-389 (For primary document see N93-12769 03-27)
Avail: CASI HC A03/MF A04

The Long Duration Exposure Facility (LDEF) provided a unique environmental exposure of a wide variety of materials. The effects of 5 years and 10 months of Low-Earth Orbit (LEO) exposure of these materials to atomic oxygen, ultraviolet and particulate radiation, meteoroid and debris, vacuum, contamination, and thermal cycling is providing a data base unparalleled in the history of space environment research. Working though the Environmental Effects on Materials Special Investigation Group (MSIG), a number of polymeric materials in various processed forms have been assembled from LDEF investigators for analysis at the NASA Langley Research Center. This paper reports the status of on-going chemical characterization of these materials. Author

N93-12788*# Marquette Univ., Milwaukee, WI. Dept. of Mechanical and Industrial Engineering.
EFFECTS OF ORBITAL EXPOSURE ON HALAR DURING THE LDEF MISSION
William E. Brower, Jr., Harish Holla, and Robert A. Bauer *In* NASA. Langley Research Center, LDEF Materials Workshop 1991, Part 1 Sep. 1992 p 391-415 (For primary document see N93-12769 03-27)
Avail: CASI HC A03/MF A04

Thermomechanical Analysis (TMA), Differential Scanning Calorimetry (DSC), and Thermogravimetric Analysis (TGA) were performed on samples of Halar exposed on the LDEF Mission for 6 years in orbit and unexposed Halar control samples. Sections 10-100 microns thick were removed from the exposed surface down to a depth of 1,000 microns through the 3 mm thick samples. The TMA and DSC results, which arise from the entire slice and not just its surface, showed no differences between the LDEF and the control samples. TMA scans were run from ambient to 300 C; results were compared by a tabulation of the glass transition temperatures. DSC scans were run from ambient to 700 C; the enthalpy of melting was compared for the samples as a function of section depth with the sample. The TGA results, which arise from the surface of the sample initially, showed a sharp increase in the topmost 50 micron section (the exposed, discolored side) in the weight loss of 170 C in oxygen. This weight loss dropped to bulk values in the range of depth of 50-200 microns. The control sample showed only a slight increase in weight loss as the top surface was approached. The LDEF Halar sample appears to be mechanically undamaged, with a surface layer which oxidizes faster as a result of orbital exposure. Author

N93-12789*# Dayton Univ. Research Inst., OH.
LONG DURATION EXPOSURE FACILITY M0003-5 RECENT RESULTS ON POLYMERIC FILMS
Charles J. Hurley and Michele D. Jones (Wright Lab., Wright-Patterson AFB, OH.) *In* NASA. Langley Research Center, LDEF Materials Workshop 1991, Part 1 Sep. 1992 p 417-447 (For primary document see N93-12769 03-27)
Avail: CASI HC A03/MF A04

The M0003-5 polymeric film specimens orbited on the LDEF M0003 Space Environment Effects on Spacecraft Materials were a part of a Wright Laboratories Materials Directorate larger thermal control materials experiment. They were selected from new materials which emerged from development programs during the 1978-1982 time frame. Included were materials described in the technical literature which were being considered or had been applied to satellites. Materials that had been exposed on previous satellite materials experiments were also included to provide data correlation with earlier space flight experiments. The objective was to determine the effects of the LDEF environment on the physical and optical properties of polymeric thin film thermal control materials, the interaction of the LDEF environment with silvered spacecraft surfaces, and the performance of low outgassing adhesives. Sixteen combinations of various polymeric films, metallized and unmetallized, adhesively bonded and unbonded films were orbited on LDEF in the M0003-5 experiment. The films were exposed in two separate locations on the vehicle. One set was exposed on the direct leading edge of the satellite. The other set was exposed on the direct trailing edge of the vehicle. The purpose of the experiment was to understand the changes in the properties of materials before and after exposure to the space environment and to compare the changes with predictions based on laboratory experiments. The basic approach was to measure the optical and physical properties of materials before and after long-term exposure to a low earth orbital environment comprised of UV, VUV, electrons, protons, atomic oxygen, thermal cycling, vacuum, debris and micrometeoroids. Due to the unanticipated extended orbital flight of LDEF, the polymeric film materials were exposed for a full five years and ten months to the space environment. Author

N93-12821# Oak Ridge National Lab., TN.
COST-EFFECTIVE SINTERED REACTION-BONDED SILICON NITRIDE (SRBSN) FOR STRUCTURAL CERAMICS
T. N. Tiegs, J. O. Kiggans, Jr., and K. L. Ploetz 1992 14 p Presented at the 94th Annual Meeting and Exposition of the American Ceramic Society, Minneapolis, MN, 12-16 Apr. 1992
(Contract DE-AC05-84OR-21400)
(DE92-019285; CONF-920448-7) Avail: CASI HC A03/MF A01

Sintered silicon nitride has many superior properties; however, for most applications these materials are too expensive to compete with metal parts. Sintered reaction-bonded silicon nitride (SRBSN) is more economical, with raw materials costs greater than 20 percent of those of comparable high-purity materials, making it competitive with metal parts. Conventional processing of SRBSN requires long nitridation times and a two-step firing process. Microwave (MW) heating reduces the reaction times and is performed in a one-step process, thereby simplifying the operation. The

mechanical properties of the MW-SRBSN are not equal to those from the higher-cost powders, but are appropriate for a number of applications at lower temperatures and stress levels. At ambient temperature, typical strength, toughness (K(sub Ic) and hardness values are 480 MPa, 4.8 MPa(sq. rt of m), and 14 GPa, respectively. DOE

N93-12858# Virginia Polytechnic Inst. and State Univ., Blacksburg. Dept. of Engineering Science and Mechanics.
INVESTIGATION OF PROPERTIES AND PERFORMANCE OF CERAMIC COMPOSITE COMPONENTS
W. W. Stinchcomb, K. L. Reifsnider, and T. J. Dunyak 15 Jun. 1992 162 p Prepared for Oak Ridge National Lab., TN
(Contract DE-AC05-84OR-21400)
(DE92-019911; ORNL/Sub-87-SA946/02; CCMS-92-14) Avail: CASI HC A08/MF A02

The objective of the work reported herein is to develop an understanding of the mechanical behavior of advanced ceramic composites subjected to elevated temperature and dynamic (cyclic) loading, to develop a test system and test methods to obtain the properties and performance information required to design engineering components made from ceramic composite materials, and to provide critical and comprehensive evaluations of such materials to material synthesizers and developers to support and enhance progress in ceramic composite material development. The accomplishments of the investigation include the design, development, and demonstration of a high temperature, biaxial mechanical test facility for ceramic composite tubes and the development and validation of a performance simulation model (MRLife) for ceramic composites. DOE

N93-12888# Lawrence Livermore National Lab., CA.
DETERMINATION OF THE PERMEABILITY OF CARBON AEROGELS BY GAS FLOW MEASUREMENTS
F. M. Kong, S. S. Hulsey, C. T. Alviso, and R. W. Pekala Apr. 1992 *11 p Presented at the Material Research Society Spring Meeting, San* Francisco, CA, 27 Apr. - 2 May 1992
(Contract W-7405-eng-48)
(DE92-019574; UCRL-JC-108831; CONF-920402-54) Avail: CASI HC A03/MF A01

Carbon aerogels are synthesized via the polycondensation of resorcinol and formaldehyde, followed by supercritical drying and pyrolysis at 1050 C in nitrogen. Because of their interconnected porosity, ultrafine cell structure and high surface area, carbon aerogels have many potential applications, such as in supercapacitors, battery electrodes, catalyst supports, and gas filters. The performance of carbon aerogels in the latter two applications depends on the permeability or gas flow conductance in these materials. By measuring the pressure differential across a thin specimen and the nitrogen gas flow rate in the viscous regime, we calculated the permeability of carbon aerogels from equations based upon Darcy's law. Our measurements show that carbon aerogels have apparent permeabilities on the order of 10(exp -12)to 10(exp -10) cm(exp 2) for densities ranging from 0.44 to 0.05 g/cm(exp 3). Like their mechanical properties, the permeability of carbon aerogels follows a power law relationship with density and average pore size. Such findings help us to estimate the average pore sizes of carbon aerogels once their densities are known. This paper reveals the relationships among permeability, pore size, and density in carbon aerogels. DOE

N93-12917# Sandia National Labs., Albuquerque, NM.
BONDING IN SIMPLE PHOSPHATE GLASS
R. K. Brow 1992 6 p Presented at the International Congress on Glass, Madrid, Spain, 4-9 Oct. 1992
(Contract DE-AC04-76DP-00789)
(DE92-019437; SAND-92-1342C; CONF-921073-1) Avail: CASI HC A02/MF A01

The bonding configurations for simple phosphate glasses are quantitatively described by both the relative concentrations of different polyhedral phosphate sites (i.e., the Q(sup n) description) determined by (sup 31)p magic angle spinning nuclear magnetic resonance (MAS NMR) spectroscopy and by the relative concentrations of bridging and nonbridging oxygen as measured by x-ray photoelectron spectroscopy (XPS). Both spectroscopies illustrate the depolymerizing effects of modifier additions in two series of Na2O and ZnO-P2O5 glasses. DOE

N93-12931# Lawrence Livermore National Lab., CA.
AEROGELS, EMULSIONS, AND COMPOSITES: CONTROLLING STRUCTURE WITH ORGANIC SOL-GEL CHEMISTRY
R. W. Pekala, C. T. Alviso, S. S. Hulsey, and F. M. Kong Apr. 1992 12 p Presented at the Winter Annual Meeting of the ASME, Anaheim, CA, 8-13 Nov. 1992
(Contract W-7405-eng-48)
(DE92-019575; UCRL-JC-109956; CONF-921110-25) Avail: CASI HC A03/MF A01

The sol-gel polymerization of resorcinol with formaldehyde is a proven synthetic route for the formation of organic aerogels. These materials can also be pyrolyzed in an inert atmosphere to form vitreous carbon aerogels. Both resorcinol-formaldehyde and carbon aerogels are characterized by high porosity (50-98 percent) ultrafine cell/pore sizes (less than 100 mn), high surface area (400-1000 m(exp 2)/g), and a solid matrix composed of interconnected colloidal-like particles or fibrous chains with characteristic diameters of 10 nm. While this nanostructure and the low Z (atomic number) composition are responsible for the unique optical, thermal, acoustic, mechanical, and electrical properties of organic aerogels, there are certain applications in which a larger scale structure is also desired in combination with the unique features of the aerogel. In order to achieve this goal, we have been emulsifying our resorcinol-formaldehyde sols to form foams which retain the aerogel framework but have some cells/pores as large as 2 micron. In another approach, we have infused an emulsion-derived polystryene foam with a resorcinol-formaldehyde sol to form a new composite foam. This paper addresses the chemistry-structure-property relationships of organic aerogels, their emulsion-derived derivatives, and composite foams. DOE

N93-12999# Los Alamos National Lab., NM.
DISLOCATION AND PORES IN MULLITE FROM DIPHASIC GELS
Wen-Cheng J. Wei (National Taiwan Univ., Taipei.), T. E. Mitchell, and J. W. Halloran (Michigan Univ., Ann Arbor.) 1992 14 p Presented at the 5th Asia-Pacific Electron Microscopy Conference, Beijing, China, 1-6 Aug. 1992
(Contract W-7405-eng-36)
(DE92-040384; LA-UR-92-2557; CONF-920891-3) Avail: CASI HC A03/MF A01

Stoichiometric mullite prepared from the reactions of nanometer-sized pseudo-bochmite and acidic-catalysed silica gel has non-sinterable pores and dislocations. The formation of the pores is accompanied by densification and reactions of the diphasic alumino-silicate gel matrix. These pores tend to be faceted and show low-index crystallographic planes: /110/ and /211/. After heat treatment at greater than or equal to 1400 C for 24 hr. Dislocations are identified by weak-beam, dark-field, and 2-beam techniques. The possible atomic models near last two dislocations are proposed. But the direct observation needs more TEM work. DOE

N93-13026# Southwestern Univ., Georgetown, TX. Dept. of Chemistry.
SYNTHESIS OF DERIVATIVES OF ALPHA, OMEGA DIFUNCTIONAL PERFLUOROALIPHATIC COMPOUNDS FOR LOW DIELECTRIC CONSTANT RESINS *Final Report, 1 Apr. - 31 Dec. 1991*
Robert L. Soulen 6 Mar. 1992 6 p
(Contract N00014-91-J-1617)
(AD-A254928) Avail: CASI HC A02/MF A01

Copper coupling reactions of perfluoroalkyl iodides with certain aryl iodides have been studied. Simple trial tests were carried out between perfluorooctyl iodide and idobenzene and between perfluorohexyl iodide and 4-odophenol. The desired product were obtained in good yield. However, the coupling of 1,6-diiodoperfluorohexane and 4-iodophenol gave a product which could not be isolated or purified. Protection of the phenolic OH by methylation or acetylation gave the coupled alpha, omega products in good yield. GRA

N93-13035# Westinghouse Savannah River Co., Aiken, SC.
ALUMINUM OXIDE FILM THICKNESS AND EMITTANCE
J. K. Thomas and R. S. Ondrejcin Nov. 1991 40 p
(Contracts DE-AC09-89SR-18035; DE-AC09-76SR-00001)
(DE92-019931; WSRC-RD-91-24) Avail: CASI HC A03/MF A01

Aluminum reactor components which are not actively cooled could be subjected to high temperatures due to gamma heating after the core coolant level dropped during the ECS phase of a hypothetical LOCA event. Radiative

heat transfer is the dominant heat transfer process in this scenario and therefore the emittance of these components is of interest. Of particular interest are the safety rod thimbles and Mark 60B blanket assemblies; for the K Reactor, these components have been exposed to low temperature (less than 55 C) moderator for about a year. The average moderator temperature was assumed to be 30 C. The Al oxide film thickness at this temperature, after one year of exposure, is predicted to be 6.4 microns +/- 10 percent; this value is insensitive to exposure time. Dehydration of the film during the gamma heating accident would result in a film thickness of 6.0 microns +/- 11 percent. Total hemispherical emittance is predicted to be 0.69 at 96 C, decreasing to 0.45 at 600 C. Some phenomena which would tend to yield thicker oxide films in the reactor environment relative to those obtained under experimental conditions were neglected and the predicted film thickness values are therefore conservative. The emittance values predicted for a given film thickness are also conservative. The conservativisms inherent in the predicted emittance are particularly relevant for uncertainty analysis of temperatures generated using these values.

DOE

N93-13101# Department of the Navy, Washington, DC.

MOLTEN SALT REACTOR FOR POTENTIOSTATIC ELECTROPLATING Patent Application

Kurt H. Stern, inventor (to Navy) (Courtney and Co., Philadelphia, PA.) and *Ralph M. Hess, inventor (to Navy) (Courtney and Co., Philadelphia, PA.)* 12 Mar. 1992 19 p

(AD-D015358; US-Patent-Appl-SN-850107; Navy-Case-72535) Avail: CASI HC A03/MF A01

A molten salt reactor for potentiostatic electroplating that includes a reactor chamber defined by a peripheral wall, a bottom wall and a top cover. The bottom wall of the reactor chamber has an opening, to which a first end of a gas inlet conduit is attached so as to be in fluid communication with the reactor chamber. A crucible support platform is positioned within the reactor chamber, and a crucible for holding a molten salt is mounted thereon. A furnace substantially surrounds the peripheral wall of the reactor chamber and the first end of the gas inlet conduit. The crucible support platform is electrically insulated from the reactor chamber. An inert gas flows from the gas inlet conduit, through a lower portion of the reactor chamber, past the crucible support platform, through an upper portion of the reactor chamber, and to a gas outlet in the upper portion of the reactor chamber. The inert gas is heated within the first end of the gas inlet conduit prior to flowing into the lower portion of the reaction chamber.

GRA

N93-13115*# National Aeronautics and Space Administration. Marshall Space Flight Center, Huntsville, AL.

GLASS FIBER PROCESSING FOR THE MOON/MARS PROGRAM: CENTER DIRECTOR'S DISCRETIONARY FUND FINAL REPORT

D. S. Tucker, E. Ethridge, and P. Curreri Oct. 1992 22 p

(NASA-TM-108379; NAS 1.15:108379) Avail: CASI HC A03/MF A01

Glass fiber has been produced from two lunar soil simulants. These two materials simulate lunar mare soil and lunar highland soil compositions, respectively. Short fibers containing recrystallized areas were produced from the as-received simulants. Doping the highland simulant with 8 weight percent B2-O3 yielded a material which could be spun continuously. The effects of lunar gravity on glass fiber formation were studied utilizing NASA's KC-135 aircraft. Gravity was found to play a major role in final fiber diameter.

Author

N93-13150*# Howard Univ., Washington, DC. Dept. of Physics.

GLASS CORROSION IN NATURAL ENVIRONMENTS Progress Report, Jan. - Jun. 1992

Arthur N. Thorpe and Aaron Barkatt Jun. 1992 27 p Prepared in cooperation with Catholic Univ. of America, Washington, DC

(Grant NAG5-1057)

(NASA-CR-191234; NAS 1.26:191234) Avail: CASI HC A03/MF A01

Experiments carried out during the progress period are summarized. Experiments carried out involving glass samples exposed to solutions of Tris have shown the appearance of 'spikes' upon monitoring glass dissolution as a function of time. The periodic 'spikes' observed in Tris-based media were interpreted in terms of cracking due to excessive stress in the surface region of the glass. Studies of the interactions of silicate glasses with metal ions in buffered media were extended to systems containing Al. Caps buffer was used to establish the pH. The procedures used are described and the results are given. Preliminary studies were initiated as to the feasibility of adding a slowly dissolving solid compound of the additive to the glass-water system to maintain a supply of dissolved additive. It appears that several magnesium compounds have a suitable combination of solubility and affinity towards silicate glass surfaces to have a pronounced retarding effect on the extraction of uranium from the glass. These preliminary findings raise the possibility that introducing a magnesium source into geologic repositories for nuclear waste glass in the form of a sparingly soluble Mg-based backfill material may cause a substantial reduction in the extent of long-term glass corrosion. The studies described also provide mechanistic understanding of the roles of various metal solutes in the leachant. Such understanding forms the basis for developing long-term predictions of nuclear waste glass durability under repository conditions. From what is known about natural highly reduced glasses such as tektites, it is clear that iron is dissolved as ferrous iron with little or no ferric iron. The reducing conditions were high enough to cause metallic iron to exsolve out of the glass in the form of submicroscopic spherules. As the nuclear waste glass is much less reduced, a study was initiated on other natural glasses in addition to the nuclear waste glass. Extensive measurements were carried out on these glasses in order to characterize their magnetic properties. Results of these studies are described.

L.R.R.

N93-13259# Army Engineer Waterways Experiment Station, Vicksburg, MS. Geotechnical Lab.

POLYPROPYLENE FIBERS IN PORTLAND CEMENT CONCRETE PAVEMENTS Final Report, Oct. 1989 - Mar. 1992

James E. Shoenberger and Joe G. Tom Aug. 1992 115 p Submitted for publication

(Contract DTFA01-90-Z-02069)

(DOT/FAA/RD-92/9) Avail: CASI HC A06/MF A02

This report provides the information obtained from a literature search, site visits, and a laboratory study of polypropylene fibers in portland cement concrete (PCC). The literature search yielded information from numerous laboratory studies of the material properties of polypropylene fiber reinforced concrete (PFRC). The literature showed that, for the low fiber volumes (0.1 percent) recommended by most manufacturers, there was marginal improvement in toughness, fatigue, impact resistance, permeability, shrinkage, and wear resistance. Limited construction has taken place on PFRC suitable for airport construction. Most construction has been of slabs-on-grade and structural slabs. The laboratory study showed that, at 0.1 percent by volume of fibers, the reinforced concrete did not provide appreciable enhancement of material properties over non-reinforced PCC.

Author

N93-13315# Los Alamos National Lab., NM.

DUCTILE PHASE TOUGHENING OF MOLYBDENUM DISILICIDE BY LOW PRESSURE PLASMA SPRAYING

R. G. Castro, A. D. Rollett, P. W. Stanek, and R. W. Smith (Drexel Univ., Philadelphia, PA.) 1992 22 p Presented at the Workshop on High Temperature Structural Silicides, Gaithersburg, MD, 4-6 Nov. 1992

(Contract W-7405-eng-36)

(DE92-007409; LA-UR-92-313; CONF-921184-1) Avail: CASI HC A03/MF A01

The low fracture toughness of MoSi2 at ambient temperature has prompted investigations into new processing methods in order to impart some degree of fracture toughness into this inherently brittle material. In the following investigation, low pressure plasma spraying was employed as a fabricating technique to produce spray-formed deposits of MoSi2 and ductile reinforced MoSi2 composites containing approximately 10 and 20 volume percent of a discontinuous tantalum lamelli reinforcement. Fracture toughness (K(sub IC)) measurements of MoSi2 and the MoSi2/Ta composites were done using a chevron notched 4-point bend fracture toughness test in both the as-sprayed condition and after hot isostatic pressing at 1200 C/206 MPa for 1 hour. Results from the ductile reinforced MoSi2/Ta composites have shown fracture toughness increases on the order of 200 percent over the as-sprayed MoSi2. In addition, a marked anisotropy in fracture toughness was observed in the spray-formed deposits due to the layered splat structure produced by the low pressure plasma spray process.

DOE

N93-13325# Duke Univ., Durham, NC. Dept. of Mechanical Engineering and Materials Science.
CHARACTERIZATION OF THERMOTROPIC LIQUID CRYSTALLINE POLYMER BLENDS BY POSITRON ANNIHILATION LIFETIME SPECTROSCOPY Final Report, 1 Jun. 1989 - 31 May 1992
Robert A. Naslund and Phillip L. Jones 17 Jul. 1992 9 p
(Contract DAAL03-89-C-0020)
(AD-A253616; ARO-26647.3-MS) Avail: CASI HC A02/MF A01

Positron annihilation lifetime spectroscopy (PALS) has been used to investigate polymer-based molecular composites of two separate thermotropic liquid crystalline polymers (TLCP's) and the thermoplastic matrix polyetherimide. Variations in PALS spectral components were observed as a function of both TLCP content and temperature and are discussed as a function of free volume and molecular structure. It has been shown that these differences, between the matrix and reinforcing phase, has substantial influence on the localization and annihilation of o-Ps. The more miscible HX4000 composites exhibited TLCP dominated lifetime characteristics at room temperature. Differential scanning calorimetry, used as a complementary characterization technique to PALS to investigate the differences in miscibility of the two systems and possible effects on lifetime values, has shown that the greater miscibility exhibited by the HX4000 system over the Vectra system provides the potential to form composites on a size scale closer to the molecular level. GRA

N93-13328 Case Western Reserve Univ., Cleveland, OH.
MICROSTRUCTURAL EVOLUTION IN REACTION BONDED ALUMINA/MULLITE CERAMICS Ph.D. Thesis
Timothy Duane Fletcher 1992 322 p
Avail: Univ. Microfilms Order No. DA9220039

Alumina, Al, and SiC powders were milled, compacted and heat-treated during which both the Al and SiC are oxidized. The Al2O3 and SiO2 that form then react to produce mullite, 3Al2O3*2SiO2. The goal of this process was to compensate for shrinkage that occurs during densification by expansion that occurs during oxidation and mullite formation to produce a body with little or no shape change during firing. The microstructure that developed during reaction bonding was in most cases not uniform and exhibited a complicated ring structure on polished cross-sections observed using polarized light optical microscopy. The outer surface was composed of a relatively dense ceramic bounded by a ring of porosity located just inside the dense layer. Inside the porous ring were many rings of alternating contrast and a black oval in the center of the body. The ring structure was more pronounced as the green density, SiC content and component size was increased. The phase distribution across the ring structure was investigated using XRD and XPS analyses. The results of these studies showed the presence of unoxidized SiC and ZrO in the center of fully heat-treated bodies. The ZrO comes from reduction of ZrO2 present in the milled powders due to wear of the ZrO2 milling media. These results indicate that the body was not completely reacted during the heat treatment and that a reducing environment existed inside of the ceramic during reaction bonding. The reducing environment is generated by densification of the outer surface before the SiC has been completely oxidized. The accumulation of CO gas that evolves during SiC oxidation and the reduction in oxygen diffusion into the body are believed to cause the observed reduction of zirconia. The microstructure of fully and partially reacted bodies was characterized by TEM. The dense region of the fully reacted bodies consisted of fine grained Al2O3 and mullite (less than 0.1 micron) with inter- and intragranular ZrO2 particles (0.1-1.0 micron). The extent of oxidation of the SiC in the partially reacted bodies was found to be function of position and increases toward the outer surface. Dissert. Abstr.

N93-13350# Massachusetts Inst. of Tech., Cambridge. Dept. of Materials Science and Engineering.
RADIATION-DISORDER AND APERIODICITY IN IRRADIATED CERAMICS
L. W. Hobbs 1992 79 p
(Contract DE-FG02-89ER-45396)
(DE92-015051; DOE/ER-45396/3) Avail: CASI HC A05/MF A01

This final technical report documents the accomplishments of the program of research entitled 'Radiation Disorder and Aperiodicity in Irradiated Ceramics' for the period June 22, 1989-June 21, 1992. This research forms the latest part on an on-going program, begun at MIT in 1983 under DOE support, which has had as its objectives the investigation of the responses in radiation environments of ceramics heavily-irradiated with electrons, neutrons, and ions, with potential applications to fusion energy technology and high-level nuclear waste storage. Materials investigated have included SiO2, MgAl2O4, Al23O27N5, SiC, BeO, LiAlO2, Li2ZrO3, CaTiO3KTaO3, and Ca(Zr, Pu)Ti2O7. The program initially proposed for 1989 had as its major objectives two main thrusts: (1) research on defect aggregation in irradiated non-oxide ceramics; and (2) research on irradiation-induced amorphization of network silicas and phosphates. DOE

N93-13414# Department of the Navy, Washington, DC.
HERMETIC SEALING AND EMI SHIELDING GASKET Patent Application
Ramanathan Panayappan, inventor (to Navy) (Courtney and Co., Philadelphia, PA.) and John C. Cooper, inventor (to Navy) (Courtney and Co., Philadelphia, PA.) 2 Apr. 1992 15 p
(AD-D015359; US-Patent-Appl-SN-864812; Navy-Case-70723) Avail: CASI HC A03/MF A01

A composition is disclosed for forming an electromagnetic interference (EMI) shielding gasket for installation against a metal object, such as an aluminum frame member of an aircraft, wherein the composition is comprised of a mixture of a prepolymer composition of a flexible polyurethane material, a sacrificial metallic material which provides electrical conductivity and anodic protection against corrosion of the metal object, and a curing agent for curing the prepolymer composition. The sacrificial metallic material can be a metal salt selected from the group consisting of water soluble zinc and cadmium salts. Water can also be present to serve two functions, as a curing agent for the polyurethane and as a foaming agent, producing carbon dioxide. A method is also providing for installing an EMI shielding gasket on an aircraft between a graphite skin panel and a metal frame member. The composition for forming the EMI shielding gasket on a metal surface can also include an agent that cleans the metal surface to which the gasket is applied. GRA

N93-13441*# National Aeronautics and Space Administration. Langley Research Center, Hampton, VA.
OXIDATIVE STABILITY OF LARC (TM)-TPI FILMS
Jeffrey A. Hinkley Oct. 1992 20 p
(RTOP 506-43-11)
(NASA-TM-107696; NAS 1.15:107696) Avail: CASI HC A03/MF A01

The oxidative aging of 50-micron-thick films of LARC-TPI was studied using conventional thermogravimetric techniques and measurements of plane-stress fracture toughness. It was shown that at high temperature, most of the toughness loss occurred very early relative to the weight loss. The difficulties of interpreting TGA results in this regime and the problems of extrapolations to long times are discussed. Author

N93-13459*# Rutgers - The State Univ., New Brunswick, NJ. Dept. of Chemistry.
THE EFFECTS OF MOLECULAR STRUCTURE ON THE ELECTRICAL CONDUCTIVITY OF POLYMERS Final Technical Report
Luke A. Burke [1992] 12 p
(Grant NAG3-956)
(NASA-CR-191265; NAS 1.26:191265) Avail: CASI HC A03/MF A01

The role of Quantum Theoretical Methods is both predictive and supportive of experimental results in Chemistry. Present day methods are able to calculate vibrational spectra and stereochemical interactions for molecules of moderate size (up to 20 atoms). As for the predictive side, the electronic structure of molecules and polymers can be calculated in order to narrow down the field of many potential candidates, which would have the novel properties looked for. The following has been accomplished at the Rutgers Camden Chemistry Department as results of calculations on molecular and polymeric systems of interest to the Polymers Branch of the NASA Lewis Research Center, under Grant NAG3-956. Author

N93-13538# Lawrence Livermore National Lab., CA.
PREPARATION AND PROPERTIES OF LOW DENSITY REPLICA CARBON FOAMS
S. S. Hulsey and P. K. Poco Apr. 1992 7 p Presented at the Material Research Society Spring Meeting, San Francisco, CA, 27 Apr. - 2 May 1992
(Contract W-7405-eng-48)
(DE92-019573; UCRL-JC-108836; CONF-920402-55) Avail: CASI HC A02/MF A01

Low density foams are used for a variety of applications, including catalytic supports, battery anodes, microporous membranes, and laser fusion targets. The technique for making replica carbon foams described in this paper has been previously reported and involves a process in which an inorganic substrate (sodium chloride) is infused with a carbonizable polymer. After carbonization, the substrate is removed by a leaching process and the wet foam is dried; the resultant foam is referred to as replica carbon. This paper describes improvements in the processing which result in a smaller pore size and improved foam homogeneity. The original substrate is the single most important factor affecting the resultant structure. Techniques to improve the uniformity of the substrate and the translation of substrate anomalies into the final product are described. In addition, correlations observed between the original particle size distribution of a variety of different salts as compared to the final pore size of the resultant foam are discussed. DOE

N93-13649# National Inst. of Standards and Technology, Gaithersburg, MD. Ceramics Div.

CERAMIC MACHINING: ASSESSMENT OF CURRENT PRACTICE AND RESEARCH NEEDS IN THE US Final Report

S. Jahanmir, L. K. Ives, A. W. Ruff, and M. B. Peterson Jun. 1992 115 p

(PB92-213511; NIST/SP-834) Avail: CASI HC A06/MF A02; SOD HC

Advanced structural ceramics, such as silicon nitride, are attractive for many advanced applications due to their high strength at elevated temperatures, resistance to chemical degradation, wear resistance, and low density. Despite these advantages, there are considerable impediments to the introduction of advanced ceramics. With current technology, fabrication costs are high, compared to other materials, and component reliability is uncertain. A study was conducted to assess the current state-of-the-art in the machining of advanced ceramics and to identify research areas which could lead to significant improvements. In conducting the assessment, an extensive literature search was carried out, visits and discussions were held with industrial companies interested in ceramic machining, a telephone survey was conducted on ceramic machining shops, a research-in-progress database was consulted, individuals were invited to visit NIST and discuss different aspects of ceramic machining. The ultimate goal of the program is to further the utilization of advanced structural ceramics in industrial applications by increasing the cost-effectiveness of ceramic components. It is recommended that these projects be carried out jointly by government laboratories and industry to facilitate technology transfer, and that all research activities funded by the government be coordinated to minimize the possibility of duplication of effort. GRA

N93-13716*# National Aeronautics and Space Administration. Marshall Space Flight Center, Huntsville, AL.

AN EVALUATION OF CORROSION PROTECTION BY TWO EPOXY PRIMERS ON 2219-T87 AND 7075-T73 ALUMINUM

M. J. Mendrek Oct. 1992 42 p Original contains color illustrations

(NASA-TM-108376; NAS 1.15:108376) Avail: CASI HC A03/MF A01; 13 functional color pages

A comparison of the corrosion protection provided by two amine epoxy primers was made using salt fog, alternate immersion, and total immersion as exposure media. The study is the result of a request to use an unqualified low volatile organic carbon (VOC) primer (AKZO 463-6-78) in place of the current primer (AKZO 463-6-3) because environmental regulations have eliminated use of the current primer in many states. Primed, scribed samples of 2219-T87 and 7075-T73 aluminum were exposed to 5-percent NaCl salt fog and 3.5-percent NaCl alternate immersion for a period of 90 days. In addition, electrode samples immersed in 3.5-percent NaCl were tested using electrochemical impedance spectroscopy (EIS). The EG&G model 368 ac impedance measurement system was used to monitor changing properties of AKZO 463-6-78 and AKZO 463-6-3 primed 2219-T87 aluminum for a period of 30 days. The response of the corroding system of a frequency scan can be modeled in terms of an equivalent circuit consisting of resistors and capacitors in a specific arrangement. Each resistor/capacitor combination represents physical processes taking place within the electrolyte, at the electrolyte/primer surface, within the coating, and at the coating/substrate surface. Values for the resistors and capacitors are assigned following a nonlinear least squares fit of the data to the equivalent circuit. Changes in the values of equivalent circuit parameters during the 30-day exposure allow assessment of the time to and mechanism of coating breakdown. Author

N93-13780 Missouri Univ., Rolla.

TOUGHENING MECHANISMS IN WEAK MATRIX CERAMIC COMPOSITES Ph.D. Thesis

Jowoong Ha 1991 123 p

Avail: Univ. Microfilms Order No. DA9133819

Tough behavior of ceramic matrix composites is closely related to the weak interface between fiber and matrix. The weak interfaces in composites were produced by reducing the chemical bonding and the residual thermal stresses between constituents. A new way to introduce the weak interface by induced porosity or damaged zones, porosity toughening or damage toughening respectively, was proposed to provide the rationale for guiding the development of oxide/oxide composites. The existence of porosity toughening was examined by qualitative theoretical consideration and experiments. Porous oxide/oxide composites were fabricated using alumino-silcate fibers (Nextel 440) and magnesium alumino-silicate matrix (1:1 mixture of kaolinite and talc), and sintered at 1100 and 1200 C. Both types of composites failed non-catastrophically in bending and tensile tests. The porous matrix composites showed the low ultimate strength of 12.7 +/- 3.4 MPa, but showed high work of fracture of 630 +/- 206 J/sq m for the specimens fired at 1100 C when tested in tension. Damaged zones or porous phases were introduced into the interface region of model composites and effects were determined using a single fiber pullout specimen or a single rod pullout specimen. Single fiber pullout specimens with a damaged zone (by the oxidation of SiC fiber in situ) produced higher frictional stress than debonding strength. Frictional stresses increased up to 6.4 +/- 3.4 MPa as pullout of the damaged fiber proceeded. The porous phase was produced by coating alumina rods with zirconia or alumino-silicates fired at various temperatures. Distinct changes in pullout behavior were observed in data for the specimens with an alumino-silicate coating fired at 1450 C. Magnitudes of frictional stress and debonding strength of the interface were both less than 2 MPa. Both coatings produced a gradual change of the pullout load during the pullout tests.

Dissert. Abstr.

N93-13785# National Inst. of Standards and Technology, Gaithersburg, MD. Polymers Div.

DETERMINATION OF THE WEIGHT AVERAGE MOLECULAR WEIGHT OF SRM 1480

Charles M. Guttman, John R. Maurey, and Peter H. Verdier Jul. 1992 27 p Sponsored by FDA

(PB92-222934; NISTIR-4837) Avail: CASI HC A03/MF A01

The characterization of a polyurethane standard reference material, SRM 1480, is described. The weight-average molecular weight of SRM 1480 by light scattering was determined. The intrinsic viscosity of SRM 1480 in tetrahydrofuran (THF) was also measured. The Size Exclusion Chromatography (SEC) of SRM 1480 in THF as received in the bottle was found to exhibit concentration dependent peak positions even for low concentrations. The addition of 0.05 moles per liter LiBr to the THF was found to alleviate this problem. This low concentration of LiBr did not change the polystyrene calibration of the SEC columns. GRA

N93-13836# Army Lab. Command, Watertown, MA. Material Technology Lab.

ASSESSMENT OF JAPANESE TECHNOLOGY IN ADVANCED GLASS AND CERAMIC FIBERS Final Report

Donald R. Messier Jun. 1992 30 p

(AD-A255229; MTL-MS-92-1) Avail: CASI HC A03/MF A01

Summarized herein are the findings from a two month trip to Japan from mid-September to mid-November 1991 to evaluate Japanese technology in oxynitride glasses and fibers and in carbide and nitride fibers and whiskers. The information discussed was obtained through visits to universities, companies, Government institutes, and through attendence at three conferences. It was learned that the development of a process for the production of oxynitride glass fibers is still being actively pursued and that, while high temperature instability problems are well-recognized, the production of carbide or nitride fibers with good high temperature stability is still several years away. Also discussed are new developments in several research areas including ceramic matrix composites, sol-gel technology, ceramic powder preparation, and high strength ceramics. GRA

N93-13862# Naval Research Lab., Washington, DC.
ION-BEAM-ASSISTED DEPOSITION OF MoS2 AND OTHER LOW-FRICTION FILMS Interim Report, Jun. 1988 - Jun. 1992
Robert N. Bolster 11 Sep. 1992 33 p
(AD-A255222; NRL/MR/6176-92-7135) Avail: CASI HC A03/MF A01

Vacuum-deposited films of molybdenum disulfide (MoS2) are effective as solid lubricants. Ion-beam-assisted deposition, which employs ion beam sputtering with an assist beam impinging on the growing film, has been investigated as a means of preparing low-friction high endurance coatings. The apparatus used and some of the techniques involved are described. Ion source operating parameters were optimized and the assist beam ion flux was quantified and found to follow a power-law relationship with beam power. The best way to produce MoS2 films was found to be cosputtering from separate Mo and S targets with deposition rates adjusted to obtain the desired stoichiometry. Deposition rates were found to also follow a power-law relationship with beam power, and formulae are given for predicting them, the ratio of assist ions to film atoms, and the effect of assist beam sputtering on film thickness. Inverse formulae are given for determining process parameters needed to achieve a selected film thickness and composition. A composite target for simultaneous Mo and S sputtering was developed. Deposition rates were determined for other metals: W, Ni, Co, Cu, and Pb. Formulae relating target-to-substrate distance to deposition rate are given. GRA

N93-13873# Air Force Inst. of Tech., Wright-Patterson AFB, OH. Foreign Aerospace Science and Technology Center.
HEAT RESISTANT DIFFUSION COATING FOR NIOBIUM ALLOY
G. V. Zemskov, R. L. Kogan, and V. M. Lukyanov 3 Jun. 1992 11 p Transl. into ENGLISH from Akademiya Nauk SSSR, Zharostoykiye i Teplostoykiye Pokrytiya (Russia), 1968 p 152-158
(AD-A255542; FASTC-ID(RS)T-0992-91) Avail: CASI HC A03/MF A01

The question of protecting niobium and its alloy from high-temperature corrosion is a current one at the present time. Diffusion coatings are receiving ever more widespread application for this purpose. Silicide diffusion coatings possess high durability. Much attention is being given abroad to a coating of chromium, titanium and silicon obtained by the method of vacuum treatment in an alloy of titanium with chromium, with subsequent siliconization. However, the indicated works do not present the results of the study for the purpose of selecting the optimal technological process ensuring a diffusion layer of maximal durability. We studied the possibility of using a simpler technological process as compared with that described for obtaining a tri-component coating containing titanium, chromium and silicon and protecting the niobium against oxidation at a temperature of 1100-1200 deg C. GRA

N93-14029# American Chemical Society, Washington, DC.
SYMPOSIUM ON POLYMERIC MATERIALS FOR PHOTONIC AND OPTICAL APPLICATIONS Final Report, 1 Jun. - 31 Aug. 1991
Gary C. Bjorklund Sep. 1992 118 p Symposium held in New York, NY, 25-30 Aug. 1991
(Grant AF-AFOSR-0275-91)
(AD-A255820; AFOSR-92-0884TR) Avail: CASI HC A06/MF A02

A symposium on Polymeric Materials for Photonic and Optical Applications was held as part of the 4th Chemical Congress of North America and 202nd ACS National Meeting during August 25-30, 1991 in New York, N.Y. This symposium was sponsored by the ACS Division of Polymer Chemistry and the ACS Division of Polymeric Materials: Science and Technology with the cooperation of the Optical Society of America. The symposium organizers were G.C. Bjorklund, G. Hadziioannou, J. Torkelson, and M.A. Winnik. The goal of the symposium was to cover in depth the chemistry, characterization, and device application of polymers for photonics and optics. The major objective was to bring together leading experts from around the world to elucidate the major scientific challenges and hurdles that must be overcome for photonic polymers to reach their full potential and find major device applications. The symposium consisted of a tutorial session, a poster session, and five oral sessions, extending over three full days. A total of 32 distinguished scientists presented invited papers. Of these, 21 were from North America, 9 from Europe, and 2 from Japan. In addition, 28 contributed papers were presented. Interactions among the attendees were quite good and the overall attendance was strong, with some of the sessions being held by more than 250 people. GRA

N93-14074 California Univ., Santa Barbara.
FRACTURE OF A METAL/CERAMIC COUPLE: TANTALUM (TITANIUM)/SAPPHIRE Ph.D. Thesis
Andrew Hughes Bartlett 1991 136 p
Avail: Univ. Microfilms Order No. DA9218419

A study of the fracture behavior of a model metal/ceramic diffusion bonded couple was performed using the system Ta(Ti)/Al2O3. Residual stress cracking due to thermal expansion misfit between the metal and ceramic was examined. Depending on composition, the alloy could have a coefficient of thermal expansion (CTE) greater than or less than that of the sapphire. When the CTE of the alloy was greater than that of the sapphire, cracking occurred in the ceramic upon cooling down from bonding temperatures. The initial orientation of the cracking was consistent with the direction of principal tension. Conversely, when the CTE of the metal was less than the sapphire, failure occurred along the metal/ceramic interface. Mechanical test specimens were fabricated in order to study fracture along a metal/ceramic interface containing reaction products. The formation of these reaction products was in accord with the Ti-Ta-Al ternary phase diagram. Periodic cracking of the reaction layer occurred either by kinking of the parent interface crack or by tunnel cracks forming ahead of it. Residual stress within the layer played a critical role in these cracking behaviors. Despite the low fracture energy of the main interface crack, periodic cracking of the reaction products dominated overall fracture energy. Dissert. Abstr.

N93-14099# Aerospace Corp., El Segundo, CA.
SPACE ENVIRONMENTAL EFFECTS ON SILVERED TEFLON THERMAL CONTROL SURFACES
C. S. Hemminger, W. K. Stuckey, and J. C. Uht 15 Sep. 1991 32 p Previously announced as N92-24822
(Contract F04701-88-C-0089)
(AD-A255909; TR-0091(6935-03)-1; SSD-TR-92-28) Avail: CASI HC A03/MF A01

Cumulative space environmental effects on silvered Teflon (fluorinated ethylene propylene, FEP) (Ag/FEP) were a function of exposure orientation. Samples from 19 Ag/FEP thermal control surfaces recovered from the Long Duration Exposure Facility (LDEF) have been analyzed to determine changes in this material as a function of position on the spacecraft. Although solar absorptance and infrared emittance of measured thermal blanket specimens are relatively unchanged from control specimen values, significant changes in surface morphology, composition, and chemistry were observed. All Ag/FEP surfaces exposed to high atomic oxygen flux (rows 7-11), irrespective of exact angle, had a uniformly cloudy appearance due to surface erosion. Scanning electron microscopy (SEM) showed a surface topography with sharp peaks and valleys, while x-ray photoelectron spectroscopy (XPS) detected a surface composition corresponding to contamination-free FEP, with less than 1 mole percent oxygen. GRA

N93-13163*# Morgan State Univ., Baltimore, MD.
IIaO ULTRAVIOLET AND NUCLEAR EMULSION FILMS RESPONSES TO ORBITAL FLIGHTS ON STS-3, STS-7, STS-8, AND STS-40
E. C. Hammond, Jr., K. A. Peters, S. M. Blake, Y. Bailey, D. Johnson, S. Robancho, and A. Stober *In* NASA. Goddard Space Flight Center, The 1992 Shuttle Small Payloads Symposium Oct. 1992 p 39-45 (For primary document see N93-13158 03-12)
Avail: CASI HC A02/MF A03

N93-13987*# Construction Technology Labs., Skokie, IL.
PHYSICAL PROPERTIES OF CONCRETE MADE WITH APOLLO 16 LUNAR SOIL SAMPLE
T. D. Lin, H. Love, and D. Stark *In* NASA. Johnson Space Center, The Second Conference on Lunar Bases and Space Activities of the 21st Century, Volume 2 Sep. 1992 p 483-487 (For primary document see N93-13972 03-91)
Avail: CASI HC A01/MF A03

N93-13988*# Shimizu Corp. (Japan). Inst. of Technology.
THE POSSIBILITY OF CONCRETE PRODUCTION ON THE MOON
Noboru Ishikawa, Hiroshi Kanamori, and Takeji Okada *In* NASA. Johnson Space Center, The Second Conference on Lunar Bases and Space Activities of the 21st Century, Volume 2 Sep. 1992 p 489-491 (For primary

document see N93-13972 03-91)
Avail: CASI HC A01/MF A03

N93-13990*# National Aeronautics and Space Administration. Lyndon B. Johnson Space Center, Houston, TX.
LUNAR CONCRETE FOR CONSTRUCTION
Hatice S. Cullingford and M. Dean Keller (Los Alamos National Lab., NM.) *In its* The Second Conference on Lunar Bases and Space Activities of the 21st Century, Volume 2 Sep. 1992 p 497-499 Sponsored in part by DOE (For primary document see N93-13972 03-91)
Avail: CASI HC A01/MF A03

28 PROPELLANTS AND FUELS

Includes rocket propellants, igniters, and oxidizers; their storage and handling procedures; and aircraft fuels.

For related information see also *07 Aircraft Propulsion and Power, 20 Spacecraft Propulsion and Power,* and *44 Energy Production and Conversion.*

N93-12563# Sandia Labs., Albuquerque, NM.
A SMOKE PRODUCING ROCKET MOTOR FOR ATMOSPHERIC WIND PROFILING
M. C. Grubelich and J. Rowland 1991 10 p Presented at the Smoke and Obscurants Symposium, Laurel, MD, 14-16 Apr. 1992
(Contract DE-AC04-76DP-00789)
(DE92-018264; SAND-91-2768C; CONF-9204190-1) Avail: CASI HC A02/MF A01

A composite propellant was developed to produce a dense plume from a rocket motor. The development of this propellant combined the smoke producing capabilities of a smoke generator with a rocket motor, thereby integrating the separate systems into one unit. A rocket motor was designed for use with this propellant to produce a high density particulate plume. This plume could then be used to determine the wind profile in the atmosphere by using a light detection and ranging system. Additionally, this smoke producing propellant could be used for rapid screening or identification. The burn rate characteristics of the propellant were measured and static firings of rocket motors were conducted to determine the performance of the propellant. The results of these tests are presented as well as theoretical performance predictions of a flight vehicle. DOE

N93-12568# Sandia National Labs., Albuquerque, NM.
AUTOMATED DRY POWDER DISPENSER FOR EXPLOSIVE COMPONENTS
P. Garcia and J. C. Salmonson (Edgerton, Germeshausen and Grier, Inc., Idaho Falls, ID.) 1992 14 p Presented at the JOWOG 39F and SUBWOG F-Robotics Joint Meeting, Monterey, CA, 14-18 Sep. 1992
(Contract DE-AC04-76DP-00789)
(DE92-019425; SAND-92-1775C; CONF-9209171-2) Avail: CASI HC A03/MF A01

Sandia and Mound are developing a workcell that will automate the assembly of explosive components. Sandia is responsible for the automated powder dispenser subsystem. Automated dispensing of explosive powders in the past resulted in separation or segregation of powder constituents. The Automated Dry Powder Dispenser designed by Sandia achieves weight tolerances of +/- 0.1 mg while keeping powder oxidizer separation to a minimum. A software control algorithm compensates for changes in powder flow due to lot variations, temperature, humidity, and the amount of powder left in the system. DOE

N93-12933# Lawrence Livermore National Lab., CA.
MEASUREMENTS OF CELLULAR STRUCTURE IN SPRAY DETONATION
J. Papavassiliou (McGill Univ., Montreal, Quebec), A. Makris (McGill Univ., Montreal, Quebec), R. Knystautas (McGill Univ., Montreal, Quebec), J. H. Lee (McGill Univ., Montreal, Quebec), C. K. Westbrook, and W. J. Pitz Oct. 1991 35 p Presented at the 13th International Colloquium on Dynamics of Explosives and Reactive Systems, Nagoya, Japan, 28 Jul. - 31 Aug. 1991
(Contract W-7405-eng-48)
(DE92-019580; UCRL-JC-108710; CONF-9107160-3) Avail: CASI HC A03/MF A01

The cellular structure of heterogeneous detonations in a low vapor pressure fuel (decane) droplet mixture with oxygen and oxygen-nitrogen was studied in the present investigation. The aerosol was generated by an ultrasonic nebulizer and the fuel concentration of the mixture was regulated by monitoring the volume flow rate of oxygen and nitrogen through the nebulizer. The vertical detonation tube is 64 mm in diameter and 3 m long and ignition was by a powerful spark (120 joules stored energy) or a high explosive detonator. Velocity was measured with ionization probes, pressure by a PCB piezoelectric transducer, and cell size by a smoked metallic foil inserted into the top end or center of the detonation tube. The initial pressure of all the experiments was 1 atmosphere. In order to compare the time scales associated with the physical processes of droplet breakup, heat transfer, evaporation, and mixing experiments were also carried out in the tube heated to 100 and 185 C, using electrical heating tape, to ensure a homogeneous gas phase mixture of decane-oxygen-nitrogen. Comparison of the cell size for the same mixture in the cold and the heated tube permits one to separate the time scales associated with the physical processes and the chemical kinetic rate processes. The results from the heated tube for the homogeneous vapor phase decane detonations are similar to those for the common gaseous fuels in the alkane group (i.e., ethane, propane, butane). Corresponding results for the heterogeneous case (cold tube) of aerosol decane detonation indicate that the cell size is larger by a factor of about 2, for the present case of a 5 micron particle size. The measurements of cellular structure obtained experimentally have been compared to the computed results determined using the ZND chemical kinetic detonation model. DOE

N93-12939# Clemson Univ., SC. Dept. of Chemistry and Geology.
PHYSICAL PROPERTY DATA ON FLUORINATED PROPANES AND BUTANES AS CFC AND HCFC ALTERNATIVES Report, Aug. 1988 - Jun. 1991
Adolph L. Beyerline, Darryl D. DesMarteau, Sun Hee Hwang, N. Dean Smith (Environmental Protection Agency, Research Triangle Park, NC.), and Powell Joyner (Electric Power Research Inst., Palo Alto, CA.) 1992 12 p Presented at the International Conference on CFC and Halon Alternatives, Baltimore, MD, 3-5 Dec. 1991
(Grant EPA-R-815134)
(PB92-206507; EPA/600/A-92/150) Avail: CASI HC A03/MF A01

The paper discusses results of the measurement and estimation of the physical properties of fluorinated propane derivatives as second generation alternatives for currently used CFC and HCFC chemicals. One fluorinated ether was also studied. A total of 22 compounds were investigated with boiling points of -34.6 to 76.7 C. The measured properties presented for these compounds are as follows: melting point, boiling point, vapor pressure below the boiling point, heat of vaporization, critical properties (temperature, density, and pressure), liquid densities, and liquid-phase heat capacities. Measured vapor pressures are reported from below the boiling point to the critical point for two of these compounds: CF3OCF2H (b.p. = 34.6 C and T(sub c) = 80.7 C) and CF3CHFCF2H (b.p. = 6.5 C and T(sub c) = 141.1 C). Vapor pressures and liquid-phase densities were also measured for CFC-12 in order to judge the accuracy of the experimental methods used. The measured vapor pressures were also compared with vapor pressures estimated using modified corresponding states methods to evaluate the accuracy of the estimation methods. GRA

N93-13081# EG and G Mound Applied Technologies, Miamisburg, OH.
DEVELOPMENT OF A LASER IGNITED ALL SECONDARY EXPLOSIVE DDT DETONATOR
C. M. Woods, E. M. Spangler, T. M. Beckman, and D. P. Kramer 1992 10 p Presented at the 18th International Pyrotechnics Seminar, Breckenridge, CO, 13-17 Jul. 1992
(Contract DE-AC04-88DP-43495)
(DE92-019340; MLM-3757(OP); CONF-920796-7) Avail: CASI HC A02/MF A01

A hermetic, stand alone, laser-ignited deflagration-to-detonation transition (DDT) detonator has been developed. The detonator uses the secondary explosive HMX (cyclo- tetramethylene-tetranitramine) and was originally developed for use with the U.S. Navy's Laser Initiated Transfer Energy subsystem (LITES). The design of the new detonator allows for its use with a variety of laser fire sets. A high density blend of 830 sq cm/g HMX

with 3 percent carbon black by weight was used for the ignition charge. Deflagration-to-detonation transition was achieved with a transition charge of undoped 830 sq cm/g HMX. Using a 12-ms ND-YAG laser pulse coupled to the detonator via a 1-mm diameter optical fiber, the ignition threshold was determined to be approximately 30 mJ. Full detonating outputs were demonstrated by function testing in Navy detonation sensitivity fittings. Finally, the detonator was tested in several configurations with shielded mild detonating chord (SNMC) endrips to determine its capability for lighting transfer lines. DOE

N93-13471# Department of the Navy, Washington, DC.
BOOSTER EXPLOSIVE RINGS Patent Application
Patrick F. Spahn, inventor (to Navy) 14 May 1992 12 p
(AD-D015375; US-Patent-Appl-SN-882721; Navy-Case-74315) Avail: CASI HC A03/MF A01

This invention relates to explosive devices and more particularly to boosters for explosive devices. To reduce the change of accidental explosions and fires, the Navy, Air Force, and Army are replacing existing main charge explosives with new, more insensitive explosives such as PBXN-103 and PBXN-109. Additionally, future underwater and bombfill explosives will have critical diameters greater than one inch. Existing booster explosives and fuses have insufficient energy output to reliably initiate the new insensitive main charge explosives. Increasing the amount of booster explosive will increase the weapon's sensitivity and the chance of an accidental detonation. Moreover, the existing Department of Defense (DOD) inventory of fuses and booster explosives is very large and cannot be replaced without considerable cost. GRA

N93-13924 Tennessee Univ., Knoxville.
BIPROPELLANT SPRAY COMBUSTION MODELING IN SMALL ROCKET ENGINES Ph.D. Thesis
Louis Marie Larosiliere 1991 151 p
Avail: Univ. Microfilms Order No. DA9221779

A CFD-based model for bipropellant spray combustion in small rocket engine combustors is formulated and developed into a predictive computational tool. This model is comprised of a two-component interacting liquid phase imbedded within a turbulent chemically reactive gas. The liquid phase is assumed to be composed of two immiscible collections of quasi-spherical material volumes called 'globules'. This allows a conservation equation similar to the well-known spray equation to be formulated for the globule number density distribution. A pair of unlike globules are allowed to interact through impingement collision which results in a collision induced oscillation of the globule surface. The amplitude of the oscillation can cause the globule surface to deform and eventually breakup into spray droplets. Thus, a simulation of the gross effects of atomization via impinging liquid streams is possible. Furthermore, secondary breakup due to aerodynamic forces are also included. Various other sub-models are developed for droplet combustion, and spray/wall collision. State-of-the-art sub-models are employed for globule acceleration, turbulence dispersion, and spray droplet coalescence. The conservation equations for a continuum gas with imbedded condensed liquid phase elements are derived via a formal averaging procedure. A standard k-epsilon turbulence model along with a gas phase chemistry model are incorporated. The formulated model is integrated within the computational framework of the KIVA-II reactive flow code. An efficient coupling of the various sub-models with the ALE scheme is obtained. Applications to three problems related to small bipropellant spray rocket combustion are demonstrated. A simulation of the spray structure from a like-doublet impinging stream injector is presented. The computed spray structures showing the effects of impingement angle and injection velocity compare favorably with photographs taken by Heidmann. Unlike-doublet stream impingement is also presented for N2H4 and N204 in a confined chamber. Simulations of bipropellant spray combustion via an unlike-doublet impinging stream injector are investigated. Two bipropellant systems (N2H4/N204 and N2H4/LOX) are studied. Finally, an investigation of the combustion flow structure with a single-element coaxial pintle injector is presented. Dissert. Abstr.

N93-13983*# Technische Univ., Berlin (Germany). Aerospace Inst.
THE INFLUENCE OF LUNAR PROPELLANT PRODUCTION ON THE COST-EFFECTIVENESS OF CISLUNAR TRANSPORTATION SYSTEMS
H. H. Koelle *In* NASA. Johnson Space Center, The Second Conference on Lunar Bases and Space Activities of the 21st Century, Volume 2 Sep. 1992 p 447-452 (For primary document see N93-13972 03-91)
Avail: CASI HC A02/MF A03

29 MATERIALS PROCESSING

Includes space-based development of products and processes for commercial applications.

For biological materials see *55 Space Biology.*

N93-12699*# Ball Aerospace Systems Div., Boulder, CO.
ZERO-GRAVITY QUANTITY GAGING SYSTEM Final Report
18 Dec. 1989 509 p
(Contract NAS9-17378)
(NASA-CR-185602; NAS 1.26:185602; DRD-MA-129T; F89-08) Avail: CASI HC A22/MF A04

The Zero-Gravity Quantity Gaging System program is a technology development effort funded by NASA-LeRC and contracted by NASA-JSC to develop and evaluate zero-gravity quantity gaging system concepts suitable for application to large, on-orbit cryogenic oxygen and hydrogen tankage. The contract effective date was 28 May 1985. During performance of the program, 18 potential quantity gaging approaches were investigated for their merit and suitability for gaging two-phase cryogenic oxygen and hydrogen in zero-gravity conditions. These approaches were subjected to a comprehensive trade study and selection process, which found that the RF modal quantity gaging approach was the most suitable for both liquid oxygen and liquid hydrogen applications. This selection was made with NASA-JSC concurrence. Author

N93-12728*# Colorado Univ., Boulder. Dept. of Chemical Engineering.
MODELING OF COALESCENCE, AGGLOMERATION, AND PHASE SEGREGATION IN MICROGRAVITY PROCESSING OF BIMETALLIC COMPOSITE MATERIALS Final Report, 2 Feb. 1989 - 30 Sep. 1992
Robert H. Davis 10 Nov. 1992 10 p
(Grant NAG3-993)
(NASA-CR-191247; NAS 1.26:191247) Avail: CASI HC A02/MF A01

The overall objective of this research is to develop models to predict drop-size-distribution evolutions due to droplet collisions and coalescence during processing within the miscibility gap of bimetallic liquid-phase-miscibility-gap materials. The individual and collective action of gravitational and nongravitational mechanisms on the relative motion and coalescence of drops are considered. Author

N93-12799*# National Academy of Sciences - National Research Council, Washington, DC. Commission on Physical Sciences, Mathematics, and Applications.
TOWARD A MICROGRAVITY RESEARCH STRATEGY
1992 69 p
(Contract NASw-4627)
(NASA-CR-190820; NAS 1.26:190820) Avail: CASI HC A04/MF A01

Recommendations of the Committee on Microgravity Research (CMGR) of the Space Studies Board of the National Research Council are found in the Summary and Recommendations in the front of the report. The CMGR recommends a long-range research strategy. The main rationale for the microgravity research program should be to improve our fundamental scientific and technical knowledge base, particularly in the areas that are likely to lead to improvements in processing and manufacturing on earth. The CMGR recommends research be categorized as Biological science and technology, Combustion, Fluid science, Fundamental phenomena, Materials, and Processing science and technology. The committee also recommends that NASA apply a set of value criteria and measurement indicators to define the research and analysis program more clearly. The CMGR recommends that the funding level for research and analysis in microgravity science be established as a fixed percentage of the total program of NASA's Microgravity Science and Applications Division in order to build a strong scientific base for future experiments. The committee also recommends a cost-effective approach to experiments. Finally the CMGR recommends that a thorough technical review of the centers for commercial development of space be conducted to determine the quality of their activities and to ascertain to what degree their original mission has been accomplished. R.L.B.

N93-12951*# National Aeronautics and Space Administration. Marshall Space Flight Center, Huntsville, AL.
THE FIRST UNITED STATES MICROGRAVITY LABORATORY
C. Blake Powers, ed. (Essex Corp., Huntsville, AL.), Charlotte Shea (Essex Corp., Huntsville, AL.), Tracy McMahan (Essex Corp., Huntsville, AL.), Denise Accardi (Essex Corp., Huntsville, AL.), and Jeff Mikatarian (Essex Corp., Huntsville, AL.) 1991 42 p LIMITED REPRODUCIBILITY: More than 20% of this document may be affected by color photographs Original contains color illustrations
(NASA-TM-107980; NAS 1.15:107980) Avail: CASI HC A03/MF A01; 28 functional color pages

The United States Microgravity Laboratory (USML-1) is one part of a science and technology program that will open NASA's next great era of discovery and establish the United States' leadership in space. A key component in the preparation for this new age of exploration, the USML-1 will fly in orbit for extended periods, providing greater opportunities for research in materials science, fluid dynamics, biotechnology, and combustion science. The major components of the USML-1 are the Crystal Growth Furnace, the Surface Tension Driven Convection Experiment (STDCE) Apparatus, and the Drop Physics Module. Other components of USML-1 include Astroculture, Generic Bioprocessing Apparatus, Extended Duration Orbiter Medical Project, Protein Crystal Growth, Space Acceleration Measurement System, Solid Surface Combustion Experiment, Zeolite Crystal Growth and Spacelab Glovebox provided by the European Space Agency.
R.L.B.

N93-13168*# Science Applications International Corp., Glendora, CA.
INVESTIGATION OF MICROGRAVITY EFFECTS ON SOLIDIFICATION PHENOMENA OF SELECTED MATERIALS
Carl R. Maag and Patricia A. Hansen (Engineering and Economics Research, Inc., Seabrook, MD.) *In* NASA. Goddard Space Flight Center, The 1992 Shuttle Small Payloads Symposium Oct. 1992 p 95-101 (For primary document see N93-13158 03-12)
Avail: CASI HC A02/MF A03

N93-13169*# Sverdrup Technology, Inc., Brook Park, OH.
ENVIRONMENTAL QUALIFICATION TESTING OF PAYLOAD G-534, THE POOL BOILING EXPERIMENT
J. Andrew Sexton *In* NASA. Goddard Space Flight Center, The 1992 Shuttle Small Payloads Symposium Oct. 1992 p 103-113 (For primary document see N93-13158 03-12)
(Contract NAS3-25266)
Avail: CASI HC A03/MF A03

N93-13170*# National Aeronautics and Space Administration. Lewis Research Center, Cleveland, OH.
ELECTRICAL DESIGN OF PAYLOAD G-534: THE POOL BOILING EXPERIMENT
David R. Francisco *In* NASA. Goddard Space Flight Center, The 1992 Shuttle Small Payloads Symposium Oct. 1992 p 115-124 (For primary document see N93-13158 03-12)
Avail: CASI HC A02/MF A03

N93-13172*# Sierra Coll., Sacramento, CA. Dept. of Computer Science.
TAGGING INSULIN IN MICROGRAVITY
Michael Dobeck and Ronald S. Nelson (Nelson, Ronald S., Fresno, CA) *In* NASA. Goddard Space Flight Center, The 1992 Shuttle Small Payloads Symposium Oct. 1992 p 133-141 (For primary document see N93-13158 03-12)
Avail: CASI HC A02/MF A03

N93-13174*# Utah State Univ., Logan.
G254 UNDERGRADUATE EXPERIMENT
Doran Barton, Karilyn Bogh, Brett Evans, Steve Folkman, Marc Hammond, Casey Hatch, Neva Herr, Tina Hubble, Jeff Humpherys, and Steve Johnson et al *In* NASA. Goddard Space Flight Center, The 1992 Shuttle Small Payloads Symposium Oct. 1992 p 151-163 Prepared in cooperation with Kinkaid High School, UT (For primary document see N93-13158 03-12)
Avail: CASI HC A03/MF A03

N93-13178*# Alabama Univ., Huntsville. Consortium for Materials Development.
CONCAP 4: A COMPLEX AUTONOMOUS PAYLOAD (CAP) FOR GROWING ORGANIC THIN FILMS IN MICROGRAVITY
W. E. Carswell and F. C. Wessling *In* NASA. Goddard Space Flight Center, The 1992 Shuttle Small Payloads Symposium Oct. 1992 p 195-204 (For primary document see N93-13158 03-12)
Avail: CASI HC A02/MF A03

N93-14011*# Los Alamos National Lab., NM.
UNIT OPERATIONS FOR GAS-LIQUID MASS TRANSFER IN REDUCED GRAVITY ENVIRONMENTS
Donald R. Pettit and David T. Allen (California Univ., Los Angeles.) *In* NASA. Johnson Space Center, The Second Conference on Lunar Bases and Space Activities of the 21st Century, Volume 2 Sep. 1992 p 647-651 Sponsored in part by DOE (For primary document see N93-13972 03-91)
Avail: CASI HC A01/MF A03

N93-14012*# Science Applications International Corp., Torrance, CA. Thermal Sciences Div.
COMBUSTION OF GASEOUS FUELS UNDER REDUCED-GRAVITY CONDITIONS
M. Yousef Bahadori and Raymond B. Edelman (Rockwell International Corp., Canoga Park, CA.) *In* NASA. Johnson Space Center, The Second Conference on Lunar Bases and Space Activities of the 21st Century, Volume 2 Sep. 1992 p 653-658 (For primary document see N93-13972 03-91)
(Contract NAS3-22822)
Avail: CASI HC A02/MF A03

31 ENGINEERING (GENERAL)

Includes vacuum technology; control engineering; display engineering; cryogenics; and fire prevention.

N93-12922# Los Alamos National Lab., NM.
NEW TECHNOLOGIES FOR REFRIGERATION WITHOUT CFC'S
G. W. Swift 1992 5 p Presented at the New Mexico Conference on the Environment: Toward A Sustainable Environment, Albuquerque, NM, 13-15 Sep. 1992
(Contract W-7405-eng-36)
(DE92-018886; LA-UR-92-2183; CONF-9209164-2) Avail: CASI HC A01/MF A01

Today the appliance industry and other cooling industries are facing the double challenge of eliminating environmentally harmful CFC's while simultaneously improving energy efficiency. These challenges will force this industry to make tremendous changes and to work out many difficult problems, ranging from choice of technology through production-line retooling to product-liability concerns. Three new cooling technologies--sonic compression, thermoacoustic refrigeration, and Malone refrigeration--have been developed at least in part at Los Alamos National Laboratory. We discuss the principles, features, and status of each of these three technologies. With these three examples we hope to show that mechanical compression and subsequent evaporation of CFC's is not the only potentially practical way to produce cooling. These examples are only three of many alternative cooling technologies. No new technology can be guaranteed a success before development is complete, from either an economic or engineering point of view. But enough alternative cooling technologies exist, and the probability for success of each technology is high enough, that one or more of these technologies can almost certainly be produced at reasonable cost, eliminate CFC's, and reduce the consumption of electricity.
DOE

N93-12934# European Space Agency, Paris (France). Materials and Processes Labs.
TOUCHSTONE FOR SUCCESS
Norman Longdon, ed., J. Dauphin, B. D. Dunn, M. D. Judd, F. G. Levadou, and A. Zwaal Apr. 1992 28 p Revised LIMITED REPRODUCIBILITY: More than 20% of this document may be affected by color photographs

Original contains color illustrations
(ESA-BR-52) Copyright Avail: CASI HC A03/MF A01

This booklet is addressed to the users of the Materials and Processes Laboratories of the European Space Research and Technology Centre (ESTEC). The revised edition updates the July 1988 edition featuring the enhancement of existing laboratories and the establishment of a ceramics laboratory. Information on three ESTEC laboratories is presented as well as a look into the future. The three laboratories are the Environmental Effects Laboratory, the Metallic Materials Laboratory, and the Non-metallic Laboratory. The booklet reports on the effects of the space environment on radiation effects (UV and particles), outgassing and contamination, charging-up and discharges, particulate contaminants, atomic oxygen and debris/impacts. Applications of metallic materials to space hardware are covered in the areas of mechanical properties, corrosion/stress corrosion, fracture testing and interpretation, metallurgical processes and failure analysis. Particular applications of non metallic materials to space hardware that are covered are advanced and reinforced polymers, advanced ceramics, thermal properties, manned ambiance, polymer processing, non-destructive tests (NDT), and failure analysis. Future emphasis will be on the measurement of thermo-optical properties for the Infrared Space Observatory (ISO) and other infrared telescopes, support of the Columbus program, Hermes related problems such as 'warm' composites and 'hot' reinforced ceramics for thermal insulation, materials for extravehicular activity (EVA), and NDT. R.L.B.

N93-12976# Illinois Univ., Urbana-Champaign. Dept. of Civil Engineering.
IDENTIFICATION OF PARAMETRIC FINITE ELEMENT MODELS USING EXPERIMENTAL MODAL DATA
David J. Alcoe and Keith D. Hjelmstad Jan. 1992 111 p
(PB92-217819; UILU-ENG-92-2003; SRS-566) Avail: CASI HC A06/MF A02

A general parametric form of a dynamic finite-element model of a linear elastic structure with small deformations is presented, with the model consisting of a set of scalar parameters multiplying element kernel matrices. The parameters of the finite-element model can represent stiffness and inertia properties, as well as axial forces if linearized buckling is assumed. Optimization of an orthogonality-based objective functional is employed to estimate parameters, using nondestructively measured experimental eigenpair data, allowing for the finite dimensional unnormalized, sparse, truncated, and inaccurate natures of experimental modal data. The method enables the use of incomplete eigenvectors, i.e., modes shapes with sparsely measured displacements. Although not vital to the parameter identification method, a procedure for combining modal data from numerous separate experiments is discussed, with the purpose of improving accuracy of the parameters. Given a sufficient number of completely measured eigenvectors with associated eigenvalues, an optimum set of parameters of the finite-element model are obtainable by solution of a linear set of equations. Some simple parameter constraint (e.g., known total mass), is used, without any explicit a priori parameter values. Arbitrary weighting factors are included in the method to take advantage of a priori knowledge of error distributions. The accuracy of the estimated parameters is shown to be function of the accuracy of the experimental modal data employed, independent of any a priori parameter estimates. The effects of missing modal data, especially lower frequency modes, is numerically demonstrated, better parameter accuracy is found with higher frequency modes despite missing lower frequency modes. GRA

N93-12980# National Inst. of Standards and Technology, Gaithersburg, MD. Building and Fire Research Lab.
IMPLICITLY COUPLING HEAT CONDUCTION INTO A ZONE FIRE MODEL
William F. Moss (Clemson Univ., SC.) and Glenn P. Forney Jul. 1992 35 p
(PB92-222769; NISTIR-4886) Avail: CASI HC A03/MF A01

The report examines several methods for coupling the partial differential equations that arise in conductive heat transfer with the ordinary differential equations that arise in zone fire modeling. Two existing algorithms (method of lines and time splitting) are discussed and a new strategy is proposed for performing this coupling. This strategy couples the wall surface temperature rather than the entire wall temperature profile with the other zone fire modeling solution variables by requiring that the wall surface temperature gradient and the incident heat flux (sum of convective and net radiative flux) satisfy Fourier's law. GRA

N93-13021*# Thiokol Corp., Brigham City, UT. Space Operations.
QUALIFICATION OF THE GRITBLAST ASSEMBLY AND PROCESS FOR THE INSIDE DIAMETER OF THE RSRM FORWARD AND AFT DOMES Final Test Report
Michael J. Nolan 1992 39 p
(Contract NAS8-38100)
(NASA-CR-184462; NAS 1.26:184462; TWR-63286) Avail: CASI HC A03/MF A01

This gritblast assembly shall be used when refurbishing the Inside Diameter (ID) of RSRM forward and aft domes. Initial blasting is used to remove corrosion and adhesive not removed during the insulation washout. Final blasting is conducted just prior to part finalization in order to remove residual contamination and prepare the ID surface for bonding. The media used in this gritblaster is DuPont Zirclean Blasting Abrasive. It is possible to use other media in this gritblast assembly, however the only facility that has the control capability for this assembly is the Zirclean blast booth. This blast booth can not use other media without the occurrence of contamination. This automated process shall replace the manually controlled gritblasting that is currently in operation. Manual gritblasting does not provide the consistency, control, and safety that an automated process is capable of delivering. Author

N93-13298# Ames Lab., IA.
SIMULATION OF FORWARD-BACKWARD EXTRUSION WITH NUMERICAL AND MODEL MATERIAL TECHNIQUES
S. B. Biner 1992 13 p Presented at the Conference on Concurrent Engineering Approaches To Materials Processing, Chicago, IL, 2 Nov. 1992
(Contract W-7405-eng-82)
(DE92-016299; IS-M-713; CONF-921166-1) Avail: CASI HC A03/MF A01

In this study, a simple and computationally efficient procedure is introduced for determination of the strain distribution during the simulations of forming processes using model material techniques. Forward-backward extrusion process is analyzed by using FEM and the model material techniques. The strain fields obtained from both methods compared favorably with each other. The advantages and the limitations of the techniques are elucidated together with suggested recommendations. DOE

N93-13404*# Alabama Cryogenic Engineering, Inc., Huntsville.
A SMALL, SINGLE STAGE ORIFICE PULSE TUBE CRYOCOOLER DEMONSTRATION Final Report, 2 Mar. 1988 - 2 Aug. 1990
John B. Hendricks 28 Aug. 1990 98 p
(Contract NAS7-1031; SBIR-08.03-8629)
(NASA-CR-190859; NAS 1.26:190859) Avail: CASI HC A05/MF A02

This final report summarizes and presents the analytical and experimental progress in the present effort. The principal objective of this effort was the demonstration of a 0.25 Watt, 80 Kelvin orifice pulse tube refrigerator. The experimental apparatus is described. The design of a partially optimized pulse tube refrigerator is included. The refrigerator demonstrates an ultimate temperature of 77 K, has a projected cooling power of 0.18 Watts at 80 K, and has a measured cooling power of 1 Watt at 97 K, with an electrical efficiency of 250 Watts/Watt, much better than previous pulse tube refrigerators. A model of the pulse tube refrigerator that provides estimates of pressure ratio and mass flow within the pulse tube refrigerator, based on component physical characteristics is included. A model of a pulse tube operation based on generalized analysis which is adequate to support local optimization of existing designs is included. A model of regenerator performance based on an analogy to counterflow heat exchangers is included. Author

N93-13422* National Aeronautics and Space Administration. Pasadena Office, CA.
THREE-STAGE SORPTION TYPE CRYOGENIC REFRIGERATION SYSTEMS AND METHODS EMPLOYING HEAT REGENERATION Patent
Steven Bard, inventor (to NASA) (Jet Propulsion Lab., California Inst. of Tech., Pasadena.) and Jack A. Jones, inventor (to NASA) (Jet Propulsion Lab., California Inst. of Tech., Pasadena.) 27 Oct. 1992 11 p Filed

22 Oct. 1991 Supersedes N92-17674 (30 - 8, p 1277)
(NASA-Case-NPO-18366-1-CU; US-Patent-5,157,938;
US-Patent-Appl-SN-781520; US-Patent-Class-62-335;
US-Patent-Class-62-434; US-Patent-Class-62-467;
Int-Patent-Class-F25B-1/00) Avail: US Patent and Trademark Office

A three-stage sorption type cryogenic refrigeration system, each stage containing a fluid having a respectively different boiling point, is presented. Each stage includes a compressor in which a respective fluid is heated to be placed in a high pressure gaseous state. The compressor for that fluid which is heated to the highest temperature is enclosed by the other two compressors to permit heat to be transferred from the inner compressor to the surrounding compressors. The system may include two sets of compressors, each having the structure described above, with the interior compressors of the two sets coupled together to permit selective heat transfer therebetween, resulting in more efficient utilization of input power. Official Gazette of the U.S. Patent and Trademark Office

N93-13434*# Interstel, Inc., Beltsville, MD.
TEST PLAN AND REPORT FOR SPACE SHUTTLE LAUNCH ENVIRONMENT TESTING OF BERGEN CABLE TECHNOLOGY SAFETY CABLE
John Ralph Washington Nov. 1992 83 p Sponsored by NASA. Goddard Space Flight Center
(Contract NAS5-30375)
(NASA-CR-4473; NAS 1.26:4473; Rept-93B00003) Avail: CASI HC A05/MF A01

Bergen Cable Technology (BCT) has introduced a new product they refer to as 'safety cable'. This product is intended as a replacement for lockwire when installed per Aerospace Standard (AS) 4536 (included in Appendix D of this document). Installation of safety cable is reportedly faster and more uniform than lockwire. NASA/GSFC proposes to use this safety cable in Shuttle Small Payloads Project (SSPP) applications on upcoming Shuttle missions. To assure that BCT safety cable will provide positive locking of fasteners equivalent to lockwire, the SSPP will conduct vibration and pull tests of the safety cable. Author

N93-13604*# Creare, Inc., Hanover, NH.
ALL-METAL, COMPACT HEAT EXCHANGER FOR SPACE CRYOCOOLERS Final Report, Sep. 1987 - Jun. 1990
Walter L. Swift, Javier Valenzuela, and Herbert Sixsmith Nov. 1990 42 p
(Contract NAS5-30172; Proj. 3307; SBIR-09.07-3800)
(NASA-CR-190861; NAS 1.26:190861; TM-1450) Avail: CASI HC A03/MF A01

This report describes the development of a high performance, all metal compact heat exchanger. The device is designed for use in a reverse Brayton cryogenic cooler which provides five watts of refrigeration at 70 K. The heat exchanger consists of a stainless steel tube concentrically assembled within a second stainless steel tube. Approximately 300 pairs of slotted copper disks and matching annular slotted copper plates are positioned along the centerline axis of the concentric tubes. Each of the disks and plates has approximately 1200 precise slots machined by means of a special electric discharge process. Positioning of the disk and plate pairs is accomplished by means of dimples in the surface of the tubes. Mechanical and thermal connections between the tubes and plate/disk pairs are made by solder joints. The heat exchanger assembly is 9 cm in diameter by 50 cm in length and has a mass of 10 kg. The predicted thermal effectiveness is greater than 0.985 at design conditions. Pressure loss at design conditions is less than 5 kPa in both fluid passages. Tests were performed on a subassembly of plates integrally soldered to two end headers. The measured thermal effectiveness of the test article exceeded predicted levels. Pressure losses were negligibly higher than predictions. Author

N93-13640# National Inst. of Standards and Technology, Gaithersburg, MD. Building and Fire Research Lab.
CORRIDOR: A ROUTINE FOR ESTIMATING THE INITIAL WAVE FRONT RESULTING FROM HIGH TEMPERATURE FIRE EXPOSURE TO A CORRIDOR
Harold E. Nelson and Scot Deal Jul. 1992 40 p Sponsored in cooperation with GSA, Washington, DC
(PB92-213347; NISTIR-4869) Avail: CASI HC A03/MF A01

A first order model and computer program implementing previously developed procedures for estimating the speed, depth, and temperature of a fire produced gravity wave front in a corridor have been developed. The program has been incorporated into FPETOOL and adjustments made to accommodated fires that occur in the corridor or in a room adjacent to the corridor. Comparisons to test results are presented and show reasonable correlation. A users' guide is included. GRA

N93-13642# Rutgers - The State Univ., New Brunswick, NJ.
FLOW THROUGH HORIZONTAL VENTS AS RELATED TO COMPARTMENT FIRE ENVIRONMENTS Report, 29 Sep. 1990 - 30 Sep. 1991
Qing Tan and Yogesh Jaluria Jun. 1992 106 p
(Grant NIST-60NANB7D0743)
(PB92-213388; NIST-GCR-92-607) Avail: CASI HC A06/MF A02

A detailed investigation has been carried out on the flow exchange through a hoizontal vent in a compartment containing a fire. A plexiglass tank with a vented horizontal partition in the middle was constructed to simulate the warmer interior environment due to a fire and the cooler ambient environment by filling the upper and lower compartment with brine and pure water, respectively. Experiments have been carried out on the combined natural and forced convection flow by imposing a pressure difference across the vent. The flow rates through the vent were determined over wide ranges of the governing variables, such as the pressure difference across the opening, density difference across the opening and the opening length to diameter ratio. The basic characteristics of the flow, particularly whether it is unidirectional or bidirectional, was also studied. Volume flow rates were obtained as functions of the governing parameters in terms of correlating equations, from which quantitative information of the effect of parameters on the flow exchange through the vent can be determined. These results can thus be applied to the modeling of fire growth in vented rooms. GRA

N93-13648# North Carolina State Univ., Raleigh. Water Resources Research Inst.
APPLICATION OF PASSIVE DOSIMETRY FOR DETECTION OF LEAKING UNDERGROUND STORAGE TANKS
Francis A. DeGiano (North Carolina Univ., Chapel Hill.), David Leith (North Carolina Univ., Chapel Hill.), Daniel W. Elliott (North Carolina Univ., Chapel Hill.), Bruce Pate (North Carolina Univ., Chapel Hill.), Claudia M. Napfel (North Carolina Univ., Chapel Hill.), and T. Renee Anthony (North Carolina Univ., Chapel Hill.) Jun. 1992 100 p
(Proj. 70085)
(PB92-218270; UNC-WRRI-92-268; Rept-268) Avail: CASI HC A05/MF A02

Several modifications to conventional uses of passive dosimetry in industrial hygiene were explored to make the method attractive for both long-term monitoring of underground storage tanks and short-term site assessments of ground water contamination. Methods for both vapor and aqueous phase measurements were of interest. In addition, a colorimetric method was tried to eliminate the need for return of the dosimeter to the laboratory for chemical analysis. The results suggest that passive dosimetry can be a useful qualitative tool for the mapping of the sub-surface of a contaminated area. It is recommended that the dosimeter be used for short-term site-assessments, rather than long-term compliance monitoring applications. A more extensive comparison with other methods of leak detection than was possible in the research may be needed before convincing the private sector to develop a product based on commercial use of these prototype dosimetry devices. GRA

N93-13989*# Shimizu Corp. (Japan).
CONCRETE STRUCTURE CONSTRUCTION ON THE MOON
Shinji Matsumoto, Haruyuki Namba, Yoshiro Kai, and Tetsuji Yoshida *In* NASA. Johnson Space Center, The Second Conference on Lunar Bases and Space Activities of the 21st Century, Volume 2 Sep. 1992 p 493-496 (For primary document see N93-13972 03-91)
Avail: CASI HC A01/MF A03

N93-14009*# Georgia Inst. of Tech., Atlanta. School of Mechanical Engineering.
MOBILE WORK PLATFORM FOR INITIAL LUNAR BASE CONSTRUCTION

James W. Brazell, Brice K. MacLaren, Gary V. McMurray, and Wendell M. Williams *In* NASA. Johnson Space Center, The Second Conference on Lunar Bases and Space Activities of the 21st Century, Volume 2 Sep. 1992 p 633-535 (For primary document see N93-13972 03-91)
Avail: CASI HC A01/MF A03

32 COMMUNICATIONS AND RADAR

Includes radar; land and global communications; communications theory; and optical communications.

For related information see also *04 Aircraft Communications and Navigation* and *17 Space Communications, Spacecraft Communications, Command and Tracking.* For search and rescue see *03 Air Transportation and Safety,* and *16 Space Transportation.*

N93-12551# Dynamics Research Corp., Wilmington, MA.
INTRODUCTORY REVIEW OF TARGET DISCRIMINATION CRITERIA Final Report, 16 Apr. - 31 Dec. 1991
John Donohue 31 Dec. 1991 34 p
(Contract F19628-89-D-0011)
(AD-A254954; E-19290U; PL-TR-92-2129; AD-E201161) Avail: CASI HC A03/MF A01

This report presents results of investigations to determine the validity of certain assumptions and criteria used in the development of the Sensor Performance Model (SPM), which is part of the Electro-Optical Tactical Decision Aids (EOTDA) Software Program. The investigations were based upon a literature review of works by John Johnson, Herschel Self, Lucien Biberman, David Schmieder, and other authors knowledgeable in the electro-optical field. The investigations sought to answer several issues related to target discrimination criteria and the role of Johnson's criteria in defining target discrimination. Among the issues to be addressed were: the levels of target discrimination; the definition of each target discrimination level; the definition of Johnson's criteria; the use of Johnson's criteria in target discrimination; the factors that influence the accuracy of Johnson's criteria; and the implication of Johnson's criteria inaccuracies on the application of these criteria to the Electro-Optical Tactical Decision Aids. GRA

N93-12574# Institute for Defense Analyses, Alexandria, VA.
ANGLE OF ARRIVAL FLUCTUATIONS FOR MILLIMETER WAVES PROPAGATING IN A TURBULENT ATMOSPHERE NEAR THE EARTH Final Report, Jan. - May 1992
Irvin W. Kay Jun. 1992 28 p
(Contract MDA903-89-C-0003)
(AD-A254478; IDA-D-1173; IDA/HQ-92-41742; AD-E501561) Avail: CASI HC A03/MF A01

This document is concerned with the effect of atmospheric turbulence on the tracking error of a millimeter wave radar transmitting over a propagation path near the ground, as in the case of one used for the guidance of a direct-fire, surface-to-surface, anti-tank missile. The objective is to estimate the likely angle-of-arrival error, and, based on general theory and specific experimental results found in the literature, to assess the reliability of the estimate. The document discusses the appropriateness and limitations of the Rytov approximation used by V.I. Tatarsky and others for theoretical calculations relevant to the error estimate. It also discusses the applicability of certain data obtained by the National Oceanic and Atmospheric Administration and the Georgia Institute of Technology in a measurement program at Flatville, Illinois. The primary conclusion is that the angle-of-arrival error will probably be significant. A program to perform measurements in a greater variety of environmental conditions than those encountered at Flatville and to include direct angle-of-arrival measurements is recommended. GRA

N93-12581# Massachusetts Univ., Lowell. Research Foundation.
BISTATIC CLUTTER RCS SIMULATION USING SCALE MODEL ROUGH SURFACES Final Report
Z. Fried, G. Phillips, and J. Waldman Jun. 1992 147 p
(Contract F19628-88-K-0020)
(AD-A254932; RL-TR-92-123) Avail: CASI HC A07/MF A02

Bistatic scattering cross section measurements of CO2 laser radiation from roughened metal and dielectric surfaces were made and compared to predictions given by the facet model. The scattered polarization state was analyzed along two directions, perpendicular (HH) and parallel (HV) to the scattering plane. The sigma sub HH nulls predicted by the facet model have been verified at steep incident angles for both metallic and dielectric surfaces. Agreement is generally better for metals than dielectrics. At shallower angles measurements diverge from theoretical predictions. A number of calculations of polarization dependent scattering cross sections from metal and dielectric cylinders of radius r as a function of r/lambda have been performed. These calculations suggest that even for large radii surfaces, rapid amplitude, and phase variations are responsible for the onset of depolarization at shallower incident and scattering angles, leading to the disagreement with the tangent plane model predictions. They also clearly demonstrate why the facet model is a better approximation, in the region of validity, for metals than dielectrics. The experimental measurements are described in detail and data for both roughened metals, and dielectrics are presented for several scattering aspect and depression angles. GRA

N93-12585# Naval Command, Control and Ocean Surveillance Center, San Diego, CA. Processing Research and Development Branch.
A NEW MATRIX FORMULATION OF CLASSICAL ELECTRODYNAMICS. PART 2: WAVE PROPAGATION IN OPTICAL MATERIALS OF INFINITE EXTENT Final Report
R. P. Bocker Jul. 1992 42 p
(AD-A255032; NRAD-TD-2320-Pt-2) Avail: CASI HC A03/MF A01

The development of a new matrix description of electromagnetic wave propagation in optical media of infinite extent is presented. This material will interest individuals desiring a description of electromagnetic wave propagation that deviates from the traditional vector calculus approach. Our starting point will be with the fundamental equations of classical electrodynamics, namely the Maxwell field equations. From the vector form of Maxwell's equations, and 8-by-8 differential matrix operator formulation of Maxwell's equations will be developed. The matrix form of the Maxwell field equations allows for simple and direct derivation of matrix representations of the electromagnetic wave and charge continuity equations, the Lorentz conditions and definition of the electromagnetic potentials, the electromagnetic potential wave equations, and Poynting's conservation of energy theorem. The matrix form of the Maxwell field equations and the electromagnetic wave and continuity equations will be used to solve a variety of wave-propagation problems dealing with linear, homogeneous, anisotropic optical media of infinite extent in the presence of monochromatic plane-wave electromagnetic fields. The indices of refraction as well as corresponding states of polarization, associated with wave propagation in crystalline, optically active, and electrooptical media, are determined by using these matrix representations. GRA

N93-12608# Massachusetts Inst. of Tech., Cambridge. Research Lab. of Electronics.
ADAPTIVE ARRAY PROCESSING IN UNCERTAIN INHOMOGENEOUS MEDIA Annual Technical Report, 1 May 1991 - 30 Apr. 1992
Alan Oppenehim and Arthur Baggeroer 18 Aug. 1992 15 p
(Contract N00014-91-J-1628)
(AD-A254418) Avail: CASI HC A03/MF A01

Adaptive array processing algorithms have achieved widespread use because they are very effective at rejecting unwanted signals (i.e., controlling sidelobe levels) and in general have very good resolution (i.e., have narrow mainlobes). However, many adaptive high-resolution array processing algorithms suffer a significant degradation in performance in the presence of environmental mismatch. This sensitivity to environmental mismatch is of particular concern in problems such as long-range acoustic array processing in the ocean where the array processor's knowledge of the propagation characteristics of the ocean is imperfect. An Adaptive Minmax Matched Field Processor has been developed which combines adaptive matched field processing and minmax approximation techniques to achieve the effective interference rejection characteristic of adaptive processors while limiting the sensitivity of the processor to environmental mismatch. The derivation of the algorithm is carried out within the framework of minmax signal processing. The optimal array weights are those which minimize the maximum conditional mean squared estimation error at the output of a linear-weight-and-sum beamformer. The error is conditioned on the propagation characteristics of the environment and the maximum is

evaluated over the range of environmental conditions in which the processor is expected to operate. GRA

N93-12615# Pennsylvania State Univ., University Park. Dept. of Electrical and Computer Engineering.

APPLICATION OF SMOOTHING TECHNIQUES FOR TRACKING MANEUVERING TARGETS. MULTIPLE TARGET TRACKING IN CLUTTER: NEW APPROACHES Final Report, Jun. 1986 - May 1992

N. K. Bose Jul. 1992 96 p

(Contract N00014-86-K-0542)

(AD-A254609) Avail: CASI HC A05/MF A01

The project was concerned with development of fast algorithms for clustering and data association and then applying fixed-lag smoothers for tracking maneuvering and non-maneuvering multitargets in clutter. The data association was done by a depth-first search (DFS) technique which extends naturally to three dimensional validation matrices which occur in Markov models of system parameters for maneuvering targets and also in multiscan correlation. A faster algorithm is then suggested for computing approximately the a posteriori probabilities without generating the data association hypotheses. This algorithm is suitable for implementation with multiprocessors in mobile airborne or seaborne distributed tracking facilities, while the DFS-based approach is suitable for ground-based trackers. Simulation studies have been conducted to demonstrate the advantages of the algorithms developed in this project over comparable ones existing in the literature. GRA

N93-12620# North Carolina State Univ., Raleigh. Dept. of Electrical and Computer Engineering.

STATE SPACE METHODS IN MULTIDIMENSIONAL DIGITAL SIGNAL PROCESSING Final Technical Report

Winser E. Alexander 1991 39 p

(Contract N00014-91-J-1151)

(AD-A254646) Avail: CASI HC A03/MF A01

This report summarizes the results of an extensive research program on the real-time implementation of multidimensional (M-D) digital signal processing algorithms. We began our study on the efficient implementation of M-D digital filters. We mapped the M-D digital filter to a state space model because the state space model supports local data communications. We studied various approaches to implementing the state space model for M-D digital signal processing applications. We found that the best approach involves mapping the state space model onto a generalized linear finite state machine which facilitates the hardware implementation. Using this approach, we were able to develop a multiprocessor system architecture which is scalable, which is modular, and which has a high efficiency. Based upon these results, we developed the architecture for an application specific computing system which we call a Block Data Flow Architecture (BDFA). We are currently studying the mapping of several other M-D signal processing algorithms and matrix operations to the BDFA. These studies show that multiprocessor systems using the BDFA can achieve high throughput and high efficiency at a modest cost. GRA

N93-12623# Naval Research Lab., Washington, DC.

DESIGN OF A DIGITAL DATA RECORDING SYSTEM (DRS)

Greory C. Tavik and James J. Alter 21 Aug. 1992 31 p

(NR Proj. S01-66)

(AD-A255088; NRL/MR/5327-92/7117) Avail: CASI HC A03/MF A01

The Data Recording System (DRS) for the Delayed Digital Side Lobe Canceler (DDSLC) radar signal processor is a 4 MByte digital data recorder capable of a 10.67 Mword/s data rate (1 word = 32 bits). The recorder may be employed to collect live digitized radar data and store it on high volume data devices such as a Bernoulli cartridge or an optical disk to make it available for future off-line processing. This paper describes the hardware design, controlling software, and implementation of the data recording system developed at NRL. GRA

N93-12633 Texas A&M Univ., College Station.

AN ANALYSIS OF THE LOW-EARTH-ORBIT COMMUNICATIONS ENVIRONMENT Ph.D. Thesis

Robert Joseph Diersing 1991 259 p

Avail: Univ. Microfilms Order No. DA9216919

Advances in microprocessor technology and availability of launch opportunities have caused interest in low-earth-orbit satellite based communications systems to increase dramatically during the past several years. In this research the capabilities of two low-cost, store-and-forward LEO communications satellites operating in the public domain are examined--PACSAT-1 (operated by the Radio Amateur Satellite Corporation) and UoSAT-3 (operated by the University of Surrey, England, Electrical Engineering Department). The file broadcasting and file transfer facilities are examined in detail and a simulation model of the downlink traffic pattern is developed. The simulator will aid the assessment of changes in design and implementation for other systems. The development of the downlink traffic simulator is based on three major parts. First, is a characterization of the low-earth-orbit operating environment along with preliminary measurements of the PACSAT-1 and UoSAT-3 systems including: satellite visibility constraints on communications, monitoring equipment configuration, link margin computations, determination of block and bit error rates, and establishing typical data capture rates for ground stations using computer-pointed directional antennas and fixed omni-directional antennas. Second, arrival rates for successful and unsuccessful file server connections are established along with transaction service times. Downlink traffic has been further characterized by measuring: frame and byte counts for all data-link layer traffic; 30-second interval average response time for all traffic and for file server traffic only; file server response time on a per-connection basis; and retry rates for information and supervisory frames. Finally, the model is verified by comparison with measurements of actual traffic not previously used in the model building process. The simulator is then used to predict operation of the PACSAT-1 satellite with modifications to the original design. Dissert. Abstr.

N93-12646# Washington Univ., Seattle. Dept. of Electrical Engineering.

WAVE PROPAGATION AND SCATTERING IN DENSE GEOPHYSICAL MEDIA Final Report, 1 Apr. 1987 - 31 Mar. 1992

Akira Ishimaru 15 Jun. 1992 36 p

(Contract DAAL03-87-K-0032)

(AD-A254573; ARO-24713.20-GS) Avail: CASI HC A03/MF A01

This final report summarizes our study of the propagation and scattering characteristics of waves in geophysical media. We have conducted theoretical and experimental studies of enhanced backscattering from very rough surfaces, millimeter wave, and optical experiments on scattering from random media, vector radiative transfer studies, including rough surface effects and pulse scattering from rough surfaces. GRA

N93-12655*# Virginia Polytechnic Inst. and State Univ., Blacksburg. Satellite Communications Group.

FEASIBILITY STUDY OF A SYNTHESIS PROCEDURE FOR ARRAY FEEDS TO IMPROVE RADIATION PERFORMANCE OF LARGE DISTORTED REFLECTOR ANTENNAS Semiannual Status Report

W. L. Stutzman, K. Takamizawa, P. Werntz, J. LaPean, R. Barts, and B. Shen Sep. 1992 84 p

(Grant NAG1-859)

(NASA-CR-190948; NAS 1.26:190948; SATCOM-92-4) Avail: CASI HC A05/MF A01

Virginia Tech has several articles which support the NASA Langley effort in the area of large aperture radiometric antenna systems. This semi-annual report reports on the following activities: a feasibility study of a synthesis procedure for array feeds to improve radiation performance of large distorted reflector antennas and the design of array feeds for large reflector antennas. Author

N93-12679*# Arizona State Univ., Tempe. Dept. of Electronics and Computer Technology.

ADVANCED COMMUNICATIONS TECHNOLOGY SATELLITE (ACTS). PHASE 1: INDUSTRIAL/ACADEMIC EXPERIMENTERS Final Technical Report, 1 Apr. 1991 - 31 Dec. 1992

James E. Maisel and Robert W. Nowlin 1992 32 p

(Grant NAGw-2389)

(NASA-CR-191211; NAS 1.26:191211) Avail: CASI HC A03/MF A01

This report presents the work done at Arizona State University under the ACTS Experimenters Program. The main thrust of the Program was to develop experiments to test, evaluate, and prove the commercial worthiness of the ACTS satellite which is scheduled for launch in 1993. To accomplish this goal, meetings were held with various governmental, industrial, and academic units to discuss the ACTS satellite and its technology and possible experiments that would generate industrial interest and support for ASU's

efforts. Several local industries generated several experiments of their own. The investigators submitted several experiments of educational, medical, commercial, and technical value and interest. The disposition of these experimental proposals is discussed in this report. Author

N93-12747# California Univ., Berkeley.
MULTIDIMENSIONAL SIGNALS, DATA AND PROCESSES Final Report, 1 Aug. 1989 - 31 Jan. 1992
Eugene Wong and Jean Walrand 15 May 1992 6 p
(Contract DAAL03-89-K-0128)
(AD-A254797; ARO-26144.1-MA) Avail: CASI HC A02/MF A01

The first part of the work yielded new results on simulated annealing and neural networks while the second part focused on large deviations in high-speed communication networks. GRA

N93-12867# California Inst. of Tech., Pasadena. Dept. of Electrical Engineering.
TERAHERTZ HORN ANTENNAS ON THIN MEMBRANES Final Report, Sep. 1987 - Oct. 1991
David Rutledge May 1992 39 p
(Contract F19628-87-K-0051)
(AD-A254772; RL-TR-92-92) Avail: CASI HC A03/MF A01

The Terahertz frequency range offers significant potential advantages for satellite systems. The use of miniature hollow metal waveguide at these high frequencies has made construction of such systems difficult and expensive. The goal of this program has been to apply integrated circuit fabrication techniques to increase flexibility and reliability, and to reduce cost. The focus of this effort has been the thin-membrane supported antenna in an etched horn. The horns are constructed in silicon using an anisotropic etch which naturally forms pyramidal holes. The antenna is supported within the horn on a membrane of silicon oxynitride, typically 1 m thick. Fabrication techniques have been developed for the production of individual horns, as well as linear and two-dimensional arrays for 93 and 242 GHz. Theoretical and measured patterns for the horns have been compared. A thin-film power-density meter has been designed. Imaging has been demonstrated at 93 GHz, using two-dimensional arrays. GRA

N93-12909*# National Aeronautics and Space Administration. Marshall Space Flight Center, Huntsville, AL.
PROGRAM SUPPORT COMMUNICATIONS NETWORK (PSCN) FACSIMILE SYSTEM DIRECTORY
Aug. 1992 85 p
(NASA-TM-108051; NAS 1.15:108051) Avail: CASI HC A05/MF A01

This directory provides a system description, a station listing, and operating procedures for the Program Support Communications Network (PSCN) NASA Facsimile System. The NASA Facsimile System is a convenient and efficient means of spanning the distance, time, and cost of transmitting documents from one person to another. In the spectrum of communication techniques, facsimile bridges the gap between mail and data transmission. Facsimile can transmit in a matter of minutes or seconds what would take a day or more by mail delivery. The NASA Facsimile System is composed of several makes and models of facsimile machines. The system also supports the 3M FaxXchange network controllers located at Marshall Space Flight Center (MSFC). Author

N93-12948# ARCO Power Technologies, Inc., Washington, DC.
EXTREMELY LOW FREQUENCY/VERY LOW FREQUENCY GENERATOR Scientific Report No. 2
Robert D. Short and Dennis Papadopoulos 31 Aug. 1991 89 p
(Contract F19628-89-C-0174)
(AD-A254347; PL-TR-91-2270; AD-E201121) Avail: CASI HC A05/MF A01

A preliminary analysis of the results of the ELF experimental campaigns conducted in the May to September 1990 time frame using the HIPAS transmitter in conjunction with the UCLA ELF receiver at the NOAA site and the mobile NUSC receiver is presented. Following a discussion of the critical physics issues and scalings relating to practical implementation of ionospherically generated ELF to submarine communications, the results of the two campaigns are presented. The data show conclusively that the measured ELF are low frequency signals generated by modulated ionospheric currents and not by nonlinear interference effects of the modulated HF. For the HIPAS parameters the received ELF signals are consistent with an equivalent Horizontal Magnetic Dipole (HMD) located at an altitude of 75 km radiating with an average dipole moment M 6x10(exp 8) A-m(exp 2). The maximum M value achieved during the campaign was 9x10(exp 8) A-m(exp 2). Results related to conversion efficiency scaling with HF polarization, low duty and painting operation, ELF frequency and ionospheric conditions, along with suggestions for future studies are also presented. GRA

N93-12950*# Space Systems/Loral, Palo Alto, CA. Communications System Lab.
APPLICATIONS OF SATELLITE TECHNOLOGY TO BROADBAND ISDN NETWORKS Final Report
Kent M. Price, Robert K. Kwan, D. M. Chitre (Communications Satellite Corp., Clarksburg, MD.), T. R. Henderson (Communications Satellite Corp., Clarksburg, MD.), L. W. White (Communications Satellite Corp., Clarksburg, MD.), and W. L. Morgan (Communications Satellite Corp., Clarksburg, MD.) Mar. 1992 145 p
(Contract NAS3-25092; RTOP 144-50-50)
(NASA-CR-189199; NAS 1.26:189199; Loral-SS/L-TR00823) Avail: CASI HC A07/MF A02

Two satellite architectures for delivering broadband integrated services digital network (B-ISDN) service are evaluated. The first is assumed integral to an existing terrestrial network, and provides complementary services such as interconnects to remote nodes as well as high-rate multicast and broadcast service. The interconnects are at a 155 Mbs rate and are shown as being met with a nonregenerative multibeam satellite having 10-1.5 degree spots. The second satellite architecture focuses on providing private B-ISDN networks as well as acting as a gateway to the public network. This is conceived as being provided by a regenerative multibeam satellite with on-board ATM (asynchronous transfer mode) processing payload. With up to 800 Mbs offered, higher satellite EIRP is required. This is accomplished with 12-0.4 degree hopping beams, covering a total of 110 dwell positions. It is estimated the space segment capital cost for architecture one would be about $190M whereas the second architecture would be about $250M. The net user cost is given for a variety of scenarios, but the cost for 155 Mbs services is shown to be about $15-22/minute for 25 percent system utilization. Author

N93-12979# National Oceanic and Atmospheric Administration, Boulder, CO. Space Environment Lab.
A RADIO FREQUENCY USER'S GUIDE TO THE SPACE ENVIRONMENT SERVICES CENTER GEOPHYSICAL ALERT BROADCASTS
David A. Rosenthal and Joseph W. Hirman May 1992 23 p Revised
(PB92-220631; NOAA-TM-ERL-SEL-80-Rev) Avail: CASI HC A03/MF A01

The National Oceanic and Atmospheric Administration's hourly short-wave radio bulletins provide continually updated information on solar-activity-induced effects on the near-Earth space environment. Bulletins are 45 seconds or less in duration and contain a large amount of useful data. The User's Guide explains the standardized format and terminology of the bulletins. Specific terms are highlighted in bold type the first time they appear, and are defined in an appendix. GRA

N93-13024# National Science Foundation, Washington, DC.
RESEARCH PRIORITIES IN NETWORKING AND COMMUNICATIONS
Apr. 1992 33 p Workshop held in Warrenton, VA, 9-11 Apr. 1992
(NSF-92-109) Avail: CASI HC A03/MF A01

The NSF Division of Networking and Communications Research and Infrastructure was established in 1987, shortly after the creation of the CISE Directorate. In 1989, a workshop was convened to assess the overall program and to suggest directions for networking and communications research. A similar group reconvened in April 1992 to consider the research program in the light of the evolution of technology, to update the suggestions made by the previous workshop, to reconsider the assessment of research directions vis-a-vis research opportunities and national needs, and to evaluate the educational and research base in these areas in the U.S. This document is the report of the April 1992 workshop. The principal findings of the workshop participants are the fields of networking and communications are developing rapidly, and their importance is continually increasing; major new applications of both communications and networking have emerged in the past three years; significant research progress has occurred; important

new research problems have sprung up; and funding levels are still well short of the needs of the field relative to its national importance. Author

N93-13042# George Washington Univ., Washington, DC. Center for Nuclear Studies.

INVESTIGATIONS OF THE STRUCTURE AND ELECTROMAGNETIC INTERACTIONS OF FEW-BODY SYSTEMS

D. R. Lehman, H. Haberzettl, L. C. Maximon, and W. C. Parke Jul. 1992 43 p

(Contract DE-FG05-86ER-40270)

(DE92-040011; DOE/ER-40270/36) Avail: CASI HC A03/MF A01

In order to make it easy for the reader to see the specific research carried out and the progress made, the report of progress is done by topic. Each item has a format layout of Topic, Investigators, Objective, Significance, and Description of Progress, followed at the end by the relevant references. The emphasis of the George Washington University (GWU) theory group has been on the structure and electromagnetic interactions of few-body nuclei. Both low- and intermediate-energy electromagnetic disintegration of these nuclei is considered. When the excitation energy of the target nucleus is low, the aim has been to handle the continuum part of the theoretical work numerically with no approximations, that is, by means of full three- or four-body dynamics. When structure questions axe the issue, numerically accurate calculations axe always carried through, limited only by the underlying two-body or three-body interactions used as input. Implicit in our work is the question of how far one can go within the traditional nuclear physics framework, i.e., nucleons and mesons in a nonrelativistic setting. Our central goal is to carry through state-of-the-art fewbody calculations that wig serve as a means of determining at what point standard nuclear physics requires quark degrees of freedom in order to understand the phenomena in question. So far, in the problems considered, there has been no evidence of the necessity to go beyond the traditional approach, though we always keep in mind that possibility. As our work is involved with questions in the intermediate-energy realm, moving from a nonrelativistic framework to a relativistic one is always a consideration. Currently, for the problems that have been pursued in this domain of energy, the issues concern far more the mechanisms of the reactions and structural questions than the need to move to relativistic dynamics. DOE

N93-13045# Los Alamos National Lab., NM.

RF SYSTEM DESCRIPTION FOR THE GROUND TEST ACCELERATOR RADIO-FREQUENCY QUADRUPOLE

A. H. Regan, D. Brittain, D. E. Rees, and D. Ziomek 1992 8 p Presented at the 16th International LINAC Conference, Ottawa, Ontario, 23-28 Aug. 1992

(Contract W-7405-eng-36)

(DE92-040239; LA-UR-92-2706; CONF-9208109-12) Avail: CASI HC A02/MF A01

This paper describes the RF system being used to provide RF power and to control the cavity field used for the ground test accelerator (GTA) radio-frequency quadrupole (RFQ). The RF system consists of a low-level RF (LLRF) control system that uses a tetrode as a high-power amplifier (HPA) as part of its plant to deliver up to 300 kW of peak power to the RFQ at a 2 percent duty factor. The LLRF control system implements in-phase and quadrature (I&Q) control to maintain the cavity field within tolerances of 0.5 percent in amplitude and 0.5 degrees in phase in the presence of beam-induced instabilities. This paper describes the identified components and presents measured performance data. The user interface with the systems is described, and cavity field measurements are included. DOE

N93-13049# Advisory Group for Aerospace Research and Development, Neuilly-Sur-Seine (France). Avionics Panel.

FUNDAMENTALS AND SPECIAL PROBLEMS OF SYNTHETIC APERTURE RADAR (SAR) [LES ASPECTS FONDAMENTAUX ET LES PROBLEMES SPECIFIQUES AUX RADARS A OUVERTURE SYNTHETIQUE (SAR)]

Aug. 1992 196 p Lecture series held in Bad Neuenahr, Germany, 5-6 Oct. 1992, in Gebze-Kocaeli, Turkey, 8-9 Oct. 1992, and in Ottawa, Ontario, 26-27 Oct. 1992

(AGARD-LS-182; ISBN-92-835-0683-9) Copyright Avail: CASI HC A09/MF A03

The influence of the antenna parameters on specification and capabilities of SAR and the advantages, necessities, and limits will be considered. Digital SAR processing is indispensable for SAR. Theories and special algorithms will be given along with basic processor configurations and different processing techniques on a hardware and software basis. The simulation of SAR-systems as well as SAR-products will also be a topic of the Lecture Series. A presentation of the present state of the art, giving examples of presently planned and realized airborne and spaceborne SAR with its foreseen applications will conclude the Lecture Series. This Lecture Series was sponsored by the Avionics Panel of AGARD and the Consultant and Exchange Program of AGARD. For individual titles, see N93-13050 through N93-13060.

N93-13050# Deutsche Forschungsanstalt fuer Luft- und Raumfahrt, Oberpfaffenhofen (Germany). Inst. fuer Hochfrequenztechnik.

BASIC PRINCIPLES OF SAR

Wolfgang Keydel *In* AGARD, Fundamentals and Special Problems of Synthetic Aperture Radar (SAR) Aug. 1992 13 p (For primary document see N93-13049 03-32)

Copyright Avail: CASI HC A03/MF A03

The basic principles of SAR will be explained. Equations for geometric and radiometric resolution and their inter-relations will be given in addition to a range equation. The difference between focussed and unfocussed SAR and the conception of beam sharpening will be explained. Author

N93-13051# Deutsche Forschungsanstalt fuer Luft- und Raumfahrt, Oberpfaffenhofen (Germany). Inst. fuer Hochfrequenztechnik.

SAR PECULIARITIES, AMBIGUITIES AND CONSTRAINTS

Wolfgang Keydel *In* AGARD, Fundamentals and Special Problems of Synthetic Aperture Radar (SAR) Aug. 1992 10 p (For primary document see N93-13049 03-32)

Copyright Avail: CASI HC A02/MF A03

A synthetic aperture radar (SAR) is basically a coherent scatterometer that employs a coherent real aperture radar with highly sophisticated data evaluation and image processing capabilities. Therefore, the coherence of the system is very important; furthermore, the keypoints for SAR are data storage, evaluation, and processing. These facts entail peculiarities of SAR and special ambiguities which are different from those arising with real aperture radar (RAR). The objective of this paper is to point out the special peculiarities and ambiguities of SAR in comparison to the corresponding properties of RAR. Main topics in this connection are as follows: basic peculiarities like range dependency of signal to noise ratio; azimuth resolution; influence of platform velocity; range and azimuth ambiguities; pulse repetition frequency limitations; velocity effects; and phase error influence, on SAR-image, that can cause motion compensation problems. All these effects will be explained together with different contrast-equations between the target and clutter signals of SAR and RAR. Author

N93-13052# Deutsche Forschungsanstalt fuer Luft- und Raumfahrt, Oberpfaffenhofen (Germany). Inst. fuer Hochfrequenztechnik.

MOTION ERRORS AND COMPENSATION POSSIBILITIES

David Hounam *In* AGARD, Fundamentals and Special Problems of Synthetic Aperture Radar (SAR) Aug. 1992 12 p (For primary document see N93-13049 03-32)

Copyright Avail: CASI HC A03/MF A03

The synthetic aperture radar (SAR) technique relies on knowledge of the relative motion between the sensor and the target. If the flight path of the sensor is not accurately known or the SAR processor is limited in its ability to take the flight data into account, the SAR image will be degraded. Motion errors are particularly critical for SAR sensors on small, low-flying aircraft, due to turbulence, and where high spatial resolution is required. The lecture discusses the effects of motion errors on image quality and the requirements on the sensor and processor to compensate for motion errors. The DLR airborne sensor, E-SAR, and associated image processor will be used as examples. Techniques using a priori knowledge of the flight path from independent sensors, e.g., inertial navigation systems (INS), and by extracting the flight data from the SAR data, e.g., autofocus and reflectivity displacement method (RDM), are treated. Author

N93-13053# Deutsche Forschungsanstalt fuer Luft- und Raumfahrt, Oberpfaffenhofen (Germany). Inst. fuer Hochfrequenztechnik.
THE REAL APERTURE ANTENNA OF SAR, A KEY ELEMENT FOR PERFORMANCE
Herwig Oettl *In* AGARD, Fundamentals and Special Problems of Synthetic Aperture Radar (SAR) Aug. 1992 8 p (For primary document see N93-13049 03-32)
Copyright Avail: CASI HC A02/MF A03

For a SAR system flying on an airborne or spaceborne platform, the real antenna must be designed in such a way so as to avoid ambiguities and achieve the envisaged resolution. Although a SAR is, with respect to geometric azimuth resolution, independent of its distance from a target, the ground range resolution depends on the incidence angle and, of course, on the bandwidth dependent slant range resolution. The antenna size and its half power beam width (HPBW) in azimuth and elevation define its azimuth resolution and, for a given off-nadir angle and chosen altitude, the swath width. The minimum antenna size, measured in wavelengths, depends on the altitude, velocity of the platform, and chosen off-nadir angle. In real antenna design, the aperture size will be somewhat larger in order to allow for amplitude taper (at least in elevation), for electronic beam steering and possibly for beam shaping. This paper explains the interdependence of antenna parameters with SAR system performance. Author

N93-13054*# Jet Propulsion Lab., California Inst. of Tech., Pasadena.
POLARIZATION EFFECTS AND MULTIPOLARIZATION SAR
Anthony Freeman *In* AGARD, Fundamentals and Special Problems of Synthetic Aperture Radar (SAR) Aug. 1992 13 p (For primary document see N93-13049 03-32)
Copyright Avail: CASI HC A03/MF A03

Imaging radar polarimeters are usually implemented using a Synthetic Aperture Radar (SAR) approach to give a high resolution image in two dimensions: range and azimuth. For each pixel in the image a polarimetric SAR gives sufficient information to characterize the polarimetric scattering properties of the imaged area (or target) as seen by the radar. Using a polarimetric SAR system as opposed to a single-polarization SAR system provides significantly more information about the target scattering mechanisms and allows better discrimination between different types of surfaces. In these notes a brief overview of SAR polarimetry is offered. The notes are intended as a text to accompany a lecture on SAR polarimetry as part of an AGARD-NATO course. Covered in the notes are the following: the polarization properties of electromagnetic waves; the concepts of radar scattering and measuring radar backscatter with a SAR; polarization synthesis; scattering matrix, Stokes matrix, and covariance matrix representations of polarimetric SAR data; polarization signature plots; design and calibration of polarimetric SAR systems; polarization filtering for target detection; fitting a simple model to polarimetric SAR measurements of naturally occurring features; and supervised classification of polarimetric SAR data. Author

N93-13055# Deutsche Forschungsanstalt fuer Luft- und Raumfahrt, Oberpfaffenhofen (Germany). Inst. fuer Hochfrequenztechnik.
RADIOMETRIC CALIBRATION OF SAR SYSTEMS
Herwig Oettl *In* AGARD, Fundamentals and Special Problems of Synthetic Aperture Radar (SAR) Aug. 1992 9 p (For primary document see N93-13049 03-32)
Copyright Avail: CASI HC A02/MF A03

Most SAR image interpretation performed in recent years was based on data which were often insufficiently calibrated. Ground truth data were used for comparison and interpretation. The importance of calibration was recognized by the need for reproducible data, by the introduction of multifrequency and multipolarization systems (interchannel calibration), and the long term scope of remote sensing. Hydrologists, especially, requested an absolute calibration with tolerances of less than 1 dB. Internal calibration schemes, as well as the use of external passive and active calibrators, were introduced to achieve this goal over the wide dynamic range. The in-flight measurement of the antenna pattern by means of ground based receivers became increasingly important due to pattern changes caused by electronic beam steering and the necessity of beam alignment in case of multifrequency and/or polarimetric operation modes. The use of radiometric corrections to compensate for near range/far range differences caused by the antenna pattern and geometry of illumination will be explained in the lecture. The impact of geocoding on radiometric levels will also be mentioned, including the phenomenon of over-/underexposing hilly regions, caused by incidence angle changes. Author

N93-13056# Deutsche Forschungsanstalt fuer Luft- und Raumfahrt, Oberpfaffenhofen (Germany). Inst. fuer Hochfrequenztechnik.
SAR SIMULATION
David Hounam *In* AGARD, Fundamentals and Special Problems of Synthetic Aperture Radar (SAR) Aug. 1992 16 p (For primary document see N93-13049 03-32)
Copyright Avail: CASI HC A03/MF A03

The use of software tools as an investigative method is particularly important in the case of synthetic aperture radar sensors, as the geometry cannot be reproduced in the laboratory. Also, the complete SAR system, from the target via the propagation path, sensor and image processor to the final image, represents a highly complex data chain, which cannot be treated in part. The lecture discusses different approaches from parametric analysis tools to full-blown simulators capable of analyzing all elements of the SAR system. The latter will be illustrated with the aid of the SARSIM simulator, which was used for confirming parameters of the ERS-1 Active Microwave Instrument (AMI). Particular emphasis will be placed on the simulation of target scattering mechanisms, the understanding of which is essential if the potential of SAR systems is to be fully exploited, and on the modelling of sensor characteristics. Author

N93-13057*# Jet Propulsion Lab., California Inst. of Tech., Pasadena.
MULTI-FREQUENCY MULTI-POLARIZATION PROCESSING FOR SPACEBORNE SAR
John C. Curlander and C. Y. Chang *In* AGARD, Fundamentals and Special Problems of Synthetic Aperture Radar (SAR) Aug. 1992 7 p (For primary document see N93-13049 03-32)
Copyright Avail: CASI HC A02/MF A03

The Shuttle Imaging Radar-C (SIR-C) is the third in a series of space shuttle based synthetic aperture radars (SAR) sponsored by the National Aeronautics and Space Administration (NASA). The SIR-C ground data processing system is to process the playbacked SAR signal data into a variety of data products for distribution to the science community. An overview of the end-to-end ground data processing system with emphasis on the unique characteristics involved in the system design is presented. Included in the discussion are science requirements, radar system specifications, input data format specifications, system operations design, data products design, processing algorithm design, hardware architecture design, and software design. Author

N93-13058# Thomson-CSF, Malakoff (France).
INVERSE SYNTHETIC APERTURE RADAR
Jean-Philippe Hardange *In* AGARD, Fundamentals and Special Problems of Synthetic Aperture Radar (SAR) Aug. 1992 14 p (For primary document see N93-13049 03-32)
Copyright Avail: CASI HC A03/MF A03

ISAR is a technique, based on time and Doppler frequency analysis, which is used for imaging of targets having rotational motions with regard to the radar. In the sixties, observation of the Moon and planets by a radar located on the Earth was one of the first applications. Closely derived from these first trials, imaging of objects in terrestrian orbit by ISAR techniques is performed with interesting results. However, the most current domains of application of ISAR are now measurements of target signatures and target recognition. Author

N93-13059# Canada Centre for Remote Sensing, Ottawa (Ontario). RADARSAT Project Office.
SPECIAL SAR TECHNIQUES AND APPLICATIONS
R. Keith Raney *In* AGARD, Fundamentals and Special Problems of Synthetic Aperture Radar (SAR) Aug. 1992 15 p (For primary document see N93-13049 03-32)
Copyright Avail: CASI HC A03/MF A03

SAR systems as considered in these lectures are fully coherent and are characterized by large time/bandwidth signal structure in both range and azimuth. These properties allow additional and specialized performance to be achieved through innovative system variations. Author

N93-13060# Canada Centre for Remote Sensing, Ottawa (Ontario). RADARSAT Project Office.
REVIEW OF SPACEBORNE AND AIRBORNE SAR SYSTEMS
R. Keith Raney *In* AGARD, Fundamentals and Special Problems of Synthetic Aperture Radar (SAR) Aug. 1992 20 p (For primary document see N93-13049 03-32)
Copyright Avail: CASI HC A03/MF A03

This Lecture provides a concise summary of the state of the art in SAR systems, both spaceborne and airborne. The first civilian SAR mission in space was the United States' SEASAT (L-band), operating Jul. - Sep. 1978. It was followed by two Shuttle missions of one week duration each, SIR-A (L-band, Nov. 1981), and SIR-B (L-band, Oct. 1984). The 1990's are witnessing a flurry of orbital SAR activity, with Almaz (USSR, S-band, Mar. 1991), ERS-1 (ESA, C-band, Jul. 1991), J-ERS-1 (Japan, L-band, Feb. 1992), SIR-C/X-SAR (USA/Germany and Italy, L-, C- and X-bands, three launches planned after 1993), ERS-2 (ESA, repeat mission), and RADARSAT (Canada, C-band, 1995) taking place in the decade. System parameters are included in Tables, and general characteristics of these radars are compared and contrasted. The lecture also provides an overview of airborne SAR systems, including those of NASA (USA), CCRS (Canada), Intera/MDA (Canada), DLR (Germany), and TUD (Denmark), among others. Author

N93-13354*# Michigan Univ., Ann Arbor. Radiation Lab.
ELECTROMAGNETIC SCATTERING AND RADIATION FROM MICROSTRIP PATCH ANTENNAS AND SPIRALS RESIDING IN A CAVITY
J. L. Volakis, J. Gong, A. Alexanian, and A. Woo Nov. 1992 48 p
(Contract NCA2-653)
(NASA-CR-191284; NAS 1.26:191284; UMICH-028918-2-T) Avail: CASI HC A03/MF A01

A new hybrid method is presented for the analysis of the scattering and radiation by conformal antennas and arrays comprised of circular or rectangular elements. In addition, calculations for cavity-backed spiral antennas are given. The method employs a finite element formulation within the cavity and the boundary integral (exact boundary condition) for terminating the mesh. By virtue of the finite element discretization, the method has no restrictions on the geometry and composition of the cavity or its termination. Furthermore, because of the convolutional nature of the boundary integral and the inherent sparseness of the finite element matrix, the storage requirement is kept very low at O(n). These unique features of the method have already been exploited in other scattering applications and have permitted the analysis of large-size structures with remarkable efficiency. In this report, we describe the method's formulation and implementation for circular and rectangular patch antennas in different superstrate and substrate configurations which may also include the presence of lumped loads and resistive sheets/cards. Also, various modelling approaches are investigated and implemented for characterizing a variety of feed structures to permit the computation of the input impedance and radiation pattern. Many computational examples for rectangular and circular patch configurations are presented which demonstrate the method's versatility, modeling capability and accuracy. Author

N93-13357# Lawrence Livermore National Lab., CA.
DIAGNOSTIC OF SHOCK WAVE PROCESSES
P. A. Urtiew May 1992 36 p Presented at the International Seminar on Physics and Gas Dynamics of Shock Waves, Minsk, Russia, 27 May - 2 Jun. 1992
(Contract W-7405-eng-48)
(DE92-018059; UCRL-JC-110355; CONF-9205137-2) Avail: CASI HC A03/MF A01

Experimental measurements of high rate processes taking place in a shock wave dynamic environment require that the diagnostic systems have fast response and high resolution. This is not a trivial requirement considering the fact that under shock loading one can expect not only sudden changes of state across the shock discontinuity but also subsequent changes in pressure, temperature and volume due to chemical reaction, phase change and other transformations which may also take place behind the shock wave. Among the various parameters which provide direct ties to theoretical studies of the equation of state and at the same time yield to relatively accurate experimental measurements are shock velocity, particle velocity and pressure. Described here are the optical techniques VISAR and Fabry Perot interferometer for observing particle and free surface velocities in transparent media as well as in situ foil gauges for measuring pressure and particle velocity within the sample. Although these techniques are not new they have been continuously improved and upgraded at our facility to yield greater accuracy, reliability and state of the art performance. The emphasis in this paper is on the operational features of the measuring techniques, but examples of experimental results are also included. DOE

N93-13375*# Illinois Univ., Urbana. Coordinated Science Lab.
LAZY CHECKPOINT COORDINATION FOR BOUNDING ROLLBACK PROPAGATION
Yi-Min Wang and W. Kent Fuchs 20 Nov. 1992 23 p
(Contract NAG1-613; N00014-91-J-1283)
(NASA-CR-191281; NAS 1.26:191281; UILU-ENG-92-2245; CRHC-92-27)
Avail: CASI HC A03/MF A01

Independent checkpointing allows maximum process autonomy but suffers from potential domino effects. Coordinated checkpointing eliminates the domino effect by sacrificing a certain degree of process autonomy. In this paper, we propose the technique of lazy checkpoint coordination which preserves process autonomy while employing communication-induced checkpoint coordination for bounding rollback propagation. The introduction of the notion of laziness allows a flexible trade-off between the cost for checkpoint coordination and the average rollback distance. Worst-case overhead analysis provides a means for estimating the extra checkpoint overhead. Communication trace-driven simulation for several parallel programs is used to evaluate the benefits of the proposed scheme for real applications. Author

N93-13411*# Notre Dame Univ., IN. Dept. of Electrical Engineering.
ERROR CONTROL TECHNIQUES FOR SATELLITE AND SPACE COMMUNICATIONS Annual Progress Report
Daniel J. Costello, Jr. Nov. 1992 63 p
(Grant NAG5-557)
(NASA-CR-191229; NAS 1.26:191229) Avail: CASI HC A04/MF A01

Worked performed during the reporting period is summarized. Construction of robustly good trellis codes for use with sequential decoding was developed. The robustly good trellis codes provide a much better trade off between free distance and distance profile. The unequal error protection capabilities of convolutional codes was studied. The problem of finding good large constraint length, low rate convolutional codes for deep space applications is investigated. A formula for computing the free distance of 1/n convolutional codes was discovered. Double memory (DM) codes, codes with two memory units per unit bit position, were studied; a search for optimal DM codes is being conducted. An algorithm for constructing convolutional codes from a given quasi-cyclic code was developed. Papers based on the above work are included in the appendix. L.R.R.

N93-13506# Sandia National Labs., Albuquerque, NM.
THE PROTECTION OF THE FACSIMILE (FAX) MACHINE AGAINST THE INSIDER THREAT
I. G. Waddoups and M. D. Tucker 1992 8 p Presented at the Institute of Nuclear Materials Management (INMM) Annual Meeting, Orlando, FL, 19-22 Jul. 1992
(Contract DE-AC04-76DP-00789)
(DE92-019424; SAND-92-0152C; CONF-9207102-56) Avail: CASI HC A02/MF A01

This paper discusses the major issues associated with protecting FAX machines from being used to transmit classified information. After discussing the ideal approach to addressing this problem, a practical solution is presented, and a description of a prototype system is given. DOE

N93-13510# Los Alamos National Lab., NM.
SPECIAL MAFIA POSTPROCESSORS FOR THE ANALYSIS OF RF STRUCTURES
M. J. Browman 1992 4 p Presented at the 16th International LINAC Conference, Ottawa, Ontario, 23-28 Aug. 1992
(Contract W-7405-eng-36)
(DE92-040248; LA-UR-92-2677; CONF-9208109-6) Avail: CASI HC A01/MF A01

This paper describes three stand-alone programs that use the electromagnetic fields generated by the MAFIA 2.04 codes to analyze radio-frequency (RF) cavities. Illustrations are provided that show how these

codes are used to do the following: (1) analyze the effect of the coupling slots on the electric and magnetic fields of the linacs for the APLE Prototype Experiment (APEX) and the Advanced Free-Electron Laser (AFEL); (2) verify the Panofsky-Wenzel theorem for a high-energy deflecting cavity proposed for the Accelerator Transmutation of Waste (ATW) project; and (3) study the effectiveness of that deflecting cavity. DOE

N93-13512# Sandia National Labs., Albuquerque, NM.
ANALYSIS AND EXPERIMENTAL RESULTS FOR AN EXTRACTION CAVITY FOR THE SPLIT-CAVITY OSCILLATOR
L. D. Bacon and R. P. Toth 1992 4 p Presented at the 6th National Conference on High Power Microwave Technologies, Lackland AFB, TX, 24-28 Aug. 1992
(Contract DE-AC04-76DP-00789)
(DE92-040262; SAND-92-0876C; CONF-9208127-1) Avail: CASI HC A01/MF A01

The kinetic energy in a split-cavity oscillator's (SCO's) modulated beam must be converted into microwave energy in a waveguide. The efficiency of this conversion process is a major factor in the overall efficiency of this source. The low-impedance beam used with the SCO--typically a few kiloamperes at 140 kV--with the accompanying space-charge effects and beam loading of the output gap, differentiates the extractor design for an SCO from that of more conventional beam-modulation tubes. This paper will discuss an analytical and experimental effort to design an extractor cavity for a 1 GHz SCO that has optimum Q and shunt impedance. Our approach was to build a rectangular extraction cavity of known, variable Q. This serves the dual purpose of enabling us to search the parameter space for an optimum coupler and to evaluate the modulation characteristics of the beam, since the power output at optimum Q is related to the beam's energy and modulation characteristics. We will discuss a chain-parameter matrix model of the cavity, beam loading effects, and experimental results for power output as a function of extraction cavity parameters. DOE

N93-13813 Polytechnic Univ., Brooklyn, NY.
GUIDANCE AND SCATTERING OF ELECTROMAGNETIC WAVES BY NONLINEAR LAYERS Ph.D. Thesis
Roger Lida Lin 1992 152 p
Avail: Univ. Microfilms Order No. DA9216055

This dissertation examines wave phenomena in nonlinear media, specifically the guidance and scattering of monochromatic electromagnetic waves in layered structures consisting of materials with Kerr-like nonlinearity. The interaction of plane waves with a single nonlinear interface is investigated first. By using a rigorous analysis, switching phenomena for plane waves incident onto a nonlinear interface are studied. Unlike previous work, the new results can be applied to both TE and TM wave incident at any angle. The results show that plane waves guided by a nonlinear interface give soliton type field profiles. Using the 'potential function' method, approximate field solutions for plane waves in nonlinear layers are obtained. With these solutions, the power-dependent dispersion relation for waves guided by nonlinear layers is calculated. The reflection and transmission coefficients for plane waves incident on nonlinear layers are derived and bistability is thus revealed for certain incident angles. The linear limit of the field solution is also examined. A new wave type referred to as a 'nonlinear leaky wave mode' is developed in the thesis. THe mode is characterized by a complex propagation constant and is helpful in studying the output field profile of nonlinear prism couplers. The studies presented here and their results show promise for applications in optical communications, optical signal processing and all-optical computers.
Dissert. Abstr.

N93-13838# Howard Univ., Washington, DC. Dept. of Electrical Engineering.
RADAR SIGNAL PROCESSING FOR OVER RESOLVED TARGETS Final Report, Jul. 1990 - Dec. 1991
Ajit K. Choudhury and Mifang Ruan May 1992 98 p
(Contract F33615-90-C-1443)
(AD-A255256; WL-TR-92-1028) Avail: CASI HC A05/MF A02

Many formulas involved in the computation of radar detection performance, such as incomplete Toronto function and modified Bessel function, have very bad numerical behaviors. This fact leads to errors of the computed results. We developed and presented in this report the numerical methods which greatly improve the accuracy of the results. Another major work in this report is to investigate the effects of the energy distribution on the radar detection performance. In contrast to ordinary assumption of uniformly distributed energy, we allow the resolution cells to have different energy. Many results are obtained based on the new energy distribution model, and the relationship between uniformly and non-uniformly distributed energy is discussed. GRA

N93-13868# Naval Research Lab., Washington, DC.
HIGH-RESOLUTION ARRAY WITH PRONY, MUSIC, AND ESPRIT ALGORITHMS Final Report
B. T. Root 25 Aug. 1992 77 p
(AD-A255514; NRL/FR/5324-92-9397) Avail: CASI HC A05/MF A01

This report investigates the array high-resolution properties of three algorithms: the Prony algorithm the MUSIC algorithm, and the ESPRIT algorithm. MUSIC has been much studied due to its excellent high-resolution properties in all but the most correlated cases. A variation of it called spatially averaged MUSIC performs well even in the case of perfectly correlated signals. The Prony technique has been less studied in an array processing context, but is shown to perform as well as spatially averaged MUSIC. ESPRIT is a recently developed eigenspace-based technique that has the same excellent resolution properties as MUSIC, but is much more computationally efficient. It can also be adapted to the correlated case.
GRA

N93-13869# Stanford Univ., CA. Space Telecommunications and Radioscience Lab.
LONG-TERM AVERAGES OF GLOBALLY-MEASURED ELF/VLF RADIO NOISE
M. M. Bowen, A. C. Fraser-Smith, and P. R. McGill Mar. 1992 58 p
(Contracts N00014-81-K-0382; N00014-90-J-1080)
(AD-A255518; SU-TR-E450-2) Avail: CASI HC A04/MF A01

In this report we present the results of a statistical study of a year of data obtained as part of the STAR Laboratory's global survey of ELF/VLF radio noise (frequencies in the range 10 Hz to 32 kHz). The data included in the study were obtained from seven measurement instruments (radiometers) located at both high and low latitudes. Average amplitude and voltage deviation (d) statistics from each of the six stations were first divided into four three-month seasons and then averaged at every measurement frequency to give two separate sets of long-term averages. Long-term averages show characteristic trends in the measurements due to the manner in which noise propagates in the earth-ionosphere waveguide. The average amplitudes of the measurements decrease with frequency, reaching a minimum around 1 kHz, and rise again towards 10 kHz. The voltage deviation amplitudes generally rise with frequency except for a depression of values around 1 kHz. GRA

N93-13871# Naval Research Lab., Washington, DC.
WR-10 BAND NOISE MEASUREMENT Final Report, 1989 - 1992
J. A. Molnar, T. V. Mai, and J. J. ONeill 21 Aug. 1992 38 p
(AD-A255526; NRL/FR/5524-92-9399) Avail: CASI HC A03/MF A01

A WR-10 band (75 to 110 GHz) noise measurement system was developed to evaluate a solid state noise source in this band. The system was characterized with a gas discharge tube that provided a stable output Excess Noise Ratio (ENR) of 14.2 dB + 0.5 dB throughout the band. To ensure the accuracy of the system characterization, the results were correlated with the results of noise temperature measurements, obtained from a load maintained at ambient and liquid nitrogen temperatures. The principles of noise measurement, method and limitations of each technique, and results of receiver characterization are discussed. The results of the receiver characterization are applied to the evaluation of solid-state noise sources. The resulting double sideband (DSB) ENR of the noise sources are presented and discussed. The accuracy of this DSB evaluation was compared to a single sideband (SSB) measurement using the Three Point Measurement method. Two WR-10 band noise sources were evaluated with the noise measurement system developed at NRL. The device performance was specified as an ENR of 15 dB + 1 dB and full waveguide coverage. The actual performance results indicate that ENR values in excess of 15 dB are available, but the devices lacked a flat output over the band. GRA

N93-13875# Army Command and General Staff Coll., Fort Leavenworth, KS.
THE JOINT SURVEILLANCE TARGET ATTACK RADAR SYSTEM: CAN PROCEDURES BE DEVELOPED TO SUPPORT THE REQUIREMENTS OF THE LAND AND AIR COMPONENT COMMANDERS? M.S. Thesis
Leonard J. Samborowski 4 May 1992 186 p
(AD-A255555) Avail: CASI HC A09/MF A02

This thesis examines the warfighting capabilities of the Joint Surveillance Target Attack Radar System (Joint STARS). Joint STARS effectiveness in DESERT STORM is examined as a case study. Additionally, an analysis of Joint STARS against the Department of Defense's Seven Threat Scenarios highlight the future potential of the system. This thesis contends that Joint STARS did not simultaneously support the requirements of the Land and Air Component Commanders, during DESERT STORM. Although a contributor to success in the war, Joint STARS supported the Army and the Air Force at different times and with different radar products. The primary, but not exclusive, reason for this limitation was the technological immaturity of a weapon system still in Full Scale Development. The strengths and weakness of Joint STARS are examined throughout this thesis. This study concludes that Joint STARS procedures can be developed to support the requirements of the Land and Air Component Commanders. Recommendations for the increased effectiveness of Joint STARS support to operational warfare is provided in the final chapter. GRA

N93-13878# Massachusetts Inst. of Tech., Lexington. Lincoln Lab.
MULTIFREQUENCY MEASUREMENTS OF RADAR GROUND CLUTTER AT 42 SITES. VOLUME 2: APPENDICES A THROUGH D
J. B. Billingsley and J. F. Larrabee 15 Nov. 1991 295 p
(Contract F19628-90-C-0002)
(AD-A246711; ESD-TR-91-175-Vol-2) Avail: CASI HC A13/MF A03

Phase One sites for multifrequency radar ground clutter measurement equipment are listed. Besides measuring backscatter from terrain, attention was devoted to characterizing and describing the terrain at each site, a necessary requirement in the development of ground clutter predictive and modeling capabilities. A description of the measurement equipment and the method of calibration used is included. Two topics associated with multipath propagation are discussed. It is shown how to get intuitive insight into the multifrequency effects of multipath in the repeat sector measurements by considering multipath from a flat surface local to the Phase One antenna but tilted at the hillside slope where the measurements are taken. Long range mountain clutter measurements are discussed. Selected groups of experiment-by-experiment repeat sector mean clutter strength at three sites are shown holding the main radar parameters of frequency, polarization, and resolution constant within each group. Clutter computations of measured clutter amplitude distributions are included. Tabulated values of mean and ratio of standard deviation to mean in repeat sector clutter amplitude distributions for 49 Phase One setups are included. L.R.R.

N93-13939# Air Force Inst. of Tech., Wright-Patterson AFB, OH.
DEVELOPMENT OF TWO-DIMENSIONAL PARAMETRIC RADAR SIGNAL MODELING AND ESTIMATION TECHNIQUES WITH APPLICATION TO TARGET IDENTIFICATION Ph.D. Thesis
Joseph J. Sacchini 1992 302 p
(AD-A252602; AFIT/CI/CIA-92-004D) Avail: CASI HC A14/MF A03

One and two dimensional signal processing models and algorithms which are utilized in the Radar Target Identification Problem are developed. A basic assumption of this work is that the high-frequency scattering from a radar target, such as an aircraft, land-based vehicle, or ship, is comprised of the sum of the scattering from a finite number of canonical scattering centers, each with a specific location and identity. By high-frequency it is meant that the overall size of the target is at least one wavelength. The scattering center assumption is more valid as the individual scattering centers become more electrically isolated. If two individual scattering centers are electrically close, then their combined response is, in general, not the sum of their individual responses. First, this dissertation investigates the electromagnetic scattering characteristics of canonical scattering centers. Canonical scattering centers are scattering centers on a target which account for the vast majority of the scattering from that target in the high-frequency case. Some of the targets of interest in this work are aircraft, tanks, trucks, automobiles, and ships. Predominant scattering centers on these targets include corners, edges, plates, dihedrals, trihedrals, and cylinders. The scattering centers are described by their scattering characteristics as functions of angle, frequency, and polarization. Second, this dissertation develops a two-dimensional (2-D) signal processing technique for locating and characterizing scattering centers from radar data. The radar gathers scattering data of a target at both multiple frequencies and multiple angles. This type of data is gathered (in raw form) by both Synthetic Aperture Radars and Inverse Synthetic Aperture Radars. The 2-D signal processing technique developed here is based on a 2-D extension of a total least squares (TLS) solution to a Prony Model and is called the 2-D TLS-Prony Technique. This technique can use single or multiple-polarization data. With full-polarization data, polarimetric characteristics of the scattering centers are found using the transient polarization response concept. This concept uses an ellipse to characterize the polarimetric characteristics of each scattering center. The abilities of the 2-D TLS-Prony Technique are demonstrated utilizing simulated 2-D radar data. Author

N93-14042 Illinois Univ. at Urbana-Champaign, Savoy.
COMPUTER-AIDED DESIGN-BASED HIGH-FREQUENCY ELECTROMAGNETIC WAVE SCATTERING FROM COMPLEX BODIES Ph.D. Thesis
John Eric Baldauf 1991 132 p
Avail: Univ. Microfilms Order No. DA9210735

This work investigates the use of high frequency electromagnetic scattering techniques, such as the physical theory of diffraction (PTD) and the geometrical theory of diffraction (GTD) and the shooting and bouncing rays (SBR) method combined with computer aided design (CAD) compatible geometries, to perform the electromagnetic scattering analysis of complex arbitrary bodies. The use of CAD formats such as solid modelled bodies and bodies modelled with triangular patch surface elements allows the scattering analysis of arbitrary bodies which can be constructed using CAD packages. The scattering analyses are applied to radar cross section (RCS) problems, cavity radiation problems, and antenna pattern predictions of complex electrically large structures, thereby showing that it is feasible to accurately approximate the electromagnetic wave scattering from general complex bodies using CAD techniques and high frequency scattering techniques. First, the RCS of large targets which involve multiple geometric optics (GO) interactions are investigated by comparing the RCS calculated using CAD designed radar targets and the SBR method and PTD for targets such as trihedral corner reflectors and an idealized military vehicle model with the experimentally obtained RCS. The comparisons between the calculated and measured results demonstrate that the SBR and PTD can provide accurate approximations of the RCS for targets which have complex multiple GO interactions. Second, the problem of interior cavity radiation for closed cavities is approached using a ray tracing and GO method based on the SBR method and triangular surface patch described geometries. Comparisons between the ray-based calculations and more exact techniques such as the method of moments (MM) for two-dimensional cavities demonstrate that ray-based methods can provide good approximations for the field behavior inside of nonresonant cavities. A three-dimensional case is shown to demonstrate that this technique can be easily applied to three-dimensional problems. Third, the GTD is applied to the problem of three-dimensional electromagnetic wave propagation in complex environments. These environments are described using triangular patch surface models compatible with CAD packages. This technique is applied to two different types of propagation problems: antenna pattern prediction in complex realistic environments and long distance radio wave propagation. Comparisons between theoretical GTD results and those for experimental and other theoretical methods demonstrate that using GTD and CAD based models, the electromagnetic wave propagation can be accurately predicted for complex problems. Dissert. Abstr.

N93-14043 Illinois Univ. at Urbana-Champaign, Savoy.
RECURSIVE ALGORITHMS FOR COMPUTATIONAL ELECTROMAGNETICS Ph.D. Thesis
Levent Gurel 1991 192 p
Avail: Univ. Microfilms Order No. DA9210822

Efficient and fast recursive algorithms for both the spectral-domain and the space-domain solutions of the electromagnetic scattering problems have been developed. These algorithms have less than O(N(sup 3)) computational complexities and less than O(N(sup 2)) memory requirements for arbitrary geometries of scatterers clustered together. Although the algorithms are discussed as they are applied to the electromagnetic

scattering problems, their domains of applicability can be extended to other types of electromagnetic problems (e.g., guidance, resonance, and radiation) and also to other types of field and wave equations (e.g., acoustic, elastic, and Schrodinger). The applications of these algorithms to the conducting strip and patch geometries have been demonstrated. Dielectric and magnetic materials can also be incorporated into conductor geometries. Due to the availability of the spectral Green's function, spectral-domain algorithms can efficiently handle geometries consisting of an arbitrary number of infinitely thin, conducting strips and flat patches of any shape embedded in arbitrarily layered media, in which the layers are infinitely large in the transverse directions. On the other hand, the space-domain algorithms presented in this dissertation are the recursive T-matrix algorithms, and due to the nature of the T-matrix formulations, they can easily handle geometries consisting of conductors, dielectrics and magnetic materials of finite size. Therefore, various problems defined in broad classes of geometries can be solved with these spectral-domain and space-domain algorithms. A recursive implementation of the method of moments is also presented. This algorithm is based on the principle of inversion of a general matrix by partitioning. Since it is a recursive algorithm, and since each recursion step requires O(N(sup 2)) operations, it can efficiently solve the problems in which one has to modify or perturb some parts of a main body whose solution is already known. When solving the electromagnetic scattering problem, these algorithms give the full-wave solution without having to make any approximations. Being computational algorithms, they are 'exact' in the numerical sense. These algorithms also give the solution for all possible incident waves or 'right-hand sides' at once, a property that is not shared by some other fast solution techniques such as the conjugate-gradient method. Futhermore, as opposed to some other formulation schemes such as the finite-element method, these algorithms naturally incorporate the radiation condition at infinity; therefore, they can handle geometries in unbounded media. Dissert. Abstr.

N93-14044 Illinois Univ. at Urbana-Champaign, Savoy.
THEORETICAL AND NUMERICAL STUDIES OF WAVE PROPAGATION AND SCATTERING IN INHOMOGENEOUS MEDIA Ph.D. Thesis
Yuan-Liang Li 1991 164 p
Avail: Univ. Microfilms Order No. DA9210892

Using the path-integral technique, an analytical expression of the three-dimensional Green's function for the background inhomogeneous medium with the linear refractive index profile is obtained. The technique is extended to treat the three-dimensional and range-dependent media with or without turning points. Two analytical expressions of the Green's functions are also obtained for such media. For a line source in the medium with the linear sound speed profile, the analytical expression of the Green's function is simply obtained using a mathematical identity. For a general background medium with the refractive index varying in only one direction, one can replace the refractive index profile with many fine layers. In this case, the Green's functions can be expressed as the Sommerfeld-type integral and evaluated by numerical techniques. However, all of the conventional techniques determine the minimum number of integration points required to evaluate the integral on the trial-and-error basis and do not allow the user to choose the precise location of the desired observation points. To improve this, a new algorithm based on the chirp z-transform, called the CFFP, has been introduced. The new algorithm is called the CFFP. With this modification, the user can select the precise locations of the range of detectors. Furthermore, the new algorithm can adaptively increase the number of integration points for evaluation of the Sommerfeld-type integral. These features make the CFFP particularly useful for studying the problems of wave propagation and scattering in layered background media. Using the analytical expression of the Green's function due to a point source embedded in a background medium with the linear refractive index profile and the Born approximation, the scattered fields from random irregularities are represented as a multiple integral. A new algorithm for efficiently computing the multiple integral has been derived. Numerical results shows that the total field level in the shadow zone can be drastically affected by the scattered fields from random irregularities. To study the problem of scattering of acoustic waves from a rough ground, the analytical expression of the Green's function due to a line source embedded in a background medium with the linear sound-speed probe has also been successfully incorporated into the Helmholtz-Kirchhoff integral equation. The integral equation has been solved by the moment method. Numerical results show that the penetration of the shadow zone by the scattered fields usually is from the diffraction and back scattering of acoustic waves from a rough surface. The effects of scattering are also dependent on the inhomogeneities of the background medium. Dissert. Abstr.

N93-14048 Ohio State Univ., Columbus.
SCATTERING FROM A FINITE COLLECTION OF TRANSVERSE DIPOLE AND AXIAL SLOT ARRAYS WITH EDGE EFFECTS Ph.D. Thesis
J. Paul Skinner 1991 275 p
Avail: Univ. Microfilms Order No. DA9211224

A moment method based solution for the electromagnetic radiation and scattering from geometries composed to transverse dipole column arrays and a finite collection of axial slot arrays is developed. Each 'array' is an infinite column of periodic elements, with transverse referring to a dipole orientation perpendicular to the infinite axis and axial denoting that thin linear slots are directed along the infinite axis. The slots are mounted in infinite ground planes, which may be surrounded by an arbitrary stack of infinite lossless dielectric slabs, simulating a hybrid frequency selective radome (i.e., periodic surface) in one linear polarization, which is infinite in one dimension and finite in another. Transverse dipole arrays are used to simulate phased array antennas in a similar 'finite by infinite' model. Independent modes in scattering current expansions are defined along single columns of periodic elements, with Floquet's theorem governing the current fluctuation along the infinite axis. A coupling matrix is developed with nine sub-blocks, representing mutual admittances, mutual impedances, unitless voltage gains, and unitless current gains. Efficient methods for calculating coupling terms are developed, using both spatial and spectral domain methods (transformable via the Poisson sum formula) in free space, and using the Array Scanning Method to circumvent the application of Sommerfeld integrals with planar dielectric interfaces. Summation acceleration techniques, such as Shanks' transformation, are used to enhance efficiency. Asymptotic solutions are also developed for coupling between widely separated columns of elements. Coupling calculations are validated by spatially adding a large number of column-to-column terms to simulate the coupling from a doubly-infinite array of elements to a test element, which may be found directly in a plane wave expansion. Validation of the entire moment method procedure is also provided by comparing far zone field calculations with those expected from using solution currents from doubly-infinite arrays with the approximation of using physical optics to correct for the finite aperture width. Dissert. Abstr.

N93-14050 Pennsylvania Univ., Philadelphia.
COHERENT FRAME ANALYSIS OF SYNTHETIC APERTURE RADAR (SAR) OCEAN IMAGERY Ph.D. Thesis
Joseph George Teti, Jr. 1991 220 p
Avail: Univ. Microfilms Order No. DA9212015

This dissertation describes the decomposition and reconstruction of SAR ocean image azimuth cuts using coherent frame theory. The motivation for this work arose from the need to develop new and alternate techniques to approach speckle reduction and feature identification or extraction. Since the ocean is a non-stationary process, the simultaneous time-frequency or space-wavenumber localization characteristics are considerably important. The two dimensional space described by time and frequency or space and wavenumber is called phase space. The methods described provide optimum phase space localization in the sense that they meet the lower limit of the uncertainty principle. To realize optimum phase space localization, the decomposition and reconstruction requires the use of functions that are based on the Gaussian function. Using functions with infinite support on the decomposition process produces non-orthogonal (coupled) coherent states which present serious numerical difficulties for the reconstruction process. To overcome these difficulties, coherent frames are used with oversampling to represent both the Weyl-Heisenberg and the Affine or Wavelet coherent states. The successful reconstruction requires the numerical evaluation and use of the corresponding 'dual' frame. The tools are first exercised on a collection of 'familiar' waveforms, and are shown to provide unique phase space signatures which illustrate the time (spatial) evolution of a waveform's frequency (wavenumber) content with both types of coherent frames. The tools are then exercised on two different SAR ocean image azimuth cuts. The effects of performing filtering based on the phase space signatures of the SAR ocean image cuts are investigated and demonstrated to extract dominant waveform features. Based on theoretical considerations, a new type of multilevel waveform representation

is presented and demonstrated to optimize either the rate of power recovery or minimization of mean square error during the reconstruction process. This new type of filtering technique is a waveform approximation based on using the waveform's coherent states according to magnitude, and is very robust and efficient at recovering dominant waveform features.

Dissert. Abstr.

N93-14052 Illinois Univ. at Urbana-Champaign, Savoy.
ELECTROMAGNETIC SCATTERING SIMULATIONS USING EQUIVALENT BOUNDARY CONDITION MODELS Ph.D. Thesis
Keith Wayne Whites 1991 290 p
Avail:. Univ. Microfilms Order No. DA9211030

Equivalent boundary condition models are one approach to simplifying electromagnetic (EM) scattering problems while retaining a high degree of solution accuracy in the domain of interest. These models are successful when the dominant EM characteristics of the scattering body are captured within the model, and they are robust when the parameters in the model are capable of adjustment, in a systematic manner, to accurately simulate the scattering for physical variations in the target. Both of these properties are successfully integrated to model two important classes of scatterers used in the modern low observable vehicle: dielectrically filled cavity-backed apertures and periodic structures at lower frequencies. The reason for using the simulation models fall into two general categories. The first is the large reduction in the computational expense as compared to more exact numerical approaches. The second is the potential for expanding the size of the target which can be analyzed beyond the capabilities of more exact solution methodologies. For the first class of structures, filled cavity-backed apertures, the Impedance Boundary Condition (IBC) is used for high contrast dielectrics in an infinite impedance plane. In a thorough study, the solutions obtained using this simulation model are compared to more exact numerical approaches to precisely define when such a model is a valid approximation. In addition to the great computational savings, this model also lends insight into methods for significant reductions in the backscattering for plane wave illumination near grazing angles of incidence. Models for the second class of structure, periodic geometries at lower frequencies (meaning only the lowest ordered Floquet harmonic lies in the visible region), are divided into simulations for arrays of planar and nonplanar elements. For planar elemental arrays, a Tensor Resistive Boundary Condition (TRBC) simulation is developed for structures possessing at least two-fold rotational symmetry in the plane of periodicity. Examples of this include strip gratings, and 2-D periodic arrays of patches, crosses and slots. The nonplanar elemental arrays (possessing the same rotational symmetry) are simulated using a Tensor Impedance Boundary Condition (TIBC) model and a Resistive/Modified Conductive (RMC) sheet approximation for thin periodic arrays. Dissert. Abstr.

N93-14066 Manitoba Univ., Winnipeg.
NUMERICAL ANALYSIS OF SCATTERING FROM CERTAIN CONDUCTING AND DIELECTRIC BODIES OF ARBITRARY SHAPE Ph.D. Thesis
Hamid Moheb 1990 163 p
(ISBN-0-315-63282-8) Avail: Univ. Microfilms Order No. DANN63282

A numerical method is developed to study the electromagnetic scattering from three-dimensional geometries, which is a generalization of the method previously used for bodies of revolution. On the object's surface two orthogonal tangent vectors are defined. Along one, the surface currents are represented by discrete triangular basis functions and along the other by a finite set of entire domain basis functions. To enable the latter expansion two different techniques are adopted. In one, called the method of coordinate transformation, the object's cross-section is conformally transformed onto a circle, and cylindrical basis functions are selected in the new space. In the second technique Fourier type basis functions are used directly in the physical coordinates of the object. The developed methods are then applied to study the scattering from geometries such as cubes and plates. The behavior of the solutions with a different number of modes are investigated to determine their coupling. The conformal transformation method is applicable to any geometry of arbitrary cross-section, but it needs the transformation function to be useful. The direct method, on the other hand, does not have such a restriction. Both methods are, however, limited in use to small objects when their size is in order of the wavelength. The developed methods are then extended to treat dielectric geometries of arbitrary shape. The surface integral equations are formulated in terms of the equivalent electric and magnetic currents over the object's surface. The surface currents are obtained from the tangential components of the fields and related to the integral operators of the conducting objects. The resulting integral equations are solved similarly. Finally, the developed techniques are also applied to the antenna problems, in particular, for handling the radiation from rectangular waveguides. An x-directed dipole is used as a source of excitation and the radiation characteristics of the rectangular waveguides are determined.

Dissert. Abstr.

N93-13087*# Massachusetts Inst. of Tech., Cambridge. Dept. of Electrical Engineering and Computer Science.
VARIANCE OF PHASE FLUCTUATIONS OF WAVES PROPAGATING THROUGH A RANDOM MEDIUM
Nelson C. Chu, Jin Au Kong, Simon H. Yueh, Son V. Nghiem, Jack G. Fleischman (Massachusetts Inst. of Tech., Lexington.), Serpil Ayasli (Massachusetts Inst. of Tech., Lexington.), and Robert T. Shin (Massachusetts Inst. of Tech., Lexington.) *In its* Remote Sensing of Earth Terrain 30 Sep. 1992 15 p Repr. from Journal of Electromagnetic Waves and Applications (VSP), v. 6, no. 2, 1992 p 169-197 (For primary document see N93-13084 03-43)
(Contracts JPL-958461; MDA972-90-C-0021; DAAL03-88-J-0057; N00014-89-J-1107)
Avail: CASI HC A03/MF A01

N93-13088*# Washington Univ., Seattle. Electromagnetics and Remote Sensing Lab.
POLARIMETRIC SIGNATURES OF A CANOPY OF DIELECTRIC CYLINDERS BASED ON FIRST AND SECOND ORDER VECTOR RADIATIVE TRANSFER THEORY
Leung Tsang, Chi Hou Chan, Jin Au Kong (Massachusetts Inst. of Tech., Cambridge.), and James Joseph (General Electric Co., Schenectady, NY.) *In* MIT, Remote Sensing of Earth Terrain 30 Sep. 1992 17 p Repr. from Journal of Electromagnetic Waves and Applications (VSP), v. 1, no. 1, 1992 p 19-51 Sponsored in part by ARO and NSF (For primary document see N93-13084 03-43)
Avail: CASI HC A03/MF A01

33 ELECTRONICS AND ELECTRICAL ENGINEERING

Includes test equipment and maintainability; components, e.g., tunnel diodes and transistors; microminiaturization; and integrated circuitry.

For related information see also *60 Computer Operations and Hardware* and *76 Solid-State Physics.*

N93-12561# Oak Ridge National Lab., TN.
MODEL FOR IMPEDANCE OF AN IONIC CONDUCTOR SANDWICHED BETWEEN BLOCKING ELECTRODES
J. C. Wang 24 Jun. 1992 14 p Presented at the Second International Symposium on Electrochemical Impedance Spectroscopy, Santa Barbara, CA, 12-17 Jul. 1992
(Contract DE-AC05-84OR-21400)
(DE92-017812; CONF-9207124-1) Avail: CASI HC A03/MF A01

The simplest model for the impedance of an ionic conductor sandwiched between two blocking electrodes is a resistor in series with a capacitor (rc pair) representing the bulk material and the conductor-electrode interface, respectively, and a second capacitor parallel to the rc pair representing the electronic dielectric response of the system. In practice, to describe the experimental data satisfactorily, one needs to replace the interface capacitor with a constant-phase-angle (CPA) element and to add a non-Debye dielectric element parallel to the resistor to represent the local ionic movement. In this paper, some of the existing physical models for the CPA and non-Debye dielectric elements are discussed, and an example is presented for analyzing the impedance data using the resultant circuit model. DOE

N93-12650# *Pennsylvania Univ., Philadelphia. Dept. of Chemistry.*
PROTON TRANSPORT ON MODIFIED SULFONATED POLYANILINE ELECTRODES
J. Yue and A. J. Epstein 25 Jun. 1992 14 p
(Contract N00014-90-J-1559)
(AD-A254917; TR-1992-11) Avail: CASI HC A03/MF A01

The pH in the vicinity of a thin self-doped conducting polyaniline electrode was electrochemically modulated in aqueous solutions using both cyclic voltammetry and step potential techniques. Changes in pH were measured directly by using a microcombination pH probe. The experimental evidences verify the mechanism that the polymer behaves as a proton ejectors during oxidation and absorbers during reduction. This potential controlled pH change near the polymer coated electrode may be applied to many fields such as an electric controller of the proton environment near the electrode surface. GRA

N93-12674*# National Aeronautics and Space Administration, Washington, DC.
REQUIREMENTS FOR SOLDERED ELECTRICAL CONNECTIONS
Jan. 1992 114 p
(NHB-5300.4(3A-2); NAS 1.18:5300.4(3A-2)) Avail: CASI HC A06/MF A02

This publication is applicable to NASA programs involving solder connections for flight hardware, mission essential support equipment, and elements thereof. This publication sets forth hand and wave soldering requirements for reliable electrical connections. The prime consideration is the physical integrity of solder connections. Special requirements may exist which are not in conformance with the requirements of this publication. Design documentation contains the detail for these requirements, and they take precedence over conflicting portions of this publication when they are approved in writing by the procuring NASA installation. Author

N93-12725# Naval Command, Control and Ocean Surveillance Center, San Diego, CA. Fluid Mechanics and Energy Research Branch.
Li/SOCl BATTERY TECHNOLOGY: PROBLEMS AND SOLUTIONS Final Technical Report, Oct. 1990 - Sep. 1991
P. A. Mosier-Boss and S. J. Szpak Mar. 1992 95 p
(NR Proj. RV3-6121)
(AD-A254514; NRAD-TR-1484) Avail: CASI HC A05/MF A01

This report illustrates the advantages of using a rational transition process when developing an electrochemical power source designed to operate at its limits by summarizing the approach and results based on such a transition philosophy. The thionyl chloride electrolyte system has a complex composition that determines the elementary reactions that occur on discharge. Electroreduction rarely involves free thionyl chloride; rather, adducts with AlCl3 and Li undergo electroreduction, preferentially. Modeling the Li/SOCl2 system has contributed significantly to an understanding of battery operation of providing the basis for both the design and understanding of electrode thickness and porosity, catalytic effects, thermal management, and intercell currents. Modeling also guided the development of quality control (QC) procedures and considerations. Li/SOCl2 technology has come a long way since the initial recognition of its value as a battery chemistry. Much of this progress has resulted from efforts to pursue a logical progression of transitions through the R and D cycle. These efforts have elucidated the chemistry of the system, the best design features of cells and modules, the assembly of these cells or modules, and the resultant characteristics of these assemblies. The Li/SOCl2 is used only as an example. Other battery technology developments could benefit from such an approach. GRA

N93-12731# Columbia Univ., New York, NY. Dept. of Electrical Engineering.
MULTICHIP MODULE HIGH SPEED TESTING Quarterly Progress Report, 1 Jul. - 30 Sep. 1991
David H. Auston 30 Sep. 1991 17 p
(Contract N00014-91-J-4045)
(AD-A254825) Avail: CASI HC A03/MF A01

In collaboration with Allied Signal Inc., have investigated the ultrafast electro-optic response and sensitivity of a poled side chain polymer film by a femtosecond electro-optic sampling technique. A 760 fs rise-time electrical transient was observed corresponding to a 460 GHz bandwidth. The measurement was made in a high speed coplanar transmission line structure using the electro-optic polymer as the dielectric. This result has important implications for the use of electro-optic polymers for probing signals in multi-chip module interconnection circuits. A paper describing this work (preprint enclosed) has been accepted for publication in Applied Physics Letters. A second area of activity during the past quarter has been the establishment of a new experimental facility which will be used for the high speed testing of materials and devices for applications to multichip modules. GRA

N93-12866# Illinois Univ., Urbana. Coordinated Science Lab.
DESIGN FOR RELIABILITY: CURRENT DENSITY Final Report, Apr. 1990 - Jul. 1991
Ibrahim N. Hajj, Vasant B. Rao, Richard Burch, Hungse Cha, and Russell Iimura Jun. 1992 50 p
(Contract F30602-88-C-0028)
(AD-A254770; RL-TR-92-122) Avail: CASI HC A03/MF A01

This work describes the computation of expected and variance current density waveforms in sections of the power/ground bus for the purpose of estimating MTF due to electromigration. This work involves three main tasks: (1) further development and enhancement of probabilistic simulation methods for computing current and voltage waveform statistics; (2) development of hierarchical extraction software for the generation of the circuit netlist and parasitics from hierarchically described layouts; and (3) computation of expected value and variance current density waveforms in the RC model of the bus. The probabilistic approach for computing current and voltage statistics has been made more general and refined especially as related to the variance of the current waveforms. The extraction software reads hierarchically described layouts, and generated circuit descriptions with the same hierarchy. An approach for computing the expected value and variance of the current density for electromigration evaluation has been implemented which uses network reduction and sparse matrix techniques. The advances are described and applied to test cases for evaluation. GRA

N93-12868# Air Force Inst. of Tech., Wright-Patterson AFB, OH.
AN ANALYSIS OF THE FIELD SERVICE FUNCTION OF SELECTED ELECTRONICS FIRMS Ph.D. Thesis
Dennis Lee Hull 1992 400 p
(AD-A255003; AFIT/CI/CIA-92-009D) Avail: CASI HC A17/MF A04

For the purposes of this study, field service was defined as the function concerned with the servicing and maintaining, by the manufacturer or supplier, of products (usually owned by customers) used away from the manufacturer's or supplier's site. Field service is an important component of the service sector and of customer service. Field service availability and quality of this service are increasingly being used by customers as a means of product selection. Many companies have recognized this trend and have identified field service as a competitive edge. A review of the field service literature and discussions with field service consultants and professionals indicated a lack of field service research--more specifically, a systems analysis of the area was lacking. The purpose of this research was to examine, utilizing a systems perspective, the field service practices of leading electronics firms in order to develop field service management propositions (empirical generalizations) and a prescriptive model of best practice. The electronics industry was selected due to the critical relation of service-based competition to company profitability. GRA

N93-12978# National Inst. of Standards and Technology, Gaithersburg, MD. Semiconductor Electronics Div.
SEMICONDUCTOR MEASUREMENT TECHNOLOGY: VERSION 2.0 OF THE TXYZ THERMAL ANALYSIS PROGRAM: TXYZ20 Final Report
John Albers Jun. 1992 35 p
(PB92-217603; NIST/SP-400/89) Avail: CASI HC A03/MF A01; SOD HC

The TXYZ computer program has been used for a number of years for the thermal analysis of semiconductor devices and packages. The program makes use of the closed form, Fourier series solutions of the steady-state heat flow equation for the general case of a rectangular three-layer structure with multiple heat sources on the top surface. TXYZ provides for the calculation of the temperature at any set of points in the structure and has proven useful for the determination of the steady-state temperature distribution of semiconductor chips and packages. The report presents TXYZ20 (TXYZ Version 2.0) which is a revised and updated

version of the original TXYZ program. The TXYZ20 program incorporates more flexible handling of input data, assignment of positive or negative noninteger weights to the various heat sources or heat sinks, and improved evaluation of limiting forms in the code. The first part of the report consists of a discussion of the general elements in the TXYZ code and the particular changes which have been made to it to obtain TXYZ20. The second part of the report contains a discussion of several examples of the running of the code. Several annotated input data files are presented and discussed to show both the increased flexibility of the input data and the actual use of the updated code. Running the TXYZ20 code for one of the input files provides a benchmark for several machines. GRA

N93-13196# Jet Propulsion Lab., California Inst. of Tech., Pasadena.
EFFICIENCY OF AN AMTEC RECIRCULATING TEST CELL, EXPERIMENTS, AND PROJECTIONS
M. L. Underwood, D. OConnor, R. M. Williams, B. Jeffries-Nakamura, and M. A. Ryan May 1992 6 p Presented at the 27th Intersociety Energy Conversion Engineering Conference, San Diego, CA, 3-7 Aug. 1992
(Contract DE-AI01-86CE-90237)
(DE92-016811; CONF-920801-9) Avail: CASI HC A02/MF A01

The alkali metal thermal to electric converter (AMTEC) is an electrochemical device for the direct conversion of heat to electrical energy with efficiencies potentially near Carnot. The future usefulness of AMTEC for space power conversion depends on the efficiency of the devices. Systems studies have projected from 15 to 35 percent thermal to electric conversion efficiencies, and one experiment has demonstrated 19 percent efficiency for a short period of time. Recent experiments in a recirculating test cell (RTC) have demonstrated sustained conversion efficiencies as high as 10.2 percent early in cell life and 9.7 percent after maturity. Extensive thermal and electrochemical analysis of the cell during several experiments demonstrated that the efficiency could be improved in two ways. First, the electrode performance could be improved. The electrode for these tests operated at about one third the power density of state of the art electrodes. The low power density was caused by a combination of high series resistance and high mass flow resistance. Reducing these resistances could improve the efficiency to greater than 10 percent. Second, the cell thermal perform ance could be improved. Efficiencies greater than 14 percent could be realized through reducing the radiative thermal loss. Further improvements to the efficiency range predicted by systems studies can be accomplished through the development and use of an advanced condenser with improved reflectivity, close to that of a smooth sodium film, and the series connecting of individual cells to further reduce thermal losses. DOE

N93-13197# Jet Propulsion Lab., California Inst. of Tech., Pasadena.
REVERSIBLE THERMODYNAMIC CYCLE FOR AMTEC POWER CONVERSION
C. B. Vining, R. M. Williams, M. L. Underwood, M. A. Ryan, and J. W. Suitor 1992 6 p Presented at the 27th Intersociety Energy Conversion Engineering Conference, San Diego, CA, 3-7 Aug. 1992
(Contract DE-AI01-86CE-90237)
(DE92-016814; CONF-920801-10) Avail: CASI HC A02/MF A01

The thermodynamic cycle appropriate to an AMTEC (alkali metal thermal-to-electric converter) cell is discussed for both liquid- and vapor-fed modes of operation, under the assumption that all processes can be performed reversibly. In the liquid-fed mode, the reversible efficiency is greater than 89.6 percent of Carnot efficiency for heat input and rejection temperatures (900-1300 K and 400-800 K, respectively) typical of practical devices. Vapor-fed cells can approach the efficiency of liquid-fed cells. Quantitative estimates confirm that the efficiency is insensitive to either the work required to pressurize the sodium liquid or the details of the state changes associated with cooling the low pressure sodium gas to the heat rejection temperature. DOE

N93-13286*# National Aeronautics and Space Administration. Lewis Research Center, Cleveland, OH.
ANOMALOUS TWTA OUTPUT POWER SPIKES AND THEIR EFFECT ON A DIGITAL SATELLITE COMMUNICATIONS SYSTEM
Brian D. May, Robert J. Kerczewski, and James S. Svoboda (Sverdrup Technology, Inc., Brook Park, OH.) Oct. 1992 14 p
(Contract NAS3-25266; RTOP 679-40-00)
(NASA-TM-105875; E-6558; NAS 1.15:105875) Avail: CASI HC A03/MF A01

Several 30 GHz, 60 W traveling wave tube amplifiers (TWTA) were manufactured for the NASA Lewis Research Center's High Burst Rate Link Evaluation Terminal Project. An unusual operating problem characterized by anomalous nonperiodic output power spikes, common to all of the TWTAs proved during testing to significantly affect the performance of a digitally-modulated data transmission test system. Modifications made to the TWTAs significantly curtailed the problem and allowed acceptable system performance to be obtained. This paper presents a discussion of the TWTA output power spike problem, possible causes of the problem, and the solutions implemented by the manufacturer which improved the TWTA performance to an acceptable level. The results of the testing done at NASA Lewis on the TWTAs both before and after the improvement made by Hughes are presented, and the effects of the output power spikes on the performance of the test system are discussed. Author

N93-13300# Sandia National Labs., Albuquerque, NM.
EDDY CURRENT POWER DISSIPATION AT SHARP CORNERS
L. K. Warne 1992 8 p Presented at the Union Radio Science International (URSI) Electromagnetic Theory Symposium, Sydney, Australia, 17 Aug. 1992
(Contract DE-AC04-76DP-00789)
(DE92-016890; SAND-92-1501C; CONF-9208116-1) Avail: CASI HC A02/MF A01

This paper develops corrections to the impedance per unit length when the conductor cross section includes sharp corners. The case of a right internal angle is treated in detail. Corrections are given for all values of the ratio of internal to external magnetic permeabilities. Both the real and imaginary parts of the corrections are determined. Application of the results to a conductor of square cross section is given. Higher order terms are developed and compared to a numerical solution. DOE

N93-13358# Brookhaven National Lab., Upton, NY.
LONGITUDINAL IMPEDANCE OF CAPACITIVE PICK-UP ELECTRODES: CALCULATIONS AND COMPARISON WITH MEASUREMENTS
M. Blaskiewicz, A. Luccio, A. Ratti, and T. J. Shea 1992 3 p Presented at the 15th International Conference on High Energy Accelerators, Hamburg, Germany, 20-24 Jul. 1992
(Contract DE-AC02-76CH-00016)
(DE92-019499; BNL-47103; CONF-920706-19) Avail: CASI HC A01/MF A01

In order to obtain high sensitivity over a broad frequency range, split cylinder capacitive pick-up electrodes have been adopted as the beam position monitors (BPMs) for the AGS booster. Numerical simulation and prototype measurements have been employed to find the coupling impedance of a BPM. The impedance was calculated using the MAFIA computer codes, and measurements were made using a coaxial wire. We found that the measured impedance depended strongly on external electronics, which could not be modeled using the computer code. Additionally, the calculated impedance is a function of beam velocity, which was not studied in the measurements. Only by using both could a reliable bound on the shunt impedance be obtained. We find that the longitudinal impedance of the BPMs is negligible for normal operating conditions in the booster. DOE

N93-13430*# Colorado Research Development Corp., Denver.
NARROW BANDGAP SEMICONDUCTING SILICIDES: INTRINSIC INFRARED DETECTORS ON A SILICON CHIP Final Report
John E. Mahan 30 May 1990 24 p
(Contract NAS7-994; SBIR-08.06-4131)
(NASA-CR-190882; NAS 1.26:190882) Avail: CASI HC A03/MF A01

Work done during the final report period is presented. The main technical objective was to achieve epitaxial growth on silicon of two semiconducting silicides, ReSi2 and CrSi2. ReSi2 thin films were grown on (001) silicon wafers by vacuum evaporation of rhenium onto hot substrates in ultrahigh vacuum. The preferred epitaxial relationship was found to be ReSi2(100)/Si(001) with ReSi2(010) parallel to Si(110). The lattice matching consists of a common unit mesh of 120 A(sup 2) area, and a mismatch of 1.8 percent. Transmission electron microscopy revealed the existence of rotation twins corresponding to two distinct but equivalent azimuthal orientations of the common unit mesh. MeV He(+) backscattering

spectrometry revealed a minimum channeling yield of 2 percent for an approximately 1,500 A thick film grown at 650 C. Although the lateral dimension of the twins is on the order of 100 A, there is a very high degree of alignment between the ReSi2(100) and the Si(001) planes. Highly oriented films of CrSi2 were grown on (111) silicon substrates, with the matching crystallographic faces being CrSi2(001)/Si(111). The reflection high-energy electron diffraction (RHEED) patterns of the films consist of sharp streaks, symmetrically arranged. The predominant azimuthal orientation of the films was determined to be CrSi2(210) parallel to Si(110). This highly desirable heteroepitaxial relationship has been obtained previously by others; it may be described with a common unit mesh of 51 A(sup 2) and mismatch of 0.3 percent. RHEED also revealed the presence of limited film regions of a competing azimuthal orientation, CrSi2(110) parallel to Si(110). A channeling effect for MeV He(+) ions was not found for this material. Potential commercial applications of this research may be found in silicon-integrated infrared detector arrays. Optical characterizations showed that semiconducting ReSi2 is a strong absorber of infrared radiation, with the adsorption constant increasing above 2 x 10(exp 4) cm(sup -1) for photon energies above 0.2 eV. CrSi2 is of potential utility for detection at photon energies above approximately 0.3 eV. L.R.R.

N93-13448*# Georgia Inst. of Tech., Atlanta. School of Electrical Engineering.

AN ACOUSTIC CHARGE TRANSPORT IMAGER FOR HIGH DEFINITION TELEVISION APPLICATIONS Final Technical Report, 1 Oct. 1991 - 30 Sep. 1992

William D. Hunt, Kevin F. Brennan, and Chris J. Summers (Georgia Tech Research Inst., Atlanta.) Nov. 1992 65 p

(Grant NAGw-2753)

(NASA-CR-191295; NAS 1.26:191295; E21-687) Avail: CASI HC A04/MF A01

In this report we present the progress during the second six month period of the project. This includes both experimental and theoretical work on the acoustic charge transport (ACT) portion of the chip, the theoretical program modelling of both the avalanche photodiode (APD) and the charge transfer and overflow transistor and the materials growth and fabrication part of the program. Author

N93-13472# Department of the Army, Washington, DC.

TRANSDUCER CIRCUIT Patent Application

Michael Sullivan, inventor (to Army) and Douglas Dussault, inventor (to Army) 1 Jun. 1992 12 p

(AD-D015376; US-Patent-Appl-SN-891120) Avail: CASI HC A03/MF A01

Accordingly, it is a general purpose and object of the present invention to provide a means for providing a circuit including a tuning inductor for use with an acoustic transducer that automatically varies inductance with frequency to keep the transducer tuned over a wide operating frequency. A still further object is the provision of a transducer circuit which is simple and rugged in design, which is capable of being easily manufactured from readily-available materials, and which is capable of a long life of useful service with a minimum of maintenance. GRA

N93-13473# Department of the Army, Washington, DC.

PREAMPLIFIER WITH ADJUSTABLE INPUT RESISTANCE Patent Application

Timothy B. Straw, inventor (to Army) and Patricia G. Murphy, inventor (to Army) 1 Jun. 1992 14 p

(AD-D015377; US-Patent-Appl-SN-891119) Avail: CASI HC A03/MF A01

The present invention overcomes the above briefly discussed deficiencies and other disadvantages of the prior art and, in so doing, employs a metal oxide semiconductor field effect transistor operated in the triode region to approximate a linear input resistance for a preamplifier employed with a capacitive transducer. The present invention thus encompasses the unobvious use of a device known to be non-linear in an application where the prior art has universally attempted to achieve linearization. The invention is based upon the discovery that the distortion of an amplified capacitive transducer output signal can be maintained within an acceptable range when the capacitive transducer and a non-linear MOSFET resistance combine to form a high-pass filter which, in effect, masks non-linearities. GRA

N93-13519# Sandia National Labs., Albuquerque, NM.

THE ESTIMATION OF ELECTRICAL CABLE FIRE-INDUCED DAMAGE LIMITS

S. P. Nowlen and M. J. Jacobus 1992 10 p Presented at the 1st International Conference and Exhibition on Fire and Materials, Washington, DC, 24-25 Sep. 1992

(Contract DE-AC04-76DP-00789)

(DE92-040100; SAND-92-1404C; CONF-9209187-1) Avail: CASI HC A02/MF A01

Sandia National Laboratories has, for several years, been engaged in the performance of both fire safety and electrical equipment qualification research under independent programs sponsored by the US Nuclear Regulatory Commission. Recent comparisons between electrical cable thermal damageability data gathered independently in these two efforts indicate that a direct correlation exists between certain of the recent cable thermal vulnerability information gathered under equipment qualification conditions and thermal damageability in a fire environment. This direct correlation allows for a significant expansion of the data base on estimated cable thermal vulnerability limits in a fire environment because of the wide range of cable types and products that have been evaluated as a part of the equipment qualification research. This paper provides a discussion of the basis for the derived correlation, and presents estimated cable thermal damage limits for a wide range of generic cable types and specific cable products. The supposition that a direct correlation exists is supported through direct comparisons of the test results for certain specific cable products. The proposed supplemental cable fire vulnerability data gained from examination of the equipment qualification results is presented. These results should be of particular interest to those engaged in the evaluation of fire risk for industrial facilities, including nuclear power plants. DOE

N93-13563*# Microwave Monolithics, Inc., Simi Valley, CA.

ADVANCED ON-CHIP DIVIDER FOR MONOLITHIC MICROWAVE VCO'S Final Report

Weddell C. Peterson May 1989 101 p

(Contract NAS7-1000; SBIR-14.06-6642A)

(NASA-CR-191355; NAS 1.26:191355) Avail: CASI HC A06/MF A02

High frequency division on a monolithic circuit is a critical technology required to significantly enhance the performance of microwave and millimeter-wave phase-locked sources. The approach used to meet this need is to apply circuit design practices which are essentially 'microwave' in nature to the basically 'digital' problem of high speed division. Following investigation of several promising circuit approaches, program phase 1 culminated in the design and layout of an 8.5 GHz (Deep Space Channel 14) divide by four circuit based on a dynamic mixing divider circuit approach. Therefore, during program phase 2, an 8.5 GHz VCO with an integral divider which provides a phase coherent 2.125 GHz reference signal for phase locking applications was fabricated and optimized. Complete phase locked operation of the monolithic GaAs devices (VCO, power splitter, and dynamic divider) was demonstrated both individually and as an integrated unit. The fully functional integrated unit in a suitable test fixture was delivered to NASA for engineering data correlation. Based on the experience gained from this 8.5 GHz super component, a monolithic GaAs millimeter-wave dynamic divider for operation with an external VCO was also designed, fabricated, and characterized. This circuit, which was also delivered to NASA, demonstrated coherent division by four at an input frequency of 24.3 GHz. The high performance monolithic microwave VCO with a coherent low frequency reference output described in this report and others based on this technology will greatly benefit advanced communications systems in both the DoD and commercial sectors. Signal processing and instrumentation systems based on phase-locking loops will also attain enhanced performance at potentially reduced cost. Author

N93-13569*# Illinois Univ., Urbana. Coordinated Science Lab.

BETA: BEHAVIORAL TESTABILITY ANALYZER AND ITS APPLICATION TO HIGH-LEVEL TEST GENERATION AND SYNTHESIS FOR TESTABILITY Ph.D. Thesis

Chung-Hsing Chen 19 Nov. 1992 113 p

(Contract NAG1-1613; SRC-92-DP-109)

(NASA-CR-191282; NAS 1.26:191282; UILU-ENG-92-2243; CRHC-92-25)

Copyright Avail: CASI HC A06/MF A02

In this thesis, a behavioral-level testability analysis approach is presented. This approach is based on analyzing the circuit behavioral description

(similar to a C program) to estimate its testability by identifying controllable and observable circuit nodes. This information can be used by a test generator to gain better access to internal circuit nodes and to reduce its search space. The results of the testability analyzer can also be used to select test points or partial scan flip-flops in the early design phase. Based on selection criteria, a novel Synthesis for Testability approach call Test Statement Insertion (TSI) is proposed, which modifies the circuit behavioral description directly. Test Statement Insertion can also be used to modify circuit structural description to improve its testability. As a result, Synthesis for Testability methodology can be combined with an existing behavioral synthesis tool to produce more testable circuits. Author

N93-13607 Iowa State Univ. of Science and Technology, Ames.
THE USE OF DEGRADATION MEASURES IN ASSESSING RELIABILITY Ph.D. Thesis
Chi-Hsien Joseph Lu 1992 242 p
Avail: Univ. Microfilms Order No. DA9223943

With today's high technology, traditional life tests for highly reliable products often result in few or even no failures. This makes it difficult to assess product reliability. For some products, degradation measures taken over time are useful for reliability assessment. By defining product failure in terms of a specified level of degradation, we study the distribution of time to failure for the degradation measures. We develop general statistical methods for using degradation measures to estimate a time-to-failure distribution. These methods employ Monte Carlo simulation to obtain point estimates and confidence intervals for reliability assessment and these can be used with a much more general and practical class of degradation models. An important application for degradation analysis, as an alternate approach in assessing reliability is in problems where few or even no failures are expected in a life test. It is thus of interest to know how degradation analysis compares with failure time analysis. We make such a comparison, in terms of relative efficiency: the ratio of the asymptotic variances of an estimated p quantile of time-to-failure distribution, by using a simple, by physically reasonable, degradation model. Even for such a simple model, the comparison is impossible to do analytically and we use numerical evaluation. We also look at how the number of inspections, the amount of measurement error, and the quantile of interest affect the asymptotic variance factor of the estimated percentile. We also describe and illustrate the computational and graphical methods for such a degradation analysis, and present the computer programs developed in the S language. We use fatigue crack growth data and a special case of Paris Law as degradation path model to illustrate the methods. Dissert. Abstr.

N93-13610*# Covalent Associates, Inc., Woburn, MA.
THERMALLY STABLE ELECTROLYTES FOR RECHARGEABLE LITHIUM BATTERIES, PHASE 2 Final Report, 1 Jan. - 31 Aug. 1989
L. A. Dominey, J. L. Goldman, and V. R. Koch 13 Sep. 1989 16 p
(Contract NAS7-967; SBIR-10.08-1140)
(NASA-CR-190878; NAS 1.26:190878) Avail: CASI HC A03/MF A01

During the second year of research under NASA SBIR Contract NAS7-967, Covalent Associates and NASA contract monitors at the Jet Propulsion Laboratory agreed to perform an evaluation of the three best electrolytes developed during Phase 2. Due to the extensive period of time required to collect meaningful cycling data, we realized the study would extend well beyond the original formal end of the Phase 2 program (August 31, 1988). The substitution of this effort in lieu of an earlier proposed 20-cell final deliverable is formally documented in Modification No. 1 of Contract NAS7-967 as task 7. This Addendum contains the results of the cycling studies performed at Covalent Associates. In addition, sealed ampoules of each of these three electrolytes were delivered to the Jet Propulsion Laboratory Electrochemical Power Group. Their concurrent evaluation in a different test vehicle has also been recently concluded and their results are also summarized herein. Author

N93-13650# Michigan Univ., Ann Arbor.
EXPLANATION-BASED KNOWLEDGE ACQUISITION OF ELECTRONICS Final Report
David E. Kieras 30 Aug. 1992 15 p
(Contract N00014-88-K-0133; DA Proj. RR0-4206)
(AD-A255069; FR-92/ONR-36) Avail: CASI HC A03/MF A01

This is the final report in a project that examined how knowledge of practical electronics could be acquired from materials similar to that appearing in electronics training textbooks, from both an artificial intelligence perspective and an experimental psychology perspective. Practical electronics training materials present a series of basic circuits accompanied by an explanation of how the circuit performs the desired function. More complex circuits are then explained in terms of these basic circuits. This material thus presents schema knowledge for individual circuit types in the form of explanations of circuit behavior. Learning from such material would thus consist of first instantiating any applicable schemas, and then constructing a new schema based on the circuit structure and behavior described in the explanation. If the basic structure of the material is an effective approach to learning, learning about a new circuit should be easier if the relevant schemas are available than not. This result was obtained for both an artificial intelligence system that used standard explanation-based learning mechanisms and with human learners in a laboratory setting, but the benefits of already having the relevant schemas were not large in these materials. The close examination of learning in this domain, and the structure of knowledge, should be useful to future cognitive analyses of training in technical domains. GRA

N93-13805 Colorado State Univ., Fort Collins.
A UNIFIED APPROACH TO THE ANALYSIS AND DESIGN OF MANIPULATOR SYSTEMS WITH ENVIRONMENTAL CONTACT Ph.D. Thesis
Thomas Michael Depkovich 1991 144 p
Avail: Univ. Microfilms Document No. DA9216184

While a great deal of emphasis has been placed on the development of higher performance manipulator systems, much less emphasis has been placed on techniques for the design of a manipulator system that accomplishes a set of specified tasks while minimizing system cost and maximizing system reliability. A major part of the reason for this is the difficulty of accurately modeling interactive tasks. Quasi-static models have developed previously, but these are insufficient for the design of a full manipulator system. More advanced strategies are required that take into account the dynamic performance of the manipulator system as a function of task performance. One primary result of this dissertation is to show that, given knowledge of the task geometry, environmental reaction forces can be naturally incorporated into the equations of motion for a manipulator system. This result is then extended to show that task success or failure can be determined as a function of the integrated equations of motion. This result establishes the framework for an optimal design process that selects subsystem parameters as function of key system states that determine task success or failure. Trial-and-error, approximation, and analytical approaches to this general problem are discussed, and two simplified manipulator system examples are presented to illustrate the basic concepts. Finally, it is shown that the results established extend naturally to the six-DOF cases. This extension to six-DOF includes both the general theory as well as the extension to tasks more complicated than simple insertion tasks laying the foundation for future work in this area.
Dissert. Abstr.

N93-13837# Massachusetts Inst. of Tech., Lexington.
PHYSICS AND TECHNOLOGY OF RESONANT-TUNNELING DEVICES Final Report, 1 May 1989 - 30 Apr. 1992
E. R. Brown 20 Jul. 1992 250 p
(AF Proj. 2305)
(AD-A255233; AFOSR-PD-89-0005) Avail: CASI HC A11/MF A03

Over the three-year course of this program, several issues in the device physics of resonant-tunneling diodes (RTDs) have been investigated, including the small-signal admittance, the shot noise, and the transport through multiple-quantum well structures. A large quantum-well inductance has been measured in the negative-differential-resistance region (NDR), but not in the positive-differential-resistance (PDR) region. The microwave shot-noise has been found to be suppressed relative to normal shot-noise in the PDR region, but enhanced in the NDR region. Triple-well RTDs have displayed a much wider NDR region in voltage than conventional single-well RTDs. Several new RTD material systems have been demonstrated including Type-2 InAS/AlSb and Type-1 GaSb/AlSb, the first of which has yielded excellent properties for high-speed device applications. Studies of highly lattice mismatched InAs/AlSb RTDs on GaAs substrates have proven that the RTD characteristics are insensitive to a high density of dislocations. Finally, these results have been incorporated into the design of RTDs in high-frequency oscillators and high-speed switches. The

InGaAs/AlAs RTD has been optimized for application in a quasioptical fundamental-frequency oscillator operating above 200 GHz. The same material system has been used to make a low-power RTD load for heterojunction field-effect and bipolar transistors in high-performance digital integrated circuits. GRA

N93-13839# Army Lab. Command, Fort Monmouth, NJ. Electronics Technology and Devices Lab.
FIRST YEAR TESTING OF PROTOTYPE MAGNESIUM/MANGANESE DIOXIDE BA-4590/U BATTERY Research and Development Technical Report, Sep. 1990 - Sep. 1991
Louis P. Jarvis Jun. 1992 27 p
(AD-A255503; SLCET-TR-92-4) Avail: CASI HC A03/MF A01

A prototype magnesium/manganese dioxide battery, the BA-4590/U, was developed as a training battery replacement for the costly lithium BA-5590/U. At room temperature (21.1 C) the magnesium battery is cost-effective at 1.50 amperes and below. During continuous usage, delivered capacity of the lithium BA-5590/U exceeded that of the magnesium battery by at least 62 percent. Under SINCGARS radio simulation testing, delivered capacity of the lithium battery exceeded that of the magnesium battery by at least 300 percent. GRA

N93-13865# Magnavox Government and Industrial Electronics Co., Mahwah, NJ. Electro-Optical Systems.
MILLIMETER-WAVE QUASI-OPTICAL AND SPATIAL POWER COMBINING TECHNIQUES Final Report
Kai Chang 10 Aug. 1992 66 p
(Contract DAAL03-89-K-0085)
(AD-A255438) Avail: CASI HC A04/MF A01

This report summarizes the research activities carried out in Electromagnetics and Microwave Laboratory, Department of Electrical Engineering, Texas A and M University. The project was sponsored by the U.S. Army Research Office under contract No. DAALO389-K-0085. The topics of investigation included active antenna elements, spatial power combining and injection-locking, quasi-optical components, novel planar slotline and coplanar waveguide circuits, and other circuit developments and analyses. A list of publications and a report of invention are included. GRA

N93-14034# State Univ. of New York, Buffalo. Space Power Insulation Inst.
[ACTIVITIES OF SPACE POWER INSULATION INST.] Annual Report No. 1
W. J. Sarjeant 14 Aug. 1992 38 p
(Contract N00014-91-J-4114)
(AD-A255825) Avail: CASI HC A03/MF A01

High frequency, high voltage properties of electrical insulation for space applications have been characterized for the first time at high field and voltage levels - to frequencies up to 30 kilohertz and voltages to 5 kilovolts. Degradation has been observed at these high frequencies (as will be used in voltage converters or are present in high frequency oscillations observed under insulation fault conditions - such as clearing in metallized capacitors) in the voltage withstand level implying significantly reduced life in such systems. This may be minimized for fluid impregnated systems as work this year shows marked reductions an aging rates for such systems wherein the fluid dielectric constants match or exceed those of the insulating materials. GRA

N93-14093 Purdue Univ., West Lafayette, IN.
MODELLING FLEXIBLE LINK MANIPULATORS IN THE THREE-DIMENSIONAL SPACE Ph.D. Thesis
David Kozel 1991 237 p
Avail: Univ. Microfilms Order No. DA9215586

The force/torque relationship between the joints and the end effector of flexible link manipulators is affected not only by the motion of the joints but also by translations and rotations of the links due to their bending and torsion effects. These inaccuracies in the force/torque relationship for flexible manipulators in the three-dimensional space are addressed. This thesis presents the development of a systematic technique for determining for force/torque relationship between the joints and the end effector for flexible link manipulators. The proposed technique accounts for link bending and torsion in the kinematic equations of a flexible manipulator while considering rigid hubs and tools attached to the ends of the links. A procedure for modelling link bending and torsion to within a desired accuracy has also been developed. The resulting model is independent of manipulator configuration. In this technique, vector cross products are used instead of partial derivatives. This reduces inaccuracies which result from approximations made in the kinematic equations when modeiling bending and torsion of the links. The magnitude and location of these inaccuracies are characterized. The validity of the proposed technique/procedure and the inaccuracies noted are demonstrated for link bending of a single-link planar manipulator by comparing simulations of the resulting force/torque relationships to results obtained experimentally; however, the experiments were not able to illustrate the torsion effect in the proposed model. Results indicate that the magnitude and location of the errors in the force/torque relationship are dependent upon the rotation due to link deformation, the 'length' of the rest of the manipulator, and the configuration of the manipulator. Although the proposed technique is able to account for the link bending and torsion effects in the kinematic equations of a flexible manipulator, it also suffers from several limitations. These include: translations and rotations due to link deformation are required to be 'small'; no analytical equation is given for determining the amount of error required to divide a link into elements nor is the exact location of the division given for the bending and torsion models; and the 'body forces' due to the weight of the links are not considered in the force/torque relationship. Dissert. Abstr.

N93-13176*# Hernandez Engineering, Inc., Greenbelt, MD.
PROPER BATTERY SYSTEM DESIGN FOR GAS EXPERIMENTS
Stephen A. Calogero *In* NASA. Goddard Space Flight Center, The 1992 Shuttle Small Payloads Symposium Oct. 1992 p 175-184 (For primary document see N93-13158 03-12)
Avail: CASI HC A02/MF A03

N93-13184*# National Aeronautics and Space Administration. Lewis Research Center, Cleveland, OH.
BATTERY SELECTION FOR SPACE EXPERIMENTS
David R. Francisco *In* NASA. Goddard Space Flight Center, The 1992 Shuttle Small Payloads Symposium Oct. 1992 p 267-276 (For primary document see N93-13158 03-12)
Avail: CASI HC A02/MF A03

34 FLUID MECHANICS AND HEAT TRANSFER

Includes boundary layers; hydrodynamics; fluidics; mass transfer; and ablation cooling.

For related information see also *02 Aerodynamics* and *77 Thermodynamics and Statistical Physics.*

N93-12569# Wisconsin Univ., Madison.
FLUID DYNAMICS OF SUPERCRITICAL HELIUM WITHIN CABLE-IN-CONDUIT CONDUCTORS
S. W. VanSciver 1 Jul. 1992 7 p
(Contract DE-FG02-88ER-52149)
(DE92-019516; DOE/ER-52149/4) Avail: CASI HC A02/MF A01

The enclosed report summarizes work carried out under DOE/MFE support during the past four years. Emphasis is placed on progress within the last year. Results of experiments on pressure drop and heat transfer within several cable-in-conduit conductors are described. These results are compared to models for flow in similar geometrics. The work provides a basis for design of magnets using the CIC conductor concept. DOE

N93-12617# Iowa Univ., Iowa City. Inst. of Hydraulic Research.
INTERACTION AND IMPACT OF FLOATING BODIES
Allen T. Chwang and Louis Landweber Jul. 1992 13 p
(Contract N00014-89-J-1581)
(AD-A254627; IIHR-357) Avail: CASI HC A03/MF A01

On the basis of two 1983 OPNAV instructions, S34705A entitled 'U.S. Navy Policy Regarding Arctic Polar Region' and S3470.6 entitled 'U.S. Navy Warfare program,' the U.S. Navy is preparing to operate its surface ships at high latitudes on a routine basis in support of the nation's Maritime Strategy. In addressing these operating requirements, the U.S. Navy must

evaluate the ability of its surface ships to fulfill their mission when operating near the ice edge in the marginal ice zone, and when entering an ice covered port with icebreaker assistance. As the Arctic has become a principal strategic location, knowledge and prediction of sea-ice conditions and the ability to cope with them have become essential to the U.S. Navy. The long-term goal of our research project is to investigate the hydrodynamic interactions, including central and oblique impact, between two floating bodies, or between a floating body and a fixed body. The floating body is usually an ice flow, and the fixed body is an offshore structure. GRA

N93-12677*# Old Dominion Univ., Norfolk, VA. Dept. of Chemistry and Biochemistry.

AB INITIO ATOMIC RECOMBINATION REACTION ENERGETICS ON MODEL HEAT SHIELD SURFACES Final Report, period ending 31 Aug. 1992

Fredrick Senese and Robert Ake Oct. 1992 24 p Submitted for publication

(Contract NCC1-147)

(NASA-CR-191210; NAS 1.26:191210) Avail: CASI HC A03/MF A01

Ab initio quantum mechanical calculations on small hydration complexes involving the nitrate anion are reported. The self-consistent field method with accurate basis sets has been applied to compute completely optimized equilibrium geometries, vibrational frequencies, thermochemical parameters, and stable site labilities of complexes involving 1, 2, and 3 waters. The most stable geometries in the first hydration shell involve in-plane waters bridging pairs of nitrate oxygens with two equal and bent hydrogen bonds. A second extremely labile local minimum involves out-of-plane waters with a single hydrogen bond and lies about 2 kcal/mol higher. The potential in the region of the second minimum is extremely flat and qualitatively sensitive to changes in the basis set; it does not correspond to a true equilibrium structure. Author

N93-12688*# Alabama Univ., Huntsville.

COMPUTATIONAL FLUID DYNAMICS COMBUSTION ANALYSIS EVALUATION Final Report

Y. M. Kim, H. M. Shang, C. P. Chen, and J. P. Ziebarth Apr. 1992 94 p

(Contract NAS8-36955)

(NASA-CR-184326; NAS 1.26:184326; CCFD-92-02) Avail: CASI HC A05/MF A01

This study involves the development of numerical modelling in spray combustion. These modelling efforts are mainly motivated to improve the computational efficiency in the stochastic particle tracking method as well as to incorporate the physical submodels of turbulence, combustion, vaporization, and dense spray effects. The present mathematical formulation and numerical methodologies can be casted in any time-marching pressure correction methodologies (PCM) such as FDNS code and MAST code. A sequence of validation cases involving steady burning sprays and transient evaporating sprays will be included. For individual titles, see N93-12689 through N93-12689.

N93-12689*# SECA, Inc., Huntsville, AL.

ADAPTATION OF MULTIDIMENSIONAL GROUP PARTICLE TRACKING AND PARTICLE WALL-BOUNDARY CONDITION MODEL TO THE FDNS CODE Final Report

Y. S. Chen and R. C. Farmer *In* Alabama Univ., Computational Fluid Dynamics Combustion Analysis Evaluation Apr. 1992 22 p (For primary document see N93-12688 03-34)

(SECA-TR-92-06) Avail: CASI HC A03/MF A01

A particulate two-phase flow CFD model was developed based on the FDNS code which is a pressure based predictor plus multi-corrector Navier-Stokes flow solver. Turbulence models with compressibility correction and the wall function models were employed as submodels. A finite-rate chemistry model was used for reacting flow simulation. For particulate two-phase flow simulations, a Eulerian-Lagrangian solution method using an efficient implicit particle trajectory integration scheme was developed in this study. Effects of particle-gas reaction and particle size change to agglomeration or fragmentation were not considered in this investigation. At the onset of the present study, a two-dimensional version of FDNS which had been modified to treat Lagrangian tracking of particles (FDNS-2DEL) had already been written and was operational. The FDNS-2DEL code was too slow for practical use, mainly because it had not been written in a form amenable to vectorization on the Cray, nor was the full three-dimensional form of FDNS utilized. The specific objective of this study was to reorder to calculations into long single arrays for automatic vectorization on the Cray and to implement the full three-dimensional version of FDNS to produce the FDNS-3DEL code. Since the FDNS-2DEL code was slow, a very limited number of test cases had been run with it. This study was also intended to increase the number of cases simulated to verify and improve, as necessary, the particle tracking methodology coded in FDNS. Author

N93-12708# Grenoble Univ. (France).

NATO ADVANCED RESEARCH WORKSHOP: VORTEX FLOWS AND RELATED NUMERICAL METHODS. LIST OF PARTICIPANTS, BOOK OF ABSTRACTS, AND INSTRUCTIONS FOR SUBMISSION TO THE PROCEEDINGS [ECOULEMENTS TOURBILLONNAIRES ET METHODES NUMERIQUES. LISTE DES PARTICIPANTS, RESUMES, ET FORMAT POUR LES ACTES]

Jun. 1992 55 p Workshop held in Grenoble-St. Pierre de Chartreuse, France, 15-19 Jun. 1992

(Contract DAJA45-92-M-0240)

(AD-A255015; R/D-6944-AN-03) Avail: CASI HC A04/MF A01

The following topics are covered: Vortex generation by suction in a rotating tank; Viscous splitting of the Navier-Stokes equation with boundaries; A Particle in Cell Method for the compressible Euler equation; A hybrid vortex method with deterministic diffusion; Three-dimensional(3D) vortex dynamic in a free shear flows; and Dynamics of vortex tubes in 3D turbulence. Additionally, a list of the confer ence's participants is provided. GRA

N93-12711# Pacific Northwest Lab., Richland, WA.

CAPILLARY ELECTROPHORESIS: ELECTROSPRAY IONIZATION MASS SPECTROMETRY IN SMALL DIAMETER CAPILLARIES

J. H. Wahl, D. R. Goodlett, H. R. Udseth, and R. D. Smith Jun. 1992 3 p Presented at the 40th ASMS Conference on Mass Spectrometry and Allied Topics, Washington, DC, 31 May - 2 Jun. 1992

(Contract DE-AC06-76RL-01830)

(DE92-019123; PNL-SA-20440; CONF-9205196-6) Avail: CASI HC A01/MF A01

Methods (such as small inner diameter capillaries) are being explored to increase analyte sensitivity in capillary electrophoresis-electrospray ionization/mass spectroscopy (CE-ESI/MS). Results are reported for melittin in a protein mixture, with 10 to 100 micron ID capillaries and for a mixture of aprotinin, cytochrome c, myoglobin, and carbonic anhydrase, with 5 to 50 micron ID capillaries. It is shown that an increase in solute sensitivity occurs when small ID capillaries (less than 20 microns) are used in CE-ESI/MS for both a peptide and a protein mixture. DOE

N93-12717*# Institute for Computer Applications in Science and Engineering, Hampton, VA.

ON THE PREDICTION OF TURBULENT SECONDARY FLOWS Final Report

C. G. Speziale, R. M. C. So (Arizona State Univ., Tempe.), and B. A. Younis (City Univ., London, England) Oct. 1992 22 p Submitted for publication

(Contract NAS1-19480; RTOP 505-90-52-01)

(NASA-CR-189722; NAS 1.26:189722; ICASE-92-57) Avail: CASI HC A03/MF A01

The prediction of turbulent secondary flows, with Reynolds stress models, in circular pipes and non-circular ducts is reviewed. Turbulence-driven secondary flows in straight non-circular ducts are considered along with turbulent secondary flows in pipes and ducts that arise from curvature or a system rotation. The physical mechanisms that generate these different kinds of secondary flows are outlined and the level of turbulence closure required to properly compute each type is discussed in detail. Illustrative computations of a variety of different secondary flows obtained from two-equation turbulence models and second-order closures are provided to amplify these points. Author

N93-12761# Westinghouse Idaho Nuclear Co., Inc., Idaho Falls.

FLUIDIC SAMPLING

E. D. Houck 20 Apr. 1992 11 p Presented at the Spectrum 1992 Nuclear and Hazardous Waste Management International Topical Meeting,

Boise, ID, 23-27 Aug. 1992
(Contract DE-AC07-84ID-12435)
(DE92-017266; WINCO-11813; CONF-920851-50) Avail: CASI HC A03/MF A01

This paper covers the development of the fluidic sampler and its testing in a fluidic transfer system. The major findings of this paper are as follows. Fluidic jet samples can dependably produce unbiased samples of acceptable volume. The fluidic transfer system with a fluidic sampler in-line will transfer water to a net lift of 37.2-39.9 feet at an average ratio of 0.02-0.05 gpm (77-192 cc/min). The fluidic sample system circulation rate compares very favorably with the normal 0.016-0.026 gpm (60-100 cc/min) circulation rate that is commonly produced for this lift and solution with the jet-assisted airlift sample system that is normally used at ICPP. The volume of the sample taken with a fluidic sampler is dependant on the motive pressure to the fluidic sampler, the sample bottle size and on the fluidic sampler jet characteristics. The fluidic sampler should be supplied with fluid having the motive pressure of the 140-150 percent of the peak vacuum producing motive pressure for the jet in the sampler. Fluidic transfer systems should be operated by emptying a full pumping chamber to nearly empty or empty during the pumping cycle, this maximizes the solution transfer rate. DOE

N93-12825# Lawrence Livermore National Lab., CA.
HEAT TRANSFER IN A LIQUID METAL CRUCIBLE WITH AN INTEGRAL BLACKBODY CAVITY
M. A. Havstad 15 May 1992 39 p
(Contract W-7405-eng-48)
(DE92-019640; UCRL-LR-110322) Avail: CASI HC A03/MF A01

Calculations of the heat transfer in a liquid metal crucible with an integral blackbody cavity have been made using two- and three-dimensional finite element techniques. Computations of thermal gradients and radiant heat exchange out of the cavity are combined to estimate cavity apparent emissivity (or quality) in a total hemispherical sense. We adjusted the model to estimate quality in a normal total sense, and then we used the Planck function to estimate normal spectral quality over the wavelength range 0.4 to 10 microns. Because of the small cavity size, its proximity to the crucible's heat source, and the conductivity of the crucible material, the estimated cavity quality is high, greater than 98 percent. The crucible design analyzed here was employed in an apparatus for the measurement of the normal spectral emissivity and optical constants of liquid uranium and aluminum. We found the results to be conservative. DOE

N93-12839# Lawrence Livermore National Lab., CA.
AN ATTEMPT AT A STATUS REPORT ON A FAST-MOVING TARGET: CFD
P. M. Gresho 22 Apr. 1992 18 p Presented at the First World Conference in Applied Computational Fluid Dynamics, Basel, Switzerland, 24-28 May 1992
(Contract W-7405-eng-48)
(DE92-017432; UCRL-JC-110809; CONF-9205119-1) Avail: CASI HC A03/MF A01

It is of course impossible for a single individual to give an objective state of the art report on all interesting topic - CFD or otherwise. Even a committee would probably be somewhat 'subjective' or at least biased. Thus the following semi-objective report is limited to those items about which I have at least a passing interest in and - hopefully - a modicum of knowledge about. It is also limited by time constraints, both for preparation of this abstract and for presentation at the meeting. The following items are addressed - to some extent below and to some other extent in the lecture: (1) Some Important Issues in Viscous Incompressible Flow; (2) Outflow Boundary Conditions; (3) The Differential-Algebraic Equations of Incompressible Flow; (4) Advection-Diffusion; (5) Control Volume/Finite Volume vis-a-vis Finite Element; (6) The Dynamics of Numerics; and (7) Contemporary Quotations concerning CFD. While incomplete, it is hoped that a reasonable sampling of some of the key issues in incompressible CFD are addressed. DOE

N93-12912# Lawrence Livermore National Lab., CA.
COMPARISON OF TWO STOCHASTIC MODELS OF SCALAR DIFFUSION IN TURBULENT FLOW
H. C. Rodean, R. Lange, J. S. Nasstrom (EG and G Energy Measurements, Inc., Pleasanton, CA.), and V. P. Gavrilov (Institute of Experimental Meteorology, Obninsk, USSR) Jul. 1992 6 p Presented at the 10th Symposium on Turbulence and Diffusion, Portland, OR, 29 Sep. - 2 Oct. 1992
(Contracts W-7405-eng-48; DE-AC08-88NV-10617)
(DE92-019381; UCRL-JC-110377; CONF-9209158-3) Avail: CASI HC A02/MF A01

This report describes and compares two Lagrangian stochastic models for turbulent diffusion: (1) the random velocity increment model based on the Langevin equation; and (2) the random displacement model. We apply both models to identical test problems for one-dimensional (vertical) diffusion, using identical parameterizations of turbulence statistics as inputs. We compare the results and discuss the advantages and disadvantages of each model. This work is part of an effort to improve the ADPIC dispersion model which is based on the eddy diffusivity model. It is also part of a cooperative research effort on the transport and dispersion of hazardous materials in the atmosphere by the Lawrence Livermore National Laboratory and the Institute of Experimental Meteorology (USSR). DOE

N93-12975# Maryland Univ., College Park. Dept. of Mechanical Engineering.
DIFFUSION-ABSORPTION HEAT PUMP Annual Report, Nov. 1990 - Oct. 1991
Lie Wang and Keith E. Herold Jun. 1992 119 p
(Contract GRI-5090-260-2041)
(PB92-217538; GRI-92/0262) Avail: CASI HC A06/MF A02

The diffusion-absorption heat pump offers advantages including no moving parts, noise and vibration free operation and operation without electric power. An example of such a cycle is the gas-fired domestic refrigerator. The cycle is similar to an absorption cycle but differs in that an auxiliary gas is used to equalize the pressures throughout the system and to allow a heat driven bubble pump. A modeling study of several cycle variations of diffusion-absorption heat pump technology was conducted to calculate the potential for improving cycle performance. A computer simulation model was developed for each of the cycle variations. Thermodynamic and transport property models were developed for the ammonia/water working fluid with both hydrogen and helium as the pressure equalizing gas. The modeling results are presented for helium. The major conclusions of the study are also valid for hydrogen. The inert gas charge pressure as well as the effectiveness of the auxiliary gas heat exchanger (AGHX) were found to have a significant influence on coefficient of performance (COP). Detailed modeling of the influence of the AGHX on the COP of the cycle was performed. In addition to the thermodynamic model, fluid and heat transfer models for the AGHX have been developed. The integration of cycle fluid and heat transfer models was performed in order to examine the coupling of the components. GRA

N93-12996# EG and G Energy Measurements, Inc., Idaho Falls.
TURBULENT NATURAL CONVECTION BETWEEN A PERFORATED VERTICAL CYLINDER AND A SURROUNDING ARRAY
D. M. McEligot, C. M. Stoots, W. A. Christenson, J. E. OBrien, D. C. Mecham, and W. G. Lussie 1992 10 p Presented at the Winter Annual Meeting of the ASME, Anaheim, CA, 8-13 Nov. 1992
(Contract DE-AC07-76ID-01570)
(DE92-019766; EGG-M-92200; CONF-921110-24) Avail: CASI HC A02/MF A01

A number of situations can be hypothesized to occur in an advanced or special purpose nuclear reactor such that the core is filled with a gas but there is no forced flow to remove the thermal energy evolved. Experiments were conducted by resistively heating a vertical circular cylinder of length-to-diameter ratio of about 160 centered inside a concentric perforated tube which was, in turn, surrounded by three larger diameter tubes cooled internally with water flow. The ratio of the test section temperature to the cooling tube temperature was varied up to 2.6; and the Rayleigh number, based on tube diameter and properties evaluated at the cooling tube temperature, ranged from 2.9(10)(exp 4) to 9.2(10)(exp 5). Results indicate that the convective heat transfer parameters for the perforated tube are about fifteen percent higher than for the smooth bare tube centered in the same position relative to the array. The Nusselt number for convective heat transfer across the annulus between the heated test section and the perforated tube corresponded to parallel laminar flow. DOE

N93-13017 Miami Univ., Coral Gables, FL.
QUANTITATIVE ANALYSIS OF THREE-DIMENSIONAL STEADY FLOW FIELD BY USING PARTICLE IMAGE VELOCIMETRY AND DIGITAL IMAGE PROCESSING METHOD Ph.D. Thesis
Jianxin Huang 1992 289 p
Avail: Univ. Microfilms Order No. DA9227204

An approach has been developed to quantitatively analyze steady incompressible flow field by using particle image velocimetry and digital image processing techniques. The fundamental laws of physics have been applied to analyze the image data. The accuracy of the results has been improved by calibrating camera in the analysis of the flow images. The images of the particles that visualize the field of a water channel flow are captured by using a CCD camera connected to an image processor and illuminated with a portable laser sheet. The images were taken from two orthogonal directions. Microsoft C language programs have been developed to manipulate the image grabbing and processing and extracting velocity data from the images. A procedure of camera calibration has been given. A uniform flow experiment and a two-dimensional flow experiment have been done to verify the method. The results of the experiment of flow past a half-body are analyzed by the comparison between the theoretical data and the experimental results. Dissert. Abstr.

N93-13074# Florida Univ., Gainesville.
STUDIES OF GRANULAR FLOW DOWN AN INCLINED CHUTE
D. M. Hanes 1992 21 p
(Contract DE-AC22-91PC-90182)
(DE92-018871; DOE/PC-90182/T5) Avail: CASI HC A03/MF A01

A preliminary series of experiments were run in order to examine the effects sidewalls have on the steady-state mass flow rate of granular material in a rectangular, inclined chute. These experiments also serve to assess the problems associated with the initial operation of the granular flow apparatus. Presumably, the friction between the sidewalls and the flowing material will slow the flow rate of that material. The relative effect of the sidewalls should decrease with increasing width for a given flow entrance condition. For instance, when the width of the chute is at a minimum (one grain diameter), the sidewalls will have a maximum frictional effect. And as the width approaches infinity, the sidewalls will have a minimum frictional effect. It is desired to know at what chute widths the sidewall effects will reasonably approach this minimum, if this condition can even be approached with the existing apparatus. The relationship between chute width and flow rate will be important to know during more involved experiments which will follow this initial investigation. These experiments will include the measurement of localized grain density, local velocity and individual grain dynamics (rotation and translation) and collisions. The secondary objective, to observe and correct problems with the system, is a more general and qualitative goal. DOE

N93-13120 Arizona Univ., Tucson.
SPANWISE-NONUNIFORM EXCITATION OF A PLANE MIXING LAYER Ph.D. Thesis
Kris Jacob Nygaard 1991 165 p
Avail: Univ. Microfilms Order No. DA9127713

The formation and evolution of secondary vortical structures in a plane mixing layer subjected to spanwise-nonuniform excitation was studied in a closed-return water facility. It is shown that secondary vortices may result from spanwise-nonuniformities in the nominally two-dimensional vorticity layer close to the flow partition, or from spanwise core deformations of the primary vortices further downstream. These distinctly different mechanisms are excited by time-harmonic wavetrains with spanwise amplitude or phase variations, respectively, synthesized by a mosaic of surface film heaters flush-mounted on the flow partition. The appearance of the secondary vortical structures is accompanied by significant distortions in transverse distributions of the streamwise velocity component. Inflection points, which are not present in corresponding velocity distributions of the unforced flow, suggest the formation of locally unstable regions of large shear in which broadband perturbations, already present in the base flow, undergo rapid amplification. This amplification is followed by breakdown to turbulence thus producing the small-scale motion necessary for mixing transition. The present investigation further shows that the flow is extremely receptive to spanwise-periodic amplitude excitation at any wavelength synthesizable by the heater mosaic. Spanwise-periodic phase excitation leads to substantial deformations of the primary vortices, although the receptivity of the flow appears to have a short wavelength cutoff. Spanwise-nonuniform amplitude and phase excitations at a subharmonic frequency of the Kelvin-Helmholtz instability result in complex pairing interactions of the primary vortices. Dissert. Abstr.

N93-13199# Advisory Group for Aerospace Research and Development, Neuilly-Sur-Seine (France). Fluid Dynamics Panel.
AERODYNAMIC ENGINE/AIRFRAME INTEGRATION FOR HIGH PERFORMANCE AIRCRAFT AND MISSILES [L'INTEGRATION AERODYNAMIQUE DES MOTEURS ET DES CELLULES DANS LES AVIONS ET LES MISSILES A HAUTES PERFORMANCES]
Sep. 1992 449 p In ENGLISH and FRENCH Symposium held in Fort Worth, TX, 7-10 Oct. 1991
(AGARD-CP-498; ISBN-92-835-0672-3) Copyright Avail: CASI HC A19/MF A04

The objective of the symposium was to review the state-of-the-art in aerodynamic engine/airframe integration techniques and to report on the progress which has been achieved during engineering project work in recent years. Because the treatment of this subject requires an interdisciplinary approach, both experimentalists and theoreticians were invited to contribute to the meeting. Six sessions were organized to cover the essential subdisciplines requiring aerodynamic engine/airframe integration during the concept-assessment and design phases for new aerospace vehicles. For individual titles, see N93-13200 through N93-13231.

N93-13200# Aircraft Research Association Ltd., Bedford (England).
TEST TECHNIQUES FOR ENGINE/AIRFRAME INTEGRATION
A. E. Harris *In* AGARD, Aerodynamic Engine/Airframe Integration for High Performance Aircraft and Missiles Sep. 1992 17 p (For primary document see N93-13199 03-34)
Copyright Avail: CASI HC A03/MF A04

The paper traces a path through modern experimental techniques in use for the study of installation performance in the context of military and civil engine/airframe integration studies. For military and civil transport designs it is shown that separate treatment of air intake and exhaust regions is generally undertaken in contemporary methods. An early entry into the aerodynamics of the complete engine/airframe is emphasized in order to avoid costly integration difficulties. Using examples largely drawn from direct experience gained during the period 1960 to 1990 the author presents a set of 'most preferred methods' for use in high speed configuration development model tests. It is noted that current trends in civil and military designs require increased attention to be paid to off-axis thrust/drag/lift variations in the engine/airframe integration process. Methods of flow visualization are briefly reviewed and the emerging laser methods are also identified. The paper closes with a conceptual configuration for a year 2000 totally integrated engine/airframe to meet 21st century civil transport mass transit requirements. Author

N93-13201# Office National d'Etudes et de Recherches Aerospatiales, Paris (France).
TESTS OF MODELS EQUIPPED WITH TPS IN LOW SPEED ONERA F1 PRESSURIZED WIND TUNNEL [ESSAIS DE MAQUETTES MOTORISEES EQUIPEES DE SIMULATEURS DE REACTEURS DANS LA SOUFFLERIE BASSE VITESSE PRESSURISEE F1, DE L'ONERA]
J. Leynaert *In* AGARD, Aerodynamic Engine/Airframe Integration for High Performance Aircraft and Missiles Sep. 1992 5 p In FRENCH Previously announced in IAA as A92-26371 (For primary document see N93-13199 03-34)
Copyright Avail: CASI HC A01/MF A04

The particular conditions of tests of models equipped with a turbofan powered simulator (TPS) at high Reynolds numbers in a pressurized wind tunnel are presented. The high-pressure air supply system of the wind tunnel, the equipment of the balance with the high-pressure traversing flow and its calibration, and the thrust calibration method of the TPS and its verification in the wind tunnel are described. Author

N93-13202# Societe Nationale d'Etudes et de Construction de Moteurs Aeronautiques, Moissy-Cramayel (France). Centre de Villaroche.
NUMERIC SIMULATION OF THE AERODYNAMIC FLOWS AROUND NACELLES [SIMULATION NUMERIQUE DE L'ECOULEMENT AERODYNAMIQUE AUTOUR DES NACELLES]
J. L. Lecordix, J. G. Fratello, and J. M. Gippet *In* AGARD, Aerodynamic

Engine/Airframe Integration for High Performance Aircraft and Missiles Sep. 1992 14 p In FRENCH (For primary document see N93-13199 03-34)

Copyright Avail: CASI HC A03/MF A04

With the aim of reducing the number and the cost of its tests, SNECMA obtained a three-dimensional Euler code. This code solves the Euler compressible equations put into conservative form, and at convergence is able to predict the aerodynamic flows around complex multidomain geometries. The numerical algorithm is of the finite volume type and is second order in time with a 2-step predictor-corrector approach. In addition, it uses a local time step and an artificial viscosity of the TURKEL-JAMESON type. This method was validated by calculations on isolated nacelles and the numerical results obtained reflected in a satisfactory manner those resulting from the tests. This code has been industralized and today allows the analysis of the aerodynamic lines of nacelles. Transl. by FLS

N93-13203# Office National d'Etudes et de Recherches Aerospatiales, Paris (France).

DETAILED ANALYSIS OF WING-NACELLE INTERACTION FOR COMMERCIAL TRANSPORT AIRCRAFT [ANALYSE DETAILLEE DE L'INTERACTION VOILURE-NACELLE D'UN AVION DE TRANSPORT CIVIL]

J. L. Godard, O.-P. Jacquotte, and D. Gisquet (Aerospatiale, Toulouse, France) *In* AGARD, Aerodynamic Engine/Airframe Integration for High Performance Aircraft and Missiles Sep. 1992 11 p In FRENCH Previously announced in IAA as A92-16122 (For primary document see N93-13199 03-34)

Copyright Avail: CASI HC A03/MF A04

An experimental setup has been developed to study the wing-nacelle interaction of commercial transports during transonic operation. This stand allows the measurement of the overall loads, pressure distribution on the model, and velocities in the field by laser velocimetry. The analysis gives a better understanding of the wing-nacelle interaction and provides the best comparative elements for modeling calculations. IAA

N93-13204# Deutsche Forschungsanstalt fuer Luft- und Raumfahrt, Brunswick (Germany). Inst. fuer Entwurfsaerodynamik.

INVESTIGATION OF INTERFERENCE PHENOMENA OF MODERN WING-MOUNTED HIGH-BYPASS-RATIO ENGINES BY THE SOLUTION OF THE EULER-EQUATIONS

C.-C. Rossow and A. Ronzhelmer *In* AGARD, Aerodynamic Engine/Airframe Integration for High Performance Aircraft and Missiles Sep. 1992 11 p (For primary document see N93-13199 03-34)

Copyright Avail: CASI HC A03/MF A04

With the development of Ultra-High Bypass (UHB) engines the aerodynamic interference between airframe and engine becomes increasingly important. In this study the solution of the Euler equations is used to simulate the flow field around the DLR-ALVAST wing-body combination with different wing-mounted engines. For a CFM-56 engine, which is taken here to represent a conventional engine, the contributions of single components like engine, pylon, and jet to the aerodynamic interference were investigated. The comparison with the flow field around the wing-body combination without engine showed that the presence of the engine alone lead to a forward movement of the shock on the complete upper surface of the wing. The pylon mainly influenced the lower surface and caused an additional loss of lift which is of the same order of magnitude as the loss due to the engine. The simulation of an inviscid jet showed no significant influence for the conventional engine. A further comparison of the interference effects of the CFM-56 engine and a UHB engine was made. The geometry of the UHB engine corresponds to the DLR-CRUF simulator for Ultra-High Bypass engines. Due to the closer installation to the wing and the larger dimensions, the UHB engine caused a local flow acceleration on the lower surface of the wing. This lead to a significant loss of lift at the engine position, compared to the conventional engine. Simulation with and without jet revealed that the jet was mainly responsible for this behavior. In case of the UHB engine the jet passed very closely under the wing and the displacement effect of the jet caused a strong flow acceleration.

Author

N93-13205# National Aerospace Lab., Amsterdam (Netherlands).

AERODYNAMIC ANALYSIS OF SLIPSTREAM/WING/NACELLE INTERFERENCE FOR PRELIMINARY DESIGN OF AIRCRAFT CONFIGURATIONS **c02**

C. M. vanBeek, W. J. Piers, and B. Oskam *In* AGARD, Aerodynamic Engine/Airframe Integration for High Performance Aircraft and Missiles Sep. 1992 20 p Sponsored by Netherlands Agency for Aerospace Programs (For primary document see N93-13199 03-34)

Copyright Avail: CASI HC A03/MF A04

A panel method based model for the computation of the time-averaged influence of a propeller slipstream on the aerodynamic characteristics of an aircraft configuration is described. The slipstream model is based on the simplifications that the single-rotating propeller is replaced by an actuator disk and that all the vorticity of the slipstream is represented on a cylindrical sheet of fixed geometry which envelops the slipstream in combination with a discrete vortex at the axis of the slipstream. Appropriate jump conditions across the actuator disk and boundary conditions on the cylindrical sheet, solved simultaneously with the boundary conditions on the aircraft configuration, yield the mutual influence of the propeller and the slipstream on the aerodynamic characteristics of the aircraft configuration. This slipstream model is incorporated in a three-dimensional panel method. Computed lift increments due to the slipstream are presented for a realistic wing/nacelle/fuselage-configuration and compared with wind-tunnel data for several thrust coefficients and angles of attack of the aircraft. Author

N93-13206# Vigyan Research Associates, Inc., Hampton, VA.

EULER ANALYSIS OF TURBOFAN/SUPERFAN INTEGRATION FOR A TRANSPORT AIRCRAFT

D. A. Naik, H. C. Chen (Boeing Co., Seattle, WA.), T. Y. Su (Boeing Co., Seattle, WA.), and T. J. Kao (Boeing Co., Seattle, WA.) *In* AGARD, Aerodynamic Engine/Airframe Integration for High Performance Aircraft and Missiles Sep. 1992 12 p (For primary document see N93-13199 03-34)

Copyright Avail: CASI HC A03/MF A04

A three-dimensional general multi-block Euler solver (GMBE) has been developed to analyze the propulsion integration effects of turbofan/superfan installations. Either flow-through or powered nacelles can be modelled. The code is demonstrated on a generic NASA low wing transport model with an advanced turbofan flow-through nacelle. The results compare favorably with experimental data obtained in the NASA Langley 16-Foot (4.88 m) Transonic Tunnel. The computed pressure distributions are used to identify, in terms of pressure coefficient peaks (maximum negative values) and gradients, undesirable flow regions in the vicinity of the pylon and nacelle. The results suggest that a change in toe angle and pylon trailing edge closure geometry will improve the propulsion integration. Author

N93-13207# Deutsche Airbus G.m.b.H., Bremen (Germany).

RECENT DEVELOPMENTS IN LOW-SPEED TPS-TESTING FOR ENGINE INTEGRATION DRAG AND INSTALLED THRUST REVERSR SIMULATION **c05**

W. Burgsmueller, C. Castan (Aerospatiale, Toulouse, France), J. W. Kooi (Duits-Nederlandse Windtunnel, North East Polder.), and J. P. Becle (Office National d'Etudes et de Recherches Aerospatiales, Paris, France) *In* AGARD, Aerodynamic Engine/Airframe Integration for High Performance Aircraft and Missiles Sep. 1992 15 p (For primary document see N93-13199 03-34)

Copyright Avail: CASI HC A03/MF A04

In accordance with the steady increase in bypass ratio and hence fan nacelle diameter of engines for modern transport aircraft, also the investigation of engine-airframe interference effects is of increasing importance. This covers not only the interferences between the wing and nacelle plus pylon bodies, but also the effects due to the presence of the engine jet flow field. In the low speed range of an aircraft, i.e., take-off, second segment climb, landing and roll out with thrust reversing, the jet interference investigations require wind tunnels with special high quality equipment, highly instrumented models with engine simulators and test setups outside the tunnel for special investigations. Concerning the different possibilities for engine simulation, the use of turbine-powered-simulators (TPS) has proven as the best and most flexible instrument. The paper presented here describes the technical progress made in the last years in testing techniques, based on close cooperation between Deutsche Airbus, Aerospatiale, DNW and ONERA. Further, a survey about the possible

applications for low speed jet interference testing is given, mainly based on the Airbus A340 development program. Finally, some of these recent test results concerning performances and understanding of the aerodynamic and thermodynamic phenomena, especially concerning second segment climb jet interference, thrust reverser efficiency and plume reingestion effects are shown and discussed. It can be summarized, that a high level of technical test standard has been achieved and this together with a better understanding of the flow phenomena gives a viable basis for the integration of the coming generations of aircraft and engines. Author

N93-13208# Fokker B.V., Schipol-Oost (Netherlands). Aerodynamics and Aeroelasticity Dept.

AERODYNAMIC INTEGRATION OF THRUST REVERSERS ON THE FOKKER 100 **c05**

J. vanHengst *In* AGARD, Aerodynamic Engine/Airframe Integration for High Performance Aircraft and Missiles Sep. 1992 9 p (For primary document see N93-13199 03-34)

Copyright Avail: CASI HC A02/MF A04

The Fokker 100 is a twin engined T-tailed aircraft developed as a short to medium haul passenger and cargo transport. The engines are located on the aft fuselage. The development of thrust reversers on this type of aircraft was accomplished through different types of wind tunnel model tests and full scale tests. Model tests on an isolated exhaust configuration, scale 1:5, were conducted at Fluidyne in order to establish nozzle suppression and thrust reverser efficiency and side plume effects. Effects on directional and longitudinal stability characteristics were investigated by model tests on a complete mode, scale 1:12, in the LST of NLR. Reingestion tests were performed on the same complete model in the RR low speed facility at Hucknall. Attached photographs show the model in the NLR and RR facilities. This paper discusses the integration process, showing test results from wind tunnel model tests as well as full scale boiler plate and flight tests. A successful means to control side plume effects on the directional stability and a configuration change to suppress induced reverse plume empennage buffet is also discussed. Author

N93-13209# Universitaet der Bundeswehr Muenchen, Neubiberg (Germany). Inst. fuer Strahlantriebe.

OVERVIEW ON TEST CASES FOR COMPUTATION OF INTERNAL FLOWS IN TURBOMACHINES

Leonhard Fottner *In* AGARD, Aerodynamic Engine/Airframe Integration for High Performance Aircraft and Missiles Sep. 1992 5 p (For primary document see N93-13199 03-34)

Copyright Avail: CASI HC A01/MF A04

Aero engine component design and development makes increasing use of computer codes for flow field calculations, such as two- or three-dimensional flow fields and flow fields with strong viscous effects. The accuracy of these calculation methods depends on the mathematical models and numerical schemes used to describe the physical reality. The proof of validity and the refinement of such methods depend on verification against relevant test cases, primarily experimental test cases. The AGARD Propulsion and Energetics Panel established Working Group 18 to specify relevant reference test cases to serve as validation bases for new methods, but also as check for existing production codes. The present paper gives an overview on the results of the Working Group and briefly describes the different test cases. These test cases refer to analytical and experimental test cases for steady flow in linear compressor and turbine cascades, single blade rows, single and multistage axial compressors and turbines and ducts. In addition, suggestions for future tests designed to reduce the limitations are discussed. Author

N93-13210# Vrije Univ., Brussels (Belgium). Dept. of Fluid Mechanics.

THE PEP SYMPOSIUM ON CFD TECHNIQUES FOR PROPULSION APPLICATIONS

Ch. Hirsch *In* AGARD, Aerodynamic Engine/Airframe Integration for High Performance Aircraft and Missiles Sep. 1992 18 p (For primary document see N93-13199 03-34)

Copyright Avail: CASI HC A03/MF A04

This is part of the PEP contribution to the 69th FDP meeting on Aerodynamic Engine/Airframe Integration for High Performance Aircraft and Missiles. It presents an overview of the main outcomes of the last PEP meeting dealing with CFD techniques for propulsion applications. The emphasis was given to computational work on realistic 3D configurations, covering the four following topics: full 3D validations; full 3D numerical techniques; unsteady flows and multidimensional reacting flows. In addition, an invited paper from FDP on the state of the art of computational techniques for 3D Navier-Stokes equations and a technical evaluation of the meeting were presented. The most widely stressed conclusion was the urgent need for a large scale effort on validation of numerical accuracy and of physical models. Author

N93-13211# Motoren- und Turbinen-Union Muenchen G.m.b.H. (Germany).

THE INFLUENCE OF INTAKE SWIRL DISTORTION ON THE STEADY-STATE PERFORMANCE OF A LOW BYPASS, TWIN-SPOOL ENGINE

W. Meyer, W. Pazur (Universitaet der Bundeswehr Muenchen, Neubiberg, Germany), and Leonhard Fottner (Universitaet der Bundeswehr Muenchen, Neubiberg, Germany) *In* AGARD, Aerodynamic Engine/Airframe Integration for High Performance Aircraft and Missiles Sep. 1992 20 p (For primary document see N93-13199 03-34)

Copyright Avail: CASI HC A03/MF A04

Intakes of supersonic aircraft can produce intake swirl configurations in front of the engine which are important for intake/engine compatibility assessment throughout the flight envelope. The main objective of this investigation was to get more information about the influence of intake twin swirl on the steady-state engine behavior. The twin swirl was simulated using a movable delta wing positioned between the bellmouth intake and the engine. By changing the angle of attack of the delta wing, the intensity of the intake swirl could be varied. Increasing the intensity of the twin swirl resulted in a deterioration of engine performance. The analysis of the test results showed that these effects on engine performance were mainly due to a modified characteristic of the low pressure compressor (LPC). Therefore, it was very important to investigate the changed LPC performance to be able to understand the effects of an intake swirl distortion on the engine performance. Hence, an experimental method was set up to measure the performance map of the installed LPC by defined changing of the engine operating line. An analysis of experimentally determined compressor maps for varying intensities showed that the performance parameters of the LPC decrease. However, there is essentially no variation of the engine's working line due to an intake twin-swirl distortion. Semi-empirical calculations which took account of this influence of the generated swirl on the performance of the LPC confirmed the loss of engine performance observed during the engine tests. Author

N93-13212# Societe Nationale d'Etudes et de Construction de Moteurs Aeronautiques, Moissy-Cramayel (France).

FLIGHT ANALYSIS OF AIR INTAKE/ENGINE COMPATIBILITY [ANALYSE EN VOL DE LA COMPATIBILITE ENTREE D'AIR-MOTEUR] **c05**

H. Joubert and J. L. Eyraud *In* AGARD, Aerodynamic Engine/Airframe Integration for High Performance Aircraft and Missiles Sep. 1992 12 p In FRENCH (For primary document see N93-13199 03-34)

Copyright Avail: CASI HC A03/MF A04

Performance improvement of the combat aircraft/engine unit rests on the optimization of intake/engine compatibility. This optimization requires specific flight tests in which the loss of the pumping margin of the compressors due to distortion is determined. The general methodology for the intake/engine compatibility analysis is described from the first wind tunnel tests to the flight tests. In order to determine the loss of the pumping margin due to the distortion of the air intake, an extensive instrumentation set was installed on the Mirage 2000 (Dassault Aviation) aircraft equipped with the M53-P2 (SNECMA) engine. The test procedures as well as the processing of the nonstationary signals are described. The correlations binding the nonstationary coefficients of distortion to the loss of pumping margin of the low pressure compressor are presented. It is shown that a correlation to only one parameter makes it possible to reach an accuracy of plus or minus 2 percent. On the other hand, the use of a correlation of two parameters (circumferential and radial) makes it possible to reduce the precision to plus or minus 1 percent. The use of an engine test stand in an altitude chamber with channels simulating nonstationary distortion makes it possible to reproduce in a satisfactory way the phenomena observed in flight and, in particular, to measure values of sensitivity to the

distortion similar to the values obtained in flight. This method makes it possible to improve the optimization of the engine while reducing the number of flight tests. Transl. by FLS

N93-13213# Aircraft Research Association Ltd., Bedford (England).
ASTOVL MODEL ENGINE SIMULATORS FOR WIND TUNNEL RESEARCH **c09**
A. E. Harris, G. L. Wilde (TKD Ltd., England), V. J. Smith (TKD Ltd., England), A. R. G. Mundell (Defence Research Agency, Farnborough, England), and D. P. Davidson (Rotadata Ltd., Derby, England) *In* AGARD, Aerodynamic Engine/Airframe Integration for High Performance Aircraft and Missiles Sep. 1992 10 p (For primary document see N93-13199 03-34)
Copyright Avail: CASI HC A02/MF A04

Feasibility studies have been conducted into the use of military turbine powered simulators (MTPS) for wind tunnel research on typical Harrier/AV8B and ASTOVL aircraft. The MTPS approach has shown significant promise for full simulation of inlet airflow ratio and nozzle thrust representations. The studies were made in two parts. In the first instance, simulation of the basic Pegasus of the Harrier/AV8B was examined. A simulator at 1 to 7.5 model scale using compressed air drive has been shown to be feasible. The design develops 467 SHP and is well adapted for use in available high-speed and low-speed wind tunnels. In the low-speed facility, a strut mounted arrangement coupled to the existing external force balance presents only minor difficulties; for the high-speed tunnel further work is required to develop/refine an internal balance/sting arrangement. Overboard bleed is used in an optimized manner to match cycle requirements to the need for minimum compressed air feed and bleed cross sectional area. In subsequent studies, cycles and layouts appropriate to the evolving ASTOVL powerplants have been examined. It is shown that MTPS designs can be developed to match a representative ASTOVL layout although compromises may be required to the support strut design to suit airfeed and bleed requirements. This paper concludes with a recommendation for a staged evolution of ASTOVL model simulations which is geared to a realistic ASTOVL project timescale in a cost effective manner. Author

N93-13214# Alenia Aeronautica, Torino (Italy). Defence Aircraft Div.
MASS FLOW EFFECTS ON THE LOW SPEED CHARACTERISTICS OF AN ADVANCED COMBAT AIRCRAFT **c02**
E. Barbantini, A. Ferretti, and A. Gatti *In* AGARD, Aerodynamic Engine/Airframe Integration for High Performance Aircraft and Missiles Sep. 1992 7 p (For primary document see N93-13199 03-34)
Copyright Avail: CASI HC A02/MF A04

The experimental results obtained on a low speed six components wind tunnel model representative of a delta-canard configuration and featuring an ejector based internal flow augmentation system are described in order to outline at what extent the near field distortions induced by the intake operating conditions can modify the aircraft aerodynamic stability characteristics and foreplane control effectiveness. Author

N93-13215# Messerschmitt-Boelkow-Blohm G.m.b.H., Munich (Germany). Military Aircraft Div.
A NOVEL-HIGH-PERFORMANCE SYSTEM FOR RECORDING AND ANALYSING INSTANTANEOUS TOTAL PRESSURE DISTORTION IN AIR INTAKES **c35**
K. W. Lotter and R.-D. Scherbaum *In* AGARD, Aerodynamic Engine/Airframe Integration for High Performance Aircraft and Missiles Sep. 1992 16 p (For primary document see N93-13199 03-34)
Copyright Avail: CASI HC A03/MF A04

Instantaneous intake total pressure distortion parameters are generally used to assess aerodynamic intake-engine compatibility. Different distortion parameters are applied by the various engine manufacturers. Distortion boundaries are specified which are not to be exceeded in the intake during the whole flight regime. The quantification of those parameters is generally made in intake wind-tunnel model tests. In these tests the instantaneous total pressure is measured in the Aerodynamic Interface Plane (AIP) (a short distance upstream of the engine compressor face) by high-response pressure transducers, typically installed on an eight-arm rake with five probes on each arm. In the past, after having undergone the relevant signal conditioning process, the signals from the transducers were combined to the above-mentioned distortion parameters by the use of an analog computer. Later on, this was supplemented by limited digital analysis of the high-frequency signals. Because of the large amount of data, the digital analysis was only applied over a predetermined short time period. The evolution of high-performance digital data storage facilities combined with highspeed analog-digital conversion now allows a major step forward to longtime digital recording and analysis during intake distortion tests. The novel system that has been installed at MBB and successfully applied during various intake wing-tunnel test campaigns is described. Dynamic signals from up to 144 high-response differential transducers can be recorded. Individual control lines are used for sensing, power supply, and in-situ calibration. A specially configured computer system is used to control the signal frequency band, the number of signal channels, the control lines, and the sample rate. The computer is also used to control the storage of the digitized data on an advanced high density tape recording system that allows continuous recording of up to 1 hour on a cassette tape. The data rate for tape storage is as high as 107 Mbits/s. Parallel to this storage process it is possible to calculate, in an on-line real-time mode, the desired instantaneous distortion parameters using an analog computer. For recording times of up to 5 seconds for each data point, digital on-line analysis is also possible. The data can be displayed on a screen and are also plotted during the test, thus allowing the test engineer to react quickly and alter or adapt the test program. Typical results from tests with different intake models in various wind-tunnel facilities are presented. The effect of digitization rate and recording time on the error of the calculated instantaneous distortion parameters is shown. Author

N93-13216# Aeronautica Macchi S.p.A., Varese (Italy). Aerodynamics Div.
WATER TUNNEL STUDIES OF INLET/AIRFRAME INTERFERENCE PHENOMENA
R. Maggio *In* AGARD, Aerodynamic Engine/Airframe Integration for High Performance Aircraft and Missiles Sep. 1992 12 p (For primary document see N93-13199 03-34)
Copyright Avail: CASI HC A03/MF A04

Some experimental studies of inlet/airframe interference, conducted at the Aermacchi's Water Tunnel facility about aircraft configurations under consideration for an Advanced Trainer Project, are presented. The chin inlet and the bifurcated inlet configurations have been considered, and the following phenomena have been investigated: inlet/forebody interference at low incidence; inlet/ground interference at take off conditions; and inlet/airframe interference. All the above mentioned studies are based on flow visualizations in water tunnel, merged with theoretical studies, semiempirical, and handbook methods. Author

N93-13217# Kingston Polytechnic, Kingston-Upon-Thames (England). School of Mechanics, Aeronautics, and Product Engineering.
EXPERIMENTAL STUDIES OF THE FLOWFIELDS AND THEIR EFFECTS DUE TO A PAIR OF LIFT JETS DISCHARGING IN THE GROUND EFFECT REGION
L. J. Hope and E. C. P. Ransom *In* AGARD, Aerodynamic Engine/Airframe Integration for High Performance Aircraft and Missiles Sep. 1992 19 p (For primary document see N93-13199 03-34)
Copyright Avail: CASI HC A03/MF A04

A small rig has been designed and made to study fountain flows formed by subsonic jets impinging onto a ground plane. A series of tests was carried out to investigate three dimensional flow patterns and pressure distributions in the fountain flows. A program of tests was then devised to establish fountain flow pressures and normal forces on rectangular blocking trays of various designs. Most tests were carried out at ambient temperature but some tests were carried out with pre-heated compressed air. The effect of the distance between the jets and the trays from the ground plane was examined and recorded. Moving ground board tests were also performed. Author

N93-13218# Deutsche Forschungsanstalt fuer Luft- und Raumfahrt, Brunswick (Germany). Inst. fuer Entwurfsaerodynamik.
THE JET BEHAVIOUR OF AN ACTUAL HIGH-BYPASS ENGINE AS DETERMINED BY LDA-MEASUREMENTS IN GROUND TESTS **c07**
H. Hoheisel, K. A. Buetefisch (Deutsche Forschungs- und Versuchsanstalt fuer Luft- und Raumfahrt, Goettingen, Germany), B. Lehmann (Deutsche Forschungs- und Versuchsanstalt fuer Luft- und Raumfahrt, Berlin, Germany), R. Henke (Deutsche Airbus G.m.b.H., Bremen, Germany), H. J. Roscher, and U. Seelhorst (Deutsche Forschungs- und Versuchsanstalt fuer Luft-

und Raumfahrt, Goettingen, Germany) *In* AGARD, Aerodynamic Engine/Airframe Integration for High Performance Aircraft and Missiles Sep. 1992 14 p (For primary document see N93-13199 03-34)
Copyright Avail: CASI HC A03/MF A04

The present contribution describes the measurements of a three-component laser Doppler anenometer (LDA) within the jet of a bypass engine CFM56-5 installed on an A320, in the form of ground tests. The aerodynamic data obtained at the fan exit and in two sections at the turbine nozzle exit near cruise condition allow an insight into the complete jet behavior. The velocity components in the specified position for all three coordinate directions are discussed allowing the evaluation of the radial velocity distribution and the swirl components. In addition, the important parameters of the turbulence intensity and the direction of the thrust vector are considered. Author

N93-13219# Aircraft Research Association Ltd., Bedford (England).
SOME ASPECTS OF INTAKE DESIGN, PERFORMANCE AND INTEGRATION WITH THE AIRFRAME **c05**
E. L. Goldsmith *In* AGARD, Aerodynamic Engine/Airframe Integration for High Performance Aircraft and Missiles Sep. 1992 19 p (For primary document see N93-13199 03-34)
Copyright Avail: CASI HC A03/MF A04

A selection of topics has been made from the state of the art review in the Fluid Dynamics Panel Working Group 13 Report on Intakes for High Speed Vehicles. The first topic is a brief account of results from a program of research on internal and external flow in pitot intakes conducted in the UK over the period 1978-88. The main topic is that of intake airframe integration and is illustrated by examples from systematic work done in the USA and Europe on agile strike fighters and multi-intake missiles. Author

N93-13220*# National Aeronautics and Space Administration. Lewis Research Center, Cleveland, OH.
AGARD WG13 AERODYNAMICS OF HIGH SPEED AIR INTAKES: ASSESSMENT OF CFD RESULTS
N. C. Bissinger (Messerschmitt-Boelkow-Blohm G.m.b.H., Munich, Germany), T. J. Benson, and R. G. Bradley, Jr. (General Dynamics Corp., Fort Worth, TX.) *In* AGARD, Aerodynamic Engine/Airframe Integration for High Performance Aircraft and Missiles Sep. 1992 24 p (For primary document see N93-13199 03-34)
Copyright Avail: CASI HC A03/MF A04

A brief review of the work accomplished by the numerical subgroup of AGARD Working Group 13 on the aerodynamics of high speed air intakes is presented. This work comprised the selection of test cases for which experimental data were available. The test cases were chosen to range in complexity from normal-shock/boundary-layer interaction to full forebody-inlet combinations. Computations for these test cases were solicited from a large number of organizations and individual researchers within the NATO countries. The computation methods reached from Euler solvers (with and without boundary layer corrections) to full Reynolds averaged Navier-Stokes codes. The group compared these results with the test data available for each test case. A short overview of the CFD methods employed, a description of the test cases selected, and some of the comparisons between CFD solutions and test data are presented. The conclusions and recommendations drawn from this assessment are given. Author

N93-13221# Deutsche Forschungs- und Versuchsanstalt fuer Luft- und Raumfahrt, Goettingen (Germany).
COMPARATIVE PERFORMANCE TESTS OF A PITOT-INLET IN SEVERAL EUROPEAN WIND-TUNNELS AT SUBSONIC AND SUPERSONIC SPEEDS **c02**
P.-A. Mackrodt, E. L. Goldsmith (Aircraft Research Association Ltd., Bedford, England), I. McGregor (Royal Aircraft Establishment, Bedford, England), J. Leynaert (Office National d'Etudes et de Recherches Aerospatiales, Paris, France), F. Garcon (Office National d'Etudes et de Recherches Aerospatiales, Modane, France), and J. Brill (Messerschmitt-Boelkow-Blohm G.m.b.H., Munich, Germany) *In* AGARD, Aerodynamic Engine/Airframe Integration for High Performance Aircraft and Missiles Sep. 1992 14 p (For primary document see N93-13199 03-34)
Copyright Avail: CASI HC A03/MF A04

A common design of inlet model (RAE Model 742L Cowl 2), but built to slightly different scales (convenient to the specific wind tunnel), was investigated in the RAE 8 ft x 8 ft tunnel, the ONERA S2MA-tunnel (1.75 m x 1.77 m), and the transonic 1 m x 1 m wind tunnel (TWG) of DLR. The measurements were carried out at subsonic and supersonic Mach numbers, at several Reynolds numbers and angles of attack. The paper presents--aside of a short description of the wind tunnels and the models--details of the instrumentation and the formulae used to calculate the steady-state and the instantaneous distortion parameters. A brief description of the data acquisition and reduction systems is also given. Results of the three tests are presented in the usual format, and from the comparison of the results the differences are analyzed and the main origins of the discrepancies discussed and explained. Finally some recommendations are given for reducing those discrepancies in further tests. Author

N93-13222# Aerospatiale, Verrieres-L-Buisson (France). Div. Engins Tactiques.
AERODYNAMIC STUDIES OF SUPERSONIC AIR INTAKES [ETUDES AERODYNAMIQUES DE PRISES D'AIR SUPERSONIQUES] **c02**
P. Garnero and R. G. Lacau *In* AGARD, Aerodynamic Engine/Airframe Integration for High Performance Aircraft and Missiles Sep. 1992 16 p In FRENCH (For primary document see N93-13199 03-34)
Copyright Avail: CASI HC A03/MF A04

The Tactical Missile Division has been using ramjets on its missiles for more than thirty years. The adaptation of this type of propulsion to very high speed aircraft and airbreathing launchers is investigated. We must study vehicles designed for higher and higher speeds, and we need to optimize more rapidly, and at a lower cost, our airbreathing missile configurations. We completed our supersonic air intake design methodology by using CFD for our work in external and internal aerodynamics. These CFD tools involving Euler and Navier-Stokes codes and mesh generators are complementary to wind tunnel tests. Author

N93-13223# Nangia Associates, Bristol (England).
APPLICATION OF SUBSONIC FIRST-ORDER PANEL METHODS FOR PREDICTION OF INLET AND NOZZLE AERODYNAMIC INTERACTIONS WITH AIRFRAME **c02**
R. K. Nangia and M. E. Palmer *In* AGARD, Aerodynamic Engine/Airframe Integration for High Performance Aircraft and Missiles Sep. 1992 16 p (For primary document see N93-13199 03-34)
Copyright Avail: CASI HC A03/MF A04

Modern aircraft require intake and nozzle flows to be closely integrated with the airframe, and various layouts are possible. In some cases, the intake/nozzle is integral with the fuselage providing a relatively 'compact' layout. This contrasts with configurations in which the nacelles are displaced from the fuselage but are near lifting surfaces. Engine intake flow conditions may range from very high Mass Flow Ratio (MFR) at take-off, to very low MFR on approach, and may include zero MFR during inflight shut-downs. The effect of the intake flows on adjacent components will vary with intake MFR, aircraft attitude, and Mach number. Designers need to know the magnitude of these effects to ensure that they can be contained to satisfactory levels within the available control parameters. A first-order panel method was used to analyze the MFR effects on several configurations. These range from simple 'generic' types to complex, Canard-Delta configurations and include various intake and nozzle arrangements. Mach number and asymmetric effects were studied in particular cases. Author

N93-13224# Wright Lab., Wright-Patterson AFB, OH.
SURVEY ON TECHNIQUES USED IN AERODYNAMIC NOZZLE/AIRFRAME INTEGRATION **c05**
Douglas L. Bowers and James A. Laughrey *In* AGARD, Aerodynamic Engine/Airframe Integration for High Performance Aircraft and Missiles Sep. 1992 11 p (For primary document see N93-13199 03-34)
Copyright Avail: CASI HC A03/MF A04

Building on a survey conducted in 1984 of the state-of-the-art of experimental and computational tools used to evaluate aerodynamic nozzle/airframe integration, this paper critically re-assesses these techniques in 1991. For experimental techniques, there have not been significant developments in the intervening seven years, and these mature techniques still serve the design engineer well. On the computational side, Euler techniques are now being applied as design tools in nozzle problems where there are not strong viscous interactions. Computation of the viscous regions, especially the nozzle boattail, with Navier-Stokes algorithms is still lacking. Author

N93-13225# General Dynamics Corp., Fort Worth, TX.
CALIBRATION OF 2D UNSTRUCTURED GRID METHODS ON PROPULSIVE FLOWFIELDS
Steve L. Karman, Jr. and Gregory S. Spragle *In* AGARD, Aerodynamic Engine/Airframe Integration for High Performance Aircraft and Missiles Sep. 1992 12 p (For primary document see N93-13199 03-34)
Copyright Avail: CASI HC A03/MF A04

A computational fluid dynamics (CFD) method is presented for the analysis of complex two-dimensional (2D) geometries using unstructured grid techniques. The grid generation procedure uses a split tree technique for subdividing the domain and generating internal mesh points. A Delaunay triangulation method is employed to triangulate the points, then iteratively refines the mesh based on cell aspect ratios and area variation to improve the quality of the initial mesh. The full Navier-Stokes equations are solved using an upwind flux difference splitting scheme for the inviscid flux and a central differencing scheme for the viscous flux. A two equation turbulence model is included for analyzing turbulent flows. A Jacobi iteration procedure is used to solve the linear set of implicit equations at each time step. Two 2D propulsive flowfields are analyzed and compared with experimental data. The grids are adapted to the flowfield by refinement based on the flowfield gradients. Improved resolution of the pertinent flowfield features were a result of the grid adaption employed. Author

N93-13226# General Dynamics Corp., Fort Worth, TX.
CFD CALIBRATION FOR THREE-DIMENSIONAL NOZZLE/AFTERBODY CONFIGURATIONS
Christopher L. Reed and Arnold Muyshondt *In* AGARD, Aerodynamic Engine/Airframe Integration for High Performance Aircraft and Missiles Sep. 1992 11 p (For primary document see N93-13199 03-34)
Copyright Avail: CASI HC A03/MF A04

The current trend in fighter aircraft design is toward highly integrated propulsive exhaust systems. In order to achieve this level of integration, extensive testing and analysis is required. Modern computational fluid dynamics (CFD) techniques have become popular in performing a part of the required analyses. Because of the complexity of most nozzle/afterbody type flow fields, Navier-Stokes codes are generally the preferred CFD methods. To gain confidence in these solvers ability to provide useful design information, a number of calibration analyses must be conducted. Extensive test data are available for these comparisons. This paper describes three such analyses which were used to calibrate two Navier-Stokes codes. The first case deals with the internal flow through a vectored nozzle. The second case looks at the development of an exhaust plume issuing from a rectangular nozzle. The third case considers the flow over an afterbody with a high-aspect-ratio rectangular nozzle. In all cases, both qualitative and quantitative comparisons are made between the test data and the CFD data. Good comparisons are obtained and additional confidence is gained in these CFD codes ability to provide useful engineering data.
Author

N93-13227# Deutsche Forschungsanstalt fuer Luft- und Raumfahrt, Brunswick (Germany).
INVESTIGATION OF THE FLOWFIELD AROUND AN ISOLATED BYPASS ENGINE WITH FAN AND CORE JET
R. Rudnik, A. Ronzheimer, C.-C. Rossow, and H. Hoheisel *In* AGARD, Aerodynamic Engine/Airframe Integration for High Performance Aircraft and Missiles Sep. 1992 8 p (For primary document see N93-13199 03-34)
Copyright Avail: CASI HC A02/MF A04

A finite-volume scheme for the discretization of the three-dimensional Euler equations is extended for the purpose of calculating the flowfield around an isolated bypass engine with fan- and core-jet. Flow calculations for a typical high bypass engine are performed for take-off and cruise conditions under consideration of realistic operational jet parameters. Several variations of the jet pressure and temperature ratio show that the jet flowfield is dominated by the pressure ratio as far as inviscid flow is concerned. A comparison of the numerical results to experimental investigations, which are carried out with a turbine powered simulator for low speeds, exhibits good agreement. The influence of numerical parameters on the solution in the region of the jet flow is analyzed by varying the coefficients of the artificial dissipation. Author

N93-13228# Wright Lab., Wright-Patterson AFB, OH.
PROPULSION INTEGRATION RESULTS OF THE STOL AND MANEUVER TECHNOLOGY DEMONSTRATOR **c05**
J. A. Laughrey and D. J. Moorhouse *In* AGARD, Aerodynamic Engine/Airframe Integration for High Performance Aircraft and Missiles Sep. 1992 12 p (For primary document see N93-13199 03-34)
Copyright Avail: CASI HC A03/MF A04

The STOL and Maneuver Technology Demonstrator program has achieved its original goals established to demonstrate the benefits of thrust vectoring and reversing on a fighter aircraft. It has been shown that thrust vectoring will enhance up-and-away aircraft maneuverability at low speeds and can be used to improve tracking and capture tasks plus contribute significantly to improve takeoff performance and rough or damaged runway operations. Thrust reversing has been shown to permit quicker changes in energy states that could provide an advantage in tactical arena and can greatly reduce landing distances. It was also demonstrated that an integrated flight and propulsion control system that incorporates the appropriate control laws can significantly simplify pilot workload during all vectoring and reversing operations, including the approach, landing, and stopping tasks. Results of this program are being used to transition these proven technologies into future fighter systems. Author

N93-13229# Wright Lab., Wright-Patterson AFB, OH.
HYPERSONIC PROPULSION SYSTEM FORCE ACCOUNTING **c07**
K. Numbers *In* AGARD, Aerodynamic Engine/Airframe Integration for High Performance Aircraft and Missiles Sep. 1992 p 15 (For primary document see N93-13199 03-34)
Copyright Avail: CASI HC A03/MF A04

A generic matrix of propulsion force accounting procedures was developed from a survey of the U.S. aerospace community. The matrix includes definitions for propulsion system and control volume boundary specification. Aerodynamic reference conditions are also discussed relative to off-design performance. The advantages and disadvantages of each of the force accounting procedures are discussed as they apply to some typical hypersonic force accounting problems. Author

N93-13230# Messerschmitt-Boelkow-Blohm G.m.b.H., Munich (Germany).
INTEGRATION OF TURBO-RAMJET ENGINES FOR HYPERSONIC AIRCRAFT **c07**
O. Herrmann *In* AGARD, Aerodynamic Engine/Airframe Integration for High Performance Aircraft and Missiles Sep. 1992 7 p (For primary document see N93-13199 03-34)
Copyright Avail: CASI HC A02/MF A04

The integration of turbo-ramjet engines for hypersonic transport vehicles operating in the Mach 0 to 6+ regime represents one of the most important development tasks. A survey over the variety of interacting problem areas and faculties, which have to be integrated to lead to an optimized propulsion/airframe system, is presented Author

N93-13231# Office National d'Etudes et de Recherches Aerospatiales, Paris (France).
AIR INLET WITH VARIABLE INTAKE SECTION: APPLICATION TO AIR BREATHING LAUNCH VEHICLES [PRISES D'AIR A SECTION DE CAPTATION VARIABLE APPLICATION AUX LANCEURS AEROBIES]
F. Falempin and Ph. Duveau *In* AGARD, Aerodynamic Engine/Airframe Integration for High Performance Aircraft and Missiles Sep. 1992 8 p In FRENCH (For primary document see N93-13199 03-34)
Copyright Avail: CASI HC A02/MF A04

The feasibility of air breathing propulsion for future space launch vehicles largely depends on the possibility of designing air intakes that will give the best trade-off between internal performance and which will provide suitable air supply to the engine, weight reduction, and aerodynamic drag. The trade-off can be markedly improved by using air intake designs with variable absorption sections. The design concepts are defined and their application to space launch vehicles is analyzed with respect to internal performance, mass, and aerodynamic drag. Transl. by L.B.

N93-13247# Sandia National Labs., Livermore, CA.
FUNDAMENTALS OF ENHANCED SCALAR TRANSPORT IN STRONGLY OSCILLATING AND/OR RESONANT FLOW FIELDS AS CREATED BY PULSE COMBUSTION
J. O. Keller, R. S. Gemmen (Department of Energy, Morgantown, WV.),

and R. W. Ozer (Bepex Corp., Minneapolis, MN.) 1992 20 p Presented at the 8th International Drying Symposium, Montreal, Ottawa, 2-5 Aug. 1992
(Contract DE-AC04-76DR-00789)
(DE92-012147; SAND-92-8405C; CONF-920871-1) Avail: CASI HC A03/MF A01

In this paper, we discuss the major features of strongly oscillating flow fields as they pertain to scalar transport. The flow fields to be discussed have been created by the acoustic resonance of a pulse combustor. Discussions of the fluid-dynamic flow field in the tailpipe where the flow is in acoustic resonance, and out of the end of the tailpipe where the flow is a pulsating free jet are presented. The flow fields to be discussed are full of intriguing features that are responsible for significantly increasing the convective transport of scalars. These features are a direct result of velocity oscillations that are sufficiently large to create flow reversal. The fundamental mechanisms that cause the increased transport of mass, momentum, and energy are discussed. We end this paper with some examples of practical systems which exploit the physics described here. DOE

N93-13277*# MCAT Inst., San Jose, CA.
A FUNDAMENTAL STUDY OF SUCTION FOR LAMINAR FLOW CONTROL (LFC) Progress Report, Nov. 1991 - Oct. 1992
Jonathan H. Watmuff Oct. 1992 7 p
(Contract NCC2-698)
(NASA-CR-191276; NAS 1.26:191276; MCAT-92-019) Avail: CASI HC A02/MF A01

This report covers the period forming the first year of the project. The aim is to experimentally investigate the effects of suction as a technique for Laminar Flow Control. Experiments are to be performed which require substantial modifications to be made to the experimental facility. Considerable effort has been spent developing new high performance constant temperature hot-wire anemometers for general purpose use in the Fluid Mechanics Laboratory. Twenty instruments have been delivered. An important feature of the facility is that it is totally automated under computer control. Unprecedently large quantities of data can be acquired and the results examined using the visualization tools developed specifically for studying the results of numerical simulations on graphics works stations. The experiment must be run for periods of up to a month at a time since the data is collected on a point-by-point basis. Several techniques were implemented to reduce the experimental run-time by a significant factor. Extra probes have been constructed and modifications have been made to the traverse hardware and to the real-time experimental code to enable multiple probes to be used. This will reduce the experimental run-time by the appropriate factor. Hot-wire calibration drift has been a frustrating problem owing to the large range of ambient temperatures experienced in the laboratory. The solution has been to repeat the calibrations at frequent intervals. However the calibration process has consumed up to 40 percent of the run-time. A new method of correcting the drift is very nearly finalized and when implemented it will also lead to a significant reduction in the experimental run-time. Author

N93-13318# Oak Ridge National Lab., TN.
A NEW APPARATUS FOR CONTINUOUS COUNTERCURRENT FLOW OF SOLIDS AND LIQUIDS
P. A. Haas 1992 18 p Presented at the American Institute of Chemical Engineers Annual Meeting, Miami, FL, 1-6 Nov. 1992
(Contract DE-AC05-84OR-21400)
(DE92-011675; CONF-921104-2) Avail: CASI HC A03/MF A01

A contactor was developed to provide true countercurrent, continuous flow of gel spheres and liquid in a moving bed. To provide smooth and controlled movement of solids, the key features consisted of a common cross section for the moving bed and a small fluidized bed, a jet to give a slurry at the bottom of the moving bed, and a controlled flow of part of this slurry to the fluidized bed. A completely continuous pilot plant for preparation of nuclear fuel by a gel-sphere process was operated with three of these moving-bed fluidized-bed contactors. Different control procedures and good countercurrent washing results were demonstrated. DOE

N93-13334 Yale Univ., New Haven, CT.
FEATURES OF VORTICITY IN FULLY TURBULENT FLOWS Ph.D. Thesis
Mark Shiaoyi Fan 1991 218 p
Avail: Univ. Microfilms Order No. DA9218782

Measurements of the longitudinal component of vorticity in several fully developed turbulent flows have been made using a modified, Kovasznay-type vorticity probe. Flows investigated include grid turbulence, a boundary layer, a cylinder wake and the atmospheric surface layer. The measured results are assessed for their accuracy in several ways. It is shown that they are in essential agreement with the semi-empirical prediction of the vorticity decay with the downstream distance in grid turbulence and with the classical data of multicomponent velocity as well as Reynolds stress distributions in a turbulent boundary layer. These latter quantities can be derived as byproducts of measurements from the probe. These comparisons serve to show that the vorticity measurements are reliable. For nearly isotropic grid turbulence and for locally isotropic atmospheric flow, it is shown that the one-dimensional vorticity spectrum calculated from one-dimensional velocity spectrum agrees well with the measured spectrum. Other statistical characteristics of vorticity distributions are also investigated. It has been found that the probability distribution functions of vorticity measured in laboratory flows at moderate Reynolds number are close to Gaussian except in the tail regions, where they tend towards exponential. However, in the large Reynolds-number case, namely, the atmospheric flow, the probability distribution of vorticity is nearly completely exponential. The exponential distribution reveals the intermittent nature of high-Reynolds-number vorticity field. Of particular interest is the multifractal analysis of turbulent vorticity. Recently, the multifractal nature of turbulence has attracted attention as a fundamental characteristic for understanding the structure of turbulence. Multifractality also appears in a number of nonlinear physical phenomena. It is already clear that the turbulent energy dissipation field can be well described by multifractal. Since enstrophy is directly related to dissipation, we conjectured that turbulent enstrophy can also be described as multifractal. The work described here confirms that conjecture. Also, the multifractal formalism for a multivariable distribution is briefly described. Moreover, on the basis of high-Reynolds-number vorticity measurements, we are not able to find divergence of moments. The fractal dimension of vorticity interface is determined to be about 2.35 using box-counting method. The issue of the epsilon-support of vorticity is also addressed. Dissert. Abstr.

N93-13356# Edgerton, Germeshausen and Grier, Inc., Idaho Falls, ID.
TWO-PHASE FLOW MODELING WITH DISCRETE PARTICLES
G. A. Mortensen and J. A. Trapp (Colorado Univ., Denver.) 23 Mar. 1992 30 p Presented at the Winter Annual Meeting of the American Society of Mechanical Engineers, Anaheim, CA, 8-13 Nov. 1992
(Contract DE-AC07-76ID-01570)
(DE92-017850; EGG-M-92026; CONF-921110-10) Avail: CASI HC A03/MF A01

The design of efficient heat exchangers in which the working fluid changes phase requires accurate modeling of two-phase fluid flow. The local Navier-Stokes equations form the basic continuum equations for this flow situation. However, the local instantaneous model using these equations is intractable for all but the simplest problems. All the practical models for two-phase flow analysis are based on equations that have been averaged over control volumes. These models average out the detailed description within the control volumes and rely on flow regime maps to determine the distribution of the two phases within a control volume. Flow regime maps depend on steady state models and probably are not correct for dynamic models. Numerical simulations of the averaged two-phase flow models are usually performed using a two-fluid Eulerian description for the two phases. Eulerian descriptions have the advantage of having simple boundary conditions, but the disadvantage of introducing numerical diffusion, i.e., sharp interfaces are not maintained as the flow develops, but are diffused. Lagrangian descriptions have the advantage of being able to track sharp interfaces without diffusion, but they have the disadvantage of requiring more complicated boundary conditions. This paper describes a numerical scheme and attendant computer program, DISCON2, for the calculation of two-phase flows that does not require the use of flow regime maps. This model is intermediate between the intractable local instantaneous and the averaged two-fluid model. This new model uses a combination of an Eulerian and a Lagrangian representation of the two phases. The dispersed particles

(bubbles or drops) are modeled individually using a large representative number of particles, each with their own Lagrangian description. The continuous phases (liquid or gas) use an Eulerian description. DOE

N93-13383 State Univ. of New York, Buffalo.
BOUNDARY ELEMENT METHODS FOR TWO-DIMENSIONAL, COUPLED, THERMOVISCOUS FLOW Ph.D. Thesis
Keith Alan Honkala 1992 281 p
Avail: Univ. Microfilms Order No. DA9222063

Boundary element methods are developed for various forms of two-dimensional, coupled, thermoviscous flow. The coupling arises from the nonlinear convective terms in the Navier-Stokes equations, from the thermal buoyancy effect, from non-Newtonian fluid models, and from the viscous heating effect. Theoretical and numerical details are presented. Both steady and transient problems are considered, as well as linear and nonlinear problems. One area of concentrated research involves an investigation of several boundary integration techniques. Previous numerical integration methods did not prove satisfactory for solving incompressible fluid flow problems. Problems with incompressibility require more accurate integration than problems of scalar heat transfer or elasticity. A new integration scheme is detailed, which represents a significant advance in BEM technology for incompressible fluid flow problems. This new integration scheme is very robust, allowing a wide variety of problems to be accurately solved. In the case of buoyancy-driven flows, a new boundary element formulation is presented. The buoyancy effect is incorporated using two distinct formulations. First, buoyancy is incorporated in a coupled fundamental solution. Second, buoyancy is left as a pseudo-body force. The two formulations are compared theoretically and computationally. The theoretical presentation has been enriched by incorporation of the theory into a general purpose boundary element program, called 'GPBEST'. This has allowed a wide variety of thermoviscous problems to be solved by the boundary element method, and also validated the theoretical presentation. Throughout this thesis, the boundary element method and finite element method are extensively compared and contrasted in the field of incompressible thermoviscous flow. These two methods are compared as to theoretical details, computational efficiency, accuracy, and ease of model preparation. This is the first comprehensive comparison of the boundary element method and the finite element method for this class of problems. Fundamental solutions for linear problems are at the heart of the boundary element method. Hormander's method is used extensively in this thesis to derive appropriate fundamental solutions. The method is presented in this thesis in a uniform, understandable manner, which can easily be extended to other coupled problems. Dissert. Abstr.

N93-13385*# National Aeronautics and Space Administration. Lewis Research Center, Cleveland, OH.
THE FOURTH ANNUAL THERMAL AND FLUIDS ANALYSIS WORKSHOP
1992 276 p Workshop held in Cleveland, OH, 17-21 Aug. 1992 (NASA-CP-10106; E-7346; NAS 1.55:10106) Avail: CASI HC A13/MF A03

The Fourth Annual Thermal and Fluids Analysis Workshop was held from August 17-21, 1992, at NASA Lewis Research Center. The workshop consisted of classes, vendor demonstrations, and paper sessions. The classes and vendor demonstrations provided participants with the information on widely used tools for thermal and fluids analysis. The paper sessions provided a forum for the exchange of information and ideas among thermal and fluids analysts. Paper topics included advances and uses of established thermal and fluids computer codes (such as SINDA and TRASYS) as well as unique modeling techniques and applications. For individual titles, see N93-13386 through N93-13403.

N93-13386*# Battelle Columbus Labs., OH.
APPLICATIONS OF CFD AND VISUALIZATION TECHNIQUES
James H. Saunders, Susan T. Brown, Jeffrey J. Crisafulli, and Leslie A. Southern (Ohio State Univ., Columbus.) *In* NASA. Lewis Research Center, The Fourth Annual Thermal and Fluids Analysis Workshop 1992 p 1-8 (For primary document see N93-13385 03-34)
Avail: CASI HC A02/MF A03

In this paper, three applications are presented to illustrate current techniques for flow calculation and visualization. The first two applications use a commercial computational fluid dynamics (CFD) code, FLUENT, performed on a Cray Y-MP. The results are animated with the aid of data visualization software, apE. The third application simulates a particulate deposition pattern using techniques inspired by developments in nonlinear dynamical systems. These computations were performed on personal computers. Author

N93-13387*# Superconducting Super Collider Lab., Dallas, TX. Accelerator Systems Div.
THERMAL ISSUES AT THE SSC
Raj P. Ranganathan and Bui V. Dao *In* NASA. Lewis Research Center, The Fourth Annual Thermal and Fluids Analysis Workshop 1992 p 9-29 (For primary document see N93-13385 03-34)
Avail: CASI HC A03/MF A03

A variety of heat transfer problems arise in the design of the Superconducting Super Collider (SSC). One class of problems is to minimize heat leak from the ambient to the SSC rings, since the rings contain superconducting magnets maintained at a temperature of 4 K. Another arises from the need to dump the beam of protrons (traveling around the SSC rings) on to absorbers during an abort of the collider. Yet another category of problems is the cooling of equipment to dissipate the heat generated during operation. An overview of these problems and sample heat transfer results are given in this paper. Author

N93-13388*# Ishikawajima-Harima Heavy Industries Co. Ltd., Yokohama (Japan).
NUMERICAL STUDY ON MIXING OF SPRAYED LIQUID IN AN LNG STORAGE TANK
Hiroyuki Uchida, Tatsuya Arai, Makoto Sugihara, and Mariko Nakayama *In* NASA. Lewis Research Center, The Fourth Annual Thermal and Fluids Analysis Workshop 1992 p 31-35 (For primary document see N93-13385 03-34)
Avail: CASI HC A01/MF A03

This paper presents a numerical method to simulate the mixing of heavier LNG sprayed on lighter layer. Numerical results for evolutions of flow field and density field are obtained in a rectangular computational domain which includes the vicinity of the liquid surface. At the surface boundary, uniform distributions of the fluid velocity and the density are assumed. Detail structure of flow caused by impingements of liquid drops are neglected. But, to trigger a realistic motion, a series of random numbers is employed. It is used as an initial distribution of the density near the surface. This method successfully gives a realistic simulation of the mixing process. Numerical results for mixing velocity shows good agreement with experimental data. Author

N93-13389*# McDonnell-Douglas Space Systems Co., Huntington Beach, CA.
ANALYSIS OF A SPACE EMERGENCY AMMONIA DUMP USING THE FLOW-NET TWO-PHASE FLOW PROGRAM
J. Navickas and W. C. Rivard (Maine Univ., Orono.) *In* NASA. Lewis Research Center, The Fourth Annual Thermal and Fluids Analysis Workshop 1992 p 37-45 (For primary document see N93-13385 03-34)
Avail: CASI HC A02/MF A03

Venting of cryogenic and non-cryogenic fluids to a vacuum or a very low pressure will take place in many space-based systems that are currently being designed. This may cause liquid freezing either internally within the flow circuit or on external spacecraft surfaces. Typical ammonia flow circuits were investigated to determine the effect of the geometric configuration and initial temperature, pressure, and void fraction on the freezing characteristics of the system. The analysis was conducted also to investigate the ranges of applicability of the FLOW-NET program. It was shown that a typical system can be vented to very low liquid fractions before freezing occurs. However, very small restrictions in the flow circuit can hasten the inception of freezing. The FLOW-NET program provided solutions over broad ranges of system conditions, such as venting of an ammonia tank, initially completely filled with liquid, through a series of contracting and expanding line cross sections to near-vacuum conditions. Author

N93-13390*# Sverdrup Technology, Inc., Huntsville, AL.
RUNNING SINDA '85/FLUINT INTERACTIVE ON THE VAX **c61**
Boris Simmonds *In* NASA. Lewis Research Center, The Fourth Annual

Thermal and Fluids Analysis Workshop 1992 p 47-70 (For primary document see N93-13385 03-34)
Avail: CASI HC A03/MF A03

Computer software as engineering tools are typically run in three modes: Batch, Demand, and Interactive. The first two are the most popular in the SINDA world. The third one is not so popular, due probably to the users inaccessibility to the command procedure files for running SINDA '85, or lack of familiarity with the SINDA '85 execution processes (pre-processor, processor, compilation, linking, execution and all of the file assignment, creation, deletions and de-assignments). Interactive is the mode that makes thermal analysis with SINDA '85 a real-time design tool. This paper explains a command procedure sufficient (the minimum modifications required in an existing demand command procedure) to run SINDA '85 on the VAX in an interactive mode. To exercise the procedure a sample problem is presented exemplifying the mode, plus additional programming capabilities available in SINDA '85. Following the same guidelines the process can be extended to other SINDA '85 residence computer platforms. Author

N93-13391*# Jet Propulsion Lab., California Inst. of Tech., Pasadena.
TRASYS FORM FACTOR MATRIX NORMALIZATION
Glenn T. Tsuyuki *In* NASA. Lewis Research Center, The Fourth Annual Thermal and Fluids Analysis Workshop 1992 p 71-82 (For primary document see N93-13385 03-34)
Avail: CASI HC A03/MF A03

A method has been developed for adjusting a TRASYS enclosure form factor matrix to unity. This approach is not limited to closed geometries, and in fact, it is primarily intended for use with open geometries. The purpose of this approach is to prevent optimistic form factors to space. In this method, nodal form factor sums are calculated within 0.05 of unity using TRASYS, although deviations as large as 0.10 may be acceptable, and then, a process is employed to distribute the difference amongst the nodes. A specific example has been analyzed with this method, and a comparison was performed with a standard approach for calculating radiation conductors. In this comparison, hot and cold case temperatures were determined. Exterior nodes exhibited temperature differences as large as 7 C and 3 C for the hot and cold cases, respectively when compared with the standard approach, while interior nodes demonstrated temperature differences from 0 C to 5 C. These results indicate that temperature predictions can be artificially biased if the form factor computation error is lumped into the individual form factors to space. Author

N93-13392*# Aerojet-General Corp., Covina, CA.
A SIMPLE NODE AND CONDUCTOR DATA GENERATOR FOR SINDA
Ronald R. Gottula *In* NASA. Lewis Research Center, The Fourth Annual Thermal and Fluids Analysis Workshop 1992 p 83-93 (For primary document see N93-13385 03-34)
Avail: CASI HC A03/MF A03

This paper presents a simple, automated method to generate NODE and CONDUCTOR DATA for thermal match modes. The method uses personal computer spreadsheets to create SINDA inputs. It was developed in order to make SINDA modeling less time consuming and serves as an alternative to graphical methods. Anyone having some experience using a personal computer can easily implement this process. The user develops spreadsheets to automatically calculate capacitances and conductances based on material properties and dimensional data. The necessary node and conductor information is then taken from the spreadsheets and automatically arranged into the proper format, ready for insertion directly into the SINDA model. This technique provides a number of benefits to the SINDA user such as a reduction in the number of hand calculations, and an ability to very quickly generate a parametric set of NODE and CONDUCTOR DATA blocks. It also provides advantages over graphical thermal modeling systems by retaining the analyst's complete visibility into the thermal network, and by permitting user comments anywhere within the DATA blocks. Author

N93-13393*# National Aeronautics and Space Administration. Lyndon B. Johnson Space Center, Houston, TX.
DEVELOPMENT STATUS OF SINDA/FLUINT AND SINAPS
Brent A. Cullimore (Martin Marietta Corp., Denver, CO.), Steven G. Ring (Martin Marietta Corp., Denver, CO.), and Eugene K. Ungar *In* NASA. Lewis Research Center, The Fourth Annual Thermal and Fluids Analysis Workshop 1992 p 95-107 (For primary document see N93-13385 03-34)
(Contracts NAS9-17053; NAS9-17448; NAS9-18411)
Avail: CASI HC A03/MF A03

SINDA/FLUINT (Systems Improved Numerical Differencing Analyzer/Fluid Integrator, formerly SINDA '85) is a computer code used to analyze thermal/fluid systems that can be represented in lumped parameter form. In addition to conduction and radiation heat transfer, the code is capable of modeling both single- and two-phase flow networks, their associated hardware, and their heat transfer processes. In this paper, recent improvements to SINDA/FLUINT are described, as are those in progress that will be available in the fall of 1992 in Version 2.5. Also, a preview of planned enhancements is provided. This paper also introduces SINAPS (SINDA Application Programming System), a powerful graphical pre- and postprocessor that will also be available in the fall of 1992. Author

N93-13394*# Sverdrup Technology, Inc., Huntsville, AL.
A SINDA THERMAL MODEL USING CAD/CAE TECHNOLOGIES
Jose A. Rodriguez and Steve Spencer *In* NASA. Lewis Research Center, The Fourth Annual Thermal and Fluids Analysis Workshop 1992 p 109-115 (For primary document see N93-13385 03-34)
Avail: CASI HC A02/MF A03

The approach to thermal analysis described by this paper is a technique that incorporates Computer Aided Design (CAD) and Computer Aided Engineering (CAE) to develop a thermal model that has the advantages of Finite Element Methods (FEM) without abandoning the unique advantages of Finite Difference Methods (FDM) in the analysis of thermal systems. The incorporation of existing CAD geometry, the powerful use of a pre and post processor and the ability to do interdisciplinary analysis, will be described. Author

N93-13395*# National Aeronautics and Space Administration. Lewis Research Center, Cleveland, OH.
A COMPRESSIBLE BOUNDARY LAYER ALGORITHM FOR USE WITH SINDA '85
Barbara Sakowski, Douglas Darling, and Allan vandeWall (Case Western Reserve Univ., Cleveland, OH.) *In its* The Fourth Annual Thermal and Fluids Analysis Workshop 1992 p 117-130 (For primary document see N93-13385 03-34)
Avail: CASI HC A03/MF A03

It is useful to interface a high-speed-flow solution and SINDA to analyze the thermal behavior of systems that include both conduction and high speed flows. When interfacing a high-speed-flow solution to SINDA, it may be necessary to include the viscous effects in the energy equations. Boundary layer effects of interest include heat transfer coefficients (including convection and viscous dissipation) and friction coefficients. To meet this need, a fast, uncoupled, compressible, two-dimensional, boundary layer algorithm was developed that can model flows with and without separation. This algorithm was used as a subroutine with SINDA. Given the core flow properties and the wall heat flux from SINDA, the boundary layer algorithm returns a wall temperature to SINDA and boundary layer algorithm are iterated until they predict the same wall temperature. Author

N93-13396*# National Aeronautics and Space Administration. Lewis Research Center, Cleveland, OH.
THE PROTEUS NAVIER-STOKES CODE
Charles E. Towne, Trong T. Bui, Richard H. Cavicchi, Julianne M. Conley, Frank B. Molls, and John R. Schwab *In its* The Fourth Annual Thermal and Fluids Analysis Workshop 1992 p 131-154 (For primary document see N93-13385 03-34)
Avail: CASI HC A03/MF A03

An effort is currently underway at NASA Lewis to develop two- and three-dimensional Navier-Stokes codes, called Proteus, for aerospace propulsion applications. The emphasis in the development of Proteus is not algorithm development or research on numerical methods, but rather the development of the code itself. The objective is to develop codes that are user-oriented, easily-modified, and well-documented. Well-proven, state-of-the-art solution algorithms are being used. Code readability, documentation (both internal and external), and validation are being emphasized. This paper is a status report on the Proteus development effort. The analysis and solution procedure are described briefly, and the

various features in the code are summarized. The results from some of the validation cases that have been run are presented for both the two- and three-dimensional codes. Author

N93-13397*# National Aeronautics and Space Administration. Lyndon B. Johnson Space Center, Houston, TX.

ANALYSIS OF FLUID/MECHANICAL SYSTEMS USING EASY5

Robert W. Clark, Jr. (McDonnell-Douglas Space Systems Co., Houston, TX.), Scott D. Arndt (McDonnell-Douglas Space Systems Co., Houston, TX.), and Eric A. Hurlbert *In* NASA. Lewis Research Center, The Fourth Annual Thermal and Fluids Analysis Workshop 1992 p 155-167 (For primary document see N93-13385 03-34)

Avail: CASI HC A03/MF A03

This paper illustrates how the use of a general analysis package can simplify modeling and analyzing fluid/mechanical systems. One such package is EASY5, a Boeing Computer Services product. The basic transmission line equations for modeling piped fluid systems are presented, as well as methods of incorporating these equations into the EASY5 environment. The paper describes how this analysis tool has been used to model several fluid subsystems of the Space Shuttle Orbiter. Author

N93-13398*# McDonnell-Douglas Space Systems Co., Houston, TX.

ACOUSTIC MODES IN FLUID NETWORKS

C. D. Michalopoulos, Robert W. Clark, Jr., and Harold H. Doiron *In* NASA. Lewis Research Center, The Fourth Annual Thermal and Fluids Analysis Workshop 1992 p 169-185 (For primary document see N93-13385 03-34)

Avail: CASI HC A03/MF A03

Pressure and flow rate eigenvalue problems for one-dimensional flow of a fluid in a network of pipes are derived from the familiar transmission line equations. These equations are linearized by assuming small velocity and pressure oscillations about mean flow conditions. It is shown that the flow rate eigenvalues are the same as the pressure eigenvalues and the relationship between line pressure modes and flow rate modes is established. A volume at the end of each branch is employed which allows any combination of boundary conditions, from open to closed, to be used. The Jacobi iterative method is used to compute undamped natural frequencies and associated pressure/flow modes. Several numerical examples are presented which include acoustic modes for the Helium Supply System of the Space Shuttle Orbiter Main Propulsion System. It should be noted that the method presented herein can be applied to any one-dimensional acoustic system involving an arbitrary number of branches. Author

N93-13399*# Tri-State Univ., Angola, IN. Dept. of Aerospace and Mechanical Engineering.

THE PROGRAM FANS-3D (FINITE ANALYTIC NUMERICAL SIMULATION 3-DIMENSIONAL) AND ITS APPLICATIONS

Ramiro H. Bravo and Ching-Jen Chen (Iowa Univ., Iowa City.) *In* NASA. Lewis Research Center, The Fourth Annual Thermal and Fluids Analysis Workshop 1992 p 187-205 (For primary document see N93-13385 03-34)

Avail: CASI HC A03/MF A03

In this study, the program named FANS-3D (Finite Analytic Numerical Simulation-3 Dimensional) is presented. FANS-3D was designed to solve problems of incompressible fluid flow and combined modes of heat transfer. It solves problems with conduction and convection modes of heat transfer in laminar flow, with provisions for radiation and turbulent flows. It can solve singular or conjugate modes of heat transfer. It also solves problems in natural convection, using the Boussinesq approximation. FANS-3D was designed to solve heat transfer problems inside one, two and three dimensional geometries that can be represented by orthogonal planes in a Cartesian coordinate system. It can solve internal and external flows using appropriate boundary conditions such as symmetric, periodic and user specified. Author

N93-13400*# National Aeronautics and Space Administration. Lewis Research Center, Cleveland, OH.

ONE-DIMENSIONAL TRANSIENT FINITE DIFFERENCE MODEL OF AN OPERATIONAL SALINITY GRADIENT SOLAR POND

Michael C. Hicks and Peter Golding (Texas Univ., El Paso.) *In its* The Fourth Annual Thermal and Fluids Analysis Workshop 1992 p 207-219 (For primary document see N93-13385 03-34)

Avail: CASI HC A03/MF A03

This paper describes the modeling approach used to simulate the transient behavior of a salinity gradient solar pond. A system of finite difference equations are used to generate the time dependent temperature and salinity profiles within the pond. The stability of the pond, as determined by the capacity of the resulting salinity profile to suppress thermal convection within the primary gradient region of the pond, is continually monitored and when necessary adjustments are made to the thickness of the gradient zone. Results of the model are then compared to measurements taken during two representative seasonal periods at the University of Texas at El Paso's (UTEP's) research solar pond. Author

N93-13401*# National Aeronautics and Space Administration. Lyndon B. Johnson Space Center, Houston, TX.

AEROSPACE APPLICATIONS OF SINDA/FLUINT AT THE JOHNSON SPACE CENTER

Michael K. Ewert, Phillip E. Bellmore (McDonnell-Douglas Space Systems Co., Houston, TX.), Kambiz K. Andish (Lockheed Engineering and Sciences Co., Houston, TX.), and John R. Keller (Lockheed Engineering and Sciences Co., Houston, TX.) *In* NASA. Lewis Research Center, The Fourth Annual Thermal and Fluids Analysis Workshop 1992 p 221-256 (For primary document see N93-13385 03-34)

Avail: CASI HC A03/MF A03

SINDA/FLUINT has been found to be a versatile code for modeling aerospace systems involving single or two-phase fluid flow and all modes of heat transfer. Several applications of SINDA/FLUINT are described in this paper. SINDA/FLUINT is being used extensively to model the single phase water loops and the two-phase ammonia loops of the Space Station Freedom active thermal control system (ATCS). These models range from large integrated system models with multiple submodels to very detailed subsystem models. An integrated Space Station ATCS model has been created with ten submodels representing five water loops, three ammonia loops, a Freon loop and a thermal submodel representing the air loop. The model, which has approximately 800 FLUINT lumps and 300 thermal nodes, is used to determine the interaction between the multiple fluid loops which comprise the Space Station ATCS. Several detailed models of the flow-through radiator subsystem of the Space Station ATCS have been developed. One model, which has approximately 70 FLUINT lumps and 340 thermal nodes, provides a representation of the ATCS low temperature radiator array with two fluid loops connected only by conduction through the radiator face sheet. The detailed models are used to determine parameters such as radiator fluid return temperature, fin efficiency, flow distribution and total heat rejection for the baseline design as well as proposed alternate designs. SINDA/FLUINT has also been used as a design tool for several systems using pressurized gasses. One model examined the pressurization and depressurization of the Space Station airlock under a variety of operating conditions including convection with the side walls and internal cooling. Another model predicted the performance of a new generation of manned maneuvering units. This model included high pressure gas depressurization, internal heat transfer and supersonic thruster equations. The results of both models were used to size components, such as the heaters and gas bottles and also to point to areas where hardware testing was needed. Author

N93-13402*# North Carolina Univ., Charlotte. Dept. of Mechanical Engineering.

TWO-PHASE/TWO-PHASE HEAT EXCHANGER SIMULATION ANALYSIS

Rhyn H. Kim *In* NASA. Lewis Research Center, The Fourth Annual Thermal and Fluids Analysis Workshop 1992 p 257-270 (For primary document see N93-13385 03-34)

(Grant NAG5-1503)

Avail: CASI HC A03/MF A03

The capillary pumped loop (CPL) system is one of the most desirable devices to dissipate heat energy in the radiation environment of the Space Station providing a relatively easy control of the temperature. A condenser, a component of the CPL system, is linked with a buffer evaporator in the form of an annulus section of a double tube heat exchanger arrangement: the concentric core of the double tube is the condenser; the annulus section is used as a buffer between the conditioned space and the radiation surrounding but works as an evaporator. A CPL system with this type of

condenser is modeled to simulate its function numerically. Preliminary results for temperature variations of the system are shown and more investigations are suggested for further improvement. Author

N93-13403*# National Aeronautics and Space Administration. Lewis Research Center, Cleveland, OH.

A SINDA '85 NODAL HEAT TRANSFER RATE CALCULATION USER SUBROUTINE

Derrick J. Cheston *In its* The Fourth Annual Thermal and Fluids Analysis Workshop 1992 p 271-281 (For primary document see N93-13385 03-34)

Avail: CASI HC A03/MF A03

This paper describes a subroutine, GETQ, which was developed to compute the heat transfer rates through all conductors attached to a node within a SINDA '85 thermal submodel. The subroutine was written for version 2.3 of SINDA '85. Upon calling GETQ, the user supplies the submodel name and node number which the heat transfer rate computation is desired. The returned heat transfer rate values are broken down into linear, nonlinear, source and combined heat loads. Author

N93-13406*# California Univ., Los Angeles. Dept. of Mechanical, Aerospace and Nuclear Engineering.

FLUID FLOW AND HEAT CONVECTION STUDIES FOR ACTIVELY COOLED AIRFRAMES Report, May - Oct. 1992

A. F. Mills Oct. 1992 9 p

(Contract NCC2-374)

(NASA-CR-190956; NAS 1.26:190956) Avail: CASI HC A02/MF A01

The work done during the progress report period from May-October 1992 is summarized. The effect of wall thermal boundary conditions on flows over a step or rib when repeated rib roughness is used for heating augmentation is examined. In numerical investigations of various such laminar and turbulent flows, the local heat transfer coefficients on a forward-facing step or on a rib were found to be very sensitive to the wall thermal boundary condition. For the computation of constant property laminar flow, the wall thermal boundary conditions were either a uniform heat flux or a uniform temperature. Results (Nusselt number and isotherms) of the studies are included. The second part of the work consisted of using PHOENICS to solve the conjugate heat transfer problem of flow over a rib in channel. Finally, the algebraic stress model in the TEAM (Turbulent Elliptic Algorithm-Manchester) code was tested for jet impingement flow, but there needs to be an addition of the energy equation to the code. L.R.R.

N93-13453*# California Univ., Davis. Dept. of MAME.

A PDF CLOSURE MODEL FOR COMPRESSIBLE TURBULENT CHEMICALLY REACTING FLOWS Final Report

W. Kollmann 1992 191 p

(Grant NAG3-836)

(NASA-CR-191209; NAS 1.26:191209) Avail: CASI HC A09/MF A02

The objective of the proposed research project was the analysis of single point closures based on probability density function (pdf) and characteristic functions and the development of a prediction method for the joint velocity-scalar pdf in turbulent reacting flows. Turbulent flows of boundary layer type and stagnation point flows with and without chemical reactions were be calculated as principal applications. Pdf methods for compressible reacting flows were developed and tested in comparison with available experimental data. The research work carried in this project was concentrated on the closure of pdf equations for incompressible and compressible turbulent flows with and without chemical reactions. Author

N93-13517 Iowa State Univ. of Science and Technology, Ames.

WALL FUNCTIONS FOR THE KAPPA-EPSILON TURBULENCE MODEL IN GENERALIZED NONORTHOGONAL CURVILINEAR COORDINATES Ph.D. Thesis

Douglas L. Sondak 1992 172 p

Avail: Univ. Microfilms Order No. DA9223968

Wall functions are often employed to model turbulent flow near solid walls. A method has not been available, however, for the application of wall functions to generalized curvilinear coordinate systems, particularly those with nonorthogonal grids. A general method for this application is developed herein. A kappa-epsilon turbulence model suitable for compressible flow, including the new wall function formulation, was incorporated into an existing compressible Reynolds-averaged Navier-Stokes code, F3D. The low-Reynolds-number kappa-epsilon model of Chien (1982) was added for comparison with the present method. A number of features were also added to F3D, including improved far-field boundary conditions and viscous terms in the streamwise direction. A series of computations of increasing complexity was run to test the effectiveness of the new formulation. Flow over a flat plate was computed using both orthogonal and nonorthogonal grids, and the friction coefficients and velocity profiles were compared with a semi-empirical equation. Flow over a body of revolution at zero angle of attack was then computed to test the method's ability to handle flow over a curved surface. Friction coefficients and velocity profiles were compared to test data. The same case was also computed using the Chien (1982) low-Reynolds-number kappa-epsilon model and the Baldwin-Lomax (1978) algebraic model for comparison. All three models gave good results on a relatively fine grid, but only the wall function formulation was effective with coarser grids. Finally, in order to demonstrate the method's ability to handle complex flow fields, separated flow over a prolate spheroid at angle of attack was computed, and results were compared to test data. The results were also compared to the computation of Kim and Patel (1991), in which a kappa-epsilon model with a one-equation model patched in at the wall was employed. Both models gave reasonable solutions, but they require improvement for accurate prediction of friction coefficients in the separated regions. Dissert. Abstr.

N93-13532 Arizona State Univ., Tempe.

STUDIES ON TURBULENT MIXING IN STRATIFIED TURBULENT PATCHES Ph.D. Thesis

Induruwage Prabhath DeSilva 1991 236 p

Avail: Univ. Microfilms Order No. DA9210371

A research program aimed towards understanding turbulent mixing in stably stratified fluids and the possible causes of such mixing was carried out giving particular attention to turbulent patches that are ubiquitous in stratified environments. The research program consists of three interrelated investigations of laboratory experimental nature, namely: (1) mixing in non-collapsing stratified turbulent patches; (2) mixing in collapsing turbulent patches; and (3) generation of turbulence owing to the interaction between the mean velocity shear and internal gravity waves (critical-layer phenomena). In the first two cases sustained oscillations of a monoplanar grid were used to generate turbulence. The third series of experiments was conducted in a stratified shear flow tank and the waves were artificially introduced. In the latter case only preliminary test runs were conducted and the major task was to complete the development of a novel Richardson number probe to be used in future experiments. Various properties of oscillating grid turbulence in homogeneous fluids were investigated as a precursor to the stratified turbulence studies. These included spatial and temporal decay laws and the influence of wall-induced secondary circulations. The results were found to be in conformity with previous theoretical predictions. The studies on noncollapsing turbulent patches in stratified fluids revealed that the initial stages of patch growth are unaffected by the stratification, but as the patch grows stratification becomes important and arrests the turbulent front propagating drastically, at a time of order 4N(sub 0)(exp -1) where N(sub 0) is the buoyancy frequency. Thereafter the patch grows slowly owing to the local mixing events at the interfaces caused by wave breaking. The time evolution of the buoyance frequency N within the patch, the buoyancy lengthscale, the overturning lengthscale, the Thorpe lengthscale, the maximum Thorpe displacement, Available Potential Energy Fluctuations within the patch and the r.m.s. amplitudes and frequencies of interfacial wave distortions were measured and their interrelationships were examined, wherever possible, using simple theoretical arguments. Various aspects of energy radiation from the patch into the outer stratified layer and the influence of the grid parameters on the universality of the results were also studied. The formation of an intrusion carrying the mixed fluid during the collapsing experiments introduces additional complexities. This is associated with the formation of complex secondary flows in the outer stratified layer. The initial development of the turbulent layer was found to be similar to the non-collapsing case, but after the collapse begins the behavior of the collapsing patch was much different. The properties of the intrusion and the return currents were measured in this case, in addition to various lengthscales and other system parameters described above. Attempts are also made to explain the results using simple theoretical models. Dissert. Abstr.

N93-13575# Sandia National Labs., Albuquerque, NM.
SUMMARY ON COMPARISON OF RADIATIVE HEAT TRANSFER SOLUTIONS FOR A SPECIFIED PROBLEM
T. W. Tong and R. D. Skocypec (Arizona State Univ., Tempe.) 1992 12 p Presented at the American Society of Mechanical Engineers National Heat Transfer Conference and Exposition, San Diego, CA, 9-12 Aug. 1992
(Contract DE-AC04-76DP-00789)
(DE92-040098; SAND-92-1745C; CONF-920804-22) Avail: CASI HC A03/MF A01

To assess the current capability for solving non-gray, anisotropically scattering multidimensional radiation problems, a specific problem was formulated for several participating authors to solve. They each applied their own methods to solve the problem, which was relevant to the modeling of heat transfer in coal-fired furnaces. This paper is a summary of the comparison of the results. Areas where future modeling efforts should address are identified. DOE

N93-13609 Iowa State Univ. of Science and Technology, Ames.
SOLUTION OF VISCOUS FLOW PROBLEMS BY USING THE BOUNDARY ELEMENT METHOD Ph.D. Thesis
Abdel-Magid Abdel-La Abdalla 1992 109 p
Avail: Univ. Microfilms Order No. DA9223911

A scheme based on the Boundary Element Method (BEM) for solving the problem of steady flow of an incompressible viscous fluid is presented in this thesis. The problem is governed by both Navier-Stokes (N-S) equations and the continuity equation. The fundamental solution of the two-dimensional N-S is derived, and the partial differential equations are converted to an integral equation. The computer code is flexible enough to handle a variety of boundary and domain elements with different degrees of interpolation polynomial. Boundary and domain integrals over corresponding elements are evaluated analytically. The Newton-Raphson iteration scheme accompanied by a relaxation factor is used to solve the nonlinear equations. The code includes a post processor that calculates the velocity components at any point inside the domain. The scheme has been applied to three test problems. The first concerns Couette flow, which has been used as a test case for testing the rate of convergence and accuracy. The second and the third concern the driven cavity and the flow in a stepped channel, respectively. In the integral equation formulation, the primary unknowns are tractions on the domain boundary and velocities in the interior. Because the shear stress, drag, and lift can be simply computed from the values of tractions along the boundary, such a formulation is markedly superior to either the finite-difference or the finite-element formulation. In customary pressure-velocity of streamfunction-vorticity formulations, employed in the finite-difference or finite-element methods, calculation of stress, drag, and lift involves extensive post processing. Dissert. Abstr.

N93-13743 Kentucky Univ., Lexington.
TRANSIENT BEHAVIOR OF HEAT PIPE WITH THERMAL ENERGY STORAGE UNDER PULSE HEAT LOADS Ph.D. Thesis
Ming-Jr Chang 1991 204 p
Avail: Univ. Microfilms Order No. DA9212968

Future space missions will require thermal transport devices with the ability to handle transient pulse heat loads. A novel design of a high-temperature axially grooved heat pipe (HP) which incorporates thermal energy storage (TES) to migrate pulse heat loads was presented. A phase-change material (PCM) which is encapsulated in cylindrical containers was used for the thermal energy storage. The transient response of the HP/TES system under two different types of pulse heat loads was studied analytically. The first type is pulse heat loads applied at the heat pipe evaporator, the second type is reversed-pulse heat loads applied at the condenser. In this research, a new three-dimensional alternating-direction-implicit (ADI) method was developed to model the heat conduction through the heat pipe wall and wicks, including the liquid flow in grooves. A very important characteristic of this new ADI method is that it is consistent with physical considerations. Compared with the well-known Brian's and Douglas's ADI methods, this new ADI method had higher accuracy and requires less computer storage. In the numerical solution of heat transfer problems with phase change (Stefan-type problem), a modified Pham's method which includes features from enthalpy and heat capacity methods was used to simulate the melting and solidification processes of the PCG. The vapor flow was assumed quasi-steady and one-dimensional, and was coupled with the evaporation and condensation on the heat pipe inside wall surface and the surfaces of the PCM containers. The transient responses of three different HP/TES configurations were compared: (1) a heat pipe with a large empty cylinder installed in the vapor core, (2) a heat pipe with a large PCM cylinder, and (3) a heat pipe with six small PCM cylinders. From the numerical results, it was found that the PCM is very effective in mitigrating the adverse effect of pulse heat loads. The six small PCM cylinders are more efficient than the large PCM cylinder in relaxing the heat pipe temperature increase under pulse heat loads. Also, the small PCM cylinders can handle periodic, pulse heat loads better because the small PCM cylinders can solidify faster after each periodic, pulse heat load is terminated. A simple lumped-heat-capacity model was also used to predict the transient behavior of the heat pipe without PCM. Compared with the results from the finite-difference solution, it was found that the lumped model can predict the average heat pipe temperature and the heat input/output as the evaporator and condenser for the heat pipe without PCM quite well. Dissert. Abstr.

N93-13749 Lehigh Univ., Bethlehem, PA.
THE THREE-DIMENSIONAL TURBULENT BOUNDARY LAYER: THEORY AND APPLICATION Ph.D. Thesis
Ammar Taher Degani 1991 366 p
Avail: Univ. Microfilms Order No. DA9207008

The objective of the present study is twofold: (1) to derive the basic structure of a three-dimensional turbulent boundary layer through an asymptotic analysis in the limit of large Reynolds number, and (2) to design and implement an embedded-function method to calculate turbulent boundary-layer flow efficiently. A two-layer structure exists in which the streamwise velocity is brought to rest through an outer defect layer and an inner wall layer in a manner similar to that in a two-dimensional boundary layer. The cross-stream velocity also behaves logarithmically in the overlap region but this behavior is associated with a higher-order term. Although the pressure gradient is of higher order in the wall layer, at large but finite Reynolds numbers, its effect is not negligible. The wall skew angle is shown to scale on the friction velocity. The out-layer self-similar solutions are calculated and matched to a wall-layer solution; the composite profiles so constructed describe the velocity profiles from the wall to the boundary-layer edge. It is shown that a two-parameter family of self-similar solutions exist. The effects of Reynolds number and cross-stream pressure gradient on the cross-stream velocity profile are investigated and discussed. In conventional calculation schemes, a substantial number of mesh points are required in the near-wall region to resolve the intense variation in velocity and enthalpy. In the embedded-function method developed in this study, mesh points within the wall layer are discarded and the velocity and enthalpy are represented analytically. The flow in the outer layer is calculated in the usual manner with the no-slip and heat-transfer condition at the wall being replace by the requirement that the velocity and enthalpy asymptote in a manner dictated by the theory. It is shown that up to a 50 percent reduction in the total number of mesh points and computational time may be realized without any degradation in the accuracy of the computed results. It is demonstrated that the present methodology is capable of calculating bi-directionally skewed cross-stream velocity profiles.
Dissert. Abstr.

N93-13765 Arizona State Univ., Tempe.
LINEAR STABILITY THEORY OF HYPERSONIC, CHEMICALLY REACTING VISCOUS FLOWS Ph.D. Thesis
Gregory Kent Stuckert 1991 383 p
Avail: Univ. Microfilms Order No. DA9134891

The linear stability of hypersonic, chemically reacting viscous shock layer on a sharp cone is studied subject to different approximations of the flow geometry and physics. The basic state laminar flows investigated are usually obtained using a Parabolized Navier-Stokes (PNS) code specifically developed for this purpose. It uses a shock-fitting scheme to capture the bow shock and thus avoids spurious numerical oscillations in the solution which could adversely affect the stability analysis. Consistent with this, the stability analyses which used these basic states then employed at the basic state shock location the linearized inviscid shock jump conditions (allowing for a disturbance in the shock location and slope as well) as boundary conditions for the disturbance state. The stability analyses subsequently carried out used different co-ordinate systems for a sharp cone with corresponding different disturbance state variables. The first of these approximates the surface of the cone as planar (i.e., Cartesian

co-ordinates are used). Another is the body-instrinsic co-ordinate system of the cone. The last one investigated is the nonorthogonal basic state shock-fit co-ordinate system. It is shown that as long as one defines the disturbance state variables appropriately, the first two co-ordinate systems produce almost identical results. However, although the results obtained using the basic static shock-fit co-ordinates are very similar for the higher inviscid modes, they predict that the first mode is unstable for the case studied--a result contrary to that obtained with either of the other two co-ordinate systems. Finally, the effects of chemical reactions on the flow were also investigated by making three different approximations of the physics: ideal gas; chemical equilibrium air; and chemical nonequilibrium air. Thermal equilibrium is always assumed and only the dissociation (not ionization) of air is considered. The results show that the equilibrium air results are radically different from those of the ideal gas and nonequilibrium air calculations. In particular, in a band of frequencies near the second mode, the equilibrium air disturbances become supersonic relative to the boundary layer edge velocity and hence exhibit much different properties. In both the equilibrium air and nonequilibrium air calculations, however, the second mode is shifted to a lower frequency relative to the perfect gas solution even though the corresponding boundary layers are thinner.

Dissert. Abstr.

N93-13767 Princeton Univ., NJ.

NUMERICAL CALCULATION OF TURBOMACHINERY CASCADE FLOWS Ph.D. Thesis

Feng Liu 1991 171 p

Avail: Univ. Microfilms Order No. DA9127102

A numerical method for solving both the Euler and the Reynolds-averaged Navier-Stokes equations for flows in turbomachinery cascades is presented and verified. The method is based on a finite volume method with an explicit multi-stage time-stepping scheme originally developed by Jameson for the Euler equations. Modified discretization schemes, based on Martinelli's work for the second order derivatives in the Navier-Stokes equations, are proposed for both the cell-vertex and the cell-centered schemes. The new schemes avoid a potential discretization problem with kinked meshes. Use of artificial dissipation to stabilize a central difference scheme and capture shocks is discussed. Local time stepping and residual smoothing are used to increase the allowable time steps for stability. A multigrid method is employed to accelerate convergence to steady state. For steady inviscid flows enthalpy damping is also used. The method is capable of handling flows of low Mach number (lower than 0.3), and transonic and supersonic flows. Both laminar and turbulent flows are calculated in solving the Reynolds-averaged equations. The Reynolds number may range from order 1 to 10(exp 7) or even higher as long as enough mesh resolution and a proper turbulence model are provided. The Baldwin-Lomax algebraic turbulence model is used in the current work. An elliptic mesh generator is used to generate H-type meshes for cascades. The cell-centered scheme is programmed in both two- and three-dimensions for the Euler equations. Numerical results included a two-dimensional Hobson cascade, a supersonic wedge cascade and the VKI turbine cascade. The three-dimensional code is used to calculate the flow in a low pressure turbine cascade. Results compare well with experimental data at design conditions. At off-design conditions, the Euler method fails in regions of large separations. Given an entrance boundary layer velocity distribution, it is confirmed that the Euler solver is able to capture three-dimensional vortex transport within a cascade passage. Numerical results of secondary flow developments agree qualitatively with experiment. The method for the Reynolds-averaged Navier-Stokes equations was tested for two-dimensional flows. Perfect agreement with the Blasius solution was obtained for low-speed laminar flow over a flat plate. Results for a turbulent flow over a flat plate compare well with empirical correlations. The method is used to calculate the flows at mid-span through the same low pressure turbine cascade for which the Euler method was tested. Calculated results compare well with experimental data not only at the design condition but also at off-design conditions. Skin friction plots show separation bubbles which agree with experiments. Dissert. Abstr.

N93-13781 Oxford Univ. (England).

VARIATIONAL CHARACTERIZATIONS OF STEADY TWO-DIMENSIONAL VORTEX MOTIONS Ph.D. Thesis

Anna Theresa Unwin 1991 130 p

Avail: Univ. Microfilms Order No. BRD-95165

The investigation concerns variational properties that relate to the stability of steady two-dimensional flows with vorticity in an inviscid, incompressible fluid. A general variational characterization of steady motions is developed following ideas of Kelvin and V. I. Arnol'd. The variational procedure amounts to an example of Liapunov's direct method applied to a continuous system. It is used to prove the nonlinear stability of an annular patch of constant vorticity and to establish sufficient conditions for stability with respect to infinitesimal, axially uniform disturbances of steady axisymmetric flows with uniform axial vorticity in a circular cylinder. A conditional variational principle is introduced: namely, a motion in a circular cylinder that is steady in a rotating reference frame realizes a conditional extremum of the kinetic energy with respect to variations in the class of rearrangements of some non-negative function and subject to the condition that the impulsive couple is constant. The existence of a conditional maximizer is proved. A stability criterion for steadily rotating vorticity distributions is derived by use of the conditional variational principle and spectral methods. Explicit second-order approximate solutions of the conditional variational principle that are small but finite-amplitude perturbations from circular and annular patches of constant vorticity are obtained, together with the respective approximate angular velocities. Numerical solutions are sought by means of a quadratic programming algorithm. Dissert. Abstr.

N93-13806 Stanford Univ., CA.

AN EXPERIMENTAL INVESTIGATION OF THE THREE-DIMENSIONAL BOUNDARY LAYER ON A ROTATING DISK Ph.D. Thesis

Howard Steven Littell 1992 255 p

Avail: Univ. Microfilms Order No. DA9217850

The velocity field above a large spinning disk has been studied using pressure probes and hotwire anemometers. The flowfield consists of a three-dimensional boundary layer due to a crossflow caused by centrifugal forces. The disk was 1 m in diameter and was spun at speeds up to 1500 rpm, giving momentum thickness Reynolds numbers in excess of 6000. The mean flow in both the laminar and turbulent regimes compares well with previous studies of 'infinite' smooth rotating disks. All six Reynolds stresses and the ten triple products have been measured using established crosswire anemometry techniques. These results are compared to previous three-dimensional boundary layer measurements and several key differences are noted. The ratio of the shear stress vector magnitude to the turbulent kinetic energy is a common descriptor of boundary layer flow and is used in many modeling efforts because it is usually a constant over most of a two-dimensional boundary layer. Three-dimensionality has been observed to depress this parameter near the wall in many pressure-driven boundary layers. In the disk flow, this parameter was at a maximum near the wall at close to the 2-D value, but dropped off almost linearly away from the wall. Two-point velocity correlations were also measured using a pair of crosswire anemometers to gain insight into the structure of the turbulence. These measurements were obtained at two different heights at momentum thickness Reynolds numbers of 2650 and 5000 to test for possible scaling effects. These measurements showed that the turbulence exhibits asymmetry in the crossflow direction, which cannot occur in two-dimensional boundary layers. A mechanism by which the crossflow may be modifying the turbulence structure is proposed which exhibits several features of the asymmetric two-point correlations. Dissert. Abstr.

N93-13825 Texas Univ., Austin.

COMPUTER MODELING OF FLOW AND TRANSPORT INTERACTIONS FOR COMPRESSIBLE NAVIER-STOKES EQUATIONS Ph.D. Thesis

Mohamed Mizanur Rahman 1992 222 p

Avail: Univ. Microfilms Order No. DA9225703

A unified numerical algorithm to simulate viscous flow with heat transfer over a wide range of Mach number and Reynolds number is developed. The governing equations used to model the numerical simulations are the 2-D compressible viscous Navier-Stokes equations. The numerical procedure is based on MacCormack's explicit 'predictor corrector' time dependent finite difference scheme. For an explicit scheme, a great number of iterations is required to get a converged steady solution because of a small time step. Vectorizing and parallelizing the code greatly alleviates this problem by reducing the total job running time manifold. The numerical algorithm, thus developed, is used to simulate such demanding and interacting flow problems as convection heat transfer in a cavity flow heat transfer enhancement by eddy-promoters, laminar/turbulent shock boundary layer

interactions and unsteady shock boundary layer interactions over a compression corner. A detailed analysis of all important flow features that characterize such flows and the mechanisms that are involved, is performed for each individual case. The flow physics are discussed and new insights are provided. Results are compared with experimental data where available and the empirical relations between different flow properties or parameters are either established or verified where possible. Apart from these, some algorithm related questions, such as grid sensitivity, boundary conditions, convergence criteria, effects of artificial viscosity and the numerical stability are investigated. Dissert. Abstr.

N93-13826 Texas Univ., Austin.

AN EXPERIMENTAL/COMPUTATIONAL STUDY OF HEAT TRANSFER IN SHARP FIN INDUCED SHOCK WAVE/TURBULENT BOUNDARY LAYER INTERACTIONS AT LOW HYPERSONIC MACH NUMBERS Ph.D. Thesis

Patrick Elroy Rodi 1992 302 p

Avail: Univ. Microfilms Order No. DA9225710

A combined experimental and computational study has been performed of sharp fin induced shock wave/turbulent boundary layer interactions at Mach numbers of 5, 6, and 11. New experimental data were obtained at Mach 5 and include mean surface heat transfer and pressure distributions and surface flow visualization for fin angles of attack of 6, 8, 10, 12, 14 and 16 degrees. Detailed heat transfer measurements were also taken radially at 8 and 16 degrees to study the flowfield's conical nature. Conical Navier-Stokes calculations have been performed using the Baldwin/Lomax turbulence model. Computations were made for two angles of attack at each of the three Mach numbers. The Mach 6 and 11 data used for comparison with the computations, were from the earlier experimental studies of Law and Holden. Careful evaluation of the performance of this numerical approach has been carried out with an emphasis on the surface heat transfer predictions. The new experimental results are described in detail and compared with existing empirical correlations. Comparisons of the experimental data with the computations reveal that the conical Navier-Stokes/Baldwin-Lomax approach underpredicts the physical extent of the interactions for the lower two Mach numbers. However, this trend is reversed at Mach 11. The numerical results overpredict peak heat transfer, although the outer scaling of the Baldwin-Lomax model prevent a grid independent solution. The computed flowfields reveal a large primary vortex located adjacent to the surface just beneath the inviscid shock wave and a smaller corner vortex located very near the fin/surface junction.

Dissert. Abstr.

N93-13898 Stanford Univ., CA.

INTERACTION OF ISOTROPIC TURBULENCE WITH A SHOCK WAVE Ph.D. Thesis

Sangsan Lee 1992 243 p

Avail: Univ. Microfilms Order No. DA9221635

As a first step to understand the compressibility effects, the interaction of isotropic quasi-incompressible turbulence with a weak shock wave was studied by three-dimensional time-dependent simulations. In addition, linear analysis was used to study interaction of isotropic turbulence with shock waves of a wide range of strengths. The effects of the fluctuation Mach number M(sub t) and the average Mach number M(sub 1)(sup U) of the upstream turbulence statistics were investigated. Both numerical simulations and linear analyses of the interaction show that turbulences is enhanced during the interaction with a shock wave. Turbulent kinetic energy (TKE) and transverse vorticity components are amplified, and turbulent length scales are decreased. The predictions of the linear analyses compare favorably with simulation results for flows with M(sub t) less than M(sub 1)(sup U)-1, which suggests that the amplification mechanism is mainly linear. Rapid evolution of TKE just downstream of the shock was not, however, reproduced by the linear analysis. Investigation of the budget of the TKE transport shows that this behavior of TKE is manifested in the pressure transport term which is nonlinear. The budgets of enstrophy components show that their amplifications through the shock are mainly caused by the distortion due to the mean flow compression, and that effect of baroclinic torque is not significant. Shock waves were found to be distorted by the upstream turbulence, but still have a well-defined shock front for M(sub t) less than M(sub 1)(sup U)-1. In this regime, the statistics of the displacement and inclination of the shock front compare favorably with the linear analysis predictions. For flows with M(sub t) greater than M(sub 1)(sup U)-1, shock waves no longer have well-defined fronts: shock wave thickness and strength vary widely along the transverse directions. Multiple peaks in pressure are found along the mean streamline where the local thickness of a shock wave has increased significantly.

Dissert. Abstr.

N93-13899 Oxford Univ. (England).

DYNAMICAL INSTABILITIES IN A FLUID SPIN-UP AND IN AN OPEN FLOW SYSTEM Ph.D. Thesis

Francis Madden 1991 176 p

Avail: Univ. Microfilms Order No. BRD-96229

The dynamics of two different fluid flow systems are studied. First, an open system is modulated flow through a sudden symmetric expansion. Here, there are 3 control parameters: the mean flow rate, the amplitude, and frequency of modulation. A rich variety of finite dimensional behavior is observed as the amplitude of modulation, measured as a percentage of the mean flow rate, is increased from 0 to 10 percent. The behavior consists of frequency locking to 1/2 of the driving frequency, quasi-periodicity, hysteresis, homoclinicity with an associated irregular mode and period doubling. These dynamics exist in the flow modulation experiment whereas no indication of finite dimensional behavior is found in the steady flow case. The spin-up from rest of a fluid filled torus was studied both experimentally and numerically. The dynamics of the transient phenomenon in an unstable spin-up configuration are examined in this closed system. The spin-up process is found to progress through a sequence of states as the final rotational rate is increased. These states are viscous diffusion, establishment of a significant secondary flow, appearance of fronts, breaking of axisymmetry and nonuniqueness, and also an inner wall phenomenon. As the final rotational rate is changed, the fractional spin-up time behaves anomalously near transitions between these states but it does not give any other indication of the fluid's dynamical condition. A technique is described which allows the phase portraits of many equivalent experimental runs to be constructed together. The results produced are a useful device for comparing flow paths in the spin-up process. The time dependent Navier-Stokes equations are solved numerically for axisymmetric spin-up flows. The quantitative and qualitative agreement with experimental results is excellent for values of the dynamical control parameter less than 500.

Dissert. Abstr.

N93-13900 California Univ., San Diego.

STRUCTURES, SPECTRA AND INERTIAL RANGE TRANSFER IN TWO-DIMENSIONAL AND BETA-PLANE TURBULENCE Ph.D. Thesis

Mathew Einar Maltrud 1992 116 p

Avail: Univ. Microfilms Order No. DA9222242

A wide range of numerical simulations have been performed to study the behavior of coherent structures in a steady, forced-dissipative, homogeneous, incompressible, two-dimensional (2D) turbulent fluid, a model system of importance in the study of geophysical fluid dynamics. Flow regimes are examined and compared with classical inertial range theories of 2D turbulence. In the enstrophy inertial range, strong vortices are found at the forcing scale and smaller. Energy spectra in this inertial range typically display two distinct subranges, one (at small length scale) that is close to the predicted slope (k(exp -3), where k is the wavenumber), and one (at largest scales) that is steeper than predicted. As the strength of vortices is reduced, either through friction or the addition of differential rotation (the 'beta-effect'), the steep part of the spectrum shallows. Coherent vortices may be eliminated with very strong friction, in which case the entire inertial range spectrum has the predicted slope and a universal Kolmogorov constant may be found with a modification to the classical phenomenology. In the energy inertial range, vortices are found only near the forcing scale, and not at larger scales in the inertial range. If the vortices are strong, the spectral slope is steeper than predicted. The predicted spectral slope (k(exp -5/3)) is recovered when vortex strength is reduced by frictional effects and the Kolmogorov constant appears universal. When forcing is applied at both large and small scales, we find stable coexistent inertial ranges with no need for intermediate range dissipation. If the Beta-effect is sufficiently strong, vortices are replaced by persistent zonal jets and enstrophy inertial range spectra are steeper than k(exp -3), while energy inertial range spectra remain close to k(exp -5/3). Investigation of energy and enstrophy transfer and flux in the enstrophy inertial range shows that interactions are due to very elongated wavevector triads. It is found that the actual enstrophy transfer and flux are local in wavenumber

space, but the energy flux has an important nonlocal component. In the energy inertial range, a wider array of triads are active and both local and nonlocal components of the flux are important. Dissert. Abstr.

N93-13901 McGill Univ., Montreal (Quebec).
CASCADE PROCESSES AND FULLY DEVELOPED TURBULENCE Ph.D. Thesis
Antoine Saucier 1991 264 p
Avail: Univ. Microfilms Order No. DANN67833

The energy cascade process in turbulent flows is studied. Kolmogorov inertial range theories are critically reviewed and the multifractal characterization is discussed. Multiplicative cascade models are compared to the energy dissipation field (EDF) measured in the atmosphere. Landau's objection to the 1941 Kolmogorov theory is extended to the predictions of statistical fluid mechanics. The hypothesis Delta v(lambda(L)) d/= lambda 1/3 Delta v (L) is rejected with a statistical test. The moments ((log epsilon(L)) sup p), where epsilon (L) denotes the EDF averaged over a volume of size L, are shown to be Gaussian. For the EDF: Convergence tests showed that the exponents r(q) were not reliable for q less than 0; the correlations obey ((mu sub x(delta)) sup p(mu sub x + delta(delta)) sup q) infinity delta sup gamma(p,q) but gamma does not always equal the value obtained with a multinominal measure; a privileged scale ratio r approx. = 1/2 is suggested by the prefactor oscillations of the correlation function. The implications of these results for the modelling of the EDF are discussed. Dissert. Abstr.

N93-13918 Tennessee Univ., Knoxville.
NUMERICAL INVESTIGATION OF NON-SPHERICAL DROPLET DYNAMICS IN VISCOUS CONVECTIVE FLOWS Ph.D. Thesis
Zhengtao Deng 1991 165 p
Avail: Univ. Microfilms Order No. DA9221749

A comprehensive computational model based on the Arbitrary Lagrangian Eulerian (ALE) numerical algorithm was developed for the numerical simulation of nonspherical (deforming) evaporating droplet dynamics in viscous convective flows. This model has the ability to solve both incompressible and compressible (two-phase) fluid flows separated by a free surface where surface tension forces, phase change, mass and heat transfer are very important. Special treatment of surface tension forces and interface jump conditions were carefully developed in the modeling effort. This model has been used to study the dynamics of cylindrical/spherical droplet shape free oscillation, nonevaporating and evaporating droplets undergoing 'deformation breakup' and oscillation dynamics under inviscid and/or viscous convective flows. The model developed was validated by comparisons of droplet shape oscillation simulations to theoretical analysis. It was shown that the numerically predicted droplet shape oscillation frequencies agree closely with those derived from linear theory. The surface pressure formula works well for the interface discontinuity. The results of spherical droplet deformation/oscillation were also compared to experimental results yielding good agreement. In the droplet deformation/breakup dynamics study, the numerically predicted breakup mode agrees well with experimentally derived criteria. The effects of droplet deformation on evaporation rates were examined indicating that the nonspherical droplet evaporation rates are significantly different from that of spherical droplets. Imposed inflow velocity fluctuations have a significant effect on the droplet evaporation rate both for spherical and nonspherical droplets. Potential applications of the present code to high pressure droplet dynamics, and microgravity free surface dynamics are discussed. Dissert. Abstr.

N93-13920 Wichita State Univ., KS.
COMPUTATIONAL FLUID DYNAMICS OF THE BASE FLOW ON A PLANE BODY BETWEEN A SUBSONIC FLOW ON ONE SIDE AND A SUPERSONIC FLOW ON THE OTHER Ph.D. Thesis
Mohammad Javad Izadi 1991 133 p
Avail: Univ. Microfilms Order No. DA9221970

Base flow characteristics are very important for determination of drag in aircraft propulsive systems. Since the performance of these systems must be known before actual production, and it is very costly to build and test every system in order to select the best design, a computational approach is an inexpensive way of determining that best design. There have been several approaches toward a variety of base flow problems but the problem of base flows at subsonic flight with supersonic central jet has not yet been approached computationally. Yet this is a commonly occurring condition. Therefore, in this project a computational scheme was developed using paneling and modeling methods to determine the flow behavior at and around a plane base. Such a method is not as accurate as a finite-difference Navier Stokes CFD solution, but is very much easier and faster to compute, thus qualifying as a good tool for design work. Using a combination of two singularities, sources plus vortices or doublets, a model of a plane body and the wake behind the base is generated. After inviscid modeling of the body and the wake, the viscous mixing of the subsonic flow and the supersonic jet are superimposed on this model as boundary conditions. The three general areas (subsonic outer flow, supersonic jet flow, and base area which is bounded by the nozzle body, the outer flow and the jet flow) are simulated using a paneling method, and the Chapman-Korst method for simulation of the mixing boundaries. In this project, pressure and velocity distribution around a plane 2-dimensional base at several flight and jet speeds are calculated. These results are in a good correlation with the expected results known from the physics of body and flow outside and inside the wake. It is regretted that no applicable experimental results could be found for comparison with this computation. This lack of data is surprising and should be remedied. Dissert. Abstr.

N93-13937 Michigan State Univ., East Lansing.
A MULTIPLE-VIEW VISUAL STUDY OF THE INNER/OUTER REGION INTERACTIONS OF COHERENT MOTIONS IN A TURBULENT BOUNDARY LAYER Ph.D. Thesis
Kue Pan 1992 198 p
Avail: Univ. Microfilms Order No. DA9223234

A time resolved multiple-view laser sheet and multiple location, multicolor dye injection flow visualization technique was used to observe the interactions between sublayer motions and the coherent motions above the wall in a turbulent flat-plate flow at R sub theta approximately = 805. Pairs of low-speed streaks were observed to form and evolve underneath passing typical eddies in the log region and lower portion of the outer region. The pairs of streaks were also found to be associated with the formation of a pocket between the streaks near their downstream end. Statistical characteristics of the observed coherent features and their interactions are presented. The streak pair spacing was found to be on average l sub + approximately = 75. Observations in laser sheets perpendicular to the flow direction consistently showed counter-rotating vortex pairs. Because of the highly resolved temporal record and the complementary spatial information, it was determined that the streamwise extent of these pairs was similar to the length characteristic of the typical eddies. Thus, they were not long axial vortices, or stretched hairpin legs. Instead they were identified as typical eddies. This was confirmed both by the dye with which they were colored, which indicated they were not connected to the wall, and by visual identification in the side view laser sheet of the typical eddy pattern. Correlations of the concurrent occurrences of the typical eddies and the sublayer features, pockets, and streak pairs, below them were examined. Results show that the average sizes of these coherent motions are similar, and that the dimensions of both sublayer features increase as the spanwise diameter of the typical eddy increases. The sampling of low-speed streaks using a classical counting method was also performed to confirm the universal mean streak spacing. An argument utilizing the statistical results of the typical eddy spanwise distribution spacing and the streak pair spacing enables one to recover the results that the overall streaky structure has a spacing of lambda sup + approximately = 100 at this Reynolds number. An overall picture of the inner/outer region interactions and the pinch-off phenomena of hairpin vortices at low Reynolds numbers is also presented. Dissert. Abstr.

N93-13938 Stanford Univ., CA.
TURBULENT BOUNDARY LAYERS WITH HIGH TURBULENCE: EXPERIMENTAL HEAT TRANSFER AND STRUCTURE ON FLAT AND CONVEX WALLS Ph.D. Thesis
Michael Kenneth Sahm 1992 433 p
Avail: Univ. Microfilms Order No. DA9221658

Experimental measurements of the effects of high levels of free stream turbulence on convex wall boundary layers were made. Using three different means of turbulence generation, intensities from 6 percent to 30 percent and length scales, L sub u/delta from 0.2 to 3 were achieved. The degree of curvature was strong for all cases, ranging from 0.12 to 0.15. Both the attenuating effects of convex wall curvature and the augmenting effects of

turbulence were observed for all cases. The augmentation in Stanton number is about two or three times the local turbulence intensity present. The exponential Reynolds number dependence in the upstream flat plate flow maintains a -0.25 slope and in the curve maintains a -1 slope. Skin friction is also augmented by free stream turbulence. Increases in skin friction are comparable to those in heat transfer but do not correspond exactly for each case. Based on length scales determined, it is concluded that smaller relative scales are more effective in augmenting skin friction and larger scales are more effective in augmenting heat transfer. Careful flow field control upstream of the curve resulted in typical curved potential core behavior. An important effect of turbulence on the velocity profile in the curve is the broadening of the transition between the boundary layer and the potential core profile. This transition grows wider and flatter as the turbulence level is increased. With the highest level of turbulence achieved, the outer region profile, transition becomes very wide and flat and a previously unreported viscid/inviscid interaction takes place which leads to rapid boundary layer growth in the curve. The correlation of the present data was examined. The Ludwieg-Tillmann correlation for skin friction was found to predict the present baseline data and the data for all three turbulence cases to about +/- 6 percent including the effects of curvature. A thermal analogy to the LT correlation was developed for use with free stream turbulence and curvature. A two dimensional boundary layer prediction program employing three different turbulence closure methods was used to model the current data. A low Reynolds number model is seen to produce the best overall prediction. Dissert. Abstr.

N93-13948 Stanford Univ., CA.
STABILITY OF THE COMPRESSIBLE REACTING MIXING LAYER Ph.D. Thesis
Dongshin Shin 1992 231 p
Avail: Univ. Microfilms Order No. DA9221665

Linear stability analysis is used to understand the behavior of compressible reacting mixing layers. The chemistry model is a single step, irreversible, finite rate reaction between the fuel in the upper stream and oxidizer in the lower stream. Laminar flows calculated from the compressible boundary-layer equations serve as inputs to the stability study, and illustrate the structure of laminar diffusion flames. For incompressible free shear layers with density variation, new inflectional modes of instability (outer modes) occur in the outer part of the mixing layer when there is significant heat release. Heat release stabilizes the center mode (Kelvin Helmholtz mode) but hardly affects the outer modes. For heat release typical of combustion flows, the outer modes are more amplified than the center mode. However, the outer modes do not cause the flow to roll up in the manner of an incompressible non-reacting mixing layer, so the mixing between fuel and oxidizer is reduced. In compressible free shear layers, supersonic unstable modes can exist, provided there is a region of the laminar flow supersonic relative to the disturbance phase velocity. The most unstable modes are the center modes at low Mach numbers, but the outer modes at high Mach numbers. The growth rate of the mixing layer drops with increasing Mach number and approaches an asymptotic value at high Mach numbers. Heat release destabilizes high-speed flows. Supersonic disturbances do not mix the reactants very well because they are largely confined to one side of the flow. For reacting flows, the most unstable modes are two-dimensional outer modes even at high Mach numbers. Reflection of supersonic disturbances by the walls makes the confined supersonic mixing layer more unstable than the unconfined free shear layer. Decreasing the distance between the walls makes the flow more unstable. However, subsonic disturbances are relatively unaffected by the walls. The most unstable supersonic disturbances are two-dimensional in rectangular channel flows, but three-dimensional in partially confined flows. Finally, the reactants are not strongly mixed by supersonic instabilities which mainly disturb one side of the layer. Dissert. Abstr.

N93-13952 Catholic Univ. of America, Washington, DC.
ORGANIZED TURBULENT STRUCTURES AND THEIR INDUCED WALL PRESSURE FLUCTUATIONS Ph.D. Thesis
Vincent Wilczynski 1992 283 p
Avail: Univ. Microfilms Order No. DA9220786

The interaction between the velocity fluctuations within and the wall pressure below a turbulent boundary layer has been experimentally studied. The fluid flow within a turbulent boundary layer has quasi-periodic patterns of organized motion that are responsible for the production and dissipation of turbulence. These coherent motions occur intermittently and exhibit a broad range of spatial and temporal scales, thereby preventing the use of a single detection method to identify all structures. The objectives were to identify the coherent structures within the boundary layer and study the contributions of these structures to the wall pressure signature. Simultaneous measurements of the velocity and wall pressure fluctuations were obtained using hot-wire anemometers and an acoustic microphone. The spectral, statistical, and temporal characteristics of the data were analyzed using long time averaging techniques and event detection methods. Five of the known classes of coherent structure were identified in the collected data by more than one signal processing method. Large scale structure was observed outside the boundary layer transmitted across the boundary layer and produced low frequency oscillations in the wall pressure signature. Intermittent, short duration velocity events, which are related to the production and dissipation of turbulence, were identified across the boundary layer. These fluctuations produced a discernable pattern in the wall pressure signature and the observations were used to produce a model of the wall pressure fluctuations during the turbulence production process. Dissert. Abstr.

N93-13953 Salford Univ. (England).
FLOW PREDICTION FOR THREE-DIMENSIONAL INTAKES AND DUCTS USING VISCOUS-INVISCID INTERACTION METHODS Ph.D. Thesis
Ian Edward Wrisdale 1991 391 p
Avail: Univ. Microfilms Order No. BRD-96502

A numerical scheme for the prediction of flows in engine intakes is presented. The scheme, which employs a viscous-inviscid interaction approach, is aimed at the treatment of high Reynolds number flows in which a significant region of inviscid core flow exists in the intake. The scheme is restricted to the treatment of attached flows; however, it is suitable for the treatment of highly rotational flows. The subsonic core flow calculations in the intake duct are performed using an Euler space marching scheme. Accurate flow prediction using the scheme requires the specification of detailed boundary conditions at the inlet plane of the duct. Appropriate conditions have been obtained by using a finite volume time marching scheme to calculate the flow field around inlet cowls at incidence. Hence, the boundary conditions for the duct calculations take account of the lip flows which are dependent on free stream conditions, incidence, and the mass flow ratio. Careful matching of the cowl and duct calculations provides a solution of the complete inviscid flow field both internal and external. The viscous-inviscid interaction scheme couples the inviscid solutions to a fully three-dimensional boundary layer method using a displacement surface model. The integral boundary layer method is aimed at the treatment of attached, turbulent boundary layers and includes the effects of rotational outer flows. Although the method is restricted to attached flows it may be used to indicate the onset of three-dimensional flow separation. The coupling of the inviscid flows and the boundary layers on the internal and external surface of the intake provide a complete description of the entire flow field. Numerical examples are presented throughout the work to illustrate the various methods. The complete scheme is then used to calculate the flow in an S-shaped intake duct operating under choked conditions at varying angles of incidence. Dissert. Abstr.

N93-13964 Colorado Univ., Boulder.
COHERENT STRUCTURES IN COMPRESSIBLE CONVECTION Ph.D. Thesis
Xin Xie 1991 202 p
Avail: Univ. Microfilms Order No. DA9220460

An issue of some debate in numerical simulations of compressible convection is concerned with whether the flows break up into multiple cells in the vertical, or whether coherent flow structures exist which span much of the depth range. We have carried out a series of two-dimensional simulations to determine whether vertically coherent flow patterns found in some of the earlier studies persist as the convective motions are required to carry an ever greater fraction of the total energy flux upward (in the limit of very 'efficient' convection), or when the density contrast across the convective layer is high (factor of approximately 100), or when an eddy viscosity is employed instead of a constant dynamic viscosity. Such circumstances were thought by some to be responsible for the compressible convection breaking up into multiple cells, in a manner favored by mixing-length models. In all the cases that we have studied, the convection consists of flows coherent over the entire depth of the computational

domain, with no tendency to form a series of cells in the vertical, contrary to the basic assumption of mixing-length approaches. The convective flows are often supersonic near the upper boundary. In some cases fluttering shocks form on the sides of the downflows, and significant modulation of the enthalpy and kinetic fluxes by vertical acoustic pulsations is observed. It appears that sufficient thermal diffusion and a high density contrast create a situation that favors the formation of supersonic regions near the upper boundary. Yet substantial thermal diffusion may also broaden the shocks into smooth transition regions, and large pressure fluctuations found near the top of downflows serve to decelerate the fast horizontal flows. Pressure fluctuations often can result in positive density fluctuations and thus cause buoyancy braking throughout the upflows, even though the fluid there is warmer than its surroundings. Since vigorous (and often supersonic) motions were encountered, we then turned to examine ways to account for effects of subgrid-scale (SGS) turbulence expected to coexist with such shearing flows. Preliminary experiments with a promising numerical technique known as large-eddy simulations (LES) were performed which incorporated SGS terms. These two-dimensional LES simulations again yield flow patterns much like our other results. However, interesting properties of the SGS models that may affect gross structures of the flows (such as flow symmetry) have been revealed, though the overall SGS effects are modest within such two-dimensional treatments. The SGS terms considered here can be incorporated readily into future three-dimensional LES simulations of compressible convection. Dissert. Abstr.

N93-13965 California Univ., Santa Barbara.
INSTABILITIES AND PATTERNS IN TAYLOR-COUETTE FLOW Ph.D. Thesis
Li Ning 1991 227 p
Avail: Univ. Microfilms Order No. DA9218460

Experimental results on two separate experiments in Taylor-Couette flow and some theoretical results pertinent to the second experiment are presented. In the first experiment, wavenumber selection in Taylor-vortex flow with slow spatial ramps of the Reynolds number was investigated. The spatial ramps drastically reduce the range of wavenumbers from the Eckhaus-stable range for homogeneous systems, but the selected wavenumber depends on the detailed nature of the ramps. For a particular ramp, wavenumbers outside the Eckhaus-stable band were selected, leading to a periodic state of drifting vortices. The selected wavenumbers and the frequencies of the periodic state agree well with a phase-dynamical calculation by Riecke and Paap. A comprehensive review of previous theoretical and experimental results on wavenumber selection is included. In the second experiment, I studied externally rotating Taylor-Couette flow. In addition to the inner cylinder rotating about the common cylindrical axis with angular velocity omega, the system rotates about an axis perpendicular to the cylinders' axis with angular velocity Omega. The effect of the Coriolis force gives rise to a surprising richness of bifurcation phenomena. At small Omega, the first bifurcation upon increasing omega was to tilted vortices. A secondary bifurcation to tilted rotation-modified wavy vortices followed at a slightly higher omega. The two bifurcation lines met at higher Omega. The initial bifurcation became one to time-dependent states of what I believe to be either tilted wavy vortices or tilted spiral vortices. For even larger values of Omega, the flow immediately above the initial bifurcation was disordered, and eventually became featureless turbulence. The linear stability of the rotation modified Couette flow was analyzed perturbatively for small Omega. The results for the critical Reynolds number, critical wavenumber and tilt angle of the vortices agree quantitatively with the experimental data. Attempts were made to explain the dynamic states observed based on linear stability analysis of time-dependent perturbations and weakly nonlinear analysis. Some speculations on open issues are given. Dissert. Abstr.

N93-14025 Mississippi State Univ., State College.
UNSTEADY THREE-DIMENSIONAL THIN-LAYER NAVIER-STOKES SOLUTIONS FOR TURBOMACHINERY IN TRANSONIC FLOW Ph.D. Thesis
Jen Ping Chen 1991 131 p
Avail: Univ. Microfilms Order No. DA9218186

This dissertation concerns the development of a numerical scheme to simulate the flow field generated by rotating machinery. The implicit Euler solver 'TURBO' developed at MSU and in use at NASA Lewis Research Center for analyzing compressible flows in general rotating machinery was augmented by including viscous effects. This was accomplished by making the thin-layer approximation with a Baldwin-Lomax turbulence model to simplify the Reynolds-averaged Navier-Stokes equations. This code is an implicit finite volume scheme with flux Jacobians evaluated by flux-vector-splitting and residual fluxes by Roe's flux-difference-splitting. Diffusive flux terms were treated explicitly in order to preserve the existing code structure. A modified two pass matrix solver based on the Gauss-Seidel iterative method was used in place of the standard LU approximate factorization to enhance the code's stability. Newton subiterations were used for unsteady flow computations. A localized grid distortion technique was applied for data communication between blocks in relative motion. An inlet boundary condition for preserving total reservoir conditions and a new approach for computing wall shear stress for nonorthogonal grids are also presented. Three engineering problems have been examined by this computational technique with fair results. Hamilton-Standard's advanced propfan design SR7 served as a test case for external flows. NASA's Rotor 67 with a rotating blade now and NASA's Stage 67 with both rotating and static blade rows with a different number of blades in each row test the code's ability for internal flow. Although some improvements are still needed for this code to become a real engineering design tool, the decent results obtained from applying this code to the above three real-world engineering problems suggest that it is moving in the right direction. Dissert. Abstr.

N93-14041 Mississippi State Univ., State College.
SOLUTION OF COMPRESSIBLE NAVIER-STOKES EQUATIONS USING SPECTRAL METHODS ON ARBITRARY TWO-DIMENSIONAL DOMAINS Ph.D. Thesis
George Paulose Koomullil 1991 75 p
Avail: Univ. Microfilms Order No. DA9218201

A method is developed for obtaining higher order accurate solutions of the Navier-Stokes equations on arbitrary two-dimensional domains. The development of a method of solving grid generation equations using spectral methods and the solution of the compressible Navier-Stokes equations by spectral methods on these coordinates is discussed. Further, an analysis was conducted to establish the order of accuracy of the solutions in transformed coordinates. Grid generation equations are solved for two-dimensional domains including simply-connected and doubly-connected regions. For simply-connected domains, Chebyshev polynomials are used in spectral methods along both coordinate directions. For doubly-connected domains Chebyshev polynomial expansions are used along the non-periodic direction and Fourier expansions along the periodic direction. Results and convergence rates are shown in various figures. The Navier-Stokes equations are first transformed to a general curvilinear coordinate system and kept in the fully conservative form. Metric coefficients are derived from the grid generation routines. The numerical scheme uses a spectral collocation method with Fourier and Chebyshev expansions along the periodic and non-periodic directions, respectively. Solutions of the governing equations are given both for a circular cylinder and a NACA0012 airfoil. Comparison of the Navier-Stokes solutions obtained on an exact grid, where the metric coefficients are obtained analytically, and a numerical grid, where the metric coefficients are derived from the spectral grid generation routine, is given. Both solutions match very closely. This type of comparison was possible only for a circular cylinder but it gives credence to the accuracy of the numerically generated grids by spectral methods. Time accuracy of the solution is tested with the results from a finite volume scheme and the experimental values at low Reynolds numbers. Also given is a comparison of the solution over NACA0012 airfoil at a moderately high Reynolds number of 10000 with finite difference and finite element results. The order of accuracy of the solution scheme is analyzed and is shown that for sustaining the solution accuracy as that of the numerical scheme, the metric coefficients should at least be of the same order of accuracy. The present solution technique permits the high order accuracy to be retained because the metric coefficients are also obtained from a high order accurate spectral scheme. Dissert. Abstr.

N93-14057 Clarkson Univ., Potsdam, NY.
A LOW-DIMENSIONAL DYNAMICAL SYSTEMS DESCRIPTION OF COHERENT STRUCTURES IN THE AXISYMMETRIC JET MIXING LAYER Ph.D. Thesis
Xiaowei Zheng 1992 148 p
Avail: Univ. Microfilms Order No. DA9214566

The near field jet mixing layer is studied using a Proper Orthogonal Decomposition (POD) based dynamical systems model similar to that applied by Aubry et al (1988) to the near wall region of the turbulent boundary layer. The instantaneous velocity field is expanded in terms of the empirical eigenfunctions obtained by Glauser and George (1987) which were obtained by application of the POD to the measured cross spectral tensor. Galerkin projection is then applied to the Navier-Stokes equations in conjunction with this representation, resulting in low-dimensional sets of ordinary differential equations. In particular, a 36 equation model is developed where the neglected modes are accounted for by a Heisenberg type model. With this 36 equation model the sequence by which the various modes contribute in time is examined for several values of a bifurcation parameter which is introduced into the system of truncated equations through the Heisenberg model. The solutions exhibit periodic, intermittent, and chaotic behavior depending on the value of the bifurcation parameter. At one particular value a cascade phenomena occurs where various streamwise wavenumbers interact and transfer energy into azimuthal modes 4, 5, and 6. It is argued that this is related to the production of turbulence in the jet shear layer. The velocity field was reconstructed from the solutions of the ODE's for various values of the bifurcation parameter. There is clear evidence of pairs of vortices interacting in the streamwise direction resulting in a transfer of azimuthal to streamwise vorticity. Spectra were computed from the reconstructed velocity field and the so called preferred mode obtained experimentally in the same jet is captured here as well. This indicates that the dynamical systems model is properly predicating the large scale temporal dynamics of the jet shear layer. Dissert. Abstr.

N93-14061 Illinois Univ. at Urbana-Champaign, Savoy.
A NUMERICAL STUDY OF HYPERSONIC FLOWS USING THE FULL NAVIER-STOKES EQUATIONS WITH DIFFERENT AIR MODELS Ph.D. Thesis
Moon-Sang Kim 1991 158 p
Avail: Univ. Microfilms Order No. DA9210867

A two-dimensional, axisymmetric, full Navier-Stokes solver has been developed with equilibrium and nonequilibrium air models. The effects of a real gas are investigated numerically in the hypersonic flow regime. The code employs several different upwind schemes to examine their effect on the accuracy and stability of the numerical solutions. A finite volume method is used with curvilinear coordinates, and the first-order, up wind schemes are extended to second-order accuracy in space. The steady-state solutions are obtained using an approximately factorized implicit scheme, including fully implicit boundary conditions, to accelerate the convergence. The numerical accuracy is improved by introducing the closed-control-volume concept in the metric quantity calculations. This idea is verified by a blunt-nosed flow case with a scrambled grid. In general, the fastest convergence in an implicit scheme is obtained when the same residual and correction operators are applied. A new simplified Jacobian matrix is derived for Roe's flux difference splitting scheme because of the complexity involved in deriving the full Jacobian matrix, and which yields a faster convergence compared to the use of a different correction operator such as Steger-Warming's. Dissert. Abstr.

N93-14067 Windsor Univ. (Ontario).
APPLICATION OF COMPLEX VARIABLES IN ELECTROMAGNETOFLUID DYNAMIC, MAGNETOFLUID DYNAMIC AND FLUID DYNAMIC FLOWS: VISCOELASTIC BOUNDARY-LAYER THEORY Ph.D. Thesis
Phu Van Nguyen 1991 308 p
(ISBN-0-315-65141-5) Avail: Univ. Microfilms Order No. DANN65141

This thesis is devoted to a theoretical investigation of steady plane electromagnetofluid dynamic (EMFD), magnetofluid dynamic (MFD) and ordinary fluid dynamic flows and a numerical study of boundary layer viscoelastic flows. In the theoretical study the complex conjugate method is employed to obtain the geometries and solutions for various EMFD, MFD and non-MFD flows. Fluid motions with different assumptions such as isometry, circulation preserving, velocity magnitude being constant on each individual streamline and vorticity being a function of the real part of an analytic function of a complex variable are considered. The flow problems that have been considered in this part are: (1) Isometric orthogonal, constantly-inclined and aligned MFD flows of an electrically conducting incompressible second-grade fluid of finite electrical conductivity and of infinite electrical conductivity, (2) Isometric constantly-inclined EMFD flows of an electrically conducting incompressible second-grade fluid with non-zero charge density, (3) Circulation-preserving constantly-inclined, orthogonal and aligned EMFD flows of an electrically conducting incompressible second-grade fluid with non-zero charge density, (4) Circulation-preserving aligned MFD flows with finite electrical conductivity, (5) Constantly-inclined and aligned magnetogasdynamic and gas dynamic flows with the assumption that the velocity magnitude is constant on each individual streamline, and (6) Jeffrey flows for incompressible viscous and second-grade fluids. The numerical study deals with viscoelastic steady plane boundary layer flows. The model for viscoelastic fluid is taken to be the second-grade fluid. A general theory of viscoelastic boundary-layer theory is developed, and as illustrations, the shooting method and the Box scheme are adopted to obtain solutions for: (1) flow near a stagnation point with suction, (2) flow due to stretching boundary with suction, (3) flow past a semi-infinite flat plate with zero pressure gradient and with exponential pressure gradient, (4) flow past a wedge, and (5) flow past a symmetrical circular cylinder. Finally, the viscoelastic boundary-layer flow is extended to study a magnetofluid dynamic boundary-layer motion due to the stretching of the wall. Dissert. Abstr.

N93-14069 California State Univ., San Diego.
EXPERIMENTS ON THE STATISTICAL NATURE OF STABLY STRATIFIED TURBULENCE Ph.D. Thesis
Sigurdur Tryggvi Thoroddsen 1991 347 p
Avail: Univ. Microfilms Order No. DA9216480

This dissertation describes experiments on the evolution of grid-generated turbulence in the presence of linear stable stratification. The experiments were conducted in a thermally stratified wind tunnel. Stratification strengths as high as N = 4.0 rad/s were attained. The configuration of the turbulence generating grid was found not to be important in the turbulence evolution, which disputes the theory of Gargett (1988) and her reinterpretations of earlier experimental results. The buoyancy forces were found to induce anisotropies in the velocity gradients causing them to become anisotropic much faster than previously thought. The mean-square values of delta(w)/delta(x) were reduced to as low as 1/4 of those predicted from delta(u)/delta(x) using isotropic relations. The rms velocity anisotropy of the vertical component was shown to scale very well with the internal Froude number. Similar buoyancy induced anisotropy does not appear in the temperature gradients, showing that the mean-square values of delta(theta)/delta(z) become as much as 2.2 times larger than those of delta(theta)/delta(x). The probability density functions (PDFs) of temperature and temperature gradients were extensively studied. The PDF of temperature remains Gaussian while the PDF of temperature gradients is shown to have strongly exponential tails. The PDF of delta(theta)/delta(z) shows strong skewness in the direction of the mean temperature gradient, which is explained by a simple phenomenological model based on the heat flux correlation. The PDF of the buoyancy flux is found to be very skewed in the direction of the mean flux and have near-exponential tails which are analytically derived from the joint-Gaussian statistics of the vertical velocity and temperature. Wavelet treatment of the buoyancy flux in the restratification regime was used to study the topology of restratification and mixing. Stratified turbulence was also passed through a contraction in the vertical direction, causing rapid fluctuation and leading to strong restratification down-stream of the contraction. The restratification rejuvinates the vertical velocity fluctuations at the large scales. Dissert. Abstr.

N93-14077 Colorado Univ., Boulder.
NUMERICAL SIMULATION OF COMPRESSIBLE COUETTE FLOW STABILITY: NON-LINEAR AND THREE-DIMENSIONAL EFFECTS Ph.D. Thesis
Abdulmannan Abdulham Saati 1991 189 p
Avail: Univ. Microfilms Order No. DA9220449

The direct numerical simulation of the stability and transition of compressible Couette flow is studied. The effects of a constant body force along the vertical direction are also studied. Cartesian geometry is adopted to approximate Couette flow produced in the gap between two coaxial cylinders rotating at high-speed, with the body force representing the effects of the centrifugal force. A new, compressible flow solver for two- and three-dimensional, time dependent Navier-Stokes equations, using both the MacCormack and the high-order Two-Four methods was developed. In order to facilitate the simulations with greater detail and accuracy, a high-speed supercomputer with large core memory is required. Thus, the computer code was written in FORTRAN for its execution on the CRAY2,

at NASA Langley. In a concurrent effort, in order to study the feasibility and efficiency of massively parallel super-computers and to speed up the computations, the work was further extended by rewriting the computer code in both C* and PARIS languages, for execution on the massively parallel Connection Machine CM 2 at the University of Colorado. Extensive testing of this new computer code was performed using wave propagation problems involving small- and large-amplitude two- and three-dimensional disturbances. Numerical simulations on the stability of compressible Couette flow between two infinite, parallel plates, with the inclusion of (1) a sudden body force, and (2) a body force in equilibrium, were performed. First, two-dimensional disturbances were considered and then the work was extended by considering three-dimensional disturbances on the rectangular Couette flow problem. Effects of body force magnitude, Mach number, and Reynolds number were also investigated. The simulations provide excellent agreement with the linear theory, thus documenting the phase and amplitude accuracy of the computed results; the overall amplitude error remains less than one percent. The results show that, for the equilibrium case, the Couette flow is stable to small and large amplitude two- and three-dimensional initial disturbances. The application of a sudden body force above a critical amplitude leads to the destabilization of the Couette flow through the formation of a shock wave. As a result of the body force, the vortex sheet that forms an elongated tube moves downward towards the location of the shock. Dissert. Abstr.

N93-14097 Iowa Univ., Iowa City.
AN EXPERIMENTAL AND COMPUTATIONAL STUDY OF LONGITUDINAL VORTICES IN TURBULENT BOUNDARY LAYERS Ph.D. Thesis
Wu Joan Kim 1991 298 p
Avail: Univ. Microfilms Order No. DA9217167

The experimental and computational study of longitudinal vortices in turbulent boundary layers are reported. Three types of flow were considered. In the first, flow in a curved duct with a 90 degree bend was measured and calculated to study a naturally occurring longitudinal vortex near the corner of the convex wall. In the second, contrarotating (common-up and common-down) pairs of vortices artificially introduced in a zero-pressure gradient boundary layer were calculated and compared with experiments to see the behavior of longitudinal vortices and their modification of otherwise 2-D turbulent boundary layer. Finally, the same configuration of vortices was introduced on either the convex or the concave wall of the 90 degree bend duct to study the joint effects of the pressure gradient and streamwise curvature on the longitudinal vortices in turbulent boundary layers along curved surfaces. In the experimental study, a five-hole pressure probe and a Preston tube were used to measure three mean-flow velocities and wall shear stresses. All Reynolds stresses but one (0/vw) were documented using a two-sensor hotwire probe. In the computational study, a numerical method was applied to solve Reynolds-averaged Navier-Stokes equation. The conservation equations of the fluid motion were obtained by transforming the dependent variables, namely, coordinates as well as the dependent variables, the velocity components. The velocity components are aligned with algebraically generated non-staggered (collocated) regular grids. The governing equations were discretized using Âfinite-analytic' scheme. For turbulence closure, the two-layered turbulence model was employed. A semi-empirical, analytic vortex model is proposed for the computational study and is confirmed to be very useful. Extensive comparisons are made between calculations and experimental data for a naturally occurring longitudinal vortex near the convex wall of a curved duct and artificially introduced vortices in the flat or curved turbulent boundary layers. The present study clarifies most salient features of flows in which curvature effect plays an important role in the development and decay of longitudinal vortices. Furthermore, the numerical method employed here describes most of the main features of the flow. Dissert. Abstr.

N93-13181*# National Aeronautics and Space Administration. Goddard Space Flight Center, Greenbelt, MD.
THE CAPILLARY PUMPED LOOP FLIGHT EXPERIMENT (CAPL): A PATHFINDER FOR EOS
D. Butler and T. Hoang (NSI Technology Services Corp., Greenbelt, MD.) *In its* The 1992 Shuttle Small Payloads Symposium Oct. 1992 p 233-245 (For primary document see N93-13158 03-12)
Avail: CASI HC A03/MF A03

N93-13182*# Martin Marietta Corp., Denver, CO.
THE VTRE PROGRAM: AN OVERVIEW
William J. Bailey and John P. Gille *In* NASA. Goddard Space Flight Center, The 1992 Shuttle Small Payloads Symposium Oct. 1992 p 247-256 (For primary document see N93-13158 03-12)
(Contract NAS3-25977)
Avail: CASI HC A02/MF A03

N93-13664*# Ohio State Univ., Columbus. Aeronautical and Astronautical Research Lab.
TIME DEPENDENT HEAT TRANSFER RATES IN HIGH REYNOLDS NUMBER HYPERSONIC FLOWFIELDS
Michael J. Flanagan *In* NASA. Langley Research Center, The 1992 NASA Langley Measurement Technology Conference: Measurement Technology for Aerospace Applications in High-Temperature Environments Sep. 1992 p 51-68 Sponsored in part by AFFDL (For primary document see N93-13661 03-35)
Avail: CASI HC A03/MF A04

N93-13670*# Virginia Polytechnic Inst. and State Univ., Blacksburg. Dept. of Aerospace and Ocean Engineering.
SKIN FRICTION MEASUREMENTS IN HIGH TEMPERATURE HIGH SPEED FLOWS
J. A. Schetz, Thomas E. Diller, and A. L. Wicks *In* NASA. Langley Research Center, The 1992 NASA Langley Measurement Technology Conference: Measurement Technology for Aerospace Applications in High-Temperature Environments Sep. 1992 p 171-188 (For primary document see N93-13661 03-35)
Avail: CASI HC A03/MF A04

N93-13685*# Stanford Univ., CA. High Temperature Gasdynamics Lab.
PLANAR LASER-INDUCED FLUORESCENCE MEASUREMENTS OF HIGH-ENTHALPY FREE JET FLOW WITH NITRIC OXIDE
Jennifer L. Palmer, Brian K. McMillin, and Ronald K. Hanson *In* NASA. Langley Research Center, The 1992 NASA Langley Measurement Technology Conference: Measurement Technology for Aerospace Applications in High-Temperature Environments Sep. 1992 p 375-386 Sponsored in part by AFOSR (For primary document see N93-13661 03-35)
Avail: CASI HC A03/MF A04

35 INSTRUMENTATION AND PHOTOGRAPHY

Includes remote sensors; measuring instruments and gages; detectors; cameras and photographic supplies; and holography.

For aerial photography see *43 Earth Resources and Remote Sensing*. For related information see also *06 Aircraft Instrumentation*, and *19 Spacecraft Instrumentation*.

N93-12619# Colorado State Univ., Fort Collins. Dept. of Chemistry.
CHEMICAL SENSORS BASED ON ULTRATHIN FILM COMPOSITE MEMBRANES
B. Ballarin, C. J. Brumhk, D. R. Lawson, W. Liang, and L. S. VanDyke 20 Aug. 1992 27 p
(Contract N00014-82-K-0612)
(AD-A254644; TR-77-ONR) Avail: CASI HC A03/MF A01

This paper introduces a new approach for designing chemical sensors. This approach is based on a concept borrowed from the membrane-based separations area--ultra thin film composite membranes. Ultrathin film composite membranes consist of an ultrathin (less than ca. 100 nm-thick) polymer skin coated onto the surface of a microporous support membrane. These composite membranes have made a tremendous impact on the field of membrane-based separations because they can offer high permeate flux without sacrificing chemical selectivity. These two qualities (high permeate flux and high chemical selectivity) are also required in polymeric barrier layers in chemical sensors. Therefore, the ultrathin film composite membrane concept should be applicable to sensor design. In this paper we present proof of this concept by showing the response characteristics of a prototype glucose sensor based on an ultrathin film composite membrane. GRA

N93-12639# Tokyo Univ. (Japan). Inst. of Space and Astronautical Science.

ARM LENGTH MATCHING IN 10 m DELAY-LINE INTERFEROMETER

R. Takahashi (Tohoku Univ., Sendai, Japan), J. Mizuno (Tokyo Univ., Sagamihara, Japan), and N. Kawashima (Tokyo Univ., Sagamihara, Japan) Sep. 1992 12 p

(ISAS-TN-649) Avail: CASI HC A03/MF A01

The noise due to laser frequency fluctuation in a Michelson interferometer can be suppressed by making the arm length difference equal to zero. But it is difficult to match the arm lengths in the interferometers with a large number of reflections in delay-lines. In this paper we show that it is possible to achieve CMRR (Common Mode Rejection Ratio) of 119 dB for the noise due to laser frequency fluctuation, by using the mirrors with small relative difference to radii of curvature and most tiltless surfaces. Author

N93-12653# Chemical Research and Development Center, Aberdeen Proving Ground, MD.

CORRELATION FOR NON-LINEAR INFRARED CALIBRATION CURVES Final Report, Aug. - Nov. 1989

John J. Mahle, Leonard C. Buettner, and David E. Tevault Aug. 1992 19 p

(AD-A255098; CRDEC-TR-399) Avail: CASI HC A03/MF A01

An analytical expression has been identified which can be used to correlate absorbance versus concentration for gas phase infrared monitors. This expression can be used to correlate both positive and negative deviations from Beer's Law. Calibration data for several vapors has been measured. Correlation of this data provided a good fit over a wide range of concentration and absorbance. GRA

N93-12681*# National Aeronautics and Space Administration. Hugh L. Dryden Flight Research Center, Edwards, CA.

THE CONSTANT CURRENT LOOP: A NEW PARADIGM FOR RESISTANCE SIGNAL CONDITIONING

Karl F. Anderson Oct. 1992 21 p

(RTOP 505-63-40)

(NASA-TM-104260; H-1861; NAS 1.15:104260) Avail: CASI HC A03/MF A01

A practical single constant current loop circuit for the signal conditioning of variable resistance transducers has been synthesized, analyzed, and demonstrated. The strain gage and the resistance temperature device are examples of variable resistance sensors. Lead wires connect variable resistance sensors to remotely located signal conditioning hardware. The presence of lead wires in the conventional Wheatstone bridge signal conditioning circuit introduces undesired effects that reduce the quality of the data from the remote sensors. A practical approach is presented for suppressing essentially all lead wire resistance effects while indicating only the change in resistance value. Theoretical predictions supported by laboratory testing confirm the following features of the approach: (1) dc response; (2) the electrical output is unaffected by extremely large variations in the resistance of any or all lead wires; (3) the electrical output remains zero for no change in gage resistance; (4) the electrical output is inherently linear with respect to gage resistance change; (5) the sensitivity is double that of a Wheatstone bridge circuit; and (6) the same excitation wires can serve multiple independent gages. An adaptation of current loop circuit is presented that simultaneously provides an output signal voltage directly proportional to transducer resistance change and provides temperature information that is unaffected by transducer and lead wire resistance variations. These innovations are the subject of NASA patent applications. Author

N93-12762# Lawrence Livermore National Lab., CA.

WIDE RANGE, PERMANENT MAGNET COMPTON SPECTROMETER

K. E. Sale and J. Kammeraad 12 Jun. 1992 9 p Presented at the SPIE International Symposium on Optical Applied Science and Engineering, San Diego, CA, 19-24 Jul. 1992

(Contract W-7405-eng-48)

(DE92-017312; UCRL-JC-109170; CONF-920792-10) Avail: CASI HC A02/MF A01

We are using a Sm-Co based permanent magnet spectrometer to analyze Compton electrons ejected from a Be converter foil that is illuminated by a gamma-ray beam. The distance along the focal plane at which a mono-energetic electron beam entering the spectrometer will cross the focal plane is proportional to the square root of the electron momentum. This design achieves a very broad range of energies that are analyzed (from momentum of about 1 MeV/c up to 30 MeV/c) while maintaining good energy resolution (the electron momentum resolution is the larger of 0.1 MeV/c or 1 percent of the momentum). In addition this design has a fairly large acceptance. By restricting the angular acceptance of the spectrometer for the Compton electrons, incoming gamma-ray energies and ejected electron momenta are simply related. The electron optical properties of this spectrometer will be discussed as well as some aspects of the overall system design and testing. DOE

N93-12831# Lawrence Livermore National Lab., CA.

THE VELOPT CODE FOR ESTIMATING PERFORMANCE OF A FABRY-PEROT VELOCIMETER

D. R. Goosman Apr. 1992 13 p

(Contract W-7405-eng-48)

(DE92-015566; UCRL-LR-109886) Avail: CASI HC A03/MF A01

The VELOPT code calculates an estimate of the performance of a Fabry-Perot (FP) velocimeter. The code is a macro-driven, Symphony spreadsheet written for an IBM PC. VELOPT is designed to be used in conjunction with the POWER codes, which estimate the amount of light entering a collection fiber and the ratio of collected light to light leaving the laser fiber. In this model a velocimeter system, single-frequency laser output illuminates a moving test surface through a lens. Reflected light from the test surface is concentrated by a lens into an optical collection fiber. The collected light is presented to a mode scrambler, a cylinder lens, a filter, and then to a striped Fabry-Perot interferometer (FPI). Light leaving the FPI is imaged via spherical lenses and one mirror onto the slit of an electronic streak camera. The image is intensified within the camera, and then is recorded on film. VELOPT takes 47 user inputs that describe the FP velocimeter system. The primary outputs from the code include the following estimates for each of the first four fringes: Energy per unit area reaching the film; optical density expected on both Polaroid 667 and TMAX3200 films; velocity and time resolution; and statistical smoothness of the streak records. Twenty-six other secondary output quantities for each fringe are also calculated. The finesse limitation due to the finite size of the mirrors is calculated in detail by the routine WALKOFF, which is internal to VELOPT. An estimate of the reduction in effective fill time of the FPI due to the finite spatial resolution of the streak camera is also calculated by VELPOPT. DOE

N93-12844# Army Electronics Technology and Devices Lab., Fort Monmouth, NJ.

TUTORIALS FROM THE 23RD ANNUAL PRECISE TIME AND TIME INTERVAL (PTTI) APPLICATIONS AND PLANNING MEETING

G. Lutes, R. Logan, J. Barnes, C. Fox, and G. A. Gifford Sep. 1992 156 p Meeting held in Pasadena, CA, 3-5 Dec. 1991

(AD-A254745) Avail: CASI HC A08/MF A02

The tutorial papers in this document are: 'Introduction to Quartz Frequency Standards,' J. Vig, Army Research Laboratory; 'Tutorial on High Performance Analog Fiber Optic Systems,' G. Lutes and R. Logan, Jet Propulsion Laboratory; 'Introduction to the Time Domain Characterization of Frequency Standards,' J. Jespersen, NIST; 'Noise Models for Time and Frequency,' J. Barnes, Austron, Inc., 'GPS Time Determination and Dissemination,' Lt. C. Fox, U.S. Air Force; G. A. Gifford, Naval Research Laboratory; and S. R. Stein, Timing Solutions. GRA

N93-12921# Ames Lab., IA.

ENHANCEMENT OF ION TRANSMISSION AND REDUCTION OF BACKGROUND AND INTERFERENCES IN INDUCTIVELY COUPLED PLASMA MASS SPECTROMETRY Ph.D. Thesis

Ke Hu Jun. 1992 174 p

(Contract W-7405-eng-82)

(DE92-018805; IS-T-1606) Avail: CASI HC A08/MF A02

An inductively coupled plasma-mass spectrometer (ICP-MS) (four stages of differential pumping) is described. The large sampling orifice (1.31 mm dia.) improves signals for metal ions and resists plugging. The ion lens deflects ions off center and then back on center into the differential pumping orifice; there is no photon stop in the center. Ion trajectories calculations SIMION show that only those ions that leave the skimmer on center are transmitted, whereas most other lenses used in ICP-MS transmit only ions

that leave the skimmer off axis. Background with the Daly detector is 4 counts s(exp -1). This ICP-MS yields low levels of many troublesome polyatomic ions. Signals from refractory metal oxide ions are about 1 percent of the corresponding metal ion signals. Grounding the first electrode of the ion lens reduces matrix effects to approximately less than 20 percent loss in signal for Co(+), Y(+), or Cs(+) in presence of 10 mM Sr, Tm, or Pb. This latter lens setting causes only 30 percent loss in sensitivity compared to biassing the first lens. Matrix effects can also be mitigated by re-adjusting the voltage on the first lens with matrix present. Floating the metal cones at various potentials can improve the ion transmission by a factor of at least four to six. Also, floating the cones extends the upper end of linearity. Net result is more sensitivity and higher ion beam intensity than with a grounded skimmer and sampler. Furthermore, mass discrimination can be reduced. DOE

N93-13267# Westinghouse Idaho Nuclear Co., Inc., Idaho Falls.
PRECISION LIQUID-LEVEL MEASUREMENT IN DEEP TANKS USING A SWEPT-RF RESONANT CAVITY
T. C. Piper 18 Mar. 1992 12 p Presented at the COCO Engineering Managers Meeting, Idaho Falls, ID, 23-26 Mar. 1992
(Contract DE-AC07-84ID-12435)
(DE92-017236; WINCO-11800; CONF-9203171-1) Avail: CASI HC A03/MF A01

The Idaho Chemical Processing Plant (ICPP) has several large, temporary-liquid-storage tanks (50 feet diameter and 30 feet height). The tanks are located in separate underground cells. Because of the huge tank storage capacity per inch (1225 gallons), extremely accurate liquid depth measurement is required to observe normal additions (or to become aware of other than large leaks). In roughly 1970, Glenn Booman, then the header of the advanced instrumentation group of ICPP, began a program to develop what in a few years became known as 'IRF tank probes'. The initial probe was installed in tank WM-189 in 1975 and ten more were installed in other tanks in 1976. Though the RF components were fairly costly at that time, they were readily available and the system has, in general, operated without incident. Three of the most desirable features of the system not found in most other continuous reading level systems are that it exhibits no hysteresis, no creep and requires no calibration. In the years since installation the RF distribution system has been upgraded and the method of data processing has been changed somewhat. Presently, the need for more probes for more tanks has renewed interest. The original development work was never fully documented. The present talk is taken from a report being written to comprehensively describe the theory and operation of the RF probe. DOE

N93-13307*# National Aeronautics and Space Administration. Lewis Research Center, Cleveland, OH.
EXPERIMENTAL TESTING OF FOUR CORRECTION ALGORITHMS FOR THE FORWARD SCATTERING SPECTROMETER PROBE
Edward A. Hovenac (Sverdrup Technology, Inc., Brook Park, OH.), John R. Oldenburg, and James A. Lock (Cleveland State Univ., OH.) Oct. 1992 31 p Sponsored in part by FAA
(RTOP 505-62-50)
(NASA-TM-105906; E-7374; NAS 1.15:105906; DOT/FAA/CT-TN92/29)
Avail: CASI HC A03/MF A01

Three number density correction algorithms and one size distribution correction algorithm for the Forward Scattering Spectrometer Probe (FSSP) were compared with data taken by the Phase Doppler Particle Analyzer (PDPA) and an optical number density measuring instrument (NDMI). Of the three number density correction algorithms, the one that compared best to the PDPA and NDMI data was the algorithm developed by Baumgardner, Strapp, and Dye (1985). The algorithm that corrects sizing errors in the FSSP that was developed by Lock and Hovenac (1989) was shown to be within 25 percent of the Phase Doppler measurements at number densities as high as 3000/cc. Author

N93-13373*# Lockheed Engineering and Sciences Co., Houston, TX. Flight Science Support Dept.
MANNED OBSERVATIONS TECHNOLOGY DEVELOPMENT, FY 1992 REPORT
Steven Israel Nov. 1992 35 p
(Contract NAS9-17900)
(NASA-CR-185704; NAS 1.26:185704; JSC-26032; LESC-30460) Avail: CASI HC A03/MF A01

This project evaluated the suitability of the NASA/JSC developed electronic still camera (ESC) digital image data for Earth observations from the Space Shuttle, as a first step to aid planning for Space Station Freedom. Specifically, image resolution achieved from the Space Shuttle using the current ESC system, which is configured with a Loral 15 mm x 15 mm (1024 x 1024 pixel array) CCD chip on the focal plane of a Nikon F4 camera, was compared to that of current handheld 70 mm Hasselblad 500 EL/M film cameras. Author

N93-13410*# National Aeronautics and Space Administration. Lewis Research Center, Cleveland, OH.
EFFECT OF VAPORIZATION ON CRYOGENIC SPRAY DROPSIZE MEASUREMENT
Robert D. Ingebo Oct. 1992 10 p Proposed for presentation at the 31st Aerospace Sciences Meeting and Exhibit, Reno, NV, 11-14 Jan. 1993; sponsored by AIAA
(RTOP 505-62-21-00)
(NASA-TM-105909; E-7387; NAS 1.15:105909; AIAA Paper 93-0692)
Copyright Avail: CASI HC A02/MF A01

The fluid mechanics of multi-phase flow breakup of liquid nitrogen, LN2, jets injected into sonic velocity nitrogen gasflow, was experimentally investigated. A scattered-light scanning instrument was used to measure the characteristic dropsize, D(sub v.5), of LN2 sprays and to determine the effect of droplet vaporization on experimental dropsize measurements. Under sonic gas-velocity conditions, liquid-jet breakup occurred in the regime of aerodynamic stripping. As a result, the following correlation of volume-median drop diameter, D(sub v.5), with atomizing gas flowrate, W(sub g), was derived for two-fluid atomizers; with atomizing gas flowrate, W(sub g), was derived for two-fluid atomizers; (D(sub v.5))(exp -1) = k(sub c)(W(sub g))(sup n), where proportionally constant k(sub c) and exponent n are functions of droplet vaporization rate. Partially vaporized sprays were investigated and it was found that n = 1.11, which is considerably less than the value of 1.33 that is predicted by atomization theory. This was attributed to the evaporative loss of very small droplets. As a result, the following expression was obtained experimentally: (D(sub v.5e))(exp -1) = 301(W(sub g))(sup 1.11). Values of D(sub v.5), that existed prior to partial vaporization of the LN2 sprays, were calculated and the following expression was derived for originally unvaporized LN2 sprays: (D(sub v.5))(exp -1) = 285(W(sub g))(sup 1.33). This expression agrees well with atomization theory that predicts n = 1.33, for liquid jet breakup in high-velocity gasflow.
Author

N93-13424*# SETS Technology, Inc., Mililani, HI.
IMAGING IR SPECTROMETER, PHASE 2 Final Report, 15 Apr. 1988 - 15 Apr. 1990
Jonathan Gradie, Ralph Lewis, Thomas Lundeen, and Shu-i Wang 10 May 1990 67 p
(Contract NAS7-1029; SBIR-08.27-8712)
(NASA-CR-190848; NAS 1.26:190848) Avail: CASI HC A04/MF A01

The development is examined of a prototype multi-channel infrared imaging spectrometer. The design, construction and preliminary performance is described. This instrument is intended for use with JPL Table Mountain telescope as well as the 88 inch UH telescope on Mauna Kea. The instrument is capable of sampling simultaneously the spectral region of 0.9 to 2.6 um at an average spectral resolution of 1 percent using a cooled (77 K) optical bench, a concave holographic grating and a special order sorting filter to allow the acquisition of the full spectral range on a 128 x 128 HgCdTe infrared detector array. The field of view of the spectrometer is 0.5 arcsec/pixel in mapping mode and designed to be 5 arcsec/pixel in spot mode. The innovative optical design has resulted in a small, transportable spectrometer, capable of remote operation. Commercial applications of this spectrometer design include remote sensing from both space and aircraft platforms as well as groundbased astronomical observations. Author

N93-13501# Department of the Army, Washington, DC.
ELECTRONIC TRIPLE POINT CELL Patent Application
John M. Ball, inventor (to Army) 29 Jun. 1992 16 p
(AD-D015374; US-Patent-Appl-SN-905706) Avail: CASI HC A03/MF A01

An electronic triple point calibration system comprising in combination triple-point-of-water cells provided with means for sealing; a central thermowell provided in the heat conducting fixture for inserting thermometer being calibrated; a temperature probe installed on heat conducting fixture; and a housing for enclosing the heat conducting fixture and intimately mounted cells in a mounted combination. The cells are prepared from glass, polytetrafluoroethylene, or other material which does not react with water. After thoroughly cleaning, the cells are partially filled with pure water and vacuum sealed. A plurality of cells are intimately mounted on the heat conducting feature designed to accommodate the outer contours of the cells equally spaced around the central thermowell. The mounted combination with cells installed is frozen prior to testing. The electronic triple point calibration system temperature probe during testing is connected to measuring means for measuring millivolt output equivalent to temperature values in determining the triple-point-of-water temperature. The electronic triple point calibration system further comprises for automated operation a DC control system electrically connected to the temperature probe, a DC switching means for receiving millivolts output, from the temperature probe, and refrigeration means including control system for freeze control with operational circuitry including associated DC switches, relays, and contacts for generating and maintaining the triple-point-of water temperature in the central thermowell. GRA

N93-13567*# West Virginia Univ., Morgantown. Dept. of Electrical and Computer Engineering.

CAPACITIVE SKIN CHARACTERIZATION

Robert McConnell and Michael Manzo 29 Oct. 1992 11 p

(Grant NAG5-1488)

(NASA-CR-191261; NAS 1.26:191261) Avail: CASI HC A03/MF A01

NASA is currently involved in research that utilizes a capacitive sensor that is used for proximity detection of objects. This sensor is sensitive to conductive and dielectric materials including metal objects and humans. The range of the sensor has been found to be about twelve inches. It is the goal of this research project to further characterize the sensor so that it can be tailored to specific requirements. The characterization of the sensor should be with respect to shield size, sensor size, object size, and object distance. The method of finite elements to calculate the capacitance of the sensor while varying different parameters was used. Each of the parameters was varied in turn, often by selecting data points from different runs. The plotted results are shown and an apparent functionality developed for each. L.R.R.

N93-13656*# Daedalus Enterprises, Inc., Ann Arbor, MI.

DEVELOPMENT OF A PORTABLE INFRARED EMISSION SPECTROMETER AA460 PIRES Final Report

James P. Lehotsky and Steven D. Cach 12 Jul. 1990 27 p

(Contract NAS7-1030; SBIR-08.26-5649)

(NASA-CR-190849; NAS 1.26:190849) Avail: CASI HC A03/MF A01

The purpose of this Phase 2 research effort was to design and build a prototype field portable thermal infrared emission spectrometer (PIRES). This phase of work would build on the design concepts and analysis completed during Phase 1. The AA460 PIRES System is a field-portable thermal emission spectral radiometer which operates over the 2.5-14.5 microns wavelength range. Its primary function is to characterize the spectral emission signatures of objects at reasonable terrestrial temperatures (0 deg to 50 deg). However, the instrument design is flexible enough to allow useful data collection to occur from objects outside this temperature range or from sources other than thermal radiators. While ideally suited for two-man operation in the field, the instrument can be transported and operated effectively by a single user. The AA460 Pires System gives the user the capability to collect and display processed thermal emission data on-site. This eliminates the need for the user/researcher to remove a sample from its natural setting in order to accommodate laboratory analysis. The AA460 PIRES instrument was fabricated, assembled, tested, and documented during this Phase 2 work period. Software development included a user friendly menu structure, control, and communications process. Testing included optical and spectral characterization of the instrument and general performance. The test results concluded that the instrument met most of the original design goals set forward in the Phase 1 work including size, weight, portability, rugged, menu driven operation, and in-field analysis. The area in which the instrument did not meet our design goals is in the signal-to-noise (SNR) performance. Testing concluded that this poor SNR performance was due primarily to data collection scheme and our inability to properly amplify and stabilize the detector signals. Modification to this collection scheme could improve the SNR performance and verification is necessary before implementation of a redesign to the optical head and its present data collection scheme. Author

N93-13661*# National Aeronautics and Space Administration. Langley Research Center, Hampton, VA.

THE 1992 NASA LANGLEY MEASUREMENT TECHNOLOGY CONFERENCE: MEASUREMENT TECHNOLOGY FOR AEROSPACE APPLICATIONS IN HIGH-TEMPERATURE ENVIRONMENTS

Jag J. Singh, ed. and Richard R. Antcliff, ed. Washington Sep. 1992 435 p Confernece held in Hampton, VA, 22-23 Apr. 1992; sponsored by NASA, AIAA, and the Instrument Society of America

(RTOP 505-59-54-02)

(NASA-CP-3161; L-17127; NAS 1.55:3161) Avail: CASI HC A19/MF A04

An intensive 2-day conference to discuss the current status of measurement technology in the areas of temperature/heat flux, stress/strain, pressure, and flowfield diagnostics for high temperature aerospace applications was held at Langley Research Center, Hampton, Virginia, on April 22 and 23, 1993. Complete texts of the papers presented at the Conference are included in these proceedings. For individual titles, see N93-13662 through N93-13687.

N93-13662*# Dayton Univ. Research Inst., OH.

TEMPERATURE AND HEAT FLUX MEASUREMENTS: CHALLENGES FOR HIGH TEMPERATURE AEROSPACE APPLICATION

Richard D. Neumann *In* NASA. Langley Research Center, The 1992 NASA Langley Measurement Technology Conference: Measurement Technology for Aerospace Applications in High-Temperature Environments Sep. 1992 p 1-30 (For primary document see N93-13661 03-35)

Avail: CASI HC A03/MF A04

The measurement of high temperatures and the influence of heat transfer data is not strictly a problem of either the high temperatures involved or the level of the heating rates to be measured at those high temperatures. It is a problem of duration during which measurements are made and the nature of the materials in which the measurements are made. Thermal measurement techniques for each application must respect and work with the unique features of that application. Six challenges in the development of measurement technology are discussed: (1) to capture the character and localized peak values within highly nonuniform heating regions; (2) to manage large volumes of thermal instrumentation in order to efficiently derive critical information; (3) to accommodate thermal sensors into practical flight structures; (4) to broaden the capabilities of thermal survey techniques to replace discrete gages in flight and on the ground; (5) to provide supporting instrumentation conduits which connect the measurement points to the thermally controlled data acquisition system; and (6) to develop a class of 'vehicle tending' thermal sensors to assure the integrity of flight vehicles in an efficient manner. M.G.

N93-13663*# Calspan Corp., Arnold AFS, TN.

HIGH HEAT FLUX MEASUREMENTS AND EXPERIMENTAL CALIBRATIONS/CHARACTERIZATIONS

Carl T. Kidd *In* NASA. Langley Research Center, The 1992 NASA Langley Measurement Technology Conference: Measurement Technology for Aerospace Applications in High-Temperature Environments Sep. 1992 p 31-50 (For primary document see N93-13661 03-35)

Avail: CASI HC A03/MF A04

Recent progress in techniques employed in the measurement of very high heat-transfer rates in reentry-type facilities at the Arnold Engineering Development Center (AEDC) is described. These advances include thermal analyses applied to transducer concepts used to make these measurements; improved heat-flux sensor fabrication methods, equipment, and procedures for determining the experimental time response of individual sensors; performance of absolute heat-flux calibrations at levels above 2,000 Btu/cu ft-sec (2.27 kW/cu cm); and innovative methods of performing in-situ run-to-run characterizations of heat-flux probes installed in the test facility. Graphical illustrations of the results of extensive thermal analyses of the null-point calorimeter and coaxial surface thermocouple concepts with application to measurements in aerothermal test environments are presented. Results of time response experiments and absolute calibrations of null-point

calorimeters and coaxial thermocouples performed in the laboratory at intermediate to high heat-flux levels are shown. Typical AEDC high-enthalpy arc heater heat-flux data recently obtained with a Calspan-fabricated null-point probe model are included. Author

N93-13664*# Ohio State Univ., Columbus. Aeronautical and Astronautical Research Lab.

TIME DEPENDENT HEAT TRANSFER RATES IN HIGH REYNOLDS NUMBER HYPERSONIC FLOWFIELDS c34

Michael J. Flanagan *In* NASA. Langley Research Center, The 1992 NASA Langley Measurement Technology Conference: Measurement Technology for Aerospace Applications in High-Temperature Environments Sep. 1992 p 51-68 Sponsored in part by AFFDL (For primary document see N93-13661 03-35)

Avail: CASI HC A03/MF A04

Time dependent heat transfer rates have been calculated from time dependent temperature measurements in the vicinity of shock-wave boundary-layer interactions due to conical compression ramps on an axisymmetric body. The basic model is a cylindrical body with a 10 degree conical nose. Four conical ramps, 20, 25, 30, and 35 degrees serve as shock wave generators. Flowfield surveys have been made in the vicinity of the conical ramp vertex, the separation point, and the reattachment point. A significant effort was made to characterize the natural frequencies and relative powers of the resulting fluctuations in heat transfer rates. This research effort, sponsored jointly by NASA and the Air Force, was conducted in the Air Force Flight Dynamics Directorate High Reynolds Facility. The nominal freestream Mach number was 6, and the freestream Reynolds numbers ranged from 2.2 million/ft to 30.0 million/ft. Experimental results quantify temperature response and the resulting heat transfer rates as a function of ramp angle and Reynolds number. The temperature response within the flowfield appears to be steady-state for all compression ramp angles and all Reynolds numbers, and hence, the heat transfer rates appear to be steady-state. Author

N93-13665*# Vatell Corp., Blacksburg, VA.

HEAT FLUX MICROSENSOR MEASUREMENTS AND CALIBRATIONS

James P. Terrell, Jon M. Hager, Shinzo Onishi (Virginia Polytechnic Inst. and State Univ., Blacksburg.), and Thomas E. Diller (Virginia Polytechnic Inst. and State Univ., Blacksburg.) *In* NASA. Langley Research Center, The 1992 NASA Langley Measurement Technology Conference: Measurement Technology for Aerospace Applications in High-Temperature Environments Sep. 1992 p 69-80 Sponsored in part by AF (For primary document see N93-13661 03-35)

Avail: CASI HC A03/MF A04

A new thin-film heat flux gage has been fabricated specifically for severe high temperature operation using platinum and platinum-10 percent rhodium for the thermocouple elements. Radiation calibrations of this gage were performed at the AEDC facility over the available heat flux range (approx. 1.0 - 1,000 W/cu cm). The gage output was linear with heat flux with a slight increase in sensitivity with increasing surface temperature. Survivability of gages was demonstrated in quench tests from 500 C into liquid nitrogen. Successful operation of gages to surface temperatures of 750 C has been achieved. No additional cooling of the gages is required because the gages are always at the same temperature as the substrate material. A video of oxyacetylene flame tests with real-time heat flux and temperature output is available. Author

N93-13666*# National Aeronautics and Space Administration. Lewis Research Center, Cleveland, OH.

THIN FILM THERMOCOUPLES FOR HIGH TEMPERATURE MEASUREMENT ON CERAMIC MATERIALS

Raymond Holanda *In* NASA. Langley Research Center, The 1992 NASA Langley Measurement Technology Conference: Measurement Technology for Aerospace Applications in High-Temperature Environments Sep. 1992 p 81-96 (For primary document see N93-13661 03-35)

Avail: CASI HC A03/MF A04

Thin film thermocouples have been developed for use on metal parts in jet engines to 1000 C. However, advanced propulsion systems are being developed that will use ceramic materials and reach higher temperatures. The purpose of this work is to develop thin film thermocouples for use on ceramic materials. The thin film thermocouples are Pt13Rh/Pt fabricated by the sputtering process. Lead wires are attached using the parallel-gap welding process. The ceramic materials are silicon nitride, silicon carbide, aluminum oxide, and mullite. Both steady state and thermal cycling furnace tests were performed in the temperature range to 1500 C. High-heating-rate tests were performed in an arc lamp heat-flux-calibration facility. The fabrication of the thin film thermocouples is described. The thin film thermocouple output was compared to a reference wire thermocouple. Drift of the thin film thermocouples was determined, and causes of drift are discussed. The results of high-heating-rate tests up to 2500 C/sec are presented. The stability of the ceramic materials is examined. It is concluded that Pt13Rh/Pt thin film thermocouples are capable of meeting lifetime goals of 50 hours or more up to temperatures of 1500 C depending on the stability of the particular ceramic substrate. Author

N93-13667*# National Aeronautics and Space Administration. Lewis Research Center, Cleveland, OH.

FABRICATION OF THIN FILM HEAT FLUX SENSORS

Herbert A. Will *In* NASA. Langley Research Center, The 1992 NASA Langley Measurement Technology Conference: Measurement Technology for Aerospace Applications in High-Temperature Environments Sep. 1992 p 97-106 (For primary document see N93-13661 03-35)

Avail: CASI HC A02/MF A04

Prototype thin film heat flux sensors have been constructed and tested. The sensors can be applied to propulsion system materials and components. The sensors can provide steady state and fast transient heat flux information. Fabrication of the sensor does not require any matching of the mounting surface. Heat flux is proportional to the temperature difference across the upper and lower surfaces of an insulation material. The sensor consists of an array of thermocouples on the upper and lower surfaces of a thin insulating layer. The thermocouples for the sensor are connected in a thermopile arrangement. A 100 thermocouple pair heat flux sensor has been fabricated on silicon wafers. The sensor produced an output voltage of 200-400 microvolts when exposed to a hot air heat gun. A 20 element thermocouple pair heat flux sensor has been fabricated on aluminum oxide sheet. Thermocouples are Pt-Pt/Rh with silicon dioxide as the insulating material. This sensor produced an output of 28 microvolts when exposed to the radiation of a furnace operating at 1000 C. Work is also underway to put this type of heat flux sensor on metal surfaces. Author

N93-13668*# National Aeronautics and Space Administration. Lewis Research Center, Cleveland, OH.

GAS TEMPERATURE MEASUREMENTS USING THE DUAL-LINE DETECTION RAYLEIGH SCATTERING TECHNIQUE

M. Volkan Otugen (Polytechnic Univ., Brooklyn, NY.), Richard G. Seasholtz, and Kurt D. Annen (Aerodyne Research, Inc., Billerica, MA.) *In* NASA. Langley Research Center, The 1992 NASA Langley Measurement Technology Conference: Measurement Technology for Aerospace Applications in High-Temperature Environments Sep. 1992 p 107-126 (For primary document see N93-13661 03-35)

(Grant NAG3-1301)

Avail: CASI HC A03/MF A04

A new laser-induced Rayleigh scattering method is presented for the improved temperature diagnostics of gas flows. In the present technique, the two lines of a copper vapor laser are used to obtain the time and space resolved temperature. A single set of optics is used to form the optical probe and to collect the signal simultaneously from both the 510 nm and the 578 nm lines. The dual-line detection allows for the determination and removal of surface-scattered laser light from a Rayleigh signal thereby improving the applicability of Rayleigh scattering to near wall flows with a high degree of glare. An optical system using the dual-line detection technique is built, calibrated and tested in a hot air jet under various levels of background contamination. The results indicate that highly accurate temperature measurements are possible even when the laser-line background intensity, captured by the collecting optics, is five times that of the Rayleigh signal. Author

N93-13669*# PRC Systems Services Co., Edwards, CA.

HIGH-TEMPERATURE STRAIN MEASUREMENT TECHNIQUES: CURRENT DEVELOPMENTS AND CHALLENGES

M. M. Lemcoe *In* NASA. Langley Research Center, The 1992 NASA Langley Measurement Technology Conference: Measurement Technology for Aerospace Applications in High-Temperature Environments Sep. 1992

p 127-169 (For primary document see N93-13661 03-35)
Avail: CASI HC A03/MF A04

Since 1987, a very substantial amount of R&D has been conducted in an attempt to develop reliable strain sensors for the measurements of structural strains during ground testing and hypersonic flight, at temperatures up to at least 2000 deg F. Much of the effort has been focused on requirements of the NASP Program. This presentation is limited to the current sensor development work and characterization studies carried out within that program. It is basically an assessment as to where we are now and what remains to be done in the way of technical accomplishments to meet the technical challenges posed by the requirements and constraints established for the NASP Program. The approach for meeting those requirements and constraints has been multi-disciplinary in nature. It was recognized early on that no one sensor could meet all these requirements and constraints, largely because of the large temperature range (cryogenic to at least 2000 deg F) and many other factors, including the most challenging requirement that the sensor system be capable of obtaining valid 'first cycle data'. Present candidate alloys for resistance-type strain gages include Fe-Cr-Al and Pd-Cr. Although they have superior properties regarding withstanding very high temperatures, they exhibit large apparent strains that must either be accounted for or cancelled out by various techniques, including the use of a dual-element, half-bridge dummy gage, or electrical compensation networks. A significant effort is being devoted to developing, refining, and evaluating the effectiveness of those techniques over a broad range in temperature and time. In the quest to obtain first-cycle data, ways must be found to eliminate the need to prestabilize or precondition the strain gage, before it is attached to the test article. It should be noted that present NASP constraints do not permit prestabilization of the sensor, in situ. Gages are currently being 'heat treated' during manufacture in both the wire- and foil-type resistance strain gages, and evaluation is in progress. In addition, the 'gage-on-shim' concept is being revisited. That concept will permit heat treatment of the gage during manufacture, before attachment on the test article. Also, it may permit the individual calibration of each gage regarding gage factor and apparent strain. Candidate alloys for the NASP include titanium metal-matrix and carbon-carbon composites. Although those materials have very attractive properties at elevated temperatures in terms of strength and weight, they pose significant attachment problems. Methods for making reliable strain gage and thermocouple attachments to them are currently under development. Experience to date indicates that Rokide attachment of the sensor directly to the protective coating is easier than to the base material itself. However, interpreting strain data from gages attached in this way may prove difficult because of possible cracks in the coating that form 'islands' and the mobility of those 'islands'. It is concluded, therefore, that major technical challenges lie ahead as we proceed to meet the stringent strain sensor requirements and constraints of the NASP Program. Author

N93-13670*# Virginia Polytechnic Inst. and State Univ., Blacksburg. Dept. of Aerospace and Ocean Engineering.

SKIN FRICTION MEASUREMENTS IN HIGH TEMPERATURE HIGH SPEED FLOWS **c34**

J. A. Schetz, Thomas E. Diller, and A. L. Wicks *In* NASA. Langley Research Center, The 1992 NASA Langley Measurement Technology Conference: Measurement Technology for Aerospace Applications in High-Temperature Environments Sep. 1992 p 171-188 (For primary document see N93-13661 03-35)
Avail: CASI HC A03/MF A04

An experimental investigation was conducted to measure skin friction along the chamber walls of supersonic combustors. A direct force measurement device was used to simultaneously measure an axial and transverse component of the small tangential shear force passing over a non-intrusive floating element. The floating head is mounted to a stiff cantilever beam arrangement with deflection due to the flow on the order of 0.00254 mm (0.0001 in.). This allowed the instrument to be a non-nulling type. A second gauge was designed with active cooling of the floating sensor head to eliminate non-uniform temperature effects between the sensor head and the surrounding wall. Samples of measurements made in combustor test facilities at NASA Langley Research Center and at the General Applied Science Laboratory (GASL) are presented. Skin friction coefficients between 0.001 - 0.005 were measured dependent on the facility and measurement location. Analysis of the measurement uncertainties indicate an accuracy to within +/- 10-15 percent of the streamwise component. Author

N93-13671*# Sverdrup Technology, Inc., Cleveland, OH.

PALLADIUM-CHROMIUM STATIC STRAIN GAGES FOR HIGH TEMPERATURES

Jih-Fen Lei *In* NASA. Langley Research Center, The 1992 NASA Langley Measurement Technology Conference: Measurement Technology for Aerospace Applications in High-Temperature Environments Sep. 1992 p 189-209 (For primary document see N93-13661 03-35)
Avail: CASI HC A03/MF A04

An electrical resistance strain gage that can provide accurate static strain measurement to a temperature of 1500 F or above is being developed both in fine wire and thin film forms. The gage is designed to be temperature compensated on any substrate material. It has a dual element: the gage element is a special alloy, palladium-13wt percent chromium (PdCr), and the compensator element is platinum (Pt). Earlier results of a PdCr based wire gage indicated that the apparent strain of this gage can be minimized and the repeatability of the apparent strain can be improved by prestabilizing the gage on the substrate for a long period of time. However, this kind of prestabilization is not practical in many applications and therefore the development of a wire gage which is prestabilized before installation on the substrate is desirable. This paper will present our recent progress in the development of a prestabilized wire gage which can provide meaningful strain data for the first thermal cycle. A weldable PdCr gage is also being developed for field testing where conventional flame-spraying installation can not be applied. This weldable gage is narrower than a previously reported gage, thereby allowing the gage to be more resistant to buckling under compressive loads. Some preliminary results of a prestabilized wire gage flame-sprayed directly on IN100, an engine material, and a weldable gage spot-welded on IN100 and SCS-6/(beta)21-S Titanium Matrix Composite (TMC), a National Aero-Space Plane (NASP) structure material, will be reported. Progress on the development of a weldable thin film gage will also be addressed. The measurement technique and procedures and the lead wire effect will be discussed. Author

N93-13672*# National Aeronautics and Space Administration. Langley Research Center, Hampton, VA.

HIGH TEMPERATURE STRAIN GAGE APPARENT STRAIN COMPENSATION

Harlan K. Holmes and T. C. Moore, Sr. *In its* The 1992 NASA Langley Measurement Technology Conference: Measurement Technology for Aerospace Applications in High-Temperature Environments Sep. 1992 p 211-222 (For primary document see N93-13661 03-35)
Avail: CASI HC A03/MF A04

Once an installed strain gage is connected to a strain indicating device and the instrument is balanced, a subsequent change in temperature of the gage installation will generally produce a resistance change in the gage. This purely temperature-induced resistance will be registered by the indicating device as a strain and is referred to as 'apparent strain' to distinguish it from strain due to applied stress. One desirable technique for apparent strain compensation is to employ two identical gages with identical mounting procedures which are connected with a 'half bridge' configuration where gages see the same thermal environment but only one experiences a mechanical strain input. Their connection in adjacent arms of the bridge will then balance the thermally induced apparent strains and, in principle, only the mechanical strain remains. Two approaches that implement this technique are discussed. Author

N93-13673*# State Univ. of New York, Stony Brook. Lab. for Experimental Mechanics Research.

ELASTIC AND PLASTIC STRAIN MEASUREMENT IN HIGH TEMPERATURE ENVIRONMENT USING LASER SPECKLE

Fu-Pen Chiang *In* NASA. Langley Research Center, The 1992 NASA Langley Measurement Technology Conference: Measurement Technology for Aerospace Applications in High-Temperature Environments Sep. 1992 p 223-235 (For primary document see N93-13661 03-35)
(Contract DAAL03-88-K-0033)
Avail: CASI HC A03/MF A04

Two laser speckle methods are described to measure strain in high temperature environment and thermal strain caused by high temperature.

Both are non-contact, non-destructive and remote sensing techniques that can be automated. The methods have different but overlapping ranges of application with one being more suitable for large plastic deformation.
Author

N93-13674*# National Aeronautics and Space Administration. Marshall Space Flight Center, Huntsville, AL.
DETERMINATION OF HIGH TEMPERATURE STRAINS USING A PC BASED VISION SYSTEM
Stephen R. McNeill (South Carolina Univ., Columbia.), Michael A. Sutton (South Carolina Univ., Columbia.), and Samuel S. Russell *In* NASA. Langley Research Center, The 1992 NASA Langley Measurement Technology Conference: Measurement Technology for Aerospace Applications in High-Temperature Environments Sep. 1992 p 237-243 (For primary document see N93-13661 03-35)
Avail: CASI HC A02/MF A04

With the widespread availability of video digitizers and cheap personal computers, the use of computer vision as an experimental tool is becoming common place. These systems are being used to make a wide variety of measurements that range from simple surface characterization to velocity profiles. The Sub-Pixel Digital Image Correlation technique has been developed to measure full field displacement and gradients of the surface of an object subjected to a driving force. The technique has shown its utility by measuring the deformation and movement of objects that range from simple translation to fluid velocity profiles to crack tip deformation of solid rocket fuel. This technique has recently been improved and used to measure the surface displacement field of an object at high temperature. The development of a PC based Sub-Pixel Digital Image Correlation system has yielded an accurate and easy to use system for measuring surface displacements and gradients. Experiments have been performed to show the system is viable for measuring thermal strain. Author

N93-13675*# Sverdrup Technology, Inc., Brook Park, OH.
LASER-BASED STRAIN MEASUREMENTS FOR HIGH TEMPERATURE APPLICATIONS
Christian T. Lant *In* NASA. Langley Research Center, The 1992 NASA Langley Measurement Technology Conference: Measurement Technology for Aerospace Applications in High-Temperature Environments Sep. 1992 p 245-249 (For primary document see N93-13661 03-35)
Avail: CASI HC A01/MF A04

The Instrumentation and Control Technology Division at NASA Lewis Research Center has developed a high performance optical strain measurement system for high temperature applications using wires and fibers. The system is based on Yamaguchi's two-beam speckle-shift strain measurement technique. The system automatically calculates surface strains at a rate of 5 Hz using a digital signal processor in a high speed micro-computer. The system is fully automated, and can be operated remotely. This report describes the speckle-shift technique and the latest NASA system design. It also shows low temperature strain test results obtained from small diameter tungsten, silicon carbide, and sapphire specimens. These specimens are of interest due to their roles in composite materials research at NASA Lewis. Author

N93-13676*# Novasensor, Inc., Fremont, CA.
TECHNOLOGY TRENDS IN HIGH TEMPERATURE PRESSURE TRANSDUCERS: THE IMPACT OF MICROMACHINING
Joseph R. Mallon, Jr. *In* NASA. Langley Research Center, The 1992 NASA Langley Measurement Technology Conference: Measurement Technology for Aerospace Applications in High-Temperature Environments Sep. 1992 p 251-254 (For primary document see N93-13661 03-35)
Avail: CASI HC A01/MF A04

This paper discusses the implications of micromachining technology on the development of high temperature pressure transducers. The introduction puts forth the thesis that micromachining will be the technology of choice for the next generation of extended temperature range pressure transducers. The term micromachining is defined, the technology is discussed and examples are presented. Several technologies for high temperature pressure transducers are discussed, including silicon on insulator, capacitive, optical, and vibrating element. Specific conclusions are presented along with recommendations for development of the technology. Author

N93-13677*# Kulite Semi-Conductor Products, Inc., Leonia, NJ.
SiC DEVICE DEVELOPMENT FOR HIGH TEMPERATURE SENSOR APPLICATIONS
J. S. Shor, David Goldstein, A. D. Kurtz, and R. M. Osgood (Columbia Univ., New York, NY.) *In* NASA. Langley Research Center, The 1992 NASA Langley Measurement Technology Conference: Measurement Technology for Aerospace Applications in High-Temperature Environments Sep. 1992 p 255-264 (For primary document see N93-13661 03-35)
Avail: CASI HC A02/MF A04

Progress made in the processing and characterization of 3C-SiC for high temperature sensor applications is reviewed. Piezoresistance properties of silicon carbide and the temperature coefficient of resistivity of n-type beta-SiC are presented. In addition, photoelectrical etching and dopant selective etch-stops in SiC and high temperature Ohmic contacts for n-type beta-SiC sensors are discussed. Author

N93-13678*# Kaman Sciences Corp., Colorado Springs, CO.
THE TRADE-OFF CHARACTERISTICS OF ACOUSTIC AND PRESSURE SENSORS FOR THE NASP Final Report
Martin Winkler and Chuck Bush *In* NASA. Langley Research Center, The 1992 NASA Langley Measurement Technology Conference: Measurement Technology for Aerospace Applications in High-Temperature Environments Sep. 1992 p 265-289 Prepared in cooperation with General Dynamics Corp., Saint Louis, MO (For primary document see N93-13661 03-35)
Avail: CASI HC A03/MF A04

Results of a trade study for the development of pressure and acoustic sensors for use on the National Aerospace Plane (NASP) are summarized. Pressure sensors are needed to operate to 100 psia; acoustic sensors are needed that can give meaningful information about a 200 dB sound pressure level (SPL) environment. Both sensors will have to operate from a high temperature of 2000 F down to absolute zero. The main conclusions of the study are the following: (1) Diaphragm materials limit minimum size and maximum frequency response attainable. (2) No transduction is available to meet all the NASP requirements with existing technology. (3) Capacitive sensors are large relative to the requirement, have limited resolution and frequency response due to noise, and cable length is limited to approximately 20 feet. (4) Eddy current sensors are large relative to the requirement and have limited cable lengths. (5) Fiber optic sensors provide the possibility for a small sensor, even though present developments do not exhibit that characteristic. The need to use sapphire at high temperature complicates the design. Present high temperature research sensors suffer from poor resolution. A significant development effort will be required to realize the potential of fiber optics. (6) Short-term development seems to favor eddy current techniques with the penalty of larger size and reduced dynamic range for acoustic sensors. (7) Long-term development may favor fiber optics with the penalties of cost, schedule, and uncertainty. Author

N93-13679*# Kulite Semi-Conductor Products, Inc., Leonia, NJ.
VERY HIGH TEMPERATURE SILICON ON SILICON PRESSURE TRANSDUCERS
Anthony D. Kurtz, Timothy A. Nunn, Stephen A. Briggs, and Alexander Ned *In* NASA. Langley Research Center, The 1992 NASA Langley Measurement Technology Conference: Measurement Technology for Aerospace Applications in High-Temperature Environments Sep. 1992 p 291-300 (For primary document see N93-13661 03-35)
Avail: CASI HC A02/MF A04

A silicon on silicon pressure sensor has been developed for use at very high temperatures (1000 F). The design principles used to fabricate the pressure sensor are outlined and results are presented of its high temperature performance. Author

N93-13680*# National Aeronautics and Space Administration. Langley Research Center, Hampton, VA.
DEVELOPMENTS ON HIGH TEMPERATURE FIBER OPTIC MICROPHONE
Kenneth D. Wright, II and Allan J. Zuckerwar *In its* The 1992 NASA Langley Measurement Technology Conference: Measurement Technology for Aerospace Applications in High-Temperature Environments Sep. 1992 p 301-304 (For primary document see N93-13661 03-35)
Avail: CASI HC A01/MF A04

A fiber optic microphone, based on the principle of the fiber optic

lever, features small size, extended bandwidth, and capability to operate at high temperatures. These are requirements for measurements in hypersonic flow. This paper describes the principles of operation of fiber optic sensors, a discussion of the design of a fiber optic microphone, the functional elements and packaging techniques of the optoelectronic circuitry, and the calibration techniques used in the development of the high temperature fiber optic microphone. Author

N93-13681*# Calspan Corp., Arnold AFS, TN.
ELECTRON BEAM FLUORESCENCE MEASUREMENTS IN THE BOEING HYPERSONIC SHOCK TUNNEL
Linwood L. Price, W. Dan Williams, and H. M. Powell (Tennessee Technological Univ., Cookeville.) *In* NASA. Langley Research Center, The 1992 NASA Langley Measurement Technology Conference: Measurement Technology for Aerospace Applications in High-Temperature Environments Sep. 1992 p 305-320 (For primary document see N93-13661 03-35)
Avail: CASI HC A03/MF A04

The Calspan electron beam fluorescence (EBF) measurement system is described along with the results of measurements made in hypersonic flow. Numerous self-emitting metallic species were identified, many of which may be associated with an aging/erosion process within the B30HST. Because there were only 16 tunnel runs, it was only possible to obtain spectral measurements over a limited range of wavelengths and time sampling periods. Many spectral features of the flow remain uninvestigated. Because flow self-emission is important to all optical diagnostic techniques, it is recommended that additional spectral studies by performed. The three electron beam-excited species that were identified are nitrogen, helium, and nitric oxide. The high metallic radiation background interfered with attempts to obtain the time-wise variation of N2 density and He radiation with the optical fiber/PMT channels. In the case of the N2 density measurements the result of interference was increased uncertainty. Unfortunately, the interference caused the time-wise He measurements to fail completely. It is recommended that the electron beam be modulated to provide discrimination against the background radiation in future N2 density measurements. Careful data reduction produced useful measurements of N2 vibrational temperature, even though the high background from metallic species significantly increased measurement uncertainty. Perhaps the recommended additional spectral studies would reveal N2(+) First Negative System band-pair regions having less background. Detection of the He arrival was easily accomplished with the spectrometer/array detector system. Because of this, it is recommended that this means of detecting He arrival be used in the future. With proper calibrations of the system an He number density could be obtained. Although the flow conditions were out of limits for the run in which the NO spectrum was recorded, the usefulness of the NO spectrum for determination of free-stream rotational temperature was demonstrated and should be exploited in future experiments. Indeed, based on the strong NO signals, it is recommended that lower resolution NO spectra be obtained to provide a measure of NO vibrational temperature in the same manner that the N2 temperature was obtained. Author

N93-13682*# General Applied Science Labs., Inc., Ronkonkoma, NY.
RESONANCE LAMP ABSORPTION MEASUREMENT OF OH NUMBER DENSITY AND TEMPERATURE IN EXPANSION TUBE SCRAMJET ENGINE TESTS
Walter R. Lempert (Princeton Univ., NJ.), Richard E. Trucco, and Robert D. Bittner (Analytical Services and Materials, Inc., Hampton, VA.) *In* NASA. Langley Research Center, The 1992 NASA Langley Measurement Technology Conference: Measurement Technology for Aerospace Applications in High-Temperature Environments Sep. 1992 p 321-338 (For primary document see N93-13661 03-35)
(Contract NAS1-18450)
Avail: CASI HC A03/MF A04

In this paper, we report results of hydroxyl radical and static temperature measurements performed in the General Applied Science Laboratories-NASA HYPULSE expansion tube facility using the microwave resonance lamp absorption technique. Data were obtained as part of a series of hydrogen/air and hydrogen/oxygen combustion tests at stagnation enthalpies corresponding to Mach 17 flight speeds. Data from a representative injector configuration is compared to a full Navier-Stokes CFD solution. Author

N93-13683*# National Aeronautics and Space Administration. Lewis Research Center, Cleveland, OH.
VISUALIZATION OF HYDROGEN INJECTION IN A SCRAMJET ENGINE BY SIMULTANEOUS PLIF IMAGING AND LASER HOLOGRAPHIC IMAGING
Robert C. Anderson, Richard E. Trucco (General Applied Science Labs., Inc., Ronkonkoma, NY.), L. F. Rubin (Rockwell International Corp., Canoga Park, CA.), and D. M. Swain (Rockwell International Corp., Canoga Park, CA.) *In* NASA. Langley Research Center, The 1992 NASA Langley Measurement Technology Conference: Measurement Technology for Aerospace Applications in High-Temperature Environments Sep. 1992 p 339-354 (For primary document see N93-13661 03-35)
Avail: CASI HC A03/MF A04

Flowfield characterization has been accomplished for several fuel injector configurations using simultaneous planar laser induced fluorescence (PLIF) and laser holographic imaging (LHI). The experiments were carried out in the GASL-NASA HYPULSE real gas expansion tube facility, a pulsed facility with steady test times of about 350 microsec. The tests were done at simulated Mach numbers 13.5 and 17. The focus of this paper is on the measurement technologies used and their application in a research facility. The HYPULSE facility, the models used for the experiments, and the setup for the LHI and PLIF measurements are described. Measurement challenges and solutions are discussed. Results are presented for experiments with several fuel injector configurations and several equivalence ratios. Author

N93-13684*# National Aeronautics and Space Administration. Lewis Research Center, Cleveland, OH.
GAS TEMPERATURE AND DENSITY MEASUREMENTS BASED ON SPECTRALLY RESOLVED RAYLEIGH-BRILLOUIN SCATTERING
Richard G. Seasholtz and James A. Lock (Cleveland State Univ., OH.) *In* NASA. Langley Research Center, The 1992 NASA Langley Measurement Technology Conference: Measurement Technology for Aerospace Applications in High-Temperature Environments Sep. 1992 p 355-374 (For primary document see N93-13661 03-35)
Avail: CASI HC A03/MF A04

The use of molecular Rayleigh scattering for measurements of gas density and temperature is evaluated. The technique used is based on the measurement of the spectrum of the scattered light, where both temperature and density are determined from the spectral shape. Planar imaging of Rayleigh scattering from air using a laser light sheet is evaluated for ambient conditions. The Cramer-Rao lower bounds for the shot-noise limited density and temperature measurement uncertainties are calculated for an ideal optical spectrum analyzer and for a planar mirror Fabry-Perot interferometer used in a static, imaging mode. With this technique, a single image of the Rayleigh scattered light can be analyzed to obtain density (or pressure) and temperature. Experimental results are presented for planar measurements taken in a heated air stream. Author

N93-13685*# Stanford Univ., CA. High Temperature Gasdynamics Lab.
PLANAR LASER-INDUCED FLUORESCENCE MEASUREMENTS OF HIGH-ENTHALPY FREE JET FLOW WITH NITRIC OXIDE **c34**
Jennifer L. Palmer, Brian K. McMillin, and Ronald K. Hanson *In* NASA. Langley Research Center, The 1992 NASA Langley Measurement Technology Conference: Measurement Technology for Aerospace Applications in High-Temperature Environments Sep. 1992 p 375-386 Sponsored in part by AFOSR (For primary document see N93-13661 03-35)
Avail: CASI HC A03/MF A04

Planar laser-induced fluorescence (PLIF) measurements of property fields in a high-enthalpy, supersonic, underexpanded free jet generated in a reflection-type shock tunnel are reported. PLIF images showing velocity and temperature sensitivity are presented. The inferred radial velocity and relative rotational temperature fields are found to be in agreement with those predicted by a numerical simulation of the flowfield using the method of characteristics. Author

N93-13686*# Sandia National Labs., Albuquerque, NM. Combustion Research Facility.
PLANAR LASER-INDUCED FLUORESCENCE IMAGING OF OH IN THE EXHAUST OF A BI-PROPELLANT THRUSTER
Phillip H. Paul, N. T. Clemens, and D. B. Makel (GenCorp Aerojet,

Sacramento, CA.) *In* NASA. Langley Research Center, The 1992 NASA Langley Measurement Technology Conference: Measurement Technology for Aerospace Applications in High-Temperature Environments Sep. 1992 p 387-401 Sponsored in part by DOE (For primary document see N93-13661 03-35)
Avail: CASI HC A03/MF A04

Planar laser-induced fluorescence imaging of the hydroxyl radical has been performed on the flow produced by the exhaust of a subscale H2/O2 fueled bi-propellant rocket engine. Measurements were made to test the feasibility of OH (0,0) and (3,0) excitation strategies by using injection seeded XeCl and KrF excimer lasers, respectively. The flow is produced with hydrogen and oxygen reacting at a combustor chamber pressure of 5 atm which then exhausts to the ambient. The hydroxyl concentration in the exhaust flow is approximately 8 percent. Fluorescence images obtained by pumping the Q1(3) transition in the (0,0) band exhibited very high signals but also showed the effect of laser beam absorption. To obtain images when pumping the P1(8) transition in the (3,0) band it was necessary to use exceptionally fast imaging optics and unacceptably high intensifier gains. The result was single-shot images which displayed a signal-to-noise ratio of order unity or less when measured on a per pixel basis. Author

N93-13687*# Physical Sciences, Inc., Andover, MA.
EXIT PLANE H2O CONCENTRATION MEASUREMENTS CORRELATED WITH OH PLIF NEAR-INJECTOR MIXING MEASUREMENTS FOR SCRAMJET FLOWS
T. E. Parker, Mark G. Allen, R. R. Foutter, D. M. Sonnenfroh, and W. T. Rawlins *In* NASA. Langley Research Center, The 1992 NASA Langley Measurement Technology Conference: Measurement Technology for Aerospace Applications in High-Temperature Environments Sep. 1992 p 403-425 (For primary document see N93-13661 03-35)
(Contract F33615-91-C-2204)
Avail: CASI HC A03/MF A04

Mixing and combusting high enthalpy flows, similar to those encountered in scramjet engines, were investigated using a shock tunnel to produce the flow in conjunction with non-intrusive optical diagnostics which monitored the performance of two injector configurations. The shock tunnel is configured to produce Mach 3 flow and stagnation enthalpies corresponding to flight equivalent Mach numbers between 7 and 11. A pulsed hydrogen injection capability and interchangeable injector blocks provide a means of examining high speed, high enthalpy reacting flows. Planar laser induced fluorescence (PLIF) of OH molecules in the near injector region produced images which show the combusting and mixing zones for the reacting flow. Line-of-sight exit plane measurement of water concentration and temperature were used to provide a unique method of monitoring exit plane products. These results demonstrated that a velocity matched axial injection system produced a fuel jet that lifted off the floor of the duct. Mixing was observed to increase for this system as a velocity mismatch was introduced. Comparison of exit plane water concentrations for a wall jet injection system and a velocity matched injection system indicated similar mixing performance but an accurate pressure measurement is necessary to further validate the result. In addition, exit plane measurements indicated an approximate steady-state condition was achieved during the 1 to 2 ms test times. Author

N93-13709*# Millitech Corp., South Deerfield, MA.
SPACE-QUALIFIED SUBMILLIMETER RADIOMETER Final Report
G. R. Huguenin 14 Jan. 1987 170 p
(Contract NAS7-933; SBIR-08.02-8591)
(NASA-CR-190886; NAS 1.26:190886) Avail: CASI HC A08/MF A02

The purpose of this research was to develop a reliable submillimeter wave spectrometer for space-borne high frequency spectral line work. The emphasis was on improving the efficiency of frequency multipliers to limit the system components to rugged, low power consumption solid-state devices. This research has allowed Millitech to develop increased efficiency and performance in Millitech's existing line of submillimeter components and systems. Millitech has fabricated and tested a complete solid-state spectrometer front end for use at 560 GHz (the 1(sub 10) to 1(sub 01) transition of water vapor). The spectrometer was designed with the rigors of flight conditions in mind. The spectrometer uses a phase-locked, solid-state Gunn diode oscillator as the local oscillator, employing a tripler to produce about 3 mW of power at 285 GHz, and a low noise second harmonic waveguide mixer which requires less than 2 mW of LO power. The LO (and the signal) is injected into the mixer by means of a quasioptical diplexer. The measured system noise temperature is 2800 K (DSB) over 400 MHz. The whole spectrometer front end is compact (21 cm by 21 cm by 24 cm), light (7.4 kg), and has a power consumption of less than 8 W. Other topics explored in this work include compact frequency agile phase lock loops, optical filters, and InP Gunn oscillators for low noise applications. As a result of this research, the improvement in the design of multipliers and harmonic mixers will allow their use as the LO power for a variety of satellite-borne receivers operating in the 200 to 600 GHz frequency range. Author

N93-14086# Aerospace Corp., El Segundo, CA. Engineering and Technology Group.
TEMPERATURE MEASUREMENTS WITH MICROMETER SPATIAL RESOLUTION
Francisco Izaguirre, Geza Csanky, and Gary F. Hawkins 24 Jul. 1992 27 p
(Contract F04701-88-C-0089)
(AD-A255897; TR-0090(5935-08)-1; SMC-TR-92-40) Avail: CASI HC A03/MF A01

A novel technique has been developed to measure temperatures with a spatial resolution less than 10 micron. This method uses the temperature-sensitive time decay fluorescence of a phosphor as a surface sensor. The spatial resolution is obtained by using an electron beam to excite individual phosphor grains deposited on the surface of interest. The phosphor selected for its dynamic range and chemical stability is the inorganic compound magnesium fluorogermanate activated with manganese. The time decay constant of its fluorescence decreases monotonically with temperature between -200 to 450 C. This method was verified on a cross-sectioned Zener diode. A description of the technique and a temperature map of the sectioned area of an operating diode are presented. GRA

N93-13215# Messerschmitt-Boelkow-Blohm G.m.b.H., Munich (Germany). Military Aircraft Div.
A NOVEL-HIGH-PERFORMANCE SYSTEM FOR RECORDING AND ANALYSING INSTANTANEOUS TOTAL PRESSURE DISTORTION IN AIR INTAKES
K. W. Lotter and R.-D. Scherbaum *In* AGARD, Aerodynamic Engine/Airframe Integration for High Performance Aircraft and Missiles Sep. 1992 16 p (For primary document see N93-13199 03-34)
Copyright Avail: CASI HC A03/MF A04

36 LASERS AND MASERS

Includes parametric amplifiers.
For related information see also *76 Solid-State Physics.*

N93-12560# Los Alamos National Lab., NM.
DEVELOPMENT OF XUV PROJECTION LITHOGRAPHY AT 60 TO 80 nm
B. E. Newnam and V. K. Viswanathan 1992 19 p Presented at the Society Photography Institute of Engineers Microlithography 1992, San Jose, CA, 8-13 Mar. 1992
(Contract W-7405-eng-36)
(DE92-017517; LA-UR-92-1901; CONF-9203177-1) Avail: CASI HC A03/MF A01

The rationale, design, component properties, properties, and potential capabilities of extreme-ultraviolet (XUV) projection lithography systems using 60-80 nm illumination and single-surface reflectors are described. These systems are evaluated for potential application to high-volume production of future generations of gigabit chips. DOE

N93-12570# Lawrence Livermore National Lab., CA.
EXPERIMENTS ON RESONANTLY PHOTO-PUMPED X RAY LASERS
J. Nilsen, J. L. Porter, L. B. DaSilva, B. MacGowan, P. Beiersdorfer, S. R. Elliott, and B. K. Young 23 Jun. 1992 8 p Presented at the 3rd International Colloquium on X Ray Lasers, Schliersee, Germany, 18-22 May 1992
(Contract W-7405-eng-48)

(DE92-019542; UCRL-JC-109844; CONF-920523-3) Avail: CASI HC A02/MF A01

We describe our recent effort to identify and study a promising resonantly photopumped x-ray laser scheme. In particular, we will describe a scheme which uses the strong emission lines of a nickel-like ion to resonantly photo-pump a neon-like ion and enhance the lasing of the neon-like 3p to 3s transitions. DOE

N93-12610# Army Environmental Hygiene Agency, Aberdeen Proving Ground, MD.

LASER MEASUREMENT TECHNIQUES GUIDE FOR A HAZARD EVALUATION

Terry Lyon Aug. 1992 26 p

(AD-A254545; USAEHA-TG-192) Avail: CASI HC A03/MF A01

This technical guide provides uniform DOD guidance when performing radiometric measurements upon laser systems to conduct a hazard evaluation. This guide was prepared for the Laser System Safety Working Group to provide some joint service standardized techniques for laser measurements and the hazard evaluation of military laser systems. This technical guide should facilitate acceptance of hazard evaluations performed by other services. Although this technical guide could be applied to any laser system, it was developed primarily for outdoor military combat and training lasers and should be used when evaluating the engineering development, advanced development, and production models. GRA

N93-12644# Manchester Univ. (England). Dept. of Physics.

LASER DENSIFICATION AND DOPING OF SOL-GEL GLASSES Final Report, 1 Sep. 1990 - 31 Dec. 1991

Terence A. King 29 Feb. 1992 51 p

(Grant AF-AFOSR-0338-90)

(AD-A254566; AFOSR-92-0803TR) Avail: CASI HC A04/MF A01

An investigation into undoped and doped sol-gel glasses has been carried out for laser, optical, and optoelectronic applications. Methods for the doping and characterization of sol-gel glasses have been developed. Lasers based on gel-silica glass doped with organic molecules and operating from the near UV to the near IR have been produced. The basic properties of the composite materials have been measured including dopant distribution, optical quality, and photostability. Fundamental parameters and mechanisms for the doped systems of fluorescence lifetime, quantum efficiency, and uniformity have been investigated. Controlled densification of the sol-gel glass to give increased refractive index has been demonstrated. This enables the writing of optical waveguides in bulk arid thin films which open up many applications in optoelectronics and the surface densification of sol-gel glass for lightweight optics. New methods of densification of photosensitized sol-gel glass to give high spatial resolution micron size waveguides is described. Applications for the types of systems resulting from this work are reviewed and areas of future development described. GRA

N93-12656*# Alabama Univ., Huntsville. Center for Applied Optics.

CO2 LASER MODELING Final Report

Barry Johnson Jul. 1992 163 p

(Contract NAS8-36955)

(NASA-CR-184455; NAS 1.26:184455) Avail: CASI HC A08/MF A02

The topics covered include the following: (1) CO2 laser kinetics modeling; (2) gas lifetimes in pulsed CO2 lasers; (3) frequency chirp and laser pulse spectral analysis; (4) LAWS A' Design Study; and (5) discharge circuit components for LAWS. The appendices include LAWS Memos, computer modeling of pulsed CO2 lasers for lidar applications, discharge circuit considerations for pulsed CO2 lidars, and presentation made at the Code RC Review. Author

N93-12734# Lawrence Livermore National Lab., CA.

WORKSHOP ON SUPER-INTENSE LASER-ATOM PHYSICS Final Report, 23 Apr. 1991 - 22 Apr. 1992

Kenneth C. Kulander Aug. 1992 71 p Workshop held in Big Sky, MT, 22-25 Jun. 1991

(Contract MIPR-ARO-147-91)

(AD-A254833; ARO-28819.1-PH-CF) Avail: CASI HC A04/MF A01

The workshop on super-intense laser-atom physics consisted of 22 invited talks and 32 presentations in the poster session. GRA

N93-12744# Massachusetts Inst. of Tech., Cambridge. Research Lab. of Electronics.

SMALL-SCALE X RAY LASER SYSTEMS

S. Basu, M. Muendel, J. Goodberlet, S. Kaushik, and P. L. Hagelstein 1991 10 p Presented at the Society of Photo-Optical Instrumentation Engineers Meeting, San Diego, CA, 21-26 Jul. 1991

(Contract DE-FG02-89ER-14012)

(DE92-018442; CONF-9107115-77) Avail: CASI HC A02/MF A01

We are constructing a small-scale XUV laser to operate at near 191 Angstroms at a repetition rate of 6 ppm. For this project, we have chosen the Ni-like collision excitation scheme. To date, collisional excitation schemes have been used to generate gain in high Z materials at wavelengths as short as 43.18 Angstroms. High Z materials require very high electron temperatures to match the 'steady state' production of sufficient number of Ni-like ions and the 3d-4d excitation energy. Based on an earlier idea, we are attempting to demonstrate gain in a low Z material, which is to be pumped with a series of short pulses rather than with one long pulse. In this case, it is predicted that favorable density and temperature conditions will be present after a few initial pulses to generate gain of the order of 5-10 cm(sup -1). In this paper, we summarize the status of our experiments. DOE

N93-12915# Sandia National Labs., Albuquerque, NM.

LATENT IMAGE EXPOSURE MONITOR USING SCATTEROMETRY

L. M. Milner (New Mexico Univ., Albuquerque.), K. C. Hickman (New Mexico Univ., Albuquerque.), S. M. Gaspar (New Mexico Univ., Albuquerque.), K. P. Bishop (New Mexico Univ., Albuquerque.), S. S. Naqvi (New Mexico Univ., Albuquerque.), J. R. McNeil (New Mexico Univ., Albuquerque.), M. Blain, and B. L. Draper 1992 10 p Presented at the Society Photography Institute of Engineers (SPIE) Microlithography 1992, San Jose, CA, 8-13 Mar. 1992

(Contract DE-AC04-76DP-00789)

(DE92-019427; SAND-92-0971C; CONF-9203177-2) Avail: CASI HC A02/MF A01

We discuss the use of light scattered from a latent image to control photoresist exposure dose and focus conditions which results in improved control of the critical dimension (CD) of the developed photoresist. A laser at a non-exposing wavelength is used to illuminate a latent image grating. The light diffracted from the grating is directly related to the exposure dose and focus and thus to the resultant CD in the developed resist. Modeling has been done using rigorous coupled wave analysis to predict the diffraction from a latent image as a function of the substrate optical properties and the photoactive compound (PAC) concentration distribution inside the photoresist. It is possible to use the model to solve the inverse problem: given the diffraction, to predict the parameters of the latent image and hence the developed pattern. This latent image monitor can be implemented in a stepper to monitor exposure in situ, or prior to development to predict the developed CD of a wafer for early detection of bad devices. Experimentation has been conducted using various photoresists and substrates with excellent agreement between theoretical and experimental results. The technique has been used to characterize a test pattern with a focused spot as small as 36 micron in diameter. Using diffracted light from a simulated closed-loop control of exposure dose, CD control was improved by as much as 4 times for substrates with variations in underlying film thickness, compared to using fixed exposure time. The latent image monitor has also been applied to wafers with rough metal substrates and focus optimization. DOE

N93-12925# Lawrence Livermore National Lab., CA.

TABLE-TOP X RAY LASING BASED ON OPTICAL-FIELD-INDUCED IONIZATION

D. C. Eder, P. Amendt, P. R. Bolton, G. Guethlein, R. A. London, M. D. Rosen, and S. C. Wilks 2 Jul. 1992 8 p Presented at the 3rd International Colloquium on X Ray Lasers, Schliersee, Germany, 18-22 May 1992

(Contract W-7405-eng-48)

(DE92-019374; UCRL-JC-110043; CONF-920523-2) Avail: CASI HC A02/MF A01

Table-top x-ray laser schemes in H- and Li-like ions following optical-field-induced ionization are discussed. The use of ultrashort ionizing pulses is shown to be necessary to keep secondary heating mechanisms, e.g., stimulated Raman scattering, at acceptable levels. The combination

of longitudinal pumping and ultrashort pulses gives modest energy requirements. The effects of plasma dispersion and longitudinal pumping, on the relative speeds of the ionizing laser pulse and the x- ray photons, are included in our calculations. The x-ray laser scheme is calculated to have relatively high energy efficiencies in Li-like Ne at 98 A. Two approaches for creating the initial high-density gas/plasma using a laser heated thin film and a high-density gas jet are described. Applications in material science and chemistry, e.g., photoelectron spectroscopy, requiring the high-repetition rate (10-100 Hz) of the proposed x-ray laser are discussed. DOE

N93-13249# Sandia National Labs., Albuquerque, NM.
RADIATION-INDUCED INFRARED ABSORPTION IN NUCLEAR-PUMPED LASER CAVITY COMPONENTS
P. J. Brannon, D. E. Bodette, and D. A. McArthur Jul. 1992 39 p
(Contract DE-AC04-76DP-00789)
(DE92-017346; SAND-92-1255) Avail: CASI HC A03/MF A01

The transient transmission of laser activity cavity materials has been measured when they are subjected to 20 ms, fat, and nominal $3 nuclear radiation pulses from Sandia National Laboratories ACRR reactor. Infrasil and 7940 fused silica, and AR and high reflectance coatings have been transient tested at 1.06, 1.73, and 2.03 microns for gamma doses ranging from 0.3 to 0.65 Mrad and neutron fluences ranging from 4.0 to 1.5 10(sup 14) n/cm(sup 2). pulse widths range from 12 to 250 ms. Transient absorption in 7940 silica and the AR coatings is less than the noise for the conditions of this experiment. At the wavelengths listed above the upper bound for the absorption coefficient of 17940 is 0.00158 cm(sup -1) for single pulse operation. The reflectivity of the HR coating does not change when it is irradiated. Infrasil has both a transient and a permanent induced absorption when it is subjected to radiation. For single pulse operation the absorption coefficients at 1.06, 1.73, and 2.03 microns are 0.0115, 0.0026, and 0.0039 cm(sup -1), respectively. DOE

N93-13365 Dartmouth Coll., Hanover, NH.
THE SAPPHIRE CERENKOV LASER Ph.D. Thesis
Emily Elizabeth Fisch 1991 140 p
Avail: Univ. Microfilms Order No. DA9213738

The theory and experimental performance of the Cerenkov Free Electron Laser (CFEL) is treated. Emphasis is on low-voltage (less than 100 keV) operation. The CFEL is an 'electron beam drive', 'dielectric resonator based' source of tunable radiation. The Cerenkov mechanism for spontaneous emission is introduced. Geometric optics and electromagnetic theory are invoked to determine the critical resonator properties of a device designed to produce stimulated emission. The gain is quantified by adapting the dimensionless FEL formalism for the first time to low energy CFEL's. Saturation and power are explored by extending the dimensionless equation of motion. The experimental results for sapphire planar resonators are presented. The experiments corroborate the theoretical predictions in all cases. Radiation was also obtained from lanthanum aluminate, quartz, boron nitride, and stycast and these results are discussed briefly. The lack of any radiation from silicon resonators is explained. The sapphire CFEL has produced up to 100 W of radiation in a approximately 1 microseconds pulse at wavelengths ranging from 3.7 to 1.4 mm (80 to 220 GHz). The sapphire Cerenkov laser could be adapted for far-infrared output (100 microns/1 mm) using the theory presented to determine the design parameters. Dissert. Abstr.

N93-13418* National Aeronautics and Space Administration. Pasadena Office, CA.
QUANTUM WELL, BEAM DEFLECTING SURFACE EMITTING LASERS Patent
Jae H. Kim, inventor (to NASA) (Jet Propulsion Lab., California Inst. of Tech., Pasadena.) 27 Oct. 1992 7 p Filed 5 Jun. 1991 Supersedes N91-32489 (29 - 24, p 4024)
(NASA-Case-NPO-18243-1-CU; US-Patent-5,159,603;
US-Patent-Appl-SN-710424; US-Patent-Class-372-45;
US-Patent-Class-372-46; Int-Patent-Class-H01S-3/19) Avail: US Patent and Trademark Office

This invention relates to surface emitting semiconductor lasers (SELs), with integrated 45 deg. beam deflectors. A SEL is formed on a wafer including vertical mirrors and 45 deg. beam deflectors formed in grooves by tilted ion beam etching. A SEL is a lattice matched, or unstrained, AlGaAs/GaAs GRINSCH SQW SEL. An alternate embodiment is shown, in which a SEL is lattice mismatched, strained or pseudomorphic, or InGaAs/AlGaAs GRINSCH SQW SEL which emits radiation at a wavelength to which its substrate is transparent. Both SELs exhibit high output power, low threshold current density, and relatively high efficiency, and each are processing compatible with conventional large scale integration technology. Such SELs may be fabricated in large numbers from single wafers. The novel features of this invention include the use of tilted ion beam etching to form a pair of grooves each including vertical mirrors and 45 deg. beam deflectors. The embodiment provides substantial circuit design flexibility because radiation may be coupled both up and/or down through the substrate. Official Gazette of the U.S. Patent and Trademark Office

N93-13497 Drexel Univ., Philadelphia, PA.
THEORY OF LASING WITHOUT POPULATION INVERSION Ph.D. Thesis
Heide Maria Doss 1992 214 p
Avail: Univ. Microfilms Order No. DA9223713

The amplification of coherent radiation from an active medium under conditions which require no population inversion between the energy levels is discussed. Gain without population inversion may be obtained by creating a sufficiently strong correlation between pairs of atomic states, usually with the help of external sources of resonant electromagnetic radiation. The main objective is to investigate two possible selections for the active medium: a three level atom in a lambda configuration and a Raman-driven four level model. For both, the conditions that lead to inversionless laser action are identified, the small signal gain is calculated, and the physical mechanisms which are responsible for the emergence of gain are investigated. While the ultimate cause of the gain is quantum interference, attractive alternative pictures based on the dressed states of the coupled atom-driving field systems are proposed. The important practical issue of the effect of atomic motion and related Doppler broadening on the inversionless gain profile is addressed and the transient response of each laser model with the help of the appropriate Maxwell-Bloch equations is analyzed. Finally, a fully quantum mechanical description of the lambda model is developed and it is found that the radiated field can display unique quantum features which manifest themselves with sub-Poissonian photon fluctuations. Dissert. Abstr.

N93-13507# Los Alamos National Lab., NM.
INITIAL PERFORMANCE OF LOS ALAMOS ADVANCED FREE ELECTRON LASER
D. C. Nguyen, D. M. Baca, K. C. D. Chan, R. B. Cheairs, C. M. Fortgang, S. M. Gierman, W. J. D. Johnson, D. E. Holcomb, J. Kinross-Wright, and S. W. McCann et al 1992 8 p Presented at the 16th International LINAC Conference, Ottawa, Ontario, 23-28 Aug. 1992
(Contract W-7405-eng-36)
(DE92-040214; LA-UR-92-2803; CONF-9208109-25) Avail: CASI HC A02/MF A01

We report recent results on the high-brightness electron linac and initial performance of the Advanced FEL at Los Alamos. The design and construction of the Advanced FEL beamline are based upon integration of advanced technologies such as high-brightness photoinjector, high-gradient compact linac, and permanent-magnet beamline components. With the use of microwiggler, both permanent magnet and pulsed electromagnet, and compact optical resonator, the Advanced FEL will be the first of its kind small enough to be mounted on an optical table and yet capable of providing highpower optical output spanning the near-IR and visible regions. A schematic of the Advanced FEL is shown. The source of high-current electron pulses is a laser-gated photoelectron injector which forms an integral part of a high-gradient 1.2-m long RF linear accelerator. The latter is capable of accelerating electrons up to 20 MeV with room temperature operation and 25 MeV at 77K. The electrons are produced in 10-ps pulses with peak currents as high as 300 A. These electron pulses are transported in a brightness-preserving beamline consisting of permanent magnet dipoles and quadrupoles. The beamline has three 30 deg bends. The first bend allows for the photocathode drive laser input, the second allows for the FEL output, and the third turns the electron beam into the floor for safety reasons. Additional information on the design physics of the Advanced FEL can be found elsewhere. DOE

N93-13514# Oregon Univ., Eugene.
MONITORING INTERFACIAL DYNAMICS BY PULSED LASER TECHNIQUES
G. L. Richmond 1991 10 p
(Contract DE-FG06-86ER-45273)
(DE92-040302; DOE/ER-45273/6) Avail: CASI HC A02/MF A01

The goal is to develop new optical methods for the study of dynamic processes at the electrode/electrolyte interface. In the past year, optical second harmonic generation was used for time resolved measurements of thallium electrodeposition on Cu(111). Other studies included the following: the study of the photochemistry involved in a GaAs surface treatment known as photowashing; and the study of picosecond time resolved luminescence decays from GaAs in electrochemical environments (power dependent effects). DOE

N93-13534# Lawrence Livermore National Lab., CA.
NUMERICAL MODELLING OF THE SUPPRESSION OF STIMULATED BRILLOUIN SCATTERING DUE TO FINITE LASER BANDWIDTH
S. N. Dixit Apr. 1992 14 p Presented at the Society of Photo-Optical Instrumentation Engineers' International Symposium on Laser Spectroscopy, Los Angeles, CA, 19-24 Jan. 1992
(Contract W-7405-eng-48)
(DE92-018064; UCRL-JC-107973; CONF-920124-27) Avail: CASI HC A03/MF A01

We present numerical simulations of transverse stimulated Brillouin scattering (SBS) in large aperture optical elements and investigate its suppression due to finite laser bandwidth. A specific model for the laser bandwidth, namely, a sinusoidal phase modulation of the electric field, is considered. Our calculations indicate that bandwidths larger than the SBS linewidth lead to significant reduction in the SBS gain. We also investigate the dependence of the SBS gain on the modulation frequency and find that for a fixed overall bandwidth, a modulation frequency of the order of the SBS linewidth leads to an optimal reduction of the SBS gain. DOE

N93-13626 Stanford Univ., CA.
METHODS FOR EFFICIENT PUMPING OF VACUUM ULTRAVIOLET LASERS Ph.D. Thesis
Steven J. Benerofe 1992 80 p
Avail: Univ. Microfilms Order No. DA9217795

Methods for improving the gain and reducing the pump requirements of VUV lasers is discussed. Experimental results are presented for two laser systems: the Xe III 109 nm Auger laser and the 116 nm Werner band H2 laser. Using the Xe III laser we demonstrate a scaling of a travelling wave pumping geometry to oblique angles. This allows us to operate the Xe III laser (saturated) at 2 Hz. We also demonstrate the use of a modified Quanta-ray laser (400 mJ in 2.5 nsec.) as the pump source for the 109 nm Xe III laser. We report the use of a laser plasma produced Photoionization Electron Source (PES) to pump (and saturate) lines in the Lyman and Werner bands of H2. Calculations are presented to support the hypothesis of PES pumping, and thereby providing the first conclusive evidence of a PES-pumped laser. Optimization of the pumping configuration is presented which has allowed 2 Hz operation and saturation of the 116 nm Werner band laser as an example, we quantitatively demonstrate the advantages of PES pumping over conventional discharge or e-beam pumping. We have measured a small signal gain coefficient of approximately cm(exp -1), an improvement of more than a factor of 10 over previously reported results. We also report results showing that the small signal gain coefficient can be increased by cooling the lasing medium, thereby reducing the Doppler width of the laser transition. Dissert. Abstr.

N93-13629 Southampton Univ. (England).
A STUDY OF TECHNIQUES FOR SINGLE FREQUENCY OPERATION OF DIODE-PUMPED Nd:YAG LASERS Ph.D. Thesis
William Andrew Clarkson 1990 245 p
Avail: Univ. Microfilms Order No. BRDX95464

The use of diode lasers to longitudinally pump Nd:YAG lasers and other solid-state lasers is becoming an increasingly widespread practice. In this thesis various aspects of the operation of these lasers are studied and in particular, techniques by which single frequency operation can be achieved. In the first part of this thesis the effects of the non-uniform transverse mode profiles for the pump laser and lasing mode on the performance of a four-level laser are considered. Expressions for threshold pump power, slope efficiency and relaxation oscillation frequency are derived using a simple rate equation model. The resulting expressions provide sufficient insight into laser behaviour to allow the design of efficient diode-laser-pumped solid-state lasers. The thesis then goes on to consider various techniques for single axial mode selection in low-gain diode-pumped solid state lasers. The two most attractive techniques, which involve the use of a 'twisted-mode' resonator or a unidirectional ring laser, have been investigated experimentally for the case of a diode-pumped Nd:YAG laser. The design and performance of each of these lasers for both continuous-wave (CW) and Q-switched single frequency operation is discussed. In the case of the ring laser, by using a novel low-loss resonator design, CW single frequency powers of 80mW and Q-switched pulse energies of 20 micro-J were achieved by pumping with a 500 mW diode laser array. Subsequent amplification of the Q-switched pulses by double-passing a conventional, high-gain, flashlamp-pumped Nd:YAG amplifier resulted in pulse energies of 12mJ. Theory predicts that pulse energies in excess of 40 mJ should be possible for an optimized system. This suggests that the combination of a miniature, Q-switched, diode-pumped ring laser and a simple amplifier may be an attractive alternative to an injection-seeded Nd:YAG laser for the production of single frequency Q-switched pulse energies in the range 10mj to 100mJ. Dissert. Abstr.

N93-13653# Lawrence Livermore National Lab., CA.
DEMONSTRATION OF A NEON-LIKE RUBIDIUM X RAY LASER
J. Nilsen, J. L. Porter, L. B. DaSilva, and B. J. MacGowan 23 Jun. 1992 7 p Presented at the 3rd International Colloquium on X Ray Lasers, Schliersee, Germany, 18-22 May 1992
(Contract W-7405-eng-48)
(DE92-019576; UCRL-JC-109845; CONF-920523-5) Avail: CASI HC A02/MF A01

We demonstrate a rubidium ion laser with two strong laser lines at 173 and 176 A. The lasing transitions are 3p yields 3s transitions in neon-like rubidium. Several weaker lasing transitions are also observed. Wavelengths of the five lasing transitions are reported. Gains of 1.9 and 1.4 cm(exp -1) are measured for the two strongest lines. The weaker gain than other neon-like laser systems is ascribed to poor target quality coupled with the dilution associated with using RbCl. DOE

N93-13747 Council for National Academic Awards (England).
PARAMETER STUDIES OF HELIUM-NEON LASERS AT 543 nm Ph.D. Thesis
B. S. Gray 1991 215 p
Avail: Univ. Microfilms Order No. BRDX94338

Previously, there have been little other than empirical reports on the 543 nm helium-neon laser, these have usually revolved around commercial laser tubes. An attempt to describe the behavior of this transition, by measuring the optical gain at 543 nm under different discharge conditions and explaining the results, is made. Initially, empirical results of commercial laser tubes are presented, in an attempt to clarify previously published reports on this transition. A commercial 543 nm laser, oscillating in a single mode, was frequency stabilized to a Zeeman stabilized 633 nm helium-neon laser in a scanning Fabry-Perot interferometer. The long term stability of this laser was estimated as being roughly 1MHz. The output from this laser was used to probe various helium-neon discharges, with the amplification of the beam's intensity being used to measure the variation of optical gain at 543 nm as a function of discharge gas fill and current. This method of measuring the optical gain could resolve changes in the probe beam's intensity of less than 0.001 percent. This experimental technique yielded results for the optical gain at 543 nm, which did not mimic those seen at 633 nm. The optimum total gas pressure of the discharge was found to lie at roughly 2/3 of that seen at 633 nm (measured using the same method), and furthermore the optical gain at 543 nm at the optimum total gas pressure for the 633 nm transition was almost zero. This behavior was explained as being caused by an electron resonance peak at 219 eV observed in the electron excitation cross section to the lower laser state of the 543 nm transition, which is not seen in the 633 nm transition. A numerical model is developed to show the effects of this resonance peak on the optical gain of the laser system as a function of gas pressure, and this predicts a similar result to that observed by the above experiments. Unsuccessful attempts to absorb 19 eV electrons and thus remove the effects of this resonance peak are also described. The

behavior of the optical gain at 543 nm as a function of discharge current is found to be explicable using existing helium-neon laser theory.
Dissert. Abstr.

N93-13773 North Carolina State Univ., Raleigh.
STRAINED-LAYER InGaAs-GaAs-AlGaA QUANTUM WELL LASERS AND TRANSVERSE JUNCTION STRIPE LASERS Ph.D. Thesis
Yongkun Sin 1991 133 p
Avail: Univ. Microfilms Order No. DA9123395

Strained-layer InGaAs-GaAs-AlGaAs quantum well lasers, transverse junction stripe lasers, and laser diodes incorporating low temperature (LT) GaAs as a current blocking layer are discussed. First, photoluminescence characteristics of uniformly silicon- and beryllium-doped pseudomorphic InGaAs-GaAs-AlGaAs single quantum well and multiple quantum well heterostructures grown by molecular beam epitaxy are studied. Second, the first detailed experimental investigation on the effect of the chemical treatments on the electrical characteristics and laser thresholds of transverse junction stripe (TJS) lasers is reported. Surface treatments of (NH4)2S are demonstrated that reduce surface leakage currents in current injection lasers. The laser thresholds of lattice-matched TJS lasers are reduced by 12mA (16 percent) after the chemical treatments. Also, the first experimental investigation on the effect of isoelectronic In doping on the current-voltage characteristics of Zn-diffused lateral p-n junctions is reported. The trap density in an In-doped AlGaAs layer is reduced greatly compared to that in an AlGaAs layer without In doping. Third, the diffusion of zinc into LT GaAs grown by MBE at 200 C, the problems associated with using a silicon nitride film directly deposited on the LT GaAs as a Zn diffusion mask, and several schemes to avoid the problems are reported. The Zn diffusion coefficient is measured to be about one order of magnitude higher in the LT GaAs than in normal GaAs, attributed to a large quantity of defects including arsenic antisites in the LT GaAs. The effectiveness of silicon nitride as a Zn diffusion mask depends on whether the mask is deposited directly on the LT GaAs. The failure of the nitride to stop the Zn is attributed to arsenic atoms outdiffusing from the As-rich LT GaAs (about 1 atomic percent excess As) into the nitride. Several structures are introduced including a 100 A thick GaAs layer on the LT GaAs that are effective in preserving the diffusion mask properties of the silicon nitride.
Dissert. Abstr.

N93-13777 California Univ., Berkeley.
THEORY OF THE ION-CHANNEL LASER Ph.D. Thesis
David Harvey Whittum 1990 305 p
Avail: Univ. Microfilms Order No. DA9126832

A relativistic electron beam propagating through a plasma in the ion-focussed regime exhibits an electromagnetic instability with peak growth rate near a resonant frequency omega is approximately 2(gamma)(exp 2)(omega(sub beta)), where gamma is the Lorentz factor and omega(sub beta) is the betatron frequency. The physical basis for this instability is that an ensemble of relativistic simple harmonic oscillators, weakly driven by an electromagnetic wave, will lose energy to the wave through axial bunching. This 'bunching' corresponds to the development of an rf component in the beam current, and a coherent centroid oscillation. The subject of this thesis is the theory of a laser capitalizing on this electromagnetic instability. In Chapter 1, a historical perspective is offered. In Chapter 2, the basic features of relativistic electron beam propagation in the iron-focussed regime are reviewed. In Chapter 3, the ion-channel laser (ICL) instability is explored theoretically through an eikonal formalism, analogous to the 'KMR' formalism for the free-electron laser (FEL). The dispersion relation is derived, and the dependence of growth rate on three key parameters (detuning--delta, Pierce parameter--rho, and betatron parameter--alpha(sub beta)) is explored. Finite temperature effects are assessed. From this work it is found that the typical gain length for amplification is longer than the Rayleigh length, and we go on to consider three mechanisms which will tend to guide the radiation. First, we consider the effect of the ion channel as a dielectric waveguide. We consider next the use of a conducting waveguide, appropriate for a microwave amplifier. Finally, we examine a form of 'optical guiding' analogous to that found in the FEL. In Chapter 4, the eikonal formalism is used to model numerically the instability through and beyond saturation. Results are compared with the numerical simulation of the full equations of motion, and with analytic scalings. The analytical requirement on detuning spread is confirmed. In Chapter 5, results are summarized, and prospects for future work are considered.
Dissert. Abstr.

N93-13797*# Alabama Univ., Huntsville. Center for Applied Optics.
CO2 LASER PRE!ONISATION Final Report, 1990
Gary D. Spiers 1991 61 p
(Contract NAS8-36955)
(NASA-CR-184424; NAS 1.26:184424) Avail: CASI HC A04/MF A01

The final report for work done during the reporting period of January 25, 1990 to January 24, 1991 is presented. A literature survey was conducted to identify the required parameters for effective preionization in TEA CO2 lasers and the methods and techniques for characterizing preionizers are reviewed. A numerical model of the LP-140 cavity was used to determine the cause of the transverse mode stability improvement obtained when the cavity was lengthened. The measurement of the voltage and current discharge pulses on the LP-140 were obtained and their subsequent analysis resulted in an explanation for the low efficiency of the laser. An assortment of items relating to the development of high-voltage power supplies is also provided. A program for analyzing the frequency chirp data files obtained with the HP time and frequency analyzer is included. A program to calculate the theoretical LIMP chirp is also included and a comparison between experiment and theory is made. A program for calculating the CO2 linewidth and its dependence on gas composition and pressure is presented. The program also calculates the number of axial modes under the FWHM of the line for a given resonator length. A graphical plot of the results is plotted.
L.R.R.

N93-13812 Hull Univ. (England).
PHASE CONJUGATION USING CO2 LASERS Ph.D. Thesis
Jonathan Stewart Leggatt 1989 196 p
Avail: Univ. Microfilms Order No. BRDX95684

CO2 lasers have an even longer history than phase conjugation. This thesis reviews some of the work on phase conjugation that has been done up to the present, concentrating on the work with CO2 lasers. Gaseous SF(sub 6) is studied as a medium for generating phase conjugate returns using degenerate four-wave mixing, a technique analogous to real-time holography. These data are discussed and compared to previously published work. An energy reflectivity of more than 100 percent is one novel aspect of the experimental data. Liquids have not been used to make phase conjugate CO2 radiation in the past. This has been achieved using CS2, in this work. The dramatic nature of the temporal pulse reshaping is explained as the result of a thermal-acoustic effect in the liquid. A full mathematical model of the size and shape of the phase conjugate return is constructed from the thermo-elastic wave equation by making use of a Fourier transform technique. The work with liquid CS2 is extended to use of a long duration low power, laser. For these studies, a new type of pyroelectric laser detector was designed and constructed. This was then used to measure the power levels and reflectivities in this experiment. The high reflectivities found are explained in terms of a simple mathematical model. Reasons why the reflectivity is not even higher are put forward. Some ideas for further consideration are made, including liquid crystal interaction media.
Dissert. Abstr.

N93-13814 Heriot-Watt Univ., Edinburgh (Scotland).
A STUDY OF SMALL SOLID-STATE SWITCHED TEA CO2 LASERS Ph.D. Thesis
Alan Sylvan 1991 357 p
Avail: Univ. Microfilms Order No. BRDX95739

The results of a theoretical and experimental investigation into the use of all solid-state exciters with small corona preionized TEA CO2 lasers are presented. To overcome the limitations of existing semiconductor devices, energy pulse compression techniques were utilized. High energy efficiency at low repetition rates was provided by the use of unreset ferrite magnetic cores in a magnetic pulse compressor. A high repetition rate laser system was also produced and operated at 1 KHz producing 18 W of optical power. In order to further improve energy efficiency, a number of different laser exciter topologies were evaluated. The successful operation of a thyristor stack driven laser enabled a comparative study with a conventional hydrogen thyratron drive circuit to be undertaken. It was found that all solid-state exciters could be as energy efficient as conventional drive techniques. The desire to minimize the amount of pulse energy switched by semiconductor elements leads to an examination of photoswitching

methods in which the laser head acts as its own switch. Finally, long optical pulse generation was achieved by the use of pulser sustainer techniques which enabled optical pulses over 20 microns long to be produced. Dissert. Abstr.

N93-13846 Oxford Univ. (England).
LASER SPECTROSCOPY OF RARE EARTH IONS Ph.D. Thesis
Peter C. Hansen 1990 353 p
Avail: Univ. Microfilms Order No. BRD-96204

The main part of this thesis reports on the study of a wide range of EuVO4 samples grown from different starting flux materials, and doped with different rare earth ions. Conventional optical absorption and emission spectroscopy was used to measure the energies of the 5D and 7F levels of the Eu(3+) ion in the different growths. Related optical absorption work was carried out on the Ho(3+) ion, in the two cases 1 percent Ho:EuVO4 (one of the doped EuVO4 growths) and 10 percent Ho:YVO4 (as a aid to understanding HoVO4). The absorption spectrum of Eu(3+) in the immediate vicinity of the forbidden 7F(sub 0)-5D(sub 0) transition was recorded by low resolution laser spectroscopy for all the sample growths. Samples from each growth revealed up to fifty different absorption lines, believed due to the presence of Eu(3+) at defect sites. The behavior of the forbidden intrinsic line, which is allowed when magnetic fields is applied, was examined in the different growth. This was compared with the predictions of perturbation theory. A search was made for Eu(3+) ions at defect sites that were inequivalent with respect to the application of magnetic field along the a and a' axes in the basal plane. Optical holeburning was applied in zero-field to determine the nuclear quadrupole parameters for the 5D(sub 0) excited state of all the defect sites in all the growth. In this thesis, a detailed recalculation of the predicted values for the nuclear quadrupole parameter P and the dependence of (P,eta) upon energy, based upon the nuclear quadrupole Hamiltonian, is put forward. Radio frequency optically detected nuclear quadrupole resonance (ODNQR) experiments were carried out on certain selected Eu(3+) defect sites in some of the sample growth. High precision measurements of the nuclear parameters (P,eta) for the 7F(sub 0) ground state of Eu(3+) was made. A brief report is made of some experimental and theoretical work on the compound HoF3.
Dissert. Abstr.

N93-13864# Illinois Univ., Urbana. Dept. of Electrical and Computer Engineering.
THE THREE TO FIVE SEMICONDUCTOR QUANTUM WELL LASERS AND RELATED OPTOELECTRONIC DEVICES ON SILICON Final Report, 15 Nov. 1988 - 31 May 1992
N. Holonyak, Jr., K. C. Hsieh, and G. E. Stillman Jun. 1992 39 p
(Contract DAAL03-89-K-0008)
(AD-A255368; ARO-26434.4-EL) Avail: CASI HC A03/MF A01

Since the beginning of this project (10+ years ago) we have been concerned with quantum well heterostructures (QWH's) and their use in advanced forms of lasers, light emitting diodes (LED's), and more generally in optoelectronics. This has led us into a wide range of studies and discoveries, including the commercially important process (patented) of impurity-induced layer disordering (which can be employed to change a QWH, in whatever pattern desired, from QW lower gap to bulk-crystal higher energy band gap). GRA

N93-13883# Optical Society of America, Washington, DC.
COMPACT BLUE-GREEN LASERS: SUMMARIES OF PAPERS PRESENTED AT THE TOPICAL MEETING. VOLUME 6: TECHNICAL DIGEST SERIES Quarterly Report, 19 Feb. - 21 Feb. 1992
Jarus W. Quinn 21 Feb. 1992 173 p Meeting held in Santa Fe, NM, 20-21 Feb. 1992
(Contract F49620-92-J-0264)
(AD-A255001; AFOSR-92-0736TR-Vol-6) Avail: CASI HC A08/MF A02

Summaries of papers presented at the Compact Blue-Green Lasers Topical Meeting held in Santa Fe, New Mexico on February 20-21, 1992 are presented. Topics covered are blue-green laser applications, IR pumped visible lasers, blue-green diode emitters, materials, frequency conversion in bulk devices, gas lasers, and frequency conversion in guided-wave devices. L.R.R.

N93-14023# Columbia Univ., New York, NY. Dept. of Physics.
TWO-PHOTON COOPERATIVE CASCADE SUPERFLUORESCENCE Final Report, 1 May 1989 - 30 Apr. 1992
S. R. Hartmann Jun. 1992 10 p
(AD-A255690; ARO-26462.1-PH) Avail: CASI HC A02/MF A01

The time evolution of the radiation field spontaneously emitted by an ensemble of many atoms as they proceed from some particular excited atomic state to a lower one (initially unpopulated) and then on to the round state is studied. A short laser pulse, two-photon resonant with an even parity optical transition, produces the excited atomic population which is forbidden (by symmetry) to radiate directly back to the ground state and must therefore radiate first to an intermediate state. If the gain is high, laser action should rapidly deplete the excited state and with sufficient population build-up on the intermediate state, one can expect laser action to appear on the transition to the ground state. This scenario becomes more interesting when the short laser pulse coherently excites the atoms into a coherent superposition of the ground and uppermost resonant state. Now laser action on the uppermost transition directly induces laser action on the lower transition even though no population inversion is present there. The effect is to modify the laser action on the uppermost transition. We have used a mode locked laser to produce pulses short enough to coherently excite the 6D(sub 3/2)-6S(sub 1/2) transition in Cs vapor. Our observations indicate that the induced coherence inhibits superfluorescence and that laser action on the uppermost transition in the backwards direction (opposite to the direction of the short excitation pulse) strongly perturbs this interference. The theoretical analysis is highly nonlinear and numerical techniques are applied. GRA

N93-14085# Scitec, Inc., Princeton, NJ.
RESULTS OF THE LASER SENSOR TECHNOLOGY TRANSITION INVESTIGATION Final Report
Richard Preston Jun. 1992 71 p
(Contract F30602-88-D-0026)
(AD-A255845; RL-TR-92-157) Avail: CASI HC A04/MF A01

This report summarizes experiments carried out at Rome Laboratory (RL) under a Laboratory Director Funds (LDF) effort. Experiments were carried out at both SCITEC and RL in conjunction with the Intelligence and Reconnaissance Directorate and the Photonics Center. Experimental results are described regarding the sensitivity and noise characteristics of commercially available mercury cadmium telluride (MCT) detectors and preamps. Also presented are some measurements of potential ways to reject false alarms. GRA

N93-13161*# Saint Mary's Hospital, Milwaukee, WI. Laser Lab.
POST FLIGHT OPERATION OF A HIGH PEAK POWER NEODYMIUM YAG LASER ABOARD THE G-449 PAYLOAD FLOWN ON SPACE SHUTTLE COLUMBIA MISSION 61-C
M. C. Muckerheide *In* NASA. Goddard Space Flight Center, The 1992 Shuttle Small Payloads Symposium Oct. 1992 p 21-27 (For primary document see N93-13158 03-12)
Avail: CASI HC A02/MF A03

N93-14010*# National Aeronautics and Space Administration. Goddard Space Flight Center, Greenbelt, MD.
ENGINEERING PLANETARY LASERS FOR INTERSTELLAR COMMUNICATION
Brent Sherwood, Michael J. Mumma, and Bruce K. Donaldson (Maryland Univ., College Park.) *In* NASA. Johnson Space Center, The Second Conference on Lunar Bases and Space Activities of the 21st Century, Volume 2 Sep. 1992 p 637-645 (For primary document see N93-13972 03-91)
(Grant NGT-21-002-823)
Avail: CASI HC A02/MF A03

37 MECHANICAL ENGINEERING

Includes auxiliary systems (nonpower); machine elements and processes; and mechanical equipment.

N93-12555# Georgia Inst. of Tech., Atlanta.
APPLICATION OF CONCURRENT ENGINEERING METHODS TO THE DESIGN OF AN AUTONOMOUS AERIAL ROBOT M.S. Thesis
Stephen A. Ingalls Dec. 1991 162 p
(AD-A254968) Avail: CASI HC A08/MF A02

This paper documents the year-long efforts of a multidisciplinary design team to design, build, and support an autonomous aerial robotics system. The system was developed to participate in the Association for Unmanned Vehicle System's (AUVS) First International Aerial Robotics Competition which was held in Atlanta, Georgia on the Georgia Tech campus on July 29th, 1991. As development time and budget were extremely limited, the team elected to attempt the design using concurrent engineering design methods. These methods were validated in an IDA study by Winner 1 in the late- 1980's to be particularly adept at handling the difficulties to design presented by these limitations. GRA

N93-12565# Los Alamos National Lab., NM.
CHARACTERIZING LASER FUSION WELDED ALUMINUM USING SYNCHROTRON X RAY MICROTOMOGRAPHY
J. O. Milewski, A. B. Hmelo, K. L. DAmico, J. H. Dunsmuir, and S. R. Ferguson 1992 14 p Presented at the 8th International Conference on TMS Beam Processing of Advanced Materials, Chicago, IL, 5 Nov. 1992
(Contracts W-7405-eng-36; DE-AC02-76CH-00016)
(DE92-018608; LA-UR-92-2464; CONF-921183-1) Avail: CASI HC A03/MF A01

Preliminary research into the application of high power Nd-YAG lasers for welding indicate a dependency of the occurrence of weld discontinuities on processing parameters such as pulse duty cycle, travel speed, etc. The size and distribution of weld features have been characterized using synchrotron microtomography, using facilities at the National Synchrotron Light Source. The ability of this technique to image defects, such as gross and minor porosity, and centerline cracking, enables a metrology of interior surfaces which cannot be provided by metallurgical sectioning techniques alone. DOE

N93-12600# Southwest Research Inst., San Antonio, TX. Belvoir Fuels and Lubricants Research Facility.
DIESEL INJECTOR FOULING BENCH TEST METHODOLOGY Interim Report, Feb. 1986 - Jun. 1992
Leon L. Stavinoha, Douglas M. Yost, and Sidney J. Lestz Jun. 1992 103 p
(Contracts DAAK70-85-C-0007; DAAK70-87-C-0043; DA Proj. 1L7-62786-AH-20)
(AD-A254532; BFLRF-267) Avail: CASI HC A06/MF A02

Compared to conventional compression ignition (CI) engine operation with the fuel being delivered at approximately 149 C (300 F), adiabatic engine operation potentially may deliver the fuel at temperatures as high as 260 C (500 F). Hypergolic CI engine combustion systems now in theoretical design stages will deliver fuel at temperatures approaching 427 to 538 C (800 to 1000 F). The ability of a fuel to resist formation of deposits on internal injector system surfaces is a form of thermal oxidative stability for which test methodology will be required. The injector Fouling Bench Test (IFBT) methodology evaluated in this report will assist in defining fuel contribution to injector fouling and control of fuel thermal stability in procurement specifications. The major observations from this project are discussed. Forty-hour cyclic IFB tests employing both Bosch APE 113 and Detroit Diesel (DD) N70 injectors are viable procedures for evaluating fuel effects on injector fouling. Cyclic operation appears to be superior to steady-state operation for both type injectors. Eighty-hour cyclic tests are more discriminating than 40-hour cyclic tests using the Bosch APE 113 injectors. JFTOT tests of fuels provide directional information on thermal stability-related deposits and filter plugging but show limited good correlation with IFBT DD N70 ratings, and none with IFBT Bosch APE 113 injector ratings. Deposition on injector pintles was more realistically rated by optical microscopy and Scanning Electron Microscopy (SEM) than conventional visual and bench rating methods. High-sulfur fuel readily caused sticking of Detroit Diesel injectors. Injector sticking is an important mode of injector fouling. GRA

N93-12604# Stanford Univ., CA. Dept. of Mechanical Engineering.
TACTILE SENSING AND CONTROL IN HUMANS AND ROBOTIC/TELEOPERATED SYSTEMS Final Report
Mark R. Cutkosky, Robert Howe, Roland Johansson, Goran Westling, and Benoni Edin 4 Aug. 1992 7 p
(Contract N00014-90-J-4014)
(AD-A254408) Avail: CASI HC A02/MF A01

The most significant result of the Stanford/Harvard/Umea collaboration is a promising new approach to grasp force control in manipulation with robots and teleoperators. Experiments at Umea showed that human subjects control grasp forces and apply manipulation strategies using information from fast-acting (FA1 and FA2) tactile afferents which signal events such as the onset of slipping between the fingers and a grasped object. An information exchange between Umea and Stanford led to experiments that demonstrated that the output of these FA1 and FA2 sensors is occasionally accompanied by small, but detectable, redistributions in the tangential contact forces between the fingertips of the human subjects and the objects that they were grasping. Dynamic tactile sensors, specifically the skin acceleration and the stress rate sensors, were developed at Stanford for robotic and teleoperated hands to provide information similar to the human PA sensors. Triggering off the microslip information provided by these sensors, a manipulator's force control algorithm can then quickly adjust the grasp force so that no gross sliding occurs. GRA

N93-12682*# National Aeronautics and Space Administration. Marshall Space Flight Center, Huntsville, AL.
DESIGN OF A WELDED JOINT FOR ROBOTIC, ON-ORBIT ASSEMBLY OF SPACE TRUSSES
W. K. Rule (Alabama Univ., Huntsville.) and F. P. Thomas Oct. 1992 35 p
(NASA-TM-108380; NAS 1.15:108380) Avail: CASI HC A03/MF A01

A preliminary design for a weldable truss joint for on-orbit assembly of large space structures is described. The joint was designed for ease of assembly, for structural efficiency, and to allow passage of fluid (for active cooling or other purposes) along the member through the joint. The truss members were assumed to consist of graphite/epoxy tubes to which were bonded 2219-T87 aluminum alloy end fittings for welding on-orbit to truss nodes of the same alloy. A modified form of gas tungsten arc welding was assumed to be the welding process. The joint was designed to withstand the thermal and structural loading associated with a 120-ft diameter tetrahedral truss intended as an aerobrake for a mission to Mars. Author

N93-12698# Maryland Univ., College Park.
TORQUE RESOLVER DESIGN FOR TENDON-DRIVEN MANIPULATORS
J. J. Lee and Lung-Wen Tsai 1992 8 p Presented at the 22nd ASME Biennial Mechanisms Conference, Scottsdale, AZ, Sep. 1992
(Contract DE-FG05-88ER-13977)
(DE92-017395; CONF-9209143-3) Avail: CASI HC A02/MF A01

Given a set of desired joint torques in an n-DOF tendon-driven manipulator with $n + 1$ control tendons, the determination of tendon forces is an indeterminate problem. Usually, the pseudo-inverse technique is used to solve for such a problem. In this paper, rather than using the pseudo-inverse technique, an efficient methodology for transforming joint torques (n elements) to motor torques ($n + 1$ elements) has been developed. This technique called 'torque resolver', utilizes two circuit-like operators to transform torques between the two different vector spaces. It can be easily programmed on a digital computer or implemented into an analog-circuit system. It is hoped that this technique will make real-time computed-torque control feasible. The technique has been demonstrated through the dynamic simulation of a three-DOF manipulator. DOE

N93-12724# Tecogen, Inc., Waltham, MA.
A NOVEL DIESEL-FUELED ENGINE FOR MICROCLIMATE COOLING FOR THE INDIVIDUAL SOLDIER Final Report, Jul. 1991 - Jan. 1992
T. K. Chen, W. K. Lam, and R. J. Raymond Jul. 1992 66 p
(DA Proj. 1L1-62786-AH-98)
(AD-A254510; Natick/TR-92/036) Avail: CASI HC A04/MF A01

Military mission performance in a chemically contaminated environment

necessitates the wearing of chemically impermeable protective garments. Soldiers encapsulated in these protective garments in a hot environment will succumb to heat stress. Consequently a microclimate cooling system is being developed. In the present design, a vapor compression cycle chills water which is then circulated over the body to absorb heat via a cooling garment. One of the major components of the vapor compression cycle system is the prime mover, i.e., the engine. For battlefield use, the engine shall utilize battlefield fuel, JP-8. Commercially available engines of the required size, approximately 0.5 hp at 4000 rpm, such as model aircraft engines and small outdoor power equipment (string trimmers) engines do not start and run on JP-8. This effort established the technical feasibility of starting and operating a small, lightweight engine on diesel fuel and JP-8. A commercially available 1.09 cubic inch displacement was used; however, the stock head was replaced with a custom designed head employing a fuel injector and pre-chamber. The engine started by hand cranking from ambient temperature (70 F) and ran without aids. The engine developed 0.42 brake hp at 3700 rpm. Brake specific fuel consumption was 0.76 lb/bbp-hr. GRA

N93-12727# National Aerospace Lab., Kakuda (Japan).
AN EXPERIMENTAL STUDY OF A SMALL HIGH-SPEED LH2 PUMP FOR ROCKETS: FLUID DYNAMIC PERFORMANCE Report No. 3 [ROKETTO YOU KOGATA LH2 PONPU NO KENKYUU SHISAKU. SONO 3: RYUURYOKU SEINOU]
Hitoshi Yamada, Yoshiaki Watanabe, and Kunio Hirota (National Space Development Agency, Tokyo, Japan) Nov. 1991 12 p In JAPANESE
(NAL-TR-1131; JTN-92-80399) Avail: CASI HC A03/MF A01

A small high speed rocket engine hydrogen pump was designed, fabricated, and tested at the National Aerospace Laboratory (NAL)/National Space Development Agency (NASDA) turbopump test facility. The pump uses liquid nitrogen and liquid hydrogen as the working fluid in order to determine its associated fluid dynamic performance. The focus is on the overall and the suction performance. The overall performance was judged to be good. However, at high speed and high pressure conditions (50,000 rpm) a clearance occurred between the pump casing and the pump outlet guide vane. This resulted in the pump outlet guide vane showing reduced performance as compared to the low speed conditions (30,000 rpm). Design of the pump outlet guide vane is subsequently necessary to improve high speed pump performance. Prediction of the impeller performance was found to be in good agreement with the experimental results when pump efficiency is taken into consideration. In addition, the inducer showed a smaller required Net Positive Suction Head (NPSH) value than the design value, in fact, it could operate even in a two phase flow condition at the pump inlet. Author

N93-12736*# National Aeronautics and Space Administration. Lewis Research Center, Cleveland, OH.
SPLIT TORQUE TRANSMISSION LOAD SHARING
T. L. Krantz, M. Rashidi (Cleveland State Univ., OH.), and J. G. Kish (Sikorsky Aircraft, Stratford, CT.) Oct. 1992 25 p Presented at the Gearbox Configurations of the 1990's, Solihull, England, 28 Oct. 1992; sponsored by the Institute of Mechanical Engineers
(DA Proj. 1L1-62211-A-47-A; RTOP 505-63-36)
(NASA-TM-105884; E-7350; NAS 1.15:105884; AVSCOM-TR-92-C-030)
Avail: CASI HC A03/MF A01

Split torque transmissions are attractive alternatives to conventional planetary designs for helicopter transmissions. The split torque designs can offer lighter weight and fewer parts but have not been used extensively for lack of experience, especially with obtaining proper load sharing. Two split torque designs that use different load sharing methods have been studied. Precise indexing and alignment of the geartrain to produce acceptable load sharing has been demonstrated. An elastomeric torque splitter that has large torsional compliance and damping produces even better load sharing while reducing dynamic transmission error and noise. However, the elastomeric torque splitter as now configured is not capable over the full range of operating conditions of a fielded system. A thrust balancing load sharing device was evaluated. Friction forces that oppose the motion of the balance mechanism are significant. A static analysis suggests increasing the helix angle of the input pinion of the thrust balancing design. Also, dynamic analysis of this design predicts good load sharing and significant torsional response to accumulative pitch errors of the gears. Author

N93-12760 Ottawa Univ. (Ontario).
A FUNDAMENTAL STUDY OF THE EFFECT OF GRAVITY ON THE STATIC AND DYNAMIC BEHAVIOR OF ROBOTS Ph.D. Thesis
Mohamed E. Mahjoub 1991 228 p
Avail: Univ. Microfilms Order No. DANN68053

The gravity induced force on revolute robot links is generally comparable to the dynamic induced forces at high operational speeds. At low speeds this force dominates over the dynamic forces. in the process of study of the static and dynamic behavior of manipulators through the overall measures such as the force ellipsoid, the dynamic manipulability ellipsoid, and the generalized ellipsoid of inertia the effect of gravity is ignored due to the complexity that the inclusion of this force brings to the analysis. This study presents a method to include the effect of gravity in the static and dynamic analysis of robot arms. Using the concept of fields, the gravity induced forces acting on individual links are replaced by a single force, called here the generalized weight of the arm. The generalized weight is a force that acts at the end effector and its magnitude and direction are functions of the configuration of the manipulator. Since the system is conservative, the generalized weight is considered to be the gradient of a potential field that will be called here the generalized gravitational field (GGF). This field alone can illustrate the overall effect of gravity on the manipulator throughout its work volume. The generalized weight field is then integrated with the force ellipsoid to display the true force that a manipulator can apply to its environment. Based on the generalized inertia tensor the generalized gravitational acceleration field is introduced. The dynamic manipulability ellipsoid is then superimposed on this field to demonstrate the true acceleration capability of the end effector. The relation between the generalized weight and the generalized ellipsoid of inertia is investigated. Effect of change of physical parameters of the arm are also discussed. It is shown that for a particular design of manipulators the generalized gravitational field is absolutely flat, and in general the manipulator's physical parameters may be used to tailor the GGF for a particular application.
Dissert. Abstr.

N93-12793# EG and G Energy Measurements, Inc., Idaho Falls.
AN INTEGRATED OPTICAL SENSOR FOR GMAW FEEDBACK CONTROL
P. L. Taylor, A. D. Watkins, E. D. Larsen, and H. B. Smartt 1992 5 p Presented at the 3rd International Conference on Trends in Welding Research, Gatlinburg, TN, 1-5 Jun. 1992
(Contract DE-AC07-76ID-01570)
(DE92-018019; EGG-M-92300; CONF-9206173-7) Avail: CASI HC A01/MF A01

The integrated optical sensor (IOS) is a multifunction feedback control sensor for arc welding, that is computer automated and independent of significant operator interaction. It is based on three major 'off-the-shelf' components: a charged coupled device (CCD) camera, a diode laser, and a processing computer. The sensor head is compact and lightweight to avoid interference with weld head mobility, hardened to survive the harsh operating environment, and free of specialized cooling and power requirements. The sensor is positioned behind the GMAW torch and measures weld pool position and width, standoff distance, and postweld centerline cooling rate. Weld pool position and width are used in a feedback loop, by the weld controller, to track the weld pool relative to the weld joint, thus allowing compensation for such phenomena as arc blow. Sensor stand off distance is used in a feedback loop to control the contact tip to base metal distance during the welding process. Cooling rate information is used to infer the final metallurgical state of the weld bead and heat affected zone, thereby providing a means of controlling post weld mechanical properties. DOE

N93-12904*# Georgia Inst. of Tech., Atlanta.
DYNAMIC CONTROL MODIFICATION TECHNIQUES IN TELEOPERATION OF A FLEXIBLE MANIPULATOR M.S. Thesis
David Patrick Magee 18 Nov. 1991 160 p
(Grant NAG1-623)
(NASA-CR-190984; NAS 1.26:190984) Avail: CASI HC A08/MF A02

The objective of this research is to reduce the end-point vibration of a large, teleoperated manipulator while preserving the usefulness of the system motion. A master arm is designed to measure desired joint angles as the user specifies a desired tip motion. The desired joint angles from the master arm are the inputs to an adaptive PD control algorithm that positions

the end-point of the manipulator. As the user moves the tip of the master, the robot will vibrate at its natural frequencies which makes it difficult to position the end-point. To eliminate the tip vibration during teleoperated motions, an input shaping method is presented. The input shaping method transforms each sample of the desired input into a new set of impulses that do not excite the system resonances. The method is explained using the equation of motion for a simple, second-order system. The impulse response of such a system is derived and the constraint equations for vibrationless motion are presented. To evaluate the robustness of the method, a different residual vibration equation from Singer's is derived that more accurately represents the input shaping technique. The input shaping method is shown to actually increase the residual vibration in certain situations when the system parameters are not accurately specified. Finally, the implementation of the input shaping method to a system with varying parameters is shown to induce a vibration into the system. To eliminate this vibration, a modified command shaping technique is developed. The ability of the modified command shaping method to reduce vibration at the system resonances is tested by varying input perturbations to trajectories in a range of possible user inputs. By comparing the frequency responses of the transverse acceleration at the end-point of the manipulator, the modified method is compared to the original PD routine. The control scheme that produces the smaller magnitude of resonant vibration at the first natural frequency is considered the more effective control method. Author

N93-12906# International Society for Terrain-Vehicle Systems, Hanover, NH.

PROCEEDINGS OF THE FIFTH EUROPEAN INTERNATIONAL SOCIETY FOR TERRAIN-VEHICLE SYSTEMS, VOLUME 1

Sep. 1991 343 p Conference held in Budapest, Hungary, 4-6 Sep. 1991

(Contract DAJA45-91-M-0211)

(AD-A254619; R/D-6659-EN-02-Vol-1) Avail: CASI HC A15/MF A03

Papers given at the 5th European Conference on the International Society for Terrain Vehicle Systems are presented. The following topics are discussed: soil properties; soil vehicle interaction, tires and tracks; instrumentation and computer control of traction and transport systems; simulation and modeling for the prediction of the performance of cross-country vehicles; and new cross-country vehicles. GRA

N93-12908# Tecogen, Inc., Waltham, MA.

UTILIZATION OF COMPRESSED NATURAL GAS IN MEDIUM- AND HEAVY-DUTY ENGINE ROUTE VEHICLES Final Report, Sep. 1989 - Sep. 1990

M. Koplow and T. Norman 2 Dec. 1991 99 p

(Contract GRI-5089-291-1835)

(PB92-217546; TR4480-074-91; GRI-92/0153) Avail: CASI HC A05/MF A02

The final report describes the early development process of a dedicated compressed natural gas medium-duty truck. The three key technological developments successfully undertaken were: (1) The design and implementation of an optimized CNG spark ignition engine to meet the performance requirements of the marketplace. (2) The design and development of an electronically controlled, electronically injected fuel system specifically for compressed natural gas utilizing pulse width modulated fuel injector technology. (3) The adaptation of a production OEM electronic engine controller to perform closed loop engine control for the CNG engine. The overarching technical goal was to provide a clear path to OEM production levels of performance reliability and economy for CNG vehicles. In this way it was intended that the OEM would commit to a production intent CNG vehicle program. The successful completion of the three technological tasks described in the report allowed the integration into a first test vehicle which has performed well. The manufacturer, by witnessing and participating in the rapid progress, has committed to pursue production of CNG vehicles. A brief description of this follow-on effort is also found in the report. GRA

N93-12919*# Nichols Research Corp., Huntsville, AL.

VPPA WELD MODEL EVALUATION Final Report, 28 Sep. 1990 - 31 Jul. 1992

Kimble D. McCutcheon, Stephen S. Gordon, and Paul A. Thompson 31 Jul. 1992 151 p

(Contract NAS8-38812)

(NASA-CR-184460; NAS 1.26:184460) Avail: CASI HC A08/MF A02

NASA uses the Variable Polarity Plasma Arc Welding (VPPAW) process extensively for fabrication of Space Shuttle External Tanks. This welding process has been in use at NASA since the late 1970's but the physics of the process have never been satisfactorily modeled and understood. In an attempt to advance the level of understanding of VPPAW, Dr. Arthur C. Nunes, Jr., (NASA) has developed a mathematical model of the process. The work described in this report evaluated and used two versions (level-0 and level-1) of Dr. Nunes' model, and a model derived by the University of Alabama at Huntsville (UAH) from Dr. Nunes' level-1 model. Two series of VPPAW experiments were done, using over 400 different combinations of welding parameters. Observations were made of VPPAW process behavior as a function of specific welding parameter changes. Data from these weld experiments was used to evaluate and suggest improvements to Dr. Nunes' model. Experimental data and correlations with the model were used to develop a multi-variable control algorithm for use with a future VPPAW controller. This algorithm is designed to control weld widths (both on the crown and root of the weld) based upon the weld parameters, base metal properties, and real-time observation of the crown width. The algorithm exhibited accuracy comparable to that of the weld width measurements for both aluminum and mild steel welds. Author

N93-12936# Southwest Research Inst., San Antonio, TX. Engine, Fuel, and Vehicle Research Div.

EFFECTS OF GAS COMPOSITION ON ENGINE PERFORMANCE AND EMISSIONS Report, Jan. 1990 - Dec. 1991

T. W. Ryan and T. J. Callahan Dec. 1991 129 p

(Contract GRI-5089-293-1848; SwRI Proj 3178-2.9)

(PB92-217561; GRI-92/0054) Avail: CASI HC A07/MF A02

The use of natural gas as a fuel for internal combustion engines that are used in highway transportation applications presents several engine and vehicle design problems. One of the main concerns is whether a fuel specification is needed to accommodate the special requirements that these vehicle applications create. The objective of this project was to determine the role of gas composition on the performance and emissions from natural gas fueled engines. A special gas mixing and control system was developed to supply blends of pure gases to a single cylinder research engine. A statistically designed test matrix of 31 gas mixtures was used to develop relationships between the composition and the knock resistance, measured as methane number, of the gas mixture. The range of composition of the test gases was selected to be representative of natural gases found in the United States. An abbreviated test matrix of six gas mixtures was used to examine the effects of composition on the performance and emissions. The results showed that the direct chemical effects of composition on the combustion process and the emissions were secondary to the effects caused by the corresponding variations in stoichiometric air-fuel ratio. The measurements were performed at different representative equivalence ratios and operating conditions. GRA

N93-12952*# Georgia Inst. of Tech., Atlanta. School of Mechanical Engineering.

MANIPULATION STRATEGIES FOR MASSIVE SPACE PAYLOADS Semiannual Progress Report, 15 May - 14 Nov. 1991

Wayne J. Book 14 Nov. 1991 46 p

(Grant NAG1-623)

(NASA-CR-190844; NAS 1.26:190844) Avail: CASI HC A03/MF A01

The industrial and environmental applications for robots with a relatively large workspace has increased significantly in the last few years. To accommodate the demands, the manipulator is usually designed with long, lightweight links that are inherently flexible. Ongoing research at Georgia Tech into the behavior and design of these flexible links is discussed. For individual titles, see N93-12953 through N93-12955.

N93-12953*# Georgia Inst. of Tech., Atlanta. School of Mechanical Engineering.

NUMERICAL ANALYSIS OF NONMINIMUM PHASE ZERO FOR NONUNIFORM LINK DESIGN

Douglas L. Girvin and Wayne J. Book *In its* Manipulation Strategies for Massive Space Payloads 14 Nov. 1991 12 p (For primary document

see N93-12952 03-37)
Avail: CASI HC A03/MF A01

As the demand for light-weight robots that can operate in a large workspace increases, the structural flexibility of the links becomes more of an issue in control. When the objective is to accurately position the tip while the robot is actuated at the base, the system is nonminimum phase. One important characteristic of nonminimum phase systems is system zeros in the right half of the Laplace plane. The ability to pick the location of these nonminimum phase zeros would give the designer a new freedom similar to pole placement. This research targets a single-link manipulator operating in the horizontal plane and modeled as a Euler-Bernoulli beam with pinned-free end conditions. Using transfer matrix theory, one can consider link designs that have variable cross-sections along the length of the beam. A FORTRAN program was developed to determine the location of poles and zeros given the system model. The program was used to confirm previous research on nonminimum phase systems, and develop a relationship for designing linearly tapered links. The method allows the designer to choose the location of the first pole and zero and then defines the appropriate taper to match the desired locations. With the pole and zero location fixed, the designer can independently change the link's moment of inertia about its axis of rotation by adjusting the height of the beam. These results can be applied to the inverse dynamic algorithms that are currently under development. Author

N93-12954*# Georgia Inst. of Tech., Atlanta. School of Mechanical Engineering.
THE APPLICATION OF INPUT SHAPING TO A SYSTEM WITH VARYING PARAMETERS
David P. Magee and Wayne J. Book *In its* Manipulation Strategies for Massive Space Payloads 14 Nov. 1991 21 p (For primary document see N93-12952 03-37)
Avail: CASI HC A03/MF A01

The original input shaping technique, that was developed in earlier work, is summarized, and a different definition for residual vibration is proposed. The new definition gives better insight into the ability of the input shaping method to reduce vibration. The extension of input shaping to a system with varying parameters, e.g., natural frequency, is discussed, and the effect of these variations is shown to induce vibration. A modified command shaping technique is developed to eliminate this unwanted motion. Author

N93-12955*# Georgia Inst. of Tech., Atlanta. School of Mechanical Engineering.
EXPERIMENTAL VERIFICATION OF MODIFIED COMMAND SHAPING USING A FLEXIBLE MANIPULATOR
David P. Magee and Wayne J. Book *In its* Manipulation Strategies for Massive Space Payloads 14 Nov. 1991 6 p Presented at the 1st International Conference on Motion and Vibration Control, Yokohama, Japan, 7-11 Sep. 1992 (For primary document see N93-12952 03-37)
Avail: CASI HC A02/MF A01

A brief discussion introduces the original input shaping method applied to a system with varying parameters. A change in parameters causes a vibration in the system and a modified command shaping technique is created to eliminate this unwanted motion. Using a two degree of freedom (DOF) flexible manipulator, experiments are conducted by varying perturbations to input trajectories to compare the modified method to a previously used adaptive proportional plus derivative (P.D.) control method. The control scheme that produces the smaller magnitude of resonant vibration at the first natural frequency of the robot is considered the more effective control method. Author

N93-12977# Northern Research and Engineering Corp., Woburn, MA.
ALTERNATIVE SYSTEMS FOR FUEL GAS BOOSTERS FOR SMALL GAS TURBINE ENGINES Final Report, Nov. 1989 - Dec. 1991
Henry B. Faulkner Apr. 1992 98 p
(Contract GRI-5086-233-1436)
(PB92-223049; NREC-1626-3; GRI-92/0239) Avail: CASI HC A05/MF A02

The study was done to investigate alternative technologies for fuel gas boosters for gas turbine engines under 5 MW output. The goal was to identify concepts which would significantly reduce the overall life cycle cost of these boosters. In a broad review of alternative systems, centrifugal compressors were found to be most promising. Electrically driven centrifugals, either direct drive or gear driven, were found to be quite limited in speed. Therefore they require many stages for these applications, and no cost advantage was indicated. Considerable promise was indicated for centrifugals driven by bleed air from the engine compressor, using turbocompressor units which are conversions of existing turbochargers for internal combustion engines. A first cost advantage of 30 to 80 percent was indicated for applications with an annual market size of at least ten units. Considerable savings in installation and maintenance costs are expected in addition.
GRA

N93-13018 Pennsylvania State Univ., University Park.
INITIAL EXPERIMENTS IN END-POINT CONTROL OF A FLEXIBLE, TWO-LINK MANIPULATOR Ph.D. Thesis
Mark David Whalen 1992 177 p
Avail: Univ. Microfilms Order No. DA9226803

A two-link, flexible manipulator has been designed and constructed to study en-point vibration and control problems. The manipulator has two activated rotary joints and operates in the horizontal plane. It has been designed for minimal join flexibility and very flexible links. Further, the links have been designed so that the first natural frequencies of each link are very close. The manipulator vibratory characteristics have been quantified through a series of frequency response and modal analysis tests using external excitation sources as well as internal excitation supplied by the manipulator joint actuators. By performing tests for various manipulator postures, the vibratory responses of the manipulator links are shown to become uncoupled as the elbow angle approaches 90 degrees. Further, the internal excitation tests have shown that some vibratory modes cannot be excited by the rotary joint actuators. An analytical model of the manipulator has been developed using Kane's equations with Bernoulli-Euler assumed modes. Because the modal analysis has shown that the manipulator vibratory response varies with the elbow joint angle, assumed modes of the individual links are used to model flexibility effects rather than manipulator assumed modes. Unfortunately, no experimental results suitable for confirming the analytical model are available yet. A PID baseline controller of the manipulator is presented with experimental results. Recommendations for improving the PID controller are presented. Alternate controller schemes are presented and discussed. Dissert. Abstr.

N93-13103# Department of Energy, Morgantown, WV. Energy Technology Center.
DEVELOPMENT OF ADVANCED TURBINE SYSTEMS: MEETING TOMORROW'S NEEDS
H. A. Webb and R. A. Bajura 1992 12 p Presented at the Advanced Turbine Conference, Washington, DC, 25-26 Jun. 1992
(DE92-017339; DOE/METC-C/92/7021; CONF-9206216-1) Avail: CASI HC A03/MF A01

The National Energy Strategy calls for increased efficiency in all sectors of energy use. It also projects a significant increase in natural gas consumption by the year 2000, due in part to increased use of natural gas for electric power generation. Consistent with the NES, a Department of Energy program is being formulated to develop Advanced Turbine Systems (ATS) which will be: ultra-high efficiency, environmentally superior, and cost competitive. The ATS program is to be a comprehensive effort involving DOE Fossil Energy, DOE Conservation and Renewable Energy, turbine manufacturers, the Gas Research Institute, the Electric Power Research Institute and others. A ten-year plan is being formulated to develop natural-gas-fired baseload power systems for commercial offering by 2002. Systems will be developed to serve both central power (utility and independent power producer) and industrial applications. The central power systems will be suitable for future adaptation to coal firing. DOE

N93-13236# Argonne National Lab., IL.
THE USE OF FINITE ELEMENTS TO MODEL SOIL/TRACK INTERACTIONS IN COUPLED MULTI-BODY DYNAMIC SIMULATIONS: IS REAL TIME SIMULATION FEASIBLE?
T. R. Canfield and M. J. Murray (Packer Engineering, Naperville, IL.) 1 May 1992 3 p Presented at the 1992 Summer Computer Simulation Conference, Reno, NV, 27-30 Jul. 1992
(Contract W-31-109-eng-38)
(DE92-016184; ANL/CP-76184; CONF-920771-4) Avail: CASI HC A01/MF A01

Finite element methods (FEM) employing the arbitrary Lagrangian-Eulerian (ALE) formulation may be used to model soil in contact with the wheels or the tracks of vehicles in off-road mobility simulations. Coupling ALE finite element methods with recursive multi-body dynamics may allow real-time simulation of vehicles off-road provided sufficient computational resources are available. The requirements of this approach will be discussed with emphasis on parallel implementation. Estimates of expected performance are calculated based on the current trend in the development of advanced computer architectures. Factors important in estimating the feasibility of using finite element methodology in real time will be considered. Among these factors are the element size, the number of elements and the rate of computation, as well as the physical requirements of the simulations.
DOE

N93-13321# Los Alamos National Lab., NM.
A PRELIMINARY STUDY OF THE EFFECT OF EQUIVALENCE RATIO ON A LOW EMISSIONS GAS TURBINE COMBUSTOR USING KIVA-2
S. L. Yang (Michigan Technological Univ., Houghton.), R. Chen (Michigan Technological Univ., Houghton.), and M. C. Cline 1992 12 p Presented at the Winter Annual Meeting of the American Society of Mechanical Engineers, Anaheim, CA, 8-13 Nov. 1992
(Contract W-7405-eng-36)
(DE92-018616; LA-UR-92-2391; CONF-921110-14) Avail: CASI HC A03/MF A01

The staged turbine combustor (STC) concept has drawn more and more attention since the late 70's because of its potential in reducing pollutant emissions where a high power output is required. A numerical study is performed to investigate the chemically reactive flow with sprays inside a STC combustor using a modified version of the KIVA-II code. This STC combustor consists of a fuel nozzle (FN), a rich-burn (RB) zone, a converging connecting section, a quick-quench (QQ) zone, a diverging connecting section, and a lean-combustion (LC) zone. An advanced airblast fuel nozzle, which has two fuel injection passages and four air flow passages for providing swirl, is used in this study. The effect of the equivalence ratio phi on the performance of the STC combustor is reported in this paper for phi range of 1.2 to 2.0. Preliminary results reveal some major features of the flow and temperature fields inside the STC combustor. Distributions of velocity, temperature, and some critical species information inside the FN/RB zone illustrate the effect of phi on the flame temperature and the NO(x) formation in rich burning. The co- and counter-rotating bulk flow, and the sandwiched-ring-shape temperature field in the QQ/LC zone, typical of the confined inclined jet-in-cross flow, are clearly shown from the computation. The predicted mass-weighted standard deviation and the pattern factor of temperature show that the mixing performance of the STC combustor is very good. The temperature of the fluid leaving the LC zone is very uniform. As expected. lower value of the emission index of NO can be achieved with larger value of phi. Prediction of the NO(x) emission shows that there is no excessive thermal NO(x) produced in the QQ/LC zone for all the cases studied.
DOE

N93-13329 Texas Univ., Austin.
DESIGN, CONSTRUCTION AND DEMONSTRATION OF MODULAR, RECONFIGURABLE ROBOTS Ph.D. Thesis
Robert Owen Ambrose 1991 611 p
Avail: Univ. Microfilms Order No. DA9212481

This report provides a framework for the design and configuration of joints and links for the assembly of modular robots. This report is founded on two premises. First, that a modular strategy will improve the robot design process, by narrowing the focus to manageable and experimentally verifiable joint and link modules. The second premise is that a module data base can be used to evaluate combinations of joints and links to identify the best modular arm for a user specified task. These modules were tested in isolation using the UT Modular Robotics Testbed developed specifically for this effort. A set of four joint modules and seven link modules was designed for this effort, in addition to dozens of mounting accessories for a total of over seventy separate components. A supporting electronics facility was designed to derive the actuators and sensors built into these modules, along with the operational software required for the initial experiments. Given these modules and their experimentally verified performance, a design process has been described for matching module combinations with user specified task requirements. Two design space formulations are described, within which nine optimization methods are used to search for the best solution. These design methodologies are evaluated on the basis of run time, reliability, and sensitivity to changes in the scale of the design problem. Recommendations for future module designs have been suggested based on the experimental results, with an emphasis on improving the drive trains that were found to limit the performance of most actuators. A series of concept drawings will be described as starting points for future design teams, such as those at UT that are now focusing on the design of joint and link prototypes. Recommendations for improving the modular configuration methodology are described in terms of increasing the number of performance criteria and expanding the design process to include broader architectures of manipulators. Finally, future experiments are proposed to use the UT Modular Robotics Testbed to answer many of the questions uncovered during this effort.
Dissert. Abstr.

N93-13331 Michigan Technological Univ., Houghton.
THE INFLUENCE OF MIXTURE PREPARATION IN THE INTAKE PORT ON THE PERFORMANCE OF A SPARK-IGNITED FOUR-STROKE ENGINE Ph.D. Thesis
Charles Howard Daniels 1991 250 p
Avail: Univ. Microfilms Order No. DA9220738

An experimental technique is developed for evaluating the influence of mixture preparation in the intake port on the performance of a spark ignited engine. The preparation components studied are fuel vapor, droplets, and liquid streams. The fuel in these three distinct forms are produced and varied in a specially designed mixture preparation system, which delivers an air/fuel mixture to a test cylinder of an engine. Incorporated in the preparation system are devices for measuring the flow rates of fuel in these forms. A method of estimating the vapor concentration of a gasoline in the preparation channel by the use of simple temperature measurements is also presented. The effect of these fuel forms on in-cylinder pressure performance and exhaust gas concentrations are investigated in a 1.9 L Ford engine. A matrix of engine operations are studied along with two gasolines of different volatilities. The results of this investigation show that the operation of the engine at low speeds and low manifold absolute pressures is most susceptible to the effects mixture preparation. For those engine operating conditions affected, the results show that by increasing the amount of fuel in liquid stream form, the performance of the engine is generally diminished. In addition, 'equivalent' mixtures resulting from a conventional injector and a pneumatic atomizer in the intake port are identified relative to engine performance.
Dissert. Abstr.

N93-13335 California Univ., Santa Barbara.
END-POINT POSITION CONTROL OF MULTI-LINK FLEXIBLE MANIPULATOR ARMS Ph.D. Thesis
Masoud Sahraian 1991 122 p
Avail: Univ. Microfilms Order No. DA9218478

In this thesis the problem of positioning the end-effector of a flexible manipulator arm along a desired path is discussed. The application of nonlinear inversion method as a potential solution is considered first. Since the inverse system is not stable, an alternative approach is presented: based on the assumption of small elastic deflection of the flexible links, the equations of motion are linearized. The solution of linear optimal control equations yields a noncausal control, which approximately reproduces the end-point trajectory for the nominal nonlinear system. The assumed mode method is used to model the elastic deformation in the links of the manipulator. Simulation results for very flexible single-link and two-link arms are given. Convergence of the optimal solution with the number of modes used in the modal expansion is shown. Accurate tracking is achieved for fast motion of the end-point. To have accurate and stable tracking for an off-nominal flexible arm, several closed-loop scheme is given which uses a simple proportional plus derivative (PD) joint feedback. The optimal solution, used as a feedforward, is essential for the implementation of this method. Simulation results for a single-link flexible arm are shown to illustrate the above ideas.
Dissert. Abstr.

N93-13384 Michigan Univ., Ann Arbor.
FORCE AND MOTION CONTROL OF A CONSTRAINED FLEXIBLE MANIPULATOR Ph.D Thesis
Fon-Lin Hu 1992 155 p
Avail: Univ. Microfilms Order No. DA9226919

This dissertation reports the results of a comprehensive research study

on the combined joint motion control, vibration control, and force control of a constrained rigid-flexible robot arm. An efficient and accurate approach to modeling for controller design is provided. Both regulation and tracking problems are considered, and a modified version of a Corless-Leitmann controller is developed. Experimental studies, which demonstrate the effectiveness of the proposed methods, are presented. In this work, the dynamic modeling of a constrained spherical coordinate robot arm, whose last link is very flexible, is studied for the purpose of combined force and motion control. The model is derived using a consistent modeling procedure which accounts for the axial force effects due to contract, and the coupling due to the effects of flexible motions on the rigid body motions. These effects are shown to be important in the prediction of the vibration frequencies. Galerkin's method is employed for spatial discretization of the flexible link deflections. A convergence study is presented to evaluate the appropriateness of the spatial approximating functions and to determine the number of modes required for obtaining accurate simulation results. Linear control design methods are shown to be adequate for solving the problem of hybrid force and position regulation for the constrained flexible robot arm. However, nonlinear control strategies show advantages (i.e., good response of the joint motion and contact force, and small magnitude of the structural vibration) in the tracking control of motion and force. A modified Corless-Leitmann controller is presented to enhance the control of the flexible motion using only joint actuators. Finally, an experimental implementation is used to validate the proposed controller designs, to assess the merit of measuring and feeding back the flexible motion and the contact force, and to evaluate the feasibility of combined force and motion control strategies for the constrained flexible robot arm. These experimental results are in good agreement with the theory, and demonstrate the effectiveness of the proposed control strategies. Dissert. Abstr.

N93-13417* National Aeronautics and Space Administration. Lyndon B. Johnson Space Center, Houston, TX.

PRELOADED LATCHING DEVICE Patent

Clarence J. Wesselski, inventor (to NASA) and Kornel Nagy, inventor (to NASA) 27 Oct. 1992 10 p Filed 25 Feb. 1991 Supersedes N91-23493 (29 - 15, p 2435)

(NASA-Case-MSC-21730-1; US-Patent-5,158,331; US-Patent-Appl-SN-660755; US-Patent-Class-294-94; US-Patent-Class-294-89; Int-Patent-Class-N66L-1/66) Avail: US Patent and Trademark Office

A latching device is disclosed which is lever operated sequentially to actuate a set of collet fingers to provide a radial expansion and to actuate a force mechanism to provide a compressive gripping force for attaching first and second devices to one another. The latching device includes a body member having elongated collet fingers which, in a deactuated condition, is insertable through bores on the first and second devices so that gripping terminal portions on the collet fingers are proximate to the end of the bore of the first device while a spring assembly on the body member is located proximate to the outer surface of a second device. A lever is rotatable through 90 deg to move a latching rod to sequentially actuate and expand collet fingers and to actuate the spring assembly by compressing it. During the first 30 deg of movement of the lever, the collet fingers are actuated by the latching rod to provide a radial expansion and during the last 60 deg of movement of the lever, the spring assembly acts as a force mechanism and is actuated to develop a compressive latching force on the devices. The latching rod and lever are connected by a camming mechanism. The amount of spring force in the spring assembly can be adjusted; the body member can be permanently attached by a telescoping assembly to one of the devices; and the structure can be used as a pulling device for removing annular bearings or the like from blind bores. Official Gazette of the U.S. Patent and Trademark Office

N93-13423* National Aeronautics and Space Administration. Lyndon B. Johnson Space Center, Houston, TX.

FASTENING APPARATUS HAVING SHAPE MEMORY ALLOY ACTUATOR

Darin N. McKinnis, inventor (to NASA) 3 Nov. 1992 9 p Filed 13 May 1992 Supersedes N92-29762 (30 - 20, p 3479)

(NASA-Case-MSC-21935-1; US-Patent-5,160,233; US-Patent-Appl-SN-882408; US-Patent-Class-411-433; US-Patent-Class-411-267; US-Patent-Class-411-909; Int-Patent-Class-F16B-37/08; Int-Patent-Class-F16B-39/36) Avail: US Patent and Trademark Office

A releasable fastening apparatus is presented. The device includes a connecting member and a housing. The housing supports a gripping mechanism that is adapted to engage the connecting member. A triggering member is movable within the housing between a first position in which it constrains the gripping mechanism in locked engagement with the connecting member, and a second position in which the gripping mechanism is disengaged from the connecting member. A shaped memory alloy actuator is employed for translating the triggering member from its first to its second position. The actuator is designed to expand longitudinally when transitioned from a martensitic to an austenitic state.

Official Gazette of the U.S. Patent and Trademark Office

N93-13436*# Alabama Univ., Huntsville. Dept. of Electrical and Computer Engineering.

ROBOT WELDING PROCESS CONTROL Final Technical Report, 25 Feb. 1990 - 25 Feb. 1991

Peter L. Romine 22 Jul. 1991 72 p

(Contract NAS8-36955)

(NASA-CR-184428; NAS 1.26:184428) Avail: CASI HC A04/MF A01

This final report documents the development and installation of software and hardware for Robotic Welding Process Control. Primary emphasis is on serial communications between the CYRO 750 robotic welder, Heurikon minicomputer running Hunter & Ready VRTX, and an IBM PC/AT, for offline programming and control and closed-loop welding control. The requirements for completion of the implementation of the Rocketdyne weld tracking control are discussed. The procedure for downloading programs from the Intergraph, over the network, is discussed. Conclusions are made on the results of this task, and recommendations are made for efficient implementation of communications, weld process control development, and advanced process control procedures using the Heurikon. Author

N93-13452# Georgia Inst. of Tech., Atlanta. School of Mechanical Engineering.

ROBUST CONTROL OF A FLEXIBLE LINK ROBOT AND RIGID LINK ROBOT: THEORY, SIMULATION, AND EXPERIMENT Ph.D. Thesis

Soo Han Lee Mar. 1992 203 p

Avail: CASI HC A10/MF A03

The goal of this research is to design a controller for multi-link flexible robots that ensures accurate joint trajectory tracking and fast vibration damping. This research follows two methods, theoretical and experimental. The theoretical approach comprises derivation of dynamic model, design of a robust controller, stability analysis of the designed controller, and computer simulations. The experimental approach includes verifications of the dynamic model and real time implementations of the controller. The experiments are performed with two physical robots, a rigid link robot and flexible link robot. The rigid link robot is designated SAM (Small Articulated Manipulator) and the flexible link robot is designated RALF (Robotic Arm, Large and Flexible). Dynamic equations are derived using Hamilton's principle and Lagrange's equations. Author

N93-13488 Minnesota Univ., Minneapolis.

PERFORMANCE AND STABILITY OF TELEMANIPULATORS USING BILATERAL IMPEDANCE CONTROL Ph.D. Thesis

Christopher Lane Moore 1991 194 p

Avail: Univ. Microfilms Order No. DA9212073

The research investigates a new method of control for telemanipulators called bilateral impedance control. This new method differs from previous approaches in that interaction forces are used as the communication signals between the master and slave robots. The new control architecture has several advantages: (1) It allows the master robot and the slave robot to be stabilized independently without becoming involved in the overall system dynamics. (2) It permits the system designers to arbitrarily specify desired performance characteristics such as the force and position ratios between the master and slave. (3) The impedance at both ends of the telerobotic system can be modulated to suit the requirements of the task. The main goals of the research are to characterize the performance and stability of the new control architecture. The dynamics of the telerobotic system are described by a bond graph model that illustrates how energy is transformed, stored, and dissipated. Performance can be completely described by a set of three independent parameters. These parameters are fundamentally

related to the structure of the H matrix that regulates the communication of force signals within the system. By tailoring the H matrix, the performance parameters can be arbitrarily specified to achieve desired performance characteristics. The only limitations on the choice of these parameters are imposed by system stability. Stability is analyzed with two mathematical techniques: the Small Gain Theorem and the Multivariable Nyquist Criterion. The Small Gain Theorem is used to arrive at a general set of stability conditions that is equally valid for linear as well as nonlinear systems. The Multivariable Nyquist Criterion is used to analyze the stability of linear systems with transfer function matrix operators. The theoretical predictions for performance and stability are experimentally verified by implementing the new control architecture on a multi-degree-of-freedom telemanipulator. The frequency response of the performance parameters is measured, and the absolute stability bounds are determined. Robustness to modeling uncertainties is demonstrated from the shape of the frequency response. Dissert. Abstr.

N93-13540 Pennsylvania Univ., Philadelphia.
ROBOTIC EXPLORATION OF SURFACES AND ITS APPLICATION TO LEGGED LOCOMOTION Ph.D. Thesis
Pramath Raj Sinha 1991 130 p
Avail: Univ. Microfilms Order No. DA9212004

Material properties like penetrability, compliance, and surface roughness are important in the characterization of the environment. While concentrating on issues of geometry and shape, researchers in perceptual robotics, until recently, have not quite addressed the issue of the extraction of material properties from the environment. The goal of this research is to design and implement a robotic system that will actively explore a surface to extract its material characteristics. Further the relevance of material properties in the legged locomotion of robots is also recognized and our research objectives are extended towards building a robotic system for exploration such that is actively perceives material properties during the process of legged locomotion. The chosen approach to the design and implementation of such a robotic system is to first select an appropriate environment model and then to design exploratory procedures salient to each attribute of interest. These exploratory procedures are then implemented through an experimental setup and the results show that material properties can be reliably measured. The design, implementation, and results of a framework for surface exploration to recover material properties are presented. Further, the exploratory procedures for exploration are integrated into an active perceptual scheme for legged locomotion. The perceptual scheme is designed around creating the ability for the robot to sense variations in terrain properties while it is walking, so that it may be able to avoid sinking, slipping, and falling due to unexpected changes in the terrain properties, and make suitable changes in its foot forces to continue locomotion. Finite element simulations of the foot-terrain interaction are used to justify some of the strategies used in this active perceptual scheme. The active perceptual scheme is implemented by simulating a leg-ankle-foot system with a PUMA arm-complaint wrist-foot system and an accelerometer mounted on the foot to detect slip. Details of implementation and experimental results are presented. Dissert. Abstr.

N93-13541 Iowa State Univ. of Science and Technology, Ames.
CONTROL OF A VERY FLEXIBLE ROBOT IN GRAVITY Ph.D. Thesis
Jay Eric Shannan 1991 133 p
Avail: Univ. Microfilms Order No. DA9212187

This thesis presents several algorithms used to control a very flexible robot in gravity. The flexible arm is modelled using an assumed modes method to characterize the elastic behavior. Gravity is included in the model. Control algorithms are developed and simulated numerically. The control schemes include proportional-derivative (PD), linear quadratic regulator (LQR), and linear quadratic regulator with a prescribed degree of stability algorithms. The PD algorithms use only hub position and velocity for feedback. Simulations show fast response times with large overshoot and long settling times. The LQR algorithms have the benefit of modal feedback. These responses settle quicker than the responses obtained using PD controllers. The LQR responses are sensitive to the weighting factors used to derive the feedback gains. As expected, the simulation results indicated that the weighting factors, and consequently the feedback gains, should be modified for each payload. The LQR with the prescribed degree of stability gives improved results compared to the previous LQR. However, this scheme results in unstable responses for large prescribed degrees of stability due to system nonlinearities. The flexible arm robot used for the simulation study is then implemented in a test bed. The flexible arm is in the vertical plane. The PD control schemes give experimental results that are similar to the simulation results. Control algorithms with modal feedback yield shorter settling times than the PD algorithms. The experiments show higher order modes can become unstable as the hub velocity and first mode feedback gains are increased. The second mode feedback gain is found to have a stabilizing effect on these instabilities. A nonlinear controller based on varying the first mode feedback gain with position is presented. This controller results in smaller overshoot in some cases. Dissert. Abstr.

N93-13608*# SatCon Technology Corp., Cambridge, MA.
MAGNETIC BEARINGS FOR A HIGH-PERFORMANCE OPTICAL DISK BUFFER, VOLUME 2 Final Report, May 1988 - Apr. 1990
May 1990 63 p
(Contract NAS5-30309; SBIR-08.01-0540A)
(NASA-CR-190874; NAS 1.26:190874; SatCon-R05-90-Vol-2) Avail: CASI HC A04/MF A01

The operating instructions for the magnetic bearings of a high-performance optical disk buffer are provided. Among the topics that are discussed are the following: front panel layout, turn-on procedure, shut-down procedure, and latch-up protection. Additionally, comprehensive engineering drawings are presented for the design. D.R.D.

N93-13638 California Univ., Santa Barbara.
NONHOLONOMIC MOTION OF FREE-FLYING SPACE ROBOTS Ph.D. Thesis
Ranjan Mukherjee 1991 172 p
Avail: Univ. Microfilms Order No. DA9218468

A free-flying space vehicle with one or more manipulators is expected to perform various tasks in space, like the construction of space stations, deployment of large antennas and solar power stations, and the servicing and maintenance of satellites. The kinematics and dynamics of these space robots are significantly different from terrestrial robots. This is because of the nonholonomic nature of the momentum constraints that govern their motion. We describe a 6-DOF space robot by nine state variables: the six joint angles of the manipulator and the three dependent Euler angles describing the orientation of the space vehicle. The nonholonomy in the mechanical structure manifests itself when we show that it is possible to converge all the nine state variables to their desired values by controlling only the six joints of the manipulator. We plan this trajectory using a Liapunov function and by adopting a bi-directional approach. Another interesting feature of free-flying space robots is the presence of a special kind of redundancy in its mechanical structure. This redundancy, which we term as nonholonomic redundancy, exhibits itself only after a global motion and is shown to exist in the absence of ordinary kinematic redundancy. We establish methods to utilize nonholonomic redundancy for avoiding obstacles and joint limits, while planning a trajectory for the end-effector. Finally we discuss the inverse dynamics problem of multibody systems in space. While solving for the inverse dynamics, the computations for the inverse kinematics are considered simultaneously, and both computations are developed on the basis of momentum constraints. This reduces the computational time significantly. We establish an efficient algorithm for the real time computation of the inverse dynamics. We also discuss the scope of parallel recursion for further reduction of the time for computing the inverse dynamics. Dissert. Abstr.

N93-13644# Acurex Corp., Mountain View, CA. Environmental Systems Div.
WHITE PAPER: PRELIMINARY ASSESSMENT OF LNG VEHICLE TECHNOLOGY, ECONOMICS, AND SAFETY ISSUES, REVISION 1 Report, Apr. - Aug. 1991
Charles Powars, Dan Lucher, Carl Moyer, and Lou Browning 10 Jan. 1992 87 p Revised
(Contract GRI-5091-292-2153)
(PB92-212943; GRI-91/0347-Rev-1) Avail: CASI HC A05/MF A01

The objective of the study is to evaluate the potential of liquified natural gas (LNG) as a vehicle fuel, to determine market inches, and to identify needed technology improvements. The white paper is being issued when the work is approximately 30 percent complete to preview the study direction, draw preliminary conclusions, and make initial recommendations.

Interim findings relative to LNG vehicle technology, economics, and safety are presented. It is important to decide if heavier hydrocarbons should be allowed in LNG vehicle fuel. Development of suitable refueling couplings and vehicle fuel supply pressure systems are recommended. Initial economics analyses considered transit buses and pickup and delivery trucks fueled via onsite liquefiers and imported LNG. Net user costs were more than (but in some cases close to) those for diesel fuel and gasoline. Lowering the cost of small-scale liquefiers would significantly improve the economics of LNG vehicles. New emissions regulations may introduce considerations beyond simple cost comparisons. LNG vehicle safety and available accident data are reviewed. Consistent codes for LNG vehicles and refueling facilities are needed. GRA

N93-13706*# SatCon Technology Corp., Cambridge, MA.
MAGNETIC BEARINGS FOR A HIGH-PERFORMANCE OPTICAL DISK BUFFER, VOLUME 1 Final Report, May 1988 - Apr. 1990
Richard Hockney, Karen Adler, George Anastas, Jr., James Downer, Frederick Flynn, James Goldie, Vijay Gondhalekar, Timothy Hawkey, and Bruce Johnson May 1990 128 p
(Contract NAS5-30309; SBIR-08.01-0540A)
(NASA-CR-190873; NAS 1.26:190873; SatCon-R05-90-Vol-1) Avail: CASI HC A07/MF A02

The innovation investigated in this project was the application of magnetic bearing technology to the translator head of an optical-disk data storage device. Both the capability for space-based applications and improved performance are expected to result. The phase 1 effort produced: (1) detailed specifications for both the translator-head and rotary-spindel bearings; (2) candidate hardware configurations for both bearings with detail definition for the translator head; (3) required characteristics for the magnetic bearing control loops; (4) position sensor selection; and (5) definition of the required electronic functions. The principal objective of Phase 2 was the design, fabrication, assembly, and test of the magnetic bearing system for the translator head. The scope of work included: (1) mechanical design of each of the required components; (2) electrical design of the required circuitry; (3) fabrication of the component parts and bread-board electronics; (4) generation of a test plan; and (5) integration of the prototype unit and performance testing. The project has confirmed the applicability of magnetic bearing technology to suspension of the translator head of the optical disk device, and demonstrated the achievement of all performance objectives. The magnetic bearing control loops perform well, achieving 100 Hz nominal bandwidth with phase margins between 37 and 63 degrees. The worst-case position resolution is 0.02 micron in the displacement loops and 1 micron rad in the rotation loops, The system is very robust to shock disturbances, recovering smoothly even when collisions occur between the translator and frame. The unique start-up/shut-down circuit has proven very effective. Author

N93-13720 State Univ. of Iowa, Iowa City.
AUTOMATIC PROGRAMMING OF ARC WELDING ROBOTS Ph.D. Thesis
Srikanth Padmanabhan 1991 231 p
Avail: Univ. Microfilms Order No. DA9207252

Automatic programming of arc welding robots requires the geometric description of a part from a solid modeling system, expert weld process knowledge and the kinematic arrangement of the robot and positioner automatically. Current commercial solid models are incapable of storing explicitly product and process definitions of weld features. This work presents a paradigm to develop a computer-aided engineering environment that supports complete weld feature information in a solid model and to create an automatic programming system for robotic arc welding. In the first part, welding features are treated as properties or attributes of an object, features which are portions of the object surface--the topological boundary. The structure for representing the features and attributes is a graph called the Welding Attribute Graph (WAGRAPH). The method associates appropriate weld features to geometric primitives, adds welding attributes, and checks the validity of welding specifications. A systematic structure is provided to incorporate welding attributes and coordinate system information in a CSG tree. The specific implementation of this structure using a hybrid solid modeler (IDEAS) and an object-oriented programming paradigm is described. The second part provides a comprehensive methodology to acquire and represent weld process knowledge required for the proper selection of welding schedules. A methodology of knowledge acquisition using statistical methods is proposed. It is shown that these procedures did little to capture the private knowledge of experts (heuristics), but helped in determining general dependencies, and trends. A need was established for building the knowledge-based system using handbook knowledge and to allow the experts further to build the system. A methodology to check the consistency and validity for such knowledge addition is proposed. A mapping shell designed to transform the design features to application specific weld process schedules is described. A new approach using fixed path modified continuation methods is proposed in the final section to plan continuously the trajectory of weld seams in an integrated welding robot and positioner environment. The joint displacement, velocity, and acceleration histories all along the path as a function of the path parameter for the best possible welding condition are provided for the robot and the positioner to track various paths normally encountered in arc welding. Dissert. Abstr.

N93-13742 Pennsylvania Univ., Philadelphia.
FORCE-CLOSURE GRASPING WITH TWO HANDS Ph.D. Thesis
Jose-Antonio Navarro Caraza 1991 133 p
Avail: Univ. Microfilms Order No. DA9211917

This thesis addresses grasping of large (but not necessarily heavy) objects by using two hands. The objective is to determine force-closure grasps of rigid objects of unknown shape. A grasp is force-closure if it can completely constrain the movement of the object. In seeking force-closure conditions, the approach taken in this study is to establish useful sufficient conditions rather than necessary and sufficient conditions since the later requires the complete knowledge of the contact parameters. Based on the friction coefficient between hands and object, and on the grasp configuration (defined as the relative position and orientation of fingers and palms), a sufficient condition under which the two hands form a force-closure grasp has been established. The salient feature of this approach is that shape, orientation and location of the object, and contact points location are not assumed in this condition. This makes it possible to use simple sensors and algorithms. A configuration of two hands in contact with the object satisfying this condition is called force-closure grasp configuration (FCGC). The two hands in a FCGC are capable of picking up and moving the object by applying appropriate forces. The two-dimensional (2-D) case is initially studied. Later, the study is extended to the three-dimensional (3-D) case. The hands considered are either flat-surface palms or grippers with two angular-motion fingers. An algorithm has been developed to check the condition for FCGC in terms of the position and orientation of the hands. The algorithm was implemented on TRACS, an experimental multiagent robotic system developed at the GRASP Laboratory at the University of Pennsylvania. The results obtained are readily applicable to grasping large but lightweight objects. The simplicity of the conditions and the practical assumptions make it feasible to implement these results in real time. Dissert. Abstr.

N93-13761# Environmental Protection Agency, Ann Arbor, MI. Technology Development Group.
THE 1992 NATURAL GAS VEHICLE CHALLENGE: EPA EMISSIONS AND FUEL ECONOMY TESTING
Robert I. Bruetsch and Martin E. Reineman Jun. 1992 73 p
(PB92-217926; EPA/AA/TDG-92/05) Avail: CASI HC A04/MF A01

The report describes the results of a student alternative fuels engineering design competition called the 1992 Natural Gas Vehicle Challenge which was held April 22 through June 1, 1992. Students from eighteen universities in the United States and four universities in Canada competed. the objective of this competition for each participating team was to convert a gaseoline-fueled General Motors (GM) Sierra pickup truck to natural gas operation and complete with students from other universities in the areas of exhaust emissions, fuel economy, performance, and design. This report also includes the comparisons between the results of the student compressed natural gas pickup truck conversions and the test results of similar gasoline-powered trucks and a dedicated compressed natural gas truck provided by General Motors. GRA

N93-13772 Wisconsin Univ., Madison.
THE EFFECTS OF PRESSURE GRADIENTS ON CONVECTIVE HEAT FLUX PREDICTIONS IN ENGINE ENVIRONMENTS Ph.D. Thesis
I-Ping Chang 1991 234 p
Avail: Univ. Microfilms Order No. DA9120038

Accurate convective heat transfer predictions inside engines is important

to improvements in performance, reduction of harmful exhaust emissions, and structural and material design. Current heat transfer models used in engine simulations do not incorporate the effects of pressure gradients. In this study, wall functions that use local pressure gradients to correct the friction velocity, wall shear stress, and heat flux were developed. The pressure-gradient-corrected (PGC) model predictions of nondimensional velocity and temperature were validated by experimental data available in the literature and were also compared with other models. Results showed reasonable agreement with the experimental data for both accelerated and decelerated flows before flow separation. The drag law relations predicted by the PGC wall function gave good trend analysis of skin coefficient variation over the local Reynolds number for different local pressure gradient conditions. The piecewise linear correlations between the skin friction coefficient and the Stanton number for different pressure gradients were observed. The PGC model wall function parameters which include a modified friction velocity, wall shear stress, and heat flux were calculated using the engine hydrodynamic simulation code KIVA-II. The predictions exhibited appropriate response to a variety of engine flow and operating conditions. The PGC model wall function predictions of friction velocity and wall shear stress were compared with two different models for a flat-piston and a deep-bowl engine at the same operating conditions and location. The wall heat flux predictions from the PGC model were compared with four different models for the different flow, geometry, and operating conditions from a flat-piston engine and a deep-bowl piston engine. Results of different model predictions were compared with experimental data. For the flat-piston engine, the PGC model predictions underestimated peaks and valleys in the compression process whereas they rendered fair agreement in the expansion processes. For the deep-bowl piston engine, the heat fluxes predicted with the PGC model were the most accurate in the high squish region near the bowl edge and annular region between the piston top and cylinder head but were less accurate near the center of the chamber. Dissert. Abstr.

N93-13808 West Virginia Univ., Morgantown.
ENHANCED ACCURACY FOR CLOSED-LOOP ROBOT Ph.D. Thesis
Jing Tian 1991 145 p
Avail: Univ. Microfilms Order No. DA9217959

The main objective of this dissertation was to improve the accuracy performance of a closed-loop robot for which kinematic parameter errors exist in its manipulator. Theoretical developments have studied the effect of the link/joint parameter errors on the kinematic and the dynamic performances of the closed-loop robot. A kinematic model calibration method has also been developed. Kinematic error computation schemes have been systematically developed for a closed-loop robot manipulator with a planar RRRRR mechanism. The developed error function, an extension of previous research work for an open-loop robot manipulator, is based on the perturbation methods. The kinematic parameter errors have been defined as kinematic deviations from the nominal link/joint parameters that are widely used for robot kinematic studies. A kinematic model calibration algorithm has been developed for a closed-loop robot manipulator with an RRRRR mechanism. A nonlinear optimization method was used to develop such an algorithm. This algorithm uses the least square method to formulate an objective function to minimize the robot's end effector pose error within the robot work envelope and applies the Newton iteration method to solve the nonlinear kinematic equations for their unknown kinematic parameters. An inverse dynamic computation scheme that considers kinematic parameter errors has been developed for a closed-loop robot manipulator. This computation scheme was developed based on the application of a d'Alembert principle to solve the closed-loop constraints by taking each partial derivative of an unactuated joint with respect to an actuated joint in the closed-loop mechanism. A computational scheme has also been developed to determine the torque deviations due to the kinematic parameter errors in a closed-loop robot manipulator Dissert. Abstr.

N93-13809 Virginia Polytechnic Inst. and State Univ., Blacksburg.
APPLICATION OF ADAPTIVE TRUSSES TO VIBRATION ISOLATION IN FLEXIBLE STRUCTURES Ph.D. Thesis
William Walker Clark 1991 191 p
Avail: Univ. Microfilms Order No. DA9218019

This dissertation presents techniques for using adaptive trusses for active vibration isolation in flexible structures. Passive methods have been used almost exclusively in the past for vibration isolation, although in the more recent literature active techniques have been proposed in an attempt to achieve greater isolation performance. Most of the active techniques, however, require either detailed knowledge of the system or of the disturbance to be isolated. This work focuses on techniques in which knowledge of the disturbance is minimal, and in some cases, knowledge of the system is not necessary. Two new active vibration isolation methods are presented which are based on feedback of transmitted forces in the system. The methods include force feedback through a high gain, and state feedback using the LQR method with disturbance modelling. A third method which has been demonstrated in the literature, force feedback through a classical compensator, is also presented for comparison. For the purpose of discussion, each of the methods is applied to a system which includes a single active mount. The methods are then applied analytically to an adaptive truss, which essentially contains multiple mounts, to demonstrate multi-degree-of-freedom active vibration isolation. It is shown that force feedback provides two-way isolation, and its effects are independent of the type of active mount used (whether it is a force or displacement-commanded mount). The most promising technique proves to be the simplest, the high-gain feedback method. This technique is a stable, model-free method of vibration isolation which places no restrictions on the type of system disturbance, other than that it must be within the actuator's bandwidth. The high-gain approach is applied experimentally and shown to agree with the simulated results. Dissert. Abstr.

N93-13931 Stanford Univ., CA.
EXPERIMENTS IN TWO-COOPERATING-ARM MANIPULATION FROM A PLATFORM WITH UNKNOWN MOTION Ph.D. Thesis
Roberto Luis Vasquez 1992 155 p
Avail: Univ. Microfilms Order No. DA9221680

This dissertation makes several contributions to the effective control of single and cooperative manipulators situated on a moving platform. In particular, an extended computed-torque controller is developed. The controller does not require direct sensing of platform position or velocity: a practical attribute. (In practice, the platform position and velocity are difficult to measure, and these signals are thus often unavailable.) Two types of systems coupling are considered: one-way coupling and two-way coupling. In a system with one-way coupling, the platform motion is not affected by manipulator motions; but manipulator motions are affected by their dynamic coupling to the platform. In a system with two-way dynamic coupling, the platform motion and manipulator motions are each affected by the other: they are totally coupled dynamically. Formulations of dynamic controllers for manipulators mounted on each type of moving platform are developed. An interesting aspect of the problem is that driven-platform oscillation produces parametric excitation of the (two-link) arm's motion. The dissertation also presents multiple-manipulator cooperative control from a moving platform. This has been achieved, for the first time, (and demonstrated experimentally) by combining the extended computed-torque controllers with a high-level object-impedance controller. Finally, the Sensitivity Map is introduced. The Sensitivity Map is a graphical representation that indicates regions in operational space where the manipulator endpoint is most sensitive to base accelerations. In particular, for example the map enables the designer to determine regions in the workspace where given endpoint position performance specifications can be met even when base acceleration is measured. The control strategies designed here have been experimentally verified on a pair of planar, cooperating manipulations situated on a light-weight, spring-mounted moving platform. Dissert. Abstr.

N93-13936 Texas Univ., Austin.
DYNAMIC MODELING AND OPTIMAL JOINT TORQUE COORDINATION OF ADVANCED ROBOTIC SYSTEMS Ph.D. Thesis
Hee-Jun Kang 1991 269 p
Avail: Univ. Microfilms Order No. DA9212561

The development is documented of an efficient dynamic modeling algorithm and the subsequent optimal joint input load coordination of advanced robotic systems for industrial application. A closed-form dynamic modeling algorithm for the general closed-chain robotic linkage systems is presented. The algorithm is based on the transfer of system dependence from a set of open chain Lagrangian coordinates to any desired system generalized coordinate set of the closed-chain. Three different techniques for evaluation of the kinematic closed chain constraints allow the representation of the dynamic modeling parameters in terms of system generalized coordinates and have no restriction with regard to kinematic redundancy. The total computational requirement of the closed-chain system

model is largely dependent on the computation required for the dynamic model of an open kinematic chain. In order to improve computational efficiency, modification of an existing open-chain KIC based dynamic formulation is made by the introduction of the generalized augmented body concept. This algorithm allows a 44 pct. computational saving over the current optimized one (O(N4), 5995 when N = 6). As means of resolving redundancies in advanced robotic systems, local joint torque optimization is applied for effectively using actuator power while avoiding joint torque limits. The stability problem in local joint torque optimization schemes is eliminated by using fictitious dissipating forces which act in the necessary null space. The performance index representing the global torque norm is shown to be satisfactory. In addition, the resulting joint motion trajectory becomes conservative, after a transient stage, for repetitive cyclic end-effector trajectories. The effectiveness of the null space damping method is shown. The modular robot, which is built of well defined structural modules from a finite-size inventory and is controlled by one general computer system, is another class of evolving, highly versatile, advanced robotic systems. Therefore, finally, a module based dynamic modeling algorithm is presented for the dynamic coordination of such reconfigurable modular robotic systems. A user interactive module based manipulator analysis program (MBMAP) has been coded in C language running on 4D/70 Silicon Graphics. Dissert. Abstr.

N93-13949 Rensselaer Polytechnic Inst., Troy, NY.
FRICTION, WEAR AND RAMAN SPECTROSCOPIC CHARACTERISTICS OF CARBON LUBRICATED SURFACES Ph.D. Thesis
Brian Lee Vlcek 1991 179 p
Avail: Univ. Microfilms Order No. DA9220914

As engineering applications demand higher operating temperatures, ceramics quickly become the designers' material of choice. Innovative lubricating techniques are consequentially required. While the lubricating properties of carbon have been recognized for decades, typically applications have been only in the form of powders or thin films that have a limited lifetime. A replenishable carbon layer can be established by the dehydrogenation of hydrocarbon vapors in high temperature wear contacts. During this effort, a high temperature pin-on-disc tester was modified to determine the lubricating properties of carbonaceous deposits that form in the wear track at high pressures. Reduction in the coefficient of friction from approximately 0.7 to 0.2 was realized under some test conditions. Wear of the pin was commonly reduced by thirty percent when the wear contact was exposed to ethylene. Ceramics, steels, and nickel oxide-coated steels were tested at increasing pressures (in the gigapascal range), increasing temperatures (as high as 650 deg Celsius), and varied ethylene concentrations. A four-ball wear tester was also modified during this research effort to operate at high temperatures (550 C), to test ceramics, and to lubricate the wear contact with ethylene. Wear and friction were reduced as lubricating carbon deposits formed in the wear track. Raman spectroscopy was used to study the varied and distinct carbonaceous deposits that formed in weak tracks tribologically, that formed out of wear tracks pyrolytically, and that formed on pin wear scars. A cataloging of Raman spectra, wear rate, structural appearance, and test parameters was undertaken. By the intensity ratio of the Disorder peak (1360 Rcm(exp-1) and the Graphite peak (1580 RCM(exp-1) it was shown that the carbon on the pin was ground to finer crystals than that found in the wear track on the disc. As the carbon layer became thinner, the spectra indicated more diamond-like structure. This process has been demonstrated to be an effective means of reducing wear and friction in high temperature ceramic contacts. Dissert. Abstr.

N93-14075 Ohio State Univ., Columbus.
DEXTEROUS GRASP AND MANIPULATION Ph.D. Thesis
Sudipto Mukherjee 1992 153 p
Avail: Univ. Microfilms Order No. DA9219002

This dissertation addresses some of the fundamental issues in multifingered cooperative manipulation. The problems investigated were stimulated by the need to devise a motion and force allocation planner for the four fingered DIGITS system. In motion planning, the emphasis has been on determining finger trajectories that generate smooth object motion in free space. A screw motion has been prescribed to be followed between two configurations of the object, in order to obtain simultaneous rotary and translatory motion. The effect of the joint motion limits on the path following capability of the fingers has been analyzed. It has been shown that knowledge of the direction of the surface normal at the contact point, coupled with the use of a spherical fingertip can be used to circumvent some contact uncertainty problems. The geometry of the force system in the multi-point contact situation has been investigated using crew theory. Conditions for which the system is underspecified have been identified. An efficient solution to the minimum norm solution, the equilibrating forces, has been presented. It has been shown that the pairs of equal and opposite forces acting along the lines joining points of contact can be used to span the space of the homogeneous solutions of the underconstrained problem. Techniques to selectively superpose the interaction forces to orient the net contact forces in desired directions have been developed. This leads to the development of a closed form solution to the optimum grasp problem in three dimensions. It has been shown that the local minimum of the maximum friction angle is characterized by a polynomial which can be symbolically enumerated. Solutions to the minimum friction angle problem can be obtained from the roots of the polynomial. The DIGITS system is instrumented to obtain six axis contact force data from the fingertip. Efficient, stable closed form algorithms have been developed to compute the location of the contact point based on the six axis force data for cylindrical and spherical fingertip geometry. It has been shown that for fingertip surfaces made of piecewise ellipsoids, as opposed to a single ellipsoid, the solution may be non-unique. The conditions for such non-uniqueness to occur have been identified. A simulation of the DIGITS system was implemented on a Symbolics 3650 running Genera 7.2. The modelling package, SuperSketch is used to generate the modelling primitives and rendering. Dissert. Abstr.

N93-14094 Texas Univ., Arlington.
A COLLISION AVOIDANCE ALGORITHM FOR THE MOBILE ROBOT AND THE ROBOT MANIPULATOR IN MULTI-ROBOT SYSTEM Ph.D. Thesis
Yeung-Jaw Joe Jih 1991 135 p
Avail: Univ. Microfilms Order No. DA9217635

As the modern, highly automated factory becomes more and more complicated, the collision avoidance between robots and other obstacles in the work space becomes increasingly important as well. A local collision avoidance algorithm which was developed based on the general structure of the Artificial Potential Field Force along with the Strategy Force and the Pseudo Distance Function is presented. In this algorithm, a goal attracting force is defined in order to drive the robot from the starting position to the goal position. When the distance between a robot and obstacle becomes smaller than a pre-defined effective avoidance distance, an artificial repulsion force is generated as a function of the distance resulting in repulsion between the two closing objects. The commanding force (by combining goal attracting force and the repulsion force) drives the robot toward the goal position without colliding with other objects in the work space. Since the repulsion force, developed here, depends on the distance only, the complicated geometric function for the object model is less important in the algorithm used in this dissertation. The simplicity of this improved artificial force collision algorithm would make it possible to be used on a real-time basis within a time variant environment. Further improvement is realized by introducing a Strategy Force within the Artificial Force whenever a locking situation is detected. The Euclidean distance between the objects normally used in this algorithm is also replaced by a defined Pseudo Distance calculated by a Pseudo Distance Function. The Pseudo Distance Function uses basic geometric information between two objects to calculate the Pseudo Distance. The Pseudo Distance is always smaller than the true minimum distance. This greatly simplified robot collision avoidance algorithm is applicable not only on a two-dimensional mobile robot system but on a three-dimensional multi-robot system as well. Simulations are performed on both mobile robot collision avoidance and multi-robot collision avoidance. Dissert. Abstr.

N93-13165*# Rockwell International Corp., Cocoa Beach, FL. Space Systems Div.
A PATH TO IN-SPACE WELDING AND TO OTHER IN-SPACE METAL PROCESSING TECHNOLOGIES USING SPACE SHUTTLE SMALL PAYLOADS
David Tamir *In* NASA. Goddard Space Flight Center, The 1992 Shuttle Small Payloads Symposium Oct. 1992 p 57-76 (For primary document see N93-13158 03-12)
Avail: CASI HC A03/MF A03

N93-13179*# National Aeronautics and Space Administration. Goddard Space Flight Center, Greenbelt, MD.
THE ROMPS ROBOT IN HITCHHIKER
George Voellmer *In its* The 1992 Shuttle Small Payloads Symposium Oct. 1992 p 205-219 (For primary document see N93-13158 03-12)
Avail: CASI HC A03/MF A03

N93-14006*# National Aeronautics and Space Administration. Langley Research Center, Hampton, VA.
AUTOMATION AND ROBOTICS CONSIDERATIONS FOR A LUNAR BASE
Nancy E. Sliwa, F. Wallace Harrison, Jr., Donald I. Soloway, William S. McKinney, Jr., Karin Cornils, William R. Doggett (Planning Research Corp., Hampton, VA.), Eric G. Cooper (Planning Research Corp., Hampton, VA.), and Thomas E. Alberts (Old Dominion Univ., Norfolk, VA.) *In* NASA. Johnson Space Center, The Second Conference on Lunar Bases and Space Activities of the 21st Century, Volume 2 Sep. 1992 p 603-608 (For primary document see N93-13972 03-91)
Avail: CASI HC A02/MF A03

N93-14008*# National Aeronautics and Space Administration. Marshall Space Flight Center, Huntsville, AL.
THE LUNAR ROVING VEHICLE: HISTORICAL PERSPECTIVE
Saverio F. Morea *In* NASA. Johnson Space Center, The Second Conference on Lunar Bases and Space Activities of the 21st Century, Volume 2 Sep. 1992 p 619-632 (For primary document see N93-13972 03-91)
Avail: CASI HC A03/MF A03

38 QUALITY ASSURANCE AND RELIABILITY

Includes product sampling procedures and techniques; and quality control.

N93-12692*# Alabama Univ., Huntsville. Lab. for Inline Process Analyses.
REAL-TIME QUALITY ASSURANCE TESTING USING PHOTONIC TECHNIQUES: APPLICATION TO IODINE WATER SYSTEM Final Report, Aug. 1989 - Aug. 1990
W. F. Arendale, Richard Hatcher, Yadilett Garlington, Jack Harwell, and Tracey Everett Jul. 1990 62 p
(Contract NAS8-36955)
(NASA-CR-184413; NAS 1.26:184413; JRC-90-28) Avail: CASI HC A04/MF A01

A feasibility study of the use of inspection systems incorporating photonic sensors and multivariate analyses to provide an instrumentation system that in real-time assures quality and that the system in control has been conducted. A system is in control when the near future of the product quality is predictable. Off-line chemical analyses can be used for a chemical process when slow kinetics allows time to take a sample to the laboratory and the system provides a recovery mechanism that returns the system to statistical control without intervention of the operator. The objective for this study has been the implementation of do-it-right-the-first-time and just-in-time philosophies. The Environment Control and Life Support Systems (ECLSS) water reclamation system that adds iodine for biocidal control is an ideal candidate for the study and implementation of do-it-right-the-first-time technologies. Author

N93-12794# Oak Ridge Y-12 Plant, TN.
FUNCTIONAL SYSTEM DESIGN DOCUMENT FOR THE INTELLIGENT INSPECTION SYSTEM (IIS)
21 Jan. 1992 106 p
(Contract DE-AC05-84OS-21400)
(DE92-018240; Y/CSD/INF-92/8) Avail: CASI HC A06/MF A02

IIS (Intelligent Inspection System) is a Martin Marietta Energy Systems Quality Services division project to design and implement a new generation inspection workstation/machine system to be used on all new and upgraded inspection machines for the next several years. The initial implementation will be on upgraded YZ inspection machines. These machines now utilize the dual processor (PDP-II/Allen Bradley combination) hardware and software. Portions of the hardware for these current systems are no longer available. Future implementations will include dual YZ, CMM and OMM systems, both upgrades and new. IIS project scope includes all of the inspection machine control hardware and software, all software to receive a part program, collect inspection data, analyze the data, output results, and the operator interface. Also included in the IIS scope are the operator interface and electronic data handling for the part programming interface and the shop floor interface. DOE

N93-12864# Army Armament Research, Development and Engineering Center, Picatinny Arsenal, NJ.
SPREADSHEET-LIKE IMAGE ANALYSIS
Paul Wilson Aug. 1992 12 p
(AD-A254395; ARPAD-TR-92002) Avail: CASI HC A03/MF A01

This report describes the design of a new software system being built by the Army to support and augment automated nondestructive inspection (NDI) on-line equipment implemented by the Army for detection of defective manufactured items. The new system recalls and post-processes (off-line) the NDI data sets archived by the on-line equipment for the purpose of verifying the correctness of the inspection analysis paradigms, of developing better analysis paradigms and to gather statistics on the defects of the items inspected. The design of the system is similar to that of a spreadsheet, i.e., an array of cells which may be programmed to contain functions with arguments being data from other cells and whose resultant is the output of that cell's function. Unlike a spreadsheet, the arguments and the resultants of a cell may be a matrix such as a two-dimensional matrix of picture elements (pixels). Functions include matrix mathematics, neural networks and image processing as well as those ordinarily found in spreadsheets. The system employs all of the common environmental supports of the Macintosh computer, which is the hardware platform. The system allows the resultant of a cell to be displayed in any of multiple formats such as a matrix of numbers, text, an image, or a chart. Each cell is a window onto the resultant. Like a spreadsheet if the input value of any cell is changed its effect is cascaded into the resultants of all cells whose functions use that value directly or indirectly. The system encourages the user to play what-of games, as ordinary spreadsheets do. GRA

N93-12875*# Alabama Univ., Huntsville.
AUTOMATED EDDY CURRENT ANALYSIS OF MATERIALS Final Report
Gary L. Workman 18 Jul. 1991 22 p
(Contract NAS8-36955)
(NASA-CR-184432; NAS 1.26:184432) Avail: CASI HC A03/MF A01

The use of eddy current techniques for characterizing flaws in graphite-based filament-wound cylindrical structures is described. A major emphasis was also placed upon incorporating artificial intelligence techniques into the signal analysis portion of the inspection process. Developing an eddy current scanning system using a commercial robot for inspecting graphite structures (and others) was a goal in the overall concept and is essential for the final implementation for the expert systems interpretation. Manual scans, as performed in the preliminary work here, do not provide sufficiently reproducible eddy current signatures to be easily built into a real time expert system. The expert systems approach to eddy current signal analysis requires that a suitable knowledge base exist in which correct decisions as to the nature of a flaw can be performed. A robotic workcell using eddy current transducers for the inspection of carbon filament materials with improved sensitivity was developed. Improved coupling efficiencies achieved with the E-probes and horseshoe probes are exceptional for graphite fibers. The eddy current supervisory system and expert system was partially developed on a MacIvory system. Continued utilization of finite element models for predetermining eddy current signals was shown to be useful in this work, both for understanding how electromagnetic fields interact with graphite fibers, and also for use in determining how to develop the knowledge base. Sufficient data was taken to indicate that the E-probe and the horseshoe probe can be useful eddy current transducers for inspecting graphite fiber components. The lacking component at this time is a large enough probe to have sensitivity in both the far and near field of a thick graphite epoxy component. L.R.R.

N93-13036# Westinghouse Savannah River Co., Aiken, SC.
STATISTICAL PROCESS MANAGEMENT: AN ESSENTIAL ELEMENT OF QUALITY IMPROVEMENT
M. R. Buckner 1992 8 p Presented at the 1992 Westinghouse

Electronic Systems Group Statistics Symposium, Baltimore, MD, 7 Aug. 1992
(Contract DE-AC09-89SR-18035)
(DE92-019934; WSRC-MS-92-249; CONF-9208123-1) Avail: CASI HC A02/MF A01

Successful quality improvement requires a balanced program involving the three elements that control quality: organization, people and technology. The focus of the SPC/SPM User's Group is to advance the technology component of Total Quality by networking within the Group and by providing an outreach within Westinghouse to foster the appropriate use of statistic techniques to achieve Total Quality. SPM encompasses the disciplines by which a process is measured against its intrinsic design capability, in the face of measurement noise and other obscuring variability. SPM tools facilitate decisions about the process that generated the data. SPM deals typically with manufacturing processes, but with some flexibility of definition and technique it accommodates many administrative processes as well. The techniques of SPM are those of Statistical Process Control, Statistical Quality Control, Measurement Control, and Experimental Design. In addition, techniques such as job and task analysis, and concurrent engineering are important elements of systematic planning and analysis that are needed early in the design process to ensure success. The SPC/SPM User's Group is endeavoring to achieve its objectives by sharing successes that have occurred within the member's own Westinghouse department as well as within other US and foreign industry. In addition, failures are reviewed to establish lessons learned in order to improve future applications. In broader terms, the Group is interested in making SPM the accepted way of doing business within Westinghouse. DOE

N93-13071# Ames Lab., IA.
REVIEW OF PROGRESS IN QUANTITATIVE NDE Abstracts Only
1992 255 p Presented at the Review of Progress in Quantitative Non Destructive Evaluation (NDE), La Jolla, CA, 19-24 Jul. 1992
(Contract W-7405-eng-82)
(DE92-018814; IS-5081; CONF-920799-Absts) Avail: CASI HC A12/MF A03

Abstracts of 386 papers and plenary presentations are included. The plenary sessions are related to the national technology initiative. The other sessions covered the following NDE topics: corrosion, electromagnetic arrays, elastic wave scattering and backscattering/noise, civil structures, material properties, holography, shearography, UT wave propagation, eddy currents, coatings, signal processing, radiography, computed tomography, EM imaging, adhesive bonds, NMR, laser ultrasonics, composites, thermal techniques, magnetic measurements, nonlinear acoustics, interface modeling and characterization, UT transducers, new techniques, joined materials, probes and systems, fatigue cracks and fracture, imaging and sizing, NDE in engineering and process control, acoustics of cracks, and sensors. An author index is included. DOE

N93-13435*# Washington Univ., Saint Louis, MO. Lab. for Ultrasonics.
PHYSICAL INTERPRETATION AND DEVELOPMENT OF ULTRASONIC NONDESTRUCTIVE EVALUATION TECHNIQUES APPLIED TO THE QUANTITATIVE CHARACTERIZATION OF TEXTILE COMPOSITE MATERIALS Semiannual Progress Report, 15 Mar. - 14 Sep. 1992
James G. Miller 1992 28 p
(Grant NsG-1601)
(NASA-CR-190962; NAS 1.26:190962) Avail: CASI HC A03/MF A01

The development and implementation of advanced ultrasonic nondestructive evaluation methods applied to the characterization of composite materials requires a better understanding of the physics underlying the interaction of ultrasound with the material. The purpose of this investigation is to identify and characterize the features of complex, three dimensional materials that limit the ability of ultrasound to detect flaws in this broad class of emerging materials. In order to explore the interaction of ultrasound with such complex media, we investigate the characteristics of ultrasonic fields which have propagated through samples with complex geometries and/or internal architecture. We focus on the physics that underlies the detection of flaws in such materials. Author

N93-13710 Florida State Univ., Gainesville.
IDENTIFIABILITY IN THE AUTOPSY MODEL OF RELIABILITY THEORY Ph.D. Thesis
Robin Michael Antoine 1992 74 p
Avail: Univ. Microfilms Order No. DA9222356

Let S be a coherent system of m components acting independently. Two statistical modes are considered. In the autopsy model S is observed until it fails. The set of failed components and the failure time of the system are noted. The failure times of the dead components are not known. In the second model, which was considered by Doss, Freitag and Proschan (Ann. Statist., 1989), the failure times of the dead components are also known. In the autopsy model, it is not always possible to estimate or identify the component lifelengths from the observed data. A sufficient condition for the identifiability of the component distributions is given for the case in which the distributions are assumed to be analytic. Necessary and sufficient conditions are given for the case in which the distributions are assumed to belong to certain parametric families. The model of Doss, Freitag and Proschan is considered in two special cases. In the first of these the component distributions are known to be identical. In the second, the distributions are known to be exponential. Estimators of the component and system life lengths are given for each of these cases, and the asymptotic relative efficiency of each with respect to the corresponding estimator of Doss, Freitag and Proschan is calculated. Dissert. Abstr.

N93-13876# Naval Postgraduate School, Monterey, CA.
AN EXAMINATION OF THE TOTAL QUALITY MANAGEMENT (TQM) CONCEPT GIVEN CURRENT FEDERAL/DOD COMPETITION INITIATIVES M.S. Thesis
Michael E. Stabile Jun. 1992 138 p
(AD-A255556) Avail: CASI HC A07/MF A02

Quality is vital to our defense and quality improvement is key to increasing productivity. The Department of Defense (DoD) Total Quality Management (TQM) effort has been given top priority by the Secretary of Defense. Many questions exist concerning the problems encountered when implementing TQM throughout DoD. This thesis looks at the compatibility of the TQM philosophy with current Federal Acquisition Regulation competition requirements. The writer concludes that the TQM philosophy implementation is compatible with existing competition policy. GRA

N93-13906 Missouri Univ., Columbia.
BAYESIAN ESTIMATION OF SYSTEM RELIABILITY UNDER ASYMMETRIC LOSS Ph.D. Thesis
Ronald David Thompson 1991 102 p
Avail: Univ. Microfilms Order No. DA9220847

This research is concerned with estimating the reliability of a k-out-of-p system when the lifetimes of its p components are iid, when subjective beliefs about the behavior of the system's individual components are available, and when losses corresponding to overestimation and underestimation errors can be approximated by a suitable family of asymmetric loss functions. Point estimates for such systems are discussed in the context of Bayes estimation with respect to loss functions. A set of properties is proposed as being minimal properties that all loss functions appropriate to reliability estimation might satisfy. Several families of asymmetric loss functions that satisfy these minimal properties are discussed, and their corresponding posterior Bayes estimators are derived. One of these families, squarex loss functions, is a generalization of linex loss functions. The concept of loss robustness is discussed in the context of parametric families of asymmetric loss functions. As an application, the reliability of O-rings critical to the 1986 catastrophic failure of the Space Shuttle Challenger is estimated. Point estimation of negative exponential stress-strength k-out-of-p systems with respect to reference priors is discussed in this context of asymmetric loss functions. Dissert. Abstr.

39 STRUCTURAL MECHANICS

Includes structural element design and weight analysis; fatigue; and thermal stress.

For applications see *05 Aircraft Design, Testing and Performance* and *18 Spacecraft Design, Testing and Performance.*

N93-12580# Army Armament Research, Development and Engineering Center, Watervliet, NY.
NOTCH DIMENSIONS FOR THREE-POINT BEND FRACTURE

SPECIMENS BASED ON COMPLIANCE ANALYSES Final Report
Francis I. Baratta and John H. Underwood Jun. 1992 24 p
(AD-A254641; ARCCB-TR-92029) Avail: CASI HC A03/MF A01

Load one was calculated for various three-point bend specimens containing finite width notches and cutouts. The load was calculated using methods of engineering strength of materials and elastic superposition. Comparing compliance results for notched specimens with results for the ideal zero thickness crack promoted the use of two basic notch configurations for fracture testing. A relatively wide notch which could be produced by conventional manufacturing methods resulted in load-line compliance values 10 percent or more above those of the ideal crack case. A narrow notch which could be produced by electric-discharge resulted in compliance values much closer to those of the ideal crack case. GRA

N93-12606# Wright Lab., Wright-Patterson AFB, OH.
LARGE-AMPLITUDE PLATE VIBRATION IN AN ELEVATED THERMAL ENVIRONMENT Final Report, May - Dec. 1991
Jon Lee Jun. 1992 98 p
(AD-A254411; WL-TR-92-3049) Avail: CASI HC A05/MF A02

At elevated temperatures the dynamics of a vibrating plate (or shell) must include the three thermal effects: (1) the global expansion that is due to uniform plate temperature; (2) the local expansion by temperature variation over the plate; and (3) the thermal moment induced by temperature gradient across the plate thickness. Using the single-mode model of Galerkin representation, we have shown that (1) and (2) give rise to the combined stiffness responsible for thermal buckling, whereas (3) contributes to the combined forcing of thermal and mechanical excitations. Anticipating the high-temperature sonic fatigue test facility being fabricated at the structural dynamics Branch (WL/FIBG) in support of NASP program, the present study attempts to estimate the mean square displacement and root-mean-square stress and strain components by using the equivalent linearization technique of stochastic dynamics. GRA

N93-12627 Michigan State Univ., East Lansing.
A STUDY OF THE INTERLAMINAR STRESS CONTINUITY THEORIES FOR COMPOSITE LAMINATES Ph.D. Thesis
Chun-Ying Lee 1991 143 p
Avail: Univ. Microfilms Order No. DA9134145

In this study, two stress continuity theories are presented. The first one, named interlaminar stress continuity theory (ISCT), accounts for the variation of transverse displacement through the laminate thickness. The continuity of interlaminar shear stresses and normal stress across the laminate interfaces and traction conditions on laminate surfaces are satisfied exactly. The second, interlaminar shear stress continuity (ISSCT), simplifies ISCT by assuming constant transverse displacement through the thickness. Thus, only the continuity of interlaminar shear stresses and shear traction conditions on laminate surfaces are enforced. The merit of these stress continuity theories is the direct calculation of interlaminar stresses from constitutive equations instead of equilibrium equations. The numerical examples for composite laminates with aspect ratio higher than five in cylindrical bending and bidirectional bending using both theories show excellent accuracy compared with elasticity solutions. ISCT provides significant improvement over ISSCT for composite analysis only when the aspect ratio is lower than five. The comparison among other displacement-based laminate theories and present theories is also performed. The further applications of ISSCT in composite analysis, e.g., vibration, buckling, nonlinear bending, nonlinear vibration, and free-edge stresses are studied. The associated numerical examples show the feasibility and potential of using this new theory in the study of composite laminates.
Dissert. Abstr.

N93-12628 Wisconsin Univ., Madison.
SMALL-STRAIN AND FINITE-STRAIN FINITE ELEMENT ANALYSES OF PLANE-STRAIN TENSILE ELASTIC-PLASTIC CRACK GROWTH Ph.D. Thesis
Meng R. Liu 1991 154 p
Avail: Univ. Microfilms Order No. DA9209325

The first part of this thesis presents a small-strain/finite element study of plane strain quasistatic crack growth in fully incompressible elastic-ideally plastic material. To facilitate precise comparisons with previous analytical results, a fully incompressible, nonhardening material model is employed. A reduced/selected integration procedure is successfully used to enforce the elastic and plastic incompressibility of the material. For crack growth under bending dominant conditions, an experimentally-measured prescribed external load versus crack length history for a compact tension specimen is employed. A constant crack tip opening angle crack growth criterion is employed to investigate crack growth under tension dominant loadings in the same geometry. A small-scale yielding crack growth simulation is conducted employing a very refined mesh. Several stationary crack solutions are produced to explore the effect of different far-field loading combinations. Correlation of the finite element results with Drugan and Chen's (1989) 'm-family' of asymptotic analytical solutions is made in an effort to identify their indeterminate parameters m and R as a function of crack growth history. Parameter m has an approximate constant value of 1.23 for the entire crack growth process under bending-dominant loading. Estimation from the small-scale yielding results gives R approximately = 0.28(EJ/sigma sub 0 squared). Another set of analyses deals with plane-strain quasistatic crack growth in the same material under small-scale yielding conditions admitting finite strain and large geometry changes. A kinematic formulation originating from a concise rate equilibrium statement and constitutive laws using appropriate frame indifferent stress and strain measures are employed. Excellent agreement in near-tip slip lines is shown between Rice and Johnson's (1970) and our stationary crack solution. For the growing crack case, the stress and plastic strain distributions are subject to a 'softening effect' by the finite-strain analysis. Dissert. Abstr.

N93-12631 Kentucky Univ., Lexington.
EXPERIMENTAL VALIDATION OF FINITE ELEMENT AND BOUNDARY ELEMENT METHODS FOR PREDICTING STRUCTURAL VIBRATION AND RADIATED NOISE Ph.D. Thesis
Xuefeng Wu 1992 133 p
Avail: Univ. Microfilms Order No. DA9222861

The research presented in this dissertation is reported in three parts. In the first part, acoustical analyses were performed on modes of vibration of the housing of a transmission of a gear test rig developed by NASA. The modes of vibration of the transmission housing were measured using experimental modal analysis. The boundary element method (BEM) was used to calculate the sound pressure and sound intensity on the surface of the housing, and the radiation efficiency of each mode. The radiation efficiency of the transmission housing modes was then compared to theoretical results for finite, baffled plate. In the second part, analytical and experimental validation of methods to predict structural vibration and radiated noise are presented. A rectangular box excited by a mechanical shaker was used as a vibrating structure. Combined finite element method (FEM) and boundary element method (BEM) models of the apparatus were used to predict the noise level expected to be radiated from the box. The FEM was used to predict the vibration, while the BEM was used to predict the sound intensity and total radiated sound power using surface vibration as the input data. Vibration predicted by the FEM model was validated by experimental modal analysis, noise predicted by the BEM was validated by measurements of sound intensity. Three types of results are presented for the total radiated sound power: (1) sound power predicted by the BEM model using vibration data measured on the surface of the box; (2) sound power predicted by the FEM/BEM model; and (3) sound power measured by an acoustic intensity scan. In the third part, the structure used in part two was modified. A rib was attached to the top plate of the structure. The FEM and BEM were then used to predict structural vibration and radiated noise respectively. The predicted vibration and radiated noise were then validated through experimentation. Dissert. Abstr.

N93-12632 Virginia Polytechnic Inst. and State Univ., Blacksburg.
SCALE EFFECTS IN BUCKLING, POSTBUCKLING AND CRIPPLING OF GRAPHITE-EPOXY Z-SECTION STIFFENERS Ph.D. Thesis
Todd Michael Wieland 1991 209 p
Avail: Univ. Microfilms Order No. DA9214616

Scale model testing improves the cost effectiveness of composite structures by reducing reliance on full size component testing. Validation of the scalability of responses was performed using graphite-epoxy laminated composite Z-section stiffeners under compressive loading. The prebuckling, local buckling, postbuckling and crippling responses were studied. A mechanistic approach to scaling was used, in which scalability was evaluated relative to governing mechanics models. This permitted determination of the scalability and the parametric sensitivity of the responses. A linked-plate analytical model was developed for initial local buckling. The buckling and

postbuckling responses were also predicted using finite elements. An experimental program involving 52 specimens of 17 basic geometrical configurations and 3 stacking sequences was completed. The responses were largely determined by the flange-to-web width ratio and both the absolute and relative values of the bending stiffnesses. Buckling loads increased with decreasing flange width, and increasing flange-to-web corner radii and laminate thickness. The postbuckling load range was the greatest for wider flanged specimens. Failure stresses were greatest among narrower specimens. The crippling mechanisms included flange free edge delamination at both nodal and anti-nodal positions, material crushing in the flange-to-web corner at nodal positions, and ply splitting in the flange-to-web corner at anti-nodal locations. A nondimensional load parameter obtained from the analytical model normalized the buckling and postbuckling loads for all the geometric and material variables. No scale effects were observed in the buckling response. The quality of the postbuckling load predictions degraded with the extent of the postbuckling load range. Limitations in the finite element modelling of the structural and material nonlinearities, and other effects such as damage development in the specimens are believed responsible. Local material strain development was related to the structural deformation characteristics. Individual strain values did not indicate which of several competing failure modes would determine the actual crippling response. Conventional maximum strain failure theories discussed in the literature were shown to be incapable of providing a quantitative prediction of crippling loads. Dissert. Abstr.

N93-12643# Army Armament Research, Development and Engineering Center, Watervliet, NY. Benet Lab.

IMPROVED WIDE RANGE EXPRESSIONS FOR DISPLACEMENTS AND INVERSE DISPLACEMENTS FOR STANDARD FRACTURE TOUGHNESS SPECIMENS Final Report

Joseph A. Kapp Jun. 1992 25 p

(AD-A254561; ARCCB-TR-92027) Avail: CASI HC A03/MF A01

Wide range expressions (interpolating polynomials) for displacements for standard ASTM fracture testing specimens have been developed. The strategy for fitting was to fit displacements as a function of crack length for all of the specimens using a similar form of nondimensional displacement. Different forms appear in different ASTM Standards for the same or similar specimens. The criterion used to establish the degree of polynomial fit and number of significant figures for the coefficients of the polynomial was for the polynomial to agree with the best available numerical displacement solutions within one percent or better. Once the polynomials for displacement as a function of crack length were developed, inverted forms of the specific interpolating polynomials were obtained to determine relative crack length (a/W) as a function of displacement. Since the inverted polynomial will be used in tandem with the interpolating polynomial, the inverted polynomial was fit to the interpolating polynomial and not to the numerical solution for displacement. Three forms of nondimensional displacements were used to invert the interpolating polynomials. The criterion used to establish the degree of polynomial and the number of significant figures of the coefficients of the polynomial was for the predicted relative crack length to agree with the actual relative crack depth to within 0.0005 W. A sensitivity analysis was performed to suggest which form of interpolating polynomial should be used for standards. GRA

N93-12652# Morgan State Univ., Baltimore, MD. Dept. of Civil Engineering.

ANALYSIS OF A STRUCTURE-EQUIPMENT SYSTEM SUBJECTED TO IMPACT LOADING Final Report, May - Sep. 1991

Bunu Alibe Sep. 1992 44 p Prepared in cooperation with Battelle Memorial Inst., Columbus, OH

(Contract DAAL03-86-D-0001)

(AD-A255097; BRL-CR-694) Avail: CASI HC A03/MF A01

The response of a coupled structure-equipment system subjected to a projectile impact is analyzed. The system consists of a simply supported plate coupled to damped oscillators. The analysis follows classical modal methods in which the mode shapes are expressed in terms of the Green's function of the system. The Green's function for the plate with homogeneous boundary conditions is obtained by Laplace transformation method arid using a symbolic mathematics program such as MACSYMA. Using an example problem of a single attached oscillator, it is shown that all parameters of the secondary system contribute to the interaction between the plate and the oscillator. GRA

N93-12735*# National Aeronautics and Space Administration. Lewis Research Center, Cleveland, OH.

PROBABILISTIC EVALUATION OF FUSELAGE-TYPE COMPOSITE STRUCTURES

Michael C. Shiao (Sverdrup Technology, Inc., Brook Park, OH.) and Christos C. Chamis Nov. 1991 20 p Presented at the Ninth DOD/NASA/FAA Conference on Fibrous Composites, Reno, NV, 3-7 Nov. 1991

(RTOP 553-13-00)

(NASA-TM-105881; E-7348; NAS 1.15:105881) Avail: CASI HC A03/MF A01

A methodology is developed to computationally simulate the uncertain behavior of composite structures. Uncertain behavior is the consequence of the random variation (scatter) of the primitive (independent random) variables at the constituent, ply, laminate and structural levels. This methodology is implemented in the IPACS (Integrated Probabilistic Assessment of Composite Structures) computer code. A fuselage-type composite structure is analyzed to demonstrate the code's capability. The probability distribution functions of structural responses are computed. Sensitivity of a given structural response to each primitive variable is also determined from the analyses. Author

N93-12738*# National Aeronautics and Space Administration. Lewis Research Center, Cleveland, OH.

NUMERICAL CALIBRATION OF THE STABLE POISSON LOADED SPECIMEN

Louis J. Ghosn (Sverdrup Technology, Inc., Brook Park, OH.), Anthony M. Calomino, and Dave N. Brewer (Army Aviation Systems Command, Cleveland, OH.) Oct. 1992 15 p

(RTOP 505-63-5B)

(NASA-TM-105609; E-7335; NAS 1.15:105609) Avail: CASI HC A03/MF A01

An analytical calibration of the Stable Poisson Loaded (SPL) specimen is presented. The specimen configuration is similar to the ASTM E-561 compact-tension specimen with displacement controlled wedge loading used for R-Curve determination. The crack mouth opening displacements (CMOD's) are produced by the diametral expansion of an axially compressed cylindrical pin located in the wake of a machined notch. Due to the unusual loading configuration, a three-dimensional finite element analysis was performed with gap elements simulating the contact between the pin and specimen. In this report, stress intensity factors, CMOD's, and crack displacement profiles are reported for different crack lengths and different contacting conditions. It was concluded that the computed stress intensity factor decreases sharply with increasing crack length, thus making the SPL specimen configuration attractive for fracture testing of brittle, high modulus materials. Author

N93-12739*# National Aeronautics and Space Administration. Lewis Research Center, Cleveland, OH.

ON BILINEARITY OF MANSON-COFFIN LOW-CYCLE-FATIGUE RELATIONSHIP

V. M. Radhakrishnan (Indian Inst. of Tech., Madras.) Oct. 1992 14 p

(RTOP 553-13-00)

(NASA-TM-105840; E-7283; NAS 1.15:105840) Avail: CASI HC A03/MF A01

Some alloy systems, such as aluminum-lithium alloys and dual-phase steels, have been found to show a bilinear Manson-Coffin low-cycle-fatigue relationship. This paper shows that such bilinear behavior is related to the cyclic stress-strain curve. A bilinear cyclic stress-strain curve is a likely indication of a bilinear Manson-Coffin relationship. It is shown that materials other than aluminum-lithium alloys and dual-phase steels also may exhibit bilinear Manson-Coffin behavior. Implications for design are discussed. Author

N93-12843# Drexel Univ., Philadelphia, PA. Geosynthetic Research Inst.

STRESS CRACK TESTING OF POLYETHYLENE GEOMEMBRANES

Y. H. Halse, R. M. Koerner, and A. E. Lord, Jr. 1992 15 p

(Contract EPA-R-815692)

(PB92-217132; EPA/600/A-92/178) Avail: CASI HC A03/MF A01

The sensitivity of high density polyethylene (HDPE) geomembranes to stress cracking is evaluated under accelerated conditions at a constant stress. The test specimens are in accordance with ASTM D-1822, and are of the dumbbell shape with a constant length in the central section. The

accelerated testing conditions consist of a 10 percent Igepal wetting solution in tap water, at a constant temperature of 50 C. The applied stresses are from 30 to 50 percent of the yield stress. It was found that most commercially available HDPE sheet material performs quite well in this type of test. Only one specimen in 80 showed any evidence of cracking and this may have been caused by other reasons. Testing of field fabricated seams, however, resulted in relatively large numbers of cracked specimens. Many of these test specimens showed signs of overgrinding and/or overheating. The results indicate that great care and excellent workmanship are required in the field fabrication of HDPE seams. GRA

N93-12863# Illinois Univ., Chicago. Dept. of Civil Engineering Mechanics and Metallurgy.

THEORETICAL AND EXPERIMENTAL STUDIES ON THE FOUNDATION OF MESOMECHANICS Final Report, Nov. 1989 - Apr. 1992

A. Chudnovsky and S. Wu 28 Jun. 1992 130 p

(Grant AF-AFOSR-0105-89)

(AD-A254385) Avail: CASI HC A07/MF A02

The report summarizes a closely coupled experimental and theoretical investigation of various stages of Fracture Process: (1) accumulation of 'damage' on submicroscopical and microscopical scales leading to crack initiation; (2) slow (subcritical) crack growth and an evolution of the damage zone; (3) transition to dynamic crack growth and the catastrophic failure. The experimental part of the program is focused on the observation and quantitative characterization of damage preceding and accompanying crack initiation and growth. A special experimental setup for studying the fracture process under variable stress field is reported in Chapter 2. A leading role of crack-damage interaction in fracture process is well documented. A new formalism for solution of crack-microcrack array interaction problem and its successful implementation in the evaluation of crack layer driving forces is presented in Chapter 3. A new model of the process zone, which generalizes the well-known Dagdale-Barenblatt model is presented in Chapter 4. A new measure for material toughness and the prediction of R-curve behavior illustrate the practical application of our model. Experimental examinations of our model under various test conditions are reported in Chapters 4, 5 and 6. The development of the constitutive equations for Crack Layer evolution and their experimental examinations under stress relaxation, fatigue and creep conditions are reported in Chapters 5 and 6. An accelerated test procedure and the formulation of crack layer instability criteria as a substitution for the conventional fracture toughness parameters are also discussed in Chapter 6. GRA

N93-12911*# Utah Univ., Salt Lake City. Dept. of Materials Science and Engineering.

MICROCRACKING, MICROCRACK-INDUCED DELAMINATION, AND LONGITUDINAL SPLITTING OF ADVANCED COMPOSITE STRUCTURES Final Report

John A. Nairn Washington Nov. 1992 153 p Sponsored by NASA. Langley Research Center

(Contract NAS1-18833; RTOP 505-63-50)

(NASA-CR-4472; NAS 1.26:4472) Avail: CASI HC A08/MF A02

A combined analytical and experimental study was conducted to analyze microcracking, microcrack-induced delamination, and longitudinal splitting in polymer matrix composites. Strain energy release rates, calculated by a variational analysis, were used in a failure criterion to predict microcracking. Predictions and test results were compared for static, fatigue, and cyclic thermal loading. The longitudinal splitting analysis accounted for the effects of fiber bridging. Test data are analyzed and compared for longitudinal splitting and delamination under mixed-mode loading. This study emphasizes the importance of using fracture mechanics analyses to understand the complex failure processes that govern composite strength and life.

Author

N93-12981# National Inst. of Standards and Technology, Gaithersburg, MD. Building and Fire Research Lab.

NONDESTRUCTIVE EVALUATION OF THE IN-PLACE COMPRESSIVE STRENGTH OF CONCRETE BASED UPON LIMITED DESTRUCTIVE TESTING

Kenneth A. Snyder, James R. Clifton, and Nicholas J. Carino Jul. 1992 67 p Sponsored by Nuclear Regulatory Commission Prepared for Oak Ridge National Lab., TN

(PB92-222751; NISTIR-4874) Avail: CASI HC A04/MF A01

Regression analysis was performed on published data from nondestructive and cylinder compressive strength testing of concrete. The nondestructive tests investigated were: rebound hammer, probe penetration, pulse velocity, pullout, and break-off. Regression analysis accounted for the error in both the nondestructive and the compressive strength data and their constant coefficient of variation. Data for each nondestructive test were grouped by coarse aggregate type and aggregate mass fraction. The results of the regression analysis are given, along with the parameters required to estimate compressive strength from subsequent nondestructive tests. A common format for the analysis and reporting of nondestructive-destructive regression experiments is suggested. GRA

N93-12989# Polish Academy of Sciences, Warsaw. Inst. Podstawowych Problemow Techniki.

DIAGNOSTIC OF MATERIAL DEFECTS FOUND IN PIPELINES MADE OF 13 HMF STEEL ON THE BASIS OF ACOUSTIC EMISSION [DIAGNOSTYKA DEFEKTOW MATERIALOWYCH WYSTEPUJACYCH W RUROCIAGACII WYKONANYCH ZE STALI 13 HMF NA PODSTAWIE EMISJI AKUSTYCZNEJ]

Jerzy Skubis (Engineering Coll., Opole, Poland), Grzegorz Jeziorski (Elektrownia, Opole S.A., Poland), and Jerzy Ranachowski 1992 24 p In POLISH

Avail: CASI HC A03/MF A01

Preparatory work performed in developing a diagnostic method for testing welded joints in pressure pipelines made of 13 HMF steel by means of acoustic emission (AE) measurements is described. Within the framework of these studies the mechanical strength characteristic of the 13 HMF steel was determined in a tension test with simultaneous AE measurements. Later AE measurements were conducted on real pipeline sections with joints, during heat treatment. Acoustic emission was investigated according to the requirements of the ASME standard. Preliminary analysis of the results indicated that the AE method may be used for diagnoses of welded joints in pressure pipelines. Technical specifications of a three-channel AE analyzer manufactured by IPPT PAN (Institute of Basic Technological Problems, Polish Academy of Sciences) and used for test are sufficient for such measurements. A detailed physical interpretation of the phenomena occurring during the tests is presented. Transl. by L.S.H.

N93-13003# Superconducting Super Collider Lab., Dallas, TX.

MAGNETIC FIELD PERTURBATION CAUSED BY BENDING VIBRATIONS OF A QUADRUPOLE

V. Lebedev and G. Stupakov Jul. 1992 9 p

(Contract DE-AC35-89ER-40486)

(DE92-040644; SSCL-580) Avail: CASI HC A02/MF A01

Bending vibration of a magnet body supported at two symmetric points is studied. The magnet is modeled by a slender elastic beam. The resonant frequencies are found and the averaged displacement of the magnet is calculated as a function of the frequency. DOE

N93-13009 Akron Univ., OH.

LINEAR AND NONLINEAR FINITE ELEMENT ANALYSIS OF LAMINATED COMPOSITE STRUCTURES AT HIGH TEMPERATURES Ph.D. Thesis

Thomas Edmund Wilt 1992 209 p

Avail: Univ. Microfilms Order No. DA9217248

The use of composite materials in aerospace applications, particularly engine components, is becoming more prevalent due to the materials high strength, yet low weight. In addition to thermomechanical deformation response, life prediction and damage modeling analysis is also required to assess the component's service life. These complex and computationally intensive analyses require the development of simple, efficient and robust finite element analysis capabilities. A simple robust finite element which can effectively model the multi-layer composite material is developed. This will include thermal gradient capabilities necessary for a complete thermomechanical analysis. In order to integrate the numerically stiff rate dependent viscoplastic equations, efficient, stable numerical algorithms are developed. In addition, consistent viscoplastic/plastic tangent matrices will also be formulated. The finite element is formulated based upon a generalized mixed variational principle with independently assumed displacements and layer number independent strains. A unique scheme utilizing nodal

temperatures is used to model a linear thermal gradient through the thickness of the composite. The numerical integration algorithms are formulated in the context of a fully implicit backward Euler scheme. The consistent tangent matrices arise directly from the formulation. The multi-layer composite finite element demonstrates good performance in terms of static displacement and stress predictions, and dynamic response. Also, the element appears to be relatively insensitive to mesh distortions. The robustness and efficiency of the fully implicit integration algorithms is effectively demonstrated in the numerical results. That is, large time steps and a significant reduction in global iterations, as a direct result of utilizing the consistent tangent matrices, is shown. Dissert. Abstr.

N93-13016 Cranfield Inst. of Tech., Bedford (England).
THE APPLICATION OF THE FINITE ELEMENT METHOD AND THE BOUNDARY ELEMENT METHOD TO FATIGUE AND FRACTURE, VOLUMES 1 AND 2 Ph.D. Thesis
Thomas Hinks 1991 520 p
Avail: Univ. Microfilms Order No. BRDX96677

This work introduces for the first time the use of the boundary element method for the analysis of cyclic plasticity, high cycle fatigue and low cycle fatigue. Incorporation of several yield criteria and hardening rules into elasto-plastic analysis was carried out such as: Von Mises and Tresca yield criteria, and isotropic, kinematic and mixed hardening rules. An efficient numerical algorithm for the evaluation of the J-integral parameter, based upon boundary and domain discretization was developed. A number of criteria for the estimation of the effect of mean stress on fatigue life, and for the evaluation of equivalent stress measures for multi-axial fatigue, were employed in fatigue analysis. A sophisticated finite element and boundary element programming package called FEBEFAT used for the evaluation of linear elastic fracture mechanics, elasto-plastic fracture mechanics, high cycle fatigue and low cycle fatigue analyses has been developed and tested on VAX mainframe computers, SUN and DIGITAL work stations and on an IBM compatible personal computer. A number of case studies with known solutions have been analyzed and employed for the validation of the developed theory and programming package. It was found that the package provides an efficient and reliable tool for fatigue and fracture analysis. Dissert. Abstr.

N93-13019*# Virginia Polytechnic Inst. and State Univ., Blacksburg. Dept. of Aerospace and Ocean Engineering.
COMPRESSION STRENGTH OF COMPOSITE PRIMARY STRUCTURAL COMPONENTS Semiannual Status Report, 1 May - 31 Oct. 1992
Eric R. Johnson Oct. 1992 23 p
(Grant NAG1-537)
(NASA-CR-190949; NAS 1.26:190949) Avail: CASI HC A03/MF A01

A status report of work performed during the period May 1, 1992 to October 31, 1992 is presented. Research was conducted in three areas: delamination initiation in postbuckled dropped-ply laminates; stiffener crippling initiated by delamination; and pressure pillowing of an orthogonally stiffened cylindrical shell. The geometrically nonlinear response and delamination initiation of compression-loaded dropped-ply laminates is analyzed. A computational model of the stiffener specimens that includes the capability to predict the interlaminar response at the flange free edge in postbuckling is developed. The distribution of the interacting loads between the stiffeners and the shell wall, particularly at the load transfer at the stiffener crossing point, is determined. L.R.R.

N93-13029*# Northwestern Univ., Evanston, IL. Dept. of Mechanical Engineering.
PROBABILISTIC FINITE ELEMENTS FOR FATIGUE AND FRACTURE ANALYSIS Final Report
Ted Belytschko and Wing Kam Liu [1992] 62 p
(Grant NAG3-822)
(NASA-CR-191246; NAS 1.26:191246) Avail: CASI HC A04/MF A01

Attenuation is focused on the development of Probabilistic Finite Element Method (PFEM), which combines the finite element method with statistics and reliability methods, and its application to linear, nonlinear structural mechanics problems and fracture mechanics problems. The computational tool based on the Stochastic Boundary Element Method is also given for the reliability analysis of a curvilinear fatigue crack growth. The existing PFEM's have been applied to solve for two types of problems: (1) determination of the response uncertainty in terms of the means, variance and correlation coefficients; and (2) determination the probability of failure associated with prescribed limit states. Author

N93-13065 Texas Univ., Austin.
SYSTEM IDENTIFICATION AND MODEL UPDATING FOR SUBSTRUCTURES Ph.D. Thesis
Hsin-Hsen Huang 1992 151 p
Avail: Univ. Microfilms Order No. DA9225608

Two model updating methods are proposed in this investigation. The first one is based on the constrained minimization theory. The second one is based on the sensitivities of system mass and stiffness matrices. The first formulation of the constrained minimization algorithm starts with a squared weighted Euclidean norm of mass and stiffness matrices which are subject to orthogonality, dynamic equation and symmetry constraints. The element mass matrix is first adjusted. The element stiffness matrix is then updated. The structural connectivity is always preserved in the process of model updating. However, since the mass matrix and stiffness matrix are not updated simultaneously, the interaction effects of mass and stiffness matrices are not considered. The second formulation, a constrained minimization algorithm, starts with the same squared weighted Euclidean norms and constraints. Additional constraints, for example, the lower bound and upper bound of structural parameters to be adjusted, can be entered into the minimization equation. The minimization algorithm is then carried out on the structural parameter level. Dissert. Abstr.

N93-13072# Sandia National Labs., Albuquerque, NM.
BIFURCATIONS IN ELASTIC-DAMAGING MATERIALS
M. K. Neilsen and H. L. Schreyer (New Mexico Univ., Albuquerque.) 1992 15 p Presented at the Winter Annual Meeting of the American Society of Mechanical Engineers, Anaheim, CA, 8-13 Nov. 1992
(Contract DE-AC04-76DP-00789)
(DE92-018818; SAND-92-1571C; CONF-921110-13) Avail: CASI HC A03/MF A01

Continuum damage theories describe the progressive reduction in stiffness and strength of brittle materials resulting from the initiation and growth of microcracks and microvoids. When brittle materials are loaded into the nonlinear regime, they often exhibit localized zones of intense deformation and the eventual formation of macrocracks. Criteria for diffuse and discontinuous bifurcations have previously been developed and used to study the initiation of necking and localization in elastic-plastic materials. In this investigation, the same bifurcation criteria are applied to continuum damage theories. Since the bifurcation criteria depend on the fourth-order tangent modulus tensor, the first step in this investigation is the derivation of the tangent modulus tensor for a general continuum damage theory. An eigenanalysis of the symmetric part of the tangent modulus tensor is then shown to fully characterize the potential diffuse and discontinuous bifurcations associated with a given continuum damage theory. DOE

N93-13077# Allied-Signal Aerospace Co., Kansas City, MO.
DEVELOPMENT OF A 1000 g, 10 ms MECHANICAL SHOCK TEST CAPABILITY
L. F. Thorne Aug. 1992 19 p
(Contract DE-AC04-76DP-00613)
(DE92-019193; KCP-613-4679) Avail: CASI HC A03/MF A01

A test capability has been developed to subject manufactured products to a mechanical shock pulse of 1000 g (gravitational units), 10 milliseconds. A dual carriage impact device was used with a horizontal pneumatic actuator and an 80 foot track system to perform the shock pulse by impact test techniques. A spread sheet was assembled to predict various mechanical shock test parameters using thermoplastic as the shock spring. The dual carriage device was modified so that a thermoplastic column 4.375 inches in diameter and 97 inches long could be used to produce a haversine shaped shock pulse. This new test capability has been used to shock 80 pound test packages within the tolerances of the 1000 g, 10 ms requirement. DOE

N93-13097 Cranfield Inst. of Tech., Bedford (England).
BOUNDARY ELEMENT METHOD FOR AXISYMMETRIC THERMOELASTIC ANALYSIS Ph.D. Thesis
R. S. Gordon 1991 211 p
Avail: Univ. Microfilms Order No. BRDX96747

The axisymmetric structure is common in engineering. Cylindrical and spherical pressure vessels, pipes, turbine and compressor discs to name but a few. In most of these examples the operating conditions include working at high temperatures. In this work an attempt has been made to develop the steady and transient boundary element method for thermoelastic analysis of axisymmetric structures. As the objective of this project is to investigate the coupling effect using the finite element method. Further to develop boundary element programs to solve transient thermoelastic problems in axisymmetric structures and to investigate the validity and accuracy of the boundary element formulation. A finite element program for coupled thermoelastic analysis was developed and it was found that coupling effects were negligible in linear thermoelastic analysis. Boundary element theory and programs for steady state and uncoupled transient thermoelastic analysis of axisymmetric structures with conductive and radiative boundary conditions were developed. Case studies with known solutions, either analytically or by means of ABAQUS FEM package have been analysed and proved that the developed theory and software are accurate and reliable. Dissert. Abstr.

N93-13125*# National Aeronautics and Space Administration. Langley Research Center, Hampton, VA.

IDENTIFIABILITY OF LINEAR SYSTEMS IN PHYSICAL COORDINATES

Tzu-Jeng Su (National Academy of Sciences - National Research Council, Hampton, VA.) and Jer-Nan Juang Oct. 1992 16 p

(RTOP 469-01-11-02)

(NASA-TM-107695; NAS 1.15:107695) Avail: CASI HC A03/MF A01

Identifiability of linear, time-invariant systems in physical coordinates is discussed. It is shown that identification of the system matrix in physical coordinates can be accomplished by determining a transformation matrix that relates the physical locations of actuators and sensors to the test-data-derived input and output matrices. For systems with symmetric matrices, the solution of a constrained optimization problem is used to characterize all the possible solutions of the transformation matrix. Conditions for the existence of a unique transformation matrix are established easily from the explicit form of the solutions. For systems with limited inputs and outputs, the question about which part of the system can be uniquely identified is also answered. A simple mass-spring system is used to verify the conclusions of this study. Author

N93-13127 Lehigh Univ., Bethlehem, PA.

AXISYMMETRIC AND ANTIPLANE SHEAR CRACK PROBLEMS IN BONDED NONHOMOGENEOUS MATERIALS Ph.D. Thesis

Murat Ozturk 1992 242 p

Avail: Univ. Microfilms Order No. DA9226077

In this dissertation the basic axisymmetric and antiplane crack problems in a nonhomogeneous solid with continuously varying elastic properties are considered. The problem is encountered in studying the fracture mechanics of certain geophysical materials such as shale-sandstone interfaces, tailored materials with graded properties such as the nonhomogeneous cermets, and interfacial zones in a variety of bonded materials. In this study the effect of the material nonhomogeneity parameters on the stress intensity factors in 'functionally gradient materials' containing a crack parallel to the nominal interface is investigated. By using Hankel integral transform for the displacements in axisymmetric crack problems and Fourier integral transform for the displacement in the antiplane crack problems, the mixed boundary conditions are first reduced to a system of dual integral equations, and then, by a systematic approach, to a system of singular integral equations. Finally, by using certain approximate techniques, the resulting system is converted to a system of functional equations. In the numerical examples, such physically important quantities as stress intensity factors and the strain energy release rates are obtained and plotted. A detailed discussion of the results is given. Dissert. Abstr.

N93-13142 Cranfield Inst. of Tech., Bedford (England).

FINITE ELEMENT VERSUS BOUNDARY ELEMENT ANALYSIS OF TWO-DIMENSIONAL COUPLED THERMOELASTICITY Ph.D. Thesis

Sulaiman Salih Al-Rushudi 1991 245 p

Avail: Univ. Microfilms Order No. BRDX96704

In this work an attempt has been made to develop efficient boundary element theory and programs for the analysis of two-dimensional decoupled, and coupled, quasistatic thermoelasticity. Some finite element work is developed and employed for comparison between the finite- and boundary-element methods. Modified time-marching schemes have been developed and programmed and proved to be efficient for transient thermo-elastic analysis. A complete theory for two-dimensional boundary element analysis of coupled thermo-elasticity is derived and employed in the developed program. Non-linear boundary conditions of convection and radiation have been successfully dealt with. A number of case studies have been analyzed and the results were assessed against analytical solutions and solutions obtained by means of PAFEC and ABAQUS finite-element packages. It was clear that theory and programs developed in this work are correct and reliable. A modified time-integral marching scheme has proved to be very efficient compared to others. The boundary element method has proved to be an efficient and powerful tool for dealing with decoupled thermoelastic analysis, and within the elastic range of engineering materials thermal coupling effects are anyway negligible. Dissert. Abstr.

N93-13153*# National Aeronautics and Space Administration. Lewis Research Center, Cleveland, OH.

IN-PHASE AND OUT-OF-PHASE AXIAL-TORSIONAL FATIGUE BEHAVIOR OF HAYNES 188 AT 760 C

Sreeramesh Kalluri and Peter J. Bonacuse Oct. 1991 22 p Presented at the Symposium on Multiaxial Fatigue, San Diego, CA, 14-15 Oct. 1991; sponsored by the American Society for Testing and Materials

(DA Proj. 1L1-61102-AH-45; RTOP 553-13-00)

(NASA-TM-105765; E-7182; NAS 1.15:105765; AVSCOM-TR-91-C-046)

Avail: CASI HC A03/MF A01

Isothermal, in-phase and out-of-phase axial-torsional fatigue experiments have been conducted at 760 C on uniform gage section, thin-walled tubular specimens of a wrought cobalt-base superalloy, Haynes 188. Test-control and data acquisition were accomplished with a minicomputer. Fatigue lives of the in- and out-of-phase axial-torsional fatigue tests have been estimated with four different multiaxial fatigue life prediction models that were developed primarily for predicting axial-torsional fatigue lives at room temperature. The models investigated were: (1) the von Mises equivalent strain range; (2) the Modified Multiaxiality Factor Approach; (3) the Modified Smith-Watson-Topper Parameter; and (4) the critical shear plane method of Fatemi, Socie, and Kurath. In general, life predictions by the von Mises equivalent strain range model were within a factor of 2 for a majority of the tests and the predictions by the Modified Multiaxiality Factor Approach were within a factor of 2, while predictions of the Modified Smith-Watson-Topper Parameter and of the critical shear plane method of Fatemi, Socie, and Kurath were unconservative and conservative, respectively, by up to factors of 4. In some of the specimens tested under combined axial-torsional loading conditions, fatigue cracks initiated near extensometer indentations. Two design modifications have been proposed to the thin-walled tubular specimen to overcome this problem. Author

N93-13157*# National Aeronautics and Space Administration. Lewis Research Center, Cleveland, OH.

STRUCTURAL OPTIMIZATION OF THIN SHELLS USING FINITE ELEMENT METHOD

Pascal K. Gotsis Oct. 1992 26 p

(RTOP 510-01-0A)

(NASA-TM-105903; E-7139; NAS 1.15:105903) Avail: CASI HC A03/MF A01

The objective of the present work was the structural optimization of thin shell structures that are subjected to stress and displacement constraints. In order to accomplish this, the structural optimization computer program DESAP1 was modified and improved. In the static analysis part of the DESAP1 computer program the torsional spring elements, which are used to analyze thin, shallow shell structures, were eliminated by modifying the membrane stiffness matrix of the triangular elements in the local coordinate system and adding a fictitious rotational stiffness matrix. This simplified the DESAP1 program input, improved the accuracy of the analysis, and saved computation time. In the optimization part of the DESAP1 program the stress ratio formula, which redesigns the thickness of each finite element of the structure, was solved by an analytical method. This scheme replaced the iterative solution that was previously used in the DESAP1 program, thus increasing the accuracy and speed of the design. The modified program was used to design a thin, cylindrical shell structure with optimum weight, and the results are reported in this paper. Author

N93-13260*# National Aeronautics and Space Administration. Lewis Research Center, Cleveland, OH.

ANALYSIS OF LARGE QUASISTATIC DEFORMATIONS OF INELASTIC SOLIDS BY A NEW STRESS BASED FINITE ELEMENT METHOD Ph.D. Thesis Final Report

Kenneth W. Reed Sep. 1992 253 p

(Grant NAG3-38; RTOP 590-21-11)

(NASA-CR-189235; NAS 1.26:189235) Avail: CASI HC A12/MF A03

A new hybrid stress finite element algorithm suitable for analyses of large quasistatic deformation of inelastic solids is presented. Principal variables in the formulation are the nominal stress rate and spin. The finite element equations which result are discrete versions of the equations of compatibility and angular momentum balance. Consistent reformulation of the constitutive equation and accurate and stable time integration of the stress are discussed at length. Examples which bring out the feasibility and performance of the algorithm conclude the work. Author

N93-13290*# Michigan Univ., Ann Arbor. Dept. of Mechanical Engineering.

COMPUTATIONAL SIMULATION OF PROBABILISTIC LIFETIME STRENGTH FOR AEROSPACE MATERIALS SUBJECTED TO HIGH TEMPERATURE, MECHANICAL FATIGUE, CREEP AND THERMAL FATIGUE Final Report

Lola Boyce (Texas Univ., San Antonio.), Callie C. Bast (Texas Univ., San Antonio.), and Greg A. Trimble (Texas Univ., San Antonio.) Nov. 1992 33 p

(Grant NAG3-867; RTOP 590-21-11)

(NASA-CR-190794; E-7415; NAS 1.26:190794) Avail: CASI HC A03/MF A01

This report presents the results of a fourth year effort of a research program, conducted for NASA-LeRC by the University of Texas at San Antonio (UTSA). The research included on-going development of methodology that provides probabilistic lifetime strength of aerospace materials via computational simulation. A probabilistic material strength degradation model, in the form of a randomized multifactor interaction equation, is postulated for strength degradation of structural components of aerospace propulsion systems subject to a number of effects or primitive variables. These primitive variables may include high temperature, fatigue or creep. In most cases, strength is reduced as a result of the action of a variable. This multifactor interaction strength degradation equation has been randomized and is included in the computer program, PROMISS. Also included in the research is the development of methodology to calibrate the above-described constitutive equation using actual experimental materials data together with regression analysis of that data, thereby predicting values for the empirical material constants for each effect or primitive variable. This regression methodology is included in the computer program, PROMISC. Actual experimental materials data were obtained from industry and the open literature for materials typically for applications in aerospace propulsion system components. Material data for Inconel 718 has been analyzed using the developed methodology. Author

N93-13301# Sandia National Labs., Albuquerque, NM.

NUMERICAL SIMULATIONS OF STEEL PLATE PERFORATION

E. P. Chen 1992 11 p Presented at the Winter Annual Meeting of the American Society of Mechanical Engineers, Anaheim, CA, 8-13 Nov. 1992

(Contract DE-AC04-76DP-00789)

(DE92-017058; SAND-92-1543C; CONF-921110-8) Avail: CASI HC A03/MF A01

Numerical simulations of perforation in steel plates involve the treatment of material failure during the perforation process. One way to model physical material separation is to delete failed elements from the analysis based on an appropriate failure criterion. Different algorithms were used in different transient finite element codes to delete failed elements. This investigation compares the results of PRONTO 2D and LS-DYNA2D codes for a specific steel plate perforation problem. Influences of the deletion algorithms on material parameters are discussed. DOE

N93-13320# Oak Ridge National Lab., TN.

SHALLOW-CRACK TOUGHNESS RESULTS FOR REACTOR PRESSURE VESSEL STEEL

T. J. Theiss, D. K. M. Shum, and S. T. Rolfe (Kansas Univ., Lawrence.) 1992 11 p Presented at the International Conference on Shallow Crack Fracture Mechanics Tests and Applications, Cambridge, England, 26 Sep. 1992

(Contract DE-AC05-84OR-21400)

(DE92-017813; CONF-9209174-1) Avail: CASI HC A03/MF A01

The Heavy Section Steel Technology Program (HSST) is investigating the influence of flaw depth on the fracture toughness of reactor pressure vessel (RPV) steel. To complete this investigation, techniques were developed to determine the fracture toughness from shallow-crack specimens. A total of 38 deep and shallow-crack tests have been performed on beam specimens about 100 mm deep loaded in 3-point bending. Two crack depths (a is approximately equal to 50 and 9 mm) and three beam thicknesses (B is approximately equal to 50, 100, and 150 mm) have been tested. Techniques were developed to estimate the toughness in terms of both the J-integral and crack-tip opening displacement (CTOD). Analytical J-integral results were consistent with experimental J-integral results, confirming the validity of the J-estimation schemes used and the effect of flaw depth on fracture toughness. Test results indicate a significant increase in the fracture toughness associated with the shallow flaw specimens in the lower transition region compared to the deep-crack fracture toughness. There is, however, little or no difference in toughness on the lower shelf where linear-elastic conditions exist for specimens with either deep or shallow flaws. The increase in shallow-flaw toughness compared with deep-flaw results appears to be well characterized by a temperature shift of 35 C. DOE

N93-13420* National Aeronautics and Space Administration. Langley Research Center, Hampton, VA.

METHOD AND APPARATUS FOR MINIMIZING MULTIPLE DEGREE OF FREEDOM VIBRATION TRANSMISSION BETWEEN TWO REGIONS OF A STRUCTURE Patent

Richard J. Silcox, inventor (to NASA), Chris R. Fuller, inventor (to NASA), and Gary P. Gibbs, inventor (to NASA) 20 Oct. 1992 13 p Filed 4 Mar. 1991 Supersedes N92-10202 (30 - 1, p 39)

(NASA-Case-LAR-14508-1-CU; US-Patent-5,156,370;
US-Patent-Appl-SN-664194; US-Patent-Class-248-550;
US-Patent-Class-73-579; US-Patent-Class-73-668; US-Patent-Class-318-649;
US-Patent-Class-318-648; Int-Patent-Class-G05D-15/01;
Int-Patent-Class-G05D-19/01) Avail: US Patent and Trademark Office

Arrays of actuators are affixed to structural elements to impede the transmission of vibrational energy. A single pair is used to provide control of bending and extensional waves and two pairs are used to control torsional motion. The arrays are applied to a wide variety of structural elements such as a beam structure that is part of a larger framework that may or may not support a rigid or non-rigid skin. Electrical excitation is applied to the actuators that generate forces on the structure. These electrical inputs may be adjusted in their amplitude and phase by a controller in communication with appropriate vibrational wave sensors to impede the flow of vibrational power in all of the above mentioned wave forms beyond the actuator location. Additional sensor elements can be used to monitor the performance and adjust the electrical inputs to maximize the attenuation of vibrational energy.

Official Gazette of the U.S. Patent and Trademark Office

N93-13443*# General Electric Co., Cincinnati, OH. Engineering Mechanics and Life Management Section.

COUPLED STRUCTURAL/THERMAL/ELECTROMAGNETIC ANALYSIS/TAILORING OF GRADED COMPOSITE STRUCTURES Annual Status Report No. 1

R. L. McKnight, P. C. Chen, L. T. Dame, and H. Huang Apr. 1992 99 p

(Contract NAS3-24538; RTOP 505-62-91)

(NASA-CR-189150; NAS 1.26:189150) Avail: CASI HC A05/MF A02

Accomplishments are described for the first year effort of a 5-year program to develop a methodology for coupled structural/thermal/electromagnetic analysis/tailoring of graded composite structures. These accomplishments include: (1) the results of the selective literature survey; (2) 8-, 16-, and 20-noded isoparametric plate and shell elements; (3) large deformation structural analysis; (4) eigenanalysis; (5) anisotropic heat transfer analysis; and (6) anisotropic electromagnetic analysis. Author

N93-13444*# General Electric Co., Cincinnati, OH. Engineering Mechanics and Life Management Section.
COUPLED STRUCTURAL/THERMAL/ELECTROMAGNETIC ANALYSIS/TAILORING OF GRADED COMPOSITE STRUCTURES
Annual Status Report No. 2
R. L. McKnight, H. Huang, and M. Hartle Apr. 1992 109 p
(Contract NAS3-24538; RTOP 505-62-91)
(NASA-CR-189151; NAS 1.26:189151) Avail: CASI HC A06/MF A02

Accomplishments are described for the third years effort of a 5-year program to develop a methodology for coupled structural/thermal/electromagnetic analysis/tailoring of graded composite structures. These accomplishments include: (1) structural analysis capability specialized for graded composite structures including large deformation and deformation position eigenanalysis technologies; (2) a thermal analyzer specialized for graded composite structures; (3) absorption of electromagnetic waves by graded composite structures; and (4) coupled structural thermal/electromagnetic analysis of graded composite structures.
Author

N93-13445*# General Electric Co., Cincinnati, OH. Life Analysis and Methods Technology Section.
COUPLED STRUCTURAL/THERMAL/ELECTROMAGNETIC ANALYSIS/TAILORING OF GRADED COMPOSITE STRUCTURES
Annual Status Report No. 3
R. L. McKnight, H. Huang, and M. Hartle Apr. 1992 56 p
(Contract NAS3-24538; RTOP 505-62-91)
(NASA-CR-189152; NAS 1.26:189152) Avail: CASI HC A04/MF A01

Accomplishments are described for the fourth years effort of a 5-year program to develop a methodology for coupled structural/thermal/electromagnetic analysis/tailoring of graded composite structures. These accomplishments include: (1) demonstration of coupled solution capability; (2) alternate CSTEM electromagnetic technology; (3) CSTEM acoustic capability; (4) CSTEM tailoring; (5) CSTEM composite micromechanics using ICAN; and (6) multiple layer elements in CSTEM.
Author

N93-13484 Stanford Univ., CA.
A FOURIER SERIES METHOD FOR POLYGONAL DOMAINS: LARGE ELEMENT COMPUTATION FOR PLATES Ph.D. Thesis
Long-Chyuan Kang 1992 159 p
Avail: Univ. Microfilms Order No. DA9221632

An efficient approach using the Fourier series for boundary value problems on polygonal domains was developed. The method is applied to (1) a reduced wave equation and the potential problems, (2) the classical plate bending problems, and (3) the bending problems of elastic plates considering transverse shear. For a problem with convex domain, which is treated as a large element, the Levy-type solution for an infinite strip can be obtained first. Then, the problem can be solved by superimposing the solution functions and matching the Fourier harmonics of the prescribed boundary conditions. For a non-convex domain, the domain can be cut into a few convex elements and connected back together using the continuity condition. Since the number of elements is much smaller than that of most existing methods, time is saved in both setting up the input data and solving the problem. To demonstrate its accuracy and effectiveness, several examples are presented and compared with the available results. These include a heat conduction problem, a mode 3 crack problem, a plate bending problem, and the bending problem of a stiffened plate.
Dissert. Abstr.

N93-13515# Sandia National Labs., Albuquerque, NM.
THERMODYNAMICALLY CONSISTENT THEORIES FOR ELASTOPLASTICITY COUPLED WITH DAMAGE
N. R. Hansen and H. L. Schreyer (New Mexico Univ., Albuquerque.) 1992 15 p Presented at the Winter Annual Meeting of the American Society of Mechanical Engineers, Anaheim, CA, 8-13 Nov. 1992
(Contract DE-AC04-76DP-00789)
(DE92-018283; SAND-92-1603C; CONF-921110-12) Avail: CASI HC A03/MF A01

A framework for coupled elastoplastic and damage theories is developed, following a rigorous thermodynamic procedure. This framework is sufficiently general to include anisotropic plasticity and damage formulations. Both the plastic yield and damage functions are constructed using homogeneous functions of degree one. The principle of maximum dissipation or maximum entropy production is used to derive the evolution relations together with the loading and unloading conditions. In addition, the convexity of the undamaging elastic domain is shown. For plasticity the resulting evolution of the plastic strains corresponds to an associative flow. This general framework is shown to be sufficiently general to describe several popular theories for both plasticity and damage. Limitations of some existing damage theories are discussed.
DOE

N93-13524# Midwest Research Inst., Golden, CO.
USER'S GUIDE FOR THE NREL FORCE AND LOADS ANALYSIS PROGRAM
A. D. Wright Aug. 1992 238 p
(Contract DE-AC02-83CH-10093)
(DE92-010579; NREL/TP-257-4674) Avail: CASI HC A11/MF A03

The following report gives the reader an overview of and instructions on the proper use of the National Renewable Energy Laboratory Force and Loads Analysis Program (FLAP, version 2.2). It is intended as a tool for prediction of rotor and blade loads and response for two- or three-bladed rigid hub wind turbines. The effects of turbulence are taken into account. The objectives of the report are to give an overview of the code and also show the methods of data input and correct code execution steps in order to model an example two-bladed rigid hub turbine. A large portion of the discussion is devoted to the subject of inputting and running the code for wind turbulence effects. The ability to include turbulent wind effects is perhaps the biggest change in the code since the release of FLAP version 2.01 in 1988. This report is intended to be a user's guide. It does not contain a theoretical discussion on equations of motion, assumptions, underlying theory, etc. It is intended to be used in conjunction with Wright, Buhl, and Thresher (1988).
DOE

N93-13525# Midwest Research Inst., Golden, CO.
USER'S GUIDE FOR THE NREL TEETERING ROTOR ANALYSIS PROGRAM (STRAP)
A. D. Wright Aug. 1992 212 p
(Contract DE-AC02-83CH-10093)
(DE92-010580; NREL/TP-257-4671) Avail: CASI HC A10/MF A03

The following report gives the reader an overview of instructions on the proper use of the National Renewable Energy Laboratory (formerly the Solar Energy Research Institute, or SERI) teetering Rotor Analysis Program (STRAP version 2.20). STRAP is a derivative of the Force and Loads Analysis program (FLAP). It is intended as a tool for prediction of rotor and blade loads and response for only two-bladed teetering hub wind turbines. The effects of delta-3, undersling, hub mass, and wind turbulence are taken into account. The objectives of the report are to give an overview of the code and also show the methods of data input and correct code execution steps in order to model an example two-bladed teetering hub turbine. A large portion of the discussion (Sections 6.0, 7.0, and 8.0) is devoted to the subject of inputting and running the code for wind turbulence effects. The ability to include turbulent wind effects is perhaps the biggest change in the code since the release of FLAP version 2.01 in 1988. This report is intended to be a user's guide. It does not contain a theoretical discussion on equations of motion, assumptions, underlying theory, etc. It is intended to be used in conjunction with Wright, Buhl, and Thresher (1988).
DOE

N93-13539 Drexel Univ., Philadelphia, PA.
MATRIX CRACKING INITIATION STRESS IN FIBER-REINFORCED CERAMIC MATRIX COMPOSITES Ph.D. Thesis
Pramod Balkrishna Kangutkar 1991 253 p
Avail: Univ. Microfilms Order No. DA9208262

One of the important design parameters in CMC's in the Matrix Cracking Initiation Stress (MCIS) which corresponds to the stress at which first matrix cracks are observed. Above the MCIS, the fibers will be exposed to the oxidizing environment which may degrade the mechanical property of the fibers and thus of the composite. In this thesis a systematic study to explore the effects of matrix toughness and inherent strength, fiber diameter, stiffness and volume fraction, temperature and interfacial bonding on the MCIS was carried out. Composites were fabricated using three different matrices--borosilicate glass, aluminosilicate glass and polycrystalline zirconium silicate (or zircon), and two different reinforcing fibers--an SiC monofilament (140 micron diameter) and an SiC yarn (16 micron diameter).

In-situ observations during 3-point bend test inside the SEM indicate that matrix cracking is a local phenomenon and occurs first in the matrix between widest spaced fibers. In all composites the MCIS was found to increase with fiber additions and scaled with the monolithic strength. The relative increase in MCIS over the monolithic strength with fiber volume fraction, however, was found to depend strongly on the a(sub 0)/S ratio, where a(sub 0) is the inherent unreinforced matrix flaw size and S is the inter-fiber spacing. For small ratios, the effect of fiber additions on enhancing MCIS are minimal. As the ratio approaches unity, the role of the fibers in constraining the inherent flaw increases, thereby increasing the MCIS. Thermal residual stresses were also seen to play an important role in determining the MCIS; systems with compressive residual stresses in the matrix show higher MCIS at room temperature than at a higher temperature. In systems such as the 7740/Nicalon, which had negligible thermal stresses, MCIS showed minimal changes on testing at 520 C. Several theoretical models were reviewed and the predictions were compared to the experimental results. It was shown that the local-flaw model predictions seem to correlate well with the observed data for the different systems considered in this study. Dissert. Abstr.

N93-13630 Virginia Polytechnic Inst. and State Univ., Blacksburg.
THE SHEAR GAGE AND COMPACT SHEAR SPECIMEN FOR SHEAR PROPERTY MEASUREMENTS OF COMPOSITE MATERIALS Ph.D. Thesis
Peter Geza Ifju 1992 179 p
Avail: Univ. Microfilms Order No. DA9226033

Techniques for shear property measurements for composite and isotropic materials were studied. A new strain gage called the shear gage was conceived, designed, and tested for routine shear characterization on notched shear specimens. The shear gage integrates the shear strain in the entire test section of the losipescu and compact shear specimens. The result was consistent and accurate determination of the shear stress/strain response of materials. Prior knowledge of material in the losipescu shear test were automatically compensated when shear gages were placed on the two faces of the specimen. The shear gages were tested on composite and isotropic materials and produced higher accuracy and consistency than could be produced using current technology. Moire interferometry was used to evaluate the ability of the shear gage to measure the average shear strains. The results from the evaluation program confirmed the attributes of the concept. The compact shear specimen was evaluated for the shear testing of laminated composite materials. Advantages of the compact specimen include its compact size, large test section, simple fixturing, and the ability to determine the shear response of a wide range of materials. The specimen produced accurate modulus measurements when used with the shear gages. The specimen compared favorably to the losipesu specimen. Moire interferometry was used to evaluate the strain fields on the compact and losipescu specimens. It was shown that the shear strain distributions of the two specimens were similar although the compact specimen produced less deleterious normal strains in the test action. The compact and losipescu specimens were evaluated for shear strength measurements. Dissert. Abstr.

N93-13634 Illinois Univ., Chicago.
TRANSVERSE WAVE MOTION IN CONSTRAINED MECHANICAL SYSTEMS Ph.D. Thesis
Wei-Cheng Hsu 1992 179 p
Avail: Univ. Microfilms Order No. DA9226242

The effect of the finite rotation on the propagation of impact-induced transverse waves in the passive system is examined. The partial differential equations of motion of kinematically driven rotating beams are obtained using the principle of virtual work in dynamics. This system is classified as a passive system which does not normally respond in the case of zero initial conditions. This system, however, is ideally suited for examining the effect of the finite rotation on the propagation of impact-induced transverse waves. The jump discontinuity in the system parameters as the result of impact is predicted using the algebraic generalized impulse momentum equations that involve the coefficient of restitution. The dispersion relationship is defined and used to demonstrate the effect of the angular velocity and the flexural rigidity of the beam on the phase and the group velocities of the dispersive transverse waves. The analysis presented shows that as the angular velocity increases the phase velocities of the transverse waves decreases and in general, the finite rotation has more significant effect on the phase velocity of the low frequency waves as compared to the high frequency waves. As the result of the finite rotation, the phase velocities of the transverse waves is significantly different from the phase velocities predicted using the classical beam theory of nonrotating beams. A finite element computational procedure for the analysis of impact-induced transverse waves in articulated mechanical and structural systems is also developed. In order to establish the accuracy of the numerical procedure developed, the solution obtained using the finite element method is compared with the solution obtained using the partial differential equation and the method of the separation of variables. Numerical results show that there is a good agreement between the finite element and the eigenfunction solutions. Dissert. Abstr.

N93-13637# Defense Nuclear Agency, Washington, DC.
PROCEEDINGS OF THE 62ND SHOCK AND VIBRATION SYMPOSIUM, VOLUME 2
31 Oct. 1991 12 p Symposium held at Springfield, VA, 29-31 Oct. 1991
(AD-A249267) Avail: CASI HC A03/MF A01

This paper reports on the degree of success that may be achieved by using simple equipment-vehicle models that produce time history responses which are equivalent to the responses that would be achieved using spectral design values employed by the Dynamic Analysis Method. The equipment models studied herein are limited to one and two-degree of freedom systems; the vehicle to which the equipment is attached consists solely of rigid mass; and the shock excitation is produced by an ideal impulse that is applied to the vehicle mass so as to produce an initial velocity. Although the case of the single-degree of freedom equipment presents no difficulties in performing a transient analysis that reproduces the DDAM-like response, it is shown that there are no unique values for the vehicle mass and for the magnitude of the impulse, but that they are interrelated. In the case of the two-degree of freedom equipment, the transient analysis duplicates the response that would be experienced using the DDAM-like input values, provided that shock design values in the first mode is less than the shock design value in the second mode. Otherwise, solutions are not possible. Brief comments are also provided for the special case of equipment composed of a very light mass attached to a large mass, and for the case of equipment with repeated natural frequencies. Author

N93-13707*# Anco Engineers, Inc., Culver City, CA.
PROVIDING STRUCTURAL MODULES WITH SELF-INTEGRITY MONITORING SOFTWARE USER'S MANUAL Final Report
Apr. 1990 97 p
(Contract NAS7-961; SBIR-04.90-5050)
(NASA-CR-190877; NAS 1.26:190877) Avail: CASI HC A05/MF A02

National Aeronautics and Space Administration (NASA) Contract NAS7-961 (A Small Business Innovation and Research (SBIR) contract from NASA) involved research dealing with remote structural damage detection using the concept of substructures. Several approaches were developed. The main two were: (1) the module (substructure) transfer function matrix (MTFM) approach; and (2) modal strain energy distribution method (MSEDM). Either method can be used with a global structure; however, the focus was on substructures. As part of the research contract, computer software was to be developed which would implement the developed methods. This was done and it was used to process all the finite element generated numerical data for the research. The software was written for the IBM AT personal computer. Copies of it were placed on floppy disks. This report serves as a user's manual for the two sets of damage detection software. Sections 2.0 and 3.0 discuss the use of the MTFM and MSEDM software, respectively. Author

N93-13728 Marquette Univ., Milwaukee, WI.
AN ELASTICITY SOLUTION FOR A TRANSVERSELY ISOTROPIC MATERIAL CONTAINING A SPHERICAL SHELL UNDER AXISYMMETRIC LOADING Ph.D. Thesis
Jiun-Yih John Wang 1991 153 p
Avail: Univ. Microfilms Order No. DA9226226

A three-dimensional elasticity solution is obtained for a transversely isotropic solid containing an isotropic spherical shell. The shell is assumed to behave as a membrane which is perfectly bonded to the surrounding medium. The applied loading may consist of any arbitrary axisymmetric traction distribution applied to the inner shell surface and/or infinity. The

solution method is based on the superposition of two fundamental solutions: those corresponding to (1) the spherical cavity problem for transverse isotropy, and (2) the spherical membrane shell problem. Each solution is expressed in the form of Legendre series, and the displacement continuity conditions are then utilized to generate an infinite system of linear algebraic equations in terms of the unknown series coefficients. The solution of this system is obtained by means of an explicitly limiting procedure. Numerical results generated by the solution provide the opportunity to investigate the influence of geometric parameters, material constants, and loading type on the displacements and stresses at the interface of the shell and surrounding medium, as well as the internal shell forces. In general, the maximum stress concentration for mildly anisotropic materials (e.g., magnesium and zinc) and isotropic materials under the loading at infinity. For more highly anisotropic materials such as graphite, the stiffest shell was found to minimize the stress concentration. Dissert. Abstr.

N93-13754 Harvard Univ., Cambridge, MA.
LOAD-TRANSFER AND CRACK BRIDGING IN FIBER-TOUGHENED CERAMIC COMPOSITES Ph.D. Thesis
William Shewen Slaughter 1991 65 p
Avail: Univ. Microfilms Order No. DA9211749

Two models are proposed to help in trying to understand the behavior of fiber-toughened ceramic composites. The first model is for approximating load-diffusion from axially loaded fibers embedded in elastic matrices. The fundamental elastostatic solutions used are for a point force and a point dilatation in either a fully-infinite or semi-infinite space. Tangential tractions across the fiber-matrix interface are included explicitly in the analysis. The model is applied to the three-dimensional analogs of Melan's first problem and Reissner's problem and comparisons are made with exact results in the case of the former to help establish the validity of the model. The second proposal is a self-consistent model for determining the equivalent spring stiffness in fiber crack-bridging problems. The model is compared with the shear-lag model for ideal bonding of the fiber-matrix interface in which the springs have a linear spring constant. A comparison is also made, in the homogeneous limit when fiber and matrix elastic properties are identical, with results from particle and ligament crack-bridging analyses. The self-consistent model is seen to agree with these other models. A simplified parametric equation is given which approximates the results over the considered range of material properties. Dissert. Abstr.

N93-13769 Virginia Polytechnic Inst. and State Univ., Blacksburg.
TRANSONIC AEROELASTIC ANALYSIS OF SYSTEMS WITH STRUCTURAL NONLINEARITIES Ph.D. Thesis
I. Wayan Tjatra 1991 211 p
Avail: Univ. Microfilms Order No. DA9126888

Wing structures often contain nonlinearities which affect their aeroelastic behavior and performance characteristics. Aerodynamic flows at the transonic Mach numbers generate nonlinear aerodynamic forces on the wing affecting the aeroelastic response of the wing. Analysis techniques accounting for these structural and aero-dynamic nonlinearities, and an understanding of their potential influence on the flutter mechanism of two-dimensional and three-dimensional wing-structure models are the main objective of this study. Two different categories of structural nonlinearities are considered: (1) distributed nonlinearity and (2) concentrated nonlinearity. The concentrated nonlinearities are mathematically modeled using the Asymptotic Expansion method which is based on the Krylov-Bogoliubov-Mitropolski technique. The effective stiffness coefficient of a nonlinear element is defined as the ratio of the amplitude of the Fourier series expansion of the load and the amplitude of the displacement of that element. The effects of distributed nonlinearities on the aeroelastic characteristic of a three-dimensional wing model are also investigated. The influences of this type of nonlinearity are treated in a quasi-nonlinear approach which allows the variation of the natural frequencies and damping factor of the structure model with respect to the amplitude of the motion. The transonic aerodynamic pressure distributions were obtained by solving the unsteady Transonic Small Disturbance (TSD) flow equation using finite-difference techniques. An Alternating Direction Implicit (ADI) algorithm was used for the two-dimensional flow model, and an Approximate Factorization (AF) algorithm was used for the three-dimensional flow model. The finite-state generalized aerodynamic forces used in the aeroelastic analysis were calculated by employing the Method of Harmonic Oscillation and the Pulse Transfer Function analysis. The solution of the aeroelastic equation in the frequency domain is obtained by representing the equation in a finite-state form through the modal approach using Lagrange's equation. The flutter boundary is obtained by solving this equation using the classical U-g method and root locus analysis. Flutter analysis of two degree-of-freedom, two-dimensional typical wing sections with nonlinear torsional springs is studied. The aeroelastic responses of the system are obtained by integrating the nonlinear structural terms and aerodynamic terms simultaneously using Newmark-beta and Wilson-theta methods. Flutter results obtained from both the time integration and eigenvalue solutions are compared. These two results, in general, are in agreement. Flutter behavior of a simple three-dimensional swept wing model is also investigated. Comparison of the flutter boundary obtained by using the eigenvalue solution with flutter data from wind-tunnel experiments is made. Dissert. Abstr.

N93-13804 Purdue Univ., West Lafayette, IN.
ANALYSIS OF CRACKED PLATES SUBJECTED TO OUT-OF-PLANE LOADINGS Ph.D. Thesis
Min-Jho Young 1991 171 p
Avail: Univ. Microfilms Order No. DA9215701

Stress singularity near a crack tip is one of the most important parameters in structural design. Fracture parameters such as stress intensity factors or strain energy release rates are often required in design considerations. This research aims to find those fracture parameters for through-the-thickness cracks in plates subjected to out-of-plane loadings. For the thin plate assumption, classical plate theory and Reissner's plate theory are employed to solve the problems. Modified crack closure method in combination with finite element method is also investigated. The research can be divided into four major topics: (1) Although the stress intensity factor and near-tip stress distributions given by the Reissner's plate theory are different from classical plate solutions, the total strain energy release rate based on Reissner's plate theory is shown to approach the classical plate solutions at the ratio of plate thickness to crack size approaches zero. (2) For plate subjected to uniform bending moment, the stress-free conditions along the crack face lead to interpenetration of te crack faces. A constraint model using plate theories in combination with plane elasticity assumption is investigated. The constraint conditions relate crack rotation and inplane displacement along the crack faces to satisfy the compatibility condition at compressive edges. The influence of the closure on the stress intensity factors is evaluated. (3) For plate subjected to transverse shear forces, the problem is solved using classical plate theory and the strain energy release rates associated with mode II and mode III are evaluated. Two plate solutions are compared. (4) The modified crack closure method in combination with the finite element method is investigated for different loading conditions. The accuracy of the method is evaluated. The results based on classical plate element and Mindlin's plate element are also compared. Dissert. Abstr.

N93-13811 California Univ., Los Angeles.
THREE-DIMENSIONAL BOUNDARY ELEMENT ANALYSIS OF RESIDUAL STRESSES IN A CROSS-PLY FIBER COMPOSITE MODEL Ph.D. Thesis
Sang Soon Lee 1992 157 p
Avail: Univ. Microfilms Order No. DA9218170

The residual stress distribution in cross-ply laminates is investigated at the microstress level within the scope of linear viscoelasticity. A three-dimensional model is presented and analyzed to estimate the residual stresses induced during the polymerization and the cool-down phases. Matrix and fibers are treated as subzones coupled with displacement continuity and traction equilibrium conditions along the interface. This problem is preceded by a unidirectional laminate problem which is a preliminary step to analyzing the three-dimensional model. In this research, a three-dimensional boundary element method appropriate to estimate residual stresses in a cross-ply laminate model is presented, in which the time domain method for viscoelastic analysis of matrix zone is used. In order to achieve an accurate and efficient integration scheme, a modified Simpson's rule with respect to time is employed. New two-dimensional BEM computer programs (BEM2DV) and three-dimensional BEM programs (BEM3DV) have been developed. Analysis capabilities of these new computer codes include stress analysis of two-dimensional and three-dimensional elastic, viscoelastic, and thermoviscoelastic objects with subregions of different materials. PATRAN is used as a pre and post processor for the BEM2DV and BEM3DV codes. Final results are presented in colored contour maps to

illustrate the residual stress distribution in the matrix zone. The resulting residual stresses are the same order of magnitude as that of the matrix strength. Dissert. Abstr.

N93-13823 Brigham Young Univ., Provo, UT.
IMPROVED DAMPING IN COMPOSITE STRUCTURES THROUGH STRESS COUPLING, CO-CURED DAMPING LAYERS, AND SEGMENTED STIFFNESS LAYERS Ph.D. Thesis
Dennis Duane Olcott 1992 127 p
Avail: Univ. Microfilms Order No. DA9222816

A unique damping concept applicable to a wide range of engineering structures was devised and analyzed. A computer program, DAMSEG, was written to conduct parametric studies on the non-dimensionalized analytical models of both flat membrane and cylindrical damped components. The damping concept uses the stress coupling effects inherent in composite materials to induce large shear strains in co-cured damping layers. Varying the ply orientation angle of the composite material in segments along the length of the component creates multiple regions of high shear, thus inducing high damping loss factors in the component. Several damped cylinders and I-beams were built to test the theory and validate the model. The model predicted the natural vibration frequency and damping loss factors of cylinders within 5 percent for most cases and predicted the vibration frequency and damping of I-beams within 10 percent for most cases. Cylinders with loss factors up to 8.5 percent and I-beams with loss factors up to 5.7 percent have been built and tested. Dissert. Abstr.

N93-13921 Stanford Univ., CA.
FAST OPTIMIZATION OF STATIC AXISYMMETRIC SHELL STRUCTURES Ph.D. Thesis
Jeffrey Jacoby 1992 189 p
Avail: Univ. Microfilms Order No. DA9221628

An axisymmetric shell optimization procedure is developed which is a fast, user-friendly and practical tool for design use in disciplines including aerospace, mechanical and civil engineering. The shape and thickness of a shell can be optimized to minimize shell mass, mass/volume ratio or stress with constraints imposed on von Mises stress and local buckling. The procedure was created with the aid of the GENOPT optimization development system (Dr. D. Bushnell, Lockheed Missiles and Space Co) and uses the FAST1 shell analysis program (Prof. C. R. Steele, Stanford University) to perform the constraint analysis. The optimization method used is the modified method of feasible directions. The procedure is fast because exact analysis methods allow complex shells to be modelled with only a few large shell elements and still retain a sufficiently accurate solution. This is of particular advantage near shell boundaries and intersections which can have small regions of very detailed variation in the solution. Finite element methods would require many small elements to capture accurately this detail with a resulting increase in computation time and model complexity. Reducing the complexity of the model also reduces the size of the required input and contributes to the simplicity of the procedure. Optimization design variables are the radial and axial coordinates of nodes and the shape parameters and thicknesses of the elements. Thickness distribution within an element can be optimized by specifying the thickness at evenly spaced control points. Spline interpolation is used to provide a smooth thickness variation between the control points. An effective method is developed for reducing the number of required stress constraint equations. Various shells have been optimized and include models for comparison with published results. Shape, thickness and shape/thickness optimization has been performed on examples including a simple aerobrake, sphere-nozzle intersections, ring reinforced cylinder and elliptical and torispherical tank heads. Convergence of different initial designs to one final design is demonstrated for a shape, thickness and shape/thickness optimization problem. The sphere-nozzle intersection is investigated in detail and the equal area replacement rule for reinforcement is verified for most intersection geometries. Dissert. Abstr.

N93-13923 Texas Univ., Austin.
BIFURCATION AND LOCALIZATION INSTABILITIES IN PLASTIC BENDING OF CYLINDRICAL SHELLS Ph.D. Thesis
Gwo-Tarng Ju 1991 169 p
Avail: Univ. Microfilms Order No. DA9212560

This study is concerned with the response and various instabilities which govern the behavior of circular shells under pure bending. Of particular interest are shells with low diameter-to-thickness ratios whose behavior is strongly influenced by the plastic characteristics of the material. Experiments were conducted on long aluminum 6061-T6 shells with eleven different diameter-to-thickness ratios ranging from 60.5 to 19.5. The experiments involve shells of length of at least 18 diameters long. The experiments were performed in a four point bending machine under curvature controlled loading. Thinner shells were found to develop short wavelength periodic ripples on the compressed side of the shell. Although this was not directly associated with catastrophic collapse, the shells buckled locally and collapsed catastrophically soon after the appearance of the ripples. The collapse buckling mode was in the form of a local kink with circumferential waves on the compressed side of the shells. Thicker shells were found to exhibit a limit load instability as a direct consequence of the ovalization induced to the shell cross section by bending. Following the limit load, the ovalization along the length ceased to be uniform; the deformation started to localize in a region a few diameters long. The localization led to the eventual collapse of the shells. For shells with intermediate D/t values, short wavelength ripples developed at the same time that localization of ovalization was recorded. The interaction of the two resulted in local buckling and catastrophic collapse following the development of a limit load. The analytical/numerical part of the study is concerned with the prediction of the response and of the various instabilities observed in the experiments. A special deformation composition scheme coupled with Sanders' nonlinear shell equations was developed for analyzing the problem. The three types of behavior observed in the experiments, involving bifurcation into short wavelength ripples, localization following the attainment of a natural limit load and interaction of the two were simulated. In each case the predicted response was found to be in good agreement with the experimental result. Dissert. Abstr.

N93-13935 Virginia Univ., Charlottesville.
THE FREE AND FORCED VIBRATIONS OF STRUCTURES USING THE FINITE DYNAMIC ELEMENT METHOD Ph.D. Thesis
Neil J. Fergusson 1991 204 p
Avail: Univ. Microfilms Order No. DA9221107

The Finite Dynamic Element Method, which has been available since 1966, provides a useful and efficient method for the analysis of freely vibrating structures. In particular, the retention of extra terms in the dynamic stiffness matrix has been shown to provide a matrix method for converging with a high rate to the natural frequencies. The current research includes the derivation of several formulas which simplify the method. The higher ordered terms in the mass matrix are shown proportional to those in the stiffness matrix. In addition, the consistent mass matrix and the quasi-static mass matrix are shown to be equivalent, in the sense that the terms in their respective Taylor expansions are proportional to one another, and that they both lead to the same dynamic stiffness matrix when used with the appropriate stiffness matrix. Futhermore, the calculation of the 2 jth order term for either of these, can be accomplished with the knowledge of the jth order shape function term. A formula is also provided which shows the dependence of the four matrices (mass, stiffness, quasi-static mass, and dynamic stiffness) on the values of the shape functions at the boundary of the element. A dynamic element is constructed for the symmetric bending of an annular Kirchoff plate, and it is shown that a second expansion in powers of the aspect ratio provides the tractability necessary to overcome the numerical instability of the otherwise transcendental expressions. The typical high convergence rate associated with the dynamic element method is exhibited for natural frequency calculations. The study also looks at forced vibrations using dynamic elements. In considering a cantilevered beam subject to a time-dependent end load, the appropriate modal superposition results in a more efficient response calculation than that associated with the traditional finite element method. A dynamic element is also constructed for coupled thermoelasticity. A Macsyma program generates the required matrices based on the heat displacement method. The work concludes with a few words on the numerical calculation of the various structural matrices. Two methods are described, based on assumed shape elements, and first order numerical integrators, respectively. Circular plate tests, not included herein, showed the feasibility of using the methods for higher ordered shell elements. Dissert. Abstr.

N93-13947 Oregon Graduate Inst. of Science and Technology, Beaverton.
EFFECTS OF RESIDUAL STRESS, WELD TOE NOTCH AND WELD DEFECTS ON FATIGUE OF WELDED STEEL STRUCTURES Ph.D. Thesis
Wenyu Shen 1992 232 p
Avail: Univ. Microfilms Order No. DA9222639

In studying the fatigue behavior of fillet welded railroad tank car shell structures, the effects of welding residual stress, weld toe notch, and weld defects on the fatigue of fillet welded A515 steel specimens were evaluated. Both hole-drilling and sectioning measurement techniques were used to obtain residual stress information. Pad-on-plate weld specimens were designed to simulate the tank car structure for welding residual stress measurement. Simple bead-on-plate and fillet weld specimens, which have similar welding residual stresses near the weld end toe to the pad-on-plate specimens, were designed to be as compact as possible for fatigue testing. As-welded and stress-relieved simple weld specimens were tested under pulsed tension and alternating cyclic load conditions to determine stress-life and fatigue crack propagation properties. Weld toe stress concentration effects were determined by strain gage measurement. Fracture surface features and crack initiation sites were studied by visual analysis, scanning electron microscopy, and optical microscopy. Welding residual stresses were found to be biaxial tension-compression near the weld end toe and biaxial tension-tension near the weld center toe. Longitudinal tensile residual stress was significantly relieved when the applied longitudinal tensile cyclic load was greater than 14 Ksi. Test results did not show a consistent effect of tensile residual stress on the fatigue strength under pulsed tension loads. However, tensile residual stress had a significant influence on the fatigue strength under alternating cyclic loads. The weld end toe was associated with a stress concentration factor of approximately 3 and was the most critical factor in initiating fatigue cracks. Weld defects, such as slag inclusions, lack of fusion, and porosity were found to significantly affect the fatigue strength of a welded joint when the load magnitude or mean stress was low. An equivalent crack concept, based on linear elastic fracture mechanics theory, was introduced to quantify the weld toe stress concentration effect. This concept was shown to be effective for fatigue design life prediction of welded structures. Dissert. Abstr.

N93-13951 Kentucky Univ., Lexington.
BOUNDARY ELEMENT ANALYSIS OF ACOUSTICAL THIN-BODY AND NONUNIQUENESS PROBLEMS USING A NORMAL DERIVATIVE INTEGRAL EQUATION Ph.D. Thesis
Guang-Cheng Wan 1992 117 p
Avail: Univ. Microfilms Order No. DA9222858

An efficient procedure to numerically evaluate a normal derivative integral equation in a three-dimensional isoparametric element environment is presented. This normal derivative equation was originally derived by Maue and later by Mitzner using a difference approach. The original hypersingular normal derivative integral equation converges in the finite-part sense only. However, Maue's equation is less-singular and converges in the Cauchy principle value sense. The Cauchy principle value integral is locally transformed into a regular integral so that it is amendable to standard Gaussian quadrature. Quadratic isoparametric elements with collocation points inside each element are used to satisfy the continuity conditions required for the convergence of Maue's equation. Maue's equation is then combined with the Helmholtz integral equation in the formulation proposed by Burton and Miller to overcome the nonuniqueness problem. A very popular method to overcome the nonuniqueness problem is the CHIEF method proposed by Schenck. Its performance is adversely affected by the interior nodal surface problem and the rank deficiency problem. Compared to the CHIEF method, Burton and Miller's formulation is theoretically robust. Numerical examples including radiation and scattering from a sphere are given to show the accuracy and effectiveness of Burton and Miller's method with Maue's equation. The final part of this dissertation is devoted to the acoustical radiation and scattering from thin bodies. By applying both the Helmholtz integral equation and Maue's equation simultaneously, it is possible to solve a thin-body problem by modeling its neutral surface only. The quarter-point technique is applied to model the 1/square root of r singularity associated with the tangential velocities at the knife edge of a thin body. The thin-body boundary element method (BEM) results compare very well with an available analytical solution and an axisymmetric multi-domain BEM solution. Dissert. Abstr.

N93-13966 Virginia Polytechnic Inst. and State Univ., Blacksburg.
DETERMINISTIC AND STOCHASTIC RESPONSES OF NONLINEAR SYSTEMS Ph.D. Thesis
Ashraf Mohamed Abou-Rayan 1992 201 p
Avail: Univ. Microfilms Order No. DA9220622

The responses of nonlinear systems to both deterministic and stochastic excitations are discussed. For a single degree of freedom system, the response of a simply supported buckled beam to parametric excitations is investigated. Two types of excitations are examined: deterministic and random. For the nonlinear response to a harmonic axial load, the method of multiple scales is used to determine to second order the amplitude and phase modulation equations. Floquet theory is used to analyze the stability of periodic responses. The perturbation results are verified by integrating the governing equation using both digital and analog computers. For small excitation amplitudes, the analytical results are in good agreement with the numerical solutions. The large amplitude responses are investigated by using simulations on a digital computer and are compared with results obtained using an analog computer. For the stochastic response to a wide-band random excitation, the Gaussian and non-Gaussian closure schemes are used to determine the response statistics. The results are compared with those obtained from real-time analysis (analog-computer simulation). The normality assumption is examined. A comparison between the responses to deterministic and random excitation is presented. For two degree of freedom systems, two methods are used to study the response under the action of broad-band random excitations. The first method is applicable to systems having cubic nonlinearities. It involves an averaging approach to reduce the number of moment equations for the non-Gaussian closure scheme from 69 to 14 equations. The results are compared with those obtained from numerical integrations of the moment equations and the exact stationary solution of the Fokker-Planck-Komologorov equation. The second method is applicable to systems having quadratic and cubic nonlinearities. Stationary solutions of the moment equations are determined and their stability is ascertained by examining the eigenvalues of the Jacobian matrix. This analysis is applied to both Gaussian and non-Gaussian closure schemes. The stochastic stability approach locates initial conditions needed to land on the desired stable or unstable manifold, which is a very difficult task for high-dimensional spaces. The results are compared with those obtained by numerically integrating the moment equations for the cases of Gaussian and non-Gaussian closure schemes. The methods used drastically reduce the computer effort and time. Dissert. Abstr.

N93-14022 Cleveland State Univ., OH.
X RAY ATTENUATION MEASUREMENTS FOR HIGH-TEMPERATURE MATERIALS CHARACTERIZATION AND IN SITU MONITORING OF DAMAGE ACCUMULATION
George Youssef Baaklini 1991 228 p
Avail: Univ. Microfilms Order No. DA9212688

The development and application is examined of x ray attenuation measurement systems that are capable of (1) characterizing density variations in high temperature materials, e.g., monolithic ceramics, ceramic and intermetallic matrix composites and (2) noninvasively monitoring damage accumulation and failure sequences in ceramic matrix composites under room temperature tensile testing. Results are presented in the development of (1) a point scan digital radiography system and (2) an in-situ x ray material testing system. The former is used to characterize silicon carbide and silicon nitride specimens and the latter is used to image the failure behavior of silicon carbide fiber reinforced reaction bonded silicon nitride matrix composites. Further, state of the art x ray computed tomography is studied to determine its capabilities and limitations in characterizing density variations of subscale engine components, e.g., a silicon carbide rotor, a silicon nitride blade, and a silicon carbide fiber reinforced beta titanium matrix rod, rotor, and ring. Microfocus radiography, conventional radiography, scanning acoustic microscopy, and metallography are used to substantiate the x ray computed tomography findings. Point scan digital radiography is a viable technique for characterization density variations in monolithic ceramic specimens. But it is very limited and time consuming in characterizing ceramic matrix composities. Precise x ray attenuation measurements, reflecting minute density variations, are achieved by photon counting and

by using micro collimators at the source and the detector. X ray computed tomography is found to be a unique x ray attenuation measurement technique capable of providing cross sectional spatial density information in monolithic ceramics and metal matrix composites. X ray computed tomography is proven to accelerate generic composite component development. Radiographic evaluation before, during and after loading show the effect of preexisting volume flaws on the fracture behavior of composites. Results from one ply, three ply, five ply, and eight ply ceramic composite specimens show that x ray film radiography can monitor damage accumulation during tensile loading. Dissert. Abstr.

N93-13175*# Hernandez Engineering, Inc., Greenbelt, MD.
STRUCTURAL VERIFICATION FOR GAS EXPERIMENTS
Mark Daniel Peden *In* NASA. Goddard Space Flight Center, The 1992 Shuttle Small Payloads Symposium Oct. 1992 p 165-174 (For primary document see N93-13158 03-12)
Avail: CASI HC A02/MF A03

42 GEOSCIENCES (GENERAL)

N93-13833*# Colorado Univ., Boulder. Center for Space and Geosciences Policy.
RESEARCH IN GEOSCIENCES POLICY Final Report, 1 Jan. 1991 - 30 Jun. 1992
Ronald D. Brunner 30 Jun. 1992 183 p
(Grant NAGw-1415)
(NASA-CR-190470; NAS 1.26:190470) Avail: CASI HC A09/MF A02

The general task was to look beyond the adverse physical impacts and to defining the policy problem. In order for policy actions to be effective, they must address the right policy problems, which will be different from and broader than the physical problems. We will work on defining the policy problems with a view to indicating how practical solutions might be implemented. In particular, public officials need advice on what should be said, and done, and for what purposes. That advice needs to be based on systematic analysis of: (1) the scholarly literature in the social sciences, and related disciplines; (2) the charging content of the policy debate at the center of attention; and (3) how citizens perceive and understand issues related to global change. We will conduct this analysis. Chapter 1 and 2 each reports work on defining the policy problem and analyzing the scholarly literature. Chapters 3 and 4, respectively, address the policy debate and citizen viewpoints in issues related to global change. Author

43 EARTH RESOURCES AND REMOTE SENSING

Includes remote sensing of earth resources by aircraft and spacecraft; photogrammetry; and aerial photography.

For instrumentation see *35 Instrumentation and Photography.*

N93-12550# New Mexico State Univ., Las Cruces. Dept. of Mathematical Sciences.
COORDINATES IN DIFFERENTIAL GEODESY
J. D. Zund 22 Jun. 1992 15 p
(Contract F19628-89-K-0044)
(AD-A254951; PL-TR-92-2072; AD-E201156) Avail: CASI HC A03/MF A01

This is a written version of an abstract of the same title which was presented at the 20th General Assembly of the International Association of Geodesy (Vienna, August 1991). It addresses the various roles of coordinates in theoretical geodesy: determinative coordinates in classical geodesy, descriptive coordinates in the Marussi-Hotine formulation of differential geodesy, and our new notion of permissible coordinates in a reformulation of the Marussi-Hotine theory. GRA

N93-12598# Army Engineer Topographic Labs., Fort Belvoir, VA.
SATELLITE IMAGERY GOES TO THE FIELD
George N. Simcox 1991 6 p
(AD-A254449; TEC-R-180) Avail: CASI HC A02/MF A01

There was a time, not long ago, when topographic terrain support to Army forces in the field was either nonexistent or woefully inadequate due to the compilation date of the available map products. Field units were devoted to providing expedient products based on old source agents reports and personnel reconnaissance. If no base materials were available, best guess products were produced to fill gaps. GRA

N93-12800*# Remote Sensing Systems, Inc., Santa Rosa, CA.
PRODUCTION OF SSM/I DATA SETS Final Report, 1 Sep. 1989 - 1 Sep. 1992
Frank J. Wentz 1 Sep. 1992 87 p Original contains color illustrations
(Contract NAS8-38075)
(NASA-CR-190944; NAS 1.26:190944; RSS-TR-090192) Avail: CASI HC A05/MF A01; 6 functional color pages

This Final Report is a summary of the work that was performed under Contract NAS8-38075 between NASA Marshall Space Flight Center and Remote Sensing Systems from September 1989 to September 1992. The primary accomplishment was the delivery of Special Sensor Microwave/Imager (SSM/I) data tapes containing sensor and geophysical products. In all, 515 tapes (80 gigabytes) were delivered. These tapes contained the F08 SSM/I data for the period from July 1988 through December 1991 and the F10 SSM/I data for the period from December 1990 through December 1991. For the F08 SSM/I, a data inventory was compiled and an engineering assessment was done. Ephemeris tables for the F08 and F10 spacecrafts were computed. Scientific studies on the oceanic wind vector and water vapor field were published, and color atlases of monthly ocean products were produced. This investigation was part of NASA's WETNET program. Author

N93-12869# Coast Guard Research and Development Center, Groton, CT.
DIGITAL CHART DATABASE CONVERSION INTO A SYSTEM ELECTRONIC NAVIGATIONAL CHART Final Report, Feb. 1991 - Mar. 1992
B. D. MacRae, R. Stephenson, T. Leadholm, and I. Gronin Mar. 1992 44 p
(Contract N61331-89-D-0021)
(AD-A255007; ERIM-215055-1-F; CG-D-15-92) Avail: CASI HC A03/MF A01

The Environmental Research Institute of Michigan (ERIM) was contracted by the United States Coast Guard Research and Development Center through the Naval Coastal Systems Center to prepare a set of technical and functional specifications that detail the means/ processes required to perform the conversion of an Electronic Navigational Chart (ENC) in the DX90 Data Transfer Standard format into a System Electronic Navigational Chart (SENC). This report details the activities associated with transforming the DX90 data structures to an intermediary ENC format, developing the software to transform this intermediary ENC to a form which could be displayed (SENC), and developing display software to allow an operator to interact with the data. Based on these activities, insights were gained into the current status of the implementation of the DX90 standard as well as the strengths and limitations of this format to support Electronic Chart Display and Information System (ECDIS) applications. Outputs from this contract include this report and software to perform the data conversion and display functions on an IBM-compatible personal computer. Software may be requested through the Coast Guard Research and Development Center. GRA

N93-13005# Instituto de Pesquisas Espaciais, Sao Jose dos Campos (Brazil).
AN ION BUDGET FOR A TERRA FIRME RAINFOREST IN CENTRAL AMAZONIA
Maria Cristina Forti and Lycia Maria Moreira-Nordemann 1992 10 p Presented at the International Seminar on Hydrology and Water Management of the Amazon Basin, Manaus, Brazil, 5-9 Aug. 1990
(INPE-5365-PRE/1745) Avail: CASI HC A02/MF A01

The ion budget for a 'terra firma' rainforest ecosystem in Central Amazonia, during two periods of contrasting rainfall, is discussed. The samples (rainwater, throughfall, litter solution, soil solution, and river water) were collected during Apr. - May and Aug. - Sep. 1987, at Reserva Ducke (2 deg 57 min S, 59 deg 58 min W), near Manaus. The budget indicates that the ionic species (Na(+), K(+), Mg(++), NH4(+), Cl(-), and SO4(--))

are found mainly in the portions of the hydrological cycles which cross the aerial phytomass and percolate throughout the root zone, showing the existence of a closed mineral cycle. Author

N93-13084*# Massachusetts Inst. of Tech., Cambridge. Center for Electromagnetic Theory and Applications.

REMOTE SENSING OF EARTH TERRAIN Progress Report, 1 Jan. - 30 Sep. 1992

J. A. Kong 30 Sep. 1992 77 p

(Grant NAGw-1617)

(NASA-CR-190908; NAS 1.26:190908) Avail: CASI HC A05/MF A01

Research findings are summarized for projects dealing with the following: application of theoretical models to active and passive remote sensing of saline ice; radiative transfer theory for polarimetric remote sensing of pine forest; scattering of electromagnetic waves from a dense medium consisting of correlated Mie scatterers with size distribution and applications to dry snow; variance of phase fluctuations of waves propagating through a random medium; theoretical modeling for passive microwave remote sensing of earth terrain; polarimetric signatures of a canopy of dielectric cylinders based on first and second order vector radiative transfer theory; branching model for vegetation; polarimetric passive remote sensing of periodic surfaces; composite volume and surface scattering model; and radar image classification. For individual titles, see N93-13085 through N93-13088.

N93-13085*# Massachusetts Inst. of Tech., Cambridge.

RADIATIVE TRANSFER THEORY FOR POLARIMETRIC REMOTE SENSING OF PINE FOREST

C. C. Hsu, H. C. Han, Robert T. Shin, Jin Au Kong, A. Beaudoin (Centre d'Etude Spatiale des Rayonnements, Toulouse, France), and T. LeToan (Centre d'Etude Spatiale des Rayonnements, Toulouse, France) *In its* Remote Sensing of Earth Terrain 30 Sep. 1992 3 p Repr. from International Journal of Remote Sensing (IEEE), 1992 p 1129-1131 (For primary document see N93-13084 03-43)

(Contracts JPL-958461; ESA-AO/1-2413/90-NL-PB; N00014-89-J-1107)

Avail: CASI HC A01/MF A01

The radiative transfer theory is applied to interpret polarimetric radar backscatter from pine forest with clustered vegetation structures. To take into account the clustered structures with the radiative transfer theory, the scattering function of each cluster is calculated by incorporating the phase interference of scattered fields from each component. Subsequently, the resulting phase matrix is used in the radiative transfer equations to evaluate the polarimetric backscattering coefficients from random medium layers embedded with vegetation clusters. Upon including the multi-scale structures, namely, trunks, primary and secondary branches, as well as needles, we interpret and simulate the polarimetric radar responses from pine forest for different frequencies and looking angles. The preliminary results are shown to be in good agreement with the measured backscattering coefficients at the Landes maritime pine forest during the MAESTRO-1 experiment. Author

N93-13086*# Massachusetts Inst. of Tech., Cambridge.

APPLICATION OF THEORETICAL MODELS TO ACTIVE AND PASSIVE REMOTE SENSING OF SALINE ICE

H. C. Han, Jin Au Kong, Robert T. Shin, Son V. Nghiem (Jet Propulsion Lab., California Inst. of Tech., Pasadena.), and R. Kwok (Jet Propulsion Lab., California Inst. of Tech., Pasadena.) *In its* Remote Sensing of Earth Terrain 30 Sep. 1992 3 p Presented at the International Geoscience and Remote Sensing Symposium, Houston, TX, 26-29 May 1992 Submitted for publication (For primary document see N93-13084 03-43)

(Contracts JPL-958461; N00014-89-J-1107)

Avail: CASI HC A01/MF A01

The random medium model is used to interpret the polarimetric active and passive measurements of saline ice. The ice layer is described as a host ice medium embedded with randomly distributed inhomogeneities, and the underlying sea water is considered as a homogeneous half-space. The scatterers in the ice layer are modeled with an ellipsoidal correlation function. The orientation of the scatterers is vertically aligned and azimuthally random. The strong permittivity fluctuation theory is employed to calculate the effective permittivity and the distorted Born approximation is used to obtain the polarimetric scattering coefficients. We also calculate the thermal emissions based on the reciprocity and energy conservation principles. The effects of the random roughness at the air-ice, and ice-water interfaces are accounted for by adding the surface scattering to the volume scattering return incoherently. The above theoretical model, which has been successfully applied to analyze the radar backscatter data of the first-year sea ice near Point Barrow, AK, is used to interpret the measurements performed in the CRRELEX program. Author

N93-13087*# Massachusetts Inst. of Tech., Cambridge. Dept. of Electrical Engineering and Computer Science.

VARIANCE OF PHASE FLUCTUATIONS OF WAVES PROPAGATING THROUGH A RANDOM MEDIUM **c32**

Nelson C. Chu, Jin Au Kong, Simon H. Yueh, Son V. Nghiem, Jack G. Fleischman (Massachusetts Inst. of Tech., Lexington.), Serpil Ayasli (Massachusetts Inst. of Tech., Lexington.), and Robert T. Shin (Massachusetts Inst. of Tech., Lexington.) *In its* Remote Sensing of Earth Terrain 30 Sep. 1992 15 p Repr. from Journal of Electromagnetic Waves and Applications (VSP), v. 6, no. 2, 1992 p 169-197 (For primary document see N93-13084 03-43)

(Contracts JPL-958461; MDA972-90-C-0021; DAAL03-88-J-0057; N00014-89-J-1107)

Avail: CASI HC A03/MF A01

As an electromagnetic wave propagates through a random scattering medium, such as a forest, its energy is attenuated and random phase fluctuations are induced. The magnitude of the random phase fluctuations induced is important in estimating how well a Synthetic Aperture Radar (SAR) can image objects within the scattering medium. The two-layer random medium model, consisting of a scattering layer between free space and ground, is used to calculate the variance of the phase fluctuations induced between a transmitter located above the random medium and a receiver located below the random medium. The scattering properties of the random medium are characterized by a correlation function of the random permittivity fluctuations. The effective permittivity of the random medium is first calculated using the strong fluctuation theory, which accounts for large permittivity fluctuations of the scatterers. The distorted Born approximation is used to calculate the first-order scattered field. A perturbation series for the phase of the received field in the Rytov approximation is then introduced and the variance of the phase fluctuations is also calculated assuming that the transmitter and receiver are in the paraxial limit of the random medium, which allows an analytic solution to be obtained. Results are compared using the paraxial approximation, scalar Green's function formulation, and dyadic Green's function formulation. The effects studied are the dependence of the variance of the phase fluctuations on receiver location in lossy and lossless regions, medium thickness, correlation length and fractional volume of scatterers, depolarization of the incident wave, ground layer permittivity, angle of incidence, and polarization. Author

N93-13088*# Washington Univ., Seattle. Electromagnetics and Remote Sensing Lab.

POLARIMETRIC SIGNATURES OF A CANOPY OF DIELECTRIC CYLINDERS BASED ON FIRST AND SECOND ORDER VECTOR RADIATIVE TRANSFER THEORY **c32**

Leung Tsang, Chi Hou Chan, Jin Au Kong (Massachusetts Inst. of Tech., Cambridge.), and James Joseph (General Electric Co., Schenectady, NY.) *In* MIT, Remote Sensing of Earth Terrain 30 Sep. 1992 17 p Repr. from Journal of Electromagnetic Waves and Applications (VSP), v. 1, no. 1, 1992 p 19-51 Sponsored in part by ARO and NSF (For primary document see N93-13084 03-43)

Avail: CASI HC A03/MF A01

Complete polarimetric signatures of a canopy of dielectric cylinders overlying a homogeneous half space are studied with the first and second order solutions of the vector radiative transfer theory. The vector radiative transfer equations contain a general nondiagonal extinction matrix and a phase matrix. The energy conservation issue is addressed by calculating the elements of the extinction matrix and the elements of the phase matrix in a manner that is consistent with energy conservation. Two methods are used. In the first method, the surface fields and the internal fields of the dielectric cylinder are calculated by using the fields of an infinite cylinder. The phase matrix is calculated and the extinction matrix is calculated by summing the absorption and scattering to ensure energy conservation. In the second method, the method of moments is used to calculate the elements of the extinction and phase matrices. The Mueller matrix based on the first order and second order multiple scattering solutions of the

vector radiative transfer equation are calculated. Results from the two methods are compared. The vector radiative transfer equations, combined with the solution based on method of moments, obey both energy conservation and reciprocity. The polarimetric signatures, copolarized and depolarized return, degree of polarization, and phase differences are studied as a function of the orientation, sizes, and dielectric properties of the cylinders. It is shown that second order scattering is generally important for vegetation canopy at C band and can be important at L band for some cases. Author

N93-13094*# National Oceanic and Atmospheric Administration, Boulder, CO. Wave Propagation Lab.

REMOTE SENSING DATA FROM CLARET: A PROTOTYPE CART DATA SET

Wynn L. Eberhard, Taneil Uttal, Kurt A. Clark, Richard E. Cupp, Ellsworth G. Dutton, Leonard Fedor, S., Janet M. Intrieri (Colorado Univ., Boulder.), Sergey Y. Matrosov (Colorado Univ., Boulder.), Jack B. Snider, and Ron J. Willis (Colorado Univ., Boulder.) Jun. 1992 65 p Sponsored by NASA, Washington

(Contract Proj. 40220-CL-378; DE-AI06-91RL-12089)

(NASA-CR-191294; NAS 1.26:191294; PB92-206853;

NOAA-TM-ERL-WPL-223) Avail: CASI HC A04/MF A01

The data set containing radiation, meteorological , and cloud sensor observations is documented. It was prepared for use by the Department of Energy's Atmospheric Radiation Measurement (ARM) Program and other interested scientists. These data are a precursor of the types of data that ARM Cloud And Radiation Testbed (CART) sites will provide. The data are from the Cloud Lidar And Radar Exploratory Test (CLARET) conducted by the Wave Propagation Laboratory during autumn 1989 in the Denver-Boulder area of Colorado primarily for the purpose of developing new cloud-sensing techniques on cirrus. After becoming aware of the experiment, ARM scientists requested archival of subsets of the data to assist in the developing ARM program. Five CLARET cases were selected: two with cirrus, one with stratus, one with mixed-phase clouds, and one with clear skies. Satellite data from the stratus case and one cirrus case were analyzed for statistics on cloud cover and top height. The main body of the selected data are available on diskette from the Wave Propagation Laboratory or Los Alamos National Laboratory. Author

N93-13258# Instituto de Pesquisas Espaciais, Sao Jose dos Campos (Brazil).

FIELD SPECTRORADIOMETRY AND SAIL MODEL APPLICATION TO IRRIGATED WHEAT (TRITICUM AESTIVUM, L) CANOPIES SPECTRAL REFLECTANCE Thesis [REFLECTANCIA ESPECTRAL DO TRIGO IRRIGADO (TRITICUM AESTIVUM, L) POR ESPECTRORRADIOMETRIA DE CAMPO E APLICACAO DO MODELO SAIL]

Marcio deMorissonValeriano 1992 141 p In PORTUGESE

(INPE-5426-TDI/483) Avail: CASI HC A07/MF A02

Experimental data and results of SAIL model supported a study relating the spectral reflectance of wheat canopies (Triticum aestivum, L.) to their biophysical parameters which included an evaluation of the model potential for investigating such relationships. The SAIL model calculates the spectral reflectance of vegetation as a function of canopy biophysical and spectral parameters and of the viewing/illuminating geometry. Data were taken over 7 varieties on 14 plots, placed in Planaltina (DF), under homogeneous management, and irrigation schedules. The measurements taken from spectroradiometer in the visible to the near-infrared portion of the electromagnetic spectrum (from 547 to 823 nm) and the agronomic data were determined together on 13 dates throughout the growing season (from May - Sep. 1989). The red and the near-infrared reflectance showed strong relationship to the leaf area index (LAI) under logarithmic regression, mainly before LAI reaches its maximum. The model was applied with experimental field data complemented by data found in literature, and the model simulations and the measured data had similar behavior. Canopy single component spectral data were considered of great importance as quantitative basis for studies concerning spectral-agronomic relationships. Author

N93-13333# Army Topographic Engineering Center, Fort Belvoir, VA.

IMPACT OF DIGITAL TERRAIN ELEVATION DATA (DTED) RESOLUTION ON TERRAIN VISUALIZATION: SIMULATION VERSUS REALITY

Louis A. Fatale and James R. Ackeret 2 Dec. 1991 9 p

(AD-A254237; TEC-R-167) Avail: CASI HC A02/MF A01

This study provides evidence of the influence of DTED resolution (in regions with different terrain roughness) on Army terrain data applications. The report documents results of the U.S. Army Topographic Engineering Center's DTED resolution analysis including extensive field work and terrain visualization undertaken to investigate DTED integrity in comparison to the actual terrain. Finally, the report offers conclusions regarding DTED support for Army tactical and simulation applications. GRA

N93-13345# Army Topographic Engineering Center, Fort Belvoir, VA.

USING ITERATIVE ORTHOPHOTO REFINEMENTS TO CORRECT DIGITAL ELEVATION MODELS (DEM'S)

Raye Norvelle 1991 10 p

(AD-A254625; TEC-R-179) Avail: CASI HC A02/MF A01

A new technique is described that can be used to correct the digital elevation data obtained using digital correlation methods on terrain stereoimages. The new technique takes advantage of the speed of modern computers and the inherent geometric relationship between elevation data and orthophotographs to provide speedy, accurate and nearly automatic methods for both generating and correcting digital elevation models (DEM's). GRA

N93-13371 Colorado State Univ., Fort Co!lins.

MICROWAVE REMOTE SENSING OF A PRECIPITATING ATMOSPHERE Ph.D. Thesis

Francis Joseph Turk 1991 196 p

Avail: Univ. Microfilms Order No. DA9216222

Throughout the 10 to 100 GHz spectrum, the scattering and absorption properties of atmospheric hydrometeors and gases vary widely. As a result, multifrequency techniques for passive microwave estimation of precipitation have been proposed. The emission-based, lower frequency observations (less than 37 GHz) effectively respond at lower altitudes, while the scattering based higher frequencies (greater than 37 GHz) respond at higher altitudes, thus providing a potential means to link self-consistent precipitation estimates to the multifrequency brightness temperatures (T sub B). Unlike many schemes which link T sub B to the liquid water content, this study emphasis the use of scattering based channels to infer information on the ice water content. The high altitude ice region remains fairly unobscured to a spaceborne sensor, suggesting the implementation of the scattering-based channels in a top-down methodology as the first step in a retrieval of the cloud vertical structure. Extensive model simulations of the upwelling T sub B were performed throughout clouds whose bulk microphysical properties were deduced from multiparameter radar data and cloud model output obtained during the 1986 Cooperative Huntsville Meteorological Experiment (COHMEX). A highly accurate plane-parallel microwave radiative transfer model with Mie phase matrices was used to solve the equation of transfer in a scattering atmosphere with a land surface. COHMEX aircraft radiometer measurements at 18, 37, and 92 GHz were compared with the output of the multiparameter radar-initialized radiative transfer model. Deviations at 92 GHz were compared with the output of the multiparameter radar-initialized radiative transfer model. Deviations at 92 GHz were attributed to uncertanties in the bulk density and size distribution of the ice region. Using both multiparameter radar observations and cloud model output, the 37-85 GHz T sub B difference (delta T sub B) was found to be sensitive to the amount of integrated ice water path (IWP) lying above the rain, independent of ice density. Presence of coexisting cloud water and ice had the net effect of compressing the delta T sub B depressions greater than 200 K were noted to be relatively insensitive to the amount of underlying liquid water content, and mainly dependent upon the thickness of the ice layer. Dissert. Abstr.

N93-13412# Instituto de Pesquisas Espaciais, Sao Jose dos Campos (Brazil).

BRAZILIAN REMOTE SENSING COMMUNITY: HISTORICAL, GEOGRAPHICAL AND ECONOMIC ASPECTS

Tania Maria Sausen 1992 8 p

(INPE-5421-PRE/1763) Avail: CASI HC A02/MF A01

Since 1968 the National Institute for Space Research (INPE) in Brazil has been working on remote sensing. After 24 years, the number of remote sensing users registered at INPE data base is around 3000 people.

This paper presents a study of the historical, geographical and economic aspects that determine the distribution of remote sensing community in Brazil and its behavior during the past fourteen years. In this study the following topics are analyzed: papers presented in the Brazilian Remote Sensing Symposiums, training courses that have been developed since October 1985 and user questionnares. With this piece of information, it was possible to identify that 50 percent of Brazilian Remote Sensing Community is located in the Southeast region. The Southeast and South regions together represent 80 percent of Brazilian Remote Sensing Community. Both these regions represent only 25 percent of the country area, but they are the richest and most developed regions in Brazil.

Author

N93-13440# Lockheed Electronics Co., Houston, TX.
THE CORRELATION OF ACTIVE AND PASSIVE MICROWAVE OUTPUTS FOR THE SKYLAB S-193 SENSOR
K. Krishen Jan. 1976 24 p
(LEC-7819) Avail: CASI HC A03/MF A01

This paper presents the results of the correlation analysis of the Skylab S-193 13.9 GHz Radiometer/Scatterometer data. Computer analysis of the S-193 data shows more than 50 percent of the radiometer and scatterometer data are uncorrelated. The correlation coefficients computed for the data gathered over various ground scenes indicates the desirability of using both active and passive sensors for the determination of various Earth phenomena.

Author

N93-13840 Utah State Univ., Logan.
THE USE OF REMOTELY SENSED DATA IN DELINEATION OF HYDROLOGIC RESPONSE UNITS AND ESTIMATION OF THEIR RAINFALL-RUNOFF MODEL PARAMETERS Ph.D. Thesis
Chi-Chung Lau 1991 239 p
Avail: Univ. Microfilms Order No. DA9222281

Estimation of parameters of the Stanford Watershed Model (SWM) was attempted from LANDSAT Thematic Mapper (TM) and Digital Elevation Model (DEM) data. Three parameters, BMIR (infiltration), LZC (soil depth), and ETLF (evapotranspiration), were found to be correlated with remotely sensed data in the San Dimas watershed in southern California. The study procedure was to partition the watershed into small hydrologic response units (HRU) with similar physical properties; estimate properties of each HRU from LANDSAT and DEM data; and calibrate the model parameters for corresponding area. Relationships between the calibrated parameters and the physical variables were explored. Five physical variables highly related to the rainfall-runoff process were used for dividing the catchment into HRU. Three of them were topographic variables: elevation, aspect, and topographic index; and the other two were soils and vegetation information: brightness and greenness. A k-mean clustering algorithm was applied to divide the watershed into two units by minimizing the total variances of the five variables. Divisions into three, four, and five units were also examined. Brightness, elevation, and aspect were found to be the three most important variables contributing to differentiate HRUs in the study area. The physical properties of each HRU were represented by the average values of the included pixels. Elevation, slope, and area were read directly as input parameters to the SWM to calibrate other model parameters. In each unit, elevation was used to estimate rainfall and temperature; slope was used to compute overland flow; and area was used to determine runoff volume. Watershed runoff was summed over the units to fit recorded streamflow. In the study area, relative position of a unit on hillslope was found to strongly impact the parameter-variable relationships for BMIR and LZC. BMIR had a positive correlation with brightness in the units located in uplands, and correlated negatively with brightness in the units located in bottom lands. LZC correlated positively with greenness when units were separated into two categories of upland and bottom land. ETLF was estimated from elevation with an exponential equation. Studies on other watersheds are likely to lead to different relationships, and additional work is necessary before reaching definitive conclusions.

Dissert. Abstr.

N93-13867# EG and G Energy Measurements, Inc., Las Vegas, NV.
DECIDUOUS FOREST SCENE COMPLEXITY IN HIGH-RESOLUTION MULTISPECTRAL SCANNER IMAGERY Final Report
Lee K. Balick Aug. 1992 75 p
(DA Proj. 4A1-62719-AT-40)
(AD-A255511; WES/TR/EL-92-26) Avail: CASI HC A04/MF A01

This report summarizes within-scene variability and spectral relationships of high-resolution, multitemporal, multispectral scanner images of a deciduous forest in eastern Tennessee. The data were obtained using a helicopter-mounted Daedalus D-1268 multispectral scanner with a 1.25-milliradian instantaneous field of view at 175 ft (53.34 m) above ground level (agl) and 350 ft (106.7 m) agl. Flights were made under generally clear skies at predawn twilight, mid-morning, and near solar noon in the north and west direction at both altitudes. In the mid-morning and solar noon data, spectral bands of yellow-green, red, near-infrared, and thermal infrared energy were analyzed. Additional thermal infrared data from a Daedalus D-1261 scanner flown at 150 ft (45.7 m) agl under overcast skies were also available. Within-scene variability was analyzed to extract parameters for autoregression models of texture for scene modeling and to provide validation data for physically based models of remotely sensed temperature variation of forests.

GRA

N93-13956 Oklahoma State Univ., Stillwater.
AN EVALUATION OF THE USE AND FUTURE NEED OF REMOTELY SENSED IMAGES IN GRADES K-12 Ph.D. Thesis
Kevin Patrick Allen 1991 129 p
Avail: Univ. Microfilms Order No. DA9220541

During the spring of 1991, a study was conducted to evaluate the use and future need of remotely sensed images in elementary and secondary education. Surveys, distributed by the Aerospace Education Service Program at Oklahoma State University, were sent to 951 K-12 educators that receive the Journal of Geography. This research population was chosen because the National Council for Geography Education inserted eight remotely sensed images in Journal of Geography. These surveys were completed and returned directly to the NASA/AESP office at Oklahoma State University. Three hundred and twenty-one surveys were returned and responses were analyzed to assess the status of remote sensing in K-12 education. The results of this study indicate that teachers at the elementary and secondary levels of education are now knowledgeable in the principles of remote sensing and, therefore, are not using remotely sensed materials as educational tools. Survey responses indicated that educators would be interested in using these materials if they were easily available and reasonably priced. The cost of remotely sensed materials was perceived by the respondents to be the greatest barrier to their adoption in the classroom. Lack of teacher training in the concepts of remote sensing was perceived as the second largest barrier to incorporating remotely sensed images into the classroom. Survey participants suggest that workshops and in-service programs on the principles of remote sensing be conducted to train educators to effectively use these materials in the classroom. Participants indicated they would be willing to attend educational workshops on the principles of remote sensing and its integration into the classroom. A large percentage of the respondents were unsure if their school administration would be receptive to adopting these materials for educational purposes. The majority of the teachers possess undergraduate degrees in one of the social studies fields and three quarters of the responding educators had attained advanced degrees. Results from the chi-square test revealed no significant difference in the responses of educators possessing B.S. and M.S. degrees to selected research questions.

Dissert. Abstr.

N93-13969 Colorado Univ., Boulder.
APPLICATION OF SATELLITE ALTIMETRY TO STUDY THE GULF OF ALASKA GYRE Ph.D. Thesis
Shyamkumar Bhaskaran 1991 174 p
Avail: Univ. Microfilms Order No. DA9220393

Satellite altimetry has demonstrated the capability to observe a wide range of ocean phenomena. Satellite altimetry was used to examine the Gulf of Alaska region, where the signals of the ocean circulation are fairly small. The research had two components: the first analyzed the variability while the second involved computing a mean sea surface. For the first portion of the study, crossover data from the GEOSAT Geodetic Mission (GM) and colinear data from the Exact Repeat Mission (ERM) were processed separately to form time series at grid points located at the ERM crossover locations. The time series from the GM and ERM were then combined to produce a 3.75 year data set. A portion of the analysis was dedicated to performing a sensitivity study to see the effects of different orbit error models, water vapor, and tidal error corrections. It was

then shown that the altimetric time series agreed fairly well with the in situ data, lending confidence to the processing techniques. The altimetric time series during the complete, GM, and ERM time spans were anlyzed using Empirical Orthogonal Functions (EOF). Examination of the EOF spatial patterns and amplitudes revealed variability that occurs primarily on annual and interannual time scales. A comparison with EOF analysis of the pressure field during the same time period showed that the primary annual mode in each of the time spans correlated highly with the annual variation in the pressure field. A second annual mode present in the ERM data set was found to correlate well with sea level at Seward. Regarding the interannual modes, the amplitude time series of the first mode in the complete data set was very similar to the North Pacific pressure index during the 1985-1989 time frame. The maximum correlation was at a lag of 250 days. Finally, an interannual mode was present in all three data sets which was closely linked to the baroclinic variations measured by the hydrographic data. The second component of the study involved computing a mean sea surface using statistical knowledge of the orbit errors which contaminate the data. To verify the procedure and test its accuracy, simulations were performed. The simulations showed that the mean sea surface can be recovered to an accuracy of 15 to 25 cm in a root mean square sense. These values are too large for absolute dynamic topography studies in the Gulf of Alaska, but improved geoids and orbits should prove the technique to be feasible in the future. Dissert. Abstr.

N93-14051 New Brunswick Univ., Fredericton.
ON THE SPACE-TIME OCEAN CURRENT VARIABILITY AND ITS EFFECTS ON THE LENGTH-OF-DAY Ph.D. Thesis
Nikolaos Theodoros Christou 1990 355 p
Avail: Univ. Microfilms Order No. DANN59510

Earth rotation (polar motion and length-of-day) studies have embarked on a new era with the contributions from space geodesy observation techniques (higher accuracy, higher temporal resolution) and the availability of new, global data bases of atmospheric and oceanic observables. Irregular variations in the earth's rotation rate (length-of-day (LOD) variations) on time scales of 5 years or less are associated with changes in the angular momentum of the solid earth. The problem of transfer of angular momentum between the Earth System components (consisting of the solid earth, the oceans, and the atmosphere) has emerged today as a problem of great scientific interest, because of the geophysical and environmental implications associated with LOD variations. This thesis research chiefly investigates the time-dependent perturbations of LOD on time scales of about two years or less, associated with the space-time fluctuations of the global ocean circulation. Estimates of the space-time variations of ocean currents were derived from both in-situ oceanographic data and two years of satellite altimetry observations from the GEOSAT Exact Repeat Mission. A new technique for extracting ocean current variability from satellite altimetry was developed. The technique is based on the gradient operator and offers advantages in that it is conceptually simple and computationally efficient. Through the analysis of ocean current variability, it is established that the oceanic excitation of LOD is at least at the level of 0.1 milliseconds. Variations in the oceanic excitation of delta-LOD have been identified and quantified at periods of 1 year and 0.5 years. At the annual period, the results indicate that the oceanic excitation appears large enough to account for the existing discrepancy between the observed (non-tidal) delta-LOD and the atmospheric contribution. No significant oceanic excitation of delta-LOD is found at the semi-annual period. The results also indicate that there exist statistically significant higher frequency variations at approximately 121-day, 107-day, and 89-day periods. The analysis of the GEOSAT altimetry data generated many new questions regarding the oceanic behavior and its dynamical link to LOD variations that require further investigations. Dissert. Abstr.

N93-13164*# Medical Univ. of South Carolina, Charleston.
EARTH OBSERVATION PHOTOGRAPHY: LOOKING BACK 20 YEARS AFTER SKYLAB
James H. Nicholson *In* NASA. Goddard Space Flight Center, The 1992 Shuttle Small Payloads Symposium Oct. 1992 p 47-56 (For primary document see N93-13158 03-12)
Avail: CASI HC A02/MF A03

44 ENERGY PRODUCTION AND CONVERSION

Includes specific energy conversion systems, e.g., fuel cells; global sources of energy; geophysical conversion; and windpower.

For related information see also *07 Aircraft Propulsion and Power, 20 Spacecraft Propulsion and Power,* and *28 Propellants and Fuels.*

N93-12683# Westinghouse Electric Corp., Pittsburgh, PA. Nuclear and Advanced Technology Div.
GAS COOLED FUEL CELL SYSTEMS TECHNOLOGY DEVELOPMENT Final Report
Mar. 1992 195 p
(Contract DE-AC21-82MC-24223)
(DE92-0012983-3103; DOE/MC/24223-3103) Avail: CASI HC A09/MF A03

This report documents in detail the work performed by Westinghouse Electric Corporation and the Energy Research Corporation during the fourth phase of a planned multiphase program to develop a Phosphoric Acid Fuel Cell (PAFC) for electric utility or industrial power plant applications. The results of this effort include (1) development of a baseline rolled electrode technology; (2) advancement of fuel cell technology through innovative improvements in the areas of acid management, catalyst selection, electrode and plate materials and processes, component designs, and quality assurance programs; (3) demonstration of improved fuel cell and stack performance and endurance; (4) successful scaleup of cell and stack design features into full height 100 kW stacks; and (5) demonstration of combining stacks into a 400 kW module that will be the building block for power plants, including the development of testing facilities and operating procedures applicable to plant operations. Author

N93-12812# Texas A&M Univ., College Station. Dept. of Chemical Engineering.
OXYGEN ELECTRODE REACTION IN MOLTEN CARBONATE FUEL CELLS Ph.D. Thesis
A. J. Appleby and R. E. White Jul. 1992 166 p
(Contract DE-FG22-87PC-79931)
(DE92-040180; DOE/PC-79931/T13) Avail: CASI HC A08/MF A02

The molten carbonate fuel cell system is a leading candidate for the utility power generation because of its high efficiency for fuel to AC power conversion, capability for an internal reforming, and a very low environmental impact. However, the performance of the molten carbonate fuel cell is limited by the oxygen reduction reaction and the cell life time is limited by the stability of the cathode material. An elucidation of oxygen reduction reaction in molten alkali carbonate is essential because overpotential losses in the molten carbonate fuel cell are considerably greater at the oxygen cathode than at the fuel anode. Oxygen reduction on a fully-immersed gold electrode in a lithium carbonate melt was investigated by electrochemical impedance spectroscopy and cyclic voltammetry to determine electrode kinetic and mass transfer parameters. The dependences of electrode kinetic and mass transfer parameters on gas composition and temperature were examined to determine the reaction orders and the activation energies. The results showed that oxygen reduction in a pure lithium carbonate melt occurs via the peroxide mechanism. A mass transfer parameter, D(sub O)(sup 1/2)C(sub O), estimated by the cyclic voltammetry concurred with that calculated by the EIS technique. The temperature dependence of the exchange current density and the product D(sub O)(sup 1/2)C(sub O) were examined and the apparent activation energies were determined to be about 122 and 175 kJ/ mol, respectively. DOE

N93-12837# Midwest Research Inst., Golden, CO.
OCEAN ENERGY PROGRAM OVERVIEW, FISCAL YEARS 1990-1991
May 1992 9 p
(Contract DE-AC02-83CH-10093)
(DE91-002176; DOE/CH-10093/99) Avail: CASI HC A02/MF A01

The oceans are the world's largest solar energy collector and storage system. Covering 71 percent of the earth's surface, the oceans collect and store this energy as waves, currents, and thermal and salinity gradients. The purpose of the US Department of Energy's (DOE) Ocean Energy Program is to develop techniques that harness ocean energy cost effectively and in ways that do not harm the environment. The program seeks to develop ocean energy technology to a point at which industry can accurately

assess whether the applications of the technology are viable energy conversion alternatives, or supplements to current power-generating systems. In past studies, DOE identified ocean thermal energy conversion (OTEC), which uses the temperature difference between warm surface water and cold deep water, as the most promising of the ocean energy technologies. As a result, the Ocean Energy Program has concentrated research that advances OTEC technology. The program also monitored developments in wave energy, ocean current, and salinity gradient concepts. It is not actively developing these technologies now. The mission of the Ocean Energy Program is to develop techniques to harness the vast solar energy stored in the oceans' waves, currents, and thermal and salinity gradients. DOE

N93-12838# Midwest Research Inst., Golden, CO.
DEVELOPMENT OF LARGE-AREA MONOLITHICALLY INTEGRATED SILICON-FILM PHOTOVOLTAIC MODULES
J. A. Rand (Astropower, Inc., Newark, DE.), C. Bacon (Astropower, Inc., Newark, DE.), J. E. Cotter (Astropower, Inc., Newark, DE.), T. H. Lampros (Astropower, Inc., Newark, DE.), A. E. Ingram (Astropower, Inc., Newark, DE.), T. R. Ruffins (Astropower, Inc., Newark, DE.), R. B. Hall (Astropower, Inc., Newark, DE.), and A. M. Barnett (Astropower, Inc., Newark, DE.)
Jul. 1992 26 p
(Contract DE-AC02-83CH-10093)
(DE92-010600; NREL/TP-413-4996) Avail: CASI HC A03/MF A01

This report describes work to develop Silicon-Film Product 3 into a low-cost, stable device for large-scale terrestrial power applications. The Product 3 structure is a thin (less than 100 micron) polycrystalline silicon layer on a non-conductive supporting ceramic substrate. The presence of the substrate allows cells to be isolated and interconnected monolithically in various series/parallel configurations. The long-term goal for the product is efficiencies over 18 percent on areas greater than 1200 cm(exp 2). The high efficiency is made possible through the benefits of using polycrystalline thin silicon incorporated into a light-trapping structure with a passivated back surface. Short-term goals focused on the development of large-area ceramics, a monolithic interconnection process, and 100 cm(exp 2) solar cells. Critical elements of the monolithically integrated device were developed, and an insulating ceramic substrate was developed and tested. A monolithic interconnection process was developed that will isolate and interconnect individual cells on the ceramic surface. Production-based, low-cost process steps were used, and the process was verified using free-standing silicon wafers to achieve an open-circuit voltage (V(sub oc)) of 8.25 V over a 17-element string. The overall efficiency of the silicon-film materials was limited to 6percent by impurities. Improved processing and feedstock materials are under investigation. DOE

N93-12923# Los Alamos National Lab., NM.
INDUSTRIAL APPLICATIONS OF HOT DRY ROCK GEOTHERMAL ENERGY
D. V. Duchane 1992 9 p Presented at the International Conference on Industrial Uses of Geothermal Energy, Reykjavik, Iceland, 2-4 Sep. 1992
(Contract W-7405-eng-36)
(DE92-018903; LA-UR-92-2380; CONF-9209147-1) Avail: CASI HC A02/MF A01

Geothermal resources in the form of naturally occurring hot water or steam have been utilized for many years. While these hydrothermal resources are found in many places, the general case is that the rock at depth is hot, but does not contain significant amounts of mobile fluid. An extremely large amount of geothermal energy is found around the world in this hot dry rock (HDR). Technology has been under development for more than twenty years at the Los Alamos National Laboratory in the United States and elsewhere to develop the technology to extract the geothermal energy from HDR in a form useful for electricity generation, space heating, or industrial processing. HDR technology is especially attractive for industrial applications because of the ubiquitous distribution of the HDR resource and the unique aspects of the process developed to recover it. In the HDR process, as developed at Los Alamos, water is pumped down a well under high pressure to open up natural joints in hot rock and create an artificial geothermal reservoir. Energy is extracted by circulating water through the reservoir. Pressurized hot water is returned to the surface through the production well, and its thermal energy is extracted for practical use. The same water is then recirculated through the system to mine more geothermal heat. Construction of a pilot HDR facility at Fenton Hill, NM, USA, has recently been completed by the Los Alamos National Laboratory. It consists of a large underground reservoir, a surface plant, and the connecting wellbores. This paper describes HDR technology and the current status of the development program. Novel industrial applications of geothermal energy based on the unique characteristics of the HDR energy extraction process are discussed. DOE

N93-12937# Department of Energy, Washington, DC.
WORLD ENERGY PROJECTION SYSTEM (WEPS), MARCH 1992. MODEL INSTALLATION MANUAL, DISTRIBUTION DISK LAYOUT
Mar. 1992 21 p
(PB92-169572; DOE/SW/DK-92/044A) Avail: CASI HC A03/MF A01

The World Energy Projection System (WEPS) is a set of Lotus 1-2-3 spreadsheet programs furnished by the Energy Information Administration (EIA) that link the following: international energy data published in the International Energy Annual 1990, assumptions and estimates concerning world energy resources, production capacities, utilization rates, and oil-export revenues; projections of gross domestic product (GDP); and assumptions about the intensity of economic activity over time to produce projections of world energy consumption by major energy source (oil, natural gas, coal, nuclear power, and 'other' energy sources) and assumptions about world oil production capacities. Projections from 1991 to 2010 are presented for selected countries, country groups, and the world as a whole. GRA

N93-12987# National Inst. of Standards and Technology, Gaithersburg, MD. Office of Technology Evaluation and Assessment.
ENERGY RELATED INVENTIONS PROGRAM. A JOINT PROGRAM OF THE DEPARTMENT OF ENERGY AND THE NATIONAL INSTITUTE OF STANDARDS AND TECHNOLOGY. STATUS REPORT FOR RECOMMENDATIONS 1 THROUGH 300
Dec. 1991 177 p Sponsored by DOE
(PB92-226265; NISTIR-4898) Avail: CASI HC A09/MF A02

The Energy-Related Inventions Program was established in 1975. Since its inception, over 29,000 inventions have been evaluated. As of the printing of this report, 563 have been recommended to the Department of Energy. This report supercedes NISTIR 4533 and summarizes the status of recommended inventions 1 through 300. A companion report, NISTIR 4899, summarizes the remainder of the recommended inventions. GRA

N93-12988# National Inst. of Standards and Technology, Gaithersburg, MD. Office of Technology Evaluation and Assessment.
ENERGY RELATED INVENTIONS PROGRAM. A JOINT PROGRAM OF THE DEPARTMENT OF ENERGY AND THE NATIONAL INSTITUTE OF STANDARDS AND TECHNOLOGY. STATUS REPORT FOR RECOMMENDATIONS 301-563
Dec. 1991 242 p Sponsored by DOE
(PB92-226273; NISTIR-4899) Avail: CASI HC A11/MF A03

The Energy-Related Inventions Program was established in 1975. Since its inception, over 29,000 inventions have been evaluated. As of the printing of this report, 563 have been recommended to the Department of Energy. This report supercedes NISTIR 4534 and summarizes the status of recommended inventions 301 through 563. A companion report (NISTIR 4898) summarizes recommended inventions 1 through 300. GRA

N93-13001# Department of Energy, Washington, DC. Advanced Energy Projects Div.
ADVANCED ENERGY PROJECTS FY 1992 RESEARCH SUMMARIES
Sep. 1992 61 p
(DE92-040442; DOE/ER-0558T) Avail: CASI HC A04/MF A01

The Division of Advanced Energy Projects (AEP) provides support to explore the feasibility of novel, energy-related concepts that evolve from advances in basic research. These concepts are typically at an early stage of scientific definition and, therefore, are beyond the scope of ongoing applied research or technology development programs. The Division provides a mechanism for converting basic research findings to applications that eventually could impact the Nation's energy economy. Technical topics include physical, chemical, materials, engineering, and biotechnologies. Projects can involve interdisciplinary approaches to solve energy-related problems. Projects are supported for a finite period of time, which is typically three years. Annual funding levels for projects are usually about $300,000 but can vary from approximately $50,000 to $500,000. It is expected that, following AEP support, each concept will be sufficiently

developed and promising to attract further funding from other sources in order to realize its full potential. There were 39 research projects in the Division of Advanced Energy Projects during Fiscal Year 1992. The abstracts of those projects are provided to introduce the overall program in Advanced Energy Projects. Further information on a specific project may be obtained by contacting the principal investigator, who is listed below the project title. Projects completed during FY-1992 are indicated. DOE

N93-13039# Energy Research Corp., Danbury, CT.
UNDERSTANDING OF CARBONATE FUEL CELL RESISTANCE ISSUES FOR PERFORMANCE IMPROVEMENT
C. Y. Yuh, M. Farooque, and R. Johnsen 1992 8 p Presented at the US Department of Energy Contractors Review Meeting on Fuel Cells, Morgantown, WV, 14-15 Jul. 1992
(Contract DE-AC21-90MC-27168)
(DE92-019976; DOE/MC-27168/92/C0051; CONF-920748-9) Avail: CASI HC A02/MF A01

The overall objective of the current Task 6 under Contract AC21-90MC27168 is to develop understanding as well as quantification of cell ohmic resistance in carbonate fuel cell. The important resistance-contributing interfaces and elements are being investigated in high-temperature out-of-cell resistance experiments, using an AC-impedance technique. Ohmic resistance loss in a state-of-the-art carbonate fuel cell contributes about 65 mV loss at BOL (beginning-of-life). It may increase to about as much as 145 mV after 40,000 hours. Its reduction will offer further improvement in fuel cell power plant efficiency. The important resistance contributing elements/interfaces are illustrated. . The majority of the ohmic loss attributed to electrolyte matrix (ionic) and cathode-side hardware (electronic). The ohmic loss due to anode-side hardware can generally be neglected because the anode-side hardware is surface protected resulting in very little surface oxide formation. The ohmic resistance of the electrodes is also negligible. The matrix ionic resistance is influenced by many factors: electrolyte conductivity, matrix porosity, tortuosity, electrolyte fill level and matrix thickness. At present, matrix contributes to greater than 300 m-Omega cm(sup 2) (greater than 70 percent of the total cell ohmic resistance) and is the major resistance contributor. DOE

N93-13040# International Fuel Cells Corp., South Windsor, CT.
ADVANCED WATER-COOLED PHOSPHORIC ACID FUEL CELL DEVELOPMENT
G. W. Scheffler and F. S. Kemp 1992 4 p Presented at the US Department of Energy Contractors Review Meeting on Fuel Cells, Morgantown, WV, 14-15 Jul. 1992
(Contract DE-AC21-88MC-24221)
(DE92-019979; DOE/MC-24221/92/C0056; CONF-920748-5) Avail: CASI HC A01/MF A01

The final task of the program addressed the testing of the three short stacks described above. The overall objective of this series of short stack tests was to verify the operation of the advanced cell design at both on-site and electric utility operating conditions. The small area development stack was operated first at atmosphenc pressure (to compare its characteristics to previous atmospheric tests) and then at 120 psia to examine its ability to operate at electric utility conditions. The 10-ft(sup 2) stack was also run at pressurized conditions to verify the scaling characteristics of the features developed in this program. The small area development stack was assembled and successfully tested for 3050 hours. The first 2380 hours of testing was conducted at atmospheric pressure, and the final 670 hours was at 120 psia pressurized conditions. Performance was stable throughout testing. Intermediate and post test inspections of the stack showed parts to be in generally good condition with no anomalies. DOE

N93-13041# Eltron Research, Inc., Aurora, IL.
PEROVSKITE SOLID ELECTROLYTES FOR SOFC
A. F. Sammells 1992 10 p Presented at the US Department of Energy Contractors Review Meeting on Fuel Cells, Morgantown, WV, 14-15 Jul. 1992
(Contract DE-FG02-90ER-80910)
(DE92-019981; DOE/ER-80910/92/C0058; CONF-920748-7) Avail: CASI HC A02/MF A01

Selected perovskite solid electrolytes incorporated into research size fuel cells have shown stability for greater than 4000 hours at 600 C. Perovskite lattice requirements which favor low E(sub a) for ionic conduction include (1) that the perovskite lattice possess a moderate enthalpy of formation, (2) perovskite lattice possess large free volumes, (3) that the lattice minimally polarizes the mobile ion and (4) that the crystallographic saddle point r(sub c) for ionic conduction is approx equal 1. DOE

N93-13069# Argonne National Lab., IL.
PROCEEDINGS OF THE TENTH SYMPOSIUM ON ENERGY ENGINEERING SCIENCES: SYNERGISM OF ANALYSIS, MODELING, AND EXPERIMENT
Jul. 1992 293 p Symposium held in Argonne, IL, 11-13 May 1992
(Contract W-31-109-eng-38)
(DE92-018777; CONF-9205147) Avail: CASI HC A13/MF A03

The Tenth Symposium on Energy Engineering Sciences was held on May 11-13, 1992, at the Argonne National Laboratory, Argonne, Illinois. These proceedings include the program, list of participants, and the papers that were presented during the seven technical sessions held at this meeting. This was the tenth annual symposium sponsored by the Engineering Research Program of the Office of Basic Energy Sciences of the U.S. Department of Energy. The central theme of this year's meeting was synergism of analysis, modeling, and experiment and related topics. Each year a group of selected researchers in the DOE/BES Engineering Research Program are invited to present their research findings in such an open forum. This Symposium was organized into seven technical sessions: fluid mechanics (two sessions); solid mechanics; analysis, nonlinear systems (two sessions); chemical processing; and instrumentation and diagnostics. Separate abstracts were prepared for individual papers in this report. DOE

N93-13082# Pacific Northwest Lab., Richland, WA.
ALTERNATIVE MATERIALS FOR SOLID OXIDE FUEL CELLS: FACTORS AFFECTING AIR-SINTERING OF CHROMITE INTERCONNECTIONS
L. A. Chick and J. L. Bates Jul. 1992 12 p Presented at the US Department of Energy Contractors Review Meeting on Fuel Cells, Morgantown, WV, 14-15 Jul. 1992
(Contract DE-AC06-76RL-01830)
(DE92-019356; PNL-SA-21162; CONF-920748-4) Avail: CASI HC A03/MF A01

The purpose of this research is to develop alternative materials for solid oxide fuel cell (SOFC) interconnections and electrodes with improved electrical, thermal, and electrochemical properties. Another objective is to develop synthesis and fabrication processes for these materials whereby they can be consolidated in air into SOFCs. The approach is as follows: (1) develop modifications of the current, state-of-the-art materials used in SOFCs; (2) minimize the number of cations used in the SOFC materials to reduce potential deleterious interactions; (3) improve thermal, electrical, and electrochemical properties; (4) develop methods to synthesize both state-of-the-art and alternative materials for the simultaneous fabrication and consolidation in air of the interconnections and electrodes with the solid electrolyte; and (5) understand electrochemical reactions at materials interfaces and the effects of component compositions and processing on those reactions. DOE

N93-13102# Department of Energy, Washington, DC. Office of Industrial Technologies.
ENERGY FROM MUNICIPAL WASTE PROGRAM
May 1992 53 p
(Contract DE-AC02-83CH-10093)
(DE92-010578; DOE/CH-10093/153) Avail: CASI HC A04/MF A01

Each year Americans throw away 3 quads of energy in the form of municipal waste and pay 6 billion dollars for the privilege. Only about 21 percent of our municipal wastes are used productively to generate electricity or produce new products by recycling. In 1990, waste-to-energy (WTE) plants and recycling efforts contributed roughly half a quad of energy in the form of electricity and reduced energy use. This productive use of waste avoided the disposal of about 50 million tons of wastes to landfills in that year. The Administration National Energy Strategy (NES) estimates that with proper Federal, State, local, and private action the electric generating capacity of WTE facilities could increase 600 percent by 2010 and by over 1200 percent by 2030, compared to 1990 capacity. This would result in about 55 gigawatts (GW) of capacity by 2030, up from

roughly 4 GW today. The Department of Energy (DOE) supports an integrated approach to waste management that includes source reduction, WTE, recycling, and landfilling as complementary pieces of a solution to the municipal waste disposal problem. The Energy from Municipal Waste Program, described in this plan, seeks to minimize the productive use of municipal waste as an energy resource to improving its economic and environmental characteristics. While the Program focuses on WTE systems, it is conducted as part of a larger Federal effort that includes source reduction and recycling of wastes to save energy. DOE

N93-13313# Los Alamos National Lab., NM.
MCFC DIAGNOSTICS: HCl DETECTION
B. A. Palmer, R. C. Oldenborgn, and D. J. Funk 1992 11 p Presented at the US Department of Energy Contractors Review Meeting on Fuel Cells, Morgantown, WV, 14-15 Jul. 1992
(Contract W-7405-eng-36)
(DE92-001292; CONF-920748-14) Avail: CASI HC A03/MF A01

Molten carbonate fuel cells (MCFC) are being developed for large-scale power generation. One source of fuel is coal gasifiers, which presents the problem of coal gas contaminants and their effect on MCFC; HCl is the most serious and hence needs to be monitored. Different methods of detecting HCl in the gas phase were evaluated, and laser diode absorption is the most suitable. Temperature sensitivity and spectral interferences are discussed; it is shown that the P10 spectral line is the best. A diode for the P10 line is on order; experiments using the P5 line show the line to be unacceptable (overlap with CH4 line). Future planned work is outlined briefly. DOE

N93-13427# Energy Research Corp., Danbury, CT.
EFFECTS OF COAL-DERIVED TRACE SPECIES ON PERFORMANCE OF MOLTEN CARBONATE FUEL CELLS Final Report, Oct. 1988 - Jun. 1992
May 1992 204 p
(Contract DE-AC21-88MC-25009)
(DE93-000203; DOE/MC/25009-3123) Avail: CASI HC A10/MF A03

The Carbonate Fuel Cell (CFC) is a promising option for efficient generation of electricity from many fuels. If coal-gas is to be used, the interactions of coal-derived impurities on various fuel cell (FC) components need to be understood. Thus the coal-derived contaminants (viz., NH3, H2S, HCl, H2Se, AsH3, Zn, Pb, Cd, Sn, and Hg) were studied. Both experimental and theoretical evaluations were performed, which have led to mechanistic insights and initial estimation of qualitative tolerance levels for each species individually and in combination with other species. Possible coal-gas contaminant effects on the anode side of the CFC was examined, using both out-of-cell thermogravimetric analysis by isothermal TGA, and FC testing in bench scale cells. Separate experiments detailing performance decay in these cells with high levels of ammonia contamination (1 vol. pct.) and with trace levels of Cd, Hg, and Sn, have indicated that, on the whole, these elements do not affect CFC performance. However, some performance decay may result when a number of the other six species are present, singly or simultaneously, as contaminants in fuel gas. In all cases, tolerance levels have been estimated for each of the 10 species and preliminary models have been developed for six of them. At this stage the models are limited to isothermal, bench-scale (300 sq cm size) single cells. The information obtained is expected to assist in the development of coal-gas cleanup systems, while the contaminant performance effects data will provide useful basic information for modeling FC endurance in conjunction with integrated gasifier/fuel-cell systems (IGFC). Author

N93-13528# Midwest Research Inst., Golden, CO.
COST ANALYSIS METHODOLOGY: PHOTOVOLTAIC MANUFACTURING TECHNOLOGY PROJECT
R. A. Whisnant (Research Triangle Inst., Research Triangle Park, NC.) Sep. 1992 23 p
(Contract DE-AC02-83CH-10093)
(DE92-016441; NREL/TP-411-5017) Avail: CASI HC A03/MF A01

This report describes work done under Phase 1 of the Photovoltaic Manufacturing Technology (PVMaT) Project. PVMaT is a five-year project to support the translation of research and development in PV technology into the marketplace. PVMaT, conceived as a DOE/industry partnership, seeks to advance PV manufacturing technologies, reduce PV module production costs, increase module performance, and expand US commercial production capacities. Under PVMaT, manufacturers will propose specific manufacturing process improvements that may contribute to the goals of the project, which is to lessen the cost, thus hastening entry into the larger scale, grid-connected applications. Phase 1 of the PVMaT project is to identify obstacles and problems associated with manufacturing processes. This report describes the cost analysis methodology required under Phase 1 that will allow subcontractors to be ranked and evaluated during Phase 2. DOE

N93-13529# Midwest Research Inst., Golden, CO.
DEVELOPMENT OF A COMPUTER MODEL FOR POLYCRYSTALLINE THIN-FILM CuInSe2 AND CdTe SOLAR CELLS
J. L. Gray (Purdue Univ., West Lafayette, IN.), R. J. Schwartz (Purdue Univ., West Lafayette, IN.), and Y. J. Lee (Purdue Univ., West Lafayette, IN.) Sep. 1992 44 p
(Contract DE-AC02-83CH-10093)
(DE92-016444; NREL/TP-413-5092) Avail: CASI HC A03/MF A01

This report describes work to develop an accurate numerical model for CuInSe2 (CIS) and CdTe-based solar cells capable of running on a personal computer. Such a model will aid researchers in designing and analyzing CIS- and CdTe-based solar cells. ADEPT (A Device Emulation Pregrain and Tool) was used as the basis for this model. An additional objective of this research was to use the models developed to analyze the performance of existing and proposed CIS- and CdTe-based solar cells. The development of accurate numerical models for CIS- and CdTe-based solar cells required the compilation of cell performance data (for use in model verification) and the compilation of measurements of material parameters. The development of the numerical models involved implementing the various physical models appropriate to CIS and CdTe, as well as some common window. A version of the model capable of running on an IBM-compatible personal computer was developed (primary code development is on a SUN workstation). A user-friendly interface with pop-up menus is being developed for release with the IBM-compatible model. DOE

N93-13611 University of South Florida, Tampa.
THIN FILMS AND SOLAR CELLS OF CADMIUM TELLURIDE AND CADMIUM ZINC TELLURIDE Ph.D. Thesis
Christos Savva Ferekides 1991 124 p
Avail. Univ. Microfilms Order No. DA9212220

The objectives of this dissertation are to investigate (1) the metalorganic chemical vapor deposition (MOCVD) and properties of cadmium telluride (CdTe) and cadmium zinc telluride (Cd(1-x)Zn(z)Te) films and junctions, and their potential application to solar cells, and (2) the fabrication and characterization of CdTe solar cells by the close spaced sublimation (CSS) technique. CdTe and Cd(1-x)Zn(x)Te films have been deposited by MOCVD on a variety of substrates at 300-400 C. The effect of the deposition parameters and post deposition heat treatments on the electrical, optical, and structural properties have been investigated. Heterojunctions of the configuration CdTe/transparent conducting semiconductor (TCS) and Cd(1-x)Zn(x)Te/TCS have been prepared and characterized. CdTe(MOCVD)/CdS and Cd(1-x)Zn(x)Te(E sub g = 1.65eV)/Cd(1-x)Zn(x)S solar cells with efficiencies of 9.9 percent and 2.4 percent, respectively have been fabricated. The as-deposited CdTe(MOCVD)/CdS junctions exhibited high dark current densities due to deflects at the interface associated with small grain size. Their characteristics of the Cd(1-x)Zn(x)Te junctions degraded with increasing Zn concentration due to the crystalline quality and very small grain size (0.3 microns) in films with high ZnTe contents (greater than 25 percent). No effective post-deposition heat treatment has been developed. CdTe/CdS solar cells have also been fabricated by the close spaced sublimation (CSS). Significant improvements in material and processing have been made, and in collaboration with fellow researchers an AM1.5 conversion efficiency of 13.4 percent has been demonstrated, the highest efficiency ever measured for such devices. The highest conversion efficiency for the CdTe(CSS)/CdS solar cell was achieved by reaching high open-circuit voltages and fill factors, while the short-circuit current densities were moderate. These results indicate that further improvements to increase the short-circuit current densities can result in conversion efficiencies over 15 percent. Dissert. Abstr.

N93-13618# Sandia National Labs., Albuquerque, NM.
BOILER EFFICIENCY METHODOLOGY FOR SOLAR HEAT APPLICATIONS
D. Maples (Louisiana State Univ., Baton Rouge.), J. C. Conwell (Louisiana State Univ., Baton Rouge.), and J. E. Pacheco Aug. 1992 87 p
(Contract DE-AC04-76DP-00789)
(DE92-019805; SAND-91-1282) Avail: CASI HC A05/MF A01

This report contains a summary of boiler efficiency measurements which can be applied to evaluate the performance of steam-generating boilers via both the direct and indirect methods. This methodology was written to assist industries in calculating the boiler efficiency for determining the applicability and value of thermal industrial heat, as part of the efforts of the Solar Thermal Design Assistance Center (STDAC) funded by Sandia National Laboratories. Tables of combustion efficiencies are enclosed as functions of stack temperatures and the amount of carbon dioxide and carbon monoxide in the gas stream. DOE

N93-13621# Energy Research Corp., Danbury, CT.
AN UPDATE OF ERC'S CARBONATE FUEL CELL DEVELOPMENT PROGRAM
M. Farooque, R. Bernard, J. Doyon, L. Paetsch, P. Patel, A. Skok, C. Yuh, G. Steinfield, and T. OShea 1992 10 p Presented at the US Department of Energy Contractors Review Meeting on Fuel Cells, Morgantown, WV, 14-15 Jul. 1992
(Contract DE-AC21-90MC-27168)
(DE92-019971; DOE/MC-27168/92/C0046; CONF-920748-12) Avail: CASI HC A02/MF A01

Energy Research Corporation's molten carbonate fuel goals are commercialization of the MW-class natural gas units and 100 MW-class coal gas/natural gas dual fuel units (long-term). Accomplishments have been made in stack height scale-up, issues relevant to attaining a long useful life for the carbonate fuel cell have been resolved, and organizational and financial aspects of power plant demonstration have been addressed. DOE

N93-13622# Electric Power Research Inst., Palo Alto, CA.
CONSIDERATIONS FOR THE TRANSITION FROM FUEL CELL R/D TO MANUFACTURING
M. S. Cobb and G. B. K. Meacham 1992 10 p Presented at the US Department of Energy Contractors Review Meeting on Fuel Cells, Morgantown, WV, 14-15 Jul. 1992
(Contract DE-FG21-91MC-27414)
(DE92-019977; DOE/MC-27414/92/C0053; CONF-920748-15) Avail: CASI HC A02/MF A01

This paper has discussed some considerations important to making a successful transition from R&D to manufacturing. It has described a product commercialization framework and discussed the importance of business analyses, especially product cost analysis, in determining the future potential of an emerging technology. Careful attention to the major elements discussed in this report should help both developers and venture sponsors to reduce the risks inherent in new business ventures. DOE

N93-13623# Westinghouse Electric Corp., Large, PA.
WESTINGHOUSE PAFC PROGRAM UPDATE
J. M. Feret, J. L. Kelly, A. J. Pereira, M. K. Wright, and A. K. Kush (Energy Research Corp., Danbury, CT.) 1992 10 p Presented at the US Department of Energy Contractors Review Meeting on Fuel Cells, Morgantown, WV, 14-15 Jul. 1992
(Contract DE-AC21-82MC-24223)
(DE92-019978; DOE/MC-24223/92/C0055; CONF-920748-8) Avail: CASI HC A02/MF A01

The objective was to develop and demonstrate the air-cooled phosphoric acid fuel cell performance and economics. Completion of cell technology and manufacturing process developments and the supporting cell/stack engineering effort have culminated in the end product module. Two modules were built and tested: the Engineering Model Module and the Demonstration Module. DOE

N93-13932 University of South Florida, Tampa.
TWO TO SIX COMPOUND THIN FILMS BY MOCVD FOR TANDEM SOLAR CELLS Ph.D. Thesis
Jeffrey Scott Britt 1992 150 p
Avail: Univ. Microfilms Order No. DA9222587

Polycrystalline Cd(1-x)Zn(x)S and Hg(x)Zn(1-x)Te films have been deposited on a variety of substrates by MOCVD. Deposition conditions have been adjusted based on measurements of the material properties. Heterojunction solar cells have been formed from these materials and their potential application as the upper member of a tandem solar cell has been examined. The evaluation and optimization of a high efficiency CdTe/CdS solar cell has also been accomplished. Polycrystalline Cd(1-x)Zn(x)S films were deposited at 350-425 C by the reaction between DMCd, DEZn, and the novel source, propanethiol (PM) in a H2 flow. The growth rate and bandgap energy are strongly dependent on the growth temperature, DMCd/DEZn molar ratio, and the II/VI molar ratio. TMAl and octyl-chloride have been introduced into the reaction mixture to lower resistivities to values suitable for device operation. Polycrystalline ZnTe films have been deposited at 270-400 C by the reaction between DIPTe and DMZn or DEZn in a H2 flow. ZnTe films have been deposited by photoenhanced and conventional MOCVD. Polycrystalline Hg(x)Zn(1-x)Te films have been deposited at 350-410 C by the reaction between elemental Hg, DIPTe, and DMZn in a H2 flow. AsH3 was introduced to the reaction mixture to control the resistivity. Heterojunctions have been formed with Cd(1-x)Zn(x)S and ZnSe. The films and junctions have been characterized by x-ray, optical transmission, low temperature photoluminescence, SEM, and electrical measurements. The evaluation and optimization of a CSS CdTe/CdS solar cell has been formed. A technique for the formation of low-resistance contacts to CdTe with HgTe has also been developed. A pre-deposition heat treatment of CdS in H2 has been demonstrated beneficial to the photovoltaic characteristics of the junction. A post-deposition CdCl2 treatment has been shown to have a profound influence on the electrical characteristics of CSS CdTe/CdS junctions. The identification of optical losses in CSS CdTe/CdS solar cells has been helpful in improving efficiences. Window losses have been ameliorated by reducing the CdS thickness. Reflection losses have been minimized by applying MgF2 AR coating to the glass surface. As a result of group effort, a record thin film solar cell efficiency of 14.6 percent has been achieved through these steps. Dissert. Abstr.

N93-13934 Arizona State Univ., Tempe.
NEW POWER-CONDITIONING SYSTEMS FOR SUPERCONDUCTING MAGNETIC ENERGY STORAGE Ph.D. Thesis
Byung Moon Han 1992 172 p
Avail: Univ. Microfilms Order No. DA9223102

This dissertation presents the development of new power-conditioning systems for superconducting magnetic energy storage (SMES), which can regulate fast and independently the active and reactive powers demanded in the ac network. Three new power-conditioning systems were developed through a systematic approach to match the requirements of the superconducting coil and the ac power network. Each of these new systems is composed of ten 100-MW modules connected in parallel to handle the large current through the superconducting coil. The first system, which was published in the IEEE Transactions on Energy Conversion, consists of line-commutated 24-pulse converter, a thyristor-switched tap-changing transformer, and a thyristor-switched capacitor bank. The second system, which was accepted for publication in the IEEE Transactions on Energy Conversion, consists of a 12-pulse GTO (gate turn-off thyristor) converter and a thyristor-switched tap-changing transformer. The third system, which was submitted to the International Journal of Energy System, consists of a dc chopper and a voltage-source PWM (pulse width modulation) converter. The operational concept of each new system is verified through mathematical analyses and computer simulations. The dynamic interaction of each new system with the ac network and the superconducting coil is analyzed using a simulation model with EMTP (electro-magnetic transients program). The analysis results prove that each new system is feasible and realizable. Each system can regulate the active and reactive powers of the utility network rapidly and independently, and each offer a significant reduction of the system rating by reducing the reactive power demand in the converter. Feasible design for each new system was introduced using a modular design approach based on the 1000 MW/5000 MWH plant, incorporating commercially available components and proven technologies.
Dissert. Abstr.

N93-14078 Brunel Univ., Uxbridge (England).
SOLAR ENERGY UTILISATION AND EVACUATED TUBULAR SOLAR COLLECTORS Ph.D. Thesis
Foroutan Parand 1991 473 p
Avail: Univ. Microfilms Order No. BRDX95894

Four types of evacuated tubular solar collectors have been constructed and their performance evaluated. The characteristics of the collectors are then compared and their design strengths assessed. One of the designs, a flat absorber with a single glass cover using glass to metal seals was found to have the best performance among the four designs which included a dewar vessel type collector, a heat pipe collector and a black liquid collector with an optical efficiency of 87.7 pct. and an overall heat loss coefficient of 12.3 Wm(exp -2)/C. The performance of the dewar vessel type and black liquid collectors was found to be comparable to the glass to metal seal collector. A detailed analysis of the optical and thermal processes in evacuated tubular collectors was made. On the basis of this analysis a computer simulation model using a finite difference technique has been developed to predict the performance of evacuated tubular collectors. The computer simulation results are then compared with the test results. For the majority of the tests the discrepancy between the simulation and the test results was within the error band of the test results (maximum 12 pct.). For the published test results the maximum discrepancy for operating temperature below 100 C was found to be 6 pct. The computer simulation model was compared with other published models and its advantages and disadvantages discussed. In some analytical and semi-analytical simulation models the energy absorbed by the glass cover and the heat loss from joints and supports has to be ignored. The present model has none of these deficiencies and more complex designs can be simulated. The developed computer simulation program might be used as an aid in the design of evacuated tubular collectors. Using the computer simulation, a parametric study of the three commmercially available collectors was made. The results are discussed and the areas of improvement are identified. Dissert. Abstr.

N93-14004*# National Aeronautics and Space Administration. Lewis Research Center, Cleveland, OH.
ADVANCED PHOTOVOLTAIC POWER SYSTEM TECHNOLOGY FOR LUNAR BASE APPLICATIONS
David J. Brinker and Dennis J. Flood *In* NASA. Johnson Space Center, The Second Conference on Lunar Bases and Space Activities of the 21st Century, Volume 2 Sep. 1992 p 593-596 Previously announced as N88-26402 (For primary document see N93-13972 03-91)
Avail: CASI HC A01/MF A03

N93-14005*# Remtech, Inc., Huntsville, AL.
SOLAR WATER HEATING SYSTEM FOR A LUNAR BASE
Richard E. Somers and R. Daniel Haynes *In* NASA. Johnson Space Center, The Second Conference on Lunar Bases and Space Activities of the 21st Century, Volume 2 Sep. 1992 p 597-602 (For primary document see N93-13972 03-91)
Avail: CASI HC A02/MF A03

45 ENVIRONMENT POLLUTION

Includes atmospheric, noise, thermal, and water pollution.

N93-12624 State Univ. of New York, Stony Brook.
THE BROAD BAND OVERLAP PROBLEM IN ATMOSPHERIC TRACE GASES Ph.D. Thesis
Bedrettin Subasilar 1991 127 p
Avail: Univ. Microfilms Order No. DA9205290

In relation to a better understanding of climate change and the related greenhouse problem, one way of projecting for the next decades is through general circulation models (GCMs). The only input as a driving force in the changing atmospheric and oceanic circulation patterns is the amount of heat perturbation either due to natural or man-caused activities. Among these, CO2 concentrations resulting from the latter has been observed to be accelerating at alarmingly high rates especially after the advent of the industrialization which just began in the last century. In addition to that, collective effects of other greenhouse gases are as important as CO2. Hence, it is evident from the above considerations that, in the predictions of climate models, the heat input which triggers changes in the atmospheric patterns, should be formulated accurately. In order to realize this objective, in this research, beginning with the available line parameter data, the problems of absorption have been investigated and attacked in the frame known as the broad band modeling since that is the only best and fastest manageable representation for GCMs. The first step was the construction of a full broad band (intra band overlap) model that was also flexible enough to accommodate the individual peculiarities of the bands. Before, the well known and very useful Ramanathan model had a limited applicability in the concentration scale, and it was also not systematically or successfully incorporated into an inter band overlap picture. Then, the established ideas that served as bases up to present, have been employed but found to have a limited practical applicability when it came to predict the inter band overlaps. This followed by the clarification of the probabilistic approach, taking into account the proper band segments, each of which are already shown to be expressible in terms of full broad bands, gave rise to the recognition of the transmittance multiplication principle being applicable to the wider than narrow-band segments or the whole bands. At the end, an example of a flux application is added. Dissert. Abstr.

N93-12684# Los Alamos National Lab., NM.
PREFERRED SETS OF STATES, PREDICTABILITY, CLASSICALITY, AND THE ENVIRONMENT-INDUCED DECOHERENCE
W. H. Zurek 22 Jun. 1992 38 p Presented at the Workshop on Physical Origins of Time Asymmetry, Mazagon, Spain, Oct. 1991
(Contract W-7405-eng-36)
(DE92-017447; LA-UR-92-2051; CONF-9110397-2) Avail: CASI HC A03/MF A01

Selection of the preferred classical set of states in the process of decoherence -- so important for cosmological considerations -- is discussed with an emphasis on the role of information loss and entropy. Persistence of correlations between the observables of two systems (for instance, a record and a state of a system evolved from the initial conditions described by that record) in the presence of the environment is used to define classical behavior. From the view point of an observer (or any system capable of maintaining records) predictability is a measure of such persistence. Predictability sieve -- a procedure which employs both the statistical and algorithmic entropies to systematicaly explore all of the Hilbert space of open system in order to eliminate the majority of the unpredictable and non-classical states and to locate the islands of predictability including the preferred pointer basis -- is proposed. Predictably evolving states of decohering systems along with the time-ordered sequences of records of their evolution define the effectively classical branches of the universal wavefunction in the context of the 'Many Worlds Interpretation'. The relation between the consistent histories approach and the preferred basis is considered. It is demonstrated that histories of sequences of events corresponding to projections onto the states of the pointer basis are consistent. DOE

N93-12685# Los Alamos National Lab., NM.
CHARACTERIZATION OF SITE GEOCHEMISTRY IN SUPPORT OF ENVIRONMENTAL RESTORATION
D. E. Morris, S. D. Conradson, C. D. Tait, C. J. Chisholm-Brause, J. M. Berg, and J. Musgrave 1992 7 p Presented at the Information Exchange Meeting on Characterization Sensors and Monitoring, Dallas, TX, 15-16 Jul. 1992
(Contract W-7405-eng-36)
(DE92-017512; LA-UR-92-1948; CONF-920791-4) Avail: CASI HC A02/MF A01

The objective of this analytical support task is to characterize the chemical speciation and physical properties of actinides and other toxic metals together with organic cocontaminants in contaminated soils at DOLE facilities. The target information for chemical speciation will be the oxidation state of the metal, the chemical structure and stoichiometry of the metal complexes, and the binding mechanism(s) of the metal complexes to the soil substrates. The physical state of the metal complexes in the soils is also important. We will determine if they exist as surface precipitates, mineral coatings, and/or clay adsorbates. The chemical speciation and physical state of the actinides and toxic metal define the chemistry of these contaminants as they presently exist at the DOE sites. This information is made available to parties involved in devising and implementing remediation strategies so that appropriate, efficient, timely, and cost-effective

remediation technologies will be brought to bear on the problem. Speciation characterization is also undertaken following the application of remediation technologies. This information is made available to parties involved with risk assessment so that judgments concerning the extent of decontamination and the long-term stability of any remaining contamination can be made and documented on the basis of sound chemical data. DOE

N93-12726# Research Triangle Inst., Research Triangle Park, NC.
THE NATIONAL ATMOSPHERIC DEPOSITION PROGRAM/NATIONAL TRENDS NETWORK (NADP/NTN) SITE VISITATION PROGRAM
Summary Report, Oct 1989 - Sep. 1990
W. C. Eaton, C. E. Moore, R. W. Murdoch, R. C. Shores, and D. A. Ward Feb. 1992 93 p
(Contract EPA-68-D8-0001)
(PB92-217298; EPA/600/R-92/151) Avail: CASI HC A05/MF A01

The proper collection of precipitation and the accurate measurement of its constituents are important steps in attaining a better understanding of the distribution and effects of acid rain in the United States. One of NAPAP Task Group 4's major programs concerns wet deposition monitoring. One of that program's projects, 4A-15, 'Quality Assurance Support for Wet Deposition Monitoring,' is sponsored by the U.S. Environmental Protection Agency (EPA) to evaluate the sample collection process and provide technical assistance to the NADP/NTN network through a site visitation program. If deficiencies or nonstandard procedures are noted, the site operator and supervisor are notified. All NADP/NTN sites were visited in 1985-1986. A second round of visits began in October 1986, with the goal of visiting approximately one-third of the 200 sites each year over the next three years. The document is a summary report of the findings from the 1989-1990 (Fiscal Year 1990) site visitation program to 67 of the sites of the NADP/NTN network. GRA

N93-12828# Oak Ridge National Lab., TN.
FOREST DECLINES: SOME PERSPECTIVES ON LINKING PROCESSES AND PATTERNS
S. B. McLaughlin 1992 30 p Presented at the Air Pollutants and Plant Metabolism Conference, Blacksburg, VA, 13-16 Jun. 1992
(Contract DE-AC05-84OR-21400)
(DE92-019946; CONF-9206254-2) Avail: CASI HC A03/MF A01

The regional decline in vigor of some species of forest trees has become an important component in the ecological, aesthetic, and economic criteria by which the costs of anthropogenic pollution are weighed. Because declines are often complex and virtually never without significant natural environmental modifiers, determining the role of specific anthropogenic stresses in initiating or enhancing the rate and direction of change in forest condition represents a significant research challenge. Separation of primary mechanisms that point to principal causes from secondary responses that result from internal feedbacks and the milieu of modifying agents is a critical issue in diagnosing forest decline. Air pollutant stress may have its most significant effects on forest processes by accelerating or amplifying natural stresses. Studies of changes in forest metabolic processes have played an important role in evaluating the role of air pollution in four regional forest declines that are the focus of this paper. The decline of ponderosa pine in the San Bernardino Mountains of California, Norway spruce and silver fir in Europe, loblolly and shortleaf pine in the Southeastern United States, and red spruce in the Eastern Appalachian Mountains provide case studies in which physiological responses to air pollutants under field and laboratory conditions have provided important analytical tools for assessing likely causes. These tools are most effective when both mechanistic explanations and larger scale patterns of response are evaluated in an iterative feedback loop that examines plausible mechanisms and patterns of response at levels ranging from cell membranes to plant populations. DOE

N93-12870# Bigelow Lab. for Ocean Sciences, West Boothbay Harbor, ME.
CHARACTERISTICS OF PHYTOPLANKTON AS MONITORS OF THE PHYSICAL ENVIRONMENT
John J. Cullen 1992 4 p
(Contract N00014-89-J-1239)
(AD-A255009) Avail: CASI HC A01/MF A01

The goal of this project was to understand the responses of phytoplankton to variations in irradiance so as to describe how physiological and optical characteristics of phytoplankton reflect physical forcing and particle dynamics. The application of this understanding is in using optical measurements to describe physical-biological coupling in the sea. The objectives of the program were to interpret measurements of fluorescence, beam attenuation, and photosynthesis versus irradiance (P-I) in terms of primary productivity, photoadaptation and particle dynamics in the euphotic zone. The context was photic variability induced by vertical mixing. Consideration was also given to the artifacts of experimental work at sea, including those associated with static bottle incubations that do not mimic vertical mixing in nature. Effort was expended principally on novel analysis of previously-collected data from laboratory experiments and field sampling. Some collaborative experiments were also performed, and measurements were made during a multidisciplinary cruise to study a Gulf Stream meander. In addition, the principal investigator acted as co-chair of and contributor to an international scientific symposium to examine the controversial hypothesis that iron limits the growth of phytoplankton in large parts of the ocean. This contract also supported a continuing and productive collaboration with Marlon R. Lewis of Dalhousie University. GRA

N93-12880# Lawrence Livermore National Lab., CA.
THE ROLE OF HUMAN ACTIVITY AND LAND USE CHANGE IN ATMOSPHERIC CHEMISTRY AND AIR QUALITY
J. E. Penner Jul. 1992 45 p Presented at the SNOWMASS Meeting, Denver, CO, 21 Jul - 10 Aug. 1991
(Contract W-7405-eng-48)
(DE92-019622; UCRL-JC-110922-Rev-1; CONF-9107235-1-Rev-1) Avail: CASI HC A03/MF A01

In this report, the importance of CO2, CH4, N2O, and COS for atmospheric chemistry, air quality, and climate is discussed. Current estimates of the sources for each specie, deriving the fraction of each source that is due to specific land use practices or land cover categories, are reviewed. Understanding the current trends of those species with known increasing abundances and projecting increases into the future is possible if the estimated sources from human activity and land use change can be projected and if the known atmospheric sinks and the interactions in atmospheric chemistry and climate change are appropriately taken into account. Regional trends in the short-lived species can be projected as well, assuming the estimated sources and sinks are correct. However, significant uncertainties continue to surround the estimated budgets for most of these species. Uncertainties and the estimated ranges in different source strength estimates for each specie are also discussed. DOE

N93-12884# Lawrence Livermore National Lab., CA.
DENSE-GAS DISPERSION ADVECTION-DIFFUSION MODEL
D. L. Ermak Jul. 1992 10 p Presented at the 1992 JANNAF Safety and Environmental Subcommittee Meeting, Monterey, CA, 10-14 Aug. 1992
(Contract W-7405-eng-48)
(DE92-019617; UCRL-JC-109697; CONF-9208112-2) Avail: CASI HC A02/MF A01

A dense-gas version of the ADPIC particle-in-cell, advection-diffusion model was developed to simulate the atmospheric dispersion of denser-than-air releases. In developing the model, it was assumed that the dense-gas effects could be described in terms of the vertically-averaged thermodynamic properties and the local height of the cloud. The dense-gas effects were treated as a perturbation to the ambient thermodynamic properties (density and temperature), ground level heat flux, turbulence level (diffusivity), and windfield (gravity flow) within the local region of the dense-gas cloud. These perturbations were calculated from conservation of energy and conservation of momentum principles along with the ideal gas law equation of state for a mixture of gases. ADPIC, which is generally run in conjunction with a mass-conserving wind flow model to provide the advection field, contains all the dense-gas modifications within it. This feature provides the versatility of coupling the new dense-gas ADPIC with alternative wind flow models. The new dense-gas ADPIC has been used to simulate the atmospheric dispersion of ground-level, colder-than-ambient, denser-than-air releases, andhas compared favorably with the results of field-scale experiments. DOE

N93-12885# Argonne National Lab., IL.
MEETING FUTURE EXHAUST EMISSIONS STANDARDS USING NATURAL GAS AS A VEHICLE FUEL: LESSONS LEARNED FROM THE NATURAL GAS VEHICLE CHALLENGE 1992

W. A. Rimkus and R. P. Larsen 1992 11 p Presented at the International Symposium on Energy, Environment and Information Management, Argonne, IL, 15-18 Sep. 1992
(Contract W-31-109-eng-38)
(DE92-019670; ANL/CP-76765; CONF-9209160-6) Avail: CASI HC A03/MF A01

The Natural Gas Vehicle Challenge '92, organized by Argonne National Laboratory and sponsored by the US Department of Energy; the Energy, Mines, and Resources - Canada; the Society of Automotive Engineers; and many others resulted in 20 varied approaches to the conversion of a gasoline-fueled, spark-ignited, internal combustion engine to dedicated natural gas use. Starting with a GMC Sierra 2500 pickup truck, donated by General Motors, teams of college and university student engineers strived to optimize Chevrolet V-8 engines operating on natural gas for improved emissions, fuel economy, performance, and advanced design features. This paper focuses on the results of the emission event and compares engine mechanical configurations, engine management systems, catalyst configurations and locations, and approaches to fuel control and the relationship of these parameters to engine-out and tailpipe emissions of regulated exhaust constituents. Nine of the student-modified trucks passed the current levels of exhaust emission standards, and some exceeded the strictest future emissions standards envisioned by the US Environmental Protection Agency. Factors in achieving good emissions control using natural gas are summarized, and observations concerning necessary components of a successful emissions control strategy are presented. DOE

N93-12926*# National Aeronautics and Space Administration. Ames Research Center, Moffett Field, CA.
A CORRELATED k-DISTRIBUTION MODEL OF THE HEATING RATES FOR CH4 AND N2O IN THE ATMOSPHERE BETWEEN 0 AND 60 km
K. Grant (Lawrence Livermore National Lab., CA.), A. S. Grossman (Lawrence Livermore National Lab., CA.), J. B. Pollack, and R. Freedman 1 Jun. 1992 20 p Presented at the 15th Annual Review Conference on Atmospheric Transmission Models, Bedford, MA, 2-3 Jun. 1992
(Contract W-7405-eng-48)
(NASA-TM-108062; NAS 1.15:108062; DE92-019376; UCRL-JC-110364; CONF-9206257-1) Avail: CASI HC A03/MF A01

An infrared radiative transfer model using the correlated-k technique is being developed for use in atmospheric chemistry and climate models at LLNL, as well as for stand-alone radiative diagnostics. This implementation of the correlated-k algorithm will provide a computationally efficient means to calculate atmospheric radiative fluxes and heating rates. It will also allow for both time-varying gas concentrations and for the rapid inclusion of new gases into the model. We present both a general background of the c-k method and the results of applying our prototype model to absorption by CH4 and N2O in the 7-9 micron wavelength band. The correlated-k algorithm maps the highly structured absorption coefficient versus wavelength relationship into a substantially smoother monotonic relationship between the absorption coefficient and its cumulative probability distribution. This provides a substantial reduction in computational complexity, relative to line-byline calculations, while maintaining a high degree of accuracy. DOE

N93-12927# Lawrence Livermore National Lab., CA.
A COMPUTER SIMULATION OF ECOSYSTEM PROCESSES IN FORESTS FOR APPLICATION TO AIR POLLUTION, ACID PRECIPITATION, AND GLOBAL CHANGE
J. R. Kercher and P. D. Anderson (California Univ., Berkeley.) 17 Jul. 1992 9 p Presented at the 1992 Summer Computer Simulation Conference, Reno, NV, 27-30 Jul. 1992
(Contract W-7405-eng-48)
(DE92-019616; UCRL-JC-108957; CONF-920771-5) Avail: CASI HC A02/MF A01

We have developed a simulation model, TREE, of the effects of gaseous air pollutants and acid precipitation on the forest ecosystem processes of tree productivity and growth. This model is based on an existing general model of forest ecosystem processes developed for regional application (FOREST-BGC) combined with an existing model of plant productivity and transpiration (BACROS). The former model uses daily and annual time-steps; BACROS uses hourly time-steps and computes gaseous pollutant (ozone) uptake. In FOREST-BGC, we model the effects of ozone by reducing productivity based on the cumulative uptake for each leaf age-class. The model computations convert this reduction in productivity to a reduction in growth. This version of the model restricts consideration of acid precipitation to possible effects on productivity due to foliar exposure. Basic model performance has been studied for ponderosa pine exposed to ozone at the USFS Chico Tree Improvement Center. The model simulates observed phenomena such as draw down of soil water during summer months. For ozone levels for the Chico Field Site for the 1990 season, maximum daily ozone uptake occurred in August with peak of 2.2 x 10(exp -5) kg m(exp - 2) d(sup 1). Cumulative annual ozone uptake for current year needles was 3.2 x 10(exp -2) kg m(exp -2) producing a 12.6 percent reduction in productivity for current year needles and a 13.3 percent reduction in chlorophyll and effective leaf area. Total transpiration was 0.95 m. The model is now being used to develop a terrestrial ecosystem submodel for a global scale Earth System Model (ESM) that integrates interacting atmospheric, oceanic, and land system components. Algorithms from the forest model will support feedback calculation of the effect of forests on atmospheric physics and chemistry as well as calculate effects of climate- and CO2-change on forest productivity. DOE

N93-12938# Research Triangle Inst., Research Triangle Park, NC. Center for Aerosol Technology.
ESPVI 4.0 ELECTROSTATIC PRECIPITATOR V-I AND PERFORMANCE MODEL: USER'S MODEL Final Report, Aug. 1989 - Feb. 1992
Phil A. Lawless Jun. 1992 83 p
(PB92-169614; EPA/600/R-92/104A; EPA/SW/DK-92/044) Avail: CASI HC A05/MF A01

The manual is the companion document for the microcomputer program ESPVI 4.0, Electrostatic Precipitation V-I and Performance Model. The program was developed to provide a user-friendly interface to an advanced model of electrostatic precipitation (ESP) performance. The program is capable of modeling standard ESP configurations as well as those that might be proposed for improved performance. It incorporates many of the latest developments in prediction of ESP performance, including electrical waveform effects, non-rapping reentrainment, and electrode misalignment. The manual provides the documentation needed to load the program from its disk, sets up the computer configuration for optimal operation, and introduces the operation of the program. The user is expected to be familiar with the operation of an ESP and know the important factors that affect it. An example ESP is provided with the program to help with the manual's exposition: it provides a direct comparison of the model's predictions. The program consists of a series of menu screens; the document is similarly organized, with increasing levels of detail provided as the menus become more specific. Finally, a section on the underlying algorithms discusses typical values that might be encountered with the model. GRA

N93-12940# Environmental Protection Agency, Research Triangle Park, NC. Technical Support Div.
INTERAGENCY WORKGROUP ON AIR QUALITY MODELING (IWAQM) WORK PLAN RATIONALE
John S. Irwin May 1992 26 p
(PB92-213248; EPA/454/R-92/001) Avail: CASI HC A03/MF A01

The document presents a status report and workplan rationale for the operation of the Interagency Workgroup on Air Quality Modeling (IWAQM). The workgroup was formed to provide a focus for development of technically sound regional air quality models for regulatory assessments of pollutant source impacts on Federal class 1 areas. The paper was published in an effort to inform the sponsoring Agencies and other interested parties about IWAQM activities. GRA

N93-12941# University of Southern California, Los Angeles. School of Medicine.
TRANSACTIONS: TROPOSPHERIC OZONE AND THE ENVIRONMENT. PAPERS FROM AN INTERNATIONAL CONFERENCE
Ronald L. Berglund, ed., Douglas R. Lawson, ed., and David J. McKee, ed. 1991 22 p
(Contracts EPA-68-D8-0017; ARB-A6-202-33)
(PB92-217017; EPA/600/A-92/164) Avail: CASI HC A03/MF A01

The role that air pollution plays in causing, promoting, facilitating, and/or exacerbating the lung disease that is present in all adults is discussed. The present study is a first step in the direction of inventory, an assessment of pathologically overt injury to a key unit of the acinus, the centriacinar region (CAR). The lungs of 107 of 118 youths (14-25 years of age), who died in vehicular accidents or were homicide victims, were suitable for

pathologic examination, and the extent and severity of disease was determined. Of the 107 youths, 29 (27 percent) had severe CAR disease as judged by scores of 5 or more (on a scale of 1-10) for both severity and extent. The high incidence and severity of CAR disease in youths is unprecedented and cannot be attributed to any single agent. The pathogenesis is undoubtedly multifactorial, with socioeconomic factor dominant, in particular a suboptimal level of health care, greater impact of respiratory tract infections, high levels of air pollution, and heavy smoking and some illicit drug use. Air pollution is highly suspect for a substantial contributory role. GRA

N93-12974# National Oceanic and Atmospheric Administration, Research Triangle Park, NC. Atmospheric Sciences Modeling Div.

NOAA ATMOSPHERIC SCIENCES MODELING DIVISION SUPPORT TO THE US ENVIRONMENTAL PROTECTION AGENCY Summary Report, Fiscal Year 1991

Evelyn M. Poole-Kober, ed. and Herbert J. Viebrock, ed. Jun. 1992 86 p Prepared in cooperation with Environmental Protection Agency, Silver Spring, MD

(PB92-217835; NOAA-TM-ERL-ARL-194) Avail: CASI HC A05/MF A01

The Atmospheric Sciences Modeling Division provided meteorological research and operational support to the U.S. Environmental Protection Agency during FY-1991. Meteorological support consisted of the application of dispersion models, and the conduct of dispersion studies and model evaluations. The primary research effort was the development and evaluation of air quality simulation models using numerical and physical techniques supported by field studies. This included development of the Regional Acid Deposition Model - Version 2.6, the Tagged Species Engineering Model and the Asymmetrical Convective Model; examination of the effect of oxidant limitations on emission changes; publication of the Regional Oxidant Model user's guides; study of the effect of biogenic emissions on ozone concentrations; incorporation of a new method describing aerosol dynamics into the Regional Particulate Model; participation in a field study of sustained stagnation conditions; conduct of a wind tunnel study of the dispersion of dense gas jets; and a study of flow and dispersion through an urban industrial complex. GRA

N93-13031*# Michigan Univ., Ann Arbor. Space Physics Research Lab.

HOW LIFE AFFECTS THE GEOCHEMICAL CYCLE OF CARBON Technical Status Report, Jan. - Dec. 1992

James C. G. Walker 30 Nov. 1992 10 p

(Grant NAGw-176)

(NASA-CR-191241; NAS 1.26:191241) Avail: CASI HC A02/MF A01

Developing a quantitative understanding of the biogeochemical cycles of carbon as they have worked throughout Earth history on various time scales, how they have been affected by biological evolution, and how changes in the carbon content of ocean and atmosphere may have affected climate and the evolution of life are the goals of the research. Theoretical simulations were developed that can be tuned to reproduce such data as exist and, once tuned, can be used to predict properties that have not yet been observed. This is an ongoing process, in which models and results are refined as new data and interpretations become available and as understanding of the global system improves. Results of the research are described in several papers which were published or submitted for publication. These papers are summarized. Future research plans are presented. L.R.R.

N93-13098# Balkema (A. A.) Publishers, Brookfield, VT.

PROCEEDINGS OF THE MEDITERRANEAN CONFERENCE ON ENVIRONMENTAL GEOTECHNOLOGY

Mumtaz A. Usmen and Yalcin B. Acar 1992 603 p Proceedings held in Izmir, Turkey, 25-27 May 1992

(Contract DAJA45-92-M-0123)

(AD-A253672; R/D-6870-EN-02) Avail: CASI HC A99/MF A01

The rapidly increasing rate of industrialization and urbanization around the globe and the unsafe practices in waste disposal, use and management endanger the ecology of the planet, and the health and the well being of her inhabitants. The scope of the technical contributions spans a wide variety of topics, which are organized here in eight sections. The first section 'Perspectives on science and regulation' provides an excellent series of views on the present and the future of scientific and regulatory considerations in environmental management. Eight papers are presented in the second section 'Contaminant transport and soil/waste interactions'. 'Performance and compliance evaluation of barriers' are treated in the subsequent fourth section. In-situ and remote contaminant detection techniques and selected facility monitoring technologies are covered in the fifth section on 'Detection and monitoring of contamination', followed by the sixth section on 'Remediation' covering the geotechnical aspects of established and emerging in-situ and ex-situ remediation technologies. GRA

N93-13121 Portland State Univ., OR.

STEADY STATE ANALYSIS OF TROPOSPHERIC CHEMISTRY Ph.D. Thesis

Wen Hsiung Pan 1991 248 p

Avail: Univ. Microfilms Order No. DA9213876

Hydroxyl radical HO plays a central role in controlling chemical processes in the troposphere. Current mechanisms are believed to accurately describe its formation, destruction and interaction with other atmospheric trace gases in clean air. Hydroperoxyl radical HO2 is linked to HO in several chain processes and serves among other roles as a reservoir for HO. The relative concentration (HO2/HO) in clean air is believed to be the order of 10(exp 2). We here examine the conditions under which steady-state kinetics apply to HO(sub x) chemistry and derive simple relationships which can be used to predict HO and HO2 concentration from measurable concentrations of the more stable trace gases. The equations assume a simple form for conditions where the ambient nitrogen oxide concentration is less than 1 ppb. These equations allow closed-form evaluation of the sensitivity of (HO) and (HO2) to changes in the concentrations of the controlling species and allow assignment of models. Although most current efforts to test fast tropospherical photochemistry center upon measurements of ambient (HO), our equations indicate that tropospheric (HO2) determinations may provide a more direct and accurate initial test of our knowledge of HO(sub x) chemistry in the unpolluted lower atmosphere. Overall the goal of this study is to benefit the experimenter by providing the information of insight and simple but reliable equations and to understand the conditions under which these measurements should be made and how best to interpret their results. Dissert. Abstr.

N93-13254*# Georgia Univ., Griffin. Dept. of Agronomy.

PERFORMANCE OF THE BOWEN RATIO SYSTEMS ON A 22 DEG SLOPE Final Report

D. Nie (Kansas State Univ., Manhattan.), I. Flitcroft, and E. T. Kanemasu 1990 34 p

(Grants NAG5-389; NAG5-1192)

(NASA-CR-191278; NAS 1.26:191278) Avail: CASI HC A03/MF A01

The Bowen ratio energy balance technique was used to assess the energy fluxes on inclined surfaces during the First ISLSCP Field Experiment (FIFE). Since air flow over sloping surface may differ from that over flat terrain, it is important to examine whether Bowen ratio measurements taken on sloping surfaces are valid. In this study, the suitability of using the Bowen ratio technique on sloping surfaces was tested by examining the assumptions that the technique requires for valid measurements. This was accomplished by studying the variation of Bowen ratio measurements along a selected slope at the FIFE site. In September 1988, four Bowen ratio systems were set up in a line along the 22 degree north-facing slope with northerly air flow (wind went up the slope). In July of 1989, six Bowen ratio systems were similarly installed with southerly air flow (the wind went down slope). Results indicated that, at distances between 10 to 40 meters from the top of the slope, no temperature or vapor pressure gradient parallel to the slope was detected. Uniform Bowen ratio values were obtained on the slope, and thus the sensible or latent heat flux should be similar along the slope. This indicates that the assumptions for valid flux measurements are reasonably met at the slope. The Bowen ratio technique should give the best estimates of the energy fluxes on slopes similar to that in this study. Author

N93-13270# Brookhaven National Lab., Upton, NY.

THE IGAC ACTIVITY FOR THE DEVELOPMENT OF GLOBAL EMISSIONS INVENTORIES: DESCRIPTION AND INITIAL RESULTS

C. M. Benkovitz and T. E. Graedel (Bell Telephone Labs., Inc., Murray Hill, NJ.) Feb. 1992 10 p Presented at the Annual Meeting of the Air and Waste Management Association (AWMA), Kansas City, MO, 21-26 Jun. 1992 Revised

(Contract DE-AC02-76CH-00016)
(DE92-016010; BNL-47273-Rev; CONF-9206114-12-Rev) Avail: CASI HC A02/MF A01

Modeling assessments of the atmospheric chemistry, air quality, and climatic conditions of the past, present, and future require, as input, inventories of emissions of the appropriate chemical species constructed on appropriate spatial and temporal scales. The task of the Global Emissions Inventories Activity (GEIA) of the International Global Atmospheric Chemistry Project (IGAC) is the production of global inventories suitable for a range of research applications. Current GEIA programs are generally based on addressing emissions by species; these include CO2, NH3/N2O, SO2/NO(x), CFC, volatile organic compounds, and radioisotopes. In addition, a separate program to inventory emissions from biomass burning and a program to address data management issues for all the developing inventories are being structured. Program priorities are based on current knowledge and tasks needed to produce the desired inventories. This paper will discuss the different types of global inventories to be developed by the GEIA programs, their key characteristics, and areas to be addressed in the compilation of such inventories. Results of the first GEIA task, a survey of existing inventories and auxiliary data, is presented. The survey included status assessments for the available inventory information for nineteen different atmospheric species or groups of species on global and regional scales and over time. Of this entire body of information, the only inventory regarded as satisfactory was that for the global emissions of CFC's. An implication of the results of these assessments is that properly gridded emissions inventories are badly needed to support atmospheric modeling calculations on a variety of spatial and temporal scales. Initial studies in the development of global inventories of sulfur dioxide, currently the most advanced GEIA program, are presented and discussed. DOE

N93-13274*# Smithsonian Astrophysical Observatory, Cambridge, MA.
ABSOLUTE ABSORPTION CROSS SECTIONS OF OZONE AT 300 K, 228 K AND 195 K IN THE WAVELENGTH REGION 185-240 nm Final Report, 1 Jun. 1989 - 31 May 1992
K. Yoshino, W. H. Parkinson, and D. E. Freeman Sep. 1992 24 p
(Grant NAGw-1788)
(NASA-CR-191267; NAS 1.26:191267) Avail: CASI HC A03/MF A01

An account is given of progress of work on absorption cross section measurements of ozone at 300 K, 228 K and 195 K in the wavelength region 185-240 nm. In this wavelength region, the penetration of solar radiation into the Earth's atmosphere is controlled by O2 and O3. The transmitted radiation is available to dissociate trace species such as halocarbons and nitrous oxide. We have recently measured absolute absorption cross sections of O3 in the wavelength region 240-350 nm (Freeman et al., 1985; Yoshino et al., 1988). We apply these proven techniques to the determination of the absorption cross section of O3 at 300 K, 228 K and 195 K throughout the wavelength region 185-240 nm. A paper titled 'Absolute Absorption Cross Section Measurements of Ozone in the Wavelength Region 185-254 nm and the Temperature Dependence' has been submitted for publication in the Journal of Geophysical Research. Author

N93-13413# National Oceanic and Atmospheric Administration, Washington, DC.
REPORTS TO THE NATION ON OUR CHANGING PLANET: OUR OZONE SHIELD Fall 1992, No. 2
Daniel L. Albritton, ed., Richard Monastersky, John A. Eddy, ed. (Consortium for International Earth Science Information Network, Ann Arbor, MI.), J. Michael Hall, ed., Eileen Shea, Francis Bretherton, ed. (Wisconsin Univ., Madison.), Robert Dickinson, ed. (Arizona Univ., Tucson.), and Stephen Schneider, ed. (National Center for Atmospheric Research, Boulder, CO.) 1992 23 p LIMITED REPRODUCIBILITY: More than 20% of this document may be affected by color photographs Original contains color illustrations
Avail: CASI HC A03/MF A01

Life as we know it is possible in part because of the protection afforded by the ozone layer. Gradually, it has become clear to scientists and to governments alike that human activities are threatening our ozone shield. Behind this environmental problem lies a tale of twin challenges: the scientific quest to understand our ozone shield and the debate among governments over how to best protect it. The affects of human activity on the stratospheric ozone layer and the world's attempt to protect it are described. L.R.R.

N93-13479# Argonne National Lab., IL.
ENVIRONMENTAL COMPLIANCE MANAGEMENT SYSTEM
L. W. Brownson (Argonne National Lab., Idaho Falls, ID.), T. Krsul (Argonne National Lab., Idaho Falls, ID.), R. A. Peralta (Argonne National Lab., Idaho Falls, ID.), D. A. Knudson, and C. L. Rosignolo 1992 12 p Presented at the International Symposium on Energy, Environment and Information Management, Argonne, IL, 15-18 Sep. 1992
(Contract W-31-109-eng-38)
(DE92-019595; ANL/CP-76558; CONF-9209160-1) Avail: CASI HC A03/MF A01

Argonne National Laboratory (ANL) is developing the Environmental Compliance Management System (ECMS) as a comprehensive, cost-effective tool to ensure the following: (1) that the Laboratory complies with all applicable federal and state environmental laws and regulations; (2) that environmental issues and concerns are recognized and considered in the early phases of projects; and (3) that Laboratory personnel conduct Laboratory operations in the most environmentally acceptable manner. The ECMS is an expert computer system which is designed to allow project engineers to perform an environmental evaluation of their projects. The system includes the following: a Master Program which collects basic project information, provides utility functions, and accesses the environmental expert modules; environmental expert system modules for each federal and state environmental law which allows the user to obtain specific information on how an individual law may affect the project; and site-specific databases which contain information necessary for effective management of the site under environmental regulations. The ECMS will have the capability to complete and print many of the necessary environmental forms required by federal and state agencies, including the Department of Energy. DOE

N93-13505# EG and G Rocky Flats, Inc., Golden, CO.
REDUCTION OF CHLOROFLUOROCARBON EMISSIONS FROM REFRIGERATION SYSTEMS
A. Cordova and M. A. Kennicott 1992 11 p Presented at the Hazardous Materials Control Resource Institute Conference, Arlington, VA, 22-24 Sep. 1992
(Contract DE-AC34-90DP-62349)
(DE92-019360; RFP-4609; CONF-9209169-1) Avail: CASI HC A03/MF A01

Recently enacted State and Federal legislation, (The Clean Air Act and Colorado Senate Bill 77), and the implementation of regulations for each, forbid the intentional release of ozone depleting chlorofluorocarbons (CFC's) from refrigeration and air conditioning systems to the atmosphere. In addition, an international agreement (The Montreal Protocol), calls for CFC manufacturing reductions, which began in 1991, and eventual discontinuation. The declining supply and resultant escalating costs of CFC's are additional driving forces toward conservation and reuse of present refrigerant resources. Rocky Flats Plant (RFP) currently has an estimated 42,000 pounds of CFC's in refrigeration and air conditioning systems. The purpose of this paper is to discuss steps being taken at RFP toward the abatement of CFC releases. The main thrust of our efforts is the use of a refrigerant management system, used to recover and recycle our current CFC stock. Additional methods of further reducing CFC emissions will also be discussed. These include the installation of state-of-the-art oil filtration systems on major chiller units, installation of spring-loaded pressure relief valves, and the retrofitting of major chiller units to accept less harmful, alternative refrigerants. DOE

N93-13615# Lawrence Livermore National Lab., CA.
AN INVESTIGATION OF THE PROCESSES CONTROLLING OZONE IN THE UPPER STRATOSPHERE
K. O. Patten, Jr., P. S. Connell, D. E. Kinnison, D. J. Wuebbles, J. Waters (Jet Propulsion Lab., California Inst. of Tech., Pasadena.), L. Froidevaux (Jet Propulsion Lab., California Inst. of Tech., Pasadena.), and T. G. Slanger (SRI International Corp., Menlo Park, CA.) Jul. 1992 7 p Presented at the 1992 Quadrennial Ozone Symposium, Charlottesville, VA, 4-13 Jun. 1992
(Contract W-7405-eng-48)
(DE92-019621; UCRL-JC-108954; CONF-9206262-3) Avail: CASI HC A02/MF A01

Photolysis of vibrationally excited oxygen produced by ultraviolet photolysis of ozone in the upper stratosphere is incorporated into the Lawrence Livermore National Laboratory 2-D zonally averaged

chemical-radiative-transport model of the troposphere and stratosphere. The importance of this potential contributor of odd oxygen to the concentration of ozone is evaluated based upon recent information on vibrational distributions of excited oxygen and upon preliminary studies of energy transfer from the excited oxygen. When the energy transfer rate constants of previous work are assumed, increases in model ozone concentrations of up to 40 percent in the upper stratosphere are found, and the ozone concentrations of the model agree with measurements, including data from the Upper Atmosphere Research Satellite. However, the increase is about 0.4 percent when the larger energy transfer rate constants suggested by more recent experimental work are applied in the model. This indicates the importance of obtaining detailed information on vibrationally excited oxygen properties, particularly the state-specific energy transfer rate constants, to evaluation of tills precess for stratospheric modeling. DOE

N93-13624 Wayne State Univ., Detroit, MI.
AN EXPERIMENTAL AND THEORETICAL STUDY OF DEGRADATION PATHWAYS FOR ATMOSPHERIC HALOCARBONS Ph.D. Thesis
Zhuangjie Li 1991 193 p
Avail: Univ. Microfilms Order No. DA9215113

The issue of ozone depletion by chlorofluorocarbons (CFCs) is of great current concern. UV photodissociation of CFCs in the stratosphere produces a chlorine atom and a trihalomethyl radical. While the catalytic role of atomic chlorine in ozone depletion processes has been well studied, the part played by the other fragment of the dissociation remains largely unknown. Two possible catalytic cycles initiated by CX3 (X = F, Cl) have been proposed, in which CX3O and CX3O2 are the key species to understand these cycles. The dissociation pathway of CX3O radicals have been studied using Hartree-Fock theory, Moller-Plesset and spin projection correlation methods. The dissociation barrier heights and the heat of reaction for these processes have been determined. CF3O has received extensive study both theoretically (using ab initio theory) and experimentally (using laser-induced fluorescence technique). The experimental observations for CF3O are consistent with the theoretical predictions. A detailed theoretical study has been carried out on dissociation pathways of carbonyl halides resulting from the degradation of CX3O radicals, and on the molecular properties of some electronic excited states of CF2O using ab initio theory. It was found that the first electronic excited state of CF2O is due to the (sup 1)(n yields pi*) transition, and possesses a non-planar configuration. The study on the dissociation barrier heights for carbonyl halides suggests that chlorofluoromethane with less than two fluorine atoms degrades to carbon monoxide; those with at least two fluorine atoms yield carbon dioxide in the stratosphere. The laser photolysis/infrared chemiluminescence technique has been applied to the kinetic study of the reaction of CF(3) with NO2. The absolute reaction rate constant was measured at 300 plus or minus 4 K to be (2.5 plus or minus 0.4) x 10(exp -11) cu cm molecule(exp -1) s(exp -1) from monitoring the rise time of CF2O time-resolved vibrational fluorescence. C2 in triplet state has been produced by infrared multiphoton dissociation of CF3OOCF3. Both high resolution excitation spectrum and dispersed spectra of C2 Swan band were collected and analyzed. The newly observed 2-0 transition of the Swan band has been identified and assigned. Dissert. Abstr.

N93-13646# Lawrence Livermore National Lab., CA.
EFFECTS OF STRATOSPHERIC AEROSOL SURFACE PROCESSES ON THE LLNL TWO-DIMENSIONAL ZONALLY AVERAGED MODEL
P. S. Connell, D. E. Kinnison, D. J. Wuebbles, J. D. Burley (California Univ., Berkeley.), and H. S. Johnston (California Univ., Berkeley.) Jul. 1992 5 p Presented at the 1992 Quadrennial Ozone Symposium, Charlottesville, VA, 4-13 Jun. 1992
(Contract W-7405-eng-48)
(DE92-019620; UCRL-JC-108955; CONF-9206262-2) Avail: CASI HC A01/MF A01

We have investigated the effects of incorporating representations of heterogeneous chemical processes associated with stratospheric sulfuric acid aerosol into the LLNL two-dimensional, zonally averaged, model of the troposphere and stratosphere. Using distributions of aerosol surface area and volume density derived from SAGE 11 satellite observations, we were primarily interested in changes in partitioning within the Cl- and N-families in the lower stratosphere, compared to a model including only gas phase photochemical reactions. DOE

N93-13647# Environmental Protection Agency, Research Triangle Park, NC. Standards Div.
DOCUMENTATION FOR DEVELOPING THE INITIAL SOURCE CATEGORY LIST Final Report
Jul. 1992 368 p
(Contract EPA-68-D1-0117)
(PB92-218429; EPA/450/3-91/030) Avail: CASI HC A16/MF A03

Section 112 of Title III (Air Toxics) of the Clean Air Act (CAA) as amended in 1990 identifies a list of 189 hazardous air pollutants (HAP's) and requires the U.S. Environmental Protection Agency (EPA) to publish, within one year of enactment, an initial list of all categories and subcategories of major and area sources of HAP's. The purpose of this report is to (1) describe the methodology used to identify sources that emit HAP's, (2) document the technical references that support EPA's conclusion that one or more of the listed HAP's is emitted from a specified source category, (3) provide broad descriptions of the categories of major sources included on the list, and (4) present the responses to public comments received regarding a preliminary draft list of source categories that was published in the Federal Register on June 21, 1991. GRA

N93-13654# Lawrence Livermore National Lab., CA.
EFFECTS OF THE MT. PINATUBO ERUPTION ON THE RADIATIVE AND CHEMICAL PROCESSES IN THE TROPOSPHERE AND STRATOSPHERE
D. E. Kinnison, K. E. Grant, P. S. Connell, and D. J. Wuebbles Jul. 1992 5 p Presented at the 1992 Quadrennial Ozone Symposium, Charlottesville, VA, 4-13 Jun. 1992
(Contract W-7405-eng-48)
(DE92-019618; UCRL-JC-108956; CONF-9206262-4) Avail: CASI HC A01/MF A01

The LLNL 2-D zonally averaged chemical-radiative transport model of the global atmosphere was used to study the effects of the June 15, 1991 eruption of the Mt. Pinatubo volcano on stratospheric processes. SAGE-11 time-dependent aerosol surface area density and optical extinction data were used as input into the model. By the winter solstice, 1991, a maximum change in column ozone was observed in the equatorial region of -2 percent (with heterogeneous chemical reactions on sulfuric acid aerosols) and -5.5 percent (including heterogeneous reactions plus radiative feedbacks). Maximum local ozone decreases of 12 percent were derived in the equatorial region, at 25 km, for winter solstice 1991. Column NO2 peaked (-14 percent) at 30 S in October 1991. Local concentrations of NO(x), Cl(x), and HO(x), in the lower stratosphere, were calculated to have changed between 30 S and 30 N by -40, +80, and +60 percent respectively. DOE

N93-13655# Lawrence Livermore National Lab., CA.
IMPACT OF SUPERSONIC AND SUBSONIC AIRCRAFT ON OZONE: INCLUDING HETEROGENEOUS CHEMICAL REACTION MECHANISMS
D. E. Kinnison and D. J. Wuebbles Jul. 1992 4 p Presented at the 1992 Quadrennial Ozone Symposium, Charlottesville, VA, 4-13 Jun. 1992
(Contract W-7405-eng-48)
(DE92-019619; UCRL-JC-108951; CONF-9206262-1) Avail: CASI HC A01/MF A01

Preliminary calculations suggest that heterogeneous reactions are important in calculating the impact on ozone from emissions of trace gases from aircraft fleets. In this study, three heterogeneous chemical processes that occur on background sulfuric acid aerosols are included and their effects on O3, NO(x), Cl(x), HCl, N2O5, ClONO2 are calculated. DOE

N93-13721 Arizona Univ., Tucson.
INTEGRATION OF VEGETATION INDICES AND THERMAL MEASUREMENTS FOR ECOSYSTEM MODELING Ph.D. Thesis
Jiang Li 1992 219 p
Avail: Univ. Microfilms Order No. DA9223561

This study represents a continuation of the historical trend in the analysis of the relationships between climate and vegetation. The focus of the work is on an examination of the association of functioning plants and climatic processes and on the interaction of structured vegetation communities with their environment. Satellite observations and remote sensing technology provide new opportunities for studying the geo-biosphere at high temporal frequencies and for large geographic areas. Integration of

spectral vegetation indices and thermal measurements from space is the prime methodology used in their study. The integration of thermal information with vegetation indices has the potential to result in an important contribution to ecological remote sensing. This study has investigated the triangular distribution pattern which has been repetitively observed in spectral domains defined by thermal measurements and vegetation indices. Results show that the triangular shape of an AVHHR data cluster can be consistently observed on different continents and at different times of the year. The triangular data pattern has also been observed using a seasonally averaged data set, representing the mean thermal and biomass conditions of a growing season. The triangular shape of the data spread in feature space clearly suggests an ecosystem triangle model for simulation of the global ecology. A closer analysis of 15 test sites representing the major biomes in the U.S. Southwest study area has shown that each biome has a stable territory in the two dimensional space of temperature and biomass. If the territory of each test site in the triangle can be viewed as a vegetation cell, the ecosystem as a whole may be modeled by using this cell structure. The ecosystem triangle model and the concept of the cell structure have been applied in a vegetation classification exercise. The significant improvement achieved in the vegetation classification supports the conclusion that the ecosystem triangle model is a reflection of surface biomes, and may be used as a tool to study the structure, organization, and function of the biosphere. Dissert. Abstr.

N93-13723 Denver Univ., CO.
APPLICATION OF IMPROVED HNO3 BAND MODEL PARAMETERS TO SOUTH POLE ATMOSPHERIC EMISSION MEASUREMENTS Ph.D. Thesis
Nicholas Brian Jones 1992 211 p
Avail: Univ. Microfilms Order No. DA9219825

Nitric acid column amounts retrieved from absorption and emission measurements over Antarctica has been reported in the literature to disagree by as much as a factor of 2. Many aspects of these measurements differed. The task was to use a common approach in terms of the analysis method. Both band model and line by line calculations were employed. The 1978 emission measurements of Williams et al., (1982) were investigated to determine whether a common analysis method could account for the higher HNO3 column amounts retrieved from emission data with respect to later absorption studies. A multilayer, temperature dependent calculation using both band model and line by line parameters indicated that the South Pole emission measurements were consistent with the ground based absorption measurements of Murcray et al. (1987). Evaluation of the assumed HNO3 temperature used in the original analysis indicated that this was a major contributer to the overestimate of the HNO3 column. It was also concluded, therefore, that the original band model parameters did not significantly contribute to the initial discrepencies. A significant part of the work was the derivation of band model parameters using the best available line parameters and experimental data. Quantum mechanical parameters were used for the central region of the 11.3 microns HNO3 band. Temperature coefficients were calculated along with the use of experimental cross-sections to extend the useful range of band model parameters into the HNO3 wings. It was concluded that with small absorber/emitter amounts, the new parameters were in good agreement with line by line calculations. Dissert. Abstr.

N93-13741 North Carolina State Univ., Raleigh.
CLOUD ACIDITY AND ACIDIC DEPOSITION IN THE LOWER TROPOSPHERE AND OZONE DEPLETION IN THE ANTARCTIC STRATOSPHERE: MODELING AND DATA ANALYSIS REGARDING THE ROLE OF ATMOSPHERIC AEROSOL Ph.D. Thesis
Neng-Huei Lin 1991 213 p
Avail: Univ. Microfilms Order No. DA9206141

This study is focused on the role of atmospheric aerosols in determining the cloud acidity and acidic deposition in the lower troposphere and the ozone depletion in the Antarctic stratosphere. For the former, a cloud chemistry model is developed to study the in-cloud chemistry and acidity in cloud droplets. The cloud chemistry model includes the absorption of trace gases, the oxidation of aqueous phase SO2, and the scavenging of atmospheric aerosols. A new scheme is developed to differentiate the acidity and chemical composition distributing in individual cloud droplets. The above cloud chemistry model is incorporated into a two-layer flow model in order to investigate the effects of mountain waves on the cloud acidity. Using the three-year (1986-1988) database acquired at Mt. Mitchell site, the in-cloud chemistry and acidic deposition through dry, wet and cloud deposition pathways are investigated. The in-cloud scavenging of submicron aerosols such as sulfates and nitrates is parameterized as a function of cloud deposition rate. The deposition fluxes of sulfur (S) compounds are found primarily contributed by cloud capture mechanism (60 percent) followed by incident precipitation (25 percent) and dry deposition (15 percent). A comparison of deposition estimates at Mt. Mitchell with those at other sites shows that the sulfate deposition at sites exceeding 1,200 m MSL in elevation in Bavaria (Germany) and eastern USA is almost identical within error limits. The features of the Antarctic stratospheric aerosols during the ozone depletion episode of October 1987 are investigated based on the SAGE II (Stratospheric Aerosol and Gas Experiment II) data. The study focuses on (1) inferring the aerosol size spectrum using a modified randomized minimization search technique (RMST), and (2) investigating the vertical, zonal and columnar averages of aerosol properties, together with the ozone concentration. The aerosol size distribution is found to be bimodal in several instances. An enhanced aerosol layer of relatively larger particles at altitudes between 21-23 km was found in the Antarctic region. Relatively abundant population of smaller particles is associated with the region of severe ozone depletion. Smaller and larger particles dominate at higher and lower latitudes, respectively. It is pointed out that the reported features of the stratospheric aerosols in Antarctic region are useful in providing insights into the mechanisms for ozone depletion. Dissert. Abstr.

N93-13758 California Univ., Los Angeles.
INFRARED SPECTROSCOPY OF SIZE RESOLVED FINE AEROSOL Ph.D. Thesis
Edward John Palen 1991 358 p
Avail: Univ. Microfilms Order No. DA9200921

This dissertation describes the development and implementation of a new analytical technique for atmospheric aerosols based on infrared spectroscopy. In this technique, aerosols are size segregated and collected using a low pressure impactor (LPI) equipped with ZnSe impaction surfaces, which are transparent to infrared radiation. The LPI samples at a flowrate of 1 L/min, and collects 8 size fractions with aerodynamic diameter cut points of 4.0, 2.0, 1.0, 0.5, 0.26, 0.12, 0.075 and 0.05 microns. Samples are analyzed using transmission Fourier Transform Infrared (FTIR) spectroscopy or microscopy over the spectrum 4000-575 cm(exp -1) (2.5-17.4 microns). Detection limits for each size fraction are as low as 10 picograms. Infrared absorption spectra of ambient urban aerosol contain absorptions due to sulfate, bisulfate, nitrate, ammonium and silicate ions. Organic absorptions due to aliphatic carbon, carbonyl carbons and organonitrates are also observed. Atmospheric loadings of these functional groups are estimated from the infrared absorbance areas based on model compound and field calibrations. Field calibration data were collected during the 1987 Southern California Air Quality Study (SCAQS). Intermethod comparisons were made using SCAQS data. Characteristic loadings and mass size distributions of sulfate ions, bisulfate ions, nitrate ions, aliphatic carbon, carbonyl carbons and organonitrates in Southern California ambient aerosol are reported in this thesis. It is shown that infrared active functional groups account for the majority of the mass present in ambient aerosols. The LPI-FTIR technique can also be applied in the analysis of aerosol generated in smog chamber studies. In separate experiments 1-octene, isoprene and beta-pinene were photooxidized in a flexible outdoor smog chamber. Initial hydrocarbon concentrations ranged from 0.34-20.0 ppm. Hydrocarbon to NO(x) ratios ranged from 2.0-10.5. Aerosols were again size segregated and collected using LPIs with ZnSe impaction surfaces for direct analysis. The mole fractions of aliphatic carbon, ketones, aldehydes, carboxylic acids, alcohols and organonitrates in the photooxidation aerosol were quantified. Molecular weights and molecular structures were estimated. Dissert. Abstr.

N93-13893 East Anglia Univ., Norwich (England).
THE SEASONAL VARIATIONS AND INTERRELATIONSHIPS OF OZONE, PEROXYACETYL NITRATE AND NITROGEN DIOXIDE IN THE TROPOSPHERE Ph.D. Thesis
Chloe Nikitas 1991 380 p
Avail: Univ. Microfilms Order No. BRDX96080

A method has been developed to measure peroxyacetyl nitrate (PAN) by thermal conversion to nitrogen dioxide (NO2) which enabled the PAN

to be measured as NO2 by a Scintrex LMA-3 NO2 Analyser. The thermal converter developed to carry out this conversion was found to be efficient in decomposing the PAN in tests carried out using a gas chromatograph. Interference tests on nitric oxide and carbon monoxide revealed that nitric oxide gave rise to the generation of NO2 in the thermal converter but this could be corrected for if nitric oxide concentrations were known or could be computed. Carbon monoxide was found to have no effect at ambient atmospheric concentrations. The LMA-3 and thermal converter were operated successfully on an aircraft and used to make airborne measurements of PAN in late April, 1990. High concentrations of 600 pptv of PAN were found in clean free tropospheric air at 10,000 feet altitude. Clean air ozone measurements from the ground-based West Beckham site, located near the North Norfolk coast, showed peak concentrations at the time of year that these flight measurements of high PAN concentrations were made. The LMA-3 and thermal converter were also operated at the West Beckham site. Concurrent measurements of ozone and PAN showed that these species were well correlated in summer photochemical episodes but in winter, some elevated PAN concentrations not associated with high ozone concentrations were measured. The EMEP-ozone model was used to simulate ozone, PAN and NO2 concentrations at the West Beckham site. Comparisons with the data measured at the site revealed that the model did not perform very well tending to overproduce ozone and underpredict NO2. Nitrate radical hydrocarbon oxidation processes were added to the EMEP model which enabled the model to be used to evaluate the effect of nitrate radical chemistry in generating the elevated winter PAN concentrations measured at the West Beckham site. The model calculations, which have to be treated with caution due to the poor performance of the model in predicting the ozone and NO2 concentrations at the site, indicate that hydroxyl radical oxidation processes rather than nitrate radical processes dominated even in the winter high PAN episodes. Dissert. Abstr.

N93-14096 Arizona Univ., Tucson.
STATISTICAL RELATIONSHIPS BETWEEN TREE GROWTH AND CLIMATE IN WESTERN NORTH AMERICA Ph.D. Thesis
Xuemei Shao 1992 195 p
Avail: Univ. Microfilms Order No. DA9225186

The objective of this study is to examine large-scale spatial patterns of tree growth and climatic variation and to investigate the possible role of climate in determining tree growth patterns over space. This study represents one of the first uses of geostatistical methods to extract information about the spatial variation of climate from tree rings in western North America. It is also one of the first uses of data in spatial series to study the relationships of spatial variations between climate and tree growth. Geostatistics analyzes the spatial structure of the variables by assuming that adjoining data are correlated with each other over space and that the particular relationship expressing the extent of spatial correlation can be analytically and statistically captured in a function. It is applied to both June Palmer Drought Severity Index (PDSI) and ring-width index data from western North America. One basic assumption of applying geostatistics in this study is that the spatially uncorrelated small-scale variations are insignificant and represent background noise in large-scale dendroclimatic studies. The statistical relationships between the spatial variations of June PDSI and ring-width index are studied by simple scatter diagrams and correlation analysis. This is done in terms of yearly variations and variations of spatial patterns. Both of them support the contention that the large-scale spatial variations in ring-width index data can be used to infer the spatial variations of climate variables. Based upon the results of this research it can be concluded that geostatistics is a viable method to characterize the spatially correlated variations in dendroclimatology. By applying geostatistics to data sets, information about the spatial variations of climate contained in tree-ring data are enhanced, and the large-scale variations of climate are emphasized. The analysis of yearly relationships over space is particularly useful for identifying statistical relationships between climate and tree growth in a geographic region. The main factors of climate controlling ring-width index are identified as well as the less frequent limiting events. Once the statistical relationships are validated, they can be used to infer the spatial variations of past climate from variations in tree-ring index. Dissert. Abstr.

N93-13995*# Texas Univ., Austin. Dept. of Zoology.
LONG-TERM LUNAR STATIONS: SOME ECOLOGICAL CONSIDERATIONS
Bassett Maguire, Jr. and Kelly W. Scott *In* NASA. Johnson Space Center, The Second Conference on Lunar Bases and Space Activities of the 21st Century, Volume 2 Sep. 1992 p 531-536 Sponsored in part by Savannah River Ecological Lab. (For primary document see N93-13972 03-91)
Avail: CASI HC A02/MF A03

46 GEOPHYSICS

Includes aeronomy; upper and lower atmosphere studies; ionospheric and magnetospheric physics; and geomagnetism.
For space radiation see *93 Space Radiation.*

N93-12621# Lockheed Missiles and Space Co., Palo Alto, CA. Research Lab.
COMPREHENSIVE MAPPINGS OF ELECTRON PRECIPITATION AND ITS EFFECTS ON THE COMPREHENSIVE MAPPINGS OF ELECTRON PRECIPITATION AND ITS EFFECTS ON THE ATMOSPHERE Final Report, Jul. 1988 - Jun. 1992
H. D. Voss, J. Mobilia, R. R. Vondrak, E. E. Gaines, and D. W. Datlowe Jun. 1992 54 p
(Contract F49620-88-C-0072)
(AD-A254665; LMSC/F247098; AFOSR-92-0732TR) Avail: CASI HC A04/MF A01

Precipitation of energetic electrons is an important energy input to the earth's upper atmosphere and can alter the chemistry and dynamics of that region. The precipitation can be studied on a global basis using a satellite x-ray imager to make maps of the x-rays produced when the electrons stop in the atmosphere. We have used 4-40 keV x-ray data from the S81-1 SEEP satellite instrument to classify the patterns of precipitation at high latitudes; the three principal types are strong auroral arcs on the nightside, extended dawnside arcs, and isolated pitches inside the polar cap. We also studied the characteristics of high energy (relativistic) electron precipitation with data from instruments that directly detect the electrons. This very penetrating radiation is important because the electrons deposit their energy down to altitudes as low as approximately 55 km. This study found that the precipitation was confined to narrow latitude bands, often at the outer boundary of the belt of trapped electrons, and that it occurs more often at midnight local time than at noontime. GRA

N93-12626 Leicester Univ. (England).
RADAR STUDIES OF HIGH LATITUDE CONVECTION FLOWS Ph.D. Thesis
Mark David Burrage 1988 223 p
Avail: Univ. Microfilms Order No. BRD-94257

Studies of the electrodynamics of the high latitude ionosphere contribute to the understanding of the coupling between the solar wind, magnetosphere and upper atmosphere. This thesis describes an experimental investigation of high latitude E-region convection flows carried out with the Sweden And Britain auroral Radar Experiment (SABRE). The ionospheric observations have been related to satellite measurements of the interplanetary medium and hence interpreted in terms of models of solar wind-magnetosphere-ionosphere coupling processes. A close relationship has been established between various solar wind parameters and the daily mean SABRE backscatter intensity, a quantity which is rarely employed in geophysical studies. Empirical IMF-dependent models of the convection flows observed by SABRE are developed and statistical studies of the occurrence time of the Harang discontinuity are presented. High spatial resolution, two dimensional maps of the ionospheric projection of the dayside merging region, for both polarities of the azimuthal component of the IMF, are obtained for the first time. Two examples of strong nightside convection flows observed throughout the SABRE latitude range indicate that the convection flows may penetrate at least as far south as 61.5 degrees N, geomagnetic latitude, during strongly northward IMF. The study indicates that, in the long term, the structure of the solar wind can be deduced from the mean backscatter intensity measured by a SABRE radar. In addition, the azimuthal component of the IMF exerts a crucial influence on the convection flows observed by SABRE in the cusp region. This effect is not confined to the noon sector but is also apparent in the vicinity of the Harang discontinuity. In general, the convection pattern exhibits a dependence on the north-south component of the IMF consistent with

established reconnection mechanisms. However, there is evidence that existing models are insufficient to explain the anomalous convection flows observed under conditions of strongly northward IMF. Dissert. Abstr.

N93-12661*# Massachusetts Inst. of Tech., Cambridge. Dept. of Earth, Atmospheric, and Planetary Sciences.

ANALYSIS OF SPACE GEODETIC MEASUREMENTS FOR STUDYING THE DYNAMICS OF THE SOLID EARTH Annual Status Report, 1 Jan. - 31 Dec. 1992

Thomas A. Herring 13 Nov. 1992 19 p

(Grant NAGw-3007)

(NASA-CR-191215; NAS 1.26:191215) Avail: CASI HC A03/MF A01

During the last decade, there has been an unprecedented improvement in both the accuracy and the temporal resolution of Earth rotation measurements. Determination of the position of the Earth's rotation axis both in inertial space and with respect to the crust with accuracies of about 0.3 milliarcseconds (mas) are now routine. In recent years, there has been an emphasis on the determination of short-period (daily and less) variations in Earth rotation. Two space based geodetic systems, very long baseline interferometry (VLBI) and the global positioning system (GPS) have proved to be very successful in this endeavor. Results for the tidally coherent part of the subdaily Earth rotation variations determined from the analysis of VLBI data are discussed. The magnitude of other subdaily variations are also considered. Author

N93-12704# Slovak Academy of Sciences, Bratislava (Czechoslovakia). Inst. of Geography.

ABSTRACTS OF PAPERS PRESENTED AT THE INTERNATIONAL SYMPOSIUM ON TIME, FREQUENCY, AND DATING IN GEOMORPHOLOGY Abstracts Only

Miloes Stankoviansky 21 Jun. 1992 52 p Symposium held in Bratislava, Czechoslovakia, 16-21 Jun. 1992

(Contract DAJA37-92-M-0126)

(AD-A254927; R/D-6857-EN-02) Avail: CASI HC A04/MF A01

Topics discussed in this report include the following: Contribution to the stage and rate of biogenic calcrete formation using C-14 measurements by liquid scintillation counting method; Effect of time on the evolution of two geomorphic systems: proximal braided river in the Polish Carpathian and torrential fan in the Tryn Basin of Bulgaria; Some new aspects of denudation chronology of the West Carpathians; Dating marine and eolian sequences in the Rabat region, Morocco; Lichenometry: some difficulties in the establishment of reliable lichen growth curves; Application opportunities for cosmogenic dating methods in the study of diamicton deposits, Central Appalachian Mountains; Matuyama boundary and geomorphological development of the Middle - Moravian Carpathians; Development of the Slovak Western Carpathian relief in space and time; Dating of the longest paleokarst period in the Western Carpathians; Some comments on the potential for using cesium radionuclides to investigate overbank sedimentation in Carpathian rivers; and Glacial stratigraphy and dating of the Quaternary accumulation forms and deposits on the foreland of the Tatra Mts. GRA

N93-12718*# Alabama Univ., Huntsville.

CHEMICAL RELEASE AND RADIATION EFFECTS EXPERIMENT ADVANCED PLANNING AND COORDINATION Final Technical Report, 31 May 1990 - 4 Apr. 1991

William W. Vaughan and Melanie Alzmann 30 May 1991 39 p

(Contract NAS8-36955)

(NASA-CR-184439; NAS 1.26:184439; UAH-5-32417) Avail: CASI HC A03/MF A01

The efforts conducted to provide assessments and planning support for the Chemical Release and Radiation Effects Satellite (CRRES) Experiments are summarized. Included are activities regarding scientific working group and workshop development including the preparation of descriptive information on the CRRES Project. Author

N93-12804# National Geophysical Data Center, Boulder, CO. World Data Center A for Solid Earth Geophysics.

A REPORT ON GEOMAGNETIC OBSERVATORY OPERATIONS, 1990

K. L. Svendsen, W. M. Davis, S. J. McLean, and H. Meyers Feb. 1991 54 p Prepared in cooperation with International Council of Scientific Unions, Paris, France

(PB92-224781; SE-45) Avail: CASI HC A04/MF A01

Contents: A report On Geomagnetic Observatory Operations, 1990; Tables--Geomagnetic Observatories in Operation During 1990, Annual Means Available (as of April 1990), Notes on Observatories (as of April 1990), Digital Geomagnetic Observatories, 1990; MAPS--Geomagnetic Observatories in Operation During 1990, Geomagnetic Observatories in Operation During 1990 (area enlarged), Observatories Providing Timely Results as of April 1990, Observatories Providing Results as of April 1990 (area enlarged), Digital Geomagnetic Observatories, 1990, Digital Geomagnetic Observatories, 1990 (area enlarged); APPENDICES--Addresses to Use in Requesting Data or Information, The World Data Center System. GRA

N93-12818# National Center for Atmospheric Research, Boulder, CO. Atmospheric Technology Div.

MEETING REVIEW: THIRD NCAR RESEARCH AIRCRAFT FLEET WORKSHOP

Lawrence F. Radke and Paul Spyers-Duran May 1992 104 p Workshop held in Boulder, CO, 27-28 Feb. 1992 Sponsored by NSF

(PB92-222710; NCAR/TN-374+PROC) Avail: CASI HC A06/MF A02

The Third NCAR Research Aircraft Fleet Workshop was held at NCAR on February 27-28, 1992, to examine and forecast the evolving needs for geosciences research aircraft to the end of the 20th century and to recommend how the configuration of the NCAR aircraft fleet should change to meet the perceived needs. The broad spectrum of participants included geoscientists with a strong history of research aircraft usage, leaders from the Atmospheric Technology Division, and other users from groups within NCAR. Because of the desire to receive the broadest possible viewpoints, distinguished representatives from outside of the usual National Science Foundation supported groups were also included. The workshops consisted of a briefing by RAF staff on the current fleet, an overview of forecast science needs, and a review of new aircraft and options under consideration. The briefing was followed by presentations from the user community of their perceived future science needs as they relate to airborne platform capabilities. The workshop then broke into five working groups that focused on options and opportunities for the future NCAR/RAF fleet changes. GRA

N93-12841# Los Alamos National Lab., NM.

EFFECTS OF SOURCE-REGION PHENOMENOLOGY ON SEISMIC DISCRIMINATION

S. R. Taylor 15 Jun. 1992 11 p Presented at the DOE/LLNL Verification Symposium on Technologies for Monitoring Nuclear Tests Related to Weapons Proliferation, Las Vegas, NV, 6-7 May 1992

(Contract W-7405-eng-36)

(DE92-017441; LA-UR-92-2085; CONF-9205166-2) Avail: CASI HC A03/MF A01

Seismic discrimination and yield-estimation studies have demonstrated the importance of explosion-source region phenomenology to the monitoring of nuclear test ban treaties. In this paper, we examine source-region factors that control spectral ratio discrimination of NTS nuclear explosions and western US earthquakes. We discuss how near-source geology controls the shape of the spectral-ratio curve for explosions. An explosion-source model derived by Denny and Johnson (1991) is used to fit the spectral-ratio data and illustrates the dependence of the pressure-time history acting at the elastic radius on the physical state of the materials on the near-source region. We then summarize two detailed studies of a missed violation (a nuclear explosion that looks like an earthquake) and a false alarm (a naturally occurring event that looks like a nuclear explosion). In both cases, source-region effects could be modeled that resulted in the radiation of anomalous seismic spectrum. These studies underscore the importance that an improved understanding of source-region phenomenology has on predicting monitoring capabilities in widely different geologic environments, assessing opportunities for evasion, and for the resolution of false alarms. DOE

N93-12845# Washington Univ., Seattle. Dept. of Geophysics.
INVESTIGATIONS OF THE DYNAMICS AND THERMODYNAMICS OF THE MESOSPHERE LOWER THERMOSPHERE AND UPPER THERMOSPHERE AT THE POLAR REGIONS WITH OPTICAL GROUND-BASED REMOTE SENSING Final Report, 15 Apr. 1989 - 14 Jul. 1992
G. Hernandez and K. C. Clark 1 Aug. 1992 11 p
(Grant AF-AFOSR-0316-89)
(AD-A254746; AFOSR-92-0824TR) Avail: CASI HC A03/MF A01

The advances in diagnostic techniques and basic studies concerning the Earth's atmosphere made under the auspices of AFOSR are described in this report. Highlights of the investigations are the following: (1) The development and exploitation of a new field of atmospheric investigations using molecular species as passive tracers of the motion and temperature of the mesosphere. This new development is the first method devised to measure simultaneously the winds and temperatures of this poorly understood region of the atmosphere. (2) The attainment of a working, stable, rugged, monolithic electrooptic solid-state cavity whose spacing can be arbitrarily and precisely manipulated by applied electric field. This breakthrough in interference optics provides the opportunity to use small high-luminosity, high-resolution Fabry-Perot spectrometers which require no adjustments for their operation. Such instruments will make it possible to make unmanned observations of unique geophysical events at isolated stations. (3) Because of the proven robustness of our AFOSR-supported developments in teleautonomous operation of instrumentation, we have installed and are conducting two high-resolution diagnostic ground-based atmospheric experiments in the Southern Hemisphere at South Pole (Antarctica) and New Zealand. Neither of these experiments is accessible to the investigators more than twice yearly; they have been successfully operated for six instrument-years. The data obtained from the field experiments have increased the basic understanding of upper atmosphere dynamics and circulation in the two polar regions. The results of these investigations are published in the open literature, and have contributed to current global semi-empirical models of these regions of the atmosphere. GRA

N93-12877*# Chicago Univ., IL.
STATISTICAL ANALYSIS OF STRATOSPHERIC TEMPERATURE AND OZONE PROFILE DATA FOR TRENDS AND MODEL COMPARISON Final Report, 1 Jul. 1990 - 30 Jun. 1992
G. C. Tiao Nov. 1992 27 p
(Grant NAGw-2057)
(NASA-CR-191248; NAS 1.26:191248) Avail: CASI HC A03/MF A01

Work performed during the project period July 1, 1990 to June 30, 1992 on the statistical analysis of stratospheric temperature data, rawinsonde temperature data, and ozone profile data for the detection of trends is described. Our principal topics of research are trend analysis of NOAA stratospheric temperature data over the period 1978-1989; trend analysis of rawinsonde temperature data for the period 1964-1988; trend analysis of Umkehr ozone profile data for the period 1977-1991; and comparison of observed ozone and temperature trends in the lower stratosphere. Analysis of NOAA stratospheric temperature data indicates the existence of large negative trends at 0.4 mb level, with magnitudes increasing with latitudes away from the equator. Trend analysis of rawinsonde temperature data over 184 stations shows significant positive trends about 0.2 C per decade at surface to 500 mb range, decreasing to negative trends about -0.3 C at 100 to 50 mb range, and increasing slightly at 30 mb level. There is little evidence of seasonal variation in trends. Analysis of Umkehr ozone data for 12 northern hemispheric stations shows significant negative trends about -.5 percent per year in Umkehr layers 7-9 and layer 3, but somewhat less negative trends in layers 4-6. There is no pronounced seasonal variation in trends, especially in layers 4-9. A comparison was made of empirical temperature trends from rawinsonde data in the lower stratosphere with temperature changes determined from a one-dimensional radiative transfer calculation that prescribed a given ozone change over the altitude region, surface to 50 km, obtained from trend analysis of ozonsonde and Umkehr profile data. The empirical and calculated temperature trends are found in substantive agreement in profile shape and magnitude. Author

N93-12943# Massachusetts Inst. of Tech., Cambridge. Earth Resources Lab.
REGIONAL SEISMOGRAMS: ATTENUATION AND SCATTERING Final Report, 1 Jul. 1989 - 31 Dec. 1991
M. N. Toksoz, E. E. Charrette, N. Cheng, A. M. Dainty, and B. Mandal 6 Mar. 1992 364 p
(Contract F19628-89-K-0020)
(AD-A254348; Rept-72237; PL-TR-92-2069; AD-E201133) Avail: CASI HC A16/MF A03

The objective of this study was to examine the influence of attenuation and scattering on regional high frequency seismograms. This report consists of a Ph.D. thesis, a paper, and three preprints of papers either submitted or in preparation, on work supported by this project; they include both basic work on attenuation, scattering and anisotropy, and applications to regional seismograms. The Ph.D. thesis discusses the application of the finite difference method to problems in scattering and attenuation due to scattering in a random medium. In the first three chapters of the thesis, the application of Born theory to scattering and scattering attenuation is assessed. The fourth chapter to explain the observed scattering phenomena at the NORSAR and NORESS arrays in Norway. The second section is a paper that examines the radiation pattern of explosive sources in anisotropic media. The third section evaluates the problem of Lg blockage across crustal extension zones by the method of coupled modes. The fourth section is concerned with the fundamental problem of scattering of the reflected wave from a rough interface. The final section applies transport theory to Rg data from a U.S. Geological Survey experiment in Maine. GRA

N93-12944# RADEX, Inc., Bedford, MA.
ANALYSIS AND MODELING OF THE CRRES SATELLITE DATA Scientific Report No. 10
J. N. Bass, C. A. Hein, C. E. Jordan, and R. P. Vancour 20 Mar. 1992 110 p
(Contract F19628-89-C-0068)
(AD-A254349; RXR-92031; PL-TR-92-2086; AD-E201136) Avail: CASI HC A06/MF A02

The radiation belts consist of energetic charged particles trapped by the Earth's magnetic field which consists of an internal field and an external field. The external field dominates the non-dipole portions of the internal field at and above geosynchronous altitude. External field modeling usually begins with models of the various current systems from which the field is derived. CRRES data provides for a generation of new models of the radiation belts. A Strawman proposal was developed for the CRRES static radiation belt model Product Associated Data Base. Several groups of models were studied in preparation for working with the CRRES data. The models and software to run them constitute a suite of routines divided into five categories. A B(sub MIN) survey data base was constructed to study the effects of magnetic latitude and local time at B(sub MIN). The behavior of the PROTEL instrument on CRRES was modeled in its hostile environment to evaluate its performance. Predictions of the developed Contamination Code compared very well with the results from the Harvard Cyclotron experiments. The CRRES Dosimeters were modeled for an isotropic, a mirror plane and the sin(sup N)alpha pitch angle distributions. GRA

N93-12946# North Carolina Central Univ., Durham.
HIGH RESOLUTION MOLECULAR SPECTROSCOPY OF ATMOSPHERIC SPECIES Final Report, 1 Jul. 1991 - 30 Jun. 1992
Jyotsna M. Dutta and Charles R. Jones 30 Jun. 1992 15 p
(Contract F49620-89-C-0080)
(AD-A254360; AFOSR-92-0797TR) Avail: CASI HC A03/MF A01

The pressure-broadening of the 2(1,1) - 2(1,2), 3(1,3) - 2(2,1), and 7(3,4) - 6(4,3) transitions of HDO were studied between 90 K and 600 K. The broadening gases were He, H2, O2, and N2. Results for the temperature dependence of the pressure broadening parameters and collisional cross sections are discussed. The HDO transitions selected for study belong to widely different lower state energies. Such a selection allows to observe any dependence that 300 K broadening parameters and temperature coefficients may have on the rotational quantum numbers. All these have considerable theoretical interest. GRA

N93-12969# National Center for Atmospheric Research, Boulder, CO. Mesoscale and Microscale Meteorology Div.
CONVECTIVE SCALE 4-D DATA ASSIMILATION USING SIMULATED SINGLE DOPPLER RADAR OBSERVATIONS Ph.D. Thesis
Juanzhen Sun 1992 191 p Prepared in cooperation with Oklahoma Univ., Norman
(Contract NSF ATM-83-04330; NSF ATM-85-11316; NSF ATM-85-01380; DAAG29-85-K-0198)
(PB92-218726; NCAR/CT-135) Avail: CASI HC A09/MF A02

The adjoint method of variational data assimilation is applied to retrieve the 3-dimensional wind and thermal dynamic variables from simulated single Doppler radar data. The constraining numerical model simulates dry thermal convection with incompressible Boussinesq dynamics. It is demonstrated that the method is able to determine satisfactorily the initial state of the unobserved velocity components and temperature as well as the mean profiles. The incorporation of the boundary conditions into the optimization algorithm results in better retrieved initial fields than specifying the boundary conditions in some artificial way. It is demonstrated that the algorithm is robust to data increments, random observational errors, and model errors. Studies on the behavior of cost function with respect to length of assimilation indicate that the width of the global minimum is large enough to allow the algorithm to start from a rough first guess as long as the assimilation period is shorter than the initial error doubling time. GRA

N93-13143 Pennsylvania State Univ., University Park.
ACOUSTIC TOMOGRAPHIC MONITORING OF THE ATMOSPHERIC BOUNDARY LAYER Ph.D. Thesis
David Keith Wilson 1992 326 p
Avail: Univ. Microfilms Order No. DA9226804

Acoustic tomography is proposed as a method for monitoring atmospheric temperature and wind velocity fields. Basic issues relating to the feasibility and implementation of tomography are discussed. Among these issues are the causes of fluctuations in acoustic signals propagated through the atmosphere; signal detection and processing techniques; mathematical inverse techniques and their numerical implementation; and whether or not tomography can provide information of interest to atmospheric scientists. Three possible tomography schemes are discussed: vertical- and horizontal-slice schemes for studying thermals and gravity waves in the surface layer, and a long-baseline array for studying evolution of the stable boundary layer. Numerical simulations are used to assess the performance of surface-layer tomography. Surface-layer horizontal-slice tomography is implemented experimentally, as an array with three sources and seven receivers, distributed over a region approximately 200 meters square. Travel-time fluctuations at the receivers are used to reconstruct the temperature and wind fields with 50 m resolution in the horizontal plane. Analysis of the measured travel-time fluctuations also suggests that turbulent eddies having horizontal length scale approaching the boundary-layer thickness (several hundred meters) are a primary cause of fluctuations in acoustic signals. Dissert. Abstr.

N93-13149 Dartmouth Coll., Hanover, NH.
RING CURRENT OXYGEN INTERACTION WITH MICROPULSATIONS Ph.D. Thesis
Xinlin Li 1992 98 p
Avail: Univ. Microfilms Order No. DA9226547

The key issue of this thesis work is to present a new loss mechanism for ring current O(+) ions due to the combined effects of convection and corotation electric fields and interaction with geomagnetic pulsations via a magnetic drift-bounce resonance. We have found that this loss mechanism can contribute significantly to the loss of ring current O(+) with intermediate energies (20-60 keV). The behavior of ring current ions in low-frequency geomagnetic pulsations is investigated analytically and numerically, with particular emphasis on O(+) ions whose flux increases dramatically during geomagnetic storms and decays at a rate which is not fully explained by collisional processes. A test-particle code is developed to calculate the motion of the ring current O(+) ions in a time-independent dipole magnetic field, convection and corotation electric fields, plus Pc 5 wave fields, for which a simple analytical model was formulated based on spacecraft observations. For given fields, whether a particle gains or loses energy depends on its initial kinetic energy, pitch angle at the equatorial plane, and the position of its guiding center with respect to azimuthal phase of the wave. The simulated ring current O(+) distribution function shows a dispersion to higher and lower energies and L values with decreasing local time across the dayside, and a bulk shift to lower energies and higher L values. The former is due to wave-particle interaction causing the ion to lose or gain energy, while the latter is due to the convection electric field. Our simulations show that once the particle's kinetic energy drops below that required to overcome the convection potential, the particle will be lost to the dayside magnetopause. Dissert. Abstr.

N93-13276# Boston Univ., MA. Coll. of Engineering.
SELF-CONSISTENT MODELING OF THE IONOSPHERE-THERMOSPHERE-MAGNETOSPHERE SYSTEM Final Technical Report, 1 Aug. 1988 - 31 Dec. 1991
Jeffrey M. Forbes 31 May 1992 5 p
(Contract F49620-88-C-0111)
(AD-A253232; AFOSR-92-0701TR) Avail: CASI HC A01/MF A01

One of the most significant results to emerge from this contract is the systems theory approach to thermospheric dynamics which was developed as part of the dissertation research of a Ph.D. student supported by AFOSR. The basic components of the computational approach are a piecewise linearization method capable of preserving nonlinear features of a dynamical system (in this case, the NCAR TIGCM) and a response function 'library' consisting of quasi-steady state and sample response functions characteristic of the system. A typical usage would be approximating the dynamical thermospheric response to an arbitrary change in forcing by performing a specialized convolution between the specified forcing and an appropriate set of response functions from the 'library'. This methodology may provide the basis for computationally efficient real-time (operational) predictions without on-line use of a TIGCM. GRA

N93-13285# National Inst. of Polar Research, Tokyo (Japan).
JARE DATA REPORTS NO. 175 (IONOSPHERE 46). RECORDS OF RADIO AURORA AT SYOWA STATION, ANTARCTICA IN 1990
Kazuhiro Ohtaka (Ministry of Posts and Telecommunications, Tokyo, Japan) and Kiyoshi Igarashi (Ministry of Posts and Telecommunications, Tokyo, Japan) Mar. 1992 38 p
Avail: CASI HC A03/MF A01

This report presents a summary of data obtained during the period of 1990 with the auroral radar at Syowa Station, Antarctica. Three kinds of data are available: (1) chart records of the time variation of echo intensity; (2) digital MT; and (3) 35 mm film records of radio auroral echo intensity (A-scope) and range-time intensity (A'-scope). Author

N93-13310# Instituto de Pesquisas Espaciais, Sao Jose dos Campos (Brazil).
CHARACTERIZATION OF ELECTRIC DISCHARGE IN AIR PRODUCED BY AN ENVIRONMENTAL IONIZATOR [CARACTERIZACAO DA DESCARGA ELETRICA PRODUZIDA NO AR POR UM IONIZADOR AMBIENTAL]
Gilberto M. Sandonato Oct. 1991 29 p In POLISH
(INPE-5310-NTC/299) Avail: CASI HC A03/MF A01

The characterization of a negative point discharge in air produced by an environmental ionizator prototype from HD Sistemas Eletronicos Inc. eCom LTDA is presented. The tests aimed at determining the discharge regime and ion density produced by this equipment in the environment. Author

N93-13326*# National Aeronautics and Space Administration, Washington, DC.
USE OF ANTARCTIC ANALOGS TO SUPPORT THE SPACE EXPLORATION INITIATIVE
Robert Wharton, Barney Roberts (National Aeronautics and Space Administration. Lyndon B. Johnson Space Center, Houston, TX.), Erick Chiang, John Lynch, Carol Roberts, Corinne Buoni (Science Applications International Corp., La Jolla, CA.), and Dale Andersen (Lockheed Engineering and Sciences Co., Hampton, VA.) Dec. 1990 22 p Prepared in cooperation with National Science Foundation, Washington, DC Original contains color illustrations
(NASA-TM-108000; NAS 1.15:108000) Avail: CASI HC A03/MF A01; 4 functional color pages

This report has discussed the Space Exploration Initiative (SEI) and the U.S. Antarctic Program (USAP) in the context of assessing the potential rationale and strategy for conducting a cooperative NASA/NSF (National

Science Foundation) effort. Specifically, such an effort would address shared research and data on living and conducting scientific research in isolated, confined, hostile, and remote environments. A review of the respective goals and requirements of NASA and the NSF indicates that numerous opportunities exist to mutually benefit from sharing relevant technologies, data, and systems. Two major conclusions can be drawn: (1) The technologies, experience, and capabilities existing and developing in the aerospace community would enhance scientific research capabilities and the efficiency and effectiveness of operations in Antarctica. The transfer and application of critical technologies (e.g., power, waste management, life support) and collaboration on crew research needs (e.g., human behavior and medical support needs) would streamline the USAP operations and provide the scientific community with advancements in facilities and tools for Antarctic research. (2) Antarctica is the most appropriate earth analog for the environments of the the Moon and Mars. Using Antarctica in this way would contribute substantially to near- and long-term needs and plans for the SEI. Antarctica is one of the few ground-based analogs that would permit comprehensive and integrated studies of three areas deemed critical to productive and safe operations on the Moon and Mars: human health and productivity; innovative scientific research techniques; and reliable, efficient technologies and facilities. Author

N93-13405# Tokyo Univ. (Japan). Inst. of Space and Astronautical Science.

MONTE CARLO CALCULATION OF IONIZATION AND EXCITATION RATES IN ELECTRON AURORA

Kunizo Onda, Makoto Hayashi (Nagoya Inst. of Tech., Japan), and Kazuo Takayanagi Jun. 1992 41 p

(ISAS-RN-645) Avail: CASI HC A03/MF A01

Ionization and excitation of atmospheric N2, O, and O2 in electron aurora are studied numerically in the Monte Carlo approach. Electrons are assumed to be injected downward into the upper atmosphere at the altitude of 250 km. The initial electron energy is 3, 5, or 7.5 keV. Time variation of the energy- and altitude-distribution of the electrons (primary and secondary electrons) is studied and the numbers of various collision processes are counted. Particularly, the number of photo-emission of the first-negative band system of molecular nitrogen and the red and green lines of atomic oxygen, and the number of ion-electron pairs created are found as functions of the altitude. The continuous-slowing-down (CSD) approximation, which was used earlier in the same problem by one of the present authors (K.T.), is tested. In the intensity of the above-mentioned photo-emissions and the ionization rate as functions of the height, good agreement is obtained between the Monte Carlo and the CSD calculations, except in the lowest region of the altitude. Author

N93-13432# National Inst. of Polar Research, Tokyo (Japan).

JARE DATA REPORTS NO. 170 (IONOSPHERE 45). HF FIELD STRENGTH DATA MEASURED AT SYOWA STATION, ANTARCTICA FROM JANUARY TO DECEMBER 1988

Shoji Kainuma (Ministry of Posts and Telecommunications, Tokyo, Japan), Kohji Inamori (Ministry of Posts and Telecommunications, Tokyo, Japan), and Atsushi Otsuka (Ministry of Posts and Telecommunications, Tokyo, Japan) Nov. 1991 22 p

Avail: CASI HC A03/MF A01

The field strength of JJY (standard frequency waves) transmitted from Japan has been measured at Syowa Station, Antarctica, since 1958. The receiver detects only the upper sideband component of signals in order to avoid the co-channel interference. This report summarizes the results of field strength measurements of JJY 8 MHz, for the interval from January to December, 1988. Author

N93-13460*# Utah State Univ., Logan. Space Dynamics Lab.

EXPERIMENTAL STUDIES OF IONOSPHERIC IRREGULARITIES AND RELATED PLASMA PROCESSES Final Report, Mar. 1982 - Dec. 1992

Kay D. Baker 1992 34 p

(Grant NAG5-603)

(NASA-CR-191271; NAS 1.26:191271; SDL/92-116) Avail: CASI HC A03/MF A01

Utah State University (USU) continued its program of measuring and interpreting electron density and its variations in a variety of ionospheric conditions with the Experimental Studies of Ionospheric Irregularities and Related Plasma Processes program. The program represented a nearly ten year effort to provide key measurements of electron density and its fluctuations using sounding rockets. The program also involved the joint interpretation of the results in terms of ionospheric processes. A complete campaign summary and a brief description of the major rocket campaigns are also included. Author

N93-13481 Columbia Univ., New York, NY.

THE MORPHOTECTONIC FABRIC OF THE EAST PACIFIC RISE: IMPLICATIONS FOR FAULT GENERATION AND CRUSTAL ACCRETION Ph.D. Thesis

Margo Helen Edwards 1991 172 p

Avail: Univ. Microfilms Order No. DA9221146

Optical and acoustic data are used to describe the morphology of the fast spreading East Pacific Rise between 10 deg N and 15 deg N. Image analysis and statistical techniques characterize volcanic and tectonic features on the axis and flanks at a variety of spatial scales. Faults on the rise axis are shorter, more closely spaced, have smaller vertical throw, and dissimilar orientations from faults on the flanks. Distinct models of formation are therefore proposed for the on-and off-axis faults. Because of their en echelon offsets, well correlated along-strike azimuths and association with collapse features, faults on the axis are modeled as initiating by gravitational collapse with subsequent evolution controlled predominantly by extension. Faults on the rise flanks nucleate within a few kilometers of the axis, but are noticeable absent from 0 km to 1.8 km. Faults on the flanks also mimic the 50-100 along-strike segmentation of the ridge axis. These observations correlate well with the suggested shape of the axial magma chamber which is 3-4 km wide and interrupted at second and third order axial discontinuities in the study area. A model is therefore proposed in which faults on the flanks are generated by inflationary cycles of the magma chamber. This model is also used to describe the formation of abyssal hills. Finally, because fresh volcanics are concentrated in the axial summit graben, evidence of multiple flooding and drainback events occur in these locales, and sediment cover on terrain just outside the bounding walls of the summit graben is quite high a model is proposed in which a large proportion of crustal layer 2A is created right at the rise axis.

Dissert. Abstr.

N93-13482 Oxford Univ. (England).

RADIATIVE TRANSFER IN THE MIDDLE ATMOSPHERE Ph.D. Thesis

Amanda J. L. Manning 1990 248 p

Avail: Univ. Microfilms Order No. BRD-94158

In recent years, much debate has surrounded phenomena such as the depletion of the ozone layer and the onset of greenhouse warming, which have occurred due to the changing concentrations of various constituents in the earth's atmosphere. The influx into the middle atmosphere of unnatural quantities of trace gases such as carbon dioxide and methane is likely to affect global climate both adversely and irreversibly. In order to model the response of the atmosphere to these changes, and to evaluate the relative importance of various gases in the interlinked radiative, dynamical, and chemical processes taking place, it is vital that we understand as fully as possible the role played by radiative transfer. To this end, a detailed yet flexible numerical model, covering the entire infrared spectrum, was developed for the study of radiative transfer processes in the stratosphere and mesosphere. The scheme is intended to be as accurate as possible within the constraints of available computer resources, and to produce reference heating rates against which those derived using more approximate methods may be checked. Particular consideration was given to minor constituents, including water vapor, methane, and nitrous oxide, whose roles were underestimated in many previous studies, and to minor spectral bands of major constituents, such as the 4.3 micron and 10 micron bands of carbon dioxide and the 14.3 micron band of ozone, whose importance with regard to the radiative balance of the middle atmosphere has not yet been fully evaluated. Considerable attention is paid to the calculation of atmospheric transmittance: the sensitivity of the heating rates to the choice of narrow band Goody or Malkmus model transmittances, as opposed to those generated using the high-resolution GENLN2 line-by-line model is assessed. Diffuse radiation is accounted for by explicit Gaussian integration over zenith angle, and the way in which heating rates thus generated differ from those derived with the more commonly used constant diffusivity factor is investigated. Both fixed-point and adaptive integration methods are discussed, with respect to the evaluation of the vertical term of the radiative transfer equation. An investigation is carried out, from the radiative

point of view, into the changes in carbon dioxide, ozone, and methane concentrations which have occurred or are expected to take place due to human activities. The results lend weight to the theory that the estimated effects on global climate of increases in anthropogenic trace gases are indeed substantial. Dissert. Abstr.

N93-13485 Wisconsin Univ., Madison.
A THEORETICAL INVESTIGATION OF THE GROWTH RATES OF ICE CRYSTALS IN CLOUDS Ph.D. Thesis
Wusheng Ji 1991 220 p
Avail: Univ. Microfilms Order No. DA9209229

A theoretical investigation of diffusional and collisional growth rates of freely falling columnar ice crystals, hexagonal ice plates, and broad-branch ice crystals in air is presented. A numerical model for unsteady flow past those three types of ice crystals was recently developed. The Navier-Stokes equations of motion for three-dimensional, viscous, unsteady, incompressible flow past those ice crystals were solved by finite difference method for Reynolds numbers ranging from 0.2 to 140. The dynamic characteristics of the velocity and vorticity fields including unsteady laminar wakes behind ice crystals are investigated and analyzed. The water vapor density profiles were then obtained by solving the convection-diffusion equation around the same falling ice crystals, and the corresponding diffusional growth rates were calculated. Furthermore, a theoretical model for studying the collision efficiencies of ice crystals interacting with supercooled water drops of radii between 1 and 100 microns in a three-dimensional flow and incorporating gravitational, inertial forces, and the electrostatic forces for a columnar ice crystal at Reynolds number of 0.5 has been formulated. The results of the present study, which provides a set of mathematical fitting functions for the growth rates of typical ice crystals, should be useful to cloud dynamical models. They also contribute to the further understanding of ice microphysical processes in atmospheric clouds. Dissert. Abstr.

N93-13491 Utah State Univ., Logan.
MAGNETIC HOLES NEAR THE MAGNETOPAUSE Ph.D. Thesis
Lane R. Brostrom 1992 150 p
Avail: Univ. Microfilms Order No. DA9222263

A search for magnetic holes, discrete spatial regions characterized by a distinct drop in magnetic field strength, has been made through the data taken during the magnetopause crossings of the AMPTE IRM satellite. In this search, the September 4, 1984 magnetic hole was used as a model for establishing a set of criteria for distinguishing magnetic holes. Holes similar to that of September 4, 1984 were observed in at least 13 percent of all AMPTE IRM passages through the magnetopause region. Plasma densities inside the magnetic hole suggest that the plasma is of magnetosheath origin. The increase in number density inside the hole compensates for the decrease in magnetic field strength such that pressure balance is maintained with the ambient magnetospheric plasma. Inside a magnetic hole, plasma waves between the ion cyclotron frequency f(sub ci) and the plasma frequency f(sub pe) are observed to fall below instrument noise levels. A related structure often encountered in the search for magnetic holes, previously called a crater flux transfer event (CFTE), is nearly identical to magnetic holes in its magnetic field and plasma characteristics. However, observations show a general enhancement of wave activity inside the CFTE in all frequencies between the ion cyclotron frequency f(sub ci) and the plasma frequency f(sub pe). Here, it is discovered that the basic difference between magnetic holes and CFTEs appears to be a critical beta level (beta(sub cr) is greater than or = 10). It is proposed that the lower hybrid drift instability plays a major role in the generation or damping of waves inside the magnetic hole; this instability, which is highly likely to be present under these conditions, is stabilized above beta(sub cr). The beta level in magnetic holes exceeds beta(sub cr) and in CFTEs it does not. In at least 22 percent of the crossings of the magnetopause region, magnetic holes or CFTE's, or both, were observed. The absence of waves above the lower hybrid frequency inside the magnetic hole suggests that the lower hybrid drift instability plays a key role in the chain of nonlinear cascading within typical magnetopause turbulence. From the perspective of the bulk flow velocity, the magnetic hole and CFTE appear to be plasma vortices which have entered the magnetosphere from the magnetosheath. Although they are similar in many respects to the flux transfer event (FTE), evidence indicates they are not reconnection phenomena. Among the various models considered, the kinetic theory model of impulsive penetration of the magnetopause offers a likely explanation for the origin of the magnetic hole. Dissert. Abstr.

N93-13492 Saint Louis Univ., MO.
LATERAL VARIATIONS OF SHEAR VELOCITY AND ANELASTICITY IN THE UPPER MANTLE OF THE WESTERN US FROM RAYLEIGH WAVE OBSERVATIONS Ph.D. Thesis
Hanan Hassan Mahdi Al-Khatib 1991 283 p
Avail: Univ. Microfilms Order No. DA9215925

Rayleigh wave phase and group velocities and attenuation coefficients in the period range 18 to 120 sec were determined for three regions along nine paths across the western United States using a two-station technique. The attenuation coefficients were found to increase systematically from east to west between the Rocky Mountains and Pacific coast. This contrasts with the results for the eastern and central United States where no systematic variation of long-period Rayleigh wave attenuation could be discerned in earlier studies. The Rayleigh wave group and phase velocities were simultaneously inverted, using a differential inversion procedure, to obtain shear wave velocity models. These velocity models were then used in an inversion process to obtain internal friction (Q(sub beta))(exp -1) as a function of depth from attenuation measurements. Both shear wave velocities and Q(sub beta) values decrease from east to west at all depths. The decrease in Q(sub beta) values is much more severe than the decrease in velocities. The inversion results show that Q(sub beta) values in the western United States are lowest for the coastal regions and westernmost Basin and Range, highest for the Rocky Mountains and western Great Plains, and intermediate for the Basin and Range, Columbia and Colorado Plateaus. Low values of Q(sub beta) (70-30) occur in the upper crust, higher values occur in the lower crust (230-90), and highest values occur in the uppermost 20 km of the mantle (835-300). These overlie a low-Q zone which is shallower than the low-velocity zone in all regions. This is consistent with a mechanism for low velocities and low Q values which is controlled by temperature. Dissert. Abstr.

N93-13513# Oregon State Univ., Corvallis. Coll. of Oceanography.
NEW APPROACHES TO ESTIMATION OF MAGNETOTELLURIC PARAMETERS
G. D. Egbert 1991 53 p
(Contract DE-FG06-89ER-14057)
(DE92-040280; DOE/ER-14057/2) Avail: CASI HC A04/MF A01

Fully efficient robust data processing procedures were developed and tested for single station and remote reference magnetotelluric (MT) data. Substantial progress was made on development, testing, and comparison of optimal procedures for single station data. A principal finding of this phase of the research was that the simplest robust procedures can be more heavily biased by noise in the (input) magnetic fields, than standard least squares estimates. To deal with this difficulty we developed a robust processing scheme which combined the regression M-estimate with coherence presorting. This hybrid approach greatly improves impedance estimates, particularly in the low signal-to-noise conditions often encountered in the 'dead band' (0.1-0.0 Hz). The methods and the results of comparisons of various single station estimators are described in detail. Progress was made on developing methods for estimating static distortion parameters and for testing hypotheses about the underlying dimensionality of the geological section. DOE

N93-13614 Colorado State Univ., Fort Collins.
MEASUREMENT OF TROPOSPHERIC TEMPERATURE AND AEROSOL EXTINCTION USING HIGH SPECTRAL RESOLUTION LIDAR Ph.D. Thesis
Raul John Alvarez, II 1991 110 p
Avail: Univ. Microfilms Order No. DA9216168

A high spectral resolution Rayleigh-Mie lidar system capable of measuring relative temperature and aerosol profiles in the troposphere was developed. The use of a narrowband laser transmitter along with an atomic vapor cell as a variable width bandstop filter allows for the separation of molecular and aerosol scattering signals. Using two of these filters with different widths and a newly developed lidar inversion method it is possible to determine relative temperature, pressure, and density profiles of the troposphere. This separation also makes a quantitative measurement of aerosol extinction coefficient profiles possible. In principle, the information required in addition to the lidar signals for determining atmospheric and

aerosol properties with this Rayleigh-Mie lidar is the theoretical Rayleigh-Brillouin spectrum for scattering of narrow bandwidth laser light, independent measurements of the filter transmission functions, the assumption that the atmosphere acts as an ideal gas in hydrostatic equilibrium, and an approximate atmospheric pressure at one reference altitude. Profiles of the tropospheric state variables of temperature, pressure, and density are determined from signals averaged over 20 minutes. Once profiles of the atmospheric variables are determined, the aerosol extinction coefficient profiles are calculated. However, a systematic offset in the lidar temperature profiles is seen in practice when compared to balloon sonde measurements. Further laboratory experiments have established that the systematic offset is real and is consistent between laboratory and field measurements. This repeatable offset can be eliminated by normalizing the temperature at a reference altitude to an independently measured or estimated value. The development and implementation of this high spectral resolution lidar and the first simultaneous measurements of tropospheric temperature and aerosol profiles from 0.2 km to 8 km are presented. The precision at 1 km altitude is plus or minus 10 K for temperature measurement, plus or minus 3 percent for backscatter ratio, and plus or minus 5 percent for aerosol extinction coefficient. At 5 km, these values are plus or minus 12 K for temperature, plus or minus 4 percent for backscatter ratio, and plus or minus 100 percent for extinction coefficient. Suggestions to determine the cause of the offset and to reduce the relative uncertainties are also discussed. Dissert. Abstr.

N93-13719*# North Carolina State Univ., Raleigh. Dept. of Marine, Earth and Atmospheric Sciences.

MESO-BETA SCALE NUMERICAL SIMULATION STUDIES OF TERRAIN-INDUCED JET STREAK MASS/MOMENTUM PERTURBATIONS Semiannual Report, Nov. 1992

Yuh-Lang Lin and Michael L. Kaplan Nov. 1992 86 p

(Grant NAG5-1790)

(NASA-CR-191365; NAS 1.26:191365) Avail: CASI HC A05/MF A01

Work performed during the report period is summarized. The first numerical experiment which was performed on the North Carolina Supercomputer Center's CRAY-YMP machine during the second half of FY92 involved a 36 hour simulation of the CCOPE case study. This first coarse-mesh simulation employed the GMASS model with a 178 x 108 x 32 matrix of grid points spaced approximately 24 km apart. The initial data was comprised of the global 2.5 x 2.5 degree analyses as well as all available North American rawinsonde data valid at 0000 UTC 11 July 1981. Highly-smoothed LFM-derived terrain data were utilized so as to determine the mesoscale response of the three-dimensional atmosphere to weak terrain forcing prior to including the observed highly complex terrain of the northern Rocky Mountain region. It was felt that the model should be run with a spectrum of terrain geometries, ranging from observed complex terrain to no terrain at all, to determine how crucial the terrain was in forcing the mesoscale phenomena. Both convection and stratiform (stable) precipitation were not allowed in this simulation so that their relative importance could be determined by inclusion in forth-coming simulations. A full suite of planetary boundary layer forcing was allowed in the simulation, including surface sensible and latent heat fluxes employing the Blakadar PBL formulation. The details of this simulation, which in many ways could be considered the control simulation, including the important synoptic-scale, meso-alpha scale, and meso-beta scale circulations is described. These results are compared to the observations diagnosed by Koch and his colleagues as well as hypotheses set forth in the project proposal for terrain-influences upon the jet stream and their role in the generation of mesoscale wave phenomenon. The fundamental goal of the analyses being the discrimination among background geostrophic adjustment, terrain influences, and shearing instability in the initiation and maintainance of mesoscale internal wave phenomena. Based upon these findings, FY93 plans are discussed. A review of linear theory and theoretical modeling of a geostrophic zonal wind anomaly is included. L.R.R.

N93-13722 State Univ. of New York, Stony Brook.

A STUDY OF THE EARTH RADIATION BUDGET EXPERIMENT: SHORTWAVE MEASUREMENTS AND BIDIRECTIONAL REFLECTANCE MODELS FOR THE OCEAN SURFACE Ph.D. Thesis

Rose Marie Dlhopolsky 1991 159 p

Avail: Univ. Microfilms Order No. DA9219319

Shortwave radiances from the Earth Radiation Budget Experiment (ERBE) satellites are converted to fluxes using bidirectional reflectance models created from Nimbus 7 data. These models describe the dependence of a shortwave measurement on the angle at which a scene is being observed and the position of the sun relative to that scene and the satellite. In this study, reflectances are derived from Earth Radiation Budget Satellite (ERBS) shortwave radiances and sorted according to the range of angles at which they were measured. This range is called the angular bin size. The Nimbus 7 Bidirectional Reflectance Models were created using this same procedure. In this study, the size of the angular bins is made smaller than the sizes in the Nimbus 7 Bidirectional Reflectance Models in order to more accurately describe the angular dependence of the shortwave reflection. Results indicate that the size of the Nimbus 7 angular bins causes the ERBE shortwave fluxes to be overestimated when the satellite views specular reflection from the ocean surface. This is especially severe for solar zenith angles less than 25 degrees. Clear sky shortwave radiances measured under specular geometries are very large and are therefore not included in the processing. However, these radiances are sometimes identified as clouds and included in the data set. This occurs because shortwave radiances reflected from clouds do not exhibit as strong a dependence on viewing geometry as the clear sky ocean surface. Therefore, a large shortwave radiance is identified as a cloud. Examples are given where this affects the regional data. Dissert. Abstr.

N93-13725 Columbia Univ., New York, NY.

DEEP CONVECTION AND ITS RELATION TO THE LARGE-SCALE CIRCULATION IN THE TROPICAL PACIFIC Ph.D. Thesis

Rong Fu 1991 196 p

Avail: Univ. Microfilms Order No. DA9209822

Behavior of deep convection and its relation to sea surface temperature (SST), surface wind divergence and convective instability are analyzed by using ISCCP cloud data, conventional SST and surface wind data and rawinsonde data in the tropical Pacific for July 1983-July 1985. The intensive deep convective clouds (DCC) and surface wind convergence areas shift latitudinally in phase with the maximum solar radiation. The warm SST area lags them one to three months in equinox seasons in the central Pacific. SST has major impact on the atmospheric conditional instability. When SST is greater than or equal to 28 C, surface wind divergence only affect the planetary boundary layer (PBL) instability. When SST is less than 27 C, strong surface wind convergence destabilizes inversion layer and moisten PBL so that atmosphere becomes convectively neutral stable. DCC is enhanced only in the area of warm SST exceed 10 percent of a region. When the fractional area of warm SST is smaller than 10 percent in a region, DCC is enhanced in cold SST (less than 27 C) when strong surface wind convergence occurs. DCC areas are latitudinally narrower than warm SST areas in the western Pacific due to lower relative humidity in PBL or inversion capped on the top of trade cumulus boundary layer (TCBL). The area with dry PBL that separates north and south branches of DCC area may be caused by subsidence and easterly advection of dry air. In warm SST areas, DCC occurs more frequently, and DCC top rises due to increase of PBL. The mean cirrus/anvil clouds (CAC) over the western and central Pacific are colder and optically thinner in El Nino months. This behavior of CAC introduces an anomaly warming effect on atmosphere-ocean system during El Nino events. The EOF analysis suggests that the vertical temperature and humidity variations are dominated by variations of large-scale vertical motion and shallow convections associated with easterly waves and perturbations of Walker and Hadley circulations. The occurrence of deep convection is mainly regulated by temperature change in the trade inversion layer on short time scales. Dissert. Abstr.

N93-13726 East Anglia Univ., Norwich (England).

KINETIC AND SPECTROSCOPIC STUDIES OF PEROXY RADICAL REACTIONS RELATED TO TROPOSPHERIC PHOTO-OXIDATION CHEMISTRY Ph.D. Thesis

Michael Edwin Jenkin 1991 283 p

Avail: Univ. Microfilms Order No. BRDX94731

Over the past 30 years, man has become increasingly aware that the presence of relatively small quantities of pollutants in the atmosphere as a result of his activities, can have a profound impact on both its chemistry, and its meteorology. Photochemistry in the atmosphere is not restricted to the behavior of pollutants; indeed, certain photochemical phenomena necessarily occur naturally in a 'pollution free' atmosphere. It is the interaction of the photochemistry of trace pollutants with the naturally established

chemistry, either inhibiting or exaggerating natural processes, which has given rise to the environment threatening consequences. The chemistry that leads to the phenomena mentioned above is complex, involving many hundreds of chemical reactions of reactive atomic and radical species. Over the years, a great deal of chemical kinetic data for elementary atmospheric reactions has accumulated, and the fundamental gas phase chemistry is well established. Computer models provide a useful means of assembling these data, and describing the likely behavior and interconversion of various atmospheric pollutants, thereby enabling policy decision. For these models to be truly predictive, however, they must be based, first on reliable field measurements of primary trace pollutants and, secondly, on accurate kinetic and mechanistic data for key reactions of atmospheric importance. The work presented in this dissertation is concerned with the kinetics and mechanisms of reactions of the hydroperoxy radial (HO2), and various organic peroxy radicals (RO2), which are formed as intermediates in the atmospheric oxidation of volatile organic compounds. In the sections that follow, our current understanding of the chemistry in general of the lower atmosphere (0-50 km) will be discussed in some detail, but with particular reference to the role played by HO2 and RO2 radicals.

Dissert. Abstr.

N93-13731 Harvard Univ., Cambridge, MA.
RADIATIVE CONSTRAINTS ON THE ENERGY BUDGET OF THE ATMOSPHERE Ph.D. Thesis
Kenneth Robert Minschwaner 1992 162 p
Avail: Univ. Microfilms Order No. DA9228246

An infrared radiative code has been developed and applied to studies of the steady state energy balance of the atmosphere. The model utilizes the correlated-k method to carry out spectral integrations and includes an improved treatment of the finite-difference approximation to the vertical radiative flux integral. Absorption coefficients are calculated directly from archived spectroscopic data. Radiative cooling rates computed with the model agree with benchmark line-by-line calculations to better than 5 percent; top of the atmosphere fluxes agree to within 1 percent. The sensitivity of clear-sky flux components to changes in sea surface temperature, atmospheric lapse rate, and relative humidity are examined. Comparison with satellite measurements indicates that a 6.5 K/km lapse rate model cannot reproduce observed infrared fluxes. Agreement is improved by employing a parameterization in which the static stability is related empirically to the surface temperature. Assumption of a constant profile of relative humidity yields results consistent with observations for surface temperatures less than 298 K, but comparison with measurements at higher temperatures suggests that significant increases in middle and upper tropospheric humidity must accompany warmer ocean temperatures. The enhanced greenhouse forcing at higher temperatures is felt primarily in the atmosphere, rather than at the surface. A simple one-dimensional model is presented to describe the energy budget of the tropical atmosphere. The heating of the tropical atmosphere due to deep cumulus convection is accounted for by clear-sky subsidence acting on a stable lapse rate of temperature. Results suggest that the strength of the subsidence field may be sensitive to changes in atmospheric composition, specifically variations in the altitude distribution of H2O and changes in the abundance of greenhouse gases such as CO2. Buoyancy considerations suggest that there may be an upper limit to the range of permissible values for surface temperature in the tropics. Simulations of tropical temperatures implied by paleo-climatic data for the last glacial maximum require either a reduction in the surface relative humidity or a weakening of the cumulus-induced subsidence field. Changes in the abundance of O3 in the lower stratosphere in the tropics can have significant implications for climate. The relatively warm climates of the Eocene and Cretaceous and the cold climates of recent glacial epochs may be associated with shallower and deeper stratospheres, respectively, with related expansion and contraction of the Hadley circulation. Changes in lower stratospheric O3 may be related to variations in stratospheric circulation corresponding to different levels of CO2, with additional contributions for the contemporary environment due to elevated levels of industrial chlorine and bromine. Dissert. Abstr.

N93-13755 Pennsylvania State Univ., University Park.
A JOINT STUDY OF THE LOWER IONOSPHERE BY RADAR, LIDAR, AND SPECTROMETER Ph.D. Thesis
Qihou Zhou 1991 173 p
Avail: Univ. Microfilms Order No. DA9204332

The dynamics and associated phenomena occurring in the lower ionospheric-E region, especially the mesopause region between 80 km to 110 km at low latitude, are studied. In particular, incoherent scatter radar (ISR), sodium lidar and airglow spectrometry are used to study the ionospheric structure and neutral sodium structure. The simultaneous study of the ionospheric plasma and neutral atomic sodium is unprecedented in scope and detail. The joint study of the mesopause region reveals that plasma, neutral densities and temperature are interconnected through the same atmospheric dynamics. The theme of the thesis is to explain the formation of the controversial sporadic sodium layer (SSL) events. Strong correlation is established between the average total ion and sodium concentrations, and between sporadic-E and SSL events. The mechanism proposed in the thesis, which invokes temperature fluctuations induced by tides and gravity waves, finds good agreement with observations. Tides and gravity waves can converge ions into thin layers through the windshear mechanisms and can influence the concentration of atomic sodium through temperature fluctuations. Sodium abundance is shown to augment rapidly when the temperature is increased. Gravity wave theory states that the ion convergence node coincides with a temperature maximum for a westward propagating gravity wave, and coincides with a temperature minimum for an eastward propagating wave. Because tidal winds propagate westward, the ion layer coincides with the temperature maximum which consequently induces higher sodium concentration. This can account for the general correlation between sodium and total ion concentration and is supported by the O2(0-1) rotational temperature. Gravity waves and their interaction with tidal winds are believed to be responsible for the close association between sudden sodium layers and sporadic-E layers. It is hypothesized that there may exist a sodium dust layer with peak amplitude around the mesopause height. When this dust layer is pushed up or down, sodium may be released from the dust to cause the structural change in the sodium layer. An effective and fast ISR interference detection and correction scheme is presented. The O2(0-1) and OH(6-2) rotational densities and temperatures of the airglow have been derived and studied.

Dissert. Abstr.

N93-13757 Pennsylvania State Univ., University Park.
NONLINEAR HYDROSTATIC CONDITIONAL SYMMETRIC INSTABILITY: SOME THEORETICAL AND MODELING CONSIDERATIONS Ph.D. Thesis
Ola Per Gustav Persson 1991 306 p
Avail: Univ. Microfilms Order No. DA9204271

A two-dimensional, meridional version of the Penn State/NCAR mesoscale model (MM4) has been used to simulate the entire life cycle of conditional symmetric instability (CSI) under conditions of no deformational or planetary boundary layer forcing. Various features of interest develop during life cycle. These include local area of potential and inertial instability, as well as specific patterns of ageostrophic zonal flow. The modeled updraft slope is approximately along surfaces of constant momentum, since the viscosity and finite grid spacing yield an unstable mode with a finite updraft width. Such a mode differs from the inviscid mode, which has the CSI characteristics frequently discussed in the literature. Local areas of increased and decreased dry potential vorticity (q), including areas of negative q, develop from the initially everywhere positive q field principally because of the horizontally differential diabatic heating. The cessation of the CSI is not due to the removal of the area of negative moist potential vorticity, but rather to the removal of unstable modes with resolvable updraft widths and to the depletion of the water vapor supply. Model-output soundings along m-surfaces show that lower-tropospheric thermodynamic stabilization occurs during the simulation. During the growth stage transverse perturbation kinetic energy (TPKE) is equally generated from the basic state kinetic energy (BSKE) and from the perturbation potential energy (PPE). During the decay stage, the generation of PKE from BSKE still occurs, but PKE is converted back to PPE. During the post-CSI stage, energy conversions between TPKE and zonal perturbation kinetic energy (ZPKE) are associated with the propagation of symmetric waves. These weak waves have a period, phasing, and amplitude consistent with linear theory. Sensitivity studies indicate that consistent horizontal and vertical grid resolutions, the ability to resolve the updraft widths of the unstable modes, and the inclusion of a Richardson number-dependent vertical diffusion scheme are important model characteristics for the simulation

CSI. Idealized studies such as these may be useful as an aid in interpreting observational data and/or numerical model simulations of real-atmosphere cases. Dissert. Abstr.

N93-13771 Texas Univ., Austin.
THE DETERMINATION AND ERROR ASSESSMENT OF THE EARTH'S GRAVITY FIELD MODEL Ph.D. Thesis
Dah-Ning Yuan 1991 448 p
Avail: Univ. Microfilms Order No. DA9128407

Precision orbit determination methods, along with a new technique to compute relative data weights, were applied to the determination of the Earth's gravity field and other geophysical parameters from the combination of satellite ground-based tracking data, satellite altimetry data, and the surface gravimetry data. The University of Texas' Earth's gravity field model, TEG-2, was determined from data sets collected from fifteen satellites, spanning the inclination ranges from 15 to 115 deg, and surface gravity data. The satellite measurements include laser ranging data, Doppler range-rate data, and satellite-to-ocean radar altimeter data, which include the direct height measurement and the differenced measurements at ground track crossings (crossover measurements). The terrestrial gravimetry data used in the TEG-2 solution were provided from the Ohio State University 1 deg x 1 deg area-mean free-air gravity anomaly data and elevation data. The estimated parameters in the TEG-2 solution include GM-gravitational constant of the Earth, geopotential coefficients complete to degree and order 50, selected dynamical tide coefficients, coordinates of the Doppler tracking stations, and two separate sets of surface spherical harmonics coefficients complete to degree and order 10 for Seasat and Geosat altimeter-derived quasistationary sea surface topography. Error assessment and calibration of the TEG-2 solution and formal error covariance were performed. Observation residual combined with covariance prediction analysis indicate that a level of internal consistency has been achieved in the TEG-2 solution, and a calibration factor was determined for the TEG-2 formal error covariance matrix so that the resulting covariance presents a realistic accuracy of TEG-2 solution. The improvement of the TEG-2 geopotential solution presented in this investigation is due in large part to the optimal weighting technique applied to the simultaneous solution for the topography, the gravity field, and the satellite orbit. The accuracy of the geographically correlated mean for Topex's radial orbit predicted from the 36 x 36 part of the TEG-2 geopotential error covariance is about 11 cm, and the global accuracy of geoid undulation predicted from the 50 x 50 part of the TEG-2 geopotential error covariance is about 1.6 m. Dissert. Abstr.

N93-13782 California Inst. of Tech., Pasadena.
ASPECTS OF ATMOSPHERIC TRANSPORT AND DISPERSION WITHIN AN AIR BASIN Ph.D. Thesis
Robin Scott Horrell 1991 347 p
Avail: Univ. Microfilms Order No. DA9137243

Atmospheric transport and dispersion relating to observed pollution levels are analyzed using three methods. Two traditional methods, dimensional analysis and atmospheric sulfur hexafluoride tracer experiments are applied to new problems; the third, neural computation is a new method of looking at incomplete ozone data reconstruction and short term ozone forecasting. A comprehensive dimensional analysis of buoyantly driven slope wind is presented to unify the subject. The relationship between thickness, velocity, Reynolds, Froude, Rossby, and Richardson numbers of the buoyant layer and the characteristic slope parameters is established. A detailed study of the velocity and temperature profiles is done using the Von Karman-Pohlhausen (KP) integral technique. The technique is extended for transient slope flows using a combination of the KP method and the method of characteristics. The transport and dispersion of airborn emissions from Los Angeles were studied using tracer methods during the Southern California Air Quality Study of 1987. Analysis of tracer trajectories indicates emission transport from downtown Los Angeles was by two routes, and the relative importance of each route was determined by a diurnally occurring divergence zone. This zone, resulting from geography and pressure gradients, was shown to migrate east to west in the air space above Los Angeles. The zone routes a majority of morning emissions northwest of Los Angeles, contrary to the commonly held belief that morning emissions were routed east. Neural computational strategies are applied to two ozone data sets for the purpose of data reconstruction and forecasting. The Madaline III algorithm is used to reconstruct data at a single site. The reconstruction is done to add missing data. This method is advantageous when peaks in the data are missing, and traditional interpolation methods inapplicable. A recurrent algorithm is used to make short-term ozone forecasts at a single location based on past history of ozone observations at that site. The results are systematically better than regression methods. Dissert. Abstr.

N93-13784 Michigan Univ., Ann Arbor.
PHOTOCHEMICAL KINETICS OF EXCITED STATES OF O3 AND O2: LABORATORY STUDIES AND ATMOSPHERIC IMPLICATIONS Ph.D. Thesis
Jichun Shi 1991 266 p
Avail: Univ. Microfilms Order No. DA9135692

The photochemistry of O3 has matured through the extensive research efforts of the last two decades, but its completeness has been questioned by several laboratory and atmospheric observations, including the unusually complex kinetics for the ozone three-body recombination reaction at high pressures, the unexplained heavy ozone isotope enhancement in the stratosphere, and the deficiencies of current chemical models at 90-120 km. The model deficiencies may be related to several of the excited states of O3 and O2. In this dissertation, the photochemical kinetics of these excited species were studied in a series of laboratory measurements, which are divided into two groups: (1) the study of the excited intermediates formed in the ozone recombination reaction; and (2) the investigation of the unusual odd oxygen formation in O2 under laser irradiation at 248 nm. The ozone recombination reaction was investigated at room temperature by monitoring the time-resolved infrared chemiluminescence of ozone at 9.6, 4.7, and 3.4 microns. These studies have indicated that the recombination reaction (O + O2 + M) apparently proceeds through an intermediate complex OM, and, for M = O2, the recombination also involves the participation of a metastable electronic state, O3(E). The three infrared emissions were also used to analyze the deactivation of vibrationally excited O3(v). The unusual odd oxygen formation in O2 at 248 nm was studied in both pure O2 and O2 + N2 and O2 + Ar mixtures at pressures between 200 and 1600 torr and at temperatures between 298 and 370 K. The results have indicated that this odd oxygen formation is initiated by O2 absorption in the Herzberg continuum, and it is autocatalytically accelerated by the photodissociation of vibrationally excited O2(v) at 248 nm. These kinetics results were used to study the possible roles of excited O3 and O2 species in the sources and sinks of odd oxygen at 90-120 km, and in the heavy ozone isotope enhancement in the stratosphere. Dissert. Abstr.

N93-13789 Michigan Univ., Ann Arbor.
A NEW INSTRUMENT FOR THE STUDY OF MESOSPHERIC GRAVITY WAVES THROUGH NIGHTGLOW OBSERVATIONS Ph.D. Thesis
Mingzhao Luo 1991 229 p
Avail: Univ. Microfilms Order No. DA9135642

The observations of the mesospheric nightglow have been used to study the characteristics of propagating gravity waves for two decades. This study involves the design and construction of an optical instrument with high spatial and temporal resolutions and the development of proper observation mode and data analysis techniques. A new variety of low resolution spectrometer is developed in this dissertation. This device, an Image Plane Detector Spectrophotometer (IPDS), measures the rotational temperature and brightness of molecular band emission or the brightness of an atomic line. It uses an interference filter as a dispersive element and an Image Plane Detector (IPD) as the photon collecting device. The IPDS can measure a spectrum as twelve wavelength position simultaneously without mechanical scan. Therefore, it has the advantage of increasing temporal resolution in nightglow observations. The IPDS has high throughput compared to traditional spectroscopic instrument, and it is compact in size and portable. This dissertation describes the principle, design, construction and calibrations of a ground-based IPDS. Although the commercial filter used did not fully meet our specifications, the instrument performed reasonably well. The data reduction technique is described. This technique is used to recover the rotational temperature and brightness of molecular band emissions from observed spectral signals. The errors in recovered parameters are also examined. The ground-based IPDS was set up to measure night-time mesosopheric emissions in Ann Arbor, Michigan. The rotational temperature and brightness of the O2(0-1) and OH(6-2) bands were obtained as a function of local time at one position in the sky. Oscillations in the temperature and brightness are clearly revealed, indicating the presence of gravity waves. Some degrees of co-variances showed in

the brightness and temperature trends. A four-position observation mode of measuring (OI) green line intensity is described. This measurement is conducted in order to examine the possibility of determining gravity wave parameters. A discussion is given about obtaining wave propagation direction and horizontal wavelength using time delays among the observed intensities at four positions. The result shows that by using only time delays, one cannot uniquely identify the wave. A criterion of eliminating some of possible waves is presented, which is based upon the wave-airglow interaction theory. The effect of background wind is also discussed. As a conclusion, a multi-instrument observation is suggested to completely study the characteristics of gravity waves in the mesosphere. Dissert. Abstr.

N93-13793 Dartmouth Coll., Hanover, NH.
STRUCTURE OF AND DYNAMICAL PROCESSES IN THE EARTH'S MAGNETOPAUSE AND BOUNDARY LAYER REGIONS Ph.D. Thesis
Tai-Duc Phan 1991 91 p
Avail: Univ. Microfilms Order No. DA9130835

The structure of and dynamical processes in the magnetopause and boundary layer regions are investigated. A two-dimensional, steady state, viscous model of the dawnside and duskside low-latitude boundary layer was developed. It incorporates coupling to the conducting ionosphere via field-aligned currents and associated fields and plasma flow in a self-consistent manner. The currents in the layer are regulated by coupling to the ionosphere. The boundary layer structure is governed by a fourth-order, nonlinear, ordinary differential equation. Numerical results from the models are presented, and the possible use of observations to determine the model parameters is discussed. This study of the magnetopause is concerned with the structure and stability of a current sheet in the presence of resistive and viscous stagnation point flows. Such a current sheet may constitute the magnetopause when the interplanetary magnetic field is due south. Exact equilibrium solutions of a current sheet in the presence of two-dimensional, incompressible stagnation point flows are presented. The flow toward the current sheet may have an arbitrary angle of incidence and an arbitrary amount of divergence from or convergence toward the stagnation point. The role of viscosity in determining the flow and field configuration is examined. For magnetospheric applications, the effect of viscosity is found to be small. Finally, the stability against tearing modes is analyzed of a field-reversing current sheet with stagnation point flow in the plane perpendicular to the magnetic field. It is found that long wavelength perturbations are completely stabilized by the stagnation-point flow so that unstable regime falls between a short wavelength and a long wavelength marginal state. In addition, the equilibrium flow has the effect of damping the growth of the instability, the effect being more important when the Lundquist number, S, i.e., the magnetic Reynolds number based on the Alfven speed, is low. Below S(sub critical) = 12.25, the current sheet is found to be stable to all perturbations. Dissert. Abstr.

N93-13794 Stanford Univ., CA.
SEISMIC STUDIES OF CRUSTAL STRUCTURE AND TECTONIC EVOLUTION ACROSS THE CENTRAL CALIFORNIA MARGIN AND THE COLORADO PLATEAU MARGIN Ph.D. Thesis
John Mark Howie 1992 273 p
Avail: Univ. Microfilms Order No. DA9221627

This thesis presents results from two integrated deep-crustal seismic-reflection and wide-angle-reflection/refraction studies that improve our understanding of crustal structure and tectonic evolution in two tectonically active areas of the western United States. A multi-faceted approach to the study of crustal structure includes the use of compressional and shear wave seismic data. Supplementing the controlled source seismic observations with seismicity, gravity, heat flow, laboratory measurements and available geologic information allows a much improved understanding of crustal structure and tectonic evolution than would be available from the seismic data alone. Chapter 1 introduces the data integration strategy applied to the studies completed. In Chapter 2, an integrated crustal-velocity model across the south-central California margin west of the San Adreas fault is presented. The crustal structure defines tectonostratigraphic terranes 15 to 20 km thick underlain by a 6-km-thick high-velocity layer (6.8-7.0 km/s) interpreted as tectonically underplated oceanic crust. Structures defined in the oceanic crust indicate significant compressional and strike-slip deformation within the oceanic crust that probably formed during the final stages of subduction from 24-16 Ma. In Chapter 3, the crustal model from Chapter 2 is used as a constraint for models of the tectonic evolution of the Pacific-North American transform plate boundary. By combining the crustal structure with thermal models for asthenospheric upwelling associated with a slab-free window, I find that the mantle lithosphere east of the coast beneath south-central California probably delaminated from the oceanic crust, stranding the oceanic crust beneath the margin. In Chapter 4, results from a high-resolution reflection experiment in central Arizona across the southwestern edge of the Colorado Plateau address the relationship between strength of the crust and localization of extensional tectonism. A low Poisson's ratio (0.20 plus or minus 0.05) in the middle crust probably indicates high quartz content. The presence of quartz in large amounts would make the middle crust rheologically weak. The localization of reflectivity within the middle crust probably results from a focusing of shear strain and magmatic intrusions in this rheologically weak zone. Lateral variation of reflectivity in the middle crust between the unextended and non-reflective Colorado Plateau and the extended and reflective Transition Zone illustrates the effect of Miocene and younger extensional tectonism on crustal reflectivity. Dissert. Abstr.

N93-13796 Yale Univ., New Haven, CT.
TROPOPAUSE FOLD INVESTIGATIONS: SECONDARY CIRCULATION, WATER VAPOR AND OZONE ANALYSES Ph.D. Thesis
Jielun Sun 1991 187 p
Avail: Univ. Microfilms Order No. DA9221445

Tropopause folds are investigated in three parts. In the first part, the three-dimensional secondary circulation which is responsible for forcing the tropopause fold is studied in two curved jet flows. The two curved flows result from an axisymmetric, barocline vortex sheared in two ways, horizontally and vertically. The secondary circulation in cylindrical coordinates are derived under both the geostrophic and gradient balance assumptions. Beyond the geostrophic momentum (GM) approximation, momentum equations up to the second order of Rossby number are used. Model results indicate that the geostrophic advection of ageostrophic winds, curvature vorticities, which are ignored in the GM approximation could increase the aspect ratio of secondary circulation and make the secondary circulation narrower horizontally. The temperature advection along the jet can shift transverse secondary circulation horizontally depending on the sign of the advection, while the temperature advection across the jet determines the secondary circulation along the jet. In the second part, characteristics of tropopause folds on satellite 6.7-micron water vapor images are studied with observed data and theoretical models. The dark (dry) bands on satellite water vapor images can come from anywhere on the equatorial side of the tropopause break depending on the amount of water vapor in the upper troposphere above the fold. A simple cloud radiation model was studied and we found that the opaqueness of cloud depends on the amount of saturated water vapor and the size of the cloud particles. A layer of saturated water vapor is more transparent than a cloud layer of small cloud particles and less transparent than that of large particles. In the third part, patterns of vertically integrated total ozone near tropopause folds are studied with aircraft-observing ozone and two stratospheric ozone models. Comparing satellite TOMS total ozone with aircraft observed ozone, we found that the extra ozone in the tropopause fold cannot account for the strong gradient seen by TOMS. The total ozone integrated from the aircraft ozone and the idealized stratospheric ozone show that the gradient of ozone concentration at the tropopause height cannot fully explain the TOMS gradient either. The main contribution to the total ozone comes from the lower stratosphere, the ozone layer 3-4 km above the tropopause where the maximum ozone density is. Dissert. Abstr.

N93-13830 Minnesota Univ., Minneapolis.
A STUDY OF THE LUMINOSITY PRODUCED BY AN ELECTRON BEAM-EMITTING ROCKET IN THE POLAR IONOSPHERE: ECHO 7 Ph.D. Thesis
Robert Curtis Franz 1991 270 p
Avail: Univ. Microfilms Order No. DA9212051

Optical observations made during the ECHO 7 experiment show for the first time the luminous manifestations of the Beam-Plasma-Interaction in a space environment. The optical observations were made using photometers and a low-light-level television camera over an altitude range of 90 to 290 km. Imagery, obtained for the first time in the ECHO series, show the luminous spatial characteristics of the BPI including the formation of diffuse luminous columns extending along the magnetic field in the same and opposite directions as beam propagation. The

beam-plasma-discharge (BPD) evolved from the BPI, igniting first about 140 km, and quenching at 115 km. The BPD appeared as discrete enhancements in the intensity of portions of the diffuse columns extending 200 to 225 m along the magnetic field line. Relaxations oscillations, or non-steady BPD with frequencies between 20 and 45 Hz were observed prior to BPD initiation. At 108 km, the distinct Larmor spiral structure of the beam became visible for distance of about 300 meters along the field. Periodic attitude control system (ACS) Nitrogen gas releases producing spectacular luminosity patterns were seen during the gun operation throughout the flight. The injected gas affected the vehicle neutralization current flow pattern causing current to be concentrated in the gas plume as it flowed toward the MAIN payload. In the absence of ACS gas, the luminosity pattern surrounding the MAIN payload showed an asymmetry, being brighter at the opposite end of the MAIN away from the electron gun. Dissert. Abstr.

N93-13887 Washington Univ., Saint Louis, MO.
THE GROWTH OF DISTURBANCES IN BAROTROPIC MODELS OF THE ATMOSPHERE Ph.D. Thesis
Mark Daniel Borges 1992 214 p
Avail: Univ. Microfilms Order No. DA9222985

An eigenvalue analysis of a divergent barotropic model on a sphere is extended to the formulation of a global optimization problem, whose solution selects an initial perturbation that experiences the greatest possible growth over a finite time interval, tau. The evolution of this optimal perturbation is obtained from companion linear and nonlinear spectral time-dependent models. The two methods of analysis are compared using idealized nonzonal flows and three zonally asymmetric flows defined by time-mean global 300 mb analyses. The results using the idealized flows illustrate the application and insights provided by the optimization problem. For finite time intervals of ten days or less, the optimal perturbations grow much more rapidly than the eigenmodes. This is particularly true for basic flows whose meridional absolute vorticity gradient is negative over a limited sector of the hemisphere. These latter idealized flows support the development of quasi-stationary dipole structures. The initial growth is dominated by the shear in the basic state, while the less rapid growth and persistence at later times is associated with the diffluence of the basic flow. The observed flows are used to investigate the applicability of the eigenanalysis and optimization problem to large amplitude, long duration anomalies in the midlatitude flow that are known to develop quickly. The optimal perturbations to these more complicated flows evolve into large anomalies that look very much like the observed anomalies in both linear and nonlinear models. Some of the optimal perturbations grow rapidly in the strong shear of the jet stream, propagate along the jet axis, slow down and subsequently form dipole structures in the jet exit region of diffluence. Reasonable finite amplitude perturbations are found to be affected by nonlinearity after a relatively short time, supporting the focus on the initial growth. The dependence of the eigenanalysis and optimal perturbations on the model parameters is examined. Dissert. Abstr.

N93-13888 Cincinnati Univ., OH.
OPTICAL MODEL ANALYSIS OF GRAVITY WAVE-CRITICAL LAYER INTERACTION Ph.D. Thesis
Fan He 1992 115 p
Avail: Univ. Microfilms Order No. DA9224019

In this paper our primary concern is to determine the degree of reflection of the original incident wave when the background wind is (1) stable, (2) unstable. To determine such reflections we use the optical model treatment, a method which is especially designed for problems involving diverse and relatively unstructured absorption mechanisms. As a first attempt, we use an analytic model for our wind profile to obtain analytic solution in order to be sure to take care of the various hydrodynamic singularities as well as to obtain a better understanding of the various complicated processes, especially for the case of over reflection. We have found that the dissipations from viscosity and heat conduction losses are very small in comparison with other absorption except very close to the actual critical level. So we model only the absorption due to nonlinearity and turbulence, leaving the reflection at the critical layer as a variable parameter. In this way, our approach takes into consideration the absorption mechanisms from (a) to (d). For (e) (the excitation and re-radiation), we have found that the gravity wave-critical layer interaction in the presence of an unstable background wind is equivalent to the corresponding interaction in a stable background wind with an emission instead of an absorption mechanism. In other words, with an emission mechanism the absorbing optical model 'potential' changes sign and becomes a 'source' for radiating gravity waves instead of a 'sink' for absorbing gravity waves. The over reflection whose occurrences depends on the phase of the reflection from the optical 'potential' serves as an example for energy-momentum transfer from the background winds back into the gravity waves; the opposite to the absorption into the mean flow. All this can be analytically demonstrated by incorporating the optical model into our Sturm-Liouville equation and derive a generalized form of the Eliassen and Palm theorem.
Dissert. Abstr.

N93-13889 Oxford Univ. (England).
GAS-PHASE REACTIONS OF HALOGEN SPECIES OF ATMOSPHERIC IMPORTANCE Ph.D. Thesis
Anne C. Heard 1991 234 p
Avail: Univ. Microfilms Order No. BRD-96210

A low-pressure discharge-flow technique, with various optical detection methods, has been used to determine bimolecular rate coefficients for a number of reactions in the gas-phase between OH radicals and organic halogen-containing molecules and between NO3 radicals and the iodine species I2 and I. These experiments have shown that: (1) the reaction of methyl iodide with OH accounts for approximately 2 percent of the removal of CH3I from the troposphere as compared with photolysis; (2) abstraction of I-atoms from a C-I bond by OH is probable in the gas-phase; (3) the halogen-containing anaesthetic substances halothane CF3CClBrH, enflurane CF2HOCF2CFClH, isoflurane CF2HOCClHCF3 and sevoflurane (CF3)2CHOCFH2 have significantly shorter tropospheric lifetimes than the fully halogenated CFCs and halons because of reaction with the OH radical and are thus unlikely to be transported up to the stratosphere where they could contribute to the depletion of ozone. Data obtained for reactions between OH and some 'CFC alternatives' along with measurements of the integrated absorption cross-sections of the compounds in the spectral region 800-1200 cm(exp -1) were used to calculate ozone depletion potentials (ODP) and greenhouse warming potentials relative to CFCl3 for each compound. The study of the reactions between OH and CF3CFBrH and CF2BrH was used to provide a useful first estimate of the environmental acceptability of these compounds in the context of their possible use as replacements for the conventional CFCs. A method was developed to provide a first estimate of the ODP of a halogenated alkane without use of a complicated (and expensive) computer modeling scheme. A reaction between molecular iodine and the nitrate radical in the gas-phase was discovered and the kinetics of this reaction have been studied. No temperature or pressure dependence was observed for the rate of reaction, the rate constant of which was found to be (1.5 +/- 0.5) x 10(exp -12)/cu cm/molecule/s. The reaction between I and NO3 was found to occur at a rate of about 60 percent of the hard-sphere collision frequency for the two species. The rate constant for reaction between I and NO3 was found to be (4.5 +/- 1.9) x 10(exp -10)/cu cm/molecule/s. An upper limit for the heat of formation of IONO2 of (21 +/- 3) kJmol(exp -1) was also derived. Dissert. Abstr.

N93-13891 Arizona Univ., Tucson.
SPECTROSCOPIC OBSERVATIONS OF THE NIGHT AIRGLOW FROM 3000 A TO 9200 A Ph.D. Thesis
Jeffrey Eric Johnston 1992 133 p
Avail: Univ. Microfilms Order No. DA9223559

Spectroscopic measurements of the night airglow were taken at mid-latitude over a period of four months. The use of intensified CCD spectrographs allowed simultaneous data to be taken from 3000 to 9200 A in 3300 contiguous spectral elements with a resolution (full width at half max.) of 6 to 15 A. The average intensities for a 6.5 hour integration period on March 16, 1991 of the O2 Herzbert I, Chamberlain, Herzberg II, and Atmospheric (0-1) emissions were 230 + or - 20 R, 80 + or - 10 R, 80 + or - 40 R, and 350 + or - 20 R respectively. For the OH Meinel (9-4), (8-3), (7-2), (7-3), (6-2), (5-1), (4-0) emissions the intensities were 450 + or - 50 R, 450 + or - 20 R, 90 + or - 20 R, 1620 + or - 200 R, 970 + or - 50 R, 680 + or - 15 R, and 190 + or - 20 R respectively. The OI 5577 and 6300 A emissions were 320 + or - 10 R and 160 + or - 10 R respectively. These simultaneous emission intensities were compared, with an atmospheric model which revealed that the O2 (A cu Sigma, A' cu delta, (c sup 1)Sigma, (b sup 1)Sigma) states and the OH(X(exp 2)II)

state, and dynamic intensity fluctuations of their related emission features provided independent confirmation of the conclusion that the O2(A cu Sigma, A' cu Delta, (c sup 1)Sigma) states and the OH(X(exp 2)II) state were heavily quenched. Dissert. Abstr.

N93-13955 Colorado Univ., Boulder.
ATMOSPHERIC LOADING RESPONSE OF THE SOLID EARTH AND OCEANS Ph.D. Thesis
Tonie M. VanDam 1991 143 p
Avail: Univ. Microfilms Order No. DA9220458

Atmospheric mass loads and deforms the earth's crust and oceans. By performing a convolution sum between daily, global surface pressure data and Farrell's mass loading Green's functions, the time dependent effects of the atmospheric loading of short-term synoptic storms on surface point positioning measurements and surface gravity observations are estimated. The load responses for both an oceanless earth and an earth with an inverted barometer ocean are calculated. Load responses for near-coastal stations are significantly affected by the inclusion of an inverted barometer ocean. Peak to peak vertical displacements are frequently 15-20 mm with accompanying gravity perturbations of 3-6 micro-Gal. Baseline changes can be as large as 20 mm or more. These amplitudes are consistent with the results of Rabbel and Zschau (1985), who modeled synoptic pressure disturbances as Gaussian functions of radius around a central point. Load responses can be adequately computed using real pressure data from points within about 1000 km of the station. Knowledge of local pressure, alone, is not sufficient. The response of the oceans to atmospheric pressure forcing is investigated by comparing one year of Geosat derived sea surface height with surface atmospheric pressure. Removing the pressure signal from altimeter derived sea level by assuming an inverted barometer response of the oceans does not significantly reduce the RMS variability of the sea surface height. By fitting pressure to the sea surface height, the empirically determined response is found to be approximately -.6 cm/mbar. Winds driven by the pressure gradients of synoptic storms induce a sea surface height response that is opposite in direction to that caused by the pressure cell. The wind driven response is estimated for a stationary storm over a barotropic ocean and a moving storm over a two-layer baroclinic ocean by modeling the pressure as an idealized Gaussian distribution. The model results indicate that the wind induced sea surface height response depends on the radius and the velocity of the pressure cell. The winds associated with storms moving at average speeds of 10 m/sec lower the theoretical pressure response by approximately .1 cm/mbar. Dissert. Abstr.

N93-14053 Oxford Univ. (England).
RADICAL REACTIONS OF ATMOSPHERIC IMPORTANCE Ph.D. Thesis
A. Douglas Parr 1991 248 p
Avail: Univ. Microfilms Order No. BRD-95147

This thesis describes experiments to measure the rate coefficients for some reactions of atmospherically important radicals. The discharge-flow technique coupled with resonance fluorescence, optical absorption and mass spectrometry was used to measure the rate constants for reactions of OH, NO3 and ClO. The rate constant for the reaction of OH with ketene was measured over the temperature range 193-423 K. The reaction displays a negative temperature dependence (E(a) = 4.2 plus or minus 3.5 kJ mol(exp -1)) and an independence of pressure. An explanation for these observations is presented which is consistent with previous work on the reaction, and the implications are discussed. The temperature dependence of the rate constants for the reaction of OH with some hydrochlorofluorocarbons (HCFC's) have been measured together with the infra-red spectra of the HCFC's in the 800-1600 cm(-1) wavenumber range. Ozone depletion potentials and greenhouse warming potentials are calculated. The measured rate constants are compared with a recent evaluation of all previous laboratory data determining the rate of reaction of OH with HCFC's. The rate constants for the reaction of NO3 with a series of alkanes have been studied between the temperatures 289 K and 553 K. Analysis of the rate constants for the reaction of NO3 with enthane, n-butane and i-butane allowed expressions for the temperature dependence for the rate of abstraction of an H atom at primary, secondary and tertiary sites to be determined. The validity of the use of these expressions was tested by comparing the measured rate of reaction of NO3 with i-pentane with that predicted using these expressions. The agreement was found to be good. The reaction between NO3 and ClO has been found to display little or no temperature dependence over the temperature range 210-353 K. An average over all the data gives a temperature-independent rate constant of (5.0 plus or minus 1.4) x 10(exp -13) cm(exp 3) molecule(exp -1) s(exp -1) in agreement with previous room temperature results. Product branching ratios have been investigated and a minor channel producing OClO has been directly observed. The overall rate constant is small for a radical-radical reaction, and possible explanations are discussed. Modulated photolysis has been used to measure for the first time the rate constant for the recombination of ClO with OClO. The low-pressure limiting rate constant at 226 K was found to be (3.0 plus or minus 0.6) x 10(exp -31) cm(exp 3) molecule(exp -1) s(exp -1). The implications for polar stratospheres are discussed. Dissert. Abstr.

N93-14054 Oxford Univ. (England).
SPECTROSCOPY FOR REMOTE SOUNDING OF THE ATMOSPHERE Ph.D. Thesis
J. J. Remedios 1990 256 p
Avail: Univ. Microfilms Order No. BRD-95155

The Improved Stratospheric and Mesospheric Sounder (ISAMS) uses the technique of pressure modulation radiometry to obtain information on the temperature, pressure and chemical composition of the middle atmosphere. This thesis describes an experimental investigation of the spectroscopy of the H2O nu(2) band undertaken to provide spectral data necessary to interpret ISAMS measurements of atmospheric H2O concentrations. The range of instruments on the Upper Atmosphere Research Satellite (UARS), on which ISAMS will fly, is considered in chapter 1 to illustrate the importance of molecular spectroscopy to remote sensing. The relevant spectral parameters are then introduced and discussed in chapter 2. The sensitivity of the signals measured by ISAMS to uncertainties in spectral data of the target gases is calculated in chapter 3 for those channels which measure chemical composition in the atmosphere. The need for improved spectral data, particularly self-broadened widths at 296K and air-broadened widths at atmospheric temperatures, is demonstrated for H2O. The H2O spectral data was recorded by absorption spectroscopy using a high resolution Fourier transform spectrometer. The theory behind its operation, the importance of radiative transfer in an interferometer and the absorption cells used are discussed in chapter 4. The experiments undertaken are described in chapter 5. A method for improving the stability of H2O in an absorption cell is investigated and its success demonstrated. The measured H2O spectral parameters discussed in chapter 6 represent the first measurements of these parameters for many of the lines considered. The temperature dependences of air-broadened widths are found to be greater than those of N2-broadened widths, and line strengths are found to be larger on average than those on the HITRAN database. The improvement in the accuracy of ISAMS H2O measurements resulting from the measured spectral data is discussed in chapter 7, and additional work recommended to improve the accuracy further. Dissert. Abstr.

N93-14062 Colorado State Univ., Fort Collins.
CONVECTIVE PARAMETERIZATION IN MESOSCALE MODELS Ph.D. Thesis
Michael Jeffrey Weissbluth 1991 225 p
Avail: Univ. Microfilms Order No. DA9216226

Currently, there is no adequate cumulus parameterization that is suitable for use in mesoscale models having horizontal resolutions between five and fifty kilometers. Based on the similarity of the temporal and spatial evolution of the vertical variances between a CCOPE supercell and a generic tropical squall line as explicitly simulated by the Colorado State University Regional Atmospheric Modeling System (CSURAMS), a modified second order closure scheme has been developed which allows the prediction of deep convective fluxes. The Mellor and Yamada 2.5 level closure has been modified to predict solely on (bar-omega')(bar-omega') using Zeman and Lumley's formulation of the buoyancy-driven mixed layer to close the pressure terms and the eddy-transport term. The extension to the free atmosphere has been accomplished by representing the deep cumulus fluxes as proportional to the difference between a cloud model derived property and the environmental value. This cloud model has been calibrated and generalized by comparisons with conditionally sampled data from the two explicitly simulated storms. The deep cumulus tendencies of heat, moisture and hydrometeors are specified by a mesoscale compensation term and a convective adjustment term. As above, the convective adjustment term is specified as the difference between a cloud model derived property

and its environmental value, but is modulated by a time scale determined by an integrated value of (bar-omega')(bar-omega'). The mesoscale compensation term is a product of the vertical gradient of the appropriate scalar and a constant determined through a moist static energy balance. One unique feature of this approach is that the parameterization is not simply a local grid column scheme; (bar-omega')(bar-omega') is transported by the turbulence as well as the mean horizontal and vertical winds. Thus, the scheme responds to shear and is more global in nature than current cumulus parameterizations. Furthermore, the scheme provides explicit cumulus source functions for all hydrometeor species. Results of an explicit simulation of two dimensional sea-breeze convection over the Florida peninsula will be compared to simulations on coarser grids using the generalized cumulus parameterization. Dissert. Abstr.

N93-14064 California Univ., Davis.
SPATIAL CHARACTERISTICS OF COHERENT TURBULENT STRUCTURES AND EXCHANGE PROCESSES IN THE ATMOSPHERIC SURFACE LAYER WITHIN AND ABOVE AN ORCHARD CANOPY Ph.D. Thesis
Changan Zhang 1991 217 p
Avail: Univ. Microfilms Order No. DA9217609

Spatial features of coherent turbulent structures and the associated exchange processes in the atmospheric surface layer within and above an orchard canopy were investigated, based on field measurements and data analyses. The experiment was conducted using longitudinal (along-wind) and then a transverse (cross-wind) setup in an English walnut orchard near Winters, California in July and August, 1989. Five towers were set along the prevailing wind direction in the longitudinal setup and seven towers were located in the cross-wind direction in the transverse setup. Arrays of fast response sonic anemometers, thermometers, hygrometers, and a CO2/H2O sensor were mounted at multiple levels. The translation speed of coherent structures was almost independent of height and distance with magnitude of 1.6 times the mean wind speed at the canopy top in a narrow range of unstable conditions, based on calculations using conditional sampling, correlation, and phase coherence. A vortex structure behind the microfront may be responsible for maintaining a constant translation speed. The time scale of the structures was 15 s for ejection and sweeps. Sizes of the coherent structures were approximately 9-12 times the canopy height (h) in the longitudinal dimension and at least 3-4 h in the transverse dimension. Microfront angles were almost constant from 2/3 h up to about 2 h with a value of 32 deg, and decreased to 17 deg at 1/3 h. Microfront angles were modified by the mean wind shear. The coherent structures were dominant and efficient in the exchange of momentum and scalars. While structures occupied 44-51 percent of the total time, they were associated with 65-70 percent of the momentum and scalar fluxes. Sweeps were more efficient than ejections inside the canopy, but ejections became as important as sweeps at 2 h. Triple products connected with the coherent structures were slightly asymmetric. Further study is needed to determine the translation speed under a larger stability range, and to examine the filtering effect on the structure's asymmetry. Dissert. Abstr.

N93-14068 New Hampshire Univ., Durham.
A STATISTICAL STUDY OF NARROW BANDWIDTH, HIGH-LATITUDE GEOMAGNETIC PULSATIONS Ph.D. Thesis
Mark Andrew Popecki 1991 205 p
Avail: Univ. Microfilms Order No. DA9209586

This study is a survey of micropulsations at three high-latitude ground stations. Results concerning the source region of Pc1/2 waves are discussed. The study revealed a diurnal occurrence pattern for waves in the 0.1-0.4 Hz band (Pc1/2), and showed that the pattern was not due to the effects of sunlight on the ionosphere, but instead from a postnoon magnetospheric source region. The importance of He+ ions in the magnetosphere to wave growth is also indicated. Based on the diurnal and seasonal occurrence patterns of the wave above and below 0.4 Hz, it is concluded that the waves observed on the ground above 0.4 Hz come primarily from plasmapause latitudes. Those below 0.4 Hz, in the Pc1/2 band, come from farther out. The different source locations for waves above and below 0.4 Hz, combined with the typically sharp, approximately 0.4 Hz upper frequency limit of Pc1/2 spectra, suggest strongly that He+ ions in the outer magnetosphere influence wavegrowth and propagation. This fits well with the observations of Anderson, et al. (1990), who showed with spacecraft study that waves above the He+ gyrofrequency are more commonly observed beyond L = 7 than in regions closer to the Earth. This ground study shows that waves above the He+ gyrofrequency from the outer magnetosphere do not readily reach the ground. The organization of ground observations by He+ has never been shown before in previous ground studies. An extensive search for correlations between Pc1/2 occurrence and solar wind pressure and magnetic field orientation rules out the solar wind as a direct source of Pc1/2 generation. They may instead be amplified by plasma sheet ions that drift sunward on the dusk side of the magnetosphere (Kaye and Kivelson, 1979; Anderson et al., 1991) and undergo ion-cyclotron resonance in the afternoon sector. This mechanism is consistent with the diurnal pattern and apparent source location of the Pc1/2. Dissert. Abstr.

47 METEOROLOGY AND CLIMATOLOGY

Includes weather forecasting and modification.

N93-12558# Arizona Univ., Tucson. Inst. of Atmospheric Physics.
SOURCES OF CLOUD NUCLEI AND DEVELOPMENT OF REMOTE SENSING TECHNIQUES FOR CLOUD PARAMETERS Final Report
Sean A. Twomey Jun. 1992 2 p
(Contract N00014-90-J-1288)
(AD-A255016) Avail: CASI HC A01/MF A01

The research focused on the problem of remotely determining the effective drop radius and optical thickness of marine stratus, and interpreting the results in terms of cloud susceptibility. Cloud susceptibility is defined here as the increase in albedo resulting from the addition of one cloud drop per cubic centimeter holding the cloud liquid water constant. The employed remote sensing technique made use of the AVHRR spectral channels on board the NOAA polar orbiting satellites. The method required an assumption of the cloud liquid water content which, for the marine stratus studied, was assumed to be 0.3 g/cubic meter. As by-products of cloud susceptibility, cloud optical thickness and effective droplet radius was also determined. The values of these two parameters were compared to in situ measurements. Some discrepancies were noted, particularly in cloud optical thickness. Author

N93-12596# Air Force Inst. of Tech., Wright-Patterson AFB, OH.
THE ROLE OF LATENT HEAT RELEASE IN EXPLOSIVE CYCLOGENESIS M.S. Thesis
Donald M. Rinderknecht 1992 78 p
(AD-A254436; AFIT/CI/CIA-92-052) Avail: CASI HC A05/MF A01

Extratropical cyclones and their attendant fronts are the primary cause of day to day weather changes at any given location in middle and higher latitudes. Storms that deepen at least 24 mb in a period of 24 hours or less are rapid developing storms. This research attempts to analyze the role of latent heating in explosive cyclogenesis, using the Sutcliffe Development Equation (SDE). The SDE describes cyclone development in terms of absolute vorticity advection, thickness advection, stability, and latent heating. The basic premise to be tested is that latent heating, including stable and convective components, plays a significant role in the rapid development of extratropical cyclones. The Sutcliffe Equation Analysis Model (SEAM), developed to study these storms, uses a grid of 27 points (x axis) by 18 points (y axis) with a spacing of 190.5 km. Verticcal resolution in the SEAM consists of 19 levels from 1000 mb to 100 mb in 50 mb increments. The model atmosphere extends to 100 mb to accommodate moisture convergence and subordinate parameters needed to calculate latent heating, which is parameterized into two basic types: stable and convective latent heat release. Stable latent heat release (SLHR) is a large scale effect while convective latent heat release (CLHR) is a sub-grid scale effect. Analysis of results show that CLHR values were virtually non-existent in the normal case and very small in the bomb case. Comparison of Sutcliffe values and storm tracks show that areas of positive values downstream of the surface center indicate movement of either type of storm. The explosive storm followed along the Sutcliffe value ridge, while the normal storm moved perpendicular to the ridge. GRA

N93-12622# Massachusetts Inst. of Tech., Lexington.
STORM TRACKING FOR TDWR: A CORRELATION ALGORITHM DESIGN AND EVALUATION
Edward S. Chornoboy 14 Jul. 1992 91 p

(Contracts F19628-90-C-0002; DTFA01-89-Z-02033)
(AD-A254701; ATC-182; DOT/FAA/NR-91/8) Avail: CASI HC A05/MF A01

Storm Movement Prediction (SMP) is a proposed (future) product for Terminal Doppler Weather Radar (TDWR), aiding controllers by tracking storms approaching and passing through the terminal environment. Because the scan strategy (data acquisition) of TDWR has been critically designed to meet the needs of its primary function, which is the detection of hazardous low-altitude wind shear, there is the question of whether reliable storm tracking can be obtained from the TDWR data set. The objectives of storm tracking involve a scope (spatial range) much larger than that required for the wind-shear algorithms where volume coverage is confined (in off-airport sited radars) to a sector covering the important approach and departure corridors and the only 360-degree scans are near-surface scans for gust-front detection. This report examines the application of a correlation based method of detecting storm motion, testing the notion that reliable storm motion can be inferred from existing TDWR data. In particular, storm motion derived from an analysis of the TDWR Precipitation product (PCP) is studied. A summary description of the algorithm is presented along with an analysis of its performance using data from MIT Lincoln Laboratory's TDWR testbed operations in Denver (1988) and Kansas City (1989). GRA

N93-12700*# National Aeronautics and Space Administration. Goddard Space Flight Center, Greenbelt, MD.
NIMBUS-7 TOTAL OZONE MAPPING SPECTROMETER (TOMS) ANTARCTIC OZONE ATLAS: AUGUST THROUGH NOVEMBER 1991
Arlin J. Krueger, Lanning M. Penn (Research and Data Systems, Inc., Greenbelt, MD.), Courtney J. Scott (Hughes STX, Inc., Greenbelt, MD.), and David E. Larko (Hughes STX, Inc., Greenbelt, MD.) Washington Aug. 1992 172 p
(Contract NAS5-31331)
(NASA-RP-1283; Rept-92B00101; NAS 1.61:1283) Avail: CASI HC A08/MF A02

Because of the great environmental significance of stratospheric ozone, and to support continuing research at the Antarctic Southern Hemisphere stations, the development of the 1991 ozone hole was monitored using data from the Nimbus-7 Total Ozone Mapping Spectrometer (TOMS) instrument, produced in near-real-time. This atlas provides a complete set of daily polar orthographic projections of the TOMS total ozone measurements over the Southern Hemisphere for the period August 1 through November 30, 1991. The 1991 ozone hole developed in a manner similar to that of the 1987, 1989, and 1990 holes, reaching a comparable depth in early October. However, the 1991 ozone hole filled far more rapidly than in 1987 or 1989, and nearly 4 weeks earlier than in 1990. Author

N93-12817# National Center for Atmospheric Research, Boulder, CO. Climate and Global Dynamics Div.
POINT CORRELATIONS OF GEOPOTENTIAL HEIGHT AND TEMPERATURE AT 30 mb AND BETWEEN 500 mb AND 30 mb
Dennis J. Shea, Harry vanLoon, and Karin Labitzke (Freie Univ., Berlin, Germany) Jan. 1992 296 p Sponsored by NSF
(PB92-222694; NCAR/TN-368+STR) Avail: CASI HC A13/MF A03

An atlas of point correlations (teleconnections) of geopotential heights and temperature in the stratosphere of the Northern Hemisphere is presented. The atlas is modeled on Namias's but uses 500 mb heights and 30 mb heights and temperatures. The correlations are shown separately for November-December, January-February, March-April, and July-August. The teleconnection patterns are most marked during the colder part of the year, which is why the emphasis is on the months November-April. The division into two-month periods was made because of the peculiarities of the interseasonal march in the stratosphere. The correlations are meant to elucidate the degree and sign of the relationship between different regions-horizontally at 30 mb and vertically between 500 mb and 30 mb by relating the time series of anomalies at a given point to the corresponding series at all other points. GRA

N93-12833 State Univ. of New York, Stony Brook.
SULFATE IMPACT UPON LOW-LEVEL CLOUD ALBEDO OVER OCEANS Ph.D. Thesis
Yongseung Kim 1991 178 p
Avail: Univ. Microfilms Order No. DA9220338

The Earth Radiation Budget Experiment (ERBE) NOAA-9 scanner measurements have been employed for the purpose of identifying cloud albedo change due to continental sulfur emissions at the Northern Hemisphere. Comparison of cloud albedo over two hemispheric oceans has been made based on the hemispheric imbalance of the anthropogenic sulfur emissions that exists. The present study shows that cloud albedo, particularly in the broad maximum region of sulfur emission off the east coasts of North America and Asia, appears to be affected by the land-transported sulfate aerosols. Although the continental sulfate aerosols substantially modify the marine low-level cloud albedo off the coasts, their dominance over the central ocean appears to be uncertain. The primary sources of cloud albedo variations over the central ocean are considered to be phytoplankton chlorophyll concentrations, sea surface temperatures (SST) and solar zenith angle (SZA). The correlation analysis, using chlorophyll concentrations derived from the Coastal Zone Color Scanner (CZSC) and the climatological SST data, respectively, demonstrates that these two variables explain substantial variations of cloud albedo over the central ocean. However, the SZA effect upon the cloud albedo vs. longitude pattern is shown to be negligible. Dissert. Abstr.

N93-12861# Air Force Inst. of Tech., Wright-Patterson AFB, OH.
SPATIAL RESOLUTION ENHANCEMENT OF SSM/I MICROWAVE BRIGHTNESS TEMPERATURES AND ITS IMPACT ON RAINFALL RETRIEVAL ALGORITHMS M.S. Thesis
Michael R. Farrar 1991 84 p
(AD-A254382; AFIT/CI/CIA-92-057) Avail: CASI HC A05/MF A01

In this study the impact of spatial resolution enhancement is tested on estimates of typhoon rainfall using microwave measurements from the Special Sensor Microwave/Imager (SSM/I). Passive microwave estimates of rainfall are susceptible to errors from non-complete beam filling. The SSM/I ground footprints for the 19, 22, and 37 GHz channels have considerable overlap and thus deconvolution techniques can be applied to enhance spatial resolution. A Backus-Gilbert matrix transform approach is utilized to accomplish the deconvolution so as to minimize noise amplification as suggested by Stogryn (1978). Various validation procedures are performed to demonstrate the effectiveness of the method. The deconvolution scheme is evaluated in terms of its impact on integrated rainfall throughout the life cycle of a number of tropical storms which occurred during the 1987 hurricane and typhoon season. This evaluation was performed for a single frequency emission algorithm, a single frequency scattering algorithm, and three multiple frequency algorithms, each with different properties and scientific approaches. While rainfall patterns detected by all algorithms were qualitatively enhanced, quantitative responses were different for each algorithm. GRA

N93-12862# Air Force Inst. of Tech., Wright-Patterson AFB, OH.
AN ANALYSIS OF THE TORNADO-PRODUCING RALEIGH THUNDERSTORM OF NOVEMBER 28, 1988 M.S. Thesis
Carl S. Funk 1992 135 p
(AD-A254384; AFIT/CI/CIA-92-045) Avail: CASI HC A07/MF A02

The purpose of this research was to document the synoptic and local environment of the North Carolina-Virginia tornado outbreak of November 28, 1988, and to present evidence of the coupling of the existing Raleigh thunderstorm mesocyclone with strong surface vorticity fields as a possible explanation for the sudden spin-up of the very strong (Fujita Scale 4) Raleigh Tornado. Conventional surface, upper-air, and satellite data were analyzed on the Man-Computer Interactive Data Access System (McIDAS) computer system to study the changes in the synoptic environment prior to the tornado event. Radar data were obtained to determine if characteristic storm signatures were present. In addition, various other types of data from local sources were obtained and used in the analysis. Results of the analysis indicated that despite marginal severe weather conditions just six hours prior to the Raleigh Tornado, the atmosphere rapidly changed and exhibited the classic severe weather characteristics necessary for tornado production. GRA

N93-12928# Colorado State Univ., Fort Collins. Dept. of Atmospheric Science.
EXTENDED RANGE FORECAST OF ATLANTIC SEASONAL HURRICANE ACTIVITY FOR 1993
William M. Gray 24 Nov. 1992 9 p Sponsored by NOAA and NSF
Avail: CASI HC A02/MF A01

Details of a 6-11 month extended range seasonal forecast of the tropical cyclone activity that might be expected to occur in the Atlantic Ocean basin during 1993 are presented. This forecast is based on new research which allows an estimate of the amount of next season's Atlantic tropical cyclone activity to be made by late November of the prior year. The forecast scheme is based upon a 10-month extrapolation of the Quasi-Biennial Oscillation (QBO) of equatorial stratospheric zonal wind, two measures of West African rainfall through late November, and an extended range estimate of El Nino conditions for next year. Information up to late November, 1992, indicates that the 1993 Atlantic hurricane activity will likely be somewhat above average with about 6 hurricanes, 11 named storms, 25 hurricane days, 3 intense hurricanes, and a hurricane destruction potential of 75. The 1993 season should be more active than the two recent hurricane seasons of 1991 and 1992 and particular more active in the tropical regions where no hurricanes occurred the last two years. The 1993 season should be more similar to the hurricane seasons of 1988 and 1989 which produced hurricanes Gilbert and Hugo and three other Category 4 hurricanes. The probability of hurricane destruction along the US East Coast Peninsula, Florida, and within the Caribbean basin for 1993 is projected to be somewhat above the last 40-year average. It is expected that the long running West African drought will somewhat abate for next season and be less of an inhibiting influence on tropical cyclone activity than has occurred in recent years. This assessment is based on an anticipated cold ENSO event for next year in combination of stratospheric QBO winds being in a rainfall enhancing westerly phase. Author

N93-13028# Colorado State Univ., Fort Collins. Dept. of Atmospheric Science.

SUMMARY OF 1992 ATLANTIC TROPICAL CYCLONE ACTIVITY AND VERIFICATION OF AUTHOR'S FORECAST (A YEAR OF NO HURRICANE ACTIVITY IN THE TROPICS BUT EXCEPTIONAL SOUTH FLORIDA DESTRUCTION FROM AN UNUSUAL HIGHER LATITUDE INTENSE HURRICANE)

William M. Gray 24 Nov. 1992 18 p Sponsored by NSF and NOAA
Avail: CASI HC A03/MF A01

This paper summarized the tropical cyclone (TC) activity which occurred in the Atlantic Basin during 1992, and verifies the author's seasonal forecasts of such activity which were issued on 26 November of last year and on 5 June and 5 August of this year. Information received by the author as of 26 November, 1991, indicated that the Atlantic should experience a below average season with about 4 hurricanes, 8 named storms of hurricane and tropical storm intensity, 15 hurricane days, 35 named storm days, one intense hurricane of Saffir/Simpson category 3-4-5, and a Hurricane Destruction Potential (HDP) of 35. The 5 June and 5 August updated forecasts, utilizing a variety of late spring and early summer meteorological data, maintained the late November forecast with no change. The forecast verified very well. Five of the seven forecast parameters were unusually accurate. There were no hurricanes in the tropics and no tropical cyclone activity at all in the Caribbean. The key to this inactive season (except for hurricane Andrew) was the lack of the development of African wave systems. The one major hurricane (Andrew of maximum Category 4) intensified above 25 degree N. Besides the lack of low latitude hurricanes, the 1992 season was characterized by an especially large number (4) of high latitude forming hurricanes whose development (except for Andrew) was influenced by middle-latitude baroclinic processes. Author

N93-13066# National Environmental Satellite Service, Washington, DC. Office of Research and Applications.

NOAA WORKSHOP ON CLIMATE SCALE OPERATIONAL PRECIPITATION AND WATER VAPOR PRODUCTS

Ralph Ferraro, ed. Oct. 1992 70 p Workshop held in Camp Springs, MD, 1-3 Apr. 1992
(NOAA-TR-NESDIS-62) Avail: CASI HC A04/MF A01

The NOAA Workshop on Climate Scale Operational Precipitation and Water Vapor Products was held on April 1-3, 1992, in the NOAA Science Center in Camp Springs, Maryland. The three day workshop was sponsored by the Operational Measurements Element of the NOAA Climate and Global Change Program. The workshop was organized by a program committee containing the following members: Ralph Ferraro, NOAA/NESDIS; Roderick Scofield, NOAA/NESDIS; Phillip Arkin, NOAA/NWS; John Bates, NOAA/OAR; James Smith, Princeton University. The main objectives of the workshop were: assess the state of the art for climate scale rainfall and water vapor estimates from satellites, determine the suitability of the available algorithms for operational implementation to produce ongoing climate products, and recommend a course of action with regard to algorithm selection, validation, and implementation. The workshop consisted of talks by invited speakers and working group discussions and recommendations. This report summarizes the findings of the working groups and briefly summarizes the presentations from the invited speakers. Author

N93-13075# Los Alamos National Lab., NM.

TRIBUTARY AND GAP NIGHTTIME AIR FLOW COMPARISONS

W. M. Porch 1992 9 p Presented at the 6th American Meteorological Society Conference on Mountain Meteorology, Portland, OR, 29 Sep. - 2 Oct. 1992
(Contract W-7405-eng-36)
(DE92-018875; LA-UR-92-2212; CONF-9209163-1) Avail: CASI HC A02/MF A01

Air flow studies in valleys at night have led to the concept of a drainage flow related to the 'air shed' area defined by ridge lines surrounding the valley (e.g. Clements et al., 1989). The concept of an 'air shed', when taken to an illogical extreme, would imply extreme drainage flows in a valley surrounded by a very large nearly flat ridge slope. A hypothesis to be tested is that, because of water erosion of gently sloping land surfaces into tributaries, the concept of an 'air shed' is really equivalent to saying that the drainage flow in a valley at night is mainly related to the number and size of tributaries feeding the main valley. Why is this distinction important? Because, if tributaries are dominating the valley drainage flow, it is important to place pollution sources so that their plumes avoid major tributaries rather than gentle ridge slopes. An experiment was conducted in March 1990 to study the relationship between nighttime winds down the Tennessee Valley (northeast to southwest) and flow out of a gap between one valley containing the city of Oak Ridge and another valley (Bear Creek Valley) containing the oak Ridge radioactive material processing facility Y-12 (Scarboro Gap). Optical cross-path wind sensors were used across the main valley and gap. The cross-valley optical paths measured a component of the cross-valley wind. Wind direction measurements at three levels (10, 30 and 100 m) from a meteorological tower near the center of the valley path was used to determine the long term (1 hour average) effect of cross valley winds. DOE

N93-13099# Computer Data Systems, Inc., Fort Worth, TX.

CLOUD CURVE ALGORITHM TEST PROGRAM Final Report, 10 Jul. 1989 - 28 Feb. 1992

Robert N. Trapnell, Jr. 28 Feb. 1992 170 p
(AD-A253918; PL-TR-92-2052; AD-E201051) Avail: CASI HC A08/MF A01

This project had three main objectives: (1) to test variations in the cloud curve algorithm (CCA) methodology to determine the superior algorithm configuration for use with the Air Force Weather Central, Global Spectral Model (AFGWC GSM), (2) to perform inter-model comparisons between CCA (using the AFGWC GSM) and AFGWC's current cloud forecast models (5LAYER in the extratropics and TRONEW in the tropics), persistence and diurnal persistence (used in TRONEW), and (3) to perform inter-model comparisons between CCA (using the AFGWC GSM) and the Geleyn scheme used until May 1985 by the European Centre for Medium-range Weather Forecasts (ECMWF) and using the AFGWC GSM. The basic-CCA approach is to generate relative humidity (RH)-to-cloud conversion curves by relating cumulative frequencies of NWP model forecasted RH to cumulative frequencies of analyzed cloud amount. Once the curves are computed, they can be used to convert an RH forecast to a cloud forecast. The cloud forecast skill of CCA (using the AFGWC GSM) compared to 5LAYER (extratropics) and TRONEW (tropics) varied by season, geographical region and forecast interval. GRA

N93-13124 Purdue Univ., West Lafayette, IN.

NUMERICAL SIMULATION OF A SQUALL LINE: TESTS OF A NEW CUMULUS PARAMETERIZATION SCHEME Ph.D. Thesis

Patrick Albert Haines 1992 433 p
Avail: Univ. Microfilms Order No. DA9229121

A new cumulus parameterization scheme (CPS) is developed and tested. The CPS includes a cloud model that is shown to favorably replicate mass, moisture and heat fluxes calculated by a time dependent non-hydrostatic three-dimensional cloud model. The CPS was tested

semi-prognostically with SESAME V data and the Q1 and Q2 values diagnosed by the CPS compare very favorably to those observed. This is true for comparisons at all convectively active grid points. The CPS is incorporated into the Purdue mesoscale model to simulate the SESAME IV squall line. The resulting simulation captures many of the observed features of this case including the backing of the low-level wind out ahead of the dryline and initial formation of the squall line in the Texas panhandle. It also shows the dryline moving westward at night as observed and shows the later extension of the squall line to the south. Dissert. Abstr.

N93-13287# National Inst. of Polar Research, Tokyo (Japan).
JARE DATA REPORTS NO. 179 (METEOROLOGY 29).
METEOROLOGICAL DATA AT ASUKA STATION, ANTARCTICA IN 1990
Akira Iwasaki (Japan Meteorological Agency, Tokyo.) and Takashi Yamanouchi Mar. 1992 113 p
Avail: CASI HC A06/MF A02

Surface meteorological observations have been made continuously since Jan. 1987 at Asuka Station. The station was established as the third Japanese Antarctic station in Dec. 1984 at 71 deg 32 min S and 24 deg 08 min E at an elevation of 965 m a.s.l. The automatic meteorological observation system was installed at the station at the beginning of Jan. 1987. The international index number (WMO) 89524 was given. The surface synoptic data taken by the 31st Japanese Antarctic Research Expedition (JARE-31) in 1990 are presented. The observer was Akira Iwasaki from the Japan Meteorological Agency. Surface synoptic reports (FM12-VIII-EXT.-SYNOP) at 00, 03, 06, 09, 12, 15, 18 and 21 UTC and monthly summaries (FM71-VI-CLIMAT) were sent to Darmstadt, F. R. G. through Geostationary Satellite (METOSAT). Data of the present report were also published in the Data Report by Japan Meteorological Agency (1992). Author

N93-13288*# National Aeronautics and Space Administration. Hugh L. Dryden Flight Research Facility, Edwards, CA.
STRATOSPHERIC TURBULENCE MEASUREMENTS AND MODELS FOR AEROSPACE PLANE DESIGN
L. J. Ehernberger Dec. 1992 28 p Proposed for presentation at the AIAA Fourth International Aerospace Planes Conference, Orlando, FL, 1-4 Dec. 1992
(RTOP 763-21-51)
(NASA-TM-104262; H-1865; NAS 1.15:104262) Copyright Avail: CASI HC A03/MF A01

Progress in computational atmospheric dynamics is exhibiting the ability of numerical simulation to describe instability processes associated with turbulence observed at altitudes between 15 and 25 km in the lower stratosphere. As these numerical simulation tools mature, they can be used to extend estimates of atmospheric perturbations from the present gust database for airplane design at altitudes below 15 km to altitudes between 25 and 50 km where aerospace plane operation would be at hypersonic speeds. The amount of available gust data and number of temperature perturbation observations are limited at altitudes between 15 and 25 km. On the other hand, in-situ gust data at higher altitudes are virtually nonexistent. The uncertain potential for future airbreathing hypersonic flight research vehicles to encounter strong turbulence at higher altitudes could penalize the design of these vehicles by undue cost or limitations on performance. Because the atmospheric structure changes markedly with altitude, direct extrapolation of gust magnitudes and encounter probabilities to the higher flight altitudes is not advisable. This paper presents a brief review of turbulence characteristics observed in the lower stratosphere and highlights the progress of computational atmospheric dynamics that may be used to estimate the severity of atmospheric transients at higher altitudes. Author

N93-13361 Princeton Univ., NJ.
BAROCLINIC WAVE PACKETS IN MODELS AND OBSERVATIONS
Ph.D. Thesis
Sukyoung Lee 1991 218 p
Avail: Univ. Microfilms Order No. DA9202535

Coherent baroclinic wave packets are found in a hierarchy of models of nonlinear baroclinic instability--a two-layer quasi-geostrophic (QG) model on a beta-plane, a two-level primitive equation (PE) model, and a general circulation model (GCM)--as well as in observations from the Southern Hemisphere (SH). The flows are chaotic but the packet itself can remain remarkably coherent, despite the complex evolution of the flow within the packet. In both QG and PE models, the packets become more robust as the supercriticality of the flow is reduced. Consistent with the model results, the packets are more often found in the summer season of the SH due to its weaker baroclinicity than in winter. In both the models and the observations, the packets move with a group velocity that is greater than the phase speed of the individual disturbances, and exhibit a downstream development. The structure of the baroclinic waves in the packet as a function of longitude resembles the life-cycles of sinusoidal baroclinic waves as a function of time. In the weakly nonlinear flow of the QG model, we illustrate direct analogies between the two in terms of eddy and mean flow evolution. More than one packet can exist in the domain at the same time. In a fully nonlinear flow, experiments with the QG model using an unrealistically long channel demonstrate that the number of packets increases in a systematic way as the length of the channel increases. In the weakly nonlinear flow, however, the existence of the packet depends on the quantization of the zonal wavenumber; only if there are two unstable zonal waves whose linear growth rates are comparable to each other do arbitrary small perturbations emerge into coherent wave packets. A qualitative comparison is made with the solutions of a nonlinear Schroedinger equation. As predicted by the solution, there is a negative correlation between the maximum amplitude of the packet and the half-width of the packet. This correlation diminishes as the flow becomes chaotic, even if the coherent packet remains a salient feature of the flow. The relationship between the nonlinear baroclinic wave packets and the climatological storm tracks is discussed. The velocity of the packets seems to be modulated by stationary waves. It is unclear, however, to what extent this kind of modulation of the wave packet can account for the location of the storm track.
Dissert. Abstr.

N93-13446# National Inst. of Polar Research, Tokyo (Japan).
JARE DATA REPORTS NO. 173 (METEOROLOGY 28). ANTARCTIC CLIMATE RESEARCH DATA. PART 5: PPI RADAR DATA AT SYOWA STATION, ANTARCTICA FROM FEBRUARY TO DECEMBER 1989
Hiroyuki Konishi (Osaka Kyoiku Univ., Japan) Mar. 1992 63 p
Avail: CASI HC A04/MF A01

A five-year program of Antarctic Climate Research (ACR) is carried out at Syowa, Asuka and Mizuho Stations surrounding the ice sheet and sea ice area from 1987 to 1991 by the Japanese Antarctic Research Expedition (JARE) as part of the international cooperating World Climate Research Program (WCRP) (Yamanouchi, 1989). The main research subjects are: (1) interannual variation of Antarctic atmosphere; (2) sea ice - atmosphere interaction, (3) variation of the ice sheet and the ice shelf; (4) ice core analysis. In JARE-29 and -30 (the 2nd and 3rd year of this program), we have mainly observed the items related to the interannual variation of Antarctic atmosphere. The data of precipitating clouds by using PPI (Plane Position Indicator) radar in 1989 are shown in this report and short- and long-term variations of clouds and precipitation will be analyzed using these data in the future. The data of clouds and precipitation in 1988 and 1989 observed by vertical pointing radar and microwave radiometer were already published (Wada, 1990; Konishi and Wada, 1991). Author

N93-13489 Wisconsin Univ., Madison.
A PARAMETERIZED QUASI-FIVE-CYLINDER CONVECTIVE CLOUD MODEL AND ITS APPLICATION TO REMOTE SENSING OF RAINFALL
Ph.D. Thesis
James Alan Ridout 1991 316 p
Avail: Univ. Microfilms Order No. DA9205564

The problem of remotely sensing rainfall from satellite data is investigated with the use of a quasi-one-dimensional cloud model. A time-dependent, nonhydrostatic cloud model is presented which models vertical velocity in one cylindrical region and other variables in a total of five such regions. The calculation of vertical velocity avoids error due to averaging the equations of motion over the entire updraft region normally associated with one-dimensional models. A parameterization in the model for the effects of vertical shear of the largescale winds on convection relates wind-shear-enhanced entrainment to cumulus scale effects. Comparisons with results from several three-dimensional cloud model simulations and radar observations show that the model does fairly well in predicting quantities of interest for remote sensing of rainfall. An investigation into applications of the model to remote sensing of rainfall focuses on two central topics. One study considers the implications of cloud model results for the retrieval of rainfall over land using microwave data. Both high

resolution and large-scale rainfall retrievals are studied. Results show that retrieved hail amounts can be useful for such retrievals, provided that cloud model simulations can be run to establish the ratio of surface rainfall to the amount of hail aloft. For high resolution retrievals based on these results, the model shows that cloud top height information available from infrared satellite data is essential. A second rainfall retrieval study concerns methods of inferring area-wide rainfall rates or total storm rainfall volume from measurements of the area of rain fields. Lognormal rainfall volume distributions fitted to model-predicted rain fields are used to estimate the slope parameter governing the relationship between area-wide rainfall rate and the fractional area above a given threshold rainfall rate. Calculated values of the slope parameter are shown to agree fairly well with values derived from observations. The significance of hail in determining the slope parameter is demonstrated. Finally, two parameters that may be used to estimate the slope parameter from satellite observations are presented.
Dissert. Abstr.

N93-13631 North Carolina Univ., Chapel Hill.
RELATIONSHIPS BETWEEN CONTINENTAL-SCALE CIRCULATION AND RAINFALL EVENT ATTRIBUTES IN THE SOUTHEASTERN US Ph.D. Thesis
Keith Glenn Henderson 1991 190 p
Avail: Univ. Microfilms Order No. DA9216726

Precipitation event attributes defined as the amount, duration, and frequency of individual rainstorms vary considerably from place to place and season to season. Event variability is caused by a combination of large-scale and local climate processes. Historical relationships between continental-scale circulation and local rainfall event attributes could be used to augment General Circulation Model results, thus providing useful information for future climate impact studies. Results indicate that specific areas in the southeastern United States display significant correlations between individual event attributes and the zonal/meridional flow across North America. Shifts in circulation regimes affect both the number of events and event size. Relationships are strongest with the number of events. The total number of events in some regions changes by as many as ten to twelve storms per season with shifts in continental-scale circulation. An analysis of attribute distributions shows that the percentage of total storms falling into important intensity categories may also change by as much as ten percent between flow regimes. Relationships have both temporal and spatial patterns. Shifts in large-scale circulation affect event attributes most strongly in winter with more events occurring in zonal years. Larger events are found east of the Appalachians in meridional years and west of the mountains in zonal years. It is concluded that modelled atmospheric flow could be used in conjunction with these relationships to create functional rainfall event scenarios for the southeastern United States. Dissert. Abstr.

N93-13643 Pennsylvania State Univ., University Park.
A SYNOPTIC CLIMATOLOGY OF THE ELEVATED MIXED LAYER INVERSION OVER THE SOUTHERN GREAT PLAINS IN SPRING Ph.D. Thesis
John Michael Lanicci 1991 314 p
Avail: Univ. Microfilms Order No. DA9204240

A synoptic climatology is presented of atmospheric conditions associated with the creation of the lid over the southern Great Plains of the U.S. during four spring seasons from 1983 - 1986. The lid sounding is created through the superposition of a potentially warm, nearly dry-adiabatic elevated mixed layer (EML) over a latently unstable moist layer. This study examines the synoptic patterns associated with the creation and evolution of the EML, the moist layer, and the lid, utilizing lid-occurrence statistics, analyses of the EML and moist layer, and a subjective synoptic typing system based on the thermal-wind relationship between the surface and 500 mb. The periodicity of lid-occurrence is determined, and relationships between different stages of lid development and specific synoptic flow types are examined, as are those relationships between lid occurrence and severe storm outbreaks over the study region. The lid-coverage area over the southern Great Plains responds to seasonal changes in the mean locations of the EML source region and the low level moist tongue. The classic airstream configuration associated with lid formation (southwesterly flow) occurs most frequently in Apr. and May, and is replaced in late spring by flow types mainly associated with large scale subsidence, such as midlevel northwesterly and anticyclonic flows. In late spring, the mean lidbase sinks downstream from the source region, in contrast to the early spring configuration in which the lidbase rises and weakens downstream from the source region. A life cycle of lid development is defined, and two seasonally dependent cycle types are identified. The relationship between antecedent lid-coverage area and the size of a severe storm outbreak is best defined in early spring. A conventional-data and modeling study of an early-spring lid cycle is performed. The Penn State/NCAR mesoscale model is employed to examine the important physical processes involved in the creation and evolution of the EML and moist layer. The results identify case-dependent aspects of the lid cycle that the synoptic climatology alone is unable to reveal. Dissert. Abstr.

N93-13718*# Columbia Univ., New York, NY.
ATMOSPHERIC, CLIMATIC AND ENVIRONMENTAL RESEARCH Semiannual Progress Report, Apr. - Sep. 1992
Wallace S. Broecker (Lamont-Doherty Geological Observatory, Palisades, NY.) and Vivien M. Gornitz (Lamont-Doherty Geological Observatory, Palisades, NY.) Sep. 1992 56 p
(Contract NCC5-29)
(NASA-CR-191367; NAS 1.26:191367) Avail: CASI HC A04/MF A01

Work performed on the three tasks during the report period is summarized. The climate and atmospheric modeling studies included work on climate model development and applications, paleoclimate studies, climate change applications, and SAGE II. Climate applications of Earth and planetary observations included studies on cloud climatology and planetary studies. Studies on the chemistry of the Earth and the environment are briefly described. Publications based on the above research are listed; two of these papers are included in the appendices. L.R.R.

N93-13736 Michigan Univ., Ann Arbor.
A METEOROLOGY-BASED APPROACH TO DETECTING RESPONSE SOURCE-RECEPTOR RELATIONSHIPS Ph.D. Thesis
Jeffrey Robert Brook 1991 331 p
Avail: Univ. Microfilms Order No. DA9135560

The wet deposition of SO4(2-) in eastern North America varies substantially from year to year, season to season and event to event. A large fraction of the variability is due to changing meteorological conditions. This meteorological 'noise' obscures the relationship between SO2 emissions and SO4(2-) amounts in precipitation. For example, from 1979 to 1986 annual emissions from eastern North America decreased by 18 percent while the mean annual concentrations of SO4(2-) at numerous locations varied by up to 35 percent. The hypothesis tested by this study was that by accounting for the variability related to meteorology a portion of the remaining variability in SO4(2-) concentrations could be linked to changes in SO2 emissions. A method for 'controlling' the effects of meteorology was developed and tested on the observations of precipitation chemistry collected at six Utility Acid Precipitation Study Program (UAPSP) monitoring sites. This technique involved multiple regression models correlating SO4(2-) concentrations in precipitation (and ln(SO4(2-))) with precipitation amount, temperature, upwind SO2 emissions, and other meteorological factors known to influence precipitation chemistry. Application of the models to study source-receptor relationships insured that relationships detected between SO2 emissions and SO4(2-) concentrations were not simply an artifact of variations in meteorology. Accounting for meteorological variability strengthened the relationship between SO2 emission changes and SO4(2-) concentrations in precipitation at 3 of the UAPSP sites. At 2 Midwestern sites, source-receptor relationships were detected, with 95 percent confidence. At Raleigh, NC, a weak relationship (P less than 0.1) was found to exist. At the other sites, the relationships were not statistically significant and at the two northeastern sites there was essentially no evidence that the SO4(2-) concentrations in precipitation responded to the emission changes between 1979 and 1986. The concentration to emission relationships quantified by the statistical models were deployed to estimate the changes in mean annual SO4(2-) concentrations in precipitation responded to the emission changes between 1979 and 1986. At the sites exhibiting relationships with at least 90 percent confidence, concentration decreases ranged from 10 to 23 percent depending upon location and the form of the regression model. Dissert. Abstr.

N93-13740 Texas A&M Univ., College Station.
THE KINETIC ENERGY BUDGET OF TROPICAL PLUMES AND ENSO IN NMC AND ECMWF ANALYSES Ph.D. Thesis

Jae Gyoo Lee 1991 195 p
Avail: Univ. Microfilms Order No. DA9206525

The regional eddy kinetic energy (EKE) budget primarily at 200 mb is calculated over the topical eastern Pacific Ocean to identify and quantify the physical processes related to the evolution of tropical plumes. In addition, energy processes in the wavenumber domain are investigated to quantify scale interactions within the tropical band between 2.5 degrees and 20 degrees N around the globe. Energetics are based on daily operational analyses prepared by ECMWF and NMC. Comparisons between the resultant analyses provide an estimate of the reliability and uncertainty of tropical kinetic energy computations. March 1983 and 1984 are examined to test sensitivity to differing general circulation regimes. The main physical difference in maintaining the area-averaged EKE over the eastern Pacific Ocean between March 1983 (ENSO period) and March 1984 (non-ENSO period) is that ENSO is dominated by flux convergence of EKE. Anticyclonic systems over the eastern Pacific Ocean strengthen during ENSO, causing influxes of kinetic energy into the domain to weaken. The main change to the regional EKE budget during most of the 8 tropical plumes examined is an increase of EKE flux across the northern boundary, indicating the importance of tropical and mid-latitude interactions. Locally within the plume, the primary contribution to the increase of EKE is due mainly to potential energy fluxes by cross-contour flow. Plumes are generally barotropically and baroclinically stable in both NMC and ECMWF analyses. During March 1983 and March 1984, the tropical wave systems are driven mainly by flux convergence of EKE from wavenumbers 1 to 8. Differences between March 1984 and March 1983 are observed mainly in the extra-long waves for all the physical process terms. During active plume period fluxes shift more to the synoptic scale and wave-wave interactions transfer EKE to the synoptic scale, as well. Disparities between different plumes and between different analyses leave some doubt as to the normal role of long waves in plume formation and the actual magnitude and direction of baroclinic and barotropic processes. Comparisons of ECMWF and NMC wind fields show that 10 ms(exp -1) discrepancies are common in synoptically active periods. Uncertainties in processes result and interpretation of the residuals, which become larger during plume events, also become a major uncertainty. With these exceptions the two model analyses confirm the major processes. Finally, the comparisons of the results from the ECMWF and NMC analyses show general agreement in the main features, even though there exist some differences in amplitudes locally, in certain waves, and, particularly, in the baroclinic terms. Dissert. Abstr.

N93-13744 Colorado State Univ., Fort Collins.
THE RELATIONSHIP BETWEEN SST ANOMALIES AND CLOUDS, WATER VAPOR, AND THEIR RADIATIVE EFFECTS Ph.D. Thesis
Thomas Carl Peterson 1991 273 p
Avail: Univ. Microfilms Order No. DA9207342

An observational study of climatological relationships between sea surface temperature anomalies (SSTAs) and clouds, water vapor, and their radiative effects was conducted. The goal of this research project was to identify and quantify cloud and water vapor radiative feedback loops through an observational study, using SSTAs as a surrogate for global climate change. The relationship of an atmospheric variable to the SSTA was determined by using a Least Absolute Deviations (LAD) regression analysis between 6 year monthly anomaly data sets of both variables at each grid point over the open ocean. The slope of the LAD regression line was used to define the relationship. The radiative effects of the relationships between clear sky water vapor anomalies and SSTAs was determined by using a two stream radiative transfer model at each grid point. The results of this research indicate that there are strong, regionally varying relationships between SSTAs and cloud anomalies, water vapor anomalies, and their radiative effects. For example, in much of the tropics and South Pacific Convergence Zone, high clouds increased with increases in SSTA while in the subtropical stratocumulus regions low clouds decreased with increases in SSTAs. Averaged over the entire data set region, total cloudiness increased with increases in SSTAs. Yet, because optically thick low clouds decreased while optically thin high clouds increased, the average reflected flux decreased. Over most of the open ocean, clear sky water vapor increased at all levels in association with increases in SSTAs. However, the decrease in OLR caused by increases in clear sky water vapor was only a small portion of the change in OLR that occurred in association with increases in SSTAs. In response to decreases in both OLR and reflected flux, net flux averaged over the data set region increased with increases in SSTAs, indicating a positive radiative feedback loop. Dissert. Abstr.

N93-13760 Florida State Univ., Tallahassee.
INTRASEASONAL VARIABILITY OF INFRARED COOLING RATES DURING THE ASIAN SUMMER MONSOON AND THEIR INFLUENCE ON INTRASEASONAL WAVES Ph.D. Thesis
Amita Vikram Mehta 1991 185 p
Avail: Univ. Microfilms Order No. DA9202307

Infrared cooling rates over the Asian monsoon domain between 5 S to 20 N and 40 E to 135 E were calculated for the summer seasons of 1984 and 1987, using a medium band resolution infrared radiative transfer model. Cloudiness is specified using INSAT infrared measurements. Intraseasonal variability of cloudiness and cooling rates are examined. INSAT-derived cloud amounts have 20 to 50 percent of total variance in intraseasonal frequency band and the centers of maximum variance are found over the Arabian Sea, equatorial Indian Ocean, Bay of Bengal, South China Sea, and western Pacific Ocean. Intraseasonal variability of cloudiness is primarily due to variations in deep convective clouds on intraseasonal time scales. Infrared cooling rates are between 1 to 5 C(day(exp -1)), and intraseasonal cooling rate anomalies have magnitudes between 0.5 to 1.5 C(day(exp -1)). The centers of large intraseasonal variability of cooling rates are co-located with the centers of cloudiness variability. The cooling rate anomalies are directly associated with variability of deep convection such that cooling rates are maximum between 200 and 400 mb when deep convective clouds are present. In the absence of deep convective clouds, cooling rates are maximum lower in the troposphere. The dominant vertical mode of cooling rate anomalies has the structure in which lower and upper troposperes have opposite phases. The difference between the 1984 and the 1987 monsoon seasons are primarily in the amplitudes and time periods associated with intraseasonal cloudiness and cooling rate anomalies. A conceptual model of equatorial Kelvin waves, with first baroclinic mode structure, is used to show that cooling rate anomalies can modify phase speeds of planetary scale Kelvin waves by up to 12 percent. The change in phase speed is maximum for wave number 1 and for the faster radiative time scales. Dissert. Abstr.

N93-13776 Pennsylvania State Univ., University Park.
AN OBSERVATIONAL AND NUMERICAL INVESTIGATION OF MESO-SCALE COASTAL PROCESSES DURING GALE IOP 2 Ph.D. Thesis
James Daniel Doyle 1991 272 p
Avail: Univ. Microfilms Order No. DA9127316

A detailed analysis of the conventional special observations taken during Intensive Observation Period 2 (IOP 2) of the Genesis of Atlantic Lows Experiment (GALE) and results from one- (1-D), two- (2-D), and three-dimensional (3-D) numerical model simulations using idealized and observed data are used to examine the structure, evolution, dynamics, and interactions of the coastal low-level jet (LLJ), marine atmospheric boundary layer (MABL), coastal front, and coastal cyclone, during a 72-hr period between 23-26 Jan. 1986. In one series of experiments, the Penn State/National Center for Atmospheric Research (PSU/NNCAR) mesoscale model is initialized with idealized data to study the MABL near the Gulf Stream. Important contributors to the MABL response and frontal structure are the horizontal resolution of the sea surface temperature analysis, latent heat release in the lower troposphere, sea-surface fluxes of moisture, and high wind speeds near the MABL front. During GALE IOP 2, a diurnally varying, low-level northeasterly jet was observed along the Carolina Coastal Plain. Results from a 3-D real-data simulation and from a 1-D planetary boundary layer model show that the LLJ is a manifestation of strong low-level geostrophic forcing, with its strength and direction forcing, with its strength and direction modulated by inertial accelerations. A large daytime speed reduction results from a rapid increase in the frictional stress at the jet level. Coastal frontogenesis takes place near the eastern edge of the Gulf Stream, coincident with a preexisting low-level coastal trough. Large sensible heat and moisture fluxes, present along the Gulf Stream, contribute directly to the trough formation. The ageostrophic deformation associated with the coastal trough formation may initiate the coastal frontogenesis. In the formative stage of the coastal front, the frontogenetical deformation over the Gulf Stream is opposed by the frontolytical differential diabatic effects. As the coastal front moves near the coastline, the deformation

and differential diabatic terms act in concert to intensify the baroclinic zone. Along the coastal front, a small-scale, shallow, warm-core cyclone develops in a region of weak quasi-geostrophic forcing. The baroclinic zone to the rear of the cyclone is substantially weakened and embedded in an environment less conducive for subsequent rapid cyclogenesis.
Dissert. Abstr.

N93-13786 Wisconsin Univ., Madison.
NUMERICAL STUDY OF NONLINEAR CONVECTIVE-SYMMETRIC INSTABILITY IN A ROTATING BAROCLINIC ATMOSPHERE Ph.D. Thesis
Charles Jacob Seman 1991 196 p
Avail: Univ. Microfilms Order No. DA9123865

The finite-amplitude behavior of deep, moist convection in a vertically-sheared atmosphere is studied as an initial value problem using a two-dimensional (y,z) nonlinear, nonhydrostatic numerical mesoscale/cloud mode. Three eight-hour simulations are performed to analyze the relative importance of baroclinicity and Coriolis rotation in the evolution of a mesoscale convective system. They are as follows: (1) a baroclinic shear environment in thermal and wind balance, with rotation on the modeled convection; (2) same environment as in (1), but without rotation on the convection; and (3) a barotropic shear environment without rotation on the convection. The baroclinic and barotropic atmospheres each have the same center-domain thermal sounding and the same constant tropospheric zonal vertical wind shear of 20 ms s(exp -1) per 10 km. The mid-tropospheric symmetric stability is about 32.5 in the baroclinic environment. A center-domain warm, moist thermal initiates the convection for each simulation. Analysis of the simulation shows that nonlinear convective-symmetric instability occurs within the rotating, baroclinic mesoscale convective system. This mode represents a new hybrid mesoscale instability concept in which the effects of momentum transport and Coriolis rotation are essential. Vertical transport of zonal momentum in the convective updraft creates negative isentropic absolute vorticity on the baroclinically cool-side aloft which is susceptible to symmetric instability. Inertial forces due to Coriolis rotation allow the symmetric instability to be released. A meridional mesoscale outflow jet grows as a result of the symmetric instability, providing upper level divergence and a mesoscale updraft for further development of deep convection. With time, this positive feedback process contributes to an upscale development of a mesoscale circulation which resembles that of a squall-line Mesoscale Convective Complex. By eight hours, the baroclinically cool-side circulation is stronger, with anticyclonic zonal shear aloft. The system is warm-core, with high pressure aloft and low pressure near the surface. Comparison of the rotating baroclinic system to the other two simulations shows that overall, Coriolis, rotation tends to stabilize the mesoscale convective system, while baroclinicity enhances its growth.
Dissert. Abstr.

N93-13790 Illinois Univ., Urbana-Champaign.
A LABORATORY INVESTIGATION OF RAINDROP OSCILLATIONS Ph.D. Thesis
Rodney Joseph Kubesh 1991 134 p
Avail: Univ. Microfilms Order No. DA9136642

Knowledge of raindrop shape is crucial to analyses of microwave scattering from precipitation, including the use of polarization radar in inferring the rainfall rate. The equilibrium shape of a water drop falling in air is nearly a sphere for millimetric drops, while larger drops are increasingly oblate with size; oscillations of the drop cause its shape to vary in time about the equilibrium shape. Oscillations are excited by collisions with other drops, or may be self-excited by aerodynamic effects arising from the airflow around the drop. The latter mechanism was studied with two experiments, one for water drops 1.1 to 1.5 mm diameter, and the other for 2.0 and 2.5 mm drops. Drops of the desired size were produced using a computer-controlled drop generator, and stroboscopic photographs of the drops a distance below the generator yielded instantaneous axis ratios. Measurements of the oscillation frequency for 2.0 and 2.5 mm drops were made from photographs of interruptions in the backscattered light of the primary rainbow. Significant variations in axis ratio were observed (as large as 15 percent, with standard deviations of up to 3 percent of the mean axis ratio), indicating oscillations were present for each dropsize. In addition, the axis ratios were shifted higher than the equilibrium value by as much as 3.5 percent, making oscillating drops more spherical on average than quiescent drops. A large fraction of the drops did not possess symmetry about the vertical axis, due to forcing caused by the detachment of eddies that form in the drop wake. Drops around 1.5 mm diameter were the exception--they displayed a strong axisymmetric component as well. The oscillation measurements showed the presence of both the fundamental frequency and the first harmonic. The research revealed that equilibrium axis ratios should not be used in differential reflectivity calculations, as the observed axis ratio shift translates into Z(DR) changes of up to 30 percent.
Dissert. Abstr.

N93-13791 Council for National Academic Awards (England).
TRANSHORIZON MICROWAVE PROPAGATION AND ITS RELATIONSHIP WITH METEOROLOGICAL CONDITIONS Ph.D. Thesis
Candida Spillard 1990 207 p
Avail: Univ. Microfilms Order No. BRDX93192

The measurement and modelling of X-Band transhorizon propagation of microwaves beyond the horizon can occur by the mechanism of scattering from eddies of atmospheric turbulence or from hydrometeors, partial reflection from stable atmospheric layers, diffraction, and 'ducting', in which the radiation is trapped in a layer of atmosphere of rapidly decreasing refractivity. The dominant mechanism operating on a link at any given time is dependent upon the state of the atmosphere. From a network of X-Band links across the English Channel, examples of propagation due to turbulent scatter, hydrometeor scatter, partial reflections, and ducting were identified. The author has developed models for propagation due to turbulent and hydrometeor scatter and due to partial reflections and compared predictions of the received signal level based on these models with cumulative distributions of the actual signal levels received when each mechanism was operating. The author has also developed a method for identifying which mechanism is operating over a link at a given time from the meteorological synoptic chart for that time. The method is based on the principle that for clear air propagation, stable air which gives rise to propagation by partial or total reflections is identifiable by anticyclonic curvature of the isobars, advection of dry air from the continent out over the sea, or both. Ducting was modelled as total reflection. Turbulent scatter is the dominant mechanism when the link is under the influence of depressions or fronts. Both models give good agreement with measured signal levels. The meteorological classification method was applied to 12 months of data. Although most of the synoptic charts are relatively easily classified, discrete categories are not always easily applied to the continuous range of meteorological conditions.
Dissert. Abstr.

N93-13816 Purdue Univ., West Lafayette, IN.
ON THE RELATIONSHIP BETWEEN THE INTENSITY OF EXTRATROPICAL FRONTAL CYCLONE SYSTEMS AND WATER LEVELS IN THE GULF OF MEXICO Ph.D. Thesis
Andrew W. Garcia 1991 138 p
Avail: Univ. Microfilms Order No. DA9215553

The effects of winter season frontal cyclone systems on tidal-period Gulf of Mexico water levels are investigated. The passage of a series of hypothetical and observed frontal cyclone systems across the Gulf of Mexico is simulated using a Gulf-wide hydrodynamic model driven by a synoptic-scale, balanced flow wind model. The observed frontal cyclone systems were selected to represent a fast moving front, a slow moving front, and a frontal system which involved Gulf cyclogenesis. Evaluation of the model simulations was based upon comparison of tidal anomalies acquired at National Ocean Service tidal monitoring stations. Results of the model simulations show generally good qualitative agreement with the tidal anomalies. Because the wind model used routinely available meteorological data, forecasts of surge levels in the Gulf may be possible.
Dissert. Abstr.

N93-13817 Illinois Univ. at Urbana-Champaign, Savoy.
CLIMATE SENSITIVITY STUDY WITH ENERGY BALANCE MODELS Ph.D. Thesis
Jin Huang 1991 141 p
Avail: Univ. Microfilms Order No. DA9210843

The sensitivity of the Earth's climate is studied by modeling past climatic variations with two-dimensional seasonal energy balance model. Two parts are presented. The first part is a study of the interaction between the seasonal cycle and the small ice cap instability, which is a possible mechanism for the initiation of glaciation in the Northern Hemisphere and Southern Hemisphere. Results from a two-dimensional energy balance model

with a realistic land-ocean distribution show that the small ice cap instability exists in the Southern Hemisphere, but not in the Northern Hemisphere. A series of experiments with a one-dimensional energy balance model with idealized geography is used to study the roles of the seasonal cycle and the land-ocean distribution. The results indicate that the seasonal cycle and land-ocean distribution can influence the strength of the albedo feedback, which is responsible for the small ice cap instability, through two factors: the temperature gradient and the amplitude of the seasonal cycle. The second part is a study of the CO2 climate feedback and its possible role in the 41 kyr sea surface temperature oscillation during the Matuyama chron (2.4 to 0.7 Myr BP). The CO2-climate feedback is parameterized as an internal longwave radiation-polar temperature feedback in the energy balance model. Other physical processes are treated as boundary conditions. It is found that the CO2-climate feedback can increase climate sensitivity to orbital parameters, especially to the obliquity changes, which have a 41 kyr cycle. The model results indicate that the CO2-climate feedbak is one of possible mechanisms for the dominant 41 kyr climate change during the Matuyama. Dissert. Abstr.

N93-13877# Naval Oceanographic and Atmospheric Research Lab., Bay Saint Louis, MS.

THE ASSIMILATION OF MARINE SURFACE DATA INTO THE NAVY OPERATIONAL GLOBAL ATMOSPHERIC PREDICTION SYSTEM

Patricia A. Phoebus and James S. Goerss 1992 17 p Submitted for publication

(AD-A255559; NOARL-JA-431-040-92) Avail: CASI HC A03/MF A01

As numerical models of the ocean and the atmosphere become more sophisticated, it becomes necessary to account for the interchange of energy at the air/sea interface. Meteorological models require accurate estimates of sea surface temperature and ice fields. Oceanographic models require accurate estimates of the surface winds and heat fluxes. Thus, it is beneficial for scientists in each discipline, to have some level of understanding and appreciation for how these various parameters are obtained. With that in mind, we will describe how a meteorological analysis/forecast system uses marine data to estimate the surface wind field, with particular emphasis on the analysis process and the resulting nowcast product. The Navy's data analysis system uses the multivariate optimum interpolation technique to produce updates to background fields provided by the forecast model. The advantage of this technique is that the relative weights given the background and the observations are determined by taking into account the estimated error properties of each. As new data sources become available, the appropriate statistics defining the errors of the observations must be determined. Since we have recently added several new data sources to the assimilation cycle, new values of the observation errors have been determined for all marine surface data. The improvements made by these new data sources, including special sensor microwave/imager wind speeds and synthetic tropical observations, will also be illustrated. GRA

N93-13890 California Univ., Los Angeles.

FRONTOGENESIS PROCESSES IN THE TROPOSPHERE Ph.D. Thesis

Keith Martin Hines 1992 201 p

Avail: Univ. Microfilms Order No. DA9221858

This investigation addresses basic issues regarding simulated tropospheric frontogenesis, including the influence of initial conditions, model resolution, and the extent to which frontal features emphasized in recent observational studies of cyclone development can be obtained in a nearly adiabatic framework. A three-dimensional primitive-equation model on the sphere is used for this investigation. The model domain is restricted to a sector of one hemisphere, and physics are reduced to surface drag, horizontal diffusion, and dry convective adjustment. Spatial discretizations range from 4.0 deg lat x 5.0 deg long to 0.6 deg lat x 0.75 deg long in the horizontal, and from 14 to 35 layers in the vertical. Simulations with several symmetric initial profiles produce strongest temperature gradients in the middle troposphere downstream of the trough of growing disturbances. Stronger temperature gradients originating upstream of the wave trough, in basic agreement with the observed configuration of upper-level fronts, are obtained when initial conditions are selected so that the growing waves have small meridional phase tilt. Simulated upper-level frontogenesis primarily results fron tilting kinematically associated with variations of across-jet ageostrophic flow. No definitive evidence is found that simulated frontogenesis is enhanced by a positive-feedback process similar to that suggested by Murdrick (1974). The results do indicate, however, that vertical advection of momentum, a component of this feedback, is an important contributor to the frontal intensification. At the surface, shallow bend-back warm fronts develop in simulations with small surface drag. Horizontal advection is primarily responsible for the resulting bend-back structure of the warm front. Additional simulations with higher horizontal resolution, slightly different initial conditions, and small surface drag produce bent-back fronts in the form of spirals, similar to that in a recently proposed ocean cyclone model. Surface cold fronts are mostly insensitive to surface drag. Increasing surface drag, however, reduces intensities of surface warm fronts, apparently by weakening positive feedback between fronts and their vertical circulations. These results are consistent with the observed weakness of warm fronts over land. Dissert. Abstr.

N93-13892 Oxford Univ. (England).

MIDDLE ATMOSPHERE WATER VAPOUR Ph.D. Thesis

Rosemary Munro 1991 211 p

Avail: Univ. Microfilms Order No. BRD-96228

The data from the B2 channel of the Stratospheric and Mesospheric Sounder (SAMS) were intended to provide water vapor cross-sections ranging from 45 deg S - 65 deg N in latitude and from 4.4 - 9.2 scale heights in the vertical. However, previous analyses have shown that the transmittance behavior of the SAMS B2 channel in-flight was poorly characterized. As a result, a two-stage retrieval process was used to obtain an improved estimate of the transmittance behavior of the B2 channel and subsequently the required water vapor cross-sections. Information could only be obtained regarding the latitudinal and seasonal variations of water vapor; no deductions could be drawn about the vertical structure or long-term trends. Although the first stage of the two-stage retrieval process provided an improved estimate of the transmittance behavior of the SAMS B2 channel in-flight, it has not provided a physical reason for the original anomalous behavior. The water vapor cross-sections obtained over the three year period from January 1979 to December 1981, clearly show the presence of a high-latitude summer maximum in water vapor at approximately 6 scale heights, accompanied by a poleward decrease in volume mixing ratio below approximately 5 scale heights in the winter hemisphere. A secondary maximum is also seen in the summer hemisphere at approximately 9 scale heights in the lower mesosphere. In addition a less distinct equatorial minimum is observed at approximately 4.4 scale heights. The decrease in water vapor volume mixing ratios in the winter hemisphere is thought to result from the downward transport of mesospheric air rich in molecular hydrogen and poor in water vapor. This molecular hydrogen is subsequently oxidized thus replenishing the water vapor volume mixing ratios and producing the high latitude summer maximum at approximately 6 scale heights. In addition the seasonal variation in water vapor volume mixing ratios in the lower mesosphere indicates a dominance of advective over diffusive control in the determination of the vertical structure of water vapor in this region. Dissert. Abstr.

N93-13894 Universitaire Instelling Antwerpen, Wilrijk (Belgium).

STUDY OF THE CONCENTRATION AND DEPOSITION OF TROPOSPHERIC AEROSOLS USING X RAY EMISSION TECHNIQUES

Carlos Manuel Rojas-Palma 1992 226 p

Avail: Univ. Microfilms Order No. DA9223526

Since the early 1980's receptor models have been a useful tool for identifying the various aerosol sources present in a given airshed. The theoretical background of receptor oriented approach such as principal factor analysis is described, while its potentialities have been reviewed through its application to identify and apportion the aerosol sources present in urban, remote, and marine areas is included. The identification of the various atmospheric particulate matter sources was based upon the elemental concentrations provided by x-ray emission techniques such as particle induced x-ray emission and energy-dispersive x-ray fluorescence, whereas the information provided by microanalytical techniques such as electron probe x-ray microanalysis and laser mass microprobe analysis was proven to be very useful for a more accurate source apportionment. The study of aerosol sampling effects, namely, penetration of aerosol particles within the fibrous structure of cellulose filters was conducted using secondary ion mass spectrometry. The outcomes contribute to a better understanding of this particular problem and provide a quantitative aid to spectroscopists who need to account for this effect. The fundamentals of deposition modeling and the development of an approach to calculate

the various parameters used in dry deposition modeling are discussed. Several dry deposition models were tested using the data from measurement carried out at the southern bight of the North Sea. The results indicated that either of the models used can provide satisfactory results, taking into account the current state-of-the-art in deposition estimates based on dispersion models. The micro and macroscopic features of the southern bight of the North Sea were studied as a function of height and wind direction. The different particle classes were individualized using multivariate techniques such as cluster analysis, whereas a novel approach to data reduction provided satisfactory results. From the aerosol elemental concentrations and dry deposition modeling, the dry and wet deposition rates into the southern bight of the North Sea were estimated. The associated uncertainties are also discussed. Dissert. Abstr.

N93-14055 Council for National Academic Awards (England).
KINETIC STUDIES OF SOME FREE RADICAL REACTIONS INVOLVED IN CLOUDWATER CHEMISTRY Ph.D. Thesis
Steven John Waygood 1991 214 p
Avail: Univ. Microfilms Order No. BRDX95362

The SO3(-), SO4(-) and SO5(-) radicals have been proposed as key intermediates in the mechanisms proposed for the oxidation of dissolved SO2 initiated by both the OH radical and transition metal ions. This study has investigated the reactivity of these radicals in solution using laser flash photolysis and steady-state photolysis techniques. Photolytic precursors for the radicals have been established. Gated diode array spectroscopy has been used to determine the absorption spectra of the radicals. Kinetic spectrophotometric techniques have been employed to investigate the decay of each radical in aqueous solution in the absence of other species. The reactions of the sulphate radical anion, SO4(-), with other cloudwater constituents, such as ferrous iron, formaldehyde, formic acid and the hydrogen carbonate anion, have also been studied. When possible, ion chromatography has been used to identify the aqueous-phase reaction products. In addition, it has been proposed that the reaction of OH radicals with hydrated formaldehyde is a major source of tropospheric formic acid, the major acidic component of precipitation at remote sites. This reaction has been studied and a mechanism proposed which accounts for the observed dependence of the rate of oxidation on the oxygen content of the solution. It was necessary to study this reaction before the reaction between the sulphate radical anion and formaldehyde could be rationalized. Using the results of this study, a better characterized mechanism is proposed for the OH-initiated oxidation of dissolved S(IV). When this scheme is used to predict the rate of formation of S(VI) adopting typical cloudwater concentrations, it is shown that the process could be an important route in the acidification of cloudwater. The study of the reaction between SO4(-) and Fe(II) shows that current cloud chemistry models greatly overpredict the rate of production of Fe(III) by this route and demonstrate that the role of transition metal ions in cloud chemistry is not fully characterized. It has been confirmed that, under atmospheric conditions, formic acid is the only product of the aqueous oxidation of formaldehyde by the OH radical. The SO4(-) radical has also been shown to be an oxidant for both formaldehyde and formic acid, but reaction mechanisms which explain all the empirical facts are not obvious. Dissert. Abstr.

N93-14063 Colorado State Univ., Fort Collins.
AN INVESTIGATION OF THE EFFECTS OF TOPOGRAPHY ON COLORADO FRONT RANGE WINTER STORMS Ph.D. Thesis
Douglas Alan Wesley 1991 209 p
Avail: Univ. Microfilms Order No. DA9216227

This study utilizes both an extensive set of observations and mesoscale model simulations to isolate and describe the important influences of complex terrain on Colorado Front Range winter storms, with an emphasis on snowfall distributions. Specifically, the interaction of various types of cold, low-level air masses with topography and the larger-scale flow is described. Field measurements of several snowstorms during the 1987-89 time period include special CLASS (Cross-chain Loran Atmospheric Sounding System) vertical profiles, standard National Weather Service (NWS) and National Meteorological Center (NMC) surface and rawinsonde data, surface observations collected by a trained snow-spotter network, profiler data, Doppler reflectivity and velocity scans, and Geostationary Operational Environmental Satellite (GOES) images. The numerical predictions are produced by the Regional Atmospheric Modeling System (RAMS) developed at Colorado State University, using two- and three-dimensional non-hydrostatic simulations. The versions of the model employed in this study utilized both horizontally homogeneous initializations and initial fields made up of NMC upper-air grids and rawinsondes. Most simulations employed full microphysics. A comparison between model predicted dynamic and microphysical fields and observational data is described for the 30-31 March 1988 snowstorm along the Colorado Front Range. Of particular interest in this study is the role of trapped cold air masses over the foothills and adjacent plains during the evolution of snow-producing synoptic scale disturbances. Specifically, these include two types of precipitating easterly ('upslope') flows along the Colorado Front Range: cold-air damming situations and arctic outbreaks. The investigation includes detailed case studies of each storm type. The cold air damming process concentrates snowfall, typically in the foothills and adjacent areas to the east. A blocked low-level stable layer causes overrunning in a north-south band over and near the foothills. A quite different scenario, the cold outbreak requires the establishment of an arctic air mass in the low levels. In this case, overrunning occurs as moist westerly winds aloft flow over the arctic air mass, producing snowfall in the foothills and plains. Dissert. Abstr.

N93-14082# Army Lab. Command, White Sands Missile Range, NM. Atmospheric Sciences Lab.
A SURFACE PRESSURE ALTITUDE PREDICTION MODEL Final Report
Elton P. Avara Aug. 1992 149 p
(AD-A255834; ASL-TR-0319) Avail: CASI HC A07/MF A02

A surface pressure altitude (SPA) prediction model has been developed that is totally empirical and based on SPA data from 556 meteorological observation stations in the free world. This model is simple and can be executed very quickly on a microcomputer. The model estimates the mean SPA perturbation (SPAP) or difference between the SPA and the surface elevation of a station by a sum of numbers that represent the additive effects of month, time of day, station location, interaction of month with station location, interaction of time of day with station location, and an additive constant. A prediction of SPA at a later time is made by taking the current SPA and adding the difference between the modelled mean SPAP for the later time and the modelled mean SPAP at the current time. The model predicts SPA well in the near term at an observing site when the current SPA is known. The quality of the prediction decays with prediction lay time until about 50 percent of actual SPA variation is accounted for by the predicted SPA at a lag time of 24 h. GRA

48 OCEANOGRAPHY

Includes biological, dynamic, and physical oceanography; and marine resources.

For related information see also *43 Earth Resources and Remote Sensing.*

N93-12556# Naval Oceanographic and Atmospheric Research Lab., Bay Saint Louis, MS.
OCEAN OPTICAL DATABASE Final Report
R. A. Arnone, R. A. Oriol, G. Terrie, and L. Estep May 1992 41 p
(AD-A254969; NOARL-TN-254) Avail: CASI HC A03/MF A01

The global ocean optical property of the diffuse attenuation coefficient at 490 nm k(490), has been assembled into a database using satellite ocean color data from the Coastal Zone Color Scanner. The database representing 6 years of satellite coverage from 1978 to 1986 is at a spatial resolution of 20 km and is represented in monthly composites. The assemblage and format of the data are defined. Problems and limitations of using satellite ocean color for retrieving ocean k(490) values are examined. The validation of the optical database from the satellite is accessed through comparison with in situ ship measurements of chlorophyll and diffuse attenuation coefficient. GRA

N93-12577# Washington Univ., Seattle. Applied Physics Lab.
NEAR-NORMAL INCIDENCE SCATTERING FROM ROUGH, FINITE SURFACES: KIRCHHOFF THEORY AND DATA COMPARISON FOR ARCTIC SEA ICE
P. D. Mourad and K. L. Williams 10 Feb. 1992 54 p
(Contracts N00014-91-J-1647; N00039-91-C-0072)
(AD-A254525) Avail: CASI HC A04/MF A01

We apply Kirchhoff theory for the target strength of a rough, circular

surface whose roughness is characterized by a two-dimensional, isotropic power-law wavenumber spectrum W(sub 2)(kappa) = eta(sub 2)kappa(exp (-)p)(sub 2). Three nondimensional parameters are found that govern the target strength: zeta = kappa(sub 0)a, eta = eta(sub 2)a(exp p(sub 2)-4), and p(sub 1) = p(sub 2)-1, where kappa(sub 0) is the acoustic wavenumber, a is the radius of the surface, and p(sub 1) is the spectral exponent of the one-dimensional power-law wavenumber spectrum. First, we discuss the general influence of zeta, p(sub 1), and eta on the target strength. Following that are calculations of average target strength of the ice/water interface of a submerged cylindrical block of ice, which are compared with individual realizations of measured target strengths of ice blocks for frequencies between 20 kHz and 80 kHz. Data and theory show that the (smooth surface) form function for a finite surface does not describe the observed diffraction pattern. Instead, the lobes of the pattern diminish and the nulls fill in--i.e., the total backscatter becomes more incoherent--as frequency increases or as the large wavenumber components of the roughness spectrum contribute more to the total acoustic return. These comparisons also allowed us to infer the rough surface statistics of the ice surface and the compressional sound speed structure within the skeletal zone of the ice. GRA

N93-12599# Washington Univ., Seattle. Applied Physics Lab.
EXPERIMENTAL EXAMINATION OF GROWING AND NEWLY SUBMERGED SEA ICE INCLUDING ACOUSTIC PROBING OF THE SKELETAL LAYER
K. L. Williams, G. R. Garrison, and P. D. Mourad 2 Apr. 1992 59 p Submitted for publication
(Contract N00014-91-J-1647)
(AD-A254526) Avail: CASI HC A04/MF A01

The acoustic properties of sea ice are inherently important to studies of sound propagation and scattering in the Arctic. The richness of the acoustic behavior of sea ice stems from its saline nature. In particular, sea ice is the result of the solidification of a sub-eutectic melt. This accounts for the high porosity layer at the ice/water interface, known as the skeletal layer. The high porosity makes measurements of the acoustic properties in the skeletal layer extremely sensitive to perturbations. Because this layer is a few centimeters thick, it is of primary importance for modeling the scattering of high frequency (above 10 kHz) acoustic energy from the underside of the ice. GRA

N93-12742# Institute of Ocean Sciences, Sidney (British Columbia).
ACOUSTIC TRACKING OF NEUTRALLY BUOYANT FLOAT
David Farmer 14 Aug. 1992 30 p
(Contract N00014-91-J-1964)
(AD-A255086) Avail: CASI HC A03/MF A01

This report summarizes work done on the development and testing of the acoustically tracked drifter. The overall goal of the drifter is to acquire Lagrangian measurements of water motion so as to study mixed layer processes such as Langmuir circulation. The float was developed jointly with Eric D'Asaro (Applied Physics Laboratory, University of Washington), with D'Asaro focusing primarily on the mechanical aspects of the float and our group focusing primarily on the acoustical tracking. Tests were carried out in Haro Strait in March 1991 and in Georgia Strait in November 1991, in addition to some preliminary open ocean tests. Basically, the tests were very successful, although they did point out a number of changes that must be made to subsequent versions

of the fundamental physical and chemical attributes of these systems, and consider the implications of high-temperature, fluid-driven processes for organic synthesis. Information about submarine hydrothermal systems comes from many directions. Measurements made directly on venting fluids provide useful, but remarkably limited, clues about processes operating at depth. The oceanic crust has been drilled to approximately 2.0 km depth providing many other pieces of information, but drilling technology has not allowed the bore holes and core samples to reach the maximum depths to which aqueous fluids circulate in oceanic crust. Such determinations rely on studies of pieces of deep oceanic crust uplifted by tectonic forces such as along the Southwest Indian Ridge, or more complete sections of oceanic crust called ophiolite sequences which are presently exposed on continents owing to tectonic emplacement. Much of what is thought to happen in submarine hydrothermal systems is inferred from studies of ophiolite sequences, and especially from the better-exposed ophiolites in Oman, Cyprus and North America. The focus of much that follows is on a few general features: pressure, temperature, oxidation states, fluid composition and mineral alteration, because these features will control whether organic synthesis can occur in hydrothermal systems. Author

N93-13483 California Univ., San Diego.
THE NORTH ATLANTIC CIRCULATION: COMBINING SIMPLIFIED DYNAMICS WITH HYDROGRAPHIC DATA Ph.D. Thesis
Philip Stuart Bogden 1991 112 p
Avail: Univ. Microfilms Order No. DA9222241

The time-averaged velocity field in the North Atlantic is estimated from observations of density, wind stress and bottom topography. The flow is taken to satisfy geostrophic dynamics, with the effects of a wind-driven Ekman layer prescribed at the surface and a no-normal-flow boundary condition imposed at the bottom. Data and dynamics determine velocity up to an arbitrary function of f/h, the dynamical 'free mode', where h is the total depth of the ocean. The free mode is selected to minimize mixing of potential density at middepth. Vertical velocity in the model is particularly sensitive to variations in the free mode and to errors in density. In contrast, horizontal velocities are relatively robust. Below the thermocline, the model predicts a strong O(1 cm/sec) westward flow across the entire North Atlantic in a narrow range of latitude (roughly 25 deg N to 32 deg N). On the bottom, mid-latitude flows tend to follow isobaths with shoaling bathymetry to the right; equatorward flows occur along the western boundary and eastern flank of the Mid-Atlantic Ridge, with poleward flows along the eastern boundary and western flank of the ridge. Long-term current measurements substantiate the predictions. Also, model flows provide a framework for explaining a variety of property distributions in terms of advection by the time-averaged circulation. The results conflict with previous oceanographic-inverse models, which predict middepth flows an order of magnitude smaller and often in other directions. The novelty of our approach involves the use of continuous representations for spatially averaged data fields, and the enforcement of the dynamics without misfit over the entire North Atlantic. This involves the plausible, although tenuous, assertion that the flow 'feels' only the large-scale features of the bottom topography. Agreement between model predictions and direct observations supports the validity of the simplified dynamics. Dissert. Abstr.

N93-13633 North Carolina Univ., Chapel Hill.
THE GULF STREAM DOWNSTREAM OF CAPE HATTERAS: MODEL/DATA COMPARISONS Ph.D. Thesis
Wei Wang 1991 123 p
Avail: Univ. Microfilms Order No. DA9216778

One year of simulation from a selected model realization of the Naval Oceanographic and Atmospheric Research Laboratory Limited-Area, North Atlantic Model (1/8 degree horizontal resolution) has been compared with historical observations in the Gulf Stream region and with data from the UNC/URI Gulf Stream Dynamics Experiment (1983-1985) and the URI Pegasus Program (1980-1983) conducted in the Gulf Stream near 73 deg W. The comparisons covered a variety of aspects of Gulf Stream variability and were carried out in two parts: basinwide comparisons and regional comparisons. The basinwide comparisons focused on climatological features of the Gulf Stream system over much of the model domain, including Gulf Stream mean position and path variability (meandering activity), statistics of Gulf Stream rings, eddy kinetic energy fields, and Gulf Stream transport. The regional comparisons focused on characteristics of the Gulf Stream current near 73 deg W, including velocity and path meander spectra, path features, coherence between meandering motion and local deep ocean flows, kinematic parameters (i.e., transport, width, and axis speed), and cross-stream structure. Agreements and disagreements between the observations and the model realization are discussed. In addition, model-produced, small-amplitude, approximately 6 day meanders northeast of Cape Hatteras have been investigated for their resemblance to often-observed, near-weekly period meanders of the Gulf Stream along the Carolinas and downstream of Cape Hatteras. The various comparisons conducted in this study provide a reference for future model/data comparison studies. Dissert. Abstr.

N93-13708*# Biospherical Instruments, Inc., San Diego, CA.
DEVELOPMENT OF MOORED OCEANOGRAPHIC SPECTRORADIOMETER Final Report
Charles R. Booth, B. Greg Mitchell, and O. Holm-Hansen 30 Jun. 1987 69 p
(Contract NAS7-934; SBIR-08.15-1315)
(NASA-CR-190883; NAS 1.26:190883) Avail: CASI HC A04/MF A01

Biospherical Instruments has successfully completed a NASA sponsored SBIR (Small Business Innovational Research Program) project to develop spectroradiometers capable of being deployed in the ocean for long periods of time. The completion of this project adds a valuable tool for the calibration of future spaceborne ocean color sensors and enables oceanographers to extend remote sensing optical techniques beyond the intermittent coverage of spaceborne sensors. Highlights of the project include two moorings totalling 8 months generating extensive sets of optical, biological, and physical data sets in the ocean off La Jolla, California, and a 70 day operational deployment of the resulting commercial product by the ONR and NASA sponsored BIOWATT program. Based on experience gained in these moorings, Biospherical Instruments has developed a new line of spectroradiometers designed to support the oceanographic remote sensing missions of NASA, the Navy, and various oceanographers. Author

N93-13714*# Princeton Univ., NJ.
ASSIMILATION OF SATELLITE COLOR OBSERVATIONS IN A COUPLED OCEAN GCM-ECOSYSTEM MODEL Progress Report
Jorge L. Sarmiento 15 Oct. 1992 5 p Original contains color illustrations
(Grant NAGw-3137)
(NASA-CR-191218; NAS 1.26:191218) Avail: CASI HC A01/MF A01; 1 functional color page

Monthly average coastal zone color scanner (CZCS) estimates of chlorophyll concentration were assimilated into an ocean global circulation model(GCM) containing a simple model of the pelagic ecosystem. The assimilation was performed in the simplest possible manner, to allow the assessment of whether there were major problems with the ecosystem model or with the assimilation procedure. The current ecosystem model performed well in some regions, but failed in others to assimilate chlorophyll estimates without disrupting important ecosystem properties. This experiment gave insight into those properties of the ecosystem model that must be changed to allow data assimilation to be generally successful, while raising other important issues about the assimilation procedure. L.R.R.

N93-13841 Washington Univ., Saint Louis, MO.
MODELING AND OBSERVATIONS OF DEEP CIRCULATION IN THE EASTERN SOUTH PACIFIC OCEAN Ph.D. Thesis
Susan L. Hautala 1992 251 p
Avail: Univ. Microfilms Order No. DA9223001

Theoretical and observational constraints on the large-scale deep mean flow in the South Pacific Ocean between Tahiti and Easter Island are investigated. Of particular interest is the question of whether the circulation in the depth range 2000 to 3000 dbars is driven by buoyancy forcing from the East Pacific Rise. The theoretical component of the study involves a reinterpretation of the Stommel and Arons (1962) abyssal circulation framework, expanding it into a three-layer, steady, planetary geostrophic model that merges the Stommel-Arons theory with the thermocline theory of Luyten, Pedlosky and Stommel (1983) and Rhines and Young (1982). This model allows an exploration of the effects upon abyssal flow of mass sources, as well as mass sinks of variable structure, topography and wind-driven circulation. The model is used specifically to investigate flow beneath the subtropical gyre driven by mass sources on the East Pacific Rise. Two different overdetermined inverse techniques are then applied to

a set of observations made in this region during October-December, 1987 (Riser, et al., 1990). The mean circulation is obtained from a nonconservative beta-spatial inverse method, applied to the hydrographic data. The nonconservative, diapycnal flux term is shown to be an essential part of the deep potential vorticity balance and, hence, proper resolution of this term is critical to the success of the beta-spiral inverse. An inverse of conservation equations for He-3, SiO4 and O2 quantitatively confirms the beta-spiral circulation. Furthermore, the tracer balance inverse method yields the fields of epipycnal and diapycnal diffusivities, and in situ tracer sources and sink, which are found to be reasonable. The balance of terms in the tracer conservation equations is explored in detail. The model circulation arising from buoyancy flux at the East Pacific Rise bears close resemblance to the observations. Furthermore, the inverse fields of diapycnal flux divergence and horizontal flow are in accord with the model physics. These facts, and the existence of several indicators of the hydrothermal origin of this water mass, lead to a conclusion that low latitude East Pacific Rise buoyancy flux does drive large-scale deep circulation. Dissert. Abstr.

N93-13842 Oxford Univ. (England).
TEST AND CALIBRATION OF THE ALONG TRACK SCANNING RADIOMETER, A SATELLITE-BORNE INFRARED RADIOMETER DESIGNED TO MEASURE SEA SURFACE TEMPERATURE Ph.D. Thesis
Graeme Mason 1991 269 p
Avail: Univ. Microfilms Order No. BRD-96208

The Along Track Scanning Radiometer (ATSR) is a multichannel infrared radiometer designed to measure sea surface temperature from space to an accuracy of better than +/- 0.5 K (2 sigma). ATSR forms part of the payload of the ERS-1 spacecraft, which was launched on the 17th of July 1991. A small team at Oxford University was responsible for the pre-launch testing and calibration of ATSR. The instrument performance requirements and test objectives are presented. In particular, ATSR is required to measure brightness temperature in the infrared to an accuracy of +/- 0.1 K to achieve the desired accuracy in the sea surface temperature measurements. The test and calibration program covered field of view determination, radiometer calibration, thermal balance tests, thermal vacuum temperature cycling and orbital simulations. A test facility was designed and built specifically for these tests. This is described in detail. The results of the test and calibration program are presented and discussed. The measured instantaneous fields of view are presented and a method of calculating the actual fields of view from these data given. Features observed in these data are described and explained. The initial radiometric calibration results show a non-linearity in each channel. The non-linearity in the 10.8 micron and 12.0 micron channels is attributed for Auger recombination in the HgCdTe detectors. Correction factors for these two channels are calculated from the calibration measurements. Using these correction factors ATSR meets the +/- 0.1 K accuracy requirements in all channels (without any correction for the 3.7 micron channel non-linearity). A possible explanation for the observed 3.7 micron channel non-linearity (based on a spectral shift) is also presented. The measured noise levels in each channel are shown to be within the design requirements. The results of this calibration program show that ATSR should measure sea surface temperature significantly more accurately than other existing space-borne instruments.
Dissert. Abstr.

N93-13943# Naval Oceanographic and Atmospheric Research Lab., Bay Saint Louis, MS.
ADDING EXPLANATION CAPABILITY TO A KNOWLEDGE-BASED SYSTEM FOR INTERPRETATION OF OCEANOGRAPHIC IMAGES Final Report
Susan Bridges Sep. 1992 70 p
(AD-A255887; NOARL-TN-296) Avail: CASI HC A04/MF A01

An explanation component has been developed for an existing oceanographic expert system that predicts the movement of mesoscale features associated with the Gulf Stream. The information provided by the expert system is used by image processing analysts when the oceanographic features cannot be observed by satellite data due to interference such as cloud cover. The addition of an explanation capability gives users a basis for judging the quality of the system's decision making process. GRA

51 LIFE SCIENCES (GENERAL)

N93-12768# Georgia Univ., Athens.
NITROGEN CONTROL OF CHLOROPLAST DEVELOPMENT AND DIFFERENTIATION
G. W. Schmidt Dec. 1991 5 p
(Contract DE-FG09-84ER-13188)
(DE92-017392; DOE/ER-13188/7) Avail: CASI HC A01/MF A01

The growth and development of plants and photosynthetic microorganisms is commonly limited by the availability of nitrogen. Our work concerns understanding the mechanisms by which plants and algae that are subjected to nitrogen deprivation alter the composition of photosynthetic membranes and enzymes involved in photosynthetic carbon metabolism. Toward these ends, we study biosynthetic and gene expression processes in the unicellular green alga Chlamydomonas reinhardtii which is grown in an ammonium-limited continuous culture system. We have found that the expression of nuclear genes, including those encoding for light-harvesting proteins, are severely repressed in nitrogen-limited cells whereas, in general, chloroplast protein synthesis is attenuated primarily at the level of mRNA translation. Conversely, nitrogen deprivation appears to lead to enhanced synthesis of enzymes that are involved in starch and storage lipid deposition. In addition, as a possible means by which photosynthetic electron transport activities and ATP synthesis is sustained during chronic periods of nitrogen deprivation, thylakoid membranes become enriched with components for chlororespiration. Characterization of the chlororespiratory electron transport constituents, including cytochrome complexes and NAD(P)H dehydrogenase is a major current effort. Also, we are striving to isolate the genes encoding chlororespiration proteins toward determining how they and others that are strongly responsive to nutrient availability are regulated. DOE

N93-12871# Mote Marine Lab., Sarasota, FL.
PHYTOPLANKTON PHOTOSYNTHESIS IN NATURAL MIXED LAYERS Final Technical Report
Gary Kirkpatrick 1992 1 p
(Contract N00014-91-J-1653)
(AD-A255010) Avail: CASI HC A01/MF A01

This report describes the technical accomplishments of the subject grant. This work forms a part of a broader, ongoing effort to more completely describe the physiological responses of marine phytoplankton species to the time-course of natural solar radiation variation on time scales of minutes to days. The investigative approach involves in situ instrumentation, laboratory observations and computer models. Collaborators on this ongoing project include Daniel Kamykowski, Thomas Curtin, Gerald Janowitz and Hidekatsu Yamazaki. The objective of the work under the subject grant was to develop the capability to conduct simultaneous, in situ comparison studies of the photosynthetic responses within and between selected phytoplankton species under natural irradiance fluctuation utilizing the Self-contained Underwater Photosynthesis Apparatus (SUPA). This objective was met by fabricating a twin SUPA based on the existing design and incorporating the necessary modifications to hardware and software to permit simultaneous operation from existing support equipment. GRA

N93-12901*# Alabama Univ., Huntsville. Dept. of Biological Sciences.
ESTABLISHING LABORATORY STANDARDS FOR BIOLOGICAL FLIGHT EXPERIMENTS Final Report
Ronald B. Young and Debra M. Moriarity [1989] 4 p
(Contract NAS8-36955)
(NASA-CR-184402; NAS 1.26:184402) Avail: CASI HC A01/MF A01

The general objective of this research was to assess the effects of exposure to simulated microgravity on ultrastructural aspects of the contractile system in chicken skeletal muscle cells. This general objective had two specific experimental components: (1) the progression of changes in cell morphology, fusion, and patterns of contractile filament organization in muscle cell cultures grown in hollow fibers in the Clinostat were evaluated, with appropriate controls; (2) to initiate experiments in which muscle cells were grown on the surface of microcarrier beads. The ultimate objective of this second portion of the work is to determine if these beads can be rotated in a bioreactor and thereby obtain a more accurate approximation

of the effects of simulated microgravity on differentiated muscle cells.
Author

N93-12949*# Alabama Univ., Huntsville. Environmental Lab. Section.
METHODS DEVELOPMENT FOR TOTAL ORGANIC CARBON ACCOUNTABILITY Final Report, 1 Nov. 1990 - 30 Apr. 1991
Brian L. Benson and Melvin V. Kilgore, Jr. 30 Apr. 1991 140 p
(Contract NAS8-36955)
(NASA-CR-184438; NAS 1.26:184438) Avail: CASI HC A07/MF A02

This report describes the efforts completed during the contract period beginning November 1, 1990 and ending April 30, 1991. Samples of product hygiene and potable water from WRT 3A were supplied by NASA/MSFC prior to contract award on July 24, 1990. Humidity condensate samples were supplied on August 3, 1990. During the course of this contract chemical analyses were performed on these samples to qualitatively determine specific components comprising, the measured organic carbon concentration. In addition, these samples and known standard solutions were used to identify and develop methodology useful to future comprehensive characterization of similar samples. Standard analyses including pH, conductivity, and total organic carbon (TOC) were conducted. Colorimetric and enzyme linked assays for total protein, bile acid, B-hydroxybutyric acid, methylene blue active substances (MBAS), urea nitrogen, ammonia, and glucose were also performed. Gas chromatographic procedures for non-volatile fatty acids and EPA priority pollutants were also performed. Liquid chromatography was used to screen for non-volatile, water soluble compounds not amenable to GC techniques. Methods development efforts were initiated to separate and quantitate certain chemical classes not classically analyzed in water and wastewater samples. These included carbohydrates, organic acids, and amino acids. Finally, efforts were initiated to identify useful concentration techniques to enhance detection limits and recovery of non-volatile, water soluble compounds.
Author

N93-13033# Joint Publications Research Service, Arlington, VA.
JPRS REPORT: SCIENCE AND TECHNOLOGY. CENTRAL EURASIA: LIFE SCIENCES
30 Oct. 1992 63 p Transl. into ENGLISH from various Russian articles
(JPRS-ULS-92-024) Avail: CASI HC A04/MF A01

Papers on the following topics are presented: the environment; epidemiology; medicine; molecular biology; pharmacology and toxicology; public health; phychology; and radiation biology.
L.R.R.

N93-13034# Louisiana State Univ., Baton Rouge.
A PHYSICO-CHEMICAL STUDY OF SOME AREAS OF FUNDAMENTAL SIGNIFICANCE TO BIOPHYSICS
S. P. McGlynn and D. Kumar 30 Apr. 1992 66 p
(Contract DE-FG05-87ER-60503)
(DE92-019917; DOE/ER-60503/353) Avail: CASI HC A04/MF A01

This report discusses the following topics on biophysics: radiation signatures; electronic structure of steroids and vitamins; laser optogalvanic effect; vacuum ultraviolet spectroscopy; and ozone.
DOE

N93-13083# Louisiana State Univ., Baton Rouge. Dept. of Chemistry.
A PHYSICO-CHEMICAL STUDY OF SOME AREAS OF FUNDAMENTAL SIGNIFICANCE TO BIOPHYSICS
S. P. McGlynn and D. Kumar 30 Apr. 1992 99 p
(Contract DE-FG05-87ER-60503)
(DE92-019916; DOE/ER-60503/352) Avail: CASI HC A05/MF A02

This report discusses the following topics: radiation signatures; photoelectron spectroscopy of biologically active molecules; laser optogalvanic effect; magnetic circular dichroism; photochemistry of halogenated molecules; and density effects on high-n rydbergs.
DOE

N93-13269# Arkansas Univ., Fayetteville. Coll. of Engineering.
BIOLOGICAL CONVERSION OF SYNTHESIS GAS
1 Apr. 1992 23 p
(Contract DE-FG21-90MC-27225)
(DE92-017673; DOE/MC-27225/T5) Avail: CASI HC A03/MF A01

The anaerobic, photosynthetic bacterium Rhodospirillum rubrum has been chosen for catalysis of the biological water gas shift reaction. In addition, two other anaerobic, photosynthetic bacteria, Chlorobium thiosulfatophilum and Chloroblum phaeobacteroides, have been evaluated as candidates for H2S conversion to elemental sulfur. Growth and H2S uptake studies in the presence of basal medium indicated that C. thiosulfatophilum is a much superior organism. C. phaeobacteroides showed sporatic growth at best, with growth always slower than C. thiosulfatophilum. Also, when C. phaeobacteroides experienced slow growth, no H2S consumption was observed. C. thiosulfatophilum always showed superior growth and H2S uptake, and thus will be selected as the bacterium for H2S conversion to elemental sulfur.
DOE

N93-13327*# National Academy of Sciences - National Research Council, Washington, DC. Commission on Physical Sciences, Mathematics, and Applications.
ASSESSMENT OF PROGRAMS IN SPACE BIOLOGY AND MEDICINE
1991 79 p
(Contract NASw-4102)
(NASA-CR-190930; NAS 1.26:190930) Avail: CASI HC A05/MF A01

Over the past 30 or more years, the National Research Council Space Studies Board and its various committees have published hundreds of recommendations concerning life sciences research. Several particularly noteworthy themes appear consistently: (1) Balance - the need for a well-balanced research program in terms of ground versus flight, basic versus clinical, and internal versus extramural; (2) Excellence - because of the extremely limited number of flight opportunities (as well as their associated relative costs), the need for absolute excellence in the research that is conducted, in terms of topic, protocol, and investigator, and (3) Facilities - the single most important facility for life sciences research in space, an on-board, variable force centrifuge. In this first assessment report, the Committee on Space Biology and Medicine emphasizes that these long-standing themes remain as essential today as when first articulated. On the brink of the twenty-first century, the nation is contemplating the goal of human space exploration; consequently, the themes bear repeating. Each is a critical component of what will be necessary to successfully achieve such a goal.
Author

N93-13457*# Washington Univ., Saint Louis, MO. Dept. of Earth and Planetary Sciences.
HYDROTHERMAL ORGANIC SYNTHESIS EXPERIMENTS
Everett L. Shock 1992 12 p
(Grants NAGw-2818; NSF EAR-90-18468)
(NASA-CR-191257; NAS 1.26:191257) Avail: CASI HC A03/MF A01

The serious scientific debate about spontaneous generation which raged for centuries reached a climax in the nineteenth century with the work of Spallanzani, Schwann, Tyndall, and Pasteur. These investigators demonstrated that spontaneous generation from dead organic matter does not occur. Although no aspects of these experiments addressed the issue of whether organic compounds could be synthesized abiotically, the impact of the experiments was great enough to cause many investigators to assume that life and its organic compounds were somehow fundamentally different than inorganic compounds. Meanwhile, other nineteenth-century investigators were showing that organic compounds could indeed be synthesized from inorganic compounds. In 1828 Friedrich Wohler synthesized urea in an attempt to form ammonium cyanate by heating a solution containing ammonia and cyanic acid. This experiment is generally recognized to be the first to bridge the artificial gap between organic and inorganic chemistry, but it also showed the usefulness of heat in organic synthesis. Not only does an increase in temperature enhance the rate of urea synthesis, but Walker and Hambly showed that equilibrium between urea and ammonium cyanate was attainable and reversible at 100 C. Wohler's synthesis of urea, and subsequent syntheses of organic compounds from inorganic compounds over the next several decades dealt serious blows to the 'vital force' concept which held that: (1) organic compounds owe their formation to the action of a special force in living organisms; and (2) forces which determine the behavior of inorganic compounds play no part in living systems. Nevertheless, such progress was overshadowed by Pasteur's refutation of spontaneous generation which nearly extinguished experimental investigations into the origins of life for several decades. Vitalism was dealt a deadly blow in the 1950's with Miller's famous spark-discharge experiments which were undertaken in the framework of the Oparin and Haldane hypotheses concerning the origin of life. These hypotheses were constructed on some basic assumptions which included a reduced atmosphere, and a low surface temperature for the early Earth. These ideas meshed well with the prevailing hypothesis of the 1940's and

50's that the Earth had formed through heterogeneous accretion of dust from a condensing solar nebula. Miller's experiments were extremely successful, and were followed by numerous other experiments by various investigators who employed a wide variety of energy sources for abiotic synthesis including spark discharges, ultra-violet radiation, heat, shock waves, plasmas, gamma rays, and other forms of energy. The conclusion reached from this body of work is that energy inputs can drive organic synthesis from a variety of inorganic starting materials. Author

N93-13503# Southwest Research Inst., San Antonio, TX.
INVESTIGATION OF EFFECTS OF 60-Hz ELECTRIC AND MAGNETIC FIELDS ON OPERANT AND SOCIAL BEHAVIOR AND ON THE NEUROENDOCRINE SYSTEM OF NONHUMAN PRIMATES, PART 2
J. W. Rhodes 14 Jul. 1992 233 p
(Contract DE-AC02-80RA-50219)
(DE92-040153; DOE/RA-50219/21-Pt-2) Avail: CASI HC A11/MF A03

This volume contains detailed experimental data to accompany quarterly report, dated July 14, 1992, by this group entitled 'Investigation of Effects of 60-Hz Electric Fields on Operant and Social Behavior and on the Neuroendocrine System of Nonhuman Primates.' This volume is a collection of Appendices which are entitled: Appendix A- Field Mapping Data Forms, Appendix B- Exposure Area (East Side) Electric Field Data, Appendix C- Exposure Area (East Side) Magnetic Field Data, Appendix D- Sham Area (West Side) Magnetic Field Data, Appendix E- Memoranda Concerning Field Onset During Experiment 4 and the Crossover Experiment, Appendix F- Exposure Area (East Side) Electric Field Data, Appendix G- Exposure Area (East Side) Magnetic Field Data, Appendix H- Sham Area (west Side) Magnetic Field Data, Appendix 1- Compiled Data and Anovas for Experiment 3 Social Data, Appendix J -Written Comments Provided by Statistician Dr. Robert Mason, and Appendix K- Reference Text Provided by Dr. Coelho. DOE

N93-13520# Southwest Research Inst., San Antonio, TX.
INVESTIGATION OF EFFECTS OF 60-Hz ELECTRIC AND MAGNETIC FIELDS ON OPERANT AND SOCIAL BEHAVIOR AND ON THE NEUROENDOCRINE SYSTEM OF NONHUMAN PRIMATES, PART 1
J. W. Rhodes 14 Jul. 1992 169 p
(Contract DE-AC02-80RA-50219)
(DE92-040152; DOE/RA-50219/21-Pt-1) Avail: CASI HC A08/MF A02

The objective of this program is to investigate behavioral and neuroendocrine effects associated with exposure to 60-Hz electric and magnetic fields, using the baboon (Papio cynocephalus). Results from this program are used to estimate consequences of human exposure to the electric and magnetic fields associated with electric power transmission. Electric and magnetic field measurements for Experiment 3A (Confirmatory), Experiment 4 and Social Behavior portion of Experiment 3 are presented. The systems for the production and monitoring of the fields performed satisfactorily during Experiment 3A and during all but the last part of Experiment 4. In Experiment 3, two-way repeated analyses of variance revealed statistically significant Group (Exposed and Sham Exposed) and Period (Baseline, Exposure, and Post-Exposure) main effects. Two significant Period by Group interactions were also found. Seven of the ten behavioral categories showed a main effect of Period. Two-sample t-test comparisons of the two groups for each period indicated that performance rates in two behavioral categories (Stereotypy and Posture) were significantly lower in the Exposure Group. In general, the Exposed subjects exhibited a trend of progressively lower performance rates across the three periods. Specific accomplishments reported in this document were: measurement of electric and magnetic fields for Experiments 3A and 4, completed analysis of the Social Behavioral data from Experiment 3, and a detailed discussion of statistical methods employed on the Social Behavioral portion of Experiment 3, and hematology data were collected and recorded for Operant and Social Behavioral subjects for Experiment 4. DOE

N93-13612*# Biospherical Instruments, Inc., San Diego, CA.
NEW APPROACHES TO THE MEASUREMENT OF CHLOROPHYLL, RELATED PIGMENTS AND PRODUCTIVITY IN THE SEA Final Report, 1 Apr. 1986 - 31 May 1989
C. R. Booth and D. A. Keifer (University of Southern California, Los Angeles.) Sep. 1989 200 p
(Contract NAS7-969; SBIR-08.15-1315)
(NASA-CR-190879; NAS 1.26:190879; TR-89-2) Avail: CASI HC A09/MF A03

In the 1984 SBIR Call for Proposals, NASA solicited new methods to measure primary production and chlorophyll in the ocean. Biospherical Instruments Inc. responded to this call with a proposal first to study a variety of approaches to this problem. A second phase of research was then funded to pursue instrumentation to measure the sunlight stimulated naturally occurring fluorescence of chlorophyll in marine phytoplankton. The monitoring of global productivity, global fisheries resources, application of above surface-to-underwater optical communications systems, submarine detection applications, correlation, and calibration of remote sensing systems are but some of the reasons for developing inexpensive sensors to measure chlorophyll and productivity. Normally, productivity measurements are manpower and cost intensive and, with the exception of a very few expensive multiship research experiments, provide no contemporaneous data. We feel that the patented, simple sensors that we have designed will provide a cost effective method for large scale, synoptic, optical measurements in the ocean. This document is the final project report for a NASA sponsored SBIR Phase 2 effort to develop new methods for the measurements of primary production in the ocean. This project has been successfully completed, a U.S. patent was issued covering the methodology and sensors, and the first production run of instrumentation developed under this contract has sold out and been delivered. Author

N93-13700# National Science Foundation, Washington, DC.
DIVERSITY IN BIOLOGICAL RESEARCH
1992 9 p Workshop held in Washington, DC, 11-12 Jul. 1991
(NSF-92-19) Avail: CASI HC A02/MF A01

The Workshop on Diversity in Biological Research met in Washington, D.C. on July 11 and 12, 1991. The purpose of the workshop was to provide advice to the National Science Foundation (NSF) on how the number of underrepresented minorities in science and engineering can be increased and on what can be done to optimize professional growth of current minority scientists. A summary of the workshop discussions including the issues to be addressed, the goals to be achieved, and the strategies for reaching these goals is presented. L.R.R.

N93-13863# Iowa Univ., Iowa City. Dept. of Microbiology.
MOLECULAR BIOLOGY OF ANAEROBIC AROMATIC BIODEGRADATION Final Report, 15 Jun. 1989 - 14 Jun. 1992
Caroline S. Harwood 14 Aug. 1992 4 p
(Contract DAAL03-89-K-0121)
(AD-A255213; ARO-26576.3-LS) Avail: CASI HC A01/MF A01

Aromatic acids are intermediates in the biodegradation of structurally diverse aromatic compounds, including lignin monomers and environmental pollutants, by many metabolic types of anaerobic bacteria. They are also the starting compounds for central pathways of anaerobic benzene ring reduction and fission. We have identified and developed molecular tools that can be used to manipulate and clone genes for aromatic acid degradation from the bacterium, Rhodopseudomonas palustris. These tools have enabled us to identify genes specifying two enzymes that initiate the degradation of the compounds benzoate and 4-hydroxybenzoate, and we have also cloned, sequenced, and characterized a regulatory gene required for the expression of aromatic acid degradation enzymes. GRA

N93-13167*# National Aeronautics and Space Administration. Marshall Space Flight Center, Huntsville, AL.
A STUDY OF THE EFFECTS OF MICRO-GRAVITY ON SEED GERMINATION
Lynn Suzanne Klein (Washington Univ., Seattle.), Mark McKibben (Ohio Univ., Athens.), David A. Brain (Rice Univ., Houston, TX.), Theodore C. Johnson (Stanford Univ., CA.), and Konrad K. Dannenberg *In* NASA. Goddard Space Flight Center, The 1992 Shuttle Small Payloads Symposium Oct. 1992 p 85-94 (For primary document see N93-13158 03-12)
Avail: CASI HC A02/MF A03

52 AEROSPACE MEDICINE

Includes physiological factors; biological effects of radiation; and effects of weightlessness on man and animals.

N93-12566# Los Alamos National Lab., NM.
FUNCTIONAL MRI STUDIES OF HUMAN VISION ON A CLINICAL IMAGER
J. S. George, J. D. Lewine, C. J. Aine, D. vanHulsteyn, C. C. Wood, J. Sanders, E. Maclin, and J. W. Belliveau 1992 3 p Presented at the 14th Annual International Conference on IEEE Engineering in Medicine and Biology Society, Paris (France), 29 Oct. - 1 Nov. 1992
(Contract W-7405-eng-36)
(DE92-017448; LA-UR-92-2039; CONF-9210149-1) Avail: CASI HC A01/MF A01

During the past decade, Magnetic Resonance Imaging (MRI) has become the method of choice for imaging the anatomy of the human brain. Recently, Belliveau and colleagues have reported the use of echo planar magnetic resonance imaging (EPI) to image patterns of neural activity. Here, we report functional MR imaging in response to visual stimulation without the use of contrast agents, and without the extensive hardware modifications required for EPI. Regions of activity were observed near the expected locations of V1, V2, and possibly V3 and another active region was observed near the parietal-occipital sulcus on the superior surface of the cerebrum. These locations are consistent with sources observed in neuromagnetic studies of the human visual response. DOE

N93-12612# Federal Aviation Administration, Washington, DC. Office of Aviation Medicine.
THE IDENTIFICATION AND QUANTITATION OF TRIAMTERENE IN BLOOD AND URINE FROM A FATAL AIRCRAFT ACCIDENT Final Report
Vicky L. White, Dennis V. Canfield, and Jerry R. Hordinsky Jul. 1992 7 p
(AD-A254550; DOT/FAA/AM-92/23) Avail: CASI HC A02/MF A01

Triamterene, a diuretic drug used in combination with other drugs for the treatment of hypertension, was found in the blood and urine of a fatal aircraft accident victim. The extraction and identification of triamterene is difficult. It exhibits poor extraction efficiency using some standard base extraction procedures and the parent drug is unsuitable for analysis using gas chromatography. In this case a thin layer chromatography solvent system and high performance liquid chromatography were used to identify and quantitate triamterene in blood and urine. Triamterene is a strong absorber in the ultraviolet region and has an unusual UV spectrum, which simplifies the identification and quantitation of this substance by High Performance Liquid Chromatography. GRA

N93-12649# Armed Forces Radiobiology Research Inst., Bethesda, MD.
AFRRI REPORTS Report, Apr. - Jul. 1992
Jul. 1992 93 p Sponsored by DNA
(AD-A254581; AFRRI-SR92-16; AFRRI-SR92-17) Avail: CASI HC A05/MF A01

This report includes the following topics: short and long courses of ofloxacin therapy of Klebsiella pneumoniae sepsis following irradiation; possible 'accelerated striatal aging' induced by 56Fe heavy-particle irradiation--implications for manned space flights; modulation of mortality by tissue trauma and sepsis in mice after radiation injury; cytokine therapy in canine and primate models of radiation-induced marrow aplasia; comparison of behavioral and radioprotective effects of WR-2721 and WR-3689; energy transfer mechanisms in DNA--relationship to energy deposition in sub-microscopic volumes; role of interleukin 6 (IL-6) in protection from lethal irradiation and in endocrine responses to IL-1 and tumor necrosis factor; effects on enhancing hemopoietic reconstitution and increasing survival following exposure to ionizing radiation; and radioprotection of hematopoietic tissues in mice by lipoic acid. GRA

N93-12751# Air Force Inst. of Tech., Wright-Patterson AFB, OH.
PHYSIOLOGICAL EFFECTS OF POSITIVE PRESSURE VENTILATION M.S. Thesis
Dennis L. Oakes May 1992 80 p
(AD-A254809) Avail: CASI HC A05/MF A01

Respiratory insufficiency is caused by numerous physiological aberrations, some of which can be treated by mechanical ventilatory support. This paper presents the more common forms of mechanical ventilatory support with the adjuncts of PEEP and CPAP. Physiological effects of positive pressure ventilation are explained with emphasis on major organ systems. This paper concludes with a discussion of the clinical nurse specialist's role in providing care for the patient who is mechanically ventilated. GRA

N93-12756# Chemical Research and Development Center, Aberdeen Proving Ground, MD.
SILICON NEURON Final Report, Sep. 1991 - Jun. 1992
Richard G. Vanderbeek Aug. 1992 27 p
(AD-A255091; CRDEC-TR-400) Avail: CASI HC A03/MF A01

Many researchers have developed neural architectures based on extremely simplified models of neurons. Recently, researchers have developed an analog electronic model of a neuron that more accurately reproduces its biological counterpart. This electronic neuron was designed to emulate the ionic currents present in biological neurons. Based on this neural model, we designed and fabricated an eight input neuron on a 2mm by 2mm 40 pin VLSI (very large scale integrated) chip. This neuron had four excitatory and four inhibitory inputs and was approximately 330 microns by 330 microns in size. In this report I describe how the neuron operates, some of the specifics of our design, our testing procedures, and the results of our tests. GRA

N93-12905# Krug Life Sciences, Inc., San Antonio, TX.
COMPLEMENT PROTEINS AND DECOMPRESSION SICKNESS SUSCEPTIBILITY Final Report, Feb. 1990 - Feb. 1992
James T. Webb Jul. 1992 13 p
(Contract F33615-89-C-0603)
(AD-A254448; AL-TR-1992-0068) Avail: CASI HC A03/MF A01

Researcher's reports have indicated that decompression sickness (DCS) is mediated via activation of the complement system as a result of venous gas emboli (VGE) introduced during the ascent phase of a dive. Activation of complement leads to inflammation which can result in symptons similar to those of DCS. If the VGE-complement relationship theorized by researchers could be validated, tests for complement activation could predict susceptibility to DCS. GRA

N93-12945# Jefferson Medical Coll., Philadelphia, PA. Dept. of Medicine.
A CORE FACILITY FOR THE STUDY OF NEUROTOXINS OF BIOLOGICAL ORIGIN Final Report, 15 May 1986 - 15 Aug. 1991
Lance L. Simpson 15 Feb. 1992 185 p
(Contract DAMD17-86-C-6161; DA Proj. 3M1-61102-BS-12)
(AD-A254359) Avail: CASI HC A09/MF A02

Studies have been done on the variety of toxins that affect the nervous system. The toxins of major interest have been dendrotoxin, tetrotoxin, saxitoxin, botulinum neurotoxin, tetanus toxin and crotoxin. Experiments have been conducted mainly on three types of tissue preparations: (1) brain synaptosomes; (2) phrenic nerve-hemidiaphragm; and (3) cells grown in tissue culture, including neuroblastoma cells and adrenal medullary tumor cells. The major accomplishments have been: (1) isolation of homogeneous preparations of dendrotoxin; (2) partial characterization of dendrotoxin binding sites; (3) partial characterization of tetrotoxin and saxitoxin binding properties using channels inserted into lipid membranes; (4) further characterization of the intracellular actions of clostridial toxins; (5) development of binding assays for clostridial toxins; and (6) study of structure-function relationships in clostridial neurotoxins and snake neurotoxins. GRA

N93-13023*# National Aeronautics and Space Administration. Langley Research Center, Hampton, VA.
KATZ MODEL PREDICTION OF CAENORHABDITIS ELEGANS MUTAGENESIS ON STS-42
Francis A. Cucinotta, John W. Wilson, Robert Katz (Nebraska Univ., Lincoln.), and Gautam D. Badhwar (National Aeronautics and Space Administration. Lyndon B. Johnson Space Center, Houston, TX.) Nov. 1992 10 p
(RTOP 199-04-16-11)
(NASA-TM-4383; L-17090; NAS 1.15:4383) Avail: CASI HC A02/MF A01

Response parameters that describe the production of recessive lethal mutations in C. elegans from ionizing radiation are obtained with the Katz

track structure model. The authors used models of the space radiation environment and radiation transport to predict and discuss mutation rates for C. elegans on the IML-1 experiment aboard STS-42. Author

N93-13061*# Arkansas Univ., Pine Bluff.
THE NEUROCHEMICAL AND NEUROPHARMACOLOGICAL BASIS OF MOTION SICKNESS Final Technical Report, 15 Dec. 1988 - 31 Aug. 1990
C. A. Walker 31 Aug. 1990 12 p
(Grant NAG2-427)
(NASA-CR-190957; NAS 1.26:190957) Avail: CASI HC A03/MF A01

An apparatus suitable for producing motion sickness in laboratory animals and constructed at the university is herein described. The apparatus is a modified version of that previously described by Fox and Daunton. It consists of a 66-inch steel arm anchored at the center to a wooden platform and attached to a motor that makes the arm move in a see-saw fashion. At each end of the steel arm is mounted an aluminum disc that can be rotated by a motorized device. Detachable cages are mounted on each disc for animal holding. The animal can then be exposed to rotational motion by rotation of the aluminum disc, or to see-saw motion simultaneously (Cross-coupled). The apparatus is presently being used in our laboratory to study the neuropharmacological basis of motion sickness in the rat. The device can be adapted for use with other animal species by modifying the cage mounted on the aluminum discs. Author

N93-13116# Georgia State Univ., Atlanta.
NEUROCHEMICAL CONTROL OF CIRCADIAN RHYTHMS Final Report, 1 Apr. 1986 - 31 Oct. 1991
H. E. Albers 2 Sep. 1992 10 p
(Contract N00014-89-J-1640; DA Proj. RR0-4108)
(AD-A255054) Avail: CASI HC A02/MF A01

The central aim of this grant was to identify which of the various neurotransmitters found within the suprachiasmatic nucleus (SCN) are involved in synchronizing circadian rhythms with the day-night cycle. Our approach was to determine which SCN neurotransmitters are both influenced by light and capable of shifting the phase of circadian rhythms. We have investigated the possible role of a number of neurotransmitters in circadian control (e.g. vasopressin, GABA, neuropeptide Y). However, our primary focus has been on the circadian functions of vasoactive intestinal peptide (VIP), peptide histidine isoleucine (PHI), and gastrin releasing peptide (GRP). As a result of our work on VIP, PHI, and GRP, we have developed a working hypothesis of the neurochemical mechanisms underlying the synchronization of circadian rhythms with the day-night cycle. The hypothesis, called the ratio hypothesis, states that light communicated to the SCN via afferent pathways sets the ratio of VIP/PHI to GRP available for release from SCN neurons by altering the cellular levels of VIP/PHI mRNA and/or GRP mRNA, and that the ratio of VIP/PHI to GRP released from SCN neurons in response to light determines how the circadian clock is reset by light. GRA

N93-13252# Rice Univ., Houston, TX. Dept. of Electrical and Computer Engineering.
SIMULATION OF EXCITATORY/INHIBITORY INTERACTIONS IN SINGLE AUDITORY NEURONS Progress Report, 1 Apr. - 30 Sep. 1992
Don H. Johnson 30 Sep. 1992 1 p
(Contract N00014-92-J-1558)
(AD-A253614) Avail: CASI HC A02/MF A01

Characterization of the function of single neurons has become essential for developing advanced nodes for massively parallel computational structures. The lateral superior olive (LSO) is a nucleus located early in the ascending auditory pathway. Anatomically, each LSO neuron receives input from both ears; this fact led researchers to hypothesize that the LSO is involved in binaural hearing. Recordings from this nucleus not only confirm that LSO neurons are responsive to sounds presented in either ear, but in a particularly interesting and simple way: sounds presented in one ear excite an LSO neuron (increase its discharge rate) while sounds present at the other ear inhibit the neuron (discharge rate decreases). This mode of operation-the interaction of excitatory an inhibitory inputs to produce neural output-is the fundamental mode of neural processing. Thus, modeling LSO neurons represents a particularly clear-cut opportunity to understand basic neural processing. The approach taken in this research is to create anatomical and biophysical models of single LSO neurons and demand that the discharge patterns produced statistically match single-neuron recordings. With this strategy, this project seeks to (1) understand the neural mechanisms that underly basic LSO response patterns (transient chopping response to tone bursts and serial interspike interval correlations), (2) understand the transformation of fractal inputs by the LSO neuron, and (3) characterize excitatory/inhibitory interactions. GRA

N93-13449*# Colorado State Univ., Fort Collins. Dept. of Physiology.
EFFECTS OF SPACEFLIGHT ON THE PROLIFERATION OF JEJUNAL MUCOSAL CELLS Final Report, 1 Nov. 1989 - 30 Apr. 1991
Robert W. Phillips, C. L. Moeller, Heywood R. Sawyer, and K. L. Smirnov (Institute of Biomedical Problems, Moscow, USSR) 30 Apr. 1991 15 p
(Grant NAG2-610; Proj. K7-17)
(NASA-CR-191303; NAS 1.26:191303) Avail: CASI HC A03/MF A01

The purpose of this project was to test the hypothesis that the generalized, whole body decrease in synthetic activity due to microgravity conditions encountered during spaceflight would be demonstrable in cells and tissues characterized by a rapid rate of turnover. Jejunal mucosal cells were chosen as a model since these cells are among the most rapidly proliferating in the body. Accordingly, the percentage of mitotic cells present in the crypts of Lieberkuhn in each of 5 rats flown on the COSMOS 2044 mission were compared to the percentage of mitotic cells present in the crypts in rats included in each of 3 ground control groups (i.e., vivarium, synchronous and caudal-elevated). No significant difference (p greater than .05) was detected in mitotic indices between the flight and vivarium group. Although the ability of jejunal mucosal cells to divide by mitosis was not impaired in flight group, there was, however, a reduction in the length of villi and depth of crypts. The concommitant reduction in villus length and crypth depth in the flight group probably reflects changes in connective tissue components within the core of villi. Author

N93-13522# Los Alamos National Lab., NM.
A WEIGHTED ITERATIVE ALGORITHM FOR NEUROMAGNETIC IMAGING
I. Gorodnitsky, J. S. George, H. A. Schlitt, and P. S. Lewis 1992 6 p
Presented at the 14th Annual International IEEE in Medicine and Biology Society, Lyon, France, 2-4 Nov. 1992
(Contract W-7405-eng-36)
(DE92-040244; LA-UR-92-2698; CONF-921197-1) Avail: CASI HC A02/MF A01

The goal of neuromagnetic source reconstruction is high resolution 3-D mapping of the current distribution within the brain. However, the neuromagnetic inverse problem is ill-posed and typically underdetermined. The Moore-Penrose pseudoinverse provides a linear algebraic inverse calculation that simultaneously minimizes chisquare and the Euclidean norm of the component currents. Such 'minimum norm' reconstructions tend to produce diffuse and superficial current distributions because voxels nearer the sensor array can account for more power in the data with less current than deeper voxels. We describe an algorithm that overcomes the bias of minimum norm procedures toward superficial solutions by using weights chosen to compensate for the distance dependence of magnetic signal strength. We also apply a Bayesian weighting strategy in an iterative pseudoinverse computation, to address the bias of the linear estimator procedure toward diffuse solutions. This strategy produces a progressively more focal current distribution while accommodating distributed current sources, and appears to effectively reduce the problems associated with the under-determined linear system. DOE

N93-13941# Army Environmental Hygiene Agency, Aberdeen Proving Ground, MD.
PROCEDURES FOR THE DIAGNOSTIC DOSE RESISTANCE TEST KITS FOR MOSQUITOES, BODY LICE, AND BEETLE PESTS OF STORED PRODUCTS
Brian Zeichner 1 Aug. 1992 38 p
(AD-A255224; USAEHA-TG-189) Avail: CASI HC A03/MF A01

In military operations, the control of medically important insect pests (such a mosquitoes, body lice, and beetle pests of stored products) is essential in preventing disease and the loss of food. The use of effective insecticides will maximize the control success. Public health insect pests' resistance to insecticides has been documented from around the world. The possibility of resistance affecting control should be considered before any disease vector control operation. This technical guide assists

entomologists and preventive medicine specialists working under the supervision of an entomologist in using the diagnostic dose resistance test kits for several medically important insect pests. GRA

N93-14027# Aerospace Medical Research Labs., Brooks AFB, TX.
THERMAL STRESS IN US AIR FORCE OPERATIONS Final Report, 1 Apr. 1990 - 31 Mar. 1992
Sarah A. Nunneley Aug. 1992 6 p
(AD-A255785; AL-TP-1992-0034) Avail: CASI HC A02/MF A01

Topics include issues raised by deployment to the Persian Gulf, aircrew heat stress guidance, real-time heat stress monitors, and clothing effects on human thermoregulation. A bibliography is included. GRA

N93-14028# Aerospace Medical Research Labs., Brooks AFB, TX.
PHYSIOLOGICAL STRESS FROM CHEMICAL DEFENSE CLOTHING AND EQUIPMENT Final Report, 1 Apr. 1990 - 31 Mar. 1992
Sarah A. Nunneley Aug. 1992 7 p
(AD-A255786; AL-TP-1992-0033) Avail: CASI HC A02/MF A01

Topics include groundcrew heat stress in Chemical Defense Ensemble (CDE), validation of the heat-humidity index for work in CDE, evaluation of CDE made with various materials, groundcrew cooling devices, and aircrew guidelines. A bibliography is included. GRA

N93-14084# Air Force Inst. of Tech., Wright-Patterson AFB, OH. Foreign Aerospace Science and Technology Center.
POSTOPERATIVE HYPERBARIC OXYGEN TREATMENT OF PERIPHERAL NERVE DAMAGE
Zhao Dewei and Cui Zhenjiang 28 Aug. 1992 9 p Transl. into ENGLISH from Chung-Hua Wai Ko Tsa Chih (China), v. 29, no. 2, 1991 p 118-120
(AD-A255842; FASTC-ID(RS)T-0064-92) Avail: CASI HC A02/MF A01

This article reports on the results of 114 cases of surgical repair of peripheral nerve damage. Of these, 54 cases involving 65 nerves were given hyperbaric oxygen treatments following surgery. This article uses the other 60 cases as a control group, to explore the results of hyperbaric oxygen treatments for peripheral nerve damage. The excellent recovery rate for the hyperbaric oxygen treatment group was 89.2 percent and for the control group it was 73.2 percent (P less than 0.05). In observing the recovery of different treatment methods, the average excellent recovery rate for the hyperbaric oxygen was higher than that of the control group, and the nerve transplant group excellent recovery rate was raised even higher to 24.9 percent (P less than 0.05). In the results of the observation during the different types of recovery, in cases of emergency recovery., the two group treatment results were about the same. As time was extended, the excellent recovery rate of the hyperbaric oxygen treatment group tended to gradually increase over that of the control group. GRA

N93-14002*# Vanderbilt Univ., Nashville, TN. Dept. of Mechanical Engineering.
BONE LOSS AND HUMAN ADAPTATION TO LUNAR GRAVITY
T. S. Keller and A. M. Strauss *In* NASA. Johnson Space Center, The Second Conference on Lunar Bases and Space Activities of the 21st Century, Volume 2 Sep. 1992 p 569-576 (For primary document see N93-13972 03-91)
Avail: CASI HC A02/MF A03

53 BEHAVIORAL SCIENCES

Includes psychological factors; individual and group behavior; crew training and evaluation; and psychiatric research.

N93-12662# Dayton Univ., OH. Research Inst.
PERCEPTUAL DIMENSIONS OF VISUAL SCENES RELEVANT FOR SIMULATING LOW-ALTITUDE FLIGHT Interim Report, Jun. 1988 - Nov. 1991
James A. Kleiss Jun. 1992 52 p
(Contract F33615-90-C-0005)
(AD-A254645; AL-TR-1992-0011) Avail: CASI HC A04/MF A01

Multidimensional scaling was used to identify the features of real-world terrain that are salient to pilots during low-altitude flight. The subjects were pilots experienced flying in the Southwest United States (Experiment 1) and pilots experienced flying in Europe (Experiment 2). The stimuli were videotape segments (Dynamic Presentation) and still photographs (Static Presentation) depicting low-altitude flight over a variety of real-world terrains. Pilots rated pairs of terrains with respect to similarity of visual cues for low-altitude flight. Terrains were also rated on eight bipolar rating scales representing a variety of terrain characteristics thought to be of possible relevance to pilots. Similarity ratings were submitted to a multidimensional scaling analysis using the procedure ALSCAL. Two-dimensional solutions were deemed most appropriate in all cases. Bipolar ratings were submitted to a multiple regression analysis in which ratings on each scale were regressed over dimensional coordinates. Results of Experiment 1, Dynamic Presentation, revealed dimensions corresponding to the following: (1) terrain contour; and (2) object size and spacing. Results for Static Presentation were less interpretable suggesting the possibility of a single dimension capturing the presence/absence of global scene detail. In Experiment 2, results for both presentation modes replicated Experiment 1, Dynamic Presentation, although the fit of the data remained superior with Dynamic Presentation. Taken together, these results provide consistent evidence that pilots flying at low altitudes perceive variation in terrain contour and object size and spacing. GRA

N93-14020*# National Aeronautics and Space Administration. Lyndon B. Johnson Space Center, Houston, TX.
THE LUNAR COMMUNITY CHURCH: CONTRIBUTIONS TO LUNAR LIVING AND TO EVOLUTION OF ETHICAL AND SPIRITUAL THINKING
J. H. Allton *In its* The Second Conference on Lunar Bases and Space Activities of the 21st Century, Volume 2 Sep. 1992 p 703-705 (For primary document see N93-13972 03-91)
Avail: CASI HC A01/MF A03

54 MAN/SYSTEM TECHNOLOGY AND LIFE SUPPORT

Includes human engineering; biotechnology; and space suits and protective clothing.

For related information see also *16 Space Transportation.*

N93-12545# Anacapa Sciences, Inc., Fort Rucker, AL.
OPERATOR WORKLOAD PREDICTIONS FOR THE REVISED AH-64A WORKLOAD PREDICTION MODEL. VOLUME 2: APPENDIXES A THROUGH H Interim Report, Sep. 1988 - Dec. 1991
David B. Hamilton and Carl R. Bierbaum Jul. 1992 414 p
(Contract MDA903-87-C-0523)
(AD-A254939; ASI690-354-92-Vol-2; ARI-RN-92-62-Vol-2) Avail: CASI HC A18/MF A04

Under a previous contract, researchers used a composite scenario to conduct a comprehensive task analysis of the AH-64A attack mission. The analysis produced workload estimates and decision rules for developing an AH-64A workload prediction model. For this research, the task analysis/workload (TAWL) methodology was used to construct a workload prediction model. The TAWL Operator Simulation System (TOSS) was used to implement the model on an IBM-compatible microcomputer, and the original function and task analysis was refined to produce a more accurate simulation of crew task activity. In addition, the ordinal workload rating scales used in the original analysis were replaced with equal-interval scales. The predictions generated by the model constructed for this research indicate that under optimum conditions (1) neither the pilot nor the copilot/gunner experiences excessive workload, (2) the pilot has higher overall workload than the copilot/gunner in most mission segments, and (3) AH-64A workload is high relative to other Army aircraft that have been analyzed for workload. This model can be used as a baseline for analyzing future modifications to the aircraft. Volume 1 (ARI Research Note 92-61) of the report summarizes the results of the research, and contains a 5.25-inch floppy diskette with model data files. This report (Volume 2) contains the appendixes, which present the AH-64A mission/task/workload analysis, decision rules, and workload predictions. GRA

N93-12576# Mitre Corp., Bedford, MA.
MEASURES OF USER-SYSTEM INTERFACE EFFECTIVENESS: ASSESSMENT OF STRUCTURED JUDGMENT EVALUATION TECHNIQUES FOR GRAPHICAL, DIRECT-MANIPULATION STYLE INTERFACES
Donna L. Cuomo and Charles D. Bowen Jul. 1992 44 p
(AD-A254493; MTR-92B0000047V2) Avail: CASI HC A03/MF A01

The results of the second phase of the MITRE sponsored research project on developing measures of user-system interface effectiveness are presented. This project is concerned with developing methods and measures of user-system interface effectiveness for command and control systems with graphical, direct manipulation style interfaces. Due to the increased use of user interface prototyping during concept definition and demonstration/validation phases, the opportunity exists for human factors engineers to apply evaluation methodologies early enough in the life cycle to make an impact on system design. Understanding and improving user-system interface (USI) evaluation techniques is critical to this process. In 1986, Norman proposed a descriptive stages of user activity model of human-computer interaction (HCI). Hutchins, Hollin, and Norman (1986) proposed concepts of measures based on the model which would assess the directness of the engagements between the user and the interface at each stage of the model. This phase of our research program involved applying three USI evaluation techniques to a single interface, and assessing which, if any, provided information on the directness of engagement at each stage of Norman's model. We also classified the problem types identified according to the Smith and Mosier (1986) functional areas. The three techniques used were cognitive walkthrough, heuristic evaluation, and guidelines. GRA

N93-12609# Anacapa Sciences, Inc., Fort Rucker, AL.
HUMAN FACTORS RESEARCH IN AIRCREW PERFORMANCE AND TRAINING: 1986-1991 Final Summary Report, Oct. 1986 - Dec. 1991
D. M. McAnulty Jul. 1992 170 p
(Contract MDA903-87-C-0523)
(AD-A254455; ASI690-348-91; ARI-TR-954) Avail: CASI HC A08/MF A02

This report presents summary descriptions of the research performed by Anacapa Sciences, Inc., for the U.S. Army Research Institute for the Behavioral and Social Sciences Fort Rucker Field Unit. This effort was entitled Human Factors Research in Aircrew Performance and Training. From 9 Oct. 1986 - 31 Dec. 1991, Anacapa personnel worked on 42 research projects and 20 technical advisory services in emerging aviation systems design, manpower and personnel programs, aviator training, and aviation safety research. The report also describes research and development projects that were conducted under 17 subcontracts to Anacapa Sciences. These descriptions contain the following: (1) a background section that describes the rationale for the project and specifies the research objectives; (2) a research approach section that describes the tasks and activities required to meet the project objectives; and (3) a work completed section that may include research findings or, in the case of developmental activities, a description of the research products. GRA

N93-12712# Pacific Northwest Lab., Richland, WA.
HUMAN PERCEPTUAL DEFICITS AS FACTORS IN COMPUTER INTERFACE TEST AND EVALUATION
S. E. Bowser Jun. 1992 6 p Presented at the 1992 Industrial Ergonomics and Safety Conference, Denver, CO, 10-14 Jun. 1992
(Contract DE-AC06-76RL-01830)
(DE92-019124; PNL-SA-20626; CONF-9206237-1) Avail: CASI HC A02/MF A01

Issues related to testing and evaluating human computer interfaces are usually based on the machine rather than on the human portion of the computer interface. Perceptual characteristics of the expected user are rarely investigated, and interface designers ignore known population perceptual limitations. For these reasons, environmental impacts on the equipment will more likely be defined than will user perceptual characteristics. The investigation of user population characteristics is most often directed toward intellectual abilities and anthropometry. This problem is compounded by the fact that some deficits capabilities tend to be found in higher-than-overall population distribution in some user groups. The test and evaluation community can address the issue from two primary aspects. First, assessing user characteristics should be extended to include tests of perceptual capability. Secondly, interface designs should use multimode information coding. DOE

N93-12732# Naval Air Warfare Center, Patuxent River, MD. Aircraft Div.
INTEGRATION OF EXTERIOR LIGHTING SYSTEMS AND NIGHT VISION IMAGING SYSTEMS
S. Kinney and R. Simpson 3 Jun. 1992 42 p
(AD-A254826; NAWCADPAX-TM-92-37-SY) Avail: CASI HC A03/MF A01

The use of Night Vision Imaging Systems (NVIS) by military aviators has had a major impact on the design and integration philosophy of interior and exterior lighting systems. The integration of NVIS exterior lighting systems to meet the associated mission requirements is in the early stages of development. Operational performance and military specification requirements have not been updated and established. This technical memorandum presents information and lessons learned from development, test, and evaluation (DT and E) support of the A-12 program and development of test procedures to evaluate exterior lighting systems. During the DT and E support of the A-12 program, major exterior lighting issues had to be resolved. This evolution generated experience associated with exterior lighting and NVIS performance requirements. The information presented is not all inclusive but contains information to be used for updating exterior lighting Military Specifications requirements and test procedures. The additional integration requirements and design considerations will improve the utility of NVIS thus improving aircraft combat survivability and performance for various mission requirements. GRA

N93-12860# Catholic Univ. of America, Washington, DC. Cognitive Science Lab.
ADAPTIVE AUTOMATION AND HUMAN PERFORMANCE. 3: EFFECTS OF PRACTICE ON THE BENEFITS AND COSTS OF AUTOMATION SHIFTS Final Report
Raja Parasuraman, Brian Hilburn, Robert Molloy, and Indramani Singh Oct. 1991 42 p Sponsored by Naval Air Warfare Center
(AD-A254381; NAWCADWAR-92037-60) Avail: CASI HC A03/MF A01

Adaptive automation, or adaptive function allocation, is thought to maximize the benefits associated with cockpit automation while maintaining pilot involvement, enhancing situation awareness, and regulating workload. These claims have not been tested empirically. The present study examined the effects of short-cycle adaptive automation and practice on performance-of flight-related functions in a multi-task environment. Twenty four non pilot subjects were tested on a PC-based flight-simulation task that included three primary flight functions -- tracking, monitoring, and fuel management. Each function could be automated or performed manually. The results provide preliminary evidence that dynamic automation shifts over short cycles, of the type likely in adaptive systems, benefit performance of flight-related tasks, with no evidence of costs to performance following the return to manual control. Benefits are realized despite the added workload of supervisory control of automated functions. However, training procedures other than simple practice may be necessary to maximize and maintain the performance benefits associated with adaptive automation. GRA

N93-12960# Army Research Inst. of Environmental Medicine, Natick, MA.
EFFECT OF PROTECTIVE CLOTHING ENSEMBLES ON ARTILLERY BATTERY CREW PERFORMANCE Final Report
Patricia C. Szlyk, David M. Caretti, Ingrid V. Sils, Orest Zubal, and Jim A. Faughn 17 Jul. 1992 41 p
(AD-A254327; USARIEM-T8-92) Avail: CASI HC A03/MF A01

Performance of three 9-man crews was evaluated while firing 90 rounds in a safe and expedient manner, with swabbing of the breech after each round. Each 9-man crew fired on three non-consecutive days; the independent variable among days was the MOPP level worn (BDU vs MOPP 4 vs MOPP 4 with cooling). All 90 rounds were fired by all three crews when wearing BDU. Despite similar climatic conditions, 2 of the 3 MOPP 4 iterations were prematurely terminated due to high rectal temperatures and/or presyncopal symptoms. During the MOPP 4 trial average time to fire one round increased from the first to the second 45 rounds. In contrast crews wearing BDU did not increase firing time. When cooling was added to the MOPP 4 configuration (cool MOPP), all iterations were completed and performance was enhanced despite warmer

environmental conditions. As in the BDU trials, the time to fire a single round was unchanged over time, and was significantly less than that for MOPP 4. Significantly higher sweat losses in MOPP 4 were reflected in the crew's enhanced perception of sweatiness, thirst, hyperthermia, and headache. Full encapsulation of crew members in chemical protective gear imposed a heat stress which reduced work tolerance and performance, but these decrements were lessened by microclimate cooling to the thorax and face. GRA

N93-12966*# Alabama Univ., Huntsville. Consortium for the Space Life Sciences.

MICROBIOLOGICAL METHODS FOR THE WATER RECOVERY SYSTEMS TEST, REVISION 1.1 Final Report

Tim Rhoads, M. V. Kilgore, Jr., and A. T. Mikell, Jr. 23 Feb. 1990 116 p Revised

(Contract NAS8-36955)

(NASA-CR-184390; NAS 1.26:184390; UAH-835-Rev-1.1) Avail: CASI HC A06/MF A02

Current microbiological parameters specified to verify microbiological quality of Space Station Freedom water quality include the enumeration of total bacteria, anaerobes, aerobes, yeasts and molds, enteric bacteria, gram positives, gram negatives, and E. coli. In addition, other parameters have been identified as necessary to support the Water Recovery Test activities to be conducted at the NASA/MSFC later this year. These other parameters include aerotolerant eutrophic mesophiles, legionellae, and an additional method for heterotrophic bacteria. If inter-laboratory data are to be compared to evaluate quality, analytical methods must be eliminated as a variable. Therefore, each participating laboratory must utilize the same analytical methods and procedures. Without this standardization, data can be neither compared nor validated between laboratories. Multiple laboratory participation represents a conservative approach to insure quality and completeness of data. Invariably, sample loss will occur in transport and analyses. Natural variance is a reality on any test of this magnitude and is further enhanced because biological entities, capable of growth and death, are specific parameters of interest. The large variation due to the participation of human test subjects has been noted with previous testing. The resultant data might be dismissed as 'out of control' unless intra-laboratory control is included as part of the method or if participating laboratories are not available for verification. The purpose of this document is to provide standardized laboratory procedures for the enumeration of certain microorganisms in water and wastewater specific to the water recovery systems test. The document consists of ten separate cultural methods and one direct count procedure. It is not intended nor is it implied to be a complete microbiological methods manual. Author

N93-12983# HydroQual, Inc., Mahwah, NJ.

ULTRAVIOLET DISINFECTION TECHNOLOGY ASSESSMENT

O. Karl Scheible, Ashok Gupta, and Dennis Scannell Sep. 1992 108 p

(Contract EPA-68-08-0023)

(PB92-222868; EPA/832/R-92/004) Avail: CASI HC A06/MF A02

Ultraviolet (UV) disinfection systems are being widely considered for application to treated wastewaters, for both new plants and retrofitting existing plants in lieu of conventional chlorination facilities. The technology is relatively new, with most systems installed over the past three to four years. The report presents an assessment of the status of the technology relative to the type and size of UV facilities that are currently operating, and discusses the trends in system design, configuration, and operations. The design and operation of selected plants are reviewed; this information and current practices are then summarized to give a perspective of key considerations that should be incorporated into the design of UV facilities. Finally, a review of costs associated with the construction and operation of UV systems is presented, based on data generated from this assessment. GRA

N93-12990*# Spectra Research Systems, Inc., Huntsville, AL. Systems Technology Group.

ECLSS EVOLUTION: ADVANCED INSTRUMENTATION INTERFACE REQUIREMENTS. VOLUME 3: APPENDIX C

3 Sep. 1991 40 p

(Contract NAS8-38781)

(NASA-CR-184367; NAS 1.26:184367; SRS/STG-TR92-01-Vol-3-App-C) Avail: CASI HC A03/MF A01

An Advanced ECLSS (Environmental Control and Life Support System) Technology Interfaces Database was developed primarily to provide ECLSS analysts with a centralized and portable source of ECLSS technologies interface requirements data. The database contains 20 technologies which were previously identified in the MDSSC ECLSS Technologies database. The primary interfaces of interest in this database are fluid, electrical, data/control interfaces, and resupply requirements. Each record contains fields describing the function and operation of the technology. Fields include: an interface diagram, description applicable design points and operating ranges, and an explaination of data, as required. A complete set of data was entered for six of the twenty components including Solid Amine Water Desorbed (SAWD), Thermoelectric Integrated Membrane Evaporation System (TIMES), Electrochemical Carbon Dioxide Concentrator (EDC), Solid Polymer Electrolysis (SPE), Static Feed Electrolysis (SFE), and BOSCH. Additional data was collected for Reverse Osmosis Water Reclaimation-Potable (ROWRP), Reverse Osmosis Water Reclaimation-Hygiene (ROWRH), Static Feed Solid Polymer Electrolyte (SFSPE), Trace Contaminant Control System (TCCS), and Multifiltration Water Reclamation - Hygiene (MFWRH). A summary of the database contents is presented in this report. Author

N93-13450*# Analytics, Inc., Willow Grove, PA.

OCULAR ATTENTION-SENSING INTERFACE SYSTEM Final Technical Report, 1977

Allen Zaklad, Floyd A. Glenn, III, Helene P. Iavecchia, and James M. Stokes Dec. 1986 76 p

(Contract NAS7-932; SBIR-06.05-4100)

(NASA-CR-190884; NAS 1.26:190884) Avail: CASI HC A05/MF A01

The purpose of the research was to develop an innovative human-computer interface based on eye movement and voice control. By eliminating a manual interface (keyboard, joystick, etc.), OASIS provides a control mechanism that is natural, efficient, accurate, and low in workload. Author

N93-13464 Institute of Sound and Vibration Research, Southampton (England).

DESIGN GUIDE FOR THE ERGONOMIC ASPECTS OF HELICOPTER CREW SEATING

A. J. Messenger, R. Stratford, and M. J. Griffin Oct. 1992 60 p

(ISVR-TR-209) Copyright Avail: CASI HC A04/MF A01

This Design Guide provides an aid to the design of new helicopter crew seats, the improvement of existing seats and the comparison of alternative seats. Methods of measuring seat dimensions, angles and contouring are defined. Recommendations for the dimensions, angles and contouring of the seat pan, backrest, armrests and headrest are based on the principle of matching seat dimensions to the relevant dimensions of the user population. The dimensions suggested are appropriate for British males and females aged between 19 and 45 years. The Design Guide has been formulated so that the suggested dimensions can be replaced by those appropriate to a different user population. Cushion material, cushion coverings, routing of harnessing, the positioning of seat controls, eye position, the operation of controls and ingress and egress from the seat are also considered. The Design Guide also contains recommendations for the subjective testing of seat comfort and the dynamic testing of the transmission of vibration through helicopter crew seats. Author

N93-13486 Minnesota Univ., Minneapolis.

DESIGN, CONSTRUCTION, AND CONTROL OF A TWO DEGREE-OF-FREEDOM ELECTRIC DIRECT-DRIVE HUMAN POWER AMPLIFIER Ph.D. Thesis

Ming-guo Her 1991 130 p

Avail: Univ. Microfilms Order No. DA9212057

This thesis describes the design, construction, and control of a class of computer controlled human-assisted robotic systems. This robotic system is a robot worn by a human to increase human mechanical ability. The system is referred to as an extender since it extends the human's mechanical ability to maneuvering objects. Commands are transferred to the extender via the contact forces between the human and the extender, eliminating the need for joystick, push-button or keyboard to transfer such commands. Instead, the operator becomes an integral part of the extender while executing the task. When the worker uses the extender to touch and manipulate a load, the extender transfers to her/his arm, and natural feedback, a scaled-down value of the actual load weight which the extender

is manipulating: the human 'feels' the load weight in the manipulations. An experimental electric two-degree-of-freedom direct-drive extender has been designed and constructed to this Ph.D. study. With high-torque/wide-bandwidth actuators, and the direct-drive architecture, this experimental extender can track the human arm maneuvers to the extent that the human feels minimum restriction in his motions. The extender is interfaced with an 486/25 IBM AT compatible computer for control. The human and environment dynamics play significant roles in the performance and stability of an extender. Modelling the human environment dynamics inside a control loop were performed first. Then expressions for the performance and stability were derived based on the human and environment dynamic models. The stability analysis, and the performance specifications lead to the controller design methods. The dynamic models, the control technique, and the trade-off between the stability and performance specification were verified experimentally by using the prototype 2 degree of freedom extender. Dissert. Abstr.

N93-13571*# National Aeronautics and Space Administration. Lyndon B. Johnson Space Center, Houston, TX.

A HEALTH CARE SYSTEM FOR THE SPACE STATION

[1992] 15 p Prepared in cooperation with Krug International, Houston, TX LIMITED REPRODUCIBILITY: More than 20% of this document may be affected by color photographs Original contains color illustrations

(NASA-TM-108093; NAS 1.15:108093) Avail: CASI HC A03/MF A01; 15 functional color pages

Life science will be one of the pacing technologies for long duration manned spaceflight. The ability to effectively deliver state-of-the-art inflight medical care will have a major impact on crew health and mission success. The future Space Station crews will participate in missions of extended duration with limited capability for emergency return. This factor alone places great responsibility on program designers to ensure the health, safety, and well-being of the crews. The Health Maintenance Facility (HMF) under development at the Johnson Space Center is described. L.R.R.

N93-13692*# National Aeronautics and Space Administration, Washington, DC.

SUITED FOR SPACEWALKING: A TEACHER'S GUIDE WITH ACTIVITIES

Gregory L. Vogt, ed. (National Aeronautics and Space Administration. Lyndon B. Johnson Space Center, Houston, TX.) and Cheryl A. Manning, ed. Mar. 1992 65 p

(NASA-EP-279; NAS 1.19:279) Avail: CASI HC A04/MF A01

This publication is an activity guide for teachers on spacesuits and spacewalking. It uses the intensive interest many children have in space exploration as a launching point for hands-on-opportunities. The guide begins with brief discussions of the space environment, the history of space walking, the Space Shuttle spacesuit, and working in space. These are followed by a series of activities that enable children to explore the space environment as well as the science and technology behind the functions of spacesuits. The activities are not rated for specific grade levels because they can be adapted for students of many ages. The guide concludes with a brief glossary as well as references and resources. R.L.B.

N93-13717*# Arizona Univ., Tucson. Aerospace and Mechanical Engineering.

THERMAL CONTROL SYSTEMS FOR LOW-TEMPERATURE HEAT REJECTION ON A LUNAR BASE Progress Report

K. R. Sridhar and Matthias Gottmann Oct. 1992 63 p

(Grant NAG5-1572)

(NASA-CR-191286; NAS 1.26:191286) Avail: CASI HC A04/MF A01

In this report, Rankine-cycle heat pumps and absorption heat pumps (ammonia-water and lithium bromide-water) have been analyzed and optimized for a lunar base cooling load of 100 kW. For the Rankine cycle, a search of several commonly used commercial refrigerants provided R11 and R717 as possible working fluids. Hence, the Rankine-cycle analysis has been performed for both R11 and R717. Two different configurations were considered for the system--one in which the heat pump is directly connected to the rejection loop and another in which a heat exchanger connects the heat pump to the rejection loop. For a marginal increase in mass, the decoupling of the rejection loop and the radiator from the heat pump provides greater reliability of the system and better control. Hence, the decoupled system is the configuration of choice. The optimal TCS mass for a 100 kW cooling load at 270 K was 5940 kg at a radiator temperature of 362 K. R11 was the working fluid in the heat pump, and R717 was the transport fluid in the rejection loop. Two TCS's based on an absorption-cycle heat pump were considered, one with an ammonia-water mixture and the other with a lithium bromide-water mixture as the working fluid. A complete cycle analysis was performed for these systems. The system components were approximated as heat exchangers with no internal pressure drop for the mass estimate. This simple approach underpredicts the mass of the systems, but is a good 'optimistic' first approximation to the TCS mass in the absence of reliable component mass data. The mass estimates of the two systems reveal that, in spite of this optimistic estimate, the absorption heat pumps are not competitive with the Rankine-cycle heat pumps. Future work at the systems level will involve similar analyses for the Brayton- and Stirling-cycle heat pumps. The analyses will also consider the operation of the pump under partial-load conditions. On the component level, a capillary evaporator will be designed, built, and tested in order to investigate its suitability in lunar base TCS and microgravity two-phase applications. Author

N93-13874# Aerospace Medical Research Labs., Wright-Patterson AFB, OH.

HYBRID 2 AND HYBRID 3 DUMMY NECK PROPERTIES FOR COMPUTER MODELING Interim Report, Jan. 1991 - Feb. 1992

Eric K. Spittle, Donna J. Miller, Buford W. Shipley, Jr., and Ints Kaleps Feb. 1992 138 p

(AF Proj. 7231)

(AD-A255544; AL-TR-1992-0049) Avail: CASI HC A07/MF A02

Existing rigid body dynamics and finite element computer codes do not have adequate databases for manikin neck structures to properly model head/neck system dynamics occurring in crash or ejection testing. This report describes measured static stiffness and dynamic damping and stiffness characteristics of the Hybrid 2 and Hybrid 3 manikin necks and uses these data to improve the current manikin neck data sets of the Articulated Total Body (ATB) model and the Head Spine Model (HSM). The Hybrid 2 and Hybrid 3 manikin necks are used extensively throughout the automotive industry, the Department of Transportation, and the Department of Defense for safety testing. Static stiffness characteristics were determined from loading and unloading the necks in flexion, extension, and lateral bending. Dynamic damping and stiffness characteristics were determined from abrupt deceleration tests in the 'X' and 'Y' directions. Current computer data sets for the Hybrid 2 and Hybrid 3 necks were compared to the experimental dynamic results to determine inconsistencies. The data sets were, then revised using the results obtained experimentally. Finally, the new data sets were compared to the experimental dynamic results to show improvements. GRA

N93-13909 Oxford Univ. (England).

FORMAL ASPECTS OF HUMAN-COMPUTER INTERACTION Ph.D. Thesis

Gregory D. Abowd 1991 246 p

Avail: Univ. Microfilms Order No. BRD-96182

A constructive application of formal methods to the study of human-computer interaction is addressed. Specifically, we are interested in promoting a principled approach to the analysis and design of interactive systems that will accompany existing heuristic techniques. Previous formal approaches have concentrated on general and abstract mathematical models of interactive systems, proving that psychologically valid principles of interaction can be expressed in a language suitable for computation. These abstract models, however, are too far removed from an actual design practice which is strongly influenced by common sense and liable to break down in the face of complexity. Our efforts are focussed toward retaining the mathematical grounding of previous formalisms while providing additional insight and direction for design practice. We introduce a unifying framework for the informal description of a user, a system, and the interface that sits between them. This interaction framework provides the context for our research and motivates the properties of interaction that we wish to formalize. We adopt the view of an interactive system as a collection of agents based on the stimulus-response model. We provide a mathematical model of the agent capable of expressing interactive properties relating the goals of interaction with the visible consequences of that interaction. We also provide a language for agents which allows a natural expression of an agent's internal state-based behavior and its external event-based behavior.

We contribute further to practical design issues by introducing templates to relate a task analysis to a specification of a system to support the tasks and an interface to adequately portray that functionality to the user. Finally, we initiate the formal investigation of multiagent architectures. This concludes the mapping of properties on abstract models of interactive systems down to properties on more implementation-based models. Dissert. Abstr.

N93-14090# Army Aeromedical Research Lab., Fort Rucker, AL.
THE RELATIONSHIP BETWEEN ENVIRONMENTAL CONDITIONS AND UH-60 COCKPIT TEMPERATURE Final Report, May 1990 - May 1992
Robert Thornton and Frank Guardiani Jul. 1992 51 p
(AD-A255918; USAARL-92-25) Avail: CASI HC A04/MF A01

Data have been collected in the UH-60 helicopter in various flight configurations (hover, contour (250 ft), and cruise (650 ft)) to relate the thermal conditions found in the cockpit to data available to commanders and researchers in the field. These have been used to develop equations for use in future thermal modeling studies and to provide information to increase the fidelity of helicopter environmental simulations. GRA

N93-13991*# National Aeronautics and Space Administration. Langley Research Center, Hampton, VA.
THE ENVIRONMENTAL CONTROL AND LIFE-SUPPORT SYSTEM FOR A LUNAR BASE: WHAT DRIVES ITS DESIGN
Warren D. Hypes (Bionetics Corp., Hampton, VA.) and John B. Hall, Jr. *In* NASA. Johnson Space Center, The Second Conference on Lunar Bases and Space Activities of the 21st Century, Volume 2 Sep. 1992 p 503-511 (For primary document see N93-13972 03-91)
Avail: CASI HC A02/MF A03

N93-13992*# Institute of Ecotechnics, London (England).
LIFE SYSTEMS FOR A LUNAR BASE
Mark Nelson, Philip B. Hawes (Sarbid Ltd., Oracle, AZ.), and Margret Augustine (Space Biospheres Ventures, Oracle, AZ.) *In* NASA. Johnson Space Center, The Second Conference on Lunar Bases and Space Activities of the 21st Century, Volume 2 Sep. 1992 p 513-518 (For primary document see N93-13972 03-91)
Avail: CASI HC A02/MF A03

N93-13993*# Walt Disney World Co., Lake Buena Vista, FL. EPCOT Center.
LUNAR BASE CELSS: A BIOREGENERATIVE APPROACH
G. W. Easterwood, J. J. Street (Florida Univ., Gainesville.), J. B. Sartain (Florida Univ., Gainesville.), D. H. Hubbell (Florida Univ., Gainesville.), and H. A. Robitaille *In* NASA. Johnson Space Center, The Second Conference on Lunar Bases and Space Activities of the 21st Century, Volume 2 Sep. 1992 p 519-523 (For primary document see N93-13972 03-91)
Avail: CASI HC A01/MF A03

N93-13994*# National Aeronautics and Space Administration. Lyndon B. Johnson Space Center, Houston, TX.
CROP GROWTH AND ASSOCIATED LIFE SUPPORT FOR A LUNAR FARM
Tyler Volk (New York Univ., New York.) and Hatice Cullingford *In its* The Second Conference on Lunar Bases and Space Activities of the 21st Century, Volume 2 Sep. 1992 p 525-530 (For primary document see N93-13972 03-91)
Avail: CASI HC A02/MF A03

N93-13996*# National Aeronautics and Space Administration. John F. Kennedy Space Center, Cocoa Beach, FL.
ENGINEERING VERIFICATION OF THE BIOMASS PRODUCTION CHAMBER
R. P. Prince, W. M. Knott, III, J. C. Sager, and J. D. Jones (National Aeronautics and Space Administration. Goddard Space Flight Center, Greenbelt, MD.) *In* NASA. Johnson Space Center, The Second Conference on Lunar Bases and Space Activities of the 21st Century, Volume 2 Sep. 1992 p 537-542 (For primary document see N93-13972 03-91)
Avail: CASI HC A02/MF A03

N93-13997*# National Aeronautics and Space Administration. John F. Kennedy Space Center, Cocoa Beach, FL.
SCENARIOS FOR OPTIMIZING POTATO PRODUCTIVITY IN A LUNAR CELSS
R. M. Wheeler, R. C. Morrow (Wisconsin Univ., Madison.), T. W. Tibbitts (Wisconsin Univ., Madison.), and R. J. Bula (Wisconsin Univ., Madison.) *In* NASA. Johnson Space Center, The Second Conference on Lunar Bases and Space Activities of the 21st Century, Volume 2 Sep. 1992 p 543-546 (For primary document see N93-13972 03-91)
Avail: CASI HC A01/MF A03

N93-13998*# Wisconsin Univ., Madison. Center for Space Automation and Robotics.
POTENTIAL OF DERIVED LUNAR VOLATILES FOR LIFE SUPPORT
R. J. Bula, L. J. Wittenberg, T. W. Tibbitts, and G. L. Kulcinski *In* NASA. Johnson Space Center, The Second Conference on Lunar Bases and Space Activities of the 21st Century, Volume 2 Sep. 1992 p 547-550 (For primary document see N93-13972 03-91)
Avail: CASI HC A01/MF A03

N93-13999*# National Aeronautics and Space Administration. Lyndon B. Johnson Space Center, Houston, TX.
TECHNOLOGY DEVELOPMENT FOR LUNAR BASE WATER RECYCLING
John R. Schultz (Krug International, Houston, TX.) and Richard L. Sauer *In its* The Second Conference on Lunar Bases and Space Activities of the 21st Century, Volume 2 Sep. 1992 p 551-557 (For primary document see N93-13972 03-91)
Avail: CASI HC A02/MF A03

N93-14000*# North Dakota Univ., Grand Forks. Energy and Environmental Research Center.
PLASMA REACTOR WASTE MANAGEMENT SYSTEMS
Robert O. Ness, Jr., John R. Rindt, and Sumitra R. Ness *In* NASA. Johnson Space Center, The Second Conference on Lunar Bases and Space Activities of the 21st Century, Volume 2 Sep. 1992 p 559-562 (For primary document see N93-13972 03-91)
Avail: CASI HC A01/MF A03

N93-14001*# North Dakota Univ., Grand Forks.
DISTRIBUTION OF HUMAN WASTE SAMPLES IN RELATION TO SIZING WASTE PROCESSING IN SPACE
Dick Parker and S. K. Gallagher (Agricultural Research Service, Grand Forks, ND.) *In* NASA. Johnson Space Center, The Second Conference on Lunar Bases and Space Activities of the 21st Century, Volume 2 Sep. 1992 p 563-568 (For primary document see N93-13972 03-91)
Avail: CASI HC A02/MF A03

N93-14003*# National Aeronautics and Space Administration. Langley Research Center, Hampton, VA.
CONCEPTUAL DESIGN OF A LUNAR BASE THERMAL CONTROL SYSTEM
Lisa C. Simonsen, Marc J. DeBarro (Rockwell International Corp., Downey, CA.), and Jeffery T. Farmer *In* NASA. Johnson Space Center, The Second Conference on Lunar Bases and Space Activities of the 21st Century, Volume 2 Sep. 1992 p 579-591 (For primary document see N93-13972 03-91)
Avail: CASI HC A03/MF A03

N93-14013*# Lockheed Engineering and Sciences Co., Houston, TX.
OCCUPATIONAL ERGONOMICS IN SPACE
J. Stramler *In* NASA. Johnson Space Center, The Second Conference on Lunar Bases and Space Activities of the 21st Century, Volume 2 Sep. 1992 p 659-663 (For primary document see N93-13972 03-91)
Avail: CASI HC A01/MF A03

N93-14014*# Schmitt (Harrison H.), Albuquerque, NM.
THE REAL WORLD AND LUNAR BASE ACTIVATION SCENARIOS
Harrison H. Schmitt *In* NASA. Johnson Space Center, The Second Conference on Lunar Bases and Space Activities of the 21st Century, Volume 2 Sep. 1992 p 667-671 (For primary document see N93-13972

03-91)
Avail: CASI HC A01/MF A03

N93-14018*# North Dakota Univ., Grand Forks. Dept. of Space Studies.
THE PROVINCE AND HERITAGE OF MANKIND RECONSIDERED: A NEW BEGINNING
J. I. Gabrynowicz *In* NASA. Johnson Space Center, The Second Conference on Lunar Bases and Space Activities of the 21st Century, Volume 2 Sep. 1992 p 691-695 (For primary document see N93-13972 03-91)
Avail: CASI HC A01/MF A03

55 SPACE BIOLOGY

Includes exobiology; planetary biology; and extraterrestrial life.

No abstracts in this category.

59 MATHEMATICAL AND COMPUTER SCIENCES (GENERAL)

N93-13438# National Science Foundation, Washington, DC. Div. of Mathematical Sciences.
SUMMARY OF AWARDS: APPLIED MATHEMATICS. FISCAL YEAR 1991
1991 83 p
(NSF-92-38) Avail: CASI HC A05/MF A01

The National Science Foundation, Directorate for Mathematical and Physical Sciences, Division of Mathematical Sciences (DMS) fosters the creation and development of mathematical ideas, methods, and techniques and promotes their use in improving our understanding of physical, biological, engineering, and social phenomena. DMS's support for significant research in the mathematical sciences serves to ensure continuing vitality and long range scientific health of the discipline. DMS fashions its program of research support activities around awards to single investigators or teams of investigators following the merit review of research proposals submitted by these investigators. There are eight disciplinary research programs within the Division of Mathematical Sciences: Classical Analysis, Modern Analysis, Geometric Analysis, Topology and Foundations, Algebra and Number Theory, Applied Mathematics, Statistics and Probability, and Computational Mathematics. These programs recommend awards for the support of research programs of high quality. Award listings do not include abstracts. They only list titles. R.L.B.

60 COMPUTER OPERATIONS AND HARDWARE

Includes hardware for computer graphics, firmware, and data processing.

For components see *33 Electronics and Electrical Engineering.*

N93-12641# Carnegie-Mellon Univ., Pittsburgh, PA. School of Computer Science.
PROGRAM STRUCTURE AS A BASIS FOR THE PARALLELIZATION OF GLOBAL COMPILER OPTIMIZATIONS Ph.D. Thesis
Angelika Zobel 15 May 1992 144 p
(Contract MDA903-90-C-0035; ARPA Order 7330)
(AD-A254554; CMU-CS-92-137) Avail: CASI HC A07/MF A02

Optimizing compilers can produce very efficient code but incur a high compilation cost. Because interactions between arbitrary points in a program are possible, global compiler organizations are inherently expensive and in general there is no easy way to partition the data processed during global compiler optimizations into independent components. This thesis explores how program structure can be used to provide a basis for the parallelization for global compiler optimizations. Two concepts to obtain data parallelism in global compiler optimizations are described. The first concept uses program structure explicitly for the parallelization. This is demonstrated by the program structure analytically to establish data partitioning points. The effectiveness of this concept is demonstrated in the parallelization of global register allocation via optimal coloring of a graph denoting register conflicts, an NP complete problem. A model for global register allocation in which program structure is used to analyze a register conflict graph is presented. The purpose of this analysis is to detect clique separators that partition a conflict graph into independent components that can be colored independently and combined to an overall coloring by renaming. Properties of live ranges in loops and conditionals are linked to characteristics of the conflict graph. GRA

N93-12707# Texas Univ., Austin.
TESTING AND FAULT-TOLERANT DESIGN TECHNIQUES FOR ADVANCED DIGITAL ARCHITECTURES Final Technical Report, 1 Jan. 1989 - 31 Dec. 1991
Miroslaw Malek and M. R. Mercer 31 Dec. 1991 10 p
(Contract N00014-86-K-0554)
(AD-A255013) Avail: CASI HC A02/MF A01

We have continued working on our new concept, topological testing, and we have demonstrated several applications in the area of multiprocessor testing. Topological testing uses graph theoretic optimization methods, such as the Traveling Salesman Problem, the Chinese Postman Problem, coloring, path covering, and partitioning to minimize the test time. The topological testing techniques can be applied to test a system's behavior and its organization at each level of the system's hierarchy: circuit, logic, register transfer, instruction, and processor-memory-switch levels. Specifically, the topological testing approach was demonstrated by developing tests for the multistage interconnection network and the hypercube network. We have also developed optimal test sets for mesh networks and further increased a test coverage by including solutions for priority circuits. GRA

N93-12823# Argonne National Lab., IL.
MEMORY ACCESS IN SHARED VIRTUAL MEMORY
R. Berrendorf (Forschungszentrum Juelich G.m.b.H., Germany) 1992 13 p Presented at the CONPAR 1992: International Conference on Parallel Processing, Lyon, France, 1-4 Sep. 1992
(Contract W-31-109-eng-38)
(DE92-019594; ANL/CP-76324; CONF-9209180-1) Avail: CASI HC A03/MF A01

Shared virtual memory (SVM) is a virtual memory layer with a single address space on top of a distributed real memory on parallel computers. We examine the behavior and performance of SVM running a parallel program with medium-grained, loop-level parallelism on top of it. A simulator for the underlying parallel architecture can be used to examine the behavior of SVM more deeply. The influence of several parameters, such as the number of processors, page size, cold or warm start, and restricted page replication, is studied. DOE

N93-12886# Westinghouse Savannah River Co., Aiken, SC.
REVIEWS OF COMPUTING TECHNOLOGY: FIBER DISTRIBUTED DATA INTERFACE
A. J. Johnson 1 Apr. 1992 36 p Revised
(Contract DE-AC09-89SR-18035)
(DE92-019927; WSRC-IM-90-83-6-Rev) Avail: CASI HC A03/MF A01

This technology report describes Fiber Distributed Data Interface (FDDI) as a technology, looks at the applications of this technology, examines the current economics of using it, and describe activities and plans by the Information Resource Management Department to implement this technology at the Savannah River Site. DOE

N93-13431# National Science Foundation, Washington, DC. Div. of Microelectronic Information Processing Systems.
SUMMARY OF AWARDS. FISCAL YEAR 1991
1991 89 p
(NSF-92-36) Avail: CASI HC A05/MF A01

This is a Summary of Awards, Fiscal Year 1991, of the National Science Foundation Division of Microelectronic Information Processing Systems of the Directorate for Computer and Information Science and Engineering. The listing of awards given includes informative abstracts which elaborate

on the basic award. Awards are grouped by subsections of five basic programs. These include the following: Design, Tools and Test Program, Systems Prototyping and Fabrication Program, Microelectronics Systems Architecture Program, Circuits and Signal Processing Program, and Experimental Systems Program. Each entry also includes institution, principal investigator, dollar amount, and duration. R.L.B.

N93-13759*# Digital Analysis Corp., Reston, VA.
DNET: A COMMUNICATIONS FACILITY FOR DISTRIBUTED HETEROGENEOUS COMPUTING Final Report
John Tole, S. Nagappan, J. Clayton, P. Ruotolo, C. Williamson, and H. Solow 1989 358 p
(Contract NAS5-30085; SBIR-07.10-0396)
(NASA-CR-190863; NAS 1.26:190863) Avail: CASI HC A16/MF A03

This document describes DNET, a heterogeneous data communications networking facility. DNET allows programs operating on hosts on dissimilar networks to communicate with one another without concern for computer hardware, network protocol, or operating system differences. The overall DNET network is defined as the collection of host machines/networks on which the DNET software is operating. Each underlying network is considered a DNET 'domain'. Data communications service is provided between any two processes on any two hosts on any of the networks (domains) that may be reached via DNET. DNET provides protocol transparent, reliable, streaming data transmission between hosts (restricted, initially to DECnet and TCP/IP networks). DNET also provides variable length datagram service with optional return receipts. Author

61 COMPUTER PROGRAMMING AND SOFTWARE

Includes computer programs, routines, alogorithms, and specific applications, e.g., CAD/CAM.

N93-12554# Pennsylvania Univ., Philadelphia. Dept. of Computer and Information Sciences.
ACTION COMPOSITION FOR THE ANIMATION OF NATURAL LANGUAGE INSTRUCTIONS Final Report, Nov. 1990 - Oct. 1991
Libby Levison Mar. 1992 23 p
(Contract FQ7624-91-C-0019)
(AD-A254963; MS-CIS-91-28; AL-TP-1992-0020) Avail: CASI HC A03/MF A01

This report is an investigation of issues encountered in generating a short maintenance task simulation from a set of instructions. A method for specifying simulations at a task level, rather than by individual motion, is discussed. The research was conducted using a set of instructions that describe the removal of a fuel control valve from an aircraft. The agent for performing this simulation was the JACK human modeling environment, developed at the University of Pennsylvania. GRA

N93-12614# Advanced Decision Systems, Mountain View, CA.
VERIFICATION AND VALIDATION OF AI SOFTWARE Final Report, Sep. 1989 - Sep. 1991
R. A. Riemenschneider, Theodore A. Linden, Karen Morgan, and William Vrotney May 1992 145 p
(Contract F30602-89-C-0201)
(AD-A254601; RL-TR-92-118) Avail: CASI HC A07/MF A02

This document provides practical advice on how to improve V and V on AI projects. Part 1 lays a firm foundation by defining terms such as verification, validation, and artificial intelligence. Also, a new representation of system lifecycles is presented which we believe you will find useful in analyzing your organization's AI development efforts. In Part 2 the focus shifts to providing advice, with sections addressed to project leaders, system specifiers, designers, programmers, and documenters. Each role contributes in a different way to the overall V and V process, so we present a set of guidelines specific to each role. Part 3 is a collection of three appendices: (1) a user's manual for a software tool, ASP, developed under this contract which supports the V and V process by allowing programmers to better integrate formal testing with code development; (2) a glossary of V and V terms; and (3) a guide to commercially available CASE tools. GRA

N93-12645# Carnegie-Mellon Univ., Pittsburgh, PA. School of Computer Science.
EXPERT-SYSTEM DEVELOPMENT IN SOAR: A TUTORIAL
Erik Altmann and Gregg R. Yost Jun. 1992 60 p
(Contract F33615-90-C-1465; ARPA Order 7597)
(AD-A254571; CMU-CS-92-151) Avail: CASI HC A04/MF A01

This is a tutorial for building an expert system in Soar using the TAQL programming language. It provides a self-contained reference for the end-to-end development of a Sonar system that accomplishes a particular task. It presents a natural-language task description, a system design, and a smple implementation, including a documented code listing. It also discusses chunking (Soar's learning mechanism) in the context of the sample implementation. GRA

N93-12647# Imperial Coll. of Science and Technology, London (England).
NUMERICAL OPTIMIZATION Final Technical Report
Francesco Zirilli 1992 71 p
(Contract DAJA45-85-C-0028)
(AD-A254575; AFOSR-92-0707TR) Avail: CASI HC A04/MF A01

In the framework of the proposed continuous approach to constrained optimization problems, we describe two new solution methods which resulted from the research. The first is a continuous inexact method for solving systems of nonlinear equations and complementarity problems (along the lines of the DAFNE method), and the second is a continuous method for solving the linear programming problems (along the lines of Karmarkar's method) which is shown to be quadratically convergent. Some numerical experience on a number of test problems is reported. GRA

N93-12654*# Mississippi State Univ., Mississippi State. Dept. of Electrical and Computer Engineering.
AN INVESTIGATION OF ERROR CORRECTING TECHNIQUES FOR OMV DATA Final Report, May 1988 - Sep. 1992
Frank Ingels and John Fryer 15 Sep. 1992 121 p
(Grant NAG8-104)
(NASA-CR-190942; NAS 1.26:190942) Avail: CASI HC A06/MF A02

Papers on the following topics are presented: considerations of testing the Orbital Maneuvering Vehicle (OMV) system with CLASS; OMV CLASS test results (first go around); equivalent system gain available from R-S encoding versus a desire to lower the power amplifier from 25 watts to 20 watts for OMV; command word acceptance/rejection rates for OMV; a memo concerning energy-to-noise ratio for the Viterbi-BSC Channel and the impact of Manchester coding loss; and an investigation of error correcting techniques for OMV and Advanced X-ray Astrophysics Facility (AXAF). Author

N93-12675*# Alabama Univ., Huntsville.
USERS MANUAL FOR PROGRAM SSFREQ INTERMEDIATE MODE STABILITY CURVES: DEVELOPED FOR USE ON A PC COMPUTER Final Report
Wilbur C. Armstrong Jun. 1992 85 p
(Contract NAS8-36955)
(NASA-CR-184452; NAS 1.26:184452) Avail: CASI HC A05/MF A01

The piping in a liquid rocket can assume complex configurations due to multiple tanks, multiple engines, and structures that must be piped around. The capability to handle some of these complex configurations have been incorporated into the SSFREQ code. The capability to modify the input on line has been implemented. The configurations allowed include multiple tanks, multiple engines, the splitting of a pipe into equal segments going to different (or the same) engines. This program will handle the following type elements: straight pipes, bends, inline accumulators, tuned stub accumulators, Helmholtz resonators, parallel resonators, pumps, split pipes, multiple tanks, and multiple engines. Author

N93-12676*# Alabama Univ., Huntsville.
USERS MANUAL FOR PROGRAM ADMIT: ADMITTANCE AND PRESSURE TRANSFER FUNCTION DEVELOPED FOR USE ON A PC COMPUTER Final Report
Wilbur C. Armstrong Jun. 1992 103 p
(Contract NAS8-36955)
(NASA-CR-184450; NAS 1.26:184450) Avail: CASI HC A06/MF A02

The piping in a liquid rocket can assume complex configurations due to

multiple tanks, multiple engines, and structures that must be piped around. The capability to handle some of these complex configurations have been incorporated into the ADMIT code. The capability to modify the input on line has been implemented. The configurations allowed include multiple tanks, multiple engines, the splitting of a pipe into unequal segments going to different (or the same) engines. This program will handle the following type elements: straight pipes, bends, inline accumulators, tuned stub accumulators, Helmholtz resonators, parallel resonators, pumps, split pipes, multiple tanks, and multiple engines. Author

N93-12686# Argonne National Lab., IL. Environmental Assessment and Information Sciences Div.

APPLICATION INTERFACE ENGINE LANGUAGE AND OBJECT REFERENCE MANUAL

R. S. Fuja and M. A. Widing Feb. 1992 292 p

(Contract W-31-109-eng-38)

(DE92-017555; ANL/EAIS/TM-72) Avail: CASI HC A13/MF A03

The Application Interface Engine (AIE) is a software tool that provides an environment for application development. In particular, the AIE system facilitates development of applications making use of graphical display and database access. Using the AIE, a developer can isolate the components of an application to provide portability and maintainability. The control structure of the application is written in a special object-oriented language provided with the system and described in this manual. The AIE Language (AIEL) contains objects that abstract the various application components. High-level objects are defined for implementing details of the user interface, database access, and process communication. The language and library of run-time system objects provided allow applications that use windowing and database systems to be prototyped and developed quickly, with emphasis on the design of generic, reusable, and self-contained code. DOE

N93-12693# National Science Foundation, Washington, DC. Div. of Computer and Computation Research.

SUMMARY OF AWARDS, FISCAL YEAR 1990

1992 104 p

(NSF-92-70) Avail: CASI HC A06/MF A02

Computer science research awards for fiscal year 1990 are given with abstracts. Awards are grouped by the following categories: Computer and Computation Theory, Numeric and Symbolic Computation, Computer Systems Architecture, Software Systems and Software Engineering. Indexes are provided for grantee institutions, principal investigators, presidential young investigators, and research initiation awardees. R.L.B.

N93-12719*# National Aeronautics and Space Administration. Ames Research Center, Moffett Field, CA.

THE MULTIDIMENSIONAL SELF-ADAPTIVE GRID CODE, SAGE

Carol B. Davies (Sterling Software, Palo Alto, CA.) and Ethiraj Venkatapathy (Eloret Corp., Sunnyvale, CA.) Jul. 1992 76 p

(RTOP 506-40-00)

(NASA-TM-103905; A-92019; NAS 1.15:103905) Avail: CASI HC A05/MF A01

This report describes the multidimensional self-adaptive grid code SAGE. A two-dimensional version of this code was described in an earlier report by the authors. The formulation of the multidimensional version is described in the first section of this document. The second section is presented in the form of a user guide that explains the input and execution of the code and provides many examples. Successful application of the SAGE code in both two and three dimensions for the solution of various flow problems has proven the code to be robust, portable, and simple to use. Although the basic formulation follows the method of Nakahashi and Deiwert, many modifications have been made to facilitate the use of the self-adaptive grid method for complex grid structures. Modifications to the method and the simplified input options make this a flexible and user-friendly code. The new SAGE code can accommodate both two-dimensional and three-dimensional flow problems. Author

N93-12722# Department of Defence, Canberra (Australia). Analytical Studies Unit.

OBTAINING MEDIANS AND OTHER QUANTILES WITH LIMITED MEMORY SPACE

B. K. McMillan May 1992 20 p

(AD-A254506; ASU-TN-4(Medians 1); DODA-AR-007-148) Avail: CASI HC A03/MF A01

This paper provides some basic methodologies for determining medians and other quantiles of data. They are applicable to data more numerous than conventional techniques can manage efficiently. The origins of the work are in ionospheric propagation assessment, but the results are generally applicable. Because these problems push computing facilities to their limit, the final implementation depends on the available facilities. Thus a complete solution cannot be presented, although important factors and techniques have been identified and potential effort savings estimated. GRA

N93-12730# Texas Univ., Austin. Center for Cybernetic Studies.

SENSITIVITY ANALYSIS OF THE SIMULTANEOUS PROPORTIONATE CHANGE OF INPUTS AND OUTPUTS IN DATA ENVELOPMENT ANALYSIS

A. Charnes and L. Neralic Aug. 1991 13 p

(Contract N00014-82-K-0295; NSF SES-84-08134)

(AD-A254821; CCS-RR-667) Avail: CASI HC A03/MF A01

Sensitivity analysis in data envelopment analysis for the Charnes-Cooper-Rhodes ratio model is studied for the case of the simultaneous proportionate increase of all inputs and proportionate decrease of all outputs of an efficient decision making unit for which efficiency is preserved. Sufficient conditions which preserve efficiency are found and a numerical example illustrating the results is provided. GRA

N93-12740# Army Lab. Command, Watertown, MA. Material Technology Lab.

AN INTERACTIVE OFFICE ACCOUNTING PROGRAM WRITTEN IN UNIX AND C Final Report

Karen M. Kinsley Jul. 1992 235 p

(AD-A255077; MTL-MS-92-2) Avail: CASI HC A11/MF A03

This program is written in UNIX (Version 5.1, POI) and C (pre-ANSI) and provides an office with the ability to create and maintain labor and non-labor accounts without requiring anyone in the office (except for the installer) to learn a computer language. Security for the accounts and account directories is automatically provided, and menus are used to create the accounts and to specify the charges to them. The program also includes creation of a summary file for all accounts, key word search functions for both the summary file and general accounts, and a printout program. A separate program, which allows an operator to view, print, and/or search the accounts for key words, but which will not allow the addition of charges to the accounts, is also provided. GRA

N93-12763# Massachusetts Univ., Amherst. Dept. of Computer and Information Science.

GRAPHICS-BASED PARALLEL PROGRAMMING TOOLS Final Report

Janice E. Cuny Sep. 1991 14 p

(Contract N00014-89-J-1492)

(AD-A254406) Avail: CASI HC A03/MF A01

Highly parallel architectures will be useful in meeting the demands of computationally intensive tasks only to the extent that it is possible to write efficient parallel software. The problems are enormous. The parallel programmer must simultaneously code for multiple processes, orchestrating their communication and synchronization; she must efficiently map logical processes onto disparate hardware configurations and schedule their execution. Further, she must debug-both for correctness and performance-in spite of a potentially overwhelming amount of relevant information and in the absence of reproducibility or consistent global state. If it is not possible to provide sophisticated programming support for these activities, it is unlikely that highly parallel computation will be generally available to either the scientific or the commercial communities. In our research, we have investigated aspects of parallel computation that are specific to massive parallelism. GRA

N93-12792# EG and G Energy Measurements, Inc., Idaho Falls.

YOU NEED THIS DONE BY WHEN? INCREASING YOUR EFFICIENCY WITH THE SAS SYSTEM

M. S. DeHaan 1992 4 p Presented at the 17th Annual Atomic Spectroscopy Safeguards and Security Users Group International Symposium, Honolulu, HI, 12 Apr. 1992

(Contract DE-AC07-76ID-01570)
(DE92-017894; EGG-M-91471; CONF-920426-3) Avail: CASI HC A01/MF A01

The SAS Institute publication -- SAS Programming Tips: A Guide to Efficient SAS Processing defines efficiency as 'obtaining more results from fewer computer or human resources.' While this publication contains many very useful tips, it seems to concentrate mostly on computer efficiency. This paper will focus on ways of increasing your efficiency in developing, writing, and debugging SAS programs, i.e., increasing human efficiency. In my job as a consulting statistician, my programs are usually one-run programs. That is, I develop and test a program, then I run them once to get the results I need, and the program is typically never used again. Even for multiple run jobs, the greatest expense by far is the time used to develop a program, and any CPU/hardware 'expense' is relatively insignificant. I believe that this is true for most SAS system users and that not enough attention has been given to this aspect of 'cost'. While most of these tips and techniques were developed under the PC platform, nearly all are applicable and useful under all SAS supported platforms. Some of the tips the experienced SAS programmer may already be familiar with, but many should be new and useful to both novice and veteran users.
DOE

N93-12795# Sandia National Labs., Albuquerque, NM.
RHALE: A MMALE SHOCK PHYSICS CODE WRITTEN IN C++
K. G. Budge and J. S. Peery 1991 19 p Presented at the Hypervelocity Impact Symposium, Austin, TX, 17-20 Nov. 1992
(Contract DE-AC04-76DP-00789)
(DE92-018271; SAND-91-2907C; CONF-921162-5) Avail: CASI HC A03/MF A01

This paper describes RHALE, a multi-material arbitrary Lagrangian-Eulerian (MMALE) shock physics code. RHALE is the successor to CTH, Sandia's 3-D Eulerian shock physics code, and will be capable of solving problems that CTH cannot adequately address. We discuss the new Lagrangian capabilities of HALE, which include arbitrary mesh connectivity, superior artificial viscosity, and improved equations of state. We also discuss some of the issues we have encountered in the choice of an axisymmetric element technology and our resolution of these issues. We discuss the MALE algorithms that have been extended for arbitrary grids in both two and three dimensions and present the results of calculations that are of interest to the hypervelocity impact community. The MALE addition to HALE provides the accuracy of a Lagrangian code while allowing a calculation to proceed under very large distortions. Coupling an arbitrary quadrilateral or hexahedral grid to the MALE solution facilitates modeling of complex shapes with a minimum number of computational cells. HALE allows regions of a problem to be modeled with Lagrangian, Eulerian or ALE meshes. In addition, regions can switch from Lagrangian to ALE to Eulerian based on user input or mesh distortion. For ALE meshes, new node locations are determined with equipotential schemes. Element quantities are advected with donor, van Leer, or Super-B algorithms. Nodal quantities are advected with the second order SHALE or HIS algorithms. To facilitate the development of such a lengthy code, we choose to write in the C++ programming language. We feel that object-oriented programming techniques are superior to conventional programming techniques. However, we discuss a few of the efficiency problems we have encountered using these techniques and how we have addressed these problems.
DOE

N93-12801*# Research Inst. for Advanced Computer Science, Moffett Field, CA.
IMPLEMENTATION DETAILS OF THE COUPLED QMR ALGORITHM
Roland W. Freund and Noel M. Nachtigal Oct. 1992 18 p
(Contract NCC2-387)
(NASA-CR-191213; NAS 1.26:191213; RIACS-TR-92-19) Avail: CASI HC A03/MF A01

The original quasi-minimal residual method (QMR) relies on the three-term look-ahead Lanczos process, to generate basis vectors for the underlying Krylov subspaces. However, empirical observations indicate that, in finite precision arithmetic, three-term vector recurrences are less robust than mathematically equivalent coupled two-term recurrences. Therefore, we recently proposed a new implementation of the QMR method based on a coupled two-term look-ahead Lanczos procedure. In this paper, we describe implementation details of this coupled QMR algorithm, and we present results of numerical experiments.
Author

N93-12851# Wickersheimer Engineers, Inc., Champaign, IL.
USER'S GUIDE: COMPUTER-AIDED STRUCTURAL MODELING (CASM), VERSION 3.00 Final Report
David Wickersheimer, Gene McDermott, Carl Roth, and Michael E. Pace Apr. 1992 364 p
(Contract DACA39-86-C-0024)
(AD-A255074; WES/IR/ITL-92-4) Avail: CASI HC A16/MF A03

CASM stands for Computer Aided Structural Modeling. It is a program designed to aid the structural engineer in the preliminary design and evaluation of structural building systems by the use of 3-D interactive graphics. Think of this program as a scratch pad for the structural decision process that would have been done on paper before you went to the computer to do the final numerical analysis of structural members. CASM will let you change your mind quickly and give you results that previously might have taken hours to obtain. By allowing quick changes, CASM allows you to make more informed decisions in the initial structural evaluation process. The purpose of this manual is to help you understand the CASM program. The CASM program is designed by structural engineers for structural engineers. Its purpose is to help solve those basic early problems that all engineers face when trying to fit a structural system into a building.
GRA

N93-12872# Wickersheimer Engineers, Inc., Champaign, IL.
COMPUTER-AIDED STRUCTURAL ENGINEERING (CASE) PROJECT. TUTORIAL GUIDE: COMPUTER-AIDED STRUCTURAL MODELING (CASM). VERSION 3.00 Final Report
David Wickersheimer, Gene McDermott, Carl Roth, and Michael E. Pace Apr. 1992 303 p Supersedes WES/IS/ITL-90-4
(Contract DACA39-86-C-0024)
(AD-A255075; WES/IR/ITL-92-5; WES/IS/ITL-90-4) Avail: CASI HC A14/MF A03

This tutorial describes version 3.00 of the computer program CASM, which is designed to aid the structural engineer in the preliminary design and evaluation of structural building systems by the use of three-dimensional interactive graphics. CASM is a preliminary structural design program that incorporates a Structural Planning philosophy. Structural Planning is the study of structural system alternatives within the context of each project's unique set of program criteria. The goal of structural planning, and thus CASM, is to select the most appropriate, efficient, and economical structural system which satisfies established program criteria while integrating the mechanical requirements and complementing the intended aesthetics.
GRA

N93-12957*# National Aeronautics and Space Administration. Langley Research Center, Hampton, VA.
THE SECOND NASA FORMAL METHODS WORKSHOP 1992
Sally C. Johnson, comp., C. Michael Holloway, comp., and Ricky W. Butler, comp. Nov. 1992 232 p Workshop held in Hampton, VA, 11-13 Aug. 1992
(RTOP 505-64-10-05)
(NASA-CP-10110; NAS 1.55:10110) Avail: CASI HC A11/MF A03

The primary goal of the workshop was to bring together formal methods researchers and aerospace industry engineers to investigate new opportunities for applying formal methods to aerospace problems. The first part of the workshop was tutorial in nature. The second part of the workshop explored the potential of formal methods to address current aerospace design and verification problems. The third part of the workshop involved on-line demonstrations of state-of-the-art formal verification tools. Also, a detailed survey was filled in by the attendees; the results of the survey are compiled. For individual titles, see N93-12958 through N93-12958.

N93-12958*# National Aeronautics and Space Administration. Langley Research Center, Hampton, VA.
A BRIEF OVERVIEW OF NASA LANGLEY'S RESEARCH PROGRAM IN FORMAL METHODS
In its The Second NASA Formal Methods Workshop 1992 Nov. 1992 p 9-22 Revised (For primary document see N93-12957 03-61)
Avail: CASI HC A03/MF A03

An overview of NASA Langley's research program in formal methods is

presented. The major goal of this work is to bring formal methods technology to a sufficiently mature level for use by the United States aerospace industry. Towards this goal, work is underway to design and formally verify a fault-tolerant computing platform suitable for advanced flight control applications. Also, several direct technology transfer efforts have been initiated that apply formal methods to critical subsystems of real aerospace computer systems. The research team consists of six NASA civil servants and contractors from Boeing Military Aircraft Company, Computational Logic Inc., Odyssey Research Associates, SRI International, University of California at Davis, and Vigyan Inc. Author

N93-12961# Stanford Univ., CA. Dept. of Computer Science.
FAST APPROXIMATION ALGORITHMS FOR MULTICOMMODITY FLOW PROBLEMS
Tom Leighton, Fillia Makedon, Serge Plotkin, Clifford Stein, and Eva Tardos Aug. 1991 28 p
(Contracts N00014-88-K-0166; DAAL03-91-G-0102)
(AD-A254335; SU-CSL-STAN-91-1375) Avail: CASI HC A03/MF A01

In this paper, we describe the first polynomial-time combinatorial algorithms for approximately solving the multicommodity flow problem. Our algorithms are significantly faster than the best previously known algorithms, that were based on linear programming. For a k-commodity multicommodity flow problem, the running time of our randomized algorithm is (up to log factors) the same as the time needed to solve k single-commodity flow problems, thus giving the surprising result that approximately computing a k-commodity maximum-flow is not much harder than computing about k single-commodity maximum-flows in isolation. Given any multicommodity flow problem as input, our algorithm is guaranteed to provide a feasible solution to a modified flow problem in which all capacities are increased by a (1 + epsilon)-factor, or to provide a proof that there is no feasible solution to the original problem. We also describe faster approximation algorithms for multicommodity flow problems with a special structure, such as those that arise in the sparsest cut problems and the uniform concurrent flow problems if k is less than m. GRA

N93-13004*# Research Inst. for Computing and Information Systems, Houston, TX.
FRAMEWORK PROGRAMMABLE PLATFORM FOR THE ADVANCED SOFTWARE DEVELOPMENT WORKSTATION (FPP/ASDW). DEMONSTRATION FRAMEWORK DOCUMENT. VOLUME 2: FRAMEWORK PROCESS DESCRIPTION
Richard J. Mayer (Knowledge Based Systems, Inc. College Station, TX.), Thomas M. Blinn (Knowledge Based Systems, Inc. College Station, TX.), Paula S. deWitte (Knowledge Based Systems, Inc. College Station, TX.), John W. Crump (Knowledge Based Systems, Inc. College Station, TX.), and Keith A. Ackley (Knowledge Based Systems, Inc. College Station, TX.) 16 Apr. 1992 66 p
(Contract NCC9-16; RICIS Proj. SE-37)
(NASA-CR-190275; NAS 1.26:190275) Avail: CASI HC A04/MF A01

In the second volume of the Demonstration Framework Document, the graphical representation of the demonstration framework is given. This second document was created to facilitate the reading and comprehension of the demonstration framework. It is designed to be viewed in parallel with Section 4.2 of the first volume to help give a picture of the relationships between the UOB's (Unit of Behavior) of the model. The model is quite large and the design team felt that this form of presentation would make it easier for the reader to get a feel for the processes described in this document. The IDEF3 (Process Description Capture Method) diagrams of the processes of an Information System Development are presented. Volume 1 describes the processes and the agents involved with each process, while this volume graphically shows the precedence relationships among the processes. Author

N93-13030*# Texas Univ., Austin. Center for Aeromechanics Research.
APPLICATION OF LANCZOS VECTORS TO CONTROL DESIGN OF FLEXIBLE STRUCTURES, PART 2 Final Report, Jan. 1991 - Jun. 1992
Roy R. Craig, Jr. and Tzu-Jeng Su Nov. 1992 37 p
(Grant NAG9-357)
(NASA-CR-191244; NAS 1.26:191244; CAR-92-3-Pt-2) Avail: CASI HC A03/MF A01

This report covers the period of the grant from January 1991 until its expiration in June 1992. Together with an Interim Report (Ref. 9), it summarizes the research conducted under NASA Grant NAG9-357 on the topic 'Application of Lanczos Vectors to Control Design of Flexible Structures.' The research concerns various ways to obtain reduced-order mathematical models of complex structures for use in dynamics analysis and in the design of control systems for these structures. This report summarizes the research. Author

N93-13063*# Research Inst. for Advanced Computer Science, Moffett Field, CA.
INTRODUCTION TO IND AND RECURSIVE PARTITIONING, VERSION 1.0
Wray Buntine and Rich Caruana (San Jose State Univ., Moffett Field, CA.) 23 Sep. 1991 99 p
(Contract NCC2-387)
(NASA-CR-191220; NAS 1.26:191220; RIACS-TR-91-23) Avail: CASI HC A05/MF A02

This manual describes the IND package for learning tree classifiers from data. The package is an integrated C and C shell re-implementation of tree learning routines such as CART, C4, and various MDL and Bayesian variations. The package includes routines for experiment control, interactive operation, and analysis of tree building. The manual introduces the system and its many options, gives a basic review of tree learning, contains a guide to the literature and a glossary, lists the manual pages for the routines, and instructions on installation. Author

N93-13261*# Colorado Univ., Boulder. Dept. of Computer Science.
VISUALIZATION TECHNIQUES TO AID IN THE ANALYSIS OF MULTI-SPECTRAL ASTROPHYSICAL DATA SETS Annual Report, Sep. 1991 - Oct. 1992
Gitta Domik, Salim Alam, and Paul Pinkney 15 Nov. 1992 46 p
(Grant NAGw-1902)
(NASA-CR-191260; NAS 1.26:191260) Avail: CASI HC A03/MF A01

This report describes our project activities for the period Sep. 1991 - Oct. 1992. Our activities included stabilizing the software system STAR, porting STAR to IDL/widgets (improved user interface), targeting new visualization techniques for multi-dimensional data visualization (emphasizing 3D visualization), and exploring leading-edge 3D interface devices. During the past project year we emphasized high-end visualization techniques, by exploring new tools offered by state-of-the-art visualization software (such as AVS3 and IDL4/widgets), by experimenting with tools still under research at the Department of Computer Science (e.g., use of glyphs for multidimensional data visualization), and by researching current 3D input/output devices as they could be used to explore 3D astrophysical data. As always, any project activity is driven by the need to interpret astrophysical data more effectively. Author

N93-13291*# Analex Corp., Brook Park, OH.
TEST AND CONTROL COMPUTER USER'S GUIDE FOR A DIGITAL BEAM FORMER TEST SYSTEM Final Report
Robert E. Alexovich and Paul G. Mallasch Jul. 1992 81 p
(Contract NAS3-25776; RTOP 316-60-13)
(NASA-CR-189208; E-7176; NAS 1.26:189208) Avail: CASI HC A05/MF A01

A Digital Beam Former Test System was developed to determine the effects of noise, interferers and distortions, and digital implementations of beam forming as applied to the Tracking and Data Relay Satellite 2 (TDRS 2) architectures. The investigation of digital beam forming with application to TDRS 2 architectures, as described in TDRS 2 advanced concept design studies, was conducted by the NASA/Lewis Research Center for NASA/Goddard Space Flight Center. A Test and Control Computer (TCC) was used as the main controlling element of the digital Beam Former Test System. The Test and Control Computer User's Guide for a Digital Beam Former Test System provides an organized description of the Digital Beam Former Test System commands. It is written for users who wish to conduct tests of the Digital Beam forming Test processor using the TCC. The document describes the function, use, and syntax of the TCC commands available to the user while summarizing and demonstrating the use of the commands wtihin DOS batch files. Author

N93-13293*# North Carolina State Univ., Raleigh. Dept. of Computer Science.

SOFTWARE RELIABILITY THROUGH FAULT-AVOIDANCE AND FAULT-TOLERANCE Technical Report - 1 Mar. 1991 - 29 Feb. 1992

Mladen A. Vouk and David F. McAllister 1992 83 p

(Grant NAG1-983)

(NASA-CR-189880; NAS 1.26:189880) Avail: CASI HC A05/MF A01

Accomplishments in the following research areas are summarized: structure based testing, reliability growth, and design testability with risk evaluation; reliability growth models and software risk management; and evaluation of consensus voting, consensus recovery block, and acceptance voting. Four papers generated during the reporting period are included as appendices. Author

N93-13295*# Texas Univ., Austin. Dept. of Aerospace Engineering and Engineering Mechanics.

UNSYMMETRIC LANCZOS MODEL REDUCTION AND LINEAR STATE FUNCTION OBSERVER FOR FLEXIBLE STRUCTURES

Tzu-Jeng Su and Roy R. Craig, Jr. Sep. 1991 62 p

(Grant NAG9-357)

(NASA-CR-191231; NAS 1.26:191231; CAR-91-4) Avail: CASI HC A04/MF A01

This report summarizes part of the research work accomplished during the second year of a two-year grant. The research, entitled 'Application of Lanczos Vectors to Control Design of Flexible Structures' concerns various ways to use Lanczos vectors and Krylov vectors to obtain reduced-order mathematical models for use in the dynamic response analyses and in control design studies. This report presents a one-sided, unsymmetric block Lanczos algorithm for model reduction of structural dynamics systems with unsymmetric damping matrix, and a control design procedure based on the theory of linear state function observers to design low-order controllers for flexible structures. Author

N93-13296*# Texas Univ., Austin. Center for Aeromechanics Research.

APPLICATION OF LANCZOS VECTORS TO CONTROL DESIGN OF FLEXIBLE STRUCTURES Interim Report

Roy R. Craig, Jr. and Tzu-Jeng Su Dec. 1990 24 p

(Grant NAG9-357)

(NASA-CR-191230; NAS 1.26:191230; CAR-90-3) Avail: CASI HC A03/MF A01

This report covers research conducted during the first year of the two-year grant. The research, entitled 'Application of Lanczos Vectors to Control Design of Flexible Structures' concerns various ways to obtain reduced-order mathematical models for use in dynamic response analyses and in control design studies. This report summarizes research described in several reports and papers that were written under this contract. Extended abstracts are presented for technical papers covering the following topics: controller reduction by preserving impulse response energy; substructuring decomposition and controller synthesis; model reduction methods for structural control design; and recent literature on structural modeling, identification, and analysis. Author

N93-13338 Nova Univ., Fort Lauderdale, FL.

USING DIALOG CIP AT WINONA STATE UNIVERSITY TO EDUCATE END-USERS Ph.D. Thesis

Kathryn Ann Sullivan 1991 300 p

Avail: Univ. Microfilms Order No. DA9217762

Graduate students need to know the resources of their university library in order to do research and cannot be expected to remember any library training they may have received as undergraduates. A class offered by the library on how to search databases available through DIALOG's Classroom Instruction Program (CIP) was proposed, in cooperation with existing research classes in the student's field. A study was conducted at Winona State University, Winona, MN, with research classes offered by two professors in the field of special education. The study was to determine whether the information presented in an instruction session based on six learning objectives-choosing a database, choosing search terms and connectors, using search commands, modifying the search online printing search results and logging out-would enable graduate students to conduct an online search. Eighteen graduate students were provided with an hour's free searching on DIALOG in order to locate citations on their own choice of topic as part of an assignment from their instructor. Questionnaires were used to gather student assessments of their skills before and after their DIALOG search, while observation of the student during the search and examination of the actual printout of the search were used in conjunction with performance indicators to rate the actual skill in using DIALOG. All of the students were able to search DIALOG and print out citations but, based on performance indicators, none had the skill to be fully independent searchers. Dissert. Abstr.

N93-13355*# Intellicorp, Mountain View, CA.

COMPILING KNOWLEDGE-BASED SYSTEMS TO Ada, PHASE 2 Final Report

Robert E. Filman and Paul H. Morris Oct. 1992 67 p

(Contract NAS8-38488)

(NASA-CR-191273; NAS 1.26:191273) Avail: CASI HC A04/MF A01

This document is the final report of Phase Two of the PrkAda project. PrkAda is a system for delivering, in a pure-Ada environment, artificial intelligence and object-oriented applications developed in the C-based ProKappa system. This involves developing (1) a compiler from ProKappa's high-level, backtracking-based language, ProTalk, to Ada, and (2) creating a run-time, Ada-language, object-system core. Novel components of this implementation include our approach to automatic storage management in Ada, achieving dynamic instance method binding in Ada, and compilation of a backtracking language to a generator model using Ada tasks. Author

N93-13408*# Research Inst. for Advanced Computer Science, Moffett Field, CA.

IMPLICIT APPLICATION OF POLYNOMIAL FILTERS IN A k-STEP ARNOLDI METHOD

D. C. Sorensen (Rice Univ., Houston, TX.) 18 Oct. 1990 58 p

(Contract NCC2-387; NSF CCR-88-09615)

(NASA-CR-191237; NAS 1.26:191237; RIACS-TR-90-43) Avail: CASI HC A04/MF A01

The Arnoldi process is a well known technique for approximating a few eigenvalues and corresponding eigenvectors of a general square matrix. Numerical difficulties such as loss of orthogonality and assessment of the numerical quality of the approximations as well as a potential for unbounded growth in storage have limited the applicability of the method. These issues are addressed by fixing the number of steps in the Arnoldi process at a prescribed value k and then treating the residual vector as a function of the initial Arnoldi vector. This starting vector is then updated through an iterative scheme that is designed to force convergence of the residual to zero. The iterative scheme is shown to be a truncation of the standard implicitly shifted QR-iteration for dense problems and it avoids the need to explicitly restart the Arnoldi sequence. The main emphasis of this paper is on the derivation and analysis of this scheme. However, there are obvious ways to exploit parallelism through the matrix-vector operations that comprise the majority of the work in the algorithm. Preliminary computational results are given for a few problems on some parallel and vector computers. Author

N93-13494 New York Univ., New York.

JAPANESE/ENGLISH MACHINE TRANSLATION USING SUBLANGUAGE PATTERNS AND REVERSIBLE GRAMMARS Ph.D. Thesis

Ping Peng 1992 177 p

Avail: Univ. Microfilms Order No. DA9222910

A Japanese/English machine translation system with reversible components was designed and implemented in PROLOG. Sublanguage co-occurrence patterns have been used to address the problems of lexical and structural selection in the transfer between the internal representations of a pair of natural languages. The sysem was tested translating Japanese into English in the domain of programming language manuals. The evaluation of the test outputs provides some assessment of the utility of the sublanguage approach as a method for the development and refinement of a machine translation system. The thesis also explores the roles that a reversible grammar would play in sharing linguistic knowledge between parsing and generation. The system was developed with the goal of using sublanguage word co-occurrence patterns to simplify the description of syntactic/semantic knowledge needed in both the transfer rules and the analysis of the source language. In particular, sublanguage co-occurrence patterns are introduced to provide semantic constraints and ellipsis recovery in parsing Japanese. This thesis introduces a right-to-left parsing scheme for Japanese. The idea for the right-to-left parsing algorithm evolved from

the desire to produce partial syntactic analyses of Japanese in a more deterministic manner than was achieved by conventional left-to-right parsing schemes. The algorithm makes efficient use of sublanguage co-occurrence patterns as semantic knowledge to help disambiguate Japanese parses. The enforcement of syntactic and semantic constraints is tightly interwoven during the course of parsing. The performance in parsing Japanese was thereby significantly enhanced. A procedure was implemented for translating a Definite Clause Grammer dually into a PROLOG parser and PROLOG generator, so that one grammar can be used for parsing and generation. In current natural language processing systems, separate grammars are used for parsing and generation. However, there has long been an interest in designing a single grammar for both parsing and synthesis for reasons of efficiency and integrity, as well as linguistic elegance and perspicuity. As part of the current implementation, a strategy was developed for creating efficient grammars for both parsing and generation using a goal reordering technique within the logic programming framework. Dissert. Abstr.

N93-13694*# Research Inst. for Advanced Computer Science, Moffett Field, CA.

RESEARCH SUMMARY, JANUARY 1989 - JUNE 1990 Report, 1 Jan. 1989 - 30 Jun. 1990

Jun. 1990 105 p

(Contract NCC2-387)

(NASA-CR-190960; NAS 1.26:190960) Avail: CASI HC A06/MF A02

The Research Institute for Advanced Computer Science (RIACS) was established at NASA ARC in June of 1983. RIACS is privately operated by the Universities Space Research Association (USRA), a consortium of 62 universities with graduate programs in the aerospace sciences, under a Cooperative Agreement with NASA. RIACS serves as the representative of the USRA universities at ARC. This document reports our activities and accomplishments for the period 1 Jan. 1989 - 30 Jun. 1990. The following topics are covered: learning systems, networked systems, and parallel systems. Author

N93-13695*# Cornell Univ., Ithaca, NY. Dept. of Computer Science.

MONITORING AND CONTROLLING DISTRIBUTED APPLICATIONS USING LOMITA (POSITION PAPER)

Keith Marzullo and Ida M. Szafranska 16 Oct. 1992 8 p

(Contract NAG2-593; N00140-87-C-8904)

(NASA-CR-190971; NAS 1.26:190971; CU-TR-92-1306) Avail: CASI HC A02/MF A01

Over the last four years, the Meta toolkit was developed for controlling distributed applications. This toolkit has been publicly available as part of the academic ISIS release, and has been used for building various system monitoring and control applications. One major stumbling block with using Meta has been the language (called NPL) it supports. NPL is very low-level and using it is difficult, in the same way it is difficult to write machine language programs or raw Postscript programs. Hence, a higher level language was built along with a runtime environment. The hope is that with this higher-level approach, more complicated Meta applications will be written and thereby concentrate more on the use (and limitations) of Meta as an architecture. The Meta toolkit is reviewed with its intended use. Next, the goals with Lomita and an overview is given of its architecture and language syntax. A detailed example is given of Lomita's use by presenting a complete program for a load-adaptable service. Author

N93-13734*# Rutgers - The State Univ., New Brunswick, NJ. Lab. for Computer Science Research.

CIRCUIT DESIGN TOOL. USER'S MANUAL, REVISION 2

Keith M. Miyake and Donald E. Smith Oct. 1992 55 p

(Grant NAG2-668)

(NASA-CR-191361; NAS 1.26:191361; LCSR-TR-191-Rev-2) Avail: CASI HC A04/MF A01

The CAM chip design was produced in a UNIX software environment using a design tool that supports definition of digital electronic modules, composition of these modules into higher level circuits, and event-driven simulation of these circuits. Our design tool provides an interface whose goals include straightforward but flexible primitive module definition and circuit composition, efficient simulation, and a debugging environment that facilitates design verification and alteration. The tool provides a set of primitive modules which can be composed into higher level circuits. Each module is a C-language subroutine that uses a set of interface protocols understood by the design tool. Primitives can be altered simply by recoding their C-code image; in addition new primitives can be added allowing higher level circuits to be described in C-code rather than as a composition of primitive modules--this feature can greatly enhance the speed of simulation. Author

N93-13835# Naval Postgraduate School, Monterey, CA. Dept. of Computer Science.

USER INTERFACE OF DFQL: AN OBJECT-ORIENTED APPROACH M.S. Thesis

Chang-Tsun Li Jun. 1992 181 p

(AD-A255225) Avail: CASI HC A09/MF A02

In recent years, many graphical approaches have been proposed to lift the inconvenience of text-based query, language among end-users. The new query language called DFQL (DataFlow Query Language) is a fully graphical interface to the relational model based on a dataflow paradigm. It only requires users to connect some well-defined operators which have been given an equivalent one-to-one correspondent functionality (or construct) in traditional query language (SQL in this case). All of the power of current query languages and sufficient expressive power and functionality are retained. But some shortcomings of DFQL user interface still exist. This thesis is to introduce a more ease-to-use and ease-to-learn user interface, so the shortcomings we found in DFQL user interface can be lifted and the productivity and power of the new version of DFQL can be increased. We have adopted object-oriented programming approach in our implementation and the benefits of using object-oriented programming in our development are also discussed. GRA

N93-13880*# Advanced System Technologies, Inc., Falls Church, VA.

INTEGRATED MODELING TOOL FOR PERFORMANCE ENGINEERING OF COMPLEX COMPUTER SYSTEMS Final Report, Mar. 1987 - 29 Jun. 1989

Gary Wright, Duane Ball, Susan Hoyt, and Oscar Steele 29 Jun. 1989 231 p

(Contract NAS7-995; SBIR-06.06-4242)

(NASA-CR-190881; NAS 1.26:190881; Rept-0002) Avail: CASI HC A11/MF A03

This report summarizes Advanced System Technologies' accomplishments on the Phase 2 SBIR contract NAS7-995. The technical objectives of the report are: (1) to develop an evaluation version of a graphical, integrated modeling language according to the specification resulting from the Phase 2 research; and (2) to determine the degree to which the language meets its objectives by evaluating ease of use, utility of two sets of performance predictions, and the power of the language constructs. The technical approach followed to meet these objectives was to design, develop, and test an evaluation prototype of a graphical, performance prediction tool. The utility of the prototype was then evaluated by applying it to a variety of test cases found in the literature and in AST case histories. Numerous models were constructed and successfully tested. The major conclusion of this Phase 2 SBIR research and development effort is that complex, real-time computer systems can be specified in a non-procedural manner using combinations of icons, windows, menus, and dialogs. Such a specification technique provides an interface that system designers and architects find natural and easy to use. In addition, PEDESTAL's multiview approach provides system engineers with the capability to perform the trade-offs necessary to produce a design that meets timing performance requirements. Sample system designs analyzed during the development effort showed that models could be constructed in a fraction of the time required by non-visual system design capture tools. I.I.C.

N93-13913 Dundee Univ. (Scotland).

AUTOMATIC PATTERN RECOGNITION TECHNIQUES FOR GEOMETRICAL CORRECTION ON SATELLITE DATA Ph.D. Thesis

Kitti Paithoonwattanakij 1989 153 p

Avail: Univ. Microfilms Order No. BRD-96045

Work involving processing digital image data obtained from remote-sensing satellites is presented. The first objective was the design of an interactive image processing package based on many specifications such as user friendliness, menu-driven program, flexibility for future modification without involving modification of all the program, optimized storage usage, etc. In order to provide users with a wide range of image

processing techniques, some modifications were made to the new version of IMAGE which introduce many new options. The second objective, which is the main focus of this research work, involves the design of automatic geometrical correction algorithms to facilitate the registration and rectification of Advanced Very High Resolution Radiometer (AVHRR) data on the TIROS-N and NOAA-n series of polar-orbiting meteorological satellites. It is based on the specification that it must achieve sub-pixel accuracy and it must be fast in computation. The first stage in the work is the development of a semi-automatic geometrical correction procedure which uses a ground control point library. This procedure requires only three pairs of ground control points as a prerequisite stage and the rest are left for automatic relocation instead of being located manually as in the normal method; the procedure can achieve one pixel accuracy. The final achievement is related to the problem of automatic geometrical rectification of AVHRR image data to within a fraction of a pixel accuracy. This involves using an orbital model as an assistant for the prediction of the approximate coordinates and then employs the new high precision ground control points library to locate the more accurate position by searching to subpixel location of the interpolated coordinates. To increase the precision of our ground control point library, we adapted a method previously used by Torlegard for Landsat MSS data. The reduction of registration time can also be tackled by using heuristic planning to reduce the excessive searching. The method reduces the search space to a less detailed, compact size, which is later used as a plan for finding exact coordinates and confines the search window to a small region. The developed algorithm works very well on cloud-free images and for images with only a modest amount of cloud. In some cases where images have heavy cloudcover, preprocessing by an adapted NDVI (Normalized Difference Vegetation Index) technique is used.

Dissert. Abstr.

N93-13942# Naval Research Lab., Washington, DC.
TALKING TO INTERFIS: ADDING SPEECH INPUT TO A NATURAL LANGUAGE INTERFACE
Stephanie S. Everett, Kenneth Wauchope, and Dennis Perzanowski 11 Sep. 1992 15 p
(DA Proj. RS3-4-C-74)
(AD-A255865; NRL/FR-5510-92-9515) Avail: CASI HC A03/MF A01

This report discusses the addition of speech recognition capabilities to InterFIS (the natural language interface to the Fault Isolation Shell (FIS)), an expert system for troubleshooting electronics equipment. Because of the limitations of today's speech recognition technology, the addition of this capability affects the structure and flexibility of the interface; the consequences and implications of this are discussed in detail in this report. The speech recognition module is described, and a brief evaluation of system performance is presented. GRA

N93-13944# Carnegie-Mellon Univ., Pittsburgh, PA. Dept. of Computer Science.
RECENT DEVELOPMENTS IN THE NL-SOAR GARDEN PATH THEORY
Richard L. Lewis 21 May 1992 32 p
(Contract F33615-90-C-1465; ARPA Order 7597)
(AD-A255889; CMU-CS-92-141) Avail: CASI HC A03/MF A01

This report describes a theory of garden path phenomena that is emerging from work on NL-Soar, a computational model of language comprehension embedded within the Soar architecture. The theory is constrained by a corpus of two kinds of sentences: garden paths (GP), which reveal the limitations of human comprehension in dealing with local ambiguities, and non-garden-paths (NGP), which reveal its power in handling local ambiguities. NL-Soar in a single-path comprehender with a limited capacity to repair misanalyzed input. A space of repair mechanisms is explored by hand simulation on the corpus. The importance of phonology and plausible search control is established, leading to a theory up to 95 percent accurate (76 percent worst case) in predicting performance on 37 distinct GP and NGP types. GRA

N93-13390*# Sverdrup Technology, Inc., Huntsville, AL.
RUNNING SINDA '85/FLUINT INTERACTIVE ON THE VAX
Boris Simmonds *In* NASA. Lewis Research Center, The Fourth Annual Thermal and Fluids Analysis Workshop 1992 p 47-70 (For primary document see N93-13385 03-34)
Avail: CASI HC A03/MF A03

62 COMPUTER SYSTEMS

Includes computer networks and special application computer systems.

N93-12549# Institute for Defense Analyses, Alexandria, VA.
SEAMLESS SIMULATION LITERATURE SURVEY Final Report, Jan. - Mar. 1992
Stephen Downes-Martin Apr. 1992 80 p
(Contract MDA903-89-C-0003)
(AD-A254950; IDA-D-1109; IDA/HQ-92-41242; AD-E501563) Avail: CASI HC A05/MF A01

This report is a summary review of people and organizations developing ideas for Seamless Simulation. Seamless Simulation is defined as the linking of heterogeneous systems on a simulation network. The current Distributed Interactive Simulation (DIS) technology supports a network of hundreds of vehicles at the battalion tactical level. Systems such as computer generated forces interact at the vehicle level via a network protocol, and current efforts to produce a DIS network standard are aimed at homogeneous objects (vehicle simulators) implemented in a heterogeneous manner (by different manufacturers). Seamless Simulation seeks to extend this technology to heterogeneous objects (vehicle simulators and unit level wargames, for example). Recommendations are to strengthen DoD support of Seamless Simulation projects; to extend the current DARPA/PMTRADE (Program Manager for Training Devices) sponsored workshop on DoD/Industry standards for the interoperability of defense simulations from the vehicle level to the general defense simulation and system level;to allow the Seamless Simulation effort to take advantage of modern software engineering and become explicitly object oriented; and to integrate the DoD effort with the business Object Management Group Architecture effort. GRA

N93-12710# Calspan-Buffalo Univ. Research Center, NY.
BLACKBOARD ARCHITECTURES FOR MULTI-AGENT PLANNING Final Report, Apr. 1991 - Jan. 1992
William B. Day (Auburn Univ., AL.) Jun. 1992 44 p
(Contract F30602-88-D-0026)
(AD-A255035; RL-TR-92-121) Avail: CASI HC A03/MF A01

This report describes investigations into the application of Distributed DataLog (DDL) multi-agent planning domains. The DDL is a distributed extension to the Prolog language. The blackboard architecture is examined as a potential representation to support the DDL as an execution model. Additionally, there are discussions regarding the nature of AND- and OR-parallelism as well as the ramifications of employing the blackboard model in KB planning domains. GRA

N93-12733# Georgia Inst. of Tech., Atlanta. School of Electrical Engineering.
MASSIVELY PARALLEL OPTICAL-TO-ELECTRONIC DATA TRANSFER Final Report, 1 Oct. 1988 - 31 Mar. 1992
C. M. Verber, J. P. Uyemura, and U.-S. Rhee 27 Jul. 1992 41 p
(Contract DAAL03-88-K-0175)
(AD-A254831; E-21-651) Avail: CASI HC A03/MF A01

The design and experimental verification of a system composed of a page-oriented holographic binary memory and a compatible CMOS chip for receiving the stored data are presented. The optical retrieval system is novel in that the Bragg cell for selecting positions in the memory plane is coupled to the angle-selecting Bragg cell by an optical fiber array. This relieves several optical constraints and allows compact packaging of the system. The design, analysis, and fabrication of the electronic RAM array was performed using the 2-micron CMOS process available through MOSIS. A high-speed integrated CMOS process was chosen for its logic-integration capabilities. Adding the photodetector and associated circuitry to the normal design procedures provides for direct optical-to-electronic interfacing. Based on the measured efficiency of the optical system and the measured sensitivity of the CMOS detectors, it is 5 predicted that a memory with a page size of 128 x 128 bits and a read rate of 5 x 10(exp 5) pages per second could be constructed. A variety of applications beyond ROM-to-RAM data transfer are discussed. GRA

N93-12797# Oak Ridge National Lab., TN.
SPEEDUP PROPERTIES OF PHASES IN THE EXECUTION PROFILE OF DISTRIBUTED PARALLEL PROGRAMS
B. M. Carlson (Toronto Univ., Ontario), T. D. Wagner (Vanderbilt Univ., Nashville, TN.), L. W. Dowdy (Vanderbilt Univ., Nashville, TN.), and P. H. Worley Aug. 1992 25 p
(Contract DE-AC05-84OR-21400)
(DE92-019301; ORNL/TM-11900) Avail: CASI HC A03/MF A01

The execution profile of a distributed-memory parallel program specifies the number of busy processors as a function of time. Periods of homogeneous processor utilization are manifested in many execution profiles. These periods can usually be correlated with the algorithms implemented in the underlying parallel code. Three families of methods for smoothing execution profile data are presented. These approaches simplify the problem of detecting end points of periods of homogeneous utilization. These periods, called phases, are then examined in isolation, and their speedup characteristics are explored. A specific workload executed on an Intel iPSC/860 is used for validation of the techniques described. DOE

N93-12810# Oak Ridge National Lab., TN.
SPEEDUP PROPERTIES OF PHASES IN THE EXECUTION PROFILE OF DISTRIBUTED PARALLEL PROGRAMS
B. M. Carlson (Torrey Research Station, Aberdeen, Scotland) and T. D. Wagner (Vanderbilt Univ., Nashville, TN.) 1992 14 p Presented at the 6th International Conference on Modelling Techniques and Tools for Performance Evaluation, Edinburgh, Scotland, 16-18 Sep. 1992
(Contract DE-AC05-84OR-21400)
(DE92-019965; CONF-9209109-2) Avail: CASI HC A03/MF A01

The execution profile of a distributed-memory parallel program specifies the number of busy processors as a function of time. Periods of homogeneous processor utilization are manifested in many execution profiles. These periods can usually be correlated with the algorithms implemented in the underlying parallel code. Three families of methods for smoothing execution profile data are presented. These approaches simplify the problem of detecting end points of periods of homogeneous utilization. These periods, called phases, are then examined in isolation, and their speedup characteristics are explored. A specific workload executed on an Intel iPSC/860 is used for validation of the techniques described. DOE

N93-12846# California Univ., San Diego, La Jolla. Center for Research in Language.
TRANSPUTER IMPLEMENTATION OF THE TRACE MODEL OF SPEECH RECOGNITION Final Report, 1 May 1987 - 31 Mar. 1992
Jeffrey L. Elman, Paul S. Smith, and Mark Dolson Aug. 1992 24 p
(Contract DAAB07-87-C-H027)
(AD-A254747) Avail: CASI HC A03/MF A01

We describe the accomplishments of the five-year project to develop an extended version of the TRACE model of speech recognition and to port it to a Transputer platform. We begin with an over view of the project. We then describe the TRACE Model. TRACE is an artificial neural network which attempts to model the processing of speech from acoustic input to word extraction, in a manner consistent with what is known of human perceptual abilities. Following that, we discuss the work done to extend and develop the model in the direction of real-time performance with an extended phonemic inventory. This includes algorithm changes to TRACE, software for managing the Transputer processors, a new acoustic/phonetic front-end, debugging and testing tools, and graphics visualization software. GRA

N93-12848# Naval Undersea Warfare Center, New London, CT.
ECONOMICAL DEVELOPMENT OF COMPLEX COMPUTER SYSTEMS
Thomas C. Choinski 15 Aug. 1992 13 p
(AD-A254752; NUWC-NL-RR-10125) Avail: CASI HC A03/MF A01

This paper proposes a product development methodology (PDM) for complex systems evolving within the current economic climate of the United States, as well as the unstable state of world affairs envisioned throughout the decade. The PDM facilitates the development of systems that are multipurpose, flexible, highly mobile, and incorporate maximum bang for the buck. Ironically, the unstable nature of the development environment within the defense community parallels the one encountered by the commercial sector over the last 20 years. Successful companies have responded by adopting a product development methodology that adapts to ever changing market demands and the concern for near term returns (profit). The PDM exploits lessons learned from the commercial market analogy to establish a flexible, low risk, cost effective approach for technological progress. The approach suits systems development, especially those involving complex mission critical computer systems. Examination of the commercial product development process reveals a strategy that can achieve the procurement flexibility needed by DoD. This strategy concentrates on leveraging the state-of-the-art in a cost effective manner. The strategy also addresses risk management. GRA

N93-12852# Syracuse Univ., NY. Northeast Parallel Architectures Center.
PARALLEL COMPUTING SYSTEMS Final Report, Sep. 1988 - Sep. 1991
Daniel Pease Jun. 1992 404 p
(Contract F30602-88-C-0136)
(AD-A255076; RL-TR-92-131) Avail: CASI HC A18/MF A04

This effort developed a Parallel Assessment Window System (PAWS) which uses a user's existing ADA applications to select the best parallel system for the application. PAWS allows comparison between vastly different machine architectures running a common application on a SUN workstation under X-windows. ADA and LISP based application are transferred into machine independent data flow graphs and graphically displayed to expose the inherent parallelism inherent in the application. Profile plots are generated showing both the parallelism of the partitioned data flow graph, and predicted parallelism of the partitioned data flow graph running on the target machine. GRA

N93-13046# Los Alamos National Lab., NM.
HIPPI AND FIBRE CHANNEL
D. E. Tolmie 1992 4 p Presented at the 10th Conference on Computing in High Energy Physics, Annecy, France, 21-25 Sep. 1992
(Contract W-7405-eng-36)
(DE92-040346; LA-UR-92-2580; CONF-920966-1) Avail: CASI HC A01/MF A01

The High-Performance Parallel Interface (HIPPI) and Fiber Channel are near-gigabit per second data communications interfaces being developed in ANSI standards Task Group X3T9.3. HIPPI is the current interface of choice in the high-end and supercomputer arena, and Fiber Channel is a follow-on effort. HIPPI came from a local area network background, and Fiber Channel came from a mainframe to peripheral interface background. DOE

N93-13154*# National Aeronautics and Space Administration. Lewis Research Center, Cleveland, OH.
TURBOMACHINERY CFD ON PARALLEL COMPUTERS
Richard A. Blech, Edward J. Milner, Angela Quealy (Sverdrup Technology, Inc., Brook Park, OH.), and Scott E. Townsend (Sverdrup Technology, Inc., Brook Park, OH.) Nov. 1992 22 p Proposed for presentation at the Symposium on High-Performance Computing for Flight Vehicles, Washington, DC, 7-9 Dec. 1992
(RTOP 505-62-52)
(NASA-TM-105932; E-7443; NAS 1.15:105932) Avail: CASI HC A03/MF A01

The role of multistage turbomachinery simulation in the development of propulsion system models is discussed. Particularly, the need for simulations with higher fidelity and faster turnaround time is highlighted. It is shown how such fast simulations can be used in engineering-oriented environments. The use of parallel processing to achieve the required turnaround times is discussed. Current work by several researchers in this area is summarized. Parallel turbomachinery CFD research at the NASA Lewis Research Center is then highlighted. These efforts are focused on implementing the average-passage turbomachinery model on MIMD, distributed memory parallel computers. Performance results are given for inviscid, single blade row and viscous, multistage applications on several parallel computers, including networked workstations. Author

N93-13198# National Inst. of Standards and Technology, Gaithersburg, MD.
REJECT MECHANISMS FOR MASSIVELY PARALLEL NEURAL NETWORK CHARACTER RECOGNITION SYSTEMS

Michael D. Garris and Charles L. Wilson Jun. 1992 16 p
(PB92-213412; NISTIR-4863) Avail: CASI HC A03/MF A01

Two reject mechanisms are compared using a massively parallel character recognition system implemented at the National Institute of Standards and Technology (NIST). The recognition system was designed to study the feasibility of automatically recognizing hand-printed text in a loosely constrained environment. The first method is a simple scalar threshold on the output activation of the winning neurode from the character classifier network. The second method uses an additional neural network trained on all outputs from the character classifier network to accept or reject assigned classifications. The neural network rejection method was expected to perform with greater accuracy than the scalar threshold method, but this was not supported by the test results. The scalar threshold method, even though arbitrary, is shown to be a viable reject mechanism for use with neural network character classifiers. Upon studying the performance of the neural network rejection method, analyses show that the two neural networks, the character classifier network and the rejection network, perform very similarly. This can be explained by the strong non-linear function of the character classifier network which effectively removes most of the correlation between character accuracy and all activations other than the winning activation. This suggests that any effective rejection network must receive information from the system which was not filtered through the non-linear classifier. GRA

N93-13620# Westinghouse Savannah River Co., Aiken, SC.
REVIEWS OF COMPUTING TECHNOLOGY: SECURING NETWORK APPLICATIONS, KERBEROS, AND RSA
S. M. Johnson 1 Jun. 1992 15 p
(Contract DE-AC09-89SR-18035)
(DE92-019928; WSRC-IM-90-83-7) Avail: CASI HC A03/MF A01

This paper will focus on the first step in establishing network security, authentication, and describe the basic function of both RSA and Kerberos as used to provide authentication and confidential data transfer services. It will also discuss the Digital Signature Standard and the market acceptance of each. Proper identification of the principals involved in a network dialog is a necessary first step in providing network-wide security comparable to that of stand-alone systems. DOE

N93-13961 Colorado Univ., Boulder.
COMPRESSIBLE CONVECTION AND PULSATIONS ON PARALLEL COMPUTERS Ph.D. Thesis
Philip Wiley Jones 1991 213 p
Avail: Univ. Microfilms Order No. DA9220420

Two-dimensional numerical simulations on the massively parallel Connection Machine CM-2 are used to study fully compressible fluid convention and its interaction with acoustic waves. Finite difference methods are very efficient on the CM-2, yielding performances exceeding 2.4 Gflops. Spectral codes are also found to be competitive with similar codes on vector machines. Finite difference simulations are used to study vigorous time dependent convection in a polytropic system in which a convectively unstable layer is bounded above and below by stable layers. In one series of simulations, acoustic waves are artificially driven at the lower boundary and their energy exchange with the fluid is analyzed using a work integral formulation. We find that wave driving due to turbulent pressure variations is comparable to that due to gas pressure and increases rapidly with wave frequency due to wave focusing effects. These results are applicable to the extended envelopes of red giant stars. Time dependent convection also introduces a stochastic component of wave driving which may result in irregular variations observed in some pulsating red giants. Another simulation is used to examine large amplitude acoustic modes excited by supersonic penetrative convection. Turbulent pressure variations result in significant damping in the penetrative region due to wave focusing effects. Gas pressure driving occurs where the transition from diffusive to convective transport is made. We speculate on the implications of these results for the envelopes of red giants where supersonic turbulence is observed. Also presented is an examination of the effects of magnetic fields on gravity wave pulsations of white dwarf stars. Results from a linear analysis show that weak fields split the frequencies of otherwise degenerate modes in a unique pattern which can be separated from the effects of rotation. Applying these results to typical white dwarf models, we find that current observations should be able to detect magnetic fields as low as 10(exp 5) Gauss. Some candidate stars are discussed. Lastly, a catalog of line profile variations due to nonradial pulsations of stars is computed. The series of line profiles shows that while Doppler imaging provides some information on the velocity fields at the surface of stars, unique mode identifications can not be made for the slowly rotating 53 Per stars. Dissert. Abstr.

63 CYBERNETICS

Includes feedback and control theory, artificial intelligence, robotics and expert systems.

For related information see also *54 Man/System Technology and Life Support.*

N93-12547# Maryland Univ., Baltimore.
OPTIMAL DESIGN AND CONTROL OF DISTRIBUTED PARAMETER SYSTEMS Final Report, 1 Oct. 1990 - 3 Sep. 1991
Thomas I. Seidman 3 Sep. 1991 8 p LIMITED REPRODUCIBILITY: Availability: Document partially illegible
(Grant AF-AFOSR-0008-91)
(AD-A254947; AFOSR-92-0823TR) Avail: CASI HC A02/MF A01

Research has been conducted on nonlinear optimization in the areas of (1) dual based methods and decomposition, (2) regularization and approximation techniques, (3) nonsmooth optimization, and (4) algorithms development for large-scale optimization. The methods developed are applicable to a wide range of important applications including optimal shape design, structural optimization, and image reconstruction. GRA

N93-12548# Wright Lab., Wright-Patterson AFB, OH.
AN APPLICATION OF EXPONENTIAL NEURAL NETWORKS TO EVENT-TRAIN RECOGNITION Final Report, 5 Jan. 1990 - 8 May 1992
Peter G. Raeth 8 May 1992 104 p
(AF Proj. 7633)
(AD-A254948; WL-TR-92-1060) Avail: CASI HC A06/MF A02

The purpose of this project is to investigate neural networks for specific applications in passive electronic warfare (EW) involving restoration of deinterleaved pulse trains to their original broadcast form. The project took a generic event-train approach and focused on event-train recognition. It was determined that backpropagation neural networks did not represent a logistically supportable means of training. Gaussian radial basis functions were found to be far superior. This report is composed of three chapters: (1) a summary of early experiments, (2) an introduction to exponential neural networks, and (3) an application to event-train recognition. GRA

N93-12559# Los Alamos National Lab., NM.
ARTIFICIAL INTELLIGENCE AND NEURAL NETWORKS APPLIED TO ION MOBILITY SPECTROMETRY
S. E. Bell and W. C. Mead 1992 34 p Presented at the Symposium on Computer-Enhanced Analytical Spectroscopy, Snowbird, UT, 19 Jun. 1992
(Contract W-7405-eng-36)
(DE92-017508; LA-UR-92-1978; CONF-9206244-1) Avail: CASI HC A03/MF A01

Pattern recognition techniques trace their history back at least 40 years. Applications of pattern recognition techniques to analytical chemistry originated in the 1950's. Several excellent textbooks, articles, and reviews are available to the interested reader. An abbreviated discussion of pattern recognition and relevant applications is presented. DOE

N93-12564# Los Alamos National Lab., NM.
A DISTRIBUTED TIMING SYSTEM FOR SYCHRONIZING CONTROL AND DATA CORRELATION
M. Stettler, M. Thout, L. R. Dalesio, R. Cole, C. Fite, G. Slentz, and D. Warren 1992 4 p Presented at the 16th International LINAC Conference, Ottawa, Ontario, 23-28 Aug. 1992
(Contract W-7405-eng-36)
(DE92-018603; LA-UR-92-2422; CONF-9208109-3) Avail: CASI HC A01/MF A01

Synchronization is necessary in experimental physics machines to provide positive control over related events. The Ground Test Accelerator (GTA) timing system provides this function through a distributed control system, known as the Experimental Physics and Industrial Control System (EPICS). The EPICS timing system was designed to take advantage of a distributed

architecture, and provides time stamping for synchronous data correlation as well as event control. The system has been successfully demonstrated on over a dozen controller nodes for operation and data analysis. The design of the hardware, software, and operational results are discussed. DOE

N93-12607# Science Applications International Corp., San Diego, CA.
DATA TO TEST AND EVALUATE THE PERFORMANCE OF NEURAL NETWORK ARCHITECTURES FOR SEISMIC SIGNAL DISCRIMINATION, VOLUME 1 Scientific Report No. 1
Thomas J. Sereno, Jr. and Gagan B. Patnaik 27 Sep. 1991 64 p
(Contract F19628-90-C-0156)
(AD-A254413; SAIC-91/1236-Vol-1; PL-TR-92-2110-Vol-1; AD-E201102)
Avail: CASI HC A04/MF A01

This report describes a data set that was developed to test and evaluate the performance of neural networks for automated processing and interpretation of seismic data. This data set may also be valuable for many other studies related to seismic monitoring of nuclear explosion testing at regional distance. It includes waveform and parametric data from 241 regional events recorded by the short-period elements of the NORESS and ARCESS arrays in Norway (33 channels/array). The waveform data are stored in SAC binary format, and the parametric data are stored in ASCII files. The event epicentral distances are 200-1800 km, and the event Lg magnitudes are approximately 1.5-3.2. Most of the events are mining explosions in western USSR, Sweden, and Finland. However, 18 of the events are earthquakes, and 22 are presumed underwater explosions. Detailed documentation has been developed for each event and is included in eight separate database reports. GRA

N93-12791# Los Alamos National Lab., NM.
ANALYSIS OF IMS SPECTRA USING NEURAL NETWORKS
S. E. Bell 1992 16 p Presented at the Workshop on Ion Mobility Spectrometry, Ruidoso, NM, 22-26 Jun. 1992
(Contract W-7405-eng-36)
(DE92-017511; LA-UR-92-1953; CONF-9206243-2) Avail: CASI HC A03/MF A01

Ion mobility spectrometry (IMS) has been used for over 20 years, and IMS coupled to gas chromatography (GC/IMS) has been used for over 10 years. There still is no systematic approach to IMS spectral interpretation such as exists for mass spectrometry and infrared spectrometry. Neural networks, a form of adaptive pattern recognition, were examined as a method of data reduction for IMS and GC/IMS. A wide variety of volatile organics were analyzed using IMS and GC/IMS and submitted to different networks for identification. Several different networks and data preprocessing algorithms were studied. A network was linked to a simple rule-based expert system and analyzed. The expert system was used to filter out false positive identifications made by the network using retention indices. The various network configurations were compared to other pattern recognition techniques, including human experts. The network performance was comparable to human experts, but responded much faster. Preliminary comparison of the network to other pattern recognition showed comparable performance. Linkage of the network output to the rule-based retention index system yielded the best performance. DOE

N93-13079# Oak Ridge National Lab., TN.
A NEURAL NETWORK APPROACH FOR THE INVESTIGATION OF CHEMICAL PHENOMENA
J. A. Darsey (Arkansas Univ., Little Rock.), B. G. Sumpter, C. Getino, and D. W. Noid 1992 9 p Presented at the 1992 World of Neural Networks, Houston, TX, 4-7 Nov. 1992
(Contract DE-AC05-84OR-21400)
(DE92-019205; CONF-921186-1) Avail: CASI HC A02/MF A01

Neural networks are coupled with other computational methods (molecular dynamics, Monte Carlo, etc.) in order to obtain information on the structure and atomistic dynamics of chemical systems. Several aspects of this research are discussed: (1) the prediction of multidimensional potential-energy surfaces from vibrational spectra and constant volume heat capacities, (2) mechanisms and rates for energy flow and redistribution, and (3) prediction of physical properties of organic and polymeric systems. The overall results obtained demonstrate the computational power and accuracies that can be achieved by coupling other computational methods with neural networks, as well as providing intriguing results on the internal dynamics of chemical systems. DOE

N93-13129 Purdue Univ., West Lafayette, IN.
ROBUST CONTROL OF UNCERTAIN AEROSPACE AND MECHANICAL SYSTEMS WITH UNMODELLED FLEXIBILITIES: A SINGULAR PERTURBATION APPROACH Ph.D. Thesis
Dong Da 1992 150 p
Avail: Univ. Microfilms Order No. DA9229102

The effect of the flexibility of aerospace/mechanical elements is becoming more significant in engineering applications, e.g., light highspeed robotic manipulators and flexible space structures. In designing a controller for a flexible aerospace/mechanical system, one quite often neglects some of the dynamics of the flexible elements in order to obtain a suitable lower order model. The singular perturbation approach is one approach for developing a controller design methodology based on a lower order model for uncertain flexible aerospace/mechanical systems which guarantees robustness with respect to the uncertainties and the unmodelled dynamics. The main objectives of this thesis are: (1) to obtain several important results for singularly perturbed uncertain systems; and (2) to develop a controller design methodology for uncertain flexible aerospace/mechanical systems described by singularly perturbed systems and to obtain criteria which guarantee that the desired properties of the feedback controlled systems are robust with respect to uncertainty and the unmodelled dynamics. New results in singularly perturbed systems and controller design methods are applicable not only to aerospace/mechanical systems but to all dynamical systems. Dissert. Abstr.

N93-13130 Michigan Univ., Ann Arbor.
COMBINED DESIGN OF STRUCTURES AND CONTROLLERS FOR OPTIMAL MANEUVERABILITY Ph.D. Thesis
Jer Richard Ling 1992 170 p
Avail: Univ. Microfilms Order No. DA9226956

This dissertation develops a theoretical and practical framework for solving problems of optimal structural design and optimal control in an itegrated fashion. This formalism calls for optimization of control objective functions with respect to control and structural design variables; it is applied to time optimal maneuvers of flexible spacecraft. Issues related to the problem formulation, analysis and development of the problem solving procedures, and computational feasibility have been emphasized. The maneuverability index, defined to reflect the time required to perform a rest-to-rest attitude maneuver for a set of given angles, is the primary design objective. The performance degradation of the system, defined to reflect the attitude error after a maneuver, is the secondary objective. We have investigated the performance degradation coming from the uncontrolled dynamics of the structure and from the effect of faults. The performance degradation from the uncontrolled dynamics has been taken into account by the design constraint that the post-maneuver spillover be within a specified bound. In order to account for the performance degradation from the effect of faults, fault tolerance of the system has been considered as a part of the design problem, leading to a multicriterion design problem. The fault tolerant design is to minimize the worst performance degradation from all admissible faults by adjusting the structural design variables of the spacecraft. Adaptive approximate design methods have been developed to overcome the computational difficulties. Numerical examples suggest that optimization of design can provide significant improvement of maneuverability and that it is possible to improve the fault tolerance substantially as well with relatively little loss in the primary objective. Dissert. Abstr.

N93-13156*# National Aeronautics and Space Administration. Marshall Space Flight Center, Huntsville, AL.
AN INTELLIGENT POSITION-SPECIFIC TRAINING SYSTEM FOR MISSION OPERATIONS Final Report
M. P. Schneider Oct. 1992 34 p
(Proj. 9020)
(NASA-TM-108381; NAS 1.15:108381) Avail: CASI HC A03/MF A01

Marshall Space Flight Center's (MSFC's) payload ground controller training program provides very good generic training; however, ground controller position-specific training can be improved by including position-specific training systems in the training program. This report explains why MSFC needs to improve payload ground controller position-specific training. The report describes a generic syllabus for position-specific training

systems, a range of system designs for position-specific training systems, and a generic development process for developing position-specific training systems. The report also describes a position-specific training system prototype that was developed for the crew interface coordinator payload operations control center ground controller position. The report concludes that MSFC can improve the payload ground controller training program by incorporating position-specific training systems for each ground controller position; however, MSFC should not develop position-specific training systems unless payload ground controller position experts will be available to participate in the development process. Author

N93-13238# Advisory Group for Aerospace Research and Development, Neuilly-Sur-Seine (France). Guidance and Control Panel.

MACHINE PERCEPTION [LA PERCEPTION DE L'ENVIRONNEMENT PAR SENSEURS AUTOMATIQUES]

Aug. 1992 205 p Lecture series held in Hamton, VA, 3-4 Sep. 1992, in Neubiberg, Germany, 14-15 Sep. 1992, and in Madrid, Spain, 17-18 Sep. 1992

(AGARD-LS-185; ISBN-92-835-0684-7) Copyright Avail: CASI HC A10/MF A03

Human perceptual capabilities involve the extraction of task-oriented information from environmental stimuli through physical sensing and the use of background knowledge. There are many activities underway aimed at providing similar capabilities of artificial machine perception. Some success is achieved by exploiting what is known of corresponding human cognitive processes and by making use of the increasing power of information processing techniques. For this purpose, the recognition of sharply contrasted as well as fuzzy patterns (stationary or dynamically changing) plays an important role along with other aspects of processing of complex information structures. This lecture series covers the following subjects: pattern recognition techniques; real time visual machine perception, principles and applications in guidance and control (G&C); and real time speech recognition and understanding in the G&C domain. For individual titles, see N93-13239 through N93-13245.

N93-13239# Daimler-Benz A.G., Ulm (Germany). Inst. for Information Technology.

PERCEPTION-BASED AND MACHINE-ORIENTED SIGNAL PROCESSING WITHIN SPEECH UNDERSTANDING SYSTEMS

Helmut Mangold *In* AGARD, Machine Perception Aug. 1992 16 p (For primary document see N93-13238 03-63)

Copyright Avail: CASI HC A03/MF A03

Automatic recognition and understanding of speech signals is one of the key issues of advanced information technology. Language and speech are the relevant topics of cognition and therefore to understand spoken and written language offers basic capabilities for universal processing of information. Speech is man's generic communication medium. Information transfer is widely done by speech communication between humans. There is a basic commonality of understanding each other's spoken messages. This common understanding must be the basis of machine understanding too. Automatic recognition and understanding of spoken language is done in a multistep approach, which starts with the low level signal processing. The output of the recognition step is word recognition. Many possible words, the so called word hypotheses are the basis for intensive linguistic processing. Linguistic processing includes syntactic analysis and semantic analysis. The semantic analysis needs, again, many additional parameters from spoken language, like intonation and prosody to derive the meaning of a spoken phrase. All the processing of natural speech is narrowly related to human information processing. It is therefore possible to learn much from our human processing or from models of this processing. On the other side, statistical methods of information processing offer rather systematic and in many cases advanced methods for handling much of the information contained in speech using purely statistical approaches. To estimate the advantages of the more statistical approaches or more rule based approaches will be a great challenge for future research. Human perception will always be a guide for how to process speech with machines. Author

N93-13240# Carnegie-Mellon Univ., Pittsburgh, PA. School of Computer Science.

SENSING AND INTERPRETATION OF 3-D SHAPE AND MOTION

Takeo Kanade *In* AGARD, Machine Perception Aug. 1992 36 p (For primary document see N93-13238 03-63)

Copyright Avail: CASI HC A03/MF A03

Robotics is where artificial intelligence meets the physical world. Computer vision provides robots with the perceptual capabilities which are especially critical for robots that operate in an unconstrained natural environment. In computer vision, recovery of 3D shape and motion is the key to understanding scenes. Thus, the problem has attracted much of the attention of vision researchers over the last decade, and many sophisticated algorithms have been developed. I address three recently developed methods for sensing and interpreting 3D shape and motion: the factorization method for image sequence analysis; very fast range imaging by analog VLSI smart chip; and the multi-baseline stereo method. It is interesting to note that while the performance of these methods has exceeded that of previous methods, the algorithms, themselves are simpler and more straightforward. In addition to enhanced performance, these algorithms are suitable for real-time parallel implementation by special hardware or VLSI. A detailed description of these methods is presented. Author

N93-13241# SRI International Corp., Menlo Park, CA. Artificial Intelligence Center.

BUILDING AND USING SCENE REPRESENTATIONS IN IMAGE UNDERSTANDING

H. Harlyn Baker *In* AGARD, Machine Perception Aug. 1992 12 p Sponsored in part by Fujitsu System Integration Lab. (For primary document see N93-13238 03-63)

(Contracts DACA76-85-C-0004; DACA76-90-C-0021; DACA76-92-C-0003)

Copyright Avail: CASI HC A03/MF A03

The task of having computers able to understand their environments through direct imaging has proved to be formidable. With its beginnings about 30 years ago, the field of computer vision has grown as a major part of the pursuit for artificial intelligence. Most elements of this pursuit - language understanding, reasoning and planning, speech - are very difficult challenges, but vision, with its high dimensionality of space, time, scale, color, dynamics, and so forth, may be the most challenging. Early attempts to develop computer vision focused on restricted situations in which it was feasible to provide the computer with fairly complete descriptions of what it would encounter. In such cases, single images provided the sensory information for analysis. As the domains of application grew, the requirements for more competent descriptions of the world increased. Dealing with three-dimensional (3D) dynamic structures (the real world) from 3D dynamic platforms (we humans) calls for greater capabilities on both the analysis and synthesis sides of the issue. The analysis side is the processing of sensory data for such tasks as recognition and navigation, and a number of techniques are discussed here for dealing with these two-, three-, and higher-dimensional data. The synthesis side is the construction of 'internal' descriptions of what is seen in the environment - constructed now so that they may be used subsequently for the above tasks. This latter issue is the underlying theme we pose in this paper - developing representations from vision that will later enable effective automated operations in our 3D dynamic environments. Author

N93-13242# Paris-Sud Univ., Orsay (France). Inst. d'Electronique Fondamentale.

SILICON VISION: ELEMENTARY FUNCTIONS TO BE IMPLEMENTED ON ELECTRONIC RETINAS

B. Zavidovique and T. Bernard *In* AGARD, Machine Perception Aug. 1992 17 p (For primary document see N93-13238 03-63)

Copyright Avail: CASI HC A03/MF A03

A smart retina is a device which intimately associates an optoelectronic layer with processing facilities. The rapprochement between acquisition and processing is particularly suited for the emergence of novel kinds of interaction, between analog and digital massive computations. Therefore, several attempts of analog, possibly neural, computations linked to the vision process are listed and discussed. But analog is not enough for really smartening retinas. Then, an additional plausible coat of cellular boolean iterative processing in these 'human size' vision machines is described, and commented on through examples. Author

N93-13243# Elettronica San Giorgio S.p.A., Genoa (Italy). Research and Development Dept.

3-D COMPUTER VISION FOR NAVIGATION/CONTROL OF MOBILE ROBOTS

G. B. Garibotto and S. Masciangelo *In* AGARD, Machine Perception Aug. 1992 13 p (For primary document see N93-13238 03-63)
(ESPRIT Proj. P-940; ESPRIT Proj. P-2502)
Copyright Avail: CASI HC A03/MF A03

The aim of this lecture is to investigate how much visual sensors may be effective in supporting autonomous navigation of mobile robots. Although in practical realizations, with robustness and reliability constraints, it is always necessary to integrate multi-sensor modalities, the discussion here is limited to an analysis of computer vision advantages and disadvantages, with particular attention given to: (1) a binocular stereo vision module for obstacle detection, with no precise calibration (reactive process to operate at a fast rate, from 5 to 10 Hz); trinocular stereovision based on segment primitives for the reconstruction of free space for navigation, in which case an acccurate calibration procedure is requested; and landmark detection for self-positioning and orientation of a mobile vehicle, using perspective invariants, for indoor navigation. Some comments are also provided on computer vision architectures to support real time implementations. A real-time front end vision subsystem is described, which is able to compute 3D segment based stereovision at 5 Hz and segment token tracking at 10 Hz. Finally, some demo arrangements are briefly discussed where an intense experimentation of such results is in progress, as a test bed for different industrial applications. Author

N93-13244# Universitaet der Bundeswehr Muenchen, Neubiberg (Germany). Dept. of Aerospace Technology.

MACHINE PERCEPTION EXPLOITING HIGH-LEVEL SPATIO-TEMPORAL MODELS

E. D. Dickmanns *In* AGARD, Machine Perception Aug. 1992 17 p (For primary document see N93-13238 03-63)
Copyright Avail: CASI HC A03/MF A03

A paradigm for machine perception is presented which takes time and 3D space in an integrated manner as the underlying framework for internal representation of the sensorially observed outside world. This world is considered to consist of material and mental processes evolving over time. The concept of state and control variables developed in the natural sciences and engineering over the last three centuries is exploited to find a new, more natural access to dynamic real-time vision and intelligence. Schopenhauer's conjecture of 'The world as evolving process and internal representation' (1819) is combined with modern recursive estimation techniques (Kalman 60) and some components from geometry and AI in order to arrive at a very efficient scheme for autonomous robotic agents dealing with evolving processes in the real world in real time. Application to autonomous mobile robots is discussed. Author

N93-13245# Roke Manor Research Ltd., Romsey (England).

THE 3-D COMPUTER VISION TECHNIQUES FOR OBJECT FOLLOWING AND OBSTACLE AVOIDANCE

Richard Evans *In* AGARD, Machine Perception Aug. 1992 24 p Sponsored in part by Commission of the European Communities (For primary document see N93-13238 03-63)
Copyright Avail: CASI HC A03/MF A03

Imaging sensors are powerful tools enabling remote control, by tele-operation, of numerous tasks where the operator requires an appreciation of the three-dimensional structure of the viewed scene. Passive video sensors also lend themselves to tasks where covert operation or electromagnetic compatibility is required. A commonly mooted tele-operational task is that of driving a known vehicle through an unknown terrain - or keeping station on a known object moving through an unknown terrain. The computer vision aspects of automating this task are divided into two separate vision functions, which are the subjects of this paper: (1) analysis of image sequences of a general scene to extract its three dimensional (3D) structure without any prior information; and (2) analysis of images of a well defined object, to extract its 3D position and orientation relative to the sensor. For both these functions, the paper provides a brief introduction to possible techniques followed by further descriptions of particular systems, DROID and RAPiD, developed by Roke Manor Research Limited. DROID is a general, feature-based 3D vision system using the structure-from-motion principle. That is, it uses the apparent image-plane movement of localized features viewed by a moving sensor to extract the three-dimensional structure of the scene. RAPiD is a model-based real-time tracker which extracts the position (X,Y,Z) and orientation (roll, pitch, yaw) of a known object from image data. The system operates iteratively, using prediction of object pose (position and orientation) to cue the search for selected edge features in subsequent imagery. This approach results in minimal processing of image pixels, so that the system can be implemented at full video rate using modest hardware. Author

N93-13289*# National Aeronautics and Space Administration. Marshall Space Flight Center, Huntsville, AL.

OPTIMAL CONTROL COMPUTER PROGRAMS

F. Kuo Nov. 1992 57 p
(NASA-TM-108384; NAS 1.15:108384) Avail: CASI HC A04/MF A01

The solution of the optimal control problem, even with low order dynamical systems, can usually strain the analytical ability of most engineers. The understanding of this subject matter, therefore, would be greatly enhanced if a software package existed that could simulate simple generic problems. Surprisingly, despite a great abundance of commercially available control software, few, if any, address the part of optimal control in its most generic form. The purpose of this paper is, therefore, to present a simple computer program that will perform simulations of optimal control problems that arise from the first necessary condition and the Pontryagin's maximum principle. Author

N93-13336 Florida Atlantic Univ., Boca Raton.

OPTIMAL COORDINATION OF ROBOTIC SYSTEMS WITH REDUNDANCY Ph.D. Thesis

K. R. Hareendra Varma 1992 178 p
Avail: Univ. Microfilms Order No. DA9218820

The research work described in this dissertation is primarily aimed at developing efficient algorithms for the rate allocation problem in redundant serial chain manipulators. While the problem of redundancy resolution in the context of robot manipulators, had been a well researched one, search for optimality in computational efficiency has caught the attention only recently. Further, the idea of modifying the already developed performance criteria to improve computational efficiency, had rarely been treated with the importance it deserves. The present work in fact, provides many alternative formulations to the existing performance criteria. As a result of the present investigation, we developed a mathematical tool for the minimum norm solution for underdetermined systems of linear equations, using the orthogonal null space. Closed form equations were provided for cases with two or three degrees of redundancy. Detailed study of computational efficiency showed substantial reduction in the arithmetic operations necessary for such a solution. The above concept was later generalized to utilize the self motion characteristics of redundant manipulators, to provide alternate solutions. The duality concept between the Jacobian and the null space, established in this work, enabled the authors to develop a highly efficient formulation as an alternative to the commonly used pseudoinverse-based solution. In addition, by providing the example of a 7R anthropomorphic arm, the feasibility of obtaining analytical formulation of null space coefficient matrix and the transformed end effector velocity vector for any geometry has been demonstrated. By utilizing the duality between the Jacobian and its null space, different performance criteria commonly used in the redundancy resolution problem have been modified, increasing the computational efficiency. Various simulations performed as part of the present work, utilizing the analytical null space coefficient matrix and the transformed end effector velocity vector for 3R planar case and 7R spatial anthropomorphic arm corroborates the theories. Another practical application has been demonstrated by the example of a Titan 7F arm mounted on a mobile base. The work is consolidated by reiterating the insight obtained to the physical aspects of the redundancy resolution problem and providing a direction for future work. Suggestions are given for extending the work for high d.o.r. systems, with relevant mathematical foundations. Future work in the area of dynamic modelling, is delineated which also includes an example of modified dynamic manipulability measure.
Dissert. Abstr.

N93-13366*# Research Inst. for Advanced Computer Science, Moffett Field, CA.

MYTHS AND LEGENDS IN LEARNING CLASSIFICATION RULES

Wray Buntine (Turing Inst., Glasgow, Scotland) May 1990 10 p

Submitted for publication
(Contract NCC2-387)
(NASA-CR-191236; NAS 1.26:191236; RIACS-TR-90-23) Avail: CASI HC A02/MF A01

This paper is a discussion of machine learning theory on empirically learning classification rules. The paper proposes six myths in the machine learning community that address issues of bias, learning as search, computational learning theory, Occam's razor, 'universal' learning algorithms, and interactive learnings. Some of the problems raised are also addressed from a Bayesian perspective. The paper concludes by suggesting questions that machine learning researchers should be addressing both theoretically and experimentally. Author

N93-13370*# Information and Control Systems, Inc., Hampton, VA.
A STOCHASTIC OPTIMAL FEEDFORWARD AND FEEDBACK CONTROL METHODOLOGY FOR SUPERAGILITY Final Report
Nesim Halyo, Haldun Direskeneli, and Deborah B. Taylor Washington Nov. 1992 150 p Sponsored by NASA. Langley Research Center
(Contract NAS1-19091; RTOP 324-02-01-01)
(NASA-CR-4471; NAS 1.26:4471; FR-692101) Avail: CASI HC A07/MF A02

A new control design methodology is developed: Stochastic Optimal Feedforward and Feedback Technology (SOFFT). Traditional design techniques optimize a single cost function (which expresses the design objectives) to obtain both the feedforward and feedback control laws. This approach places conflicting demands on the control law such as fast tracking versus noise atttenuation/disturbance rejection. In the SOFFT approach, two cost functions are defined. The feedforward control law is designed to optimize one cost function, the feedback optimizes the other. By separating the design objectives and decoupling the feedforward and feedback design processes, both objectives can be achieved fully. A new measure of command tracking performance, Z-plots, is also developed. By analyzing these plots at off-nominal conditions, the sensitivity or robustness of the system in tracking commands can be predicted. Z-plots provide an important tool for designing robust control systems. The Variable-Gain SOFFT methodology was used to design a flight control system for the F/A-18 aircraft. It is shown that SOFFT can be used to expand the operating regime and provide greater performance (flying/handling qualities) throughout the extended flight regime. This work was performed under the NASA SBIR program. ICS plans to market the software developed as a new module in its commercial CACSD software package: ACET. Author

N93-13376*# Illinois Univ., Urbana. Coordinated Science Lab.
RESOURCE CONSTRAINED DESIGN OF ARTIFICIAL NEURAL NETWORKS USING COMPARATOR NEURAL NETWORK
Benjamin W. Wah and Tanay S. Karnik 19 Nov. 1992 20 p
(Contract NCC2-481)
(NASA-CR-191280; NAS 1.26:191280; UILU-ENG-92-2242; CRHC-92-24)
Avail: CASI HC A03/MF A01

We present a systematic design method executed under resource constraints for automating the design of artificial neural networks using the back error propagation algorithm. Our system aims at finding the best possible configuration for solving the given application with proper tradeoff between the training time and the network complexity. The design of such a system is hampered by three related problems. First, there are infinitely many possible network configurations, each may take an exceedingly long time to train; hence, it is impossible to enumerate and train all of them to completion within fixed time, space, and resource constraints. Second, expert knowledge on predicting good network configurations is heuristic in nature and is application dependent, rendering it difficult to characterize fully in the design process. A learning procedure that refines this knowledge based on examples on training neural networks for various applications is, therefore, essential. Third, the objective of the network to be designed is ill-defined, as it is based on a subjective tradeoff between the training time and the network cost. A design process that proposes alternate configurations under different cost-performance tradeoff is important. We have developed a Design System which schedules the available time, divided into quanta, for testing alternative network configurations. Its goal is to select/generate and test alternative network configurations in each quantum, and find the best network when time is expended. Since time is limited, a dynamic schedule that determines the network configuration to be tested in each quantum is developed. The schedule is based on relative comparison of predicted training times of alternative network configurations using comparator network paradigm. The comparator network has been trained to compare training times for a large variety of traces of TSSE-versus-time collected during back-propagation learning of various applications. Author

N93-13442*# National Aeronautics and Space Administration. Langley Research Center, Hampton, VA.
SPACE ROBOTICS: RECENT ACCOMPLISHMENTS AND OPPORTUNITIES FOR FUTURE RESEARCH Annual Report, 1991 - 1992
Raymond C. Montgomery, Carey S. Buttrill, John T. Dorsey, Jer-Nan Juang, Frederick J. Lallman, Daniel D. Moerder, Michael A. Scott, Patrick Troutman, and Robert L. Williams, II Sep. 1992 23 p
(RTOP 590-14-11-01)
(NASA-TM-107675; NAS 1.15:107675) Avail: CASI HC A03/MF A01

The Langley Guidance, Navigation, and Control Technical Committee (GNCTC) was one of six technical committees created in 1991 by the Chief Scientist, Dr. Michael F. Card. During the kickoff meeting Dr. Card charged the chairmen to: (1) establish a cross-Center committee; (2) support at least one workshop in a selected discipline; and (3) prepare a technical paper on recent accomplishments in the discipline and on opportunities for future research. The Guidance, Navigation, and Control Committee was formed and selected for focus on the discipline of Space robotics. This report is a summary of the committee's assessment of recent accomplishments and opportunities for future research. The report is organized as follows. First is an overview of the data sources used by the committee. Next is a description of technical needs identified by the committee followed by recent accomplishments. Opportunities for future research ends the main body of the report. It includes the primary recommendation of the committee that NASA establish a national space facility for the development of space automation and robotics, one element of which is a telerobotic research platform in space. References 1 and 2 are the proceedings of two workshops sponsored by the committee during its June 1991, through May 1992 term. The focus of the committee for the June 1992 - May 1993 term will be to further define to the recommended platform in space and to add an additional discipline which includes aircraft related GN&C issues. To the latter end members performing aircraft related research will be added to the committee. (A preliminary assessment of future opportunities in aircraft-related GN&C research has been included as appendix A.) Author

N93-13925 Stanford Univ., CA.
ROBUST CONTROLLER AND ESTIMATOR DESIGN USING MINIMAX METHODS Ph.D. Thesis
Raymond Arthur Mills 1992 215 p
Avail: Univ. Microfilms Order No. DA9221645

Optimal control methods yield high performance for the plant model used to design the controller, but the resulting closed-loop system is sometimes sensitive to plant parameter variations. This sensitivity causes performance degradation and even instability when the control is applied to the actual plant, since the plant parameters are never known exactly. Such sensitivity occurs especially in plants containing lightly damped oscillatory modes, which are common in aerospace systems. We propose a minimax algorithm for designing controllers that give the best closed-loop linear-quadratic-gaussian (LQG) performance over a set of worst plant parameter changes from nominal. The algorithm combines a multi-plant optimal control design code, SANDY, with a worst-parameter algorithm that uses an ellipsoidal norm on parameter changes. The minimax algorithm is unique in the way it weights worst plants to expand the stable region in the parameter space. A new LQG derivation is used to derive saddle-point necessary conditions which are stopping criteria for the minimax algorithm. The minimax derivation suggests a calculus of variations H(infinity) derivation, which shows that the H(infinity) controller is simply a differential game between the control and the worst bounded disturbance. Minimax control design compares favorably with H(infinity)-based 'mu-synthesis'. The optimal LQG estimator (Kalman filter) is formulated as a special case of the LQG controller, making all controller results equally valid for estimation. Thus, the worst-parameter algorithm also assesses estimator robustness and the minimax algorithm also designs robust estimators. The minimax algorithm is applied to a three-parameter two-mass/spring benchmark problem, a six-parameter helicopter near hover, and a four-parameter space telescope.

The results show that minimax control provides near-optimal nominal performance with significant robustness and parameter margin improvements. Surprisingly the minimax controllers differ relatively little from the nominal LQG controllers. Dissert. Abstr.

N93-14021 Texas A&M Univ., College Station.
ON A ROBUST CONTROLLER DESIGN USING A MINIMAX OPTIMIZATION APPROACH Ph.D. Thesis
Shih-Tein Hsu 1991 182 p
Avail: Univ. Microfilms Order No. DA9216942

An extension of the Linear Quadratic Regulator, and Linear Quadratic Gaussian methodology is proposed to design a robust controller from the viewpoint of eigenvalue sensitivity. The resulting system is optimal under the worst case of norm-bounded initial condition uncertainty, norm-bounded deterministic noise, and norm-bounded parameter uncertainty. The uncertainties are modelled such that we can formulate the problem on a zero-sum, two-sided minimax game. The minimax solution is proved to be a saddle point solution under either the positivity of control-disturbance authority, or the strict concavity of the open loop system. The existence of the solution is proven by using the successive approximation technique. The theory considers both finite dimensional and infinite dimensional systems. By using the trace operator of the product of two Hilbert-Schmidt operators, all the matrix theory in the finite dimensional minimax control theory can be extended to distributed parameter systems. A finite dimensional approximation scheme also is developed. It is proven that the minimax solution of the infinite dimensional problem can exactly be specified by a convergent sequence of minimax solutions of finite dimensional approximations of the problem. Examples that provide verification of the theory presented include (1) scalar minimax controller design, (2) finite dimensional output feedback minimax robust controller design, and (3) minimax controller design of a parabolic heat problem by spline approximation. Results are (1) to broaden the application of minimax control theory and make it a straightforward engineering tool for robust controller design by using eigenvalue sensitivity approach and (2) to show the feasibility of finite dimensional approximation of the worst case distributed parameter system robust control. Dissert. Abstr.

N93-14039 Texas A&M Univ., College Station.
NEAR-MINIMUM-TIME CONTROL OF A FLEXIBLE ARM Ph.D. Thesis
Norman Karl Hecht 1991 74 p
Avail: Univ. Microfilms Order No. DA9216935

Near-minimum-time control of flexible manipulators can be accomplished by designing a controller that tracks a reference maneuver. The control method presented here uses a near-minimum-time rigid link reference maneuver, and a Liapunov controller to make the flexible manipulator track the reference maneuver while reducing and eventually eliminating flexible motions. The near-minimum-time reference maneuvers have been developed using a function-space gradient method to derive optimal smoothed switch times for the control torques for a rigid arm. This method maintains much of the performance of the true bang-bang minimum time control, while the smoothing of the changes in torque level reduces the energy delivered to the flexible motion of the links. The Liapunov function for the tracking controller is a weighted sum of the energies of the elements of the flexible manipulator and the control law is chosen to make the rate of change of the Liapunov function negative. The Liapunov function is bounded during a maneuver, and decays asymptotically after the maneuver ends. The tracking controller is demonstrated using a numerical simulation of a flexible arm. The equations of motion are solved by a new implicit, second-order integration scheme that efficiently solves the equations of motion of flexible, multi-body structures. These techniques show that rigid-body reference motions are adequate, but that including one flexible mode per link of the arm would improve performance. Smoothing proves to be valuable in reducing the energy in higher-order modes, in both open- and closed-loop motions. The combination of a simple flexible reference motion with a smooth control-torque profile would give excellent results in executing rapid motions of flexible robots. Dissert. Abstr.

N93-14045 Purdue Univ., West Lafayette, IN.
Q-MARKOV COVER IDENTIFICATION AND INTEGRATED MCA-OVC CONTROLLER DESIGN FOR FLEXIBLE STRUCTURES Ph.D. Thesis
Ketao Liu 1991 215 p
Avail: Univ. Microfilms Order No. DA9215600

The main objective is to develop methods for indentification and control of flexible structures. The specific problems this research focused upon are the following, (1) applying the Q-Markov Cover theory to the indentification of flexible structures, (2) developing an integrated model reduction and controller design method, and (3) developing a controller design method to accommodate finite wordlength errors for flexible structure controls at fast sampling rates. This research takes linear algebra approach to simplify the existing solutions of the Q-Markov Cover indentification algorithm and to analyze its indentification errors due to measurement noises. Under the assumption that measurement noises have rational spectrums, analytic formulas of the errors are obtained. These formulas reveal that under certain conditions, some system parameters (eigenvalues for example) can be correctly identified. Based upon this analytical result, a new algorithm which is capable of identifying some system parameters correctly is developed. The MCA model reduction and OVC controller design algorithms are integrated into an iterative method for low order high performance controller designs based upon high order models. The resulting integrated MCA-OVC controller design method is a heuristic method which probes the stability boundaries of the closed loop systems formed by the high order model and low order controllers and searches for the maximum accuracy of the low order controllers. This research studies the effects of the finite wordlength errors on the LQC controllers. Under the assumptions that the controls are computed by fix point computations and that the external excitations are white, the lower and upper bounds of the influences of the finite wordlength errors on control systems are analyzed. An optimal control design method which is capable of accommodating the finite wordlength errors is developed. NASA's ACES structure is a ground test facility for flexible space structure controls. The effectiveness of the Q-Markov Cover identification and the integrated MCA-OVC controller design algorithms are successfully shown by the identification and control experiments on the ACES structure. Dissert. Abstr.

N93-14065 Texas Univ., Arlington.
POSITION AND FORCE CONTROL OF FLEXIBLE AND RIGID MANIPULATORS USING THE SLIDING-MODE TECHNIQUE Ph.D. Thesis
Jesus Flores-Morfin 1991 134 p
Avail: Univ. Microfilms Order No. DA9217629

A robust control to achieve position tracking and force regulation for multi-link manipulators is presented. The cases of rigid and flexible manipulators are considered. The sliding-mode technique is used in both cases for obtaining a control law which is robust to parameter variations of the manipulator and its environment. For both cases, rigid and flexible, the main features of the proposed algorithm are: (1) The formulation of the control law is simple; (2) It is not required to invert the inertial matrix or the Jacobian matrix; (3) The control law does not require the derivative of the force signal; and (4) The designed sliding-mode controller is robust to variations of the payload and the stiffness of the environment. As a consequence, the control law requires no payload forecast or estimation of the stiffness of the environment. For both cases of rigid and flexible manipulators, the Lagrangian formulation is used to derive the models of the manipulators. In the flexible case, the deformation of the flexible link is formulated using the clamped-loaded Euler-Bernoulli beam theory and the assumed-modes method. Results of simulation studies verify the effectiveness of this controller. Also, robustness of the controller against both payload and stiffness variations is verified. Dissert. Abstr.

64 NUMERICAL ANALYSIS

Includes iteration, difference equations, and numerical approximation.

N93-12582# Cornell Univ., Ithaca, NY.
ANALYSIS OF A LINEARLY CONSTRAINED LEAST SQUARES ALGORITHM FOR ADAPTIVE BEAMFORMING
Franklin T. Luk and Sanzheng Qiao Aug. 1992 13 p Prepared in cooperation with Rensselaer Polytechnic Inst., Troy, NY
(Contract DAAL03-90-G-0104)
(AD-A255017; ARO-26930.1-MA-SDI) Avail: CASI HC A03/MF A01

The problem of linearly constrained least squares has many applications in signal processing. In this paper, we present a perturbation analysis of a linearly constrained least squares algorithm for adaptive beamforming. The

perturbation bounds for the solution as well as for the latest residual element are derived. We also propose an error estimation scheme for the residual element, which can be incorporated into a systolic array implementation of the algorithm. GRA

N93-12594# Wisconsin Univ., Madison. Center for Mathematical Sciences.
HYPERBOLIC CONSERVATION LAWS WITH UMBILIC POINTS, 1
Gui-Qiang Chen and Pui T. Kan Aug. 1992 61 p
(Contract N00014-91-J-1384)
(AD-A254431; CMS-TSR-92-3) Avail: CASI HC A04/MF A01

In this paper a compactness framework for approximate solutions to nonlinear hyperbolic systems with umbilic points is established by combining ideas in modern nonlinear analysis with classical methods and by a detailed analysis of a highly singular Euler-Poisson-Darboux-type equation. Then this framework is successfully applied to prove the convergence of the Lax-Friedrichs scheme, the Godunov scheme, and the viscosity method, and the existence of global entropy solutions for the Cauchy problem with large initial data for a canonical class of the quadratic flux systems and other related systems. In forthcoming papers we apply (a variant of) this framework to solve the other three canonical classes of the quadratic flux systems, the system of three-phase flow in porous media, and other related systems with umbilic points. GRA

N93-12625 Cincinnati Univ., OH.
AN INVESTIGATION OF NEW SEARCH TECHNIQUES FOR THE TRAVELING SALESMAN PROBLEM Ph.D. Thesis
Shigeru Tsubakitani 1991 244 p
Avail: Univ. Microfilms Order No. DA9205407

The traveling salesman problem (TSP) is one of the most widely-studied problems in combinatorial optimization. The problem is to seek the minimum tour of N nodes visiting every node exactly once and coming back to the starting node. The TSP belongs to the class of NP-complete problems for which polynomial algorithms have not yet been developed. Since the computational effort demanded by optimal procedures grows exponentially with the problem size, many heuristic procedures have been developed. Tabu search, which employs the artificial intelligence concepts of short or long term memory, is believed to be the state of the art heuristic procedure for the TSP. A new heuristic search procedure for the TSP is developed. The new procedure, called 'jump search', is designed to diversify the search in the solution space. Jump search is a meta-heuristic that provides guidance to prevent certain local search procedures from being trapped at local optima. Unlike tabu search, which continuously moves from one solution to another in a 2-opt or 3-opt neighborhood, jump search jumps from local optima to new solutions outside the neighborhood thereby covering more diverse areas of the solution space. The effectiveness of jump search is examined empirically on 157 problems, seven published in the literature and the rest randomly generated problems having 50, 100, and 150 nodes. Jump search is compared with tabu search and iterative local search with random starting points for fixed computational times using 2-opt and 3-opt heuristics. A statistical analysis is used to compare the effectiveness of these three meta-heuristics. The computational experiments reveal that jump search significantly outperformed tabu search and iterative local search for all computational time limits tested in this dissertation. In these cases, the 2-opt and 3-opt based jump search procedures find better (and sometimes much better) solutions at an early stage of the search process, and improve somewhat the incumbent solution as the search process progresses. Two-opt and 3-opt based jump search procedures do not differ significantly in their performance for given computational times.
Dissert. Abstr.

N93-12640# Carnegie-Mellon Univ., Pittsburgh, PA. Graduate School of Industrial Administration.
FROM TOTALLY UNIMODULAR TO BALANCED 0, +/- 1 MATRICES: A FAMILY OF INTEGER POLYTOPES
Michele Conforti, Gwrard Cornuwjols, and Klaus Truemper 7 Jul. 1992 6 p
(Grants NSF DDM-92-01340; NSF DDM-90-01750; NSF DMS-90-00376)
(AD-A254552) Avail: CASI HC A02/MF A01

In this paper we introduce a family of integer polytopes and characterize them in terms of forbidden submatrices. The two extreme cases in this family arise when the constraint matrix is totally unimodular and balanced, respectively. This generalizes results of Truemper-Chandrasekaran and Conforti-Cornuejols. GRA

N93-12701# Maryland Univ., College Park. Inst. for Physical Science and Technology.
QUALITY ASSESSMENT OF THE A-POSTERIORI ERROR ESTIMATION IN FINITE ELEMENTS Final Report
Ivo Babuska, Lothar Plank, and Rodolfo Rodriguez Aug. 1991 30 p
(Contract N00014-90-J-1030; NSF CCR-88-20279)
(AD-A254767; BN-1127) Avail: CASI HC A03/MF A01

The paper addresses results of numerical experimentation with an a-posteriori error estimator which was theoretically analyzed in an earlier work. The paper concentrates on the problems of the selection of benchmarks which is directed to a numerical verification of basic theoretical features of the estimator. GRA

N93-12847# Wisconsin Univ., Madison. Center for Mathematical Sciences.
ON ASCERTAINING INDUCTIVELY THE DIMENSION OF THE JOINT KERNEL OF CERTAIN COMMUTING LINEAR OPERATORS
Carl DeBoor, Amos Ron, and Zuowei Shen Jun. 1992 32 p
(Contract DAAL03-90-G-0090; NSF DMS-90-00053)
(AD-A254748; CMS-TSR-92-13) Avail: CASI HC A03/MF A01

Given a linear space S (over some field), we attempt to determine the dimension of spaces of a certain form with a L(a)(finite) sequence of linear endomorphisms of S, i.e., a sequence in L(S). GRA

N93-12889# Institut des Hautes Etudes Scientifiques, Bures-sur-Yvette (France).
SOLUTIONS WITHOUT PHASE-SLIP FOR THE GINSBURG-LANDAU EQUATION
P. Collet (Ecole Polytechnique, Palaiseau, France) and J.-P. Eckmann (Geneva Univ., Switzerland) Sep. 1991 21 p Sponsored in part by Direction des Recherches, Etudes et Techniques and Schweizenischer Nationalfonds zur Foederung der Wissenschaftlichen Forschung
(PB92-115575; IHES/P/91/64) Avail: CASI HC A03/MF A01

The authors consider the Ginsburg-Landau equation for a complex scalar field in one dimension and consider initial data which have two different stationary solutions as their limits in space as x approaches plus or minus infinity. If these solutions are not very different, then it is shown that the initial data will evolve to a stationary solution by a 'phase melting' process which avoids 'phase slips', i.e., which does not go through zero amplitude. GRA

N93-12942*# Institute for Computer Applications in Science and Engineering, Hampton, VA.
FAST MULTIRESOLUTION ALGORITHMS FOR MATRIX-VECTOR MULTIPLICATION Final Report
Ami Harten (Tel-Aviv Univ., Israel) and Itai Yad-Shalom (Tel-Aviv Univ., Israel) Oct. 1992 44 p Submitted for publication
(Contracts NAS1-18605; NAS1-19480; N00014-91-J-1034; NSF DMS-91-03104; RTOP 505-90-52-01)
(NASA-CR-189721; NAS 1.26:189721; ICASE-92-55) Avail: CASI HC A03/MF A01

In this paper we present a class of multiresolution algorithms for fast application of structured dense matrices to arbitrary vectors, which includes the fast wavelet transform of Beylkin, Coifman and Rokhlin and the multilevel matrix multiplication of Brandt and Lubrecht. In designing these algorithms we first apply data compression techniques to the matrix and then show how to compute the desired matrix-vector multiplication from the compressed form of the matrix. In describing this class we pay special attention to an algorithm which is based on discretization by cell-averages as it seems to be suitable for discretization of integral transforms with integrably singular kernels. Author

N93-13027# Columbia Univ., New York, NY. Dept. of Applied Physics.
ANALYTICAL STUDIES OF NONLINEAR PARTIAL DIFFERENTIAL EQUATIONS OF INTEREST IN NONLINEAR OPTICS Final Report, 1 Mar. 1991 - 31 Mar. 1992
M. J. Potasek 5 May 1992 21 p

(Contract DAAL03-91-G-0090)
(AD-A254931; ARO-28803.4-MA) Avail: CASI HC A03/MF A01

We use the time-dependent Hartree approximation to obtain solutions to a quantized higher-order nonlinear Schroedinger equation. This equation describes pulses propagating, in nonlinear optical fibers and, under certain conditions, has femtosecond soliton solutions. These solitons travel at velocities that differ from those of the picosecond solitons obtained from the standard quantized nonlinear Schroedinger equation. Furthermore, we find that quadruple-clad fibers are required for the propagation of these solitons, unlike the solitons of the standard nonlinear Schroedinger equation which can propagate in graded-index optical fibers. From the quantum solution, we find that the soliton experiences phase-spreading and self-squeezing as it propagates. GRA

N93-13271# Geophysical Observatory, Helsinki (Finland). Dept. of Mathematics.
RECURSIVE CONSTRUCTION OF FRACTALS Thesis
Leif M. Andersson 1992 50 p Sponsored in part by Finnish Society of Sciences; Finnish Cultural Foundation; and Academy of Finland
(ISBN-951-41-0689-X) Avail: CASI HC A03/MF A01

A general theory for the setting up of recursive constructions involving contractions in complete metric space is presented. In this context, the following topics are discussed: the convergence of recursive models to limit sets; and the Hausdorff and similarity dimensions of these sets. The first chapter focuses on the convergence of recursive sequences and characterizes the limit points. The second chapter deals with the convergence behavior of the whole model and examines the limit sets in different cases. The third and fourth chapters concentrate on the relation between the Hausdorf and similarity dimensions of the fractal set. The fifth provides some applications of the theory. Author

N93-13363 Tennessee Univ., Knoxville.
A METHODOLOGY FOR THE SOLUTION OF NONLINEAR TWO-POINT BOUNDARY VALUE INVERSE PROBLEMS IN PHYSICS AND ENGINEERING Ph.D. Thesis
Daniele Ugolini 1991 172 p
Avail: Univ. Microfilms Order No. DA9221818

The development is examined of a new methodology for the solution of two-point boundary value inverse problems and on its application to solve inverse problems in science and engineering. The new methodology, derived from the parallel shooting method, attempts to improve the performance time of the original method by modifying the convergence iteration procedure. In an effort to further improve the speed of the calculation, the algorithm was also implemented on a shared memory parallel computer. The new methodology is used to solve inverse problems in (1) optimal control, to calculate the xenon concentration buildup in a nuclear reactor, the optimal fuel distribution in a slab reactor and to solve the stationary Schrodinger equation, (2) computer simulation, to determine the heat transfer coefficients in a sodium to water heat exchanger, and (3) applied quantum physics, to design semiconductor devices. The results show that the new methodology achieves a much faster performance time compared to the one of the traditional parallel shooting method. Also, the new methodology shows to be very reliable since highly nonlinear two-point boundary value inverse problems could be quite easily solved.
Dissert. Abstr.

N93-13409*# Research Inst. for Advanced Computer Science, Moffett Field, CA.
EFFICIENT SOLUTION OF PARABOLIC EQUATIONS BY KRYLOV APPROXIMATION METHODS
E. Gallopoulos (Illinois Univ., Urbana-Champaign.) and Y. Saad (Minnesota Univ., Minneapolis.) Mar. 1990 30 p Sponsored in part by American Telephone and Telegraph Co.
(Contracts NCC2-387; DE-FG02-85ER-25001; AF-AFOSR-0044-90; NSF CCR-87-17942)
(NASA-CR-191235; NAS 1.26:191235; RIACS-TR-90-14) Avail: CASI HC A03/MF A01

Numerical techniques for solving parabolic equations by the method of lines is addressed. The main motivation for the proposed approach is the possibility of exploiting a high degree of parallelism in a simple manner. The basic idea of the method is to approximate the action of the evolution operator on a given state vector by means of a projection process onto a Krylov subspace. Thus, the resulting approximation consists of applying an evolution operator of a very small dimension to a known vector which is, in turn, computed accurately by exploiting well-known rational approximations to the exponential. Because the rational approximation is only applied to a small matrix, the only operations required with the original large matrix are matrix-by-vector multiplications, and as a result the algorithm can easily be parallelized and vectorized. Some relevant approximation and stability issues are discussed. We present some numerical experiments with the method and compare its performance with a few explicit and implicit algorithms.
Author

N93-13886# Naval Oceanographic and Atmospheric Research Lab., Bay Saint Louis, MS.
ESTIMATION OF EOF EXPANSION COEFFICIENTS FROM INCOMPLETE DATA
J. D. Boyd, E. P. Kennelly, and P Pistek Aug. 1992 46 p
(AD-A255252; NOARL-TN-291) Avail: CASI HC A03/MF A01

A least-squares minimization technique for estimating principal components (empirical orthogonal function (EOF) expansion coefficients) from incomplete ocean profile data is developed, and its use for interpolating or extrapolating these profiles is described. GRA

N93-14036# Naval Postgraduate School, Monterey, CA. Dept. of Mathematics.
ON COMPUTING ACCURATE SINGULAR VALUES AND EIGENVALUES OF ACYCLIC MATRICES Technical Report, 1 Oct. 1991 - 31 Mar. 1992
James W. Demmel and William Gragg 7 Aug. 1992 16 p
(AD-A255892; NPS-MA-92-010) Avail: CASI HC A03/MF A01

It is known that small relative perturbations in the entries of a bidiagonal matrix only cause small relative perturbations in its singular values, independent of the values of the matrix entries. In this paper we show that a matrix has this property if and only if its associated bipartite graph is acyclic. We also show how to compute the singular values of such a matrix to high relative accuracy. The same algorithm can compute eigenvalues of symmetric acyclic matrices with tiny component-wise relative backward error. This class includes tridragonal matrices, arrow matrices, and exponentially many others. GRA

N93-14081# Naval Surface Warfare Center, Dahlgren, VA.
FIXED-GAIN, TWO-STAGE ESTIMATORS FOR TRACKING MANEUVERING TARGETS Final Report
W. D. Blair Jul. 1992 64 p
(AD-A255832; NSWCDD/TR-92/297) Avail: CASI HC A04/MF A01

The two-stage Alpha-Beta-Gamma estimator is proposed as an alternative to adaptive gain versions of the Alpha-Beta and Alpha-Beta-Gamma filters for tracking maneuvering targets. This report accomplishes fixed-gain, variable dimension filtering with a two-stage Alpha-Beta-Gamma estimator. The two-stage Alpha-Beta-Gamma estimator is derived from the two-stage Kalman estimator, and the noise variance and reduction matrix and steady-state error covariance matrix are given as a function of the steady-state gains. A procedure for filter parameter selection is also given along with a technique for maneuver response and a gain scheduling technique for initialization. The kinematic constraint for constant speed targets is also incorporated into the two-stage estimator to form the two-stage Alpha-Beta-Gamma-Lambda estimator. Simulation results are given for a comparison of the performances of estimators with that of the Alpha-Beta-Gamma filter. GRA

65 STATISTICS AND PROBABILITY

Includes data sampling and smoothing; Monte Carlo method; and stochastic processes.

N93-12702# Stanford Univ., CA. Dept. of Statistics.
BAYESIAN ANALYSIS OF LINEAR AND NONLINEAR POPULATION MODELS USING THE GIBBS SAMPLER
J. C. Wakefield, A. F. Smith, A. Racine-Poon, and A. E. Gelfand 21 Jul. 1992 40 p
(Contract N00014-92-J-1254)
(AD-A254769; SU-TR-456) Avail: CASI HC A03/MF A01

A fully Bayesian analysis of linear and nonlinear population models has

previously been unavailable, as a consequence of the seeming impossibility of performing the necessary numerical integrations in the complex multi-parameter structures typically arising in such models. It is demonstrated that, for a variety of linear and nonlinear population models, a fully Bayesian analysis can be implemented in a straightforward manner using the Gibbs sampler. The approach is illustrated with examples involving challenging problems of outliers and mean-variance relationships in population modelling. GRA

N93-12709# California Univ., Davis.
MODELING AND ESTIMATION OF RECIPROCAL DIFFUSION AND GAUSS-MARKOV RANDOM FIELDS Final Report
5 Aug. 1992 4 p
(Contract N00014-89-J-3153)
(AD-A255034) Avail: CASI HC A01/MF A01

The basic goal of this research was to develop a theory of second order stochastic differential equations as a class of models for problems of filtering and estimation. This goal has been achieved for both continuous and discrete time linear-Gaussian reciprocal processes. GRA

N93-13064# Texas A&M Univ., College Station. Dept. of Statistics.
FROM COMPARISON DENSITY TO TWO SAMPLE ANALYSIS
Emanuel Parzen May 1992 20 p
(Contract DAAL03-90-G-0069)
(AD-A253866; TR-169; ARO-27574.8-MA) Avail: CASI HC A03/MF A01

Contents of the paper are: 1. Introduction. 2. Quantile domain functions: F,Q; 3. Mid distribution and quantile functions: Fmid, Fmid; 4. Sample distribution and quantile: F-, Q-; 5. Comparison distribution and comparison density for discrete F,G; 7. Information measures: Renyi, Chi-square; 8. Information for comparison density function; 9. Information measures and entropy tests of fit; 10. Continuous versions of discrete distribution functions: Fc, Qc; 11. Comparison distributions of one sample (continuous data); 12. One sample parameter estimation; 13. Comparison distributions of two samples, (continuous) data; 14. Two sample comparison density estimation, statistical modeling, information measures, entropy* quantile functions, density estimation, quantile' density estimate, comparison density, maximum spacings parameter estimation, minimum information parameter estimation, goodness of fit. GRA

66 SYSTEMS ANALYSIS

Includes mathematical modeling; network analysis; and operations research.

No abstracts in this category.

67 THEORETICAL MATHEMATICS

Includes topology and number theory.

No abstracts in this category.

70 PHYSICS (GENERAL)

For precision time and time interval (PTTI) see *35 Instrumentation and Photography;* for geophysics, astrophysics or solar physics see *46 Geophysics, 90 Astrophysics,* or *92 Solar Physics.*

N93-12805# National Inst. of Standards and Technology, Gaithersburg, MD.
JOURNAL OF RESEARCH OF THE NATIONAL INSTITUTE OF STANDARDS AND TECHNOLOGY, MAY-JUNE 1992, VOLUME 97, NUMBER 3
Barry N. Taylor, ed., J. W. Gallagher, ed., Richard J. VanBrunt, ed., Theodore V. Vorburger, ed., Patrick A. G. OHare, ed., Chris E. Kuyatt, ed., Daniel B. Butrymowicz, ed., Richard G. Gann, ed., Alan H. Goldfine, ed., and Joan R. Rosenblatt, ed. et al 1992 89 p
(PB92-217637; LC-89-656121) Avail: CASI HC A05/MF A01; SOD HC

Contents: A radiometer for precision coherent radiation measurements; ITS-90 density of water formulation for volumetric standards calibration; Heat capacity and thermodynamic properties of poly(chlorotribluoroethylene) from 2.5 to 620 K; Precipitation and solubility of calcium hydrogenurate hexahydrate; The NIST SPIDER, a robot crane. GRA

N93-12865# Delaware Univ., Newark. Dept. of Physics and Astronomy.
MAGNETIC HARDENING STUDIES AND NOVEL TECHNIQUES FOR PREPARATION OF HIGH PERFORMANCE MAGNETS Final Report, 1 Jan. 1990 - 25 Jan. 1992
George C. Hadjipanayis 28 Apr. 1992 12 p
(Contract DAAL03-90-G-0026)
(AD-A254761; ARO-27794.1-MS) Avail: CASI HC A03/MF A01

Our efforts in permanent magnets have been focused on the search for new phases and alloys with high magnetization, large anisotropy, and high Curie temperature that can be used for permanent magnet development and on the magnetic hardening behavior of R-FE-B magnets. The systems studied include Fe-Mo, Co-Zr-B and as-cast Nd(Pr)-rich alloys with coercivities exceeding 6 kOe obtained in the latter two samples. Small additions of Al and Cu have been found to increase the coercivity of melt-spun R-FE-B magnets substantially (by as much as 8 kOe). The microstructure of the substituted samples is more homogeneous with the secondary Nd-Al(Cu)-rich phases uniformly distributed throughout the sample. In addition, disturbed lattice regions were observed at most of the grain boundaries. In Cu-substituted melt-spun samples several faults have been observed inside the 2:14:1 grains. This is the first time that defects were observed in a 2:14:1 matrix and they have been attributed to the small solubility of Cu on Fe. As-cast Nd(Pr)-Fe(1-x)Mn(x)-B samples have been found to have large coercivities at cryogenic temperatures. The large coercivities observed are due to domain wall pinning at atomic-size defects caused by the random Mn site occupation (leading to sites with fluctuations in exchange and anisotropy) because of the extremely thin domain walls. GRA

N93-12890# Helsinki Univ. of Technology, Espoo (Finland). Inst. of Mathematics.
STABILIZATION AND PROJECTION METHODS FOR MULTIBODY DYNAMICS
Edda Eich (Augsburg Univ., Germany), Claus Fuehrer (Deutsche Forschungs- und Versuchsanstalt fuer Luft- und Raumfahrt, Oberpfaffenhofen, Germany), Benedict Leimkuhler, and Sebastian Reich (Deutsche Akademie der Wissenschaften, Berlin, German D.R.) Aug. 1990 21 p
(PB92-133883; RR-A281; ISBN-951-22-0332-4) Avail: CASI HC A03/MF A01

In recent years, there has been growing interest in stabilized index reduction techniques for differential-algebraic equations (DAE) of multibody dynamics. A number of the proposals which incorporate the idea of a projection onto the constraint manifold are discussed. The methods are divided into classes based on whether the projection is performed on the residuals of the discretized DAE or on the numerical solution itself, and demonstrate relationships between the methods of each class. GRA

N93-13303# Joint Publications Research Service, Arlington, VA.
JPRS REPORT: SCIENCE AND TECHNOLOGY. CENTRAL EURASIA: PHYSICS AND MATHEMATICS
9 Nov. 1992 31 p Transl. into ENGLISH from various Russian articles
(JPRS-UPM-92-006) Avail: CASI HC A03/MF A01

Translations are presented of articles from Russian publications. The areas of study are: Crystals, laser glasses, semiconductors; Fluid dynamics; Lasers; Nuclear physics; Optics, spectroscopy; Plasma physics; Superconductivity; and Theoretical physics. Some representative titles are as follows: High conducting state in thin polymer films; On solitons with small number of time or space periods; Stimulated emission dynamics analysis of Ti doped Sapphire laser under double mode locking and limited ultrashort pump pulse train; Emission of charged particles during slow negative pion capture by uranium nuclei; Coherent spectroscopy of Raman and hyper-Raman light scattering of excited and autoionized atomic states in gaseous discharge plasma of copper and copper bromide vapor lasers'

active media; On possibility of determining spatial plasma oscillation spectrum by enhanced microwave scattering method; and Magnetic ordering and phase separation in high temperature superconductors. E.R.

N93-13851 New York Univ., New York.
ATOMS AND MOLECULES IN SUPERNOVA 1987A Ph.D. Thesis
Weihong Liu 1992 234 p
Avail: Univ. Microfilms Order No. DA9222896

About 163,000 years ago, the core of blue supergiant star Sanduleak-69 deg 202 in the Large Magellanic Cloud collapsed and the star exploded to become SN1987A, the neutrinos and photons from which were detected on February 23, 1987. The HeI(1.0830 micron) line was observed in SN1987A early as a P-Cygni profile. The recombination of He(+) ions produced by fast electron impact is mainly responsible for populating the helium metastable states, the abundances of which are calculated. The line profile of the transition HeI(2(exp 3)S - 2(exp 3)P(exp 0) is constructed. In comparison with the observed spectrum at 135 days, 10 percent of the energy released by the radioactive species in SN1987A is deposited in the He gas. The detection of CO and SiO provides the first evidence of molecular formation in supernova ejecta. I explore the molecular formation and destruction mechanisms in SN1987A to determine the molecular abundances. The CO masses are derived using the first overtone emission band at 2.3 microns observed during the first year. It is found that the delta-v = 2 line of CO in SN1987A is optically thick at early times and that the vibrational level populations fall out of thermal equilibrium at later times. A careful interpretation of the observational data allowing departure from LTE and allowing optical depth effects yields the order of 10(exp 3) solar mass of CO in SN1987A. The mixed chemistry is inefficient in producing CO and fails to account for the observed abundances of CO by three orders of magnitude whereas the unmixed chemistry predicts the order of 10(exp -2) solar mass of CO. Thus the CO masses implied from the observations can be reproduced by assuming that the regions without microscopic mixing occupy 10 percent of the ejects. The chemistry predicts that SiO is substantially more abundant than that derived from its fundamental band assuming LTE. As for CO, departures from LTE and optical depth effects may have led to a severe underestimate of the SiO abundance. In the first year, a weak feature at 1.334 micron is tentatively attributed to the fundamental band of SiS, whose mass in SN1987A is predicted as about 10(exp -7) solar mass. Dissert. Abstr.

N93-13907 Iowa State Univ. of Science and Technology, Ames.
EFFECTS OF STINGER AXIAL DYNAMICS AND MASS COMPENSATION METHODS ON EXPERIMENTAL MODAL ANALYSIS Ph.D. Thesis
Ximing Hu 1992 125 p
Avail: Univ. Microfilms Order No. DA9223932

A longitudinal bar model that includes both stinger elastic and inertia properties is used to analyze the stinger's axial dynamics as well as the mass compensation that is required to obtain accurate input forces when a stinger is installed between the excitation source, force transducer, and the structure under test. Stinger motion transmissibility and force transmissibility, axial resonance and excitation energy transfer problems are discussed in detail. Stinger mass compensation problems occur when the force transducer is mounted on the exciter end of the stinger. These problems are studied theoretically, numerically, and experimentally. It is found that the measured Frequency Response Function (FRF) can be underestimated if mass compensation is based on the stinger exciter-end acceleration and can be overestimated if the mass compensation is based on the structure-end acceleration due to the stinger's compliance. A new mass compensation method that is based on two accelerations is introduced and is seen to improve the accuracy considerably. The effects of the force transducer's compliance on the mass compensation are also discussed. A theoretical model is developed that describes the measurement system's FRD around a test structure's resonance. The model shows that very large measurement errors occur when there is a small relative phase shift between the force and acceleration measurements. These errors can be in hundreds of percent corresponding to a phase error on the order of one or two degrees. The physical reasons for this unexpected error pattern are explained. This error is currently unknown to the experimental modal analysis community. Two sample structures consisting of a rigid mass and a double cantilever beam are used in the numerical calculations and experiments. Dissert. Abstr.

71 ACOUSTICS

Includes sound generation, transmission and attenuation.
For noise pollution see *45 Environmental Pollution.*

N93-12601# Naval Command, Control and Ocean Surveillance Center, San Diego, CA. Research, Development, Test and Evaluation Div.
VISUALIZATION OF SCATTERING STRENGTH OF ELASTIC BODIES IN A FLUID Final Report
H. A. Schenck and J. L. Fales Jul. 1992 72 p
(AD-A254535; NRAD-TD-2287) Avail: CASI HC A04/MF A01

As Part of the Submarine Technology Program, the Defense Advanced Research Projects Agency (DARPA) recently sponsored a Low-Frequency Structural Acoustics Benchmark Exercise. The purpose of the exercise was to test and validate several major computational codes that have been developed to solve acoustic scattering problems of elastic objects in a fluid. This report describes some of the visualization techniques and procedures that were developed to review, compare, and analyze the large amount of computational data generated in the exercise. GRA

N93-12714 Institute of Sound and Vibration Research, Southampton (England). Fluid Dynamics and Acoustics Group.
INTAKE AND EXHAUST NOISE
P. O. A. L. Davies Jul. 1992 33 p
(ISVR-TR-207) Copyright Avail: Issuing Activity

The basic mechanisms by which intake and exhaust noise is generated are described as a combination of the unsteady flow processes associated with engine breathing interacting with the acoustic characteristics of the corresponding flow paths. Quantitative descriptions are given of the relationship between the spectral characteristics of the emitted sound, system geometry, and the flow characteristics. These are assessed on the basis of current design objectives for intake and exhaust noise control. Author

N93-12986*# Institute for Computer Applications in Science and Engineering, Hampton, VA.
REPORT ON THE FINAL PANEL DISCUSSION ON COMPUTATIONAL AEROACOUSTICS Final Report
James Lighthill (University Coll., London, England) Oct. 1992 15 p Proceedings held at the ICASE/NASA Workshop on Computational Aeroacoustics, 6-9 Apr. 1992
(Contract NAS1-18605; RTOP 505-90-52-01)
(NASA-CR-189718; NAS 1.26:189718; ICASE-92-53) Avail: CASI HC A03/MF A01

Some important conclusions about future prospects for aeroacoustics in general, and for computational aeroacoustics in particular, that were reached in the course of the Final Panel Discussion of the Workshop on Computational Aeroacoustics held from 6 to 9 April 1992 by ICASE and NASA Langley Research Center are summarized by the panel chairman. Aeroacoustics must now be involved in interactions with computational fluid dynamics (as applied not only to deterministic flows but also to the statistical characteristics of turbulence), while additionally incorporating rigorous comparisons with experiment. The new Computational Aeroacoustics will press forward in two parallel ways. In one of them, CFD will be used to determine aeroacoustic source strengths, the associated radiation being derived by the Acoustic Analogy approach in one of its forms. In the other, a direct Computational Aeroacoustics will apply CFD techniques over a region extending beyond the flow field so as to include at least the beginnings of the acoustic far field. There are some particularly important areas of study, including rotor noise, boundary-layer noise, and the noise of supersonic jets, where it is strongly recommended that use of both methods is continued. On the other hand, important problems of the diffraction of radiation from aeroacoustic sources around complicated aircraft shapes will require the use of comprehensively Computational Aeroacoustics, while Acoustic Analogy methods seem better suited to estimating subsonic jet noise. The study of model problems to allow comparisons with experiment will be valuable in both lines of attack. L.R.R.

N93-13262# Sandia National Labs., Livermore, CA.
NONLINEAR STABILITY OF COMBUSTION-DRIVEN ACOUSTIC OSCILLATIONS IN RESONANCE TUBES
S. B. Margolis 1992 50 p Presented at the American Physical Society (APS) Division of Fluid Dynamics Annual Meeting, Tallahassee, FL,

23-25 Nov. 1992
(Contract DE-AC04-76DR-00789)
(DE92-012153; SAND-92-8491; CONF-921143-1) Avail: CASI HC A03/MF A01

The leading-order fluid motions and frequencies in resonance tubes coupled to a combustion-driven flow source, such as occurs in various types of pulse combustors, are usually strongly related to those predicted by linear acoustics. However, in order to determine the amplitudes of the infinite number of classical acoustic modes predicted by linear theory alone, and hence the complete solution, a nonlinear analysis is required. In the present work, we adopt a formal perturbation approach based on the smallness of the mean-flow Mach number which, as a consequence of solvability conditions at higher orders in the analysis, results in an infinitely-coupled system of nonlinear evolution equations for the amplitudes of the linear acoustic modes. An analysis of these amplitude equations then shows that the combination of inertial processes that supply energy to the acoustic oscillations and those, such as viscosity, that dampen such motions, in conjunction with the manner in which the resonance tube is coupled to its flow source, provides an effective mode-selection mechanism that inhibits the growth of all but a few of the lower-frequency modes. For the common case of long resonance tubes, the lowest frequencies correspond to purely longitudinal modes, and we analyze in detail the solution behavior for a typical situation in which only the first of these has a positive linear growth rate. Basic truncation strategies for the infinitely-coupled amplitudes are discussed, and we demonstrate, based on analyses with both two and three modes, the stable bifurcation of an acoustic oscillation, or limit cycle, at a critical value of an appropriate bifurcation parameter. In addition, we show that the bifurcated solution branch has a turning point at a second critical value of the bifurcation parameter beyond which no stable bounded solutions exist. DOE

N93-13421* National Aeronautics and Space Administration. Pasadena Office, CA.
ACOUSTIC DEVICE AND METHOD FOR MEASURING GAS DENSITIES Patent
Parthasarathy Shakkottai, inventor (to NASA) (Jet Propulsion Lab., California Inst. of Tech., Pasadena.), Eug Y. Kwack, inventor (to NASA) (Jet Propulsion Lab., California Inst. of Tech., Pasadena.), and Lloyd Back, inventor (to NASA) (Jet Propulsion Lab., California Inst. of Tech., Pasadena.) 3 Nov. 1992 19 p Filed 19 Feb. 1991 Supersedes N92-10609 (30 - 1, p 105)
(NASA-Case-NPO-18155-1-CU; US-Patent-5,159,843;
US-Patent-Appl-SN-658477; US-Patent-Class-73-24.05;
US-Patent-Class-73-24.06; US-Patent-Class-73-24.01;
Int-Patent-Class-G01N-29/00; Int-Patent-Class-G01N-29/22) Avail: US Patent and Trademark Office

Density measurements can be made in a gas contained in a flow through enclosure by measuring the sound pressure level at a receiver or microphone located near a dipole sound source which is driven at constant velocity amplitude at low frequencies. Analytical results, which are provided in terms of geometrical parameters, wave numbers, and sound source type for systems of this invention, agree well with published data. The relatively simple designs feature a transmitter transducer at the closed end of a small tube and a receiver transducer on the circumference of the small tube located a small distance away from the transmitter. The transmitter should be a dipole operated at low frequency with the kL value preferable less that about 0.3.
Official Gazette of the U.S. Patent and Trademark Office

N93-13439 Institute of Sound and Vibration Research, Southampton (England). Fluid Dynamics and Acoustics Group.
MINT: THE MULTIPLE ERROR LMS ALGORITHM, AND THE DESIGN OF INVERSE FILTERS FOR MULTI-CHANNEL SOUND REPRODUCTION SYSTEMS
P. A. Nelson, F. Orduna-Bustamante, and H. Hamada Nov. 1992 21 p (ISVR-TR-211) Copyright Avail: Issuing Activity

A discussion is presented of two techniques for designing inverse filters for use in multi-channel sound reproduction systems. The first is the Multiple-Input/Output Inverse Filtering Theorem which uses direct inversion of a matrix containing the coefficients of filters used to specify the electroacoustic transmission paths. The second is an adaptive technique based on the Multiple Error LMS algorithm. The theory presented reconciles the two approaches and furthermore, derives explicit conditions which must be fulfilled if an exact inverse is to exist. A formula is presented which gives the number of coefficients required in the inverse filters in terms of the number of coefficients used to represent the transmission paths.
Author

N93-13635 Mississippi Univ., University.
CANCELLATION OF AIR-BORNE ACOUSTIC PLANE WAVES OBLIQUELY INCIDENT UPON A PLANAR PHASED-ARRAY OF ACTIVE SURFACE ELEMENTS Ph.D. Thesis
Timothy Harry Ruppel 1991 116 p
Avail: Univ. Microfilms Order No. DA9216074

The active reduction of sound inside and outside an enclosure is of much interest to researchers in acoustics. The approach most often used is to control the sound in a given region (sensed by a series of point microphones) with destructive interference from a set of point sources whose strengths, phases, and locations can be adjusted. However, the Active Surfaces Research Group at the National Center for Physical Acoustics has designed surfaces which react to an incident wave in a prescribed manner. If this reaction is such that the surface moves with a velocity that coincides with the normal particle velocity of the incoming wave, reflections are eliminated. Active surfaces have been built by this group for the control of normally incident plane waves. This dissertation reports on the construction and testing of a planar active surface capable of cancelling the reflections of obliquely incident acoustic plane waves. Theoretical analysis of the potential performance of the surface is given. The viscosity and thermal conductivity of the medium in which the surface operates are found to have negligible effect on the surface's performance. Since the phase of an obliquely incident wave varies over the active surface, an array of transducers is required to accomplish the desired control. The surface was shown to perform well for 30-50 kHz of sound. The cancellation covers a broad angular range. Dissert. Abstr.

N93-13770 George Washington Univ., Washington, DC.
A TIME DOMAIN NUMERICAL THEORY FOR STUDYING STEADY-STATE ACOUSTIC DISTURBANCE IN FLOW Ph.D. Thesis
Willie Ross Watson 1991 122 p
Avail: Univ. Microfilms Order No. DA9125033

The interaction of steady-state sound with subsonic flows in the presence of complicated geometries has become a major concern in the design of most new aircraft. There is growing recognition by the aeroacoustic community in both industry and government that understanding this phenomenon is likely to be achieved only through application of numerical methods. This dissertation was motivated by the lack of a theory for studying these types of acoustic problems numerically. The work develops a time dependent numerical theory for studying the interaction of steady-state acoustic disturbances with viscous compressible mean flows. All effects, except the effects of viscosity on the acoustic disturbance are thus included. First, the equations governing the nonlinear acoustic perturbations in the flow are separated from the Navier Stokes Equations. These equations are then analyzed, to determine the number and form of the acoustic boundary conditions required for a well-posed problem. A new set of acoustic boundary conditions based upon knowledge of the inflow vorticity and normal impedance are derived and tested. The perturbation equations are then solved numerically using an unsplit MacCormack predictor-corrector method. Also included is the development of a new method for evolving the acoustic system to a steady-state. The method, referred to here as a 'Two-Step-Method', eliminates the need to develop nonreflecting boundary conditions in order to obtain steady-state acoustic solutions. Calculated results demonstrate that the method is very effective in eliminating transients. In addition, the superiority of solving the perturbation equations rather than solving for the disturbance and mean flow together is demonstrated.
Dissert. Abstr.

N93-13774 Iowa Univ., Iowa City.
FINITE ELEMENT STUDY OF ULTRASONIC IMAGING Ph.D. Thesis
Zhongqing You 1991 216 p
Avail: Univ. Microfilms Order No. DA9126275

An increasing requirement for engineering system reliability provides the motivation for further development of nondestructive evaluation (NDE) techniques. An important objective of NDE system measurements is related to the inverse process which either images the defect or sizes and locates

the defect from the detected signals. Many inverse algorithms involve assumptions and approximations which are not realistic. Evaluation of these effects on the reconstructed images has always been difficult, as experimentally, these different factors cannot be easily distinguished. Thus, a powerful test bed is essential to study the sensitivity of an inverse algorithm. Numerical models are the most suitable technique for this purpose. The development and use of finite element analysis to model ultrasonic wave propagation phenomena and to study diffraction tomography is discussed. The nature of the finite element model allows the accurate prediction of the displacement field for complicated situations including arbitrary anisotropy, inhomogeneity, and attenuation. Basic formulations are presented for general three-dimensional (3-D) geometries and verified by comparing to analytical solutions. To optimize computer resources, the combination of central difference and forward difference schemes is chosen to approximate the time derivatives and a lumped mass scheme is introduced to avoid the expensive matrix inversion. The 2-D and axisymmetric formulations discussed at length in this thesis effectively model problems satisfying either plane strain or axisymmetric conditions. Absorbing boundary conditions are introduced for large geometries and applied to some typical test situations. Using this finite element model as a test bed, the diffraction tomographic algorithm is studied with regard to finite aperture effects and material anisotropy. Extensive comparison of the finite element results with analytic solutions proves the validity of the 2-D, axisymmetric and 3-D models. Applications of the 2-D and axisymmetric formulations correctly predict useful phenomena associated with wave/defect interactions and the anisotropic property of the material. Dissert. Abstr.

72 ATOMIC AND MOLECULAR PHYSICS

Includes atomic structure, electron properties, and molecular spectra.

N93-12572# Fermi National Accelerator Lab., Batavia, IL.
PARTICLE PRODUCTION AND SURVIVAL IN MUON ACCELERATION
R. J. Noble Jun. 1992 9 p Presented at the Advanced Accelerator Concepts Workshop, Port Jefferson, NY, 14-20 Jun. 1992
(Contract DE-AC02-76CH-03000)
(DE92-019553; FNAL/C-92/165; CONF-9206193-6) Avail: CASI HC A02/MF A01

Because of the relative immunity of muons to synchrotron radiation, the idea of using them instead of electrons as probes in high-energy physics experiments has existed for some time, but applications were limited by the short muon lifetime. The production and survival of an adequate supply of low-emittance muons will determine the available luminosity in a high-energy physics collider. In this paper, the production of pions by protons, their decay to muons, and the survival of muons during acceleration are studied. Based on a combination of the various efficiencies, the number of protons needed at the pion source for every muon required in the final high-energy collider is estimated. DOE

N93-12588# Los Alamos National Lab., NM.
NEUTRINO MASS
R. G. H. Robertson 1992 12 p Presented at the Franklin Symposium, Philadelphia, PA, 29 Apr. - 1 May 1992
(Contract W-7405-eng-36)
(DE92-017411; LA-UR-92-1768; CONF-9204182-1) Avail: CASI HC A03/MF A01

Despite intensive experimental work since the neutrino's existence was proposed by Pauli 60 years ago, and its first observation by Reines and Cowan almost 40 years ago, the neutrino's fundamental properties remain elusive. Among those properties are the masses of the three known flavors, properties under charge conjugation, parity and time-reversal, and static and dynamic electromagnetic moments. Mass is perhaps the most fundamental, as it constrains the other properties. The present status of the search for neutrino mass is briefly reviewed. DOE

N93-12745# Rochester Univ., NY. Dept. of Chemistry.
INTERMOLECULAR POTENTIAL FUNCTIONS FROM SPECTROSCOPIC PROPERTIES OF WEAKLY BOUND COMPLEXES Progress Report No. 3, 1 Jul. 1991 - 30 Jun. 1992
John S. Muenter 1992 25 p
(Contract DE-FG02-87ER-60514)
(DE92-018643; DOE/ER-60514/6) Avail: CASI HC A03/MF A01

The goal is to consolidate the information from high resolution spectroscopy of weakly bound cluster molecules through a theoretical model of intermolecular potential energy surfaces. The ability to construct analytic intermolecular potential functions that accurately predict the interaction energy between small molecules will have a major impact in chemistry, biochemistry, and biology. This document presents the evolution and capabilities of a potential function model developed here, and then describes plans for future developments and applications. This potential energy surface (PES) model was first used on (HCCH)(sub 2), (CO2)(sub 2), HCCH - CO2; it had to be modified to work with HX dimers and CO2-HX complexes. Potential functions have been calculated for 15 different molecular complexes containing 7 different monomer molecules. Current questions, logical extensions and new applications of the model are discussed. The questions are those raised by changing the repulsion and dispersion terms. A major extension of the PES model will be the inclusion of induction effects. Projects in progress include PES calculations on (HCCH)(sub 3), CO2 containing complexes, HX(sub 2), HX - CO2, CO2 - CO, (CO2)(sub 3), and OCS(sub 2). The first PES calculation for a nonlinear molecule will be for water and ammonia complexes. Possible long-term applications for biological molecules are discussed. Differences between computer programs used for molecular mechanics and dynamics in biological systems are discussed, as is the problem of errors. DOE

N93-12806# Lawrence Livermore National Lab., CA.
C60 TRANSFORMATIONS AT HIGH PRESSURES
C. S. Yoo, W. J. Nellis, M. L. Sattler, R. G. Musket, N. Hinsey, and W. Brocious Apr. 1992 6 p Presented at the Material Research Society Spring Meeting, San Francisco, CA, 27 Apr. - 2 May 1992
(Contract W-7405-eng-48)
(DE92-019546; UCRL-JC-110324; CONF-920402-52) Avail: CASI HC A02/MF A01

C60 molecules have been studied at both shock and static high pressures. Under shock compressions C60 fullerenes are stable into the 13-17 GPa pressure range. The onset of a fast (approximately 0.5 micro-s) reconstructive Information to graphite occurs near 17 GPa. The graphite recovered from 27 GPa and about 900 K is relatively well with L(sub a) = 100 A. Above 50 GPa a continuous transformation to an amorphous state is observed in recovered specimens. A transparent, metastable carbon phase was recovered from thin films of C60, shocked to 69 GPa and 2200 K and then rapidly quenched to 1000 K. The selected area diffraction patterns indicate that the metastable carbon contains an amorphous diamond and n-diamond. Under hydrostatic compressions C60 molecules transform reversibly to a semi-transform phase in the pressure range of 15-25 GPa with a large pressure hysteresis. The high pressure phase consists of interconnected strongly interacting C60 agglomerates, or networks of fullerenes, whose stability continuously increases with increase of pressure. Above 27 GPa the transition becomes irreversible, and the material recovered from high pressure is metastable and diamond-like at ambient conditions. These pressure-induced transitions are explained in terms of pi-electron rehybridization between C60 molecules, which occurs at substantially decreased intermolecular distances. DOE

N93-12832# Brookhaven National Lab., Upton, NY.
LECTURE NOTES FOR CRITICALITY SAFETY
R. Fullwood Mar. 1992 91 p
(Contract DE-AC02-76CH-00016)
(DE92-016009; BNL-47594) Avail: CASI HC A05/MF A01

These lecture notes for criticality safety are prepared for the training of Department of Energy supervisory, project management, and administrative staff. Technical training and basic mathematics are assumed. The notes are designed for a two-day course, taught by two lecturers. Video tapes may be used at the options of the instructors. The notes provide all the materials that are necessary but outside reading will assist in the fullest understanding. The course begins with a nuclear physics overview. The reader is led from the macroscopic world into the microscopic world of atoms and the elementary particles that constitute atoms. The particles, their masses and sizes and properties associated with radioactive decay and fission are introduced along with Einstein's mass-energy equivalence. Radioactive decay, nuclear reactions, radiation penetration,

shielding and health-effects are discussed to understand protection in case of a criticality accident. Fission, the fission products, particles and energy released are presented to appreciate the dangers of criticality. Nuclear cross sections are introduced to understand the effectiveness of slow neutrons to produce fission. Chain reactors are presented as an economy; effective use of the neutrons from fission leads to more fission resulting in a power reactor or a criticality excursion. The six-factor formula is presented for managing the neutron budget. This leads to concepts of material and geometric buckling which are used in simple calculations to assure safety from criticality. Experimental measurements and computer code calculations of criticality are discussed. To emphasize the reality, historical criticality accidents are presented in a table with major ones discussed to provide lessons-learned. Finally, standards, NRC guides and regulations, and DOE orders relating to criticality protection are presented. DOE

N93-12855# Arizona Univ., Tucson.
ELEMENTARY PARTICLE PHYSICS RESEARCH
J. Rutherfoord 1 Apr. 1992 57 p
(Contract DE-AC02-91ER-40605)
(DE92-019746; DOE/ER-40605/2) Avail: CASI HC A04/MF A01

This summary of our activities supported by our DOE contract covers the period from 1-31 Jan. 1992. The major areas which consumed most of our time are D0 at the Fermilab collider, E800 at the Fermilab fixed target facility, and SSC work on major detectors and in detector R&D. The research in these areas is discussed in this report. DOE

N93-12900*# National Aeronautics and Space Administration. Ames Research Center, Moffett Field, CA.
THE 2S(+) - 2P SEPARATION IN KO
Charles W. Bauschlicher, Jr., Harry Partridge, and Kenneth G. Dyall (Eloret Corp., Palo Alto, CA.) [1991] 9 p
(NASA-TM-108086; NAS 1.15:108086) Avail: CASI HC A02/MF A01

The 2S(+) - 2P separation in KO is investigated using large basis sets and high levels of correlation treatment. Relativistic effects are included at the Dirac-Fock level and reduce the separation only slightly. The basis set superposition error is considered in detail. On the basis of these calculations, our best estimate places the 2p sub 3/2 state about 200 cm(exp -1) above the ground 2 sigma(+) state in agreement with our previous estimate. Author

N93-12947# Pennsylvania Univ., Philadelphia. Dept. of Materials Science and Engineering.
ATOMIC STRUCTURE OF MIXED FERROELECTRICS Report, 1 Oct. 1990 - 30 Sep. 1991
Takeshi Egami 28 Jul. 1992 8 p
(Contract N00014-91-J-1036)
(AD-A254369) Avail: CASI HC A02/MF A01

The purpose of this project is to determine the local atomic structure of mixed ferroelectric solids such as Pb(Mg(1/3)Nb(2/3))O3 (PMN) by diffraction experiments, in order to obtain better understanding of the basis for their relaxor ferroelectric behavior. In particular we use pulsed neutron and synchrotron x-ray scattering measurements, and analyze the results in terms of the atomic pair distribution function. Anomalous x-ray scattering measurements were carried out for PMN at the Nb K-edge. The x-ray scattering intensity of an element depends strongly upon energy near the absorption edge, due to the anomalous dispersion effect. By making use of this phenomenon it is possible to differentiate contributions from different elements to the total scattering intensity. This technique is called the x-ray anomalous scattering study. The experiment was carried out at X-7A beamline of the National Synchrotron Light Source (NSLS) of Brookhaven National Laboratory. GRA

N93-13037# Oak Ridge National Lab., TN.
NEUTRON SCATTERING STUDIES OF THE SPIN DYNAMICS IN La(2-x)Sr(x)O4
S. M. Hayden (Bristol Univ., England), T. E. Mason (Risoe National Lab., Roskilde, Denmark), G. Aeppli (Bell Telephone Labs., Inc., Murray Hill, NJ.), and S.-W. Cheong (Bell Telephone Labs., Inc., Murray Hill, NJ.) 1992 10 p Presented at the Conference on Phase Separation in Cuprate Superconductors, Sicily, Italy, 6-12 May 1992
(Contract DE-AC05-84OR-21400)
(DE92-019952; CONF-9205236-3) Avail: CASI HC A02/MF A01

Inelastic neutron scattering has determined the modulation vectors and correlation lengths for the low-energy incommensurate magnetic fluctuations observed in La(2-x)Sr(x)CuO4 for x approx. greater than 0.075. On entering the superconducting state a strong suppression of the low-energy fluctuations is observed. These results are discussed with reference to a two-dimensional band structure model. DOE

N93-13067# National Center for Atmospheric Research, Boulder, CO.
PHOTODISSOCIATION PROCESSES Ph.D. Thesis
Coleen M. Roehl 1992 220 p Sponsored by NSF Prepared in cooperation with California Univ., Santa Barbara
(PB92-222702; NCAR/CT-133) Avail: CASI HC A10/MF A03

Photodissociation studies were carried out on the molecular ion CO3(1-), the ionic clusters Ar3(1+), CO2(1+)-(H2O) and CO3(-1)-H2O, and the neutral molecule NO2. For experiments involving the ionic species, a reverse geometry double focusing mass spectrometer and an argon ion/dye laser system was used. Investigations were conducted by crossing a mass-selected, 8 keV ion beam with a linearly polarized laser beam, and measuring the kinetic energy distributions of the charged photodissociation products. By varying the angle between the ion beam and the laser polarization, angular distributions were obtained. Product branching ratios and photodissociation cross sections were also measured when possible. Based on the data obtained, dissociation dynamics, relative lifetimes, surface symmetries, energy partitioning, and structural information were suggested. In several cases, ab initio calculations focusing on geometric structure and vibrational frequencies of a ground state ion were performed. Statistical phase space modeling was also employed when applicable. GRA

N93-13070# Argonne National Lab., IL.
MINIATURE NEUTRON SOURCES: THERMAL NEUTRON SOURCES AND THEIR USERS IN THE ACADEMIC FIELD
P. A. Egelstaff (Guelph Univ., Ontario) and J. M. Carpenter 1992 14 p Presented at the Conference on Physics and Engineering of Advanced Detectors and Collection/Focusing Systems, San Diego, CA, 19-24 Jul. 1992
(Contract W-31-109-eng-38)
(DE92-018793; ANL/CP-76789; CONF-920768-3) Avail: CASI HC A03/MF A01

The three levels of thermal neutron sources are introduced - University laboratory sources, infrastructure sources and world-class sources - and the needs for each kind and their inter-dependence will be emphasized. A description of the possibilities for University sources based on (alpha)-Be reactions or spontaneous fission emission is given, and current experience with them is described. A new generation of infrastructure sources is needed to continue the regional programs based on small reactors. Some possibilities for accelerator sources that could meet this need are considered. DOE

N93-13073# Yale Univ., New Haven, CT. Dept. of Physics.
THE SPIN OF THE NUCLEON IN DEEP INELASTIC LEPTON SCATTERING EXPERIMENTS
G. K. Mallot (European Organization for Nuclear Research, Geneva, Switzerland) 1992 12 p Presented at the 13th International Conference on Few Body Problems in Physics, Adelaide, Australia, 5-11 Jan. 1992
(Contract DE-FG02-92ER-40704)
(DE92-018854; CONF-920126-4) Avail: CASI HC A03/MF A01

The current experimental status of the spin dependent structure functions as measured in polarized deep inelastic scattering of charged leptons from nucleons is reviewed. The proposals for new experiments at CERN, SLAC and HERA are discussed with special emphasis on the experiment of the Spin Muon collaboration at CERN which has started data taking. DOE

N93-13076# Los Alamos National Lab., NM.
THE USE OF RING RATIOS TO DETECT SAMPLE DIFFERENCES IN PASSIVE NEUTRON COUNTING
D. F. Langner, M. S. Krick, and D. W. Miller 1992 9 p Presented at the Institute of Nuclear Materials Management (INMM) Annual Meeting, Orlando, FL, 19-22 Jul. 1992
(Contract W-7405-eng-36)
(DE92-018920; LA-UR-92-2327; CONF-9207102-46) Avail: CASI HC A02/MF A01

In passive thermal neutron counting, the detection efficiency of a neutron

counter is susceptible to changes in the neutron energy spectrum emitted by a sample. Variable levels of moisture and impurities in samples can cause such changes and thus affect the accuracy of an assay. In this work, we use Monte Carlo simulations of thermal neutron measurements in the four-ring pyrochemical multiplicity counter to study the effect of sample-to-sample changes in the emitted neutron spectrum on the ratios of total neutron counts from the different rings. We also present ring ratio data obtained in the pyrochemical multiplicity counter for several pure and impure plutonium bearing samples. DOE

N93-13092# Stanford Univ., CA. Linear Accelerator Center.
SEARCH FOR DOUBLY CABIBBO SUPPRESSED DECAYS OF THE CHARGED D MESON Ph.D. Thesis
J. F. Labs Mar. 1992 322 p
(Contract DE-AC03-76SF-00515)
(DE92-018588; SLAC-382) Avail: CASI HC A14/MF A03

The doubly Cabibbo suppressed decays D(+) yields K(sup asterisk)(+)pi(-)pi(+), D(+) yields K(+)pi(sup 0) and D(+) yields K(sup asterisk)(+)pi(sup 0) are searched for in a 9.56 pb(exp -1) data sample of e(+)e(-) annihilation events collected near the psi(3770) resonance with the Mark 3 detector at the SPEAR storage ring, at the Stanford Linear Accelerator Center. These rare weak decays are naively expected at a rate of tan(exp 4)theta(sub c) relative to corresponding Cabibbo allowed decays. In the context of presently accepted models of hadronic weak decays, however, they are anticipated to be enhanced, making their experimental detection feasible in the Mark 3 data set. The experimentally simplest decay channel D(+) yields K(+)pi(-)pi(+) is searched for inclusively through conventional analysis techniques. A signal of approximately 2.5 sigma significance is obtained. An independent analysis is performed to establish examples of this decay of D(+) yields K(+)pi(0) and K(sup asterisk)t(sup asterisk)(+)pi(0) by full reconstruction of D(+)D(-) e vents. Exploiting the two body kinematics of psi(3770) yields D(bar-D), this second approach obtains significantly smaller backgrounds than the inclusive study. Consistent with the inclusive results, three D(+) yields K(+)pi(-)pi(+) candidate events are observed. No events are observed for either D(+) yields K(+)pi(sup 0) or K(sup asterisk)(+)pi(sup 0). The branching fraction for D(sup +) yields K(+)pi(-)pi(+) is measured, and limits are established on the branching fractions for D(+) yields K(+)pi(sup 0) and K(sup asterisk)(+)(pi)(sup 0). These results are used to confront the theoretical predictions from models of the weak hadronic decays of charmed mesons. DOE

N93-13095# Tokyo Univ. (Japan). Inst. of Space and Astronautical Science.
CROSS SECTIONS AND RATE COEFFICIENTS FOR THE ELECTRON-IMPACT EXCITATION OF He-LIKE IONS
Leonid A. Vainshtein (Academy of Sciences, USSR, Moscow) and Yukikazu Itikawa Sep. 1992 29 p
(ISAS-RN-647) Avail: CASI HC A03/MF A01

Electron-impact excitation of He-like ions is theoretically studied. Cross sections are calculated for the transitions 1s(2)-1s2(l) l = (0,1) and 1s(2)-1s3(l) (l = 0, 1, 2) of the ions with the nuclear charge Z = 6(2)46. With the use of the resulting cross section, rate coefficients are obtained. A simple approximation is used to reduce the cross section calculation to one-electron problem, which is solved with a perturbation theory. A relativistic effect is taken into account so that each fine-structure state is considered separately. Author

N93-13106# Cornell Univ., Ithaca, NY. Lab. of Atomic and Solid State Physics.
PHOTOCHEMICAL DYNAMICS OF SURFACE ORIENTED MOLECULES
W. Ho 1992 6 p
(Contract DE-FG02-91ER-14205)
(DE92-019813; DOE/ER-14205/1) Avail: CASI HC A02/MF A01

The period 8/01/91-7/31/92 is the first year of a new project titled 'Photochemical Dynamics of Surface Oriented Molecules', initiated with DOE Support. The main objective of this project is to understand the dynamics of elementary chemical reactions by studying photochemical dynamics of surface-oriented molecules. In addition, the mechanisms of photon-surface interactions need to be elucidated. The strategy is to carry out experiments to measure the translational energy distribution, as a function of the angle from the surface normal, of the photoproducts by time-of-flight (TOF) technique by varying the photon wavelength, intensity, polarization, and pulse duration. By choosing adsorbates with different bonding configuration, the effects of adsorbate orientation on surface photochemical dynamics can be studied. DOE

N93-13114# Oak Ridge National Lab., TN.
TRANSITION PROBABILITIES UP TO I = 36(+)IN Yb-160
N. R. Johnson, F. K. McGowan, D. F. Winchell, C. Baktash, J. D. Garrett, I. Y. Lee, and J. C. Wells 1992 8 p Presented at the International Conference on Nuclear Structure at High Angular Momentum, Ottawa, Ontario, 18-21 May 1992
(Contract DE-AC05-84OR-21400)
(DE92-017191; CONF-9205108-5) Avail: CASI HC A02/MF A01

During the past dozen years or so, numerous groups have worked on the properties of the ytterbium nuclei and we at Oak Ridge have been actively involved in the study of many of these nuclei. We have concentrated on lifetime measurements of their high-spin states because it is from the lifetime of a state that one can determine Q(sub t), the transition quadrupole moment. The importance of obtaining a Q(sub t) value is in that it reflects the intrinsic part of the wave function and, hence, provides an indicator of the collectivity. This paper presents the results from recent Doppler broadened line shape measurements in Yb-160 at very large rotational frequencies of bar-H(omega) approx. 0.36 - 0.50 MeV (I = 22(+) -36(+)). DOE

N93-13187# Washington Univ., Seattle. Dept. of Physics.
FERMI MOLECULAR DYNAMICS
L. Wilets and W. Beck 1991 4 p Presented at the 7th Winter Workshop on Nuclear Dynamics, Key West, FL, 27 Jan. - 2 Feb. 1991
(Contract DE-FG06-88ER-40427)
(DE92-015351; DOE/ER-40427/40-N91; CONF-910135-6) Avail: CASI HC A01/MF A01

Classical many body models supplemented by repulsive momentum-dependent potentials to simulate the Pauli and Heisenberg principles have been used with some success for nuclear and atomic bound state and collision problems. They are capable of describing mean ground state properties, hydrodynamics, shocks (if warranted by the physics), viscosity, correlations, clustering, and fragmentation. We have become interested in the Feldmeier Gaussian packet formulation since it is based on a variational principle using trial wave functions. We discuss some limitations of the model and discuss further directions of investigation. DOE

N93-13194# Argonne National Lab., IL.
STUDY OF SHORT-RANGE MOTION OF ATOMIC HYDROGEN IN AMORPHOUS SILICON BY NEUTRON REFLECTOMETRY
W. D. Dozier, K. W. Herwig (Missouri Univ., Columbia.), and R. Shinar (Iowa State Univ. of Science and Technology, Ames.) May 1992 7 p Presented at the Material Research Society Spring Meeting, San Francisco, CA, 27 Apr. - 2 May 1992
(Contract W-31-109-eng-38)
(DE92-016392; ANL/CP-76336; CONF-920402-36) Avail: CASI HC A02/MF A01

Preliminary results of neutron reflectometry (NR) measurements on rf sputter-deposited a-Si:H/a-Si:D bilayers indicate that this technique may be used to monitor H and D motions over distances of approximately 10 to 200 A with a nominal resolution of 5-10 A. In studying RF sputter-deposited thin films containing a high density of microvoids annealed at 270 C, we found that the hydrogen diffused a distance of only approximately 100 A. Further annealing at 270 and 280 C produced no additional motion. This result is consistent with a model of this system in which the hydrogen is trapped in microvoids after moving a relatively short distance. DOE

N93-13246# Argonne National Lab., IL.
A FRESH LOOK AT (E,E(PRIME)) SCATTERING FROM LIGHT NUCLEI: A GFMC APPROACH
R. Schiavilla (Istituto Nazionale di Fisica Nucleare, Lecce, Italy) 1992 11 p Presented at the National Conference on Physics of Few-Body and Quark-Hadronic Systems, Ukraine, 1-5 Jun. 1992
(Contract W-31-109-eng-38)
(DE92-016377; ANL/CP-76332; CONF-9206199-1) Avail: CASI HC A03/MF A01

Green's function Monte Carlo methods are used to calculate, in light nuclei, the Euclidean proton response, defined as the Laplace transform of the longitudinal response function measured in inclusive electron scattering. The calculations are based on a realistic Hamiltonian containing two- and three-nucleon interactions. Final-state-interaction effects are exactly included in this approach. The calculated Euclidean proton response functions for the He-4 nucleus are found to be in excellent agreement with those obtained from an analysis of the Bates and Saclay longitudinal data. DOE

N93-13250# Stanford Linear Accelerator Center, CA.
RECENT DEVELOPMENTS IN THE THEORY OF HEAVY-QUARK DECAYS
M. Neubert Jun. 1992 6 p Presented at the B Factories: State of the Art in Accelerators, Detectors, and Physics, Stanford, CA, 6-10 Apr. 1992
(Contract DE-AC03-76SF-00515)
(DE92-017598; SU-SLAC-PUB-5842; CONF-9204126-2) Avail: CASI HC A02/MF A01

I report on recent developments in the heavy-quark effective theory and its application to B meson decays. The parameters of the effective theory, the spin-flavor symmetry limit, and the leading symmetry-breaking corrections to it are discussed. The results of a QCD sum rule analysis of the universal Isgur-Wise functions that appear at leading and subleading order in the 1/m(sub Q) expansion are presented. I illustrate the phenomenological applications of this formalism by focusing on two specific examples: the determination of V(sub cb) from the endpoint spectrum in semileptonic decays, and the study of spin-symmetry violating effects in ratios of form facts. I also briefly comment on nonleptonic decays. DOE

N93-13251# Brandeis Univ., Waltham, MA. Dept. of Physics.
RESEARCH IN ELEMENTARY PARTICLE PHYSICS
L. E. Kirsch, H. J. Schnitzer, J. R. Bensinger, and C. A. Blocker 1992 13 p
(Contract DE-FG02-92ER-40706)
(DE92-017869; DOE/ER-40706/1) Avail: CASI HC A03/MF A01

This report discusses research in the following areas of high energy physics: B meson mixing; CDF response to low energy jets; jet scaling behavior; search for pair produced leptoquarks at CDF; SSC program; quantum field theory; and neural networks. DOE

N93-13263# New Jersey Inst. of Tech., Newark.
ON DEVELOPMENT OF A THREE-DIMENSIONAL PARTICLE MOTION TRACKING SYSTEM
R. N. Dave, A. S. Ashok, and B. G. Bukiet 1992 26 p Presented at the Winter Annual Meeting of the American Society of Mechanical Engineers, Anaheim, CA, 8-13 Nov. 1992
(Contract DE-AC22-91PC-90181)
(DE92-015846; CONF-921110-6) Avail: CASI HC A03/MF A01

Development of a non-intrusive particle tracking technique is considered. Evaluation of the existing methods show that they are not suitable for three-dimensional motion tracking. A novel system based on the principle of magnetic induction coupling is presented. This technique can be used to track the position and orientation of a single particle in a three-dimensional flow of a mass of particles. The system consists of two or more small transmitters, powered by small batteries, mounted inside the particle, and six or more receivers which acquire the induced voltages. This paper presents details of the techniques used to derive the position and orientation information from the voltages induced in the receivers. The feasibility of the proposed technique is established through simulated and actual experiments. Practical issues such as the effect of signal noise are considered. The technique presented here has a wide range of applications due to its non-intrusive nature, and is particularly useful when optical techniques are not feasible. Directions for future work are provided. DOE

N93-13281# Los Alamos National Lab., NM.
APPLICATIONS OF THE LOS ALAMOS HIGH ENERGY TRANSPORT CODE
L. Waters, A. Gavron, and R. E. Prael 1992 11 p Presented at the American Nuclear Society Meeting, Jackson Hole, WY, 16-19 Aug. 1992
(Contract W-7405-eng-36)
(DE92-017408; LA-UR-92-1805; CONF-9208114-2) Avail: CASI HC A03/MF A01

Simulation codes reliable through a large range of energies are essential to analyze the environment of vehicles and habitats proposed for space exploration. The LAHET monte carlo code has recently been expanded to track high energy hadrons with FLUKA, while retaining the original Los Alamos version of HETC at lower energies. Electrons and photons are transported with EGS4, and an interface to the MCNP monte carlo code is provided to analyze neutrons with kinetic energies less than 20 MeV. These codes are benchmarked by comparison of LAHET/MCNP calculations to data from the Brookhaven experiment E814 participant calorimeter. DOE

N93-13319# Oak Ridge Y-12 Plant, TN.
A STOCHASTIC/DETERMINISTIC METHOD FOR TRANSIENT, THREE-DIMENSIONAL NEUTRON TRANSPORT
M. W. Waddell, Jr. and H. L. Dodds (Tennessee Univ., Knoxville.) 11 Jun. 1992 8 p Presented at the Joint American Nuclear Society/European Nuclear Society International Meeting, Chicago, IL, 15-20 Nov. 1992
(Contract DE-AC05-84OS-21400)
(DE92-016690; Y/DD-564; CONF-921102-14) Avail: CASI HC A02/MF A01

The development of a method for solving the time-dependent, three-dimensional Boltzmann transport model is described. A hybrid stochastic/deterministic technique is utilized with a Monte Carlo code embedded inside of a quasi-static kinetics framework. The amplitude function is computed deterministically by a conventional point kinetics algorithm. The point kinetics parameters, reactivity, and generation time, as well as the flux shape, are computed stochastically during the random walk of the Monte Carlo calculation. The code, which has been developed based on this new method, could serve as a benchmarking tool for other more approximate and less expensive kinetics codes. It would also be useful for modeling transients of systems with complex geometries. Furthermore, a 3-D transport theory is needed in areas such as reactor accident studies which involve coolant voiding and/or core disassembly. Preliminary results are presented in this paper. The code is applied to a standard benchmark problem, and the results are compared to another method. DOE

N93-13369 Boston Univ., MA.
ENERGETICS AND DYNAMICS OF EXCESS ELECTRONS IN SIMPLE FLUIDS Ph.D. Thesis
Brian Space 1992 163 p
Avail: Univ. Microfilms Order No. DA9223512

Excess electronic dynamical and equilibrium properties are modeled in both polarizable and nonpolarizable noble gas fluids. Explicit dynamical calculations are carried out for excess electrons in fluid helium, where excess electronic eigenstates are localized. Energetics and dynamics are considered for fluids which span the entire range of polarizability present in the rare gases. Excess electronic eigenstates and eigenvalues are calculated for fluids of helium, argon and xenon. Both equilibrium and dynamical information is obtained from the calculation of these wavefunctions. A surface hopping trajectory method for studying nonadiabatic excess electronic relaxation in condensed systems is used to explore the nonadiabatic relaxation after photoexciting an equilibrated excess electron in dense fluid helium. The different types on nonadiabatic phenomena which are important in excess electronic relaxation are surveyed. The same surface hopping trajectory method is also used to study the rapid nonadiabatic relaxation after an excess electron is injected into unperturbed fluid helium. Several distinctively different relaxation processes, characterized by their relative importance at different times during the relaxation to a localized equilibrium state, are detailed. Though the dynamical properties of excess electrons under the conditions considered here have never been studied before, the behavior is remarkably similar to that observed in both experimental and theoretical studies of electron hydration dynamics, indicating that the processes described may be very general relaxation mechanisms for localization and trapping in fluids. Additionally, ground state energies of an excess electron, e(sub 0), are computed as a function of solvent density using model electron-atom pseudopotentials in fluid helium, argon, and xenon. The nonuniqueness of the pseudopotential description of electron-molecule interactions is demonstrated. It is found that when many-body polarization effects are included, the calculated e(sub 0) results are in close agreement with experimental v(sub 0) values. If the many-body nature of the polarization interaction is ignored the ground state energies deviate significantly from the V(sub 0) results. The extent of the ground

state wave function as a function of solvent density is correlated with the density dependence of both V(sub 0) and the electron mobility.
Dissert. Abstr.

N93-13531# Argonne National Lab., IL.
EFFECTS OF IONIZING RADIATION ON SCINTILLATORS AND OTHER PARTICLE DETECTORS
J. Proudfoot 1992 11 p Presented at the International Conference of Radiation-Tolerant Scintillators and Detectors, Tallahassee, FL, 28 Apr. - 2 May 1992
(Contract W-31-109-eng-38)
(DE92-018184; ANL-HEP-CP-92-46; CONF-9204138-Summ) Avail: CASI HC A03/MF A01

It is my task to summarize the great variety of topics (covering a refreshing mix of physics, chemistry, and technology) presented at this conference, which has focused on the effects of ionizing radiation on scintillators and other particle detectors. The central interest of many of the participants was the use of such detectors in experiments at two future large hadron colliders: the Superconducting Super Collider, which is to be operating outside of Dallas by the end of the decade; and its European counterpart the Large Hadron Collider which is to be operating outside of Geneva on a similar time scale. These accelerators are the 'apple of the high energy physicist's eye.' Their goal is to uncover the elusive Higgs particle and thereby set the cornerstone in our current knowledge of elementary particle interactions. This is the Quest, and from this lofty height the presentations rapidly moved on to the specific questions of experimental science: how such an experiment is carried out; why radiation damage is an issue; how radiation damage affects detectors; which factors affect radiation damage characteristics; which factors are not affected by radiation damage; and how better detectors may be constructed. These were the substance of this conference. DOE

N93-13537# Fermi National Accelerator Lab., Batavia, IL.
HEAVY GAUGE BOSON AND LAMBDA(b) BARYON SEARCHES AT CDF
K. Maeshima Jun. 1992 8 p Presented at the 27th Rencontres De Moriond, QCD and High Energy Hadronic Interactions, Les Arcs, France, 22-28 Mar. 1992
(Contract DE-AC02-76CH-03000)
(DE92-019551; FNAL/C-92/160-E; CONF-9203154-7) Avail: CASI HC A02/MF A01

We have searched for new gauge bosons (W' yields l nu, Z' yields ll) and b baryons (Lambda(sub b) yields psi Lambda(sup 0) in p bar-p collisions at square root of zeta = 1.8 TeV from the 1988-1989 run of the Collider Detector at Fermilab (CDF). We present 95 percent confidence level (C.L.) limits on the W' and Z' production cross section in leptonic decay modes. The nonobservation of these processes leads to limits of M(sub W') greater than 520 GeV/c(exp 2) and M(sub Z') greater than 412 GeV/c(sub 2) (95 percent C.L.), assuming Standard Model coupling strengths. We see no evidence for the signal (Lambda(sub b) yields psi Lambda(sup 0)) in our psi sample (psi yields mu mu) around the Lambda(sub b) mass region of 5600 MeV. We set an upper limit on F(Lambda(sub b)B(sub tau) (Lambda(sub b) yields psi Lambda(sup 0) of 0.55 x 10(exp -3) (90 percent C.L.), assuming that b baryons and mesons are produced in the fragmentation process in similar ways. The CDF Ai, search is also reported in the QCD session of this conference. This paper summarizes our result briefly; the details can be found in the other talk. DOE

N93-13546# Argonne National Lab., IL.
EVIDENCE FOR ALPHA-PARTICLE CHAIN CONFIGURATIONS IN Mg-24
A. H. Wuosmaa, B. B. Back, R. R. Betts, M. Ferre, J. Gehring, P. G. Glagola, T. Happ, D. J. Henderson, P. Wilt, and I. G. Bearden (Purdue Univ., West Lafayette, IN.) 1992 8 p Presented at the 2nd International Nuclear Physics Conference, Wiesbaden, Germany, 26 Jul. - 1 Aug. 1992
(Contract W-31-109-eng-38)
(DE92-018790; ANL/CP-74960; CONF-920708-1) Avail: CASI HC A02/MF A01

Many theoretical models have been employed to describe the structure of the nucleus Mg-24. Among these are the Cranked Shell model (CSM), the Cranked Cluster Model (CCM), and calculations have also been performed using the Hartree-Fock formalism. One very striking prediction of these calculations is that in this nucleus there exist very unusual configurations, with structures reminiscent of linear chains of alpha particles. In the CSM, for instance, such a configuration is identified with a pronounced minimum in the potential energy energy at very large prolate deformation. In the CCM, several very different alpha-particle duster configurations are identified, many having rather large deformations. These cluster configurations can be associated with the different potential-energy minima obtained in the CSM results. In the case of the CCM, a 6(alpha) chain-like configuration is predicted to occur at excitation energies between 40 and 50 MeV, with predicted rotational spacing given by Dirac-h(sup 2)/2I = 22 keV. At this excitation energy, such a chain configuration would lie well above the threshold for the decay of Mg-24 into 6 alpha particles, and its identification poses a difficult experimental challenge. This report discusses this challenge. DOE

N93-13606*# Quantex Corp., Rockville, MD.
LARGE AREA NUCLEAR PARTICLE DETECTORS USING ET MATERIALS, PHASE 2 Final Report, 9 May 1988 - 9 May 1990
Charles Y. Wrigley, George M. Storti, Lee Walter, and Scott Mathews May 1990 40 p
(Contract NAS5-30310; SBIR-08.04-2701)
(NASA-CR-190866; NAS 1.26:190866) Avail: CASI HC A03/MF A01

This report presents work done under a Phase 2 SBIR contract for demonstrating large area detector planes utilizing Quantex electron trapping materials as a film medium for storing high-energy nuclide impingement information. The detector planes utilize energy dissipated by passage of the high-energy nuclides to produce localized populations of electrons stored in traps. Readout of the localized trapped electron populations is effected by scanning the ET plane with near-infrared, which frees the trapped electrons and results in optical emission at visible wavelengths. The effort involved both optimizing fabrication technology for the detector planes and developing a readout system capable of high spatial resolution for displaying the recorded nuclide passage tracks. Author

73 NUCLEAR AND HIGH-ENERGY PHYSICS

Includes elementary and nuclear particles; and reactor theory. For space radiation see *93 Space Radiation*.

N93-12713# Texas Univ., Austin. Inst. for Fusion Studies.
FAST ION-DRIVEN BERNSTEIN INSTABILITIES
K. R. Chen 20 Jul. 1992 14 p
(Contract DE-FG05-80ET-53088)
(DE92-019393; DOE/ET-53088/556; IFSR-556) Avail: CASI HC A03/MF A01

We investigate a new mechanism, the two-energy-stream cyclotron instability, for fast ions (e.g., fusion products) to drive electrostatic waves and to slow down. The instability comes from a relativistic effect, which dominates conventional phase overtaking as the axial phase velocity exceeds the speed of light. Both a single particle model and a dispersion relation are developed in order to illuminate the physics insights and scaling laws. We present numerical results and discuss nonlinear processes. The mechanism is essential for the dynamics of the fast ions in both D-D and D-T devices. DOE

N93-12715*# Aerospace Corp., El Segundo, CA. Engineering and Technology Group.
ION RADIAL DIFFUSION IN AN ELECTROSTATIC IMPULSE MODEL FOR STORMTIME RING CURRENT FORMATION
Margaret W. Chen, Michael Schulz, Larry R. Lyons, and David J. Gorney 15 Sep. 1992 9 p
(Grant NAGw-2126)
(NASA-CR-190941; NAS 1.26:190941; ATR-92(7190)-3) Avail: CASI HC A02/MF A01

Guiding-center simulations of stormtime transport of ring-current and radiation-belt ions having first adiabatic invariants mu is approximately greater than 15 MeV/G (E is approximately greater than 165 keV at L is approximately 3) are surprisingly well described (typically within a factor of approximately less than 4) by the quasilinear theory of radial diffusion. This holds even for the case of an individual model storm characterized by substorm-associated impulses in the convection electric field, provided that the actual spectrum of the electric field is incorporated in the quasilinear

theory. Correction of the quasilinear diffusion coefficient D(sub LL)(sup ql) for drift-resonance broadening (so as to define D(sub LL)(sup ql)) reduced the typical discrepancy with the diffusion coefficients D(sub LL)(sup sim) deduced from guiding-center simulations of representative-particle trajectories to a factor of approximately 3. The typical discrepancy was reduced to a factor of approximately 1.4 by averaging D(sub LL)(sup sim), D(sub LL)(sup ql), and D(sub LL)(sup rb) over an ensemble of model storms characterized by different (but statistically equivalent) sets of substorm-onset times.

Author

N93-12822# Colorado Univ., Boulder.

THEORETICAL NUCLEAR PHYSICS

E. Rost and J. R. Shephard Aug. 1992 79 p

(Contract DE-FG02-87ER-40335)

(DE92-019286; DOE/ER-40335/13) Avail: CASI HC A05/MF A01

This report discusses the following topics: Exact 1-loop vacuum polarization effects in 1 + 1 dimensional QHD; exact 1-fermion loop contributions in 1 + 1 dimensional solitons; exact scalar 1-loop contributions in 1 + 3 dimensions; exact vacuum calculations in a hyper-spherical basis; relativistic nuclear matter with self-consistent correlation energy; consistent RHA-RPA for finite nuclei; transverse response functions in the (triangle)-resonance region; hadronic matter in a nontopological soliton model; scalar and vector contributions to (bar p)p yields (bar lambda)lambda reaction; 0+ and 2+ strengths in pion double-charge exchange to double giant-dipole resonances; and nucleons in a hybrid sigma model including a quantized pion field. DOE

N93-12829# Oak Ridge National Lab., TN.

ELECTROMAGNETIC LEPTON-PAIR PRODUCTION IN RELATIVISTIC COLLISIONS

C. J. Albert (Texas A&M Univ., College Station.), D. J. Ernst (Texas A&M Univ., College Station.), M. R. Strayer, and C. Bottcher 1991 13 p Presented at the Conference on Computational Quantum Physics, Nashville, TN, 22-25 May 1991

(Contract DE-AC05-84OR-21400)

(DE92-011069; CONF-9105238-7) Avail: CASI HC A03/MF A01

Electromagnetic lepton-pair production in relativistic collisions is studied in an ab initio approach with no free parameters. After a semi-classical approximation to the relative motion of the two incident particles is made, the resulting second-order diagram is calculated using a Monte Carlo technique to evaluate the resulting seven-dimensional integral. We examine the case of electron-positron pair production in pi(-)p collisions at p(sub pi) = 17 GeV. We find that a significant fraction of the measured pairs in this reaction are produced via the magnetic spin-flip current of the proton. Approaches, such as the equivalent photon approximation, which neglect this part of the current predict much too small a cross section. This feature is traced to the cuts imposed in taking the experimental data. Lepton-pair production in the scattering of He-3, He-4 and He-4, He-4 is proposed as a clean way of experimentally separating the spin-flip and non-flip processes; predictions are made for these systems. DOE

N93-12830# Sandia National Labs., Albuquerque, NM.

LONG PULSE ELECTRON BEAM PROPAGATION

J. R. Smith (Titan Technologies, Albuquerque, NM.), R. B. Miller (Titan Technologies, Albuquerque, NM.), I. R. Shokair, P. Kiekel, I. Molina, B. N. Turman, and K. W. Struve (Mission Research Corp., Albuquerque, NM.) 1992 9 p Presented at the 9th International Conference on High Power Particle Beams, Washington, DC, 25-29 May 1992

(Contract DE-AC04-76DP-00789)

(DE92-014948; SAND-91-2477C; CONF-920515-3) Avail: CASI HC A02/MF A01

Propagation of a 1 microsec electron beam over a distance of 90 m has been investigated in the EPOCH Laboratory at Sandia National Laboratories. The mode of propagation is Ion Focused Regime (IFR) transport. The plasma channel, which is required for IFR transport, is obtained by photoionization of trimethylamine gas with a krypton-fluoride laser. Beam voltage is 2.5 MV, and beam current is 1 to 2 kA. Propagation efficiencies better than 90 percent have been recorded. The ion hose instability is a key issue concerning long-pulse beam propagation. In previous work, growth of transverse beam oscillations (due to the ion hose instability) and moderate damping (due to phase-mixing) were measured in the first 6 m of beam propagation. Detailed displacement measurements in this region were used to determine the ion hose growth rate. Damping of beam oscillations is accompanied by an increase in beam radius as measured from head-to-tail. Measurement of radius growth has been one of the key tasks of FY 91. Several new features which improve these radius measurements as compared to those taken in FY 90 are: slice radius growth measured on a single shot, improved accuracy due to reduction in camera to target distance, improved accuracy due to diagnostic calibrations, and improved software analysis. The recent measurements may be separated into two categories, each characterized by different beam parameters. Category 1 has an initial radius of 1 to 2 cm, and a peak current of 1.1 kA. The initial radius for Category 2 has not yet been measured; we estimate that it lies in the range from 2 to 3 cm. Category 2 peak current is 1.6 kA. The space charge neutralization (channel strength) used in obtaining data for both cases is in the range 0.5 less than f less than 1.3.

DOE

N93-12924# Kent State Univ., OH. Dept. of Physics.

HEAVY-ION COLLISIONS AND THE NUCLEAR EQUATION OF STATE

D. Keane 1992 14 p

(Contract DE-FG02-89ER-40531)

(DE92-019364; DOE/ER-40531/3) Avail: CASI HC A03/MF A01

The overall goal of this project is to study nucleus-nucleus collisions experimentally at intermediate and relativistic energies. with emphasis on measurement and interpretation of correlation effects that provide insight into the nuclear phase diagram and the nuclear equation of state. During the past year, the PI has been on leave at Lawrence Berkeley Lab and has worked on this research project full-time. A large fraction of the effort of the PI and graduate students has gone into preparing for experiments using the Time Projection Chamber at LBL's Bevalac accelerator; in March 1992, this device successfully took data in production mode for the first time, and the first physics analysis is now under way. The PI has carried out simulations that help to define the physics performance and engineering specifications of the recently-approved STAR detector for the Relativistic Heavy Ion Collider, and has identified a new capability of this device with the potential for being an important quark-gluon plasma signature. A Postdoctoral Fellow, jointly supported by this grant and Kent State University, has been recruited to augment these efforts. Since May 1991, 11 journal papers have been published or submitted for publication; 2 conference proceedings and 9 reports or abstracts have also been published during the past year. DOE

N93-12970# Lawrence Livermore National Lab., CA.

ALTERNATE ELECTRODE MATERIALS FOR THE SP100 REACTOR

E. Randich May 1992 11 p

(Contract W-7405-eng-48)

(DE92-019570; UCRL-CR-111008) Avail: CASI HC A03/MF A01

This work was performed in response to a request by the Astro-Space Division of the General Electric Co. to develop alternate electrodes materials for the electrodes of the PD2 modules to be used in the SP100 thermoelectric power conversion system. Initially, the project consisted of four tasks: (1) development of a ZrB2 (C) CVD coating on SiMo substrates; (2) development of a ZrB2 (C) CVD coating on SiGe substrates; (3) development of CVI W for porous graphite electrodes; and (4) technology transfer of pertinent developed processes. The project evolved initially into developing only ZrB2 coatings on SiGe and graphite substrates, and later into developing ZrB2 coatings only on graphite substrates. Several sizes of graphite and pyrolytic carbon-coated graphite substrates were coated with ZrB2 during the project. For budgetary reasons, the project was terminated after half the allotted time had passed. Apart from the production of coated specimens for evaluation, the major accomplishment of the project was the development of the CVD processing to produce the desired coatings. DOE

N93-12992# Stanford Linear Accelerator Center, CA.

A SIMPLE MODEL FOR SLC POSITRON STABILITY ISSUES

P. Krejcik and V. Ziemann Jun. 1992 9 p Presented at the Spring Meeting of the American Physical Society, Washington, DC, 12-20 Apr. 1992

(Contract DE-AC03-76SF-00515)

(DE92-019644; SU-SLAC-PUB-5725; CONF-920405-1) Avail: CASI HC A02/MF A01

A simple model is constructed for the SLC positron system to describe the intensity variations induced by beam loading in the linac. It is found

that the system can be described by the well known logistic equation. This allows us to use results from the stability analysis to characterize the positron system, to place tolerances on fluctuations, and to slow variations on the scavenger beam intensity. DOE

N93-12993# Stanford Linear Accelerator Center, CA.
TEST OF QED USING A LASER AT THE SLAC FINAL FOCUS TEST BEAM
J. E. Spencer Apr. 1992 4 p Presented at the 9th International Workshop on Photon-Photon Collisions, San Diego, CA, 22-26 Mar. 1992
(Contract DE-AC03-76SF-00515)
(DE92-019647; SU-SLAC-PUB-5819; CONF-9203159-7) Avail: CASI HC A01/MF A01

Experiment no. 144 at SLAC has three parts: the search for low-mass states excited in gamma(gamma) collisions and observed in pair decay; the study of nonlinear, nonperturbative QED in (gamma)e and gamma(gamma) collisions; and its possible applications to general purpose linear colliders. Such colliders could produce the full range of J(sub q(dot)(dot)(bar-q))/(sup PC) states, leptoquarks J(sub l(dot)(dot)(bar-q))/(sup PC), the particles of supersymmetry, the top quark, or Higgs. However, to realize them, a number of technical problems need resolution that are addressed in E144 together with interesting possibilities for highly polarized, high brightness bar-gamma and bar-e(sup +/-) beams that are needed for electroweak studies. DOE

N93-13002# Indiana Univ., Bloomington. Dept. of Physics.
INDIANA UNIVERSITY HIGH ENERGY PHYSICS GROUP, TASK C
C. Bower, R. Heinz, S. Mufson, and J. Musser 24 Apr. 1992 39 p
(Contract DE-FG02-91ER-40661)
(DE92-040458; DOE/ER-40661/3) Avail: CASI HC A03/MF A01

We are participating in the experiments GEM at the SSC and MACRO at the Gran Sasso. After introducing GEM in chapter 2, we present some results from GEM work we have done during the current contract period. Other significant GEM activities by our group such as participation in the evolution of GEM (as founding fathers), GEM proposal writing, and the design of GEM electronics for the Interpolating Pad Chambers for the Central Tracker are not included in this report. In chapter 3 we introduce MACRO and give a brief status report. Instead of a survey of our many ongoing contributions to MACRO, we choose in this technical report to concentrate on reporting results of some MACRO data analysis headed by our group (with important contributions by our collaborators, of course). This analysis, in chapter 4V, concerns Point Sources. DOE

N93-13090# Stanford Univ., CA. Linear Accelerator Center.
DAMPING THE (PI)-MODE INSTABILITY IN THE SLC DAMPING RINGS WITH A PASSIVE CAVITY
Y. Chao, P. Corredoura, A. Hill, P. Krejcik, T. Limberg, M. Minty, M. Nordby, F. Pedersen, H. Schwarz, and W. Spence et al Jul. 1992 3 p Presented at the 15th International Conference on High Energy Accelerators, Hamburg, Germany, 20-24 Jul. 1992
(Contract DE-AC03-76SF-00515)
(DE92-018153; SLAC-Pub-5868; CONF-920706-6) Avail: CASI HC A01/MF A01

Operating the Stanford Linear Collider (SLC) at 120 Hz repetition rate requires the presence of two bunches in both the electron and the positron damping ring. The pi-mode instability, a coupled bunch instability where the two bunches oscillate with a phase difference of 180 deg, had been observed in both rings with low current thresholds of 7 x 10(exp 9) particles per bunch. To avoid the instability, the RF system had to be operated in ways which in general reduced the cavity gap voltages and required constant operational attention. For the 1992 running cycle a passive cavity was installed and successfully tested. It is tuned to the frequency of the lower synchrotron oscillation sideband of an odd revolution harmonic. The impedance of the cavity then damps pi-mode oscillations very similar to the Robinson damping provided by the main RF cavities which damps O-mode synchrotron oscillations. In this report we describe the motivation and physical considerations that led to the final design parameters and the experience obtained from the performance of these cavities. DOE

N93-13108# Superconducting Super Collider Lab., Dallas, TX.
LONGITUDINAL BEAM DYNAMICS WITH RF NOISE
H. J. Shih, J. A. Ellison, R. Cogburn (New Mexico Univ., Albuquerque.), and B. S. Newberger (Texas Univ., Austin.) Jul. 1992 44 p
(Contract DE-AC35-89ER-40486)
(DE92-040645; SSCL-578) Avail: CASI HC A03/MF A01

The Dome-Krinsky-Wang (DKW) diffusion-in-action theory for rf-noise-induced emittance dilution is reviewed and related to recent work on the approximation of stochastic processes by Markov processes. An accurate and efficient numerical procedure is developed to integrate the diffusion equation of the DKW theory. Tracking simulations are undertaken to check the validity of the theory in the parameter range of the Superconducting Super Collider (SSC) and to provide additional information. The study of effects of rf noise is applied to two problems of interest at the SSC: (1) determination of noise tolerance levels in the rf system, and (2) feasibility of beam extraction using crystal channeling. DOE

N93-13189# Columbia Univ., New York, NY.
THEORETICAL HIGH ENERGY PHYSICS Progress Report
T. D. Lee 1992 26 p
(Contract DE-FG02-92ER-40699)
(DE92-015480; DOE/ER-40699/1) Avail: CASI HC A03/MF A01

This progress report discusses research by Columbia University staff in high energy physics. Some of the topics discussed are as follows: lattice gauge theory; quantum chromodynamics; parity doublets; solitons; baryon number violation; black holes; magnetic monopoles; gluon plasma; Chern-Simons theory; and the inflationary universe. DOE

N93-13192# Brookhaven National Lab., Upton, NY.
POWER EXCITATION BY THE USE OF A RF WIGGLER
A. G. Ruggiero 1992 14 p Presented at the Advanced Accelerator Concepts Workshop, Port Jefferson, NY, 14-20 Jun. 1992
(Contract DE-AC02-76CH-00016)
(DE92-016097; BNL-47616; CONF-9206193-1) Avail: CASI HC A03/MF A01

It is well-known that it is difficult to obtain RF power sources for frequencies larger than 3 GHz. Yet, RF sources in the centimeter/millimeter wavelength range would be very useful to drive, for example, high-gradient accelerating linacs for electron-positron linear colliders. We would like to propose an alternative method to produce such radiation. It makes use of a short electron bunch traveling along the axis of a waveguide which is at the same time excited by a TM propagating electromagnetic wave. It is well known that radiation can be obtained by wiggling the motion of the electrons in a direction perpendicular to the main one. The wiggling action can be induced by electromagnetic fields in a fashion similar to the one caused by wiggler magnets. We found that an interesting mode of operation is to drive the waveguide with an excitation frequency very close to the cut off. For such excitation, the corresponding e.m. wave travels with a very large phase velocity which in turn has the effect to increase the wiggling action on the electron bunch. Our method, to be effective, relies also on the coherence of the radiation; that is the bunch length is taken to be considerably shorter than the radiated wavelength. In this case, the total power radiated should be proportional to the square of the total number of electrons in the bunch. The paper concludes with possible modes of operation, a list of performance parameters, and a proposed experimental set-up. DOE

N93-13235# Fermi National Accelerator Lab., Batavia, IL.
RF VOLTAGE MODULATION AT DISCRETE FREQUENCIES WITH APPLICATIONS TO CRYSTAL CHANNELING EXTRACTION
W. Gabella (California Univ., Los Angeles.), J. Rosenzweig (California Univ., Los Angeles.), R. Kick (Illinois Mathematics and Science Academy, Aurora.), and S. Peggs May 1992 26 p
(Contract DE-AC02-76CH-03000)
(DE92-015567; FNAL-TM-1783) Avail: CASI HC A03/MF A01

RF voltage modulation at a finite number of discrete frequencies is described in a Hamiltonian resonance framework. The theory is applied to the problem of parasitic extraction of a fixed target beam from a high energy proton collider, using a bent crystal as a thin 'septum' within an effective width of about one micron. Three modes of employment of discrete resonances are proposed. First, a single relatively strong static 'drive' resonance may be used to excite a test proton so that it will penetrate deeply into the channeling crystal. Second, a moderately strong 'feed' resonance with a ramped modulation tune may be used to adiabatically trap protons near the edge of the beam core, and transport them to the

drive resonance. Third, several weak resonances may be overlapped to create a chaotic amplitude band, either to transport protons to the drive resonance, or to provide a 'pulse stretching' buffer between a feed resonance and the drive resonance. Extraction efficiency is semi- quantitatively described in terms of characteristic 'penetration,' 'depletion,' and 'repetition' times. Simulations are used to quantitatively confirm the fundamental results of the theory, and to show that a prototypical extraction scheme using all three modes promises good extraction performance. DOE

N93-13284# Continuous Electron Beam Accelerator Facility, Newport New, VA.

TEST OF A NEW RF SEPARATOR STRUCTURE FOR CEBAF

Reza Kazimi, J. Fugitt, A. Krycuk, C. K. Sinclair, and L. Turlington Aug. 1992 5 p

(Contract DE-AC05-84ER-40150)

(CEBAF-PR-92-024) Avail: CASI HC A01/MF A01

A prototype of the RF separator for CEBAF was made and successfully beam tested. This structure is a new design which has a high transverse shunt impedance together with a small transverse dimension compared to more conventional structures. Five RF separators will be used at CEBAF to allow a beam from any one of the five recirculation passes to be delivered to any of the three experimental halls. The basic design of the structure, and the theoretical, RF, and beam-test results are presented. Author

N93-13508# Los Alamos National Lab., NM.

DESIGN AND OPERATION OF A BUNCHED-BEAM, PHASE-SPREAD MEASUREMENT

J. D. Gilpatrick, H. Marquez, J. Power, and V. Yuan 1992 9 p Presented at the 16th International LINAC Conference, Ottawa, Ontario, 23-28 Aug. 1992

(Contract W-7405-eng-36)

(DE92-040230; LA-UR-92-2728; CONF-9208109-20) Avail: CASI HC A02/MF A01

A bunch-length monitor system has measured the relative changes in the temporal beam-bunch length of an H(-), 2.5 MeV beam. This system includes a non interceptive electromagnetic probe, associated RF processing electronics, and a software algorithm. The probe is an axial symmetric capacitive pickup whose output signal is proportional to the bunched beam image currents traveling through its bore. The RF electronics processes the beam-induced signal into a ratio of its fundamental and fifth-harmonic Fourier components and provides a time-varying output voltage proportional to the phase length of the beam-bunch. This paper reviews the measurement hardware, software algorithm, and operational experience. DOE

N93-13574# Oak Ridge National Lab., TN.

THE ORNL RADIOACTIVE ION BEAM PROJECT WITH THE ORIC ACCELERATOR

D. K. Olsen, G. D. Alton, C. Baktash, D. T. Dowling, J. D. Garrett, D. L. Haynes, C. M. Jones, R. C. Juras, S. N. Lane, and I. Y. Lee et al 1992 4 p Presented at the Conference on Cyclotrons and Their Applications, Vancouver, British Columbia, 10-16 Jul. 1992

(Contract DE-AC05-84OR-21400)

(DE92-040027; CONF-920741-1) Avail: CASI HC A01/MF A01

The ORNL project to produce medium-intensity, proton-rich, radioactive ion beams (RIBS) for astrophysics, nuclear physics, and applied research with the Holifield Heavy Ion Research Facility (HHIRF) accelerators has been approved. Radioactive atoms will be produced by fusion reactions in an Isotope Separator On-Line (ISOL) type target-ion source assembly using light ion beams from the Oak Ridge Isochronous Cyclotron (ORIC). The radioactive atoms will be converted to negative ions using either (1) direct-surface ionization, or (2) charge exchange following positive ionization. After acceleration to approximately 300 keV from a high-voltage platform, these negative ions will be injected into the 25-MV tandem accelerator for acceleration to higher energies. Beams of up to mass 80 will be accelerated to energies greater than 5 MeV/nucleon. For some radioactive beams. intensities greater than I pnA are possible. DOE

N93-14089# Aerospace Corp., El Segundo, CA. Engineering and Technology Group.

COMPARISON OF HEAVY ION AND ELECTRON-BEAM UPSET DATA FOR GaAs

L. D. Flesner, R. Zuleeg, and W. A. Kolasinski 16 Jul. 1992 19 p

(Contract F04701-88-C-0089)

(AD-A255901; TR-0090(5940-05)-5; SMC-TR-92-37) Avail: CASI HC A03/MF A01

We report the results of experiments designed to evaluate the extent to which focused electron-beam pulses simulate energetic ion upset phenomena in GaAs memory circuits fabricated by the McDonnell Douglas Astronautics Company. The results of two experimental methods were compared, irradiation by heavy-ion particle beams, and upset mapping using focused electron pulses. Linear energy transfer (LET) thresholds and upset cross sections are derived from the data for both methods. A comparison of results shows good agreement, indicating that for these circuits electron-beam pulse mapping is a viable simulation technique. GRA

74 OPTICS

Includes light phenomena; and optical devices.
For lasers see *36 Lasers and Masers.*

N93-12591*# Eastman Kodak Co., Rochester, NY. Government Systems Div.

LARGE DEPLOYABLE REFLECTOR (LDR) SYSTEM CONCEPT AND TECHNOLOGY DEFINITION STUDY. VOLUME 1: EXECUTIVE SUMMARY, ANALYSES AND TRADES, AND SYSTEM CONCEPTS Final Technical Report

Donald L. Agnew and Peter A. Jones Apr. 1989 375 p

(Contract NAS2-11861; RTOP 506-62-21)

(NASA-CR-177413-Vol-1; NAS 1.26:177413-Vol-1) Avail: CASI HC A16/MF A03

A study was conducted to define reasonable and representative large deployable reflector (LDR) system concepts for the purpose of defining a technology development program aimed at providing the requisite technological capability necessary to start LDR development by the end of 1991. This volume includes the executive summary for the total study, a report of thirteen system analysis and trades tasks (optical configuration, aperture size, reflector material, segmented mirror, optical subsystem, thermal, pointing and control, transportation to orbit, structures, contamination control, orbital parameters, orbital environment, and spacecraft functions), and descriptions of three selected LDR system concepts. Supporting information is contained in appendices. Author

N93-12593*# Eastman Kodak Co., Rochester, NY. Government Systems Div.

LARGE DEPLOYABLE REFLECTOR (LDR) SYSTEM CONCEPT AND TECHNOLOGY DEFINITION STUDY. VOLUME 2: TECHNOLOGY ASSESSMENT AND TECHNOLOGY DEVELOPMENT PLAN Final Technical Report

Donald L. Agnew and Peter A. Jones Apr. 1989 117 p

(Contract NAS2-11861; RTOP 506-62-21)

(NASA-CR-177413-Vol-2; NAS 1.26:177413-Vol-2) Avail: CASI HC A06/MF A02

A study was conducted to define reasonable and representative LDR system concepts for the purpose of defining a technology development program aimed at providing the requisite technological capability necessary to start LDR development by the end of 1991. This volume presents thirteen technology assessments and technology development plans, as well as an overview and summary of the LDR concepts. Twenty-two proposed augmentation projects are described (selected from more than 30 candidates). The five LDR technology areas most in need of supplementary support are: cryogenic cooling; astronaut assembly of the optically precise LDR in space; active segmented primary mirror; dynamic structural control; and primary mirror contamination control. Three broad, time-phased, five-year programs were synthesized from the 22 projects, scheduled, and funding requirements estimated. Author

N93-12642# Air Force Inst. of Tech., Wright-Patterson AFB, OH.

FIBRE-OPTIC SENSORS USING ADIABATICALLY TAPERED SINGLE-MODE FIBRES Ph.D. Thesis

Zoe M. Hale May 1992 45 p

(AD-A254555; AFIT/CI/CIA-92-047) Avail: CASI HC A03/MF A01

A tapered single-mode fiber optic device was investigated for use as

an intrinsic pH sensor. The sensing process is based on the detection of evanescent-wave excited fluorescence energy from an indicator dye circulating the taper. Appropriate selection of dye and taper parameters have allowed the sensor to perform well in harsh chemical environments, with near-real-time response. Future work could include immobilization schemes for the indicator as well as other sensor types, such as pCa. Further optical properties of the tapered fiber are also investigated. GRA

N93-12666# Optical Society of America, Washington, DC.
ORGANIZATION OF THE OPTICAL SOCIETY OF AMERICA PHOTONIC SCIENCE TOPICAL MEETING SERIES. VOLUME 8: INTEGRATED PHOTONICS RESEARCH. LIFORNIA ON 9-11 APRIL 1991 Final Report, 1 Jan. - 31 Dec. 1991
Jarus W. Quinn 22 May 1992 233 p Workshop on Active and Passive Fiber Components held in Monterey, CA, 9-11 Apr. 1991
(Grant AF-AFOSR-0176-91)
(AD-A254682; AFOSR-92-0513TR-Vol-8) Avail: CASI HC A11/MF A03

The attached list of reports is presented by the by Optical Society of America. The following topics are discussed: Photorefractive Materials, Effects, and Devices; Integrated Photonics Research; Nonlinear Guided Wave Phenomena Optical Amplifiers and their Applications; Optical Computing Picosecond Electronics and Optoelectronics; Quantum Optoelectronics; Photonic Switching; Microphysics of Surfaces: Beam Induced Processes; Soft X-ray Projection Lithography; Short Wavelength Coherent Radiation, Generation and Applications; and Persistent Spectral Hole-Burning: Science and Applications. GRA

N93-12850# Optical Society of America, Washington, DC.
SOFT X RAY PROJECTION LITHOGRAPHY TOPICAL MEETING. VOLUME 8: TECHNICAL DIGEST Quarterly Report
8 Apr. 1992 162 p Meeting held in Monterey, CA, 6-8 Apr. 1992
(Contract F49620-92-J-0264)
(AD-A254756; AFOSR-92-0738TR-Vol-8) Avail: CASI HC A08/MF A02

Since the first suggestion of doing projection lithography with soft x-rays was made by Hawryluk and Seppala, and Silvfast and Wood nearly 4 years ago, there has been a flood of activity on many of the basic principles and technologies. Foremost among these has been the development of high reflectivity coatings for mirrors that operate near 130 angstroms, the demonstration of diffraction-limited reduction imaging over a small field, and the design of high efficiency laser plasmas for compact illumination sources. Current work includes construction and repair of reflection masks, designs for large field cameras, and illuminators to couple them to the source, and development of advanced methods to measure and ultimately fabricate precision spherical and aspherical mirrors for large field cameras. Yet a great deal of work has to be done before soft x-ray projection lithography can become even a prototype lithography system, much less a commercial competitor. GRA

N93-12894*# Alabama Univ., Huntsville. Center for Applied Optics.
CONTAMINATION ANALYSIS OF SSF CANDIDATE MATERIALS Final Report
R. Barry Johnson Aug. 1991 52 p
(Contract NAS8-36955)
(NASA-CR-184431; NAS 1.26:184431; UAH-5-32391) Avail: CASI HC A04/MF A01

NASA's In Situ Contamination Effects Facility, Marshall Space Flight Center, has been used to test several candidate materials for use upon Space Station Freedom. Optical measurements were made in the vacuum ultraviolet (VUV) as test mirrors were contaminated by materials in a space-like environment. This was done to determine the effects of the contamination and subsequent exposure to VUV radiation upon optical components that will be used upon the space station. Author

N93-12918# Sandia National Labs., Albuquerque, NM.
PROCESS DESIGNED FOR EXPERIMENTATION FOR INCREASED-CALIPER FRESNEL LENSES
A. J. Zderad (Minnesota Mining and Mfg. Co., Saint Paul.) Apr. 1992 18 p
(Contract DE-AC04-76DP-00789)
(DE92-019464; SAND-91-7017) Avail: CASI HC A03/MF A01

The feasibility of producing increased caliper linear and point focus Fresnel lenses in a continuous sheet is described. Both a 8.16-inch-square radial 2 x 7 parquet, and a 22-inch-wide linear lens were produced at .11-inch in caliper. The primary purpose of this experimentation is to determine the replication effectiveness and production rate of the polymeric web process at increased thickness. The results demonstrated that both radial and linear lenses, at increased caliper, can be replicated with performance comparable to that of the current state-of-the-art 3M laminated lenses; however, the radial parquets were bowed on the edges. Additional process development is necessary to solve this problem. Current estimates are that the .11-inch caliper parquets cost significantly more than customer laminated parquets using 0.022-inch thick lensfilm. DOE

N93-12984 Rhode Island Univ., Kingston.
FIBER OPTIC SENSORS FOR STATIC FRACTURE STUDIES AND DYNAMIC WAVE PROPAGATION PROBLEMS Ph.D. Thesis
Nadarajah Narendran 1991 177 p
Avail: Univ. Microfilms Order No. DA9217535

An experimental study is conducted to investigate the applicability of fiber-optic sensors for static fracture and dynamic wave propagation problems. The type of sensor considered for fracture studies is the Mach-Zehnder interferometer. Mode I stress intensity factors, which completely define the stress field near a crack tip, are obtained using surface attached and embedded fiber-optic sensors in single edge notched specimens. The experimental results compare well with the theoretical predictions. In dynamic applications it is important to know both the magnitude as well as the sign of the strain field. The results from the Mach-Zehnder interferometer are difficult to interpret if the strain changes sign during the observations period. To overcome this problem a novel combined interference and polarization technique is developed. The performance of the Mach-Zehnder interferometer is extremely good at very low frequencies, but at higher frequencies it failed to give meaningful results. Thus a polarimetric sensor is used for high frequency wave propagation studies. A distributed fiber-optic sensor based on polarmetric technique is developed to study acoustic wave propagation in materials. The feasibility of using this sensor to detect flaws and characterize materials is performed. Dissert. Abstr.

N93-12985*# Texas A&M Univ., College Station. Dept. of Mechanical Engineering.
AUTOMATION OF THE TARGETING AND REFLECTIVE ALIGNMENT CONCEPT Final Report, Sep. 1989 - Aug. 1992
Robin C. Redfield Oct. 1992 43 p
(Grant NAG9-374)
(NASA-CR-190964; NAS 1.26:190964) Avail: CASI HC A03/MF A01

The automated alignment system, described herein, employs a reflective, passive (requiring no power) target and includes a PC-based imaging system and one camera mounted on a six degree of freedom robot manipulator. The system detects and corrects for manipulator misalignment in three translational and three rotational directions by employing the Targeting and Reflective Alignment Concept (TRAC), which simplifies alignment by decoupling translational and rotational alignment control. The concept uses information on the camera and the target's relative position based on video feedback from the camera. These relative positions are converted into alignment errors and minimized by motions of the robot. The system is robust to exogenous lighting by virtue of a subtraction algorithm which enables the camera to only see the target. These capabilities are realized with relatively minimal complexity and expense. Author

N93-13062*# Alabama Univ., Huntsville. Center for Applied Optics.
OPTICAL DESIGN FOR A BALLOON-BORNE MAGNETOGRAPH Final Report, 18 Oct. 1991 - 17 Jun. 1992
James B. Hadaway and Chen Feng 6 Oct. 1992 170 p
(Contract NAS8-38609)
(NASA-CR-191003; NAS 1.26:191003; UAH-5-32794) Avail: CASI HC A08/MF A02

This report details activities performed in order to accomplish the optical design of a balloon-borne solar vector magnetograph. Author

N93-13419* National Aeronautics and Space Administration. Pasadena Office, CA.
INTEGRATED FILTER AND DETECTOR ARRAY FOR SPECTRAL IMAGING Patent
Clayton C. LaBaw, inventor (to NASA) (Jet Propulsion Lab., California Inst.

of Tech., Pasadena.) 27 Oct. 1992 10 p Filed 12 Aug. 1991
Supersedes N91-32926 (29 - 24, p 4103)
(NASA-Case-NPO-18317-1-CU; US-Patent-5,159,199;
US-Patent-Appl-SN-744197; US-Patent-Class-250-339;
US-Patent-Class-356-328; US-Patent-Class-357-30;
US-Patent-Class-359-859; Int-Patent-Class-G01N-21/27;
Int-Patent-Class-G02B-5/20) Avail: US Patent and Trademark Office

A spectral imaging system having an integrated filter and photodetector array is disclosed. The filter has narrow transmission bands which vary in frequency along the photodetector array. The frequency variation of the transmission bands is matched to, and aligned with, the frequency variation of a received spectral image. The filter is deposited directly on the photodetector array by a low temperature deposition process. By depositing the filter directly on the photodetector array, permanent alignment is achieved for all temperatures, spectral crosstalk is substantially eliminated, and a high signal to noise ratio is achieved.

Official Gazette of the U.S. Patent and Trademark Office

N93-13500# Department of the Army, Washington, DC.
INFRARED IMAGE PROJECTOR UTILIZING A DEFORMABLE MIRROR DEVICE SPATIAL LIGHT MODULATOR Patent Application
Don A. Gregory, inventor (to Army), David J. Lanteigne, inventor (to Army), Joseph J. Booth, inventor (to Army), and Scottie B. Mobley, inventor (to Army) 4 Jun. 1992 18 p
(AD-D015373; US-Patent-Appl-SN-863908) Avail: CASI HC A03/MF A01

The mirror elements of a deformable mirror device spatial light modulator are selectively deflected. Such deflection causes incident infrared radiation to be reflected in selected directions. The number of deflected mirror elements as well as the degree of deflection determines the amount of reflected radiation which travels through an aperture and is collimated by suitable imaging optics, thus creating an infrared image that appears to be at infinity. GRA

N93-13509# Los Alamos National Lab., NM.
VIDEO PROFILE MONITOR DIAGNOSTIC SYSTEM FOR GTA
D. P. Sandoval, R. C. Garcia, J. D. Gilpatrick, K. F. Johnson, M. A. Shinas, R. Wright, V. Yuan, and M. E. Zander 1992 4 p Presented at the 16th International LINAC Conference, Ottawa, Ontario, 23-28 Aug. 1992
(Contract W-7405-eng-36)
(DE92-040231; LA-UR-92-2727; CONF-9208109-19) Avail: CASI HC A01/MF A01

This paper describes a video diagnostic system used to measure the beam profile and position of the Ground Test Accelerator 2.5-MeV H(-) ion beam as it exits the intermediate matching section. Inelastic collisions between H-ions and residual nitrogen in the vacuum chamber cause the nitrogen to fluoresce. The resulting light is captured through transport optics by an intensified CCD camera and is digitized. Real-time beam-profile images are displayed and stored for detailed analysis. Analyzed data showing resolutions for both position and profile measurements will also be presented. DOE

N93-13576# Westinghouse Savannah River Co., Aiken, SC.
FIBER OPTIC SENSORS FOR ENVIRONMENTAL APPLICATIONS: A BRIEF REVIEW
J. Rossabi Apr. 1992 17 p
(Contract DE-AC09-89SR-18035)
(DE92-040170; WSRC-RP-92-471) Avail: CASI HC A03/MF A01

Understanding the flow and transport of contaminants in the subsurface is vital to a complete knowledge of groundwater quality. This understanding is achieved by measurement of the appropriate chemical and physical subsurface parameters. The ideal measurement would accurately assess a parameter without affecting the parameter or its environment. Fiber optic spectroscopy offers some of the most promising techniques for accurate, non-invasive measurements of environmental parameters. Fiber optic sensors for subsurface applications are currently being developed by several Department of Energy laboratories. Some of these sensors have been successfully deployed in the field and are attaining the goals of accurate, noninvasive, real time measurements in the subsurface. DOE

N93-13652# Brookhaven National Lab., Upton, NY.
DEVELOPMENT OF OPTICAL SURFACE PROFILING INSTRUMENTATION
Yao Lin, P. Takacs, T. Tsang, K. Furenlid, and Run-Wen Wang (Academia Sinica, Shanghai, China) Jun. 1992 10 p Presented at the SPIE International Symposium on Optical Applied Science and Engineering, San Diego, CA, 19-24 Jul. 1992
(Contract DE-AC02-76CH-00016)
(DE92-019252; BNL-47797; CONF-920792-24) Avail: CASI HC A02/MF A01

A non-contact optical profiler described in this paper is designed and made for measuring the surface characteristics of optical parts. Measurements are based on a combination of an optical heterodyne technique and a precise phase measurement procedure without the need of a inference surface. A Zeeman-split He-Ne laser is employed as the light source which offers two common-path polarized beams. The frequency difference between the beams is 1.8 MHz. A special optical head is designed and fashioned as a beam splitter which contains a birefringent lens and an objective. The whole optical system is completely common-path. This allows the optical common-mode injection technique to be applied in the system for minimizing the environmental effects in measurements such as air turbulence, vibrations and temperature variations. To keep the sample surface focused to the ordinary rays in the optical head, an astigmatic autofocus system is employed. A stepping micro-stepping system can move the optical head in the range of 25 mm with 0.1 micron resolution. A data acquisition system is made to control the auto-focus system, data receiving, and analyses. This makes the measurement automatically while the sample is being scanned. The characteristics of the surface can be displayed on the computer screen. The theoretical and experimental analyses of the profiler are completed. The profiler measures samples with 1.1 A height accuracy and 4 micron lateral resolution when a 4OX objective is used in the optical head. The accuracy comparisons of the profiler with different objectives 5X, 1OX, 2OX, and 4OX are shown in a good agreement. The advantages of the present profiler are presented. Based on the autofocus system, the profiler optical system will be designed to mount on a large linear air-bearing slide, so that it is capable of scanning over a distance covering from 4 microns to 1 m. DOE

N93-13696*# Alabama Univ., Huntsville. Dept. of Electrical and Computer Engineering.
DEVELOPMENT OF A STABLE ELECTRO-OPTICAL MODULATOR Final Report
Mustafa A. G. Abushagur [1992] 3 p
(Contract NAS8-36955)
(NASA-CR-184404; NAS 1.26:184404) Avail: CASI HC A01/MF A01

The activity of the sun can be studied through the measurement of its magnetic field. The measurement of the polarization state of the sunlight in a narrow spectral bandwidth can be related to the magnetic fields strengths and directions over the active sunspots. Measuring the polarization state can be done using the vector magnetograph. The essential component of the vector magnetograph is the polarization modulators. Electro-optical modulators are used as dynamic retarders. KDP (potassium dideuterium phosphate) crystals provide variable retardation which can be controlled by the applied voltage. KDP's have a high contrast ratio but suffer some problems; they require a high voltage and have a limited modulation lifetime. The KDP modulator forms the heart of the polarimeter assembly which is used for carrying out accurate measurements of linear polarization of the sun. It is therefore important to study the optical and electrical behavior of the KDP crystals so that the ultimate goal of making stable electro-optical modulators in the laboratory is achieved. A number of activities were performed in coating and testing the KDP crystals. A summary of these activities is given. Author

N93-13705*# Radiation Monitoring Devices, Inc., Watertown, MA.
SOFT X RAY WINDOW ENCAPSULANT FOR HgI2 DETECTORS Final Report
G. Entine, K. Shah, and M. Squillante 30 Jun. 1987 62 p
(Contract NAS7-931; SBIR-08.07-1167)
(NASA-CR-190850; NAS 1.26:190850) Avail: CASI HC A04/MF A01

HgI2 is an excellent semiconductor material for a low energy, room temperature x-ray spectrometer. The high values of the atomic numbers for its constituent elements gives high x-ray and gamma ray stopping

power. The band gap of HgI2 is significantly higher than other commonly used semiconductors. Owing to the large value band gap, the leakage current for HgI2 devices is smaller, thus allowing low noise performance. Devices fabricated from HgI2 crystals have demonstrated energy resolution sufficient to distinguish the x-ray emission from the neighboring elements on the periodic table. Also the power requirements of HgI2 are very low. These characteristics make a HgI2 spectrometer an ideal component in a satellite based detection system. Unfortunately, HgI2 crystals tend to deteriorate with time, even if protected by standard semiconductor encapsulants. This degradation ruins the performance of the device in terms of its energy resolution and pulse amplitude. The degrading mechanism is believed to be material loss occurring from below the electrodes, due to high vapor pressure of HgI2 at room temperature. To address this major obstacle to rapid expansion of HgI2 technology, a research program aimed at improving device stability by encapsulation with inert polymeric materials was carried out. The program focused specifically on optimizing the encapsulant materials and their deposition techniques. The principal objectives for this program were device encapsulation, device testing, and accelerated testing to ensure very long term stability of these high resolution sensors. A variety of encapsulants were investigated with the selection criteria based on their chemical diffusion barrier properties, mechanical stability, reactivity, and morphology of encapsulant films. The investigation covered different classes of encapsulants including solvent based encapsulants, vapor deposited encapsulants, and plasma polymerized encapsulants. A variety of characterization techniques were employed to examine their effectiveness in stabilizing HgI2 devices; these included permeability evaluation, vacuum and heat testing, scanning electron microscopy (SEM) as well as studying the detector performance of coated detectors. The plasma polymerized films appear to have entirely solved the HgI2 degradation problem. Another achievement of this program was the development of an accelerated testing technique which correlates extremely well with long term tesing. L.R.R.

N93-13711* National Aeronautics and Space Administration. Pasadena Office, CA.

LARGE AREA PROJECTION LIQUID-CRYSTAL VIDEO DISPLAY SYSTEM WITH INHERENT GRID PATTERN OPTICALLY REMOVED Patent

Hua-Kuang Liu, inventor (to NASA) (Jet Propulsion Lab., California Inst. of Tech., Pasadena.) 3 Nov. 1992 4 p Filed 21 Dec. 1990 Continuation of abandoned application US-Patent-Appl-SN-913433, filed 30 Sep. 1986

(NASA-Case-NPO-16932-2-CU; US-Patent-5,161,027; US-Patent-Appl-SN-632408; US-Patent-Appl-SN-913433; US-Patent-Class-358-231; US-Patent-Class-358-61; US-Patent-Class-358-232; Int-Patent-Class-H04N-5/74; Int-Patent-Class-H04N-9/31) Avail: US Patent and Trademark Office

A relatively small and low-cost system is provided for projecting a large and bright television image onto a screen. A miniature liquid crystal array is driven by video circuitry to produce a pattern of transparencies in the array corresponding to a television image. Light is directed against the rear surface of the array to illuminate it, while a projection lens lies in front of the array to project the image of the array onto a large screen. Grid lines in the liquid crystal array are eliminated by a spacial filter which comprises a negative of the Fourier transform of the grid.

Official Gazette of the U.S. Patent and Trademark Office

N93-13762*# General Electric Co., Evendale, OH.

ELECTRO-OPTIC ARCHITECTURE FOR SERVICING SENSORS AND ACTUATORS IN ADVANCED AIRCRAFT PROPULSION SYSTEMS Final Report, Apr. 1988 - Jan. 1989

G. L. Poppel (General Electric Co., Cincinnati, OH.) and W. M. Glasheen (General Electric Co., Cincinnati, OH.) Jun. 1989 98 p

(Contract NAS3-25344)

(NASA-CR-182269; NAS 1.26:182269; GE-R89AEB208) Avail: CASI HC A05/MF A02

A detailed design of a fiber optic propulsion control system, integrating favored sensors and electro-optics architecture is presented. Layouts, schematics, and sensor lists describe an advanced fighter engine system model. Components and attributes of candidate fiber optic sensors are identified, and evaluation criteria are used in a trade study resulting in favored sensors for each measurand. System architectural ground rules were applied to accomplish an electro-optics architecture for the favored sensors. A key result was a considerable reduction in signal conductors. Drawings, schematics, specifications, and printed circuit board layouts describe the detailed system design, including application of a planar optical waveguide interface. Author

N93-13866# Vanderbilt Univ., Nashville, TN.

INTRINSIC BISTABLE PHOTONIC MATERIALS BY COPPER COLLOID FORMATION IN SILICA Final Report, 1 Mar. 1991 - 31 May 1992

Robert H. Magruder, III 31 Jul. 1992 17 p

(Contract DAAL03-91-G-0028)

(AD-A255505; ARO-28109.8-MS) Avail: CASI HC A03/MF A01

Ion implantation has been used to assemble planar thin films of metallic nanoclusters embedded in a dielectric. Gold and copper were both found to produce nanosize metal clusters in silica. Both the size and size distribution of the metallic nanoclusters were characterized by transmission electron microscopy. The size and size distribution were found to be controlled by implantation protocols and post implantation processing. The linear and nonlinear optical properties were measured and found to be a function of the cluster size and size distribution. The nonlinear response was electronic in character and has a response time which is no longer than 15 ps. The nonlinear index of refraction of these materials has a magnitude of approximately 10(exp -10) cm(exp 2) W(exp -1), comparing favorably to semi-conductor microcrystallites. The linear optical properties were well described by Mie theory while the nonlinear responses can be described by effective medium theory. GRA

N93-13879# Optical Society of America, Washington, DC.

OSA PROCEEDINGS OF THE TOPICAL MEETING ON OPTICAL AMPLIFIERS AND THEIR APPLICATIONS, VOLUME 13 Final Report, 1 Jan. - 31 Dec. 1991

Jarus W. Quinn 22 May 1992 309 p Meeting held in Snowmass Village, CO, 24-26 Jul. 1991

(Grant AF-AFOSR-0176-91)

(AD-A252974; AFOSR-92-0521TR-Vol-13) Avail: CASI HC A14/MF A03

Summaries of papers presented at the Optical Amplifiers and Their Applications Topical Meeting held in Snowmass Village, Colorado on July 24-26, 1991 are included. Topics covered are optical amplifiers, doped fiber amplifiers, laser diode pump sources, material effects in fiber amplifiers, semiconductor optical amplifiers, ultra-long distance transmission systems, spectral characteristics of fiber amplifiers, carrier dynamics and nonlinearities in semiconductor amplifiers, components and amplifier configurations, high efficiency and saturated amplifiers, system performance considerations, broadband optical network applications, applications of semiconductor optical amplifiers, fiber amplifier engineering, and system techniques and applications. L.R.R.

N93-14031# Naval Research Lab., Washington, DC.

FIBER OPTIC DATA BUS RADIATION EFFECTS STUDY Report, 1 Oct. 1990 - 30 Sep. 1991

E. J. Frieble, P. W. Marshall, G. P. Summers, Y. J. Chen, and A. B. Campbell 28 Sep. 1992 90 p

(AD-A255821; NRL/MR/4613-92-6982) Avail: CASI HC A05/MF A01

This report summarizes a study of radiation effects in components of a proposed fiber optic data bus for space, including models of the natural radiation environment. This test procedure outlines methods for measuring both the steady state response of optical fibers and cables exposed to continuous radiation and the transient response of optical fibers and cables exposed to a pulse of radiation. It can be used to determine the level of radiation-induced attenuation produced in single-mode or multimode optical fibers, in either cabled or uncabled form. GRA

N93-14032# Dynetics, Inc., Huntsville, AL.

ACOUSTO-OPTIC APPLICATIONS FOR MULTICHANNEL ADAPTIVE OPTICAL PROCESSOR Final Technical Report, Feb. 1991 - Feb. 1992

Merv C. Budge, Robert J. Bertinato, and Michael C. Zari Jun. 1992 162 p

(Contract F30602-91-D-0001)

(AD-A255823; RL-TR-92-160) Avail: CASI HC A08/MF A02

This final report describes the design and hardware implementation of an acousto-optic (AO) multichannel adaptive optical processor (MADOP) for application to the cancellation of multipath jamming interference in advanced surveillance radars. The primary objective of this effort was the design and preliminary fabrication of a multichannel adaptive system that

can perform cancellation of multiple wide (10 MHz) jamming interference in the presence of multipath. The MADOP system is composed of three primary subsystems. A multichannel time-integrating AO correlator performs a correlation between the residual cancellation error and each of the auxiliary omnidirectional antennas to arrive at updates for each of the adaptive weight functions. A digital interface accepts this update information and generates the appropriate adaptive weight functions for performing auxiliary channel filtering. Finally, a multichannel AO tapped delay line (AOTDL) filter system accepts these weight functions through an AO spatial light modulator (AOSLM) and taps the auxiliary channel inputs to form the estimate of the noise signal in the main receiver channel. This noise signal estimate is then subtracted from the main receiver channel at the system intermediate frequency to form the residual cancellation error for input to the multichannel time AO correlator, thereby closing the adaptive loop. GRA

N93-14100 Exeter Univ. (England).
ACOUSTO-OPTIC DEVICES AND APPLICATIONS Ph.D. Thesis
Paul Antony Gass 1991 242 p
Avail: Univ. Microfilms Order No. BRDX96613

When an acoustic wave propagates in a transparent medium the strain associated with the wave can perturb the optical permittivity of the medium. By varying the amplitude and wavelength of the acoustic wave it is possible to control the intensity, wavelength and propagation direction of the diffracted optical wave. A number of useful optical devices are based on acousto-optic diffraction. The acousto-optic tunable filter (AOTF) and the acousto-optic deflector (AOD) respectively control the wavelength or the propagation direction of the diffracted beam. Prototypes of the AOTF and the AOD have been designed and evaluated. Modified analyses which avoided inaccuracies in the literature have been developed and verified against the experimental results. Using the AOD and AOTF to rapidly modulate the angle or wavelength of a probe beam a method of directly measuring the differential optical properties of a sample has been developed. Applying the system to the study of vapor adsorption and the measurement of the electro-optic response of Langmuir-Blodgett films allowed the detection of sub-monolayer adsorption and 10(exp -5) degree shifts in optical features. This was an improvement of several orders of magnitude over the sensitivity which had previously been possible. One of the drawbacks of acousto-optic devices is that they require high drive powers. It was found that the combined acousto-optic Fabry-Perot device performed best at modulating the intensity of the undiffracted beam. It has also been established that successful Fabry-Perot enhanced acousto-optic devices require very high levels of thermal stability and optical quality. If these conditions are met significant reductions in the drive power can be achieved. Dissert. Abstr.

N93-14101 Worcester Polytechnic Inst., MA.
DIGITAL FLUOROSCOPY WITH AN OPTICALLY COUPLED CHARGE-COUPLED DEVICE Ph.D. Thesis
Hong Liu 1992 252 p
Avail: Univ. Microfilms Order No. DA9224089

This research was aimed at investigating the potential of developing an optically coupled charge-coupled device (CCD) imaging system for some digital fluoroscopic applications. The viability of this concept for fluoroscopic imaging was studied with respect to image intensifier-television (II-TV) techniques. The anticipated advantages of the optically coupled CCD, compared with II-TV, include higher contrast sensitivity, larger dynamic range, moderate spatial resolution and clinically acceptable dose. Following an investigation of some theoretical and practical issues concerning the optical coupling efficiency between the intensifying screen and the CCD imager, mathematical methods were developed to relate the signal, signal-to-noise ratio, and x-ray quantum efficiency of the optically coupled CCD imaging chain. The spatial resolution of the system was also analyzed. Using an ultra-sensitive CCD, as well as improved scintillating and optical coupling techniques, we built a laboratory system for experiments. We conducted measurements of the modulation transfer function (MTF), contrast sensitivity, contrast-detail detectability and detector contrast. The results suggest that the lesion detectability of our sub-optimal system was comparable to that of a screen-film technique under the same radiation dose, and was significantly better than II-TV fluoroscopy. Potential clinical applications of our system include mammography, pre-operational localization, pediatric chest radiography, and single tracer autoradiography. Images of selected phantoms, pathological specimens and small animals were acquired to demonstrate the radiologic quality attainable for such procedures. We conclude that developing an x-ray quantum limited, pseudo-real time, digital fluoroscopic imaging system (for some applications) without an II appears to be theoretically and technically feasible. The successful development of optically coupled CCD fluoroscopy has the potential for improving the quality of many clinical procedures in radiology. Dissert. Abstr.

75 PLASMA PHYSICS

Includes magnetohydrodynamics and plasma fusion.

For ionospheric plasmas see *46 Geophysics*. For space plasmas see *90 Astrophysics*.

N93-12571# Lawrence Livermore National Lab., CA.
SELF-CONSISTENT ONE-DIMENSIONAL MODELLING OF X RAY LASER PLASMAS
A. S. Wan, R. S. Walling, H. A. Scott, R. W. Mayle, and A. L. Osterheld 23 Jun. 1992 4 p Presented at the 3rd International Colloquium on X Ray Lasers, Schliersee, Germany, 18-22 May 1992
(Contract W-7405-eng-48)
(DE92-019543; UCRL-JC-109843; CONF-920523-4) Avail: CASI HC A01/MF A01

This paper presents the simulation of a planar, one-dimensional expanding Ge x-ray laser plasma using a new code which combines hydrodynamics, laser absorption, and detailed level population calculations within the same simulation. Previously, these simulations were performed in separate steps. We present the effect of line transfer on gains and excited level populations and compare the line transfer result with simulations using escape probabilities. We also discuss the impact of different atomic models on the accuracy of our simulation. DOE

N93-12687# General Atomic Co., San Diego, CA.
A QUANTITATIVE ANALYSIS OF THE EFFECT OF ELMs ON H-MODE THERMAL ENERGY CONFINEMENT IN DIII-D
D. P. Schissel, T. H. Osborne, T. N. Carlstrom, and H. Zohm (Max-Planck-Inst. fuer Plasmaphysik, Garching, Germany) Jun. 1992 4 p Presented at the 14th International Conference on Plasma and 19th EPS Conference on Controlled Fusion and Plasma Physics, Innsbruck, Austria, 29 Jun. - 3 Jul. 1992
(Contract DE-AC03-89ER-51114)
(DE92-017704; GA-A-20942; CONF-920610-11) Avail: CASI HC A01/MF A01

The desire to reach ignition in future tokamaks makes the energy confinement time a critical parameter. The most promising enhanced (over L-mode) confinement regime is the H-mode, discovered on ASDEX with neutral beam heating, and then confirmed with various auxiliary heating sources on numerous machines. The knowledge of how H-mode tau(sub E) depends on different parameters is of chemical importance to the performance predictions for next generation devices. Inter-machine H-mode total and thermal energy confinement (tau(sub th)) scalings, which are being utilized to predict ITER thermal energy confinement, have been created for discharges where the Edge Localized Mode (ELM) instability has not been present. Confinement scaling research has concentrated on this ELM-free H-mode phase mostly owing to the difficulty of characterizing ELM behavior. To date, long pulse H-mode operation has only been achieved by utilizing ELMs to flush out impurities and prevent radiative collapse of the discharge. Unfortunately, accompanying the ELMS is a decrease of the plasma stored energy due to the expulsion of particles near the edge of the discharge resulting in a reduction of the steep edge electron density gradient. In order to predict ITER's H-mode tau(sub th) in the presence of ELMs, an estimated 25 percent confinement degradation factor has been applied to the ELM-free predictions. Our work, summarized in this paper, indicates that this 25 percent reduction factor is too large and instead a value of approximately 15 percent would be more appropriate. DOE

N93-12705# Aerospace Corp., El Segundo, CA. Technology Operations.
OBSERVATIONS OF CORRELATED BROADBAND ELECTROSTATIC NOISE AND ELECTRON CYCLOTRON EMISSIONS IN THE PLASMA SHEET

J. L. Roeder, V. Angelopoulos, W. Baumjohann, and R. R. Anderson 15 Nov. 1991 20 p
(Contract F04701-88-C-0089)
(AD-A255002; TR-92(2940)-1; SSD-TR-92-27) Avail: CASI HC A03/MF A01

Electric field wave observations in the central plasma sheet of the earth's magnetosphere show the correlated occurrence of broadband electrostatic noise and electrostatic electron cyclotron harmonic emissions. A model is proposed in which the broadband emissions are electron acoustic waves generated by an observed low energy electron beam, and the cyclotron emissions are generated by the hot electron loss cone instability. The high degree of correlation between the two emissions is provided in the model by the presence of the cold electron beam population, which allows both of the plasma instabilities to grow. GRA

N93-12809# Los Alamos National Lab., NM.
ADVANCED HIGH-EXPLOSIVE FLUX COMPRESSION GENERATOR DEVELOPMENT: THE CN-3 SERIES
B. L. Freeman, M. G. Sheppard, and C. M. Fowler Aug. 1992 44 p
(Contract W-7405-eng-36)
(DE92-019962; LA-12348) Avail: CASI HC A03/MF A01

A very successful series of three flux compression generator (FCG) experiments and one hydro-only test, designed to quantify the performance capabilities and limitations of high-current, high-field, high-power coaxial FCG's, is reported. In the last test, the CN-3 FCG produced a peak current of greater than 150 MA with a final doubling time of less than 10 micro-s into a 2-nH inductive load. Experimental results are in excellent agreement with extensive preshot and postshot one-dimensional (1D) and two-dimensional (2D) magnetohydrodynamic (MHD) calculations. DOE

N93-12811# New York Univ., New York. Courant Inst. of Mathematical Sciences.
PLASMA PROPERTIES
H. Weitzner Aug. 1992 42 p
(Contract DE-FG02-86ER-53223)
(DE92-019982; DOE/ER-53223/194) Avail: CASI HC A03/MF A01

The Magneto-Fluid Dynamics Division works on a wide range of problems originating in plasma physics, with the primary focus being on problems from magnetic fusion plasma physics. This report discusses the following topics: MHD Equilibrium and Stability; MHD Transport; Statistical Analysis; Edge Physics Studies; Wave Propagation; Basic Plasma Physics; and Space Plasma Physics. DOE

N93-12856# Edgerton, Germeshausen and Grier, Inc., Idaho Falls, ID.
INVESTIGATION OF COMPONENT FAILURE RATES FOR PULSED VERSUS STEADY STATE TOKAMAK OPERATION
L. C. Cadwallader Jul. 1992 39 p
(Contract DE-AC07-76ID-01570)
(DE92-019758; EGG-FSP-10262) Avail: CASI HC A03/MF A01

This report presents component failure rate data sources applicable to magnetic fusion systems, and defines multiplicative factors to adjust these data for specific use on magnetic fusion experiment designs. The multipliers address both long pulse and steady state tokamak operation. Thermal fatigue and radiation damage are among the leading reasons for large multiplier values in pulsed operation applications. Field failure rate values for graphite protective tiles are presented, and beryllium tile failure rates in laboratory testing are also given. All of these data can be used for reliability studies, safety analyses, design tradeoff studies, and risk assessments. DOE

N93-12873# Texas Univ., Austin. Inst. for Fusion Studies.
THE ELECTROSTATIC WAKE OF A SUPERTHERMAL TEST ELECTRON IN A MAGNETIZED PLASMA
A. A. Ware and J. C. Wiley Jul. 1992 16 p
(Contract DE-FG05-80ET-53088)
(DE92-019394; IFSR-561; DOE/ET-53088/561) Avail: CASI HC A03/MF A01

The electrostatic potential is determined for a test electron with v(sub parallel) much greater than than v(sub Te), in a uniform magnetized plasma (omega(sub ce) much greater than than omega(sub pe)). In the frame of the test electron, part of the spatially oscillatory potential has spherical symmetry over the hemisphere to the rear of the electron and is zero ahead of the electron. A second part of different character, which makes the potential continuous at the plane containing the electron, is oscillatory in the radial direction but decreases almost monotonically in the axial direction. DOE

N93-12878# Wisconsin Univ., Madison.
MEASUREMENT OF CURRENT DENSITY FLUCTUATIONS AND AMBIPOLAR PARTICLE FLUX DUE TO MAGNETIC FLUCTUATIONS IN MST Ph.D. Thesis
Weimin Shen Aug. 1992 119 p
(Contract DE-FG02-85ER-53198)
(DE92-041013; DOE/ER-53198/201) Avail: CASI HC A06/MF A02

Studies of magnetic fluctuation induced particle transport on reversed field pinch plasmas were done on the Madison Symmetric Torus. Plasma current density and current density fluctuations were measured using a multi-coil magnetic probe. The low frequency (f less than 50 kHz) current density fluctuations are consistent with the global resistive tearing instabilities predicted by 3-D MHD simulations. At frequencies above 50 kHz, the magnetic fluctuations were detected to be localized with a radial correlation length of about 1-2 cm. These modes are locally resonant modes since the measured dominant mode number spectra match the local safety factor q. The net charged particle flux induced by magnetic fluctuations was obtained by measuring the correlation term ((tilde j)(sub parallel) (tilde B)(sub r)). The result of zero net charged particle loss was obtained, meaning the flux is ambipolar. The ambipolarity of low frequency global tearing modes is satisfied through the phase relations determined by tearing instabilities. The ambipolarity of high frequency localized modes could be partially explained by the simple model of Waltz based on the radial average of small scale turbulence. DOE

N93-12882# Wisconsin Univ., Madison. Dept. of Physics.
ANOMALOUS ION HEATING AND SUPERTHERMAL ELECTRONS IN THE MST REVERSED-FIELD PINCH
S. Hokin, A. Almagri, S. Assadi, M. Cekic, B. Chapman, G. Chartas, N. Crocker, M. Cudzinovic, D. J. DenHartog, and R. Dexter et al Sep. 1992 10 p Presented at the 14th International Conference on Plasma Physics and Controlled Nuclear Fusion Research, Wuerzburg, Germany, 30 Sep. - 7 Oct. 1992
(Contract DE-FG02-85ER-53198)
(DE92-041011; DOE/ER-53198/203; IAEA-CN-56/C-3-2; CONF-920913-9)
Avail: CASI HC A02/MF A01

Anomalous ion heating and superthermal electron populations have been studied in the MST reversed-field pinch. The ion heating is much stronger than that given by classical electron-ion friction, and is particularly strong during dynamo bursts. The heating displays a marked density dependence: in a 350-kA discharge with a maximum (bar n) = 0.9 x 10(exp 13) cm(exp -3), T(sub i) rises sharply as (bar n) drops below 0.4 x 10(exp 13) cm(exp -3) late in the discharge. Superthermal electrons are produced in the core, with temperatures of T(sub eh), = 350-700 eV while the bulk core temperature is T(sub e)o = 130-230 eV. The fraction of superthermal electrons decreases with increasing density, from 40 percent at (bar n) = 0.5 x 10(exp 13) cm(exp -3) to 8 percent at (bar n) = 1.9 x 10(exp 13) cm(exp -3) at I = 350 kA. However, data with similar plasma parameters but higher oxygen impurity content had a lower T(sub eh) and higher hot fraction. The edge superthermal electron distribution is well fit by a drifted bi-Maxwellian distribution with T(sub parallel) approximately T(sub e0) and relative drift speed v(sub d)/v(sub th) = 0.4. With the assumption that the parallel heat flux measured with a pyroelectric probe is carried by superthermal electrons, the measured electron current is consistent with T(sub perpendicular) approximately T(sub ea) approximately T(sub e0)/3 and accounts for over half of the total edge parallel current measured with magnetic probes. DOE

N93-12883# Wisconsin Univ., Madison. Dept. of Physics.
CURRENT DENSITY FLUCTUATIONS, NONLINEAR COUPLING, AND TRANSPORT IN MST
S. C. Prager, A. F. Almagri, S. Assadi, M. Cekic, B. E. Chapman, N. Crocker, D. J. DenHartog, R. N. Dexter, G. Fiksel, and R. J. Fonck et al Sep. 1992 10 p Presented at the 14th International Conference on Plasma Physics and Controlled Nuclear Fusion Research, Wuerzburg, Germany, 30 Sep. - 7 Oct. 1992

(Contract DE-FG02-85ER-53198)
(DE92-041012; DOE/ER-53198/202; IAEA-CN-56/C-3-1; CONF-920913-10) Avail: CASI HC A02/MF A01

New information on magnetic fluctuations and transport in toroidal devices has been obtained in the MST reversed field pinch through measurement of nonlinear coupling of three waves in k-space, and measurement of current density fluctuations. Measurements of nonlinear coupling of magnetic fluctuations reveals that (1) two poloidal mode number $m = 1$ modes couple strongly to an $m = 2$ mode, (2) toroidal mode coupling is broad extending up to $n = 20$, (3) these features agree with predictions for tearing fluctuations from a nonlinear MHD code, and (4) during a sawtooth crash the number of modes involved in nonlinear interactions increases dramatically and the k-spectrum broadens simultaneously. Measurements of current density fluctuations over the outer 20 percent of the minor radius reveal that (1) low frequency fluctuations are consistent with tearing modes, (2) high frequency fluctuations are localized turbulence which maintains resonance with the equilibrium field as q changes with radius, and (3) particle transport from magnetic fluctuations is ambipolar. DOE

N93-12913# Texas Univ., Austin. Inst. for Fusion Studies.
NONLINEAR STUDIES OF m = 1 MODES IN HIGH-TEMPERATURE PLASMAS
A. Y. Aydemir Jul. 1992 13 p
(Contract DE-FG05-80ET-53088)
(DE92-019395; IFSR-560; DOE/ET-53088/560) Avail: CASI HC A03/MF A01

Nonlinear evolution of the $m = 1$ mode is examined in high-temperature plasmas where the mode is in the semi-collisional or collisionless regime. Unlike the resistive $m = 1$ mode, both the semi-collisional mode, with a very weak resistivity dependence, and the collisionless mode, driven by finite electron inertia, can be robustly unstable in today's large tokamaks. And unlike the finite-(Delta')(m is greater than or equal to 2) tearing modes, the nonlinear evolution of which is collisional, both the semi-collisional and collisionless $m = 1$ modes exhibit nonlinearly enhanced growth rates that far exceed their linear values, thus making their nonlinear evolution collisionless; this accelerated growth of a collisionless $m = 1$ mode may explain the fast sawtooth-crashes observed in large tokamaks. DOE

N93-12914# Texas Univ., Austin. Inst. for Fusion Studies.
DYNAMICS OF THE ION-ION ACOUSTIC INSTABILITY IN THE THERMALIZATION OF ION BEAMS
J. H. Han, W. Horton, and J. N. Leboeuf (Oak Ridge National Lab., TN.) Jul. 1992 44 p
(Contract DE-FG05-80ET-53088)
(DE92-019396; IFSR-562; DOE/ET-53088/562) Avail: CASI HC A03/MF A01

Particle simulation using a nonlinear adiabatic electron response with two streaming ion species and nonlinear theory are used to study the collisionless thermalization of ion beams in a hot electron plasma. The slow beam or subsonic regime is investigated and the criterion for the transition from predominantly light ion to predominantly heavy ion heating is developed. Long-lived ion hole structures are observed in the final state. DOE

N93-12932# Lawrence Livermore National Lab., CA.
A DESIGN FOR AN ADVANCED DIVERTOR FOR D3D AND ITER: THE RADIATIVE SLOT DIVERTOR
S. L. Allen, M. E. Rensink, D. N. Hill, R. Wood, D. Nilson, B. G. Logan, R. Stambaugh, T. W. Petrie, G. M. Staebler, and M. A. Mahdavi Mar. 1992 19 p Presented at the 10th International Conference on Plasma-Surface Interactions in Controlled Fusion Devices, Monterey, CA, 30 Mar. - 3 Apr. 1992
(Contracts W-7405-eng-48; DE-AC03-89ER-51114; DE-AC04-76DP-00789)
(DE92-019579; UCRL-JC-108860; CONF-920311-24) Avail: CASI HC A03/MF A01

Reduction of the divertor heat load is an important issue for future tokamaks, particularly during the technology phase of ITER. We discuss a conceptual design for one type of advanced divertor: the radiative slot divertor. The goal of this divertor configuration is to enhance the radiation in the divertor region and thereby reduce the heat load at the strike points. At the same time, any effects on the core plasma must be minimized. Proof-of-principle experiments to enhance the radiation in the DIII-D divertor have been performed both with deuterium and impurity injection. We compare several computer models with results from these experiments to predict performance and thereby guide designs of radiative divertors for future machines. We have estimated impurity radiation using calculations of the background plasma with the 2-dimensional code B2 coupled with non-coronal models of impurity radiation. The DEGAS code has been used to estimate hydrogenic transport, charge exchange, and radiation losses. Estimates of impurity transport are provided by 1-1/2 dimensional models and calculations of impurity frictional-force terms. These model results are in qualitative agreement with the approximately 1MW reduction of measured divertor power in D3-D during divertor impurity puffing experiments. Specific designs, including engineering details, for applications to DIII-D and ITER are discussed. DOE

N93-12971# Lawrence Livermore National Lab., CA.
DIII-D EDGE PHYSICS DATABASE
R. A. Jong, G. D. Porter, D. N. Hill, D. A. Buchenauer (Sandia National Labs., Albuquerque, NM.), and G. Bramson (General Atomic Co., San Diego, CA.) Mar. 1992 15 p Presented at the 10th International Conference on Plasma-Surface Interactions in Controlled Fusion Devices, Monterey, CA, 30 Mar. - 3 Apr. 1992
(Contracts W-7405-eng-48; DE-AC04-76DP-00789; DE-AC03-89ER-51114)
(DE92-019577; UCRL-JC-108861; CONF-920311-25) Avail: CASI HC A03/MF A01

We have developed an edge-physics database containing data for the plasma in the divertor region and the scrape-off layer (SOL) for the DIII-D tokamak. The database provides many of the parameters necessary to model the power flow to the divertor and other plasma processes in the plasma edge. It will also facilitate the analysis of DIII-D data for comparison with other divertor tokamaks. In addition to the core plasma parameters, edge-specific data are included in this database. Initial results using the database show good agreement between the pressure profiles measured by the Langmuir probes and those determined from the Thomson data for the inner strike point, but not for the outer strike point region. We also find that the ratio of separatrix density to average core density, as well as the in/out asymmetry in the SOL power at the divertor in DIII-D do not agree with values currently assumed in modeling the International Thermonuclear Experimental Reactor (ITER). DOE

N93-12982# Science Applications International Corp., San Diego, CA.
RETECH, INC., PLASMA CENTRIFUGAL FURNACE: APPLICATIONS ANALYSIS REPORT
Trevor Jackson Jun. 1992 52 p
(Contract EPA-68-CO-0048)
(PB92-218791; EPA/540/A5-91/007) Avail: CASI HC A04/MF A01

The document is an evaluation of the performance of the Retech Inc. Plasma Centrifugal Furnace (PCF) and its applicability as a treatment technique for soils contaminated with organic and/or inorganic compounds. Both the technical and economic aspects of the technology were examined. A demonstration of the Retech furnace was conducted under the Superfund Innovative Technology Evaluation Program and the Department of Energy's Component Development and Integration Facility in Butte, Montana. Operational data, along with sampling and analysis information, were carefully complied to establish a data base against which other available data, as well as the vendor's claims for the technology, have been compared and evaluated. Conclusions concerning the technology's suitability for use in immobilizing contaminants in the feed soil were reached, and extrapolations regarding applications at other sites with different contaminants and soil types were made. GRA

N93-12997# Los Alamos National Lab., NM.
SUPPRESSION OF THE e(-) COEXTRACTED FROM A PENNING SURFACE-PLASMA H(-) SOURCE
H. V. Smith, Jr. and P. Allison 1992 4 p Presented at the 16th International LINAC Conference, Ottawa, Ontario, 23-28 Aug. 1992
(Contract W-7405-eng-36)
(DE92-040350; LA-UR-92-2553; CONF-9208109-9) Avail: CASI HC A01/MF A01

The ratio of electrons to negative ions extracted from Penning surface-plasma sources (SPS) such as the 8X source is low even before any steps are taken to suppress the electrons. For the 8X source the

e(sup -)/H(sup -) ratio is typically four or five to one for H(sup -) operation and nine to one for D(sup -) operation. Because the coextracted e(sup -) present a power-loading problem to the 8X source extraction system, methods to dissipate and/or reduce the power in the e(sup -) beam must be developed before extracting a dc H(sup -) or D(sup -) beam. Thus, an experiment was run to see if a collar installed in the near extraction region of the 8X source suppresses the electrons extracted from that source. DOE

N93-13006# Institute of Plasma Physics, Prague (Czechoslovakia).
PHASE MIXING AND SURFACE WAVE DECAY IN AN INHOMOGENEOUS PLASMA
Paul S. Cally (Monash Univ., Clayton, Australia) and Zdenek Sedlacek Feb. 1992 22 p
(IPPCZ-320) Avail: CASI HC A03/MF A01

The decay rate of an Alfven or plasma surface wave propagating along an inhomogeneous layer of plasma is calculated. The inhomogeneous profile is thin and odd, but otherwise arbitrary. The wave's decay rate is determined using two fundamentally different methods, the integro-differential equation approach of Sedlacek and the Fourier expansion technique of Cally, and found by both to depend only on the slope of the Alven or plasma frequency profile at the 'resonant point', and not on other details of its shape. The result is verified numerically. This problem represents a good example with which to compare and contrast the two methods. Author

N93-13038# New York Univ., New York. Courant Inst. of Mathematical Sciences.
TOKAMAK EQUILIBRIA AND TRANSPORT BASED ON GRAD'S THIRTEEN MOMENT DESCRIPTION
M. K. Tippett Jun. 1992 103 p
(Contract DE-FG02-86ER-53223)
(DE92-019960; DOE/ER-53223/180; MF-124) Avail: CASI HC A06/MF A02

In this thesis, I study collisional transport of a hot magnetically confined plasma in a tokamak. The weakly collisional plasma is modeled by Grad's two-fluid thirteen moment equations. This model provides a better treatment of the stresses and the heat fluxes than do collisional fluid models such as Braginski's. Using physical parameters for a typical tokamak, I estimate the orders of magnitude of various effects. I obtain a reduced system by neglecting small terms in the two-fluid thirteen moment equations. This reduced model includes small particle flows, pressure anisotropy and temperature variation within flux surfaces. The reduced model is compared with standard fluid models. To understand better the behavior of solutions of this system, I expand the solution in a formal series in powers of the small parameter (m(sub e)/m(sub i))(sup 1/4). Flux coordinates are used to solve the equations in a general axisymmetric geometry. In lowest order, the equilibrium solution consists of a number of arbitrary flux functions together with a Grad-Shafranov equation relating the poloidal flux and the toroidal current. The energy dynamics of the system is complicated and requires determining the solution to high order. As corrections to the lowest order solution are calculated, the equilibrium is extended to successively longer time scales until on the time scale tau(sub e)m(sub i)/m(sub e), time independent solutions are in general not possible. I calculate the time evolution of the lowest order solution on the time scale tau(sub e)m(sub i)/m(sub e), a time scale consistent with experiment. DOE

N93-13044# General Atomic Co., San Diego, CA.
FUTURE DEVELOPMENT OF THE D3-D TOKAMAK PROGRAM
T. C. Simonen Jul. 1992 14 p Presented at the Fusion Power Associates Annual Meeting and Symposium, Pleasanton, CA, 9 Apr. 1992
(Contracts DE-AC03-89ER-51114; W-7405-eng-48; DE-AC03-89ER-52153; DE-AC05-84OR-21400)
(DE92-040051; GA-A-20914; CONF-9204146-4) Avail: CASI HC A03/MF A01

The D3-D long range research program focuses on diverter and advanced tokamak issues. Our D3-D goal is to provide an integrated demonstration of well-confined high-beta diverter plasma with non-inductive current drive. Our reference scenario is 5 percent beta with 2MA for 10's. Implementation of this plan will resolve many ITER R&D issues, validate many aspects of the ITER engineering design, possibly open new ITER operating options, and identify engineering design concepts for an attractive DEMO to follow the success of ITER. The D3-D plan for implementation of new research tools is discussed. To implement this program will require additional research tools, in particular, a radiative divertor configuration and higher power RF systems for non-inductive current profile control. DOE

N93-13047# Los Alamos National Lab., NM.
APPLICATIONS OF GROUP-INVARIANT ANALYTIC SOLUTIONS TO INERTIAL CONFINEMENT FUSION
S. V. Coggeshall 1992 6 p Presented at the 14th International Conference on Plasma Physics and Controlled Nuclear Fusion Research, Wuerzburg, Germany, 30 Sep. - 7 Oct. 1992
(Contract W-7405-eng-36)
(DE92-040347; LA-UR-92-2582; CONF-920913-11) Avail: CASI HC A02/MF A01

Analytic solutions to 1-,2-, and 3-D hydrodynamics are presented which can be applied to specific aspects of inertial confinement fusion target evolutions. These solutions include drive source time profiles for 1-D isentropic implosions, 2-D P(sub 2) asymmetric compressions, 1- and 2-D solutions for the stagnation phase of implosions, and a 3-D spinning (mixing) solution. DOE

N93-13091# Institute of Plasma Physics, Prague (Czechoslovakia).
ON THE BOOTSTRAP CURRENT CALCULATIONS BASED ON VALUES OF THE RADIAL ELECTRON TRANSPORT
V. Petrzilka Jan. 1992 12 p Presented at the ICPP 1992, Innsbruck, Austria, 1992
(IPPCZ-317) Avail: CASI HC A03/MF A01

A method of computation of anomalous bootstrap current is suggested which uses calculated or experimentally found values of the radial transport velocity. The underlying theory is the drift kinetic equation approach of Shaing to anomalous plasma transport in a toroidal configuration and/or the MHD approach of Klima and Petrzilka to convection and diffusion in a plasma cylinder under the influence of RF fields. Author

N93-13093# Institute of Plasma Physics, Prague (Czechoslovakia).
FLUCTUATION STUDIES ON CASTOR AND ASDEX TOKAMAKS AT LOWER HYBRID CURRENT DRIVE
F. Zacek, J. Stoeckel, J. Badalec, L. Dvoracek, K. Jakubka, P. Kletecka, L. Kryska, P. Magula, J. Mlynar, and F. Soeldner (Max-Planck-Inst. fuer Plasmaphysik, Garching, Germany) et al Jan. 1992 18 p Presented at the IAEA Technical Committee Meeting on Research Using Small Tokamaks, Hefei, China, Oct. 1991
(Contract IAEA-6702/RB)
(IPPCZ-319) Avail: CASI HC A03/MF A01

An improvement of the global confinement is reported from CASTOR and ASDEX tokamaks during lower hybrid current drive (LHCD) regimes at moderate LH powers (P sub LH) less than 1.5 P(0) sub OH, P(0)sub OH is the initial ohmic heating power). Simultaneously a significant reduction of edge electrostatic fluctuations is observed. The best global confinement and the maximum reduction of the edge fluctuations is reached when the total power P(TOT) delivered into the plasma is minimum (P(TOT) = P sub LH + P(0)sub OH). Behavior of the edge plasma parameters, namely the level, frequency spectra and poloidal velocity of electrostatic fluctuations, are documented for CASTOR tokamak. Author

N93-13105# Lawrence Livermore National Lab., CA.
RECENT NOVA EXPERIMENTAL RESULTS
J. D. Kilkenny, H. A. Baldis, S. H. Batha, M. D. Cable, E. M. Campbell, R. C. Cook, C. B. Darrow, T. Dittrich, R. J. Ellis, and S. G. Glendinning et al 16 Mar. 1992 5 p Presented at the 10th Topical Meeting on Technology of Fusion Energy, Boston, MA, 7-12 Jun. 1992
(Contract W-7405-eng-48)
(DE92-019783; UCRL-JC-110036; CONF-920607-19) Avail: CASI HC A01/MF A01

The Inertial Confinement Fusion (ICF) Program and the Lawrence Livermore National Laboratory has made substantial progress in understanding the details of the radiation drive and the dynamics of capsules imploded by the Nova laser. A detailed understanding, validated by Nova experiments of the crucial physics for implosions is necessary before a new facility is started. A National Academy of Science Review Committee on ICF has recently endorsed a 12 point technical contract for the Nova program. Recent experiments have achieved a substantial number of these goals. A decrease in the level of plasma instabilities has been demonstrated

by the use of phase plates. Neutron measurements have been used to demonstrate high densities in well understood implosions. A detailed understanding of the Rayleigh-Taylor instability at the ablation front of x-ray driven planar foil targets with large hydrodynamic growth factors has been proven. X-ray spectroscopy has been used to demonstrate a high fuel density and an improvement in the compression ratio of targets when a shaped pulse is used to keep a pusher on a low rho-r trajectory. DOE

N93-13107# Texas Univ., Austin. Inst. for Fusion Studies.
FUSION: MAGNETIC CONFINEMENT
H. L. Berk Aug. 1992 109 p
(Contract DE-FG05-80ET-53088)
(DE92-019876; IFSR-565; DOE/ET-53088/565) Avail: CASI HC A06/MF A02

An overview is presented of the principles of magnetic confinement of plasmas for the purpose of achieving controlled fusion conditions. Sec. 1 discusses the different nuclear fusion reactions which can be exploited in prospective fusion reactors and explains why special technologies need to be developed for the supply of tritium or He-3, the probable fuels. In Sec. 2 the Lawson condition, a criterion that is a measure of the quality of confinement relative to achieving fusion conditions, is explained. In Sec. 3 fluid equations are used to describe plasma confinement. Specific confinement configurations are considered. In Sec. 4 the orbits of particles in magnetic and electric fields are discussed. In Sec. 5 stability considerations are discussed. It is noted that confinement systems usually need to satisfy stability constraints imposed by ideal magnetohydrodynamic (MHD) theory. The paper culminates with a summary of experimental progress in magnetic confinement. Present experiments in tokamaks have reached the point that the conditions necessary to achieve fusion are being satisfied. DOE

N93-13191# Sandia National Labs., Albuquerque, NM.
LASER FORMATION OF LITHIUM PLASMA ION SOURCES FOR APPLIED-B ION DIODES ON THE PBFA-2 ACCELERATOR
G. C. Tisone, T. J. Renk, D. J. Johnson, R. A. Gerber, and R. G. Adams 1992 6 p Presented at the 9th International Conference on High Power Particle Beams, Washington, DC, 25-29 May 1992
(Contract DE-AC04-76DP-00789)
(DE92-016091; SAND-92-1242C; CONF-920515-21) Avail: CASI HC A02/MF A01

An active ion source, LEVIS (Laser EVaporation Ion Source), using a short pulsed Nd laser (1.06 m, 8 ns) to form a thin Li vapor layer and a tuned dye laser (670.8 nm, 1 micro-sec) for ionization is being developed at Sandia. The LEVIS process has been developed and characterized in the laboratory. Initial experiments using these ion sources on PBFA-II produced ion beams with a low fraction of lithium ions and with low voltages. Recent experiments using improved distribution optics and anode cleaning techniques are described. DOE

N93-13193# General Atomic Co., San Diego, CA.
FAST WAVE CURRENT DRIVE EXPERIMENT ON THE D3-D TOKAMAK
C. C. Petty, R. I. Pinsker, S. C. Chiu, J. S. deGrassie, R. W. Harvey, J. Lohr, T. C. Luce, M. J. Mayberry, R. Prater, and M. Porkolab (Massachusetts Inst. of Tech., Cambridge.) Jun. 1992 4 p Presented at the 14th International Conference on Plasma and 19th EPS Conference on Controlled Fusion and Plasma Physics, Innsbruck (Austria), 29 Jun. - 3 Jul. 1992
(Contracts DE-AC03-89ER-51114; DE-AC02-78ET-51013; DE-AC02-76CH-03073; DE-AC05-84OR-21400)
(DE92-016253; GA-A-20930; CONF-920610-6) Avail: CASI HC A01/MF A01

One method of radio-frequency heating which shows theoretical promise for both heating and current drive in tokamak plasmas is the direct absorption by electrons of the fast Alfven wave (FW). Electrons can directly absorb fast waves via electron Landau damping and transit-time magnetic pumping when the resonance condition omega- kappa(sub parallel)(upsilon)(sub (parallel)e) = O is satisfied. Since the FW accelerates electrons traveling the same toroidal direction as the wave, the plasma current can be generated non-inductively by launching FW's which propagate in one toroidal direction. Fast wave current drive (FWCD) is considered an attractive means of sustaining the plasma current in reactor-grade tokamaks due to the potentially high current drive efficiency achievable and excellent penetration of the wave power to the high temperature plasma core. Ongoing experiments on the D3-D tokamak are aimed at a demonstration of FWCD in the ion cyclotron range of frequencies (ICRF). Using frequencies in the ICRF avoids the possibility of mode conversion between the fast and slow wave branches which characterized early tokamak FWCD experiments in the lower hybrid range of frequencies. Previously on D3-D, efficient direct electron heating by FW was found using symmetric (non-current drive) antenna phasing. However, high FWCD efficiencies are not expected due to the relatively low electron temperatures (compared to a reactor) in D3-D. DOE

N93-13257# Instituto de Pesquisas Espaciais, Sao Jose dos Campos (Brazil).
DIAGNOSTICS SYSTEMS FOR THE TBR-E TOKAMAK
M. Ueda, J. L. Ferreira, Y. Aso, and J. G. Ferreira 1992 36 p
(INPE-5428-RPQ/662) Avail: CASI HC A03/MF A01

A general view of the several diagnostic systems proposed for the TBR-E tokamak is given. This project is a joint undertaking of INPE, USP and UNICAMP plasma laboratories. The requirements for the measurements of the plasma produced parameters are described. Special attention is given for diagnostics used to investigate new physical issues on a low aspect ratio tokamak such as TBR-E. Author

N93-13297# Oak Ridge National Lab., TN.
PERFORMANCE OF A PLASMA FLUID CODE ON THE INTEL PARALLEL COMPUTERS
V. E. Lynch (Martin Marietta Energy Systems, Inc., Oak Ridge, TN.), B. A. Carreras, J. B. Drake, J. N. Leboeuf, and P. Liewer (Jet Propulsion Lab., California Inst. of Tech., Pasadena.) 1992 26 p Presented at the ACM/IEEE Supercomputing Conference, Minneapolis, MN, 14-21 Nov. 1992
(Contract DE-AC05-84OR-21400)
(DE92-011680; CONF-921125-1) Avail: CASI HC A03/MF A01

One approach to improving the real-time efficiency of plasma turbulence calculations is to use a parallel algorithm. A parallel algorithm for plasma turbulence calculations was tested on the Intel iPSC/860 hypercube and the Touchtone Delta machine. Using the 128 processors of the Intel iPSC/860 hypercube, a factor of 5 improvement over a single-processor CRAY-2 is obtained. For the Touchtone Delta machine, the corresponding improvement factor is 16. For plasma edge turbulence calculations, an extrapolation of the present results to the Intel (sigma) machine gives an improvement factor close to 64 over the single-processor CRAY-2. DOE

N93-13330# Institute of Plasma Physics, Prague (Czechoslovakia).
MEASUREMENTS OF THE TEMPERATURE IN THE EDGE PLASMA OF THE CASTOR TOKAMAK BY A TRIPLE LANGMUIR PROBE
K. Jakubka, J. Stoeckel, and F. Zacek Jan. 1992 6 p
(IAEA-6702/RB)
(IPPCZ-318) Avail: CASI HC A02/MF A01

The triple Langmuir probe is an array of three identical Langmuir probes, in which two biased tips work in a regime of a double Langmuir probe and the third is at the floating potential (floating tip). The potential difference between the floating tip and the positively charged tip is proportional to the electron temperature of plasma. In the case of a tokamak plasma, the measurement has to be made on the same magnetic field surface, at which the electron temperature is constant. Fulfilling of this condition gives the limit of accuracy of the measurement by the triple probe. In comparison with other Langmuir probe methods, this one does not require any voltage sweeps or switching and it gives directly the temporal evolution of electron temperature. Moreover, the triple probe is a kind of a floating probe and it does not disturb plasma so much as it is in the case of the single Langmuir probe. Author

N93-13359# National Academy of Sciences - National Research Council, Washington, DC. Board on Physics and Astronomy.
PLASMA SCIENCE COMMITTEE (PLSC) AND STUDY ON NEW OPPORTUNITIES IN PLASMA SCIENCE AND TECHNOLOGY
1992 10 p
(Contract DE-FG05-88ER-53279)
(DE92-019507; DOE/ER-53279/2) Avail: CASI HC A02/MF A01

The Plasma Science Committee (PLSC) of the National Research Council (NRC) is charged with monitoring the health of the field of plasma science in the United States. Accordingly, the Committee identifies and examines both broad and specific issues affecting the field. Regular meetings, teleconferences, briefings from agencies and the scientific community, the

formation of study panels to prepare reports, and special symposia are among the mechanisms used by the PLSC to meet its charge. This progress report presents a review of PLSC activities from July 15, 1991 to May 31, 1992. The details of prior activities are discussed in earlier reports. This report also includes the status of activities associated with the PLSC study on opportunities in plasma science and technology. During the above period, the PLSC has continued to track and participate in, when requested, discussions on the health of the field. Much of the perspective of the PLSC has been presented in the recently-published report Research Briefing on Contemporary Problems in Plasma Science. That report has served as the basis for briefings to representatives of the federal government as well as the community-at-large. In keeping with its charge to identify and highlight specific areas for scientific and technological opportunities, the PLSC completed publication of the report Plasma Processing of Materials: Scientific and Technological Opportunities and launched a study on new opportunities in plasma science and technology. DOE

N93-13495 Maryland Univ., College Park.
EXPERIMENTAL STUDIES OF HIGH-POWER PLASMA-FILLED BACKWARD WAVE OSCILLATORS Ph.D. Thesis
Weiran Lou 1991 195 p
Avail: Microfilms Order No. DA9222724

High power X-band microwave radiation from a plasma filled backward wave oscillator (BWO) driven by an intense relativistic electron beam was studied experimentally. It was demonstrated that a plasma filled BWO can operate at an enhanced efficiency of 40 percent compared with a typical efficiency of 20 percent in a vacuum BWO under the same conditions at low current regime. The radiation frequency was coherent (delta f/f is approximately 0.35 percent) and could be tuned by changing the plasma density. The plasma BWO was found to operate efficiently at magnetic fields as low as 800 G, and with a wide range of magnetic fields, except at the two cyclotron absorption dips, which probably correspond to the first and third harmonic cyclotron waves. The start oscillation current was obtained experimentally for vacuum BWO and plasma loaded BWO. It was also show that the spectrum of the conventional low frequency (omega less than omega(sub p)) Trivelpiece-Gould modes was drastically modified by the periodicity of the structure in a way that produced a fundamentally new sort of spectral behavior, the 'dense spectrum'. The radiation leaking out of the plasma was measured. Dissert. Abstr.

N93-13496 Texas Univ., Austin.
LOW-FREQUENCY FLUCTUATIONS OF PLASMA MAGNETIC FIELDS Ph.D. Thesis
Samuel Benjamin Cable 1992 166 p
Avail: Univ. Microfilms Order No. DA9225538

The fluctuation-dissipation theorem is used to study fluctuation power spectra in various plasmas, particularly at low frequencies. Gaseous and degenerate plasmas are studied. Careful application of the theorem shows that a cold, non-magnetized plasma has a sharp zero-frequency peak in its magnetic field power spectrum. When a uniform magnetic field is applied to the plasma, the energy under the zero-frequency peak is shifted into the Alfven and cyclotron modes. A simple relation between the fluctuation spectra and dispersion relations of electromagnetic waves is found in deriving this result. Using a kinetic theory treatment, a warm isotropic plasma is shown to exhibit a zero-frequency peak in its magnetic power spectrum, with a different functional dependence on frequency. In a stationary degenerate plasma, the magnetic power spectrum again has a zero-frequency peak. In a degenerate plasma with net drift velocity, a white noise spectrum in voltage fluctuation is found. This spectrum is similar to shot noise. Effects of fluid expansion on the Rayleigh-Taylor instability are studied. Overall fluid expansion often has a retarding effect on the growth of Rayleigh-Taylor (RT) instabilities. Two new analytical examples of this phenomenon of reduced growth or stabilization are given. Confirmation of this phenomenon is also obtained from a new magnetohydrodynamic (MHD) code constructed specifically for modelling fluids undergoing nearly homogeneous expansion or contraction. In the code, expansion is treated by making each point of the computational grid co-moving with a predetermined overall expansion. Short-range force effects on the Rayleigh-Taylor instability are also studied with the help of a new particle-in-cell (PIC) MHD code. It is to be expected that short-range forces would effect the instability much like surface tension, slowing the growth of the instability. Comparisons of simulations with and without short-range forces do not give unambiguous confirmation of this expectation, however. Limitations to the accuracy of the code exist at short wavelengths, where the effects of the short-range forces would be expected to be most pronounced. Dissert. Abstr.

N93-13502# Texas Univ., Austin. Inst. for Fusion Studies.
ESTABLISHMENT OF AN INSTITUTE FOR FUSION STUDIES
R. D. Hazeltine Jul. 1992 29 p
(Contract DE-FG05-80ET-53088)
(DE92-040014; DOE/ET-53088/8) Avail: CASI HC A03/MF A01

The Institute for Fusion Studies is a national center for theoretical fusion plasma physics research. Its purposes are: (1) to conduct research on theoretical questions concerning the achievement of controlled fusion energy by means of magnetic confinement--including both fundamental problems of long-range significance, as well as shorter-term issues; (2) to serve as a center for information exchange, nationally and internationally, by hosting exchange visits, conferences, and workshops; (3) and to train students and postdoctoral research personnel for the fusion energy program and plasma physics research areas. The theoretical research results that are obtained by the Institute contribute mainly to the progress of national and international efforts in nuclear fusion research, whose goal is the development of fusion power as a basic energy source. In addition to its primary focus on fusion physics, the Institute is also involved with research in related fields, such as advanced computing techniques, nonlinear dynamics, plasma astrophysics, and accelerator physics. The work of EFS scientists continued to receive national and international recognition. Numerous invited papers were given during the past year at workshops, conferences, and scientific meetings. Last year IFS scientists published 95 scientific articles in technical journals and monographs. DOE

N93-13511# Sandia National Labs., Albuquerque, NM.
A FAST SCANNING PROBE FOR D3-D
J. G. Watkins, J. Salmonson (Edgerton, Germeshausen and Grier, Inc., Albuquerque, NM.), R. Doerner (California Univ., Los Angeles.), R. Lehmer (California Univ., Los Angeles.), R. Moyer (California Univ., Los Angeles.), L. Schmitz (California Univ., Los Angeles.), and D. N. Hill (Lawrence Livermore National Lab., CA.) 1991 13 p Presented at the 9th Topical Conference on High-Temperature Plasma Diagnostics, Santa Fe, NM, 15-19 Mar. 1992
(Contract DE-AC04-76DP-00789)
(DE92-040260; SAND-91-2625C; CONF-920362-42) Avail: CASI HC A03/MF A01

A fast reciprocating probe was developed for D3-D which can penetrate the separatrix during H - mode with up to 5MW of NBI heating. The probe was designed to carry various sensor tips into the scrape-off layer at a velocity of 3 m/sec and dwell motionless for a programmed period of time. The driving force is provided by a pneumatic cylinder charged with helium to facilitate greater mass flow. The first series of experiments were done using a Langmuir probe head with 5 graphite tips to measure radial profiles of n(sub e), T(sub e), phi(sub f), (n tilde)(sub e), and (phi tilde)(sub f). The amplitude and phase of the fluctuating quantities are measured by using specially constructed vacuum compatible 5 kV coaxial transmission lines which allow us to extend the measurements into the MHz range. TTZ ceramic bearings and fast stroke bellows were also specially designed for the D3-D probe. Initial measurements will be presented. DOE

N93-13518# Oak Ridge National Lab., TN.
BIASING EXPERIMENTS ON THE ADVANCED TOROIDAL FACILITY
T. Uckan, R. C. Isler, T. C. Jernigan, J. F. Lyon, P. K. Mioduszewski, M. Murakami, D. A. Rasmussen, J. B. Wilgen, S. C. Aceto (Rensselaer Polytechnic Inst., Troy, NY.), and J. J. Zielinski (Rensselaer Polytechnic Inst., Troy, NY.) 1992 22 p Presented at the International Atomic Energy Agency (IAEA) Technical Committee Meeting on Tokamak Plasma Biasing, Montreal, Quebec, 8-10 Sep. 1992
(Contract DE-AC05-84OR-21400)
(DE92-040033; CONF-9209181-1) Avail: CASI HC A03/MF A01

Biasing experiments have been carried out in 1 T plasmas with approximately 200 kW of electron cyclotron heating (ECH) in the current-fire Advanced Toroidal Facility (ATF) torsatron. Two rail limiters, one at the top and one at the bottom of the device, located at the last closed flux surface (LCFS), are, biased at positive and negative potentials with respect to the vacuum vessel. When the limiters are positively biased at up to 300

V and the plasma density is controlled with a significantly reduced gas feed, the H(sub alpha) radiation from both the limiter and the wall drops, indicating reduced particle recycling as a result of improved particle confinement. For bias voltages around +100 V, there is almost no change of plasma stored energy W(sub p), but W(sub p) then drops with the higher biasing voltages. Positive biasing has caused the core plasma density profile to become peaked and the electric field to become more negative inside the LCFS. At the same time, edge plasma fluctuations are reduced significantly and their power spectrum becomes less broad. The propagation direction of these electrostatic fluctuations reverses to the ion diamagnetic direction, and their wavelengths become longer. The resulting fluctuation-induced particle flux is also reduced. Power deposition on the limiters is lower as a result of reduced edge plasma density and temperature. Negative biasing yields somewhat less improvement in the particle confinement while having almost no apparent effect on W(sub p) or on the core and the edge plasma density and temperature profiles. Simultaneous measurements of the plasma potential profile indicate almost no significant change. Biasing has almost no effect on the intrinsic impurity levels in the plasma. DOE

N93-13535# Columbia Univ., New York, NY.
ACHIEVING HIGH Q(SUB DD) OPERATION IN HIGH POLOIDAL BETA DISCHARGES IN TFTR
M. E. Mauel, G. A. Navratil, S. A. Sabbagh, M. G. Bell (Princeton Univ., NJ.), R. Bell (Princeton Univ., NJ.), R. V. Budny (Princeton Univ., NJ.), C. E. Bush (Princeton Univ., NJ.), A. Cavallo (Princeton Univ., NJ.), M. S. Chance (Princeton Univ., NJ.), and P. C. Efthimion (Princeton Univ., NJ.) et al 1992 2 p Presented at the 14th International Conference on Plasma Physics and Controlled Nuclear Fusion Research, Wuerzburg, Germany, 30 Sep. - 7 Oct. 1992
(Contracts DE-FG02-89ER-53297; DE-AC02-76CH-03073; DE-FG02-90ER-54084)
(DE92-019494; CONF-920913-8) Avail: CASI HC A01/MF A01

Tokamak operation at high poloidal beta (epsilon beta(sub p) approximately 1, epsilon = a/R) offers several important advantages to future fusion reactors: low plasma current, high bootstrap current fraction, and the possibility of improved confinement due to equilibrium modification. However, since the plasma current is low at high epsilon beta(sub p), the achievement of high fusion reactivity generally requires operation at a high Troyon-normalized beta, beta(sub N) = 10(exp 8) (beta) aB(sub t)/I(sub p), and a high L-mode normalized confinement, H = tau E / tau (sub E, ITER(sub p)). The TFTR high poloidal beta experiments have explored this advanced operating regime in reactor-like conditions, and we have demonstrated techniques that can be used to achieve high Q(sub DD) at high epsilon beta(sub p). In this paper, we present new results showing that Q(sub DD) as high as 1.3 x 10(exp -3), can be achieved at epsilon beta(sub p) approximately 0.85 using transient current profile modification techniques, which nevertheless, maintain high Q(sub DD) for an alpha slowing down time. Future DT experiments in TFTR will be able to study collective alpha-particle physics in discharges having high epsilon beta(sub p), high beta(sub N), and evolving current profiles. This paper also illustrates the need for steady-state current profile control to sustain high Q(sub DD) at high epsilon beta(sub p) by presenting recent observations of long-pulse, high beta(sub p) discharges in which the current density is allowed to relax naturally to a broad, bootstrap-dominated profile. DOE

N93-13651# Oak Ridge National Lab., TN.
REVIEW OF STELLARATOR RESEARCH: IN SEARCH OF THE MAGIC MAGNETIC BOTTLE
N. Dominguez 1992 113 p Presented at the 5th Latin American Workshop on Plasma Physics, Mexico City, Mexico, 20-31 Jul. 1992
(Contract DE-AC05-84OR-21400)
(DE92-019045; CONF-920728-1) Avail: CASI HC A06/MF A02

The current work on stellarators being carried out in fusion research laboratories around the world is summarized. The theoretical aspects of the stellarator research are emphasized. DOE

N93-13732# Lawrence Livermore National Lab., CA.
ELECTRON TEMPERATURE OF Gd PLASMA PRODUCED BY LASER RESONANCE IONIZATION
Koichi Ogura (Japan Atomic Energy Research Inst., Tokai.), Takashi Arisawa (Japan Atomic Energy Research Inst., Tokai.), Akira Kobana (Japan Atomic Energy Research Inst., Tokai.), and Takemasa Shibata (Japan Atomic Energy Research Inst., Tokai.) 14 Nov. 1990 21 p
(Contract W-7405-eng-48)
(DE91-017785; UCRL-TT-105571; JAERI-M-90-162) Avail: CASI HC A03/MF A01

In Atomic Vapor Laser Isotope Separation (AVLIS), it is necessary to extract ions efficiently from plasma produced by laser resonance ionization. It is important to know electron temperature of the plasma, once the aimed isotope ions are accelerated by electric potential of the order of electron temperature in the plasma. The electron temperature of Gd plasma produced by laser resonance ionization was measured by a Langmuir probe. This measured electron temperature, 0.05-0.08 eV, is much lower than the release electron energy and is close to the atomic excitation temperature of Gd. This result seems to show that electrons collide with Gd atoms with excited or de-excited ground or metastable Gd atoms, and the electron temperature becomes close to the atomic excitation temperature. DOE

N93-13750 Princeton Univ., NJ.
INTERACTION OF ENERGETIC RING CURRENT PROTONS WITH MAGNETOSPHERIC HYDROMAGNETIC WAVES Ph.D. Thesis
Anthony Arthur Chan 1991 143 p
Avail: Univ. Microfilms Order No. DA9202513

A theoretical study of the interaction of energetic (approximately greater than 10 keV) ring current protons with hydromagnetic waves in the Earth's magnetosphere is described. The focus is on the highly energetic (approximately greater than 100 keV) protons, which can undergo magnetic drift-bounce resonances with the waves. A set of gyrokinetic eigenmode equations which describe the linear stability of antisymmetric coupled transverse and compressional magnetic perturbations in an isotropic beta = 0 (1) plasma is analyzed. Using a geomagnetic field model obtained from a perturbation expansion of the Grad-Shafranov equation, and assuming an adiabatically-injected locally-Maxwellian distribution of ring current ions near synchronous orbit, numerical solutions of the eigenmode equations yield the following main results: (1) For beta greater than 0.2, drift-bounce resonant destabilization due to the highly energetic protons can overcome bounce resonant stabilization due to the warm ions, resulting in modes which propagate in the direction of the energetic ion diamagnetic drift; (2) as beta is increased, the drift-bounce resonance instability evolves from a slowly-growing dissipative instability to a rapidly-growing reactive ballooning instability that occurs for beta approximately greater than 1; (3) the drift-bounce resonance instability is sharply maximized at kappa(perpendicular) rho is approximately 0.8, where kappa(perpendicular) is the azimuthal wave number and rho is the equatorial gyroradius of the energetic protons; (4) the lowest-frequency antisymmetric mode is the most easily excited; and (5) the field-aligned eigenmode structure is fairly insensitive to changes in beta or changes in the steepness of the radial pressure gradient. In order to study the effect of the waves on the resonant particles we have used the phase-space Lagrangian Lie transform perturbation methods to derive Hamiltonian gyrophase-independent test-particle equations of motion which include finite gyroradius effects. Analysis and numerical solutions of these equations for the drift-bounce resonance protons yield the following main results: (1) the expected phase-space island structure is obtained; (2) the observed wave amplitudes exceed the Chirikov overlap criterion by roughly two orders of magnitude; (3) the motion in a wave packet consisting of more than about 10 azimuthal mode numbers is well approximated by a quasilinear diffusion coefficient; and (4) the observed wave amplitudes are consistent with nonlinear saturation by quasilinear diffusion from the free-energy source region. Dissert. Abstr.

N93-13792 Wisconsin Univ., Madison.
FLUIDLIKE STUDIES OF THE SHEATH AND PRESHEATH REGIONS OF A PLASMA Ph.D. Thesis
Bong Ju Lee 1991 135 p
Avail: Univ. Microfilms Order No. DA9124677

We investigate the problem of a collisional plasma flowing into a perfectly absorbing wall. Both the collisional presheath and the collisionless sheath regions are modelled by fluid-like moment equations that are derived from kinetic theory. Previous work was based primarily on a collisionless kinetic theory or collisional Braginskii equations which have singularities at the sheath edge. The electron distribution function is obtained here from

the solution of a Pastukhov type problem instead of a simple Boltzmann relation. For the ions a kinetic theory is required to determine the ion viscous stress tensor and heat flux because the collisional mean free path is comparable to the characteristic gradient scale length in the presheath region. A boundary layer analysis is applied for determining the distribution function of the ions in the velocity space region corresponding to no net return flux from the wall. This analysis provides a continuous solution over the entire region of interest. The viscous force deduced from this distribution function, which is a cutoff Maxwellian relaxed by collisions, is comparable to the electric field force everywhere and removes the singularity between the presheath and the sheath regions in the ion momentum equation. The total heat flux obtained using the same method as for the viscous force removes the singularity in the ion energy conservation equation. Four different numerical calculation cases are presented in this thesis. Dissert. Abstr.

N93-13897 Council for National Academic Awards (England).
LASER ABLATION FOR SAMPLE INTRODUCTION IN INDUCTIVELY COUPLED PLASMA SPECTROMETRY Ph.D. Thesis
Peter Booth 1991 437 p
Avail: Univ. Microfilms Order No. BRDX96074

Laser ablation as a means of sample introduction for the Inductively Coupled Plasma (ICP) was investigated. This involved the configuration of an ICP spectrometer, a laser, and a laser ablation chamber. The latter offered the facility the option of electrothermally heating samples before or during laser ablation. Several operating conditions associated with the ablation process were investigated and optimized. These optimization studies utilized a variety of metallurgical materials. It was found that the Q-Switched mode of laser operation provided greater sensitivity than long pulsed operation. Laser ablation ICP studies on paints and polymers were reported. Ablation of paints was found to provide good precision. This was attributed to a combination of homogeneity and viscosity effect. Operation conditions associated with the ablation process were again examined and found to be independent of sample type. Calibration studies were performed using laser ablation of synthetic aqueous standards. The wide dynamic range associated with conventional ICP was also evident for laser ablation. Calibration followed by analysis of samples provided semi-quantitative data for paints and polymers. Limits of detection were inferior to solutions nebulization ICP. Dissert. Abstr.

N93-13985*# Wisconsin Univ., Madison. Fusion Technology Inst.
FUSION ENERGY FROM THE MOON FOR THE TWENTY-FIRST CENTURY
G. L. Kulcinski, E. N. Cameron, J. F. Santarius, I. N. Sviatoslavsky, L. J. Wittenberg, and Harrison H. Schmitt (Schmitt, Harrison H., Albuquerque, NM) *In* NASA. Johnson Space Center, The Second Conference on Lunar Bases and Space Activities of the 21st Century, Volume 2 Sep. 1992 p 459-474 Sponsored in part by EPRI; Wisconsin Electric Utilities Research Foundation; and Granger Foundation (For primary document see N93-13972 03-91)
Avail: CASI HC A03/MF A03

76 SOLID-STATE PHYSICS

Includes superconductivity.

For related information, see also *33 Electronics and Electrical Engineering* and *36 Lasers and Masers.*

N93-12544# Princeton Univ., NJ. Dept. of Electrical Engineering and Computer Science.
GROUP 2 CUBIC FLUORIDES DIELECTRICS FOR 3-D INTEGRATION AND GaAs-BASED OPTOELECTRONIC STRUCTURES Final Report, Jun. 1989 - May 1992
Antoine Kahn 3 Aug. 1992 8 p
(Contract DAAL03-89-K-0035)
(AD-A254937; ARO-26666.10-EL) Avail: CASI HC A02/MF A01

The epitaxial growth of Ca(x)Sr(1-x)F2/GaAs(100) GaAs/Ca(x)Sr(1-x) F2(100) is investigated. Optimum growth temperature of 530 C growth rate of 1 A/sec and composition x = 0.47 lead to very high crystallinity layers of mixed fluorides on GaAs. The growth of GaAs/Ca(0.47)SrO(.053)F2(100), rendered much more difficult by the morphology and faceting of the insulating surface, is substantially improved by modifying the fluoride surface by electron irradiation prior to GaAs growth, and by a two-step growth sequence where the interface GaAs is grown at low temperature (300 C). Finally, the patterning of the fluoride layer is performed by e-beam exposure. Features as small as 1 micron are drawn and developed on a 2000 A thick CaF2 layer, opening the possibility of using the fluorides for wave-guides or re-growth of small 3-5 features. GRA

N93-12562# Argonne National Lab., IL.
THERMAL IMAGING OF SYNCHROTRON BEAMS ON SILICON CRYSTALS
R. K. Smither Jun. 1992 7 p Presented at the Quantitative Infrared Thermography, Chatillon Cedex, France, 7-9 Jul. 1992
(Contract W-31-109-eng-38)
(DE92-018182; ANL/CP-76582; CONF-9207128-1) Avail: CASI HC A02/MF A01

The Advanced Photon Source, a next generation synchrotron source, currently under construction at Argonne National Laboratory, will deliver large thermal loads of 1 to 10 kW to the first optical elements (usually a silicon crystal) in the synchrotron, x-ray beam lines. The first optical elements will distort and attenuate the x-ray beam if they are not extremely well cooled. An infrared camera is used to monitor the temperature distribution of the first optical elements. This measurement is complicated because the silicon crystal is transparent to the infrared radiation and requires a special approach to the analysis of the data to get a meaningful temperature for the crystal. DOE

N93-12586# Sandia National Labs., Albuquerque, NM.
USES OF MONTE CARLO COMPUTER SIMULATIONS IN UNDERSTANDING EPITAXIAL GROWTH AND ION BOMBARDMENT OF Si(001)
E. Chason 1992 3 p Presented at the DOE Workshop in Surface Diffusion in the Growth of Materials, Santa Fe, NM, 1-3 Jun. 1992
(Contract DE-AC04-76DP-00789)
(DE92-016944; SAND-92-1267C; CONF-9206250-1) Avail: CASI HC A01/MF A01

Understanding the mechanisms of growth during vapor-phase deposition is critical for the precise control of surface morphology required by advanced electronic device structures. Yet only relatively recently have the tools for observing this growth on an atomic-level scale become available (via scanning tunneling microscopy (STM) reflection high energy electron diffraction (RHEED) and low-energy electron microscopy (LEEM)). We present results from our own RHEED and STM measurements in which we use computer simulations to aid in determining the fundamental surface processes which contribute to the observed structures. In this study of low-energy ion bombardment and growth on Si(001), it is demonstrated how simulations enable us to determine the dominant atomistic process. DOE

N93-12648# California Univ., San Diego, La Jolla. Dept. of Electrical and Computer Engineering.
SYNTHESIS AND PROPERTIES OF MISMATCHED HETEROJUNCTION/SUBSTRATE INTERFACES Annual Report, 27 Aug. 1991 - 1 Aug. 1992
Harry H. Wieder 1 Aug. 1992 54 p
(Contract N00014-91-K-2019)
(AD-A254577) Avail: CASI HC A04/MF A01

Unstrained In(x)Ga(1-x)As and In(y)Al(1-y)As layers and heterostructures lattice matched to each other but mismatched with respect to their GaAs substrates were grown by molecular beam epitaxy using compositionally step graded buffer layers to relax the mismatch strain by more than 90 percent and their structure, composition, and electrical and optical properties were investigated. For x = 0.3, the buffer layer is stabilized by dislocation loops. Two-dimensional electron gas in modulation doped heterostructures exhibit a 300 K mobility rising from 9 x 10 exp 3 sq. cm/V-s for x = 0.3 to 1.1 x 10 exp 4 sq. cm/V-s for x = 0.45 and an estimated conduction band offset, delta Ec - 0.67 x the bandgap difference between the quantum well and the barrier layer. GRA

N93-12691*# Alabama Univ., Huntsville.
HIGH TEMPERATURE SUPERCONDUCTOR MATERIALS AND APPLICATIONS Final Technical Report, 12 Jul. 1990 - 11 Jan. 1991

George B. Doane, III., ed., Curtis Banks, and John Golben 11 Jan. 1991 24 p
(Contract NAS8-36955)
(NASA-CR-184437; NAS 1.26:184437; UAH-5-32425) Avail: CASI HC A03/MF A01

One of the areas concerned itself with the investigation of the phenomena involved in formulating and making in the laboratory new and better superconductor material with enhanced values of critical current and temperature. Of special interest were the chemistry, physical processes, and environment required to attain these enhanced desirable characteristics. The other area concerned itself with producing high temperature superconducting thin films by pulsed laser deposition techniques. Such films are potentially very useful in the detection of very low power signals. To perform this research high vacuum is required. In the course of this effort, older vacuum chambers were maintained and used. In addition, a new facility is being brought on line. This latter activity has been replete with the usual problems of bringing a new facility into service. Some of the problems are covered in the main body of this report. Author

N93-12748# Purdue Univ., West Lafayette, IN. School of Electrical Engineering.
GaAs GATE DYNAMIC MEMORY TECHNOLOGY Final Report, 1 Feb. 1989 - 31 Dec. 1991
M. R. Melloch and J. A. Cooper, Jr. Jun. 1992 91 p
(Contract N00014-89-J-1864)
(AD-A254801) Avail: CASI HC A05/MF A01

During the course of this work the charge storage times of isolated GaAs pn-junction storage capacitors was increased from 20 minutes to over 10 hours at room temperature. This was accomplished through a combination of improved epitaxy, device processing, and device structure. Furthermore complete DRAM cells were demonstrated using JFET-, MESFET-, MODFET-, and HBT-access transistors. The research supported by this contract has resulted in 21 journal publications and 18 conference papers. GRA

N93-12750# Virginia Commonwealth Univ., Richmond.
ELECTRONIC STRUCTURE OF MICROCLUSTERS AND DEFECT COMPLEXES Final Report, 1 Feb. 1989 - 31 Mar. 1992
P. Jena, S. N. Khanna, and B. K. Rao 10 Aug. 1992 17 p
(Contract DAAL03-89-K-0015)
(AD-A254807; ARO-25906.7-PH) Avail: CASI HC A03/MF A01

A study was made of the electronic and structural properties of atomic clusters and defects in metals. Five main areas were considered: (1) magnetism of clusters, low dimensional systems and transition metal superlattices, (2) interaction of hydrogen with metals and hydrogen absorption around metal ions, (3) defects and defect complexes, (4) electronic structure of LiMgH3 class of compounds and (5) super-shell structure in clusters. The final report provides an outline of the accomplishments in each of these areas as well as the professional accomplishments. GRA

N93-12758# Rockwell International Corp., Thousand Oaks, CA. Science Center.
ELECTRODEPOSITION OF HIGH TEMPERATURE SUPERCONDUCTORS Quarterly Report No. 7, 1 Apr. - 30 Jun. 1992
D. M. Tench 11 Aug. 1992 3 p
(Contract N00014-90-C-0225)
(AD-A255095) Avail: CASI HC A01/MF A01

The overall objective of this project is to develop a process for direct electrodeposition of Y-Ba-Cu superconducting oxides from a molten salt at relatively low temperatures (300-550 deg C). The approach entails establishing a sequence of electrochemical steps for the layered deposition of Y, Ba and Cu oxide species from a eutectic Na-K nitrate melt. GRA

N93-12807# Argonne National Lab., IL.
OXYGEN DIFFUSION IN HIGH-T(c) SUPERCONDUCTORS
S. J. Rothman and J. L. Routbort Jul. 1992 14 p Presented at the 2nd Iketani International Conference on Diffusion in Materials (DIMAT-92), Kyoto, Jpan, 7-11 Sep. 1992
(Contract W-31-109-eng-38)
(DE92-019597; ANL/CP-76698; CONF-9209179-2) Avail: CASI HC A03/MF A01

The cuprate superconductors are fascinating not only because of their technical promise, but also because of their structures, especially the anisotropy of the crystal lattice. There are some structural similarities among these compounds, but also significant differences. Measurements of the oxygen tracer diffusion coefficients was carried out as a function of temperature, oxygen partial pressure, crystal orientation, and doping in the La-Sr-Cu-0, Y-Ba-Cu-0, and Bi-Sr-Ca-Cu-0 systems. These measurements revealed a variety of defect mechanisms operating in these compounds; the exact nature of the mechanism depends on the details of the structure. DOE

N93-12819# Argonne National Lab., IL.
THERMAL EFFECTS ON THE FREQUENCY RESPONSE OF PIEZOELECTRIC CRYSTALS
T. R. Canfield, M. T. Jones, P. E. Plassmann, and M. S. H. Tang (Motorola, Inc., Schaumburg, IL.) 10 Jun. 1992 15 p Presented at the Winter Annual Meeting of the American Society of Mechanical Engineers, Anaheim, CA, 8-13 Nov. 1992
(Contract W-31-109-eng-38)
(DE92-019039; ANL/CP-76560; CONF-921110-17) Avail: CASI HC A03/MF A01

We describe a solution strategy to determine the natural frequencies of piezoelectric crystals subject to moderate changes in temperature and a variety of boundary constraints. The finite element equations governing piezoelectricity are derived based upon a Galerkin formulation of the problem. Suitable assumptions are made to linearize the steady-state (static) problem leading to an iteration scheme that can be used to refine the solution and include nonlinear geometric effects caused by deformation. The eigenvalue problem is cast in this perturbed state to allow more accurate prediction of resonant frequencies. DOE

N93-12827# Harvard Univ., Cambridge, MA. Div. of Applied Sciences.
MEASUREMENTS OF CRYSTAL GROWTH KINETICS AT EXTREME DEVIATIONS FROM EQUILIBRIUM
M. J. Aziz 14 Jul. 1992 6 p
(Contract DE-FG02-89ER-45401)
(DE92-019744; DOE/ER-45401/3) Avail: CASI HC A02/MF A01

We have measured solute trapping of several solutes in Al and Ni during rapid solidification. We have also made preliminary measurements of solute trapping of As in Si, trapped 20 atomic percent As in Si, and made a preliminary measurement of the T(sub o) curve in Si-As. DOE

N93-12853# Los Alamos National Lab., NM.
BIPOLARONIC CHARGE DENSITY WAVES, POLARONIC SPIN DENSITY WAVES AND HIGH T(c) SUPERCONDUCTIVITY
S. Aubry 1992 33 p Presented at the Conference on Phase Separation in Cuprate Superconductors, Sicily (Italy), 6-12 May 1992
(Contract W-7405-eng-36)
(DE92-017403; LA-UR-92-1844; CONF-9205236-2) Avail: CASI HC A03/MF A01

At large enough electron phonon coupling, the existence of bipolaronic, polaronic and mixed states is rigorously proven for the adiabatic Holstein model at any dimension and any band filling. The ground-state is one of them which then prove the existence of insulating Bipolaronic Charge Density Waves. The role of the quantum lattice fluctuations is analyzed and found to be neglegible in that regime but to become essential in case of phonon softening then favoring the occurrence of superconductivity. When a strong Hubbard term is also present, the bipolarons break into polorons and the ground state is expected to be a polaronic spin density wave. If the repulsive Hubbard term is comparable to the electron-phonon coupling, the energy for breaking a bipoloron into two polarons can become small and we get instead of these two degenerate structures, a pait of polarons bounded by a spin resonance which we call 'spin resonant bipolaron'. This resonant bipolaron is still strongly bound, but the role of the quantum lattice fluctuations becomes now very important and yields a sharp broadening of the bandwidth of this resonant bipolarona. Thus, the strong quantum character of these resonant bipolarons could prevent their localization into real space structures which could be insulating bipolaronic CDWs or polaronic SDWS, then favoring the formation of a superconducting coherent state with a possible high T(c). DOE

N93-12854# Argonne National Lab., IL.
HIGH-TEMPERATURE DEFORMATION AND DIFFUSION IN OXIDES

J. L. Routbort Jun. 1992 7 p Presented at the 2nd Iketani International Conference on Diffusion in Materials (DIMAT-92), Kyoto, Japan, 7-11 Sep. 1992
(Contract W-31-109-eng-38)
(DE92-019593; ANL/CP-75064; CONF-9209179-1) Avail: CASI HC A02/MF A01

High-temperature, steady-state deformation is usually controlled by diffusion of the slowest moving ion along its fastest diffusion path. Therefore, measurements of steady-state deformation can, in principle, be used to obtain information concerning diffusion. This paper will briefly review the assumptions that relate creep, defect chemistry, and diffusion. Steady-state deformation of the NaCl-structured oxides, Co(1-x)O and Mn(1-x)O, and the perovskite-structured high-temperature superconductors YBa2Cu3O(x) and Bi2Sr2CaCu2O(x) will be discussed, emphasizing diffusion of the minority defects. DOE

N93-12881# Argonne National Lab., IL.
EMITTANCE, BRILLIANCE, AND BANDPASS ISSUES RELATED TO AN INCLINED CRYSTAL MONOCHROMATOR
A. T. Macrander, D. R. Haeffner, and P. L. Cowan Jul. 1992 10 p Presented at the SPIE International Symposium on Optical Applied Science and Engineering, San Diego, CA, 19-24 Jul. 1992
(Contract W-31-109-eng-38)
(DE92-019671; ANL/CP-76870; CONF-920792-26) Avail: CASI HC A02/MF A01

The inclined double crystal monochromator arrangement is very effective in handling high heat loads and holds considerable promise as a monochromator for undulator beams at third generation synchrotrons. Results for the ideal inclined crystal case have been obtained by dynamical diffraction calculations, and diffraction results for the (111) reflection of silicon are presented for an inclination angle of 85 degrees and energies of 5 key and 13.84 key. The diffraction characteristics resemble closely diffraction from-asymmetric (111) plane of silicon. However, the inclined and noninclined cases are not identical. Diffraction in the inclined case is slightly different due to refraction. The full width at half maximum of the Darwin-Prins reflectivity curve is slightly increased (approximately 1 percent) and the angles of the outgoing beam after one reflection are slightly altered. That is, except for a wave incident at the Laue point in reciprocal space, the diffraction is always slightly asymmetric. The effect can be exactly reversed by an identical second crystal in the (+,-) arrangement. DOE

N93-12887# SRI International Corp., Menlo Park, CA.
STIMULATED BRILLOUIN PROCESSES IN CRYSTALS AND GLASSES Final Report, 17 Sep. 1986 - 31 Oct. 1991
G. W. Faris and A. P. Hickman Feb. 1992 25 p Prepared in cooperation with SRI International, Menlo Park, CA
(Contract W-7405-eng-48)
(DE92-019549; UCRL-JC-110478; MP-91-278) Avail: CASI HC A03/MF A01

The basic physics and material properties needed to describe and predict the Brillouin gain for a variety of materials have been investigated. Lawrence Livermore National Laboratory (LLNL) has identified transverse stimulated Brillouin scattering (SBS) as an important limiting mechanism in high power laser fusion systems. At sufficiently high laser intensities, SBS drives acoustic vibrations that can damage optical components. SRI has performed measurements and developed the corresponding theory for stimulated Brillouin gain spectroscopy in anisotropic crystals. Absolute Brillouin steady-state gain coefficients, linewidths, and frequency shifts have been determined at 532 nm for a number of optical materials of interest to LLNL. This knowledge can be used to select optical materials and devise suppression schemes that will allow much higher laser fluences to be used in laser fusion. DOE

N93-12972# Lawrence Livermore National Lab., CA.
SILICIDE LAYER GROWTH RATES IN Mo/Si MULTILAYERS
R. S. Rosen, D. G. Stearns, M. A. Viliardos, M. E. Kassner, S. P. Vernon, and Yuanda Cheng Apr. 1992 21 p Presented at the Soft X Ray Projection Lithography Topical Meeting, Monterey, CA, 6-8 Apr. 1992
(Contract W-7405-eng-48)
(DE92-019581; UCRL-JC-110360; CONF-9204120-3) Avail: CASI HC A03/MF A01

The thermal stability of sputter-deposited Mo/Si multilayers was investigated by annealing studies at relatively low temperatures (approximately 250 to 350 C) for various times (0.5 to 2000 h). Two distinct stages of thermally-activated interlayer growth were found: a primary 'surge' of approximately 0.3 nm, followed by a (slower) secondary 'steady-state' growth where the interdiffusion coefficient is constant. The interdiffusion coefficients for the interlayer formed by deposition of Mo-on-Si are 200 times greater than those of the interlayer formed by deposition of Si-on-Mo. The interdiffusion coefficient, D(sub 0) approximately equal to 100 cm(exp 2)/s and apparent activation energy, E(exp a) approximately equal to 2.5 eV for the secondary stage of Mo-on-Si interlayer growth are comparable to values for diffusion of Si in h-MoSi2. DOE

N93-13022*# North Carolina State Univ., Raleigh. Coll. of Textiles.
THE CRYSTALLIZATION AND CRYSTALLINE PROPERTIES OF LARC-TPI Final Technical Report, 1 Jan. 1987 - 31 Dec. 1988
Michael H. Theil and Pravin D. Gangal 1992 36 p
(Grant NAG1-723)
(NASA-CR-191001; NAS 1.26:191001) Avail: CASI HC A03/MF A01

LARC-TPI, a thermoplastic polyimide, has been studied in order to develop an understanding of its crystalline phase transition. Our experiments suggest that samples synthesized in different laboratories apparently had different degrees of imidization and their thermal behaviors differed accordingly. When the most crystalline of these polyimides was studied in some detail, we found that it melted irreversibly in that once a sample was completely melted it would not recrystallize. A polymer that did not recrystallize displayed a glass transition, which increased in temperature upon subsequent cooling and reheating. Solubility experiments indicated that heating above the crystalline melting temperature led to network formation in the polymer, a conclusion that is consistent with other behavior just mentioned. Differential calorimetric studies revealed that annealing at slow heating rates or under isothermal conditions resulted in dual melting transitions. These studies, supported by X-ray diffraction results, strongly indicate that the annealing process involves a solid-liquid-solid transformation. From an existing phenomenological model for the kinetics of phase transitions, kinetic parameters for these crystallizations have been evaluated. The Avrami exponents n increased with the annealing temperature in the protocol used in this study. Their values were about 2 or lower, thus indicating that crystallization may have followed a mechanism that included heterogeneous nucleation of a low dimensional order in which all the embryonic crystallites formed at the beginning of the process. A positive temperature coefficient for these crystallizations indicated that diffusion may have had a rate controlling influence and affected the values of n.
Author

N93-13089# Ames Lab., IA.
OXYGEN DEFICIENCIES AT DEFECTS IN YBa2Cu3O(7-DELTA) AS DETERMINED BY HIGH RESOLUTION PARALLEL ELECTRON ENERGY LOSS
M. J. Kramer and R. W. McCallum 1992 6 p Presented at the Material Research Society Spring Meeting, San Francisco, CA, 27 Apr. - 2 May 1992
(Contract W-7405-eng-82)
(DE92-016301; IS-M-717; CONF-920402-34) Avail: CASI HC A02/MF A01

There has been considerable discussion on the exact nature of the pinning defects in the high temperature ceramic superconductors, and the YBa2Cu3O(7-delta) (Y123) structure in particular. High resolution parallel electron energy loss spectrometry (PEELS) allows for fine spatial resolution (less than 17 nm) and fast acquisition times to probe the oxygen content of defects (i.e., dislocations, stacking faults, twin boundaries and grain boundaries), all which have been proposed as potential pinning sites or weak-links. Oxygen deficiencies up to 13 percent were measured at twin boundaries, and 20 percent at grain boundaries while stacking faults showed an increase in oxygen and copper content. Regions of low oxygen (0.5 less than delta less than 1) were usually confined to an area within approximately 50 nm of the defect, which is within the spacial resolution of the measurements. Examination of the fine structure of the oxygen K-edge suggests that the oxygen holes are absent at the twin and ground boundaries. DOE

N93-13100# Advanced Technology Materials, Inc., Danbury, CT.
SINGLE LIQUID SOURCE PLASMA ENHANCED METALORGANIC CHEMICAL VAPOR DEPOSITION OF YBa2Cu3O(7-x) THIN FILMS
Jiming Zhang, Robin Gardiner, Peter S. Kirlin, Robert W. Boerstler, and John Steinbeck 29 Jul. 1992 13 p
(Contract N00014-90-C-0201)
(AD-A254119; ATM-52) Avail: CASI HC A02/MF A01

High quality YBa2Cu3O(7-x) films were grown in-situ on LaAlO3 (100) by a novel single liquid source plasma-enhanced metalorganic chemical vapor deposition process. The metalorganic complexes M(thd)(sub n), (thd = 2,2,6,6-tetramethyl-3,5-heptanedionate; M = Y, Ba, Cu) were dissolved in an organic solution and injected into a vaporizer immediately upstream of the reactor inlet. The single liquid source technique dramatically simplifies current CVD processing and can significantly improve the process reproducibility. X-ray diffraction. measurements indicated that single phase, highly c-axis oriented YBa2Cu3O(7-x) was formed in-situ at a substrate temperature 680 C. The as-deposited films exhibited a mirror-like surface, had transition temperature T(sub c0) approximately equal to 89 K, Delta T(sub c) less than 1 K, and Jc (77 K) = 10(exp 6) A/sq cm. GRA

N93-13104# Argonne National Lab., IL.
ION-CHANNELING OBSERVATION OF CORRELATED ATOMIC DISPLACEMENTS BELOW Tc IN YBa2Cu3O(7-x) AND Pb-DOPED Bi2Sr2CaCu2O(x)
L. E. Rehn, R. P. Sharma, and P. M. Baldo Jul. 1992 7 p Presented at the Lattice Effects in High (Tc) Superconductors, Santa Fe, NM, 13-15 Jan. 1992
(Contract W-31-109-eng-38)
(DE92-018186; ANL/CP-74688; CONF-920141-9) Avail: CASI HC A02/MF A01

Temperature dependent studies of ion channeling in high-quality, high-Tc single-crystals are summarized. The measurements revealed an abrupt change across Tc in displacements in the a-b plane of the Cu(1 and 2) and O(4) atoms; normal 'Debye-like' vibrations were found for the Y and Ba atoms. The anomalous atomic displacements were found for both proton and He channeling, and manifested themselves as an abrupt increase in the critical angle and a simultaneous decrease in the minimum yield. The anomalous change in Cu-O displacements shifted directly with stoichiometry-induced changes in Tc, implying a causal link between the observed phonon anomaly and the superconducting state. An apparently identical anomaly was found in (Bi(1.7)Pb(0.3))Sr(2)CaCu(2)O(x), indicating that it is a general feature of high-Tc superconductivity. A comparison with other experimental measurements in YBa(2)Cu(3)O(7-x), including a detailed neutron diffraction study, indicates that the anomaly is not due to an overall reduction in average vibrational amplitude, but arises instead from a strongly correlated sequence of Cu(1 and 2) and 04 displacements that appears with the onset of superconductivity. These strongly correlated displacements are either dynamic, or they are static distortions that fail to preserve the overall crystal symmetry. DOE

N93-13118# Los Alamos National Lab., NM.
MAGNETIC BEHAVIOR OF A BI(SUB 2)Sr(SUB 2)Ca(SUB 1)Cu(SUB 2)O(SUB x) SINGLE CRYSTAL BY DIRECT MAGNETO-OPTICAL OBSERVATIONS
S. Gotoh (Kawasaki Steel Corp., Chiba, Japan), K. Takamuku, N. Nakamura, N. Koshizuka, and J. O. Willis 1992 5 p Presented at the International Conference on Ferrites, Tokyo, Japan, 29 Sep. - 2 Oct. 1992
(Contract W-7405-eng-36)
(DE92-018612; LA-UR-92-2444; CONF-9209175-1) Avail: CASI HC A01/MF A01

Magnetization and the spatial variation of magnetic flux in a single crystal of Bi2Sr2Ca1Cu2O(x) were studied by using a high contrast magneto-optical observation method (HICOM). Flux penetration, temperature dependence of trapped flux and flux creep have been observed by HICOM. Results show the breakdown of flux pinning and the spatial pinning variation related to sample inhomogeneities. DOE

N93-13195# Argonne National Lab., IL.
ATOMIC RELAXATION MODES IN GRAIN BOUNDARIES
K. L. Merkle and D. Wolf 1992 5 p Presented at the 6th International Conference on Intergranular and Interphase Boundaries in Materials, Thessaloniki (Greece), 22-26 Jun. 1992
(Contract W-31-109-eng-38)
(DE92-016781; ANL/CP-75277; CONF-920670-1) Avail: CASI HC A01/MF A01

High-resolution electron microscopy (HREM) in combination with computer simulations of the fully relaxed atomic structures and energies of symmetric and asymmetric grain boundaries (GB's) in Au (110) tilt bicrystals has been applied to a study of atomic relaxation modes. These investigations indicate the following: (1) atomic relaxations are typically dominated by short-range interactions and the tendency of the solid to assume a local atomic environment similar to the bulk; (2) misfit localizations are likely within a structural unit whenever the GB unit cell is large; (3) when there is a length mismatch along the GB the atomic relaxations can assume quasiperiodic character, generating densely spaced regions of structural disorder, akin to misfit dislocations; and (4) atomic relaxations can take the form of stacking disorder. DOE

N93-13268 Tel-Aviv Univ. (Israel). Dept. of Physics and Astronomy.
EPITAXIAL GROWTH OF SILICON AND GERMANIUM FOR SOLAR CELLS M.S. Thesis
Edmond Redmard Oct. 1990 132 p In HEBREW
(ITN-92-85168) Copyright Avail: Tel-Aviv Univ., Exact Sciences Library, Ramat Aviv, 69978, Israel

In this work we present the epitaxial growth of thin (up to 20 microns) single crystal silicon and germanium films. The growth was carried out via evaporation from an electron gun in an ultra-high vacuum (UHV) chamber. Thin silicon films were deposited directly upon single crystal susbtrates: Silicon wafers with orientations (111) and (100) or heterostructure substrates which consisted of silicon wafers with intermediate (buffer) water-soluble CaF2 layers, in order to obtain self-supporting single crystal films by dissolving the salt layers after the growth of the silicon films upon them. Single crystal sapphire (Al2O3) wafers with their polished faces directed toward the (1 -1 0 2) direction were used as substrates for single crystal germanium films. An intermediate salt layer was used in this case also, in order to separate the germanium film from the substrate. In the course of the work evidence of reactions between the semiconductor film and the buffer layers at high temperatures was found. The reactions were detected by the electron microscope and their nature was discussed. We tried to obtain solar cells from the silicon films by doping them properly during growth (in situ) of the films. The electrical properties of the cells were determined and discussed. The crystalline structure and surface morphology of the films were determined by transmission electron diffraction (TED) and scanning electron microscope (SEM), respectively. The chemical composition and chemical changes of the film surfaces, due to reactions, were studied using EDAX (Energy Dispersive Analysis by means of X-ray) and the junction electrical activities were studied by the special mode of Electron Beam Induced Current (EBIC) of the SEM. Author (ISA)

N93-13323# Sandia National Labs., Albuquerque, NM.
EFFECT OF O2 PARTIAL PRESSURE ON POST ANNEALED Ba2YCu3O(7-DELTA) THIN FILMS
J. M. Phillps (Bell Telephone Labs., Inc., Murray Hill, NJ.), M. P. Siegal (Bell Telephone Labs., Inc., Murray Hill, NJ.), S. Y. Hou (Bell Telephone Labs., Inc., Murray Hill, NJ.), T. H. Tiefel (Bell Telephone Labs., Inc., Murray Hill, NJ.), and J. H. Marshall (Bell Telephone Labs., Inc., Murray Hill, NJ.) 1992 9 p Presented at the Material Research Society Spring Meeting, San Francisco, CA, 27 Apr. - 2 May 1992
(Contract DE-AC04-76DP-00789)
(DE92-014949; SAND-92-1154C; CONF-920402-21) Avail: CASI HC A02/MF A01

Epitaxial films of Ba2YCu3O(7-delta) (BYCO) as thin as 250 A and with J(sub c)'s approaching those of the best in situ grown films can be formed by co-evaporating BaF2, Y, and Cu followed by a two-stage anneal. High quality films of these thicknesses become possible if low oxygen partial pressure (p(O2) = 4.3 Torr) is used during the high temperature portion of the anneal (T(sub a)). The BYCO melt line is the upper limit for T(sub a). The use of low p(O2) shifts the window for stable BYCO film growth to lower temperature, which allows the formation of smooth films with greater microstructural disorder than is found in films grown in p(O2) = 740 Torr at higher T(sub a). The best films annealed in p(O2) = 4.3 Torr have J(sub c) values a factor of four higher than do comparable films annealed in p(O2) = 740 Torr. The relationship between the T(sub a) required to grow films with the strongest pinning force and p(O2) is log

(p(O2)) proportional to T(sub a) exp(1 exp a) independent of growth method (in situ or ex situ) over a range of five orders of magnitude of p(O2).
DOE

N93-13332 Southampton Univ. (England).
SCATTERING AND ORDER IN THERMOTROPIC LIQUID CRYSTALS Ph.D. Thesis
Ian William Hamley 1990 343 p
Avail: Univ. Microfilms Order No. BRDX96012

The information on ordering in nematic and smectic liquid crystals provided by neutron and x-ray diffraction is discussed. Both orientational and positional molecular ordering is considered, the latter to a lesser extent. Theoretical treatments used to quantify molecular orientational order for rigid nematogens are introduced and the molecular field theories for nematics are described. The theory for neutron, x-ray, or electron scattering from fluid phases is outlined. Mesogenic molecules are invariably of low symmetry and non-rigid. Calculations of the intramolecular neutron diffraction from biaxial molecules is included and it is shown that the deviations from cylindrical symmetry have a minor effect on this scattering. An analogy with nuclear magnetic resonance (NMR) is developed where order parameters for internuclear vectors are specified. The influence of molecular flexibility on the anisotropic intramolecular neutron scattering components extracted at low Q from scattering by mixtures of protonated and deuterated nematogens containing a single terminal alkyl chain is shown. The magnitudes of these anisotropic terms depend on the ordering and weightings of individual conformers. An analysis of experimental intramolecular neutron diffraction data extracted at low Q to determine orientational order parameters is presented. Singlet distribution functions calculated from the order parameters via the maximum entropy method often show maxima away from the direction of preferred orientation. The splitting of the wide angle peak observed in the neutron diffraction pattern from 4-methoxy-4'-cyanobiphenyl may be due to local molecular biaxial packing. Molecular mechanics calculations are used to model possible dimers. Results of a computer simulation are used in calculations of the diffraction pattern from ensembles of linear molecules in isotropic, nematic, smectic A and smectic B phases. The intra- and inter-molecular scattering is readily separated so that the separate influence of molecular orientational order and positional organization on the diffraction pattern may be studied. Thus, information on molecular packing is readily obtained which may not be obvious from the simulation. The features of the calculated diffraction patterns resemble those for real mesogens. Dissert. Abstr.

N93-13347# Oak Ridge National Lab., TN.
DEFECTS NEAR THE Y2BaCuO5/YBa2Cu3O(7-x) INTERFACE AND THEIR EFFECT ON FLUX-PINNING IN MELT-PROCESSED AND QUENCH-MELT-GROWTH PROCESSED YBa2Cu3O(7-x)
Z. L. Wang (Tennessee Univ., Knoxville.), A. Goyal, D. M. Kroeger, and T. Armstrong (Allied-Signal Aerospace Co., Torrance, CA.) 1992 6 p Presented at the Material Research Society Spring Meeting, San Francisco, CA, 27 Apr. - 2 May 1992
(Contract DE-AC05-84OR-21400)
(DE92-014463; CONF-920402-10) Avail: CASI HC A02/MF A01

A detailed examination of the Y2BaCuO5 (211)/YBa2CuO(7-x) (123) interface in several melt-processed 123 samples prepared using different methods was undertaken using analytical electron microscopy. It is found that there exists a significant increase in the a-b planar stacking fault density in 123, near the 211/123 interface. When viewed along zone axes (001), these faults appear as disks with diameter from a few to 30 nm and are bounded by dislocation loops. Most stacking faults are confined to the (001) basal plane. The size and density of defects around the 211 particles suggest that these defects could act as effective flux-pinning sites and may explain the observations of increased J(sub c) with increasing volume fraction of 211 and a maximum in J(sub c) when the applied field parallel to the c-axis. DOE

N93-13349# Argonne National Lab., IL.
ELECTRON STIMULATED DESORPTION OF THE METALLIC SUBSTRATE AT MONOLAYER COVERAGE: SENSITIVE DETECTION VIA 193 nm LASER PHOTOIONIZATION OF NEUTRAL ALUMINUM DESORBED FROM CH3O/Al(111)
C. E. Young, J. E. Whitten, M. J. Pellin, D. M. Gruen, and P. L. Jones (Spectra Technology, Inc., Bellevue, WA.) 1992 9 p Presented at the Workshop on Desorption Induced By Electronic Transitions, Taos, NM, 1-4 Apr. 1992
(Contract W-31-109-eng-38)
(DE92-014858; ANL/CP-75386; CONF-920462-2) Avail: CASI HC A02/MF A01

A fortuitous overlap between the gain profile of the 193 nm ArF excimer laser and the Al autoionizing transition (sup 2)S(sub 1/2) (512753/cm) yields to the left (sup 2)P(sup 0)J has been exploited in the direct observation of substrate metal atoms in an electron simulated desorption (ESD) process from the monolayer adsorbate system CH3O/Al(111). The identity of the mass 27 photoion was established as Al(+) by (1) isotopic substitution of C-13 in the methanol employed for methoxy formation, and (2) tunable laser scans utilizing the DJ-2 (J = 3/2, 5/2) intermediate levels at approximately 32436/cm and a 248 nm ionization step. An ESD yield of approximately x 10(exp -6) Al atoms/(electron at 1 keV) was established by comparison with a sputtering experiment in the same apparatus. Velocity distributions measured for the desorbed Al species showed some differences in comparison with methoxy velocity data: a slightly lower peak velocity and a significantly less prominent high-velocity component. DOE

N93-13362 Tel-Aviv Univ. (Israel). School of Physics and Astronomy.
Y1Ba2Cu3O(7-DELTA) THIN FILM DC SQUIDS (SUPERCONDUCTING QUANTUM INTERFERENCE DEVICE) M.S. Thesis
Daniel Racah Mar. 1991 87 p
(ITN-92-85167) Copyright Avail: Tel-Aviv Univ., Exact Sciences Library, Ramat Aviv, 69978, Israel

Direct current superconducting quantum interferometers (SQUIDs) based on HTSC thin films have been measured and characterized. The thin films used were of different quality: (1) Granular films on Sapphire substrates, prepared either by e-gun evaporation, by laser ablation or by MOCVD (metal oxide chemical vapor deposition), (2) Epitaxial films on MgO substrates. Modulations of the voltage on the SQUIDs as a function of the applied flux have been observed in a wide range of temperatures. The nature of the modulation was found to be strongly dependent on the morphology of the film and on its critical current. The SQUIDs based on granular films were relatively noisy, hysteretic and with a complicated V-phi shape. Those devices based on low quality (lowIc) granular films could be measured only at low temperatures (much lower than 77 K). While those of higher quality (granular films with high Ic) could be measured near to the superconductive transition. The SQUID based on high quality epitaxial film was measured near Tc and showed an anomalous, time dependent behavior. ISA

N93-13526# Midwest Research Inst., Golden, CO.
NOVEL THIN-FILM CuInSe2 FABRICATION
A. Gabor and A. Hermann (Colorado Univ., Boulder.) Sep. 1992 20 p
(Contract DE-AC02-83CH-10093)
(DE92-016440; NREL/TP-451-5014) Avail: CASI HC A03/MF A01

This report describes the formation of thin films of CuInSe2 (CIS) by annealing precursor films containing Cu, In, and Se in a rapid thermal processor. This involves two steps: (1) a precursor containing Cu, In, and Se is deposited on unheated substrates such that CIS does not form during this deposition step; and (2) the precursor is annealed in a rapid thermal processor to crystallize the CIS. Advantages of this process are as follows: (1) no H2Se is used; (2) concentration gradients can potentially be built into the film due to the rapid annealing; and (3) the precursor can potentially be deposited using scalable methods such as sputtering, solution growth, and electrodeposition. The deposition method used was three-source, elemental physical vapor deposition. At room temperature, such a method was considered to be a flexible way to deposit a precursor that would be fairly typical of precursors deposited by more scalable techniques. Precursors were made both by the stacked elemental layer approach, where one element at a time was evaporated, as well as by a co-evaporation method. Adhesion problems limited device performance, and the co-evaporated precursors displayed unintended segregation of Cu and I in a direction normal to the film plane. The best cell efficiency was 3.5 percent. DOE

N93-13547# Argonne National Lab., IL.
ACTIVATION ENERGY AND CRITICAL CURRENT DENSITY IN Bi-Sr-Ca-Cu-O
Donglu Shi, S. Sengupta, M. Smith, and Z. Wang Jul. 1992 7 p

Presented at the International Cryogenic Engineering Conference and the International Cryogenic Materials Conference, Kiev, Ukraine, 8-12 Jun. 1992

(Contract W-31-109-eng-38)
(DE92-018795; ANL/CP-76805; CONF-920614-2) Avail: CASI HC A02/MF A01

Flux creep in a Bi-Sr-Ca-Cu-O system has been investigated in wide temperature and field regimes. Previously reported studies of the flux-creep activation energy U have been controversial in terms of the temperature and field dependence, and the U values have not been consistent with the macroscopically measured critical current density, J(sub c). We have developed a new approach to obtain the activation energy by considering the nonlinearity between U and J. We find that the activation energy is considerably increased in liquid-quenched Bi-Sr-Ca-Cu-O, as a result of enhanced pinning by finely dispersed precipitates. Our results are consistent with the increased macroscopic parameter J(sub c). DOE

N93-13570*# Eloret Corp., Sunnyvale, CA.
SIMULATION STUDIES FOR SURFACES AND MATERIALS STRENGTH Semiannual Progress Report, 1 May - 31 Oct. 1992
Timur Halicioglu 31 Oct. 1992 61 p
(Contract NCC2-297)
(NASA-CR-191289; NAS 1.26:191289) Avail: CASI HC A04/MF A01

The progress report for the period May 1, 1992 to October 31, 1992 is presented. During this period investigations were carried out in three areas. Binding energies and high energy binding sites were calculated for carbon atoms deposited on a (2 x 1) dimerized Si(100) surface. Structure- and energy-related properties of defects formed on relaxed diamond surfaces were investigated. Tersoff-type model functions for Si were employed to investigate the energetics of the following processes: (1) neutral monovacancy and divacancy formation and migration energies; (2) neutral bond-centered, site sharing, tetrahedral, and hexagonal self-interstitial formation and migration energies; and (3) the variation of these energies with distance from a bulk site of Frenkel defect formation and from (100) and (111) surfaces. Calculations are included in the appendices. L.R.R.

N93-13577# City Coll. of the City Univ. of New York, NY. Dept. of Physics.
DYNAMICS AND PATTERN SELECTION AT THE CRYSTAL-MELT INTERFACE
H. Z. Cummins 1992 6 p
(Contract DE-FG02-84ER-45132)
(DE92-040210; DOE/ER-45132/7) Avail: CASI HC A02/MF A01

This report discusses the following topics: morphological instability and pattern selection; sidebranching; planar-to-cellular transition; and dynamic light scattering at the crystal-melt interface. DOE

N93-13628 Washington State Univ., Pullman.
POINT DEFECTS QUENCHED IN NiAl AND RELATED INTERMETALLIC COMPOUNDS Ph.D. Thesis
Jiawen Fan 1991 103 p
Avail: Univ. Microfilms Order No. DA9226145

Point defects in the highly ordered B2 compounds NiAl, CoAl and FeAl were studied using the perturbed gamma-gamma angular correlations (PAC) technique. Quadrupole interactions detected at dilute In-111 probes on Al sites in NiAl and CoAl were identified with complexes containing one or two vacancies in the first atomic shell. Measurements on rapidly quenched NiAl and CoAl exhibited increases in site fractions of vacancy-probe complexes caused by formation of thermal defects. Site fractions were analyzed using the law of mass action to obtain absolute vacancy concentrations. PAC is shown to be a powerful new technique for the quantitative study of equilibrium defects in solids. For NiAl, the vacancy concentration quenched-in from a given temperature was found to be independent of composition over the range 50.4 to 53.5 at. pct. Ni, identifying the Schottky defect (vacancy pair) as the dominant equilibrium defect, and ruling out the so-called triple defect. Formation energies and entropies of Schottky pairs were determined to be 2.66(8) and 3.48(12) eV, and 12(1) and 17(2) k sub B, respectively, for NiAl and CoAl. The entropies suggest huge vacancy concentrations, 13 pct. at the melting temperatures of NiAl and CoAl. Migration energies of Ni and Co vacancies were found to be 1.8(2) and 2.5(2) eV, respectively. FeAl exhibited complex behavior. A low temperature regime was detected in NiAl and CoAl within which vacancies are mobile but do not anneal out, so that the vacancy concentration remains constant. In NiAl, this 'bottleneck' regime extends from 350 to 700 C. Vacancies were found to be bound to the In probes with an energy very close to 0.20 eV in NiAl and CoAl. An explanation of the bottleneck is proposed in terms of saturation of all lattice sinks. This annealing bottleneck should exist in a wide range of intermetallic compounds when there is a sufficiently high vacancy concentration. Dissert. Abstr.

N93-13730 Maryland Univ., College Park.
ELECTRONIC TRANSPORT PROPERTIES OF SEMICONDUCTOR MICROSTRUCTURES Ph.D. Thesis
Tetsuo Kawamura 1991 136 p
Avail: Univ. Microfilms Order No. DA9222707

In this dissertation we investigate the momentum and energy relaxation properties of a 2D EG at the interface of a high-mobility, modulation doped Al(x)Ga(1-x)As/GaAs heterojunction. Our work consists of four main parts. In the first part we study the bulk phonon scattering contribution to the transport properties of a two-dimensional electron gas formed at the interface of an ultra-pure Al(x)Ga(1-x)As/GaAs heterojunction. Our work encompasses three physically distinct temperature ranges with respect to phonon scattering: the Bloch-Grueneisen (BG), equipartition (EP), and inelastic scattering regimes. To evaluate the mobility in the inelastic scattering regime at high temperatures above T approximately equal to 40 K, where the scattering from polar LO-phonons becomes important, we compute that first order perturbation distribution phi(E) as function of the carrier energy E by directly solving the linearized Boltzmann equation by an interactive method. In part two we investigate in detail the temperature dependence of the mobility at low temperatures in the range T = 4 - 40 K, and density range (0.3 - 6.0) x 10(exp 11) cm(exp -2) due to acoustic-phonon scattering. In agreement with experimental results, we show that the linear coefficient of the temperature dependence alpha = d(mu)(exp -1) (T)/dT has a shallow minimum as a function of the electron density. The energy relaxation properties of a 2D EG in Al(x)Ga(1-x)As/GaAs heterojunctions are investigated in part three. The total average energy-loss rate at low temperatures is calculated for various densities and temperatures. We take into account the inelastic-scattering mechanisms due to acoustic phonons by deformation-potential and piezoelectric coupling, and the low-energy phonons associated with the coupling of quasiparticle excitations to the LO phonons. Finally, in the fourth part we study the effects of impurity scattering from the remote donors on a 2D EG using the Born approximation. We carry out a simple model calculation to investigate the spatial correlation effect of the ionized scattering sites on the electron mobility. Dissert. Abstr.

N93-13739 Wisconsin Univ., Madison.
HEAT TRANSFER, FLUID FLOW AND INTERFACE SHAPES IN FLOATING-ZONE CRYSTAL GROWTH Ph.D. Thesis
Chung-Wen Lan 1991 394 p
Avail: Univ. Microfilms Order No. DA9135475

The main objectives of the present study are: (1) to better understand the conventional floating-zone process, and (2) to overcome some of the difficulties in this process, including zone stability, and control of the melt/crystal interface and crystal diameter. In order to achieve these objectives, single crystal were grown using a material (i.e., NaNO3) whose melt is transparent, so that the melt/sold interfaces and the flow pattern in the melt could be visualized during crystal growth. Furthermore, computer simulation was conducted, so that heat transfer and fluid flow during crystal growth can be described quantitatively. Growth of 0.6 cm-diameter crystal was unsuccessful due to poor zone stability. In order to improve the zone stability, a simple method for shortening and hence significantly improving the stability of a floating melt zone was proposed and applied to crystal growth. NaNO3 single crystals of 0.6 and 1.0 cm in diameter were grown successfully. Flow visualization and computer simulation were conducted to explain why this method works. A procedure for correcting optical distortions in flow visualization was proposed and verified. Two modified floating-zone processes were also developed in which a heated shaper in contact with the melt is used. It was demonstrated that crystals with a very uniform diameter and smooth surface can be grown by this modified process, and thermocapillary convection can be reduced significantly. Computer simulation of these processes was also conducted.

Dissert. Abstr.

N93-13783# National Inst. of Standards and Technology, Gaithersburg, MD. Electronics and Electrical Engineering Lab.
SEMICONDUCTOR MEASUREMENT TECHNOLOGY: INSTANT (IGBT NETWORK SIMULATION AND TRANSIENT ANALYSIS TOOL)
Allen R. Hefner, Jr. Jun. 1992 163 p
(PB92-213529; NIST/SP-400-88) Avail: CASI HC A08/MF A02; SOD HC

The IGBT (Insulated Gate Bipolar Transistor) is a power semiconductor device that has gained acceptance among power electronic circuit design engineers for motor drive and power converter applications. these devices have the best features of both power MOSFET's and power bipolar transistors, i.e., efficient voltage gate drive requirements and high current density capability. When designing circuits and systems that utilize IGBT's or other power semiconductor devices, circuit simulations are needed to examine how the devices affect the behavior of the circuit. However, the semiconductor device models available in most circuit simulators were originally intended to describe microelectronic devices and cannot adequately describe the characteristics of power devices. In the publication, a compact IGBT model suitable for incorporation in circuit simulators is described, and a circuit simulation program called INSTANT is presented that simulates the dynamic behavior of IGBT's within any external drive, load, and feedback circuit configuration. The INSTANT simulator solves the systems of differential equations (state equations) that describe each component of the circuit, where the equations for the individual components are coupled by the circuit configuration. The publication also describes the automated measurement methods developed to extract the IGBT device model parameters from terminal electrical measurements. GRA

N93-13843 Southampton Univ. (England).
MOLECULAR THEORIES AND COMPUTER SIMULATIONS OF LIQUID CRYSTALS Ph.D. Thesis
Andrew Peter John Emerson 1991 254 p
Avail: Univ. Microfilms Order No. BRDX96159

Two different approaches are adopted for the study of the properties of liquid-crystalline systems: molecular theories and computer simulations. The development is described of a molecular field theory for calculating the thermodynamic properties of liquid crystals containing flexible chains. The application of this theory to a variety of flexible model mesogens is discussed and the results compared with experimental data. In an attempt to rectify the deficiencies in this model, an alternative parameterization is presented of the molecular field theory based on the molecular moment of inertia tensor. The predictions of this new parameterization are compared with those of the previous approach and thermodynamic data obtained from experiment. The conformational probabilities calculated with the original theory are used in a study into possible visual representations for flexible mesogens. Techniques involving fixed and conformational dependent reference frames are explored and the results analyzed with the aid of computer graphics. The possible relationships between the graphics images and order parameters determined from NMR spectroscopy are discussed. Next, a molecular dynamics simulation of particles is presented in the microcanonical ensemble interacting via a single-site anisotropic potential which has been parameterized to model both rod-like and disc-like mesogens. The phase behavior together with the static and dynamic properties of these systems are discussed and compared with results of other simulations of liquid crystals and experiments. Dissert. Abstr.

N93-13844 State Univ. of New York at Buffalo, Amherst.
EFFECT OF HYDROGEN REDUCTION AND DOPING ON THE CHARACTERISTICS OF HIGH-TEMPERATURE SUPERCONDUCTORS Ph.D. Thesis
Min Qi 1992 108 p
Avail: Univ. Microfilms Order No. DA9222098

The CuO2 layers in oxide superconductors have been recognized as essential for high T(sub c) superconductivity. A useful approach to study superconductivity is to modify the charge carrier concentration in the active CuO2 layers through chemical modification such as annealing under different atmospheres or substitutions of ions in charge reservoirs. In order to avoid possible structural changes caused by doping or annealing at high temperature, low temperature reduction with hydrogen was used for the reversible removal of excess oxygen from high T(sub c) superconductors without observable changes in structure. From the chemical analysis of excess oxygen, the determination of crystal structure, and other physical properties, a simple correlation between T(sub c) and hole concentration in the CuO2 planes was established. High T(sub c) superconducting materials represent a rewarding but formidable challenge for application. One of the technical difficulties is that the low magnetic flux-pinning energies severely limit their critical current density. Compressive reorientation and doping were shown to be useful methods for enhancing the critical current density of ceramic superconductors. The results show that the observed increase in J(sub c) is mainly due to the strengthening of weak-links by improving the coupling between individual grains. Dissert. Abstr.

N93-13845 Nottingham Univ. (England).
STUDIES OF ORBITAL DOUBLET AND MODELLING OF ORBITAL TRIPLET JAHN-TELLER SYSTEMS IN 3 TO 5 SEMICONDUCTORS Ph.D. Thesis
Rashad Ibrahim Badran 1991 190 p
Avail: Univ. Microfilms Order No. BRD-96370

The method of an initial unitary transformation followed by an energy minimization is used to study the tensor product of E x e Jahn-Teller (JT) system in the strong coupling limit. The positions of the wells in the potential energy surface are found when this surface is warped by either anharmonicity or quadratic coupling. The cubic ground and first excited vibronic states are obtained and their energies are derived by analytical methods. The inversion splitting and reduction factors are also obtained by analytical procedures. Anisotropic corrections are then added to both the vibronic states and their energies. The inversion splittings and reduction factors are recalculated. It is shown that the results obtained for the inversion splittings and reduction factors are in agreement with the previously published numerical and analytical results. An analysis of the structure of the zero-phonon lines (ZPL's) of transitions within V(sup 3+) ions in GaAs, GaP, and InP under the effects of spin-orbit coupling, uniaxial stress and external magnetic field which are accompanied by Jahn-Teller effects, are also studied and discussed. The theoretical results are compared to the experimental data and other theoretical results. Dissert. Abstr.

N93-13847 Lancaster Univ. (England).
USE OF PHONON ECHOES IN THE STUDY OF 2-6 COMPOUNDS AND DIELECTRIC Bi12GeO20:Cr Ph.D. Thesis
Nacer-Eddine Bensaid 1990 177 p
Avail: Univ. Microfilms Order No. BRDX96003

Wavevector-reversed phonon echoes in single crystals are generated by the nonlinear interaction between a forward propagating acoustic wave (w, k), launched by the first microwave pulse (w, O), with the uniform electric field of the second pulse (w, O). In piezoelectric semi-conductors, the nonlinearities are derivable on the basis of field induced ionization of shallow impurity states. At low temperatures (approximately 1.3K), the space charge gratings may be formed in shallow traps through charge transfer by field assisted tunnelling induced by the sum of the acoustic and electric fields. In CdS, the charge gratings could be stored as a hologram for a considerable length of time. A novel technique (echo erasure technique) has been used successfully in the determination of trap distribution in CdS. For the first time, storage echoes were observed in the semimagnetic Cd(1-x)Mn(x)Te (x = 0.1, 10 percent) and ternary Cd(1-x)Zn(x)Te (x = 4 percent) semiconductor compounds. Also investigated are samples of CdTe prepared by a number of different growth techniques (Bridgman, SET and THM) and CdTe doped with indium (100ppm). In contrast with CdS, the common feature of the storage echoes observed in these materials is their relatively short lifetime (T(sub 1) is greater than or equal to 100 microseconds). There is some evidence to suggest that concentration of recombination inhibitors may be very small in CdTe samples. It is suggested that hopping conductivity may contribute to the formation of the charge grating. This thesis reports also on investigations of the dielectric Bi12GeO20:Cr subject to a magnetic field with strength up to 8kGauss. The echoes observed in these materials are thought to be closely related to ultrasonic spin echoes where the magnetic character of the chromium atoms play a dominant role. Dissert. Abstr.

N93-13881# California Univ., Los Angeles. Dept. of Physics.
TRANSPORT ON FRACTAL NETWORKS Final Report, 1 Oct. 1990 - 30 Sep. 1991
Raymond L. Orbach 30 Sep. 1991 11 p
(Contract N00014-91-J-1063)
(AD-A253797) Avail: CASI HC A03/MF A01

The dynamics of transport on fractal networks was studied. Progress was made towards understanding the ac conductivity of a fractal network ((Na(+), Ba(2+))beta''-alumina). Mixed (Na(+),Ba(2+))beta''-alumina crystals are near ideal examples of ionic motion in a two dimensional percolating network. At low temperatures, the Na(+) ions move along a two dimensional percolation network in a sea of frozen Ba(2+) ions, the latter blocking available sites for the Na(+) ions. For sufficient Ba(2+) concentration, the number of available sites for Na(+) ion motion falls below the critical percolation concentration, p(sub c). This implies a vanishing dc conductivity. The extrapolated dc conductivity for a range of compositions and over a temperature range of 173 K to 373 K were measured. The conductivity exhibits activated behavior, with an unusual dependence of the activation energy on (Na(+), Ba(2+)) concentration. The activation energy rises rapidly from the pure Na(+) and Ba(2+) values to two plateaus of energy delta = 0.48 eV and delta = 0.67 eV respectively. The plateaus cross over from one to the other between 40 percent and 50 percent Ba(2+) exchange. The plateau values of delta are interpreted to be the bare-potential-well minima depths for the Na(+) and Ba(2+) ions. The smaller values for the pure Na(+) and Ba(2+) material are interpreted as the consequence of interplay between the single ion attractive potential and the inter-ionic repulsive Coulomb potential which results in a collective state. The competing interactions lead to off-site ionic positions, thereby reducing delta from its bare value. The screening of the inter-ionic Coulomb interaction by the minority ions in the mixed materials allows the majority ions to move independently, thereby exhibiting the full bare value of delta in conductivity measurments. L.R.R.

N93-13895 Oxford Univ. (England).
HIGH MAGNETIC FIELD STUDIES OF STRAINED LAYER SUPERLATTICES Ph.D. Thesis
Richard John Warburton 1991 191 p
Avail: Univ. Microfilms Order No. BRD-96243

Strained layer quantum wells were investigated experimentally at high magnetic field and at high pressure, and with k.p theory calculations. Cyclotron resonance of p-type In(x)Ga(1-x)Sb/GaSb quantum wells showed that the valence band is reconstructed by the strain such that the absolute value of M(sub J) = 3/2 subband has a light mass. Masses as low as 0.07 were recorded. Simple inter-band spectra were observed. Strain reconstruction gives a simple set of selection rules for the inter-band process. Agreement of the experiments with k.p theory calculations was good. The valence band of p-type In(0.18)Ga(0.82)As/GaAs quantum wells was studied. Masses of 0.16 were measured. Filling factor related anomalies in the cyclotron resonance were observed and interpreted in terms of hole-hole interactions combined with the presence of localizing potentials. The magneto-exciton and band-filling were considered in the interpretation of the inter-band results. Magneto-transport experiments on the p-type In(0.18)Ga(0.82)As/GaAs samples in tilted fields showed that the valence band spin has two dimensional behavior. The effect was found to apply over a wide range of filling Landau level calculations determined an upper limit to the value of kappa(sup L), the spin-magnetic field coupling parameter. Photoluminescence at high pressure was used to measure the pressure coefficient and L(sub c) - Gamma(sub c) crossover pressure of bulk GaSb. In(0.15)Ga(1-x)Sb/GaSb quantum wells had the same Gamma-gap pressure coefficient as bulk GaSb, a consequence of the similarity of GaSb and In(0.15)Ga(0.85)Sb. Both quantum well L(sub c) - Gamma(sub c) and X(sub c) - L(sub c) crossovers were observed. High pressure photoluminescence measurements were carried out on highly strained GaSb/GaAs heterostructures. The pressure coefficient implies that the electrons are in Gamma(sub c) band, and the X(sub c) - Gamma(sub c) crossover implies that the band alignment is type-2. The transition energy suggests that alloying of As into the GaSb layers has occurred. Dissert. Abstr.

N93-13904 Stanford Univ., CA.
THE HETEROEPITAXIAL GROWTH OF YBCO AND OTHER METAL OXIDES ON SILICON AND GaAs BY PULSED LASER DEPOSITION Ph.D. Thesis
David Kirtland Fork 1992 203 p
Avail: Univ. Microfilms Order No. DA9221614

Earlier attempts to produce high quality thin films of YBa2Cu307-delta (YBCO) on Si substrates were thwarted by their reactivity and thermal expansion behavior. This research has demonstrated several epitaxial buffer layer systems including yttria-stabilized zirconia and MgO which allow the epitaxial growth of YBCO on Si without chemical reaction. All of the materials may be grown in a single process by laser deposition. Pulsed laser deposition has been proven to be a rapid and versatile technique for exploring new epitaxial systems on a variety of substrates; this work has provided the first extension of pulsed laser deposition to epitaxy on semiconductor substrates. Although direct epitaxy of YBCO on silicon may not be possible, buffer layers permit the growth of device quality YBCO films with critical current densities in excess of 10(exp 6) A/sq cm at 77 K. Methods have been developed to pattern these films in-situ by removing the buffer layer in selected areas to produce isolated superconducting mesas. The complications of thermally induced tensile stress have been eliminated through the use of silicon-on-sapphire instead of silicon. This work has revealed methods for controlling the in-plane epitaxy of YBCO films on zirconia via homoepitaxy and nucleation-initiating monolayers. Recent research has demonstrated that some of the epitaxial growth processes developed for Si may be adapted to produce similar results on GaAs substrates. Dissert. Abstr.

N93-13905 State Univ. of Iowa, Iowa City.
MAGNETIC PROPERTIES OF HIGH-T(SUB c) SUPERCONDUCTORS Ph.D. Thesis
Junho Gohng 1992 128 p
Avail: Univ. Microfilms Order No. DA9223928

Magnetic properties of high-T(sub c) superconductors have been studied in order to determine the free-energy surface, the characteristic critical fields, order parameters structure, and the grain size effect on magnetization. Studies of the thermodynamic reversibility for YBa2Cu3O(7-delta) show the rounding in magnetization vs. temperature curves is a reflection of the thermodynamic fluctuations near T(sub c). Specific heat jump C(0)-C(H) values that have been calculated from the free-energy surfaces show good agreement with the direct calorimetric measurements. Comparative studies of the free-energy surfaces, flux creep and critical currents for both melt-textured and grain-aligned YBa2Cu3O(7-delta) samples have been undertaken in order to evaluate the difference caused by different micro structures in these samples. The free energy per unit length of a vortex is found to be essentially the same in the melt-textured sample as for the single crystals in the grain-aligned sample, suggesting that the line energy is the same for these rather different samples. The specific heat jump values calculated from the free-energy surfaces also show close agreement between the two samples. Magnetic field and temperature dependence of the average Ginzburg-Landau order parameter (f) is evaluated by fitting the magnetization data of grain-aligned YBa2Cu3O(7-delta) to the Hao-Clem model in the region of thermodynamic reversibility. H(sub C)(T) and H(sub c2)(T) were also determined from the fitting along with the kappa(sub c)(T) values. The study reveals the kappa(sub c) is a slowly decreasing function of temperature near T(sub c). Fittings of the same model to Bi2Sr2Ca2Cu3O10 have been carried out. The 2-D nature of bismuth family superconductors introduces some difficulties in applying Hao-Clem model and it is discussed in comparison with YBa2Cu3O(7-delta) results. Lastly, studies on the grain size effect on free energy and specific heat jump in grain aligned YBa2Cu3O(7-delta) samples show that the free energy is reduced by about 15 percent as the average grain size changes from 37.5 to 12.7 microns. The twin spacing d is related to the average grain size D by d varies as square root of D and is thought to be the major factor that causes the decrease in the free energy. Dissert. Abstr.

N93-13933 University of South Florida, Tampa.
NOISE MEASUREMENTS OF YBa2Cu3O7 THIN FILM HIGH-TEMPERATURE SUPERCONDUCTORS Ph.D. Thesis
James Joseph Hall 1992 255 p
Avail: Univ. Microfilms Order No. DA9222593

The characteristics of thin-film YBa2Cu3O7 superconductors were studied from the superconducting region through the transition region and into the normal region. The properties studied included the resistance-temperature, current-voltage, and electrical noise with concentration of measurements in the transition region. The resistance vs. temperature measurements show a zero resistance followed by a small rise in magnitude at the onset of resistance followed by a sharp increase until the resistance tapers off in the fully normal region. The a-axis films had a larger normal resistivity, a lower critical temperature, and a broader transition than the similar c-axis films. The current(I) - voltage(V) measurements were concentrated in the transition region. A power relation

between I and V was found to be V varies as I(sup a(T)) where a(T) is temperature dependent starting high the onset of vortex formation, approaches 3 at the vortex unbinding temperature, and goes to 1 when fully normal. This behavior was predicted by the Kosterlitz-Thouless theory and was found experimentally in all four films measured. The current-induced electrical noise characteristics were measured for four samples varying in thickness and axis orientation. Each film exhibited a widely varying magnitude of the noise voltage spectral density (S(sub V)) in the transition region with a leveling off when fully normal. The normalized noise (S(sub V)/V squared) showed a sharp decrease in magnitude from the onset of measurable noise continually decreasing until flattening out when fully normal. The a-axis films exhibited S(sub V)/V squared over 3 order of magnitude larger than the c-axis films in the transition and normal regions. The normalized temperature coefficient of resistance (beta) was plotted against S(sub V)/V squared on a log-log scale to see if the noise generated was due to temperature fluctuations (slope = 2). The four films all had slopes of greater than 4 revealing that the temperature fluctuations were not the cause of the noise in the transition region. The generating mechanisms behind 1/f-squared voltage spectra were investigated. The traditional voltage ramp, usually considered the cause of the 1/f-squared signal, was shown both theoretically and experimentally to show no measurable output signal when using an amplification system. The 1/f-squared signal was generated using a changing resistance and exhibited a 1/f-squared spectrum with a magnitude attenuated about 75 db from the no amplification value.

Dissert. Abstr.

N93-14073 Stanford Univ., CA.
DIFFUSION OF ION-IMPLANTED GROUP 4 n-TYPE DOPANTS IN GALLIUM ARSENIDE AND GALLIUM/ARSENIDE-BASED SUPERLATTICES Ph.D. Thesis
Emily Lin Allen 1992 168 p
Avail: Univ. Microfilms Order No. DA9217790

As semiconductor device dimensions shrink, understanding and controlling dopant diffusion becomes increasingly important. For submicron FET's made in GaAs, dopant diffusion during post-implant anneal is undesirable. In addition, impurity induced intermixing of III-V heterostructures for optoelectronic devices requires a series of carefully controlled diffusion steps. A more complete understanding of the diffusion mechanisms of dopants and point defects in both GaAs and Al(x)Ga(1-x)As is thus required for several advanced technologies. Most of the published parameters for diffusion of dopants in III-V compound semiconductors are from thin film or vapor source diffusions. The effect of implant damage and extended defects on diffusion of implanted dopants in GaAs and Al(x)Ga(1-x)As has not been extensively studied. In this work we measure the carrier concentrations and diffusivities of the ion-implanted Group IV dopants Sn, Ge and Si in GaAs and Al(x)Ga(1-x)As, using SIMS, polaron and SUPREM 3.5 simulations. In the substrate, diffusion is modeled by an effective diffusivity which depends on the square of the electron concentration (n), due to enhancement of the negatively charged Ga vacancy concentration by the n-type doping. In the near-surface implanted region diffusion is suppressed for doses greater than 1 x 10(exp 14)/sq cm. The carrier concentrations for Sn implants are anomalously high in this region, and anomalously low for Ge and Si. Transmission electron microscopy shows that precipitates and dislocations form in the implanted region during annealing for doses greater than 1 x 10(exp 14)/sq cm. These extended defects may influence dopant diffusion by controlling the generation and recombination of point defects. The carrier concentration-dependent diffusion model is applied to interdiffusion of Al and Ga in AlAs/Al(x)Ga(1-x)As superlattice structures. We show that interdiffusion is enhanced more under an oxide film than under a nitride film, while a tungsten nitride film suppresses disordering. These effects are due to Fermi level enhancement of the vacancy concentration and vacancy injection from the encapsulant.

Dissert. Abstr.

N93-14083# Aerospace Corp., El Segundo, CA. Technology Operations.
SURFACE PHONON DISPERSION OF MoS2
P. A. Bertrand 31 Jul. 1992 23 p
(Contract F04701-88-C-0089)
(AD-A255835; TR-0091(6945-03)-2; SMC-TR-92-41) Avail: CASI HC A03/MF A01

The dispersion of phonons on the (0001) surface of MoS2 was measured by high-resolution electron energy loss spectroscopy along both the groups of zone axes (010) and (110) azimuths (i.e., r to K and r to M, respectively). The surface phonons have lower energies than the corresponding bulk phonons, which indicates that the bonding interactions of the surface atoms are different from those of the bulk even in a layer lattice compound. Since sputtered MoS2 lubricant films are composed of many small crystallites, the relative number of surface atoms in a film is much higher than in a single crystal. The stronger bonding of the surface layer may affect the amount of inter- vs intracrystalline slip in the lubrication mechanism. This work also demonstrates the use and usefulness of a new technique (high-resolution electron energy loss spectroscopy) in this laboratory.

GRA

N93-13177*# Pennsylvania State Univ., University Park. Dept. of Engineering and Science.
A PENNSYLVANIA STATE UNIVERSITY/GENERAL ELECTRIC GET AWAY SPECIAL (GAS) EXPERIMENT
George Evanisko, Theodore Grosch, Milad Youssef, and Jim Yurack *In* NASA. Goddard Space Flight Center, The 1992 Shuttle Small Payloads Symposium Oct. 1992 p 185-193 Sponsored in part by GE (For primary document see N93-13158 03-12)
Avail: CASI HC A02/MF A03

77 THERMODYNAMICS AND STATISTICAL PHYSICS

Includes quantum mechanics; theoretical physics; and Bose and Fermi statistics.

For related information see also *25 Inorganic and Physical Chemistry* and *34 Fluid Mechanics and Heat Transfer.*

N93-12546# Wright Lab., Wright-Patterson AFB, OH.
A HEAT PIPE COUPLED PLANAR THERMIONIC CONVERTER: PERFORMANCE CHARACTERIZATION, NONDESTRUCTIVE TESTING, AND EVALUATION Final Report, 1 Aug. 1990 - 30 Nov. 1991
Timothy J. Young, Thomas R. Lamp, Bang-Hung Tsao, and Mysore L. Ramalingam 15 Mar. 1992 121 p
(AD-A254941; WL-TR-92-2033) Avail: CASI HC A06/MF A02

This report provides the technical details on the research activities conducted by Wright Laboratory and UES, Inc. personnel during the period of August 1990 to November 1991. The performance of two heat pipe coupled, planar thermionic energy converters was characterized using experimental and analytical methods. Nondestructive failure analysis was performed to evaluate the causes for the failure of a molybdenum-rhenium converter. The experimentation was carded out at the thermionic facilities at the USAF Wright Laboratory while the computer simulations were performed at Wright Laboratory and the University of Central Florida. A maximum current density of 10.1 amps/sq. cm and a peak power density of 7.7 watts/sq. cm were obtained from the rhenium-rhenium diode operating in the ignited mode.

GRA

N93-12796# Harvard Univ., Cambridge, MA.
MATHEMATICS AND STRING THEORY
1992 6 p
(Contract DE-FG02-88ER-25065)
(DE92-019292; DOE/ER-25065/3) Avail: CASI HC A02/MF A01

Over the past year our research activities concentrated around: (1) non-commutative differential geometry and its connections with quantum physics, and (2) 2-dimensional (super) conformal quantum field theories and related nonlinear sigma-models. This paper discusses these topics.

DOE

N93-12826# Stanford Linear Accelerator Center, CA.
SECOND QUANTIZATION IN BIT-STRING PHYSICS
H. P. Noyes Aug. 1992 6 p Presented at the Workshop on Harmonic Oscillators, Baltimore, MD, 25-28 Mar. 1992 Revised
(Contract DE-AC03-76SF-00515)
(DE92-019645; SU-SLAC-PUB-5733-Rev; CONF-9203181-1-Rev) Avail: CASI HC A02/MF A01

Using a new fundamental theory based on bit-strings, we derived a finite and discrete version of the solutions of the free one particle Dirac

equation as segmented trajectories with steps of length h/mc along the forward and backward light cones executed at velocity +/- c. Interpreting the statistical fluctuations which cause the bends in these segmented trajectories as emission and absorption of radiation, these solutions are analagous to a fermion propagator in a second quantized theory. This allows us to interpret the mass parameter in the step length as the physical mass of the free particle. The radiation in interaction with it has the usual harmonic oscillator structure of a second quantized theory. We sketch how these free particle masses can be generated gravitationally using the combinatorial hierarchy sequence (3,10,137,2(exp 127)+136), and some of the predictive consequences. DOE

N93-12857# Edgerton, Germeshausen and Grier, Inc., Idaho Falls, ID.
NATURAL CONVECTION BETWEEN A VERTICAL CYLINDER AND A SURROUNDING ARRAY
D. M. McEligot, J. E. OBrien, C. M. Stoots, T. K. Larson, W. A. Christenson, D. C. Mecham, and W. G. Lussie 1992 8 p Presented at the International Topical Meeting on Reactor Thermal Hydraulics: Towards the Next Generation of Nuclear Power Plants, Salt Lake City, UT, 20-24 Sep. 1992
(Contract DE-AC07-76ID-01570)
(DE92-019763; EGG-M-91505; CONF-920903-16) Avail: CASI HC A02/MF A01

The generic situation considered is natural convection between a single heated, vertical cylinder and a surrounding array of cooler vertical cylinders in a triangular pattern. The ratio of the test section temperature to the cooling tube temperature was varied up to 2.6 by adjusting the electrical power. The Rayleigh number, based on test section diameter and air properties evaluated at cooling tube temperature, ranged from 2.9(10)(exp 4) - 4.6(10)(exp 5). Results indicate that the convective heat transfer data could be approximated as Nu(sub D) (T(sub ts)/T(sub ct))(exp 0.14) = 0.156(Ra(sub D)(sup 1/3)) in the apparent turbulent region for Ra(sub L) greater than 1.2(10)(exp 11). DOE

N93-12967*# National Aeronautics and Space Administration. Lewis Research Center, Cleveland, OH.
COMPUTER PROGRAM FOR CALCULATING AND FITTING THERMODYNAMIC FUNCTIONS
Bonnie J. McBride and Sanford Gordon (Gordon, Sanford, Cleveland, OH) Nov. 1992 91 p Sponsored in cooperation with Sverdrup Technology, Inc., Brook Park, OH
(Contract NAS3-25266; RTOP 505-62-52)
(NASA-RP-1271; E-5894; NAS 1.61:1271) Avail: CASI HC A05/MF A01

A computer program is described which (1) calculates thermodynamic functions (heat capacity, enthalpy, entropy, and free energy) for several optional forms of the partition function, (2) fits these functions to empirical equations by means of a least-squares fit, and (3) calculates, as a function of temperture, heats of formation and equilibrium constants. The program provides several methods for calculating ideal gas properties. For monatomic gases, three methods are given which differ in the technique used for truncating the partition function. For diatomic and polyatomic molecules, five methods are given which differ in the corrections to the rigid-rotator harmonic-oscillator approximation. A method for estimating thermodynamic functions for some species is also given. Author

N93-13498 Texas Univ., Austin.
DUAL MASS AND TORSION Ph.D. Thesis
Steven Douglas Breed 1992 160 p
Avail: Univ. Microfilms Order No. DA9225533

Dual mass is considered as a gravitational analog of magnetic charge in electrodynamics. It is defined by its effect on the trajectories of spinless test particles. It is found that extended bodies of dual mass cannot exist in general relativity theory due to violation of the cyclic identity of the Riemann curvature tensor. Expanded theories of gravitation incorporating torsion as well as a metric are therefore examined. By studying the conservation law of energy-momentum, it is shown that, contrary to widespread opinion, torsion does influence the motion of spinless test particles. From the influence on test particles, a stress-energy tensor for dual matter is derived. The stress-energy is found to be primary a divergence of the torsion field, along with additional terms linear in the torsion. Three other approaches to dual matter in the presence of torsion are explored. Two of them are found to be the same, although different from that defined in this work. The third defines only a topological form of dual mass, not the extended variety. Dissert. Abstr.

N93-13751 Pennsylvania State Univ., University Park.
QUANTUM INFLATIONARY MINISUPERSPACE COSMOLOGICAL MODELS Ph.D. Thesis
Sangpyo Kim 1991 176 p
Avail: Univ. Microfilms Order No. DA9204231

The Wheeler-DeWitt equations for the Friedmann-Robertson-Walker cosmology conformally and minimally coupled to scalar fields with power-law potentials are expanded in the eigenstates of the scalar field parts. The gravitational parts become a diagonal matrix-valued differential equation for a conformal scalar field, and a coupled matrix-valued differential equation for a minimally coupled scalar field. The coupling matrix for the minimal scalar field is found to be a dimensionless quantity by the Symanzik scaling law, invalidating the Born-Oppenheimer approximation. There also occur returning points depending on the energy eigenvalues of the scalar field, contrary to the WKB approximation obtained by neglecting the kinetic energy term for the scalar field. The Cauchy initial value problem is defined with respect to the intrinsic timelike coordinate, and the wavefunctions incorporating initial data are constructed using the product integral formulation. The packetlike wavefunctions around classical turning points are shown possible in the product integral formulation, and the returning wavepackets near the returning point of the classical Friedmann-Robertson-Walker cosmology are constructed. The wavefunctions to the Wheeler-DeWitt equation minimally coupled to the scalar field are constructed by two different methods, the master equation and the enlarged matrix equation. The spectrum for the wavefunctions regular at the infinite size of universe is found, and these are interpreted as the Hawking-Page spectrum of wormholes connecting two asymptotically Euclidean regions. The quantum Friedmann-Robertson-Walker cosmology is extended to the minimal scalar field with the inflationary potential having a first order phase transition. The Wheeler-DeWitt equation is expanded in the eigenstates of the scalar field, and the gravitational part becomes a coupled matrix-valued differential equation. When the symmetry of the scalar field is broken at a certain stage of evolution of the universe, the relative energy difference of a local minimum to the global minimum (absolute zero) behaves as an effective cosmological constant responsible for inflation for the modes whose eigenvalues are almost determined by the local minimum. As the universe evolves further, the effective cosmological constant vanishes due to disappearance of the local minimum. This quantum inflationary cosmological model avoids not only ad hoc potentials having very weak-coupling but also the a priori cosmological constant. Dissert. Abstr.

N93-13753 Princeton Univ., NJ.
SOLITONS AND INSTANTONS IN STRING THEORY Ph.D. Thesis
Ramzi Raja Khuri 1991 79 p
Avail: Univ. Microfilms Order No. DA9202532

We constructed higher loop instanton solutions in string theory and studied the dynamics of analogous soliton solutions. In chapter two we extend to O(alpha') in bosonic string theory the tree-level exterior heterotic instanton solution and present several related non-supersymmetric solutions. For the spherically symmetric solution, the corresponding Weyl invariant sigma model is the product of a Wess-Zumino-Witten model and a Feigin-Fuks Coulomb gas. An exact single instanton solution is obtained by fixing the metric and antisymmetric tensor field in lowest order form and rescaling the dilation order by order in alpha'. An exact multi-instanton solution for the heterotic string can be obtained by combining generic properties of the heterotic string with a simple extension of the methods used to construct the bosonic solution. In chapter three, a test string approach is adopted to study the dynamics of soliton solutions to string theory. Like BPS magnetic monopoles, these solutions exert zero static force on each other and can be superposed to form multi-soliton solutions. We show that in contradistinction to the BPS case, the velocity-dependent forces between these strings also vanish in the test-string approximation. A similar result is found for fivebrane solutions of the supergravity equations. The trivial scattering result is consistent with a Veneziano amplitude calculation for macroscopic fundamental strings in the limit of large winding radius. These results provide dynamical evidence for the identification of the string solitons with the fundamental string and support the conjecture of duality between strings and fivebranes. In chapter four we calculate the

Manton metric on moduli space for the scattering of a class of heterotic string solitons with the structure of fivebranes. The geodesics of this metric represent the trajectories of multi-soliton solutions in the static solution manifold, and give a low-velocity approximation to the dynamics of the solitons. From the metric, we determine the scattering angle of the two-soliton interaction to leading order in the impact parameter. Dissert. Abstr.

N93-13832 Texas Univ., Austin.
THE NONEQUILIBRIUM STATISTICAL MECHANICS OF CHAOTIC MAPS Ph.D. Thesis
William Cooper Saphir 1992 128 p
Avail: Univ. Microfilms Order No. DA9225719

We discuss the nonequilibrium statistical mechanics of highly chaotic dynamical systems. Such systems can exhibit transport and display an approach to equilibrium--behavior which is usually associated with large or many-body systems. We show that this thermodynamic behavior can be seen as a spectral property of the associated Perron-Frobenius operator. We present a method, based on the subdynamics approach of the Brussels group, for constructing a spectral decomposition for the Perron-Frobenius operator in terms of exponentially decaying generalized eigenstates. This representation, which we call the 'physical spectral representation' introduces thermodynamic properties and time symmetry breaking into the description of the system at a fundamental level. We use our method to analyze the Bernoulli and baker maps, constructing the physical spectral representation explicitly. We show that the representation is valid on a space of smooth test functions which does not include Dirac distributions. Trajectories are therefore excluded from consideration. We discuss the relation between the physical spectral representation and the usual representation in Hilbert space. Finally, we use our method to discuss diffusion in the standard map in the large K limit, deriving the detailed dependence of the diffusion constant on the kick parameter. Dissert. Abstr.

N93-13896 Connecticut Univ., Storrs.
NON-PERTURBATIVE STUDIES IN QUANTUM ELECTRODYNAMICS Ph.D. Thesis
Saeid Vafaeisefat 1991 196 p
Avail: Univ. Microfilms Order No. DA9221555

Investigations of a possible new, non-perturbative phase of Quantum Electrodynamics (QED) are presented. This new phase may have been seen in the heavy-ion collision experiments at GSI (Germany): The narrow peaks in the e(+)e(-) coincidence data are well explained as composite states of e(+)e(-) in this new phase of QED. Some new direct evidence is presented, based on computer simulations (modified spectral density method) of the proper-time path integral and monitoring the chiral order parameter, (bar-psi(x)psi(x)), that background electromagnetic field configurations similar to those in the experiments (E x B = 0, Gaussian shaped fields in space-time and colliding particles carrying positive charge) can induce the phase transition via spontaneous mass generation. The result of the calculations seems to indicate that the attributes of the external (background) electromagnetic fields that cause the phase transition are their duration, asymptotic behavior, and locality in space. Furthermore, a static Coulomb field makes the phase transition harder to achieve. The calculation of the first four orders in the inverse coupling g, (1/g(exp 8)), of time-independent (Rayleigh-Schroedinger) strong-coupling perturbation theory in (3 + 1) dimensions (using Kogut-Susskind fermions) for the e(+)e(-) bound state is presented. A new numerical algorithm is presented to calculate fourth and higher order coefficients in the perturbation expansion. Poles in the Pade approximants are monitored to find the critical coupling g(sub c), using programs employing algebra manipulations (MACSYMA). The calculated spectrum is in a good agreement with the observed peaks and predicts some additional states. Dissert. Abstr.

N93-13957 California Univ., Los Angeles.
CONNECTION OF MICROSCOPIC WITH MACROSCOPIC DYNAMICS: TOWARDS A HYDRODYNAMICAL DESCRIPTION OF QUANTUM MECHANICS Ph.D. Thesis
Antonio Boulhosa Nassar 1992 166 p
Avail: Univ. Microfilms Order No. DA9213657

An approach to the problem of tunneling through sharp-edged potential barriers with and without dissipation was developed. Boundary conditions can be matched without assuming continuity of the wave function. The effect of a small friction mechanism on the tunneling of a particle through a single, sharp-edged rectangular barrier diminishes the transmission coefficient. This work provides a quantum kinetics approach to the problem of irreversibility and its connection with macroscopic equations of quantum hydrodynamics. We also study the effect of the quantum potential and friction mechanism on nonadiabatic transport corrections to the geometric phase acquired by a wave packet undergoing an excursion in its parameter space. The macroscopic hydrodynamical equations are also applied to the study of parametric oscillations of charged particle driven by an external monochromatic wave having large phase velocity. A new approach to the problem of scattering through arbitrarily-shaped potential wells is presented via the exact invariants of quantum hydrodynamics, where the solution preserves information about the quantum potential which accounts for quantum-wave features such as interference and diffraction effects. Within this formalism, a formula for the transmission coefficient of a steady flux of fluid-particles scattered by an arbitrarily-shaped potential well is derived and discussed for some exact and approximate solutions. This approach is extended to the problem of scattering in multilayer sharp-edged systems. Further, the so-called Ermakov problem in the theory of invariants is derived and solved within the framework of Nelson's stochastic mechanics: a natural and straightforward particle interpretation of quantum hydrodynamics by allowing a random character to the underlying trajectories, that is, a stochastic interpretation of quantum mechanics in terms of subquantum random fluctuations resulting from the action of a stochastic invariant thermostat. Within the formalism, we investigate special types of solutions of the hydrodynamical version of a generalized Schroedinger-Langevin equation (GNLSLE) via quantum hydrodynamics. Within the same scheme of hydrodynamical differential equations, we decompose the physical process, associated with the GNLSLE, into two independent processes: a classical Langevin-type process and a pure quantum Nelson-type process. Dissert. Abstr.

80 SOCIAL SCIENCES (GENERAL)

Includes educational matters.

N93-12694# National Science Foundation, Washington, DC. Div. of Science Resources Studies.
SCIENCE AND ENGINEERING DEGREES, BY RACE/ETHNICITY OF RECIPIENTS: 1977-1990
Susan T. Hill and Millicent V. Gough, ed. 1992 111 p *Its* Surveys of Science Resources Series
(Grant NSF SRS-91-00714)
(NSF-92-327) Avail: CASI HC A06/MF A02

This publication is based on data obtained by the National Center for Educational Statistics (NCES), U.S. Department of Education. Five racial/ethnic categories are used in Federal Government surveys of institutions. These categories are Black (non-Hispanic), American Indian or Alaskan Native, Asian or Pacific Islander, Hispanic, and White (non-Hispanic). Forty six bar charts summarize data given in detail in the remainder of the report showing results of the survey regarding science and engineering degrees by race/ethnicity of recipients between 1977-1990. R.L.B.

N93-12802# National Science Foundation, Washington, DC. Div. of Science Resources Studies.
ACADEMIC SCIENCE AND ENGINEERING: GRADUATE ENROLLMENT AND SUPPORT, FALL 1990
J. G. Huckenpoehler Aug. 1992 337 p Sponsored in part by NIH
Its Survey of Science Resources Series
(Grant NSF SRS-91-00714)
(NSF-92-323) Avail: CASI HC A15/MF A03

Total graduate enrollment in the science, engineering and health fields reached nearly 459,000 in the fall of 1990, the largest single-year increase in recent years -- more than 4 percent over the fall 1989 total. The increase was sharpest in the health fields, more than 6 percent, compared to a 4 percent growth in both science fields and engineering fields. Psychology students increased the most rapidly of those in any science field, 6 percent. Growth was slowest in the agricultural sciences, just over 1 percent. The social sciences continued to be the most popular field, with 78,600 graduate students or more than one-sixth of the total. Nearly one-third of engineering graduate students, 34,900, were enrolled in electrical engineering. The number of graduate students enrolled part time increased

at a more rapid rate than did the number enrolled full time, 6 percent compared to just over 3 percent. Part-time students made up about one-third of all science and engineering graduate students. Enrollment in doctorate-granting institutions at 398,400 represented 87 percent of all graduate students. This proportion has varied only slightly since the survey series began in 1975. R.L.B.

N93-12907# National Science Foundation, Washington, DC.
WOMEN AND MINORITIES IN SCIENCE AND ENGINEERING: AN UPDATE
Patricia E. White Jan. 1992 194 p
(NSF-92-303) Avail: CASI HC A09/MF A03

The Science and Technology Equal Opportunities Act, passed in December 1980, calls for the National Science Foundation (NSF) to promote the full use of human resources in science and technology through a comprehensive and continuing program to increase substantially the contribution and advancement of woman and minorities in scientific, professional, and technical careers, and for other purposes. Under this act, NSF is required to report to Congress on the status of women and minorities in science and engineering (S&E) professions on a biennial basis. This report is the sixth in the series, and, like its predecessors, it provides a comprehensive overview of the participation of women, minorities (including Hispanics), and persons with physical disabilities in S&E employment and training. The report has been designated as a reference document that allows readers to easily locate information on particular subgroups or specific aspects of participation and utilization. The Status Update provides a concise overview; summary findings are presented in the introductory overviews of each chapter. Author

N93-13015# National Science Foundation, Washington, DC. Div. of Science Resources Studies.
BLACKS IN UNDERGRADUATE SCIENCE AND ENGINEERING EDUCATION Special Report
Susan T. Hill Apr. 1992 108 p
(NSF-92-305) Avail: CASI HC A06/MF A02

Data is presented for Black undergraduate science and engineering enrollment from 1977 through 1989. Chapters include Introduction, High School to College Transition, the Undergraduate Process, Degree Awards, and Undergraduate Origins of S&E Doctorates. Appendices include sources of data and S&E degrees awarded to Blacks by institution. In the area of undergraduate education, the goal of the National Science Foundation is to increase the number of minorities earning bachelor's degrees in science and engineering fields by the year 2000. A special report on Minorities in Science states that 'to meet these goals, the alliances are going to have to dramatically plug some important leaks in the pipeline that produces science and engineering professionals.' This report provides useful information to those joined in this effort. R.L.B.

N93-13248*# National Aeronautics and Space Administration, Washington, DC.
NASA INDUSTRY EDUCATION INITIATIVE. EDUCATION PROGRAMS REPORT, 1991
1991 32 p
(NASA-NP-158; NAS 1.83:158) Avail: CASI HC A03/MF A01

Findings from the initial inventory of education programs show that support for the NASA-Industry Education Initiative (NIEI) appears to be strong among the organizations surveyed. In addition, the range, depth and historical baselines of NIEI education programs are encouraging. It is also apparent that there is a significant level of cooperation between NIEI members and other organizations. Heavily focused towards science, engineering, mathematics and technology achievement, NIEI activities appear to be aligned with national education goals. Three criticisms are revealed: (1) the majority of programs are targeted fairly late in the education cycle; (2) the number of initiatives geared towards adult literacy and adult skills-enhancement appears to be relatively low; (3) the majority of NIEI activities involve traditional education-assistance programs, but the number of critical assessment and systematic reform initiatives is low. Four Working Group recommendations resulted from this activity: (1) NIEI Working Group operations should continue for an indefinite period, with participation open to other like-minded private-sector organization; (2) the report should be periodically updated; (3) an analysis of ongoing education programs should be conducted; (4) American corporations should continue to support education and evaluate in-house programs periodically. R.L.B.

N93-13278# National Science Foundation, Washington, DC. Directorate for Education and Human Resources.
GATEWAY TO DIVERSITY IN THE SCIENTIFIC AND TECHNOLOGICAL WORKFORCE
Sep. 1992 89 p
(NSF-92-99) Avail: CASI HC A05/MF A01

The National Science Foundation's (NSF) Division of Human Resource Development (HRD), within the Directorate for Education and Human Resources, has primary responsibility for broadening participation of minority groups underrepresented in science, engineering, and mathematics (SEM). The NSF minority programs reflect the Foundation's growing commitment to develop the resources of the scientific and technological community as a whole and to ensure an adequately trained research and development workforce in the next decade. The Education and Human Resources Directorate has five major long-range goals: to help ensure that a high-quality school education in science is available to every child in the United States and is of sufficient quality to enable those who are interested and talented to pursue technical careers at all levels; to help ensure that the educational pipelines carrying students to careers in science, mathematics, and engineering yield enough well-educated individuals to meet the needs of the U.S. technical workforce; to help ensure that those who select science and engineering careers have available the best possible professional education in their discipline; to help ensure that opportunities are available at the college level for interested nonspecialists to broaden their scientific backgrounds; and to support informal science education programs and to maintain public interest in, and awareness of, scientific and technological developments. The Division of Human Resource Development is one of the six divisions of the Education and Human Resources Directorate. HRD activities reflect NSF's commitment to developing the resources of the scientific and technical community as a whole. Objectives of the programs profiled in this publication are as follows: to increase opportunities for participation in the nation's scientific and technical enterprise for investigators who are monorities; young persons who are minorities; and faculty from predominantly undergraduate colleges and universities; to strengthen the capabilities of institutions that have significant minority enrollments; and to foster comprehensive approaches and build effective coalitions that address the development of scientific and engineering talent, drawing from underrepresented minority groups on a nationwide basis. NSF's goals are to increase the number of minorities underrepresented in NSF-supported fields receiving B.S. degrees to more than 50,000 annually by the year 2000 and to increase the minority Ph.D. attainment to more than 2,000 annually by the same year. Minorities that are underrepresented in science and engineering are: Black's, Hispanics, American Indians, Native Alaskans, and Native Pacific Islanders (Micronesian and Polynesian). Minority programs at individual universities throughout the country are also described.
Author

N93-13437# National Science Foundation, Washington, DC. Div. of Science Resource Studies.
SCIENTISTS, ENGINEERS, AND TECHNICIANS IN MANUFACTURING INDUSTRIES: 1989. DETAILED STATISTICAL TABLES
Millicent V. Gough, ed. 1992 84 p
(NSF-92-312) Avail: CASI HC A05/MF A01

In this report, estimates are presented on the total numbers of scientists, engineers, and technicians (SET's) who were employed in manufacturing industries in 1989. The estimates were developed from the Labor Department's Occupational Employment Statistics (OES) Survey, a Federal/State program that produces national and State estimates of employment by industry for nonfarm wage and salary workers. The Bureau of Labor Statistics (BLS) has the primary responsibility for developing OES survey procedures and providing technical guidance and assistance with survey problems. State Employment Security Agencies implement the survey at State levels and prepare current and projected employment statistics for these labor markets. Some States also prepare sub-State estimates. The National Science Foundation (NSF) has enhanced the BLS effort since 1977 by financing the collection of full details on the types of scientific and technical jobs filled by industry. Analysis of this information provides insight into the dynamics of the labor market. Author

N93-13454# National Science Foundation, Washington, DC. Div. of Science Resources Studies.
CHARACTERISTICS OF RECENT SCIENCE AND ENGINEERING GRADUATES: 1990. DETAILED STATISTICAL TABLES
Millicent V. Gough, ed. 1992 153 p
(NSF-92-316) Avail: CASI HC A08/MF A02

In these tables, data are presented on the characteristics of men and women who received a bachelor's or master's degree in a science or engineering field from U.S. institutions during the 1987/88 (1988) and 1988/89 (1989) academic years. The data were collected in 1990 and reflect the characteristics of individuals as of the spring of that year. In addition to disclosing the demographic attributes of recent science and engineering (S&E) graduates, the data reveal early career employment experiences, such as the extent to which recent graduates entered the labor force, whether they were able to find employment, and the attributes of that employment. Results of this survey are presented separately for bachelor's and master's degree recipients, and most results are presented separately also for the two graduating years. To overcome some of the limitations of small cell size information the data on certain salary and selected employment characteristics are combined for the graduating classes at each degree level. This report comprises three sections: the technical notes on survey methodology, coverage, concepts, definitions, and sampling errors; detailed tabulations from the survey; and the questionnaire used in the survey. Author

N93-13698# National Science Foundation, Washington, DC. Div. of Science Resources Studies.
SELECTED DATA ON SCIENCE AND ENGINEERING DOCTORATE AWARDS: 1991
Susan T. Hill Apr. 1992 62 p
(NSF-92-309) Avail: CASI HC A04/MF A01

The data presented in this report were derived from the Survey of Earned Doctorates (SED). They show trends in doctorate production by science and engineering (S&E) field and recipient characteristics, institutions awarding doctorates, and postgraduation plans of recipients. The SED is conducted annually for the National Science Foundation (NSF) and other Federal agencies by the National Research Council. Information from this survey becomes part of the Doctorate Records File, which is a census of doctorates awarded since 1920 by regionally-accredited universities and colleges. Data for the SED are collected directly from the individual doctorate recipients. Approximately 94 percent of the annual cohort of doctorate recipients responded to the questionnaire, which is distributed to them through the cooperation of the Graduate Deans. These tables present detailed data on S&E doctorates recipients, with some totals provided for non-S&E fields. Author

N93-13699# National Science Foundation, Washington, DC. Div. of Undergraduate Science Engineering and Mathematics Education.
AWARDS: 1991 UNDERGRADUATE COURSE AND CURRICULUM DEVELOPMENT PROGRAM
1992 61 p
(NSF-92-45) Avail: CASI HC A04/MF A01

Undergraduate education in the sciences and mathematics is fundamental in the preparation of our Nation's future scientists, engineers, mathematicians, and teachers, and provides literacy essential for all citizens. In recognition of this critical role, the National Science Foundation (NSF) through the Division of Undergraduate Science, Engineering, and Mathematics Education (USEME) in the Directorate of Education and Human Resources (EHR), supports the development of improved and innovative undergraduate courses and curricula in the sciences, engineering, and mathematics. The goals of the undergraduate Course and Curriculum Development (UCC) program are to encourage course and curriculum development to meet the Nation's need for high quality scientists, engineers, mathematicians, dedicated and able teachers of pre-college and college science and mathematics, and scientifically and technically literate citizens; and to inspire faculty to devote creative energy to educational activities that address the needs of their students and the Nation, and that enhance the faculty's professional and scholarly interests. The introductory-level courses, curricula, and laboratory projects which recieved awards in FY 1991 are described. L.R.R.

N93-13701# National Science Foundation, Washington, DC. Div. of Science Resources Studies.
SCIENCE AND ENGINEERING DEGREES: 1966-1990
1992 69 p *Its* Surveys of Science Resources Series
(Grant NSF SRS-91-00714)
(NSF-92-326) Avail: CASI HC A04/MF A01

An analysis of science and engineering degrees awarded from 1966 to 1990 is presented. Statistical charts and tables which show the number of bachelor's, master's, and doctorate degrees awarded by field and by sex of the recipient for the years studied are included. The analysis is based upon final data from several federal surveys. Current classification schemes for fields of study are listed along with changes in the classification system during the time period studied. L.R.R.

N93-13702# National Science Foundation, Washington, DC. Div. of Undergraduate Science, Engineering, and Mathematics Education.
FISCAL YEAR 1991 HIGHLIGHTS
1992 44 p
(NSF-92-23; OMB-3145-0058) Avail: CASI HC A03/MF A01

The National Science Foundation's (NSF) undergraduate program is an agency-wide effort involving all program directorates. The division of Undergraduate Science, Engineering, and Mathematics Education (USEME within the Directorate for Education and Human Resources (EHR) serves as the focal point for NSF undergraduate activities. Presented are summaries of the FY-91 accomplishments of the programs. The following topics are discussed: the Instrumentation and Laboratory Improvement Program; the Undergraduate Course and Curriculum Development Program; the Undergraduate Curriculum Development in Mathematics: Calculus (CALC); the Undergraduate Faculty Enhancement Program; and the staff and program structure. Author

N93-13834# Mitre Corp., Bedford, MA.
APPLICATION OF INFORMATION SYSTEM TECHNOLOGY TO K-12 EDUCATION
Barry M. Horowitz, Nelson E. Bolen, and Peter J. Negroni Aug. 1992 24 p
(AD-A255223; M92-B0000088) Avail: CASI HC A03/MF A01

Information system technology has revolutionized how modern business and government organizations operate. That same technology holds great promise for helping to improve K-12 education, but for a variety of reasons the public schools lag other sectors in taking advantage of the technology that is already available. If technology is to make a difference in public education, it must be integrated into the overall curriculum in the schools, and it must be implemented in ways that are both affordable and sustainable. This paper argues that key steps in this process are establishing a set of flexible standards for educational technology, promoting the sharing and reuse of educational technology materials, and creating a peer review process for the selection of educational technology products. The paper concludes by describing how these ideas are being pursued in partnership with MITRE and the Springfield, Massachusetts school system. GRA

81 ADMINISTRATION AND MANAGEMENT

Includes management planning and research.

N93-12637# National Science Foundation, Washington, DC. Div. of Polar Programs.
US ANTARCTIC PROGRAM. PERSONNEL MANUAL, 1992
1992 73 p
(NSF-92-63) Avail: CASI HC A04/MF A01

This manual was written primarily for National Science Foundation (NSF) grantees and their assistants, and also as an aid for employees of the Antarctic Program support contractor and for military personnel. In addition to helping employees in their personal and professional objectives, the manual describes legal responsibilities resulting from participation in the Antarctic Program. These responsibilities include actions required of employees to (1) ensure U.S. compliance with the Antarctic Treaty's provisions for protecting the environment, and (2) aid in complying with U.S. public law and program procedures. Major concerns addressed are safety, health, and the environment. Also discussed are pre-travel

preparations, transportation to the Antarctic, communications and mail, working at U.S. Antarctic facilities, and sources of further information.
J.P.S.

N93-13109# General Accounting Office, Washington, DC. National Security and International Affairs Div.
LARGE PROGRAMS MAY CONSUME INCREASING SHARE OF LIMITED FUTURE BUDGETS. REPORT TO CONGRESSIONAL REQUESTERS
Sep. 1992 18 p
(GAO/NSIAD-92-278; B-247693) Avail: CASI HC A03/MF A01; GAO, PO Box 6015, Gaithersburg, MD 20877 HC

NASA's largest programs may require an increasing share of its limited future budgets. If NASA receives funding averaging about $15 billion annually for the next 5 years (a total of about $75 billion), as reflected in the executive branch's fiscal year 1993 budget submission, its largest programs may consume increasing shares of the agency's annual appropriations. Additional unplanned cost growth typical of NASA research and development programs may push funding requirements for these programs even higher. Under this scenario, NASA would have to reduce funds originally intended for other programs. NASA is in the process of reviewing the costs of all its major programs and plans to make appropriate adjustments to ensure a balanced overall space and aeronautics program within budget realities. The results of this effort, however, may not be known until NASA submits its fiscal year 1994 budget proposal. NASA's strategic plan (called Vision 21), prepared last year before the appointment of the current Administrator, did not address the mismatch between the agency's 5-year program plan and potential budgetary resources. The new Administrator said that he is going to give top priority to the creation of a new strategic plan. NASA wrote Vision 21 because the Senate Committee on Appropriations had directed that the agency complete an agencywide strategic plan by the time the President submitted his fiscal year 1993 budget. The Committee set forth eight criteria on which it expected NASA to base its plan. These criteria focus on setting priorities, coming to grips more honestly with accurate cost estimates, and anticipating more modest future budget growth. However, NASA did not fully respond to these issues. Information provided to Congress on NASA's future program cost estimates could be improved. Although program plans cover 5 years, NASA's biannual Project Status Reports, the agency's principal mechanism for reporting program costs to Congress, provide funding estimates for only 1 year beyond the current budget request. This time frame is too short to provide Congress with the broad view necessary to anticipate program funding needs and make forward-looking decisions. Author

N93-13111# General Accounting Office, Washington, DC. National Security and International Affairs Div.
SPACE STATION: RESOLVING CONFLICT OVER INTEGRATION CONTRACTOR'S ROLE. BRIEFING REPORT TO THE CHAIRMAN, SUBCOMMITTEE ON INVESTIGATIONS AND OVERSIGHT, COMMITTEE ON SCIENCE, SPACE, AND TECHNOLOGY, HOUSE OF REPRESENTATIVES
10 Sep. 1992 16 p
(GAO/NSIAD-92-291BR; B-249568) Avail: CASI HC A03/MF A01; GAO, PO Box 6015, Gaithersburg, MD 20877 HC

NASA and Grumman's working relationship has been turbulent over much of the contract period primarily because of (1) NASA's belief that Grumman did not quickly change its role from a program support contractor to an engineering and integration contractor when asked to do so and (2) Grumman's belief that NASA's failure to resolve issues stemming from the changes in its organization following the Challenger accident had adversely affected Grumman's ability to quickly step up to the program integration role. NASA's concern with Grumman's program management became so acute by early 1990 that the Fee Determination Official significantly reduced Grumman's award fee. Since that time, NASA and Grumman have made progress in redefining Grumman's role as the engineering and integration contractor. Both parties currently believe they have a mutual understanding of their roles and that there are no barriers to the contractor fully performing in that capacity. Author

N93-13693# Committee on Science, Space and Technology (U.S. House).
WINDOW ON WASTE: ATROPHY IN NASA MANAGEMENT
Washington GPO 1992 155 p Hearing before the Committee on Science, Space, and Technology, 102nd Congress, 2nd Session, No. 142, 7 May 1992
(GPO-57-273; ISBN-0-16-039083-4) Avail: CASI HC A08/MF A02; Subcommittee on Investigations and Oversight, House of Representatives, Washington, DC 20515 HC; SOD HC

This House Congressional Hearing on waste at NASA focuses on problems in the contracting area as well as other affected areas. Particular problems noted were cost overruns and time delays. The hearing points to a new NASA administration as being able to deal with these problems in the future. R.L.B.

N93-13703# National Science Foundation, Washington, DC. Div. of Industrial Innovation Interface.
ABSTRACTS OF PHASE 1 AWARDS: NSF SMALL BUSINESS INNOVATION RESEARCH PROGRAM (SBIR): 1992
Jun. 1992 87 p
(NSF-92-80; OMB-3145-0058) Avail: CASI HC A05/MF A01

This brochure contains abstracts of Phase 1 awards made under the National Science Foundations's Small Business Innovation Research (SBIR) Program in 1992 as a result of the 1991 solicitation for proposals. SBIR supports creative advanced research in important scientific and engineering areas and is designed to encourage the conversion of that R&D into technological innovation and commercial applications for its potential economic benefits to the nation. Author

N93-13185*# Brigham Young Univ., Provo, UT. Dept. of Physics and Astronomy.
THE UNIQUE CHALLENGE OF MANAGING AN UNDERGRADUATE GET-AWAY-SPECIAL EXPERIMENT
Peter W. A. Roming, Mark K. Spute, and Memorie K. Williams *In* NASA. Goddard Space Flight Center, The 1992 Shuttle Small Payloads Symposium Oct. 1992 p 277-284 (For primary document see N93-13158 03-12)
(Grant NAGw-2612)
Avail: CASI HC A02/MF A03

N93-13186*# National Aeronautics and Space Administration. Goddard Space Flight Center, Greenbelt, MD.
PREPARING SAFETY DATA PACKAGES FOR EXPERIMENTERS USING THE GET AWAY SPECIAL (GAS) CARRIER SYSTEM
Jerome Kosko *In its* The 1992 Shuttle Small Payloads Symposium Oct. 1992 p 285-292 (For primary document see N93-13158 03-12)
Avail: CASI HC A02/MF A03

N93-14017*# National Aeronautics and Space Administration. Lyndon B. Johnson Space Center, Houston, TX.
CREATING A FOUNDATION FOR A SYNERGISTIC APPROACH TO PROGRAM MANAGEMENT
Karyn T. Knoll *In its* The Second Conference on Lunar Bases and Space Activities of the 21st Century, Volume 2 Sep. 1992 p 683-689 (For primary document see N93-13972 03-91)
Avail: CASI HC A02/MF A03

82 DOCUMENTATION AND INFORMATION SCIENCE

Includes information management; information storage and retrieval technology; technical writing; graphic arts; and micrography.

For computer documentation see *61 Computer Programming and Software.*

N93-12553# Louisiana State Univ., Baton Rouge. Dept. of Computer Science.
A GENERAL THEORY OF SIGNAL INTEGRATION FOR FAULT-TOLERANT DYNAMIC DISTRIBUTED SENSOR NETWORKS Annual Report No. 2, 1 Oct. 1991 - 30 Sep. 1992
S. S. Iyengar and B. J. Jones 1 Oct. 1992 7 p
(Contract N00014-91-J-1306)
(AD-A254961) Avail: CASI HC A02/MF A01

The computational issues related to information integration in multisensor

systems and distributed sensor networks has become an active area of research. In recent years, a number of significant advances in the field of sensor integration have been made. This interest in the development of Distributed Sensor Networks (DSNs) for information gathering has partly emerged because of (1) the availability of new technology which makes the DSN's economically feasible to implement, and (2) the increasing complexity of today's information gathering tasks to which they are applied. From a computational viewpoint, the efficient extraction of information from noisy and faulty signals emanating from many sensors requires the solution of problems related to (1) the architecture and fault-tolerance of the distributed sensor network, (2) the proper synchronization of sensor signals, (3) the integration of information to keep the communication and the processing requirements small, and (4) the design of efficient computational techniques to abstractly represent and integrate sensor information. The following issues were studied and worked upon this year: computational frameworks for distributed sensing and fault-tolerant sensor integration; design of fault-tolerant architectures for distributed sensor integration; computational complexities of the problem of distributed detection; wavelet based distributed sensing and fault-tolerant sensor integration; and issues related to recording of events and synchronization in distributed sensor networks. GRA

N93-12567# Los Alamos National Lab., NM.
REAL-TIME DATA ARCHIVING FOR GTA
R. A. Cole and W. H. Atkins 1992 4 p Presented at the 16th International LINAC Conference, Ottawa, Ontario, 23-28 Aug. 1992
(Contract W-7405-eng-36)
(DE92-018613; LA-UR-92-2420; CONF-9208109-2) Avail: CASI HC A01/MF A01

The architecture of the GTA control system, the nature of a typical GTA commissioning activity, and the varied interests of those analyzing the data make it challenging to develop a general-purpose scheme for archiving data and making the data available to those who will use it. Addressing the needs of those who develop and trouble-shoot hardware and software increases the challenge. This paper describes the aspects of GTA that affect archiving operations and discusses how the features of the EPICS archiving module meet a variety of needs for storing and accessing data. DOE

N93-12597# Air Univ., Maxwell AFB, AL. Airpower Research Inst.
PRINCIPLES OF INFORMATION RESOURCE MANAGEMENT: A FOUNDATION FOR THE FUTURE
Paul D. Condit Jun. 1992 116 p
(AD-A254447; AU-ARI-91-1) Avail: CASI HC A06/MF A02

The Department of Defense (DOD) is dependent on many automated information systems which have been implemented over several decades. These systems represent widely diverse technology in the form of fragmented, inflexible, and often inconsistent information resources such as software, hardware, and data. Although technology has advanced rapidly, efficient and effective management of DOD's total information resources has not yet been realized. The DOD information resource management (IRM) program, initiated in the early 1980's, attempted to bring order to this chaotic environment. Less than a decade later the corporate information management (CIM) program has been established for the very same reason. The CIM program is focused on actions to improve the quality of DOD information systems, actions deemed essential to cope with budget and force reduction, and actions in harmony with DOD's total quality management (TQM) initiative and its fundamental principle of continuous process improvement. Information systems, whether manual or automated, are mechanisms to integrate the processes of enterprises (an industry or government agency), whose efficiency and effectiveness are determined to a large extent by the level of integration achieved. To understand TQM and IRM is to understand that an enterprise is a complex system that requires design through the application of sound engineering practice. This paper presents a cohesive set of principles and motivating concepts for IRM with the principles of TQM as the nucleus. Together, TQM and IRM provide the general principles for engineering enterprises with information systems treated as an integral part of the enterprise and information used as the primary integrating agent. GRA

N93-12634*# National Aeronautics and Space Administration, Washington, DC.
COORDINATING COUNCIL. SECOND MEETING: INTERNATIONAL ACQUISITIONS
1990 97 p Meeting held in Washington, DC, 23 Jul. 1990
(NASA-TM-108015; NAS 1.15:108015) Avail: CASI HC A05/MF A02

The theme of this NASA Scientific and Technical Information Program Coordinating Council was International Acquisitions. Included are both visuals for presentations and reports on discussions related to the topics. Presentations were made on the following topics: Coordination council organization international plan, STI global network, International aerospace climate, Foreign exchange program, Foreign activities RMS & AIAA, NASA translation program, A.F. machine translation system, and CIRC cooperation. R.L.B.

N93-12635*# National Aeronautics and Space Administration, Washington, DC.
COORDINATING COUNCIL. FIFTH MEETING: QUALITY
1991 77 p Meeting held in Arlington, VA, 1 Jul. 1991
(NASA-TM-108018; NAS 1.15:108018) Avail: CASI HC A05/MF A01

This NASA Scientific and Technical Information Program Coordinating Council meeting had a theme of Quality. Four presentations were made with the following titles: How much quality can you pay for?, What the Center for AeroSpace Information has done to improve quality, Quality from the user standpoint, and Database quality: user views test producer perception. Visuals as well as discussion summaries are also included. R.L.B.

N93-12636*# National Aeronautics and Space Administration, Washington, DC.
COORDINATING COUNCIL. SEVENTH MEETING: ACQUISITIONS
1992 57 p Meeting held in Arlington, VA, 23 Jan. 1992
(NASA-TM-108020; NAS 1.15:108020) Avail: CASI HC A04/MF A01

The theme for this NASA Scientific and Technical Information Program Coordinating Council meeting was Acquisitions. In addition to NASA and the NASA Center for AeroSpace Information (CASI) presentations, the report contains fairly lengthy visuals about acquisitions at the Defense Technical Information Center. CASI's acquisitions program and CASI's proactive acquisitions activity were described. There was a presentation on the document evaluation process at CASI. A talk about open literature scope and coverage at the American Institute of Aeronautics and Astronautics was also given. An overview of the STI Program's Acquisitions Experts Committee was given next. Finally acquisitions initiatives of the NASA STI program were presented. R.L.B.

N93-12660*# Consortium for International Earth Science Information Network, Ann Arbor, MI.
EARTH SCIENCE INFORMATION: PLANNING FOR THE INTEGRATION AND USE OF GLOBAL CHANGE INFORMATION Semiannual Status Report, 1 Jan. - 30 Jun. 1992
Jack R. Lousma Oct. 1992 10 p
(Grant NAGw-2901)
(NASA-CR-191217; NAS 1.26:191217) Avail: CASI HC A02/MF A01

Activities and accomplishments of the first six months of the Consortium for International Earth Science Information Network (CIESIN's) 1992 technical program have focused on four main missions: (1) the development and implementation of plans for initiation of the Socioeconomic Data and Applications Center (SEDAC) as part of the EOSDIS Program; (2) the pursuit and development of a broad-based global change information cooperative by providing systems analysis and integration between natural science and social science data bases held by numerous federal agencies and other sources; (3) the fostering of scientific research into the human dimensions of global change and providing integration between natural science and social science data and information; and (4) the serving of CIESIN as a gateway for global change data and information distribution through development of the Global Change Research Information Office and other comprehensive knowledge sharing systems. Author

N93-12670*# National Aeronautics and Space Administration, Washington, DC.
COORDINATING COUNCIL. THIRD MEETING: STI STRATEGIC PLANS

1990 43 p Meeting held 29 Nov. 1990
(NASA-TM-108016; NAS 1.15:108016) Avail: CASI HC A03/MF A01

The NASA Scientific and Technical Information Program Coordinating Council conducts meetings after which both modified transcripts of presentations and interactive discussions are published. The theme for the November 1990 meeting was 'STI Strategic Plans'. This theme was the focus of recorded discussions by members of the council. The last section of the report presents visuals on strategic goals for the STI Information Division. NASA's vision is to be at the forefront of advancements in aeronautics, space science, and exploration. More specific NASA goals are listed followed by the STI Division mission statement. The Strategic Goals for the STI Division are outlined as follows: Implement effective management strategies, Accomplish rapid deployment of the NASA STI Network, Seek out and develop cooperative partnerships, Establish the STI Program as an integral part of the NASA R&D effort, Enhance the quality of our products and services through a focus on the customer, Build an attitude of quality throughout the enterprise, Expand the existing participant community, Assert a NASA leadership role for STI policy, and Develop a program for information science R&D. The STI division mission statement appears on the document cover as follows 'The mission of the NASA STI Program is to advance aerospace knowledge, contribute to U.S. competitiveness, and become an integral partner in NASA R&D programs to support NASA goals.' R.L.B.

N93-12671*# National Aeronautics and Space Administration, Washington, DC.
COORDINATING COUNCIL. FOURTH MEETING: NACA DOCUMENTS DATABASE PROJECT
1991 87 p Meeting held in Arlington, VA, 7 Feb. 1991
(NASA-TM-108017; NAS 1.15:108017) Avail: CASI HC A05/MF A01

This NASA Scientific and Technical Information Coordination Council meeting dealt with the topic 'NACA Documents Database Project'. The following presentations were made and reported on: NACA documents database project study plan, AIAA study, the Optimal NACA database, Deficiencies in online file, NACA documents: Availability and Preservation, the NARA Collection: What is in it? and What to do about it?, and NACA foreign documents and availability. Visuals are available for most presentations. R.L.B.

N93-12672*# National Aeronautics and Space Administration, Washington, DC.
COORDINATING COUNCIL. SIXTH MEETING: WHO ARE OUR KEY USERS?
1991 101 p Meeting held in Arlington, VA, 25 Oct. 1991
(NASA-TM-108021; NAS 1.15:108021) Avail: CASI HC A06/MF A02

This NASA Scientific and Technical Information Program Coordinating Council meeting deals with the topic 'Who are our key users?' Presentations were made on the following subtopics: Key users: Who uses the system the most, Who orders the most documents, Users: What do we know about them?, NASA/DOD Aerospace Knowledge Diffusion research project on 'Potential key users', How we meet the user's needs, and STI Council user requirements update. Summaries of discussions after the presentations are included along with visuals for the presentations. R.L.B.

N93-12673*# National Aeronautics and Space Administration, Washington, DC.
COORDINATING COUNCIL. EIGHTH MEETING: USING THE INTERNET
1992 52 p Meeting held in Arlington, VA, 5 Jun. 1992
(NASA-TM-108019; NAS 1.15:108019) Avail: CASI HC A04/MF A01

This NASA Scientific and Technical Information Program Coordinating Council meeting theme was entitled 'Using Internet'. Individual topics included STI LAN migration, NSF and NREN (National Science Foundation and the National Research and Education Network), and the New NASA Headquarters LAN. Discussions are recorded for each topic and visuals are provided for STI LAN migration and NSI - NASA Science Internet. R.L.B.

N93-12680*# Consortium for International Earth Science Information Network, Ann Arbor, MI.
EARTH SCIENCE INFORMATION: PLANNING FOR THE INTEGRATION AND USE OF GLOBAL CHANGE INFORMATION Final Technical Report, 1 Apr. 1991 - 31 Mar. 1992
Jack R. Lousma Oct. 1992 5 p
(Grant NAGw-2010)
(NASA-CR-191208; NAS 1.26:191208) Avail: CASI HC A01/MF A01

The Consortium for International Earth Science Information Network (CIESIN) was founded in 1989 as a non-profit corporation dedicated to facilitating access to, use and understanding of global change information worldwide. The Consortium was created to cooperate and coordinate with organizations and researchers throughout the global change community to further access the most advanced technology, the latest scientific research, and the best information available for critical environmental decision making. CIESIN study efforts are guided by Congressional mandates to 'convene key present and potential users to assess the need for investment in integration of earth science information,' to 'outline the desirable pattern of interaction with the scientific and policy community,' and to 'develop recommendations and draft plans to achieve the appropriate level of effort in the use of earth science data for research and public policy purposes.' In addition, CIESIN is tasked by NASA to develop a data center that would extend the benefits of Earth Observing System (EOS) to the users of global change information related to human dimensions issues. For FY 1991, CIESIN focused on two main objectives. The first addressed the identification of information needs of global change research and non-research user groups worldwide. The second focused on an evaluation of the most efficient mechanisms for making this information available in usable forms. Author

N93-12703# Rome Lab., Griffiss AFB, NY.
PROCEEDINGS OF JOINT RL/AFOSR WORKSHOP ON INTELLIGENT INFORMATION SYSTEMS
Raymond A. Liuzzi and Abraham Waksman Apr. 1992 369 p Workshop held in Griffiss AFB, NY, 22-23 Oct. 1991
(AF Proj. 5581)
(AD-A254795; RL-TR-92-57) Avail: CASI HC A16/MF A03

The RL/AFOSR Intelligence Information System Workshop (IIS) brought together researchers in the field of Artificial Intelligence and Data Bases. Represented were various government agencies, leading university groups, and government contractors. The workshop agenda included an integrated set of tutorial presentations, individual research thrusts, and panel discussions, general agreement was reached that Intelligent Information Systems will play a major role in future C3I application areas. GRA

N93-12723# Florida State Univ., Tallahassee. Dept. of Educational Research.
EFFICACY OF MULTIMEDIA INSTRUCTION AND AN INTRODUCTION TO DIGITAL MULTIMEDIA TECHNOLOGY Interim Technical Report, Jun. - Aug. 1991
Mark J. Gavora Jul. 1992 28 p
(Contract F49620-90-C-0076)
(AD-A254509; AL-TP-1992-0031) Avail: CASI HC A03/MF A01

This paper describes research on the use of multimedia delivery to improve learning. A literature review was conducted to gauge support for the belief that multimedia presentations influence learning and to identify criteria needed for a multimedia presentation to enhance learning. Research contributing to the effective design of multimedia presentations is discussed. A description of digital multimedia technology and its advantages over older technologies is provided. Critical components of digital multimedia technology, applications best suited for the technology, and resources required for successful development of digital multimedia presentations are addressed. Future trends affecting digital multimedia technology are projected. An explanation of the two dominant digital multimedia products (Digital Video Interactive and Compact Disc Interactive) is also featured. GRA

N93-12759# Federal Library and Information Center Committee, Washington, DC.
PROCEEDINGS OF FLICC FORUMS ON FEDERAL INFORMATION POLICIES. COMBINED SUMMARIES OF PROCEEDINGS. THE 1990 7TH FORUM, ACCESS IS THE KEY AND THE 1991 8TH FORUM, BUILDING INFORMATION SUPERHIGHWAYS: SUPERCOMPUTING NETWORKS AND LIBRARIES
1992 101 p The 1990 7th Forum held 20 Mar. 1990; and the 1991 8th Forum held on 21 Mar. 1991
(PB92-147370) Copyright Avail: CASI HC A06/MF A02

Summaries are provided for the following papers: The changing information landscape: opportunities for better management; Managing scientific and technical information in the 1990's; Future trends in Government Information Issues; The future of the GPO Depository Library Program: Issues and strategies; Access to government information: A Canadian perspective; The medical community's views on open access; Public needs for Federal information; The State's view of access issues; What industry expects from Federal Information Providers; Information science and changing needs; NREN and other information Networks: The Federal role; Future directions for Federal Libraries and Information Centers; Balancing the E and R in NREN: The educational imperative; Supporting the modern researcher; Future implications for the profit and not-for-profit sectors. GRA

N93-12808# Argonne National Lab., IL.
UTILIZATION OF DATABASES TO MANAGE RESOURCES
T. Sheridan 1992 8 p Presented at the International Symposium on Energy, Environment and Information Management, Argonne, IL, 15-18 Sep. 1992
(Contract W-31-109-eng-38)
(DE92-019598; ANL/CP-76667; CONF-9209160-4) Avail: CASI HC A02/MF A01

A description of how databases are used by the Advanced Photon Source (APS) Project at Argonne National Laboratory to help manage the project and its resources is presented. It documents our experiences in implementing database technology in a large scientific project. Some of the topics that will be discussed include: the APS database environment; decentralizing databases; extending the database environment (graphical, spreadsheet, and barcode interfaces); choosing a database; and software development issues. DOE

N93-12813# Sandia National Labs., Albuquerque, NM.
NONIDEAL THERMOEQUILIBRIUM CALCULATIONS USING A LARGE PRODUCT SPECIES DATA BASE
M. L. Hobbs and M. R. Baer Jun. 1992 127 p
(Contract DE-AC04-76DP-00789)
(DE92-040839; SAND-92-0482) Avail: CASI HC A07/MF A02

Thermochemical data fits for approximately 900 gaseous and 600 condensed species found in the JANAF tables have been completed for use with the TIGER nonideal thermoequilibrium code. The TIGER code has been modified to allow systems containing up to 400 gaseous and 100 condensed constituents composed of up to 50 elements. Gaseous covolumes have been estimated following the procedure outlined by Mader using estimates of van der Waals radii for 48 elements and three-dimensional molecular mechanics. Molecular structures for all gaseous components were explicitly defined in terms of atomic coordinates in A. The Becker-Kistiakowsky-Wilson equation of state (BKW-EOS) has been calibrated near C-J states using detonation temperatures measured in liquid and solid explosives and a large product species data base. Detonation temperatures for liquid and solid explosives were predicted adequately with a single set of BKW parameters. Values for the empirical BKW constants alpha, beta, kappa, and theta were 0.5, 0.174, 11.85, and 5160, respectively. Values for the covolume factors, k(sub i), were assumed to be invariant. The liquid explosives included mixtures of hydrazine nitrate with hydrazine, hydrazine hydrate, and water; mixtures of tetranitromethane with nitromethane; liquid isomers ethyl nitrate and 2-nitroethanol; and nitroglycerine. The solid explosives included HMX, RDX, PETN, Tetryl, and TNT. Color contour plots of HMX equilibrium products as well as thermodynamic variables are shown in pressure and temperature space. Similar plots for a pyrotechnic reaction composed of TiH2 and KClO4 are also reported. Calculations for a typical HMX-based propellant are also discussed. DOE

N93-12824# Argonne National Lab., IL.
INCREASING THE END USER'S PRODUCTIVITY THROUGH SEAMLESS INTEGRATION OF APPLICATIONS WITH THE DATABASE
K. Parizadeh 1992 7 p Presented at the International Symposium on Energy, Environment and Information Management, Argonne, IL, 15-18 Sep. 1992
(Contract W-31-109-eng-38)
(DE92-019599; ANL/CP-76725; CONF-9209160-3) Avail: CASI HC A02/MF A01

End user's productivity is a critical issue in modern day offices. The first section of this paper will present some guidelines and methods to improve end user's productivity. The second section presents an actual system. DOE

N93-12991*# National Aeronautics and Space Administration. Goddard Space Flight Center, Greenbelt, MD.
REPORT ON PHASE 2 OF 1990 OSSA DATA CENSUS
Joseph H. King Oct. 1991 64 p
(NASA-TM-107992; NAS 1.15:107992; NSSDCA/WDC-A-R/S-91-23)
Avail: CASI HC A04/MF A01

The 1990 NASA Office of Space Science and Applications (OSSA) data census contributed significantly to a database intended to identify and briefly describe all archived data and potentially archive-desirable data from active and inactive NASA/OSSA spaceflight investigations. This database is being created at the National Space Science Data Center (NSSDC) and will be more comprehensive than the databases describing data held at individual sites such as NSSDC. Active investigations are defined as those flying on currently operational spacecraft or those that flew on recently operational spacecraft for which project-coordinated data archiving is continuing. Inactive investigations are those that flew on spacecraft that are no longer operational, and for which systematic archiving has ended. The principal purpose of this report is to describe phase two of the 1990 census. The previously reported phase one of this census, as well as a relevant 1981 census, are briefly discussed. The phase two survey instrument is described, those surveyed and respondents/reponses are identified, and data sets from inactive OSSA investigations discovered during the 1990 census (phase two) are briefly discussed individually.
Author

N93-12994# Argonne National Lab., IL.
EVOLUTION OF THE SCIENTIFIC PAPER
J. E. Harmon 1992 12 p Presented at the IEEE International Professional Communications Conference: Crossing Frontiers, Santa Fe, NM, 30 Sep. 1992
(Contract W-31-109-eng-38)
(DE92-019696; ANL/CP-76315; CONF-9209142-6) Avail: CASI HC A03/MF A01

The first papers reporting original research results in technical periodicals and proceedings appeared in the late 17th century. Since that time, the typical scientific paper has evolved from a fairly simple document, accessible to a general audience, to a much more complex one, aimed at a specialized audience. The purpose of this article is to give an overview of what the first scientific papers were like and how they evolved to their present form and style. To facilitate this discussion, the scientific paper's development has arbitrarily been divided into four stages: the origin and formative years of the scientific paper (1665-1765), emergence of scientific papers written for specialized publications (1765-1865), development of the modern scientific paper (1865-1965), and hyperspecialization and computerization of the modern scientific paper (1965-?). DOE

N93-13000# Lawrence Livermore National Lab., CA.
DATA: HOW TO GENERATE, STORE, RETRIEVE, COMMUNICATE, AND INTERPRET IT: PROCEEDINGS
R. E. Carlson, ed. Jul. 1992 245 p Presented at the High Speed Computing Conference, Glenenden Beach, OR, 11-14 May 1992
(Contract W-7405-eng-48)
(DE92-040405; CONF-9205214) Avail: CASI HC A11/MF A03

This report contains viewgraphs covering the following topics: Considerations for the evolution of high speed networking; gigabit networks; status of LLNL's prototype gigabit/sec Lan; distributed data server infrastructure for seismic processing on a new spectrum of computing platforms; sequoia 2000: computer science applied to global change research; toward transparent, distributed storage systems; LANL's high-performance data system; the data millieu for climate modeling at the national center for atmospheric research; the pass project: database computing for the SSC; a comparison of three application dependent mass storage systems; striped arrays of tertiary storage devices; abstracts: a technique for hiding latency in a mass-storage system; marching cubes on the CM-2; A carpetbagger's guide to the human genome project; global change research, large data sets, and landsat pathfinder; organizing and interpreting data in a modeling and simulation environment; high- resolution

adaptive methods for compressible flow; future computers--an intellectual power grid; and high speed computing in the '90's: the technologies and the delivery. DOE

N93-13048# Oak Ridge K-25 Site, TN.
ENGINEERING DESIGN INFORMATION SYSTEM (EDIS) INFORMATION SERVICES DIVISION (ISD) INDEX FUNCTION: USER'S MANUAL
R. K. Schwarz, ed. Aug. 1992 77 p
(Contract DE-AC05-84OT-21400)
(DE92-041242; K/CSD/TM-101) Avail: CASI HC A05/MF A01

The Engineering Design Information System (EDIS) Information Services Division (ISD) Index Function is an interactive system developed for ISD personnel to perform indexing, maintenance, and retrieval of information about engineering documents. Section 2.0 of this manual gives an overview of the system structure, data, and functionality, as well as the hardware and security environment within which the system operates. Section 3.0 gives a detailed description of the interactive menus, screens, and prompts that provide access to the system functions and the requirements for data entry. Appendixes A-F are included to display data definitions, modification rules, help screen formats, explanation of system help and informational messages, code translations, and a report format. DOE

N93-13078# Allied-Signal Aerospace Co., Kansas City, MO.
DIGITAL IMAGING SYSTEMS
S. G. Mozzano and C. E. Watterson Aug. 1992 46 p
(Contract DE-AC04-76DP-00613)
(DE92-019194; KCP-613-4669) Avail: CASI HC A03/MF A01

The Advanced Vision Information System (AVIS) was a long-term development project for the engineering technical thrust for intelligent vision systems. The goal of the project was to develop an image processing capability in the laboratory through which advanced automated image analysis techniques could be achieved. From the many instruments in the Materials Evaluation laboratory which provide video output data, three were selected for initial development activities. The instruments selected were the infrared camera, the metallograph, and electron optics. To the application development activities for these instruments were added the development of the laboratory network for transferring image data, the development of a standardized image processing workstation, and a nondestructive measurement capability. Since the project had such a broad scope, each of six activities was established as a subproject. DOE

N93-13112# General Accounting Office, Washington, DC. Information Management and Technology Div.
EARTH OBSERVING SYSTEM: INFORMATION ON NASA'S INCORPORATION OF EXISTING DATA INTO EOSDIS. REPORT TO THE CHAIRMAN, COMMITTEE ON SCIENCE, SPACE, AND TECHNOLOGY, HOUSE OF REPRESENTATIVES
25 Sep. 1992 12 p
(GAO/IMTEC-92-79; B-249927) Avail: CASI HC A03/MF A01; GAO, PO Box 6015, Gaithersburg, MD 20877 HC

NASA plans to include a variety of data in the early EOSDIS (EOS Data/Information System), including reprocessed versions of certain key large-volume data sets that have been collected over many years. However, few of the data sets earmarked for reprocessing will be sufficiently reworked to be available for users to test early EOSDIS capabilities and provide feedback. Although EOSDIS Version 0 is scheduled to become operational in 1994, none of the six large data sets selected for inclusion by the scientific community is likely to be fully reprocessed by that date. Many projects remain in the preliminary planning phase, with few details worked out regarding how their data sets will be made available through EOSDIS. Others do not even have preliminary plans or milestones because scientists are still debating various alternatives for reprocessing their data to make it useful within EOSDIS. Author

N93-13117# Michigan Univ., Ann Arbor.
SEMANTICS-BASED REFERENCE RESOLUTION IN TECHNICAL TEXT PROCESSING: AN EXPLORATION OF USING THE WORD NET DATABASE IN THE COMPUTERIZED COMPREHENSIBILITY SYSTEM
Interim Technical Report
David E. Kieras 30 Aug. 1992 19 p
(Contract N00014-88-K-0133; DA Proj. RR0-4206)
(AD-A255068; TR-92/ONR-35) Avail: CASI HC A03/MF A01

The Computerized Comprehensibility System (CCS) provides an automated copy editing function, generating a 'mark-up' of a draft of a technical document by simulating the simpler comprehension processes of a human reader, and then criticizing the text when these simple processes cannot successfully comprehend the material. A key CCS function is criticizing the coherence of the material by tracking which objects are mentioned in the passage. A common comprehensibility problem is that the text mentions a new object using the syntactic structures appropriate for an already-known object. If the reader must make an inference that presence of the new object is implied by earlier-mentioned object, the result is a potential break in the coherence of the text. CCS criticizes all such coherence breaks. However, many such inferences are actually easy for most readers, since only general knowledge is required to make the inference, rather than specialized knowledge about the domain. If so, then the CCS criticism of a coherence break is a false alarm. This report describes exploratory work with an augmented form of CCS, in which the WordNet database is used as a source of general knowledge to allow CCS to make the same kind of general knowledge inferences that human readers do to overcome coherence breaks. GRA

N93-13131*# National Aeronautics and Space Administration. Goddard Space Flight Center, Greenbelt, MD.
NSSDC CONFERENCE ON MASS STORAGE SYSTEMS AND TECHNOLOGIES FOR SPACE AND EARTH SCIENCE APPLICATIONS, VOLUME 1
Benjamin Kobler, ed., P. C. Hariharan, ed. (ST Systems Corp., Lanham, MD.), and L. G. Blasso, ed. (ST Systems Corp., Lanham, MD.) Washington Sep. 1992 205 p Conference held in Greenbelt, MD, 23-25 Jul. 1991
(RTOP 656-80-02-26)
(NASA-CP-3165-Vol-1; Rept-92B00093-Vol-1; NAS 1.55:3165-Vol-1) Avail: CASI HC A10/MF A03

Papers and viewgraphs from the conference are presented. This conference served as a broad forum for the discussion of a number of important issues in the field of mass storage systems. Topics include magnetic disk and tape technologies, optical disks and tape, software storage and file management systems, and experiences with the use of a large, distributed storage system. The technical presentations describe, among other things, integrated mass storage systems that are expected to be available commercially. Also included is a series of presentations from Federal Government organizations and research institutions covering their mass storage requirements for the 1990's. For individual titles, see N93-13132 through N93-13139.

N93-13132*# Storage Technology Corp., Louisville, CO. Strategic Planning Div.
ENTERPRISE STORAGE REPORT FOR THE 1990'S
Fred Moore *In* NASA. Goddard Space Flight Center, NSSDC Conference on Mass Storage Systems and Technologies for Space and Earth Science Applications, Volume 1 Sep. 1992 30 p (For primary document see N93-13131 03-82)
Avail: CASI HC A03/MF A03

Data processing has become an increasingly vital function, if not the most vital function, in most businesses today. No longer only a mainframe domain, the data processing enterprise also includes the midrange and workstation platforms, either local or remote. This expanded view of the enterprise has encouraged more and more businesses to take a strategic, long-range view of information management rather than the short-term tactical approaches of the past. This paper will highlight some of the significant aspects of data storage in the enterprise for the 1990's. Author

N93-13133*# Alphatronix, Inc., Research Triangle Park, NC.
OPTICAL DISKS BECOME ERASABLE
Robert P. Freese *In* NASA. Goddard Space Flight Center, NSSDC Conference on Mass Storage Systems and Technologies for Space and Earth Science Applications, Volume 1 Sep. 1992 35 p (For primary document see N93-13131 03-82)
Avail: CASI HC A03/MF A03

The topics covered include the following: optical recording; how does it work?; why all the fuss?; state of the industry; sample applications; and future directions. Author

N93-13134*# Mallinson Magnetics, Inc., Carlsbad, CA.
MAGNETIC DISK
John C. Mallinson *In* NASA. Goddard Space Flight Center, NSSDC Conference on Mass Storage Systems and Technologies for Space and Earth Science Applications, Volume 1 Sep. 1992 10 p (For primary document see N93-13131 03-82)
Avail: CASI HC A02/MF A03

Magnetic disk recording was invented in 1953 and has undergone intensive development ever since. As a result of this 38 years of development, the cost per byte and the areal density have halved and doubled respectively every 2-2 1/2 years. Today, the cost per byte is lower than 10(exp -6) dollars per byte and area densities exceed 100 10(exp 6) bits per square inch. In this talk, the recent achievements in magnetic disk recording are first surveyed briefly. Then, the principal areas of current technical development are outlined. Finally, some comments are made about the future of magnetic disk recording. Author

N93-13135*# Datatape, Inc., Pasadena, CA.
MAGNETIC TAPE
Harriss Robinson *In* NASA. Goddard Space Flight Center, NSSDC Conference on Mass Storage Systems and Technologies for Space and Earth Science Applications, Volume 1 Sep. 1992 28 p (For primary document see N93-13131 03-82)
Avail: CASI HC A03/MF A03

The move to visualization and image processing in data systems is increasing the demand for larger and faster mass storage systems. The technology of choice is magnetic tape. This paper briefly reviews the technology past, present, and projected. A case is made for standards and the value of the standards to users. Author

N93-13136*# General Atomic Co., San Diego, CA. Distributed Computing Solutions Div.
STORAGE SYSTEM SOFTWARE SOLUTIONS FOR HIGH-END USER NEEDS
Carole B. Hogan *In* NASA. Goddard Space Flight Center, NSSDC Conference on Mass Storage Systems and Technologies for Space and Earth Science Applications, Volume 1 Sep. 1992 32 p (For primary document see N93-13131 03-82)
Avail: CASI HC A03/MF A03

Today's high-end storage user is one that requires rapid access to a reliable terabyte-capacity storage system running in a distributed environment. This paper discusses conventional storage system software and concludes that this software, designed for other purposes, cannot meet high-end storage requirements. The paper also reviews the philosophy and design of evolving storage system software. It concludes that this new software, designed with high-end requirements in mind, provides the potential for solving not only the storage needs of today but those of the foreseeable future as well. Author

N93-13137*# San Diego Supercomputer Center, CA.
FILE SERVERS, NETWORKING, AND SUPERCOMPUTERS
Reagan W. Moore *In* NASA. Goddard Space Flight Center, NSSDC Conference on Mass Storage Systems and Technologies for Space and Earth Science Applications, Volume 1 Sep. 1992 18 p (For primary document see N93-13131 03-82)
Avail: CASI HC A03/MF A03

One of the major tasks of a supercomputer center is managing the massive amount of data generated by application codes. A data flow analysis of the San Diego Supercomputer Center is presented that illustrates the hierarchical data buffering/caching capacity requirements and the associated I/O throughput requirements needed to sustain file service and archival storage. Usage paradigms are examined for both tightly-coupled and loosely-coupled file servers linked to the supercomputer by high-speed networks. Author

N93-13138*# National Center for Atmospheric Research, Boulder, CO. Scientific Computing Div.
MASS STORAGE SYSTEM EXPERIENCES AND FUTURE NEEDS AT THE NATIONAL CENTER FOR ATMOSPHERIC RESEARCH
Bernard T. OLear *In* NASA. Goddard Space Flight Center, NSSDC Conference on Mass Storage Systems and Technologies for Space and Earth Science Applications, Volume 1 Sep. 1992 19 p Sponsored in part by NSF (For primary document see N93-13131 03-82)
Avail: CASI HC A03/MF A03

This presentation is designed to relate some of the experiences of the Scientific Computing Division at NCAR dealing with the 'data problem'. A brief history and a development of some basic Mass Storage System (MSS) principles are given. An attempt is made to show how these principles apply to the integration of various components into NCAR's MSS. There is discussion of future MSS needs for future computing environments. Author

N93-13139*# National Archives and Records Service, Washington, DC. Center for Electronic Records.
THE LONG HOLD: STORING DATA AT THE NATIONAL ARCHIVES
Kenneth Thibodeau *In* NASA. Goddard Space Flight Center, NSSDC Conference on Mass Storage Systems and Technologies for Space and Earth Science Applications, Volume 1 3 p(SEE N93-13131 03-82) Sep. 1992 (For primary document see N93-13131 03-82)
Avail: CASI HC A01/MF A03

The National Archives is, in many respects, in a unique position. For example, I find people from other organizations describing an archival medium as one which will last for three to five years. At the National Archives, we deal with the centuries, not years. From our perspective, there is no archival medium for data storage, and we do not expect there will ever be one. Predicting the long-term future of information technology beyond a mere five or ten years approaches the occult arts. But one prediction is probably safe. It is that the technology will continue to change, at least until analysts start talking about the post-information age. If we did have a medium which lasted a hundred years or longer, we probably would not have a device capable of reading it. The issue of obsolescence, as opposed to media stability, is more complex and more costly. It is especially complex at the National Archives because of two other aspects of our peculiar position. The first aspect is that we deal with incoherent data. The second is that we are charged with satisfying unknown and unknowable requirements. A brief overview of these aspects is presented. Author

N93-13275# Stanford Univ., CA. Linear Accelerator Center.
GUIDE TO QSPIRES AND THE PARTICLE PHYSICS DATABASES ON SLACVM
H. Galic Jun. 1992 219 p
(Contract DE-AC03-76SF-00515)
(DE92-018099; SU-SLAC-393) Avail: CASI HC A10/MF A03

SLAC, in collaboration with DESY, LBL, and several other institutions, maintains many databases of interest to the high energy physics community. You do not need a computer account at SLAC to search through some of these databases, they can be reached via the remote server QSPIRES, set at the BITNET node SLACVM. This text describes, in great detail, how to search in the popular HEP database via QSPIRES; HEP contains bibliographic summaries of more than 200,000 particle physics papers. Other remotely available databases are also reviewed, and the registration procedure for those who would like to use QSPIRES is explained. To utilize QSPIRES, you must have access to a large computer network. It is not necessary that the network be BITNET; however, a gateway must exist between your network and BITNET. It should be mentioned that BITNET users have some advantages in searching, e.g., the possibility of interactive communication with QSPIRES. Therefore, if you have a choice, let a BITNET machine be your base for QSPIRES searches. You will also need an authorization to use HEP and other databases, and you should know the set of relevant commands and rules. The authorization is free, the commands are simple, and BITNET can be reached from all over the world. DOE

N93-13368# National Aeronautical Lab., Bangalore (India). Information Centre for Aeronautics.
COMPOSITES: A CATALOGUE OF BOOKS AND CONFERENCE PROCEEDINGS AVAILABLE IN THE NAL LIBRARY
G. Shashikala and V. Bhanumathi Mar. 1992 15 p
(NAL Proj. ST-1-166)
(NAL-SP-IC-9201) Avail: CASI HC A03/MF A01

Books and conference proceedings on composite materials held by the National Aeronautical Laboratory in Bangalore, India are listed. Author

N93-13415# National Inst. of Standards and Technology, Gaithersburg, MD. Office of Information Services.

ABSTRACT AND INDEX COLLECTION IN THE RESEARCH INFORMATION CENTER OF THE NATIONAL INSTITUTE OF STANDARDS AND TECHNOLOGY Final Report

Diane Cunningham Jun. 1992 40 p

(PB92-217587; NIST/SP-836) Avail: CASI HC A03/MF A01; SOD HC

An alphabetical arrangement of abstracts and indexes available in the Research Information Center (RIC) of the National Institute of Standards and Technology (NIST) is listed by most current title of the publication. Other information includes description of the abstract or index, RIC holdings, principal sources, publisher or association, corresponding RIC database and CD-ROM availability and the classification number. A general subject and former title/database name index follow the main text of the report. GRA

N93-13619# Lawrence Livermore National Lab., CA.

ENGINEERING DATA TRANSFER TEST WITH EDMICS USING MIL-R-28002 (RASTER)

1 May 1992 318 p Prepared for Air Force Systems Command, Wright-Patterson AFB, OH

(Contract W-7405-eng-48)

(DE92-019808; UCRL-ID-110448; AITI-1168; CTN-92-008) Avail: CASI HC A14/MF A03

This paper documents the results of a sequence of tests conducted to evaluate the DoD Computer-aided Acquisition and Logistic Support (CALS) data interchange capability of the Navy Electronic Data Management Information and Control System (EDMICS). The CABS initiative specifies a standard digital interface to streamline the interchange of technical data between the DoD and the commercial sector. The CABS Test Network (CTN) is tasked to conduct tests of the military standards which specify this digital interface. The testing results outlined in this report are intended to evaluate the EDMICS systems ability to support CALS data interchanges and establish the level of technical data interoperability implemented at this DoD engineering data repository. DOE

N93-13737*# Research Inst. for Computing and Information Systems, Houston, TX.

PERFORMANCE MEASUREMENT FOR INFORMATION SYSTEMS: INDUSTRY PERSPECTIVES Final Report

Peter C. Bishop (Houston Univ., Clear Lake, TX.), Cissy Yoes (Houston Univ., Clear Lake, TX.), and Kay Hamilton (Houston Univ., Clear Lake, TX.) 30 Oct. 1992 41 p

(Contract NCC9-16; RICIS Proj. IR-01a)

(NASA-CR-191369; NAS 1.26:191369) Avail: CASI HC A03/MF A01

Performance measurement has become a focal topic for information systems (IS) organizations. Historically, IS performance measures have dealt with the efficiency of the data processing function. Today, the function of most IS organizations goes beyond simple data processing. To understand how IS organizations have developed meaningful performance measures that reflect their objectives and activities, industry perspectives on IS performance measurement was studied. The objectives of the study were to understand the state of the practice in IS performance techniques for IS performance measurement; to gather approaches and measures of actual performance measures used in industry; and to report patterns, trends, and lessons learned about performance measurement to NASA/JSC. Examples of how some of the most forward looking companies are shaping their IS processes through measurement is provided. Thoughts on the presence of a life-cycle to performance measures development and a suggested taxonomy for performance measurements are included in the appendices. L.R.R.

N93-13884# Syracuse Univ., NY. School of Information Studies.

IDENTIFYING AND DESCRIBING FEDERAL INFORMATION INVENTORY/LOCATOR SYSTEMS: DESIGN FOR NETWORKED-BASED LOCATORS, VOLUME 1 Final Report

Charles R. McClure, Joe Ryan, and William E. Moen 25 Aug. 1992 148 p

Avail: CASI HC A07/MF A02

This study identified and described Federal information inventory/locator systems. Such locator systems provide an important means of accessing a range of government information not previously available to the public or other government officials. The report should be considered as Phase 2 to the study Federal Information Inventory/Locator Systems: From Burden to Benefit: Final Report (McClure, et al., 1990). The 1990 report contains background information about Federal locator systems and the recommendation for a Government-Wide Information Inventory/Locator System (GIILS). The goal of Phase 2 was to improve access to and use of U.S. government information. The project's methodology relied on multiple data collection and analysis strategies employing primarily a qualitative approach with the following specific objectives: (1) to identify existing and planned Federal locators; (2) to identify critical success factors in the design, development and maintenance of a Federal agency locator; and (3) to identify and discuss key issues and policy recommendations related to the design and development of a government-wide locator system. I.I.C.

N93-13885*# National Aeronautics and Space Administration, Washington, DC.

COORDINATING COUNCIL. NINTH MEETING: TOTAL QUALITY MANAGEMENT

1992 129 p Meeting held in Arlington, VA, 28 Oct. 1992

(NASA-TM-108106; NAS 1.15:108106) Avail: CASI HC A07/MF A02

This report summarizes the 9th meeting of the STI Coordinating Council. The council listened to the speakers' understanding of Total Quality Management (TQM) principles and heard stories of successful applications of these principles. Definitions of quality stated were focused on customer satisfaction. Reports presented by the speakers are also included. I.I.C.

N93-13910 Aberdeen Univ. (Scotland).

MAKING OBJECT-ORIENTED DATABASES MORE KNOWLEDGEABLE (FROM ADAM TO ABEL) Ph.D. Thesis

Oscar DiazGarcia 1992 198 p

Avail: Univ. Microfilms Order No. BRDX96273

The salient points of this thesis are as follows: (1) Object-Oriented Databases can help in solving the impedance mismatch problem by introducing methods. However, methods have sometimes been overused in the sense that the code encapsulated refers not only to how the operation is implemented but also to other kinds of knowledge that are implicit in the code. The disadvantages of this approach for modelling integrity constraints, user-defined relationships and active behavior are pointed out. (2) The ADAM Object-Oriented Database has been extended to allow the designer to specify integrity constraints declaratively. A constraint equation approach is implemented that supports the inheritance of constraints. (3) A need for semantic-rich user defined relationships has been identified. In this thesis, relationships are represented as objects. An approach to enhance the semantics of relationships in both its structural and behavioral aspects is presented. The most novel idea of the approach presented is the support of the inferred properties and the operational semantics of relationships. (4) Active Databases have recently become an important area of research. This thesis shows how to extend an Object-Oriented Database with active capabilities. The principal contribution lies in representing as 'first-class' objects not only the active rules but also the rule manager itself. Hence, besides handling active rules as any other object in the system, future requirements can be supported just by specializing the current rule manager. (5) Active rules have been proposed for several purposes. Several examples are given of the direct use of rules. However, higher level tools can be provided of which rules are simply a vehicle for implementation. This is shown by generating rules from the declarative specification of integrity constraints and it has also been applied to generate rules for enforcing the operational semantics of relationships. (6) Metaclasses are a valuable mechanism for enhancing the uniformity, accessibility and extensibility of the system. This is demonstrated by showing how ADAM has been extended with integrity constraints, semantic-rich user-defined relationships and active behavior. Dissert. Abstr.

N93-13911 Florida State Univ., Gainesville.

APPLYING AN OBJECT-ORIENTED DATABASE MODEL TO A SCIENTIFIC DATABASE PROBLEM: MANAGING EXPERIMENTAL DATA AT CEBAF Ph.D. Thesis

Bryon K. Ehlmann 1992 143 p

Avail: Univ. Microfilms Order No. DA9222380

Current scientific experiments are often characterized by massive amounts of very complex data and the need for complex data analysis

software. Object-oriented database (OODB) systems have the potential of improving the description of the structure and semantics of this data and of integrating the analysis software with the data. This dissertation results from research to enhance OODB functionality and methodology to support scientific databases (SDB's) and, more specifically, to support a nuclear physics experiments database for the Continuous Electron Beam Accelerator Facility (CEBAF). This research to date identified a number of problems related to the practical application of OODB technology to the conceptual design of the CEBAF experiments database and other SDB's: the lack of a generally accepted OODB design methodology, the lack of a standard OODB model, the lack of a clear conceptual level in existing OODB models, and the limited support in existing OODB systems for many common object relationships inherent in SDB's. To address these problems, the dissertation describes an Object-Relationship Diagram (ORD) and an Object-oriented Database Definition Language (ODDL) that provide tools that allow SDB design and development to proceed systematically and independently of existing OODB systems. These tools define multi-level, conceptual data models for SDB design, which incorporate a simple notation for describing common types of relationships that occur in SDB's. ODDL allows these relationships and other desirable SDB capabilities to be supported by an extended OODB system. A conceptual model of the CEBAF experiments database is presented in terms of ORD's and the ODDL to demonstrate their functionality and use and provide a foundation for future development of experimental nuclear physics software using an OODB approach. Dissert. Abstr.

N93-13912 Universitaire Instelling Antwerpen, Wilrijk (Belgium).
A THEORY OF REFERENCE GRAPHS IN RELATIONAL DATABASES
Hans Janssens 1991 295 p
Avail: Univ. Microfilms Order No. DA9223516

This work is an attempt at enhancing the data modeling and query capabilities of the standard relational model. To this end, reference graphs are defined as larger meaningful units than simple tables are, and referential SQL is introduced as a new query language. A reference graph has tables at its nodes and its edges model a kind of referential integrity constraint. The structure of a reference graph can be chosen freely, and in particular is not required to be a tree. On these reference graphs, a so-called referential algebra and a referential calculus are defined. Much of the current database research focuses on object-orientation. The latter actually provides a framework in which reference graphs nicely fit. Many typical concepts of the object-oriented paradigm, such as inheritance, object sharing, and the manipulation of structured data are indeed easily implemented with reference graphs. A parallel is drawn between the standard relational model and its extension with reference graphs: a table is a special case of a reference graph, the relational algebra and calculus are special cases of their referential counterparts, and like the relational algebra and calculus are equivalent, so are the referential algebra and calculus. This equivalence theorem is a central theorem in the present theory of reference graphs. Referential SQL is in appearance very similar to relational SQL. Like relational SQL is mathematically founded on the relational algebra and calculus, so does referential SQL rest on the referential algebra and calculus. As could be expected, queries involving aggregate functions are often much simpler to write in referential SQL than in relational SQL. Dissert. Abstr.

N93-14058 Lancaster Univ. (England).
LEARNING AND USING METHODOLOGIES IN INFORMATION SYSTEMS ANALYSIS AND DESIGN Ph.D. Thesis
Peter Axel Nielsen 1990 221 p
Avail: Univ. Microfilms Order No. BRDX95148

The question is addressed: 'Which methodologies in which situations.' Action Research has served as the primary research approach, i.e. the thesis is based on documented and practical experience. The argumentation throughout is rooted in this practice; the lessons learned, the interpretation and the reflection refer explicitly hereto or to the theoretical framework of the thesis. The thesis refers to three levels of practice: (1) The individual level: Based on qualitative interviews with three systems developers, lessons have been learned on the richness and diversity of individual use of methodologies; (2) The project level: Based on the use of methodologies in three similar projects (documented in project diaries) several lessons have been learned. Some of the lessons address the question of the domain of usefulness of the involved methodologies. The remaining lessons address the question of how methodologies may be used: using only a single methodology; using a theory as a methodology; and using a combination of methodologies. (3) The organizational level: Based on an inquiry structured by Soft Systems Methodology lessons have been learned on: the process of introducing new methodologies; a DP department; and the process of choosing methodology in a particular situation. Each of the lessons learned are argued with explicit reference to the interview, the diaries, or the soft systems models. The implications drawn from this practice as to how to anwser the fundamental question are twofold. On the one hand, it is possible and useful to have a framework to explicate differences between domains where different methodologies are useful. This has been done as a set of Use-Criteria related to: context of use, conditions for use, and characteristics of use. On the other hand, such a framework has itself limited usefulness as it is stable and general. A new dynamic and situational approach for learning and using methodologies is outlined. The approach is based on Soft Systems Methodology and integrates the Use-Criteria. Dissert. Abstr.

N93-14076 Texas Woman's Univ., Denton.
A STUDY OF TRADITIONAL INFORMATION ACCESS MODELS APPLIED IN A HYPERTEXT INFORMATION SYSTEM Ph.D. Thesis
Ernest Raoul Perez 1991 259 p
Avail: Univ. Microfilms Order No. DA9219620

Hypertext is an effective computer interface technology showing promise for information retrievel system applications. The ease of use and totally self-directed nature of navigating a hypertext information system using embedded associative links has drawn favorable reactions from system developers and implementors. However, many information retrieval specialists and librarians are concerned about the absence of planning for effective, consistent, controlled means of information organization and access. This exploratory study investigated the potential for transferring traditional, print-based methods of information retrieval to the hypertext medium. An extensive literature review provided background for construction of a conceptual model of traditional information access methods. The study used the established case study procedure of comparing a subject system against a proposed model, to establish the degree of agreement or disagreement with the hypothesis. The investigator selected an MS-DOS hypertext authoring system which apparently used some traditional information organization and structuring methods. Data collection methods included interview of the system developer and associates, examination of system documentation, informal interview of hypertext system developers using the system, and use of the subject system authoring tools for construction of a small hypertext system. Multiple means of data collection were used, allowing for cross-checking and verification of information. The data was interpreted by tabulation and examination of results against the traditional information access model. The study conclusively supported the hypothesis of the transferability of nearly all traditional information access and retrieval methods to the hypertext medium. It identified the hierarchical taxonomy matrix tool used in the subject authoring system as an accepted method of organizing information structure, and found it to be an effective hypertext authoring approach. It recommended the use of methods for insuring structured information organization, and tools to provide for consistency and control of access means. The study concluded that it would be productive for hypertext system authors to adopt a highly integrative approach, using a mixture of traditional information access methodologies to complement hypertext associative linking access and sophisticated information retrieval software approaches. Dissert. Abstr.

N93-14080 Claremont Graduate School, CA.
HUMAN MEMORY FOR THE SPATIAL LOCATIONS OF ITEMS ON PULL-DOWN COMPUTER MENUS Ph.D. Thesis
Frederick Joseph Condo, Jr. 1992 209 p
Avail: Univ. Microfilms Order No. DA9220594

Software whose design incorporates pull-down menus is in widespread use. A user searching for a menu item can employ one of three strategies: exhaustively searching menus; forming mnemonic associations between menu titles and items; or remembering the locations of menu items. The conditions under which each strategy might be used have implications for interface design. A pilot study and two experiments examined how the representation of items on pull-down menus affects speed of access to menu items. Menu items were represented as an icon, a word, or an icon plus a word. Novices participated for about 30 minutes on each of two consecutive days. After a training session they were presented a prompt

on the computer screen; their task was to locate that prompt as quickly as possible within the menus listed at the top of the screen. It was found that response times were significantly faster with icon displays than with word-only displays and that there was no difference in reaction time between the icon-alone and icon-plus-word conditions. These results are discussed in terms of automatic versus effortful processes in memory and in terms of mental and motor processes, and are related to the field of human-computer-interface design. A program for future research addresses issues of screen space used by icons, design costs related to the design of distinctive icons, the role of the semantic content of icons in user responses, the role icons might play in training, and the applicability of the present results to realistic situations. Four lessons arise from this work. First, automatic cognitive processes may not proceed optimally, so design can affect their operation. Second, because pull-down menus are invisible grids that associate commands with spatial locations, knowledge about human responses to such grids is applicable to menu design. Third, memory for the locations of icons is superior to memory for the locations of words alone; hence response times can be improved by using icons in the design of pull-down menus. Fourth, despite their sophistication, current writings on human-interface design do not address low-level details of human cognition that affect human performance in computer use. Dissert. Abstr.

N93-14088 Florida State Univ., Gainesville.
A STUDY REGARDING INFORMATION-SEEKING BEHAVIOR, VALUATION OF INFORMATION INCLUDING PERCEPTIONS OF INFORMATION ATTRIBUTES, AND ASSOCIATED CORRELATES PERTAINING TO INFORMATION USAGE Ph.D. Thesis
Marsha Kay Turner 1992 357 p
Avail: Univ. Microfilms Order No. DA9222427

The purpose of this research study was to gather and examine data on the relationships among individuals' demographic and use environment characteristics; information seeking behavior; valuation of information; and impact and usage of information. The research design methodology employed to accomplish this purpose included two techniques of descriptive research, the questionnaire and in-depth interview. The collected data were used to test the specified five study hypotheses in an effort to specify the nature of these relationships. The following null hypotheses were tested: (1) Perceptual valuation of selection attributes of received information by recipients/users is independent of their information seeking behavior (requesting/not requesting/receiving without opportunity to request information). (2) Information impact and usage is independent of recipient's/user's information seeking behavior. (3) Recipient's/user's perceptual valuation of information attributes associated with the quality of information content and/or the information channel is independent of their usage of the received information. (4) Perceptual valuation of information attributes associated with the quality of information content and the information channel is independent of selected demographic and personal characteristics for recipients/users. (5) Usage of received information is independent of selected demographic and personal characteristics for recipients/users. The hypothesized model of the reflected factors of information usage with the associated variables includes the following components: Information Seeking Behavior: Requestors, Non-Requestors, and Recipients Only. Information Channel Attributes: Ease of Use, Readability, Availability, Accessibility, Response Time, Procedures to Receive Information, and Instructions for Information Use. Information Content Attributes: Completeness, Accuracy, Relevancy, Timeliness, Volume, Currency, and Value of Information. Information Impacts: Increases in Productivity, Saves Time, Necessary Part of Work Activity, Confirms Existing Knowledge, Stimulus for Action, etc. Information Usages: Discarded, Considered and Rej ected, Redirected, Communicated, Filed, Read then Filed, Stimulus for Action, etc., Transformed into Another Information Product, Analyzed and Combined with Other Information, and Other Usages. Demographic and Use Environment Characteristics: Type of Work Environment-Public or Private. Management Level-Manager or Non-Manager. Gender-Male or Female. Education Levels-High School through Graduate School Degree. Findings and conclusions are based on analysis and interpretation of the critical functions and relationships among the identified variables of the information transfer and utilization processes, and in the valuation activities accomplished by recipients/users. Dissert. Abstr.

83 ECONOMICS AND COST ANALYSIS

Includes cost effectiveness studies.

N93-12814*# Rockwell International Corp., Pittsburgh, PA. Space Transportation Systems Div.
ORBITAL SPACECRAFT CONSUMABLES RESUPPLY SYSTEM (OSCRS). VOLUME 3: PROGRAM COST ESTIMATE Final Report
D. L. Perry Oct. 1986 24 p
(Contract NAS9-17584)
(NASA-CR-185685; NAS 1.26:185685; STS-86-0302-3-Vol-3; MA-1023T-Vol-3) Avail: CASI HC A03/MF A01

A cost analysis for the design, development, qualification, and production of the monopropellant and bipropellant Orbital Spacecraft Consumable Resupply System (OSCRS) tankers, their associated avionics located in the Orbiter payload bay, and the unique ground support equipment (GSE) and airborne support equipment (ASE) required to support operations is presented. Monopropellant resupply for the Gamma Ray Observatory (GRO) in calendar year 1991 is the first defined resupply mission with bipropellant resupply missions expected in the early to mid 1990's. The monopropellant program estimate also includes contractor costs associated with operations support through the first GRO resupply mission. Author

N93-12920# National Science Foundation, Washington, DC. Div. of Science Resources Studies.
SELECTED DATA ON FEDERAL SUPPORT TO UNIVERSITIES AND COLLEGES: FISCAL YEAR 1990
Apr. 1992 33 p
(NSF-92-310) Avail: CASI HC A03/MF A01

The data presented in this summary are derived from the Survey of Federal Support to Universities, Colleges, and Nonprofit Institutions--Fiscal Year 1990 (hereafter referred to as the Federal Support Survey), and are being released in advance of the publication that contains more comprehensive detailed statistical tables. Among the available data excluded from this summary are academic totals by type of institutional control, by highest degree granted, and by field of science and engineering (S&E) discipline; data on historically black colleges; data on nonprofit institutions; and data on university and nonprofit-administered federally funded research and development centers (FFRDC's). Author

N93-13280# General Accounting Office, Washington, DC.
NASA BUDGET: POTENTIAL SHORTFALLS IN FUNDING NASA'S 5-YEAR PLAN. TESTIMONY BEFORE THE SUBCOMMITTEE ON SCIENCE, TECHNOLOGY, AND SPACE, COMMITTEE ON COMMERCE, SCIENCE, AND TRANSPORTATION, UNITED STATES SENATE
1992 7 p
(GAO/T-NSIAD-92-18) Avail: CASI HC A02/MF A01; GAO, PO Box 6015, Gaithersburg, MD 20877 HC

This GAO congressional report represents testimony before the Subcommittee on Science, Technology, and Space, Committee on Commerce, Science, and Transportation, United States Senate. The potential shortfalls in funding NASA's 5-year plan are described in text and charts. Reconciliation of budget realities and the 5-year plan show shortfalls with three different methods of comparison. NASA's Program Plan calls for a total budget for FY 93-97 of 92.4 billion. When compared with a Base Funding Level (14.3 billion per year) the shortfall would be 20.9 billion. Using an extension of the President's budget of 15 billion per year, the shortfall would be 17.4 billion. Finally using a growth for inflation only, the shortfall would be 12.9 billion. Two programs proposed for elimination, the Advanced Solid Rocket Motor (ASRM) and the Comet Rendevous Asteroid Flyby (CRAF) are excluded from the projections even though $2 billion dollars would be saved since termination is uncertain and due to costs due to termination. R.L.B.

N93-13312# National Science Foundation, Washington, DC. Div. of Science Resources Studies.
FEDERAL R/D FUNDING BY BUDGET FUNCTION: FISCAL YEARS 1991-1993 Annual Report
John E. Jankowski, Jr. Jun. 1992 45 p
(NSF-92-318) Avail: CASI HC A03/MF A01

Table 1 of this report lists by dollar amount 16 types of spending for the 1993 budget. The top five budget functions in descending order are

National Defense, Health, Space Research and Technology, Energy, and General Science. The NASA R&D budget is proposed to increase in 1993 by 12 percent, or $0.8 billion, for a total of $7.5 billion. One-third of the increase is proposed for continuing development of the Space Station Freedom. Highlights from the NASA budget include a proposed funding level of $2.4 billion for the Space Station Freedom which represents 31 percent of total R&D budget authority. Other areas of space activity which show increases are: space transportation capability development - 17 percent to $963 million; space science - 5 percent to $2.0 billion; space and terrestrial applications - 18 percent to $1.3 billion; and space commercialization - 15 percent to $189 million. R.L.B.

N93-13543# National Science Foundation, Washington, DC. Div. of Science Resources Studies.
FEDERAL SUPPORT TO UNIVERSITIES, COLLEGES, AND NONPROFIT INSTITUTIONS: FISCAL YEAR 1990. A REPORT TO THE PRESIDENT AND CONGRESS Report, 1 Oct. 1989 - 30 Sep. 1990
Richard Bennof Jul. 1992 213 p *Its* Surveys of Science Resources Series
(NSF-92-324) Avail: CASI HC A10/MF A03

Summary tables are given for various government agencies as follows: AID (Agency for International Development), COM (Dept. of Commerce), DOD (Dept. of Defense), DOT (Dept. of Transportation), ED (Dept. of Education), HHS (Dept. of Health and Human Services), HUD (Dept. of Housing and Urban Development), INT (Dept. of the Interior), LABOR (Dept. of Labor), NASA (National Aeronautics and Space Administration), NRC (Nuclear Regulatory Commission), NSF (National Science Foundation), and USDA (Dept. of Agriculture). In addition, more specific breakdowns of federal support for HHS divisions are also given. Most of the data is arranged by state. Because of the nature of this congressional report, most federal support is in science and engineering. R.L.B.

N93-13544# National Science Foundation, Washington, DC. Div. of Science Resources Studies.
ACADEMIC SCIENCE AND ENGINEERING: R/D EXPENDITURES, FISCAL YEAR 1990
Jul. 1992 192 p
(Grant NSF SRS-91-00672)
(NSF-92-321) Avail: CASI HC A09/MF A02

University expenditures in science and engineering are arranged in groupings by rank according to expenditures. Summaries preceding institutional listings are grouped by subject, state, and geographical region. The data presented in this report were compiled from the National Science Foundation's (NSF) fiscal year 1990 Survey of Scientific and Engineering Expenditures at Universities and Colleges. They refer to science and engineering expenditures for separately budgeted research and development. The term 'separately budgeted research and development expenditures' includes all funds expended for activities specifically organized to produce research outcomes and commissioned by an agency either external to the institution or separately budgeted by an organizational unit within the institution. R.L.B.

N93-13657# National Science Foundation, Washington, DC. Science and Engineering Activities Program.
SELECTED DATA ON FEDERAL FUNDS FOR RESEARCH AND DEVELOPMENT: FISCAL YEARS 1990, 1991, AND 1992
Jul. 1992 31 p
(NSF-92-319) Avail: CASI HC A03/MF A01

The summary data in these tables show R&D funding levels as reported by 33 Federal agencies and their subdivisions--104 individual respondents--in Mar. - Oct. 1991. All agencies with R&D programs were covered. The amounts reported for each year of this survey include the obligations or outlays incurred in that year, regardless of when the funds were authorized, appropriated, or received by an agency, and regardless of whether the funds are identified in an agency's budget specifically for research, development, or R&D plant. Author

N93-13658# National Science Foundation, Washington, DC. Div. of Science Resources Studies.
RESEARCH AND DEVELOPMENT IN INDUSTRY: 1989. FUNDS, 1989. SCIENTISTS AND ENGINEERS, JANUARY 1990
John R. Gawalt 1992 157 p *Its* Surveys of Science Resources Series
(NSF-92-307) Avail: CASI HC A08/MF A02

The Survey of Research and Development in Industry provides national estimates of the total expenditures on R&D performed within the United States by industrial firms, whether U.S.- or foreign-owned. It is a sample survey in which it is intended that all R&D-performing companies, including privately-held firms, are included or represented. All companies that are identified in the sample year as annually spending more than $1 million on R&D in the United States receive a survey form every year. Information from individual companies in the sample is used to develop national estimates on an industry-by-industry basis. Author

N93-14019*# Los Alamos National Lab., NM. Earth and Space Science Div.
A BASIS OF SETTLEMENT: ECONOMIC FOUNDATIONS OF PERMANENT PIONEER COMMUNITIES
Eric M. Jones *In* NASA. Johnson Space Center, The Second Conference on Lunar Bases and Space Activities of the 21st Century, Volume 2 Sep. 1992 p 697-701 (For primary document see N93-13972 03-91)
Avail: CASI HC A01/MF A03

84 LAW, POLITICAL SCIENCE AND SPACE POLICY

Includes NASA appropriation hearings; aviation law; space law and policy; international law; international cooperation; and patent policy.

N93-13788# Commerce Dept., Washington, DC. Japan Technology Program.
US INDUSTRY ACCESS TO JAPANESE SCIENCE AND TECHNOLOGY: PROCEEDINGS OF A CONFERENCE
Phyllis Genther, William Herrmann, Tamami Kusuda, and Ann Reed Apr. 1992 23 p Conference held 27-28 Mar. 1991
(PB92-167964) Avail: CASI HC A03/MF A01

A summary is provided of a conference which was intended to acquaint high-level U.S. executives and policy makers with the importance of Japanese scientific and technical (S&T) literature. It was also intended to help them to begin to address the complicated issues of how a company gathers and monitors such information, and to explain what benefits can result from such efforts. A secondary objective was to explain the framework established by the 1988 U.S./Japan S&T Agreement, and how the agreement affects the bilateral S&T relationship. The topics covered range from corporate evaluation programs for Japanese S&T to tracking Japanese technical information from the viewpoint of major U.S. corporations. Other topics include access for U.S. industrial researchers to Japanese national and private laboratories; using industry, university and government partnerships to respond to the Japanese; and defining the national interest through cooperation and competition. GRA

N93-13798# Committee on Commerce, Science, and Transportation (U.S. Senate).
NATIONAL AERONAUTICS AND SPACE ADMINISTRATION AUTHORIZATION ACT, FISCAL YEAR 1993
Ernest F. Hollings Washington GPO 1992 49 p Report on H.R. 4364 presented by the Committee on Commerce, Science, and Transportation, 102d Congress, 2d Session, 10 Aug. 1992
(S-Rept-102-364; GPO-59-010) Avail: CASI HC A03/MF A01; Document Room, Senate, Washington, DC 20510 HC; SOD HC

A report of the Senate Committee on Commerce, Science, and Transportation on a bill to authorize fiscal year 1993 appropriations for NASA is presented along with the budget estimates. A detailed summary of the programs funded by this budget is included. L.R.R.

N93-13799# Committee on Science, Space and Technology (U.S. House).
NASA AUTHORIZATION, 1993, VOLUME 2
Washington GPO 1992 592 p Hearings before the Subcommittee on Space, 102d Congress, 2d Session, No. 137, 19 Feb., 26-27 Feb., 4-5

Mar., and 24 Mar. 1992
(GPO-56-943-Vol-2; ISBN-0-16-038977-1) Avail: CASI HC A25/MF A06; Subcommittee on Space, House of Representatives, Washington, DC 20515 HC; SOD HC

Hearings before a subcommittee of the House Committee on Science, Space, and Technology are presented on NASA's 1993 budget request. All written testimony and submittals for the record are included. L.R.R.

N93-13800# Committee on Commerce, Science, and Transportation (U.S. Senate).
NASA'S FISCAL YEAR 1993 BUDGET
Washington GPO 1992 81 p Hearing before the Committee on Commerce, Science, and Transportation, 102d Congress, 2d Session, 17 Mar. 1992
(S-Hrg-102-707; GPO-57-099; ISBN-0-16-038961-5) Avail: CASI HC A05/MF A01; Subcommittee on Science, Technology, and Space, Senate, Washington, DC 20510 HC; SOD HC

Hearings before a subcommittee of the Senate Committee on Commerce, Science, and Transportation are presented on NASA's fiscal year 1993 budget. All written testimony and submittals for the record are included. L.R.R.

85 URBAN TECHNOLOGY AND TRANSPORTATION

Includes applications of space technology to urban problems; technology transfer; technology assessment; and surface and mass transportation.

For related information see also *03 Air Transportation and Safety, 16 Space Transportation,* and *44 Energy Production and Conversion.*

N93-13433*# National Aeronautics and Space Administration, Washington, DC.
COMMERCIAL NON-AEROSPACE TECHNOLOGY TRANSFER PROGRAM FOR THE 2000S: STRATEGIC ANALYSIS AND IMPLEMENTATION
Gary A. P. Horsham Nov. 1992 48 p
(NASA-TM-4424; NAS 1.15:4424) Avail: CASI HC A03/MF A01

This report presents a strategic analysis and implementation plan for NASA's Office of Commercial Programs (OCP), Technology Transfer Division's (TTD), Technology Transfer Program. The main objectives of this study are to: (1) characterize the NASA TTD's environment and past organizational structure; (2) clearly identify current and prospective programmatic efforts; (3) determine an evolutionary view of an organizational structure which could lead to the accomplishment of NASA's future technology transfer aims; and (4) formulate a strategy and plan to improve NASA's (and other federal agencies) ability to transfer technology to the non-aerospace sectors of the U.S. economy. The planning horizon for this study extends through the remainder of the 1990s to the year 2000. Author

N93-14049 Simon Fraser Univ., Burnaby (British Columbia).
THE INFORMED CITIZEN: TECHNOLOGY AND RESPONSIBILITY IN THE INFORMATION AGE Ph.D. Thesis
Peter Geoffrey Cook 1989 213 p
Avail: Univ. Microfilms Order No. DANN59307

This thesis explores the justification and possibility of informed citizenship in the affluent liberal-democratic states. The approach is interdisciplinary, drawing upon literature in communication studies, the philosophy of technology, and political theory. The study focuses on how modern science and technology, and information technology in particular, affect the citizen's parameters of knowledge and action in unprecedented ways. It is argued that the main difficulty for informed citizenship is not the lack of availability of information as such, but rather the pattern of citizen attention to it, and this pattern is itself an outcome of specific social relations of information. In the affluent liberal-democratic states the social relations of information are primarily geared to privatism, i.e., an orientation to intensive commodity consumption, as a way of life. In this context, information procured through advanced technology serves not only to disclose the problems and suffering of a common world, but also to insulate citizens from these same problems. The thesis argues that as a first step toward a deeper understanding of the prospects for informed citizenship, the concept of information should be reformulated to reflect its ambiguous status within contemporary technological civilization. The study first of all outlines three perspectives on the citizen inherited from the modern Enlightenment: the citizen as pursuer of rational self-interest, as a member of a reasoning public, and as an object of technocratic manipulation. The following chapter discusses different approaches within democratic political theory to the question of informed citizenship and in particular the grounds for the citizen's deference to expert knowledge. Then, there is a consideration of the prospects for world citizenship in the light of global technological threats to the conditions for sustaining human life, and the global electronic matrix of instant communication. The next chapter focuses on debates about the role of mass media, and television in particular, in stultifying rather than enhancing informed citizenship. Finally, four themes implicit in the concept of information are highlighted for their relevance to informed citizenship: information as fact, as form, as commodity, and as self-formation. Dissert. Abstr.

88 SPACE SCIENCES (GENERAL)

No abstracts in this category.

89 ASTRONOMY

Includes radio, gamma-ray, and infrared astronomy, and astrometry.

N93-12592*# Eastman Kodak Co., Rochester, NY. Government Systems Div.
LARGE DEPLOYABLE REFLECTOR (LDR) SYSTEM CONCEPT AND TECHNOLOGY DEFINITION STUDY. ANALYSIS OF SPACE STATION REQUIREMENTS FOR LDR Final Technical Report
Donald L. Agnew, Victor F. Vinkey, and Fritz C. Runge (McDonnell-Douglas Astronautics Co., Huntington Beach, CA.) Apr. 1989 116 p
(Contract NAS2-11861; RTOP 506-62-21)
(NASA-CR-177414; NAS 1.26:177414) Avail: CASI HC A06/MF A02

A study was conducted to determine how the Large Deployable Reflector (LDR) might benefit from the use of the space station for assembly, checkout, deployment, servicing, refurbishment, and technology development. Requirements that must be met by the space station to supply benefits for a selected scenario are summarized. Quantitative and qualitative data are supplied. Space station requirements for LDR which may be utilized by other missions are identified. A technology development mission for LDR is outlined and requirements summarized. A preliminary experiment plan is included. Space Station Data Base SAA 0020 and TDM 2411 are updated. Author

N93-12657*# Alabama Univ., Huntsville. Center for Applied Optics.
SOFT X RAY TELESCOPE (SXT) FOCUS ERROR ANALYSIS Final Report No. 3, Dec. 1990 - Mar. 1991
Anees Ahmad 4 Mar. 1991 29 p
(Contract NAS8-36955)
(NASA-CR-184443; NAS 1.26:184443; UAH-5-32527) Avail: CASI HC A03/MF A01

The analysis performed on the soft x-ray telescope (SXT) to determine the correct thickness of the spacer to position the CCD camera at the best focus of the telescope and to determine the maximum uncertainty in this focus position due to a number of metrology and experimental errors, and thermal, and humidity effects is presented. This type of analysis has been performed by the SXT prime contractor, Lockheed Palo Alto Research Lab (LPARL). The SXT project office at MSFC formed an independent team of experts to review the LPARL work, and verify the analysis performed by them. Based on the recommendation of this team, the project office will make a decision if an end to end focus test is required for the SXT

prior to launch. The metrology and experimental data, and the spreadsheets provided by LPARL are used at the basis of the analysis presented. The data entries in these spreadsheets have been verified as far as feasible, and the format of the spreadsheets has been improved to make these easier to understand. The results obtained from this analysis are very close to the results obtained by LPARL. However, due to the lack of organized documentation the analysis uncovered a few areas of possibly erroneous metrology data, which may affect the results obtained by this analytical approach. Author

N93-12898*# George Washington Univ., Washington, DC.
PUBLICATIONS OF THE SPACE PHYSIOLOGY AND COUNTERMEASURES PROGRAM, MUSCULOSKELETAL DISCIPLINE: 1980-1990
Elizabeth L. Hess, Janice Wallace-Robinson, Katherine J. Dickson, and Janet V. Powers Oct. 1992 103 p
(Contract NASw-4324)
(NASA-CR-4468; NAS 1.26:4468) Avail: CASI HC A06/MF A02

A 10-year cumulative bibliography of publications resulting from research supported by the musculoskeletal discipline of the space physiology and countermeasures program of NASA's Life Sciences Division is provided. Primary subjects are bone, mineral, and connective tissue, and muscle. General physiology references are also included. Principal investigators whose research tasks resulted in publication are identified by asterisk. Publications are identified by a record number corresponding with their entry in the life sciences bibliographic database, maintained by the George Washington University. Author

N93-13272*# Pennsylvania State Univ., University Park. Dept. of Astronomy and Astrophysics.
PROBING THE GALACTIC HALO WITH ROSAT Semiannual Report
David N. Burrows and J. A. Mendenhall 1992 19 p
(Grants NAG5-1535; NAG5-1786)
(NASA-CR-191268; NAS 1.26:191268) Avail: CASI HC A03/MF A01

We discuss the current status of ROSAT shadowing observations designed to search for emission from million degree gas in the halo of the Milky Way galaxy. Preliminary results indicate that million degree halo gas is observed in the 1/4 keV band in some directions, most notably toward the Draco cloud at (l,b) = (92 deg, +38 deg), but that the halo emission is patchy and highly anisotropic. Our current understanding of this halo emission is based on a small handful of observations which have been analyzed to date. Many more observations are currently being analyzed or are scheduled for observation within the next year, and we expect our understanding of this component of the galactic halo to improve dramatically in the near future. Author

N93-13273# Royal Observatory, Edinburgh (Scotland).
UNITED KINGDOM INFRARED TELESCOPE Annual Report, 1991
1991 57 p Prepared in cooperation with Joint Astronomy Centre, Hilo, HI
Avail: CASI HC A04/MF A01

The cooled grating spectrometer CGS4, which is an infrared array spectrometer with its novel design and atmospheric optics, gives UK Infrared Telescope (UKIRT) a substantial lead over its competitores. The system has a sensitivity capable of measuring infrared spectra of cosmologically interesting objects such as high redshift quasars. The greatly increased resolving power also enables the infrared study of nearby objects in unprecedented detail and has, for example, enabled the detection of frozen carbon monoxide and carbon dioxide on Tritron. These and other scientific results are described, showing the wide range of science to which UKIRT contributes. Operations report, instrumentation development, and financial statement are also described. I.I.C.

N93-13339# Los Alamos National Lab., NM.
RADIAL AND NONRADIAL PERIODS AND GROWTH RATES OF AN AI VELORUM MODEL
J. A. Guzik 1992 5 p Presented at the International Astronomical Union Meeting, Mito (Japan), 6-10 Jan. 1992
(Contract W-7405-eng-36)
(DE92-011369; LA-UR-92-861; CONF-920184-3) Avail: CASI HC A01/MF A01

Walraven, Walraven, and Balona recently discovered several new periodicities in addition to the well-known fundamental and first overtone periods of the high-amplitude delta Scuti star AI Velorum. Linear nonadiabatic pulsation calculations were performed for an AI Velorum model of mass 1.96 solar mass, 24.05 solar luminosity, and T(sub eff) 7566 K for the radial and low-degree nonradial modes to help verify the tentative identifications made by Walraven, et al. Comparison of the calculated periods with the observations suggests some alternatives to the identifications proposed by Walraven, et al. DOE

N93-13342# Los Alamos National Lab., NM.
UNIFORMITY RESULTS OF THE MULTILAYER MIRRORS USED IN THE ALEXIS ULTRASOFT X RAY TELESCOPES
D. Roussel-Dupre and F. Ameduri 1992 10 p Presented at the SPIE International Symposium on Optical Applied Science and Engineering, San Diego, CA, 19-24 Jul. 1992
(Contract W-7405-eng-36)
(DE92-018611; LA-UR-92-2457; CONF-920792-27) Avail: CASI HC A02/MF A01

The Array of Low Energy X-ray Imaging Sensors (ALEXIS) experiment, a mini-satellite containing six wide angle EUV/ultrasoft X-ray telescopes, is scheduled to be launched by a Pegasus rocket into a 425 nautical mile orbit in 1992 to observe cosmic X-rays. The telescopes utilize near normal incidence optics featuring a 12.8 cm diameter, 13.52 cm radius of curvature spherical mirror with a Mo/Si multilayer coating. The multilayer coatings are tuned to wavelengths of 133, 171, and 186 A. In addition, the top layers are comprised of a unique 'wavetrap' designed to suppress the dominate background radiation at 304 A from the geocorona. We present measured performance data for these mirrors including the two dimensional uniformity of the multilayer as a function of both radius and angular rotation, the measured reflectivity at the primary wavelength and the effectiveness of the 'wavetrap'. We also discuss problems encountered due to contamination and design changes that have been made to mitigate the effect of contamination. DOE

N93-13343 Arizona Univ., Tucson.
NOVEL TECHNIQUES OF WAVEFRONT SENSING FOR ADAPTIVE OPTICS WITH ARRAY TELESCOPES USING AN ARTIFICIAL NEURAL NETWORK Ph.D. Thesis
Michael Lloyd-Hart 1992 169 p
Avail: Univ. Microfilms Order No. DA9220676

Atmospheric turbulence causes severe degradation of the resolving and signal-to-noise properties of present optical telescopes. Diffraction-limited resolution can be recovered through the use of a deformable ('adaptive') optical element to correct the atmospheric wavefront error. An adaptive optics system operating in the near infrared (1.7 - 3.5 microns) has been developed for use at the Multiple Mirror Telescope (MMT), an array of six co-mounted 1.8 m telescopes, in which six flat mirrors are used to correct the wavefront tilt across each aperture, and the phase differences between apertures. This can reduce the error sufficiently to achieve a diffraction-limited image with a central peak of 0.06 arcseconds full width at half maximum at 2.2 microns wavelength. A number of algorithms are used to drive the adaptive mirror in a closed servo loop, including a trained artificial neural network which deduces the wavefront aberration from a pair of simultaneous in- and out-of-focus images of a star, taken at the combined focal plane of the telescope. Computer simulations have shown that the net is capable of deriving the wavefront for the full six-mirror aperture, and in practice, the net has been demonstrated in the lab to maintain two- and three-aperture diffraction-limited beam profiles in the presence of distorting effects. On the sky, with a real star, the net has successfully restored the diffraction limit for two adjacent MMT segments. High resolution images have been obtained of various objects with a wide-field camera looking in the field around the wavefront reference star. Work has also been carried out to characterize the wavefront aberration at the MMT, which confirms the Kolmogorov model of turbulence. Finally, a new algorithm is discussed which shows great promise for correction of phase errors in array telescopes. Dissert. Abstr.

N93-13352*# Johns Hopkins Univ., Baltimore, MD. Dept. of Physics and Astronomy.
THE MASS AND DYNAMICS OF cD CLUSTERS WITH COOLING FLOWS. 1: ROSAT OBSERVATIONS OF A 496 Progress Report

Gerard A. Kriss 24 Nov. 1992 11 p
(Grant NAG5-1636)
(NASA-CR-191240; NAS 1.26:191240) Avail: CASI HC A03/MF A01

As a part of a program to determine the mass distribution of cD galaxy clusters with cooling flows, we obtained a ROSAT image of the cluster A 496. The image reveals sharply peaked emission centered on the cD galaxy. Both the peaked cooling flow emission and the more extended emission filling the cluster are centered on the cD galaxy to within 15 sec. The surface brightness profile is consistent with previous Einstein HRI observations. We measure spatially resolved spectra for the x-ray emission, and find a significant decline in temperature in the innermost 2 to 4 min. We also find a gradient in absorption due to cold neutral gas, with excess absorption, however, is far below previously reported values. We caution that this is a progress report, and that our results are preliminary. Author

N93-13461*# National Aeronautics and Space Administration. Goddard Space Flight Center, Greenbelt, MD.
INTERNATIONAL ULTRAVIOLET EXPLORER (IUE) ULTRAVIOLET SPECTRAL ATLAS OF SELECTED ASTRONOMICAL OBJECTS
Chi-Chao Wu (Computer Sciences Corp., Beltsville, MD.), Gail A. Reichert (Computer Sciences Corp., Beltsville, MD.), Thomas B. Ake (Computer Sciences Corp., Beltsville, MD.), Albert Boggess, Albert V. Holm (Computer Sciences Corp., Beltsville, MD.), Catherine L. Imhoff (Computer Sciences Corp., Beltsville, MD.), Yoji Kondo, Jaylee M. Mead, and Steven N. Shore (Computer Sciences Corp., Beltsville, MD.) Nov. 1992 419 p
(NASA-RP-1285; NAS 1.61:1285; Rept-92B00114) Avail: CASI HC A18/MF A04

The IUE Ultraviolet Spectral Atlas of Selected Astronomical Objects (or 'the Atlas'), is based on the data that were available in the IUE archive in 1986, and is intended to be a quick reference for the ultraviolet spectra of many categories of astronomical objects. It shows reflected sunlight from the Moon, planets, and asteroids, and also shows emission from comets. Comprehensive compilations of UV spectra for main sequence, subgiant, giant, bright giant, and supergiant stars are published elsewhere. This Atlas contains the spectra for objects occupying other areas of the Hertzsprung-Russell diagram: pre-main sequence stars, chemically peculiar stars, pulsating variables, subluminous stars, and Wolf-Rayet stars. This Atlas also presents phenomena such as the chromospheric and transition region emissions from late-type stars; composite spectra of stars, gas streams, accretion disks and gas envelopes of binary systems; the behavior of gas ejecta shortly after the outburst of novac and supernovac; and the H II regions, planetary nebulae, and supernova remnants. Population 2 stars, globular clusters, and luminous stars in the Magellanic Clouds, M31, and M33, are also included in this publication. Finally, the Atlas gives the ultraviolet spectra of galaxies of different Hubble types and of active galaxies. Author

N93-13480 Columbia Univ., New York, NY.
A HIGH-RESOLUTION RADIO SURVEY OF THE GALACTIC PLANE
Ph.D. Thesis
Saeid Zoonematkermani 1990 186 p
Avail: Univ. Microfilms Order No. DA9128016

A multi-frequency high resolution survey of the Galactic plane was carried out using the Very Large Array. The 1400 MHz (20 cm) survey was divided into inner and outer portions. We present here a catalog of the 1992 discrete sources detected in the inner portion of the 20 cm survey which is approximately 75 percent complete to 25 mJy for sources smaller than approximately 20 in. in diameter. The catalog includes for each entry a position accurate to approximately less than 3 in., peak and integrated flux densities, source extent, and information on counterparts both from earlier radio surveys of the plan and from the Infrared Astronomical Satellite (IRAS) point source catalog. An extensive analysis of the integrity and completeness of the survey is presented. This survey has revealed a strong concentration of low-latitude objects with 50 deg of the Galactic center with a scale height of approximately 25 pc. This extreme Population 1 subset of the catalog is dominated by sources with diameters between 3-20 arcsec; most are associated with strong far infrared sources and are compact and ultracompact (UC) H 2 regions. Most of the sources are UC H 2 regions distributed with the amazingly small scale height of only approximately 25 pc. Only 23 of the 64 known planetary nebulae (PNe) are detected in our survey; however, practically all of the radio-selected PNe have essentially identical IRAS colors, suggesting that they are in very similar evolutionary states. The other 19 sources with similar infrared colors in our survey are likely to be previously unrecognized, highly reddened PNe. A total of 297 sources were detected in the 6 cm survey which is 90 percent complete to 5 mJy. More than 30 percent of these sources have infrared counterparts, and we have identified 117 matches to our 20 cm sources. Dissert. Abstr.

N93-13579*# New Mexico Univ., Albuquerque. Inst. for Astrophysics.
A LUNAR OPTICAL-ULTRAVIOLET-INFRARED SYNTHESIS ARRAY (LOUISA)
Jack O. Burns, ed. (New Mexico State Univ., Las Cruces.), Stewart W. Johnson, ed. (BDM Corp., Albuquerque, NM.), and Nebojsa Duric, ed. Washington NASA Nov. 1992 294 p Workshop held in Albuquerque, NM, 8-10 Feb. 1989 Sponsored by NASA. Washington
(NASA-CP-3066; NAS 1.55:3066) Avail: CASI HC A13/MF A03

This document contains papers presented at a workshop held to consider 'optical ultraviolet infrared' interferometric observations from the moon. Part 1 is an introduction. Part 2 is a description of current and planned ground-based interferometers. Part 3 is a description of potential space-based interferometers. Part 4 addresses the potential for interferometry on the moon. Part 5 is the report of the workshop's working groups. Concluding remarks, summary, and conclusions are presented in Part 6. For individual titles, see N93-13580 through N93-13601.

N93-13580*# National Radio Astronomy Observatory, Socorro, NM.
RADIO AND OPTICAL INTERFEROMETRIC IMAGING
Tim J. Cornwell *In* New Mexico Univ., A Lunar Optical-Ultraviolet-Infrared Synthesis Array (LOUISA) Nov. 1992 p 7-17 (For primary document see N93-13579 03-89)
(Grant NSF AST-88-14515)
Avail: CASI HC A03/MF A03

Since diffraction-limited imaging with a single aperture yields angular resolution approx. lambda/D, the attainment of high angular resolution with single apertures requires the construction of correspondingly large monolithic apertures, the whole surface of which must be figured to much less than a wavelength. At the longer wavelengths, it is impossible to build a sufficiently large single aperture: for example, at lambda 21 cm, arcsec resolution requires an aperture of diameter approx. 50 km. At the shorter wavelengths, the atmosphere imposes a natural limit in resolution of about one arcsec. However, another route is possible; that is, using synthetic apertures to image the sky. Synthetic apertures are now in use in many fields, e.g., radio interferometry, radar imaging, and magnetic-resonance imaging. Radio-interferometric techniques developed in radio astronomy over the past 40 years are now being applied to optical and IR astronomical imaging by a number of groups. Furthermore, the problem of figuring synthetic apertures is considerably simpler, and can be implemented in a computer: new 'self-calibration' techniques allow imaging even in the presence of phase errors due to the atmosphere. Author

N93-13581*# Georgia State Univ., Atlanta. Center for High Angular Resolution Astronomy.
THE CHARA OPTICAL ARRAY
Harold A. McAlister *In* New Mexico Univ., A Lunar Optical-Ultraviolet-Infrared Synthesis Array (LOUISA) Nov. 1992 p 18-34 (For primary document see N93-13579 03-89)
(Grant NSF AST-84-21304)
Avail: CASI HC A03/MF A03

The Center for High Angular Resolution Astronomy (CHARA) was established in the College of Arts and Sciences at Georgia State University in 1984 with the goals of designing, constructing, and then operating a facility for very high spatial resolution astronomy. The interest in such a facility grew out of the participants' decade of activity in speckle interferometry. Although speckle interferometry continues to provide important astrophysical measurements of a variety of objects, many pressing problems require resolution far beyond that which can be expected from single aperture telescopes. In early 1986, CHARA received a grant from the National Science Foundation which has permitted a detailed exploration of the feasibility of constructing a facility which will provide a hundred-fold increase in angular resolution over what is possible by speckle interferometry at the largest existing telescopes. The design concept for the CHARA Array was developed initially with the contractural collaboration of United Technologies Optical Systems, Inc., in West Palm Beach, Florida, an

arrangement that expired in August 1987. In late November 1987, the Georgia Tech Research Institute joined with CHARA to continue and complete the design concept study. Very high-resolution imaging at optical wavelengths is clearly coming of age in astronomy. The CHARA Array and other related projects will be important and necessary milestones along the way toward the development of a major national facility for high-resolution imaging--a true optical counterpart to the Very Large Array. Ground-based arrays and their scientific output will lead to high resolution facilities in space and, ultimately, on the Moon. Author

N93-13582*# Hulburt (E. O.) Center for Space Research, Washington, DC.

THE MOUNT WILSON OPTICAL INTERFEROMETER: THE FIRST AUTOMATED INSTRUMENT AND THE PROSPECTS FOR LUNAR INTERFEROMETRY

Ken J. Johnston, D. Mozurkewich, R. S. Simon, Michael Shao (Smithsonian Astrophysical Observatory, Cambridge, MA.), and M. Colavita (Smithsonian Astrophysical Observatory, Cambridge, MA.) *In* New Mexico Univ., A Lunar Optical-Ultraviolet-Infrared Synthesis Array (LOUISA) Nov. 1992 p 35-48 (For primary document see N93-13579 03-89)

Avail: CASI HC A03/MF A03

Before contemplating an optical interferometer on the Moon one must first review the accomplishments achieved by this technology in scientific applications for astronomy. This will be done by presenting the technical status of optical interferometry as achieved by the Mount Wilson Optical Interferometer. The further developments needed for a future lunar-based interferometer are discussed. Author

N93-13583*# Observatoire de la Cote d'Azur, Nice (France).

THE OPTICAL VERY LARGE ARRAY AND ITS MOON-BASED VERSION

Antoine Labeyrie *In* New Mexico Univ., A Lunar Optical-Ultraviolet-Infrared Synthesis Array (LOUISA) Nov. 1992 p 49-58 (For primary document see N93-13579 03-89)

Avail: CASI HC A02/MF A03

An Optical Very Large Array (OVLA) is currently in early prototyping stages for ground-based sites, such as Mauna Kea and perhaps the VLT site in Chile. Its concept is also suited for a moon-based interferometer. With a ring of bi-dimensionally mobile telescopes, there is maximal flexibility in the aperture pattern, and no need for delay lines. A circular configuration of many free-flying telescopes, TRIO, is also considered for space interferometers. Finally, the principle of gaseous mirrors may become applicable for moon-based optical arrays. Fifteen years after the first coherent linkage of two optical telescopes, the design of an ambitious imaging array, the OVLA, is now well advanced. Two 1.5 m telescopes have been built and now provide astronomical results. Elements of the OVLA are under construction. Although primarily conceived for ground-based sites, the OVLA structure appears to meet the essential requirements for operation on the Moon. Autnor

N93-13584*# California Inst. of Tech., Pasadena. Palomar Observatory.

HIGH RESOLUTION IMAGING AT PALOMAR

Shrinivas R. Kulkarni *In* New Mexico Univ., A Lunar Optical-Ultraviolet-Infrared Synthesis Array (LOUISA) Nov. 1992 p 59-74 Sponsored in part by W. M. Keck Foundation (For primary document see N93-13579 03-89)

Avail: CASI HC A03/MF A03

For the last two years we have embarked on a program of understanding the ultimate limits of ground-based optical imaging. We have designed and fabricated a camera specifically for high resolution imaging. This camera has now been pressed into service at the prime focus of the Hale 5 m telescope. We have concentrated on two techniques: the Non-Redundant Masking (NRM) and Weigelt's Fully Filled Aperture (FFA) method. The former is the optical analog of radio interferometry and the latter is a higher order extension of the Labeyrie autocorrelation method. As in radio Very Long Baseline Interferometry (VLBI), both these techniques essentially measure the closure phase and, hence, true image construction is possible. We have successfully imaged binary stars and asteroids with angular resolution approaching the diffraction limit of the telescope and image quality approaching that of a typical radio VLBI map. In addition, we have carried out analytical and simulation studies to determine the ultimate limits of ground-based optical imaging, the limits of space-based interferometric imaging, and investigated the details of imaging tradeoffs of beam combination in optical interferometers. Author

N93-13585*# California Univ., Berkeley. Space Sciences Lab.

RECENT ASTRONOMICAL RESULTS FROM THE INFRARED SPATIAL INTERFEROMETER AND THEIR IMPLICATIONS FOR LOUISA

William C. Danchi, M. Bester, and C. H. Townes *In* New Mexico Univ., A Lunar Optical-Ultraviolet-Infrared Synthesis Array (LOUISA) Nov. 1992 p 75-92 Sponsored in part by New York Academy of Sciences (For primary document see N93-13579 03-89)

(Contract N00014-82-C-0700)

Avail: CASI HC A03/MF A03

A new heterodyne interferometer for the atmospheric window from 9 to 12 microns was developed during the past five years. This instrument, called the Infrared Spatial Interferometer (ISI), was designed to use earth rotation aperture synthesis techniques developed in radio interferometry. It was moved to Mt. Wilson, California, in January 1988 and first fringes were obtained in June of that year. Systematic observations of some of the brighter late-type stars began shortly after the first fringes were obtained. We describe the basic principles and design of the ISI and give an overview of some of the initial results obtained from these observations. The implications of our work to the proposed Lunar Optical/UV/IR Synthesis Array (LOUISA) are discussed. We also analyze the conditions for the maximum signal-to-noise ratio of such an interferometer as a function of wavelength. The optimum wavelength is found to depend on the assumed scaling relation between telescope area and wavelength. Author

N93-13586*# New Mexico Univ., Albuquerque. Center for Advanced Studies.

SHOT NOISE LIMITS TO SENSITIVITY OF OPTICAL INTERFEROMETRY

Sudhakar Prasad *In its* A Lunar Optical-Ultraviolet-Infrared Synthesis Array (LOUISA) Nov. 1992 p 93-107 (For primary document see N93-13579 03-89)

Avail: CASI HC A03/MF A03

By arguing that the limiting noise is the photoelectron shot noise, we show that the sensitivity of image synthesis by an ideal optical interferometer is independent of the details of beam-splitting and recombination. The signal-to-noise ratio of the synthesized image is proportional to the square root of the total number of photoelectrons detected by the entire array. For non-ideal interferometers, which are forced to employ a closure-phase method of indirect inference of the visibility data, essentially the same result holds for strong sources, but at weak light levels beam-splitting degrades sensitivity. Author

N93-13587*# Jet Propulsion Lab., California Inst. of Tech., Pasadena.

ORBITING SPACE INTERFEROMETER (OSI): A FIRST GENERATION SPACE INTERFEROMETER

Michael Shao *In* New Mexico Univ., A Lunar Optical-Ultraviolet-Infrared Synthesis Array (LOUISA) Nov. 1992 p 109-113 (For primary document see N93-13579 03-89)

Avail: CASI HC A01/MF A03

The technical requirements and performance of a first generation space interferometer is discussed. The performance of an interferometer, sensitivity, field of view, dynamic range, astrometric accuracy, etc, in space is set by what cannot be achieved for a ground-based instrument. For the Orbiting Space Interferometer (OSI), the nominal performance parameters are 20 mag sensitivity, field of view of approximately 500*500 pixels, a 1000:1 dynamic range in the image with one milliarcsec resolution, and an astrometric accuracy of 0.1 milliarcsec for wide angle astrometry and 10 microarcsec accuracy for narrow field astrometry (few degrees). OSI is a fully phased interferometer where all critical optical paths are controlled to 0.05 wavelengths. The instrument uses two guide interferometers locked on bright stars several degrees away to provide the spacecraft attitude information needed to keep the fringes from the faint science object stable on the detector. Author

N93-13588*# Space Telescope Science Inst., Baltimore, MD.

HARDI: A HIGH ANGULAR RESOLUTION DEPLOYABLE INTERFEROMETER FOR SPACE

Pierre Y. Bely (European Space Agency. European Space Research and Technology Center, ESTEC, Noordwijk, Netherlands), Christopher Burrows

(European Space Agency. European Space Research and Technology Center, ESTEC, Noordwijk, Netherlands), Francois Roddier (Hawaii Univ., Honolulu.), and Gerd Weigelt (Max-Planck-Inst. fuer Radioastronomie, Bonn, Germany) *In* New Mexico Univ., A Lunar Optical-Ultraviolet-Infrared Synthesis Array (LOUISA) Nov. 1992 p 114-126 (For primary document see N93-13579 03-89)
Avail: CASI HC A03/MF A03

We describe here a proposed orbiting interferometer covering the UV, visible, and near-IR spectral ranges. With a 6-m baseline and a collecting area equivalent to about a 1.4 m diameter full aperture, this instrument will offer significant improvements in resolution over the Hubble Space Telescope, and complement the new generation of ground-based interferometers with much better limiting magnitude and spectral coverage. On the other hand, it has been designed as a considerably less ambitious project (one launch) than other current proposals. We believe that this concept is feasible given current technological capabilities, yet would serve to prove the concepts necessary for the much larger systems that must eventually be flown. The interferometer is of the Fizeau type. It therefore has a much larger field (for guiding) better UV throughout (only 4 surfaces) than phased arrays. Optimize aperture configurations and ideas for the cophasing and coalignment system are presented. The interferometer would be placed in a geosynchronous or sunsynchronous orbit to minimize thermal and mechanical disturbances and to maximize observing efficiency.
Author

N93-13589*# Lockheed Missiles and Space Co., Sunnyvale, CA. Astronautics Div.
SUPPORT AND SERVICING REQUIREMENTS FOR LARGE OBSERVATORIES IN SPACE
Thomas E. Styczynski *In* New Mexico Univ., A Lunar Optical-Ultraviolet-Infrared Synthesis Array (LOUISA) Nov. 1992 p 127-131 (For primary document see N93-13579 03-89)
Avail: CASI HC A01/MF A03

The concept of lunar optical and IR observatories is a natural step in the total utilization of the space environment for the benefit of science. Among the challenges associated with this remote observatory concept is the requirement for the support and servicing of the facility. This presentation will draw on the experience of the Hubble Space Telescope (HST) program on-orbit maintenance design requirements plus the Lockheed on-orbit servicing and assembly activity to develop requirements for the maintenance and construction of a lunar observatory.
Author

N93-13590*# National Optical Astronomy Lab. Tucson, AZ.
SCIENCE OBJECTIVES FOR GROUND- AND SPACE-BASED OPTICAL/IR INTERFEROMETRY
Stephen T. Ridgway *In* New Mexico Univ., A Lunar Optical-Ultraviolet-Infrared Synthesis Array (LOUISA) Nov. 1992 p 132-143 Sponsored in part by NSF (For primary document see N93-13579 03-89)
Avail: CASI HC A03/MF A03

Ground-based interferometry will make spectacular strides in the next decade. However, it will always be limited by the turbulence of the terrestrial atmosphere. Some of the most exciting and subtle problems may only be addressed from a stable platform above the atmosphere. The lunar surface offers such a platform, nearly ideal in many respects. Once built, such a telescope array will not only resolve key fundamental problems, but will revolutionize virtually every topic in observational astronomy. Estimates of the possible performance of lunar and ground-based interferometers of the 21st century shows that the lunar interferometer reaches the faintest sources of all wavelengths, but has the most significant advantage in the infrared.
Author

N93-13591*# National Aeronautics and Space Administration, Washington, DC.
TELESCOPES ON THE MOON OR PIE IN THE SKY?
Carl B. Pilcher *In* New Mexico Univ., A Lunar Optical-Ultraviolet-Infrared Synthesis Array (LOUISA) Nov. 1992 p 145-156 Revised (For primary document see N93-13579 03-89)
Avail: CASI HC A03/MF A03

The question is examined of whether it makes sense to believe that there will one day be an interferometric array of telescopes on the Moon. The question is really one of national commitment to a lunar base, since it is not likely that a scientific undertaking of this magnitude would occur in the absence of permanent human presence on the Moon. A discussion is also given of the real possibility if the exploration of space should be a multinational effort.
E.R.

N93-13592*# Arizona Univ., Tucson. Steward Observatory.
LUNAR INTERFEROMETRIC ASTRONOMY: SOME BASIC QUESTIONS
Neville Woolf *In* New Mexico Univ., A Lunar Optical-Ultraviolet-Infrared Synthesis Array (LOUISA) Nov. 1992 p 157-162 (For primary document see N93-13579 03-89)
Avail: CASI HC A02/MF A03

The author examines some basic questions as to why there should be astronomical facilities on the far side of the moon. The questions are ones of appropriateness, i.e., is this a proper use for human resources, what the real goals are, and are the present concepts the best match for the goals.
E.R.

N93-13593*# BDM International, Inc., Albuquerque, NM.
LUNAR OPTICAL TELESCOPES: AN HISTORICAL PERSPECTIVE
Stewart W. Johnson *In* New Mexico Univ., A Lunar Optical-Ultraviolet-Infrared Synthesis Array (LOUISA) Nov. 1992 p 163-182 (For primary document see N93-13579 03-89)
(Grant NAG9-245)
Avail: CASI HC A03/MF A03

There is a long history of thought and discussion on the possibilities of astronomical observatories on the Moon. Numerous ideas have been suggested and a variety of concepts have resulted for lunar optical telescopes. This paper reviews some of the ideas and efforts of individuals and working groups including Hershel, Clarke, Malina, Herbig, and Hess; working groups of the 1960s; and recent initiatives of Burke, Burns, and others. The enhanced technologies of the 1980s and 1990s can make past dreams of lunar observatories come to reality in the 21st century.
Author

N93-13594*# Hawaii Univ., Honolulu. Inst. of Geophysics.
THE LUNAR ENVIRONMENT AND ITS EFFECT ON OPTICAL ASTRONOMY
G. Jeffrey Taylor *In* New Mexico Univ., A Lunar Optical-Ultraviolet-Infrared Synthesis Array (LOUISA) Nov. 1992 p 183-195 (For primary document see N93-13579 03-89)
(Grant NAG9-245)
Avail: CASI HC A03/MF A03

The Moon's geologic environment features: (1) gravity field one-sixth that of Earth; (2) sidereal rotation period of 27.3 days; (3) surface with greater curvature than Earth's surface (a chord along a 10 km baseline would have a bulge of 7.2 m); (4) seismically and tidally stable platform on which to make astronomical observations (most moonquakes have magnitudes of 1 to 2 on the Richter scale, within the earth's seismic noise, resulting in ground motions only 1 nm); (5) tenuous atmosphere (the total mass at night is only 10(exp 4) kg) that has an optical depth of 10(exp -6) and does not cause wind induced stresses and vibrations on structures; (6) large diurnal temperature variation (100 to 385 K in equatorial regions), which telescopes must be designed to withstand; (7) weak magnetic field, ranging from 3 to 330 x 10(exp -9) T, compared to 3 x 10(exp -5) T on Earth at the equator; (8) surface exposed to radiation, the most dangerous of which are high energy (1 to 100 Mev) particles resulting from solar flares; (9) high flux of micrometeorites which are not slowed down from their cosmic velocities because of the lack of air (data indicate that microcraters greater than 10 microns across will form at the rate of 3000/sq m/yr); (10) regolith 2 to 30 m thick which blankets the entire lunar surface (this layer is fine-grained (average grain sizes range from 40 to 268 microns), has a low density (800 to 1000 kg/cu m in the upper few mm, rising to 1500 to 1800 kg/cu m at depths of 10 to 20 cm), is porous (35 to 45 pct), cohesive (0.1 to 1.0 kN/sq m), and has a low thermal diffusivity (0.7 to 1.0 x 110-8 sq m/sec); about 29 pct of the regolith is less than 20 micron in size (this dust could pose a hazard to optical telescopes); (11) rubbly upper several hundred meters in which intact bedrock is uncommon, especially in the lunar highlands; and (12) craters with diameter-to-depth ratios of 5 if fresh and less than km across (larger and eroded craters have diameter-to-depth ratios greater than 5).
Author

N93-13595*# BDM International, Inc., Albuquerque, NM.
ENVIRONMENTAL EFFECTS ON AN OPTICAL-UV-IR SYNTHESIS ARRAY
Stewart W. Johnson, G. Jeffrey Taylor (Hawaii Univ., Honolulu.), and John P. Wetzel *In* New Mexico Univ., A Lunar Optical-Ultraviolet-Infrared Synthesis Array (LOUISA) Nov. 1992 p 196-209 (For primary document see N93-13579 03-89)
(Grant NAG9-245)
Avail: CASI HC A03/MF A03

The Moon offers a stable platform with excellent seeing conditions for the Lunar Optical-UV-IR Synthesis Array (LOUISA). Some troublesome aspects of the lunar environment will need to be overcome to realize the full potential of the Moon as an observatory site. Mitigation of negative effects of vacuum, thermal radiation, dust, and micrometeorite impact is feasible with careful engineering and operational planning. Shields against impact, dust, and solar radiation need to be developed. Means of restoring degraded surfaces are probably essential for optical and thermal control surfaces deployed in long-lifetime lunar facilities. Precursor missions should be planned to validate and enhance the understanding of the lunar environment (e.g., dust behavior without and with human presence and to determine environmental effects on surfaces and components. Precursor missions should generate data useful in establishing keepout zones around observatory facilities while rocket launches and landings, mining, and vehicular traffic could be detrimental to observatory operation. Author

N93-13596*# Massachusetts Inst. of Tech., Cambridge. Dept. of Physics.
AN OPTICAL VLA ON THE MOON
Bernard F. Burke *In* New Mexico Univ., A Lunar Optical-Ultraviolet-Infrared Synthesis Array (LOUISA) Nov. 1992 p 210-224 (For primary document see N93-13579 03-89)
Avail: CASI HC A03/MF A03

Optical observations on the Earth must cope with the refractive disturbances of the atmosphere, perturbations by the day-to-night thermal cycle, vibrations induced by the wind, and the bending of the telescope by gravity. These all conspire to limit telescope performance. In particular, in trying to improve angular resolution, there seems to be a practical limit of the order of a few tenths of an arc-second for the realizable angular resolution of single-aperture telescopes, largely imposed by the atmosphere, although other structural limitations would appear as limits at one-tenth of an arc-second or so. Author

N93-13597*# Massachusetts Inst. of Tech., Cambridge. Dept. of Physics.
APPENDIX: LIMITS ON THE USE OF HETERODYNING AND AMPLIFICATION IN OPTICAL INTERFEROMETRY
Bernard F. Burke *In* New Mexico Univ., A Lunar Optical-Ultraviolet-Infrared Synthesis Array (LOUISA) Nov. 1992 p 225-226 (For primary document see N93-13579 03-89)
Avail: CASI HC A01/MF A03

The development of optical fibers, lasers, and mixers at optical frequencies has offered the hope that active methods can contribute to optical interferometry. Heterodyning, in particular, looks attractive, even though bandwidths are narrower than one would like at present; one might expect this limitation to lessen as technology develops. That expectation, unfortunately, is not likely to benefit interferometry at optical wavelengths because of the intervention of quantum mechanics and the second law of thermodynamics, as Burke (1985a) pointed out. So much 'second quantization' noise is generated that only at infrared frequencies, somewhere in the 10-100 micron range, can one look forward to heterodyning in any realistic sense. The reason is easily understood. Every amplifier, in the quantum limit, works by stimulated emission, even though this basic truth is not obvious at radio frequencies. This means that there must be spontaneous emission occurring within every amplifier, and Strandberg (1957) showed that this implied a limiting noise temperature, T sub N = h nu/k, for any amplifier. Burke (1969) used this result to demonstrate that, if it were not for this quantum noise, the VLBI method would allow one to tell which slit a photon went through before forming an interference pattern, thus violating basic tenants of quantum mechanics. In essence, the second quantization condition Delta N Delta phi greater than or = 1 saves one from paradox. One can state the conclusion simply: any amplifier produces approximately one photon per Hertz of bandwidth. In optical interferometry, one will certainly want bandwidth in the 10(exp 12) to 10(exp 14) Hz range, and that implies an intolerable cacophony of noise photons. Only at infrared frequencies can one tolerate the quantum noise, where the natural noise background may be high and the mixers are not as efficient as one would hope for. The crossover at present is about 10 or 20 microns, but the boundary will shift to longer wavelengths as noise performance improves. One might guess that ultimately a wavelength of about 100 microns will mark the limit of useful amplification and heterodyning in astronomical aperture synthesis interferometry. Author

N93-13598*# BDM International, Inc., Albuquerque, NM. Advanced Basing Systems.
REQUIRED TECHNOLOGIES FOR A LUNAR OPTICAL UV-IR SYNTHESIS ARRAY
Stewart W. Johnson and John P. Wetzel *In* New Mexico Univ., A Lunar Optical-Ultraviolet-Infrared Synthesis Array (LOUISA) Nov. 1992 p 227-241 (For primary document see N93-13579 03-89)
(Grant NAG9-245)
Avail: CASI HC A03/MF A03

A Lunar Optical UV-IR Synthesis Array (LOUISA) proposed to take advantage of the characteristics of the lunar environment requires appropriate advances in technology. These technologies are in the areas of contamination/interference control, test and evaluation, manufacturing, construction, autonomous operations and maintenance, power and heating/cooling, stable precision structures, optics, parabolic antennas, and communications/control. LOUISA needs to be engineered to operate for long periods with minimal intervention by humans or robots. What is essential for LOUISA operation is enforcement of a systems engineering approach that makes compatible all lunar operations associated with habitation, resource development, and science. Author

N93-13599*# New Mexico Univ., Albuquerque.
REPORT OF THE WORKING GROUP ON SPACE/LUNAR TRADEOFFS
In its A Lunar Optical-Ultraviolet-Infrared Synthesis Array (LOUISA) Nov. 1992 p 243-248 (For primary document see N93-13579 03-89)
Avail: CASI HC A02/MF A03

The group discussed the advantages and disadvantages of five locations for an optical/infrared array: low-Earth orbit (LEO), Sun-synchronous Earth-orbit, geosynchronous orbit (GEO), Lagrangian points (L4 and L5), and the lunar surface. The factors affecting an array and our assessments of them are given and briefly discussed. In the discussions, two axioms are assumed: (1) Human expansion into space and to the Moon will occur; and (2) The Space Station will be constructed and operational. The major conclusion reached is that baselines of moderate size (greater than 300 m) are best done on the Moon and that large baselines (greater than 10 km) can be done only on the Moon. Three areas needing additional research were identified as follows. (1) Studies are needed on methods to steer long-baseline systems in orbit. This involves learning how to control free-flyers. It is not clear how the difficulty of control varies with orbital elevation. (2) More work is needed on the internal metrology of array systems, both orbital and lunar-surface systems.(3) We need to understand the radiation effects on detectors and electronics and learn how to mitigate them. Author

N93-13600*# New Mexico Univ., Albuquerque.
REPORT OF THE SCIENCE WORKING GROUP: SCIENCE WITH A LUNAR OPTICAL INTERFEROMETER
In its A Lunar Optical-Ultraviolet-Infrared Synthesis Array (LOUISA) Nov. 1992 p 249-255 (For primary document see N93-13579 03-89)
Avail: CASI HC A02/MF A03

Resolution is the greatest constraint in observational astronomy. The Earth's atmosphere causes on optical image to blur to about 1 arcsec or greater. Interferometric techniques have been developed to overcome atmospheric limitations for both filled aperture conventional telescopes and for partially filled aperture telescopes, such as the Michelson or the radio interferometer. The Hubble Space Telescope (HST) represents the first step toward space based optical astronomy. The HST represents an immediate short term evolution of observational optical astronomy. A longer time scale of evolution is focused on and the benefits are considered to astronomy of placing an array of telescopes on the Moon at a time when a permanent base may exist there. E.R.

N93-13601*# New Mexico Univ., Albuquerque.
REPORT OF THE WORKING DESIGN GROUP
In its A Lunar Optical-Ultraviolet-Infrared Synthesis Array (LOUISA) Nov. 1992 p 256-279 (For primary document see N93-13579 03-89)
Avail: CASI HC A03/MF A03

The engineering study group in the LOUISA workshop was responsible for producing a preliminary general design for an optical synthetic aperture telescope on the Moon. This design is intended to be a test case for focusing continuing design studies. The scope of the design included consideration of the array geometry, individual telescopes, metrology, site attributes, and construction. However, no attempt was made to go into further depth in the design than to cover the essential characteristics of the instrument. The starting point for the array design was the lunar optical array discussed by Burke (1985). His array geometry followed the design and correlation procedure of the 27-element Very Large Array (VLA) radio telescopes near Socorro, New Mexico. Author

N93-13659*# Colorado Univ., Boulder.
B SUPERGIANTS IN OPEN CLUSTERS AND ASSOCIATIONS Final Technical Report
C. D. Garmany [1990] 4 p
(Grant NAG5-78)
(NASA-CR-191275; NAS 1.26:191275) Avail: CASI HC A01/MF A01

The final report on project NAG5-78, 'IUE Observations of B Supergiants in the Large Magellanic Cloud', a collaborative effort between Garmany (U. of Colorado), Sonneborn (Goddard Space Flight Center) and Fitzpatrick (Princeton Univ.) is presented. Over 90 B supergiants in the Large Magellanic Cloud with the IUE satellite, using the low dispersion mode were observed. These stars were chosen because they resemble the precursor star to SN 1987a, and a data base in the continuing effort to understand why the precursor star was a blue, not a red supergiant was needed. The observations were all reduced and made into an atlas, and efforts to understand the evolutionary history of stars of the H-R diagram are underway. Author

N93-13660*# Eckerd Coll., Saint Petersburg, FL. Dept. of Chemistry.
EXPERIMENTAL STUDIES OF THE FAR-INFRARED SPECTRA OF COSMIC-TYPE ICES Interim Report, Jan. - Nov. 1992
Reggie L. Hudson 24 Nov. 1992 27 p
(Grant NAG5-1843)
(NASA-CR-191300; NAS 1.26:191300) Avail: CASI HC A03/MF A01

Work performed during the period is reported. The abstract of a paper presented at the Second International Workshop on the Nature of Cometary Organic Matter is included. Far infrared spectra of amorphous and crystalline water ice before and after proton irradiation is presented. Also, a study of clathrate hydrates was conducted in which a methanol (CH3OH) clathrate hydrate was prepared and its far-infrared spectrum investigated. This paper is also included. L.R.R.

N93-13688 Texas Univ., Austin.
MOLECULAR GAS TEMPERATURE AND DENSITY IN SPIRAL GALAXIES Ph.D. Thesis
William Frank Wall 1991 132 p
Avail: Univ. Microfilms Order No. DA9200744

Beam-matched (13)CO, (12)CO J = 3 approaches 2 and J = 2 approaches 1 line data are combined to infer the molecular gas excitation conditions in the central 500 to 1600 pc diameters of a small sample of infrared-bright spiral galaxies: NGC 253, IC 342, M 83, Maffei 2, and NGC 6946. We find the central 200 to 500 pc diameter regions can have molecular gas densities ranging from approximately 10(exp 4) cm(exp -3) (in M 83) to approximately 10(exp 5) cm(exp -3) (in NGC 253), and outside of these regions, the densities are likely to be approximately less than 10(exp 4) cm(exp -3) and the molecular clouds, in this outer region, are at least as warm as the molecular clouds in our Galaxy. Column densities derived from integrated (13)CO line strengths and H(alpha) surface brightnesses suggest that the star formation rate is enhanced in the central 200 to 500 pc diameters by an order-of-magnitude over that inferred for the outer star-forming disks in spiral galaxies. The total luminosity of each sample galaxy over all CO rotational lines is approximately 10(exp 5) - 10(exp 6) solar luminosity which is within an order of magnitude of that of the important cooling line of (C 2) at 158 micron; CO is a major gas coolant in the ISM of infrared-bright galaxies. Additional observations of the J = 1 approaches 0 lines of CO-18 and (13)CO suggest that the central kiloparsec of spiral galaxies may be optically thick in the (13)CO J = 1 approaches 0 line. If so, our estimates of molecular gas mass using (13)CO integrated line strengths could then be too low, partly accounting for the disagreement with the mass estimates of previous work. Dissert. Abstr.

N93-13852 Aberdeen Univ. (Scotland).
A SUBMILLIMETRE POLARIMETER FOR THE CONTINUUM RECEIVER UKT14 ON THE JAMES CLERK MAXWELL TELESCOPE Ph.D. Thesis
Alexander G. Murray 1991 185 p
Avail: Univ. Microfilms Order No. BRDX95973

The submillimeter continuum radiation from astronomical sources is often linearly polarized due either to the synchrotron radiation from relativistic electrons spiraling along magnetic field lines or thermal radiation from aspherical magnetically aligned dust grains. Measurements of the degree and direction of linear polarization can yield useful and unique information on the physical conditions prevailing in the source and its environs. This thesis describes the development of a submillimeter polarimeter for the continuum receiver UKT14 on the James Clerk Maxwell Telescope (JCMT). The polarimeter is of the rotating half-wave plate design and the theoretical performance of such an instrument is considered under ideal and various non-ideal conditions. The mechanical, electronic and software systems engineered to convert this measurement concept into a useful instrument are detailed. High efficiency half-wave plates for submillimeter wavelengths were developed and their design, construction and testing is described. The results from extensive laboratory testing of the complete polarimeter are presented. Some general issues regarding polarization measurement with UKT14 and the JCMT are considered before the observing methods used during the polarimeter commissioning tests at the JCMT are outlined. Successful submillimeter polarization measurements were made on a variety of astronomical objects at 450, 800 and 1100 microns with many of these being first detections. In combination with UKT14 and the JCMT the polarimeter has achieved a significant increase in the available sensitivity and angular resolution of astronomical polarization measurements at submillimeter wavelengths. Dissert. Abstr.

N93-13960 Massachusetts Univ., Amherst.
AN OPTICAL STUDY OF THE FAINT END OF THE STELLAR LUMINOSITY FUNCTION Ph.D. Thesis
Thomas Harold Jarrett 1992 347 p
Avail: Univ. Microfilms Order No. DA9219451

A new method is implemented by which to study the faint end of the field star luminosity function. The method relies on deep, multicolor photometry of fields projected against highly obscured, nearby molecular clouds. The clouds act as nearly opaque screens and delimit a well defined survey sample volume free of the problem of distinguishing nearby, intrinsically faint dwarf stars from more distant red giants. It is shown that with this technique it is possible to probe the faint end of the field star luminosity function down to the hydrogen burning main sequence out to distance much further than have been previously attempted. This study is based upon deep photographic and CCD photometry at optical (V, R, I) bandpasses towards the most obscured portions of the Taurus and Ophiuchus molecular clouds. The fields comprise a total area of approx. 0.63 sq degs, and the total volume delimited by the cloud distances is approx. 198 cu pc. Within this volume, the survey is complete for all stars brighter than M sub v = 16-17 mag; at R and I, the survey is complete down to the lowest mass stars capable of sustaining core hydrogen burning. Color-color criteria are used to distinguish between background, highly reddened stars and stars located in front of the clouds. The method of photometric parallax is used to deduce the absolute magnitude and spectral type of those stars found to lie in front of the luminosity function rises beyond M sub v approx. 16; there appears to be little doubt that the luminosity function at least remains flat for the lowest mass stars. Our provisional finding that the luminosity function rises again beyond its well known peak at M sub v approx. 12 to 13, also implies that the IMF probably rises beyond the turnover point associated with this peak. The IMF must at least remain flat down to the edge of the hydrogen burning main sequence. Dissert. Abstr.

N93-14070 Arizona Univ., Tucson.
A SYSTEMATIC SEARCH FOR LOW-MASS COMPANIONS ORBITING NEARBY STARS AND THE CALIBRATION OF THE END OF THE STELLAR MAIN SEQUENCE Ph.D. Thesis
Todd Jackson Henry 1991 362 p
Avail: Univ. Microfilms Order No. DA9210296

We have completed a search for low luminosity companions, including high mass brown dwarfs, to all M dwarfs known within eight parsecs of the sun, and north of -25 degrees. We found six new companions orbiting the survey stars. The masses of the six new secondaries fall between 0.39 and 0.05 M-circle. Three of the new companions, G208-44B, GL 623B and LHS 1047B, and one previously known secondary in the survey, Ross 614B, are brown dwarf candidates with masses approximately 80 Jupiters (0.08 solar mass), the dividing line between stars and brown dwarfs. In addition, we provide infrared photometry at J, H, and K for all 99 survey members, and spectral types on standard system for half. Analysis of the entire sample indicates that 50 percent of the stars in the more distant half of the survey volume remain undetected, as is supported by the steadily growing M dwarf census over the last 45 years. The binary fraction of M dwarfs, 30-40 percent, is lower than that of earlier type main sequence stars, and there are more companions to M dwarf found between 1 and 10 AU than in any other decade interval. We find that the luminosity function of the lowest mass stars is flat or rising to the end of the main sequence, and that the mass function undoubtedly rises to the stellar/substellar break. We illustrate that the resolution of close binaries is crucial if accurate luminosity and mass functions are to be determined. Finally, we estimate 0.02 solar mass/pc(exp 3) to be the amount of mass contributed by M dwarfs to the galactic mass. Based upon new mass-luminosity relations developed at infrared wavelengths using a sample of stars with well-determined masses between 1.2 and 0.08 solar mass, we are able to define empirically the end of the main sequence. We present absolute magnitudes, colors and spectral types for objects at the theoretical lowest stellar mass. Using these relations, we conclude that a few brown dwarfs may have already been discovered. Dissert. Abstr.

N93-13171*# Brigham Young Univ., Provo, UT. Dept. of Physics and Astronomy.
G-133: A SOFT X RAY SOLAR TELESCOPE
Memorie K. Williams, Branton Campbell, Peter W. A. Roming, Mark K. Spute, and J. Ward Moody *In* NASA. Goddard Space Flight Center, The 1992 Shuttle Small Payloads Symposium Oct. 1992 p 125-131 (For primary document see N93-13158 03-12)
(Grant NAGw-2612)
Avail: CASI HC A02/MF A03

90 ASTROPHYSICS

Includes cosmology; celestial mechanics; space plasmas; and interstellar and interplanetary gases and dust.

For related information see also *75 Plasma Physics*.

N93-12587# Los Alamos National Lab., NM.
APPROXIMATING THE r-PROCESS ON EARTH WITH THERMONUCLEAR EXPLOSIONS
S. A. Becker 1992 5 p Presented at the Origin and Evolution of the Elements Conference, Paris (France), 22-25 Jun. 1992
(Contract W-7405-eng-36)
(DE92-017409; LA-UR-92-1783; CONF-9206249-1) Avail: CASI HC A01/MF A01

The astrophysical r-process can be approximately simulated in certain types of thermonuclear explosions. Between 1952 and 1969 twenty-three nuclear tests were fielded by the United States which had as one of their objectives the production of heavy transuranic elements. Of these tests, fifteen were at least partially successful. Some of these shots were conducted under the project Plowshare Peaceful Nuclear Explosion Program as scientific research experiments. A review of the program, target nuclei used, and heavy element yields achieved is presented as well as discussion of plans for a new experiment in a future nuclear test. DOE

N93-12956# Los Alamos National Lab., NM.
AIRBLAST DAMAGE FROM SMALL ASTEROIDS
J. G. Hills and M. P. Goda 22 Jun. 1992 13 p Presented at the ECA Intercept Conference, Los Alamos, NM, 14-16 Jan. 1992
(Contract W-7405-eng-36)
(DE92-017834; LA-UR-92-2049; CONF-920191-2) Avail: CASI HC A03/MF A01

The fragmentation of a small asteroid in the atmosphere greatly increases its cross sections from aerodynamic braking and energy dissipation. At a typical impact velocity of 22 km/s, the atmosphere absorbs more than half the kinetic energy of stony meteoroids with diameters, D(sub M) less than 250 meters and iron meteoroids with D(sub M) less than 60 meters. Most of this energy dissipation occurs in a fraction of a scale height, which causes large meteoroids to appear to 'explode' or 'flare' at the end of their visible paths. The dissipation of energy in the atmosphere reduces the damage due to direct impacts (e.g., craters and tsunamis), but it produces a blast wave than can cause considerable damage to structures on the ground. The area of destruction around the impact point in which the over pressure in the blast wave exceeds 4 pounds/inch(exp 2) = 2.8x10(exp 5) dynes/cm(exp 3), which is enough to knock over trees and destroy buildings, increases rapidly from zero for chondritic asteroids less than 50 meters in diameter (9 megatons) to about 2000 square km for those 80 meters in diameter (40 megatons), the approximate diameter of the Tunguska impactor of 1908. The area of destruction produced by the blast wave from the impact of stony asteroids between 70 meters and 200 meters in diameter is up to twice as great as it would be without fragmentation. DOE

N93-12965# European Space Agency, Paris (France).
GIOTTO: THE SECOND ENCOUNTER
Gerhard Schwehm (European Space Agency. European Space Research and Technology Center, ESTEC, Noordwijk, Netherlands), Manfred Grensemann (European Space Agency. European Space Research and Technology Center, ESTEC, Noordwijk, Netherlands), and Norman Longdon, ed. 1992 24 p Original contains color illustrations
(ESA-BR-83; ISBN-92-9092-111-0) Copyright Avail: CASI HC A03/MF A01

This colorful booklet features the Giotto mission and its comet targets. The new target is the Comet Grigg-Skjellerup due to meet on July 10, 1992. After some general discussions on comets and the solar system, technical descriptions of Giotto's interaction with Halley's Comet and subsequent analyses are presented. Orbits of Giotto, earth, and Grigg Skjellerup are described. Next a technical description of the Giotto spacecraft is presented. The instruments in the scientific payload and their experimenters are discussed. Finally there is a description of communicating with Giotto. R.L.B.

N93-13011 Wisconsin Univ., Madison.
A CATALOG OF MODERATELY DISTANT GALAXY CLUSTERS Ph.D. Thesis
Mark Joseph Abbott 1991 94 p
Avail: Univ. Microfilms Order No. DA9207543

A new magnitude-limited catalog of galaxy clusters complete to z approximately 0.35 is presented. The clusters in this catalog are candidates for inclusion in a volume-limited sample of clusters. The catalog contains 38 clusters, selected from a catalog of stars and galaxies which was produced from PDS scans of a Schmidt plate. Candidate clusters were detected by software which used a thresholding algorithm on filtered maps of the star/galaxy catalog, and the significance of each candidate was estimated by its signal-to-noise ratio. The cluster catalog was limited to those candidates with S/N greater than 4.5 which were found by subsequent visual inspection not to be plate defects. Simulated fields were produced to investigate the behavior of the cluster algorithm. These tests indicated that the sensitivity of cluster detection was maximized by including the entire star/galaxy catalog in the search. Classification of objects did not substantially increase the sensitivity, and performing the detection in a position-magnitude space with a limited range in magnitude significantly lowered the sensitivity. New redshift measurements are presented for 24 clusters in this field, 7 of which are in the catalog. Eleven clusters in the catalog have available redshifts. The redshifts already acquired indicate that the limiting redshift will be approximately 0.35. The clusters visually detected by Gunn et al. (1986) using the same plate material were compared to those detected by the automated algorithm to clarify the selection criteria

of the former catalog. The results indicate that Gunn et al. may have been biased toward the detection of clusters with a high central concentration and that their catalog extends to a similar limiting redshift. Dissert. Abstr.

N93-13122 Michigan Univ., Ann Arbor.
THE DYNAMICAL EVOLUTION OF CLUSTERS OF GALAXIES Ph.D. Thesis
Diab Heinrich Jerius 1992 167 p
Avail: Univ. Microfilms Order No. DA9226928

The temporal dynamical and structural evolution of clusters of galaxy is studied using N-body simulations of cosmological evolution in order to determine whether the observed structure of clusters can aid in distinguishing between different cosmological scenarios. Three different cosmological scenarios are studied: a pancake scenario with a density power spectral index of n = 1 and a low mass cut-off of 30 Mpc and two hierarchical models with spectral indices of n = -2 and n = -1. A catalogue of clusters is assembled using a percolation technique with an effective density contrast over the mean background density of 250. The temporal evolution of the clusters' velocity dispersions and particle distributions as a function of cluster mass is studied. Individual clusters are examined to investigate the importance of mergers vs infall in determining the observable characteristics of the clusters. The results are compared against available observations. The models predict steady evolution with redshift of both the velocity dispersion and the mass distribution. Comparisons with observations indicate that while the models are not inconsistent with them, the incompleteness in the observed parameters and deficiencies in the models prevent the unique determination of a specific cosmological scenario. The results are clouded by the uncertain role of mergers and infall in the growth of clusters, and the dependence of these processes upon the initial density power spectrum. Dissert. Abstr.

N93-13123 Ohio State Univ., Columbus.
COSMOLOGICAL CONSTRAINTS ON EARLY-DECAYING PARTICLES Ph.D. Thesis
Ho-Shik Kang 1992 153 p
Avail: Univ. Microfilms Order No. DA9227297

We have derived a simple set of Boltzmann equations to study cosmological effects of early-decaying particles. Early-decaying particles are defined as those particles whose decay has been finished effectively before or at about the nucleosynthesis epochs. The inverse decay and the time dilation were included in the Boltzmann equations. From these Boltzmann equations we have studied the time evolution of the abundances for a generic early-decaying particle and its decay products. Further, for a massive tau-neutrino which decays into a light neutrino and a majoron we have calculated the time evolution of the abundances for the particles as a function of the mass (M) and proper lifetime (tau) of the tau-neutrino. It was noticed that the inverse decay is important if the massive particle decays when relativistic. In addition, the time evolution of the effective number of neutrino species (N(sub nu)) was calculated as a function of the mass and lifetime of the tau-neutrino. Since He-4 abundance increases as (N(sub nu)) increases, the observational constraints on both He-4 and D + He-3 abundances limit (N(sub nu)) to less than or equal to 3.3. We have derived constraints on a massive tau-neutrino for M less than or equal to 35 MeV from this upper limit to N(sub nu). For example, a 17 keV tau-neutrino should be excluded if its lifetime is shorter than about 10(exp -3) sec. Dissert. Abstr.

N93-13148 Johns Hopkins Univ., Baltimore, MD.
EVOLUTION OF GALAXIES IN COMPACT GROUPS Ph.D. Thesis
Stephen Edward Zepf 1992 216 p
Avail: Univ. Microfilms Order No. DA9229433

We investigate the role of mergers and interactions in the evolution of galaxies by studying galaxies in compact groups. Compact groups of galaxies have high spatial densities and low velocity dispersions making these regions ideal laboratories in which to study the effect of interactions and mergers on galaxies. We present a large multicolor survey of the elliptical galaxies in compact groups and show that several of the elliptical galaxies in these groups have unusually blue colors indicative of recent interactions or mergers. We also find that a small fraction of galaxies in these groups are currently merging, based on their disturbed optical morphologies, warm far-infrared colors, and unusual dynamics. However, unusually blue elliptical galaxies and currently merging systems are relatively rare, indicating that the timescale for a compact group to evolve through merging into a single object is at least 3 Gyr. Although merging is not occurring rapidly, the elliptical galaxies appear to be affected by tidal interactions within the group. We find that compact group elliptical galaxies are less likely than similar galaxies in other environments to have boxy isophotes and more likely to have irregular isophotal shapes indicative of a recent tidal encounter. The most striking difference between elliptical galaxies in compact groups and those in other regions is that the elliptical galaxies in compact groups appear to have systematically low velocity dispersions for their effective radii, average surface brightnesses, absolute magnitudes, and colors, and therefore do not lie on the fundamental plane defined by elliptical galaxies in other environments. Dissert. Abstr.

N93-13279# Instituto de Pesquisas Espaciais, Sao Jose dos Campos (Brazil).
ALTERNATIVE METHODS FOR DETERMINATION OF THE TEMPERATURE OF CENTRAL STARS OF PLANETARY NEBULAE M.S. Thesis [METODOS ALTERNATIVOS PARA DETERMINACAO DA TEMPERATURA DE ESTRELAS CENTRAIS DE NEBULOSAS PLANETARIAS]
Flavio Elizalde Mar. 1992 88 p In PORTUGESE
(INPE-5434-TDI/485) Avail: CASI HC A05/MF A01

This work presents the formulation and application of three methods for determining the temperature of central stars in planetary nebulae. The methods are based on global spectroscopic indices for comparing objects with models. The spectroscopic data are taken from the literature, while models were calculated with the CLOUDY code. The three methods are: the I(sub r) method compares the ratio of helium to hydrogen lines; the S-N(sub 1/2) method generalizes the energy balance method for different metalicity classes and different gas densities; the TIN method makes a direct comparison between the spectroscopic indices of the model and the object, minimizing their differences. In this method the chemical abundances of the main elements are calculated. The I(sub r) method was applied to 78 objects; the S-N(sub 1/2) method was applied to 85 objects while the TIN method was used upon 8 nebulae. The results are discussed and compared to other determinations in the literature. One of the main conclusions is that only about half of the objects are optically thick. Finally, future developments and applications are suggested. Author

N93-13294 Keele Univ. (England).
X RAY SCATTERING BY COSMIC DUST GRAINS Ph.D. Thesis
George A. Norwell 1990 242 p
Avail: Univ. Microfilms Order No. BRDX96593

This thesis reports work carried out to investigate ways of observing X-ray haloes produced by scattering of X-rays by cosmic dust grains. It also examines how the haloes can give information about the properties of dust grains. The first part of the thesis discusses the important properties of dust grains already obtained at wavelengths ranging from the infrared to the ultra-violet. The thesis then reviews classical scattering theory and applies it to X-ray wavelengths and spherical particles. This theory is then used to simulate situations in which X-ray haloes might be expected to arise and discusses the feasibility of observing such haloes. The thesis then presents a new technique for extracting a scattered X-ray halo from the surface brightness distribution of a variable X-ray source and presents results of the detection of a halo using this novel technique. The work establishes that there is great potential in using X-rays as probes of the properties of cosmic dust grains. Dissert. Abstr.

N93-13340 Princeton Univ., NJ.
THE DYNAMICS OF DENSE GALACTIC NUCLEI Ph.D. Thesis
Man Hoi Lee 1992 123 p
Avail: Univ. Microfilms Order No. DA9219847

In this thesis, two topics on the dynamics of dense galactic nuclei are studied. They are relevant to the formation of massive black holes and the observations of several nearby galactic nuclei. An overview of the observations is given in Chapter 1. In Chapter 2, the dynamical evolution of dense clusters of compact stars is studied. The formation of binaries and their subsequent merging by gravitational radiation emission is important to the evolution of such clusters. Aaseth's NBODY5 N-body simulation code, which is modified to include these processes, is used to simulate small N clusters with different initial velocity dispersions. The initial evolution is similar to previous results from Fokker-Planck simulations and shows

orderly formation of heavy objects. However, the late evolution shows runaway growth for the most massive object in the cluster. We present arguments to show that merger by gravitational radiation (and possibly hydrodynamic merger of normal stars) is expected to be unstable to runaway growth. These results suggest that a seed massive black hole can be formed by runaway growth in a dense cluster of compact stars. In Chapter 3, the effects of stellar encounters on rotating stellar systems with central massive black holes are studied. For axisymmetric stellar systems with distribution functions that depend only on the energy E and the angular momentum about one axis J(sub x), the steady-state stellar distribution is found by directly integrating the Fokker-Planck equation in E, J subx) space. Two sets of models with simple assumptions about the loss cone in phase space (due to loss of stars to the central black hole) are presented: the loss cone in the J(sub x) direction is either ignored or completely empty. We find that the depletion of stars due to an empty loss cone is significant. Density and kinematic profiles are also presented. The ratio of rotation velocity to velocity dispersion, V/sigma at small radii is higher than that of the background isothermal core with solid body rotation. However, only the empty loss cone models have V/sigma that rises inward. Possible future refinements, especially toward a more realistic loss cone boundary condition, are discussed. Dissert. Abstr.

N93-13360 California Univ., Berkeley.
H I SHELLS AND SUPERSHELLS: OBSERVATIONS AND THEORY Ph.D. Thesis
Bon-Chul Koo 1990 234 p
Avail: Univ. Microfilms Order No. DA9126642

A study of the dynamics of dense neutral shells formed by stellar winds and SN explosions is presented. The shells are formed by single SN explosions and the supershells are formed by the combined action of stellar winds and sequential SN explosions. We have detected a fast, approximately 70 km s(exp -1), expanding H I shell around the old SNR CTB 80. The H I shell's expansion velocity and size imply that it is a SNR shell, with an estimated dynamical age of approximately 8 x 10(exp 4) yr. Among 103 SNRs, we detected 15 SNRs that have associated high-velocity HI gas. We also detected 12 SNRs that possibly have associated H I shells. The expansion velocity of H I gas in 15 sources ranges from 70 to 160 km s(exp -1) and their dynamical ages range from 3 x 10(exp 4) to 5 x 10(exp 5) yr. In four sources, G24.7-0.6, W51, CTB 80, and HB 21, the velocity structure implies that the high-velocity gas is a portion of an expanding shell. We obtained the mass per unit line-of-sight velocity v(sub l) in these four sources, and it varies as M(v(sub l) alpha v(sub v)(-3). We detected the 'Galactic worms' in H I, infrared, and radio continuum, which are believed to be the broken-through supershells. We identified and cataloged 118 worm candidates that appear in both H I and infrared. The infrared and the radio continuum properties of the worm candidates suggest that some worms have associated ionized gas. According to our results, the area filling factor of the hot gas in the inner galaxy is greater than approximately 0.1. We developed a simple and general formulation to describe the integrated properties of nonrelativistic adiabatic blastwaves in media with a finite total mass, such as media with an exponentially decreasing density. We studied the overall evolution of wind bubbles and superbubbles. The results in a uniform medium are applied to the evolution of bubbles in media with a finite total mass, e.g., superbubbles in a galactic disk. We discuss the evolution of three types of winds, e.g., the neutral stellar wind in HH 7-11 region, the North Polar Spur, and the galactic winds in starburst galaxies, based on our results. Dissert. Abstr.

N93-13374 Victoria Univ. (British Columbia).
A STUDY OF THE STRUCTURE, EVOLUTION AND OBSERVATION OF HORIZONTAL BRANCH STARS Ph.D. Thesis
Benjamin Dorman 1990 370 p
(ISBN-0-315-62655-0) Avail: Univ. Microfilms Order No. DANN62655

The dissertation presents a detailed study of many aspects of the Horizontal Branch (HB) phase of stellar evolution. The chief conclusions from this work are firstly, that the total mass of the envelope sensitively affects the luminosity of the hydrogen-burning shell and the equilibrium of the helium-rich core. Secondly, the rapid progression of models across the Hertzsprung-Russell diagram with decreasing mass is the result of important changes in the hydrostatic structure of the stars. Thirdly, the luminosity-metallicity relationship of the Zero Age models results from the change in the core equilibrium luminosity with the CNO abundance of the shell region, together with the decrease in stellar mass at fixed effective temperature. The evolution of the stars is then considered, and the analysis of the interior structures provides a reclassification of HB track morphology into three categories, depending on whether the model contains an outer convection zone or a radiative outer envelope, and on the luminosity of the hydrogen-burning shell. Lastly, the question of the formation of red-giant stars is considered. Next, the evolution of the convective core of HB stars is reviewed, together with a detailed account of the numerical techniques developed for modelling semi-convection. The problems associated with the late phase of HB evolution are also discussed. A brief review of the physical inputs and numerical methods used in the interior is presented, focussing on the calculation and implementation of the Equation of State. The calculations performed for this study are then presented in detail. The effects of oxygen enhancement on zero-age sequences are illustrated for a range in metallicity, and theoretical relations between luminosity and metallicity for the ZAHBs are demonstrated. The evolutionary tracks computed are illustrated and summarized in extensive tabulations in the Appendices. The final chapter reproduces previously published studies of globular clusters. The first of these investigates the globular cluster NGC104 (47 Tucanae). The second study presents an investigation of the horizontal branch of M15. Detailed matches of our theoretical sequences to the cluster observations indicate that high envelope helium abundances are imcompatible with the observed morphology. Dissert. Abstr.

N93-13380 Virginia Univ., Charlottesville.
EVIDENCE FOR COOL GAS AND STAR FORMATION IN CLUSTER COOLING FLOWS Ph.D. Thesis
Brian Robert McNamara 1991 177 p
Avail: Univ. Microfilms Order No. DA9217323

X-ray observations of clusters of galaxies have established the presence of hot (T approximately 10(exp 7) K) intracluster atmosphere in clusters of galaxies. The cooling time of the gas in the inner approximately 150 kpc of many clusters is less than the Hubble time. Therefore, the gas is expected to cool and accrete onto the centrally dominant galaxies (CFD's) of these clusters at rates of approximately 100 solar mass per year. This dissertation is an investigation of the optical properties and neutral hydrogen content of CFS's. The results of three observational surveys of cluster cooling flows are presented. We have obtained lambda 3400-5100 spectrophotometry of the nuclei of 13 CFD's, 21-cm radio observations of 14 cooling flow clusters, and U-, b-, V-, and I-band CCD imagery of 19 CFD's. Results for a smaller sample of non-accreting objects are presented as well. The spectrophotometry and 21-cm results are presented in their published form. They were written in collaboration with my advisers: Dr. R. W. O'Connell, and Dr. Joel N. Bregman. The results of the CCD imaging are presented in preprint form. This section will be expanded and separated into three papers for publication. Included in these papers will be a discussion of the morphology of star formation in CFD's, and new emission-line and color imagery of NGC 1275. The most important result of this dissertation has been to establish a firm connection between the presence of cooling, x-ray-emitting intracluster gas, and cool gas and star formation for a sample of CFD's. In two clusters, we have detected neutral hydrogen (H I) in absorption against background radio sources. The H I appears to be falling into the CFD's. The detection of infalling cold gas is an important link in the processes of cooling from x-ray-emitting temperatures to the cold temperatures required for accretion and star formation. The limits on the cold gas content and star-formation rates suggest that star formation occurs more rapidly and efficiently in CFS's than in disk galaxies. If gas is accreting at rates comparable to those inferred from x-ray observations, then star formation with an initial mass function unlike that in the Galaxy is implied. In addition, new results on the underlying properties of centrally dominant galaxies (i.e., metallicity and color gradients) are presented.

Dissert. Abstr.

N93-13465*# Lockheed Missiles and Space Co., Sunnyvale, CA.
A STUDY OF ION COMPOSITION AND DYNAMICS AT COMET HALLEY Final Report
E. G. Shelley and S. A. Fuselier 31 Mar. 1991 226 p
(Contract NASw-4336)
(NASA-CR-188478; NAS 1.26:188478) Avail: CASI HC A11/MF A03

This report details the participation by Lockheed co-investigators in the reduction, analysis, and interpretation of data obtained by the Ion Mass Spectrometer onboard the Giotto mission to Comet Halley. The data analysis

activities and much of the scientific collaboration was shared by this team. One objective of the effort under this contract was to use data obtained by the Giotto Ion Mass Spectrometer (IMS) during the encounter with comet Halley for the purpose of advancing our understanding of the chemistry and physics of the interaction of the solar wind with comets and obtaining new information on the comet's composition. An additional objective was to make this unique data set available in a format which can be easily used by the reset of the cometary science community for other analysis in the future. The IMS has two sensors: the High Intensity Spectrometer (HIS) and the High Energy Range Spectrometer (HERS). For individual titles, see N93-13466 through N93-13469.

N93-13466*# Jet Propulsion Lab., California Inst. of Tech., Pasadena.
DENSITIES AND ABUNDANCES OF HOT COMETARY IONS IN THE COMA OF P/HALLEY

M. Neugebauer, R. Goldstein, B. E. Goldstein, S. A. Fuselier (Lockheed Missiles and Space Co., Palo Alto, CA.), H. Balsiger (Bern Univ., Switzerland), and W.-H. Ip (Max-Planck-Inst. fuer Aeronomie, Katlenburg-Lindau, Germany) *In* LMSC, A Study of Ion Composition and Dynamics at Comet Halley 31 Mar. 1991 34 p Submitted for publication (For primary document see N93-13465 03-90)
Avail: CASI HC A03/MF A03

On its flight by P/Halley, the Giotto spacecraft carried a High Energy Range Spectrometer (HERS) for measuring the properties of cometary ions picked up by the solar wind in the nearly collisionless regions of the coma. Preliminary estimates of the ion densities observed by HERS were reevaluated and extended; density profiles along the Giotto trajectory are presented for 13 values of ion mass/charge. Comparison with the physical-chemical model of the interaction of sunlight and the solar wind with the comet by other researchers reveals that, with the exception of protons and H2(+), all ion densities were at least an order of magnitude higher than predicted. The high ion densities cannot be explained on the basis of compression of the plasma, but require additional or stronger ionization mechanisms. Ratios of the densities of different ion species reveal an overabundance of carbonaceous material and an underabundance of H2(+) compared to the predictions of the Schmidt. While the densities of solar wind ions (H(+) and He(++)) changed sharply across a magnetic discontinuity located 1.35(10)(exp 5) km from the comet, this feature, which has been called both the 'cometopause' and the 'magnetic pileup boundary' was barely distinguishable in the density profiles of hot cometary ions. This result is consistent with the interpretation that the magnetic pileup boundary detected by Giotto was caused by a discontinuity in the solar wind and is not an intrinsic feature of the interaction of the solar wind with an active comet. Author

N93-13467*# Jet Propulsion Lab., California Inst. of Tech., Pasadena.
OBSERVATIONS OF SOLAR WIND ION CHARGE EXCHANGE IN THE COMET HALLEY COMA

S. A. Fuselier (Lockheed Missiles and Space Co., Palo Alto, CA.), E. G. Shelley (Lockheed Missiles and Space Co., Palo Alto, CA.), B. E. Goldstein, R. Goldstein, M. Neugebauer, W.-H. Ip (Max-Planck-Inst. fuer Aeronomie, Katlenburg-Lindau, Germany), H. Balsiger (Bern Univ., Switzerland), and H. Reme (Centre d'Etude Spatiale des Rayonnements, Toulouse, France) *In* LMSC, A Study of Ion Composition and Dynamics at Comet Halley 31 Mar. 1991 25 p (For primary document see N93-13465 03-90)
(Contract NAS5-4336; CNES-1212)
Avail: CASI HC A03/MF A03

Giotto Ion Mass Spectrometer/High Energy Range Spectrometer (IMS/HERS) observations of solar wind ions show charge exchange effects and solar wind compositional changes in the coma of comet Halley. As the comet was approached, the He(++) to proton density ratio increased until about 1 hour before closest approach after which time it decreased. Abrupt increases in this ratio were also observed in the beginning and near the end of the so-called Mystery Region (8.6 - 5.5(10)(exp 5) km from the comet along the spacecraft trajectory). These abrupt increases in the density ratio were well correlated with enhanced fluxes of keV electrons as measured by the Giotto plasma electron spectrometer. The general increase and then decrease of the He(++) to proton density ratio is quantitatively consistent with a combination of the addition of protons of cometary origin to the plasma and loss of plasma through charge exchange of protons and He(++). In general agreement with the solar wind proton and He(++) observations, solar wind oxygen and carbon ions were observed to charge exchange from higher to lower charge states with decreasing distance to the comet. The more abrupt increases in the He(++) to proton and the He(++) to O(6+) density ratios in the mystery region require a change in the solar wind ion composition in this region while the correlation with energetic electrons indicates processes associated with the comet. Author

N93-13468*# Jet Propulsion Lab., California Inst. of Tech., Pasadena.
OBSERVATIONS OF PLASMA DYNAMICS IN THE COMA OF P/HALLEY BY THE GIOTTO ION MASS SPECTROMETER

B. E. Goldstein, R. Goldstein, M. Neugebauer, S. A. Fuselier (Lockheed Missiles and Space Co., Palo Alto, CA.), E. G. Shelley (Lockheed Missiles and Space Co., Palo Alto, CA.), H. Balsiger (Bern Univ., Switzerland), G. Kettmann (Max-Planck-Inst. fuer Aeronomie, Katlenburg-Lindau, Germany), W.-H. Ip (Max-Planck-Inst. fuer Aeronomie, Katlenburg-Lindau, Germany), H. Rosenbauer (Max-Planck-Inst. fuer Aeronomie, Katlenburg-Lindau, Germany), and R. Schwenn (Max-Planck-Inst. fuer Aeronomie, Katlenburg-Lindau, Germany) *In* LMSC, A Study of Ion Composition and Dynamics at Comet Halley 31 Mar. 1991 23 p Submitted for publication (For primary document see N93-13465 03-90)
(Contract NASw-4336)
Avail: CASI HC A03/MF A03

Observations in the coma of P/Halley by the Giotto Ion Mass Spectrometer (IMS) are reported. The High Energy Range Spectrometer (HERS) of the IMS obtained measurements of protons and alpha particles from the far upstream region to the near ionopause region and of ions from mass 12 to 32 at distances of about 250,000 to 40,000 km from the nucleus. Plasma parameters from the High Intensity Spectrometer (HIS) of the IMS obtained between 150,000 to 5000 km from the nucleus are also discussed. The distribution functions of water group ions (water group will be used to refer to ions of 16 to 18 m/q, where m is in AMU and q is in unit charges) are observed to be spherically symmetric in velocity space, indicating strong pitch angle scattering. The discontinuity known as the magnetic pile-up boundary (MPB) is apparent only in proton, alpha, and magnetometer data, indicating that it is a tangential discontinuity of solar wind origin. HERS observations show no significant change in the properties of the heavy ions across the MPB. A comparison of the observations to an MHD model is made. The plasma flow directions at all distances greater than 30,000 km from the nucleus are in agreement with MHD calculations. However, despite the agreement in flow direction, within 200,000 km of the nucleus the magnitude of the velocity is lower than predicted by the MHD model and the density is much larger (a factor of 4). Within 30,000 km of the nucleus there are large theoretical differences between the MHD model flow calculations for the plane containing the magnetic field and for the plane perpendicular to the magnetic field. The observations agreed much better with the pattern calculated for the plane perpendicular to the magnetic field. The data obtained by the High Energy Range Spectrometer (HERS) of the IMS that are published herein were provided to the International Halley Watch archive. Author

N93-13469*# Jet Propulsion Lab., California Inst. of Tech., Pasadena.
INTERPRETATION OF THE ION MASS SPECTRA IN THE MASS RANGE 25-35 OBTAINED IN THE INNER COMA OF HALLEY'S COMET BY THE HIS-SENSOR OF THE GIOTTO IMS EXPERIMENT

J. Geiss (Bern Univ., Switzerland), K. Altwegg (Bern Univ., Switzerland), E. Anders (Bern Univ., Switzerland), H. Balsiger (Bern Univ., Switzerland), W.-H. Ip (Max-Planck-Inst. fuer Aeronomie, Katlenburg-Lindau, Germany), A. Meier (Bern Univ., Switzerland), M. Neugebauer, H. Rosenbauer (Max-Planck-Inst. fuer Aeronomie, Katlenburg-Lindau, Germany), and E. G. Shelley (Bern Univ., Switzerland) *In* LMSC, A Study of Ion Composition and Dynamics at Comet Halley 31 Mar. 1991 34 p Submitted for publication (For primary document see N93-13465 03-90)
Avail: CASI HC A03/MF A03

The IMS-HIS double-focussing mass spectrometer that flew on the Giotto spacecraft covered the mass per charge range from 12 to 56 (AMU/e). By comparing flight data, calibration data, and results of model calculations of the ion population in the inner coma, the absolute mass scale is established, and ions in the mass range 25 to 35 are identified. Ions resulting from protonation of molecules with high proton affinity are relatively abundant, enabling us to estimate relative source strengths for H2CO, CH3OH, HCN, and H2S, providing for the first time a positive in situ

measurement of methanol. Also, upper limits for NO and some hydrocarbons are derived. Author

N93-13487 Ohio State Univ., Columbus.
THE EMISSION-LINE PROPERTIES OF QUASARS Ph.D. Thesis
Michael R. Corbin 1991 161 p
Avail: Univ. Microfilms Order No. DA9201640

The broad emission lines in the spectra of quasars and related objects indicate the physical conditions close to the central massive object that is believed to serve as their power source. An effort to determine what these conditions are and how they may differ between the different classes of broad-line objects is made through the statistical analysis of the emission-like properties of samples of quasars, QSO's, and active galactic nuclei that have been obtained from both new and previous observations, with an observational emphasis on quasars at high redshift (z is approximately 2). An analysis of pre-existing samples of spectra of high-redshift objects reveals that the magnitudes of the differences in redshift objects reveals that the magnitudes of the differences in redshift between the prominent ultraviolet broad lines C 4 lambda1549, C 3 lambda1909, and Mg 2 lambda2800 are in several cases much larger than had been previously measured, and are also correlated with one another. The available evidence also suggests that the magnitude of these differences is weakly correlated with the luminosity of the underlying continuum, as is the asymmetry of the C 4 line. A comparison of the properties of these lines between samples of high-redshift quasars having steep radio spectra and those having flat radio spectra reveals differences which suggest that the ionization of the regions producing these lines is anisotropic, such that the gas is most strongly ionized in the direction of the quasar's radio axis. A comparison of the properties of the C 4 lambda1549 and H(beta) emission-line profiles among objects at lower redshift reveals that these profiles are fundamentally similar. This result is contrary to previously favored models in which these lines arise in physically distinct regions. A comparison of the ultraviolet broad lines between samples of radio-loud and radio-quiet objects at high redshift reveals no strong differences related to their different radio or x-ray continuum luminosities. This suggests that the broad-line regions to both classes of objects are fundamentally similar, with the line-emitting gas being relatively unaffected by the production of the radio-emitting plasma. Dissert. Abstr.

N93-13499 Wisconsin Univ., Madison.
SPECTROSCOPIC STUDIES OF LOW-DENSITY GAS IN THE GALACTIC DISK AND HALO Ph.D. Thesis
Kenneth Russell Sembach 1992 323 p
Avail: Univ. Microfilms Order No. DA9218367

The distribution and physical properties of low density gas in the Galactic disk and halo are discussed. The two major topics addressed are (1) issues related to the formation of highly ionized gas in the Galaxy, and (2) the distribution of neutral gas along low density interarm and Galactic center sight lines. It is anticipated that the results will help to constrain current theories of gas energetics and kinematics associated with phenomena such as Galactic fountains or large scale gas flows. Highly ionized gas is studied via International Ultraviolet Explorer satellite observations of the Si IV, C IV, and N V doublets. The detection of N V indicates that hot (T is approximately 2 x 10(exp 4) deg K) gas exists along the sight lines. Of the species detectable with operational space-based satellites, it provides the best diagnostic of collisionally ionized gas in the interstellar medium (ISM) because it is extremely difficult to produce by photoionization. The N V profiles are compared to the C IV and Si IV profiles along individual sight lines. A trend for increasing line width as the ionization level increases is found. In many cases, the profile widths are broader than expected from thermal line broadening alone, suggesting that large scale flows of hot gas may exist along some of the sight lines. Portions of the high ion profiles agree with each other, indicating that all three ions may be formed in collisionally ionized gas in some regions. The high ion profiles have very different shapes than the Al III profiles. Al III is a tracer of photoionized gas. The general results of a survey of Na I and Ca II absorption over 57 extended low density paths in the Galactic disk and halo are described. It is found that Na I and Ca II trace different phases of the ISM along the sight lines. Na I traces a cloudy medium, whereas Ca II traces both the clouds and a more smoothly distributed intercloud medium. Dissert. Abstr.

N93-13523# Los Alamos National Lab., NM.
NUCLEOSYNTHESIS IN NOVA EXPLOSIONS
S. Starrfield (Arizona State Univ., Tempe.), M. Politano (Arizona State Univ., Tempe.), J. W. Truran (Chicago Univ., IL.), W. M. Sparks, I. Nofar (Technion - Israel Inst. of Tech., Haifa.), and G. Shaviv (Technion - Israel Inst. of Tech., Haifa.) 1992 5 p Presented at the Origin and Evolution of the Elements Conference, Paris, France, 22-25 Jun. 1992
(Contract W-7405-eng-36)
(DE92-040349; LA-UR-92-2548; CONF-9206249-2) Avail: CASI HC A01/MF A01

This paper examines the consequences of accretion of hydrogen rich material onto ONeMg white dwarfs with masses of 1.0, 1.25, and 1.35 solar mass. Our results demonstrate that novae produce both Na-22 and Al-26 in astrophysically interesting amounts. Hot hydrogen burning on ONeMg white dwarfs can produce as much as 2 percent of the ejected material as Al-26 and 3 percent as Na-22. The largest amount of Na-22 is produced by the highest mass ONeMg white dwarfs nova systems which are predicted to be the fastest and most luminous of all types of novae. The largest amount of Al-26 is produced in the lowest mass white dwarfs, which according to our evolutionary calculations, should eject the largest amount of material. In support of this prediction, the observations of QU Vul, a slow ONeMg nova, indicate that it has ejected about 10(exp -3) solar mass. However, such a large amount of ejected mass is inconsistent with a typical ONeMg white dwarf mass greater than 1.25 solar mass. DOE

N93-13536# Lawrence Livermore National Lab., CA.
STUDY OF HELIUMLIKE NEON USING AN ELECTRON BEAM ION TRAP
B. J. Wargelin (California Univ., Berkeley.), S. M. Kahn (California Univ., Berkeley.), and P. Beiersdorfer 1992 6 p Presented at the 10th International Colloquium on Ultra Violet and X Ray Spectroscopy of Astrophysical and Laboratory Plasmas, Berkeley, CA, 3-5 Feb. 1992
(Contract W-7405-eng-48)
(DE92-019544; UCRL-JC-110494; CONF-9202103) Avail: CASI HC A02/MF A01

The 2-to-1 spectra of several astrophysically abundant He-like ions are being studied using the Electron Beam Ion Trap (EBIT) at Lawrence Livermore National Laboratory. Spectra are recorded for a broad range of plasma parameters, including electron density, energy, and ionization balance. We describe the experimental equipment and procedure and present some typical data. DOE

N93-13602 Kent Univ., Canterbury (England).
IN SITU DUST MASS DISTRIBUTION MEASUREMENTS FROM THE GIOTTO ENCOUNTER WITH COMET P/HALLEY Ph.D. Thesis
Christopher H. Perry 1990 246 p
Avail: Univ. Microfilms Order No. BRDX93626

On the night of 13-14 March 1986 the Giotto spacecraft passed within 600km of the nucleus of comet P/Halley. On board the spacecraft was an array of experiments designed to study all aspects of the cometary coma and provide high resolution images of the nucleus. The principle experiment designed to measure the coma dust mass distribution was called the Dust Impact Detection System (DIDSY). The design operation and performance of this experiment are considered and details are provided of post-mission recalibration, including the development of a software simulation to aid in the interpretation of the returned data. The faulty operation of one of the DIDSY sensors resulted in the use of the front end channels of the Particulate Impact Analyser Experiment (PIA) to provide information on particles of mass 10(exp -19) kg less than or equal to m less than or equal 10(exp -15) kg. The techniques used to extract the required information and calibrate the sensor using encounter data and the inter-relationship between different operating modes is described. The analysis of impacts which caused multiple detection by two or more of the DIDSY sensors is described and the results from these multi-sensor events are used to extend the measured mass range up to 10(exp -5) kg. A mass distribution representative of the coma passed through by Giotto was constructed and this is combined with a simple model to obtain the dust production rate and dust to gas ratio. Dissert. Abstr.

N93-13603 Johns Hopkins Univ., Baltimore, MD.
COMPARISON OF COMETARY COMAE USING ULTRAVIOLET

SPECTROSCOPY: COMPOSITION AND VARIATION Ph.D. Thesis
Elizabeth Ellen Roettger 1991 249 p
Avail: Univ. Microfilms Order No. DA9132723

Ultraviolet spectroscopy (1150-3300 A) of cometary comae from the International Ultraviolet Explorer (IUE) satellite shows features of both gas and dust. Photometry of visible light is also obtained with the satellite. Visual magnitudes, as well as data from rocket-borne and ground-based instruments, the Pioneer Venus Orbiter, and the Soviet satellite ASTRON, supplement the IUE observations. The temporal evolution of four comets, before and after perihelion, is compared. Water production rates calculated from OH emissions represent the comets' activity; as expected from ground-based observations of dust and minor species, pre/postperihelion asymmetries are observed in the water production rates for these comets. Visual magnitudes reveal similar trends when reduced to an estimated water production rate. Remaining differences between these data sets are attributed to the spatial and temporal variation of dust relative to gas. Comparison of a comet fresh from the Oort Cloud with a periodic comet reveals great differences in activity (attributed to processes in the nucleus's surface layer), but few differences in chemical composition. Observations representing complete wavelength coverage for 13 comets were selected from spectra of 38 comets obtained with the IUE between Oct. 1978 and May 1990. This database is relatively stable over time, permitting a direct evaluation of the effects of the variation of solar radiation over a complete 11 year solar cycle. Observed species were compared using both model-dependent and model-independent methods. Relative abundances of OH, CO2(+), CO, CS, O, S, and C are compared; water is confirmed as the dominant species of the comets studied. Solar cycle effects are apparent in O and possible C; optical depth effects are noted in the atomic emissions. The comets appear to be a single population or continuous distribution, not two distinct populations. New details are added to the 'carbon puzzle'; H2S is proposed as a second source of S. Two features due to S are identified and compared to recent calculations of sulfur oscillator strengths. The S:O ratio in detected gaseous species is low compared to cosmic abundances. Dissert. Abstr.

N93-13636 Princeton Univ., NJ.
LIMITS ON GALACTIC DYNAMO THEORY DUE TO MAGNETIC FLUCTUATIONS Ph.D. Thesis
Stephen William Anderson 1992 159 p
Avail: Univ. Microfilms Order No. DA9216789

Spiral galaxies have weak magnetic fields, and the accepted explanation for their origin is that a dynamo must be responsible. The dynamo equation employed to predict galactic field strength and shape is derived from the mean field approach developed by Vainshtein who shows how an ensemble of turbulent flows can act on an initial field to give an exponentially increasing ensemble average field (B). We show that this theory is not applicable to galactic magnetic fields for two reasons. First, the high magnetic Reynolds number means that small scale tangles in the magnetic field are not damped effectively, and therefore grow more quickly than the ensemble average field. The mean field (B) is therefore a poor representative because each realization of turbulent flow that makes up the ensemble has a field dominated by small scale tangles, while the average does not. Our second criticism is related to the first; mean field dynamo theory uses the kinematic assumption that the field is too weak to affect the flow. Since the total energy is much greater than indicated by the mean field, equipartition is reached when the mean field has not grown significantly. We substatiate these points by showing that the average energy (B(exp 2)) increases much more quickly than (B)(exp 2) does, and that the energy is concentrated in small scale fields. We find a spectrum of magnetic energy M(k,t) approximately k(sup 3/2)e(sup 3v(sub 2)t/4), where v(sup 2) is the turnover rate of the smallest eddies. We consider three possible mechanisms to cut off the spectrum for short wavelengths; resistivity, magnetic reconnection, and ambipolar diffusion, but our main result that the mean field is dominated by energy on small scales is unaffected. We find that an initial seed field of 10(exp -17) G grows to a strength sufficient for the kinematic assumption to break down, square root of (B(sup 2)) is approximately equal to 10(exp -8) G in roughly 1 Myr, before the mean field (B) has changed significantly. We find that the field continues to grow, suppressing all the turbulence after 10 Myr, when the mean field has grown to a strength of 2 x 10(exp -17) G. At this point our theory breaks down, but we are left with a mean field that contains 10(exp 20) times less energy than the small scale random fields. We conclude that a mean field dynamo theory as it stands cannot explain the observed galactic magnetic fields. Dissert. Abstr.

N93-13645 Boston Univ., MA.
THE PLANETARY NEBULA SYSTEM AND THE DYNAMICS OF THE GALAXY CENTAURUS A Ph.D. Thesis
Xiaohui Hui 1992 193 p
Avail: Univ. Microfilms Order No. DA9216085

Centaurus A (Cen A, or NGC 5128) is a giant elliptical galaxy with a conspicuous dust lane lying along its photometric minor axis. Previous dynamical studies have been restricted to the bright central region of the galaxy and the ionized gas of the dust lane. The stellar dynamics in the halo of Cen A is explored in this thesis using planetary nebulae (PNe) as test particles. The Cen A planetary nebulae were observed through a characteristic emission line of doubly ionized oxygen. The original survey was made with a prime focus CCD camera on the 4-meter telescope of the Cerro Tololo Inter-American Observatory (CTIO), and the spectra of the PNe were observed with spectrographs on both the Anglo-Australian 4-m Telescope (AAT) and the CTIO 4-m telescope. The main results of the thesis are (1) A total of 784 PNe were identified in the survey fields which cover a strip along the photometric major axis out to 20 kiloparsecs (kpc) from the center of the galaxy, and the entire galaxy to a distance of 10 kpc. Velocities of 433 PNe were measured from the spectra with a typical 1 sigma error of plus or minus 4 km s(exp -1) for the AAT data and plus or minus 30 km s(exp -1) for the CTIO data. (2) A complete sample of 224 PNe defines the brightest 1.5 magnitudes of the Cen A planetary nebula luminosity function. A Cen A distance of 3.5 plus or minus 0.2 megaparsecs is derived. (3) The planetary nebula velocity field shows distinctive characteristics of a triaxial potential: the galaxy's rotation axis is offset from its photometric minor axis by 39 degrees and the rotation axis and the line of maximum rotation are not orthogonal. With increasing radius, the ordered motions of the stars become more important compared to their random motions. The rotation reaches approximately 100 km s(exp -1) and 50 km s(exp -1) along the major and minor axes, giving a local ratio of rotation to velocity dispersion of about 1.0 and 0.5 respectively. (4) The mass-to-light ratio (M/LB) is 3.9 in the central region of Cen A. If the stellar velocity dispersion is isotropic, the mass-to-light ratio increases with radius, suggesting the presence of dark matter in the halo. Within 25 kpc radius, the total mass of the galaxy is 3.1 x 10(exp 11) solar masses and M/LB = 10. (5) The observer's viewing direction is uniquely determined with respect to the intrinsic shape of the galaxy. The true shape of Cen A is nearly spherical, yet sufficiently triaxial to impose a distinctive gravitational signature on the kinematics. Dissert. Abstr.

N93-13727 Yale Univ., New Haven, CT.
ENCOUNTERS WITH PROTOSTELLAR DISKS Ph.D. Thesis
Clayton H. Heller 1991 113 p
Avail: Univ. Microfilms Order No. DA9224348

We have completed a numerical study of encounters between a star and star/disk system. Cross sections and rates for disk tilt, disk disruption, and binary formation are estimated using a large database of encounter simulations. The consequences of these results for star forming regions and our Solar System are discussed. A numerical code is developed which is capable of evolving a mixture of stars and gas in three dimensions. The algorithm is based on the method of smoothed particle hydrodynamics combined with the hierarchical tree method of computing gravitational forces. The code is tested by simulating the collision between two sheets of gas and the radial pulsations of a polytropic gas sphere. A protostellar disk model is developed based on simple assumptions. Test encounters are performed to determine the sensitivity of measured quantities on algorithm parameters, such as the gravitational tolerance and viscosity. This study shows that the Solar System could have had an encounter shortly after its formation of sufficient strength to generate the observed obliquity yet retain enough mass and radial extent to form the planetary system. A circumstellar disk will survive a typical encounter, approximately retaining its initial size and 50 percent of its mass. Even in dense environments the characteristic lifetime of a disk due to disruptive encounters is many millions of years. An average encounter that penetrates the disk will dissipate an amount of orbital energy equal to approximately 50 percent of the initial binding energy of the disk. An encounter with m = 1 solar mass, V(sub 0) = 1 km/s, and r(sub per) is less than 250 AU will result in a capture 27

percent of the time for a disk mass of 0.1 solar mass. For the inner region of the Trapezium cluster we estimate star-disk and disk-disk capture rates of 0.02 and greater than or = 0.04 Myr(exp -1), respectively. All of the estimated rates are lower limits. The number densities and velocity dispersions used are global values, which may not be appropriate if hierarchical structure exists in the clusters or if encounters are a natural outcome of the formation of binaries and higher order systems.

Dissert. Abstr.

N93-13764 Cornell Univ., Ithaca, NY.
HYDRODYNAMICAL CALCULATIONS OF STELLAR INTERACTIONS Ph.D. Thesis
Frederic Armand Rasio 1991 170 p
Avail: Univ. Microfilms Order No. DA9203887

Collisions and close encounters between a compact object and a giant star are studied by means of fully three-dimensional numerical simulations. Our astrophysical motivation is the formation of binary sources in dense stellar systems and, in particular, binary pulsars and x-ray sources in globular clusters. Using simple N-body simulations, we have performed a survey of a large number of encounters, varying all relevant parameters over wide ranges. We show how the numerical data on individual encounters can be used to calculate the binary formation rate and the probability distribution of the orbital parameters. Using smooth particle hydrodynamics (SPH), we have studied parabolic encounters between a 0.8 solar mass giant star and a 1.4 solar mass compact object. Our results can be summarized as follows. All encounters with periastron distance r(sub p) is less than or approximately equal to 2.5R, where R is the stellar radius, lead to significant disruption of the stellar envelope, including some mass loss. When r(sub p) is less than or approximately equal to 0.5R, the envelope is completely destroyed during the collision. About 40 percent of the gas escapes, while the rest forms a massive disk around the compact object, leaving behind the bare stellar core on a highly eccentric orbit. Subsequent close passages lead to continuous extraction of gas from the disk at a large rate, and the binary orbit may eventually stabilize while still retaining a large eccentricity. For 0.5R is less than or approximately equal to r(sub p) is less than or approximately equal to 2.5R, complete destruction of the envelope is avoided during the first close passage. However, nonlinear effects tend to make the envelope expand by a large factor, so that subsequent close passages will likely destroy it. In particular, all captures of a neutron star by a red giant in the core of a globular cluster are likely to result in the eventual destruction of the red giant envelope. We discuss the implications of our results in light of recent new detections of millisecond pulsars in globular clusters. Most importantly, we suggest that many globular cluster pulsars may have been spun-up by accretion from a massive disk rather than from a binary companion, thereby providing a possible solution to the birthrate problem. Dissert. Abstr.

N93-13795 Newcastle-upon-Tyne Univ. (England).
THE IMPLICATIONS OF THE MAGNETISM OF ORDINARY CHONDRITES Ph.D. Thesis
Simon James Morden 1990 234 p
Avail: Univ. Microfilms Order No. BRDX96322

Eleven ordinary chondrites (including ALHA77278 (LL3), ALH84086 (LL3), Appley Bridge (LL6), Crumlin (L5), Dalgety Downs (L4), Khanpur (LL5), Oberline (LL5), and Parnallee (LL3)) were studied in order to determine (1) the magnetic mineralogy, (2) the shape of the metal grains, and (3) the nature of the Natural Remanent Magnetization (NRM). Response to alternating field demagnetization, high-field isothermal remanent magnetization (IRM), magnetic hysteresis, and thermal demagnetization were all measured. It was found that the magnetic mineralogy of the chondrites was dominated by the FeNi alloy system. Alpha-kamacite, gamma-taenite, and gamma'-tetrataenite were all found in varying quantities. It was shown that tetrataenite was the dominant magnetic carrier, possessing a high coercivity (greater than 500 mT) and high remanence. On heating, tetrataenite became magnetically soft taenite. Since tetrataenite can only form as the result of very slow cooling, the transition was irreversible. No tetrataenite was found in the type 3 chondrites studied. The orientation of the stable NRM in the samples was shown to be random. The stable remanence was held by tetrataenite, where present. A magnetic fabric was found in all the samples. In all but two, the fabric was a distinct foliation; Tuxtuac and Wold Cottage showed lineations. It was concluded that the magnetic carriers were magnetized before emplacement in the rock, and that the rock was not a fine-scale breccia. Planetary magnetic fields were discounted as the source of the magnetizing field. Thermal demagnetizations of NRM showed a definite trend towards higher blocking temperatures for type 6 chondrites over types 3-5, and a tentative trend for lower blocking temperatures of type 3 against 4-5. Hot accretion of chondrites was favored and it is possible that this accretion occurred after a catastrophic impact between two large bodies. The plasma cloud thus formed might enhance any magnetic field present, and may have been able to support its own transient field. Chondrites may therefore possibly be secondary objects, and not direct condensates from a solar nebula. Dissert. Abstr.

N93-13828 Illinois Univ. at Urbana-Champaign, Savoy.
THE ROLE OF AMBIPOLAR DIFFUSION IN THE FORMATION OF INTERSTELLAR CLOUD CORES AND PROTOSTARS Ph.D. Thesis
Scott Allyn Morton 1991 348 p
Avail: Univ. Microfilms Order No. DA9210926

The formation of stars is a fundamental unsolved problem in astrophysics. Interstellar molecular clouds, observed to be the birth place of stars, have masses much larger than those of typical stars. Observed densities, temperatures, and strengths of well-ordered magnetic fields imply that magnetic forces, transmitted to the neutral fluid through collisions with ions, dominate thermal forces in supporting these objects against self-gravity. The anisotropy of the Lorentz force, which is always perpendicular to the magnetic field, allows a simplified treatment of the dynamics involving motion along the magnetic field. We derive a reduced system of non-linear, non-ideal magnetohydrodynamic equations by assuming a balance of thermal and gravitational forces along the magnetic field. We then study both the stability of dense clouds as well as their non-linear evolution/contraction owing to ambipolar diffusion. An important result is the selection by ambipolar diffusion of a characteristic mass comparable to a solar mass.

Dissert. Abstr.

N93-13829 Illinois Univ. at Urbana-Champaign, Savoy.
SOME PROBLEMS OF QUANTUM COSMOLOGY AND DARK MATTER PHYSICS Ph.D. Thesis
Jin Wang 1991 131 p
Avail: Univ. Microfilms Order No. DA9211025

The quantum cosmology is studied of the string universe obtained by embedding the Robertson-Walker metric in the nonlinear sigma model. It was found that initially the universe exists in a series of metastable bound states with the scale factor taking discrete values. Then it tunnels through a barrier and comes out in an inflationary state. This tunneling (or evolution in imaginary time) also has the effect of heating up the matter field so that we have a condition of chaotic inflation. The asymptotic solutions agree with those obtained from the classical Einstein equations. Quantum cosmology was considered of a 4-D universe using the effective action of superstrings. Both Hartle-Hawking and Vilenkin boundary conditions were applied to the solution of Wheeler-DeWitt equation. Under certain conditions (fermions added) the universe was found to tunnel through to the Lorentzian regime from the Euclidean regime and time is dynamically generated. Chudnovsky and Vilenkin's idea was applied to possible existence of cosmic strings in the Sun. Stellar evolution with cosmic strings at solar age gives a radius and luminosity of the star which are in contradiction with observation. The astrophysical bound was studied on the change of gravitational constant with time. It was found that (G/G) less than 10(exp -12)yr(exp -1) is the condition that has to be satisfied in order not to cause the conflict with observation. The effect was studied of axions on the steller evolution of a 10 solar mass star model. If the axion mass is larger than .1 ev the star's age is significantly different at late stages, compared to the star without axions. It is argued that if cosmions (or WIMPS) solve the solar neutrino problem, then they must also play an important role in the evolution of low mass star main sequence stars. If they do so, then a simple (long mean free path) model for the interaction of cosmions with baryons leads to changes in the structure of the nuclear-burning core which may in principle be observable. Dissert. Abstr.

N93-13848 Stanford Univ., CA.
GRAVITATIONAL LENSING BY GALAXY CLUSTERS: THE GIANT ARCS IN ABELL 370 AND CI2244-02 Ph.D. Thesis
Anton George Bergmann 1992 160 p
Avail: Univ. Microfilms Order No. DA9221596

We construct lens models of the giant arcs discovered recently in the

galaxy clusters Abell 370 and C12244-02. Using these models we show that the minimum mass to blue light ratio within the central 150 kpc of these clusters is approximately 400 solar mass/solar luminosity. Furthermore, we demonstrate that the location and extent of the arc in A370 cannot be modeled by mass distribution in which the dark matter in the cluster is colocated with the luminous galaxies. We investigate the surface brightness fluctuations along the C12244 arc. These fluctuations could be either due to lensing by small masses superimposed on the arc or they could be due to bright regions of the background source being multiply imaged along the arc. We explore these models in detail and find that we cannot dismiss either model. Finally we calculate the relative probability distribution of high magnification to low magnification gravitational lens events. We first provide an analytic discussion of the magnification probability for point sources and then explore numerically the magnification probability for extended sources. For realistic lens models and sources we find that for every highly tangentially magnified image such as the giant arcs one would expect to find approximately ten small arclets. This ratio depends on the assumed central density of the model. The lensing model favored by our calculation to produce a large number of highly magnified images has a central mass density that is approximately three times larger than the mass density obtained by extrapolating x-ray brightness measurements to the center of clusters. This disagreement between two methods of determining the cluster potential is still tentative since the sample of lensing events is very small, but it may indicate that the dark matter in clusters is more centrally condensed than the hot intracluster gas producing the x-rays. Dissert. Abstr.

N93-13850 California Univ., Los Angeles.
DENSITY CONTRAST SHELL MODELS FOR PLANETARY NEBULAE Ph.D. Thesis
Siek Hyung 1992 193 p
Avail: Univ. Microfilms Order No. DA9221026

Chemical compositions of planetary nebulae are of interest for several reasons: checking on predictions of nucleosynthesis in late stages of stellar evolution and for elemental contributions to the interstellar medium of reprocessed elements since possibly a large fraction of stars in 1.0-5 solar mass range go through this stage. One of the methods for getting chemical composition is construction of theoretical models, a task of enormous difficulty involving geometrical complexities and a variety of physical processes. The validity of a model as judged from among several factors must be how well it represents spectroscopic observations. The excellent theoretical models produced by Harrington, Clegg (1987) and others give the radiation contributed by the whole image. However, except for the strongest lines, which can be measured with a photoelectric scanner using a large entrance slot, we do not observe the radiation integrated over the whole image. When we look for strategically important, often weak, lines we use a slit spectrograph or an image tube scanner and take a narrow pencil through the image. We must, therefore, use the model to predict the emission from this pencil and compare it with the relevant observations. Different observers may select different regions in the nebular image. The model program should accommodate this circumstance as long as observers precisely described the regions they have selected. Thus, the present investigation involves not just the calculation of improved models putting in all the best available physics but also development of procedures for predicting the emission from cross-sections taken through the nebular image. Spherically symmetrical shells pose no great difficulty by nebulae with bilateral symmetry are less easily handled since the pencil may pass through zones of different density. Although presently available spherically symmetric nebular models can well accommodate round planetary nebulae, the nonspherical shape of most of objects implies that these models are too simplistic. The thesis emphasizes the treatment of non-spherically symmetrical planetaries. The vast majority of planetary nebulae are of this type. An improved agreement with observations can be obtained by adopting theoretical models with bilateral symmetry. Results are presented for two well observed high excitation planetary nebulae IC 2165 and NSG 7027 for which it is believed substantially improved chemical compositions are found; some abundances differ considerably from those estimated by previous study. Dissert. Abstr.

N93-13853 Oklahoma Univ., Norman.
A STUDY OF THE NEUTRAL AND IONIZED GAS IN THE INTERSTELLAR MEDIUM AND GALACTIC H 2 REGIONS Ph.D. Thesis
Douglas Alan Roberts 1992 193 p
Avail: Univ. Microfilms Order No. DA9217967

High resolution radio spectral line imaging has been carried out towards a number of galactic sources in order to investigate the properties of the sources themselves as well as the properties of the interstellar medium (ISM). In the case of the supernova remnant 3C 58, H I spectral line observations using both the Westerbork Synthesis Radio Telescope and the Effelsberg 100 m telescope have been carried out at an angular resolution of approximately 1 min. Significant small scale structure in the ISM towards 3C 58 has been detected in H I emission. These emission features have densities in the range 1 to 9 cu cm, masses 30-1200 solar mass and brightness temperatures 15-35 K. The star-forming region DR21 has been observed in H I absorption in a 12(sup h) observation, using the Very Large Array (VLA) B configuration, and a short 2(sup h) observation, using the C configuration. The goals of this project were the investigation of the distribution of H I in front of DR21 and the detection of the Zeeman splitting of the 21 cm line. The Zeeman effect has been successfully observed in the 21 cm line of H I towards W3 using the VLA. The line-of-sight magnetic field in the W3 'core' has been imaged at approximately 25 sec. resolution with a noise of 3 mJy beam(exp -1). A model of a pinched magnetic field due to the collapse of the molecular cloud is proposed. A large portion of this research has been a series of H 92 alpha recombination line observations of the H II region in the center of the galaxy, Sagittarius A (Sgr A) West. The first of these observations was carried out to detect the Zeeman splitting of the H 92 alpha line. With a resolution of 2.4 sec. and an r.m.s. noise of 0.4 Mjy beam(exp -1), the northern arm and bar of Sgr A West have been observed in the H 92 alpha line at 8.3 GHz using the VLA. The most extensive study that was undertaken was multi-configuration VLA project to observe the 92 H alpha line in Sgr A West with an angular resolution of approximately 1 sec., a velocity resolution of 14 km/s and an r.m.s. noise of approximately 0.15 mJy beam(exp -1). The global kinematics and electron temperatures of the H II region have been determined. Dissert. Abstr.

N93-13959 Yale Univ., New Haven, CT.
GALAXIES WITH SPECTRAL ENERGY DISTRIBUTIONS PEAKING AT 60 MICROMETERS: MORPHOLOGY AND ACTIVITY EXPLAINED BY INTERACTIONS Ph.D. Thesis
Charlene Anne Heisler 1991 293 p
Avail: Univ. Microfilms Order No. DA9218787

We present a multiwavelength investigation of galaxies with far-infrared (FIR) spectral energy distributions peaking near 60 microns. Over half of the 60 micron Peakers were previously unidentified in optical catalogues, thus the first step towards understanding these galaxies is through morphological classification. CCD images taken with broadband optical filters, and digitally enhanced images reveal that the galaxies have either an amorphous appearance or a peculiar morphology. All of the 60 micron Peakers are strong emission line galaxies with spectroscopic types ranging from starburst to seyfert. The paucity of spiral structure among the 60 micron Peakers is a very striking result as optically-selected emission line galaxies are typically spirals. The qualitative appearance of the 60 micron Peakers is well correlated with quantitative morphology parameters, both model-dependent (i.e., bulge-to-disk ratio) and model-independent (i.e., concentration index, effective surface brightness). The amorphous galaxies are bulge-dominated, have larger concentration indices, smaller effective radii, warmer FIR colors, smaller FIR-to-Blue luminosity ratios and a more active spectroscopic type (i.e., seyfert 1), compared with the peculiar galaxies. Narrowband H-alpha images reveal that the ionized gas emission in the 60 micron Peakers is centrally concentrated (less than a few kpc). Radio continuum maps demonstrate that the radio sources are also compact (less than a kpc), with radio fluxes intermediate to that of radio loud quasars and normal spiral galaxies. This together with the H-alpha FIR and radio-FIR correlations, implies that the FIR emission also originates from a central, compact region as the result of a circumnuclear dust shroud obscuring the central radiation source. The observational results and trends are well explained in terms of an evolutionary sequence in galaxy morphology and nuclear activity. An interaction plays two crucial roles: (1) triggering nuclear activity by driving gas and dust to the central regions of the galaxy, and (2) directly creating the initial peculiar features

and subsequent amorphous morphology. We conclude that the 60 micron Peakers represent a short-lived phase of nuclear activity, triggered by an interaction. Dissert. Abstr.

N93-13962 Colorado Univ., Boulder.
HYDRODYNAMICS AND SPECTRA FORMATION OF INTERACTING MASSIVE BINARIES AND THE YOUNG REMNANT OF SN1987A Ph.D. Thesis
Ding Luo 1991 144 p
Avail: Univ. Microfilms Order No. DA9220426

Massive stars interact with the interstellar medium through stellar winds and supernova explosions. These processes provide useful information on the evolution and the explosions of massive stars. The interactions were studies between the steady stellar winds of close massive binaries, the formation of the circumstellar structure of SN1987A through the stellar winds of the progenitor star, the illumination of this circumstellar structure by SN1987A, and the young remnant of SN1987A. A stellar wind from a massive OB or Wolf-Rayet star in a binary system will strike the surface or stellar wind of its companion, forming shocked gas that can radiate X rays. The X ray spectrum from the shocked winds will vary in a predictable way with orbital phase, owing to photoelectric absorption by the stellar winds. Using a 2D hydro code, ZEUS2D, we calculate detailed models for the hydrodynamics and X ray emission from two such systems. We describe how our results can be scaled to other such systems, and we discuss prospects for future observations. The progenitor star of type II supernova evolves from a blue giant main sequence star to a red giant and, in the case of SN1987A, to a second blue giant stage before it finally explodes. At each stage it loses mass through stellar winds; the interactions between these winds form the circumstellar structure. The thin shell Kompaneets approximation is used to model the interaction between the fast stellar wind of the blue giant and the slow, anisotropic relic stellar wind of the red giant. It is shown that this interaction forms an hourglass-shaped circumstellar shell. This hourglass shell was ionized by the soft X ray and UV flash at the outburst of SN1987A. The ionization, recombination and cooling of the shell was studied and the resulting light curves of the narrow emission were compared with observations. This study put useful constraints on the flux and spectrum of the ionizing flash, which was not directly observed. The rapidly expanding envelope of SN1987A will strike the hourglass shell at about 20 years after the explosion. The young supernova remnant will then become a strong source of soft X ray and UV radiation. Dissert. Abstr.

N93-13963 Harvard Univ., Cambridge, MA.
SUPERNOVA REMNANTS, SHOCKS, AND THE INTERSTELLAR MEDIUM Ph.D. Thesis
Robert Christopher Smith 1992 211 p
Avail: Univ. Microfilms Order No. DA9220145

Supernova remnants (SNR's) can provide information about not only their energetics and evolution but also about supernovae, interstellar shocks, and the interstellar medium. Observations are presented along with analysis of SNR's ranging from studies of a sample of extragalactic SNRs to detailed analysis of shocks in Balmer-dominated SNRs. Optical spectra for the 42 SNR's and SNR candidates identified in a previous imaging survey of M33 confirm that all have spectral characteristics similar to those of galactic and LMC SNR's. There is, however, no evidence of the correlations of emission-line ratios with SNR diameter seen in previous samples. The abundance gradients derived are consistent with those obtained from observations of H II regions, but the nitrogen abundances are systematically larger by about 0.4 dex. This discrepancy remains unexplained. The sample is shown to be consistent with Sedov-Taylor expansion both in the number-diameter distribution and through simple evolutionary modeling. Analysis of the energy-diameter relation provides no evidence to support the reported energy increase with increasing diameter. Only evolved remnants with strong (S II) emission have been included in the above M33 sample. We also report on the observations of six Balmer-dominated SNR's which show little or no forbidden line emission: the galactic remnants of SN 1572 (Tycho) and SN 1006, and four remnants in the LMC, 0505-67.9, 0509-67.5, 0519-69.0, and 0548-70.4. Line widths are reported and compared to models for a collisionless shock interacting with a partially neutral medium. Although previous analyses used the ratio of broad to narrow intensity as an indicator of shock velocity, our models show that this is not reliable. Combining shock velocity estimates based on the line widths with observed proper motions, the distances to Tycho and SN 1006 are estimated to be 1.5-3.1 kpc and 1.4-2.8 kpc respectively. The shock velocities derived for the LMC remnants allow us to estimate their ages. The ages range from approx. 10(exp 4) years for 0505-67.9 and 0548-70.4 to less than 1500 years for the small remnants 0509-67.5 and 0519-69.0. Dissert. Abstr.

N93-14059 Washington Univ., Saint Louis, MO.
THE STELLAR ANGULAR CORRELATION: CLUES TO WIDE BINARY STAR PROPERTIES Ph.D. Thesis
Peter Marcus Garnavich 1991 319 p
Avail: Univ. Microfilms Order No. DA9211556

The angular distribution of stars brighter than visual magnitude 14 is analyzed for evidence of gravitationally bound systems with widely separated components. Binary stars with separations on the order of 0.1 parsec are interesting as probes of Galactic dynamics, disk dark matter, the Oort comet cloud and the postulated Solar compannion star, Nemesis. Catalogs of stars, complete to a resolution limit of four arcseconds, were constructed from digitized Schmidt telescope plates covering over 600 square degrees of the sky in four directions. I analyze the clustering properties of stars and star pairs using two-point and three-point angular correlation functions. Significant correlation (assumed to be due to binary stars) is detected only for angular separations less than 40 arcseconds. No significant numbers of ternary systems are detected. Employing a modified Wasserman-Weinberg technique, I directly compare the angular correlation functions with a simple model of wide binary star properties. The wide binary semimajor axis distribution at low Galactic latitudes is best described as a single power law of index -1.3. Near the north Galactic pole (NGP), the power law is less steep and the distribution is consistent with a cutoff near 0.1 parsec. The derived wide binary density is unrealistically large, suggesting that the basic model inadequately characterizes wide binary properties. I also study a sample of stars from the Space Telescope Guide Star Catalog (GSC). The region analyzed lies within thirty degrees of the NGP and covers 2500 square degrees of sky. This large, low resolution sample complements the smaller, more uniform plate catalogs. I identify many systematic errors in the GSC and attempt to account for image misclassifications and poorly defined resolution limits. The corrected stellar correlation function from the GSC is found to be consistent with a wide binary separation cutoff 0.1 parsec. The dissolution of a poor Galactic cluster at the NGP may explain the observed wide binary distribution in that direction. Evidence for weak clustering on scales of one degree is seen in the pair-pair correlation function. The unphysically large wide binary density derived from magnitude-limited samples is explained well by luminosity correlation between the binary components. An alternative solution requires all F to K dwarfs to be members of wide binaries. Based on the observed properties of wide binary stars, the probability that the Sun has a stellar companion capable of inducing periodic mass extinctions on Earth is only 0.05 percent. In an analogy with Oort cloud dynamics, I suggest a mechanism that can substantially reduce the number wide binaries with separations greater than 0.1 parsec. Dissert. Abstr.

N93-14071 Princeton Univ., NJ.
THE INTERSTELLAR MEDIUM OF ELLIPTICAL GALAXIES Ph.D. Thesis
Joanna Frances Lees 1992 280 p
Avail: Univ. Microfilms Order No. DA9216837

Initial investigations showed elliptical galaxies to be deficient in gas compared to their spiral cousins. However, in the past decade more sensitive observations have revealed a varied interstellar medium in many ellipticals--from a hot 10(exp 7) K corona to disks of cold neutral and molecular gas. In this thesis, both the cold and hot gaseous components are investigated and compared. The presence of gas in elliptical galaxies may give important clues to their recent history; the balance of the various phases may indicate the relevant energy input mechanisms; the gas kinematics trace the gravitational potential of these systems. First, observations of CO(2-1) emissions from FIR-bright elliptical galaxies, of which 40 percent are detected, are described. Typical molecular masses are similar to that of the atomic gas, about 10(exp 7) to 10(exp -9) solar mass. The ellipticals display a power-law distribution of M(sub H2)/L(sub B), increasing slowly toward the lower values of the gas-to-luminosity ratio, implying that most elliptical galaxies may contain small quantities of cold gas. They display the same M(sub H2) - L(sub FIR) and M(sub H2) - M(sub HI) relationships as do spiral galaxies, so that the global interstellar medium properties of early-type systems appear to be similar to those of

the late-type galaxies, although for gas masses over an order of magnitude smaller. Second, the x-ray and FIR data for elliptical galaxies are compared, and it is shown that ellipticals obey a L(sub X) - L(sub B) - L(sub FIR) relationship such that L(sub X) is proportional to L(sub B)(exp 2.3) L(sub FIR)(exp -0.3). Furthermore, the ratio of cold-to-hot gas mass shows a bimodal distribution with field ellipticals containing more cold than hot gas and cluster ellipticals having cold gas masses only a few percent of their hot gas mass. Finally, VLA HI21 cm observations of the atomic gas disk in the nearby elliptical galaxy NGC 4278, and other members of the group, are presented. NGC 4278 shows a very extended cold gas disk in well ordered rotation, ideal for mapping the potential of this system. Models of the gas kinematics using spherical, oblate, and triaxial mass distributions are employed to constrain the mass-to-light ratio out to over ten half-light radii.
Dissert. Abstr.

N93-14091 Harvard Univ., Cambridge, MA.
THERMAL AND NONTHERMAL STAR FORMATION: AN INVESTIGATION INTO THE PROCESS OF STAR FORMATION AS A FUNCTION OF STELLAR MASS Ph.D. Thesis
Edwin Fremont Ladd 1991 394 p
Avail: Univ. Microfilms Order No. DA9211709

In this thesis, we examine the process of star formation as a function of stellar mass. We present broadband far infrared and submillimeter wavelength maps of 11 embedded sources of low luminosity (L is less than 30 L solar magnitude) and eight sources of intermediate luminosity (30 is less than L is less than 3000 L solar magnitude), acquired with the Kuiper Airborne Observatory, the NASA Infrared Telescope Facility, and the James Clerk Maxwell Telescope. We compare the spatial and spectral distribution of flux and find that the emission is consistent with a centrally condensed model envelope whose temperature and density structure varies as a power law with radius. We also conclude that dust column density, and not total luminosity, plays a central role in determining the shapes of the spectral energy distributions of these sources. We present microwave spectral line observations of dense gas associated with embedded sources of varying luminosity, using the J = (1 approaches 0) rotational transitions of (C-13)(O-16) and (C-12)(O-18), as well as the (J,K) = (1,1) and (2,2) in inversion transitions of NH(sub 3). We compare the linewidth, temperature, and mass of these dense cores and conclude that all three properties scale with the luminosity of the associated source. We conclude that while the cores which are associated with stars of low and intermediate mass are quite different, the process by which stars form is not a strong function of luminosity for sources with L is less than 3000 L solar magnitude.
Dissert. Abstr.

N93-14095 Harvard Univ., Cambridge, MA.
MOLECULAR CLOUDS IN THE DISTANT OUTER GALAXY Ph.D. Thesis
Seth William Digel 1991 162 p
Avail: Univ. Microfilms Order No. DA9211674

The first large-scale CO J = 1 approaches 0 survey with sensitivity and angular resolution sufficient for study of individual giant molecular clouds in the Outer Arm of the Galaxy is presented. Also analyzed here is the composite of all recent CO observations of the outer Galaxy with the CfA 1.2 m telescope. This data set covers nearly one-seventh of the Galactic equator and is the largest and most sensitive to date for study of the large-scale distribution of molecular gas in the outer Galaxy. The essential conclusion from the CO survey of the Outer Arm is that the Outer Arm is a well-defined, continuous feature in CO that contains GMCs as large as those in the inner Galaxy. The molecular clouds in the Arm do not appear deficient in massive star formation nor unusual in any way other than faint in CO for their H2 content. Several lines of evidence support the assertion that the ratio of the column density of molecular hydrogen to the integrated intensity of the CO line, denoted X, is a factor of 4 larger in the Outer Arm than in the molecular ring, most importantly analysis of the luminosity-line width relation of individual clouds in the arm and comparison of the far-infrared emissivities of the dust associated with the atomic and molecular gas there. The observed distribution of CO in the outer Galaxy probably differs significantly from the distribution of IRAS point sources with infrared colors characteristic of star-forming regions. In particular, the radial extent of the CO distribution is greater than that of the point sources, especially if X increases markedly beyond the solar circle. However, the difference may be due only to inadequate observations of the point sources. The composite data show the increasing warp and flare of the plane beyond the solar circle and indicate significant CO emission to Galactocentric distance R = 14 kpc, the distribution of emission matching smoothly that known for the inner Galaxy. The analysis of the data is limited most by the requirement of extremely flat baselines in the observations. On the assumption X = 9.2 x 10(exp 20) cm(exp -2) (K km s(exp -1))(exp -1) for R is greater than or equal to 12.5 kpc, the molecular mass extrapolated to the range R = 11-14 kpc is about 3 x 10(exp 8) solar mass, a significant fraction of the total molecular mass of the Galaxy, which may be estimated as 1.4 x 10(exp 9) solar mass, including a correction for helium.
Dissert. Abstr.

91 LUNAR AND PLANETARY EXPLORATION

Includes planetology; and manned and unmanned flights.

For spacecraft design or space stations see *18 Spacecraft Design, Testing and Performance.*

N93-13337 State Univ. of New York, Stony Brook.
THE JOVIAN IONOSPHERE Ph.D. Thesis
Yong Ha Kim 1991 234 p
Avail: Univ. Microfilms Order No. DA9220352

The Jovian ionosphere has been modeled for both auroral and nonauroral regions in this dissertation. The model utilizes updated data on chemical reactions of ion chemistry among ions in the ionosphere, photo-process cross sections for major neutrals and hydrocarbons, and electron impact cross sections for major neutrals in the Jovian upper atmosphere. The absorption of solar ultraviolet flux between 846 and 1116 A by H2 has been calculated at high resolution, which results in previously-ignored ionization of hydrocarbons near the methane homopause by strong solar UV emission lines and the continuum flux in the wings of the H2 lines. The non-auroral model shows that the Jovian ionosphere at mid-latitudes should have a hydrocarbon ion layer at lower altitudes, which may correspond to the E region in the terrestrial ionosphere. In the auroral model, a multi-stream transport code is employed for the precipitation of 10 keV electrons into the Jovian upper atmosphere. An upper atmosphere model for auroral regions is constructed from the mid-latitude neutral atmosphere model derived from the Voyager data, modified with higher temperatures based on ground-based infrared observations of the auroral regions. It is found form the auroral model that vibrationally excited H2 affects the vibrational distribution of H3(+) that can be probed by infrared emission spectra. Results of the auroral model include densities of major ions as well as vibrational distributions of H2 keV electrons with an energy flux of 1 erg cm(exp -2)s(exp -1). The computed column densities of H3(+)(v1 = 0, v2 = 1) and H3(+)(v1 = 0, v2 = 2) are consistent with the infrared observations of H3(+). Finally we investigate the time variation of ion densities in response to electron precipitation in the auroral regions. We find that the electron densities from the time-dependent auroral model could differ by up to an order of magnitude from those of steady-state models depending on the time scale of variations in the precipitating energy flux.
Dissert. Abstr.

N93-13344*# Southwest Research Inst., San Antonio, TX. Space Sciences Div.
SO2 ON VENUS: A FINAL CROSS-CALIBRATION WITH PIONEER VENUS Semiannual Progress Report No. 1
S. Alan Stern 1 Sep. 1992 19 p
(Grant NAG5-1913; SwRI Proj. 15-4914)
(NASA-CR-191256; NAS 1.26:191256) Avail: CASI HC A03/MF A01

In our previous report, we noted that we had successfully completed all of the IUE observations which were proposed. A total of 7 Venus spectra were obtained. In the present reporting period, essentially all of the associated data reduction and analysis activities were completed, and Drs. Stern, Barker, and Na met to collaborate on data interpretation. The model atmosphere used in this analysis is similar to the one used in the analysis of the Pioneer Venus observations (Esposito, et al. 1979, 1988) and the previous IUE observations (Na, et al. 1990). In this model, sulfuric acid aerosols with a radius of about 1 micron are mixed uniformly with Rayleigh scattering gases throughout the cloud layer. There are two wavelength-independent absorbers. First, the aerosols are assumed to have a single scattering albedo of 0.98, and second a pure absorbing layer with an optical depth of 0.2 is added at an altitude of 75 mbar. The variable

parameters in this model are the mixing ratios of SO2 at the cloud top (40 mbar level), and the scale height of SO2 at the same altitude. Model spectra were calculated using a radiative transfer code utilizing a Markov Chain method. Each model calculation takes into account the multiple scattering and the vertical inhomogeneity of the atmosphere. We reported those initial results at the 1992 meeting of the AAS Division of Planetary Sciences (Barker, Stern, and Na 1992) The important finding we have reached is that the 1991 IUE observations indicate that the long-term decline in Venus SO2 abundance has either halted or reversed. Our simultaneous groundbased measurements made on the McDonald Observatory 2.7 m corroborate this result. We are now preparing a paper describing these IUE results for publication in Icarus. With the IUE results reduced, we are also beginning a project to compare the 1991 IUE results to Pioneer Venus UV spectra made on the same dates. Author

N93-13504# EG and G Mound Applied Technologies, Miamisburg, OH.
ISOTOPIC SEPARATION OF He-3/He-4 FROM SOLAR WIND GASES EVOLVED FROM THE LUNAR REGOLITH
W. R. Wilkes and L. J. Wittenberg (Wisconsin Univ., Madison.) 1992 8 p Presented at the 3rd International Conference on Engineering Construction and Operations in Space, Denver, CO, 31 May - 4 Jun. 1992 (Contract DE-AC04-88DP-43495)
(DE92-019339; MLM-3759(OP); CONF-9205239-1) Avail: CASI HC A02/MF A01

The potential benefits of He-3 when utilized in a nuclear fusion reactor to provide clean, safe electricity in the 21st century for the world's inhabitants has been documented. Unfortunately, He is scarce on earth. Large quantities of He-3, perhaps a million tons, are embedded in the lunar regolith, presumably implanted by the solar wind together with other elements, notably He-4, H, C, and N. Several studies have suggested processing the lunar regolith and recovering these valuable solar wind gases. Once released, these gases can be separated for use. The separation of helium isotopes is described in this paper. He-3 constitutes only 400 at. ppm of lunar He, too dilute to separate economically by distillation alone. A 'superfluid' separator is being considered to preconcentrate the He-3. The superfluid separator consists of a porous filter in a tube maintained at a temperature of 2.17 K or less. Although the He-4, which is superfluid below 2.17 K, flows readily through the filter, the He is blocked by the filter, and becomes enriched at the feed end. He can be enriched to about 10 percent in such a system. The enriched product from the superfluid separation serves as a feed to a distillation apparatus operating at a pressure of 9 kPa, with a boiler temperature of 2.4 K, and a condenser temperature of 1.6 K. Under constant flow conditions, a 99.9 percent enriched He product can be produced in this apparatus. The heat rejection load of the refrigeration equipment necessary to cool the separation operations would be conducted during the lunar nights. DOE

N93-13568*# Southwest Research Inst., San Antonio, TX. Instrumentation and Space Research Div.
CHAIRMANSHIP OF THE NEPTUNE/PLUTO OUTER PLANETS SCIENCE WORKING GROUP Annual Report
S. Alan Stern 1 Nov. 1992 43 p
(Grant NAGw-2914; SwRI Proj. 15-4945)
(NASA-CR-191288; NAS 1.26:191288) Avail: CASI HC A03/MF A01

The Outer Planets Science Working Group (OPSWG) is the NASA Solar System Exploration Division (SSED) scientific steering committee for the Outer Solar Systems missions. The FY92 activities of OPSWG are summarized. A set of objectives for OPSWG over FY93 are described. OPSWG's activities for subsequent years are outlined. A paper which examines scientific questions motivating renewed exploration of the Neptune/Triton system and which reviews the technical results of the mission studies completed to date is included in the appendix. L.R.R.

N93-13625 Johns Hopkins Univ., Baltimore, MD.
THE JOVIAN ULTRAVIOLET AURORA OBSERVED WITH THE IUE SPACECRAFT: BRIGHTNESS AND COLOR DISTRIBUTION WITH LONGITUDE Ph.D. Thesis
Timothy Austin Livengood 1992 434 p
Avail: Univ. Microfilms Order No. DA9216595

Ultraviolet auroral emissions from Jupiter's poles are produced by excitation of fundamental electronic transitions of H2. The UV spectrum provides a direct measure of the auroral power without significant dependence on chemical composition or temperature in the emission region. The aurora deposits approximately 6 x 10(exp 13) W at the north and south poles combined, an order of magnitude greater than the total solar EUV irradiance. The aurora is thus significant in the global upper atmospheric energy budget. The aurora is powered by precipitating magnetospheric charged particles, so auroral activity reflects plasma production, energization, and loss from the magnetosphere. This work analyzes 509 International Ultraviolet Explorer satellite spectra of the Jovian aurorae. This large data set is used to establish the distribution on the auroral oval of luminosity and of the hydrocarbon abundance overlying the emission as functions of Jovigraphic magnetic longitude. The distributions correlate for each pole, with maxima and minima at about the same longitudes. The northern maximum of luminosity and hydrocarbon column is at approximately 180 deg - 190 deg System III (1965) magnetic longitude and the southern maxima are at approximately 30 deg - 70 deg. Either vertical winds driven by auroral heating or longitude-dependent primary particle energy can explain the correlated distributions of luminosity and overlying hydrocarbon abundance. Sufficient power is deposited in the aurora to plausibly support winds of the necessary magnitude, whereas the contrast in particle energies estimated here appears insufficient to support the luminosity contrast. This work favors heavy ions as the probable auroral primaries, in preference to electrons or protons. This work also fits individual auroral observations with models of the luminosity distribution on the auroral oval. The results favor the auroral oval mapped by the Voyager ultaviolet experiment as the probable northern oval and identify a best-fit southern oval based on magnetic field models. Variations in the north and south auroral luminosity and in the longitude of maximum luminosity are correlated between the poles. There are no systematic trends in the auroral brightness or morphology over the lifetime of the data set, ruling out correlation of Jovian auroral brightness with solar EUV irradiance, which is part of a suggested mechanism for energization of heavy ion primary particles. Dissert. Abstr.

N93-13831 Washington Univ., Saint Louis, MO.
MODEL STUDIES OF THE MIDDLE ATMOSPHERE OF VENUS Ph.D. Thesis
Matthew Newman 1991 509 p
Avail: Univ. Microfilms Order No. DA9211575

Zonal winds reach in excess of 100 m/s in the middle atmosphere of Venus; the cloud-level atmosphere takes little more than 4 days to complete one rotation, while the solid planet below has a 243-day rotation period. This phenomenon, known as superrotation, is the central problem of the Venus atmosphere. The question we address is how the superrotation maintains itself against friction in the middle atmosphere, and in particular, what are the eddy processes that maintain equatorial superrotation. Also of interest is the cloud-top atmosphere is a feature known as the polar dipole, a pair of hot spots that orbit the pole with a period of about 3 days. Previous linear analyses have suggested that the dipole could be due to barotropic instability. In the first part of the thesis we examine the interaction of barotropically unstable polar Rossby wave with the mean cloud-top zonal circulation. Linear, quasi-linear, and nonlinear regimes are investigated in order to isolate the factors that control the properties of these waves. We find that the observed properties of the dipole at high latitudes on Venus may not be explained by barotropic instability theory. In the second part of the thesis we employ a zonally-truncated-three-dimensional mode of the Venus middle atmosphere. We find that the interaction of the diurnal and semidiurnal thermal tides with the zonal mean flow can maintain the observed cloud top superrotation. The model system tends toward a zonal wind pattern similar to that observed, despite model initializations that were either faster or slower than the final winds. Moreover, our model suggests that the origin of the observed midlatitude '5-day wave' is baroclinic instability within the lower cloud. Finally, the diurnal tidal winds have large amplitude at the cloud tops. This may distort the interpretation of cloud-tracked winds, which use dayside observations only. Dissert. Abstr.

N93-13958 California Univ., Santa Barbara.
ACCRETION RATES OF PROTOPLANETS Ph.D. Thesis
Yuval Greenzweig 1991 228 p
Avail: Univ. Microfilms Order No. DA9211510

The giant planets' solid cores must have formed prior to the dispersal of the primordial solar nebula, to allow the capture of their massive, gaseous envelopes from the nebula. Recent observations of disks of dust surrounding

nearby solar-like stars lead to estimates of nebula lifetimes at 10(exp 6) to 10(exp 7) years. Thus, theories of solid particle accretion must explain how the solid cores of the giant planets may have formed within comparable timescales. Calculations are presented which support the sole currently hypothesized mechanism of planetary accretion in which the duration of the stage of growth from planetesimals (1 to 10 km size bodies) to moon- or planet-size bodies lies within the widely accepted time constraint mentioned above. It has been shown that under certain conditions a growth advantage is given to the larger bodies of a swarm of Sun-orbiting planetesimals, resulting in runaway growth of the largest body (or bodies) in the swarm. The gravitational cross section of the protoplanet (the largest body in the swarm) increases with its size, eventually requiring the inclusion of the effect of the solar tidal force on the interaction between it and a passing planetesimal. Thus, numerical integrations of the three-body problem (Sun, protoplanet and planetesimal) are needed to determine the accretion rates of protoplanets. Existing analytical formulas are refined for the two-body (no solar tidal force) accretion rates of planetesimals or small protoplanets, and numerically derives the three-body accretion rates of large protoplanets. The three-body accretion rates calculated span a wide range of protoplanetary orbital radii, masses, and densities, and a wide range of planetesimal orbital eccentricities and inclinations. The most useful numerical results are approximated by algebraic expressions, to facilitate their use in accretion calculations, particularly by numerical codes. Since planetary accretion rates depend strongly on planetesimal random velocities, the effect of the three body encounter on the velocity dispersion was also studied. It was found that protoplanets are more effective perturbers of planetesimal eccentricities than previously noted. Dissert. Abstr.

N93-13972*# National Aeronautics and Space Administration. Lyndon B. Johnson Space Center, Houston, TX.

THE SECOND CONFERENCE ON LUNAR BASES AND SPACE ACTIVITIES OF THE 21ST CENTURY, VOLUME 2

Wendell W. Mendell, ed., John W. Alred, ed. (Eagle Engineering, Inc., Houston, TX.), Larry S. Bell, ed. (Houston Univ., TX.), Mark J. Cintala, ed., Thomas M. Crabb, ed. (Orbital Technologies Corp., Madison, WI.), Robert H. Durrett, ed. (National Aeronautics and Space Administration. Marshall Space Flight Center, Huntsville, AL.), Ben R. Finney, ed. (Hawaii Univ., Honolulu.), H. Andrew Franklin, ed. (Bechtel National, Inc., San Francisco, CA.), James R. French, ed. (JRF Engineering Services, La Canada, CA.), and Joel S. Greenberg, ed. (Princeton Synergetics, Inc., NJ.) et al Washington Sep. 1992 355 p Conference held in Houston, TX, 5-7 Apr. 1988 Prepared in cooperation with Lunar and Planetary Inst., Houston, TX

(NASA-CP-3166-Vol-2; S-684-Vol-2; NAS 1.55:3166-Vol-2) Avail: CASI HC A16/MF A03

These 92 papers comprise a peer-reviewed selection of presentations by authors from NASA, the Lunar and Planetary Institute (LPI), industry, and academia at the Second Conference on Lunar Bases and Space Activities of the 21st Century. These papers go into more technical depth than did those published from the first NASA-sponsored symposium on the topic, held in 1984. Session topics included the following: (1) design and operation of transportation systems to, in orbit around, and on the Moon; (2) lunar base site selection; (3) design, architecture, construction, and operation of lunar bases and human habitats; (4) lunar-based scientific research and experimentation in astronomy, exobiology, and lunar geology; (5) recovery and use of lunar resources; (6) environmental and human factors of and life support technology for human presence on the Moon; and (7) program management of human exploration of the Moon and space. For individual titles, see N93-13973 through N93-14020.

N93-13973*# Tennessee Univ., Knoxville. Dept. of Geological Sciences.

RESOURCES FOR A LUNAR BASE: ROCKS, MINERALS, AND SOIL OF THE MOON

Lawrence A. Taylor *In* NASA. Johnson Space Center, The Second Conference on Lunar Bases and Space Activities of the 21st Century, Volume 2 Sep. 1992 p 361-377 (For primary document see N93-13972 03-91)

(Grant NAG9-62)

Avail: CASI HC A03/MF A03

The rocks and minerals of the Moon will be included among the raw materials used to construct a lunar base. The lunar regolith, the fragmental material present on the surface of the Moon, is composed mostly of disaggregated rocks and minerals, but also includes glassy fragments fused together by meteorite impacts. The finer fraction of the regolith (i.e., less than 1 cm) is informally referred to as soil. The soil is probably the most important portion of the regolith for use at a lunar base. For example, soil can be used as insulation against cosmic rays, for lunar ceramics and abodes, or for growing plants. The soil contains abundant solar-wind-implanted elements as well as various minerals, particularly oxide phases, that are of potential economic importance. For example, these components of the soil are sources of oxygen and hydrogen for rocket fuel, helium for nuclear energy, and metals such as Fe, Al, Si, and Ti.

Author

N93-13974*# Tennessee Univ., Knoxville. Dept. of Geological Sciences.

THE FORMATION OF ORE MINERAL DEPOSITS ON THE MOON: A FEASIBILITY STUDY

Lawrence A. Taylor and Fengxiang Lu *In* NASA. Johnson Space Center, The Second Conference on Lunar Bases and Space Activities of the 21st Century, Volume 2 Sep. 1992 p 379-383 (For primary document see N93-13972 03-91)

(Grant NAG9-62)

Avail: CASI HC A01/MF A03

Most of the ore deposits on Earth are the direct result of formation by hydrothermal solutions. Analogous mineral concentrations do not occur on the Moon, however, because of the absence of water. Stratified ore deposits form in layered instrusives on Earth due to fractional crystallization of magma and crystal settling of high-density minerals, particularly chromium in the mineral chromite. We have evaluated the possibility of such mineral deposition on the Moon, based upon considerations of 'particle settling velocities' in lunar vs. terrestrial magmas. A first approximation of Stoke's Law would seem to indicate that the lower lunar gravity (1/6 terrestrial) would result in slower crystal settling on the Moon. However, the viscosity of the silicate melt is the most important factor affecting the settling velocity. The viscosities of typical lunar basaltic melts are 10-100 times less than their terrestrial analogs. These lower viscosities result from two factors: (1) lunar basaltic melts are typically higher in FeO and lower in Al2O3, Na2O, and K2O than terrestrial melts; and (2) lunar igneous melts and phase equilibria tend to be 100-150 C higher than terrestrial, largely because of the general paucity of water and other volatile phases on the Moon. Therefore, particle settling velocities on the Moon are 5-10 times greater than those on Earth. It is highly probable that stratiform ore deposits similar to those on Earth exist on the Moon. The most likely ore minerals involved are chromite, ilmenite, and native FeNi metal. In addition, the greater settling velocities of periodotite in lunar magmas indicate that the buoyancy effects of the melt are less than on Earth. Consequently, the possibility is considerably less than on Earth of deep-seated volcanism transporting upper mantle/lower crustal xenoliths to the surface of the Moon, such as occurs in kimberlites on Earth. Author

N93-13975*# National Aeronautics and Space Administration. Lyndon B. Johnson Space Center, Houston, TX.

APPLICATIONS FOR SPECIAL-PURPOSE MINERALS AT A LUNAR BASE

Douglas W. Ming *In its* The Second Conference on Lunar Bases and Space Activities of the 21st Century, Volume 2 Sep. 1992 p 385-391 (For primary document see N93-13972 03-91)

Avail: CASI HC A02/MF A03

Maintaining a colony on the Moon will require the use of lunar resources to reduce the number of launches necessary to transport goods from the Earth. It may be possible to alter lunar materials to produce minerals or other materials that can be used for applications in life support systems at a lunar base. For example, mild hydrothermal alteration of lunar basaltic glasses can produce special-purpose minerals (e.g., zeolites, smectites, and tobermorites) that in turn may be used in life support, construction, waste renovation, and chemical processes. Zeolites, smectites, and tobermorites have a number of potential applications at a lunar base. Zeolites are hydrated aluminosilicates of alkali and alkaline earth cations that possess infinite, three-dimensional crystal structures. They are further characterized by an ability to hydrate and dehydrate reversibly and to exchange some of their constituent cations, both without major change of structure. Based on their unique absorption, cation exchange, molecular sieving, and catalytic properties, zeolites may be used as a solid support medium for the growth of plants, as an adsorption medium for separation

of various gases (e.g., N2 from O2), as catalysts, as molecular sieves, and as a cation exchanger in sewage-effluent treatment, in radioactive waste disposal, and in pollution control. Smectites are crystalline, hydrated 2:1 layered aluminosilicates that also have the ability to exchange some of their constituent cations. Like zeolites, smectites may be used as an adsorption medium for waste renovation, as adsorption sites for important essential plant growth cations in solid support plant growth mediums (i.e., 'soils'), as cation exchangers, and in other important application. Tobermorites are cystalline, hydrated single-chained layered silicates that have cation-exchange and selectivity properties between those of smectites and most zeolites. Tobermorites may be used as a cement in building lunar base structures, as catalysts, as media for nuclear and hazardous waste disposal, as exchange media for waste-water treatment, and in other potential applications. Special-purpose minerals synthesized at a lunar base may also have important applications at a space station and for other planetary missions. New technologies will be required at a lunar base to develop life support systems that are self-sufficient, and the use of special-purpose minerals may help achieve this self-sufficiency. Author

N93-13976*# Washington Univ., Saint Louis, MO. Dept. of Earth and Planetary Sciences.

WATER AND CHEESE FROM THE LUNAR DESERT: ABUNDANCES AND ACCESSIBILITY OF H, C, AND N ON THE MOON

L. A. Haskin *In* NASA. Johnson Space Center, The Second Conference on Lunar Bases and Space Activities of the 21st Century, Volume 2 Sep. 1992 p 393-396 (For primary document see N93-13972 03-91)

(Grant NAG9-56)

Avail: CASI HC A01/MF A03

The Moon has been underrated as a source of H, N, C, and other elements essential to support life and to provide fuel for rockets. There is enough of these elements in each cubic meter of typical lunar soil to provide a substantial lunch for two, if converted to edible forms. The average amount of C per square meter of the lunar surface to a depth of 2 m is some 35 percent of the average amount per square meter tied up in living organisms on Earth. The water equivalent of H in the upper 2 m of the regolith averages at least 1.3 million liters per square kilometer. Mining of H from a small fraction of the regolith would provide all the rocket fuel needed for thousands of years. These elements can be removed from the soil by heating it to high temperature. Some favor the unproven resources of Phobos, Deimos, or near-Earth asteroids instead of the Moon as a source of extraterrestrial material for use in space, or Mars over the Moon as a site for habitation, partly on the basis that the chemical elements needed for life support and propellant are readily abundant on those bodies, but not on the Moon. Well, the Moon is not as barren of H, C, and N as is commonly perceived. In fact, the elements needed for life support and for rocket fuel are plentiful there, although the ore grades are low. Furthermore, the proximity of the Moon and consequent lower cost of transportation and shorter trip and communication times favor that body as the logical site for early acquisition of resources and extraterrestrial living. Author

N93-13977*# Space Studies Inst., Princeton, NJ.

FIRST STEPS TO LUNAR MANUFACTURING: RESULTS OF THE 1988 SPACE STUDIES INSTITUTE LUNAR SYSTEMS WORKSHOP

Gregg E. Maryniak *In* NASA. Johnson Space Center, The Second Conference on Lunar Bases and Space Activities of the 21st Century, Volume 2 Sep. 1992 p 397-406 (For primary document see N93-13972 03-91)

Avail: CASI HC A02/MF A03

Prior studies by NASA and the Space Studies Institute have looked at the infrastructure required for the construction of solar power satellites (SPS) and other valuable large space systems from lunar materials. This paper discusses the results of a Lunar Systems Workshop conducted in January 1988. The workshop identified components of the infrastructure that could be implemented in the near future to create a revenue stream. These revenues could then be used to 'bootstrap' the additional elements required to begin the commercial use of nonterrestrial materials. Author

N93-13978*# Pennsylvania State Univ., University Park. Coll. of Earth and Mineral Sciences.

LUNAR RESOURCE RECOVERY: A DEFINITION OF REQUIREMENTS

D. Elsworth, J. L. Kohler, and S. S. Alexander *In* NASA. Johnson Space Center, The Second Conference on Lunar Bases and Space Activities of the 21st Century, Volume 2 Sep. 1992 p 407-410 (For primary document see N93-13972 03-91)

Avail: CASI HC A01/MF A03

The capability to locate, mine, and process the natural resources of the Moon will be an essential requirement for lunar base development and operation. The list of materials that will be necessary is extensive and ranges from oxygen and hydrogen for fuel and life support to process tailings for emplacement over habitats. Despite the resources need, little is known about methodologies that might be suitable for utilizing lunar resources. This paper examines some of the requirements and constraints for resource recovery and identifies key areas of research needed to locate, mine, and process extraterrestrial natural resources. Author

N93-13979*# Washington Univ., Saint Louis, MO. Dept. of Earth and Planetary Sciences.

ELECTROLYTIC SMELTING OF LUNAR ROCK FOR OXYGEN, IRON, AND SILICON

Larry A. Haskin, Russell O. Colson, David J. Lindstrom, Robert H. Lewis, and Krystyna W. Semkow *In* NASA. Johnson Space Center, The Second Conference on Lunar Bases and Space Activities of the 21st Century, Volume 2 Sep. 1992 p 411-422 (For primary document see N93-13972 03-91)

(Grants NAG9-56; NSF DAR-79-24705)

Avail: CASI HC A03/MF A03

Preliminary studies of the electrochemical properties of silicate melts such as those available from heating of lunar mare soils indicate that conductivities are high enough for design of a practical electrolytic cell. The nature and kinetics of the electrode reactions, which involve reduction of Fe(++) and Si(IV) and oxidation of silicate anions as the primary, product-forming reactions, are also satisfactory. A survey of the efficiencies for production (amount of product for a given current) of O2, Fe(sup 0), and Si(sup 0) as functions of potential and of electrolyte composition indicate that conditions can be chosen to yield high production efficiencies. We also conclude that electronic conductivity does not occur to a significant extent. Based on these data, a cell with electrodes of 30 sq m in area operating between 1 and 5V with a current between 1.6 and 3.5(10)(exp 5) A for a mean power requirement of 0.54 MW and total energy use of approximately 13 MWhr per 24-hr day would produce 1 ton of O2, 0.81 ton of Fe(sup 0), 0.65 ton of Si(sup 0) (as Fe(sup 0)-Si(sup 0) alloy), and about 3.5 tons of silicate melt of altered composition per 24 hr. Adjustable distance between electrodes could offer flexibility with respect to feedstock and power source. Author

N93-13980*# Lunar and Planetary Inst., Houston, TX.

LUNAR MINING OF OXYGEN USING FLUORINE

Donald M. Burt (Arizona State Univ., Tempe.) *In* NASA. Johnson Space Center, The Second Conference on Lunar Bases and Space Activities of the 21st Century, Volume 2 Sep. 1992 p 423-428 (For primary document see N93-13972 03-91)

(Contract NASw-4066)

(LPI-748) Avail: CASI HC A02/MF A03

An important aspect of lunar mining will be the extraction of volatiles, particularly oxygen, from lunar rocks. Thermodynamic data show that oxygen could readily be recovered by fluorination of abundant lunar anorthite, CaAl2Si2O8. Fluorine is the most reactive element, and the only reagent able to extract 100 percent of the oxygen from any mineral, yet it can safely be stored or reacted in nickel or iron containers. The general fluorination reaction, mineral + 2F2 = mixed fluorides = O2, has been used for more than 30 years at a laboratory scale by stable-isotope geochemists. For anorthite, metallic Al and Si may be recovered from the mixed fluorides by Na-reduction, and CaO via exchange with Na2O; the resulting NaF may be recycled into F2 and Na by electrolysis, using lanthanide-doped CaF2 as the inert anode. Author

N93-13981*# Los Alamos National Lab., NM.

USES OF LUNAR SULFUR

D. Vaniman, D. Pettit, and G. Heiken *In* NASA. Johnson Space Center, The Second Conference on Lunar Bases and Space Activities of the 21st Century, Volume 2 Sep. 1992 p 429-435 Sponsored in part by DOE (For primary document see N93-13972 03-91)

Avail: CASI HC A02/MF A03

Sulfur and sulfur compounds have a wide range of applications for their fluid, electrical, chemical, and biochemical properties. Although known abundances on the Moon are limited (approximately 0.1 percent in mare soils), sulfur is relatively extractable by heating. Coproduction of sulfur during oxygen extraction from ilmenite-rich mare soils could yield sulfur in masses up to 10 percent of the mass of oxygen produced. Sulfur deserves serious consideration as a lunar resource. Author

N93-13982*# National Aeronautics and Space Administration. Lyndon B. Johnson Space Center, Houston, TX.
AVAILABILITY OF HYDROGEN FOR LUNAR BASE ACTIVITIES
Roberta Bustin (Arkansas Coll., Batesville.) and Everett K. Gibson, Jr. *In its* The Second Conference on Lunar Bases and Space Activities of the 21st Century, Volume 2 Sep. 1992 p 437-445 Previously announced as N91-11644 (For primary document see N93-13972 03-91)
Avail: CASI HC A02/MF A03

Hydrogen will be needed on a lunar base to make water for consumables, to provide fuel, and to serve as a reducing agent in the extraction of oxygen from lunar minerals. This study was undertaken in order to learn more about the abundance and distribution of solar-wind-implanted hydrogen. Hydrogen was found in all samples studied, with concentrations, varying widely depending on soil maturity, grain size, and mineral composition. Seven cores returned from the Moon were studied. Although hydrogen was implanted in the upper surface layer of the regolith, it was found throughout the cores due to micrometeorite reworking of the soil. Author

N93-13983*# Technische Univ., Berlin (Germany). Aerospace Inst.
THE INFLUENCE OF LUNAR PROPELLANT PRODUCTION ON THE COST-EFFECTIVENESS OF CISLUNAR TRANSPORTATION SYSTEMS **c28**
H. H. Koelle *In* NASA. Johnson Space Center, The Second Conference on Lunar Bases and Space Activities of the 21st Century, Volume 2 Sep. 1992 p 447-452 (For primary document see N93-13972 03-91)
Avail: CASI HC A02/MF A03

It is well known that propellants produced at the points of destination such as the Moon or Mars will help the economy of space transportation, particularly if round trips with a crew are involved. The construction and operation of a lunar base shortly after the turn of the century is one of the space programs under serious consideration at the present time. Space transportation is one of the major cost drivers. With present technology, if expendable launchers were employed, the specific transportation costs of one-way cargo flights would be approximately 10,000 dollars/kg (1985) at life-cycle cumulative 100,000 ton payload to the lunar surface. A fully reusable space transportation system using lunar oxygen and Earth-produced liquid hydrogen (LH2) would reduce the specific transportation costs by one order of magnitude to less than 1000 dollars/kg at the same payload volume. Another case of primary interest is the delivery of construction material and consumables from the lunar surface to the assembly site of space solar power plants in geostationary orbit (GEO). If such a system were technically and economically feasible, a cumulative payload of about 1 million tons or more would be required. At this level a space freighter system could deliver this material from Earth for about 300 dollars/kg (1985) to GEO. A lunar space transportation system using lunar oxygen and a fuel mixture of 50 percent Al and 50 percent LH2 (that has to come from Earth) could reduce the specific transportation costs to less than half, approximately 150 dollars/kg. If only lunar oxygen were available, these costs would come down to 200 dollars/kg. This analysis indicates a sizable reduction of the transportation burden on this type of mission. It should not be overlooked, however, that there are several uncertainties in such calculations. It is quite difficult at this point to calculate the cost of lunar-produced O and/or Al. This will be a function of production rate and life-cycle length. In quoting any cost of this nature, it is very important to state the cumulative transportation volume, since this is a very sensitive parameter. Nevertheless, cost models must be developed now to understand fully the interdependencies of a large number of parameters and to provide the best possible data for planning purposes. Without such data, mission modes and vehicle designs or sizes cannot be selected intelligently. Author

N93-13984*# Spectra Research Systems, Inc., Huntsville, AL.
IMPACT OF LUNAR OXYGEN PRODUCTION ON DIRECT MANNED MARS MISSIONS **c25**
Roy M. Young, Jr. and William B. Tucker (Nichols Research Corp., Huntsville, AL.) *In* NASA. Johnson Space Center, The Second Conference on Lunar Bases and Space Activities of the 21st Century, Volume 2 Sep. 1992 p 453-458 (For primary document see N93-13972 03-91)
Avail: CASI HC A02/MF A03

A manned Mars program made up of six missions is evaluated to determine the impact of using lunar liquid oxygen (LOX) as a propellant. Two departure and return nodes, low Earth orbit and low lunar orbit, are considered, as well as two return vehicle configurations, a full 70,000-kg vehicle and a 6800-kg capsule. The cost of lunar LOX delivered to orbit is expressed as a ratio of Earth launch cost. Author

N93-13985*# Wisconsin Univ., Madison. Fusion Technology Inst.
FUSION ENERGY FROM THE MOON FOR THE TWENTY-FIRST CENTURY **c75**
G. L. Kulcinski, E. N. Cameron, J. F. Santarius, I. N. Sviatoslavsky, L. J. Wittenberg, and Harrison H. Schmitt (Schmitt, Harrison H., Albuquerque, NM) *In* NASA. Johnson Space Center, The Second Conference on Lunar Bases and Space Activities of the 21st Century, Volume 2 Sep. 1992 p 459-474 Sponsored in part by EPRI; Wisconsin Electric Utilities Research Foundation; and Granger Foundation (For primary document see N93-13972 03-91)
Avail: CASI HC A03/MF A03

It is shown in this paper that the D-He-3 fusion fuel cycle is not only credible from a physics standpoint, but that its breakeven and ignition characteristics could be developed on roughly the same time schedule as the DT cycle. It was also shown that the extremely low fraction of power in neutrons, the lack of significant radioactivity in the reactants, and the potential for very high conversion efficiencies, can result in definite advantages for the D-He-3 cycle with respect to DT fusion and fission reactors in the twenty-first century. More specifically, the D-He-3 cycle can accomplish the following: (1) eliminate the need for deep geologic waste burial facilities and the wastes can qualify for Class A, near-surface land burial; (2) allow 'inherently safe' reactors to be built that, under the worst conceivable accident, cannot cause a civilian fatality or result in a significant (greater than 100 mrem) exposure to a member of the public; (3) reduce the radiation damage levels to a point where no scheduled replacement of reactor structural components is required, i.e., full reactor lifetimes (approximately 30 FPY) can be credibly claimed; (4) increase the reliability and availability of fusion reactors compared to DT systems because of the greatly reduced radioactivity, the low neutron damage, and the elimination of T breeding; and (5) greatly reduce the capital costs of fusion power plants (compared to DT systems) by as much as 50 percent and present the potential for a significant reduction on the COE. The concepts presented in this paper tie together two of the most ambitious high-technology endeavors of the twentieth century: the development of controlled thermonuclear fusion for civilian power applications and the utilization of outer space for the benefit of mankind on Earth. Author

N93-13986*# Orbital Technologies Corp., Madison, WI.
SYNERGISM OF He-3 ACQUISITION WITH LUNAR BASE EVOLUTION **c25**
T. M. Crabb and M. K. Jacobs (Science Applications International Corp., Schaumburg, IL.) *In* NASA. Johnson Space Center, The Second Conference on Lunar Bases and Space Activities of the 21st Century, Volume 2 Sep. 1992 p 475-482 Previously announced as N89-14852 (For primary document see N93-13972 03-91)
Avail: CASI HC A02/MF A03

Researchers have discovered that the lunar surface contains a valuable fusion fuel element that is relatively scarce on Earth. This element, He-3, originates from the solar wind that has bombarded the surface of the Moon over geologic time. Mining operations to recover this resource would allow the by-product acquisition of hydrogen, water, carbon dioxide, carbon monoxide, methane, and nitrogen from the lunar surface with relatively minimal additional resource investment when compared to the costs to supply these resources from Earth. Two configurations for the He-3 mining system are discussed, and the impacts of these mining operations on a projected lunar base scenario are assessed. We conclude that the acquisition of He-3 is feasible with minimal advances in current state-of-the-art technologies and could support a terrestrial nuclear fusion power economy with the lowest hazard risk of any nuclear reaction known. Also, the availability of the by-products of He-3 acquisition from the Moon could

significantly reduce the operational requirements of a lunar base and increase the commercialization potential of the base through consumable resupply of the lunar base itself, other components of the space infrastructure, and other space missions. Author

N93-13987*# Construction Technology Labs., Skokie, IL.
PHYSICAL PROPERTIES OF CONCRETE MADE WITH APOLLO 16 LUNAR SOIL SAMPLE **c27**
T. D. Lin, H. Love, and D. Stark *In* NASA. Johnson Space Center, The Second Conference on Lunar Bases and Space Activities of the 21st Century, Volume 2 Sep. 1992 p 483-487 (For primary document see N93-13972 03-91)
Avail: CASI HC A01/MF A03

This paper describes the first phase of the long-term investigation for the construction of concrete lunar bases. In this phase, petrographic and scanning electron microscope examinations showed that the morphology and elemental composition of the lunar soil made it suitable for use as a fine aggregate for concrete. Based on this finding, calcium aluminate cement and distilled water were mixed with the lunar soil to fabricate test specimens. The test specimens consisted of a 1-in cube, a 1/2-in cube, and three 0.12 x 0.58 x 3.15-in beam specimens. Tests were performed on these specimens to determine compressive strength, modulus of rupture, modulus of elasticity, and thermal coefficient of expansion. Based on examination of the material and test results, it is concluded that lunar soil can be used as a fine aggregate for concrete. Author

N93-13988*# Shimizu Corp. (Japan). Inst. of Technology.
THE POSSIBILITY OF CONCRETE PRODUCTION ON THE MOON **c27**
Noboru Ishikawa, Hiroshi Kanamori, and Takeji Okada *In* NASA. Johnson Space Center, The Second Conference on Lunar Bases and Space Activities of the 21st Century, Volume 2 Sep. 1992 p 489-491 (For primary document see N93-13972 03-91)
Avail: CASI HC A01/MF A03

When a long-term lunar base is constructed, most of the materials for the construction will be natural resources on the Moon, mainly for economic reasons. In terms of economy and exploiting natural resources, concrete would be the most suitable material for construction. This paper describes the possibility of concrete production on the Moon. The possible production methods are derived from the results of a series of experiments that were carried out taking two main environmental features, low gravity acceleration and vacuum, into consideration. Author

N93-13989*# Shimizu Corp. (Japan).
CONCRETE STRUCTURE CONSTRUCTION ON THE MOON **c31**
Shinji Matsumoto, Haruyuki Namba, Yoshiro Kai, and Tetsuji Yoshida *In* NASA. Johnson Space Center, The Second Conference on Lunar Bases and Space Activities of the 21st Century, Volume 2 Sep. 1992 p 493-496 (For primary document see N93-13972 03-91)
Avail: CASI HC A01/MF A03

This paper describes a precast prestressed concrete structure system on the Moon and erection methods for this system. The horizontal section of the structural module is hexagonal so that various layouts of the modules are possible by connecting the adjacent modules to each other. For erection of the modules, specially designed mobile cranes are used. Author

N93-13990*# National Aeronautics and Space Administration. Lyndon B. Johnson Space Center, Houston, TX.
LUNAR CONCRETE FOR CONSTRUCTION **c27**
Hatice S. Cullingford and M. Dean Keller (Los Alamos National Lab., NM.) *In its* The Second Conference on Lunar Bases and Space Activities of the 21st Century, Volume 2 Sep. 1992 p 497-499 Sponsored in part by DOE (For primary document see N93-13972 03-91)
Avail: CASI HC A01/MF A03

Feasibility of using concrete for lunar base construction was discussed recently without relevant data for the effects of vacuum on concrete. Our experimental studies performed earlier at Los Alamos have shown that concrete is stable in vacuum with no deterioration of its quality as measured by the compressive strength. Various considerations of using concrete successfully on the Moon are provided in this paper, along with specific conclusions from the existing database. Author

N93-13991*# National Aeronautics and Space Administration. Langley Research Center, Hampton, VA.
THE ENVIRONMENTAL CONTROL AND LIFE-SUPPORT SYSTEM FOR A LUNAR BASE: WHAT DRIVES ITS DESIGN **c54**
Warren D. Hypes (Bionetics Corp., Hampton, VA.) and John B. Hall, Jr. *In* NASA. Johnson Space Center, The Second Conference on Lunar Bases and Space Activities of the 21st Century, Volume 2 Sep. 1992 p 503-511 (For primary document see N93-13972 03-91)
Avail: CASI HC A02/MF A03

The purpose of this paper is to identify and briefly discuss some of the ground rules and mission scenario details that become drivers of the environmental control and life support (ECLS) system design and of the logistics related to the design. This paper is written for mission planners and non-ECLS system engineers to inform them of the details that will be important to the ECLS engineer when the design phase is reached. In addition, examples illustrate the impact of some selected mission characteristics on the logistics associated with ECLS systems. The last section of this paper focuses on the ECLS system technology development sequence and highlights specific portions that need emphasis. Author

N93-13992*# Institute of Ecotechnics, London (England).
LIFE SYSTEMS FOR A LUNAR BASE **c54**
Mark Nelson, Philip B. Hawes (Sarbid Ltd., Oracle, AZ.), and Margret Augustine (Space Biospheres Ventures, Oracle, AZ.) *In* NASA. Johnson Space Center, The Second Conference on Lunar Bases and Space Activities of the 21st Century, Volume 2 Sep. 1992 p 513-518 (For primary document see N93-13972 03-91)
Avail: CASI HC A02/MF A03

The Biosphere 2 project is pioneering work on life systems that can serve as a prototype for long-term habitation on the Moon. This project will also facilitate the understanding of the smaller systems that will be needed for initial lunar base life-support functions. In its recommendation for a policy for the next 50 years in space, the National Commission on Space urged, 'To explore and settle the inner Solar System, we must develop biospheres of smaller size, and learn how to build and maintain them' (National Commission on Space, 1986). The Biosphere 2 project, along with its Biospheric Research and Development Center, is a materially closed and informationally and energetically open system capable of supporting a human crew of eight, undertaking work to meet this need. This paper gives an overview of the Space Biospheres Ventures' endeavor and its lunar applications. Author

N93-13993*# Walt Disney World Co., Lake Buena Vista, FL. EPCOT Center.
LUNAR BASE CELSS: A BIOREGENERATIVE APPROACH **c54**
G. W. Easterwood, J. J. Street (Florida Univ., Gainesville.), J. B. Sartain (Florida Univ., Gainesville.), D. H. Hubbell (Florida Univ., Gainesville.), and H. A. Robitaille *In* NASA. Johnson Space Center, The Second Conference on Lunar Bases and Space Activities of the 21st Century, Volume 2 Sep. 1992 p 519-523 (For primary document see N93-13972 03-91)
Avail: CASI HC A01/MF A03

During the twenty-first century, human habitation of a self-sustaining lunar base could become a reality. To achieve this goal, the occupants will have to have food, water, and an adequate atmosphere within a carefully designed environment. Advanced technology will be employed to support terrestrial life-sustaining processes on the Moon. One approach to a life support system based on food production, waste management and utilization, and product synthesis is outlined. Inputs include an atmosphere, water, plants, biodegradable substrates, and manufacutured materials such as fiberglass containment vessels from lunar resources. Outputs include purification of air and water, food, and hydrogen (H2) generated from methane (CH4). Important criteria are as follows: (1) minimize resupply from Earth; and (2) recycle as efficiently as possible. Author

N93-13994*# National Aeronautics and Space Administration. Lyndon B. Johnson Space Center, Houston, TX.
CROP GROWTH AND ASSOCIATED LIFE SUPPORT FOR A LUNAR FARM **c54**
Tyler Volk (New York Univ., New York.) and Hatice Cullingford *In its* The Second Conference on Lunar Bases and Space Activities of the 21st Century, Volume 2 Sep. 1992 p 525-530 (For primary document see

N93-13972 03-91)
Avail: CASI HC A02/MF A03

Supporting human life on a lunar base will require growing many different food crops. This paper investigates the growth dynamics of four crops (wheat, soybeans, potatoes, and lettuce) for general similarities and differences, along with associated material flows of the gases, liquids, and solids in a lunar farm. The human dietary requirements are compared with the protein, carbohydrate, and lipid contents of these hydroponically grown, high-productivity crops to derive a lunar farm diet. A simple and general analytical model is used to calculate the mass fluxes of CO2, H2O, HNO3, and O2 during the life cycle of each of the four crops. The resulting farm crop areas and corresponding biomass production rates are given. One significant conclusion of this study is that there is a 'lipid problem' associated with the incorporation of these four crops into a viable diet. Author

N93-13995*# Texas Univ., Austin. Dept. of Zoology.
LONG-TERM LUNAR STATIONS: SOME ECOLOGICAL CONSIDERATIONS **c45**
Bassett Maguire, Jr. and Kelly W. Scott *In* NASA. Johnson Space Center, The Second Conference on Lunar Bases and Space Activities of the 21st Century, Volume 2 Sep. 1992 p 531-536 Sponsored in part by Savannah River Ecological Lab. (For primary document see N93-13972 03-91)
Avail: CASI HC A02/MF A03

A major factor for long-term success of a lunar station is the ability to keep an agroecosystem functioning at a desirable, stable steady-state with ecological stability and reliability. Design for a long-lived extraterrestrial manned station must take into account interactions among its subsystems to insure that overall functionality is enhanced (or at least not compromised). Physical isolation of feed production, human living areas, recycling, and other systems may be straightforward, however, microbiological isolation will be very difficult. While it is possible to eliminate plant-associated microbiological communities by growing the plants asepticallly, it is not practical to keep plants germ-free on a large scale if humans are working with them. Ecological theory strongly suggests that some kinds of communities or organisms effectively increase the stability of ecosystems and will protect the plants from potential pathogens. A carefully designed and maintained (lunar-derived) soil can provide a variety of habitats for effective microbial buffers while adding structure to the agroecosystem. A soil can also increase ecosystem reliability through buffering otherwise large element and compound fluctuations (of nutrients, wastes, etc.) as well as buffering temperature level and atmosphere composition. We are doing experiments in ecological dynamics and attempting to extend the relevant theories. Author

N93-13996*# National Aeronautics and Space Administration. John F. Kennedy Space Center, Cocoa Beach, FL.
ENGINEERING VERIFICATION OF THE BIOMASS PRODUCTION CHAMBER **c54**
R. P. Prince, W. M. Knott, III, J. C. Sager, and J. D. Jones (National Aeronautics and Space Administration. Goddard Space Flight Center, Greenbelt, MD.) *In* NASA. Johnson Space Center, The Second Conference on Lunar Bases and Space Activities of the 21st Century, Volume 2 Sep. 1992 p 537-542 (For primary document see N93-13972 03-91)
Avail: CASI HC A02/MF A03

The requirements for life support systems, both biological and physical-chemical, for long-term human attended space missions are under serious study throughout NASA. The KSC 'breadboard' project has focused on biomass production using higher plants for atmospheric regeneration and food production in a special biomass production chamber. This chamber is designed to provide information on food crop growth rate, contaminants in the chamber that alter plant growth requirements for atmospheric regeneration, carbon dioxide consumption, oxygen production, and water utilization. The shape and size, mass, and energy requirements in relation to the overall integrity of the biomass production chamber are under constant study. Author

N93-13997*# National Aeronautics and Space Administration. John F. Kennedy Space Center, Cocoa Beach, FL.
SCENARIOS FOR OPTIMIZING POTATO PRODUCTIVITY IN A LUNAR CELSS **c54**
R. M. Wheeler, R. C. Morrow (Wisconsin Univ., Madison.), T. W. Tibbitts (Wisconsin Univ., Madison.), and R. J. Bula (Wisconsin Univ., Madison.) *In* NASA. Johnson Space Center, The Second Conference on Lunar Bases and Space Activities of the 21st Century, Volume 2 Sep. 1992 p 543-546 (For primary document see N93-13972 03-91)
Avail: CASI HC A01/MF A03

The use of controlled ecological life support system (CELSS) in the development and growth of large-scale bases on the Moon will reduce the expense of supplying life support materials from Earth. Such systems would use plants to produce food and oxygen, remove carbon dioxide, and recycle water and minerals. In a lunar CELSS, several factors are likely to be limiting to plant productivity, including the availability of growing area, electrical power, and lamp/ballast weight for lighting systems. Several management scenarios are outlined in this discussion for the production of potatoes based on their response to irradiance, photoperiod, and carbon dioxide concentration. Management scenarios that use 12-hr photoperiods, high carbon dioxide concentrations, and movable lamp banks to alternately irradiate halves of the growing area appear to be the most efficient in terms of growing area, electrical power, and lamp weights. However, the optimal scenario will be dependent upon the relative 'costs' of each factor. Author

N93-13998*# Wisconsin Univ., Madison. Center for Space Automation and Robotics.
POTENTIAL OF DERIVED LUNAR VOLATILES FOR LIFE SUPPORT **c54**
R. J. Bula, L. J. Wittenberg, T. W. Tibbitts, and G. L. Kulcinski *In* NASA. Johnson Space Center, The Second Conference on Lunar Bases and Space Activities of the 21st Century, Volume 2 Sep. 1992 p 547-550 (For primary document see N93-13972 03-91)
Avail: CASI HC A01/MF A03

The lunar regolith contains small quantities of solar wind implanted volatile compounds that have vital, basic uses for maintaining life support systems of lunar or space settlements. Recent proposals to utilize the helium-3 isotope (He-3) derived from the lunar regolith as a fuel for fusion reactors would result in the availability of large quantities of other lunar volatile compounds. The quantities obtained would provide the annual life support replacement requirements of 1150 to 23,000 inhabitants per ton of He-3 recovered, depending on the volatile compound. Utilization of the lunar volatile compounds for life support depends on the costs, in terms of materials and energy, associated with their extraction from the lunar regolith as compared to the delivery costs of these compounds from Earth resources. Considering today's conservative estimated transportation costs ($10,000 dollars per kilogram) and regolith mining costs ($5 dollars per ton), the life support replacement requirements could be more economically supplied by recovering the lunar volatile compounds than transporting these materials from Earth resources, even before He-3 will be utilized as a fusion fuel. In addition, availability of lunar volatile compounds could have a significant cost impact on maintaining the life support systems of the space station and a Mars base. Author

N93-13999*# National Aeronautics and Space Administration. Lyndon B. Johnson Space Center, Houston, TX.
TECHNOLOGY DEVELOPMENT FOR LUNAR BASE WATER RECYCLING **c54**
John R. Schultz (Krug International, Houston, TX.) and Richard L. Sauer *In its* The Second Conference on Lunar Bases and Space Activities of the 21st Century, Volume 2 Sep. 1992 p 551-557 (For primary document see N93-13972 03-91)
Avail: CASI HC A02/MF A03

This paper will review previous and ongoing work in aerospace water recycling and identify research activities required to support development of a lunar base. The development of a water recycle system for use in the life support systems envisioned for a lunar base will require considerable research work. A review of previous work on aerospace water recycle systems indicates that more efficient physical and chemical processes are needed to reduce expendable and power requirements. Development work on biological processes that can be applied to microgravity and lunar environments also needs to be initiated. Biological processes are inherently more efficient than physical and chemical processes and may be used to minimize resupply and waste disposal requirements. Processes for recovering and recycling nutrients such as nitrogen, phosphorus, and sulfur also need

to be developed to support plant growth units. The development of efficient water quality monitors to be used for process control and environmental monitoring also needs to be initiated. Author

N93-14000*# North Dakota Univ., Grand Forks. Energy and Environmental Research Center.

PLASMA REACTOR WASTE MANAGEMENT SYSTEMS **c54**

Robert O. Ness, Jr., John R. Rindt, and Sumitra R. Ness *In* NASA. Johnson Space Center, The Second Conference on Lunar Bases and Space Activities of the 21st Century, Volume 2 Sep. 1992 p 559-562 (For primary document see N93-13972 03-91)

Avail: CASI HC A01/MF A03

The University of North Dakota is developing a plasma reactor system for use in closed-loop processing that includes biological, materials, manufacturing, and waste processing. Direct-current, high-frequency, or microwave discharges will be used to produce plasmas for the treatment of materials. The plasma reactors offer several advantages over other systems, including low operating temperatures, low operating pressures, mechanical simplicity, and relatively safe operation. Human fecal material, sunflowers, oats, soybeans, and plastic were oxidized in a batch plasma reactor. Over 98 percent of the organic material was converted to gaseous products. The solids were then analyzed and a large amount of water and acid-soluble materials were detected. These materials could possibly be used as nutrients for biological systems. Author

N93-14001*# North Dakota Univ., Grand Forks.

DISTRIBUTION OF HUMAN WASTE SAMPLES IN RELATION TO SIZING WASTE PROCESSING IN SPACE **c54**

Dick Parker and S. K. Gallagher (Agricultural Research Service, Grand Forks, ND.) *In* NASA. Johnson Space Center, The Second Conference on Lunar Bases and Space Activities of the 21st Century, Volume 2 Sep. 1992 p 563-568 (For primary document see N93-13972 03-91)

Avail: CASI HC A02/MF A03

Human waste processing for closed ecological life support systems (CELSS) in space requires that there be an accurate knowledge of the quantity of wastes produced. Because initial CELSS will be handling relatively few individuals, it is important to know the variation that exists in the production of wastes rather than relying upon mean values that could result in undersizing equipment for a specific crew. On the other hand, because of the costs of orbiting equipment, it is important to design the equipment with a minimum of excess capacity because of the weight that extra capacity represents. A considerable quantity of information that had been independently gathered on waste production was examined in order to obtain estimates of equipment sizing requirements for handling waste loads from crews of 2 to 20 individuals. The recommended design for a crew of 8 should hold 34.5 liters per day (4315 ml/person/day) for urine and stool water and a little more than 1.25 kg per day (154 g/person/day) of human waste solids and sanitary supplies. Author

N93-14002*# Vanderbilt Univ., Nashville, TN. Dept. of Mechanical Engineering.

BONE LOSS AND HUMAN ADAPTATION TO LUNAR GRAVITY **c52**

T. S. Keller and A. M. Strauss *In* NASA. Johnson Space Center, The Second Conference on Lunar Bases and Space Activities of the 21st Century, Volume 2 Sep. 1992 p 569-576 (For primary document see N93-13972 03-91)

Avail: CASI HC A02/MF A03

Long-duration space missions and establishment of permanently manned bases on the Moon and Mars are currently being planned. The weightless environment of space and the low-gravity environments of the Moon and Mars pose an unknown challenge to human habitability and survivability. Of particular concern in the medical research community today is the effect of less than Earth gravity on the human skeleton, since the limits, if any, of human endurance in low-gravity environments are unknown. This paper provides theoretical predictions on bone loss and skeletal adaptation to lunar and other nonterrestrial-gravity environments based upon the experimentally derived relationship, density approximately (mass x gravity)(exp 1/8). The predictions are compared to skeletal changes reported during bed rest, immobilization, certrifugation, and spaceflight. Countermeasures to reduce bone losses in fractional gravity are also discussed. Author

N93-14003*# National Aeronautics and Space Administration. Langley Research Center, Hampton, VA.

CONCEPTUAL DESIGN OF A LUNAR BASE THERMAL CONTROL SYSTEM **c54**

Lisa C. Simonsen, Marc J. DeBarro (Rockwell International Corp., Downey, CA.), and Jeffery T. Farmer *In* NASA. Johnson Space Center, The Second Conference on Lunar Bases and Space Activities of the 21st Century, Volume 2 Sep. 1992 p 579-591 (For primary document see N93-13972 03-91)

Avail: CASI HC A03/MF A03

Space station and alternate thermal control technologies were evaluated for lunar base applications. The space station technologies consisted of single-phase, pumped water loops for sensible and latent heat removal from the cabin internal environment and two-phase ammonia loops for the transportation and rejection of these heat loads to the external environment. Alternate technologies were identified for those areas where space station technologies proved to be incompatible with the lunar environment. Areas were also identified where lunar resources could enhance the thermal control system. The internal acquisition subsystem essentially remained the same, while modifications were needed for the transport and rejection subsystems because of the extreme temperature variations on the lunar surface. The alternate technologies examined to accommodate the high daytime temperatures incorporated lunar surface insulating blankets, heat pump system, shading, and lunar soil. Other heat management techniques, such as louvers, were examined to prevent the radiators from freezing. The impact of the geographic location of the lunar base and the orientation of the radiators was also examined. A baseline design was generated that included weight, power, and volume estimates. Author

N93-14004*# National Aeronautics and Space Administration. Lewis Research Center, Cleveland, OH.

ADVANCED PHOTOVOLTAIC POWER SYSTEM TECHNOLOGY FOR LUNAR BASE APPLICATIONS **c44**

David J. Brinker and Dennis J. Flood *In* NASA. Johnson Space Center, The Second Conference on Lunar Bases and Space Activities of the 21st Century, Volume 2 Sep. 1992 p 593-596 Previously announced as N88-26402 (For primary document see N93-13972 03-91)

Avail: CASI HC A01/MF A03

The development of an advanced photovoltaic power system that would have application for a manned lunar base is currently planned under the Surface Power element of Pathfinder. Significant mass savings over state-of-the-art photovoltaic/battery systems are possible with the use of advanced lightweight solar arrays coupled with regenerative fuel cell storage. The solar blanket, using either ultrathin GaAs or amorphous silicon solar cells, would be integrated with a reduced-g structure. Regenerative fuel cells with high-pressure gas storage in filament-wound tanks are planned for energy storage. An advanced PV/RFC power system is a leading candidate for a manned lunar base as it offers a tremendous weight advantage over state-of-the-art photovoltaic/battery systems and is comparable in mass to other advanced power generation technologies. Author

N93-14005*# Remtech, Inc., Huntsville, AL.

SOLAR WATER HEATING SYSTEM FOR A LUNAR BASE **c44**

Richard E. Somers and R. Daniel Haynes *In* NASA. Johnson Space Center, The Second Conference on Lunar Bases and Space Activities of the 21st Century, Volume 2 Sep. 1992 p 597-602 (For primary document see N93-13972 03-91)

Avail: CASI HC A02/MF A03

An investigation of the feasibility of using a solar water heater for a lunar base is described. During the investigation, computer codes were developed to model the lunar base configuration, lunar orbit, and heating systems. Numerous collector geometries, orientation variations, and system options were identified and analyzed. The results indicate that the recommended solar water heater could provide 88 percent of the design load and would not require changes in the overall lunar base design. The system would give a 'safe-haven' water heating capability and use only 7 percent to 10 percent as much electricity as an electric heating system. As a result, a fixed position photovoltaic array can be reduced by 21 sq m. Author

N93-14006*# National Aeronautics and Space Administration. Langley Research Center, Hampton, VA.

AUTOMATION AND ROBOTICS CONSIDERATIONS FOR A LUNAR BASE **c37**

Nancy E. Sliwa, F. Wallace Harrison, Jr., Donald I. Soloway, William S. McKinney, Jr., Karin Cornils, William R. Doggett (Planning Research Corp., Hampton, VA.), Eric G. Cooper (Planning Research Corp., Hampton, VA.), and Thomas E. Alberts (Old Dominion Univ., Norfolk, VA.) *In* NASA. Johnson Space Center, The Second Conference on Lunar Bases and Space Activities of the 21st Century, Volume 2 Sep. 1992 p 603-608 (For primary document see N93-13972 03-91)

Avail: CASI HC A02/MF A03

An envisioned lunar outpost shares with other NASA missions many of the same criteria that have prompted the development of intelligent automation techniques with NASA. Because of increased radiation hazards, crew surface activities will probably be even more restricted than current extravehicular activity in low Earth orbit. Crew availability for routine and repetitive tasks will be at least as limited as that envisioned for the space station, particularly in the early phases of lunar development. Certain tasks are better suited to the untiring watchfulness of computers, such as the monitoring and diagnosis of multiple complex systems, and the perception and analysis of slowly developing faults in such systems. In addition, mounting costs and constrained budgets require that human resource requirements for ground control be minimized. This paper provides a glimpse of certain lunar base tasks as seen through the lens of automation and robotic (A&R) considerations. This can allow a more efficient focusing of research and development not only in A&R, but also in those technologies that will depend on A&R in the lunar environment. Author

N93-14007*# Wisconsin Univ., Madison. Center for Space Automation and Robotics.

LUNAR SURFACE MINING FOR AUTOMATED ACQUISITION OF HELIUM-3: METHODS, PROCESSES, AND EQUIPMENT

Y. T. Li and L. J. Wittenberg *In* NASA. Johnson Space Center, The Second Conference on Lunar Bases and Space Activities of the 21st Century, Volume 2 Sep. 1992 p 609-617 (For primary document see N93-13972 03-91)

Avail: CASI HC A02/MF A03

In this paper, several techniques considered for mining and processing the regolith on the lunar surface are presented. These techniques have been proposed and evaluated based primarily on the following criteria: (1) mining operations should be relatively simple; (2) procedures of mineral processing should be few and relatively easy; (3) transferring tonnages of regolith on the Moon should be minimized; (4) operations outside the lunar base should be readily automated; (5) all equipment should be maintainable; and (6) economic benefit should be sufficient for commercial exploitation. The economic benefits are not addressed in this paper; however, the energy benefits have been estimated to be between 250 and 350 times the mining energy. A mobile mining scheme is proposed that meets most of the mining objectives. This concept uses a bucket-wheel excavator for excavating the regolith, several mechanical electrostatic separators for beneficiation of the regolith, a fast-moving fluidized bed reactor to heat the particles, and a palladium diffuser to separate H2 from the other solar wind gases. At the final stage of the miner, the regolith 'tailings' are deposited directly into the ditch behind the miner and cylinders of the valuable solar wind gases are transported to a central gas processing facility. During the production of He-3, large quantities of valuable H2, H2O, CO, CO2, and N2 are produced for utilization at the lunar base. For larger production of He-3 the utilization of multiple-miners is recommended rather than increasing their size. Multiple miners permit operations at more sites and provide redundancy in case of equipment failure. Author

N93-14008*# National Aeronautics and Space Administration. Marshall Space Flight Center, Huntsville, AL.

THE LUNAR ROVING VEHICLE: HISTORICAL PERSPECTIVE **c37**

Saverio F. Morea *In* NASA. Johnson Space Center, The Second Conference on Lunar Bases and Space Activities of the 21st Century, Volume 2 Sep. 1992 p 619-632 (For primary document see N93-13972 03-91)

Avail: CASI HC A03/MF A03

As NASA proceeds with its studies, planning, and technology efforts in preparing for the early twenty-first century, it seems appropriate to reexamine past programs for potential applicability in meeting future national space science and exploration goals and objectives. Both the National Commission on Space (NCOS) study and NASA's 'Sally Ride study' suggest future programs involving returning to the Moon and establishing man's permanent presence there, and/or visiting the planet Mars in both the unmanned and manned mode. Regardless of when and which of these new bold initiatives is selected as our next national space goal, implementing these potentially new national thrusts in space will undoubtedly require the use of both manned and remotely controlled roving vehicles. Therefore, the purpose of this paper is to raise the consciousness level of the current space exploration planners to what, in the early 1970s, was a highly successful roving vehicle. During the Apollo program the vehicle known as the Lunar Roving Vehicle (LRV) was designed for carrying two astronauts, their tools, and the equipment needed for rudimentary exploration of the Moon. This paper contains a discussion of the vehicle, its characteristics, and its use on the Moon. Conceivably, the LRV has the potential to meet some future requirements, either with relatively low cost modifications or via an evolutionary route. This aspect, however, is left to those who would choose to further study these options. Author

N93-14009*# Georgia Inst. of Tech., Atlanta. School of Mechanical Engineering.

MOBILE WORK PLATFORM FOR INITIAL LUNAR BASE CONSTRUCTION **c31**

James W. Brazell, Brice K. MacLaren, Gary V. McMurray, and Wendell M. Williams *In* NASA. Johnson Space Center, The Second Conference on Lunar Bases and Space Activities of the 21st Century, Volume 2 Sep. 1992 p 633-535 (For primary document see N93-13972 03-91)

Avail: CASI HC A01/MF A03

Described is a system of equipment intended for site preparation and construction of a lunar base. The proximate era of lunar exploration and the initial phase of outpost habitation are addressed. Drilling, leveling, trenching, and cargo handling are within the scope of the system's capabilities. The centerpiece is a three-legged mobile work platform, named SKITTER. Using standard interfaces, the system is modular in nature and analogous to the farmer's tractor and implement set. Conceptually somewhat different from their Earthbound counterparts, the implements are designed to take advantage of the lunar environment as well as the capabilities of the work platform. The proposed system is mechanically simple and weight efficient. Author

N93-14010*# National Aeronautics and Space Administration. Goddard Space Flight Center, Greenbelt, MD.

ENGINEERING PLANETARY LASERS FOR INTERSTELLAR COMMUNICATION **c36**

Brent Sherwood, Michael J. Mumma, and Bruce K. Donaldson (Maryland Univ., College Park.) *In* NASA. Johnson Space Center, The Second Conference on Lunar Bases and Space Activities of the 21st Century, Volume 2 Sep. 1992 p 637-645 (For primary document see N93-13972 03-91)

(Grant NGT-21-002-823)

Avail: CASI HC A02/MF A03

Spacefaring skills evolved in the twenty-first century will enable missions of unprecedented complexity. One such elaborate project might be to develop tools for efficient interstellar data transfer. Informational links to other star systems would facilitate eventual human expansion beyond our solar system, as well as intercourse with potential extraterrestrial intelligence. This paper reports the major findings of a 600-page, 3-year, NASA-funded study examining in quantitative detail the requirements, some seemingly feasible methods, and implications of achieving reliable extrasolar communications. Author

N93-14011*# Los Alamos National Lab., NM.

UNIT OPERATIONS FOR GAS-LIQUID MASS TRANSFER IN REDUCED GRAVITY ENVIRONMENTS **c29**

Donald R. Pettit and David T. Allen (California Univ., Los Angeles.) *In* NASA. Johnson Space Center, The Second Conference on Lunar Bases and Space Activities of the 21st Century, Volume 2 Sep. 1992 p 647-651 Sponsored in part by DOE (For primary document see N93-13972 03-91)

Avail: CASI HC A01/MF A03

Basic scaling rules are derived for converting Earth-based designs of

mass transfer equipment into designs for a reduced gravity environment. Three types of gas-liquid mass transfer operations are considered: bubble columns, spray towers, and packed columns. Application of the scaling rules reveals that the height of a bubble column in lunar- and Mars-based operations would be lower than terrestrial designs by factors of 0.64 and 0.79 respectively. The reduced gravity columns would have greater cross-sectional areas, however, by factors of 2.4 and 1.6 for lunar and Martian settings. Similar results were obtained for spray towers. In contract, packed column height was found to be nearly independent of gravity.

Author

N93-14012*# Science Applications International Corp., Torrance, CA. Thermal Sciences Div.

COMBUSTION OF GASEOUS FUELS UNDER REDUCED-GRAVITY CONDITIONS **c29**

M. Yousef Bahadori and Raymond B. Edelman (Rockwell International Corp., Canoga Park, CA.) *In* NASA. Johnson Space Center, The Second Conference on Lunar Bases and Space Activities of the 21st Century, Volume 2 Sep. 1992 p 653-658 (For primary document see N93-13972 03-91)

(Contract NAS3-22822)

Avail: CASI HC A02/MF A03

The need for an improved understanding of fires is becoming critically important with increased space travel and utilization. While the control of fires in low-gravity environments is not well understood, it is known that buoyancy significantly affects flame behavior and characteristics. The objective of this research is to gain a more fundamental understanding of fires, and to quantify flame behavior under reduced-gravity levels. Non-premixed flames of gaseous fuels are considered in this study because they are relatively simple and easy to control, yet embody mechanisms found in all types of combustion processes ranging from uncontrolled fires to practical combustion systems. This paper presents some recent results from microgravity studies of these flames. In addition, the potential usefulness of lunar- and Martian-based laboratories is discussed in order to understand the characteristics and behavior of fires in reduced-gravity environments.

Author

N93-14013*# Lockheed Engineering and Sciences Co., Houston, TX.

OCCUPATIONAL ERGONOMICS IN SPACE **c54**

J. Stramler *In* NASA. Johnson Space Center, The Second Conference on Lunar Bases and Space Activities of the 21st Century, Volume 2 Sep. 1992 p 659-663 (For primary document see N93-13972 03-91)

Avail: CASI HC A01/MF A03

Ergonomics is often defined simply as the study of work. Related or synonymous terms include human factors, human engineering, engineering psychology, and others. Occupational ergonomics is a term that has been proposed to describe the study of the working environment, including the physical consequences resulting from having an improperly designed workplace. The routine space working environment presents some problems not found in the typical Earthbound workplace. These include radiation, intravehicular contamination/pollution, temperature extremes, impact with other objects, limited psychosocial relationships, sensory deprivation, and reduced gravity. These are important workplace considerations, and may affect astronauts either directly at work or at some point during their life as a result of their work under these conditions. Some of the major issues associated with each of these hazards are presented. Author

N93-14014*# Schmitt (Harrison H.), Albuquerque, NM.

THE REAL WORLD AND LUNAR BASE ACTIVATION SCENARIOS **c54**

Harrison H. Schmitt *In* NASA. Johnson Space Center, The Second Conference on Lunar Bases and Space Activities of the 21st Century, Volume 2 Sep. 1992 p 667-671 (For primary document see N93-13972 03-91)

Avail: CASI HC A01/MF A03

A lunar base or a network of lunar bases may have highly desirable support functions in a national or international program to explore and settle Mars. In addition, He-3 exported from the Moon could be the basis for providing much of the energy needs of humankind in the twenty-first century. Both technical and managerial issues must be addressed when considering the establishment of a lunar base that can serve the needs of human civilization in space. Many of the technical issues become evident in the consideration of hypothetical scenarios for the activation of a network of lunar bases. Specific and realistic assumptions must be made about the conduct of various types of activities in addition to the general assumptions given above. These activities include landings, crew consumables, power production, crew selection, risk management, habitation, science station placement, base planning, science, agriculture, resource evaluation, readaptation, plant activation and test, storage module landings, resource transport module landings, integrated operations, maintenance, Base 2 activation, and management. The development of scenarios for the activation of a lunar base or network of bases will require close attention to the 'real world' of space operations. That world is defined by the natural environment, available technology, realistic objectives, and common sense.

Author

N93-14015*# Tokyo Univ., Sagamihara (Japan). Inst. of Space and Astronautical Science.

MOON PARK: A RESEARCH AND EDUCATIONAL FACILITY **c14**

Kyoichi Kuriki, Takao Saito (Obayashi Corp., Tokyo, Japan), and Yukimasa Ogawa (Obayashi Corp., Tokyo, Japan) *In* NASA. Johnson Space Center, The Second Conference on Lunar Bases and Space Activities of the 21st Century, Volume 2 Sep. 1992 p 673-676 (For primary document see N93-13972 03-91)

Avail: CASI HC A01/MF A03

Moon Park has been proposed as an International Space Year (ISY) event for international cooperative efforts. Moon Park will serve as a terrestrial demonstration of a prototype lunar base and provide research and educational opportunities. The kind of data that can be obtained in the Moon Park facilities is examined taking the minimum number of lunar base residents as an example. Author

N93-14016*# Eagle Engineering, Inc., Houston, TX.

LUNAR STEPPING STONES TO A MANNED MARS EXPLORATION SCENARIO

W. L. Davidson and W. R. Stump *In* NASA. Johnson Space Center, The Second Conference on Lunar Bases and Space Activities of the 21st Century, Volume 2 Sep. 1992 p 677-681 (For primary document see N93-13972 03-91)

Avail: CASI HC A01/MF A03

The initial trips to Mars by humans will be the first real severing of our dependence on Earth's environment. Common sense dictates that a human departure from Earth measured in years, to explore a distant planet, requires systems, techniques, and operations that have solid credibility proven with space experience. The space test and verification experience must occur with Mars-like conditions but under proving-ground conditions with good instrumentation, close monitoring, and fast emergency recovery capabilities. The lunar environment is the only arena that satisfies the requirements of a space recovery capabilities. The lunar environment is the only arena that satisfies the requirements of a space planetary proving-ground. The objective of this scenario is to demonstrate a program planning approach that has human presence at Mars as the goal but, prudently, capitalizes on manned lunar project facilities, operations, and experience to enable a safe journey for the first Mars crews. The emphasis in lunar application objectives is to perform productive science and resources exploitation missions. Most of the Mars mission aspects can be proven in the lunar environment providing 'stepping stones' to conducting the first human mission to travel to Mars and return safely to Earth. Author

N93-14017*# National Aeronautics and Space Administration. Lyndon B. Johnson Space Center, Houston, TX.

CREATING A FOUNDATION FOR A SYNERGISTIC APPROACH TO PROGRAM MANAGEMENT **c81**

Karyn T. Knoll *In its* The Second Conference on Lunar Bases and Space Activities of the 21st Century, Volume 2 Sep. 1992 p 683-689 (For primary document see N93-13972 03-91)

Avail: CASI HC A02/MF A03

In order to accelerate the movement of humans into space within reasonable budgetary constraints, NASA must develop an organizational structure that will allow the agency to efficiently use all the resources it has available for the development of any program the nation decides to undertake. This work considers the entire set of tasks involved in the successful development of any program. Areas that hold the greatest promise of accelerating programmatic development and/or increasing the efficiency of the use of available resources by being dealt with in a centralized

manner rather than being handled by each program individually are identified. Using this information, an agency organizational structure is developed that will allow NASA to promote interprogram synergisms. In order for NASA to efficiently manage its programs in a manner that will allow programs to benefit from one another and thereby accelerate the movement of humans into space, several steps must be taken. First, NASA must develop an organizational structure that will allow potential interprogram synergisms to be identified and promoted. Key features of the organizational structure are recommended in this paper. Second, NASA must begin to develop the requirements for a program in a manner that will promote overall space program goals rather than achieving only the goals that apply to the program for which the requirements are being developed. Finally, NASA must consider organizing the agency around the functions required to support NASA's goals and objectives rather than around geographic locations. Author

N93-14018*# North Dakota Univ., Grand Forks. Dept. of Space Studies.

THE PROVINCE AND HERITAGE OF MANKIND RECONSIDERED: A NEW BEGINNING **c54**

J. I. Gabrynowicz *In* NASA. Johnson Space Center, The Second Conference on Lunar Bases and Space Activities of the 21st Century, Volume 2 Sep. 1992 p 691-695 (For primary document see N93-13972 03-91)

Avail: CASI HC A01/MF A03

The central problem of our time -- one that is shared by all races and nationalities -- is to discover the things, the qualities, and interest that people have in common so that durable institutions can be designed for mankind's survival. The 'common heritage of mankind' and the 'province of all mankind' are different legal concepts developed in international space law during the last quarter of a century. Since the initial appearance of these provisions, controversy has arisen regarding their intent and meaning as applied to a nation's right to explore and use a common environment such as space or the high seas and a nation's obligation to share benefits derived from those environments with the rest of the world. As can be expected, different interpretations are currently competing for acceptance. This is so, in part, because, in the case of the Outer Space Treaty, although a general principle was articulated, rules for acceptance and application of the principles were not. In the case of the Moon and Sea Treaties, although an effort has been made to clarify both meaning and application, the articulations are still too vague for legal certainty. This paper focuses on the fact that these concepts are already currently available tools for the advancement of both global and U.S. interests but, because of the labyrinthine legal arguments that have been generated and some assumptions being held, they are in danger of being lost as such tools. The tendency of many observers in the U.S. to confuse the concept of 'province of all mankind' and 'common heritage of mankind' and to assume that both are incompatible with U. S. commercial space interests is also addressed. It is suggested that reconsidering these provisions can yield positions compatible with U.S. interests and that it can and should actively seek the use of these provisions as a basis for global cooperation and commercial benefit. Author

N93-14019*# Los Alamos National Lab., NM. Earth and Space Science Div.

A BASIS OF SETTLEMENT: ECONOMIC FOUNDATIONS OF PERMANENT PIONEER COMMUNITIES **c83**

Eric M. Jones *In* NASA. Johnson Space Center, The Second Conference on Lunar Bases and Space Activities of the 21st Century, Volume 2 Sep. 1992 p 697-701 (For primary document see N93-13972 03-91)

Avail: CASI HC A01/MF A03

High transport costs will dominate the course of lunar development. During the earliest phases, when lunar facilities consist of a research and resource development complex with staff serving tours of a few months, transport costs will encourage local production of fuel, food, and building materials. Once these capabilities are in place and the number of personnel grows to a few hundred, staff rotation might well dominate transport budgets. At that point it would make economic sense to encourage some members of staff to become permanent residents. By analogy with early British settlement in Australia, a vigorous private sector economy could emerge if the lunar organization provided quasi-export earnings through its role as the community's major employer and as the major buyer of locally produced goods. By providing such a market for goods and services, the lunar organization would not only provide a means whereby permanent residents could support themselves, but could also accelerate the process of replacing imported goods with local manufacturers, thereby reducing the cost of operations. By analogy with recent Alaskan experience, if the resource development activity started making money from sales to orbital customers, export taxes and/or royalty payments could also provide means by which a lunar community could support itself. Author

N93-14020*# National Aeronautics and Space Administration. Lyndon B. Johnson Space Center, Houston, TX.

THE LUNAR COMMUNITY CHURCH: CONTRIBUTIONS TO LUNAR LIVING AND TO EVOLUTION OF ETHICAL AND SPIRITUAL THINKING **c53**

J. H. Allton *In its* The Second Conference on Lunar Bases and Space Activities of the 21st Century, Volume 2 Sep. 1992 p 703-705 (For primary document see N93-13972 03-91)

Avail: CASI HC A01/MF A03

Should religious institutions get interested in lunar settlement? Would their participation make positive contributions or would it discourage creative diversity and interfere with science and good technical judgement? Among the spacefaring nations of today, religion is distinctly separated from the governments that plan and pay for space exploration. However, as we move off the Earth, our art and philosophy will follow our science and technology. Spiritual thinking will follow as part of our culture. It is time to consider in what ways this can occur constructively. Transport of religious values to a lunar base may have positive effects in two ways. First, the social structure of a 'community church' as found in today's United States, supports its members psychologically. Mutual psychological and social support will be needed in a lunar community. Second, our space pioneers will experience a unique view of the universe which may, in their philosophical discussions, forge new ideas in the spiritual realm. Author

N93-14072 Johns Hopkins Univ., Baltimore, MD.

AN ANALYSIS OF THE VOYAGER 2 ULTRAVIOLET SPECTROMETER OCCULTATION DATA AT URANUS AND TRITON: INFERRING HEAT SOURCES AND MODEL ATMOSPHERES Ph.D. Thesis

Michael Hugh Stevens 1992 182 p

Avail: Univ. Microfilms Order No. DA9216634

In January 1986, the Voyager 2 Ultraviolet Spectrometer (UVS) observed a stellar entrance and exit occultation and a solar occultation by Uranus. Temperatures inferred near the top of the atmosphere of Uranus from these occultations are much higher (872 K) than could be explained by solar extreme ultraviolet heating alone. One purpose of this thesis is to analyze the UVS stellar and solar occultation data at Uranus and to determine the best thermospheric temperature profile consistent with UVS occultation data. This analysis yields the first smooth thermospheric temperature profile for Uranus and significantly different results for the thermal structure than those obtained in preliminary work by Herbert et al. (1987). One may infer from the work of Herbert et al. that there are two heat sources, one at the 1 micro-bar level with an integrated heating rate of about 0.20 erg/sq cm/s and one near 10(exp -4) micro-bar with an integrated heating rate of about 0.03 erg/sq cm/s. This analysis, however, yields one heat source between 3 x 10(exp -5) and 6 x 10(exp -7) micro-bar with an integrated heating rate of about 0.06 plus or minus 0.02 erg/sq cm/s micro-bar as the least squares best fit to all UVS occultation data. In contrast to preliminary work, the inferred temperature for the stellar entrance occultation (63.7 degrees S) is at least 45 degrees K cooler near 50 micro-bar than for the stellar exit occultation (69.7 degrees N), whereas at about 1 micro-bar the temperature contrast is near 30 degrees K. Voyager 2 observed a solar entrance and exit occultation at Triton in August, 1989. The same model atmosphere is inferred from the solar entrance occultation at 26 degrees N and the solar exit occultation at 44 degrees S. This atmosphere has a heat source at 500 km with an integrated heating rate referenced to the surface of 1.3 x 10(exp-3) erg/sq cm/s. Dissert. Abstr.

N93-14092 Arizona State Univ., Tempe.

VOLCANISM IN THE EASTERN HELLAS REGION OF MARS: THE GEOLOGY OF HADRIACA AND TYRRHENA PATERAE Ph.D. Thesis

David Arden Crown 1991 242 p

Avail: Univ. Microfilms Order No. DA9210368

Photogeologic analyses of Viking Orbiter images and analytical models

based on terrestrial volcanic processes are used to determine the types, distribution, and mode(s) of formation of the materials composing two ancient Martian volcanoes. Hadriaca Patera and Tyrrhena Patera are large, low-relief features located in the southern highlands of Mars northeast of the Hellas basin. Layered, dissected deposits compose the extensive channeled flanks of these volcanoes. The erosional characteristics, lack of lava flow features, and friable nature of the materials indicate that the paterae consist predominantly of pyroclastic deposits. Morphologic similarities between Hadriaca and Tyrrhena Paterae suggest similar volcanic histories, with an early phyroclastic-dominated, shield-building phase followed by effusive eruptions at their summit calderas and on the southwest flank of Tyrrhena Patera. Geomorphic analyses and crater statistics constrain the evolution of the eastern Hellas region. Relative ages of the geologic units support morphologic evidence for interactions between volcanic, tectonic, and volatile-driven processes. Degradation by fluvial erosion was widespread and dominated the region surrounding Hadriaca Patera. Application of gravity-driven flow models demonstrates that the distribution of units at Hadriaca and Tyrrhena Paterae can be attributed to the emplacement of pyroclastic flows. Explosive eruptions driven by either magmatic volatiles or groundwater could provide sufficient energy. Large volumes of groundwater could accumulate rapidly at flow rates determined for Mars to drive hydrovolcanism. Analysis of cooling during transport indicates that welding of pyroclastic flows can occur at large distances from a source vent on Mars and could explain the layering observed within the paterae. The volcanic evolution of the highland paterae and subsequent dominance of the ridged plains of Hesperia Planum suggest a transition from explosive to effusive volcanism in the eastern Hellas region. A progressive depletion of volatiles on Mars is consistent with the morphologic properties of the highland paterae and other central-vent volcanoes. The prevalence of hydrovolcanic eruptions in the development of the paterae would imply that the transition in volcanic eruption style can be attributed to a volatile depletion of the Martian crust, whereas magmatic eruptions at the paterae would be indicative of temporal changes in Martian magmas.

Dissert. Abstr.

92 SOLAR PHYSICS

Includes solar activity, solar flares, solar radiation and sunspots. For related information see *93 Space Radiation*.

N93-12658*# Alabama Univ., Huntsville.
SCIENTIFIC STUDY OF DATA ANALYSIS Final Report
S. T. Wu [1990] 35 p
(Contract NAS8-36955)
(NASA-CR-184435; NAS 1.26:184435) Avail: CASI HC A03/MF A01

We present a comparison between two numerical methods for the extrapolation of nonlinear force-free magnetic fields, the Iterative Method (IM) and the Progressive Extension Method (PEM). The advantages and disadvantages of these two methods are summarized and the accuracy and numerical instability are discussed. On the basis of this investigation, we claim that the two methods do resemble each other qualitatively.

Author

N93-12669*# Southwest Research Inst., San Antonio, TX. Instrumentation and Space Research Div.
STUDIES OF EXTRA-SOLAR OORT CLOUDS AND THE KUIPER DISK Semiannual Report No. 1
S. Alan Stern 23 Sep. 1992 22 p
(Grant NAGw-3023; SwRI Proj. 15-4971)
(NASA-CR-190958; NAS 1.26:190958) Avail: CASI HC A03/MF A01

In 1991 we detected extended 1.1 mm emission around Fomalhaut (alpha PsA) at distances in order of magnitude beyond previous detections. This emission is plausibly related to the presence of an extended comet cloud, like our Oort Cloud, and may therefore represent indirect evidence for the formation of a planetary system at Fomalhaut. We propose now to extend this work to create a map of the angular and spatial extent of this emission. Fomalhaut is the only known main-sequence, submm-resolved IR excess source besides beta Pic.

Author

N93-12803# National Geophysical Data Center, Boulder, CO.
SOLAR-GEOPHYSICAL DATA NUMBER 574, JUNE 1992. PART 1: (PROMPT REPORTS). DATA FOR MAY, APRIL 1992 AND LATE DATA
Helen E. Coffey, ed. Jun. 1992 130 p
(PB92-218759; SGD-574-Pt-1; LC-79-640375) Avail: CASI HC A07/MF A02

Detailed index for 1991-1992; Data for May 1992 -- Solar-terestrial environment, IUWDS alert periods (Advance and Worldwide), Solar activity indices, Solar flares, Solar radio emission, Stanford mean solar magnetic field; Data for April 1992 -- Solar active regions, Sudden ionospheric disturbances, Solar radio spectral observations, Cosmic ray measurements by neutron monitor, Geomagnetic indices; Late data -- Geomagnetic activity indices Mar. 92.

GRA

N93-12930*# New Hampshire Univ., Durham. Space Science Center.
STUDY OF SMM FLARES IN GAMMA-RAYS AND NEUTRONS Final Technical Report, 1 Nov. 1991 - 31 Oct. 1992
Philip P. Dunphy and Edward L. Chupp 31 Oct. 1992 51 p
(Grant NAGw-2755)
(NASA-CR-191249; NAS 1.26:191249) Avail: CASI HC A04/MF A01

This report summarizes the results of the research supported by NASA grant NAGW-2755 and lists the papers and publications produced through the grant. The objective of the work was to study solar flares that produced observable signals from high-energy (greater than 10 MeV) gamma-rays and neutrons in the Solar Maximum Mission (SMM) Gamma-Ray Spectrometer (GRS). In 3 of 4 flares that had been studied previously, most of the neutrons and neutral pions appear to have been produced after the 'main' impulsive phase as determined from hard x-rays and gamma-rays. We, therefore, proposed to analyze the timing of the high-energy radiation, and its implications for the acceleration, trapping, and transport of flare particles. It was equally important to characterize the spectral shapes of the interacting energetic electrons and protons - another key factor in constraining possible particle acceleration mechanisms. In section 2.0, we discuss the goals of the research. In section 3.0, we summarize the results of the research. In section 4.0, we list the papers and publications produced under the grant. Preprints or reprints of the publications are attached as appendices.

Author

N93-13014*# Alabama Univ., Huntsville. Center for Space Plasma and Aeronomic Research.
SOLAR PREDICTION ANALYSIS Final Report
Jesse B. Smith 7 May 1992 5 p
(Contract NAS8-36955)
(NASA-CR-184422; NAS 1.26:184422) Avail: CASI HC A01/MF A01

Solar Activity prediction is essential to definition of orbital design and operational environments for space flight. This task provides the necessary research to better understand solar predictions being generated by the solar community and to develop improved solar prediction models. The contractor shall provide the necessary manpower and facilities to perform the following tasks: (1) review, evaluate, and assess the time evolution of the solar cycle to provide probable limits of solar cycle behavior near maximum end during the decline of solar cycle 22, and the forecasts being provided by the solar community and the techniques being used to generate these forecasts; and (2) develop and refine prediction techniques for short-term solar behavior flare prediction within solar active regions, with special emphasis on the correlation of magnetic shear with flare occurrence.

Author

N93-13475*# Alabama Univ., Huntsville. Dept. of Mechanical Engineering.
DATA EVALUATION, ANALYSIS, AND SCIENTIFIC STUDY Final Report
S. T. Wu 1991 173 p
(Contract NAS8-36955)
(NASA-CR-184396; NAS 1.26:184396) Avail: CASI HC A08/MF A02

Extensive work was performed in data analysis and modeling of solar active phenomena. The work consisted in the study of UV data from the Ultraviolet Spectrometer and Polarimeter (UVSP) instrument on board the Solar Maximum Mission satellite. These data were studied in conjunction with X-rays from the Hard X-ray Imaging Spectrometer (HXIS) instrument, and with H-alpha and magnetographic data from ground-based observatories. The processes we studied are the active phenomena which result from the interaction of the solar magnetic fields with the plasma in the outer

regions of the solar atmosphere. These processes include some very dynamic processes such as the prominence eruptions and the 'microflares'. Our research aimed at characterizing the following: the observed phenomena, the possible physical models, and the relevance to the chromospheric and coronal heating. For individual titles, see N93-13476 through N93-13478.

N93-13476*# Smithsonian Astrophysical Observatory, Cambridge, MA.
THE ROLE OF PARTICLE DIFFUSION IN THE LOWER TRANSITION REGION: REVISED INTERPRETATION OF EMISSION MEASURES
Eugene H. Avrett and Juan M. Fontenla (Alabama Univ., Huntsville.) *In* Alabama Univ., Data Evaluation, Analysis, and Scientific Study 1991 2 p Submitted for publication (For primary document see N93-13475 03-92)
Avail: CASI HC A01/MF A02

Our energy-balance models of the lower transit ion region were presented in a previous paper (New Models of the Chromosphere and Transition Region). Here we show the influence of particle diffusion on the calculated hydrogen and helium number densities for a given temperature-density model (model C in the preceding paper). We have also solved the statistical equilibrium and radiative transfer equations for a 13-level He I atom (22 radiative transitions) and a 6-level He II ion (15 radiative transitions) together with He III. The resulting He I and He II level-1 number densities and He III density are shown as functions of temperature. Diffusion substantially increases eta(sub HeI) for T greater than 35,000 K and decreases eta(sub HeI) (while increasing eta(sub(HeII)) between 9,000 and 25,000 K. Including the effects of diffusion also increases eta(sub HeIII) for T less than 60,000 K. Author

N93-13477*# National Aeronautics and Space Administration. Marshall Space Flight Center, Huntsville, AL.
THE 3-D DESCRIPTION OF VERTICAL CURRENT SHEETS WITH APPLICATION TO SOLAR FLARES
Juan M. Fontenla (Alabama Univ., Huntsville.) and J. M. Davis *In* Alabama Univ., Data Evaluation, Analysis, and Scientific Study 1991 24 p Submitted for publication (For primary document see N93-13475 03-92)
(SSL-Preprint-90-119) Avail: CASI HC A03/MF A02

Following a brief review of the processes which have been suggested for explaining the occurrence of solar flares we suggest a new scenario which builds on the achievements of the previous suggestion that the current sheets, which develop naturally in 3-D cases with gravity from impacting independent magnetic structures (i.e., approaching current systems), do not consist of horizontal currents but are instead predominantly vertical current systems. This suggestion is based on the fact that as the subphotospheric sources of the magnetic field displace the upper photosphere and lower chromosphere regions, where plasma beta is near unity, will experience predominantly horizontal mass motions which will lead to a distorted 3-D configurations of the magnetic field having stored free energy. In our scenario, a vertically flowing current sheet separates the plasma regions associated with either of the subphotospheric sources. This reflects the balanced tension of the two stressed fields which twist around each other. This leads naturally to a metastable or unstable situation as the twisted field emerges into a low beta region where vertical motions are not inhibited by gravity. In our flare scenario the impulsive energy release occurs, initially, not by reconnection but mainly by the rapid change of the magnetic field which has become unstable. During the impulsive phase the field lines contort in such way as to realign the electric current sheet into a minimum energy horizontal flow. This contortion produces very large electric fields which will accelerate particles. As the current evolves to a horizontal configuration the magnetic field expands vertically, which can be accompanied by eruptions of material. The instability of a horizontal current is well known and causes the magnetic field to undergo a rapid outward expansion. In our scenario, fast reconnection is not necessary to trigger the flare, however, slow reconnection would occur continuously in the current layer at the locations of potential flaring. During the initial rearrangement of the field strong plasma turbulence develops. Following the impulsive phase, the final current sheet will experience faster reconnection which we believe responsible for the gradual phase of the flare. The reconnection will dissipate part of the current and will produce sustained and extended heating in the flare region and in the postflare loops. Author

N93-13478*# National Aeronautics and Space Administration. Goddard Space Flight Center, Greenbelt, MD.
ELECTRON IMPACT POLARIZATION EXPECTED IN SOLAR EUV LINES FROM FLARING CHROMOSPHERES/TRANSITION REGIONS
S. Fineschi (National Academy of Sciences - National Research Council, Washington, DC.), Juan M. Fontenla (Alabama Univ., Huntsville.), P. MacNeice, and N. N. Ljepojevic (Cambridge Univ., England) *In* Alabama Univ., Data Evaluation, Analysis, and Scientific Study 1991 9 p Submitted for publication (For primary document see N93-13475 03-92)
(Grant NAGw-2096)
(SSL-Preprint-90-124) Avail: CASI HC A02/MF A02

We have evaluated lower bounds on the degree of impact Extreme Ultraviolet/Ultraviolet (EUV/UV) line polarization expected during solar flares. This polarization arises from collisional excitation by energetic electrons with non-Maxwellian velocity distributions. Linear polarization was observed in the S I 1437 A line by the Ultraviolet Spectrometer and Polarimeter/Solar Maximum Mission (UVSP/SMM) during a flare on 15 July 1980. An early interpretation suggested that impact excitation by electrons propagating through the steep temperature gradient of the flaring transition region/high chromosphere produced this polarization. Our calculations show that the observed polarization in this UV line cannot be due to this effect. We find instead that, in some flare models, the energetic electrons can produce an impact polarization of a few percent in EUV neutral helium lines (i.e., lambda lambda 522, 537, and 584 A). Author

N93-13605 Saint Andrew's Univ. (Scotland).
EQUILIBRIUM AND ERUPTION OF SOLAR CORONAL MAGNETIC STRUCTURES Ph.D. Thesis
C. D. C. Steele 1989 321 p
Avail: Univ. Microfilms Order No. BRDX93487

Magnetostatic and thermal equilibria of several coronal magnetic structures are considered. A model is set up for the eruption of a prominence (modelled as a twisted flux tube) magnetically coupled to a coronal mass ejection. Two different prominence models are considered. In one a globally stable equilibrium becomes unstable and, in the other, equilibrium ceases to exist. In both cases, the components accelerate upwards before reaching constant velocities in a manner consistent with observations. A cylindrically symmetric magnetic arcade in equilibrium with its axis on the photosphere is subjected to a base pressure perturbation. The perturbation is examined with the aim of seeking equilibrium configurations close to the original equilibrium. It is found that equilibria can only be found when the integral of the excess base pressure is zero. For an initial arcade whose field increases linearly with radial distance from the axis, neighboring equilibria were found. Equations of thermal equilibrium along coronal loops with footpoint temperatures of 2 x 10(exp 4) are solved. Three fundamentally different categories are found, namely hot loops (corresponding to the hot corona), cool loops (relevant to fibrils, cool cores, and active-region prominences), and hot-cool loops with cool summits but much hotter parts between the summit and the footpoints. Quiescent prominences may be modelled as hot-cool loops inclined to the prominence axis. Furthermore, warm loops at intermediate summit temperatures (8 x 10(exp 4) K - 4 x 10(exp 5) K) can exist, but the observed differential emission measure suggests these are uncommon. Thermal catastrophe may occur when the loop length or pressure is too small. Many loops can be superimposed to form a coronal arcade. Two types of arcade are considered--one has its axis on the photosphere; the other is isobaric and has its axis below photosphere. In both cases, cool material can exist high in the corona as is observed for prominences. Dissert. Abstr.

N93-13627 Maryland Univ., College Park.
AN INFRARED POLARIMETRIC STUDY OF SUNSPOTS Ph.D. Thesis
Tilak Hewagama 1991 244 p
Avail: Univ. Microfilms Order No. DA9222696

A polarimetric study of the extremely Zeeman sensitive 12.32 microns neutral magnesium (Mg I) emission line from sunspots is discussed. A single blocked impurity band (BIB) detector in a cryogenic grating postdisperser was used to limit the McMath Fourier transform spectrometer (FTS) bandpass and obtain high signal/noise spectra at 0.005 cm(exp -1) spectral resolution with 4.5 sec spatial resolution. A polarization analyzer preceded the FTS and consisted of an anti-reflection coated CdS 1/4 waveplate and a thin film Ge linear polarizer. A second 1/4 waveplate was mounted at 45 deg to the linear polarizer to eliminate dependence on

the polarization properties of the FTS optics and postdisperser grating. The instrument polarization introduced by the McMath telescope is shown to be negligible for the purpose of 12 microns polarimetry, and theoretical arguments are presented to show that the 12 microns observations are not corrupted by magneto-optical effects. Stokes I,Q,U, and V profiles were generated by subtracting successive interferograms. The time resolution of a set of Stokes parameters was 12 minutes. Within the sunspot the Zeeman triplet was fully resolved. Since the line is optically thin, it was possible to derive vector fields by non-linear least squares fits of the Seares formulae to the observed Stokes profiles. The observations of a visually symmetric sunspot (23-28 Oct. 1989) show that the 12 microns emission is completely polarized. This implies that the sunspot magnetic field at the 12 microns altitude is not filamentary in the sense of containing field-free regions nor is there cancellation of field, over any spatial scale, in the beam area. The sunspot field strength varied from 2050 G in the umbra to 650 G at the outer penumbral edge, and the magnetic structure extended well beyond the photometric edge of the sunspot. Vector magnetograms obtained for the same spot by the Haleakala Stokes polarimeter, operating at 6302.5 A, show an umbral field strength which is larger by 400 G. On this basis the altitude of formation for the Mg I line is estimated to be approximately 600 km above tau approximately 1 for the 6302.5 A line. Dissert. Abstr.

N93-13639 North Carolina Univ., Chapel Hill.
A THERMAL/NONTHERMAL APPROACH TO SOLAR FLARES Ph.D. Thesis
Stephen G. Benka 1991 109 p
Avail: Univ. Microfilms Order No. DA9216685

A new approach for modeling solar flare high energy emissions is developed in which both thermal and nonthermal particles coexist and contribute to the radiation. The thermal/nonthermal distribution function is interpreted physically by postulating the existence of DC sheets in the flare region. These current sheets then provide both primary plasma heating through Joule dissipation, and runaway electron acceleration. The physics of runaway acceleration is discussed. Several methods are presented for obtaining approximations to the thermal/nonthermal distribution function, both within the current sheets and outside of them. Theoretical hard x-ray spectra are calculated, allowing for thermal bremsstrahlung from the heated plasma external to the current sheets, as well as thick-target bremsstrahlung from runaway electrons impinging on the chromosphere. A simple model for hard-x ray images of two-ribbon flares is presented. Theoretical microwave gyrosynchrotron spectra are calculated and analyzed, uncovering important new effects caused by the interplay of thermal and nonthermal particles. The theoretical spectra are compared with observed high resolution spectra of solar flares, and excellent agreement is found, in both hard x-ray and microwaves. The future detailed application of this approach to solar flares is discussed, as are possible refinements of this theory. Dissert. Abstr.

N93-13849 Columbia Univ., New York, NY.
THERMOCONVECTIVE INSTABILITY IN THE SOLAR CORE Ph.D. Thesis
Sandip Ghosal 1992 220 p
Avail: Univ. Microfilms Order No. DA9221153

Models of the present sun have a thin shell of He-3 at the edge of the core. The rates of nuclear burning of He-3 are very temperature sensitive and this can lead to thermal instability. Thermal instability in a stably stratified medium results in growing oscillations (overstability of gravity waves). The excitation of gravity modes by thermal instability is classically studied as a quasiadiabatic problem. However, the period of adiabatic oscillations increases with decreasing vertical to horizontal aspect ratio of these modes while the local thermal diffusion time decrease. It is shown through the study of a simplified example that such slow gravity modes can be trapped in a thin layer due to thermal effects, contrary to expectations based on quasiadiabatic arguments, which are not applicable to such slow modes. Using the smallness of the aspect ratio, amplitude equations can be derived for the wave amplitude under mildly unstable conditions. The amplitude equations admit nonlinear waves. Stationary wave solutions are also possible and these are described by a Hopf bifurcation that is subcritical in the thin layer limit, possibly leading to overturning motions. It is shown that if such monotonic or oscillatory convection of large horizontal scale exists in the solar core, the central temperature and therefore the high energy neutrino flux will be lower than that expected from the standard solar models. These 'shellular' modes are expected to have periods of about two hours. If such modes are detected in the sun, they will be a powerful tool for seismic probing of the solar interior. Dissert. Abstr.

93 SPACE RADIATION

Includes cosmic radiation; and inner and outer earth's radiation belts.

For biological effects of radiation see *52 Aerospace Medicine.* For theory see *73 Nuclear and High-Energy Physics.*

N93-13020*# National Aeronautics and Space Administration. Langley Research Center, Hampton, VA.
FULLY ENERGY-DEPENDENT HZETRN (A GALACTIC COSMIC-RAY TRANSPORT CODE)
Judy L. Shinn, Sarah John (Vigyan Research Associates, Inc., Hampton, VA.), Ram K. Tripathi (Vigyan Research Associates, Inc., Hampton, VA.), John W. Norbury (Rider Coll., Lawrenceville, NJ.), John W. Wilson, and Lawrence W. Townsend Washington Nov. 1992 18 p
(RTOP 593-42-21-01)
(NASA-TP-3243; L-17103; NAS 1.61:3243) Avail: CASI HC A03/MF A01

For extended manned space missions, the radiation shielding design requires efficient and accurate cosmic-ray transport codes that can handle the physics processes in detail. The Langley Research Center galactic cosmic-ray transport code (HZETRN) is currently under development for such design use. The cross sections for the production of secondary nucleons in the existing HZETRN code are energy dependent only for nucleon collisions. The approximation of energy-independent, heavy-ion fragmentation cross section is now removed by implementing a mathematically simplified energy-dependent stepping formalism for heavy ions. The cross section at each computational grid is obtained by linear interpolation from a few tabulated data to minimize computing time. Test runs were made for galactic cosmic-ray transport through a liquid hydrogen shield and a water shield at solar minimum. The results show no appreciable change in total fluxes or computing time compared with energy-independent calculations. Differences in high LET (linear energy transfer) spectra are noted, however, because of the large variation in cross sections at the low-energy region. The high LET components are significantly higher in the new code and have important implications on biological risk estimates for heavy-ion exposure. Author

N93-13126*# National Aeronautics and Space Administration. Langley Research Center, Hampton, VA.
GALACTIC COSMIC RAY EXPOSURE ESTIMATES FOR SAGE-3 MISSION IN POLAR ORBIT
John E. Nealy and Bryan E. Tipton (Pennsylvania State Univ., University Park.) Oct. 1992 17 p
(RTOP 593-42-31-01)
(NASA-TM-107678; NAS 1.15:107678) Avail: CASI HC A03/MF A01

An analysis of the effects of galactic cosmic ray (GCR) exposures on charge-coupled devices (CCDs) was performed for the SAGE-III 5-year mission in sun-synchronous orbit between 1996 and 2001. A detailed environment model used in conjunction with a geomagnetic vertical cut-off code provides the predicted 5-year fluence of GCR ions. A computerized solid model of the spacecraft was used to define the effective shield thickness distribution around the CCD detector. The particle fluences at the detector location are calculated with the Langley heavy-ion transport code, and these fluences are used in conjunction with estimated nuclear stopping powers to evaluate dosimetric quantities related to the detector degradation. A previous study analyzing effects of trapped particle and solar flare protons indicated an approximate 20 percent reduction in detector sensitivity for the mission. The galactic cosmic ray contribution was thought to be relatively small and therefore was not previously analyzed. The present study provides quantification of the GCR effects, which are found to contribute less than 1 percent of the total environment degradation.
Dissert. Abstr.

N93-13145 California Univ., Berkeley.
THE MILLIMETER AND SUBMILLIMETER WAVELENGTH DIFFUSE BACKGROUNDS: MEASUREMENTS OF THE SPECTRUM AND ANISOTROPY Ph.D. Thesis
David Charles Alsop 1991 193 p
Avail: Univ. Microfilms Order No. DA9228553

The results of two experiments to study the diffuse background at millimeter and submillimeter wavelengths are reported. The first experiment was a rocket-borne photometer designed to measure the spectrum of the background. The background was observed in six bands centered at 7, 13, 20, 30, 40, and 50 cm(exp -1). After the flight, a systematic error was detected in the flight data. A model for the error was developed and an attempt at correction was made, but indications that the correction was not complete were found. The second experiment was a search for anisotropy in the Cosmic Microwave Background at one degree angular scales. The search employed a multiband, bolometric receiver mounted on a balloon-borne telescope. The search achieved the highest statistical sensitivity at this angular scale, which is of crucial importance for constraining theories of structure formation in the universe. Signals in excess of random were detected but concern over possible systematic error sources prevents the interpretation of the signals as uniquely cosmological in origin.
Dissert. Abstr.

N93-13146 California Univ., Berkeley.
MEASUREMENTS OF THE COSMIC MICROWAVE BACKGROUND TEMPERATURE AT 1.47 GHz Ph.D. Thesis
Marc John Bensadoun 1991 143 p
Avail: Univ. Microfilms Order No. DA9228572

A radiofrequency-gain total power radiometer measured the intensity of the cosmic microwave background (CMB) at a frequency of 1.47 GHz (20.4 cm wavelength) from White Mountain, California, in Sep. 1988 and from the South Pole, Antarctica, in Dec. 1989. The CMB thermodynamic temperature, T(sub CMB), is 2.27 +/- 0.25 K (68 percent C.L.) measured from White Mountain and 2.26 +/- 0.21 K from the South Pole site. The combined result is 2.27 +/- 0.19 K. The correction for galactic emission was derived from scaled low-frequency maps and constitutes the main source of error. The atmospheric signal is found by extrapolation from zenith scan measurements at higher frequencies. The result is consistent with previous low-frequency measurements, including a measurement at 1.41 GHz made with an earlier version of this instrument. The result is approximately 2.5 sigma (approximately 1 percent probability) from the 2.74 +/- 0.02 K global average CMB temperature. Dissert. Abstr.

N93-13147 California Univ., Berkeley.
ZODIACAL EMISSION Ph.D. Thesis
William Thomas Reach 1991 209 p
Avail: Univ. Microfilms Order No. DA9228828

This thesis is devoted to the study of small particles in the Solar System and their contribution to the brightness of the sky. In the three chapters comprising the main body of the thesis, observations of the sky brightness by the Infrared Astronomical Satellite (IRAS) are analyzed and compared to models of the emission spectrum and spatial distribution of interplanetary dust. The IRAS observations revolutionized the study of the infrared sky by providing the first complete maps at 12, 25, 60, and 100 micrometer wavelengths. These observations were used to measure the following: (1) the emission spectrum of dust near the Earth's orbit; (2) the temporal and angular variations of the brightness of the ecliptic; and (3) the properties of the zodiacal dust bands. The zodiacal dust bands were an unanticipated IRAS discovery, and have led to a new view of the source of interplanetary dust: the asteroid belt. In the Appendix to the thesis, the possibility that a large amount of interplanetary dust was produced, either by a comet or in an asteroid collision, within recorded history is examined using the Chinese astronomical records. Dissert. Abstr.

N93-13255# National Inst. of Polar Research, Tokyo (Japan).
JARE DATA REPORTS NO. 176 (IONOSPHERE 47). RIOMETER RECORDS OF 30 MHz COSMIC NOISE AT SYOWA STATION, ANTARCTICA IN 1990
Kazuhiro Ohtaka (Ministry of Posts and Telecommunications, Tokyo, Japan) and Manabu Kunitake (Ministry of Posts and Telecommunications, Tokyo, Japan) Mar. 1992 208 p
Avail: CASI HC A10/MF A03

At Syowa Station, Antarctica, absorption of cosmic radio noise has been observed with a standard riometer (relative ionospheric opacity meter) at 30 MHz, since February 1966. This report presents data observed from January 1 to December 31, 1990, in the format of hourly values and combined data plots. Besides riometer data, other observation data are also presented in the combined data plots for reference. These plots include geomagnetic field, HF, VLF, and radar observations. In case of lack of the combined plots, riometer, and geomagnetic field observation data are presented. Author

N93-13306*# Arizona Univ., Tucson. Dept. of Physics.
A PROGRAM TO STUDY ANTIPROTONS IN THE COSMIC RAYS: ARIZONA COLLABORATION Final Progress Report
Theodore Bowen 30 Nov. 1992 24 p
(Grant NAG5-879)
(NASA-CR-191272; NAS 1.26:191272) Avail: CASI HC A03/MF A01

The Cherenkov detector designed and built for the LEAP (Low Energy AntiProton) experiment utilized a novel design to achieve appreciable sensitive area (02. sq m) with a refractive index of 1.25 in a magnetic fringe field region (500-1000 Gauss). The weight was held to only 64 kg by using 16 unshielded Hamamatsu R2490-01 photomultiplier tubes, each aligned with its local magnetic field. A filling and reservoir system for the highly volatile FC-72 liquid Cherenkov radiator also presented many design challenges. Relativistic particles yielded about 72 photoelectrons, total.
Author

N93-13533# Washington Univ., Seattle. Inst. for Nuclear Theory.
NEUTRINO(e) APPEARANCE FOR NEUTRINO(MU)-NEUTRINO(TAU) OSCILLATIONS IN MATTER
J. Pantaleone 1992 9 p
(Contract DE-FG06-90ER-40561)
(DE92-040303; DOE/ER-40561/59) Avail: CASI HC A02/MF A01

New ranges of neutrino oscillation parameters can be probed by sending accelerator produced nu(sub mu) to large neutrino detectors thousands of kilometers away. Since the neutrino propagation is through the Earth, the nu(sub e) - nu(sub tau) mixing can be enhanced by matter effects. Then a neutrino coupled dominantly to the nu, with a mass squared of 10(exp -3) eV(exp 2) to 10(exp -1) eV(exp 2), may most easily be observed by a nu(sub e) appearance experiment. DOE

N93-13572*# National Aeronautics and Space Administration. Langley Research Center, Hampton, VA.
A STUDY OF THE GENERATION OF LINEAR ENERGY TRANSFER SPECTRA FOR SPACE RADIATIONS
John W. Wilson and Francis F. Badavi (Christopher Newport Coll., Newport News, VA.) Dec. 1992 9 p
(RTOP 199-04-16-11)
(NASA-TM-4410; L-17137; NAS 1.15:4410) Avail: CASI HC A02/MF A01

The conversion of particle-energy spectra into a linear energy transfer (LET) distribution is a guide in assessing biologically significant components. The mapping of LET to energy is triple valued and can be defined only on open subintervals. A well-defined numerical procedure is found to allow generation of LET spectra on the open subintervals that are integrable in spite of their singular nature. Author

N93-13689 California Univ., Berkeley.
ANISOTROPY MEASUREMENTS OF THE COSMIC BACKGROUND RADIATION AT 3 mm WAVELENGTH AND AN ANGULAR SCALE OF 30 ARCMINUTES Ph.D. Thesis
Peter Russell Meinhold 1990 119 p
Avail: Univ. Microfilms Order No. DA9126703

Measurements of the anisotropy in the Cosmic Background Radiation (CBR), at 3mm wavelength, on angular scales from 5 arcminutes to 1 degree, are discussed. The data give an upper limit at 95 percent confidence to fluctuations in the cosmic Background Radiation of delta(T)/T less than 3.0 x 10(exp -5) for Gaussian autocorrelation functions with dispersions from 20 to 30 arcminutes and weaker limits on smaller and larger scales. In addition, measurements of the galactic plane show unexpectedly high emission at 3 mm, inconsistent with the previously accepted single component galactic dust model with a scaling index of 2. These measurements were carried out with a 1 meter off axis telescope designed

for operation from a stratospheric Helium filled balloon, but also used on the ground from the South Pole. The detector is a superconducting mixer with a sensitivity of 1.7 mK/the square root of Hz (before chopping), and telescope pointing performance is demonstrated to be better than 1 arcminute in both azimuth and elevation. The development of the instrument is described, and details of the optical system, detector, and servo system are given. Discussions of the performance of the various subsystems, along with the limitations of the instrument are included. Two balloon flights and an expedition to the South Pole are described, and the data from the South Pole expedition are discussed in detail. The method used to produce upper limits to CBR fluctuations is explained, and the relevance of these limits to current theories of structure formation is discussed.

Dissert. Abstr.

N93-13738 Indiana Univ., Bloomington.
A SEARCH FOR POINT SOURCES OF COSMIC RAY MUONS USING THE MACRO DETECTOR Ph.D. Thesis
John Peter Petrakis 1990 237 p
Avail: Univ. Microfilms Order No. DA9119752

This dissertation describes a search for small scale anisotropies in the cosmic ray muon flux above 1 TeV using the monopole Astrophysics and Cosmic Ray Observatory (MACRO). From February 28 to May 30, 1989, MACRO detector collected data during its maiden run. Using these data, a search of the entire sky visible to MACRO was performed in an effort to find a small scale flux of cosmic ray muons. The results of this search indicates that no small scale anisotropies in the cosmic ray muon flux exist greater than or equal to 5.8 x 10(exp -12) cm(exp -2)s(exp -1) down to 3 x 10(exp -3) sr. Periodic effects in the muon flux are searched for in two cases: Cygnus X-3 and Hercules X-1. These two x-ray eclipsing binary stars have been detected in TeV and PeV gamma-rays by air shower experiments. Observations suggest that other high energy particles, such as cosmic ray primaries, may be produced in x-ray binary stars. Cygnus X-3 in particular may be a source of cosmic ray primary particles. By observing muons presumably produced by atmospheric interactions, it may be possible to determine if systems such as Cygnus X-3 are indeed cosmic ray accelerators. Two experiments claim to have observed time dependent muon excesses pointing back to Cygnus X-3. The findings of this dissertation suggests that no periodic flux of cosmic ray muon from Cygnus X-3 or Hercules X-1 exists to greater than or equal to 3 x 10(exp -12) cm(exp -2)s(exp -2) over the time period of MACRO's maiden run. Dissert. Abstr.

N93-13173*# California Inst. of Tech., Pasadena. Dept. of Physics, Mathematics, and Astronomy.
GAMCIT: A GAMMA RAY BURST DETECTOR
Derek M. Surka, John M. Grunsfeld, and Brett A. Warneke *In* NASA. Goddard Space Flight Center, The 1992 Shuttle Small Payloads Symposium Oct. 1992 p 143-149 (For primary document see N93-13158 03-12)
Avail: CASI HC A02/MF A03

99 GENERAL

N93-12663# Universal Energy Systems, Inc., Dayton, OH.
USAF 1990 RESEARCH INITIATION PROGRAM, VOLUME 2 Annual Report, 1 Jan. - 31 Dec. 1991
Rod Darrah 25 Jun. 1992 432 p
(Contract F49620-88-C-0053)
(AD-A254654; AFOSR-92-0708TR-Vol-2) Avail: CASI HC A19/MF A04

This program is for follow-on research efforts for the participants in the Summer Faculty Research Program. Funding is provided to establish RIP awards to about half the number of participants in the SFRP. Participants in the 1990 SFRP competed for funding under the 1990 RIP. Evaluation of the proposals were made by the contractor. Evaluation criteria consisted of the following: (1) technical excellence of the proposal; (2) continuation of the SFRP effort; and (3) cost sharing by the university. The list of proposals selected for award was forwarded to AFOSR for approval of funding and for research efforts to be completed by 31 Dec. 1991. The following summarizes the events for the evaluation of proposals and award of funding under the RIP. RIP proposals were submitted to the contractor by 1 Nov. 1991. The proposals were limited to $20,000 plus cost sharing by the universities. The universities were encouraged to cost share, since this is an effort to establish a long term effort between the Air Force and the university. Proposals were evaluated on the criteria listed above and the final award approval was given by AFOSR after consultation with the Air Force Laboratories. Subcontracts were negotiated with the Universities. There were a total of 92 RIP awards made under the 1990 program.

GRA

N93-12664# Universal Energy Systems, Inc., Dayton, OH.
USAF 1990 RESEARCH INITIATION PROGRAM, VOLUME 4 Annual Report, 1 Jan. - 31 Dec. 1991
Rod Darrah 25 Jun. 1992 795 p
(Contract F49620-88-C-0053)
(AD-A254655; AFOSR-92-0710TR-Vol-4) Avail: CASI HC A99/MF A06

This program is for follow-on research efforts for the participants in the Summer Faculty Research Program. Funding is provided to establish RIP awards to about half the number of participants in the SFRP. Participants in the 1990 SFRP competed for funding under the 1990 RIP. Evaluation of the proposals were made by the contractor. Evaluation criteria consisted of the following: (1) technical excellence of the proposal; (2) continuation of the SFRP effort; and (3) cost sharing by the university. The list of proposals selected for award was forwarded to AFOSR for approval of funding and for research efforts to be completed by 31 Dec. 1991. The following summarizes the events for the evaluation of proposals and award of funding under the RIP. RIP proposals were submitted to the contractor by 1 Nov. 1991. The proposals were limited to $20,000 plus cost sharing by the universities. The universities were encouraged to cost share, since this is an effort to establish a long term effort between the Air Force and the university. Proposals were evaluated on the criteria listed above, and the final award approval was given by AFOSR after consultation with the Air Force Laboratories. Subcontracts were negotiated with the Universities. There were a total of 92 RIP awards made under the 1990 program.

GRA

N93-12665# Universal Energy Systems, Inc., Dayton, OH.
USAF 1990 RESEARCH INITIATION PROGRAM, VOLUME 1 Annual Report, 1 Jan. - 31 Dec. 1991
Rod Darrah 25 Jun. 1992 811 p
(Contract F49620-88-C-0053)
(AD-A254656; AFOSR-92-0707TR-Vol-1) Avail: CASI HC A99/MF A06

This program is for follow-on research efforts for the participants in the Summer Faculty Research Program. Funding is provided to establish RIP awards to about half the number of participants in the SFRP. Participants in the 1990 SFRP competed for funding under the 1990 RIP. Evaluation of the proposals were made by the contractor. Evaluation criteria consisted of the following: (1) technical excellence of the proposal; (2) continuation of the SFRP effort; and (3) cost sharing by the university. The list of proposals selected for award was forwarded to AFOSR for approval of funding and for research efforts to be completed by 31 Dec. 1991. The following summarizes the events for the evaluation of proposals and award of funding under the RIP. RIP proposals were submitted to the contractor by 1 Nov. 1991. The proposals were limited to $20,000 plus cost sharing by the universities. The universities were encouraged to cost share, since this is an effort to establish a long term effort between the Air Force and the university. Proposals were evaluated on the criteria listed above and the final award approval was given by AFOSR after consultation with the Air Force Laboratories. Subcontracts were negotiated with the Universities. There were a total of 92 RIP awards made under the 1990 program.

GRA

N93-12667# National Science Foundation, Washington, DC. Div. of Science Resources Studies.
SELECTED DATA ON RESEARCH AND DEVELOPMENT IN INDUSTRY: 1990 Report, Jan. 1981 - Jan. 1991
John R. Gawalt Jun. 1992 37 p
(NSF-92-317) Avail: CASI HC A03/MF A01

The Survey of Research and Development in Industry provides national estimates of the total expenditures on R&D performed within the United States by industrial firms, whether U.S.- or foreign-owned. It is a sample survey in which it is intended that all R&D-performing companies, including privately held firms, are included or represented. All companies that are

identified in the sample year as spending more than $1 million annually on R&D in the United States receive a survey form each year. Information from individual companies in the sample is used to develop national estimates on an industry-by-industry basis. The industry R&D survey does not cover trade associations. Although their primary mission is to serve industry, these associations are established as nonprofit organizations, and it is estimated that their R&D expenditures are less than one percent of the industry R&D total. It is an enterprise-based rather than an establishment-based survey. Therefore, all R&D data for each enterprise are reported in the major Standard Industrial Classification (SIC) code of the firm. Data are aggregated in this manner for all tables in this report. Data are based on probability samples selected about every five years. In intervening years, a subset of the last sample, called a 'panel', is used. The latest probability sample was selected and first used for survey year 1987. The Bureau of the Census, Department of Commerce, has conducted the annual Survey of Industrial Research and Development for the National Science Foundation (NSF) since 1957. Census staff conduct the survey under Title 13 of the U.S. Code, which prohibits publication or release of data that may reveal information about individual companies. Therefore, on some tables of this report, the symbol '(D)' is used as a footnote reference to indicate that data are being withheld to avoid possible disclosure of information about operations of individual companies. The data presented in this summary are part of a larger data set containing more comprehensive detailed statistical tables, and are derived from the 1990 Survey of Industrial Research and Development. This report provides data on research and development (R&D) funding for the years 1980-90, and R&D personnel for the period from January 1981 to January 1991. Author

N93-12696# Texas Univ., Austin. Applied Research Lab.
ONR BASIC RESEARCH PROGRAM: SUMMARY AND BIBLIOGRAPHIES, FY 1990 AND 1991 Annual Report, 1 Oct. 1989 - 30 Sep. 1991
Thomas G. Muir 19 May 1992 32 p
(Contract N00014-90-J-1366)
(AD-A253038; ARL-TR-92-9) Avail: CASI HC A03/MF A01

Research conducted under the subject contract is surveyed from a bibliographical perspective based on an inventory of published research. This survey is intended to be useful in managerial evaluation of the funded research program. GRA

N93-12706# United Engineering Trustees, Inc., New York, NY. Engineering Foundation.
AIR FORCE ENGINEERING RESEARCH INITIATION GRANTS (1990-1991) Final Report, 1 Aug. 1989 - 31 Aug. 1991
Charles V. Freiman 16 Jul. 1992 130 p
(Grant AF-AFOSR-0464-89; AF Proj. 2302)
(AD-A255004; AFOSR-92-0764TR) Avail: CASI HC A07/MF A02

This work unit covers the Air Force Research Initiation Grant (AFERIG) Program for the Academic Year 1990-1991. It was announced in the Fall of 1990 for up to 25 AFERIG's carrying a stipend of $20,000. The Engineering Foundation's five Founder Societies received a total of 262 proposals. Fifty-six of these were selected for referral to AFOSR. AFOSR selected 25 with 10 alternates. This report contains abstracts and papers for each of the 25 grants. GRA

N93-12764# Universal Energy Systems, Inc., Dayton, OH.
US AIR FORCE 1989 RESEARCH INITIATION PROGRAM, VOLUME 1 Annual Report, 1 Jan. - 31 Dec. 1990
Rod Darrah 25 Jun. 1992 1113 p
(Contract F49620-88-C-0053)
(AD-A254457; AFOSR-92-0704TR-Vol-1) Avail: CASI HC A99/MF A10

This program is for follow-on efforts for the participants in the Summer Faculty Research Program. Funding is provided to establish RIP awards to about half the number of participants in the SFRP. Participants in the 1989 SFRP competed for funding under the 1989 RIP. Evaluation of the proposals were made by the contractor. Evaluation criteria consisted of the following: (1) technical excellence of the proposal; (2) continuation of the SFRP effort; and (3) cost sharing by the university. The list of proposals selected for award was forwarded to AFOSR for approval of funding and for research efforts to be completed by 31 December 1990. The following summarizes the events for the evaluation of proposals and award of funding under the RIP. RIP proposals were submitted to the contractor by 1 November 1990. The proposals were limited to $20,000 plus cost by the universities. The universities were encouraged to cost share, since this is an effort to establish a long term effort between the Air Force and the university. Proposals were evaluated on the criteria listed above and the final award approval was given by AFOSR after consultation with the Air Force Laboratories. Subcontracts were negotiated with the Universities. There were a total of 122 REP awards made under the 1989 program. GRA

N93-12765# Universal Energy Systems, Inc., Dayton, OH.
US AIR FORCE 1989 RESEARCH INITIATION PROGRAM, VOLUME 4 Annual Report, 1 Jan. - 31 Dec. 1990
Rod Darrah 25 Jun. 1992 861 p
(Contract F49620-88-C-0053)
(AD-A254458; AFOSR-92-0719TR-Vol-4) Avail: CASI HC A99/MF A10

This program is for follow-on research efforts for the participants in the Summer Faculty Research Program. Funding is provided to establish RIP awards to about half the number of participants in the SFRP. Participants in the 1989 SFRP competed for funding under the 1989 RIP. Evaluation of the proposals were made by the contractor. Evaluation criteria consisted of the following: (1) technical excellence of the proposal; (2) continuation of the SFRP effort; and (3) cost sharing by the university. The list of proposals selected for award was forwarded to AFOSR for approval of funding and for research efforts to be completed by 31 December 1990. The following summarizes the events for the evaluation of proposals and award of funding under the RIP. RIP proposals were submitted to the contractor by 1 November 1990. The proposals were limited to $20,000 plus cost sharing by the universities. The universities were encouraged to cost share, since this is an effort to establish a long term effort between the Air Force and the university. Proposals were evaluated on the criteria listed above and the final award approval was given by AFOSR after consultation with the Air Force Laboratories. Subcontracts were negotiated with the Universities. There were a total of 122 RIP awards made under the 1989 program. GRA

N93-12766# Universal Energy Systems, Inc., Dayton, OH.
US AIR FORCE 1989 RESEARCH INITIATION PROGRAM, VOLUME 2 Annual Report, 1 Jan. - 31 Dec. 1990
Rod Darrah 25 Jun. 1992 545 p
(Contract F49620-88-C-0053)
(AD-A254459; AFOSR-92-0705TR-Vol-2) Avail: CASI HC A23/MF A04

This program is for follow-on research efforts for the participants in the Summer Faculty Research Program. Funding is provided to establish RIP awards to about half the number of participants in the SFRP. Participants in the 1989 SFRP competed for funding under the 1989 RIP. Evaluation of the proposals were made by the contractor. Evaluation criteria consisted of the following: (1) technical excellence of the proposal; (2) continuation of the SFRP effort; and (3) cost sharing by the university. The list of proposals selected for award was forwarded to AFOSR for approval of funding and for research efforts to be completed by 31 December 1990. The following summarizes the events for the evaluation of proposals and award of funding under the RIP. RIP proposals were submitted to the contractor by 1 November 1990. The proposals were limited to $20,000 plus cost sharing by the universities. The universities were encouraged to cost share, since this is an effort to establish a long term effort between the Air Force and the university. Proposals were evaluated on the criteria fisted above and the final award approval was given by AFOSR after conclusion with the Air Force Laboratories. Subcontracts were negotiated with the Universities. There were a total of 122 RIP awards made under the 1989 program. GRA

N93-12767# Universal Energy Systems, Inc., Dayton, OH.
US AIR FORCE 1989 RESEARCH INITIATION PROGRAM, VOLUME 3 Annual Report, 1 Jan. - 31 Dec. 1990
Rod Darrah 25 Jun. 1992 1377 p
(Contract F49620-88-C-0053)
(AD-A254460; AFOSR-92-0706TR-Vol-3) Avail: CASI HC A99/MF A10

This program for follow-on research efforts for the participants in the Summer Faculty Research Funding is provided to establish RIP awards to about half the number of participants in the SFRP. Participants in the 1989 SFRP competed for funding under the 1989 RIP. Evaluation of the proposals were made by the contractor. Evaluation criteria consisted of

the following: (1) technical excellence of the proposal; (2) continuation of the SFRP effort; and (3) cost sharing by the university. The list of proposals selected for award was forwarded to AFOSR for approval of funding and for research efforts to be completed by 31 December 1990. The following summarizes the events for the evaluation of proposals and award of funding under the RIP. RIP proposals were submitted to the contractor by 1 November 1990. The proposals were limited to $20,000 plus cost by the universities. The universities were encouraged to cost share, since this is an effort to establish a long term effort between the Air Force and the university. Proposals were evaluated on the criteria listed above and the final award approval was given by AFOSR after consultation with the Air Force Laboratories. Subcontracts were negotiated with the Universities. There were a total of 122 REP awards made under the 1989 program. GRA

N93-12849# Universal Energy Systems, Inc., Dayton, OH.
USAF 1990 RESEARCH INITIATION PROGRAM, VOLUME 3 Annual Report, 1 Jan. 1991 - 31 Dec. 1991
Rod Darrah 25 Jun. 1992 1318 p
(Contract F49620-88C-0053)
(AD-A254755; AFOSR-92-0709TR-Vol-3) Avail: CASI HC A99/MF A10

This program is for follow-on research efforts for the participants in the Summer Faculty Research Program. Funding is provided to establish RIP awards to about half the number of participants in the SFRP. Participants, in the 1990 SFRP competed for funding under the 1990 RIP. Evaluation of the proposals were made by the contractor. Evaluation criteria consisted of: (1) Technical excellence of the proposal; (2) Continuation of the SFRP effort; (3) Cost sharing by the university. The list of proposals selected for award was forwarded to AFOSR for approval of funding and for research efforts to be completed by 31 December 1991. The following summarizes the events for the evaluation of proposals and award of funding under the RIP. RIP proposals were submitted to the contractor by 1 November 1991. The proposals were limited to $20,000 plus cost sharing by the universities. The universities were encouraged to cost share, since this is an effort to establish a long term effort between the Air Force and the university. Proposals were evaluated on the criteria listed above and the final award approval was given by AFOSR after consultation with the Air Force Laboratories. Subcontracts were negotiated with the Universities. There were a total of 92 RIP awards made under the 1990 program. GRA

N93-12859# Air Force Office of Scientific Research, Bolling AFB, Washington, DC.
AIR FORCE OFFICE OF SCIENTIFIC RESEARCH TECHNICAL REPORT SUMMARIES Quarterly Report, Jan. - Mar. 1992
Debra L. Tyrrell 1992 324 p
(AD-A254380; AFOSR-92-0812TR) Avail: CASI HC A14/MF A03

The AFOSR Technical Report Summaries are published quarterly of each calendar year. They consist of a brief summary of each AFOSR technical report received in the Technical Information Division and submitted to the Defense Technical Information Center for that quarter. GRA

N93-13381# National Science Foundation, Washington, DC.
STATE AWARD SUMMARY: FISCAL YEAR 1991
1992 116 p
(NSF-92-3) Avail: CASI HC A06/MF A02

This congressional report is produced to accompany the budget submission to the Congress. The report reflects the number and dollar value of National Science Foundation (NSF) programs and contracts made in Fiscal Year 1991. It is arranged by state and then by university or institution. Four principal program activities are included from appropriations for these activities: (1) Research Activities; (2) Education and Human Resources; (3) Antarctic Program; and (4) Academic Infrastructure. R.L.B.

N93-13474# Advisory Group for Aerospace Research and Development, Neuilly-Sur-Seine (France).
AGARD HIGHLIGHTS 92/2, SEPTEMBER 1992
Sep. 1992 36 p
(AGARD-Highlights-92/2) Copyright Avail: CASI HC A03/MF A01

In this issue of AGARD (Advisory Group for Aerospace Research & Development) HIGHLIGHTS 92/2 several sections of general information are provided. They are as follows: Pictures from Paris, AGARDoday 92, Twenty Years On, AGARD family, Time Off..., President's letter to CASI (Canadian Aeronautics and Space Institute), and This really is the end. Announcements of this year's winners of the von Karman Medal and the Scientific Achievement Award are made. Professor Otto Gerlach won this year's von Karman Medal. Professor K C Yeh won this years's Scientific Achievement Award. Lastly, three articles are presented: Open Skies Ahead, The Role of the IEPG (Independent European Program Group), and EUCLID (European Cooperation for the Long Term in Defense). D.R.D.

N93-13704# National Science Foundation, Washington, DC.
DIRECTORY OF AWARDS, FISCAL YEAR 1991. DIRECTORATE FOR ENGINEERING
1992 292 p
(NSF-92-55) Avail: CASI HC A13/MF A03

The Engineering Directory of Awards provides bibliographic data on the engineering awards granted each fiscal year by the National Science Foundation's (NSF's) Directorate for Engineering (ENG). All awards are listed under their primary division and within division by program or sub-program. Within each sub-program is an alphabetical listing of awards by the Principal Investigator's last name. Split funded awards are listed under primary programs and under those programs which contributed to that award. All data is reconciled with NSF's Office of Information Systems (OIS). The following subject areas are covered: biological and critical systems (BCS), chemical and thermal systems (CTS), design and manufacturing systems (DDM), electrical and communications systems (ECS), engineering centers division (ECD), engineering infrastructure development (EID), and mechanical and structural systems (MSS). Author

N93-13713# National Science Foundation, Washington, DC. Div. of Polar Programs.
ARCTIC SCIENCE, ENGINEERING, AND EDUCATION. DIRECTORY OF AWARDS, FISCAL YEAR 1991 Report, 1 Oct. 1990 - 30 Sep. 1991
1992 67 p
(NSF-92-60) Avail: CASI HC A04/MF A01

As part of the Arctic Research and Policy Act of 1984, a report on Arctic grants awarded by the National Science Foundation (NSF) during FY 1991 are described. Bibliographic data and an abstract are included. Topics covered by the projects which received awards are the following: atmospheric sciences, behavioral and cognitive sciences, biological sciences, earth science, engineering infrastructure development, industrial science and technological innovation, education, mechanical and structural systems, ocean sciences, social and economic science, glaciology, arctic system science, and arctic coordination. L.R.R.

Typical Subject Index Listing

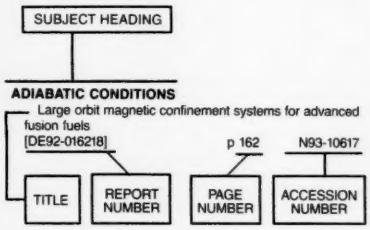

The subject heading is a key to the subject content of the document. Titles, report numbers, and accession numbers of pertinent documents are provided under each subject heading. When the title is insufficiently descriptive of the document content, a title extension has been added, separated from the title by three hyphens. The report number helps to indicate the type of document cited (e.g., NASA report, NASA translation, NASA contractor report). The accession number is the number by which the document abstracts are arranged in this journal and by which the document is sold or requested. The page number helps you locate the the citation in the abstract section. The titles, with title extensions if present, are arranged under each subject heading in ascending accession number order. The subject headings have been selected from the latest revision of the *NASA Thesaurus*.

A

A STARS
A catalog of moderately distant galaxy clusters p 749 N93-13011

ABRASIVES
Qualification of the gritblast assembly and process for the inside diameter of the RSRM forward and aft domes [NASA-CR-184462] p 558 N93-13021

ABSORBENTS
Structure sensitive reactions over Co, Fe and mixed metal clusters in zeolites [DE92-040359] p 542 N93-12998

ABSORPTANCE
Correlation for non-linear infrared calibration curves [AD-A255098] p 596 N93-12653

ABSORPTION CROSS SECTIONS
Absolute absorption cross sections of ozone at 300 K, 228 K and 195 K in the wavelength region 185-240 nm [NASA-CR-191267] p 645 N93-13274

ABSORPTION SPECTRA
MCFC diagnostics: HCl detection [DE92-001292] p 639 N93-13313
Application of improved HNO3 band model parameters to South Pole atmospheric emission measurements p 647 N93-13723
Laser spectroscopy of rare earth ions p 608 N93-13846

ABSORPTION SPECTROSCOPY
MCFC diagnostics: HCl detection [DE92-001292] p 639 N93-13313
Resonance lamp absorption measurement of OH number density and temperature in expansion tube scramjet engine tests p 602 N93-13682
Spectroscopy for remote sounding of the atmosphere p 659 N93-14054

ABSORPTIVITY
Optical model analysis of gravity wave-critical layer interaction p 658 N93-13888

ABSTRACTS
AFOSR Contractors Meeting in Propulsion [AD-A254484] p 525 N93-12575
Abstracts of papers presented at the International Symposium on Time, Frequency, and Dating in Geomorphology [AD-A254927] p 649 N93-12704
Air Force engineering research initiation grants (1990-1991) [AD-A255004] p 774 N93-12706
NATO Advanced Research Workshop: Vortex Flows and Related Numerical Methods. List of participants, book of abstracts, and instructions for submission to the proceedings [AD-A255015] p 575 N93-12708
DATA: How to generate, store, retrieve, communicate, and interpret it: Proceedings [DE92-040405] p 735 N93-13000
Advanced energy projects FY 1992 research summaries [DE92-040442] p 637 N93-13001
Abstract and index collection in the Research Information Center of the National Institute of Standards and Technology [PB92-217587] p 738 N93-13415
Abstracts of phase 1 awards: NSF Small Business Innovation Research Program (SBIR): 1992 [NSF-92-80] p 732 N93-13703
Arctic science, engineering, and education. Directory of awards, fiscal year 1991 [NSF-92-60] p 775 N93-13713

ABUNDANCE
Densities and abundances of hot cometary ions in the coma of P/Halley p 752 N93-13466
Atoms and molecules in supernova 1987A p 699 N93-13851
Supernova remnants, shocks, and the interstellar medium p 757 N93-13963

ACCELERATED LIFE TESTS
AFRRI reports [AD-A254581] p 674 N93-12649
Stress crack testing of polyethylene geomembranes [PB92-217132] p 622 N93-12843

ACCELERATION (PHYSICS)
Effects of stinger axial dynamics and mass compensation methods on experimental modal analysis p 699 N93-13907

ACCESS CONTROL
Memory access in shared virtual memory [DE92-019594] p 681 N93-12823
Reviews of computing technology: Securing network applications, Kerberos, and RSA [DE92-019928] p 690 N93-13620

ACCOUNTING
An interactive office accounting program written in UNIX and C [AD-A255077] p 683 N93-12740
Space Station: Resolving conflict over integration contractor's role. Briefing report to the Chairman, Subcommittee on Investigations and Oversight, Committee on Science, Space, and Technology, House of Representatives [GAO/NSIAD-92-291BR] p 732 N93-13111

ACCRETION DISKS
Encounters with protostellar disks p 754 N93-13727

ACCUMULATORS
Solar energy utilisation and evacuated tubular solar collectors p 641 N93-14078

ACID RAIN
The National Atmospheric Deposition Program/National Trends Network (NADP/NTN) site visitation program [PB92-217298] p 642 N93-12726
A computer simulation of ecosystem processes in forests for application to air pollution, acid precipitation, and global change [DE92-019616] p 643 N93-12927

ACIDITY
Cloud acidity and acidic deposition in the lower troposphere and ozone depletion in the Antarctic stratosphere: Modeling and data analysis regarding the role of atmospheric aerosol p 647 N93-13741

ACOUSTIC EMISSION
Diagnostic of material defects found in pipelines made of 13 HMF steel on the basis of acoustic emission p 623 N93-12989

ACOUSTIC FATIGUE
Large-amplitude plate vibration in an elevated thermal environment [AD-A254411] p 621 N93-12606

ACOUSTIC INSTABILITY
Dynamics of the ion-ion acoustic instability in the thermalization of ion beams [DE92-019396] p 714 N93-12914
Numerical simulation of the acoustic instability in the spatially developing, confined, supersonic mixing layer p 494 N93-13521

ACOUSTIC MEASUREMENT
Adaptive array processing in uncertain inhomogeneous media [AD-A254418] p 560 N93-12608
Review of progress in quantitative NDE [DE92-018814] p 620 N93-13071
Acoustic device and method for measuring gas densities [NASA-CASE-NPO-18155-1-CU] p 700 N93-13421
The trade-off characteristics of acoustic and pressure sensors for the NASP p 601 N93-13678
Developments on high temperature fiber optic microphone p 601 N93-13680

ACOUSTIC PROPAGATION
Acoustic tomographic monitoring of the atmospheric boundary layer p 651 N93-13143
Acoustic radiation from a point excited infinite bilaminar plate p 531 N93-13144

ACOUSTIC PROPERTIES
Experimental examination of growing and newly submerged sea ice including acoustic probing of the skeletal layer [AD-A254526] p 669 N93-12599
Acoustic modes in fluid networks p 586 N93-13398

ACOUSTIC SCATTERING
Visualization of scattering strength of elastic bodies in a fluid [AD-A254535] p 699 N93-12601
Boundary element analysis of acoustical thin-body and nonuniqueness problems using a normal derivative integral equation p 631 N93-13951

ACOUSTIC VELOCITY
Near-normal incidence scattering from rough, finite surfaces: Kirchhoff theory and data comparison for Arctic sea ice [AD-A254525] p 668 N93-12577

ACOUSTICS
Cancellation of air-borne acoustic plane waves obliquely incident upon a planar phased-array of active surface elements p 700 N93-13635

ACOUSTO-OPTICS
Acousto-optic applications for multichannel adaptive optical processor [AD-A255823] p 711 N93-14032
Acousto-optic devices and applications p 712 N93-14100

ACTIVATION ENERGY
Is there a unique effective interaction profile for dislocations? [DE92-018615] p 543 N93-13545
Activation energy and critical current density in Bi-Sr-Ca-Cu-O [DE92-018795] p 723 N93-13547
Transport on fractal networks [AD-A253797] p 725 N93-13881

ACTIVE CONTROL
Active flutter suppression using dipole filters [NASA-TM-107594] p 504 N93-13367
Method and apparatus for minimizing multiple degree of freedom vibration transmission between two regions of a structure [NASA-CASE-LAR-14508-1-CU] p 626 N93-13420
An investigation of dynamic stress reduction of multi-body aircraft using active gust control p 505 N93-13916

ACTIVE GALACTIC NUCLEI
The emission-line properties of quasars
p 753 N93-13487
ACTIVITY CYCLES (BIOLOGY)
Scenarios for optimizing potato productivity in a lunar CELSS
p 680 N93-13997
ACTS
Anomalous TWTA output power spikes and their effect on a digital satellite communications system
[NASA-TM-105875] p 571 N93-13286
ACTUATORS
Development of a 1000 g, 10 ms mechanical shock test capability
[DE92-019193] p 624 N93-13077
Preloaded latching device
[NASA-CASE-MSC-21730-1] p 614 N93-13417
Method and apparatus for minimizing multiple degree of freedom vibration transmission between two regions of a structure
[NASA-CASE-LAR-14508-1-CU] p 626 N93-13420
Fastening apparatus having shape memory alloy actuator
[NASA-CASE-MSC-21935-1] p 614 N93-13423
Design, construction, and control of a two degree-of-freedom electric direct-drive human power amplifier
p 678 N93-13486
Electro-optic architecture for servicing sensors and actuators in advanced aircraft propulsion systems
[NASA-CR-182269] p 711 N93-13762
Model reduction, sensor/actuator selection and control system redesign for large flexible structures
p 523 N93-14040
ADA (PROGRAMMING LANGUAGE)
Compiling knowledge-based systems to Ada, phase 2
[NASA-CR-191273] p 686 N93-13355
ADAPTATION
Specification of adaptive aiding systems
[AD-A254537] p 499 N93-12602
Theory and design of adaptive automation in aviation systems
[AD-A254595] p 499 N93-12613
The multidimensional self-adaptive grid code, SAGE
[NASA-TM-103905] p 683 N93-12719
Bone loss and human adaptation to lunar gravity
p 676 N93-14002
ADAPTIVE CONTROL
Specification of adaptive aiding systems
[AD-A254537] p 499 N93-12602
Adaptive array processing in uncertain inhomogeneous media
[AD-A254418] p 560 N93-12608
Theory and design of adaptive automation in aviation systems
[AD-A254595] p 499 N93-12613
Adaptive automation and human performance. 3: Effects of practice on the benefits and costs of automation shifts
[AD-A254381] p 677 N93-12860
Subsonic flight test evaluation of a propulsion system parameter estimation process for the F100 engine
[NASA-TM-4426] p 502 N93-13155
Application of adaptive trusses to vibration isolation in flexible structures
p 617 N93-13809
ADAPTIVE OPTICS
Novel techniques of wavefront sensing for adaptive optics with array telescopes using an artificial neural network
p 743 N93-13343
ADDITIVES
Laser densification and doping of sol-gel glasses
[AD-A254566] p 604 N93-12644
ADHESION
EURECA
[ESA-F-26] p 522 N93-12964
ADIABATIC CONDITIONS
A synoptic climatology of the elevated mixed layer inversion over the southern Great Plains in spring
p 664 N93-13643
ADSORPTION
Halogen surface chemistry on Si(100)-(2x1)
[AD-A254643] p 536 N93-12618
Kinetics and dynamics of oxidation reactions involving an adsorbed CO species
[DE92-019745] p 537 N93-12995
Acousto-optic devices and applications
p 712 N93-14100
ADVANCED LAUNCH SYSTEM (STS)
Approximate optimal guidance for the Advanced Launch System
p 519 N93-13819
ADVANCED SOLID ROCKET MOTOR (STS)
Large programs may consume increasing share of limited future budgets. Report to Congressional Requesters
[GAO/NSIAD-92-278] p 732 N93-13109
NASA budget: Potential shortfalls in funding NASA's 5-year plan. Testimony before the Subcommittee on Science, Technology, and Space, Committee on Commerce, Science, and Transportation, United States Senate
[GAO/T-NSIAD-92-18] p 740 N93-13280
ADVANCED VERY HIGH RESOLUTION RADIOMETER
Automatic pattern recognition techniques for geometrical correction on satellite data
p 687 N93-13913
ADVECTION
Dense-gas dispersion advection-diffusion model
[DE92-019617] p 642 N93-12884
Transhorizon microwave propagation and its relationship with meteorological conditions
p 666 N93-13791
AEROACOUSTICS
Report on the final panel discussion on computational aeroacoustics
[NASA-CR-189718] p 699 N93-12986
A time domain numerical theory for studying steady-state acoustic disturbance in flow
p 700 N93-13770
AEROBRAKING
Physiologically constrained aerocapture for manned Mars missions
[NASA-TM-103954] p 521 N93-12720
Weight optimization of an aerobrake structural concept for a lunar transfer vehicle
[NASA-TP-3262] p 519 N93-13379
Control algorithms for aerobraking in the Martian atmosphere
p 524 N93-14046
AEROCAPTURE
Physiologically constrained aerocapture for manned Mars missions
[NASA-TM-103954] p 521 N93-12720
AERODYNAMIC BALANCE
Trim analysis by shooting and finite elements and Floquet eigenanalysis by QR and subspace iterations in helicopter dynamics
p 501 N93-13914
AERODYNAMIC CHARACTERISTICS
X-29 linear aerodynamic perturbation model
[AD-A254810] p 500 N93-12752
Determination of the stability and control derivatives of the F/A-18 HARV from flight data using the maximum likelihood method
[NASA-CR-191216] p 503 N93-12903
Test techniques for engine/airframe integration
p 577 N93-13200
Aerodynamic analysis of slipstream/wing/nacelle interference for preliminary design of aircraft configurations
p 497 N93-13205
Mass flow effects on the low speed characteristics of an advanced combat aircraft
p 497 N93-13214
The jet behaviour of an actual high-bypass engine as determined by LDA-measurements in ground tests
p 503 N93-13218
AGARD WG13 aerodynamics of high speed air intakes: Assessment of CFD results
p 581 N93-13220
Survey on techniques used in aerodynamic nozzle/airframe integration
p 502 N93-13224
Effects of forebody strakes and Mach number on overall aerodynamic characteristics of configuration with 55 deg cropped delta wing
[NASA-TP-3253] p 493 N93-13353
High-speed aerodynamics of upper surface blowing aircraft configurations
p 494 N93-13729
A laboratory investigation of raindrop oscillations
p 666 N93-13790
AERODYNAMIC CONFIGURATIONS
New methods for predicting nonlinear lift, center of pressure, and pitching moment on missile configurations
[AD-A255078] p 492 N93-12741
Water tunnel studies of inlet/airframe interference phenomena
p 580 N93-13216
Application of subsonic first-order panel methods for prediction of inlet and nozzle aerodynamic interactions with airframe
p 497 N93-13223
AERODYNAMIC DRAG
Dynamic stall effects on hingeless rotor stability with experimental correlation
p 492 N93-13010
Hypersonic propulsion system force accounting
p 503 N93-13229
High-speed aerodynamics of upper surface blowing aircraft configurations
p 494 N93-13729
AERODYNAMIC FORCES
Transonic aeroelastic analysis of systems with structural nonlinearities
p 629 N93-13769
AERODYNAMIC HEAT TRANSFER
Fluid flow and heat convection studies for actively cooled airframes
[NASA-CR-190956] p 587 N93-13406
AERODYNAMIC HEATING
Physiologically constrained aerocapture for manned Mars missions
[NASA-TM-103954] p 521 N93-12720
Time dependent heat transfer rates in high Reynolds number hypersonic flowfields
p 595 N93-13664
AERODYNAMIC INTERFERENCE
Investigation of interference phenomena of modern wing-mounted high-bypass-ratio engines by the solution of the Euler-equations
p 578 N93-13204
Aerodynamic analysis of slipstream/wing/nacelle interference for preliminary design of aircraft configurations
p 497 N93-13205
Recent developments in low-speed TPS-testing for engine integration drag and installed thrust reversr simulation
p 502 N93-13207
Hypersonic propulsion system force accounting
p 503 N93-13229
AERODYNAMIC LOADS
User's Guide for the NREL Force and Loads Analysis Program
[DE92-010579] p 627 N93-13524
User's Guide for the NREL Teetering Rotor Analysis Program (STRAP)
[DE92-010580] p 627 N93-13525
An investigation of dynamic stress reduction of multi-body aircraft using active gust control
p 505 N93-13916
Hypersonic panel flutter in a rarefied atmosphere
p 505 N93-13928
The unsteady aerodynamics of a delta wing undergoing large-amplitude pitching motions
p 496 N93-13929
AERODYNAMIC NOISE
Report on the final panel discussion on computational aeroacoustics
[NASA-CR-189718] p 699 N93-12986
AERODYNAMIC STABILITY
X-29 linear aerodynamic perturbation model
[AD-A254810] p 500 N93-12752
The Orbiter Stability Experiment on STS-40
p 508 N93-13159
AERODYNAMIC STALLING
Nonlinear stall flutter of wings with bending-torsion coupling
[AD-A254323] p 503 N93-12959
Dynamic stall effects on hingeless rotor stability with experimental correlation
p 492 N93-13010
AERODYNAMICS
JPRS report: Science and technology. Central Eurasia: Space
[JPRS-USP-92-005] p 513 N93-13304
JPRS report: Science and technology. USSR: Space
[JPRS-USP-91-004] p 516 N93-13756
Formulation and validation of high-order mathematical models of helicopter flight dynamics
p 501 N93-13821
An investigation of jet engine test cell aerodynamics by means of scale model test studies with comparisons to full-scale test results
p 507 N93-14060
AEROELASTICITY
Nonlinear stall flutter of wings with bending-torsion coupling
[AD-A254323] p 503 N93-12959
Dynamic stall effects on hingeless rotor stability with experimental correlation
p 492 N93-13010
Active flutter suppression using dipole filters
[NASA-TM-107594] p 504 N93-13367
Transonic aeroelastic analysis of systems with structural nonlinearities
p 629 N93-13769
Hypersonic panel flutter in a rarefied atmosphere
p 505 N93-13928
AEROEMBOLISM
Complement proteins and decompression sickness susceptibility
[AD-A254448] p 674 N93-12905
AEROGELS
Determination of the permeability of carbon aerogels by gas flow measurements
[DE92-019574] p 550 N93-12888
Aerogels, emulsions, and composites: Controlling structure with organic sol-gel chemistry
[DE92-019575] p 550 N93-12931
AERONAUTICAL ENGINEERING
NASA Mission: The Universe
[NASA-NP-141] p 508 N93-12891
Advanced technology for America's future in space. Executive summary
[NASA-TM-107969] p 513 N93-13308
AERONAUTICS
Coordinating Council. Fourth Meeting: NACA Documents Database Project
[NASA-TM-108017] p 734 N93-12671
Coordinating Council. Sixth Meeting: Who Are Our Key Users?
[NASA-TM-108021] p 734 N93-12672
NASA aeronautics: Research and technology program highlights
[NASA-NP-159] p 491 N93-13110
AERONOMY
Aeronomy coexperiments on drag-free satellites with proportional thrusters: GP-B and STEP
p 518 N93-13922

AEROSOLS
Sulfate impact upon low-level cloud albedo over oceans p 661 N93-12833
Measurement of tropospheric temperature and aerosol extinction using high spectral resolution lidar p 653 N93-13614
Effects of stratospheric aerosol surface processes on the LLNL two-dimensional zonally averaged model [DE92-019620] p 646 N93-13646
Cloud acidity and acidic deposition in the lower troposphere and ozone depletion in the Antarctic stratosphere: Modeling and data analysis regarding the role of atmospheric aerosol p 647 N93-13741
Infrared spectroscopy of size resolved fine aerosol p 647 N93-13758
Study of the concentration and deposition of tropospheric aerosols using x ray emission techniques p 667 N93-13894

AEROSPACE ENGINEERING
USAF 1990 research initiation program, volume 2 [AD-A254654] p 773 N93-12663
USAF 1990 research initiation program, volume 4 [AD-A254655] p 773 N93-12664
USAF 1990 research initiation program, volume 1 [AD-A254656] p 773 N93-12665
Air Force engineering research initiation grants (1990-1991) [AD-A255004] p 774 N93-12706
US Air Force 1989 research initiation program, volume 1 [AD-A254457] p 774 N93-12764
US Air Force 1989 research initiation program, volume 4 [AD-A254458] p 774 N93-12765
US Air Force 1989 research initiation program, volume 2 [AD-A254459] p 774 N93-12766
US Air Force 1989 research initiation program, volume 3 [AD-A254460] p 774 N93-12767
NASA Mission: The Universe [NASA-NP-141] p 508 N93-12891
Space Station: Resolving conflict over integration contractor's role. Briefing report to the Chairman, Subcommittee on Investigations and Oversight, Committee on Science, Space, and Technology, House of Representatives [GAO/NSIAD-92-291BR] p 732 N93-13111
JPRS report: Science and technology. Central Eurasia: Space [JPRS-USP-92-006] p 508 N93-13151
JPRS report: Science and technology. Central Eurasia: Space [JPRS-USP-92-004] p 513 N93-13282
JPRS report: Science and technology. Central Eurasia: Space [JPRS-USP-92-005] p 513 N93-13304
Advanced technology for America's future in space. Executive summary [NASA-TM-107969] p 513 N93-13308
Highlights 92/2 p 775 N93-13474
JPRS report: Science and technology. USSR: Space [JPRS-USP-91-004] p 516 N93-13756
Recent developments in the NL-Soar garden path theory [AD-A255889] p 688 N93-13944

AEROSPACE ENVIRONMENTS
Preferred sets of states, predictability, classicality, and the environment-induced decoherence [DE92-017447] p 641 N93-12684
Touchstone for success [ESA-BR-52] p 557 N93-12934
A radio frequency user's guide to the Space Environment Services Center geophysical alert broadcasts [PB92-220631] p 562 N93-12979
A path to in-space welding and to other in-space metal processing technologies using Space Shuttle small payloads p 509 N93-13165
Environmental qualification testing of payload G-534, the Pool Boiling Experiment p 510 N93-13169
G254 undergraduate experiment p 511 N93-13174
The VTRE Program: An overview p 512 N93-13182
The LDCE Particle Impact Experiment as flown on STS-46 --- limited duration space environment candidate materials exposure (LDCE) p 512 N93-13183
Report of the Working Group on Space/Lunar Tradeoffs p 747 N93-13599
Suited for spacewalking: A teacher's guide with activities [NASA-EP-279] p 679 N93-13692
A study of the luminosity produced by an electron beam-emitting rocket in the polar ionosphere: ECHO 7 p 657 N93-13830
Occupational ergonomics in space p 680 N93-14013
Space environmental effects on silvered teflon thermal control surfaces [AD-A255909] p 554 N93-14099

AEROSPACE INDUSTRY
Use of antarctic analogs to support the space exploration initiative [NASA-TM-108000] p 651 N93-13326

AEROSPACE MEDICINE
Publications of the space physiology and countermeasures program, Musculoskeletal Discipline: 1980-1990 [NASA-CR-4468] p 743 N93-12898
Advanced technology for America's future in space. Executive summary [NASA-TM-107969] p 513 N93-13308
Assessment of programs in space biology and medicine [NASA-CR-190930] p 672 N93-13327
A health care system for the Space Station [NASA-TM-108093] p 679 N93-13571
Postmortem alcohol production in fatal aircraft accidents [AD-A255766] p 498 N93-14026

AEROSPACE PLANES
NASA aeronautics: Research and technology program highlights [NASA-NP-159] p 491 N93-13110
Air inlet with variable intake section: Application to air breathing launch vehicles p 582 N93-13231
National Aero-Space Plane: Key issues facing the program. Testimony before the Subcommittee on Technology and Competitiveness, Committee on Science, Space, and Technology, House of Representatives [GAO/T-NSIAD-92-26] p 500 N93-13253
Stratospheric turbulence measurements and models for aerospace plane design [NASA-TM-104262] p 663 N93-13288
An inverse dynamics approach to trajectory optimization for an aerospace plane [NASA-CR-191277] p 500 N93-13305
Performance and control of ascending trajectories to minimize heat load for transatmospheric aero-space planes p 495 N93-13745

AEROSPACE SAFETY
Preparing safety data packages for experimenters using the Get Away Special (GAS) carrier system p 512 N93-13186
Findings of a review of spacecraft fire safety needs [NASA-CR-189181] p 523 N93-13715
Occupational ergonomics in space p 680 N93-14013

AEROSPACE SCIENCES
Coordinating Council. Fifth Meeting: Quality [NASA-TM-108018] p 733 N93-12635
Coordinating Council. Sixth Meeting: Who Are Our Key Users? [NASA-TM-108021] p 734 N93-12672
NASA Mission: The Universe [NASA-NP-141] p 508 N93-12891
Europe qualifies for space [ESA-BR-64] p 508 N93-12892
NSSDC Conference on Mass Storage Systems and Technologies for Space and Earth Science Applications, volume 1 [NASA-CP-3165-VOL-1] p 736 N93-13131
Federal R/D funding by budget function: Fiscal years 1991-1993 [NSF-92-318] p 740 N93-13312
JPRS report: Science and technology. USSR: Space [JPRS-USP-91-004] p 516 N93-13756

AEROSPACE SYSTEMS
Advanced technology for America's future in space. Executive summary [NASA-TM-107969] p 513 N93-13308
Activities of Space Power Insulation Inst. [AD-A255825] p 574 N93-14034

AEROSPACE TECHNOLOGY TRANSFER
Legal and political issues raised by the International Asteroid Mission p 514 N93-13555

AEROSPACE VEHICLES
Applications of the Los Alamos High Energy Transport code [DE92-017408] p 704 N93-13281

AFFINITY
Interpretation of the ion mass spectra in the mass range 25-35 obtained in the inner coma of Halley's comet by the HIS-sensor of the Giotto IMS Experiment p 752 N93-13469

AFTERBODIES
Survey on techniques used in aerodynamic nozzle/airframe integration p 502 N93-13224
CFD calibration for three-dimensional nozzle/afterbody configurations p 582 N93-13226

AGGLOMERATION
Modeling of coalescence, agglomeration, and phase segregation in microgravity processing of bimetallic composite materials [NASA-CR-191247] p 556 N93-12728

AGGREGATES
Physical properties of concrete made with Apollo 16 lunar soil sample p 554 N93-13987

AGING (BIOLOGY)
AFRRI reports [AD-A254581] p 674 N93-12649

AGING (MATERIALS)
Transverse flexural tests as a tool for assessing damage to PMR-15 composites from isothermal aging in air at elevated temperatures [NASA-TM-105848] p 529 N93-12737
Influence of cold work level on the irradiation creep and creep rupture of titanium-modified austenitic stainless steels [DE92-019078] p 541 N93-12820
Oxidative stability of LARC (tm)-TPI films [NASA-TM-107696] p 552 N93-13441
The estimation of electrical cable fire-induced damage limits [DE92-040100] p 572 N93-13519

AGRICULTURE
Academic science and engineering: Graduate enrollment and support, Fall 1990 [NSF-92-323] p 729 N93-12802
Field spectroradiometry and sail model application to irrigated wheat (Triticum aestivum, L) canopies spectral reflectance [INPE-5426-TDI/483] p 634 N93-13258
Federal support to universities, colleges, and nonprofit institutions: Fiscal year 1990. A report to the President and Congress [NSF-92-324] p 741 N93-13543

AH-64 HELICOPTER
Operator workload predictions for the revised AH-64A workload prediction model. Volume 2: Appendixes A through H [AD-A254939] p 676 N93-12545

AIR BREATHING ENGINES
Aerodynamic studies of supersonic air intakes p 497 N93-13222
Air inlet with variable intake section: Application to air breathing launch vehicles p 582 N93-13231
Performance and control of ascending trajectories to minimize heat load for transatmospheric aero-space planes p 495 N93-13745

AIR CONDITIONING
Applications of CFD and visualization techniques p 584 N93-13386

AIR CONDITIONING EQUIPMENT
Reduction of chlorofluorocarbon emissions from refrigeration systems [DE92-019360] p 645 N93-13505

AIR FLOW
Tributary and gap nighttime air flow comparisons [DE92-018875] p 662 N93-13075
ASTOVL model engine simulators for wind tunnel research p 507 N93-13213
Performance of the Bowen ratio systems on a 22 deg slope [NASA-CR-191278] p 644 N93-13254
A preliminary study of the effect of equivalence ratio on a low emissions gas turbine combustor using KIVA-2 [DE92-018616] p 613 N93-13321
Applications of CFD and visualization techniques p 584 N93-13386

AIR INTAKES
A novel-high-performance system for recording and analysing instantaneous total pressure distortion in air intakes p 580 N93-13215
AGARD WG13 aerodynamics of high speed air intakes: Assessment of CFD results p 581 N93-13220
Aerodynamic studies of supersonic air intakes p 497 N93-13222
Air inlet with variable intake section: Application to air breathing launch vehicles p 582 N93-13231

AIR LAND INTERACTIONS
Climate sensitivity study with energy balance models p 666 N93-13817

AIR POLLUTION
Forest declines: Some perspectives on linking processes and patterns [DE92-019946] p 642 N93-12828
The role of human activity and land use change in atmospheric chemistry and air quality [DE92-019622] p 642 N93-12880
Dense-gas dispersion advection-diffusion model [DE92-019617] p 642 N93-12884
New technologies for refrigeration without CFC's [DE92-018886] p 557 N93-12922

A computer simulation of ecosystem processes in forests for application to air pollution, acid precipitation, and global change
[DE92-019616] p 643 N93-12927
Interagency Workgroup on Air Quality Modeling (IWAQM) work plan rationale
[PB92-213248] p 643 N93-12940
Transactions: Tropospheric ozone and the environment. Papers from an international conference
[PB92-217017] p 643 N93-12941
NOAA Atmospheric Sciences Modeling Division support to the US Environmental Protection Agency
[PB92-217835] p 644 N93-12974
The IGAC activity for the development of global emissions inventories: Description and initial results
[DE92-016010] p 644 N93-13270
An experimental and theoretical study of degradation pathways for atmospheric halocarbons
p 646 N93-13624
Documentation for developing the initial source category list
[PB92-218429] p 646 N93-13647
Impact of supersonic and subsonic aircraft on ozone: Including heterogeneous chemical reaction mechanisms
[DE92-019619] p 646 N93-13655
Kinetic and spectroscopic studies of peroxy radical reactions related to tropospheric photo-oxidation chemistry p 654 N93-13726
Infrared spectroscopy of size resolved fine aerosol
p 647 N93-13758
Aspects of atmospheric transport and dispersion within an air basin p 656 N93-13782
The seasonal variations and interrelationships of ozone, peroxyacetyl nitrate and nitrogen dioxide in the troposphere p 647 N93-13893
Radical reactions of atmospheric importance
p 659 N93-14053
Kinetic studies of some free radical reactions involved in cloudwater chemistry p 668 N93-14055

AIR PURIFICATION
Lunar base CELSS: A bioregenerative approach
p 680 N93-13993

AIR QUALITY
The role of human activity and land use change in atmospheric chemistry and air quality
[DE92-019622] p 642 N93-12880
Interagency Workgroup on Air Quality Modeling (IWAQM) work plan rationale
[PB92-213248] p 643 N93-12940
The IGAC activity for the development of global emissions inventories: Description and initial results
[DE92-016010] p 644 N93-13270
Reduction of chlorofluorocarbon emissions from refrigeration systems
[DE92-019360] p 645 N93-13505
Aspects of atmospheric transport and dispersion within an air basin p 656 N93-13782

AIR SEA ICE INTERACTIONS
JARE data reports no. 173 (meteorology 28). Antarctic climate research data. Part 5: PPI radar data at Syowa Station, Antarctica from February to December 1989
p 663 N93-13446

AIR TRAFFIC
A NASPAC-based analysis of the delay and cost effects of the Dallas/Fort Worth metroplex plan
[DOT/FAA/CT-TN92/21] p 507 N93-13447

AIR TRAFFIC CONTROL
Limited production Precision Runway Monitor (PRM) master test plan
[DOT/FAA/CT-TN92/23] p 506 N93-12899
Prototype stop bar system evaluation at John F. Kennedy International Airport
[DOT/FAA/CT-92/24] p 506 N93-12902

AIR TRANSPORTATION
Report to Congress: State Block Grant Program
[AD-A254569] p 507 N93-13882

AIR WATER INTERACTIONS
Sulfate impact upon low-level cloud albedo over oceans p 661 N93-12833
Deep convection and its relation to the large-scale circulation in the tropical Pacific p 654 N93-13725
An observational and numerical investigation of meso-scale coastal processes during GALE IOP 2
p 665 N93-13776
The assimilation of marine surface data into the Navy operational global atmospheric prediction system
[AD-A255559] p 667 N93-13877

AIRBORNE EQUIPMENT
Cancellation of air-borne acoustic plane waves obliquely incident upon a planar phased-array of active surface elements p 700 N93-13635

AIRBORNE/SPACEBORNE COMPUTERS
The Second NASA Formal Methods Workshop 1992
[NASA-CP-10110] p 684 N93-12957
A brief overview of NASA Langley's research program in formal methods p 684 N93-12958

AIRCRAFT ACCIDENT INVESTIGATION
Aircraft accident report: Britt Airways, Inc., d/b/a, Continental Express Flight 2574, in-flight structural breakup, EMB-120RT, N33701, Eagle Lake, Texas, September 11, 1991
[PB92-910405] p 498 N93-13426
Postmortem alcohol production in fatal aircraft accidents
[AD-A255766] p 498 N93-14026

AIRCRAFT ACCIDENTS
The identification and quantitation of triamterene in blood and urine from a fatal aircraft accident
[AD-A254550] p 674 N93-12612
Aircraft accident report: Britt Airways, Inc., d/b/a, Continental Express Flight 2574, in-flight structural breakup, EMB-120RT, N33701, Eagle Lake, Texas, September 11, 1991
[PB92-910405] p 498 N93-13426
Aircraft accident/incident summary report: Controlled flight into terrain, Bruno's Inc., Beechjet, N25BR, Rome, Georgia, December 11, 1991
[PB92-910404] p 498 N93-13470
Postmortem alcohol production in fatal aircraft accidents
[AD-A255766] p 498 N93-14026

AIRCRAFT CONFIGURATIONS
Water tunnel studies of inlet/airframe interference phenomena p 580 N93-13216
Some aspects of intake design, performance and integration with the airframe p 502 N93-13219
High-speed aerodynamics of upper surface blowing aircraft configurations p 494 N93-13729

AIRCRAFT CONSTRUCTION MATERIALS
Compression strength of composite primary structural components
[NASA-CR-190949] p 624 N93-13019

AIRCRAFT CONTROL
Application of concurrent engineering methods to the design of an autonomous aerial robot
[AD-A254968] p 609 N93-12555
Adaptive automation and human performance. 3: Effects of practice on the benefits and costs of automation shifts
[AD-A254381] p 677 N93-12860
Determination of the stability and control derivatives of the F/A-18 HARV from flight data using the maximum likelihood method
[NASA-CR-191216] p 503 N93-12903
The Second NASA Formal Methods Workshop 1992
[NASA-CP-10110] p 684 N93-12957
A stochastic optimal feedforward and feedback control methodology for superagility
[NASA-CR-4471] p 694 N93-13370
Ideal aircraft handling quality models: Longitudinal axis
[NAL-PD-FC-9203] p 504 N93-13566
Multiplexing electro-optic architectures for advanced aircraft integrated flight control systems
[NASA-CR-182268] p 504 N93-13735
Sequential quadratic programming solutions to related aircraft trajectory optimization problems
p 505 N93-13926

AIRCRAFT DESIGN
Aerodynamic Engine/Airframe Integration for High Performance Aircraft and Missiles
[AGARD-CP-498] p 577 N93-13199
Test techniques for engine/airframe integration
p 577 N93-13200
Aerodynamic analysis of slipstream/wing/nacelle interference for preliminary design of aircraft configurations p 497 N93-13205
Euler analysis of turbofan/superfan integration for a transport aircraft p 578 N93-13206
Aerodynamic integration of thrust reversers on the Fokker 100 p 502 N93-13208
Some aspects of intake design, performance and integration with the airframe p 502 N93-13219
AGARD WG13 aerodynamics of high speed air intakes: Assessment of CFD results p 581 N93-13220
Survey on techniques used in aerodynamic nozzle/airframe integration p 502 N93-13224
CFD calibration for three-dimensional nozzle/afterbody configurations p 582 N93-13226
Optimum design of aircraft structures with manufacturing and buckling constraints p 501 N93-13815

AIRCRAFT ENGINES
Overview on test cases for computation of internal flows in turbomachines p 579 N93-13209
Electro-optic architecture for servicing sensors and actuators in advanced aircraft propulsion systems
[NASA-CR-182269] p 711 N93-13762

AIRCRAFT ICING
Icing prevention by ultrasonic nucleation of supercooled water droplets in front of subsonic aircraft
[DOT/FAA/CT-TN92/38] p 497 N93-12816

AIRCRAFT MAINTENANCE
Action composition for the animation of natural language instructions
[AD-A254963] p 682 N93-12554
Aircraft accident report: Britt Airways, Inc., d/b/a, Continental Express Flight 2574, in-flight structural breakup, EMB-120RT, N33701, Eagle Lake, Texas, September 11, 1991
[PB92-910405] p 498 N93-13426

AIRCRAFT MANEUVERS
Application of smoothing techniques for tracking maneuvering targets. Multiple target tracking in clutter: New approaches
[AD-A254609] p 561 N93-12615
Propulsion integration results of the STOL and Maneuver Technology Demonstrator p 502 N93-13228

AIRCRAFT MODELS
Operator workload predictions for the revised AH-64A workload prediction model. Volume 2: Appendixes A through H
[AD-A254939] p 676 N93-12545
Design philosophy for wind tunnel model positioning systems
[AD-A254958] p 506 N93-12552
ASTOVL model engine simulators for wind tunnel research p 507 N93-13213

AIRCRAFT NOISE
Report on the final panel discussion on computational aeroacoustics
[NASA-CR-189718] p 699 N93-12986

AIRCRAFT PERFORMANCE
Subsonic flight test evaluation of a propulsion system parameter estimation process for the F100 engine
[NASA-TM-4426] p 502 N93-13155
A stochastic optimal feedforward and feedback control methodology for superagility
[NASA-CR-4471] p 694 N93-13370
Sequential quadratic programming solutions to related aircraft trajectory optimization problems
p 505 N93-13926

AIRCRAFT PILOTS
Operator workload predictions for the revised AH-64A workload prediction model. Volume 2: Appendixes A through H
[AD-A254939] p 676 N93-12545
Adaptive automation and human performance: Multi-task performance characteristics
[AD-A254596] p 503 N93-12578
Human factors research in aircrew performance and training: 1986-1991
[AD-A254455] p 677 N93-12609

AIRCRAFT PRODUCTION
Optimum design of aircraft structures with manufacturing and buckling constraints p 501 N93-13815

AIRCRAFT RELIABILITY
Structural fatigue aspects of the P-3 Orion
[ARL-STRUC-TM-558] p 500 N93-13256

AIRCRAFT SAFETY
Public-sector aviation issues: Graduate research award papers, 1990 - 1991
[PB92-222629] p 498 N93-13787

AIRCRAFT STABILITY
Mass flow effects on the low speed characteristics of an advanced combat aircraft p 497 N93-13214

AIRCRAFT STRUCTURES
Probabilistic evaluation of fuselage-type composite structures
[NASA-TM-105881] p 622 N93-12735
Structural fatigue aspects of the P-3 Orion
[ARL-STRUC-TM-558] p 500 N93-13256
Hermetic sealing and EMI shielding gasket
[AD-D015359] p 552 N93-13414
Optimum design of aircraft structures with manufacturing and buckling constraints p 501 N93-13815
Hypersonic panel flutter in a rarefied atmosphere
p 505 N93-13928

AIRFOIL PROFILES
Overall effects of separation on thin aerofoils
[ISBN-0-315-67464-4] p 496 N93-13930

AIRFOILS
Fatigue in single crystal nickel superalloys
[AD-A254704] p 541 N93-12746
Airfoil-vortex interaction and the wake of an oscillating airfoil p 495 N93-13803
Solution of compressible Navier-Stokes equations using spectral methods on arbitrary two-dimensional domains
p 593 N93-14041

AIRFRAMES
Water tunnel studies of inlet/airframe interference phenomena p 580 N93-13216
Some aspects of intake design, performance and integration with the airframe p 502 N93-13219
Structural fatigue aspects of the P-3 Orion
[ARL-STRUC-TM-558] p 500 N93-13256

AIRLINE OPERATIONS
Future regional transport aircraft market, constraints, and technology stimuli
[NASA-TM-107669] p 491 N93-13025
A NASPAC-based analysis of the delay and cost effects of the Dallas/Fort Worth metroplex plan
[DOT/FAA/CT-TN92/21] p 507 N93-13447
Public-sector aviation issues: Graduate research award papers, 1990 - 1991
[PB92-222629] p 498 N93-13787

AIRPORT LIGHTS
Prototype stop bar system evaluation at John F. Kennedy International Airport
[DOT/FAA/CT-92/24] p 506 N93-12902

AIRPORT PLANNING
Report to Congress: State Block Grant Program
[AD-A254569] p 507 N93-13882

AIRSPEED
An investigation of the dynamic response of lifting surfaces with concentrated structural nonlinearities p 501 N93-13807

ALBEDO
Sources of cloud nuclei and development of remote sensing techniques for cloud parameters
[AD-A255016] p 660 N93-12558

ALGEBRA
Summary of awards: Applied mathematics. Fiscal year 1991
[NSF-92-38] p 681 N93-13438
A weighted iterative algorithm for neuromagnetic imaging
[DE92-040244] p 675 N93-13522
Systematic chemical equation balancing
[DE92-017234] p 539 N93-13530
An elasticity solution for a transversely isotropic material containing a spherical shell under axisymmetric loading p 628 N93-13728
A theory of reference graphs in relational databases p 739 N93-13912

ALGORITHMS
Analysis of a linearly constrained least squares algorithm for adaptive beamforming
[AD-A255017] p 695 N93-12582
Storm tracking for TDWR: A correlation algorithm design and evaluation
[AD-A254701] p 660 N93-12622
An investigation of new search techniques for the traveling salesman problem p 696 N93-12625
Torque resolver design for tendon-driven manipulators
[DE92-017395] p 609 N93-12698
Implementation details of the coupled QMR algorithm
[NASA-CR-191213] p 684 N93-12801
Equations of motion of slung-load systems, including multilift systems
[NASA-TP-3280] p 503 N93-12815
Spatial resolution enhancement of SSM/I microwave brightness temperatures and its impact on rainfall retrieval algorithms
[AD-A254382] p 661 N93-12861
Dynamic control modification techniques in teleoperation of a flexible manipulator
[NASA-CR-190984] p 610 N93-12904
VPPA weld model evaluation
[NASA-CR-184460] p 611 N93-12919
A correlated k-distribution model of the heating rates for CH4 and N2O in the atmosphere between 0 and 60 km
[NASA-TM-108062] p 643 N93-12926
Fast multiresolution algorithms for matrix-vector multiplication
[NASA-CR-189721] p 696 N93-12942
Fast approximation algorithms for multicommodity flow problems
[AD-A254335] p 685 N93-12961
Convective scale 4-D data assimilation using simulated single Doppler radar observations
[PB92-218726] p 651 N93-12969
Implicitly coupling heat conduction into a zone fire model
[PB92-222769] p 558 N93-12980
Solar prediction analysis
[NASA-CR-184422] p 769 N93-13014
Application of Lanczos vectors to control design of flexible structures, part 2
[NASA-CR-191244] p 685 N93-13030
NOAA Workshop on Climate Scale Operational Precipitation and Water Vapor Products
[NOAA-TR-NESDIS-62] p 662 N93-13066
Cloud curve algorithm test program
[AD-A253918] p 662 N93-13099
Performance of a plasma fluid code on the Intel parallel computers
[DE92-011680] p 716 N93-13297
Experimental testing of four correction algorithms for the forward scattering spectrometer probe
[NASA-TM-105906] p 597 N93-13307
A methodology for the solution of nonlinear two-point boundary value inverse problems in physics and engineering p 697 N93-13363
Simulation of two-dimensional icing, de-icing and anti-icing phenomena p 498 N93-13364
SeaWiFS technical report series. Volume 4, an analysis of GAC sampling algorithms: A case study
[NASA-TM-104566-VOL-4] p 669 N93-13382
A compressible boundary layer algorithm for use with SINDA '85 p 585 N93-13395
MINT: The multiple error LMS algorithm, and the design of inverse filters for multi-channel sound reproduction systems
[ISVR-TR-211] p 700 N93-13439
Design and operation of a bunched-beam, phase-spread measurement
[DE92-040230] p 708 N93-13508
A weighted iterative algorithm for neuromagnetic imaging
[DE92-040244] p 675 N93-13522
Control of a very flexible robot in gravity p 615 N93-13541
Ideal aircraft handling quality models: Longitudinal axis
[NAL-PD-FC-9203] p 504 N93-13566
BETA: Behavioral testability analyzer and its application to high-level test generation and synthesis for testability
[NASA-CR-191282] p 572 N93-13569
Nonholonomic motion of free-flying space robots p 615 N93-13638
Computer modeling of flow and transport interactions for compressible Navier-Stokes equations p 589 N93-13825
High-resolution array with Prony, MUSIC, and ESPRIT algorithms
[AD-A255514] p 566 N93-13868
Non-perturbative studies in quantum electrodynamics p 729 N93-13896
Dynamic modeling and optimal joint torque coordination of advanced robotic systems p 617 N93-13936
Model reduction, sensor/actuator selection and control system redesign for large flexible structures p 523 N93-14040
Recursive algorithms for computational electromagnetics p 567 N93-14043
Theoretical and numerical studies of wave propagation and scattering in inhomogeneous media p 568 N93-14044
Q-Markov cover identification and integrated MCA-OVC controller design for flexible structures p 695 N93-14045
Control algorithms for aerobraking in the Martian atmosphere p 524 N93-14046
Dexterous grasp and manipulation p 618 N93-14075
A collision avoidance algorithm for the mobile robot and the robot manipulator in multi-robot system p 618 N93-14094

ALIGNMENT
Automation of the targeting and reflective alignment concept
[NASA-CR-190964] p 709 N93-12985
Magnetic properties of high-T(sub c) superconductors p 726 N93-13905

ALKALIES
Oxygen electrode reaction in molten carbonate fuel cells
[DE92-040180] p 636 N93-12812

ALKALINE BATTERIES
Proper battery system design for GAS experiments p 511 N93-13176
Battery selection for space experiments p 512 N93-13184

ALLOCATIONS
National Aeronautics and Space Administration Authorization Act, fiscal year 1993
[S-REPT-102-364] p 741 N93-13798
NASA authorization, 1993, volume 2
[GPO-56-943-VOL-2] p 741 N93-13799
NASA's fiscal year 1993 budget
[S-HRG-102-707] p 742 N93-13800

ALLOYS
Experimental studies of cascade phenomena in metals
[DE92-019586] p 540 N93-12573

ALPHA PARTICLES
Observations of plasma dynamics in the coma of P/Halley by the Giotto Ion Mass Spectrometer p 752 N93-13468
Evidence for alpha-particle chain configurations in Mg-24
[DE92-018790] p 705 N93-13546

ALTERNATING CURRENT
Oxygen electrode reaction in molten carbonate fuel cells
[DE92-040180] p 636 N93-12812

ALTERNATIVES
Physical property data on fluorinated propanes and butanes as CFC and HCFC alternatives
[PB92-206507] p 555 N93-12939

ALTITUDE
A surface pressure altitude prediction model
[AD-A255834] p 668 N93-14082

ALUMINIDES
Development of weldable high-strength iron aluminides
[DE92-016018] p 542 N93-13190
Point defects quenched in NiAl and related intermetallic compounds p 724 N93-13628
An investigation of the interatomic bonding characteristics of a Ti - 51 atomic percent Al alloy by x ray diffraction
[AD-A245362] p 544 N93-13945

ALUMINUM
Characterizing laser fusion welded aluminum using synchrotron x ray microtomography
[DE92-018608] p 609 N93-12565
Anodized aluminum on LDEF: A current status of measurements on chromic acid anodized aluminum p 544 N93-12779
Measurements of crystal growth kinetics at extreme deviations from equilibrium
[DE92-019744] p 720 N93-12827
Electron stimulated desorption of the metallic substrate at monolayer coverage: Sensitive detection via 193 nm laser photoionization of neutral aluminum desorbed from CH3O/Al(111)
[DE92-014858] p 723 N93-13349
An evaluation of corrosion protection by two epoxy primers on 2219-T87 and 7075-T73 aluminum
[NASA-TM-108376] p 553 N93-13716

ALUMINUM ALLOYS
Fatigue and fracture of intermetallic alloys
[AD-A254543] p 540 N93-12603
Ordering energies and mechanisms in beta-phase NiAl
[DE92-040031] p 542 N93-13043
Environmental effects on iron aluminides
[DE92-016341] p 542 N93-13237
FNAS modify matric and transparent experiments
[NASA-CR-184442] p 531 N93-13311
A comparison of chromic acid and sulfuric acid anodizing
[NASA-TM-108383] p 543 N93-13378
Fatigue studies in Al-Mg-Si alloys p 543 N93-13690
An investigation of the interatomic bonding characteristics of a Ti - 51 atomic percent Al alloy by x ray diffraction
[AD-A245362] p 544 N93-13945

ALUMINUM ARSENIDES
Synthesis and properties of mismatched heterojunction/substrate interfaces
[AD-A254577] p 719 N93-12648

ALUMINUM BORON COMPOSITES
Thermoviscoplastic analysis of metal matrix composites p 535 N93-13954

ALUMINUM GALLIUM ARSENIDES
Electronic transport properties of semiconductor microstructures p 724 N93-13730
Strained-layer InGaAs-GaAs-AlGaAs quantum well lasers and transverse junction stripe lasers p 607 N93-13773
Diffusion of ion-implanted group 4 n-type dopants in gallium arsenide and gallium/arsenide-based superlattices p 727 N93-14073

ALUMINUM GRAPHITE COMPOSITES
Thermoviscoplastic analysis of metal matrix composites p 535 N93-13954

ALUMINUM OXIDES
Sol-gel synthesis and densification of aluminoborosilicate powders. Part 1: Synthesis
[NASA-TM-103964] p 527 N93-12895
Sol-gel synthesis and densification of aluminoborosilicate powders. Part 2: Densification
[NASA-TM-103969] p 528 N93-12896
Aluminum oxide film thickness and emittance
[DE92-019931] p 550 N93-13035
Microstructural evolution in reaction bonded alumina/mullite ceramics p 552 N93-13328
Experimental characterization of continuous alumina fiber/epoxy p 533 N93-13775
Transport on fractal networks
[AD-A253797] p 725 N93-13881
Mechanical properties of epoxy/alumina trihydrate-filled compositions p 534 N93-13950

ALUMINUM SILICATES
Sol-gel synthesis and densification of aluminoborosilicate powders. Part 1: Synthesis
[NASA-TM-103964] p 527 N93-12895
Sol-gel synthesis and densification of aluminoborosilicate powders. Part 2: Densification
[NASA-TM-103969] p 528 N93-12896

Applications for special-purpose minerals at a lunar base p 760 N93-13975

ALUMINUM-LITHIUM ALLOYS

On bilinearity of Manson-Coffin low-cycle-fatigue relationship
[NASA-TM-105840] p 622 N93-12739

AMAZON REGION (SOUTH AMERICA)

An ion budget for a terra firme rainforest in Central Amazonia
[INPE-5365-PRE/1745] p 632 N93-13005

AMBIENT TEMPERATURE

Electrochemical and chemical characteristics of a new ambient temperature Li(I) polymer electrolyte
[AD-A254918] p 545 N93-12651

Ductile phase toughening of molybdenum disilicide by low pressure plasma spraying
[DE92-007409] p 551 N93-13315

Experimental characterization of continuous alumina fiber/epoxy p 533 N93-13775

The relationship between environmental conditions and UH-60 cockpit temperature
[AD-A255918] p 680 N93-14090

AMBIGUITY

SAR peculiarities, ambiguities and constraints p 563 N93-13051

AMBIPOLAR DIFFUSION

The role of ambipolar diffusion in the formation of interstellar cloud cores and protostars p 755 N93-13828

AMMONIA

Analysis of a space emergency ammonia dump using the FLOW-NET two-phase flow program p 584 N93-13389

Hydrothermal organic synthesis experiments
[NASA-CR-191257] p 672 N93-13457

AMORPHOUS MATERIALS

Electrochemical and chemical characteristics of a new ambient temperature Li(I) polymer electrolyte
[AD-A254918] p 545 N93-12651

AMORPHOUS SILICON

Study of short-range motion of atomic hydrogen in amorphous silicon by neutron reflectometry
[DE92-016392] p 703 N93-13194

AMPLIFICATION

Theory of lasing without population inversion p 605 N93-13497

Appendix: Limits on the use of heterodyning and amplification in optical interferometry p 747 N93-13597

AMPLITUDE DISTRIBUTION ANALYSIS

Multifrequency measurements of radar ground clutter at 42 sites. Volume 2: Appendices A through D
[AD-A246711] p 567 N93-13878

AMPLITUDE MODULATION

Dynamical instabilities in a fluid spin-up and in an open flow system p 590 N93-13899

ANAEROBES

Biological conversion of synthesis gas
[DE92-017673] p 672 N93-13269

Molecular biology of anaerobic aromatic biodegradation
[AD-A255213] p 673 N93-13863

ANALOG CIRCUITS

Torque resolver design for tendon-driven manipulators
[DE92-017395] p 609 N93-12698

Silicon neuron
[AD-A255091] p 674 N93-12756

Talking to InterFIS: Adding speech input to a natural language interface
[AD-A255865] p 688 N93-13942

ANALOG TO DIGITAL CONVERTERS

A novel-high-performance system for recording and analysing instantaneous total pressure distortion in air intakes p 580 N93-13215

ANALYSIS (MATHEMATICS)

Applications of group-invariant analytic solutions to inertial confinement fusion
[DE92-040347] p 715 N93-13047

ANALYZERS

Coupled structural/thermal/electromagnetic analysis/tailoring of graded composite structures
[NASA-CR-189151] p 627 N93-13444

ANELASTICITY

Lateral variations of shear velocity and anelasticity in the upper mantle of the western US from Rayleigh wave observations p 653 N93-13492

ANGLE OF ATTACK

The influence of intake swirl distortion on the steady-state performance of a low bypass, twin-spool engine p 579 N93-13211

Comparative performance tests of a pitot-inlet in several European wind-tunnels at subsonic and supersonic speeds p 497 N93-13221

In-flight flow visualization results from the X-29A aircraft at high angles of attack
[NASA-TM-4430] p 493 N93-13322

Airfoil-vortex interaction and the wake of an oscillating airfoil p 495 N93-13803

The unsteady aerodynamics of a delta wing undergoing large-amplitude pitching motions p 496 N93-13929

ANGLES (GEOMETRY)

Cancellation of air-borne acoustic plane waves obliquely incident upon a planar phased-array of active surface elements p 700 N93-13635

ANGULAR CORRELATION

The stellar angular correlation: Clues to wide binary star properties p 757 N93-14059

ANGULAR DISTRIBUTION

Halogen surface chemistry on Si(100)-(2x1)
[AD-A254643] p 536 N93-12618

Photodissociation processes
[PB92-222702] p 702 N93-13067

The stellar angular correlation: Clues to wide binary star properties p 757 N93-14059

ANGULAR RESOLUTION

Radio and optical interferometric imaging p 744 N93-13580

The CHARA optical array p 744 N93-13581

High resolution imaging at Palomar p 745 N93-13584

HARDI: A high angular resolution deployable interferometer for space p 745 N93-13588

ANGULAR VELOCITY

Transverse wave motion in constrained mechanical systems p 628 N93-13634

Instabilities and patterns in Taylor-Couette flow p 593 N93-13965

ANILINE

Proton transport on modified sulfonated polyaniline electrodes
[AD-A254917] p 570 N93-12650

ANIONS

Ab initio atomic recombination reaction energetics on model heat shield surfaces
[NASA-CR-191210] p 575 N93-12677

Kinetic studies of some free radical reactions involved in cloudwater chemistry p 668 N93-14055

ANISOTROPIC MEDIA

Regional seismograms: Attenuation and scattering
[AD-A254348] p 650 N93-12943

Theoretical and numerical studies of wave propagation and scattering in inhomogeneous media p 568 N93-14044

ANISOTROPIC PLATES

Finite element analysis of anisotropic viscoelastic composite structures and analytical determination of optimum viscoelastic material properties p 530 N93-13007

ANISOTROPY

Experiments, theory, and simulation on the evolution of fabric in granular materials
[AD-A254820] p 545 N93-12729

Oxygen diffusion in high-T(c) superconductors
[DE92-019597] p 720 N93-12807

Anisotropy measurements of the cosmic background radiation at 3 mm wavelength and an angular scale of 30 arcminutes p 772 N93-13689

ANNEALING

Silicide layer growth rates in Mo/Si multilayers
[DE92-019581] p 721 N93-12972

The crystallization and crystalline properties of LARC-TPI
[NASA-CR-191001] p 721 N93-13022

Effect of O2 partial pressure on post annealed Ba2YCu3O(7-delta) thin films
[DE92-014949] p 722 N93-13323

Novel thin-film CuInSe2 fabrication
[DE92-016440] p 723 N93-13526

Diffusion of ion-implanted group 4 n-type dopants in gallium arsenide and gallium/arsenide-based superlattices p 727 N93-14073

ANNIHILATION REACTIONS

Search for doubly Cabibbo suppressed decays of the charged D meson
[DE92-018588] p 703 N93-13092

ANNUAL VARIATIONS

Statistical analysis of stratospheric temperature and ozone profile data for trends and model comparison
[NASA-CR-191248] p 650 N93-12877

Cloud curve algorithm test program
[AD-A253918] p 662 N93-13099

JARE data reports no. 173 (meteorology 28). Antarctic climate research data. Part 5: PPI radar data at Syowa Station, Antarctica from February to December 1989 p 663 N93-13446

A synoptic climatology of the elevated mixed layer inversion over the southern Great Plains in spring p 664 N93-13643

Long-term averages of globally-measured ELF/VLF radio noise
[AD-A255518] p 566 N93-13869

Middle atmosphere water vapour p 667 N93-13892

The seasonal variations and interrelationships of ozone, peroxyacetyl nitrate and nitrogen dioxide in the troposphere p 647 N93-13893

Application of satellite altimetry to study the Gulf of Alaska gyre p 635 N93-13969

ANODES

Anode power deposition in applied-field MPD thrusters
[NASA-CR-190790] p 526 N93-13283

ANODIZING

Anodized aluminum on LDEF: A current status of measurements on chromic acid anodized aluminum p 544 N93-12779

A comparison of chromic acid and sulfuric acid anodizing
[NASA-TM-108383] p 543 N93-13378

ANOMALIES

The relationship between SST anomalies and clouds, water vapor, and their radiative effects p 665 N93-13744

ANTARCTIC REGIONS

US Antarctic program. Personnel manual, 1992
[NSF-92-63] p 731 N93-12637

Nimbus-7 Total Ozone Mapping Spectrometer (TOMS) Antarctic ozone atlas: August through November 1991
[NASA-RP-1283] p 661 N93-12700

JARE data reports no. 176 (Ionosphere 47). Riometer records of 30 MHz cosmic noise at Syowa Station, Antarctica in 1990 p 772 N93-13255

JARE data reports no. 175 (ionosphere 46). Records of radio aurora at Syowa Station, Antarctica in 1990 p 651 N93-13285

JARE data reports no. 179 (meteorology 29). Meteorological data at Asuka Station, Antarctica in 1990 p 663 N93-13287

Use of antarctic analogs to support the space exploration initiative
[NASA-TM-108000] p 651 N93-13326

State award summary: Fiscal Year 1991
[NSF-92-3] p 775 N93-13381

JARE data reports no. 170 (ionosphere 45). HF field strength data measured at Syowa Station, Antarctica from January to December 1988 p 652 N93-13432

JARE data reports no. 173 (meteorology 28). Antarctic climate research data. Part 5: PPI radar data at Syowa Station, Antarctica from February to December 1989 p 663 N93-13446

Application of improved HNO3 band model parameters to South Pole atmospheric emission measurements p 647 N93-13723

Cloud acidity and acidic deposition in the lower troposphere and ozone depletion in the Antarctic stratosphere: Modeling and data analysis regarding the role of atmospheric aerosol p 647 N93-13741

ANTENNA ARRAYS

Adaptive array processing in uncertain inhomogeneous media
[AD-A254418] p 560 N93-12608

Electromagnetic scattering and radiation from microstrip patch antennas and spirals residing in a cavity
[NASA-CR-191284] p 565 N93-13354

Phased array feed design technology for Large Aperture Microwave Radiometer (LAMR) Earth observations
[NASA-CR-189727] p 519 N93-13462

Scattering from a finite collection of transverse dipole and axial slot arrays with edge effects p 568 N93-14048

ANTENNA COMPONENTS

Millimeter-wave quasi-optical and spatial power combining techniques
[AD-A255438] p 574 N93-13865

ANTENNA DESIGN

Feasibility study of a synthesis procedure for array feeds to improve radiation performance of large distorted reflector antennas
[NASA-CR-190948] p 561 N93-12655

ILS mathematical modeling study of the effects of an ASR-9 structure at the Long Island MacArthur Airport, Islip, NY
[DOT/FAA/CT-TN92/25] p 506 N93-12668

The real aperture antenna of SAR, a key element for performance p 564 N93-13053

ANTENNA FEEDS

Feasibility study of a synthesis procedure for array feeds to improve radiation performance of large distorted reflector antennas
[NASA-CR-190948] p 561 N93-12655

ANTENNA RADIATION PATTERNS

Electromagnetic scattering and radiation from microstrip patch antennas and spirals residing in a cavity
[NASA-CR-191284] p 565 N93-13354

Scattering from a finite collection of transverse dipole and axial slot arrays with edge effects p 568 N93-14048

ANTHROPOMETRY
Human perceptual deficits as factors in computer interface test and evaluation
[DE92-019124] p 677 N93-12712
ANTIPROTONS
Theoretical nuclear physics
[DE92-019286] p 706 N93-12822
A program to study antiprotons in the cosmic rays: Arizona collaboration
[NASA-CR-191272] p 772 N93-13306
APERTURES
Phased array feed design technology for Large Aperture Microwave Radiometer (LAMR) Earth observations
[NASA-CR-189727] p 519 N93-13462
Radio and optical interferometric imaging
p 744 N93-13580
The CHARA optical array p 744 N93-13581
High resolution imaging at Palomar
p 745 N93-13584
APPLICATIONS OF MATHEMATICS
Fast approximation algorithms for multicommodity flow problems
[AD-A254335] p 685 N93-12961
Summary of awards: Applied mathematics. Fiscal year 1991
[NSF-92-38] p 681 N93-13438
APPLICATIONS PROGRAMS (COMPUTERS)
Application interface engine language and object reference manual
[DE92-017555] p 683 N93-12686
An interactive office accounting program written in UNIX and C
[AD-A255077] p 683 N93-12740
The VELOPT code for estimating performance of a Fabry-Perot velocimeter
[DE92-015566] p 596 N93-12831
User's guide: Computer-Aided Structural Modeling (CASM), version 3.00
[AD-A255074] p 684 N93-12851
Computer program for calculating and fitting thermodynamic functions
[NASA-RP-1271] p 728 N93-12967
Semiconductor measurement technology: Version 2.0 of the TXYZ thermal analysis program: TXYZ20
[PB92-217603] p 570 N93-12978
Fully energy-dependent HZETRN (a galactic cosmic-ray transport code)
[NASA-TP-3243] p 771 N93-13020
Introduction to IND and recursive partitioning, version 1.0
[NASA-CR-191220] p 685 N93-13063
Visualization techniques to aid in the analysis of multi-spectral astrophysical data sets
[NASA-CR-191260] p 685 N93-13261
Optimal control computer programs
[NASA-TM-108384] p 693 N93-13289
Development status of SINDA/FLUINT and SINAPS
p 585 N93-13393
A compressible boundary layer algorithm for use with SINDA '85 p 585 N93-13395
Analysis of fluid/mechanical systems using EASY5
p 586 N93-13397
Aerospace applications of SINDA/FLUINT at the Johnson Space Center p 586 N93-13401
Two-phase/two-phase heat exchanger simulation analysis p 586 N93-13402
A SINDA '85 nodal heat transfer rate calculation user subroutine p 587 N93-13403
Special MAFIA postprocessors for the analysis of RF structures
[DE92-040248] p 565 N93-13510
User's Guide for the NREL Force and Loads Analysis Program
[DE92-010579] p 627 N93-13524
User's Guide for the NREL Teetering Rotor Analysis Program (STRAP)
[DE92-010580] p 627 N93-13525
Ideal aircraft handling quality models: Longitudinal axis
[NAL-PD-FC-9203] p 504 N93-13566
Scientific predictability of solid rocket performance: Analyses of the processing parameters
p 526 N93-13824
APPROPRIATIONS
Large programs may consume increasing share of limited future budgets. Report to Congressional Requesters
[GAO/NSIAD-92-278] p 732 N93-13109
State award summary: Fiscal Year 1991
[NSF-92-3] p 775 N93-13381
National Aeronautics and Space Administration Authorization Act, fiscal year 1993
[S-REPT-102-364] p 741 N93-13798
NASA authorization, 1993, volume 2
[GPO-56-943-VOL-2] p 741 N93-13799
NASA's fiscal year 1993 budget
[S-HRG-102-707] p 742 N93-13800
APPROXIMATION
Implicit application of polynomial filters in a k-step Arnoldi method
[NASA-CR-191237] p 686 N93-13408
Efficient solution of parabolic equations by Krylov approximation methods
[NASA-CR-191235] p 697 N93-13409
ARC DISCHARGES
Study of plasma environments for the integrated Space Station electromagnetic analysis system
[NASA-CR-191263] p 522 N93-13152
ARC JET ENGINES
AFOSR Contractors Meeting in Propulsion
[AD-A254484] p 525 N93-12575
ARC WELDING
An integrated optical sensor for GMAW feedback control
[DE92-018019] p 610 N93-12793
Automatic programming of arc welding robots
p 616 N93-13720
ARCHITECTURE (COMPUTERS)
A general theory of signal integration for fault-tolerant dynamic distributed sensor networks
[AD-A254961] p 732 N93-12553
A distributed timing system for sychronizing control and data correlation
[DE92-018603] p 690 N93-12564
State space methods in multidimensional digital signal processing
[AD-A254646] p 561 N93-12620
Summary of awards, fiscal year 1990
[NSF-92-70] p 683 N93-12693
Parallel computing systems
[AD-A255076] p 689 N93-12852
Summary of awards. Fiscal year 1991
[NSF-92-36] p 681 N93-13431
Reviews of computing technology: Securing network applications, Kerberos, and RSA
[DE92-019928] p 690 N93-13620
Research summary, January 1989 - June 1990
[NASA-CR-190960] p 687 N93-13694
Monitoring and controlling distributed applications using Lomita (position paper)
[NASA-CR-190971] p 687 N93-13695
Integrated modeling tool for performance engineering of complex computer systems
[NASA-CR-190881] p 687 N93-13880
ARCS
Gravitational lensing by galaxy clusters: The giant arcs in Abell 370 and Cl2244-02 p 755 N93-13848
ARCTIC OCEAN
Near-normal incidence scattering from rough, finite surfaces: Kirchhoff theory and data comparison for Arctic sea ice
[AD-A254525] p 668 N93-12577
ARCTIC REGIONS
Experimental examination of growing and newly submerged sea ice including acoustic probing of the skeletal layer
[AD-A254526] p 669 N93-12599
Interaction and impact of floating bodies
[AD-A254627] p 574 N93-12617
Arctic science, engineering, and education. Directory of awards, fiscal year 1991
[NSF-92-60] p 775 N93-13713
ARIANE LAUNCH VEHICLE
Reaching for the skies: The next generation
[ESA-BR-37-G] p 516 N93-13859
ARM (ANATOMY)
Control of a very flexible robot in gravity
p 615 N93-13541
ARMED FORCES (UNITED STATES)
USAF 1990 research initiation program, volume 2
[AD-A254654] p 773 N93-12663
US Air Force 1989 research initiation program, volume 1
[AD-A254457] p 774 N93-12764
AROMATIC COMPOUNDS
Molecular biology of anaerobic aromatic biodegradation
[AD-A255213] p 673 N93-13863
ARRAYS
United Kingdom Infrared Telescope
p 743 N93-13273
ARSENIC ALLOYS
Measurements of crystal growth kinetics at extreme deviations from equilibrium
[DE92-019744] p 720 N93-12827
ARTEMIA
A decade of discovery: Experiments with the Get Away Special (GAS) canister p 509 N93-13162
ARTIFICIAL INTELLIGENCE
Artificial intelligence and neural networks applied to ion mobility spectrometry
[DE92-017508] p 690 N93-12559
Verification and validation of AI software
[AD-A254601] p 682 N93-12614
Proceedings of Joint RL/AFOSR Workshop on Intelligent Information Systems
[AD-A254795] p 734 N93-12703
Automated eddy current analysis of materials
[NASA-CR-184432] p 619 N93-12875
Digital imaging systems
[DE92-019194] p 736 N93-13078
Machine Perception
[AGARD-LS-185] p 692 N93-13238
Building and using scene representations in image understanding p 692 N93-13241
Machine perception exploiting high-level spatio-temporal models p 693 N93-13244
Robotic exploration of surfaces and its application to legged locomotion p 615 N93-13540
Explanation-based knowledge acquisition of electronics
[AD-A255069] p 573 N93-13650
ARTIFICIAL SATELLITES
Terahertz horn antennas on thin membranes
[AD-A254772] p 562 N93-12867
Infrared emission from the water outgas cloud of an orbiting vehicle induced by collisions with atmospheric gases p 521 N93-13854
Resonance studies of artificial earth satellites
p 523 N93-14037
On the suitability of non-hardened high density SRAMs for space applications
[AD-A255898] p 524 N93-14087
ARTILLERY
Effect of protective clothing ensembles on artillery battery crew performance
[AD-A254327] p 677 N93-12960
ARTILLERY FIRE
Effect of protective clothing ensembles on artillery battery crew performance
[AD-A254327] p 677 N93-12960
ASCENT TRAJECTORIES
Performance and control of ascending trajectories to minimize heat load for transatmospheric aero-space planes p 495 N93-13745
ASIA
Intraseasonal variability of infrared cooling rates during the Asian summer monsoon and their influence on intraseasonal waves p 665 N93-13760
ASPECT RATIO
Calibration of 2D unstructured grid methods on propulsive flowfields p 582 N93-13225
ASSAYING
Methods development for total organic carbon accountability
[NASA-CR-184438] p 672 N93-12949
ASSEMBLING
Qualification of the gritblast assembly and process for the inside diameter of the RSRM forward and aft domes
[NASA-CR-184462] p 558 N93-13021
ASSEMBLY
Automated dry powder dispenser for explosive components
[DE92-019425] p 555 N93-12568
Design, construction and demonstration of modular, reconfigurable robots p 613 N93-13329
ASSURANCE
Verification and validation of TMAP4
[DE92-019684] p 539 N93-13616
ASTEROID MISSIONS
International Asteroid Mission p 513 N93-13548
Introduction to the International Asteroid Mission
p 513 N93-13549
The program plan: An overview of the development and implementation of the International Asteroid Mission
p 514 N93-13553
Business analysis: The commercial mission of the International Asteroid Mission p 514 N93-13554
Legal and political issues raised by the International Asteroid Mission p 514 N93-13555
Engineering and architectural issues associated with the asteroid mission p 514 N93-13556
Human factors dealing with the International Asteroid Mission p 515 N93-13559
Ground operations and logistics in the context of the International Asteroid Mission p 515 N93-13560
Scientific experimentation afforded by the International Asteroid Mission p 515 N93-13561
Research and technology in support of IAM
p 515 N93-13562
ASTEROIDS
Airblast damage from small asteroids
[DE92-017834] p 749 N93-12956
International Asteroid Mission p 513 N93-13548
Introduction to the International Asteroid Mission
p 513 N93-13549
Asteroid search program p 514 N93-13550

Summary of literature on unmanned probes to asteroids and precursor data requirements for IAM
p 514 N93-13551
Conceptual design of a human piloted mining mission
p 514 N93-13552
Mining equipment and operations for mining the 1982HR (Orpheus) asteroid p 515 N93-13557

ASTRODYNAMICS
The mass and dynamics of cD clusters with cooling flows. 1: ROSAT observations of A 496
[NASA-CR-191240] p 743 N93-13352
The planetary nebula system and the dynamics of the galaxy Centaurus A p 754 N93-13645

ASTROMETRY
Orbiting Space Interferometer (OSI): A first generation space interferometer p 745 N93-13587

ASTRONAUTS
Radiation dose to critical body organs for October 1989 proton event
[NASA-TP-3237] p 520 N93-12876

ASTRONOMICAL CATALOGS
A catalog of moderately distant galaxy clusters
p 749 N93-13011
A high-resolution radio survey of the galactic plane
p 744 N93-13480

ASTRONOMICAL MODELS
Anisotropy measurements of the cosmic background radiation at 3 mm wavelength and an angular scale of 30 arcminutes p 772 N93-13689
Quantum inflationary minisuperspace cosmological models p 728 N93-13751

ASTRONOMICAL OBSERVATORIES
A Lunar Optical-Ultraviolet-Infrared Synthesis Array (LOUISA)
[NASA-CP-3066] p 744 N93-13579
Lunar optical telescopes: An historical perspective
p 746 N93-13593
Environmental effects on an optical-UV-IR synthesis array p 747 N93-13595
Report of the Working Group on Space/Lunar Tradeoffs p 747 N93-13599
Report of the Science Working Group: Science with a lunar optical interferometer p 747 N93-13600
Report of the Working Design Group
p 748 N93-13601

ASTRONOMICAL POLARIMETRY
An infrared polarimetric study of sunspots
p 770 N93-13627

ASTRONOMICAL SPECTROSCOPY
Anisotropy measurements of the cosmic background radiation at 3 mm wavelength and an angular scale of 30 arcminutes p 772 N93-13689
Galaxies with spectral energy distributions peaking at 60 micrometers: Morphology and activity explained by interactions p 756 N93-13959

ASTRONOMY
Visualization techniques to aid in the analysis of multi-spectral astrophysical data sets
[NASA-CR-191260] p 685 N93-13261

ASTROPHYSICS
Visualization techniques to aid in the analysis of multi-spectral astrophysical data sets
[NASA-CR-191260] p 685 N93-13261
The role of ambipolar diffusion in the formation of interstellar cloud cores and protostars
p 755 N93-13828

ASYMMETRY
Bayesian estimation of system reliability under asymmetric loss p 620 N93-13906

ASYMPTOTIC METHODS
Eddy current power dissipation at sharp corners
[DE92-016890] p 571 N93-13300
The three-dimensional turbulent boundary layer: Theory and application p 588 N93-13749

ATLANTIC OCEAN
Extended range forecast of Atlantic seasonal hurricane activity for 1993 p 661 N93-12928
The North Atlantic circulation: Combining simplified dynamics with hydrographic data p 670 N93-13483

ATMOSPHERIC BOUNDARY LAYER
Comparison of two stochastic models of scalar diffusion in turbulent flow
[DE92-019381] p 576 N93-12912
Acoustic tomographic monitoring of the atmospheric boundary layer p 651 N93-13143

ATMOSPHERIC CHEMISTRY
Meeting review: Third NCAR Research Aircraft Fleet Workshop
[PB92-222710] p 649 N93-12818
The role of human activity and land use change in atmospheric chemistry and air quality
[DE92-019622] p 642 N93-12880
A computer simulation of ecosystem processes in forests for application to air pollution, acid precipitation, and global change
[DE92-019616] p 643 N93-12927
Steady state analysis of tropospheric chemistry
p 644 N93-13121
The IGAC activity for the development of global emissions inventories: Description and initial results
[DE92-016010] p 644 N93-13270
An investigation of the processes controlling ozone in the upper stratosphere
[DE92-019621] p 645 N93-13615
An experimental and theoretical study of degradation pathways for atmospheric halocarbons
p 646 N93-13624
Effects of stratospheric aerosol surface processes on the LLNL two-dimensional zonally averaged model
[DE92-019620] p 646 N93-13646
Effects of the Mt. Pinatubo eruption on the radiative and chemical processes in the troposphere and stratosphere
[DE92-019618] p 646 N93-13654
Impact of supersonic and subsonic aircraft on ozone: Including heterogeneous chemical reaction mechanisms
[DE92-019619] p 646 N93-13655
Kinetic and spectroscopic studies of peroxy radical reactions related to tropospheric photo-oxidation chemistry p 654 N93-13726
Thermochemistry of atmospheric metal reactions
[AD-A248651] p 543 N93-13733
Cloud acidity and acidic deposition in the lower troposphere and ozone depletion in the Antarctic stratosphere: Modeling and data analysis regarding the role of atmospheric aerosol p 647 N93-13741
Gas-phase reactions of halogen species of atmospheric importance p 658 N93-13889
The seasonal variations and interrelationships of ozone, peroxyacetyl nitrate and nitrogen dioxide in the troposphere p 647 N93-13893
Radical reactions of atmospheric importance
p 659 N93-14053
Kinetic studies of some free radical reactions involved in cloudwater chemistry p 668 N93-14055

ATMOSPHERIC CIRCULATION
A smoke producing rocket motor for atmospheric wind profiling
[DE92-018264] p 555 N93-12563
Meeting review: Third NCAR Research Aircraft Fleet Workshop
[PB92-222710] p 649 N93-12818
Investigations of the dynamics and thermodynamics of the mesosphere lower thermosphere and upper thermosphere at the polar regions with optical ground-based remote sensing
[AD-A254746] p 650 N93-12845
NOAA Atmospheric Sciences Modeling Division support to the US Environmental Protection Agency
[PB92-217835] p 644 N93-12974
Self-consistent modeling of the ionosphere-thermosphere-magnetosphere system
[AD-A253232] p 651 N93-13276
Deep convection and its relation to the large-scale circulation in the tropical Pacific p 654 N93-13725
Radiative constraints on the energy budget of the atmosphere p 655 N93-13731
Nonlinear hydrostatic conditional symmetric instability: Some theoretical and modeling considerations
p 655 N93-13757
Aspects of atmospheric transport and dispersion within an air basin p 656 N93-13782
Tropopause fold investigations: Secondary circulation, water vapor and ozone analyses p 657 N93-13796
The growth of disturbances in barotropic models of the atmosphere p 658 N93-13887
Frontogenesis processes in the troposphere
p 667 N93-13890
Middle atmosphere water vapour p 667 N93-13892

ATMOSPHERIC COMPOSITION
The broad band overlap problem in atmospheric trace gases p 641 N93-12624
Nimbus-7 Total Ozone Mapping Spectrometer (TOMS) Antarctic ozone atlas: August through November 1991
[NASA-RP-1283] p 661 N93-12700
Studies of radiative emission from the simulated shock layer of the Huygens probe p 521 N93-12834
High resolution molecular spectroscopy of atmospheric species
[AD-A254360] p 650 N93-12946
Absolute absorption cross sections of ozone at 300 K, 228 K and 195 K in the wavelength region 185-240 nm
[NASA-CR-191267] p 645 N93-13274
Microwave remote sensing of a precipitating atmosphere p 634 N93-13371
Reports to the Nation on our changing planet: Our ozone shield p 645 N93-13413
A study of ion composition and dynamics at Comet Halley
[NASA-CR-188478] p 751 N93-13465
Radiative transfer in the middle atmosphere
p 652 N93-13482
Application of improved HNO3 band model parameters to South Pole atmospheric emission measurements
p 647 N93-13723
Radiative constraints on the energy budget of the atmosphere p 655 N93-13731
Cloud acidity and acidic deposition in the lower troposphere and ozone depletion in the Antarctic stratosphere: Modeling and data analysis regarding the role of atmospheric aerosol p 647 N93-13741
Infrared spectroscopy of size resolved fine aerosol
p 647 N93-13758
Tropopause fold investigations: Secondary circulation, water vapor and ozone analyses p 657 N93-13796
The seasonal variations and interrelationships of ozone, peroxyacetyl nitrate and nitrogen dioxide in the troposphere p 647 N93-13893
Engineering verification of the biomass production chamber p 680 N93-13996
Spectroscopy for remote sounding of the atmosphere
p 659 N93-14054

ATMOSPHERIC DENSITY
Aeronomy coexperiments on drag-free satellites with proportional thrusters: GP-B and STEP
p 518 N93-13922

ATMOSPHERIC DIFFUSION
Dense-gas dispersion advection-diffusion model
[DE92-019617] p 642 N93-12884
Interagency Workgroup on Air Quality Modeling (IWAQM) work plan rationale
[PB92-213248] p 643 N93-12940

ATMOSPHERIC EFFECTS
Environmental qualification testing of payload G-534, the Pool Boiling Experiment p 510 N93-13169
The lunar environment and its effect on optical astronomy p 746 N93-13594
Environmental effects on an optical-UV-IR synthesis array p 747 N93-13595
An optical VLA on the Moon p 747 N93-13596
Report of the Science Working Group: Science with a lunar optical interferometer p 747 N93-13600

ATMOSPHERIC ELECTRICITY
Characterization of electric discharge in air produced by an environmental ionizator
[INPE-5310-NTC/299] p 651 N93-13310

ATMOSPHERIC ENTRY
Control algorithms for aerobraking in the Martian atmosphere p 524 N93-14046

ATMOSPHERIC GENERAL CIRCULATION MODELS
The broad band overlap problem in atmospheric trace gases p 641 N93-12624
Baroclinic wave packets in models and observations
p 663 N93-13361
Relationships between continental-scale circulation and rainfall event attributes in the southeastern US
p 664 N93-13631
Assimilation of satellite color observations in a coupled ocean GCM-ecosystem model
[NASA-CR-191218] p 670 N93-13714
Meso-beta scale numerical simulation studies of terrain-induced jet streak mass/momentum perturbations
[NASA-CR-191365] p 654 N93-13719
Convective parameterization in mesoscale models
p 659 N93-14062

ATMOSPHERIC HEATING
Dense-gas dispersion advection-diffusion model
[DE92-019617] p 642 N93-12884
A correlated k-distribution model of the heating rates for CH4 and N2O in the atmosphere between 0 and 60 km
[NASA-TM-108062] p 643 N93-12926
Radiative transfer in the middle atmosphere
p 652 N93-13482

ATMOSPHERIC MODELS
The role of latent heat release in explosive cyclogenesis
[AD-A254436] p 660 N93-12596
A correlated k-distribution model of the heating rates for CH4 and N2O in the atmosphere between 0 and 60 km
[NASA-TM-108062] p 643 N93-12926
A computer simulation of ecosystem processes in forests for application to air pollution, acid precipitation, and global change
[DE92-019616] p 643 N93-12927
NOAA Atmospheric Sciences Modeling Division support to the US Environmental Protection Agency
[PB92-217835] p 644 N93-12974
Summary of 1992 Atlantic tropical cyclone activity and verification of author's forecast (a year of no hurricane activity in the tropics but exceptional South Florida destruction from an unusual higher latitude intense hurricane) p 662 N93-13028
How life affects the geochemical cycle of carbon
[NASA-CR-191241] p 644 N93-13031
Cloud curve algorithm test program
[AD-A253918] p 662 N93-13099

Numerical simulation of a squall line: Tests of a new cumulus parameterization scheme p 662 N93-13124
The IGAC activity for the development of global emissions inventories: Description and initial results [DE92-016010] p 644 N93-13270
Self-consistent modeling of the ionosphere-thermosphere-magnetosphere system [AD-A253232] p 651 N93-13276
Stratospheric turbulence measurements and models for aerospace plane design [NASA-TM-104262] p 663 N93-13288
The Jovian ionosphere p 758 N93-13337
SO2 on Venus: A final cross-calibration with Pioneer Venus [NASA-CR-191256] p 758 N93-13344
A parameterized quasi-five-cylinder convective cloud model and its application to remote sensing of rainfall p 663 N93-13489
Effects of stratospheric aerosol surface processes on the LLNL two-dimensional zonally averaged model [DE92-019620] p 646 N93-13646
Effects of the Mt. Pinatubo eruption on the radiative and chemical processes in the troposphere and stratosphere [DE92-019618] p 646 N93-13654
Impact of supersonic and subsonic aircraft on ozone: Including heterogeneous chemical reaction mechanisms [DE92-019619] p 646 N93-13655
Atmospheric, climatic and environmental research [NASA-CR-191367] p 664 N93-13718
Application of improved HNO3 band model parameters to South Pole atmospheric emission measurements p 647 N93-13723
Cloud acidity and acidic deposition in the lower troposphere and ozone depletion in the Antarctic stratosphere: Modeling and data analysis regarding the role of atmospheric aerosol p 647 N93-13741
Nonlinear hydrostatic conditional symmetric instability: Some theoretical and modeling considerations p 655 N93-13757
Numerical study of nonlinear convective-symmetric instability in a rotating baroclinic atmosphere p 666 N93-13786
Model studies of the middle atmosphere of Venus p 759 N93-13831
The growth of disturbances in barotropic models of the atmosphere p 658 N93-13887
Frontogenesis processes in the troposphere p 667 N93-13890
Study of the concentration and deposition of tropospheric aerosols using x ray emission techniques p 667 N93-13894

ATMOSPHERIC MOISTURE
Sources of cloud nuclei and development of remote sensing techniques for cloud parameters [AD-A255016] p 660 N93-12558
The relationship between SST anomalies and clouds, water vapor, and their radiative effects p 665 N93-13744
Tropopause fold investigations: Secondary circulation, water vapor and ozone analyses p 657 N93-13796
Spectroscopy for remote sounding of the atmosphere p 659 N93-14054

ATMOSPHERIC PHYSICS
Studies of radiative emission from the simulated shock layer of the Huygens probe p 521 N93-12834
The kinetic energy budget of tropical plumes and ENSO in NMC and ECMWF analyses p 664 N93-13740

ATMOSPHERIC PRESSURE
SAC contrail formation study [AD-A254410] p 499 N93-12605
An analysis of the tornado-producing Raleigh thunderstorm of November 28, 1988 [AD-A254384] p 661 N93-12862
Atmospheric loading response of the solid earth and oceans p 659 N93-13955
A surface pressure altitude prediction model [AD-A255834] p 668 N93-14082

ATMOSPHERIC RADIATION
Remote sensing data from CLARET: A prototype CART data set [NASA-CR-191294] p 634 N93-13094
A study of the Earth Radiation Budget Experiment: Shortwave measurements and bidirectional reflectance models for the ocean surface p 654 N93-13722
Radiative constraints on the energy budget of the atmosphere p 655 N93-13731
The relationship between SST anomalies and clouds, water vapor, and their radiative effects p 665 N93-13744

ATMOSPHERIC REFRACTION
Angle of arrival fluctuations for millimeter waves propagating in a turbulent atmosphere near the Earth [AD-A254478] p 560 N93-12574

ATMOSPHERIC SOUNDING
CO2 laser modeling [NASA-CR-184455] p 604 N93-12656
Spectroscopy for remote sounding of the atmosphere p 659 N93-14054

ATMOSPHERIC STRATIFICATION
Transhorizon microwave propagation and its relationship with meteorological conditions p 666 N93-13791
Spatial characteristics of coherent turbulent structures and exchange processes in the atmospheric surface layer within and above an orchard canopy p 660 N93-14064

ATMOSPHERIC TEMPERATURE
SAC contrail formation study [AD-A254410] p 499 N93-12605
Point correlations of geopotential height and temperature at 30 mb and between 500 mb and 30 mb [PB92-222694] p 661 N93-12817
Investigations of the dynamics and thermodynamics of the mesosphere lower thermosphere and upper thermosphere at the polar regions with optical ground-based remote sensing [AD-A254746] p 650 N93-12845
Statistical analysis of stratospheric temperature and ozone profile data for trends and model comparison [NASA-CR-191248] p 650 N93-12877
Acoustic tomographic monitoring of the atmospheric boundary layer p 651 N93-13143
Two-phase/two-phase heat exchanger simulation analysis p 586 N93-13402
Measurement of tropospheric temperature and aerosol extinction using high spectral resolution lidar p 653 N93-13614
A synoptic climatology of the elevated mixed layer inversion over the southern Great Plains in spring p 664 N93-13643
Integration of vegetation indices and thermal measurements for ecosystem modeling p 646 N93-13721
An analysis of the Voyager 2 ultraviolet spectrometer occultation data at Uranus and Triton: Inferring heat sources and model atmospheres p 768 N93-14072
The relationship between environmental conditions and UH-60 cockpit temperature [AD-A255918] p 680 N93-14090

ATMOSPHERIC TURBULENCE
Angle of arrival fluctuations for millimeter waves propagating in a turbulent atmosphere near the Earth [AD-A254478] p 560 N93-12574
Stratospheric turbulence measurements and models for aerospace plane design [NASA-TM-104262] p 663 N93-13288
Novel techniques of wavefront sensing for adaptive optics with array telescopes using an artificial neural network p 743 N93-13343
Science objectives for ground- and space-based optical/IR interferometry p 746 N93-13590
Transhorizon microwave propagation and its relationship with meteorological conditions p 666 N93-13791
The growth of disturbances in barotropic models of the atmosphere p 658 N93-13887
Spatial characteristics of coherent turbulent structures and exchange processes in the atmospheric surface layer within and above an orchard canopy p 660 N93-14064

ATMOSPHERIC WINDOWS
Recent astronomical results from the infrared spatial interferometer and their implications for LOUISA p 745 N93-13585

ATMOSPHERICS
G-133: A soft x ray solar telescope p 510 N93-13171

ATOMIC COLLISIONS
Fermi molecular dynamics [DE92-015351] p 703 N93-13187

ATOMIC ENERGY LEVELS
Experiments on resonantly photo-pumped x ray lasers [DE92-019542] p 603 N93-12570
The 2S(+) - 2P separation in KO [NASA-TM-108086] p 702 N93-12900
Theory of lasing without population inversion p 605 N93-13497
Two-photon cooperative cascade superfluorescence [AD-A255690] p 608 N93-14023

ATOMIC EXCITATIONS
Experiments on resonantly photo-pumped x ray lasers [DE92-019542] p 603 N93-12570
Self-consistent one-dimensional modelling of x ray laser plasmas [DE92-019543] p 712 N93-12571
Workshop on Super-Intense Laser-Atom Physics [AD-A254833] p 604 N93-12734
Cross sections and rate coefficients for the electron-impact excitation of He-like ions [ISAS-RN-647] p 703 N93-13095
Atomic relaxation modes in grain boundaries [DE92-016781] p 722 N93-13195
Monte Carlo calculation of ionization and excitation rates in electron aurora [ISAS-RN-645] p 652 N93-13405
Two-photon cooperative cascade superfluorescence [AD-A255690] p 608 N93-14023

ATOMIC RECOMBINATION
Ab initio atomic recombination reaction energetics on model heat shield surfaces [NASA-CR-191210] p 575 N93-12677

ATOMIC STRUCTURE
Electronic structure of microclusters and defect complexes [AD-A254807] p 720 N93-12750
Atomic structure of mixed ferroelectrics [AD-A254369] p 702 N93-12947
Ordering energies and mechanisms in beta-phase NiAl [DE92-040031] p 542 N93-13043
Atomic relaxation modes in grain boundaries [DE92-016781] p 722 N93-13195
An investigation of the interatomic bonding characteristics of a Ti - 51 atomic percent Al alloy by x ray diffraction [AD-A245362] p 544 N93-13945

ATOMS
Theory of lasing without population inversion p 605 N93-13497

ATTENUATION COEFFICIENTS
Lateral variations of shear velocity and anelasticity in the upper mantle of the western US from Rayleigh wave observations p 653 N93-13492

AUDIO EQUIPMENT
Acoustic device and method for measuring gas densities [NASA-CASE-NPO-18155-1-CU] p 700 N93-13421

AUDITORY SENSATION AREAS
Simulation of excitatory/inhibitory interactions in single auditory neurons [AD-A253614] p 675 N93-13252

AURORAL IONIZATION
Monte Carlo calculation of ionization and excitation rates in electron aurora [ISAS-RN-645] p 652 N93-13405

AURORAL ZONES
JARE data reports no. 175 (ionosphere 46). Records of radio aurora at Syowa Station, Antarctica in 1990 p 651 N93-13285
The Jovian ionosphere p 758 N93-13337

AURORAS
Monte Carlo calculation of ionization and excitation rates in electron aurora [ISAS-RN-645] p 652 N93-13405
The Jovian ultraviolet aurora observed with the IUE spacecraft: Brightness and color distribution with longitude p 759 N93-13625

AUSTENITE
Fastening apparatus having shape memory alloy actuator [NASA-CASE-MSC-21935-1] p 614 N93-13423

AUSTENITIC STAINLESS STEELS
Influence of cold work level on the irradiation creep and creep rupture of titanium-modified austenitic stainless steels [DE92-019078] p 541 N93-12820

AUTOIONIZATION
Electron stimulated desorption of the metallic substrate at monolayer coverage: Sensitive detection via 193 nm laser photoionization of neutral aluminum desorbed from CH3O/Al(111) [DE92-014858] p 723 N93-13349

AUTOMATIC CONTROL
Design philosophy for wind tunnel model positioning systems [AD-A254958] p 506 N93-12552
Application of concurrent engineering methods to the design of an autonomous aerial robot [AD-A254968] p 609 N93-12555
Theory and design of adaptive automation in aviation systems [AD-A254595] p 499 N93-12613
Adaptive automation and human performance. 3: Effects of practice on the benefits and costs of automation shifts [AD-A254381] p 677 N93-12860
Robot welding process control [NASA-CR-184428] p 614 N93-13436
Automation and robotics considerations for a lunar base p 619 N93-14006

AUTOMATION
Space robotics: Recent accomplishments and opportunities for future research [NASA-TM-107675] p 694 N93-13442
Mining equipment and operations for mining the 1982HR (Orpheus) asteroid p 515 N93-13557

AUTOMOBILE FUELS
The 1992 natural gas vehicle challenge: EPA emissions and fuel economy testing
[PB92-217926] p 616 N93-13761
AUTONOMOUS NAVIGATION
Application of concurrent engineering methods to the design of an autonomous aerial robot
[AD-A254968] p 609 N93-12555
3-D computer vision for navigation/control of mobile robots p 693 N93-13243
AUTONOMY
On-orbit supervisor for controlling spacecraft
[AD-A254342] p 522 N93-12962
AUTORADIOGRAPHY
Tagging insulin in microgravity p 510 N93-13172
AUXILIARY POWER SOURCES
Proper battery system design for GAS experiments p 511 N93-13176
AVALANCHE DIODES
A payload to evaluate photodiodes for the detection of soft and hard x rays in a space environment using a Get Away Special p 509 N93-13166
An acoustic charge transport imager for high definition television applications
[NASA-CR-191295] p 572 N93-13448
Temperature measurements with micrometer spatial resolution
[AD-A255897] p 603 N93-14086
AVIATION PSYCHOLOGY
Specification of adaptive aiding systems
[AD-A254537] p 499 N93-12602
Theory and design of adaptive automation in aviation systems
[AD-A254595] p 499 N93-12613
AVIONICS
The Second NASA Formal Methods Workshop 1992
[NASA-CP-10110] p 684 N93-12957
A brief overview of NASA Langley's research program in formal methods p 684 N93-12958
AWARDS
Summary of awards, fiscal year 1990
[NSF-92-70] p 683 N93-12693
State award summary: Fiscal Year 1991
[NSF-92-3] p 775 N93-13381
Summary of awards. Fiscal year 1991
[NSF-92-36] p 681 N93-13431
Summary of awards: Applied mathematics. Fiscal year 1991
[NSF-92-38] p 681 N93-13438
Directory of awards, fiscal year 1991. Directorate for engineering
[NSF-92-55] p 775 N93-13704
AXES OF ROTATION
Numerical analysis of nonminimum phase zero for nonuniform link design p 611 N93-12953
AXIAL LOADS
In-phase and out-of-phase axial-torsional fatigue behavior of Haynes 188 at 760 C
[NASA-TM-105765] p 625 N93-13153
Load-transfer and crack bridging in fiber-toughened ceramic composites p 629 N93-13754
AXISYMMETRIC BODIES
Boundary element method for axisymmetric thermoelastic analysis p 624 N93-13097
Fast optimization of static axisymmetric shell structures p 630 N93-13921
AXISYMMETRIC FLOW
Dynamical instabilities in a fluid spin-up and in an open flow system p 590 N93-13899
AZIMUTH
The real aperture antenna of SAR, a key element for performance p 564 N93-13053
Polarization effects and multipolarization SAR p 564 N93-13054
GPS azimuth determination
[AD-A254687] p 499 N93-13348

B

B STARS
B supergiants in open clusters and associations
[NASA-CR-191275] p 748 N93-13659
BACKGROUND RADIATION
The millimeter and submillimeter wavelength diffuse backgrounds: Measurements of the spectrum and anisotropy p 772 N93-13145
Measurements of the cosmic microwave background temperature at 1.47 GHz p 772 N93-13146
Uniformity results of the multilayer mirrors used in the ALEXIS ultrasoft x ray telescopes
[DE92-018611] p 743 N93-13342
Anisotropy measurements of the cosmic background radiation at 3 mm wavelength and an angular scale of 30 arcminutes p 772 N93-13689
BACKSCATTERING
Near-normal incidence scattering from rough, finite surfaces: Kirchhoff theory and data comparison for Arctic sea ice
[AD-A254525] p 668 N93-12577
BACKWARD FACING STEPS
Velocity and temperature measurements in a non-premixed reacting flow behind a backward facing step p 494 N93-13632
BACKWARD WAVES
Experimental studies of high-power plasma-filled backward wave oscillators p 717 N93-13495
BACTERIA
Biological conversion of synthesis gas
[DE92-017673] p 672 N93-13269
BAINITE
Tempering effects for lower bainite, martensite, and mixed microstructures on impact, fracture, and related mechanical properties of ASTM A723 steel
[AD-A254617] p 541 N93-12616
BALANCING
Systematic chemical equation balancing
[DE92-017234] p 539 N93-13530
BALLISTIC RANGES
Investigation of hypersonic shock-induced combustion in a hydrogen-air system
[NASA-CR-191239] p 538 N93-13456
BALLOON-BORNE INSTRUMENTS
Optical design for a balloon-borne magnetograph
[NASA-CR-191003] p 709 N93-13062
BALLOONING MODES
Interaction of energetic ring current protons with magnetospheric hydromagnetic waves p 718 N93-13750
BANDWIDTH
The real aperture antenna of SAR, a key element for performance p 564 N93-13053
Numerical modelling of the suppression of stimulated Brillouin scattering due to finite laser bandwidth
[DE92-018064] p 606 N93-13534
BAROCLINIC WAVES
Baroclinic wave packets in models and observations p 663 N93-13361
BAROCLINITY
Summary of 1992 Atlantic tropical cyclone activity and verification of author's forecast (a year of no hurricane activity in the tropics but exceptional South Florida destruction from an unusual higher latitude intense hurricane) p 662 N93-13028
Baroclinic wave packets in models and observations p 663 N93-13361
Intraseasonal variability of infrared cooling rates during the Asian summer monsoon and their influence on intraseasonal waves p 665 N93-13760
An observational and numerical investigation of meso-scale coastal processes during GALE IOP 2 p 665 N93-13776
Numerical study of nonlinear convective-symmetric instability in a rotating baroclinic atmosphere p 666 N93-13786
BAROTROPIC FLOW
Model studies of the middle atmosphere of Venus p 759 N93-13831
BAROTROPISM
Numerical study of nonlinear convective-symmetric instability in a rotating baroclinic atmosphere p 666 N93-13786
The growth of disturbances in barotropic models of the atmosphere p 658 N93-13887
BARRIER LAYERS
Chemical sensors based on ultrathin film composite membranes
[AD-A254644] p 595 N93-12619
BARYONS
Heavy gauge boson and lambda(b) baryon searches at CDF
[DE92-019551] p 705 N93-13537
BASE FLOW
Spanwise-nonuniform excitation of a plane mixing layer p 577 N93-13120
Computational fluid dynamics of the base flow on a plane body between a subsonic flow on one side and a supersonic flow on the other p 591 N93-13920
BAYES THEOREM
Bayesian analysis of linear and nonlinear population models using the Gibbs sampler
[AD-A254769] p 697 N93-12702
Bayesian estimation of system reliability under asymmetric loss p 620 N93-13906
BEAM CURRENTS
Design and operation of a bunched-beam, phase-spread measurement
[DE92-040230] p 708 N93-13508
Theory of the ion-channel laser p 607 N93-13777
BEAM INJECTION
Test of a new RF separator structure for CEBAF
[CEBAF-PR-92-024] p 708 N93-13284
Longitudinal impedance of capacitive pick-up electrodes: Calculations and comparison with measurements
[DE92-019499] p 571 N93-13358
A fast scanning probe for D3-D
[DE92-040260] p 717 N93-13511
BEAM INTERACTIONS
Longitudinal beam dynamics with rf noise
[DE92-040645] p 707 N93-13108
BEAM PLASMA AMPLIFIERS
A study of the luminosity produced by an electron beam-emitting rocket in the polar ionosphere: ECHO 7 p 657 N93-13830
BEAM SPLITTERS
Test of a new RF separator structure for CEBAF
[CEBAF-PR-92-024] p 708 N93-13284
Shot noise limits to sensitivity of optical interferometry p 745 N93-13586
BEAM WAVEGUIDES
Long pulse electron beam propagation
[DE92-014948] p 706 N93-12830
BEAMFORMING
Analysis of a linearly constrained least squares algorithm for adaptive beamforming
[AD-A255017] p 695 N93-12582
Test and control computer user's guide for a digital beam former test system
[NASA-CR-189208] p 685 N93-13291
BEAMS (RADIATION)
Longitudinal impedance of capacitive pick-up electrodes: Calculations and comparison with measurements
[DE92-019499] p 571 N93-13358
Design and operation of a bunched-beam, phase-spread measurement
[DE92-040230] p 708 N93-13508
Video profile monitor diagnostic system for GTA
[DE92-040231] p 710 N93-13509
BEAMS (SUPPORTS)
Finite elements for free edge delaminations and delaminated anisotropic beams p 535 N93-13967
BEECHCRAFT AIRCRAFT
Aircraft accident/incident summary report: Controlled flight into terrain, Bruno's Inc., Beechjet, N25BR, Rome, Georgia, December 11, 1991
[PB92-910404] p 498 N93-13470
BEHAVIOR
Investigation of effects of 60-Hz electric and magnetic fields on operant and social behavior and on the neuroendocrine system of nonhuman primates, part 2
[DE92-040153] p 673 N93-13503
Investigation of effects of 60-Hz electric and magnetic fields on operant and social behavior and on the neuroendocrine system of nonhuman primates, part 1
[DE92-040152] p 673 N93-13520
BEND TESTS
Transverse flexural tests as a tool for assessing damage to PMR-15 composites from isothermal aging in air at elevated temperatures
[NASA-TM-105848] p 529 N93-12737
Matrix cracking initiation stress in fiber-reinforced ceramic matrix composites p 627 N93-13539
BENDING
Notch dimensions for three-point bend fracture specimens based on compliance analyses
[AD-A254641] p 620 N93-12580
Small-strain and finite-strain finite element analyses of plane-strain tensile elastic-plastic crack growth p 621 N93-12628
Finite element analysis of anisotropic viscoelastic composite structures and analytical determination of optimum viscoelastic material properties p 530 N93-13007
Bifurcation and localization instabilities in plastic bending of cylindrical shells p 630 N93-13923
BENDING VIBRATION
Magnetic field perturbation caused by bending vibrations of a quadrupole
[DE92-040644] p 623 N93-13003
BENZENE
Molecular biology of anaerobic aromatic biodegradation
[AD-A255213] p 673 N93-13863
BERNSTEIN ENERGY PRINCIPLE
Fast ion-driven Bernstein instabilities
[DE92-019393] p 705 N93-12713
BETATRONS
Theory of the ion-channel laser p 607 N93-13777
BIBLIOGRAPHIES
ONR basic research program: Summary and bibliographies, FY 1990 and 1991
[AD-A253038] p 774 N93-12696

Publications of the space physiology and countermeasures program, Musculoskeletal Discipline: 1980-1990
[NASA-CR-4468] p 743 N93-12898
Composites: A catalogue of books and conference proceedings available in the NAL library
[NAL-SP-IC-9201] p 737 N93-13368
Directory of awards, fiscal year 1991. Directorate for engineering
[NSF-92-55] p 775 N93-13704
Arctic science, engineering, and education. Directory of awards, fiscal year 1991
[NSF-92-60] p 775 N93-13713

BICRYSTALS
Atomic relaxation modes in grain boundaries
[DE92-016781] p 722 N93-13195

BIDIRECTIONAL REFLECTANCE
A study of the Earth Radiation Budget Experiment: Shortwave measurements and bidirectional reflectance models for the ocean surface p 654 N93-13722

BIG BANG COSMOLOGY
Cosmological constraints on early-decaying particles p 750 N93-13123

BIMETALS
Modeling of coalescence, agglomeration, and phase segregation in microgravity processing of bimetallic composite materials
[NASA-CR-191247] p 556 N93-12728

BINARY ALLOYS
The nature of scales grown on binary Cr-Nb alloys
[DE92-019283] p 542 N93-13080

BINARY DATA
Data to test and evaluate the performance of neural network architectures for seismic signal discrimination, volume 1
[AD-A254413] p 691 N93-12607

BINARY MIXTURES
Chemical potentials in dilute, multicomponent solutions
[DE92-011041] p 538 N93-13317

BINARY STARS
The stellar angular correlation: Clues to wide binary star properties p 757 N93-14059

BINARY SYSTEMS (MATERIALS)
Fatigue and fracture of intermetallic alloys
[AD-A254543] p 540 N93-12603

BINAURAL HEARING
Simulation of excitatory/inhibitory interactions in single auditory neurons
[AD-A253614] p 675 N93-13252

BINDERS (MATERIALS)
A new route for fibre management in metal matrix composites p 534 N93-13779
Improving the temperature resistance of aluminum-matrix composites by using an acid phosphate binder p 536 N93-14056

BINOCULAR VISION
3-D computer vision for navigation/control of mobile robots p 693 N93-13243

BIOASTRONAUTICS
Occupational ergonomics in space p 680 N93-14013

BIOCHEMISTRY
A physico-chemical study of some areas of fundamental significance to biophysics
[DE92-019917] p 672 N93-13034
A physico-chemical study of some areas of fundamental significance to biophysics
[DE92-019916] p 672 N93-13083
Resonance ionization mass spectrometry in biochemical analysis
[DE92-017407] p 538 N93-13341

BIOCONVERSION
Biological conversion of synthesis gas
[DE92-017673] p 672 N93-13269

BIODEGRADATION
Molecular biology of anaerobic aromatic biodegradation
[AD-A255213] p 673 N93-13863

BIOGEOCHEMISTRY
How life affects the geochemical cycle of carbon
[NASA-CR-191241] p 644 N93-13031

BIOINSTRUMENTATION
Chemical sensors based on ultrathin film composite membranes
[AD-A254644] p 595 N93-12619

BIOLOGICAL EFFECTS
Radiation dose to critical body organs for October 1989 proton event
[NASA-TP-3237] p 520 N93-12876
Establishing laboratory standards for biological flight experiments
[NASA-CR-184402] p 671 N93-12901
A computer simulation of ecosystem processes in forests for application to air pollution, acid precipitation, and global change
[DE92-019616] p 643 N93-12927
Effects of spaceflight on the proliferation of jejunal mucosal cells
[NASA-CR-191303] p 675 N93-13449
Investigation of effects of 60-Hz electric and magnetic fields on operant and social behavior and on the neuroendocrine system of nonhuman primates, part 2
[DE92-040153] p 673 N93-13503
Investigation of effects of 60-Hz electric and magnetic fields on operant and social behavior and on the neuroendocrine system of nonhuman primates, part 1
[DE92-040152] p 673 N93-13520
Human factors dealing with the International Asteroid Mission p 515 N93-13559
A study of the generation of linear energy transfer spectra for space radiations
[NASA-TM-4410] p 772 N93-13572

BIOLOGICAL EVOLUTION
Hydrothermal organic synthesis experiments
[NASA-CR-191257] p 672 N93-13457
Chemical environments of submarine hydrothermal systems
[NASA-CR-191258] p 669 N93-13458

BIOLOGICAL MODELS (MATHEMATICS)
Simulation of excitatory/inhibitory interactions in single auditory neurons
[AD-A253614] p 675 N93-13252

BIOMAGNETISM
A weighted iterative algorithm for neuromagnetic imaging
[DE92-040244] p 675 N93-13522

BIOMASS
Engineering verification of the biomass production chamber p 680 N93-13996

BIOPHYSICS
A physico-chemical study of some areas of fundamental significance to biophysics
[DE92-019917] p 672 N93-13034
A physico-chemical study of some areas of fundamental significance to biophysics
[DE92-019916] p 672 N93-13083

BIOPROCESSING
The First United States Microgravity Laboratory
[NASA-TM-107980] p 557 N93-12951

BIOSPHERE
An ion budget for a terra firme rainforest in Central Amazonia
[INPE-5365-PRE/1745] p 632 N93-13005
Life systems for a lunar base p 680 N93-13992

BIOSYNTHESIS
Nitrogen control of chloroplast development and differentiation
[DE92-017392] p 671 N93-12768
Biological conversion of synthesis gas
[DE92-017673] p 672 N93-13269
Effects of spaceflight on the proliferation of jejunal mucosal cells
[NASA-CR-191303] p 675 N93-13449

BIOTECHNOLOGY
Toward a microgravity research strategy
[NASA-CR-190820] p 556 N93-12799
The First United States Microgravity Laboratory
[NASA-TM-107980] p 557 N93-12951

BIPOLAR TRANSISTORS
Semiconductor measurement technology: INSTANT (IGBT network simulation and transient Analysis tool)
[PB92-213529] p 725 N93-13783

BIRDS
Birds mimicking microbursts on 2 June 1990 in Orlando, Florida
[AD-A255703] p 498 N93-14024

BISMUTH OXIDES
Ion-channeling observation of correlated atomic displacements below Tc in YBa2Cu3O(7-x) and Pb-doped Bi2Sr2CaCu2O(x)
[DE92-018186] p 722 N93-13104
Magnetic behavior of a Bi(sub 2)Sr(sub 2)Ca(sub 1)Cu(sub 2)O(sub x) single crystal by direct magneto-optical observations
[DE92-018612] p 722 N93-13118
Activation energy and critical current density in Bi-Sr-Ca-Cu-O
[DE92-018795] p 723 N93-13547

BLACK BODY RADIATION
Heat transfer in a liquid metal crucible with an integral blackbody cavity
[DE92-019640] p 576 N93-12825

BLACK HOLES (ASTRONOMY)
The dynamics of dense galactic nuclei p 750 N93-13340

BLASTS
Qualification of the gritblast assembly and process for the inside diameter of the RSRM forward and aft domes
[NASA-CR-184462] p 558 N93-13021

BLOCKING
Model for impedance of an ionic conductor sandwiched between blocking electrodes
[DE92-017812] p 569 N93-12561

BLOOD
The identification and quantitation of triamterene in blood and urine from a fatal aircraft accident
[AD-A254550] p 674 N93-12612

BLOOD PLASMA
Complement proteins and decompression sickness susceptibility
[AD-A254448] p 674 N93-12905

BLOWING
A numerical study of hypersonic flow with strong surface blowing p 492 N93-13128

BLUNT BODIES
Computation of steady and unsteady shock-induced combustion over hypervelocity blunt bodies p 536 N93-12836

BODIES OF REVOLUTION
Wall functions for the kappa-epsilon turbulence model in generalized nonorthogonal curvilinear coordinates p 587 N93-13517

BODY CENTERED CUBIC LATTICES
Experimental studies of cascade phenomena in metals
[DE92-019586] p 540 N93-12573

BODY FLUIDS
Methods development for total organic carbon accountability
[NASA-CR-184438] p 672 N93-12949

BODY TEMPERATURE
Effect of protective clothing ensembles on artillery battery crew performance
[AD-A254327] p 677 N93-12960

BOILERS
Boiler efficiency methodology for solar heat applications
[DE92-019805] p 640 N93-13618

BOLOMETERS
The millimeter and submillimeter wavelength diffuse backgrounds: Measurements of the spectrum and anisotropy p 772 N93-13145

BOLTZMANN TRANSPORT EQUATION
A stochastic/deterministic method for transient, three-dimensional neutron transport
[DE92-016690] p 704 N93-13319

BONDING
Bonding in simple phosphate glass
[DE92-019437] p 550 N93-12917
Toughening mechanisms in weak matrix ceramic composites p 553 N93-13780
An investigation of the interatomic bonding characteristics of a Ti - 51 atomic percent Al alloy by x ray diffraction
[AD-A245362] p 544 N93-13945
Fracture of a metal/ceramic couple: Tantalum (titanium)/sapphire p 554 N93-14074

BONE DEMINERALIZATION
Bone loss and human adaptation to lunar gravity p 676 N93-14002

BONE MARROW
AFRRI reports
[AD-A254581] p 674 N93-12649

BONES
Assessment of programs in space biology and medicine
[NASA-CR-190930] p 672 N93-13327

BOOSTERS (EXPLOSIVES)
Booster explosive rings
[AD-D015375] p 556 N93-13471

BORIDES
Alternate electrode materials for the SP100 reactor
[DE92-019570] p 706 N93-12970
Elevated temperature tensile properties of borated 304 stainless steel: Effect of boride dispersion on strength and ductility
[DE92-040096] p 542 N93-13302

BORN-OPPENHEIMER APPROXIMATION
Quantum inflationary minisuperspace cosmological models p 728 N93-13751

BORON ALLOYS
Elevated temperature tensile properties of borated 304 stainless steel: Effect of boride dispersion on strength and ductility
[DE92-040096] p 542 N93-13302

BOROSILICATE GLASS
Sol-gel synthesis and densification of aluminoborosilicate powders. Part 1: Synthesis
[NASA-TM-103964] p 527 N93-12895

Sol-gel synthesis and densification of aluminoborosilicate powders. Part 2: Densification
[NASA-TM-103969] p 528 N93-12896
Glass corrosion in natural environments
[NASA-CR-191234] p 551 N93-13150

BOSONS
Heavy gauge boson and lambda(b) baryon searches at CDF
[DE92-019551] p 705 N93-13537

BOUNDARY CONDITIONS
Analysis of a structure-equipment system subjected to impact loading
[AD-A255097] p 622 N93-12652
Adaptation of multidimensional group particle tracking and particle wall-boundary condition model to the FDNS code
[SECA-TR-92-06] p 575 N93-12689
Convective scale 4-D data assimilation using simulated single Doppler radar observations
[PB92-218726] p 651 N93-12969
Fluid flow and heat convection studies for actively cooled airframes
[NASA-CR-190956] p 587 N93-13406
A Fourier series method for polygonal domains: Large element computation for plates p 627 N93-13484
A time domain numerical theory for studying steady-state acoustic disturbance in flow p 700 N93-13770
Scientific predictability of solid rocket performance: Analyses of the processing parameters p 526 N93-13824
Some problems of quantum cosmology and dark matter physics p 755 N93-13829
Electromagnetic scattering simulations using equivalent boundary condition models p 569 N93-14052

BOUNDARY ELEMENT METHOD
Experimental validation of finite element and boundary element methods for predicting structural vibration and radiated noise p 621 N93-12631
The application of the finite element method and the boundary element method to fatigue and fracture, volumes 1 and 2 p 624 N93-13016
Boundary element method for axisymmetric thermoelastic analysis p 624 N93-13097
Finite element versus boundary element analysis of two-dimensional coupled thermoelasticity p 625 N93-13142
Boundary element methods for two-dimensional, coupled, thermoviscous flow p 584 N93-13383
Solution of viscous flow problems by using the boundary element method p 588 N93-13609
Three-dimensional boundary element analysis of residual stresses in a cross-ply fiber composite model p 629 N93-13811
Boundary element analysis of acoustical thin-body and nonuniqueness problems using a normal derivative integral equation p 631 N93-13951

BOUNDARY INTEGRAL METHOD
Electromagnetic scattering and radiation from microstrip patch antennas and spirals residing in a cavity
[NASA-CR-191284] p 565 N93-13354

BOUNDARY LAYER COMBUSTION
A PDF closure model for compressible turbulent chemically reacting flows
[NASA-CR-191209] p 587 N93-13453

BOUNDARY LAYER CONTROL
A numerical study of hypersonic flow with strong surface blowing p 492 N93-13128
A fundamental study of suction for Laminar Flow Control (LFC)
[NASA-CR-191276] p 583 N93-13277

BOUNDARY LAYER FLOW
The three-dimensional turbulent boundary layer: Theory and application p 588 N93-13749
An experimental investigation of the three-dimensional boundary layer on a rotating disk p 589 N93-13806
Application of complex variables in electromagnetofluid dynamic, magnetofluid dynamic and fluid dynamic flows: Viscoelastic boundary-layer theory
[ISBN-0-315-65141-5] p 594 N93-14067

BOUNDARY LAYER SEPARATION
Time dependent heat transfer rates in high Reynolds number hypersonic flowfields p 595 N93-13664

BOUNDARY LAYERS
Report on the final panel discussion on computational aeroacoustics
[NASA-CR-189718] p 699 N93-12986
AGARD WG13 aerodynamics of high speed air intakes: Assessment of CFD results p 581 N93-13220
Fluidlike studies of the sheath and presheath regions of a plasma p 718 N93-13792
An experimental/computational study of heat transfer in sharp fin induced shock wave/turbulent boundary layer interactions at low hypersonic Mach numbers p 590 N93-13826

BOUNDARY VALUE PROBLEMS
A methodology for the solution of nonlinear two-point boundary value inverse problems in physics and engineering p 697 N93-13363
A Fourier series method for polygonal domains: Large element computation for plates p 627 N93-13484

BOUSSINESQ APPROXIMATION
Convective scale 4-D data assimilation using simulated single Doppler radar observations
[PB92-218726] p 651 N93-12969

BRAGG CELLS
Massively parallel optical-to-electronic data transfer
[AD-A254831] p 688 N93-12733

BRAIN
A core facility for the study of neurotoxins of biological origin
[AD-A254359] p 674 N93-12945
The neurochemical and neuropharmacological basis of motion sickness
[NASA-CR-190957] p 675 N93-13061
A weighted iterative algorithm for neuromagnetic imaging
[DE92-040244] p 675 N93-13522

BRANCHING (MATHEMATICS)
Instabilities and patterns in Taylor-Couette flow p 593 N93-13965

BRAZIL
Brazilian remote sensing community: Historical, geographical and economic aspects
[INPE-5421-PRE/1763] p 634 N93-13412

BRAZILIAN SPACE PROGRAM
Brazilian remote sensing community: Historical, geographical and economic aspects
[INPE-5421-PRE/1763] p 634 N93-13412

BREADBOARD MODELS
Engineering verification of the biomass production chamber p 680 N93-13996

BREATHING APPARATUS
Physiological effects of positive pressure ventilation
[AD-A254809] p 674 N93-12751

BRIGHTNESS DISTRIBUTION
Evolution of galaxies in compact groups p 750 N93-13148
X ray scattering by cosmic dust grains p 750 N93-13294
The Jovian ultraviolet aurora observed with the IUE spacecraft: Brightness and color distribution with longitude p 759 N93-13625

BRIGHTNESS TEMPERATURE
Spatial resolution enhancement of SSM/I microwave brightness temperatures and its impact on rainfall retrieval algorithms
[AD-A254382] p 661 N93-12861
Deciduous forest scene complexity in high-resolution multispectral scanner imagery
[AD-A255511] p 635 N93-13867

BRILLOUIN EFFECT
Stimulated Brillouin processes in crystals and glasses
[DE92-019549] p 721 N93-12887
Numerical modelling of the suppression of stimulated Brillouin scattering due to finite laser bandwidth
[DE92-018064] p 606 N93-13534

BRITTLE MATERIALS
Fracture toughness of short fiber/brittle matrix composites p 528 N93-12630
Numerical calibration of the stable poisson loaded specimen
[NASA-TM-105609] p 622 N93-12738
Bifurcations in elastic-damaging materials
[DE92-018818] p 624 N93-13072

BROADBAND
Observations of correlated broadband electrostatic noise and electron cyclotron emissions in the plasma sheet
[AD-A255002] p 712 N93-12705
Applications of satellite technology to broadband ISDN networks
[NASA-CR-189199] p 562 N93-12950

BROADCASTING
An application of exponential neural networks to event-train recognition
[AD-A254948] p 690 N93-12548
A radio frequency user's guide to the Space Environment Services Center geophysical alert broadcasts
[PB92-220631] p 562 N93-12979
SeaWiFS technical report series. Volume 4, an analysis of GAC sampling algorithms: A case study
[NASA-TM-104566-VOL-4] p 669 N93-13382

BROMIDES
Determination of the weight average molecular weight of SRM 1480
[PB92-222934] p 553 N93-13785

BROWN DWARF STARS
A systematic search for low-mass companions orbiting nearby stars and the calibration of the end of the stellar main sequence p 749 N93-14070

BUBBLES
Diffusion-absorption heat pump
[PB92-217538] p 576 N93-12975
A decade of discovery: Experiments with the Get Away Special (GAS) canister p 509 N93-13162
Two-phase flow modeling with discrete particles
[DE92-017850] p 583 N93-13356
H I shells and supershells: Observations and theory p 751 N93-13360
Overall effects of separation on thin aerofoils
[ISBN-0-315-67464-4] p 496 N93-13930

BUCKLING
Scale effects in buckling, postbuckling and crippling of graphite-epoxy Z-section stiffeners p 621 N93-12632
Optimum design of aircraft structures with manufacturing and buckling constraints p 501 N93-13815

BUCKMINSTERFULLERENE
C60 transformations at high pressures
[DE92-019546] p 701 N93-12806

BUDGETING
NASA budget: Potential shortfalls in funding NASA's 5-year plan. Testimony before the Subcommittee on Science, Technology, and Space, Committee on Commerce, Science, and Transportation, United States Senate
[GAO/T-NSIAD-92-18] p 740 N93-13280
Academic science and engineering: R/D expenditures, fiscal year 1990
[NSF-92-321] p 741 N93-13544
Lunar interferometric astronomy: Some basic questions p 746 N93-13592
Selected data on Federal funds for research and development: Fiscal years 1990, 1991, and 1992
[NSF-92-319] p 741 N93-13657
Research and development in industry: 1989. Funds, 1989. Scientists and engineers, January 1990
[NSF-92-307] p 741 N93-13658

BUFFER STORAGE
Magnetic bearings for a high-performance optical disk buffer, volume 2
[NASA-CR-190874] p 615 N93-13608
Magnetic bearings for a high-performance optical disk buffer, volume 1
[NASA-CR-190873] p 616 N93-13706

BUNCHING
Damping the (pi)-mode instability in the SLC damping rings with a passive cavity
[DE92-018153] p 707 N93-13090

BUOYANCY
Boundary element methods for two-dimensional, coupled, thermoviscous flow p 584 N93-13383

BURAN SPACE SHUTTLE
JPRS report: Science and technology. Central Eurasia: Space
[JPRS-USP-92-005] p 513 N93-13304

BURNING RATE
Semi-quantitative model for the burning rate of solid materials
[PB92-213362] p 539 N93-13641

BURNTHROUGH (FAILURE)
The estimation of electrical cable fire-induced damage limits
[DE92-040100] p 572 N93-13519

BUS CONDUCTORS
Fiber optic data bus radiation effects study
[AD-A255821] p 711 N93-14031

BUTANES
Physical property data on fluorinated propanes and butanes as CFC and HCFC alternatives
[PB92-206507] p 555 N93-12939

BY-PRODUCTS
Synergism of He-3 acquisition with lunar base evolution p 540 N93-13986

BYPASS RATIO
Investigation of the flowfield around an isolated bypass engine with fan and core jet p 582 N93-13227

C

C (PROGRAMMING LANGUAGE)
An interactive office accounting program written in UNIX and C
[AD-A255077] p 683 N93-12740
Introduction to IND and recursive partitioning, version 1.0
[NASA-CR-191220] p 685 N93-13063
Compiling knowledge-based systems to Ada, phase 2
[NASA-CR-191273] p 686 N93-13355
Circuit design tool. User's manual, revision 2
[NASA-CR-191361] p 687 N93-13734

C BAND
Review of spaceborne and airborne SAR systems p 565 N93-13060

Polarimetric signatures of a canopy of dielectric cylinders based on first and second order vector radiative transfer theory p 569 N93-13088

CABIN ATMOSPHERES

Conceptual design of a lunar base thermal control system p 680 N93-14003

The relationship between environmental conditions and UH-60 cockpit temperature

[AD-A255918] p 680 N93-14090

CABLES (ROPES)

Test plan and report for Space Shuttle launch environment testing of Bergen cable technology safety cable

[NASA-CR-4473] p 559 N93-13434

CADMIUM SULFIDES

Two to six compound thin films by MOCVD for tandem solar cells p 640 N93-13932

CADMIUM TELLURIDES

Development of a computer model for polycrystalline thin-film CuInSe2 and CdTe solar cells

[DE92-016444] p 639 N93-13529

Thin films and solar cells of cadmium telluride and cadmium zinc telluride p 639 N93-13611

Two to six compound thin films by MOCVD for tandem solar cells p 640 N93-13932

CALCIUM FLUORIDES

Group 2 cubic fluorides dielectrics for 3-D integration and GaAs-based optoelectronic structures

[AD-A254937] p 719 N93-12544

Lunar mining of oxygen using fluorine

[LPI-748] p 761 N93-13980

CALCIUM OXIDES

Magnetic behavior of a Bi(sub 2)Sr(sub 2)Ca(sub 1)Cu(sub 2)O(sub x) single crystal by direct magneto-optical observations

[DE92-018612] p 722 N93-13118

Activation energy and critical current density in Bi-Sr-Ca-Cu-O

[DE92-018795] p 723 N93-13547

CALCULUS

A theory of reference graphs in relational databases p 739 N93-13912

CALIBRATING

Correlation for non-linear infrared calibration curves

[AD-A255098] p 596 N93-12653

Numerical calibration of the stable poisson loaded specimen

[NASA-TM-105609] p 622 N93-12738

Journal of Research of the National Institute of Standards and Technology, May-June 1992, volume 97, number 3

[PB92-217637] p 698 N93-12805

Radiometric calibration of SAR systems p 564 N93-13055

Calibration of 2D unstructured grid methods on propulsive flowfields p 582 N93-13225

CFD calibration for three-dimensional nozzle/afterbody configurations p 582 N93-13226

SO2 on Venus: A final cross-calibration with Pioneer Venus

[NASA-CR-191256] p 758 N93-13344

Interpretation of the ion mass spectra in the mass range 25-35 obtained in the inner coma of Halley's comet by the HIS-sensor of the Giotto IMS Experiment p 752 N93-13469

Electronic triple point cell

[AD-D015374] p 597 N93-13501

High heat flux measurements and experimental calibrations/characterizations p 598 N93-13663

Heat flux microsensor measurements and calibrations p 599 N93-13665

Determination of the weight average molecular weight of SRM 1480

[PB92-222934] p 553 N93-13785

Test and calibration of the along track scanning radiometer, a satellite-borne infrared radiometer designed to measure sea surface temperature p 671 N93-13842

A systematic search for low-mass companions orbiting nearby stars and the calibration of the end of the stellar main sequence p 749 N93-14070

CALIFORNIA

GPS measurements at Vandenberg AFB

[AD-A254978] p 499 N93-12557

Seismic studies of crustal structure and tectonic evolution across the central California margin and the Colorado Plateau margin p 657 N93-13794

CALORIMETERS

High heat flux measurements and experimental calibrations/characterizations p 598 N93-13663

CAMERAS

Soft X Ray Telescope (SXT) focus error analysis

[NASA-CR-184443] p 742 N93-12657

Digital imaging systems

[DE92-019194] p 736 N93-13078

Manned observations technology development, FY 1992 report

[NASA-CR-185704] p 597 N93-13373

CANCELLATION

Cancellation of air-borne acoustic plane waves obliquely incident upon a planar phased-array of active surface elements p 700 N93-13635

CANOPIES (VEGETATION)

Polarimetric signatures of a canopy of dielectric cylinders based on first and second order vector radiative transfer theory p 569 N93-13088

Deciduous forest scene complexity in high-resolution multispectral scanner imagery

[AD-A255511] p 635 N93-13867

CANTILEVER BEAMS

Results of ASTM round robin testing for mode 1 interlaminar fracture toughness of composite materials

[NASA-TM-104222] p 532 N93-13428

Vibration damping response of composite materials p 533 N93-13748

Finite elements for free edge delaminations and delaminated anisotropic beams p 535 N93-13967

CAPACITANCE

Preamplifier with adjustable input resistance

[AD-D015377] p 572 N93-13473

Capacitive skin characterization

[NASA-CR-191261] p 598 N93-13567

CAPACITORS

Model for impedance of an ionic conductor sandwiched between blocking electrodes

[DE92-017812] p 569 N93-12561

GaAs gate dynamic memory technology

[AD-A254801] p 720 N93-12748

Capacitive skin characterization

[NASA-CR-191261] p 598 N93-13567

Numerical analysis of permittivity with loss in isotropic binary composites

[AD-A255203] p 534 N93-13940

CAPILLARY FLOW

The Capillary Pumped Loop Flight Experiment (CAPL): A pathfinder for EOS p 512 N93-13181

CARBON

Determination of the permeability of carbon aerogels by gas flow measurements

[DE92-019574] p 550 N93-12888

Aerogels, emulsions, and composites: Controlling structure with organic sol-gel chemistry

[DE92-019575] p 550 N93-12931

Methods development for total organic carbon accountability

[NASA-CR-184438] p 672 N93-12949

Preparation and properties of low density replica carbon foams

[DE92-019573] p 552 N93-13538

Simulation studies for surfaces and materials strength

[NASA-CR-191289] p 724 N93-13570

Friction, wear and Raman spectroscopic characteristics of carbon lubricated surfaces p 618 N93-13949

CARBON DIOXIDE

Kinetics and dynamics of oxidation reactions involving an adsorbed CO species

[DE92-019745] p 537 N93-12995

The MAGSORB process for bulk separation of carbon dioxide

[DE92-001296] p 538 N93-13314

CARBON DIOXIDE CONCENTRATION

How life affects the geochemical cycle of carbon

[NASA-CR-191241] p 644 N93-13031

Climate sensitivity study with energy balance models p 666 N93-13817

CARBON DIOXIDE LASERS

Bistatic clutter RCS simulation using scale model rough surfaces

[AD-A254932] p 560 N93-12581

CO2 laser modeling

[NASA-CR-184455] p 604 N93-12656

CO2 laser preionisation

[NASA-CR-184424] p 607 N93-13797

Phase conjugation using CO2 lasers p 607 N93-13812

A study of small solid-state switched TEA CO2 lasers p 607 N93-13814

Results of the laser sensor technology transition investigation

[AD-A255845] p 608 N93-14085

CARBON FIBER REINFORCED PLASTICS

Physical interpretation and development of ultrasonic nondestructive evaluation techniques applied to the quantitative characterization of textile composite materials

[NASA-CR-190962] p 620 N93-13435

Investigations of the mechanical behavior of graphite/PEEK (APC-2) composites p 534 N93-13908

CARBON FIBERS

Properties of five toughened matrix composite materials

[NASA-TP-3254] p 528 N93-12590

Results of ASTM round robin testing for mode 1 interlaminar fracture toughness of composite materials

[NASA-TM-104222] p 532 N93-13428

CARBON MONOXIDE

Molecular clouds in the distant outer galaxy p 758 N93-14095

CARBON STEELS

Wastage-resistant FBC evaporator tubing through microalloying

[DE92-001256] p 541 N93-12790

CARBON 12

Evidence for alpha-particle chain configurations in Mg-24

[DE92-018790] p 705 N93-13546

CARBONACEOUS CHONDRITES

Asteroid search program p 514 N93-13550

CARBONATES

Effect of plasticizers on the properties of new ambient temperature solid polymer electrolytes

[AD-A254817] p 545 N93-12754

Oxygen electrode reaction in molten carbonate fuel cells

[DE92-040180] p 636 N93-12812

Understanding of carbonate fuel cell resistance issues for performance improvement

[DE92-019976] p 638 N93-13039

Microwave and infrared dielectric relaxation of alkylcarbonates, chloroform and their mixtures at 25 C

[AD-A253606] p 537 N93-13096

Effects of coal-derived trace species on performance of molten carbonate fuel cells

[DE93-000203] p 639 N93-13427

An update of ERC's carbonate fuel cell development program

[DE92-019971] p 640 N93-13621

CARBONYL COMPOUNDS

Microwave and infrared dielectric relaxation of alkylcarbonates, chloroform and their mixtures at 25 C

[AD-A253606] p 537 N93-13096

CARDIOVASCULAR SYSTEM

Assessment of programs in space biology and medicine

[NASA-CR-190930] p 672 N93-13327

CARIBBEAN REGION

Extended range forecast of Atlantic seasonal hurricane activity for 1993 p 661 N93-12928

CARNOT CYCLE

Reversible thermodynamic cycle for AMTEC power conversion

[DE92-016814] p 571 N93-13197

CARRIER DENSITY (SOLID STATE)

Effect of hydrogen reduction and doping on the characteristics of high-temperature superconductors p 725 N93-13844

CASCADE FLOW

Overview on test cases for computation of internal flows in turbomachines p 579 N93-13209

Numerical calculation of turbomachinery cascade flows p 589 N93-13767

Cascade processes and fully developed turbulence p 591 N93-13901

CAST ALLOYS

Magnetic hardening studies and novel techniques for preparation of high performance magnets

[AD-A254761] p 698 N93-12865

CATALOGS (PUBLICATIONS)

A catalog of moderately distant galaxy clusters p 749 N93-13011

Composites: A catalogue of books and conference proceedings available in the NAL library

[NAL-SP-IC-9201] p 737 N93-13368

CATALYSIS

Structure sensitive reactions over Co, Fe and mixed metal clusters in zeolites

[DE92-040359] p 542 N93-12998

Studies of the kinetics and mechanisms of perfluoroether reactions on iron and oxidized iron surfaces

[NASA-CR-191363] p 539 N93-13763

CATALYSTS

Oligomer and mixed-metal compounds potential multielectron transfer catalysts

[DE92-011347] p 543 N93-13346

A novel process for methanol synthesis

[DE92-019719] p 539 N93-13617

Applications for special-purpose minerals at a lunar base p 760 N93-13975

CATIONS

Alternative materials for solid oxide fuel cells: Factors affecting air-sintering of chromite interconnections

[DE92-019356] p 638 N93-13082

CAUCHY PROBLEM
Hyperbolic conservation laws with umbilic points, 1
[AD-A254431] p 696 N93-12594
CAVITIES
Navier-Stokes simulations of unsteady transonic flow phenomena
[NASA-TM-103962] p 491 N93-12721
Heat transfer in a liquid metal crucible with an integral blackbody cavity
[DE92-019640] p 576 N93-12825
Damping the (pi)-mode instability in the SLC damping rings with a passive cavity
[DE92-018153] p 707 N93-13090
CO2 laser preionisation
[NASA-CR-184424] p 607 N93-13797
CAVITY FLOW
Navier-Stokes simulations of unsteady transonic flow phenomena
[NASA-TM-103962] p 491 N93-12721
Application of a solution adaptive grid to flow over an embedded cavity p 492 N93-13141
Computer modeling of flow and transport interactions for compressible Navier-Stokes equations p 589 N93-13825
CAVITY RESONATORS
Damping the (pi)-mode instability in the SLC damping rings with a passive cavity
[DE92-018153] p 707 N93-13090
Nonlinear stability of combustion-driven acoustic oscillations in resonance tubes
[DE92-012153] p 699 N93-13262
Precision liquid-level measurement in deep tanks using a swept-RF resonant cavity
[DE92-017236] p 597 N93-13267
Special MAFIA postprocessors for the analysis of RF structures
[DE92-040248] p 565 N93-13510
Analysis and experimental results for an extraction cavity for the split-cavity oscillator
[DE92-040262] p 566 N93-13512
CELLS (BIOLOGY)
Establishing laboratory standards for biological flight experiments
[NASA-CR-184402] p 671 N93-12901
Tagging insulin in microgravity p 510 N93-13172
Assessment of programs in space biology and medicine
[NASA-CR-190930] p 672 N93-13327
Effects of spaceflight on the proliferation of jejunal mucosal cells
[NASA-CR-191303] p 675 N93-13449
CEMENTS
Polypropylene fibers in portland cement concrete pavements
[DOT/FAA/RD-92/9] p 551 N93-13259
Physical properties of concrete made with Apollo 16 lunar soil sample p 554 N93-13987
CENSUS
Report on phase 2 of 1990 OSSA data census
[NASA-TM-107992] p 735 N93-12991
Selected data on Science and Engineering Doctorate Awards: 1991
[NSF-92-309] p 731 N93-13698
CENTAURUS CONSTELLATION
The planetary nebula system and the dynamics of the galaxy Centaurus A p 754 N93-13645
CENTER OF MASS
Dynamics and control of a tumbling satellite retrieval device p 522 N93-13119
CENTER OF PRESSURE
New methods for predicting nonlinear lift, center of pressure, and pitching moment on missile configurations
[AD-A255078] p 492 N93-12741
CENTRAL NERVOUS SYSTEM
A core facility for the study of neurotoxins of biological origin
[AD-A254359] p 674 N93-12945
CENTRIFUGAL COMPRESSORS
Alternative systems for fuel gas boosters for small gas turbine engines
[PB92-223049] p 612 N93-12977
CENTRIFUGES
ReTech, Inc., Plasma Centrifugal Furnace: Applications analysis report
[PB92-218791] p 714 N93-12982
Assessment of programs in space biology and medicine
[NASA-CR-190930] p 672 N93-13327
CERAMIC COATINGS
Thermal barrier coating life prediction model development, phase 2
[NASA-CR-189111] p 544 N93-12589
Fracture of a metal/ceramic couple: Tantalum (titanium)/sapphire p 554 N93-14074
CERAMIC FIBERS
Experimental characterization of continuous alumina fiber/epoxy p 533 N93-13775
A new route for fibre management in metal matrix composites p 534 N93-13779
Assessment of Japanese technology in advanced glass and ceramic fibers
[AD-A255229] p 553 N93-13836
CERAMIC MATRIX COMPOSITES
Investigation of properties and performance of ceramic composite components
[DE92-019911] p 550 N93-12858
Mechanical behaviour of fiber-reinforced ceramic matrix composites p 532 N93-13527
Matrix cracking initiation stress in fiber-reinforced ceramic matrix composites p 627 N93-13539
Load-transfer and crack bridging in fiber-toughened ceramic composites p 629 N93-13754
Toughening mechanisms in weak matrix ceramic composites p 553 N93-13780
Assessment of Japanese technology in advanced glass and ceramic fibers
[AD-A255229] p 553 N93-13836
X ray attenuation measurements for high-temperature materials characterization and in situ monitoring of damage accumulation p 631 N93-14022
Fracture of a metal/ceramic couple: Tantalum (titanium)/sapphire p 554 N93-14074
CERAMICS
Cost-effective Sintered Reaction-Bonded Silicon Nitride (SRBSN) for structural ceramics
[DE92-019285] p 549 N93-12821
Touchstone for success
[ESA-BR-52] p 557 N93-12934
Microstructural evolution in reaction bonded alumina/mullite ceramics p 552 N93-13328
Radiation-disorder and aperiodicity in irradiated ceramics
[DE92-015051] p 552 N93-13350
Ceramic machining: Assessment of current practice and research needs in the US
[PB92-213511] p 553 N93-13649
Thin film thermocouples for high temperature measurement on ceramic materials p 599 N93-13666
X ray attenuation measurements for high-temperature materials characterization and in situ monitoring of damage accumulation p 631 N93-14022
CEREBRAL CORTEX
Functional MRI studies of human vision on a clinical imager
[DE92-017448] p 674 N93-12566
CERENKOV COUNTERS
A program to study antiprotons in the cosmic rays: Arizona collaboration
[NASA-CR-191272] p 772 N93-13306
The sapphire Cerenkov laser p 605 N93-13365
CERENKOV RADIATION
The sapphire Cerenkov laser p 605 N93-13365
CHALLENGER (ORBITER)
Space Station: Resolving conflict over integration contractor's role. Briefing report to the Chairman, Subcommittee on Investigations and Oversight, Committee on Science, Space, and Technology, House of Representatives
[GAO/NSIAD-92-291BR] p 732 N93-13111
CHANNELS (DATA TRANSMISSION)
HIPPI and Fibre Channel
[DE92-040346] p 689 N93-13046
Fiber optic data bus radiation effects study
[AD-A255821] p 711 N93-14031
CHAOS
Chaotic vortical motion in the near region of a plane jet p 493 N93-13493
CHARACTER RECOGNITION
Reject mechanisms for massively parallel neural network character recognition systems
[PB92-213412] p 689 N93-13198
CHARACTERIZATION
Capacitive skin characterization
[NASA-CR-191261] p 598 N93-13567
CHARGE CARRIERS
Effect of hydrogen reduction and doping on the characteristics of high-temperature superconductors p 725 N93-13844
CHARGE COUPLED DEVICES
Soft X Ray Telescope (SXT) focus error analysis
[NASA-CR-184443] p 742 N93-12657
Galactic cosmic ray exposure estimates for SAGE-3 mission in polar orbit
[NASA-TM-107678] p 771 N93-13126
GAMCIT: A gamma ray burst detector p 510 N93-13173
Video profile monitor diagnostic system for GTA
[DE92-040231] p 710 N93-13509
Digital fluoroscopy with an optically coupled charge-coupled device p 712 N93-14101
CHARGE EFFICIENCY
Thermally stable electrolytes for rechargeable lithium batteries, phase 2
[NASA-CR-190878] p 573 N93-13610
CHARGE EXCHANGE
Observations of solar wind ion charge exchange in the comet Halley coma p 752 N93-13467
Particle simulation of grid erosion in an ion thruster p 527 N93-13927
CHARGE TRANSFER
An acoustic charge transport imager for high definition television applications
[NASA-CR-191295] p 572 N93-13448
Use of phonon echoes in the study of 2-6 compounds and dielectric Bi12GeO20:Cr p 725 N93-13847
CHARM (PARTICLE PHYSICS)
Search for doubly Cabibbo suppressed decays of the charged D meson
[DE92-018588] p 703 N93-13092
CHARTS
Digital chart database conversion into a system electronic navigational chart
[AD-A255007] p 632 N93-12869
CHEMICAL ANALYSIS
Fiber optic sensors for environmental applications: A brief review
[DE92-040170] p 710 N93-13576
Application of passive dosimetry for detection of leaking underground storage tanks
[PB92-218270] p 559 N93-13648
CHEMICAL BONDS
Halogen surface chemistry on Si(100)-(2x1)
[AD-A254643] p 536 N93-12618
Intermolecular potential functions from spectroscopic properties of weakly bound complexes
[DE92-018643] p 701 N93-12745
CHEMICAL COMPOSITION
Noninvasive probing of the ocean surface using laser-based nonlinear optical methods
[DE92-019431] p 669 N93-12916
A neural network approach for the investigation of chemical phenomena
[DE92-019205] p 691 N93-13079
The nature of scales grown on binary Cr-Nb alloys
[DE92-019283] p 542 N93-13080
Comparison of cometary comae using ultraviolet spectroscopy: Composition and variation p 753 N93-13603
Density contrast shell models for planetary nebulae p 756 N93-13850
Water and cheese from the lunar desert: Abundances and accessibility of H, C, and N on the Moon p 761 N93-13976
Physical properties of concrete made with Apollo 16 lunar soil sample p 554 N93-13987
CHEMICAL DEFENSE
Physiological stress from chemical defense clothing and equipment
[AD-A255786] p 676 N93-14028
CHEMICAL EFFECTS
Chemical release and radiation effects experiment advanced planning and coordination
[NASA-CR-184439] p 649 N93-12718
CHEMICAL EVOLUTION
Hydrothermal organic synthesis experiments
[NASA-CR-191257] p 672 N93-13457
Chemical environments of submarine hydrothermal systems
[NASA-CR-191258] p 669 N93-13458
CHEMICAL EXPLOSIONS
Nonideal thermoequilibrium calculations using a large product species data base
[DE92-040839] p 735 N93-12813
Development of a laser ignited all secondary explosive DDT detonator
[DE92-019340] p 555 N93-13081
CHEMICAL MACHINING
Ceramic machining: Assessment of current practice and research needs in the US
[PB92-213511] p 553 N93-13649
CHEMICAL PROPERTIES
High temperature superconductor materials and applications
[NASA-CR-184437] p 719 N93-12691
Synthesis and properties of novel cluster phases
[DE92-017388] p 545 N93-12697
CHEMICAL REACTIONS
The reactions of imidogen with nitric oxide and molecular oxygen
[DE92-006697] p 537 N93-13233
Systematic chemical equation balancing
[DE92-017234] p 539 N93-13530
Thermochemistry of atmospheric metal reactions
[AD-A248651] p 543 N93-13733
Applications for special-purpose minerals at a lunar base p 760 N93-13975

The chemistry of the extreme pressure lubricant additive lead naphthenate on steel surfaces
[AD-A255828] p 544 N93-14098

CHEMICAL REACTORS
Molten salt reactor for potentiostatic electroplating
[AD-D015358] p 551 N93-13101

CHEMILUMINESCENCE
Photochemical kinetics of excited states of O3 and O2: Laboratory studies and atmospheric implications
p 656 N93-13784

CHEMISORPTION
The chemistry of the extreme pressure lubricant additive lead naphthenate on steel surfaces
[AD-A255828] p 544 N93-14098

CHILDREN
Suited for spacewalking: A teacher's guide with activities
[NASA-EP-279] p 679 N93-13692

CHIPS (ELECTRONICS)
Multichip module high speed testing
[AD-A254825] p 570 N93-12731
Massively parallel optical-to-electronic data transfer
[AD-A254831] p 688 N93-12733
Silicon neuron
[AD-A255091] p 674 N93-12756
Semiconductor measurement technology: Version 2.0 of the TXYZ thermal analysis program: TXYZ20
[PB92-217603] p 570 N93-12978
Circuit design tool. User's manual, revision 2
[NASA-CR-191361] p 687 N93-13734

CHIRP
CO2 laser preionisation
[NASA-CR-184424] p 607 N93-13797
Theoretical and numerical studies of wave propagation and scattering in inhomogeneous media
p 568 N93-14044

CHLORIDES
Li/SOCl battery technology: Problems and solutions
[AD-A254514] p 570 N93-12725

CHLOROFLUOROCARBONS
Effects of orbital exposure on Halar during the LDEF mission p 549 N93-12788
New technologies for refrigeration without CFC's
[DE92-018886] p 557 N93-12922
Physical property data on fluorinated propanes and butanes as CFC and HCFC alternatives
[PB92-206507] p 555 N93-12939
Reduction of chlorofluorocarbon emissions from refrigeration systems
[DE92-019360] p 645 N93-13505
An experimental and theoretical study of degradation pathways for atmospheric halocarbons
p 646 N93-13624
Gas-phase reactions of halogen species of atmospheric importance p 658 N93-13889

CHLOROFORM
Microwave and infrared dielectric relaxation of alkylcarbonates, chloroform and their mixtures at 25 C
[AD-A253606] p 537 N93-13096

CHLOROPHYLLS
New approaches to the measurement of chlorophyll, related pigments and productivity in the sea
[NASA-CR-190879] p 673 N93-13612

CHLOROPLASTS
Nitrogen control of chloroplast development and differentiation
[DE92-017392] p 671 N93-12768

CHONDRITES
The implications of the magnetism of ordinary chondrites p 755 N93-13795

CHROMIC ACID
Anodized aluminum on LDEF: A current status of measurements on chromic acid anodized aluminum
p 544 N93-12779
A comparison of chromic acid and sulfuric acid anodizing
[NASA-TM-108383] p 543 N93-13378

CHROMIUM
Palladium-chromium static strain gages for high temperatures p 600 N93-13671

CHROMIUM ALLOYS
Weak-beam imaging of dissociated dislocations in HVEM-irradiated Fe-Ni-Cr alloys
[DE92-019587] p 541 N93-12798

CHROMIUM OXIDES
Alternative materials for solid oxide fuel cells: Factors affecting air-sintering of chromite interconnections
[DE92-019356] p 638 N93-13082

CHROMIUM STEELS
Influence of cold work level on the irradiation creep and creep rupture of titanium-modified austenitic stainless steels
[DE92-019078] p 541 N93-12820

CHROMOSPHERE
Data evaluation, analysis, and scientific study
[NASA-CR-184396] p 769 N93-13475
The role of particle diffusion in the lower transition region: Revised interpretation of emission measures
p 770 N93-13476
The 3-D description of vertical current sheets with application to solar flares
[SSL-PREPRINT-90-119] p 770 N93-13477
Electron impact polarization expected in solar EUV lines from flaring chromospheres/transition regions
[SSL-PREPRINT-90-124] p 770 N93-13478

CHUTES
Studies of granular flow down an inclined chute
[DE92-018871] p 577 N93-13074

CIRCADIAN RHYTHMS
Neurochemical control of circadian rhythms
[AD-A255054] p 675 N93-13116

CIRCUIT DIAGRAMS
Testing and fault-tolerant design techniques for advanced digital architectures
[AD-A255013] p 681 N93-12707

CIRCUIT RELIABILITY
Requirements for soldered electrical connections
[NHB-5300.4(3A-2)] p 570 N93-12674
Design for reliability: Current density
[AD-A254770] p 570 N93-12866

CIRCUITS
Summary of awards. Fiscal year 1991
[NSF-92-36] p 681 N93-13431
Transducer circuit
[AD-D015376] p 572 N93-13472
Explanation-based knowledge acquisition of electronics
[AD-A255089] p 573 N93-13650
Circuit design tool. User's manual, revision 2
[NASA-CR-191361] p 687 N93-13734

CIRCULAR CYLINDERS
Turbulent natural convection between a perforated vertical cylinder and a surrounding array
[DE92-019766] p 576 N93-12996
Solution of compressible Navier-Stokes equations using spectral methods on arbitrary two-dimensional domains
p 593 N93-14041

CIRCULAR ORBITS
Robust rendezvous maneuver point conditions
[NASA-CR-190996] p 517 N93-12690

CIRCULAR PLATES
Contact of orthotropic laminates with a rigid spherical indentor p 533 N93-13778

CIRCULAR SHELLS
Bifurcation and localization instabilities in plastic bending of cylindrical shells p 630 N93-13923

CIRCULATION CONTROL AIRFOILS
Navier-Stokes flowfield computation of wing/rotor interaction for a tilt rotor aircraft in hover
p 497 N93-14035

CISLUNAR SPACE
A guidance methodology for the cislunar transfer of low-thrust spacecraft p 517 N93-13766
The influence of lunar propellant production on the cost-effectiveness of cislunar transportation systems
p 556 N93-13983

CIVIL AVIATION
Public-sector aviation issues: Graduate research award papers, 1990 - 1991
[PB92-222629] p 498 N93-13787
Report to Congress: State Block Grant Program
[AD-A254569] p 507 N93-13882
Postmortem alcohol production in fatal aircraft accidents
[AD-A255766] p 498 N93-14026

CLASSIFICATIONS
Myths and legends in learning classification rules
[NASA-CR-191236] p 693 N93-13366

CLASSIFIERS
Reject mechanisms for massively parallel neural network character recognition systems
[PB92-213412] p 689 N93-13198

CLATHRATES
Experimental studies of the far-infrared spectra of cosmic-type ices
[NASA-CR-191300] p 748 N93-13660

CLEAN ROOMS
Europe qualifies for space
[ESA-BR-64] p 508 N93-12892

CLIMATE
A computer simulation of ecosystem processes in forests for application to air pollution, acid precipitation, and global change
[DE92-019616] p 643 N93-12927
The IGAC activity for the development of global emissions inventories: Description and initial results
[DE92-016010] p 644 N93-13270
Relationships between continental-scale circulation and rainfall event attributes in the southeastern US
p 664 N93-13631
Atmospheric, climatic and environmental research
[NASA-CR-191367] p 664 N93-13718
Integration of vegetation indices and thermal measurements for ecosystem modeling
p 646 N93-13721
Statistical relationships between tree growth and climate in western North America p 648 N93-14096

CLIMATE CHANGE
The broad band overlap problem in atmospheric trace gases p 641 N93-12624
Earth science information: Planning for the integration and use of global change information
[NASA-CR-191217] p 733 N93-12660
A computer simulation of ecosystem processes in forests for application to air pollution, acid precipitation, and global change
[DE92-019616] p 643 N93-12927
How life affects the geochemical cycle of carbon
[NASA-CR-191241] p 644 N93-13031
NOAA Workshop on Climate Scale Operational Precipitation and Water Vapor Products
[NOAA-TR-NESDIS-62] p 662 N93-13066
Atmospheric, climatic and environmental research
[NASA-CR-191367] p 664 N93-13718
The relationship between SST anomalies and clouds, water vapor, and their radiative effects
p 665 N93-13744
Climate sensitivity study with energy balance models
p 666 N93-13817

CLIMATOLOGY
Performance of the Bowen ratio systems on a 22 deg slope
[NASA-CR-191278] p 644 N93-13254
The IGAC activity for the development of global emissions inventories: Description and initial results
[DE92-016010] p 644 N93-13270
A synoptic climatology of the elevated mixed layer inversion over the southern Great Plains in spring
p 664 N93-13643
Atmospheric, climatic and environmental research
[NASA-CR-191367] p 664 N93-13718

CLINICAL MEDICINE
A health care system for the Space Station
[NASA-TM-108093] p 679 N93-13571

CLOSED CYCLES
Plasma reactor waste management systems
p 680 N93-14000
Conceptual design of a lunar base thermal control system p 680 N93-14003

CLOSED ECOLOGICAL SYSTEMS
Real-time quality assurance testing using photonic techniques: Application to iodine water system
[NASA-CR-184413] p 619 N93-12692
An ion budget for a terra firme rainforest in Central Amazonia
[INPE-5365-PRE/1745] p 632 N93-13005
The environmental control and life-support system for a lunar base: What drives its design
p 680 N93-13991
Life systems for a lunar base p 680 N93-13992
Lunar base CELSS: A bioregenerative approach
p 680 N93-13993
Long-term lunar stations: Some ecological considerations p 648 N93-13995
Scenarios for optimizing potato productivity in a lunar CELSS p 680 N93-13997
Distribution of human waste samples in relation to sizing waste processing in space p 680 N93-14001
Moon Park: A research and educational facility
p 519 N93-14015

CLOUD COVER
Remote sensing data from CLARET: A prototype CART data set
[NASA-CR-191294] p 634 N93-13094
The relationship between SST anomalies and clouds, water vapor, and their radiative effects
p 665 N93-13744
Intraseasonal variability of infrared cooling rates during the Asian summer monsoon and their influence on intraseasonal waves p 665 N93-13760

CLOUD PHYSICS
Microwave remote sensing of a precipitating atmosphere p 634 N93-13371

CLOUDS (METEOROLOGY)
Sulfate impact upon low-level cloud albedo over oceans p 661 N93-12833
Remote sensing data from CLARET: A prototype CART data set
[NASA-CR-191294] p 634 N93-13094
Numerical simulation of a squall line: Tests of a new cumulus parameterization scheme p 662 N93-13124
Microwave remote sensing of a precipitating atmosphere p 634 N93-13371
Cloud acidity and acidic deposition in the lower troposphere and ozone depletion in the Antarctic stratosphere: Modeling and data analysis regarding the role of atmospheric aerosol p 647 N93-13741

Kinetic studies of some free radical reactions involved in cloudwater chemistry p 668 N93-14055

CLUSTERS

Synthesis and properties of novel cluster phases [DE92-017388] p 545 N93-12697

Electronic structure of microclusters and defect complexes [AD-A254807] p 720 N93-12750

Structure sensitive reactions over Co, Fe and mixed metal clusters in zeolites [DE92-040359] p 542 N93-12998

Photodissociation processes [PB92-222702] p 702 N93-13067

CLUTTER

Bistatic clutter RCS simulation using scale model rough surfaces [AD-A254932] p 560 N93-12581

Application of smoothing techniques for tracking maneuvering targets. Multiple target tracking in clutter: New approaches [AD-A254609] p 561 N93-12615

Multifrequency measurements of radar ground clutter at 42 sites. Volume 2: Appendices A through D [AD-A246711] p 567 N93-13878

CMOS

Massively parallel optical-to-electronic data transfer [AD-A254831] p 688 N93-12733

COAL

Summary on comparison of radiative heat transfer solutions for a specified problem [DE92-040098] p 588 N93-13575

COAL DERIVED GASES

High octane ethers from synthesis gas-derived alcohols [DE92-015467] p 537 N93-13188

MCFC diagnostics: HCl detection [DE92-001292] p 639 N93-13313

Effects of coal-derived trace species on performance of molten carbonate fuel cells [DE93-000203] p 639 N93-13427

COAL GASIFICATION

The MAGSORB process for bulk separation of carbon dioxide [DE92-001296] p 538 N93-13314

An update of ERC's carbonate fuel cell development program [DE92-019971] p 640 N93-13621

COAL UTILIZATION

Development of advanced turbine systems: Meeting tomorrow's needs [DE92-017339] p 612 N93-13103

COALESCING

Modeling of coalescence, agglomeration, and phase segregation in microgravity processing of bimetallic composite materials [NASA-CR-191247] p 556 N93-12728

COASTAL PLAINS

An observational and numerical investigation of meso-scale coastal processes during GALE IOP 2 p 665 N93-13776

COASTAL ZONE COLOR SCANNER

Ocean optical database [AD-A254969] p 668 N93-12556

SeaWiFS technical report series. Volume 4, an analysis of GAC sampling algorithms: A case study [NASA-TM-104566-VOL-4] p 669 N93-13382

COASTS

Digital chart database conversion into a system electronic navigational chart [AD-A255007] p 632 N93-12869

COATING

Alternate electrode materials for the SP100 reactor [DE92-019570] p 706 N93-12970

COATINGS

Chemical sensors based on ultrathin film composite membranes [AD-A254644] p 595 N93-12619

Proton transport on modified sulfonated polyaniline electrodes [AD-A254917] p 570 N93-12650

COBALT ALLOYS

In-phase and out-of-phase axial-torsional fatigue behavior of Haynes 188 at 760 C [NASA-TM-105765] p 625 N93-13153

COBALT COMPOUNDS

Solvation of cobalt salts by oligomeric polyethers [AD-A254815] p 545 N93-12753

COCKPITS

Theory and design of adaptive automation in aviation systems [AD-A254595] p 499 N93-12613

Adaptive automation and human performance. 3: Effects of practice on the benefits and costs of automation shifts [AD-A254381] p 677 N93-12860

The relationship between environmental conditions and UH-60 cockpit temperature [AD-A255918] p 680 N93-14090

COEFFICIENT OF FRICTION

Wall functions for the kappa-epsilon turbulence model in generalized nonorthogonal curvilinear coordinates p 587 N93-13517

COEFFICIENTS

Cross sections and rate coefficients for the electron-impact excitation of He-like ions [ISAS-RN-647] p 703 N93-13095

Estimation of EOF expansion coefficients from incomplete data [AD-A255252] p 697 N93-13886

COERCIVITY

Magnetic hardening studies and novel techniques for preparation of high performance magnets [AD-A254761] p 698 N93-12865

COGNITION

Recent developments in the NL-Soar garden path theory [AD-A255889] p 688 N93-13944

COHERENCE

Radio and optical interferometric imaging p 744 N93-13580

COHERENT RADAR

SAR peculiarities, ambiguities and constraints p 563 N93-13051

COHERENT RADIATION

Organization of the Optical Society of America Photonic Science Topical Meeting Series. Volume 8: Integrated photonics research. lifornia on 9-11 april 1991 [AD-A254682] p 709 N93-12666

Theory of lasing without population inversion p 605 N93-13497

Two-photon cooperative cascade superfluorescence [AD-A255690] p 608 N93-14023

COLD FLOW TESTS

Planar measurement of flow field parameters in nonreacting supersonic flows with laser-induced iodine fluorescence p 495 N93-13801

COLD GAS

Evidence for cool gas and star formation in cluster cooling flows p 751 N93-13380

The interstellar medium of elliptical galaxies p 757 N93-14071

COLD WORKING

Influence of cold work level on the irradiation creep and creep rupture of titanium-modified austenitic stainless steels [DE92-019078] p 541 N93-12820

COLLISION AVOIDANCE

A collision avoidance algorithm for the mobile robot and the robot manipulator in multi-robot system p 618 N93-14094

COLLISIONAL PLASMAS

Fluidlike studies of the sheath and presheath regions of a plasma p 718 N93-13792

COLLISIONS

Hydrodynamical calculations of stellar interactions p 755 N93-13764

Non-perturbative studies in quantum electrodynamics p 729 N93-13896

COLLOIDS

Intrinsic bistable photonic materials by copper colloid formation in silica [AD-A255505] p 711 N93-13866

COLOR

The Jovian ultraviolet aurora observed with the IUE spacecraft: Brightness and color distribution with longitude p 759 N93-13625

COLORADO

An investigation of the effects of topography on Colorado front range winter storms p 668 N93-14063

COLORADO PLATEAU (US)

Seismic studies of crustal structure and tectonic evolution across the central California margin and the Colorado Plateau margin p 657 N93-13794

COLORIMETRY

Methods development for total organic carbon accountability [NASA-CR-184438] p 672 N93-12949

Application of passive dosimetry for detection of leaking underground storage tanks [PB92-218270] p 559 N93-13648

COLUMBUS SPACE STATION

A home port in space [ESA-BR-37-E] p 516 N93-13858

A growing dimension in space [ESA-BR-37-F] p 517 N93-13902

COMBINATORIAL ANALYSIS

An investigation of new search techniques for the traveling salesman problem p 696 N93-12625

Fast approximation algorithms for multicommodity flow problems [AD-A254335] p 685 N93-12961

COMBUSTIBLE FLOW

Computation of steady and unsteady shock-induced combustion over hypervelocity blunt bodies p 536 N93-12836

Velocity and temperature measurements in a non-premixed reacting flow behind a backward facing step p 494 N93-13632

Exit plane H2O concentration measurements correlated with OH PLIF near-injector mixing measurements for scramjet flows p 603 N93-13687

COMBUSTION

Toward a microgravity research strategy [NASA-CR-190820] p 556 N93-12799

The First United States Microgravity Laboratory [NASA-TM-107980] p 557 N93-12951

Semi-quantitative model for the burning rate of solid materials [PB92-213362] p 539 N93-13641

COMBUSTION CHAMBERS

Pressure fed thrust chamber technology program [NASA-CR-184461] p 526 N93-12968

A preliminary study of the effect of equivalence ratio on a low emissions gas turbine combustor using KIVA-2 [DE92-018616] p 613 N93-13321

Skin friction measurements in high temperature high speed flows p 595 N93-13670

Planar laser-induced fluorescence imaging of OH in the exhaust of a bi-propellant thruster p 602 N93-13686

COMBUSTION CHEMISTRY

The reactions of imidogen with nitric oxide and molecular oxygen [DE92-006697] p 537 N93-13233

Modelling combustion zones in porous media p 540 N93-13802

COMBUSTION EFFICIENCY

Development of advanced turbine systems: Meeting tomorrow's needs [DE92-017339] p 612 N93-13103

COMBUSTION PHYSICS

Measurements of cellular structure in spray detonation [DE92-019580] p 555 N93-12933

Findings of a review of spacecraft fire safety needs [NASA-CR-189181] p 523 N93-13715

Modelling combustion zones in porous media p 540 N93-13802

Combustion of gaseous fuels under reduced-gravity conditions p 557 N93-14012

COMBUSTION PRODUCTS

A smoke producing rocket motor for atmospheric wind profiling [DE92-018264] p 555 N93-12563

The role of human activity and land use change in atmospheric chemistry and air quality [DE92-019622] p 642 N93-12880

Meeting future exhaust emissions standards using natural gas as a vehicle fuel: Lessons learned from the natural gas vehicle challenge 1992 [DE92-019670] p 642 N93-12885

Effects of gas composition on engine performance and emissions [PB92-217561] p 611 N93-12936

High-resolution investigation of degenerate four-wave mixing in the (gamma)(0,0) band of nitric oxide [DE92-005312] p 537 N93-13232

The IGAC activity for the development of global emissions inventories: Description and initial results [DE92-016010] p 644 N93-13270

COMBUSTION STABILITY

Stability codes for a liquid rocket implemented for use on a PC [NASA-CR-184453] p 525 N93-12659

Nonlinear stability of combustion-driven acoustic oscillations in resonance tubes [DE92-012153] p 699 N93-13262

COMBUSTION VIBRATION

Fundamentals of enhanced scalar transport in strongly oscillating and/or resonant flow fields as created by pulse combustion [DE92-012147] p 582 N93-13247

COMET NUCLEI

In situ dust mass distribution measurements from the Giotto encounter with comet P/Halley p 753 N93-13602

COMET RENDEZVOUS ASTEROID FLYBY MISSION

NASA budget: Potential shortfalls in funding NASA's 5-year plan. Testimony before the Subcommittee on Science, Technology, and Space, Committee on Commerce, Science, and Transportation, United States Senate [GAO/T-NSIAD-92-18] p 740 N93-13280

Summary of literature on unmanned probes to asteroids and precursor data requirements for IAM p 514 N93-13551

COMET TAILS

Observations of solar wind ion charge exchange in the comet Halley coma p 752 N93-13467

COMETARY ATMOSPHERES
A study of ion composition and dynamics at Comet Halley
[NASA-CR-188478] p 751 N93-13465
Densities and abundances of hot cometary ions in the coma of P/Halley p 752 N93-13466
In situ dust mass distribution measurements from the Giotto encounter with comet P/Halley p 753 N93-13602
Comparison of cometary comae using ultraviolet spectroscopy: Composition and variation p 753 N93-13603

COMETS
Studies of extra-solar Oort Clouds and the Kuiper disk
[NASA-CR-190958] p 769 N93-12669
Giotto: The second encounter
[ESA-BR-83] p 749 N93-12965
Comparison of cometary comae using ultraviolet spectroscopy: Composition and variation p 753 N93-13603

COMMAND AND CONTROL
Measures of user-system interface effectiveness: Assessment of structured judgment evaluation techniques for graphical, direct-manipulation style interfaces
[AD-A254493] p 677 N93-12576
Proceedings of Joint RL/AFOSR Workshop on Intelligent Information Systems
[AD-A254795] p 734 N93-12703

COMMERCE
Federal support to universities, colleges, and nonprofit institutions: Fiscal year 1990. A report to the President and Congress
[NSF-92-324] p 741 N93-13543
Abstracts of phase 1 awards: NSF Small Business Innovation Research Program (SBIR): 1992
[NSF-92-80] p 732 N93-13703
Research in geosciences policy
[NASA-CR-190470] p 632 N93-13833
Application of information system technology to K-12 education
[AD-A255223] p 731 N93-13834

COMMERCIAL AIRCRAFT
Future regional transport aircraft market, constraints, and technology stimuli
[NASA-TM-107669] p 491 N93-13025
Detailed analysis of wing-nacelle interaction for commercial transport aircraft p 578 N93-13203

COMMINUTION
Fatigue and fracture of intermetallic alloys
[AD-A254543] p 540 N93-12603

COMMUNICATION CABLES
Fiber optic data bus radiation effects study
[AD-A255821] p 711 N93-14031

COMMUNICATION NETWORKS
A general theory of signal integration for fault-tolerant dynamic distributed sensor networks
[AD-A254961] p 732 N93-12553
Reviews of computing technology: Fiber distributed data interface
[DE92-019927] p 681 N93-12886
Program Support Communications Network (PSCN) facsimile system directory
[NASA-TM-108051] p 562 N93-12909
Applications of satellite technology to broadband ISDN networks
[NASA-CR-189199] p 562 N93-12950
DATA: How to generate, store, retrieve, communicate, and interpret it: Proceedings
[DE92-040405] p 735 N93-13000
Research priorities in networking and communications
[NSF-92-109] p 562 N93-13024
DNET: A communications facility for distributed heterogeneous computing
[NASA-CR-190863] p 682 N93-13759

COMMUNICATION SATELLITES
An analysis of the low-earth-orbit communications environment p 561 N93-12633

COMMUNICATIONS TECHNOLOGY SATELLITE
Advanced Communications Technology Satellite (ACTS). Phase 1: Industrial/academic experimenters
[NASA-CR-191211] p 561 N93-12679

COMPACT GALAXIES
Evolution of galaxies in compact groups p 750 N93-13148

COMPANION STARS
A systematic search for low-mass companions orbiting nearby stars and the calibration of the end of the stellar main sequence p 749 N93-14070

COMPARISON
From comparison density to two sample analysis
[AD-A253866] p 698 N93-13064

COMPARTMENTS
Flow through horizontal vents as related to compartment fire environments
[PB92-213388] p 559 N93-13642

COMPATIBILITY
Flight analysis of air intake/engine compatibility p 502 N93-13212

COMPETITION
The 1992 natural gas vehicle challenge: EPA emissions and fuel economy testing
[PB92-217926] p 616 N93-13761

COMPILERS
Program structure as a basis for the parallelization of global compiler optimizations
[AD-A254554] p 681 N93-12641
Compiling knowledge-based systems to Ada, phase 2
[NASA-CR-191273] p 686 N93-13355

COMPLEX COMPOUNDS
Oligomer and mixed-metal compounds potential multielectron transfer catalysts
[DE92-011347] p 543 N93-13346

COMPLEX SYSTEMS
Integrated modeling tool for performance engineering of complex computer systems
[NASA-CR-190881] p 687 N93-13880

COMPLEX VARIABLES
Application of complex variables in electromagnetofluid dynamic, magnetofluid dynamic and fluid dynamic flows: Viscoelastic boundary-layer theory
[ISBN-0-315-65141-5] p 594 N93-14067

COMPONENT RELIABILITY
Investigation of component failure rates for pulsed versus steady state tokamak operation
[DE92-019758] p 713 N93-12856
A unified approach to the analysis and design of manipulator systems with environmental contact p 573 N93-13805
Bayesian estimation of system reliability under asymmetric loss p 620 N93-13906

COMPOSITE MATERIALS
Compression test simulation of thick-section composite materials
[AD-A255021] p 528 N93-12583
Performance of thermal control tape in the protection of composite materials p 536 N93-12780
Aerogels, emulsions, and composites: Controlling structure with organic sol-gel chemistry
[DE92-019575] p 550 N93-12931
Composites: A catalogue of books and conference proceedings available in the NAL library
[NAL-SP-IC-9201] p 737 N93-13368
Three-dimensional boundary element analysis of residual stresses in a cross-ply fiber composite model p 629 N93-13811
Improved damping in composite structures through stress coupling, co-cured damping layers, and segmented stiffness layers p 630 N93-13823
Numerical analysis of permittivity with loss in isotropic binary composites
[AD-A255203] p 534 N93-13940

COMPOSITE PROPELLANTS
A smoke producing rocket motor for atmospheric wind profiling
[DE92-018264] p 555 N93-12563

COMPOSITE STRUCTURES
Probabilistic evaluation of fuselage-type composite structures
[NASA-TM-105881] p 622 N93-12735
Investigation of properties and performance of ceramic composite components
[DE92-019911] p 550 N93-12858
Microcracking, microcrack-induced delamination, and longitudinal splitting of advanced composite structures
[NASA-CR-4472] p 623 N93-12911
Large-deflection analysis of cord composite plates p 530 N93-13008
Linear and nonlinear finite element analysis of laminated composite structures at high temperatures p 623 N93-13009
Coupled structural/thermal/electromagnetic analysis/tailoring of graded composite structures
[NASA-CR-189150] p 626 N93-13443
Coupled structural/thermal/electromagnetic analysis/tailoring of graded composite structures
[NASA-CR-189151] p 627 N93-13444
Coupled structural/thermal/electromagnetic analysis/tailoring of graded composite structures
[NASA-CR-189152] p 627 N93-13445
Optimum design of aircraft structures with manufacturing and buckling constraints p 501 N93-13815
Improved damping in composite structures through stress coupling, co-cured damping layers, and segmented stiffness layers p 630 N93-13823
Numerical analysis of permittivity with loss in isotropic binary composites
[AD-A255203] p 534 N93-13940

COMPRESSED AIR
ASTOVL model engine simulators for wind tunnel research p 507 N93-13213

COMPRESSED GAS
Utilization of compressed natural gas in medium- and heavy-duty engine route vehicles
[PB92-217546] p 611 N93-12908

COMPRESSIBILITY EFFECTS
Interaction of isotropic turbulence with a shock wave p 590 N93-13898

COMPRESSIBLE BOUNDARY LAYER
A compressible boundary layer algorithm for use with SINDA '85 p 585 N93-13395

COMPRESSIBLE FLOW
Application of a solution adaptive grid to flow over an embedded cavity p 492 N93-13141
A PDF closure model for compressible turbulent chemically reacting flows
[NASA-CR-191209] p 587 N93-13453
Wall functions for the kappa-epsilon turbulence model in generalized nonorthogonal curvilinear coordinates p 587 N93-13517
Development and computation of continuum higher order constitutive relations for high-altitude hypersonic flow p 494 N93-13578
Stability of the compressible reacting mixing layer p 592 N93-13948
Coherent structures in compressible convection p 592 N93-13964
Solution of compressible Navier-Stokes equations using spectral methods on arbitrary two-dimensional domains p 593 N93-14041
Numerical simulation of compressible Couette flow stability: Non-linear and three-dimensional effects p 594 N93-14077

COMPRESSIBLE FLUIDS
Compressible convection and pulsations on parallel computers p 690 N93-13961

COMPRESSING
Preloaded latching device
[NASA-CASE-MSC-21730-1] p 614 N93-13417

COMPRESSION LOADS
Scale effects in buckling, postbuckling and crippling of graphite-epoxy Z-section stiffeners p 621 N93-12632
The effects of compressive preloads on the compression-after-impact strength of carbon/epoxy
[NASA-TP-3303] p 529 N93-12678
New technologies for refrigeration without CFC's
[DE92-018886] p 557 N93-12922
Aerogels, emulsions, and composites: Controlling structure with organic sol-gel chemistry
[DE92-019575] p 550 N93-12931
Effects of layer waviness on compression-loaded thermoplastic composite laminates p 532 N93-13724

COMPRESSION TESTS
Compression test simulation of thick-section composite materials
[AD-A255021] p 528 N93-12583
Properties of five toughened matrix composite materials
[NASA-TP-3254] p 528 N93-12590
Scale effects in buckling, postbuckling and crippling of graphite-epoxy Z-section stiffeners p 621 N93-12632
Compression strength of composite primary structural components
[NASA-CR-190949] p 624 N93-13019

COMPRESSIVE STRENGTH
The effects of compressive preloads on the compression-after-impact strength of carbon/epoxy
[NASA-TP-3303] p 529 N93-12678
Nondestructive evaluation of the in-place compressive strength of concrete based upon limited destructive testing
[PB92-222751] p 623 N93-12981
Compression strength of composite primary structural components
[NASA-CR-190949] p 624 N93-13019
Effects of layer waviness on compression-loaded thermoplastic composite laminates p 532 N93-13724
Experimental characterization of continuous alumina fiber/epoxy p 533 N93-13775
Lunar concrete for construction p 555 N93-13990
Delamination initiation in postbuckled dropped-ply laminates p 535 N93-14030

COMPRESSOR EFFICIENCY
Flight analysis of air intake/engine compatibility p 502 N93-13212

COMPRESSORS
The influence of intake swirl distortion on the steady-state performance of a low bypass, twin-spool engine p 579 N93-13211
A novel-high-performance system for recording and analysing instantaneous total pressure distortion in air intakes p 580 N93-13215

COMPTON EFFECT
Wide range, permanent magnet Compton spectrometer
[DE92-017312] p 596 N93-12762

COMPUTATION
Summary of awards, fiscal year 1990
[NSF-92-70] p 683 N93-12693
Fast approximation algorithms for multicommodity flow problems
[AD-A254335] p 685 N93-12961
COMPUTATIONAL ASTROPHYSICS
Hydrodynamical calculations of stellar interactions p 755 N93-13764
COMPUTATIONAL CHEMISTRY
The vibrational spectrum of H2O3: An ab initio investigation
[NASA-CR-190968] p 537 N93-12935
A neural network approach for the investigation of chemical phenomena
[DE92-019205] p 691 N93-13079
COMPUTATIONAL FLUID DYNAMICS
Computational fluid dynamics combustion analysis evaluation
[NASA-CR-184326] p 575 N93-12688
Adaptation of multidimensional group particle tracking and particle wall-boundary condition model to the FDNS code
[SECA-TR-92-06] p 575 N93-12689
The multidimensional self-adaptive grid code, SAGE
[NASA-TM-103905] p 683 N93-12719
Computation of steady and unsteady shock-induced combustion over hypervelocity blunt bodies p 536 N93-12836
An attempt at a status report on a fast-moving target: CFD --- computational fluid dynamics
[DE92-017432] p 576 N93-12839
Report on the final panel discussion on computational aeroacoustics
[NASA-CR-189718] p 699 N93-12986
NASA aeronautics: Research and technology program highlights
[NASA-NP-159] p 491 N93-13110
A numerical study of hypersonic flow with strong surface blowing p 492 N93-13128
Application of a solution adaptive grid to flow over an embedded cavity p 492 N93-13141
Turbomachinery CFD on parallel computers
[NASA-TM-105932] p 689 N93-13154
Numeric simulation of the aerodynamic flows around nacelles p 577 N93-13202
Investigation of interference phenomena of modern wing-mounted high-bypass-ratio engines by the solution of the Euler-equations p 578 N93-13204
Aerodynamic analysis of slipstream/wing/nacelle interference for preliminary design of aircraft configurations p 497 N93-13205
Euler analysis of turbofan/superfan integration for a transport aircraft p 578 N93-13206
The PEP Symposium on CFD Techniques for Propulsion Applications p 579 N93-13210
AGARD WG13 aerodynamics of high speed air intakes: Assessment of CFD results p 581 N93-13220
Calibration of 2D unstructured grid methods on propulsive flowfields p 582 N93-13225
CFD calibration for three-dimensional nozzle/afterbody configurations p 582 N93-13226
Boundary element methods for two-dimensional, coupled, thermoviscous flow p 584 N93-13383
The Fourth Annual Thermal and Fluids Analysis Workshop
[NASA-CP-10106] p 584 N93-13385
Applications of CFD and visualization techniques p 584 N93-13386
Numerical study on mixing of sprayed liquid in an LNG storage tank p 584 N93-13388
Analysis of a space emergency ammonia dump using the FLOW-NET two-phase flow program p 584 N93-13389
The Proteus Navier-Stokes code p 585 N93-13396
Fluid flow and heat convection studies for actively cooled airframes
[NASA-CR-190956] p 587 N93-13406
A theoretical investigation of the growth rates of ice crystals in clouds p 653 N93-13485
Wall functions for the kappa-epsilon turbulence model in generalized nonorthogonal curvilinear coordinates p 587 N93-13517
Numerical simulation of the acoustic instability in the spatially developing, confined, supersonic mixing layer p 494 N93-13521
Development and computation of continuum higher order constitutive relations for high-altitude hypersonic flow p 494 N93-13578
The three-dimensional turbulent boundary layer: Theory and application p 588 N93-13749
Linear stability theory of hypersonic, chemically reacting viscous flows p 588 N93-13765
Variational characterizations of steady two-dimensional vortex motions p 589 N93-13781
Structures, spectra and inertial range transfer in two-dimensional and beta-plane turbulence p 590 N93-13900
Computational fluid dynamics of the base flow on a plane body between a subsonic flow on one side and a supersonic flow on the other p 591 N93-13920
Bipropellant spray combustion modeling in small rocket engines p 556 N93-13924
Flow prediction for three-dimensional intakes and ducts using viscous-inviscid interaction methods p 592 N93-13953
Unsteady three-dimensional thin-layer Navier-Stokes solutions for turbomachinery in transonic flow p 593 N93-14025
Navier-Stokes flowfield computation of wing/rotor interaction for a tilt rotor aircraft in hover p 497 N93-14035
Solution of compressible Navier-Stokes equations using spectral methods on arbitrary two-dimensional domains p 593 N93-14041
Application of complex variables in electromagnetofluid dynamic, magnetofluid dynamic and fluid dynamic flows: Viscoelastic boundary-layer theory
[ISBN-0-315-65141-5] p 594 N93-14067
COMPUTATIONAL GEOMETRY
A Fourier series method for polygonal domains: Large element computation for plates p 627 N93-13484
COMPUTATIONAL GRIDS
The multidimensional self-adaptive grid code, SAGE
[NASA-TM-103905] p 683 N93-12719
Calibration of 2D unstructured grid methods on propulsive flowfields p 582 N93-13225
Numerical calculation of turbomachinery cascade flows p 589 N93-13767
COMPUTER AIDED DESIGN
Verification and validation of AI software
[AD-A254601] p 682 N93-12614
Stability codes for a liquid rocket implemented for use on a PC
[NASA-CR-184453] p 525 N93-12659
Users manual for program SSFREQ intermediate mode stability curves: Developed for use on a PC computer
[NASA-CR-184452] p 682 N93-12675
Users manual for program ADMIT: Admittance and pressure transfer function developed for use on a PC computer
[NASA-CR-184450] p 682 N93-12676
Application interface engine language and object reference manual
[DE92-017555] p 683 N93-12686
User's guide: Computer-Aided Structural Modeling (CASM), version 3.00
[AD-A255074] p 684 N93-12851
Computer-Aided Structural Engineering (CASE) project. Tutorial guide: Computer-Aided Structural Modeling (CASM). Version 3.00
[AD-A255075] p 684 N93-12872
Structural optimization of thin shells using finite element method
[NASA-TM-105903] p 625 N93-13157
A SINDA thermal model using CAD/CAE technologies p 585 N93-13394
Analysis and design of planar and non-planar wings for induced drag minimization
[NASA-CR-191274] p 493 N93-13463
Automatic programming of arc welding robots p 616 N93-13720
Semiconductor measurement technology: INSTANT (IGBT network simulation and transient Analysis tool)
[PB92-213529] p 725 N93-13783
Optimum design of aircraft structures with manufacturing and buckling constraints p 501 N93-13815
Integrated modeling tool for performance engineering of complex computer systems
[NASA-CR-190881] p 687 N93-13880
Computer-aided design-based high-frequency electromagnetic wave scattering from complex bodies p 567 N93-14042
COMPUTER ASSISTED INSTRUCTION
Seamless simulation literature survey
[AD-A254950] p 688 N93-12549
Human factors research in aircrew performance and training: 1986-1991
[AD-A254455] p 677 N93-12609
Efficacy of multimedia instruction and an introduction to digital multimedia technology
[AD-A254509] p 734 N93-12723
An intelligent position-specific training system for mission operations
[NASA-TM-108381] p 691 N93-13156
Application of information system technology to K-12 education
[AD-A255223] p 731 N93-13834
COMPUTER COMPONENTS
A decade of discovery: Experiments with the Get Away Special (GAS) canister p 509 N93-13162
COMPUTER DESIGN
Resource constrained design of artificial neural networks using comparator neural network
[NASA-CR-191280] p 694 N93-13376
Formal aspects of human-computer interaction p 679 N93-13909
COMPUTER GRAPHICS
Stability codes for a liquid rocket implemented for use on a PC
[NASA-CR-184453] p 525 N93-12659
User's guide: Computer-Aided Structural Modeling (CASM), version 3.00
[AD-A255074] p 684 N93-12851
Spreadsheet-like image analysis
[AD-A254395] p 619 N93-12864
Computer-Aided Structural Engineering (CASE) project. Tutorial guide: Computer-Aided Structural Modeling (CASM). Version 3.00
[AD-A255075] p 684 N93-12872
Visualization techniques to aid in the analysis of multi-spectral astrophysical data sets
[NASA-CR-191260] p 685 N93-13261
A simple node and conductor data generator for SINDA p 585 N93-13392
COMPUTER INFORMATION SECURITY
Reviews of computing technology: Securing network applications, Kerberos, and RSA
[DE92-019928] p 690 N93-13620
COMPUTER NETWORKS
Seamless simulation literature survey
[AD-A254950] p 688 N93-12549
A general theory of signal integration for fault-tolerant dynamic distributed sensor networks
[AD-A254961] p 732 N93-12553
Real-time data archiving for GTA
[DE92-018613] p 733 N93-12567
Earth science information: Planning for the integration and use of global change information
[NASA-CR-191208] p 734 N93-12680
Proceedings of FLICC forums on federal information policies. Combined summaries of proceedings. The 1990 7th Forum, Access is the Key and the 1991 8th Forum, Building Information Superhighways: Supercomputing Networks and Libraries
[PB92-147370] p 734 N93-12759
Reviews of computing technology: Fiber distributed data interface
[DE92-019927] p 681 N93-12886
DATA: How to generate, store, retrieve, communicate, and interpret it: Proceedings
[DE92-040405] p 735 N93-13000
Research priorities in networking and communications
[NSF-92-109] p 562 N93-13024
File servers, networking, and supercomputers p 737 N93-13137
Guide to QSPIRES and the particle physics databases on SLACVM
[DE92-018099] p 737 N93-13275
Engineering data transfer test with EDMICS using MIL-R-28002 (Raster)
[DE92-019808] p 738 N93-13619
Reviews of computing technology: Securing network applications, Kerberos, and RSA
[DE92-019928] p 690 N93-13620
Research summary, January 1989 - June 1990
[NASA-CR-190960] p 687 N93-13694
Monitoring and controlling distributed applications using Lomita (position paper)
[NASA-CR-190971] p 687 N93-13695
DNET: A communications facility for distributed heterogeneous computing
[NASA-CR-190863] p 682 N93-13759
COMPUTER PROGRAMMING
Seamless simulation literature survey
[AD-A254950] p 688 N93-12549
Verification and validation of AI software
[AD-A254601] p 682 N93-12614
Program structure as a basis for the parallelization of global compiler optimizations
[AD-A254554] p 681 N93-12641
Expert-system development in Soar: A tutorial
[AD-A254571] p 682 N93-12645
Numerical optimization
[AD-A254575] p 682 N93-12647
Summary of awards, fiscal year 1990
[NSF-92-70] p 683 N93-12693
Compiling knowledge-based systems to Ada, phase 2
[NASA-CR-191273] p 686 N93-13355
Running SINDA '85/FLUINT interactive on the VAX p 584 N93-13390
A SINDA '85 nodal heat transfer rate calculation user subroutine p 587 N93-13403
Automatic programming of arc welding robots p 616 N93-13720

COMPUTER PROGRAMS
Introductory review of target discrimination criteria
[AD-A254954] p 560 N93-12551
A distributed timing system for sychronizing control and data correlation
[DE92-018603] p 690 N93-12564
Design of a digital Data Recording System (DRS)
[AD-A255088] p 561 N93-12623
Analysis of a structure-equipment system subjected to impact loading
[AD-A255097] p 622 N93-12652
Stability codes for a liquid rocket implemented for use on a PC
[NASA-CR-184453] p 525 N93-12659
Users manual for program SSFREQ intermediate mode stability curves: Developed for use on a PC computer
[NASA-CR-184452] p 682 N93-12675
Users manual for program ADMIT: Admittance and pressure transfer function developed for use on a PC computer
[NASA-CR-184450] p 682 N93-12676
Probabilistic evaluation of fuselage-type composite structures
[NASA-TM-105881] p 622 N93-12735
You need this done by when? Increasing your efficiency with the SAS system
[DE92-017894] p 683 N93-12792
RHALE: A MMALE shock physics code written in C++
[DE92-018271] p 684 N93-12795
Spreadsheet-like image analysis
[AD-A254395] p 619 N93-12864
Digital chart database conversion into a system electronic navigational chart
[AD-A255007] p 632 N93-12869
Computer-Aided Structural Engineering (CASE) project. Tutorial guide: Computer-Aided Structural Modeling (CASM). Version 3.00
[AD-A255075] p 684 N93-12872
Analysis and modeling of the CRRES satellite data
[AD-A254349] p 650 N93-12944
High Energy Propulsion System (HEPS) analysis
[AD-A254343] p 525 N93-12963
Cloud curve algorithm test program
[AD-A253918] p 662 N93-13099
Software reliability through fault-avoidance and fault-tolerance
[NASA-CR-189880] p 686 N93-13293
A computer program for engineering simulations of space reactor system performance
[DE92-016400] p 526 N93-13299
Numerical simulations of steel plate perforation
[DE92-017058] p 626 N93-13301
A stochastic/deterministic method for transient, three-dimensional neutron transport
[DE92-016690] p 704 N93-13319
The Fourth Annual Thermal and Fluids Analysis Workshop
[NASA-CP-10106] p 584 N93-13385
Analysis of a space emergency ammonia dump using the FLOW-NET two-phase flow program
p 584 N93-13389
Running SINDA '85/FLUINT interactive on the VAX
p 584 N93-13390
TRASYS form factor matrix normalization
p 585 N93-13391
A simple node and conductor data generator for SINDA
p 585 N93-13392
The Proteus Navier-Stokes code p 585 N93-13396
The program FANS-3D (finite analytic numerical simulation 3-dimensional) and its applications
p 586 N93-13399
Robot welding process control
[NASA-CR-184428] p 614 N93-13436
Multiple-function multi-input/multi-output digital control and on-line analysis
[NASA-TM-107697] p 500 N93-13565
Verification and validation of TMAP4
[DE92-019684] p 539 N93-13616
CORRIDOR: A routine for estimating the initial wave front resulting from high temperature fire exposure to a corridor
[PB92-213347] p 559 N93-13640
Providing structural modules with self-integrity monitoring software user's manual
[NASA-CR-190877] p 628 N93-13707
Semiconductor measurement technology: INSTANT (IGBT network simulation and transient Analysis tool)
[PB92-213529] p 725 N93-13783
Improved damping in composite structures through stress coupling, co-cured damping layers, and segmented stiffness layers p 630 N93-13823
Solar water heating system for a lunar base
p 641 N93-14005
Recursive algorithms for computational electromagnetics p 567 N93-14043
Human memory for the spatial locations of items on pull-down computer menus p 739 N93-14080

COMPUTER STORAGE DEVICES
GaAs gate dynamic memory technology
[AD-A254801] p 720 N93-12748
NSSDC Conference on Mass Storage Systems and Technologies for Space and Earth Science Applications, volume 1
[NASA-CP-3165-VOL-1] p 736 N93-13131
Storage system software solutions for high-end user needs p 737 N93-13136
Mass storage system experiences and future needs at the National Center for Atmospheric Research
p 737 N93-13138

COMPUTER SYSTEMS DESIGN
Testing and fault-tolerant design techniques for advanced digital architectures
[AD-A255013] p 681 N93-12707
Economical development of complex computer systems
[AD-A254752] p 689 N93-12848
Research summary, January 1989 - June 1990
[NASA-CR-190960] p 687 N93-13694
Integrated modeling tool for performance engineering of complex computer systems
[NASA-CR-190881] p 687 N93-13880
A study of traditional information access models applied in a hypertext information system p 739 N93-14076

COMPUTER SYSTEMS PERFORMANCE
Memory access in shared virtual memory
[DE92-019594] p 681 N93-12823
Parallel computing systems
[AD-A255076] p 689 N93-12852
Storage system software solutions for high-end user needs p 737 N93-13136
Performance of a plasma fluid code on the Intel parallel computers
[DE92-011680] p 716 N93-13297
A methodology for the solution of nonlinear two-point boundary value inverse problems in physics and engineering p 697 N93-13363
Integrated modeling tool for performance engineering of complex computer systems
[NASA-CR-190881] p 687 N93-13880

COMPUTER SYSTEMS PROGRAMS
Summary of awards, fiscal year 1990
[NSF-92-70] p 683 N93-12693
The Second NASA Formal Methods Workshop 1992
[NASA-CP-10110] p 684 N93-12957
Storage system software solutions for high-end user needs p 737 N93-13136

COMPUTER SYSTEMS SIMULATION
Parallel computing systems
[AD-A255076] p 689 N93-12852
Summary: Experimental validation of real-time fault-tolerant systems
[NASA-CR-190985] p 503 N93-13697

COMPUTER TECHNIQUES
Obtaining medians and other quantiles with limited memory space
[AD-A254506] p 683 N93-12722

COMPUTER VISION
Machine Perception
[AGARD-LS-185] p 692 N93-13238
Sensing and interpretation of 3-D shape and motion
p 692 N93-13240
Building and using scene representations in image understanding p 692 N93-13241
Silicon vision: Elementary functions to be implemented on electronic retinas p 692 N93-13242
3-D computer vision for navigation/control of mobile robots p 693 N93-13243
Machine perception exploiting high-level spatio-temporal models p 693 N93-13244
The 3-D computer vision techniques for object following and obstacle avoidance p 693 N93-13245
Determination of high temperature strains using a PC based vision system p 601 N93-13674

COMPUTERIZED SIMULATION
Seamless simulation literature survey
[AD-A254950] p 688 N93-12549
Action composition for the animation of natural language instructions
[AD-A254963] p 682 N93-12554
Experimental studies of cascade phenomena in metals
[DE92-019586] p 540 N93-12573
Bistatic clutter RCS simulation using scale model rough surfaces
[AD-A254932] p 560 N93-12581
Compression test simulation of thick-section composite materials
[AD-A255021] p 528 N93-12583
Uses of Monte Carlo computer simulations in understanding epitaxial growth and ion bombardment of Si(001)
[DE92-016944] p 719 N93-12586
An analysis of the low-earth-orbit communications environment p 561 N93-12633
Navier-Stokes simulations of unsteady transonic flow phenomena
[NASA-TM-103962] p 491 N93-12721
Probabilistic evaluation of fuselage-type composite structures
[NASA-TM-105881] p 622 N93-12735
X-29 linear aerodynamic perturbation model
[AD-A254810] p 500 N93-12752
Theoretical and experimental studies on the foundation theoretical and experimental studies on the foundation of mesomechanics
[AD-A254385] p 623 N93-12863
Design for reliability: Current density
[AD-A254770] p 570 N93-12866
Radiation dose to critical body organs for October 1989 proton event
[NASA-TP-3237] p 520 N93-12876
Proceedings of the Fifth European International Society for Terrain-Vehicle Systems, volume 1
[AD-A254619] p 611 N93-12906
NOAA Atmospheric Sciences Modeling Division support to the US Environmental Protection Agency
[PB92-217835] p 644 N93-12974
Diffusion-absorption heat pump
[PB92-217538] p 576 N93-12975
DATA: How to generate, store, retrieve, communicate, and interpret it: Proceedings
[DE92-040405] p 735 N93-13000
Fundamentals and Special Problems of Synthetic Aperture Radar (SAR)
[AGARD-LS-182] p 563 N93-13049
SAR simulation p 564 N93-13056
NASA aeronautics: Research and technology program highlights
[NASA-NP-159] p 491 N93-13110
Turbomachinery CFD on parallel computers
[NASA-TM-105932] p 689 N93-13154
The use of finite elements to model soil/track interactions in coupled multi-body dynamic simulations: Is real time simulation feasible?
[DE92-016184] p 612 N93-13236
Simulation of excitatory/inhibitory interactions in single auditory neurons
[AD-A253614] p 675 N93-13252
Applications of the Los Alamos High Energy Transport code
[DE92-017408] p 704 N93-13281
Simulation of forward-backward extrusion with numerical and model material techniques
[DE92-016299] p 558 N93-13298
A computer program for engineering simulations of space reactor system performance
[DE92-016400] p 526 N93-13299
Numerical simulations of steel plate perforation
[DE92-017058] p 626 N93-13301
A methodology for the solution of nonlinear two-point boundary value inverse problems in physics and engineering p 697 N93-13363
Simulation of two-dimensional icing, de-icing and anti-icing phenomena p 498 N93-13364
Two-phase/two-phase heat exchanger simulation analysis p 586 N93-13402
A SINDA '85 nodal heat transfer rate calculation user subroutine p 587 N93-13403
Robust control of a flexible link robot and rigid link robot: Theory, simulation, and experiment p 614 N93-13452
Development of a computer model for polycrystalline thin-film CuInSe2 and CdTe solar cells
[DE92-016444] p 639 N93-13529
Control of a very flexible robot in gravity
p 615 N93-13541
An investigation of the processes controlling ozone in the upper stratosphere
[DE92-019621] p 645 N93-13615
Heat transfer, fluid flow and interface shapes in floating-zone crystal growth p 724 N93-13739
Application of a vectorized particle simulation to the study of plates and wedges in high-speed rarefied flow
p 495 N93-13746
On the relationship between the intensity of extratropical frontal cyclone systems and water levels in the Gulf of Mexico p 666 N93-13816
Computer modeling of flow and transport interactions for compressible Navier-Stokes equations
p 589 N93-13825
Molecular theories and computer simulations of liquid crystals p 725 N93-13843
Computer simulation of a space-based infrared surveillance sensor
[AD-A255521] p 524 N93-13870

Hybrid 2 and hybrid 3 dummy neck properties for computer modeling
[AD-A255544] p 679 N93-13874
Non-perturbative studies in quantum electrodynamics p 729 N93-13896
Interaction of isotropic turbulence with a shock wave p 590 N93-13898
Particle simulation of grid erosion in an ion thruster p 527 N93-13927
Recent developments in the NL-Soar garden path theory
[AD-A255889] p 688 N93-13944
Deterministic and stochastic responses of nonlinear systems p 631 N93-13966
Convective parameterization in mesoscale models p 659 N93-14062
An investigation of the effects of topography on Colorado front range winter storms p 668 N93-14063

COMPUTERS
Summary of awards, fiscal year 1990
[NSF-92-70] p 683 N93-12693
Economical development of complex computer systems
[AD-A254752] p 689 N93-12848
Summary of awards. Fiscal year 1991
[NSF-92-36] p 681 N93-13431

CONCENTRATORS
Process designed for experimentation for increased-caliper Fresnel lenses
[DE92-019464] p 709 N93-12918

CONCRETE STRUCTURES
Concrete structure construction on the Moon p 559 N93-13989

CONCRETES
Nondestructive evaluation of the in-place compressive strength of concrete based upon limited destructive testing
[PB92-222751] p 623 N93-12981
Polypropylene fibers in portland cement concrete pavements
[DOT/FAA/RD-92/9] p 551 N93-13259
Physical properties of concrete made with Apollo 16 lunar soil sample p 554 N93-13987
The possibility of concrete production on the Moon p 554 N93-13988
Lunar concrete for construction p 555 N93-13990

CONDENSATES
Methods development for total organic carbon accountability
[NASA-CR-184438] p 672 N93-12949

CONDUCTING FLUIDS
Application of complex variables in electromagnetofluid dynamic, magnetofluid dynamic and fluid dynamic flows: Viscoelastic boundary-layer theory
[ISBN-0-315-65141-5] p 594 N93-14067

CONDUCTING POLYMERS
Electrochemical and chemical characteristics of a new ambient temperature Li(I) polymer electrolyte
[AD-A254918] p 545 N93-12651
Synthesis and properties of novel cluster phases
[DE92-017388] p 545 N93-12697
Electronic phenomena in polyanilines
[AD-A254803] p 545 N93-12749
Effect of plasticizers on the properties of new ambient temperature solid polymer electrolytes
[AD-A254817] p 545 N93-12754
Studies of plasticized-polymer electrolytes containing mixed Zn(2) and Li(1)
[AD-A254818] p 545 N93-12755
The effects of molecular structure on the electrical conductivity of polymers
[NASA-CR-191265] p 552 N93-13459

CONDUCTION BANDS
Synthesis and properties of mismatched heterojunction/substrate interfaces
[AD-A254577] p 719 N93-12648

CONDUCTIVE HEAT TRANSFER
Implicitly coupling heat conduction into a zone fire model
[PB92-222769] p 558 N93-12980
Development status of SINDA/FLUINT and SINAPS p 585 N93-13393
A SINDA '85 nodal heat transfer rate calculation user subroutine p 587 N93-13403
Transient behavior of heat pipe with thermal energy storage under pulse heat loads p 588 N93-13743

CONDUCTIVITY
High temperature oxidation and electrochemical studies related to hot corrosion
[AD-A254435] p 540 N93-12595

CONFERENCES
Proceedings of Joint RL/AFOSR Workshop on Intelligent Information Systems
[AD-A254795] p 734 N93-12703
Abstracts of papers presented at the International Symposium on Time, Frequency, and Dating in Geomorphology
[AD-A254927] p 649 N93-12704
NATO Advanced Research Workshop: Vortex Flows and Related Numerical Methods. List of participants, book of abstracts, and instructions for submission to the proceedings
[AD-A255015] p 575 N93-12708
Workshop on Super-Intense Laser-Atom Physics
[AD-A254833] p 604 N93-12734
Proceedings of FLICC forums on federal information policies. Combined summaries of proceedings. The 1990 7th Forum, Access is the Key and the 1991 8th Forum, Building Information Superhighways: Supercomputing Networks and Libraries
[PB92-147370] p 734 N93-12759
Soft X Ray Projection Lithography Topical Meeting. Volume 8: Technical digest
[AD-A254756] p 709 N93-12850
Proceedings of the Fifth European International Society for Terrain-Vehicle Systems, volume 1
[AD-A254619] p 611 N93-12906
Transactions: Tropospheric ozone and the environment. Papers from an international conference
[PB92-217017] p 643 N93-12941
DATA: How to generate, store, retrieve, communicate, and interpret it: Proceedings
[DE92-040405] p 735 N93-13000
Proceedings of the Tenth Symposium on Energy Engineering Sciences: Synergism of Analysis, Modeling, and Experiment
[DE92-018777] p 638 N93-13069
Review of progress in quantitative NDE
[DE92-018814] p 620 N93-13071
NSSDC Conference on Mass Storage Systems and Technologies for Space and Earth Science Applications, volume 1
[NASA-CP-3165-VOL-1] p 736 N93-13131
Aerodynamic Engine/Airframe Integration for High Performance Aircraft and Missiles
[AGARD-CP-498] p 577 N93-13199
Highlights 92/2 p 775 N93-13474
Effects of ionizing radiation on scintillators and other particle detectors
[DE92-018184] p 705 N93-13531
The 1992 NASA Langley Measurement Technology Conference: Measurement Technology for Aerospace Applications in High-Temperature Environments
[NASA-CP-3161] p 598 N93-13661
Diversity in biological research
[NSF-92-19] p 673 N93-13700
Symposium proceedings on Quantitative Feedback Theory
[AD-A255527] p 505 N93-13872
OSA proceedings of the topical meeting on optical amplifiers and their applications, volume 13
[AD-A252974] p 711 N93-13879
Compact Blue-Green Lasers: Summaries of papers presented at the topical meeting. Volume 6: Technical digest series
[AD-A255001] p 608 N93-13883
Coordinating Council. Ninth Meeting: Total Quality Management
[NASA-TM-108106] p 738 N93-13885
The Second Conference on Lunar Bases and Space Activities of the 21st Century, volume 2
[NASA-CP-3166-VOL-2] p 760 N93-13972
Informal Conference on Photochemistry
[AD-A255824] p 540 N93-14033

CONFORMAL MAPPING
Numerical analysis of scattering from certain conducting and dielectric bodies of arbitrary shape
[ISBN-0-315-63282-8] p 569 N93-14066

CONGRESSIONAL REPORTS
Large programs may consume increasing share of limited future budgets. Report to Congressional Requesters
[GAO/NSIAD-92-278] p 732 N93-13109
Space Station: Resolving conflict over integration contractor's role. Briefing report to the Chairman, Subcommittee on Investigations and Oversight, Committee on Science, Space, and Technology, House of Representatives
[GAO/NSIAD-92-291BR] p 732 N93-13111
Earth observing system: Information on NASA's incorporation of existing data into EOSDIS. Report to the Chairman, Committee on Science, Space, and Technology, House of Representatives
[GAO/IMTEC-92-79] p 736 N93-13112
Small planetary mission plan: Report to Congress
[NASA-TM-107809] p 513 N93-13266
NASA budget: Potential shortfalls in funding NASA's 5-year plan. Testimony before the Subcommittee on Science, Technology, and Space, Committee on Commerce, Science, and Transportation, United States Senate
[GAO/T-NSIAD-92-18] p 740 N93-13280
State award summary: Fiscal Year 1991
[NSF-92-3] p 775 N93-13381
Window on waste: Atrophy in NASA management
[GPO-57-273] p 732 N93-13693
National Aeronautics and Space Administration Authorization Act, fiscal year 1993
[S-REPT-102-364] p 741 N93-13798
NASA authorization, 1993, volume 2
[GPO-56-943-VOL-2] p 741 N93-13799
NASA's fiscal year 1993 budget
[S-HRG-102-707] p 742 N93-13800

CONIFERS
Forest declines: Some perspectives on linking processes and patterns
[DE92-019946] p 642 N93-12828
Radiative transfer theory for polarimetric remote sensing of pine forest p 633 N93-13085

CONNECTORS
Fastening apparatus having shape memory alloy actuator
[NASA-CASE-MSC-21935-1] p 614 N93-13423

CONSERVATION LAWS
Hyperbolic conservation laws with umbilic points, 1
[AD-A254431] p 696 N93-12594

CONSOLIDATION
Consolidation of powder coated thermoplastic preform process modeling
[AD-A255094] p 529 N93-12757
Enabling technologies for economical manufacturing of composites
[AD-A253615] p 531 N93-13324

CONSTITUTIVE EQUATIONS
The 3-D nonlinear constitutive modeling approach for composite materials
[AD-A255022] p 528 N93-12584
Analysis of large quasistatic deformations of inelastic solids by a new stress based finite element method
[NASA-CR-189235] p 626 N93-13260

CONSTRAINTS
Optimum design of aircraft structures with manufacturing and buckling constraints p 501 N93-13815

CONSTRUCTION
Scientific and engineering research facilities at universities and colleges: 1992
[NSF-92-325] p 506 N93-13407
The Second Conference on Lunar Bases and Space Activities of the 21st Century, volume 2
[NASA-CP-3166-VOL-2] p 760 N93-13972
Physical properties of concrete made with Apollo 16 lunar soil sample p 554 N93-13987
The possibility of concrete production on the Moon p 554 N93-13988
Concrete structure construction on the Moon p 559 N93-13989
Lunar concrete for construction p 555 N93-13990

CONSTRUCTION MATERIALS
Polypropylene fibers in portland cement concrete pavements
[DOT/FAA/RD-92/9] p 551 N93-13259
The possibility of concrete production on the Moon p 554 N93-13988
Concrete structure construction on the Moon p 559 N93-13989
Lunar concrete for construction p 555 N93-13990

CONSUMABLES (SPACECRAFT)
The influence of lunar propellant production on the cost-effectiveness of cislunar transportation systems p 556 N93-13983

CONTACTORS
A new apparatus for continuous countercurrent flow of solids and liquids
[DE92-011675] p 583 N93-13318

CONTAMINANTS
The broad band overlap problem in atmospheric trace gases p 641 N93-12624
Characterization of site geochemistry in support of environmental restoration
[DE92-017512] p 641 N93-12685
Materials SIG quantification and characterization of surface contaminants p 546 N93-12773
Z306 molecular contamination ad hoc committee results p 546 N93-12774
Surface contamination on LDEF exposed materials p 547 N93-12776
Sources and transport of silicone NVR p 547 N93-12777
Skylab D024 thermal control coatings and polymeric films experiment p 548 N93-12784

Interagency Workgroup on Air Quality Modeling (IWAQM) work plan rationale
[PB92-213248] p 643 N93-12940
ReTech, Inc., Plasma Centrifugal Furnace: Applications analysis report
[PB92-218791] p 714 N93-12982
MCFC diagnostics: HCl detection
[DE92-001292] p 639 N93-13313
Effects of coal-derived trace species on performance of molten carbonate fuel cells
[DE93-000203] p 639 N93-13427
Documentation for developing the initial source category list
[PB92-218429] p 646 N93-13647
Kinetic and spectroscopic studies of peroxy radical reactions related to tropospheric photo-oxidation chemistry p 654 N93-13726
Infrared spectroscopy of size resolved fine aerosol p 647 N93-13758

CONTAMINATION
Characterization of site geochemistry in support of environmental restoration
[DE92-017512] p 641 N93-12685
A novel diesel-fueled engine for microclimate cooling for the individual soldier
[AD-A254510] p 609 N93-12724
Touchstone for success
[ESA-BR-52] p 557 N93-12934

CONTINUITY EQUATION
A Fourier series method for polygonal domains: Large element computation for plates p 627 N93-13484

CONTINUOUS SPECTRA
A submillimetre polarimeter for the continuum receiver UKT14 on the James Clerk Maxwell Telescope p 748 N93-13852

CONTINUUM FLOW
A new apparatus for continuous countercurrent flow of solids and liquids
[DE92-011675] p 583 N93-13318

CONTINUUM MECHANICS
Thermodynamically consistent theories for elastoplasticity coupled with damage
[DE92-018283] p 627 N93-13515

CONTINUUMS
Development and computation of continuum higher order constitutive relations for high-altitude hypersonic flow p 494 N93-13578

CONTOURS
Perceptual dimensions of visual scenes relevant for simulating low-altitude flight
[AD-A254645] p 676 N93-12662

CONTRACT MANAGEMENT
An examination of the Total Quality Management (TQM) concept given current Federal/DoD competition initiatives
[AD-A255556] p 620 N93-13876

CONTRACTORS
AFOSR Contractors Meeting in Propulsion
[AD-A254484] p 525 N93-12575
USAF 1990 research initiation program, volume 2
[AD-A254654] p 773 N93-12663
USAF 1990 research initiation program, volume 4
[AD-A254655] p 773 N93-12664
USAF 1990 research initiation program, volume 1
[AD-A254656] p 773 N93-12665
Orbital Spacecraft Consumables Resupply System (OSCRS). Volume 3: Program cost estimate
[NASA-CR-185685] p 740 N93-12814
Space Station: Resolving conflict over integration contractor's role. Briefing report to the Chairman, Subcommittee on Investigations and Oversight, Committee on Science, Space, and Technology, House of Representatives
[GAO/NSIAD-92-291BR] p 732 N93-13111

CONTRACTS
USAF 1990 research initiation program, volume 2
[AD-A254654] p 773 N93-12663
USAF 1990 research initiation program, volume 4
[AD-A254655] p 773 N93-12664
USAF 1990 research initiation program, volume 1
[AD-A254656] p 773 N93-12665
USAF 1990 research initiation program, volume 3
[AD-A254755] p 775 N93-12849

CONTRAILS
SAC contrail formation study
[AD-A254410] p 499 N93-12605

CONTROL EQUIPMENT
RF system description for the ground test accelerator radio-frequency quadrupole
[DE92-040239] p 563 N93-13045
Electrical design of payload G-534: The Pool Boiling Experiment p 510 N93-13170

CONTROL SIMULATION
A multiple pointing-mount control strategy for space platforms
[NASA-CR-184448] p 522 N93-12893

CONTROL SURFACES
Space environmental effects on silvered teflon thermal control surfaces
[AD-A255909] p 554 N93-14099

CONTROL SYSTEMS DESIGN
Design philosophy for wind tunnel model positioning systems
[AD-A254958] p 506 N93-12552
Application of concurrent engineering methods to the design of an autonomous aerial robot
[AD-A254968] p 609 N93-12555
Limited production Precision Runway Monitor (PRM) master test plan
[DOT/FAA/CT-TN92/23] p 506 N93-12899
Dynamic control modification techniques in teleoperation of a flexible manipulator
[NASA-CR-190984] p 610 N93-12904
Numerical analysis of nonminimum phase zero for nonuniform link design p 611 N93-12953
Experimental verification of modified command shaping using a flexible manipulator p 612 N93-12955
The Second NASA Formal Methods Workshop 1992
[NASA-CP-10110] p 684 N93-12957
A brief overview of NASA Langley's research program in formal methods p 684 N93-12958
Application of Lanczos vectors to control design of flexible structures, part 2
[NASA-CR-191244] p 685 N93-13030
Hypersonic vehicle control law development using H infinity and mu-synthesis
[NASA-TM-107689] p 504 N93-13068
Robust control of uncertain aerospace and mechanical systems with unmodelled flexibilities: A singular perturbation approach p 691 N93-13129
Combined design of structures and controllers for optimal maneuverability p 691 N93-13130
Unsymmetric Lanczos model reduction and linear state function observer for flexible structures
[NASA-CR-191231] p 686 N93-13295
Active flutter suppression using dipole filters
[NASA-TM-107594] p 504 N93-13367
A stochastic optimal feedforward and feedback control methodology for superagility
[NASA-CR-4471] p 694 N93-13370
Robust control of a flexible link robot and rigid link robot: Theory, simulation, and experiment p 614 N93-13452
Design, construction, and control of a two degree-of-freedom electric direct-drive human power amplifier p 678 N93-13486
Robust controller and estimator design using minimax methods p 694 N93-13925
Experiments in two-cooperating-arm manipulation from a platform with unknown motion p 617 N93-13931
Near-minimum-time control of a flexible arm p 695 N93-14039
Q-Markov cover identification and integrated MCA-OVC controller design for flexible structures p 695 N93-14045

CONTROL THEORY
Hypersonic vehicle control law development using H infinity and mu-synthesis
[NASA-TM-107689] p 504 N93-13068
Symposium proceedings on Quantitative Feedback Theory
[AD-A255527] p 505 N93-13872
On a robust controller design using a minimax optimization approach p 695 N93-14021
Model reduction, sensor/actuator selection and control system redesign for large flexible structures p 523 N93-14040
Position and force control of flexible and rigid manipulators using the sliding-mode technique p 695 N93-14065

CONTROL VALVES
Action composition for the animation of natural language instructions
[AD-A254963] p 682 N93-12554

CONTROLLED ATMOSPHERES
Use of antarctic analogs to support the space exploration initiative
[NASA-TM-108000] p 651 N93-13326

CONTROLLED FUSION
A design for an advanced divertor for D3D and ITER: The radiative slot divertor
[DE92-019579] p 714 N93-12932
Fusion energy from the Moon for the twenty-first century p 719 N93-13985

CONTROLLERS
Design philosophy for wind tunnel model positioning systems
[AD-A254958] p 506 N93-12552
Manipulation strategies for massive space payloads
[NASA-CR-190844] p 611 N93-12952
Numerical analysis of nonminimum phase zero for nonuniform link design p 611 N93-12953
Robust control of uncertain aerospace and mechanical systems with unmodelled flexibilities: A singular perturbation approach p 691 N93-13129
Unsymmetric Lanczos model reduction and linear state function observer for flexible structures
[NASA-CR-191231] p 686 N93-13295
Application of Lanczos vectors to control design of flexible structures
[NASA-CR-191230] p 686 N93-13296
Force and motion control of a constrained flexible manipulator p 613 N93-13384
Ocular attention-sensing interface system
[NASA-CR-190884] p 678 N93-13450
Design, construction, and control of a two degree-of-freedom electric direct-drive human power amplifier p 678 N93-13486
Performance and stability of telemanipulators using bilateral impedance control p 614 N93-13488
Control of a very flexible robot in gravity p 615 N93-13541
Multiple-function multi-input/multi-output digital control and on-line analysis
[NASA-TM-107697] p 500 N93-13565
Robust controller and estimator design using minimax methods p 694 N93-13925
Experiments in two-cooperating-arm manipulation from a platform with unknown motion p 617 N93-13931
On a robust controller design using a minimax optimization approach p 695 N93-14021
Near-minimum-time control of a flexible arm p 695 N93-14039
Model reduction, sensor/actuator selection and control system redesign for large flexible structures p 523 N93-14040
Q-Markov cover identification and integrated MCA-OVC controller design for flexible structures p 695 N93-14045
Control algorithms for aerobraking in the Martian atmosphere p 524 N93-14046
Position and force control of flexible and rigid manipulators using the sliding-mode technique p 695 N93-14065

CONVECTION
The First United States Microgravity Laboratory
[NASA-TM-107980] p 557 N93-12951
Turbulent natural convection between a perforated vertical cylinder and a surrounding array
[DE92-019766] p 576 N93-12996
On the bootstrap current calculations based on values of the radial electron transport
[IPPCZ-317] p 715 N93-13091
Deep convection and its relation to the large-scale circulation in the tropical Pacific p 654 N93-13725
Coherent structures in compressible convection p 592 N93-13964
Convective parameterization in mesoscale models p 659 N93-14062

CONVECTION CELLS
Coherent structures in compressible convection p 592 N93-13964

CONVECTION CLOUDS
A parameterized quasi-five-cylinder convective cloud model and its application to remote sensing of rainfall p 663 N93-13489

CONVECTIVE FLOW
Radar studies of high latitude convection flows p 648 N93-12626
Flow through horizontal vents as related to compartment fire environments
[PB92-213388] p 559 N93-13642
Numerical investigation of non-spherical droplet dynamics in viscous convective flows p 591 N93-13918
Coherent structures in compressible convection p 592 N93-13964
Convective parameterization in mesoscale models p 659 N93-14062

CONVECTIVE HEAT TRANSFER
The role of latent heat release in explosive cyclogenesis
[AD-A254436] p 660 N93-12596
Natural convection between a vertical cylinder and a surrounding array
[DE92-019763] p 728 N93-12857
Turbulent natural convection between a perforated vertical cylinder and a surrounding array
[DE92-019766] p 576 N93-12996
The program FANS-3D (finite analytic numerical simulation 3-dimensional) and its applications p 586 N93-13399
The effects of pressure gradients on convective heat flux predictions in engine environments p 616 N93-13772
Computer modeling of flow and transport interactions for compressible Navier-Stokes equations p 589 N93-13825

CONVERGENCE
Hyperbolic conservation laws with umbilic points, 1
[AD-A254431] p 696 N93-12594
A methodology for the solution of nonlinear two-point boundary value inverse problems in physics and engineering p 697 N93-13363
CONVOLUTION INTEGRALS
Error control techniques for satellite and space communications
[NASA-CR-191229] p 565 N93-13411
COOLING
Natural convection between a vertical cylinder and a surrounding array
[DE92-019763] p 728 N93-12857
Effect of protective clothing ensembles on artillery battery crew performance
[AD-A254327] p 677 N93-12960
Radial turbine cooling
[NASA-TM-105658] p 492 N93-13292
Thermal issues at the SSC p 584 N93-13387
Intraseasonal variability of infrared cooling rates during the Asian summer monsoon and their influence on intraseasonal waves p 665 N93-13760
Solar energy utilisation and evacuated tubular solar collectors p 641 N93-14078
COOLING FLOWS (ASTROPHYSICS)
The mass and dynamics of cD clusters with cooling flows. 1: ROSAT observations of A 496
[NASA-CR-191240] p 743 N93-13352
Evidence for cool gas and star formation in cluster cooling flows p 751 N93-13380
COOLING SYSTEMS
A novel diesel-fueled engine for microclimate cooling for the individual soldier
[AD-A254510] p 609 N93-12724
New technologies for refrigeration without CFC's
[DE92-018886] p 557 N93-12922
Turbulent natural convection between a perforated vertical cylinder and a surrounding array
[DE92-019766] p 576 N93-12996
Reduction of chlorofluorocarbon emissions from refrigeration systems
[DE92-019360] p 645 N93-13505
Physiological stress from chemical defense clothing and equipment
[AD-A255786] p 676 N93-14028
COORDINATE TRANSFORMATIONS
Numerical analysis of scattering from certain conducting and dielectric bodies of arbitrary shape
[ISBN-0-315-63282-8] p 569 N93-14066
COORDINATES
Identifiability of linear systems in physical coordinates
[NASA-TM-107695] p 625 N93-13125
Automatic programming of arc welding robots p 616 N93-13720
COORDINATION
Chemical release and radiation effects experiment advanced planning and coordination
[NASA-CR-184439] p 649 N93-12718
Optimal coordination of robotic systems with redundancy p 693 N93-13336
COPPER
Recession of FEP specimens from trays D11 and B7 p 549 N93-12786
Synthesis of derivatives of alpha, omega difunctional perfluoroaliphatic compounds for low dielectric constant resins
[AD-A254928] p 550 N93-13026
All-metal, compact heat exchanger for space cryocoolers
[NASA-CR-190861] p 559 N93-13604
Intrinsic bistable photonic materials by copper colloid formation in silica
[AD-A255505] p 711 N93-13866
COPPER ALLOYS
A study of the vacancy loop formation probability in Ni-Cu and Ag-Pd alloys
[DE92-019584] p 541 N93-12879
COPPER OXIDES
Neutron scattering studies of the spin dynamics in La(2-x)Sr(x)O4
[DE92-019952] p 702 N93-13037
Magnetic behavior of a Bi(sub 2)Sr(sub 2)Ca(sub 1)Cu(sub 2)O(sub x) single crystal by direct magneto-optical observations
[DE92-018612] p 722 N93-13118
Activation energy and critical current density in Bi-Sr-Ca-Cu-O
[DE92-018795] p 723 N93-13547
COPPER SELENIDES
Novel thin-film CuInSe2 fabrication
[DE92-016440] p 723 N93-13526
Development of a computer model for polycrystalline thin-film CuInSe2 and CdTe solar cells
[DE92-016444] p 639 N93-13529
CORDAGE
Large-deflection analysis of cord composite plates p 530 N93-13008
CORES
The role of ambipolar diffusion in the formation of interstellar cloud cores and protostars p 755 N93-13828
CORIOLIS EFFECT
Numerical study of nonlinear convective-symmetric instability in a rotating baroclinic atmosphere p 666 N93-13786
CORONAL LOOPS
Equilibrium and eruption of solar coronal magnetic structures p 770 N93-13605
CORONAS
Equilibrium and eruption of solar coronal magnetic structures p 770 N93-13605
CORRELATION
Point correlations of geopotential height and temperature at 30 mb and between 500 mb and 30 mb
[PB92-222694] p 661 N93-12817
Variance of phase fluctuations of waves propagating through a random medium p 569 N93-13087
CORRELATION COEFFICIENTS
The correlation of active and passive microwave outputs for the Skylab S-193 sensor
[LEC-7819] p 635 N93-13440
CORRIDORS
CORRIDOR: A routine for estimating the initial wave front resulting from high temperature fire exposure to a corridor
[PB92-213347] p 559 N93-13640
CORROSION PREVENTION
Glass corrosion in natural environments
[NASA-CR-191234] p 551 N93-13150
A comparison of chromic acid and sulfuric acid anodizing
[NASA-TM-108383] p 543 N93-13378
Hermetic sealing and EMI shielding gasket
[AD-D015359] p 552 N93-13414
An evaluation of corrosion protection by two epoxy primers on 2219-T87 and 7075-T73 aluminum
[NASA-TM-108376] p 553 N93-13716
Heat resistant diffusion coating for niobium alloy
[AD-A255542] p 554 N93-13873
CORROSION RESISTANCE
A comparison of chromic acid and sulfuric acid anodizing
[NASA-TM-108383] p 543 N93-13378
CORROSION TESTS
Touchstone for success
[ESA-BR-52] p 557 N93-12934
Environmental effects on iron aluminides
[DE92-016341] p 542 N93-13237
An evaluation of corrosion protection by two epoxy primers on 2219-T87 and 7075-T73 aluminum
[NASA-TM-108376] p 553 N93-13716
COSMIC DUST
X ray scattering by cosmic dust grains p 750 N93-13294
COSMIC GASES
Evidence for cool gas and star formation in cluster cooling flows p 751 N93-13380
COSMIC NOISE
JARE data reports no. 176 (Ionosphere 47). Riometer records of 30 MHz cosmic noise at Syowa Station, Antarctica in 1990 p 772 N93-13255
COSMIC RAYS
Solar-geophysical data number 574, June 1992. Part 1: (Prompt reports). Data for May, April 1992 and late data
[PB92-218759] p 769 N93-12803
Katz model prediction of Caenorhabditis elegans mutagenesis on STS-42
[NASA-TM-4383] p 674 N93-13023
IIaO ultraviolet and nuclear emulsion films responses to orbital flights on STS-3, STS-7, STS-8, and STS-40 p 509 N93-13163
A program to study antiprotons in the cosmic rays: Arizona collaboration
[NASA-CR-191272] p 772 N93-13306
Large area nuclear particle detectors using ET materials, phase 2
[NASA-CR-190866] p 705 N93-13606
A search for point sources of cosmic ray muons using the MACRO detector p 773 N93-13738
COSMIC X RAYS
Uniformity results of the multilayer mirrors used in the ALEXIS ultrasoft x ray telescopes
[DE92-018611] p 743 N93-13342
COSMOLOGY
Preferred sets of states, predictability, classicality, and the environment-induced decoherence
[DE92-017447] p 641 N93-12684
The dynamical evolution of clusters of galaxies p 750 N93-13122
Theoretical high energy physics
[DE92-015480] p 707 N93-13189
Anisotropy measurements of the cosmic background radiation at 3 mm wavelength and an angular scale of 30 arcminutes p 772 N93-13689
Quantum inflationary minisuperspace cosmological models p 728 N93-13751
COST ANALYSIS
Orbital Spacecraft Consumables Resupply System (OSCRS). Volume 3: Program cost estimate
[NASA-CR-185685] p 740 N93-12814
Hydrogen Program Plan, FY 1993 - 1997
[DE92-010556] p 538 N93-13316
Cost analysis methodology: Photovoltaic Manufacturing Technology Project
[DE92-016441] p 639 N93-13528
Impact of lunar oxygen production on direct manned Mars missions p 540 N93-13984
A basis of settlement: Economic foundations of permanent pioneer communities p 741 N93-14019
Model reduction, sensor/actuator selection and control system redesign for large flexible structures p 523 N93-14040
COST EFFECTIVENESS
Cost-effective Sintered Reaction-Bonded Silicon Nitride (SRBSN) for structural ceramics
[DE92-019285] p 549 N93-12821
Economical development of complex computer systems
[AD-A254752] p 689 N93-12848
Ceramic machining: Assessment of current practice and research needs in the US
[PB92-213511] p 553 N93-13649
The influence of lunar propellant production on the cost-effectiveness of cislunar transportation systems p 556 N93-13983
Synergism of He-3 acquisition with lunar base evolution p 540 N93-13986
COST ESTIMATES
Orbital Spacecraft Consumables Resupply System (OSCRS). Volume 3: Program cost estimate
[NASA-CR-185685] p 740 N93-12814
Large programs may consume increasing share of limited future budgets. Report to Congressional Requesters
[GAO/NSIAD-92-278] p 732 N93-13109
National Aero-Space Plane: Key issues facing the program. Testimony before the Subcommittee on Technology and Competitiveness, Committee on Science, Space, and Technology, House of Representatives
[GAO/T-NSIAD-92-26] p 500 N93-13253
Business analysis: The commercial mission of the International Asteroid Mission p 514 N93-13554
COST REDUCTION
Aerodynamic studies of supersonic air intakes p 497 N93-13222
National Aero-Space Plane: Key issues facing the program. Testimony before the Subcommittee on Technology and Competitiveness, Committee on Science, Space, and Technology, House of Representatives
[GAO/T-NSIAD-92-26] p 500 N93-13253
A NASPAC-based analysis of the delay and cost effects of the Dallas/Fort Worth metroplex plan
[DOT/FAA/CT-TN92/21] p 507 N93-13447
COSTS
Adaptive automation and human performance. 3: Effects of practice on the benefits and costs of automation shifts
[AD-A254381] p 677 N93-12860
Process designed for experimentation for increased-caliper Fresnel lenses
[DE92-019464] p 709 N93-12918
Development of advanced turbine systems: Meeting tomorrow's needs
[DE92-017339] p 612 N93-13103
National Aero-Space Plane: Key issues facing the program. Testimony before the Subcommittee on Technology and Competitiveness, Committee on Science, Space, and Technology, House of Representatives
[GAO/T-NSIAD-92-26] p 500 N93-13253
The influence of lunar propellant production on the cost-effectiveness of cislunar transportation systems p 556 N93-13983
COUETTE FLOW
Navier-Stokes simulations of unsteady transonic flow phenomena
[NASA-TM-103962] p 491 N93-12721
Solution of viscous flow problems by using the boundary element method p 588 N93-13609
Instabilities and patterns in Taylor-Couette flow p 593 N93-13965
Numerical simulation of compressible Couette flow stability: Non-linear and three-dimensional effects p 594 N93-14077

COUNTER ROTATION
Investigation of advanced counterrotation blade configuration concepts for high speed turboprop systems. Task 4: Advanced fan section aerodynamic analysis
[NASA-CR-187128] p 502 N93-12695
A multiple-view visual study of the inner/outer region interactions of coherent motions in a turbulent boundary layer p 591 N93-13937
COUNTERMEASURES
Publications of the space physiology and countermeasures program, Musculoskeletal Discipline: 1980-1990
[NASA-CR-4468] p 743 N93-12898
COVALENT BONDS
Halogen surface chemistry on Si(100)-(2x1)
[AD-A254643] p 536 N93-12618
COVARIANCE
The use of consider covariance analysis in choosing data weights to reduce the effect of errors in model parameters on satellite orbit determination accuracy p 518 N93-13768
Orbit determination error analysis and station-keeping for liberation point trajectories p 518 N93-14038
CRACK CLOSURE
Studies on numerical and experimental determination of energy release rate for composite laminates p 533 N93-13752
Analysis of cracked plates subjected to out-of-plane loadings p 629 N93-13804
CRACK INITIATION
Theoretical and experimental studies on the foundation theoretical and experimental studies on the foundation of mesomechanics
[AD-A254385] p 623 N93-12863
Fatigue studies in Al-Mg-Si alloys p 543 N93-13690
Delamination initiation in postbuckled dropped-ply laminates p 535 N93-14030
CRACK OPENING DISPLACEMENT
Improved wide range expressions for displacements and inverse displacements for standard fracture toughness specimens
[AD-A254561] p 622 N93-12643
Numerical calibration of the stable poisson loaded specimen
[NASA-TM-105609] p 622 N93-12738
CRACK PROPAGATION
Small-strain and finite-strain finite element analyses of plane-strain tensile elastic-plastic crack growth p 621 N93-12628
Improved wide range expressions for displacements and inverse displacements for standard fracture toughness specimens
[AD-A254561] p 622 N93-12643
Numerical calibration of the stable poisson loaded specimen
[NASA-TM-105609] p 622 N93-12738
Theoretical and experimental studies on the foundation theoretical and experimental studies on the foundation of mesomechanics
[AD-A254385] p 623 N93-12863
Shallow-crack toughness results for reactor pressure vessel steel
[DE92-017813] p 626 N93-13320
The use of degradation measures in assessing reliability p 573 N93-13607
Fatigue studies in Al-Mg-Si alloys p 543 N93-13690
CRACK TIPS
Notch dimensions for three-point bend fracture specimens based on compliance analyses
[AD-A254641] p 620 N93-12580
Shallow-crack toughness results for reactor pressure vessel steel
[DE92-017813] p 626 N93-13320
Studies on numerical and experimental determination of energy release rate for composite laminates p 533 N93-13752
Analysis of cracked plates subjected to out-of-plane loadings p 629 N93-13804
CRACKING (FRACTURING)
Fracture toughness of short fiber/brittle matrix composites p 528 N93-12630
Stress crack testing of polyethylene geomembranes
[PB92-217132] p 622 N93-12843
Axisymmetric and antiplane shear crack problems in bonded nonhomogeneous materials p 625 N93-13127
Mechanical behaviour of fiber-reinforced ceramic matrix composites p 532 N93-13527
Matrix cracking initiation stress in fiber-reinforced ceramic matrix composites p 627 N93-13539
Load-transfer and crack bridging in fiber-toughened ceramic composites p 629 N93-13754
CRACKS
Notch dimensions for three-point bend fracture specimens based on compliance analyses
[AD-A254641] p 620 N93-12580
Stress crack testing of polyethylene geomembranes
[PB92-217132] p 622 N93-12843
Bifurcations in elastic-damaging materials
[DE92-018818] p 624 N93-13072
Micromechanics of finite length fibers in composite materials p 532 N93-13490
Finite elements for free edge delaminations and delaminated anisotropic beams p 535 N93-13967
CRASH LANDING
The identification and quantitation of triamterene in blood and urine from a fatal aircraft accident
[AD-A254550] p 674 N93-12612
CRASHES
Aircraft accident/incident summary report: Controlled flight into terrain, Bruno's Inc., Beechjet, N25BR, Rome, Georgia, December 11, 1991
[PB92-910404] p 498 N93-13470
CRAY COMPUTERS
Performance of a plasma fluid code on the Intel parallel computers
[DE92-011680] p 716 N93-13297
CREEP PROPERTIES
Influence of cold work level on the irradiation creep and creep rupture of titanium-modified austenitic stainless steels
[DE92-019078] p 541 N93-12820
High-temperature deformation and diffusion in oxides
[DE92-019593] p 720 N93-12854
Theoretical and experimental studies on the foundation theoretical and experimental studies on the foundation of mesomechanics
[AD-A254385] p 623 N93-12863
An investigation of the thermoviscoplastic behavior of a metal matrix composite at elevated temperatures
[NASA-CR-189706] p 530 N93-12929
Finite element analysis of anisotropic viscoelastic composite structures and analytical determination of optimum viscoelastic material properties p 530 N93-13007
Computational simulation of probabilistic lifetime strength for aerospace materials subjected to high temperature, mechanical fatigue, creep and thermal fatigue
[NASA-CR-190794] p 626 N93-13290
Investigations of the mechanical behavior of graphite/PEEK (APC-2) composites p 534 N93-13908
Thermoviscoplastic analysis of metal matrix composites p 535 N93-13954
CREEP RUPTURE STRENGTH
Development of weldable high-strength iron aluminides
[DE92-016018] p 542 N93-13190
CREWS
Effect of protective clothing ensembles on artillery battery crew performance
[AD-A254327] p 677 N93-12960
First International Microgravity Laboratory
[NASA-TM-108007] p 518 N93-13113
CRITICAL TEMPERATURE
Physical property data on fluorinated propanes and butanes as CFC and HCFC alternatives
[PB92-206507] p 555 N93-12939
Chemical potentials in dilute, multicomponent solutions
[DE92-011041] p 538 N93-13317
Effect of hydrogen reduction and doping on the characteristics of high-temperature superconductors p 725 N93-13844
CROP GROWTH
Crop growth and associated life support for a lunar farm p 680 N93-13994
Engineering verification of the biomass production chamber p 680 N93-13996
Scenarios for optimizing potato productivity in a lunar CELSS p 680 N93-13997
CROSS FLOW
Dynamics of vortex rings in cross-flow p 496 N93-13917
CROSS SECTIONS
Cross sections and rate coefficients for the electron-impact excitation of He-like ions
[ISAS-RN-647] p 703 N93-13095
CROSSLINKING
A tough high performance composite matrix
[NASA-CASE-LAR-14338-1] p 531 N93-13416
CROSSTALK
Integrated filter and detector array for spectral imaging
[NASA-CASE-NPO-18317-1-CU] p 709 N93-13419
CRUCIBLES
Heat transfer in a liquid metal crucible with an integral blackbody cavity
[DE92-019640] p 576 N93-12825
CRYOGENIC COOLING
A small, single stage orifice pulse tube cryocooler demonstration
[NASA-CR-190859] p 558 N93-13404
Three-stage sorption type cryogenic refrigeration systems and methods employing heat regeneration
[NASA-CASE-NPO-18366-1-CU] p 558 N93-13422
All-metal, compact heat exchanger for space cryocoolers
[NASA-CR-190861] p 559 N93-13604
CRYOGENIC FLUIDS
Fluid dynamics of supercritical helium within cable-in-conduit conductors
[DE92-019516] p 574 N93-12569
Effect of vaporization on cryogenic spray dropsize measurement
[NASA-TM-105909] p 597 N93-13410
CRYOGENIC ROCKET PROPELLANTS
Zero-gravity quantity gaging system
[NASA-CR-185602] p 556 N93-12699
CRYOGENIC STORAGE
Zero-gravity quantity gaging system
[NASA-CR-185602] p 556 N93-12699
CRYOGENIC TEMPERATURE
Experimental characterization of continuous alumina fiber/epoxy p 533 N93-13775
CRYPTOGRAPHY
Reviews of computing technology: Securing network applications, Kerberos, and RSA
[DE92-019928] p 690 N93-13620
CRYSTAL DEFECTS
Weak-beam imaging of dissociated dislocations in HVEM-irradiated Fe-Ni-Cr alloys
[DE92-019587] p 541 N93-12798
Oxygen diffusion in high-T(c) superconductors
[DE92-019597] p 720 N93-12807
Influence of dilute impurities on the evolution of defect cascades in nickel
[DE92-019585] p 542 N93-12973
Oxygen deficiencies at defects in YBa2Cu3O(7-delta) as determined by high resolution parallel electron energy loss
[DE92-016301] p 721 N93-13089
CONCAP 4: A Complex Autonomous Payload (CAP) for growing organic thin films in microgravity p 511 N93-13178
Defects near the Y2BaCuO5/YBa2Cu3O(7-x) interface and their effect on flux-pinning in melt-processed and quench-melt-growth processed YBa2Cu3O(7-x)
[DE92-014463] p 723 N93-13347
Simulation studies for surfaces and materials strength
[NASA-CR-191289] p 724 N93-13570
CRYSTAL DISLOCATIONS
Experimental studies of cascade phenomena in metals
[DE92-019586] p 540 N93-12573
Defects near the Y2BaCuO5/YBa2Cu3O(7-x) interface and their effect on flux-pinning in melt-processed and quench-melt-growth processed YBa2Cu3O(7-x)
[DE92-014463] p 723 N93-13347
CRYSTAL GROWTH
Measurements of crystal growth kinetics at extreme deviations from equilibrium
[DE92-019744] p 720 N93-12827
The First United States Microgravity Laboratory
[NASA-TM-107980] p 557 N93-12951
Silicide layer growth rates in Mo/Si multilayers
[DE92-019581] p 721 N93-12972
Spaceflight payload design flight experience G-408 p 508 N93-13160
CONCAP 4: A Complex Autonomous Payload (CAP) for growing organic thin films in microgravity p 511 N93-13178
A theoretical investigation of the growth rates of ice crystals in clouds p 653 N93-13485
Dynamics and pattern selection at the crystal-melt interface
[DE92-040210] p 724 N93-13577
Soft x ray window encapsulant for HgI2 detectors
[NASA-CR-190850] p 710 N93-13705
Heat transfer, fluid flow and interface shapes in floating-zone crystal growth p 724 N93-13739
Laser spectroscopy of rare earth ions p 608 N93-13846
CRYSTAL LATTICES
Oxygen diffusion in high-T(c) superconductors
[DE92-019597] p 720 N93-12807
Ion-channeling observation of correlated atomic displacements below Tc in YBa2Cu3O(7-x) and Pb-doped Bi2Sr2CaCu2O(x)
[DE92-018186] p 722 N93-13104
CRYSTAL OSCILLATORS
Tutorials from the 23rd Annual Precise Time and Time Interval (PTTI) Applications and Planning Meeting
[AD-A254745] p 596 N93-12844
CRYSTAL STRUCTURE
Experimental studies of cascade phenomena in metals
[DE92-019586] p 540 N93-12573

C60 transformations at high pressures
[DE92-019546] p 701 N93-12806
Oxygen diffusion in high-T(c) superconductors
[DE92-019597] p 720 N93-12807
Ordering energies and mechanisms in beta-phase NiAl
[DE92-040031] p 542 N93-13043
Defects near the Y2BaCuO5/YBa2Cu3O(7-x) interface and their effect on flux-pinning in melt-processed and quench-melt-growth processed YBa2Cu3O(7-x)
[DE92-014463] p 723 N93-13347
Radiation-disorder and aperiodicity in irradiated ceramics
[DE92-015051] p 552 N93-13350
Influence of surface defects and local structure on oxygenate reaction pathways over metal oxide surfaces
[DE92-040013] p 539 N93-13573
Effect of hydrogen reduction and doping on the characteristics of high-temperature superconductors p 725 N93-13844

CRYSTALLINITY
The crystallization and crystalline properties of LARC-TPI
[NASA-CR-191001] p 721 N93-13022
Single liquid source plasma enhanced metalorganic chemical vapor deposition of YBa2Cu3O(7-x) thin films
[AD-A254119] p 722 N93-13100
Investigations of the mechanical behavior of graphite/PEEK (APC-2) composites p 534 N93-13908

CRYSTALLIZATION
EURECA
[ESA-F-26] p 522 N93-12964
Eureca: A first for Europe
[ESA-BR-85] p 516 N93-13691
The formation of ore mineral deposits on the Moon: A feasibility study p 760 N93-13974

CRYSTALS
Thermal imaging of synchrotron beams on silicon crystals
[DE92-018182] p 719 N93-12562
Emittance, brilliance, and bandpass issues related to an inclined crystal monochromator
[DE92-019671] p 721 N93-12881
Stimulated Brillouin processes in crystals and glasses
[DE92-019549] p 721 N93-12887
Development of a stable electro-optical modulator
[NASA-CR-184404] p 710 N93-13696
The formation of ore mineral deposits on the Moon: A feasibility study p 760 N93-13974

CUBES (MATHEMATICS)
DATA: How to generate, store, retrieve, communicate, and interpret it: Proceedings
[DE92-040405] p 735 N93-13000

CULTURE TECHNIQUES
Phytoplankton photosynthesis in natural mixed layers
[AD-A255010] p 671 N93-12871
Establishing laboratory standards for biological flight experiments
[NASA-CR-184402] p 671 N93-12901
Microbiological methods for the water recovery systems test, revision 1.1
[NASA-CR-184390] p 678 N93-12966

CURING
Influence of cure shrinkage on process-induced stress and deformation in thick thermosetting composites
[AD-A254325] p 529 N93-12842

CURRENT DENSITY
Oxygen electrode reaction in molten carbonate fuel cells
[DE92-040180] p 636 N93-12812
Design for reliability: Current density
[AD-A254770] p 570 N93-12866
Measurement of current density fluctuations and ambipolar particle flux due to magnetic fluctuations in MST
[DE92-041013] p 713 N93-12878
Current density fluctuations, nonlinear coupling, and transport in MST
[DE92-041012] p 713 N93-12883
Effect of O2 partial pressure on post annealed Ba2YCu3O(7-delta) thin films
[DE92-014949] p 722 N93-13323
Activation energy and critical current density in Bi-Sr-Ca-Cu-O
[DE92-018795] p 723 N93-13547

CURRENT SHEETS
The 3-D description of vertical current sheets with application to solar flares
[SSL-PREPRINT-90-119] p 770 N93-13477
A thermal/nonthermal approach to solar flares p 771 N93-13639
Structure of and dynamical processes in the Earth's magnetopause and boundary layer regions p 657 N93-13793

CURVE FITTING
Improved wide range expressions for displacements and inverse displacements for standard fracture toughness specimens
[AD-A254561] p 622 N93-12643

CURVES
Users manual for program SSFREQ intermediate mode stability curves: Developed for use on a PC computer
[NASA-CR-184452] p 682 N93-12675

CYANATES
Hydrothermal organic synthesis experiments
[NASA-CR-191257] p 672 N93-13457

CYCLES
Thermally stable electrolytes for rechargeable lithium batteries, phase 2
[NASA-CR-190878] p 573 N93-13610

CYCLIC ACCELERATORS
Heavy-ion collisions and the nuclear equation of state
[DE92-019364] p 706 N93-12924

CYCLIC LOADS
On bilinearity of Manson-Coffin low-cycle-fatigue relationship
[NASA-TM-105840] p 622 N93-12739
Investigation of properties and performance of ceramic composite components
[DE92-019911] p 550 N93-12858

CYCLOGENESIS
The role of latent heat release in explosive cyclogenesis
[AD-A254436] p 660 N93-12596

CYCLONES
The role of latent heat release in explosive cyclogenesis
[AD-A254436] p 660 N93-12596
Extended range forecast of Atlantic seasonal hurricane activity for 1993 p 661 N93-12928
An observational and numerical investigation of meso-scale coastal processes during GALE IOP 2 p 665 N93-13776
On the relationship between the intensity of extratropical frontal cyclone systems and water levels in the Gulf of Mexico p 666 N93-13816
Frontogenesis processes in the troposphere p 667 N93-13890

CYCLOPROPANE
Structure sensitive reactions over Co, Fe and mixed metal clusters in zeolites
[DE92-040359] p 542 N93-12998

CYCLOTRON RADIATION
Observations of correlated broadband electrostatic noise and electron cyclotron emissions in the plasma sheet
[AD-A255002] p 712 N93-12705

CYCLOTRON RESONANCE
High magnetic field studies of strained layer superlattices p 726 N93-13895

CYCLOTRONS
The ORNL radioactive ion beam project with the ORIC accelerator
[DE92-040027] p 708 N93-13574

CYLINDRICAL BODIES
Natural convection between a vertical cylinder and a surrounding array
[DE92-019763] p 728 N93-12857
Dynamics and control of a tumbling satellite retrieval device p 522 N93-13119

CYLINDRICAL SHELLS
Structural optimization of thin shells using finite element method
[NASA-TM-105903] p 625 N93-13157
Fast optimization of static axisymmetric shell structures p 630 N93-13921
Bifurcation and localization instabilities in plastic bending of cylindrical shells p 630 N93-13923

CYTOCHROMES
Capillary electrophoresis: Electrospray ionization mass spectrometry in small diameter capillaries
[DE92-019123] p 575 N93-12711
Nitrogen control of chloroplast development and differentiation
[DE92-017392] p 671 N93-12768

D

DAMAGE
A study of the vacancy loop formation probability in Ni-Cu and Ag-Pd alloys
[DE92-019584] p 541 N93-12879
Bifurcations in elastic-damaging materials
[DE92-018818] p 624 N93-13072
Thermodynamically consistent theories for elastoplasticity coupled with damage
[DE92-018283] p 627 N93-13515
Providing structural modules with self-integrity monitoring software user's manual
[NASA-CR-190877] p 628 N93-13707
Toughening mechanisms in weak matrix ceramic composites p 553 N93-13780
Postoperative hyperbaric oxygen treatment of peripheral nerve damage
[AD-A255842] p 676 N93-14084

DAMAGE ASSESSMENT
The effects of compressive preloads on the compression-after-impact strength of carbon/epoxy
[NASA-TP-3303] p 529 N93-12678
Transverse flexural tests as a tool for assessing damage to PMR-15 composites from isothermal aging in air at elevated temperatures
[NASA-TM-105848] p 529 N93-12737
Thermal control surfaces on the MSFC LDEF experiments p 547 N93-12778
Debris/ice/TPS assessment and integrated photographic analysis for Shuttle mission STS-47
[NASA-TM-107553] p 520 N93-13032
Application of passive dosimetry for detection of leaking underground storage tanks
[PB92-218270] p 559 N93-13648

DARK MATTER
Some problems of quantum cosmology and dark matter physics p 755 N93-13829

DATA
Earth observing system: Information on NASA's incorporation of existing data into EOSDIS. Report to the Chairman, Committee on Science, Space, and Technology, House of Representatives
[GAO/IMTEC-92-79] p 736 N93-13112

DATA ACQUISITION
Real-time data archiving for GTA
[DE92-018613] p 733 N93-12567
Data acquisition applications for long duration electromagnetic launcher experiments
[AD-A254546] p 519 N93-12611
Design of a digital Data Recording System (DRS)
[AD-A255088] p 561 N93-12623
Multi-frequency multi-polarization processing for spaceborne SAR p 564 N93-13057
Development of a portable infrared emission spectrometer AA460 PIRES
[NASA-CR-190849] p 598 N93-13656

DATA BASE MANAGEMENT SYSTEMS
Application interface engine language and object reference manual
[DE92-017555] p 683 N93-12686
Utilization of databases to manage resources
[DE92-019598] p 735 N93-12808
Increasing the end user's productivity through seamless integration of applications with the database
[DE92-019599] p 735 N93-12824
Applying an object-oriented database model to a scientific database problem: Managing experimental data at CEBAF p 738 N93-13911

DATA BASES
Ocean optical database
[AD-A254969] p 668 N93-12556
Data to test and evaluate the performance of neural network architectures for seismic signal discrimination, volume 1
[AD-A254413] p 691 N93-12607
Coordinating Council. Fifth Meeting: Quality
[NASA-TM-108018] p 733 N93-12635
Earth science information: Planning for the integration and use of global change information
[NASA-CR-191217] p 733 N93-12660
Coordinating Council. Fourth Meeting: NACA Documents Database Project
[NASA-TM-108017] p 734 N93-12671
Proceedings of Joint RL/AFOSR Workshop on Intelligent Information Systems
[AD-A254795] p 734 N93-12703
Utilization of databases to manage resources
[DE92-019598] p 735 N93-12808
Nonideal thermoequilibrium calculations using a large product species data base
[DE92-040839] p 735 N93-12813
Increasing the end user's productivity through seamless integration of applications with the database
[DE92-019599] p 735 N93-12824
Publications of the space physiology and countermeasures program, Musculoskeletal Discipline: 1980-1990
[NASA-CR-4468] p 743 N93-12898
DIII-D edge physics database
[DE92-019577] p 714 N93-12971
ECLSS evolution: Advanced instrumentation interface requirements. Volume 3: Appendix C
[NASA-CR-184367] p 678 N93-12990
Report on phase 2 of 1990 OSSA data census
[NASA-TM-107992] p 735 N93-12991

DATA: How to generate, store, retrieve, communicate, and interpret it: Proceedings
[DE92-040405] p 735 N93-13000
Earth observing system: Information on NASA's incorporation of existing data into EOSDIS. Report to the Chairman, Committee on Science, Space, and Technology, House of Representatives
[GAO/IMTEC-92-79] p 736 N93-13112
Semantics-based reference resolution in technical text processing: An exploration of using the Word Net database in the computerized comprehensibility system
[AD-A255068] p 736 N93-13117
Guide to QSPIRES and the particle physics databases on SLACVM
[DE92-018099] p 737 N93-13275
Abstract and index collection in the Research Information Center of the National Institute of Standards and Technology
[PB92-217587] p 738 N93-13415
Identifying and describing Federal information inventory/locator systems: Design for networked-based locators, volume 1 p 738 N93-13884
Making object-oriented databases more knowledgeable (from ADAM to ABEL) p 738 N93-13910
Applying an object-oriented database model to a scientific database problem: Managing experimental data at CEBAF p 738 N93-13911
A theory of reference graphs in relational databases p 739 N93-13912

DATA CONVERSION ROUTINES
Digital chart database conversion into a system electronic navigational chart
[AD-A255007] p 632 N93-12869

DATA CORRELATION
A distributed timing system for sychronizing control and data correlation
[DE92-018603] p 690 N93-12564
Correlation for non-linear infrared calibration curves
[AD-A255098] p 596 N93-12653
Long Duration Exposure Facility M0003-5 thermal control coatings on DoD flight experiment p 548 N93-12782
Long Duration Exposure Facility M0003-5 recent results on polymeric films p 549 N93-12789
Using iterative orthophoto refinements to correct Digital Elevation Models (DEM's)
[AD-A254625] p 634 N93-13345

DATA FLOW ANALYSIS
Parallel computing systems
[AD-A255076] p 689 N93-12852
File servers, networking, and supercomputers p 737 N93-13137

DATA INTEGRATION
Applying an object-oriented database model to a scientific database problem: Managing experimental data at CEBAF p 738 N93-13911

DATA MANAGEMENT
Principles of information resource management: A foundation for the future
[AD-A254447] p 733 N93-12597
Functional system design document for the Intelligent Inspection System (IIS)
[DE92-018240] p 619 N93-12794
Utilization of databases to manage resources
[DE92-019598] p 735 N93-12808
Report on phase 2 of 1990 OSSA data census
[NASA-TM-107992] p 735 N93-12991
Engineering Design Information System (EDIS) Information Services Division (ISD) index function: User's manual
[DE92-041242] p 736 N93-13048
File servers, networking, and supercomputers p 737 N93-13137

DATA PROCESSING
Analysis of IMS spectra using neural networks
[DE92-017511] p 691 N93-12791
Reviews of computing technology: Fiber distributed data interface
[DE92-019927] p 681 N93-12886
Convective scale 4-D data assimilation using simulated single Doppler radar observations
[PB92-218726] p 651 N93-12969
SAR peculiarities, ambiguities and constraints p 563 N93-13051
Multi-frequency multi-polarization processing for spaceborne SAR p 564 N93-13057
Enterprise storage report for the 1990's p 736 N93-13132
Mass storage system experiences and future needs at the National Center for Atmospheric Research p 737 N93-13138

DATA PROCESSING EQUIPMENT
Multi-frequency multi-polarization processing for spaceborne SAR p 564 N93-13057

DATA RECORDERS
Design of a digital Data Recording System (DRS)
[AD-A255088] p 561 N93-12623

DATA RECORDING
Design of a digital Data Recording System (DRS)
[AD-A255088] p 561 N93-12623
Optical disks become erasable p 736 N93-13133
Magnetic disk p 737 N93-13134
Magnetic tape p 737 N93-13135
A novel-high-performance system for recording and analysing instantaneous total pressure distortion in air intakes p 580 N93-13215

DATA REDUCTION
Speedup properties of phases in the execution profile of distributed parallel programs
[DE92-019301] p 689 N93-12797
Production of SSM/I data sets
[NASA-CR-190944] p 632 N93-12800
An analysis of the tornado-producing Raleigh thunderstorm of November 28, 1988
[AD-A254384] p 661 N93-12862
Applications of the Los Alamos High Energy Transport code
[DE92-017408] p 704 N93-13281
SO2 on Venus: A final cross-calibration with Pioneer Venus
[NASA-CR-191256] p 758 N93-13344

DATA RETRIEVAL
Earth observing system: Information on NASA's incorporation of existing data into EOSDIS. Report to the Chairman, Committee on Science, Space, and Technology, House of Representatives
[GAO/IMTEC-92-79] p 736 N93-13112
Guide to QSPIRES and the particle physics databases on SLACVM
[DE92-018099] p 737 N93-13275

DATA SAMPLING
From comparison density to two sample analysis
[AD-A253866] p 698 N93-13064

DATA SIMULATION
SAR simulation p 564 N93-13056

DATA STORAGE
Design of a digital Data Recording System (DRS)
[AD-A255088] p 561 N93-12623
Massively parallel optical-to-electronic data transfer
[AD-A254831] p 688 N93-12733
SAR peculiarities, ambiguities and constraints p 563 N93-13051
NSSDC Conference on Mass Storage Systems and Technologies for Space and Earth Science Applications, volume 1
[NASA-CP-3165-VOL-1] p 736 N93-13131
Enterprise storage report for the 1990's p 736 N93-13132
Optical disks become erasable p 736 N93-13133
Storage system software solutions for high-end user needs p 737 N93-13136
File servers, networking, and supercomputers p 737 N93-13137
Mass storage system experiences and future needs at the National Center for Atmospheric Research p 737 N93-13138
The long hold: Storing data at the National Archives p 737 N93-13139
Magnetic bearings for a high-performance optical disk buffer, volume 1
[NASA-CR-190873] p 616 N93-13706

DATA SYSTEMS
DATA: How to generate, store, retrieve, communicate, and interpret it: Proceedings
[DE92-040405] p 735 N93-13000
NSSDC Conference on Mass Storage Systems and Technologies for Space and Earth Science Applications, volume 1
[NASA-CP-3165-VOL-1] p 736 N93-13131
Magnetic tape p 737 N93-13135
Mass storage system experiences and future needs at the National Center for Atmospheric Research p 737 N93-13138
Applying an object-oriented database model to a scientific database problem: Managing experimental data at CEBAF p 738 N93-13911

DATA TRANSFER (COMPUTERS)
Massively parallel optical-to-electronic data transfer
[AD-A254831] p 688 N93-12733

DATA TRANSMISSION
State space methods in multidimensional digital signal processing
[AD-A254646] p 561 N93-12620
Anomalous TWTA output power spikes and their effect on a digital satellite communications system
[NASA-TM-105875] p 571 N93-13286
The protection of the Facsimile (FAX) machine against the insider threat
[DE92-019424] p 565 N93-13506
Engineering data transfer test with EDMICS using MIL-R-28002 (Raster)
[DE92-019808] p 738 N93-13619
DNET: A communications facility for distributed heterogeneous computing
[NASA-CR-190863] p 682 N93-13759

DAYTIME
NOAA Workshop on Climate Scale Operational Precipitation and Water Vapor Products
[NOAA-TR-NESDIS-62] p 662 N93-13066

DEACTIVATION
The MAGSORB process for bulk separation of carbon dioxide
[DE92-001296] p 538 N93-13314

DECAY
Recent developments in the theory of heavy-quark decays
[DE92-017598] p 704 N93-13250

DECAY RATES
Phase mixing and surface wave decay in an inhomogeneous plasma
[IPPCZ-320] p 715 N93-13006

DECELERATION
Physiologically constrained aerocapture for manned Mars missions
[NASA-TM-103954] p 521 N93-12720

DECIDUOUS TREES
Deciduous forest scene complexity in high-resolution multispectral scanner imagery
[AD-A255511] p 635 N93-13867

DECISION MAKING
Specification of adaptive aiding systems
[AD-A254537] p 499 N93-12602
Earth science information: Planning for the integration and use of global change information
[NASA-CR-191208] p 734 N93-12680
Sensitivity analysis of the simultaneous proportionate change of inputs and outputs in data envelopment analysis
[AD-A254821] p 683 N93-12730

DECOMPRESSION SICKNESS
Complement proteins and decompression sickness susceptibility
[AD-A254448] p 674 N93-12905

DECONTAMINATION
Characterization of site geochemistry in support of environmental restoration
[DE92-017512] p 641 N93-12685
ReTech, Inc., Plasma Centrifugal Furnace: Applications analysis report
[PB92-218791] p 714 N93-12982

DEFECTS
Electronic structure of microclusters and defect complexes
[AD-A254807] p 720 N93-12750
Spreadsheet-like image analysis
[AD-A254395] p 619 N93-12864
Diagnostic of material defects found in pipelines made of 13 HMF steel on the basis of acoustic emission p 623 N93-12989
Finite element study of ultrasonic imaging p 700 N93-13774
Effects of residual stress, weld toe notch and weld defects on fatigue of welded steel structures p 631 N93-13947

DEFENSE PROGRAM
Principles of information resource management: A foundation for the future
[AD-A254447] p 733 N93-12597
An examination of the Total Quality Management (TQM) concept given current Federal/DoD competition initiatives
[AD-A255556] p 620 N93-13876

DEFLECTORS
Quantum well, beam deflecting surface emitting lasers
[NASA-CASE-NPO-18243-1-CU] p 605 N93-13418
Acousto-optic devices and applications p 712 N93-14100

DEFORESTATION
Forest declines: Some perspectives on linking processes and patterns
[DE92-019946] p 642 N93-12828

DEFORMATION
Experiments, theory, and simulation on the evolution of fabric in granular materials
[AD-A254820] p 545 N93-12729
RHALE: A MMALE shock physics code written in C++
[DE92-018271] p 684 N93-12795
Influence of cure shrinkage on process-induced stress and deformation in thick thermosetting composites
[AD-A254325] p 529 N93-12842
High-temperature deformation and diffusion in oxides
[DE92-019593] p 720 N93-12854
Acoustic radiation from a point excited infinite bilaminar plate p 531 N93-13144

Analysis of large quasistatic deformations of inelastic solids by a new stress based finite element method
[NASA-CR-189235] p 626 N93-13260
An investigation into thermomechanical fatigue of metal matrix composites p 534 N93-13810

DEGRADATION
An experimental and theoretical study of degradation pathways for atmospheric halocarbons
p 646 N93-13624

DEGREES OF FREEDOM
Torque resolver design for tendon-driven manipulators
[DE92-017395] p 609 N93-12698
Design, construction, and control of a two degree-of-freedom electric direct-drive human power amplifier p 678 N93-13486

DEICING
Icing prevention by ultrasonic nucleation of supercooled water droplets in front of subsonic aircraft
[DOT/FAA/CT-TN92/38] p 497 N93-12816
Simulation of two-dimensional icing, de-icing and anti-icing phenomena p 498 N93-13364

DELAMINATING
Scale effects in buckling, postbuckling and crippling of graphite-epoxy Z-section stiffeners p 621 N93-12632
Microcracking, microcrack-induced delamination, and longitudinal splitting of advanced composite structures
[NASA-CR-4472] p 623 N93-12911
Results of ASTM round robin testing for mode 1 interlaminar fracture toughness of composite materials
[NASA-TM-104222] p 532 N93-13428
Effects of layer waviness on compression-loaded thermoplastic composite laminates p 532 N93-13724
Finite elements for free edge delaminations and delaminated anisotropic beams p 535 N93-13967
Delamination initiation in postbuckled dropped-ply laminates p 535 N93-14030

DELAY
A NASPAC-based analysis of the delay and cost effects of the Dallas/Fort Worth metroplex plan
[DOT/FAA/CT-TN92/21] p 507 N93-13447

DELAY LINES
Arm length matching in 10 m delay-line interferometer
[ISAS-TN-649] p 596 N93-12639

DELTA WINGS
The influence of intake swirl distortion on the steady-state performance of a low bypass, twin-spool engine p 579 N93-13211
Effects of forebody strakes and Mach number on overall aerodynamic characteristics of configuration with 55 deg cropped delta wing
[NASA-TP-3253] p 493 N93-13353
An experimental and computational investigation of slender wings undergoing wing rock
p 505 N93-13915
The unsteady aerodynamics of a delta wing undergoing large-amplitude pitching motions p 496 N93-13929

DEMAGNETIZATION
The implications of the magnetism of ordinary chondrites p 755 N93-13795

DEMOGRAPHY
A study regarding information-seeking behavior, valuation of information including perceptions of information attributes, and associated correlates pertaining to information usage p 740 N93-14088

DENSIFICATION
Laser densification and doping of sol-gel glasses
[AD-A254566] p 604 N93-12644
Sol-gel synthesis and densification of aluminoborosilicate powders. Part 1: Synthesis
[NASA-TM-103964] p 527 N93-12895
Sol-gel synthesis and densification of aluminoborosilicate powders. Part 2: Densification
[NASA-TM-103969] p 528 N93-12896
Microstructural evolution in reaction bonded alumina/mullite ceramics p 552 N93-13328

DENSIMETERS
Experimental testing of four correction algorithms for the forward scattering spectrometer probe
[NASA-TM-105906] p 597 N93-13307

DENSITY (MASS/VOLUME)
Determination of the permeability of carbon aerogels by gas flow measurements
[DE92-019574] p 550 N93-12888

DENSITY DISTRIBUTION
From comparison density to two sample analysis
[AD-A253866] p 698 N93-13064

DENSITY MEASUREMENT
Zero-gravity quantity gaging system
[NASA-CR-185602] p 556 N93-12699
Acoustic device and method for measuring gas densities
[NASA-CASE-NPO-18155-1-CU] p 700 N93-13421
Electron beam fluorescence measurements in the Boeing hypersonic shock tunnel p 602 N93-13681
Resonance lamp absorption measurement of OH number density and temperature in expansion tube scramjet engine tests p 602 N93-13682
Gas temperature and density measurements based on spectrally resolved Rayleigh-Brillouin scattering
p 602 N93-13684

DEOXYRIBONUCLEIC ACID
AFRRI reports
[AD-A254581] p 674 N93-12649

DEPLOYMENT
Tether deployment monitoring system, phase 2
[NASA-CR-184098] p 522 N93-13425

DEPOLYMERIZATION
Bonding in simple phosphate glass
[DE92-019437] p 550 N93-12917

DEPOSITION
High temperature superconductor materials and applications
[NASA-CR-184437] p 719 N93-12691
The National Atmospheric Deposition Program/National Trends Network (NADP/NTN) site visitation program
[PB92-217298] p 642 N93-12726
Integrated filter and detector array for spectral imaging
[NASA-CASE-NPO-18317-1-CU] p 709 N93-13419
A meteorology-based approach to detecting response source-receptor relationships p 664 N93-13736
Study of the concentration and deposition of tropospheric aerosols using x ray emission techniques
p 667 N93-13894
The heteroepitaxial growth of YBCO and other metal oxides on silicon and GaAs by pulsed laser deposition
p 726 N93-13904

DEPOSITS
Diesel injector fouling bench test methodology
[AD-A254532] p 609 N93-12600
Sources and transport of silicone NVR
p 547 N93-12777

DEPTH MEASUREMENT
Precision liquid-level measurement in deep tanks using a swept-RF resonant cavity
[DE92-017236] p 597 N93-13267

DESERTS
Water and cheese from the lunar desert: Abundances and accessibility of H, C, and N on the Moon
p 761 N93-13976

DESIGN ANALYSIS
Optimal design and control of distributed parameter systems
[AD-A254947] p 690 N93-12547
Pressure fed thrust chamber technology program
[NASA-CR-184461] p 526 N93-12968
Optical design for a balloon-borne magnetograph
[NASA-CR-191003] p 709 N93-13062
Design, construction and demonstration of modular, reconfigurable robots p 613 N93-13329
Phased array feed design technology for Large Aperture Microwave Radiometer (LAMR) Earth observations
[NASA-CR-189727] p 519 N93-13462
Design guide for the ergonomic aspects of helicopter crew seating
[ISVR-TR-209] p 678 N93-13464
All-metal, compact heat exchanger for space cryocoolers
[NASA-CR-190861] p 559 N93-13604
The environmental control and life-support system for a lunar base: What drives its design
p 680 N93-13991
Validation test of 125 Ah advanced design IPV nickel-hydrogen flight cells
[NASA-TM-105912] p 527 N93-14079

DESORPTION
Halogen surface chemistry on Si(100)-(2x1)
[AD-A254643] p 536 N93-12618
Photochemical dynamics of surface oriented molecules
[DE92-019813] p 703 N93-13106
Electron stimulated desorption of the metallic substrate at monolayer coverage: Sensitive detection via 193 nm laser photoionization of neutral aluminum desorbed from CH3O/Al(111)
[DE92-014858] p 723 N93-13349

DESTRUCTIVE TESTS
Stress crack testing of polyethylene geomembranes
[PB92-217132] p 622 N93-12843
Nondestructive evaluation of the in-place compressive strength of concrete based upon limited destructive testing
[PB92-222751] p 623 N93-12981
Development of a 1000 g, 10 ms mechanical shock test capability
[DE92-019193] p 624 N93-13077

DETECTION
Capacitive skin characterization
[NASA-CR-191261] p 598 N93-13567
Application of passive dosimetry for detection of leaking underground storage tanks
[PB92-218270] p 559 N93-13648

DETERIORATION
Lunar concrete for construction p 555 N93-13990

DETONATION
Measurements of cellular structure in spray detonation
[DE92-019580] p 555 N93-12933
Development of a laser ignited all secondary explosive DDT detonator
[DE92-019340] p 555 N93-13081

DETONATORS
Development of a laser ignited all secondary explosive DDT detonator
[DE92-019340] p 555 N93-13081
Booster explosive rings
[AD-D015375] p 556 N93-13471

DEUTERIUM
Fusion energy from the Moon for the twenty-first century p 719 N93-13985

DIAMAGNETISM
Interaction of energetic ring current protons with magnetospheric hydromagnetic waves
p 718 N93-13750

DIAMETERS
Booster explosive rings
[AD-D015375] p 556 N93-13471

DIAMONDS
Simulation studies for surfaces and materials strength
[NASA-CR-191289] p 724 N93-13570

DIATOMIC MOLECULES
Computer program for calculating and fitting thermodynamic functions
[NASA-RP-1271] p 728 N93-12967

DIELECTRIC PROPERTIES
Model for impedance of an ionic conductor sandwiched between blocking electrodes
[DE92-017812] p 569 N93-12561
Polarimetric signatures of a canopy of dielectric cylinders based on first and second order vector radiative transfer theory p 569 N93-13088

DIELECTRICS
Group 2 cubic fluorides dielectrics for 3-D integration and GaAs-based optoelectronic structures
[AD-A254937] p 719 N93-12544
Bistatic clutter RCS simulation using scale model rough surfaces
[AD-A254932] p 560 N93-12581
Synthesis of derivatives of alpha, omega difunctional perfluoroaliphatic compounds for low dielectric constant resins
[AD-A254928] p 550 N93-13026
Polarimetric signatures of a canopy of dielectric cylinders based on first and second order vector radiative transfer theory p 569 N93-13088
Microwave and infrared dielectric relaxation of alkylcarbonates, chloroform and their mixtures at 25 C
[AD-A253606] p 537 N93-13096
Numerical analysis of permittivity with loss in isotropic binary composites
[AD-A255203] p 534 N93-13940
Electromagnetic scattering simulations using equivalent boundary condition models p 569 N93-14052

DIESEL ENGINES
Diesel injector fouling bench test methodology
[AD-A254532] p 609 N93-12600
A novel diesel-fueled engine for microclimate cooling for the individual soldier
[AD-A254510] p 609 N93-12724

DIESEL FUELS
White paper: Preliminary assessment of LNG vehicle technology, economics, and safety issues, revision 1
[PB92-212943] p 615 N93-13644

DIETS
Crop growth and associated life support for a lunar farm p 680 N93-13994

DIFFERENCE EQUATIONS
Numerical calculation of turbomachinery cascade flows p 589 N93-13767

DIFFERENTIAL EQUATIONS
Stabilization and projection methods for multibody dynamics
[PB92-133883] p 698 N93-12890

DIFFERENTIAL GEOMETRY
Coordinates in differential geodesy
[AD-A254951] p 632 N93-12550
Mathematics and string theory
[DE92-019292] p 727 N93-12796

DIFFRACTION PATTERNS
Near-normal incidence scattering from rough, finite surfaces: Kirchhoff theory and data comparison for Arctic sea ice
[AD-A254525] p 668 N93-12577
Narrow bandgap semiconducting silicides: Intrinsic infrared detectors on a silicon chip
[NASA-CR-190882] p 571 N93-13430

DIFFUSE RADIATION
Radiative transfer in the middle atmosphere
p 652 N93-13482
DIFFUSION
Modeling and estimation of reciprocal diffusion and Gauss-Markov random fields
[AD-A255034] p 698 N93-12709
High-temperature deformation and diffusion in oxides
[DE92-019593] p 720 N93-12854
On grain boundary transport of hydrogen and mechanism of hydrogen-induced intergranular fracture
p 544 N93-14047
Diffusion of ion-implanted group 4 n-type dopants in gallium arsenide and gallium/arsenide-based superlattices p 727 N93-14073
DIFFUSION COEFFICIENT
Ion radial diffusion in an electrostatic impulse model for stormtime ring current formation
[NASA-CR-190941] p 705 N93-12715
Oxygen diffusion in high-T(c) superconductors
[DE92-019597] p 720 N93-12807
DIFFUSION FLAMES
Stability of the compressible reacting mixing layer
p 592 N93-13948
DIFFUSION THEORY
Longitudinal beam dynamics with rf noise
[DE92-040645] p 707 N93-13108
DIGITAL COMPUTERS
Reviews of computing technology: Fiber distributed data interface
[DE92-019927] p 681 N93-12886
DIGITAL DATA
Satellite imagery goes to the field
[AD-A254449] p 632 N93-12598
Design of a digital Data Recording System (DRS)
[AD-A255088] p 561 N93-12623
A novel-high-performance system for recording and analysing instantaneous total pressure distortion in air intakes p 580 N93-13215
Automatic pattern recognition techniques for geometrical correction on satellite data
p 687 N93-13913
DIGITAL FILTERS
State space methods in multidimensional digital signal processing
[AD-A254646] p 561 N93-12620
DIGITAL SYSTEMS
Design of a digital Data Recording System (DRS)
[AD-A255088] p 561 N93-12623
The Second NASA Formal Methods Workshop 1992
[NASA-CP-10110] p 684 N93-12957
Fundamentals and Special Problems of Synthetic Aperture Radar (SAR)
[AGARD-LS-182] p 563 N93-13049
Digital imaging systems
[DE92-019194] p 736 N93-13078
Test and control computer user's guide for a digital beam former test system
[NASA-CR-189208] p 685 N93-13291
Multiple-function multi-input/multi-output digital control and on-line analysis
[NASA-TM-107697] p 500 N93-13565
Digital fluoroscopy with an optically coupled charge-coupled device p 712 N93-14101
DIGITAL TELEVISION
Efficacy of multimedia instruction and an introduction to digital multimedia technology
[AD-A254509] p 734 N93-12723
DILUTION
Chemical potentials in dilute, multicomponent solutions
[DE92-011041] p 538 N93-13317
DIMENSIONAL ANALYSIS
Heat transfer in a liquid metal crucible with an integral blackbody cavity
[DE92-019640] p 576 N93-12825
Aspects of atmospheric transport and dispersion within an air basin p 656 N93-13782
DIMERS
Halogen surface chemistry on Si(100)-(2x1)
[AD-A254643] p 536 N93-12618
DIODES
Laser formation of lithium plasma ion sources for applied-B ion diodes on the PBFA-2 accelerator
[DE92-016091] p 716 N93-13191
DIPOLE ANTENNAS
ILS mathematical modeling study of the effects of an ASR-9 structure at the Long Island MacArthur Airport, Islip, NY
[DOT/FAA/CT-TN92/25] p 506 N93-12668
Scattering from a finite collection of transverse dipole and axial slot arrays with edge effects
p 568 N93-14048
DIRAC EQUATION
Second quantization in bit-string physics
[DE92-019645] p 727 N93-12826
DIRECT CURRENT
A thermal/nonthermal approach to solar flares
p 771 N93-13639
DIRECT POWER GENERATORS
A heat pipe coupled planar thermionic converter: Performance characterization, nondestructive testing, and evaluation
[AD-A254941] p 727 N93-12546
DIRECTIONAL STABILITY
Aerodynamic integration of thrust reversers on the Fokker 100 p 502 N93-13208
DIRECTORIES
Program Support Communications Network (PSCN) facsimile system directory
[NASA-TM-108051] p 562 N93-12909
Directory of awards, fiscal year 1991. Directorate for engineering
[NSF-92-55] p 775 N93-13704
DISABILITIES
Women and minorities in science and engineering: An update
[NSF-92-303] p 730 N93-12907
DISCONNECT DEVICES
Fastening apparatus having shape memory alloy actuator
[NASA-CASE-MSC-21935-1] p 614 N93-13423
DISCRETE FUNCTIONS
From comparison density to two sample analysis
[AD-A253866] p 698 N93-13064
DISCRIMINANT ANALYSIS (STATISTICS)
SAC contrail formation study
[AD-A254410] p 499 N93-12605
DISILICIDES
Ductile phase toughening of molybdenum disilicide by low pressure plasma spraying
[DE92-007409] p 551 N93-13315
DISK GALAXIES
Spectroscopic studies of low-density gas in the Galactic disk and halo p 753 N93-13499
DISLOCATIONS (MATERIALS)
Is there a unique effective interaction profile for dislocations?
[DE92-018615] p 543 N93-13545
DISPENSERS
Automated dry powder dispenser for explosive components
[DE92-019425] p 555 N93-12568
DISPERSIONS
Elevated temperature tensile properties of borated 304 stainless steel: Effect of boride dispersion on strength and ductility
[DE92-040096] p 542 N93-13302
DISPLACEMENT
A study of the interlaminar stress continuity theories for composite laminates p 621 N93-12627
Axisymmetric and antiplane shear crack problems in bonded nonhomogeneous materials
p 625 N93-13127
Acoustic radiation from a point excited infinite bilaminar plate p 531 N93-13144
DISPLACEMENT MEASUREMENT
Determination of high temperature strains using a PC based vision system p 601 N93-13674
DISPLAY DEVICES
Human memory for the spatial locations of items on pull-down computer menus p 739 N93-14080
DISSIPATION
Connection of microscopic with macroscopic dynamics: Towards a hydrodynamical description of quantum mechanics p 729 N93-13957
DISSOLVING
Glass corrosion in natural environments
[NASA-CR-191234] p 551 N93-13150
DISTILLATION
Technology development for lunar base water recycling p 680 N93-13999
DISTRIBUTED PARAMETER SYSTEMS
Optimal design and control of distributed parameter systems
[AD-A254947] p 690 N93-12547
A general theory of signal integration for fault-tolerant dynamic distributed sensor networks
[AD-A254961] p 732 N93-12553
On a robust controller design using a minimax optimization approach p 695 N93-14021
DISTRIBUTED PROCESSING
Seamless simulation literature survey
[AD-A254950] p 688 N93-12549
A distributed timing system for sychronizing control and data correlation
[DE92-018603] p 690 N93-12564
Speedup properties of phases in the execution profile of distributed parallel programs
[DE92-019301] p 689 N93-12797
Speedup properties of phases in the execution profile of distributed parallel programs
[DE92-019965] p 689 N93-12810
Memory access in shared virtual memory
[DE92-019594] p 681 N93-12823
Reviews of computing technology: Fiber distributed data interface
[DE92-019927] p 681 N93-12886
Lazy checkpoint coordination for bounding rollback propagation
[NASA-CR-191281] p 565 N93-13375
Monitoring and controlling distributed applications using Lomita (position paper)
[NASA-CR-190971] p 687 N93-13695
DIURETICS
The identification and quantitation of triamterene in blood and urine from a fatal aircraft accident
[AD-A254550] p 674 N93-12612
DIURNAL VARIATIONS
Cloud curve algorithm test program
[AD-A253918] p 662 N93-13099
Neurochemical control of circadian rhythms
[AD-A255054] p 675 N93-13116
JARE data reports no. 170 (ionosphere 45). HF field strength data measured at Syowa Station, Antarctica from January to December 1988 p 652 N93-13432
Deciduous forest scene complexity in high-resolution multispectral scanner imagery
[AD-A255511] p 635 N93-13867
Long-term averages of globally-measured ELF/VLF radio noise
[AD-A255518] p 566 N93-13869
A statistical study of narrow bandwidth, high-latitude geomagnetic pulsations p 660 N93-14068
DIVERTERS
A design for an advanced divertor for D3D and ITER: The radiative slot divertor
[DE92-019579] p 714 N93-12932
Future development of the D3-D tokamak program
[DE92-040051] p 715 N93-13044
DIVIDERS
Advanced on-chip divider for monolithic microwave VCO's
[NASA-CR-191355] p 572 N93-13563
DOCUMENTS
Coordinating Council. Seventh Meeting: Acquisitions
[NASA-TM-108020] p 733 N93-12636
Publications of the space physiology and countermeasures program, Musculoskeletal Discipline: 1980-1990
[NASA-CR-4468] p 743 N93-12898
Evolution of the scientific paper
[DE92-019696] p 735 N93-12994
The long hold: Storing data at the National Archives
p 737 N93-13139
DOMAINS
A Fourier series method for polygonal domains: Large element computation for plates p 627 N93-13484
DOMES (STRUCTURAL FORMS)
Qualification of the gritblast assembly and process for the inside diameter of the RSRM forward and aft domes
[NASA-CR-184462] p 558 N93-13021
DOPED CRYSTALS
Laser densification and doping of sol-gel glasses
[AD-A254566] p 604 N93-12644
Proton transport on modified sulfonated polyaniline electrodes
[AD-A254917] p 570 N93-12650
Measurements of crystal growth kinetics at extreme deviations from equilibrium
[DE92-019744] p 720 N93-12827
Effect of hydrogen reduction and doping on the characteristics of high-temperature superconductors
p 725 N93-13844
Laser spectroscopy of rare earth ions
p 608 N93-13846
DOPPLER RADAR
Storm tracking for TDWR: A correlation algorithm design and evaluation
[AD-A254701] p 660 N93-12622
Convective scale 4-D data assimilation using simulated single Doppler radar observations
[PB92-218726] p 651 N93-12969
Terminal Doppler Weather Radar (TDWR) Operational Test and Evaluation (OT/E) integration test plan
[DOT/FAA/CT-TN92/6] p 499 N93-13377
Birds mimicking microbursts on 2 June 1990 in Orlando, Florida
[AD-A255703] p 498 N93-14024
DOSAGE
Procedures for the diagnostic dose resistance test kits for mosquitoes, body lice, and beetle pests of stored products
[AD-A255224] p 675 N93-13941

DOSIMETERS
Application of passive dosimetry for detection of leaking underground storage tanks
[PB92-218270] p 559 N93-13648
DOWNBURSTS
The modelling of turbulence and downbursts for flight simulators p 507 N93-13542
DOWNLINKING
An analysis of the low-earth-orbit communications environment p 561 N93-12633
DOWNWASH
Navier-Stokes flowfield computation of wing/rotor interaction for a tilt rotor aircraft in hover p 497 N93-14035
DRAG
Recent developments in low-speed TPS-testing for engine integration drag and installed thrust reversr simulation p 502 N93-13207
DRAG MEASUREMENT
Aeronomy coexperiments on drag-free satellites with proportional thrusters: GP-B and STEP p 518 N93-13922
DRAG REDUCTION
Analysis and design of planar and non-planar wings for induced drag minimization
[NASA-CR-191274] p 493 N93-13463
DRAINAGE PATTERNS
The use of remotely sensed data in delineation of hydrologic response units and estimation of their rainfall-runoff model parameters p 635 N93-13840
DRIFT (INSTRUMENTATION)
Thin film thermocouples for high temperature measurement on ceramic materials p 599 N93-13666
DRONE AIRCRAFT
Application of concurrent engineering methods to the design of an autonomous aerial robot
[AD-A254968] p 609 N93-12555
DROP SIZE
Effect of vaporization on cryogenic spray dropsize measurement
[NASA-TM-105909] p 597 N93-13410
A laboratory investigation of raindrop oscillations p 666 N93-13790
DROPS (LIQUIDS)
Sources of cloud nuclei and development of remote sensing techniques for cloud parameters
[AD-A255016] p 660 N93-12558
Computational fluid dynamics combustion analysis evaluation
[NASA-CR-184326] p 575 N93-12688
Modeling of coalescence, agglomeration, and phase segregation in microgravity processing of bimetallic composite materials
[NASA-CR-191247] p 556 N93-12728
Experimental testing of four correction algorithms for the forward scattering spectrometer probe
[NASA-TM-105906] p 597 N93-13307
Numerical study on mixing of sprayed liquid in an LNG storage tank p 584 N93-13388
Numerical investigation of non-spherical droplet dynamics in viscous convective flows p 591 N93-13918
DRUGS
The identification and quantitation of triamterene in blood and urine from a fatal aircraft accident
[AD-A254550] p 674 N93-12612
DUCTED FLOW
An experimental and computational study of longitudinal vortices in turbulent boundary layers p 595 N93-14097
DUCTILITY
Development of weldable high-strength iron aluminides
[DE92-016018] p 542 N93-13190
Ductile fracture process of discontinuous fiber reinforced composites
[DE92-016298] p 531 N93-13264
Elevated temperature tensile properties of borated 304 stainless steel: Effect of boride dispersion on strength and ductility
[DE92-040096] p 542 N93-13302
Ductile phase toughening of molybdenum disilicide by low pressure plasma spraying
[DE92-007409] p 551 N93-13315
DUCTS
On the prediction of turbulent secondary flows
[NASA-CR-189722] p 575 N93-12717
DUMMIES
Hybrid 2 and hybrid 3 dummy neck properties for computer modeling
[AD-A255544] p 679 N93-13874
DWARF NOVAE
Nucleosynthesis in nova explosions
[DE92-040349] p 753 N93-13523
DWARF STARS
An optical study of the faint end of the stellar luminosity function p 748 N93-13960
A systematic search for low-mass companions orbiting nearby stars and the calibration of the end of the stellar main sequence p 749 N93-14070
DYNAMIC CHARACTERISTICS
A fundamental study of the effect of gravity on the static and dynamic behavior of robots p 610 N93-12760
Self-consistent modeling of the ionosphere-thermosphere-magnetosphere system
[AD-A253232] p 651 N93-13276
Hybrid 2 and hybrid 3 dummy neck properties for computer modeling
[AD-A255544] p 679 N93-13874
DYNAMIC CONTROL
Innovative methods in the dynamics of large space structures
[AD-A254630] p 521 N93-12579
Dynamic control modification techniques in teleoperation of a flexible manipulator
[NASA-CR-190984] p 610 N93-12904
Application of Lanczos vectors to control design of flexible structures, part 2
[NASA-CR-191244] p 685 N93-13030
Dynamics and control of a tumbling satellite retrieval device p 522 N93-13119
Robust control of uncertain aerospace and mechanical systems with unmodelled flexibilities: A singular perturbation approach p 691 N93-13129
Unsymmetric Lanczos model reduction and linear state function observer for flexible structures
[NASA-CR-191231] p 686 N93-13295
Application of Lanczos vectors to control design of flexible structures
[NASA-CR-191230] p 686 N93-13296
End-point position control of multi-link flexible manipulator arms p 613 N93-13335
Force and motion control of a constrained flexible manipulator p 613 N93-13384
Experiments in two-cooperating-arm manipulation from a platform with unknown motion p 617 N93-13931
Q-Markov cover identification and integrated MCA-OVC controller design for flexible structures p 695 N93-14045
DYNAMIC LOADS
Analysis of a structure-equipment system subjected to impact loading
[AD-A255097] p 622 N93-12652
Investigation of properties and performance of ceramic composite components
[DE92-019911] p 550 N93-12858
The use of finite elements to model soil/track interactions in coupled multi-body dynamic simulations: Is real time simulation feasible?
[DE92-016184] p 612 N93-13236
An investigation of dynamic stress reduction of multi-body aircraft using active gust control p 505 N93-13916
DYNAMIC MODELS
A multiple pointing-mount control strategy for space platforms
[NASA-CR-184448] p 522 N93-12893
Approximate optimal guidance for the Advanced Launch System p 519 N93-13819
Formulation and validation of high-order mathematical models of helicopter flight dynamics p 501 N93-13821
A low-dimensional dynamical systems description of coherent structures in the axisymmetric jet mixing layer p 593 N93-14057
DYNAMIC PRESSURE
Performance and control of ascending trajectories to minimize heat load for transatmospheric aero-space planes p 495 N93-13745
DYNAMIC PROGRAMMING
Optimal control computer programs
[NASA-TM-108384] p 693 N93-13289
Approximate optimal guidance for the Advanced Launch System p 519 N93-13819
DYNAMIC RESPONSE
Innovative methods in the dynamics of large space structures
[AD-A254630] p 521 N93-12579
Initial experiments in end-point control of a flexible, two-link manipulator p 612 N93-13018
Robust control of uncertain aerospace and mechanical systems with unmodelled flexibilities: A singular perturbation approach p 691 N93-13129
Self-consistent modeling of the ionosphere-thermosphere-magnetosphere system
[AD-A253232] p 651 N93-13276
Proceedings of the 62nd Shock and Vibration Symposium, Volume 2
[AD-A249267] p 628 N93-13637
Transonic aeroelastic analysis of systems with structural nonlinearities p 629 N93-13769
An investigation of the dynamic response of lifting surfaces with concentrated structural nonlinearities p 501 N93-13807
Formulation and validation of high-order mathematical models of helicopter flight dynamics p 501 N93-13821
DYNAMIC STRUCTURAL ANALYSIS
Innovative methods in the dynamics of large space structures
[AD-A254630] p 521 N93-12579
A multiple pointing-mount control strategy for space platforms
[NASA-CR-184448] p 522 N93-12893
Application of Lanczos vectors to control design of flexible structures, part 2
[NASA-CR-191244] p 685 N93-13030
NASA aeronautics: Research and technology program highlights
[NASA-NP-159] p 491 N93-13110
Acoustic radiation from a point excited infinite bilaminar plate p 531 N93-13144
A domain decomposition method for parallel transient response calculations p 504 N93-13827
An investigation of dynamic stress reduction of multi-body aircraft using active gust control p 505 N93-13916
DYNAMIC TESTS
Europe qualifies for space
[ESA-BR-64] p 508 N93-12892
Design guide for the ergonomic aspects of helicopter crew seating
[ISVR-TR-209] p 678 N93-13464
Hybrid 2 and hybrid 3 dummy neck properties for computer modeling
[AD-A255544] p 679 N93-13874
DYNAMICAL SYSTEMS
Robust control of uncertain aerospace and mechanical systems with unmodelled flexibilities: A singular perturbation approach p 691 N93-13129
Applications of CFD and visualization techniques p 584 N93-13386
The nonequilibrium statistical mechanics of chaotic maps p 729 N93-13832
A low-dimensional dynamical systems description of coherent structures in the axisymmetric jet mixing layer p 593 N93-14057
DYNAMO THEORY
Limits on galactic dynamo theory due to magnetic fluctuations p 754 N93-13636

E

E REGION
Radar studies of high latitude convection flows p 648 N93-12626
A joint study of the lower ionosphere by radar, lidar, and spectrometer p 655 N93-13755
EARTH ALBEDO
Sulfate impact upon low-level cloud albedo over oceans p 661 N93-12833
EARTH ATMOSPHERE
A correlated k-distribution model of the heating rates for CH4 and N2O in the atmosphere between 0 and 60 km
[NASA-TM-108062] p 643 N93-12926
Airblast damage from small asteroids
[DE92-017834] p 749 N93-12956
Report of the Science Working Group: Science with a lunar optical interferometer p 747 N93-13600
EARTH CRUST
GPS measurements at Vandenberg AFB
[AD-A254978] p 499 N93-12557
Seismic studies of crustal structure and tectonic evolution across the central California margin and the Colorado Plateau margin p 657 N93-13794
Atmospheric loading response of the solid earth and oceans p 659 N93-13955
EARTH ENVIRONMENT
JPRS report: Science and technology. Central Eurasia: Life sciences
[JPRS-ULS-92-024] p 672 N93-13033
Remote sensing of Earth terrain
[NASA-CR-190908] p 633 N93-13084
Atmospheric, climatic and environmental research
[NASA-CR-191367] p 664 N93-13718
EARTH GRAVITATION
The determination and error assessment of the Earth's gravity field model p 656 N93-13771
Resonance studies of artificial earth satellites p 523 N93-14037
EARTH HYDROSPHERE
On the space-time ocean current variability and its effects on the length-of-day p 636 N93-14051

EARTH IONOSPHERE
Radar studies of high latitude convection flows
p 648 N93-12626
Self-consistent modeling of the ionosphere-thermosphere-magnetosphere system
[AD-A253232] p 651 N93-13276
JARE data reports no. 170 (ionosphere 45). HF field strength data measured at Syowa Station, Antarctica from January to December 1988 p 652 N93-13432
Experimental studies of ionospheric irregularities and related plasma processes
[NASA-CR-191271] p 652 N93-13460
EARTH MAGNETOSPHERE
Observations of correlated broadband electrostatic noise and electron cyclotron emissions in the plasma sheet
[AD-A255002] p 712 N93-12705
Analysis and modeling of the CRRES satellite data
[AD-A254349] p 650 N93-12944
Self-consistent modeling of the ionosphere-thermosphere-magnetosphere system
[AD-A253232] p 651 N93-13276
Interaction of energetic ring current protons with magnetospheric hydromagnetic waves
p 718 N93-13750
A statistical study of narrow bandwidth, high-latitude geomagnetic pulsations p 660 N93-14068
EARTH MANTLE
Lateral variations of shear velocity and anelasticity in the upper mantle of the western US from Rayleigh wave observations p 653 N93-13492
EARTH OBSERVATIONS (FROM SPACE)
Earth observation photography: Looking back 20 years after Skylab p 509 N93-13164
Manned observations technology development, FY 1992 report
[NASA-CR-185704] p 597 N93-13373
Taking a global view
[ESA-BR-37-C] p 516 N93-13856
A home port in space
[ESA-BR-37-E] p 516 N93-13858
EARTH OBSERVING SYSTEM (EOS)
Earth science information: Planning for the integration and use of global change information
[NASA-CR-191208] p 734 N93-12680
Earth observing system: Information on NASA's incorporation of existing data into EOSDIS. Report to the Chairman, Committee on Science, Space, and Technology, House of Representatives
[GAO/IMTEC-92-79] p 736 N93-13112
The Capillary Pumped Loop Flight Experiment (CAPL): A pathfinder for EOS p 512 N93-13181
EARTH ORBITAL ENVIRONMENTS
LDEF Materials Workshop 1991, part 1
[NASA-CP-3162-PT-1] p 545 N93-12769
LDEF materials: An overview of the interim findings
p 546 N93-12770
LDEF atomic oxygen fluence update
p 546 N93-12771
LDEF yaw and pitch angle estimates
p 524 N93-12772
Surface contamination on LDEF exposed materials
p 547 N93-12776
Thermal control surfaces on the MSFC LDEF experiments p 547 N93-12778
Anodized aluminum on LDEF: A current status of measurements on chromic acid anodized aluminum
p 544 N93-12779
Performance of thermal control tape in the protection of composite materials p 536 N93-12780
Fluorescence of thermal control coatings on S0069 and A0114 p 548 N93-12781
Long Duration Exposure Facility M0003-5 thermal control coatings on DoD flight experiment
p 548 N93-12782
Element Material Exposure Experiment by EFFU
p 548 N93-12783
Skylab D024 thermal control coatings and polymeric films experiment p 548 N93-12784
Effects of the LDEF environment on the Ag/FEP thermal blankets p 548 N93-12785
Recession of FEP specimens from trays D11 and B7
p 549 N93-12786
Characterization of selected LDEF: Exposed polymer films and resins p 549 N93-12787
Effects of orbital exposure on Halar during the LDEF mission p 549 N93-12788
Long Duration Exposure Facility M0003-5 recent results on polymeric films p 549 N93-12789
Analysis and modeling of the CRRES satellite data
[AD-A254349] p 650 N93-12944
Study of plasma environments for the integrated Space Station electromagnetic analysis system
[NASA-CR-191263] p 522 N93-13152
Ground operations and logistics in the context of the International Asteroid Mission p 515 N93-13560
Studies of surface-induced luminescence relevant to spacecraft glow, using a seeded arc-jet
p 523 N93-13919
Wake characterization: Full flow simulation of space structures in low earth orbit p 497 N93-13970
EARTH ORBITS
EURECA
[ESA-F-26] p 522 N93-12964
The LDCE Particle Impact Experiment as flown on STS-46 --- limited duration space environment candidate materials exposure (LDCE) p 512 N93-13183
Report of the Working Group on Space/Lunar Tradeoffs p 747 N93-13599
A guidance methodology for the cislunar transfer of low-thrust spacecraft p 517 N93-13766
Infrared emission from the water outgas cloud of an orbiting vehicle induced by collisions with atmospheric gases p 521 N93-13854
EARTH RADIATION BUDGET
A study of the Earth Radiation Budget Experiment: Shortwave measurements and bidirectional reflectance models for the ocean surface p 654 N93-13722
EARTH RADIATION BUDGET EXPERIMENT
A study of the Earth Radiation Budget Experiment: Shortwave measurements and bidirectional reflectance models for the ocean surface p 654 N93-13722
EARTH ROTATION
On the space-time ocean current variability and its effects on the length-of-day p 636 N93-14051
EARTH SCIENCES
Earth science information: Planning for the integration and use of global change information
[NASA-CR-191217] p 733 N93-12660
Earth science information: Planning for the integration and use of global change information
[NASA-CR-191208] p 734 N93-12680
NSSDC Conference on Mass Storage Systems and Technologies for Space and Earth Science Applications, volume 1
[NASA-CP-3165-VOL-1] p 736 N93-13131
EARTH SURFACE
Earth observation photography: Looking back 20 years after Skylab p 509 N93-13164
A surface pressure altitude prediction model
[AD-A255834] p 668 N93-14082
EARTH-MOON SYSTEM
Introduction to the International Asteroid Mission
p 513 N93-13549
A guidance methodology for the cislunar transfer of low-thrust spacecraft p 517 N93-13766
EARTHQUAKES
Data to test and evaluate the performance of neural network architectures for seismic signal discrimination, volume 1
[AD-A254413] p 691 N93-12607
Effects of source-region phenomenology on seismic discrimination
[DE92-017441] p 649 N93-12841
ECLIPSING BINARY STARS
A search for point sources of cosmic ray muons using the MACRO detector p 773 N93-13738
ECONOMIC ANALYSIS
Earth science information: Planning for the integration and use of global change information
[NASA-CR-191217] p 733 N93-12660
Future regional transport aircraft market, constraints, and technology stimuli
[NASA-TM-107669] p 491 N93-13025
Business analysis: The commercial mission of the International Asteroid Mission p 514 N93-13554
Considerations for the transition from fuel cell R/D to manufacturing
[DE92-019977] p 640 N93-13622
Westinghouse PAFC program update
[DE92-019978] p 640 N93-13623
A basis of settlement: Economic foundations of permanent pioneer communities p 741 N93-14019
ECONOMIC DEVELOPMENT
Research and development in industry: 1989. Funds, 1989. Scientists and engineers, January 1990
[NSF-92-307] p 741 N93-13658
A basis of settlement: Economic foundations of permanent pioneer communities p 741 N93-14019
ECONOMIC FACTORS
Economical development of complex computer systems
[AD-A254752] p 689 N93-12848
ECONOMICS
World Energy Projection System (WEPS), March 1992. Model installation manual, distribution disk layout
[PB92-169572] p 637 N93-12937
Energy from Municipal Waste Program
[DE92-010578] p 638 N93-13102
White paper: Preliminary assessment of LNG vehicle technology, economics, and safety issues, revision 1
[PB92-212943] p 615 N93-13644
A basis of settlement: Economic foundations of permanent pioneer communities p 741 N93-14019
ECOSYSTEMS
An ion budget for a terra firme rainforest in Central Amazonia
[INPE-5365-PRE/1745] p 632 N93-13005
Proceedings of the Mediterranean Conference on Environmental Geotechnology
[AD-A253672] p 644 N93-13098
Assimilation of satellite color observations in a coupled ocean GCM-ecosystem model
[NASA-CR-191218] p 670 N93-13714
Integration of vegetation indices and thermal measurements for ecosystem modeling
p 646 N93-13721
Long-term lunar stations: Some ecological considerations p 648 N93-13995
Scenarios for optimizing potato productivity in a lunar CELSS p 680 N93-13997
EDDY CURRENTS
Automated eddy current analysis of materials
[NASA-CR-184432] p 619 N93-12875
Eddy current power dissipation at sharp corners
[DE92-016890] p 571 N93-13300
EDITING
Semantics-based reference resolution in technical text processing: An exploration of using the Word Net database in the computerized comprehensibility system
[AD-A255068] p 738 N93-13117
EDUCATION
Coordinating Council. Eighth Meeting: Using the Internet
[NASA-TM-108019] p 734 N93-12673
Science and engineering degrees, by race/ethnicity of recipients: 1977-1990
[NSF-92-327] p 729 N93-12694
Efficacy of multimedia instruction and an introduction to digital multimedia technology
[AD-A254509] p 734 N93-12723
Lecture notes for criticality safety
[DE92-016009] p 701 N93-12832
Women and minorities in science and engineering: An update
[NSF-92-303] p 730 N93-12907
Blacks in undergraduate science and engineering education
[NSF-92-305] p 730 N93-13015
An intelligent position-specific training system for mission operations
[NASA-TM-108381] p 691 N93-13156
NASA industry education initiative. Education programs report, 1991
[NASA-NP-158] p 730 N93-13248
Advanced technology for America's future in space. Executive summary
[NASA-TM-107969] p 513 N93-13308
Using DIALOG CIP at Winona State University to educate end-users p 686 N93-13338
State award summary: Fiscal Year 1991
[NSF-92-3] p 775 N93-13381
Systematic chemical equation balancing
[DE92-017234] p 539 N93-13530
The modelling of turbulence and downbursts for flight simulators p 507 N93-13542
Federal support to universities, colleges, and nonprofit institutions: Fiscal year 1990. A report to the President and Congress
[NSF-92-324] p 741 N93-13543
Explanation-based knowledge acquisition of electronics
[AD-A255069] p 573 N93-13650
Suited for spacewalking: A teacher's guide with activities
[NASA-EP-279] p 679 N93-13692
Selected data on Science and Engineering Doctorate Awards: 1991
[NSF-92-309] p 731 N93-13698
Fiscal Year 1991 highlights
[NSF-92-23] p 731 N93-13702
NSF Science and Technology Centers
[NSF-92-104] p 507 N93-13712
Application of information system technology to K-12 education
[AD-A255223] p 731 N93-13834
An evaluation of the use and future need of remotely sensed images in grades K-12 p 635 N93-13956
The informed citizen: Technology and responsibility in the information age p 742 N93-14049
EIGENVALUES
Acoustic modes in fluid networks p 586 N93-13398
Implicit application of polynomial filters in a k-step Arnoldi method
[NASA-CR-191237] p 686 N93-13408
Quantum inflationary minisuperspace cosmological models p 728 N93-13751

The growth of disturbances in barotropic models of the atmosphere p 658 N93-13887
Trim analysis by shooting and finite elements and Floquet eigenanalysis by QR and subspace iterations in helicopter dynamics p 501 N93-13914
On computing accurate singular values and eigenvalues of acyclic matrices
[AD-A255892] p 697 N93-14036

EIGENVECTORS
Implicit application of polynomial filters in a k-step Arnoldi method
[NASA-CR-191237] p 686 N93-13408
Quantum inflationary minisuperspace cosmological models p 728 N93-13751

EJECTA
Atoms and molecules in supernova 1987A p 699 N93-13851

EL NINO
Extended range forecast of Atlantic seasonal hurricane activity for 1993 p 661 N93-12928

ELASTIC BENDING
Nonlinear stall flutter of wings with bending-torsion coupling
[AD-A254323] p 503 N93-12959

ELASTIC BODIES
Visualization of scattering strength of elastic bodies in a fluid
[AD-A254535] p 699 N93-12601
Identification of parametric finite element models using experimental modal data
[PB92-217819] p 558 N93-12976
Analysis of large quasistatic deformations of inelastic solids by a new stress based finite element method
[NASA-CR-189235] p 626 N93-13260

ELASTIC DEFORMATION
Bifurcations in elastic-damaging materials
[DE92-018818] p 624 N93-13072
Elastic and plastic strain measurement in high temperature environment using laser speckle p 600 N93-13673

ELASTIC PLATES
A Fourier series method for polygonal domains: Large element computation for plates p 627 N93-13484

ELASTIC PROPERTIES
A study of the interlaminar stress continuity theories for composite laminates p 621 N93-12627
Large-deflection analysis of cord composite plates p 530 N93-13008
Axisymmetric and antiplane shear crack problems in bonded nonhomogeneous materials p 625 N93-13127
An elasticity solution for a transversely isotropic material containing a spherical shell under axisymmetric loading p 628 N93-13728
Effects of stinger axial dynamics and mass compensation methods on experimental modal analysis p 699 N93-13907

ELASTOPLASTICITY
The application of the finite element method and the boundary element method to fatigue and fracture, volumes 1 and 2 p 624 N93-13016
Bifurcations in elastic-damaging materials
[DE92-018818] p 624 N93-13072
Analysis of large quasistatic deformations of inelastic solids by a new stress based finite element method
[NASA-CR-189235] p 626 N93-13260
Thermodynamically consistent theories for elastoplasticity coupled with damage
[DE92-018283] p 627 N93-13515

ELECTRIC BATTERIES
Li/SOCl battery technology: Problems and solutions
[AD-A254514] p 570 N93-12725
Electrical design of payload G-534: The Pool Boiling Experiment p 510 N93-13170
Thermally stable electrolytes for rechargeable lithium batteries, phase 2
[NASA-CR-190878] p 573 N93-13610
First year testing of prototype magnesium/manganese dioxide BA-4590/U battery
[AD-A255503] p 574 N93-13839

ELECTRIC CONDUCTORS
Model for impedance of an ionic conductor sandwiched between blocking electrodes
[DE92-017812] p 569 N93-12561
Fluid dynamics of supercritical helium within cable-in-conduit conductors
[DE92-019516] p 574 N93-12569
Eddy current power dissipation at sharp corners
[DE92-016890] p 571 N93-13300

ELECTRIC CONNECTORS
Requirements for soldered electrical connections
[NHB-5300.4(3A-2)] p 570 N93-12674

ELECTRIC CURRENT
Effect of O2 partial pressure on post annealed Ba2YCu3O(7-delta) thin films
[DE92-014949] p 722 N93-13323

ELECTRIC DISCHARGES
Characterization of electric discharge in air produced by an environmental ionizator
[INPE-5310-NTC/299] p 651 N93-13310
CO2 laser preionisation
[NASA-CR-184424] p 607 N93-13797

ELECTRIC FIELDS
Investigation of effects of 60-Hz electric and magnetic fields on operant and social behavior and on the neuroendocrine system of nonhuman primates, part 2
[DE92-040153] p 673 N93-13503
Investigation of effects of 60-Hz electric and magnetic fields on operant and social behavior and on the neuroendocrine system of nonhuman primates, part 1
[DE92-040152] p 673 N93-13520
Use of phonon echoes in the study of 2-6 compounds and dielectric Bi12GeO20:Cr p 725 N93-13847

ELECTRIC GENERATORS
Advanced high-explosive flux compression generator development: The CN-3 series
[DE92-019962] p 713 N93-12809

ELECTRIC MOTORS
Semiconductor measurement technology: INSTANT (IGBT network simulation and transient Analysis tool)
[PB92-213529] p 725 N93-13783

ELECTRIC POTENTIAL
Design and operation of a bunched-beam, phase-spread measurement
[DE92-040230] p 708 N93-13508

ELECTRIC POWER PLANTS
Industrial applications of hot dry rock geothermal energy
[DE92-018903] p 637 N93-12923

ELECTRIC POWER SUPPLIES
Electrical design of payload G-534: The Pool Boiling Experiment p 510 N93-13170
Advanced photovoltaic power system technology for lunar base applications p 641 N93-14004

ELECTRIC ROCKET ENGINES
AFOSR Contractors Meeting in Propulsion
[AD-A254484] p 525 N93-12575
Anode power deposition in applied-field MPD thrusters
[NASA-CR-190790] p 526 N93-13283

ELECTRIC WIRE
The estimation of electrical cable fire-induced damage limits
[DE92-040100] p 572 N93-13519

ELECTRICAL FAULTS
Talking to InterFIS: Adding speech input to a natural language interface
[AD-A255865] p 688 N93-13942

ELECTRICAL GROUNDING
Recession of FEP specimens from trays D11 and B7 p 549 N93-12786

ELECTRICAL IMPEDANCE
Model for impedance of an ionic conductor sandwiched between blocking electrodes
[DE92-017812] p 569 N93-12561
Briefing notes on propulsion stability codes ADMIT, NYQUIST, and SSFREQ
[NASA-CR-184449] p 525 N93-12874
Eddy current power dissipation at sharp corners
[DE92-016890] p 571 N93-13300
Longitudinal impedance of capacitive pick-up electrodes: Calculations and comparison with measurements
[DE92-019499] p 571 N93-13358
Analysis and experimental results for an extraction cavity for the split-cavity oscillator
[DE92-040262] p 566 N93-13512

ELECTRICAL INSULATION
Activities of Space Power Insulation Inst.
[AD-A255825] p 574 N93-14034

ELECTRICAL PROPERTIES
Synthesis and properties of mismatched heterojunction/substrate interfaces
[AD-A254577] p 719 N93-12648
Electronic phenomena in polyanilines
[AD-A254803] p 545 N93-12749

ELECTRICAL RESISTANCE
The constant current loop: A new paradigm for resistance signal conditioning
[NASA-TM-104260] p 596 N93-12681
Understanding of carbonate fuel cell resistance issues for performance improvement
[DE92-019976] p 638 N93-13039

ELECTRICAL RESISTIVITY
High temperature oxidation and electrochemical studies related to hot corrosion
[AD-A254435] p 540 N93-12595
Electrochemical and chemical characteristics of a new ambient temperature Li(I) polymer electrolyte
[AD-A254918] p 545 N93-12651
Effect of plasticizers on the properties of new ambient temperature solid polymer electrolytes
[AD-A254817] p 545 N93-12754
Studies of plasticized-polymer electrolytes containing mixed Zn(2) and Li(1)
[AD-A254818] p 545 N93-12755
The effects of molecular structure on the electrical conductivity of polymers
[NASA-CR-191265] p 552 N93-13459
Transport on fractal networks
[AD-A253797] p 725 N93-13881

ELECTRICITY
Eddy current power dissipation at sharp corners
[DE92-016890] p 571 N93-13300

ELECTRO-OPTICS
Group 2 cubic fluorides dielectrics for 3-D integration and GaAs-based optoelectronic structures
[AD-A254937] p 719 N93-12544
Introductory review of target discrimination criteria
[AD-A254954] p 560 N93-12551
Organization of the Optical Society of America Photonic Science Topical Meeting Series. Volume 8: Integrated photonics research. Iifornia on 9-11 april 1991
[AD-A254682] p 709 N93-12666
Multichip module high speed testing
[AD-A254825] p 570 N93-12731
Multiplexing electro-optic architectures for advanced aircraft integrated flight control systems
[NASA-CR-182268] p 504 N93-13735
Electro-optic architecture for servicing sensors and actuators in advanced aircraft propulsion systems
[NASA-CR-182269] p 711 N93-13762

ELECTROACOUSTIC TRANSDUCERS
Transducer circuit
[AD-D015376] p 572 N93-13472

ELECTROACOUSTICS
MINT: The multiple error LMS algorithm, and the design of inverse filters for multi-channel sound reproduction systems
[ISVR-TR-211] p 700 N93-13439

ELECTROCHEMICAL CORROSION
An evaluation of corrosion protection by two epoxy primers on 2219-T87 and 7075-T73 aluminum
[NASA-TM-108376] p 553 N93-13716

ELECTROCHEMICAL OXIDATION
Electrochemical and chemical characteristics of a new ambient temperature Li(I) polymer electrolyte
[AD-A254918] p 545 N93-12651

ELECTROCHEMISTRY
High temperature oxidation and electrochemical studies related to hot corrosion
[AD-A254435] p 540 N93-12595
Electrochemical and chemical characteristics of a new ambient temperature Li(I) polymer electrolyte
[AD-A254918] p 545 N93-12651
Oligomer and mixed-metal compounds potential multielectron transfer catalysts
[DE92-011347] p 543 N93-13346

ELECTRODE MATERIALS
Alternate electrode materials for the SP100 reactor
[DE92-019570] p 706 N93-12970

ELECTRODEPOSITION
Electrodeposition of high temperature superconductors
[AD-A255095] p 720 N93-12758
Molten salt reactor for potentiostatic electroplating
[AD-D015358] p 551 N93-13101
Monitoring interfacial dynamics by pulsed laser techniques
[DE92-040302] p 606 N93-13514

ELECTRODES
Model for impedance of an ionic conductor sandwiched between blocking electrodes
[DE92-017812] p 569 N93-12561
Proton transport on modified sulfonated polyaniline electrodes
[AD-A254917] p 570 N93-12650
Li/SOCl battery technology: Problems and solutions
[AD-A254514] p 570 N93-12725
Oxygen electrode reaction in molten carbonate fuel cells
[DE92-040180] p 636 N93-12812
ESPVI 4.0 electrostatic precipitator V-I and performance model: User's model
[PB92-169614] p 643 N93-12938
Alternative materials for solid oxide fuel cells: Factors affecting air-sintering of chromite interconnections
[DE92-019356] p 638 N93-13082
Efficiency of an AMTEC recirculating test cell, experiments, and projections
[DE92-016811] p 571 N93-13196

ELECTRODYNAMICS
A new matrix formulation of classical electrodynamics. Part 2: Wave propagation in optical materials of infinite extent
[AD-A255032] p 560 N93-12585

ELECTROENCEPHALOGRAPHY
A weighted iterative algorithm for neuromagnetic imaging
[DE92-040244] p 675 N93-13522
ELECTROLYSIS
A microgravity processing plant for the manufacturing of propellant and water from asteroid ore p 515 N93-13558
Lunar mining of oxygen using fluorine
[LPI-748] p 761 N93-13980
ELECTROLYTES
Electrochemical and chemical characteristics of a new ambient temperature Li(I) polymer electrolyte
[AD-A254918] p 545 N93-12651
Li/SOCl battery technology: Problems and solutions
[AD-A254514] p 570 N93-12725
Solvation of cobalt salts by oligomeric polyethers
[AD-A254815] p 545 N93-12753
Thermally stable electrolytes for rechargeable lithium batteries, phase 2
[NASA-CR-190878] p 573 N93-13610
ELECTROLYTIC CELLS
Electrolytic smelting of lunar rock for oxygen, iron, and silicon p 761 N93-13979
ELECTROMAGNETIC ABSORPTION
Laser spectroscopy of rare earth ions p 608 N93-13846
ELECTROMAGNETIC COUPLING
Coupled structural/thermal/electromagnetic analysis/tailoring of graded composite structures
[NASA-CR-189150] p 626 N93-13443
Coupled structural/thermal/electromagnetic analysis/tailoring of graded composite structures
[NASA-CR-189151] p 627 N93-13444
Coupled structural/thermal/electromagnetic analysis/tailoring of graded composite structures
[NASA-CR-189152] p 627 N93-13445
ELECTROMAGNETIC FIELDS
A new matrix formulation of classical electrodynamics. Part 2: Wave propagation in optical materials of infinite extent
[AD-A255032] p 560 N93-12585
Workshop on Super-Intense Laser-Atom Physics
[AD-A254833] p 604 N93-12734
Study of plasma environments for the integrated Space Station electromagnetic analysis system
[NASA-CR-191263] p 522 N93-13152
Power excitation by the use of a RF wiggler
[DE92-016097] p 707 N93-13192
New approaches to estimation of magnetotelluric parameters
[DE92-040280] p 653 N93-13513
ELECTROMAGNETIC INTERACTIONS
Electromagnetic lepton-pair production in relativistic collisions
[DE92-011069] p 706 N93-12829
Investigations of the structure and electromagnetic interactions of few-body systems
[DE92-040011] p 563 N93-13042
ELECTROMAGNETIC INTERFERENCE
A Pennsylvania State University/General Electric Get Away Special (GAS) experiment p 511 N93-13177
Hermetic sealing and EMI shielding gasket
[AD-D015359] p 552 N93-13414
ELECTROMAGNETIC NOISE
Observations of correlated broadband electrostatic noise and electron cyclotron emissions in the plasma sheet
[AD-A255002] p 712 N93-12705
Longitudinal beam dynamics with rf noise
[DE92-040645] p 707 N93-13108
Long-term averages of globally-measured ELF/VLF radio noise
[AD-A255518] p 566 N93-13869
WR-10 band noise measurement
[AD-A255526] p 566 N93-13871
ELECTROMAGNETIC RADIATION
IIaO ultraviolet and nuclear emulsion films responses to orbital flights on STS-3, STS-7, STS-8, and STS-40 p 509 N93-13163
Low-frequency fluctuations of plasma magnetic fields p 717 N93-13496
Theory of lasing without population inversion p 605 N93-13497
Guidance and scattering of electromagnetic waves by nonlinear layers p 566 N93-13813
Recursive algorithms for computational electromagnetics p 567 N93-14043
Scattering from a finite collection of transverse dipole and axial slot arrays with edge effects p 568 N93-14048
ELECTROMAGNETIC SCATTERING
Electromagnetic scattering and radiation from microstrip patch antennas and spirals residing in a cavity
[NASA-CR-191284] p 565 N93-13354
Development of two-dimensional parametric radar signal modeling and estimation techniques with application to target identification
[AD-A252602] p 567 N93-13939
Computer-aided design-based high-frequency electromagnetic wave scattering from complex bodies p 567 N93-14042
Recursive algorithms for computational electromagnetics p 567 N93-14043
Scattering from a finite collection of transverse dipole and axial slot arrays with edge effects p 568 N93-14048
Electromagnetic scattering simulations using equivalent boundary condition models p 569 N93-14052
Numerical analysis of scattering from certain conducting and dielectric bodies of arbitrary shape
[ISBN-0-315-63282-8] p 569 N93-14066
ELECTROMAGNETIC SHIELDING
Hermetic sealing and EMI shielding gasket
[AD-D015359] p 552 N93-13414
ELECTROMAGNETIC SURFACE WAVES
Guidance and scattering of electromagnetic waves by nonlinear layers p 566 N93-13813
ELECTROMAGNETIC WAVE TRANSMISSION
A new matrix formulation of classical electrodynamics. Part 2: Wave propagation in optical materials of infinite extent
[AD-A255032] p 560 N93-12585
Variance of phase fluctuations of waves propagating through a random medium p 569 N93-13087
ELECTROMAGNETISM
Eddy current power dissipation at sharp corners
[DE92-016890] p 571 N93-13300
Recursive algorithms for computational electromagnetics p 567 N93-14043
ELECTROMAGNETS
Initial performance of Los Alamos Advanced Free Electron Laser
[DE92-040214] p 605 N93-13507
ELECTROMIGRATION
Design for reliability: Current density
[AD-A254770] p 570 N93-12866
ELECTRON ACCELERATORS
Test of a new RF separator structure for CEBAF
[CEBAF-PR-92-024] p 708 N93-13284
ELECTRON BEAMS
Weak-beam imaging of dissociated dislocations in HVEM-irradiated Fe-Ni-Cr alloys
[DE92-019587] p 541 N93-12798
Long pulse electron beam propagation
[DE92-014948] p 706 N93-12830
Suppression of the e(-) coextracted from a Penning surface-plasma H(-) source
[DE92-040350] p 714 N93-12997
Damping the (pi)-mode instability in the SLC damping rings with a passive cavity
[DE92-018153] p 707 N93-13090
Test of a new RF separator structure for CEBAF
[CEBAF-PR-92-024] p 708 N93-13284
Study of heliumlike neon using an electron beam ion trap
[DE92-019544] p 753 N93-13536
Methods for efficient pumping of vacuum ultraviolet lasers p 606 N93-13626
Electron beam fluorescence measurements in the Boeing hypersonic shock tunnel p 602 N93-13681
A study of the luminosity produced by an electron beam-emitting rocket in the polar ionosphere: ECHO 7 p 657 N93-13830
Comparison of heavy ion and electron-beam upset data for GaAs
[AD-A255901] p 708 N93-14089
ELECTRON BUNCHING
Power excitation by the use of a RF wiggler
[DE92-016097] p 707 N93-13192
Design and operation of a bunched-beam, phase-spread measurement
[DE92-040230] p 708 N93-13508
ELECTRON CYCLOTRON HEATING
Biasing experiments on the Advanced Toroidal Facility
[DE92-040033] p 717 N93-13518
ELECTRON DENSITY (CONCENTRATION)
Electronic transport properties of semiconductor microstructures p 724 N93-13730
ELECTRON DENSITY PROFILES
The electrostatic wake of a superthermal test electron in a magnetized plasma
[DE92-019394] p 713 N93-12873
ELECTRON DIFFRACTION
Uses of Monte Carlo computer simulations in understanding epitaxial growth and ion bombardment of Si(001)
[DE92-016944] p 719 N93-12586
Narrow bandgap semiconducting silicides: Intrinsic infrared detectors on a silicon chip
[NASA-CR-190882] p 571 N93-13430
ELECTRON DIFFUSION
On the bootstrap current calculations based on values of the radial electron transport
[IPPCZ-317] p 715 N93-13091
ELECTRON DISTRIBUTION
Fluidlike studies of the sheath and presheath regions of a plasma p 718 N93-13792
ELECTRON ENERGY
Wide range, permanent magnet Compton spectrometer
[DE92-017312] p 596 N93-12762
The electrostatic wake of a superthermal test electron in a magnetized plasma
[DE92-019394] p 713 N93-12873
Anomalous ion heating and superthermal electrons in the MST reversed-field pinch
[DE92-041011] p 713 N93-12882
Table-top x ray lasing based on optical-field-induced ionization
[DE92-019374] p 604 N93-12925
Oxygen deficiencies at defects in YBa2Cu3O(7-delta) as determined by high resolution parallel electron energy loss
[DE92-016301] p 721 N93-13089
Energetics and dynamics of excess electrons in simple fluids p 704 N93-13369
Electron temperature of Gd plasma produced by laser resonance ionization
[DE91-017785] p 718 N93-13732
Surface phonon dispersion of MoS2
[AD-A255835] p 727 N93-14083
ELECTRON IMPACT
Cross sections and rate coefficients for the electron-impact excitation of He-like ions
[ISAS-RN-647] p 703 N93-13095
Electron impact polarization expected in solar EUV lines from flaring chromospheres/transition regions
[SSL-PREPRINT-90-124] p 770 N93-13478
ELECTRON IRRADIATION
Radiation-disorder and aperiodicity in irradiated ceramics
[DE92-015051] p 552 N93-13350
ELECTRON MICROSCOPY
Uses of Monte Carlo computer simulations in understanding epitaxial growth and ion bombardment of Si(001)
[DE92-016944] p 719 N93-12586
Influence of dilute impurities on the evolution of defect cascades in nickel
[DE92-019585] p 542 N93-12973
ELECTRON MOBILITY
Electronic transport properties of semiconductor microstructures p 724 N93-13730
ELECTRON OPTICS
Digital imaging systems
[DE92-019194] p 736 N93-13078
ELECTRON ORBITALS
Studies of orbital doublet and modelling of orbital triplet Jahn-Teller systems in 3 to 5 semiconductors p 725 N93-13845
ELECTRON PLASMA
The electrostatic wake of a superthermal test electron in a magnetized plasma
[DE92-019394] p 713 N93-12873
Dynamics of the ion-ion acoustic instability in the thermalization of ion beams
[DE92-019396] p 714 N93-12914
Observations of solar wind ion charge exchange in the comet Halley coma p 752 N93-13467
ELECTRON PRECIPITATION
Comprehensive mappings of electron precipitation and its effects on the comprehensive mappings of electron precipitation and its effects on the atmosphere
[AD-A254665] p 648 N93-12621
Monte Carlo calculation of ionization and excitation rates in electron aurora
[ISAS-RN-645] p 652 N93-13405
ELECTRON SCATTERING
A fresh look at (e,e(prime)) scattering from light nuclei: A GFMC approach
[DE92-016377] p 703 N93-13246
Scattering and order in thermotropic liquid crystals p 723 N93-13332
ELECTRON STATES
The 2S(+) - 2P separation in KO
[NASA-TM-108086] p 702 N93-12900
Studies of orbital doublet and modelling of orbital triplet Jahn-Teller systems in 3 to 5 semiconductors p 725 N93-13845
ELECTRON TRAJECTORIES
Energetics and dynamics of excess electrons in simple fluids p 704 N93-13369
ELECTRON TRANSFER
Oligomer and mixed-metal compounds potential multielectron transfer catalysts
[DE92-011347] p 543 N93-13346

ELECTRON TRANSITIONS
Demonstration of a neon-like rubidium x ray laser
[DE92-019576] p 606 N93-13653
ELECTRONIC EQUIPMENT
Analysis of a structure-equipment system subjected to impact loading
[AD-A255097] p 622 N93-12652
An analysis of the field service function of selected electronics firms
[AD-A255003] p 570 N93-12868
ELECTRONIC EQUIPMENT TESTS
BETA: Behavioral testability analyzer and its application to high-level test generation and synthesis for testability
[NASA-CR-191282] p 572 N93-13569
Talking to InterFIS: Adding speech input to a natural language interface
[AD-A255865] p 688 N93-13942
ELECTRONIC MODULES
Circuit design tool. User's manual, revision 2
[NASA-CR-191361] p 687 N93-13734
ELECTRONIC PACKAGING
Semiconductor measurement technology: Version 2.0 of the TXYZ thermal analysis program: TXYZ20
[PB92-217603] p 570 N93-12978
ELECTRONIC SPECTRA
Surface phonon dispersion of MoS2
[AD-A255835] p 727 N93-14083
ELECTRONIC WARFARE
An application of exponential neural networks to event-train recognition
[AD-A254948] p 690 N93-12548
ELECTRONS
Suppression of the e(-) coextracted from a Penning surface-plasma H(-) source
[DE92-040350] p 714 N93-12997
Monte Carlo calculation of ionization and excitation rates in electron aurora
[ISAS-RN-645] p 652 N93-13405
ELECTROPHORESIS
Capillary electrophoresis: Electrospray ionization mass spectrometry in small diameter capillaries
[DE92-019123] p 575 N93-12711
ELECTROPLATING
Molten salt reactor for potentiostatic electroplating
[AD-D015358] p 551 N93-13101
ELECTROSTATIC PRECIPITATORS
ESPVI 4.0 electrostatic precipitator V-I and performance model: User's model
[PB92-169614] p 643 N93-12938
ELECTROSTATIC PROBES
Measurements of the temperature in the edge plasma of the CASTOR tokamak by a triple Langmuir probe
[IPPCZ-318] p 716 N93-13330
A fast scanning probe for D3-D
[DE92-040260] p 717 N93-13511
ELECTROSTATIC WAVES
Fast ion-driven Bernstein instabilities
[DE92-019393] p 705 N93-12713
ELEMENTARY PARTICLE INTERACTIONS
Research in elementary particle physics
[DE92-017869] p 704 N93-13251
Effects of ionizing radiation on scintillators and other particle detectors
[DE92-018184] p 705 N93-13531
Neutrino(e) appearance for neutrino(mu)-neutrino(tau) oscillations in matter
[DE92-040303] p 772 N93-13533
Heavy gauge boson and lambda(b) baryon searches at CDF
[DE92-019551] p 705 N93-13537
ELEMENTARY PARTICLES
Theoretical nuclear physics
[DE92-019286] p 706 N93-12822
Elementary particle physics research
[DE92-019746] p 702 N93-12855
Indiana University High Energy Physics Group, task C
[DE92-040458] p 707 N93-13002
Guide to QSPIRES and the particle physics databases on SLACVM
[DE92-018099] p 737 N93-13275
ELEVATION
Impact of Digital Terrain Elevation Data (DTED) resolution on terrain visualization: Simulation versus reality
[AD-A254237] p 634 N93-13333
Using iterative orthophoto refinements to correct Digital Elevation Models (DEM's)
[AD-A254625] p 634 N93-13345
ELLIPTICAL GALAXIES
Evolution of galaxies in compact groups
p 750 N93-13148
The planetary nebula system and the dynamics of the galaxy Centaurus A p 754 N93-13645
The interstellar medium of elliptical galaxies
p 757 N93-14071
ELLIPTICAL ORBITS
Robust rendezvous maneuver point conditions
[NASA-CR-190996] p 517 N93-12690
ELONGATION
Mechanical properties of epoxy/alumina trihydrate-filled compositions p 534 N93-13950
EMERGENCIES
Assured crew return vehicle post landing configuration design and test
[NASA-CR-191253] p 520 N93-12910
EMISSION SPECTRA
Studies of extra-solar Oort Clouds and the Kuiper disk
[NASA-CR-190958] p 769 N93-12669
Zodiacal emission p 772 N93-13147
G-133: A soft x ray solar telescope
p 510 N93-13171
Field spectroradiometry and sail model application to irrigated wheat (Triticum aestivum, L) canopies spectral reflectance
[INPE-5426-TDI/483] p 634 N93-13258
The emission-line properties of quasars
p 753 N93-13487
An infrared polarimetric study of sunspots
p 770 N93-13627
Anisotropy measurements of the cosmic background radiation at 3 mm wavelength and an angular scale of 30 arcminutes p 772 N93-13689
Application of improved HNO3 band model parameters to South Pole atmospheric emission measurements
p 647 N93-13723
Laser spectroscopy of rare earth ions
p 608 N93-13846
Spectroscopic observations of the night airglow from 3000 A to 9200 A p 658 N93-13891
EMITTANCE
Emittance, brilliance, and bandpass issues related to an inclined crystal monochromator
[DE92-019671] p 721 N93-12881
Longitudinal beam dynamics with rf noise
[DE92-040645] p 707 N93-13108
EMULSIONS
Aerogels, emulsions, and composites: Controlling structure with organic sol-gel chemistry
[DE92-019575] p 550 N93-12931
ENCAPSULATING
Soft x ray window encapsulant for HgI2 detectors
[NASA-CR-190850] p 710 N93-13705
END EFFECTORS
Tactile sensing and control in humans and robotic/teleoperated systems
[AD-A254408] p 609 N93-12604
The ROMPS robot in HitchHiker p 511 N93-13179
End-point position control of multi-link flexible manipulator arms p 613 N93-13335
Preloaded latching device
[NASA-CASE-MSC-21730-1] p 614 N93-13417
Force-closure grasping with two hands
p 616 N93-13742
Enhanced accuracy for closed-loop robot
p 617 N93-13808
Dynamic modeling and optimal joint torque coordination of advanced robotic systems p 617 N93-13936
Dexterous grasp and manipulation
p 618 N93-14075
Modelling flexible link manipulators in the three-dimensional space p 574 N93-14093
END-TO-END DATA SYSTEMS
Multi-frequency multi-polarization processing for spaceborne SAR p 564 N93-13057
ENDOCRINOLOGY
AFRRI reports
[AD-A254581] p 674 N93-12649
ENERGY ABSORPTION
Atomic structure of mixed ferroelectrics
[AD-A254369] p 702 N93-12947
ENERGY BUDGETS
Sulfate impact upon low-level cloud albedo over oceans p 661 N93-12833
Performance of the Bowen ratio systems on a 22 deg slope
[NASA-CR-191278] p 644 N93-13254
Radiative constraints on the energy budget of the atmosphere p 655 N93-13731
The kinetic energy budget of tropical plumes and ENSO in NMC and ECMWF analyses p 664 N93-13740
Climate sensitivity study with energy balance models
p 666 N93-13817
ENERGY CONSERVATION
Hydrogen Program Plan, FY 1993 - 1997
[DE92-010556] p 538 N93-13316
ENERGY CONSUMPTION
World Energy Projection System (WEPS), March 1992. Model installation manual, distribution disk layout
[PB92-169572] p 637 N93-12937
ENERGY CONVERSION
Energy from Municipal Waste Program
[DE92-010578] p 638 N93-13102
High octane ethers from synthesis gas-derived alcohols
[DE92-015467] p 537 N93-13188
Hydrogen Program Plan, FY 1993 - 1997
[DE92-010556] p 538 N93-13316
Analysis and experimental results for an extraction cavity for the split-cavity oscillator
[DE92-040262] p 566 N93-13512
ENERGY CONVERSION EFFICIENCY
Efficiency of an AMTEC recirculating test cell, experiments, and projections
[DE92-016811] p 571 N93-13196
Hydrogen Program Plan, FY 1993 - 1997
[DE92-010556] p 538 N93-13316
Boiler efficiency methodology for solar heat applications
[DE92-019805] p 640 N93-13618
Fusion energy from the Moon for the twenty-first century p 719 N93-13985
ENERGY DISSIPATION
Airblast damage from small asteroids
[DE92-017834] p 749 N93-12956
Oxygen deficiencies at defects in YBa2Cu3O(7-delta) as determined by high resolution parallel electron energy loss
[DE92-016301] p 721 N93-13089
Hydrogen Program Plan, FY 1993 - 1997
[DE92-010556] p 538 N93-13316
Cascade processes and fully developed turbulence
p 591 N93-13901
Surface phonon dispersion of MoS2
[AD-A255835] p 727 N93-14083
ENERGY DISTRIBUTION
Photodissociation processes
[PB92-222702] p 702 N93-13067
Radar signal processing for over resolved targets
[AD-A255256] p 566 N93-13838
Galaxies with spectral energy distributions peaking at 60 micrometers: Morphology and activity explained by interactions p 756 N93-13959
ENERGY OF FORMATION
Point defects quenched in NiAl and related intermetallic compounds p 724 N93-13628
ENERGY POLICY
Research in geosciences policy
[NASA-CR-190470] p 632 N93-13833
ENERGY SPECTRA
The use of ring ratios to detect sample differences in passive neutron counting
[DE92-018920] p 702 N93-13076
Oxygen deficiencies at defects in YBa2Cu3O(7-delta) as determined by high resolution parallel electron energy loss
[DE92-016301] p 721 N93-13089
A study of the generation of linear energy transfer spectra for space radiations
[NASA-TM-4410] p 772 N93-13572
ENERGY STORAGE
High Energy Propulsion System (HEPS) analysis
[AD-A254343] p 525 N93-12963
Advanced photovoltaic power system technology for lunar base applications p 641 N93-14004
ENERGY TECHNOLOGY
Gas cooled fuel cell systems technology development
[DE92-0012983-3103] p 636 N93-12683
Energy related inventions program. A joint program of the Department of Energy and the National Institute of Standards and Technology. Status report for recommendations 1 through 300
[PB92-226265] p 637 N93-12987
Energy related inventions program. A joint program of the Department of Energy and the National Institute of Standards and Technology. Status report for recommendations 301-563
[PB92-226273] p 637 N93-12988
Advanced energy projects FY 1992 research summaries
[DE92-040442] p 637 N93-13001
Proceedings of the Tenth Symposium on Energy Engineering Sciences: Synergism of Analysis, Modeling, and Experiment
[DE92-018777] p 638 N93-13069
Considerations for the transition from fuel cell R/D to manufacturing
[DE92-019977] p 640 N93-13622
ENERGY TRANSFER
Structures, spectra and inertial range transfer in two-dimensional and beta-plane turbulence
p 590 N93-13900
Effects of stinger axial dynamics and mass compensation methods on experimental modal analysis
p 699 N93-13907

ENGINE AIRFRAME INTEGRATION
Aerodynamic Engine/Airframe Integration for High Performance Aircraft and Missiles
[AGARD-CP-498] p 577 N93-13199
Test techniques for engine/airframe integration p 577 N93-13200
Investigation of interference phenomena of modern wing-mounted high-bypass-ratio engines by the solution of the Euler-equations p 578 N93-13204
Aerodynamic analysis of slipstream/wing/nacelle interference for preliminary design of aircraft configurations p 497 N93-13205
Euler analysis of turbofan/superfan integration for a transport aircraft p 578 N93-13206
Recent developments in low-speed TPS-testing for engine integration drag and installed thrust reversr simulation p 502 N93-13207
Aerodynamic integration of thrust reversers on the Fokker 100 p 502 N93-13208
The PEP Symposium on CFD Techniques for Propulsion Applications p 579 N93-13210
Flight analysis of air intake/engine compatibility p 502 N93-13212
Water tunnel studies of inlet/airframe interference phenomena p 580 N93-13216
Some aspects of intake design, performance and integration with the airframe p 502 N93-13219
Application of subsonic first-order panel methods for prediction of inlet and nozzle aerodynamic interactions with airframe p 497 N93-13223
Survey on techniques used in aerodynamic nozzle/airframe integration p 502 N93-13224
Hypersonic propulsion system force accounting p 503 N93-13229
Integration of turbo-ramjet engines for hypersonic aircraft p 503 N93-13230

ENGINE CONTROL
Subsonic flight test evaluation of a propulsion system parameter estimation process for the F100 engine
[NASA-TM-4426] p 502 N93-13155

ENGINE DESIGN
Application interface engine language and object reference manual
[DE92-017555] p 683 N93-12686
Investigation of advanced counterrotation blade configuration concepts for high speed turboprop systems. Task 4: Advanced fan section aerodynamic analysis
[NASA-CR-187128] p 502 N93-12695
A novel diesel-fueled engine for microclimate cooling for the individual soldier
[AD-A254510] p 609 N93-12724
Effects of gas composition on engine performance and emissions
[PB92-217561] p 611 N93-12936
Alternative systems for fuel gas boosters for small gas turbine engines
[PB92-223049] p 612 N93-12977
An investigation of jet engine test cell aerodynamics by means of scale model test studies with comparisons to full-scale test results p 507 N93-14060

ENGINE INLETS
Aerodynamic Engine/Airframe Integration for High Performance Aircraft and Missiles
[AGARD-CP-498] p 577 N93-13199
Test techniques for engine/airframe integration p 577 N93-13200
The influence of intake swirl distortion on the steady-state performance of a low bypass, twin-spool engine p 579 N93-13211
Flight analysis of air intake/engine compatibility p 502 N93-13212
Water tunnel studies of inlet/airframe interference phenomena p 580 N93-13216
Some aspects of intake design, performance and integration with the airframe p 502 N93-13219
Application of subsonic first-order panel methods for prediction of inlet and nozzle aerodynamic interactions with airframe p 497 N93-13223
Air inlet with variable intake section: Application to air breathing launch vehicles p 582 N93-13231
Flow prediction for three-dimensional intakes and ducts using viscous-inviscid interaction methods p 592 N93-13953

ENGINE PARTS
Thermal barrier coating life prediction model development, phase 2
[NASA-CR-189111] p 544 N93-12589
Linear and nonlinear finite element analysis of laminated composite structures at high temperatures p 623 N93-13009

ENGINE TESTS
The influence of intake swirl distortion on the steady-state performance of a low bypass, twin-spool engine p 579 N93-13211
Flight analysis of air intake/engine compatibility p 502 N93-13212
Resonance lamp absorption measurement of OH number density and temperature in expansion tube scramjet engine tests p 602 N93-13682
An investigation of jet engine test cell aerodynamics by means of scale model test studies with comparisons to full-scale test results p 507 N93-14060

ENGINEERING
Women and minorities in science and engineering: An update
[NSF-92-303] p 730 N93-12907
NASA industry education initiative. Education programs report, 1991
[NASA-NP-158] p 730 N93-13248
Scientific and engineering research facilities at universities and colleges: 1992
[NSF-92-325] p 506 N93-13407
Academic science and engineering: R/D expenditures, fiscal year 1990
[NSF-92-321] p 741 N93-13544
Awards: 1991 undergraduate course and curriculum development program
[NSF-92-45] p 731 N93-13699
Diversity in biological research
[NSF-92-19] p 673 N93-13700
Science and engineering degrees: 1966-1990
[NSF-92-326] p 731 N93-13701

ENGINEERING DRAWINGS
Magnetic bearings for a high-performance optical disk buffer, volume 2
[NASA-CR-190874] p 615 N93-13608

ENGINEERS
Science and engineering degrees, by race/ethnicity of recipients: 1977-1990
[NSF-92-327] p 729 N93-12694
Air Force engineering research initiation grants (1990-1991)
[AD-A255004] p 774 N93-12706
Academic science and engineering: Graduate enrollment and support, Fall 1990
[NSF-92-323] p 729 N93-12802
Blacks in undergraduate science and engineering education
[NSF-92-305] p 730 N93-13015
Gateway to diversity in the scientific and technological workforce
[NSF-92-99] p 730 N93-13278
Characteristics of recent science and engineering graduates: 1990. Detailed statistical tables
[NSF-92-316] p 731 N93-13454
Highlights 92/2 p 775 N93-13474
Research and development in industry: 1989. Funds, 1989. Scientists and engineers, January 1990
[NSF-92-307] p 741 N93-13658
Selected data on Science and Engineering Doctorate Awards: 1991
[NSF-92-309] p 731 N93-13698

ENGLISH LANGUAGE
Japanese/English machine translation using sublanguage patterns and reversible grammars p 686 N93-13494

ENTOMOLOGY
Procedures for the diagnostic dose resistance test kits for mosquitoes, body lice, and beetle pests of stored products
[AD-A255224] p 675 N93-13941

ENTROPY
From comparison density to two sample analysis
[AD-A253866] p 698 N93-13064
Point defects quenched in NiAl and related intermetallic compounds p 724 N93-13628

ENVIRONMENT EFFECTS
Touchstone for success
[ESA-BR-52] p 557 N93-12934
Environmental effects on an optical-UV-IR synthesis array p 747 N93-13595
Effects of the Mt. Pinatubo eruption on the radiative and chemical processes in the troposphere and stratosphere
[DE92-019618] p 646 N93-13654
Research in geosciences policy
[NASA-CR-190470] p 632 N93-13833
Space environmental effects on silvered teflon thermal control surfaces
[AD-A255909] p 554 N93-14099

ENVIRONMENT MANAGEMENT
Proceedings of the Mediterranean Conference on Environmental Geotechnology
[AD-A253672] p 644 N93-13098

ENVIRONMENT MODELS
Interagency Workgroup on Air Quality Modeling (IWAQM) work plan rationale
[PB92-213248] p 643 N93-12940
Katz model prediction of Caenorhabditis elegans mutagenesis on STS-42
[NASA-TM-4383] p 674 N93-13023
How life affects the geochemical cycle of carbon
[NASA-CR-191241] p 644 N93-13031
Galactic cosmic ray exposure estimates for SAGE-3 mission in polar orbit
[NASA-TM-107678] p 771 N93-13126
Robotic exploration of surfaces and its application to legged locomotion p 615 N93-13540
Assimilation of satellite color observations in a coupled ocean GCM-ecosystem model
[NASA-CR-191218] p 670 N93-13714
Integration of vegetation indices and thermal measurements for ecosystem modeling p 646 N93-13721

ENVIRONMENT POLLUTION
ReTech, Inc., Plasma Centrifugal Furnace: Applications analysis report
[PB92-218791] p 714 N93-12982
Reports to the Nation on our changing planet: Our ozone shield p 645 N93-13413
Documentation for developing the initial source category list
[PB92-218429] p 646 N93-13647

ENVIRONMENT PROTECTION
NOAA Atmospheric Sciences Modeling Division support to the US Environmental Protection Agency
[PB92-217835] p 644 N93-12974
Proceedings of the Mediterranean Conference on Environmental Geotechnology
[AD-A253672] p 644 N93-13098
Reports to the Nation on our changing planet: Our ozone shield p 645 N93-13413
Environmental Compliance Management System
[DE92-019595] p 645 N93-13479
Documentation for developing the initial source category list
[PB92-218429] p 646 N93-13647

ENVIRONMENT SIMULATION
The relationship between environmental conditions and UH-60 cockpit temperature
[AD-A255918] p 680 N93-14090

ENVIRONMENTAL CONTROL
ECLSS evolution: Advanced instrumentation interface requirements. Volume 3: Appendix C
[NASA-CR-184367] p 678 N93-12990
Use of antarctic analogs to support the space exploration initiative
[NASA-TM-108000] p 651 N93-13326
The environmental control and life-support system for a lunar base: What drives its design p 680 N93-13991
Life systems for a lunar base p 680 N93-13992

ENVIRONMENTAL MONITORING
The National Atmospheric Deposition Program/National Trends Network (NADP/NTN) site visitation program
[PB92-217298] p 642 N93-12726
Remote sensing of Earth terrain
[NASA-CR-190908] p 633 N93-13084
Reports to the Nation on our changing planet: Our ozone shield p 645 N93-13413
Technology development for lunar base water recycling p 680 N93-13999

ENVIRONMENTAL TESTS
LDEF Materials Workshop 1991, part 1
[NASA-CP-3162-PT-1] p 545 N93-12769
LDEF materials: An overview of the interim findings p 546 N93-12770
LDEF atomic oxygen fluence update p 546 N93-12771
Surface contamination on LDEF exposed materials p 547 N93-12776
Anodized aluminum on LDEF: A current status of measurements on chromic acid anodized aluminum p 544 N93-12779
Performance of thermal control tape in the protection of composite materials p 536 N93-12780
Fluorescence of thermal control coatings on S0069 and A0114 p 548 N93-12781
Long Duration Exposure Facility M0003-5 thermal control coatings on DoD flight experiment p 548 N93-12782
Element Material Exposure Experiment by EFFU p 548 N93-12783
Skylab D024 thermal control coatings and polymeric films experiment p 548 N93-12784
Effects of the LDEF environment on the Ag/FEP thermal blankets p 548 N93-12785
Recession of FEP specimens from trays D11 and B7 p 549 N93-12786
Characterization of selected LDEF: Exposed polymer films and resins p 549 N93-12787
Effects of orbital exposure on Halar during the LDEF mission p 549 N93-12788
Long Duration Exposure Facility M0003-5 recent results on polymeric films p 549 N93-12789
Europe qualifies for space
[ESA-BR-64] p 508 N93-12892

Studies of surface-induced luminescence relevant to spacecraft glow, using a seeded arc-jet
p 523 N93-13919

ENZYMES
Nitrogen control of chloroplast development and differentiation
[DE92-017392] p 671 N93-12768
Complement proteins and decompression sickness susceptibility
[AD-A254448] p 674 N93-12905

EPITAXY
Uses of Monte Carlo computer simulations in understanding epitaxial growth and ion bombardment of Si(001)
[DE92-016944] p 719 N93-12586
Narrow bandgap semiconducting silicides: Intrinsic infrared detectors on a silicon chip
[NASA-CR-190882] p 571 N93-13430
The heteroepitaxial growth of YBCO and other metal oxides on silicon and GaAs by pulsed laser deposition
p 726 N93-13904

EPOXY MATRIX COMPOSITES
Results of ASTM round robin testing for mode 1 interlaminar fracture toughness of composite materials
[NASA-TM-104222] p 532 N93-13428
Physical interpretation and development of ultrasonic nondestructive evaluation techniques applied to the quantitative characterization of textile composite materials
[NASA-CR-190962] p 620 N93-13435
Vibration damping response of composite materials
p 533 N93-13748
Experimental characterization of continuous alumina fiber/epoxy p 533 N93-13775
Mechanical properties of epoxy/alumina trihydrate-filled compositions p 534 N93-13950

EPOXY RESINS
An evaluation of corrosion protection by two epoxy primers on 2219-T87 and 7075-T73 aluminum
[NASA-TM-108376] p 553 N93-13716
Experimental characterization of continuous alumina fiber/epoxy p 533 N93-13775

EQUATIONS OF MOTION
Equations of motion of slung-load systems, including multilift systems
[NASA-TP-3280] p 503 N93-12815

EQUATIONS OF STATE
Nonideal thermoequilibrium calculations using a large product species data base
[DE92-040839] p 735 N93-12813

EQUILIBRIUM EQUATIONS
The role of particle diffusion in the lower transition region: Revised interpretation of emission measures
p 770 N93-13476

EQUIPARTITION THEOREM
Limits on galactic dynamo theory due to magnetic fluctuations p 754 N93-13636

EQUIPMENT
Conceptual design of a human piloted mining mission
p 514 N93-13552
Mining equipment and operations for mining the 1982HR (Orpheus) asteroid p 515 N93-13557

EQUIPMENT SPECIFICATIONS
Magnetic bearings for a high-performance optical disk buffer, volume 2
[NASA-CR-190874] p 615 N93-13608
Development of a portable infrared emission spectrometer AA460 PIRES
[NASA-CR-190849] p 598 N93-13656
Distribution of human waste samples in relation to sizing waste processing in space p 680 N93-14001

EQUIVALENCE
A preliminary study of the effect of equivalence ratio on a low emissions gas turbine combustor using KIVA-2
[DE92-018616] p 613 N93-13321

EQUIVALENT CIRCUITS
Model for impedance of an ionic conductor sandwiched between blocking electrodes
[DE92-017812] p 569 N93-12561
An evaluation of corrosion protection by two epoxy primers on 2219-T87 and 7075-T73 aluminum
[NASA-TM-108376] p 553 N93-13716

EREP
Earth observation photography: Looking back 20 years after Skylab p 509 N93-13164

EROSION
Wastage-resistant FBC evaporator tubing through microalloying
[DE92-001256] p 541 N93-12790
Particle simulation of grid erosion in an ion thruster
p 527 N93-13927

ERROR ANALYSIS
Angle of arrival fluctuations for millimeter waves propagating in a turbulent atmosphere near the Earth
[AD-A254478] p 560 N93-12574
Analysis of a linearly constrained least squares algorithm for adaptive beamforming
[AD-A255017] p 695 N93-12582
Soft X Ray Telescope (SXT) focus error analysis
[NASA-CR-184443] p 742 N93-12657
Robust rendezvous maneuver point conditions
[NASA-CR-190996] p 517 N93-12690
Quality assessment of the A-posteriori error estimation in finite elements
[AD-A254767] p 696 N93-12701
Radar signal processing for over resolved targets
[AD-A255256] p 566 N93-13838
Orbit determination error analysis and station-keeping for liberation point trajectories p 518 N93-14038
Fixed-gain, two-stage estimators for tracking maneuvering targets
[AD-A255832] p 697 N93-14081

ERROR CORRECTING CODES
An investigation of error correcting techniques for OMV data
[NASA-CR-190942] p 682 N93-12654
Error control techniques for satellite and space communications
[NASA-CR-191229] p 565 N93-13411

ERROR DETECTION CODES
Error control techniques for satellite and space communications
[NASA-CR-191229] p 565 N93-13411

ERRORS
Motion errors and compensation possibilities
p 563 N93-13052
The millimeter and submillimeter wavelength diffuse backgrounds: Measurements of the spectrum and anisotropy p 772 N93-13145
The use of consider covariance analysis in choosing data weights to reduce the effect of errors in model parameters on satellite orbit determination accuracy
p 518 N93-13768

ERS-1 (ESA SATELLITE)
Test and calibration of the along track scanning radiometer, a satellite-borne infrared radiometer designed to measure sea surface temperature
p 671 N93-13842

ESTIMATES
Selected data on research and development in industry: 1990
[NSF-92-317] p 773 N93-12667
World Energy Projection System (WEPS), March 1992. Model installation manual, distribution disk layout
[PB92-169572] p 637 N93-12937
Large programs may consume increasing share of limited future budgets. Report to Congressional Requesters
[GAO/NSIAD-92-278] p 732 N93-13109
Galactic cosmic ray exposure estimates for SAGE-3 mission in polar orbit
[NASA-TM-107678] p 771 N93-13126

ESTIMATING
GPS measurements at Vandenberg AFB
[AD-A254978] p 499 N93-12557
From comparison density to two sample analysis
[AD-A253866] p 698 N93-13064
Scientific and engineering research facilities at universities and colleges: 1992
[NSF-92-325] p 506 N93-13407
Robust controller and estimator design using minimax methods p 694 N93-13925

ESTIMATORS
Fixed-gain, two-stage estimators for tracking maneuvering targets
[AD-A255832] p 697 N93-14081

ETCHING
Terahertz horn antennas on thin membranes
[AD-A254772] p 562 N93-12867

ETHERS
High octane ethers from synthesis gas-derived alcohols
[DE92-015467] p 537 N93-13188
Studies of the kinetics and mechanisms of perfluoroether reactions on iron and oxidized iron surfaces
[NASA-CR-191363] p 539 N93-13763

ETHICS
The lunar community church: Contributions to lunar living and to evolution of ethical and spiritual thinking
p 676 N93-14020

ETHYL ALCOHOL
Vapor to liquid ratio test as an indicator of volatility
[DOT/FAA/CT-TN92/40] p 537 N93-12897
Postmortem alcohol production in fatal aircraft accidents
[AD-A255766] p 498 N93-14026

ETHYLENE
Effect of plasticizers on the properties of new ambient temperature solid polymer electrolytes
[AD-A254817] p 545 N93-12754

ETHYLENE COMPOUNDS
Studies of plasticized-polymer electrolytes containing mixed Zn(2) and Li(1)
[AD-A254818] p 545 N93-12755
Recession of FEP specimens from trays D11 and B7
p 549 N93-12786
Effects of orbital exposure on Halar during the LDEF mission p 549 N93-12788

ETIOLOGY
Complement proteins and decompression sickness susceptibility
[AD-A254448] p 674 N93-12905

EULER EQUATIONS OF MOTION
Numeric simulation of the aerodynamic flows around nacelles p 577 N93-13202
Investigation of interference phenomena of modern wing-mounted high-bypass-ratio engines by the solution of the Euler-equations p 578 N93-13204
Euler analysis of turbofan/superfan integration for a transport aircraft p 578 N93-13206
Two-phase flow modeling with discrete particles
[DE92-017850] p 583 N93-13356
Numerical simulation of the acoustic instability in the spatially developing, confined, supersonic mixing layer
p 494 N93-13521

EULER-LAGRANGE EQUATION
RHALE: A MMALE shock physics code written in C++
[DE92-018271] p 684 N93-12795
Stabilization and projection methods for multibody dynamics
[PB92-133883] p 698 N93-12890

EURECA (ESA)
EURECA
[ESA-F-26] p 522 N93-12964
Eureca: A first for Europe
[ESA-BR-85] p 516 N93-13691

EUROPE
Europe qualifies for space
[ESA-BR-64] p 508 N93-12892

EUROPEAN SPACE AGENCY
Europe qualifies for space
[ESA-BR-64] p 508 N93-12892
Horizon 2000: Seven years on
[ESA-BR-37-B] p 516 N93-13855
Taking a global view
[ESA-BR-37-C] p 516 N93-13856
Messengers in space
[ESA-BR-37-D] p 516 N93-13857
A home port in space
[ESA-BR-37-E] p 516 N93-13858
Reaching for the skies: The next generation
[ESA-BR-37-G] p 516 N93-13859
Preparing for the future
[ESA-BR-37-H] p 517 N93-13860
The next step forward
[ESA-BR-37-A] p 517 N93-13861
A growing dimension in space
[ESA-BR-37-F] p 517 N93-13902
Ever watchful
[ESA-BR-37-I] p 517 N93-13903

EUROPEAN SPACE PROGRAMS
Eureca: A first for Europe
[ESA-BR-85] p 516 N93-13691
Horizon 2000: Seven years on
[ESA-BR-37-B] p 516 N93-13855
Taking a global view
[ESA-BR-37-C] p 516 N93-13856
Messengers in space
[ESA-BR-37-D] p 516 N93-13857
A home port in space
[ESA-BR-37-E] p 516 N93-13858
Reaching for the skies: The next generation
[ESA-BR-37-G] p 516 N93-13859
Preparing for the future
[ESA-BR-37-H] p 517 N93-13860
The next step forward
[ESA-BR-37-A] p 517 N93-13861
A growing dimension in space
[ESA-BR-37-F] p 517 N93-13902
Ever watchful
[ESA-BR-37-I] p 517 N93-13903

EUROPIUM COMPOUNDS
Laser spectroscopy of rare earth ions
p 608 N93-13846

EUTECTICS
The nature of scales grown on binary Cr-Nb alloys
[DE92-019283] p 542 N93-13080

EVALUATION
Verification and validation of TMAP4
[DE92-019684] p 539 N93-13616

EVAPORATORS
Wastage-resistant FBC evaporator tubing through microalloying
[DE92-001256] p 541 N93-12790

EVAPOTRANSPIRATION
Performance of the Bowen ratio systems on a 22 deg slope
[NASA-CR-191278] p 644 N93-13254
EXCIMER LASERS
Electron stimulated desorption of the metallic substrate at monolayer coverage: Sensitive detection via 193 nm laser photoionization of neutral aluminum desorbed from CH3O/Al(111)
[DE92-014858] p 723 N93-13349
EXCITATION
Large-amplitude plate vibration in an elevated thermal environment
[AD-A254411] p 621 N93-12606
Spanwise-nonuniform excitation of a plane mixing layer p 577 N93-13120
Power excitation by the use of a RF wiggler
[DE92-016097] p 707 N93-13192
Effects of stinger axial dynamics and mass compensation methods on experimental modal analysis p 699 N93-13907
Deterministic and stochastic responses of nonlinear systems p 631 N93-13966
EXHAUST EMISSION
Meeting future exhaust emissions standards using natural gas as a vehicle fuel: Lessons learned from the natural gas vehicle challenge 1992
[DE92-019670] p 642 N93-12885
Effects of gas composition on engine performance and emissions
[PB92-217561] p 611 N93-12936
A preliminary study of the effect of equivalence ratio on a low emissions gas turbine combustor using KIVA-2
[DE92-018616] p 613 N93-13321
EXHAUST GASES
Meeting future exhaust emissions standards using natural gas as a vehicle fuel: Lessons learned from the natural gas vehicle challenge 1992
[DE92-019670] p 642 N93-12885
Effects of gas composition on engine performance and emissions
[PB92-217561] p 611 N93-12936
Documentation for developing the initial source category list
[PB92-218429] p 646 N93-13647
EXHAUST NOZZLES
Survey on techniques used in aerodynamic nozzle/airframe integration p 502 N93-13224
CFD calibration for three-dimensional nozzle/afterbody configurations p 582 N93-13226
EXHAUST SYSTEMS
Intake and exhaust noise
[ISVR-TR-207] p 699 N93-12714
EXOBIOLOGY
EURECA
[ESA-F-26] p 522 N93-12964
Assessment of programs in space biology and medicine
[NASA-CR-190930] p 672 N93-13327
EXPEDITIONS
JARE data reports no. 179 (meteorology 29). Meteorological data at Asuka Station, Antarctica in 1990 p 663 N93-13287
EXPERIMENT DESIGN
Large Deployable Reflector (LDR) system concept and technology definition study. Analysis of space station requirements for LDR
[NASA-CR-177414] p 742 N93-12592
The effects of compressive preloads on the compression-after-impact strength of carbon/epoxy
[NASA-TP-3303] p 529 N93-12678
Chemical release and radiation effects experiment advanced planning and coordination
[NASA-CR-184439] p 649 N93-12718
Element Material Exposure Experiment by EFFU p 548 N93-12783
The 1992 Shuttle Small Payloads Symposium
[NASA-CP-3171] p 508 N93-13158
Spaceflight payload design flight experience G-408 p 508 N93-13160
A decade of discovery: Experiments with the Get Away Special (GAS) canister p 509 N93-13162
G254 undergraduate experiment p 511 N93-13174
Proper battery system design for GAS experiments p 511 N93-13176
CONCAP 4: A Complex Autonomous Payload (CAP) for growing organic thin films in microgravity p 511 N93-13178
The Capillary Pumped Loop Flight Experiment (CAPL): A pathfinder for EOS p 512 N93-13181
The VTRE Program: An overview p 512 N93-13182
The unique challenge of managing an undergraduate Get-Away-Special experiment p 512 N93-13185
Preparing safety data packages for experimenters using the Get Away Special (GAS) carrier system p 512 N93-13186
EXPERIMENTATION
Scientific experimentation afforded by the International Asteroid Mission p 515 N93-13561
EXPERT SYSTEMS
Expert-system development in Soar: A tutorial
[AD-A254571] p 682 N93-12645
Analysis of IMS spectra using neural networks
[DE92-017511] p 691 N93-12791
Automated eddy current analysis of materials
[NASA-CR-184432] p 619 N93-12875
On-orbit supervisor for controlling spacecraft
[AD-A254342] p 522 N93-12962
An intelligent position-specific training system for mission operations
[NASA-TM-108381] p 691 N93-13156
Compiling knowledge-based systems to Ada, phase 2
[NASA-CR-191273] p 686 N93-13355
Environmental Compliance Management System
[DE92-019595] p 645 N93-13479
Talking to InterFIS: Adding speech input to a natural language interface
[AD-A255865] p 688 N93-13942
Adding explanation capability to a knowledge-based system for interpretation of oceanographic images
[AD-A255887] p 671 N93-13943
A study of traditional information access models applied in a hypertext information system p 739 N93-14076
EXPLOSIONS
Booster explosive rings
[AD-D015375] p 556 N93-13471
Nucleosynthesis in nova explosions
[DE92-040349] p 753 N93-13523
EXPLOSIVE DEVICES
Booster explosive rings
[AD-D015375] p 556 N93-13471
EXPLOSIVES
Automated dry powder dispenser for explosive components
[DE92-019425] p 555 N93-12568
Nonideal thermoequilibrium calculations using a large product species data base
[DE92-040839] p 735 N93-12813
EXPONENTS
An application of exponential neural networks to event-train recognition
[AD-A254948] p 690 N93-12548
EXPOSURE
Latent image exposure monitor using scatterometry
[DE92-019427] p 604 N93-12915
EXTERNAL TANKS
VPPA weld model evaluation
[NASA-CR-184460] p 611 N93-12919
EXTINGUISHING
Semi-quantitative model for the burning rate of solid materials
[PB92-213362] p 539 N93-13641
EXTRACTION
The identification and quantitation of triamterene in blood and urine from a fatal aircraft accident
[AD-A254550] p 674 N93-12612
RF voltage modulation at discrete frequencies with applications to crystal channeling extraction
[DE92-015567] p 707 N93-13235
Analysis and experimental results for an extraction cavity for the split-cavity oscillator
[DE92-040262] p 566 N93-13512
Lunar mining of oxygen using fluorine
[LPI-748] p 761 N93-13980
Availability of hydrogen for lunar base activities p 762 N93-13982
EXTRAPOLATION
Scientific study of data analysis
[NASA-CR-184435] p 769 N93-12658
EXTRATERRESTRIAL RADIATION
Chemical release and radiation effects experiment advanced planning and coordination
[NASA-CR-184439] p 649 N93-12718
A study of the generation of linear energy transfer spectra for space radiations
[NASA-TM-4410] p 772 N93-13572
EXTRAVEHICULAR ACTIVITY
JPRS report: Science and technology. Central Eurasia: Space
[JPRS-USP-92-005] p 513 N93-13304
Suited for spacewalking: A teacher's guide with activities
[NASA-EP-279] p 679 N93-13692
EXTREME ULTRAVIOLET RADIATION
Development of XUV projection lithography at 60 to 80 nm
[DE92-017517] p 603 N93-12560
The Orbiter Stability Experiment on STS-40 p 508 N93-13159
Electron impact polarization expected in solar EUV lines from flaring chromospheres/transition regions
[SSL-PREPRINT-90-124] p 770 N93-13478
EXTREMELY HIGH FREQUENCIES
The DSI small satellite launcher p 511 N93-13180
EXTREMELY LOW FREQUENCIES
Extremely low frequency/very low frequency Generator
[AD-A254347] p 562 N93-12948
EXTREMELY LOW RADIO FREQUENCIES
Long-term averages of globally-measured ELF/VLF radio noise
[AD-A255518] p 566 N93-13869
EXTRUDING
Simulation of forward-backward extrusion with numerical and model material techniques
[DE92-016299] p 558 N93-13298
EYE MOVEMENTS
Ocular attention-sensing interface system
[NASA-CR-190884] p 678 N93-13450

F

F-18 AIRCRAFT
Determination of the stability and control derivatives of the F/A-18 HARV from flight data using the maximum likelihood method
[NASA-CR-191216] p 503 N93-12903
A stochastic optimal feedforward and feedback control methodology for superagility
[NASA-CR-4471] p 694 N93-13370
FABRICATION
Development of XUV projection lithography at 60 to 80 nm
[DE92-017517] p 603 N93-12560
Consolidation of powder coated thermoplastic preform process modeling
[AD-A255094] p 529 N93-12757
Development of large-area monolithically integrated silicon-film photovoltaic modules
[DE92-010600] p 637 N93-12838
Terahertz horn antennas on thin membranes
[AD-A254772] p 562 N93-12867
Pressure fed thrust chamber technology program
[NASA-CR-184461] p 526 N93-12968
Glass fiber processing for the Moon/Mars program: Center director's discretionary fund final report
[NASA-TM-108379] p 551 N93-13115
Novel thin-film CuInSe2 fabrication
[DE92-016440] p 723 N93-13526
All-metal, compact heat exchanger for space cryocoolers
[NASA-CR-190861] p 559 N93-13604
Thin films and solar cells of cadmium telluride and cadmium zinc telluride p 639 N93-13611
Ceramic machining: Assessment of current practice and research needs in the US
[PB92-213511] p 553 N93-13649
Fabrication of thin film heat flux sensors p 599 N93-13667
Technology trends in high temperature pressure transducers: The impact of micromachining p 601 N93-13676
FABRICS
Experiments, theory, and simulation on the evolution of fabric in granular materials
[AD-A254820] p 545 N93-12729
FABRY-PEROT INTERFEROMETERS
The VELOPT code for estimating performance of a Fabry-Perot velocimeter
[DE92-015566] p 596 N93-12831
Parameter studies of helium-neon lasers at 543 nm p 606 N93-13747
Acousto-optic devices and applications p 712 N93-14100
FACSIMILE COMMUNICATION
Program Support Communications Network (PSCN) facsimile system directory
[NASA-TM-108051] p 562 N93-12909
The protection of the Facsimile (FAX) machine against the insider threat
[DE92-019424] p 565 N93-13506
FACTOR ANALYSIS
Study of the concentration and deposition of tropospheric aerosols using x ray emission techniques p 667 N93-13894
FAILURE
Microcracking, microcrack-induced delamination, and longitudinal splitting of advanced composite structures
[NASA-CR-4472] p 623 N93-12911
Identifiability in the autopsy model of reliability theory p 620 N93-13710
FAILURE ANALYSIS
A heat pipe coupled planar thermionic converter: Performance characterization, nondestructive testing, and evaluation
[AD-A254941] p 727 N93-12546

Compression test simulation of thick-section composite materials
[AD-A255021] p 528 N93-12583
The 3-D nonlinear constitutive modeling approach for composite materials
[AD-A255022] p 528 N93-12584
Thermal barrier coating life prediction model development, phase 2
[NASA-CR-189111] p 544 N93-12589
Touchstone for success
[ESA-BR-52] p 557 N93-12934
Structural integrity of composites under load and thermal insult p 530 N93-13012
BETA: Behavioral testability analyzer and its application to high-level test generation and synthesis for testability
[NASA-CR-191282] p 572 N93-13569
The use of degradation measures in assessing reliability p 573 N93-13607
Effects of layer waviness on compression-loaded thermoplastic composite laminates p 532 N93-13724

FAILURE MODES
Theoretical and experimental studies on the foundation theoretical and experimental studies on the foundation of mesomechanics
[AD-A254385] p 623 N93-12863
Structural integrity of composites under load and thermal insult p 530 N93-13012

FAINT OBJECTS
Orbiting Space Interferometer (OSI): A first generation space interferometer p 745 N93-13587
An optical study of the faint end of the stellar luminosity function p 748 N93-13960

FAN BLADES
Investigation of advanced counterrotation blade configuration concepts for high speed turboprop systems. Task 4: Advanced fan section aerodynamic analysis
[NASA-CR-187128] p 502 N93-12695

FAR INFRARED RADIATION
Experimental studies of the far-infrared spectra of cosmic-type ices
[NASA-CR-191300] p 748 N93-13660
The interstellar medium of elliptical galaxies p 757 N93-14071
Thermal and nonthermal star formation: An investigation into the process of star formation as a function of stellar mass p 758 N93-14091

FAR ULTRAVIOLET RADIATION
Contamination analysis of SSF candidate materials
[NASA-CR-184431] p 709 N93-12894

FASTENERS
Structural verification for GAS experiments p 511 N93-13175

FATIGUE (MATERIALS)
Fatigue and fracture of intermetallic alloys
[AD-A254543] p 540 N93-12603
The application of the finite element method and the boundary element method to fatigue and fracture, volumes 1 and 2 p 624 N93-13016
Probabilistic finite elements for fatigue and fracture analysis
[NASA-CR-191246] p 624 N93-13029
The use of degradation measures in assessing reliability p 573 N93-13607
Fatigue studies in Al-Mg-Si alloys p 543 N93-13690

FATIGUE LIFE
On bilinearity of Manson-Coffin low-cycle-fatigue relationship
[NASA-TM-105840] p 622 N93-12739
The application of the finite element method and the boundary element method to fatigue and fracture, volumes 1 and 2 p 624 N93-13016
In-phase and out-of-phase axial-torsional fatigue behavior of Haynes 188 at 760 C
[NASA-TM-105765] p 625 N93-13153
Structural fatigue aspects of the P-3 Orion
[ARL-STRUC-TM-558] p 500 N93-13256
Computational simulation of probabilistic lifetime strength for aerospace materials subjected to high temperature, mechanical fatigue, creep and thermal fatigue
[NASA-CR-190794] p 626 N93-13290
Fatigue studies in Al-Mg-Si alloys p 543 N93-13690
Effects of layer waviness on compression-loaded thermoplastic composite laminates p 532 N93-13724
An investigation into thermomechanical fatigue of metal matrix composites p 534 N93-13810

FATIGUE TESTS
On bilinearity of Manson-Coffin low-cycle-fatigue relationship
[NASA-TM-105840] p 622 N93-12739

FAULT TOLERANCE
A general theory of signal integration for fault-tolerant dynamic distributed sensor networks
[AD-A254961] p 732 N93-12553
Testing and fault-tolerant design techniques for advanced digital architectures
[AD-A255013] p 681 N93-12707
Reviews of computing technology: Fiber distributed data interface
[DE92-019927] p 681 N93-12886
A brief overview of NASA Langley's research program in formal methods p 684 N93-12958
On-orbit supervisor for controlling spacecraft
[AD-A254342] p 522 N93-12962
Software reliability through fault-avoidance and fault-tolerance
[NASA-CR-189880] p 686 N93-13293
Lazy checkpoint coordination for bounding rollback propagation
[NASA-CR-191281] p 565 N93-13375
Summary: Experimental validation of real-time fault-tolerant systems
[NASA-CR-190985] p 503 N93-13697

FEASIBILITY ANALYSIS
Feasibility study of a synthesis procedure for array feeds to improve radiation performance of large distorted reflector antennas
[NASA-CR-190948] p 561 N93-12655
Real-time quality assurance testing using photonic techniques: Application to iodine water system
[NASA-CR-184413] p 619 N93-12692
ASTOVL model engine simulators for wind tunnel research p 507 N93-13213
The formation of ore mineral deposits on the Moon: A feasibility study p 760 N93-13974
Lunar concrete for construction p 555 N93-13990
Solar water heating system for a lunar base p 641 N93-14005

FECES
Distribution of human waste samples in relation to sizing waste processing in space p 680 N93-14001

FEDERAL BUDGETS
Selected data on federal support to universities and colleges: Fiscal year 1990
[NSF-92-310] p 740 N93-12920
Federal R/D funding by budget function: Fiscal years 1991-1993
[NSF-92-318] p 740 N93-13312
Selected data on Federal funds for research and development: Fiscal years 1990, 1991, and 1992
[NSF-92-319] p 741 N93-13657
Window on waste: Atrophy in NASA management
[GPO-57-273] p 732 N93-13693
National Aeronautics and Space Administration Authorization Act, fiscal year 1993
[S-REPT-102-364] p 741 N93-13798
NASA authorization, 1993, volume 2
[GPO-56-943-VOL-2] p 741 N93-13799
NASA's fiscal year 1993 budget
[S-HRG-102-707] p 742 N93-13800
Research in geosciences policy
[NASA-CR-190470] p 632 N93-13833

FEEDBACK
Forest declines: Some perspectives on linking processes and patterns
[DE92-019946] p 642 N93-12828

FEEDBACK CONTROL
Design philosophy for wind tunnel model positioning systems
[AD-A254958] p 506 N93-12552
An integrated optical sensor for GMAW feedback control
[DE92-018019] p 610 N93-12793
The application of input shaping to a system with varying parameters p 612 N93-12954
RF system description for the ground test accelerator radio-frequency quadrupole
[DE92-040239] p 563 N93-13045
Robust control of uncertain aerospace and mechanical systems with unmodelled flexibilities: A singular perturbation approach p 691 N93-13129
End-point position control of multi-link flexible manipulator arms p 613 N93-13335
Novel techniques of wavefront sensing for adaptive optics with array telescopes using an artificial neural network p 743 N93-13343
A stochastic optimal feedforward and feedback control methodology for superagility
[NASA-CR-4471] p 694 N93-13370
Robust control of a flexible link robot and rigid link robot: Theory, simulation, and experiment p 614 N93-13452
Design, construction, and control of a two degree-of-freedom electric direct-drive human power amplifier p 678 N93-13486
Control of a very flexible robot in gravity p 615 N93-13541
Ideal aircraft handling quality models: Longitudinal axis
[NAL-PD-FC-9203] p 504 N93-13566
Performance and control of ascending trajectories to minimize heat load for transatmospheric aero-space planes p 495 N93-13745
Enhanced accuracy for closed-loop robot p 617 N93-13808
Application of adaptive trusses to vibration isolation in flexible structures p 617 N93-13809
Symposium proceedings on Quantitative Feedback Theory
[AD-A255527] p 505 N93-13872
Robust controller and estimator design using minimax methods p 694 N93-13925
Model reduction, sensor/actuator selection and control system redesign for large flexible structures p 523 N93-14040

FEEDFORWARD CONTROL
A stochastic optimal feedforward and feedback control methodology for superagility
[NASA-CR-4471] p 694 N93-13370

FEMALES
Women and minorities in science and engineering: An update
[NSF-92-303] p 730 N93-12907
NASA industry education initiative. Education programs report, 1991
[NASA-NP-158] p 730 N93-13248

FERROELECTRICITY
Atomic structure of mixed ferroelectrics
[AD-A254369] p 702 N93-12947

FIBER COMPOSITES
Properties of five toughened matrix composite materials
[NASA-TP-3254] p 528 N93-12590
Fracture toughness of short fiber/brittle matrix composites p 528 N93-12630
Transverse flexural tests as a tool for assessing damage to PMR-15 composites from isothermal aging in air at elevated temperatures
[NASA-TM-105848] p 529 N93-12737
Consolidation of powder coated thermoplastic preform process modeling
[AD-A255094] p 529 N93-12757
Predictive forming of advanced thermoplastic composite structures p 529 N93-12835
Microcracking, microcrack-induced delamination, and longitudinal splitting of advanced composite structures
[NASA-CR-4472] p 623 N93-12911
Polypropylene fibers in portland cement concrete pavements
[DOT/FAA/RD-92/9] p 551 N93-13259
Ductile fracture process of discontinuous fiber reinforced composites
[DE92-016298] p 531 N93-13264
Nonlinear mechanics of composite materials with periodic microstructure
[NASA-CR-190750] p 531 N93-13309
Results of ASTM round robin testing for mode 1 interlaminar fracture toughness of composite materials
[NASA-TM-104222] p 532 N93-13428
Micromechanics of finite length fibers in composite materials p 532 N93-13490
Mechanical behaviour of fiber-reinforced ceramic matrix composites p 532 N93-13527
Load-transfer and crack bridging in fiber-toughened ceramic composites p 629 N93-13754
Experimental characterization of continuous alumina fiber/epoxy p 533 N93-13775
Thermoviscoplastic analysis of metal matrix composites p 535 N93-13954
X ray attenuation measurements for high-temperature materials characterization and in situ monitoring of damage accumulation p 631 N93-14022

FIBER OPTICS
Fibre-optic sensors using adiabatically tapered single-mode fibres
[AD-A254555] p 708 N93-12642
Tutorials from the 23rd Annual Precise Time and Time Interval (PTTI) Applications and Planning Meeting
[AD-A254745] p 596 N93-12844
Reviews of computing technology: Fiber distributed data interface
[DE92-019927] p 681 N93-12886
Fiber optic sensors for static fracture studies and dynamic wave propagation problems p 709 N93-12984
HIPPI and Fibre Channel
[DE92-040346] p 689 N93-13046
Fiber optic sensors for environmental applications: A brief review
[DE92-040170] p 710 N93-13576
Developments on high temperature fiber optic microphone p 601 N93-13680
Multiplexing electro-optic architectures for advanced aircraft integrated flight control systems
[NASA-CR-182268] p 504 N93-13735

Electro-optic architecture for servicing sensors and actuators in advanced aircraft propulsion systems
[NASA-CR-182269] p 711 N93-13762
OSA proceedings of the topical meeting on optical amplifiers and their applications, volume 13
[AD-A252974] p 711 N93-13879
Fiber optic data bus radiation effects study
[AD-A255821] p 711 N93-14031

FIBER VOLUME FRACTION
Matrix cracking initiation stress in fiber-reinforced ceramic matrix composites p 627 N93-13539
Thermoviscoplastic analysis of metal matrix composites p 535 N93-13954

FIBERS
Micromechanics of finite length fibers in composite materials p 532 N93-13490

FIELD ALIGNED CURRENTS
Structure of and dynamical processes in the Earth's magnetopause and boundary layer regions p 657 N93-13793

FIELD EFFECT TRANSISTORS
GaAs gate dynamic memory technology
[AD-A254801] p 720 N93-12748
Preamplifier with adjustable input resistance
[AD-D015377] p 572 N93-13473
Semiconductor measurement technology: INSTANT (IGBT network simulation and transient Analysis tool)
[PB92-213529] p 725 N93-13783

FIELD OF VIEW
SeaWiFS technical report series. Volume 4, an analysis of GAC sampling algorithms: A case study
[NASA-TM-104566-VOL-4] p 669 N93-13382

FIELD STRENGTH
JARE data reports no. 170 (ionosphere 45). HF field strength data measured at Syowa Station, Antarctica from January to December 1988 p 652 N93-13432
An infrared polarimetric study of sunspots p 770 N93-13627
Limits on galactic dynamo theory due to magnetic fluctuations p 754 N93-13636

FIELD THEORY (PHYSICS)
Mathematics and string theory
[DE92-019292] p 727 N93-12796

FIGHTER AIRCRAFT
Specification of adaptive aiding systems
[AD-A254537] p 499 N93-12602
The PEP Symposium on CFD Techniques for Propulsion Applications p 579 N93-13210
Mass flow effects on the low speed characteristics of an advanced combat aircraft p 497 N93-13214
Some aspects of intake design, performance and integration with the airframe p 502 N93-13219
CFD calibration for three-dimensional nozzle/afterbody configurations p 582 N93-13226
Propulsion integration results of the STOL and Maneuver Technology Demonstrator p 502 N93-13228
Ideal aircraft handling quality models: Longitudinal axis
[NAL-PD-FC-9203] p 504 N93-13566
Electro-optic architecture for servicing sensors and actuators in advanced aircraft propulsion systems
[NASA-CR-182269] p 711 N93-13762

FILAMENT WINDING
Process comparison study. MSFC Center Director's Discretionary Fund (CDDF)
[NASA-TM-108382] p 526 N93-13429

FILE MAINTENANCE (COMPUTERS)
File servers, networking, and supercomputers p 737 N93-13137

FILLERS
Mechanical properties of epoxy/alumina trihydrate-filled compositions p 534 N93-13950

FILLETS
Effects of residual stress, weld toe notch and weld defects on fatigue of welded steel structures p 631 N93-13947

FILM THICKNESS
Latent image exposure monitor using scatterometry
[DE92-019427] p 604 N93-12915

FINANCIAL MANAGEMENT
NASA budget: Potential shortfalls in funding NASA's 5-year plan. Testimony before the Subcommittee on Science, Technology, and Space, Committee on Commerce, Science, and Transportation, United States Senate
[GAO/T-NSIAD-92-18] p 740 N93-13280
Business analysis: The commercial mission of the International Asteroid Mission p 514 N93-13554
Window on waste: Atrophy in NASA management
[GPO-57-273] p 732 N93-13693

FINE STRUCTURE
Oxygen deficiencies at defects in YBa2Cu3O(7-delta) as determined by high resolution parallel electron energy loss
[DE92-016301] p 721 N93-13089

FINGERS
Dexterous grasp and manipulation p 618 N93-14075

FINITE DIFFERENCE THEORY
Regional seismograms: Attenuation and scattering
[AD-A254348] p 650 N93-12943
A SINDA thermal model using CAD/CAE technologies p 585 N93-13394
One-dimensional transient finite difference model of an operational salinity gradient solar pond p 586 N93-13400

FINITE ELEMENT METHOD
Innovative methods in the dynamics of large space structures
[AD-A254630] p 521 N93-12579
Compression test simulation of thick-section composite materials
[AD-A255021] p 528 N93-12583
The 3-D nonlinear constitutive modeling approach for composite materials
[AD-A255022] p 528 N93-12584
Small-strain and finite-strain finite element analyses of plane-strain tensile elastic-plastic crack growth p 621 N93-12628
Experimental validation of finite element and boundary element methods for predicting structural vibration and radiated noise p 621 N93-12631
Analysis of a structure-equipment system subjected to impact loading
[AD-A255097] p 622 N93-12652
Quality assessment of the A-posteriori error estimation in finite elements
[AD-A254767] p 696 N93-12701
Numerical calibration of the stable poisson loaded specimen
[NASA-TM-105609] p 622 N93-12738
Heat transfer in a liquid metal crucible with an integral blackbody cavity
[DE92-019640] p 576 N93-12825
Identification of parametric finite element models using experimental modal data
[PB92-217819] p 558 N93-12976
Finite element analysis of anisotropic viscoelastic composite structures and analytical determination of optimum viscoelastic material properties p 530 N93-13007
Linear and nonlinear finite element analysis of laminated composite structures at high temperatures p 623 N93-13009
The application of the finite element method and the boundary element method to fatigue and fracture, volumes 1 and 2 p 624 N93-13016
Compression strength of composite primary structural components
[NASA-CR-190949] p 624 N93-13019
Probabilistic finite elements for fatigue and fracture analysis
[NASA-CR-191246] p 624 N93-13029
Finite element versus boundary element analysis of two-dimensional coupled thermoelasticity p 625 N93-13142
Structural optimization of thin shells using finite element method
[NASA-TM-105903] p 625 N93-13157
The use of finite elements to model soil/track interactions in coupled multi-body dynamic simulations: Is real time simulation feasible?
[DE92-016184] p 612 N93-13236
Analysis of large quasistatic deformations of inelastic solids by a new stress based finite element method
[NASA-CR-189235] p 626 N93-13260
Simulation of forward-backward extrusion with numerical and model material techniques
[DE92-016299] p 558 N93-13298
Numerical simulations of steel plate perforation
[DE92-017058] p 626 N93-13301
Electromagnetic scattering and radiation from microstrip patch antennas and spirals residing in a cavity
[NASA-CR-191284] p 565 N93-13354
A SINDA thermal model using CAD/CAE technologies p 585 N93-13394
Coupled structural/thermal/electromagnetic analysis/tailoring of graded composite structures
[NASA-CR-189150] p 626 N93-13443
Coupled structural/thermal/electromagnetic analysis/tailoring of graded composite structures
[NASA-CR-189151] p 627 N93-13444
Coupled structural/thermal/electromagnetic analysis/tailoring of graded composite structures
[NASA-CR-189152] p 627 N93-13445
Robotic exploration of surfaces and its application to legged locomotion p 615 N93-13540
Finite element study of ultrasonic imaging p 700 N93-13774
Trim analysis by shooting and finite elements and Floquet eigenanalysis by QR and subspace iterations in helicopter dynamics p 501 N93-13914
The free and forced vibrations of structures using the finite dynamic element method p 630 N93-13935
Finite elements for free edge delaminations and delaminated anisotropic beams p 535 N93-13967
Delamination initiation in postbuckled dropped-ply laminates p 535 N93-14030

FINITE VOLUME METHOD
Numeric simulation of the aerodynamic flows around nacelles p 577 N93-13202
Unsteady three-dimensional thin-layer Navier-Stokes solutions for turbomachinery in transonic flow p 593 N93-14025
A numerical study of hypersonic flows using the full Navier-Stokes equations with different air models p 594 N93-14061

FIRE DAMAGE
The estimation of electrical cable fire-induced damage limits
[DE92-040100] p 572 N93-13519

FIRE FIGHTING
Flow through horizontal vents as related to compartment fire environments
[PB92-213388] p 559 N93-13642
Combustion of gaseous fuels under reduced-gravity conditions p 557 N93-14012

FIRE PREVENTION
Findings of a review of spacecraft fire safety needs
[NASA-CR-189181] p 523 N93-13715

FIRES
Implicitly coupling heat conduction into a zone fire model
[PB92-222769] p 558 N93-12980
CORRIDOR: A routine for estimating the initial wave front resulting from high temperature fire exposure to a corridor
[PB92-213347] p 559 N93-13640
Semi-quantitative model for the burning rate of solid materials
[PB92-213362] p 539 N93-13641
Flow through horizontal vents as related to compartment fire environments
[PB92-213388] p 559 N93-13642
Findings of a review of spacecraft fire safety needs
[NASA-CR-189181] p 523 N93-13715
Combustion of gaseous fuels under reduced-gravity conditions p 557 N93-14012

FLAME TEMPERATURE
A preliminary study of the effect of equivalence ratio on a low emissions gas turbine combustor using KIVA-2
[DE92-018616] p 613 N93-13321

FLAMMABILITY
The estimation of electrical cable fire-induced damage limits
[DE92-040100] p 572 N93-13519
Findings of a review of spacecraft fire safety needs
[NASA-CR-189181] p 523 N93-13715

FLAPPING
User's Guide for the NREL Force and Loads Analysis Program
[DE92-010579] p 627 N93-13524
User's Guide for the NREL Teetering Rotor Analysis Program (STRAP)
[DE92-010580] p 627 N93-13525

FLAT PLATES
Wall functions for the kappa-epsilon turbulence model in generalized nonorthogonal curvilinear coordinates p 587 N93-13517
Application of a vectorized particle simulation to the study of plates and wedges in high-speed rarefied flow p 495 N93-13746

FLAVOR (PARTICLE PHYSICS)
Neutrino mass
[DE92-017411] p 701 N93-12588

FLEXIBILITY
Numerical analysis of nonminimum phase zero for nonuniform link design p 611 N93-12953
Large-deflection analysis of cord composite plates p 530 N93-13008
Initial experiments in end-point control of a flexible, two-link manipulator p 612 N93-13018
Position and force control of flexible and rigid manipulators using the sliding-mode technique p 695 N93-14065

FLEXIBLE BODIES
Manipulation strategies for massive space payloads
[NASA-CR-190844] p 611 N93-12952
The application of input shaping to a system with varying parameters p 612 N93-12954
Experimental verification of modified command shaping using a flexible manipulator p 612 N93-12955
Application of Lanczos vectors to control design of flexible structures, part 2
[NASA-CR-191244] p 685 N93-13030

Robust control of uncertain aerospace and mechanical systems with unmodelled flexibilities: A singular perturbation approach p 691 N93-13129
Unsymmetric Lanczos model reduction and linear state function observer for flexible structures
[NASA-CR-191231] p 686 N93-13295
Application of Lanczos vectors to control design of flexible structures
[NASA-CR-191230] p 686 N93-13296
Application of adaptive trusses to vibration isolation in flexible structures p 617 N93-13809
Q-Markov cover identification and integrated MCA-OVC controller design for flexible structures
p 695 N93-14045
Modelling flexible link manipulators in the three-dimensional space p 574 N93-14093

FLEXIBLE SPACECRAFT
Robust control of uncertain aerospace and mechanical systems with unmodelled flexibilities: A singular perturbation approach p 691 N93-13129
Combined design of structures and controllers for optimal maneuverability p 691 N93-13130

FLEXIBLE WINGS
Active flutter suppression using dipole filters
[NASA-TM-107594] p 504 N93-13367

FLEXING
Transverse flexural tests as a tool for assessing damage to PMR-15 composites from isothermal aging in air at elevated temperatures
[NASA-TM-105848] p 529 N93-12737

FLIGHT CHARACTERISTICS
X-29 linear aerodynamic perturbation model
[AD-A254810] p 500 N93-12752
Trim analysis by shooting and finite elements and Floquet eigenanalysis by QR and subspace iterations in helicopter dynamics p 501 N93-13914

FLIGHT CONDITIONS
Stratospheric turbulence measurements and models for aerospace plane design
[NASA-TM-104262] p 663 N93-13288

FLIGHT CONTROL
The Second NASA Formal Methods Workshop 1992
[NASA-CP-10110] p 684 N93-12957
A brief overview of NASA Langley's research program in formal methods p 684 N93-12958
A stochastic optimal feedforward and feedback control methodology for superagility
[NASA-CR-4471] p 694 N93-13370
Aircraft accident/incident summary report: Controlled flight into terrain, Bruno's Inc., Beechjet, N25BR, Rome, Georgia, December 11, 1991
[PB92-910404] p 498 N93-13470
Formulation and validation of high-order mathematical models of helicopter flight dynamics
p 501 N93-13821

FLIGHT CREWS
Operator workload predictions for the revised AH-64A workload prediction model. Volume 2: Appendixes A through H
[AD-A254939] p 676 N93-12545
Adaptive automation and human performance: Multi-task performance characteristics
[AD-A254596] p 503 N93-12578
Human factors research in aircrew performance and training: 1986-1991
[AD-A254455] p 677 N93-12609
Thermal stress in US Air Force operations
[AD-A255785] p 676 N93-14027

FLIGHT OPERATIONS
Element Material Exposure Experiment by EFFU
p 548 N93-12783
EURECA
[ESA-F-26] p 522 N93-12964
Post flight operation of a high peak power neodymium YAG laser aboard the G-449 payload flown on Space Shuttle Columbia mission 61-C p 508 N93-13161

FLIGHT OPTIMIZATION
Minimum-time flight paths of supersonic aircraft
p 500 N93-13140

FLIGHT PATHS
Minimum-time flight paths of supersonic aircraft
p 500 N93-13140

FLIGHT SAFETY
Structural verification for GAS experiments
p 511 N93-13175
Aircraft accident report: Britt Airways, Inc., d/b/a, Continental Express Flight 2574, in-flight structural breakup, EMB-120RT, N33701, Eagle Lake, Texas, September 11, 1991
[PB92-910405] p 498 N93-13426

FLIGHT SIMULATION
Adaptive automation and human performance: Multi-task performance characteristics
[AD-A254596] p 503 N93-12578
Perceptual dimensions of visual scenes relevant for simulating low-altitude flight
[AD-A254645] p 676 N93-12662
The modelling of turbulence and downbursts for flight simulators p 507 N93-13542

FLIGHT TESTS
Subsonic flight test evaluation of a propulsion system parameter estimation process for the F100 engine
[NASA-TM-4426] p 502 N93-13155
Flight analysis of air intake/engine compatibility
p 502 N93-13212
National Aero-Space Plane: Key issues facing the program. Testimony before the Subcommittee on Technology and Competitiveness, Committee on Science, Space, and Technology, House of Representatives
[GAO/T-NSIAD-92-26] p 500 N93-13253

FLIGHT TRAINING
Human factors research in aircrew performance and training: 1986-1991
[AD-A254455] p 677 N93-12609

FLIP-FLOPS
BETA: Behavioral testability analyzer and its application to high-level test generation and synthesis for testability
[NASA-CR-191282] p 572 N93-13569

FLOAT ZONES
Heat transfer, fluid flow and interface shapes in floating-zone crystal growth p 724 N93-13739

FLOATING
Interaction and impact of floating bodies
[AD-A254627] p 574 N93-12617

FLOATS
Acoustic tracking of neutrally buoyant float
[AD-A255086] p 669 N93-12742

FLOQUET THEOREM
Trim analysis by shooting and finite elements and Floquet eigenanalysis by QR and subspace iterations in helicopter dynamics p 501 N93-13914
Deterministic and stochastic responses of nonlinear systems p 631 N93-13966

FLORIDA
Extended range forecast of Atlantic seasonal hurricane activity for 1993 p 661 N93-12928

FLOW CHARACTERISTICS
Numeric simulation of the aerodynamic flows around nacelles p 577 N93-13202
Overview on test cases for computation of internal flows in turbomachines p 579 N93-13209
Effects of forebody strakes and Mach number on overall aerodynamic characteristics of configuration with 55 deg cropped delta wing
[NASA-TP-3253] p 493 N93-13353
Chaotic vortical motion in the near region of a plane jet p 493 N93-13493
Computational fluid dynamics of the base flow on a plane body between a subsonic flow on one side and a supersonic flow on the other p 591 N93-13920
The unsteady aerodynamics of a delta wing undergoing large-amplitude pitching motions p 496 N93-13929

FLOW DISTRIBUTION
Quantitative analysis of three-dimensional steady flow field by using particle image velocimetry and digital image processing method p 577 N93-13017
A numerical study of hypersonic flow with strong surface blowing p 492 N93-13128
Application of a solution adaptive grid to flow over an embedded cavity p 492 N93-13141
Detailed analysis of wing-nacelle interaction for commercial transport aircraft p 578 N93-13203
Investigation of interference phenomena of modern wing-mounted high-bypass-ratio engines by the solution of the Euler-equations p 578 N93-13204
Euler analysis of turbofan/superfan integration for a transport aircraft p 578 N93-13206
Recent developments in low-speed TPS-testing for engine integration drag and installed thrust reversr simulation p 502 N93-13207
Experimental studies of the flowfields and their effects due to a pair of lift jets discharging in the ground effect region p 580 N93-13217
Calibration of 2D unstructured grid methods on propulsive flowfields p 582 N93-13225
Investigation of the flowfield around an isolated bypass engine with fan and core jet p 582 N93-13227
Fundamentals of enhanced scalar transport in strongly oscillating and/or resonant flow fields as created by pulse combustion
[DE92-012147] p 582 N93-13247
Mathematical problems in inviscid hypersonic flow
p 493 N93-13451
A theoretical investigation of the growth rates of ice crystals in clouds p 653 N93-13485
Wall functions for the kappa-epsilon turbulence model in generalized nonorthogonal curvilinear coordinates
p 587 N93-13517
Velocity and temperature measurements in a non-premixed reacting flow behind a backward facing step p 494 N93-13632
Planar laser-induced fluorescence measurements of high-enthalpy free jet flow with nitric oxide
p 595 N93-13685
Planar measurement of flow field parameters in nonreacting supersonic flows with laser-induced iodine fluorescence p 495 N93-13801
An experimental investigation of the three-dimensional boundary layer on a rotating disk p 589 N93-13806
Numerical investigation of the flow field in the head-end, star grain section of a solid rocket motor during ignition transients p 526 N93-13818
Assessment of potential aerodynamic benefits from spanwise blowing at the wing tip p 496 N93-13822
An experimental/computational study of heat transfer in sharp fin induced shock wave/turbulent boundary layer interactions at low hypersonic Mach numbers
p 590 N93-13826
Numerical investigation of non-spherical droplet dynamics in viscous convective flows
p 591 N93-13918
Overall effects of separation on thin aerofoils
[ISBN-0-315-67464-4] p 496 N93-13930
Turbulent boundary layers with high turbulence: Experimental heat transfer and structure on flat and convex walls p 591 N93-13938
Organized turbulent structures and their induced wall pressure fluctuations p 592 N93-13952
Flow prediction for three-dimensional intakes and ducts using viscous-inviscid interaction methods
p 592 N93-13953
Coherent structures in compressible convection
p 592 N93-13964
Instabilities and patterns in Taylor-Couette flow
p 593 N93-13965
Wake characterization: Full flow simulation of space structures in low earth orbit p 497 N93-13970
Unsteady three-dimensional thin-layer Navier-Stokes solutions for turbomachinery in transonic flow
p 593 N93-14025
Navier-Stokes flowfield computation of wing/rotor interaction for a tilt rotor aircraft in hover
p 497 N93-14035

FLOW EQUATIONS
An experimental and computational investigation of slender wings undergoing wing rock
p 505 N93-13915

FLOW MEASUREMENT
Determination of the permeability of carbon aerogels by gas flow measurements
[DE92-019574] p 550 N93-12888
Quantitative analysis of three-dimensional steady flow field by using particle image velocimetry and digital image processing method p 577 N93-13017
The jet behaviour of an actual high-bypass engine as determined by LDA-measurements in ground tests
p 503 N93-13218
A fundamental study of suction for Laminar Flow Control (LFC)
[NASA-CR-191276] p 583 N93-13277
The 1992 NASA Langley Measurement Technology Conference: Measurement Technology for Aerospace Applications in High-Temperature Environments
[NASA-CP-3161] p 598 N93-13661
Gas temperature and density measurements based on spectrally resolved Rayleigh-Brillouin scattering
p 602 N93-13684
Planar laser-induced fluorescence measurements of high-enthalpy free jet flow with nitric oxide
p 595 N93-13685
Planar laser-induced fluorescence imaging of OH in the exhaust of a bi-propellant thruster p 602 N93-13686
Airfoil-vortex interaction and the wake of an oscillating airfoil p 495 N93-13803

FLOW NETS
Analysis of a space emergency ammonia dump using the FLOW-NET two-phase flow program
p 584 N93-13389

FLOW STABILITY
Investigation of hypersonic shock-induced combustion in a hydrogen-air system
[NASA-CR-191239] p 538 N93-13456
Development and computation of continuum higher order constitutive relations for high-altitude hypersonic flow p 494 N93-13578
Linear stability theory of hypersonic, chemically reacting viscous flows p 588 N93-13765
Variational characterizations of steady two-dimensional vortex motions p 589 N93-13781
Dynamical instabilities in a fluid spin-up and in an open flow system p 590 N93-13899
Stability of the compressible reacting mixing layer
p 592 N93-13948

Experiments on the statistical nature of stably stratified turbulence p 594 N93-14069
Numerical simulation of compressible Couette flow stability: Non-linear and three-dimensional effects p 594 N93-14077

FLOW VELOCITY
The jet behaviour of an actual high-bypass engine as determined by LDA-measurements in ground tests p 503 N93-13218
The influence of mixture preparation in the intake port on the performance of a spark-ignited four-stroke engine p 613 N93-13331
Velocity and temperature measurements in a non-premixed reacting flow behind a backward facing step p 494 N93-13632
Planar laser-induced fluorescence measurements of high-enthalpy free jet flow with nitric oxide p 595 N93-13685
Dynamical instabilities in a fluid spin-up and in an open flow system p 590 N93-13899
Dynamics of vortex rings in cross-flow p 496 N93-13917

FLOW VISUALIZATION
Quantitative analysis of three-dimensional steady flow field by using particle image velocimetry and digital image processing method p 577 N93-13017
In-flight flow visualization results from the X-29A aircraft at high angles of attack [NASA-TM-4430] p 493 N93-13322
Applications of CFD and visualization techniques p 584 N93-13386
Visualization of hydrogen injection in a scramjet engine by simultaneous PLIF imaging and laser holographic imaging p 602 N93-13683
Planar laser-induced fluorescence imaging of OH in the exhaust of a bi-propellant thruster p 602 N93-13686
Exit plane H2O concentration measurements correlated with OH PLIF near-injector mixing measurements for scramjet flows p 603 N93-13687
Heat transfer, fluid flow and interface shapes in floating-zone crystal growth p 724 N93-13739
A multiple-view visual study of the inner/outer region interactions of coherent motions in a turbulent boundary layer p 591 N93-13937

FLUCTUATION THEORY
Chemical potentials in dilute, multicomponent solutions [DE92-011041] p 538 N93-13317

FLUENCE
LDEF atomic oxygen fluence update p 546 N93-12771

FLUID DYNAMICS
Fluid dynamics of supercritical helium within cable-in-conduit conductors [DE92-019516] p 574 N93-12569
An experimental study of a small high-speed LH2 pump for rockets: Fluid dynamic performance [NAL-TR-1131] p 610 N93-12727
The First United States Microgravity Laboratory [NASA-TM-107980] p 557 N93-12951
JPRS report: Science and technology. Central Eurasia: Physics and mathematics [JPRS-UPM-92-006] p 698 N93-13303

FLUID FLOW
A decade of discovery: Experiments with the Get Away Special (GAS) canister p 509 N93-13162
Analysis of fluid/mechanical systems using EASY5 p 586 N93-13397
Heat transfer, fluid flow and interface shapes in floating-zone crystal growth p 724 N93-13739
Application of complex variables in electromagnetofluid dynamic, magnetofluid dynamic and fluid dynamic flows: Viscoelastic boundary-layer theory [ISBN-0-315-65141-5] p 594 N93-14067

FLUID MANAGEMENT
The VTRE Program: An overview p 512 N93-13182

FLUID MECHANICS
Fluid dynamics of supercritical helium within cable-in-conduit conductors [DE92-019516] p 574 N93-12569
Proceedings of the Tenth Symposium on Energy Engineering Sciences: Synergism of Analysis, Modeling, and Experiment [DE92-018777] p 638 N93-13069
A computer program for engineering simulations of space reactor system performance [DE92-016400] p 526 N93-13299

FLUID TRANSMISSION LINES
Fluidic sampling [DE92-017266] p 575 N93-12761

FLUIDICS
Fluidic sampling [DE92-017266] p 575 N93-12761

FLUIDIZED BED PROCESSORS
Wastage-resistant FBC evaporator tubing through microalloying [DE92-001256] p 541 N93-12790

FLUORESCENCE
Fluorescence of thermal control coatings on S0069 and A0114 p 548 N93-12781
New approaches to the measurement of chlorophyll, related pigments and productivity in the sea [NASA-CR-190879] p 673 N93-13612
Electron beam fluorescence measurements in the Boeing hypersonic shock tunnel p 602 N93-13681

FLUORIDES
Group 2 cubic fluorides dielectrics for 3-D integration and GaAs-based optoelectronic structures [AD-A254937] p 719 N93-12544

FLUORINATION
Lunar mining of oxygen using fluorine [LPI-748] p 761 N93-13980

FLUORINE
Lunar mining of oxygen using fluorine [LPI-748] p 761 N93-13980

FLUORINE ORGANIC COMPOUNDS
Recession of FEP specimens from trays D11 and B7 p 549 N93-12786

FLUOROPOLYMERS
Synthesis of derivatives of alpha, omega difunctional perfluoroaliphatic compounds for low dielectric constant resins [AD-A254928] p 550 N93-13026

FLUOROSCOPY
Digital fluoroscopy with an optically coupled charge-coupled device p 712 N93-14101

FLUTTER
Nonlinear stall flutter of wings with bending-torsion coupling [AD-A254323] p 503 N93-12959
Active flutter suppression using dipole filters [NASA-TM-107594] p 504 N93-13367
Transonic aeroelastic analysis of systems with structural nonlinearities p 629 N93-13769
An investigation of the dynamic response of lifting surfaces with concentrated structural nonlinearities p 501 N93-13807

FLUX (RATE)
Measurement of current density fluctuations and ambipolar particle flux due to magnetic fluctuations in MST [DE92-041013] p 713 N93-12878

FLUX DENSITY
The LDCE Particle Impact Experiment as flown on STS-46 --- limited duration space environment candidate materials exposure (LDCE) p 512 N93-13183
Battery selection for space experiments p 512 N93-13184

FLUX PINNING
Defects near the Y2BaCuO5/YBa2Cu3O(7-x) interface and their effect on flux-pinning in melt-processed and quench-melt-growth processed YBa2Cu3O(7-x) [DE92-014463] p 723 N93-13347

FLUX TRANSFER EVENTS
Magnetic holes near the magnetopause p 653 N93-13491

FLUX VECTOR SPLITTING
Unsteady three-dimensional thin-layer Navier-Stokes solutions for turbomachinery in transonic flow p 593 N93-14025

FLY BY LIGHT CONTROL
Multiplexing electro-optic architectures for advanced aircraft integrated flight control systems [NASA-CR-182268] p 504 N93-13735

FLYING PLATFORMS
Meeting review: Third NCAR Research Aircraft Fleet Workshop [PB92-222710] p 649 N93-12818
The real aperture antenna of SAR, a key element for performance p 564 N93-13053

FOAMS
Aerogels, emulsions, and composites: Controlling structure with organic sol-gel chemistry [DE92-019575] p 550 N93-12931
Preparation and properties of low density replica carbon foams [DE92-019573] p 552 N93-13538

FOCUSING
Soft X Ray Telescope (SXT) focus error analysis [NASA-CR-184443] p 742 N93-12657
Long pulse electron beam propagation [DE92-014948] p 706 N93-12830

FOKKER AIRCRAFT
Aerodynamic integration of thrust reversers on the Fokker 100 p 502 N93-13208

FOKKER-PLANCK EQUATION
The dynamics of dense galactic nuclei p 750 N93-13340

FOOD PRODUCTION (IN SPACE)
A decade of discovery: Experiments with the Get Away Special (GAS) canister p 509 N93-13162
Lunar base CELSS: A bioregenerative approach p 680 N93-13993
Crop growth and associated life support for a lunar farm p 680 N93-13994
Long-term lunar stations: Some ecological considerations p 648 N93-13995

FORBIDDEN TRANSITIONS
Laser spectroscopy of rare earth ions p 608 N93-13846

FORCE DISTRIBUTION
Hypersonic propulsion system force accounting p 503 N93-13229

FORCE-FREE MAGNETIC FIELDS
Scientific study of data analysis [NASA-CR-184435] p 769 N93-12658

FORCED CONVECTION
Flow through horizontal vents as related to compartment fire environments [PB92-213388] p 559 N93-13642

FORCED VIBRATION
The free and forced vibrations of structures using the finite dynamic element method p 630 N93-13935

FOREBODIES
Effects of forebody strakes and Mach number on overall aerodynamic characteristics of configuration with 55 deg cropped delta wing [NASA-TP-3253] p 493 N93-13353

FORECASTING
Meeting review: Third NCAR Research Aircraft Fleet Workshop [PB92-222710] p 649 N93-12818

FORESTS
Forest declines: Some perspectives on linking processes and patterns [DE92-019946] p 642 N93-12828
Radiative transfer theory for polarimetric remote sensing of pine forest p 633 N93-13085
Variance of phase fluctuations of waves propagating through a random medium p 569 N93-13087
Deciduous forest scene complexity in high-resolution multispectral scanner imagery [AD-A255511] p 635 N93-13867

FORM FACTORS
TRASYS form factor matrix normalization p 585 N93-13391

FORMALISM
Theory of the ion-channel laser p 607 N93-13777
Formal aspects of human-computer interaction p 679 N93-13909

FORMING TECHNIQUES
Predictive forming of advanced thermoplastic composite structures p 529 N93-12835

FORTRAN
High Energy Propulsion System (HEPS) analysis [AD-A254343] p 525 N93-12963

FORWARD SCATTERING
Experimental testing of four correction algorithms for the forward scattering spectrometer probe [NASA-TM-105906] p 597 N93-13307

FOSSIL FUELS
The role of human activity and land use change in atmospheric chemistry and air quality [DE92-019622] p 642 N93-12880

FOULING
Diesel injector fouling bench test methodology [AD-A254532] p 609 N93-12600

FOUR-WAVE MIXING
High-resolution investigation of degenerate four-wave mixing in the (gamma)(0,0) band of nitric oxide [DE92-005312] p 537 N93-13232
High-resolution resonant degenerate 4-wave mixing spectroscopy [DE92-012146] p 538 N93-13234
Phase conjugation using CO2 lasers p 607 N93-13812

FOURIER ANALYSIS
Implicitly coupling heat conduction into a zone fire model [PB92-222769] p 558 N93-12980

FOURIER SERIES
A Fourier series method for polygonal domains: Large element computation for plates p 627 N93-13484

FOURIER TRANSFORMATION
Phase conjugation using CO2 lasers p 607 N93-13812

FRACTALS
Recursive construction of fractals [ISBN-951-41-0689-X] p 697 N93-13271
Features of vorticity in fully turbulent flows p 583 N93-13334
Transport on fractal networks [AD-A253797] p 725 N93-13881

FRACTURE MECHANICS
The application of the finite element method and the boundary element method to fatigue and fracture, volumes 1 and 2 p 624 N93-13016
Probabilistic finite elements for fatigue and fracture analysis
[NASA-CR-191246] p 624 N93-13029
Proceedings of the Tenth Symposium on Energy Engineering Sciences: Synergism of Analysis, Modeling, and Experiment
[DE92-018777] p 638 N93-13069
Axisymmetric and antiplane shear crack problems in bonded nonhomogeneous materials p 625 N93-13127
Shallow-crack toughness results for reactor pressure vessel steel
[DE92-017813] p 626 N93-13320
Fracture of a metal/ceramic couple: Tantalum (titanium)/sapphire p 554 N93-14074

FRACTURE STRENGTH
Fracture toughness of short fiber/brittle matrix composites p 528 N93-12630
Improved wide range expressions for displacements and inverse displacements for standard fracture toughness specimens
[AD-A254561] p 622 N93-12643
Numerical calibration of the stable poisson loaded specimen
[NASA-TM-105609] p 622 N93-12738
Ductile phase toughening of molybdenum disilicide by low pressure plasma spraying
[DE92-007409] p 551 N93-13315
Shallow-crack toughness results for reactor pressure vessel steel
[DE92-017813] p 626 N93-13320
Results of ASTM round robin testing for mode 1 interlaminar fracture toughness of composite materials
[NASA-TM-104222] p 532 N93-13428
Mechanical behaviour of fiber-reinforced ceramic matrix composites p 532 N93-13527
Matrix cracking initiation stress in fiber-reinforced ceramic matrix composites p 627 N93-13539
Three-dimensional boundary element analysis of residual stresses in a cross-ply fiber composite model p 629 N93-13811

FRACTURES (MATERIALS)
Ductile fracture process of discontinuous fiber reinforced composites
[DE92-016298] p 531 N93-13264
Micromechanics of finite length fibers in composite materials p 532 N93-13490

FRACTURING
Notch dimensions for three-point bend fracture specimens based on compliance analyses
[AD-A254641] p 620 N93-12580
Tempering effects for lower bainite, martensite, and mixed microstructures on impact, fracture, and related mechanical properties of ASTM A723 steel
[AD-A254617] p 541 N93-12616
Fatigue in single crystal nickel superalloys
[AD-A254704] p 541 N93-12746
Theoretical and experimental studies on the foundation theoretical and experimental studies on the foundation of mesomechanics
[AD-A254385] p 623 N93-12863
Touchstone for success
[ESA-BR-52] p 557 N93-12934
Fiber optic sensors for static fracture studies and dynamic wave propagation problems p 709 N93-12984
The application of the finite element method and the boundary element method to fatigue and fracture, volumes 1 and 2 p 624 N93-13016
Structural verification for GAS experiments p 511 N93-13175
Mechanical properties of epoxy/alumina trihydrate-filled compositions p 534 N93-13950
On grain boundary transport of hydrogen and mechanism of hydrogen-induced intergranular fracture p 544 N93-14047

FRAGMENTATION
Airblast damage from small asteroids
[DE92-017834] p 749 N93-12956

FREE CONVECTION
Natural convection between a vertical cylinder and a surrounding array
[DE92-019763] p 728 N93-12857
Convective scale 4-D data assimilation using simulated single Doppler radar observations
[PB92-218726] p 651 N93-12969
One-dimensional transient finite difference model of an operational salinity gradient solar pond p 586 N93-13400
Numerical study of nonlinear convective-symmetric instability in a rotating baroclinic atmosphere p 666 N93-13786

FREE ELECTRON LASERS
Development of XUV projection lithography at 60 to 80 nm
[DE92-017517] p 603 N93-12560
The sapphire Cerenkov laser p 605 N93-13365
Initial performance of Los Alamos Advanced Free Electron Laser
[DE92-040214] p 605 N93-13507
Special MAFIA postprocessors for the analysis of RF structures
[DE92-040248] p 565 N93-13510
Theory of the ion-channel laser p 607 N93-13777

FREE ENERGY
Magnetic properties of high-T(sub c) superconductors p 726 N93-13905

FREE FLOW
Application of a vectorized particle simulation to the study of plates and wedges in high-speed rarefied flow p 495 N93-13746

FREE JETS
Planar laser-induced fluorescence measurements of high-enthalpy free jet flow with nitric oxide p 595 N93-13685

FREE RADICALS
Kinetic studies of some free radical reactions involved in cloudwater chemistry p 668 N93-14055

FREE VIBRATION
The free and forced vibrations of structures using the finite dynamic element method p 630 N93-13935

FREEZING
Analysis of a space emergency ammonia dump using the FLOW-NET two-phase flow program p 584 N93-13389

FRENKEL DEFECTS
Simulation studies for surfaces and materials strength
[NASA-CR-191289] p 724 N93-13570

FREQUENCIES
Transducer circuit
[AD-D015376] p 572 N93-13472

FREQUENCY CONVERTERS
Compact Blue-Green Lasers: Summaries of papers presented at the topical meeting, Volume 6: Technical digest series
[AD-A255001] p 608 N93-13883

FREQUENCY DIVIDERS
Advanced on-chip divider for monolithic microwave VCO's
[NASA-CR-191355] p 572 N93-13563

FREQUENCY MEASUREMENT
Multifrequency measurements of radar ground clutter at 42 sites. Volume 2: Appendices A through D
[AD-A246711] p 567 N93-13878

FREQUENCY MODULATION
RF voltage modulation at discrete frequencies with applications to crystal channeling extraction
[DE92-015567] p 707 N93-13235

FREQUENCY MULTIPLIERS
Space-qualified submillimeter radiometer
[NASA-CR-190886] p 603 N93-13709

FREQUENCY RANGES
Inverse Synthetic Aperture Radar p 564 N93-13058

FREQUENCY RESPONSE
Thermal effects on the frequency response of piezoelectric crystals
[DE92-019039] p 720 N93-12819

FREQUENCY SHIFT
Low-frequency fluctuations of plasma magnetic fields p 717 N93-13496

FREQUENCY STABILITY
Arm length matching in 10 m delay-line interferometer
[ISAS-TN-649] p 596 N93-12639

FREQUENCY STANDARDS
Tutorials from the 23rd Annual Precise Time and Time Interval (PTTI) Applications and Planning Meeting
[AD-A254745] p 596 N93-12844

FRESNEL LENSES
Process designed for experimentation for increased-caliper Fresnel lenses
[DE92-019464] p 709 N93-12918

FRICTION
Mechanical behaviour of fiber-reinforced ceramic matrix composites p 532 N93-13527
Ion-beam-assisted deposition of MoS2 and other low-friction films
[AD-A255222] p 554 N93-13862
Friction, wear and Raman spectroscopic characteristics of carbon lubricated surfaces p 618 N93-13949
Dexterous grasp and manipulation p 618 N93-14075

FRICTION DRAG
Overall effects of separation on thin aerofoils
[ISBN-0-315-67464-4] p 496 N93-13930

FRICTION MEASUREMENT
Skin friction measurements in high temperature high speed flows p 595 N93-13679

FRONTS (METEOROLOGY)
An observational and numerical investigation of meso-scale coastal processes during GALE IOP 2 p 665 N93-13776
On the relationship between the intensity of extratropical frontal cyclone systems and water levels in the Gulf of Mexico p 666 N93-13816
Frontogenesis processes in the troposphere p 667 N93-13890
An investigation of the effects of topography on Colorado front range winter storms p 668 N93-14063

FROUDE NUMBER
Aspects of atmospheric transport and dispersion within an air basin p 656 N93-13782

FUEL CELL POWER PLANTS
An update of ERC's carbonate fuel cell development program
[DE92-019971] p 640 N93-13621

FUEL CELLS
Gas cooled fuel cell systems technology development
[DE92-0012983-3103] p 636 N93-12683
Oxygen electrode reaction in molten carbonate fuel cells
[DE92-040180] p 636 N93-12812
Understanding of carbonate fuel cell resistance issues for performance improvement
[DE92-019976] p 638 N93-13039
Perovskite solid electrolytes for SOFC
[DE92-019981] p 638 N93-13041
Alternative materials for solid oxide fuel cells: Factors affecting air-sintering of chromite interconnections
[DE92-019356] p 638 N93-13082
MCFC diagnostics: HCl detection
[DE92-001292] p 639 N93-13313
Effects of coal-derived trace species on performance of molten carbonate fuel cells
[DE93-000203] p 639 N93-13427
An update of ERC's carbonate fuel cell development program
[DE92-019971] p 640 N93-13621
Considerations for the transition from fuel cell R/D to manufacturing
[DE92-019977] p 640 N93-13622

FUEL COMBUSTION
Diesel injector fouling bench test methodology
[AD-A254532] p 609 N93-12600
Computational fluid dynamics combustion analysis evaluation
[NASA-CR-184326] p 575 N93-12688
The role of human activity and land use change in atmospheric chemistry and air quality
[DE92-019622] p 642 N93-12880
Meeting future exhaust emissions standards using natural gas as a vehicle fuel: Lessons learned from the natural gas vehicle challenge 1992
[DE92-019670] p 642 N93-12885
Measurements of cellular structure in spray detonation
[DE92-019580] p 555 N93-12933
Effects of gas composition on engine performance and emissions
[PB92-217561] p 611 N93-12936
Velocity and temperature measurements in a non-premixed reacting flow behind a backward facing step p 494 N93-13632

FUEL CONSUMPTION
Meeting future exhaust emissions standards using natural gas as a vehicle fuel: Lessons learned from the natural gas vehicle challenge 1992
[DE92-019670] p 642 N93-12885

FUEL CONTROL
Action composition for the animation of natural language instructions
[AD-A254963] p 682 N93-12554

FUEL FLOW
Visualization of hydrogen injection in a scramjet engine by simultaneous PLIF imaging and laser holographic imaging p 602 N93-13683
Exit plane H2O concentration measurements correlated with OH PLIF near-injector mixing measurements for scramjet flows p 603 N93-13687

FUEL INJECTION
Diesel injector fouling bench test methodology
[AD-A254532] p 609 N93-12600
A preliminary study of the effect of equivalence ratio on a low emissions gas turbine combustor using KIVA-2
[DE92-018616] p 613 N93-13321
The influence of mixture preparation in the intake port on the performance of a spark-ignited four-stroke engine p 613 N93-13331
Visualization of hydrogen injection in a scramjet engine by simultaneous PLIF imaging and laser holographic imaging p 602 N93-13683
Exit plane H2O concentration measurements correlated with OH PLIF near-injector mixing measurements for scramjet flows p 603 N93-13687

FUEL PUMPS
An experimental study of a small high-speed LH2 pump for rockets: Fluid dynamic performance
[NAL-TR-1131] p 610 N93-12727
FUEL SPRAYS
Measurements of cellular structure in spray detonation
[DE92-019580] p 555 N93-12933
The influence of mixture preparation in the intake port on the performance of a spark-ignited four-stroke engine
p 613 N93-13331
Effect of vaporization on cryogenic spray dropsize measurement
[NASA-TM-105909] p 597 N93-13410
FUEL TANKS
Acoustic modes in fluid networks p 586 N93-13398
FUEL TESTS
Vapor to liquid ratio test as an indicator of volatility
[DOT/FAA/CT-TN92/40] p 537 N93-12897
The 1992 natural gas vehicle challenge: EPA emissions and fuel economy testing
[PB92-217926] p 616 N93-13761
FULL SCALE TESTS
Aerodynamic integration of thrust reversers on the Fokker 100 p 502 N93-13208
An investigation of jet engine test cell aerodynamics by means of scale model test studies with comparisons to full-scale test results p 507 N93-14060
FUNCTIONAL ANALYSIS
Operator workload predictions for the revised AH-64A workload prediction model. Volume 2: Appendixes A through H
[AD-A254939] p 676 N93-12545
FUNCTIONAL DESIGN SPECIFICATIONS
Functional system design document for the Intelligent Inspection System (IIS)
[DE92-018240] p 619 N93-12794
FUNCTIONALLY GRADIENT MATERIALS
Axisymmetric and antiplane shear crack problems in bonded nonhomogeneous materials
p 625 N93-13127
FUNCTIONS (MATHEMATICS)
Bayesian estimation of system reliability under asymmetric loss p 620 N93-13906
FURNACES
The First United States Microgravity Laboratory
[NASA-TM-107980] p 557 N93-12951
EURECA
[ESA-F-26] p 522 N93-12964
ReTech, Inc., Plasma Centrifugal Furnace: Applications analysis report
[PB92-218791] p 714 N93-12982
FNAS modify matric and transparent experiments
[NASA-CR-184442] p 531 N93-13311
Summary on comparison of radiative heat transfer solutions for a specified problem
[DE92-040098] p 588 N93-13575
FUSELAGES
Probabilistic evaluation of fuselage-type composite structures
[NASA-TM-105881] p 622 N93-12735
FUSES (ORDNANCE)
Booster explosive rings
[AD-D015375] p 556 N93-13471
FUSION REACTORS
A design for an advanced divertor for D3D and ITER: The radiative slot divertor
[DE92-019579] p 714 N93-12932
Verification and validation of TMAP4
[DE92-019684] p 539 N93-13616
Fusion energy from the Moon for the twenty-first century p 719 N93-13985

G

GADOLINIUM
Electron temperature of Gd plasma produced by laser resonance ionization
[DE91-017785] p 718 N93-13732
GALACTIC CLUSTERS
A catalog of moderately distant galaxy clusters
p 749 N93-13011
The dynamical evolution of clusters of galaxies
p 750 N93-13122
Evolution of galaxies in compact groups
p 750 N93-13148
The mass and dynamics of cD clusters with cooling flows. 1: ROSAT observations of A 496
[NASA-CR-191240] p 743 N93-13352
Evidence for cool gas and star formation in cluster cooling flows p 751 N93-13380
Gravitational lensing by galaxy clusters: The giant arcs in Abell 370 and Cl2244-02 p 755 N93-13848
GALACTIC COSMIC RAYS
Fully energy-dependent HZETRN (a galactic cosmic-ray transport code)
[NASA-TP-3243] p 771 N93-13020
Galactic cosmic ray exposure estimates for SAGE-3 mission in polar orbit
[NASA-TM-107678] p 771 N93-13126
GALACTIC EVOLUTION
The dynamical evolution of clusters of galaxies
p 750 N93-13122
Evolution of galaxies in compact groups
p 750 N93-13148
Anisotropy measurements of the cosmic background radiation at 3 mm wavelength and an angular scale of 30 arcminutes p 772 N93-13689
GALACTIC MASS
The mass and dynamics of cD clusters with cooling flows. 1: ROSAT observations of A 496
[NASA-CR-191240] p 743 N93-13352
GALACTIC NUCLEI
The dynamics of dense galactic nuclei
p 750 N93-13340
GALACTIC STRUCTURE
Probing the galactic halo with ROSAT
[NASA-CR-191268] p 743 N93-13272
Galaxies with spectral energy distributions peaking at 60 micrometers: Morphology and activity explained by interactions p 756 N93-13959
GALAXIES
Galaxies with spectral energy distributions peaking at 60 micrometers: Morphology and activity explained by interactions p 756 N93-13959
GALERKIN METHOD
Large-amplitude plate vibration in an elevated thermal environment
[AD-A254411] p 621 N93-12606
GALLIUM ANTIMONIDES
High magnetic field studies of strained layer superlattices p 726 N93-13895
GALLIUM ARSENIDES
Group 2 cubic fluorides dielectrics for 3-D integration and GaAs-based optoelectronic structures
[AD-A254937] p 719 N93-12544
Synthesis and properties of mismatched heterojunction/substrate interfaces
[AD-A254577] p 719 N93-12648
GaAs gate dynamic memory technology
[AD-A254801] p 720 N93-12748
Electronic transport properties of semiconductor microstructures p 724 N93-13730
Studies of orbital doublet and modelling of orbital triplet Jahn-Teller systems in 3 to 5 semiconductors
p 725 N93-13845
High magnetic field studies of strained layer superlattices p 726 N93-13895
The heteroepitaxial growth of YBCO and other metal oxides on silicon and GaAs by pulsed laser deposition
p 726 N93-13904
Comparison of heavy ion and electron-beam upset data for GaAs
[AD-A255901] p 708 N93-14089
GALLIUM COMPOUNDS
Group 2 cubic fluorides dielectrics for 3-D integration and GaAs-based optoelectronic structures
[AD-A254937] p 719 N93-12544
GALLIUM PHOSPHIDES
Studies of orbital doublet and modelling of orbital triplet Jahn-Teller systems in 3 to 5 semiconductors
p 725 N93-13845
GAMMA RAY BURSTS
GAMCIT: A gamma ray burst detector
p 510 N93-13173
GAMMA RAY SPECTROMETERS
Wide range, permanent magnet Compton spectrometer
[DE92-017312] p 596 N93-12762
Study of SMM flares in gamma-rays and neutrons
[NASA-CR-191249] p 769 N93-12930
GAMCIT: A gamma ray burst detector
p 510 N93-13173
GAMMA RAYS
Study of SMM flares in gamma-rays and neutrons
[NASA-CR-191249] p 769 N93-12930
GAMCIT: A gamma ray burst detector
p 510 N93-13173
GAS ANALYSIS
Correlation for non-linear infrared calibration curves
[AD-A255098] p 596 N93-12653
Analysis of IMS spectra using neural networks
[DE92-017511] p 691 N93-12791
Infrared spectroscopy of size resolved fine aerosol
p 647 N93-13758
GAS CHROMATOGRAPHY
Analysis of IMS spectra using neural networks
[DE92-017511] p 691 N93-12791
Methods development for total organic carbon accountability
[NASA-CR-184438] p 672 N93-12949
GAS COMPOSITION
Nonideal thermoequilibrium calculations using a large product species data base
[DE92-040839] p 735 N93-12813
Effects of gas composition on engine performance and emissions
[PB92-217561] p 611 N93-12936
GAS COOLING
Gas cooled fuel cell systems technology development
[DE92-0012983-3103] p 636 N93-12683
GAS DENSITY
Acoustic device and method for measuring gas densities
[NASA-CASE-NPO-18155-1-CU] p 700 N93-13421
The role of particle diffusion in the lower transition region: Revised interpretation of emission measures
p 770 N93-13476
Electron beam fluorescence measurements in the Boeing hypersonic shock tunnel p 602 N93-13681
Resonance lamp absorption measurement of OH number density and temperature in expansion tube scramjet engine tests p 602 N93-13682
Gas temperature and density measurements based on spectrally resolved Rayleigh-Brillouin scattering
p 602 N93-13684
Molecular gas temperature and density in spiral galaxies p 748 N93-13688
Molecular clouds in the distant outer galaxy
p 758 N93-14095
GAS DETECTORS
Correlation for non-linear infrared calibration curves
[AD-A255098] p 596 N93-12653
GAS DYNAMICS
Development and computation of continuum higher order constitutive relations for high-altitude hypersonic flow p 494 N93-13578
GAS FLOW
Determination of the permeability of carbon aerogels by gas flow measurements
[DE92-019574] p 550 N93-12888
Mathematical problems in inviscid hypersonic flow
p 493 N93-13451
Spectroscopic studies of low-density gas in the Galactic disk and halo p 753 N93-13499
GAS GIANT PLANETS
Chairmanship of the Neptune/Pluto Outer Planets Science Working Group
[NASA-CR-191288] p 759 N93-13568
Accretion rates of protoplanets p 759 N93-13958
GAS JETS
Experimental studies of the flowfields and their effects due to a pair of lift jets discharging in the ground effect region p 580 N93-13217
Effect of vaporization on cryogenic spray dropsize measurement
[NASA-TM-105909] p 597 N93-13410
GAS LASERS
Radiation-induced infrared absorption in nuclear-pumped laser cavity components
[DE92-017346] p 605 N93-13249
Compact Blue-Green Lasers: Summaries of papers presented at the topical meeting. Volume 6: Technical digest series
[AD-A255001] p 608 N93-13883
GAS MIXTURES
Effects of gas composition on engine performance and emissions
[PB92-217561] p 611 N93-12936
GAS PATH ANALYSIS
Spectroscopic studies of low-density gas in the Galactic disk and halo p 753 N93-13499
GAS PRESSURE
Diffusion-absorption heat pump
[PB92-217538] p 576 N93-12975
GAS TEMPERATURE
Gas temperature measurements using the dual-line detection Rayleigh scattering technique
p 599 N93-13668
Gas temperature and density measurements based on spectrally resolved Rayleigh-Brillouin scattering
p 602 N93-13684
Molecular gas temperature and density in spiral galaxies p 748 N93-13688
GAS TUNGSTEN ARC WELDING
Design of a welded joint for robotic, on-orbit assembly of space trusses
[NASA-TM-108380] p 609 N93-12682
GAS TURBINE ENGINES
AFOSR Contractors Meeting in Propulsion
[AD-A254484] p 525 N93-12575
Thermal barrier coating life prediction model development, phase 2
[NASA-CR-189111] p 544 N93-12589

Alternative systems for fuel gas boosters for small gas turbine engines
[PB92-223049] p 612 N93-12977
Overview on test cases for computation of internal flows in turbomachines p 579 N93-13209
A preliminary study of the effect of equivalence ratio on a low emissions gas turbine combustor using KIVA-2
[DE92-018616] p 613 N93-13321

GAS TURBINES
Development of advanced turbine systems: Meeting tomorrow's needs
[DE92-017339] p 612 N93-13103

GAS WELDING
An integrated optical sensor for GMAW feedback control
[DE92-018019] p 610 N93-12793

GAS-LIQUID INTERACTIONS
Unit operations for gas-liquid mass transfer in reduced gravity environments p 557 N93-14011

GASEOUS FUELS
Effects of coal-derived trace species on performance of molten carbonate fuel cells
[DE93-000203] p 639 N93-13427
Combustion of gaseous fuels under reduced-gravity conditions p 557 N93-14012

GASIFICATION
High octane ethers from synthesis gas-derived alcohols
[DE92-015467] p 537 N93-13188

GASKETS
Hermetic sealing and EMI shielding gasket
[AD-D015359] p 552 N93-13414

GASOLINE
White paper: Preliminary assessment of LNG vehicle technology, economics, and safety issues, revision 1
[PB92-212943] p 615 N93-13644

GAUGE THEORY
Theoretical high energy physics
[DE92-015480] p 707 N93-13189
Heavy gauge boson and lambda(b) baryon searches at CDF
[DE92-019551] p 705 N93-13537

GELS
Aerogels, emulsions, and composites: Controlling structure with organic sol-gel chemistry
[DE92-019575] p 550 N93-12931
A new apparatus for continuous countercurrent flow of solids and liquids
[DE92-011675] p 583 N93-13318

GENES
Molecular biology of anaerobic aromatic biodegradation
[AD-A255213] p 673 N93-13863

GENETIC ENGINEERING
Molecular biology of anaerobic aromatic biodegradation
[AD-A255213] p 673 N93-13863

GEOCHEMISTRY
Characterization of site geochemistry in support of environmental restoration
[DE92-017512] p 641 N93-12685

GEOCHRONOLOGY
Abstracts of papers presented at the International Symposium on Time, Frequency, and Dating in Geomorphology
[AD-A254927] p 649 N93-12704

GEOCORONAL EMISSIONS
Uniformity results of the multilayer mirrors used in the ALEXIS ultrasoft x ray telescopes
[DE92-018611] p 743 N93-13342

GEODESY
Coordinates in differential geodesy
[AD-A254951] p 632 N93-12550
GPS measurements at Vandenberg AFB
[AD-A254978] p 499 N93-12557
Analysis of space geodetic measurements for studying the dynamics of the solid Earth
[NASA-CR-191215] p 649 N93-12661

GEODETIC COORDINATES
Coordinates in differential geodesy
[AD-A254951] p 632 N93-12550

GEODETIC SURVEYS
GPS measurements at Vandenberg AFB
[AD-A254978] p 499 N93-12557
Analysis of space geodetic measurements for studying the dynamics of the solid Earth
[NASA-CR-191215] p 649 N93-12661

GEODYNAMICS
Analysis of space geodetic measurements for studying the dynamics of the solid Earth
[NASA-CR-191215] p 649 N93-12661
The morphotectonic fabric of the East Pacific Rise: Implications for fault generation and crustal accretion
p 652 N93-13481
On the space-time ocean current variability and its effects on the length-of-day p 636 N93-14051

GEOGRAPHY
An evaluation of the use and future need of remotely sensed images in grades K-12 p 635 N93-13956

GEOLOGICAL FAULTS
GPS measurements at Vandenberg AFB
[AD-A254978] p 499 N93-12557
The morphotectonic fabric of the East Pacific Rise: Implications for fault generation and crustal accretion
p 652 N93-13481

GEOLOGICAL SURVEYS
New approaches to estimation of magnetotelluric parameters
[DE92-040280] p 653 N93-13513

GEOLOGY
Meeting review: Third NCAR Research Aircraft Fleet Workshop
[PB92-222710] p 649 N93-12818

GEOMAGNETIC MICROPULSATIONS
Ring current oxygen interaction with micropulsations
p 651 N93-13149
A statistical study of narrow bandwidth, high-latitude geomagnetic pulsations p 660 N93-14068

GEOMAGNETIC PULSATIONS
Ring current oxygen interaction with micropulsations
p 651 N93-13149

GEOMAGNETISM
Solar-geophysical data number 574, June 1992. Part 1: (Prompt reports). Data for May, April 1992 and late data
[PB92-218759] p 769 N93-12803
A report on geomagnetic observatory operations, 1990
[PB92-224781] p 649 N93-12804
Galactic cosmic ray exposure estimates for SAGE-3 mission in polar orbit
[NASA-TM-107678] p 771 N93-13126
JARE data reports no. 176 (Ionosphere 47). Riometer records of 30 MHz cosmic noise at Syowa Station, Antarctica in 1990 p 772 N93-13255
Magnetic holes near the magnetopause
p 653 N93-13491
New approaches to estimation of magnetotelluric parameters
[DE92-040280] p 653 N93-13513

GEOMETRICAL OPTICS
The sapphire Cerenkov laser p 605 N93-13365

GEOMETRICAL THEORY OF DIFFRACTION
Computer-aided design-based high-frequency electromagnetic wave scattering from complex bodies
p 567 N93-14042

GEOMETRY
Summary of awards: Applied mathematics. Fiscal year 1991
[NSF-92-38] p 681 N93-13438

GEOMORPHOLOGY
Abstracts of papers presented at the International Symposium on Time, Frequency, and Dating in Geomorphology
[AD-A254927] p 649 N93-12704
The morphotectonic fabric of the East Pacific Rise: Implications for fault generation and crustal accretion
p 652 N93-13481

GEOPHYSICAL FLUIDS
Structures, spectra and inertial range transfer in two-dimensional and beta-plane turbulence
p 590 N93-13900

GEOPHYSICS
Wave propagation and scattering in dense geophysical media
[AD-A254573] p 561 N93-12646
Production of SSM/I data sets
[NASA-CR-190944] p 632 N93-12800
Solar-geophysical data number 574, June 1992. Part 1: (Prompt reports). Data for May, April 1992 and late data
[PB92-218759] p 769 N93-12803
Meeting review: Third NCAR Research Aircraft Fleet Workshop
[PB92-222710] p 649 N93-12818
A radio frequency user's guide to the Space Environment Services Center geophysical alert broadcasts
[PB92-220631] p 562 N93-12979
Research in geosciences policy
[NASA-CR-190470] p 632 N93-13833

GEOPOTENTIAL
The determination and error assessment of the Earth's gravity field model p 656 N93-13771

GEOPOTENTIAL HEIGHT
Point correlations of geopotential height and temperature at 30 mb and between 500 mb and 30 mb
[PB92-222694] p 661 N93-12817

GEOSYNCHRONOUS ORBITS
Report of the Working Group on Space/Lunar Tradeoffs p 747 N93-13599

GEOTECHNICAL ENGINEERING
Proceedings of the Mediterranean Conference on Environmental Geotechnology
[AD-A253672] p 644 N93-13098

GEOTECHNICAL FABRICS
The morphotectonic fabric of the East Pacific Rise: Implications for fault generation and crustal accretion
p 652 N93-13481

GEOTHERMAL ENERGY CONVERSION
Industrial applications of hot dry rock geothermal energy
[DE92-018903] p 637 N93-12923

GEOTHERMAL RESOURCES
Industrial applications of hot dry rock geothermal energy
[DE92-018903] p 637 N93-12923

GERMANIUM
Epitaxial growth of silicon and germanium for solar cells
[ITN-92-85168] p 722 N93-13268

GERMINATION
A study of the effects of micro-gravity on seed germination p 510 N93-13167

GET AWAY SPECIALS (STS)
The 1992 Shuttle Small Payloads Symposium
[NASA-CP-3171] p 508 N93-13158
Spaceflight payload design flight experience G-408
p 508 N93-13160
Investigation of microgravity effects on solidification phenomena of selected materials p 510 N93-13168
GAMCIT: A gamma ray burst detector
p 510 N93-13173
Structural verification for GAS experiments
p 511 N93-13175
A Pennsylvania State University/General Electric Get Away Special (GAS) experiment p 511 N93-13177
The ROMPS robot in HitchHiker p 511 N93-13179
The unique challenge of managing an undergraduate Get-Away-Special experiment p 512 N93-13185
Preparing safety data packages for experimenters using the Get Away Special (GAS) carrier system
p 512 N93-13186

GIOTTO MISSION
Giotto: The second encounter
[ESA-BR-83] p 749 N93-12965
A study of ion composition and dynamics at Comet Halley
[NASA-CR-188478] p 751 N93-13465
Densities and abundances of hot cometary ions in the coma of P/Halley p 752 N93-13466
Observations of plasma dynamics in the coma of P/Halley by the Giotto Ion Mass Spectrometer
p 752 N93-13468
Interpretation of the ion mass spectra in the mass range 25-35 obtained in the inner coma of Halley's comet by the HIS-sensor of the Giotto IMS Experiment
p 752 N93-13469
In situ dust mass distribution measurements from the Giotto encounter with comet P/Halley
p 753 N93-13602

GLASS
Stimulated Brillouin processes in crystals and glasses
[DE92-019549] p 721 N93-12887
Bonding in simple phosphate glass
[DE92-019437] p 550 N93-12917

GLASS FIBER REINFORCED PLASTICS
Matrix cracking initiation stress in fiber-reinforced ceramic matrix composites p 627 N93-13539
Vibration damping response of composite materials
p 533 N93-13748

GLASS FIBERS
Test equipment data package for the KC-135 fiber pulling apparatus
[NASA-CR-184446] p 506 N93-13013
Glass fiber processing for the Moon/Mars program: Center director's discretionary fund final report
[NASA-TM-108379] p 551 N93-13115
A new route for fibre management in metal matrix composites p 534 N93-13779
Assessment of Japanese technology in advanced glass and ceramic fibers
[AD-A255229] p 553 N93-13836

GLOBAL POSITIONING SYSTEM
GPS measurements at Vandenberg AFB
[AD-A254978] p 499 N93-12557
Analysis of space geodetic measurements for studying the dynamics of the solid Earth
[NASA-CR-191215] p 649 N93-12661
GPS azimuth determination
[AD-A254687] p 499 N93-13348

GLOBAL WARMING
Earth science information: Planning for the integration and use of global change information
[NASA-CR-191217] p 733 N93-12660

GLOBULAR CLUSTERS
Hydrodynamical calculations of stellar interactions
p 755 N93-13764
GLYCOLS
Solvation of cobalt salts by oligomeric polyethers
[AD-A254815] p 545 N93-12753
Studies of plasticized-polymer electrolytes containing mixed Zn(2) and Li(1)
[AD-A254818] p 545 N93-12755
GOGGLES
Integration of exterior lighting systems and night vision imaging systems
[AD-A254826] p 677 N93-12732
GOODNESS OF FIT
From comparison density to two sample analysis
[AD-A253866] p 698 N93-13064
GOVERNMENT PROCUREMENT
Selected data on federal support to universities and colleges: Fiscal year 1990
[NSF-92-310] p 740 N93-12920
GOVERNMENT/INDUSTRY RELATIONS
Abstracts of phase 1 awards: NSF Small Business Innovation Research Program (SBIR): 1992
[NSF-92-80] p 732 N93-13703
GRADIENTS
One-dimensional transient finite difference model of an operational salinity gradient solar pond
p 586 N93-13400
GRAIN BOUNDARIES
Atomic relaxation modes in grain boundaries
[DE92-016781] p 722 N93-13195
On grain boundary transport of hydrogen and mechanism of hydrogen-induced intergranular fracture
p 544 N93-14047
GRAIN SIZE
Magnetic properties of high-T(sub c) superconductors
p 726 N93-13905
GRAMMARS
Japanese/English machine translation using sublanguage patterns and reversible grammars
p 686 N93-13494
GRANTS
Selected data on Federal funds for research and development: Fiscal years 1990, 1991, and 1992
[NSF-92-319] p 741 N93-13657
Awards: 1991 undergraduate course and curriculum development program
[NSF-92-45] p 731 N93-13699
Fiscal Year 1991 highlights
[NSF-92-23] p 731 N93-13702
Abstracts of phase 1 awards: NSF Small Business Innovation Research Program (SBIR): 1992
[NSF-92-80] p 732 N93-13703
Directory of awards, fiscal year 1991. Directorate for engineering
[NSF-92-55] p 775 N93-13704
Arctic science, engineering, and education. Directory of awards, fiscal year 1991
[NSF-92-60] p 775 N93-13713
GRANULAR MATERIALS
Experiments, theory, and simulation on the evolution of fabric in granular materials
[AD-A254820] p 545 N93-12729
Studies of granular flow down an inclined chute
[DE92-018871] p 577 N93-13074
On development of a three-dimensional particle motion tracking system
[DE92-015846] p 704 N93-13263
GRAPH THEORY
Testing and fault-tolerant design techniques for advanced digital architectures
[AD-A255013] p 681 N93-12707
GRAPHITE-EPOXY COMPOSITES
The 3-D nonlinear constitutive modeling approach for composite materials
[AD-A255022] p 528 N93-12584
Scale effects in buckling, postbuckling and crippling of graphite-epoxy Z-section stiffeners p 621 N93-12632
The effects of compressive preloads on the compression-after-impact strength of carbon/epoxy
[NASA-TP-3303] p 529 N93-12678
Design of a welded joint for robotic, on-orbit assembly of space trusses
[NASA-TM-108380] p 609 N93-12682
Influence of cure shrinkage on process-induced stress and deformation in thick thermosetting composites
[AD-A254325] p 529 N93-12842
Automated eddy current analysis of materials
[NASA-CR-184432] p 619 N93-12875
Compression strength of composite primary structural components
[NASA-CR-190949] p 624 N93-13019
Vibration damping response of composite materials
p 533 N93-13748
Delamination initiation in postbuckled dropped-ply laminates p 535 N93-14030
GRAPHITE-POLYIMIDE COMPOSITES
Transverse flexural tests as a tool for assessing damage to PMR-15 composites from isothermal aging in air at elevated temperatures
[NASA-TM-105848] p 529 N93-12737
GRAPHS (CHARTS)
Stability codes for a liquid rocket implemented for use on a PC
[NASA-CR-184453] p 525 N93-12659
JARE data reports no. 175 (ionosphere 46). Records of radio aurora at Syowa Station, Antarctica in 1990
p 651 N93-13285
A theory of reference graphs in relational databases
p 739 N93-13912
GRASSLANDS
Performance of the Bowen ratio systems on a 22 deg slope
[NASA-CR-191278] p 644 N93-13254
GRATINGS (SPECTRA)
United Kingdom Infrared Telescope
p 743 N93-13273
GRAVIMETRY
The determination and error assessment of the Earth's gravity field model p 656 N93-13771
GRAVITATION
Second quantization in bit-string physics
[DE92-019645] p 727 N93-12826
Control of a very flexible robot in gravity
p 615 N93-13541
The determination and error assessment of the Earth's gravity field model p 656 N93-13771
Atmospheric loading response of the solid earth and oceans p 659 N93-13955
GRAVITATION THEORY
Second quantization in bit-string physics
[DE92-019645] p 727 N93-12826
Dual mass and torsion p 728 N93-13498
GRAVITATIONAL CONSTANT
Some problems of quantum cosmology and dark matter physics p 755 N93-13829
GRAVITATIONAL EFFECTS
A fundamental study of the effect of gravity on the static and dynamic behavior of robots p 610 N93-12760
Test equipment data package for the KC-135 fiber pulling apparatus
[NASA-CR-184446] p 506 N93-13013
Glass fiber processing for the Moon/Mars program: Center director's discretionary fund final report
[NASA-TM-108379] p 551 N93-13115
A study of the effects of micro-gravity on seed germination p 510 N93-13167
Investigation of microgravity effects on solidification phenomena of selected materials p 510 N93-13168
Effects of spaceflight on the proliferation of jejunal mucosal cells
[NASA-CR-191303] p 675 N93-13449
Eureca: A first for Europe
[ESA-BR-85] p 516 N93-13691
Bone loss and human adaptation to lunar gravity
p 676 N93-14002
GRAVITATIONAL FIELDS
The lunar environment and its effect on optical astronomy p 746 N93-13594
The determination and error assessment of the Earth's gravity field model p 656 N93-13771
Resonance studies of artificial earth satellites
p 523 N93-14037
GRAVITATIONAL LENSES
Gravitational lensing by galaxy clusters: The giant arcs in Abell 370 and Cl2244-02 p 755 N93-13848
GRAVITATIONAL PHYSIOLOGY
SLS-1 flight experiments preliminary significant results
[NASA-TM-108033] p 520 N93-13613
Bone loss and human adaptation to lunar gravity
p 676 N93-14002
GRAVITATIONAL WAVES
The dynamics of dense galactic nuclei
p 750 N93-13340
GRAVITY ANOMALIES
The determination and error assessment of the Earth's gravity field model p 656 N93-13771
GRAVITY PROBE B
Aeronomy coexperiments on drag-free satellites with proportional thrusters: GP-B and STEP
p 518 N93-13922
GRAVITY WAVES
CORRIDOR: A routine for estimating the initial wave front resulting from high temperature fire exposure to a corridor
[PB92-213347] p 559 N93-13640
A new instrument for the study of mesospheric gravity waves through nightglow observations
p 656 N93-13789
Optical model analysis of gravity wave-critical layer interaction p 658 N93-13888
GREAT PLAINS CORRIDOR (NORTH AMERICA)
A synoptic climatology of the elevated mixed layer inversion over the southern Great Plains in spring
p 664 N93-13643
GREEN'S FUNCTIONS
Analysis of a structure-equipment system subjected to impact loading
[AD-A255097] p 622 N93-12652
Variance of phase fluctuations of waves propagating through a random medium p 569 N93-13087
A fresh look at (e,e(prime)) scattering from light nuclei: A GFMC approach
[DE92-016377] p 703 N93-13246
Theoretical and numerical studies of wave propagation and scattering in inhomogeneous media
p 568 N93-14044
GREENHOUSE EFFECT
The role of human activity and land use change in atmospheric chemistry and air quality
[DE92-019622] p 642 N93-12880
A correlated k-distribution model of the heating rates for CH4 and N2O in the atmosphere between 0 and 60 km
[NASA-TM-108062] p 643 N93-12926
Radiative transfer in the middle atmosphere
p 652 N93-13482
Radiative constraints on the energy budget of the atmosphere p 655 N93-13731
Gas-phase reactions of halogen species of atmospheric importance p 658 N93-13889
GRID GENERATION (MATHEMATICS)
The multidimensional self-adaptive grid code, SAGE
[NASA-TM-103905] p 683 N93-12719
Calibration of 2D unstructured grid methods on propulsive flowfields p 582 N93-13225
Solution of compressible Navier-Stokes equations using spectral methods on arbitrary two-dimensional domains
p 593 N93-14041
GRIGG-SKJELLERUP COMET
Giotto: The second encounter
[ESA-BR-83] p 749 N93-12965
GRIT
Qualification of the gritblast assembly and process for the inside diameter of the RSRM forward and aft domes
[NASA-CR-184462] p 558 N93-13021
GROUND BASED CONTROL
An intelligent position-specific training system for mission operations
[NASA-TM-108381] p 691 N93-13156
Ground operations and logistics in the context of the International Asteroid Mission p 515 N93-13560
GROUND EFFECT (AERODYNAMICS)
Experimental studies of the flowfields and their effects due to a pair of lift jets discharging in the ground effect region p 580 N93-13217
GROUND EFFECT (COMMUNICATIONS)
Multifrequency measurements of radar ground clutter at 42 sites. Volume 2: Appendices A through D
[AD-A246711] p 567 N93-13878
GROUND OPERATIONAL SUPPORT SYSTEM
Ground operations and logistics in the context of the International Asteroid Mission p 515 N93-13560
Ever watchful
[ESA-BR-37-I] p 517 N93-13903
GROUND STATE
The 2S(+) - 2P separation in KO
[NASA-TM-108086] p 702 N93-12900
Fermi molecular dynamics
[DE92-015351] p 703 N93-13187
GROUND STATIONS
Giotto: The second encounter
[ESA-BR-83] p 749 N93-12965
GROUND SUPPORT EQUIPMENT
Ground operations and logistics in the context of the International Asteroid Mission p 515 N93-13560
GROUND TESTS
RF system description for the ground test accelerator radio-frequency quadrupole
[DE92-040239] p 563 N93-13045
The jet behaviour of an actual high-bypass engine as determined by LDA-measurements in ground tests
p 503 N93-13218
On the suitability of non-hardened high density SRAMs for space applications
[AD-A255898] p 524 N93-14087
GROUND TRUTH
Radiometric calibration of SAR systems
p 564 N93-13055
GROUND WATER
Fiber optic sensors for environmental applications: A brief review
[DE92-040170] p 710 N93-13576
GROUP VELOCITY
Baroclinic wave packets in models and observations
p 663 N93-13361

Lateral variations of shear velocity and anelasticity in the upper mantle of the western US from Rayleigh wave observations p 653 N93-13492

GULF OF ALASKA

Application of satellite altimetry to study the Gulf of Alaska gyre p 635 N93-13969

GULF OF MEXICO

On the relationship between the intensity of extratropical frontal cyclone systems and water levels in the Gulf of Mexico p 666 N93-13816

GULF STREAM

The Gulf Stream downstream of Cape Hatteras: Model/data comparisons p 670 N93-13633

An observational and numerical investigation of meso-scale coastal processes during GALE IOP 2 p 665 N93-13776

GUN LAUNCHERS

Data acquisition applications for long duration electromagnetic launcher experiments [AD-A254546] p 519 N93-12611

GUSTS

Stratospheric turbulence measurements and models for aerospace plane design [NASA-TM-104262] p 663 N93-13288

GYRES

Application of satellite altimetry to study the Gulf of Alaska gyre p 635 N93-13969

H

H I REGIONS

H I shells and supershells: Observations and theory p 751 N93-13360

H II REGIONS

A study of the neutral and ionized gas in the interstellar medium and galactic H 2 regions p 756 N93-13853

H-INFINITY CONTROL

Hypersonic vehicle control law development using H infinity and mu-synthesis [NASA-TM-107689] p 504 N93-13068

HABITATS

The Second Conference on Lunar Bases and Space Activities of the 21st Century, volume 2 [NASA-CP-3166-VOL-2] p 760 N93-13972

Lunar resource recovery: A definition of requirements p 761 N93-13978

HALLEY'S COMET

Giotto: The second encounter [ESA-BR-83] p 749 N93-12965

A study of ion composition and dynamics at Comet Halley [NASA-CR-188478] p 751 N93-13465

Densities and abundances of hot cometary ions in the coma of P/Halley p 752 N93-13466

Observations of solar wind ion charge exchange in the comet Halley coma p 752 N93-13467

Observations of plasma dynamics in the coma of P/Halley by the Giotto Ion Mass Spectrometer p 752 N93-13468

Interpretation of the ion mass spectra in the mass range 25-35 obtained in the inner coma of Halley's comet by the HIS-sensor of the Giotto IMS Experiment p 752 N93-13469

In situ dust mass distribution measurements from the Giotto encounter with comet P/Halley p 753 N93-13602

HALOCARBONS

An experimental and theoretical study of degradation pathways for atmospheric halocarbons p 646 N93-13624

HALOGENS

Halogen surface chemistry on Si(100)-(2x1) [AD-A254643] p 536 N93-12618

Gas-phase reactions of halogen species of atmospheric importance p 658 N93-13889

HALOS

Probing the galactic halo with ROSAT [NASA-CR-191268] p 743 N93-13272

Spectroscopic studies of low-density gas in the Galactic disk and halo p 753 N93-13499

HAMILTON-JACOBI EQUATION

Approximate optimal guidance for the Advanced Launch System p 519 N93-13819

HANDLING EQUIPMENT

Automated dry powder dispenser for explosive components [DE92-019425] p 555 N93-12568

HARDENING (MATERIALS)

Magnetic hardening studies and novel techniques for preparation of high performance magnets [AD-A254761] p 698 N93-12865

HARMONIC GENERATIONS

Monitoring interfacial dynamics by pulsed laser techniques [DE92-040302] p 606 N93-13514

HARMONIC OSCILLATORS

Theory of the ion-channel laser p 607 N93-13777

HARTREE APPROXIMATION

Analytical studies of nonlinear partial differential equations of interest in nonlinear optics [AD-A254931] p 696 N93-13027

HAULING

Equations of motion of slung-load systems, including multilift systems [NASA-TP-3280] p 503 N93-12815

HAZARDS

Laser measurement techniques guide for a hazard evaluation [AD-A254545] p 604 N93-12610

Occupational ergonomics in space p 680 N93-14013

HEALTH

US Antarctic program. Personnel manual, 1992 [NSF-92-63] p 731 N93-12637

Academic science and engineering: Graduate enrollment and support, Fall 1990 [NSF-92-323] p 729 N93-12802

A health care system for the Space Station [NASA-TM-108093] p 679 N93-13571

HEAT EXCHANGERS

Diffusion-absorption heat pump [PB92-217538] p 576 N93-12975

A small, single stage orifice pulse tube cryocooler demonstration [NASA-CR-190859] p 558 N93-13404

All-metal, compact heat exchanger for space cryocoolers [NASA-CR-190861] p 559 N93-13604

HEAT FLUX

Heat transfer in a liquid metal crucible with an integral blackbody cavity [DE92-019640] p 576 N93-12825

Anomalous ion heating and superthermal electrons in the MST reversed-field pinch [DE92-041011] p 713 N93-12882

Implicitly coupling heat conduction into a zone fire model [PB92-222769] p 558 N93-12980

Performance of the Bowen ratio systems on a 22 deg slope [NASA-CR-191278] p 644 N93-13254

Temperature and heat flux measurements: Challenges for high temperature aerospace application p 598 N93-13662

High heat flux measurements and experimental calibrations/characterizations p 598 N93-13663

Heat flux microsensor measurements and calibrations p 599 N93-13665

Fabrication of thin film heat flux sensors p 599 N93-13667

The effects of pressure gradients on convective heat flux predictions in engine environments p 616 N93-13772

HEAT MEASUREMENT

Effects of orbital exposure on Halar during the LDEF mission p 549 N93-12788

HEAT PIPES

A heat pipe coupled planar thermionic converter: Performance characterization, nondestructive testing, and evaluation [AD-A254941] p 727 N93-12546

Transient behavior of heat pipe with thermal energy storage under pulse heat loads p 588 N93-13743

Solar energy utilisation and evacuated tubular solar collectors p 641 N93-14078

HEAT PUMPS

Diffusion-absorption heat pump [PB92-217538] p 576 N93-12975

Thermal control systems for low-temperature heat rejection on a lunar base [NASA-CR-191286] p 679 N93-13717

HEAT RESISTANT ALLOYS

Fatigue in single crystal nickel superalloys [AD-A254704] p 541 N93-12746

In-phase and out-of-phase axial-torsional fatigue behavior of Haynes 188 at 760 C [NASA-TM-105765] p 625 N93-13153

Computational simulation of probabilistic lifetime strength for aerospace materials subjected to high temperature, mechanical fatigue, creep and thermal fatigue [NASA-CR-190794] p 626 N93-13290

HEAT SHIELDING

Ab initio atomic recombination reaction energetics on model heat shield surfaces [NASA-CR-191210] p 575 N93-12677

HEAT STORAGE

Transient behavior of heat pipe with thermal energy storage under pulse heat loads p 588 N93-13743

HEAT TOLERANCE

A novel diesel-fueled engine for microclimate cooling for the individual soldier [AD-A254510] p 609 N93-12724

Thermal stress in US Air Force operations [AD-A255785] p 676 N93-14027

Physiological stress from chemical defense clothing and equipment [AD-A255786] p 676 N93-14028

HEAT TRANSFER

Fluid dynamics of supercritical helium within cable-in-conduit conductors [DE92-019516] p 574 N93-12569

Heat transfer in a liquid metal crucible with an integral blackbody cavity [DE92-019640] p 576 N93-12825

A correlated k-distribution model of the heating rates for CH4 and N2O in the atmosphere between 0 and 60 km [NASA-TM-108062] p 643 N93-12926

Diffusion-absorption heat pump [PB92-217538] p 576 N93-12975

Environmental qualification testing of payload G-534, the Pool Boiling Experiment p 510 N93-13169

Electrical design of payload G-534: The Pool Boiling Experiment p 510 N93-13170

Simulation of two-dimensional icing, de-icing and anti-icing phenomena p 498 N93-13364

Boundary element methods for two-dimensional, coupled, thermoviscous flow p 584 N93-13383

Thermal issues at the SSC p 584 N93-13387

The program FANS-3D (finite analytic numerical simulation 3-dimensional) and its applications p 586 N93-13399

Aerospace applications of SINDA/FLUINT at the Johnson Space Center p 586 N93-13401

Coupled structural/thermal/electromagnetic analysis/tailoring of graded composite structures [NASA-CR-189150] p 626 N93-13443

High heat flux measurements and experimental calibrations/characterizations p 598 N93-13663

Heat transfer, fluid flow and interface shapes in floating-zone crystal growth p 724 N93-13739

The effects of pressure gradients on convective heat flux predictions in engine environments p 616 N93-13772

An experimental/computational study of heat transfer in sharp fin induced shock wave/turbulent boundary layer interactions at low hypersonic Mach numbers p 590 N93-13826

Turbulent boundary layers with high turbulence: Experimental heat transfer and structure on flat and convex walls p 591 N93-13938

Stability of the compressible reacting mixing layer p 592 N93-13948

HEAT TREATMENT

Dislocation and pores in mullite from diphasic gels [DE92-040384] p 550 N93-12999

HEAVY IONS

Heavy-ion collisions and the nuclear equation of state [DE92-019364] p 706 N93-12924

Galactic cosmic ray exposure estimates for SAGE-3 mission in polar orbit [NASA-TM-107678] p 771 N93-13126

Observations of plasma dynamics in the coma of P/Halley by the Giotto Ion Mass Spectrometer p 752 N93-13468

Non-perturbative studies in quantum electrodynamics p 729 N93-13896

Comparison of heavy ion and electron-beam upset data for GaAs [AD-A255901] p 708 N93-14089

HEISENBERG THEORY

Fermi molecular dynamics [DE92-015351] p 703 N93-13187

HELICOPTER CONTROL

Trim analysis by shooting and finite elements and Floquet eigenanalysis by QR and subspace iterations in helicopter dynamics p 501 N93-13914

HELICOPTER DESIGN

Split torque transmission load sharing [NASA-TM-105884] p 610 N93-12736

HELICOPTER PERFORMANCE

Trim analysis by shooting and finite elements and Floquet eigenanalysis by QR and subspace iterations in helicopter dynamics p 501 N93-13914

HELICOPTER PROPELLER DRIVE

Split torque transmission load sharing [NASA-TM-105884] p 610 N93-12736

HELICOPTERS

Human factors research in aircrew performance and training: 1986-1991 [AD-A254455] p 677 N93-12609

Equations of motion of slung-load systems, including multilift systems [NASA-TP-3280] p 503 N93-12815

Design guide for the ergonomic aspects of helicopter crew seating
[ISVR-TR-209] p 678 N93-13464
Formulation and validation of high-order mathematical models of helicopter flight dynamics
p 501 N93-13821

HELIUM
Fluid dynamics of supercritical helium within cable-in-conduit conductors
[DE92-019516] p 574 N93-12569
A fast scanning probe for D3-D
[DE92-040260] p 717 N93-13511

HELIUM IONS
A statistical study of narrow bandwidth, high-latitude geomagnetic pulsations p 660 N93-14068

HELIUM ISOTOPES
Cosmological constraints on early-decaying particles
p 750 N93-13123
The role of particle diffusion in the lower transition region: Revised interpretation of emission measures
p 770 N93-13476
Isotopic separation of He-3/He-4 from solar wind gases evolved from the lunar regolith
[DE92-019339] p 759 N93-13504
Thermoconvective instability in the solar core
p 771 N93-13849
Fusion energy from the Moon for the twenty-first century p 719 N93-13985
Synergism of He-3 acquisition with lunar base evolution p 540 N93-13986
Potential of derived lunar volatiles for life support
p 680 N93-13998
Lunar surface mining for automated acquisition of helium-3: Methods, processes, and equipment
p 766 N93-14007

HELIUM-NEON LASERS
Parameter studies of helium-neon lasers at 543 nm
p 606 N93-13747

HELMHOLTZ EQUATIONS
Boundary element analysis of acoustical thin-body and nonuniqueness problems using a normal derivative integral equation p 631 N93-13951

HEMATOLOGY
Investigation of effects of 60-Hz electric and magnetic fields on operant and social behavior and on the neuroendocrine system of nonhuman primates, part 1
[DE92-040152] p 673 N93-13520

HERMES MANNED SPACEPLANE
Reaching for the skies: The next generation
[ESA-BR-37-G] p 516 N93-13859

HERMETIC SEALS
Hermetic sealing and EMI shielding gasket
[AD-D015359] p 552 N93-13414

HERTZSPRUNG-RUSSELL DIAGRAM
International Ultraviolet Explorer (IUE) ultraviolet spectral atlas of selected astronomical objects
[NASA-RP-1285] p 744 N93-13461

HETERODYNING
Recent astronomical results from the infrared spatial interferometer and their implications for LOUISA
p 745 N93-13585
Appendix: Limits on the use of heterodyning and amplification in optical interferometry
p 747 N93-13597

HETEROGENEITY
DNET: A communications facility for distributed heterogeneous computing
[NASA-CR-190863] p 682 N93-13759

HETEROJUNCTION DEVICES
Two to six compound thin films by MOCVD for tandem solar cells p 640 N93-13932

HETEROJUNCTIONS
Synthesis and properties of mismatched heterojunction/substrate interfaces
[AD-A254577] p 719 N93-12648
Electronic transport properties of semiconductor microstructures p 724 N93-13730
Physics and technology of resonant-tunneling devices
[AD-A255233] p 573 N93-13837

HEURISTIC METHODS
Measures of user-system interface effectiveness: Assessment of structured judgment evaluation techniques for graphical, direct-manipulation style interfaces
[AD-A254493] p 677 N93-12576
An investigation of new search techniques for the traveling salesman problem p 696 N93-12625
Automatic programming of arc welding robots
p 616 N93-13720
Formal aspects of human-computer interaction
p 679 N93-13909
Q-Markov cover identification and integrated MCA-OVC controller design for flexible structures
p 695 N93-14045

HIERARCHIES
Hierarchic models for laminated plates
p 528 N93-12629

HIGH ALTITUDE
Development and computation of continuum higher order constitutive relations for high-altitude hypersonic flow p 494 N93-13578

HIGH CURRENT
Advanced high-explosive flux compression generator development: The CN-3 series
[DE92-019962] p 713 N93-12809

HIGH DEFINITION TELEVISION
An acoustic charge transport imager for high definition television applications
[NASA-CR-191295] p 572 N93-13448

HIGH ENERGY ELECTRONS
Comprehensive mappings of electron precipitation and its effects on the comprehensive mappings of electron precipitation and its effects on the atmosphere
[AD-A254665] p 648 N93-12621

HIGH ENERGY INTERACTIONS
Particle production and survival in muon acceleration
[DE92-019553] p 701 N93-12572
Electromagnetic lepton-pair production in relativistic collisions
[DE92-011069] p 706 N93-12829
Indiana University High Energy Physics Group, task C
[DE92-040458] p 707 N93-13002
Search for doubly Cabibbo suppressed decays of the charged D meson
[DE92-018588] p 703 N93-13092
Theoretical high energy physics
[DE92-015480] p 707 N93-13189
Guide to QSPIRES and the particle physics databases on SLACVM
[DE92-018099] p 737 N93-13275

HIGH FREQUENCIES
Terahertz horn antennas on thin membranes
[AD-A254772] p 562 N93-12867
JARE data reports no. 170 (ionosphere 45). HF field strength data measured at Syowa Station, Antarctica from January to December 1988 p 652 N93-13432
Activities of Space Power Insulation Inst.
[AD-A255825] p 574 N93-14034
Computer-aided design-based high-frequency electromagnetic wave scattering from complex bodies
p 567 N93-14042

HIGH PASS FILTERS
Preamplifier with adjustable input resistance
[AD-D015377] p 572 N93-13473

HIGH POWER LASERS
Test of QED using a laser at the SLAC final focus test beam
[DE92-019647] p 707 N93-12993

HIGH PRESSURE
Pressure fed thrust chamber technology program
[NASA-CR-184461] p 526 N93-12968

HIGH RESOLUTION
High resolution molecular spectroscopy of atmospheric species
[AD-A254360] p 650 N93-12946
Motion errors and compensation possibilities
p 563 N93-13052
Oxygen deficiencies at defects in YBa2Cu3O(7-delta) as determined by high resolution parallel electron energy loss
[DE92-016301] p 721 N93-13089
United Kingdom Infrared Telescope
p 743 N93-13273
A high-resolution radio survey of the galactic plane
p 744 N93-13480

HIGH REYNOLDS NUMBER
Time dependent heat transfer rates in high Reynolds number hypersonic flowfields p 595 N93-13664
Flow prediction for three-dimensional intakes and ducts using viscous-inviscid interaction methods
p 592 N93-13953

HIGH SPEED
Investigation of advanced counterrotation blade configuration concepts for high speed turboprop systems. Task 4: Advanced fan section aerodynamic analysis
[NASA-CR-187128] p 502 N93-12695
Multichip module high speed testing
[AD-A254825] p 570 N93-12731
A compressible boundary layer algorithm for use with SINDA '85 p 585 N93-13395
Physics and technology of resonant-tunneling devices
[AD-A255233] p 573 N93-13837

HIGH SPEED PHOTOGRAPHY
Debris/ice/TPS assessment and integrated photographic analysis for Shuttle mission STS-47
[NASA-TM-107553] p 520 N93-13032

HIGH TEMPERATURE
High temperature oxidation and electrochemical studies related to hot corrosion
[AD-A254435] p 540 N93-12595
High-temperature deformation and diffusion in oxides
[DE92-019593] p 720 N93-12854
An investigation of the thermoviscoplastic behavior of a metal matrix composite at elevated temperatures
[NASA-CR-189706] p 530 N93-12929
Linear and nonlinear finite element analysis of laminated composite structures at high temperatures
p 623 N93-13009
Oxidative stability of LARC (tm)-TPI films
[NASA-TM-107696] p 552 N93-13441

HIGH TEMPERATURE ENVIRONMENTS
Large-amplitude plate vibration in an elevated thermal environment
[AD-A254411] p 621 N93-12606
A novel diesel-fueled engine for microclimate cooling for the individual soldier
[AD-A254510] p 609 N93-12724
Investigation of properties and performance of ceramic composite components
[DE92-019911] p 550 N93-12858
The 1992 NASA Langley Measurement Technology Conference: Measurement Technology for Aerospace Applications in High-Temperature Environments
[NASA-CP-3161] p 598 N93-13661
Temperature and heat flux measurements: Challenges for high temperature aerospace application
p 598 N93-13662
High heat flux measurements and experimental calibrations/characterizations p 598 N93-13663
Heat flux microsensor measurements and calibrations
p 599 N93-13665
Thin film thermocouples for high temperature measurement on ceramic materials p 599 N93-13666
Fabrication of thin film heat flux sensors
p 599 N93-13667
Gas temperature measurements using the dual-line detection Rayleigh scattering technique
p 599 N93-13668
High-temperature strain measurement techniques: Current developments and challenges
p 599 N93-13669
Skin friction measurements in high temperature high speed flows p 595 N93-13670
Palladium-chromium static strain gages for high temperatures p 600 N93-13671
High temperature strain gage apparent strain compensation p 600 N93-13672
Elastic and plastic strain measurement in high temperature environment using laser speckle
p 600 N93-13673
Determination of high temperature strains using a PC based vision system p 601 N93-13674
Laser-based strain measurements for high temperature applications p 601 N93-13675
Technology trends in high temperature pressure transducers: The impact of micromachining
p 601 N93-13676
SiC device development for high temperature sensor applications p 601 N93-13677
The trade-off characteristics of acoustic and pressure sensors for the NASP p 601 N93-13678
Very high temperature silicon on silicon pressure transducers p 601 N93-13679
Developments on high temperature fiber optic microphone p 601 N93-13680

HIGH TEMPERATURE GASES
Spectroscopic studies of low-density gas in the Galactic disk and halo p 753 N93-13499
The interstellar medium of elliptical galaxies
p 757 N93-14071

HIGH TEMPERATURE PLASMAS
Nonlinear studies of m = 1 modes in high-temperature plasmas
[DE92-019395] p 714 N93-12913
Fast wave current drive experiment on the D3-D tokamak
[DE92-016253] p 716 N93-13193
Establishment of an Institute for Fusion Studies
[DE92-040014] p 717 N93-13502

HIGH TEMPERATURE SUPERCONDUCTORS
High temperature superconductor materials and applications
[NASA-CR-184437] p 719 N93-12691
Electrodeposition of high temperature superconductors
[AD-A255095] p 720 N93-12758
Oxygen diffusion in high-T(c) superconductors
[DE92-019597] p 720 N93-12807
Bipolaronic charge density waves, polaronic spin density waves and high T(c) superconductivity
[DE92-017403] p 720 N93-12853
High-temperature deformation and diffusion in oxides
[DE92-019593] p 720 N93-12854
Neutron scattering studies of the spin dynamics in La(2-x)Sr(x)O4
[DE92-019952] p 702 N93-13037

Ion-channeling observation of correlated atomic displacements below Tc in YBa2Cu3O(7-x) and Pb-doped Bi2Sr2CaCu2O(x)
[DE92-018186] p 722 N93-13104
Effect of O2 partial pressure on post annealed Ba2YCu3O(7-delta) thin films
[DE92-014949] p 722 N93-13323
Activation energy and critical current density in Bi-Sr-Ca-Cu-O
[DE92-018795] p 723 N93-13547
Effect of hydrogen reduction and doping on the characteristics of high-temperature superconductors p 725 N93-13844

HIGH VOLTAGES
Activities of Space Power Insulation Inst.
[AD-A255825] p 574 N93-14034

HILBERT SPACE
Preferred sets of states, predictability, classicality, and the environment-induced decoherence
[DE92-017447] p 641 N93-12684

HISTIDINE
Neurochemical control of circadian rhythms
[AD-A255054] p 675 N93-13116

HISTORIES
Evolution of the scientific paper
[DE92-019696] p 735 N93-12994
The Lunar Roving Vehicle: Historical perspective p 619 N93-14008

HMX
Development of a laser ignited all secondary explosive DDT detonator
[DE92-019340] p 555 N93-13081

HOLE DISTRIBUTION (ELECTRONICS)
Effect of hydrogen reduction and doping on the characteristics of high-temperature superconductors p 725 N93-13844

HOLES (ELECTRON DEFICIENCIES)
Effect of hydrogen reduction and doping on the characteristics of high-temperature superconductors p 725 N93-13844
High magnetic field studies of strained layer superlattices p 726 N93-13895

HOLOGRAPHY
Massively parallel optical-to-electronic data transfer
[AD-A254831] p 688 N93-12733
Visualization of hydrogen injection in a scramjet engine by simultaneous PLIF imaging and laser holographic imaging p 602 N93-13683

HORIZONTAL BRANCH STARS
A study of the structure, evolution and observation of Horizontal Branch stars
[ISBN-0-315-62655-0] p 751 N93-13374

HORN ANTENNAS
Terahertz horn antennas on thin membranes
[AD-A254772] p 562 N93-12867

HOT CORROSION
High temperature oxidation and electrochemical studies related to hot corrosion
[AD-A254435] p 540 N93-12595

HOT ELECTRONS
Observations of correlated broadband electrostatic noise and electron cyclotron emissions in the plasma sheet
[AD-A255002] p 712 N93-12705
Anomalous ion heating and superthermal electrons in the MST reversed-field pinch
[DE92-041011] p 713 N93-12882
Dynamics of the ion-ion acoustic instability in the thermalization of ion beams
[DE92-019396] p 714 N93-12914

HOT ISOSTATIC PRESSING
Fatigue and fracture of intermetallic alloys
[AD-A254543] p 540 N93-12603

HOT PRESSING
An investigation of the thermoviscoplastic behavior of a metal matrix composite at elevated temperatures
[NASA-CR-189706] p 530 N93-12929

HOT-WIRE ANEMOMETERS
A fundamental study of suction for Laminar Flow Control (LFC)
[NASA-CR-191276] p 583 N93-13277

HOUSINGS
Experimental validation of finite element and boundary element methods for predicting structural vibration and radiated noise p 621 N93-12631

HOVERING
Navier-Stokes flowfield computation of wing/rotor interaction for a tilt rotor aircraft in hover p 497 N93-14035

HUBBLE SPACE TELESCOPE
Support and servicing requirements for large observatories in space p 746 N93-13589
Report of the Science Working Group: Science with a lunar optical interferometer p 747 N93-13600

HUMAN BEHAVIOR
Use of antarctic analogs to support the space exploration initiative
[NASA-TM-108000] p 651 N93-13326
Moon Park: A research and educational facility p 519 N93-14015

HUMAN BEINGS
Tactile sensing and control in humans and robotic/teleoperated systems
[AD-A254408] p 609 N93-12604
Transactions: Tropospheric ozone and the environment. Papers from an international conference
[PB92-217017] p 643 N93-12941
Assessment of programs in space biology and medicine
[NASA-CR-190930] p 672 N93-13327

HUMAN BODY
Assessment of programs in space biology and medicine
[NASA-CR-190930] p 672 N93-13327

HUMAN FACTORS ENGINEERING
Action composition for the animation of natural language instructions
[AD-A254963] p 682 N93-12554
Measures of user-system interface effectiveness: Assessment of structured judgment evaluation techniques for graphical, direct-manipulation style interfaces
[AD-A254493] p 677 N93-12576
Human factors research in aircrew performance and training: 1986-1991
[AD-A254455] p 677 N93-12609
Human perceptual deficits as factors in computer interface test and evaluation
[DE92-019124] p 677 N93-12712
Adaptive automation and human performance. 3: Effects of practice on the benefits and costs of automation shifts
[AD-A254381] p 677 N93-12860
Human factors dealing with the International Asteroid Mission p 515 N93-13559
Occupational ergonomics in space p 680 N93-14013
Moon Park: A research and educational facility p 519 N93-14015

HUMAN PERFORMANCE
Adaptive automation and human performance: Multi-task performance characteristics
[AD-A254596] p 503 N93-12578
Adaptive automation and human performance. 3: Effects of practice on the benefits and costs of automation shifts
[AD-A254381] p 677 N93-12860
Effect of protective clothing ensembles on artillery battery crew performance
[AD-A254327] p 677 N93-12960
Human memory for the spatial locations of items on pull-down computer menus p 739 N93-14080

HUMAN REACTIONS
Human factors dealing with the International Asteroid Mission p 515 N93-13559

HUMAN RESOURCES
Women and minorities in science and engineering: An update
[NSF-92-303] p 730 N93-12907
Gateway to diversity in the scientific and technological workforce
[NSF-92-99] p 730 N93-13278
State award summary: Fiscal Year 1991
[NSF-92-3] p 775 N93-13381
Diversity in biological research
[NSF-92-19] p 673 N93-13700
Fiscal Year 1991 highlights
[NSF-92-23] p 731 N93-13702

HUMIDITY
Methods development for total organic carbon accountability
[NASA-CR-184438] p 672 N93-12949

HUMIDITY MEASUREMENT
Middle atmosphere water vapour p 667 N93-13892

HURRICANES
Extended range forecast of Atlantic seasonal hurricane activity for 1993 p 661 N93-12928
Summary of 1992 Atlantic tropical cyclone activity and verification of author's forecast (a year of no hurricane activity in the tropics but exceptional South Florida destruction from an unusual higher latitude intense hurricane) p 662 N93-13028

HYBRID COMPOSITES
Micromechanics of finite length fibers in composite materials p 532 N93-13490

HYDRATES
Experimental studies of the far-infrared spectra of cosmic-type ices
[NASA-CR-191300] p 748 N93-13660

HYDRATION
Ab initio atomic recombination reaction energetics on model heat shield surfaces
[NASA-CR-191210] p 575 N93-12677

HYDROCHLORIC ACID
MCFC diagnostics: HCl detection
[DE92-001292] p 639 N93-13313

HYDRODYNAMICS
The Capillary Pumped Loop Flight Experiment (CAPL): A pathfinder for EOS p 512 N93-13181
Hydrodynamical calculations of stellar interactions p 755 N93-13764
Connection of microscopic with macroscopic dynamics: Towards a hydrodynamical description of quantum mechanics p 729 N93-13957
Hydrodynamics and spectra formation of interacting massive binaries and the young remnant of SN1987A p 757 N93-13962

HYDROGEN
Study of short-range motion of atomic hydrogen in amorphous silicon by neutron reflectometry
[DE92-016392] p 703 N93-13194
Effect of hydrogen reduction and doping on the characteristics of high-temperature superconductors p 725 N93-13844
Availability of hydrogen for lunar base activities p 762 N93-13982
On grain boundary transport of hydrogen and mechanism of hydrogen-induced intergranular fracture p 544 N93-14047

HYDROGEN BONDS
Ab initio atomic recombination reaction energetics on model heat shield surfaces
[NASA-CR-191210] p 575 N93-12677

HYDROGEN FUELS
Visualization of hydrogen injection in a scramjet engine by simultaneous PLIF imaging and laser holographic imaging p 602 N93-13683

HYDROGEN OXYGEN FUEL CELLS
Investigation of hypersonic shock-induced combustion in a hydrogen-air system
[NASA-CR-191239] p 538 N93-13456

HYDROGEN PEROXIDE
The vibrational spectrum of H2O3: An ab initio investigation
[NASA-CR-190968] p 537 N93-12935

HYDROGEN SULFIDE
Environmental effects on iron aluminides
[DE92-016341] p 542 N93-13237
Biological conversion of synthesis gas
[DE92-017673] p 672 N93-13269

HYDROGEN-BASED ENERGY
Hydrogen Program Plan, FY 1993 - 1997
[DE92-010556] p 538 N93-13316

HYDROGENATION
A novel process for methanol synthesis
[DE92-019719] p 539 N93-13617

HYDROGRAPHY
The North Atlantic circulation: Combining simplified dynamics with hydrographic data p 670 N93-13483

HYDROLOGY
An ion budget for a terra firme rainforest in Central Amazonia
[INPE-5365-PRE/1745] p 632 N93-13005
Radiometric calibration of SAR systems p 564 N93-13055

HYDROLOGY MODELS
The use of remotely sensed data in delineation of hydrologic response units and estimation of their rainfall-runoff model parameters p 635 N93-13840

HYDROSTATICS
Nonlinear hydrostatic conditional symmetric instability: Some theoretical and modeling considerations p 655 N93-13757

HYDROTHERMAL SYSTEMS
Hydrothermal organic synthesis experiments
[NASA-CR-191257] p 672 N93-13457
Chemical environments of submarine hydrothermal systems
[NASA-CR-191258] p 669 N93-13458

HYDROXYL EMISSION
Comparison of cometary comae using ultraviolet spectroscopy: Composition and variation p 753 N93-13603
Spectroscopic observations of the night airglow from 3000 A to 9200 A p 658 N93-13891

HYDROXYL RADICALS
The vibrational spectrum of H2O3: An ab initio investigation
[NASA-CR-190968] p 537 N93-12935
Steady state analysis of tropospheric chemistry p 644 N93-13121
Resonance lamp absorption measurement of OH number density and temperature in expansion tube scramjet engine tests p 602 N93-13682

Planar laser-induced fluorescence imaging of OH in the exhaust of a bi-propellant thruster p 602 N93-13686
Gas-phase reactions of halogen species of atmospheric importance p 658 N93-13889
Radical reactions of atmospheric importance p 659 N93-14053
Kinetic studies of some free radical reactions involved in cloudwater chemistry p 668 N93-14055

HYPERBOLIC DIFFERENTIAL EQUATIONS
Hyperbolic conservation laws with umbilic points, 1 [AD-A254431] p 696 N93-12594

HYPERCUBE MULTIPROCESSORS
Testing and fault-tolerant design techniques for advanced digital architectures [AD-A255013] p 681 N93-12707
Performance of a plasma fluid code on the Intel parallel computers [DE92-011680] p 716 N93-13297

HYPERSONIC AIRCRAFT
Integration of turbo-ramjet engines for hypersonic aircraft p 503 N93-13230

HYPERSONIC BOUNDARY LAYER
Time dependent heat transfer rates in high Reynolds number hypersonic flowfields p 595 N93-13664

HYPERSONIC COMBUSTION
Investigation of hypersonic shock-induced combustion in a hydrogen-air system [NASA-CR-191239] p 538 N93-13456

HYPERSONIC FLIGHT
Hypersonic vehicle control law development using H infinity and mu-synthesis [NASA-TM-107689] p 504 N93-13068
Hypersonic propulsion system force accounting p 503 N93-13229
High-temperature strain measurement techniques: Current developments and challenges p 599 N93-13669

HYPERSONIC FLOW
A numerical study of hypersonic flow with strong surface blowing p 492 N93-13128
Mathematical problems in inviscid hypersonic flow p 493 N93-13451
Development and computation of continuum higher order constitutive relations for high-altitude hypersonic flow p 494 N93-13578
Time dependent heat transfer rates in high Reynolds number hypersonic flowfields p 595 N93-13664
Resonance lamp absorption measurement of OH number density and temperature in expansion tube scramjet engine tests p 602 N93-13682
Exit plane H2O concentration measurements correlated with OH PLIF near-injector mixing measurements for scramjet flows p 603 N93-13687
Application of a vectorized particle simulation to the study of plates and wedges in high-speed rarefied flow p 495 N93-13746
Linear stability theory of hypersonic, chemically reacting viscous flows p 588 N93-13765
A numerical study of hypersonic flows using the full Navier-Stokes equations with different air models p 594 N93-14061

HYPERSONIC FORCES
Hypersonic propulsion system force accounting p 503 N93-13229

HYPERSONIC HEAT TRANSFER
Time dependent heat transfer rates in high Reynolds number hypersonic flowfields p 595 N93-13664

HYPERSONIC SHOCK
Electron beam fluorescence measurements in the Boeing hypersonic shock tunnel p 602 N93-13681
Linear stability theory of hypersonic, chemically reacting viscous flows p 588 N93-13765

HYPERSONIC SPEED
An experimental/computational study of heat transfer in sharp fin induced shock wave/turbulent boundary layer interactions at low hypersonic Mach numbers p 590 N93-13826

HYPERSONIC VEHICLES
Hypersonic vehicle control law development using H infinity and mu-synthesis [NASA-TM-107689] p 504 N93-13068
A numerical study of hypersonic flow with strong surface blowing p 492 N93-13128
Application of a vectorized particle simulation to the study of plates and wedges in high-speed rarefied flow p 495 N93-13746

HYPERSONICS
Hypersonic panel flutter in a rarefied atmosphere p 505 N93-13928

HYPERTENSION
The identification and quantitation of triamterene in blood and urine from a fatal aircraft accident [AD-A254550] p 674 N93-12612

HYPERVELOCITY IMPACT
RHALE: A MMALE shock physics code written in C++ [DE92-018271] p 684 N93-12795
A Pennsylvania State University/General Electric Get Away Special (GAS) experiment p 511 N93-13177

HYPERVELOCITY PROJECTILES
Computation of steady and unsteady shock-induced combustion over hypervelocity blunt bodies p 536 N93-12836

HYPOTHALAMUS
Neurochemical control of circadian rhythms [AD-A255054] p 675 N93-13116

I

ICE
Microwave remote sensing of a precipitating atmosphere p 634 N93-13371
Experimental studies of the far-infrared spectra of cosmic-type ices [NASA-CR-191300] p 748 N93-13660

ICE ENVIRONMENTS
Interaction and impact of floating bodies [AD-A254627] p 574 N93-12617

ICE FLOES
Interaction and impact of floating bodies [AD-A254627] p 574 N93-12617

ICE FORMATION
Debris/ice/TPS assessment and integrated photographic analysis for Shuttle mission STS-47 [NASA-TM-107553] p 520 N93-13032
Simulation of two-dimensional icing, de-icing and anti-icing phenomena p 498 N93-13364
A theoretical investigation of the growth rates of ice crystals in clouds p 653 N93-13485

ICE NUCLEI
Icing prevention by ultrasonic nucleation of supercooled water droplets in front of subsonic aircraft [DOT/FAA/CT-TN92/38] p 497 N93-12816

ICE PREVENTION
Icing prevention by ultrasonic nucleation of supercooled water droplets in front of subsonic aircraft [DOT/FAA/CT-TN92/38] p 497 N93-12816
Simulation of two-dimensional icing, de-icing and anti-icing phenomena p 498 N93-13364

ICE REPORTING
Application of theoretical models to active and passive remote sensing of saline ice p 633 N93-13086
JARE data reports no. 173 (meteorology 28). Antarctic climate research data. Part 5: PPI radar data at Syowa Station, Antarctica from February to December 1989 p 663 N93-13446

IDEAL GAS
Navier-Stokes simulations of unsteady transonic flow phenomena [NASA-TM-103962] p 491 N93-12721
Mathematical problems in inviscid hypersonic flow p 493 N93-13451

IGNITION
Development of a laser ignited all secondary explosive DDT detonator [DE92-019340] p 555 N93-13081
Numerical investigation of the flow field in the head-end, star grain section of a solid rocket motor during ignition transients p 526 N93-13818

ILLUMINATING
Integration of exterior lighting systems and night vision imaging systems [AD-A254826] p 677 N93-12732

IMAGE ANALYSIS
Spreadsheet-like image analysis [AD-A254395] p 619 N93-12864
Digital imaging systems [DE92-019194] p 736 N93-13078
Sensing and interpretation of 3-D shape and motion p 692 N93-13240
Building and using scene representations in image understanding p 692 N93-13241
The 3-D computer vision techniques for object following and obstacle avoidance p 693 N93-13245
The use of remotely sensed data in delineation of hydrologic response units and estimation of their rainfall-runoff model parameters p 635 N93-13840
Deciduous forest scene complexity in high-resolution multispectral scanner imagery [AD-A255511] p 635 N93-13867
Coherent frame analysis of Synthetic Aperture Radar (SAR) ocean imagery p 568 N93-14050

IMAGE CORRELATORS
Determination of high temperature strains using a PC based vision system p 601 N93-13674

IMAGE ENHANCEMENT
Large area projection liquid-crystal video display system with inherent grid pattern optically removed [NASA-CASE-NPO-16932-2-CU] p 711 N93-13711

IMAGE INTENSIFIERS
Digital fluoroscopy with an optically coupled charge-coupled device p 712 N93-14101

IMAGE PROCESSING
Thermal imaging of synchrotron beams on silicon crystals [DE92-018182] p 719 N93-12562
Quantitative analysis of three-dimensional steady flow field by using particle image velocimetry and digital image processing method p 577 N93-13017
Fundamentals and Special Problems of Synthetic Aperture Radar (SAR) [AGARD-LS-182] p 563 N93-13049
SAR peculiarities, ambiguities and constraints p 563 N93-13051
Special SAR techniques and applications p 564 N93-13059
Magnetic tape p 737 N93-13135
IIaO ultraviolet and nuclear emulsion films responses to orbital flights on STS-3, STS-7, STS-8, and STS-40 p 509 N93-13163
Impact of Digital Terrain Elevation Data (DTED) resolution on terrain visualization: Simulation versus reality [AD-A254237] p 634 N93-13333
Using iterative orthophoto refinements to correct Digital Elevation Models (DEM's) [AD-A254625] p 634 N93-13345
A weighted iterative algorithm for neuromagnetic imaging [DE92-040244] p 675 N93-13522
Automatic pattern recognition techniques for geometrical correction on satellite data p 687 N93-13913
Adding explanation capability to a knowledge-based system for interpretation of oceanographic images [AD-A255887] p 671 N93-13943
Coherent frame analysis of Synthetic Aperture Radar (SAR) ocean imagery p 568 N93-14050

IMAGE RESOLUTION
Motion errors and compensation possibilities p 563 N93-13052
Manned observations technology development, FY 1992 report [NASA-CR-185704] p 597 N93-13373
High resolution imaging at Palomar p 745 N93-13584

IMAGERY
SeaWiFS technical report series. Volume 4, an analysis of GAC sampling algorithms: A case study [NASA-TM-104566-VOL-4] p 669 N93-13382

IMAGES
Introductory review of target discrimination criteria [AD-A254954] p 560 N93-12551

IMAGING RADAR
Polarization effects and multipolarization SAR p 564 N93-13054

IMAGING SPECTROMETERS
Imaging IR spectrometer, phase 2 [NASA-CR-190848] p 597 N93-13424

IMAGING TECHNIQUES
Thermal imaging of synchrotron beams on silicon crystals [DE92-018182] p 719 N93-12562
Functional MRI studies of human vision on a clinical imager [DE92-017448] p 674 N93-12566
Integration of exterior lighting systems and night vision imaging systems [AD-A254826] p 677 N93-12732
Weak-beam imaging of dissociated dislocations in HVEM-irradiated Fe-Ni-Cr alloys [DE92-019587] p 541 N93-12798
Automation of the targeting and reflective alignment concept [NASA-CR-190964] p 709 N93-12985
Quantitative analysis of three-dimensional steady flow field by using particle image velocimetry and digital image processing method p 577 N93-13017
Multi-frequency multi-polarization processing for spaceborne SAR p 564 N93-13057
Inverse Synthetic Aperture Radar p 564 N93-13058
Digital imaging systems [DE92-019194] p 736 N93-13078
Silicon vision: Elementary functions to be implemented on electronic retinas p 692 N93-13242
The 3-D computer vision techniques for object following and obstacle avoidance p 693 N93-13245
Infrared image projector utilizing a deformable mirror device spatial light modulator [AD-D015373] p 710 N93-13500

Radio and optical interferometric imaging
p 744 N93-13580
The optical very large array and its moon-based version p 745 N93-13583
Visualization of hydrogen injection in a scramjet engine by simultaneous PLIF imaging and laser holographic imaging p 602 N93-13683
Planar laser-induced fluorescence imaging of OH in the exhaust of a bi-propellant thruster p 602 N93-13686
Finite element study of ultrasonic imaging
p 700 N93-13774
Planar measurement of flow field parameters in nonreacting supersonic flows with laser-induced iodine fluorescence p 495 N93-13801
Digital fluoroscopy with an optically coupled charge-coupled device p 712 N93-14101

IMMUNOLOGY
Assessment of programs in space biology and medicine
[NASA-CR-190930] p 672 N93-13327

IMPACT
Airblast damage from small asteroids
[DE92-017834] p 749 N93-12956

IMPACT DAMAGE
Properties of five toughened matrix composite materials
[NASA-TP-3254] p 528 N93-12590
The effects of compressive preloads on the compression-after-impact strength of carbon/epoxy
[NASA-TP-3303] p 529 N93-12678

IMPACT LOADS
Analysis of a structure-equipment system subjected to impact loading
[AD-A255097] p 622 N93-12652
The effects of compressive preloads on the compression-after-impact strength of carbon/epoxy
[NASA-TP-3303] p 529 N93-12678

IMPACT TESTS
Properties of five toughened matrix composite materials
[NASA-TP-3254] p 528 N93-12590
Development of a 1000 g, 10 ms mechanical shock test capability
[DE92-019193] p 624 N93-13077

IMPEDANCE
High temperature oxidation and electrochemical studies related to hot corrosion
[AD-A254435] p 540 N93-12595
Performance and stability of telemanipulators using bilateral impedance control p 614 N93-13488
Electromagnetic scattering simulations using equivalent boundary condition models p 569 N93-14052

IMPURITIES
Structure sensitive reactions over Co, Fe and mixed metal clusters in zeolites
[DE92-040359] p 542 N93-12998

INCOHERENT SCATTER RADAR
A joint study of the lower ionosphere by radar, lidar, and spectrometer p 655 N93-13755

INCOMPRESSIBLE FLOW
An attempt at a status report on a fast-moving target: CFD --- computational fluid dynamics
[DE92-017432] p 576 N93-12839
Boundary element methods for two-dimensional, coupled, thermoviscous flow p 584 N93-13383

INCOMPRESSIBLE FLUIDS
The program FANS-3D (finite analytic numerical simulation 3-dimensional) and its applications
p 586 N93-13399
Solution of viscous flow problems by using the boundary element method p 588 N93-13609
Structures, spectra and inertial range transfer in two-dimensional and beta-plane turbulence
p 590 N93-13900

INDENTATION
Contact of orthotropic laminates with a rigid spherical indentor p 533 N93-13778

INDEXES (DOCUMENTATION)
Abstract and index collection in the Research Information Center of the National Institute of Standards and Technology
[PB92-217587] p 738 N93-13415

INDIUM COMPOUNDS
Novel thin-film CuInSe2 fabrication
[DE92-016440] p 723 N93-13526
Development of a computer model for polycrystalline thin-film CuInSe2 and CdTe solar cells
[DE92-016444] p 639 N93-13529

INDIUM GALLIUM ARSENIDES
Synthesis and properties of mismatched heterojunction/substrate interfaces
[AD-A254577] p 719 N93-12648
High magnetic field studies of strained layer superlattices p 726 N93-13895

INDIUM PHOSPHIDES
Studies of orbital doublet and modelling of orbital triplet Jahn-Teller systems in 3 to 5 semiconductors
p 725 N93-13845

INDUCED DRAG
Assessment of potential aerodynamic benefits from spanwise blowing at the wing tip p 496 N93-13822

INDUCTORS
Transducer circuit
[AD-D015376] p 572 N93-13472

INDUSTRIAL ENERGY
Industrial applications of hot dry rock geothermal energy
[DE92-018903] p 637 N93-12923

INDUSTRIAL MANAGEMENT
An analysis of the field service function of selected electronics firms
[AD-A255003] p 570 N93-12868
Performance measurement for information systems: Industry perspectives
[NASA-CR-191369] p 738 N93-13737

INDUSTRIAL PLANTS
An analysis of the field service function of selected electronics firms
[AD-A255003] p 570 N93-12868

INDUSTRIAL WASTES
Documentation for developing the initial source category list
[PB92-218429] p 646 N93-13647

INDUSTRIES
Selected data on research and development in industry: 1990
[NSF-92-317] p 773 N93-12667
An analysis of the field service function of selected electronics firms
[AD-A255003] p 570 N93-12868
Industrial applications of hot dry rock geothermal energy
[DE92-018903] p 637 N93-12923
NASA industry education initiative. Education programs report, 1991
[NASA-NP-158] p 730 N93-13248
Advanced technology for America's future in space. Executive summary
[NASA-TM-107969] p 513 N93-13308
Scientists, engineers, and technicians in manufacturing industries: 1989. Detailed statistical tables
[NSF-92-312] p 730 N93-13437
Research and development in industry: 1989. Funds, 1989. Scientists and engineers, January 1990
[NSF-92-307] p 741 N93-13658
US Industry Access to Japanese Science and Technology: Proceedings of a conference
[PB92-167964] p 741 N93-13788

INELASTIC COLLISIONS
Video profile monitor diagnostic system for GTA
[DE92-040231] p 710 N93-13509

INELASTIC SCATTERING
The spin of the nucleon in deep inelastic lepton scattering experiments
[DE92-018854] p 702 N93-13073
Electronic transport properties of semiconductor microstructures p 724 N93-13730

INERTIAL CONFINEMENT FUSION
Applications of group-invariant analytic solutions to inertial confinement fusion
[DE92-040347] p 715 N93-13047

INFECTIOUS DISEASES
Transactions: Tropospheric ozone and the environment. Papers from an international conference
[PB92-217017] p 643 N93-12941

INFORMATION
The informed citizen: Technology and responsibility in the information age p 742 N93-14049
A study regarding information-seeking behavior, valuation of information including perceptions of information attributes, and associated correlates pertaining to information usage p 740 N93-14088

INFORMATION DISSEMINATION
Proceedings of FLICC forums on federal information policies. Combined summaries of proceedings. The 1990 7th Forum, Access is the Key and the 1991 8th Forum, Building Information Superhighways: Supercomputing Networks and Libraries
[PB92-147370] p 734 N93-12759
Brazilian remote sensing community: Historical, geographical and economic aspects
[INPE-5421-PRE/1763] p 634 N93-13412
A study regarding information-seeking behavior, valuation of information including perceptions of information attributes, and associated correlates pertaining to information usage p 740 N93-14088

INFORMATION FLOW
State space methods in multidimensional digital signal processing
[AD-A254646] p 561 N93-12620
US Industry Access to Japanese Science and Technology: Proceedings of a conference
[PB92-167964] p 741 N93-13788

INFORMATION MANAGEMENT
Principles of information resource management: A foundation for the future
[AD-A254447] p 733 N93-12597
Earth science information: Planning for the integration and use of global change information
[NASA-CR-191217] p 733 N93-12660
Proceedings of FLICC forums on federal information policies. Combined summaries of proceedings. The 1990 7th Forum, Access is the Key and the 1991 8th Forum, Building Information Superhighways: Supercomputing Networks and Libraries
[PB92-147370] p 734 N93-12759
Engineering Design Information System (EDIS) Information Services Division (ISD) index function: User's manual
[DE92-041242] p 736 N93-13048
NSSDC Conference on Mass Storage Systems and Technologies for Space and Earth Science Applications, volume 1
[NASA-CP-3165-VOL-1] p 736 N93-13131
Enterprise storage report for the 1990's
p 736 N93-13132
The long hold: Storing data at the National Archives
p 737 N93-13139
The protection of the Facsimile (FAX) machine against the insider threat
[DE92-019424] p 565 N93-13506
Identifying and describing Federal information inventory/locator systems: Design for networked-based locators, volume 1 p 738 N93-13884
Coordinating Council. Ninth Meeting: Total Quality Management
[NASA-TM-108106] p 738 N93-13885

INFORMATION PROCESSING (BIOLOGY)
Simulation of excitatory/inhibitory interactions in single auditory neurons
[AD-A253614] p 675 N93-13252

INFORMATION RETRIEVAL
Coordinating Council. Second Meeting: International Acquisitions
[NASA-TM-108015] p 733 N93-12634
Using DIALOG CIP at Winona State University to educate end-users p 686 N93-13338
A study of traditional information access models applied in a hypertext information system p 739 N93-14076
A study regarding information-seeking behavior, valuation of information including perceptions of information attributes, and associated correlates pertaining to information usage p 740 N93-14088

INFORMATION SYSTEMS
Coordinating Council. Second Meeting: International Acquisitions
[NASA-TM-108015] p 733 N93-12634
Coordinating Council. Fifth Meeting: Quality
[NASA-TM-108018] p 733 N93-12635
Earth science information: Planning for the integration and use of global change information
[NASA-CR-191217] p 733 N93-12660
Coordinating Council. Third Meeting: STI Strategic Plans
[NASA-TM-108016] p 733 N93-12670
Proceedings of Joint RL/AFOSR Workshop on Intelligent Information Systems
[AD-A254795] p 734 N93-12703
Proceedings of FLICC forums on federal information policies. Combined summaries of proceedings. The 1990 7th Forum, Access is the Key and the 1991 8th Forum, Building Information Superhighways: Supercomputing Networks and Libraries
[PB92-147370] p 734 N93-12759
Increasing the end user's productivity through seamless integration of applications with the database
[DE92-019599] p 735 N93-12824
Publications of the space physiology and countermeasures program, Musculoskeletal Discipline: 1980-1990
[NASA-CR-4468] p 743 N93-12898
A radio frequency user's guide to the Space Environment Services Center geophysical alert broadcasts
[PB92-220631] p 562 N93-12979
Engineering Design Information System (EDIS) Information Services Division (ISD) index function: User's manual
[DE92-041242] p 736 N93-13048
Earth observing system: Information on NASA's incorporation of existing data into EOSDIS. Report to the Chairman, Committee on Science, Space, and Technology, House of Representatives
[GAO/IMTEC-92-79] p 736 N93-13112

NSSDC Conference on Mass Storage Systems and Technologies for Space and Earth Science Applications, volume 1
[NASA-CP-3165-VOL-1] p 736 N93-13131
Mass storage system experiences and future needs at the National Center for Atmospheric Research
p 737 N93-13138
The long hold: Storing data at the National Archives
p 737 N93-13139
Using DIALOG CIP at Winona State University to educate end-users p 686 N93-13338
Performance measurement for information systems: Industry perspectives
[NASA-CR-191369] p 738 N93-13737
Application of information system technology to K-12 education
[AD-A255223] p 731 N93-13834
Identifying and describing Federal information inventory/locator systems: Design for networked-based locators, volume 1 p 738 N93-13884
Learning and using methodologies in information systems analysis and design p 739 N93-14058
A study of traditional information access models applied in a hypertext information system p 739 N93-14076

INFORMATION THEORY
From comparison density to two sample analysis
[AD-A253866] p 698 N93-13064

INFRARED ABSORPTION
Radiation-induced infrared absorption in nuclear-pumped laser cavity components
[DE92-017346] p 605 N93-13249

INFRARED ASTRONOMY
United Kingdom Infrared Telescope
p 743 N93-13273
H I shells and supershells: Observations and theory
p 751 N93-13360
A Lunar Optical-Ultraviolet-Infrared Synthesis Array (LOUISA)
[NASA-CP-3066] p 744 N93-13579

INFRARED ASTRONOMY SATELLITE
Zodiacal emission p 772 N93-13147

INFRARED DETECTORS
Computer simulation of a space-based infrared surveillance sensor
[AD-A255521] p 524 N93-13870

INFRARED IMAGERY
Infrared image projector utilizing a deformable mirror device spatial light modulator
[AD-D015373] p 710 N93-13500
Deciduous forest scene complexity in high-resolution multispectral scanner imagery
[AD-A255511] p 635 N93-13867

INFRARED INSTRUMENTS
Correlation for non-linear infrared calibration curves
[AD-A255098] p 596 N93-12653

INFRARED INTERFEROMETERS
Recent astronomical results from the infrared spatial interferometer and their implications for LOUISA
p 745 N93-13585
Science objectives for ground- and space-based optical/IR interferometry p 746 N93-13590

INFRARED LASERS
Compact Blue-Green Lasers: Summaries of papers presented at the topical meeting. Volume 6: Technical digest series
[AD-A255001] p 608 N93-13883

INFRARED RADIATION
A correlated k-distribution model of the heating rates for CH4 and N2O in the atmosphere between 0 and 60 km
[NASA-TM-108062] p 643 N93-12926
Microwave and infrared dielectric relaxation of alkylcarbonates, chloroform and their mixtures at 25 C
[AD-A253606] p 537 N93-13096
Zodiacal emission p 772 N93-13147
Appendix: Limits on the use of heterodyning and amplification in optical interferometry
p 747 N93-13597
An infrared polarimetric study of sunspots
p 770 N93-13627
Intraseasonal variability of infrared cooling rates during the Asian summer monsoon and their influence on intraseasonal waves p 665 N93-13760
Infrared emission from the water outgas cloud of an orbiting vehicle induced by collisions with atmospheric gases p 521 N93-13854

INFRARED RADIOMETERS
Test and calibration of the along track scanning radiometer, a satellite-borne infrared radiometer designed to measure sea surface temperature
p 671 N93-13842
Computer simulation of a space-based infrared surveillance sensor
[AD-A255521] p 524 N93-13870

INFRARED SOURCES (ASTRONOMY)
Studies of extra-solar Oort Clouds and the Kuiper disk
[NASA-CR-190958] p 769 N93-12669

INFRARED SPECTRA
The millimeter and submillimeter wavelength diffuse backgrounds: Measurements of the spectrum and anisotropy p 772 N93-13145
Imaging IR spectrometer, phase 2
[NASA-CR-190848] p 597 N93-13424
Required technologies for a lunar optical UV-IR synthesis array p 747 N93-13598
Experimental studies of the far-infrared spectra of cosmic-type ices
[NASA-CR-191300] p 748 N93-13660
Galaxies with spectral energy distributions peaking at 60 micrometers: Morphology and activity explained by interactions p 756 N93-13959
Thermal and nonthermal star formation: An investigation into the process of star formation as a function of stellar mass p 758 N93-14091

INFRARED SPECTROMETERS
Imaging IR spectrometer, phase 2
[NASA-CR-190848] p 597 N93-13424
Development of a portable infrared emission spectrometer AA460 PIRES
[NASA-CR-190849] p 598 N93-13656

INFRARED SPECTROSCOPY
Kinetics and dynamics of oxidation reactions involving an adsorbed CO species
[DE92-019745] p 537 N93-12995
Infrared spectroscopy of size resolved fine aerosol
p 647 N93-13758

INFRARED TELESCOPES
United Kingdom Infrared Telescope
p 743 N93-13273
Thermal and nonthermal star formation: An investigation into the process of star formation as a function of stellar mass p 758 N93-14091

INHOMOGENEITY
Axisymmetric and antiplane shear crack problems in bonded nonhomogeneous materials
p 625 N93-13127
Theoretical and numerical studies of wave propagation and scattering in inhomogeneous media
p 568 N93-14044

INJECTION LASERS
Strained-layer InGaAs-GaAs-AlGaAs quantum well lasers and transverse junction stripe lasers
p 607 N93-13773

INJECTION LOCKING
Millimeter-wave quasi-optical and spatial power combining techniques
[AD-A255438] p 574 N93-13865

INJECTORS
Diesel injector fouling bench test methodology
[AD-A254532] p 609 N93-12600
Pressure fed thrust chamber technology program
[NASA-CR-184461] p 526 N93-12968

INLET AIRFRAME CONFIGURATIONS
Aerodynamic Engine/Airframe Integration for High Performance Aircraft and Missiles
[AGARD-CP-498] p 577 N93-13199
Aerodynamic studies of supersonic air intakes
p 497 N93-13222

INLET FLOW
Some aspects of intake design, performance and integration with the airframe p 502 N93-13219
Comparative performance tests of a pitot-inlet in several European wind-tunnels at subsonic and supersonic speeds p 497 N93-13221
Flow prediction for three-dimensional intakes and ducts using viscous-inviscid interaction methods
p 592 N93-13953

INLET NOZZLES
ASTOVL model engine simulators for wind tunnel research p 507 N93-13213
Application of subsonic first-order panel methods for prediction of inlet and nozzle aerodynamic interactions with airframe p 497 N93-13223

INLET PRESSURE
A novel-high-performance system for recording and analysing instantaneous total pressure distortion in air intakes p 580 N93-13215

INORGANIC COMPOUNDS
ReTech, Inc., Plasma Centrifugal Furnace: Applications analysis report
[PB92-218791] p 714 N93-12982

INSECTICIDES
Procedures for the diagnostic dose resistance test kits for mosquitoes, body lice, and beetle pests of stored products
[AD-A255224] p 675 N93-13941

INSECTS
Procedures for the diagnostic dose resistance test kits for mosquitoes, body lice, and beetle pests of stored products
[AD-A255224] p 675 N93-13941

INSPECTION
Functional system design document for the Intelligent Inspection System (IIS)
[DE92-018240] p 619 N93-12794

INSTALLATION MANUALS
World Energy Projection System (WEPS), March 1992. Model installation manual, distribution disk layout
[PB92-169572] p 637 N93-12937

INSTALLING
Requirements for soldered electrical connections
[NHB-5300.4(3A-2)] p 570 N93-12674

INSTANTONS
Solitons and instantons in string theory
p 728 N93-13753

INSTRUCTION SETS (COMPUTERS)
Action composition for the animation of natural language instructions
[AD-A254963] p 682 N93-12554

INSTRUCTORS
Suited for spacewalking: A teacher's guide with activities
[NASA-EP-279] p 679 N93-13692

INSTRUMENT COMPENSATION
High temperature strain gage apparent strain compensation p 600 N93-13672

INSTRUMENT LANDING SYSTEMS
ILS mathematical modeling study of the effects of an ASR-9 structure at the Long Island MacArthur Airport, Islip, NY
[DOT/FAA/CT-TN92/25] p 506 N93-12668

INSULATORS
Electronic phenomena in polyanilines
[AD-A254803] p 545 N93-12749

INSULIN
Tagging insulin in microgravity p 510 N93-13172

INTAKE SYSTEMS
Intake and exhaust noise
[ISVR-TR-207] p 699 N93-12714

INTEGERS
From totally unimodular to balanced O, +/- 1 matrices: A family of integer polytopes
[AD-A254552] p 696 N93-12640

INTEGRAL EQUATIONS
Boundary element analysis of acoustical thin-body and nonuniqueness problems using a normal derivative integral equation p 631 N93-13951
Numerical analysis of scattering from certain conducting and dielectric bodies of arbitrary shape
[ISBN-0-315-63282-8] p 569 N93-14066

INTEGRATED CIRCUITS
Development of XUV projection lithography at 60 to 80 nm
[DE92-017517] p 603 N93-12560
Development of large-area monolithically integrated silicon-film photovoltaic modules
[DE92-010600] p 637 N93-12838
Terahertz horn antennas on thin membranes
[AD-A254772] p 562 N93-12867
Advanced on-chip divider for monolithic microwave VCO's
[NASA-CR-191355] p 572 N93-13563
Physics and technology of resonant-tunneling devices
[AD-A255233] p 573 N93-13837
Comparison of heavy ion and electron-beam upset data for GaAs
[AD-A255901] p 708 N93-14089

INTERACTIONAL AERODYNAMICS
Aerodynamic Engine/Airframe Integration for High Performance Aircraft and Missiles
[AGARD-CP-498] p 577 N93-13199
Detailed analysis of wing-nacelle interaction for commercial transport aircraft p 578 N93-13203
Recent developments in low-speed TPS-testing for engine integration drag and installed thrust reversr simulation p 502 N93-13207
Aerodynamic integration of thrust reversers on the Fokker 100 p 502 N93-13208
Water tunnel studies of inlet/airframe interference phenomena p 580 N93-13216
AGARD WG13 aerodynamics of high speed air intakes: Assessment of CFD results p 581 N93-13220
Airfoil-vortex interaction and the wake of an oscillating airfoil p 495 N93-13803
Navier-Stokes flowfield computation of wing/rotor interaction for a tilt rotor aircraft in hover
p 497 N93-14035

INTERFACE STABILITY
Monitoring interfacial dynamics by pulsed laser techniques
[DE92-040302] p 606 N93-13514

INTERFACIAL TENSION
The First United States Microgravity Laboratory
[NASA-TM-107980] p 557 N93-12951
INTERFEROMETERS
A Lunar Optical-Ultraviolet-Infrared Synthesis Array (LOUISA)
[NASA-CP-3066] p 744 N93-13579
The Mount Wilson optical interferometer: The first automated instrument and the prospects for lunar interferometry p 745 N93-13582
The optical very large array and its moon-based version p 745 N93-13583
High resolution imaging at Palomar p 745 N93-13584
Shot noise limits to sensitivity of optical interferometry p 745 N93-13586
HARDI: A high angular resolution deployable interferometer for space p 745 N93-13588
Report of the Working Group on Space/Lunar Tradeoffs p 747 N93-13599
INTERFEROMETRY
A Lunar Optical-Ultraviolet-Infrared Synthesis Array (LOUISA)
[NASA-CP-3066] p 744 N93-13579
Shot noise limits to sensitivity of optical interferometry p 745 N93-13586
Science objectives for ground- and space-based optical/IR interferometry p 746 N93-13590
Telescopes on the Moon or pie in the sky? p 746 N93-13591
Lunar interferometric astronomy: Some basic questions p 746 N93-13592
Lunar optical telescopes: An historical perspective p 746 N93-13593
An optical VLA on the Moon p 747 N93-13596
INTERGALACTIC MEDIA
Evidence for cool gas and star formation in cluster cooling flows p 751 N93-13380
INTERLAMINAR STRESS
A study of the interlaminar stress continuity theories for composite laminates p 621 N93-12627
INTERLAYERS
Silicide layer growth rates in Mo/Si multilayers
[DE92-019581] p 721 N93-12972
INTERMETALLICS
Fatigue and fracture of intermetallic alloys
[AD-A254543] p 540 N93-12603
INTERMOLECULAR FORCES
Intermolecular potential functions from spectroscopic properties of weakly bound complexes
[DE92-018643] p 701 N93-12745
INTERNAL COMBUSTION ENGINES
Intake and exhaust noise
[ISVR-TR-207] p 699 N93-12714
Meeting future exhaust emissions standards using natural gas as a vehicle fuel: Lessons learned from the natural gas vehicle challenge 1992
[DE92-019670] p 642 N93-12885
Utilization of compressed natural gas in medium- and heavy-duty engine route vehicles
[PB92-217546] p 611 N93-12908
Effects of gas composition on engine performance and emissions
[PB92-217561] p 611 N93-12936
The influence of mixture preparation in the intake port on the performance of a spark-ignited four-stroke engine p 613 N93-13331
INTERNAL FRICTION
Lateral variations of shear velocity and anelasticity in the upper mantle of the western US from Rayleigh wave observations p 653 N93-13492
INTERNATIONAL COOPERATION
Coordinating Council. Second Meeting: International Acquisitions
[NASA-TM-108015] p 733 N93-12634
Coordinating Council. Fourth Meeting: NACA Documents Database Project
[NASA-TM-108017] p 734 N93-12671
First International Microgravity Laboratory
[NASA-TM-108007] p 518 N93-13113
The IGAC activity for the development of global emissions inventories: Description and initial results
[DE92-016010] p 644 N93-13270
Introduction to the International Asteroid Mission p 513 N93-13549
Legal and political issues raised by the International Asteroid Mission p 514 N93-13555
Horizon 2000: Seven years on
[ESA-BR-37-B] p 516 N93-13855
Moon Park: A research and educational facility p 519 N93-14015
INTERNATIONAL LAW
Legal and political issues raised by the International Asteroid Mission p 514 N93-13555
INTERPLANETARY DUST
In situ dust mass distribution measurements from the Giotto encounter with comet P/Halley p 753 N93-13602
Comparison of cometary comae using ultraviolet spectroscopy: Composition and variation p 753 N93-13603
INTERPLANETARY MAGNETIC FIELDS
Chemical release and radiation effects experiment advanced planning and coordination
[NASA-CR-184439] p 649 N93-12718
INTERPLANETARY SPACE
JPRS report: Science and technology. Central Eurasia: Space
[JPRS-USP-92-006] p 508 N93-13151
INTERPOLATION
Improved wide range expressions for displacements and inverse displacements for standard fracture toughness specimens
[AD-A254561] p 622 N93-12643
INTERPROCESSOR COMMUNICATION
Lazy checkpoint coordination for bounding rollback propagation
[NASA-CR-191281] p 565 N93-13375
DNET: A communications facility for distributed heterogeneous computing
[NASA-CR-190863] p 682 N93-13759
INTERSTELLAR COMMUNICATION
Engineering planetary lasers for interstellar communication p 608 N93-14010
INTERSTELLAR GAS
Probing the galactic halo with ROSAT
[NASA-CR-191268] p 743 N93-13272
H I shells and supershells: Observations and theory p 751 N93-13360
The interstellar medium of elliptical galaxies p 757 N93-14071
Molecular clouds in the distant outer galaxy p 758 N93-14095
INTERSTELLAR MAGNETIC FIELDS
Limits on galactic dynamo theory due to magnetic fluctuations p 754 N93-13636
INTERSTELLAR MATTER
The role of ambipolar diffusion in the formation of interstellar cloud cores and protostars p 755 N93-13828
A study of the neutral and ionized gas in the interstellar medium and galactic H 2 regions p 756 N93-13853
Hydrodynamics and spectra formation of interacting massive binaries and the young remnant of SN1987A p 757 N93-13962
Supernova remnants, shocks, and the interstellar medium p 757 N93-13963
INTERSTITIALS
Oxygen diffusion in high-T(c) superconductors
[DE92-019597] p 720 N93-12807
INVENTIONS
Energy related inventions program. A joint program of the Department of Energy and the National Institute of Standards and Technology. Status report for recommendations 1 through 300
[PB92-226265] p 637 N93-12987
Energy related inventions program. A joint program of the Department of Energy and the National Institute of Standards and Technology. Status report for recommendations 301-563
[PB92-226273] p 637 N93-12988
INVENTORIES
ONR basic research program: Summary and bibliographies, FY 1990 and 1991
[AD-A253038] p 774 N93-12696
NASA industry education initiative. Education programs report, 1991
[NASA-NP-158] p 730 N93-13248
The IGAC activity for the development of global emissions inventories: Description and initial results
[DE92-016010] p 644 N93-13270
Identifying and describing Federal information inventory/locator systems: Design for networked-based locators, volume 1 p 738 N93-13884
INVERSE KINEMATICS
Nonholonomic motion of free-flying space robots p 615 N93-13638
INVERSIONS
A synoptic climatology of the elevated mixed layer inversion over the southern Great Plains in spring p 664 N93-13643
INVISCID FLOW
Calibration of 2D unstructured grid methods on propulsive flowfields p 582 N93-13225
Investigation of the flowfield around an isolated bypass engine with fan and core jet p 582 N93-13227
Mathematical problems in inviscid hypersonic flow p 493 N93-13451
Numerical calculation of turbomachinery cascade flows p 589 N93-13767
Numerical investigation of non-spherical droplet dynamics in viscous convective flows p 591 N93-13918
Flow prediction for three-dimensional intakes and ducts using viscous-inviscid interaction methods p 592 N93-13953
IODIDES
Synthesis of derivatives of alpha, omega difunctional perfluoroaliphatic compounds for low dielectric constant resins
[AD-A254928] p 550 N93-13026
IODINE
Real-time quality assurance testing using photonic techniques: Application to iodine water system
[NASA-CR-184413] p 619 N93-12692
Planar measurement of flow field parameters in nonreacting supersonic flows with laser-induced iodine fluorescence p 495 N93-13801
Gas-phase reactions of halogen species of atmospheric importance p 658 N93-13889
ION ACCELERATORS
Laser formation of lithium plasma ion sources for applied-B ion diodes on the PBFA-2 accelerator
[DE92-016091] p 716 N93-13191
The ORNL radioactive ion beam project with the ORIC accelerator
[DE92-040027] p 708 N93-13574
ION BEAMS
Uses of Monte Carlo computer simulations in understanding epitaxial growth and ion bombardment of Si(001)
[DE92-016944] p 719 N93-12586
A study of the vacancy loop formation probability in Ni-Cu and Ag-Pd alloys
[DE92-019584] p 541 N93-12879
Dynamics of the ion-ion acoustic instability in the thermalization of ion beams
[DE92-019396] p 714 N93-12914
Enhancement of ion transmission and reduction of background and interferences in inductively coupled plasma mass spectrometry
[DE92-018805] p 596 N93-12921
Influence of dilute impurities on the evolution of defect cascades in nickel
[DE92-019585] p 542 N93-12973
Photodissociation processes
[PB92-222702] p 702 N93-13067
Laser formation of lithium plasma ion sources for applied-B ion diodes on the PBFA-2 accelerator
[DE92-016091] p 716 N93-13191
Video profile monitor diagnostic system for GTA
[DE92-040231] p 710 N93-13509
Study of heliumlike neon using an electron beam ion trap
[DE92-019544] p 753 N93-13536
The ORNL radioactive ion beam project with the ORIC accelerator
[DE92-040027] p 708 N93-13574
Ion-beam-assisted deposition of MoS2 and other low-friction films
[AD-A255222] p 554 N93-13862
Comparison of heavy ion and electron-beam upset data for GaAs
[AD-A255901] p 708 N93-14089
ION CHARGE
Observations of solar wind ion charge exchange in the comet Halley coma p 752 N93-13467
ION CURRENTS
Electrochemical and chemical characteristics of a new ambient temperature Li(I) polymer electrolyte
[AD-A254918] p 545 N93-12651
Silicon neuron
[AD-A255091] p 674 N93-12756
ION DENSITY (CONCENTRATION)
An ion budget for a terra firme rainforest in Central Amazonia
[INPE-5365-PRE/1745] p 632 N93-13005
A study of ion composition and dynamics at Comet Halley
[NASA-CR-188478] p 751 N93-13465
Interpretation of the ion mass spectra in the mass range 25-35 obtained in the inner coma of Halley's comet by the HIS-sensor of the Giotto IMS Experiment p 752 N93-13469
A statistical study of narrow bandwidth, high-latitude geomagnetic pulsations p 660 N93-14068
ION DISTRIBUTION
Halogen surface chemistry on Si(100)-(2x1)
[AD-A254643] p 536 N93-12618
ION ENGINES
Particle simulation of grid erosion in an ion thruster p 527 N93-13927

ION IMPLANTATION
Enhancement of ion transmission and reduction of background and interferences in inductively coupled plasma mass spectrometry
[DE92-018805] p 596 N93-12921
Intrinsic bistable photonic materials by copper colloid formation in silica
[AD-A255505] p 711 N93-13866
ION IRRADIATION
Experimental studies of cascade phenomena in metals
[DE92-019586] p 540 N93-12573
Uses of Monte Carlo computer simulations in understanding epitaxial growth and ion bombardment of Si(001)
[DE92-016944] p 719 N93-12586
Radiation-disorder and aperiodicity in irradiated ceramics
[DE92-015051] p 552 N93-13350
ION PROPULSION
Particle simulation of grid erosion in an ion thruster
p 527 N93-13927
ION SOURCES
Enhancement of ion transmission and reduction of background and interferences in inductively coupled plasma mass spectrometry
[DE92-018805] p 596 N93-12921
Laser formation of lithium plasma ion sources for applied-B ion diodes on the PBFA-2 accelerator
[DE92-016091] p 716 N93-13191
Ion-beam-assisted deposition of MoS2 and other low-friction films
[AD-A255222] p 554 N93-13862
ION TEMPERATURE
Recent Nova experimental results
[DE92-019783] p 715 N93-13105
ION TRAPS (INSTRUMENTATION)
Study of heliumlike neon using an electron beam ion trap
[DE92-019544] p 753 N93-13536
IONIC COLLISIONS
Heavy-ion collisions and the nuclear equation of state
[DE92-019364] p 706 N93-12924
Spectroscopic studies of low-density gas in the Galactic disk and halo p 753 N93-13499
IONIC CRYSTALS
Transport on fractal networks
[AD-A253797] p 725 N93-13881
IONIC MOBILITY
Artificial intelligence and neural networks applied to ion mobility spectrometry
[DE92-017508] p 690 N93-12559
Enhancement of ion transmission and reduction of background and interferences in inductively coupled plasma mass spectrometry
[DE92-018805] p 596 N93-12921
IONIZATION
Capillary electrophoresis: Electrospray ionization mass spectrometry in small diameter capillaries
[DE92-019123] p 575 N93-12711
Resonance ionization mass spectrometry in biochemical analysis
[DE92-017407] p 538 N93-13341
Densities and abundances of hot cometary ions in the coma of P/Halley p 752 N93-13466
Electron temperature of Gd plasma produced by laser resonance ionization
[DE91-017785] p 718 N93-13732
CO2 laser preionisation
[NASA-CR-184424] p 607 N93-13797
IONIZED GASES
Spectroscopic studies of low-density gas in the Galactic disk and halo p 753 N93-13499
A study of the neutral and ionized gas in the interstellar medium and galactic H 2 regions p 756 N93-13853
IONIZERS
Characterization of electric discharge in air produced by an environmental ionizator
[INPE-5310-NTC/299] p 651 N93-13310
IONIZING RADIATION
Katz model prediction of Caenorhabditis elegans mutagenesis on STS-42
[NASA-TM-4383] p 674 N93-13023
Effects of ionizing radiation on scintillators and other particle detectors
[DE92-018184] p 705 N93-13531
IONOPAUSE
Observations of plasma dynamics in the coma of P/Halley by the Giotto Ion Mass Spectrometer
p 752 N93-13468
IONOSPHERIC CURRENTS
Extremely low frequency/very low frequency Generator
[AD-A254347] p 562 N93-12948
IONOSPHERIC DISTURBANCES
Extremely low frequency/very low frequency Generator
[AD-A254347] p 562 N93-12948
Experimental studies of ionospheric irregularities and related plasma processes
[NASA-CR-191271] p 652 N93-13460
IONOSPHERIC ION DENSITY
A joint study of the lower ionosphere by radar, lidar, and spectrometer p 655 N93-13755
IONOSPHERIC PROPAGATION
Obtaining medians and other quantiles with limited memory space
[AD-A254506] p 683 N93-12722
IONS
Fast ion-driven Bernstein instabilities
[DE92-019393] p 705 N93-12713
Structure sensitive reactions over Co, Fe and mixed metal clusters in zeolites
[DE92-040359] p 542 N93-12998
Cross sections and rate coefficients for the electron-impact excitation of He-like ions
[ISAS-RN-647] p 703 N93-13095
Ring current oxygen interaction with micropulsations
p 651 N93-13149
Densities and abundances of hot cometary ions in the coma of P/Halley p 752 N93-13466
IRON
Studies of the kinetics and mechanisms of perfluoroether reactions on iron and oxidized iron surfaces
[NASA-CR-191363] p 539 N93-13763
Electrolytic smelting of lunar rock for oxygen, iron, and silicon p 761 N93-13979
IRON ALLOYS
Weak-beam imaging of dissociated dislocations in HVEM-irradiated Fe-Ni-Cr alloys
[DE92-019587] p 541 N93-12798
Development of weldable high-strength iron aluminides
[DE92-016018] p 542 N93-13190
Environmental effects on iron aluminides
[DE92-016341] p 542 N93-13237
The implications of the magnetism of ordinary chondrites p 755 N93-13795
IRON OXIDES
Studies of the kinetics and mechanisms of perfluoroether reactions on iron and oxidized iron surfaces
[NASA-CR-191363] p 539 N93-13763
IRRADIATION
Influence of cold work level on the irradiation creep and creep rupture of titanium-modified austenitic stainless steels
[DE92-019078] p 541 N93-12820
Influence of dilute impurities on the evolution of defect cascades in nickel
[DE92-019585] p 542 N93-12973
IRREVERSIBLE PROCESSES
Connection of microscopic with macroscopic dynamics: Towards a hydrodynamical description of quantum mechanics p 729 N93-13957
IRRIGATION
Field spectroradiometry and sail model application to irrigated wheat (Triticum aestivum, L) canopies spectral reflectance
[INPE-5426-TDI/483] p 634 N93-13258
ISOELECTRONIC SEQUENCE
Strained-layer InGaAs-GaAs-AlGaAs quantum well lasers and transverse junction stripe lasers
p 607 N93-13773
ISOLATION
A core facility for the study of neurotoxins of biological origin
[AD-A254359] p 674 N93-12945
ISOMERIZATION
Structure sensitive reactions over Co, Fe and mixed metal clusters in zeolites
[DE92-040359] p 542 N93-12998
ISOPARAMETRIC FINITE ELEMENTS
Predictive forming of advanced thermoplastic composite structures p 529 N93-12835
Coupled structural/thermal/electromagnetic analysis/tailoring of graded composite structures
[NASA-CR-189150] p 626 N93-13443
Boundary element analysis of acoustical thin-body and nonuniqueness problems using a normal derivative integral equation p 631 N93-13951
ISOTHERMAL PROCESSES
Transverse flexural tests as a tool for assessing damage to PMR-15 composites from isothermal aging in air at elevated temperatures
[NASA-TM-105848] p 529 N93-12737
ISOTOPE SEPARATION
Isotopic separation of He-3/He-4 from solar wind gases evolved from the lunar regolith
[DE92-019339] p 759 N93-13504
ISOTOPIC ENRICHMENT
Isotopic separation of He-3/He-4 from solar wind gases evolved from the lunar regolith
[DE92-019339] p 759 N93-13504
ISOTROPIC MEDIA
An elasticity solution for a transversely isotropic material containing a spherical shell under axisymmetric loading
p 628 N93-13728
Interaction of energetic ring current protons with magnetospheric hydromagnetic waves
p 718 N93-13750
ISOTROPIC TURBULENCE
Interaction of isotropic turbulence with a shock wave
p 590 N93-13898
ISOTROPY
Contact of orthotropic laminates with a rigid spherical indentor p 533 N93-13778
ITERATION
A methodology for the solution of nonlinear two-point boundary value inverse problems in physics and engineering p 697 N93-13363
Computer modeling of flow and transport interactions for compressible Navier-Stokes equations
p 589 N93-13825
ITERATIVE SOLUTION
Speedup properties of phases in the execution profile of distributed parallel programs
[DE92-019301] p 689 N93-12797
Implementation details of the coupled QMR algorithm
[NASA-CR-191213] p 684 N93-12801
Speedup properties of phases in the execution profile of distributed parallel programs
[DE92-019965] p 689 N93-12810
Implicit application of polynomial filters in a k-step Arnoldi method
[NASA-CR-191237] p 686 N93-13408
Trim analysis by shooting and finite elements and Floquet eigenanalysis by QR and subspace iterations in helicopter dynamics p 501 N93-13914
IUE
SO2 on Venus: A final cross-calibration with Pioneer Venus
[NASA-CR-191256] p 758 N93-13344
International Ultraviolet Explorer (IUE) ultraviolet spectral atlas of selected astronomical objects
[NASA-RP-1285] p 744 N93-13461
Comparison of cometary comae using ultraviolet spectroscopy: Composition and variation
p 753 N93-13603
The Jovian ultraviolet aurora observed with the IUE spacecraft: Brightness and color distribution with longitude p 759 N93-13625

J

J INTEGRAL
Shallow-crack toughness results for reactor pressure vessel steel
[DE92-017813] p 626 N93-13320
JAHN-TELLER EFFECT
Studies of orbital doublet and modelling of orbital triplet Jahn-Teller systems in 3 to 5 semiconductors
p 725 N93-13845
JAMMING
Acousto-optic applications for multichannel adaptive optical processor
[AD-A255823] p 711 N93-14032
JAPAN
JARE data reports no. 179 (meteorology 29). Meteorological data at Asuka Station, Antarctica in 1990
p 663 N93-13287
US Industry Access to Japanese Science and Technology: Proceedings of a conference
[PB92-167964] p 741 N93-13788
Assessment of Japanese technology in advanced glass and ceramic fibers
[AD-A255229] p 553 N93-13836
JAPANESE SPACE PROGRAM
Spacelab J: Microgravity and life sciences
[NASA-CR-191353] p 516 N93-13564
JET ENGINES
An investigation of jet engine test cell aerodynamics by means of scale model test studies with comparisons to full-scale test results p 507 N93-14060
JET FLOW
Chaotic vortical motion in the near region of a plane jet p 493 N93-13493
Dynamics of vortex rings in cross-flow
p 496 N93-13917
JET MIXING FLOW
Exit plane H2O concentration measurements correlated with OH PLIF near-injector mixing measurements for scramjet flows p 603 N93-13687

A low-dimensional dynamical systems description of coherent structures in the axisymmetric jet mixing layer p 593 N93-14057

JET STREAMS (METEOROLOGY)
Meso-beta scale numerical simulation studies of terrain-induced jet streak mass/momentum perturbations [NASA-CR-191365] p 654 N93-13719
An observational and numerical investigation of meso-scale coastal processes during GALE IOP 2 p 665 N93-13776

JOINTS (JUNCTIONS)
Dynamic modeling and optimal joint torque coordination of advanced robotic systems p 617 N93-13936
Modelling flexible link manipulators in the three-dimensional space p 574 N93-14093

JUDGMENTS
Measures of user-system interface effectiveness: Assessment of structured judgment evaluation techniques for graphical, direct-manipulation style interfaces [AD-A254493] p 677 N93-12576

JUNCTION DIODES
Physics and technology of resonant-tunneling devices [AD-A255233] p 573 N93-13837

JUPITER ATMOSPHERE
The Jovian ionosphere p 758 N93-13337
The Jovian ultraviolet aurora observed with the IUE spacecraft: Brightness and color distribution with longitude p 759 N93-13625

K

K-EPSILON TURBULENCE MODEL
On the prediction of turbulent secondary flows [NASA-CR-189722] p 575 N93-12717
Wall functions for the kappa-epsilon turbulence model in generalized nonorthogonal curvilinear coordinates p 587 N93-13517

KALMAN FILTERS
Fixed-gain, two-stage estimators for tracking maneuvering targets [AD-A255832] p 697 N93-14081

KELVIN-HELMHOLTZ INSTABILITY
Spanwise-nonuniform excitation of a plane mixing layer p 577 N93-13120

KERNEL FUNCTIONS
On ascertaining inductively the dimension of the joint kernel of certain commuting linear operators [AD-A254748] p 696 N93-12847
Identification of parametric finite element models using experimental modal data [PB92-217819] p 558 N93-12976

KINEMATIC EQUATIONS
Enhanced accuracy for closed-loop robot p 617 N93-13808

KINEMATICS
Nonholonomic motion of free-flying space robots p 615 N93-13638

KINETIC ENERGY
Airblast damage from small asteroids [DE92-017834] p 749 N93-12956
Ring current oxygen interaction with micropulsations p 651 N93-13149
Analysis and experimental results for an extraction cavity for the split-cavity oscillator [DE92-040262] p 566 N93-13512
The kinetic energy budget of tropical plumes and ENSO in NMC and ECMWF analyses p 664 N93-13740
An experimental investigation of the three-dimensional boundary layer on a rotating disk p 589 N93-13806

KINETIC HEATING
Mechanical behaviour of fiber-reinforced ceramic matrix composites p 532 N93-13527

KINETIC THEORY
Fluidlike studies of the sheath and presheath regions of a plasma p 718 N93-13792

KINETICS
CO2 laser modeling [NASA-CR-184455] p 604 N93-12656
Measurements of crystal growth kinetics at extreme deviations from equilibrium [DE92-019744] p 720 N93-12627

KITS
Procedures for the diagnostic dose resistance test kits for mosquitoes, body lice, and beetle pests of stored products [AD-A255224] p 675 N93-13941

KLEBSIELLA
AFRRI reports [AD-A254581] p 674 N93-12649

KNUDSEN FLOW
Application of a vectorized particle simulation to the study of plates and wedges in high-speed rarefied flow p 495 N93-13746

KOLMOGOROFF THEORY
Cascade processes and fully developed turbulence p 591 N93-13901

KRYPTON
Influence of dilute impurities on the evolution of defect cascades in nickel [DE92-019585] p 542 N93-12973

KUIPER AIRBORNE OBSERVATORY
Thermal and nonthermal star formation: An investigation into the process of star formation as a function of stellar mass p 758 N93-14091

L

LABOR
Federal support to universities, colleges, and nonprofit institutions: Fiscal year 1990. A report to the President and Congress [NSF-92-324] p 741 N93-13543

LABORATORIES
Environmental Compliance Management System [DE92-019595] p 645 N93-13479
US Industry Access to Japanese Science and Technology: Proceedings of a conference [PB92-167964] p 741 N93-13788

LAMINAR BOUNDARY LAYER
Application of a solution adaptive grid to flow over an embedded cavity p 492 N93-13141
A fundamental study of suction for Laminar Flow Control (LFC) [NASA-CR-191276] p 583 N93-13277

LAMINAR FLOW
The program FANS-3D (finite analytic numerical simulation 3-dimensional) and its applications p 586 N93-13399

LAMINAR WAKES
A theoretical investigation of the growth rates of ice crystals in clouds p 653 N93-13485

LAMINATES
Properties of five toughened matrix composite materials [NASA-TP-3254] p 528 N93-12590
A study of the interlaminar stress continuity theories for composite laminates p 621 N93-12627
Hierarchic models for laminated plates p 528 N93-12629
Scale effects in buckling, postbuckling and crippling of graphite-epoxy Z-section stiffeners p 621 N93-12632
Probabilistic evaluation of fuselage-type composite structures [NASA-TM-105881] p 622 N93-12735
Consolidation of powder coated thermoplastic preform process modeling [AD-A255094] p 529 N93-12757
Predictive forming of advanced thermoplastic composite structures p 529 N93-12835
Influence of cure shrinkage on process-induced stress and deformation in thick thermosetting composites [AD-A254325] p 529 N93-12842
Microcracking, microcrack-induced delamination, and longitudinal splitting of advanced composite structures [NASA-CR-4472] p 623 N93-12911
Process designed for experimentation for increased-caliper Fresnel lenses [DE92-019464] p 709 N93-12918
An investigation of the thermoviscoplastic behavior of a metal matrix composite at elevated temperatures [NASA-CR-189706] p 530 N93-12929
Finite element analysis of anisotropic viscoelastic composite structures and analytical determination of optimum viscoelastic material properties p 530 N93-13007
Structural integrity of composites under load and thermal insult p 530 N93-13012
Compression strength of composite primary structural components [NASA-CR-190949] p 624 N93-13019
Enabling technologies for economical manufacturing of composites [AD-A253615] p 531 N93-13324
The shear gage and compact shear specimen for shear property measurements of composite materials p 628 N93-13630
Effects of layer waviness on compression-loaded thermoplastic composite laminates p 532 N93-13724
Studies on numerical and experimental determination of energy release rate for composite laminates p 533 N93-13752
Contact of orthotropic laminates with a rigid spherical indentor p 533 N93-13778
Investigations of the mechanical behavior of graphite/PEEK (APC-2) composites p 534 N93-13908
Finite elements for free edge delaminations and delaminated anisotropic beams p 535 N93-13967
The role of the fiber/matrix interphase in the static and fatigue behavior of polymeric matrix composite laminates p 535 N93-13968
Delamination initiation in postbuckled dropped-ply laminates p 535 N93-14030

LAND USE
The role of human activity and land use change in atmospheric chemistry and air quality [DE92-019622] p 642 N93-12880

LANDAU DAMPING
Fast wave current drive experiment on the D3-D tokamak [DE92-016253] p 716 N93-13193

LANDAU-GINZBURG EQUATIONS
Solutions without phase-slip for the Ginsburg-Landau equation [PB92-115575] p 696 N93-12889

LANDFILLS
Energy from Municipal Waste Program [DE92-010578] p 638 N93-13102

LANDSAT SATELLITES
Satellite imagery goes to the field [AD-A254449] p 632 N93-12598

LANGUAGES
Japanese/English machine translation using sublanguage patterns and reversible grammars p 686 N93-13494

LANTHANUM COMPOUNDS
Neutron scattering studies of the spin dynamics in La(2-x)Sr(x)O4 [DE92-019952] p 702 N93-13037

LAPLACE TRANSFORMATION
Analysis of a structure-equipment system subjected to impact loading [AD-A255097] p 622 N93-12652

LARGE DEPLOYABLE REFLECTOR
Large Deployable Reflector (LDR) system concept and technology definition study. Volume 1: Executive summary, analyses and trades, and system concepts [NASA-CR-177413-VOL-1] p 708 N93-12591
Large Deployable Reflector (LDR) system concept and technology definition study. Analysis of space station requirements for LDR [NASA-CR-177414] p 742 N93-12592
Large Deployable Reflector (LDR) system concept and technology definition study. Volume 2: Technology assessment and technology development plan [NASA-CR-177413-VOL-2] p 708 N93-12593

LARGE SPACE STRUCTURES
Innovative methods in the dynamics of large space structures [AD-A254630] p 521 N93-12579
Large Deployable Reflector (LDR) system concept and technology definition study. Volume 1: Executive summary, analyses and trades, and system concepts [NASA-CR-177413-VOL-1] p 708 N93-12591
Large Deployable Reflector (LDR) system concept and technology definition study. Analysis of space station requirements for LDR [NASA-CR-177414] p 742 N93-12592
Large Deployable Reflector (LDR) system concept and technology definition study. Volume 2: Technology assessment and technology development plan [NASA-CR-177413-VOL-2] p 708 N93-12593
Feasibility study of a synthesis procedure for array feeds to improve radiation performance of large distorted reflector antennas [NASA-CR-190948] p 561 N93-12655
Design of a welded joint for robotic, on-orbit assembly of space trusses [NASA-TM-108380] p 609 N93-12682
First steps to lunar manufacturing: Results of the 1988 Space Studies Institute Lunar Systems Workshop p 761 N93-13977

LASER ABLATION
Laser ablation for sample introduction in inductively coupled plasma spectrometry p 719 N93-13897

LASER ANEMOMETERS
The jet behaviour of an actual high-bypass engine as determined by LDA-measurements in ground tests p 503 N93-13218

LASER APPLICATIONS
Laser measurement techniques guide for a hazard evaluation [AD-A254545] p 604 N93-12610
Laser densification and doping of sol-gel glasses [AD-A254566] p 604 N93-12644
CO2 laser modeling [NASA-CR-184455] p 604 N93-12656
Noninvasive probing of the ocean surface using laser-based nonlinear optical methods [DE92-019431] p 669 N93-12916
Development of a laser ignited all secondary explosive DDT detonator [DE92-019340] p 555 N93-13081

Gas temperature measurements using the dual-line detection Rayleigh scattering technique
p 599 N93-13668
Laser-based strain measurements for high temperature applications p 601 N93-13675
Parameter studies of helium-neon lasers at 543 nm
p 606 N93-13747
Compact Blue-Green Lasers: Summaries of papers presented at the topical meeting. Volume 6: Technical digest series
[AD-A255001] p 608 N93-13883
Engineering planetary lasers for interstellar communication p 608 N93-14010
Results of the laser sensor technology transition investigation
[AD-A255845] p 608 N93-14085

LASER BEAMS
Workshop on Super-Intense Laser-Atom Physics
[AD-A254833] p 604 N93-12734
Photodissociation processes
[PB92-222702] p 702 N93-13067
Quantum well, beam deflecting surface emitting lasers
[NASA-CASE-NPO-18243-1-CU] p 605 N93-13418

LASER CAVITIES
Radiation-induced infrared absorption in nuclear-pumped laser cavity components
[DE92-017346] p 605 N93-13249

LASER DOPPLER VELOCIMETERS
The jet behaviour of an actual high-bypass engine as determined by LDA-measurements in ground tests
p 503 N93-13218
Airfoil-vortex interaction and the wake of an oscillating airfoil p 495 N93-13803

LASER FUSION
Characterizing laser fusion welded aluminum using synchrotron x ray microtomography
[DE92-018608] p 609 N93-12565
Recent Nova experimental results
[DE92-019783] p 715 N93-13105

LASER INDUCED FLUORESCENCE
Visualization of hydrogen injection in a scramjet engine by simultaneous PLIF imaging and laser holographic imaging p 602 N93-13683
Planar laser-induced fluorescence measurements of high-enthalpy free jet flow with nitric oxide
p 595 N93-13685
Planar laser-induced fluorescence imaging of OH in the exhaust of a bi-propellant thruster p 602 N93-13686
Exit plane H2O concentration measurements correlated with OH PLIF near-injector mixing measurements for scramjet flows p 603 N93-13687
Planar measurement of flow field parameters in nonreacting supersonic flows with laser-induced iodine fluorescence p 495 N93-13801
Two-photon cooperative cascade superfluorescence
[AD-A255690] p 608 N93-14023

LASER INTERFEROMETRY
Elastic and plastic strain measurement in high temperature environment using laser speckle
p 600 N93-13673

LASER MATERIALS
Stimulated Brillouin processes in crystals and glasses
[DE92-019549] p 721 N93-12887
Radiation-induced infrared absorption in nuclear-pumped laser cavity components
[DE92-017346] p 605 N93-13249
JPRS report: Science and technology. Central Eurasia: Physics and mathematics
[JPRS-UPM-92-006] p 698 N93-13303

LASER MODES
A study of techniques for single frequency operation of diode-pumped Nd:YAG lasers p 606 N93-13629

LASER OUTPUTS
Arm length matching in 10 m delay-line interferometer
[ISAS-TN-649] p 596 N93-12639
Small-scale x ray laser systems
[DE92-018442] p 604 N93-12744
Numerical modelling of the suppression of stimulated Brillouin scattering due to finite laser bandwidth
[DE92-018064] p 606 N93-13534
A study of techniques for single frequency operation of diode-pumped Nd:YAG lasers p 606 N93-13629
Demonstration of a neon-like rubidium x ray laser
[DE92-019576] p 606 N93-13653
Parameter studies of helium-neon lasers at 543 nm
p 606 N93-13747
CO2 laser preionisation
[NASA-CR-184424] p 607 N93-13797

LASER PLASMA INTERACTIONS
Laser ablation for sample introduction in inductively coupled plasma spectrometry p 719 N93-13897

LASER PLASMAS
Development of XUV projection lithography at 60 to 80 nm
[DE92-017517] p 603 N93-12560
Self-consistent one-dimensional modelling of x ray laser plasmas
[DE92-019543] p 712 N93-12571
Table-top x ray lasing based on optical-field-induced ionization
[DE92-019374] p 604 N93-12925
Laser formation of lithium plasma ion sources for applied-B ion diodes on the PBFA-2 accelerator
[DE92-016091] p 716 N93-13191
Methods for efficient pumping of vacuum ultraviolet lasers p 606 N93-13626
Electron temperature of Gd plasma produced by laser resonance ionization
[DE91-017785] p 718 N93-13732
Laser ablation for sample introduction in inductively coupled plasma spectrometry p 719 N93-13897

LASER PUMPING
Radiation-induced infrared absorption in nuclear-pumped laser cavity components
[DE92-017346] p 605 N93-13249
Methods for efficient pumping of vacuum ultraviolet lasers p 606 N93-13626
A study of techniques for single frequency operation of diode-pumped Nd:YAG lasers p 606 N93-13629

LASER SPECTROSCOPY
High-resolution investigation of degenerate four-wave mixing in the (gamma)(0,0) band of nitric oxide
[DE92-005312] p 537 N93-13232
High-resolution resonant degenerate 4-wave mixing spectroscopy
[DE92-012146] p 538 N93-13234
Resonance ionization mass spectrometry in biochemical analysis
[DE92-017407] p 538 N93-13341
Methods for efficient pumping of vacuum ultraviolet lasers p 606 N93-13626
Laser spectroscopy of rare earth ions
p 608 N93-13846
Laser ablation for sample introduction in inductively coupled plasma spectrometry p 719 N93-13897

LASER STABILITY
Arm length matching in 10 m delay-line interferometer
[ISAS-TN-649] p 596 N93-12639

LASER TARGET INTERACTIONS
Workshop on Super-Intense Laser-Atom Physics
[AD-A254833] p 604 N93-12734

LASER TARGETS
Recent Nova experimental results
[DE92-019783] p 715 N93-13105

LASER WELDING
Characterizing laser fusion welded aluminum using synchrotron x ray microtomography
[DE92-018608] p 609 N93-12565

LASERS
Laser measurement techniques guide for a hazard evaluation
[AD-A254545] p 604 N93-12610
Numerical modelling of the suppression of stimulated Brillouin scattering due to finite laser bandwidth
[DE92-018064] p 606 N93-13534
Compact Blue-Green Lasers: Summaries of papers presented at the topical meeting. Volume 6: Technical digest series
[AD-A255001] p 608 N93-13883

LASING
Table-top x ray lasing based on optical-field-induced ionization
[DE92-019374] p 604 N93-12925
Theory of lasing without population inversion
p 605 N93-13497

LATCH-UP
On the suitability of non-hardened high density SRAMs for space applications
[AD-A255898] p 524 N93-14087

LATCHES
Preloaded latching device
[NASA-CASE-MSC-21730-1] p 614 N93-13417

LATENT HEAT
The role of latent heat release in explosive cyclogenesis
[AD-A254436] p 660 N93-12596
Performance of the Bowen ratio systems on a 22 deg slope
[NASA-CR-191278] p 644 N93-13254
Conceptual design of a lunar base thermal control system p 680 N93-14003

LATERAL STABILITY
Effects of forebody strakes and Mach number on overall aerodynamic characteristics of configuration with 55 deg cropped delta wing
[NASA-TP-3253] p 493 N93-13353

LATTICE PARAMETERS
An investigation of the interatomic bonding characteristics of a Ti - 51 atomic percent Al alloy by x ray diffraction
[AD-A245362] p 544 N93-13945

LATTICES (MATHEMATICS)
On ascertaining inductively the dimension of the joint kernel of certain commuting linear operators
[AD-A254748] p 696 N93-12847

LAUNCH VEHICLES
Air inlet with variable intake section: Application to air breathing launch vehicles p 582 N93-13231

LAUNCHERS
The DSI small satellite launcher p 511 N93-13180

LAUNCHING
Debris/ice/TPS assessment and integrated photographic analysis for Shuttle mission STS-47
[NASA-TM-107553] p 520 N93-13032
Space Shuttle orbiter modifications to support Space Station Freedom
[NASA-TM-108050] p 520 N93-13455

LAUNCHING BASES
Ever watchful
[ESA-BR-37-1] p 517 N93-13903

LAY-UP
Process comparison study. MSFC Center Director's Discretionary Fund (CDDF)
[NASA-TM-108382] p 526 N93-13429

LAYOUTS
World Energy Projection System (WEPS), March 1992. Model installation manual, distribution disk layout
[PB92-169572] p 637 N93-12937
Magnetic bearings for a high-performance optical disk buffer, volume 2
[NASA-CR-190874] p 615 N93-13608

LEAD ACID BATTERIES
Proper battery system design for GAS experiments
p 511 N93-13176
Battery selection for space experiments
p 512 N93-13184

LEAF AREA INDEX
Field spectroradiometry and sail model application to irrigated wheat (Triticum aestivum, L) canopies spectral reflectance
[INPE-5426-TDI/483] p 634 N93-13258

LEAKAGE
Thermal issues at the SSC p 584 N93-13387
Application of passive dosimetry for detection of leaking underground storage tanks
[PB92-218270] p 559 N93-13648

LEARNING
Learning and using methodologies in information systems analysis and design p 739 N93-14058

LEARNING THEORY
Myths and legends in learning classification rules
[NASA-CR-191236] p 693 N93-13366

LEAST SQUARES METHOD
Analysis of a linearly constrained least squares algorithm for adaptive beamforming
[AD-A255017] p 695 N93-12582
Computer program for calculating and fitting thermodynamic functions
[NASA-RP-1271] p 728 N93-12967
Estimation of EOF expansion coefficients from incomplete data
[AD-A255252] p 697 N93-13886

LECTURES
Lecture notes for criticality safety
[DE92-016009] p 701 N93-12832

LEGAL LIABILITY
US Antarctic program. Personnel manual, 1992
[NSF-92-63] p 731 N93-12637

LENSES
Large area projection liquid-crystal video display system with inherent grid pattern optically removed
[NASA-CASE-NPO-16932-2-CU] p 711 N93-13711

LEPTONS
Electromagnetic lepton-pair production in relativistic collisions
[DE92-011069] p 706 N93-12829
The spin of the nucleon in deep inelastic lepton scattering experiments
[DE92-018854] p 702 N93-13073

LEVERS
Preloaded latching device
[NASA-CASE-MSC-21730-1] p 614 N93-13417

LIBRARIES
The long hold: Storing data at the National Archives
p 737 N93-13139

LICHENS
Abstracts of papers presented at the International Symposium on Time, Frequency, and Dating in Geomorphology
[AD-A254927] p 649 N93-12704

LIE GROUPS
Applications of group-invariant analytic solutions to inertial confinement fusion
[DE92-040347] p 715 N93-13047

LIFE (DURABILITY)
Thermal barrier coating life prediction model development, phase 2
[NASA-CR-189111] p 544 N93-12589
Verification and validation of AI software
[AD-A254601] p 682 N93-12614
LIFE CYCLE COSTS
Alternative systems for fuel gas boosters for small gas turbine engines
[PB92-223049] p 612 N93-12977
Business analysis: The commercial mission of the International Asteroid Mission p 514 N93-13554
LIFE SCIENCES
Publications of the space physiology and countermeasures program, Musculoskeletal Discipline: 1980-1990
[NASA-CR-4468] p 743 N93-12898
JPRS report: Science and technology. Central Eurasia: Life sciences
[JPRS-ULS-92-024] p 672 N93-13033
First International Microgravity Laboratory
[NASA-TM-108007] p 518 N93-13113
JPRS report: Science and technology. Central Eurasia: Space
[JPRS-USP-92-004] p 513 N93-13282
Assessment of programs in space biology and medicine
[NASA-CR-190930] p 672 N93-13327
A health care system for the Space Station
[NASA-TM-108093] p 679 N93-13571
SLS-1 flight experiments preliminary significant results
[NASA-TM-108033] p 520 N93-13613
LIFE SUPPORT SYSTEMS
ECLSS evolution: Advanced instrumentation interface requirements. Volume 3: Appendix C
[NASA-CR-184367] p 678 N93-12990
Use of antarctic analogs to support the space exploration initiative
[NASA-TM-108000] p 651 N93-13326
Engineering and architectural issues associated with the asteroid mission p 514 N93-13556
Lunar resource recovery: A definition of requirements p 761 N93-13978
The environmental control and life-support system for a lunar base: What drives its design p 680 N93-13991
Life systems for a lunar base p 680 N93-13992
Lunar base CELSS: A bioregenerative approach p 680 N93-13993
Crop growth and associated life support for a lunar farm p 680 N93-13994
Engineering verification of the biomass production chamber p 680 N93-13996
Scenarios for optimizing potato productivity in a lunar CELSS p 680 N93-13997
Potential of derived lunar volatiles for life support p 680 N93-13998
Technology development for lunar base water recycling p 680 N93-13999
Plasma reactor waste management systems p 680 N93-14000
Distribution of human waste samples in relation to sizing waste processing in space p 680 N93-14001
LIFT
New methods for predicting nonlinear lift, center of pressure, and pitching moment on missile configurations
[AD-A255078] p 492 N93-12741
Dynamic stall effects on hingeless rotor stability with experimental correlation p 492 N93-13010
Investigation of interference phenomena of modern wing-mounted high-bypass-ratio engines by the solution of the Euler-equations p 578 N93-13204
LIFT DRAG RATIO
Physiologically constrained aerocapture for manned Mars missions
[NASA-TM-103954] p 521 N93-12720
LIGANDS
Oligomer and mixed-metal compounds potential multielectron transfer catalysts
[DE92-011347] p 543 N93-13346
LIGHT AMPLIFIERS
Organization of the Optical Society of America Photonic Science Topical Meeting Series. Volume 8: Integrated photonics research. Ilfornia on 9-11 april 1991
[AD-A254682] p 709 N93-12666
OSA proceedings of the topical meeting on optical amplifiers and their applications, volume 13
[AD-A252974] p 711 N93-13879
LIGHT EMITTING DIODES
Compact Blue-Green Lasers: Summaries of papers presented at the topical meeting. Volume 6: Technical digest series
[AD-A255001] p 608 N93-13883
LIGHT MODULATION
Infrared image projector utilizing a deformable mirror device spatial light modulator
[AD-D015373] p 710 N93-13500
Acousto-optic applications for multichannel adaptive optical processor
[AD-A255823] p 711 N93-14032
LIGHT SCATTERING
Numerical modelling of the suppression of stimulated Brillouin scattering due to finite laser bandwidth
[DE92-018064] p 606 N93-13534
Measurement of tropospheric temperature and aerosol extinction using high spectral resolution lidar p 653 N93-13614
LIGHTING EQUIPMENT
Integration of exterior lighting systems and night vision imaging systems
[AD-A254826] p 677 N93-12732
LINE SHAPE
High-resolution investigation of degenerate four-wave mixing in the (gamma)(0,0) band of nitric oxide
[DE92-005312] p 537 N93-13232
LINE SPECTRA
High-resolution investigation of degenerate four-wave mixing in the (gamma)(0,0) band of nitric oxide
[DE92-005312] p 537 N93-13232
MCFC diagnostics: HCl detection
[DE92-001292] p 639 N93-13313
The emission-line properties of quasars p 753 N93-13487
Methods for efficient pumping of vacuum ultraviolet lasers p 606 N93-13626
An infrared polarimetric study of sunspots p 770 N93-13627
A study of the neutral and ionized gas in the interstellar medium and galactic H 2 regions p 756 N93-13853
LINEAR ACCELERATORS
A simple model for SLC positron stability issues
[DE92-019644] p 706 N93-12992
Test of QED using a laser at the SLAC final focus test beam
[DE92-019647] p 707 N93-12993
Suppression of the e(-) coextracted from a Penning surface-plasma H(-) source
[DE92-040350] p 714 N93-12997
RF system description for the ground test accelerator radio-frequency quadrupole
[DE92-040239] p 563 N93-13045
Test of a new RF separator structure for CEBAF
[CEBAF-PR-92-024] p 708 N93-13284
Initial performance of Los Alamos Advanced Free Electron Laser
[DE92-040214] p 605 N93-13507
Design and operation of a bunched-beam, phase-spread measurement
[DE92-040230] p 708 N93-13508
Video profile monitor diagnostic system for GTA
[DE92-040231] p 710 N93-13509
Special MAFIA postprocessors for the analysis of RF structures
[DE92-040248] p 565 N93-13510
LINEAR ENERGY TRANSFER (LET)
A study of the generation of linear energy transfer spectra for space radiations
[NASA-TM-4410] p 772 N93-13572
Comparison of heavy ion and electron-beam upset data for GaAs
[AD-A255901] p 708 N93-14089
LINEAR EQUATIONS
Implementation details of the coupled QMR algorithm
[NASA-CR-191213] p 684 N93-12801
LINEAR OPERATORS
On ascertaining inductively the dimension of the joint kernel of certain commuting linear operators
[AD-A254748] p 696 N93-12847
LINEAR POLARIZATION
Electron impact polarization expected in solar EUV lines from flaring chromospheres/transition regions
[SSL-PREPRINT-90-124] p 770 N93-13478
An infrared polarimetric study of sunspots p 770 N93-13627
Development of a stable electro-optical modulator
[NASA-CR-184404] p 710 N93-13696
LINEAR PROGRAMMING
Numerical optimization
[AD-A254575] p 682 N93-12647
Sensitivity analysis of the simultaneous proportionate change of inputs and outputs in data envelopment analysis
[AD-A254821] p 683 N93-12730
Fast approximation algorithms for multicommodity flow problems
[AD-A254335] p 685 N93-12961
LINEAR QUADRATIC GAUSSIAN CONTROL
Robust controller and estimator design using minimax methods p 694 N93-13925
On a robust controller design using a minimax *optimization approach* p 695 N93-14021
LINEAR QUADRATIC REGULATOR
Control of a very flexible robot in gravity p 615 N93-13541
Application of adaptive trusses to vibration isolation in flexible structures p 617 N93-13809
LINEAR SYSTEMS
Identification of parametric finite element models using experimental modal data
[PB92-217819] p 558 N93-12976
Identifiability of linear systems in physical coordinates
[NASA-TM-107695] p 625 N93-13125
LINGUISTICS
Perception-based and machine-oriented signal processing within speech understanding systems p 692 N93-13239
Recent developments in the NL-Soar garden path theory
[AD-A255889] p 688 N93-13944
LIQUEFIED NATURAL GAS
Dense-gas dispersion advection-diffusion model
[DE92-019617] p 642 N93-12884
White paper: Preliminary assessment of LNG vehicle technology, economics, and safety issues, revision 1
[PB92-212943] p 615 N93-13644
LIQUID CHROMATOGRAPHY
Methods development for total organic carbon accountability
[NASA-CR-184438] p 672 N93-12949
LIQUID CRYSTALS
Characterization of thermotropic liquid crystalline polymer blends by positron annihilation lifetime spectroscopy
[AD-A253616] p 552 N93-13325
Scattering and order in thermotropic liquid crystals p 723 N93-13332
Large area projection liquid-crystal video display system with inherent grid pattern optically removed
[NASA-CASE-NPO-16932-2-CU] p 711 N93-13711
Phase conjugation using CO2 lasers p 607 N93-13812
Molecular theories and computer simulations of liquid crystals p 725 N93-13843
LIQUID HYDROGEN
Zero-gravity quantity gaging system
[NASA-CR-185602] p 556 N93-12699
LIQUID INJECTION
Single liquid source plasma enhanced metalorganic chemical vapor deposition of YBa2Cu3O(7-x) thin films
[AD-A254119] p 722 N93-13100
LIQUID LEVELS
Precision liquid-level measurement in deep tanks using a swept-RF resonant cavity
[DE92-017236] p 597 N93-13267
LIQUID METALS
Heat transfer in a liquid metal crucible with an integral blackbody cavity
[DE92-019640] p 576 N93-12825
Efficiency of an AMTEC recirculating test cell, experiments, and projections
[DE92-016811] p 571 N93-13196
LIQUID NITROGEN
Effect of vaporization on cryogenic spray dropsize measurement
[NASA-TM-105909] p 597 N93-13410
LIQUID OXYGEN
Zero-gravity quantity gaging system
[NASA-CR-185602] p 556 N93-12699
Impact of lunar oxygen production on direct manned Mars missions p 540 N93-13984
LIQUID PROPELLANT ROCKET ENGINES
Stability codes for a liquid rocket implemented for use on a PC
[NASA-CR-184453] p 525 N93-12659
Users manual for program SSFREQ intermediate mode stability curves: Developed for use on a PC computer
[NASA-CR-184452] p 682 N93-12675
Users manual for program ADMIT: Admittance and pressure transfer function developed for use on a PC computer
[NASA-CR-184450] p 682 N93-12676
Briefing notes on propulsion stability codes ADMIT, NYQUIST, and SSFREQ
[NASA-CR-184449] p 525 N93-12874
LIQUID ROCKET PROPELLANTS
Demand thrust pumped propulsion with automatic warm gas valving
[DE92-017435] p 525 N93-12840
Bipropellant spray combustion modeling in small rocket engines p 556 N93-13924
The influence of lunar propellant production on the cost-effectiveness of cislunar transportation systems p 556 N93-13983
Impact of lunar oxygen production on direct manned Mars missions p 540 N93-13984

LIQUID-GAS MIXTURES
The influence of mixture preparation in the intake port on the performance of a spark-ignited four-stroke engine p 613 N93-13331
LIQUID-SOLID INTERFACES
Dynamics and pattern selection at the crystal-melt interface
[DE92-040210] p 724 N93-13577
Heat transfer, fluid flow and interface shapes in floating-zone crystal growth p 724 N93-13739
LIQUIDS
Vapor to liquid ratio test as an indicator of volatility
[DOT/FAA/CT-TN92/40] p 537 N93-12897
A new apparatus for continuous countercurrent flow of solids and liquids
[DE92-011675] p 583 N93-13318
LITHIUM
Electrochemical and chemical characteristics of a new ambient temperature Li(I) polymer electrolyte
[AD-A254918] p 545 N93-12651
Li/SOCl battery technology: Problems and solutions
[AD-A254514] p 570 N93-12725
Laser formation of lithium plasma ion sources for applied-B ion diodes on the PBFA-2 accelerator
[DE92-016091] p 716 N93-13191
Thermally stable electrolytes for rechargeable lithium batteries, phase 2
[NASA-CR-190878] p 573 N93-13610
LITHIUM COMPOUNDS
Determination of the weight average molecular weight of SRM 1480
[PB92-222934] p 553 N93-13785
LITHIUM SULFUR BATTERIES
First year testing of prototype magnesium/manganese dioxide BA-4590/U battery
[AD-A255503] p 574 N93-13839
LITHOGRAPHY
Development of XUV projection lithography at 60 to 80 nm
[DE92-017517] p 603 N93-12560
Soft X Ray Projection Lithography Topical Meeting. Volume 8: Technical digest
[AD-A254756] p 709 N93-12850
LOAD DISTRIBUTION (FORCES)
Split torque transmission load sharing
[NASA-TM-105884] p 610 N93-12736
Load-transfer and crack bridging in fiber-toughened ceramic composites p 629 N93-13754
LOAD TESTS
The effects of compressive preloads on the compression-after-impact strength of carbon/epoxy
[NASA-TP-3303] p 529 N93-12678
On bilinearity of Manson-Coffin low-cycle-fatigue relationship
[NASA-TM-105840] p 622 N93-12739
LOADING
An elasticity solution for a transversely isotropic material containing a spherical shell under axisymmetric loading p 628 N93-13728
LOADS (FORCES)
Notch dimensions for three-point bend fracture specimens based on compliance analyses
[AD-A254641] p 620 N93-12580
Equations of motion of slung-load systems, including multilift systems
[NASA-TP-3280] p 503 N93-12815
Structural verification for GAS experiments p 511 N93-13175
Contact of orthotropic laminates with a rigid spherical indentor p 533 N93-13778
Atmospheric loading response of the solid earth and oceans p 659 N93-13955
LOCAL AREA NETWORKS
Coordinating Council. Eighth Meeting: Using the Internet
[NASA-TM-108019] p 734 N93-12673
DATA: How to generate, store, retrieve, communicate, and interpret it: Proceedings
[DE92-040405] p 735 N93-13000
HIPPI and Fibre Channel
[DE92-040346] p 689 N93-13046
User interface of DFQL: An object-oriented approach
[AD-A255225] p 687 N93-13835
LOCAL THERMODYNAMIC EQUILIBRIUM
Atoms and molecules in supernova 1987A p 699 N93-13851
LOG PERIODIC ANTENNAS
ILS mathematical modeling study of the effects of an ASR-9 structure at the Long Island MacArthur Airport, Islip, NY
[DOT/FAA/CT-TN92/25] p 506 N93-12668
LOGIC CIRCUITS
Testing and fault-tolerant design techniques for advanced digital architectures
[AD-A255013] p 681 N93-12707
BETA: Behavioral testability analyzer and its application to high-level test generation and synthesis for testability
[NASA-CR-191282] p 572 N93-13569
LOGIC DESIGN
Blackboard architectures for multi-agent planning
[AD-A255035] p 688 N93-12710
LOGIC PROGRAMMING
Blackboard architectures for multi-agent planning
[AD-A255035] p 688 N93-12710
LOGISTICS
Ground operations and logistics in the context of the International Asteroid Mission p 515 N93-13560
The environmental control and life-support system for a lunar base: What drives its design p 680 N93-13991
LONG DURATION EXPOSURE FACILITY
LDEF Materials Workshop 1991, part 1
[NASA-CP-3162-PT-1] p 545 N93-12769
LDEF materials: An overview of the interim findings p 546 N93-12770
LDEF atomic oxygen fluence update p 546 N93-12771
LDEF yaw and pitch angle estimates p 524 N93-12772
Materials SIG quantification and characterization of surface contaminants p 546 N93-12773
Z306 molecular contamination ad hoc committee results p 546 N93-12774
Long Duration Exposure Facility (LDEF) contamination modeling p 547 N93-12775
Surface contamination on LDEF exposed materials p 547 N93-12776
Sources and transport of silicone NVR p 547 N93-12777
Thermal control surfaces on the MSFC LDEF experiments p 547 N93-12778
Anodized aluminum on LDEF: A current status of measurements on chromic acid anodized aluminum p 544 N93-12779
Performance of thermal control tape in the protection of composite materials p 536 N93-12780
Fluorescence of thermal control coatings on S0069 and A0114 p 548 N93-12781
Long Duration Exposure Facility M0003-5 thermal control coatings on DoD flight experiment p 548 N93-12782
Skylab D024 thermal control coatings and polymeric films experiment p 548 N93-12784
Effects of the LDEF environment on the Ag/FEP thermal blankets p 548 N93-12785
Recession of FEP specimens from trays D11 and B7 p 549 N93-12786
Characterization of selected LDEF: Exposed polymer films and resins p 549 N93-12787
Effects of orbital exposure on Halar during the LDEF mission p 549 N93-12788
Long Duration Exposure Facility M0003-5 recent results on polymeric films p 549 N93-12789
Space environmental effects on silvered teflon thermal control surfaces
[AD-A255909] p 554 N93-14099
LONG DURATION SPACE FLIGHT
SLS-1 flight experiments preliminary significant results
[NASA-TM-108033] p 520 N93-13613
LONG RANGE WEATHER FORECASTING
Summary of 1992 Atlantic tropical cyclone activity and verification of author's forecast (a year of no hurricane activity in the tropics but exceptional South Florida destruction from an unusual higher latitude intense hurricane) p 662 N93-13028
LONGITUDINAL CONTROL
Ideal aircraft handling quality models: Longitudinal axis
[NAL-PD-FC-9203] p 504 N93-13566
LONGITUDINAL STABILITY
Aerodynamic integration of thrust reversers on the Fokker 100 p 502 N93-13208
Effects of forebody strakes and Mach number on overall aerodynamic characteristics of configuration with 55 deg cropped delta wing
[NASA-TP-3253] p 493 N93-13353
LOOPS
The Capillary Pumped Loop Flight Experiment (CAPL): A pathfinder for EOS p 512 N93-13181
LOSS OF COOLANT
Aluminum oxide film thickness and emittance
[DE92-019931] p 550 N93-13035
LOSSES
Bayesian estimation of system reliability under asymmetric loss p 620 N93-13906
LOSSLESS MATERIALS
Variance of phase fluctuations of waves propagating through a random medium p 569 N93-13087
LOSSY MEDIA
Variance of phase fluctuations of waves propagating through a random medium p 569 N93-13087
LOW ALTITUDE
Perceptual dimensions of visual scenes relevant for simulating low-altitude flight
[AD-A254645] p 676 N93-12662
LOW ASPECT RATIO
Diagnostics systems for the TBR-E tokamak
[INPE-5428-RPQ/662] p 716 N93-13257
LOW COST
Pressure fed thrust chamber technology program
[NASA-CR-184461] p 526 N93-12968
Large area projection liquid-crystal video display system with inherent grid pattern optically removed
[NASA-CASE-NPO-16932-2-CU] p 711 N93-13711
LOW GRAVITY MANUFACTURING
A microgravity processing plant for the manufacturing of propellant and water from asteroid ore p 515 N93-13558
LOW LEVEL TURBULENCE
Spatial characteristics of coherent turbulent structures and exchange processes in the atmospheric surface layer within and above an orchard canopy p 660 N93-14064
LOW PRESSURE
The influence of intake swirl distortion on the steady-state performance of a low bypass, twin-spool engine p 579 N93-13211
Ductile phase toughening of molybdenum disilicide by low pressure plasma spraying
[DE92-007409] p 551 N93-13315
LOW SPEED
Mass flow effects on the low speed characteristics of an advanced combat aircraft p 497 N93-13214
LOW SPEED WIND TUNNELS
Tests of models equipped with TPS in low speed ONERA F1 pressurized wind tunnel p 577 N93-13201
LUBRICANTS
Studies of the kinetics and mechanisms of perfluoroether reactions on iron and oxidized iron surfaces
[NASA-CR-191363] p 539 N93-13763
LUBRICATING OILS
The chemistry of the extreme pressure lubricant additive lead naphthenate on steel surfaces
[AD-A255828] p 544 N93-14098
LUBRICATION
Friction, wear and Raman spectroscopic characteristics of carbon lubricated surfaces p 618 N93-13949
LUMINESCENCE
Studies of surface-induced luminescence relevant to spacecraft glow, using a seeded arc-jet p 523 N93-13919
LUMINOSITY
The emission-line properties of quasars p 753 N93-13487
Molecular gas temperature and density in spiral galaxies p 748 N93-13688
A systematic search for low-mass companions orbiting nearby stars and the calibration of the end of the stellar main sequence p 749 N93-14070
LUNAR ATMOSPHERE
The Mount Wilson optical interferometer: The first automated instrument and the prospects for lunar interferometry p 745 N93-13582
The lunar environment and its effect on optical astronomy p 746 N93-13594
Environmental effects on an optical-UV-IR synthesis array p 747 N93-13595
An optical VLA on the Moon p 747 N93-13596
Required technologies for a lunar optical UV-IR synthesis array p 747 N93-13598
LUNAR BASED EQUIPMENT
Unit operations for gas-liquid mass transfer in reduced gravity environments p 557 N93-14011
LUNAR BASES
Use of antarctic analogs to support the space exploration initiative
[NASA-TM-108000] p 651 N93-13326
A Lunar Optical-Ultraviolet-Infrared Synthesis Array (LOUISA)
[NASA-CP-3066] p 744 N93-13579
Telescopes on the Moon or pie in the sky? p 746 N93-13591
Lunar interferometric astronomy: Some basic questions p 746 N93-13592
Required technologies for a lunar optical UV-IR synthesis array p 747 N93-13598
Report of the Working Group on Space/Lunar Tradeoffs p 747 N93-13599
Report of the Science Working Group: Science with a lunar optical interferometer p 747 N93-13600
Thermal control systems for low-temperature heat rejection on a lunar base
[NASA-CR-191286] p 679 N93-13717
The Second Conference on Lunar Bases and Space Activities of the 21st Century, volume 2
[NASA-CP-3166-VOL-2] p 760 N93-13972

Resources for a lunar base: Rocks, minerals, and soil of the Moon p 760 N93-13973
Applications for special-purpose minerals at a lunar base p 760 N93-13975
Water and cheese from the lunar desert: Abundances and accessibility of H, C, and N on the Moon p 761 N93-13976
Lunar resource recovery: A definition of requirements p 761 N93-13978
Availability of hydrogen for lunar base activities p 762 N93-13982
The influence of lunar propellant production on the cost-effectiveness of cislunar transportation systems p 556 N93-13983
Fusion energy from the Moon for the twenty-first century p 719 N93-13985
Synergism of He-3 acquisition with lunar base evolution p 540 N93-13986
Physical properties of concrete made with Apollo 16 lunar soil sample p 554 N93-13987
The possibility of concrete production on the Moon p 554 N93-13988
Concrete structure construction on the Moon p 559 N93-13989
Lunar concrete for construction p 555 N93-13990
The environmental control and life-support system for a lunar base: What drives its design p 680 N93-13991
Life systems for a lunar base p 680 N93-13992
Lunar base CELSS: A bioregenerative approach p 680 N93-13993
Crop growth and associated life support for a lunar farm p 680 N93-13994
Long-term lunar stations: Some ecological considerations p 648 N93-13995
Scenarios for optimizing potato productivity in a lunar CELSS p 680 N93-13997
Potential of derived lunar volatiles for life support p 680 N93-13998
Technology development for lunar base water recycling p 680 N93-13999
Conceptual design of a lunar base thermal control system p 680 N93-14003
Advanced photovoltaic power system technology for lunar base applications p 641 N93-14004
Solar water heating system for a lunar base p 641 N93-14005
Automation and robotics considerations for a lunar base p 619 N93-14006
Lunar surface mining for automated acquisition of helium-3: Methods, processes, and equipment p 766 N93-14007
Mobile work platform for initial lunar base construction p 559 N93-14009
The real world and lunar base activation scenarios p 680 N93-14014
Moon Park: A research and educational facility p 519 N93-14015
Lunar stepping stones to a manned Mars exploration scenario p 767 N93-14016
A basis of settlement: Economic foundations of permanent pioneer communities p 741 N93-14019
The lunar community church: Contributions to lunar living and to evolution of ethical and spiritual thinking p 676 N93-14020

LUNAR COMPOSITION
Resources for a lunar base: Rocks, minerals, and soil of the Moon p 760 N93-13973

LUNAR CONSTRUCTION EQUIPMENT
Mobile work platform for initial lunar base construction p 559 N93-14009

LUNAR EXCAVATION EQUIPMENT
Lunar surface mining for automated acquisition of helium-3: Methods, processes, and equipment p 766 N93-14007

LUNAR EXPLORATION
First International Microgravity Laboratory [NASA-TM-108007] p 518 N93-13113
Mobile work platform for initial lunar base construction p 559 N93-14009

LUNAR GEOLOGY
Resources for a lunar base: Rocks, minerals, and soil of the Moon p 760 N93-13973
The formation of ore mineral deposits on the Moon: A feasibility study p 760 N93-13974
Water and cheese from the lunar desert: Abundances and accessibility of H, C, and N on the Moon p 761 N93-13976

LUNAR GRAVITATION
Bone loss and human adaptation to lunar gravity p 676 N93-14002

LUNAR MARIA
Electrolytic smelting of lunar rock for oxygen, iron, and silicon p 761 N93-13979
Uses of lunar sulfur p 761 N93-13981

LUNAR MINING
Lunar mining of oxygen using fluorine [LPI-748] p 761 N93-13980
Synergism of He-3 acquisition with lunar base evolution p 540 N93-13986
Potential of derived lunar volatiles for life support p 680 N93-13998
Lunar surface mining for automated acquisition of helium-3: Methods, processes, and equipment p 766 N93-14007

LUNAR OBSERVATORIES
Support and servicing requirements for large observatories in space p 746 N93-13589
Lunar optical telescopes: An historical perspective p 746 N93-13593

LUNAR ORBITS
A guidance methodology for the cislunar transfer of low-thrust spacecraft p 517 N93-13766

LUNAR RESOURCES
Applications for special-purpose minerals at a lunar base p 760 N93-13975
Water and cheese from the lunar desert: Abundances and accessibility of H, C, and N on the Moon p 761 N93-13976
First steps to lunar manufacturing: Results of the 1988 Space Studies Institute Lunar Systems Workshop p 761 N93-13977
Lunar resource recovery: A definition of requirements p 761 N93-13978
Uses of lunar sulfur p 761 N93-13981
The influence of lunar propellant production on the cost-effectiveness of cislunar transportation systems p 556 N93-13983
Impact of lunar oxygen production on direct manned Mars missions p 540 N93-13984
Fusion energy from the Moon for the twenty-first century p 719 N93-13985
The possibility of concrete production on the Moon p 554 N93-13988
Concrete structure construction on the Moon p 559 N93-13989
Lunar base CELSS: A bioregenerative approach p 680 N93-13993
Potential of derived lunar volatiles for life support p 680 N93-13998
Conceptual design of a lunar base thermal control system p 680 N93-14003
Lunar surface mining for automated acquisition of helium-3: Methods, processes, and equipment p 766 N93-14007

LUNAR ROCKS
Isotopic separation of He-3/He-4 from solar wind gases evolved from the lunar regolith [DE92-019339] p 759 N93-13504
Resources for a lunar base: Rocks, minerals, and soil of the Moon p 760 N93-13973
Electrolytic smelting of lunar rock for oxygen, iron, and silicon p 761 N93-13979
Lunar mining of oxygen using fluorine [LPI-748] p 761 N93-13980

LUNAR ROVING VEHICLES
The Lunar Roving Vehicle: Historical perspective p 619 N93-14008

LUNAR SOIL
Test equipment data package for the KC-135 fiber pulling apparatus [NASA-CR-184446] p 506 N93-13013
Glass fiber processing for the Moon/Mars program: Center director's discretionary fund final report [NASA-TM-108379] p 551 N93-13115
Resources for a lunar base: Rocks, minerals, and soil of the Moon p 760 N93-13973
Water and cheese from the lunar desert: Abundances and accessibility of H, C, and N on the Moon p 761 N93-13976
Lunar resource recovery: A definition of requirements p 761 N93-13978
Electrolytic smelting of lunar rock for oxygen, iron, and silicon p 761 N93-13979
Uses of lunar sulfur p 761 N93-13981
Availability of hydrogen for lunar base activities p 762 N93-13982
Physical properties of concrete made with Apollo 16 lunar soil sample p 554 N93-13987
The possibility of concrete production on the Moon p 554 N93-13988
Potential of derived lunar volatiles for life support p 680 N93-13998

LUNAR SURFACE
The lunar environment and its effect on optical astronomy p 746 N93-13594
Availability of hydrogen for lunar base activities p 762 N93-13982
Synergism of He-3 acquisition with lunar base evolution p 540 N93-13986
Conceptual design of a lunar base thermal control system p 680 N93-14003
Lunar surface mining for automated acquisition of helium-3: Methods, processes, and equipment p 766 N93-14007

LUNAR SURFACE VEHICLES
Mobile work platform for initial lunar base construction p 559 N93-14009

LUNGS
Transactions: Tropospheric ozone and the environment. Papers from an international conference [PB92-217017] p 643 N93-12941

M

M STARS
A systematic search for low-mass companions orbiting nearby stars and the calibration of the end of the stellar main sequence p 749 N93-14070

MACH NUMBER
Effects of forebody strakes and Mach number on overall aerodynamic characteristics of configuration with 55 deg cropped delta wing [NASA-TP-3253] p 493 N93-13353
Investigation of hypersonic shock-induced combustion in a hydrogen-air system [NASA-CR-191239] p 538 N93-13456
An experimental/computational study of heat transfer in sharp fin induced shock wave/turbulent boundary layer interactions at low hypersonic Mach numbers p 590 N93-13826
Interaction of isotropic turbulence with a shock wave p 590 N93-13898
Stability of the compressible reacting mixing layer p 592 N93-13948

MACH-ZEHNDER INTERFEROMETERS
Fiber optic sensors for static fracture studies and dynamic wave propagation problems p 709 N93-12984

MACHINE LEARNING
Semantics-based reference resolution in technical text processing: An exploration of using the Word Net database in the computerized comprehensibility system [AD-A255068] p 736 N93-13117
Myths and legends in learning classification rules [NASA-CR-191236] p 693 N93-13366
Resource constrained design of artificial neural networks using comparator neural network [NASA-CR-191280] p 694 N93-13376
Explanation-based knowledge acquisition of electronics [AD-A255069] p 573 N93-13650
Research summary, January 1989 - June 1990 [NASA-CR-190960] p 687 N93-13694

MACHINE ORIENTED LANGUAGES
Monitoring and controlling distributed applications using Lomita (position paper) [NASA-CR-190971] p 687 N93-13695

MACHINE TRANSLATION
Japanese/English machine translation using sublanguage patterns and reversible grammars p 686 N93-13494

MACHINING
Ceramic machining: Assessment of current practice and research needs in the US [PB92-213511] p 553 N93-13649

MACROSCOPIC EQUATIONS
Connection of microscopic with macroscopic dynamics: Towards a hydrodynamical description of quantum mechanics p 729 N93-13957

MAGELLANIC CLOUDS
B supergiants in open clusters and associations [NASA-CR-191275] p 748 N93-13659
Atoms and molecules in supernova 1987A p 699 N93-13851

MAGMA
The formation of ore mineral deposits on the Moon: A feasibility study p 760 N93-13974

MAGNESIUM ALLOYS
Fatigue studies in Al-Mg-Si alloys p 543 N93-13690

MAGNESIUM ISOTOPES
Evidence for alpha-particle chain configurations in Mg-24 [DE92-018790] p 705 N93-13546

MAGNETIC ANOMALIES
Magnetic holes near the magnetopause p 653 N93-13491

MAGNETIC BEARINGS
Magnetic bearings for a high-performance optical disk buffer, volume 2 [NASA-CR-190874] p 615 N93-13608
Magnetic bearings for a high-performance optical disk buffer, volume 1 [NASA-CR-190873] p 616 N93-13706

MAGNETIC COMPRESSION
Advanced high-explosive flux compression generator development: The CN-3 series
[DE92-019962] p 713 N93-12809
MAGNETIC DISKS
Magnetic disk p 737 N93-13134
MAGNETIC EFFECTS
Investigation of effects of 60-Hz electric and magnetic fields on operant and social behavior and on the neuroendocrine system of nonhuman primates, part 2
[DE92-040153] p 673 N93-13503
Investigation of effects of 60-Hz electric and magnetic fields on operant and social behavior and on the neuroendocrine system of nonhuman primates, part 1
[DE92-040152] p 673 N93-13520
MAGNETIC ENERGY STORAGE
New power-conditioning systems for superconducting magnetic energy storage p 640 N93-13934
MAGNETIC FIELD CONFIGURATIONS
Ion radial diffusion in an electrostatic impulse model for stormtime ring current formation
[NASA-CR-190941] p 705 N93-12715
The 3-D description of vertical current sheets with application to solar flares
[SSL-PREPRINT-90-119] p 770 N93-13477
Biasing experiments on the Advanced Toroidal Facility
[DE92-040033] p 717 N93-13518
Equilibrium and eruption of solar coronal magnetic structures p 770 N93-13605
Review of stellarator research: In search of the magic magnetic bottle
[DE92-019045] p 718 N93-13651
MAGNETIC FIELD RECONNECTION
The 3-D description of vertical current sheets with application to solar flares
[SSL-PREPRINT-90-119] p 770 N93-13477
MAGNETIC FIELDS
Current density fluctuations, nonlinear coupling, and transport in MST
[DE92-041012] p 713 N93-12883
Magnetic field perturbation caused by bending vibrations of a quadrupole
[DE92-040644] p 623 N93-13003
A program to study antiprotons in the cosmic rays: Arizona collaboration
[NASA-CR-191272] p 772 N93-13306
Low-frequency fluctuations of plasma magnetic fields p 717 N93-13496
Investigation of effects of 60-Hz electric and magnetic fields on operant and social behavior and on the neuroendocrine system of nonhuman primates, part 2
[DE92-040153] p 673 N93-13503
Investigation of effects of 60-Hz electric and magnetic fields on operant and social behavior and on the neuroendocrine system of nonhuman primates, part 1
[DE92-040152] p 673 N93-13520
The lunar environment and its effect on optical astronomy p 746 N93-13594
Development of a stable electro-optical modulator
[NASA-CR-184404] p 710 N93-13696
The implications of the magnetism of ordinary chondrites p 755 N93-13795
A study of the luminosity produced by an electron beam-emitting rocket in the polar ionosphere: ECHO 7 p 657 N93-13830
High magnetic field studies of strained layer superlattices p 726 N93-13895
MAGNETIC FLUX
Advanced high-explosive flux compression generator development: The CN-3 series
[DE92-019962] p 713 N93-12809
MAGNETIC INDUCTION
On development of a three-dimensional particle motion tracking system
[DE92-015846] p 704 N93-13263
MAGNETIC MEASUREMENT
Magnetic behavior of a Bi(sub 2)Sr(sub 2)Ca(sub 1)Cu(sub 2)O(sub x) single crystal by direct magneto-optical observations
[DE92-018612] p 722 N93-13118
MAGNETIC MONOPOLES
Solitons and instantons in string theory p 728 N93-13753
MAGNETIC PERMEABILITY
Eddy current power dissipation at sharp corners
[DE92-016890] p 571 N93-13300
MAGNETIC PROPERTIES
Magnetic behavior of a Bi(sub 2)Sr(sub 2)Ca(sub 1)Cu(sub 2)O(sub x) single crystal by direct magneto-optical observations
[DE92-018612] p 722 N93-13118
Magnetic properties of high-T(sub c) superconductors p 726 N93-13905
MAGNETIC RESONANCE
Functional MRI studies of human vision on a clinical imager
[DE92-017448] p 674 N93-12566
Ring current oxygen interaction with micropulsations p 651 N93-13149
Interaction of energetic ring current protons with magnetospheric hydromagnetic waves p 718 N93-13750
MAGNETIC SIGNATURES
Optical design for a balloon-borne magnetograph
[NASA-CR-191003] p 709 N93-13062
Development of a stable electro-optical modulator
[NASA-CR-184404] p 710 N93-13696
MAGNETIC SPECTROSCOPY
Wide range, permanent magnet Compton spectrometer
[DE92-017312] p 596 N93-12762
MAGNETIC STORMS
Ion radial diffusion in an electrostatic impulse model for stormtime ring current formation
[NASA-CR-190941] p 705 N93-12715
Ring current oxygen interaction with micropulsations p 651 N93-13149
MAGNETIC SURVEYS
New approaches to estimation of magnetotelluric parameters
[DE92-040280] p 653 N93-13513
MAGNETIC TAPES
Magnetic tape p 737 N93-13135
MAGNETIC VARIATIONS
Measurement of current density fluctuations and ambipolar particle flux due to magnetic fluctuations in MST
[DE92-041013] p 713 N93-12878
MAGNETICALLY TRAPPED PARTICLES
Review of stellarator research: In search of the magic magnetic bottle
[DE92-019045] p 718 N93-13651
MAGNETIZATION
Magnetic hardening studies and novel techniques for preparation of high performance magnets
[AD-A254761] p 698 N93-12865
The implications of the magnetism of ordinary chondrites p 755 N93-13795
MAGNETO-OPTICS
Magnetic behavior of a Bi(sub 2)Sr(sub 2)Ca(sub 1)Cu(sub 2)O(sub x) single crystal by direct magneto-optical observations
[DE92-018612] p 722 N93-13118
MAGNETOHYDRODYNAMIC FLOW
Observations of plasma dynamics in the coma of P/Halley by the Giotto Ion Mass Spectrometer p 752 N93-13468
Structure of and dynamical processes in the Earth's magnetopause and boundary layer regions p 657 N93-13793
Wake characterization: Full flow simulation of space structures in low earth orbit p 497 N93-13970
Application of complex variables in electromagnetofluid dynamic, magnetofluid dynamic and fluid dynamic flows: Viscoelastic boundary-layer theory
[ISBN-0-315-65141-5] p 594 N93-14067
MAGNETOHYDRODYNAMIC STABILITY
Observations of correlated broadband electrostatic noise and electron cyclotron emissions in the plasma sheet
[AD-A255002] p 712 N93-12705
Fast ion-driven Bernstein instabilities
[DE92-019393] p 705 N93-12713
Plasma properties
[DE92-019982] p 713 N93-12811
Anomalous ion heating and superthermal electrons in the MST reversed-field pinch
[DE92-041011] p 713 N93-12882
Current density fluctuations, nonlinear coupling, and transport in MST
[DE92-041012] p 713 N93-12883
A simple model for SLC positron stability issues
[DE92-019644] p 706 N93-12992
Tokamak equilibria and transport based on Grad's thirteen moment description
[DE92-019960] p 715 N93-13038
Measurements of the temperature in the edge plasma of the CASTOR tokamak by a triple Langmuir probe
[IPPCZ-318] p 716 N93-13330
Biasing experiments on the Advanced Toroidal Facility
[DE92-040033] p 717 N93-13518
Equilibrium and eruption of solar coronal magnetic structures p 770 N93-13605
Review of stellarator research: In search of the magic magnetic bottle
[DE92-019045] p 718 N93-13651
Interaction of energetic ring current protons with magnetospheric hydromagnetic waves p 718 N93-13750
Theory of the ion-channel laser p 607 N93-13777
MAGNETOHYDRODYNAMIC WAVES
Fast wave current drive experiment on the D3-D tokamak
[DE92-016253] p 716 N93-13193
Low-frequency fluctuations of plasma magnetic fields p 717 N93-13496
Interaction of energetic ring current protons with magnetospheric hydromagnetic waves p 718 N93-13750
MAGNETOHYDRODYNAMICS
Advanced high-explosive flux compression generator development: The CN-3 series
[DE92-019962] p 713 N93-12809
Applications of group-invariant analytic solutions to inertial confinement fusion
[DE92-040347] p 715 N93-13047
Low-frequency fluctuations of plasma magnetic fields p 717 N93-13496
MAGNETOMETERS
Optical design for a balloon-borne magnetograph
[NASA-CR-191003] p 709 N93-13062
MAGNETOPAUSE
Magnetic holes near the magnetopause p 653 N93-13491
Structure of and dynamical processes in the Earth's magnetopause and boundary layer regions p 657 N93-13793
MAGNETOPLASMADYNAMICS
Scaling of 100 kW class applied-field MPD thrusters
[NASA-CR-190791] p 525 N93-12638
Anode power deposition in applied-field MPD thrusters
[NASA-CR-190790] p 526 N93-13283
MAGNETOSPHERE-IONOSPHERE COUPLING
Radar studies of high latitude convection flows p 648 N93-12626
MAGNETOSTATIC FIELDS
Analysis and modeling of the CRRES satellite data
[AD-A254349] p 650 N93-12944
MAGNETS
Fluid dynamics of supercritical helium within cable-in-conduit conductors
[DE92-019516] p 574 N93-12569
MAGNIFICATION
Gravitational lensing by galaxy clusters: The giant arcs in Abell 370 and Cl2244-02 p 755 N93-13848
MAGNITUDE
Evolution of galaxies in compact groups p 750 N93-13148
MAGNONS
Bipolaronic charge density waves, polaronic spin density waves and high T(c) superconductivity
[DE92-017403] p 720 N93-12853
MAIN SEQUENCE STARS
Studies of extra-solar Oort Clouds and the Kuiper disk
[NASA-CR-190958] p 769 N93-12669
International Ultraviolet Explorer (IUE) ultraviolet spectral atlas of selected astronomical objects
[NASA-RP-1285] p 744 N93-13461
Some problems of quantum cosmology and dark matter physics p 755 N93-13829
An optical study of the faint end of the stellar luminosity function p 748 N93-13960
MAINTENANCE
Scientific and engineering research facilities at universities and colleges: 1992
[NSF-92-325] p 506 N93-13407
MAN ENVIRONMENT INTERACTIONS
Sulfate impact upon low-level cloud albedo over oceans p 661 N93-12833
MAN MACHINE SYSTEMS
Operator workload predictions for the revised AH-64A workload prediction model. Volume 2: Appendixes A through H
[AD-A254939] p 676 N93-12545
Specification of adaptive aiding systems
[AD-A254537] p 499 N93-12602
MAN-COMPUTER INTERFACE
Measures of user-system interface effectiveness: Assessment of structured judgment evaluation techniques for graphical, direct-manipulation style interfaces
[AD-A254493] p 677 N93-12576
Human perceptual deficits as factors in computer interface test and evaluation
[DE92-019124] p 677 N93-12712
Ocular attention-sensing interface system
[NASA-CR-190884] p 678 N93-13450
User interface of DFQL: An object-oriented approach
[AD-A255225] p 687 N93-13835
Formal aspects of human-computer interaction p 679 N93-13909
Talking to InterFIS: Adding speech input to a natural language interface
[AD-A255865] p 688 N93-13942
A study of traditional information access models applied in a hypertext information system p 739 N93-14076

Human memory for the spatial locations of items on pull-down computer menus p 739 N93-14080

MANAGEMENT INFORMATION SYSTEMS

Principles of information resource management: A foundation for the future
[AD-A254447] p 733 N93-12597

Utilization of databases to manage resources
[DE92-019598] p 735 N93-12808

NSSDC Conference on Mass Storage Systems and Technologies for Space and Earth Science Applications, volume 1
[NASA-CP-3165-VOL-1] p 736 N93-13131

Engineering data transfer test with EDMICS using MIL-R-28002 (Raster)
[DE92-019808] p 738 N93-13619

MANAGEMENT METHODS

World Energy Projection System (WEPS), March 1992. Model installation manual, distribution disk layout
[PB92-169572] p 637 N93-12937

Research and technology in support of IAM p 515 N93-13562

Performance measurement for information systems: Industry perspectives
[NASA-CR-191369] p 738 N93-13737

MANAGEMENT PLANNING

Coordinating Council. Second Meeting: International Acquisitions
[NASA-TM-108015] p 733 N93-12634

Coordinating Council. Seventh Meeting: Acquisitions
[NASA-TM-108020] p 733 N93-12636

Coordinating Council. Third Meeting: STI Strategic Plans
[NASA-TM-108016] p 733 N93-12670

Energy from Municipal Waste Program
[DE92-010578] p 638 N93-13102

NASA budget: Potential shortfalls in funding NASA's 5-year plan. Testimony before the Subcommittee on Science, Technology, and Space, Committee on Commerce, Science, and Transportation, United States Senate
[GAO/T-NSIAD-92-18] p 740 N93-13280

Window on waste: Atrophy in NASA management
[GPO-57-273] p 732 N93-13693

Research in geosciences policy
[NASA-CR-190470] p 632 N93-13833

The real world and lunar base activation scenarios p 680 N93-14014

MANAGEMENT SYSTEMS

Environmental Compliance Management System
[DE92-019595] p 645 N93-13479

Performance measurement for information systems: Industry perspectives
[NASA-CR-191369] p 738 N93-13737

MANEUVERABILITY

Combined design of structures and controllers for optimal maneuverability p 691 N93-13130

MANIPULATORS

Tactile sensing and control in humans and robotic/teleoperated systems
[AD-A254408] p 609 N93-12604

Torque resolver design for tendon-driven manipulators
[DE92-017395] p 609 N93-12698

A fundamental study of the effect of gravity on the static and dynamic behavior of robots p 610 N93-12760

Dynamic control modification techniques in teleoperation of a flexible manipulator
[NASA-CR-190984] p 610 N93-12904

Manipulation strategies for massive space payloads
[NASA-CR-190844] p 611 N93-12952

Numerical analysis of nonminimum phase zero for nonuniform link design p 611 N93-12953

The application of input shaping to a system with varying parameters p 612 N93-12954

Experimental verification of modified command shaping using a flexible manipulator p 612 N93-12955

Initial experiments in end-point control of a flexible, two-link manipulator p 612 N93-13018

Robust control of uncertain aerospace and mechanical systems with unmodelled flexibilities: A singular perturbation approach p 691 N93-13129

Design, construction and demonstration of modular, reconfigurable robots p 613 N93-13329

End-point position control of multi-link flexible manipulator arms p 613 N93-13335

Optimal coordination of robotic systems with redundancy p 693 N93-13336

Force and motion control of a constrained flexible manipulator p 613 N93-13384

Robust control of a flexible link robot and rigid link robot: Theory, simulation, and experiment p 614 N93-13452

Performance and stability of telemanipulators using bilateral impedance control p 614 N93-13488

Nonholonomic motion of free-flying space robots p 615 N93-13638

Force-closure grasping with two hands p 616 N93-13742

A unified approach to the analysis and design of manipulator systems with environmental contact p 573 N93-13805

Experiments in two-cooperating-arm manipulation from a platform with unknown motion p 617 N93-13931

Dynamic modeling and optimal joint torque coordination of advanced robotic systems p 617 N93-13936

Near-minimum-time control of a flexible arm p 695 N93-14039

Position and force control of flexible and rigid manipulators using the sliding-mode technique p 695 N93-14065

Modelling flexible link manipulators in the three-dimensional space p 574 N93-14093

A collision avoidance algorithm for the mobile robot and the robot manipulator in multi-robot system p 618 N93-14094

MANNED MARS MISSIONS

Physiologically constrained aerocapture for manned Mars missions
[NASA-TM-103954] p 521 N93-12720

Impact of lunar oxygen production on direct manned Mars missions p 540 N93-13984

Lunar stepping stones to a manned Mars exploration scenario p 767 N93-14016

MANNED SPACE FLIGHT

Physiologically constrained aerocapture for manned Mars missions
[NASA-TM-103954] p 521 N93-12720

Fully energy-dependent HZETRN (a galactic cosmic-ray transport code)
[NASA-TP-3243] p 771 N93-13020

JPRS report: Science and technology. Central Eurasia: Space
[JPRS-USP-92-006] p 508 N93-13151

Introduction to the International Asteroid Mission p 513 N93-13549

Asteroid search program p 514 N93-13550

Conceptual design of a human piloted mining mission p 514 N93-13552

MANUAL CONTROL

Qualification of the gritblast assembly and process for the inside diameter of the RSRM forward and aft domes
[NASA-CR-184462] p 558 N93-13021

MANUALS

US Antarctic program. Personnel manual, 1992
[NSF-92-63] p 731 N93-12637

Computer-Aided Structural Engineering (CASE) project. Tutorial guide: Computer-Aided Structural Modeling (CASM). Version 3.00
[AD-A255075] p 684 N93-12872

A radio frequency user's guide to the Space Environment Services Center geophysical alert broadcasts
[PB92-220631] p 562 N93-12979

MANUFACTURING

Toward a microgravity research strategy
[NASA-CR-190820] p 556 N93-12799

Enabling technologies for economical manufacturing of composites
[AD-A253615] p 531 N93-13324

Design, construction and demonstration of modular, reconfigurable robots p 613 N93-13329

Process comparison study. MSFC Center Director's Discretionary Fund (CDDF)
[NASA-TM-108382] p 526 N93-13429

Scientists, engineers, and technicians in manufacturing industries: 1989. Detailed statistical tables
[NSF-92-312] p 730 N93-13437

Cost analysis methodology: Photovoltaic Manufacturing Technology Project
[DE92-016441] p 639 N93-13528

An update of ERC's carbonate fuel cell development program
[DE92-019971] p 640 N93-13621

Considerations for the transition from fuel cell R/D to manufacturing
[DE92-019977] p 640 N93-13622

Optimum design of aircraft structures with manufacturing and buckling constraints p 501 N93-13815

MANY BODY PROBLEM

Stabilization and projection methods for multibody dynamics
[PB92-133883] p 698 N93-12890

Investigations of the structure and electromagnetic interactions of few-body systems
[DE92-040011] p 563 N93-13042

Fermi molecular dynamics
[DE92-015351] p 703 N93-13187

Hydrodynamical calculations of stellar interactions p 755 N93-13764

MAPS

Satellite imagery goes to the field
[AD-A254449] p 632 N93-12598

MARANGONI CONVECTION

Modeling of coalescence, agglomeration, and phase segregation in microgravity processing of bimetallic composite materials
[NASA-CR-191247] p 556 N93-12728

MARINE BIOLOGY

Phytoplankton photosynthesis in natural mixed layers
[AD-A255010] p 671 N93-12871

MARINE CHEMISTRY

Noninvasive probing of the ocean surface using laser-based nonlinear optical methods
[DE92-019431] p 669 N93-12916

MARINE ENVIRONMENTS

Characteristics of phytoplankton as monitors of the physical environment
[AD-A255009] p 642 N93-12870

MARINE METEOROLOGY

Sources of cloud nuclei and development of remote sensing techniques for cloud parameters
[AD-A255016] p 660 N93-12558

Production of SSM/I data sets
[NASA-CR-190944] p 632 N93-12800

MARKET RESEARCH

Future regional transport aircraft market, constraints, and technology stimuli
[NASA-TM-107669] p 491 N93-13025

MARKETING

Westinghouse PAFC program update
[DE92-019978] p 640 N93-13623

MARKING

Tagging insulin in microgravity p 510 N93-13172

MARKOV PROCESSES

Modeling and estimation of reciprocal diffusion and Gauss-Markov random fields
[AD-A255034] p 698 N93-12709

Longitudinal beam dynamics with rf noise
[DE92-040645] p 707 N93-13108

MARS (PLANET)

Unit operations for gas-liquid mass transfer in reduced gravity environments p 557 N93-14011

The real world and lunar base activation scenarios p 680 N93-14014

Lunar stepping stones to a manned Mars exploration scenario p 767 N93-14016

MARS ATMOSPHERE

Control algorithms for aerobraking in the Martian atmosphere p 524 N93-14046

MARS PHOTOGRAPHS

Volcanism in the eastern Hellas region of Mars: The geology of Hadriaca and Tyrrhena Paterae p 768 N93-14092

MARS VOLCANOES

Volcanism in the eastern Hellas region of Mars: The geology of Hadriaca and Tyrrhena Paterae p 768 N93-14092

MARTENSITE

Tempering effects for lower bainite, martensite, and mixed microstructures on impact, fracture, and related mechanical properties of ASTM A723 steel
[AD-A254617] p 541 N93-12616

Ordering energies and mechanisms in beta-phase NiAl
[DE92-040031] p 542 N93-13043

Fastening apparatus having shape memory alloy actuator
[NASA-CASE-MSC-21935-1] p 614 N93-13423

MARTENSITIC TRANSFORMATION

Tempering effects for lower bainite, martensite, and mixed microstructures on impact, fracture, and related mechanical properties of ASTM A723 steel
[AD-A254617] p 541 N93-12616

MASS

Dual mass and torsion p 728 N93-13498

MASS DISTRIBUTION

Dynamics and control of a tumbling satellite retrieval device p 522 N93-13119

In situ dust mass distribution measurements from the Giotto encounter with comet P/Halley p 753 N93-13602

MASS FLOW

Efficiency of an AMTEC recirculating test cell, experiments, and projections
[DE92-016811] p 571 N93-13196

Mass flow effects on the low speed characteristics of an advanced combat aircraft p 497 N93-13214

Application of subsonic first-order panel methods for prediction of inlet and nozzle aerodynamic interactions with airframe p 497 N93-13223

A fast scanning probe for D3-D
[DE92-040260] p 717 N93-13511

MASS SPECTRA

Interpretation of the ion mass spectra in the mass range 25-35 obtained in the inner coma of Halley's comet by the HIS-sensor of the Giotto IMS Experiment p 752 N93-13469

MASS SPECTROMETERS
Enhancement of ion transmission and reduction of background and interferences in inductively coupled plasma mass spectrometry
[DE92-018805] p 596 N93-12921
Photodissociation processes
[PB92-222702] p 702 N93-13067
A study of ion composition and dynamics at Comet Halley
[NASA-CR-188478] p 751 N93-13465
Densities and abundances of hot cometary ions in the coma of P/Halley p 752 N93-13466
Observations of plasma dynamics in the coma of P/Halley by the Giotto Ion Mass Spectrometer p 752 N93-13468
Interpretation of the ion mass spectra in the mass range 25-35 obtained in the inner coma of Halley's comet by the HIS-sensor of the Giotto IMS Experiment p 752 N93-13469

MASS SPECTROSCOPY
Artificial intelligence and neural networks applied to ion mobility spectrometry
[DE92-017508] p 690 N93-12559
Capillary electrophoresis: Electrospray ionization mass spectrometry in small diameter capillaries
[DE92-019123] p 575 N93-12711
Enhancement of ion transmission and reduction of background and interferences in inductively coupled plasma mass spectrometry
[DE92-018805] p 596 N93-12921
Resonance ionization mass spectrometry in biochemical analysis
[DE92-017407] p 538 N93-13341
Thermochemistry of atmospheric metal reactions
[AD-A248651] p 543 N93-13733

MASS TO LIGHT RATIOS
Gravitational lensing by galaxy clusters: The giant arcs in Abell 370 and Cl2244-02 p 755 N93-13848
The interstellar medium of elliptical galaxies p 757 N93-14071

MASS TRANSFER
Unit operations for gas-liquid mass transfer in reduced gravity environments p 557 N93-14011

MASSIVE STARS
Hydrodynamics and spectra formation of interacting massive binaries and the young remnant of SN1987A p 757 N93-13962

MASSIVELY PARALLEL PROCESSORS
Massively parallel optical-to-electronic data transfer
[AD-A254831] p 688 N93-12733
Reject mechanisms for massively parallel neural network character recognition systems
[PB92-213412] p 689 N93-13198
Simulation of excitatory/inhibitory interactions in single auditory neurons
[AD-A253614] p 675 N93-13252
Compressible convection and pulsations on parallel computers p 690 N93-13961

MATCHED FILTERS
ACTA Aeronautica et Astronautica Sinica (selected articles)
[AD-A255070] p 491 N93-13946

MATERIALS SCIENCE
First International Microgravity Laboratory
[NASA-TM-108007] p 518 N93-13113

MATERIALS TESTS
LDEF Materials Workshop 1991, part 1
[NASA-CP-3162-PT-1] p 545 N93-12769
Element Material Exposure Experiment by EFFU p 548 N93-12783

MATHEMATICAL LOGIC
A brief overview of NASA Langley's research program in formal methods p 684 N93-12958

MATHEMATICAL MODELS
Operator workload predictions for the revised AH-64A workload prediction model. Volume 2: Appendixes A through H
[AD-A254939] p 676 N93-12545
Self-consistent one-dimensional modelling of x ray laser plasmas
[DE92-019543] p 712 N93-12571
Thermal barrier coating life prediction model development, phase 2
[NASA-CR-189111] p 544 N93-12589
Hierarchic models for laminated plates p 528 N93-12629
CO2 laser modeling
[NASA-CR-184455] p 604 N93-12656
ILS mathematical modeling study of the effects of an ASR-9 structure at the Long Island MacArthur Airport, Islip, NY
[DOT/FAA/CT-TN92/25] p 506 N93-12668
Torque resolver design for tendon-driven manipulators
[DE92-017395] p 609 N93-12698
Bayesian analysis of linear and nonlinear population models using the Gibbs sampler
[AD-A254769] p 697 N93-12702
LDEF atomic oxygen fluence update p 546 N93-12771
Long Duration Exposure Facility (LDEF) contamination modeling p 547 N93-12775
Predictive forming of advanced thermoplastic composite structures p 529 N93-12835
Effects of source-region phenomenology on seismic discrimination
[DE92-017441] p 649 N93-12841
Influence of cure shrinkage on process-induced stress and deformation in thick thermosetting composites
[AD-A254325] p 529 N93-12842
Briefing notes on propulsion stability codes ADMIT, NYQUIST, and SSFREQ
[NASA-CR-184449] p 525 N93-12874
Dense-gas dispersion advection-diffusion model
[DE92-019617] p 642 N93-12884
VPPA weld model evaluation
[NASA-CR-184460] p 611 N93-12919
Convective scale 4-D data assimilation using simulated single Doppler radar observations
[PB92-218726] p 651 N93-12969
NOAA Atmospheric Sciences Modeling Division support to the US Environmental Protection Agency
[PB92-217835] p 644 N93-12974
Diffusion-absorption heat pump
[PB92-217538] p 576 N93-12975
Implicitly coupling heat conduction into a zone fire model
[PB92-222769] p 558 N93-12980
Solar prediction analysis
[NASA-CR-184422] p 769 N93-13014
Compression strength of composite primary structural components
[NASA-CR-190949] p 624 N93-13019
Application of Lanczos vectors to control design of flexible structures, part 2
[NASA-CR-191244] p 685 N93-13030
Basic principles of SAR p 563 N93-13050
Remote sensing of Earth terrain
[NASA-CR-190908] p 633 N93-13084
Application of theoretical models to active and passive remote sensing of saline ice p 633 N93-13086
Simulation of forward-backward extrusion with numerical and model material techniques
[DE92-016299] p 558 N93-13298
A small, single stage orifice pulse tube cryocooler demonstration
[NASA-CR-190859] p 558 N93-13404
A Fourier series method for polygonal domains: Large element computation for plates p 627 N93-13484
A theoretical investigation of the growth rates of ice crystals in clouds p 653 N93-13485
Micromechanics of finite length fibers in composite materials p 532 N93-13490
Thermodynamically consistent theories for elastoplasticity coupled with damage
[DE92-018283] p 627 N93-13515
Summary on comparison of radiative heat transfer solutions for a specified problem
[DE92-040098] p 588 N93-13575
Semi-quantitative model for the burning rate of solid materials
[PB92-213362] p 539 N93-13641
Effects of stratospheric aerosol surface processes on the LLNL two-dimensional zonally averaged model
[DE92-019620] p 646 N93-13646
Meso-beta scale numerical simulation studies of terrain-induced jet streak mass/momentum perturbations
[NASA-CR-191365] p 654 N93-13719
Radiative constraints on the energy budget of the atmosphere p 655 N93-13731
An investigation of the dynamic response of lifting surfaces with concentrated structural nonlinearities p 501 N93-13807
Climate sensitivity study with energy balance models p 666 N93-13817
Formulation and validation of high-order mathematical models of helicopter flight dynamics p 501 N93-13821
Assessment of potential aerodynamic benefits from spanwise blowing at the wing tip p 496 N93-13822
Studies of orbital doublet and modelling of orbital triplet Jahn-Teller systems in 3 to 5 semiconductors p 725 N93-13845
Infrared emission from the water outgas cloud of an orbiting vehicle induced by collisions with atmospheric gases p 521 N93-13854
The growth of disturbances in barotropic models of the atmosphere p 658 N93-13887
Optical model analysis of gravity wave-critical layer interaction p 658 N93-13888
Formal aspects of human-computer interaction p 679 N93-13909
Solar water heating system for a lunar base p 641 N93-14005
Theoretical and numerical studies of wave propagation and scattering in inhomogeneous media p 568 N93-14044
Numerical simulation of compressible Couette flow stability: Non-linear and three-dimensional effects p 594 N93-14077
Solar energy utilisation and evacuated tubular solar collectors p 641 N93-14078
Fixed-gain, two-stage estimators for tracking maneuvering targets
[AD-A255832] p 697 N93-14081
A surface pressure altitude prediction model
[AD-A255834] p 668 N93-14082
The relationship between environmental conditions and UH-60 cockpit temperature
[AD-A255918] p 680 N93-14090
Volcanism in the eastern Hellas region of Mars: The geology of Hadriaca and Tyrrhena Paterae p 768 N93-14092

MATHEMATICAL PROGRAMMING
From totally unimodular to balanced O, +/- 1 matrices: A family of integer polytopes
[AD-A254552] p 696 N93-12640

MATHEMATICS
Summary of awards: Applied mathematics. Fiscal year 1991
[NSF-92-38] p 681 N93-13438
On computing accurate singular values and eigenvalues of acyclic matrices
[AD-A255892] p 697 N93-14036

MATRICES (MATHEMATICS)
A new matrix formulation of classical electrodynamics. Part 2: Wave propagation in optical materials of infinite extent
[AD-A255032] p 560 N93-12585
From totally unimodular to balanced O, +/- 1 matrices: A family of integer polytopes
[AD-A254552] p 696 N93-12640
Implementation details of the coupled QMR algorithm
[NASA-CR-191213] p 684 N93-12801
Fast multiresolution algorithms for matrix-vector multiplication
[NASA-CR-189721] p 696 N93-12942
Identifiability of linear systems in physical coordinates
[NASA-TM-107695] p 625 N93-13125
TRASYS form factor matrix normalization p 585 N93-13391
Implicit application of polynomial filters in a k-step Arnoldi method
[NASA-CR-191237] p 686 N93-13408
On computing accurate singular values and eigenvalues of acyclic matrices
[AD-A255892] p 697 N93-14036

MATRIX MANAGEMENT
A new route for fibre management in metal matrix composites p 534 N93-13779

MATRIX MATERIALS
Properties of five toughened matrix composite materials
[NASA-TP-3254] p 528 N93-12590
Fracture toughness of short fiber/brittle matrix composites p 528 N93-12630
Load-transfer and crack bridging in fiber-toughened ceramic composites p 629 N93-13754
The role of the fiber/matrix interphase in the static and fatigue behavior of polymeric matrix composite laminates p 535 N93-13968

MATRIX METHODS
Efficient solution of parabolic equations by Krylov approximation methods
[NASA-CR-191235] p 697 N93-13409
The free and forced vibrations of structures using the finite dynamic element method p 630 N93-13935

MATRIX THEORY
A new matrix formulation of classical electrodynamics. Part 2: Wave propagation in optical materials of infinite extent
[AD-A255032] p 560 N93-12585

MATTER (PHYSICS)
Theoretical nuclear physics
[DE92-019286] p 706 N93-12822

MAXIMUM LIKELIHOOD ESTIMATES
Determination of the stability and control derivatives of the F/A-18 HARV from flight data using the maximum likelihood method
[NASA-CR-191216] p 503 N93-12903

MAXIMUM PRINCIPLE
Optimal control computer programs
[NASA-TM-108384] p 693 N93-13289

MAXWELL EQUATION
A new matrix formulation of classical electrodynamics. Part 2: Wave propagation in optical materials of infinite extent
[AD-A255032] p 560 N93-12585
MEASURING INSTRUMENTS
Precision liquid-level measurement in deep tanks using a swept-RF resonant cavity
[DE92-017236] p 597 N93-13267
MECHANICAL PROPERTIES
Compression test simulation of thick-section composite materials
[AD-A255021] p 528 N93-12583
The 3-D nonlinear constitutive modeling approach for composite materials
[AD-A255022] p 528 N93-12584
Thermal barrier coating life prediction model development, phase 2
[NASA-CR-189111] p 544 N93-12589
Properties of five toughened matrix composite materials
[NASA-TP-3254] p 528 N93-12590
Transverse flexural tests as a tool for assessing damage to PMR-15 composites from isothermal aging in air at elevated temperatures
[NASA-TM-105848] p 529 N93-12737
Influence of cold work level on the irradiation creep and creep rupture of titanium-modified austenitic stainless steels
[DE92-019078] p 541 N93-12820
Investigation of properties and performance of ceramic composite components
[DE92-019911] p 550 N93-12858
Touchstone for success
[ESA-BR-52] p 557 N93-12934
Elevated temperature tensile properties of borated 304 stainless steel: Effect of boride dispersion on strength and ductility
[DE92-040096] p 542 N93-13302
Simulation studies for surfaces and materials strength
[NASA-CR-191289] p 724 N93-13570
Investigations of the mechanical behavior of graphite/PEEK (APC-2) composites p 534 N93-13908
MECHANICAL SHOCK
Development of a 1000 g, 10 ms mechanical shock test capability
[DE92-019193] p 624 N93-13077
MEDIA
Wave propagation and scattering in dense geophysical media
[AD-A254573] p 561 N93-12646
Variance of phase fluctuations of waves propagating through a random medium p 569 N93-13087
MEDICAL EQUIPMENT
Functional MRI studies of human vision on a clinical imager
[DE92-017448] p 674 N93-12566
A health care system for the Space Station
[NASA-TM-108093] p 679 N93-13571
MEDICAL SCIENCE
JPRS report: Science and technology. Central Eurasia: Life sciences
[JPRS-ULS-92-024] p 672 N93-13033
MEDICAL SERVICES
Federal support to universities, colleges, and nonprofit institutions: Fiscal year 1990. A report to the President and Congress
[NSF-92-324] p 741 N93-13543
MELTS (CRYSTAL GROWTH)
Dynamics and pattern selection at the crystal-melt interface
[DE92-040210] p 724 N93-13577
The formation of ore mineral deposits on the Moon: A feasibility study p 760 N93-13974
Electrolytic smelting of lunar rock for oxygen, iron, and silicon p 761 N93-13979
MEMBRANES
Chemical sensors based on ultrathin film composite membranes
[AD-A254644] p 595 N93-12619
Stress crack testing of polyethylene geomembranes
[PB92-217132] p 622 N93-12843
Terahertz horn antennas on thin membranes
[AD-A254772] p 562 N93-12867
An elasticity solution for a transversely isotropic material containing a spherical shell under axisymmetric loading p 628 N93-13728
MEMORY
Human memory for the spatial locations of items on pull-down computer menus p 739 N93-14080
MEMORY (COMPUTERS)
Massively parallel optical-to-electronic data transfer
[AD-A254831] p 688 N93-12733
GaAs gate dynamic memory technology
[AD-A254801] p 720 N93-12748
Speedup properties of phases in the execution profile of distributed parallel programs
[DE92-019965] p 689 N93-12810
Memory access in shared virtual memory
[DE92-019594] p 681 N93-12823
Comparison of heavy ion and electron-beam upset data for GaAs
[AD-A255901] p 708 N93-14089
MERCURY CADMIUM TELLURIDES
Results of the laser sensor technology transition investigation
[AD-A255845] p 608 N93-14085
MERCURY TELLURIDES
Two to six compound thin films by MOCVD for tandem solar cells p 640 N93-13932
MERIDIONAL FLOW
Relationships between continental-scale circulation and rainfall event attributes in the southeastern US p 664 N93-13631
MESONS
Search for doubly Cabibbo suppressed decays of the charged D meson
[DE92-018588] p 703 N93-13092
Recent developments in the theory of heavy-quark decays
[DE92-017598] p 704 N93-13250
Research in elementary particle physics
[DE92-017869] p 704 N93-13251
MESOPAUSE
A joint study of the lower ionosphere by radar, lidar, and spectrometer p 655 N93-13755
MESOSCALE PHENOMENA
A synoptic climatology of the elevated mixed layer inversion over the southern Great Plains in spring p 664 N93-13643
Nonlinear hydrostatic conditional symmetric instability: Some theoretical and modeling considerations p 655 N93-13757
Numerical study of nonlinear convective-symmetric instability in a rotating baroclinic atmosphere p 666 N93-13786
Adding explanation capability to a knowledge-based system for interpretation of oceanographic images
[AD-A255887] p 671 N93-13943
Convective parameterization in mesoscale models p 659 N93-14062
MESOSPHERE
Investigations of the dynamics and thermodynamics of the mesosphere lower thermosphere and upper thermosphere at the polar regions with optical ground-based remote sensing
[AD-A254746] p 650 N93-12845
Radiative transfer in the middle atmosphere p 652 N93-13482
A new instrument for the study of mesospheric gravity waves through nightglow observations p 656 N93-13789
Middle atmosphere water vapour p 667 N93-13892
MESSAGE PROCESSING
Lazy checkpoint coordination for bounding rollback propagation
[NASA-CR-191281] p 565 N93-13375
METABOLISM
Forest declines: Some perspectives on linking processes and patterns
[DE92-019946] p 642 N93-12828
METAL FATIGUE
On bilinearity of Manson-Coffin low-cycle-fatigue relationship
[NASA-TM-105840] p 622 N93-12739
Fatigue in single crystal nickel superalloys
[AD-A254704] p 541 N93-12746
In-phase and out-of-phase axial-torsional fatigue behavior of Haynes 188 at 760 C
[NASA-TM-105765] p 625 N93-13153
Elevated temperature tensile properties of borated 304 stainless steel: Effect of boride dispersion on strength and ductility
[DE92-040096] p 542 N93-13302
Effects of residual stress, weld toe notch and weld defects on fatigue of welded steel structures p 631 N93-13947
METAL IONS
Electrochemical and chemical characteristics of a new ambient temperature Li(I) polymer electrolyte
[AD-A254918] p 545 N93-12651
Laser formation of lithium plasma ion sources for applied-B ion diodes on the PBFA-2 accelerator
[DE92-016091] p 716 N93-13191
METAL MATRIX COMPOSITES
An investigation of the thermoviscoplastic behavior of a metal matrix composite at elevated temperatures
[NASA-CR-189706] p 530 N93-12929
Ductile fracture process of discontinuous fiber reinforced composites
[DE92-016298] p 531 N93-13264
FNAS modify matric and transparent experiments
[NASA-CR-184442] p 531 N93-13311
A new route for fibre management in metal matrix composites p 534 N93-13779
An investigation into thermomechanical fatigue of metal matrix composites p 534 N93-13810
Thermoviscoplastic analysis of metal matrix composites p 535 N93-13954
X ray attenuation measurements for high-temperature materials characterization and in situ monitoring of damage accumulation p 631 N93-14022
Improving the temperature resistance of aluminum-matrix composites by using an acid phosphate binder p 536 N93-14056
METAL OXIDE SEMICONDUCTORS
Semiconductor measurement technology: INSTANT (IGBT network simulation and transient Analysis tool)
[PB92-213529] p 725 N93-13783
METAL OXIDES
Oxygen diffusion in high-T(c) superconductors
[DE92-019597] p 720 N93-12807
Magnetic behavior of a Bi(sub 2)Sr(sub 2)Ca(sub 1)Cu(sub 2)O(sub x) single crystal by direct magneto-optical observations
[DE92-018612] p 722 N93-13118
The heteroepitaxial growth of YBCO and other metal oxides on silicon and GaAs by pulsed laser deposition p 726 N93-13904
METAL PLATES
Numerical simulations of steel plate perforation
[DE92-017058] p 626 N93-13301
METAL SURFACES
Bistatic clutter RCS simulation using scale model rough surfaces
[AD-A254932] p 560 N93-12581
Photochemical dynamics of surface oriented molecules
[DE92-019813] p 703 N93-13106
Studies of the kinetics and mechanisms of perfluoroether reactions on iron and oxidized iron surfaces
[NASA-CR-191363] p 539 N93-13763
The chemistry of the extreme pressure lubricant additive lead naphthenate on steel surfaces
[AD-A255828] p 544 N93-14098
METALLIC GLASSES
Glass corrosion in natural environments
[NASA-CR-191234] p 551 N93-13150
METALLIC PLASMAS
Laser formation of lithium plasma ion sources for applied-B ion diodes on the PBFA-2 accelerator
[DE92-016091] p 716 N93-13191
METALORGANIC CHEMICAL VAPOR DEPOSITION
Single liquid source plasma enhanced metalorganic chemical vapor deposition of YBa2Cu3O(7-x) thin films
[AD-A254119] p 722 N93-13100
Thin films and solar cells of cadmium telluride and cadmium zinc telluride p 639 N93-13611
Two to six compound thin films by MOCVD for tandem solar cells p 640 N93-13932
METALS
Experimental studies of cascade phenomena in metals
[DE92-019586] p 540 N93-12573
Electronic structure of microclusters and defect complexes
[AD-A254807] p 720 N93-12750
Simulation of forward-backward extrusion with numerical and model material techniques
[DE92-016299] p 558 N93-13298
Is there a unique effective interaction profile for dislocations?
[DE92-018615] p 543 N93-13545
Thermochemistry of atmospheric metal reactions
[AD-A248651] p 543 N93-13733
METASTABLE STATE
The 3-D description of vertical current sheets with application to solar flares
[SSL-PREPRINT-90-119] p 770 N93-13477
Some problems of quantum cosmology and dark matter physics p 755 N93-13829
METEOROLOGICAL PARAMETERS
An analysis of the tornado-producing Raleigh thunderstorm of November 28, 1988
[AD-A254384] p 661 N93-12862
NOAA Atmospheric Sciences Modeling Division support to the US Environmental Protection Agency
[PB92-217835] p 644 N93-12974
Summary of 1992 Atlantic tropical cyclone activity and verification of author's forecast (a year of no hurricane activity in the tropics but exceptional South Florida destruction from an unusual higher latitude intense hurricane) p 662 N93-13028
Remote sensing data from CLARET: A prototype CART data set
[NASA-CR-191294] p 634 N93-13094

JARE data reports no. 179 (meteorology 29). Meteorological data at Asuka Station, Antarctica in 1990
p 663 N93-13287
A meteorology-based approach to detecting response source-receptor relationships p 664 N93-13736
The assimilation of marine surface data into the Navy operational global atmospheric prediction system
[AD-A255559] p 667 N93-13877

METEOROLOGICAL RADAR
Storm tracking for TDWR: A correlation algorithm design and evaluation
[AD-A254701] p 660 N93-12622
Remote sensing data from CLARET: A prototype CART data set
[NASA-CR-191294] p 634 N93-13094
Terminal Doppler Weather Radar (TDWR) Operational Test and Evaluation (OT/E) integration test plan
[DOT/FAA/CT-TN92/6] p 499 N93-13377
Birds mimicking microbursts on 2 June 1990 in Orlando, Florida
[AD-A255703] p 498 N93-14024

METEOROLOGICAL RESEARCH AIRCRAFT
Meeting review: Third NCAR Research Aircraft Fleet Workshop
[PB92-222710] p 649 N93-12818

METEOROLOGY
Comparison of two stochastic models of scalar diffusion in turbulent flow
[DE92-019381] p 576 N93-12912
JARE data reports no. 173 (meteorology 28). Antarctic climate research data. Part 5: PPI radar data at Syowa Station, Antarctica from February to December 1989
p 663 N93-13446
A meteorology-based approach to detecting response source-receptor relationships p 664 N93-13736

METHANE
Studies of radiative emission from the simulated shock layer of the Huygens probe p 521 N93-12834

METHOD OF MOMENTS
Scattering from a finite collection of transverse dipole and axial slot arrays with edge effects
p 568 N93-14048

METHOXY SYSTEMS
Microwave and infrared dielectric relaxation of alkylcarbonates, chloroform and their mixtures at 25 C
[AD-A253606] p 537 N93-13096

METHYL ALCOHOL
Kinetics and dynamics of oxidation reactions involving an adsorbed CO species
[DE92-019745] p 537 N93-12995
High octane ethers from synthesis gas-derived alcohols
[DE92-015467] p 537 N93-13188
A novel process for methanol synthesis
[DE92-019719] p 539 N93-13617

METRIC SPACE
Recursive construction of fractals
[ISBN-951-41-0689-X] p 697 N93-13271
Solitons and instantons in string theory
p 728 N93-13753

METROLOGY
Soft X Ray Telescope (SXT) focus error analysis
[NASA-CR-184443] p 742 N93-12657

MICHELSON INTERFEROMETERS
Arm length matching in 10 m delay-line interferometer
[ISAS-TN-649] p 596 N93-12639
Radio and optical interferometric imaging
p 744 N93-13580
Report of the Science Working Group: Science with a lunar optical interferometer p 747 N93-13600

MICROBIOLOGY
Microbiological methods for the water recovery systems test, revision 1.1
[NASA-CR-184390] p 678 N93-12966
Long-term lunar stations: Some ecological considerations p 648 N93-13995

MICROCLIMATOLOGY
A novel diesel-fueled engine for microclimate cooling for the individual soldier
[AD-A254510] p 609 N93-12724

MICROCOMPUTERS
ESPVI 4.0 electrostatic precipitator V-I and performance model: User's model
[PB92-169614] p 643 N93-12938

MICROCRACKS
Microcracking, microcrack-induced delamination, and longitudinal splitting of advanced composite structures
[NASA-CR-4472] p 623 N93-12911
A tough high performance composite matrix
[NASA-CASE-LAR-14338-1] p 531 N93-13416

MICROELECTRONICS
Summary of awards. Fiscal year 1991
[NSF-92-36] p 681 N93-13431

MICROGRAVITY APPLICATIONS
Modeling of coalescence, agglomeration, and phase segregation in microgravity processing of bimetallic composite materials
[NASA-CR-191247] p 556 N93-12728
Toward a microgravity research strategy
[NASA-CR-190820] p 556 N93-12799
First International Microgravity Laboratory
[NASA-TM-108007] p 518 N93-13113
A microgravity processing plant for the manufacturing of propellant and water from asteroid ore
p 515 N93-13558
Spacelab J: Microgravity and life sciences
[NASA-CR-191353] p 516 N93-13564

MICROMECHANICS
The 3-D nonlinear constitutive modeling approach for composite materials
[AD-A255022] p 528 N93-12584
Fracture toughness of short fiber/brittle matrix composites p 528 N93-12630
Theoretical and experimental studies on the foundation theoretical and experimental studies on the foundation of mesomechanics
[AD-A254385] p 623 N93-12863
Micromechanics of finite length fibers in composite materials p 532 N93-13490
Vibration damping response of composite materials
p 533 N93-13748
Thermoviscoplastic analysis of metal matrix composites p 535 N93-13954

MICROMETEOROLOGY
Performance of the Bowen ratio systems on a 22 deg slope
[NASA-CR-191278] p 644 N93-13254

MICROMETERS
Temperature measurements with micrometer spatial resolution
[AD-A255897] p 603 N93-14086

MICROORGANISMS
Long-term lunar stations: Some ecological considerations p 648 N93-13995

MICROPARTICLES
The LDCE Particle Impact Experiment as flown on STS-46 --- limited duration space environment candidate materials exposure (LDCE) p 512 N93-13183

MICROPHONES
Developments on high temperature fiber optic microphone p 601 N93-13680

MICROPOROSITY
Chemical sensors based on ultrathin film composite membranes
[AD-A254644] p 595 N93-12619

MICROSTRIP ANTENNAS
Electromagnetic scattering and radiation from microstrip patch antennas and spirals residing in a cavity
[NASA-CR-191284] p 565 N93-13354

MICROSTRUCTURE
Fatigue and fracture of intermetallic alloys
[AD-A254543] p 540 N93-12603
Tempering effects for lower bainite, martensite, and mixed microstructures on impact, fracture, and related mechanical properties of ASTM A723 steel
[AD-A254617] p 541 N93-12616
Sol-gel synthesis and densification of aluminoborosilicate powders. Part 1: Synthesis
[NASA-TM-103964] p 527 N93-12895
Nonlinear mechanics of composite materials with periodic microstructure
[NASA-CR-190750] p 531 N93-13309
Microstructural evolution in reaction bonded alumina/mullite ceramics p 552 N93-13328
Fatigue studies in Al-Mg-Si alloys p 543 N93-13690

MICROWAVE AMPLIFIERS
Anomalous TWTA output power spikes and their effect on a digital satellite communications system
[NASA-TM-105875] p 571 N93-13286

MICROWAVE ANTENNAS
Millimeter-wave quasi-optical and spatial power combining techniques
[AD-A255438] p 574 N93-13865

MICROWAVE FREQUENCIES
Experimental studies of high-power plasma-filled backward wave oscillators p 717 N93-13495

MICROWAVE IMAGERY
Production of SSM/I data sets
[NASA-CR-190944] p 632 N93-12800
Spatial resolution enhancement of SSM/I microwave brightness temperatures and its impact on rainfall retrieval algorithms
[AD-A254382] p 661 N93-12861
Microwave remote sensing of a precipitating atmosphere p 634 N93-13371

MICROWAVE OSCILLATORS
Experimental studies of high-power plasma-filled backward wave oscillators p 717 N93-13495
Analysis and experimental results for an extraction cavity for the split-cavity oscillator
[DE92-040262] p 566 N93-13512
Space-qualified submillimeter radiometer
[NASA-CR-190886] p 603 N93-13709

MICROWAVE RADIOMETERS
Measurements of the cosmic microwave background temperature at 1.47 GHz p 772 N93-13146
The correlation of active and passive microwave outputs for the Skylab S-193 sensor
[LEC-7819] p 635 N93-13440
Phased array feed design technology for Large Aperture Microwave Radiometer (LAMR) Earth observations
[NASA-CR-189727] p 519 N93-13462

MICROWAVE RESONANCE
Resonance lamp absorption measurement of OH number density and temperature in expansion tube scramjet engine tests p 602 N93-13682

MICROWAVE SCATTERING
Transhorizon microwave propagation and its relationship with meteorological conditions p 666 N93-13791

MICROWAVE SENSORS
The correlation of active and passive microwave outputs for the Skylab S-193 sensor
[LEC-7819] p 635 N93-13440

MICROWAVE SPECTRA
A thermal/nonthermal approach to solar flares
p 771 N93-13639
A study of the neutral and ionized gas in the interstellar medium and galactic H 2 regions p 756 N93-13853

MICROWAVE TRANSMISSION
Transhorizon microwave propagation and its relationship with meteorological conditions p 666 N93-13791

MICROWAVES
Microwave and infrared dielectric relaxation of alkylcarbonates, chloroform and their mixtures at 25 C
[AD-A253606] p 537 N93-13096
The millimeter and submillimeter wavelength diffuse backgrounds: Measurements of the spectrum and anisotropy p 772 N93-13145
Measurements of the cosmic microwave background temperature at 1.47 GHz p 772 N93-13146
The correlation of active and passive microwave outputs for the Skylab S-193 sensor
[LEC-7819] p 635 N93-13440
Experimental studies of high-power plasma-filled backward wave oscillators p 717 N93-13495
Use of phonon echoes in the study of 2-6 compounds and dielectric Bi12GeO20:Cr p 725 N93-13847

MIDDLE ATMOSPHERE
Model studies of the middle atmosphere of Venus
p 759 N93-13831
Spectroscopy for remote sounding of the atmosphere
p 659 N93-14054

MIE SCATTERING
Microwave remote sensing of a precipitating atmosphere p 634 N93-13371

MILITARY AIR FACILITIES
US Air Force 1989 research initiation program, volume 4
[AD-A254458] p 774 N93-12765
US Air Force 1989 research initiation program, volume 2
[AD-A254459] p 774 N93-12766
US Air Force 1989 research initiation program, volume 3
[AD-A254460] p 774 N93-12767

MILITARY OPERATIONS
Satellite imagery goes to the field
[AD-A254449] p 632 N93-12598
A novel diesel-fueled engine for microclimate cooling for the individual soldier
[AD-A254510] p 609 N93-12724
The Joint Surveillance Target Attack Radar System: Can procedures be developed to support the requirements of the land and air component commanders?
[AD-A255555] p 567 N93-13875
Procedures for the diagnostic dose resistance test kits for mosquitoes, body lice, and beetle pests of stored products
[AD-A255224] p 675 N93-13941
Thermal stress in US Air Force operations
[AD-A255785] p 676 N93-14027

MILITARY TECHNOLOGY
Laser measurement techniques guide for a hazard evaluation
[AD-A254545] p 604 N93-12610
Proceedings of Joint RL/AFOSR Workshop on Intelligent Information Systems
[AD-A254795] p 734 N93-12703
Air Force engineering research initiation grants (1990-1991)
[AD-A255004] p 774 N93-12706
USAF 1990 research initiation program, volume 3
[AD-A254755] p 775 N93-12849

Formulation and validation of high-order mathematical models of helicopter flight dynamics
p 501 N93-13821
First year testing of prototype magnesium/manganese dioxide BA-4590/U battery
[AD-A255503] p 574 N93-13839

MILITARY VEHICLES
Seamless simulation literature survey
[AD-A254950] p 688 N93-12549

MILKY WAY GALAXY
Probing the galactic halo with ROSAT
[NASA-CR-191268] p 743 N93-13272
Molecular clouds in the distant outer galaxy
p 758 N93-14095

MILLIMETER WAVES
Angle of arrival fluctuations for millimeter waves propagating in a turbulent atmosphere near the Earth
[AD-A254478] p 560 N93-12574
Wave propagation and scattering in dense geophysical media
[AD-A254573] p 561 N93-12646
The millimeter and submillimeter wavelength diffuse backgrounds: Measurements of the spectrum and anisotropy p 772 N93-13145
Millimeter-wave quasi-optical and spatial power combining techniques
[AD-A255438] p 574 N93-13865
WR-10 band noise measurement
[AD-A255526] p 566 N93-13871

MIMO (CONTROL SYSTEMS)
Symposium proceedings on Quantitative Feedback Theory
[AD-A255527] p 505 N93-13872

MINERAL DEPOSITS
Resources for a lunar base: Rocks, minerals, and soil of the Moon p 760 N93-13973
The formation of ore mineral deposits on the Moon: A feasibility study p 760 N93-13974
Lunar surface mining for automated acquisition of helium-3: Methods, processes, and equipment
p 766 N93-14007

MINERALOGY
The implications of the magnetism of ordinary chondrites p 755 N93-13795

MINERALS
An ion budget for a terra firme rainforest in Central Amazonia
[INPE-5365-PRE/1745] p 632 N93-13005
The implications of the magnetism of ordinary chondrites p 755 N93-13795
Applications for special-purpose minerals at a lunar base p 760 N93-13975
Water and cheese from the lunar desert: Abundances and accessibility of H, C, and N on the Moon
p 761 N93-13976

MINIATURIZATION
Large area projection liquid-crystal video display system with inherent grid pattern optically removed
[NASA-CASE-NPO-16932-2-CU] p 711 N93-13711

MINIMAX TECHNIQUE
An inverse dynamics approach to trajectory optimization for an aerospace plane
[NASA-CR-191277] p 500 N93-13305
Robust controller and estimator design using minimax methods p 694 N93-13925
On a robust controller design using a minimax optimization approach p 695 N93-14021

MINING
International Asteroid Mission p 513 N93-13548
Conceptual design of a human piloted mining mission
p 514 N93-13552
Mining equipment and operations for mining the 1982HR (Orpheus) asteroid p 515 N93-13557
Water and cheese from the lunar desert: Abundances and accessibility of H, C, and N on the Moon
p 761 N93-13976

MINORITIES
Science and engineering degrees, by race/ethnicity of recipients: 1977-1990
[NSF-92-327] p 729 N93-12694
Women and minorities in science and engineering: An update
[NSF-92-303] p 730 N93-12907
Blacks in undergraduate science and engineering education
[NSF-92-305] p 730 N93-13015
NASA industry education initiative. Education programs report, 1991
[NASA-NP-158] p 730 N93-13248
Gateway to diversity in the scientific and technological workforce
[NSF-92-99] p 730 N93-13278
Diversity in biological research
[NSF-92-19] p 673 N93-13700

MIR SPACE STATION
JPRS report: Science and technology. Central Eurasia: Space
[JPRS-USP-92-004] p 513 N93-13282

MIRAGE AIRCRAFT
Flight analysis of air intake/engine compatibility
p 502 N93-13212

MIRRORS
Large Deployable Reflector (LDR) system concept and technology definition study. Volume 1: Executive summary, analyses and trades, and system concepts
[NASA-CR-177413-VOL-1] p 708 N93-12591
Large Deployable Reflector (LDR) system concept and technology definition study. Volume 2: Technology assessment and technology development plan
[NASA-CR-177413-VOL-2] p 708 N93-12593
Contamination analysis of SSF candidate materials
[NASA-CR-184431] p 709 N93-12894
EURECA
[ESA-F-26] p 522 N93-12964
Automation of the targeting and reflective alignment concept
[NASA-CR-190964] p 709 N93-12985
Uniformity results of the multilayer mirrors used in the ALEXIS ultrasoft x ray telescopes
[DE92-018611] p 743 N93-13342
Quantum well, beam deflecting surface emitting lasers
[NASA-CASE-NPO-18243-1-CU] p 605 N93-13418
Infrared image projector utilizing a deformable mirror device spatial light modulator
[AD-D015373] p 710 N93-13500

MISSILE CONFIGURATIONS
New methods for predicting nonlinear lift, center of pressure, and pitching moment on missile configurations
[AD-A255078] p 492 N93-12741
Aerodynamic studies of supersonic air intakes
p 497 N93-13222

MISSILE DESIGN
Aerodynamic Engine/Airframe Integration for High Performance Aircraft and Missiles
[AGARD-CP-498] p 577 N93-13199

MISSILE TRAJECTORIES
Angle of arrival fluctuations for millimeter waves propagating in a turbulent atmosphere near the Earth
[AD-A254478] p 560 N93-12574

MISSILES
The PEP Symposium on CFD Techniques for Propulsion Applications p 579 N93-13210
Some aspects of intake design, performance and integration with the airframe p 502 N93-13219
Aerodynamic studies of supersonic air intakes
p 497 N93-13222

MISSION PLANNING
Chemical release and radiation effects experiment advanced planning and coordination
[NASA-CR-184439] p 649 N93-12718
Element Material Exposure Experiment by EFFU
p 548 N93-12783
Earth observation photography: Looking back 20 years after Skylab p 509 N93-13164
International Asteroid Mission p 513 N93-13548
Conceptual design of a human piloted mining mission
p 514 N93-13552
The program plan: An overview of the development and implementation of the International Asteroid Mission
p 514 N93-13553
Business analysis: The commercial mission of the International Asteroid Mission p 514 N93-13554
Spacelab J: Microgravity and life sciences
[NASA-CR-191353] p 516 N93-13564
Chairmanship of the Neptune/Pluto Outer Planets Science Working Group
[NASA-CR-191288] p 759 N93-13568
The real world and lunar base activation scenarios
p 680 N93-14014
Lunar stepping stones to a manned Mars exploration scenario p 767 N93-14016

MIXING HEIGHT
Middle atmosphere water vapour p 667 N93-13892

MIXING LAYERS (FLUIDS)
Effect of the flow non-uniformity on the mixing layer at the interface of parallel supersonic flows
[ISAS-RN-646] p 491 N93-12716
Spanwise-nonuniform excitation of a plane mixing layer p 577 N93-13120
Numerical study on mixing of sprayed liquid in an LNG storage tank p 584 N93-13388
Numerical simulation of the acoustic instability in the spatially developing, confined, supersonic mixing layer
p 494 N93-13521
Stability of the compressible reacting mixing layer
p 592 N93-13948

MIXING LENGTH FLOW THEORY
Coherent structures in compressible convection
p 592 N93-13964

MODELS
Hybrid 2 and hybrid 3 dummy neck properties for computer modeling
[AD-A255544] p 679 N93-13874

MODULATION
Multiplexing electro-optic architectures for advanced aircraft integrated flight control systems
[NASA-CR-182268] p 504 N93-13735

MODULATORS
Development of a stable electro-optical modulator
[NASA-CR-184404] p 710 N93-13696

MODULES
Design, construction and demonstration of modular, reconfigurable robots p 613 N93-13329
Providing structural modules with self-integrity monitoring software user's manual
[NASA-CR-190877] p 628 N93-13707

MODULUS OF ELASTICITY
Mechanical properties of epoxy/alumina trihydrate-filled compositions p 534 N93-13950

MOISTURE CONTENT
Sources of cloud nuclei and development of remote sensing techniques for cloud parameters
[AD-A255016] p 660 N93-12558

MOLECULAR BEAM EPITAXY
Group 2 cubic fluorides dielectrics for 3-D integration and GaAs-based optoelectronic structures
[AD-A254937] p 719 N93-12544
Synthesis and properties of mismatched heterojunction/substrate interfaces
[AD-A254577] p 719 N93-12648

MOLECULAR BIOLOGY
Molecular biology of anaerobic aromatic biodegradation
[AD-A255213] p 673 N93-13863

MOLECULAR CLOUDS
United Kingdom Infrared Telescope
p 743 N93-13273
Molecular gas temperature and density in spiral galaxies p 748 N93-13688
The role of ambipolar diffusion in the formation of interstellar cloud cores and protostars
p 755 N93-13828
An optical study of the faint end of the stellar luminosity function p 748 N93-13960
Molecular clouds in the distant outer galaxy
p 758 N93-14095

MOLECULAR COLLISIONS
Monte Carlo calculation of ionization and excitation rates in electron aurora
[ISAS-RN-645] p 652 N93-13405

MOLECULAR EXCITATION
Monte Carlo calculation of ionization and excitation rates in electron aurora
[ISAS-RN-645] p 652 N93-13405
Photochemical kinetics of excited states of O3 and O2: Laboratory studies and atmospheric implications
p 656 N93-13784

MOLECULAR GASES
Molecular gas temperature and density in spiral galaxies p 748 N93-13688
Molecular clouds in the distant outer galaxy
p 758 N93-14095

MOLECULAR IONS
Photodissociation processes
[PB92-222702] p 702 N93-13067

MOLECULAR PHYSICS
Experimental studies of cascade phenomena in metals
[DE92-019586] p 540 N93-12573

MOLECULAR SPECTROSCOPY
Intermolecular potential functions from spectroscopic properties of weakly bound complexes
[DE92-018643] p 701 N93-12745
High resolution molecular spectroscopy of atmospheric species
[AD-A254360] p 650 N93-12946
High-resolution investigation of degenerate four-wave mixing in the (gamma)(0,0) band of nitric oxide
[DE92-005312] p 537 N93-13232
High-resolution resonant degenerate 4-wave mixing spectroscopy
[DE92-012146] p 538 N93-13234
Spectroscopy for remote sounding of the atmosphere
p 659 N93-14054

MOLECULAR STRUCTURE
Nonideal thermoequilibrium calculations using a large product species data base
[DE92-040839] p 735 N93-12813
Characterization of thermotropic liquid crystalline polymer blends by positron annihilation lifetime spectroscopy
[AD-A253616] p 552 N93-13325
Oligomer and mixed-metal compounds potential multielectron transfer catalysts
[DE92-011347] p 543 N93-13346

Radiation-disorder and aperiodicity in irradiated ceramics
[DE92-015051] p 552 N93-13350
The effects of molecular structure on the electrical conductivity of polymers
[NASA-CR-191265] p 552 N93-13459

MOLECULAR THEORY
Scattering and order in thermotropic liquid crystals p 723 N93-13332
Molecular theories and computer simulations of liquid crystals p 725 N93-13843

MOLECULAR WEIGHT
Determination of the weight average molecular weight of SRM 1480
[PB92-222934] p 553 N93-13785

MOLECULES
Photochemical dynamics of surface oriented molecules
[DE92-019813] p 703 N93-13106
Tagging insulin in microgravity p 510 N93-13172

MOLTEN SALT ELECTROLYTES
Oxygen electrode reaction in molten carbonate fuel cells
[DE92-040180] p 636 N93-12812

MOLTEN SALTS
Electrodeposition of high temperature superconductors
[AD-A255095] p 720 N93-12758
Molten salt reactor for potentiostatic electroplating
[AD-D015358] p 551 N93-13101

MOLYBDENUM
Small-scale x ray laser systems
[DE92-018442] p 604 N93-12744
Silicide layer growth rates in Mo/Si multilayers
[DE92-019581] p 721 N93-12972
Ductile phase toughening of molybdenum disilicide by low pressure plasma spraying
[DE92-007409] p 551 N93-13315

MOLYBDENUM COMPOUNDS
Silicide layer growth rates in Mo/Si multilayers
[DE92-019581] p 721 N93-12972

MOLYBDENUM DISULFIDES
Ion-beam-assisted deposition of MoS2 and other low-friction films
[AD-A255222] p 554 N93-13862
Surface phonon dispersion of MoS2
[AD-A255835] p 727 N93-14083

MOMENTS OF INERTIA
Numerical analysis of nonminimum phase zero for nonuniform link design p 611 N93-12953
Dynamics and control of a tumbling satellite retrieval device p 522 N93-13119

MOMENTUM THEORY
Transverse wave motion in constrained mechanical systems p 628 N93-13634

MONATOMIC GASES
Computer program for calculating and fitting thermodynamic functions
[NASA-RP-1271] p 728 N93-12967

MONITORS
Limited production Precision Runway Monitor (PRM) master test plan
[DOT/FAA/CT-TN92/23] p 506 N93-12899
Video profile monitor diagnostic system for GTA
[DE92-040231] p 710 N93-13509

MONOCHROMATORS
Emittance, brilliance, and bandpass issues related to an inclined crystal monochromator
[DE92-019671] p 721 N93-12881

MONOTECTIC ALLOYS
FNAS modify matric and transparent experiments
[NASA-CR-184442] p 531 N93-13311

MONSOONS
Intraseasonal variability of infrared cooling rates during the Asian summer monsoon and their influence on intraseasonal waves p 665 N93-13760

MONTE CARLO METHOD
Uses of Monte Carlo computer simulations in understanding epitaxial growth and ion bombardment of Si(001)
[DE92-016944] p 719 N93-12586
Robust rendezvous maneuver point conditions
[NASA-CR-190996] p 517 N93-12690
A neural network approach for the investigation of chemical phenomena
[DE92-019205] p 691 N93-13079
A fresh look at (e,e(prime)) scattering from light nuclei: A GFMC approach
[DE92-016377] p 703 N93-13246
Applications of the Los Alamos High Energy Transport code
[DE92-017408] p 704 N93-13281
Monte Carlo calculation of ionization and excitation rates in electron aurora
[ISAS-RN-645] p 652 N93-13405
The use of degradation measures in assessing reliability p 573 N93-13607
Summary: Experimental validation of real-time fault-tolerant systems
[NASA-CR-190985] p 503 N93-13697

MOON
The possibility of concrete production on the Moon p 554 N93-13988

MOORING
Development of moored oceanographic spectroradiometer
[NASA-CR-190883] p 670 N93-13708

MORPHOLOGY
Dynamics and pattern selection at the crystal-melt interface
[DE92-040210] p 724 N93-13577
Galaxies with spectral energy distributions peaking at 60 micrometers: Morphology and activity explained by interactions p 756 N93-13959
Volcanism in the eastern Hellas region of Mars: The geology of Hadriaca and Tyrrhena Paterae p 768 N93-14092

MOTION
The neurochemical and neuropharmacological basis of motion sickness
[NASA-CR-190957] p 675 N93-13061

MOTION SICKNESS
The neurochemical and neuropharmacological basis of motion sickness
[NASA-CR-190957] p 675 N93-13061

MOTOR VEHICLES
White paper: Preliminary assessment of LNG vehicle technology, economics, and safety issues, revision 1
[PB92-212943] p 615 N93-13644

MOUNTAINS
Aircraft accident/incident summary report: Controlled flight into terrain, Bruno's Inc., Beechjet, N25BR, Rome, Georgia, December 11, 1991
[PB92-910404] p 498 N93-13470

MULLITES
Dislocation and pores in mullite from diphasic gels
[DE92-040384] p 550 N93-12999
Microstructural evolution in reaction bonded alumina/mullite ceramics p 552 N93-13328

MULTIPATH TRANSMISSION
Acousto-optic applications for multichannel adaptive optical processor
[AD-A255823] p 711 N93-14032

MULTIPHASE FLOW
Effect of vaporization on cryogenic spray dropsize measurement
[NASA-TM-105909] p 597 N93-13410

MULTIPLE TARGET TRACKING
Application of smoothing techniques for tracking maneuvering targets. Multiple target tracking in clutter: New approaches
[AD-A254609] p 561 N93-12615

MULTIPLEXING
Multiplexing electro-optic architectures for advanced aircraft integrated flight control systems
[NASA-CR-182268] p 504 N93-13735

MULTIPLICATION
Fast multiresolution algorithms for matrix-vector multiplication
[NASA-CR-189721] p 696 N93-12942

MULTIPLIERS
Investigation of component failure rates for pulsed versus steady state tokamak operation
[DE92-019758] p 713 N93-12856

MULTIPOLAR FIELDS
Polarization effects and multipolarization SAR p 564 N93-13054
Radiometric calibration of SAR systems p 564 N93-13055

MULTIPROCESSING (COMPUTERS)
Application of smoothing techniques for tracking maneuvering targets. Multiple target tracking in clutter: New approaches
[AD-A254609] p 561 N93-12615
State space methods in multidimensional digital signal processing
[AD-A254646] p 561 N93-12620
Testing and fault-tolerant design techniques for advanced digital architectures
[AD-A255013] p 681 N93-12707
Speedup properties of phases in the execution profile of distributed parallel programs
[DE92-019301] p 689 N93-12797
Speedup properties of phases in the execution profile of distributed parallel programs
[DE92-019965] p 689 N93-12810
Memory access in shared virtual memory
[DE92-019594] p 681 N93-12823

MULTISENSOR APPLICATIONS
A general theory of signal integration for fault-tolerant dynamic distributed sensor networks
[AD-A254961] p 732 N93-12553

MULTISPECTRAL BAND SCANNERS
Deciduous forest scene complexity in high-resolution multispectral scanner imagery
[AD-A255511] p 635 N93-13867

MULTISPECTRAL RADAR
Multifrequency measurements of radar ground clutter at 42 sites. Volume 2: Appendices A through D
[AD-A246711] p 567 N93-13878

MULTISTATIC RADAR
Bistatic clutter RCS simulation using scale model rough surfaces
[AD-A254932] p 560 N93-12581

MULTIVARIATE STATISTICAL ANALYSIS
Real-time quality assurance testing using photonic techniques: Application to iodine water system
[NASA-CR-184413] p 619 N93-12692

MUONS
Particle production and survival in muon acceleration
[DE92-019553] p 701 N93-12572
A search for point sources of cosmic ray muons using the MACRO detector p 773 N93-13738

MUSCLES
Establishing laboratory standards for biological flight experiments
[NASA-CR-184402] p 671 N93-12901

MUSCULOSKELETAL SYSTEM
Publications of the space physiology and countermeasures program, Musculoskeletal Discipline: 1980-1990
[NASA-CR-4468] p 743 N93-12898
Bone loss and human adaptation to lunar gravity p 676 N93-14002

MUTATIONS
Katz model prediction of Caenorhabditis elegans mutagenesis on STS-42
[NASA-TM-4383] p 674 N93-13023

MYOGLOBIN
Capillary electrophoresis: Electrospray ionization mass spectrometry in small diameter capillaries
[DE92-019123] p 575 N93-12711

N

NACELLES
Numeric simulation of the aerodynamic flows around nacelles p 577 N93-13202
High-speed aerodynamics of upper surface blowing aircraft configurations p 494 N93-13729

NARROWBAND
Integrated filter and detector array for spectral imaging
[NASA-CASE-NPO-18317-1-CU] p 709 N93-13419
A statistical study of narrow bandwidth, high-latitude geomagnetic pulsations p 660 N93-14068

NASA PROGRAMS
Coordinating Council. Second Meeting: International Acquisitions
[NASA-TM-108015] p 733 N93-12634
Coordinating Council. Fifth Meeting: Quality
[NASA-TM-108018] p 733 N93-12635
Coordinating Council. Seventh Meeting: Acquisitions
[NASA-TM-108020] p 733 N93-12636
Coordinating Council. Third Meeting: STI Strategic Plans
[NASA-TM-108016] p 733 N93-12670
Coordinating Council. Fourth Meeting: NACA Documents Database Project
[NASA-TM-108017] p 734 N93-12671
Coordinating Council. Sixth Meeting: Who Are Our Key Users?
[NASA-TM-108021] p 734 N93-12672
Coordinating Council. Eighth Meeting: Using the Internet
[NASA-TM-108019] p 734 N93-12673
NASA Mission: The Universe
[NASA-NP-141] p 508 N93-12891
The First United States Microgravity Laboratory
[NASA-TM-107980] p 557 N93-12951
Large programs may consume increasing share of limited future budgets. Report to Congressional Requesters
[GAO/NSIAD-92-278] p 732 N93-13109
NASA aeronautics: Research and technology program highlights
[NASA-NP-159] p 491 N93-13110
NASA industry education initiative. Education programs report, 1991
[NASA-NP-158] p 730 N93-13248

NASA budget: Potential shortfalls in funding NASA's 5-year plan. Testimony before the Subcommittee on Science, Technology, and Space, Committee on Commerce, Science, and Transportation, United States Senate
[GAO/T-NSIAD-92-18] p 740 N93-13280
Advanced technology for America's future in space. Executive summary
[NASA-TM-107969] p 513 N93-13308
Federal R/D funding by budget function: Fiscal years 1991-1993
[NSF-92-318] p 740 N93-13312
Commercial non-aerospace technology transfer program for the 2000s: Strategic analysis and implementation
[NASA-TM-4424] p 742 N93-13433
Federal support to universities, colleges, and nonprofit institutions: Fiscal year 1990. A report to the President and Congress
[NSF-92-324] p 741 N93-13543
Window on waste: Atrophy in NASA management
[GPO-57-273] p 732 N93-13693
Research summary, January 1989 - June 1990
[NASA-CR-190960] p 687 N93-13694

NASA SPACE PROGRAMS
Solar System Exploration Division Strategic Plan, volume 1. Executive summary and overview
[NASA-TM-107843] p 513 N93-13265
Small planetary mission plan: Report to Congress
[NASA-TM-107809] p 513 N93-13266
Advanced technology for America's future in space. Executive summary
[NASA-TM-107969] p 513 N93-13308
Creating a foundation for a synergistic approach to program management p 732 N93-14017

NATIONAL AEROSPACE PLANE PROGRAM
National Aero-Space Plane: Key issues facing the program. Testimony before the Subcommittee on Technology and Competitiveness, Committee on Science, Space, and Technology, House of Representatives
[GAO/T-NSIAD-92-26] p 500 N93-13253
High-temperature strain measurement techniques: Current developments and challenges
p 599 N93-13669
The trade-off characteristics of acoustic and pressure sensors for the NASP p 601 N93-13678

NATIONAL AIRSPACE SYSTEM
Limited production Precision Runway Monitor (PRM) master test plan
[DOT/FAA/CT-TN92/23] p 506 N93-12899
Terminal Doppler Weather Radar (TDWR) Operational Test and Evaluation (OT/E) integration test plan
[DOT/FAA/CT-TN92/6] p 499 N93-13377
A NASPAC-based analysis of the delay and cost effects of the Dallas/Fort Worth metroplex plan
[DOT/FAA/CT-TN92/21] p 507 N93-13447

NATURAL GAS
Meeting future exhaust emissions standards using natural gas as a vehicle fuel: Lessons learned from the natural gas vehicle challenge 1992
[DE92-019670] p 642 N93-12885
Utilization of compressed natural gas in medium- and heavy-duty engine route vehicles
[PB92-217546] p 611 N93-12908
Effects of gas composition on engine performance and emissions
[PB92-217561] p 611 N93-12936
Development of advanced turbine systems: Meeting tomorrow's needs
[DE92-017339] p 612 N93-13103
The 1992 natural gas vehicle challenge: EPA emissions and fuel economy testing
[PB92-217926] p 616 N93-13761

NATURAL LANGUAGE (COMPUTERS)
Action composition for the animation of natural language instructions
[AD-A254963] p 682 N93-12554
Expert-system development in Soar: A tutorial
[AD-A254571] p 682 N93-12645
Talking to InterFIS: Adding speech input to a natural language interface
[AD-A255865] p 688 N93-13942

NAVIER-STOKES EQUATION
Investigation of advanced counterrotation blade configuration concepts for high speed turboprop systems. Task 4: Advanced fan section aerodynamic analysis
[NASA-CR-187128] p 502 N93-12695
NATO Advanced Research Workshop: Vortex Flows and Related Numerical Methods. List of participants, book of abstracts, and instructions for submission to the proceedings
[AD-A255015] p 575 N93-12708
Navier-Stokes simulations of unsteady transonic flow phenomena
[NASA-TM-103962] p 491 N93-12721
Application of a solution adaptive grid to flow over an embedded cavity p 492 N93-13141
The PEP Symposium on CFD Techniques for Propulsion Applications p 579 N93-13210
Boundary element methods for two-dimensional, coupled, thermoviscous flow p 584 N93-13383
The Proteus Navier-Stokes code p 585 N93-13396
Wall functions for the kappa-epsilon turbulence model in generalized nonorthogonal curvilinear coordinates
p 587 N93-13517
Solution of viscous flow problems by using the boundary element method p 588 N93-13609
Linear stability theory of hypersonic, chemically reacting viscous flows p 588 N93-13765
Unsteady three-dimensional thin-layer Navier-Stokes solutions for turbomachinery in transonic flow
p 593 N93-14025
Navier-Stokes flowfield computation of wing/rotor interaction for a tilt rotor aircraft in hover
p 497 N93-14035
Solution of compressible Navier-Stokes equations using spectral methods on arbitrary two-dimensional domains
p 593 N93-14041
A low-dimensional dynamical systems description of coherent structures in the axisymmetric jet mixing layer
p 593 N93-14057
A numerical study of hypersonic flows using the full Navier-Stokes equations with different air models
p 594 N93-14061
Numerical simulation of compressible Couette flow stability: Non-linear and three-dimensional effects
p 594 N93-14077

NAVIGATION AIDS
Digital chart database conversion into a system electronic navigational chart
[AD-A255007] p 632 N93-12869

NAVY
Interaction and impact of floating bodies
[AD-A254627] p 574 N93-12617

NEAR INFRARED RADIATION
Kinetics and dynamics of oxidation reactions involving an adsorbed CO species
[DE92-019745] p 537 N93-12995
Novel techniques of wavefront sensing for adaptive optics with array telescopes using an artificial neural network p 743 N93-13343
Initial performance of Los Alamos Advanced Free Electron Laser
[DE92-040214] p 605 N93-13507
HARDI: A high angular resolution deployable interferometer for space p 745 N93-13588

NEAR WAKES
Wake characterization: Full flow simulation of space structures in low earth orbit p 497 N93-13970

NECK (ANATOMY)
Hybrid 2 and hybrid 3 dummy neck properties for computer modeling
[AD-A255544] p 679 N93-13874

NEEDLES
Radiative transfer theory for polarimetric remote sensing of pine forest p 633 N93-13085

NEGATIVE IONS
Suppression of the e(-) coextracted from a Penning surface-plasma H(-) source
[DE92-040350] p 714 N93-12997
The ORNL radioactive ion beam project with the ORIC accelerator
[DE92-040027] p 708 N93-13574

NEGATIVE RESISTANCE CIRCUITS
Physics and technology of resonant-tunneling devices
[AD-A255233] p 573 N93-13837

NEODYMIUM LASERS
Stimulated Brillouin processes in crystals and glasses
[DE92-019549] p 721 N93-12887
Post flight operation of a high peak power neodymium YAG laser aboard the G-449 payload flown on Space Shuttle Columbia mission 61-C p 508 N93-13161
A study of techniques for single frequency operation of diode-pumped Nd:YAG lasers p 606 N93-13629

NEON
Study of heliumlike neon using an electron beam ion trap
[DE92-019544] p 753 N93-13536

NEPTUNE (PLANET)
Chairmanship of the Neptune/Pluto Outer Planets Science Working Group
[NASA-CR-191288] p 759 N93-13568

NERVOUS SYSTEM
Neurochemical control of circadian rhythms
[AD-A255054] p 675 N93-13116

NETWORK ANALYSIS
Multidimensional signals, data and processes
[AD-A254797] p 562 N93-12747
Fast approximation algorithms for multicommodity flow problems
[AD-A254335] p 685 N93-12961

NEURAL NETS
An application of exponential neural networks to event-train recognition
[AD-A254948] p 690 N93-12548
Artificial intelligence and neural networks applied to ion mobility spectrometry
[DE92-017508] p 690 N93-12559
Data to test and evaluate the performance of neural network architectures for seismic signal discrimination, volume 1
[AD-A254413] p 691 N93-12607
Multidimensional signals, data and processes
[AD-A254797] p 562 N93-12747
Silicon neuron
[AD-A255091] p 674 N93-12756
Analysis of IMS spectra using neural networks
[DE92-017511] p 691 N93-12791
Transputer implementation of the TRACE model of speech recognition
[AD-A254747] p 689 N93-12846
A neural network approach for the investigation of chemical phenomena
[DE92-019205] p 691 N93-13079
Reject mechanisms for massively parallel neural network character recognition systems
[PB92-213412] p 689 N93-13198
Simulation of excitatory/inhibitory interactions in single auditory neurons
[AD-A253614] p 675 N93-13252
Resource constrained design of artificial neural networks using comparator neural network
[NASA-CR-191280] p 694 N93-13376

NEUROLOGY
SLS-1 flight experiments preliminary significant results
[NASA-TM-108033] p 520 N93-13613

NEURONS
Silicon neuron
[AD-A255091] p 674 N93-12756
Neurochemical control of circadian rhythms
[AD-A255054] p 675 N93-13116
Simulation of excitatory/inhibitory interactions in single auditory neurons
[AD-A253614] p 675 N93-13252

NEUROPHYSIOLOGY
Functional MRI studies of human vision on a clinical imager
[DE92-017448] p 674 N93-12566
A core facility for the study of neurotoxins of biological origin
[AD-A254359] p 674 N93-12945
The neurochemical and neuropharmacological basis of motion sickness
[NASA-CR-190957] p 675 N93-13061
Investigation of effects of 60-Hz electric and magnetic fields on operant and social behavior and on the neuroendocrine system of nonhuman primates, part 2
[DE92-040153] p 673 N93-13503
Investigation of effects of 60-Hz electric and magnetic fields on operant and social behavior and on the neuroendocrine system of nonhuman primates, part 1
[DE92-040152] p 673 N93-13520

NEUROTRANSMITTERS
Neurochemical control of circadian rhythms
[AD-A255054] p 675 N93-13116

NEUTRAL ATMOSPHERES
H I shells and supershells: Observations and theory
p 751 N93-13360

NEUTRAL GASES
Spectroscopic studies of low-density gas in the Galactic disk and halo p 753 N93-13499
A study of the neutral and ionized gas in the interstellar medium and galactic H 2 regions p 756 N93-13538

NEUTRAL PARTICLES
Wake characterization: Full flow simulation of space structures in low earth orbit p 497 N93-13970

NEUTRINOS
Neutrino mass
[DE92-017411] p 701 N93-12588
Cosmological constraints on early-decaying particles
p 750 N93-13123
Neutrino(e) appearance for neutrino(mu)-neutrino(tau) oscillations in matter
[DE92-040303] p 772 N93-13533

NEUTRON COUNTERS
The use of ring ratios to detect sample differences in passive neutron counting
[DE92-018920] p 702 N93-13076

NEUTRON DIFFRACTION
Study of short-range motion of atomic hydrogen in amorphous silicon by neutron reflectometry
[DE92-016392] p 703 N93-13194
Scattering and order in thermotropic liquid crystals
p 723 N93-13332

NEUTRON IRRADIATION
Radiation-induced infrared absorption in nuclear-pumped laser cavity components
[DE92-017346] p 605 N93-13249
Radiation-disorder and aperiodicity in irradiated ceramics
[DE92-015051] p 552 N93-13350
NEUTRON SCATTERING
Atomic structure of mixed ferroelectrics
[AD-A254369] p 702 N93-12947
Neutron scattering studies of the spin dynamics in La(2-x)Sr(x)O4
[DE92-019952] p 702 N93-13037
Ordering energies and mechanisms in beta-phase NiAl
[DE92-040031] p 542 N93-13043
Scattering and order in thermotropic liquid crystals
p 723 N93-13332
NEUTRON SOURCES
Miniature neutron sources: Thermal neutron sources and their users in the academic field
[DE92-018793] p 702 N93-13070
NEUTRON SPECTRA
The use of ring ratios to detect sample differences in passive neutron counting
[DE92-018920] p 702 N93-13076
NEUTRON STARS
Hydrodynamical calculations of stellar interactions
p 755 N93-13764
NEUTRONS
A stochastic/deterministic method for transient, three-dimensional neutron transport
[DE92-016690] p 704 N93-13319
NEWTON-RAPHSON METHOD
Solution of viscous flow problems by using the boundary element method p 588 N93-13609
NICKEL
Measurements of crystal growth kinetics at extreme deviations from equilibrium
[DE92-019744] p 720 N93-12827
Influence of dilute impurities on the evolution of defect cascades in nickel
[DE92-019585] p 542 N93-12973
On grain boundary transport of hydrogen and mechanism of hydrogen-induced intergranular fracture
p 544 N93-14047
NICKEL ALLOYS
Fatigue in single crystal nickel superalloys
[AD-A254704] p 541 N93-12746
Weak-beam imaging of dissociated dislocations in HVEM-irradiated Fe-Ni-Cr alloys
[DE92-019587] p 541 N93-12798
A study of the vacancy loop formation probability in Ni-Cu and Ag-Pd alloys
[DE92-019584] p 541 N93-12879
Influence of dilute impurities on the evolution of defect cascades in nickel
[DE92-019585] p 542 N93-12973
Ordering energies and mechanisms in beta-phase NiAl
[DE92-040031] p 542 N93-13043
The implications of the magnetism of ordinary chondrites p 755 N93-13795
NICKEL CADMIUM BATTERIES
Battery selection for space experiments
p 512 N93-13184
NICKEL HYDROGEN BATTERIES
Validation test of 125 Ah advanced design IPV nickel-hydrogen flight cells
[NASA-TM-105912] p 527 N93-14079
NIGHT
Tributary and gap nighttime air flow comparisons
[DE92-018875] p 662 N93-13075
NIGHT VISION
Integration of exterior lighting systems and night vision imaging systems
[AD-A254826] p 677 N93-12732
NIGHTGLOW
A new instrument for the study of mesospheric gravity waves through nightglow observations
p 656 N93-13789
Spectroscopic observations of the night airglow from 3000 A to 9200 A p 658 N93-13891
NIMBUS 7 SATELLITE
Nimbus-7 Total Ozone Mapping Spectrometer (TOMS) Antarctic ozone atlas: August through November 1991
[NASA-RP-1283] p 661 N93-12700
NIOBIUM ALLOYS
Heat resistant diffusion coating for niobium alloy
[AD-A255542] p 554 N93-13873
NIOBIUM COMPOUNDS
The nature of scales grown on binary Cr-Nb alloys
[DE92-019283] p 542 N93-13080
NITRATES
Ab initio atomic recombination reaction energetics on model heat shield surfaces
[NASA-CR-191210] p 575 N93-12677
The seasonal variations and interrelationships of ozone, peroxyacetyl nitrate and nitrogen dioxide in the troposphere p 647 N93-13893
Radical reactions of atmospheric importance
p 659 N93-14053
NITRIC ACID
Application of improved HNO3 band model parameters to South Pole atmospheric emission measurements
p 647 N93-13723
NITRIC OXIDE
High-resolution investigation of degenerate four-wave mixing in the (gamma)(0,0) band of nitric oxide
[DE92-005312] p 537 N93-13232
The reactions of imidogen with nitric oxide and molecular oxygen
[DE92-006697] p 537 N93-13233
High-resolution resonant degenerate 4-wave mixing spectroscopy
[DE92-012146] p 538 N93-13234
Planar laser-induced fluorescence measurements of high-enthalpy free jet flow with nitric oxide
p 595 N93-13685
NITROGEN
Nitrogen control of chloroplast development and differentiation
[DE92-017392] p 671 N93-12768
Video profile monitor diagnostic system for GTA
[DE92-040231] p 710 N93-13509
NITROGEN DIOXIDE
The seasonal variations and interrelationships of ozone, peroxyacetyl nitrate and nitrogen dioxide in the troposphere p 647 N93-13893
NITROGEN HYDRIDES
The reactions of imidogen with nitric oxide and molecular oxygen
[DE92-006697] p 537 N93-13233
NOAA SATELLITES
Extremely low frequency/very low frequency Generator
[AD-A254347] p 562 N93-12948
Automatic pattern recognition techniques for geometrical correction on satellite data
p 687 N93-13913
NOISE
Noise measurements of YBa2Cu3O7 thin film high-temperature superconductors p 726 N93-13933
NOISE INTENSITY
Experimental validation of finite element and boundary element methods for predicting structural vibration and radiated noise p 621 N93-12631
NOISE MEASUREMENT
JARE data reports no. 176 (Ionosphere 47). Riometer records of 30 MHz cosmic noise at Syowa Station, Antarctica in 1990 p 772 N93-13255
NOISE REDUCTION
Intake and exhaust noise
[ISVR-TR-207] p 699 N93-12714
Report on the final panel discussion on computational aeroacoustics
[NASA-CR-189718] p 699 N93-12986
Cancellation of air-borne acoustic plane waves obliquely incident upon a planar phased-array of active surface elements p 700 N93-13635
NOISE SPECTRA
Intake and exhaust noise
[ISVR-TR-207] p 699 N93-12714
NOISE TEMPERATURE
Appendix: Limits on the use of heterodyning and amplification in optical interferometry
p 747 N93-13597
WR-10 band noise measurement
[AD-A255526] p 566 N93-13871
NONCONSERVATIVE FORCES
Nonconservative force model parameter estimation strategy for TOPEX/Poseidon precision orbit determination
[NASA-TM-104575] p 519 N93-13372
NONDESTRUCTIVE TESTS
A heat pipe coupled planar thermionic converter: Performance characterization, nondestructive testing, and evaluation
[AD-A254941] p 727 N93-12546
Characterizing laser fusion welded aluminum using synchrotron x ray microtomography
[DE92-018608] p 609 N93-12565
Spreadsheet-like image analysis
[AD-A254395] p 619 N93-12864
Automated eddy current analysis of materials
[NASA-CR-184432] p 619 N93-12875
Touchstone for success
[ESA-BR-52] p 557 N93-12934
Nondestructive evaluation of the in-place compressive strength of concrete based upon limited destructive testing
[PB92-222751] p 623 N93-12981
Review of progress in quantitative NDE
[DE92-018814] p 620 N93-13071
Structural fatigue aspects of the P-3 Orion
[ARL-STRUC-TM-558] p 500 N93-13256
Enabling technologies for economical manufacturing of composites
[AD-A253615] p 531 N93-13324
Physical interpretation and development of ultrasonic nondestructive evaluation techniques applied to the quantitative characterization of textile composite materials
[NASA-CR-190962] p 620 N93-13435
Finite element study of ultrasonic imaging
p 700 N93-13774
NONEQUILIBRIUM FLOW
Development and computation of continuum higher order constitutive relations for high-altitude hypersonic flow p 494 N93-13578
NONEQUILIBRIUM THERMODYNAMICS
The nonequilibrium statistical mechanics of chaotic maps p 729 N93-13832
NONINTRUSIVE MEASUREMENT
Elastic and plastic strain measurement in high temperature environment using laser speckle
p 600 N93-13673
Exit plane H2O concentration measurements correlated with OH PLIF near-injector mixing measurements for scramjet flows p 603 N93-13687
NONLINEAR EQUATIONS
Numerical optimization
[AD-A254575] p 682 N93-12647
Analytical studies of nonlinear partial differential equations of interest in nonlinear optics
[AD-A254931] p 696 N93-13027
Efficient solution of parabolic equations by Krylov approximation methods
[NASA-CR-191235] p 697 N93-13409
NONLINEAR OPTICS
Noninvasive probing of the ocean surface using laser-based nonlinear optical methods
[DE92-019431] p 669 N93-12916
Analytical studies of nonlinear partial differential equations of interest in nonlinear optics
[AD-A254931] p 696 N93-13027
Symposium on Polymeric Materials for Photonic and Optical Applications
[AD-A255820] p 554 N93-14029
NONLINEAR SYSTEMS
Optimal design and control of distributed parameter systems
[AD-A254947] p 690 N93-12547
The 3-D nonlinear constitutive modeling approach for composite materials
[AD-A255022] p 528 N93-12584
Hyperbolic conservation laws with umbilic points, 1
[AD-A254431] p 696 N93-12594
Correlation for non-linear infrared calibration curves
[AD-A255098] p 596 N93-12653
Scientific study of data analysis
[NASA-CR-184435] p 769 N93-12658
Organization of the Optical Society of America Photonic Science Topical Meeting Series. Volume 8: Integrated photonics research. lifornia on 9-11 april 1991
[AD-A254682] p 709 N93-12666
Current density fluctuations, nonlinear coupling, and transport in MST
[DE92-041012] p 713 N93-12883
Nonlinear stall flutter of wings with bending-torsion coupling
[AD-A254323] p 503 N93-12959
Proceedings of the Tenth Symposium on Energy Engineering Sciences: Synergism of Analysis, Modeling, and Experiment
[DE92-018777] p 638 N93-13069
Nonlinear stability of combustion-driven acoustic oscillations in resonance tubes
[DE92-012153] p 699 N93-13262
Nonlinear mechanics of composite materials with periodic microstructure
[NASA-CR-190750] p 531 N93-13309
Baroclinic wave packets in models and observations
p 663 N93-13361
Applications of CFD and visualization techniques
p 584 N93-13386
Chaotic vortical motion in the near region of a plane jet p 493 N93-13493
Nonlinear hydrostatic conditional symmetric instability: Some theoretical and modeling considerations
p 655 N93-13757
Deterministic and stochastic responses of nonlinear systems p 631 N93-13966
NONLINEARITY
Innovative methods in the dynamics of large space structures
[AD-A254630] p 521 N93-12579

Organization of the Optical Society of America Photonic Science Topical Meeting Series. Volume 8: Integrated photonics research. Iifornia on 9-11 april 1991
[AD-A254682] p 709 N93-12666
Bayesian analysis of linear and nonlinear population models using the Gibbs sampler
[AD-A254769] p 697 N93-12702
Nonlinear studies of m = 1 modes in high-temperature plasmas
[DE92-019395] p 714 N93-12913
Dynamics of the ion-ion acoustic instability in the thermalization of ion beams
[DE92-019396] p 714 N93-12914
Noninvasive probing of the ocean surface using laser-based nonlinear optical methods
[DE92-019431] p 669 N93-12916
Preamplifier with adjustable input resistance
[AD-D015377] p 572 N93-13473
Transonic aeroelastic analysis of systems with structural nonlinearities p 629 N93-13769
A time domain numerical theory for studying steady-state acoustic disturbance in flow p 700 N93-13770
Numerical study of nonlinear convective-symmetric instability in a rotating baroclinic atmosphere p 666 N93-13786

NORMAL SHOCK WAVES
AGARD WG13 aerodynamics of high speed air intakes: Assessment of CFD results p 581 N93-13220

NORMALIZING (STATISTICS)
TRASYS form factor matrix normalization p 585 N93-13391

NORTH AMERICA
A meteorology-based approach to detecting response source-receptor relationships p 664 N93-13736
Statistical relationships between tree growth and climate in western North America p 648 N93-14096

NORTH ATLANTIC TREATY ORGANIZATION (NATO)
NATO Advanced Research Workshop: Vortex Flows and Related Numerical Methods. List of participants, book of abstracts, and instructions for submission to the proceedings
[AD-A255015] p 575 N93-12708
Highlights 92/2 p 775 N93-13474

NORTHERN HEMISPHERE
Point correlations of geopotential height and temperature at 30 mb and between 500 mb and 30 mb
[PB92-222694] p 661 N93-12817
The North Atlantic circulation: Combining simplified dynamics with hydrographic data p 670 N93-13483

NOTCHES
Notch dimensions for three-point bend fracture specimens based on compliance analyses
[AD-A254641] p 620 N93-12580
Effects of residual stress, weld toe notch and weld defects on fatigue of welded steel structures p 631 N93-13947

NOVA LASER SYSTEM
Recent Nova experimental results
[DE92-019783] p 715 N93-13105

NOWCASTING
The assimilation of marine surface data into the Navy operational global atmospheric prediction system
[AD-A255559] p 667 N93-13877

NOZZLE DESIGN
Survey on techniques used in aerodynamic nozzle/airframe integration p 502 N93-13224

NOZZLE FLOW
The jet behaviour of an actual high-bypass engine as determined by LDA-measurements in ground tests p 503 N93-13218

NUCLEAR ASTROPHYSICS
Approximating the r-process on earth with thermonuclear explosions
[DE92-017409] p 749 N93-12587
Cosmological constraints on early-decaying particles p 750 N93-13123
Establishment of an Institute for Fusion Studies
[DE92-040014] p 717 N93-13502

NUCLEAR BINDING ENERGY
Simulation studies for surfaces and materials strength
[NASA-CR-191289] p 724 N93-13570

NUCLEAR DEFORMATION
Transition probabilities up to I = 36(+)in Yb-160
[DE92-017191] p 703 N93-13114

NUCLEAR EMULSIONS
IIaO ultraviolet and nuclear emulsion films responses to orbital flights on STS-3, STS-7, STS-8, and STS-40 p 509 N93-13163

NUCLEAR EXPLOSIONS
Automated dry powder dispenser for explosive components
[DE92-019425] p 555 N93-12568
Data to test and evaluate the performance of neural network architectures for seismic signal discrimination, volume 1
[AD-A254413] p 691 N93-12607
Effects of source-region phenomenology on seismic discrimination
[DE92-017441] p 649 N93-12841

NUCLEAR FISSION
Lecture notes for criticality safety
[DE92-016009] p 701 N93-12832
High Energy Propulsion System (HEPS) analysis
[AD-A254343] p 525 N93-12963

NUCLEAR FUELS
A new apparatus for continuous countercurrent flow of solids and liquids
[DE92-011675] p 583 N93-13318

NUCLEAR FUSION
Plasma properties
[DE92-019982] p 713 N93-12811
Investigation of component failure rates for pulsed versus steady state tokamak operation
[DE92-019758] p 713 N93-12856
High Energy Propulsion System (HEPS) analysis
[AD-A254343] p 525 N93-12963
Fusion: Magnetic confinement
[DE92-019876] p 716 N93-13107
Cosmological constraints on early-decaying particles p 750 N93-13123
Establishment of an Institute for Fusion Studies
[DE92-040014] p 717 N93-13502
Isotopic separation of He-3/He-4 from solar wind gases evolved from the lunar regolith
[DE92-019339] p 759 N93-13504
Nucleosynthesis in nova explosions
[DE92-040349] p 753 N93-13523
Synergism of He-3 acquisition with lunar base evolution p 540 N93-13986

NUCLEAR MAGNETIC RESONANCE
Molecular theories and computer simulations of liquid crystals p 725 N93-13843

NUCLEAR PARTICLES
Large area nuclear particle detectors using ET materials, phase 2
[NASA-CR-190866] p 705 N93-13606

NUCLEAR PHYSICS
Theoretical nuclear physics
[DE92-019286] p 706 N93-12822
Heavy-ion collisions and the nuclear equation of state
[DE92-019364] p 706 N93-12924
Investigations of the structure and electromagnetic interactions of few-body systems
[DE92-040011] p 563 N93-13042
Guide to QSPIRES and the particle physics databases on SLACVM
[DE92-018099] p 737 N93-13275
JPRS report: Science and technology. Central Eurasia: Physics and mathematics
[JPRS-UPM-92-006] p 698 N93-13303

NUCLEAR POWER PLANTS
Reviews of computing technology: Fiber distributed data interface
[DE92-019927] p 681 N93-12886

NUCLEAR PROPULSION
A computer program for engineering simulations of space reactor system performance
[DE92-016400] p 526 N93-13299

NUCLEAR QUADRUPOLE RESONANCE
Laser spectroscopy of rare earth ions p 608 N93-13846

NUCLEAR RADIATION
AFRRI reports
[AD-A254581] p 674 N93-12649

NUCLEAR REACTIONS
A fresh look at (e,e(prime)) scattering from light nuclei: A GFMC approach
[DE92-016377] p 703 N93-13246
Evidence for alpha-particle chain configurations in Mg-24
[DE92-018790] p 705 N93-13546

NUCLEAR REACTORS
DIII-D edge physics database
[DE92-019577] p 714 N93-12971
Turbulent natural convection between a perforated vertical cylinder and a surrounding array
[DE92-019766] p 576 N93-12996
Aluminum oxide film thickness and emittance
[DE92-019931] p 550 N93-13035

NUCLEAR RESEARCH
Approximating the r-process on earth with thermonuclear explosions
[DE92-017409] p 749 N93-12587

NUCLEAR STRUCTURE
Investigations of the structure and electromagnetic interactions of few-body systems
[DE92-040011] p 563 N93-13042

NUCLEATE BOILING
Environmental qualification testing of payload G-534, the Pool Boiling Experiment p 510 N93-13169
Electrical design of payload G-534: The Pool Boiling Experiment p 510 N93-13170

NUCLEATION
Icing prevention by ultrasonic nucleation of supercooled water droplets in front of subsonic aircraft
[DOT/FAA/CT-TN92/38] p 497 N93-12816

NUCLEI (NUCLEAR PHYSICS)
Heavy-ion collisions and the nuclear equation of state
[DE92-019364] p 706 N93-12924
A fresh look at (e,e(prime)) scattering from light nuclei: A GFMC approach
[DE92-016377] p 703 N93-13246

NUCLEON-NUCLEON INTERACTIONS
Fermi molecular dynamics
[DE92-015351] p 703 N93-13187

NUCLEONS
Theoretical nuclear physics
[DE92-019286] p 706 N93-12822
The spin of the nucleon in deep inelastic lepton scattering experiments
[DE92-018854] p 702 N93-13073

NUCLEOTIDES
Nitrogen control of chloroplast development and differentiation
[DE92-017392] p 671 N93-12768

NUMBER THEORY
Summary of awards: Applied mathematics. Fiscal year 1991
[NSF-92-38] p 681 N93-13438

NUMERICAL ANALYSIS
Scientific study of data analysis
[NASA-CR-184435] p 769 N93-12658
Investigation of advanced counterrotation blade configuration concepts for high speed turboprop systems. Task 4: Advanced fan section aerodynamic analysis
[NASA-CR-187128] p 502 N93-12695
NATO Advanced Research Workshop: Vortex Flows and Related Numerical Methods. List of participants, book of abstracts, and instructions for submission to the proceedings
[AD-A255015] p 575 N93-12708
Numerical analysis of nonminimum phase zero for nonuniform link design p 611 N93-12953
A time domain numerical theory for studying steady-state acoustic disturbance in flow p 700 N93-13770
Numerical analysis of permittivity with loss in isotropic binary composites
[AD-A255203] p 534 N93-13940
Deterministic and stochastic responses of nonlinear systems p 631 N93-13966
Numerical analysis of scattering from certain conducting and dielectric bodies of arbitrary shape
[ISBN-0-315-63282-8] p 569 N93-14066

NUMERICAL CONTROL
A distributed timing system for sychronizing control and data correlation
[DE92-018603] p 690 N93-12564
Real-time data archiving for GTA
[DE92-018613] p 733 N93-12567
Automated dry powder dispenser for explosive components
[DE92-019425] p 555 N93-12568
The Second NASA Formal Methods Workshop 1992
[NASA-CP-10110] p 684 N93-12957
A brief overview of NASA Langley's research program in formal methods p 684 N93-12958
Engineering data transfer test with EDMICS using MIL-R-28002 (Raster)
[DE92-019808] p 738 N93-13619

NUMERICAL DATA BASES
Earth observing system: Information on NASA's incorporation of existing data into EOSDIS. Report to the Chairman, Committee on Science, Space, and Technology, House of Representatives
[GAO/IMTEC-92-79] p 736 N93-13112

NUMERICAL STABILITY
Stabilization and projection methods for multibody dynamics
[PB92-133883] p 698 N93-12890
Efficient solution of parabolic equations by Krylov approximation methods
[NASA-CR-191235] p 697 N93-13409

NUMERICAL WEATHER FORECASTING
Cloud curve algorithm test program
[AD-A253918] p 662 N93-13099
A parameterized quasi-five-cylinder convective cloud model and its application to remote sensing of rainfall p 663 N93-13489

NUTATION
Nutational stability and passive control of symmetric spinning bodies with axial forcing and internal mass motion p 504 N93-13820

O

OBJECT-ORIENTED PROGRAMMING
Application interface engine language and object reference manual
[DE92-017555] p 683 N93-12686
Making object-oriented databases more knowledgeable (from ADAM to ABEL) p 738 N93-13910
Applying an object-oriented database model to a scientific database problem: Managing experimental data at CEBAF p 738 N93-13911
A theory of reference graphs in relational databases p 739 N93-13912

OBSERVABILITY (SYSTEMS)
BETA: Behavioral testability analyzer and its application to high-level test generation and synthesis for testability
[NASA-CR-191282] p 572 N93-13569

OBSERVATORIES
A report on geomagnetic observatory operations, 1990
[PB92-224781] p 649 N93-12804

OBSTACLE AVOIDANCE
3-D computer vision for navigation/control of mobile robots p 693 N93-13243
The 3-D computer vision techniques for object following and obstacle avoidance p 693 N93-13245

OCCULTATION
EURECA
[ESA-F-26] p 522 N93-12964

OCCUPATION
NASA Mission: The Universe
[NASA-NP-141] p 508 N93-12891
Gateway to diversity in the scientific and technological workforce
[NSF-92-99] p 730 N93-13278
Scientists, engineers, and technicians in manufacturing industries: 1989. Detailed statistical tables
[NSF-92-312] p 730 N93-13437

OCEAN BOTTOM
Adaptive array processing in uncertain inhomogeneous media
[AD-A254418] p 560 N93-12608
Chemical environments of submarine hydrothermal systems
[NASA-CR-191258] p 669 N93-13458

OCEAN CURRENTS
Acoustic tracking of neutrally buoyant float
[AD-A255086] p 669 N93-12742
Ocean Energy Program overview, fiscal years 1990-1991
[DE91-002176] p 636 N93-12837
The North Atlantic circulation: Combining simplified dynamics with hydrographic data p 670 N93-13483
The Gulf Stream downstream of Cape Hatteras: Model/data comparisons p 670 N93-13633
Modeling and observations of deep circulation in the eastern South Pacific Ocean p 670 N93-13841
Application of satellite altimetry to study the Gulf of Alaska gyre p 635 N93-13969
On the space-time ocean current variability and its effects on the length-of-day p 636 N93-14051

OCEAN DATA ACQUISITIONS SYSTEMS
Assimilation of satellite color observations in a coupled ocean GCM-ecosystem model
[NASA-CR-191218] p 670 N93-13714

OCEAN DYNAMICS
The North Atlantic circulation: Combining simplified dynamics with hydrographic data p 670 N93-13483
On the space-time ocean current variability and its effects on the length-of-day p 636 N93-14051

OCEAN MODELS
The Gulf Stream downstream of Cape Hatteras: Model/data comparisons p 670 N93-13633
Assimilation of satellite color observations in a coupled ocean GCM-ecosystem model
[NASA-CR-191218] p 670 N93-13714
Modeling and observations of deep circulation in the eastern South Pacific Ocean p 670 N93-13841

OCEAN SURFACE
Ocean optical database
[AD-A254969] p 668 N93-12556
Noninvasive probing of the ocean surface using laser-based nonlinear optical methods
[DE92-019431] p 669 N93-12916
Atmospheric loading response of the solid earth and oceans p 659 N93-13955
Application of satellite altimetry to study the Gulf of Alaska gyre p 635 N93-13969
Coherent frame analysis of Synthetic Aperture Radar (SAR) ocean imagery p 568 N93-14050

OCEAN TEMPERATURE
Ocean Energy Program overview, fiscal years 1990-1991
[DE91-002176] p 636 N93-12837

OCEAN THERMAL ENERGY CONVERSION
Ocean Energy Program overview, fiscal years 1990-1991
[DE91-002176] p 636 N93-12837

OCEANOGRAPHIC PARAMETERS
Estimation of EOF expansion coefficients from incomplete data
[AD-A255252] p 697 N93-13886

OCEANOGRAPHY
Ocean optical database
[AD-A254969] p 668 N93-12556
Meeting review: Third NCAR Research Aircraft Fleet Workshop
[PB92-222710] p 649 N93-12818
Development of moored oceanographic spectroradiometer
[NASA-CR-190883] p 670 N93-13708
Adding explanation capability to a knowledge-based system for interpretation of oceanographic images
[AD-A255887] p 671 N93-13943

OCEANS
Ocean optical database
[AD-A254969] p 668 N93-12556
Ocean Energy Program overview, fiscal years 1990-1991
[DE91-002176] p 636 N93-12837
Atmospheric loading response of the solid earth and oceans p 659 N93-13955

OHMIC DISSIPATION
Understanding of carbonate fuel cell resistance issues for performance improvement
[DE92-019976] p 638 N93-13039

OIL ADDITIVES
The chemistry of the extreme pressure lubricant additive lead naphthenate on steel surfaces
[AD-A255828] p 544 N93-14098

OLIGOMERS
Solvation of cobalt salts by oligomeric polyethers
[AD-A254815] p 545 N93-12753
Effect of plasticizers on the properties of new ambient temperature solid polymer electrolytes
[AD-A254817] p 545 N93-12754
Oligomer and mixed-metal compounds potential multielectron transfer catalysts
[DE92-011347] p 543 N93-13346

OMNIDIRECTIONAL ANTENNAS
Acousto-optic applications for multichannel adaptive optical processor
[AD-A255823] p 711 N93-14032

ON-LINE SYSTEMS
Spreadsheet-like image analysis
[AD-A254395] p 619 N93-12864
Engineering Design Information System (EDIS) Information Services Division (ISD) index function: User's manual
[DE92-041242] p 736 N93-13048
Using DIALOG CIP at Winona State University to educate end-users p 686 N93-13338
Multiple-function multi-input/multi-output digital control and on-line analysis
[NASA-TM-107697] p 500 N93-13565
Approximate optimal guidance for the Advanced Launch System p 519 N93-13819

ONBOARD EQUIPMENT
Proceedings of the 62nd Shock and Vibration Symposium, Volume 2
[AD-A249267] p 628 N93-13637

OORT CLOUD
Studies of extra-solar Oort Clouds and the Kuiper disk
[NASA-CR-190958] p 769 N93-12669

OPEN CLUSTERS
B supergiants in open clusters and associations
[NASA-CR-191275] p 748 N93-13659

OPERATING COSTS
Future regional transport aircraft market, constraints, and technology stimuli
[NASA-TM-107669] p 491 N93-13025

OPERATIONS RESEARCH
Sensitivity analysis of the simultaneous proportionate change of inputs and outputs in data envelopment analysis
[AD-A254821] p 683 N93-12730

OPERATOR PERFORMANCE
Adaptive automation and human performance: Multi-task performance characteristics
[AD-A254596] p 503 N93-12578

OPTICAL COMMUNICATION
Engineering planetary lasers for interstellar communication p 608 N93-14010

OPTICAL COMPUTERS
Acousto-optic applications for multichannel adaptive optical processor
[AD-A255823] p 711 N93-14032

OPTICAL COUPLING
Digital fluoroscopy with an optically coupled charge-coupled device p 712 N93-14101

OPTICAL DATA PROCESSING
Optical disks become erasable p 736 N93-13133

OPTICAL DATA STORAGE MATERIALS
Massively parallel optical-to-electronic data transfer
[AD-A254831] p 688 N93-12733

OPTICAL DISKS
Optical disks become erasable p 736 N93-13133
Magnetic bearings for a high-performance optical disk buffer, volume 2
[NASA-CR-190874] p 615 N93-13608
Magnetic bearings for a high-performance optical disk buffer, volume 1
[NASA-CR-190873] p 616 N93-13706

OPTICAL EQUIPMENT
Large Deployable Reflector (LDR) system concept and technology definition study. Volume 1: Executive summary, analyses and trades, and system concepts
[NASA-CR-177413-VOL-1] p 708 N93-12591
Contamination analysis of SSF candidate materials
[NASA-CR-184431] p 709 N93-12894
OSA proceedings of the topical meeting on optical amplifiers and their applications, volume 13
[AD-A252974] p 711 N93-13879
Symposium on Polymeric Materials for Photonic and Optical Applications
[AD-A255820] p 554 N93-14029

OPTICAL FIBERS
Fibre-optic sensors using adiabatically tapered single-mode fibres
[AD-A254555] p 708 N93-12642
Appendix: Limits on the use of heterodyning and amplification in optical interferometry p 747 N93-13597
Fiber optic data bus radiation effects study
[AD-A255821] p 711 N93-14031

OPTICAL FILTERS
Integrated filter and detector array for spectral imaging
[NASA-CASE-NPO-18317-1-CU] p 709 N93-13419

OPTICAL HETERODYNING
Development of optical surface profiling instrumentation
[DE92-019252] p 710 N93-13652

OPTICAL MATERIALS
A new matrix formulation of classical electrodynamics. Part 2: Wave propagation in optical materials of infinite extent
[AD-A255032] p 560 N93-12585
Intrinsic bistable photonic materials by copper colloid formation in silica
[AD-A255505] p 711 N93-13866
Symposium on Polymeric Materials for Photonic and Optical Applications
[AD-A255820] p 554 N93-14029

OPTICAL MEASUREMENT
Introductory review of target discrimination criteria
[AD-A254954] p 560 N93-12551
Diagnostic of shock wave processes
[DE92-018059] p 565 N93-13357
Gas temperature measurements using the dual-line detection Rayleigh scattering technique p 599 N93-13668
Elastic and plastic strain measurement in high temperature environment using laser speckle p 600 N93-13673
Laser-based strain measurements for high temperature applications p 601 N93-13675

OPTICAL MEASURING INSTRUMENTS
Development of XUV projection lithography at 60 to 80 nm
[DE92-017517] p 603 N93-12560
Fibre-optic sensors using adiabatically tapered single-mode fibres
[AD-A254555] p 708 N93-12642
An integrated optical sensor for GMAW feedback control
[DE92-018019] p 610 N93-12793
Fiber optic sensors for environmental applications: A brief review
[DE92-040170] p 710 N93-13576
Development of optical surface profiling instrumentation
[DE92-019252] p 710 N93-13652
Multiplexing electro-optic architectures for advanced aircraft integrated flight control systems
[NASA-CR-182268] p 504 N93-13735

OPTICAL MEMORY (DATA STORAGE)
Optical disks become erasable p 736 N93-13133

OPTICAL PATHS
Orbiting Space Interferometer (OSI): A first generation space interferometer p 745 N93-13587

OPTICAL PROPERTIES
Ocean optical database
[AD-A254969] p 668 N93-12556
Fibre-optic sensors using adiabatically tapered single-mode fibres
[AD-A254555] p 708 N93-12642

Wave propagation and scattering in dense geophysical media
[AD-A254573] p 561 N93-12646
Synthesis and properties of mismatched heterojunction/substrate interfaces
[AD-A254577] p 719 N93-12648
Long Duration Exposure Facility M0003-5 recent results on polymeric films p 549 N93-12789
Latent image exposure monitor using scatterometry
[DE92-019427] p 604 N93-12915
Process designed for experimentation for increased-caliper Fresnel lenses
[DE92-019464] p 709 N93-12918
Development of optical surface profiling instrumentation
[DE92-019252] p 710 N93-13652
Symposium on Polymeric Materials for Photonic and Optical Applications
[AD-A255820] p 554 N93-14029

OPTICAL PUMPING
Experiments on resonantly photo-pumped x ray lasers
[DE92-019542] p 603 N93-12570
Self-consistent one-dimensional modelling of x ray laser plasmas
[DE92-019543] p 712 N93-12571

OPTICAL PYROMETERS
Gas temperature measurements using the dual-line detection Rayleigh scattering technique p 599 N93-13668

OPTICAL RADAR
A smoke producing rocket motor for atmospheric wind profiling
[DE92-018264] p 555 N93-12563
CO2 laser modeling
[NASA-CR-184455] p 604 N93-12656
Remote sensing data from CLARET: A prototype CART data set
[NASA-CR-191294] p 634 N93-13094
Measurement of tropospheric temperature and aerosol extinction using high spectral resolution lidar p 653 N93-13614
A joint study of the lower ionosphere by radar, lidar, and spectrometer p 655 N93-13755

OPTICAL REFLECTION
Optical model analysis of gravity wave-critical layer interaction p 658 N93-13888

OPTICAL RESONANCE
Electron temperature of Gd plasma produced by laser resonance ionization
[DE91-017785] p 718 N93-13732

OPTICAL RESONATORS
Initial performance of Los Alamos Advanced Free Electron Laser
[DE92-040214] p 605 N93-13507

OPTICAL SCANNERS
Development of optical surface profiling instrumentation
[DE92-019252] p 710 N93-13652

OPTICAL SWITCHING
A study of small solid-state switched TEA CO2 lasers p 607 N93-13814

OPTICAL THICKNESS
Sources of cloud nuclei and development of remote sensing techniques for cloud parameters
[AD-A255016] p 660 N93-12558
Comparison of cometary comae using ultraviolet spectroscopy: Composition and variation p 753 N93-13603
Atoms and molecules in supernova 1987A p 699 N93-13851

OPTICS
Optical design for a balloon-borne magnetograph
[NASA-CR-191003] p 709 N93-13062

OPTIMAL CONTROL
Optimal design and control of distributed parameter systems
[AD-A254947] p 690 N93-12547
Dynamics and control of a tumbling satellite retrieval device p 522 N93-13119
Combined design of structures and controllers for optimal maneuverability p 691 N93-13130
Subsonic flight test evaluation of a propulsion system parameter estimation process for the F100 engine
[NASA-TM-4426] p 502 N93-13155
Optimal control computer programs
[NASA-TM-108384] p 693 N93-13289
End-point position control of multi-link flexible manipulator arms p 613 N93-13335
A stochastic optimal feedforward and feedback control methodology for superagility
[NASA-CR-4471] p 694 N93-13370
Robust controller and estimator design using minimax methods p 694 N93-13925
Sequential quadratic programming solutions to related aircraft trajectory optimization problems p 505 N93-13926

OPTIMIZATION
Optimal design and control of distributed parameter systems
[AD-A254947] p 690 N93-12547
An investigation of new search techniques for the traveling salesman problem p 696 N93-12625
Program structure as a basis for the parallelization of global compiler optimizations
[AD-A254554] p 681 N93-12641
Numerical optimization
[AD-A254575] p 682 N93-12647
Weight optimization of an aerobrake structural concept for a lunar transfer vehicle
[NASA-TP-3262] p 519 N93-13379
Fast optimization of static axisymmetric shell structures p 630 N93-13921

OPTOELECTRONIC DEVICES
Introductory review of target discrimination criteria
[AD-A254954] p 560 N93-12551
Massively parallel optical-to-electronic data transfer
[AD-A254831] p 688 N93-12733
Silicon vision: Elementary functions to be implemented on electronic retinas p 692 N93-13242
The three to five semiconductor quantum well lasers and related optoelectronic devices on silicon
[AD-A255368] p 608 N93-13864
Intrinsic bistable photonic materials by copper colloid formation in silica
[AD-A255505] p 711 N93-13866

ORBIT CALCULATION
Nonconservative force model parameter estimation strategy for TOPEX/Poseidon precision orbit determination
[NASA-TM-104575] p 519 N93-13372
The use of consider covariance analysis in choosing data weights to reduce the effect of errors in model parameters on satellite orbit determination accuracy p 518 N93-13768

ORBIT TRANSFER VEHICLES
Weight optimization of an aerobrake structural concept for a lunar transfer vehicle
[NASA-TP-3262] p 519 N93-13379
A guidance methodology for the cislunar transfer of low-thrust spacecraft p 517 N93-13766

ORBITAL ASSEMBLY
Large Deployable Reflector (LDR) system concept and technology definition study. Volume 1: Executive summary, analyses and trades, and system concepts
[NASA-CR-177413-VOL-1] p 708 N93-12591
Large Deployable Reflector (LDR) system concept and technology definition study. Analysis of space station requirements for LDR
[NASA-CR-177414] p 742 N93-12592
Design of a welded joint for robotic, on-orbit assembly of space trusses
[NASA-TM-108380] p 609 N93-12682
A path to in-space welding and to other in-space metal processing technologies using Space Shuttle small payloads p 509 N93-13165
Space Shuttle orbiter modifications to support Space Station Freedom
[NASA-TM-108050] p 520 N93-13455

ORBITAL MANEUVERING VEHICLES
An investigation of error correcting techniques for OMV data
[NASA-CR-190942] p 682 N93-12654

ORBITAL MECHANICS
Approximate optimal guidance for the Advanced Launch System p 519 N93-13819

ORBITAL POSITION ESTIMATION
Nonconservative force model parameter estimation strategy for TOPEX/Poseidon precision orbit determination
[NASA-TM-104575] p 519 N93-13372

ORBITAL SERVICING
Large Deployable Reflector (LDR) system concept and technology definition study. Analysis of space station requirements for LDR
[NASA-CR-177414] p 742 N93-12592
Orbital Spacecraft Consumables Resupply System (OSCRS). Volume 3: Program cost estimate
[NASA-CR-185685] p 740 N93-12814
Support and servicing requirements for large observatories in space p 746 N93-13589

ORGANIC COMPOUNDS
Vapor pressure data analysis methodology, statistics, and applications
[AD-A255090] p 536 N93-12743
Analysis of IMS spectra using neural networks
[DE92-017511] p 691 N93-12791
ReTech, Inc., Plasma Centrifugal Furnace: Applications analysis report
[PB92-218791] p 714 N93-12982

ORGANIC MATERIALS
Z306 molecular contamination ad hoc committee results p 546 N93-12774
CONCAP 4: A Complex Autonomous Payload (CAP) for growing organic thin films in microgravity p 511 N93-13178
Hydrothermal organic synthesis experiments
[NASA-CR-191257] p 672 N93-13457

ORGANIC PEROXIDES
Kinetic and spectroscopic studies of peroxy radical reactions related to tropospheric photo-oxidation chemistry p 654 N93-13726

ORGANISMS
Long-term lunar stations: Some ecological considerations p 648 N93-13995

ORGANIZATIONS
Verification and validation of AI software
[AD-A254601] p 682 N93-12614
Selected data on research and development in industry: 1990
[NSF-92-317] p 773 N93-12667
NASA industry education initiative. Education programs report, 1991
[NASA-NP-158] p 730 N93-13248

ORGANOMETALLIC COMPOUNDS
Oligomer and mixed-metal compounds potential multielectron transfer catalysts
[DE92-011347] p 543 N93-13346

ORIFICES
A small, single stage orifice pulse tube cryocooler demonstration
[NASA-CR-190859] p 558 N93-13404
Scientific predictability of solid rocket performance: Analyses of the processing parameters p 526 N93-13824

ORTHOGONAL FUNCTIONS
Estimation of EOF expansion coefficients from incomplete data
[AD-A255252] p 697 N93-13886

ORTHOPHOTOGRAPHY
Using iterative orthophoto refinements to correct Digital Elevation Models (DEM's)
[AD-A254625] p 634 N93-13345

OSCILLATING FLOW
Fundamentals of enhanced scalar transport in strongly oscillating and/or resonant flow fields as created by pulse combustion
[DE92-012147] p 582 N93-13247

OSCILLATION DAMPERS
Damping the (pi)-mode instability in the SLC damping rings with a passive cavity
[DE92-018153] p 707 N93-13090

OSCILLATIONS
Damping the (pi)-mode instability in the SLC damping rings with a passive cavity
[DE92-018153] p 707 N93-13090
Nonlinear stability of combustion-driven acoustic oscillations in resonance tubes
[DE92-012153] p 699 N93-13262
Neutrino(e) appearance for neutrino(mu)-neutrino(tau) oscillations in matter
[DE92-040303] p 772 N93-13533
Parameter studies of helium-neon lasers at 543 nm p 606 N93-13747
A laboratory investigation of raindrop oscillations p 666 N93-13790

OSO
Orbiting Space Interferometer (OSI): A first generation space interferometer p 745 N93-13587
HARDI: A high angular resolution deployable interferometer for space p 745 N93-13588
Support and servicing requirements for large observatories in space p 746 N93-13589

OUTER SPACE TREATY
The province and heritage of mankind reconsidered: A new beginning p 681 N93-14018

OUTGASSING
Touchstone for success
[ESA-BR-52] p 557 N93-12934
Infrared emission from the water outgas cloud of an orbiting vehicle induced by collisions with atmospheric gases p 521 N93-13854

OVER-THE-HORIZON RADAR
Obtaining medians and other quantiles with limited memory space
[AD-A254506] p 683 N93-12722

OXIDATION
High temperature oxidation and electrochemical studies related to hot corrosion
[AD-A254435] p 540 N93-12595
Kinetics and dynamics of oxidation reactions involving an adsorbed CO species
[DE92-019745] p 537 N93-12995
Oxidative stability of LARC (tm)-TPI films
[NASA-TM-107696] p 552 N93-13441
Influence of surface defects and local structure on oxygenate reaction pathways over metal oxide surfaces
[DE92-040013] p 539 N93-13573

Effect of O2 partial pressure on post annealed Ba2YCu3O(7-delta) thin films
[DE92-014949] p 722 N93-13323
Spectroscopic observations of the night airglow from 3000 A to 9200 A p 658 N93-13891
Electrolytic smelting of lunar rock for oxygen, iron, and silicon p 761 N93-13979
Lunar mining of oxygen using fluorine
[LPI-748] p 761 N93-13980
Postoperative hyperbaric oxygen treatment of peripheral nerve damage
[AD-A255842] p 676 N93-14084

OXYGEN ATOMS
LDEF atomic oxygen fluence update p 546 N93-12771
LDEF yaw and pitch angle estimates p 524 N93-12772
Touchstone for success
[ESA-BR-52] p 557 N93-12934
The LDCE Particle Impact Experiment as flown on STS-46 --- limited duration space environment candidate materials exposure (LDCE) p 512 N93-13183
Photochemical kinetics of excited states of O3 and O2: Laboratory studies and atmospheric implications p 656 N93-13784
Studies of surface-induced luminescence relevant to spacecraft glow, using a seeded arc-jet p 523 N93-13919

OXYGEN IONS
Observations of solar wind ion charge exchange in the comet Halley coma p 752 N93-13467

OXYGEN PRODUCTION
Impact of lunar oxygen production on direct manned Mars missions p 540 N93-13984

OZONE
Nimbus-7 Total Ozone Mapping Spectrometer (TOMS) Antarctic ozone atlas: August through November 1991
[NASA-RP-1283] p 661 N93-12700
Absolute absorption cross sections of ozone at 300 K, 228 K and 195 K in the wavelength region 185-240 nm
[NASA-CR-191267] p 645 N93-13274
An investigation of the processes controlling ozone in the upper stratosphere
[DE92-019621] p 645 N93-13615
Impact of supersonic and subsonic aircraft on ozone: Including heterogeneous chemical reaction mechanisms
[DE92-019619] p 646 N93-13655
Aspects of atmospheric transport and dispersion within an air basin p 656 N93-13782
Photochemical kinetics of excited states of O3 and O2: Laboratory studies and atmospheric implications p 656 N93-13784
Tropopause fold investigations: Secondary circulation, water vapor and ozone analyses p 657 N93-13796
The seasonal variations and interrelationships of ozone, peroxyacetyl nitrate and nitrogen dioxide in the troposphere p 647 N93-13893

OZONE DEPLETION
Nimbus-7 Total Ozone Mapping Spectrometer (TOMS) Antarctic ozone atlas: August through November 1991
[NASA-RP-1283] p 661 N93-12700
A computer simulation of ecosystem processes in forests for application to air pollution, acid precipitation, and global change
[DE92-019616] p 643 N93-12927
Reports to the Nation on our changing planet: Our ozone shield p 645 N93-13413
Radiative transfer in the middle atmosphere p 652 N93-13482
Reduction of chlorofluorocarbon emissions from refrigeration systems
[DE92-019360] p 645 N93-13505
An experimental and theoretical study of degradation pathways for atmospheric halocarbons p 646 N93-13624
Cloud acidity and acidic deposition in the lower troposphere and ozone depletion in the Antarctic stratosphere: Modeling and data analysis regarding the role of atmospheric aerosol p 647 N93-13741
Gas-phase reactions of halogen species of atmospheric importance p 658 N93-13889

OZONOMETRY
Nimbus-7 Total Ozone Mapping Spectrometer (TOMS) Antarctic ozone atlas: August through November 1991
[NASA-RP-1283] p 661 N93-12700
Absolute absorption cross sections of ozone at 300 K, 228 K and 195 K in the wavelength region 185-240 nm
[NASA-CR-191267] p 645 N93-13274

OZONOSPHERE
Reports to the Nation on our changing planet: Our ozone shield p 645 N93-13413
Radiative transfer in the middle atmosphere p 652 N93-13482
An investigation of the processes controlling ozone in the upper stratosphere
[DE92-019621] p 645 N93-13615
Impact of supersonic and subsonic aircraft on ozone: Including heterogeneous chemical reaction mechanisms
[DE92-019619] p 646 N93-13655

P

P-I-N JUNCTIONS
A payload to evaluate photodiodes for the detection of soft and hard x rays in a space environment using a Get Away Special p 509 N93-13166

P-N JUNCTIONS
GaAs gate dynamic memory technology
[AD-A254801] p 720 N93-12748
Investigation of microgravity effects on solidification phenomena of selected materials p 510 N93-13168

P-3 AIRCRAFT
Structural fatigue aspects of the P-3 Orion
[ARL-STRUC-TM-558] p 500 N93-13256

PACIFIC OCEAN
The morphotectonic fabric of the East Pacific Rise: Implications for fault generation and crustal accretion p 652 N93-13481
Deep convection and its relation to the large-scale circulation in the tropical Pacific p 654 N93-13725
Modeling and observations of deep circulation in the eastern South Pacific Ocean p 670 N93-13841

PACKAGING
Battery selection for space experiments p 512 N93-13184

PAINTS
Laser ablation for sample introduction in inductively coupled plasma spectrometry p 719 N93-13897

PAIR PRODUCTION
Electromagnetic lepton-pair production in relativistic collisions
[DE92-011069] p 706 N93-12829
Research in elementary particle physics
[DE92-017869] p 704 N93-13251

PALEOCLIMATOLOGY
How life affects the geochemical cycle of carbon
[NASA-CR-191241] p 644 N93-13031
Atmospheric, climatic and environmental research
[NASA-CR-191367] p 664 N93-13718

PALLADIUM
Palladium-chromium static strain gages for high temperatures p 600 N93-13671

PANEL FLUTTER
Hypersonic panel flutter in a rarefied atmosphere p 505 N93-13928

PANEL METHOD (FLUID DYNAMICS)
Aerodynamic analysis of slipstream/wing/nacelle interference for preliminary design of aircraft configurations p 497 N93-13205
Application of subsonic first-order panel methods for prediction of inlet and nozzle aerodynamic interactions with airframe p 497 N93-13223
Analysis and design of planar and non-planar wings for induced drag minimization
[NASA-CR-191274] p 493 N93-13463
Computational fluid dynamics of the base flow on a plane body between a subsonic flow on one side and a supersonic flow on the other p 591 N93-13920

PARABOLIC ANTENNAS
Required technologies for a lunar optical UV-IR synthesis array p 747 N93-13598

PARABOLIC DIFFERENTIAL EQUATIONS
Efficient solution of parabolic equations by Krylov approximation methods
[NASA-CR-191235] p 697 N93-13409

PARALLEL COMPUTERS
Parallel computing systems
[AD-A255076] p 689 N93-12852
Performance of a plasma fluid code on the Intel parallel computers
[DE92-011680] p 716 N93-13297
Research summary, January 1989 - June 1990
[NASA-CR-190960] p 687 N93-13694

PARALLEL FLOW
Effect of the flow non-uniformity on the mixing layer at the interface of parallel supersonic flows
[ISAS-RN-646] p 491 N93-12716

PARALLEL PLATES
Numerical simulation of compressible Couette flow stability: Non-linear and three-dimensional effects p 594 N93-14077

PARALLEL PROCESSING (COMPUTERS)
An application of exponential neural networks to event-train recognition
[AD-A254948] p 690 N93-12548
Program structure as a basis for the parallelization of global compiler optimizations
[AD-A254554] p 681 N93-12641
Graphics-based parallel programming tools
[AD-A254406] p 683 N93-12763
Speedup properties of phases in the execution profile of distributed parallel programs
[DE92-019301] p 689 N93-12797
Memory access in shared virtual memory
[DE92-019594] p 681 N93-12823
Parallel computing systems
[AD-A255076] p 689 N93-12852
HIPPI and Fibre Channel
[DE92-040346] p 689 N93-13046
Turbomachinery CFD on parallel computers
[NASA-TM-105932] p 689 N93-13154
Simulation of excitatory/inhibitory interactions in single auditory neurons
[AD-A253614] p 675 N93-13252
Performance of a plasma fluid code on the Intel parallel computers
[DE92-011680] p 716 N93-13297
Compressible convection and pulsations on parallel computers p 690 N93-13961

PARALLEL PROGRAMMING
Graphics-based parallel programming tools
[AD-A254406] p 683 N93-12763
Speedup properties of phases in the execution profile of distributed parallel programs
[DE92-019301] p 689 N93-12797
Speedup properties of phases in the execution profile of distributed parallel programs
[DE92-019965] p 689 N93-12810

PARAMETER IDENTIFICATION
Identifiability of linear systems in physical coordinates
[NASA-TM-107695] p 625 N93-13125
The use of consider covariance analysis in choosing data weights to reduce the effect of errors in model parameters on satellite orbit determination accuracy p 518 N93-13768

PARAMETERIZATION
A parameterized quasi-five-cylinder convective cloud model and its application to remote sensing of rainfall p 663 N93-13489

PARSING ALGORITHMS
Japanese/English machine translation using sublanguage patterns and reversible grammars p 686 N93-13494

PARTIAL DIFFERENTIAL EQUATIONS
Analytical studies of nonlinear partial differential equations of interest in nonlinear optics
[AD-A254931] p 696 N93-13027

PARTIAL PRESSURE
Effect of O2 partial pressure on post annealed Ba2YCu3O(7-delta) thin films
[DE92-014949] p 722 N93-13323

PARTICLE ACCELERATION
Particle production and survival in muon acceleration
[DE92-019553] p 701 N93-12572

PARTICLE ACCELERATORS
A distributed timing system for sychronizing control and data correlation
[DE92-018603] p 690 N93-12564
Real-time data archiving for GTA
[DE92-018613] p 733 N93-12567

PARTICLE BEAMS
A simple model for SLC positron stability issues
[DE92-019644] p 706 N93-12992
Longitudinal beam dynamics with rf noise
[DE92-040645] p 707 N93-13108

PARTICLE COLLISIONS
Particle production and survival in muon acceleration
[DE92-019553] p 701 N93-12572
Test of QED using a laser at the SLAC final focus test beam
[DE92-019647] p 707 N93-12993
Search for doubly Cabibbo suppressed decays of the charged D meson
[DE92-018588] p 703 N93-13092
Heavy gauge boson and lambda(b) baryon searches at CDF
[DE92-019551] p 705 N93-13537

PARTICLE DENSITY (CONCENTRATION)
Experimental testing of four correction algorithms for the forward scattering spectrometer probe
[NASA-TM-105906] p 597 N93-13307

PARTICLE DIFFUSION
Longitudinal beam dynamics with rf noise
[DE92-040645] p 707 N93-13108
The role of particle diffusion in the lower transition region: Revised interpretation of emission measures p 770 N93-13476

PARTICLE ENERGY
A study of the generation of linear energy transfer spectra for space radiations
[NASA-TM-4410] p 772 N93-13572

PARTICLE INTERACTIONS
Theoretical nuclear physics
[DE92-019286] p 706 N93-12822

Real-time data archiving for GTA
[DE92-018613] p 733 N93-12567

PARTICLE BEAMS
A simple model for SLC positron stability issues
[DE92-019644] p 706 N93-12992
Longitudinal beam dynamics with rf noise
[DE92-040645] p 707 N93-13108

PARTICLE COLLISIONS
Particle production and survival in muon acceleration
[DE92-019553] p 701 N93-12572
Test of QED using a laser at the SLAC final focus test beam
[DE92-019647] p 707 N93-12993
Search for doubly Cabibbo suppressed decays of the charged D meson
[DE92-018588] p 703 N93-13092
Heavy gauge boson and lambda(b) baryon searches at CDF
[DE92-019551] p 705 N93-13537

PARTICLE DENSITY (CONCENTRATION)
Experimental testing of four correction algorithms for the forward scattering spectrometer probe
[NASA-TM-105906] p 597 N93-13307

PARTICLE DIFFUSION
Longitudinal beam dynamics with rf noise
[DE92-040645] p 707 N93-13108
The role of particle diffusion in the lower transition region: Revised interpretation of emission measures p 770 N93-13476

PARTICLE ENERGY
A study of the generation of linear energy transfer spectra for space radiations
[NASA-TM-4410] p 772 N93-13572

PARTICLE INTERACTIONS
Theoretical nuclear physics
[DE92-019286] p 706 N93-12822
Electromagnetic lepton-pair production in relativistic collisions
[DE92-011069] p 706 N93-12829

PARTICLE MASS
Neutrino mass
[DE92-017411] p 701 N93-12588
In situ dust mass distribution measurements from the Giotto encounter with comet P/Halley p 753 N93-13602

PARTICLE MOTION
Proton transport on modified sulfonated polyaniline electrodes
[AD-A254917] p 570 N93-12650
On development of a three-dimensional particle motion tracking system
[DE92-015846] p 704 N93-13263
Dual mass and torsion p 728 N93-13498

PARTICLE PRODUCTION
Particle production and survival in muon acceleration
[DE92-019553] p 701 N93-12572
Heavy gauge boson and lambda(b) baryon searches at CDF
[DE92-019551] p 705 N93-13537

PARTICLE SIZE DISTRIBUTION
Experimental testing of four correction algorithms for the forward scattering spectrometer probe
[NASA-TM-105906] p 597 N93-13307

PARTICLE SPIN
The spin of the nucleon in deep inelastic lepton scattering experiments
[DE92-018854] p 702 N93-13073

PARTICLE THEORY
Research in elementary particle physics
[DE92-017869] p 704 N93-13251

PARTICLE TRAJECTORIES
Adaptation of multidimensional group particle tracking and particle wall-boundary condition model to the FDNS code
[SECA-TR-92-06] p 575 N93-12689
Ion radial diffusion in an electrostatic impulse model for stormtime ring current formation
[NASA-CR-190941] p 705 N93-12715

PARTICLES
Two-phase flow modeling with discrete particles
[DE92-017850] p 583 N93-13356

PARTICULATE REINFORCED COMPOSITES
An investigation into thermomechanical fatigue of metal matrix composites p 534 N93-13810

PARTICULATES
Touchstone for success
[ESA-BR-52] p 557 N93-12934
On development of a three-dimensional particle motion tracking system
[DE92-015846] p 704 N93-13263
Study of the concentration and deposition of tropospheric aerosols using x ray emission techniques p 667 N93-13894

PATHOGENESIS
Transactions: Tropospheric ozone and the environment. Papers from an international conference
[PB92-217017] p 643 N93-12941

PATHOGENS
Long-term lunar stations: Some ecological considerations p 648 N93-13995

PATHOLOGY
AFRRI reports
[AD-A254581] p 674 N93-12649

PATTERN RECOGNITION
Artificial intelligence and neural networks applied to ion mobility spectrometry
[DE92-017508] p 690 N93-12559
Machine Perception
[AGARD-LS-185] p 692 N93-13238
Automatic pattern recognition techniques for geometrical correction on satellite data p 687 N93-13913

PAVEMENTS
Polypropylene fibers in portland cement concrete pavements
[DOT/FAA/RD-92/9] p 551 N93-13259

PAYLOAD INTEGRATION
Spaceflight payload design flight experience G-408 p 508 N93-13160
Preparing safety data packages for experimenters using the Get Away Special (GAS) carrier system p 512 N93-13186

PAYLOADS
Manipulation strategies for massive space payloads
[NASA-CR-190844] p 611 N93-12952
The DSI small satellite launcher p 511 N93-13180
Approximate optimal guidance for the Advanced Launch System p 519 N93-13819
The influence of lunar propellant production on the cost-effectiveness of cislunar transportation systems p 556 N93-13983

PEEK
Investigations of the mechanical behavior of graphite/PEEK (APC-2) composites p 534 N93-13908

PENNING DISCHARGE
Suppression of the e(-) coextracted from a Penning surface-plasma H(-) source
[DE92-040350] p 714 N93-12997

PEPTIDES
Neurochemical control of circadian rhythms
[AD-A255054] p 675 N93-13116

PERCEPTION
Machine Perception
[AGARD-LS-185] p 692 N93-13238
Machine perception exploiting high-level spatio-temporal models p 693 N93-13244
Public perceptions of the risks of an unfamiliar technology: The case of using nuclear energy sources for space missions p 527 N93-13971

PERFLUORO COMPOUNDS
Studies of the kinetics and mechanisms of perfluoroether reactions on iron and oxidized iron surfaces
[NASA-CR-191363] p 539 N93-13763

PERFLUOROALKANE
Synthesis of derivatives of alpha, omega difunctional perfluoroaliphatic compounds for low dielectric constant resins
[AD-A254928] p 550 N93-13026

PERFORATING
Numerical simulations of steel plate perforation
[DE92-017058] p 626 N93-13301

PERFORMANCE PREDICTION
Operator workload predictions for the revised AH-64A workload prediction model. Volume 2: Appendixes A through H
[AD-A254939] p 676 N93-12545
Introductory review of target discrimination criteria
[AD-A254954] p 560 N93-12551
An experimental study of a small high-speed LH2 pump for rockets: Fluid dynamic performance
[NAL-TR-1131] p 610 N93-12727
ESPVI 4.0 electrostatic precipitator V-I and performance model: User's model
[PB92-169614] p 643 N93-12938
Identifiability in the autopsy model of reliability theory p 620 N93-13710
Sequential quadratic programming solutions to related aircraft trajectory optimization problems p 505 N93-13926

PERFORMANCE TESTS
A heat pipe coupled planar thermionic converter: Performance characterization, nondestructive testing, and evaluation
[AD-A254941] p 727 N93-12546
Diesel injector fouling bench test methodology
[AD-A254532] p 609 N93-12600
The constant current loop: A new paradigm for resistance signal conditioning
[NASA-TM-104260] p 596 N93-12681
Performance of thermal control tape in the protection of composite materials p 536 N93-12780
Speedup properties of phases in the execution profile of distributed parallel programs
[DE92-019301] p 689 N93-12797
The VELOPT code for estimating performance of a Fabry-Perot velocimeter
[DE92-015566] p 596 N93-12831
Limited production Precision Runway Monitor (PRM) master test plan
[DOT/FAA/CT-TN92/23] p 506 N93-12899
Pressure fed thrust chamber technology program
[NASA-CR-184461] p 526 N93-12968
Advanced water-cooled phosphoric acid fuel cell development
[DE92-019979] p 638 N93-13040
Cloud curve algorithm test program
[AD-A253918] p 662 N93-13099
Comparative performance tests of a pitot-inlet in several European wind-tunnels at subsonic and supersonic speeds p 497 N93-13221
Terminal Doppler Weather Radar (TDWR) Operational Test and Evaluation (OT/E) integration test plan
[DOT/FAA/CT-TN92/6] p 499 N93-13377
All-metal, compact heat exchanger for space cryocoolers
[NASA-CR-190861] p 559 N93-13604
Thermally stable electrolytes for rechargeable lithium batteries, phase 2
[NASA-CR-190878] p 573 N93-13610
Boiler efficiency methodology for solar heat applications
[DE92-019805] p 640 N93-13618
Engineering data transfer test with EDMICS using MIL-R-28002 (Raster)
[DE92-019808] p 738 N93-13619
Westinghouse PAFC program update
[DE92-019978] p 640 N93-13623
Thermal control systems for low-temperature heat rejection on a lunar base
[NASA-CR-191286] p 679 N93-13717
Validation test of 125 Ah advanced design IPV nickel-hydrogen flight cells
[NASA-TM-105912] p 527 N93-14079

PERIODIC FUNCTIONS
Deterministic and stochastic responses of nonlinear systems p 631 N93-13966

PERIODIC VARIATIONS
Radial and nonradial periods and growth rates of an Al Velorum model
[DE92-011369] p 743 N93-13339

PERIODICALS
Evolution of the scientific paper
[DE92-019696] p 735 N93-12994

PERIPHERAL NERVOUS SYSTEM
Postoperative hyperbaric oxygen treatment of peripheral nerve damage
[AD-A255842] p 676 N93-14084

PERMANENT MAGNETS
Wide range, permanent magnet Compton spectrometer
[DE92-017312] p 596 N93-12762
Magnetic hardening studies and novel techniques for preparation of high performance magnets
[AD-A254761] p 698 N93-12865
Initial performance of Los Alamos Advanced Free Electron Laser
[DE92-040214] p 605 N93-13507

PERMEABILITY
Determination of the permeability of carbon aerogels by gas flow measurements
[DE92-019574] p 550 N93-12888

PERMITTIVITY
Microwave and infrared dielectric relaxation of alkylcarbonates, chloroform and their mixtures at 25 C
[AD-A253606] p 537 N93-13096
Numerical analysis of permittivity with loss in isotropic binary composites
[AD-A255203] p 534 N93-13940

PEROVSKITES
Perovskite solid electrolytes for SOFC
[DE92-019981] p 638 N93-13041

PEROXIDES
Kinetic and spectroscopic studies of peroxy radical reactions related to tropospheric photo-oxidation chemistry p 654 N93-13726

PERSONAL COMPUTERS
Users manual for program SSFREQ intermediate mode stability curves: Developed for use on a PC computer
[NASA-CR-184452] p 682 N93-12675
Digital chart database conversion into a system electronic navigational chart
[AD-A255007] p 632 N93-12869

PERSONNEL
US Antarctic program. Personnel manual, 1992
[NSF-92-63] p 731 N93-12637

Highlights 92/2 p 775 N93-13474
A basis of settlement: Economic foundations of permanent pioneer communities p 741 N93-14019
PERSONNEL DEVELOPMENT
Human factors research in aircrew performance and training: 1986-1991
[AD-A254455] p 677 N93-12609
Women and minorities in science and engineering: An update
[NSF-92-303] p 730 N93-12907
Diversity in biological research
[NSF-92-19] p 673 N93-13700
PERTURBATION
Analysis of a linearly constrained least squares algorithm for adaptive beamforming
[AD-A255017] p 695 N93-12582
Magnetic field perturbation caused by bending vibrations of a quadrupole
[DE92-040644] p 623 N93-13003
Spanwise-nonuniform excitation of a plane mixing layer p 577 N93-13120
A time domain numerical theory for studying steady-state acoustic disturbance in flow p 700 N93-13770
On computing accurate singular values and eigenvalues of acyclic matrices
[AD-A255892] p 697 N93-14036
PERTURBATION THEORY
Cross sections and rate coefficients for the electron-impact excitation of He-like ions
[ISAS-RN-647] p 703 N93-13095
The growth of disturbances in barotropic models of the atmosphere p 658 N93-13887
PH
Fibre-optic sensors using adiabatically tapered single-mode fibres
[AD-A254555] p 708 N93-12642
Proton transport on modified sulfonated polyaniline electrodes
[AD-A254917] p 570 N93-12650
Methods development for total organic carbon accountability
[NASA-CR-184438] p 672 N93-12949
PHARMACOLOGY
JPRS report: Science and technology. Central Eurasia: Life sciences
[JPRS-ULS-92-024] p 672 N93-13033
The neurochemical and neuropharmacological basis of motion sickness
[NASA-CR-190957] p 675 N93-13061
PHASE CONJUGATION
Phase conjugation using CO2 lasers p 607 N93-13812
PHASE DIAGRAMS
Solutions without phase-slip for the Ginsburg-Landau equation
[PB92-115575] p 696 N93-12889
PHASE ERROR
Effects of stinger axial dynamics and mass compensation methods on experimental modal analysis p 699 N93-13907
PHASE LOCKED SYSTEMS
Advanced on-chip divider for monolithic microwave VCO's
[NASA-CR-191355] p 572 N93-13563
PHASE SHIFT
Design and operation of a bunched-beam, phase-spread measurement
[DE92-040230] p 708 N93-13508
Effects of stinger axial dynamics and mass compensation methods on experimental modal analysis p 699 N93-13907
PHASE TRANSFORMATIONS
Tempering effects for lower bainite, martensite, and mixed microstructures on impact, fracture, and related mechanical properties of ASTM A723 steel
[AD-A254617] p 541 N93-12616
Modeling of coalescence, agglomeration, and phase segregation in microgravity processing of bimetallic composite materials
[NASA-CR-191247] p 556 N93-12728
C60 transformations at high pressures
[DE92-019546] p 701 N93-12806
The crystallization and crystalline properties of LARC-TPI
[NASA-CR-191001] p 721 N93-13022
Chemical potentials in dilute, multicomponent solutions
[DE92-011041] p 538 N93-13317
PHASE VELOCITY
Baroclinic wave packets in models and observations p 663 N93-13361
Lateral variations of shear velocity and anelasticity in the upper mantle of the western US from Rayleigh wave observations p 653 N93-13492
Transverse wave motion in constrained mechanical systems p 628 N93-13634
PHASED ARRAYS
Phased array feed design technology for Large Aperture Microwave Radiometer (LAMR) Earth observations
[NASA-CR-189727] p 519 N93-13462
Scattering from a finite collection of transverse dipole and axial slot arrays with edge effects p 568 N93-14048
PHENOLS
Synthesis of derivatives of alpha, omega difunctional perfluoroaliphatic compounds for low dielectric constant resins
[AD-A254928] p 550 N93-13026
PHENOMENOLOGY
Effects of source-region phenomenology on seismic discrimination
[DE92-017441] p 649 N93-12841
PHILOSOPHY
The lunar community church: Contributions to lunar living and to evolution of ethical and spiritual thinking p 676 N93-14020
PHONETICS
Perception-based and machine-oriented signal processing within speech understanding systems p 692 N93-13239
PHONONS
Electronic transport properties of semiconductor microstructures p 724 N93-13730
PHOSPHATES
Bonding in simple phosphate glass
[DE92-019437] p 550 N93-12917
Improving the temperature resistance of aluminum-matrix composites by using an acid phosphate binder p 536 N93-14056
PHOSPHORESCENCE
Temperature measurements with micrometer spatial resolution
[AD-A255897] p 603 N93-14086
PHOSPHORIC ACID
Westinghouse PAFC program update
[DE92-019978] p 640 N93-13623
PHOSPHORIC ACID FUEL CELLS
Gas cooled fuel cell systems technology development
[DE92-0012983-3103] p 636 N93-12683
Advanced water-cooled phosphoric acid fuel cell development
[DE92-019979] p 638 N93-13040
Westinghouse PAFC program update
[DE92-019978] p 640 N93-13623
PHOSPHORS
Temperature measurements with micrometer spatial resolution
[AD-A255897] p 603 N93-14086
PHOTOCHEMICAL REACTIONS
A physico-chemical study of some areas of fundamental significance to biophysics
[DE92-019916] p 672 N93-13083
Photochemical dynamics of surface oriented molecules
[DE92-019813] p 703 N93-13106
Monitoring interfacial dynamics by pulsed laser techniques
[DE92-040302] p 606 N93-13514
Effects of stratospheric aerosol surface processes on the LLNL two-dimensional zonally averaged model
[DE92-019620] p 646 N93-13646
Photochemical kinetics of excited states of O3 and O2: Laboratory studies and atmospheric implications p 656 N93-13784
Informal Conference on Photochemistry
[AD-A255824] p 540 N93-14033
PHOTOCONDUCTORS
Latent image exposure monitor using scatterometry
[DE92-019427] p 604 N93-12915
PHOTODIODES
A payload to evaluate photodiodes for the detection of soft and hard x rays in a space environment using a Get Away Special p 509 N93-13166
An acoustic charge transport imager for high definition television applications
[NASA-CR-191295] p 572 N93-13448
PHOTODISSOCIATION
Photodissociation processes
[PB92-222702] p 702 N93-13067
An experimental and theoretical study of degradation pathways for atmospheric halocarbons p 646 N93-13624
PHOTOELECTRICITY
A Pennsylvania State University/General Electric Get Away Special (GAS) experiment p 511 N93-13177
PHOTOELECTRON SPECTROSCOPY
Surface contamination on LDEF exposed materials p 547 N93-12776
Table-top x ray lasing based on optical-field-induced ionization
[DE92-019374] p 604 N93-12925
PHOTOELECTRONS
Initial performance of Los Alamos Advanced Free Electron Laser
[DE92-040214] p 605 N93-13507
Shot noise limits to sensitivity of optical interferometry p 745 N93-13586
PHOTOEXCITATION
Workshop on Super-Intense Laser-Atom Physics
[AD-A254833] p 604 N93-12734
PHOTOGEOLOGY
Volcanism in the eastern Hellas region of Mars: The geology of Hadriaca and Tyrrhena Paterae p 768 N93-14092
PHOTOGRAPHIC FILM
IIaO ultraviolet and nuclear emulsion films responses to orbital flights on STS-3, STS-7, STS-8, and STS-40 p 509 N93-13163
PHOTOIONIZATION
Long pulse electron beam propagation
[DE92-014948] p 706 N93-12830
Table-top x ray lasing based on optical-field-induced ionization
[DE92-019374] p 604 N93-12925
Electron stimulated desorption of the metallic substrate at monolayer coverage: Sensitive detection via 193 nm laser photoionization of neutral aluminum desorbed from CH3O/Al(111)
[DE92-014858] p 723 N93-13349
PHOTOLITHOGRAPHY
Soft X Ray Projection Lithography Topical Meeting. Volume 8: Technical digest
[AD-A254756] p 709 N93-12850
PHOTOLUMINESCENCE
Strained-layer InGaAs-GaAs-AlGaAs quantum well lasers and transverse junction stripe lasers p 607 N93-13773
High magnetic field studies of strained layer superlattices p 726 N93-13895
PHOTOLYSIS
An investigation of the processes controlling ozone in the upper stratosphere
[DE92-019621] p 645 N93-13615
Kinetic studies of some free radical reactions involved in cloudwater chemistry p 668 N93-14055
PHOTOMETERS
Integrated filter and detector array for spectral imaging
[NASA-CASE-NPO-18317-1-CU] p 709 N93-13419
PHOTON BEAMS
Thermal imaging of synchrotron beams on silicon crystals
[DE92-018182] p 719 N93-12562
PHOTONICS
Organization of the Optical Society of America Photonic Science Topical Meeting Series. Volume 8: Integrated photonics research. Iifornia on 9-11 april 1991
[AD-A254682] p 709 N93-12666
Real-time quality assurance testing using photonic techniques: Application to iodine water system
[NASA-CR-184413] p 619 N93-12692
Symposium on Polymeric Materials for Photonic and Optical Applications
[AD-A255820] p 554 N93-14029
Fiber optic data bus radiation effects study
[AD-A255821] p 711 N93-14031
PHOTOOXIDATION
Kinetic and spectroscopic studies of peroxy radical reactions related to tropospheric photo-oxidation chemistry p 654 N93-13726
PHOTOSPHERE
The 3-D description of vertical current sheets with application to solar flares
[SSL-PREPRINT-90-119] p 770 N93-13477
PHOTOSYNTHESIS
Nitrogen control of chloroplast development and differentiation
[DE92-017392] p 671 N93-12768
Characteristics of phytoplankton as monitors of the physical environment
[AD-A255009] p 642 N93-12870
Phytoplankton photosynthesis in natural mixed layers
[AD-A255010] p 671 N93-12871
PHOTOVOLTAIC CONVERSION
Cost analysis methodology: Photovoltaic Manufacturing Technology Project
[DE92-016441] p 639 N93-13528
PHYSICAL OPTICS
Wave propagation and scattering in dense geophysical media
[AD-A254573] p 561 N93-12646
PHYSICAL PROPERTIES
High temperature superconductor materials and applications
[NASA-CR-184437] p 719 N93-12691
Synthesis and properties of novel cluster phases
[DE92-017388] p 545 N93-12697

PHYSIOLOGICAL DEFENSES
Physiological stress from chemical defense clothing and equipment
[AD-A255786] p 676 N93-14028
PHYSIOLOGICAL EFFECTS
Physiologically constrained aerocapture for manned Mars missions
[NASA-TM-103954] p 521 N93-12720
Physiological effects of positive pressure ventilation
[AD-A254809] p 674 N93-12751
SLS-1 flight experiments preliminary significant results
[NASA-TM-108033] p 520 N93-13613
Thermal stress in US Air Force operations
[AD-A255785] p 676 N93-14027
PHYSIOLOGICAL FACTORS
Characteristics of phytoplankton as monitors of the physical environment
[AD-A255009] p 642 N93-12870
PHYSIOLOGICAL RESPONSES
Functional MRI studies of human vision on a clinical imager
[DE92-017448] p 674 N93-12566
Forest declines: Some perspectives on linking processes and patterns
[DE92-019946] p 642 N93-12828
Phytoplankton photosynthesis in natural mixed layers
[AD-A255010] p 671 N93-12871
SLS-1 flight experiments preliminary significant results
[NASA-TM-108033] p 520 N93-13613
PHYTOPLANKTON
Characteristics of phytoplankton as monitors of the physical environment
[AD-A255009] p 642 N93-12870
Phytoplankton photosynthesis in natural mixed layers
[AD-A255010] p 671 N93-12871
New approaches to the measurement of chlorophyll, related pigments and productivity in the sea
[NASA-CR-190879] p 673 N93-13612
PIEZOELECTRIC CRYSTALS
Thermal effects on the frequency response of piezoelectric crystals
[DE92-019039] p 720 N93-12819
PIEZOELECTRIC TRANSDUCERS
Very high temperature silicon on silicon pressure transducers p 601 N93-13679
PIEZOELECTRICITY
Thermal effects on the frequency response of piezoelectric crystals
[DE92-019039] p 720 N93-12819
Use of phonon echoes in the study of 2-6 compounds and dielectric Bi12GeO20:Cr p 725 N93-13847
PIEZORESISTIVE TRANSDUCERS
SiC device development for high temperature sensor applications p 601 N93-13677
PILOT PERFORMANCE
Operator workload predictions for the revised AH-64A workload prediction model. Volume 2: Appendixes A through H
[AD-A254939] p 676 N93-12545
Theory and design of adaptive automation in aviation systems
[AD-A254595] p 499 N93-12613
PILOT PLANTS
A new apparatus for continuous countercurrent flow of solids and liquids
[DE92-011675] p 583 N93-13318
PILOT TRAINING
The modelling of turbulence and downbursts for flight simulators p 507 N93-13542
PINTLES
Diesel injector fouling bench test methodology
[AD-A254532] p 609 N93-12600
PIONEER VENUS SPACECRAFT
SO2 on Venus: A final cross-calibration with Pioneer Venus
[NASA-CR-191256] p 758 N93-13344
PIONS
Particle production and survival in muon acceleration
[DE92-019553] p 701 N93-12572
PIPE FLOW
Analysis of fluid/mechanical systems using EASY5 p 586 N93-13397
PIPELINES
Briefing notes on propulsion stability codes ADMIT, NYQUIST, and SSFREQ
[NASA-CR-184449] p 525 N93-12874
Diagnostic of material defects found in pipelines made of 13 HMF steel on the basis of acoustic emission p 623 N93-12989
PIPES (TUBES)
Users manual for program SSFREQ intermediate mode stability curves: Developed for use on a PC computer
[NASA-CR-184452] p 682 N93-12675
Users manual for program ADMIT: Admittance and pressure transfer function developed for use on a PC computer
[NASA-CR-184450] p 682 N93-12676
On the prediction of turbulent secondary flows
[NASA-CR-189722] p 575 N93-12717
Wastage-resistant FBC evaporator tubing through microalloying
[DE92-001256] p 541 N93-12790
Briefing notes on propulsion stability codes ADMIT, NYQUIST, and SSFREQ
[NASA-CR-184449] p 525 N93-12874
Acoustic modes in fluid networks p 586 N93-13398
PISTON ENGINES
The effects of pressure gradients on convective heat flux predictions in engine environments p 616 N93-13772
PITCH (INCLINATION)
LDEF yaw and pitch angle estimates p 524 N93-12772
PITCHING MOMENTS
New methods for predicting nonlinear lift, center of pressure, and pitching moment on missile configurations
[AD-A255078] p 492 N93-12741
Dynamic stall effects on hingeless rotor stability with experimental correlation p 492 N93-13010
PITOT TUBES
Comparative performance tests of a pitot-inlet in several European wind-tunnels at subsonic and supersonic speeds p 497 N93-13221
PIXELS
Polarization effects and multipolarization SAR p 564 N93-13054
PLANAR STRUCTURES
Analysis and design of planar and non-planar wings for induced drag minimization
[NASA-CR-191274] p 493 N93-13463
PLANE STRAIN
Small-strain and finite-strain finite element analyses of plane-strain tensile elastic-plastic crack growth p 621 N93-12628
PLANE STRESS
Oxidative stability of LARC (tm)-TPI films
[NASA-TM-107696] p 552 N93-13441
PLANE WAVES
Cancellation of air-borne acoustic plane waves obliquely incident upon a planar phased-array of active surface elements p 700 N93-13635
Guidance and scattering of electromagnetic waves by nonlinear layers p 566 N93-13813
Electromagnetic scattering simulations using equivalent boundary condition models p 569 N93-14052
PLANETARY BOUNDARY LAYER
Structure of and dynamical processes in the Earth's magnetopause and boundary layer regions p 657 N93-13793
PLANETARY COMPOSITION
Studies of radiative emission from the simulated shock layer of the Huygens probe p 521 N93-12834
PLANETARY EVOLUTION
Studies of extra-solar Oort Clouds and the Kuiper disk
[NASA-CR-190958] p 769 N93-12669
PLANETARY IONOSPHERES
The Jovian ionosphere p 758 N93-13337
PLANETARY NEBULAE
Alternative methods for determination of the temperature of central stars of planetary nebulae
[INPE-5434-TDI/485] p 750 N93-13279
A high-resolution radio survey of the galactic plane p 744 N93-13480
The planetary nebula system and the dynamics of the galaxy Centaurus A p 754 N93-13645
Density contrast shell models for planetary nebulae p 756 N93-13850
Accretion rates of protoplanets p 759 N93-13958
PLANETARY RADIATION
The Jovian ultraviolet aurora observed with the IUE spacecraft: Brightness and color distribution with longitude p 759 N93-13625
PLANETARY TEMPERATURE
An analysis of the Voyager 2 ultraviolet spectrometer occultation data at Uranus and Triton: Inferring heat sources and model atmospheres p 768 N93-14072
PLANETARY WAVES
Intraseasonal variability of infrared cooling rates during the Asian summer monsoon and their influence on intraseasonal waves p 665 N93-13760
PLANT DESIGN
Ultraviolet disinfection technology assessment
[PB92-222868] p 678 N93-12983
A microgravity processing plant for the manufacturing of propellant and water from asteroid ore p 515 N93-13558
PLASMA ARC WELDING
VPPA weld model evaluation
[NASA-CR-184460] p 611 N93-12919
PLASMA COMPOSITION
A design for an advanced divertor for D3D and ITER: The radiative slot divertor
[DE92-019579] p 714 N93-12932
PLASMA COMPRESSION
Densities and abundances of hot cometary ions in the coma of P/Halley p 752 N93-13466
PLASMA CONTROL
A quantitative analysis of the effect of ELMs on H-mode thermal energy confinement in DIII-D
[DE92-017704] p 712 N93-12687
Stimulated Brillouin processes in crystals and glasses
[DE92-019549] p 721 N93-12887
A design for an advanced divertor for D3D and ITER: The radiative slot divertor
[DE92-019579] p 714 N93-12932
Future development of the D3-D tokamak program
[DE92-040051] p 715 N93-13044
Applications of group-invariant analytic solutions to inertial confinement fusion
[DE92-040347] p 715 N93-13047
Fluctuation studies on CASTOR and ASDEX tokamaks at lower hybrid current drive
[IPPCZ-319] p 715 N93-13093
Recent Nova experimental results
[DE92-019783] p 715 N93-13105
Fusion: Magnetic confinement
[DE92-019876] p 716 N93-13107
Biasing experiments on the Advanced Toroidal Facility
[DE92-040033] p 717 N93-13518
PLASMA CORE REACTORS
Plasma reactor waste management systems p 680 N93-14000
PLASMA CURRENTS
Measurement of current density fluctuations and ambipolar particle flux due to magnetic fluctuations in MST
[DE92-041013] p 713 N93-12878
Current density fluctuations, nonlinear coupling, and transport in MST
[DE92-041012] p 713 N93-12883
On the bootstrap current calculations based on values of the radial electron transport
[IPPCZ-317] p 715 N93-13091
Fast wave current drive experiment on the D3-D tokamak
[DE92-016253] p 716 N93-13193
Achieving high Q(sub DD) operation in high poloidal beta discharges in TFTR
[DE92-019494] p 718 N93-13535
A thermal/nonthermal approach to solar flares p 771 N93-13639
PLASMA DENSITY
Measurement of current density fluctuations and ambipolar particle flux due to magnetic fluctuations in MST
[DE92-041013] p 713 N93-12878
Current density fluctuations, nonlinear coupling, and transport in MST
[DE92-041012] p 713 N93-12883
Magnetic holes near the magnetopause p 653 N93-13491
PLASMA DIAGNOSTICS
DIII-D edge physics database
[DE92-019577] p 714 N93-12971
Diagnostics systems for the TBR-E tokamak
[INPE-5428-RPQ/662] p 716 N93-13257
Measurements of the temperature in the edge plasma of the CASTOR tokamak by a triple Langmuir probe
[IPPCZ-318] p 716 N93-13330
A fast scanning probe for D3-D
[DE92-040260] p 717 N93-13511
Study of heliumlike neon using an electron beam ion trap
[DE92-019544] p 753 N93-13536
PLASMA DRIFT
On the bootstrap current calculations based on values of the radial electron transport
[IPPCZ-317] p 715 N93-13091
PLASMA DYNAMICS
Current density fluctuations, nonlinear coupling, and transport in MST
[DE92-041012] p 713 N93-12883
Tokamak equilibria and transport based on Grad's thirteen moment description
[DE92-019960] p 715 N93-13038
Observations of plasma dynamics in the coma of P/Halley by the Giotto Ion Mass Spectrometer p 752 N93-13468
PLASMA ENGINES
Scaling of 100 kW class applied-field MPD thrusters
[NASA-CR-190791] p 525 N93-12638
PLASMA EQUILIBRIUM
Anomalous ion heating and superthermal electrons in the MST reversed-field pinch
[DE92-041011] p 713 N93-12882

Tokamak equilibria and transport based on Grad's thirteen moment description
[DE92-019960] p 715 N93-13038
Fusion: Magnetic confinement
[DE92-019876] p 716 N93-13107

PLASMA FREQUENCIES
Phase mixing and surface wave decay in an inhomogeneous plasma
[IPPCZ-320] p 715 N93-13006

PLASMA HEATING
A quantitative analysis of the effect of ELMs on H-mode thermal energy confinement in DIII-D
[DE92-017704] p 712 N93-12687
Anomalous ion heating and superthermal electrons in the MST reversed-field pinch
[DE92-041011] p 713 N93-12882
Dynamics of the ion-ion acoustic instability in the thermalization of ion beams
[DE92-019396] p 714 N93-12914
ReTech, Inc., Plasma Centrifugal Furnace: Applications analysis report
[PB92-218791] p 714 N93-12982
Future development of the D3-D tokamak program
[DE92-040051] p 715 N93-13044
Fast wave current drive experiment on the D3-D tokamak
[DE92-016253] p 716 N93-13193
A fast scanning probe for D3-D
[DE92-040260] p 717 N93-13511
A thermal/nonthermal approach to solar flares
p 771 N93-13639
Laser ablation for sample introduction in inductively coupled plasma spectrometry p 719 N93-13897

PLASMA JETS
Single liquid source plasma enhanced metalorganic chemical vapor deposition of YBa2Cu3O(7-x) thin films
[AD-A254119] p 722 N93-13100

PLASMA LAYERS
Observations of correlated broadband electrostatic noise and electron cyclotron emissions in the plasma sheet
[AD-A255002] p 712 N93-12705

PLASMA PHYSICS
Plasma properties
[DE92-019982] p 713 N93-12811
JPRS report: Science and technology. Central Eurasia: Physics and mathematics
[JPRS-UPM-92-006] p 698 N93-13303
Plasma Science Committee (PLSC) and study on new opportunities in plasma science and technology
[DE92-019507] p 716 N93-13359
Establishment of an Institute for Fusion Studies
[DE92-040014] p 717 N93-13502

PLASMA PROPULSION
AFOSR Contractors Meeting in Propulsion
[AD-A254484] p 525 N93-12575
Scaling of 100 kW class applied-field MPD thrusters
[NASA-CR-190791] p 525 N93-12638
Anode power deposition in applied-field MPD thrusters
[NASA-CR-190790] p 526 N93-13283

PLASMA SHEATHS
Fluidlike studies of the sheath and presheath regions of a plasma p 718 N93-13792

PLASMA SPECTRA
Laser ablation for sample introduction in inductively coupled plasma spectrometry p 719 N93-13897

PLASMA SPRAYING
Ductile phase toughening of molybdenum disilicide by low pressure plasma spraying
[DE92-007409] p 551 N93-13315

PLASMA TEMPERATURE
Measurements of the temperature in the edge plasma of the CASTOR tokamak by a triple Langmuir probe
[IPPCZ-318] p 716 N93-13330
Electron temperature of Gd plasma produced by laser resonance ionization
[DE91-017785] p 718 N93-13732

PLASMA TURBULENCE
Fluctuation studies on CASTOR and ASDEX tokamaks at lower hybrid current drive
[IPPCZ-319] p 715 N93-13093
Performance of a plasma fluid code on the Intel parallel computers
[DE92-011680] p 716 N93-13297
The 3-D description of vertical current sheets with application to solar flares
[SSL-PREPRINT-90-119] p 770 N93-13477

PLASMA WAVES
Phase mixing and surface wave decay in an inhomogeneous plasma
[IPPCZ-320] p 715 N93-13006
Experimental studies of high-power plasma-filled backward wave oscillators p 717 N93-13495

PLASMAS (PHYSICS)
Plasma properties
[DE92-019982] p 713 N93-12811
Study of plasma environments for the integrated Space Station electromagnetic analysis system
[NASA-CR-191263] p 522 N93-13152
Theoretical high energy physics
[DE92-015480] p 707 N93-13189
Performance of a plasma fluid code on the Intel parallel computers
[DE92-011680] p 716 N93-13297
Measurements of the temperature in the edge plasma of the CASTOR tokamak by a triple Langmuir probe
[IPPCZ-318] p 716 N93-13330
Plasma Science Committee (PLSC) and study on new opportunities in plasma science and technology
[DE92-019507] p 716 N93-13359
Experimental studies of ionospheric irregularities and related plasma processes
[NASA-CR-191271] p 652 N93-13460
Low-frequency fluctuations of plasma magnetic fields
p 717 N93-13496
Theory of the ion-channel laser p 607 N93-13777
Fluidlike studies of the sheath and presheath regions of a plasma p 718 N93-13792

PLASTIC DEFORMATION
Small-strain and finite-strain finite element analyses of plane-strain tensile elastic-plastic crack growth
p 621 N93-12628
On bilinearity of Manson-Coffin low-cycle-fatigue relationship
[NASA-TM-105840] p 622 N93-12739
Elastic and plastic strain measurement in high temperature environment using laser speckle
p 600 N93-13673

PLASTIC PROPERTIES
The application of the finite element method and the boundary element method to fatigue and fracture, volumes 1 and 2 p 624 N93-13016
Is there a unique effective interaction profile for dislocations?
[DE92-018615] p 543 N93-13545
Bifurcation and localization instabilities in plastic bending of cylindrical shells p 630 N93-13923

PLASTICIZERS
Effect of plasticizers on the properties of new ambient temperature solid polymer electrolytes
[AD-A254817] p 545 N93-12754
Studies of plasticized-polymer electrolytes containing mixed Zn(2) and Li(1)
[AD-A254818] p 545 N93-12755

PLATE THEORY
Influence of cure shrinkage on process-induced stress and deformation in thick thermosetting composites
[AD-A254325] p 529 N93-12842
Acoustic radiation from a point excited infinite bilaminar plate p 531 N93-13144
Analysis of cracked plates subjected to out-of-plane loadings p 629 N93-13804

PLATES (STRUCTURAL MEMBERS)
Hierarchic models for laminated plates
p 528 N93-12629
Numerical simulations of steel plate perforation
[DE92-017058] p 626 N93-13301

PLATFORMS
Mobile work platform for initial lunar base construction
p 559 N93-14009

PLUMES
A smoke producing rocket motor for atmospheric wind profiling
[DE92-018264] p 555 N93-12563
The kinetic energy budget of tropical plumes and ENSO in NMC and ECMWF analyses p 664 N93-13740

PLUTO (PLANET)
Chairmanship of the Neptune/Pluto Outer Planets Science Working Group
[NASA-CR-191288] p 759 N93-13568

PLY ORIENTATION
Three-dimensional boundary element analysis of residual stresses in a cross-ply fiber composite model
p 629 N93-13811
Improved damping in composite structures through stress coupling, co-cured damping layers, and segmented stiffness layers p 630 N93-13823
The role of the fiber/matrix interphase in the static and fatigue behavior of polymeric matrix composite laminates
p 535 N93-13968

POINT DEFECTS
Point defects quenched in NiAl and related intermetallic compounds p 724 N93-13628
Diffusion of ion-implanted group 4 n-type dopants in gallium arsenide and gallium/arsenide-based superlattices p 727 N93-14073

POINT SOURCES
A search for point sources of cosmic ray muons using the MACRO detector p 773 N93-13738

POINTING CONTROL SYSTEMS
Large Deployable Reflector (LDR) system concept and technology definition study. Volume 1: Executive summary, analyses and trades, and system concepts
[NASA-CR-177413-VOL-1] p 708 N93-12591

POLAR ORBITS
Galactic cosmic ray exposure estimates for SAGE-3 mission in polar orbit
[NASA-TM-107678] p 771 N93-13126

POLAR REGIONS
Interaction and impact of floating bodies
[AD-A254627] p 574 N93-12617
Investigations of the dynamics and thermodynamics of the mesosphere lower thermosphere and upper thermosphere at the polar regions with optical ground-based remote sensing
[AD-A254746] p 650 N93-12845
The Jovian ionosphere p 758 N93-13337

POLARIMETERS
Polarization effects and multipolarization SAR
p 564 N93-13054
A submillimetre polarimeter for the continuum receiver UKT14 on the James Clerk Maxwell Telescope
p 748 N93-13852

POLARIMETRY
Polarization effects and multipolarization SAR
p 564 N93-13054
Remote sensing of Earth terrain
[NASA-CR-190908] p 633 N93-13084
Radiative transfer theory for polarimetric remote sensing of pine forest p 633 N93-13085
Application of theoretical models to active and passive remote sensing of saline ice p 633 N93-13086
Polarimetric signatures of a canopy of dielectric cylinders based on first and second order vector radiative transfer theory p 569 N93-13088

POLARIZATION CHARACTERISTICS
Polarization effects and multipolarization SAR
p 564 N93-13054

POLARIZED ELECTROMAGNETIC RADIATION
An infrared polarimetric study of sunspots
p 770 N93-13627

POLARONS
Bipolaronic charge density waves, polaronic spin density waves and high T(c) superconductivity
[DE92-017403] p 720 N93-12853

POLICIES
Interaction and impact of floating bodies
[AD-A254627] p 574 N93-12617
Coordinating Council. Third Meeting: STI Strategic Plans
[NASA-TM-108016] p 733 N93-12670
Proceedings of FLICC forums on federal information policies. Combined summaries of proceedings. The 1990 7th Forum, Access is the Key and the 1991 8th Forum, Building Information Superhighways: Supercomputing Networks and Libraries
[PB92-147370] p 734 N93-12759

POLITICS
The informed citizen: Technology and responsibility in the information age p 742 N93-14049

POLLUTION CONTROL
New technologies for refrigeration without CFC's
[DE92-018886] p 557 N93-12922
ESPVI 4.0 electrostatic precipitator V-I and performance model: User's model
[PB92-169614] p 643 N93-12938
Physical property data on fluorinated propanes and butanes as CFC and HCFC alternatives
[PB92-206507] p 555 N93-12939
Interagency Workgroup on Air Quality Modeling (IWAQM) work plan rationale
[PB92-213248] p 643 N93-12940

POLLUTION MONITORING
The National Atmospheric Deposition Program/National Trends Network (NADP/NTN) site visitation program
[PB92-217298] p 642 N93-12726
Documentation for developing the initial source category list
[PB92-218429] p 646 N93-13647
Infrared spectroscopy of size resolved fine aerosol
p 647 N93-13758

POLLUTION TRANSPORT
Interagency Workgroup on Air Quality Modeling (IWAQM) work plan rationale
[PB92-213248] p 643 N93-12940

POLYCRYSTALS
Development of a computer model for polycrystalline thin-film CuInSe2 and CdTe solar cells
[DE92-016444] p 639 N93-13529

POLYESTERS
IIaO ultraviolet and nuclear emulsion films responses to orbital flights on STS-3, STS-7, STS-8, and STS-40
p 509 N93-13163

POLYETHYLENES
Solvation of cobalt salts by oligomeric polyethers
[AD-A254815] p 545 N93-12753
Studies of plasticized-polymer electrolytes containing mixed Zn(2) and Li(1)
[AD-A254818] p 545 N93-12755
Stress crack testing of polyethylene geomembranes
[PB92-217132] p 622 N93-12843
POLYIMIDES
The crystallization and crystalline properties of LARC-TPI
[NASA-CR-191001] p 721 N93-13022
A tough high performance composite matrix
[NASA-CASE-LAR-14338-1] p 531 N93-13416
POLYMER BLENDS
Characterization of thermotropic liquid crystalline polymer blends by positron annihilation lifetime spectroscopy
[AD-A253616] p 552 N93-13325
POLYMER CHEMISTRY
Proton transport on modified sulfonated polyaniline electrodes
[AD-A254917] p 570 N93-12650
Symposium on Polymeric Materials for Photonic and Optical Applications
[AD-A255820] p 554 N93-14029
POLYMER MATRIX COMPOSITES
Microcracking, microcrack-induced delamination, and longitudinal splitting of advanced composite structures
[NASA-CR-4472] p 623 N93-12911
Characterization of thermotropic liquid crystalline polymer blends by positron annihilation lifetime spectroscopy
[AD-A253616] p 552 N93-13325
The role of the fiber/matrix interphase in the static and fatigue behavior of polymeric matrix composite laminates
p 535 N93-13968
POLYMERIC FILMS
Proton transport on modified sulfonated polyaniline electrodes
[AD-A254917] p 570 N93-12650
Multichip module high speed testing
[AD-A254825] p 570 N93-12731
Skylab D024 thermal control coatings and polymeric films experiment p 548 N93-12784
Characterization of selected LDEF: Exposed polymer films and resins p 549 N93-12787
Long Duration Exposure Facility M0003-5 recent results on polymeric films p 549 N93-12789
Soft x ray window encapsulant for HgI2 detectors
[NASA-CR-190850] p 710 N93-13705
Symposium on Polymeric Materials for Photonic and Optical Applications
[AD-A255820] p 554 N93-14029
POLYMERIZATION
Aerogels, emulsions, and composites: Controlling structure with organic sol-gel chemistry
[DE92-019575] p 550 N93-12931
POLYMERS
Electronic phenomena in polyanilines
[AD-A254803] p 545 N93-12749
Laser ablation for sample introduction in inductively coupled plasma spectrometry p 719 N93-13897
POLYNOMIALS
Improved wide range expressions for displacements and inverse displacements for standard fracture toughness specimens
[AD-A254561] p 622 N93-12643
Solutions without phase-slip for the Ginsburg-Landau equation
[PB92-115575] p 696 N93-12889
Implicit application of polynomial filters in a k-step Arnoldi method
[NASA-CR-191237] p 686 N93-13408
Dexterous grasp and manipulation
p 618 N93-14075
POLYPROPYLENE
Polypropylene fibers in portland cement concrete pavements
[DOT/FAA/RD-92/9] p 551 N93-13259
POLYSTYRENE
Aerogels, emulsions, and composites: Controlling structure with organic sol-gel chemistry
[DE92-019575] p 550 N93-12931
Determination of the weight average molecular weight of SRM 1480
[PB92-222934] p 553 N93-13785
POLYTOPES
From totally unimodular to balanced O, +/- 1 matrices: A family of integer polytopes
[AD-A254552] p 696 N93-12640
POLYURETHANE FOAM
Preparation and properties of low density replica carbon foams
[DE92-019573] p 552 N93-13538
POLYURETHANE RESINS
Hermetic sealing and EMI shielding gasket
[AD-D015359] p 552 N93-13414
POPULATIONS
Human perceptual deficits as factors in computer interface test and evaluation
[DE92-019124] p 677 N93-12712
Forest declines: Some perspectives on linking processes and patterns
[DE92-019946] p 642 N93-12828
POROSITY
Experimental examination of growing and newly submerged sea ice including acoustic probing of the skeletal layer
[AD-A254526] p 669 N93-12599
Dislocation and pores in mullite from diphasic gels
[DE92-040384] p 550 N93-12999
Preparation and properties of low density replica carbon foams
[DE92-019573] p 552 N93-13538
Toughening mechanisms in weak matrix ceramic composites p 553 N93-13780
POROUS MATERIALS
Preparation and properties of low density replica carbon foams
[DE92-019573] p 552 N93-13538
Modelling combustion zones in porous media
p 540 N93-13802
PORTABLE EQUIPMENT
Development of a portable infrared emission spectrometer AA460 PIRES
[NASA-CR-190849] p 598 N93-13656
POSEIDON SATELLITE
Nonconservative force model parameter estimation strategy for TOPEX/Poseidon precision orbit determination
[NASA-TM-104575] p 519 N93-13372
POSITION (LOCATION)
ILS mathematical modeling study of the effects of an ASR-9 structure at the Long Island MacArthur Airport, Islip, NY
[DOT/FAA/CT-TN92/25] p 506 N93-12668
Dexterous grasp and manipulation
p 618 N93-14075
Human memory for the spatial locations of items on pull-down computer menus p 739 N93-14080
POSITION ERRORS
Orbit determination error analysis and station-keeping for liberation point trajectories p 518 N93-14038
POSITIONING
Soft X Ray Telescope (SXT) focus error analysis
[NASA-CR-184443] p 742 N93-12657
End-point position control of multi-link flexible manipulator arms p 613 N93-13335
GPS azimuth determination
[AD-A254687] p 499 N93-13348
Tether deployment monitoring system, phase 2
[NASA-CR-184098] p 522 N93-13425
POSITIONING DEVICES (MACHINERY)
Design philosophy for wind tunnel model positioning systems
[AD-A254958] p 506 N93-12552
POSITIVE IONS
Laser spectroscopy of rare earth ions
p 608 N93-13846
POSITRON ANNIHILATION
Characterization of thermotropic liquid crystalline polymer blends by positron annihilation lifetime spectroscopy
[AD-A253616] p 552 N93-13325
POSITRONS
A simple model for SLC positron stability issues
[DE92-019644] p 706 N93-12992
Damping the (pi)-mode instability in the SLC damping rings with a passive cavity
[DE92-018153] p 707 N93-13090
POSTFLIGHT ANALYSIS
LDEF Materials Workshop 1991, part 1
[NASA-CP-3162-PT-1] p 545 N93-12769
LDEF materials: An overview of the interim findings
p 546 N93-12770
Surface contamination on LDEF exposed materials
p 547 N93-12776
Sources and transport of silicone NVR
p 547 N93-12777
Thermal control surfaces on the MSFC LDEF experiments p 547 N93-12778
Anodized aluminum on LDEF: A current status of measurements on chromic acid anodized aluminum
p 544 N93-12779
Fluorescence of thermal control coatings on S0069 and A0114 p 548 N93-12781
Long Duration Exposure Facility M0003-5 thermal control coatings on DoD flight experiment
p 548 N93-12782
Skylab D024 thermal control coatings and polymeric films experiment p 548 N93-12784
Effects of the LDEF environment on the Ag/FEP thermal blankets p 548 N93-12785
Effects of orbital exposure on Halar during the LDEF mission p 549 N93-12788
Long Duration Exposure Facility M0003-5 recent results on polymeric films p 549 N93-12789
Post flight operation of a high peak power neodymium YAG laser aboard the G-449 payload flown on Space Shuttle Columbia mission 61-C p 508 N93-13161
POTABLE WATER
Methods development for total organic carbon accountability
[NASA-CR-184438] p 672 N93-12949
POTASSIUM PHOSPHATES
Development of a stable electro-optical modulator
[NASA-CR-184404] p 710 N93-13696
POTATOES
Crop growth and associated life support for a lunar farm p 680 N93-13994
Scenarios for optimizing potato productivity in a lunar CELSS p 680 N93-13997
POTENTIAL ENERGY
Intermolecular potential functions from spectroscopic properties of weakly bound complexes
[DE92-018643] p 701 N93-12745
Energy from Municipal Waste Program
[DE92-010578] p 638 N93-13102
POTENTIAL FLOW
Overall effects of separation on thin aerofoils
[ISBN-0-315-67464-4] p 496 N93-13930
POWDER (PARTICLES)
Automated dry powder dispenser for explosive components
[DE92-019425] p 555 N93-12568
Fatigue and fracture of intermetallic alloys
[AD-A254543] p 540 N93-12603
Consolidation of powder coated thermoplastic preform process modeling
[AD-A255094] p 529 N93-12757
Sol-gel synthesis and densification of aluminoborosilicate powders. Part 1: Synthesis
[NASA-TM-103964] p 527 N93-12895
Sol-gel synthesis and densification of aluminoborosilicate powders. Part 2: Densification
[NASA-TM-103969] p 528 N93-12896
An investigation of the interatomic bonding characteristics of a Ti - 51 atomic percent Al alloy by x ray diffraction
[AD-A245362] p 544 N93-13945
Friction, wear and Raman spectroscopic characteristics of carbon lubricated surfaces p 618 N93-13949
POWDER METALLURGY
Elevated temperature tensile properties of borated 304 stainless steel: Effect of boride dispersion on strength and ductility
[DE92-040096] p 542 N93-13302
Improving the temperature resistance of aluminum-matrix composites by using an acid phosphate binder p 536 N93-14056
POWDERED ALUMINUM
A new route for fibre management in metal matrix composites p 534 N93-13779
POWER AMPLIFIERS
Design, construction, and control of a two degree-of-freedom electric direct-drive human power amplifier p 678 N93-13486
POWER CONDITIONING
New power-conditioning systems for superconducting magnetic energy storage p 640 N93-13934
POWER CONVERTERS
Semiconductor measurement technology: INSTANT (IGBT network simulation and transient Analysis tool)
[PB92-213529] p 725 N93-13783
POWER GAIN
Parameter studies of helium-neon lasers at 543 nm
p 606 N93-13747
POWER LINES
The estimation of electrical cable fire-induced damage limits
[DE92-040100] p 572 N93-13519
POWER SPECTRA
Low-frequency fluctuations of plasma magnetic fields
p 717 N93-13496
POWERED MODELS
Tests of models equipped with TPS in low speed ONERA F1 pressurized wind tunnel p 577 N93-13201
Recent developments in low-speed TPS-testing for engine integration drag and installed thrust reversr simulation p 502 N93-13207
PRE-MAIN SEQUENCE STARS
International Ultraviolet Explorer (IUE) ultraviolet spectral atlas of selected astronomical objects
[NASA-RP-1285] p 744 N93-13461

PREAMPLIFIERS
Preamplifier with adjustable input resistance
[AD-D015377] p 572 N93-13473
PRECIPITATION
The National Atmospheric Deposition Program/National Trends Network (NADP/NTN) site visitation program
[PB92-217298] p 642 N93-12726
PRECIPITATION (METEOROLOGY)
Microwave remote sensing of a precipitating atmosphere p 634 N93-13371
PREDICTION ANALYSIS TECHNIQUES
Operator workload predictions for the revised AH-64A workload prediction model. Volume 2: Appendixes A through H
[AD-A254939] p 676 N93-12545
Thermal barrier coating life prediction model development, phase 2
[NASA-CR-189111] p 544 N93-12589
LDEF atomic oxygen fluence update
p 546 N93-12771
Computational simulation of probabilistic lifetime strength for aerospace materials subjected to high temperature, mechanical fatigue, creep and thermal fatigue
[NASA-CR-190794] p 626 N93-13290
A PDF closure model for compressible turbulent chemically reacting flows
[NASA-CR-191209] p 587 N93-13453
Analysis and design of planar and non-planar wings for induced drag minimization
[NASA-CR-191274] p 493 N93-13463
PREDICTIONS
Preferred sets of states, predictability, classicality, and the environment-induced decoherence
[DE92-017447] p 641 N93-12684
An investigation of the effects of topography on Colorado front range winter storms p 668 N93-14063
A surface pressure altitude prediction model
[AD-A255834] p 668 N93-14082
PREFLIGHT ANALYSIS
Test and calibration of the along track scanning radiometer, a satellite-borne infrared radiometer designed to measure sea surface temperature
p 671 N93-13842
PREFORMS
Consolidation of powder coated thermoplastic preform process modeling
[AD-A255094] p 529 N93-12757
PRESSURE
Users manual for program ADMIT: Admittance and pressure transfer function developed for use on a PC computer
[NASA-CR-184450] p 682 N93-12676
PRESSURE BROADENING
High resolution molecular spectroscopy of atmospheric species
[AD-A254360] p 650 N93-12946
PRESSURE DISTRIBUTION
DIII-D edge physics database
[DE92-019577] p 714 N93-12971
A numerical study of hypersonic flow with strong surface blowing p 492 N93-13128
Application of a solution adaptive grid to flow over an embedded cavity p 492 N93-13141
Experimental studies of the flowfields and their effects due to a pair of lift jets discharging in the ground effect region p 580 N93-13217
An experimental/computational study of heat transfer in sharp fin induced shock wave/turbulent boundary layer interactions at low hypersonic Mach numbers
p 590 N93-13826
PRESSURE EFFECTS
Effect of the flow non-uniformity on the mixing layer at the interface of parallel supersonic flows
[ISAS-RN-646] p 491 N93-12716
C60 transformations at high pressures
[DE92-019546] p 701 N93-12806
A novel-high-performance system for recording and analysing instantaneous total pressure distortion in air intakes p 580 N93-13215
Effect of O2 partial pressure on post annealed Ba2YCu3O(7-delta) thin films
[DE92-014949] p 722 N93-13323
The effects of pressure gradients on convective heat flux predictions in engine environments
p 616 N93-13772
An experimental and computational study of longitudinal vortices in turbulent boundary layers
p 595 N93-14097
PRESSURE GRADIENTS
Effect of the flow non-uniformity on the mixing layer at the interface of parallel supersonic flows
[ISAS-RN-646] p 491 N93-12716
The effects of pressure gradients on convective heat flux predictions in engine environments
p 616 N93-13772
PRESSURE MEASUREMENT
Acoustic device and method for measuring gas densities
[NASA-CASE-NPO-18155-1-CU] p 700 N93-13421
The 1992 NASA Langley Measurement Technology Conference: Measurement Technology for Aerospace Applications in High-Temperature Environments
[NASA-CP-3161] p 598 N93-13661
Technology trends in high temperature pressure transducers: The impact of micromachining
p 601 N93-13676
The trade-off characteristics of acoustic and pressure sensors for the NASP p 601 N93-13678
Very high temperature silicon on silicon pressure transducers p 601 N93-13679
Planar measurement of flow field parameters in nonreacting supersonic flows with laser-induced iodine fluorescence p 495 N93-13801
PRESSURE OSCILLATIONS
Acoustic modes in fluid networks p 586 N93-13398
Organized turbulent structures and their induced wall pressure fluctuations p 592 N93-13952
PRESSURE RATIO
Investigation of the flowfield around an isolated bypass engine with fan and core jet p 582 N93-13227
PRESSURE REDUCTION
Fluid dynamics of supercritical helium within cable-in-conduit conductors
[DE92-019516] p 574 N93-12569
Complement proteins and decompression sickness susceptibility
[AD-A254448] p 674 N93-12905
PRESSURE SENSORS
Storm tracking for TDWR: A correlation algorithm design and evaluation
[AD-A254701] p 660 N93-12622
A novel-high-performance system for recording and analysing instantaneous total pressure distortion in air intakes p 580 N93-13215
Technology trends in high temperature pressure transducers: The impact of micromachining
p 601 N93-13676
SiC device development for high temperature sensor applications p 601 N93-13677
The trade-off characteristics of acoustic and pressure sensors for the NASP p 601 N93-13678
Very high temperature silicon on silicon pressure transducers p 601 N93-13679
PRESSURE VESSELS
Shallow-crack toughness results for reactor pressure vessel steel
[DE92-017813] p 626 N93-13320
Validation test of 125 Ah advanced design IPV nickel-hydrogen flight cells
[NASA-TM-105912] p 527 N93-14079
PRESTRESSING
The effects of compressive preloads on the compression-after-impact strength of carbon/epoxy
[NASA-TP-3303] p 529 N93-12678
PRIMARY BATTERIES
First year testing of prototype magnesium/manganese dioxide BA-4590/U battery
[AD-A255503] p 574 N93-13839
PRIMATES
Investigation of effects of 60-Hz electric and magnetic fields on operant and social behavior and on the neuroendocrine system of nonhuman primates, part 2
[DE92-040153] p 673 N93-13503
PRIMERS (COATINGS)
An evaluation of corrosion protection by two epoxy primers on 2219-T87 and 7075-T73 aluminum
[NASA-TM-108376] p 553 N93-13716
PRIORITIES
Large programs may consume increasing share of limited future budgets. Report to Congressional Requesters
[GAO/NSIAD-92-278] p 732 N93-13109
PROBABILITY DISTRIBUTION FUNCTIONS
Probabilistic evaluation of fuselage-type composite structures
[NASA-TM-105881] p 622 N93-12735
From comparison density to two sample analysis
[AD-A253866] p 698 N93-13064
PROBABILITY THEORY
Design for reliability: Current density
[AD-A254770] p 570 N93-12866
A study of the vacancy loop formation probability in Ni-Cu and Ag-Pd alloys
[DE92-019584] p 541 N93-12879
Summary of awards: Applied mathematics. Fiscal year 1991
[NSF-92-38] p 681 N93-13438
A PDF closure model for compressible turbulent chemically reacting flows
[NASA-CR-191209] p 587 N93-13453
Gravitational lensing by galaxy clusters: The giant arcs in Abell 370 and Cl2244-02 p 755 N93-13848
PROBLEM SOLVING
Fast approximation algorithms for multicommodity flow problems
[AD-A254335] p 685 N93-12961
PROCESS CONTROL (INDUSTRY)
Statistical process management: An essential element of quality improvement
[DE92-019934] p 619 N93-13036
Robot welding process control
[NASA-CR-184428] p 614 N93-13436
PROCUREMENT MANAGEMENT
Coordinating Council. Second Meeting: International Acquisitions
[NASA-TM-108015] p 733 N93-12634
Coordinating Council. Seventh Meeting: Acquisitions
[NASA-TM-108020] p 733 N93-12636
Window on waste: Atrophy in NASA management
[GPO-57-273] p 732 N93-13693
PRODUCT DEVELOPMENT
Laser measurement techniques guide for a hazard evaluation
[AD-A254545] p 604 N93-12610
Economical development of complex computer systems
[AD-A254752] p 689 N93-12848
Abstracts of phase 1 awards: NSF Small Business Innovation Research Program (SBIR): 1992
[NSF-92-80] p 732 N93-13703
PRODUCTION COSTS
Future regional transport aircraft market, constraints, and technology stimuli
[NASA-TM-107669] p 491 N93-13025
Process comparison study. MSFC Center Director's Discretionary Fund (CDDF)
[NASA-TM-108382] p 526 N93-13429
PRODUCTIVITY
Increasing the end user's productivity through seamless integration of applications with the database
[DE92-019599] p 735 N93-12824
Scenarios for optimizing potato productivity in a lunar CELSS p 680 N93-13997
PROGRAM VERIFICATION (COMPUTERS)
Verification and validation of AI software
[AD-A254601] p 682 N93-12614
The Second NASA Formal Methods Workshop 1992
[NASA-CP-10110] p 684 N93-12957
PROGRAMMERS
Graphics-based parallel programming tools
[AD-A254406] p 683 N93-12763
PROGRAMMING LANGUAGES
Blackboard architectures for multi-agent planning
[AD-A255035] p 688 N93-12710
Visualization techniques to aid in the analysis of multi-spectral astrophysical data sets
[NASA-CR-191260] p 685 N93-13261
PROJECT MANAGEMENT
Space Station: Resolving conflict over integration contractor's role. Briefing report to the Chairman, Subcommittee on Investigations and Oversight, Committee on Science, Space, and Technology, House of Representatives
[GAO/NSIAD-92-291BR] p 732 N93-13111
Environmental Compliance Management System
[DE92-019595] p 645 N93-13479
Report to Congress: State Block Grant Program
[AD-A254569] p 507 N93-13882
The Second Conference on Lunar Bases and Space Activities of the 21st Century, volume 2
[NASA-CP-3166-VOL-2] p 760 N93-13972
Creating a foundation for a synergistic approach to program management p 732 N93-14017
PROJECT PLANNING
Limited production Precision Runway Monitor (PRM) master test plan
[DOT/FAA/CT-TN92/23] p 506 N93-12899
Large programs may consume increasing share of limited future budgets. Report to Congressional Requesters
[GAO/NSIAD-92-278] p 732 N93-13109
Solar System Exploration Division Strategic Plan, volume 1. Executive summary and overview
[NASA-TM-107843] p 513 N93-13265
Small planetary mission plan: Report to Congress
[NASA-TM-107809] p 513 N93-13266
Hydrogen Program Plan, FY 1993 - 1997
[DE92-010556] p 538 N93-13316
Scientific and engineering research facilities at universities and colleges: 1992
[NSF-92-325] p 506 N93-13407
The program plan: An overview of the development and implementation of the International Asteroid Mission
p 514 N93-13553
Lunar stepping stones to a manned Mars exploration scenario p 767 N93-14016

PROJECTILES
Analysis of a structure-equipment system subjected to impact loading
[AD-A255097] p 622 N93-12652
PROJECTION
Stabilization and projection methods for multibody dynamics
[PB92-133883] p 698 N93-12890
Large area projection liquid-crystal video display system with inherent grid pattern optically removed
[NASA-CASE-NPO-16932-2-CU] p 711 N93-13711
PROJECTORS
Infrared image projector utilizing a deformable mirror device spatial light modulator
[AD-D015373] p 710 N93-13500
PROLATE SPHEROIDS
Wall functions for the kappa-epsilon turbulence model in generalized nonorthogonal curvilinear coordinates p 587 N93-13517
PROLOG (PROGRAMMING LANGUAGE)
Blackboard architectures for multi-agent planning
[AD-A255035] p 688 N93-12710
PROP-FAN TECHNOLOGY
Investigation of advanced counterrotation blade configuration concepts for high speed turboprop systems. Task 4: Advanced fan section aerodynamic analysis
[NASA-CR-187128] p 502 N93-12695
PROPAGATION (EXTENSION)
Long pulse electron beam propagation
[DE92-014948] p 706 N93-12830
PROPAGATION VELOCITY
Diagnostic of shock wave processes
[DE92-018059] p 565 N93-13357
PROPANE
Physical property data on fluorinated propanes and butanes as CFC and HCFC alternatives
[PB92-206507] p 555 N93-12939
PROPELLANT COMBUSTION
A smoke producing rocket motor for atmospheric wind profiling
[DE92-018264] p 555 N93-12563
Stability codes for a liquid rocket implemented for use on a PC
[NASA-CR-184453] p 525 N93-12659
Bipropellant spray combustion modeling in small rocket engines p 556 N93-13924
PROPELLANT GRAINS
Numerical investigation of the flow field in the head-end, star grain section of a solid rocket motor during ignition transients p 526 N93-13818
PROPELLANT SPRAYS
Bipropellant spray combustion modeling in small rocket engines p 556 N93-13924
PROPELLANT TANKS
Orbital Spacecraft Consumables Resupply System (OSCRS). Volume 3: Program cost estimate
[NASA-CR-185685] p 740 N93-12814
PROPELLANTS
Nonideal thermoequilibrium calculations using a large product species data base
[DE92-040839] p 735 N93-12813
PROPELLER SLIPSTREAMS
Aerodynamic analysis of slipstream/wing/nacelle interference for preliminary design of aircraft configurations p 497 N93-13205
PROPULSION
The PEP Symposium on CFD Techniques for Propulsion Applications p 579 N93-13210
National Aero-Space Plane: Key issues facing the program. Testimony before the Subcommittee on Technology and Competitiveness, Committee on Science, Space, and Technology, House of Representatives
[GAO/T-NSIAD-92-26] p 500 N93-13253
Electro-optic architecture for servicing sensors and actuators in advanced aircraft propulsion systems
[NASA-CR-182269] p 711 N93-13762
PROPULSION SYSTEM CONFIGURATIONS
AFOSR Contractors Meeting in Propulsion
[AD-A254484] p 525 N93-12575
Demand thrust pumped propulsion with automatic warm gas valving
[DE92-017435] p 525 N93-12840
Briefing notes on propulsion stability codes ADMIT, NYQUIST, and SSFREQ
[NASA-CR-184449] p 525 N93-12874
Aerodynamic Engine/Airframe Integration for High Performance Aircraft and Missiles
[AGARD-CP-498] p 577 N93-13199
Euler analysis of turbofan/superfan integration for a transport aircraft p 578 N93-13206
Propulsion integration results of the STOL and Maneuver Technology Demonstrator p 502 N93-13228
Integration of turbo-ramjet engines for hypersonic aircraft p 503 N93-13230
Engineering and architectural issues associated with the asteroid mission p 514 N93-13556
PROPULSION SYSTEM PERFORMANCE
Demand thrust pumped propulsion with automatic warm gas valving
[DE92-017435] p 525 N93-12840
High Energy Propulsion System (HEPS) analysis
[AD-A254343] p 525 N93-12963
Subsonic flight test evaluation of a propulsion system parameter estimation process for the F100 engine
[NASA-TM-4426] p 502 N93-13155
The influence of intake swirl distortion on the steady-state performance of a low bypass, twin-spool engine p 579 N93-13211
Some aspects of intake design, performance and integration with the airframe p 502 N93-13219
Hypersonic propulsion system force accounting p 503 N93-13229
Air inlet with variable intake section: Application to air breathing launch vehicles p 582 N93-13231
Engineering and architectural issues associated with the asteroid mission p 514 N93-13556
Scientific predictability of solid rocket performance: Analyses of the processing parameters p 526 N93-13824
PROPYLENE
Effect of plasticizers on the properties of new ambient temperature solid polymer electrolytes
[AD-A254817] p 545 N93-12754
Recession of FEP specimens from trays D11 and B7 p 549 N93-12786
PROTECTIVE CLOTHING
A novel diesel-fueled engine for microclimate cooling for the individual soldier
[AD-A254510] p 609 N93-12724
Effect of protective clothing ensembles on artillery battery crew performance
[AD-A254327] p 677 N93-12960
Physiological stress from chemical defense clothing and equipment
[AD-A255786] p 676 N93-14028
PROTECTIVE COATINGS
High temperature oxidation and electrochemical studies related to hot corrosion
[AD-A254435] p 540 N93-12595
Soft x ray window encapsulant for HgI2 detectors
[NASA-CR-190850] p 710 N93-13705
An evaluation of corrosion protection by two epoxy primers on 2219-T87 and 7075-T73 aluminum
[NASA-TM-108376] p 553 N93-13716
Heat resistant diffusion coating for niobium alloy
[AD-A255542] p 554 N93-13873
The chemistry of the extreme pressure lubricant additive lead naphthenate on steel surfaces
[AD-A255828] p 544 N93-14098
PROTEIN CRYSTAL GROWTH
The First United States Microgravity Laboratory
[NASA-TM-107980] p 557 N93-12951
PROTEINS
Capillary electrophoresis: Electrospray ionization mass spectrometry in small diameter capillaries
[DE92-019123] p 575 N93-12711
Eureca: A first for Europe
[ESA-BR-85] p 516 N93-13691
PROTOCOL (COMPUTERS)
Seamless simulation literature survey
[AD-A254950] p 688 N93-12549
Assessment of programs in space biology and medicine
[NASA-CR-190930] p 672 N93-13327
DNET: A communications facility for distributed heterogeneous computing
[NASA-CR-190863] p 682 N93-13759
PROTON BEAMS
RF voltage modulation at discrete frequencies with applications to crystal channeling extraction
[DE92-015567] p 707 N93-13235
PROTON IRRADIATION
Experimental studies of the far-infrared spectra of cosmic-type ices
[NASA-CR-191300] p 748 N93-13660
PROTONS
Particle production and survival in muon acceleration
[DE92-019553] p 701 N93-12572
Proton transport on modified sulfonated polyaniline electrodes
[AD-A254917] p 570 N93-12650
Theoretical nuclear physics
[DE92-019286] p 706 N93-12822
Interpretation of the ion mass spectra in the mass range 25-35 obtained in the inner coma of Halley's comet by the HIS-sensor of the Giotto IMS Experiment p 752 N93-13469
Interaction of energetic ring current protons with magnetospheric hydromagnetic waves p 718 N93-13750
PROTOPLANETS
Accretion rates of protoplanets p 759 N93-13958
PROTOSTARS
Encounters with protostellar disks p 754 N93-13727
The role of ambipolar diffusion in the formation of interstellar cloud cores and protostars p 755 N93-13828
PROTOTYPES
First year testing of prototype magnesium/manganese dioxide BA-4590/U battery
[AD-A255503] p 574 N93-13839
Life systems for a lunar base p 680 N93-13992
PROVING
Summary of 1992 Atlantic tropical cyclone activity and verification of author's forecast (a year of no hurricane activity in the tropics but exceptional South Florida destruction from an unusual higher latitude intense hurricane) p 662 N93-13028
PSYCHOLOGY
Academic science and engineering: Graduate enrollment and support, Fall 1990
[NSF-92-323] p 729 N93-12802
PUBLIC HEALTH
JPRS report: Science and technology. Central Eurasia: Life sciences
[JPRS-ULS-92-024] p 672 N93-13033
Procedures for the diagnostic dose resistance test kits for mosquitoes, body lice, and beetle pests of stored products
[AD-A255224] p 675 N93-13941
PUBLIC RELATIONS
Public perceptions of the risks of an unfamiliar technology: The case of using nuclear energy sources for space missions p 527 N93-13971
PULLING
Test equipment data package for the KC-135 fiber pulling apparatus
[NASA-CR-184446] p 506 N93-13013
Test plan and report for Space Shuttle launch environment testing of Bergen cable technology safety cable
[NASA-CR-4473] p 559 N93-13434
PULSARS
Hydrodynamical calculations of stellar interactions p 755 N93-13764
PULSE COMPRESSION
A study of small solid-state switched TEA CO2 lasers p 607 N93-13814
ACTA Aeronautica et Astronautica Sinica (selected articles)
[AD-A255070] p 491 N93-13946
PULSE GENERATORS
Advanced high-explosive flux compression generator development: The CN-3 series
[DE92-019962] p 713 N93-12809
PULSED LASERS
CO2 laser modeling
[NASA-CR-184455] p 604 N93-12656
High temperature superconductor materials and applications
[NASA-CR-184437] p 719 N93-12691
Development of a laser ignited all secondary explosive DDT detonator
[DE92-019340] p 555 N93-13081
Monitoring interfacial dynamics by pulsed laser techniques
[DE92-040302] p 606 N93-13514
A study of small solid-state switched TEA CO2 lasers p 607 N93-13814
PULSED RADIATION
Comparison of heavy ion and electron-beam upset data for GaAs
[AD-A255901] p 708 N93-14089
PULSES
Long pulse electron beam propagation
[DE92-014948] p 706 N93-12830
Fundamentals of enhanced scalar transport in strongly oscillating and/or resonant flow fields as created by pulse combustion
[DE92-012147] p 582 N93-13247
PULTRUSION
Process comparison study. MSFC Center Director's Discretionary Fund (CDDF)
[NASA-TM-108382] p 526 N93-13429
PUMP IMPELLERS
An experimental study of a small high-speed LH2 pump for rockets: Fluid dynamic performance
[NAL-TR-1131] p 610 N93-12727
PUMPING
Fluidic sampling
[DE92-017266] p 575 N93-12761
PUMPS
Demand thrust pumped propulsion with automatic warm gas valving
[DE92-017435] p 525 N93-12840

PURSUIT TRACKING
The 3-D computer vision techniques for object following and obstacle avoidance p 693 N93-13245
PYLONS
Investigation of interference phenomena of modern wing-mounted high-bypass-ratio engines by the solution of the Euler-equations p 578 N93-13204
Euler analysis of turbofan/superfan integration for a transport aircraft p 578 N93-13206
Recent developments in low-speed TPS-testing for engine integration drag and installed thrust reversr simulation p 502 N93-13207
PYROTECHNICS
Nonideal thermoequilibrium calculations using a large product species data base
[DE92-040839] p 735 N93-12813

Q

Q FACTORS
Achieving high Q(sub DD) operation in high poloidal beta discharges in TFTR
[DE92-019494] p 718 N93-13535
QUADRATIC PROGRAMMING
Sequential quadratic programming solutions to related aircraft trajectory optimization problems p 505 N93-13926
QUADRUPOLES
Magnetic field perturbation caused by bending vibrations of a quadrupole
[DE92-040644] p 623 N93-13003
RF system description for the ground test accelerator radio-frequency quadrupole
[DE92-040239] p 563 N93-13045
QUALIFICATIONS
Qualification of the gritblast assembly and process for the inside diameter of the RSRM forward and aft domes
[NASA-CR-184462] p 558 N93-13021
QUALITY
Coordinating Council. Fifth Meeting: Quality
[NASA-TM-108018] p 733 N93-12635
QUALITY CONTROL
Coordinating Council. Fifth Meeting: Quality
[NASA-TM-108018] p 733 N93-12635
Real-time quality assurance testing using photonic techniques: Application to iodine water system
[NASA-CR-184413] p 619 N93-12692
Li/SOCl battery technology: Problems and solutions
[AD-A254514] p 570 N93-12725
The National Atmospheric Deposition Program/National Trends Network (NADP/NTN) site visitation program
[PB92-217298] p 642 N93-12726
Functional system design document for the Intelligent Inspection System (IIS)
[DE92-018240] p 619 N93-12794
Spreadsheet-like image analysis
[AD-A254395] p 619 N93-12864
Microbiological methods for the water recovery systems test, revision 1.1
[NASA-CR-184390] p 678 N93-12966
Statistical process management: An essential element of quality improvement
[DE92-019934] p 619 N93-13036
Verification and validation of TMAP4
[DE92-019684] p 539 N93-13616
An examination of the Total Quality Management (TQM) concept given current Federal/DoD competition initiatives
[AD-A255556] p 620 N93-13876
Coordinating Council. Ninth Meeting: Total Quality Management
[NASA-TM-108106] p 738 N93-13885
QUANTILES
Obtaining medians and other quantiles with limited memory space
[AD-A254506] p 683 N93-12722
From comparison density to two sample analysis
[AD-A253866] p 698 N93-13064
QUANTITATIVE ANALYSIS
A quantitative analysis of the effect of ELMs on H-mode thermal energy confinement in DIII-D
[DE92-017704] p 712 N93-12687
QUANTUM CHROMODYNAMICS
Search for doubly Cabibbo suppressed decays of the charged D meson
[DE92-018588] p 703 N93-13092
Theoretical high energy physics
[DE92-015480] p 707 N93-13189
Recent developments in the theory of heavy-quark decays
[DE92-017598] p 704 N93-13250
QUANTUM ELECTRODYNAMICS
Test of QED using a laser at the SLAC final focus test beam
[DE92-019647] p 707 N93-12993
Non-perturbative studies in quantum electrodynamics p 729 N93-13896
QUANTUM MECHANICS
Ab initio atomic recombination reaction energetics on model heat shield surfaces
[NASA-CR-191210] p 575 N93-12677
Preferred sets of states, predictability, classicality, and the environment-induced decoherence
[DE92-017447] p 641 N93-12684
Mathematics and string theory
[DE92-019292] p 727 N93-12796
Second quantization in bit-string physics
[DE92-019645] p 727 N93-12826
Electromagnetic lepton-pair production in relativistic collisions
[DE92-011069] p 706 N93-12829
Connection of microscopic with macroscopic dynamics: Towards a hydrodynamical description of quantum mechanics p 729 N93-13957
QUANTUM NUMBERS
High resolution molecular spectroscopy of atmospheric species
[AD-A254360] p 650 N93-12946
QUANTUM OPTICS
Analytical studies of nonlinear partial differential equations of interest in nonlinear optics
[AD-A254931] p 696 N93-13027
QUANTUM THEORY
Mathematics and string theory
[DE92-019292] p 727 N93-12796
QUANTUM WELLS
Synthesis and properties of mismatched heterojunction/substrate interfaces
[AD-A254577] p 719 N93-12648
Quantum well, beam deflecting surface emitting lasers
[NASA-CASE-NPO-18243-1-CU] p 605 N93-13418
Strained-layer InGaAs-GaAs-AlGaAs quantum well lasers and transverse junction stripe lasers p 607 N93-13773
The three to five semiconductor quantum well lasers and related optoelectronic devices on silicon
[AD-A255368] p 608 N93-13864
High magnetic field studies of strained layer superlattices p 726 N93-13895
QUARKS
Test of QED using a laser at the SLAC final focus test beam
[DE92-019647] p 707 N93-12993
Recent developments in the theory of heavy-quark decays
[DE92-017598] p 704 N93-13250
QUARTZ CRYSTALS
Tutorials from the 23rd Annual Precise Time and Time Interval (PTTI) Applications and Planning Meeting
[AD-A254745] p 596 N93-12844
QUASARS
The emission-line properties of quasars p 753 N93-13487
QUERY LANGUAGES
User interface of DFQL: An object-oriented approach
[AD-A255225] p 687 N93-13835
A theory of reference graphs in relational databases p 739 N93-13912

R

RADAR ANTENNAS
Tether deployment monitoring system, phase 2
[NASA-CR-184098] p 522 N93-13425
RADAR CROSS SECTIONS
Bistatic clutter RCS simulation using scale model rough surfaces
[AD-A254932] p 560 N93-12581
RADAR DATA
Design of a digital Data Recording System (DRS)
[AD-A255088] p 561 N93-12623
Convective scale 4-D data assimilation using simulated single Doppler radar observations
[PB92-218726] p 651 N93-12969
Multi-frequency multi-polarization processing for spaceborne SAR p 564 N93-13057
Application of theoretical models to active and passive remote sensing of saline ice p 633 N93-13086
JARE data reports no. 173 (meteorology 28). Antarctic climate research data. Part 5: PPI radar data at Syowa Station, Antarctica from February to December 1989 p 663 N93-13446
RADAR DETECTION
Radar signal processing for over resolved targets
[AD-A255256] p 566 N93-13838
Birds mimicking microbursts on 2 June 1990 in Orlando, Florida
[AD-A255703] p 498 N93-14024
RADAR EQUIPMENT
Multifrequency measurements of radar ground clutter at 42 sites. Volume 2: Appendices A through D
[AD-A246711] p 567 N93-13878
RADAR IMAGERY
Fundamentals and Special Problems of Synthetic Aperture Radar (SAR)
[AGARD-LS-182] p 563 N93-13049
Special SAR techniques and applications p 564 N93-13059
Remote sensing of Earth terrain
[NASA-CR-190908] p 633 N93-13084
Variance of phase fluctuations of waves propagating through a random medium p 569 N93-13087
Coherent frame analysis of Synthetic Aperture Radar (SAR) ocean imagery p 568 N93-14050
RADAR MEASUREMENT
Bistatic clutter RCS simulation using scale model rough surfaces
[AD-A254932] p 560 N93-12581
Radar studies of high latitude convection flows p 648 N93-12626
CO2 laser modeling
[NASA-CR-184455] p 604 N93-12656
Remote sensing data from CLARET: A prototype CART data set
[NASA-CR-191294] p 634 N93-13094
JARE data reports no. 175 (ionosphere 46). Records of radio aurora at Syowa Station, Antarctica in 1990 p 651 N93-13285
A joint study of the lower ionosphere by radar, lidar, and spectrometer p 655 N93-13755
RADAR RECEIVERS
Acousto-optic applications for multichannel adaptive optical processor
[AD-A255823] p 711 N93-14032
RADAR SCATTERING
Development of two-dimensional parametric radar signal modeling and estimation techniques with application to target identification
[AD-A252602] p 567 N93-13939
Birds mimicking microbursts on 2 June 1990 in Orlando, Florida
[AD-A255703] p 498 N93-14024
RADAR SIGNATURES
Birds mimicking microbursts on 2 June 1990 in Orlando, Florida
[AD-A255703] p 498 N93-14024
RADAR TARGETS
Application of smoothing techniques for tracking maneuvering targets. Multiple target tracking in clutter: New approaches
[AD-A254609] p 561 N93-12615
Motion errors and compensation possibilities p 563 N93-13052
The real aperture antenna of SAR, a key element for performance p 564 N93-13053
Polarization effects and multipolarization SAR p 564 N93-13054
SAR simulation p 564 N93-13056
Inverse Synthetic Aperture Radar p 564 N93-13058
Special SAR techniques and applications p 564 N93-13059
Tether deployment monitoring system, phase 2
[NASA-CR-184098] p 522 N93-13425
Radar signal processing for over resolved targets
[AD-A255256] p 566 N93-13838
The Joint Surveillance Target Attack Radar System: Can procedures be developed to support the requirements of the land and air component commanders?
[AD-A255555] p 567 N93-13875
Development of two-dimensional parametric radar signal modeling and estimation techniques with application to target identification
[AD-A252602] p 567 N93-13939
Computer-aided design-based high-frequency electromagnetic wave scattering from complex bodies p 567 N93-14042
RADAR TRACKING
Angle of arrival fluctuations for millimeter waves propagating in a turbulent atmosphere near the Earth
[AD-A254478] p 560 N93-12574
Convective scale 4-D data assimilation using simulated single Doppler radar observations
[PB92-218726] p 651 N93-12969
JARE data reports no. 176 (Ionosphere 47). Riometer records of 30 MHz cosmic noise at Syowa Station, Antarctica in 1990 p 772 N93-13255
RADARSAT
Review of spaceborne and airborne SAR systems p 565 N93-13060
RADIANT FLUX DENSITY
A high-resolution radio survey of the galactic plane p 744 N93-13480

RADIANT HEATING
A correlated k-distribution model of the heating rates for CH4 and N2O in the atmosphere between 0 and 60 km
[NASA-TM-108062] p 643 N93-12926
RADIATION BELTS
Ion radial diffusion in an electrostatic impulse model for stormtime ring current formation
[NASA-CR-190941] p 705 N93-12715
Analysis and modeling of the CRRES satellite data
[AD-A254349] p 650 N93-12944
RADIATION COUNTERS
Elementary particle physics research
[DE92-019746] p 702 N93-12855
Galactic cosmic ray exposure estimates for SAGE-3 mission in polar orbit
[NASA-TM-107678] p 771 N93-13126
Applications of the Los Alamos High Energy Transport code
[DE92-017408] p 704 N93-13281
Neutrino(e) appearance for neutrino(mu)-neutrino(tau) oscillations in matter
[DE92-040303] p 772 N93-13533
Large area nuclear particle detectors using ET materials, phase 2
[NASA-CR-190866] p 705 N93-13606
RADIATION DAMAGE
Investigation of component failure rates for pulsed versus steady state tokamak operation
[DE92-019758] p 713 N93-12856
Effects of ionizing radiation on scintillators and other particle detectors
[DE92-018184] p 705 N93-13531
Fusion energy from the Moon for the twenty-first century p 719 N93-13985
On the suitability of non-hardened high density SRAMs for space applications
[AD-A255898] p 524 N93-14087
Space environmental effects on silvered teflon thermal control surfaces
[AD-A255909] p 554 N93-14099
RADIATION DETECTORS
Elementary particle physics research
[DE92-019746] p 702 N93-12855
Indiana University High Energy Physics Group, task C
[DE92-040458] p 707 N93-13002
Applications of the Los Alamos High Energy Transport code
[DE92-017408] p 704 N93-13281
RADIATION DISTRIBUTION
Two-photon cooperative cascade superfluorescence
[AD-A255690] p 608 N93-14023
RADIATION DOSAGE
Radiation dose to critical body organs for October 1989 proton event
[NASA-TP-3237] p 520 N93-12876
JPRS report: Science and technology. Central Eurasia: Life sciences
[JPRS-ULS-92-024] p 672 N93-13033
IIaO ultraviolet and nuclear emulsion films responses to orbital flights on STS-3, STS-7, STS-8, and STS-40 p 509 N93-13163
Fiber optic data bus radiation effects study
[AD-A255821] p 711 N93-14031
RADIATION EFFECTS
Experimental studies of cascade phenomena in metals
[DE92-019586] p 540 N93-12573
Chemical release and radiation effects experiment advanced planning and coordination
[NASA-CR-184439] p 649 N93-12718
Weak-beam imaging of dissociated dislocations in HVEM-irradiated Fe-Ni-Cr alloys
[DE92-019587] p 541 N93-12798
Influence of cold work level on the irradiation creep and creep rupture of titanium-modified austenitic stainless steels
[DE92-019078] p 541 N93-12820
A study of the vacancy loop formation probability in Ni-Cu and Ag-Pd alloys
[DE92-019584] p 541 N93-12879
Contamination analysis of SSF candidate materials
[NASA-CR-184431] p 709 N93-12894
Touchstone for success
[ESA-BR-52] p 557 N93-12934
Influence of dilute impurities on the evolution of defect cascades in nickel
[DE92-019585] p 542 N93-12973
Katz model prediction of Caenorhabditis elegans mutagenesis on STS-42
[NASA-TM-4383] p 674 N93-13023
A Pennsylvania State University/General Electric Get Away Special (GAS) experiment p 511 N93-13177
Radiation-induced infrared absorption in nuclear-pumped laser cavity components
[DE92-017346] p 605 N93-13249
Radiation-disorder and aperiodicity in irradiated ceramics
[DE92-015051] p 552 N93-13350
Effects of ionizing radiation on scintillators and other particle detectors
[DE92-018184] p 705 N93-13531
Human factors dealing with the International Asteroid Mission p 515 N93-13559
An investigation of the processes controlling ozone in the upper stratosphere
[DE92-019621] p 645 N93-13615
Fiber optic data bus radiation effects study
[AD-A255821] p 711 N93-14031
RADIATION HAZARDS
Radiation dose to critical body organs for October 1989 proton event
[NASA-TP-3237] p 520 N93-12876
Applications of the Los Alamos High Energy Transport code
[DE92-017408] p 704 N93-13281
Fusion energy from the Moon for the twenty-first century p 719 N93-13985
Synergism of He-3 acquisition with lunar base evolution p 540 N93-13986
RADIATION INJURIES
AFRRI reports
[AD-A254581] p 674 N93-12649
RADIATION MEASUREMENT
Neutrino mass
[DE92-017411] p 701 N93-12588
Remote sensing data from CLARET: A prototype CART data set
[NASA-CR-191294] p 634 N93-13094
A study of the Earth Radiation Budget Experiment: Shortwave measurements and bidirectional reflectance models for the ocean surface p 654 N93-13722
RADIATION PROTECTION
AFRRI reports
[AD-A254581] p 674 N93-12649
RADIATION SHIELDING
Fully energy-dependent HZETRN (a galactic cosmic-ray transport code)
[NASA-TP-3243] p 771 N93-13020
Applications of the Los Alamos High Energy Transport code
[DE92-017408] p 704 N93-13281
Human factors dealing with the International Asteroid Mission p 515 N93-13559
Fiber optic data bus radiation effects study
[AD-A255821] p 711 N93-14031
RADIATION TRANSPORT
Applications of the Los Alamos High Energy Transport code
[DE92-017408] p 704 N93-13281
A stochastic/deterministic method for transient, three-dimensional neutron transport
[DE92-016690] p 704 N93-13319
RADIATIVE HEAT TRANSFER
Studies of radiative emission from the simulated shock layer of the Huygens probe p 521 N93-12834
Development status of SINDA/FLUINT and SINAPS p 585 N93-13393
Summary on comparison of radiative heat transfer solutions for a specified problem
[DE92-040098] p 588 N93-13575
RADIATIVE TRANSFER
Radiative transfer theory for polarimetric remote sensing of pine forest p 633 N93-13085
Polarimetric signatures of a canopy of dielectric cylinders based on first and second order vector radiative transfer theory p 569 N93-13088
The role of particle diffusion in the lower transition region: Revised interpretation of emission measures p 770 N93-13476
Radiative transfer in the middle atmosphere p 652 N93-13482
The relationship between SST anomalies and clouds, water vapor, and their radiative effects p 665 N93-13744
RADICALS
An experimental and theoretical study of degradation pathways for atmospheric halocarbons p 646 N93-13624
Kinetic and spectroscopic studies of peroxy radical reactions related to tropospheric photo-oxidation chemistry p 654 N93-13726
Radical reactions of atmospheric importance p 659 N93-14053
RADII
Long pulse electron beam propagation
[DE92-014948] p 706 N93-12830
RADIO ASTRONOMY
A high-resolution radio survey of the galactic plane p 744 N93-13480
The emission-line properties of quasars p 753 N93-13487
A study of the neutral and ionized gas in the interstellar medium and galactic H 2 regions p 756 N93-13853
RADIO AURORAS
JARE data reports no. 175 (ionosphere 46). Records of radio aurora at Syowa Station, Antarctica in 1990 p 651 N93-13285
RADIO FREQUENCIES
A radio frequency user's guide to the Space Environment Services Center geophysical alert broadcasts
[PB92-220631] p 562 N93-12979
RF system description for the ground test accelerator radio-frequency quadrupole
[DE92-040239] p 563 N93-13045
Power excitation by the use of a RF wiggler
[DE92-016097] p 707 N93-13192
Test of a new RF separator structure for CEBAF
[CEBAF-PR-92-024] p 708 N93-13284
Special MAFIA postprocessors for the analysis of RF structures
[DE92-040248] p 565 N93-13510
RADIO FREQUENCY HEATING
Fast wave current drive experiment on the D3-D tokamak
[DE92-016253] p 716 N93-13193
RADIO FREQUENCY INTERFERENCE
Long-term averages of globally-measured ELF/VLF radio noise
[AD-A255518] p 566 N93-13869
RADIO INTERFEROMETERS
Report of the Science Working Group: Science with a lunar optical interferometer p 747 N93-13600
RADIO SOURCES (ASTRONOMY)
A high-resolution radio survey of the galactic plane p 744 N93-13480
RADIO SPECTRA
The emission-line properties of quasars p 753 N93-13487
RADIO TELESCOPES
Report of the Working Design Group p 748 N93-13601
RADIOACTIVE DECAY
Particle production and survival in muon acceleration
[DE92-019553] p 701 N93-12572
RADIOACTIVE ISOTOPES
The ORNL radioactive ion beam project with the ORIC accelerator
[DE92-040027] p 708 N93-13574
RADIOACTIVE MATERIALS
Lecture notes for criticality safety
[DE92-016009] p 701 N93-12832
RADIOACTIVE WASTES
Glass corrosion in natural environments
[NASA-CR-191234] p 551 N93-13150
Radiation-disorder and aperiodicity in irradiated ceramics
[DE92-015051] p 552 N93-13350
RADIOBIOLOGY
AFRRI reports
[AD-A254581] p 674 N93-12649
Katz model prediction of Caenorhabditis elegans mutagenesis on STS-42
[NASA-TM-4383] p 674 N93-13023
RADIOGRAPHY
Review of progress in quantitative NDE
[DE92-018814] p 620 N93-13071
RADIOMETERS
Feasibility study of a synthesis procedure for array feeds to improve radiation performance of large distorted reflector antennas
[NASA-CR-190948] p 561 N93-12655
EURECA
[ESA-F-26] p 522 N93-12964
Radiometric calibration of SAR systems p 564 N93-13055
Space-qualified submillimeter radiometer
[NASA-CR-190886] p 603 N93-13709
Spectroscopy for remote sounding of the atmosphere p 659 N93-14054
RADIOMETRIC RESOLUTION
Basic principles of SAR p 563 N93-13050
Test and calibration of the along track scanning radiometer, a satellite-borne infrared radiometer designed to measure sea surface temperature p 671 N93-13842
RAILGUN ACCELERATORS
Data acquisition applications for long duration electromagnetic launcher experiments
[AD-A254546] p 519 N93-12611
RAIN
Spatial resolution enhancement of SSM/I microwave brightness temperatures and its impact on rainfall retrieval algorithms
[AD-A254382] p 661 N93-12861
NOAA Workshop on Climate Scale Operational Precipitation and Water Vapor Products
[NOAA-TR-NESDIS-62] p 662 N93-13066

A parameterized quasi-five-cylinder convective cloud model and its application to remote sensing of rainfall
p 663 N93-13489
Relationships between continental-scale circulation and rainfall event attributes in the southeastern US
p 664 N93-13631

RAIN FORESTS
An ion budget for a terra firme rainforest in Central Amazonia
[INPE-5365-PRE/1745] p 632 N93-13005

RAINDROPS
A laboratory investigation of raindrop oscillations
p 666 N93-13790

RAINSTORMS
Relationships between continental-scale circulation and rainfall event attributes in the southeastern US
p 664 N93-13631

RAMAN SPECTRA
JPRS report: Science and technology. Central Eurasia: Physics and mathematics
[JPRS-UPM-92-006] p 698 N93-13303
Friction, wear and Raman spectroscopic characteristics of carbon lubricated surfaces p 618 N93-13949

RAMJET ENGINES
Aerodynamic studies of supersonic air intakes
p 497 N93-13222

RANDOM ACCESS MEMORY
On the suitability of non-hardened high density SRAMs for space applications
[AD-A255898] p 524 N93-14087

RANDOM NOISE
Modeling and estimation of reciprocal diffusion and Gauss-Markov random fields
[AD-A255034] p 698 N93-12709

RANDOM VARIABLES
The use of consider covariance analysis in choosing data weights to reduce the effect of errors in model parameters on satellite orbit determination accuracy
p 518 N93-13768

RANDOM WALK
A stochastic/deterministic method for transient, three-dimensional neutron transport
[DE92-016690] p 704 N93-13319

RANKINE CYCLE
Thermal control systems for low-temperature heat rejection on a lunar base
[NASA-CR-191286] p 679 N93-13717

RAPID QUENCHING (METALLURGY)
Measurements of crystal growth kinetics at extreme deviations from equilibrium
[DE92-019744] p 720 N93-12827
FNAS modify matric and transparent experiments
[NASA-CR-184442] p 531 N93-13311
Point defects quenched in NiAl and related intermetallic compounds p 724 N93-13628

RARE GASES
Energetics and dynamics of excess electrons in simple fluids p 704 N93-13369

RAREFIED GAS DYNAMICS
Application of a vectorized particle simulation to the study of plates and wedges in high-speed rarefied flow
p 495 N93-13746
Studies of surface-induced luminescence relevant to spacecraft glow, using a seeded arc-jet
p 523 N93-13919

RATES (PER TIME)
Cross sections and rate coefficients for the electron-impact excitation of He-like ions
[ISAS-RN-647] p 703 N93-13095

RATIOS
Vapor to liquid ratio test as an indicator of volatility
[DOT/FAA/CT-TN92/40] p 537 N93-12897

RATS
The neurochemical and neuropharmacological basis of motion sickness
[NASA-CR-190957] p 675 N93-13061

RAY TRACING
Computer-aided design-based high-frequency electromagnetic wave scattering from complex bodies
p 567 N93-14042

RAYLEIGH NUMBER
Natural convection between a vertical cylinder and a surrounding array
[DE92-019763] p 728 N93-12857

RAYLEIGH SCATTERING
Gas temperature measurements using the dual-line detection Rayleigh scattering technique
p 599 N93-13668
Gas temperature and density measurements based on spectrally resolved Rayleigh-Brillouin scattering
p 602 N93-13684

RAYLEIGH WAVES
Lateral variations of shear velocity and anelasticity in the upper mantle of the western US from Rayleigh wave observations p 653 N93-13492

RC CIRCUITS
Model for impedance of an ionic conductor sandwiched between blocking electrodes
[DE92-017812] p 569 N93-12561

REACTING FLOW
Computation of steady and unsteady shock-induced combustion over hypervelocity blunt bodies
p 536 N93-12836
A PDF closure model for compressible turbulent chemically reacting flows
[NASA-CR-191209] p 587 N93-13453
Velocity and temperature measurements in a non-premixed reacting flow behind a backward facing step p 494 N93-13632
Exit plane H2O concentration measurements correlated with OH PLIF near-injector mixing measurements for scramjet flows p 603 N93-13687
Linear stability theory of hypersonic, chemically reacting viscous flows p 588 N93-13765
Stability of the compressible reacting mixing layer
p 592 N93-13948
Wake characterization: Full flow simulation of space structures in low earth orbit p 497 N93-13970

REACTION BONDING
Microstructural evolution in reaction bonded alumina/mullite ceramics p 552 N93-13328

REACTION KINETICS
Abstracts of papers presented at the International Symposium on Time, Frequency, and Dating in Geomorphology
[AD-A254927] p 649 N93-12704
Measurements of cellular structure in spray detonation
[DE92-019580] p 555 N93-12933
Kinetics and dynamics of oxidation reactions involving an adsorbed CO species
[DE92-019745] p 537 N93-12995
The reactions of imidogen with nitric oxide and molecular oxygen
[DE92-006697] p 537 N93-13233
Systematic chemical equation balancing
[DE92-017234] p 539 N93-13530
A novel process for methanol synthesis
[DE92-019719] p 539 N93-13617
Kinetic and spectroscopic studies of peroxy radical reactions related to tropospheric photo-oxidation chemistry p 654 N93-13726
Studies of the kinetics and mechanisms of perfluoroether reactions on iron and oxidized iron surfaces
[NASA-CR-191363] p 539 N93-13763
Photochemical kinetics of excited states of O3 and O2: Laboratory studies and atmospheric implications
p 656 N93-13784
Radical reactions of atmospheric importance
p 659 N93-14053

REACTIVITY
The MAGSORB process for bulk separation of carbon dioxide
[DE92-001296] p 538 N93-13314

REACTOR DESIGN
Molten salt reactor for potentiostatic electroplating
[AD-D015358] p 551 N93-13101

REACTOR MATERIALS
Aluminum oxide film thickness and emittance
[DE92-019931] p 550 N93-13035
Radiation-disorder and aperiodicity in irradiated ceramics
[DE92-015051] p 552 N93-13350

REACTOR SAFETY
Investigation of component failure rates for pulsed versus steady state tokamak operation
[DE92-019758] p 713 N93-12856
Aluminum oxide film thickness and emittance
[DE92-019931] p 550 N93-13035
Public perceptions of the risks of an unfamiliar technology: The case of using nuclear energy sources for space missions p 527 N93-13971

REACTOR TECHNOLOGY
Plasma reactor waste management systems
p 680 N93-14000

REAL TIME OPERATION
Real-time data archiving for GTA
[DE92-018613] p 733 N93-12567
Real-time quality assurance testing using photonic techniques: Application to iodine water system
[NASA-CR-184413] p 619 N93-12692
VPPA weld model evaluation
[NASA-CR-184460] p 611 N93-12919
Performance of a plasma fluid code on the Intel parallel computers
[DE92-011680] p 716 N93-13297
SeaWiFS technical report series. Volume 4, an analysis of GAC sampling algorithms: A case study
[NASA-TM-104566-VOL-4] p 669 N93-13382
Summary: Experimental validation of real-time fault-tolerant systems
[NASA-CR-190985] p 503 N93-13697
Phase conjugation using CO2 lasers
p 607 N93-13812
Approximate optimal guidance for the Advanced Launch System p 519 N93-13819

RECEIVERS
Extremely low frequency/very low frequency Generator
[AD-A254347] p 562 N93-12948

RECOMBINATION REACTIONS
Ab initio atomic recombination reaction energetics on model heat shield surfaces
[NASA-CR-191210] p 575 N93-12677
Photochemical kinetics of excited states of O3 and O2: Laboratory studies and atmospheric implications
p 656 N93-13784

RECONNAISSANCE
Results of the laser sensor technology transition investigation
[AD-A255845] p 608 N93-14085

RECOVERY
On-orbit supervisor for controlling spacecraft
[AD-A254342] p 522 N93-12962

RECRYSTALLIZATION
The crystallization and crystalline properties of LARC-TPI
[NASA-CR-191001] p 721 N93-13022

RECTANGULAR PLATES
Large-deflection analysis of cord composite plates
p 530 N93-13008

RECTANGULAR WINGS
An investigation of the dynamic response of lifting surfaces with concentrated structural nonlinearities
p 501 N93-13807

RECURSIVE FUNCTIONS
Recursive construction of fractals
[ISBN-951-41-0689-X] p 697 N93-13271

RECYCLING
Long-term lunar stations: Some ecological considerations p 648 N93-13995
Technology development for lunar base water recycling p 680 N93-13999

RED GIANT STARS
Hydrodynamical calculations of stellar interactions
p 755 N93-13764

RED SHIFT
The emission-line properties of quasars
p 753 N93-13487

REDUCED GRAVITY
Toward a microgravity research strategy
[NASA-CR-190820] p 556 N93-12799
Establishing laboratory standards for biological flight experiments
[NASA-CR-184402] p 671 N93-12901
The First United States Microgravity Laboratory
[NASA-TM-107980] p 557 N93-12951
First International Microgravity Laboratory
[NASA-TM-108007] p 518 N93-13113
Glass fiber processing for the Moon/Mars program: Center director's discretionary fund final report
[NASA-TM-108379] p 551 N93-13115
Spaceflight payload design flight experience G-408
p 508 N93-13160
A decade of discovery: Experiments with the Get Away Special (GAS) canister p 509 N93-13162
A path to in-space welding and to other in-space metal processing technologies using Space Shuttle small payloads p 509 N93-13165
A study of the effects of micro-gravity on seed germination p 510 N93-13167
Investigation of microgravity effects on solidification phenomena of selected materials p 510 N93-13168
Tagging insulin in microgravity p 510 N93-13172
G254 undergraduate experiment p 511 N93-13174
A Pennsylvania State University/General Electric Get Away Special (GAS) experiment p 511 N93-13177
CONCAP 4: A Complex Autonomous Payload (CAP) for growing organic thin films in microgravity
p 511 N93-13178
The ROMPS robot in HitchHiker p 511 N93-13179
The Capillary Pumped Loop Flight Experiment (CAPL): A pathfinder for EOS p 512 N93-13181
The VTRE Program: An overview p 512 N93-13182
FNAS modify matric and transparent experiments
[NASA-CR-184442] p 531 N93-13311
Effects of spaceflight on the proliferation of jejunal mucosal cells
[NASA-CR-191303] p 675 N93-13449
Human factors dealing with the International Asteroid Mission p 515 N93-13559
Spacelab J: Microgravity and life sciences
[NASA-CR-191353] p 516 N93-13564
Eureca: A first for Europe
[ESA-BR-85] p 516 N93-13691
A growing dimension in space
[ESA-BR-37-F] p 517 N93-13902

The possibility of concrete production on the Moon p 554 N93-13988
Bone loss and human adaptation to lunar gravity p 676 N93-14002
Unit operations for gas-liquid mass transfer in reduced gravity environments p 557 N93-14011
Combustion of gaseous fuels under reduced-gravity conditions p 557 N93-14012

REDUCTION (CHEMISTRY)
Electrochemical and chemical characteristics of a new ambient temperature Li(I) polymer electrolyte [AD-A254918] p 545 N93-12651
Effect of hydrogen reduction and doping on the characteristics of high-temperature superconductors p 725 N93-13844

REDUNDANCY
Optimal coordination of robotic systems with redundancy p 693 N93-13336
Nonholonomic motion of free-flying space robots p 615 N93-13638

REFLECTED WAVES
Regional seismograms: Attenuation and scattering [AD-A254348] p 650 N93-12943

REFLECTOR ANTENNAS
Feasibility study of a synthesis procedure for array feeds to improve radiation performance of large distorted reflector antennas [NASA-CR-190948] p 561 N93-12655

REFRACTIVITY
An optical VLA on the Moon p 747 N93-13596
Transhorizon microwave propagation and its relationship with meteorological conditions p 666 N93-13791

REFRIGERANTS
New technologies for refrigeration without CFC's [DE92-018886] p 557 N93-12922
Reduction of chlorofluorocarbon emissions from refrigeration systems [DE92-019360] p 645 N93-13505

REFRIGERATING
New technologies for refrigeration without CFC's [DE92-018886] p 557 N93-12922

REFRIGERATORS
New technologies for refrigeration without CFC's [DE92-018886] p 557 N93-12922
Diffusion-absorption heat pump [PB92-217538] p 576 N93-12975
A small, single stage orifice pulse tube cryocooler demonstration [NASA-CR-190859] p 558 N93-13404
Three-stage sorption type cryogenic refrigeration systems and methods employing heat regeneration [NASA-CASE-NPO-18366-1-CU] p 558 N93-13422

REFUELING
Orbital Spacecraft Consumables Resupply System (OSCRS). Volume 3: Program cost estimate [NASA-CR-185685] p 740 N93-12814

REGENERATION (PHYSIOLOGY)
Lunar base CELSS: A bioregenerative approach p 680 N93-13993

REGENERATIVE COOLING
Three-stage sorption type cryogenic refrigeration systems and methods employing heat regeneration [NASA-CASE-NPO-18366-1-CU] p 558 N93-13422

REGENERATIVE FUEL CELLS
Advanced photovoltaic power system technology for lunar base applications p 641 N93-14004

REGENERATORS
A small, single stage orifice pulse tube cryocooler demonstration [NASA-CR-190859] p 558 N93-13404

REGOLITH
Isotopic separation of He-3/He-4 from solar wind gases evolved from the lunar regolith [DE92-019339] p 759 N93-13504
Resources for a lunar base: Rocks, minerals, and soil of the Moon p 760 N93-13973
Availability of hydrogen for lunar base activities p 762 N93-13982
Potential of derived lunar volatiles for life support p 680 N93-13998
Lunar surface mining for automated acquisition of helium-3: Methods, processes, and equipment p 766 N93-14007

REGRESSION ANALYSIS
Perceptual dimensions of visual scenes relevant for simulating low-altitude flight [AD-A254645] p 676 N93-12662
Nondestructive evaluation of the in-place compressive strength of concrete based upon limited destructive testing [PB92-222751] p 623 N93-12981
The relationship between SST anomalies and clouds, water vapor, and their radiative effects p 665 N93-13744

REGULATIONS
Lecture notes for criticality safety [DE92-016009] p 701 N93-12832
Reports to the Nation on our changing planet: Our ozone shield p 645 N93-13413
Environmental Compliance Management System [DE92-019595] p 645 N93-13479
Reduction of chlorofluorocarbon emissions from refrigeration systems [DE92-019360] p 645 N93-13505

REINFORCED PLASTICS
Synthesis and properties of novel cluster phases [DE92-017388] p 545 N93-12697

REINFORCING FIBERS
Fracture toughness of short fiber/brittle matrix composites p 528 N93-12630
Polypropylene fibers in portland cement concrete pavements [DOT/FAA/RD-92/9] p 551 N93-13259
Matrix cracking initiation stress in fiber-reinforced ceramic matrix composites p 627 N93-13539
Load-transfer and crack bridging in fiber-toughened ceramic composites p 629 N93-13754

REINFORCING MATERIALS
Large-deflection analysis of cord composite plates p 530 N93-13008

REISSNER THEORY
Load-transfer and crack bridging in fiber-toughened ceramic composites p 629 N93-13754

RELATIVISTIC EFFECTS
Fast ion-driven Bernstein instabilities [DE92-019393] p 705 N93-12713
The 2S(+) - 2P separation in KO [NASA-TM-108086] p 702 N93-12900
Cross sections and rate coefficients for the electron-impact excitation of He-like ions [ISAS-RN-647] p 703 N93-13095
Cosmological constraints on early-decaying particles p 750 N93-13123

RELATIVISTIC ELECTRON BEAMS
Theory of the ion-channel laser p 607 N93-13777

RELATIVISTIC PARTICLES
Comprehensive mappings of electron precipitation and its effects on the comprehensive mappings of electron precipitation and its effects on the atmosphere [AD-A254665] p 648 N93-12621

RELATIVISTIC VELOCITY
Electromagnetic lepton-pair production in relativistic collisions [DE92-011069] p 706 N93-12829

RELAXATION (MECHANICS)
Microwave and infrared dielectric relaxation of alkylcarbonates, chloroform and their mixtures at 25 C [AD-A253606] p 537 N93-13096
Atomic relaxation modes in grain boundaries [DE92-016781] p 722 N93-13195
Energetics and dynamics of excess electrons in simple fluids p 704 N93-13369

RELEASING
Chemical release and radiation effects experiment advanced planning and coordination [NASA-CR-184439] p 649 N93-12718

RELIABILITY
Advanced technology for America's future in space. Executive summary [NASA-TM-107969] p 513 N93-13308
Identifiability in the autopsy model of reliability theory p 620 N93-13710

RELIABILITY ANALYSIS
Requirements for soldered electrical connections [NHB-5300.4(3A-2)] p 570 N93-12674
Probabilistic finite elements for fatigue and fracture analysis [NASA-CR-191246] p 624 N93-13029
Software reliability through fault-avoidance and fault-tolerance [NASA-CR-189880] p 686 N93-13293

RELIABILITY ENGINEERING
Requirements for soldered electrical connections [NHB-5300.4(3A-2)] p 570 N93-12674
Software reliability through fault-avoidance and fault-tolerance [NASA-CR-189880] p 686 N93-13293
The use of degradation measures in assessing reliability p 573 N93-13607
Identifiability in the autopsy model of reliability theory p 620 N93-13710
Finite element study of ultrasonic imaging p 700 N93-13774

RELIC RADIATION
Measurements of the cosmic microwave background temperature at 1.47 GHz p 772 N93-13146

REMOTE HANDLING
Automated dry powder dispenser for explosive components [DE92-019425] p 555 N93-12568

REMOTE MANIPULATOR SYSTEM
The application of input shaping to a system with varying parameters p 612 N93-12954
Automation of the targeting and reflective alignment concept [NASA-CR-190964] p 709 N93-12985
Enhanced accuracy for closed-loop robot p 617 N93-13808
Dexterous grasp and manipulation p 618 N93-14075

REMOTE SENSING
Ocean optical database [AD-A254969] p 668 N93-12556
Sources of cloud nuclei and development of remote sensing techniques for cloud parameters [AD-A255016] p 660 N93-12558
Nimbus-7 Total Ozone Mapping Spectrometer (TOMS) Antarctic ozone atlas: August through November 1991 [NASA-RP-1283] p 661 N93-12700
Production of SSM/I data sets [NASA-CR-190944] p 632 N93-12800
Meeting review: Third NCAR Research Aircraft Fleet Workshop [PB92-222710] p 649 N93-12818
Investigations of the dynamics and thermodynamics of the mesosphere lower thermosphere and upper thermosphere at the polar regions with optical ground-based remote sensing [AD-A254746] p 650 N93-12845
Automation of the targeting and reflective alignment concept [NASA-CR-190964] p 709 N93-12985
Radiometric calibration of SAR systems p 564 N93-13055
Remote sensing of Earth terrain [NASA-CR-190908] p 633 N93-13084
Radiative transfer theory for polarimetric remote sensing of pine forest p 633 N93-13085
Application of theoretical models to active and passive remote sensing of saline ice p 633 N93-13086
Remote sensing data from CLARET: A prototype CART data set [NASA-CR-191294] p 634 N93-13094
Proceedings of the Mediterranean Conference on Environmental Geotechnology [AD-A253672] p 644 N93-13098
Performance of the Bowen ratio systems on a 22 deg slope [NASA-CR-191278] p 644 N93-13254
SeaWiFS technical report series. Volume 4, an analysis of GAC sampling algorithms: A case study [NASA-TM-104566-VOL-4] p 669 N93-13382
Brazilian remote sensing community: Historical, geographical and economic aspects [INPE-5421-PRE/1763] p 634 N93-13412
Phased array feed design technology for Large Aperture Microwave Radiometer (LAMR) Earth observations [NASA-CR-189727] p 519 N93-13462
A parameterized quasi-five-cylinder convective cloud model and its application to remote sensing of rainfall p 663 N93-13489
New approaches to the measurement of chlorophyll, related pigments and productivity in the sea [NASA-CR-190879] p 673 N93-13612
Providing structural modules with self-integrity monitoring software user's manual [NASA-CR-190877] p 628 N93-13707
Development of moored oceanographic spectroradiometer [NASA-CR-190883] p 670 N93-13708
The use of remotely sensed data in delineation of hydrologic response units and estimation of their rainfall-runoff model parameters p 635 N93-13840
Deciduous forest scene complexity in high-resolution multispectral scanner imagery [AD-A255511] p 635 N93-13867
Automatic pattern recognition techniques for geometrical correction on satellite data p 687 N93-13913
An evaluation of the use and future need of remotely sensed images in grades K-12 p 635 N93-13956
Spectroscopy for remote sounding of the atmosphere p 659 N93-14054

REMOTE SENSORS
The correlation of active and passive microwave outputs for the Skylab S-193 sensor [LEC-7819] p 635 N93-13440
Summary of literature on unmanned probes to asteroids and precursor data requirements for IAM p 514 N93-13551
Computer simulation of a space-based infrared surveillance sensor [AD-A255521] p 524 N93-13870

RENDEZVOUS SPACECRAFT
Robust rendezvous maneuver point conditions [NASA-CR-190996] p 517 N93-12690

REPLICAS
Preparation and properties of low density replica carbon foams
[DE92-019573] p 552 N93-13538
REPRODUCTION (BIOLOGY)
Assessment of programs in space biology and medicine
[NASA-CR-190930] p 672 N93-13327
REQUIREMENTS
US Antarctic program. Personnel manual, 1992
[NSF-92-63] p 731 N93-12637
RESCUE OPERATIONS
Assured crew return vehicle post landing configuration design and test
[NASA-CR-191253] p 520 N93-12910
RESEARCH AIRCRAFT
Determination of the stability and control derivatives of the F/A-18 HARV from flight data using the maximum likelihood method
[NASA-CR-191216] p 503 N93-12903
NASA aeronautics: Research and technology program highlights
[NASA-NP-159] p 491 N93-13110
RESEARCH AND DEVELOPMENT
Toward a microgravity research strategy
[NASA-CR-190820] p 556 N93-12799
USAF 1990 research initiation program, volume 3
[AD-A254755] p 775 N93-12849
Air Force Office of Scientific Research technical report summaries
[AD-A254380] p 775 N93-12859
Women and minorities in science and engineering: An update
[NSF-92-303] p 730 N93-12907
The First United States Microgravity Laboratory
[NASA-TM-107980] p 557 N93-12951
Advanced energy projects FY 1992 research summaries
[DE92-040442] p 637 N93-13001
Research priorities in networking and communications
[NSF-92-109] p 562 N93-13024
NASA industry education initiative. Education programs report, 1991
[NASA-NP-158] p 730 N93-13248
Federal R/D funding by budget function: Fiscal years 1991-1993
[NSF-92-318] p 740 N93-13312
Plasma Science Committee (PLSC) and study on new opportunities in plasma science and technology
[DE92-019507] p 716 N93-13359
State award summary: Fiscal Year 1991
[NSF-92-3] p 775 N93-13381
Highlights 92/2 p 775 N93-13474
Academic science and engineering: R/D expenditures, fiscal year 1990
[NSF-92-321] p 741 N93-13544
Research and technology in support of IAM
p 515 N93-13562
Westinghouse PAFC program update
[DE92-019978] p 640 N93-13623
Selected data on Federal funds for research and development: Fiscal years 1990, 1991, and 1992
[NSF-92-319] p 741 N93-13657
Research and development in industry: 1989. Funds, 1989. Scientists and engineers, January 1990
[NSF-92-307] p 741 N93-13658
Abstracts of phase 1 awards: NSF Small Business Innovation Research Program (SBIR): 1992
[NSF-92-80] p 732 N93-13703
Directory of awards, fiscal year 1991. Directorate for engineering
[NSF-92-55] p 775 N93-13704
NSF Science and Technology Centers
[NSF-92-104] p 507 N93-13712
Arctic science, engineering, and education. Directory of awards, fiscal year 1991
[NSF-92-60] p 775 N93-13713
JPRS report: Science and technology. USSR: Space
[JPRS-USP-91-004] p 516 N93-13756
US Industry Access to Japanese Science and Technology: Proceedings of a conference
[PB92-167964] p 741 N93-13788
Research in geosciences policy
[NASA-CR-190470] p 632 N93-13833
Assessment of Japanese technology in advanced glass and ceramic fibers
[AD-A255229] p 553 N93-13836
Preparing for the future
[ESA-BR-37-H] p 517 N93-13860
Symposium on Polymeric Materials for Photonic and Optical Applications
[AD-A255820] p 554 N93-14029
RESEARCH FACILITIES
Scientific and engineering research facilities at universities and colleges: 1992
[NSF-92-325] p 506 N93-13407
NSF Science and Technology Centers
[NSF-92-104] p 507 N93-13712
Moon Park: A research and educational facility
p 519 N93-14015
RESEARCH MANAGEMENT
ONR basic research program: Summary and bibliographies, FY 1990 and 1991
[AD-A253038] p 774 N93-12696
Elementary particle physics research
[DE92-019746] p 702 N93-12855
Air Force Office of Scientific Research technical report summaries
[AD-A254380] p 775 N93-12859
Advanced energy projects FY 1992 research summaries
[DE92-040442] p 637 N93-13001
Theoretical high energy physics
[DE92-015480] p 707 N93-13189
Federal R/D funding by budget function: Fiscal years 1991-1993
[NSF-92-318] p 740 N93-13312
RESEARCH PROJECTS
US Air Force 1989 research initiation program, volume 1
[AD-A254457] p 774 N93-12764
US Air Force 1989 research initiation program, volume 4
[AD-A254458] p 774 N93-12765
US Air Force 1989 research initiation program, volume 2
[AD-A254459] p 774 N93-12766
US Air Force 1989 research initiation program, volume 3
[AD-A254460] p 774 N93-12767
Air Force Office of Scientific Research technical report summaries
[AD-A254380] p 775 N93-12859
Research in elementary particle physics
[DE92-017869] p 704 N93-13251
Plasma Science Committee (PLSC) and study on new opportunities in plasma science and technology
[DE92-019507] p 716 N93-13359
RESIDUAL STRESS
Toughening mechanisms in weak matrix ceramic composites p 553 N93-13780
Three-dimensional boundary element analysis of residual stresses in a cross-ply fiber composite model
p 629 N93-13811
Effects of residual stress, weld toe notch and weld defects on fatigue of welded steel structures
p 631 N93-13947
Thermoviscoplastic analysis of metal matrix composites p 535 N93-13954
Fracture of a metal/ceramic couple: Tantalum (titanium)/sapphire p 554 N93-14074
RESIN MATRIX COMPOSITES
Consolidation of powder coated thermoplastic preform process modeling
[AD-A255094] p 529 N93-12757
Predictive forming of advanced thermoplastic composite structures p 529 N93-12835
Enabling technologies for economical manufacturing of composites
[AD-A253615] p 531 N93-13324
Characterization of thermotropic liquid crystalline polymer blends by positron annihilation lifetime spectroscopy
[AD-A253616] p 552 N93-13325
RESINS
Characterization of selected LDEF: Exposed polymer films and resins p 549 N93-12787
Synthesis of derivatives of alpha, omega difunctional perfluoroaliphatic compounds for low dielectric constant resins
[AD-A254928] p 550 N93-13026
RESOLVERS
Torque resolver design for tendon-driven manipulators
[DE92-017395] p 609 N93-12698
RESONANCE
Experiments on resonantly photo-pumped x ray lasers
[DE92-019542] p 603 N93-12570
Resonance ionization mass spectrometry in biochemical analysis
[DE92-017407] p 538 N93-13341
Parameter studies of helium-neon lasers at 543 nm
p 606 N93-13747
Resonance studies of artificial earth satellites
p 523 N93-14037
RESONANCE FLUORESCENCE
Two-photon cooperative cascade superfluorescence
[AD-A255690] p 608 N93-14023
RESONANT FREQUENCIES
The application of input shaping to a system with varying parameters p 612 N93-12954
Initial experiments in end-point control of a flexible, two-link manipulator p 612 N93-13018
RESONANT TUNNELING
Physics and technology of resonant-tunneling devices
[AD-A255233] p 573 N93-13837
RESONANT VIBRATION
Dynamic control modification techniques in teleoperation of a flexible manipulator
[NASA-CR-190984] p 610 N93-12904
Experimental verification of modified command shaping using a flexible manipulator p 612 N93-12955
RESOURCES MANAGEMENT
Principles of information resource management: A foundation for the future
[AD-A254447] p 733 N93-12597
RESPIRATORS
Physiological effects of positive pressure ventilation
[AD-A254809] p 674 N93-12751
RESPONSE TIME (COMPUTERS)
A methodology for the solution of nonlinear two-point boundary value inverse problems in physics and engineering p 697 N93-13363
RESTORATION
An application of exponential neural networks to event-train recognition
[AD-A254948] p 690 N93-12548
RETINA
Silicon vision: Elementary functions to be implemented on electronic retinas p 692 N93-13242
REVERSE FIELD PINCH
Measurement of current density fluctuations and ambipolar particle flux due to magnetic fluctuations in MST
[DE92-041013] p 713 N93-12878
Anomalous ion heating and superthermal electrons in the MST reversed-field pinch
[DE92-041011] p 713 N93-12882
Current density fluctuations, nonlinear coupling, and transport in MST
[DE92-041012] p 713 N93-12883
REVERSING
Propulsion integration results of the STOL and Maneuver Technology Demonstrator p 502 N93-13228
REYNOLDS NUMBER
Comparative performance tests of a pitot-inlet in several European wind-tunnels at subsonic and supersonic speeds p 497 N93-13221
A theoretical investigation of the growth rates of ice crystals in clouds p 653 N93-13485
Numerical calculation of turbomachinery cascade flows p 589 N93-13767
REYNOLDS STRESS
On the prediction of turbulent secondary flows
[NASA-CR-189722] p 575 N93-12717
RIBLETS
Fluid flow and heat convection studies for actively cooled airframes
[NASA-CR-190956] p 587 N93-13406
RIGID ROTORS
Dynamic stall effects on hingeless rotor stability with experimental correlation p 492 N93-13010
RIGID STRUCTURES
Equations of motion of slung-load systems, including multilift systems
[NASA-TP-3280] p 503 N93-12815
An investigation of the dynamic response of lifting surfaces with concentrated structural nonlinearities
p 501 N93-13807
RING CURRENTS
Ion radial diffusion in an electrostatic impulse model for stormtime ring current formation
[NASA-CR-190941] p 705 N93-12715
Ring current oxygen interaction with micropulsations
p 651 N93-13149
Interaction of energetic ring current protons with magnetospheric hydromagnetic waves
p 718 N93-13750
RIOMETERS
JARE data reports no. 176 (Ionosphere 47). Riometer records of 30 MHz cosmic noise at Syowa Station, Antarctica in 1990 p 772 N93-13255
RISK
The estimation of electrical cable fire-induced damage limits
[DE92-040100] p 572 N93-13519
The program plan: An overview of the development and implementation of the International Asteroid Mission
p 514 N93-13553
Findings of a review of spacecraft fire safety needs
[NASA-CR-189181] p 523 N93-13715
Public perceptions of the risks of an unfamiliar technology: The case of using nuclear energy sources for space missions p 527 N93-13971
ROBOT ARMS
A fundamental study of the effect of gravity on the static and dynamic behavior of robots p 610 N93-12760
Initial experiments in end-point control of a flexible, two-link manipulator p 612 N93-13018

Robust control of uncertain aerospace and mechanical systems with unmodelled flexibilities: A singular perturbation approach p 691 N93-13129
Optimal coordination of robotic systems with redundancy p 693 N93-13336
Force and motion control of a constrained flexible manipulator p 613 N93-13384
Robust control of a flexible link robot and rigid link robot: Theory, simulation, and experiment p 614 N93-13452
Enhanced accuracy for closed-loop robot p 617 N93-13808
Near-minimum-time control of a flexible arm p 695 N93-14039
A collision avoidance algorithm for the mobile robot and the robot manipulator in multi-robot system p 618 N93-14094

ROBOT CONTROL
Application of concurrent engineering methods to the design of an autonomous aerial robot [AD-A254968] p 609 N93-12555
Manipulation strategies for massive space payloads [NASA-CR-190844] p 611 N93-12952
Numerical analysis of nonminimum phase zero for nonuniform link design p 611 N93-12953
Experimental verification of modified command shaping using a flexible manipulator p 612 N93-12955
The ROMPS robot in HitchHiker p 511 N93-13179
3-D computer vision for navigation/control of mobile robots p 693 N93-13243
Robot welding process control [NASA-CR-184428] p 614 N93-13436
Automatic programming of arc welding robots p 616 N93-13720
A unified approach to the analysis and design of manipulator systems with environmental contact p 573 N93-13805
Automation and robotics considerations for a lunar base p 619 N93-14006
Near-minimum-time control of a flexible arm p 695 N93-14039
Position and force control of flexible and rigid manipulators using the sliding-mode technique p 695 N93-14065

ROBOT DYNAMICS
A fundamental study of the effect of gravity on the static and dynamic behavior of robots p 610 N93-12760
Manipulation strategies for massive space payloads [NASA-CR-190844] p 611 N93-12952
The ROMPS robot in HitchHiker p 511 N93-13179
End-point position control of multi-link flexible manipulator arms p 613 N93-13335
Optimal coordination of robotic systems with redundancy p 693 N93-13336
Force and motion control of a constrained flexible manipulator p 613 N93-13384
Force-closure grasping with two hands p 616 N93-13742
A unified approach to the analysis and design of manipulator systems with environmental contact p 573 N93-13805
Enhanced accuracy for closed-loop robot p 617 N93-13808
Experiments in two-cooperating-arm manipulation from a platform with unknown motion p 617 N93-13931

ROBOT SENSORS
Tactile sensing and control in humans and robotic/teleoperated systems [AD-A254408] p 609 N93-12604
Sensing and interpretation of 3-D shape and motion p 692 N93-13240
Silicon vision: Elementary functions to be implemented on electronic retinas p 692 N93-13242
Machine perception exploiting high-level spatio-temporal models p 693 N93-13244

ROBOTICS
Design of a welded joint for robotic, on-orbit assembly of space trusses [NASA-TM-108380] p 609 N93-12682
Torque resolver design for tendon-driven manipulators [DE92-017395] p 609 N93-12698
G-133: A soft x ray solar telescope p 510 N93-13171
Machine Perception [AGARD-LS-185] p 692 N93-13238
Building and using scene representations in image understanding p 692 N93-13241
Machine perception exploiting high-level spatio-temporal models p 693 N93-13244
Space robotics: Recent accomplishments and opportunities for future research [NASA-TM-107675] p 694 N93-13442
Design, construction, and control of a two degree-of-freedom electric direct-drive human power amplifier p 678 N93-13486
Robotic exploration of surfaces and its application to legged locomotion p 615 N93-13540
Nonholonomic motion of free-flying space robots p 615 N93-13638
Automatic programming of arc welding robots p 616 N93-13720
Position and force control of flexible and rigid manipulators using the sliding-mode technique p 695 N93-14065
Dexterous grasp and manipulation p 618 N93-14075
Modelling flexible link manipulators in the three-dimensional space p 574 N93-14093

ROBOTS
Application of concurrent engineering methods to the design of an autonomous aerial robot [AD-A254968] p 609 N93-12555
Tactile sensing and control in humans and robotic/teleoperated systems [AD-A254408] p 609 N93-12604
A fundamental study of the effect of gravity on the static and dynamic behavior of robots p 610 N93-12760
Journal of Research of the National Institute of Standards and Technology, May-June 1992, volume 97, number 3 [PB92-217637] p 698 N93-12805
Dynamic control modification techniques in teleoperation of a flexible manipulator [NASA-CR-190984] p 610 N93-12904
The ROMPS robot in HitchHiker p 511 N93-13179
3-D computer vision for navigation/control of mobile robots p 693 N93-13243
Design, construction and demonstration of modular, reconfigurable robots p 613 N93-13329
Control of a very flexible robot in gravity p 615 N93-13541
Dynamic modeling and optimal joint torque coordination of advanced robotic systems p 617 N93-13936

ROBUSTNESS (MATHEMATICS)
Robust rendezvous maneuver point conditions [NASA-CR-190996] p 517 N93-12690

ROCKET ENGINE DESIGN
Stability codes for a liquid rocket implemented for use on a PC [NASA-CR-184453] p 525 N93-12659
Users manual for program SSFREQ intermediate mode stability curves: Developed for use on a PC computer [NASA-CR-184452] p 682 N93-12675
Users manual for program ADMIT: Admittance and pressure transfer function developed for use on a PC computer [NASA-CR-184450] p 682 N93-12676

ROCKET EXHAUST
Planar laser-induced fluorescence imaging of OH in the exhaust of a bi-propellant thruster p 602 N93-13686

ROCKET PROPELLANTS
High Energy Propulsion System (HEPS) analysis [AD-A254343] p 525 N93-12963

RODS
Preloaded latching device [NASA-CASE-MSC-21730-1] p 614 N93-13417

ROLL
An experimental and computational investigation of slender wings undergoing wing rock p 505 N93-13915

ROOM TEMPERATURE
Initial performance of Los Alamos Advanced Free Electron Laser [DE92-040214] p 605 N93-13507

ROOMS
Applications of CFD and visualization techniques p 584 N93-13386

ROSAT MISSION
Probing the galactic halo with ROSAT [NASA-CR-191268] p 743 N93-13272
The mass and dynamics of cD clusters with cooling flows. 1: ROSAT observations of A 496 [NASA-CR-191240] p 743 N93-13352

ROTARY WINGS
Dynamic stall effects on hingeless rotor stability with experimental correlation p 492 N93-13010

ROTATING BODIES
Inverse Synthetic Aperture Radar p 564 N93-13058
Nutational stability and passive control of symmetric spinning bodies with axial forcing and internal mass motion p 504 N93-13820

ROTATING CYLINDERS
Instabilities and patterns in Taylor-Couette flow p 593 N93-13965

ROTATING DISKS
An experimental investigation of the three-dimensional boundary layer on a rotating disk p 589 N93-13806

ROTATING LIQUIDS
Dynamical instabilities in a fluid spin-up and in an open flow system p 590 N93-13899

ROTATION
The neurochemical and neuropharmacological basis of motion sickness [NASA-CR-190957] p 675 N93-13061
Numerical study of nonlinear convective-symmetric instability in a rotating baroclinic atmosphere p 666 N93-13786
Modelling flexible link manipulators in the three-dimensional space p 574 N93-14093

ROTATIONAL SPECTRA
High resolution molecular spectroscopy of atmospheric species [AD-A254360] p 650 N93-12946

ROTOR AERODYNAMICS
Dynamic stall effects on hingeless rotor stability with experimental correlation p 492 N93-13010
Overview on test cases for computation of internal flows in turbomachines p 579 N93-13209
Unsteady three-dimensional thin-layer Navier-Stokes solutions for turbomachinery in transonic flow p 593 N93-14025

ROTOR BLADES
Radial turbine cooling [NASA-TM-105658] p 492 N93-13292

ROTORS
User's Guide for the NREL Teetering Rotor Analysis Program (STRAP) [DE92-010580] p 627 N93-13525

RUBIDIUM
Demonstration of a neon-like rubidium x ray laser [DE92-019576] p 606 N93-13653

RUN TIME (COMPUTERS)
Monitoring and controlling distributed applications using Lomita (position paper) [NASA-CR-190971] p 687 N93-13695

RUNWAYS
Limited production Precision Runway Monitor (PRM) master test plan [DOT/FAA/CT-TN92/23] p 506 N93-12899
Prototype stop bar system evaluation at John F. Kennedy International Airport [DOT/FAA/CT-92/24] p 506 N93-12902
A NASPAC-based analysis of the delay and cost effects of the Dallas/Fort Worth metroplex plan [DOT/FAA/CT-TN92/21] p 507 N93-13447

S

S WAVES
Lateral variations of shear velocity and anelasticity in the upper mantle of the western US from Rayleigh wave observations p 653 N93-13492

SAFETY
US Antarctic program. Personnel manual, 1992 [NSF-92-63] p 731 N93-12637
Advanced technology for America's future in space. Executive summary [NASA-TM-107969] p 513 N93-13308
White paper: Preliminary assessment of LNG vehicle technology, economics, and safety issues, revision 1 [PB92-212943] p 615 N93-13644

SAFETY DEVICES
Test plan and report for Space Shuttle launch environment testing of Bergen cable technology safety cable [NASA-CR-4473] p 559 N93-13434
Physiological stress from chemical defense clothing and equipment [AD-A255786] p 676 N93-14028

SAFETY FACTORS
Laser measurement techniques guide for a hazard evaluation [AD-A254545] p 604 N93-12610
Test plan and report for Space Shuttle launch environment testing of Bergen cable technology safety cable [NASA-CR-4473] p 559 N93-13434
Booster explosive rings [AD-D015375] p 556 N93-13471

SAFETY MANAGEMENT
Lecture notes for criticality safety [DE92-016009] p 701 N93-12832
Verification and validation of TMAP4 [DE92-019684] p 539 N93-13616
Findings of a review of spacecraft fire safety needs [NASA-CR-189181] p 523 N93-13715

SALINITY
One-dimensional transient finite difference model of an operational salinity gradient solar pond p 586 N93-13400

SAMPLERS
Bayesian analysis of linear and nonlinear population models using the Gibbs sampler [AD-A254769] p 697 N93-12702

SAMPLING
Data acquisition applications for long duration electromagnetic launcher experiments
[AD-A254546] p 519 N93-12611
Selected data on research and development in industry: 1990
[NSF-92-317] p 773 N93-12667
Characterization of site geochemistry in support of environmental restoration
[DE92-017512] p 641 N93-12685
Fluidic sampling
[DE92-017266] p 575 N93-12761
SeaWiFS technical report series. Volume 4, an analysis of GAC sampling algorithms: A case study
[NASA-TM-104566-VOL-4] p 669 N93-13382

SAPPHIRE
The sapphire Cerenkov laser p 605 N93-13365
Fracture of a metal/ceramic couple: Tantalum (titanium)/sapphire p 554 N93-14074

SATELLITE ALTIMETRY
Application of satellite altimetry to study the Gulf of Alaska gyre p 635 N93-13969
On the space-time ocean current variability and its effects on the length-of-day p 636 N93-14051

SATELLITE ATMOSPHERES
Studies of radiative emission from the simulated shock layer of the Huygens probe p 521 N93-12834

SATELLITE COMMUNICATION
An analysis of the low-earth-orbit communications environment p 561 N93-12633
Applications of satellite technology to broadband ISDN networks
[NASA-CR-189199] p 562 N93-12950
Anomalous TWTA output power spikes and their effect on a digital satellite communications system
[NASA-TM-105875] p 571 N93-13286
Error control techniques for satellite and space communications
[NASA-CR-191229] p 565 N93-13411
Advanced on-chip divider for monolithic microwave VCO's
[NASA-CR-191355] p 572 N93-13563
Messengers in space
[ESA-BR-37-D] p 516 N93-13857

SATELLITE CONTROL
Dynamics and control of a tumbling satellite retrieval device p 522 N93-13119

SATELLITE DRAG
Aeronomy coexperiments on drag-free satellites with proportional thrusters: GP-B and STEP p 518 N93-13922

SATELLITE IMAGERY
Satellite imagery goes to the field
[AD-A254449] p 632 N93-12598
Production of SSM/I data sets
[NASA-CR-190944] p 632 N93-12800
Assimilation of satellite color observations in a coupled ocean GCM-ecosystem model
[NASA-CR-191218] p 670 N93-13714
The use of remotely sensed data in delineation of hydrologic response units and estimation of their rainfall-runoff model parameters p 635 N93-13840
Automatic pattern recognition techniques for geometrical correction on satellite data p 687 N93-13913
An evaluation of the use and future need of remotely sensed images in grades K-12 p 635 N93-13956

SATELLITE INSTRUMENTS
Comprehensive mappings of electron precipitation and its effects on the comprehensive mappings of electron precipitation and its effects on the atmosphere
[AD-A254665] p 648 N93-12621

SATELLITE NETWORKS
Applications of satellite technology to broadband ISDN networks
[NASA-CR-189199] p 562 N93-12950

SATELLITE OBSERVATION
Ocean optical database
[AD-A254969] p 668 N93-12556
Remote sensing data from CLARET: A prototype CART data set
[NASA-CR-191294] p 634 N93-13094
B supergiants in open clusters and associations
[NASA-CR-191275] p 748 N93-13659
Assimilation of satellite color observations in a coupled ocean GCM-ecosystem model
[NASA-CR-191218] p 670 N93-13714
The determination and error assessment of the Earth's gravity field model p 656 N93-13771
Resonance studies of artificial earth satellites p 523 N93-14037

SATELLITE ORBITS
An analysis of the low-earth-orbit communications environment p 561 N93-12633
Nonconservative force model parameter estimation strategy for TOPEX/Poseidon precision orbit determination
[NASA-TM-104575] p 519 N93-13372
The use of consider covariance analysis in choosing data weights to reduce the effect of errors in model parameters on satellite orbit determination accuracy p 518 N93-13768

SATELLITE ORIENTATION
LDEF yaw and pitch angle estimates p 524 N93-12772
The Orbiter Stability Experiment on STS-40 p 508 N93-13159

SATELLITE PERTURBATION
Nonconservative force model parameter estimation strategy for TOPEX/Poseidon precision orbit determination
[NASA-TM-104575] p 519 N93-13372
Resonance studies of artificial earth satellites p 523 N93-14037

SATELLITE TRANSMISSION
An analysis of the low-earth-orbit communications environment p 561 N93-12633

SATELLITE-BORNE INSTRUMENTS
Test and calibration of the along track scanning radiometer, a satellite-borne infrared radiometer designed to measure sea surface temperature p 671 N93-13842
Computer simulation of a space-based infrared surveillance sensor
[AD-A255521] p 524 N93-13870
Spectroscopy for remote sounding of the atmosphere p 659 N93-14054

SATELLITE-BORNE RADAR
SAR simulation p 564 N93-13056

SAWTOOTH WAVEFORMS
Current density fluctuations, nonlinear coupling, and transport in MST
[DE92-041012] p 713 N93-12883

SCALARS
Solutions without phase-slip for the Ginsburg-Landau equation
[PB92-115575] p 696 N93-12889
Comparison of two stochastic models of scalar diffusion in turbulent flow
[DE92-019381] p 576 N93-12912
Reject mechanisms for massively parallel neural network character recognition systems
[PB92-213412] p 689 N93-13198
Quantum inflationary minisuperspace cosmological models p 728 N93-13751

SCALE EFFECT
Scale effects in buckling, postbuckling and crippling of graphite-epoxy Z-section stiffeners p 621 N93-12632

SCALE MODELS
Bistatic clutter RCS simulation using scale model rough surfaces
[AD-A254932] p 560 N93-12581
Scale effects in buckling, postbuckling and crippling of graphite-epoxy Z-section stiffeners p 621 N93-12632
ASTOVL model engine simulators for wind tunnel research p 507 N93-13213
An investigation of jet engine test cell aerodynamics by means of scale model test studies with comparisons to full-scale test results p 507 N93-14060

SCALING LAWS
Scaling of 100 kW class applied-field MPD thrusters
[NASA-CR-190791] p 525 N93-12638
Quantum inflationary minisuperspace cosmological models p 728 N93-13751
Unit operations for gas-liquid mass transfer in reduced gravity environments p 557 N93-14011

SCATTERING
Experimental examination of growing and newly submerged sea ice including acoustic probing of the skeletal layer
[AD-A254526] p 669 N93-12599

SCATTERING CROSS SECTIONS
Bistatic clutter RCS simulation using scale model rough surfaces
[AD-A254932] p 560 N93-12581

SCATTEROMETERS
Latent image exposure monitor using scatterometry
[DE92-019427] p 604 N93-12915
SAR peculiarities, ambiguities and constraints p 563 N93-13051
The correlation of active and passive microwave outputs for the Skylab S-193 sensor
[LEC-7819] p 635 N93-13440

SCENE ANALYSIS
Sensing and interpretation of 3-D shape and motion p 692 N93-13240
Building and using scene representations in image understanding p 692 N93-13241
The 3-D computer vision techniques for object following and obstacle avoidance p 693 N93-13245
Deciduous forest scene complexity in high-resolution multispectral scanner imagery
[AD-A255511] p 635 N93-13867

SCHOOLS
Blacks in undergraduate science and engineering education
[NSF-92-305] p 730 N93-13015
Fiscal Year 1991 highlights
[NSF-92-23] p 731 N93-13702
Application of information system technology to K-12 education
[AD-A255223] p 731 N93-13834

SCHROEDINGER EQUATION
Analytical studies of nonlinear partial differential equations of interest in nonlinear optics
[AD-A254931] p 696 N93-13027

SCIENCE
Women and minorities in science and engineering: An update
[NSF-92-303] p 730 N93-12907
NASA industry education initiative. Education programs report, 1991
[NASA-NP-158] p 730 N93-13248
Scientific and engineering research facilities at universities and colleges: 1992
[NSF-92-325] p 506 N93-13407
Academic science and engineering: R/D expenditures, fiscal year 1990
[NSF-92-321] p 741 N93-13544
Awards: 1991 undergraduate course and curriculum development program
[NSF-92-45] p 731 N93-13699
Diversity in biological research
[NSF-92-19] p 673 N93-13700
Science and engineering degrees: 1966-1990
[NSF-92-326] p 731 N93-13701

SCIENTIFIC SATELLITES
Chemical release and radiation effects experiment advanced planning and coordination
[NASA-CR-184439] p 649 N93-12718
Element Material Exposure Experiment by EFFU p 548 N93-12783
Analysis and modeling of the CRRES satellite data
[AD-A254349] p 650 N93-12944

SCIENTISTS
USAF 1990 research initiation program, volume 4
[AD-A254655] p 773 N93-12664
USAF 1990 research initiation program, volume 1
[AD-A254656] p 773 N93-12665
Science and engineering degrees, by race/ethnicity of recipients: 1977-1990
[NSF-92-327] p 729 N93-12694
Air Force engineering research initiation grants (1990-1991)
[AD-A255004] p 774 N93-12706
US Air Force 1989 research initiation program, volume 1
[AD-A254457] p 774 N93-12764
US Air Force 1989 research initiation program, volume 4
[AD-A254458] p 774 N93-12765
US Air Force 1989 research initiation program, volume 2
[AD-A254459] p 774 N93-12766
US Air Force 1989 research initiation program, volume 3
[AD-A254460] p 774 N93-12767
Academic science and engineering: Graduate enrollment and support, Fall 1990
[NSF-92-323] p 729 N93-12802
Evolution of the scientific paper
[DE92-019696] p 735 N93-12994
Blacks in undergraduate science and engineering education
[NSF-92-305] p 730 N93-13015
Gateway to diversity in the scientific and technological workforce
[NSF-92-99] p 730 N93-13278
Characteristics of recent science and engineering graduates: 1990. Detailed statistical tables
[NSF-92-316] p 731 N93-13454
Highlights 92/2 p 775 N93-13474
Research and development in industry: 1989. Funds, 1989. Scientists and engineers, January 1990
[NSF-92-307] p 741 N93-13658
Selected data on Science and Engineering Doctorate Awards: 1991
[NSF-92-309] p 731 N93-13698

SCINTILLATION
Abstracts of papers presented at the International Symposium on Time, Frequency, and Dating in Geomorphology
[AD-A254927] p 649 N93-12704

SCINTILLATION COUNTERS
A payload to evaluate photodiodes for the detection of soft and hard x rays in a space environment using a Get Away Special p 509 N93-13166
Effects of ionizing radiation on scintillators and other particle detectors
[DE92-018184] p 705 N93-13531
SCREW DISLOCATIONS
Weak-beam imaging of dissociated dislocations in HVEM-irradiated Fe-Ni-Cr alloys
[DE92-019587] p 541 N93-12798
SEA ICE
Near-normal incidence scattering from rough, finite surfaces: Kirchhoff theory and data comparison for Arctic sea ice
[AD-A254525] p 668 N93-12577
Experimental examination of growing and newly submerged sea ice including acoustic probing of the skeletal layer
[AD-A254526] p 669 N93-12599
Interaction and impact of floating bodies
[AD-A254627] p 574 N93-12617
Application of theoretical models to active and passive remote sensing of saline ice p 633 N93-13086
SEA LEVEL
Atmospheric loading response of the solid earth and oceans p 659 N93-13955
SEA SURFACE TEMPERATURE
The relationship between SST anomalies and clouds, water vapor, and their radiative effects p 665 N93-13744
Climate sensitivity study with energy balance models p 666 N93-13817
Test and calibration of the along track scanning radiometer, a satellite-borne infrared radiometer designed to measure sea surface temperature p 671 N93-13842
The assimilation of marine surface data into the Navy operational global atmospheric prediction system
[AD-A255559] p 667 N93-13877
SEA WATER
Application of theoretical models to active and passive remote sensing of saline ice p 633 N93-13086
On the relationship between the intensity of extratropical frontal cyclone systems and water levels in the Gulf of Mexico p 666 N93-13816
SEARCH PROFILES
An investigation of new search techniques for the traveling salesman problem p 696 N93-12625
SEARCH RADAR
The Joint Surveillance Target Attack Radar System: Can procedures be developed to support the requirements of the land and air component commanders?
[AD-A255555] p 567 N93-13875
SEASAT SATELLITES
Review of spaceborne and airborne SAR systems p 565 N93-13060
SEATS
Design guide for the ergonomic aspects of helicopter crew seating
[ISVR-TR-209] p 678 N93-13464
SECONDARY FLOW
On the prediction of turbulent secondary flows
[NASA-CR-189722] p 575 N93-12717
Dynamical instabilities in a fluid spin-up and in an open flow system p 590 N93-13899
SECURITY
The protection of the Facsimile (FAX) machine against the insider threat
[DE92-019424] p 565 N93-13506
SEEDS
A study of the effects of micro-gravity on seed germination p 510 N93-13167
SEISMIC WAVES
Effects of source-region phenomenology on seismic discrimination
[DE92-017441] p 649 N93-12841
Regional seismograms: Attenuation and scattering
[AD-A254348] p 650 N93-12943
SEISMOGRAMS
Regional seismograms: Attenuation and scattering
[AD-A254348] p 650 N93-12943
SEISMOLOGY
Effects of source-region phenomenology on seismic discrimination
[DE92-017441] p 649 N93-12841
Lateral variations of shear velocity and anelasticity in the upper mantle of the western US from Rayleigh wave observations p 653 N93-13492
Seismic studies of crustal structure and tectonic evolution across the central California margin and the Colorado Plateau margin p 657 N93-13794
SELF CONSISTENT FIELDS
Ab initio atomic recombination reaction energetics on model heat shield surfaces
[NASA-CR-191210] p 575 N93-12677
SEMANTICS
Semantics-based reference resolution in technical text processing: An exploration of using the Word Net database in the computerized comprehensibility system
[AD-A255068] p 736 N93-13117
Japanese/English machine translation using sublanguage patterns and reversible grammars p 686 N93-13494
SEMICONDUCTING FILMS
Two to six compound thin films by MOCVD for tandem solar cells p 640 N93-13932
SEMICONDUCTOR DEVICES
Semiconductor measurement technology: Version 2.0 of the TXYZ thermal analysis program: TXYZ20
[PB92-217603] p 570 N93-12978
A study of small solid-state switched TEA CO2 lasers p 607 N93-13814
On the suitability of non-hardened high density SRAMs for space applications
[AD-A255898] p 524 N93-14087
SEMICONDUCTOR LASERS
Quantum well, beam deflecting surface emitting lasers
[NASA-CASE-NPO-18243-1-CU] p 605 N93-13418
A study of techniques for single frequency operation of diode-pumped Nd:YAG lasers p 606 N93-13629
Strained-layer InGaAs-GaAs-AlGaAs quantum well lasers and transverse junction stripe lasers p 607 N93-13773
The three to five semiconductor quantum well lasers and related optoelectronic devices on silicon
[AD-A255368] p 608 N93-13864
SEMICONDUCTORS (MATERIALS)
Group 2 cubic fluorides dielectrics for 3-D integration and GaAs-based optoelectronic structures
[AD-A254937] p 719 N93-12544
Investigation of microgravity effects on solidification phenomena of selected materials p 510 N93-13168
Electrical design of payload G-534: The Pool Boiling Experiment p 510 N93-13170
JPRS report: Science and technology. Central Eurasia: Physics and mathematics
[JPRS-UPM-92-006] p 698 N93-13303
Quantum well, beam deflecting surface emitting lasers
[NASA-CASE-NPO-18243-1-CU] p 605 N93-13418
Soft x ray window encapsulant for HgI2 detectors
[NASA-CR-190850] p 710 N93-13705
Electronic transport properties of semiconductor microstructures p 724 N93-13730
Studies of orbital doublet and modelling of orbital triplet Jahn-Teller systems in 3 to 5 semiconductors p 725 N93-13845
Two to six compound thin films by MOCVD for tandem solar cells p 640 N93-13932
Diffusion of ion-implanted group 4 n-type dopants in gallium arsenide and gallium/arsenide-based superlattices p 727 N93-14073
SENSITIVITY
Sensitivity analysis of the simultaneous proportionate change of inputs and outputs in data envelopment analysis
[AD-A254821] p 683 N93-12730
SENSORS
Fibre-optic sensors using adiabatically tapered single-mode fibres
[AD-A254555] p 708 N93-12642
Real-time quality assurance testing using photonic techniques: Application to iodine water system
[NASA-CR-184413] p 619 N93-12692
An integrated optical sensor for GMAW feedback control
[DE92-018019] p 610 N93-12793
Capacitive skin characterization
[NASA-CR-191261] p 598 N93-13567
Electro-optic architecture for servicing sensors and actuators in advanced aircraft propulsion systems
[NASA-CR-182269] p 711 N93-13762
SENTENCES
Recent developments in the NL-Soar garden path theory
[AD-A255889] p 688 N93-13944
SEPARATED FLOW
In-flight flow visualization results from the X-29A aircraft at high angles of attack
[NASA-TM-4430] p 493 N93-13322
The effects of pressure gradients on convective heat flux predictions in engine environments p 616 N93-13772
Overall effects of separation on thin aerofoils
[ISBN-0-315-67464-4] p 496 N93-13930
SEPARATORS
Isotopic separation of He-3/He-4 from solar wind gases evolved from the lunar regolith
[DE92-019339] p 759 N93-13504
SERVICE LIFE
Wastage-resistant FBC evaporator tubing through microalloying
[DE92-001256] p 541 N93-12790
Structural fatigue aspects of the P-3 Orion
[ARL-STRUC-TM-558] p 500 N93-13256
Identifiability in the autopsy model of reliability theory p 620 N93-13710
SERVICES
An analysis of the field service function of selected electronics firms
[AD-A255003] p 570 N93-12868
SERVOMECHANISMS
Novel techniques of wavefront sensing for adaptive optics with array telescopes using an artificial neural network p 743 N93-13343
SET THEORY
Recursive construction of fractals
[ISBN-951-41-0689-X] p 697 N93-13271
SETTLING
The formation of ore mineral deposits on the Moon: A feasibility study p 760 N93-13974
SHAPE MEMORY ALLOYS
Fastening apparatus having shape memory alloy actuator
[NASA-CASE-MSC-21935-1] p 614 N93-13423
SHAPES
A laboratory investigation of raindrop oscillations p 666 N93-13790
SHEAR FLOW
Coherent structures in compressible convection p 592 N93-13964
SHEAR LAYERS
A low-dimensional dynamical systems description of coherent structures in the axisymmetric jet mixing layer p 593 N93-14057
SHEAR PROPERTIES
Axisymmetric and antiplane shear crack problems in bonded nonhomogeneous materials p 625 N93-13127
The shear gage and compact shear specimen for shear property measurements of composite materials p 628 N93-13630
SHEAR STRAIN
The shear gage and compact shear specimen for shear property measurements of composite materials p 628 N93-13630
SHEAR STRENGTH
Transverse flexural tests as a tool for assessing damage to PMR-15 composites from isothermal aging in air at elevated temperatures
[NASA-TM-105848] p 529 N93-12737
SHEAR STRESS
A study of the interlaminar stress continuity theories for composite laminates p 621 N93-12627
SHELL THEORY
Fast optimization of static axisymmetric shell structures p 630 N93-13921
SHOCK FRONTS
Interaction of isotropic turbulence with a shock wave p 590 N93-13898
SHOCK LAYERS
Studies of radiative emission from the simulated shock layer of the Huygens probe p 521 N93-12834
AGARD WG13 aerodynamics of high speed air intakes: Assessment of CFD results p 581 N93-13220
Linear stability theory of hypersonic, chemically reacting viscous flows p 588 N93-13765
Computer modeling of flow and transport interactions for compressible Navier-Stokes equations p 589 N93-13825
SHOCK RESISTANCE
Proceedings of the 62nd Shock and Vibration Symposium, Volume 2
[AD-A249267] p 628 N93-13637
SHOCK TESTS
Development of a 1000 g, 10 ms mechanical shock test capability
[DE92-019193] p 624 N93-13077
SHOCK TUBES
Visualization of hydrogen injection in a scramjet engine by simultaneous PLIF imaging and laser holographic imaging p 602 N93-13683
SHOCK TUNNELS
Electron beam fluorescence measurements in the Boeing hypersonic shock tunnel p 602 N93-13681
SHOCK WAVE INTERACTION
AGARD WG13 aerodynamics of high speed air intakes: Assessment of CFD results p 581 N93-13220
Time dependent heat transfer rates in high Reynolds number hypersonic flowfields p 595 N93-13664
Interaction of isotropic turbulence with a shock wave p 590 N93-13898

SHOCK WAVES
Effect of the flow non-uniformity on the mixing layer at the interface of parallel supersonic flows
[ISAS-RN-646] p 491 N93-12716
RHALE: A MMALE shock physics code written in C++
[DE92-018271] p 684 N93-12795
A preliminary study of the effect of equivalence ratio on a low emissions gas turbine combustor using KIVA-2
[DE92-018616] p 613 N93-13321
Diagnostic of shock wave processes
[DE92-018059] p 565 N93-13357
An experimental/computational study of heat transfer in sharp fin induced shock wave/turbulent boundary layer interactions at low hypersonic Mach numbers
p 590 N93-13826
Interaction of isotropic turbulence with a shock wave
p 590 N93-13898
Supernova remnants, shocks, and the interstellar medium p 757 N93-13963
SHORT TAKEOFF AIRCRAFT
Propulsion integration results of the STOL and Maneuver Technology Demonstrator p 502 N93-13228
High-speed aerodynamics of upper surface blowing aircraft configurations p 494 N93-13729
SHORT WAVE RADIATION
A study of the Earth Radiation Budget Experiment: Shortwave measurements and bidirectional reflectance models for the ocean surface p 654 N93-13722
SHOT NOISE
Shot noise limits to sensitivity of optical interferometry
p 745 N93-13586
Physics and technology of resonant-tunneling devices
[AD-A255233] p 573 N93-13837
SHRINKAGE
Influence of cure shrinkage on process-induced stress and deformation in thick thermosetting composites
[AD-A254325] p 529 N93-12842
Microstructural evolution in reaction bonded alumina/mullite ceramics p 552 N93-13328
SHUTTLE IMAGING RADAR
Multi-frequency multi-polarization processing for spaceborne SAR p 564 N93-13057
Review of spaceborne and airborne SAR systems
p 565 N93-13060
SIDELOBE REDUCTION
ACTA Aeronautica et Astronautica Sinica (selected articles)
[AD-A255070] p 491 N93-13946
SIDELOBES
Adaptive array processing in uncertain inhomogeneous media
[AD-A254418] p 560 N93-12608
ACTA Aeronautica et Astronautica Sinica (selected articles)
[AD-A255070] p 491 N93-13946
SIGNAL ANALYSIS
Automated eddy current analysis of materials
[NASA-CR-184432] p 619 N93-12875
Special SAR techniques and applications
p 564 N93-13059
SIGNAL ANALYZERS
Design of a digital Data Recording System (DRS)
[AD-A255088] p 561 N93-12623
High-resolution array with Prony, MUSIC, and ESPRIT algorithms
[AD-A255514] p 566 N93-13868
SIGNAL DETECTION
Integrated filter and detector array for spectral imaging
[NASA-CASE-NPO-18317-1-CU] p 709 N93-13419
SIGNAL PROCESSING
A general theory of signal integration for fault-tolerant dynamic distributed sensor networks
[AD-A254961] p 732 N93-12553
Analysis of a linearly constrained least squares algorithm for adaptive beamforming
[AD-A255017] p 695 N93-12582
Adaptive array processing in uncertain inhomogeneous media
[AD-A254418] p 560 N93-12608
State space methods in multidimensional digital signal processing
[AD-A254646] p 561 N93-12620
Design of a digital Data Recording System (DRS)
[AD-A255088] p 561 N93-12623
The constant current loop: A new paradigm for resistance signal conditioning
[NASA-TM-104260] p 596 N93-12681
Fundamentals and Special Problems of Synthetic Aperture Radar (SAR)
[AGARD-LS-182] p 563 N93-13049
Special SAR techniques and applications
p 564 N93-13059
A novel-high-performance system for recording and analysing instantaneous total pressure distortion in air intakes p 580 N93-13215
Perception-based and machine-oriented signal processing within speech understanding systems
p 692 N93-13239
Summary of awards. Fiscal year 1991
[NSF-92-36] p 681 N93-13431
MINT: The multiple error LMS algorithm, and the design of inverse filters for multi-channel sound reproduction systems
[ISVR-TR-211] p 700 N93-13439
Radar signal processing for over resolved targets
[AD-A255256] p 566 N93-13838
High-resolution array with Prony, MUSIC, and ESPRIT algorithms
[AD-A255514] p 566 N93-13868
Development of two-dimensional parametric radar signal modeling and estimation techniques with application to target identification
[AD-A252602] p 567 N93-13939
ACTA Aeronautica et Astronautica Sinica (selected articles)
[AD-A255070] p 491 N93-13946
SIGNAL TO NOISE RATIOS
Novel techniques of wavefront sensing for adaptive optics with array telescopes using an artificial neural network p 743 N93-13343
New approaches to estimation of magnetotelluric parameters
[DE92-040280] p 653 N93-13513
Shot noise limits to sensitivity of optical interferometry
p 745 N93-13586
SIGNATURES
Polarimetric signatures of a canopy of dielectric cylinders based on first and second order vector radiative transfer theory p 569 N93-13088
SILICA GEL
Dislocation and pores in mullite from diphasic gels
[DE92-040384] p 550 N93-12999
SILICA GLASS
Laser densification and doping of sol-gel glasses
[AD-A254566] p 604 N93-12644
SILICIDES
Silicide layer growth rates in Mo/Si multilayers
[DE92-019581] p 721 N93-12972
Narrow bandgap semiconducting silicides: Intrinsic infrared detectors on a silicon chip
[NASA-CR-190882] p 571 N93-13430
SILICON
Thermal imaging of synchrotron beams on silicon crystals
[DE92-018182] p 719 N93-12562
Uses of Monte Carlo computer simulations in understanding epitaxial growth and ion bombardment of Si(001)
[DE92-016944] p 719 N93-12586
Development of large-area monolithically integrated silicon-film photovoltaic modules
[DE92-010600] p 637 N93-12838
Silicide layer growth rates in Mo/Si multilayers
[DE92-019581] p 721 N93-12972
A payload to evaluate photodiodes for the detection of soft and hard x rays in a space environment using a Get Away Special p 509 N93-13166
Narrow bandgap semiconducting silicides: Intrinsic infrared detectors on a silicon chip
[NASA-CR-190882] p 571 N93-13430
Technology trends in high temperature pressure transducers: The impact of micromachining
p 601 N93-13676
The heteroepitaxial growth of YBCO and other metal oxides on silicon and GaAs by pulsed laser deposition
p 726 N93-13904
Electrolytic smelting of lunar rock for oxygen, iron, and silicon p 761 N93-13979
SILICON ALLOYS
Weak-beam imaging of dissociated dislocations in HVEM-irradiated Fe-Ni-Cr alloys
[DE92-019587] p 541 N93-12798
Measurements of crystal growth kinetics at extreme deviations from equilibrium
[DE92-019744] p 720 N93-12827
SILICON CARBIDES
Single liquid source plasma enhanced metalorganic chemical vapor deposition of YBa2Cu3O(7-x) thin films
[AD-A254119] p 722 N93-13100
FNAS modify matric and transparent experiments
[NASA-CR-184442] p 531 N93-13311
Matrix cracking initiation stress in fiber-reinforced ceramic matrix composites p 627 N93-13539
SiC device development for high temperature sensor applications p 601 N93-13677
Improving the temperature resistance of aluminum-matrix composites by using an acid phosphate binder p 536 N93-14056
SILICON DIOXIDE
Microstructural evolution in reaction bonded alumina/mullite ceramics p 552 N93-13328
Intrinsic bistable photonic materials by copper colloid formation in silica
[AD-A255505] p 711 N93-13866
SILICON FILMS
Epitaxial growth of silicon and germanium for solar cells
[ITN-92-85168] p 722 N93-13268
SILICON NITRIDES
Cost-effective Sintered Reaction-Bonded Silicon Nitride (SRBSN) for structural ceramics
[DE92-019285] p 549 N93-12821
Ceramic machining: Assessment of current practice and research needs in the US
[PB92-213511] p 553 N93-13649
SILICON OXIDES
Radiation-induced infrared absorption in nuclear-pumped laser cavity components
[DE92-017346] p 605 N93-13249
SILICONES
Sources and transport of silicone NVR
p 547 N93-12777
SILVER ZINC BATTERIES
Proper battery system design for GAS experiments
p 511 N93-13176
Battery selection for space experiments
p 512 N93-13184
SIMULATION
Approximating the r-process on earth with thermonuclear explosions
[DE92-017409] p 749 N93-12587
Europe qualifies for space
[ESA-BR-64] p 508 N93-12892
ASTOVL model engine simulators for wind tunnel research p 507 N93-13213
A parameterized quasi-five-cylinder convective cloud model and its application to remote sensing of rainfall
p 663 N93-13489
Wake characterization: Full flow simulation of space structures in low earth orbit p 497 N93-13970
Moon Park: A research and educational facility
p 519 N93-14015
SIMULATORS
Seamless simulation literature survey
[AD-A254950] p 688 N93-12549
ASTOVL model engine simulators for wind tunnel research p 507 N93-13213
SINGLE CRYSTALS
Fatigue in single crystal nickel superalloys
[AD-A254704] p 541 N93-12746
Ion-channeling observation of correlated atomic displacements below Tc in YBa2Cu3O(7-x) and Pb-doped Bi2Sr2CaCu2O(x)
[DE92-018186] p 722 N93-13104
Magnetic behavior of a Bi(sub 2)Sr(sub 2)Ca(sub 1)Cu(sub 2)O(sub x) single crystal by direct magneto-optical observations
[DE92-018612] p 722 N93-13118
Epitaxial growth of silicon and germanium for solar cells
[ITN-92-85168] p 722 N93-13268
Heat transfer, fluid flow and interface shapes in floating-zone crystal growth p 724 N93-13739
Use of phonon echoes in the study of 2-6 compounds and dielectric Bi12GeO20:Cr p 725 N93-13847
SINGLE EVENT UPSETS
On the suitability of non-hardened high density SRAMs for space applications
[AD-A255898] p 524 N93-14087
Comparison of heavy ion and electron-beam upset data for GaAs
[AD-A255901] p 708 N93-14089
SINGLE STAGE TO ORBIT VEHICLES
Hypersonic vehicle control law development using H infinity and mu-synthesis
[NASA-TM-107689] p 504 N93-13068
SINGULARITY (MATHEMATICS)
On computing accurate singular values and eigenvalues of acyclic matrices
[AD-A255892] p 697 N93-14036
SINTERING
Cost-effective Sintered Reaction-Bonded Silicon Nitride (SRBSN) for structural ceramics
[DE92-019285] p 549 N93-12821
SITE SELECTION
Conceptual design of a human piloted mining mission
p 514 N93-13552
The Second Conference on Lunar Bases and Space Activities of the 21st Century, volume 2
[NASA-CP-3166-VOL-2] p 760 N93-13972
SITES
Characterization of site geochemistry in support of environmental restoration
[DE92-017512] p 641 N93-12685
SKIN FRICTION
Skin friction measurements in high temperature high speed flows p 595 N93-13670

SKY BRIGHTNESS
Zodiacal emission p 772 N93-13147
SKY SURVEYS (ASTRONOMY)
A systematic search for low-mass companions orbiting nearby stars and the calibration of the end of the stellar main sequence p 749 N93-14070
SKYLAB PROGRAM
Skylab D024 thermal control coatings and polymeric films experiment p 548 N93-12784
The correlation of active and passive microwave outputs for the Skylab S-193 sensor
[LEC-7819] p 635 N93-13440
SLENDER CONES
Linear stability theory of hypersonic, chemically reacting viscous flows p 588 N93-13765
SLENDER WINGS
An experimental and computational investigation of slender wings undergoing wing rock
p 505 N93-13915
SLIDING
Tactile sensing and control in humans and robotic/teleoperated systems
[AD-A254408] p 609 N93-12604
SLOT ANTENNAS
Scattering from a finite collection of transverse dipole and axial slot arrays with edge effects
p 568 N93-14048
SMALL SCIENTIFIC SATELLITES
The ALEXIS experiment: Current status and performance
[DE92-018601] p 524 N93-13516
SMELTING
Electrolytic smelting of lunar rock for oxygen, iron, and silicon p 761 N93-13979
SMOKE
A smoke producing rocket motor for atmospheric wind profiling
[DE92-018264] p 555 N93-12563
SMOOTHING
Application of smoothing techniques for tracking maneuvering targets. Multiple target tracking in clutter: New approaches
[AD-A254609] p 561 N93-12615
SNOW
A theoretical investigation of the growth rates of ice crystals in clouds p 653 N93-13485
An investigation of the effects of topography on Colorado front range winter storms p 668 N93-14063
SNOWSTORMS
An investigation of the effects of topography on Colorado front range winter storms p 668 N93-14063
SOCIAL FACTORS
Earth science information: Planning for the integration and use of global change information
[NASA-CR-191217] p 733 N93-12660
The lunar community church: Contributions to lunar living and to evolution of ethical and spiritual thinking
p 676 N93-14020
SOCIOLOGY
The informed citizen: Technology and responsibility in the information age p 742 N93-14049
SODIUM
A joint study of the lower ionosphere by radar, lidar, and spectrometer p 655 N93-13755
SOFIA (AIRBORNE OBSERVATORY)
Navier-Stokes simulations of unsteady transonic flow phenomena
[NASA-TM-103962] p 491 N93-12721
SOFTWARE ENGINEERING
Summary of awards, fiscal year 1990
[NSF-92-70] p 683 N93-12693
Utilization of databases to manage resources
[DE92-019598] p 735 N93-12808
Framework Programmable Platform for the Advanced Software Development Workstation (FPP/ASDW). Demonstration framework document. Volume 2: Framework process description
[NASA-CR-190275] p 685 N93-13004
Visualization techniques to aid in the analysis of multi-spectral astrophysical data sets
[NASA-CR-191260] p 685 N93-13261
Software reliability through fault-avoidance and fault-tolerance
[NASA-CR-189880] p 686 N93-13293
SOFTWARE TOOLS
Verification and validation of AI software
[AD-A254601] p 682 N93-12614
Graphics-based parallel programming tools
[AD-A254406] p 683 N93-12763
SAR simulation p 564 N93-13056
SOIL MECHANICS
The use of finite elements to model soil/track interactions in coupled multi-body dynamic simulations: Is real time simulation feasible?
[DE92-016184] p 612 N93-13236
SOILS
Proceedings of the Fifth European International Society for Terrain-Vehicle Systems, volume 1
[AD-A254619] p 611 N93-12906
ReTech, Inc., Plasma Centrifugal Furnace: Applications analysis report
[PB92-218791] p 714 N93-12982
SOL-GEL PROCESSES
Laser densification and doping of sol-gel glasses
[AD-A254566] p 604 N93-12644
Sol-gel synthesis and densification of aluminoborosilicate powders. Part 1: Synthesis
[NASA-TM-103964] p 527 N93-12895
Sol-gel synthesis and densification of aluminoborosilicate powders. Part 2: Densification
[NASA-TM-103969] p 528 N93-12896
Aerogels, emulsions, and composites: Controlling structure with organic sol-gel chemistry
[DE92-019575] p 550 N93-12931
SOLAR ACTIVITY
Solar-geophysical data number 574, June 1992. Part 1: (Prompt reports). Data for May, April 1992 and late data
[PB92-218759] p 769 N93-12803
EURECA
[ESA-F-26] p 522 N93-12964
Solar prediction analysis
[NASA-CR-184422] p 769 N93-13014
SOLAR ACTIVITY EFFECTS
Radar studies of high latitude convection flows
p 648 N93-12626
A radio frequency user's guide to the Space Environment Services Center geophysical alert broadcasts
[PB92-220631] p 562 N93-12979
SOLAR ARRAYS
Advanced photovoltaic power system technology for lunar base applications p 641 N93-14004
SOLAR ATMOSPHERE
Data evaluation, analysis, and scientific study
[NASA-CR-184396] p 769 N93-13475
SOLAR BLANKETS
Advanced photovoltaic power system technology for lunar base applications p 641 N93-14004
SOLAR CELLS
Development of large-area monolithically integrated silicon-film photovoltaic modules
[DE92-010600] p 637 N93-12838
Epitaxial growth of silicon and germanium for solar cells
[ITN-92-85168] p 722 N93-13268
Novel thin-film CuInSe2 fabrication
[DE92-016440] p 723 N93-13526
Cost analysis methodology: Photovoltaic Manufacturing Technology Project
[DE92-016441] p 639 N93-13528
Development of a computer model for polycrystalline thin-film CuInSe2 and CdTe solar cells
[DE92-016444] p 639 N93-13529
Thin films and solar cells of cadmium telluride and cadmium zinc telluride p 639 N93-13611
Two to six compound thin films by MOCVD for tandem solar cells p 640 N93-13932
Advanced photovoltaic power system technology for lunar base applications p 641 N93-14004
SOLAR COLLECTORS
Process designed for experimentation for increased-caliper Fresnel lenses
[DE92-019464] p 709 N93-12918
Solar energy utilisation and evacuated tubular solar collectors p 641 N93-14078
SOLAR CONSTANT
EURECA
[ESA-F-26] p 522 N93-12964
SOLAR CONVECTION (ASTRONOMY)
Thermoconvective instability in the solar core
p 771 N93-13849
SOLAR CORONA
Data evaluation, analysis, and scientific study
[NASA-CR-184396] p 769 N93-13475
Equilibrium and eruption of solar coronal magnetic structures p 770 N93-13605
SOLAR CORPUSCULAR RADIATION
Radiation dose to critical body organs for October 1989 proton event
[NASA-TP-3237] p 520 N93-12876
SOLAR COSMIC RAYS
Data evaluation, analysis, and scientific study
[NASA-CR-184396] p 769 N93-13475
SOLAR CYCLES
Solar prediction analysis
[NASA-CR-184422] p 769 N93-13014
SOLAR ELECTRONS
Study of SMM flares in gamma-rays and neutrons
[NASA-CR-191249] p 769 N93-12930
SOLAR ENERGY
Solar energy utilisation and evacuated tubular solar collectors p 641 N93-14078
SOLAR ENERGY CONVERSION
Boiler efficiency methodology for solar heat applications
[DE92-019805] p 640 N93-13618
SOLAR FLARES
Solar-geophysical data number 574, June 1992. Part 1: (Prompt reports). Data for May, April 1992 and late data
[PB92-218759] p 769 N93-12803
Radiation dose to critical body organs for October 1989 proton event
[NASA-TP-3237] p 520 N93-12876
Study of SMM flares in gamma-rays and neutrons
[NASA-CR-191249] p 769 N93-12930
Solar prediction analysis
[NASA-CR-184422] p 769 N93-13014
Data evaluation, analysis, and scientific study
[NASA-CR-184396] p 769 N93-13475
The 3-D description of vertical current sheets with application to solar flares
[SSL-PREPRINT-90-119] p 770 N93-13477
Electron impact polarization expected in solar EUV lines from flaring chromospheres/transition regions
[SSL-PREPRINT-90-124] p 770 N93-13478
A thermal/nonthermal approach to solar flares
p 771 N93-13639
SOLAR HEATING
Boiler efficiency methodology for solar heat applications
[DE92-019805] p 640 N93-13618
Solar water heating system for a lunar base
p 641 N93-14005
SOLAR INTERIOR
Thermoconvective instability in the solar core
p 771 N93-13849
SOLAR MAGNETIC FIELD
Chemical release and radiation effects experiment advanced planning and coordination
[NASA-CR-184439] p 649 N93-12718
Optical design for a balloon-borne magnetograph
[NASA-CR-191003] p 709 N93-13062
Data evaluation, analysis, and scientific study
[NASA-CR-184396] p 769 N93-13475
Equilibrium and eruption of solar coronal magnetic structures p 770 N93-13605
An infrared polarimetric study of sunspots
p 770 N93-13627
SOLAR MAXIMUM MISSION
Study of SMM flares in gamma-rays and neutrons
[NASA-CR-191249] p 769 N93-12930
SOLAR NEUTRONS
Study of SMM flares in gamma-rays and neutrons
[NASA-CR-191249] p 769 N93-12930
SOLAR PONDS (HEAT STORAGE)
One-dimensional transient finite difference model of an operational salinity gradient solar pond
p 586 N93-13400
SOLAR POWER SATELLITES
First steps to lunar manufacturing: Results of the 1988 Space Studies Institute Lunar Systems Workshop
p 761 N93-13977
SOLAR PROMINENCES
Data evaluation, analysis, and scientific study
[NASA-CR-184396] p 769 N93-13475
Equilibrium and eruption of solar coronal magnetic structures p 770 N93-13605
SOLAR PROTONS
Study of SMM flares in gamma-rays and neutrons
[NASA-CR-191249] p 769 N93-12930
JPRS report: Science and technology. Central Eurasia: Space
[JPRS-USP-92-004] p 513 N93-13282
SOLAR RADIATION
Phytoplankton photosynthesis in natural mixed layers
[AD-A255010] p 671 N93-12871
Study of SMM flares in gamma-rays and neutrons
[NASA-CR-191249] p 769 N93-12930
Environmental effects on an optical-UV-IR synthesis array p 747 N93-13595
Molecular gas temperature and density in spiral galaxies p 748 N93-13688
Deep convection and its relation to the large-scale circulation in the tropical Pacific p 654 N93-13725
Fiber optic data bus radiation effects study
[AD-A255821] p 711 N93-14031
SOLAR RADIO BURSTS
Data evaluation, analysis, and scientific study
[NASA-CR-184396] p 769 N93-13475
SOLAR RADIO EMISSION
Solar-geophysical data number 574, June 1992. Part 1: (Prompt reports). Data for May, April 1992 and late data
[PB92-218759] p 769 N93-12803

SOLAR SPECTRA
EURECA
[ESA-F-26] p 522 N93-12964
A thermal/nonthermal approach to solar flares p 771 N93-13639
SOLAR SYSTEM
Giotto: The second encounter
[ESA-BR-83] p 749 N93-12965
Zodiacal emission p 772 N93-13147
Solar System Exploration Division Strategic Plan, volume 1. Executive summary and overview
[NASA-TM-107843] p 513 N93-13265
Scientific experimentation afforded by the International Asteroid Mission p 515 N93-13561
Chairmanship of the Neptune/Pluto Outer Planets Science Working Group
[NASA-CR-191288] p 759 N93-13568
SOLAR SYSTEM EVOLUTION
Encounters with protostellar disks p 754 N93-13727
SOLAR TERRESTRIAL INTERACTIONS
Orbit determination error analysis and station-keeping for liberation point trajectories p 518 N93-14038
SOLAR WIND
A study of ion composition and dynamics at Comet Halley
[NASA-CR-188478] p 751 N93-13465
Densities and abundances of hot cometary ions in the coma of P/Halley p 752 N93-13466
Observations of solar wind ion charge exchange in the comet Halley coma p 752 N93-13467
Isotopic separation of He-3/He-4 from solar wind gases evolved from the lunar regolith
[DE92-019339] p 759 N93-13504
Availability of hydrogen for lunar base activities p 762 N93-13982
Synergism of He-3 acquisition with lunar base evolution p 540 N93-13986
SOLAR X-RAYS
Study of SMM flares in gamma-rays and neutrons
[NASA-CR-191249] p 769 N93-12930
G-133: A soft x ray solar telescope p 510 N93-13171
A thermal/nonthermal approach to solar flares p 771 N93-13639
SOLDERING
Requirements for soldered electrical connections
[NHB-5300.4(3A-2)] p 570 N93-12674
SOLDERS
Requirements for soldered electrical connections
[NHB-5300.4(3A-2)] p 570 N93-12674
SOLID ELECTROLYTES
Effect of plasticizers on the properties of new ambient temperature solid polymer electrolytes
[AD-A254817] p 545 N93-12754
Studies of plasticized-polymer electrolytes containing mixed Zn(2) and Li(1)
[AD-A254818] p 545 N93-12755
Perovskite solid electrolytes for SOFC
[DE92-019981] p 638 N93-13041
Alternative materials for solid oxide fuel cells: Factors affecting air-sintering of chromite interconnections
[DE92-019356] p 638 N93-13082
SOLID LUBRICANTS
Ion-beam-assisted deposition of MoS2 and other low-friction films
[AD-A255222] p 554 N93-13862
Surface phonon dispersion of MoS2
[AD-A255835] p 727 N93-14083
SOLID PROPELLANT COMBUSTION
Modelling combustion zones in porous media p 540 N93-13802
SOLID PROPELLANT ROCKET ENGINES
A smoke producing rocket motor for atmospheric wind profiling
[DE92-018264] p 555 N93-12563
Numerical investigation of the flow field in the head-end, star grain section of a solid rocket motor during ignition transients p 526 N93-13818
SOLID PROPELLANTS
Scientific predictability of solid rocket performance: Analyses of the processing parameters p 526 N93-13824
SOLID ROCKET PROPELLANTS
A smoke producing rocket motor for atmospheric wind profiling
[DE92-018264] p 555 N93-12563
SOLID STATE DEVICES
Space-qualified submillimeter radiometer
[NASA-CR-190886] p 603 N93-13709
SOLID STATE LASERS
A study of small solid-state switched TEA CO2 lasers p 607 N93-13814
SOLID SURFACES
The First United States Microgravity Laboratory
[NASA-TM-107980] p 557 N93-12951
SOLID-SOLID INTERFACES
Synthesis and properties of mismatched heterojunction/substrate interfaces
[AD-A254577] p 719 N93-12648
Defects near the Y2BaCuO5/YBa2Cu3O(7-x) interface and their effect on flux-pinning in melt-processed and quench-melt-growth processed YBa2Cu3O(7-x)
[DE92-014463] p 723 N93-13347
Toughening mechanisms in weak matrix ceramic composites p 553 N93-13780
SOLIDIFICATION
Measurements of crystal growth kinetics at extreme deviations from equilibrium
[DE92-019744] p 720 N93-12827
Investigation of microgravity effects on solidification phenomena of selected materials p 510 N93-13168
SOLIDS
Analysis of large quasistatic deformations of inelastic solids by a new stress based finite element method
[NASA-CR-189235] p 626 N93-13260
A new apparatus for continuous countercurrent flow of solids and liquids
[DE92-011675] p 583 N93-13318
Semi-quantitative model for the burning rate of solid materials
[PB92-213362] p 539 N93-13641
SOLIDS FLOW
Studies of granular flow down an inclined chute
[DE92-018871] p 577 N93-13074
SOLITARY WAVES
Theoretical nuclear physics
[DE92-019286] p 706 N93-12822
Analytical studies of nonlinear partial differential equations of interest in nonlinear optics
[AD-A254931] p 696 N93-13027
Solitons and instantons in string theory p 728 N93-13753
Guidance and scattering of electromagnetic waves by nonlinear layers p 566 N93-13813
SOLUTES
Chemical potentials in dilute, multicomponent solutions
[DE92-011041] p 538 N93-13317
SOLVATION
Solvation of cobalt salts by oligomeric polyethers
[AD-A254815] p 545 N93-12753
SOLVENTS
Chemical potentials in dilute, multicomponent solutions
[DE92-011041] p 538 N93-13317
SONAR
Expert-system development in Soar: A tutorial
[AD-A254571] p 682 N93-12645
Acoustic tracking of neutrally buoyant float
[AD-A255086] p 669 N93-12742
SORBENTS
The MAGSORB process for bulk separation of carbon dioxide
[DE92-001296] p 538 N93-13314
SORPTION
Three-stage sorption type cryogenic refrigeration systems and methods employing heat regeneration
[NASA-CASE-NPO-18366-1-CU] p 558 N93-13422
SOS (SEMICONDUCTORS)
Very high temperature silicon on silicon pressure transducers p 601 N93-13679
SOUND GENERATORS
Acoustic tracking of neutrally buoyant float
[AD-A255086] p 669 N93-12742
SOUND PRESSURE
Acoustic device and method for measuring gas densities
[NASA-CASE-NPO-18155-1-CU] p 700 N93-13421
SOUND PROPAGATION
Experimental examination of growing and newly submerged sea ice including acoustic probing of the skeletal layer
[AD-A254526] p 669 N93-12599
SOUND TRANSDUCERS
The trade-off characteristics of acoustic and pressure sensors for the NASP p 601 N93-13678
SOUND WAVES
Icing prevention by ultrasonic nucleation of supercooled water droplets in front of subsonic aircraft
[DOT/FAA/CT-TN92/38] p 497 N93-12816
Cancellation of air-borne acoustic plane waves obliquely incident upon a planar phased-array of active surface elements p 700 N93-13635
A time domain numerical theory for studying steady-state acoustic disturbance in flow p 700 N93-13770
Use of phonon echoes in the study of 2-6 compounds and dielectric Bi12GeO20:Cr p 725 N93-13847
Boundary element analysis of acoustical thin-body and nonuniqueness problems using a normal derivative integral equation p 631 N93-13951
Compressible convection and pulsations on parallel computers p 690 N93-13961
SOUNDING ROCKETS
Experimental studies of ionospheric irregularities and related plasma processes
[NASA-CR-191271] p 652 N93-13460
SOUTHERN HEMISPHERE
Baroclinic wave packets in models and observations p 663 N93-13361
SOVIET SATELLITES
Review of spaceborne and airborne SAR systems p 565 N93-13060
SOYBEANS
Crop growth and associated life support for a lunar farm p 680 N93-13994
SPACE BASES
The real world and lunar base activation scenarios p 680 N93-14014
Lunar stepping stones to a manned Mars exploration scenario p 767 N93-14016
SPACE CHARGE
Use of phonon echoes in the study of 2-6 compounds and dielectric Bi12GeO20:Cr p 725 N93-13847
SPACE COLONIES
The real world and lunar base activation scenarios p 680 N93-14014
Lunar stepping stones to a manned Mars exploration scenario p 767 N93-14016
A basis of settlement: Economic foundations of permanent pioneer communities p 741 N93-14019
SPACE COMMERCIALIZATION
JPRS report: Science and technology. Central Eurasia: Space
[JPRS-USP-92-006] p 508 N93-13151
Federal R/D funding by budget function: Fiscal years 1991-1993
[NSF-92-318] p 740 N93-13312
First steps to lunar manufacturing: Results of the 1988 Space Studies Institute Lunar Systems Workshop p 761 N93-13977
Lunar surface mining for automated acquisition of helium-3: Methods, processes, and equipment p 766 N93-14007
A basis of settlement: Economic foundations of permanent pioneer communities p 741 N93-14019
SPACE DEBRIS
Debris/ice/TPS assessment and integrated photographic analysis for Shuttle mission STS-47
[NASA-TM-107553] p 520 N93-13032
The LDCE Particle Impact Experiment as flown on STS-46 --- limited duration space environment candidate materials exposure (LDCE) p 512 N93-13183
SPACE ERECTABLE STRUCTURES
Large Deployable Reflector (LDR) system concept and technology definition study. Volume 1: Executive summary, analyses and trades, and system concepts
[NASA-CR-177413-VOL-1] p 708 N93-12591
Large Deployable Reflector (LDR) system concept and technology definition study. Analysis of space station requirements for LDR
[NASA-CR-177414] p 742 N93-12592
Large Deployable Reflector (LDR) system concept and technology definition study. Volume 2: Technology assessment and technology development plan
[NASA-CR-177413-VOL-2] p 708 N93-12593
SPACE EXPLORATION
First International Microgravity Laboratory
[NASA-TM-108007] p 518 N93-13113
Solar System Exploration Division Strategic Plan, volume 1. Executive summary and overview
[NASA-TM-107843] p 513 N93-13265
Use of antarctic analogs to support the space exploration initiative
[NASA-TM-108000] p 651 N93-13326
Assessment of programs in space biology and medicine
[NASA-CR-190930] p 672 N93-13327
International Asteroid Mission p 513 N93-13548
Summary of literature on unmanned probes to asteroids and precursor data requirements for IAM p 514 N93-13551
Chairmanship of the Neptune/Pluto Outer Planets Science Working Group
[NASA-CR-191288] p 759 N93-13568
Lunar interferometric astronomy: Some basic questions p 746 N93-13592
Lunar optical telescopes: An historical perspective p 746 N93-13593
Horizon 2000: Seven years on
[ESA-BR-37-B] p 516 N93-13855
Creating a foundation for a synergistic approach to program management p 732 N93-14017
SPACE FLIGHT
Effects of spaceflight on the proliferation of jejunal mucosal cells
[NASA-CR-191303] p 675 N93-13449

Human factors dealing with the International Asteroid Mission p 515 N93-13559

SPACE HABITATS

Applications of the Los Alamos High Energy Transport code
[DE92-017408] p 704 N93-13281

Concrete structure construction on the Moon p 559 N93-13989

Moon Park: A research and educational facility p 519 N93-14015

SPACE INDUSTRIALIZATION

First steps to lunar manufacturing: Results of the 1988 Space Studies Institute Lunar Systems Workshop p 761 N93-13977

SPACE LAW

JPRS report: Science and technology. Central Eurasia: Space
[JPRS-USP-92-006] p 508 N93-13151

JPRS report: Science and technology. Central Eurasia: Space
[JPRS-USP-92-004] p 513 N93-13282

JPRS report: Science and technology. Central Eurasia: Space
[JPRS-USP-92-005] p 513 N93-13304

Legal and political issues raised by the International Asteroid Mission p 514 N93-13555

JPRS report: Science and technology. USSR: Space
[JPRS-USP-91-004] p 516 N93-13756

The province and heritage of mankind reconsidered: A new beginning p 681 N93-14018

SPACE MAINTENANCE

A path to in-space welding and to other in-space metal processing technologies using Space Shuttle small payloads p 509 N93-13165

SPACE MANUFACTURING

First steps to lunar manufacturing: Results of the 1988 Space Studies Institute Lunar Systems Workshop p 761 N93-13977

Lunar resource recovery: A definition of requirements p 761 N93-13978

SPACE MISSIONS

High Energy Propulsion System (HEPS) analysis
[AD-A254343] p 525 N93-12963

Debris/ice/TPS assessment and integrated photographic analysis for Shuttle mission STS-47
[NASA-TM-107553] p 520 N93-13032

Solar System Exploration Division Strategic Plan, volume 1. Executive summary and overview
[NASA-TM-107843] p 513 N93-13265

Small planetary mission plan: Report to Congress
[NASA-TM-107809] p 513 N93-13266

Advanced technology for America's future in space. Executive summary
[NASA-TM-107969] p 513 N93-13308

Introduction to the International Asteroid Mission p 513 N93-13549

JPRS report: Science and technology. USSR: Space
[JPRS-USP-91-004] p 516 N93-13756

Engineering verification of the biomass production chamber p 680 N93-13996

SPACE OBSERVATIONS (FROM EARTH)

Asteroid search program p 514 N93-13550

SPACE PLASMAS

Plasma properties
[DE92-019982] p 713 N93-12811

SPACE PLATFORMS

A multiple pointing-mount control strategy for space platforms
[NASA-CR-184448] p 522 N93-12893

The real aperture antenna of SAR, a key element for performance p 564 N93-13053

Science objectives for ground- and space-based optical/IR interferometry p 746 N93-13590

SPACE POWER REACTORS

A computer program for engineering simulations of space reactor system performance
[DE92-016400] p 526 N93-13299

Public perceptions of the risks of an unfamiliar technology: The case of using nuclear energy sources for space missions p 527 N93-13971

Activities of Space Power Insulation Inst.
[AD-A255825] p 574 N93-14034

SPACE PROBES

Summary of literature on unmanned probes to asteroids and precursor data requirements for IAM p 514 N93-13551

Advanced on-chip divider for monolithic microwave VCO's
[NASA-CR-191355] p 572 N93-13563

SPACE PROCESSING

Modeling of coalescence, agglomeration, and phase segregation in microgravity processing of bimetallic composite materials
[NASA-CR-191247] p 556 N93-12728

Glass fiber processing for the Moon/Mars program: Center director's discretionary fund final report
[NASA-TM-108379] p 551 N93-13115

A microgravity processing plant for the manufacturing of propellant and water from asteroid ore p 515 N93-13558

Research and technology in support of IAM p 515 N93-13562

Distribution of human waste samples in relation to sizing waste processing in space p 680 N93-14001

SPACE PROGRAMS

Report on phase 2 of 1990 OSSA data census
[NASA-TM-107992] p 735 N93-12991

Advanced technology for America's future in space. Executive summary
[NASA-TM-107969] p 513 N93-13308

SPACE SHUTTLE ORBITERS

The Orbiter Stability Experiment on STS-40 p 508 N93-13159

Analysis of fluid/mechanical systems using EASY5 p 586 N93-13397

Space Shuttle orbiter modifications to support Space Station Freedom
[NASA-TM-108050] p 520 N93-13455

SPACE SHUTTLE PAYLOADS

The 1992 Shuttle Small Payloads Symposium
[NASA-CP-3171] p 508 N93-13158

The DSI small satellite launcher p 511 N93-13180

Test plan and report for Space Shuttle launch environment testing of Bergen cable technology safety cable
[NASA-CR-4473] p 559 N93-13434

SPACE SHUTTLES

VPPA weld model evaluation
[NASA-CR-184460] p 611 N93-12919

First International Microgravity Laboratory
[NASA-TM-108007] p 518 N93-13113

SPACE SIMULATORS

Europe qualifies for space
[ESA-BR-64] p 508 N93-12892

SPACE STATION FREEDOM

Element Material Exposure Experiment by EFFU p 548 N93-12783

Contamination analysis of SSF candidate materials
[NASA-CR-184431] p 709 N93-12894

Assured crew return vehicle post landing configuration design and test
[NASA-CR-191253] p 520 N93-12910

Microbiological methods for the water recovery systems test, revision 1.1
[NASA-CR-184390] p 678 N93-12966

Large programs may consume increasing share of limited future budgets. Report to Congressional Requesters
[GAO/NSIAD-92-278] p 732 N93-13109

Space Station: Resolving conflict over integration contractor's role. Briefing report to the Chairman, Subcommittee on Investigations and Oversight, Committee on Science, Space, and Technology, House of Representatives
[GAO/NSIAD-92-291BR] p 732 N93-13111

Study of plasma environments for the integrated Space Station electromagnetic analysis system
[NASA-CR-191263] p 522 N93-13152

Federal R/D funding by budget function: Fiscal years 1991-1993
[NSF-92-318] p 740 N93-13312

Aerospace applications of SINDA/FLUINT at the Johnson Space Center p 586 N93-13401

Space Shuttle orbiter modifications to support Space Station Freedom
[NASA-TM-108050] p 520 N93-13455

Taking a global view
[ESA-BR-37-C] p 516 N93-13856

Messengers in space
[ESA-BR-37-D] p 516 N93-13857

A home port in space
[ESA-BR-37-E] p 516 N93-13858

Reaching for the skies: The next generation
[ESA-BR-37-G] p 516 N93-13859

The next step forward
[ESA-BR-37-A] p 517 N93-13861

SPACE STATION POLAR PLATFORMS

A home port in space
[ESA-BR-37-E] p 516 N93-13858

SPACE STATION POWER SUPPLIES

Study of plasma environments for the integrated Space Station electromagnetic analysis system
[NASA-CR-191263] p 522 N93-13152

SPACE STATIONS

Large Deployable Reflector (LDR) system concept and technology definition study. Analysis of space station requirements for LDR
[NASA-CR-177414] p 742 N93-12592

Space robotics: Recent accomplishments and opportunities for future research
[NASA-TM-107675] p 694 N93-13442

A health care system for the Space Station
[NASA-TM-108093] p 679 N93-13571

Conceptual design of a lunar base thermal control system p 680 N93-14003

Automation and robotics considerations for a lunar base p 619 N93-14006

SPACE SUITS

Suited for spacewalking: A teacher's guide with activities
[NASA-EP-279] p 679 N93-13692

SPACE TRANSPORTATION

Federal R/D funding by budget function: Fiscal years 1991-1993
[NSF-92-318] p 740 N93-13312

The Second Conference on Lunar Bases and Space Activities of the 21st Century, volume 2
[NASA-CP-3166-VOL-2] p 760 N93-13972

SPACE TRANSPORTATION SYSTEM

Large Deployable Reflector (LDR) system concept and technology definition study. Volume 1: Executive summary, analyses and trades, and system concepts
[NASA-CR-177413-VOL-1] p 708 N93-12591

Reaching for the skies: The next generation
[ESA-BR-37-G] p 516 N93-13859

The influence of lunar propellant production on the cost-effectiveness of cislunar transportation systems p 556 N93-13983

SPACEBORNE EXPERIMENTS

Chemical release and radiation effects experiment advanced planning and coordination
[NASA-CR-184439] p 649 N93-12718

LDEF Materials Workshop 1991, part 1
[NASA-CP-3162-PT-1] p 545 N93-12769

LDEF materials: An overview of the interim findings p 546 N93-12770

LDEF atomic oxygen fluence update p 546 N93-12771

LDEF yaw and pitch angle estimates p 524 N93-12772

Surface contamination on LDEF exposed materials p 547 N93-12776

Performance of thermal control tape in the protection of composite materials p 536 N93-12780

Fluorescence of thermal control coatings on S0069 and A0114 p 548 N93-12781

Long Duration Exposure Facility M0003-5 thermal control coatings on DoD flight experiment p 548 N93-12782

Element Material Exposure Experiment by EFFU p 548 N93-12783

Skylab D024 thermal control coatings and polymeric films experiment p 548 N93-12784

Effects of the LDEF environment on the Ag/FEP thermal blankets p 548 N93-12785

Characterization of selected LDEF: Exposed polymer films and resins p 549 N93-12787

Effects of orbital exposure on Halar during the LDEF mission p 549 N93-12788

Long Duration Exposure Facility M0003-5 recent results on polymeric films p 549 N93-12789

Spaceflight payload design flight experience G-408 p 508 N93-13160

A path to in-space welding and to other in-space metal processing technologies using Space Shuttle small payloads p 509 N93-13165

Scientific experimentation afforded by the International Asteroid Mission p 515 N93-13561

Spacelab J: Microgravity and life sciences
[NASA-CR-191353] p 516 N93-13564

SPACEBORNE PHOTOGRAPHY

Earth observation photography: Looking back 20 years after Skylab p 509 N93-13164

Manned observations technology development, FY 1992 report
[NASA-CR-185704] p 597 N93-13373

SPACEBORNE TELESCOPES

Large Deployable Reflector (LDR) system concept and technology definition study. Volume 2: Technology assessment and technology development plan
[NASA-CR-177413-VOL-2] p 708 N93-12593

The ALEXIS experiment: Current status and performance
[DE92-018601] p 524 N93-13516

SPACECRAFT ANTENNAS

Feasibility study of a synthesis procedure for array feeds to improve radiation performance of large distorted reflector antennas
[NASA-CR-190948] p 561 N93-12655

SPACECRAFT CHARGING

Study of plasma environments for the integrated Space Station electromagnetic analysis system
[NASA-CR-191263] p 522 N93-13152

SPACECRAFT CONFIGURATIONS
Assured crew return vehicle post landing configuration design and test
[NASA-CR-191253] p 520 N93-12910
SPACECRAFT CONSTRUCTION MATERIALS
LDEF materials: An overview of the interim findings p 546 N93-12770
Engineering and architectural issues associated with the asteroid mission p 514 N93-13556
SPACECRAFT CONTAMINATION
LDEF Materials Workshop 1991, part 1
[NASA-CP-3162-PT-1] p 545 N93-12769
Materials SIG quantification and characterization of surface contaminants p 546 N93-12773
Z306 molecular contamination ad hoc committee results p 546 N93-12774
Long Duration Exposure Facility (LDEF) contamination modeling p 547 N93-12775
Surface contamination on LDEF exposed materials p 547 N93-12776
Sources and transport of silicone NVR p 547 N93-12777
Skylab D024 thermal control coatings and polymeric films experiment p 548 N93-12784
Characterization of selected LDEF: Exposed polymer films and resins p 549 N93-12787
Contamination analysis of SSF candidate materials
[NASA-CR-184431] p 709 N93-12894
SPACECRAFT CONTROL
A multiple pointing-mount control strategy for space platforms
[NASA-CR-184448] p 522 N93-12893
On-orbit supervisor for controlling spacecraft
[AD-A254342] p 522 N93-12962
Hypersonic vehicle control law development using H infinity and mu-synthesis
[NASA-TM-107689] p 504 N93-13068
An inverse dynamics approach to trajectory optimization for an aerospace plane
[NASA-CR-191277] p 500 N93-13305
SPACECRAFT DESIGN
Large Deployable Reflector (LDR) system concept and technology definition study. Volume 1: Executive summary, analyses and trades, and system concepts
[NASA-CR-177413-VOL-1] p 708 N93-12591
Assured crew return vehicle post landing configuration design and test
[NASA-CR-191253] p 520 N93-12910
Combined design of structures and controllers for optimal maneuverability p 691 N93-13130
Weight optimization of an aerobrake structural concept for a lunar transfer vehicle
[NASA-TP-3262] p 519 N93-13379
Engineering and architectural issues associated with the asteroid mission p 514 N93-13556
SPACECRAFT ENVIRONMENTS
Findings of a review of spacecraft fire safety needs
[NASA-CR-189181] p 523 N93-13715
SPACECRAFT EQUIPMENT
Transient behavior of heat pipe with thermal energy storage under pulse heat loads p 588 N93-13743
Preparing for the future
[ESA-BR-37-H] p 517 N93-13860
SPACECRAFT GLOW
Studies of surface-induced luminescence relevant to spacecraft glow, using a seeded arc-jet p 523 N93-13919
SPACECRAFT LAUNCHING
EURECA
[ESA-F-26] p 522 N93-12964
The DSI small satellite launcher p 511 N93-13180
SPACECRAFT MAINTENANCE
Space Shuttle orbiter modifications to support Space Station Freedom
[NASA-TM-108050] p 520 N93-13455
SPACECRAFT MANEUVERS
Robust rendezvous maneuver point conditions
[NASA-CR-190996] p 517 N93-12690
Combined design of structures and controllers for optimal maneuverability p 691 N93-13130
SPACECRAFT MODELS
Long Duration Exposure Facility (LDEF) contamination modeling p 547 N93-12775
SPACECRAFT MODULES
Assured crew return vehicle post landing configuration design and test
[NASA-CR-191253] p 520 N93-12910
SPACECRAFT ORBITS
Robust rendezvous maneuver point conditions
[NASA-CR-190996] p 517 N93-12690
SPACECRAFT POWER SUPPLIES
Alternate electrode materials for the SP100 reactor
[DE92-019570] p 706 N93-12970
Efficiency of an AMTEC recirculating test cell, experiments, and projections
[DE92-016811] p 571 N93-13196
Reversible thermodynamic cycle for AMTEC power conversion
[DE92-016814] p 571 N93-13197
Public perceptions of the risks of an unfamiliar technology: The case of using nuclear energy sources for space missions p 527 N93-13971
Activities of Space Power Insulation Inst.
[AD-A255825] p 574 N93-14034
SPACECRAFT PROPULSION
Briefing notes on propulsion stability codes ADMIT, NYQUIST, and SSFREQ
[NASA-CR-184449] p 525 N93-12874
The Proteus Navier-Stokes code p 585 N93-13396
Aeronomy coexperiments on drag-free satellites with proportional thrusters: GP-B and STEP p 518 N93-13922
SPACECRAFT SHIELDING
LDEF atomic oxygen fluence update p 546 N93-12771
SPACECRAFT STRUCTURES
Innovative methods in the dynamics of large space structures
[AD-A254630] p 521 N93-12579
Combined design of structures and controllers for optimal maneuverability p 691 N93-13130
Wake characterization: Full flow simulation of space structures in low earth orbit p 497 N93-13970
SPACECRAFT TRAJECTORIES
Robust rendezvous maneuver point conditions
[NASA-CR-190996] p 517 N93-12690
An inverse dynamics approach to trajectory optimization for an aerospace plane
[NASA-CR-191277] p 500 N93-13305
Orbit determination error analysis and station-keeping for liberation point trajectories p 518 N93-14038
SPACECREWS
A health care system for the Space Station
[NASA-TM-108093] p 679 N93-13571
The environmental control and life-support system for a lunar base: What drives its design p 680 N93-13991
SPACELAB
First International Microgravity Laboratory
[NASA-TM-108007] p 518 N93-13113
Spacelab J: Microgravity and life sciences
[NASA-CR-191353] p 516 N93-13564
SLS-1 flight experiments preliminary significant results
[NASA-TM-108033] p 520 N93-13613
SPACELAB PAYLOADS
An intelligent position-specific training system for mission operations
[NASA-TM-108381] p 691 N93-13156
SPACING
Perceptual dimensions of visual scenes relevant for simulating low-altitude flight
[AD-A254645] p 676 N93-12662
Matrix cracking initiation stress in fiber-reinforced ceramic matrix composites p 627 N93-13539
SPALLATION
The nature of scales grown on binary Cr-Nb alloys
[DE92-019283] p 542 N93-13080
SPANWISE BLOWING
Assessment of potential aerodynamic benefits from spanwise blowing at the wing tip p 496 N93-13822
SPATIAL DISTRIBUTION
Zodiacal emission p 772 N93-13147
SPATIAL RESOLUTION
Spatial resolution enhancement of SSM/I microwave brightness temperatures and its impact on rainfall retrieval algorithms
[AD-A254382] p 661 N93-12861
Motion errors and compensation possibilities p 563 N93-13052
The CHARA optical array p 744 N93-13581
Temperature measurements with micrometer spatial resolution
[AD-A255897] p 603 N93-14086
SPECIFICATIONS
Specification of adaptive aiding systems
[AD-A254537] p 499 N93-12602
Microbiological methods for the water recovery systems test, revision 1.1
[NASA-CR-184390] p 678 N93-12966
SPECIMEN GEOMETRY
Studies on numerical and experimental determination of energy release rate for composite laminates p 533 N93-13752
SPECIMENS
Numerical calibration of the stable poisson loaded specimen
[NASA-TM-105609] p 622 N93-12738
SPECKLE INTERFEROMETRY
The CHARA optical array p 744 N93-13581
Elastic and plastic strain measurement in high temperature environment using laser speckle p 600 N93-13673
SPECKLE PATTERNS
Laser-based strain measurements for high temperature applications p 601 N93-13675
SPECTRA
Organization of the Optical Society of America Photonic Science Topical Meeting Series. Volume 8: Integrated photonics research. Ilfornia on 9-11 april 1991
[AD-A254682] p 709 N93-12666
SPECTRAL BANDS
Imaging IR spectrometer, phase 2
[NASA-CR-190848] p 597 N93-13424
Application of improved HNO3 band model parameters to South Pole atmospheric emission measurements p 647 N93-13723
SPECTRAL EMISSION
Development of a portable infrared emission spectrometer AA460 PIRES
[NASA-CR-190849] p 598 N93-13656
SPECTRAL METHODS
Solution of compressible Navier-Stokes equations using spectral methods on arbitrary two-dimensional domains p 593 N93-14041
SPECTRAL REFLECTANCE
Field spectroradiometry and sail model application to irrigated wheat (Triticum aestivum, L) canopies spectral reflectance
[INPE-5426-TDI/483] p 634 N93-13258
SPECTRAL RESOLUTION
Imaging IR spectrometer, phase 2
[NASA-CR-190848] p 597 N93-13424
Measurement of tropospheric temperature and aerosol extinction using high spectral resolution lidar p 653 N93-13614
SPECTROGRAPHS
Spectroscopic observations of the night airglow from 3000 A to 9200 A p 658 N93-13891
SPECTROMETERS
Artificial intelligence and neural networks applied to ion mobility spectrometry
[DE92-017508] p 690 N93-12559
Elementary particle physics research
[DE92-019746] p 702 N93-12855
Indiana University High Energy Physics Group, task C
[DE92-040458] p 707 N93-13002
Applications of the Los Alamos High Energy Transport code
[DE92-017408] p 704 N93-13281
Experimental testing of four correction algorithms for the forward scattering spectrometer probe
[NASA-TM-105906] p 597 N93-13307
Soft x ray window encapsulant for HgI2 detectors
[NASA-CR-190850] p 710 N93-13705
SPECTROPHOTOMETERS
A new instrument for the study of mesospheric gravity waves through nightglow observations p 656 N93-13789
SPECTRORADIOMETERS
Field spectroradiometry and sail model application to irrigated wheat (Triticum aestivum, L) canopies spectral reflectance
[INPE-5426-TDI/483] p 634 N93-13258
Development of moored oceanographic spectroradiometer
[NASA-CR-190883] p 670 N93-13708
SPECTROSCOPIC ANALYSIS
Real-time quality assurance testing using photonic techniques: Application to iodine water system
[NASA-CR-184413] p 619 N93-12692
Analysis of IMS spectra using neural networks
[DE92-017511] p 691 N93-12791
High-resolution investigation of degenerate four-wave mixing in the (gamma)(0,0) band of nitric oxide
[DE92-005312] p 537 N93-13232
Characterization of thermotropic liquid crystalline polymer blends by positron annihilation lifetime spectroscopy
[AD-A253616] p 552 N93-13325
Resonance ionization mass spectrometry in biochemical analysis
[DE92-017407] p 538 N93-13341
Laser ablation for sample introduction in inductively coupled plasma spectrometry p 719 N93-13897
Friction, wear and Raman spectroscopic characteristics of carbon lubricated surfaces p 618 N93-13949
SPECTROSCOPIC TELESCOPES
High resolution imaging at Palomar p 745 N93-13584
SPECTROSCOPY
Analysis of IMS spectra using neural networks
[DE92-017511] p 691 N93-12791
Spectroscopic studies of low-density gas in the Galactic disk and halo p 753 N93-13499
Spectroscopic observations of the night airglow from 3000 A to 9200 A p 658 N93-13891

SPECTRUM ANALYSIS
CO2 laser modeling
[NASA-CR-184455] p 604 N93-12656
Field spectroradiometry and sail model application to irrigated wheat (Triticum aestivum, L) canopies spectral reflectance
[INPE-5426-TDI/483] p 634 N93-13258
A thermal/nonthermal approach to solar flares p 771 N93-13639

SPEECH RECOGNITION
Transputer implementation of the TRACE model of speech recognition
[AD-A254747] p 689 N93-12846
Machine Perception
[AGARD-LS-185] p 692 N93-13238
Perception-based and machine-oriented signal processing within speech understanding systems p 692 N93-13239
Talking to InterFIS: Adding speech input to a natural language interface
[AD-A255865] p 688 N93-13942

SPHERES
A new apparatus for continuous countercurrent flow of solids and liquids
[DE92-011675] p 583 N93-13318

SPHERICAL SHELLS
An elasticity solution for a transversely isotropic material containing a spherical shell under axisymmetric loading p 628 N93-13728

SPIN DYNAMICS
Neutron scattering studies of the spin dynamics in La(2-x)Sr(x)O4
[DE92-019952] p 702 N93-13037
Nutational stability and passive control of symmetric spinning bodies with axial forcing and internal mass motion p 504 N93-13820
Dynamical instabilities in a fluid spin-up and in an open flow system p 590 N93-13899

SPIN REDUCTION
Dynamics and control of a tumbling satellite retrieval device p 522 N93-13119

SPIN STABILIZATION
Nutational stability and passive control of symmetric spinning bodies with axial forcing and internal mass motion p 504 N93-13820

SPINNERS
Nutational stability and passive control of symmetric spinning bodies with axial forcing and internal mass motion p 504 N93-13820

SPIRAL ANTENNAS
Electromagnetic scattering and radiation from microstrip patch antennas and spirals residing in a cavity
[NASA-CR-191284] p 565 N93-13354

SPIRAL GALAXIES
Limits on galactic dynamo theory due to magnetic fluctuations p 754 N93-13636
Molecular gas temperature and density in spiral galaxies p 748 N93-13688

SPONTANEOUS EMISSION
The sapphire Cerenkov laser p 605 N93-13365

SPRAY CHARACTERISTICS
Bipropellant spray combustion modeling in small rocket engines p 556 N93-13924

SPRAYERS
Computational fluid dynamics combustion analysis evaluation
[NASA-CR-184326] p 575 N93-12688
Measurements of cellular structure in spray detonation
[DE92-019580] p 555 N93-12933

SPUTTERING
Ion-beam-assisted deposition of MoS2 and other low-friction films
[AD-A255222] p 554 N93-13862

SQUALLS
Numerical simulation of a squall line: Tests of a new cumulus parameterization scheme p 662 N93-13124

SQUID (DETECTORS)
Y1Ba2Cu3O(7-delta) thin film dc SQUIDs (superconducting quantum interference device)
[ITN-92-85167] p 723 N93-13362

STABILITY
Users manual for program SSFREQ intermediate mode stability curves: Developed for use on a PC computer
[NASA-CR-184452] p 682 N93-12675
Silicide layer growth rates in Mo/Si multilayers
[DE92-019581] p 721 N93-12972
Performance and stability of telemanipulators using bilateral impedance control p 614 N93-13488
Parameter studies of helium-neon lasers at 543 nm p 606 N93-13747

STABILITY DERIVATIVES
Determination of the stability and control derivatives of the F/A-18 HARV from flight data using the maximum likelihood method
[NASA-CR-191216] p 503 N93-12903

STABILITY TESTS
Robust control of a flexible link robot and rigid link robot: Theory, simulation, and experiment p 614 N93-13452
Stability of the compressible reacting mixing layer p 592 N93-13948

STABILIZATION
Stabilization and projection methods for multibody dynamics
[PB92-133883] p 698 N93-12890

STAGNATION POINT
Performance and control of ascending trajectories to minimize heat load for transatmospheric aero-space planes p 495 N93-13745
Structure of and dynamical processes in the Earth's magnetopause and boundary layer regions p 657 N93-13793

STAINLESS STEELS
Elevated temperature tensile properties of borated 304 stainless steel: Effect of boride dispersion on strength and ductility
[DE92-040096] p 542 N93-13302

STANDARDIZATION
Laser measurement techniques guide for a hazard evaluation
[AD-A254545] p 604 N93-12610
Microbiological methods for the water recovery systems test, revision 1.1
[NASA-CR-184390] p 678 N93-12966

STANDARDS
Improved wide range expressions for displacements and inverse displacements for standard fracture toughness specimens
[AD-A254561] p 622 N93-12643
Journal of Research of the National Institute of Standards and Technology, May-June 1992, volume 97, number 3
[PB92-217637] p 698 N93-12805

STAR CLUSTERS
The dynamics of dense galactic nuclei p 750 N93-13340

STAR DISTRIBUTION
The stellar angular correlation: Clues to wide binary star properties p 757 N93-14059

STAR FORMATION
Evidence for cool gas and star formation in cluster cooling flows p 751 N93-13380
Encounters with protostellar disks p 754 N93-13727
Thermal and nonthermal star formation: An investigation into the process of star formation as a function of stellar mass p 758 N93-14091

STATIONKEEPING
Orbit determination error analysis and station-keeping for liberation point trajectories p 518 N93-14038

STATISTICAL ANALYSIS
Quality assessment of the A-posteriori error estimation in finite elements
[AD-A254767] p 696 N93-12701
Obtaining medians and other quantiles with limited memory space
[AD-A254506] p 683 N93-12722
You need this done by when? Increasing your efficiency with the SAS system
[DE92-017894] p 683 N93-12792
Statistical analysis of stratospheric temperature and ozone profile data for trends and model comparison
[NASA-CR-191248] p 650 N93-12877
Probabilistic finite elements for fatigue and fracture analysis
[NASA-CR-191246] p 624 N93-13029
Statistical process management: An essential element of quality improvement
[DE92-019934] p 619 N93-13036
From comparison density to two sample analysis
[AD-A253866] p 698 N93-13064
Scientists, engineers, and technicians in manufacturing industries: 1989. Detailed statistical tables
[NSF-92-312] p 730 N93-13437
Characteristics of recent science and engineering graduates: 1990. Detailed statistical tables
[NSF-92-316] p 731 N93-13454
The use of degradation measures in assessing reliability p 573 N93-13607
Bayesian estimation of system reliability under asymmetric loss p 620 N93-13906
Fixed-gain, two-stage estimators for tracking maneuvering targets
[AD-A255832] p 697 N93-14081
A surface pressure altitude prediction model
[AD-A255834] p 668 N93-14082

STATISTICAL CORRELATION
Storm tracking for TDWR: A correlation algorithm design and evaluation
[AD-A254701] p 660 N93-12622

STATISTICAL DISTRIBUTIONS
The use of degradation measures in assessing reliability p 573 N93-13607

STATISTICAL MECHANICS
The nonequilibrium statistical mechanics of chaotic maps p 729 N93-13832

STATISTICS
Selected data on federal support to universities and colleges: Fiscal year 1990
[NSF-92-310] p 740 N93-12920
State award summary: Fiscal Year 1991
[NSF-92-3] p 775 N93-13381
Summary of awards: Applied mathematics. Fiscal year 1991
[NSF-92-38] p 681 N93-13438
Science and engineering degrees: 1966-1990
[NSF-92-326] p 731 N93-13701

STEADY FLOW
Quantitative analysis of three-dimensional steady flow field by using particle image velocimetry and digital image processing method p 577 N93-13017
Mathematical problems in inviscid hypersonic flow p 493 N93-13451
Solution of viscous flow problems by using the boundary element method p 588 N93-13609
Variational characterizations of steady two-dimensional vortex motions p 589 N93-13781
Dynamical instabilities in a fluid spin-up and in an open flow system p 590 N93-13899

STEADY STATE
High-temperature deformation and diffusion in oxides
[DE92-019593] p 720 N93-12854
Investigation of component failure rates for pulsed versus steady state tokamak operation
[DE92-019758] p 713 N93-12856
The influence of intake swirl distortion on the steady-state performance of a low bypass, twin-spool engine p 579 N93-13211
A time domain numerical theory for studying steady-state acoustic disturbance in flow p 700 N93-13770

STEAM
Boiler efficiency methodology for solar heat applications
[DE92-019805] p 640 N93-13618

STEEL STRUCTURES
Effects of residual stress, weld toe notch and weld defects on fatigue of welded steel structures p 631 N93-13947

STEELS
On bilinearity of Manson-Coffin low-cycle-fatigue relationship
[NASA-TM-105840] p 622 N93-12739
Diagnostic of material defects found in pipelines made of 13 HMF steel on the basis of acoustic emission p 623 N93-12989
Numerical simulations of steel plate perforation
[DE92-017058] p 626 N93-13301
The chemistry of the extreme pressure lubricant additive lead naphthenate on steel surfaces
[AD-A255828] p 544 N93-14098

STELLAR COMPOSITION
Density contrast shell models for planetary nebulae p 756 N93-13850

STELLAR CORES
Accretion rates of protoplanets p 759 N93-13958

STELLAR ENVELOPES
A study of the structure, evolution and observation of Horizontal Branch stars
[ISBN-0-315-62655-0] p 751 N93-13374
Hydrodynamics and spectra formation of interacting massive binaries and the young remnant of SN1987A p 757 N93-13962

STELLAR EVOLUTION
Approximating the r-process on earth with thermonuclear explosions
[DE92-017409] p 749 N93-12587
Radial and nonradial periods and growth rates of an Al Velorum model
[DE92-011369] p 743 N93-13339
A study of the structure, evolution and observation of Horizontal Branch stars
[ISBN-0-315-62655-0] p 751 N93-13374
Comparison of cometary comae using ultraviolet spectroscopy: Composition and variation p 753 N93-13603
B supergiants in open clusters and associations
[NASA-CR-191275] p 748 N93-13659
The role of ambipolar diffusion in the formation of interstellar cloud cores and protostars p 755 N93-13828
Supernova remnants, shocks, and the interstellar medium p 757 N93-13963

STELLAR LUMINOSITY
A study of the structure, evolution and observation of Horizontal Branch stars
[ISBN-0-315-62655-0] p 751 N93-13374

An optical study of the faint end of the stellar luminosity function p 748 N93-13960

STELLAR MAGNETIC FIELDS
Compressible convection and pulsations on parallel computers p 690 N93-13961

STELLAR MASS
The role of ambipolar diffusion in the formation of interstellar cloud cores and protostars p 755 N93-13828
Some problems of quantum cosmology and dark matter physics p 755 N93-13829
An optical study of the faint end of the stellar luminosity function p 748 N93-13960
Thermal and nonthermal star formation: An investigation into the process of star formation as a function of stellar mass p 758 N93-14091

STELLAR MASS ACCRETION
Nucleosynthesis in nova explosions [DE92-040349] p 753 N93-13523
Accretion rates of protoplanets p 759 N93-13958

STELLAR MASS EJECTION
Nucleosynthesis in nova explosions [DE92-040349] p 753 N93-13523
Equilibrium and eruption of solar coronal magnetic structures p 770 N93-13605

STELLAR MODELS
Radial and nonradial periods and growth rates of an Al Velorum model [DE92-011369] p 743 N93-13339
A thermal/nonthermal approach to solar flares p 771 N93-13639
Encounters with protostellar disks p 754 N93-13727
Density contrast shell models for planetary nebulae p 756 N93-13850

STELLAR OCCULTATION
An analysis of the Voyager 2 ultraviolet spectrometer occultation data at Uranus and Triton: Inferring heat sources and model atmospheres p 768 N93-14072

STELLAR SPECTRA
International Ultraviolet Explorer (IUE) ultraviolet spectral atlas of selected astronomical objects [NASA-RP-1285] p 744 N93-13461
The Mount Wilson optical interferometer: The first automated instrument and the prospects for lunar interferometry p 745 N93-13582
Orbiting Space Interferometer (OSI): A first generation space interferometer p 745 N93-13587
Atoms and molecules in supernova 1987A p 699 N93-13851
Supernova remnants, shocks, and the interstellar medium p 757 N93-13963

STELLAR SPECTROPHOTOMETRY
An optical study of the faint end of the stellar luminosity function p 748 N93-13960

STELLAR STRUCTURE
A study of the structure, evolution and observation of Horizontal Branch stars [ISBN-0-315-62655-0] p 751 N93-13374

STELLAR SYSTEMS
Encounters with protostellar disks p 754 N93-13727
Hydrodynamical calculations of stellar interactions p 755 N93-13764

STELLAR TEMPERATURE
Alternative methods for determination of the temperature of central stars of planetary nebulae [INPE-5434-TDI/485] p 750 N93-13279

STELLAR WINDS
H I shells and supershells: Observations and theory p 751 N93-13360
Hydrodynamics and spectra formation of interacting massive binaries and the young remnant of SN1987A p 757 N93-13962

STELLARATORS
Fusion: Magnetic confinement [DE92-019876] p 716 N93-13107
Review of stellarator research: In search of the magic magnetic bottle [DE92-019045] p 718 N93-13651

STEPS
Fluid flow and heat convection studies for actively cooled airframes [NASA-CR-190956] p 587 N93-13406

STEREOCHEMISTRY
The effects of molecular structure on the electrical conductivity of polymers [NASA-CR-191265] p 552 N93-13459

STEREOPHOTOGRAPHY
Using iterative orthophoto refinements to correct Digital Elevation Models (DEM's) [AD-A254625] p 634 N93-13345

STEREOSCOPIC VISION
3-D computer vision for navigation/control of mobile robots p 693 N93-13243

STIFFNESS
Large-deflection analysis of cord composite plates p 530 N93-13008
Improved damping in composite structures through stress coupling, co-cured damping layers, and segmented stiffness layers p 630 N93-13823
Hybrid 2 and hybrid 3 dummy neck properties for computer modeling [AD-A255544] p 679 N93-13874
Position and force control of flexible and rigid manipulators using the sliding-mode technique p 695 N93-14065

STIFFNESS MATRIX
System identification and model updating for substructures p 624 N93-13065
The free and forced vibrations of structures using the finite dynamic element method p 630 N93-13935

STIMULATED EMISSION
Experiments on resonantly photo-pumped x ray lasers [DE92-019542] p 603 N93-12570

STOCHASTIC PROCESSES
Modeling and estimation of reciprocal diffusion and Gauss-Markov random fields [AD-A255034] p 698 N93-12709
Comparison of two stochastic models of scalar diffusion in turbulent flow [DE92-019381] p 576 N93-12912
A stochastic/deterministic method for transient, three-dimensional neutron transport [DE92-016690] p 704 N93-13319
A stochastic optimal feedforward and feedback control methodology for superagility [NASA-CR-4471] p 694 N93-13370
Deterministic and stochastic responses of nonlinear systems p 631 N93-13966

STOICHIOMETRY
Dislocation and pores in mullite from diphasic gels [DE92-040384] p 550 N93-12999

STORAGE RINGS (PARTICLE ACCELERATORS)
Damping the (pi)-mode instability in the SLC damping rings with a passive cavity [DE92-018153] p 707 N93-13090
RF voltage modulation at discrete frequencies with applications to crystal channeling extraction [DE92-015567] p 707 N93-13235

STORAGE TANKS
Zero-gravity quantity gaging system [NASA-CR-185602] p 556 N93-12699
Precision liquid-level measurement in deep tanks using a swept-RF resonant cavity [DE92-017236] p 597 N93-13267
Numerical study on mixing of sprayed liquid in an LNG storage tank p 584 N93-13388
Application of passive dosimetry for detection of leaking underground storage tanks [PB92-218270] p 559 N93-13648

STORMS
Storm tracking for TDWR: A correlation algorithm design and evaluation [AD-A254701] p 660 N93-12622
An analysis of the tornado-producing Raleigh thunderstorm of November 28, 1988 [AD-A254384] p 661 N93-12862
Baroclinic wave packets in models and observations p 663 N93-13361

STRAIN DISTRIBUTION
Micromechanics of finite length fibers in composite materials p 532 N93-13490
The shear gage and compact shear specimen for shear property measurements of composite materials p 628 N93-13630
High magnetic field studies of strained layer superlattices p 726 N93-13895

STRAIN ENERGY RELEASE RATE
Microcracking, microcrack-induced delamination, and longitudinal splitting of advanced composite structures [NASA-CR-4472] p 623 N93-12911
Axisymmetric and antiplane shear crack problems in bonded nonhomogeneous materials p 625 N93-13127
Studies on numerical and experimental determination of energy release rate for composite laminates p 533 N93-13752
Finite elements for free edge delaminations and delaminated anisotropic beams p 535 N93-13967

STRAIN GAGES
The constant current loop: A new paradigm for resistance signal conditioning [NASA-TM-104260] p 596 N93-12681
Enabling technologies for economical manufacturing of composites [AD-A253615] p 531 N93-13324
The shear gage and compact shear specimen for shear property measurements of composite materials p 628 N93-13630
High-temperature strain measurement techniques: Current developments and challenges p 599 N93-13669
Palladium-chromium static strain gages for high temperatures p 600 N93-13671
High temperature strain gage apparent strain compensation p 600 N93-13672
SiC device development for high temperature sensor applications p 601 N93-13677

STRAIN MEASUREMENT
The 1992 NASA Langley Measurement Technology Conference: Measurement Technology for Aerospace Applications in High-Temperature Environments [NASA-CP-3161] p 598 N93-13661
High-temperature strain measurement techniques: Current developments and challenges p 599 N93-13669
Palladium-chromium static strain gages for high temperatures p 600 N93-13671
High temperature strain gage apparent strain compensation p 600 N93-13672
Elastic and plastic strain measurement in high temperature environment using laser speckle p 600 N93-13673
Determination of high temperature strains using a PC based vision system p 601 N93-13674
Laser-based strain measurements for high temperature applications p 601 N93-13675

STRAIN RATE
GPS measurements at Vandenberg AFB [AD-A254978] p 499 N93-12557
On bilinearity of Manson-Coffin low-cycle-fatigue relationship [NASA-TM-105840] p 622 N93-12739
An investigation of the thermoviscoplastic behavior of a metal matrix composite at elevated temperatures [NASA-CR-189706] p 530 N93-12929
Is there a unique effective interaction profile for dislocations? [DE92-018615] p 543 N93-13545

STRAKES
Effects of forebody strakes and Mach number on overall aerodynamic characteristics of configuration with 55 deg cropped delta wing [NASA-TP-3253] p 493 N93-13353

STRAPS
Recession of FEP specimens from trays D11 and B7 p 549 N93-12786

STRATIFIED FLOW
Studies on turbulent mixing in stratified turbulent patches p 587 N93-13532
Experiments on the statistical nature of stably stratified turbulence p 594 N93-14069

STRATIGRAPHY
Abstracts of papers presented at the International Symposium on Time, Frequency, and Dating in Geomorphology [AD-A254927] p 649 N93-12704

STRATOSPHERE
Point correlations of geopotential height and temperature at 30 mb and between 500 mb and 30 mb [PB92-222694] p 661 N93-12817
Statistical analysis of stratospheric temperature and ozone profile data for trends and model comparison [NASA-CR-191248] p 650 N93-12877
Stratospheric turbulence measurements and models for aerospace plane design [NASA-TM-104262] p 663 N93-13288
An experimental and theoretical study of degradation pathways for atmospheric halocarbons p 646 N93-13624
Effects of stratospheric aerosol surface processes on the LLNL two-dimensional zonally averaged model [DE92-019620] p 646 N93-13646
Effects of the Mt. Pinatubo eruption on the radiative and chemical processes in the troposphere and stratosphere [DE92-019618] p 646 N93-13654
Cloud acidity and acidic deposition in the lower troposphere and ozone depletion in the Antarctic stratosphere: Modeling and data analysis regarding the role of atmospheric aerosol p 647 N93-13741
Photochemical kinetics of excited states of O3 and O2: Laboratory studies and atmospheric implications p 656 N93-13784
Middle atmosphere water vapour p 667 N93-13892

STRATUS CLOUDS
Sources of cloud nuclei and development of remote sensing techniques for cloud parameters [AD-A255016] p 660 N93-12558

STRESS (PHYSIOLOGY)
Thermal stress in US Air Force operations [AD-A255785] p 676 N93-14027
Physiological stress from chemical defense clothing and equipment [AD-A255786] p 676 N93-14028

The relationship between environmental conditions and UH-60 cockpit temperature
[AD-A255918] p 680 N93-14090

STRESS ANALYSIS
Compression test simulation of thick-section composite materials
[AD-A255021] p 528 N93-12583
The 3-D nonlinear constitutive modeling approach for composite materials
[AD-A255022] p 528 N93-12584
A study of the interlaminar stress continuity theories for composite laminates p 621 N93-12627
Numerical calibration of the stable poisson loaded specimen
[NASA-TM-105609] p 622 N93-12738
Stress crack testing of polyethylene geomembranes
[PB92-217132] p 622 N93-12843
An investigation of the thermoviscoplastic behavior of a metal matrix composite at elevated temperatures
[NASA-CR-189706] p 530 N93-12929
Nonlinear mechanics of composite materials with periodic microstructure
[NASA-CR-190750] p 531 N93-13309
Analysis of cracked plates subjected to out-of-plane loadings p 629 N93-13804
Three-dimensional boundary element analysis of residual stresses in a cross-ply fiber composite model
p 629 N93-13811
A domain decomposition method for parallel transient response calculations p 504 N93-13827

STRESS CONCENTRATION
Effects of residual stress, weld toe notch and weld defects on fatigue of welded steel structures
p 631 N93-13947

STRESS CORROSION CRACKING
Glass corrosion in natural environments
[NASA-CR-191234] p 551 N93-13150

STRESS DISTRIBUTION
Compression test simulation of thick-section composite materials
[AD-A255021] p 528 N93-12583
Fiber optic sensors for static fracture studies and dynamic wave propagation problems
p 709 N93-12984
Nonlinear mechanics of composite materials with periodic microstructure
[NASA-CR-190750] p 531 N93-13309
Micromechanics of finite length fibers in composite materials p 532 N93-13490
Studies on numerical and experimental determination of energy release rate for composite laminates
p 533 N93-13752
Analysis of cracked plates subjected to out-of-plane loadings p 629 N93-13804
Three-dimensional boundary element analysis of residual stresses in a cross-ply fiber composite model
p 629 N93-13811

STRESS INTENSITY FACTORS
Numerical calibration of the stable poisson loaded specimen
[NASA-TM-105609] p 622 N93-12738
Fiber optic sensors for static fracture studies and dynamic wave propagation problems
p 709 N93-12984
Axisymmetric and antiplane shear crack problems in bonded nonhomogeneous materials
p 625 N93-13127
Analysis of cracked plates subjected to out-of-plane loadings p 629 N93-13804

STRESS TENSORS
Fluidlike studies of the sheath and presheath regions of a plasma p 718 N93-13792

STRESS-STRAIN RELATIONSHIPS
The 3-D nonlinear constitutive modeling approach for composite materials
[AD-A255022] p 528 N93-12584
On bilinearity of Manson-Coffin low-cycle-fatigue relationship
[NASA-TM-105840] p 622 N93-12739
The shear gage and compact shear specimen for shear property measurements of composite materials
p 628 N93-13630

STRESSES
Is there a unique effective interaction profile for dislocations?
[DE92-018615] p 543 N93-13545

STRETCHING
Finite element analysis of anisotropic viscoelastic composite structures and analytical determination of optimum viscoelastic material properties
p 530 N93-13007

STRING THEORY
Mathematics and string theory
[DE92-019292] p 727 N93-12796
Second quantization in bit-string physics
[DE92-019645] p 727 N93-12826
Solitons and instantons in string theory
p 728 N93-13753
Some problems of quantum cosmology and dark matter physics p 755 N93-13829

STRONGLY COUPLED PLASMAS
Current density fluctuations, nonlinear coupling, and transport in MST
[DE92-041012] p 713 N93-12883
Enhancement of ion transmission and reduction of background and interferences in inductively coupled plasma mass spectrometry
[DE92-018805] p 596 N93-12921
Laser ablation for sample introduction in inductively coupled plasma spectrometry p 719 N93-13897

STRONTIUM COMPOUNDS
Group 2 cubic fluorides dielectrics for 3-D integration and GaAs-based optoelectronic structures
[AD-A254937] p 719 N93-12544
Neutron scattering studies of the spin dynamics in La(2-x)Sr(x)O4
[DE92-019952] p 702 N93-13037
Magnetic behavior of a Bi(sub 2)Sr(sub 2)Ca(sub 1)Cu(sub 2)O(sub x) single crystal by direct magneto-optical observations
[DE92-018612] p 722 N93-13118

STRONTIUM OXIDES
Ion-channeling observation of correlated atomic displacements below Tc in YBa2Cu3O(7-x) and Pb-doped Bi2Sr2CaCu2O(x)
[DE92-018186] p 722 N93-13104
Activation energy and critical current density in Bi-Sr-Ca-Cu-O
[DE92-018795] p 723 N93-13547

STRUCTURAL ANALYSIS
The 3-D nonlinear constitutive modeling approach for composite materials
[AD-A255022] p 528 N93-12584
Hierarchic models for laminated plates
p 528 N93-12629
Probabilistic evaluation of fuselage-type composite structures
[NASA-TM-105881] p 622 N93-12735
User's guide: Computer-Aided Structural Modeling (CASM), version 3.00
[AD-A255074] p 684 N93-12851
Computer-Aided Structural Engineering (CASE) project. Tutorial guide: Computer-Aided Structural Modeling (CASM). Version 3.00
[AD-A255075] p 684 N93-12872
Linear and nonlinear finite element analysis of laminated composite structures at high temperatures
p 623 N93-13009
Structural integrity of composites under load and thermal insult p 530 N93-13012
Structural verification for GAS experiments
p 511 N93-13175
Weight optimization of an aerobrake structural concept for a lunar transfer vehicle
[NASA-TP-3262] p 519 N93-13379
Aircraft accident report: Britt Airways, Inc., d/b/a, Continental Express Flight 2574, in-flight structural breakup, EMB-120RT, N33701, Eagle Lake, Texas, September 11, 1991
[PB92-910405] p 498 N93-13426
Coupled structural/thermal/electromagnetic analysis/tailoring of graded composite structures
[NASA-CR-189150] p 626 N93-13443
Coupled structural/thermal/electromagnetic analysis/tailoring of graded composite structures
[NASA-CR-189151] p 627 N93-13444
Coupled structural/thermal/electromagnetic analysis/tailoring of graded composite structures
[NASA-CR-189152] p 627 N93-13445
A domain decomposition method for parallel transient response calculations p 504 N93-13827
The free and forced vibrations of structures using the finite dynamic element method p 630 N93-13935

STRUCTURAL DESIGN
Innovative methods in the dynamics of large space structures
[AD-A254630] p 521 N93-12579
Large Deployable Reflector (LDR) system concept and technology definition study. Volume 1: Executive summary, analyses and trades, and system concepts
[NASA-CR-177413-VOL-1] p 708 N93-12591
Computer-Aided Structural Engineering (CASE) project. Tutorial guide: Computer-Aided Structural Modeling (CASM). Version 3.00
[AD-A255075] p 684 N93-12872
System identification and model updating for substructures p 624 N93-13065
Combined design of structures and controllers for optimal maneuverability p 691 N93-13130
Structural optimization of thin shells using finite element method
[NASA-TM-105903] p 625 N93-13157
Unsymmetric Lanczos model reduction and linear state function observer for flexible structures
[NASA-CR-191231] p 686 N93-13295
Application of Lanczos vectors to control design of flexible structures
[NASA-CR-191230] p 686 N93-13296
Process comparison study. MSFC Center Director's Discretionary Fund (CDDF)
[NASA-TM-108382] p 526 N93-13429
Analysis and design of planar and non-planar wings for induced drag minimization
[NASA-CR-191274] p 493 N93-13463
Fast optimization of static axisymmetric shell structures p 630 N93-13921
Concrete structure construction on the Moon
p 559 N93-13989

STRUCTURAL ENGINEERING
User's guide: Computer-Aided Structural Modeling (CASM), version 3.00
[AD-A255074] p 684 N93-12851

STRUCTURAL FAILURE
Structural integrity of composites under load and thermal insult p 530 N93-13012
Compression strength of composite primary structural components
[NASA-CR-190949] p 624 N93-13019

STRUCTURAL PROPERTIES (GEOLOGY)
Abstracts of papers presented at the International Symposium on Time, Frequency, and Dating in Geomorphology
[AD-A254927] p 649 N93-12704

STRUCTURAL RELIABILITY
A domain decomposition method for parallel transient response calculations p 504 N93-13827

STRUCTURAL STABILITY
Numerical calibration of the stable poisson loaded specimen
[NASA-TM-105609] p 622 N93-12738
A multiple pointing-mount control strategy for space platforms
[NASA-CR-184448] p 522 N93-12893
Environmental effects on an optical-UV-IR synthesis array p 747 N93-13595
Bifurcation and localization instabilities in plastic bending of cylindrical shells p 630 N93-13923

STRUCTURAL STRAIN
High-temperature strain measurement techniques: Current developments and challenges
p 599 N93-13669

STRUCTURAL VIBRATION
Experimental validation of finite element and boundary element methods for predicting structural vibration and radiated noise p 621 N93-12631
Dynamic control modification techniques in teleoperation of a flexible manipulator
[NASA-CR-190984] p 610 N93-12904
Acoustic radiation from a point excited infinite bilaminar plate p 531 N93-13144
Method and apparatus for minimizing multiple degree of freedom vibration transmission between two regions of a structure
[NASA-CASE-LAR-14508-1-CU] p 626 N93-13420
Application of adaptive trusses to vibration isolation in flexible structures p 617 N93-13809

STRUCTURAL WEIGHT
Weight optimization of an aerobrake structural concept for a lunar transfer vehicle
[NASA-TP-3262] p 519 N93-13379
An investigation of dynamic stress reduction of multi-body aircraft using active gust control
p 505 N93-13916

STUDENTS
Academic science and engineering: Graduate enrollment and support, Fall 1990
[NSF-92-323] p 729 N93-12802
NASA industry education initiative. Education programs report, 1991
[NASA-NP-158] p 730 N93-13248
Gateway to diversity in the scientific and technological workforce
[NSF-92-99] p 730 N93-13278
Systematic chemical equation balancing
[DE92-017234] p 539 N93-13530
Suited for spacewalking: A teacher's guide with activities
[NASA-EP-279] p 679 N93-13692
Fiscal Year 1991 highlights
[NSF-92-23] p 731 N93-13702
The 1992 natural gas vehicle challenge: EPA emissions and fuel economy testing
[PB92-217926] p 616 N93-13761

SUBCONTRACTS
Human factors research in aircrew performance and training: 1986-1991
[AD-A254455] p 677 N93-12609

USAF 1990 research initiation program, volume 2
[AD-A254654] p 773 N93-12663

SUBLIMATION
Thin films and solar cells of cadmium telluride and cadmium zinc telluride p 639 N93-13611

SUBMARINES
Visualization of scattering strength of elastic bodies in a fluid
[AD-A254535] p 699 N93-12601
Chemical environments of submarine hydrothermal systems
[NASA-CR-191258] p 669 N93-13458

SUBMILLIMETER WAVES
The millimeter and submillimeter wavelength diffuse backgrounds: Measurements of the spectrum and anisotropy p 772 N93-13145
Space-qualified submillimeter radiometer
[NASA-CR-190886] p 603 N93-13709
A submillimetre polarimeter for the continuum receiver UKT14 on the James Clerk Maxwell Telescope p 748 N93-13852
Thermal and nonthermal star formation: An investigation into the process of star formation as a function of stellar mass p 758 N93-14091

SUBROUTINES
A SINDA '85 nodal heat transfer rate calculation user subroutine p 587 N93-13403
Circuit design tool. User's manual, revision 2
[NASA-CR-191361] p 687 N93-13734

SUBSONIC FLOW
Experimental studies of the flowfields and their effects due to a pair of lift jets discharging in the ground effect region p 580 N93-13217
Application of subsonic first-order panel methods for prediction of inlet and nozzle aerodynamic interactions with airframe p 497 N93-13223
A time domain numerical theory for studying steady-state acoustic disturbance in flow p 700 N93-13770
Assessment of potential aerodynamic benefits from spanwise blowing at the wing tip p 496 N93-13822

SUBSONIC SPEED
Comparative performance tests of a pitot-inlet in several European wind-tunnels at subsonic and supersonic speeds p 497 N93-13221

SUBSTRATES
Synthesis and properties of mismatched heterojunction/substrate interfaces
[AD-A254577] p 719 N93-12648
Latent image exposure monitor using scatterometry
[DE92-019427] p 604 N93-12915
Electron stimulated desorption of the metallic substrate at monolayer coverage: Sensitive detection via 193 nm laser photoionization of neutral aluminum desorbed from CH3O/Al(111)
[DE92-014858] p 723 N93-13349
Novel thin-film CuInSe2 fabrication
[DE92-016440] p 723 N93-13526

SUBSTRUCTURES
System identification and model updating for substructures p 624 N93-13065
Providing structural modules with self-integrity monitoring software user's manual
[NASA-CR-190877] p 628 N93-13707

SUCTION
An experimental study of a small high-speed LH2 pump for rockets: Fluid dynamic performance
[NAL-TR-1131] p 610 N93-12727
A fundamental study of suction for Laminar Flow Control (LFC)
[NASA-CR-191276] p 583 N93-13277

SULFATES
Sulfate impact upon low-level cloud albedo over oceans p 661 N93-12833
Kinetic studies of some free radical reactions involved in cloudwater chemistry p 668 N93-14055

SULFUR
Uses of lunar sulfur p 761 N93-13981

SULFUR COMPOUNDS
Uses of lunar sulfur p 761 N93-13981

SULFUR DIOXIDES
SO2 on Venus: A final cross-calibration with Pioneer Venus
[NASA-CR-191256] p 758 N93-13344
A meteorology-based approach to detecting response source-receptor relationships p 664 N93-13736
Kinetic studies of some free radical reactions involved in cloudwater chemistry p 668 N93-14055

SULFURIC ACID
A comparison of chromic acid and sulfuric acid anodizing
[NASA-TM-108383] p 543 N93-13378

SUMMER
USAF 1990 research initiation program, volume 2
[AD-A254654] p 773 N93-12663
USAF 1990 research initiation program, volume 4
[AD-A254655] p 773 N93-12664
USAF 1990 research initiation program, volume 1
[AD-A254656] p 773 N93-12665
US Air Force 1989 research initiation program, volume 1
[AD-A254457] p 774 N93-12764
US Air Force 1989 research initiation program, volume 4
[AD-A254458] p 774 N93-12765
US Air Force 1989 research initiation program, volume 2
[AD-A254459] p 774 N93-12766
US Air Force 1989 research initiation program, volume 3
[AD-A254460] p 774 N93-12767
Intraseasonal variability of infrared cooling rates during the Asian summer monsoon and their influence on intraseasonal waves p 665 N93-13760

SUNSPOTS
An infrared polarimetric study of sunspots p 770 N93-13627
Development of a stable electro-optical modulator
[NASA-CR-184404] p 710 N93-13696

SUPERCOMPUTERS
Proceedings of FLICC forums on federal information policies. Combined summaries of proceedings. The 1990 7th Forum, Access is the Key and the 1991 8th Forum, Building Information Superhighways: Supercomputing Networks and Libraries
[PB92-147370] p 734 N93-12759
HIPPI and Fibre Channel
[DE92-040346] p 689 N93-13046
File servers, networking, and supercomputers p 737 N93-13137
Mass storage system experiences and future needs at the National Center for Atmospheric Research p 737 N93-13138

SUPERCONDUCTING FILMS
High temperature superconductor materials and applications
[NASA-CR-184437] p 719 N93-12691
Effect of O2 partial pressure on post annealed Ba2YCu3O(7-delta) thin films
[DE92-014949] p 722 N93-13323
Y1Ba2Cu3O(7-delta) thin film dc SQUIDs (superconducting quantum interference device)
[ITN-92-85167] p 723 N93-13362
The heteroepitaxial growth of YBCO and other metal oxides on silicon and GaAs by pulsed laser deposition p 726 N93-13904
Noise measurements of YBa2Cu3O7 thin film high-temperature superconductors p 726 N93-13933

SUPERCONDUCTING MAGNETS
Magnetic field perturbation caused by bending vibrations of a quadrupole
[DE92-040644] p 623 N93-13003
New power-conditioning systems for superconducting magnetic energy storage p 640 N93-13934

SUPERCONDUCTING SUPER COLLIDER
Thermal issues at the SSC p 584 N93-13387

SUPERCONDUCTIVITY
Bipolaronic charge density waves, polaronic spin density waves and high T(c) superconductivity
[DE92-017403] p 720 N93-12853
Solutions without phase-slip for the Ginsburg-Landau equation
[PB92-115575] p 696 N93-12889
JPRS report: Science and technology. Central Eurasia: Physics and mathematics
[JPRS-UPM-92-006] p 698 N93-13303
Effect of hydrogen reduction and doping on the characteristics of high-temperature superconductors p 725 N93-13844

SUPERCOOLING
Icing prevention by ultrasonic nucleation of supercooled water droplets in front of subsonic aircraft
[DOT/FAA/CT-TN92/38] p 497 N93-12816

SUPERCRITICAL FLUIDS
Fluid dynamics of supercritical helium within cable-in-conduit conductors
[DE92-019516] p 574 N93-12569

SUPERCRITICAL PRESSURES
Fluid dynamics of supercritical helium within cable-in-conduit conductors
[DE92-019516] p 574 N93-12569
Chemical potentials in dilute, multicomponent solutions
[DE92-011041] p 538 N93-13317

SUPERFLUIDITY
Isotopic separation of He-3/He-4 from solar wind gases evolved from the lunar regolith
[DE92-019339] p 759 N93-13504

SUPERGIANT STARS
B supergiants in open clusters and associations
[NASA-CR-191275] p 748 N93-13659
Atoms and molecules in supernova 1987A p 699 N93-13851

SUPERGRAVITY
Solitons and instantons in string theory p 728 N93-13753

SUPERHIGH FREQUENCIES
Review of spaceborne and airborne SAR systems p 565 N93-13060
Transhorizon microwave propagation and its relationship with meteorological conditions p 666 N93-13791

SUPERLATTICES
Electronic structure of microclusters and defect complexes
[AD-A254807] p 720 N93-12750
High magnetic field studies of strained layer superlattices p 726 N93-13895
Diffusion of ion-implanted group 4 n-type dopants in gallium arsenide and gallium/arsenide-based superlattices p 727 N93-14073

SUPERNOVA REMNANTS
H I shells and supershells: Observations and theory p 751 N93-13360
Supernova remnants, shocks, and the interstellar medium p 757 N93-13963

SUPERNOVA 1987A
Atoms and molecules in supernova 1987A p 699 N93-13851
Hydrodynamics and spectra formation of interacting massive binaries and the young remnant of SN1987A p 757 N93-13962

SUPERNOVAE
H I shells and supershells: Observations and theory p 751 N93-13360

SUPERROTATION
Model studies of the middle atmosphere of Venus p 759 N93-13831

SUPERSONIC AIRCRAFT
Minimum-time flight paths of supersonic aircraft p 500 N93-13140
The PEP Symposium on CFD Techniques for Propulsion Applications p 579 N93-13210
The influence of intake swirl distortion on the steady-state performance of a low bypass, twin-spool engine p 579 N93-13211
Ideal aircraft handling quality models: Longitudinal axis
[NAL-PD-FC-9203] p 504 N93-13566
Impact of supersonic and subsonic aircraft on ozone: Including heterogeneous chemical reaction mechanisms
[DE92-019619] p 646 N93-13655

SUPERSONIC BOUNDARY LAYERS
Application of a solution adaptive grid to flow over an embedded cavity p 492 N93-13141

SUPERSONIC COMBUSTION RAMJET ENGINES
Resonance lamp absorption measurement of OH number density and temperature in expansion tube scramjet engine tests p 602 N93-13682
Visualization of hydrogen injection in a scramjet engine by simultaneous PLIF imaging and laser holographic imaging p 602 N93-13683
Exit plane H2O concentration measurements correlated with OH PLIF near-injector mixing measurements for scramjet flows p 603 N93-13687

SUPERSONIC FLOW
Effect of the flow non-uniformity on the mixing layer at the interface of parallel supersonic flows
[ISAS-RN-646] p 491 N93-12716
Computation of steady and unsteady shock-induced combustion over hypervelocity blunt bodies p 536 N93-12836
Numerical simulation of the acoustic instability in the spatially developing, confined, supersonic mixing layer p 494 N93-13521
Skin friction measurements in high temperature high speed flows p 595 N93-13670
Numerical calculation of turbomachinery cascade flows p 589 N93-13767
Planar measurement of flow field parameters in nonreacting supersonic flows with laser-induced iodine fluorescence p 495 N93-13801
Computational fluid dynamics of the base flow on a plane body between a subsonic flow on one side and a supersonic flow on the other p 591 N93-13920

SUPERSONIC INLETS
Aerodynamic studies of supersonic air intakes p 497 N93-13222

SUPERSONIC JET FLOW
Planar laser-induced fluorescence measurements of high-enthalpy free jet flow with nitric oxide p 595 N93-13685
Computational fluid dynamics of the base flow on a plane body between a subsonic flow on one side and a supersonic flow on the other p 591 N93-13920

SUPERSONIC SPEED
Comparative performance tests of a pitot-inlet in several European wind-tunnels at subsonic and supersonic speeds p 497 N93-13221

Performance and control of ascending trajectories to minimize heat load for transatmospheric aero-space planes p 495 N93-13745
SUPPORT SYSTEMS
Functional system design document for the Intelligent Inspection System (IIS)
[DE92-018240] p 619 N93-12794
Framework Programmable Platform for the Advanced Software Development Workstation (FPP/ASDW). Demonstration framework document. Volume 2: Framework process description
[NASA-CR-190275] p 685 N93-13004
The Joint Surveillance Target Attack Radar System: Can procedures be developed to support the requirements of the land and air component commanders?
[AD-A255555] p 567 N93-13875
SURFACE DEFECTS
Simulation studies for surfaces and materials strength
[NASA-CR-191289] p 724 N93-13570
Influence of surface defects and local structure on oxygenate reaction pathways over metal oxide surfaces
[DE92-040013] p 539 N93-13573
SURFACE EMITTING LASERS
Quantum well, beam deflecting surface emitting lasers
[NASA-CASE-NPO-18243-1-CU] p 605 N93-13418
SURFACE LAYERS
Availability of hydrogen for lunar base activities p 762 N93-13982
Surface phonon dispersion of MoS2
[AD-A255835] p 727 N93-14083
SURFACE NAVIGATION
Digital chart database conversion into a system electronic navigational chart
[AD-A255007] p 632 N93-12869
SURFACE PROPERTIES
Materials SIG quantification and characterization of surface contaminants p 546 N93-12773
Noninvasive probing of the ocean surface using laser-based nonlinear optical methods
[DE92-019431] p 669 N93-12916
The MAGSORB process for bulk separation of carbon dioxide
[DE92-001296] p 538 N93-13314
Simulation studies for surfaces and materials strength
[NASA-CR-191289] p 724 N93-13570
SURFACE REACTIONS
Halogen surface chemistry on Si(100)-(2x1)
[AD-A254643] p 536 N93-12618
Photochemical dynamics of surface oriented molecules
[DE92-019813] p 703 N93-13106
Influence of surface defects and local structure on oxygenate reaction pathways over metal oxide surfaces
[DE92-040013] p 539 N93-13573
Studies of the kinetics and mechanisms of perfluoroether reactions on iron and oxidized iron surfaces
[NASA-CR-191363] p 539 N93-13763
Studies of surface-induced luminescence relevant to spacecraft glow, using a seeded arc-jet p 523 N93-13919
The chemistry of the extreme pressure lubricant additive lead naphthenate on steel surfaces
[AD-A255828] p 544 N93-14098
SURFACE ROUGHNESS
Near-normal incidence scattering from rough, finite surfaces: Kirchhoff theory and data comparison for Arctic sea ice
[AD-A254525] p 668 N93-12577
Bistatic clutter RCS simulation using scale model rough surfaces
[AD-A254932] p 560 N93-12581
SURFACE TEMPERATURE
Implicitly coupling heat conduction into a zone fire model
[PB92-222769] p 558 N93-12980
Performance of the Bowen ratio systems on a 22 deg slope
[NASA-CR-191278] p 644 N93-13254
SURFACE TO SURFACE MISSILES
Angle of arrival fluctuations for millimeter waves propagating in a turbulent atmosphere near the Earth
[AD-A254478] p 560 N93-12574
SURFACE TREATMENT
Monitoring interfacial dynamics by pulsed laser techniques
[DE92-040302] p 606 N93-13514
Strained-layer InGaAs-GaAs-AlGaAs quantum well lasers and transverse junction stripe lasers p 607 N93-13773
SURFACE VEHICLES
The use of finite elements to model soil/track interactions in coupled multi-body dynamic simulations: Is real time simulation feasible?
[DE92-016184] p 612 N93-13236
SURFACE WAVES
Phase mixing and surface wave decay in an inhomogeneous plasma
[IPPCZ-320] p 715 N93-13006
SURGERY
Postoperative hyperbaric oxygen treatment of peripheral nerve damage
[AD-A255842] p 676 N93-14084
SURVEILLANCE
Computer simulation of a space-based infrared surveillance sensor
[AD-A255521] p 524 N93-13870
SURVEILLANCE RADAR
The Joint Surveillance Target Attack Radar System: Can procedures be developed to support the requirements of the land and air component commanders?
[AD-A255555] p 567 N93-13875
Acousto-optic applications for multichannel adaptive optical processor
[AD-A255823] p 711 N93-14032
SURVEYS
Selected data on research and development in industry: 1990
[NSF-92-317] p 773 N93-12667
Science and engineering degrees, by race/ethnicity of recipients: 1977-1990
[NSF-92-327] p 729 N93-12694
ONR basic research program: Summary and bibliographies, FY 1990 and 1991
[AD-A253038] p 774 N93-12696
Academic science and engineering: Graduate enrollment and support, Fall 1990
[NSF-92-323] p 729 N93-12802
Report on phase 2 of 1990 OSSA data census
[NASA-TM-107992] p 735 N93-12991
Survey on techniques used in aerodynamic nozzle/airframe integration p 502 N93-13224
Topographic surveyor: Transitioning to the 90's
[AD-A254688] p 499 N93-13351
Scientific and engineering research facilities at universities and colleges: 1992
[NSF-92-325] p 506 N93-13407
Scientists, engineers, and technicians in manufacturing industries: 1989. Detailed statistical tables
[NSF-92-312] p 730 N93-13437
Characteristics of recent science and engineering graduates: 1990. Detailed statistical tables
[NSF-92-316] p 731 N93-13454
Academic science and engineering: R/D expenditures, fiscal year 1990
[NSF-92-321] p 741 N93-13544
Selected data on Federal funds for research and development: Fiscal years 1990, 1991, and 1992
[NSF-92-319] p 741 N93-13657
Research and development in industry: 1989. Funds, 1989. Scientists and engineers, January 1990
[NSF-92-307] p 741 N93-13658
Selected data on Science and Engineering Doctorate Awards: 1991
[NSF-92-309] p 731 N93-13698
SUSPENDING (HANGING)
Equations of motion of slung-load systems, including multilift systems
[NASA-TP-3280] p 503 N93-12815
SWATH WIDTH
The real aperture antenna of SAR, a key element for performance p 564 N93-13053
SWEPT WINGS
Assessment of potential aerodynamic benefits from spanwise blowing at the wing tip p 496 N93-13822
The unsteady aerodynamics of a delta wing undergoing large-amplitude pitching motions p 496 N93-13929
SYMBOLS
Human memory for the spatial locations of items on pull-down computer menus p 739 N93-14080
SYNCHRONISM
A distributed timing system for sychronizing control and data correlation
[DE92-018603] p 690 N93-12564
Graphics-based parallel programming tools
[AD-A254406] p 683 N93-12763
Neurochemical control of circadian rhythms
[AD-A255054] p 675 N93-13116
SYNCHROTRON RADIATION
Development of XUV projection lithography at 60 to 80 nm
[DE92-017517] p 603 N93-12560
Particle production and survival in muon acceleration
[DE92-019553] p 701 N93-12572
Atomic structure of mixed ferroelectrics
[AD-A254369] p 702 N93-12947
SYNCHROTRONS
Thermal imaging of synchrotron beams on silicon crystals
[DE92-018182] p 719 N93-12562
Characterizing laser fusion welded aluminum using synchrotron x ray microtomography
[DE92-018608] p 609 N93-12565
Emittance, brilliance, and bandpass issues related to an inclined crystal monochromator
[DE92-019671] p 721 N93-12881
RF voltage modulation at discrete frequencies with applications to crystal channeling extraction
[DE92-015567] p 707 N93-13235
Longitudinal impedance of capacitive pick-up electrodes: Calculations and comparison with measurements
[DE92-019499] p 571 N93-13358
SYNOPTIC METEOROLOGY
JARE data reports no. 179 (meteorology 29). Meteorological data at Asuka Station, Antarctica in 1990 p 663 N93-13287
A synoptic climatology of the elevated mixed layer inversion over the southern Great Plains in spring p 664 N93-13643
SYNTAX
Japanese/English machine translation using sublanguage patterns and reversible grammars p 686 N93-13494
SYNTHESIS (CHEMISTRY)
Synthesis and properties of novel cluster phases
[DE92-017388] p 545 N93-12697
Sol-gel synthesis and densification of aluminoborosilicate powders. Part 1: Synthesis
[NASA-TM-103964] p 527 N93-12895
Sol-gel synthesis and densification of aluminoborosilicate powders. Part 2: Densification
[NASA-TM-103969] p 528 N93-12896
Synthesis of derivatives of alpha, omega difunctional perfluoroaliphatic compounds for low dielectric constant resins
[AD-A254928] p 550 N93-13026
High octane ethers from synthesis gas-derived alcohols
[DE92-015467] p 537 N93-13188
Oligomer and mixed-metal compounds potential multielectron transfer catalysts
[DE92-011347] p 543 N93-13346
Hydrothermal organic synthesis experiments
[NASA-CR-191257] p 672 N93-13457
A novel process for methanol synthesis
[DE92-019719] p 539 N93-13617
SYNTHETIC APERTURE RADAR
Fundamentals and Special Problems of Synthetic Aperture Radar (SAR)
[AGARD-LS-182] p 563 N93-13049
Basic principles of SAR p 563 N93-13050
SAR peculiarities, ambiguities and constraints p 563 N93-13051
Motion errors and compensation possibilities p 563 N93-13052
Polarization effects and multipolarization SAR p 564 N93-13054
Radiometric calibration of SAR systems p 564 N93-13055
SAR simulation p 564 N93-13056
Multi-frequency multi-polarization processing for spaceborne SAR p 564 N93-13057
Inverse Synthetic Aperture Radar p 564 N93-13058
Special SAR techniques and applications p 564 N93-13059
Review of spaceborne and airborne SAR systems p 565 N93-13060
Variance of phase fluctuations of waves propagating through a random medium p 569 N93-13087
Coherent frame analysis of Synthetic Aperture Radar (SAR) ocean imagery p 568 N93-14050
SYNTHETIC APERTURES
SAR peculiarities, ambiguities and constraints p 563 N93-13051
The real aperture antenna of SAR, a key element for performance p 564 N93-13053
Radio and optical interferometric imaging p 744 N93-13580
Recent astronomical results from the infrared spatial interferometer and their implications for LOUISA p 745 N93-13585
Report of the Working Design Group p 748 N93-13601
SYNTHETIC ARRAYS
Basic principles of SAR p 563 N93-13050
A Lunar Optical-Ultraviolet-Infrared Synthesis Array (LOUISA)
[NASA-CP-3066] p 744 N93-13579
An optical VLA on the Moon p 747 N93-13596
Required technologies for a lunar optical UV-IR synthesis array p 747 N93-13598
SYSTEM EFFECTIVENESS
Prototype stop bar system evaluation at John F. Kennedy International Airport
[DOT/FAA/CT-92/24] p 506 N93-12902

SYSTEM FAILURES
Summary: Experimental validation of real-time fault-tolerant systems
[NASA-CR-190985] p 503 N93-13697
SYSTEM IDENTIFICATION
Identification of parametric finite element models using experimental modal data
[PB92-217819] p 558 N93-12976
System identification and model updating for substructures p 624 N93-13065
SYSTEMS ANALYSIS
High Energy Propulsion System (HEPS) analysis
[AD-A254343] p 525 N93-12963
Summary: Experimental validation of real-time fault-tolerant systems
[NASA-CR-190985] p 503 N93-13697
SYSTEMS ENGINEERING
Optimal design and control of distributed parameter systems
[AD-A254947] p 690 N93-12547
Expert-system development in Soar: A tutorial
[AD-A254571] p 682 N93-12645
Integrated modeling tool for performance engineering of complex computer systems
[NASA-CR-190881] p 687 N93-13880
SYSTEMS INTEGRATION
Terminal Doppler Weather Radar (TDWR) Operational Test and Evaluation (OT/E) integration test plan
[DOT/FAA/CT-TN92/6] p 499 N93-13377
Multiplexing electro-optic architectures for advanced aircraft integrated flight control systems
[NASA-CR-182268] p 504 N93-13735
SYSTEMS MANAGEMENT
On-orbit supervisor for controlling spacecraft
[AD-A254342] p 522 N93-12962
SYSTEMS SIMULATION
Seamless simulation literature survey
[AD-A254950] p 688 N93-12549
SYSTOLIC ARRAYS
Analysis of a linearly constrained least squares algorithm for adaptive beamforming
[AD-A255017] p 695 N93-12582

T

TABLES (DATA)
Selected data on research and development in industry: 1990
[NSF-92-317] p 773 N93-12667
Selected data on federal support to universities and colleges: Fiscal year 1990
[NSF-92-310] p 740 N93-12920
World Energy Projection System (WEPS), March 1992. Model installation manual, distribution disk layout
[PB92-169572] p 637 N93-12937
Characteristics of recent science and engineering graduates: 1990. Detailed statistical tables
[NSF-92-316] p 731 N93-13454
Selected data on Science and Engineering Doctorate Awards: 1991
[NSF-92-309] p 731 N93-13698
Science and engineering degrees: 1966-1990
[NSF-92-326] p 731 N93-13701
TAPES
Performance of thermal control tape in the protection of composite materials p 536 N93-12780
TARGET ACQUISITION
The Joint Surveillance Target Attack Radar System: Can procedures be developed to support the requirements of the land and air component commanders?
[AD-A255555] p 567 N93-13875
TARGET RECOGNITION
Introductory review of target discrimination criteria
[AD-A254954] p 560 N93-12551
Automation of the targeting and reflective alignment concept
[NASA-CR-190964] p 709 N93-12985
Inverse Synthetic Aperture Radar p 564 N93-13058
Development of two-dimensional parametric radar signal modeling and estimation techniques with application to target identification
[AD-A252602] p 567 N93-13939
TASK COMPLEXITY
A unified approach to the analysis and design of manipulator systems with environmental contact p 573 N93-13805
TASKS
Adaptive automation and human performance: Multi-task performance characteristics
[AD-A254596] p 503 N93-12578
TAYLOR INSTABILITY
Low-frequency fluctuations of plasma magnetic fields p 717 N93-13496
TDR SATELLITES
Test and control computer user's guide for a digital beam former test system
[NASA-CR-189208] p 685 N93-13291
TEA LASERS
CO2 laser preionisation
[NASA-CR-184424] p 607 N93-13797
A study of small solid-state switched TEA CO2 lasers p 607 N93-13814
TEARING MODES (PLASMAS)
Nonlinear studies of m = 1 modes in high-temperature plasmas
[DE92-019395] p 714 N93-12913
TECHNOLOGIES
Toward a microgravity research strategy
[NASA-CR-190820] p 556 N93-12799
NASA industry education initiative. Education programs report, 1991
[NASA-NP-158] p 730 N93-13248
National Aero-Space Plane: Key issues facing the program. Testimony before the Subcommittee on Technology and Competitiveness, Committee on Science, Space, and Technology, House of Representatives
[GAO/T-NSIAD-92-26] p 500 N93-13253
NSF Science and Technology Centers
[NSF-92-104] p 507 N93-13712
US Industry Access to Japanese Science and Technology: Proceedings of a conference
[PB92-167964] p 741 N93-13788
Public perceptions of the risks of an unfamiliar technology: The case of using nuclear energy sources for space missions p 527 N93-13971
The informed citizen: Technology and responsibility in the information age p 742 N93-14049
TECHNOLOGY ASSESSMENT
Large Deployable Reflector (LDR) system concept and technology definition study. Volume 1: Executive summary, analyses and trades, and system concepts
[NASA-CR-177413-VOL-1] p 708 N93-12591
Large Deployable Reflector (LDR) system concept and technology definition study. Volume 2: Technology assessment and technology development plan
[NASA-CR-177413-VOL-2] p 708 N93-12593
Advanced Communications Technology Satellite (ACTS). Phase 1: Industrial/academic experimenters
[NASA-CR-191211] p 561 N93-12679
Ocean Energy Program overview, fiscal years 1990-1991
[DE91-002176] p 636 N93-12837
Industrial applications of hot dry rock geothermal energy
[DE92-018903] p 637 N93-12923
Applications of satellite technology to broadband ISDN networks
[NASA-CR-189199] p 562 N93-12950
Ultraviolet disinfection technology assessment
[PB92-222868] p 678 N93-12983
Future regional transport aircraft market, constraints, and technology stimuli
[NASA-TM-107669] p 491 N93-13025
Phased array feed design technology for Large Aperture Microwave Radiometer (LAMR) Earth observations
[NASA-CR-189727] p 519 N93-13462
White paper: Preliminary assessment of LNG vehicle technology, economics, and safety issues, revision 1
[PB92-212943] p 615 N93-13644
Technology trends in high temperature pressure transducers: The impact of micromachining p 601 N93-13676
The trade-off characteristics of acoustic and pressure sensors for the NASP p 601 N93-13678
Assessment of Japanese technology in advanced glass and ceramic fibers
[AD-A255229] p 553 N93-13836
TECHNOLOGY TRANSFER
Brazilian remote sensing community: Historical, geographical and economic aspects
[INPE-5421-PRE/1763] p 634 N93-13412
Commercial non-aerospace technology transfer program for the 2000s: Strategic analysis and implementation
[NASA-TM-4424] p 742 N93-13433
Research and technology in support of IAM p 515 N93-13562
Considerations for the transition from fuel cell R/D to manufacturing
[DE92-019977] p 640 N93-13622
NSF Science and Technology Centers
[NSF-92-104] p 507 N93-13712
TECHNOLOGY UTILIZATION
Advanced Communications Technology Satellite (ACTS). Phase 1: Industrial/academic experimenters
[NASA-CR-191211] p 561 N93-12679
Efficacy of multimedia instruction and an introduction to digital multimedia technology
[AD-A254509] p 734 N93-12723
Industrial applications of hot dry rock geothermal energy
[DE92-018903] p 637 N93-12923
Applications of satellite technology to broadband ISDN networks
[NASA-CR-189199] p 562 N93-12950
Energy related inventions program. A joint program of the Department of Energy and the National Institute of Standards and Technology. Status report for recommendations 1 through 300
[PB92-226265] p 637 N93-12987
Energy related inventions program. A joint program of the Department of Energy and the National Institute of Standards and Technology. Status report for recommendations 301-563
[PB92-226273] p 637 N93-12988
JPRS report: Science and technology. Central Eurasia: Space
[JPRS-USP-92-004] p 513 N93-13282
JPRS report: Science and technology. Central Eurasia: Space
[JPRS-USP-92-005] p 513 N93-13304
Commercial non-aerospace technology transfer program for the 2000s: Strategic analysis and implementation
[NASA-TM-4424] p 742 N93-13433
Research and technology in support of IAM p 515 N93-13562
Abstracts of phase 1 awards: NSF Small Business Innovation Research Program (SBIR): 1992
[NSF-92-80] p 732 N93-13703
First steps to lunar manufacturing: Results of the 1988 Space Studies Institute Lunar Systems Workshop p 761 N93-13977
Activities of Space Power Insulation Inst.
[AD-A255825] p 574 N93-14034
TECTONICS
GPS measurements at Vandenberg AFB
[AD-A254978] p 499 N93-12557
Chemical environments of submarine hydrothermal systems
[NASA-CR-191258] p 669 N93-13458
The morphotectonic fabric of the East Pacific Rise: Implications for fault generation and crustal accretion p 652 N93-13481
Seismic studies of crustal structure and tectonic evolution across the central California margin and the Colorado Plateau margin p 657 N93-13794
TEETERING
User's Guide for the NREL Teetering Rotor Analysis Program (STRAP)
[DE92-010580] p 627 N93-13525
TEFLON (TRADEMARK)
Recession of FEP specimens from trays D11 and B7 p 549 N93-12786
Space environmental effects on silvered teflon thermal control surfaces
[AD-A255909] p 554 N93-14099
TELECOMMUNICATION
Research priorities in networking and communications
[NSF-92-109] p 562 N93-13024
OSA proceedings of the topical meeting on optical amplifiers and their applications, volume 13
[AD-A252974] p 711 N93-13879
TELECONNECTIONS (METEOROLOGY)
Point correlations of geopotential height and temperature at 30 mb and between 500 mb and 30 mb
[PB92-222694] p 661 N93-12817
TELEOPERATORS
Tactile sensing and control in humans and robotic/teleoperated systems
[AD-A254408] p 609 N93-12604
Dynamic control modification techniques in teleoperation of a flexible manipulator
[NASA-CR-190984] p 610 N93-12904
The 3-D computer vision techniques for object following and obstacle avoidance p 693 N93-13245
Performance and stability of telemanipulators using bilateral impedance control p 614 N93-13488
TELEROBOTICS
Space robotics: Recent accomplishments and opportunities for future research
[NASA-TM-107675] p 694 N93-13442
Performance and stability of telemanipulators using bilateral impedance control p 614 N93-13488
Mining equipment and operations for mining the 1982HR (Orpheus) asteroid p 515 N93-13557
Automation and robotics considerations for a lunar base p 619 N93-14006
TELESCOPES
EURECA
[ESA-F-26] p 522 N93-12964
The CHARA optical array p 744 N93-13581
The optical very large array and its moon-based version p 745 N93-13583

Recent astronomical results from the infrared spatial interferometer and their implications for LOUISA p 745 N93-13585
Science objectives for ground- and space-based optical/IR interferometry p 746 N93-13590
Telescopes on the Moon or pie in the sky? p 746 N93-13591
Lunar optical telescopes: An historical perspective p 746 N93-13593
The lunar environment and its effect on optical astronomy p 746 N93-13594
An optical VLA on the Moon p 747 N93-13596
A submillimetre polarimeter for the continuum receiver UKT14 on the James Clerk Maxwell Telescope p 748 N93-13852

TELEVISION SYSTEMS
Large area projection liquid-crystal video display system with inherent grid pattern optically removed [NASA-CASE-NPO-16932-2-CU] p 711 N93-13711

TELLURIC CURRENTS
New approaches to estimation of magnetotelluric parameters [DE92-040280] p 653 N93-13513

TEMPERATURE CONTROL
Li/SOCl battery technology: Problems and solutions [AD-A254514] p 570 N93-12725
Performance of thermal control tape in the protection of composite materials p 536 N93-12780
The Capillary Pumped Loop Flight Experiment (CAPL): A pathfinder for EOS p 512 N93-13181
The LDCE Particle Impact Experiment as flown on STS-46 --- limited duration space environment candidate materials exposure (LDCE) p 512 N93-13183
Aerospace applications of SINDA/FLUINT at the Johnson Space Center p 586 N93-13401
Environmental effects on an optical-UV-IR synthesis array p 747 N93-13595
Thermal control systems for low-temperature heat rejection on a lunar base [NASA-CR-191286] p 679 N93-13717
Conceptual design of a lunar base thermal control system p 680 N93-14003
Space environmental effects on silvered teflon thermal control surfaces [AD-A255909] p 554 N93-14099

TEMPERATURE DEPENDENCE
The nature of scales grown on binary Cr-Nb alloys [DE92-019283] p 542 N93-13080
Ion-channeling observation of correlated atomic displacements below Tc in YBa2Cu3O(7-x) and Pb-doped Bi2Sr2CaCu2O(x) [DE92-018186] p 722 N93-13104
Is there a unique effective interaction profile for dislocations? [DE92-018615] p 543 N93-13545

TEMPERATURE DISTRIBUTION
Statistical analysis of stratospheric temperature and ozone profile data for trends and model comparison [NASA-CR-191248] p 650 N93-12877
Measurements of the cosmic microwave background temperature at 1.47 GHz p 772 N93-13146
A preliminary study of the effect of equivalence ratio on a low emissions gas turbine combustor using KIVA-2 [DE92-018616] p 613 N93-13321
Fluid flow and heat convection studies for actively cooled airframes [NASA-CR-190956] p 587 N93-13406
Planar laser-induced fluorescence measurements of high-enthalpy free jet flow with nitric oxide p 595 N93-13685

TEMPERATURE EFFECTS
The role of latent heat release in explosive cyclogenesis [AD-A254436] p 660 N93-12596
Large-amplitude plate vibration in an elevated thermal environment [AD-A254411] p 621 N93-12606
Thermal effects on the frequency response of piezoelectric crystals [DE92-019039] p 720 N93-12819
An investigation of the thermoviscoplastic behavior of a metal matrix composite at elevated temperatures [NASA-CR-189706] p 530 N93-12929
Structural integrity of composites under load and thermal insult p 530 N93-13012
Post flight operation of a high peak power neodymium YAG laser aboard the G-449 payload flown on Space Shuttle Columbia mission 61-C p 508 N93-13161
Computational simulation of probabilistic lifetime strength for aerospace materials subjected to high temperature, mechanical fatigue, creep and thermal fatigue [NASA-CR-190794] p 626 N93-13290
A tough high performance composite matrix [NASA-CASE-LAR-14338-1] p 531 N93-13416
Point defects quenched in NiAl and related intermetallic compounds p 724 N93-13628
High temperature strain gage apparent strain compensation p 600 N93-13672
Some problems of quantum cosmology and dark matter physics p 755 N93-13829
Investigations of the mechanical behavior of graphite/PEEK (APC-2) composites p 534 N93-13908

TEMPERATURE GRADIENTS
Large-amplitude plate vibration in an elevated thermal environment [AD-A254411] p 621 N93-12606
TRASYS form factor matrix normalization p 585 N93-13391
Fluid flow and heat convection studies for actively cooled airframes [NASA-CR-190956] p 587 N93-13406
Electron impact polarization expected in solar EUV lines from flaring chromospheres/transition regions [SSL-PREPRINT-90-124] p 770 N93-13478
Climate sensitivity study with energy balance models p 666 N93-13817

TEMPERATURE MEASUREMENT
Thermal imaging of synchrotron beams on silicon crystals [DE92-018182] p 719 N93-12562
Measurements of the cosmic microwave background temperature at 1.47 GHz p 772 N93-13146
Measurements of the temperature in the edge plasma of the CASTOR tokamak by a triple Langmuir probe [IPPCZ-318] p 716 N93-13330
Measurement of tropospheric temperature and aerosol extinction using high spectral resolution lidar p 653 N93-13614
The 1992 NASA Langley Measurement Technology Conference: Measurement Technology for Aerospace Applications in High-Temperature Environments [NASA-CP-3161] p 598 N93-13661
Temperature and heat flux measurements: Challenges for high temperature aerospace application p 598 N93-13662
High heat flux measurements and experimental calibrations/characterizations p 598 N93-13663
Time dependent heat transfer rates in high Reynolds number hypersonic flowfields p 595 N93-13664
Thin film thermocouples for high temperature measurement on ceramic materials p 599 N93-13666
Fabrication of thin film heat flux sensors p 599 N93-13667
Gas temperature measurements using the dual-line detection Rayleigh scattering technique p 599 N93-13668
Resonance lamp absorption measurement of OH number density and temperature in expansion tube scramjet engine tests p 602 N93-13682
Gas temperature and density measurements based on spectrally resolved Rayleigh-Brillouin scattering p 602 N93-13684
Planar laser-induced fluorescence measurements of high-enthalpy free jet flow with nitric oxide p 595 N93-13685
Planar measurement of flow field parameters in nonreacting supersonic flows with laser-induced iodine fluorescence p 495 N93-13801
Temperature measurements with micrometer spatial resolution [AD-A255897] p 603 N93-14086

TEMPERATURE MEASURING INSTRUMENTS
Temperature and heat flux measurements: Challenges for high temperature aerospace application p 598 N93-13662

TEMPERATURE PROBES
Electronic triple point cell [AD-D015374] p 597 N93-13501
High heat flux measurements and experimental calibrations/characterizations p 598 N93-13663
Heat flux microsensor measurements and calibrations p 599 N93-13665
Fabrication of thin film heat flux sensors p 599 N93-13667

TEMPERATURE PROFILES
SAC contrail formation study [AD-A254410] p 499 N93-12605
Measurement of tropospheric temperature and aerosol extinction using high spectral resolution lidar p 653 N93-13614
Aspects of atmospheric transport and dispersion within an air basin p 656 N93-13782
Estimation of EOF expansion coefficients from incomplete data [AD-A255252] p 697 N93-13886

TEMPERATURE RATIO
Investigation of the flowfield around an isolated bypass engine with fan and core jet p 582 N93-13227

TEMPERATURE SENSORS
The constant current loop: A new paradigm for resistance signal conditioning [NASA-TM-104260] p 596 N93-12681
SiC device development for high temperature sensor applications p 601 N93-13677

TEMPERING
Tempering effects for lower bainite, martensite, and mixed microstructures on impact, fracture, and related mechanical properties of ASTM A723 steel [AD-A254617] p 541 N93-12616

TEMPORAL DISTRIBUTION
Zodiacal emission p 772 N93-13147

TENSILE PROPERTIES
Fatigue and fracture of intermetallic alloys [AD-A254543] p 540 N93-12603
Small-strain and finite-strain finite element analyses of plane-strain tensile elastic-plastic crack growth p 621 N93-12628
Elevated temperature tensile properties of borated 304 stainless steel: Effect of boride dispersion on strength and ductility [DE92-040096] p 542 N93-13302

TENSILE STRENGTH
Development of weldable high-strength iron aluminides [DE92-016018] p 542 N93-13190
Mechanical properties of epoxy/alumina trihydrate-filled compositions p 534 N93-13950
Improving the temperature resistance of aluminum-matrix composites by using an acid phosphate binder p 536 N93-14056

TENSILE TESTS
Test plan and report for Space Shuttle launch environment testing of Bergen cable technology safety cable [NASA-CR-4473] p 559 N93-13434

TENSORS
Solitons and instantons in string theory p 728 N93-13753

TERMINAL BALLISTICS
Analysis of a structure-equipment system subjected to impact loading [AD-A255097] p 622 N93-12652

TERRAIN
Satellite imagery goes to the field [AD-A254449] p 632 N93-12598
Perceptual dimensions of visual scenes relevant for simulating low-altitude flight [AD-A254645] p 676 N93-12662
Proceedings of the Fifth European International Society for Terrain-Vehicle Systems, volume 1 [AD-A254619] p 611 N93-12906
Remote sensing of Earth terrain [NASA-CR-190908] p 633 N93-13084
Impact of Digital Terrain Elevation Data (DTED) resolution on terrain visualization: Simulation versus reality [AD-A254237] p 634 N93-13333
Using iterative orthophoto refinements to correct Digital Elevation Models (DEM's) [AD-A254625] p 634 N93-13345
Meso-beta scale numerical simulation studies of terrain-induced jet streak mass/momentum perturbations [NASA-CR-191365] p 654 N93-13719

TERRAIN ANALYSIS
Perceptual dimensions of visual scenes relevant for simulating low-altitude flight [AD-A254645] p 676 N93-12662

TEST CHAMBERS
Natural convection between a vertical cylinder and a surrounding array [DE92-019763] p 728 N93-12857

TEST EQUIPMENT
Multichip module high speed testing [AD-A254825] p 570 N93-12731
Test and control computer user's guide for a digital beam former test system [NASA-CR-189208] p 685 N93-13291

TEST FACILITIES
An investigation of jet engine test cell aerodynamics by means of scale model test studies with comparisons to full-scale test results p 507 N93-14060

TEST VEHICLES
Utilization of compressed natural gas in medium- and heavy-duty engine route vehicles [PB92-217546] p 611 N93-12908

TETHERING
Equations of motion of slung-load systems, including multilift systems [NASA-TP-3280] p 503 N93-12815
Tether deployment monitoring system, phase 2 [NASA-CR-184098] p 522 N93-13425

TETRAHYDROFURAN
Determination of the weight average molecular weight of SRM 1480
[PB92-222934] p 553 N93-13785
TEXTILES
Physical interpretation and development of ultrasonic nondestructive evaluation techniques applied to the quantitative characterization of textile composite materials
[NASA-CR-190962] p 620 N93-13435
TEXTS
Semantics-based reference resolution in technical text processing: An exploration of using the Word Net database in the computerized comprehensibility system
[AD-A255068] p 736 N93-13117
Reject mechanisms for massively parallel neural network character recognition systems
[PB92-213412] p 689 N93-13198
THALLIUM
Monitoring interfacial dynamics by pulsed laser techniques
[DE92-040302] p 606 N93-13514
THEOREMS
MINT: The multiple error LMS algorithm, and the design of inverse filters for multi-channel sound reproduction systems
[ISVR-TR-211] p 700 N93-13439
THEORETICAL PHYSICS
Theoretical nuclear physics
[DE92-019286] p 706 N93-12822
Theoretical high energy physics
[DE92-015480] p 707 N93-13189
Guide to QSPIRES and the particle physics databases on SLACVM
[DE92-018099] p 737 N93-13275
JPRS report: Science and technology. Central Eurasia: Physics and mathematics
[JPRS-UPM-92-006] p 698 N93-13303
Dual mass and torsion p 728 N93-13498
THERAPY
AFRRI reports
[AD-A254581] p 674 N93-12649
THERMAL ANALYSIS
Semiconductor measurement technology: Version 2.0 of the TXYZ thermal analysis program: TXYZ20
[PB92-217603] p 570 N93-12978
Structural integrity of composites under load and thermal insult p 530 N93-13012
The Fourth Annual Thermal and Fluids Analysis Workshop
[NASA-CP-10106] p 584 N93-13385
Running SINDA '85/FLUINT interactive on the VAX p 584 N93-13390
Development status of SINDA/FLUINT and SINAPS p 585 N93-13393
A SINDA thermal model using CAD/CAE technologies p 585 N93-13394
Analysis of fluid/mechanical systems using EASY5 p 586 N93-13397
Coupled structural/thermal/electromagnetic analysis/tailoring of graded composite structures
[NASA-CR-189150] p 626 N93-13443
Coupled structural/thermal/electromagnetic analysis/tailoring of graded composite structures
[NASA-CR-189151] p 627 N93-13444
Coupled structural/thermal/electromagnetic analysis/tailoring of graded composite structures
[NASA-CR-189152] p 627 N93-13445
THERMAL BUCKLING
Large-amplitude plate vibration in an elevated thermal environment
[AD-A254411] p 621 N93-12606
THERMAL CONDUCTORS
A simple node and conductor data generator for SINDA p 585 N93-13392
THERMAL CONTROL COATINGS
Thermal barrier coating life prediction model development, phase 2
[NASA-CR-189111] p 544 N93-12589
Z306 molecular contamination ad hoc committee results p 546 N93-12774
Thermal control surfaces on the MSFC LDEF experiments p 547 N93-12778
Anodized aluminum on LDEF: A current status of measurements on chromic acid anodized aluminum p 544 N93-12779
Fluorescence of thermal control coatings on S0069 and A0114 p 548 N93-12781
Long Duration Exposure Facility M0003-5 thermal control coatings on DoD flight experiment p 548 N93-12782
Skylab D024 thermal control coatings and polymeric films experiment p 548 N93-12784
Long Duration Exposure Facility M0003-5 recent results on polymeric films p 549 N93-12789
THERMAL CYCLING TESTS
Environmental qualification testing of payload G-534, the Pool Boiling Experiment p 510 N93-13169
Thin film thermocouples for high temperature measurement on ceramic materials p 599 N93-13666
THERMAL DIFFUSION
Thermoconvective instability in the solar core p 771 N93-13849
THERMAL EMISSION
Development of a portable infrared emission spectrometer AA460 PIRES
[NASA-CR-190849] p 598 N93-13656
THERMAL ENERGY
A quantitative analysis of the effect of ELMs on H-mode thermal energy confinement in DIII-D
[DE92-017704] p 712 N93-12687
Turbulent natural convection between a perforated vertical cylinder and a surrounding array
[DE92-019766] p 576 N93-12996
THERMAL ENVIRONMENTS
Large-amplitude plate vibration in an elevated thermal environment
[AD-A254411] p 621 N93-12606
THERMAL EXPANSION
Fracture of a metal/ceramic couple: Tantalum (titanium)/sapphire p 554 N93-14074
THERMAL FATIGUE
Fatigue in single crystal nickel superalloys
[AD-A254704] p 541 N93-12746
Investigation of component failure rates for pulsed versus steady state tokamak operation
[DE92-019758] p 713 N93-12856
Computational simulation of probabilistic lifetime strength for aerospace materials subjected to high temperature, mechanical fatigue, creep and thermal fatigue
[NASA-CR-190794] p 626 N93-13290
THERMAL INSTABILITY
Thermoconvective instability in the solar core p 771 N93-13849
THERMAL INSULATION
Effects of the LDEF environment on the Ag/FEP thermal blankets p 548 N93-12785
Touchstone for success
[ESA-BR-52] p 557 N93-12934
THERMAL MAPPING
Thermal imaging of synchrotron beams on silicon crystals
[DE92-018182] p 719 N93-12562
THERMAL NEUTRONS
Miniature neutron sources: Thermal neutron sources and their users in the academic field
[DE92-018793] p 702 N93-13070
The use of ring ratios to detect sample differences in passive neutron counting
[DE92-018920] p 702 N93-13076
THERMAL PROTECTION
Debris/ice/TPS assessment and integrated photographic analysis for Shuttle mission STS-47
[NASA-TM-107553] p 520 N93-13032
THERMAL RADIATION
TRASYS form factor matrix normalization p 585 N93-13391
A SINDA '85 nodal heat transfer rate calculation user subroutine p 587 N93-13403
THERMAL RESISTANCE
Heat resistant diffusion coating for niobium alloy
[AD-A255542] p 554 N93-13873
THERMAL STABILITY
Transverse flexural tests as a tool for assessing damage to PMR-15 composites from isothermal aging in air at elevated temperatures
[NASA-TM-105848] p 529 N93-12737
Studies of plasticized-polymer electrolytes containing mixed Zn(2) and Li(1)
[AD-A254818] p 545 N93-12755
THERMAL STRESSES
Toughening mechanisms in weak matrix ceramic composites p 553 N93-13780
Thermal stress in US Air Force operations
[AD-A255785] p 676 N93-14027
Physiological stress from chemical defense clothing and equipment
[AD-A255786] p 676 N93-14028
The relationship between environmental conditions and UH-60 cockpit temperature
[AD-A255918] p 680 N93-14090
THERMAL VACUUM TESTS
Environmental qualification testing of payload G-534, the Pool Boiling Experiment p 510 N93-13169
THERMIONIC CONVERTERS
A heat pipe coupled planar thermionic converter: Performance characterization, nondestructive testing, and evaluation
[AD-A254941] p 727 N93-12546
THERMOCHEMISTRY
Nonideal thermoequilibrium calculations using a large product species data base
[DE92-040839] p 735 N93-12813
Thermochemistry of atmospheric metal reactions
[AD-A248651] p 543 N93-13733
THERMOCOUPLES
High heat flux measurements and experimental calibrations/characterizations p 598 N93-13663
Heat flux microsensor measurements and calibrations p 599 N93-13665
Thin film thermocouples for high temperature measurement on ceramic materials p 599 N93-13666
Fabrication of thin film heat flux sensors p 599 N93-13667
THERMODYNAMIC EFFICIENCY
Efficiency of an AMTEC recirculating test cell, experiments, and projections
[DE92-016811] p 571 N93-13196
Reversible thermodynamic cycle for AMTEC power conversion
[DE92-016814] p 571 N93-13197
THERMODYNAMIC PROPERTIES
Effects of orbital exposure on Halar during the LDEF mission p 549 N93-12788
Journal of Research of the National Institute of Standards and Technology, May-June 1992, volume 97, number 3
[PB92-217637] p 698 N93-12805
Touchstone for success
[ESA-BR-52] p 557 N93-12934
Thermodynamically consistent theories for elastoplasticity coupled with damage
[DE92-018283] p 627 N93-13515
Molecular theories and computer simulations of liquid crystals p 725 N93-13843
THERMODYNAMICS
Computer program for calculating and fitting thermodynamic functions
[NASA-RP-1271] p 728 N93-12967
Structural integrity of composites under load and thermal insult p 530 N93-13012
THERMOELASTICITY
Boundary element method for axisymmetric thermoelastic analysis p 624 N93-13097
Finite element versus boundary element analysis of two-dimensional coupled thermoelasticity p 625 N93-13142
THERMOELECTRIC GENERATORS
Alternate electrode materials for the SP100 reactor
[DE92-019570] p 706 N93-12970
Efficiency of an AMTEC recirculating test cell, experiments, and projections
[DE92-016811] p 571 N93-13196
Reversible thermodynamic cycle for AMTEC power conversion
[DE92-016814] p 571 N93-13197
THERMOGRAVIMETRY
Effects of orbital exposure on Halar during the LDEF mission p 549 N93-12788
Oxidative stability of LARC (tm)-TPI films
[NASA-TM-107696] p 552 N93-13441
THERMOMECHANICAL TREATMENT
Development of weldable high-strength iron aluminides
[DE92-016018] p 542 N93-13190
THERMOMETERS
Electronic triple point cell
[AD-D015374] p 597 N93-13501
Temperature measurements with micrometer spatial resolution
[AD-A255897] p 603 N93-14086
THERMONUCLEAR EXPLOSIONS
Approximating the r-process on earth with thermonuclear explosions
[DE92-017409] p 749 N93-12587
THERMOPILES
Fabrication of thin film heat flux sensors p 599 N93-13667
THERMOPLASTIC RESINS
Consolidation of powder coated thermoplastic preform process modeling
[AD-A255094] p 529 N93-12757
Predictive forming of advanced thermoplastic composite structures p 529 N93-12835
The crystallization and crystalline properties of LARC-TPI
[NASA-CR-191001] p 721 N93-13022
Development of a 1000 g, 10 ms mechanical shock test capability
[DE92-019193] p 624 N93-13077
Enabling technologies for economical manufacturing of composites
[AD-A253615] p 531 N93-13324

Characterization of thermotropic liquid crystalline polymer blends by positron annihilation lifetime spectroscopy
[AD-A253616] p 552 N93-13325
A tough high performance composite matrix
[NASA-CASE-LAR-14338-1] p 531 N93-13416

THERMOPLASTICITY
Enabling technologies for economical manufacturing of composites
[AD-A253615] p 531 N93-13324
Effects of layer waviness on compression-loaded thermoplastic composite laminates p 532 N93-13724
Thermoviscoplastic analysis of metal matrix composites p 535 N93-13954

THERMOSETTING RESINS
Influence of cure shrinkage on process-induced stress and deformation in thick thermosetting composites
[AD-A254325] p 529 N93-12842
A tough high performance composite matrix
[NASA-CASE-LAR-14338-1] p 531 N93-13416

THERMOSPHERE
Investigations of the dynamics and thermodynamics of the mesosphere lower thermosphere and upper thermosphere at the polar regions with optical ground-based remote sensing
[AD-A254746] p 650 N93-12845
Self-consistent modeling of the ionosphere-thermosphere-magnetosphere system
[AD-A253232] p 651 N93-13276

THICKNESS
Aspects of atmospheric transport and dispersion within an air basin p 656 N93-13782

THIN BODIES
Boundary element analysis of acoustical thin-body and nonuniqueness problems using a normal derivative integral equation p 631 N93-13951

THIN FILMS
Chemical sensors based on ultrathin film composite membranes
[AD-A254644] p 595 N93-12619
Electrochemical and chemical characteristics of a new ambient temperature Li(I) polymer electrolyte
[AD-A254918] p 545 N93-12651
High temperature superconductor materials and applications
[NASA-CR-184437] p 719 N93-12691
Long Duration Exposure Facility M0003-5 recent results on polymeric films p 549 N93-12789
Development of large-area monolithically integrated silicon-film photovoltaic modules
[DE92-010600] p 637 N93-12838
Single liquid source plasma enhanced metalorganic chemical vapor deposition of YBa2Cu3O(7-x) thin films
[AD-A254119] p 722 N93-13100
CONCAP 4: A Complex Autonomous Payload (CAP) for growing organic thin films in microgravity p 511 N93-13178
Study of short-range motion of atomic hydrogen in amorphous silicon by neutron reflectometry
[DE92-016392] p 703 N93-13194
Epitaxial growth of silicon and germanium for solar cells
[ITN-92-85168] p 722 N93-13268
Effect of O2 partial pressure on post annealed Ba2YCu3O(7-delta) thin films
[DE92-014949] p 722 N93-13323
Y1Ba2Cu3O(7-delta) thin film dc SQUIDs (superconducting quantum interference device)
[ITN-92-85167] p 723 N93-13362
Narrow bandgap semiconducting silicides: Intrinsic infrared detectors on a silicon chip
[NASA-CR-190882] p 571 N93-13430
Novel thin-film CuInSe2 fabrication
[DE92-016440] p 723 N93-13526
Development of a computer model for polycrystalline thin-film CuInSe2 and CdTe solar cells
[DE92-016444] p 639 N93-13529
Thin films and solar cells of cadmium telluride and cadmium zinc telluride p 639 N93-13611
Thin film thermocouples for high temperature measurement on ceramic materials p 599 N93-13666
Fabrication of thin film heat flux sensors p 599 N93-13667
Ion-beam-assisted deposition of MoS2 and other low-friction films
[AD-A255222] p 554 N93-13862
Intrinsic bistable photonic materials by copper colloid formation in silica
[AD-A255505] p 711 N93-13866
The heteroepitaxial growth of YBCO and other metal oxides on silicon and GaAs by pulsed laser deposition p 726 N93-13904
Two to six compound thin films by MOCVD for tandem solar cells p 640 N93-13932
Noise measurements of YBa2Cu3O7 thin film high-temperature superconductors p 726 N93-13933
Friction, wear and Raman spectroscopic characteristics of carbon lubricated surfaces p 618 N93-13949
Surface phonon dispersion of MoS2
[AD-A255835] p 727 N93-14083

THIN PLATES
Analysis of cracked plates subjected to out-of-plane loadings p 629 N93-13804

THIN WALLED SHELLS
Structural optimization of thin shells using finite element method
[NASA-TM-105903] p 625 N93-13157
An elasticity solution for a transversely isotropic material containing a spherical shell under axisymmetric loading p 628 N93-13728

THREE BODY PROBLEM
Orbit determination error analysis and station-keeping for liberation point trajectories p 518 N93-14038

THREE DIMENSIONAL BODIES
Hierarchic models for laminated plates p 528 N93-12629
Sensing and interpretation of 3-D shape and motion p 692 N93-13240
Numerical analysis of scattering from certain conducting and dielectric bodies of arbitrary shape
[ISBN-0-315-63282-8] p 569 N93-14066

THREE DIMENSIONAL BOUNDARY LAYER
The three-dimensional turbulent boundary layer: Theory and application p 588 N93-13749
An experimental investigation of the three-dimensional boundary layer on a rotating disk p 589 N93-13806

THREE DIMENSIONAL COMPOSITES
Micromechanics of finite length fibers in composite materials p 532 N93-13490

THREE DIMENSIONAL FLOW
The multidimensional self-adaptive grid code, SAGE
[NASA-TM-103905] p 683 N93-12719
Quantitative analysis of three-dimensional steady flow field by using particle image velocimetry and digital image processing method p 577 N93-13017
Experimental studies of the flowfields and their effects due to a pair of lift jets discharging in the ground effect region p 580 N93-13217
Unsteady three-dimensional thin-layer Navier-Stokes solutions for turbomachinery in transonic flow p 593 N93-14025

THREE DIMENSIONAL MODELS
The 3-D nonlinear constitutive modeling approach for composite materials
[AD-A255022] p 528 N93-12584
Numerical simulation of a squall line: Tests of a new cumulus parameterization scheme p 662 N93-13124
A stochastic/deterministic method for transient, three-dimensional neutron transport
[DE92-016690] p 704 N93-13319
Thermal issues at the SSC p 584 N93-13387
Hydrodynamical calculations of stellar interactions p 755 N93-13764
Transonic aeroelastic analysis of systems with structural nonlinearities p 629 N93-13769
An observational and numerical investigation of meso-scale coastal processes during GALE IOP 2 p 665 N93-13776
Numerical simulation of compressible Couette flow stability: Non-linear and three-dimensional effects p 594 N93-14077

THREE DIMENSIONAL MOTION
Heat transfer in a liquid metal crucible with an integral blackbody cavity
[DE92-019640] p 576 N93-12825
Sensing and interpretation of 3-D shape and motion p 692 N93-13240
On development of a three-dimensional particle motion tracking system
[DE92-015846] p 704 N93-13263
A weighted iterative algorithm for neuromagnetic imaging
[DE92-040244] p 675 N93-13522

THRUST CHAMBERS
Demand thrust pumped propulsion with automatic warm gas valving
[DE92-017435] p 525 N93-12840
Pressure fed thrust chamber technology program
[NASA-CR-184461] p 526 N93-12968

THRUST REVERSAL
Recent developments in low-speed TPS-testing for engine integration drag and installed thrust reversr simulation p 502 N93-13207
Aerodynamic integration of thrust reversers on the Fokker 100 p 502 N93-13208

THRUST VECTOR CONTROL
Propulsion integration results of the STOL and Maneuver Technology Demonstrator p 502 N93-13228

THRUSTORS
Scaling of 100 kW class applied-field MPD thrusters
[NASA-CR-190791] p 525 N93-12638
Analysis of fluid/mechanical systems using EASY5 p 586 N93-13397

THUNDERSTORMS
An analysis of the tornado-producing Raleigh thunderstorm of November 28, 1988
[AD-A254384] p 661 N93-12862
The modelling of turbulence and downbursts for flight simulators p 507 N93-13542

THYRATRONS
A study of small solid-state switched TEA CO2 lasers p 607 N93-13814

THYRISTORS
A study of small solid-state switched TEA CO2 lasers p 607 N93-13814

TIDES
On the relationship between the intensity of extratropical frontal cyclone systems and water levels in the Gulf of Mexico p 666 N93-13816

TILT ROTOR AIRCRAFT
Navier-Stokes flowfield computation of wing/rotor interaction for a tilt rotor aircraft in hover p 497 N93-14035

TIME DEPENDENCE
Speedup properties of phases in the execution profile of distributed parallel programs
[DE92-019965] p 689 N93-12810
Analytical studies of nonlinear partial differential equations of interest in nonlinear optics
[AD-A254931] p 696 N93-13027
Time dependent heat transfer rates in high Reynolds number hypersonic flowfields p 595 N93-13664
A surface pressure altitude prediction model
[AD-A255834] p 668 N93-14082

TIME MEASUREMENT
A distributed timing system for sychronizing control and data correlation
[DE92-018603] p 690 N93-12564
The VELOPT code for estimating performance of a Fabry-Perot velocimeter
[DE92-015566] p 596 N93-12831
Tutorials from the 23rd Annual Precise Time and Time Interval (PTTI) Applications and Planning Meeting
[AD-A254745] p 596 N93-12844
RF system description for the ground test accelerator radio-frequency quadrupole
[DE92-040239] p 563 N93-13045

TIME SERIES ANALYSIS
A study of the luminosity produced by an electron beam-emitting rocket in the polar ionosphere: ECHO 7 p 657 N93-13830
Application of satellite altimetry to study the Gulf of Alaska gyre p 635 N93-13969

TIMING DEVICES
A distributed timing system for sychronizing control and data correlation
[DE92-018603] p 690 N93-12564
Tutorials from the 23rd Annual Precise Time and Time Interval (PTTI) Applications and Planning Meeting
[AD-A254745] p 596 N93-12844

TIN OXIDES
Influence of surface defects and local structure on oxygenate reaction pathways over metal oxide surfaces
[DE92-040013] p 539 N93-13573

TIROS N SERIES SATELLITES
Automatic pattern recognition techniques for geometrical correction on satellite data p 687 N93-13913

TISSUES (BIOLOGY)
Effects of spaceflight on the proliferation of jejunal mucosal cells
[NASA-CR-191303] p 675 N93-13449

TITAN
Studies of radiative emission from the simulated shock layer of the Huygens probe p 521 N93-12834

TITANIUM
An investigation of the thermoviscoplastic behavior of a metal matrix composite at elevated temperatures
[NASA-CR-189706] p 530 N93-12929

TITANIUM ALLOYS
Influence of cold work level on the irradiation creep and creep rupture of titanium-modified austenitic stainless steels
[DE92-019078] p 541 N93-12820
An investigation of the interatomic bonding characteristics of a Ti - 51 atomic percent Al alloy by x ray diffraction
[AD-A245362] p 544 N93-13945

TOKAMAK DEVICES
A quantitative analysis of the effect of ELMs on H-mode thermal energy confinement in DIII-D
[DE92-017704] p 712 N93-12687
Investigation of component failure rates for pulsed versus steady state tokamak operation
[DE92-019758] p 713 N93-12856

Nonlinear studies of m = 1 modes in high-temperature plasmas
[DE92-019395] p 714 N93-12913
A design for an advanced divertor for D3D and ITER: The radiative slot divertor
[DE92-019579] p 714 N93-12932
DIII-D edge physics database
[DE92-019577] p 714 N93-12971
Tokamak equilibria and transport based on Grad's thirteen moment description
[DE92-019960] p 715 N93-13038
Future development of the D3-D tokamak program
[DE92-040051] p 715 N93-13044
Fluctuation studies on CASTOR and ASDEX tokamaks at lower hybrid current drive
[IPPCZ-319] p 715 N93-13093
Fusion: Magnetic confinement
[DE92-019876] p 716 N93-13107
Fast wave current drive experiment on the D3-D tokamak
[DE92-016253] p 716 N93-13193
Diagnostics systems for the TBR-E tokamak
[INPE-5428-RPQ/662] p 716 N93-13257
Measurements of the temperature in the edge plasma of the CASTOR tokamak by a triple Langmuir probe
[IPPCZ-318] p 716 N93-13330
A fast scanning probe for D3-D
[DE92-040260] p 717 N93-13511
Biasing experiments on the Advanced Toroidal Facility
[DE92-040033] p 717 N93-13518
Achieving high Q(sub DD) operation in high poloidal beta discharges in TFTR
[DE92-019494] p 718 N93-13535

TOLERANCES (MECHANICS)
Properties of five toughened matrix composite materials
[NASA-TP-3254] p 528 N93-12590

TOMOGRAPHY
Characterizing laser fusion welded aluminum using synchrotron x ray microtomography
[DE92-018608] p 609 N93-12565
Acoustic tomographic monitoring of the atmospheric boundary layer p 651 N93-13143
X ray attenuation measurements for high-temperature materials characterization and in situ monitoring of damage accumulation p 631 N93-14022

TOPEX
Nonconservative force model parameter estimation strategy for TOPEX/Poseidon precision orbit determination
[NASA-TM-104575] p 519 N93-13372

TOPOGRAPHY
Satellite imagery goes to the field
[AD-A254449] p 632 N93-12598
Tributary and gap nighttime air flow comparisons
[DE92-018875] p 662 N93-13075
Impact of Digital Terrain Elevation Data (DTED) resolution on terrain visualization: Simulation versus reality
[AD-A254237] p 634 N93-13333
Topographic surveyor: Transitioning to the 90's
[AD-A254688] p 499 N93-13351
An investigation of the effects of topography on Colorado front range winter storms p 668 N93-14063

TOPOLOGY
Summary of awards: Applied mathematics. Fiscal year 1991
[NSF-92-38] p 681 N93-13438

TORNADOES
An analysis of the tornado-producing Raleigh thunderstorm of November 28, 1988
[AD-A254384] p 661 N93-12862

TOROIDAL PLASMAS
Biasing experiments on the Advanced Toroidal Facility
[DE92-040033] p 717 N93-13518
Achieving high Q(sub DD) operation in high poloidal beta discharges in TFTR
[DE92-019494] p 718 N93-13535

TORQUE
Torque resolver design for tendon-driven manipulators
[DE92-017395] p 609 N93-12698
Split torque transmission load sharing
[NASA-TM-105884] p 610 N93-12736
Dynamic modeling and optimal joint torque coordination of advanced robotic systems p 617 N93-13936
Modelling flexible link manipulators in the three-dimensional space p 574 N93-14093

TORSION
Nonlinear stall flutter of wings with bending-torsion coupling
[AD-A254323] p 503 N93-12959
In-phase and out-of-phase axial-torsional fatigue behavior of Haynes 188 at 760 C
[NASA-TM-105765] p 625 N93-13153
Dual mass and torsion p 728 N93-13498

TOTAL OZONE MAPPING SPECTROMETER
Nimbus-7 Total Ozone Mapping Spectrometer (TOMS) Antarctic ozone atlas: August through November 1991
[NASA-RP-1283] p 661 N93-12700

TOTAL QUALITY MANAGEMENT
Principles of information resource management: A foundation for the future
[AD-A254447] p 733 N93-12597
Statistical process management: An essential element of quality improvement
[DE92-019934] p 619 N93-13036
Performance measurement for information systems: Industry perspectives
[NASA-CR-191369] p 738 N93-13737
An examination of the Total Quality Management (TQM) concept given current Federal/DoD competition initiatives
[AD-A255556] p 620 N93-13876
Coordinating Council. Ninth Meeting: Total Quality Management
[NASA-TM-108106] p 738 N93-13885

TOUGHNESS
Notch dimensions for three-point bend fracture specimens based on compliance analyses
[AD-A254641] p 620 N93-12580
Polypropylene fibers in portland cement concrete pavements
[DOT/FAA/RD-92/9] p 551 N93-13259
Ductile phase toughening of molybdenum disilicide by low pressure plasma spraying
[DE92-007409] p 551 N93-13315
Shallow-crack toughness results for reactor pressure vessel steel
[DE92-017813] p 626 N93-13320
Oxidative stability of LARC (tm)-TPI films
[NASA-TM-107696] p 552 N93-13441
Toughening mechanisms in weak matrix ceramic composites p 553 N93-13780

TOXICOLOGY
JPRS report: Science and technology. Central Eurasia: Life sciences
[JPRS-ULS-92-024] p 672 N93-13033

TOXINS AND ANTITOXINS
A core facility for the study of neurotoxins of biological origin
[AD-A254359] p 674 N93-12945

TRACE ELEMENTS
Resonance ionization mass spectrometry in biochemical analysis
[DE92-017407] p 538 N93-13341
Effects of coal-derived trace species on performance of molten carbonate fuel cells
[DE93-000203] p 639 N93-13427
Radiative transfer in the middle atmosphere p 652 N93-13482

TRACKED VEHICLES
Proceedings of the Fifth European International Society for Terrain-Vehicle Systems, volume 1
[AD-A254619] p 611 N93-12906
The use of finite elements to model soil/track interactions in coupled multi-body dynamic simulations: Is real time simulation feasible?
[DE92-016184] p 612 N93-13236

TRACKING (POSITION)
Acoustic tracking of neutrally buoyant float
[AD-A255086] p 669 N93-12742
Automation of the targeting and reflective alignment concept
[NASA-CR-190964] p 709 N93-12985

TRACKING FILTERS
Fixed-gain, two-stage estimators for tracking maneuvering targets
[AD-A255832] p 697 N93-14081

TRACTION
Proceedings of the Fifth European International Society for Terrain-Vehicle Systems, volume 1
[AD-A254619] p 611 N93-12906

TRAINING DEVICES
Seamless simulation literature survey
[AD-A254950] p 688 N93-12549
Water tunnel studies of inlet/airframe interference phenomena p 580 N93-13216

TRAJECTORIES
Second quantization in bit-string physics
[DE92-019645] p 727 N93-12826
Experimental verification of modified command shaping using a flexible manipulator p 612 N93-12955
A guidance methodology for the cislunar transfer of low-thrust spacecraft p 517 N93-13766

TRAJECTORY CONTROL
An inverse dynamics approach to trajectory optimization for an aerospace plane
[NASA-CR-191277] p 500 N93-13305
Tether deployment monitoring system, phase 2
[NASA-CR-184098] p 522 N93-13425
A guidance methodology for the cislunar transfer of low-thrust spacecraft p 517 N93-13766
Control algorithms for aerobraking in the Martian atmosphere p 524 N93-14046

TRAJECTORY OPTIMIZATION
An inverse dynamics approach to trajectory optimization for an aerospace plane
[NASA-CR-191277] p 500 N93-13305
Sequential quadratic programming solutions to related aircraft trajectory optimization problems p 505 N93-13926

TRAJECTORY PLANNING
Robust rendezvous maneuver point conditions
[NASA-CR-190996] p 517 N93-12690
A unified approach to the analysis and design of manipulator systems with environmental contact p 573 N93-13805
Dynamic modeling and optimal joint torque coordination of advanced robotic systems p 617 N93-13936
A collision avoidance algorithm for the mobile robot and the robot manipulator in multi-robot system p 618 N93-14094

TRANSATMOSPHERIC VEHICLES
Performance and control of ascending trajectories to minimize heat load for transatmospheric aero-space planes p 495 N93-13745

TRANSDUCERS
The constant current loop: A new paradigm for resistance signal conditioning
[NASA-TM-104260] p 596 N93-12681
Preamplifier with adjustable input resistance
[AD-D015377] p 572 N93-13473
Effects of stinger axial dynamics and mass compensation methods on experimental modal analysis p 699 N93-13907

TRANSFER FUNCTIONS
Users manual for program ADMIT: Admittance and pressure transfer function developed for use on a PC computer
[NASA-CR-184450] p 682 N93-12676

TRANSFER ORBITS
Nutational stability and passive control of symmetric spinning bodies with axial forcing and internal mass motion p 504 N93-13820

TRANSIENT LOADS
Transient behavior of heat pipe with thermal energy storage under pulse heat loads p 588 N93-13743

TRANSIENT RESPONSE
A domain decomposition method for parallel transient response calculations p 504 N93-13827

TRANSISTORS
An acoustic charge transport imager for high definition television applications
[NASA-CR-191295] p 572 N93-13448

TRANSITION FLOW
Numerical simulation of the acoustic instability in the spatially developing, confined, supersonic mixing layer p 494 N93-13521

TRANSITION POINTS
Tempering effects for lower bainite, martensite, and mixed microstructures on impact, fracture, and related mechanical properties of ASTM A723 steel
[AD-A254617] p 541 N93-12616

TRANSITION PROBABILITIES
Transition probabilities up to I = 36(+)in Yb-160
[DE92-017191] p 703 N93-13114

TRANSITION TEMPERATURE
Tempering effects for lower bainite, martensite, and mixed microstructures on impact, fracture, and related mechanical properties of ASTM A723 steel
[AD-A254617] p 541 N93-12616

TRANSLATING
Modelling flexible link manipulators in the three-dimensional space p 574 N93-14093

TRANSMISSION LINES
Acoustic modes in fluid networks p 586 N93-13398

TRANSMISSIONS (MACHINE ELEMENTS)
Experimental validation of finite element and boundary element methods for predicting structural vibration and radiated noise p 621 N93-12631
Split torque transmission load sharing
[NASA-TM-105884] p 610 N93-12736

TRANSMITTERS
Extremely low frequency/very low frequency Generator
[AD-A254347] p 562 N93-12948

TRANSONIC FLOW
Navier-Stokes simulations of unsteady transonic flow phenomena
[NASA-TM-103962] p 491 N93-12721
Numerical calculation of turbomachinery cascade flows p 589 N93-13767
Transonic aeroelastic analysis of systems with structural nonlinearities p 629 N93-13769

Unsteady three-dimensional thin-layer Navier-Stokes solutions for turbomachinery in transonic flow p 593 N93-14025

TRANSPONDERS
Acoustic tracking of neutrally buoyant float [AD-A255086] p 669 N93-12742

TRANSPORT AIRCRAFT
Future regional transport aircraft market, constraints, and technology stimuli [NASA-TM-107669] p 491 N93-13025
Detailed analysis of wing-nacelle interaction for commercial transport aircraft p 578 N93-13203
Euler analysis of turbofan/superfan integration for a transport aircraft p 578 N93-13206
Aerodynamic integration of thrust reversers on the Fokker 100 p 502 N93-13208

TRANSPORT PROPERTIES
High temperature oxidation and electrochemical studies related to hot corrosion [AD-A254435] p 540 N93-12595
Proton transport on modified sulfonated polyaniline electrodes [AD-A254917] p 570 N93-12650
Tokamak equilibria and transport based on Grad's thirteen moment description [DE92-019960] p 715 N93-13038
On the bootstrap current calculations based on values of the radial electron transport [IPPCZ-317] p 715 N93-13091
Transport on fractal networks [AD-A253797] p 725 N93-13881

TRANSPORT THEORY
A stochastic/deterministic method for transient, three-dimensional neutron transport [DE92-016690] p 704 N93-13319

TRANSPORT VEHICLES
Integration of turbo-ramjet engines for hypersonic aircraft p 503 N93-13230

TRANSPORTATION
Federal support to universities, colleges, and nonprofit institutions: Fiscal year 1990. A report to the President and Congress [NSF-92-324] p 741 N93-13543

TRANSPUTERS
Transputer implementation of the TRACE model of speech recognition [AD-A254747] p 689 N93-12846

TRANSURANIUM ELEMENTS
Approximating the r-process on earth with thermonuclear explosions [DE92-017409] p 749 N93-12587

TRANSVERSE WAVES
Transverse wave motion in constrained mechanical systems p 628 N93-13634
Guidance and scattering of electromagnetic waves by nonlinear layers p 566 N93-13813

TRAPPED MAGNETIC FIELDS
Review of stellarator research: In search of the magic magnetic bottle [DE92-019045] p 718 N93-13651

TRAVELING SALESMAN PROBLEM
An investigation of new search techniques for the traveling salesman problem p 696 N93-12625

TRAVELING WAVE TUBES
Anomalous TWTA output power spikes and their effect on a digital satellite communications system [NASA-TM-105875] p 571 N93-13286

TREES (MATHEMATICS)
Introduction to IND and recursive partitioning, version 1.0 [NASA-CR-191220] p 685 N93-13063

TREES (PLANTS)
Statistical relationships between tree growth and climate in western North America p 648 N93-14096

TRELLIS CODING
Error control techniques for satellite and space communications [NASA-CR-191229] p 565 N93-13411

TREND ANALYSIS
Statistical analysis of stratospheric temperature and ozone profile data for trends and model comparison [NASA-CR-191248] p 650 N93-12877

TRENDS
Selected data on Science and Engineering Doctorate Awards: 1991 [NSF-92-309] p 731 N93-13698

TRIBOLOGY
Friction, wear and Raman spectroscopic characteristics of carbon lubricated surfaces p 618 N93-13949

TRITON
An analysis of the Voyager 2 ultraviolet spectrometer occultation data at Uranus and Triton: Inferring heat sources and model atmospheres p 768 N93-14072

TROPICAL METEOROLOGY
The kinetic energy budget of tropical plumes and ENSO in NMC and ECMWF analyses p 664 N93-13740

TROPICAL REGIONS
Deep convection and its relation to the large-scale circulation in the tropical Pacific p 654 N93-13725

TROPICAL STORMS
Extended range forecast of Atlantic seasonal hurricane activity for 1993 p 661 N93-12928

TROPOPAUSE
Tropopause fold investigations: Secondary circulation, water vapor and ozone analyses p 657 N93-13796

TROPOSPHERE
Steady state analysis of tropospheric chemistry p 644 N93-13121
Measurement of tropospheric temperature and aerosol extinction using high spectral resolution lidar p 653 N93-13614
Effects of the Mt. Pinatubo eruption on the radiative and chemical processes in the troposphere and stratosphere [DE92-019618] p 646 N93-13654
Kinetic and spectroscopic studies of peroxy radical reactions related to tropospheric photo-oxidation chemistry p 654 N93-13726
Radiative constraints on the energy budget of the atmosphere p 655 N93-13731
Cloud acidity and acidic deposition in the lower troposphere and ozone depletion in the Antarctic stratosphere: Modeling and data analysis regarding the role of atmospheric aerosol p 647 N93-13741
An observational and numerical investigation of meso-scale coastal processes during GALE IOP 2 p 665 N93-13776
Numerical study of nonlinear convective-symmetric instability in a rotating baroclinic atmosphere p 666 N93-13786
Gas-phase reactions of halogen species of atmospheric importance p 658 N93-13889
Frontogenesis processes in the troposphere p 667 N93-13890
The seasonal variations and interrelationships of ozone, peroxyacetyl nitrate and nitrogen dioxide in the troposphere p 647 N93-13893
Study of the concentration and deposition of tropospheric aerosols using x ray emission techniques p 667 N93-13894

TRUCKS
Meeting future exhaust emissions standards using natural gas as a vehicle fuel: Lessons learned from the natural gas vehicle challenge 1992 [DE92-019670] p 642 N93-12885
Utilization of compressed natural gas in medium- and heavy-duty engine route vehicles [PB92-217546] p 611 N93-12908
The 1992 natural gas vehicle challenge: EPA emissions and fuel economy testing [PB92-217926] p 616 N93-13761

TRUSSES
Design of a welded joint for robotic, on-orbit assembly of space trusses [NASA-TM-108380] p 609 N93-12682
Application of adaptive trusses to vibration isolation in flexible structures p 617 N93-13809

TUBE HEAT EXCHANGERS
Two-phase/two-phase heat exchanger simulation analysis p 586 N93-13402

TUMBLING MOTION
Dynamics and control of a tumbling satellite retrieval device p 522 N93-13119

TUNABLE LASERS
Electron stimulated desorption of the metallic substrate at monolayer coverage: Sensitive detection via 193 nm laser photoionization of neutral aluminum desorbed from CH3O/Al(111) [DE92-014858] p 723 N93-13349

TUNING
Transducer circuit [AD-D015376] p 572 N93-13472

TURBINE BLADES
Fatigue in single crystal nickel superalloys [AD-A254704] p 541 N93-12746
Overview on test cases for computation of internal flows in turbomachines p 579 N93-13209
Radial turbine cooling [NASA-TM-105658] p 492 N93-13292
User's Guide for the NREL Force and Loads Analysis Program [DE92-010579] p 627 N93-13524

TURBINE PUMPS
An experimental study of a small high-speed LH2 pump for rockets: Fluid dynamic performance [NAL-TR-1131] p 610 N93-12727

TURBINES
ASTOVL model engine simulators for wind tunnel research p 507 N93-13213
Radial turbine cooling [NASA-TM-105658] p 492 N93-13292

TURBOCOMPRESSORS
Alternative systems for fuel gas boosters for small gas turbine engines [PB92-223049] p 612 N93-12977
Overview on test cases for computation of internal flows in turbomachines p 579 N93-13209

TURBOFAN ENGINES
Subsonic flight test evaluation of a propulsion system parameter estimation process for the F100 engine [NASA-TM-4426] p 502 N93-13155
Tests of models equipped with TPS in low speed ONERA F1 pressurized wind tunnel p 577 N93-13201
Euler analysis of turbofan/superfan integration for a transport aircraft p 578 N93-13206
The influence of intake swirl distortion on the steady-state performance of a low bypass, twin-spool engine p 579 N93-13211
The jet behaviour of an actual high-bypass engine as determined by LDA-measurements in ground tests p 503 N93-13218
Investigation of the flowfield around an isolated bypass engine with fan and core jet p 582 N93-13227
An investigation of jet engine test cell aerodynamics by means of scale model test studies with comparisons to full-scale test results p 507 N93-14060

TURBOMACHINERY
Turbomachinery CFD on parallel computers [NASA-TM-105932] p 689 N93-13154
Numerical calculation of turbomachinery cascade flows p 589 N93-13767
Unsteady three-dimensional thin-layer Navier-Stokes solutions for turbomachinery in transonic flow p 593 N93-14025

TURBOPROP ENGINES
Investigation of advanced counterrotation blade configuration concepts for high speed turboprop systems. Task 4: Advanced fan section aerodynamic analysis [NASA-CR-187128] p 502 N93-12695

TURBORAMJET ENGINES
Integration of turbo-ramjet engines for hypersonic aircraft p 503 N93-13230

TURBULENCE
Natural convection between a vertical cylinder and a surrounding array [DE92-019763] p 728 N93-12857
Turbulent natural convection between a perforated vertical cylinder and a surrounding array [DE92-019766] p 576 N93-12996
Motion errors and compensation possibilities p 563 N93-13052
Studies on turbulent mixing in stratified turbulent patches p 587 N93-13532
Structures, spectra and inertial range transfer in two-dimensional and beta-plane turbulence p 590 N93-13900
Turbulent boundary layers with high turbulence: Experimental heat transfer and structure on flat and convex walls p 591 N93-13938
Experiments on the statistical nature of stably stratified turbulence p 594 N93-14069

TURBULENCE EFFECTS
Cascade processes and fully developed turbulence p 591 N93-13901
Turbulent boundary layers with high turbulence: Experimental heat transfer and structure on flat and convex walls p 591 N93-13938
An experimental and computational study of longitudinal vortices in turbulent boundary layers p 595 N93-14097

TURBULENCE MODELS
Adaptation of multidimensional group particle tracking and particle wall-boundary condition model to the FDNS code [SECA-TR-92-06] p 575 N93-12689
Calibration of 2D unstructured grid methods on propulsive flowfields p 582 N93-13225
The modelling of turbulence and downbursts for flight simulators p 507 N93-13542
Numerical calculation of turbomachinery cascade flows p 589 N93-13767
Coherent structures in compressible convection p 592 N93-13964
A low-dimensional dynamical systems description of coherent structures in the axisymmetric jet mixing layer p 593 N93-14057
An experimental and computational study of longitudinal vortices in turbulent boundary layers p 595 N93-14097

TURBULENT BOUNDARY LAYER
Features of vorticity in fully turbulent flows p 583 N93-13334
The three-dimensional turbulent boundary layer: Theory and application p 588 N93-13749
A multiple-view visual study of the inner/outer region interactions of coherent motions in a turbulent boundary layer p 591 N93-13937

Turbulent boundary layers with high turbulence: Experimental heat transfer and structure on flat and convex walls p 591 N93-13938
Organized turbulent structures and their induced wall pressure fluctuations p 592 N93-13952
Flow prediction for three-dimensional intakes and ducts using viscous-inviscid interaction methods p 592 N93-13953
A low-dimensional dynamical systems description of coherent structures in the axisymmetric jet mixing layer p 593 N93-14057
An experimental and computational study of longitudinal vortices in turbulent boundary layers p 595 N93-14097

TURBULENT DIFFUSION
Comparison of two stochastic models of scalar diffusion in turbulent flow [DE92-019381] p 576 N93-12912

TURBULENT FLOW
On the prediction of turbulent secondary flows [NASA-CR-189722] p 575 N93-12717
Comparison of two stochastic models of scalar diffusion in turbulent flow [DE92-019381] p 576 N93-12912
Calibration of 2D unstructured grid methods on propulsive flowfields p 582 N93-13225
Features of vorticity in fully turbulent flows p 583 N93-13334
The program FANS-3D (finite analytic numerical simulation 3-dimensional) and its applications p 586 N93-13399
A PDF closure model for compressible turbulent chemically reacting flows [NASA-CR-191209] p 587 N93-13453
Wall functions for the kappa-epsilon turbulence model in generalized nonorthogonal curvilinear coordinates p 587 N93-13517
Velocity and temperature measurements in a non-premixed reacting flow behind a backward facing step p 494 N93-13632
Limits on galactic dynamo theory due to magnetic fluctuations p 754 N93-13636
Numerical investigation of the flow field in the head-end, star grain section of a solid rocket motor during ignition transients p 526 N93-13818
Computer modeling of flow and transport interactions for compressible Navier-Stokes equations p 589 N93-13825
Cascade processes and fully developed turbulence p 591 N93-13901
A multiple-view visual study of the inner/outer region interactions of coherent motions in a turbulent boundary layer p 591 N93-13937
Organized turbulent structures and their induced wall pressure fluctuations p 592 N93-13952
Instabilities and patterns in Taylor-Couette flow p 593 N93-13965
Spatial characteristics of coherent turbulent structures and exchange processes in the atmospheric surface layer within and above an orchard canopy p 660 N93-14064

TURBULENT MIXING
Studies on turbulent mixing in stratified turbulent patches p 587 N93-13532

TWO DIMENSIONAL BOUNDARY LAYER
A compressible boundary layer algorithm for use with SINDA '85 p 585 N93-13395
Turbulent boundary layers with high turbulence: Experimental heat transfer and structure on flat and convex walls p 591 N93-13938
An experimental and computational study of longitudinal vortices in turbulent boundary layers p 595 N93-14097

TWO DIMENSIONAL FLOW
The multidimensional self-adaptive grid code, SAGE [NASA-TM-103905] p 683 N93-12719
Boundary element methods for two-dimensional, coupled, thermoviscous flow p 584 N93-13383
Mathematical problems in inviscid hypersonic flow p 493 N93-13451
Variational characterizations of steady two-dimensional vortex motions p 589 N93-13781
Overall effects of separation on thin aerofoils [ISBN-0-315-67464-4] p 496 N93-13930

TWO DIMENSIONAL MODELS
Effects of stratospheric aerosol surface processes on the LLNL two-dimensional zonally averaged model [DE92-019620] p 646 N93-13646
Transonic aeroelastic analysis of systems with structural nonlinearities p 629 N93-13769
Finite element study of ultrasonic imaging p 700 N93-13774
Structure of and dynamical processes in the Earth's magnetopause and boundary layer regions p 657 N93-13793
Structures, spectra and inertial range transfer in two-dimensional and beta-plane turbulence p 590 N93-13900
Development of two-dimensional parametric radar signal modeling and estimation techniques with application to target identification [AD-A252602] p 567 N93-13939
Compressible convection and pulsations on parallel computers p 690 N93-13961
Coherent structures in compressible convection p 592 N93-13964
A numerical study of hypersonic flows using the full Navier-Stokes equations with different air models p 594 N93-14061

TWO PHASE FLOW
Adaptation of multidimensional group particle tracking and particle wall-boundary condition model to the FDNS code [SECA-TR-92-06] p 575 N93-12689
An experimental study of a small high-speed LH2 pump for rockets: Fluid dynamic performance [NAL-TR-1131] p 610 N93-12727
Fundamentals of enhanced scalar transport in strongly oscillating and/or resonant flow fields as created by pulse combustion [DE92-012147] p 582 N93-13247
Two-phase flow modeling with discrete particles [DE92-017850] p 583 N93-13356
Analysis of a space emergency ammonia dump using the FLOW-NET two-phase flow program p 584 N93-13389
Development status of SINDA/FLUINT and SINAPS p 585 N93-13393
Aerospace applications of SINDA/FLUINT at the Johnson Space Center p 586 N93-13401
Two-phase/two-phase heat exchanger simulation analysis p 586 N93-13402
Numerical investigation of non-spherical droplet dynamics in viscous convective flows p 591 N93-13918

U

U.S.S.R.
JPRS report: Science and technology. USSR: Space [JPRS-USP-91-004] p 516 N93-13756

UH-60A HELICOPTER
The relationship between environmental conditions and UH-60 cockpit temperature [AD-A255918] p 680 N93-14090

ULTRAHIGH FREQUENCIES
Review of spaceborne and airborne SAR systems p 565 N93-13060
Polarimetric signatures of a canopy of dielectric cylinders based on first and second order vector radiative transfer theory p 569 N93-13088

ULTRASONIC FLAW DETECTION
Review of progress in quantitative NDE [DE92-018814] p 620 N93-13071

ULTRASONIC RADIATION
Icing prevention by ultrasonic nucleation of supercooled water droplets in front of subsonic aircraft [DOT/FAA/CT-TN92/38] p 497 N93-12816

ULTRASONIC TESTS
Physical interpretation and development of ultrasonic nondestructive evaluation techniques applied to the quantitative characterization of textile composite materials [NASA-CR-190962] p 620 N93-13435

ULTRASONICS
Finite element study of ultrasonic imaging p 700 N93-13774

ULTRAVIOLET EMISSION
The Jovian ultraviolet aurora observed with the IUE spacecraft: Brightness and color distribution with longitude p 759 N93-13625

ULTRAVIOLET LASERS
Methods for efficient pumping of vacuum ultraviolet lasers p 606 N93-13626

ULTRAVIOLET RADIATION
Z306 molecular contamination ad hoc committee results p 546 N93-12774
Ultraviolet disinfection technology assessment [PB92-222868] p 678 N93-12983

ULTRAVIOLET SPECTRA
International Ultraviolet Explorer (IUE) ultraviolet spectral atlas of selected astronomical objects [NASA-RP-1285] p 744 N93-13461
HARDI: A high angular resolution deployable interferometer for space p 745 N93-13588
Required technologies for a lunar optical UV-IR synthesis array p 747 N93-13598
An analysis of the Voyager 2 ultraviolet spectrometer occultation data at Uranus and Triton: Inferring heat sources and model atmospheres p 768 N93-14072

ULTRAVIOLET SPECTROSCOPY
Comparison of cometary comae using ultraviolet spectroscopy: Composition and variation p 753 N93-13603

ULTRAVIOLET TELESCOPES
The ALEXIS experiment: Current status and performance [DE92-018601] p 524 N93-13516

UMBRAS
An infrared polarimetric study of sunspots p 770 N93-13627

UNDERGROUND STORAGE
Application of passive dosimetry for detection of leaking underground storage tanks [PB92-218270] p 559 N93-13648

UNDERWATER ACOUSTICS
Visualization of scattering strength of elastic bodies in a fluid [AD-A254535] p 699 N93-12601
Adaptive array processing in uncertain inhomogeneous media [AD-A254418] p 560 N93-12608

UNDERWATER COMMUNICATION
Extremely low frequency/very low frequency Generator [AD-A254347] p 562 N93-12948

UNDERWATER EXPLOSIONS
Data to test and evaluate the performance of neural network architectures for seismic signal discrimination, volume 1 [AD-A254413] p 691 N93-12607

UNITED KINGDOM
United Kingdom Infrared Telescope p 743 N93-13273

UNITED STATES
Gateway to diversity in the scientific and technological workforce [NSF-92-99] p 730 N93-13278
State award summary: Fiscal Year 1991 [NSF-92-3] p 775 N93-13381
Lateral variations of shear velocity and anelasticity in the upper mantle of the western US from Rayleigh wave observations p 653 N93-13492
Federal support to universities, colleges, and nonprofit institutions: Fiscal year 1990. A report to the President and Congress [NSF-92-324] p 741 N93-13543
Academic science and engineering: R/D expenditures, fiscal year 1990 [NSF-92-321] p 741 N93-13544
US Industry Access to Japanese Science and Technology: Proceedings of a conference [PB92-167964] p 741 N93-13788

UNIVERSE
Preferred sets of states, predictability, classicality, and the environment-induced decoherence [DE92-017447] p 641 N93-12684

UNIVERSITIES
USAF 1990 research initiation program, volume 2 [AD-A254654] p 773 N93-12663
USAF 1990 research initiation program, volume 4 [AD-A254655] p 773 N93-12664
USAF 1990 research initiation program, volume 1 [AD-A254656] p 773 N93-12665
Summary of awards, fiscal year 1990 [NSF-92-70] p 683 N93-12693
Selected data on federal support to universities and colleges: Fiscal year 1990 [NSF-92-310] p 740 N93-12920
Blacks in undergraduate science and engineering education [NSF-92-305] p 730 N93-13015
Gateway to diversity in the scientific and technological workforce [NSF-92-99] p 730 N93-13278
Scientific and engineering research facilities at universities and colleges: 1992 [NSF-92-325] p 506 N93-13407
Summary of awards. Fiscal year 1991 [NSF-92-36] p 681 N93-13431
Summary of awards: Applied mathematics. Fiscal year 1991 [NSF-92-38] p 681 N93-13438
Federal support to universities, colleges, and nonprofit institutions: Fiscal year 1990. A report to the President and Congress [NSF-92-324] p 741 N93-13543
Academic science and engineering: R/D expenditures, fiscal year 1990 [NSF-92-321] p 741 N93-13544
Selected data on Science and Engineering Doctorate Awards: 1991 [NSF-92-309] p 731 N93-13698
Science and engineering degrees: 1966-1990 [NSF-92-326] p 731 N93-13701

Fiscal Year 1991 highlights
[NSF-92-23] p 731 N93-13702

UNIVERSITY PROGRAM
USAF 1990 research initiation program, volume 4
[AD-A254655] p 773 N93-12664
USAF 1990 research initiation program, volume 1
[AD-A254656] p 773 N93-12665
US Air Force 1989 research initiation program, volume 1
[AD-A254457] p 774 N93-12764
US Air Force 1989 research initiation program, volume 4
[AD-A254458] p 774 N93-12765
US Air Force 1989 research initiation program, volume 2
[AD-A254459] p 774 N93-12766
US Air Force 1989 research initiation program, volume 3
[AD-A254460] p 774 N93-12767
USAF 1990 research initiation program, volume 3
[AD-A254755] p 775 N93-12849
Selected data on federal support to universities and colleges: Fiscal year 1990
[NSF-92-310] p 740 N93-12920
Small planetary mission plan: Report to Congress
[NASA-TM-107809] p 513 N93-13266

UNIX (OPERATING SYSTEM)
An interactive office accounting program written in UNIX and C
[AD-A255077] p 683 N93-12740

UNMANNED SPACECRAFT
On-orbit supervisor for controlling spacecraft
[AD-A254342] p 522 N93-12962
Summary of literature on unmanned probes to asteroids and precursor data requirements for IAM
p 514 N93-13551

UNSTEADY AERODYNAMICS
An investigation of the dynamic response of lifting surfaces with concentrated structural nonlinearities
p 501 N93-13807
The unsteady aerodynamics of a delta wing undergoing large-amplitude pitching motions p 496 N93-13929

UNSTEADY FLOW
Intake and exhaust noise
[ISVR-TR-207] p 699 N93-12714
Navier-Stokes simulations of unsteady transonic flow phenomena
[NASA-TM-103962] p 491 N93-12721
Computation of steady and unsteady shock-induced combustion over hypervelocity blunt bodies
p 536 N93-12836
Mathematical problems in inviscid hypersonic flow
p 493 N93-13451
Numerical investigation of the flow field in the head-end, star grain section of a solid rocket motor during ignition transients p 526 N93-13818
Compressible convection and pulsations on parallel computers p 690 N93-13961

UPLINKING
Anomalous TWTA output power spikes and their effect on a digital satellite communications system
[NASA-TM-105875] p 571 N93-13286

UPPER ATMOSPHERE
Comprehensive mappings of electron precipitation and its effects on the comprehensive mappings of electron precipitation and its effects on the atmosphere
[AD-A254665] p 648 N93-12621
Infrared emission from the water outgas cloud of an orbiting vehicle induced by collisions with atmospheric gases p 521 N93-13854

UPPER ATMOSPHERE RESEARCH SATELLITE (UARS)
Spectroscopy for remote sounding of the atmosphere
p 659 N93-14054

UPPER SURFACE BLOWING
High-speed aerodynamics of upper surface blowing aircraft configurations p 494 N93-13729

UPWIND SCHEMES (MATHEMATICS)
A numerical study of hypersonic flows using the full Navier-Stokes equations with different air models
p 594 N93-14061

URANUS (PLANET)
An analysis of the Voyager 2 ultraviolet spectrometer occultation data at Uranus and Triton: Inferring heat sources and model atmospheres p 768 N93-14072

URANUS ATMOSPHERE
An analysis of the Voyager 2 ultraviolet spectrometer occultation data at Uranus and Triton: Inferring heat sources and model atmospheres p 768 N93-14072

URBAN DEVELOPMENT
Federal support to universities, colleges, and nonprofit institutions: Fiscal year 1990. A report to the President and Congress
[NSF-92-324] p 741 N93-13543

UREAS
Hydrothermal organic synthesis experiments
[NASA-CR-191257] p 672 N93-13457

URINE
The identification and quantitation of triamterene in blood and urine from a fatal aircraft accident
[AD-A254550] p 674 N93-12612
Distribution of human waste samples in relation to sizing waste processing in space p 680 N93-14001

USER MANUALS (COMPUTER PROGRAMS)
Stability codes for a liquid rocket implemented for use on a PC
[NASA-CR-184453] p 525 N93-12659
Users manual for program SSFREQ intermediate mode stability curves: Developed for use on a PC computer
[NASA-CR-184452] p 682 N93-12675
Users manual for program ADMIT: Admittance and pressure transfer function developed for use on a PC computer
[NASA-CR-184450] p 682 N93-12676
An interactive office accounting program written in UNIX and C
[AD-A255077] p 683 N93-12740
User's guide: Computer-Aided Structural Modeling (CASM), version 3.00
[AD-A255074] p 684 N93-12851
Engineering Design Information System (EDIS) Information Services Division (ISD) index function: User's manual
[DE92-041242] p 736 N93-13048
Introduction to IND and recursive partitioning, version 1.0
[NASA-CR-191220] p 685 N93-13063
Test and control computer user's guide for a digital beam former test system
[NASA-CR-189208] p 685 N93-13291
Providing structural modules with self-integrity monitoring software user's manual
[NASA-CR-190877] p 628 N93-13707
Circuit design tool. User's manual, revision 2
[NASA-CR-191361] p 687 N93-13734

USER REQUIREMENTS
Coordinating Council. Sixth Meeting: Who Are Our Key Users?
[NASA-TM-108021] p 734 N93-12672
Coordinating Council. Eighth Meeting: Using the Internet
[NASA-TM-108019] p 734 N93-12673

UTILIZATION
Utilization of databases to manage resources
[DE92-019598] p 735 N93-12808

V

V/STOL AIRCRAFT
ASTOVL model engine simulators for wind tunnel research p 507 N93-13213

VACANCIES (CRYSTAL DEFECTS)
Oxygen diffusion in high-T(c) superconductors
[DE92-019597] p 720 N93-12807
A study of the vacancy loop formation probability in Ni-Cu and Ag-Pd alloys
[DE92-019584] p 541 N93-12879
Influence of dilute impurities on the evolution of defect cascades in nickel
[DE92-019585] p 542 N93-12973

VACUUM
The possibility of concrete production on the Moon
p 554 N93-13988

VACUUM CHAMBERS
High temperature superconductor materials and applications
[NASA-CR-184437] p 719 N93-12691

VACUUM DEPOSITION
Ion-beam-assisted deposition of MoS2 and other low-friction films
[AD-A255222] p 554 N93-13862

VACUUM EFFECTS
Lunar concrete for construction p 555 N93-13990

VALLEYS
Tributary and gap nighttime air flow comparisons
[DE92-018875] p 662 N93-13075

VALVES
Demand thrust pumped propulsion with automatic warm gas valving
[DE92-017435] p 525 N93-12840

VANES
The VTRE Program: An overview p 512 N93-13182

VAPOR DEPOSITION
Thermal barrier coating life prediction model development, phase 2
[NASA-CR-189111] p 544 N93-12589
Alternate electrode materials for the SP100 reactor
[DE92-019570] p 706 N93-12970
Novel thin-film CuInSe2 fabrication
[DE92-016440] p 723 N93-13526

VAPOR PHASE EPITAXY
Epitaxial growth of silicon and germanium for solar cells
[ITN-92-85168] p 722 N93-13268

VAPOR PHASES
Correlation for non-linear infrared calibration curves
[AD-A255098] p 596 N93-12653

VAPOR PRESSURE
Vapor pressure data analysis methodology, statistics, and applications
[AD-A255090] p 536 N93-12743

VAPORIZING
Effect of vaporization on cryogenic spray dropsize measurement
[NASA-TM-105909] p 597 N93-13410

VAPORS
Correlation for non-linear infrared calibration curves
[AD-A255098] p 596 N93-12653
Vapor to liquid ratio test as an indicator of volatility
[DOT/FAA/CT-TN92/40] p 537 N93-12897
The influence of mixture preparation in the intake port on the performance of a spark-ignited four-stroke engine
p 613 N93-13331

VARIABILITY
A meteorology-based approach to detecting response source-receptor relationships p 664 N93-13736
Intraseasonal variability of infrared cooling rates during the Asian summer monsoon and their influence on intraseasonal waves p 665 N93-13760

VARIABLE STARS
Radial and nonradial periods and growth rates of an AI Velorum model
[DE92-011369] p 743 N93-13339

VARIABLE THRUST
Performance and control of ascending trajectories to minimize heat load for transatmospheric aero-space planes p 495 N93-13745

VARIANCE (STATISTICS)
Bayesian analysis of linear and nonlinear population models using the Gibbs sampler
[AD-A254769] p 697 N93-12702

VARIATIONAL PRINCIPLES
Fermi molecular dynamics
[DE92-015351] p 703 N93-13187
Variational characterizations of steady two-dimensional vortex motions p 589 N93-13781

VAX COMPUTERS
Running SINDA '85/FLUINT interactive on the VAX
p 584 N93-13390

VECTOR SPACES
A new matrix formulation of classical electrodynamics. Part 2: Wave propagation in optical materials of infinite extent
[AD-A255032] p 560 N93-12585

VECTORS (MATHEMATICS)
Implementation details of the coupled QMR algorithm
[NASA-CR-191213] p 684 N93-12801
Fast multiresolution algorithms for matrix-vector multiplication
[NASA-CR-189721] p 696 N93-12942
Application of Lanczos vectors to control design of flexible structures, part 2
[NASA-CR-191244] p 685 N93-13030
Polarimetric signatures of a canopy of dielectric cylinders based on first and second order vector radiative transfer theory p 569 N93-13088

VEGETABLES
Crop growth and associated life support for a lunar farm p 680 N93-13994

VEGETATION
Integration of vegetation indices and thermal measurements for ecosystem modeling
p 646 N93-13721

VEGETATION GROWTH
Engineering verification of the biomass production chamber p 680 N93-13996
Statistical relationships between tree growth and climate in western North America p 648 N93-14096

VELOCITY DISTRIBUTION
The electrostatic wake of a superthermal test electron in a magnetized plasma
[DE92-019394] p 713 N93-12873
Evolution of galaxies in compact groups
p 750 N93-13148
The jet behaviour of an actual high-bypass engine as determined by LDA-measurements in ground tests
p 503 N93-13218
Fundamentals of enhanced scalar transport in strongly oscillating and/or resonant flow fields as created by pulse combustion
[DE92-012147] p 582 N93-13247
Electron impact polarization expected in solar EUV lines from flaring chromospheres/transition regions
[SSL-PREPRINT-90-124] p 770 N93-13478
A theoretical investigation of the growth rates of ice crystals in clouds p 653 N93-13485

Wall functions for the kappa-epsilon turbulence model in generalized nonorthogonal curvilinear coordinates
p 587 N93-13517
Velocity and temperature measurements in a non-premixed reacting flow behind a backward facing step
p 494 N93-13632
Aspects of atmospheric transport and dispersion within an air basin
p 656 N93-13782
An experimental investigation of the three-dimensional boundary layer on a rotating disk
p 589 N93-13806
Dynamics of vortex rings in cross-flow
p 496 N93-13917
A low-dimensional dynamical systems description of coherent structures in the axisymmetric jet mixing layer
p 593 N93-14057

VELOCITY MEASUREMENT
The VELOPT code for estimating performance of a Fabry-Perot velocimeter
[DE92-015566]
p 596 N93-12831
Quantitative analysis of three-dimensional steady flow field by using particle image velocimetry and digital image processing method
p 577 N93-13017
The jet behaviour of an actual high-bypass engine as determined by LDA-measurements in ground tests
p 503 N93-13218
On development of a three-dimensional particle motion tracking system
[DE92-015846]
p 704 N93-13263
Diagnostic of shock wave processes
[DE92-018059]
p 565 N93-13357
Planar measurement of flow field parameters in nonreacting supersonic flows with laser-induced iodine fluorescence
p 495 N93-13801
Airfoil-vortex interaction and the wake of an oscillating airfoil
p 495 N93-13803

VENTILATION
Flow through horizontal vents as related to compartment fire environments
[PB92-213388]
p 559 N93-13642

VENTING
The VTRE Program: An overview
p 512 N93-13182
Analysis of a space emergency ammonia dump using the FLOW-NET two-phase flow program
p 584 N93-13389

VENTS
Flow through horizontal vents as related to compartment fire environments
[PB92-213388]
p 559 N93-13642

VENUS ATMOSPHERE
SO2 on Venus: A final cross-calibration with Pioneer Venus
[NASA-CR-191256]
p 758 N93-13344
Model studies of the middle atmosphere of Venus
p 759 N93-13831

VERTICAL AIR CURRENTS
A parameterized quasi-five-cylinder convective cloud model and its application to remote sensing of rainfall
p 663 N93-13489
Nonlinear hydrostatic conditional symmetric instability: Some theoretical and modeling considerations
p 655 N93-13757
Coherent structures in compressible convection
p 592 N93-13964

VERTICAL MOTION
SAC contrail formation study
[AD-A254410]
p 499 N93-12605
Deep convection and its relation to the large-scale circulation in the tropical Pacific
p 654 N93-13725

VERY LARGE ARRAY (VLA)
A high-resolution radio survey of the galactic plane
p 744 N93-13480
The optical very large array and its moon-based version
p 745 N93-13583
An optical VLA on the Moon
p 747 N93-13596
Report of the Working Design Group
p 748 N93-13601

VERY LARGE SCALE INTEGRATION
Silicon neuron
[AD-A255091]
p 674 N93-12756
BETA: Behavioral testability analyzer and its application to high-level test generation and synthesis for testability
[NASA-CR-191282]
p 572 N93-13569

VERY LONG BASE INTERFEROMETRY
GPS measurements at Vandenberg AFB
[AD-A254978]
p 499 N93-12557
Analysis of space geodetic measurements for studying the dynamics of the solid Earth
[NASA-CR-191215]
p 649 N93-12661
The Mount Wilson optical interferometer: The first automated instrument and the prospects for lunar interferometry
p 745 N93-13582
High resolution imaging at Palomar
p 745 N93-13584
Orbiting Space Interferometer (OSI): A first generation space interferometer
p 745 N93-13587
Appendix: Limits on the use of heterodyning and amplification in optical interferometry
p 747 N93-13597

VERY LOW FREQUENCIES
Extremely low frequency/very low frequency Generator
[AD-A254347]
p 562 N93-12948
Long-term averages of globally-measured ELF/VLF radio noise
[AD-A255518]
p 566 N93-13869

VIBRATION
Large-amplitude plate vibration in an elevated thermal environment
[AD-A254411]
p 621 N93-12606
Initial experiments in end-point control of a flexible, two-link manipulator
p 612 N93-13018
The lunar environment and its effect on optical astronomy
p 746 N93-13594
Proceedings of the 62nd Shock and Vibration Symposium, Volume 2
[AD-A249267]
p 628 N93-13637

VIBRATION DAMPING
Dynamic control modification techniques in teleoperation of a flexible manipulator
[NASA-CR-190984]
p 610 N93-12904
The application of input shaping to a system with varying parameters
p 612 N93-12954
Initial experiments in end-point control of a flexible, two-link manipulator
p 612 N93-13018
Active flutter suppression using dipole filters
[NASA-TM-107594]
p 504 N93-13367
Force and motion control of a constrained flexible manipulator
p 613 N93-13384
Method and apparatus for minimizing multiple degree of freedom vibration transmission between two regions of a structure
[NASA-CASE-LAR-14508-1-CU]
p 626 N93-13420
Vibration damping response of composite materials
p 533 N93-13748
Application of adaptive trusses to vibration isolation in flexible structures
p 617 N93-13809
Improved damping in composite structures through stress coupling, co-cured damping layers, and segmented stiffness layers
p 630 N93-13823

VIBRATION EFFECTS
The Orbiter Stability Experiment on STS-40
p 508 N93-13159
Post flight operation of a high peak power neodymium YAG laser aboard the G-449 payload flown on Space Shuttle Columbia mission 61-C
p 508 N93-13161

VIBRATION ISOLATORS
Application of adaptive trusses to vibration isolation in flexible structures
p 617 N93-13809

VIBRATION MODE
Experimental validation of finite element and boundary element methods for predicting structural vibration and radiated noise
p 621 N93-12631
Analysis of a structure-equipment system subjected to impact loading
[AD-A255097]
p 622 N93-12652

VIBRATION TESTS
Environmental qualification testing of payload G-534, the Pool Boiling Experiment
p 510 N93-13169
Test plan and report for Space Shuttle launch environment testing of Bergen cable technology safety cable
[NASA-CR-4473]
p 559 N93-13434
Design guide for the ergonomic aspects of helicopter crew seating
[ISVR-TR-209]
p 678 N93-13464

VIBRATIONAL SPECTRA
The vibrational spectrum of H2O3: An ab initio investigation
[NASA-CR-190968]
p 537 N93-12935
Studies of orbital doublet and modelling of orbital triplet Jahn-Teller systems in 3 to 5 semiconductors
p 725 N93-13845

VIDEO DATA
Digital imaging systems
[DE92-019194]
p 736 N93-13078

VIDEO DISKS
Efficacy of multimedia instruction and an introduction to digital multimedia technology
[AD-A254509]
p 734 N93-12723

VIDEO TAPES
Efficacy of multimedia instruction and an introduction to digital multimedia technology
[AD-A254509]
p 734 N93-12723

VIKING ORBITER SPACECRAFT
Volcanism in the eastern Hellas region of Mars: The geology of Hadriaca and Tyrrhena Paterae
p 768 N93-14092

VIRTUAL MEMORY SYSTEMS
Memory access in shared virtual memory
[DE92-019594]
p 681 N93-12823

VISCOELASTICITY
Finite element analysis of anisotropic viscoelastic composite structures and analytical determination of optimum viscoelastic material properties
p 530 N93-13007
Vibration damping response of composite materials
p 533 N93-13748
Application of complex variables in electromagnetofluid dynamic, magnetofluid dynamic and fluid dynamic flows: Viscoelastic boundary-layer theory
[ISBN-0-315-65141-5]
p 594 N93-14067

VISCOPLASTICITY
An investigation of the thermoviscoplastic behavior of a metal matrix composite at elevated temperatures
[NASA-CR-189706]
p 530 N93-12929
Analysis of large quasistatic deformations of inelastic solids by a new stress based finite element method
[NASA-CR-189235]
p 626 N93-13260
Thermoviscoplastic analysis of metal matrix composites
p 535 N93-13954

VISCOSITY
Scientific predictability of solid rocket performance: Analyses of the processing parameters
p 526 N93-13824
The formation of ore mineral deposits on the Moon: A feasibility study
p 760 N93-13974

VISCOUS FLOW
An attempt at a status report on a fast-moving target: CFD --- computational fluid dynamics
[DE92-017432]
p 576 N93-12839
Boundary element methods for two-dimensional, coupled, thermoviscous flow
p 584 N93-13383
A compressible boundary layer algorithm for use with SINDA '85
p 585 N93-13395
Development and computation of continuum higher order constitutive relations for high-altitude hypersonic flow
p 494 N93-13578
Solution of viscous flow problems by using the boundary element method
p 588 N93-13609
Application of a vectorized particle simulation to the study of plates and wedges in high-speed rarefied flow
p 495 N93-13746
Linear stability theory of hypersonic, chemically reacting viscous flows
p 588 N93-13765
A time domain numerical theory for studying steady-state acoustic disturbance in flow
p 700 N93-13770
Structure of and dynamical processes in the Earth's magnetopause and boundary layer regions
p 657 N93-13793
Computer modeling of flow and transport interactions for compressible Navier-Stokes equations
p 589 N93-13825
Numerical investigation of non-spherical droplet dynamics in viscous convective flows
p 591 N93-13918
Unsteady three-dimensional thin-layer Navier-Stokes solutions for turbomachinery in transonic flow
p 593 N93-14025

VISCOUS FLUIDS
Solution of viscous flow problems by using the boundary element method
p 588 N93-13609

VISION
Functional MRI studies of human vision on a clinical imager
[DE92-017448]
p 674 N93-12566

VISUAL AIDS
Efficacy of multimedia instruction and an introduction to digital multimedia technology
[AD-A254509]
p 734 N93-12723

VISUAL OBSERVATION
A study of the luminosity produced by an electron beam-emitting rocket in the polar ionosphere: ECHO 7
p 657 N93-13830

VISUAL STIMULI
Perceptual dimensions of visual scenes relevant for simulating low-altitude flight
[AD-A254645]
p 676 N93-12662

VOICE CONTROL
Ocular attention-sensing interface system
[NASA-CR-190884]
p 678 N93-13450

VOICE DATA PROCESSING
Transputer implementation of the TRACE model of speech recognition
[AD-A254747]
p 689 N93-12846
Perception-based and machine-oriented signal processing within speech understanding systems
p 692 N93-13239
MINT: The multiple error LMS algorithm, and the design of inverse filters for multi-channel sound reproduction systems
[ISVR-TR-211]
p 700 N93-13439
Talking to InterFIS: Adding speech input to a natural language interface
[AD-A255865]
p 688 N93-13942

VOID RATIO
Hyperbolic conservation laws with umbilic points, 1
[AD-A254431] p 696 N93-12594
VOIDS
Ductile fracture process of discontinuous fiber reinforced composites
[DE92-016298] p 531 N93-13264
VOLATILITY
Vapor to liquid ratio test as an indicator of volatility
[DOT/FAA/CT-TN92/40] p 537 N93-12897
VOLCANOES
The morphotectonic fabric of the East Pacific Rise: Implications for fault generation and crustal accretion
p 652 N93-13481
Effects of the Mt. Pinatubo eruption on the radiative and chemical processes in the troposphere and stratosphere
[DE92-019618] p 646 N93-13654
VOLCANOLOGY
Volcanism in the eastern Hellas region of Mars: The geology of Hadriaca and Tyrrhena Paterae
p 768 N93-14092
VOLT-AMPERE CHARACTERISTICS
Noise measurements of YBa2Cu3O7 thin film high-temperature superconductors p 726 N93-13933
VOLTAGE REGULATORS
Battery selection for space experiments
p 512 N93-13184
VOLUMETRIC ANALYSIS
Journal of Research of the National Institute of Standards and Technology, May-June 1992, volume 97, number 3
[PB92-217637] p 698 N93-12805
VORTEX GENERATORS
NATO Advanced Research Workshop: Vortex Flows and Related Numerical Methods. List of participants, book of abstracts, and instructions for submission to the proceedings
[AD-A255015] p 575 N93-12708
VORTEX RINGS
Dynamics of vortex rings in cross-flow
p 496 N93-13917
VORTICES
NATO Advanced Research Workshop: Vortex Flows and Related Numerical Methods. List of participants, book of abstracts, and instructions for submission to the proceedings
[AD-A255015] p 575 N93-12708
Spanwise-nonuniform excitation of a plane mixing layer p 577 N93-13120
The influence of intake swirl distortion on the steady-state performance of a low bypass, twin-spool engine p 579 N93-13211
The jet behaviour of an actual high-bypass engine as determined by LDA-measurements in ground tests
p 503 N93-13218
In-flight flow visualization results from the X-29A aircraft at high angles of attack
[NASA-TM-4430] p 493 N93-13322
Chaotic vortical motion in the near region of a plane jet p 493 N93-13493
The kinetic energy budget of tropical plumes and ENSO in NMC and ECMWF analyses p 664 N93-13740
Variational characterizations of steady two-dimensional vortex motions p 589 N93-13781
Airfoil-vortex interaction and the wake of an oscillating airfoil p 495 N93-13803
The growth of disturbances in barotropic models of the atmosphere p 658 N93-13887
The unsteady aerodynamics of a delta wing undergoing large-amplitude pitching motions p 496 N93-13929
A multiple-view visual study of the inner/outer region interactions of coherent motions in a turbulent boundary layer p 591 N93-13937
Instabilities and patterns in Taylor-Couette flow
p 593 N93-13965
Spatial characteristics of coherent turbulent structures and exchange processes in the atmospheric surface layer within and above an orchard canopy
p 660 N93-14064
An experimental and computational study of longitudinal vortices in turbulent boundary layers
p 595 N93-14097
VORTICITY
The role of latent heat release in explosive cyclogenesis
[AD-A254436] p 660 N93-12596
An analysis of the tornado-producing Raleigh thunderstorm of November 28, 1988
[AD-A254384] p 661 N93-12862
Spanwise-nonuniform excitation of a plane mixing layer p 577 N93-13120
Features of vorticity in fully turbulent flows
p 583 N93-13334
A theoretical investigation of the growth rates of ice crystals in clouds p 653 N93-13485
Structures, spectra and inertial range transfer in two-dimensional and beta-plane turbulence
p 590 N93-13900
VULNERABILITY
The estimation of electrical cable fire-induced damage limits
[DE92-040100] p 572 N93-13519

W

WAFERS
Latent image exposure monitor using scatterometry
[DE92-019427] p 604 N93-12915
The ROMPS robot in HitchHiker p 511 N93-13179
Quantum well, beam deflecting surface emitting lasers
[NASA-CASE-NPO-18243-1-CU] p 605 N93-13418
WAKES
The electrostatic wake of a superthermal test electron in a magnetized plasma
[DE92-019394] p 713 N93-12873
Features of vorticity in fully turbulent flows
p 583 N93-13334
Airfoil-vortex interaction and the wake of an oscillating airfoil p 495 N93-13803
WALKING
Robotic exploration of surfaces and its application to legged locomotion p 615 N93-13540
WALKING MACHINES
Robotic exploration of surfaces and its application to legged locomotion p 615 N93-13540
Mobile work platform for initial lunar base construction
p 559 N93-14009
WALL FLOW
Application of a solution adaptive grid to flow over an embedded cavity p 492 N93-13141
Skin friction measurements in high temperature high speed flows p 595 N93-13670
WALL PRESSURE
Organized turbulent structures and their induced wall pressure fluctuations p 592 N93-13952
WALL TEMPERATURE
Implicitly coupling heat conduction into a zone fire model
[PB92-222769] p 558 N93-12980
WALLS
Adaptation of multidimensional group particle tracking and particle wall-boundary condition model to the FDNS code
[SECA-TR-92-06] p 575 N93-12689
The effects of pressure gradients on convective heat flux predictions in engine environments
p 616 N93-13772
Turbulent boundary layers with high turbulence: Experimental heat transfer and structure on flat and convex walls p 591 N93-13938
WASTE DISPOSAL
Proceedings of the Mediterranean Conference on Environmental Geotechnology
[AD-A253672] p 644 N93-13098
Energy from Municipal Waste Program
[DE92-010578] p 638 N93-13102
Use of antarctic analogs to support the space exploration initiative
[NASA-TM-108000] p 651 N93-13326
Radiation-disorder and aperiodicity in irradiated ceramics
[DE92-015051] p 552 N93-13350
Technology development for lunar base water recycling p 680 N93-13999
Plasma reactor waste management systems
p 680 N93-14000
Distribution of human waste samples in relation to sizing waste processing in space p 680 N93-14001
WASTE ENERGY UTILIZATION
Energy from Municipal Waste Program
[DE92-010578] p 638 N93-13102
WASTE TREATMENT
ReTech, Inc., Plasma Centrifugal Furnace: Applications analysis report
[PB92-218791] p 714 N93-12982
Proceedings of the Mediterranean Conference on Environmental Geotechnology
[AD-A253672] p 644 N93-13098
Use of antarctic analogs to support the space exploration initiative
[NASA-TM-108000] p 651 N93-13326
Plasma reactor waste management systems
p 680 N93-14000
WASTE UTILIZATION
Lunar base CELSS: A bioregenerative approach
p 680 N93-13993
Plasma reactor waste management systems
p 680 N93-14000
WASTE WATER
Microbiological methods for the water recovery systems test, revision 1.1
[NASA-CR-184390] p 678 N93-12966
Ultraviolet disinfection technology assessment
[PB92-222868] p 678 N93-12983
WATER
Exit plane H2O concentration measurements correlated with OH PLIF near-injector mixing measurements for scramjet flows p 603 N93-13687
Infrared emission from the water outgas cloud of an orbiting vehicle induced by collisions with atmospheric gases p 521 N93-13854
Water and cheese from the lunar desert: Abundances and accessibility of H, C, and N on the Moon
p 761 N93-13976
Lunar base CELSS: A bioregenerative approach
p 680 N93-13993
Technology development for lunar base water recycling p 680 N93-13999
Conceptual design of a lunar base thermal control system p 680 N93-14003
WATER COLOR
Ocean optical database
[AD-A254969] p 668 N93-12556
WATER CURRENTS
Acoustic tracking of neutrally buoyant float
[AD-A255086] p 669 N93-12742
WATER FLOW
Turbulent natural convection between a perforated vertical cylinder and a surrounding array
[DE92-019766] p 576 N93-12996
WATER HEATING
Solar water heating system for a lunar base
p 641 N93-14005
WATER QUALITY
Real-time quality assurance testing using photonic techniques: Application to iodine water system
[NASA-CR-184413] p 619 N93-12692
Microbiological methods for the water recovery systems test, revision 1.1
[NASA-CR-184390] p 678 N93-12966
Fiber optic sensors for environmental applications: A brief review
[DE92-040170] p 710 N93-13576
Technology development for lunar base water recycling p 680 N93-13999
WATER RECLAMATION
Real-time quality assurance testing using photonic techniques: Application to iodine water system
[NASA-CR-184413] p 619 N93-12692
Microbiological methods for the water recovery systems test, revision 1.1
[NASA-CR-184390] p 678 N93-12966
WATER TREATMENT
Real-time quality assurance testing using photonic techniques: Application to iodine water system
[NASA-CR-184413] p 619 N93-12692
Ultraviolet disinfection technology assessment
[PB92-222868] p 678 N93-12983
WATER TUNNEL TESTS
Water tunnel studies of inlet/airframe interference phenomena p 580 N93-13216
WATER VAPOR
NOAA Workshop on Climate Scale Operational Precipitation and Water Vapor Products
[NOAA-TR-NESDIS-62] p 662 N93-13066
The relationship between SST anomalies and clouds, water vapor, and their radiative effects
p 665 N93-13744
Tropopause fold investigations: Secondary circulation, water vapor and ozone analyses p 657 N93-13796
Middle atmosphere water vapour p 667 N93-13892
WATERSHEDS
The use of remotely sensed data in delineation of hydrologic response units and estimation of their rainfall-runoff model parameters p 635 N93-13840
WATERWAVE ENERGY CONVERSION
Ocean Energy Program overview, fiscal years 1990-1991
[DE91-002176] p 636 N93-12837
WAVE ATTENUATION
Regional seismograms: Attenuation and scattering
[AD-A254348] p 650 N93-12943
Lateral variations of shear velocity and anelasticity in the upper mantle of the western US from Rayleigh wave observations p 653 N93-13492
WAVE DIFFRACTION
Computer-aided design-based high-frequency electromagnetic wave scattering from complex bodies
p 567 N93-14042
WAVE DISPERSION
Fast ion-driven Bernstein instabilities
[DE92-019393] p 705 N93-12713

WAVE EQUATIONS
Phase conjugation using CO2 lasers
p 607 N93-13812
Recursive algorithms for computational electromagnetics p 567 N93-14043
WAVE FRONTS
Novel techniques of wavefront sensing for adaptive optics with array telescopes using an artificial neural network p 743 N93-13343
WAVE FUNCTIONS
Fermi molecular dynamics
[DE92-015351] p 703 N93-13187
WAVE PACKETS
Baroclinic wave packets in models and observations
p 663 N93-13361
Quantum inflationary minisuperspace cosmological models p 728 N93-13751
WAVE PROPAGATION
Angle of arrival fluctuations for millimeter waves propagating in a turbulent atmosphere near the Earth
[AD-A254478] p 560 N93-12574
A new matrix formulation of classical electrodynamics. Part 2: Wave propagation in optical materials of infinite extent
[AD-A255032] p 560 N93-12585
Wave propagation and scattering in dense geophysical media
[AD-A254573] p 561 N93-12646
Fiber optic sensors for static fracture studies and dynamic wave propagation problems
p 709 N93-12984
Variance of phase fluctuations of waves propagating through a random medium p 569 N93-13087
Power excitation by the use of a RF wiggler
[DE92-016097] p 707 N93-13192
Diagnostic of shock wave processes
[DE92-018059] p 565 N93-13357
Transverse wave motion in constrained mechanical systems p 628 N93-13634
Theoretical and numerical studies of wave propagation and scattering in inhomogeneous media
p 568 N93-14044
WAVE REFLECTION
Cancellation of air-borne acoustic plane waves obliquely incident upon a planar phased-array of active surface elements p 700 N93-13635
WAVE SCATTERING
Wave propagation and scattering in dense geophysical media
[AD-A254573] p 561 N93-12646
Regional seismograms: Attenuation and scattering
[AD-A254348] p 650 N93-12943
Guidance and scattering of electromagnetic waves by nonlinear layers p 566 N93-13813
Electromagnetic scattering simulations using equivalent boundary condition models p 569 N93-14052
WAVEFORMS
Design for reliability: Current density
[AD-A254770] p 570 N93-12866
ESPVI 4.0 electrostatic precipitator V-I and performance model: User's model
[PB92-169614] p 643 N93-12938
WAVEGUIDES
Terahertz horn antennas on thin membranes
[AD-A254772] p 562 N93-12867
Power excitation by the use of a RF wiggler
[DE92-016097] p 707 N93-13192
Analysis and experimental results for an extraction cavity for the split-cavity oscillator
[DE92-040262] p 566 N93-13512
Recursive algorithms for computational electromagnetics p 567 N93-14043
WAVELENGTHS
Instabilities and patterns in Taylor-Couette flow
p 593 N93-13965
WAVES
Effects of layer waviness on compression-loaded thermoplastic composite laminates p 532 N93-13724
WEAK INTERACTIONS (FIELD THEORY)
Test of QED using a laser at the SLAC final focus test beam
[DE92-019647] p 707 N93-12993
WEAR
Friction, wear and Raman spectroscopic characteristics of carbon lubricated surfaces p 618 N93-13949
WEAR RESISTANCE
Wastage-resistant FBC evaporator tubing through microalloying
[DE92-001256] p 541 N93-12790
WEATHER
Transhorizon microwave propagation and its relationship with meteorological conditions p 666 N93-13791
WEATHER FORECASTING
The role of latent heat release in explosive cyclogenesis
[AD-A254436] p 660 N93-12596
SAC contrail formation study
[AD-A254410] p 499 N93-12605
Extended range forecast of Atlantic seasonal hurricane activity for 1993 p 661 N93-12928
Terminal Doppler Weather Radar (TDWR) Operational Test and Evaluation (OT/E) integration test plan
[DOT/FAA/CT-TN92/6] p 499 N93-13377
WEDGES
Application of a vectorized particle simulation to the study of plates and wedges in high-speed rarefied flow
p 495 N93-13746
WEIGHT REDUCTION
Weight optimization of an aerobrake structural concept for a lunar transfer vehicle
[NASA-TP-3262] p 519 N93-13379
An investigation of dynamic stress reduction of multi-body aircraft using active gust control
p 505 N93-13916
WEIGHTLESSNESS
Zero-gravity quantity gaging system
[NASA-CR-185602] p 556 N93-12699
Establishing laboratory standards for biological flight experiments
[NASA-CR-184402] p 671 N93-12901
SLS-1 flight experiments preliminary significant results
[NASA-TM-108033] p 520 N93-13613
Bone loss and human adaptation to lunar gravity
p 676 N93-14002
WELD TESTS
Characterizing laser fusion welded aluminum using synchrotron x ray microtomography
[DE92-018608] p 609 N93-12565
WELDABILITY
Development of weldable high-strength iron aluminides
[DE92-016018] p 542 N93-13190
WELDED JOINTS
Characterizing laser fusion welded aluminum using synchrotron x ray microtomography
[DE92-018608] p 609 N93-12565
Design of a welded joint for robotic, on-orbit assembly of space trusses
[NASA-TM-108380] p 609 N93-12682
VPPA weld model evaluation
[NASA-CR-184460] p 611 N93-12919
Diagnostic of material defects found in pipelines made of 13 HMF steel on the basis of acoustic emission
p 623 N93-12989
WELDED STRUCTURES
Effects of residual stress, weld toe notch and weld defects on fatigue of welded steel structures
p 631 N93-13947
WELDING
A path to in-space welding and to other in-space metal processing technologies using Space Shuttle small payloads p 509 N93-13165
Robot welding process control
[NASA-CR-184428] p 614 N93-13436
WENTZEL-KRAMER-BRILLOUIN METHOD
Quantum inflationary minisuperspace cosmological models p 728 N93-13751
WHEAT
Field spectroradiometry and sail model application to irrigated wheat (Triticum aestivum, L) canopies spectral reflectance
[INPE-5426-TDI/483] p 634 N93-13258
Crop growth and associated life support for a lunar farm p 680 N93-13994
WHEATSTONE BRIDGES
The constant current loop: A new paradigm for resistance signal conditioning
[NASA-TM-104260] p 596 N93-12681
WHISKER COMPOSITES
Improving the temperature resistance of aluminum-matrix composites by using an acid phosphate binder p 536 N93-14056
WHITE DWARF STARS
Nucleosynthesis in nova explosions
[DE92-040349] p 753 N93-13523
WIGGLER MAGNETS
Emittance, brilliance, and bandpass issues related to an inclined crystal monochromator
[DE92-019671] p 721 N93-12881
Power excitation by the use of a RF wiggler
[DE92-016097] p 707 N93-13192
WIND (METEOROLOGY)
A smoke producing rocket motor for atmospheric wind profiling
[DE92-018264] p 555 N93-12563
Production of SSM/I data sets
[NASA-CR-190944] p 632 N93-12800
Comparison of two stochastic models of scalar diffusion in turbulent flow
[DE92-019381] p 576 N93-12912
Tributary and gap nighttime air flow comparisons
[DE92-018875] p 662 N93-13075
WIND DIRECTION
Spatial characteristics of coherent turbulent structures and exchange processes in the atmospheric surface layer within and above an orchard canopy
p 660 N93-14064
WIND EFFECTS
User's Guide for the NREL Force and Loads Analysis Program
[DE92-010579] p 627 N93-13524
User's Guide for the NREL Teetering Rotor Analysis Program (STRAP)
[DE92-010580] p 627 N93-13525
WIND MEASUREMENT
CO2 laser modeling
[NASA-CR-184455] p 604 N93-12656
WIND PROFILES
A smoke producing rocket motor for atmospheric wind profiling
[DE92-018264] p 555 N93-12563
Optical model analysis of gravity wave-critical layer interaction p 658 N93-13888
WIND SHEAR
Storm tracking for TDWR: A correlation algorithm design and evaluation
[AD-A254701] p 660 N93-12622
A parameterized quasi-five-cylinder convective cloud model and its application to remote sensing of rainfall
p 663 N93-13489
Spatial characteristics of coherent turbulent structures and exchange processes in the atmospheric surface layer within and above an orchard canopy
p 660 N93-14064
WIND TUNNEL APPARATUS
Design philosophy for wind tunnel model positioning systems
[AD-A254958] p 506 N93-12552
A fundamental study of suction for Laminar Flow Control (LFC)
[NASA-CR-191276] p 583 N93-13277
WIND TUNNEL MODELS
Design philosophy for wind tunnel model positioning systems
[AD-A254958] p 506 N93-12552
Aerodynamic integration of thrust reversers on the Fokker 100 p 502 N93-13208
Mass flow effects on the low speed characteristics of an advanced combat aircraft p 497 N93-13214
A novel-high-performance system for recording and analysing instantaneous total pressure distortion in air intakes p 580 N93-13215
Multiple-function multi-input/multi-output digital control and on-line analysis
[NASA-TM-107697] p 500 N93-13565
WIND TUNNEL TESTS
Icing prevention by ultrasonic nucleation of supercooled water droplets in front of subsonic aircraft
[DOT/FAA/CT-TN92/38] p 497 N93-12816
Test techniques for engine/airframe integration
p 577 N93-13200
Tests of models equipped with TPS in low speed ONERA F1 pressurized wind tunnel p 577 N93-13201
Detailed analysis of wing-nacelle interaction for commercial transport aircraft p 578 N93-13203
Recent developments in low-speed TPS-testing for engine integration drag and installed thrust reversr simulation p 502 N93-13207
Aerodynamic integration of thrust reversers on the Fokker 100 p 502 N93-13208
Flight analysis of air intake/engine compatibility
p 502 N93-13212
ASTOVL model engine simulators for wind tunnel research p 507 N93-13213
Mass flow effects on the low speed characteristics of an advanced combat aircraft p 497 N93-13214
A novel-high-performance system for recording and analysing instantaneous total pressure distortion in air intakes p 580 N93-13215
Comparative performance tests of a pitot-inlet in several European wind-tunnels at subsonic and supersonic speeds p 497 N93-13221
Effects of forebody strakes and Mach number on overall aerodynamic characteristics of configuration with 55 deg cropped delta wing
[NASA-TP-3253] p 493 N93-13353
Time dependent heat transfer rates in high Reynolds number hypersonic flowfields p 595 N93-13664
High-speed aerodynamics of upper surface blowing aircraft configurations p 494 N93-13729
The unsteady aerodynamics of a delta wing undergoing large-amplitude pitching motions p 496 N93-13929
Experiments on the statistical nature of stably stratified turbulence p 594 N93-14069
WIND TUNNELS
Design philosophy for wind tunnel model positioning systems
[AD-A254958] p 506 N93-12552

WIND TURBINES
User's Guide for the NREL Force and Loads Analysis Program
[DE92-010579] p 627 N93-13524
User's Guide for the NREL Teetering Rotor Analysis Program (STRAP)
[DE92-010580] p 627 N93-13525
WIND VELOCITY
Acoustic tomographic monitoring of the atmospheric boundary layer p 651 N93-13143
The assimilation of marine surface data into the Navy operational global atmospheric prediction system
[AD-A255559] p 667 N93-13877
Spatial characteristics of coherent turbulent structures and exchange processes in the atmospheric surface layer within and above an orchard canopy
p 660 N93-14064
WIND VELOCITY MEASUREMENT
Stratospheric turbulence measurements and models for aerospace plane design
[NASA-TM-104262] p 663 N93-13288
WING NACELLE CONFIGURATIONS
Detailed analysis of wing-nacelle interaction for commercial transport aircraft p 578 N93-13203
Aerodynamic analysis of slipstream/wing/nacelle interference for preliminary design of aircraft configurations p 497 N93-13205
Euler analysis of turbofan/superfan integration for a transport aircraft p 578 N93-13206
Recent developments in low-speed TPS-testing for engine integration drag and installed thrust reversr simulation p 502 N93-13207
Application of subsonic first-order panel methods for prediction of inlet and nozzle aerodynamic interactions with airframe p 497 N93-13223
High-speed aerodynamics of upper surface blowing aircraft configurations p 494 N93-13729
WING OSCILLATIONS
Airfoil-vortex interaction and the wake of an oscillating airfoil p 495 N93-13803
An experimental and computational investigation of slender wings undergoing wing rock
p 505 N93-13915
WINGS
Nonlinear stall flutter of wings with bending-torsion coupling
[AD-A254323] p 503 N93-12959
Analysis and design of planar and non-planar wings for induced drag minimization
[NASA-CR-191274] p 493 N93-13463
Transonic aeroelastic analysis of systems with structural nonlinearities p 629 N93-13769
Navier-Stokes flowfield computation of wing/rotor interaction for a tilt rotor aircraft in hover
p 497 N93-14035
WINTER
On the relationship between the intensity of extratropical frontal cyclone systems and water levels in the Gulf of Mexico p 666 N93-13816
An investigation of the effects of topography on Colorado front range winter storms p 668 N93-14063
WIRE
Synthesis and properties of novel cluster phases
[DE92-017388] p 545 N93-12697
Large-deflection analysis of cord composite plates
p 530 N93-13008
WORDS (LANGUAGE)
Semantics-based reference resolution in technical text processing: An exploration of using the Word Net database in the computerized comprehensibility system
[AD-A255068] p 736 N93-13117
WORKING FLUIDS
An experimental study of a small high-speed LH2 pump for rockets: Fluid dynamic performance
[NAL-TR-1131] p 610 N93-12727
Diffusion-absorption heat pump
[PB92-217538] p 576 N93-12975
WORKLOADS (PSYCHOPHYSIOLOGY)
Operator workload predictions for the revised AH-64A workload prediction model. Volume 2: Appendixes A through H
[AD-A254939] p 676 N93-12545
Adaptive automation and human performance: Multi-task performance characteristics
[AD-A254596] p 503 N93-12578
Theory and design of adaptive automation in aviation systems
[AD-A254595] p 499 N93-12613
WORKSTATIONS
Framework Programmable Platform for the Advanced Software Development Workstation (FPP/ASDW). Demonstration framework document. Volume 2: Framework process description
[NASA-CR-190275] p 685 N93-13004
Enterprise storage report for the 1990's
p 736 N93-13132
WORLD DATA CENTERS
A report on geomagnetic observatory operations, 1990
[PB92-224781] p 649 N93-12804
WOVEN COMPOSITES
Physical interpretation and development of ultrasonic nondestructive evaluation techniques applied to the quantitative characterization of textile composite materials
[NASA-CR-190962] p 620 N93-13435
WROUGHT ALLOYS
In-phase and out-of-phase axial-torsional fatigue behavior of Haynes 188 at 760 C
[NASA-TM-105765] p 625 N93-13153
Fatigue studies in Al-Mg-Si alloys p 543 N93-13690

X

X RAY ANALYSIS
Characterizing laser fusion welded aluminum using synchrotron x ray microtomography
[DE92-018608] p 609 N93-12565
X ray attenuation measurements for high-temperature materials characterization and in situ monitoring of damage accumulation p 631 N93-14022
X RAY APPARATUS
Soft X Ray Projection Lithography Topical Meeting. Volume 8: Technical digest
[AD-A254756] p 709 N93-12850
X RAY ASTRONOMY
Probing the galactic halo with ROSAT
[NASA-CR-191268] p 743 N93-13272
The interstellar medium of elliptical galaxies
p 757 N93-14071
X RAY ASTROPHYSICS FACILITY
An investigation of error correcting techniques for OMV data
[NASA-CR-190942] p 682 N93-12654
X RAY BINARIES
A search for point sources of cosmic ray muons using the MACRO detector p 773 N93-13738
X RAY DETECTORS
A payload to evaluate photodiodes for the detection of soft and hard x rays in a space environment using a Get Away Special p 509 N93-13166
X RAY DIFFRACTION
An investigation of the interatomic bonding characteristics of a Ti - 51 atomic percent Al alloy by x ray diffraction
[AD-A245362] p 544 N93-13945
X RAY FLUORESCENCE
Study of the concentration and deposition of tropospheric aerosols using x ray emission techniques
p 667 N93-13894
X RAY IMAGERY
Uniformity results of the multilayer mirrors used in the ALEXIS ultrasoft x ray telescopes
[DE92-018611] p 743 N93-13342
Data evaluation, analysis, and scientific study
[NASA-CR-184396] p 769 N93-13475
X RAY LASERS
Experiments on resonantly photo-pumped x ray lasers
[DE92-019542] p 603 N93-12570
Self-consistent one-dimensional modelling of x ray laser plasmas
[DE92-019543] p 712 N93-12571
Small-scale x ray laser systems
[DE92-018442] p 604 N93-12744
Table-top x ray lasing based on optical-field-induced ionization
[DE92-019374] p 604 N93-12925
Demonstration of a neon-like rubidium x ray laser
[DE92-019576] p 606 N93-13653
X RAY SCATTERING
Atomic structure of mixed ferroelectrics
[AD-A254369] p 702 N93-12947
X ray scattering by cosmic dust grains
p 750 N93-13294
Scattering and order in thermotropic liquid crystals
p 723 N93-13332
X RAY SOURCES
X ray scattering by cosmic dust grains
p 750 N93-13294
Uniformity results of the multilayer mirrors used in the ALEXIS ultrasoft x ray telescopes
[DE92-018611] p 743 N93-13342
Gravitational lensing by galaxy clusters: The giant arcs in Abell 370 and Cl2244-02 p 755 N93-13848
X RAY SPECTRA
Experiments on resonantly photo-pumped x ray lasers
[DE92-019542] p 603 N93-12570
The mass and dynamics of cD clusters with cooling flows. 1: ROSAT observations of A 496
[NASA-CR-191240] p 743 N93-13352
A thermal/nonthermal approach to solar flares
p 771 N93-13639
Demonstration of a neon-like rubidium x ray laser
[DE92-019576] p 606 N93-13653
X RAY SPECTROSCOPY
Surface contamination on LDEF exposed materials
p 547 N93-12776
Soft x ray window encapsulant for HgI2 detectors
[NASA-CR-190850] p 710 N93-13705
X RAY TELESCOPES
Soft X Ray Telescope (SXT) focus error analysis
[NASA-CR-184443] p 742 N93-12657
G-133: A soft x ray solar telescope
p 510 N93-13171
The unique challenge of managing an undergraduate Get-Away-Special experiment p 512 N93-13185
Uniformity results of the multilayer mirrors used in the ALEXIS ultrasoft x ray telescopes
[DE92-018611] p 743 N93-13342
The ALEXIS experiment: Current status and performance
[DE92-018601] p 524 N93-13516
X RAYS
Thermal imaging of synchrotron beams on silicon crystals
[DE92-018182] p 719 N93-12562
Comprehensive mappings of electron precipitation and its effects on the comprehensive mappings of electron precipitation and its effects on the atmosphere
[AD-A254665] p 648 N93-12621
Organization of the Optical Society of America Photonic Science Topical Meeting Series. Volume 8: Integrated photonics research. lifornia on 9-11 april 1991
[AD-A254682] p 709 N93-12666
Soft X Ray Projection Lithography Topical Meeting. Volume 8: Technical digest
[AD-A254756] p 709 N93-12850
The Orbiter Stability Experiment on STS-40
p 508 N93-13159
X-29 AIRCRAFT
X-29 linear aerodynamic perturbation model
[AD-A254810] p 500 N93-12752
NASA aeronautics: Research and technology program highlights
[NASA-NP-159] p 491 N93-13110
In-flight flow visualization results from the X-29A aircraft at high angles of attack
[NASA-TM-4430] p 493 N93-13322
X-30 VEHICLE
National Aero-Space Plane: Key issues facing the program. Testimony before the Subcommittee on Technology and Competitiveness, Committee on Science, Space, and Technology, House of Representatives
[GAO/T-NSIAD-92-26] p 500 N93-13253

Y

YAG LASERS
Post flight operation of a high peak power neodymium YAG laser aboard the G-449 payload flown on Space Shuttle Columbia mission 61-C p 508 N93-13161
A study of techniques for single frequency operation of diode-pumped Nd:YAG lasers p 606 N93-13629
YAW
LDEF yaw and pitch angle estimates
p 524 N93-12772
YBCO SUPERCONDUCTORS
Electrodeposition of high temperature superconductors
[AD-A255095] p 720 N93-12758
High-temperature deformation and diffusion in oxides
[DE92-019593] p 720 N93-12854
Oxygen deficiencies at defects in YBa2Cu3O(7-delta) as determined by high resolution parallel electron energy loss
[DE92-016301] p 721 N93-13089
Single liquid source plasma enhanced metalorganic chemical vapor deposition of YBa2Cu3O(7-x) thin films
[AD-A254119] p 722 N93-13100
Ion-channeling observation of correlated atomic displacements below Tc in YBa2Cu3O(7-x) and Pb-doped Bi2Sr2CaCu2O(x)
[DE92-018186] p 722 N93-13104
Defects near the Y2BaCuO5/YBa2Cu3O(7-x) interface and their effect on flux-pinning in melt-processed and quench-melt-growth processed YBa2Cu3O(7-x)
[DE92-014463] p 723 N93-13347
Y1Ba2Cu3O(7-delta) thin film dc SQUIDs (superconducting quantum interference device)
[ITN-92-85167] p 723 N93-13362
The heteroepitaxial growth of YBCO and other metal oxides on silicon and GaAs by pulsed laser deposition
p 726 N93-13904
Magnetic properties of high-T(sub c) superconductors
p 726 N93-13905

Noise measurements of YBa2Cu3O7 thin film high-temperature superconductors p 726 N93-13933
YIELD STRENGTH
Development of weldable high-strength iron aluminides
[DE92-016018] p 542 N93-13190
Elevated temperature tensile properties of borated 304 stainless steel: Effect of boride dispersion on strength and ductility
[DE92-040096] p 542 N93-13302
YOUTH
Gateway to diversity in the scientific and technological workforce
[NSF-92-99] p 730 N93-13278
YTTERBIUM ISOTOPES
Transition probabilities up to I = 36(+)in Yb-160
[DE92-017191] p 703 N93-13114
YTTRIUM OXIDES
Laser spectroscopy of rare earth ions
p 608 N93-13846

Z

ZEOLITES
The First United States Microgravity Laboratory
[NASA-TM-107980] p 557 N93-12951
Structure sensitive reactions over Co, Fe and mixed metal clusters in zeolites
[DE92-040359] p 542 N93-12998
Spaceflight payload design flight experience G-408
p 508 N93-13160
Applications for special-purpose minerals at a lunar base p 760 N93-13975
ZINC TELLURIDES
Thin films and solar cells of cadmium telluride and cadmium zinc telluride p 639 N93-13611
Two to six compound thin films by MOCVD for tandem solar cells p 640 N93-13932
ZIRCONIUM COMPOUNDS
Alternate electrode materials for the SP100 reactor
[DE92-019570] p 706 N93-12970
ZIRCONIUM OXIDES
Thermal barrier coating life prediction model development, phase 2
[NASA-CR-189111] p 544 N93-12589
ZODIACAL DUST
Zodiacal emission p 772 N93-13147
ZONAL FLOW (METEOROLOGY)
Relationships between continental-scale circulation and rainfall event attributes in the southeastern US
p 664 N93-13631
Meso-beta scale numerical simulation studies of terrain-induced jet streak mass/momentum perturbations
[NASA-CR-191365] p 654 N93-13719
Nonlinear hydrostatic conditional symmetric instability: Some theoretical and modeling considerations
p 655 N93-13757
Model studies of the middle atmosphere of Venus
p 759 N93-13831

Typical Personal Author Index Listing

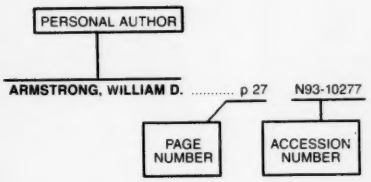

Listings in this index are arranged alphabetically by personal author. The page number helps you locate the citation in the abstract section. The accession number denotes the number by which the citation is identified.

A

ABBOTT, MARK JOSEPH ..... p 749 N93-13011
ABDALLA, ABDEL-MAGID ABDEL-LATIF ..... p 588 N93-13609
ABE, TAKASHI ..... p 491 N93-12716
ABOU-RAYAN, ASHRAF MOHAMED ..... p 631 N93-13966
ABOWD, GREGORY D. ..... p 679 N93-13909
ABUSHAGUR, MUSTAFA A. G. ..... p 710 N93-13696
ACAR, YALCIN B. ..... p 644 N93-13098
ACCARDI, DENISE ..... p 557 N93-12951
p 518 N93-13113
ACETO, S. C. ..... p 717 N93-13518
ACHAR, NAGARI SHRIRANGA ..... p 501 N93-13914
ACKERET, JAMES R. ..... p 634 N93-13333
ACKLEY, KEITH A. ..... p 685 N93-13004
ACTIS, RICARDO LUIS ..... p 528 N93-12629
ADAMS, DANIEL OHARE ..... p 532 N93-13724
ADAMS, R. G. ..... p 716 N93-13191
ADLER, KAREN ..... p 616 N93-13706
AEPPLI, G. ..... p 702 N93-13037
AGNEW, DONALD L. ..... p 708 N93-12591
p 742 N93-12592
p 708 N93-12593
AHMAD, ANEES ..... p 742 N93-12657
AHMAD, FAIZ ..... p 534 N93-13779
AHUJA, J. K. ..... p 538 N93-13456
AINE, C. J. ..... p 674 N93-12566
AKE, ROBERT ..... p 575 N93-12677
AKE, THOMAS B. ..... p 744 N93-13461
AL-GARNI, AHMED ZAFER ..... p 495 N93-13745
AL-KHATIB, HANAN HASSAN MAHDI ..... p 653 N93-13492
AL-RUSHUDI, SULAIMAN SALIH ..... p 625 N93-13142
ALAM, SALIM ..... p 685 N93-13261
ALBERS, H. E. ..... p 675 N93-13116
ALBERS, JOHN ..... p 570 N93-12978
ALBERT, C. J. ..... p 706 N93-12829
ALBERTS, THOMAS E. ..... p 619 N93-14006
ALBRITTON, DANIEL L. ..... p 645 N93-13413
ALCOE, DAVID J. ..... p 558 N93-12976
ALEXANDER, S. S. ..... p 761 N93-13978
ALEXANDER, W. MERLE ..... p 512 N93-13183
ALEXANDER, WINSER E. ..... p 561 N93-12620
ALEXANIAN, A. ..... p 565 N93-13354
ALEXOVICH, ROBERT E. ..... p 685 N93-13291
ALIBE, BUNU ..... p 622 N93-12652
ALLEN, DAVID T. ..... p 557 N93-14011
ALLEN, EMILY LIN ..... p 727 N93-14073
ALLEN, KEVIN PATRICK ..... p 635 N93-13956
ALLEN, MARK G. ..... p 603 N93-13687
ALLEN, S. L. ..... p 714 N93-12932
ALLISON, P. ..... p 714 N93-12997
ALLTON, J. H. ..... p 676 N93-14020
ALMAGRI, A. ..... p 713 N93-12882
ALMAGRI, A. F. ..... p 713 N93-12883
ALRED, JOHN W. ..... p 760 N93-13972
ALSOP, DAVID CHARLES ..... p 772 N93-13145
ALTER, JAMES J. ..... p 561 N93-12623
ALTMANN, ERIK ..... p 682 N93-12645
ALTON, G. D. ..... p 708 N93-13574
ALTWEGG, K. ..... p 752 N93-13469
ALVAREZ, RAUL JOHN, II ..... p 653 N93-13614
ALVISO, C. T. ..... p 550 N93-12888
p 550 N93-12931
ALZMANN, MELANIE ..... p 649 N93-12718
AMBROSE, ROBERT OWEN ..... p 613 N93-13329
AMEDURI, F. ..... p 743 N93-13342
AMENDT, P. ..... p 604 N93-12925
ANASTAS, GEORGE, JR. ..... p 616 N93-13706
ANDERS, E. ..... p 752 N93-13469
ANDERSEN, DALE ..... p 651 N93-13326
ANDERSON, J. E. ..... p 538 N93-13341
ANDERSON, KARL F. ..... p 596 N93-12681
ANDERSON, P. D. ..... p 643 N93-12927
ANDERSON, R. R. ..... p 712 N93-12705
ANDERSON, ROBERT C. ..... p 602 N93-13683
ANDERSON, STEPHEN WILLIAM ..... p 754 N93-13636
ANDERSSON, LEIF M. ..... p 697 N93-13271
ANDES, ROBERT C. ..... p 499 N93-12602
ANDISH, KAMBIZ K. ..... p 586 N93-13401
ANGELOPOULOS, V. ..... p 712 N93-12705
ANNEN, KURT D. ..... p 599 N93-13668
ANTCLIFF, RICHARD R. ..... p 598 N93-13661
ANTHONY, T. RENEE ..... p 559 N93-13648
ANTOINE, ROBIN MICHAEL ..... p 620 N93-13710
APOSTOLAKIS, G. E. ..... p 523 N93-13715
APPLEBY, A. J. ..... p 636 N93-12812
ARAI, TATSUYA ..... p 584 N93-13388
ARENA, ANDREW SALVATORE, JR. ..... p 505 N93-13915
ARENDALE, W. F. ..... p 619 N93-12692
ARIGA, HIRONOBU ..... p 491 N93-12716
ARISAWA, TAKASHI ..... p 718 N93-13732
ARMSTRONG, T. ..... p 723 N93-13347
ARMSTRONG, W. C. ..... p 525 N93-12874
ARMSTRONG, WILBUR ..... p 525 N93-12659
ARMSTRONG, WILBUR C. ..... p 682 N93-12675
p 682 N93-12676
ARNDT, SCOTT D. ..... p 586 N93-13397
ARNONE, R. A. ..... p 668 N93-12556
ASHER, W. E. ..... p 669 N93-12916
ASHOK, A. S. ..... p 704 N93-13263
ASO, Y. ..... p 716 N93-13257
ASSADI, S. ..... p 713 N93-12882
p 713 N93-12883
ATKINS, W. H. ..... p 733 N93-12567
ATLURI, SATYA N. ..... p 521 N93-12579
ATWELL, WILLIAM ..... p 520 N93-12876
ATWOOD, C. A. ..... p 491 N93-12721
AUBECK, KURT ..... p 516 N93-13691
AUBRY, S. ..... p 720 N93-12853
AUGUSTINE, MARGRET ..... p 680 N93-13992
AUSTON, DAVID H. ..... p 570 N93-12731
AVARA, ELTON P. ..... p 668 N93-14082
AVRETT, EUGENE H. ..... p 770 N93-13476
AYASLI, SERPIL ..... p 569 N93-13087
AYDEMIR, A. Y. ..... p 714 N93-12913
AZIZ, M. J. ..... p 720 N93-12827

B

BAAKLINI, GEORGE YOUSSEF ..... p 631 N93-14022
BAART, DOUGLAS ..... p 507 N93-13447
BABUSKA, IVO ..... p 696 N93-12701
BACA, D. M. ..... p 605 N93-13507
BACK, B. B. ..... p 705 N93-13546
BACK, LLOYD ..... p 700 N93-13421
BACON, C. ..... p 637 N93-12838
BACON, L. D. ..... p 566 N93-13512
BADALEC, J. ..... p 715 N93-13093
BADAVI, FRANCIS F. ..... p 772 N93-13572
BADHWAR, GAUTAM D. ..... p 674 N93-13023
BADRAN, RASHAD IBRAHIM ..... p 725 N93-13845
BAER, M. R. ..... p 735 N93-12813
BAGGEROER, ARTHUR ..... p 560 N93-12608
BAHADORI, M. YOUSEF ..... p 557 N93-14012
BAHRI, TOUFIK ..... p 503 N93-12578
p 499 N93-12613
BAILEY, WILLIAM J. ..... p 512 N93-13182
BAILEY, Y. ..... p 509 N93-13163
BAJURA, R. A. ..... p 612 N93-13103
BAKER, H. HARLYN ..... p 692 N93-13241
BAKER, KAY D. ..... p 652 N93-13460
BAKTASH, C. ..... p 703 N93-13114
p 708 N93-13574
BALDAUF, JOHN ERIC ..... p 567 N93-14042
BALDIS, H. A. ..... p 715 N93-13105
BALDO, P. M. ..... p 722 N93-13104
BALICK, LEE K. ..... p 635 N93-13867
BALL, DUANE ..... p 687 N93-13880
BALL, JOHN M. ..... p 597 N93-13501
BALLARIN, B. ..... p 595 N93-12619
BALLATO, ARTHUR ..... p 534 N93-13940
BALSIGER, H. ..... p 752 N93-13466
p 752 N93-13467
p 752 N93-13468
p 752 N93-13469
BANKS, BRUCE A. ..... p 524 N93-12772
BANKS, CURTIS ..... p 719 N93-12691
BARATTA, FRANCIS I. ..... p 620 N93-12580
BARBANTINI, E. ..... p 497 N93-13214
BARBIERI, A. ..... p 542 N93-13043
BARD, STEVEN ..... p 558 N93-13422
BARKATT, AARON ..... p 551 N93-13150
BARNES, J. ..... p 596 N93-12844
BARNES, MICHAEL ..... p 499 N93-12613
BARNETT, A. M. ..... p 637 N93-12838
BARRANCO, J. M. ..... p 541 N93-12616
BARTLETT, ANDREW HUGHES ..... p 554 N93-14074
BARTON, DORAN ..... p 511 N93-13174
BARTS, R. ..... p 561 N93-12655
BARWEY, DINESH ..... p 492 N93-13010
BASS, J. N. ..... p 650 N93-12944
BAST, CALLIE C. ..... p 626 N93-13290
BASU, S. ..... p 604 N93-12744
BATES, J. L. ..... p 638 N93-13082
BATHA, S. H. ..... p 715 N93-13105
BAUER, ROBERT A. ..... p 549 N93-12788
BAUMJOHANN, W. ..... p 712 N93-12705
BAUSCHLICHER, CHARLES W., JR. ..... p 702 N93-12900
BEARDEN, I. G. ..... p 705 N93-13546
BEAUDOIN, A. ..... p 633 N93-13085
BECK, W. ..... p 703 N93-13187
BECKER, S. A. ..... p 749 N93-12587
BECKMAN, T. M. ..... p 555 N93-13081
BECLE, J. P. ..... p 502 N93-13207
BEIERSDORFER, P. ..... p 603 N93-12570
p 753 N93-13536
BELL, LARRY S. ..... p 760 N93-13972
BELL, M. G. ..... p 718 N93-13535
BELL, R. ..... p 718 N93-13535
BELL, S. E. ..... p 690 N93-12559
p 691 N93-12791
BELLIVEAU, J. W. ..... p 674 N93-12566
BELLMORE, PHILLIP E. ..... p 586 N93-13401
BELY, PIERRE Y. ..... p 745 N93-13588
BELYTSCHKO, TED ..... p 624 N93-13029
BENEROFE, STEVEN J. ..... p 606 N93-13626
BENKA, STEPHEN G. ..... p 771 N93-13639
BENKOVITZ, C. M. ..... p 644 N93-13270
BENNOF, RICHARD ..... p 741 N93-13543
BENSADOUN, MARC JOHN ..... p 772 N93-13146
BENSAID, NACER-EDDINE ..... p 725 N93-13847
BENSINGER, J. R. ..... p 704 N93-13251
BENSON, BRIAN L. ..... p 672 N93-12949
BENSON, T. J. ..... p 581 N93-13220
BERG, J. M. ..... p 641 N93-12685
BERGLUND, RONALD L. ..... p 643 N93-12941
BERGMANN, ANTON GEORGE ..... p 755 N93-13848
BERK, H. L. ..... p 716 N93-13107
BERNARD, R. ..... p 640 N93-13621
BERNARD, T. ..... p 692 N93-13242
BERRENDORF, R. ..... p 681 N93-12823
BERTINATO, ROBERT J. ..... p 711 N93-14032
BERTRAND, P. A. ..... p 727 N93-14083
BESTER, M. ..... p 745 N93-13585
BETTS, R. R. ..... p 705 N93-13546
BEYERLINE, ADOLPH L. ..... p 555 N93-12939
BHANUMATHI, V. ..... p 737 N93-13368
BHASKARAN, SHYAMKUMAR ..... p 635 N93-13969
BIBRING, JEAN-PIERRE ..... p 512 N93-13183

BIERBAUM, CARL R. ..... p 676 N93-12545
BILLINGSLEY, J. B. ..... p 567 N93-13878
BINER, S. B. ..... p 531 N93-13264
p 558 N93-13298
BIRCKELBAW, LARRY DEAN ..... p 494 N93-13729
BIRKAN, M. A. ..... p 525 N93-12575
BISHOP, K. P. ..... p 604 N93-12915
BISHOP, PETER C. ..... p 738 N93-13737
BISSINGER, N. C. ..... p 581 N93-13220
BITTNER, ROBERT D. ..... p 602 N93-13682
BJORKLUND, GARY C. ..... p 554 N93-14029
BJORNSON, BRIAN M. ..... p 499 N93-12605
BLAIN, M. ..... p 604 N93-12915
BLAIR, W. D. ..... p 697 N93-14081
BLAKE, S. M. ..... p 509 N93-13163
BLASKIEWICZ, M. ..... p 571 N93-13358
BLASSO, L. G. ..... p 736 N93-13131
BLECH, RICHARD A. ..... p 689 N93-13154
BLINN, THOMAS M. ..... p 685 N93-13004
BLOCH, J. J. ..... p 524 N93-13516
BLOCKER, C. A. ..... p 704 N93-13251
BOCKER, R. P. ..... p 560 N93-12585
BODETTE, D. E. ..... p 605 N93-13249
BOERSTLER, ROBERT W. ..... p 722 N93-13100
BOGDEN, PHILIP STUART ..... p 670 N93-13483
BOGETTI, TRAVIS A. ..... p 529 N93-12842
BOGGESS, ALBERT ..... p 744 N93-13461
BOGH, KARILYN ..... p 511 N93-13174
BOLEN, NELSON E. ..... p 731 N93-13834
BOLSTER, ROBERT N. ..... p 554 N93-13862
BOLTON, P. R. ..... p 604 N93-12925
BONACUSE, PETER J. ..... p 625 N93-13153
BOOK, WAYNE J. ..... p 611 N93-12952
p 611 N93-12953
p 612 N93-12954
p 612 N93-12955
BOOTH, C. R. ..... p 673 N93-13612
BOOTH, CHARLES R. ..... p 670 N93-13708
BOOTH, JOSEPH J. ..... p 710 N93-13500
BOOTH, PETER ..... p 719 N93-13897
BORG, JANET ..... p 512 N93-13183
BORGES, MARK DANIEL ..... p 658 N93-13887
BOSE, N. K. ..... p 561 N93-12615
BOTTCHER, C. ..... p 706 N93-12829
BOURASSA, ROGER J. ..... p 546 N93-12771
BOWEN, CHARLES D. ..... p 677 N93-12576
BOWEN, M. M. ..... p 566 N93-13869
BOWEN, THEODORE ..... p 772 N93-13306
BOWER, C. ..... p 707 N93-13002
BOWERS, DOUGLAS L. ..... p 502 N93-13224
BOWLES, KENNETH J. ..... p 529 N93-12737
BOWSER, S. E. ..... p 677 N93-12712
BOYCE, LOLA ..... p 626 N93-13290
BOYD, J. D. ..... p 697 N93-13886
BRADLEY, R. G., JR. ..... p 581 N93-13220
BRAIN, DAVID A. ..... p 510 N93-13167
BRAMSON, G. ..... p 714 N93-12971
BRANNON, P. J. ..... p 605 N93-13249
BRATTON, THOMAS ..... p 506 N93-12899
BRAVO, RAMIRO H. ..... p 586 N93-13399
BRAZELL, JAMES W. ..... p 559 N93-14009
BREED, STEVEN DOUGLAS ..... p 728 N93-13498
BRENNAN, KEVIN F. ..... p 572 N93-13448
BRETHERTON, FRANCIS ..... p 645 N93-13413
BREWER, DAVE N. ..... p 622 N93-12738
BRIDGES, SUSAN ..... p 671 N93-13943
BRIENZO, ROBERT ..... p 509 N93-13162
BRIGGS, STEPHEN A. ..... p 601 N93-13679
BRILL, J. ..... p 497 N93-13221
BRINKER, DAVID J. ..... p 641 N93-14004
BRITT, JEFFREY SCOTT ..... p 640 N93-13932
BRITTAIN, D. ..... p 563 N93-13045
BROCIOUS, W. ..... p 701 N93-12806
BROECKER, WALLACE S. ..... p 664 N93-13718
BROOK, JEFFREY ROBERT ..... p 664 N93-13736
BROSTROM, LANE R. ..... p 653 N93-13491
BROW, R. K. ..... p 550 N93-12917
BROWER, WILLIAM E., JR. ..... p 549 N93-12788
BROWMAN, M. J. ..... p 565 N93-13510
BROWN, E. R. ..... p 573 N93-13837
BROWN, SUSAN T. ..... p 584 N93-13386
BROWNING, LOU ..... p 615 N93-13644
BROWNSON, L. W. ..... p 645 N93-13479
BRUETSCH, ROBERT I. ..... p 616 N93-13761
BRUMHK, C. J. ..... p 595 N93-12619
BRUNNER, RONALD D. ..... p 632 N93-13833
BUCHENAUER, D. A. ..... p 714 N93-12971
BUCKNER, M. R. ..... p 619 N93-13036
BUDGE, K. G. ..... p 684 N93-12795
BUDGE, MERV C. ..... p 711 N93-14032
BUDNY, R. V. ..... p 718 N93-13535
BUETEFISCH, K. A. ..... p 503 N93-13218
BUETTNER, LEONARD C. ..... p 596 N93-12653
BUI, TRONG T. ..... p 585 N93-13396
BUKIET, B. G. ..... p 704 N93-13263
BULA, R. J. ..... p 680 N93-13997
p 680 N93-13998
BULL, JEFFREY ..... p 527 N93-12895
p 528 N93-12896
BUNTINE, WRAY ..... p 685 N93-13063
p 693 N93-13366
BUONI, CORINNE ..... p 651 N93-13326
BURCH, RICHARD ..... p 570 N93-12866
BURGSMUELLER, W. ..... p 502 N93-13207
BURKE, BERNARD F. ..... p 747 N93-13596
p 747 N93-13597
BURKE, LUKE A. ..... p 552 N93-13459
BURLEY, J. D. ..... p 646 N93-13646
BURNS, JACK O. ..... p 744 N93-13579
BURRAGE, MARK DAVID ..... p 648 N93-12626
BURROWS, CHRISTOPHER ..... p 745 N93-13588
BURROWS, DAVID N. ..... p 743 N93-13272
BURT, DONALD M. ..... p 761 N93-13980
BUSH, C. E. ..... p 718 N93-13535
BUSH, CHUCK ..... p 601 N93-13678
BUSH, LANCE B. ..... p 519 N93-13379
BUSTIN, ROBERTA ..... p 762 N93-13982
BUTLER, D. ..... p 512 N93-13181
BUTLER, R. G. ..... p 506 N93-12552
BUTLER, RICKY W. ..... p 684 N93-12957
BUTRYMOWICZ, DANIEL B. ..... p 698 N93-12805
BUTTRILL, CAREY S. ..... p 694 N93-13442
BYRNE, HELEN M. ..... p 540 N93-13802

C

CABLE, M. D. ..... p 715 N93-13105
CABLE, SAMUEL BENJAMIN ..... p 717 N93-13496
CACH, STEVEN D. ..... p 598 N93-13656
CADE, STEVEN C. ..... p 544 N93-13945
CADWALLADER, L. C. ..... p 713 N93-12856
CALLAHAN, T. J. ..... p 611 N93-12936
CALLY, PAUL S. ..... p 715 N93-13006
CALOGERO, STEPHEN A. ..... p 511 N93-13176
CALOMINO, ANTHONY M. ..... p 622 N93-12738
CAMERON, E. N. ..... p 719 N93-13985
CAMPBELL, A. B. ..... p 711 N93-14031
CAMPBELL, BRANTON ..... p 510 N93-13171
CAMPBELL, E. M. ..... p 715 N93-13105
CANFIELD, DENNIS V. ..... p 674 N93-12612
p 498 N93-14026
CANFIELD, T. R. ..... p 720 N93-12819
p 612 N93-13236
CANO, ROBERTO J. ..... p 528 N93-12590
CARAZA, JOSE-ANTONIO NAVARRO
p 616 N93-13742
CARETTI, DAVID M. ..... p 677 N93-12960
CARINO, NICHOLAS J. ..... p 623 N93-12981
CARLSON, B. M. ..... p 689 N93-12797
p 689 N93-12810
CARLSON, R. E. ..... p 735 N93-13000
CARLSTROM, T. N. ..... p 712 N93-12687
CARMAN, GREGORY PAUL ..... p 532 N93-13490
CARPENTER, J. M. ..... p 702 N93-13070
CARRERAS, B. A. ..... p 716 N93-13297
CARSWELL, W. E. ..... p 511 N93-13178
CARTER, NELSON DAVID ..... p 492 N93-13128
CARTY, R. H. ..... p 538 N93-13314
CARUANA, RICH ..... p 685 N93-13063
CASTAN, C. ..... p 502 N93-13207
CASTRO, R. G. ..... p 551 N93-13315
CATTON, I. ..... p 523 N93-13715
CAVALLO, A. ..... p 718 N93-13535
CAVICCHI, RICHARD H. ..... p 585 N93-13396
CEKIC, M. ..... p 713 N93-12882
p 713 N93-12883
CHA, HUNGSE ..... p 570 N93-12866
CHAMIS, CHRISTOS C. ..... p 622 N93-12735
CHAN, ANTHONY ARTHUR ..... p 718 N93-13750
CHAN, CHI HOU ..... p 569 N93-13088
CHAN, K. C. D. ..... p 605 N93-13507
CHANCE, M. S. ..... p 718 N93-13535
CHANDLER, PHILLIP R. ..... p 505 N93-13872
CHANDRA. R. ..... p 537 N93-13096
CHANG, C. Y. ..... p 564 N93-13057
CHANG, I-PING ..... p 616 N93-13772
CHANG, JOHN ..... p 505 N93-13916
CHANG, KAI ..... p 574 N93-13865
CHANG, MING-JR ..... p 588 N93-13743
CHANG, YOUNG KEUN ..... p 496 N93-13917
CHAO, Y. ..... p 707 N93-13090
CHAPMAN, B. ..... p 713 N93-12882
CHAPMAN, B. E. ..... p 713 N93-12883
CHARNES, A. ..... p 683 N93-12730
CHARRETTE, E. E. ..... p 650 N93-12943
CHARTAS, G. ..... p 713 N93-12882
CHASON, E. ..... p 719 N93-12586
CHEAIRS, R. B. ..... p 605 N93-13507
CHEN, C. P. ..... p 575 N93-12688
CHEN, CHING-JEN ..... p 586 N93-13399
CHEN, CHUN-FU ..... p 533 N93-13778
CHEN, CHUNG-HSING ..... p 572 N93-13569
CHEN, E. P. ..... p 626 N93-13301
CHEN, GENGSHENG ..... p 541 N93-12879
CHEN, GUI-QIANG ..... p 696 N93-12594
CHEN, H. C. ..... p 578 N93-13206
CHEN, JEN PING ..... p 593 N93-14025
CHEN, K. R. ..... p 705 N93-12713
CHEN, MARGARET W. ..... p 705 N93-12715
CHEN, P. C. ..... p 626 N93-13443
CHEN, R. ..... p 613 N93-13321
CHEN, SHUH RONG ..... p 543 N93-13545
CHEN, T. K. ..... p 609 N93-12724
CHEN, TZI-KANG ..... p 528 N93-12583
CHEN, Y. J. ..... p 711 N93-14031
CHEN, Y. S. ..... p 575 N93-12689
CHENG, C. C. ..... p 536 N93-12618
CHENG, N. ..... p 650 N93-12943
CHENG, YUANDA ..... p 721 N93-12972
CHEONG, S.-W. ..... p 702 N93-13037
CHESTON, DERRICK J. ..... p 587 N93-13403
CHETTY, SHYAM ..... p 504 N93-13566
CHIANG, ERICK ..... p 651 N93-13326
CHIANG, FU-PEN ..... p 600 N93-13673
CHICK, L. A. ..... p 638 N93-13082
CHIOU, JENG-MAW ..... p 536 N93-14056
CHISHOLM-BRAUSE, C. J. ..... p 641 N93-12685
CHITRE, D. M. ..... p 562 N93-12950
CHIU, S. C. ..... p 716 N93-13193
CHO, CHONGDU ..... p 532 N93-13527
CHOI, G. S. ..... p 503 N93-13697
CHOINSKI, THOMAS C. ..... p 689 N93-12848
CHORNOBOY, EDWARD S. ..... p 660 N93-12622
CHOUDHURY, AJIT K. ..... p 566 N93-13838
CHOWDARI, B. V. ..... p 545 N93-12755
CHOWDHRY, RAJIV S. ..... p 504 N93-13068
CHOYKE, W. J. ..... p 536 N93-12618
CHRISTENSON, W. A. ..... p 728 N93-12857
p 576 N93-12996
CHRISTOU, NIKOLAOS THEODOROS
p 636 N93-14051
CHU, NELSON C. ..... p 569 N93-13087
CHUDNOVSKY, A. ..... p 623 N93-12863
CHUPP, EDWARD L. ..... p 769 N93-12930
CHWANG, ALLEN T. ..... p 574 N93-12617
CICOLANI, LUIGI S. ..... p 503 N93-12815
CINTALA, MARK J. ..... p 760 N93-13972
CIUCCI, ALESSANDRO ..... p 526 N93-13818
CLARK, K. C. ..... p 650 N93-12845
CLARK, KURT A. ..... p 634 N93-13094
CLARK, ROBERT W., JR. ..... p 586 N93-13397
p 586 N93-13398
CLARK, WILLIAM WALKER ..... p 617 N93-13809
CLARKSON, WILLIAM ANDREW ..... p 606 N93-13629
CLAYTON, J. ..... p 682 N93-13759
CLEMENS, N. T. ..... p 602 N93-13686
CLIFTON, JAMES R. ..... p 623 N93-12981
CLINE, M. C. ..... p 613 N93-13321
COBB, M. S. ..... p 640 N93-13622
COCHRAN, H. D. ..... p 538 N93-13317
COCHRAN, ROLAND ..... p 529 N93-12757
COFFEY, HELEN E. ..... p 769 N93-12803
COGBURN, R. ..... p 707 N93-13108
COGGESHALL, S. V. ..... p 715 N93-13047
COLAVITA, M. ..... p 745 N93-13582
COLE, R. ..... p 690 N93-12564
COLE, R. A. ..... p 733 N93-12567
COLLET, P. ..... p 696 N93-12889
COLSON, RUSSELL O. ..... p 761 N93-13979
CONDIT, PAUL D. ..... p 733 N93-12597
CONDO, FREDERICK JOSEPH, JR.
p 739 N93-14080
CONFORTI, MICHELE ..... p 696 N93-12640
CONIA, J. E. ..... p 538 N93-13341
CONLEY, JULIANNE M. ..... p 585 N93-13396
CONNELL, P. S. ..... p 645 N93-13615
p 646 N93-13646
p 646 N93-13654
CONNER, W. CURTIS ..... p 537 N93-12995
CONRADSON, S. D. ..... p 641 N93-12685
CONWELL, J. C. ..... p 640 N93-13618
COOK, PETER GEOFFREY ..... p 742 N93-14049
COOK, R. C. ..... p 715 N93-13105
COOPER, C. V. ..... p 540 N93-12603
COOPER, ERIC G. ..... p 619 N93-14006
COOPER, J. A., JR. ..... p 720 N93-12748
COOPER, JOHN C. ..... p 552 N93-13414
CORBIN, MICHAEL R. ..... p 753 N93-13487
CORDOVA, A. ..... p 645 N93-13505
CORNETTE, JAMES B. ..... p 519 N93-12611
CORNILS, KARIN ..... p 619 N93-14006
CORNUWJOLS, GWRARD ..... p 696 N93-12640
CORNWELL, TIM J. ..... p 744 N93-13580
CORREDOURA, P. ..... p 707 N93-13090
COSTELLO, DANIEL J., JR. ..... p 565 N93-13411
COSTIN, DANIEL PATRICK ..... p 501 N93-13815
COTE, P. J. ..... p 541 N93-12616
COTTER, J. E. ..... p 637 N93-12838

COWAN, P. L. ..... p 721 N93-12881
COX, D. F. ..... p 539 N93-13573
CRABB, T. M. ..... p 540 N93-13986
CRABB, THOMAS M. ..... p 760 N93-13972
CRAIG, ROY R., JR. ..... p 685 N93-13030
p 686 N93-13295
p 686 N93-13296
CRAIN, W. R. ..... p 524 N93-14087
CRANE, ROGER MICHAEL ..... p 533 N93-13748
CRISAFULLI, JEFFREY J. ..... p 584 N93-13386
CROCKER, N. ..... p 713 N93-12882
p 713 N93-12883
CROOK, ANDREW J. ..... p 502 N93-12695
CROWN, DAVID ARDEN ..... p 768 N93-14092
CRUMP, JOHN W. ..... p 685 N93-13004
CRUTCHER, E. RUSS ..... p 546 N93-12773
CSANKY, GEZA ..... p 603 N93-14086
CUCINOTTA, FRANCIS A. ..... p 520 N93-12876
p 674 N93-13023
CUDZINOVIC, M. ..... p 713 N93-12882
CULLEN, JOHN J. ..... p 642 N93-12870
CULLIMORE, BRENT A. ..... p 585 N93-13393
CULLINGFORD, HATICE ..... p 680 N93-13994
CULLINGFORD, HATICE S. ..... p 555 N93-13990
CUMMINS, H. Z. ..... p 724 N93-13577
CUNDALL, P. A. ..... p 545 N93-12729
CUNNINGHAM, DIANE ..... p 738 N93-13415
CUNY, JANICE E. ..... p 683 N93-12763
CUOMO, DONNA L. ..... p 677 N93-12576
CUPP, RICHARD E. ..... p 634 N93-13094
CURLANDER, JOHN C. ..... p 564 N93-13057
CURRERI, P. ..... p 551 N93-13115
CUTBIRTH, JAMES W. ..... p 493 N93-13493
CUTKOSKY, MARK R. ..... p 609 N93-12604

D

DA, DONG ..... p 691 N93-13129
DAINTY, A. M. ..... p 650 N93-12943
DALESIO, L. R. ..... p 690 N93-12564
DAME, L. T. ..... p 626 N93-13443
DAMICO, K. L. ..... p 609 N93-12565
DANCHI, WILLIAM C. ..... p 745 N93-13585
DANFORD, M. D. ..... p 543 N93-13378
DANIELS, CHARLES HOWARD ..... p 613 N93-13331
DANNENBERG, KONRAD K. ..... p 510 N93-13167
DAO, BUI V. ..... p 584 N93-13387
DARLING, DOUGLAS ..... p 585 N93-13395
DARRAH, ROD ..... p 773 N93-12663
p 773 N93-12664
p 773 N93-12665
p 774 N93-12764
p 774 N93-12765
p 774 N93-12766
p 774 N93-12767
p 775 N93-12849
DARROW, C. B. ..... p 715 N93-13105
DARSEY, J. A. ..... p 691 N93-13079
DASILVA, L. B. ..... p 603 N93-12570
p 606 N93-13653
DATLOWE, D. W. ..... p 648 N93-12621
DAUPHIN, J. ..... p 557 N93-12934
DAVE, R. N. ..... p 704 N93-13263
DAVID, VALERIE ..... p 508 N93-12892
p 522 N93-12964
DAVIDSON, D. P. ..... p 507 N93-13213
DAVIDSON, W. L. ..... p 767 N93-14016
DAVIES, CAROL B. ..... p 683 N93-12719
DAVIES, P. O. A. L. ..... p 699 N93-12714
DAVILA, CARLOS GUIDO ..... p 535 N93-14030
DAVIS, J. BRADLEY ..... p 520 N93-13032
DAVIS, J. M. ..... p 770 N93-13477
DAVIS, ROBERT H. ..... p 556 N93-12728
DAVIS, W. M. ..... p 649 N93-12804
DAY, WILLIAM B. ..... p 688 N93-12710
DEAL, SCOT ..... p 559 N93-13640
DEAN, GARVIN ..... p 525 N93-12659
DEATON, JOHN E. ..... p 499 N93-12613
DEBARRO, MARC J. ..... p 680 N93-14003
DEBOOR, CARL ..... p 696 N93-12847
DEGANI, AMMAR TAHER ..... p 588 N93-13749
DEGIANO, FRANCIS A. ..... p 559 N93-13648
DEGRASSIE, J. S. ..... p 716 N93-13193
DEHAAN, M. S. ..... p 683 N93-12792
DELANEY, ROBERT A. ..... p 502 N93-12695
DELFRATE, JOHN H. ..... p 493 N93-13322
DELUCA, DANIEL P. ..... p 541 N93-12746
DEMMEL, JAMES W. ..... p 697 N93-14036
DEMORISSONVALERIANO, MARCIO
p 634 N93-13258
DENG, ZHENGTAO ..... p 591 N93-13918
DENHARTOG, D. J. ..... p 713 N93-12882
p 713 N93-12883
DEPKOVICH, THOMAS MICHAEL ..... p 573 N93-13805
DESAI, UPENDRA D. ..... p 509 N93-13166
DESILVA, INDURUWAGE PRABHATH DARSHANA
p 587 N93-13532
DESMARTEAU, DARRYL D. ..... p 555 N93-12939
DEVAN, J. H. ..... p 542 N93-13080
p 542 N93-13237
DEVAN, LEROY ..... p 492 N93-12741
DEWEI, ZHAO ..... p 676 N93-14084
DEWITTE, PAULA S. ..... p 685 N93-13004
DEXTER, R. ..... p 713 N93-12882
DEXTER, R. N. ..... p 713 N93-12883
DIAZGARCIA, OSCAR ..... p 738 N93-13910
DICKINSON, ROBERT ..... p 645 N93-13413
DICKMANNS, E. D. ..... p 693 N93-13244
DICKSON, KATHERINE J. ..... p 743 N93-12898
DIDZIULIS, S. V. ..... p 544 N93-14098
DIERSING, ROBERT JOSEPH ..... p 561 N93-12633
DIGEL, SETH WILLIAM ..... p 758 N93-14095
DILLER, THOMAS E. ..... p 599 N93-13665
p 595 N93-13670
DIRESKENELI, HALDUN ..... p 694 N93-13370
DISALVO, F. ..... p 545 N93-12697
DITTRICH, T. ..... p 715 N93-13105
DIXIT, S. N. ..... p 606 N93-13534
DIXON, ANTHONY G. ..... p 508 N93-13160
DLHOPOLSKY, ROSE MARIE ..... p 654 N93-13722
DOANE, GEORGE B., III. ..... p 719 N93-12691
DOANE, GEORGE C., III ..... p 525 N93-12659
DOBECK, MICHAEL ..... p 510 N93-13172
DOBRANICH, D. ..... p 526 N93-13299
DODD, ROBERT S. ..... p 498 N93-13787
DODDS, H. L. ..... p 704 N93-13319
DOERNER, R. ..... p 717 N93-13511
DOGGETT, WILLIAM R. ..... p 619 N93-14006
DOIRON, HAROLD H. ..... p 586 N93-13398
DOLSON, MARK ..... p 689 N93-12846
DOMIK, GITTA ..... p 685 N93-13261
DOMINEY, L. A. ..... p 573 N93-13610
DOMINGUEZ, N. ..... p 718 N93-13651
DONALDSON, BRUCE K. ..... p 608 N93-14010
DONOHUE, JOHN ..... p 560 N93-12551
DORMAN, BENJAMIN ..... p 751 N93-13374
DORSEY, JOHN T. ..... p 694 N93-13442
DOSS, HEIDE MARIA ..... p 605 N93-13497
DOW, MARVIN B. ..... p 528 N93-12590
DOWDY, L. W. ..... p 689 N93-12797
DOWLING, D. T. ..... p 708 N93-13574
DOWNER, JAMES ..... p 616 N93-13706
DOWNES-MARTIN, STEPHEN ..... p 688 N93-12549
DOYLE, JAMES DANIEL ..... p 665 N93-13776
DOYON, J. ..... p 640 N93-13621
DOZIER, W. D. ..... p 703 N93-13194
DRAKE, J. B. ..... p 716 N93-13297
DRAPER, B. L. ..... p 604 N93-12915
DROLLINGER, MICHAEL T. ..... p 498 N93-13787
DUCHANE, D. V. ..... p 637 N93-12923
DUGUNDJI, JOHN ..... p 503 N93-12959
DUNN, B. D. ..... p 557 N93-12934
DUNN, GLENN M. ..... p 526 N93-12968
DUNN, PETER E. ..... p 503 N93-12959
DUNPHY, PHILIP P. ..... p 769 N93-12930
DUNSMUIR, J. H. ..... p 609 N93-12565
DUNYAK, T. J. ..... p 550 N93-12858
DURGIN, WILLIAM W. ..... p 508 N93-13160
DURIC, NEBOJSA ..... p 744 N93-13579
DURRETT, ROBERT H. ..... p 760 N93-13972
DUSSAULT, DOUGLAS ..... p 572 N93-13472
DUTHIE, R. G. ..... p 538 N93-13314
DUTTA, JYOTSNA M. ..... p 650 N93-12946
DUTTON, ELLSWORTH G. ..... p 634 N93-13094
DUVEAU, PH. ..... p 582 N93-13231
DVORACEK, L. ..... p 715 N93-13093
DYALL, KENNETH G. ..... p 702 N93-12900

E

EASTERWOOD, G. W. ..... p 680 N93-13993
EATON, W. C. ..... p 642 N93-12726
EBERHARD, WYNN L. ..... p 634 N93-13094
ECKMANN, J.-P. ..... p 696 N93-12889
EDDY, JOHN A. ..... p 645 N93-13413
EDELMAN, RAYMOND B. ..... p 557 N93-14012
EDER, D. C. ..... p 604 N93-12925
EDIN, BENONI ..... p 609 N93-12604
EDWARDS, B. C. ..... p 524 N93-13516
EDWARDS, MARGO HELEN ..... p 652 N93-13481
EFTHIMION, P. C. ..... p 718 N93-13535
EGAMI, TAKESHI ..... p 702 N93-12947
EGBERT, G. D. ..... p 653 N93-13513
EGELSTAFF, P. A. ..... p 702 N93-13070
EHERNBERGER, L. J. ..... p 663 N93-13288
EHLMANN, BRYON K. ..... p 738 N93-13911
EICH, EDDA ..... p 698 N93-12890
EIHOLZER, C. R. ..... p 541 N93-12820
ELIZALDE, FLAVIO ..... p 750 N93-13279
ELLIOTT, DANIEL W. ..... p 559 N93-13648
ELLIOTT, S. R. ..... p 603 N93-12570
ELLIS, R. J. ..... p 715 N93-13105
ELLISON, J. A. ..... p 707 N93-13108
ELMAN, JEFFREY L. ..... p 689 N93-12846
ELSWORTH, D. ..... p 761 N93-13978
EMERSON, ANDREW PETER JOHN
p 725 N93-13843
ENGLISH, C. A. ..... p 541 N93-12798
ENTINE, G. ..... p 710 N93-13705
EPSTEIN, A. J. ..... p 570 N93-12650
p 545 N93-12749
EPSTEIN, GABRIEL L. ..... p 508 N93-13159
ERICKSON, GARY E. ..... p 493 N93-13353
ERMAK, D. L. ..... p 642 N93-12884
ERNST, D. J. ..... p 706 N93-12829
ESTEP, L. ..... p 668 N93-12556
ESTLER, R. C. ..... p 538 N93-13341
ETHRIDGE, E. ..... p 551 N93-13115
EVANISKO, GEORGE ..... p 511 N93-13177
EVANS, BRETT ..... p 511 N93-13174
EVANS, RICHARD ..... p 693 N93-13245
EVERETT, STEPHANIE S. ..... p 688 N93-13942
EVERETT, TRACEY ..... p 619 N93-12692
EWERT, MICHAEL K. ..... p 586 N93-13401
EYRAUD, J. L. ..... p 502 N93-13212
EYRING, EDWARD M. ..... p 537 N93-13096

F

FALEMPIN, F. ..... p 582 N93-13231
FALES, J. L. ..... p 699 N93-12601
FAN, JIAWEN ..... p 724 N93-13628
FAN, MARK SHIAOYI ..... p 583 N93-13334
FARIS, G. W. ..... p 721 N93-12887
FARMER, DAVID ..... p 669 N93-12742
FARMER, JEFFERY T. ..... p 680 N93-14003
FARMER, R. C. ..... p 575 N93-12689
FAROOQUE, M. ..... p 638 N93-13039
p 640 N93-13621
FARRAR, MICHAEL R. ..... p 661 N93-12861
FARRINGTON, G. C. ..... p 545 N93-12651
p 545 N93-12753
p 545 N93-12754
p 545 N93-12755
FARROW, R. L. ..... p 537 N93-13232
p 538 N93-13234
FATALE, LOUIS A. ..... p 634 N93-13333
FAUGHN, JIM A. ..... p 677 N93-12960
FAULKNER, HENRY B. ..... p 612 N93-12977
FAVROW, L. H. ..... p 540 N93-12603
FEDOR, LEONARD, S. ..... p 634 N93-13094
FEELEY, O. C. ..... p 537 N93-13188
FEELEY, TIMOTHY SCOTT ..... p 519 N93-13819
FEJTEK, IAN GEORGE ..... p 497 N93-14035
FENG, CHEN ..... p 709 N93-13062
FEREKIDES, CHRISTOS SAVVA ..... p 639 N93-13611
FERET, J. M. ..... p 640 N93-13623
FERGUSON, S. R. ..... p 609 N93-12565
FERGUSSON, NEIL J. ..... p 630 N93-13935
FERRARO, RALPH ..... p 662 N93-13066
FERRE, M. ..... p 705 N93-13546
FERREIRA, J. G. ..... p 716 N93-13257
FERREIRA, J. L. ..... p 716 N93-13257
FERRETTI, A. ..... p 497 N93-13214
FIKSEL, G. ..... p 713 N93-12883
FILBY, E. E. ..... p 539 N93-13530
FILMAN, ROBERT E. ..... p 686 N93-13355
FINESCHI, S. ..... p 770 N93-13478
FINNEY, BEN R. ..... p 760 N93-13972
FIRESTONE, ELAINE R. ..... p 669 N93-13382
FIRMAN, PAUL ..... p 537 N93-13096
FISCH, EMILY ELIZABETH ..... p 605 N93-13365
FITE, C. ..... p 690 N93-12564
FLANAGAN, MICHAEL J. ..... p 595 N93-13664
FLEISCHAUER, P. D. ..... p 544 N93-14098
FLEISCHMAN, JACK G. ..... p 569 N93-13087
FLESNER, L. D. ..... p 708 N93-14089
FLETCHER, TIMOTHY DUANE ..... p 552 N93-13328
FLITCROFT, I. ..... p 644 N93-13254
FLOOD, DENNIS J. ..... p 641 N93-14004
FLORES-MORFIN, JESUS ..... p 695 N93-14065
FLYNN, FREDERICK ..... p 616 N93-13706
FOGLE, DEBRA ANN ..... p 517 N93-12690
FOLKMAN, STEVE ..... p 511 N93-13174
FONCK, R. J. ..... p 713 N93-12883
FONTENLA, JUAN M. ..... p 770 N93-13476
p 770 N93-13477
p 770 N93-13478
FORBES, JEFFREY M. ..... p 651 N93-13276
FOREMAN, BRENT ..... p 491 N93-13025
FORK, DAVID KIRTLAND ..... p 726 N93-13904
FORNEY, GLENN P. ..... p 558 N93-12980
FORTGANG, C. M. ..... p 605 N93-13507
FORTI, MARIA CRISTINA ..... p 632 N93-13005
FOTTNER, LEONHARD ..... p 579 N93-13209
p 579 N93-13211

FOUTTER, R. R.	p 603	N93-13687
FOWLER, C. M.	p 713	N93-12809
FOX, C.	p 596	N93-12844
FRANCISCO, DAVID R.	p 510	N93-13170
	p 512	N93-13184
FRANKLIN, H. ANDREW	p 760	N93-13972
FRANZ, ROBERT CURTIS	p 657	N93-13830
FRASER-SMITH, A. C.	p 566	N93-13869
FRATELLO, J. G.	p 577	N93-13202
FREEDMAN, R.	p 643	N93-12926
FREEMAN, ANTHONY	p 564	N93-13054
FREEMAN, B. L.	p 713	N93-12809
FREEMAN, D. E.	p 645	N93-13274
FREESE, ROBERT P.	p 736	N93-13133
FREIMAN, CHARLES V.	p 774	N93-12706
FRENCH, JAMES R.	p 760	N93-13972
FREULER, RICHARD JEFFREY	p 507	N93-14060
FREUND, ROLAND W.	p 684	N93-12801
FRIEBLE, E. J.	p 711	N93-14031
FRIED, Z.	p 560	N93-12581
FROIDEVAUX, L.	p 645	N93-13615
FRYER, JOHN	p 682	N93-12654
FRYSINGER, G. S.	p 669	N93-12916
FU, GARY	p 669	N93-13382
FU, RONG	p 654	N93-13725
FUCHS, W. KENT	p 565	N93-13375
FUEHRER, CLAUS	p 698	N93-12890
FUGITT, J.	p 708	N93-13284
FUJA, R. S.	p 683	N93-12686
FULLER, CHRIS R.	p 626	N93-13420
FULLWOOD, R.	p 701	N93-12832
FUNABIKI, KATSUSHI	p 491	N93-12716
FUNK, CARL S.	p 661	N93-12862
FUNK, D. J.	p 639	N93-13313
FURENLID, K.	p 710	N93-13652
FUSELIER, S. A.	p 751	N93-13465
	p 752	N93-13466
	p 752	N93-13467
	p 752	N93-13468

G

GABELLA, W.	p 707	N93-13235
GABOR, A.	p 723	N93-13526
GABRYNOWICZ, J. I.	p 681	N93-14018
GAINES, E. E.	p 648	N93-12621
GALIC, H.	p 737	N93-13275
GALLAGHER, J. W.	p 698	N93-12805
GALLAGHER, S. K.	p 680	N93-14001
GALLOPOULOS, E.	p 697	N93-13409
GANGAL, PRAVIN D.	p 721	N93-13022
GANN, RICHARD G.	p 698	N93-12805
GAO, Q.	p 536	N93-12618
GARCIA, ANDREW W.	p 666	N93-13816
GARCIA, P.	p 555	N93-12568
GARCIA, R. C.	p 710	N93-13509
GARCON, F.	p 497	N93-13221
GARDINER, ROBIN	p 722	N93-13100
GARIBOTTO, G. B.	p 693	N93-13243
GARLINGTON, YADILETT	p 619	N93-12692
GARMANY, C. D.	p 748	N93-13659
GARNAVICH, PETER MARCUS	p 757	N93-14059
GARNER, F. A.	p 541	N93-12820
GARNERO, P.	p 497	N93-13222
GARRETT, J. D.	p 703	N93-13114
	p 708	N93-13574
GARRIS, MICHAEL D.	p 689	N93-13198
GARRISON, G. R.	p 669	N93-12599
GASPAR, S. M.	p 604	N93-12915
GASS, PAUL ANTONY	p 712	N93-14100
GATELY, MICHELE	p 518	N93-13113
GATTI, A.	p 497	N93-13214
GAVORA, MARK J.	p 734	N93-12723
GAVRILOV, V. P.	p 576	N93-12912
GAVRON, A.	p 704	N93-13281
GAWALT, JOHN R.	p 773	N93-12667
	p 741	N93-13658
GEBAUER, LINDA	p 524	N93-12772
GEHRING, J.	p 705	N93-13546
GEISS, J.	p 752	N93-13469
GEIST, G. A.	p 542	N93-13043
GELFAND, A. E.	p 697	N93-12702
GEMMEN, R. S.	p 582	N93-13247
GENTHER, PHYLLIS	p 741	N93-13788
GENTRY, THOMAS A.	p 500	N93-12752
GEORGE, J. S.	p 674	N93-12566
	p 675	N93-13522
GERBER, R. A.	p 716	N93-13191
GETINO, C.	p 691	N93-13079
GHOSAL, SANDIP	p 771	N93-13849
GHOSN, LOUIS J.	p 622	N93-12738
GIAMEI, A. F.	p 540	N93-12603
GIBBONS, D.	p 511	N93-13180
GIBBS, GARY P.	p 626	N93-13420
GIBSON, EVERETT K., JR.	p 762	N93-13982
GIERMAN, S. M.	p 605	N93-13507
GIFFORD, G. A.	p 596	N93-12844
GILLE, JOHN P.	p 512	N93-13182
GILLESPIE, JOHN W., JR.	p 529	N93-12842
GILLIS, J. R.	p 546	N93-12771
GILPATRICK, J. D.	p 708	N93-13508
	p 710	N93-13509
GILTHORPE, MARK STEVEN	p 523	N93-14037
GILYARD, GLENN B.	p 502	N93-13155
GINATEMPO, B.	p 542	N93-13043
GIPPET, J. M.	p 577	N93-13202
GIPPLE, KARIN L.	p 528	N93-12584
GIRVIN, DOUGLAS L.	p 611	N93-12953
GISQUET, D.	p 578	N93-13203
GLAGOLA, P. G.	p 705	N93-13546
GLASHEEN, W. M.	p 711	N93-13762
GLENDINNING, S. G.	p 715	N93-13105
GLENN, FLOYD A., III	p 678	N93-13450
GODA, M. P.	p 749	N93-12956
GODARD, J. L.	p 578	N93-13203
GOERSS, JAMES S.	p 667	N93-13877
GOHNG, JUNHO	p 726	N93-13905
GOLBEN, JOHN	p 719	N93-12691
GOLDEN, JOHNNY L.	p 546	N93-12774
	p 544	N93-12779
GOLDEN, T.	p 526	N93-13429
GOLDFINE, ALAN H.	p 698	N93-12805
GOLDIE, JAMES	p 616	N93-13706
GOLDING, PETER	p 586	N93-13400
GOLDMAN, J. L.	p 573	N93-13610
GOLDSMITH, E. L.	p 502	N93-13219
	p 497	N93-13221
GOLDSTEIN, B. E.	p 752	N93-13466
	p 752	N93-13467
	p 752	N93-13468
GOLDSTEIN, DAVID	p 601	N93-13677
GOLDSTEIN, R.	p 752	N93-13466
	p 752	N93-13467
	p 752	N93-13468
GONDHALEKAR, VIJAY	p 616	N93-13706
GONG, J.	p 565	N93-13354
GOODBERLET, J.	p 604	N93-12744
GOODLETT, D. R.	p 575	N93-12711
GOOSMAN, D. R.	p 596	N93-12831
GORDON, R. S.	p 624	N93-13097
GORDON, SANFORD	p 728	N93-12967
GORDON, STEPHEN S.	p 611	N93-12919
GORDON, STEVEN CRAIG	p 518	N93-14038
GORDON, TIM	p 547	N93-12775
GORNEY, DAVID J.	p 705	N93-12715
GORNITZ, VIVIEN M.	p 664	N93-13718
GORODNITSKY, I.	p 675	N93-13522
GOTOH, S.	p 722	N93-13118
GOTSIS, PASCAL K.	p 625	N93-13157
GOTTMANN, MATTHIAS	p 679	N93-13717
GOTTULA, RONALD R.	p 585	N93-13392
GOUGH, MILLICENT V.	p 729	N93-12694
	p 730	N93-13437
	p 731	N93-13454
GOYAL, A.	p 723	N93-13347
GRABEN, JEAN	p 518	N93-13113
GRADIE, JONATHAN	p 597	N93-13424
GRAEDEL, T. E.	p 644	N93-13270
GRAGG, WILLIAM	p 697	N93-14036
GRANDAGE, J. M.	p 500	N93-13256
GRANT, K.	p 643	N93-12926
GRANT, K. E.	p 646	N93-13654
GRAY, B. S.	p 606	N93-13747
GRAY, J. L.	p 639	N93-13529
GRAY, WILLIAM M.	p 661	N93-12928
	p 662	N93-13028
GREENBERG, JOEL S.	p 760	N93-13972
GREENZWEIG, YUVAL	p 759	N93-13958
GREER, WILLIAM ANDREW DEREK	p 523	N93-13919
GREGORY, DON A.	p 710	N93-13500
GREGORY, IRENE M.	p 504	N93-13068
GREGORY, JOHN C.	p 547	N93-12778
	p 548	N93-12781
GRENSEMANN, MANFRED	p 749	N93-12965
GRESHO, P. M.	p 576	N93-12839
GRIFFIN, M. J.	p 678	N93-13464
GRONIN, I.	p 632	N93-12869
GROSCH, THEODORE	p 511	N93-13177
GROSSMAN, A. S.	p 643	N93-12926
GRUBELICH, M. C.	p 555	N93-12563
GRUEN, D. M.	p 723	N93-13349
GRUNSFELD, JOHN M.	p 510	N93-13173
GU, YIJUN	p 533	N93-13775
GUARDIANI, FRANK	p 680	N93-14090
GUENGOER, SALIH	p 543	N93-13690
GUETHLEIN, G.	p 604	N93-12925
GUPTA, ASHOK	p 678	N93-12983
GUREL, LEVENT	p 567	N93-14043
GUTHLEIN, PETER	p 499	N93-13377
GUTTMAN, CHARLES M.	p 553	N93-13785
GUZIK, J. A.	p 743	N93-13339
GYOERFFY, B. L.	p 542	N93-13043

H

HA, JOWOONG	p 553	N93-13780
HAAS, P. A.	p 583	N93-13318
HABERZETTL, H.	p 563	N93-13042
HADAWAY, JAMES B.	p 709	N93-13062
HADJIPANAYIS, GEORGE C.	p 698	N93-12865
HAEFFNER, D. R.	p 721	N93-12881
HAGAR, H. D.	p 506	N93-12552
HAGELSTEIN, P. L.	p 604	N93-12744
HAGER, JON M.	p 599	N93-13665
HAINES, PATRICK ALBERT	p 662	N93-13124
HAJJ, IBRAHIM N.	p 570	N93-12866
HALE, ZOE M.	p 708	N93-12642
HALICIOGLU, TIMUR	p 724	N93-13570
HALL, J. MICHAEL	p 645	N93-13413
HALL, JAMES JOSEPH	p 726	N93-13933
HALL, JOHN B., JR.	p 680	N93-13991
HALL, R. B.	p 637	N93-12838
HALL, STEPHEN W.	p 527	N93-14079
HALLORAN, J. W.	p 550	N93-12999
HALSE, Y. H.	p 622	N93-12843
HALSMER, DOMINIC MICHAEL	p 504	N93-13820
HALYO, NESIM	p 694	N93-13370
HAMADA, H.	p 700	N93-13439
HAMILTON, DAVID B.	p 676	N93-12545
HAMILTON, KAY	p 738	N93-13737
HAMILTON, M. L.	p 541	N93-12820
HAMLEY, IAN WILLIAM	p 723	N93-13332
HAMMOND, E. C., JR.	p 509	N93-13163
HAMMOND, MARC	p 511	N93-13174
HAN, BYUNG MOON	p 640	N93-13934
HAN, H. C.	p 633	N93-13085
	p 633	N93-13086
HAN, J. H.	p 714	N93-12914
HANES, D. M.	p 577	N93-13074
HANSEN, N. R.	p 627	N93-13515
HANSEN, PATRICIA A.	p 510	N93-13168
HANSEN, PETER C.	p 608	N93-13846
HANSON, RONALD K.	p 595	N93-13685
HAPP, T.	p 705	N93-13546
HARDANGE, JEAN-PHILIPPE	p 564	N93-13058
HARIHARAN, P. C.	p 736	N93-13131
HARMON, J. E.	p 735	N93-12994
HARMS, S. L.	p 539	N93-13616
HAROLD, MICHAEL P.	p 537	N93-12995
HARRIS, A. E.	p 577	N93-13200
	p 507	N93-13213
HARRISON, F. WALLACE, JR.	p 619	N93-14006
HARTEN, AMI	p 696	N93-12942
HARTFIELD, ROY JAMES, JR.	p 495	N93-13801
HARTLE, M.	p 627	N93-13444
	p 627	N93-13445
HARTMANN, S. R.	p 608	N93-14023
HARVEY, GALE A.	p 547	N93-12777
HARVEY, R. W.	p 716	N93-13193
HARVEY, W. DON	p 491	N93-13025
HARWELL, JACK	p 619	N93-12692
HARWOOD, CAROLINE S.	p 673	N93-13863
HASHIMOTO, YOSHIHIRO	p 548	N93-12783
HASKIN, L. A.	p 761	N93-13976
HASKIN, LARRY A.	p 761	N93-13979
HATCH, CASEY	p 511	N93-13174
HATCHER, RICHARD	p 619	N93-12692
HAUTALA, SUSAN L.	p 670	N93-13841
HAVSTAD, M. A.	p 576	N93-12825
HAWES, PHILIP B.	p 680	N93-13992
HAWKEY, TIMOTHY	p 616	N93-13706
HAWKINS, GARY F.	p 603	N93-14086
HAWORTH, J.	p 541	N93-12879
HAYASHI, MAKOTO	p 652	N93-13405
HAYDEN, S. M.	p 702	N93-13037
HAYNES, D. L.	p 708	N93-13574
HAYNES, R. DANIEL	p 641	N93-14005
HAZELTINE, R. D.	p 717	N93-13502
HE, FAN	p 658	N93-13888
HEARD, ANNE C.	p 658	N93-13889
HECHT, NORMAN KARL	p 695	N93-14039
HED, ZEEV	p 497	N93-12816
HEDGES, LINDA SIGALLA	p 494	N93-13521
HEFNER, ALLEN R., JR.	p 725	N93-13783
HEGWOOD, JULIE ANNE YATES	p 498	N93-13787
HEIDNER, SUSAN J.	p 498	N93-13787
HEIKEN, G.	p 761	N93-13981
HEIN, C. A.	p 650	N93-12944
HEINZ, R.	p 707	N93-13002
HEISLER, CHARLENE ANNE	p 756	N93-13959
HELLER, CLAYTON H.	p 754	N93-13727
HEMMINGER, C. S.	p 554	N93-14099
HEMMINGER, CAROL S.	p 547	N93-12776
HENDERSON, D. J.	p 705	N93-13546
HENDERSON, KEITH GLENN	p 664	N93-13631

HENDERSON, T. R. p 562 N93-12950
HENDRICKS, JOHN B. p 558 N93-13404
HENKE, R. p 503 N93-13218
HENRY, TODD JACKSON p 749 N93-14070
HER, MING-GUO p 678 N93-13486
HERMAN, R. G. p 537 N93-13188
HERMANN, A. p 723 N93-13526
HERNANDEZ, G. p 650 N93-12845
HEROLD, KEITH E. p 576 N93-12975
HERR, NEVA p 511 N93-13174
HERRING, THOMAS A. p 649 N93-12661
HERRMANN, O. p 503 N93-13230
HERRMANN, WILLIAM p 741 N93-13788
HERWIG, K. W. p 703 N93-13194
HESS, ELIZABETH L. p 743 N93-12898
HESS, ERIC p 499 N93-13377
HESS, RALPH M. p 551 N93-13101
HEWAGAMA, TILAK p 770 N93-13627
HEYSE, MARK W. p 519 N93-12611
HICKMAN, A. P. p 721 N93-12887
HICKMAN, K. C. p 604 N93-12915
HICKS, MICHAEL C. p 586 N93-13400
HIGGINBOTHAM, SCOTT A. p 520 N93-13032
HILBURN, BRIAN p 677 N93-12860
HILDENBRAND, D. L. p 543 N93-13733
HILL, A. p 707 N93-13090
HILL, D. N. p 714 N93-12932
p 714 N93-12971
p 717 N93-13511
HILL, SUSAN T. p 729 N93-12694
p 730 N93-13015
p 731 N93-13698
HILLS, J. G. p 749 N93-12956
HINES, KEITH MARTIN p 667 N93-13890
HINKLEY, JEFFREY A. p 552 N93-13441
HINKS, THOMAS p 624 N93-13016
HINSEY, N. p 701 N93-12806
HIRAOKA, KATSUMI p 491 N93-12716
HIRMAN, JOSEPH W. p 562 N93-12979
HIROTA, KUNIO p 610 N93-12727
HIRSCH, CH. p 579 N93-13210
HJELMSTAD, KEITH D. p 558 N93-12976
HMELO, A. B. p 609 N93-12565
HO, W. p 703 N93-13106
HOADLEY, SHERWOOD T. p 500 N93-13565
HOANG, T. p 512 N93-13181
HOBBS, L. W. p 552 N93-13350
HOBBS, M. L. p 735 N93-12813
HOCKNEY, RICHARD p 616 N93-13706
HOGAN, CAROLE B. p 737 N93-13136
HOHEISEL, H. p 503 N93-13218
p 582 N93-13227
HOKIN, S. p 713 N93-12882
HOLANDA, RAYMOND p 599 N93-13666
HOLCOMB, D. E. p 605 N93-13507
HOLLA, HARISH p 549 N93-12788
HOLLINGS, ERNEST F. p 741 N93-13798
HOLLOWAY, C. MICHAEL p 684 N93-12957
HOLM-HANSEN, O. p 670 N93-13708
HOLM, ALBERT V. p 744 N93-13461
HOLMES, HARLAN K. p 600 N93-13672
HOLONYAK, N., JR. p 608 N93-13864
HONKALA, KEITH ALAN p 584 N93-13383
HOOKER, STANFORD B. p 669 N93-13382
HOPE, L. J. p 580 N93-13217
HORDINSKY, JERRY R. p 674 N93-12612
HOROWITZ, BARRY M. p 731 N93-13834
HORRELL, ROBIN SCOTT p 656 N93-13782
HORSHAM, GARY A. P. p 742 N93-13433
HORTON, W. p 714 N93-12914
HOU, S. Y. p 722 N93-13323
HOUCK, E. D. p 575 N93-12761
HOUNAM, DAVID p 563 N93-13052
p 564 N93-13056
HOUPIS, CONSTANTINE H. p 505 N93-13872
HOUSTON, JAMES p 508 N93-13159
HOVENAC, EDWARD A. p 597 N93-13307
HOWE, ROBERT p 609 N93-12604
HOWIE, JOHN MARK p 657 N93-13794
HOYT, SUSAN p 687 N93-13880
HSIEH, K. C. p 608 N93-13864
HSU, C. C. p 633 N93-13085
HSU, SHIH-TEIN p 695 N93-14021
HSU, WEI-CHENG p 628 N93-13634
HU, FON-LIN p 613 N93-13384
HU, KE p 596 N93-12921
HU, XIMING p 699 N93-13907
HUANG, H. p 626 N93-13443
p 627 N93-13444
p 627 N93-13445
HUANG, HSIN-HSEN p 624 N93-13065
HUANG, JIANXIN p 577 N93-13017
HUANG, JIN p 666 N93-13817
HUBBELL, D. H. p 680 N93-13993
HUBBLE, TINA p 511 N93-13174
HUCKENPOEHLER, J. G. p 729 N93-12802
HUDSON, REGGIE L. p 748 N93-13660
HUFFINE, EDWIN F. p 498 N93-14026
HUG, R. p 545 N93-12755
HUGUENIN, G. R. p 603 N93-13709
HUI, XIAOHUI p 754 N93-13645
HULL, DENNIS LEE p 570 N93-12868
HULSEY, S. S. p 550 N93-12888
p 550 N93-12931
p 552 N93-13538
HUMPHERYS, JEFF p 511 N93-13174
HUNT, LILA p 518 N93-13113
HUNT, WILLIAM D. p 572 N93-13448
HUQ, R. p 545 N93-12651
p 545 N93-12754
HURLBERT, ERIC A. p 586 N93-13397
HURLEY, CHARLES J. p 548 N93-12782
p 548 N93-12784
p 549 N93-12789
HWANG, SUN HEE p 555 N93-12939
HYMER, TOM p 492 N93-12741
HYPES, WARREN D. p 680 N93-13991
HYUNG, SIEK p 756 N93-13850

I

IAVECCHIA, HELENE P. p 678 N93-13450
IFJU, PETER GEZA p 628 N93-13630
IGARASHI, KIYOSHI p 651 N93-13285
IIMURA, RUSSELL p 570 N93-12866
IMHOFF, CATHERINE L. p 744 N93-13461
INAMORI, KOHJI p 652 N93-13432
INGALLS, STEPHEN A. p 609 N93-12555
INGEBO, ROBERT D. p 597 N93-13410
INGELS, FRANK p 682 N93-12654
INGRAM, A. E. p 637 N93-12838
INNOCENTI, LUISA p 516 N93-13691
INOUE, H. R. p 540 N93-12603
INTRIERI, JANET M. p 634 N93-13094
IP, W.-H. p 752 N93-13466
p 752 N93-13467
p 752 N93-13468
p 752 N93-13469
IRWIN, JOHN S. p 643 N93-12940
ISAMINGER, M. A. p 498 N93-14024
ISHIBASHI, I. p 545 N93-12729
ISHII, MASAHIRO p 548 N93-12783
ISHIKAWA, NOBORU p 554 N93-13988
ISHIMARU, AKIRA p 561 N93-12646
ISLER, R. C. p 717 N93-13518
ISMAIL, SHAIK p 504 N93-13566
ISRAEL, STEVEN p 597 N93-13373
ITIKAWA, YUKIKAZU p 703 N93-13095
ITO, MASAAKI p 548 N93-12783
IVES, L. K. p 553 N93-13649
IWASAKI, AKIRA p 663 N93-13287
IYENGAR, S. S. p 732 N93-12553
IYER, R. K. p 503 N93-13697
IZADI, MOHAMMAD JAVAD p 591 N93-13920
IZAGUIRRE, FRANCISCO p 603 N93-14086

J

JACKELS, CHARLES F. p 537 N93-12935
JACKSON, TREVOR p 714 N93-12982
JACOBS, M. K. p 540 N93-13986
JACOBUS, M. J. p 572 N93-13519
JACOBY, JEFFREY p 630 N93-13921
JACQUOTTE, O.-P. p 578 N93-13203
JAFRY, YUSUF R. p 518 N93-13922
JAHANMIR, S. p 553 N93-13649
JAIN, LALIT KUMAR p 528 N93-12630
JAKUBKA, K. p 715 N93-13093
p 716 N93-13330
JALURIA, YOGESH p 559 N93-13642
JANKOWSKI, JOHN E., JR. p 740 N93-13312
JANSSENS, HANS p 739 N93-13912
JARRETT, THOMAS HAROLD p 748 N93-13960
JARVIS, LOUIS P. p 574 N93-13839
JEFFRIES-NAKAMURA, B. p 571 N93-13196
JENA, P. p 720 N93-12750
JENKIN, MICHAEL EDWIN p 654 N93-13726
JENKINS, J. T. p 545 N93-12729
JENKINS, M. L. p 540 N93-12573
p 541 N93-12798
JERIUS, DIAB HEINRICH p 750 N93-13122
JERNIGAN, T. C. p 717 N93-13518
JEZIORSKI, GRZEGORZ p 623 N93-12989
JI, WUSHENG p 653 N93-13485
JIH, YEUNG-JAW JOE p 618 N93-14094
JOHANSSON, M. A. p 537 N93-13188
JOHANSSON, ROLAND p 609 N93-12604
JOHN, SARAH p 771 N93-13020
JOHNSEN, R. p 638 N93-13039
JOHNSON, A. J. p 681 N93-12886
JOHNSON, BARRY p 604 N93-12656
JOHNSON, BRUCE p 616 N93-13706
JOHNSON, C. D. p 522 N93-12893
JOHNSON, D. p 509 N93-13163
JOHNSON, D. J. p 716 N93-13191
JOHNSON, DON H. p 675 N93-13252
JOHNSON, ERIC R. p 624 N93-13019
JOHNSON, K. F. p 710 N93-13509
JOHNSON, N. R. p 703 N93-13114
JOHNSON, R. BARRY p 709 N93-12894
JOHNSON, S. M. p 690 N93-13620
JOHNSON, SALLY C. p 684 N93-12957
JOHNSON, STEVE p 511 N93-13174
JOHNSON, STEWART W. p 744 N93-13579
p 746 N93-13593
p 747 N93-13595
p 747 N93-13598
JOHNSON, THEODORE C. p 510 N93-13167
JOHNSON, W. J. D. p 605 N93-13507
JOHNSTON, H. S. p 646 N93-13646
JOHNSTON, JEFFREY ERIC p 658 N93-13891
JOHNSTON, KEN J. p 745 N93-13582
JOHNSTON, NORMAN J. p 531 N93-13416
JONAH, D. A. p 538 N93-13317
JONES, B. J. p 732 N93-12553
JONES, C. M. p 708 N93-13574
JONES, CHARLES R. p 650 N93-12946
JONES, ERIC M. p 741 N93-14019
JONES, J. D. p 680 N93-13996
JONES, JACK A. p 558 N93-13422
JONES, M. T. p 720 N93-12819
JONES, MICHELE D. p 549 N93-12789
JONES, NICHOLAS BRIAN p 647 N93-13723
JONES, P. L. p 723 N93-13349
JONES, PETER A. p 708 N93-12591
p 708 N93-12593
JONES, PHILIP WILEY p 690 N93-13961
JONES, PHILLIP L. p 552 N93-13325
JONES, S. p 523 N93-13715
JONG, R. A. p 714 N93-12971
JORDAN, C. E. p 650 N93-12944
JORDAN, E. H. p 531 N93-13309
JOSEPH, JAMES p 569 N93-13088
JOUBERT, H. p 502 N93-13212
JOYNER, POWELL p 555 N93-12939
JU, GWO-TARNG p 630 N93-13923
JUANG, JER-NAN p 625 N93-13125
p 694 N93-13442
JUDD, M. D. p 557 N93-12934
JURAS, R. C. p 708 N93-13574
JUSTIZ, CHARLES RICHARD p 497 N93-13970

K

KAHN, ANTOINE p 719 N93-12544
KAHN, S. M. p 753 N93-13536
KAI, YOSHIRO p 559 N93-13989
KAINUMA, SHOJI p 652 N93-13432
KALEPS, INTS p 679 N93-13874
KALLURI, SREERAMESH p 625 N93-13153
KAMENETZKY, RACHEL R. p 536 N93-12780
KAMMERAAD, J. p 596 N93-12762
KAN, PUI T. p 696 N93-12594
KANADE, TAKEO p 692 N93-13240
KANAMORI, HIROSHI p 554 N93-13988
KANEMASU, E. T. p 644 N93-13254
KANG, HEE-JUN p 617 N93-13936
KANG, HO-SHIK p 750 N93-13123
KANG, LONG-CHYUAN p 627 N93-13484
KANGUTKAR, PRAMOD BALKRISHNA p 627 N93-13539
KANNING, GERD p 503 N93-12815
KAO, T. J. p 578 N93-13206
KAPLAN, MICHAEL L. p 654 N93-13719
KAPP, J. A. p 541 N93-12616
KAPP, JOSEPH A. p 622 N93-12643
KARAYAKA, METIN p 534 N93-13810
KARMAN, STEVE L., JR. p 582 N93-13225
KARNIK, TANAY S. p 694 N93-13376
KASSNER, M. E. p 721 N93-12972
KATNIK, GREGORY N. p 520 N93-13032
KATZ, ERIC S. p 506 N93-12902
KATZ, ROBERT p 674 N93-13023
KAUSHIK, S. p 604 N93-12744
KAWAMURA, TETSUO p 724 N93-13730
KAWASHIMA, N. p 596 N93-12639
KAY, IRVIN W. p 560 N93-12574
KAZIMI, REZA p 708 N93-13284
KEANE, D. p 706 N93-12924
KEIFER, D. A. p 673 N93-13612
KELLER, J. O. p 582 N93-13247
KELLER, JOHN R. p 586 N93-13401
KELLER, M. DEAN p 555 N93-13990
KELLER, T. S. p 676 N93-14002
KELLY, J. L. p 640 N93-13623

KEMP, F. S. ..... p 638 N93-13040
KENNELLY, E. P. ..... p 697 N93-13886
KENNICOTT, M. A. ..... p 645 N93-13505
KERCHER, J. R. ..... p 643 N93-12927
KERCZEWSKI, ROBERT J. ..... p 571 N93-13286
KETTMANN, G. ..... p 752 N93-13468
KEYDEL, WOLFGANG ..... p 563 N93-13050
p 563 N93-13051
KHANNA, S. N. ..... p 720 N93-12750
KHURI, RAMZI RAJA ..... p 728 N93-13753
KICK, R. ..... p 707 N93-13235
KIDD, CARL T. ..... p 598 N93-13663
KIEKEL, P. ..... p 706 N93-12830
KIERAS, DAVID E. ..... p 736 N93-13117
p 573 N93-13650
KIGGANS, J. O., JR. ..... p 549 N93-12821
KILGORE, M. V., JR. ..... p 678 N93-12966
KILGORE, MELVIN V., JR. ..... p 672 N93-12949
KILKENNY, J. D. ..... p 715 N93-13105
KIM, D.-H. ..... p 540 N93-12595
KIM, FREDERICK DONG ..... p 501 N93-13821
KIM, JAE H. ..... p 605 N93-13418
KIM, JAE HOON ..... p 523 N93-14040
KIM, MOON-SANG ..... p 594 N93-14061
KIM, RHYN H. ..... p 586 N93-13402
KIM, SANGPYO ..... p 728 N93-13751
KIM, WU JOAN ..... p 595 N93-14097
KIM, Y. M. ..... p 575 N93-12688
KIM, YONG HA ..... p 758 N93-13337
KIM, YONGSEUNG ..... p 661 N93-12833
KING, JOSEPH H. ..... p 735 N93-12991
KING, ROBERT W. ..... p 499 N93-12557
KING, S. L. ..... p 541 N93-12798
KING, TERENCE A. ..... p 604 N93-12644
KINNEY, S. ..... p 677 N93-12732
KINNISON, D. E. ..... p 645 N93-13615
p 646 N93-13646
p 646 N93-13654
p 646 N93-13655
KINROSS-WRIGHT, J. ..... p 605 N93-13507
KINSLEY, KAREN M. ..... p 683 N93-12740
KIRK, M. A. ..... p 540 N93-12573
p 541 N93-12798
p 541 N93-12879
p 542 N93-12973
KIRKPATRICK, GARY ..... p 671 N93-12871
KIRLIN, PETER S. ..... p 722 N93-13100
KIRSCH, L. E. ..... p 704 N93-13251
KISH, J. G. ..... p 610 N93-12736
KLEIN, LYNN SUZANNE ..... p 510 N93-13167
KLEISS, JAMES A. ..... p 676 N93-12662
KLETECKA, P. ..... p 715 N93-13093
KLIER, K. ..... p 537 N93-13188
KNIGHT, R. A. ..... p 538 N93-13314
KNOLL, KARYN T. ..... p 732 N93-14017
KNOTT, W. M., III ..... p 680 N93-13996
KNUDSON, D. A. ..... p 645 N93-13479
KNYSTAUTAS, R. ..... p 555 N93-12933
KOBANA, AKIRA ..... p 718 N93-13732
KOBLER, BENJAMIN ..... p 736 N93-13131
KOCH, V. R. ..... p 573 N93-13610
KOCKS, U. F. ..... p 543 N93-13545
KOELLE, H. H. ..... p 556 N93-13983
KOERNER, R. M. ..... p 622 N93-12843
KOGA, R. ..... p 524 N93-14087
KOGAN, R. L. ..... p 554 N93-13873
KOHLER, J. L. ..... p 761 N93-13978
KOKSBANG, R. ..... p 545 N93-12651
p 545 N93-12754
KOLASINSKI, W. A. ..... p 708 N93-14089
KOLLMANN, W. ..... p 587 N93-13453
KONDO, YOJI ..... p 744 N93-13461
KONG, F. M. ..... p 550 N93-12888
p 550 N93-12931
KONG, J. A. ..... p 633 N93-13084
KONG, JIN AU ..... p 633 N93-13085
p 633 N93-13086
p 569 N93-13087
p 569 N93-13088
KONISHI, HIROYUKI ..... p 663 N93-13446
KOO, BON-CHUL ..... p 751 N93-13360
KOOI, J. W. ..... p 502 N93-13207
KOOMULLIL, GEORGE PAULOSE ..... p 593 N93-14041
KOPLOW, M. ..... p 611 N93-12908
KORENOWSKI, G. M. ..... p 669 N93-12916
KORSMEYER, DAVID JEROME ..... p 517 N93-13766
KOSHIZUKA, N. ..... p 722 N93-13118
KOSINSKI, JOHN ..... p 534 N93-13940
KOSKO, JEROME ..... p 512 N93-13186
KOSTEN, SUE ..... p 506 N93-13013
KOSTEN, SUE E. ..... p 531 N93-13311
KOZEL, DAVID ..... p 574 N93-14093
KRAMER, D. P. ..... p 555 N93-13081
KRAMER, M. J. ..... p 721 N93-13089
KRANTZ, T. L. ..... p 610 N93-12736
KRAWIEC, J. ..... p 526 N93-13429
KREJCIK, P. ..... p 706 N93-12992
p 707 N93-13090
KRICK, M. S. ..... p 702 N93-13076
KRISHEN, K. ..... p 635 N93-13440
KRISS, GERARD A. ..... p 743 N93-13352
KROEGER, D. M. ..... p 723 N93-13347
KRSUL, T. ..... p 645 N93-13479
KRUEGER, ARLIN J. ..... p 661 N93-12700
KRYCUK, A. ..... p 708 N93-13284
KRYSKA, L. ..... p 715 N93-13093
KUBESH, RODNEY JOSEPH ..... p 666 N93-13790
KULANDER, KENNETH C. ..... p 604 N93-12734
KULCINSKI, G. L. ..... p 719 N93-13985
p 680 N93-13998
KULKARNI, SHRINIVAS R. ..... p 745 N93-13584
KUMAR, A. S. ..... p 541 N93-12820
KUMAR, D. ..... p 672 N93-13034
p 672 N93-13083
KUNITAKE, MANABU ..... p 772 N93-13255
KUO, F. ..... p 693 N93-13289
KUPIEC, THOMAS C. ..... p 498 N93-14026
KURIKI, KYOICHI ..... p 519 N93-14015
KURTZ, A. D. ..... p 601 N93-13677
KURTZ, ANTHONY D. ..... p 601 N93-13679
KUSH, A. K. ..... p 640 N93-13623
KUSUDA, TAMAMI ..... p 741 N93-13788
KUYATT, CHRIS E. ..... p 698 N93-12805
KWACK, EUG Y. ..... p 700 N93-13421
KWAN, ROBERT K. ..... p 562 N93-12950
KWOK, R. ..... p 633 N93-13086

L

LABAW, CLAYTON C. ..... p 709 N93-13419
LABEYRIE, ANTOINE ..... p 745 N93-13583
LABITZKE, KARIN ..... p 661 N93-12817
LABONTE, ROBERT ..... p 508 N93-13160
LABS, J. F. ..... p 703 N93-13092
LACAU, R. G. ..... p 497 N93-13222
LADD, EDWIN FREMONT ..... p 758 N93-14091
LALLMAN, FREDERICK J. ..... p 694 N93-13442
LAM, W. K. ..... p 609 N93-12724
LAMP, THOMAS R. ..... p 727 N93-12546
LAMPROS, T. H. ..... p 637 N93-12838
LAN, CHUNG-WEN ..... p 724 N93-13739
LANCE, D. G. ..... p 529 N93-12678
LANDWEBER, LOUIS ..... p 574 N93-12617
LANE, S. N. ..... p 708 N93-13574
LANGE, R. ..... p 576 N93-12912
LANGNER, D. F. ..... p 702 N93-13076
LANICCI, JOHN MICHAEL ..... p 664 N93-13643
LANT, CHRISTIAN T. ..... p 601 N93-13675
LANTEIGNE, DAVID J. ..... p 710 N93-13500
LAPEAN, J. ..... p 561 N93-12655
LARKO, DAVID E. ..... p 661 N93-12700
LAROSILIERE, LOUIS MARIE ..... p 556 N93-13924
LARRABEE, J. F. ..... p 567 N93-13878
LARSEN, E. D. ..... p 610 N93-12793
LARSEN, R. P. ..... p 642 N93-12885
LARSON, T. K. ..... p 728 N93-12857
LAU, CHI-CHUNG ..... p 635 N93-13840
LAU, D. D. ..... p 524 N93-14087
LAU, K. H. ..... p 543 N93-13733
LAUGHREY, J. A. ..... p 502 N93-13228
LAUGHREY, JAMES A. ..... p 502 N93-13224
LAWLESS, PHIL A. ..... p 643 N93-12938
LAWSON, D. R. ..... p 595 N93-12619
LAWSON, DOUGLAS R. ..... p 643 N93-12941
LEADHOLM, T. ..... p 632 N93-12869
LEBEDEV, V. ..... p 623 N93-13003
LEBOEUF, J. N. ..... p 714 N93-12914
p 716 N93-13297
LECORDIX, J. L. ..... p 577 N93-13202
LEE, BONG JU ..... p 718 N93-13792
LEE, CHUN-YING ..... p 621 N93-12627
LEE, I. Y. ..... p 703 N93-13114
p 708 N93-13574
LEE, J. H. ..... p 555 N93-12933
LEE, J. J. ..... p 609 N93-12698
LEE, JAE GYOO ..... p 664 N93-13740
LEE, JON ..... p 621 N93-12606
LEE, KYUN ..... p 534 N93-13908
LEE, MAN HOI ..... p 750 N93-13340
LEE, SANG SOON ..... p 629 N93-13811
LEE, SANGSAN ..... p 590 N93-13898
LEE, SOO HAN ..... p 614 N93-13452
LEE, SUKYOUNG ..... p 663 N93-13361
LEE, T. D. ..... p 707 N93-13189
LEE, Y. J. ..... p 639 N93-13529
LEES, JOANNA FRANCES ..... p 757 N93-14071
LEGGATT, JONATHAN STEWART ..... p 607 N93-13812
LEHMAN, D. R. ..... p 563 N93-13042
LEHMANN, B. ..... p 503 N93-13218
LEHMER, R. ..... p 717 N93-13511
LEHN, WILLIAM L. ..... p 548 N93-12782
p 548 N93-12784
LEHOTSKY, JAMES P. ..... p 598 N93-13656
LEI, JIH-FEN ..... p 600 N93-13671
LEIGHTON, TOM ..... p 685 N93-12961
LEIMKUHLER, BENEDICT ..... p 698 N93-12890
LEISER, DANIEL ..... p 527 N93-12895
p 528 N93-12896
LEITH, DAVID ..... p 559 N93-13648
LEMCOE, M. M. ..... p 599 N93-13669
LEMPERT, WALTER R. ..... p 602 N93-13682
LESTZ, SIDNEY J. ..... p 609 N93-12600
LETOAN, T. ..... p 633 N93-13085
LEVADOU, F. G. ..... p 557 N93-12934
LEVADOU, FRANCOIS ..... p 548 N93-12785
LEVISON, LIBBY ..... p 682 N93-12554
LEWINE, J. D. ..... p 674 N93-12566
LEWIS, P. S. ..... p 675 N93-13522
LEWIS, RALPH ..... p 597 N93-13424
LEWIS, RICHARD L. ..... p 688 N93-13944
LEWIS, ROBERT H. ..... p 761 N93-13979
LEYNAERT, J. ..... p 577 N93-13201
p 497 N93-13221
LI, CHANG-TSUN ..... p 687 N93-13835
LI, JIANG ..... p 646 N93-13721
LI, XINLIN ..... p 651 N93-13149
LI, Y. T. ..... p 766 N93-14007
LI, YUAN-LIANG ..... p 568 N93-14044
LI, ZHUANGJIE ..... p 646 N93-13624
LIANG, W. ..... p 595 N93-12619
LICHTENFELS, ALLYSON ..... p 520 N93-13455
LIEWER, P. ..... p 716 N93-13297
LIGHTHILL, JAMES ..... p 699 N93-12986
LIMBERG, T. ..... p 707 N93-13090
LIN, CHING-CHANG CHARLES ..... p 530 N93-13008
LIN, NENG-HUEI ..... p 647 N93-13741
LIN, ROGER LIDA ..... p 566 N93-13813
LIN, T. D. ..... p 554 N93-13987
LIN, YAO ..... p 710 N93-13652
LIN, YUH-LANG ..... p 654 N93-13719
LINDEN, THEODORE A. ..... p 682 N93-12614
LINDSTROM, DAVID J. ..... p 761 N93-13979
LING, JER RICHARD ..... p 691 N93-13130
LINTON, ROGER C. ..... p 547 N93-12778
LITTELL, HOWARD STEVEN ..... p 589 N93-13806
LIU, FENG ..... p 589 N93-13767
LIU, HONG ..... p 712 N93-14101
LIU, HUA-KUANG ..... p 711 N93-13711
LIU, KETAO ..... p 695 N93-14045
LIU, MENG R. ..... p 621 N93-12628
LIU, WEIHONG ..... p 699 N93-13851
LIU, WING KAM ..... p 624 N93-13029
LIUZZI, RAYMOND A. ..... p 734 N93-12703
LIVENGOOD, TIMOTHY AUSTIN ..... p 759 N93-13625
LJEPOJEVIC, N. N. ..... p 770 N93-13478
LLOYD-HART, MICHAEL ..... p 743 N93-13343
LOCK, JAMES A. ..... p 597 N93-13307
p 602 N93-13684
LOGAN, B. G. ..... p 714 N93-12932
LOGAN, R. ..... p 596 N93-12844
LOHR, J. ..... p 716 N93-13193
LONDON, R. A. ..... p 604 N93-12925
LONGDON, NORMAN ..... p 557 N93-12934
p 749 N93-12965
p 516 N93-13691
p 516 N93-13855
p 516 N93-13856
p 516 N93-13857
p 516 N93-13858
p 516 N93-13859
p 517 N93-13860
p 517 N93-13861
p 517 N93-13902
p 517 N93-13903
LONGHURST, G. R. ..... p 539 N93-13616
LOOFT, FRED J. ..... p 508 N93-13160
LORD, A. E., JR. ..... p 622 N93-12843
LOTTER, K. W. ..... p 580 N93-13215
LOU, WEIRAN ..... p 717 N93-13495
LOUIE, KEN ..... p 493 N93-13451
LOUSMA, JACK R. ..... p 733 N93-12660
p 734 N93-12680
LOVE, H. ..... p 554 N93-13987
LU, CHI-HSIEN JOSEPH ..... p 573 N93-13607
LU, FENGXIANG ..... p 760 N93-13974
LU, PING ..... p 500 N93-13305
LUCCIO, A. ..... p 571 N93-13358
LUCE, T. C. ..... p 716 N93-13193
LUCHER, DAN ..... p 615 N93-13644
LUCKE, R. ..... p 524 N93-13870
LUK, FRANKLIN T. ..... p 695 N93-12582
LUKYANOV, V. M. ..... p 554 N93-13873
LUNDEEN, THOMAS ..... p 597 N93-13424
LUO, DING ..... p 757 N93-13962
LUO, MINGZHAO ..... p 656 N93-13789
LUSSIE, W. G. ..... p 728 N93-12857
p 576 N93-12996
LUTES, G. ..... p 596 N93-12844

LUTHCKE, S. B. ..... p 519 N93-13372
LYNCH, JOHN ..... p 651 N93-13326
LYNCH, V. E. ..... p 716 N93-13297
LYNE, JAMES EVANS ..... p 521 N93-12720
LYON, J. F. ..... p 717 N93-13518
LYON, TERRY ..... p 604 N93-12610
LYONS, LARRY R. ..... p 705 N93-12715

M

MAAG, ANDREW J. ..... p 512 N93-13183
MAAG, CARL R. ..... p 510 N93-13168
p 512 N93-13183
MACDIARMID, A. G. ..... p 545 N93-12749
MACGOWAN, B. ..... p 603 N93-12570
MACGOWAN, B. J. ..... p 606 N93-13653
MACKRODT, P.-A. ..... p 497 N93-13221
MACLAREN, BRICE K. ..... p 559 N93-14009
MACLIN, E. ..... p 674 N93-12566
MACNEICE, P. ..... p 770 N93-13478
MACRAE, B. D. ..... p 632 N93-12869
MACRANDER, A. T. ..... p 721 N93-12881
MADDEN, FRANCIS ..... p 590 N93-13899
MAESHIMA, K. ..... p 705 N93-13537
MAGEE, DAVID P. ..... p 612 N93-12954
p 612 N93-12955
MAGEE, DAVID PATRICK ..... p 610 N93-12904
MAGGIO, R. ..... p 580 N93-13216
MAGRUDER, ROBERT H., III ..... p 711 N93-13866
MAGUIRE, BASSETT, JR. ..... p 648 N93-13995
MAGULA, P. ..... p 715 N93-13093
MAHAN, JOHN E. ..... p 571 N93-13430
MAHARIK, MICHAEL ..... p 527 N93-13971
MAHDAVI, M. A. ..... p 714 N93-12932
MAHJOUB, MOHAMED E. ..... p 610 N93-12760
MAHLE, JOHN J. ..... p 596 N93-12653
MAI, T. V. ..... p 566 N93-13871
MAISEL, JAMES E. ..... p 561 N93-12679
MAKEDON, FILLIA ..... p 685 N93-12961
MAKEL, D. B. ..... p 602 N93-13686
MAKRIS, A. ..... p 555 N93-12933
MALEK, MIROSLAW ..... p 681 N93-12707
MALLASCH, PAUL G. ..... p 685 N93-13291
MALLINSON, JOHN C. ..... p 737 N93-13134
MALLON, JOSEPH R., JR. ..... p 601 N93-13676
MALLOT, G. K. ..... p 702 N93-13073
MALTRUD, MATHEW EINAR ..... p 590 N93-13900
MANDAL, B. ..... p 650 N93-12943
MANGOLD, HELMUT ..... p 692 N93-13239
MANNING, AMANDA J. L. ..... p 652 N93-13482
MANNING, CHERYL A. ..... p 679 N93-13692
MANZO, MICHAEL ..... p 598 N93-13567
MAPLES, D. ..... p 640 N93-13618
MARGOLIS, S. B. ..... p 699 N93-13262
MARQUEZ, H. ..... p 708 N93-13508
MARSHALL, J. A. ..... p 519 N93-13372
MARSHALL, J. H. ..... p 722 N93-13323
MARSHALL, P. W. ..... p 711 N93-14031
MARTH, RICHARD B. ..... p 499 N93-13348
p 499 N93-13351
MARTIN, RODERICK H. ..... p 532 N93-13428
MARWIL, E. S. ..... p 539 N93-13616
MARYNIAK, GREGG E. ..... p 761 N93-13977
MARZULLO, KEITH ..... p 687 N93-13695
MASCIANGELO, S. ..... p 693 N93-13243
MASON, GRAEME ..... p 671 N93-13842
MASON, T. E. ..... p 702 N93-13037
MATHEWS, SCOTT ..... p 705 N93-13606
MATROSOV, SERGEY Y. ..... p 634 N93-13094
MATSUMOTO, SHINJI ..... p 559 N93-13989
MAUEL, M. E. ..... p 718 N93-13535
MAUGHMER, MARK D. ..... p 493 N93-13463
MAUREY, JOHN R. ..... p 553 N93-13785
MAXIMON, L. C. ..... p 563 N93-13042
MAY, BRIAN D. ..... p 571 N93-13286
MAYBERRY, M. J. ..... p 716 N93-13193
MAYER, RICHARD J. ..... p 685 N93-13004
MAYLE, R. W. ..... p 712 N93-12571
MAZIASZ, P. J. ..... p 542 N93-13190
MCALISTER, HAROLD A. ..... p 744 N93-13581
MCALLISTER, DAVID F. ..... p 686 N93-13293
MCANULTY, D. M. ..... p 677 N93-12609
MCARTHUR, D. A. ..... p 605 N93-13249
MCBRIDE, BONNIE J. ..... p 728 N93-12967
MCCALLUM, R. W. ..... p 721 N93-13089
MCCANN, S. W. ..... p 605 N93-13507
MCCLAIN, CHARLES R. ..... p 669 N93-13382
MCCLURE, CHARLES R. ..... p 738 N93-13884
MCCONNELL, P. ..... p 542 N93-13302
MCCONNELL, ROBERT ..... p 598 N93-13567
MCCUTCHEON, KIMBLE D. ..... p 611 N93-12919
MCDERMOTT, GENE ..... p 684 N93-12851
p 684 N93-12872
MCELIGOT, D. M. ..... p 728 N93-12857
p 576 N93-12996
MCGILL, P. R. ..... p 566 N93-13869
MCGLYNN, S. P. ..... p 672 N93-13034
p 672 N93-13083
MCGOWAN, F. K. ..... p 703 N93-13114
MCGRAW, SANDRA M. ..... p 500 N93-13565
MCGREGOR, I. ..... p 497 N93-13221
MCKAMEY, C. G. ..... p 542 N93-13190
MCKEE, DAVID J. ..... p 643 N93-12941
MCKIBBEN, MARK ..... p 510 N93-13167
MCKINNEY, WILLIAM S., JR. ..... p 619 N93-14006
MCKINNIS, DARIN N. ..... p 614 N93-13423
MCKNIGHT, R. L. ..... p 626 N93-13443
p 627 N93-13444
p 627 N93-13445
MCLAUGHLIN, S. B. ..... p 642 N93-12828
MCLEAN, S. J. ..... p 649 N93-12804
MCMAHAN, TRACY ..... p 557 N93-12951
p 518 N93-13113
MCMILLAN, B. K. ..... p 683 N93-12722
MCMILLIN, BRIAN K. ..... p 595 N93-13685
MCMINN, JOHN D. ..... p 504 N93-13068
MCMURRAY, GARY V. ..... p 559 N93-14009
MCNAMARA, BRIAN ROBERT ..... p 751 N93-13380
MCNEIL, J. R. ..... p 604 N93-12915
MCNEILL, STEPHEN R. ..... p 601 N93-13674
MEACHAM, G. B. K. ..... p 640 N93-13622
MEAD, JAYLEE M. ..... p 744 N93-13461
MEAD, W. C. ..... p 690 N93-12559
MECHAM, D. C. ..... p 728 N93-12857
p 576 N93-12996
MECKING, H. ..... p 543 N93-13545
MEESE, KENNETH J. ..... p 508 N93-13159
MEHTA, AMITA VIKRAM ..... p 665 N93-13760
MEIER, A. ..... p 752 N93-13469
MEIER, SUSAN MANNING ..... p 544 N93-12589
MEINHOLD, PETER RUSSELL ..... p 772 N93-13689
MELIUS, C. F. ..... p 537 N93-13233
MELL, RICHARD J. ..... p 548 N93-12781
MELLOCH, M. R. ..... p 720 N93-12748
MENDELL, WENDELL W. ..... p 760 N93-13972
MENDENHALL, J. A. ..... p 743 N93-13272
MENDOLIA, M. S. ..... p 545 N93-12753
MENDREK, M. J. ..... p 553 N93-13716
MERCER, M. R. ..... p 681 N93-12707
MERKLE, K. L. ..... p 722 N93-13195
MESLAND, DICKY A. M. ..... p 516 N93-13691
MESSENGER, A. J. ..... p 678 N93-13464
MESSIER, DONALD R. ..... p 553 N93-13836
MEYER, W. ..... p 579 N93-13211
MEYERS, H. ..... p 649 N93-12804
MIAKE-LYE, RICHARD ..... p 497 N93-12816
MICHALOPOULOS, C. D. ..... p 586 N93-13398
MIKATARIAN, JEFF ..... p 557 N93-12951
MIKELL, A. T., JR. ..... p 678 N93-12966
MILEWSKI, J. O. ..... p 609 N93-12565
MILKE, JAMES ALBERT ..... p 530 N93-13012
MILLER, ALAN K. ..... p 531 N93-13324
MILLER, B. G. ..... p 539 N93-13616
MILLER, D. W. ..... p 702 N93-13076
MILLER, DONNA J. ..... p 679 N93-13874
MILLER, EDGAR R. ..... p 548 N93-12781
MILLER, J. A. ..... p 537 N93-13233
MILLER, JAMES G. ..... p 620 N93-13435
MILLER, R. B. ..... p 706 N93-12830
MILLS, A. F. ..... p 587 N93-13406
MILLS, RAYMOND ARTHUR ..... p 694 N93-13925
MILNER, EDWARD J. ..... p 689 N93-13154
MILNER, L. M. ..... p 604 N93-12915
MINECK, RAYMOND EDWARD ..... p 496 N93-13822
MING, DOUGLAS W. ..... p 760 N93-13975
MINSCHWANER, KENNETH ROBERT
p 655 N93-13731
MINTY, M. ..... p 707 N93-13090
MIODUSZEWSKI, P. K. ..... p 717 N93-13518
MITCHELL, B. GREG ..... p 670 N93-13708
MITCHELL, T. E. ..... p 550 N93-12999
MIYAKE, KEITH M. ..... p 687 N93-13734
MIZUNO, J. ..... p 596 N93-12639
MLYNAR, J. ..... p 715 N93-13093
MOBILIA, J. ..... p 648 N93-12621
MOBLEY, SCOTTIE B. ..... p 710 N93-13500
MOELLER, C. L. ..... p 675 N93-13449
MOEN, WILLIAM E. ..... p 738 N93-13884
MOERDER, DANIEL D. ..... p 694 N93-13442
MOHEB, HAMID ..... p 569 N93-14066
MOLINA, I. ..... p 706 N93-12830
MOLLOY, ROBERT ..... p 503 N93-12578
p 677 N93-12860
MOLLS, FRANK B. ..... p 585 N93-13396
MOLNAR, J. A. ..... p 566 N93-13871
MONASTERSKY, RICHARD ..... p 645 N93-13413
MONTGOMERY, RAYMOND C. ..... p 694 N93-13442
MOODY, J. WARD ..... p 510 N93-13171
MOORE, C. E. ..... p 642 N93-12726
MOORE, CHRISTOPHER LANE ..... p 614 N93-13488
MOORE, FRANK G. ..... p 492 N93-12741
MOORE, FRED ..... p 736 N93-13132
MOORE, REAGAN W. ..... p 737 N93-13137
MOORE, T. C., SR. ..... p 600 N93-13672
MOORHOUSE, D. J. ..... p 502 N93-13228
MORDEN, SIMON JAMES ..... p 755 N93-13795
MOREA, SAVERIO F. ..... p 619 N93-14008
MOREIRA-NORDEMANN, LYCIA MARIA
p 632 N93-13005
MORGAN, KAREN ..... p 682 N93-12614
MORGAN, W. L. ..... p 562 N93-12950
MORIARITY, DEBRA M. ..... p 671 N93-12901
MORRIS, D. E. ..... p 641 N93-12685
MORRIS, PAUL H. ..... p 686 N93-13355
MORRISON, JEFFREY G. ..... p 499 N93-12613
MORROW, R. C. ..... p 680 N93-13997
MORTARA, KARL W. ..... p 493 N93-13463
MORTENSEN, G. A. ..... p 583 N93-13356
MORTON, SCOTT ALLYN ..... p 755 N93-13828
MOSCHINI, LARRY ..... p 508 N93-13160
MOSIER-BOSS, P. A. ..... p 570 N93-12725
MOSIER, FRANCES L. ..... p 508 N93-13158
MOSS, WILLIAM F. ..... p 558 N93-12980
MOURAD, P. D. ..... p 668 N93-12577
p 669 N93-12599
MOYER, CARL ..... p 615 N93-13644
MOYER, R. ..... p 717 N93-13511
MOZURKEWICH, D. ..... p 745 N93-13582
MOZZANO, S. G. ..... p 736 N93-13078
MUCKERHEIDE, M. C. ..... p 508 N93-13161
MUENDEL, M. ..... p 604 N93-12744
MUENTER, JOHN S. ..... p 701 N93-12745
MUFSON, S. ..... p 707 N93-13002
MUIR, THOMAS G. ..... p 774 N93-12696
MUKHERJEE, RANJAN ..... p 615 N93-13638
MUKHERJEE, SUDIPTO ..... p 618 N93-14075
MUMMA, MICHAEL J. ..... p 608 N93-14010
MUNDELL, A. R. G. ..... p 507 N93-13213
MUNEY, WILLIAM S. ..... p 508 N93-13159
MUNRO, ROSEMARY ..... p 667 N93-13892
MURAKAMI, M. ..... p 717 N93-13518
MURDOCH, R. W. ..... p 642 N93-12726
MURPHY, PATRICIA G. ..... p 572 N93-13473
MURRAY, ALEXANDER G. ..... p 748 N93-13852
MURRAY, M. J. ..... p 612 N93-13236
MUSGRAVE, J. ..... p 641 N93-12685
MUSKET, R. G. ..... p 701 N93-12806
MUSSER, J. ..... p 707 N93-13002
MUYSHONDT, ARNOLD ..... p 582 N93-13226
MYERS, ROGER M. ..... p 525 N93-12638
p 526 N93-13283

N

NACHTIGAL, NOEL M. ..... p 684 N93-12801
NACHTRIEB, ROBERT T. ..... p 525 N93-12963
NAGAPPAN, S. ..... p 682 N93-13759
NAGY, KORNEL ..... p 614 N93-13417
NAIK, D. A. ..... p 578 N93-13206
NAIRN, JOHN A. ..... p 623 N93-12911
NAKAMURA, N. ..... p 722 N93-13118
NAKAYAMA, MARIKO ..... p 584 N93-13388
NAMBA, HARUYUKI ..... p 559 N93-13989
NANGIA, R. K. ..... p 497 N93-13223
NAPFEL, CLAUDIA M. ..... p 559 N93-13648
NAPIER, MARY E. ..... p 539 N93-13763
NAPOLITANO, MARCELLO R. ..... p 503 N93-12903
NAQVI, S. S. ..... p 604 N93-12915
NARENDRAN, NADARAJAH ..... p 709 N93-12984
NASLUND, ROBERT A. ..... p 552 N93-13325
NASSAR, ANTONIO BOULHOSA ..... p 729 N93-13957
NASSTROM, J. S. ..... p 576 N93-12912
NAVICKAS, J. ..... p 584 N93-13389
NAVRATIL, G. A. ..... p 718 N93-13535
NEAL, VALERIE ..... p 518 N93-13113
NEALY, JOHN E. ..... p 520 N93-12876
p 771 N93-13126
NED, ALEXANDER ..... p 601 N93-13679
NEFF, JON MARK ..... p 522 N93-13119
NEGRONI, PETER J. ..... p 731 N93-13834
NEILSEN, M. K. ..... p 624 N93-13072
NELLESSEN, WOLFGANG ..... p 516 N93-13691
NELLIS, W. J. ..... p 701 N93-12806
NELSON, HAROLD E. ..... p 559 N93-13640
NELSON, MARK ..... p 680 N93-13992
NELSON, P. A. ..... p 700 N93-13439
NELSON, RONALD S. ..... p 510 N93-13172
NERALIC, L. ..... p 683 N93-12730
NESS, ROBERT O., JR. ..... p 680 N93-14000
NESS, SUMITRA R. ..... p 680 N93-14000
NETTLES, A. T. ..... p 529 N93-12678
NEUBERT, M. ..... p 704 N93-13250
NEUGEBAUER, M. ..... p 752 N93-13466
p 752 N93-13467
p 752 N93-13468
p 752 N93-13469

NEUMANN, RICHARD D. p 598 N93-13662
NEUPERT, WERNER M. p 508 N93-13159
NEWBERGER, B. S. p 707 N93-13108
NEWMAN, MATTHEW p 759 N93-13831
NEWNAM, B. E. p 603 N93-12560
NGHIEM, SON V. p 633 N93-13086
p 569 N93-13087
NGUYEN, D. p 511 N93-13180
NGUYEN, D. C. p 605 N93-13507
NGUYEN, PHU VAN p 594 N93-14067
NICHOLS, S. p 511 N93-13180
NICHOLSON, D. M. p 542 N93-13043
NICHOLSON, JAMES H. p 509 N93-13164
NIE, D. p 644 N93-13254
NIELSEN, PETER AXEL p 739 N93-14058
NIKITAS, CHLOE p 647 N93-13893
NILSEN, J. p 603 N93-12570
p 606 N93-13653
NILSON, D. p 714 N93-12932
NING, LI p 593 N93-13965
NISSLEY, DAVID M. p 544 N93-12589
NOBLE, R. J. p 701 N93-12572
NOFAR, I. p 753 N93-13523
NOGAR, N. S. p 538 N93-13341
NOID, D. W. p 691 N93-13079
NOLAN, MICHAEL J. p 558 N93-13021
NORBURY, JOHN W. p 771 N93-13020
NORDBY, M. p 707 N93-13090
NORMAN, T. p 611 N93-12908
NORVELLE, RAYE p 634 N93-13345
NORWELL, GEORGE A. p 750 N93-13294
NOWLEN, S. P. p 572 N93-13519
NOWLIN, ROBERT W. p 561 N93-12679
NOYES, H. P. p 727 N93-12826
NUMBERS, K. p 503 N93-13229
NUNN, TIMOTHY A. p 601 N93-13679
NUNNELEY, SARAH A. p 676 N93-14027
p 676 N93-14028
NYGAARD, KRIS JACOB p 577 N93-13120

O

OAKES, DENNIS L. p 674 N93-12751
OBRIEN, J. E. p 728 N93-12857
p 576 N93-12996
OBRIEN, T. KEVIN p 532 N93-13428
OCONNOR, D. p 571 N93-13196
OETTL, HERWIG p 564 N93-13053
p 564 N93-13055
OGAWA, YUKIMASA p 519 N93-14015
OGURA, KOICHI p 718 N93-13732
OHARE, PATRICK A. G. p 698 N93-12805
OHTAKA, KAZUHIRO p 772 N93-13255
p 651 N93-13285
OKADA, TAKEJI p 554 N93-13988
OLCOTT, DENNIS DUANE p 630 N93-13823
OLDENBORGN, R. C. p 639 N93-13313
OLDENBURG, JOHN R. p 597 N93-13307
OLEAR, BERNARD T. p 737 N93-13138
OLSEN, D. K. p 708 N93-13574
ONDA, KUNIZO p 652 N93-13405
ONDREJCIN, R. S. p 550 N93-13035
ONEILL, J. J. p 566 N93-13871
ONG, SHAW YANG p 505 N93-13926
ONISHI, SHINZO p 599 N93-13665
OPPENEHIM, ALAN p 560 N93-12608
ORBACH, RAYMOND L. p 725 N93-13881
ORDUNA-BUSTAMANTE, F. p 700 N93-13439
ORIOL, R. A. p 668 N93-12556
ORME, JOHN S. p 502 N93-13155
OSBORNE, T. H. p 712 N93-12687
OSGOOD, R. M. p 601 N93-13677
OSHEA, T. p 640 N93-13621
OSKAM, B. p 497 N93-13205
OSTERHELD, A. L. p 712 N93-12571
OTSUKA, ATSUSHI p 652 N93-13432
OTUGEN, M. VOLKAN p 599 N93-13668
OZER, R. W. p 582 N93-13247
OZTURK, MURAT p 625 N93-13127

P

PACE, MICHAEL E. p 684 N93-12851
p 684 N93-12872
PACHECO, J. E. p 640 N93-13618
PADMANABHAN, SRIKANTH p 616 N93-13720
PAETSCH, L. p 640 N93-13621
PAITHOONWATTANAKIJ, KITTI p 687 N93-13913
PALEN, EDWARD JOHN p 647 N93-13758
PALMER, B. A. p 639 N93-13313
PALMER, JENNIFER L. p 595 N93-13685
PALMER, M. E. p 497 N93-13223
PAN, KUE p 591 N93-13937
PAN, WEN HSIUNG p 644 N93-13121
PANAYAPPAN, RAMANATHAN p 552 N93-13414
PANTALEONE, J. p 772 N93-13533
PAPADOPOULOS, DENNIS p 562 N93-12948
PAPAVASSILIOU, J. p 555 N93-12933
PARAND, FOROUTAN p 641 N93-14078
PARASURAMAN, RAJA p 503 N93-12578
p 499 N93-12613
p 677 N93-12860
PARIZADEH, K. p 735 N93-12824
PARK, CHUNG SIK p 521 N93-12834
PARKE, W. C. p 563 N93-13042
PARKER, DICK p 680 N93-14001
PARKER, T. E. p 603 N93-13687
PARKINSON, W. H. p 645 N93-13274
PARR, A. DOUGLAS p 659 N93-14053
PARTRIDGE, HARRY p 702 N93-12900
PARZEN, EMANUEL p 698 N93-13064
PATE, BRUCE p 559 N93-13648
PATEL, P. p 640 N93-13621
PATER, RUTH H. p 531 N93-13416
PATNAIK, GAGAN B. p 691 N93-12607
PATTEN, K. O., JR. p 645 N93-13615
PATTON, J. p 540 N93-12595
PAUL, PHILLIP H. p 602 N93-13686
PAULOS, T. p 523 N93-13715
PAXTON, K. p 523 N93-13715
PAZUR, W. p 579 N93-13211
PEASE, DANIEL p 689 N93-12852
PECHTL, P. A. p 538 N93-13314
PEDEN, MARK DANIEL p 511 N93-13175
PEDERSEN, F. p 707 N93-13090
PEERY, J. S. p 684 N93-12795
PEGGS, S. p 707 N93-13235
PEKALA, R. W. p 550 N93-12888
p 550 N93-12931
PELLIN, M. J. p 723 N93-13349
PENG, PING p 686 N93-13494
PENG, XIAOHANG p 527 N93-13927
PENN, LANNING M. p 661 N93-12700
PENNER, J. E. p 642 N93-12880
PENSKI, ELWIN C. p 536 N93-12743
PERALTA, R. A. p 645 N93-13479
PEREIRA, A. J. p 640 N93-13623
PEREZ-LOPEZ, B. L. p 538 N93-13341
PEREZ, DANIEL LIZARRAGA p 526 N93-13824
PEREZ, ERNEST RAOUL p 739 N93-14076
PERRY, CHRISTOPHER H. p 753 N93-13602
PERRY, D. L. p 740 N93-12814
PERSSON, OLA PER GUSTAV p 655 N93-13757
PERZANOWSKI, DENNIS p 688 N93-13942
PETERS, K. A. p 509 N93-13163
PETERS, PALMER N. p 547 N93-12778
p 548 N93-12781
PETERSON, M. B. p 553 N93-13649
PETERSON, THOMAS CARL p 665 N93-13744
PETERSON, WEDDELL C. p 572 N93-13563
PETRAKIS, JOHN PETER p 773 N93-13738
PETRIE, T. W. p 714 N93-12932
PETRUCCI, SERGIO p 537 N93-13096
PETRZILKA, V. p 715 N93-13091
PETTIT, D. p 761 N93-13981
PETTIT, DONALD R. p 557 N93-14011
PETTY, C. C. p 716 N93-13193
PHAN, TAI-DUC p 657 N93-13793
PHILLIPS, G. p 560 N93-12581
PHILLIPS, ROBERT W. p 675 N93-13449
PHILLPS, J. M. p 722 N93-13323
PHOEBUS, PATRICIA A. p 667 N93-13877
PHYTHIAN, W. J. p 540 N93-12573
PIERS, W. J. p 497 N93-13205
PILCHER, CARL B. p 746 N93-13591
PINHEIRO, MARCO ANTONIO SANTOS p 535 N93-13967
PINKERTON, S. D. p 524 N93-14087
PINKNEY, PAUL p 685 N93-13261
PINSKER, R. I. p 716 N93-13193
PINSKI, F. J. p 542 N93-13043
PIPER, T. C. p 597 N93-13267
PIPPIN, H. GARY p 548 N93-12785
p 549 N93-12786
PISTEK, P p 697 N93-13886
PITZ, W. J. p 555 N93-12933
PLANK, LOTHAR p 696 N93-12701
PLASSMANN, P. E. p 720 N93-12819
PLOETZ, K. L. p 549 N93-12821
PLOTKIN, SERGE p 685 N93-12961
PLUMMER, THOMAS B. p 508 N93-13159
POCO, P. K. p 552 N93-13538
POLITANO, M. p 753 N93-13523
POLLACK, J. B. p 643 N93-12926
POMERANTZ, ARTHUR p 507 N93-13447
POOLE-KOBER, EVELYN M. p 644 N93-12974
POOLE, STEVEN ROSS p 518 N93-13768
POPECKI, MARK ANDREW p 660 N93-14068
POPPEL, G. L. p 711 N93-13762
PORCH, W. M. p 662 N93-13075
PORKOLAB, M. p 716 N93-13193
PORTER, G. D. p 714 N93-12971
PORTER, J. L. p 603 N93-12570
p 606 N93-13653
POTASEK, M. J. p 696 N93-13027
POWARS, CHARLES p 615 N93-13644
POWELL, H. M. p 602 N93-13681
POWER, J. p 708 N93-13508
POWERS, C. BLAKE p 557 N93-12951
POWERS, JANET V. p 743 N93-12898
PRAEL, R. E. p 704 N93-13281
PRAGER, S. C. p 713 N93-12883
PRASAD, SUDHAKAR p 745 N93-13586
PRATER, R. p 716 N93-13193
PRESTON, RICHARD p 608 N93-14085
PRICE, KENT M. p 562 N93-12950
PRICE, LINWOOD L. p 602 N93-13681
PRIEDHORSKY, W. C. p 524 N93-13516
PRINCE, R. P. p 680 N93-13996
PROUDFOOT, J. p 705 N93-13531

Q

QI, MIN p 725 N93-13844
QIAO, SANZHENG p 695 N93-12582
QUEALY, ANGELA p 689 N93-13154
QUINN, JARUS W. p 709 N93-12666
p 711 N93-13879
p 608 N93-13883
QUINTIERE, JAMES G. p 539 N93-13641
QUMEI, IYAD KHALIL p 501 N93-13807

R

RACAH, DANIEL p 723 N93-13362
RACINE-POON, A. p 697 N93-12702
RADHAKRISHNAN, V. M. p 622 N93-12739
RADKE, LAWRENCE F. p 649 N93-12818
RAETH, PETER G. p 690 N93-12548
RAHMAN, MOHAMED MIZANUR p 589 N93-13825
RAKESTRAW, D. J. p 537 N93-13232
p 538 N93-13234
RALPH, JOHN p 559 N93-13434
RAMALINGAM, MYSORE L. p 727 N93-12546
RAMBONE, JAMES D. p 506 N93-12668
RANACHOWSKI, JERZY p 623 N93-12989
RAND, J. A. p 637 N93-12838
RANDICH, E. p 706 N93-12970
RANEY, R. KEITH p 564 N93-13059
p 565 N93-13060
RANGANATHAN, RAJ P. p 584 N93-13387
RANSOM, E. C. P. p 580 N93-13217
RANTANEN, RAY p 547 N93-12775
RAO, B. K. p 720 N93-12750
RAO, VASANT B. p 570 N93-12866
RASHIDI, M. p 610 N93-12736
RASIO, FREDERIC ARMAND p 755 N93-13764
RASMUSSEN, D. A. p 717 N93-13518
RATTI, A. p 571 N93-13358
RAWLINS, W. T. p 603 N93-13687
RAYMOND, R. J. p 609 N93-12724
REACH, WILLIAM THOMAS p 772 N93-13147
REDFIELD, ROBIN C. p 709 N93-12985
REDMARD, EDMOND p 722 N93-13268
REED, ANN p 741 N93-13788
REED, CHRISTOPHER L. p 582 N93-13226
REED, KENNETH W. p 626 N93-13260
REES, D. E. p 563 N93-13045
REGAN, A. H. p 563 N93-13045
REHDER, JOHN J. p 519 N93-13379
REHN, L. E. p 722 N93-13104
REICH, SEBASTIAN p 698 N93-12890
REICHERT, GAIL A. p 744 N93-13461
REIDY, R. p 540 N93-12595
REIFSNIDER, K. L. p 550 N93-12858
REINEMAN, MARTIN E. p 616 N93-13761
REME, H. p 752 N93-13467
REMEDIOS, J. J. p 659 N93-14054
RENK, T. J. p 716 N93-13191
RENSINK, M. E. p 714 N93-12932
RESENDE, HUGO B. p 505 N93-13928
RHEE, KYONG YOP p 533 N93-13752
RHEE, U.-S. p 688 N93-12733
RHOADS, TIM p 678 N93-12966
RHODES, J. W. p 673 N93-13503
p 673 N93-13520
RHODES, R. p 524 N93-13870
RICHIE, JOSEPH M. p 507 N93-13447
RICHMOND, G. L. p 606 N93-13514
RIDGWAY, STEPHEN T. p 746 N93-13590
RIDOUT, JAMES ALAN p 663 N93-13489
RIEMENSCHNEIDER, R. A. p 682 N93-12614
RILLEMA, D. P. p 543 N93-13346
RIMKUS, W. A. p 642 N93-12885

RINDERKNECHT, DONALD M. ..... p 660 N93-12596
RINDT, JOHN R. ..... p 680 N93-14000
RING, STEVEN G. ..... p 585 N93-13393
RIVARD, W. C. ..... p 584 N93-13389
ROBANCHO, S. ..... p 509 N93-13163
ROBERTI, DINO ..... p 508 N93-13160
ROBERTS, BARNEY ..... p 651 N93-13326
ROBERTS, CAROL ..... p 651 N93-13326
ROBERTS, DOUGLAS ALAN ..... p 756 N93-13853
ROBERTSON, I. M. ..... p 541 N93-12879
p 542 N93-12973
ROBERTSON, R. G. H. ..... p 701 N93-12588
ROBINSON, HARRISS ..... p 737 N93-13135
ROBINSON, PAUL AARON ..... p 507 N93-13542
ROBITAILLE, H. A. ..... p 680 N93-13993
RODDIER, FRANCOIS ..... p 745 N93-13588
RODEAN, H. C. ..... p 576 N93-12912
RODI, PATRICK ELROY ..... p 590 N93-13826
RODRIGUEZ, JOSE A. ..... p 585 N93-13394
RODRIGUEZ, RODOLFO ..... p 696 N93-12701
ROEDER, J. L. ..... p 712 N93-12705
ROEHL, COLEEN M. ..... p 702 N93-13067
ROELKE, RICHARD J. ..... p 492 N93-13292
ROETTGER, ELIZABETH ELLEN .. p 753 N93-13603
ROGACKI, JOHN R. ..... p 530 N93-12929
ROGERS, LAWRENCE W. ..... p 493 N93-13353
ROJAS-PALMA, CARLOS MANUEL
p 667 N93-13894
ROLFE, S. T. ..... p 626 N93-13320
ROLLETT, A. D. ..... p 551 N93-13315
ROMINE, PETER L. ..... p 614 N93-13436
ROMING, PETER W. A. ..... p 510 N93-13171
p 512 N93-13185
RON, AMOS ..... p 696 N93-12847
RONZHEIMER, A. ..... p 582 N93-13227
RONZHELMER, A. ..... p 578 N93-13204
ROOT, B. T. ..... p 566 N93-13868
ROSCHER, H. J. ..... p 503 N93-13218
ROSEN, M. D. ..... p 604 N93-12925
ROSEN, R. S. ..... p 721 N93-12972
ROSENBAUER, H. ..... p 752 N93-13468
p 752 N93-13469
ROSENBLATT, JOAN R. ..... p 698 N93-12805
ROSENTHAL, DAVID A. ..... p 562 N93-12979
ROSENZWEIG, J. ..... p 707 N93-13235
ROSIGNOLO, C. L. ..... p 645 N93-13479
ROSSABI, J. ..... p 710 N93-13576
ROSSOW, C.-C. ..... p 578 N93-13204
p 582 N93-13227
ROST, E. ..... p 706 N93-12822
ROTH, CARL ..... p 684 N93-12851
p 684 N93-12872
ROTHMAN, S. J. ..... p 720 N93-12807
ROUSE, WILLIAM B. ..... p 499 N93-12602
ROUSSEL-DUPRE, D. ..... p 743 N93-13342
p 524 N93-13516
ROUTBORT, J. L. ..... p 720 N93-12807
p 720 N93-12854
ROWELL, LAWRENCE F. ..... p 519 N93-13379
ROWLAND, J. ..... p 555 N93-12563
RUAN, MIFANG ..... p 566 N93-13838
RUBIN, L. F. ..... p 602 N93-13683
RUDNIK, R. ..... p 582 N93-13227
RUFF, A. W. ..... p 553 N93-13649
RUFFINS, T. R. ..... p 637 N93-12838
RUGGIERO, A. G. ..... p 707 N93-13192
RULE, W. K. ..... p 609 N93-12682
RUNGE, FRITZ C. ..... p 742 N93-12592
RUOTOLO, P. ..... p 682 N93-13759
RUPPEL, TIMOTHY HARRY ..... p 700 N93-13635
RUSSELL, SAMUEL S. ..... p 601 N93-13674
RUSSO, FRANK P. ..... p 508 N93-13159
RUTHERFOORD, J. ..... p 702 N93-12855
RUTLEDGE, DAVID ..... p 562 N93-12867
RYAN, JOE ..... p 738 N93-13884
RYAN, M. A. ..... p 571 N93-13196
p 571 N93-13197
RYAN, T. W. ..... p 611 N93-12936

S

SAAD, Y. ..... p 697 N93-13409
SAATI, ABDULMANNAN ABDULHAMID
p 594 N93-14077
SABBAGH, S. A. ..... p 718 N93-13535
SACCHINI, JOSEPH J. ..... p 567 N93-13939
SACCO, ALBERT, JR. ..... p 508 N93-13160
SAGER, J. C. ..... p 680 N93-13996
SAHM, MICHAEL KENNETH ..... p 591 N93-13938
SAHRAIAN, MASOUD ..... p 613 N93-13335
SAITO, TAKAO ..... p 519 N93-14015
SAKOWSKI, BARBARA ..... p 585 N93-13395
SALE, K. E. ..... p 596 N93-12762
SALMONSON, J. ..... p 717 N93-13511
SALMONSON, J. C. ..... p 555 N93-12568
SALTZMAN, JOHN A. ..... p 493 N93-13322
SAMBOROWSKI, LEONARD J. ..... p 567 N93-13875
SAMMELLS, A. F. ..... p 638 N93-13041
SANDERS, J. ..... p 674 N93-12566
SANDONATO, GILBERTO M. ..... p 651 N93-13310
SANDOVAL, D. P. ..... p 710 N93-13509
SANTARIUS, J. F. ..... p 719 N93-13985
SAPHIR, WILLIAM COOPER ..... p 729 N93-13832
SARJEANT, W. J. ..... p 574 N93-14034
SARMIENTO, JORGE L. ..... p 670 N93-13714
SARTAIN, J. B. ..... p 680 N93-13993
SATTLER, M. L. ..... p 701 N93-12806
SAUCIER, ANTOINE ..... p 591 N93-13901
SAUER, RICHARD L. ..... p 680 N93-13999
SAUNDERS, JAMES H. ..... p 584 N93-13386
SAUSEN, TANIA MARIA ..... p 634 N93-13412
SAWYER, HEYWOOD R. ..... p 675 N93-13449
SCANNELL, DENNIS ..... p 678 N93-12983
SCHEFFLER, G. W. ..... p 638 N93-13040
SCHEIBLE, O. KARL ..... p 678 N93-12983
SCHENCK, H. A. ..... p 699 N93-12601
SCHERBAUM, R.-D. ..... p 580 N93-13215
SCHETZ, J. A. ..... p 595 N93-13670
SCHIAVILLA, R. ..... p 703 N93-13246
SCHISSEL, D. P. ..... p 712 N93-12687
SCHLITT, H. A. ..... p 675 N93-13522
SCHMIDT, G. W. ..... p 671 N93-12768
SCHMITT, HARRISON H. ..... p 719 N93-13985
p 680 N93-14014
SCHMITZ, L. ..... p 717 N93-13511
SCHNEIDER, M. P. ..... p 691 N93-13156
SCHNEIDER, STEPHEN ..... p 645 N93-13413
SCHNITZER, H. J. ..... p 704 N93-13251
SCHREYER, H. L. ..... p 624 N93-13072
p 627 N93-13515
SCHULTZ, JOHN R. ..... p 680 N93-13999
SCHULZ, MICHAEL ..... p 705 N93-12715
SCHUMAN, H. K. ..... p 519 N93-13462
SCHWAB, JOHN R. ..... p 585 N93-13396
SCHWARTZ, R. J. ..... p 639 N93-13529
SCHWARZ, H. ..... p 707 N93-13090
SCHWARZ, R. K. ..... p 736 N93-13048
SCHWEHM, GERHARD ..... p 749 N93-12965
SCHWENN, R. ..... p 752 N93-13468
SCOTT, COURTNEY J. ..... p 661 N93-12700
SCOTT, H. A. ..... p 712 N93-12571
SCOTT, KELLY W. ..... p 648 N93-13995
SCOTT, MICHAEL A. ..... p 694 N93-13442
SEAL, D. W. ..... p 504 N93-13735
SEASHOLTZ, RICHARD G. ..... p 599 N93-13668
p 602 N93-13684
SEDLACEK, ZDENEK ..... p 715 N93-13006
SEELHORST, U. ..... p 503 N93-13218
SEGERT, RANDALL ..... p 520 N93-13455
SEIDMAN, THOMAS I. ..... p 690 N93-12547
SELVADURAY, GUNA ..... p 527 N93-12895
p 528 N93-12896
SEMAN, CHARLES JACOB ..... p 666 N93-13786
SEMBACH, KENNETH RUSSELL .. p 753 N93-13499
SEMKOW, KRYSTYNA W. ..... p 761 N93-13979
SENESE, FREDRICK ..... p 575 N93-12677
SENGUPTA, S. ..... p 723 N93-13547
SERENO, THOMAS J., JR. ..... p 691 N93-12607
SEXTON, J. ANDREW ..... p 510 N93-13169
SHAFFER, W. ..... p 524 N93-13870
SHAH, K. ..... p 710 N93-13705
SHAKKOTTAI, PARTHASARATHY ..... p 700 N93-13421
SHANG, H. M. ..... p 575 N93-12688
SHANNAN, JAY ERIC ..... p 615 N93-13541
SHAO, MICHAEL ..... p 745 N93-13582
p 745 N93-13587
SHAO, XUEMEI ..... p 648 N93-14096
SHARMA, R. P. ..... p 722 N93-13104
SHASHIKALA, G. ..... p 737 N93-13368
SHAUGHNESSY, JOHN D. ..... p 504 N93-13068
SHAVIV, G. ..... p 753 N93-13523
SHEA, CHARLOTTE ..... p 557 N93-12951
p 518 N93-13113
SHEA, DENNIS J. ..... p 661 N93-12817
SHEA, EILEEN ..... p 645 N93-13413
SHEA, T. J. ..... p 571 N93-13358
SHEFFLER, KEITH D. ..... p 544 N93-12589
SHELLEY, E. G. ..... p 751 N93-13465
p 752 N93-13467
p 752 N93-13468
p 752 N93-13469
SHELTON, W. A. ..... p 542 N93-13043
SHEN, B. ..... p 561 N93-12655
SHEN, WEIMIN ..... p 713 N93-12878
SHEN, WENYU ..... p 631 N93-13947
SHEN, ZUOWEI ..... p 696 N93-12847
SHEPHARD, J. R. ..... p 706 N93-12822
SHEPPARD, M. G. ..... p 713 N93-12809
SHERIDAN, T. ..... p 735 N93-12808
SHERWOOD, BRENT ..... p 608 N93-14010
SHEU, DONGLONG ..... p 500 N93-13140
SHI, DONGLU ..... p 723 N93-13547
SHI, JICHUN ..... p 656 N93-13784
SHIAO, MICHAEL C. ..... p 622 N93-12735
SHIBATA, TAKEMASA ..... p 718 N93-13732
SHIH, H. J. ..... p 707 N93-13108
SHIN, DONGSHIN ..... p 592 N93-13948
SHIN, ROBERT T. ..... p 633 N93-13085
p 633 N93-13086
p 569 N93-13087
SHINAR, R. ..... p 703 N93-13194
SHINAS, M. A. ..... p 710 N93-13509
SHINN, JUDY L. ..... p 771 N93-13020
SHIPLEY, BUFORD W., JR. ..... p 679 N93-13874
SHIPLEY, BUFORD WILEY, JR. ... p 524 N93-14046
SHOCK, EVERETT L. ..... p 672 N93-13457
p 669 N93-13458
SHOENBERGER, JAMES E. ..... p 551 N93-13259
SHOKAIR, I. R. ..... p 706 N93-12830
SHOR, J. S. ..... p 601 N93-13677
SHORE, STEVEN N. ..... p 744 N93-13461
SHORES, R. C. ..... p 642 N93-12726
SHORT, ROBERT D. ..... p 562 N93-12948
SHULAR, DAVID ..... p 547 N93-12778
SHUM, D. K. M. ..... p 626 N93-13320
SIEGAL, M. P. ..... p 722 N93-13323
SILCOX, RICHARD J. ..... p 626 N93-13420
SILS, INGRID V. ..... p 677 N93-12960
SIMCOX, GEORGE N. ..... p 632 N93-12598
SIMKOVICH, G. ..... p 540 N93-12595
SIMMONDS, BORIS ..... p 584 N93-13390
SIMON, R. S. ..... p 745 N93-13582
SIMONEN, T. C. ..... p 715 N93-13044
SIMONSEN, LISA C. ..... p 520 N93-12876
p 680 N93-14003
SIMPSON, LANCE L. ..... p 674 N93-12945
SIMPSON, R. ..... p 677 N93-12732
SIN, YONGKUN ..... p 607 N93-13773
SINCLAIR, C. K. ..... p 708 N93-13284
SINGH, D. J. ..... p 538 N93-13456
SINGH, INDRAMANI ..... p 677 N93-12860
SINGH, JAG J. ..... p 598 N93-13661
SINGH, NAGENDRA ..... p 522 N93-13152
SINHA, PRAMATH RAJ ..... p 615 N93-13540
SIXSMITH, HERBERT ..... p 559 N93-13604
SKINNER, J. PAUL ..... p 568 N93-14048
SKOCYPEC, R. D. ..... p 588 N93-13575
SKOK, A. ..... p 640 N93-13621
SKUBIS, JERZY ..... p 623 N93-12989
SLANGER, T. G. ..... p 645 N93-13615
SLAUGHTER, WILLIAM SHEWEN ..... p 629 N93-13754
SLEMP, WAYNE S. ..... p 549 N93-12787
SLENTZ, G. ..... p 690 N93-12564
SLIWA, NANCY E. ..... p 619 N93-14006
SMALINSKAS, K. ..... p 541 N93-12879
SMARTT, H. B. ..... p 610 N93-12793
SMIRNOV, K. L. ..... p 675 N93-13449
SMITH, A. F. ..... p 697 N93-12702
SMITH, B. W. ..... p 524 N93-13516
SMITH, DONALD E. ..... p 687 N93-13734
SMITH, GUY A. ..... p 506 N93-13013
p 531 N93-13311
SMITH, H. V., JR. ..... p 714 N93-12997
SMITH, J. R. ..... p 706 N93-12830
SMITH, JESSE B. ..... p 769 N93-13014
SMITH, M. ..... p 723 N93-13547
SMITH, N. DEAN ..... p 555 N93-12939
SMITH, PAUL S. ..... p 689 N93-12846
SMITH, R. D. ..... p 575 N93-12711
SMITH, R. W. ..... p 551 N93-13315
SMITH, ROBERT CHRISTOPHER . p 757 N93-13963
SMITH, V. J. ..... p 507 N93-13213
SMITHER, R. K. ..... p 719 N93-12562
SMITHRICK, JOHN J. ..... p 527 N93-14079
SNIDER, JACK B. ..... p 634 N93-13094
SNYDER, KENNETH A. ..... p 623 N93-12981
SO, R. M. C. ..... p 575 N93-12717
SOELDNER, F. ..... p 715 N93-13093
SOLOW, H. ..... p 682 N93-13759
SOLOWAY, DONALD I. ..... p 619 N93-14006
SOMERS, RICHARD E. ..... p 641 N93-14005
SONDAK, DOUGLAS L. ..... p 587 N93-13517
SONNENFROH, D. M. ..... p 603 N93-13687
SORENSEN, D. C. ..... p 686 N93-13408
SORENSON, K. B. ..... p 542 N93-13302
SOULAS, GEORGE C. ..... p 526 N93-13283
SOULEN, ROBERT L. ..... p 550 N93-13026
SOUTHERN, LESLIE A. ..... p 584 N93-13386
SPACE, BRIAN ..... p 704 N93-13369
SPAGNUOLO, JOELLE M. ..... p 503 N93-12903
SPAHN, PATRICK F. ..... p 556 N93-13471
SPANGLER, E. M. ..... p 555 N93-13081
SPARKS, W. M. ..... p 753 N93-13523
SPENCE, W. ..... p 707 N93-13090
SPENCER, J. E. ..... p 707 N93-12993
SPENCER, STEVE ..... p 585 N93-13394
SPEZIALE, C. G. ..... p 575 N93-12717

SPIERS, GARY D. p 607 N93-13797
SPILLARD, CANDIDA p 666 N93-13791
SPITTLE, ERIC K. p 679 N93-13874
SPRAGLE, GREGORY S. p 582 N93-13225
SPRINGER, GEORGE S. p 531 N93-13324
SPUTE, MARK K. p 510 N93-13171
p 512 N93-13185
SPYERS-DURAN, PAUL p 649 N93-12818
SQUILLANTE, M. p 710 N93-13705
SRIDHAR, K. R. p 679 N93-13717
SRINATHKUMAR, S. p 504 N93-13367
STABILE, MICHAEL E. p 620 N93-13876
STAEBLER, G. M. p 714 N93-12932
STAIR, PETER C. p 539 N93-13763
STAMBAUGH, R. p 714 N93-12932
STANEK, P. W. p 551 N93-13315
STANKOVIANSKY, MILOES p 649 N93-12704
STARK, D. p 554 N93-13987
STARRFIELD, S. p 753 N93-13523
STAVINOHA, LEON L. p 609 N93-12600
STEARNS, D. G. p 721 N93-12972
STEELE, C. D. C. p 770 N93-13605
STEELE, OSCAR p 687 N93-13880
STEIN, BLAND A. p 545 N93-12769
p 546 N93-12770
STEIN, CLIFFORD p 685 N93-12961
STEIN, EARL S. p 506 N93-12902
STEINBECK, JOHN p 722 N93-13100
STEINFIELD, G. p 640 N93-13621
STEPHENS, J. J. p 542 N93-13302
STEPHENSON, R. p 632 N93-12869
STERN, KURT H. p 551 N93-13101
STERN, S. ALAN p 769 N93-12669
p 758 N93-13344
p 759 N93-13568
STETTLER, M. p 690 N93-12564
STEVENS, MICHAEL HUGH p 768 N93-14072
STEWART, AMYELIZABETH C. p 509 N93-13166
STILLMAN, G. E. p 608 N93-13864
STINCHCOMB, W. W. p 550 N93-12858
STOBER, A. p 509 N93-13163
STOCKS, G. M. p 542 N93-13043
STOECKEL, J. p 715 N93-13093
p 716 N93-13330
STOKES, JAMES M. p 678 N93-13450
STOOTS, C. M. p 728 N93-12857
p 576 N93-12996
STORTI, GEORGE M. p 705 N93-13606
STOUFFER, VIRGINIA p 498 N93-13787
STRAMLER, J. p 680 N93-14013
STRATFORD, R. p 678 N93-13464
STRAUSS, A. M. p 676 N93-14002
STRAUSSFOGEL, DENNIS M. p 493 N93-13463
STRAW, TIMOTHY B. p 572 N93-13473
STRAYER, M. R. p 706 N93-12829
STREET, J. J. p 680 N93-13993
STRUVE, K. W. p 706 N93-12830
STUCKERT, GREGORY KENT p 588 N93-13765
STUCKEY, W. K. p 554 N93-14099
STUMP, W. R. p 767 N93-14016
STUPAKOV, G. p 623 N93-13003
STUTZMAN, W. L. p 561 N93-12655
STYCZYNSKI, THOMAS E. p 746 N93-13589
SU, T. Y. p 578 N93-13206
SU, TZU-JENG p 685 N93-13030
p 625 N93-13125
p 686 N93-13295
p 686 N93-13296
SUBASILAR, BEDRETTIN p 641 N93-12624
SUGIHARA, MAKOTO p 584 N93-13388
SUIB, S. L. p 542 N93-12998
SUITOR, J. W. p 571 N93-13197
SULLIVAN, KATHRYN ANN p 686 N93-13338
SULLIVAN, MICHAEL p 572 N93-13472
SUMMERS, CHRIS J. p 572 N93-13448
SUMMERS, G. P. p 711 N93-14031
SUMPTER, B. G. p 691 N93-13079
SUN, JIELUN p 657 N93-13796
SUN, JUANZHEN p 651 N93-12969
SUPPA, EGIDIO p 516 N93-13691
SURKA, DEREK M. p 510 N93-13173
SUTTON, MICHAEL A. p 601 N93-13674
SVENDSEN, K. L. p 649 N93-12804
SVIATOSLAVSKY, I. N. p 719 N93-13985
SVOBODA, JAMES S. p 571 N93-13286
SWAIN, D. M. p 602 N93-13683
SWAIN, ROBERT EDWARD, III p 535 N93-13968
SWIFT, G. W. p 557 N93-12922
SWIFT, WALTER L. p 559 N93-13604
SYLVAN, ALAN p 607 N93-13814
SZAFRANSKA, IDA M. p 687 N93-13695
SZLYK, PATRICIA C. p 677 N93-12960
SZPAK, S. J. p 570 N93-12725

T

TAIT, C. D. p 641 N93-12685
TAKACS, P. p 710 N93-13652
TAKAHASHI, R. p 596 N93-12639
TAKAMIZAWA, K. p 561 N93-12655
TAKAMUKU, K. p 722 N93-13118
TAKAYANAGI, KAZUO p 652 N93-13405
TAMIR, DAVID p 509 N93-13165
TAN, QING p 559 N93-13642
TANG, M. S. H. p 720 N93-12819
TANNER, WILLIAM G. p 512 N93-13183
TARDOS, EVA p 685 N93-12961
TAVIK, GREORY C. p 561 N93-12623
TAYLOR, BARRY N. p 698 N93-12805
TAYLOR, DEBORAH B. p 694 N93-13370
TAYLOR, G. JEFFREY p 746 N93-13594
p 747 N93-13595
TAYLOR, LAWRENCE A. p 760 N93-13973
p 760 N93-13974
TAYLOR, P. L. p 610 N93-12793
TAYLOR, S. R. p 649 N93-12841
TENCH, D. M. p 720 N93-12758
TERRELL, JAMES P. p 599 N93-13665
TERRIE, G. p 668 N93-12556
TETI, JOSEPH GEORGE, JR. p 568 N93-14050
TEVAULT, DAVID E. p 596 N93-12653
THEIL, MICHAEL H. p 721 N93-13022
THEISS, T. J. p 626 N93-13320
THIBODEAU, KENNETH p 737 N93-13139
THOMAS, F. P. p 609 N93-12682
THOMAS, J. K. p 550 N93-13035
THOMAS, LAWRENCE R. p 508 N93-13158
THOMPSON, PAUL A. p 611 N93-12919
THOMPSON, ROBERT p 508 N93-13160
THOMPSON, RONALD DAVID p 620 N93-13906
THOMPSON, SCOTT ANDREW p 496 N93-13929
THORNE, L. F. p 624 N93-13077
THORNTON, ANTHONY LINN p 492 N93-13141
THORNTON, ROBERT p 680 N93-14090
THORODDSEN, SIGURDUR TRYGGVI p 594 N93-14069
THORPE, ARTHUR N. p 551 N93-13150
THOUT, M. p 690 N93-12564
TIAN, JING p 617 N93-13808
TIAO, G. C. p 650 N93-12877
TIBBITTS, T. W. p 680 N93-13997
p 680 N93-13998
TIDERMAN, JULIE p 518 N93-13113
TIEFEL, T. H. p 722 N93-13323
TIEGS, T. N. p 549 N93-12821
TIERNEY, J. W. p 539 N93-13617
TIPPETT, M. K. p 715 N93-13038
TIPTON, BRYAN E. p 771 N93-13126
TISHKOFF, J. M. p 525 N93-12575
TISONE, G. C. p 716 N93-13191
TIWARI, S. N. p 538 N93-13456
TJATRA, I. WAYAN p 629 N93-13769
TOKSOZ, M. N. p 650 N93-12943
TOLE, JOHN p 682 N93-13759
TOLMIE, D. E. p 689 N93-13046
TOLOCZKO, M. B. p 541 N93-12820
TOM, JOE G. p 551 N93-13259
TONDER, P. E. p 545 N93-12754
TONG, T. W. p 588 N93-13575
TORTORELLI, P. F. p 542 N93-13080
p 542 N93-13237
TOTH, R. P. p 566 N93-13512
TOWNE, CHARLES E. p 585 N93-13396
TOWNES, C. H. p 745 N93-13585
TOWNSEND, LAWRENCE W. p 771 N93-13020
TOWNSEND, SCOTT E. p 689 N93-13154
TRAPNELL, ROBERT N., JR. p 662 N93-13099
TRAPP, J. A. p 583 N93-13356
TRIMBLE, GREG A. p 626 N93-13290
TRIPATHI, RAM K. p 771 N93-13020
TROUTMAN, PATRICK p 694 N93-13442
TRUCCO, RICHARD E. p 602 N93-13682
p 602 N93-13683
TRUEMPER, KLAUS p 696 N93-12640
TRURAN, J. W. p 753 N93-13523
TSAI, LUNG-WEN p 609 N93-12698
TSANG, LEUNG p 569 N93-13088
TSANG, T. p 710 N93-13652
TSAO, BANG-HUNG p 727 N93-12546
TSE, MAN-CHUN p 496 N93-13930
TSUBAKITANI, SHIGERU p 696 N93-12625
TSUYUKI, GLENN T. p 585 N93-13391
TUCKER, D. S. p 551 N93-13115
TUCKER, DENNIS p 506 N93-13013
TUCKER, M. D. p 565 N93-13506
TUCKER, WILLIAM B. p 540 N93-13984
TURK, FRANCIS JOSEPH p 634 N93-13371
TURLINGTON, L. p 708 N93-13284
TURMAN, B. N. p 708 N93-12830
TURNER, MARSHA KAY p 740 N93-14088
TUTTLE, MARK E. p 530 N93-12929
TWOMEY, SEAN A. p 660 N93-12558
TYRRELL, DEBRA L. p 775 N93-12859

U

UCHIDA, HIROYUKI p 584 N93-13388
UCKAN, T. p 717 N93-13518
UDSETH, H. R. p 575 N93-12711
UEDA, M. p 716 N93-13257
UGOLINI, DANIELE p 697 N93-13363
UHT, J. C. p 554 N93-14099
UNAL, RESIT p 519 N93-13379
UNDERWOOD, JOHN H. p 620 N93-12580
UNDERWOOD, M. L. p 571 N93-13196
p 571 N93-13197
UNGAR, EUGENE K. p 585 N93-13393
UNWIN, ANNA THERESA p 589 N93-13781
URTIEW, P. A. p 565 N93-13357
USMEN, MUMTAZ A. p 644 N93-13098
UTTAL, TANEIL p 634 N93-13094
UYEMURA, J. P. p 688 N93-12733

V

VAFAEISEFAT, SAEID p 729 N93-13896
VAINSHTEIN, LEONID A. p 703 N93-13095
VALENZUELA, JAVIER p 559 N93-13604
VANBEEK, C. M. p 497 N93-13205
VANBRUNT, RICHARD J. p 698 N93-12805
VANCOUR, R. P. p 650 N93-12944
VANDAM, TONIE M. p 659 N93-13955
VANDERBEEK, RICHARD G. p 674 N93-12756
VANDERVOORT, RICHARD J. p 522 N93-12962
VANDERWAHL, R. L. p 538 N93-13234
VANDERWAL, R. L. p 537 N93-13232
VANDEWALL, ALLAN p 585 N93-13395
VANDYKE, L. S. p 595 N93-12619
VANHENGST, J. p 502 N93-13208
VANHULSTEYN, D. p 674 N93-12566
VANIMAN, D. p 761 N93-13981
VANLOON, HARRY p 661 N93-12817
VANSCIVER, S. W. p 574 N93-12569
VARMA, K. R. HAREENDRA p 693 N93-13336
VASQUEZ, ROBERTO LUIS p 617 N93-13931
VAUGHAN, WILLIAM W. p 649 N93-12718
VENKATAPATHY, ETHIRAJ p 683 N93-12719
VERBER, C. M. p 688 N93-12733
VERDIER, PETER H. p 553 N93-13785
VERNON, S. P. p 721 N93-12972
VETRANO, J. S. p 542 N93-12973
VIEBROCK, HERBERT J. p 644 N93-12974
VILIARDOS, M. A. p 721 N93-12972
VINING, C. B. p 571 N93-13197
VINKEY, VICTOR F. p 742 N93-12592
VISWANATHAN, V. K. p 603 N93-12560
VLCEK, BRIAN LEE p 618 N93-13949
VOELLMER, GEORGE p 511 N93-13179
VOGT, GREGORY L. p 679 N93-13692
VOLAKIS, J. L. p 565 N93-13354
VOLK, TYLER p 680 N93-13994
VONDRAK, R. R. p 648 N93-12621
VORBURGER, THEODORE V. p 698 N93-12805
VOSS, H. D. p 648 N93-12621
VOUK, MLADEN A. p 686 N93-13293
VROTNEY, WILLIAM p 682 N93-12614

W

WADDELL, M. W., JR. p 704 N93-13319
WADDOUPS, I. G. p 565 N93-13506
WAGNER, T. D. p 689 N93-12797
p 689 N93-12810
WAH, BENJAMIN W. p 694 N93-13376
WAHL, J. H. p 575 N93-12711
WAINWRIGHT, ROBIN p 534 N93-13950
WAKEFIELD, J. C. p 697 N93-12702
WAKSMAN, ABRAHAM p 734 N93-12703
WALDMAN, J. p 560 N93-12581
WALKER, C. A. p 675 N93-13061
WALKER, JAMES C. G. p 644 N93-13031
WALKER, K. P. p 531 N93-13309
WALL, WILLIAM FRANK p 748 N93-13688
WALLACE-ROBINSON, JANICE p 743 N93-12898
WALLIN, MARTA J. p 534 N93-13940
WALLIN, STEPHEN R. p 534 N93-13940
WALLING, R. S. p 712 N93-12571
WALRAND, JEAN p 562 N93-12747
WALTER, LEE p 705 N93-13606
WAN, A. S. p 712 N93-12571
WAN, GUANG-CHENG p 631 N93-13951
WANG, CONG p 529 N93-12835
WANG, J. C. p 569 N93-12561

WANG, JIN ..... p 755 N93-13829
WANG, JIUN-YIH JOHN ..... p 628 N93-13728
WANG, LIE ..... p 576 N93-12975
WANG, RUN-WEN ..... p 710 N93-13652
WANG, SHU-I ..... p 597 N93-13424
WANG, WEI ..... p 670 N93-13633
WANG, YI-MIN ..... p 565 N93-13375
WANG, Z. ..... p 723 N93-13547
WANG, Z. L. ..... p 723 N93-13347
WARBURTON, RICHARD JOHN ... p 726 N93-13895
WARD, D. A. ..... p 642 N93-12726
WARE, A. A. ..... p 713 N93-12873
WARGELIN, B. J. ..... p 753 N93-13536
WARNE, L. K. ..... p 571 N93-13300
WARNEKE, BRETT A. ..... p 510 N93-13173
WARREN, D. ..... p 690 N93-12564
WASZAK, MARTIN R. ..... p 504 N93-13367
WATANABE, YOSHIAKI ..... p 610 N93-12727
WATERS, J. ..... p 645 N93-13615
WATERS, L. ..... p 704 N93-13281
WATKINS, A. D. ..... p 610 N93-12793
WATKINS, J. G. ..... p 717 N93-13511
WATMUFF, JONATHAN H. ..... p 583 N93-13277
WATSON, WILLIE ROSS ..... p 700 N93-13770
WATTERSON, C. E. ..... p 736 N93-13078
WAUCHOPE, KENNETH ..... p 688 N93-13942
WAYGOOD, STEVEN JOHN ..... p 668 N93-14055
WEBB, H. A. ..... p 612 N93-13103
WEBB, JAMES T. ..... p 674 N93-12905
WEI, WEN-CHENG J. ..... p 550 N93-12999
WEIGELT, GERD ..... p 745 N93-13588
WEISSBLUTH, MICHAEL JEFFREY
p 659 N93-14062
WEITZNER, H. ..... p 713 N93-12811
WELLS, J. C. ..... p 703 N93-13114
WENDER, I. ..... p 539 N93-13617
WENTZ, FRANK J. ..... p 632 N93-12800
WERNTZ, P. ..... p 561 N93-12655
WESLEY, DOUGLAS ALAN ..... p 668 N93-14063
WESSELSKI, CLARENCE J. ..... p 614 N93-13417
WESSLING, F. C. ..... p 511 N93-13178
WESTBROOK, C. K. ..... p 555 N93-12933
WESTLING, GORAN ..... p 609 N93-12604
WETZEL, JOHN P. ..... p 747 N93-13595
p 747 N93-13598
WHALEN, MARK DAVID ..... p 612 N93-13018
WHARTON, ROBERT ..... p 651 N93-13326
WHEELER, R. M. ..... p 680 N93-13997
WHISNANT, R. A. ..... p 639 N93-13528
WHITAKER, ANN F. ..... p 547 N93-12778
p 536 N93-12780
WHITE, L. W. ..... p 562 N93-12950
WHITE, PATRICIA E. ..... p 730 N93-12907
WHITE, R. E. ..... p 636 N93-12812
WHITE, VICKY L. ..... p 674 N93-12612
WHITEHEAD, J. C. ..... p 525 N93-12840
WHITES, KEITH WAYNE ..... p 569 N93-14052
WHITTEN, J. E. ..... p 723 N93-13349
WHITTUM, DAVID HARVEY ..... p 607 N93-13777
WICKERSHEIMER, DAVID ..... p 684 N93-12851
p 684 N93-12872
WICKS, A. L. ..... p 595 N93-13670
WIDING, M. A. ..... p 683 N93-12686
WIEDER, HARRY H. ..... p 719 N93-12648
WIELAND, TODD MICHAEL ..... p 621 N93-12632
WIESEMAN, CAROL D. ..... p 500 N93-13565
WIGINTON, MARGARET ..... p 518 N93-13113
WILCZYNSKI, VINCENT ..... p 592 N93-13952
WILDE, G. L. ..... p 507 N93-13213
WILDER, MICHAEL CURTIS ..... p 495 N93-13803
WILETS, L. ..... p 703 N93-13187
WILEY, J. C. ..... p 713 N93-12873
WILGEN, J. B. ..... p 717 N93-13518
WILKES, DONALD R. ..... p 547 N93-12778
p 548 N93-12781
WILKES, W. R. ..... p 759 N93-13504
WILKS, S. C. ..... p 604 N93-12925
WILL, HERBERT A. ..... p 599 N93-13667
WILLIAMS, K. L. ..... p 668 N93-12577
p 669 N93-12599
WILLIAMS, MEMORIE K. ..... p 510 N93-13171
p 512 N93-13185
WILLIAMS, R. M. ..... p 571 N93-13196
p 571 N93-13197
WILLIAMS, ROBERT L., II ..... p 694 N93-13442
WILLIAMS, W. DAN ..... p 602 N93-13681
WILLIAMS, WENDELL M. ..... p 559 N93-14009
WILLIAMSON, C. ..... p 682 N93-13759
WILLIS, J. O. ..... p 722 N93-13118
WILLIS, RON J. ..... p 634 N93-13094
WILSON, CHARLES L. ..... p 689 N93-13198
WILSON, DAVID KEITH ..... p 651 N93-13143
WILSON, GREGORY JON ..... p 536 N93-12836
WILSON, JOHN W. ..... p 771 N93-13020
p 674 N93-13023
p 772 N93-13572
WILSON, PAUL ..... p 619 N93-12864
WILT, P. ..... p 705 N93-13546
WILT, THOMAS EDMUND ..... p 623 N93-13009
WINCHELL, D. F. ..... p 703 N93-13114
WINKLER, MARTIN ..... p 601 N93-13678
WINS, PAUL H. ..... p 540 N93-14033
WISE, J. ..... p 511 N93-13180
WITHERELL, C. E. ..... p 541 N93-12790
WITTENBERG, L. J. ..... p 759 N93-13504
p 719 N93-13985
p 680 N93-13998
p 766 N93-14007
WOLF, D. ..... p 722 N93-13195
WONG, EUGENE ..... p 562 N93-12747
WOO, A. ..... p 565 N93-13354
WOOD, C. C. ..... p 674 N93-12566
WOOD, R. ..... p 714 N93-12932
WOODS, C. M. ..... p 555 N93-13081
WOOLF, NEVILLE ..... p 746 N93-13592
WORKMAN, GARY ..... p 506 N93-13013
WORKMAN, GARY L. ..... p 619 N93-12875
p 531 N93-13311
WORLEY, P. H. ..... p 689 N93-12797
WORONOWICZ, MICHAEL STANLEY
p 495 N93-13746
WORSNOP, DOUGLAS R. ..... p 497 N93-12816
WRIGHT, A. D. ..... p 627 N93-13524
p 627 N93-13525
WRIGHT, GARY ..... p 687 N93-13880
WRIGHT, KENNETH D., II ..... p 601 N93-13680
WRIGHT, M. K. ..... p 640 N93-13623
WRIGHT, R. ..... p 710 N93-13509
WRIGHT, WILLIAM BENJAMIN .... p 498 N93-13364
WRIGLEY, CHARLES Y. ..... p 705 N93-13606
WRISDALE, IAN EDWARD ..... p 592 N93-13953
WU, CHI-CHAO ..... p 744 N93-13461
WU, JIANN-YUARN ..... p 504 N93-13827
WU, MEN-ZAN BILL ..... p 494 N93-13632
WU, S. ..... p 623 N93-12863
WU, S. T. ..... p 769 N93-12658
p 769 N93-13475
WU, XUEFENG ..... p 621 N93-12631
WUEBBLES, D. J. ..... p 645 N93-13615
p 646 N93-13646
p 646 N93-13654
p 646 N93-13655
WUOSMAA, A. H. ..... p 705 N93-13546

X

XIE, XIN ..... p 592 N93-13964
XU, MEIZHEN ..... p 537 N93-13096

Y

YAD-SHALOM, ITAI ..... p 696 N93-12942
YAMADA, HITOSHI ..... p 610 N93-12727
YAMANOUCHI, TAKASHI ..... p 663 N93-13287
YANG, S. L. ..... p 613 N93-13321
YAO, JING ..... p 544 N93-14047
YATES, JOHN T., JR. ..... p 536 N93-12618
YEH, EUENG-NAN ..... p 669 N93-13382
YEH, NAN-MING ..... p 535 N93-13954
YI, B. K. ..... p 524 N93-14087
YI, SUNG ..... p 530 N93-13007
YOES, CISSY ..... p 738 N93-13737
YOO, C. S. ..... p 701 N93-12806
YOSHIDA, TETSUJI ..... p 559 N93-13989
YOSHINO, K. ..... p 645 N93-13274
YOST, DOUGLAS M. ..... p 609 N93-12600
YOST, GREGG R. ..... p 682 N93-12645
YOU, ZHONGQING ..... p 700 N93-13774
YOUNG, B. K. ..... p 603 N93-12570
YOUNG, C. E. ..... p 723 N93-13349
YOUNG, MIN-JHO ..... p 629 N93-13804
YOUNG, PHILIP R. ..... p 545 N93-12769
p 549 N93-12787
YOUNG, RONALD B. ..... p 671 N93-12901
YOUNG, ROY M., JR. ..... p 540 N93-13984
YOUNG, TIMOTHY J. ..... p 727 N93-12546
YOUNIS, B. A. ..... p 575 N93-12717
YOUSSEF, MILAD ..... p 511 N93-13177
YUAN, DAH-NING ..... p 656 N93-13771
YUAN, V. ..... p 708 N93-13508
p 710 N93-13509
YUE, J. ..... p 570 N93-12650
YUEH, SIMON H. ..... p 569 N93-13087
YUH, C. ..... p 640 N93-13621
YUH, C. Y. ..... p 638 N93-13039
YUM, SI-HWAN ..... p 531 N93-13144
YURACK, JIM ..... p 511 N93-13177

Z

ZACEK, F. ..... p 715 N93-13093
p 716 N93-13330
ZACHARIA, T. ..... p 542 N93-13190
ZAKLAD, ALLEN ..... p 678 N93-13450
ZANDER, M. E. ..... p 710 N93-13509
ZARI, MICHAEL C. ..... p 711 N93-14032
ZAVIDOVIQUE, B. ..... p 692 N93-13242
ZDERAD, A. J. ..... p 709 N93-12918
ZEICHNER, BRIAN ..... p 675 N93-13941
ZEMEL, MARC ..... p 537 N93-12897
ZEMSKOV, G. V. ..... p 554 N93-13873
ZEPF, STEPHEN EDWARD ..... p 750 N93-13148
ZHANG, CHANGAN ..... p 660 N93-14064
ZHANG, JIMING ..... p 722 N93-13100
ZHENG, XIAOWEI ..... p 593 N93-14057
ZHENJIANG, CUI ..... p 676 N93-14084
ZHONG, XIAOLIN ..... p 494 N93-13578
ZHOU, KEZHENG ..... p 521 N93-13854
ZHOU, QIHOU ..... p 655 N93-13755
ZIEBARTH, J. P. ..... p 575 N93-12688
ZIELINSKI, J. J. ..... p 717 N93-13518
ZIEMANN, V. ..... p 706 N93-12992
ZIOMEK, D. ..... p 563 N93-13045
ZIRILLI, FRANCESCO ..... p 682 N93-12647
ZOBEL, ANGELIKA ..... p 681 N93-12641
ZOHM, H. ..... p 712 N93-12687
ZOONEMATKERMANI, SAEID ..... p 744 N93-13480
ZUBAL, OREST ..... p 677 N93-12960
ZUCKERWAR, ALLAN J. ..... p 601 N93-13680
ZULEEG, R. ..... p 708 N93-14089
ZUND, J. D. ..... p 632 N93-12550
ZUREK, W. H. ..... p 641 N93-12684
ZWAAL, A. ..... p 557 N93-12934
ZWIENER, JAMES M. ..... p 547 N93-12778
p 548 N93-12781

CORPORATE SOURCE INDEX

Typical Corporate Source Index Listing

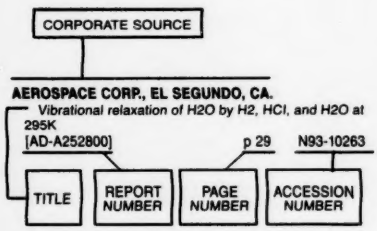

Listings in this index are arranged alphabetically by corporate source. The title of the document provides the user with a brief description of the subject matter. The report number helps to indicate the type of document cited (e.g., NASA report, translation, NASA contractor report). The accession number denotes the number by which the citation is identified. The page number helps you locate the citation in the abstract section. The titles are arranged under each corporate source in ascending accession number order.

A

ABERDEEN UNIV. (SCOTLAND).
A submillimetre polarimeter for the continuum receiver UKT14 on the James Clerk Maxwell Telescope
p 748 N93-13852
Making object-oriented databases more knowledgeable (from ADAM to ABEL) p 738 N93-13910

ACUREX CORP., MOUNTAIN VIEW, CA.
White paper: Preliminary assessment of LNG vehicle technology, economics, and safety issues, revision 1
[PB92-212943] p 615 N93-13644

ADVANCED DECISION SYSTEMS, MOUNTAIN VIEW, CA.
Verification and validation of AI software
[AD-A254601] p 682 N93-12614

ADVANCED SYSTEM TECHNOLOGIES, INC., FALLS CHURCH, VA.
Integrated modeling tool for performance engineering of complex computer systems
[NASA-CR-190881] p 687 N93-13880

ADVANCED TECHNOLOGY MATERIALS, INC., DANBURY, CT.
Single liquid source plasma enhanced metalorganic chemical vapor deposition of YBa2Cu3O(7-x) thin films
[AD-A254119] p 722 N93-13100

ADVISORY GROUP FOR AEROSPACE RESEARCH AND DEVELOPMENT, NEUILLY-SUR-SEINE (FRANCE).
Fundamentals and Special Problems of Synthetic Aperture Radar (SAR)
[AGARD-LS-182] p 563 N93-13049
Aerodynamic Engine/Airframe Integration for High Performance Aircraft and Missiles
[AGARD-CP-498] p 577 N93-13199
Machine Perception
[AGARD-LS-185] p 692 N93-13238
Highlights 92/2 p 775 N93-13474

AERODYNE RESEARCH, INC., BILLERICA, MA.
Icing prevention by ultrasonic nucleation of supercooled water droplets in front of subsonic aircraft
[DOT/FAA/CT-TN92/38] p 497 N93-12816

AEROJET-GENERAL CORP., COVINA, CA.
A simple node and conductor data generator for SINDA p 585 N93-13392

AERONAUTICA MACCHI S.P.A., VARESE (ITALY).
Water tunnel studies of inlet/airframe interference phenomena p 580 N93-13216

AERONAUTICAL RESEARCH LABS., MELBOURNE (AUSTRALIA).
Structural fatigue aspects of the P-3 Orion
[ARL-STRUC-TM-558] p 500 N93-13256

AEROSPACE CORP., EL SEGUNDO, CA.
Observations of correlated broadband electrostatic noise and electron cyclotron emissions in the plasma sheet
[AD-A255002] p 712 N93-12705
Ion radial diffusion in an electrostatic impulse model for stormtime ring current formation
[NASA-CR-190941] p 705 N93-12715
Surface contamination on LDEF exposed materials
p 547 N93-12776
Surface phonon dispersion of MoS2
[AD-A255835] p 727 N93-14083
Temperature measurements with micrometer spatial resolution
[AD-A255897] p 603 N93-14086
On the suitability of non-hardened high density SRAMs for space applications
[AD-A255898] p 524 N93-14087
Comparison of heavy ion and electron-beam upset data for GaAs
[AD-A255901] p 708 N93-14089
The chemistry of the extreme pressure lubricant additive lead naphthenate on steel surfaces
[AD-A255828] p 544 N93-14098
Space environmental effects on silvered teflon thermal control surfaces
[AD-A255909] p 554 N93-14099

AEROSPACE MEDICAL RESEARCH LABS., BROOKS AFB, TX.
Thermal stress in US Air Force operations
[AD-A255785] p 676 N93-14027
Physiological stress from chemical defense clothing and equipment
[AD-A255786] p 676 N93-14028

AEROSPACE MEDICAL RESEARCH LABS., WRIGHT-PATTERSON AFB, OH.
Hybrid 2 and hybrid 3 dummy neck properties for computer modeling
[AD-A255544] p 679 N93-13874

AEROSPATIALE, VERRIERES-L-BUISSON (FRANCE).
Aerodynamic studies of supersonic air intakes
p 497 N93-13222

AIR FORCE ENVIRONMENTAL TECHNICAL APPLICATIONS CENTER, SCOTT AFB, IL.
SAC contrail formation study
[AD-A254410] p 499 N93-12605

AIR FORCE INST. OF TECH., WRIGHT-PATTERSON AFB, OH.
The role of latent heat release in explosive cyclogenesis
[AD-A254436] p 660 N93-12596
Fibre-optic sensors using adiabatically tapered single-mode fibres
[AD-A254555] p 708 N93-12642
Physiological effects of positive pressure ventilation
[AD-A254809] p 674 N93-12751
Spatial resolution enhancement of SSM/I microwave brightness temperatures and its impact on rainfall retrieval algorithms
[AD-A254382] p 661 N93-12861
An analysis of the tornado-producing Raleigh thunderstorm of November 28, 1988
[AD-A254384] p 661 N93-12862
An analysis of the field service function of selected electronics firms
[AD-A255003] p 570 N93-12868
Heat resistant diffusion coating for niobium alloy
[AD-A255542] p 554 N93-13873
Development of two-dimensional parametric radar signal modeling and estimation techniques with application to target identification
[AD-A252602] p 567 N93-13939
ACTA Aeronautica et Astronautica Sinica (selected articles)
[AD-A255070] p 491 N93-13946
Postoperative hyperbaric oxygen treatment of peripheral nerve damage
[AD-A255842] p 676 N93-14084

AIR FORCE OFFICE OF SCIENTIFIC RESEARCH BOLLING AFB, WASHINGTON, DC.
Air Force Office of Scientific Research technical report summaries
[AD-A254380] p 775 N93-12859

AIR FORCE SYSTEMS COMMAND, WRIGHT-PATTERSON AFB, OH.
Engineering data transfer test with EDMICS using MIL-R-28002 (Raster)
[DE92-019808] p 738 N93-13619

AIR UNIV., MAXWELL AFB, AL.
Principles of information resource management: A foundation for the future
[AD-A254447] p 733 N93-12597

AIRCRAFT RESEARCH ASSOCIATION LTD., BEDFORD (ENGLAND).
Test techniques for engine/airframe integration
p 577 N93-13200
ASTOVL model engine simulators for wind tunnel research p 507 N93-13213
Some aspects of intake design, performance and integration with the airframe p 502 N93-13219

AKRON UNIV., OH.
Linear and nonlinear finite element analysis of laminated composite structures at high temperatures
p 623 N93-13009

ALABAMA CRYOGENIC ENGINEERING, INC., HUNTSVILLE.
A small, single stage orifice pulse tube cryocooler demonstration
[NASA-CR-190859] p 558 N93-13404

ALABAMA UNIV., HUNTSVILLE.
CO2 laser modeling
[NASA-CR-184455] p 604 N93-12656
Soft X Ray Telescope (SXT) focus error analysis
[NASA-CR-184443] p 742 N93-12657
Scientific study of data analysis
[NASA-CR-184435] p 769 N93-12658
Stability codes for a liquid rocket implemented for use on a PC
[NASA-CR-184453] p 525 N93-12659
Users manual for program SSFREQ intermediate mode stability curves: Developed for use on a PC computer
[NASA-CR-184452] p 682 N93-12675
Users manual for program ADMIT: Admittance and pressure transfer function developed for use on a PC computer
[NASA-CR-184450] p 682 N93-12676
Computational fluid dynamics combustion analysis evaluation
[NASA-CR-184326] p 575 N93-12688
High temperature superconductor materials and applications
[NASA-CR-184437] p 719 N93-12691
Real-time quality assurance testing using photonic techniques: Application to iodine water system
[NASA-CR-184413] p 619 N93-12692
Chemical release and radiation effects experiment advanced planning and coordination
[NASA-CR-184439] p 649 N93-12718
Briefing notes on propulsion stability codes ADMIT, NYQUIST, and SSFREQ
[NASA-CR-184449] p 525 N93-12874
Automated eddy current analysis of materials
[NASA-CR-184432] p 619 N93-12875
A multiple pointing-mount control strategy for space platforms
[NASA-CR-184448] p 522 N93-12893
Contamination analysis of SSF candidate materials
[NASA-CR-184431] p 709 N93-12894

Establishing laboratory standards for biological flight experiments
[NASA-CR-184402] p 671 N93-12901
Methods development for total organic carbon accountability
[NASA-CR-184438] p 672 N93-12949
Microbiological methods for the water recovery systems test, revision 1.1
[NASA-CR-184390] p 678 N93-12966
Test equipment data package for the KC-135 fiber pulling apparatus
[NASA-CR-184446] p 506 N93-13013
Solar prediction analysis
[NASA-CR-184422] p 769 N93-13014
Optical design for a balloon-borne magnetograph
[NASA-CR-191003] p 709 N93-13062
Study of plasma environments for the integrated Space Station electromagnetic analysis system
[NASA-CR-191263] p 522 N93-13152
CONCAP 4: A Complex Autonomous Payload (CAP) for growing organic thin films in microgravity p 511 N93-13178
FNAS modify matric and transparent experiments
[NASA-CR-184442] p 531 N93-13311
Robot welding process control
[NASA-CR-184428] p 614 N93-13436
Data evaluation, analysis, and scientific study
[NASA-CR-184396] p 769 N93-13475
Development of a stable electro-optical modulator
[NASA-CR-184404] p 710 N93-13696
CO2 laser preionisation
[NASA-CR-184424] p 607 N93-13797

ALENIA AERONAUTICA, TORINO (ITALY).
Mass flow effects on the low speed characteristics of an advanced combat aircraft p 497 N93-13214

ALLIED-SIGNAL AEROSPACE CO., KANSAS CITY, MO.
Development of a 1000 g, 10 ms mechanical shock test capability
[DE92-019193] p 624 N93-13077
Digital imaging systems
[DE92-019194] p 736 N93-13078

ALPHATRONIX, INC., RESEARCH TRIANGLE PARK, NC.
Optical disks become erasable p 736 N93-13133

AMERICAN CHEMICAL SOCIETY, WASHINGTON, DC.
Symposium on Polymeric Materials for Photonic and Optical Applications
[AD-A255820] p 554 N93-14029

AMES LAB., IA.
Enhancement of ion transmission and reduction of background and interferences in inductively coupled plasma mass spectrometry
[DE92-018805] p 596 N93-12921
Review of progress in quantitative NDE
[DE92-018814] p 620 N93-13071
Oxygen deficiencies at defects in YBa2Cu3O(7-delta) as determined by high resolution parallel electron energy loss
[DE92-016301] p 721 N93-13089
Ductile fracture process of discontinuous fiber reinforced composites
[DE92-016298] p 531 N93-13264
Simulation of forward-backward extrusion with numerical and model material techniques
[DE92-016299] p 558 N93-13298

ANACAPA SCIENCES, INC., FORT RUCKER, AL.
Operator workload predictions for the revised AH-64A workload prediction model. Volume 2: Appendixes A through H
[AD-A254939] p 676 N93-12545
Human factors research in aircrew performance and training: 1986-1991
[AD-A254455] p 677 N93-12609

ANALEX CORP., BROOK PARK, OH.
Test and control computer user's guide for a digital beam former test system
[NASA-CR-189208] p 685 N93-13291

ANALYTICS, INC., WILLOW GROVE, PA.
Ocular attention-sensing interface system
[NASA-CR-190884] p 678 N93-13450

ANCO ENGINEERS, INC., CULVER CITY, CA.
Tether deployment monitoring system, phase 2
[NASA-CR-184098] p 522 N93-13425
Providing structural modules with self-integrity monitoring software user's manual
[NASA-CR-190877] p 628 N93-13707

APPLIED SCIENCE TECHNOLOGY, INC., LITTLETON, CO.
Long Duration Exposure Facility (LDEF) contamination modeling p 547 N93-12775

ARC PROFESSIONAL SERVICE GROUP, INC., ROME, NY.
Phased array feed design technology for Large Aperture Microwave Radiometer (LAMR) Earth observations
[NASA-CR-189727] p 519 N93-13462

ARCO POWER TECHNOLOGIES, INC., WASHINGTON, DC.
Extremely low frequency/very low frequency Generator
[AD-A254347] p 562 N93-12948

ARGONNE NATIONAL LAB., IL.
Thermal imaging of synchrotron beams on silicon crystals
[DE92-018182] p 719 N93-12562
Experimental studies of cascade phenomena in metals
[DE92-019586] p 540 N93-12573
Application interface engine language and object reference manual
[DE92-017555] p 683 N93-12686
Weak-beam imaging of dissociated dislocations in HVEM-irradiated Fe-Ni-Cr alloys
[DE92-019587] p 541 N93-12798
Oxygen diffusion in high-T(c) superconductors
[DE92-019597] p 720 N93-12807
Utilization of databases to manage resources
[DE92-019598] p 735 N93-12808
Thermal effects on the frequency response of piezoelectric crystals
[DE92-019039] p 720 N93-12819
Memory access in shared virtual memory
[DE92-019594] p 681 N93-12823
Increasing the end user's productivity through seamless integration of applications with the database
[DE92-019599] p 735 N93-12824
High-temperature deformation and diffusion in oxides
[DE92-019593] p 720 N93-12854
A study of the vacancy loop formation probability in Ni-Cu and Ag-Pd alloys
[DE92-019584] p 541 N93-12879
Emittance, brilliance, and bandpass issues related to an inclined crystal monochromator
[DE92-019671] p 721 N93-12881
Meeting future exhaust emissions standards using natural gas as a vehicle fuel: Lessons learned from the natural gas vehicle challenge 1992
[DE92-019670] p 642 N93-12885
Influence of dilute impurities on the evolution of defect cascades in nickel
[DE92-019585] p 542 N93-12973
Evolution of the scientific paper
[DE92-019696] p 735 N93-12994
Proceedings of the Tenth Symposium on Energy Engineering Sciences: Synergism of Analysis, Modeling, and Experiment
[DE92-018777] p 638 N93-13069
Miniature neutron sources: Thermal neutron sources and their users in the academic field
[DE92-018793] p 702 N93-13070
Ion-channeling observation of correlated atomic displacements below Tc in YBa2Cu3O(7-x) and Pb-doped Bi2Sr2CaCu2O(x)
[DE92-018186] p 722 N93-13104
Study of short-range motion of atomic hydrogen in amorphous silicon by neutron reflectometry
[DE92-016392] p 703 N93-13194
Atomic relaxation modes in grain boundaries
[DE92-016781] p 722 N93-13195
The use of finite elements to model soil/track interactions in coupled multi-body dynamic simulations: Is real time simulation feasible?
[DE92-016184] p 612 N93-13236
A fresh look at (e,e(prime)) scattering from light nuclei: A GFMC approach
[DE92-016377] p 703 N93-13246
Electron stimulated desorption of the metallic substrate at monolayer coverage: Sensitive detection via 193 nm laser photoionization of neutral aluminum desorbed from CH3O/Al(111)
[DE92-014858] p 723 N93-13349
Environmental Compliance Management System
[DE92-019595] p 645 N93-13479
Effects of ionizing radiation on scintillators and other particle detectors
[DE92-018184] p 705 N93-13531
Evidence for alpha-particle chain configurations in Mg-24
[DE92-018790] p 705 N93-13546
Activation energy and critical current density in Bi-Sr-Ca-Cu-O
[DE92-018795] p 723 N93-13547

ARIZONA STATE UNIV., TEMPE.
Advanced Communications Technology Satellite (ACTS). Phase 1: Industrial/academic experimenters
[NASA-CR-191211] p 561 N93-12679
Studies on turbulent mixing in stratified turbulent patches p 587 N93-13532
Linear stability theory of hypersonic, chemically reacting viscous flows p 588 N93-13765
New power-conditioning systems for superconducting magnetic energy storage p 640 N93-13934
Volcanism in the eastern Hellas region of Mars: The geology of Hadriaca and Tyrrhena Paterae p 768 N93-14092

ARIZONA UNIV., TUCSON.
Sources of cloud nuclei and development of remote sensing techniques for cloud parameters
[AD-A255016] p 660 N93-12558
Elementary particle physics research
[DE92-019746] p 702 N93-12855
Spanwise-nonuniform excitation of a plane mixing layer p 577 N93-13120
A program to study antiprotons in the cosmic rays: Arizona collaboration
[NASA-CR-191272] p 772 N93-13306
Novel techniques of wavefront sensing for adaptive optics with array telescopes using an artificial neural network p 743 N93-13343
Lunar interferometric astronomy: Some basic questions p 746 N93-13592
Thermal control systems for low-temperature heat rejection on a lunar base
[NASA-CR-191286] p 679 N93-13717
Integration of vegetation indices and thermal measurements for ecosystem modeling p 646 N93-13721
Scientific predictability of solid rocket performance: Analyses of the processing parameters p 526 N93-13824
Spectroscopic observations of the night airglow from 3000 A to 9200 A p 658 N93-13891
A systematic search for low-mass companions orbiting nearby stars and the calibration of the end of the stellar main sequence p 749 N93-14070
Statistical relationships between tree growth and climate in western North America p 648 N93-14096

ARKANSAS UNIV., FAYETTEVILLE.
Biological conversion of synthesis gas
[DE92-017673] p 672 N93-13269

ARKANSAS UNIV., PINE BLUFF.
The neurochemical and neuropharmacological basis of motion sickness
[NASA-CR-190957] p 675 N93-13061

ARMED FORCES RADIOBIOLOGY RESEARCH INST., BETHESDA, MD.
AFRRI reports
[AD-A254581] p 674 N93-12649

ARMY AEROMEDICAL RESEARCH LAB., FORT RUCKER, AL.
The relationship between environmental conditions and UH-60 cockpit temperature
[AD-A255918] p 680 N93-14090

ARMY AEROSTRUCTURES DIRECTORATE, HAMPTON, VA.
Results of ASTM round robin testing for mode 1 interlaminar fracture toughness of composite materials
[NASA-TM-104222] p 532 N93-13428

ARMY ARMAMENT RESEARCH, DEVELOPMENT AND ENGINEERING CENTER, PICATINNY ARSENAL, NJ.
Spreadsheet-like image analysis
[AD-A254395] p 619 N93-12864

ARMY ARMAMENT RESEARCH, DEVELOPMENT AND ENGINEERING CENTER, WATERVLIET, NY.
Notch dimensions for three-point bend fracture specimens based on compliance analyses
[AD-A254641] p 620 N93-12580
Tempering effects for lower bainite, martensite, and mixed microstructures on impact, fracture, and related mechanical properties of ASTM A723 steel
[AD-A254617] p 541 N93-12616
Improved wide range expressions for displacements and inverse displacements for standard fracture toughness specimens
[AD-A254561] p 622 N93-12643

ARMY COMMAND AND GENERAL STAFF COLL., FORT LEAVENWORTH, KS.
The Joint Surveillance Target Attack Radar System: Can procedures be developed to support the requirements of the land and air component commanders?
[AD-A255555] p 567 N93-13875

ARMY ELECTRONICS TECHNOLOGY AND DEVICES LAB., FORT MONMOUTH, NJ.
Tutorials from the 23rd Annual Precise Time and Time Interval (PTTI) Applications and Planning Meeting
[AD-A254745] p 596 N93-12844

ARMY ENGINEER TOPOGRAPHIC LABS., FORT BELVOIR, VA.
Satellite imagery goes to the field
[AD-A254449] p 632 N93-12598

ARMY ENGINEER WATERWAYS EXPERIMENT STATION, VICKSBURG, MS.
Polypropylene fibers in portland cement concrete pavements
[DOT/FAA/RD-92/9] p 551 N93-13259

ARMY ENVIRONMENTAL HYGIENE AGENCY, ABERDEEN PROVING GROUND, MD.
Laser measurement techniques guide for a hazard evaluation
[AD-A254545] p 604 N93-12610
Procedures for the diagnostic dose resistance test kits for mosquitoes, body lice, and beetle pests of stored products
[AD-A255224] p 675 N93-13941
ARMY LAB. COMMAND, FORT MONMOUTH, NJ.
First year testing of prototype magnesium/manganese dioxide BA-4590/U battery
[AD-A255503] p 574 N93-13839
ARMY LAB. COMMAND, WATERTOWN, MA.
An interactive office accounting program written in UNIX and C
[AD-A255077] p 683 N93-12740
Assessment of Japanese technology in advanced glass and ceramic fibers
[AD-A255229] p 553 N93-13836
ARMY LAB. COMMAND, WHITE SANDS MISSILE RANGE, NM.
A surface pressure altitude prediction model
[AD-A255834] p 668 N93-14082
ARMY MATERIALS TECHNOLOGY LAB., WATERTOWN, MA.
Compression test simulation of thick-section composite materials
[AD-A255021] p 528 N93-12583
ARMY RESEARCH INST. OF ENVIRONMENTAL MEDICINE, NATICK, MA.
Effect of protective clothing ensembles on artillery battery crew performance
[AD-A254327] p 677 N93-12960
ARMY TOPOGRAPHIC ENGINEERING CENTER, FORT BELVOIR, VA.
Impact of Digital Terrain Elevation Data (DTED) resolution on terrain visualization: Simulation versus reality
[AD-A254237] p 634 N93-13333
Using iterative orthophoto refinements to correct Digital Elevation Models (DEM's)
[AD-A254625] p 634 N93-13345
GPS azimuth determination
[AD-A254687] p 499 N93-13348
Topographic surveyor: Transitioning to the 90's
[AD-A254688] p 499 N93-13351
ASTON UNIV., BIRMINGHAM (ENGLAND).
Resonance studies of artificial earth satellites
p 523 N93-14037
AUBURN UNIV., AL.
Numerical investigation of the flow field in the head-end, star grain section of a solid rocket motor during ignition transients p 526 N93-13818

B

BALKEMA (A. A.) PUBLISHERS, BROOKFIELD, VT.
Proceedings of the Mediterranean Conference on Environmental Geotechnology
[AD-A253672] p 644 N93-13098
BALL AEROSPACE SYSTEMS DIV., BOULDER, CO.
Zero-gravity quantity gaging system
[NASA-CR-185602] p 556 N93-12699
BALLISTIC RESEARCH LABS., ABERDEEN PROVING GROUND, MD.
Influence of cure shrinkage on process-induced stress and deformation in thick thermosetting composites
[AD-A254325] p 529 N93-12842
BATTELLE COLUMBUS LABS., OH.
Applications of CFD and visualization techniques
p 584 N93-13386
BATTELLE MEMORIAL INST., COLUMBUS, OH.
Numerical analysis of permittivity with loss in isotropic binary composites
[AD-A255203] p 534 N93-13940
BDM INTERNATIONAL, INC., ALBUQUERQUE, NM.
Lunar optical telescopes: An historical perspective
p 746 N93-13593
Environmental effects on an optical-UV-IR synthesis array p 747 N93-13595
Required technologies for a lunar optical UV-IR synthesis array p 747 N93-13598
BIGELOW LAB. FOR OCEAN SCIENCES, WEST BOOTHBAY HARBOR, ME.
Characteristics of phytoplankton as monitors of the physical environment
[AD-A255009] p 642 N93-12870
BIOSPHERICAL INSTRUMENTS, INC., SAN DIEGO, CA.
New approaches to the measurement of chlorophyll, related pigments and productivity in the sea
[NASA-CR-190879] p 673 N93-13612
Development of moored oceanographic spectroradiometer
[NASA-CR-190883] p 670 N93-13708
BOEING CO., KENT, WA.
Materials SIG quantification and characterization of surface contaminants p 546 N93-12773
BOEING CO., SEATTLE, WA.
LDEF atomic oxygen fluence update
p 546 N93-12771
Z306 molecular contamination ad hoc committee results p 546 N93-12774
Anodized aluminum on LDEF: A current status of measurements on chromic acid anodized aluminum
p 544 N93-12779
Recession of FEP specimens from trays D11 and B7
p 549 N93-12786
BOOKER T. WASHINGTON'S HIGH SCHOOL FOR ENGINEERING PROFESSIONS, HOUSTON, TX.
A decade of discovery: Experiments with the Get Away Special (GAS) canister p 509 N93-13162
BOSTON UNIV., MA.
Self-consistent modeling of the ionosphere-thermosphere-magnetosphere system
[AD-A253232] p 651 N93-13276
Energetics and dynamics of excess electrons in simple fluids p 704 N93-13369
The planetary nebula system and the dynamics of the galaxy Centaurus A p 754 N93-13645
BRANDEIS UNIV., WALTHAM, MA.
Research in elementary particle physics
[DE92-017869] p 704 N93-13251
BRIGHAM YOUNG UNIV., PROVO, UT.
G-133: A soft x ray solar telescope
p 510 N93-13171
The unique challenge of managing an undergraduate Get-Away-Special experiment p 512 N93-13185
Improved damping in composite structures through stress coupling, co-cured damping layers, and segmented stiffness layers p 630 N93-13823
BROOKHAVEN NATIONAL LAB., UPTON, NY.
Lecture notes for criticality safety
[DE92-016009] p 701 N93-12832
Power excitation by the use of a RF wiggler
[DE92-016097] p 707 N93-13192
The IGAC activity for the development of global emissions inventories: Description and initial results
[DE92-016010] p 644 N93-13270
Longitudinal impedance of capacitive pick-up electrodes: Calculations and comparison with measurements
[DE92-019499] p 571 N93-13358
Development of optical surface profiling instrumentation
[DE92-019252] p 710 N93-13652
BRUNEL UNIV., UXBRIDGE (ENGLAND).
A new route for fibre management in metal matrix composites p 534 N93-13779
Solar energy utilisation and evacuated tubular solar collectors p 641 N93-14078

C

CALIFORNIA INST. OF TECH., PASADENA.
Terahertz horn antennas on thin membranes
[AD-A254772] p 562 N93-12867
GAMCIT: A gamma ray burst detector
p 510 N93-13173
High resolution imaging at Palomar
p 745 N93-13584
Aspects of atmospheric transport and dispersion within an air basin p 656 N93-13782
CALIFORNIA STATE UNIV., SAN DIEGO.
Experiments on the statistical nature of stably stratified turbulence p 594 N93-14069
CALIFORNIA UNIV., BERKELEY.
Multidimensional signals, data and processes
[AD-A254797] p 562 N93-12747
The millimeter and submillimeter wavelength diffuse backgrounds: Measurements of the spectrum and anisotropy p 772 N93-13145
Measurements of the cosmic microwave background temperature at 1.47 GHz p 772 N93-13146
Zodiacal emission p 772 N93-13147
H I shells and supershells: Observations and theory
p 751 N93-13360
Recent astronomical results from the infrared spatial interferometer and their implications for LOUISA
p 745 N93-13585
Anisotropy measurements of the cosmic background radiation at 3 mm wavelength and an angular scale of 30 arcminutes p 772 N93-13689
Theory of the ion-channel laser p 607 N93-13777
CALIFORNIA UNIV., DAVIS.
Modeling and estimation of reciprocal diffusion and Gauss-Markov random fields
[AD-A255034] p 698 N93-12709
A PDF closure model for compressible turbulent chemically reacting flows
[NASA-CR-191209] p 587 N93-13453
Spatial characteristics of coherent turbulent structures and exchange processes in the atmospheric surface layer within and above an orchard canopy
p 660 N93-14064
CALIFORNIA UNIV., LOS ANGELES.
Fluid flow and heat convection studies for actively cooled airframes
[NASA-CR-190956] p 587 N93-13406
Findings of a review of spacecraft fire safety needs
[NASA-CR-189181] p 523 N93-13715
Infrared spectroscopy of size resolved fine aerosol
p 647 N93-13758
Three-dimensional boundary element analysis of residual stresses in a cross-ply fiber composite model
p 629 N93-13811
Nutational stability and passive control of symmetric spinning bodies with axial forcing and internal mass motion p 504 N93-13820
Density contrast shell models for planetary nebulae
p 756 N93-13850
Transport on fractal networks
[AD-A253797] p 725 N93-13881
Frontogenesis processes in the troposphere
p 667 N93-13890
Connection of microscopic with macroscopic dynamics: Towards a hydrodynamical description of quantum mechanics p 729 N93-13957
CALIFORNIA UNIV., SAN DIEGO.
The North Atlantic circulation: Combining simplified dynamics with hydrographic data p 670 N93-13483
Structures, spectra and inertial range transfer in two-dimensional and beta-plane turbulence
p 590 N93-13900
CALIFORNIA UNIV., SAN DIEGO, LA JOLLA.
AFOSR Contractors Meeting in Propulsion
[AD-A254484] p 525 N93-12575
Synthesis and properties of mismatched heterojunction/substrate interfaces
[AD-A254577] p 719 N93-12648
Transputer implementation of the TRACE model of speech recognition
[AD-A254747] p 689 N93-12846
CALIFORNIA UNIV., SANTA BARBARA.
Photodissociation processes
[PB92-222702] p 702 N93-13067
End-point position control of multi-link flexible manipulator arms p 613 N93-13335
Nonholonomic motion of free-flying space robots
p 615 N93-13638
Accretion rates of protoplanets p 759 N93-13958
Instabilities and patterns in Taylor-Couette flow
p 593 N93-13965
Fracture of a metal/ceramic couple: Tantalum (titanium)/sapphire p 554 N93-14074
CALSPAN-BUFFALO UNIV. RESEARCH CENTER, NY.
Blackboard architectures for multi-agent planning
[AD-A255035] p 688 N93-12710
CALSPAN CORP., ARNOLD AFS, TN.
High heat flux measurements and experimental calibrations/characterizations p 598 N93-13663
Electron beam fluorescence measurements in the Boeing hypersonic shock tunnel p 602 N93-13681
CALSPAN FIELD SERVICES, INC., ARNOLD AFS, TN.
Design philosophy for wind tunnel model positioning systems
[AD-A254958] p 506 N93-12552
CANADA CENTRE FOR REMOTE SENSING, OTTAWA (ONTARIO).
Special SAR techniques and applications
p 564 N93-13059
Review of spaceborne and airborne SAR systems
p 565 N93-13060
CARNEGIE-MELLON UNIV., PITTSBURGH, PA.
From totally unimodular to balanced O, +/- 1 matrices: A family of integer polytopes
[AD-A254552] p 696 N93-12640
Program structure as a basis for the parallelization of global compiler optimizations
[AD-A254554] p 681 N93-12641
Expert-system development in Soar: A tutorial
[AD-A254571] p 682 N93-12645
Sensing and interpretation of 3-D shape and motion
p 692 N93-13240
Recent developments in the NL-Soar garden path theory
[AD-A255889] p 688 N93-13944
Public perceptions of the risks of an unfamiliar technology: The case of using nuclear energy sources for space missions p 527 N93-13971
CASE WESTERN RESERVE UNIV., CLEVELAND, OH.
Microstructural evolution in reaction bonded alumina/mullite ceramics p 552 N93-13328
CATHOLIC UNIV. OF AMERICA, WASHINGTON, DC.
Adaptive automation and human performance: Multi-task performance characteristics
[AD-A254596] p 503 N93-12578

Theory and design of adaptive automation in aviation systems
[AD-A254595] p 499 N93-12613
Adaptive automation and human performance. 3: Effects of practice on the benefits and costs of automation shifts
[AD-A254381] p 677 N93-12860
Glass corrosion in natural environments
[NASA-CR-191234] p 551 N93-13150
Organized turbulent structures and their induced wall pressure fluctuations p 592 N93-13952

CENTRE NATIONAL D'ETUDES SPATIALES, TOULOUSE (FRANCE).
Europe qualifies for space
[ESA-BR-64] p 508 N93-12892

CHEMICAL RESEARCH AND DEVELOPMENT CENTER, ABERDEEN PROVING GROUND, MD.
Correlation for non-linear infrared calibration curves
[AD-A255098] p 596 N93-12653
Vapor pressure data analysis methodology, statistics, and applications
[AD-A255090] p 536 N93-12743
Silicon neuron
[AD-A255091] p 674 N93-12756

CHICAGO UNIV., IL.
Statistical analysis of stratospheric temperature and ozone profile data for trends and model comparison
[NASA-CR-191248] p 650 N93-12877

CINCINNATI UNIV., OH.
An investigation of new search techniques for the traveling salesman problem p 696 N93-12625
Optical model analysis of gravity wave-critical layer interaction p 658 N93-13888

CITY COLL. OF THE CITY UNIV. OF NEW YORK, NY.
Dynamics and pattern selection at the crystal-melt interface
[DE92-040210] p 724 N93-13577

CLAREMONT GRADUATE SCHOOL, CA.
Human memory for the spatial locations of items on pull-down computer menus p 739 N93-14080

CLARKSON UNIV., POTSDAM, NY.
A low-dimensional dynamical systems description of coherent structures in the axisymmetric jet mixing layer p 593 N93-14057

CLEMSON UNIV., SC.
Physical property data on fluorinated propanes and butanes as CFC and HCFC alternatives
[PB92-206507] p 555 N93-12939

CLEVELAND STATE UNIV., OH.
X ray attenuation measurements for high-temperature materials characterization and in situ monitoring of damage accumulation p 631 N93-14022

COAST GUARD RESEARCH AND DEVELOPMENT CENTER, GROTON, CT.
Digital chart database conversion into a system electronic navigational chart
[AD-A255007] p 632 N93-12869

COLORADO RESEARCH DEVELOPMENT CORP., DENVER.
Narrow bandgap semiconducting silicides: Intrinsic infrared detectors on a silicon chip
[NASA-CR-190882] p 571 N93-13430

COLORADO STATE UNIV., FORT COLLINS.
Chemical sensors based on ultrathin film composite membranes
[AD-A254644] p 595 N93-12619
Extended range forecast of Atlantic seasonal hurricane activity for 1993 p 661 N93-12928
Summary of 1992 Atlantic tropical cyclone activity and verification of author's forecast (a year of no hurricane activity in the tropics but exceptional South Florida destruction from an unusual higher latitude intense hurricane) p 662 N93-13028
Microwave remote sensing of a precipitating atmosphere p 634 N93-13371
Effects of spaceflight on the proliferation of jejunal mucosal cells
[NASA-CR-191303] p 675 N93-13449
Measurement of tropospheric temperature and aerosol extinction using high spectral resolution lidar p 653 N93-13614
The relationship between SST anomalies and clouds, water vapor, and their radiative effects p 665 N93-13744
A unified approach to the analysis and design of manipulator systems with environmental contact p 573 N93-13805
Convective parameterization in mesoscale models p 659 N93-14062
An investigation of the effects of topography on Colorado front range winter storms p 668 N93-14063

COLORADO UNIV., BOULDER.
Modeling of coalescence, agglomeration, and phase segregation in microgravity processing of bimetallic composite materials
[NASA-CR-191247] p 556 N93-12728
Theoretical nuclear physics
[DE92-019286] p 706 N93-12822
Visualization techniques to aid in the analysis of multi-spectral astrophysical data sets
[NASA-CR-191260] p 685 N93-13261
B supergiants in open clusters and associations
[NASA-CR-191275] p 748 N93-13659
Research in geosciences policy
[NASA-CR-190470] p 632 N93-13833
Atmospheric loading response of the solid earth and oceans p 659 N93-13955
Compressible convection and pulsations on parallel computers p 690 N93-13961
Hydrodynamics and spectra formation of interacting massive binaries and the young remnant of SN1987A p 757 N93-13962
Coherent structures in compressible convection p 592 N93-13964
Application of satellite altimetry to study the Gulf of Alaska gyre p 635 N93-13969
Numerical simulation of compressible Couette flow stability: Non-linear and three-dimensional effects p 594 N93-14077

COLUMBIA UNIV., NEW YORK, NY.
Multichip module high speed testing
[AD-A254825] p 570 N93-12731
Analytical studies of nonlinear partial differential equations of interest in nonlinear optics
[AD-A254931] p 696 N93-13027
Theoretical high energy physics
[DE92-015480] p 707 N93-13189
A high-resolution radio survey of the galactic plane p 744 N93-13480
The morphotectonic fabric of the East Pacific Rise: Implications for fault generation and crustal accretion p 652 N93-13481
Achieving high Q(sub DD) operation in high poloidal beta discharges in TFTR
[DE92-019494] p 718 N93-13535
Atmospheric, climatic and environmental research
[NASA-CR-191367] p 664 N93-13718
Deep convection and its relation to the large-scale circulation in the tropical Pacific p 654 N93-13725
Thermoconvective instability in the solar core p 771 N93-13849
Two-photon cooperative cascade superfluorescence
[AD-A255690] p 608 N93-14023

COMMERCE DEPT., WASHINGTON, DC.
US Industry Access to Japanese Science and Technology: Proceedings of a conference
[PB92-167964] p 741 N93-13788

COMMITTEE ON COMMERCE, SCIENCE, AND TRANSPORTATION (U.S. SENATE).
National Aeronautics and Space Administration Authorization Act, fiscal year 1993
[S-REPT-102-364] p 741 N93-13798
NASA's fiscal year 1993 budget
[S-HRG-102-707] p 742 N93-13800

COMMITTEE ON SCIENCE, SPACE AND TECHNOLOGY (U.S. HOUSE).
Window on waste: Atrophy in NASA management
[GPO-57-273] p 732 N93-13693
NASA authorization, 1993, volume 2
[GPO-56-943-VOL-2] p 741 N93-13799

COMPUTER DATA SYSTEMS, INC., FORT WORTH, TX.
Cloud curve algorithm test program
[AD-A253918] p 662 N93-13099

CONNECTICUT UNIV., STORRS.
Structure sensitive reactions over Co, Fe and mixed metal clusters in zeolites
[DE92-040359] p 542 N93-12998
Nonlinear mechanics of composite materials with periodic microstructure
[NASA-CR-190750] p 531 N93-13309
Non-perturbative studies in quantum electrodynamics p 729 N93-13896

CONSORTIUM FOR INTERNATIONAL EARTH SCIENCE INFORMATION NETWORK, ANN ARBOR, MI.
Earth science information: Planning for the integration and use of global change information
[NASA-CR-191217] p 733 N93-12660
Earth science information: Planning for the integration and use of global change information
[NASA-CR-191208] p 734 N93-12680

CONSTRUCTION TECHNOLOGY LABS., SKOKIE, IL.
Physical properties of concrete made with Apollo 16 lunar soil sample p 554 N93-13987

CONTINUOUS ELECTRON BEAM ACCELERATOR FACILITY, NEWPORT NEW, VA.
Test of a new RF separator structure for CEBAF
[CEBAF-PR-92-024] p 708 N93-13284

CORNELL UNIV., ITHACA, NY.
Analysis of a linearly constrained least squares algorithm for adaptive beamforming
[AD-A255017] p 695 N93-12582
Synthesis and properties of novel cluster phases
[DE92-017388] p 545 N93-12697
Experiments, theory, and simulation on the evolution of fabric in granular materials
[AD-A254820] p 545 N93-12729
Photochemical dynamics of surface oriented molecules
[DE92-019813] p 703 N93-13106
Monitoring and controlling distributed applications using Lomita (position paper)
[NASA-CR-190971] p 687 N93-13695
Hydrodynamical calculations of stellar interactions p 755 N93-13764

COUNCIL FOR NATIONAL ACADEMIC AWARDS (ENGLAND).
Parameter studies of helium-neon lasers at 543 nm p 606 N93-13747
Transhorizon microwave propagation and its relationship with meteorological conditions p 666 N93-13791
Laser ablation for sample introduction in inductively coupled plasma spectrometry p 719 N93-13897
Mechanical properties of epoxy/alumina trihydrate-filled compositions p 534 N93-13950
Kinetic studies of some free radical reactions involved in cloudwater chemistry p 668 N93-14055

COVALENT ASSOCIATES, INC., WOBURN, MA.
Thermally stable electrolytes for rechargeable lithium batteries, phase 2
[NASA-CR-190878] p 573 N93-13610

CRANFIELD INST. OF TECH., BEDFORD (ENGLAND).
The application of the finite element method and the boundary element method to fatigue and fracture, volumes 1 and 2 p 624 N93-13016
Boundary element method for axisymmetric thermoelastic analysis p 624 N93-13097
Finite element versus boundary element analysis of two-dimensional coupled thermoelasticity p 625 N93-13142

CREARE, INC., HANOVER, NH.
All-metal, compact heat exchanger for space cryocoolers
[NASA-CR-190861] p 559 N93-13604

D

DAEDALUS ENTERPRISES, INC., ANN ARBOR, MI.
Development of a portable infrared emission spectrometer AA460 PIRES
[NASA-CR-190849] p 598 N93-13656

DAIMLER-BENZ A.G., ULM (GERMANY).
Perception-based and machine-oriented signal processing within speech understanding systems p 692 N93-13239

DARTMOUTH COLL., HANOVER, NH.
Ring current oxygen interaction with micropulsations p 651 N93-13149
The sapphire Cerenkov laser p 605 N93-13365
Structure of and dynamical processes in the Earth's magnetopause and boundary layer regions p 657 N93-13793

DATATAPE, INC., PASADENA, CA.
Magnetic tape p 737 N93-13135

DAYTON UNIV., OH.
Perceptual dimensions of visual scenes relevant for simulating low-altitude flight
[AD-A254645] p 676 N93-12662

DAYTON UNIV. RESEARCH INST., OH.
Long Duration Exposure Facility M0003-5 thermal control coatings on DoD flight experiment p 548 N93-12782
Long Duration Exposure Facility M0003-5 recent results on polymeric films p 549 N93-12789
Temperature and heat flux measurements: Challenges for high temperature aerospace application p 598 N93-13662

DEFENSE NUCLEAR AGENCY, WASHINGTON, DC.
Proceedings of the 62nd Shock and Vibration Symposium, Volume 2
[AD-A249267] p 628 N93-13637

DEFENSE SYSTEMS, INC., MCLEAN, VA.
The DSI small satellite launcher p 511 N93-13180

DELAWARE UNIV., NEWARK.
Magnetic hardening studies and novel techniques for preparation of high performance magnets
[AD-A254761] p 698 N93-12865
Vibration damping response of composite materials p 533 N93-13748

DENVER UNIV., CO.
Application of improved HNO3 band model parameters to South Pole atmospheric emission measurements p 647 N93-13723

DEPARTMENT OF DEFENCE, CANBERRA (AUSTRALIA).
Obtaining medians and other quantiles with limited memory space
[AD-A254506] p 683 N93-12722
DEPARTMENT OF ENERGY, MORGANTOWN, WV.
Development of advanced turbine systems: Meeting tomorrow's needs
[DE92-017339] p 612 N93-13103
DEPARTMENT OF ENERGY, WASHINGTON, DC.
World Energy Projection System (WEPS), March 1992. Model installation manual, distribution disk layout
[PB92-169572] p 637 N93-12937
Advanced energy projects FY 1992 research summaries
[DE92-040442] p 637 N93-13001
Energy from Municipal Waste Program
[DE92-010578] p 638 N93-13102
DEPARTMENT OF THE ARMY, WASHINGTON, DC.
Transducer circuit
[AD-D015376] p 572 N93-13472
Preamplifier with adjustable input resistance
[AD-D015377] p 572 N93-13473
Infrared image projector utilizing a deformable mirror device spatial light modulator
[AD-D015373] p 710 N93-13500
Electronic triple point cell
[AD-D015374] p 597 N93-13501
DEPARTMENT OF THE NAVY, WASHINGTON, DC.
Molten salt reactor for potentiostatic electroplating
[AD-D015358] p 551 N93-13101
Hermetic sealing and EMI shielding gasket
[AD-D015359] p 552 N93-13414
Booster explosive rings
[AD-D015375] p 556 N93-13471
DEUTSCHE AIRBUS G.M.B.H., BREMEN (GERMANY).
Recent developments in low-speed TPS-testing for engine integration drag and installed thrust reversr simulation p 502 N93-13207
DEUTSCHE FORSCHUNGS- UND VERSUCHSANSTALT FUER LUFT- UND RAUMFAHRT, GOETTINGEN (GERMANY).
Comparative performance tests of a pitot-inlet in several European wind-tunnels at subsonic and supersonic speeds p 497 N93-13221
DEUTSCHE FORSCHUNGSANSTALT FUER LUFT- UND RAUMFAHRT, BRUNSWICK (GERMANY).
Investigation of interference phenomena of modern wing-mounted high-bypass-ratio engines by the solution of the Euler-equations p 578 N93-13204
The jet behaviour of an actual high-bypass engine as determined by LDA-measurements in ground tests p 503 N93-13218
Investigation of the flowfield around an isolated bypass engine with fan and core jet p 582 N93-13227
DEUTSCHE FORSCHUNGSANSTALT FUER LUFT- UND RAUMFAHRT, OBERPFAFFENHOFEN (GERMANY).
Basic principles of SAR p 563 N93-13050
SAR peculiarities, ambiguities and constraints p 563 N93-13051
Motion errors and compensation possibilities p 563 N93-13052
The real aperture antenna of SAR, a key element for performance p 564 N93-13053
Radiometric calibration of SAR systems p 564 N93-13055
SAR simulation p 564 N93-13056
DIGITAL ANALYSIS CORP., RESTON, VA.
DNET: A communications facility for distributed heterogeneous computing
[NASA-CR-190863] p 682 N93-13759
DRAPER (CHARLES STARK) LAB., INC., CAMBRIDGE, MA.
Robust rendezvous maneuver point conditions
[NASA-CR-190996] p 517 N93-12690
DREXEL UNIV., PHILADELPHIA, PA.
Stress crack testing of polyethylene geomembranes
[PB92-217132] p 622 N93-12843
Theory of lasing without population inversion p 605 N93-13497
Matrix cracking initiation stress in fiber-reinforced ceramic matrix composites p 627 N93-13539
DUKE UNIV., DURHAM, NC.
Characterization of thermotropic liquid crystalline polymer blends by positron annihilation lifetime spectroscopy
[AD-A253616] p 552 N93-13325
DUNDEE UNIV. (SCOTLAND).
Automatic pattern recognition techniques for geometrical correction on satellite data p 687 N93-13913
DYNACS ENGINEERING CO., INC., CLEARWATER, FL.
On-orbit supervisor for controlling spacecraft
[AD-A254342] p 522 N93-12962
DYNAMICS RESEARCH CORP., WILMINGTON, MA.
Introductory review of target discrimination criteria
[AD-A254954] p 560 N93-12551
DYNETICS, INC., HUNTSVILLE, AL.
Acousto-optic applications for multichannel adaptive optical processor
[AD-A255823] p 711 N93-14032

E

EAGLE ENGINEERING, INC., HOUSTON, TX.
Lunar stepping stones to a manned Mars exploration scenario p 767 N93-14016
EAST ANGLIA UNIV., NORWICH (ENGLAND).
Kinetic and spectroscopic studies of peroxy radical reactions related to tropospheric photo-oxidation chemistry p 654 N93-13726
The seasonal variations and interrelationships of ozone, peroxyacetyl nitrate and nitrogen dioxide in the troposphere p 647 N93-13893
EASTMAN KODAK CO., ROCHESTER, NY.
Large Deployable Reflector (LDR) system concept and technology definition study. Volume 1: Executive summary, analyses and trades, and system concepts
[NASA-CR-177413-VOL-1] p 708 N93-12591
Large Deployable Reflector (LDR) system concept and technology definition study. Analysis of space station requirements for LDR
[NASA-CR-177414] p 742 N93-12592
Large Deployable Reflector (LDR) system concept and technology definition study. Volume 2: Technology assessment and technology development plan
[NASA-CR-177413-VOL-2] p 708 N93-12593
ECKERD COLL., SAINT PETERSBURG, FL.
Experimental studies of the far-infrared spectra of cosmic-type ices
[NASA-CR-191300] p 748 N93-13660
EDGERTON, GERMESHAUSEN AND GRIER, INC., IDAHO FALLS, ID.
Investigation of component failure rates for pulsed versus steady state tokamak operation
[DE92-019758] p 713 N93-12856
Natural convection between a vertical cylinder and a surrounding array
[DE92-019763] p 728 N93-12857
Two-phase flow modeling with discrete particles
[DE92-017850] p 583 N93-13356
Verification and validation of TMAP4
[DE92-019684] p 539 N93-13616
EG AND G ENERGY MEASUREMENTS, INC., IDAHO FALLS.
You need this done by when? Increasing your efficiency with the SAS system
[DE92-017894] p 683 N93-12792
An integrated optical sensor for GMAW feedback control
[DE92-018019] p 610 N93-12793
Turbulent natural convection between a perforated vertical cylinder and a surrounding array
[DE92-019766] p 576 N93-12996
EG AND G ENERGY MEASUREMENTS, INC., LAS VEGAS, NV.
Deciduous forest scene complexity in high-resolution multispectral scanner imagery
[AD-A255511] p 635 N93-13867
EG AND G MOUND APPLIED TECHNOLOGIES, MIAMISBURG, OH.
Development of a laser ignited all secondary explosive DDT detonator
[DE92-019340] p 555 N93-13081
Isotopic separation of He-3/He-4 from solar wind gases evolved from the lunar regolith
[DE92-019339] p 759 N93-13504
EG AND G ROCKY FLATS, INC., GOLDEN, CO.
Reduction of chlorofluorocarbon emissions from refrigeration systems
[DE92-019360] p 645 N93-13505
ELECTRIC POWER RESEARCH INST., PALO ALTO, CA.
Considerations for the transition from fuel cell R/D to manufacturing
[DE92-019977] p 640 N93-13622
ELETTRONICA SAN GIORGIO S.P.A., GENOA (ITALY).
3-D computer vision for navigation/control of mobile robots p 693 N93-13243
ELORET CORP., SUNNYVALE, CA.
Simulation studies for surfaces and materials strength
[NASA-CR-191289] p 724 N93-13570
ELTRON RESEARCH, INC., AURORA, IL.
Perovskite solid electrolytes for SOFC
[DE92-019981] p 638 N93-13041
ENERGETICS, INC., COLUMBIA, MD.
Hydrogen Program Plan, FY 1993 - 1997
[DE92-010556] p 538 N93-13316
ENERGY RESEARCH CORP., DANBURY, CT.
Understanding of carbonate fuel cell resistance issues for performance improvement
[DE92-019976] p 638 N93-13039
Effects of coal-derived trace species on performance of molten carbonate fuel cells
[DE93-000203] p 639 N93-13427
An update of ERC's carbonate fuel cell development program
[DE92-019971] p 640 N93-13621
ENVIRONMENTAL PROTECTION AGENCY, ANN ARBOR, MI.
The 1992 natural gas vehicle challenge: EPA emissions and fuel economy testing
[PB92-217926] p 616 N93-13761
ENVIRONMENTAL PROTECTION AGENCY, RESEARCH TRIANGLE PARK, NC.
Interagency Workgroup on Air Quality Modeling (IWAQM) work plan rationale
[PB92-213248] p 643 N93-12940
Documentation for developing the initial source category list
[PB92-218429] p 646 N93-13647
ENVIRONMENTAL PROTECTION AGENCY, SILVER SPRING, MD.
NOAA Atmospheric Sciences Modeling Division support to the US Environmental Protection Agency
[PB92-217835] p 644 N93-12974
ESSEX CORP., HUNTSVILLE, AL.
Spacelab J: Microgravity and life sciences
[NASA-CR-191353] p 516 N93-13564
EUROPEAN SPACE AGENCY, PARIS (FRANCE).
Touchstone for success
[ESA-BR-52] p 557 N93-12934
Giotto: The second encounter
[ESA-BR-83] p 749 N93-12965
Eureca: A first for Europe
[ESA-BR-85] p 516 N93-13691
EUROPEAN SPACE AGENCY. EUROPEAN SPACE RESEARCH AND TECHNOLOGY CENTER, ESTEC, NOORDWIJK (NETHERLANDS).
Effects of the LDEF environment on the Ag/FEP thermal blankets p 548 N93-12785
Europe qualifies for space
[ESA-BR-64] p 508 N93-12892
EURECA
[ESA-F-26] p 522 N93-12964
Horizon 2000: Seven years on
[ESA-BR-37-B] p 516 N93-13855
Taking a global view
[ESA-BR-37-C] p 516 N93-13856
Messengers in space
[ESA-BR-37-D] p 516 N93-13857
A home port in space
[ESA-BR-37-E] p 516 N93-13858
Reaching for the skies: The next generation
[ESA-BR-37-G] p 516 N93-13859
Preparing for the future
[ESA-BR-37-H] p 517 N93-13860
The next step forward
[ESA-BR-37-A] p 517 N93-13861
A growing dimension in space
[ESA-BR-37-F] p 517 N93-13902
Ever watchful
[ESA-BR-37-I] p 517 N93-13903
EXETER UNIV. (ENGLAND).
Acousto-optic devices and applications p 712 N93-14100

F

FEDERAL AVIATION ADMINISTRATION, ATLANTIC CITY, NJ.
ILS mathematical modeling study of the effects of an ASR-9 structure at the Long Island MacArthur Airport, Islip, NY
[DOT/FAA/CT-TN92/25] p 506 N93-12668
Vapor to liquid ratio test as an indicator of volatility
[DOT/FAA/CT-TN92/40] p 537 N93-12897
Limited production Precision Runway Monitor (PRM) master test plan
[DOT/FAA/CT-TN92/23] p 506 N93-12899
Prototype stop bar system evaluation at John F. Kennedy International Airport
[DOT/FAA/CT-92/24] p 506 N93-12902
Terminal Doppler Weather Radar (TDWR) Operational Test and Evaluation (OT/E) integration test plan
[DOT/FAA/CT-TN92/6] p 499 N93-13377
A NASPAC-based analysis of the delay and cost effects of the Dallas/Fort Worth metroplex plan
[DOT/FAA/CT-TN92/21] p 507 N93-13447

FEDERAL AVIATION ADMINISTRATION, OKLAHOMA CITY, OK.
Postmortem alcohol production in fatal aircraft accidents
[AD-A255766] p 498 N93-14026
FEDERAL AVIATION ADMINISTRATION, WASHINGTON, DC.
The identification and quantitation of triamterene in blood and urine from a fatal aircraft accident
[AD-A254550] p 674 N93-12612
Report to Congress: State Block Grant Program
[AD-A254569] p 507 N93-13882
FEDERAL LIBRARY AND INFORMATION CENTER COMMITTEE, WASHINGTON, DC.
Proceedings of FLICC forums on federal information policies. Combined summaries of proceedings. The 1990 7th Forum, Access is the Key and the 1991 8th Forum, Building Information Superhighways: Supercomputing Networks and Libraries
[PB92-147370] p 734 N93-12759
FERMI NATIONAL ACCELERATOR LAB., BATAVIA, IL.
Particle production and survival in muon acceleration
[DE92-019553] p 701 N93-12572
RF voltage modulation at discrete frequencies with applications to crystal channeling extraction
[DE92-015567] p 707 N93-13235
Heavy gauge boson and lambda(b) baryon searches at CDF
[DE92-019551] p 705 N93-13537
FLORIDA ATLANTIC UNIV., BOCA RATON.
Dynamic stall effects on hingeless rotor stability with experimental correlation p 492 N93-13010
Optimal coordination of robotic systems with redundancy p 693 N93-13336
Trim analysis by shooting and finite elements and Floquet eigenanalysis by QR and subspace iterations in helicopter dynamics p 501 N93-13914
FLORIDA STATE UNIV., GAINESVILLE.
Identifiability in the autopsy model of reliability theory p 620 N93-13710
Applying an object-oriented database model to a scientific database problem: Managing experimental data at CEBAF p 738 N93-13911
A study regarding information-seeking behavior, valuation of information including perceptions of information attributes, and associated correlates pertaining to information usage p 740 N93-14088
FLORIDA STATE UNIV., TALLAHASSEE.
Efficacy of multimedia instruction and an introduction to digital multimedia technology
[AD-A254509] p 734 N93-12723
Intraseasonal variability of infrared cooling rates during the Asian summer monsoon and their influence on intraseasonal waves p 665 N93-13760
FLORIDA UNIV., GAINESVILLE.
Studies of granular flow down an inclined chute
[DE92-018871] p 577 N93-13074
Finite elements for free edge delaminations and delaminated anisotropic beams p 535 N93-13967
FOKKER B.V., SCHIPOL-OOST (NETHERLANDS).
Aerodynamic integration of thrust reversers on the Fokker 100 p 502 N93-13208

G

GENCORP AEROJET, SACRAMENTO, CA.
Pressure fed thrust chamber technology program
[NASA-CR-184461] p 526 N93-12968
GENERAL ACCOUNTING OFFICE, WASHINGTON, DC.
Large programs may consume increasing share of limited future budgets. Report to Congressional Requesters
[GAO/NSIAD-92-278] p 732 N93-13109
Space Station: Resolving conflict over integration contractor's role. Briefing report to the Chairman, Subcommittee on Investigations and Oversight, Committee on Science, Space, and Technology, House of Representatives
[GAO/NSIAD-92-291BR] p 732 N93-13111
Earth observing system: Information on NASA's incorporation of existing data into EOSDIS. Report to the Chairman, Committee on Science, Space, and Technology, House of Representatives
[GAO/IMTEC-92-79] p 736 N93-13112
National Aero-Space Plane: Key issues facing the program. Testimony before the Subcommittee on Technology and Competitiveness, Committee on Science, Space, and Technology, House of Representatives
[GAO/T-NSIAD-92-26] p 500 N93-13253
NASA budget: Potential shortfalls in funding NASA's 5-year plan. Testimony before the Subcommittee on Science, Technology, and Space, Committee on Commerce, Science, and Transportation, United States Senate
[GAO/T-NSIAD-92-18] p 740 N93-13280
GENERAL APPLIED SCIENCE LABS., INC., RONKONKOMA, NY.
Resonance lamp absorption measurement of OH number density and temperature in expansion tube scramjet engine tests p 602 N93-13682
GENERAL ATOMIC CO., SAN DIEGO, CA.
A quantitative analysis of the effect of ELMs on H-mode thermal energy confinement in DIII-D
[DE92-017704] p 712 N93-12687
Future development of the D3-D tokamak program
[DE92-040051] p 715 N93-13044
Storage system software solutions for high-end user needs p 737 N93-13136
Fast wave current drive experiment on the D3-D tokamak
[DE92-016253] p 716 N93-13193
GENERAL DYNAMICS CORP., FORT WORTH, TX.
Calibration of 2D unstructured grid methods on propulsive flowfields p 582 N93-13225
CFD calibration for three-dimensional nozzle/afterbody configurations p 582 N93-13226
GENERAL DYNAMICS CORP., SAINT LOUIS, MO.
The trade-off characteristics of acoustic and pressure sensors for the NASP p 601 N93-13678
GENERAL ELECTRIC CO., CINCINNATI, OH.
Coupled structural/thermal/electromagnetic analysis/tailoring of graded composite structures
[NASA-CR-189150] p 626 N93-13443
Coupled structural/thermal/electromagnetic analysis/tailoring of graded composite structures
[NASA-CR-189151] p 627 N93-13444
Coupled structural/thermal/electromagnetic analysis/tailoring of graded composite structures
[NASA-CR-189152] p 627 N93-13445
GENERAL ELECTRIC CO., EVENDALE, OH.
Electro-optic architecture for servicing sensors and actuators in advanced aircraft propulsion systems
[NASA-CR-182269] p 711 N93-13762
GENERAL MOTORS CORP., INDIANAPOLIS, IN.
Investigation of advanced counterrotation blade configuration concepts for high speed turboprop systems. Task 4: Advanced fan section aerodynamic analysis
[NASA-CR-187128] p 502 N93-12695
GEOPHYSICAL OBSERVATORY, HELSINKI (FINLAND).
Recursive construction of fractals
[ISBN-951-41-0689-X] p 697 N93-13271
GEORGE WASHINGTON UNIV., WASHINGTON, DC.
Publications of the space physiology and countermeasures program, Musculoskeletal Discipline: 1980-1990
[NASA-CR-4468] p 743 N93-12898
Investigations of the structure and electromagnetic interactions of few-body systems
[DE92-040011] p 563 N93-13042
A time domain numerical theory for studying steady-state acoustic disturbance in flow p 700 N93-13770
GEORGETOWN UNIV., WASHINGTON, DC.
Assessment of potential aerodynamic benefits from spanwise blowing at the wing tip p 496 N93-13822
GEORGIA INST. OF TECH., ATLANTA.
Application of concurrent engineering methods to the design of an autonomous aerial robot
[AD-A254968] p 609 N93-12555
Innovative methods in the dynamics of large space structures
[AD-A254630] p 521 N93-12579
Massively parallel optical-to-electronic data transfer
[AD-A254831] p 688 N93-12733
Dynamic control modification techniques in teleoperation of a flexible manipulator
[NASA-CR-190984] p 610 N93-12904
Manipulation strategies for massive space payloads
[NASA-CR-190844] p 611 N93-12952
Numerical analysis of nonminimum phase zero for nonuniform link design p 611 N93-12953
The application of input shaping to a system with varying parameters p 612 N93-12954
Experimental verification of modified command shaping using a flexible manipulator p 612 N93-12955
An acoustic charge transport imager for high definition television applications
[NASA-CR-191295] p 572 N93-13448
Robust control of a flexible link robot and rigid link robot: Theory, simulation, and experiment p 614 N93-13452
Velocity and temperature measurements in a non-premixed reacting flow behind a backward facing step p 494 N93-13632
High-speed aerodynamics of upper surface blowing aircraft configurations p 494 N93-13729
Studies on numerical and experimental determination of energy release rate for composite laminates p 533 N93-13752
Mobile work platform for initial lunar base construction p 559 N93-14009
GEORGIA STATE UNIV., ATLANTA.
Neurochemical control of circadian rhythms
[AD-A255054] p 675 N93-13116
The CHARA optical array p 744 N93-13581
GEORGIA TECH RESEARCH INST., ATLANTA.
Informal Conference on Photochemistry
[AD-A255824] p 540 N93-14033
GEORGIA UNIV., ATHENS.
Nitrogen control of chloroplast development and differentiation
[DE92-017392] p 671 N93-12768
GEORGIA UNIV., GRIFFIN.
Performance of the Bowen ratio systems on a 22 deg slope
[NASA-CR-191278] p 644 N93-13254
GRENOBLE UNIV. (FRANCE).
NATO Advanced Research Workshop: Vortex Flows and Related Numerical Methods. List of participants, book of abstracts, and instructions for submission to the proceedings
[AD-A255015] p 575 N93-12708

H

HARVARD UNIV., CAMBRIDGE, MA.
Mathematics and string theory
[DE92-019292] p 727 N93-12796
Measurements of crystal growth kinetics at extreme deviations from equilibrium
[DE92-019744] p 720 N93-12827
Radiative constraints on the energy budget of the atmosphere p 655 N93-13731
Load-transfer and crack bridging in fiber-toughened ceramic composites p 629 N93-13754
Supernova remnants, shocks, and the interstellar medium p 757 N93-13963
Thermal and nonthermal star formation: An investigation into the process of star formation as a function of stellar mass p 758 N93-14091
Molecular clouds in the distant outer galaxy p 758 N93-14095
HAWAII UNIV., HONOLULU.
The lunar environment and its effect on optical astronomy p 746 N93-13594
HELSINKI UNIV. OF TECHNOLOGY, ESPOO (FINLAND).
Stabilization and projection methods for multibody dynamics
[PB92-133883] p 698 N93-12890
HERIOT-WATT UNIV., EDINBURGH (SCOTLAND).
A study of small solid-state switched TEA CO2 lasers p 607 N93-13814
HERNANDEZ ENGINEERING, INC., GREENBELT, MD.
Structural verification for GAS experiments p 511 N93-13175
Proper battery system design for GAS experiments p 511 N93-13176
HOUSTON UNIV., TX.
Wake characterization: Full flow simulation of space structures in low earth orbit p 497 N93-13970
HOWARD UNIV., WASHINGTON, DC.
Glass corrosion in natural environments
[NASA-CR-191234] p 551 N93-13150
Radar signal processing for over resolved targets
[AD-A255256] p 566 N93-13838
HULBURT (E. O.) CENTER FOR SPACE RESEARCH, WASHINGTON, DC.
The Mount Wilson optical interferometer: The first automated instrument and the prospects for lunar interferometry p 745 N93-13582
HULL UNIV. (ENGLAND).
Phase conjugation using CO2 lasers p 607 N93-13812
HYDROQUAL, INC., MAHWAH, NJ.
Ultraviolet disinfection technology assessment
[PB92-222868] p 678 N93-12983

I

ILLINOIS UNIV., CHICAGO.
Theoretical and experimental studies on the foundation theoretical and experimental studies on the foundation of mesomechanics
[AD-A254385] p 623 N93-12863
Transverse wave motion in constrained mechanical systems p 628 N93-13634
ILLINOIS UNIV., URBANA.
Design for reliability: Current density
[AD-A254770] p 570 N93-12866
Lazy checkpoint coordination for bounding rollback propagation
[NASA-CR-191281] p 565 N93-13375
Resource constrained design of artificial neural networks using comparator neural network
[NASA-CR-191280] p 694 N93-13376

BETA: Behavioral testability analyzer and its application to high-level test generation and synthesis for testability
[NASA-CR-191282] p 572 N93-13569
Summary: Experimental validation of real-time fault-tolerant systems
[NASA-CR-190985] p 503 N93-13697
The three to five semiconductor quantum well lasers and related optoelectronic devices on silicon
[AD-A255368] p 608 N93-13864

ILLINOIS UNIV., URBANA-CHAMPAIGN.
Fatigue and fracture of intermetallic alloys
[AD-A254543] p 540 N93-12603
Identification of parametric finite element models using experimental modal data
[PB92-217819] p 558 N93-12976
A laboratory investigation of raindrop oscillations
p 666 N93-13790

ILLINOIS UNIV. AT URBANA-CHAMPAIGN, SAVOY.
Finite element analysis of anisotropic viscoelastic composite structures and analytical determination of optimum viscoelastic material properties
p 530 N93-13007
Large-deflection analysis of cord composite plates
p 530 N93-13008
An investigation into thermomechanical fatigue of metal matrix composites p 534 N93-13810
Climate sensitivity study with energy balance models
p 666 N93-13817
The role of ambipolar diffusion in the formation of interstellar cloud cores and protostars
p 755 N93-13828
Some problems of quantum cosmology and dark matter physics p 755 N93-13829
Computer-aided design-based high-frequency electromagnetic wave scattering from complex bodies
p 567 N93-14042
Recursive algorithms for computational electromagnetics p 567 N93-14043
Theoretical and numerical studies of wave propagation and scattering in inhomogeneous media
p 568 N93-14044
Electromagnetic scattering simulations using equivalent boundary condition models p 569 N93-14052
A numerical study of hypersonic flows using the full Navier-Stokes equations with different air models
p 594 N93-14061

IMPERIAL COLL. OF SCIENCE AND TECHNOLOGY, LONDON (ENGLAND).
Numerical optimization
[AD-A254575] p 682 N93-12647

INDIANA UNIV., BLOOMINGTON.
Indiana University High Energy Physics Group, task C
[DE92-040458] p 707 N93-13002
A search for point sources of cosmic ray muons using the MACRO detector p 773 N93-13738

INDUSTRIEANLAGEN-BETRIEBSGESELLSCHAFT M.B.H., MUNICH (GERMANY).
Europe qualifies for space
[ESA-BR-64] p 508 N93-12892

INFORMATION AND CONTROL SYSTEMS, INC., HAMPTON, VA.
A stochastic optimal feedforward and feedback control methodology for superagility
[NASA-CR-4471] p 694 N93-13370

INSTITUT DES HAUTES ETUDES SCIENTIFIQUES, BURES-SUR-YVETTE (FRANCE).
Solutions without phase-slip for the Ginsburg-Landau equation
[PB92-115575] p 696 N93-12889

INSTITUTE FOR COMPUTER APPLICATIONS IN SCIENCE AND ENGINEERING, HAMPTON, VA.
On the prediction of turbulent secondary flows
[NASA-CR-189722] p 575 N93-12717
Fast multiresolution algorithms for matrix-vector multiplication
[NASA-CR-189721] p 696 N93-12942
Report on the final panel discussion on computational aeroacoustics
[NASA-CR-189718] p 699 N93-12986

INSTITUTE FOR DEFENSE ANALYSES, ALEXANDRIA, VA.
Seamless simulation literature survey
[AD-A254950] p 688 N93-12549
Angle of arrival fluctuations for millimeter waves propagating in a turbulent atmosphere near the Earth
[AD-A254478] p 560 N93-12574

INSTITUTE OF ECOTECHNICS, LONDON (ENGLAND).
Life systems for a lunar base p 680 N93-13992

INSTITUTE OF GAS TECHNOLOGY, CHICAGO, IL.
The MAGSORB process for bulk separation of carbon dioxide
[DE92-001296] p 538 N93-13314

INSTITUTE OF OCEAN SCIENCES, SIDNEY (BRITISH COLUMBIA).
Acoustic tracking of neutrally buoyant float
[AD-A255086] p 669 N93-12742

INSTITUTE OF PLASMA PHYSICS, PRAGUE (CZECHOSLOVAKIA).
Phase mixing and surface wave decay in an inhomogeneous plasma
[IPPCZ-320] p 715 N93-13006
On the bootstrap current calculations based on values of the radial electron transport
[IPPCZ-317] p 715 N93-13091
Fluctuation studies on CASTOR and ASDEX tokamaks at lower hybrid current drive
[IPPCZ-319] p 715 N93-13093
Measurements of the temperature in the edge plasma of the CASTOR tokamak by a triple Langmuir probe
[IPPCZ-318] p 716 N93-13330

INSTITUTE OF SOUND AND VIBRATION RESEARCH, SOUTHAMPTON (ENGLAND).
Intake and exhaust noise
[ISVR-TR-207] p 699 N93-12714
MINT: The multiple error LMS algorithm, and the design of inverse filters for multi-channel sound reproduction systems
[ISVR-TR-211] p 700 N93-13439
Design guide for the ergonomic aspects of helicopter crew seating
[ISVR-TR-209] p 678 N93-13464

INSTITUTO DE PESQUISAS ESPACIAIS, SAO JOSE DOS CAMPOS (BRAZIL).
An ion budget for a terra firme rainforest in Central Amazonia
[INPE-5365-PRE/1745] p 632 N93-13005
Diagnostics systems for the TBR-E tokamak
[INPE-5428-RPQ/662] p 716 N93-13257
Field spectroradiometry and sail model application to irrigated wheat (Triticum aestivum, L) canopies spectral reflectance
[INPE-5426-TDI/483] p 634 N93-13258
Alternative methods for determination of the temperature of central stars of planetary nebulae
[INPE-5434-TDI/485] p 750 N93-13279
Characterization of electric discharge in air produced by an environmental ionizator
[INPE-5310-NTC/299] p 651 N93-13310
Brazilian remote sensing community: Historical, geographical and economic aspects
[INPE-5421-PRE/1763] p 634 N93-13412

INTELLICORP, MOUNTAIN VIEW, CA.
Compiling knowledge-based systems to Ada, phase 2
[NASA-CR-191273] p 686 N93-13355

INTERNATIONAL COUNCIL OF SCIENTIFIC UNIONS, PARIS (FRANCE).
A report on geomagnetic observatory operations, 1990
[PB92-224781] p 649 N93-12804

INTERNATIONAL FUEL CELLS CORP., SOUTH WINDSOR, CT.
Advanced water-cooled phosphoric acid fuel cell development
[DE92-019979] p 638 N93-13040

INTERNATIONAL SOCIETY FOR TERRAIN-VEHICLE SYSTEMS, HANOVER, NH.
Proceedings of the Fifth European International Society for Terrain-Vehicle Systems, volume 1
[AD-A254619] p 611 N93-12906

INTERNATIONAL SPACE UNIV., INC., TORONTO (ONTARIO).
International Asteroid Mission p 513 N93-13548
Introduction to the International Asteroid Mission
p 513 N93-13549
Asteroid search program p 514 N93-13550
Summary of literature on unmanned probes to asteroids and precursor data requirements for IAM
p 514 N93-13551
Conceptual design of a human piloted mining mission
p 514 N93-13552
The program plan: An overview of the development and implementation of the International Asteroid Mission
p 514 N93-13553
Business analysis: The commercial mission of the International Asteroid Mission p 514 N93-13554
Legal and political issues raised by the International Asteroid Mission p 514 N93-13555
Engineering and architectural issues associated with the asteroid mission p 514 N93-13556
Mining equipment and operations for mining the 1982HR (Orpheus) asteroid p 515 N93-13557
A microgravity processing plant for the manufacturing of propellant and water from asteroid ore
p 515 N93-13558
Human factors dealing with the International Asteroid Mission p 515 N93-13559
Ground operations and logistics in the context of the International Asteroid Mission p 515 N93-13560
Scientific experimentation afforded by the International Asteroid Mission p 515 N93-13561
Research and technology in support of IAM
p 515 N93-13562

INTERSTEL, INC., BELTSVILLE, MD.
Test plan and report for Space Shuttle launch environment testing of Bergen cable technology safety cable
[NASA-CR-4473] p 559 N93-13434

IOWA STATE UNIV. OF SCIENCE AND TECHNOLOGY, AMES.
An inverse dynamics approach to trajectory optimization for an aerospace plane
[NASA-CR-191277] p 500 N93-13305
Wall functions for the kappa-epsilon turbulence model in generalized nonorthogonal curvilinear coordinates
p 587 N93-13517
Control of a very flexible robot in gravity
p 615 N93-13541
The use of degradation measures in assessing reliability p 573 N93-13607
Solution of viscous flow problems by using the boundary element method p 588 N93-13609
Effects of stinger axial dynamics and mass compensation methods on experimental modal analysis
p 699 N93-13907
Sequential quadratic programming solutions to related aircraft trajectory optimization problems
p 505 N93-13926

IOWA UNIV., IOWA CITY.
Interaction and impact of floating bodies
[AD-A254627] p 574 N93-12617
Finite element study of ultrasonic imaging
p 700 N93-13774
Molecular biology of anaerobic aromatic biodegradation
[AD-A255213] p 673 N93-13863
An experimental and computational study of longitudinal vortices in turbulent boundary layers
p 595 N93-14097

ISHIKAWAJIMA-HARIMA HEAVY INDUSTRIES CO. LTD., TOKYO (JAPAN).
Element Material Exposure Experiment by EFFU
p 548 N93-12783

ISHIKAWAJIMA-HARIMA HEAVY INDUSTRIES CO. LTD., YOKOHAMA (JAPAN).
Numerical study on mixing of sprayed liquid in an LNG storage tank p 584 N93-13388

J

JEFFERSON MEDICAL COLL., PHILADELPHIA, PA.
A core facility for the study of neurotoxins of biological origin
[AD-A254359] p 674 N93-12945

JET PROPULSION LAB., CALIFORNIA INST. OF TECH., PASADENA.
Polarization effects and multipolarization SAR
p 564 N93-13054
Multi-frequency multi-polarization processing for spaceborne SAR p 564 N93-13057
Efficiency of an AMTEC recirculating test cell, experiments, and projections
[DE92-016811] p 571 N93-13196
Reversible thermodynamic cycle for AMTEC power conversion
[DE92-016814] p 571 N93-13197
TRASYS form factor matrix normalization
p 585 N93-13391
Quantum well, beam deflecting surface emitting lasers
[NASA-CASE-NPO-18243-1-CU] p 605 N93-13418
Integrated filter and detector array for spectral imaging
[NASA-CASE-NPO-18317-1-CU] p 709 N93-13419
Acoustic device and method for measuring gas densities
[NASA-CASE-NPO-18155-1-CU] p 700 N93-13421
Three-stage sorption type cryogenic refrigeration systems and methods employing heat regeneration
[NASA-CASE-NPO-18366-1-CU] p 558 N93-13422
Densities and abundances of hot cometary ions in the coma of P/Halley p 752 N93-13466
Observations of solar wind ion charge exchange in the comet Halley coma p 752 N93-13467
Observations of plasma dynamics in the coma of P/Halley by the Giotto Ion Mass Spectrometer
p 752 N93-13468
Interpretation of the ion mass spectra in the mass range 25-35 obtained in the inner coma of Halley's comet by the HIS-sensor of the Giotto IMS Experiment
p 752 N93-13469
Orbiting Space Interferometer (OSI): A first generation space interferometer p 745 N93-13587
Large area projection liquid-crystal video display system with inherent grid pattern optically removed
[NASA-CASE-NPO-16932-2-CU] p 711 N93-13711

JOHNS HOPKINS UNIV., BALTIMORE, MD.
Evolution of galaxies in compact groups
p 750 N93-13148

The mass and dynamics of cD clusters with cooling flows. 1: ROSAT observations of A 496
[NASA-CR-191240] p 743 N93-13352
Comparison of cometary comae using ultraviolet spectroscopy: Composition and variation
p 753 N93-13603
The Jovian ultraviolet aurora observed with the IUE spacecraft: Brightness and color distribution with longitude p 759 N93-13625
An analysis of the Voyager 2 ultraviolet spectrometer occultation data at Uranus and Triton: Inferring heat sources and model atmospheres p 768 N93-14072

JOINT ASTRONOMY CENTRE, HILO, HI.
United Kingdom Infrared Telescope
p 743 N93-13273

JOINT PUBLICATIONS RESEARCH SERVICE, ARLINGTON, VA.
JPRS report: Science and technology. Central Eurasia: Life sciences
[JPRS-ULS-92-024] p 672 N93-13033
JPRS report: Science and technology. Central Eurasia: Space
[JPRS-USP-92-006] p 508 N93-13151
JPRS report: Science and technology. Central Eurasia: Space
[JPRS-USP-92-004] p 513 N93-13282
JPRS report: Science and technology. Central Eurasia: Physics and mathematics
[JPRS-UPM-92-006] p 698 N93-13303
JPRS report: Science and technology. Central Eurasia: Space
[JPRS-USP-92-005] p 513 N93-13304
JPRS report: Science and technology. USSR: Space
[JPRS-USP-91-004] p 516 N93-13756

K

KAMAN SCIENCES CORP., COLORADO SPRINGS, CO.
The trade-off characteristics of acoustic and pressure sensors for the NASP p 601 N93-13678

KEELE UNIV. (ENGLAND).
X ray scattering by cosmic dust grains
p 750 N93-13294

KENT STATE UNIV., OH.
Heavy-ion collisions and the nuclear equation of state
[DE92-019364] p 706 N93-12924

KENT UNIV., CANTERBURY (ENGLAND).
In situ dust mass distribution measurements from the Giotto encounter with comet P/Halley
p 753 N93-13602

KENTUCKY UNIV., LEXINGTON.
Experimental validation of finite element and boundary element methods for predicting structural vibration and radiated noise p 621 N93-12631
Transient behavior of heat pipe with thermal energy storage under pulse heat loads p 588 N93-13743
Boundary element analysis of acoustical thin-body and nonuniqueness problems using a normal derivative integral equation p 631 N93-13951

KINGSTON POLYTECHNIC, KINGSTON-UPON-THAMES (ENGLAND).
Experimental studies of the flowfields and their effects due to a pair of lift jets discharging in the ground effect region p 580 N93-13217

KINKAID HIGH SCHOOL, UT.
G254 undergraduate experiment p 511 N93-13174

KRUG INTERNATIONAL, HOUSTON, TX.
A health care system for the Space Station
[NASA-TM-108093] p 679 N93-13571

KRUG LIFE SCIENCES, INC., SAN ANTONIO, TX.
Complement proteins and decompression sickness susceptibility
[AD-A254448] p 674 N93-12905

KULITE SEMI-CONDUCTOR PRODUCTS, INC., LEONIA, NJ.
SiC device development for high temperature sensor applications p 601 N93-13677
Very high temperature silicon on silicon pressure transducers p 601 N93-13679

L

LANCASTER UNIV. (ENGLAND).
Use of phonon echoes in the study of 2-6 compounds and dielectric Bi12GeO20:Cr p 725 N93-13847
Learning and using methodologies in information systems analysis and design p 739 N93-14058

LAWRENCE LIVERMORE NATIONAL LAB., CA.
Experiments on resonantly photo-pumped x ray lasers
[DE92-019542] p 603 N93-12570
Self-consistent one-dimensional modelling of x ray laser plasmas
[DE92-019543] p 712 N93-12571
Workshop on Super-Intense Laser-Atom Physics
[AD-A254833] p 604 N93-12734
Wide range, permanent magnet Compton spectrometer
[DE92-017312] p 596 N93-12762
Wastage-resistant FBC evaporator tubing through microalloying
[DE92-001256] p 541 N93-12790
C60 transformations at high pressures
[DE92-019546] p 701 N93-12806
Heat transfer in a liquid metal crucible with an integral blackbody cavity
[DE92-019640] p 576 N93-12825
The VELOPT code for estimating performance of a Fabry-Perot velocimeter
[DE92-015566] p 596 N93-12831
An attempt at a status report on a fast-moving target: CFD
[DE92-017432] p 576 N93-12839
Demand thrust pumped propulsion with automatic warm gas valving
[DE92-017435] p 525 N93-12840
The role of human activity and land use change in atmospheric chemistry and air quality
[DE92-019622] p 642 N93-12880
Dense-gas dispersion advection-diffusion model
[DE92-019617] p 642 N93-12884
Stimulated Brillouin processes in crystals and glasses
[DE92-019549] p 721 N93-12887
Determination of the permeability of carbon aerogels by gas flow measurements
[DE92-019574] p 550 N93-12888
Comparison of two stochastic models of scalar diffusion in turbulent flow
[DE92-019381] p 576 N93-12912
Table-top x ray lasing based on optical-field-induced ionization
[DE92-019374] p 604 N93-12925
A computer simulation of ecosystem processes in forests for application to air pollution, acid precipitation, and global change
[DE92-019616] p 643 N93-12927
Aerogels, emulsions, and composites: Controlling structure with organic sol-gel chemistry
[DE92-019575] p 550 N93-12931
A design for an advanced divertor for D3D and ITER: The radiative slot divertor
[DE92-019579] p 714 N93-12932
Measurements of cellular structure in spray detonation
[DE92-019580] p 555 N93-12933
Alternate electrode materials for the SP100 reactor
[DE92-019570] p 706 N93-12970
DIII-D edge physics database
[DE92-019577] p 714 N93-12971
Silicide layer growth rates in Mo/Si multilayers
[DE92-019581] p 721 N93-12972
DATA: How to generate, store, retrieve, communicate, and interpret it: Proceedings
[DE92-040405] p 735 N93-13000
Recent Nova experimental results
[DE92-019783] p 715 N93-13105
Diagnostic of shock wave processes
[DE92-018059] p 565 N93-13357
Numerical modelling of the suppression of stimulated Brillouin scattering due to finite laser bandwidth
[DE92-018064] p 606 N93-13534
Study of heliumlike neon using an electron beam ion trap
[DE92-019544] p 753 N93-13536
Preparation and properties of low density replica carbon foams
[DE92-019573] p 552 N93-13538
An investigation of the processes controlling ozone in the upper stratosphere
[DE92-019621] p 645 N93-13615
Engineering data transfer test with EDMICS using MIL-R-28002 (Raster)
[DE92-019808] p 738 N93-13619
Effects of stratospheric aerosol surface processes on the LLNL two-dimensional zonally averaged model
[DE92-019620] p 646 N93-13646
Demonstration of a neon-like rubidium x ray laser
[DE92-019576] p 606 N93-13653
Effects of the Mt. Pinatubo eruption on the radiative and chemical processes in the troposphere and stratosphere
[DE92-019618] p 646 N93-13654
Impact of supersonic and subsonic aircraft on ozone: Including heterogeneous chemical reaction mechanisms
[DE92-019619] p 646 N93-13655
Electron temperature of Gd plasma produced by laser resonance ionization
[DE91-017785] p 718 N93-13732

LEHIGH UNIV., BETHLEHEM, PA.
Axisymmetric and antiplane shear crack problems in bonded nonhomogeneous materials
p 625 N93-13127
High octane ethers from synthesis gas-derived alcohols
[DE92-015467] p 537 N93-13188
The three-dimensional turbulent boundary layer: Theory and application p 588 N93-13749

LEICESTER UNIV. (ENGLAND).
Radar studies of high latitude convection flows
p 648 N93-12626

LIEGE UNIV. (BELGIUM).
Europe qualifies for space
[ESA-BR-64] p 508 N93-12892

LOCKHEED ELECTRONICS CO., HOUSTON, TX.
The correlation of active and passive microwave outputs for the Skylab S-193 sensor
[LEC-7819] p 635 N93-13440

LOCKHEED ENGINEERING AND SCIENCES CO., HOUSTON, TX.
Manned observations technology development, FY 1992 report
[NASA-CR-185704] p 597 N93-13373
Occupational ergonomics in space
p 680 N93-14013

LOCKHEED MISSILES AND SPACE CO., PALO ALTO, CA.
Comprehensive mappings of electron precipitation and its effects on the comprehensive mappings of electron precipitation and its effects on the atmosphere
[AD-A254665] p 648 N93-12621

LOCKHEED MISSILES AND SPACE CO., SUNNYVALE, CA.
A study of ion composition and dynamics at Comet Halley
[NASA-CR-188478] p 751 N93-13465
Support and servicing requirements for large observatories in space p 746 N93-13589

LOS ALAMOS NATIONAL LAB., NM.
Artificial intelligence and neural networks applied to ion mobility spectrometry
[DE92-017508] p 690 N93-12559
Development of XUV projection lithography at 60 to 80 nm
[DE92-017517] p 603 N93-12560
A distributed timing system for sychronizing control and data correlation
[DE92-018603] p 690 N93-12564
Characterizing laser fusion welded aluminum using synchrotron x ray microtomography
[DE92-018608] p 609 N93-12565
Functional MRI studies of human vision on a clinical imager
[DE92-017448] p 674 N93-12566
Real-time data archiving for GTA
[DE92-018613] p 733 N93-12567
Approximating the r-process on earth with thermonuclear explosions
[DE92-017409] p 749 N93-12587
Neutrino mass
[DE92-017411] p 701 N93-12588
Preferred sets of states, predictability, classicality, and the environment-induced decoherence
[DE92-017447] p 641 N93-12684
Characterization of site geochemistry in support of environmental restoration
[DE92-017512] p 641 N93-12685
Analysis of IMS spectra using neural networks
[DE92-017511] p 691 N93-12791
Advanced high-explosive flux compression generator development: The CN-3 series
[DE92-019962] p 713 N93-12809
Effects of source-region phenomenology on seismic discrimination
[DE92-017441] p 649 N93-12841
Bipolaronic charge density waves, polaronic spin density waves and high T(c) superconductivity
[DE92-017403] p 720 N93-12853
New technologies for refrigeration without CFC's
[DE92-018886] p 557 N93-12922
Industrial applications of hot dry rock geothermal energy
[DE92-018903] p 637 N93-12923
Airblast damage from small asteroids
[DE92-017834] p 749 N93-12956
Suppression of the e(-) coextracted from a Penning surface-plasma H(-) source
[DE92-040350] p 714 N93-12997
Dislocation and pores in mullite from diphasic gels
[DE92-040384] p 550 N93-12999
RF system description for the ground test accelerator radio-frequency quadrupole
[DE92-040239] p 563 N93-13045
HIPPI and Fibre Channel
[DE92-040346] p 689 N93-13046

Applications of group-invariant analytic solutions to inertial confinement fusion
[DE92-040347] p 715 N93-13047
Tributary and gap nighttime air flow comparisons
[DE92-018875] p 662 N93-13075
The use of ring ratios to detect sample differences in passive neutron counting
[DE92-018920] p 702 N93-13076
Magnetic behavior of a Bi(sub 2)Sr(sub 2)Ca(sub 1)Cu(sub 2)O(sub x) single crystal by direct magneto-optical observations
[DE92-018612] p 722 N93-13118
Applications of the Los Alamos High Energy Transport code
[DE92-017408] p 704 N93-13281
MCFC diagnostics: HCl detection
[DE92-001292] p 639 N93-13313
Ductile phase toughening of molybdenum disilicide by low pressure plasma spraying
[DE92-007409] p 551 N93-13315
A preliminary study of the effect of equivalence ratio on a low emissions gas turbine combustor using KIVA-2
[DE92-018616] p 613 N93-13321
Radial and nonradial periods and growth rates of an Al Velorum model
[DE92-011369] p 743 N93-13339
Resonance ionization mass spectrometry in biochemical analysis
[DE92-017407] p 538 N93-13341
Uniformity results of the multilayer mirrors used in the ALEXIS ultrasoft x ray telescopes
[DE92-018611] p 743 N93-13342
Initial performance of Los Alamos Advanced Free Electron Laser
[DE92-040214] p 605 N93-13507
Design and operation of a bunched-beam, phase-spread measurement
[DE92-040230] p 708 N93-13508
Video profile monitor diagnostic system for GTA
[DE92-040231] p 710 N93-13509
Special MAFIA postprocessors for the analysis of RF structures
[DE92-040248] p 565 N93-13510
The ALEXIS experiment: Current status and performance
[DE92-018601] p 524 N93-13516
A weighted iterative algorithm for neuromagnetic imaging
[DE92-040244] p 675 N93-13522
Nucleosynthesis in nova explosions
[DE92-040349] p 753 N93-13523
Is there a unique effective interaction profile for dislocations?
[DE92-018615] p 543 N93-13545
Uses of lunar sulfur p 761 N93-13981
Unit operations for gas-liquid mass transfer in reduced gravity environments p 557 N93-14011
A basis of settlement: Economic foundations of permanent pioneer communities p 741 N93-14019

LOUISIANA STATE UNIV., BATON ROUGE.
A general theory of signal integration for fault-tolerant dynamic distributed sensor networks
[AD-A254961] p 732 N93-12553
A physico-chemical study of some areas of fundamental significance to biophysics
[DE92-019917] p 672 N93-13034
A physico-chemical study of some areas of fundamental significance to biophysics
[DE92-019916] p 672 N93-13083

LUNAR AND PLANETARY INST., HOUSTON, TX.
The Second Conference on Lunar Bases and Space Activities of the 21st Century, volume 2
[NASA-CP-3166-VOL-2] p 760 N93-13972
Lunar mining of oxygen using fluorine
[LPI-748] p 761 N93-13980

M

MAGNAVOX GOVERNMENT AND INDUSTRIAL ELECTRONICS CO., MAHWAH, NJ.
Millimeter-wave quasi-optical and spatial power combining techniques
[AD-A255438] p 574 N93-13865

MALLINSON MAGNETICS, INC., CARLSBAD, CA.
Magnetic disk p 737 N93-13134

MANCHESTER UNIV. (ENGLAND).
Laser densification and doping of sol-gel glasses
[AD-A254566] p 604 N93-12644

MANITOBA UNIV., WINNIPEG.
On grain boundary transport of hydrogen and mechanism of hydrogen-induced intergranular fracture p 544 N93-14047
Numerical analysis of scattering from certain conducting and dielectric bodies of arbitrary shape
[ISBN-0-315-63282-8] p 569 N93-14066

MARQUETTE UNIV., MILWAUKEE, WI.
Effects of orbital exposure on Halar during the LDEF mission p 549 N93-12788
An elasticity solution for a transversely isotropic material containing a spherical shell under axisymmetric loading p 628 N93-13728

MARTIN MARIETTA CORP., DENVER, CO.
The VTRE Program: An overview p 512 N93-13182

MARYLAND UNIV., BALTIMORE.
Optimal design and control of distributed parameter systems
[AD-A254947] p 690 N93-12547

MARYLAND UNIV., COLLEGE PARK.
Torque resolver design for tendon-driven manipulators
[DE92-017395] p 609 N93-12698
Quality assessment of the A-posteriori error estimation in finite elements
[AD-A254767] p 696 N93-12701
Diffusion-absorption heat pump
[PB92-217538] p 576 N93-12975
Structural integrity of composites under load and thermal insult p 530 N93-13012
Experimental studies of high-power plasma-filled backward wave oscillators p 717 N93-13495
An infrared polarimetric study of sunspots p 770 N93-13627
Electronic transport properties of semiconductor microstructures p 724 N93-13730
Performance and control of ascending trajectories to minimize heat load for transatmospheric aero-space planes p 495 N93-13745
Formulation and validation of high-order mathematical models of helicopter flight dynamics p 501 N93-13821

MASSACHUSETTS INST. OF TECH., CAMBRIDGE.
GPS measurements at Vandenberg AFB
[AD-A254978] p 499 N93-12557
Adaptive array processing in uncertain inhomogeneous media
[AD-A254418] p 560 N93-12608
Analysis of space geodetic measurements for studying the dynamics of the solid Earth
[NASA-CR-191215] p 649 N93-12661
Small-scale x ray laser systems
[DE92-018442] p 604 N93-12744
Regional seismograms: Attenuation and scattering
[AD-A254348] p 650 N93-12943
Nonlinear stall flutter of wings with bending-torsion coupling
[AD-A254323] p 503 N93-12959
Remote sensing of Earth terrain
[NASA-CR-190908] p 633 N93-13084
Radiative transfer theory for polarimetric remote sensing of pine forest p 633 N93-13085
Application of theoretical models to active and passive remote sensing of saline ice p 633 N93-13086
Variance of phase fluctuations of waves propagating through a random medium p 569 N93-13087
Radiation-disorder and aperiodicity in irradiated ceramics
[DE92-015051] p 552 N93-13350
An optical VLA on the Moon p 747 N93-13596
Appendix: Limits on the use of heterodyning and amplification in optical interferometry p 747 N93-13597

MASSACHUSETTS INST. OF TECH., LEXINGTON.
Storm tracking for TDWR: A correlation algorithm design and evaluation
[AD-A254701] p 660 N93-12622
Physics and technology of resonant-tunneling devices
[AD-A255233] p 573 N93-13837
Multifrequency measurements of radar ground clutter at 42 sites. Volume 2: Appendices A through D
[AD-A246711] p 567 N93-13878
Birds mimicking microbursts on 2 June 1990 in Orlando, Florida
[AD-A255703] p 498 N93-14024

MASSACHUSETTS UNIV., AMHERST.
Graphics-based parallel programming tools
[AD-A254406] p 683 N93-12763
Kinetics and dynamics of oxidation reactions involving an adsorbed CO species
[DE92-019745] p 537 N93-12995
An optical study of the faint end of the stellar luminosity function p 748 N93-13960

MASSACHUSETTS UNIV., LOWELL.
Bistatic clutter RCS simulation using scale model rough surfaces
[AD-A254932] p 560 N93-12581

MCAT INST., SAN JOSE, CA.
A fundamental study of suction for Laminar Flow Control (LFC)
[NASA-CR-191276] p 583 N93-13277

MCDONNELL AIRCRAFT CO., SAINT LOUIS, MO.
Multiplexing electro-optic architectures for advanced aircraft integrated flight control systems
[NASA-CR-182268] p 504 N93-13735

MCDONNELL-DOUGLAS SPACE SYSTEMS CO., HOUSTON, TX.
Acoustic modes in fluid networks p 586 N93-13398

MCDONNELL-DOUGLAS SPACE SYSTEMS CO., HUNTINGTON BEACH, CA.
Analysis of a space emergency ammonia dump using the FLOW-NET two-phase flow program p 584 N93-13389

MCGILL UNIV., MONTREAL (QUEBEC).
Cascade processes and fully developed turbulence p 591 N93-13901
Overall effects of separation on thin aerofoils
[ISBN-0-315-67464-4] p 496 N93-13930

MEDICAL UNIV. OF SOUTH CAROLINA, CHARLESTON.
Earth observation photography: Looking back 20 years after Skylab p 509 N93-13164

MESSERSCHMITT-BOELKOW-BLOHM G.M.B.H., MUNICH (GERMANY).
A novel-high-performance system for recording and analysing instantaneous total pressure distortion in air intakes p 580 N93-13215
Integration of turbo-ramjet engines for hypersonic aircraft p 503 N93-13230

MIAMI UNIV., CORAL GABLES, FL.
Quantitative analysis of three-dimensional steady flow field by using particle image velocimetry and digital image processing method p 577 N93-13017

MICHIGAN STATE UNIV., EAST LANSING.
A study of the interlaminar stress continuity theories for composite laminates p 621 N93-12627
A multiple-view visual study of the inner/outer region interactions of coherent motions in a turbulent boundary layer p 591 N93-13937

MICHIGAN TECHNOLOGICAL UNIV., HOUGHTON.
The influence of mixture preparation in the intake port on the performance of a spark-ignited four-stroke engine p 613 N93-13331

MICHIGAN UNIV., ANN ARBOR.
How life affects the geochemical cycle of carbon
[NASA-CR-191241] p 644 N93-13031
Semantics-based reference resolution in technical text processing: An exploration of using the Word Net database in the computerized comprehensibility system
[AD-A255068] p 736 N93-13117
The dynamical evolution of clusters of galaxies p 750 N93-13122
A numerical study of hypersonic flow with strong surface blowing p 492 N93-13128
Combined design of structures and controllers for optimal maneuverability p 691 N93-13130
Minimum-time flight paths of supersonic aircraft p 500 N93-13140
Computational simulation of probabilistic lifetime strength for aerospace materials subjected to high temperature, mechanical fatigue, creep and thermal fatigue
[NASA-CR-190794] p 626 N93-13290
Electromagnetic scattering and radiation from microstrip patch antennas and spirals residing in a cavity
[NASA-CR-191284] p 565 N93-13354
Force and motion control of a constrained flexible manipulator p 613 N93-13384
Mechanical behaviour of fiber-reinforced ceramic matrix composites p 532 N93-13527
Explanation-based knowledge acquisition of electronics
[AD-A255069] p 573 N93-13650
A meteorology-based approach to detecting response source-receptor relationships p 664 N93-13736
Photochemical kinetics of excited states of O3 and O2: Laboratory studies and atmospheric implications p 656 N93-13784
A new instrument for the study of mesospheric gravity waves through nightglow observations p 656 N93-13789

MICROWAVE MONOLITHICS, INC., SIMI VALLEY, CA.
Advanced on-chip divider for monolithic microwave VCO's
[NASA-CR-191355] p 572 N93-13563

MIDWEST RESEARCH INST., GOLDEN, CO.
Ocean Energy Program overview, fiscal years 1990-1991
[DE91-002176] p 636 N93-12837
Development of large-area monolithically integrated silicon-film photovoltaic modules
[DE92-010600] p 637 N93-12838
Hydrogen Program Plan, FY 1993 - 1997
[DE92-010556] p 538 N93-13316
User's Guide for the NREL Force and Loads Analysis Program
[DE92-010579] p 627 N93-13524

User's Guide for the NREL Teetering Rotor Analysis Program (STRAP)
[DE92-010580] p 627 N93-13525

Novel thin-film CuInSe2 fabrication
[DE92-016440] p 723 N93-13526

Cost analysis methodology: Photovoltaic Manufacturing Technology Project
[DE92-016441] p 639 N93-13528

Development of a computer model for polycrystalline *thin-film CuInSe2 and CdTe solar cells*
[DE92-016444] p 639 N93-13529

MILLITECH CORP., SOUTH DEERFIELD, MA.

Space-qualified submillimeter radiometer
[NASA-CR-190886] p 603 N93-13709

MINNESOTA UNIV., MINNEAPOLIS.

Design, construction, and control of a two degree-of-freedom electric direct-drive human power amplifier p 678 N93-13486

Performance and stability of telemanipulators using bilateral impedance control p 614 N93-13488

A study of the luminosity produced by an electron *beam-emitting rocket in the polar ionosphere: ECHO 7* p 657 N93-13830

MISSISSIPPI STATE UNIV., MISSISSIPPI STATE.

An investigation of error correcting techniques for OMV data
[NASA-CR-190942] p 682 N93-12654

MISSISSIPPI STATE UNIV., STATE COLLEGE.

Unsteady three-dimensional thin-layer Navier-Stokes solutions for turbomachinery in transonic flow p 593 N93-14025

Solution of compressible Navier-Stokes equations using spectral methods on arbitrary two-dimensional domains p 593 N93-14041

MISSISSIPPI UNIV., UNIVERSITY.

Cancellation of air-borne acoustic plane waves obliquely incident upon a planar phased-array of active surface elements p 700 N93-13635

MISSOURI UNIV., COLUMBIA.

Bayesian estimation of system reliability under asymmetric loss p 620 N93-13906

MISSOURI UNIV., ROLLA.

Toughening mechanisms in weak matrix ceramic composites p 553 N93-13780

An investigation of the dynamic response of lifting surfaces with concentrated structural nonlinearities p 501 N93-13807

MITRE CORP., BEDFORD, MA.

Measures of user-system interface effectiveness: Assessment of structured judgment evaluation techniques for graphical, direct-manipulation style interfaces
[AD-A254493] p 677 N93-12576

Application of information system technology to K-12 education
[AD-A255223] p 731 N93-13834

MORGAN STATE UNIV., BALTIMORE, MD.

Analysis of a structure-equipment system subjected to impact loading
[AD-A255097] p 622 N93-12652

IIaO ultraviolet and nuclear emulsion films responses to orbital flights on STS-3, STS-7, STS-8, and STS-40 p 509 N93-13163

MOTE MARINE LAB., SARASOTA, FL.

Phytoplankton photosynthesis in natural mixed layers
[AD-A255010] p 671 N93-12871

MOTOREN- UND TURBINEN-UNION MUENCHEN G.M.B.H. (GERMANY).

The influence of intake swirl distortion on the steady-state performance of a low bypass, twin-spool engine p 579 N93-13211

N

NANGIA ASSOCIATES, BRISTOL (ENGLAND).

Application of subsonic first-order panel methods for prediction of inlet and nozzle aerodynamic interactions with airframe p 497 N93-13223

NATIONAL ACADEMY OF SCIENCES - NATIONAL RESEARCH COUNCIL, WASHINGTON, DC.

Toward a microgravity research strategy
[NASA-CR-190820] p 556 N93-12799

Assessment of programs in space biology and medicine
[NASA-CR-190930] p 672 N93-13327

Plasma Science Committee (PLSC) and study on new opportunities in plasma science and technology
[DE92-019507] p 716 N93-13359

NATIONAL AERONAUTICAL LAB., BANGALORE (INDIA).

Composites: A catalogue of books and conference proceedings available in the NAL library
[NAL-SP-IC-9201] p 737 N93-13368

Ideal aircraft handling quality models: Longitudinal axis
[NAL-PD-FC-9203] p 504 N93-13566

NATIONAL AERONAUTICS AND SPACE ADMINISTRATION, WASHINGTON, DC.

Coordinating Council. Second Meeting: International Acquisitions
[NASA-TM-108015] p 733 N93-12634

Coordinating Council. Fifth Meeting: Quality
[NASA-TM-108018] p 733 N93-12635

Coordinating Council. Seventh Meeting: Acquisitions
[NASA-TM-108020] p 733 N93-12636

Coordinating Council. Third Meeting: STI Strategic Plans
[NASA-TM-108016] p 733 N93-12670

Coordinating Council. Fourth Meeting: NACA Documents Database Project
[NASA-TM-108017] p 734 N93-12671

Coordinating Council. Sixth Meeting: Who Are Our Key Users?
[NASA-TM-108021] p 734 N93-12672

Coordinating Council. Eighth Meeting: Using the Internet
[NASA-TM-108019] p 734 N93-12673

Requirements for soldered electrical connections
[NHB-5300.4(3A-2)] p 570 N93-12674

NASA Mission: The Universe
[NASA-NP-141] p 508 N93-12891

NASA aeronautics: Research and technology program highlights
[NASA-NP-159] p 491 N93-13110

NASA industry education initiative. Education programs report, 1991
[NASA-NP-158] p 730 N93-13248

Solar System Exploration Division Strategic Plan, volume 1. Executive summary and overview
[NASA-TM-107843] p 513 N93-13265

Small planetary mission plan: Report to Congress
[NASA-TM-107809] p 513 N93-13266

Advanced technology for America's future in space. Executive summary
[NASA-TM-107969] p 513 N93-13308

Use of antarctic analogs to support the space exploration initiative
[NASA-TM-108000] p 651 N93-13326

Commercial non-aerospace technology transfer program for the 2000s: Strategic analysis and implementation
[NASA-TM-4424] p 742 N93-13433

Space Shuttle orbiter modifications to support Space Station Freedom
[NASA-TM-108050] p 520 N93-13455

Telescopes on the Moon or pie in the sky? p 746 N93-13591

SLS-1 flight experiments preliminary significant results
[NASA-TM-108033] p 520 N93-13613

Suited for spacewalking: A teacher's guide with activities
[NASA-EP-279] p 679 N93-13692

Coordinating Council. Ninth Meeting: Total Quality Management
[NASA-TM-108106] p 738 N93-13885

NATIONAL AERONAUTICS AND SPACE ADMINISTRATION. AMES RESEARCH CENTER, MOFFETT FIELD, CA.

The multidimensional self-adaptive grid code, SAGE
[NASA-TM-103905] p 683 N93-12719

Physiologically constrained aerocapture for manned Mars missions
[NASA-TM-103954] p 521 N93-12720

Navier-Stokes simulations of unsteady transonic flow phenomena
[NASA-TM-103962] p 491 N93-12721

Equations of motion of slung-load systems, including multilift systems
[NASA-TP-3280] p 503 N93-12815

Sol-gel synthesis and densification of aluminoborosilicate powders. Part 1: Synthesis
[NASA-TM-103964] p 527 N93-12895

Sol-gel synthesis and densification of aluminoborosilicate powders. Part 2: Densification
[NASA-TM-103969] p 528 N93-12896

The 2S(+) - 2P separation in KO
[NASA-TM-108086] p 702 N93-12900

A correlated k-distribution model of the heating rates for CH4 and N2O in the atmosphere between 0 and 60 km
[NASA-TM-108062] p 643 N93-12926

NATIONAL AERONAUTICS AND SPACE ADMINISTRATION. GODDARD SPACE FLIGHT CENTER, GREENBELT, MD.

Nimbus-7 Total Ozone Mapping Spectrometer (TOMS) Antarctic ozone atlas: August through November 1991
[NASA-RP-1283] p 661 N93-12700

Report on phase 2 of 1990 OSSA data census
[NASA-TM-107992] p 735 N93-12991

NSSDC Conference on Mass Storage Systems and Technologies for Space and Earth Science Applications, volume 1
[NASA-CP-3165-VOL-1] p 736 N93-13131

The 1992 Shuttle Small Payloads Symposium
[NASA-CP-3171] p 508 N93-13158

The Orbiter Stability Experiment on STS-40 p 508 N93-13159

A payload to evaluate photodiodes for the detection of *soft and hard x rays in a space environment using a Get* Away Special p 509 N93-13166

The ROMPS robot in HitchHiker p 511 N93-13179

The Capillary Pumped Loop Flight Experiment (CAPL): A pathfinder for EOS p 512 N93-13181

Preparing safety data packages for experimenters using *the Get Away Special (GAS) carrier system* p 512 N93-13186

Nonconservative force model parameter estimation *strategy for TOPEX/Poseidon precision orbit* determination
[NASA-TM-104575] p 519 N93-13372

SeaWiFS technical report series. Volume 4, an analysis of GAC sampling algorithms: A case study
[NASA-TM-104566-VOL-4] p 669 N93-13382

International Ultraviolet Explorer (IUE) ultraviolet spectral atlas of selected astronomical objects
[NASA-RP-1285] p 744 N93-13461

Electron impact polarization expected in solar EUV lines from flaring chromospheres/transition regions
[SSL-PREPRINT-90-124] p 770 N93-13478

Engineering planetary lasers for interstellar communication p 608 N93-14010

NATIONAL AERONAUTICS AND SPACE ADMINISTRATION. HUGH L. DRYDEN FLIGHT RESEARCH CENTER, EDWARDS, CA.

The constant current loop: A new paradigm for resistance signal conditioning
[NASA-TM-104260] p 596 N93-12681

NATIONAL AERONAUTICS AND SPACE ADMINISTRATION. HUGH L. DRYDEN FLIGHT RESEARCH FACILITY, EDWARDS, CA.

Subsonic flight test evaluation of a propulsion system parameter estimation process for the F100 engine
[NASA-TM-4426] p 502 N93-13155

Stratospheric turbulence measurements and models for aerospace plane design
[NASA-TM-104262] p 663 N93-13288

In-flight flow visualization results from the X-29A aircraft at high angles of attack
[NASA-TM-4430] p 493 N93-13322

NATIONAL AERONAUTICS AND SPACE ADMINISTRATION. JOHN F. KENNEDY SPACE CENTER, COCOA BEACH, FL.

Debris/ice/TPS assessment and integrated photographic analysis for Shuttle mission STS-47
[NASA-TM-107553] p 520 N93-13032

Engineering verification of the biomass production chamber p 680 N93-13996

Scenarios for optimizing potato productivity in a lunar CELSS p 680 N93-13997

NATIONAL AERONAUTICS AND SPACE ADMINISTRATION. LYNDON B. JOHNSON SPACE CENTER, HOUSTON, TX.

Development status of SINDA/FLUINT and SINAPS p 585 N93-13393

Analysis of fluid/mechanical systems using EASY5 p 586 N93-13397

Aerospace applications of SINDA/FLUINT at the Johnson Space Center p 586 N93-13401

Preloaded latching device
[NASA-CASE-MSC-21730-1] p 614 N93-13417

Fastening apparatus having shape memory alloy actuator
[NASA-CASE-MSC-21935-1] p 614 N93-13423

A health care system for the Space Station
[NASA-TM-108093] p 679 N93-13571

The Second Conference on Lunar Bases and Space Activities of the 21st Century, volume 2
[NASA-CP-3166-VOL-2] p 760 N93-13972

Applications for special-purpose minerals at a lunar base p 760 N93-13975

Availability of hydrogen for lunar base activities p 762 N93-13982

Lunar concrete for construction p 555 N93-13990

Crop growth and associated life support for a lunar farm p 680 N93-13994

Technology development for lunar base water recycling p 680 N93-13999

Creating a foundation for a synergistic approach to program management p 732 N93-14017

The lunar community church: Contributions to lunar living and to evolution of ethical and spiritual thinking p 676 N93-14020

NATIONAL AERONAUTICS AND SPACE ADMINISTRATION. LANGLEY RESEARCH CENTER, HAMPTON, VA.
Properties of five toughened matrix composite materials
[NASA-TP-3254] p 528 N93-12590
LDEF Materials Workshop 1991, part 1
[NASA-CP-3162-PT-1] p 545 N93-12769
LDEF materials: An overview of the interim findings p 546 N93-12770
Sources and transport of silicone NVR p 547 N93-12777
Characterization of selected LDEF: Exposed polymer films and resins p 549 N93-12787
Radiation dose to critical body organs for October 1989 proton event
[NASA-TP-3237] p 520 N93-12876
The Second NASA Formal Methods Workshop 1992
[NASA-CP-10110] p 684 N93-12957
A brief overview of NASA Langley's research program in formal methods p 684 N93-12958
Fully energy-dependent HZETRN (a galactic cosmic-ray transport code)
[NASA-TP-3243] p 771 N93-13020
Katz model prediction of Caenorhabditis elegans mutagenesis on STS-42
[NASA-TM-4383] p 674 N93-13023
Future regional transport aircraft market, constraints, and technology stimuli
[NASA-TM-107669] p 491 N93-13025
Hypersonic vehicle control law development using H infinity and mu-synthesis
[NASA-TM-107689] p 504 N93-13068
Identifiability of linear systems in physical coordinates
[NASA-TM-107695] p 625 N93-13125
Galactic cosmic ray exposure estimates for SAGE-3 mission in polar orbit
[NASA-TM-107678] p 771 N93-13126
Effects of forebody strakes and Mach number on overall aerodynamic characteristics of configuration with 55 deg cropped delta wing
[NASA-TP-3253] p 493 N93-13353
Active flutter suppression using dipole filters
[NASA-TM-107594] p 504 N93-13367
Weight optimization of an aerobrake structural concept for a lunar transfer vehicle
[NASA-TP-3262] p 519 N93-13379
A tough high performance composite matrix
[NASA-CASE-LAR-14338-1] p 531 N93-13416
Method and apparatus for minimizing multiple degree of freedom vibration transmission between two regions of a structure
[NASA-CASE-LAR-14508-1-CU] p 626 N93-13420
Results of ASTM round robin testing for mode 1 interlaminar fracture toughness of composite materials
[NASA-TM-104222] p 532 N93-13428
Oxidative stability of LARC (tm)-TPI films
[NASA-TM-107696] p 552 N93-13441
Space robotics: Recent accomplishments and opportunities for future research
[NASA-TM-107675] p 694 N93-13442
Multiple-function multi-input/multi-output digital control and on-line analysis
[NASA-TM-107697] p 500 N93-13565
A study of the generation of linear energy transfer spectra for space radiations
[NASA-TM-4410] p 772 N93-13572
The 1992 NASA Langley Measurement Technology Conference: Measurement Technology for Aerospace Applications in High-Temperature Environments
[NASA-CP-3161] p 598 N93-13661
High temperature strain gage apparent strain compensation p 600 N93-13672
Developments on high temperature fiber optic microphone p 601 N93-13680
The environmental control and life-support system for a lunar base: What drives its design p 680 N93-13991
Conceptual design of a lunar base thermal control system p 680 N93-14003
Automation and robotics considerations for a lunar base p 619 N93-14006

NATIONAL AERONAUTICS AND SPACE ADMINISTRATION. LEWIS RESEARCH CENTER, CLEVELAND, OH.
Probabilistic evaluation of fuselage-type composite structures
[NASA-TM-105881] p 622 N93-12735
Split torque transmission load sharing
[NASA-TM-105884] p 610 N93-12736
Transverse flexural tests as a tool for assessing damage to PMR-15 composites from isothermal aging in air at elevated temperatures
[NASA-TM-105848] p 529 N93-12737
Numerical calibration of the stable poisson loaded specimen
[NASA-TM-105609] p 622 N93-12738
On bilinearity of Manson-Coffin low-cycle-fatigue relationship
[NASA-TM-105840] p 622 N93-12739
LDEF yaw and pitch angle estimates p 524 N93-12772
Computer program for calculating and fitting thermodynamic functions
[NASA-RP-1271] p 728 N93-12967
In-phase and out-of-phase axial-torsional fatigue behavior of Haynes 188 at 760 C
[NASA-TM-105765] p 625 N93-13153
Turbomachinery CFD on parallel computers
[NASA-TM-105932] p 689 N93-13154
Structural optimization of thin shells using finite element method
[NASA-TM-105903] p 625 N93-13157
Electrical design of payload G-534: The Pool Boiling Experiment p 510 N93-13170
Battery selection for space experiments p 512 N93-13184
AGARD WG13 aerodynamics of high speed air intakes: Assessment of CFD results p 581 N93-13220
Analysis of large quasistatic deformations of inelastic solids by a new stress based finite element method
[NASA-CR-189235] p 626 N93-13260
Anomalous TWTA output power spikes and their effect on a digital satellite communications system
[NASA-TM-105875] p 571 N93-13286
Radial turbine cooling
[NASA-TM-105658] p 492 N93-13292
Experimental testing of four correction algorithms for the forward scattering spectrometer probe
[NASA-TM-105906] p 597 N93-13307
The Fourth Annual Thermal and Fluids Analysis Workshop
[NASA-CP-10106] p 584 N93-13385
A compressible boundary layer algorithm for use with SINDA '85 p 585 N93-13395
The Proteus Navier-Stokes code p 585 N93-13396
One-dimensional transient finite difference model of an operational salinity gradient solar pond p 586 N93-13400
A SINDA '85 nodal heat transfer rate calculation user subroutine p 587 N93-13403
Effect of vaporization on cryogenic spray dropsize measurement
[NASA-TM-105909] p 597 N93-13410
Thin film thermocouples for high temperature measurement on ceramic materials p 599 N93-13666
Fabrication of thin film heat flux sensors p 599 N93-13667
Gas temperature measurements using the dual-line detection Rayleigh scattering technique p 599 N93-13668
Visualization of hydrogen injection in a scramjet engine by simultaneous PLIF imaging and laser holographic imaging p 602 N93-13683
Gas temperature and density measurements based on spectrally resolved Rayleigh-Brillouin scattering p 602 N93-13684
Advanced photovoltaic power system technology for lunar base applications p 641 N93-14004
Validation test of 125 Ah advanced design IPV nickel-hydrogen flight cells
[NASA-TM-105912] p 527 N93-14079

NATIONAL AERONAUTICS AND SPACE ADMINISTRATION. MARSHALL SPACE FLIGHT CENTER, HUNTSVILLE, AL.
The effects of compressive preloads on the compression-after-impact strength of carbon/epoxy
[NASA-TP-3303] p 529 N93-12678
Design of a welded joint for robotic, on-orbit assembly of space trusses
[NASA-TM-108380] p 609 N93-12682
Thermal control surfaces on the MSFC LDEF experiments p 547 N93-12778
Performance of thermal control tape in the protection of composite materials p 536 N93-12780
Fluorescence of thermal control coatings on S0069 and A0114 p 548 N93-12781
Program Support Communications Network (PSCN) facsimile system directory
[NASA-TM-108051] p 562 N93-12909
The First United States Microgravity Laboratory
[NASA-TM-107980] p 557 N93-12951
First International Microgravity Laboratory
[NASA-TM-108007] p 518 N93-13113
Glass fiber processing for the Moon/Mars program: Center director's discretionary fund final report
[NASA-TM-108379] p 551 N93-13115
An intelligent position-specific training system for mission operations
[NASA-TM-108381] p 691 N93-13156

NATIONAL INST. OF POLAR RESEARCH
A study of the effects of micro-gravity on seed germination p 510 N93-13167
Optimal control computer programs
[NASA-TM-108384] p 693 N93-13289
A comparison of chromic acid and sulfuric acid anodizing
[NASA-TM-108383] p 543 N93-13378
Process comparison study. MSFC Center Director's Discretionary Fund (CDDF)
[NASA-TM-108382] p 526 N93-13429
The 3-D description of vertical current sheets with application to solar flares
[SSL-PREPRINT-90-119] p 770 N93-13477
Determination of high temperature strains using a PC based vision system p 601 N93-13674
An evaluation of corrosion protection by two epoxy primers on 2219-T87 and 7075-T73 aluminum
[NASA-TM-108376] p 553 N93-13716
The Lunar Roving Vehicle: Historical perspective p 619 N93-14008

NATIONAL AERONAUTICS AND SPACE ADMINISTRATION. PASADENA OFFICE, CA.
Quantum well, beam deflecting surface emitting lasers
[NASA-CASE-NPO-18243-1-CU] p 605 N93-13418
Integrated filter and detector array for spectral imaging
[NASA-CASE-NPO-18317-1-CU] p 709 N93-13419
Acoustic device and method for measuring gas densities
[NASA-CASE-NPO-18155-1-CU] p 700 N93-13421
Three-stage sorption type cryogenic refrigeration systems and methods employing heat regeneration
[NASA-CASE-NPO-18366-1-CU] p 558 N93-13422
Large area projection liquid-crystal video display system with inherent grid pattern optically removed
[NASA-CASE-NPO-16932-2-CU] p 711 N93-13711

NATIONAL AEROSPACE LAB., AMSTERDAM (NETHERLANDS).
Aerodynamic analysis of slipstream/wing/nacelle interference for preliminary design of aircraft configurations p 497 N93-13205

NATIONAL AEROSPACE LAB., KAKUDA (JAPAN).
An experimental study of a small high-speed LH2 pump for rockets: Fluid dynamic performance
[NAL-TR-1131] p 610 N93-12727

NATIONAL ARCHIVES AND RECORDS SERVICE, WASHINGTON, DC.
The long hold: Storing data at the National Archives p 737 N93-13139

NATIONAL CENTER FOR ATMOSPHERIC RESEARCH, BOULDER, CO.
Point correlations of geopotential height and temperature at 30 mb and between 500 mb and 30 mb
[PB92-222694] p 661 N93-12817
Meeting review: Third NCAR Research Aircraft Fleet Workshop
[PB92-222710] p 649 N93-12818
Convective scale 4-D data assimilation using simulated single Doppler radar observations
[PB92-218726] p 651 N93-12969
Photodissociation processes
[PB92-222702] p 702 N93-13067
Mass storage system experiences and future needs at the National Center for Atmospheric Research p 737 N93-13138

NATIONAL ENVIRONMENTAL SATELLITE SERVICE, WASHINGTON, DC.
NOAA Workshop on Climate Scale Operational Precipitation and Water Vapor Products
[NOAA-TR-NESDIS-62] p 662 N93-13066

NATIONAL GEOPHYSICAL DATA CENTER, BOULDER, CO.
Solar-geophysical data number 574, June 1992. Part 1: (Prompt reports). Data for May, April 1992 and late data
[PB92-218759] p 769 N93-12803
A report on geomagnetic observatory operations, 1990
[PB92-224781] p 649 N93-12804

NATIONAL INST. OF POLAR RESEARCH, TOKYO (JAPAN).
JARE data reports no. 176 (Ionosphere 47). Riometer records of 30 MHz cosmic noise at Syowa Station, Antarctica in 1990 p 772 N93-13255
JARE data reports no. 175 (ionosphere 46). Records of radio aurora at Syowa Station, Antarctica in 1990 p 651 N93-13285
JARE data reports no. 179 (meteorology 29). Meteorological data at Asuka Station, Antarctica in 1990 p 663 N93-13287
JARE data reports no. 170 (ionosphere 45). HF field strength data measured at Syowa Station, Antarctica from January to December 1988 p 652 N93-13432
JARE data reports no. 173 (meteorology 28). Antarctic climate research data. Part 5: PPI radar data at Syowa Station, Antarctica from February to December 1989 p 663 N93-13446

NATIONAL INST. OF STANDARDS AND TECHNOLOGY, GAITHERSBURG, MD.
Journal of Research of the National Institute of Standards and Technology, May-June 1992, volume 97, number 3
[PB92-217637] p 698 N93-12805
Semiconductor measurement technology: Version 2.0 of the TXYZ thermal analysis program: TXYZ20
[PB92-217603] p 570 N93-12978
Implicitly coupling heat conduction into a zone fire model
[PB92-222769] p 558 N93-12980
Nondestructive evaluation of the in-place compressive strength of concrete based upon limited destructive testing
[PB92-222751] p 623 N93-12981
Energy related inventions program. A joint program of the Department of Energy and the National Institute of Standards and Technology. Status report for recommendations 1 through 300
[PB92-226265] p 637 N93-12987
Energy related inventions program. A joint program of the Department of Energy and the National Institute of Standards and Technology. Status report for recommendations 301-563
[PB92-226273] p 637 N93-12988
Reject mechanisms for massively parallel neural network character recognition systems
[PB92-213412] p 689 N93-13198
Abstract and index collection in the Research Information Center of the National Institute of Standards and Technology
[PB92-217587] p 738 N93-13415
CORRIDOR: A routine for estimating the initial wave front resulting from high temperature fire exposure to a corridor
[PB92-213347] p 559 N93-13640
Semi-quantitative model for the burning rate of solid materials
[PB92-213362] p 539 N93-13641
Ceramic machining: Assessment of current practice and research needs in the US
[PB92-213511] p 553 N93-13649
Semiconductor measurement technology: INSTANT (IGBT network simulation and transient Analysis tool)
[PB92-213529] p 725 N93-13783
Determination of the weight average molecular weight of SRM 1480
[PB92-222934] p 553 N93-13785

NATIONAL OCEANIC AND ATMOSPHERIC ADMINISTRATION, BOULDER, CO.
A radio frequency user's guide to the Space Environment Services Center geophysical alert broadcasts
[PB92-220631] p 562 N93-12979
Remote sensing data from CLARET: A prototype CART data set
[NASA-CR-191294] p 634 N93-13094

NATIONAL OCEANIC AND ATMOSPHERIC ADMINISTRATION, RESEARCH TRIANGLE PARK, NC.
NOAA Atmospheric Sciences Modeling Division support to the US Environmental Protection Agency
[PB92-217835] p 644 N93-12974

NATIONAL OCEANIC AND ATMOSPHERIC ADMINISTRATION, WASHINGTON, DC.
Reports to the Nation on our changing planet: Our ozone shield p 645 N93-13413

NATIONAL OPTICAL ASTRONOMY LAB. TUCSON, AZ.
Science objectives for ground- and space-based optical/IR interferometry p 746 N93-13590

NATIONAL RADIO ASTRONOMY OBSERVATORY, SOCORRO, NM.
Radio and optical interferometric imaging p 744 N93-13580

NATIONAL SCIENCE FOUNDATION, WASHINGTON, DC.
US Antarctic program. Personnel manual, 1992
[NSF-92-63] p 731 N93-12637
Selected data on research and development in industry: 1990
[NSF-92-317] p 773 N93-12667
Summary of awards, fiscal year 1990
[NSF-92-70] p 683 N93-12693
Science and engineering degrees, by race/ethnicity of recipients: 1977-1990
[NSF-92-327] p 729 N93-12694
Academic science and engineering: Graduate enrollment and support, Fall 1990
[NSF-92-323] p 729 N93-12802
Women and minorities in science and engineering: An update
[NSF-92-303] p 730 N93-12907
Selected data on federal support to universities and colleges: Fiscal year 1990
[NSF-92-310] p 740 N93-12920
Blacks in undergraduate science and engineering education
[NSF-92-305] p 730 N93-13015
Research priorities in networking and communications
[NSF-92-109] p 562 N93-13024
Gateway to diversity in the scientific and technological workforce
[NSF-92-99] p 730 N93-13278
Federal R/D funding by budget function: Fiscal years 1991-1993
[NSF-92-318] p 740 N93-13312
Use of antarctic analogs to support the space exploration initiative
[NASA-TM-108000] p 651 N93-13326
State award summary: Fiscal Year 1991
[NSF-92-3] p 775 N93-13381
Scientific and engineering research facilities at universities and colleges: 1992
[NSF-92-325] p 506 N93-13407
Summary of awards. Fiscal year 1991
[NSF-92-36] p 681 N93-13431
Scientists, engineers, and technicians in manufacturing industries: 1989. Detailed statistical tables
[NSF-92-312] p 730 N93-13437
Summary of awards: Applied mathematics. Fiscal year 1991
[NSF-92-38] p 681 N93-13438
Characteristics of recent science and engineering graduates: 1990. Detailed statistical tables
[NSF-92-316] p 731 N93-13454
Federal support to universities, colleges, and nonprofit institutions: Fiscal year 1990. A report to the President and Congress
[NSF-92-324] p 741 N93-13543
Academic science and engineering: R/D expenditures, fiscal year 1990
[NSF-92-321] p 741 N93-13544
Selected data on Federal funds for research and development: Fiscal years 1990, 1991, and 1992
[NSF-92-319] p 741 N93-13657
Research and development in industry: 1989. Funds, 1989. Scientists and engineers, January 1990
[NSF-92-307] p 741 N93-13658
Selected data on Science and Engineering Doctorate Awards: 1991
[NSF-92-309] p 731 N93-13698
Awards: 1991 undergraduate course and curriculum development program
[NSF-92-45] p 731 N93-13699
Diversity in biological research
[NSF-92-19] p 673 N93-13700
Science and engineering degrees: 1966-1990
[NSF-92-326] p 731 N93-13701
Fiscal Year 1991 highlights
[NSF-92-23] p 731 N93-13702
Abstracts of phase 1 awards: NSF Small Business Innovation Research Program (SBIR): 1992
[NSF-92-80] p 732 N93-13703
Directory of awards, fiscal year 1991. Directorate for engineering
[NSF-92-55] p 775 N93-13704
NSF Science and Technology Centers
[NSF-92-104] p 507 N93-13712
Arctic science, engineering, and education. Directory of awards, fiscal year 1991
[NSF-92-60] p 775 N93-13713

NATIONAL TRANSPORTATION SAFETY BOARD, WASHINGTON, DC.
Aircraft accident report: Britt Airways, Inc., d/b/a, Continental Express Flight 2574, in-flight structural breakup, EMB-120RT, N33701, Eagle Lake, Texas, September 11, 1991
[PB92-910405] p 498 N93-13426
Aircraft accident/incident summary report: Controlled flight into terrain, Bruno's Inc., Beechjet, N25BR, Rome, Georgia, December 11, 1991
[PB92-910404] p 498 N93-13470

NAVAL AIR DEVELOPMENT CENTER, WARMINSTER, PA.
Consolidation of powder coated thermoplastic preform process modeling
[AD-A255094] p 529 N93-12757

NAVAL AIR WARFARE CENTER, PATUXENT RIVER, MD.
Integration of exterior lighting systems and night vision imaging systems
[AD-A254826] p 677 N93-12732

NAVAL COMMAND, CONTROL AND OCEAN SURVEILLANCE CENTER, SAN DIEGO, CA.
A new matrix formulation of classical electrodynamics. Part 2: Wave propagation in optical materials of infinite extent
[AD-A255032] p 560 N93-12585
Visualization of scattering strength of elastic bodies in a fluid
[AD-A254535] p 699 N93-12601
Li/SOCl battery technology: Problems and solutions
[AD-A254514] p 570 N93-12725

NAVAL OCEANOGRAPHIC AND ATMOSPHERIC RESEARCH LAB., BAY SAINT LOUIS, MS.
Ocean optical database
[AD-A254969] p 668 N93-12556
The assimilation of marine surface data into the Navy operational global atmospheric prediction system
[AD-A255559] p 667 N93-13877
Estimation of EOF expansion coefficients from incomplete data
[AD-A255252] p 697 N93-13886
Adding explanation capability to a knowledge-based system for interpretation of oceanographic images
[AD-A255887] p 671 N93-13943

NAVAL POSTGRADUATE SCHOOL, MONTEREY, CA.
User interface of DFQL: An object-oriented approach
[AD-A255225] p 687 N93-13835
An examination of the Total Quality Management (TQM) concept given current Federal/DoD competition initiatives
[AD-A255556] p 620 N93-13876
An investigation of the interatomic bonding characteristics of a Ti - 51 atomic percent Al alloy by x ray diffraction
[AD-A245362] p 544 N93-13945
On computing accurate singular values and eigenvalues of acyclic matrices
[AD-A255892] p 697 N93-14036

NAVAL RESEARCH LAB., WASHINGTON, DC.
Design of a digital Data Recording System (DRS)
[AD-A255088] p 561 N93-12623
Ion-beam-assisted deposition of MoS2 and other low-friction films
[AD-A255222] p 554 N93-13862
High-resolution array with Prony, MUSIC, and ESPRIT algorithms
[AD-A255514] p 566 N93-13868
Computer simulation of a space-based infrared surveillance sensor
[AD-A255521] p 524 N93-13870
WR-10 band noise measurement
[AD-A255526] p 566 N93-13871
Talking to InterFIS: Adding speech input to a natural language interface
[AD-A255865] p 688 N93-13942
Fiber optic data bus radiation effects study
[AD-A255821] p 711 N93-14031

NAVAL SURFACE WARFARE CENTER, BETHESDA, MD.
The 3-D nonlinear constitutive modeling approach for composite materials
[AD-A255022] p 528 N93-12584

NAVAL SURFACE WARFARE CENTER, DAHLGREN, VA.
Fixed-gain, two-stage estimators for tracking maneuvering targets
[AD-A255832] p 697 N93-14081

NAVAL SURFACE WEAPONS CENTER, DAHLGREN, VA.
New methods for predicting nonlinear lift, center of pressure, and pitching moment on missile configurations
[AD-A255078] p 492 N93-12741

NAVAL UNDERSEA WARFARE CENTER, NEW LONDON, CT.
Economical development of complex computer systems
[AD-A254752] p 689 N93-12848

NEW BRUNSWICK UNIV., FREDERICTON.
On the space-time ocean current variability and its effects on the length-of-day p 636 N93-14051

NEW HAMPSHIRE UNIV., DURHAM.
Study of SMM flares in gamma-rays and neutrons
[NASA-CR-191249] p 769 N93-12930
A statistical study of narrow bandwidth, high-latitude geomagnetic pulsations p 660 N93-14068

NEW JERSEY INST. OF TECH., NEWARK.
On development of a three-dimensional particle motion tracking system
[DE92-015846] p 704 N93-13263

NEW MEXICO STATE UNIV., LAS CRUCES.
Coordinates in differential geodesy
[AD-A254951] p 632 N93-12550

NEW MEXICO UNIV., ALBUQUERQUE.
A Lunar Optical-Ultraviolet-Infrared Synthesis Array (LOUISA)
[NASA-CP-3066] p 744 N93-13579
Shot noise limits to sensitivity of optical interferometry p 745 N93-13586
Report of the Working Group on Space/Lunar Tradeoffs p 747 N93-13599
Report of the Science Working Group: Science with a lunar optical interferometer p 747 N93-13600
Report of the Working Design Group p 748 N93-13601

NEW YORK UNIV., NEW YORK.
Plasma properties
[DE92-019982] p 713 N93-12811
Tokamak equilibria and transport based on Grad's thirteen moment description
[DE92-019960] p 715 N93-13038
Japanese/English machine translation using sublanguage patterns and reversible grammars
p 686 N93-13494
Atoms and molecules in supernova 1987A
p 699 N93-13851
NEWCASTLE-UPON-TYNE UNIV. (ENGLAND).
The implications of the magnetism of ordinary chondrites p 755 N93-13795
NICHOLS RESEARCH CORP., DAYTON, OH.
Skylab D024 thermal control coatings and polymeric films experiment p 548 N93-12784
NICHOLS RESEARCH CORP., HUNTSVILLE, AL.
VPPA weld model evaluation
[NASA-CR-184460] p 611 N93-12919
NORTH CAROLINA CENTRAL UNIV., DURHAM.
High resolution molecular spectroscopy of atmospheric species
[AD-A254360] p 650 N93-12946
NORTH CAROLINA STATE UNIV., RALEIGH.
State space methods in multidimensional digital signal processing
[AD-A254646] p 561 N93-12620
The crystallization and crystalline properties of LARC-TPI
[NASA-CR-191001] p 721 N93-13022
Software reliability through fault-avoidance and fault-tolerance
[NASA-CR-189880] p 686 N93-13293
Application of passive dosimetry for detection of leaking underground storage tanks
[PB92-218270] p 559 N93-13648
Meso-beta scale numerical simulation studies of terrain-induced jet streak mass/momentum perturbations
[NASA-CR-191365] p 654 N93-13719
Cloud acidity and acidic deposition in the lower troposphere and ozone depletion in the Antarctic stratosphere: Modeling and data analysis regarding the role of atmospheric aerosol p 647 N93-13741
Strained-layer InGaAs-GaAs-AlGaAs quantum well lasers and transverse junction stripe lasers
p 607 N93-13773
NORTH CAROLINA UNIV., CHAPEL HILL.
Relationships between continental-scale circulation and rainfall event attributes in the southeastern US
p 664 N93-13631
The Gulf Stream downstream of Cape Hatteras: Model/data comparisons p 670 N93-13633
A thermal/nonthermal approach to solar flares
p 771 N93-13639
NORTH CAROLINA UNIV., CHARLOTTE.
Oligomer and mixed-metal compounds potential multielectron transfer catalysts
[DE92-011347] p 543 N93-13346
Two-phase/two-phase heat exchanger simulation analysis p 586 N93-13402
NORTH DAKOTA UNIV., GRAND FORKS.
Plasma reactor waste management systems
p 680 N93-14000
Distribution of human waste samples in relation to sizing waste processing in space p 680 N93-14001
The province and heritage of mankind reconsidered: A new beginning p 681 N93-14018
NORTHERN RESEARCH AND ENGINEERING CORP., WOBURN, MA.
Alternative systems for fuel gas boosters for small gas turbine engines
[PB92-223049] p 612 N93-12977
NORTHWESTERN UNIV., EVANSTON, IL.
Probabilistic finite elements for fatigue and fracture analysis
[NASA-CR-191246] p 624 N93-13029
Studies of the kinetics and mechanisms of perfluoroether reactions on iron and oxidized iron surfaces
[NASA-CR-191363] p 539 N93-13763
NOTRE DAME UNIV., IN.
Error control techniques for satellite and space communications
[NASA-CR-191229] p 565 N93-13411
An experimental and computational investigation of slender wings undergoing wing rock
p 505 N93-13915
The unsteady aerodynamics of a delta wing undergoing large-amplitude pitching motions p 496 N93-13929
NOTTINGHAM UNIV. (ENGLAND).
Studies of orbital doublet and modelling of orbital triplet Jahn-Teller systems in 3 to 5 semiconductors
p 725 N93-13845
NOVA UNIV., FORT LAUDERDALE, FL.
Using DIALOG CIP at Winona State University to educate end-users p 686 N93-13338
NOVASENSOR, INC., FREMONT, CA.
Technology trends in high temperature pressure transducers: The impact of micromachining
p 601 N93-13676

O

OAK RIDGE K-25 SITE, TN.
Engineering Design Information System (EDIS) Information Services Division (ISD) index function: User's manual
[DE92-041242] p 736 N93-13048
OAK RIDGE NATIONAL LAB., TN.
Model for impedance of an ionic conductor sandwiched between blocking electrodes
[DE92-017812] p 569 N93-12561
Speedup properties of phases in the execution profile of distributed parallel programs
[DE92-019301] p 689 N93-12797
Speedup properties of phases in the execution profile of distributed parallel programs
[DE92-019965] p 689 N93-12810
Cost-effective Sintered Reaction-Bonded Silicon Nitride (SRBSN) for structural ceramics
[DE92-019285] p 549 N93-12821
Forest declines: Some perspectives on linking processes and patterns
[DE92-019946] p 642 N93-12828
Electromagnetic lepton-pair production in relativistic collisions
[DE92-011069] p 706 N93-12829
Investigation of properties and performance of ceramic composite components
[DE92-019911] p 550 N93-12858
Nondestructive evaluation of the in-place compressive strength of concrete based upon limited destructive testing
[PB92-222751] p 623 N93-12981
Neutron scattering studies of the spin dynamics in La(2-x)Sr(x)O4
[DE92-019952] p 702 N93-13037
Ordering energies and mechanisms in beta-phase NiAl
[DE92-040031] p 542 N93-13043
A neural network approach for the investigation of chemical phenomena
[DE92-019205] p 691 N93-13079
The nature of scales grown on binary Cr-Nb alloys
[DE92-019283] p 542 N93-13080
Transition probabilities up to I = 36(+)in Yb-160
[DE92-017191] p 703 N93-13114
Development of weldable high-strength iron aluminides
[DE92-016018] p 542 N93-13190
Environmental effects on iron aluminides
[DE92-016341] p 542 N93-13237
Performance of a plasma fluid code on the Intel parallel computers
[DE92-011680] p 716 N93-13297
Chemical potentials in dilute, multicomponent solutions
[DE92-011041] p 538 N93-13317
A new apparatus for continuous countercurrent flow of solids and liquids
[DE92-011675] p 583 N93-13318
Shallow-crack toughness results for reactor pressure vessel steel
[DE92-017813] p 626 N93-13320
Defects near the Y2BaCuO5/YBa2Cu3O(7-x) interface and their effect on flux-pinning in melt-processed and quench-melt-growth processed YBa2Cu3O(7-x)
[DE92-014463] p 723 N93-13347
Biasing experiments on the Advanced Toroidal Facility
[DE92-040033] p 717 N93-13518
The ORNL radioactive ion beam project with the ORIC accelerator
[DE92-040027] p 708 N93-13574
Review of stellarator research: In search of the magic magnetic bottle
[DE92-019045] p 718 N93-13651
OAK RIDGE Y-12 PLANT, TN.
Functional system design document for the Intelligent Inspection System (IIS)
[DE92-018240] p 619 N93-12794
A stochastic/deterministic method for transient, three-dimensional neutron transport
[DE92-016690] p 704 N93-13319
OBSERVATOIRE DE LA COTE D'AZUR, NICE (FRANCE).
The optical very large array and its moon-based version p 745 N93-13583
OFFICE NATIONAL D'ETUDES ET DE RECHERCHES AEROSPATIALES, PARIS (FRANCE).
Tests of models equipped with TPS in low speed ONERA F1 pressurized wind tunnel p 577 N93-13201
Detailed analysis of wing-nacelle interaction for commercial transport aircraft p 578 N93-13203
Air inlet with variable intake section: Application to air breathing launch vehicles p 582 N93-13231
OHIO STATE UNIV., COLUMBUS.
Cosmological constraints on early-decaying particles
p 750 N93-13123
The emission-line properties of quasars
p 753 N93-13487
Time dependent heat transfer rates in high Reynolds number hypersonic flowfields p 595 N93-13664
Scattering from a finite collection of transverse dipole and axial slot arrays with edge effects
p 568 N93-14048
An investigation of jet engine test cell aerodynamics by means of scale model test studies with comparisons to full-scale test results p 507 N93-14060
Dexterous grasp and manipulation
p 618 N93-14075
OKLAHOMA STATE UNIV., STILLWATER.
Chaotic vortical motion in the near region of a plane jet p 493 N93-13493
An evaluation of the use and future need of remotely sensed images in grades K-12 p 635 N93-13956
OKLAHOMA UNIV., NORMAN.
Convective scale 4-D data assimilation using simulated single Doppler radar observations
[PB92-218726] p 651 N93-12969
A study of the neutral and ionized gas in the interstellar medium and galactic H 2 regions p 756 N93-13853
OLD DOMINION UNIV., NORFOLK, VA.
Ab initio atomic recombination reaction energetics on model heat shield surfaces
[NASA-CR-191210] p 575 N93-12677
Investigation of hypersonic shock-induced combustion in a hydrogen-air system
[NASA-CR-191239] p 538 N93-13456
OPEN UNIV., MILTON (ENGLAND).
Fatigue studies in Al-Mg-Si alloys p 543 N93-13690
OPTICAL SOCIETY OF AMERICA, WASHINGTON, DC.
Organization of the Optical Society of America Photonic Science Topical Meeting Series. Volume 8: Integrated photonics research. Iifornia on 9-11 april 1991
[AD-A254682] p 709 N93-12666
Soft X Ray Projection Lithography Topical Meeting. Volume 8: Technical digest
[AD-A254756] p 709 N93-12850
OSA proceedings of the topical meeting on optical amplifiers and their applications, volume 13
[AD-A252974] p 711 N93-13879
Compact Blue-Green Lasers: Summaries of papers presented at the topical meeting. Volume 6: Technical digest series
[AD-A255001] p 608 N93-13883
ORBITAL TECHNOLOGIES CORP., MADISON, WI.
Synergism of He-3 acquisition with lunar base evolution p 540 N93-13986
OREGON GRADUATE INST. OF SCIENCE AND TECHNOLOGY, BEAVERTON.
Effects of residual stress, weld toe notch and weld defects on fatigue of welded steel structures
p 631 N93-13947
OREGON STATE UNIV., CORVALLIS.
New approaches to estimation of magnetotelluric parameters
[DE92-040280] p 653 N93-13513
OREGON UNIV., EUGENE.
Monitoring interfacial dynamics by pulsed laser techniques
[DE92-040302] p 606 N93-13514
OTTAWA UNIV. (ONTARIO).
A fundamental study of the effect of gravity on the static and dynamic behavior of robots p 610 N93-12760
OXFORD UNIV. (ENGLAND).
Mathematical problems in inviscid hypersonic flow
p 493 N93-13451
Radiative transfer in the middle atmosphere
p 652 N93-13482
Variational characterizations of steady two-dimensional vortex motions p 589 N93-13781
Modelling combustion zones in porous media
p 540 N93-13802
Test and calibration of the along track scanning radiometer, a satellite-borne infrared radiometer designed to measure sea surface temperature
p 671 N93-13842
Laser spectroscopy of rare earth ions
p 608 N93-13846
Gas-phase reactions of halogen species of atmospheric importance p 658 N93-13889
Middle atmosphere water vapour p 667 N93-13892
High magnetic field studies of strained layer superlattices p 726 N93-13895
Dynamical instabilities in a fluid spin-up and in an open flow system p 590 N93-13899

Formal aspects of human-computer interaction
p 679 N93-13909
Radical reactions of atmospheric importance
p 659 N93-14053
Spectroscopy for remote sounding of the atmosphere
p 659 N93-14054

P

PACIFIC NORTHWEST LAB., RICHLAND, WA.
Capillary electrophoresis: Electrospray ionization mass spectrometry in small diameter capillaries
[DE92-019123] p 575 N93-12711
Human perceptual deficits as factors in computer interface test and evaluation
[DE92-019124] p 677 N93-12712
Influence of cold work level on the irradiation creep and creep rupture of titanium-modified austenitic stainless steels
[DE92-019078] p 541 N93-12820
Noninvasive probing of the ocean surface using laser-based nonlinear optical methods
[DE92-019431] p 669 N93-12916
Alternative materials for solid oxide fuel cells: Factors affecting air-sintering of chromite interconnections
[DE92-019356] p 638 N93-13082
PARIS-SUD UNIV., ORSAY (FRANCE).
Silicon vision: Elementary functions to be implemented on electronic retinas p 692 N93-13242
PENNSYLVANIA STATE UNIV., UNIVERSITY PARK.
High temperature oxidation and electrochemical studies related to hot corrosion
[AD-A254435] p 540 N93-12595
Application of smoothing techniques for tracking maneuvering targets. Multiple target tracking in clutter: New approaches
[AD-A254609] p 561 N93-12615
Initial experiments in end-point control of a flexible, two-link manipulator p 612 N93-13018
Acoustic tomographic monitoring of the atmospheric boundary layer p 651 N93-13143
Acoustic radiation from a point excited infinite bilaminar plate p 531 N93-13144
A Pennsylvania State University/General Electric Get Away Special (GAS) experiment p 511 N93-13177
Probing the galactic halo with ROSAT
[NASA-CR-191268] p 743 N93-13272
Analysis and design of planar and non-planar wings for induced drag minimization
[NASA-CR-191274] p 493 N93-13463
A synoptic climatology of the elevated mixed layer inversion over the southern Great Plains in spring
p 664 N93-13643
Quantum inflationary minisuperspace cosmological models p 728 N93-13751
A joint study of the lower ionosphere by radar, lidar, and spectrometer p 655 N93-13755
Nonlinear hydrostatic conditional symmetric instability: Some theoretical and modeling considerations
p 655 N93-13757
An observational and numerical investigation of meso-scale coastal processes during GALE IOP 2
p 665 N93-13776
Lunar resource recovery: A definition of requirements
p 761 N93-13978
PENNSYLVANIA UNIV., PHILADELPHIA.
Action composition for the animation of natural language instructions
[AD-A254963] p 682 N93-12554
Proton transport on modified sulfonated polyaniline electrodes
[AD-A254917] p 570 N93-12650
Electrochemical and chemical characteristics of a new ambient temperature Li(I) polymer electrolyte
[AD-A254918] p 545 N93-12651
Electronic phenomena in polyanilines
[AD-A254803] p 545 N93-12749
Solvation of cobalt salts by oligomeric polyethers
[AD-A254815] p 545 N93-12753
Effect of plasticizers on the properties of new ambient temperature solid polymer electrolytes
[AD-A254817] p 545 N93-12754
Studies of plasticized-polymer electrolytes containing mixed Zn(2) and Li(1)
[AD-A254818] p 545 N93-12755
Atomic structure of mixed ferroelectrics
[AD-A254369] p 702 N93-12947
Robotic exploration of surfaces and its application to legged locomotion p 615 N93-13540
Force-closure grasping with two hands
p 616 N93-13742
Coherent frame analysis of Synthetic Aperture Radar (SAR) ocean imagery p 568 N93-14050
PHILLIPS LAB., EDWARDS AFB, CA.
High Energy Propulsion System (HEPS) analysis
[AD-A254343] p 525 N93-12963
PHYSICAL SCIENCES, INC., ANDOVER, MA.
Exit plane H2O concentration measurements correlated with OH PLIF near-injector mixing measurements for scramjet flows p 603 N93-13687
PITTSBURGH UNIV., PA.
Halogen surface chemistry on Si(100)-(2x1)
[AD-A254643] p 536 N93-12618
A novel process for methanol synthesis
[DE92-019719] p 539 N93-13617
POLISH ACADEMY OF SCIENCES, WARSAW.
Diagnostic of material defects found in pipelines made of 13 HMF steel on the basis of acoustic emission
p 623 N93-12989
POLYTECHNIC UNIV., BROOKLYN, NY.
Guidance and scattering of electromagnetic waves by nonlinear layers p 566 N93-13813
POLYTECHNIC UNIV., FARMINGDALE, NY.
Microwave and infrared dielectric relaxation of alkylcarbonates, chloroform and their mixtures at 25 C
[AD-A253606] p 537 N93-13096
PORTLAND STATE UNIV., OR.
Steady state analysis of tropospheric chemistry
p 644 N93-13121
PRATT AND WHITNEY AIRCRAFT, EAST HARTFORD, CT.
Thermal barrier coating life prediction model development, phase 2
[NASA-CR-189111] p 544 N93-12589
PRATT AND WHITNEY AIRCRAFT, WEST PALM BEACH, FL.
Fatigue in single crystal nickel superalloys
[AD-A254704] p 541 N93-12746
PRC SYSTEMS SERVICES CO., EDWARDS, CA.
High-temperature strain measurement techniques: Current developments and challenges
p 599 N93-13669
PRINCETON UNIV., NJ.
Group 2 cubic fluorides dielectrics for 3-D integration and GaAs-based optoelectronic structures
[AD-A254937] p 719 N93-12544
The dynamics of dense galactic nuclei
p 750 N93-13340
Baroclinic wave packets in models and observations
p 663 N93-13361
Limits on galactic dynamo theory due to magnetic fluctuations p 754 N93-13636
Assimilation of satellite color observations in a coupled ocean GCM-ecosystem model
[NASA-CR-191218] p 670 N93-13714
Interaction of energetic ring current protons with magnetospheric hydromagnetic waves
p 718 N93-13750
Solitons and instantons in string theory
p 728 N93-13753
Numerical calculation of turbomachinery cascade flows p 589 N93-13767
The interstellar medium of elliptical galaxies
p 757 N93-14071
PURDUE UNIV., WEST LAFAYETTE, IN.
GaAs gate dynamic memory technology
[AD-A254801] p 720 N93-12748
Predictive forming of advanced thermoplastic composite structures p 529 N93-12835
Numerical simulation of a squall line: Tests of a new cumulus parameterization scheme p 662 N93-13124
Robust control of uncertain aerospace and mechanical systems with unmodelled flexibilities: A singular perturbation approach p 691 N93-13129
Application of a solution adaptive grid to flow over an embedded cavity p 492 N93-13141
Analysis of cracked plates subjected to out-of-plane loadings p 629 N93-13804
On the relationship between the intensity of extratropical frontal cyclone systems and water levels in the Gulf of Mexico p 666 N93-13816
Orbit determination error analysis and station-keeping for liberation point trajectories p 518 N93-14038
Model reduction, sensor/actuator selection and control system redesign for large flexible structures
p 523 N93-14040
Q-Markov cover identification and integrated MCA-OVC controller design for flexible structures
p 695 N93-14045
Modelling flexible link manipulators in the three-dimensional space p 574 N93-14093

Q

QUANTEX CORP., ROCKVILLE, MD.
Large area nuclear particle detectors using ET materials, phase 2
[NASA-CR-190866] p 705 N93-13606

R

RADEX, INC., BEDFORD, MA.
Analysis and modeling of the CRRES satellite data
[AD-A254349] p 650 N93-12944
RADIATION MONITORING DEVICES, INC., WATERTOWN, MA.
Soft x ray window encapsulant for HgI2 detectors
[NASA-CR-190850] p 710 N93-13705
REMOTE SENSING SYSTEMS, INC., SANTA ROSA, CA.
Production of SSM/I data sets
[NASA-CR-190944] p 632 N93-12800
REMTECH, INC., HUNTSVILLE, AL.
Solar water heating system for a lunar base
p 641 N93-14005
RENSSELAER POLYTECHNIC INST., TROY, NY.
Analysis of a linearly constrained least squares algorithm for adaptive beamforming
[AD-A255017] p 695 N93-12582
An investigation of dynamic stress reduction of multi-body aircraft using active gust control
p 505 N93-13916
Friction, wear and Raman spectroscopic characteristics of carbon lubricated surfaces p 618 N93-13949
Thermoviscoplastic analysis of metal matrix composites p 535 N93-13954
RESEARCH INST. FOR ADVANCED COMPUTER SCIENCE, MOFFETT FIELD, CA.
Implementation details of the coupled QMR algorithm
[NASA-CR-191213] p 684 N93-12801
Introduction to IND and recursive partitioning, version 1.0
[NASA-CR-191220] p 685 N93-13063
Myths and legends in learning classification rules
[NASA-CR-191236] p 693 N93-13366
Implicit application of polynomial filters in a k-step Arnoldi method
[NASA-CR-191237] p 686 N93-13408
Efficient solution of parabolic equations by Krylov approximation methods
[NASA-CR-191235] p 697 N93-13409
Research summary, January 1989 - June 1990
[NASA-CR-190960] p 687 N93-13694
RESEARCH INST. FOR COMPUTING AND INFORMATION SYSTEMS, HOUSTON, TX.
Framework Programmable Platform for the Advanced Software Development Workstation (FPP/ASDW). Demonstration framework document. Volume 2: Framework process description
[NASA-CR-190275] p 685 N93-13004
Performance measurement for information systems: Industry perspectives
[NASA-CR-191369] p 738 N93-13737
RESEARCH TRIANGLE INST., RESEARCH TRIANGLE PARK, NC.
The National Atmospheric Deposition Program/National Trends Network (NADP/NTN) site visitation program
[PB92-217298] p 642 N93-12726
ESPVI 4.0 electrostatic precipitator V-I and performance model: User's model
[PB92-169614] p 643 N93-12938
Phased array feed design technology for Large Aperture Microwave Radiometer (LAMR) Earth observations
[NASA-CR-189727] p 519 N93-13462
RHODE ISLAND UNIV., KINGSTON.
Fiber optic sensors for static fracture studies and dynamic wave propagation problems
p 709 N93-12984
RICE UNIV., HOUSTON, TX.
Simulation of excitatory/inhibitory interactions in single auditory neurons
[AD-A253614] p 675 N93-13252
ROCHESTER UNIV., NY.
Intermolecular potential functions from spectroscopic properties of weakly bound complexes
[DE92-018643] p 701 N93-12745
ROCKWELL INTERNATIONAL CORP., COCOA BEACH, FL.
A path to in-space welding and to other in-space metal processing technologies using Space Shuttle small payloads p 509 N93-13165
ROCKWELL INTERNATIONAL CORP., PITTSBURGH, PA.
Orbital Spacecraft Consumables Resupply System (OSCRS). Volume 3: Program cost estimate
[NASA-CR-185685] p 740 N93-12814
ROCKWELL INTERNATIONAL CORP., THOUSAND OAKS, CA.
Electrodeposition of high temperature superconductors
[AD-A255095] p 720 N93-12758
ROKE MANOR RESEARCH LTD., ROMSEY (ENGLAND).
The 3-D computer vision techniques for object following and obstacle avoidance p 693 N93-13245

ROME LAB., GRIFFISS AFB, NY.
Proceedings of Joint RL/AFOSR Workshop on Intelligent Information Systems
[AD-A254795] p 734 N93-12703
ROYAL OBSERVATORY, EDINBURGH (SCOTLAND).
United Kingdom Infrared Telescope
p 743 N93-13273
RUTGERS - THE STATE UNIV., NEW BRUNSWICK, NJ.
The effects of molecular structure on the electrical conductivity of polymers
[NASA-CR-191265] p 552 N93-13459
Flow through horizontal vents as related to compartment fire environments
[PB92-213388] p 559 N93-13642
Circuit design tool. User's manual, revision 2
[NASA-CR-191361] p 687 N93-13734

S

SAINT ANDREW'S UNIV. (SCOTLAND).
Equilibrium and eruption of solar coronal magnetic structures p 770 N93-13605
SAINT LOUIS UNIV., MO.
Lateral variations of shear velocity and anelasticity in the upper mantle of the western US from Rayleigh wave observations p 653 N93-13492
SAINT MARY'S HOSPITAL, MILWAUKEE, WI.
Post flight operation of a high peak power neodymium YAG laser aboard the G-449 payload flown on Space Shuttle Columbia mission 61-C p 508 N93-13161
SALFORD UNIV. (ENGLAND).
Flow prediction for three-dimensional intakes and ducts using viscous-inviscid interaction methods
p 592 N93-13953
SAN DIEGO SUPERCOMPUTER CENTER, CA.
File servers, networking, and supercomputers
p 737 N93-13137
SANDIA LABS., ALBUQUERQUE, NM.
A smoke producing rocket motor for atmospheric wind profiling
[DE92-018264] p 555 N93-12563
SANDIA NATIONAL LABS., ALBUQUERQUE, NM.
Automated dry powder dispenser for explosive components
[DE92-019425] p 555 N93-12568
Uses of Monte Carlo computer simulations in understanding epitaxial growth and ion bombardment of Si(001)
[DE92-016944] p 719 N93-12586
RHALE: A MMALE shock physics code written in C++
[DE92-018271] p 684 N93-12795
Nonideal thermoequilibrium calculations using a large product species data base
[DE92-040839] p 735 N93-12813
Long pulse electron beam propagation
[DE92-014948] p 706 N93-12830
Latent image exposure monitor using scatterometry
[DE92-019427] p 604 N93-12915
Bonding in simple phosphate glass
[DE92-019437] p 550 N93-12917
Process designed for experimentation for increased-caliper Fresnel lenses
[DE92-019464] p 709 N93-12918
Bifurcations in elastic-damaging materials
[DE92-018818] p 624 N93-13072
Laser formation of lithium plasma ion sources for applied-B ion diodes on the PBFA-2 accelerator
[DE92-016091] p 716 N93-13191
Radiation-induced infrared absorption in nuclear-pumped laser cavity components
[DE92-017346] p 605 N93-13249
A computer program for engineering simulations of space reactor system performance
[DE92-016400] p 526 N93-13299
Eddy current power dissipation at sharp corners
[DE92-016890] p 571 N93-13300
Numerical simulations of steel plate perforation
[DE92-017058] p 626 N93-13301
Elevated temperature tensile properties of borated 304 stainless steel: Effect of boride dispersion on strength and ductility
[DE92-040096] p 542 N93-13302
Effect of O2 partial pressure on post annealed Ba2YCu3O(7-delta) thin films
[DE92-014949] p 722 N93-13323
The protection of the Facsimile (FAX) machine against the insider threat
[DE92-019424] p 565 N93-13506
A fast scanning probe for D3-D
[DE92-040260] p 717 N93-13511
Analysis and experimental results for an extraction cavity for the split-cavity oscillator
[DE92-040262] p 566 N93-13512
Thermodynamically consistent theories for elastoplasticity coupled with damage
[DE92-018283] p 627 N93-13515
The estimation of electrical cable fire-induced damage limits
[DE92-040100] p 572 N93-13519
Summary on comparison of radiative heat transfer solutions for a specified problem
[DE92-040098] p 588 N93-13575
Boiler efficiency methodology for solar heat applications
[DE92-019805] p 640 N93-13618
Planar laser-induced fluorescence imaging of OH in the exhaust of a bi-propellant thruster p 602 N93-13686
SANDIA NATIONAL LABS., LIVERMORE, CA.
High-resolution investigation of degenerate four-wave mixing in the (gamma)(0,0) band of nitric oxide
[DE92-005312] p 537 N93-13232
The reactions of imidogen with nitric oxide and molecular oxygen
[DE92-006697] p 537 N93-13233
High-resolution resonant degenerate 4-wave mixing spectroscopy
[DE92-012146] p 538 N93-13234
Fundamentals of enhanced scalar transport in strongly oscillating and/or resonant flow fields as created by pulse combustion
[DE92-012147] p 582 N93-13247
Nonlinear stability of combustion-driven acoustic oscillations in resonance tubes
[DE92-012153] p 699 N93-13262
SATCON TECHNOLOGY CORP., CAMBRIDGE, MA.
Magnetic bearings for a high-performance optical disk buffer, volume 2
[NASA-CR-190874] p 615 N93-13608
Magnetic bearings for a high-performance optical disk buffer, volume 1
[NASA-CR-190873] p 616 N93-13706
SCHMITT (HARRISON H.), ALBUQUERQUE, NM.
The real world and lunar base activation scenarios
p 680 N93-14014
SCIENCE APPLICATIONS INTERNATIONAL CORP., GLENDORA, CA.
Investigation of microgravity effects on solidification phenomena of selected materials p 510 N93-13168
The LDCE Particle Impact Experiment as flown on STS-46 p 512 N93-13183
SCIENCE APPLICATIONS INTERNATIONAL CORP., SAN DIEGO, CA.
Data to test and evaluate the performance of neural network architectures for seismic signal discrimination, volume 1
[AD-A254413] p 691 N93-12607
ReTech, Inc., Plasma Centrifugal Furnace: Applications analysis report
[PB92-218791] p 714 N93-12982
SCIENCE APPLICATIONS INTERNATIONAL CORP., TORRANCE, CA.
Combustion of gaseous fuels under reduced-gravity conditions p 557 N93-14012
SCITEC, INC., PRINCETON, NJ.
Results of the laser sensor technology transition investigation
[AD-A255845] p 608 N93-14085
SEARCH TECHNOLOGY, INC., NORCROSS, GA.
Specification of adaptive aiding systems
[AD-A254537] p 499 N93-12602
SECA, INC., HUNTSVILLE, AL.
Adaptation of multidimensional group particle tracking and particle wall-boundary condition model to the FDNS code
[SECA-TR-92-06] p 575 N93-12689
SETS TECHNOLOGY, INC., MILILANI, HI.
Imaging IR spectrometer, phase 2
[NASA-CR-190848] p 597 N93-13424
SHIMIZU CORP. (JAPAN).
The possibility of concrete production on the Moon
p 554 N93-13988
Concrete structure construction on the Moon
p 559 N93-13989
SIERRA COLL., SACRAMENTO, CA.
Tagging insulin in microgravity p 510 N93-13172
SIMON FRASER UNIV., BURNABY (BRITISH COLUMBIA).
The informed citizen: Technology and responsibility in the information age p 742 N93-14049
SLOVAK ACADEMY OF SCIENCES, BRATISLAVA (CZECHOSLOVAKIA).
Abstracts of papers presented at the International Symposium on Time, Frequency, and Dating in Geomorphology
[AD-A254927] p 649 N93-12704
SMITHSONIAN ASTROPHYSICAL OBSERVATORY, CAMBRIDGE, MA.
Absolute absorption cross sections of ozone at 300 K, 228 K and 195 K in the wavelength region 185-240 nm
[NASA-CR-191267] p 645 N93-13274
The role of particle diffusion in the lower transition region: Revised interpretation of emission measures
p 770 N93-13476
SOCIETE NATIONALE D'ETUDES ET DE CONSTRUCTION DE MOTEURS AERONAUTIQUES, MOISSY-CRAMAYEL (FRANCE).
Numeric simulation of the aerodynamic flows around nacelles p 577 N93-13202
Flight analysis of air intake/engine compatibility
p 502 N93-13212
SOUTHAMPTON UNIV. (ENGLAND).
Scattering and order in thermotropic liquid crystals
p 723 N93-13332
A study of techniques for single frequency operation of diode-pumped Nd:YAG lasers p 606 N93-13629
Molecular theories and computer simulations of liquid crystals p 725 N93-13843
Studies of surface-induced luminescence relevant to spacecraft glow, using a seeded arc-jet
p 523 N93-13919
SOUTHWEST RESEARCH INST., SAN ANTONIO, TX.
Diesel injector fouling bench test methodology
[AD-A254532] p 609 N93-12600
Studies of extra-solar Oort Clouds and the Kuiper disk
[NASA-CR-190958] p 769 N93-12669
Effects of gas composition on engine performance and emissions
[PB92-217561] p 611 N93-12936
SO2 on Venus: A final cross-calibration with Pioneer Venus
[NASA-CR-191256] p 758 N93-13344
Investigation of effects of 60-Hz electric and magnetic fields on operant and social behavior and on the neuroendocrine system of nonhuman primates, part 2
[DE92-040153] p 673 N93-13503
Investigation of effects of 60-Hz electric and magnetic fields on operant and social behavior and on the neuroendocrine system of nonhuman primates, part 1
[DE92-040152] p 673 N93-13520
Chairmanship of the Neptune/Pluto Outer Planets Science Working Group
[NASA-CR-191288] p 759 N93-13568
SOUTHWESTERN UNIV., GEORGETOWN, TX.
Synthesis of derivatives of alpha, omega difunctional perfluoroaliphatic compounds for low dielectric constant resins
[AD-A254928] p 550 N93-13026
SPACE STUDIES INST., PRINCETON, NJ.
First steps to lunar manufacturing: Results of the 1988 Space Studies Institute Lunar Systems Workshop
p 761 N93-13977
SPACE SYSTEMS/LORAL, PALO ALTO, CA.
Applications of satellite technology to broadband ISDN networks
[NASA-CR-189199] p 562 N93-12950
SPACE TELESCOPE SCIENCE INST., BALTIMORE, MD.
HARDI: A high angular resolution deployable interferometer for space p 745 N93-13588
SPECTRA RESEARCH SYSTEMS, INC., HUNTSVILLE, AL.
ECLSS evolution: Advanced instrumentation interface requirements. Volume 3: Appendix C
[NASA-CR-184367] p 678 N93-12990
Impact of lunar oxygen production on direct manned Mars missions p 540 N93-13984
SRI INTERNATIONAL CORP., MENLO PARK, CA.
Stimulated Brillouin processes in crystals and glasses
[DE92-019549] p 721 N93-12887
Building and using scene representations in image understanding p 692 N93-13241
Thermochemistry of atmospheric metal reactions
[AD-A248651] p 543 N93-13733
STANFORD LINEAR ACCELERATOR CENTER, CA.
Second quantization in bit-string physics
[DE92-019645] p 727 N93-12826
A simple model for SLC positron stability issues
[DE92-019644] p 706 N93-12992
Test of QED using a laser at the SLAC final focus test beam
[DE92-019647] p 707 N93-12993
Recent developments in the theory of heavy-quark decays
[DE92-017598] p 704 N93-13250
STANFORD UNIV., CA.
Tactile sensing and control in humans and robotic/teleoperated systems
[AD-A254408] p 609 N93-12604
Bayesian analysis of linear and nonlinear population models using the Gibbs sampler
[AD-A254769] p 697 N93-12702

Studies of radiative emission from the simulated shock layer of the Huygens probe p 521 N93-12834
Computation of steady and unsteady shock-induced combustion over hypervelocity blunt bodies p 536 N93-12836
Fast approximation algorithms for multicommodity flow problems
[AD-A254335] p 685 N93-12961
Damping the (pi)-mode instability in the SLC damping rings with a passive cavity
[DE92-018153] p 707 N93-13090
Search for doubly Cabibbo suppressed decays of the charged D meson
[DE92-018588] p 703 N93-13092
Guide to QSPIRES and the particle physics databases on SLACVM
[DE92-018099] p 737 N93-13275
Enabling technologies for economical manufacturing of composites
[AD-A253615] p 531 N93-13324
A Fourier series method for polygonal domains: Large element computation for plates p 627 N93-13484
Development and computation of continuum higher order constitutive relations for high-altitude hypersonic flow p 494 N93-13578
Methods for efficient pumping of vacuum ultraviolet lasers p 606 N93-13626
Planar laser-induced fluorescence measurements of high-enthalpy free jet flow with nitric oxide p 595 N93-13685
Application of a vectorized particle simulation to the study of plates and wedges in high-speed rarefied flow p 495 N93-13746
Seismic studies of crustal structure and tectonic evolution across the central California margin and the Colorado Plateau margin p 657 N93-13794
An experimental investigation of the three-dimensional boundary layer on a rotating disk p 589 N93-13806
Gravitational lensing by galaxy clusters: The giant arcs in Abell 370 and Cl2244-02 p 755 N93-13848
Long-term averages of globally-measured ELF/VLF radio noise
[AD-A255518] p 566 N93-13869
Interaction of isotropic turbulence with a shock wave p 590 N93-13898
The heteroepitaxial growth of YBCO and other metal oxides on silicon and GaAs by pulsed laser deposition p 726 N93-13904
Fast optimization of static axisymmetric shell structures p 630 N93-13921
Aeronomy coexperiments on drag-free satellites with proportional thrusters: GP-B and STEP p 518 N93-13922
Robust controller and estimator design using minimax methods p 694 N93-13925
Hypersonic panel flutter in a rarefied atmosphere p 505 N93-13928
Experiments in two-cooperating-arm manipulation from a platform with unknown motion p 617 N93-13931
Turbulent boundary layers with high turbulence: Experimental heat transfer and structure on flat and convex walls p 591 N93-13938
Stability of the compressible reacting mixing layer p 592 N93-13948
Navier-Stokes flowfield computation of wing/rotor interaction for a tilt rotor aircraft in hover p 497 N93-14035
Diffusion of ion-implanted group 4 n-type dopants in gallium arsenide and gallium/arsenide-based superlattices p 727 N93-14073

STATE UNIV. OF IOWA, IOWA CITY.
Automatic programming of arc welding robots p 616 N93-13720
Magnetic properties of high-T(sub c) superconductors p 726 N93-13905

STATE UNIV. OF NEW YORK, BUFFALO.
Boundary element methods for two-dimensional, coupled, thermoviscous flow p 584 N93-13383
Activities of Space Power Insulation Inst.
[AD-A255825] p 574 N93-14034

STATE UNIV. OF NEW YORK, STONY BROOK.
The broad band overlap problem in atmospheric trace gases p 641 N93-12624
Sulfate impact upon low-level cloud albedo over oceans p 661 N93-12833
The Jovian ionosphere p 758 N93-13337
Elastic and plastic strain measurement in high temperature environment using laser speckle p 600 N93-13673
A study of the Earth Radiation Budget Experiment: Shortwave measurements and bidirectional reflectance models for the ocean surface p 654 N93-13722

STATE UNIV. OF NEW YORK AT BUFFALO, AMHERST.
Fracture toughness of short fiber/brittle matrix composites p 528 N93-12630
Effect of hydrogen reduction and doping on the characteristics of high-temperature superconductors p 725 N93-13844
Improving the temperature resistance of aluminum-matrix composites by using an acid phosphate binder p 536 N93-14056

STORAGE TECHNOLOGY CORP., LOUISVILLE, CO.
Enterprise storage report for the 1990's p 736 N93-13132

SUPERCONDUCTING SUPER COLLIDER LAB., DALLAS, TX.
Magnetic field perturbation caused by bending vibrations of a quadrupole
[DE92-040644] p 623 N93-13003
Longitudinal beam dynamics with rf noise
[DE92-040645] p 707 N93-13108
Thermal issues at the SSC p 584 N93-13387

SVERDRUP TECHNOLOGY, INC., BROOK PARK, OH.
Scaling of 100 kW class applied-field MPD thrusters
[NASA-CR-190791] p 525 N93-12638
Environmental qualification testing of payload G-534, the Pool Boiling Experiment p 510 N93-13169
Anode power deposition in applied-field MPD thrusters
[NASA-CR-190790] p 526 N93-13283
Laser-based strain measurements for high temperature applications p 601 N93-13675

SVERDRUP TECHNOLOGY, INC., CLEVELAND, OH.
Palladium-chromium static strain gages for high temperatures p 600 N93-13671

SVERDRUP TECHNOLOGY, INC., HUNTSVILLE, AL.
Running SINDA '85/FLUINT interactive on the VAX p 584 N93-13390
A SINDA thermal model using CAD/CAE technologies p 585 N93-13394

SYRACUSE UNIV., NY.
Parallel computing systems
[AD-A255076] p 689 N93-12852
Identifying and describing Federal information inventory/locator systems: Design for networked-based locators, volume 1 p 738 N93-13884

T

TECHNISCHE UNIV., BERLIN (GERMANY).
The influence of lunar propellant production on the cost-effectiveness of cislunar transportation systems p 556 N93-13983

TECOGEN, INC., WALTHAM, MA.
A novel diesel-fueled engine for microclimate cooling for the individual soldier
[AD-A254510] p 609 N93-12724
Utilization of compressed natural gas in medium- and heavy-duty engine route vehicles
[PB92-217546] p 611 N93-12908

TEL-AVIV UNIV. (ISRAEL).
Epitaxial growth of silicon and germanium for solar cells
[ITN-92-85168] p 722 N93-13268
Y1Ba2Cu3O(7-delta) thin film dc SQUIDs (superconducting quantum interference device)
[ITN-92-85167] p 723 N93-13362

TELEDYNE BROWN ENGINEERING, HUNTSVILLE, AL.
Spacelab J: Microgravity and life sciences
[NASA-CR-191353] p 516 N93-13564

TENNESSEE UNIV., KNOXVILLE.
A methodology for the solution of nonlinear two-point boundary value inverse problems in physics and engineering p 697 N93-13363
Investigations of the mechanical behavior of graphite/PEEK (APC-2) composites p 534 N93-13908
Dynamics of vortex rings in cross-flow p 496 N93-13917
Numerical investigation of non-spherical droplet dynamics in viscous convective flows p 591 N93-13918
Bipropellant spray combustion modeling in small rocket engines p 556 N93-13924
Particle simulation of grid erosion in an ion thruster p 527 N93-13927
Resources for a lunar base: Rocks, minerals, and soil of the Moon p 760 N93-13973
The formation of ore mineral deposits on the Moon: A feasibility study p 760 N93-13974

TEXAS A&M UNIV., COLLEGE STATION.
An analysis of the low-earth-orbit communications environment p 561 N93-12633
Oxygen electrode reaction in molten carbonate fuel cells
[DE92-040180] p 636 N93-12812
Automation of the targeting and reflective alignment concept
[NASA-CR-190964] p 709 N93-12985
From comparison density to two sample analysis
[AD-A253866] p 698 N93-13064
The kinetic energy budget of tropical plumes and ENSO in NMC and ECMWF analyses p 664 N93-13740
On a robust controller design using a minimax optimization approach p 695 N93-14021
Near-minimum-time control of a flexible arm p 695 N93-14039
Control algorithms for aerobraking in the Martian atmosphere p 524 N93-14046

TEXAS UNIV., ARLINGTON.
Optimum design of aircraft structures with manufacturing and buckling constraints p 501 N93-13815
Position and force control of flexible and rigid manipulators using the sliding-mode technique p 695 N93-14065
A collision avoidance algorithm for the mobile robot and the robot manipulator in multi-robot system p 618 N93-14094

TEXAS UNIV., AUSTIN.
ONR basic research program: Summary and bibliographies, FY 1990 and 1991
[AD-A253038] p 774 N93-12696
Testing and fault-tolerant design techniques for advanced digital architectures
[AD-A255013] p 681 N93-12707
Fast ion-driven Bernstein instabilities
[DE92-019393] p 705 N93-12713
Sensitivity analysis of the simultaneous proportionate change of inputs and outputs in data envelopment analysis
[AD-A254821] p 683 N93-12730
The electrostatic wake of a superthermal test electron in a magnetized plasma
[DE92-019394] p 713 N93-12873
Nonlinear studies of m = 1 modes in high-temperature plasmas
[DE92-019395] p 714 N93-12913
Dynamics of the ion-ion acoustic instability in the thermalization of ion beams
[DE92-019396] p 714 N93-12914
Application of Lanczos vectors to control design of flexible structures, part 2
[NASA-CR-191244] p 685 N93-13030
System identification and model updating for substructures p 624 N93-13065
Fusion: Magnetic confinement
[DE92-019876] p 716 N93-13107
Dynamics and control of a tumbling satellite retrieval device p 522 N93-13119
Unsymmetric Lanczos model reduction and linear state function observer for flexible structures
[NASA-CR-191231] p 686 N93-13295
Application of Lanczos vectors to control design of flexible structures
[NASA-CR-191230] p 686 N93-13296
Design, construction and demonstration of modular, reconfigurable robots p 613 N93-13329
Low-frequency fluctuations of plasma magnetic fields p 717 N93-13496
Dual mass and torsion p 728 N93-13498
Establishment of an Institute for Fusion Studies
[DE92-040014] p 717 N93-13502
Molecular gas temperature and density in spiral galaxies p 748 N93-13688
A guidance methodology for the cislunar transfer of low-thrust spacecraft p 517 N93-13766
The use of consider covariance analysis in choosing data weights to reduce the effect of errors in model parameters on satellite orbit determination accuracy p 518 N93-13768
The determination and error assessment of the Earth's gravity field model p 656 N93-13771
Approximate optimal guidance for the Advanced Launch System p 519 N93-13819
Computer modeling of flow and transport interactions for compressible Navier-Stokes equations p 589 N93-13825
An experimental/computational study of heat transfer in sharp fin induced shock wave/turbulent boundary layer interactions at low hypersonic Mach numbers p 590 N93-13826
A domain decomposition method for parallel transient response calculations p 504 N93-13827
The nonequilibrium statistical mechanics of chaotic maps p 729 N93-13832
Bifurcation and localization instabilities in plastic bending of cylindrical shells p 630 N93-13923
Dynamic modeling and optimal joint torque coordination of advanced robotic systems p 617 N93-13936
Long-term lunar stations: Some ecological considerations p 648 N93-13995

TEXAS WOMAN'S UNIV., DENTON.
A study of traditional information access models applied in a hypertext information system p 739 N93-14076

THIOKOL CORP., BRIGHAM CITY, UT.
Qualification of the gritblast assembly and process for the inside diameter of the RSRM forward and aft domes
[NASA-CR-184462] p 558 N93-13021
THOMSON-CSF, MALAKOFF (FRANCE).
Inverse Synthetic Aperture Radar p 564 N93-13058
TOKYO UNIV. (JAPAN).
Arm length matching in 10 m delay-line interferometer
[ISAS-TN-649] p 596 N93-12639
Effect of the flow non-uniformity on the mixing layer at the interface of parallel supersonic flows
[ISAS-RN-646] p 491 N93-12716
Cross sections and rate coefficients for the electron-impact excitation of He-like ions
[ISAS-RN-647] p 703 N93-13095
Monte Carlo calculation of ionization and excitation rates in electron aurora
[ISAS-RN-645] p 652 N93-13405
TOKYO UNIV., SAGAMIHARA (JAPAN).
Moon Park: A research and educational facility
p 519 N93-14015
TOLEDO UNIV., OH.
Simulation of two-dimensional icing, de-icing and anti-icing phenomena p 498 N93-13364
TORONTO UNIV. (ONTARIO).
The modelling of turbulence and downbursts for flight simulators p 507 N93-13542
TRANSPORTATION RESEARCH BOARD, WASHINGTON, DC.
Public-sector aviation issues: Graduate research award papers, 1990 - 1991
[PB92-222629] p 498 N93-13787
TRI-STATE UNIV., ANGOLA, IN.
The program FANS-3D (finite analytic numerical simulation 3-dimensional) and its applications
p 586 N93-13399

U

UNITED ENGINEERING TRUSTEES, INC., NEW YORK, NY.
Air Force engineering research initiation grants (1990-1991)
[AD-A255004] p 774 N93-12706
UNITED TECHNOLOGIES RESEARCH CENTER, EAST HARTFORD, CT.
Fatigue and fracture of intermetallic alloys
[AD-A254543] p 540 N93-12603
UNIVERSAL ENERGY SYSTEMS, INC., DAYTON, OH.
USAF 1990 research initiation program, volume 2
[AD-A254654] p 773 N93-12663
USAF 1990 research initiation program, volume 4
[AD-A254655] p 773 N93-12664
USAF 1990 research initiation program, volume 1
[AD-A254656] p 773 N93-12665
US Air Force 1989 research initiation program, volume 1
[AD-A254457] p 774 N93-12764
US Air Force 1989 research initiation program, volume 4
[AD-A254458] p 774 N93-12765
US Air Force 1989 research initiation program, volume 2
[AD-A254459] p 774 N93-12766
US Air Force 1989 research initiation program, volume 3
[AD-A254460] p 774 N93-12767
USAF 1990 research initiation program, volume 3
[AD-A254755] p 775 N93-12849
UNIVERSITAET DER BUNDESWEHR MUENCHEN, NEUBIBERG (GERMANY).
Overview on test cases for computation of internal flows in turbomachines p 579 N93-13209
Machine perception exploiting high-level spatio-temporal models p 693 N93-13244
UNIVERSITAIRE INSTELLING ANTWERPEN, WILRIJK (BELGIUM).
Study of the concentration and deposition of tropospheric aerosols using x ray emission techniques
p 667 N93-13894
A theory of reference graphs in relational databases
p 739 N93-13912
UNIVERSITY OF CENTRAL FLORIDA, ORLANDO.
Assured crew return vehicle post landing configuration design and test
[NASA-CR-191253] p 520 N93-12910
UNIVERSITY OF SOUTH FLORIDA, TAMPA.
Thin films and solar cells of cadmium telluride and cadmium zinc telluride p 639 N93-13611
Two to six compound thin films by MOCVD for tandem solar cells p 640 N93-13932
Noise measurements of YBa2Cu3O7 thin film high-temperature superconductors p 726 N93-13933
UNIVERSITY OF SOUTHERN CALIFORNIA, LOS ANGELES.
Transactions: Tropospheric ozone and the environment. Papers from an international conference
[PB92-217017] p 643 N93-12941
UTAH STATE UNIV., LOGAN.
G254 undergraduate experiment p 511 N93-13174
Experimental studies of ionospheric irregularities and related plasma processes
[NASA-CR-191271] p 652 N93-13460
Magnetic holes near the magnetopause
p 653 N93-13491
The use of remotely sensed data in delineation of hydrologic response units and estimation of their rainfall-runoff model parameters p 635 N93-13840
Infrared emission from the water outgas cloud of an orbiting vehicle induced by collisions with atmospheric gases p 521 N93-13854
UTAH UNIV., SALT LAKE CITY.
Microcracking, microcrack-induced delamination, and longitudinal splitting of advanced composite structures
[NASA-CR-4472] p 623 N93-12911

V

VANDERBILT UNIV., NASHVILLE, TN.
Intrinsic bistable photonic materials by copper colloid formation in silica
[AD-A255505] p 711 N93-13866
Bone loss and human adaptation to lunar gravity
p 676 N93-14002
VATELL CORP., BLACKSBURG, VA.
Heat flux microsensor measurements and calibrations
p 599 N93-13665
VICTORIA UNIV. (BRITISH COLUMBIA).
A study of the structure, evolution and observation of Horizontal Branch stars
[ISBN-0-315-62655-0] p 751 N93-13374
VIGYAN RESEARCH ASSOCIATES, INC., HAMPTON, VA.
Euler analysis of turbofan/superfan integration for a transport aircraft p 578 N93-13206
VIRGINIA COMMONWEALTH UNIV., RICHMOND.
Electronic structure of microclusters and defect complexes
[AD-A254807] p 720 N93-12750
VIRGINIA POLYTECHNIC INST. AND STATE UNIV., BLACKSBURG.
Scale effects in buckling, postbuckling and crippling of graphite-epoxy Z-section stiffeners p 621 N93-12632
Feasibility study of a synthesis procedure for array feeds to improve radiation performance of large distorted reflector antennas
[NASA-CR-190948] p 561 N93-12655
Investigation of properties and performance of ceramic composite components
[DE92-019911] p 550 N93-12858
Compression strength of composite primary structural components
[NASA-CR-190949] p 624 N93-13019
Micromechanics of finite length fibers in composite materials p 532 N93-13490
Influence of surface defects and local structure on oxygenate reaction pathways over metal oxide surfaces
[DE92-040013] p 539 N93-13573
The shear gage and compact shear specimen for shear property measurements of composite materials
p 628 N93-13630
Skin friction measurements in high temperature high speed flows p 595 N93-13670
Effects of layer waviness on compression-loaded thermoplastic composite laminates p 532 N93-13724
Transonic aeroelastic analysis of systems with structural nonlinearities p 629 N93-13769
Contact of orthotropic laminates with a rigid spherical indentor p 533 N93-13778
Airfoil-vortex interaction and the wake of an oscillating airfoil p 495 N93-13803
Application of adaptive trusses to vibration isolation in flexible structures p 617 N93-13809
Deterministic and stochastic responses of nonlinear systems p 631 N93-13966
The role of the fiber/matrix interphase in the static and fatigue behavior of polymeric matrix composite laminates
p 535 N93-13968
Delamination initiation in postbuckled dropped-ply laminates p 535 N93-14030
VIRGINIA UNIV., CHARLOTTESVILLE.
Evidence for cool gas and star formation in cluster cooling flows p 751 N93-13380
Planar measurement of flow field parameters in nonreacting supersonic flows with laser-induced iodine fluorescence p 495 N93-13801
The free and forced vibrations of structures using the finite dynamic element method p 630 N93-13935
VRIJE UNIV., BRUSSELS (BELGIUM).
The PEP Symposium on CFD Techniques for Propulsion Applications p 579 N93-13210

W

WAKE FOREST UNIV., WINSTON-SALEM, NC.
The vibrational spectrum of H2O3: An ab initio investigation
[NASA-CR-190968] p 537 N93-12935
WALT DISNEY WORLD CO., LAKE BUENA VISTA, FL.
Lunar base CELSS: A bioregenerative approach
p 680 N93-13993
WASHINGTON STATE UNIV., PULLMAN.
Point defects quenched in NiAl and related intermetallic compounds p 724 N93-13628
WASHINGTON UNIV., SAINT LOUIS, MO.
Hierarchic models for laminated plates
p 528 N93-12629
Physical interpretation and development of ultrasonic nondestructive evaluation techniques applied to the quantitative characterization of textile composite materials
[NASA-CR-190962] p 620 N93-13435
Hydrothermal organic synthesis experiments
[NASA-CR-191257] p 672 N93-13457
Chemical environments of submarine hydrothermal systems
[NASA-CR-191258] p 669 N93-13458
Model studies of the middle atmosphere of Venus
p 759 N93-13831
Modeling and observations of deep circulation in the eastern South Pacific Ocean p 670 N93-13841
The growth of disturbances in barotropic models of the atmosphere p 658 N93-13887
Water and cheese from the lunar desert: Abundances and accessibility of H, C, and N on the Moon
p 761 N93-13976
Electrolytic smelting of lunar rock for oxygen, iron, and silicon p 761 N93-13979
The stellar angular correlation: Clues to wide binary star properties p 757 N93-14059
WASHINGTON UNIV., SEATTLE.
Near-normal incidence scattering from rough, finite surfaces: Kirchhoff theory and data comparison for Arctic sea ice
[AD-A254525] p 668 N93-12577
Experimental examination of growing and newly submerged sea ice including acoustic probing of the skeletal layer
[AD-A254526] p 669 N93-12599
Wave propagation and scattering in dense geophysical media
[AD-A254573] p 561 N93-12646
Investigations of the dynamics and thermodynamics of the mesosphere lower thermosphere and upper thermosphere at the polar regions with optical ground-based remote sensing
[AD-A254746] p 650 N93-12845
An investigation of the thermoviscoplastic behavior of a metal matrix composite at elevated temperatures
[NASA-CR-189706] p 530 N93-12929
Polarimetric signatures of a canopy of dielectric cylinders based on first and second order vector radiative transfer theory p 569 N93-13088
Fermi molecular dynamics
[DE92-015351] p 703 N93-13187
Numerical simulation of the acoustic instability in the spatially developing, confined, supersonic mixing layer
p 494 N93-13521
Neutrino(e) appearance for neutrino(mu)-neutrino(tau) oscillations in matter
[DE92-040303] p 772 N93-13533
WAYNE STATE UNIV., DETROIT, MI.
An experimental and theoretical study of degradation pathways for atmospheric halocarbons
p 646 N93-13624
WEST VIRGINIA UNIV., MORGANTOWN.
Determination of the stability and control derivatives of the F/A-18 HARV from flight data using the maximum likelihood method
[NASA-CR-191216] p 503 N93-12903
Capacitive skin characterization
[NASA-CR-191261] p 598 N93-13567
Enhanced accuracy for closed-loop robot
p 617 N93-13808
WESTINGHOUSE ELECTRIC CORP., LARGE, PA.
Westinghouse PAFC program update
[DE92-019978] p 640 N93-13623
WESTINGHOUSE ELECTRIC CORP., PITTSBURGH, PA.
Gas cooled fuel cell systems technology development
[DE92-0012983-3103] p 636 N93-12683

WESTINGHOUSE IDAHO NUCLEAR CO., INC., IDAHO FALLS.
Fluidic sampling
[DE92-017266] p 575 N93-12761
Precision liquid-level measurement in deep tanks using a swept-RF resonant cavity
[DE92-017236] p 597 N93-13267
Systematic chemical equation balancing
[DE92-017234] p 539 N93-13530
WESTINGHOUSE SAVANNAH RIVER CO., AIKEN, SC.
Reviews of computing technology: Fiber distributed data interface
[DE92-019927] p 681 N93-12886
Aluminum oxide film thickness and emittance
[DE92-019931] p 550 N93-13035
Statistical process management: An essential element of quality improvement
[DE92-019934] p 619 N93-13036
Fiber optic sensors for environmental applications: A brief review
[DE92-040170] p 710 N93-13576
Reviews of computing technology: Securing network applications, Kerberos, and RSA
[DE92-019928] p 690 N93-13620
WICHITA STATE UNIV., KS.
Computational fluid dynamics of the base flow on a plane body between a subsonic flow on one side and a supersonic flow on the other p 591 N93-13920
WICKERSHEIMER ENGINEERS, INC., CHAMPAIGN, IL.
User's guide: Computer-Aided Structural Modeling (CASM), version 3.00
[AD-A255074] p 684 N93-12851
Computer-Aided Structural Engineering (CASE) project. Tutorial guide: Computer-Aided Structural Modeling (CASM). Version 3.00
[AD-A255075] p 684 N93-12872
WINDSOR UNIV. (ONTARIO).
Application of complex variables in electromagnetofluid dynamic, magnetofluid dynamic and fluid dynamic flows: Viscoelastic boundary-layer theory
[ISBN-0-315-65141-5] p 594 N93-14067
WISCONSIN UNIV., MADISON.
Fluid dynamics of supercritical helium within cable-in-conduit conductors
[DE92-019516] p 574 N93-12589
Hyperbolic conservation laws with umbilic points, 1
[AD-A254431] p 696 N93-12594
Small-strain and finite-strain finite element analyses of plane-strain tensile elastic-plastic crack growth p 621 N93-12628
On ascertaining inductively the dimension of the joint kernel of certain commuting linear operators
[AD-A254748] p 696 N93-12847
Measurement of current density fluctuations and ambipolar particle flux due to magnetic fluctuations in MST
[DE92-041013] p 713 N93-12878
Anomalous ion heating and superthermal electrons in the MST reversed-field pinch
[DE92-041011] p 713 N93-12882
Current density fluctuations, nonlinear coupling, and transport in MST
[DE92-041012] p 713 N93-12883
A catalog of moderately distant galaxy clusters p 749 N93-13011
A theoretical investigation of the growth rates of ice crystals in clouds p 653 N93-13485
A parameterized quasi-five-cylinder convective cloud model and its application to remote sensing of rainfall p 663 N93-13489
Spectroscopic studies of low-density gas in the Galactic disk and halo p 753 N93-13499
Heat transfer, fluid flow and interface shapes in floating-zone crystal growth p 724 N93-13739
The effects of pressure gradients on convective heat flux predictions in engine environments p 616 N93-13772
Experimental characterization of continuous alumina fiber/epoxy p 533 N93-13775
Numerical study of nonlinear convective-symmetric instability in a rotating baroclinic atmosphere p 666 N93-13786
Fluidlike studies of the sheath and presheath regions of a plasma p 718 N93-13792
Fusion energy from the Moon for the twenty-first century p 719 N93-13985
Potential of derived lunar volatiles for life support p 680 N93-13998
Lunar surface mining for automated acquisition of helium-3: Methods, processes, and equipment p 766 N93-14007
WORCESTER POLYTECHNIC INST., MA.
Spaceflight payload design flight experience G-408 p 508 N93-13160
Digital fluoroscopy with an optically coupled charge-coupled device p 712 N93-14101
WRIGHT LAB., WRIGHT-PATTERSON AFB, OH.
A heat pipe coupled planar thermionic converter: Performance characterization, nondestructive testing, and evaluation
[AD-A254941] p 727 N93-12546
An application of exponential neural networks to event-train recognition
[AD-A254948] p 690 N93-12548
Large-amplitude plate vibration in an elevated thermal environment
[AD-A254411] p 621 N93-12606
Data acquisition applications for long duration electromagnetic launcher experiments
[AD-A254546] p 519 N93-12611
X-29 linear aerodynamic perturbation model
[AD-A254810] p 500 N93-12752
Survey on techniques used in aerodynamic nozzle/airframe integration p 502 N93-13224
Propulsion integration results of the STOL and Maneuver Technology Demonstrator p 502 N93-13228
Hypersonic propulsion system force accounting p 503 N93-13229
Symposium proceedings on Quantitative Feedback Theory
[AD-A255527] p 505 N93-13872

Y

YALE UNIV., NEW HAVEN, CT.
The spin of the nucleon in deep inelastic lepton scattering experiments
[DE92-018854] p 702 N93-13073
Features of vorticity in fully turbulent flows p 583 N93-13334
Encounters with protostellar disks p 754 N93-13727
Tropopause fold investigations: Secondary circulation, water vapor and ozone analyses p 657 N93-13796
Galaxies with spectral energy distributions peaking at 60 micrometers: Morphology and activity explained by interactions p 756 N93-13959

Typical Contract Number Index Listing

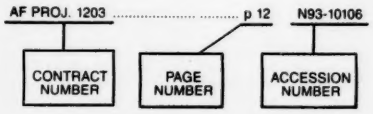

Listings in this index are arranged alphanumerically by contract number. Under each contract number the accession numbers denoting documents that have been produced as a result of research done under that contract are arranged in ascending order. The page number helps to locate the citation in the abstract section. The accession number denotes the number by which the citation is identified.

AF PROJ. 2302 ..... p 774 N93-12706
AF PROJ. 2305 ..... p 573 N93-13837
AF PROJ. 2308 ..... p 525 N93-12575
AF PROJ. 2403 ..... p 505 N93-13872
AF PROJ. 5581 ..... p 734 N93-12703
AF PROJ. 7231 ..... p 679 N93-13874
AF PROJ. 7633 ..... p 690 N93-12548
AF-AFOSR-0008-91 ..... p 690 N93-12547
AF-AFOSR-0044-90 ..... p 697 N93-13409
AF-AFOSR-0105-89 ..... p 623 N93-12863
AF-AFOSR-0159-91 ..... p 503 N93-12959
AF-AFOSR-0176-91 ..... p 709 N93-12666
p 711 N93-13879
AF-AFOSR-0275-91 ..... p 554 N93-14029
AF-AFOSR-0316-89 ..... p 650 N93-12845
AF-AFOSR-0338-90 ..... p 604 N93-12644
AF-AFOSR-0339-90 ..... p 499 N93-12557
AF-AFOSR-0464-89 ..... p 774 N93-12706
ARB-A6-202-33 ..... p 643 N93-12941
ARPA ORDER 7330 ..... p 681 N93-12641
ARPA ORDER 7597 ..... p 682 N93-12645
p 688 N93-13944
CNES-1212 ..... p 752 N93-13467
DA PROJ. RR0-4108 ..... p 675 N93-13116
DA PROJ. RR0-4206 ..... p 736 N93-13117
p 573 N93-13650
DA PROJ. RS3-4-C-74 ..... p 688 N93-13942
DA PROJ. 1L1-61101-AH-42 ..... p 528 N93-12583
DA PROJ. 1L1-61102-AH-45 ..... p 625 N93-13153
DA PROJ. 1L1-62211-A-47-A ..... p 610 N93-12736
DA PROJ. 1L1-62706-A-553 ..... p 536 N93-12743
DA PROJ. 1L1-62786-AH-98 ..... p 609 N93-12724
DA PROJ. 1L7-62786-AH-20 ..... p 609 N93-12600
DA PROJ. 3M1-61102-BS-12 ..... p 674 N93-12945
DA PROJ. 4A1-62719-AT-40 ..... p 635 N93-13867
DAAB07-87-C-H027 ..... p 689 N93-12846
DAAG29-85-K-0198 ..... p 651 N93-12969
DAAK70-85-C-0007 ..... p 609 N93-12600
DAAK70-87-C-0043 ..... p 609 N93-12600
DAAL03-86-D-0001 ..... p 622 N93-12652
p 534 N93-13940
DAAL03-87-K-0032 ..... p 561 N93-12646
DAAL03-88-J-0057 ..... p 569 N93-13087
DAAL03-88-K-0033 ..... p 600 N93-13673
DAAL03-88-K-0175 ..... p 688 N93-12733
DAAL03-89-C-0020 ..... p 552 N93-13325
DAAL03-89-K-0008 ..... p 608 N93-13864
DAAL03-89-K-0015 ..... p 720 N93-12750
DAAL03-89-K-0035 ..... p 719 N93-12544
DAAL03-89-K-0083 ..... p 531 N93-13324
DAAL03-89-K-0085 ..... p 574 N93-13865
DAAL03-89-K-0121 ..... p 673 N93-13863
DAAL03-89-K-0128 ..... p 562 N93-12747
DAAL03-89-K-0148 ..... p 537 N93-13096
DAAL03-90-G-0026 ..... p 698 N93-12865
DAAL03-90-G-0069 ..... p 698 N93-13064
DAAL03-90-G-0090 ..... p 696 N93-12847
DAAL03-90-G-0104 ..... p 695 N93-12582
DAAL03-91-G-0028 ..... p 711 N93-13866
DAAL03-91-G-0090 ..... p 696 N93-13027
DAAL03-91-G-0102 ..... p 685 N93-12961
DACA39-86-C-0024 ..... p 684 N93-12851
p 684 N93-12872
DACA76-85-C-0004 ..... p 692 N93-13241
DACA76-90-C-0021 ..... p 692 N93-13241
DACA76-92-C-0003 ..... p 692 N93-13241
DAJA37-92-M-0126 ..... p 649 N93-12704
DAJA45-85-C-0028 ..... p 682 N93-12647
DAJA45-91-M-0211 ..... p 611 N93-12906
DAJA45-92-M-0123 ..... p 644 N93-13098
DAJA45-92-M-0240 ..... p 575 N93-12708
DAMD17-86-C-6161 ..... p 674 N93-12945
DE-AC02-76CH-00016 ..... p 609 N93-12565
p 701 N93-12832
p 707 N93-13192
p 644 N93-13270
p 571 N93-13358
p 710 N93-13652
DE-AC02-76CH-03000 ..... p 701 N93-12572
p 707 N93-13235
p 705 N93-13537
DE-AC02-76CH-03073 ..... p 716 N93-13193
p 718 N93-13535
DE-AC02-78ET-51013 ..... p 716 N93-13193
DE-AC02-80RA-50219 ..... p 673 N93-13503
p 673 N93-13520
DE-AC02-83CH-10093 ..... p 636 N93-12837
p 637 N93-12838
p 638 N93-13102
p 538 N93-13316
p 627 N93-13524
p 627 N93-13525
p 723 N93-13526
p 639 N93-13528
p 639 N93-13529
DE-AC02-91ER-40605 ..... p 702 N93-12855
DE-AC03-76SF-00515 ..... p 727 N93-12826
p 706 N93-12992
p 707 N93-12993
p 707 N93-13090
p 703 N93-13092
p 704 N93-13250
DE-AC03-89ER-51114 ..... p 737 N93-13275
p 712 N93-12687
p 714 N93-12932
p 714 N93-12971
p 715 N93-13044
p 716 N93-13193
DE-AC03-89ER-52153 ..... p 715 N93-13044
DE-AC04-76DP-00613 ..... p 624 N93-13077
p 736 N93-13078
DE-AC04-76DP-00789 ..... p 555 N93-12563
p 555 N93-12568
p 719 N93-12586
p 684 N93-12795
p 735 N93-12813
p 706 N93-12830
p 604 N93-12915
p 550 N93-12917
p 709 N93-12918
p 714 N93-12932
p 714 N93-12971
p 624 N93-13072
p 716 N93-13191
p 605 N93-13249
p 526 N93-13299
p 571 N93-13300
p 626 N93-13301
p 542 N93-13302
p 722 N93-13323
p 565 N93-13506
p 717 N93-13511
p 566 N93-13512
p 627 N93-13515
p 572 N93-13519
p 588 N93-13575
p 640 N93-13618
DE-AC04-76DR-00789 ..... p 537 N93-13232
p 537 N93-13233
p 538 N93-13234
p 582 N93-13247
p 699 N93-13262
DE-AC04-88DP-43495 ..... p 555 N93-13081
p 759 N93-13504
DE-AC05-84ER-40150 ..... p 708 N93-13284
DE-AC05-84OR-21400 ..... p 569 N93-12561
p 689 N93-12797
p 689 N93-12810
p 549 N93-12821
p 642 N93-12828
p 706 N93-12829
p 550 N93-12858
p 702 N93-13037
p 542 N93-13043
p 715 N93-13044
p 691 N93-13079
p 542 N93-13080
p 703 N93-13114
p 542 N93-13190
p 716 N93-13193
p 542 N93-13237
p 716 N93-13297
p 538 N93-13317
p 583 N93-13318
p 626 N93-13320
p 723 N93-13347
p 717 N93-13518
p 708 N93-13574
p 718 N93-13651
DE-AC05-84OS-21400 ..... p 619 N93-12794
p 704 N93-13319
DE-AC05-84OT-21400 ..... p 736 N93-13048
DE-AC06-76RL-01830 ..... p 575 N93-12711
p 677 N93-12712
p 541 N93-12820
p 669 N93-12916
p 638 N93-13082
DE-AC07-76ID-01570 ..... p 683 N93-12792
p 610 N93-12793
p 713 N93-12856
p 728 N93-12857
p 576 N93-12996
p 583 N93-13356
p 539 N93-13616
DE-AC07-84ID-12435 ..... p 575 N93-12761
p 597 N93-13267
p 539 N93-13530
DE-AC08-88NV-10617 ..... p 576 N93-12912
DE-AC09-76SR-00001 ..... p 550 N93-13035
DE-AC09-89SR-18035 ..... p 681 N93-12886
p 550 N93-13035
p 619 N93-13036
p 710 N93-13576
p 690 N93-13620
DE-AC21-82MC-24223 ..... p 636 N93-12683
p 640 N93-13623
DE-AC21-88MC-24221 ..... p 638 N93-13040
DE-AC21-88MC-25009 ..... p 639 N93-13427
DE-AC21-90MC-26364 ..... p 538 N93-13314
DE-AC21-90MC-27168 ..... p 638 N93-13039
p 640 N93-13621
DE-AC22-90PC-90044 ..... p 537 N93-13188
DE-AC22-91PC-90181 ..... p 704 N93-13263
DE-AC22-91PC-90182 ..... p 577 N93-13074
DE-AC34-90DP-62349 ..... p 645 N93-13505
DE-AC35-89ER-40486 ..... p 623 N93-13003
p 707 N93-13108
DE-AI01-86CE-90237 ..... p 571 N93-13196
p 571 N93-13197
DE-AI06-91RL-12089 ..... p 634 N93-13094
DE-FG02-84ER-45132 ..... p 724 N93-13577
DE-FG02-85ER-25001 ..... p 697 N93-13409
DE-FG02-85ER-53198 ..... p 713 N93-12878
p 713 N93-12882
p 713 N93-12883
DE-FG02-86ER-13622 ..... p 542 N93-12998
DE-FG02-86ER-53223 ..... p 713 N93-12811
p 715 N93-13038
DE-FG02-87ER-13772 ..... p 537 N93-12995
DE-FG02-87ER-40335 ..... p 706 N93-12822
DE-FG02-87ER-45298 ..... p 545 N93-12697
DE-FG02-87ER-60514 ..... p 701 N93-12745
DE-FG02-88ER-25065 ..... p 727 N93-12796
DE-FG02-88ER-52149 ..... p 574 N93-12569
DE-FG02-89ER-14012 ..... p 604 N93-12744
DE-FG02-89ER-40531 ..... p 706 N93-12924
DE-FG02-89ER-45396 ..... p 552 N93-13350

DE-FG02-89ER-45401 ..... p 720 N93-12827
DE-FG02-89ER-53297 ..... p 718 N93-13535
DE-FG02-90ER-54084 ..... p 718 N93-13535
DE-FG02-90ER-80910 ..... p 638 N93-13041
DE-FG02-91ER-14205 ..... p 703 N93-13106
DE-FG02-91ER-40661 ..... p 707 N93-13002
DE-FG02-91ER-45439 ..... p 542 N93-12973
DE-FG02-92ER-40699 ..... p 707 N93-13189
DE-FG02-92ER-40704 ..... p 702 N93-13073
DE-FG02-92ER-40706 ..... p 704 N93-13251
DE-FG05-80ET-53088 ..... p 705 N93-12713
p 713 N93-12873
p 714 N93-12913
p 714 N93-12914
p 716 N93-13107
p 717 N93-13502
DE-FG05-84ER-13263 ..... p 543 N93-13346
DE-FG05-86ER-40270 ..... p 563 N93-13042
DE-FG05-87ER-60503 ..... p 672 N93-13034
p 672 N93-13083
DE-FG05-88ER-13977 ..... p 609 N93-12698
DE-FG05-88ER-53279 ..... p 716 N93-13359
DE-FG05-90ER-14129 ..... p 539 N93-13573
DE-FG06-86ER-45273 ..... p 606 N93-13514
DE-FG06-88ER-40427 ..... p 703 N93-13187
DE-FG06-89ER-14057 ..... p 653 N93-13513
DE-FG06-90ER-40561 ..... p 772 N93-13533
DE-FG09-84ER-13188 ..... p 671 N93-12768
DE-FG21-90MC-27225 ..... p 672 N93-13269
DE-FG21-91MC-27414 ..... p 640 N93-13622
DE-FG22-87PC-79931 ..... p 636 N93-12812
DE-FG22-89PC-89786 ..... p 539 N93-13617
DTFA01-89-C-00002 ..... p 499 N93-13377
DTFA01-89-Z-02033 ..... p 660 N93-12622
p 498 N93-14024
DTFA01-90-Z-02069 ..... p 551 N93-13259
DTFA03-91-C-00038 ..... p 497 N93-12816
EPA-R-815134 ..... p 555 N93-12939
EPA-R-815692 ..... p 622 N93-12843
EPA-68-CO-0048 ..... p 714 N93-12982
EPA-68-D1-0117 ..... p 646 N93-13647
EPA-68-D8-0001 ..... p 642 N93-12726
EPA-68-D8-0017 ..... p 643 N93-12941
EPA-68-08-0023 ..... p 678 N93-12983
ESA-AO/1-2413/90-NL-PB ..... p 633 N93-13085
ESPRIT PROJ. P-2502 ..... p 693 N93-13243
ESPRIT PROJ. P-940 ..... p 693 N93-13243
FAA-F2006-E ..... p 507 N93-13447
FAA-T0603-S ..... p 506 N93-12668
FQ7624-91-C-0019 ..... p 682 N93-12554
F04701-88-C-0089 ..... p 712 N93-12705
p 547 N93-12776
p 727 N93-14083
p 603 N93-14086
p 524 N93-14087
p 708 N93-14089
p 544 N93-14098
p 554 N93-14099
F19628-87-K-0051 ..... p 562 N93-12867
F19628-88-K-0020 ..... p 560 N93-12581
F19628-89-C-0068 ..... p 650 N93-12944
F19628-89-C-0174 ..... p 562 N93-12948
F19628-89-D-0011 ..... p 560 N93-12551
F19628-89-K-0020 ..... p 650 N93-12943
F19628-89-K-0044 ..... p 632 N93-12550
F19628-90-C-0002 ..... p 660 N93-12622
p 567 N93-13878
F19628-90-C-0156 ..... p 691 N93-12607
F19628-90-K-0030 ..... p 543 N93-13733
F29601-91-C-0033 ..... p 522 N93-12962
F30602-88-C-0028 ..... p 570 N93-12866
F30602-88-C-0136 ..... p 689 N93-12852
F30602-88-D-0026 ..... p 688 N93-12710
p 608 N93-14085
F30602-89-C-0201 ..... p 682 N93-12614
F30602-91-D-0001 ..... p 711 N93-14032
F33615-88-C-3612 ..... p 499 N93-12602
F33615-89-C-0603 ..... p 674 N93-12905
F33615-90-C-0005 ..... p 676 N93-12662
F33615-90-C-1443 ..... p 566 N93-13838
F33615-90-C-1465 ..... p 682 N93-12645
p 688 N93-13944
F33615-91-C-2204 ..... p 603 N93-13687
F40600-90-C-0002 ..... p 506 N93-12552
F49620-87-C-0064 ..... p 521 N93-12579
F49620-88-C-0053 ..... p 773 N93-12663
p 773 N93-12664
p 773 N93-12665
p 774 N93-12764
p 774 N93-12765
p 774 N93-12766
p 774 N93-12767
F49620-88-C-0072 ..... p 648 N93-12621
F49620-88-C-0090 ..... p 545 N93-12729
F49620-88-C-0111 ..... p 651 N93-13276
F49620-88C-0053 ..... p 775 N93-12849
F49620-89-C-0047 ..... p 540 N93-12603
F49620-89-C-0080 ..... p 650 N93-12946
F49620-90-C-0076 ..... p 734 N93-12723
F49620-92-J-0180 ..... p 540 N93-14033
F49620-92-J-0264 ..... p 709 N93-12850
p 608 N93-13883
GRI-5086-233-1436 ..... p 612 N93-12977
GRI-5089-291-1835 ..... p 611 N93-12908
GRI-5089-293-1848 ..... p 611 N93-12936
GRI-5090-260-2041 ..... p 576 N93-12975
GRI-5091-292-2153 ..... p 615 N93-13644
IAEA-6702/RB ..... p 715 N93-13093
p 716 N93-13330
JPL-958461 ..... p 633 N93-13085
p 633 N93-13086
p 569 N93-13087
MDA903-87-C-0523 ..... p 676 N93-12545
p 677 N93-12609
MDA903-89-C-0003 ..... p 688 N93-12549
p 560 N93-12574
MDA903-90-C-0035 ..... p 681 N93-12641
MDA972-90-C-0021 ..... p 569 N93-13087
MIPR-ARO-147-91 ..... p 604 N93-12734
NAGW-1331 ..... p 521 N93-12720
NAGW-1415 ..... p 632 N93-13833
NAGW-1617 ..... p 633 N93-13084
NAGW-176 ..... p 644 N93-13031
NAGW-1788 ..... p 645 N93-13274
NAGW-1902 ..... p 685 N93-13261
NAGW-2010 ..... p 734 N93-12680
NAGW-2057 ..... p 650 N93-12877
NAGW-2096 ..... p 770 N93-13478
NAGW-2126 ..... p 705 N93-12715
NAGW-2389 ..... p 561 N93-12679
NAGW-2612 ..... p 510 N93-13171
p 512 N93-13185
NAGW-2753 ..... p 572 N93-13448
NAGW-2755 ..... p 769 N93-12930
NAGW-2818 ..... p 672 N93-13457
p 669 N93-13458
NAGW-2901 ..... p 733 N93-12660
NAGW-2914 ..... p 759 N93-13568
NAGW-3007 ..... p 649 N93-12661
NAGW-3023 ..... p 769 N93-12669
NAGW-3137 ..... p 670 N93-13714
NAG1-1198 ..... p 493 N93-13463
NAG1-1255 ..... p 500 N93-13305
NAG1-1613 ..... p 572 N93-13569
NAG1-363 ..... p 538 N93-13456
NAG1-423 ..... p 538 N93-13456
NAG1-537 ..... p 624 N93-13019
NAG1-602 ..... p 503 N93-13697
NAG1-613 ..... p 565 N93-13375
NAG1-623 ..... p 610 N93-12904
p 611 N93-12952
NAG1-723 ..... p 721 N93-13022
NAG1-859 ..... p 561 N93-12655
NAG1-974 ..... p 530 N93-12929
NAG1-983 ..... p 686 N93-13293
NAG10-0103 ..... p 520 N93-12910
NAG2-427 ..... p 675 N93-13061
NAG2-593 ..... p 687 N93-13695
NAG2-610 ..... p 675 N93-13449
NAG2-668 ..... p 687 N93-13734
NAG3-1301 ..... p 599 N93-13668
NAG3-38 ..... p 626 N93-13260
NAG3-822 ..... p 624 N93-13029
NAG3-836 ..... p 587 N93-13453
NAG3-867 ..... p 626 N93-13290
NAG3-869 ..... p 539 N93-13763
NAG3-882 ..... p 531 N93-13309
NAG3-956 ..... p 552 N93-13459
NAG3-993 ..... p 556 N93-12728
NAG5-1057 ..... p 551 N93-13150
NAG5-1192 ..... p 644 N93-13254
NAG5-1488 ..... p 598 N93-13567
NAG5-1503 ..... p 586 N93-13402
NAG5-1535 ..... p 743 N93-13272
NAG5-1572 ..... p 679 N93-13717
NAG5-1636 ..... p 743 N93-13352
NAG5-1786 ..... p 743 N93-13272
NAG5-1790 ..... p 664 N93-13719
NAG5-1843 ..... p 748 N93-13660
NAG5-1913 ..... p 758 N93-13344
NAG5-389 ..... p 644 N93-13254
NAG5-557 ..... p 565 N93-13411
NAG5-603 ..... p 652 N93-13460
NAG5-78 ..... p 748 N93-13659
NAG5-879 ..... p 772 N93-13306
NAG8-104 ..... p 682 N93-12654
NAG9-245 ..... p 746 N93-13593
p 746 N93-13594
p 747 N93-13595
p 747 N93-13598
NAG9-357 ..... p 685 N93-13030
p 686 N93-13295
NAG9-374 ..... p 686 N93-13296
NAG9-56 ..... p 709 N93-12985
p 761 N93-13976
p 761 N93-13979
NAG9-62 ..... p 760 N93-13973
p 760 N93-13974
NAL PROJ. FC-8-121 ..... p 504 N93-13566
NAL PROJ. ST-1-166 ..... p 737 N93-13368
NASW-4066 ..... p 761 N93-13980
NASW-4102 ..... p 672 N93-13327
NASW-4324 ..... p 743 N93-12898
NASW-4336 ..... p 751 N93-13465
p 752 N93-13468
NASW-4627 ..... p 556 N93-12799
NAS1-18224 ..... p 546 N93-12771
NAS1-18450 ..... p 602 N93-13682
NAS1-18605 ..... p 696 N93-12942
p 699 N93-12986
NAS1-18833 ..... p 623 N93-12911
NAS1-18925 ..... p 519 N93-13462
NAS1-19091 ..... p 694 N93-13370
NAS1-19480 ..... p 575 N93-12717
p 696 N93-12942
NAS2-11861 ..... p 708 N93-12591
p 742 N93-12592
p 708 N93-12593
NAS3-22822 ..... p 557 N93-14012
NAS3-23944 ..... p 544 N93-12589
NAS3-24538 ..... p 626 N93-13443
p 627 N93-13444
p 627 N93-13445
NAS3-25092 ..... p 562 N93-12950
NAS3-25266 ..... p 728 N93-12967
p 510 N93-13169
p 571 N93-13286
NAS3-25270 ..... p 502 N93-12695
NAS3-25344 ..... p 711 N93-13762
NAS3-25345 ..... p 504 N93-13735
NAS3-25776 ..... p 685 N93-13291
NAS3-25975 ..... p 523 N93-13715
NAS3-25977 ..... p 512 N93-13182
NAS5-30085 ..... p 682 N93-13759
NAS5-30172 ..... p 559 N93-13604
NAS5-30309 ..... p 615 N93-13608
p 616 N93-13706
NAS5-30310 ..... p 705 N93-13606
NAS5-30375 ..... p 559 N93-13434
NAS5-31331 ..... p 661 N93-12700
NAS5-4336 ..... p 752 N93-13467
NAS7-1000 ..... p 572 N93-13563
NAS7-1029 ..... p 597 N93-13424
NAS7-1030 ..... p 598 N93-13656
NAS7-1031 ..... p 558 N93-13404
NAS7-931 ..... p 710 N93-13705
NAS7-932 ..... p 678 N93-13450
NAS7-933 ..... p 603 N93-13709
NAS7-934 ..... p 670 N93-13708
NAS7-961 ..... p 628 N93-13707
NAS7-967 ..... p 573 N93-13610
NAS7-969 ..... p 673 N93-13612
NAS7-994 ..... p 571 N93-13430
NAS7-995 ..... p 687 N93-13880
NAS8-36955 ..... p 604 N93-12656
p 742 N93-12657
p 769 N93-12658
p 525 N93-12659
p 682 N93-12675
p 682 N93-12676
p 575 N93-12688
p 719 N93-12691
p 619 N93-12692
p 649 N93-12718
p 525 N93-12874
p 619 N93-12875
p 522 N93-12893
p 709 N93-12894
p 671 N93-12901
p 672 N93-12949
p 678 N93-12966
p 506 N93-13013
p 769 N93-13014
p 522 N93-13152
p 531 N93-13311
p 614 N93-13436
p 769 N93-13475
p 710 N93-13696
p 607 N93-13797
NAS8-37336 ..... p 522 N93-13425
NAS8-37365 ..... p 526 N93-12968
NAS8-38075 ..... p 632 N93-12800
NAS8-38100 ..... p 558 N93-13021
NAS8-38488 ..... p 686 N93-13355
NAS8-38609 ..... p 709 N93-13062
NAS8-38781 ..... p 678 N93-12990
NAS8-38812 ..... p 611 N93-12919
NAS9-17053 ..... p 585 N93-13393

NAS9-17378 ..... p 556 N93-12699
NAS9-17448 ..... p 585 N93-13393
NAS9-17584 ..... p 740 N93-12814
NAS9-17900 ..... p 597 N93-13373
NAS9-18411 ..... p 585 N93-13393
NAS9-18426 ..... p 517 N93-12690
NCA2-653 ..... p 565 N93-13354
NCC1-147 ..... p 575 N93-12677
NCC1-55 ..... p 537 N93-12935
NCC2-297 ..... p 724 N93-13570
NCC2-374 ..... p 587 N93-13406
NCC2-387 ..... p 684 N93-12801
p 685 N93-13063
p 693 N93-13366
p 686 N93-13408
p 697 N93-13409
p 687 N93-13694
NCC2-481 ..... p 694 N93-13376
NCC2-540 ..... p 491 N93-12721
NCC2-677 ..... p 491 N93-12721
NCC2-698 ..... p 583 N93-13277
NCC2-759 ..... p 503 N93-12903
NCC5-29 ..... p 664 N93-13718
NCC9-16 ..... p 685 N93-13004
p 738 N93-13737
NGT-21-002-823 ..... p 608 N93-14010
NIST-60NANB7D0743 ..... p 559 N93-13642
NR PROJ. RV3-6121 ..... p 570 N93-12725
NR PROJ. R36-25 ..... p 528 N93-12584
NR PROJ. S01-66 ..... p 561 N93-12623
NSF AST-84-21304 ..... p 744 N93-13581
NSF AST-88-14515 ..... p 744 N93-13580
NSF ATM-83-04330 ..... p 651 N93-12969
NSF ATM-85-01380 ..... p 651 N93-12969
NSF ATM-85-11316 ..... p 651 N93-12969
NSF CCR-87-17942 ..... p 697 N93-13409
NSF CCR-88-09615 ..... p 686 N93-13408
NSF CCR-88-20279 ..... p 696 N93-12701
NSF CHE-89-13800 ..... p 537 N93-12935
NSF DAR-79-24705 ..... p 761 N93-13979
NSF DDM-90-01750 ..... p 696 N93-12640
NSF DDM-92-01340 ..... p 696 N93-12640
NSF DMS-90-00053 ..... p 696 N93-12847
NSF DMS-90-00376 ..... p 696 N93-12640
NSF DMS-91-03104 ..... p 696 N93-12942
NSF EAR-90-18468 ..... p 672 N93-13457
p 669 N93-13458
NSF SES-84-08134 ..... p 683 N93-12730
NSF SRS-91-00672 ..... p 741 N93-13544
NSF SRS-91-00714 ..... p 729 N93-12694
p 729 N93-12802
p 731 N93-13701
NSG-1601 ..... p 620 N93-13435
N00014-81-K-0382 ..... p 566 N93-13869
N00014-82-C-0280 ..... p 536 N93-12618
N00014-82-C-0700 ..... p 745 N93-13585
N00014-82-K-0295 ..... p 683 N93-12730
N00014-82-K-0612 ..... p 595 N93-12619
N00014-86-K-0542 ..... p 561 N93-12615
N00014-86-K-0554 ..... p 681 N93-12707
N00014-88-K-0133 ..... p 736 N93-13117
p 573 N93-13650
N00014-88-K-0166 ..... p 685 N93-12961
N00014-89-J-1107 ..... p 633 N93-13085
p 633 N93-13086
p 569 N93-13087
N00014-89-J-1239 ..... p 642 N93-12870
N00014-89-J-1492 ..... p 683 N93-12763
N00014-89-J-1581 ..... p 574 N93-12617
N00014-89-J-1640 ..... p 675 N93-13116
N00014-89-J-1864 ..... p 720 N93-12748
N00014-89-J-3153 ..... p 698 N93-12709
N00014-90-C-0201 ..... p 722 N93-13100
N00014-90-C-0225 ..... p 720 N93-12758
N00014-90-J-1030 ..... p 696 N93-12701
N00014-90-J-1080 ..... p 566 N93-13869
N00014-90-J-1288 ..... p 660 N93-12558
N00014-90-J-1366 ..... p 774 N93-12696
N00014-90-J-1559 ..... p 570 N93-12650
p 545 N93-12651
p 545 N93-12749
p 545 N93-12753
p 545 N93-12754
p 545 N93-12755
N00014-90-J-4014 ..... p 609 N93-12604
N00014-91-C-0124 ..... p 541 N93-12746
N00014-91-J-1034 ..... p 696 N93-12942
N00014-91-J-1036 ..... p 702 N93-12947
N00014-91-J-1063 ..... p 725 N93-13881
N00014-91-J-1151 ..... p 561 N93-12620
N00014-91-J-1283 ..... p 565 N93-13375
N00014-91-J-1306 ..... p 732 N93-12553
N00014-91-J-1384 ..... p 696 N93-12594
N00014-91-J-1528 ..... p 540 N93-12595
N00014-91-J-1617 ..... p 550 N93-13026
N00014-91-J-1628 ..... p 560 N93-12608
N00014-91-J-1647 ..... p 668 N93-12577
p 669 N93-12599
N00014-91-J-1653 ..... p 671 N93-12871
N00014-91-J-1964 ..... p 669 N93-12742
N00014-91-J-4045 ..... p 570 N93-12731
N00014-91-J-4114 ..... p 574 N93-14034
N00014-91-K-2019 ..... p 719 N93-12648
N00014-92-J-1254 ..... p 697 N93-12702
N00014-92-J-1558 ..... p 675 N93-13252
N00039-91-C-0072 ..... p 668 N93-12577
N00140-87-C-8904 ..... p 687 N93-13695
N61331-89-D-0021 ..... p 632 N93-12869
N62269-90-0022-5931 ..... p 499 N93-12613
PROJ. K7-17 ..... p 675 N93-13449
PROJ. 3307 ..... p 559 N93-13604
PROJ. 40220-CL-378 ..... p 634 N93-13094
PROJ. 70085 ..... p 559 N93-13648
PROJ. 89-03 ..... p 526 N93-13429
PROJ. 9020 ..... p 691 N93-13156
RICIS PROJ. IR-01A ..... p 738 N93-13737
RICIS PROJ. SE-37 ..... p 685 N93-13004
RTOP 144-50-50 ..... p 562 N93-12950
RTOP 199-04-16-11 ..... p 674 N93-13023
p 772 N93-13572
RTOP 316-60-13 ..... p 685 N93-13291
RTOP 324-02-01-01 ..... p 694 N93-13370
RTOP 469-01-11-02 ..... p 625 N93-13125
RTOP 505-40-61 ..... p 521 N93-12720
RTOP 505-59-00 ..... p 491 N93-12721
RTOP 505-59-54-02 ..... p 598 N93-13661
RTOP 505-62-21-00 ..... p 597 N93-13410
RTOP 505-62-50 ..... p 597 N93-13307
RTOP 505-62-52 ..... p 728 N93-12967
p 689 N93-13154
RTOP 505-62-91 ..... p 626 N93-13443
p 627 N93-13444
p 627 N93-13445
RTOP 505-63-36 ..... p 610 N93-12736
RTOP 505-63-40 ..... p 596 N93-12681
RTOP 505-63-5B ..... p 622 N93-12738
RTOP 505-63-50-04 ..... p 530 N93-12929
RTOP 505-63-50-15 ..... p 500 N93-13565
RTOP 505-63-50 ..... p 528 N93-12590
p 623 N93-12911
p 532 N93-13428
RTOP 505-64-10-05 ..... p 684 N93-12957
RTOP 505-64-40-01 ..... p 504 N93-13068
RTOP 505-64-52-03 ..... p 504 N93-13367
RTOP 505-66-01 ..... p 503 N93-12815
RTOP 505-68-30-03 ..... p 493 N93-13353
RTOP 505-69-20-01 ..... p 491 N93-13025
RTOP 505-90-52-01 ..... p 575 N93-12717
p 696 N93-12942
p 699 N93-12986
RTOP 506-32-31 ..... p 526 N93-13283
RTOP 506-40-00 ..... p 683 N93-12719
RTOP 506-41-21 ..... p 527 N93-14079
RTOP 506-42-31 ..... p 525 N93-12638
RTOP 506-43-11 ..... p 552 N93-13441
RTOP 506-43-31 ..... p 527 N93-12895
p 528 N93-12896
RTOP 506-48-4C ..... p 523 N93-13715
RTOP 506-48-91-08 ..... p 545 N93-12769
RTOP 506-49-64-01 ..... p 519 N93-13462
RTOP 506-62-21 ..... p 708 N93-12591
p 742 N93-12592
p 708 N93-12593
RTOP 510-01-0A ..... p 625 N93-13157
RTOP 510-01-50 ..... p 529 N93-12737
RTOP 533-02-36 ..... p 502 N93-13155
RTOP 533-02-38 ..... p 493 N93-13322
RTOP 535-03-10 ..... p 502 N93-12695
RTOP 535-05-10 ..... p 492 N93-13292
RTOP 553-13-00 ..... p 622 N93-12735
p 622 N93-12739
p 625 N93-13153
RTOP 590-14-11-01 ..... p 694 N93-13442
RTOP 590-21-11 ..... p 626 N93-13260
p 626 N93-13290
RTOP 593-11-11-01 ..... p 519 N93-13379
RTOP 593-42-21-01 ..... p 771 N93-13020
RTOP 593-42-31-01 ..... p 520 N93-12876
p 771 N93-13126
RTOP 656-80-02-26 ..... p 736 N93-13131
RTOP 679-40-00 ..... p 571 N93-13286
RTOP 740-00-00 ..... p 508 N93-13158
RTOP 763-21-51 ..... p 663 N93-13288
SBIR-04.90-5050 ..... p 628 N93-13707
SBIR-06.05-4100 ..... p 678 N93-13450
SBIR-06.06-4242 ..... p 687 N93-13880
SBIR-07.10-0396 ..... p 682 N93-13759
SBIR-08.01-0540A ..... p 615 N93-13608
p 616 N93-13706
SBIR-08.02-8591 ..... p 603 N93-13709
SBIR-08.03-8629 ..... p 558 N93-13404
SBIR-08.04-2701 ..... p 705 N93-13606
SBIR-08.06-4131 ..... p 571 N93-13430
SBIR-08.07-1167 ..... p 710 N93-13705
SBIR-08.15-1315 ..... p 673 N93-13612
p 670 N93-13708
SBIR-08.26-5649 ..... p 598 N93-13656
SBIR-08.27-8712 ..... p 597 N93-13424
SBIR-09.02-5050 ..... p 522 N93-13425
SBIR-09.07-3800 ..... p 559 N93-13604
SBIR-10.08-1140 ..... p 573 N93-13610
SBIR-14.06-6642A ..... p 572 N93-13563
SRC-92-DP-109 ..... p 572 N93-13569
SWRI PROJ 3178-2.9 ..... p 611 N93-12936
SWRI PROJ. 15-4914 ..... p 758 N93-13344
SWRI PROJ. 15-4945 ..... p 759 N93-13568
SWRI PROJ. 15-4971 ..... p 769 N93-12669
W-31-109-ENG-38 ..... p 719 N93-12562
p 540 N93-12573
p 683 N93-12686
p 541 N93-12798
p 720 N93-12807
p 735 N93-12808
p 720 N93-12819
p 681 N93-12823
p 735 N93-12824
p 720 N93-12854
p 541 N93-12879
p 721 N93-12881
p 642 N93-12885
p 542 N93-12973
p 735 N93-12994
p 638 N93-13069
p 702 N93-13070
p 722 N93-13104
p 703 N93-13194
p 722 N93-13195
p 612 N93-13236
p 703 N93-13246
p 723 N93-13349
p 645 N93-13479
p 705 N93-13531
p 705 N93-13546
p 723 N93-13547
W-7405-ENG-36 ..... p 690 N93-12559
p 603 N93-12560
p 690 N93-12564
p 609 N93-12565
p 674 N93-12566
p 733 N93-12567
p 749 N93-12587
p 701 N93-12588
p 641 N93-12684
p 641 N93-12685
p 691 N93-12791
p 713 N93-12809
p 649 N93-12841
p 720 N93-12853
p 557 N93-12922
p 637 N93-12923
p 749 N93-12956
p 714 N93-12997
p 550 N93-12999
p 563 N93-13045
p 689 N93-13046
p 715 N93-13047
p 662 N93-13075
p 702 N93-13076
p 722 N93-13118
p 704 N93-13281
p 639 N93-13313
p 551 N93-13315
p 613 N93-13321
p 743 N93-13339
p 538 N93-13341
p 743 N93-13342
p 605 N93-13507
p 708 N93-13508
p 710 N93-13509
p 565 N93-13510
p 524 N93-13516
p 675 N93-13522
p 753 N93-13523
p 543 N93-13545
W-7405-ENG-48 ..... p 603 N93-12570
p 712 N93-12571
p 596 N93-12762
p 541 N93-12790
p 701 N93-12806
p 576 N93-12825
p 596 N93-12831
p 576 N93-12839
p 525 N93-12840
p 642 N93-12880
p 642 N93-12884
p 721 N93-12887
p 550 N93-12888
p 576 N93-12912

p 604 N93-12925
p 643 N93-12926
p 643 N93-12927
p 550 N93-12931
p 714 N93-12932
p 555 N93-12933
p 706 N93-12970
p 714 N93-12971
p 721 N93-12972
p 735 N93-13000
p 715 N93-13044
p 715 N93-13105
p 565 N93-13357
p 606 N93-13534
p 753 N93-13536
p 552 N93-13538
p 645 N93-13615
p 738 N93-13619
p 646 N93-13646
p 606 N93-13653
p 646 N93-13654
p 646 N93-13655
p 718 N93-13732

W-7405-ENG-82 ..... p 596 N93-12921
p 620 N93-13071
p 721 N93-13089
p 531 N93-13264
p 558 N93-13298

Typical Report Number Index Listing

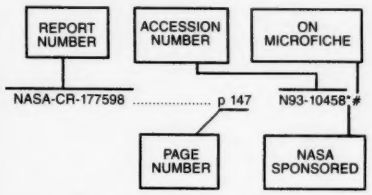

Listings in this index are arranged alphanumerically by report number. The accession number denotes the number by which the citation is identified. The page number helps to locate the citation in the abstract section. An asterisk (*) indicates that the item is a NASA report. A pound sign (#) indicates that the item is available on microfiche.

A-91099 ..... p 503 N93-12815 * #
A-92019 ..... p 683 N93-12719 * #
A-92107 ..... p 527 N93-12895 * #
A-92149 ..... p 521 N93-12720 * #
A-92159 ..... p 491 N93-12721 * #
A-92174 ..... p 528 N93-12896 * #

AD-A245362 ..... p 544 N93-13945 #
AD-A246711 ..... p 567 N93-13878 #
AD-A248651 ..... p 543 N93-13733 #
AD-A249267 ..... p 628 N93-13637 #
AD-A252602 ..... p 567 N93-13939 #
AD-A252974 ..... p 711 N93-13879 #
AD-A253038 ..... p 774 N93-12696 #
AD-A253232 ..... p 651 N93-13276 #
AD-A253606 ..... p 537 N93-13096 #
AD-A253614 ..... p 675 N93-13252 #
AD-A253615 ..... p 531 N93-13324 #
AD-A253616 ..... p 552 N93-13325 #
AD-A253672 ..... p 644 N93-13098 #
AD-A253797 ..... p 725 N93-13881 #
AD-A253866 ..... p 698 N93-13064 #
AD-A253918 ..... p 662 N93-13099 #
AD-A254119 ..... p 722 N93-13100 #
AD-A254237 ..... p 634 N93-13333 #
AD-A254323 ..... p 503 N93-12959 #
AD-A254325 ..... p 529 N93-12842 #
AD-A254327 ..... p 677 N93-12960 #
AD-A254335 ..... p 685 N93-12961 #
AD-A254342 ..... p 522 N93-12962 #
AD-A254343 ..... p 525 N93-12963 #
AD-A254347 ..... p 562 N93-12948 #
AD-A254348 ..... p 650 N93-12943 #
AD-A254349 ..... p 650 N93-12944 #
AD-A254359 ..... p 674 N93-12945 #
AD-A254360 ..... p 650 N93-12946 #
AD-A254369 ..... p 702 N93-12947 #
AD-A254380 ..... p 775 N93-12859 #
AD-A254381 ..... p 677 N93-12860 #
AD-A254382 ..... p 661 N93-12861 #
AD-A254384 ..... p 661 N93-12862 #
AD-A254385 ..... p 623 N93-12863 #
AD-A254395 ..... p 619 N93-12864 #
AD-A254406 ..... p 683 N93-12763 #
AD-A254408 ..... p 609 N93-12604 #
AD-A254410 ..... p 499 N93-12605 #
AD-A254411 ..... p 621 N93-12606 #
AD-A254413 ..... p 691 N93-12607 #
AD-A254418 ..... p 560 N93-12608 #
AD-A254431 ..... p 696 N93-12594 #
AD-A254435 ..... p 540 N93-12595 #
AD-A254436 ..... p 660 N93-12596 #
AD-A254447 ..... p 733 N93-12597 #
AD-A254448 ..... p 674 N93-12905 #
AD-A254449 ..... p 632 N93-12598 #
AD-A254455 ..... p 677 N93-12609 #
AD-A254457 ..... p 774 N93-12764 #
AD-A254458 ..... p 774 N93-12765 #
AD-A254459 ..... p 774 N93-12766 #
AD-A254460 ..... p 774 N93-12767 #
AD-A254478 ..... p 560 N93-12574 #
AD-A254484 ..... p 525 N93-12575 #
AD-A254493 ..... p 677 N93-12576 #
AD-A254506 ..... p 683 N93-12722 #
AD-A254509 ..... p 734 N93-12723 #
AD-A254510 ..... p 609 N93-12724 #
AD-A254514 ..... p 570 N93-12725 #
AD-A254525 ..... p 668 N93-12577 #
AD-A254526 ..... p 669 N93-12599 #
AD-A254532 ..... p 609 N93-12600 #
AD-A254535 ..... p 699 N93-12601 #
AD-A254537 ..... p 499 N93-12602 #
AD-A254543 ..... p 540 N93-12603 #
AD-A254545 ..... p 604 N93-12610 #
AD-A254546 ..... p 519 N93-12611 #
AD-A254550 ..... p 674 N93-12612 #
AD-A254552 ..... p 696 N93-12640 #
AD-A254554 ..... p 681 N93-12641 #
AD-A254555 ..... p 708 N93-12642 #
AD-A254561 ..... p 622 N93-12643 #
AD-A254566 ..... p 604 N93-12644 #
AD-A254569 ..... p 507 N93-13882 #
AD-A254571 ..... p 682 N93-12645 #
AD-A254573 ..... p 561 N93-12646 #
AD-A254575 ..... p 682 N93-12647 #
AD-A254577 ..... p 719 N93-12648 #
AD-A254581 ..... p 674 N93-12649 #
AD-A254595 ..... p 499 N93-12613 #
AD-A254596 ..... p 503 N93-12578 #
AD-A254601 ..... p 682 N93-12614 #
AD-A254609 ..... p 561 N93-12615 #
AD-A254617 ..... p 541 N93-12616 #
AD-A254619 ..... p 611 N93-12906 #
AD-A254625 ..... p 634 N93-13345 #
AD-A254627 ..... p 574 N93-12617 #
AD-A254630 ..... p 521 N93-12579 #
AD-A254641 ..... p 620 N93-12580 #
AD-A254643 ..... p 536 N93-12618 #
AD-A254644 ..... p 595 N93-12619 #
AD-A254645 ..... p 676 N93-12662 #
AD-A254646 ..... p 561 N93-12620 #
AD-A254654 ..... p 773 N93-12663 #
AD-A254655 ..... p 773 N93-12664 #
AD-A254656 ..... p 773 N93-12665 #
AD-A254665 ..... p 648 N93-12621 #
AD-A254682 ..... p 709 N93-12666 #
AD-A254687 ..... p 499 N93-13348 #
AD-A254688 ..... p 499 N93-13351 #
AD-A254701 ..... p 660 N93-12622 #
AD-A254704 ..... p 541 N93-12746 #
AD-A254745 ..... p 596 N93-12844 #
AD-A254746 ..... p 650 N93-12845 #
AD-A254747 ..... p 689 N93-12846 #
AD-A254748 ..... p 696 N93-12847 #
AD-A254752 ..... p 689 N93-12848 #
AD-A254755 ..... p 775 N93-12849 #
AD-A254756 ..... p 709 N93-12850 #
AD-A254761 ..... p 698 N93-12865 #
AD-A254767 ..... p 696 N93-12701 #
AD-A254769 ..... p 697 N93-12702 #
AD-A254770 ..... p 570 N93-12866 #
AD-A254772 ..... p 562 N93-12867 #
AD-A254795 ..... p 734 N93-12703 #
AD-A254797 ..... p 562 N93-12747 #
AD-A254801 ..... p 720 N93-12748 #
AD-A254803 ..... p 545 N93-12749 #
AD-A254807 ..... p 720 N93-12750 #
AD-A254809 ..... p 674 N93-12751 #
AD-A254810 ..... p 500 N93-12752 #
AD-A254815 ..... p 545 N93-12753 #
AD-A254817 ..... p 545 N93-12754 #
AD-A254818 ..... p 545 N93-12755 #
AD-A254820 ..... p 545 N93-12729 #
AD-A254821 ..... p 683 N93-12730 #
AD-A254825 ..... p 570 N93-12731 #
AD-A254826 ..... p 677 N93-12732 #
AD-A254831 ..... p 688 N93-12733 #
AD-A254833 ..... p 604 N93-12734 #
AD-A254917 ..... p 570 N93-12650 #
AD-A254918 ..... p 545 N93-12651 #
AD-A254927 ..... p 649 N93-12704 #
AD-A254928 ..... p 550 N93-13026 #
AD-A254931 ..... p 696 N93-13027 #
AD-A254932 ..... p 560 N93-12581 #
AD-A254937 ..... p 719 N93-12544 #
AD-A254939 ..... p 676 N93-12545 #
AD-A254941 ..... p 727 N93-12546 #
AD-A254947 ..... p 690 N93-12547 #
AD-A254948 ..... p 690 N93-12548 #
AD-A254950 ..... p 688 N93-12549 #
AD-A254951 ..... p 632 N93-12550 #
AD-A254954 ..... p 560 N93-12551 #
AD-A254958 ..... p 506 N93-12552 #
AD-A254961 ..... p 732 N93-12553 #
AD-A254963 ..... p 682 N93-12554 #
AD-A254968 ..... p 609 N93-12555 #
AD-A254969 ..... p 668 N93-12556 #
AD-A254978 ..... p 499 N93-12557 #
AD-A255001 ..... p 608 N93-13883 #
AD-A255002 ..... p 712 N93-12705 #
AD-A255003 ..... p 570 N93-12868 #
AD-A255004 ..... p 774 N93-12706 #
AD-A255007 ..... p 632 N93-12869 #
AD-A255009 ..... p 642 N93-12870 #
AD-A255010 ..... p 671 N93-12871 #
AD-A255013 ..... p 681 N93-12707 #
AD-A255015 ..... p 575 N93-12708 #
AD-A255016 ..... p 660 N93-12558 #
AD-A255017 ..... p 695 N93-12582 #
AD-A255021 ..... p 528 N93-12583 #
AD-A255022 ..... p 528 N93-12584 #
AD-A255032 ..... p 560 N93-12585 #
AD-A255034 ..... p 698 N93-12709 #
AD-A255035 ..... p 688 N93-12710 #
AD-A255054 ..... p 675 N93-13116 #
AD-A255068 ..... p 736 N93-13117 #
AD-A255069 ..... p 573 N93-13650 #
AD-A255070 ..... p 491 N93-13946 #
AD-A255074 ..... p 684 N93-12851 #
AD-A255075 ..... p 684 N93-12872 #
AD-A255076 ..... p 689 N93-12852 #
AD-A255077 ..... p 683 N93-12740 #
AD-A255078 ..... p 492 N93-12741 #
AD-A255086 ..... p 669 N93-12742 #
AD-A255088 ..... p 561 N93-12623 #
AD-A255090 ..... p 536 N93-12743 #
AD-A255091 ..... p 674 N93-12756 #
AD-A255094 ..... p 529 N93-12757 #
AD-A255095 ..... p 720 N93-12758 #
AD-A255097 ..... p 622 N93-12652 #
AD-A255098 ..... p 596 N93-12653 #
AD-A255203 ..... p 534 N93-13940 #
AD-A255213 ..... p 673 N93-13863 #
AD-A255222 ..... p 554 N93-13862 #
AD-A255223 ..... p 731 N93-13834 #
AD-A255224 ..... p 675 N93-13941 #
AD-A255225 ..... p 687 N93-13835 #
AD-A255229 ..... p 553 N93-13836 #
AD-A255233 ..... p 573 N93-13837 #
AD-A255252 ..... p 697 N93-13886 #
AD-A255256 ..... p 566 N93-13838 #
AD-A255368 ..... p 608 N93-13864 #
AD-A255438 ..... p 574 N93-13865 #
AD-A255503 ..... p 574 N93-13839 #
AD-A255505 ..... p 711 N93-13866 #
AD-A255511 ..... p 635 N93-13867 #
AD-A255514 ..... p 566 N93-13868 #
AD-A255518 ..... p 566 N93-13869 #
AD-A255521 ..... p 524 N93-13870 #
AD-A255526 ..... p 566 N93-13871 #
AD-A255527 ..... p 505 N93-13872 #
AD-A255542 ..... p 554 N93-13873 #
AD-A255544 ..... p 679 N93-13874 #
AD-A255555 ..... p 567 N93-13875 #
AD-A255556 ..... p 620 N93-13876 #
AD-A255559 ..... p 667 N93-13877 #
AD-A255690 ..... p 608 N93-14023 #
AD-A255703 ..... p 498 N93-14024 #
AD-A255766 ..... p 498 N93-14026 #
AD-A255785 ..... p 676 N93-14027 #
AD-A255786 ..... p 676 N93-14028 #

AD-A255820 ..... p 554 N93-14029 #
AD-A255821 ..... p 711 N93-14031 #
AD-A255823 ..... p 711 N93-14032 #
AD-A255824 ..... p 540 N93-14033 #
AD-A255825 ..... p 574 N93-14034 #
AD-A255828 ..... p 544 N93-14098 #
AD-A255832 ..... p 697 N93-14081 #
AD-A255834 ..... p 668 N93-14082 #
AD-A255835 ..... p 727 N93-14083 #
AD-A255842 ..... p 676 N93-14084 #
AD-A255845 ..... p 608 N93-14085 #
AD-A255865 ..... p 688 N93-13942 #
AD-A255887 ..... p 671 N93-13943 #
AD-A255889 ..... p 688 N93-13944 #
AD-A255892 ..... p 697 N93-14036 #
AD-A255897 ..... p 603 N93-14086 #
AD-A255898 ..... p 524 N93-14087 #
AD-A255901 ..... p 708 N93-14089 #
AD-A255909 ..... p 554 N93-14099 #
AD-A255918 ..... p 680 N93-14090 #

AD-D015358 ..... p 551 N93-13101 #
AD-D015359 ..... p 552 N93-13414 #
AD-D015373 ..... p 710 N93-13500 #
AD-D015374 ..... p 597 N93-13501 #
AD-D015375 ..... p 556 N93-13471 #
AD-D015376 ..... p 572 N93-13472 #
AD-D015377 ..... p 572 N93-13473 #

AD-E201051 ..... p 662 N93-13099 #
AD-E201102 ..... p 691 N93-12607 #
AD-E201121 ..... p 562 N93-12948 #
AD-E201133 ..... p 650 N93-12943 #
AD-E201136 ..... p 650 N93-12944 #
AD-E201154 ..... p 525 N93-12963 #
AD-E201156 ..... p 632 N93-12550 #
AD-E201161 ..... p 560 N93-12551 #
AD-E201165 ..... p 522 N93-12962 #
AD-E501561 ..... p 560 N93-12574 #
AD-E501563 ..... p 688 N93-12549 #

AFIT/CI/CIA-92-004D ..... p 567 N93-13939 #
AFIT/CI/CIA-92-009D ..... p 570 N93-12868 #
AFIT/CI/CIA-92-045 ..... p 661 N93-12862 #
AFIT/CI/CIA-92-047 ..... p 708 N93-12642 #
AFIT/CI/CIA-92-052 ..... p 660 N93-12596 #
AFIT/CI/CIA-92-057 ..... p 661 N93-12861 #

AFOSR-PD-89-0005 ..... p 573 N93-13837 #

AFOSR-92-0513TR-VOL-8 ..... p 709 N93-12666 #
AFOSR-92-0521TR-VOL-13 ..... p 711 N93-13879 #
AFOSR-92-0701TR ..... p 651 N93-13276 #
AFOSR-92-0704TR-VOL-1 ..... p 774 N93-12764 #
AFOSR-92-0705TR-VOL-2 ..... p 774 N93-12766 #
AFOSR-92-0706TR-VOL-3 ..... p 774 N93-12767 #
AFOSR-92-0707TR-VOL-1 ..... p 773 N93-12665 #
AFOSR-92-0707TR ..... p 682 N93-12647 #
AFOSR-92-0708TR-VOL-2 ..... p 773 N93-12663 #
AFOSR-92-0709TR-VOL-3 ..... p 775 N93-12849 #
AFOSR-92-0710TR-VOL-4 ..... p 773 N93-12664 #
AFOSR-92-0719TR-VOL-4 ..... p 774 N93-12765 #
AFOSR-92-0732TR ..... p 648 N93-12621 #
AFOSR-92-0736TR-VOL-6 ..... p 608 N93-13883 #
AFOSR-92-0738TR-VOL-8 ..... p 709 N93-12850 #
AFOSR-92-0740TR ..... p 525 N93-12575 #
AFOSR-92-0764TR ..... p 774 N93-12706 #
AFOSR-92-0783TR ..... p 503 N93-12959 #
AFOSR-92-0797TR ..... p 650 N93-12946 #
AFOSR-92-0798TR ..... p 540 N93-12603 #
AFOSR-92-0803TR ..... p 604 N93-12644 #
AFOSR-92-0808TR ..... p 521 N93-12579 #
AFOSR-92-0811TR ..... p 545 N93-12729 #
AFOSR-92-0812TR ..... p 775 N93-12859 #
AFOSR-92-0822TR ..... p 499 N93-12557 #
AFOSR-92-0823TR ..... p 690 N93-12547 #
AFOSR-92-0824TR ..... p 650 N93-12845 #
AFOSR-92-0880TR ..... p 540 N93-14033 #
AFOSR-92-0884TR ..... p 554 N93-14029 #

AFRRI-SR92-16 ..... p 674 N93-12649 #
AFRRI-SR92-17 ..... p 674 N93-12649 #

AGARD-CP-498 ..... p 577 N93-13199 #

AGARD-LS-182 ..... p 563 N93-13049 #
AGARD-LS-185 ..... p 692 N93-13238 #

AIAA PAPER 92-0339 ..... p 538 N93-13456 * #
AIAA PAPER 92-3462 ..... p 525 N93-12638 * #
AIAA PAPER 92-3463 ..... p 526 N93-13283 * #
AIAA PAPER 92-3745 ..... p 502 N93-13155 * #
AIAA PAPER 92-4102 ..... p 493 N93-13322 * #
AIAA PAPER 93-0692 ..... p 597 N93-13410 * #

AITI-1168 ..... p 738 N93-13619 #

AL-TP-1992-0020 ..... p 682 N93-12554 #
AL-TP-1992-0031 ..... p 734 N93-12723 #
AL-TP-1992-0033 ..... p 676 N93-14028 #
AL-TP-1992-0034 ..... p 676 N93-14027 #

AL-TR-1992-0011 ..... p 676 N93-12662 #
AL-TR-1992-0049 ..... p 679 N93-13874 #
AL-TR-1992-0068 ..... p 674 N93-12905 #

ANL-HEP-CP-92-46 ..... p 705 N93-13531 #

ANL/CP-74687 ..... p 541 N93-12798 #
ANL/CP-74688 ..... p 722 N93-13104 #
ANL/CP-74789 ..... p 542 N93-12973 #
ANL/CP-74791 ..... p 541 N93-12879 #
ANL/CP-74960 ..... p 705 N93-13546 #
ANL/CP-75064 ..... p 720 N93-12854 #
ANL/CP-75277 ..... p 722 N93-13195 #
ANL/CP-75386 ..... p 723 N93-13349 #
ANL/CP-76184 ..... p 612 N93-13236 #
ANL/CP-76315 ..... p 735 N93-12994 #
ANL/CP-76324 ..... p 681 N93-12823 #
ANL/CP-76332 ..... p 703 N93-13246 #
ANL/CP-76336 ..... p 703 N93-13194 #
ANL/CP-76480 ..... p 540 N93-12573 #
ANL/CP-76558 ..... p 645 N93-13479 #
ANL/CP-76560 ..... p 720 N93-12819 #
ANL/CP-76582 ..... p 719 N93-12562 #
ANL/CP-76667 ..... p 735 N93-12808 #
ANL/CP-76698 ..... p 720 N93-12807 #
ANL/CP-76725 ..... p 735 N93-12824 #
ANL/CP-76765 ..... p 642 N93-12885 #
ANL/CP-76789 ..... p 702 N93-13070 #
ANL/CP-76805 ..... p 723 N93-13547 #
ANL/CP-76870 ..... p 721 N93-12881 #

ANL/EAIS/TM-72 ..... p 683 N93-12686 #

AR-007-068 ..... p 500 N93-13256

ARCCB-TR-92024 ..... p 541 N93-12616 #
ARCCB-TR-92027 ..... p 622 N93-12643 #
ARCCB-TR-92029 ..... p 620 N93-12580 #

ARI-RN-92-62-VOL-2 ..... p 676 N93-12545 #

ARI-TR-954 ..... p 677 N93-12609 #

ARL-STRUC-TM-558 ..... p 500 N93-13256

ARL-TR-92-9 ..... p 774 N93-12696 #

ARO-24713.20-GS ..... p 561 N93-12646 #
ARO-25906.7-PH ..... p 720 N93-12750 #
ARO-26144.1-MA ..... p 562 N93-12747 #
ARO-26434.4-EL ..... p 608 N93-13864 #
ARO-26462.1-PH ..... p 608 N93-14023 #
ARO-26576.3-LS ..... p 673 N93-13863 #
ARO-26636.3-CH ..... p 537 N93-13096 #
ARO-26647.3-MS ..... p 552 N93-13325 #
ARO-26666.10-EL ..... p 719 N93-12544 #
ARO-26882.3-MS-A ..... p 531 N93-13324 #
ARO-26930.1-MA-SDI ..... p 695 N93-12582 #
ARO-27574.8-MA ..... p 698 N93-13064 #
ARO-27794.1-MS ..... p 698 N93-12865 #
ARO-28109.8-MS ..... p 711 N93-13866 #
ARO-28803.4-MA ..... p 696 N93-13027 #
ARO-28819.1-PH-CF ..... p 604 N93-12734 #

ARPAD-TR-92002 ..... p 619 N93-12864 #

ASI690-348-91 ..... p 677 N93-12609 #
ASI690-354-92-VOL-2 ..... p 676 N93-12545 #

ASL-TR-0319 ..... p 668 N93-14082 #

ASU-TN-4(MEDIANS 1) ..... p 683 N93-12722 #

ATC-182 ..... p 660 N93-12622 #
ATC-184 ..... p 498 N93-14024 #

ATM-52 ..... p 722 N93-13100 #

ATR-92(7190)-3 ..... p 705 N93-12715 * #

AU-ARI-91-1 ..... p 733 N93-12597 #

AVSCOM-TR-91-C-046 ..... p 625 N93-13153 * #
AVSCOM-TR-92-B-013 ..... p 532 N93-13428 * #
AVSCOM-TR-92-C-030 ..... p 610 N93-12736 * #

B-247693 ..... p 732 N93-13109 #
B-249568 ..... p 732 N93-13111 #
B-249927 ..... p 736 N93-13112 #

BFLRF-267 ..... p 609 N93-12600 #

BN-1127 ..... p 696 N93-12701 #

BNL-47103 ..... p 571 N93-13358 #
BNL-47273-REV ..... p 644 N93-13270 #
BNL-47594 ..... p 701 N93-12832 #
BNL-47616 ..... p 707 N93-13192 #
BNL-47797 ..... p 710 N93-13652 #

BRL-CR-694 ..... p 622 N93-12652 #

BRL-TR-3380 ..... p 529 N93-12842 #

CAR-90-3 ..... p 686 N93-13296 * #
CAR-91-4 ..... p 686 N93-13295 * #
CAR-92-3-PT-2 ..... p 685 N93-13030 * #

CCFD-92-02 ..... p 575 N93-12688 * #

CCMS-92-14 ..... p 550 N93-12858 #

CCS-RR-667 ..... p 683 N93-12730 #

CDNSWC-SME-92/25 ..... p 528 N93-12584 #

CEBAF-PR-92-024 ..... p 708 N93-13284 #

CG-D-15-92 ..... p 632 N93-12869 #

CMC-GIT-92-3 ..... p 521 N93-12579 #

CMS-TSR-92-13 ..... p 696 N93-12847 #
CMS-TSR-92-3 ..... p 696 N93-12594 #

CMU-CS-92-137 ..... p 681 N93-12641 #
CMU-CS-92-141 ..... p 688 N93-13944 #
CMU-CS-92-151 ..... p 682 N93-12645 #

CONF-910135-6 ..... p 703 N93-13187 #
CONF-9105238-7 ..... p 706 N93-12829 #
CONF-9107115-77 ..... p 604 N93-12744 #
CONF-9107160-3 ..... p 555 N93-12933 #
CONF-9107235-1-REV-1 ..... p 642 N93-12880 #
CONF-9110397-2 ..... p 641 N93-12684 #
CONF-920124-27 ..... p 606 N93-13534 #
CONF-920126-4 ..... p 702 N93-13073 #
CONF-920141-9 ..... p 722 N93-13104 #
CONF-920184-3 ..... p 743 N93-13339 #
CONF-920191-2 ..... p 749 N93-12956 #
CONF-9202103 ..... p 753 N93-13536 #
CONF-920305-14 ..... p 542 N93-13043 #
CONF-920311-24 ..... p 714 N93-12932 #
CONF-920311-25 ..... p 714 N93-12971 #
CONF-9203154-7 ..... p 705 N93-13537 #
CONF-9203159-7 ..... p 707 N93-12993 #
CONF-9203171-1 ..... p 597 N93-13267 #
CONF-9203177-1 ..... p 603 N93-12560 #
CONF-9203177-2 ..... p 604 N93-12915 #
CONF-9203181-1-REV ..... p 727 N93-12826 #
CONF-9203182-1 ..... p 539 N93-13530 #
CONF-920362-42 ..... p 717 N93-13511 #
CONF-920402-10 ..... p 723 N93-13347 #
CONF-920402-21 ..... p 722 N93-13323 #
CONF-920402-34 ..... p 721 N93-13089 #
CONF-920402-36 ..... p 703 N93-13194 #
CONF-920402-52 ..... p 701 N93-12806 #
CONF-920402-54 ..... p 550 N93-12888 #
CONF-920402-55 ..... p 552 N93-13538 #
CONF-920405-1 ..... p 706 N93-12992 #
CONF-9204120-3 ..... p 721 N93-12972 #
CONF-9204126-2 ..... p 704 N93-13250 #
CONF-9204138-SUMM ..... p 705 N93-13531 #
CONF-9204146-4 ..... p 715 N93-13044 #
CONF-9204182-1 ..... p 701 N93-12588 #
CONF-9204190-1 ..... p 555 N93-12563 #
CONF-920426-3 ..... p 683 N93-12792 #
CONF-920448-7 ..... p 549 N93-12821 #
CONF-920462-2 ..... p 723 N93-13349 #
CONF-9205108-5 ..... p 703 N93-13114 #
CONF-9205119-1 ..... p 576 N93-12839 #
CONF-9205123-6 ..... p 542 N93-13190 #
CONF-9205123-9 ..... p 542 N93-13237 #
CONF-9205137-2 ..... p 565 N93-13357 #
CONF-9205147 ..... p 638 N93-13069 #
CONF-920515-21 ..... p 716 N93-13191 #
CONF-920515-3 ..... p 706 N93-12830 #
CONF-9205166-2 ..... p 649 N93-12841 #
CONF-9205196-6 ..... p 575 N93-12711 #
CONF-920514 ..... p 735 N93-13000 #
CONF-920523-2 ..... p 604 N93-12925 #
CONF-920523-3 ..... p 603 N93-12570 #
CONF-920523-4 ..... p 712 N93-12571 #
CONF-920523-5 ..... p 606 N93-13653 #
CONF-9205236-2 ..... p 720 N93-12853 #
CONF-9205236-3 ..... p 702 N93-13037 #
CONF-9205239-1 ..... p 759 N93-13504 #
CONF-920574-12 ..... p 538 N93-13341 #

CONF-920607-19 ..... p 715 N93-13105 #
CONF-920610-11 ..... p 712 N93-12687 #
CONF-920610-6 ..... p 716 N93-13193 #
CONF-9206114-12-REV ..... p 644 N93-13270 #
CONF-920614-2 ..... p 723 N93-13547 #
CONF-9206173-7 ..... p 610 N93-12793 #
CONF-9206193-1 ..... p 707 N93-13192 #
CONF-9206193-6 ..... p 701 N93-12572 #
CONF-9206199-1 ..... p 703 N93-13246 #
CONF-9206216-1 ..... p 612 N93-13103 #
CONF-9206237-1 ..... p 677 N93-12712 #
CONF-9206241-1 ..... p 543 N93-13545 #
CONF-9206243-2 ..... p 691 N93-12791 #
CONF-9206244-1 ..... p 690 N93-12559 #
CONF-9206249-1 ..... p 749 N93-12587 #
CONF-9206249-2 ..... p 753 N93-13523 #
CONF-9206250-1 ..... p 719 N93-12586 #
CONF-9206254-2 ..... p 642 N93-12828 #
CONF-9206257-1 ..... p 643 N93-12926 * #
CONF-9206260-2 ..... p 669 N93-12916 #
CONF-9206262-1 ..... p 646 N93-13655 #
CONF-9206262-2 ..... p 646 N93-13646 #
CONF-9206262-3 ..... p 645 N93-13615 #
CONF-9206262-4 ..... p 646 N93-13654 #
CONF-920670-1 ..... p 722 N93-13195 #
CONF-920673-8 ..... p 541 N93-12820 #
CONF-920706-19 ..... p 571 N93-13358 #
CONF-920706-6 ..... p 707 N93-13090 #
CONF-920707-13 ..... p 537 N93-13233 #
CONF-920707-3 ..... p 537 N93-13232 #
CONF-920708-1 ..... p 705 N93-13546 #
CONF-9207102-46 ..... p 702 N93-13076 #
CONF-9207102-56 ..... p 565 N93-13506 #
CONF-9207124-1 ..... p 569 N93-12561 #
CONF-9207128-1 ..... p 719 N93-12562 #
CONF-920728-1 ..... p 718 N93-13651 #
CONF-920741-1 ..... p 708 N93-13574 #
CONF-920747-4 ..... p 525 N93-12840 #
CONF-920748-12 ..... p 640 N93-13621 #
CONF-920748-14 ..... p 639 N93-13313 #
CONF-920748-15 ..... p 640 N93-13622 #
CONF-920748-4 ..... p 638 N93-13082 #
CONF-920748-5 ..... p 638 N93-13040 #
CONF-920748-7 ..... p 638 N93-13041 #
CONF-920748-8 ..... p 640 N93-13623 #
CONF-920748-9 ..... p 638 N93-13039 #
CONF-920768-3 ..... p 702 N93-13070 #
CONF-920771-4 ..... p 612 N93-13236 #
CONF-920771-5 ..... p 643 N93-12927 #
CONF-920791-4 ..... p 641 N93-12685 #
CONF-920792-10 ..... p 596 N93-12762 #
CONF-920792-18 ..... p 524 N93-13516 #
CONF-920792-24 ..... p 710 N93-13652 #
CONF-920792-26 ..... p 721 N93-12881 #
CONF-920792-27 ..... p 743 N93-13342 #
CONF-920796-7 ..... p 555 N93-13081 #
CONF-920799-ABSTS ..... p 620 N93-13071 #
CONF-920801-10 ..... p 571 N93-13197 #
CONF-920801-9 ..... p 571 N93-13196 #
CONF-920804-22 ..... p 588 N93-13575 #
CONF-9208109-12 ..... p 563 N93-13045 #
CONF-9208109-19 ..... p 710 N93-13509 #
CONF-9208109-20 ..... p 708 N93-13508 #
CONF-9208109-25 ..... p 605 N93-13507 #
CONF-9208109-2 ..... p 733 N93-12567 #
CONF-9208109-3 ..... p 690 N93-12564 #
CONF-9208109-6 ..... p 565 N93-13510 #
CONF-9208109-9 ..... p 714 N93-12997 #
CONF-9208112-2 ..... p 642 N93-12884 #
CONF-9208114-2 ..... p 704 N93-13281 #
CONF-9208116-1 ..... p 571 N93-13300 #
CONF-9208123-1 ..... p 619 N93-13036 #
CONF-9208127-1 ..... p 566 N93-13512 #
CONF-920851-50 ..... p 575 N93-12761 #
CONF-920871-1 ..... p 582 N93-13247 #
CONF-920872-1 ..... p 538 N93-13234 #
CONF-920891-3 ..... p 550 N93-12999 #
CONF-920903-16 ..... p 728 N93-12857 #
CONF-920905-5 ..... p 542 N93-13302 #
CONF-9209109-2 ..... p 689 N93-12810 #
CONF-9209913-10 ..... p 713 N93-12883 #
CONF-9209913-11 ..... p 715 N93-13047 #
CONF-9209913-8 ..... p 718 N93-13535 #
CONF-9209913-9 ..... p 713 N93-12882 #
CONF-9209142-6 ..... p 735 N93-12994 #
CONF-9209143-3 ..... p 609 N93-12698 #
CONF-9209147-1 ..... p 637 N93-12923 #
CONF-9209158-3 ..... p 576 N93-12912 #
CONF-9209160-1 ..... p 645 N93-13479 #
CONF-9209160-3 ..... p 735 N93-12824 #
CONF-9209160-4 ..... p 735 N93-12808 #
CONF-9209160-6 ..... p 642 N93-12885 #
CONF-9209163-1 ..... p 662 N93-13075 #
CONF-9209164-2 ..... p 557 N93-12922 #
CONF-9209169-1 ..... p 645 N93-13505 #
CONF-9209171-2 ..... p 555 N93-12568 #
CONF-9209174-1 ..... p 626 N93-13320 #
CONF-9209175-1 ..... p 722 N93-13118 #
CONF-9209179-1 ..... p 720 N93-12854 #
CONF-9209179-2 ..... p 720 N93-12807 #
CONF-9209180-1 ..... p 681 N93-12823 #
CONF-9209181-1 ..... p 717 N93-13518 #
CONF-9209187-1 ..... p 572 N93-13519 #
CONF-920966-1 ..... p 689 N93-13046 #
CONF-920970-1 ..... p 540 N93-12573 #
CONF-920970-2 ..... p 541 N93-12798 #
CONF-920970-3 ..... p 541 N93-12879 #
CONF-920970-4 ..... p 542 N93-12973 #
CONF-9210149-1 ..... p 674 N93-12566 #
CONF-921036-5 ..... p 542 N93-13080 #
CONF-921073-1 ..... p 550 N93-12917 #
CONF-921102-14 ..... p 704 N93-13319 #
CONF-921102-8 ..... p 526 N93-13299 #
CONF-921104-1 ..... p 538 N93-13317 #
CONF-921104-2 ..... p 583 N93-13318 #
CONF-921110-10 ..... p 583 N93-13356 #
CONF-921110-12 ..... p 627 N93-13515 #
CONF-921110-13 ..... p 624 N93-13072 #
CONF-921110-14 ..... p 613 N93-13321 #
CONF-921110-17 ..... p 720 N93-12819 #
CONF-921110-24 ..... p 576 N93-12996 #
CONF-921110-25 ..... p 550 N93-12931 #
CONF-921110-6 ..... p 704 N93-13263 #
CONF-921110-8 ..... p 626 N93-13301 #
CONF-921125-1 ..... p 716 N93-13297 #
CONF-921143-1 ..... p 699 N93-13262 #
CONF-921162-5 ..... p 684 N93-12795 #
CONF-921166-1 ..... p 558 N93-13298 #
CONF-921172-1 ..... p 531 N93-13264 #
CONF-921183-1 ..... p 609 N93-12565 #
CONF-921184-1 ..... p 551 N93-13315 #
CONF-921186-1 ..... p 691 N93-13079 #
CONF-921197-1 ..... p 675 N93-13522 #

CRDEC-TR-386 ..... p 536 N93-12743 #
CRDEC-TR-399 ..... p 596 N93-12653 #
CRDEC-TR-400 ..... p 674 N93-12756 #

CRHC-92-24 ..... p 694 N93-13376 * #
CRHC-92-25 ..... p 572 N93-13569 * #
CRHC-92-27 ..... p 565 N93-13375 * #

CSDL-T-1134 ..... p 517 N93-12690 * #

CSL-N91-1 ..... p 503 N93-12578 #

CTN-92-008 ..... p 738 N93-13619 #

CU-TR-92-1306 ..... p 687 N93-13695 * #

DE91-002176 ..... p 636 N93-12837 #
DE91-017785 ..... p 718 N93-13732 #
DE92-001256 ..... p 541 N93-12790 #
DE92-001292 ..... p 639 N93-13313 #
DE92-001296 ..... p 538 N93-13314 #
DE92-0012983-3103 ..... p 636 N93-12683 #
DE92-005312 ..... p 537 N93-13232 #
DE92-006697 ..... p 537 N93-13233 #
DE92-007409 ..... p 551 N93-13315 #
DE92-010556 ..... p 538 N93-13316 #
DE92-010578 ..... p 638 N93-13102 #
DE92-010579 ..... p 627 N93-13524 #
DE92-010580 ..... p 627 N93-13525 #
DE92-010600 ..... p 637 N93-12838 #
DE92-011041 ..... p 538 N93-13317 #
DE92-011069 ..... p 706 N93-12829 #
DE92-011347 ..... p 543 N93-13346 #
DE92-011369 ..... p 743 N93-13339 #
DE92-011675 ..... p 583 N93-13318 #
DE92-011680 ..... p 716 N93-13297 #
DE92-012146 ..... p 538 N93-13234 #
DE92-012147 ..... p 582 N93-13247 #
DE92-012153 ..... p 699 N93-13262 #
DE92-014463 ..... p 723 N93-13347 #
DE92-014858 ..... p 723 N93-13349 #
DE92-014948 ..... p 706 N93-12830 #
DE92-014949 ..... p 722 N93-13323 #
DE92-015051 ..... p 552 N93-13350 #
DE92-015351 ..... p 703 N93-13187 #
DE92-015467 ..... p 537 N93-13188 #
DE92-015480 ..... p 707 N93-13189 #
DE92-015566 ..... p 596 N93-12831 #
DE92-015567 ..... p 707 N93-13235 #
DE92-015846 ..... p 704 N93-13263 #
DE92-016009 ..... p 701 N93-12832 #
DE92-016010 ..... p 644 N93-13270 #
DE92-016018 ..... p 542 N93-13190 #
DE92-016091 ..... p 716 N93-13191 #
DE92-016097 ..... p 707 N93-13192 #
DE92-016184 ..... p 612 N93-13236 #
DE92-016253 ..... p 716 N93-13193 #
DE92-016298 ..... p 531 N93-13264 #
DE92-016299 ..... p 558 N93-13298 #
DE92-016301 ..... p 721 N93-13089 #
DE92-016341 ..... p 542 N93-13237 #
DE92-016377 ..... p 703 N93-13246 #
DE92-016392 ..... p 703 N93-13194 #
DE92-016400 ..... p 526 N93-13299 #
DE92-016440 ..... p 723 N93-13526 #
DE92-016441 ..... p 639 N93-13528 #
DE92-016444 ..... p 639 N93-13529 #
DE92-016690 ..... p 704 N93-13319 #
DE92-016781 ..... p 722 N93-13195 #
DE92-016811 ..... p 571 N93-13196 #
DE92-016814 ..... p 571 N93-13197 #
DE92-016890 ..... p 571 N93-13300 #
DE92-016944 ..... p 719 N93-12586 #
DE92-017058 ..... p 626 N93-13301 #
DE92-017191 ..... p 703 N93-13114 #
DE92-017234 ..... p 539 N93-13530 #
DE92-017236 ..... p 597 N93-13267 #
DE92-017266 ..... p 575 N93-12761 #
DE92-017312 ..... p 596 N93-12762 #
DE92-017339 ..... p 612 N93-13103 #
DE92-017346 ..... p 605 N93-13249 #
DE92-017388 ..... p 545 N93-12697 #
DE92-017392 ..... p 671 N93-12768 #
DE92-017395 ..... p 609 N93-12698 #
DE92-017403 ..... p 720 N93-12853 #
DE92-017407 ..... p 538 N93-13341 #
DE92-017408 ..... p 704 N93-13281 #
DE92-017409 ..... p 749 N93-12587 #
DE92-017411 ..... p 701 N93-12588 #
DE92-017432 ..... p 576 N93-12839 #
DE92-017435 ..... p 525 N93-12840 #
DE92-017441 ..... p 649 N93-12841 #
DE92-017447 ..... p 641 N93-12684 #
DE92-017448 ..... p 674 N93-12566 #
DE92-017508 ..... p 690 N93-12559 #
DE92-017511 ..... p 691 N93-12791 #
DE92-017512 ..... p 641 N93-12685 #
DE92-017517 ..... p 603 N93-12560 #
DE92-017555 ..... p 683 N93-12686 #
DE92-017598 ..... p 704 N93-13250 #
DE92-017673 ..... p 672 N93-13269 #
DE92-017704 ..... p 712 N93-12687 #
DE92-017812 ..... p 569 N93-12561 #
DE92-017813 ..... p 626 N93-13320 #
DE92-017834 ..... p 749 N93-12956 #
DE92-017850 ..... p 583 N93-13356 #
DE92-017869 ..... p 704 N93-13251 #
DE92-017894 ..... p 683 N93-12792 #
DE92-018019 ..... p 610 N93-12793 #
DE92-018059 ..... p 565 N93-13357 #
DE92-018064 ..... p 606 N93-13534 #
DE92-018099 ..... p 737 N93-13275 #
DE92-018153 ..... p 707 N93-13090 #
DE92-018182 ..... p 719 N93-12562 #
DE92-018184 ..... p 705 N93-13531 #
DE92-018186 ..... p 722 N93-13104 #
DE92-018240 ..... p 619 N93-12794 #
DE92-018264 ..... p 555 N93-12563 #
DE92-018271 ..... p 684 N93-12795 #
DE92-018283 ..... p 627 N93-13515 #
DE92-018442 ..... p 604 N93-12744 #
DE92-018588 ..... p 703 N93-13092 #
DE92-018601 ..... p 524 N93-13516 #
DE92-018603 ..... p 690 N93-12564 #
DE92-018608 ..... p 609 N93-12565 #
DE92-018611 ..... p 743 N93-13342 #
DE92-018612 ..... p 722 N93-13118 #
DE92-018613 ..... p 733 N93-12567 #
DE92-018615 ..... p 543 N93-13545 #
DE92-018616 ..... p 613 N93-13321 #
DE92-018643 ..... p 701 N93-12745 #
DE92-018777 ..... p 638 N93-13069 #
DE92-018790 ..... p 705 N93-13546 #
DE92-018793 ..... p 702 N93-13070 #
DE92-018795 ..... p 723 N93-13547 #
DE92-018805 ..... p 596 N93-12921 #
DE92-018814 ..... p 620 N93-13071 #
DE92-018818 ..... p 624 N93-13072 #
DE92-018854 ..... p 702 N93-13073 #
DE92-018871 ..... p 577 N93-13074 #
DE92-018875 ..... p 662 N93-13075 #
DE92-018886 ..... p 557 N93-12922 #
DE92-018903 ..... p 637 N93-12923 #
DE92-018920 ..... p 702 N93-13076 #
DE92-019039 ..... p 720 N93-12819 #
DE92-019045 ..... p 718 N93-13651 #
DE92-019078 ..... p 541 N93-12820 #
DE92-019123 ..... p 575 N93-12711 #
DE92-019124 ..... p 677 N93-12712 #
DE92-019193 ..... p 624 N93-13077 #
DE92-019194 ..... p 736 N93-13078 #
DE92-019205 ..... p 691 N93-13079 #
DE92-019252 ..... p 710 N93-13652 #
DE92-019283 ..... p 542 N93-13080 #

DE92-019285 ..... p 549 N93-12821 #
DE92-019286 ..... p 706 N93-12822 #
DE92-019292 ..... p 727 N93-12796 #
DE92-019301 ..... p 689 N93-12797 #
DE92-019339 ..... p 759 N93-13504 #
DE92-019340 ..... p 555 N93-13081 #
DE92-019356 ..... p 638 N93-13082 #
DE92-019360 ..... p 645 N93-13505 #
DE92-019364 ..... p 706 N93-12924 #
DE92-019374 ..... p 604 N93-12925 #
DE92-019376 ..... p 643 N93-12926 * #
DE92-019381 ..... p 576 N93-12912 #
DE92-019393 ..... p 705 N93-12713 #
DE92-019394 ..... p 713 N93-12873 #
DE92-019395 ..... p 714 N93-12913 #
DE92-019396 ..... p 714 N93-12914 #
DE92-019424 ..... p 565 N93-13506 #
DE92-019425 ..... p 555 N93-12568 #
DE92-019427 ..... p 604 N93-12915 #
DE92-019431 ..... p 669 N93-12916 #
DE92-019437 ..... p 550 N93-12917 #
DE92-019464 ..... p 709 N93-12918 #
DE92-019494 ..... p 718 N93-13535 #
DE92-019499 ..... p 571 N93-13358 #
DE92-019507 ..... p 716 N93-13359 #
DE92-019516 ..... p 574 N93-12569 #
DE92-019542 ..... p 603 N93-12570 #
DE92-019543 ..... p 712 N93-12571 #
DE92-019544 ..... p 753 N93-13536 #
DE92-019546 ..... p 701 N93-12806 #
DE92-019549 ..... p 721 N93-12887 #
DE92-019551 ..... p 705 N93-13537 #
DE92-019553 ..... p 701 N93-12572 #
DE92-019570 ..... p 706 N93-12970 #
DE92-019573 ..... p 552 N93-13538 #
DE92-019574 ..... p 550 N93-12888 #
DE92-019575 ..... p 550 N93-12931 #
DE92-019576 ..... p 606 N93-13653 #
DE92-019577 ..... p 714 N93-12971 #
DE92-019579 ..... p 714 N93-12932 #
DE92-019580 ..... p 555 N93-12933 #
DE92-019581 ..... p 721 N93-12972 #
DE92-019584 ..... p 541 N93-12879 #
DE92-019585 ..... p 542 N93-12973 #
DE92-019586 ..... p 540 N93-12573 #
DE92-019587 ..... p 541 N93-12798 #
DE92-019593 ..... p 720 N93-12854 #
DE92-019594 ..... p 681 N93-12823 #
DE92-019595 ..... p 645 N93-13479 #
DE92-019597 ..... p 720 N93-12807 #
DE92-019598 ..... p 735 N93-12808 #
DE92-019599 ..... p 735 N93-12824 #
DE92-019616 ..... p 643 N93-12927 #
DE92-019617 ..... p 642 N93-12884 #
DE92-019618 ..... p 646 N93-13654 #
DE92-019619 ..... p 646 N93-13655 #
DE92-019620 ..... p 646 N93-13646 #
DE92-019621 ..... p 645 N93-13615 #
DE92-019622 ..... p 642 N93-12880 #
DE92-019640 ..... p 576 N93-12825 #
DE92-019644 ..... p 706 N93-12992 #
DE92-019645 ..... p 727 N93-12826 #
DE92-019647 ..... p 707 N93-12993 #
DE92-019670 ..... p 642 N93-12885 #
DE92-019671 ..... p 721 N93-12881 #
DE92-019684 ..... p 539 N93-13616 #
DE92-019696 ..... p 735 N93-12994 #
DE92-019719 ..... p 539 N93-13617 #
DE92-019744 ..... p 720 N93-12827 #
DE92-019745 ..... p 537 N93-12995 #
DE92-019746 ..... p 702 N93-12855 #
DE92-019758 ..... p 713 N93-12856 #
DE92-019763 ..... p 728 N93-12857 #
DE92-019766 ..... p 576 N93-12996 #
DE92-019783 ..... p 715 N93-13105 #
DE92-019805 ..... p 640 N93-13618 #
DE92-019808 ..... p 738 N93-13619 #
DE92-019813 ..... p 703 N93-13106 #
DE92-019876 ..... p 716 N93-13107 #
DE92-019911 ..... p 550 N93-12858 #
DE92-019916 ..... p 672 N93-13083 #
DE92-019917 ..... p 672 N93-13034 #
DE92-019927 ..... p 681 N93-12886 #
DE92-019928 ..... p 690 N93-13620 #
DE92-019931 ..... p 550 N93-13035 #
DE92-019934 ..... p 619 N93-13036 #
DE92-019946 ..... p 642 N93-12828 #
DE92-019952 ..... p 702 N93-13037 #
DE92-019960 ..... p 715 N93-13038 #
DE92-019962 ..... p 713 N93-12809 #
DE92-019965 ..... p 689 N93-12810 #
DE92-019971 ..... p 640 N93-13621 #
DE92-019976 ..... p 638 N93-13039 #
DE92-019977 ..... p 640 N93-13622 #
DE92-019978 ..... p 640 N93-13623 #
DE92-019979 ..... p 638 N93-13040 #
DE92-019981 ..... p 638 N93-13041 #
DE92-019982 ..... p 713 N93-12811 #
DE92-040011 ..... p 563 N93-13042 #
DE92-040013 ..... p 539 N93-13573 #
DE92-040014 ..... p 717 N93-13502 #
DE92-040027 ..... p 708 N93-13574 #
DE92-040031 ..... p 542 N93-13043 #
DE92-040033 ..... p 717 N93-13518 #
DE92-040051 ..... p 715 N93-13044 #
DE92-040096 ..... p 542 N93-13302 #
DE92-040098 ..... p 588 N93-13575 #
DE92-040100 ..... p 572 N93-13519 #
DE92-040152 ..... p 673 N93-13520 #
DE92-040153 ..... p 673 N93-13503 #
DE92-040170 ..... p 710 N93-13576 #
DE92-040180 ..... p 636 N93-12812 #
DE92-040210 ..... p 724 N93-13577 #
DE92-040214 ..... p 605 N93-13507 #
DE92-040230 ..... p 708 N93-13508 #
DE92-040231 ..... p 710 N93-13509 #
DE92-040239 ..... p 563 N93-13045 #
DE92-040244 ..... p 675 N93-13522 #
DE92-040248 ..... p 565 N93-13510 #
DE92-040260 ..... p 717 N93-13511 #
DE92-040262 ..... p 566 N93-13512 #
DE92-040280 ..... p 653 N93-13513 #
DE92-040302 ..... p 606 N93-13514 #
DE92-040303 ..... p 772 N93-13533 #
DE92-040346 ..... p 689 N93-13046 #
DE92-040347 ..... p 715 N93-13047 #
DE92-040349 ..... p 753 N93-13523 #
DE92-040350 ..... p 714 N93-12997 #
DE92-040359 ..... p 542 N93-12998 #
DE92-040384 ..... p 550 N93-12999 #
DE92-040405 ..... p 735 N93-13000 #
DE92-040442 ..... p 637 N93-13001 #
DE92-040458 ..... p 707 N93-13002 #
DE92-040644 ..... p 623 N93-13003 #
DE92-040645 ..... p 707 N93-13108 #
DE92-040839 ..... p 735 N93-12813 #
DE92-041011 ..... p 713 N93-12882 #
DE92-041012 ..... p 713 N93-12883 #
DE92-041013 ..... p 713 N93-12878 #
DE92-041242 ..... p 736 N93-13048 #
DE93-000203 ..... p 639 N93-13427 #

DODA-AR-007-148 ..... p 683 N93-12722 #

DOE/CH-10093/147 ..... p 538 N93-13316 #
DOE/CH-10093/153 ..... p 638 N93-13102 #
DOE/CH-10093/99 ..... p 636 N93-12837 #

DOE/ER-0558T ..... p 637 N93-13001 #
DOE/ER-13188/7 ..... p 671 N93-12768 #
DOE/ER-13263/8 ..... p 543 N93-13346 #
DOE/ER-13622/T2 ..... p 542 N93-12998 #
DOE/ER-13772/5 ..... p 537 N93-12995 #
DOE/ER-14057/2 ..... p 653 N93-13513 #
DOE/ER-14129/2 ..... p 539 N93-13573 #
DOE/ER-14205/1 ..... p 703 N93-13106 #
DOE/ER-25065/3 ..... p 727 N93-12796 #
DOE/ER-40270/36 ..... p 563 N93-13042 #
DOE/ER-40335/13 ..... p 706 N93-12822 #
DOE/ER-40427/40-N91 ..... p 703 N93-13187 #
DOE/ER-40531/3 ..... p 706 N93-12924 #
DOE/ER-40561/59 ..... p 772 N93-13533 #
DOE/ER-40605/2 ..... p 702 N93-12855 #
DOE/ER-40661/3 ..... p 707 N93-13002 #
DOE/ER-40699/1 ..... p 707 N93-13189 #
DOE/ER-40706/1 ..... p 704 N93-13251 #
DOE/ER-45132/7 ..... p 724 N93-13577 #
DOE/ER-45273/6 ..... p 606 N93-13514 #
DOE/ER-45298/8 ..... p 545 N93-12697 #
DOE/ER-45396/3 ..... p 552 N93-13350 #
DOE/ER-45401/3 ..... p 720 N93-12827 #
DOE/ER-52149/4 ..... p 574 N93-12569 #
DOE/ER-53198/201 ..... p 713 N93-12878 #
DOE/ER-53198/202 ..... p 713 N93-12883 #
DOE/ER-53198/203 ..... p 713 N93-12882 #
DOE/ER-53223/180 ..... p 715 N93-13038 #
DOE/ER-53223/194 ..... p 713 N93-12811 #
DOE/ER-53279/2 ..... p 716 N93-13359 #
DOE/ER-60503/352 ..... p 672 N93-13083 #
DOE/ER-60503/353 ..... p 672 N93-13034 #
DOE/ER-60514/6 ..... p 701 N93-12745 #
DOE/ER-80910/92/C0058 ..... p 638 N93-13041 #

DOE/ET-53088/556 ..... p 705 N93-12713 #
DOE/ET-53088/560 ..... p 714 N93-12913 #
DOE/ET-53088/561 ..... p 713 N93-12873 #
DOE/ET-53088/562 ..... p 714 N93-12914 #
DOE/ET-53088/565 ..... p 716 N93-13107 #
DOE/ET-53088/8 ..... p 717 N93-13502 #

DOE/MC-24221/92/C0056 ..... p 638 N93-13040 #
DOE/MC-24223/92/C0055 ..... p 640 N93-13623 #

DOE/MC-26364/3101 ..... p 538 N93-13314 #
DOE/MC-27168/92/C0046 ..... p 640 N93-13621 #
DOE/MC-27168/92/C0051 ..... p 638 N93-13039 #
DOE/MC-27225/T5 ..... p 672 N93-13269 #
DOE/MC-27414/92/C0053 ..... p 640 N93-13622 #

DOE/MC/24223-3103 ..... p 636 N93-12683 #
DOE/MC/25009-3123 ..... p 639 N93-13427 #

DOE/METC-C/92/7021 ..... p 612 N93-13103 #

DOE/NBM-92001256 ..... p 541 N93-12790 #

DOE/PC-79931/T13 ..... p 636 N93-12812 #
DOE/PC-89786/T13 ..... p 539 N93-13617 #
DOE/PC-90044/6 ..... p 537 N93-13188 #
DOE/PC-90182/T5 ..... p 577 N93-13074 #

DOE/RA-50219/21-PT-1 ..... p 673 N93-13520 #
DOE/RA-50219/21-PT-2 ..... p 673 N93-13503 #

DOE/SW/DK-92/044A ..... p 637 N93-12937 #

DOT/FAA/AM-92/23 ..... p 674 N93-12612 #
DOT/FAA/AM-92/24 ..... p 498 N93-14026 #

DOT/FAA/AOR-100-93/007 ..... p 507 N93-13447 #

DOT/FAA/CT-TN92/21 ..... p 507 N93-13447 #
DOT/FAA/CT-TN92/23 ..... p 506 N93-12899 #
DOT/FAA/CT-TN92/25 ..... p 506 N93-12668 #
DOT/FAA/CT-TN92/29 ..... p 597 N93-13307 * #
DOT/FAA/CT-TN92/38 ..... p 497 N93-12816 #
DOT/FAA/CT-TN92/40 ..... p 537 N93-12897 #
DOT/FAA/CT-TN92/6 ..... p 499 N93-13377 #

DOT/FAA/CT-92/24 ..... p 506 N93-12902 #

DOT/FAA/NR-91/8 ..... p 660 N93-12622 #

DOT/FAA/PP-92-1 ..... p 507 N93-13882 #

DOT/FAA/RD-92/9 ..... p 551 N93-13259 #

DRD-MA-129T ..... p 556 N93-12699 * #

E-19290U ..... p 560 N93-12551 #
E-21-651 ..... p 688 N93-12733 #
E-5894 ..... p 728 N93-12967 * #
E-6558 ..... p 571 N93-13286 * #
E-7022 ..... p 492 N93-13292 * #
E-7139 ..... p 625 N93-13157 * #
E-7176 ..... p 685 N93-13291 * #
E-7182 ..... p 625 N93-13153 * #
E-7283 ..... p 622 N93-12739 * #
E-7293 ..... p 529 N93-12737 * #
E-7335 ..... p 622 N93-12738 * #
E-7346 ..... p 584 N93-13385 * #
E-7348 ..... p 622 N93-12735 * #
E-7350 ..... p 610 N93-12736 * #
E-7374 ..... p 597 N93-13307 * #
E-7387 ..... p 597 N93-13410 * #
E-7393 ..... p 527 N93-14079 * #
E-7404 ..... p 526 N93-13283 * #
E-7405 ..... p 525 N93-12638 * #
E-7415 ..... p 626 N93-13290 * #
E-7443 ..... p 689 N93-13154 * #

EGG-FSP-10262 ..... p 713 N93-12856 #
EGG-FSP-10347 ..... p 539 N93-13616 #

EGG-M-91471 ..... p 683 N93-12792 #
EGG-M-91505 ..... p 728 N93-12857 #
EGG-M-92026 ..... p 583 N93-13356 #
EGG-M-92200 ..... p 576 N93-12996 #
EGG-M-92300 ..... p 610 N93-12793 #

EPA/AA/TDG-92/05 ..... p 616 N93-13761 #

EPA/SW/DK-92/044 ..... p 643 N93-12938 #

EPA/450/3-91/030 ..... p 646 N93-13647 #
EPA/454/R-92/001 ..... p 643 N93-12940 #
EPA/540/A5-91/007 ..... p 714 N93-12982 #
EPA/600/A-92/150 ..... p 555 N93-12939 #
EPA/600/A-92/164 ..... p 643 N93-12941 #
EPA/600/A-92/178 ..... p 622 N93-12843 #
EPA/600/R-92/104A ..... p 643 N93-12938 #
EPA/600/R-92/151 ..... p 642 N93-12726 #
EPA/832/R-92/004 ..... p 678 N93-12983 #

ERIM-215055-1-F ..... p 632 N93-12869 #

ESA-BR-37-A ..... p 517 N93-13861 #
ESA-BR-37-B ..... p 516 N93-13855 #
ESA-BR-37-C ..... p 516 N93-13856 #

ESA-BR-37-D ..... p 516 N93-13857 #
ESA-BR-37-E ..... p 516 N93-13858 #
ESA-BR-37-F ..... p 517 N93-13902 #
ESA-BR-37-G ..... p 516 N93-13859 #
ESA-BR-37-H ..... p 517 N93-13860 #
ESA-BR-37-I ..... p 517 N93-13903 #
ESA-BR-52 ..... p 557 N93-12934 #
ESA-BR-64 ..... p 508 N93-12892 #
ESA-BR-83 ..... p 749 N93-12965 #
ESA-BR-85 ..... p 516 N93-13691 #

ESA-F-26 ..... p 522 N93-12964 #

ESD-TR-91-175-VOL-2 ..... p 567 N93-13878 #

E21-687 ..... p 572 N93-13448 * #

FASTC-ID(RS)T-0064-92 ..... p 676 N93-14084 #
FASTC-ID(RS)T-0608-91 ..... p 491 N93-13946 #
FASTC-ID(RS)T-0992-91 ..... p 554 N93-13873 #

FNAL-TM-1783 ..... p 707 N93-13235 #

FNAL/C-92/160-E ..... p 705 N93-13537 #
FNAL/C-92/165 ..... p 701 N93-12572 #

FR-892101 ..... p 694 N93-13370 * #
FR-92/ONR-36 ..... p 573 N93-13650 #

F89-08 ..... p 556 N93-12699 * #

GA-A-20914 ..... p 715 N93-13044 #
GA-A-20930 ..... p 716 N93-13193 #
GA-A-20942 ..... p 712 N93-12687 #

GAO/IMTEC-92-79 ..... p 736 N93-13112 #

GAO/NSIAD-92-278 ..... p 732 N93-13109 #
GAO/NSIAD-92-291BR ..... p 732 N93-13111 #

GAO/T-NSIAD-92-18 ..... p 740 N93-13280 #
GAO/T-NSIAD-92-26 ..... p 500 N93-13253 #

GE-R89AEB208 ..... p 711 N93-13762 * #

GPO-56-943-VOL-2 ..... p 741 N93-13799 #
GPO-57-099 ..... p 742 N93-13800 #
GPO-57-273 ..... p 732 N93-13693 #
GPO-59-010 ..... p 741 N93-13798 #

GRI-91/0347-REV-1 ..... p 615 N93-13644 #
GRI-92/0054 ..... p 611 N93-12936 #
GRI-92/0153 ..... p 611 N93-12908 #
GRI-92/0239 ..... p 612 N93-12977 #
GRI-92/0262 ..... p 576 N93-12975 #

H-1809 ..... p 502 N93-13155 * #
H-1825 ..... p 493 N93-13322 * #
H-1861 ..... p 596 N93-12681 * #
H-1865 ..... p 663 N93-13288 * #

IAEA-CN-56/C-3-1 ..... p 713 N93-12883 #
IAEA-CN-56/C-3-2 ..... p 713 N93-12882 #

IAF-92-0689 ..... p 520 N93-13455 * #

ICASE-92-53 ..... p 699 N93-12986 * #
ICASE-92-55 ..... p 696 N93-12942 * #
ICASE-92-57 ..... p 575 N93-12717 * #

IDA-D-1109 ..... p 688 N93-12549 #
IDA-D-1173 ..... p 560 N93-12574 #

IDA/HQ-92-41242 ..... p 688 N93-12549 #
IDA/HQ-92-41742 ..... p 560 N93-12574 #

IFSR-556 ..... p 705 N93-12713 #
IFSR-560 ..... p 714 N93-12913 #
IFSR-561 ..... p 713 N93-12873 #
IFSR-562 ..... p 714 N93-12914 #
IFSR-565 ..... p 716 N93-13107 #

IHES/P/91/64 ..... p 696 N93-12889 #

IIHR-357 ..... p 574 N93-12617 #

INPE-5310-NTC/299 ..... p 651 N93-13310 #
INPE-5365-PRE/1745 ..... p 632 N93-13005 #
INPE-5421-PRE/1763 ..... p 634 N93-13412 #
INPE-5426-TDI/483 ..... p 634 N93-13258 #
INPE-5428-RPQ/662 ..... p 716 N93-13257 #
INPE-5434-TDI/485 ..... p 750 N93-13279 #

INT-PATENT-CLASS-C08J-5/08 .. p 531 N93-13416 *
INT-PATENT-CLASS-C08L-49/08 p 531 N93-13416 *

INT-PATENT-CLASS-F16B-37/08 p 614 N93-13423 *
INT-PATENT-CLASS-F16B-39/36 p 614 N93-13423 *
INT-PATENT-CLASS-F25B-1/00 . p 558 N93-13422 *

INT-PATENT-CLASS-G01N-21/27 p 709 N93-13419 *
INT-PATENT-CLASS-G01N-29/00 p 700 N93-13421 *
INT-PATENT-CLASS-G01N-29/22 p 700 N93-13421 *
INT-PATENT-CLASS-G02B-5/20 . p 709 N93-13419 *
INT-PATENT-CLASS-G05D-15/01 p 626 N93-13420 *
INT-PATENT-CLASS-G05D-19/01 p 626 N93-13420 *

INT-PATENT-CLASS-H01S-3/19 . p 605 N93-13418 *
INT-PATENT-CLASS-H04N-5/74 . p 711 N93-13711 *
INT-PATENT-CLASS-H04N-9/31 . p 711 N93-13711 *

INT-PATENT-CLASS-N66L-1/66 . p 614 N93-13417 *

IPPCZ-317 ..... p 715 N93-13091 #
IPPCZ-318 ..... p 716 N93-13330 #
IPPCZ-319 ..... p 715 N93-13093 #
IPPCZ-320 ..... p 715 N93-13006 #

IS-M-713 ..... p 558 N93-13298 #
IS-M-714 ..... p 531 N93-13264 #
IS-M-717 ..... p 721 N93-13089 #

IS-T-1606 ..... p 596 N93-12921 #

IS-5081 ..... p 620 N93-13071 #

ISAS-RN-645 ..... p 652 N93-13405 #
ISAS-RN-646 ..... p 491 N93-12716 #
ISAS-RN-647 ..... p 703 N93-13095 #

ISAS-TN-649 ..... p 596 N93-12639 #

ISBN-0-16-038961-5 ..... p 742 N93-13800 #
ISBN-0-16-038977-1 ..... p 741 N93-13799 #
ISBN-0-16-039083-4 ..... p 732 N93-13693 #
ISBN-0-309-05171-1 ..... p 498 N93-13787 #
ISBN-0-315-62655-0 ..... p 751 N93-13374
ISBN-0-315-63282-8 ..... p 569 N93-14066
ISBN-0-315-65141-5 ..... p 594 N93-14067
ISBN-0-315-67464-4 ..... p 496 N93-13930
ISBN-92-835-0672-3 ..... p 577 N93-13199 #
ISBN-92-835-0683-9 ..... p 563 N93-13049 #
ISBN-92-835-0684-7 ..... p 692 N93-13238 #
ISBN-92-9092-035-1 ..... p 508 N93-12892 #
ISBN-92-9092-111-0 ..... p 749 N93-12965 #
ISBN-92-9092-119-6 ..... p 516 N93-13691 #
ISBN-92-9092-159-5 ..... p 516 N93-13855 #
ISBN-92-9092-159-5 ..... p 516 N93-13856 #
ISBN-92-9092-159-5 ..... p 516 N93-13857 #
ISBN-92-9092-159-5 ..... p 516 N93-13858 #
ISBN-92-9092-159-5 ..... p 516 N93-13859 #
ISBN-92-9092-159-5 ..... p 517 N93-13860 #
ISBN-92-9092-159-5 ..... p 517 N93-13861 #
ISBN-92-9092-159-5 ..... p 517 N93-13902 #
ISBN-92-9092-159-5 ..... p 517 N93-13903 #
ISBN-951-22-0332-4 ..... p 698 N93-12890 #
ISBN-951-41-0689-X ..... p 697 N93-13271 #

ISVR-TR-207 ..... p 699 N93-12714
ISVR-TR-209 ..... p 678 N93-13464
ISVR-TR-211 ..... p 700 N93-13439

ITN-92-85167 ..... p 723 N93-13362
ITN-92-85168 ..... p 722 N93-13268

JAERI-M-90-162 ..... p 718 N93-13732 #

JPRS-ULS-92-024 ..... p 672 N93-13033 #

JPRS-UPM-92-006 ..... p 698 N93-13303 #

JPRS-USP-91-004 ..... p 516 N93-13758 #
JPRS-USP-92-004 ..... p 513 N93-13282 #
JPRS-USP-92-005 ..... p 513 N93-13304 #
JPRS-USP-92-006 ..... p 508 N93-13151 #

JRC-90-28 ..... p 619 N93-12692 * #

JSC-26032 ..... p 597 N93-13373 * #

JTN-92-80399 ..... p 610 N93-12727 #

K/CSD/TM-101 ..... p 736 N93-13048 #

KCP-613-4669 ..... p 736 N93-13078 #
KCP-613-4679 ..... p 624 N93-13077 #

KGG-29 ..... p 526 N93-12968 * #

L-17060 ..... p 493 N93-13353 * #
L-17078 ..... p 520 N93-12876 * #
L-17083 ..... p 528 N93-12590 * #

L-17090 ..... p 674 N93-13023 * #
L-17103 ..... p 771 N93-13020 * #
L-17120 ..... p 519 N93-13379 * #
L-17127 ..... p 598 N93-13661 * #
L-17135-PT-1 ..... p 545 N93-12769 * #
L-17137 ..... p 772 N93-13572 * #

LA-UR-92-1768 ..... p 701 N93-12588 #
LA-UR-92-1783 ..... p 749 N93-12587 #
LA-UR-92-1805 ..... p 704 N93-13281 #
LA-UR-92-1813 ..... p 538 N93-13341 #
LA-UR-92-1844 ..... p 720 N93-12853 #
LA-UR-92-1901 ..... p 603 N93-12560 #
LA-UR-92-1948 ..... p 641 N93-12685 #
LA-UR-92-1953 ..... p 691 N93-12791 #
LA-UR-92-1978 ..... p 690 N93-12559 #
LA-UR-92-2039 ..... p 674 N93-12566 #
LA-UR-92-2049 ..... p 749 N93-12956 #
LA-UR-92-2051 ..... p 641 N93-12684 #
LA-UR-92-2085 ..... p 649 N93-12841 #
LA-UR-92-2183 ..... p 557 N93-12922 #
LA-UR-92-2212 ..... p 662 N93-13075 #
LA-UR-92-2327 ..... p 702 N93-13076 #
LA-UR-92-2380 ..... p 637 N93-12923 #
LA-UR-92-2391 ..... p 613 N93-13321 #
LA-UR-92-2400 ..... p 543 N93-13545 #
LA-UR-92-2420 ..... p 733 N93-12567 #
LA-UR-92-2422 ..... p 690 N93-12564 #
LA-UR-92-2431 ..... p 524 N93-13516 #
LA-UR-92-2444 ..... p 722 N93-13118 #
LA-UR-92-2457 ..... p 743 N93-13342 #
LA-UR-92-2464 ..... p 609 N93-12565 #
LA-UR-92-2548 ..... p 753 N93-13523 #
LA-UR-92-2553 ..... p 714 N93-12997 #
LA-UR-92-2557 ..... p 550 N93-12999 #
LA-UR-92-2580 ..... p 689 N93-13046 #
LA-UR-92-2582 ..... p 715 N93-13047 #
LA-UR-92-2677 ..... p 565 N93-13510 #
LA-UR-92-2698 ..... p 675 N93-13522 #
LA-UR-92-2706 ..... p 563 N93-13045 #
LA-UR-92-2727 ..... p 710 N93-13509 #
LA-UR-92-2728 ..... p 708 N93-13508 #
LA-UR-92-2803 ..... p 605 N93-13507 #
LA-UR-92-313 ..... p 551 N93-13315 #
LA-UR-92-861 ..... p 743 N93-13339 #

LA-12348 ..... p 713 N93-12809 #

LC-79-640375 ..... p 769 N93-12803 #
LC-89-656121 ..... p 698 N93-12805 #
LC-92-15610 ..... p 498 N93-13787 #

LCSR-TR-191-REV-2 ..... p 687 N93-13734 * #

LEC-7819 ..... p 635 N93-13440 #

LESC-30460 ..... p 597 N93-13373 * #

LMSC/F247098 ..... p 648 N93-12621 #

LORAL-SS/L-TR00823 ..... p 562 N93-12950 * #

LPI-748 ..... p 761 N93-13980 * #

M-701 ..... p 529 N93-12678 * #

MA-1023T-VOL-3 ..... p 740 N93-12814 * #

MCAT-92-019 ..... p 583 N93-13277 * #

MF-124 ..... p 715 N93-13038 #

MLM-3757(OP) ..... p 555 N93-13081 #
MLM-3759(OP) ..... p 759 N93-13504 #

MP-91-278 ..... p 721 N93-12887 #

MS-CIS-91-28 ..... p 682 N93-12554 #

MTL-MS-92-1 ..... p 553 N93-13836 #
MTL-MS-92-2 ..... p 683 N93-12740 #

MTL-TR-92-25 ..... p 528 N93-12583 #

MTR-92B0000047V2 ..... p 677 N93-12576 #

M92-B0000088 ..... p 731 N93-13834 #

NADC-91116-60 ..... p 529 N93-12757 #

NAL-PD-FC-9203 ..... p 504 N93-13566 #

NAL-SP-IC-9201 ..... p 737 N93-13368 #

NAL-TR-1131 ..... p 610 N93-12727 #

NAS 1.15:103905 p 683 N93-12719 * #
NAS 1.15:103954 p 521 N93-12720 * #
NAS 1.15:103962 p 491 N93-12721 * #
NAS 1.15:103964 p 527 N93-12895 * #
NAS 1.15:103969 p 528 N93-12896 * #
NAS 1.15:104222 p 532 N93-13428 * #
NAS 1.15:104260 p 596 N93-12681 * #
NAS 1.15:104262 p 663 N93-13288 * #
NAS 1.15:104566-VOL-4 p 669 N93-13382 * #
NAS 1.15:104575 p 519 N93-13372 * #
NAS 1.15:105609 p 622 N93-12738 * #
NAS 1.15:105658 p 492 N93-13292 * #
NAS 1.15:105765 p 625 N93-13153 * #
NAS 1.15:105840 p 622 N93-12739 * #
NAS 1.15:105848 p 529 N93-12737 * #
NAS 1.15:105875 p 571 N93-13286 * #
NAS 1.15:105881 p 622 N93-12735 * #
NAS 1.15:105884 p 610 N93-12736 * #
NAS 1.15:105903 p 625 N93-13157 * #
NAS 1.15:105906 p 597 N93-13307 * #
NAS 1.15:105909 p 597 N93-13410 * #
NAS 1.15:105912 p 527 N93-14079 * #
NAS 1.15:105932 p 689 N93-13154 * #
NAS 1.15:107553 p 520 N93-13032 * #
NAS 1.15:107594 p 504 N93-13367 * #
NAS 1.15:107669 p 491 N93-13025 * #
NAS 1.15:107675 p 694 N93-13442 * #
NAS 1.15:107678 p 771 N93-13126 * #
NAS 1.15:107689 p 504 N93-13068 * #
NAS 1.15:107695 p 625 N93-13125 * #
NAS 1.15:107696 p 552 N93-13441 * #
NAS 1.15:107697 p 500 N93-13565 * #
NAS 1.15:107809 p 513 N93-13266 * #
NAS 1.15:107843 p 513 N93-13265 * #
NAS 1.15:107969 p 513 N93-13308 *
NAS 1.15:107980 p 557 N93-12951 * #
NAS 1.15:107992 p 735 N93-12991 * #
NAS 1.15:108000 p 651 N93-13326 * #
NAS 1.15:108007 p 518 N93-13113 * #
NAS 1.15:108015 p 733 N93-12634 * #
NAS 1.15:108016 p 733 N93-12670 * #
NAS 1.15:108017 p 734 N93-12671 * #
NAS 1.15:108018 p 733 N93-12635 * #
NAS 1.15:108019 p 734 N93-12673 * #
NAS 1.15:108020 p 733 N93-12636 * #
NAS 1.15:108021 p 734 N93-12672 * #
NAS 1.15:108033 p 520 N93-13613 * #
NAS 1.15:108050 p 520 N93-13455 * #
NAS 1.15:108051 p 562 N93-12909 * #
NAS 1.15:108062 p 643 N93-12926 * #
NAS 1.15:108086 p 702 N93-12900 * #
NAS 1.15:108093 p 679 N93-13571 * #
NAS 1.15:108106 p 738 N93-13885 * #
NAS 1.15:108376 p 553 N93-13716 * #
NAS 1.15:108379 p 551 N93-13115 * #
NAS 1.15:108380 p 609 N93-12682 * #
NAS 1.15:108381 p 691 N93-13156 * #
NAS 1.15:108382 p 526 N93-13429 * #
NAS 1.15:108383 p 543 N93-13378 * #
NAS 1.15:108384 p 693 N93-13289 * #
NAS 1.15:4383 p 674 N93-13023 * #
NAS 1.15:4410 p 772 N93-13572 * #
NAS 1.15:4424 p 742 N93-13433 * #
NAS 1.15:4426 p 502 N93-13155 * #
NAS 1.15:4430 p 493 N93-13322 * #
NAS 1.18:5300.4(3A-2) p 570 N93-12674 * #
NAS 1.19:279 p 679 N93-13692 * #
NAS 1.26:177413-VOL-1 p 708 N93-12591 * #
NAS 1.26:177413-VOL-2 p 708 N93-12593 * #
NAS 1.26:177414 p 742 N93-12592 * #
NAS 1.26:182268 p 504 N93-13735 * #
NAS 1.26:182269 p 711 N93-13762 * #
NAS 1.26:184098 p 522 N93-13425 * #
NAS 1.26:184326 p 575 N93-12688 * #
NAS 1.26:184367 p 678 N93-12990 * #
NAS 1.26:184390 p 678 N93-12966 * #
NAS 1.26:184396 p 769 N93-13475 * #
NAS 1.26:184402 p 671 N93-12901 * #
NAS 1.26:184404 p 710 N93-13696 * #
NAS 1.26:184413 p 619 N93-12692 * #
NAS 1.26:184422 p 769 N93-13014 * #
NAS 1.26:184424 p 607 N93-13797 * #
NAS 1.26:184428 p 614 N93-13436 * #
NAS 1.26:184431 p 709 N93-12894 * #
NAS 1.26:184432 p 619 N93-12875 * #
NAS 1.26:184435 p 769 N93-12658 * #
NAS 1.26:184437 p 719 N93-12691 * #
NAS 1.26:184438 p 672 N93-12949 * #
NAS 1.26:184439 p 649 N93-12718 * #
NAS 1.26:184442 p 531 N93-13311 * #
NAS 1.26:184443 p 742 N93-12657 * #
NAS 1.26:184446 p 506 N93-13013 * #
NAS 1.26:184448 p 522 N93-12893 * #
NAS 1.26:184449 p 525 N93-12874 * #
NAS 1.26:184450 p 682 N93-12676 * #
NAS 1.26:184452 p 682 N93-12675 * #
NAS 1.26:184453 p 525 N93-12659 * #
NAS 1.26:184455 p 604 N93-12656 * #
NAS 1.26:184460 p 611 N93-12919 * #
NAS 1.26:184461 p 526 N93-12968 * #
NAS 1.26:184462 p 558 N93-13021 * #
NAS 1.26:185602 p 556 N93-12699 * #
NAS 1.26:185685 p 740 N93-12814 * #
NAS 1.26:185704 p 597 N93-13373 * #
NAS 1.26:187128 p 502 N93-12695 * #
NAS 1.26:188478 p 751 N93-13465 * #
NAS 1.26:189111 p 544 N93-12589 * #
NAS 1.26:189150 p 626 N93-13443 * #
NAS 1.26:189151 p 627 N93-13444 * #
NAS 1.26:189152 p 627 N93-13445 * #
NAS 1.26:189181 p 523 N93-13715 * #
NAS 1.26:189199 p 562 N93-12950 * #
NAS 1.26:189208 p 685 N93-13291 * #
NAS 1.26:189235 p 626 N93-13260 * #
NAS 1.26:189706 p 530 N93-12929 * #
NAS 1.26:189718 p 699 N93-12986 * #
NAS 1.26:189721 p 696 N93-12942 * #
NAS 1.26:189722 p 575 N93-12717 * #
NAS 1.26:189727 p 519 N93-13462 * #
NAS 1.26:189880 p 686 N93-13293 * #
NAS 1.26:190275 p 685 N93-13004 * #
NAS 1.26:190470 p 632 N93-13833 * #
NAS 1.26:190750 p 531 N93-13309 * #
NAS 1.26:190790 p 526 N93-13283 * #
NAS 1.26:190791 p 525 N93-12638 * #
NAS 1.26:190794 p 626 N93-13290 * #
NAS 1.26:190820 p 556 N93-12799 * #
NAS 1.26:190844 p 611 N93-12952 * #
NAS 1.26:190848 p 597 N93-13424 * #
NAS 1.26:190849 p 598 N93-13656 * #
NAS 1.26:190850 p 710 N93-13705 * #
NAS 1.26:190859 p 558 N93-13404 * #
NAS 1.26:190861 p 559 N93-13604 * #
NAS 1.26:190863 p 682 N93-13759 * #
NAS 1.26:190866 p 705 N93-13606 * #
NAS 1.26:190873 p 616 N93-13706 * #
NAS 1.26:190874 p 615 N93-13608 * #
NAS 1.26:190877 p 628 N93-13707 * #
NAS 1.26:190878 p 573 N93-13610 * #
NAS 1.26:190879 p 673 N93-13612 * #
NAS 1.26:190881 p 687 N93-13880 * #
NAS 1.26:190882 p 571 N93-13430 * #
NAS 1.26:190883 p 670 N93-13708 * #
NAS 1.26:190884 p 678 N93-13450 * #
NAS 1.26:190886 p 603 N93-13709 * #
NAS 1.26:190908 p 633 N93-13084 * #
NAS 1.26:190930 p 672 N93-13327 * #
NAS 1.26:190941 p 705 N93-12715 * #
NAS 1.26:190942 p 682 N93-12654 * #
NAS 1.26:190944 p 632 N93-12800 * #
NAS 1.26:190948 p 561 N93-12655 * #
NAS 1.26:190949 p 624 N93-13019 * #
NAS 1.26:190956 p 587 N93-13406 * #
NAS 1.26:190957 p 675 N93-13061 * #
NAS 1.26:190958 p 769 N93-12669 * #
NAS 1.26:190960 p 687 N93-13694 * #
NAS 1.26:190962 p 620 N93-13435 * #
NAS 1.26:190964 p 709 N93-12985 * #
NAS 1.26:190968 p 537 N93-12935 * #
NAS 1.26:190971 p 687 N93-13695 * #
NAS 1.26:190984 p 610 N93-12904 * #
NAS 1.26:190985 p 503 N93-13697 * #
NAS 1.26:190996 p 517 N93-12690 * #
NAS 1.26:191001 p 721 N93-13022 * #
NAS 1.26:191003 p 709 N93-13062 * #
NAS 1.26:191208 p 734 N93-12680 * #
NAS 1.26:191209 p 587 N93-13453 * #
NAS 1.26:191210 p 575 N93-12677 * #
NAS 1.26:191211 p 561 N93-12679 * #
NAS 1.26:191213 p 684 N93-12801 * #
NAS 1.26:191215 p 649 N93-12661 * #
NAS 1.26:191216 p 503 N93-12903 * #
NAS 1.26:191217 p 733 N93-12660 * #
NAS 1.26:191218 p 670 N93-13714 * #
NAS 1.26:191220 p 685 N93-13063 * #
NAS 1.26:191229 p 565 N93-13411 * #
NAS 1.26:191230 p 686 N93-13296 * #
NAS 1.26:191231 p 686 N93-13295 * #
NAS 1.26:191234 p 551 N93-13150 * #
NAS 1.26:191235 p 697 N93-13409 * #
NAS 1.26:191236 p 693 N93-13366 * #
NAS 1.26:191237 p 686 N93-13408 * #
NAS 1.26:191239 p 538 N93-13456 * #
NAS 1.26:191240 p 743 N93-13352 * #
NAS 1.26:191241 p 644 N93-13031 * #
NAS 1.26:191244 p 685 N93-13030 * #
NAS 1.26:191246 p 624 N93-13029 * #
NAS 1.26:191247 p 556 N93-12728 * #
NAS 1.26:191248 p 650 N93-12877 * #
NAS 1.26:191249 p 769 N93-12930 * #
NAS 1.26:191253 p 520 N93-12910 * #
NAS 1.26:191256 p 758 N93-13344 * #
NAS 1.26:191257 p 672 N93-13457 * #
NAS 1.26:191258 p 669 N93-13458 * #
NAS 1.26:191260 p 685 N93-13261 * #
NAS 1.26:191261 p 598 N93-13567 * #
NAS 1.26:191263 p 522 N93-13152 * #
NAS 1.26:191265 p 552 N93-13459 * #
NAS 1.26:191267 p 645 N93-13274 * #
NAS 1.26:191268 p 743 N93-13272 * #
NAS 1.26:191271 p 652 N93-13460 * #
NAS 1.26:191272 p 772 N93-13306 * #
NAS 1.26:191273 p 686 N93-13355 * #
NAS 1.26:191274 p 493 N93-13463 * #
NAS 1.26:191275 p 748 N93-13659 * #
NAS 1.26:191276 p 583 N93-13277 * #
NAS 1.26:191277 p 500 N93-13305 * #
NAS 1.26:191278 p 644 N93-13254 * #
NAS 1.26:191280 p 694 N93-13376 * #
NAS 1.26:191281 p 565 N93-13375 * #
NAS 1.26:191282 p 572 N93-13569 * #
NAS 1.26:191284 p 565 N93-13354 * #
NAS 1.26:191286 p 679 N93-13717 * #
NAS 1.26:191288 p 759 N93-13568 * #
NAS 1.26:191289 p 724 N93-13570 * #
NAS 1.26:191294 p 634 N93-13094 * #
NAS 1.26:191295 p 572 N93-13448 * #
NAS 1.26:191300 p 748 N93-13660 * #
NAS 1.26:191303 p 675 N93-13449 * #
NAS 1.26:191353 p 516 N93-13564 * #
NAS 1.26:191355 p 572 N93-13563 * #
NAS 1.26:191361 p 687 N93-13734 * #
NAS 1.26:191363 p 539 N93-13763 * #
NAS 1.26:191365 p 654 N93-13719 * #
NAS 1.26:191367 p 664 N93-13718 * #
NAS 1.26:191369 p 738 N93-13737 * #
NAS 1.26:4468 p 743 N93-12898 * #
NAS 1.26:4471 p 694 N93-13370 * #
NAS 1.26:4472 p 623 N93-12911 * #
NAS 1.26:4473 p 559 N93-13434 * #
NAS 1.55:10106 p 584 N93-13385 * #
NAS 1.55:10110 p 684 N93-12957 * #
NAS 1.55:3066 p 744 N93-13579 * #
NAS 1.55:3161 p 598 N93-13661 * #
NAS 1.55:3162-PT-1 p 545 N93-12769 * #
NAS 1.55:3165-VOL-1 p 736 N93-13131 * #
NAS 1.55:3166-VOL-2 p 760 N93-13972 * #
NAS 1.55:3171 p 508 N93-13158 * #
NAS 1.60:3237 p 520 N93-12876 * #
NAS 1.60:3253 p 493 N93-13353 * #
NAS 1.60:3254 p 528 N93-12590 * #
NAS 1.60:3262 p 519 N93-13379 * #
NAS 1.60:3280 p 503 N93-12815 * #
NAS 1.60:3303 p 529 N93-12678 * #
NAS 1.61:1271 p 728 N93-12967 * #
NAS 1.61:1283 p 661 N93-12700 * #
NAS 1.61:1285 p 744 N93-13461 * #
NAS 1.61:3243 p 771 N93-13020 * #
NAS 1.83:141 p 508 N93-12891 *
NAS 1.83:158 p 730 N93-13248 * #
NAS 1.83:159 p 491 N93-13110 * #

NASA-CASE-LAR-14338-1 p 531 N93-13416 *
NASA-CASE-LAR-14508-1-CU p 626 N93-13420 *

NASA-CASE-MSC-21730-1 p 614 N93-13417 *
NASA-CASE-MSC-21935-1 p 614 N93-13423 *

NASA-CASE-NPO-16932-2-CU p 711 N93-13711 *
NASA-CASE-NPO-18155-1-CU p 700 N93-13421 *
NASA-CASE-NPO-18243-1-CU p 605 N93-13418 *
NASA-CASE-NPO-18317-1-CU p 709 N93-13419 *
NASA-CASE-NPO-18366-1-CU p 558 N93-13422 *

NASA-CP-10106 p 584 N93-13385 * #
NASA-CP-10110 p 684 N93-12957 * #
NASA-CP-3066 p 744 N93-13579 * #
NASA-CP-3161 p 598 N93-13661 * #
NASA-CP-3162-PT-1 p 545 N93-12769 * #
NASA-CP-3165-VOL-1 p 736 N93-13131 * #
NASA-CP-3166-VOL-2 p 760 N93-13972 * #
NASA-CP-3171 p 508 N93-13158 * #

NASA-CR-177413-VOL-1 p 708 N93-12591 * #
NASA-CR-177413-VOL-2 p 708 N93-12593 * #
NASA-CR-177414 p 742 N93-12592 * #
NASA-CR-182268 p 504 N93-13735 * #
NASA-CR-182269 p 711 N93-13762 * #
NASA-CR-184098 p 522 N93-13425 * #
NASA-CR-184326 p 575 N93-12688 * #
NASA-CR-184367 p 678 N93-12990 * #
NASA-CR-184390 p 678 N93-12966 * #
NASA-CR-184396 p 769 N93-13475 * #
NASA-CR-184402 p 671 N93-12901 * #
NASA-CR-184404 p 710 N93-13696 * #
NASA-CR-184413 p 619 N93-12692 * #
NASA-CR-184422 p 769 N93-13014 * #
NASA-CR-184424 p 607 N93-13797 * #

NASA-CR-184428 ..... p 614 N93-13436 * #
NASA-CR-184431 ..... p 709 N93-12894 * #
NASA-CR-184432 ..... p 619 N93-12875 * #
NASA-CR-184435 ..... p 769 N93-12658 * #
NASA-CR-184437 ..... p 719 N93-12691 * #
NASA-CR-184438 ..... p 672 N93-12949 * #
NASA-CR-184439 ..... p 649 N93-12718 * #
NASA-CR-184442 ..... p 531 N93-13311 * #
NASA-CR-184443 ..... p 742 N93-12657 * #
NASA-CR-184446 ..... p 506 N93-13013 * #
NASA-CR-184448 ..... p 522 N93-12893 * #
NASA-CR-184449 ..... p 525 N93-12874 * #
NASA-CR-184450 ..... p 682 N93-12676 * #
NASA-CR-184452 ..... p 682 N93-12675 * #
NASA-CR-184453 ..... p 525 N93-12659 * #
NASA-CR-184455 ..... p 604 N93-12656 * #
NASA-CR-184460 ..... p 611 N93-12919 * #
NASA-CR-184461 ..... p 526 N93-12968 * #
NASA-CR-184462 ..... p 558 N93-13021 * #
NASA-CR-185602 ..... p 556 N93-12699 * #
NASA-CR-185685 ..... p 740 N93-12814 * #
NASA-CR-185704 ..... p 597 N93-13373 * #
NASA-CR-187128 ..... p 502 N93-12695 * #
NASA-CR-188478 ..... p 751 N93-13465 * #
NASA-CR-189111 ..... p 544 N93-12589 * #
NASA-CR-189150 ..... p 626 N93-13443 * #
NASA-CR-189151 ..... p 627 N93-13444 * #
NASA-CR-189152 ..... p 627 N93-13445 * #
NASA-CR-189181 ..... p 523 N93-13715 * #
NASA-CR-189199 ..... p 562 N93-12950 * #
NASA-CR-189208 ..... p 685 N93-13291 * #
NASA-CR-189235 ..... p 626 N93-13260 * #
NASA-CR-189706 ..... p 530 N93-12929 * #
NASA-CR-189718 ..... p 699 N93-12986 * #
NASA-CR-189721 ..... p 696 N93-12942 * #
NASA-CR-189722 ..... p 575 N93-12717 * #
NASA-CR-189727 ..... p 519 N93-13462 * #
NASA-CR-189880 ..... p 686 N93-13293 * #
NASA-CR-190275 ..... p 685 N93-13004 * #
NASA-CR-190470 ..... p 632 N93-13833 * #
NASA-CR-190750 ..... p 531 N93-13309 * #
NASA-CR-190790 ..... p 526 N93-13283 * #
NASA-CR-190791 ..... p 525 N93-12638 * #
NASA-CR-190794 ..... p 626 N93-13290 * #
NASA-CR-190820 ..... p 556 N93-12799 * #
NASA-CR-190844 ..... p 611 N93-12952 * #
NASA-CR-190848 ..... p 597 N93-13424 * #
NASA-CR-190849 ..... p 598 N93-13656 * #
NASA-CR-190850 ..... p 710 N93-13705 * #
NASA-CR-190859 ..... p 558 N93-13404 * #
NASA-CR-190861 ..... p 559 N93-13604 * #
NASA-CR-190863 ..... p 682 N93-13759 * #
NASA-CR-190866 ..... p 705 N93-13606 * #
NASA-CR-190873 ..... p 616 N93-13706 * #
NASA-CR-190874 ..... p 615 N93-13608 * #
NASA-CR-190877 ..... p 628 N93-13707 * #
NASA-CR-190878 ..... p 573 N93-13610 * #
NASA-CR-190879 ..... p 673 N93-13612 * #
NASA-CR-190881 ..... p 687 N93-13880 * #
NASA-CR-190882 ..... p 571 N93-13430 * #
NASA-CR-190883 ..... p 670 N93-13708 * #
NASA-CR-190884 ..... p 678 N93-13450 * #
NASA-CR-190886 ..... p 603 N93-13709 * #
NASA-CR-190908 ..... p 633 N93-13084 * #
NASA-CR-190930 ..... p 672 N93-13327 * #
NASA-CR-190941 ..... p 705 N93-12715 * #
NASA-CR-190942 ..... p 682 N93-12654 * #
NASA-CR-190944 ..... p 632 N93-12800 * #
NASA-CR-190948 ..... p 561 N93-12655 * #
NASA-CR-190949 ..... p 624 N93-13019 * #
NASA-CR-190956 ..... p 587 N93-13406 * #
NASA-CR-190957 ..... p 675 N93-13061 * #
NASA-CR-190958 ..... p 769 N93-12669 * #
NASA-CR-190960 ..... p 687 N93-13694 * #
NASA-CR-190962 ..... p 620 N93-13435 * #
NASA-CR-190964 ..... p 709 N93-12985 * #
NASA-CR-190968 ..... p 537 N93-12935 * #
NASA-CR-190971 ..... p 687 N93-13695 * #
NASA-CR-190984 ..... p 610 N93-12904 * #
NASA-CR-190985 ..... p 503 N93-13697 * #
NASA-CR-190996 ..... p 517 N93-12690 * #
NASA-CR-191001 ..... p 721 N93-13022 * #
NASA-CR-191003 ..... p 709 N93-13062 * #
NASA-CR-191208 ..... p 734 N93-12680 * #
NASA-CR-191209 ..... p 587 N93-13453 * #
NASA-CR-191210 ..... p 575 N93-12677 * #
NASA-CR-191211 ..... p 561 N93-12679 * #
NASA-CR-191213 ..... p 684 N93-12801 * #
NASA-CR-191215 ..... p 649 N93-12661 * #
NASA-CR-191216 ..... p 503 N93-12903 * #
NASA-CR-191217 ..... p 733 N93-12660 * #
NASA-CR-191218 ..... p 670 N93-13714 * #
NASA-CR-191220 ..... p 685 N93-13063 * #
NASA-CR-191229 ..... p 565 N93-13411 * #
NASA-CR-191230 ..... p 686 N93-13296 * #
NASA-CR-191231 ..... p 686 N93-13295 * #
NASA-CR-191234 ..... p 551 N93-13150 * #
NASA-CR-191235 ..... p 697 N93-13409 * #
NASA-CR-191236 ..... p 693 N93-13366 * #
NASA-CR-191237 ..... p 686 N93-13408 * #
NASA-CR-191239 ..... p 538 N93-13456 * #
NASA-CR-191240 ..... p 743 N93-13352 * #
NASA-CR-191241 ..... p 644 N93-13031 * #
NASA-CR-191244 ..... p 685 N93-13030 * #
NASA-CR-191246 ..... p 624 N93-13029 * #
NASA-CR-191247 ..... p 556 N93-12728 * #
NASA-CR-191248 ..... p 650 N93-12877 * #
NASA-CR-191249 ..... p 769 N93-12930 * #
NASA-CR-191253 ..... p 520 N93-12910 * #
NASA-CR-191256 ..... p 758 N93-13344 * #
NASA-CR-191257 ..... p 672 N93-13457 * #
NASA-CR-191258 ..... p 669 N93-13458 * #
NASA-CR-191260 ..... p 685 N93-13261 * #
NASA-CR-191261 ..... p 598 N93-13567 * #
NASA-CR-191263 ..... p 522 N93-13152 * #
NASA-CR-191265 ..... p 552 N93-13459 * #
NASA-CR-191267 ..... p 645 N93-13274 * #
NASA-CR-191268 ..... p 743 N93-13272 * #
NASA-CR-191271 ..... p 652 N93-13460 * #
NASA-CR-191272 ..... p 772 N93-13306 * #
NASA-CR-191273 ..... p 686 N93-13355 * #
NASA-CR-191274 ..... p 493 N93-13463 * #
NASA-CR-191275 ..... p 748 N93-13659 * #
NASA-CR-191276 ..... p 583 N93-13277 * #
NASA-CR-191277 ..... p 500 N93-13305 * #
NASA-CR-191278 ..... p 644 N93-13254 * #
NASA-CR-191280 ..... p 694 N93-13376 * #
NASA-CR-191281 ..... p 565 N93-13375 * #
NASA-CR-191282 ..... p 572 N93-13569 * #
NASA-CR-191284 ..... p 565 N93-13354 * #
NASA-CR-191286 ..... p 679 N93-13717 * #
NASA-CR-191288 ..... p 759 N93-13568 * #
NASA-CR-191289 ..... p 724 N93-13570 * #
NASA-CR-191294 ..... p 634 N93-13094 * #
NASA-CR-191295 ..... p 572 N93-13448 * #
NASA-CR-191300 ..... p 748 N93-13660 * #
NASA-CR-191303 ..... p 675 N93-13449 * #
NASA-CR-191353 ..... p 516 N93-13564 * #
NASA-CR-191355 ..... p 572 N93-13563 * #
NASA-CR-191361 ..... p 687 N93-13734 * #
NASA-CR-191363 ..... p 539 N93-13763 * #
NASA-CR-191365 ..... p 654 N93-13719 * #
NASA-CR-191367 ..... p 664 N93-13718 * #
NASA-CR-191369 ..... p 738 N93-13737 * #
NASA-CR-4468 ..... p 743 N93-12898 * #
NASA-CR-4471 ..... p 694 N93-13370 * #
NASA-CR-4472 ..... p 623 N93-12911 * #
NASA-CR-4473 ..... p 559 N93-13434 * #

NASA-EP-279 ..... p 679 N93-13692 * #

NASA-NP-141 ..... p 508 N93-12891 *
NASA-NP-158 ..... p 730 N93-13248 * #
NASA-NP-159 ..... p 491 N93-13110 * #

NASA-RP-1271 ..... p 728 N93-12967 * #
NASA-RP-1283 ..... p 661 N93-12700 * #
NASA-RP-1285 ..... p 744 N93-13461 * #

NASA-TM-103905 ..... p 683 N93-12719 * #
NASA-TM-103954 ..... p 521 N93-12720 * #
NASA-TM-103962 ..... p 491 N93-12721 * #
NASA-TM-103964 ..... p 527 N93-12895 * #
NASA-TM-103969 ..... p 528 N93-12896 * #
NASA-TM-104222 ..... p 532 N93-13428 * #
NASA-TM-104260 ..... p 596 N93-12681 * #
NASA-TM-104262 ..... p 663 N93-13288 * #
NASA-TM-104566-VOL-4 ..... p 669 N93-13382 * #
NASA-TM-104575 ..... p 519 N93-13372 * #
NASA-TM-105609 ..... p 622 N93-12738 * #
NASA-TM-105658 ..... p 492 N93-13292 * #
NASA-TM-105765 ..... p 625 N93-13153 * #
NASA-TM-105840 ..... p 622 N93-12739 * #
NASA-TM-105848 ..... p 529 N93-12737 * #
NASA-TM-105875 ..... p 571 N93-13286 * #
NASA-TM-105881 ..... p 622 N93-12735 * #
NASA-TM-105884 ..... p 610 N93-12736 * #
NASA-TM-105903 ..... p 625 N93-13157 * #
NASA-TM-105906 ..... p 597 N93-13307 * #
NASA-TM-105909 ..... p 597 N93-13410 * #
NASA-TM-105912 ..... p 527 N93-14079 * #
NASA-TM-105932 ..... p 689 N93-13154 * #
NASA-TM-107553 ..... p 520 N93-13032 * #
NASA-TM-107594 ..... p 504 N93-13367 * #
NASA-TM-107669 ..... p 491 N93-13025 * #
NASA-TM-107675 ..... p 694 N93-13442 * #
NASA-TM-107678 ..... p 771 N93-13126 * #
NASA-TM-107689 ..... p 504 N93-13068 * #
NASA-TM-107695 ..... p 625 N93-13125 * #
NASA-TM-107696 ..... p 552 N93-13441 * #
NASA-TM-107697 ..... p 500 N93-13565 * #
NASA-TM-107809 ..... p 513 N93-13266 * #
NASA-TM-107843 ..... p 513 N93-13265 * #
NASA-TM-107969 ..... p 513 N93-13308 *
NASA-TM-107980 ..... p 557 N93-12951 * #
NASA-TM-107992 ..... p 735 N93-12991 * #
NASA-TM-108000 ..... p 651 N93-13326 * #
NASA-TM-108007 ..... p 518 N93-13113 * #
NASA-TM-108015 ..... p 733 N93-12634 * #
NASA-TM-108016 ..... p 733 N93-12670 * #
NASA-TM-108017 ..... p 734 N93-12671 * #
NASA-TM-108018 ..... p 733 N93-12635 * #
NASA-TM-108019 ..... p 734 N93-12673 * #
NASA-TM-108020 ..... p 733 N93-12636 * #
NASA-TM-108021 ..... p 734 N93-12672 * #
NASA-TM-108033 ..... p 520 N93-13613 * #
NASA-TM-108050 ..... p 520 N93-13455 * #
NASA-TM-108051 ..... p 562 N93-12909 * #
NASA-TM-108062 ..... p 643 N93-12926 * #
NASA-TM-108086 ..... p 702 N93-12900 * #
NASA-TM-108093 ..... p 679 N93-13571 * #
NASA-TM-108106 ..... p 738 N93-13885 * #
NASA-TM-108376 ..... p 553 N93-13716 * #
NASA-TM-108379 ..... p 551 N93-13115 * #
NASA-TM-108380 ..... p 609 N93-12682 * #
NASA-TM-108381 ..... p 691 N93-13156 * #
NASA-TM-108382 ..... p 526 N93-13429 * #
NASA-TM-108383 ..... p 543 N93-13378 * #
NASA-TM-108384 ..... p 693 N93-13289 * #
NASA-TM-4383 ..... p 674 N93-13023 * #
NASA-TM-4410 ..... p 772 N93-13572 * #
NASA-TM-4424 ..... p 742 N93-13433 * #
NASA-TM-4426 ..... p 502 N93-13155 * #
NASA-TM-4430 ..... p 493 N93-13322 * #

NASA-TP-3237 ..... p 520 N93-12876 * #
NASA-TP-3243 ..... p 771 N93-13020 * #
NASA-TP-3253 ..... p 493 N93-13353 * #
NASA-TP-3254 ..... p 528 N93-12590 * #
NASA-TP-3262 ..... p 519 N93-13379 * #
NASA-TP-3280 ..... p 503 N93-12815 * #
NASA-TP-3303 ..... p 529 N93-12678 * #

NATICK/TR-92/036 ..... p 609 N93-12724 #

NAVY-CASE-70723 ..... p 552 N93-13414 #
NAVY-CASE-72535 ..... p 551 N93-13101 #
NAVY-CASE-74315 ..... p 556 N93-13471 #

NAWCADPAX-TM-92-37-SY ..... p 677 N93-12732 #

NAWCADWAR-92033-60 ..... p 499 N93-12613 #
NAWCADWAR-92034-60 ..... p 499 N93-12602 #
NAWCADWAR-92035-60 ..... p 503 N93-12578 #
NAWCADWAR-92037-60 ..... p 677 N93-12860 #

NCAR/CT-133 ..... p 702 N93-13067 #
NCAR/CT-135 ..... p 651 N93-12969 #

NCAR/TN-368+STR ..... p 661 N93-12817 #
NCAR/TN-374+PROC ..... p 649 N93-12818 #

NHB-5300.4(3A-2) ..... p 570 N93-12674 * #

NIST-GCR-92-607 ..... p 559 N93-13642 #

NIST/SP-400-88 ..... p 725 N93-13783 #
NIST/SP-400/89 ..... p 570 N93-12978 #
NIST/SP-834 ..... p 553 N93-13649 #
NIST/SP-836 ..... p 738 N93-13415 #

NISTIR-4837 ..... p 553 N93-13785 #
NISTIR-4840 ..... p 539 N93-13641 #
NISTIR-4863 ..... p 689 N93-13198 #
NISTIR-4869 ..... p 559 N93-13640 #
NISTIR-4874 ..... p 623 N93-12981 #
NISTIR-4886 ..... p 558 N93-12980 #
NISTIR-4898 ..... p 637 N93-12987 #
NISTIR-4899 ..... p 637 N93-12988 #

NOAA-TM-ERL-ARL-194 ..... p 644 N93-12974 #

NOAA-TM-ERL-SEL-80-REV ..... p 562 N93-12979 #

NOAA-TM-ERL-WPL-223 ..... p 634 N93-13094 * #

NOAA-TR-NESDIS-62 ..... p 662 N93-13066 #

NOARL-JA-431-040-92 ..... p 667 N93-13877 #

NOARL-TN-254 ..... p 668 N93-12556 #
NOARL-TN-291 ..... p 697 N93-13886 #
NOARL-TN-296 ..... p 671 N93-13943 #

NPS-MA-92-010 ..... p 697 N93-14036 #

NRAD-TD-2287 ..... p 699 N93-12601 #
NRAD-TD-2320-PT-2 ..... p 560 N93-12585 #

NRAD-TR-1484 ..... p 570 N93-12725 #

NREC-1626-3 ..... p 612 N93-12977 #

NREL/TP-257-4671 ..... p 627 N93-13525 #
NREL/TP-257-4674 ..... p 627 N93-13524 #
NREL/TP-411-5017 ..... p 639 N93-13528 #
NREL/TP-413-4996 ..... p 637 N93-12838 #
NREL/TP-413-5092 ..... p 639 N93-13529 #
NREL/TP-451-5014 ..... p 723 N93-13526 #

NRL/FR-5510-92-9515 ..... p 688 N93-13942 #

NRL/FR/5324-92-9397 ..... p 566 N93-13868 #
NRL/FR/5524-92-9399 ..... p 566 N93-13871 #
NRL/FR/6521-92-9508 ..... p 524 N93-13870 #

NRL/MR/4613-92-6982 ..... p 711 N93-14031 #
NRL/MR/5327-92/7117 ..... p 561 N93-12623 #
NRL/MR/6176-92-7135 ..... p 554 N93-13862 #

NSF-92-104 ..... p 507 N93-13712 #
NSF-92-109 ..... p 562 N93-13024 #
NSF-92-19 ..... p 673 N93-13700 #
NSF-92-23 ..... p 731 N93-13702 #
NSF-92-303 ..... p 730 N93-12907 #
NSF-92-305 ..... p 730 N93-13015 #
NSF-92-307 ..... p 741 N93-13658 #
NSF-92-309 ..... p 731 N93-13698 #
NSF-92-310 ..... p 740 N93-12920 #
NSF-92-312 ..... p 730 N93-13437 #
NSF-92-316 ..... p 731 N93-13454 #
NSF-92-317 ..... p 773 N93-12667 #
NSF-92-318 ..... p 740 N93-13312 #
NSF-92-319 ..... p 741 N93-13657 #
NSF-92-321 ..... p 741 N93-13544 #
NSF-92-323 ..... p 729 N93-12802 #
NSF-92-324 ..... p 741 N93-13543 #
NSF-92-325 ..... p 506 N93-13407 #
NSF-92-326 ..... p 731 N93-13701 #
NSF-92-327 ..... p 729 N93-12694 #
NSF-92-36 ..... p 681 N93-13431 #
NSF-92-38 ..... p 681 N93-13438 #
NSF-92-3 ..... p 775 N93-13381 #
NSF-92-45 ..... p 731 N93-13699 #
NSF-92-55 ..... p 775 N93-13704 #
NSF-92-60 ..... p 775 N93-13713 #
NSF-92-63 ..... p 731 N93-12637 #
NSF-92-70 ..... p 683 N93-12693 #
NSF-92-80 ..... p 732 N93-13703 #
NSF-92-99 ..... p 730 N93-13278 #

NSSDCA/WDC-A-R/S-91-23 ..... p 735 N93-12991 * #

NSWCDD/TR-92/217 ..... p 492 N93-12741 #
NSWCDD/TR-92/297 ..... p 697 N93-14081 #

NTSB/AAR-92/01/SUM ..... p 498 N93-13470 #
NTSB/AAR-92/04 ..... p 498 N93-13426 #

NUWC-NL-RR-10125 ..... p 689 N93-12848 #

OMB-3145-0058 ..... p 731 N93-13702 #
OMB-3145-0058 ..... p 732 N93-13703 #
OMB-3145-0058 ..... p 507 N93-13712 #

ORNL/SUB-87-SA946/02 ..... p 550 N93-12858 #

ORNL/TM-11900 ..... p 689 N93-12797 #

PB92-115575 ..... p 696 N93-12889 #
PB92-133883 ..... p 698 N93-12890 #
PB92-147370 ..... p 734 N93-12759 #
PB92-167964 ..... p 741 N93-13788 #
PB92-169572 ..... p 637 N93-12937 #
PB92-169614 ..... p 643 N93-12938 #
PB92-206507 ..... p 555 N93-12939 #
PB92-206853 ..... p 634 N93-13094 * #
PB92-212943 ..... p 615 N93-13644 #
PB92-213248 ..... p 643 N93-12940 #
PB92-213347 ..... p 559 N93-13640 #
PB92-213362 ..... p 539 N93-13641 #
PB92-213388 ..... p 559 N93-13642 #
PB92-213412 ..... p 689 N93-13198 #
PB92-213511 ..... p 553 N93-13649 #
PB92-213529 ..... p 725 N93-13783 #
PB92-217017 ..... p 643 N93-12941 #
PB92-217132 ..... p 622 N93-12843 #
PB92-217298 ..... p 642 N93-12726 #
PB92-217538 ..... p 576 N93-12975 #
PB92-217546 ..... p 611 N93-12908 #
PB92-217561 ..... p 611 N93-12936 #
PB92-217587 ..... p 738 N93-13415 #
PB92-217603 ..... p 570 N93-12978 #
PB92-217637 ..... p 698 N93-12805 #
PB92-217819 ..... p 558 N93-12976 #

PB92-217835 ..... p 644 N93-12974 #
PB92-217926 ..... p 616 N93-13761 #
PB92-218270 ..... p 559 N93-13648 #
PB92-218429 ..... p 646 N93-13647 #
PB92-218726 ..... p 651 N93-12969 #
PB92-218759 ..... p 769 N93-12803 #
PB92-218791 ..... p 714 N93-12982 #
PB92-220631 ..... p 562 N93-12979 #
PB92-222629 ..... p 498 N93-13787 #
PB92-222694 ..... p 661 N93-12817 #
PB92-222702 ..... p 702 N93-13067 #
PB92-222710 ..... p 649 N93-12818 #
PB92-222751 ..... p 623 N93-12981 #
PB92-222769 ..... p 558 N93-12980 #
PB92-222868 ..... p 678 N93-12983 #
PB92-222934 ..... p 553 N93-13785 #
PB92-223049 ..... p 612 N93-12977 #
PB92-224781 ..... p 649 N93-12804 #
PB92-226265 ..... p 637 N93-12987 #
PB92-226273 ..... p 637 N93-12988 #
PB92-910404 ..... p 498 N93-13470 #
PB92-910405 ..... p 498 N93-13426 #

PL-TR-91-2270 ..... p 562 N93-12948 #
PL-TR-91-2280 ..... p 543 N93-13733 #
PL-TR-92-2052 ..... p 662 N93-13099 #
PL-TR-92-2069 ..... p 650 N93-12943 #
PL-TR-92-2072 ..... p 632 N93-12550 #
PL-TR-92-2086 ..... p 650 N93-12944 #
PL-TR-92-2110-VOL-1 ..... p 691 N93-12607 #
PL-TR-92-2129 ..... p 560 N93-12551 #
PL-TR-92-3024 ..... p 522 N93-12962 #
PL-TR-92-3025 ..... p 525 N93-12963 #

PNL-SA-19946 ..... p 541 N93-12820 #
PNL-SA-20440 ..... p 575 N93-12711 #
PNL-SA-20626 ..... p 677 N93-12712 #
PNL-SA-21162 ..... p 638 N93-13082 #
PNL-SA-21206 ..... p 669 N93-12916 #

PW/GESP-FR-21998-09 ..... p 541 N93-12746 #

R/D-6659-EN-02-VOL-1 ..... p 611 N93-12906 #
R/D-6857-EN-02 ..... p 649 N93-12704 #
R/D-6870-EN-02 ..... p 644 N93-13098 #
R/D-6944-AN-03 ..... p 575 N93-12708 #

REPT-0002 ..... p 687 N93-13880 * #
REPT-1992-19 ..... p 545 N93-12753 #
REPT-268 ..... p 559 N93-13648 #
REPT-72237 ..... p 650 N93-12943 #
REPT-92B00093-VOL-1 ..... p 736 N93-13131 * #
REPT-92B00101 ..... p 661 N93-12700 * #
REPT-92B00110 ..... p 508 N93-13158 * #
REPT-92B00114 ..... p 744 N93-13461 * #
REPT-93B00003 ..... p 559 N93-13434 * #
REPT-93B00013 ..... p 519 N93-13372 * #
REPT-93B00016 ..... p 669 N93-13382 * #

RFP-4609 ..... p 645 N93-13505 #

RIACS-TR-90-14 ..... p 697 N93-13409 * #
RIACS-TR-90-23 ..... p 693 N93-13366 * #
RIACS-TR-90-43 ..... p 686 N93-13408 * #
RIACS-TR-91-23 ..... p 685 N93-13063 * #
RIACS-TR-92-19 ..... p 684 N93-12801 * #

RL-TR-92-118 ..... p 682 N93-12614 #
RL-TR-92-121 ..... p 688 N93-12710 #
RL-TR-92-122 ..... p 570 N93-12866 #
RL-TR-92-123 ..... p 560 N93-12581 #
RL-TR-92-131 ..... p 689 N93-12852 #
RL-TR-92-157 ..... p 608 N93-14085 #
RL-TR-92-160 ..... p 711 N93-14032 #
RL-TR-92-57 ..... p 734 N93-12703 #
RL-TR-92-92 ..... p 562 N93-12867 #

RR-A281 ..... p 698 N93-12890 #

RSS-TR-090192 ..... p 632 N93-12800 * #

RTI/4500/017-01F ..... p 519 N93-13462 * #

RXR-92031 ..... p 650 N93-12944 #

R92-917992-3 ..... p 540 N93-12603 #

S-HRG-102-707 ..... p 742 N93-13800 #

S-REPT-102-364 ..... p 741 N93-13798 #

S-684-VOL-2 ..... p 760 N93-13972 * #

SAIC-91/1236-VOL-1 ..... p 691 N93-12607 #

SAND-91-1282 ..... p 640 N93-13618 #
SAND-91-2477C ..... p 706 N93-12830 #
SAND-91-2625C ..... p 717 N93-13511 #
SAND-91-2768C ..... p 555 N93-12563 #
SAND-91-2774C ..... p 542 N93-13302 #
SAND-91-2907C ..... p 684 N93-12795 #
SAND-91-7017 ..... p 709 N93-12918 #
SAND-91-8711 ..... p 537 N93-13232 #
SAND-91-8732 ..... p 537 N93-13233 #
SAND-92-0152C ..... p 565 N93-13506 #
SAND-92-0482 ..... p 735 N93-12813 #
SAND-92-0876C ..... p 566 N93-13512 #
SAND-92-0971C ..... p 604 N93-12915 #
SAND-92-1154C ..... p 722 N93-13323 #
SAND-92-1200C ..... p 526 N93-13299 #
SAND-92-1242C ..... p 716 N93-13191 #
SAND-92-1255 ..... p 605 N93-13249 #
SAND-92-1267C ..... p 719 N93-12586 #
SAND-92-1342C ..... p 550 N93-12917 #
SAND-92-1404C ..... p 572 N93-13519 #
SAND-92-1501C ..... p 571 N93-13300 #
SAND-92-1543C ..... p 626 N93-13301 #
SAND-92-1571C ..... p 624 N93-13072 #
SAND-92-1603C ..... p 627 N93-13515 #
SAND-92-1745C ..... p 588 N93-13575 #
SAND-92-1775C ..... p 555 N93-12568 #
SAND-92-8405C ..... p 582 N93-13247 #
SAND-92-8463C ..... p 538 N93-13234 #
SAND-92-8491 ..... p 699 N93-13262 #

SATCOM-92-4 ..... p 561 N93-12655 * #

SATCON-R05-90-VOL-1 ..... p 616 N93-13706 * #
SATCON-R05-90-VOL-2 ..... p 615 N93-13608 * #

SDL/92-116 ..... p 652 N93-13460 * #

SE-45 ..... p 649 N93-12804 #

SECA-TR-92-06 ..... p 575 N93-12689 * #

SGD-574-PT-1 ..... p 769 N93-12803 #

SLAC-PUB-5868 ..... p 707 N93-13090 #

SLAC-382 ..... p 703 N93-13092 #

SLCET-TR-92-4 ..... p 574 N93-13839 #
SLCET-TR-92-8 ..... p 534 N93-13940 #

SMC-TR-92-36 ..... p 524 N93-14087 #
SMC-TR-92-37 ..... p 708 N93-14089 #
SMC-TR-92-39 ..... p 544 N93-14098 #
SMC-TR-92-40 ..... p 603 N93-14086 #
SMC-TR-92-41 ..... p 727 N93-14083 #

SRI-1165 ..... p 543 N93-13733 #

SRS-566 ..... p 558 N93-12976 #

SRS/STG-TR92-01-VOL-3-APP-C ..... p 678 N93-12990 * #

SSCL-578 ..... p 707 N93-13108 #
SSCL-580 ..... p 623 N93-13003 #

SSD-TR-92-27 ..... p 712 N93-12705 #
SSD-TR-92-28 ..... p 554 N93-14099 #

SSL-PREPRINT-90-119 ..... p 770 N93-13477 * #
SSL-PREPRINT-90-124 ..... p 770 N93-13478 * #

STS-86-0302-3-VOL-3 ..... p 740 N93-12814 * #

SU-SLAC-PUB-5725 ..... p 706 N93-12992 #
SU-SLAC-PUB-5733-REV ..... p 727 N93-12826 #
SU-SLAC-PUB-5819 ..... p 707 N93-12993 #
SU-SLAC-PUB-5842 ..... p 704 N93-13250 #

SU-SLAC-393 ..... p 737 N93-13275 #

SU-STAN-CS-91-1375 ..... p 685 N93-12961 #

SU-TR-E450-2 ..... p 566 N93-13869 #

SU-TR-456 ..... p 697 N93-12702 #

TEC-R-156 ..... p 499 N93-13351 #
TEC-R-161 ..... p 499 N93-13348 #
TEC-R-167 ..... p 634 N93-13333 #
TEC-R-179 ..... p 634 N93-13345 #
TEC-R-180 ..... p 632 N93-12598 #

TELAC-91-16A ..... p 503 N93-12959 #

TM-1450 ..... p 559 N93-13604 * #

TR-0090(5935-08)-1 ..... p 603 N93-14086 #

TR-0090(5940-05)-5 ..... p 708 N93-14089 #
TR-0091(6935-03)-1 ..... p 554 N93-14099 #
TR-0091(6940-05)-3 ..... p 524 N93-14087 #
TR-0091(6945-03)-2 ..... p 727 N93-14083 #
TR-0091(6945-03)-3 ..... p 544 N93-14098 #
TR-169 ..... p 698 N93-13064 #
TR-1992-11 ..... p 570 N93-12650 #
TR-1992-17 ..... p 545 N93-12651 #
TR-1992-20 ..... p 545 N93-12754 #
TR-1992-21 ..... p 545 N93-12755 #
TR-1992-9 ..... p 545 N93-12749 #
TR-50 ..... p 536 N93-12618 #
TR-77-ONR ..... p 595 N93-12619 #
TR-89-2 ..... p 673 N93-13612 * #
TR-92(2940)-1 ..... p 712 N93-12705 #
TR-92/ONR-35 ..... p 736 N93-13117 #

TRB/TRR-1332 ..... p 498 N93-13787 #

TR4480-074-91 ..... p 611 N93-12908 #

TWR-63286 ..... p 558 N93-13021 * #

UAH-5-32391 ..... p 709 N93-12894 * #
UAH-5-32417 ..... p 649 N93-12718 * #
UAH-5-32425 ..... p 719 N93-12691 * #
UAH-5-32527 ..... p 742 N93-12657 * #
UAH-5-32639 ..... p 522 N93-12893 * #
UAH-5-32794 ..... p 709 N93-13062 * #
UAH-835-REV-1.1 ..... p 678 N93-12966 * #

UCLA-ENG-92-19 ..... p 523 N93-13715 * #

UCRL-CR-109002 ..... p 541 N93-12790 #
UCRL-CR-111008 ..... p 706 N93-12970 #

UCRL-ID-110448 ..... p 738 N93-13619 #

UCRL-JC-107973 ..... p 606 N93-13534 #
UCRL-JC-108710 ..... p 555 N93-12933 #
UCRL-JC-108831 ..... p 550 N93-12888 #
UCRL-JC-108836 ..... p 552 N93-13538 #
UCRL-JC-108860 ..... p 714 N93-12932 #
UCRL-JC-108861 ..... p 714 N93-12971 #
UCRL-JC-108951 ..... p 646 N93-13655 #
UCRL-JC-108954 ..... p 645 N93-13615 #
UCRL-JC-108955 ..... p 646 N93-13646 #
UCRL-JC-108956 ..... p 646 N93-13654 #
UCRL-JC-108957 ..... p 643 N93-12927 #
UCRL-JC-109170 ..... p 596 N93-12762 #
UCRL-JC-109697 ..... p 642 N93-12884 #
UCRL-JC-109843 ..... p 712 N93-12571 #
UCRL-JC-109844 ..... p 603 N93-12570 #
UCRL-JC-109845 ..... p 606 N93-13653 #
UCRL-JC-109956 ..... p 550 N93-12931 #
UCRL-JC-110036 ..... p 715 N93-13105 #
UCRL-JC-110043 ..... p 604 N93-12925 #
UCRL-JC-110324 ..... p 701 N93-12806 #
UCRL-JC-110355 ..... p 565 N93-13357 #
UCRL-JC-110360 ..... p 721 N93-12972 #
UCRL-JC-110364 ..... p 643 N93-12926 * #
UCRL-JC-110377 ..... p 576 N93-12912 #
UCRL-JC-110478 ..... p 721 N93-12887 #
UCRL-JC-110494 ..... p 753 N93-13536 #
UCRL-JC-110809 ..... p 576 N93-12839 #
UCRL-JC-110828 ..... p 525 N93-12840 #
UCRL-JC-110922-REV-1 ..... p 642 N93-12880 #

UCRL-LR-109886 ..... p 596 N93-12831 #
UCRL-LR-110322 ..... p 576 N93-12825 #

UCRL-TT-105571 ..... p 718 N93-13732 #

UILU-ENG-92-2003 ..... p 558 N93-12976 #
UILU-ENG-92-2242 ..... p 694 N93-13376 * #
UILU-ENG-92-2243 ..... p 572 N93-13569 * #
UILU-ENG-92-2245 ..... p 565 N93-13375 * #

UMICH-028918-2-T ..... p 565 N93-13354 * #

UNC-WRRI-92-268 ..... p 559 N93-13648 #

US-PATENT-APPL-SN-429514 ..... p 531 N93-13416 *
US-PATENT-APPL-SN-632408 ..... p 711 N93-13711 *
US-PATENT-APPL-SN-658477 ..... p 700 N93-13421 *
US-PATENT-APPL-SN-660755 ..... p 614 N93-13417 *
US-PATENT-APPL-SN-664194 ..... p 626 N93-13420 *
US-PATENT-APPL-SN-710424 ..... p 605 N93-13418 *
US-PATENT-APPL-SN-744197 ..... p 709 N93-13419 *
US-PATENT-APPL-SN-781520 ..... p 558 N93-13422 *
US-PATENT-APPL-SN-850107 ..... p 551 N93-13101 #
US-PATENT-APPL-SN-863908 ..... p 710 N93-13500 #
US-PATENT-APPL-SN-864812 ..... p 552 N93-13414 #
US-PATENT-APPL-SN-882408 ..... p 614 N93-13423 *
US-PATENT-APPL-SN-882721 ..... p 556 N93-13471 #
US-PATENT-APPL-SN-891119 ..... p 572 N93-13473 #
US-PATENT-APPL-SN-891120 ..... p 572 N93-13472 #
US-PATENT-APPL-SN-905706 ..... p 597 N93-13501 #
US-PATENT-APPL-SN-913433 ..... p 711 N93-13711 *

US-PATENT-CLASS-248-550 ..... p 626 N93-13420 *
US-PATENT-CLASS-250-339 ..... p 709 N93-13419 *
US-PATENT-CLASS-294-89 ..... p 614 N93-13417 *
US-PATENT-CLASS-294-94 ..... p 614 N93-13417 *
US-PATENT-CLASS-318-648 ..... p 626 N93-13420 *
US-PATENT-CLASS-318-649 ..... p 626 N93-13420 *
US-PATENT-CLASS-356-328 ..... p 709 N93-13419 *
US-PATENT-CLASS-357-30 ..... p 709 N93-13419 *
US-PATENT-CLASS-358-231 ..... p 711 N93-13711 *
US-PATENT-CLASS-358-232 ..... p 711 N93-13711 *
US-PATENT-CLASS-358-61 ..... p 711 N93-13711 *
US-PATENT-CLASS-359-859 ..... p 709 N93-13419 *
US-PATENT-CLASS-372-45 ..... p 605 N93-13418 *
US-PATENT-CLASS-372-46 ..... p 605 N93-13418 *
US-PATENT-CLASS-411-267 ..... p 614 N93-13423 *
US-PATENT-CLASS-411-433 ..... p 614 N93-13423 *
US-PATENT-CLASS-411-909 ..... p 614 N93-13423 *
US-PATENT-CLASS-525-421 ..... p 531 N93-13416 *
US-PATENT-CLASS-525-426 ..... p 531 N93-13416 *
US-PATENT-CLASS-525-432 ..... p 531 N93-13416 *
US-PATENT-CLASS-525-436 ..... p 531 N93-13416 *
US-PATENT-CLASS-525-903 ..... p 531 N93-13416 *
US-PATENT-CLASS-62-335 ..... p 558 N93-13422 *
US-PATENT-CLASS-62-434 ..... p 558 N93-13422 *
US-PATENT-CLASS-62-467 ..... p 558 N93-13422 *
US-PATENT-CLASS-73-24.01 ..... p 700 N93-13421 *
US-PATENT-CLASS-73-24.05 ..... p 700 N93-13421 *
US-PATENT-CLASS-73-24.06 ..... p 700 N93-13421 *
US-PATENT-CLASS-73-579 ..... p 626 N93-13420 *
US-PATENT-CLASS-73-668 ..... p 626 N93-13420 *

US-PATENT-5,156,370 ..... p 626 N93-13420 *
US-PATENT-5,157,938 ..... p 558 N93-13422 *
US-PATENT-5,158,331 ..... p 614 N93-13417 *
US-PATENT-5,159,029 ..... p 531 N93-13416 *
US-PATENT-5,159,199 ..... p 709 N93-13419 *
US-PATENT-5,159,603 ..... p 605 N93-13418 *
US-PATENT-5,159,843 ..... p 700 N93-13421 *
US-PATENT-5,160,233 ..... p 614 N93-13423 *
US-PATENT-5,161,027 ..... p 711 N93-13711 *

USAARL-92-25 ..... p 680 N93-14090 #

USAEHA-TG-189 ..... p 675 N93-13941 #
USAEHA-TG-192 ..... p 604 N93-12610 #

USAFETAC/PR-92/003 ..... p 499 N93-12605 #

USARIEM-T8-92 ..... p 677 N93-12960 #

WES/IR/ITL-92-4 ..... p 684 N93-12851 #
WES/IR/ITL-92-5 ..... p 684 N93-12872 #

WES/IS/ITL-90-4 ..... p 684 N93-12872 #

WES/TR/EL-92-26 ..... p 635 N93-13867 #

WINCO-11795 ..... p 539 N93-13530 #
WINCO-11800 ..... p 597 N93-13267 #
WINCO-11813 ..... p 575 N93-12761 #

WL-TM-92-338-FIGC ..... p 500 N93-12752 #

WL-TP-92-007 ..... p 519 N93-12611 #

WL-TR-92-1028 ..... p 566 N93-13838 #
WL-TR-92-1060 ..... p 690 N93-12548 #
WL-TR-92-2033 ..... p 727 N93-12546 #
WL-TR-92-3049 ..... p 621 N93-12606 #
WL-TR-92-3063 ..... p 505 N93-13872 #

WSRC-IM-90-83-6-REV ..... p 681 N93-12886 #
WSRC-IM-90-83-7 ..... p 690 N93-13620 #

WSRC-MS-92-249 ..... p 619 N93-13036 #

WSRC-RD-91-24 ..... p 550 N93-13035 #

WSRC-RP-92-471 ..... p 710 N93-13576 #

Y/CSD/INF-92/8 ..... p 619 N93-12794 #

Y/DD-564 ..... p 704 N93-13319 #

Appendix

NASA SCIENTIFIC AND TECHNICAL INFORMATION PROGRAM PRODUCTS AND SERVICES

The NASA Scientific and Technical Information (STI) Program provides for the collection and announcement of aerospace-related reports and literature obtained worldwide through agreements and exchanges. The result of the collection is the comprehensive NASA STI Database that covers aeronautics, space, and supporting disciplines.

The STI Database, documents generated or obtained by NASA, and products and services derived from or supporting the database are made available to the NASA research community and to the public. Descriptions and sources of these items are presented in the following pages.

Scientific and Technical Aerospace Reports (*STAR*) is an abstract journal, listing citations with abstracts for aerospace-related reports obtained from worldwide sources. *STAR* is issued on the first of each month, and announces current documents that have been entered into the NASA STI Database during the previous month. The reports are of the following types:

- NASA, NASA contractor, and NASA grantee reports;
- Reports issued by other U.S. Government agencies, domestic and foreign institutions, universities, and private firms;
- Translations in report form;
- NASA-owned patents and patent applications;
- Other U.S. Government agency and foreign patents and patent applications;
- Domestic and foreign dissertations and theses.

Journal, book, and conference literature, journal translations, and certain foreign dissertations having the same subject scope as *STAR* are announced in a companion journal, *International Aerospace Abstracts* (*IAA*). *IAA* is issued on the 1st and 15th of each month and is available from the American Institute of Aeronautics and Astronautics, Technical Information Service, 555 West 57th Street, 12th Floor, New York, NY 10019.

ELIGIBILITY AND REGISTRATION FOR NASA STI PRODUCTS AND SERVICES

Organizations of the type listed below that have registered with NASA can receive products and services.

- NASA offices and installations, contractors, subcontractors, grantees, and consultants;
- Other U.S. Government agencies and their contractors;
- Libraries in the United States that have arrangements with NASA to maintain collections of NASA documents for public reference;
- Other organizations in the United States having a need for NASA documents in work related to aeronautics and space research;
- Organizations abroad that have established reciprocal documents exchange arrangements with NASA.

The central service points — central points of document acquisition and control within qualified organizations — or individuals are eligible to register for NASA STI products and services. Domestic organizations or individuals may be eligible to receive various classes of NASA publications and services and should address their requests for registration or further information to:

ATTN: Registration Services
NASA Center for AeroSpace Information
800 Elkridge Landing Road
Linthicum Heights, MD 21090-2934
301-621-0390

Organizations abroad should direct requests to:

National Aeronautics and Space Administration
Scientific and Technical Information Program (JTT)
International STI Program
Washington, DC 20546-0001
USA
703-271-5640

SUBJECT SCOPE

The subject scope of *STAR* and *IAA* includes all aspects of aeronautics and space research and development, supporting basic and applied research, and applications. Aerospace aspects of Earth resources, energy development, conservation, oceanography, environmental protection, urban transportation, and other topics of high national priority are also covered.

HOW TO USE *STAR* SUBJECT CATEGORIES

Abstracts in *STAR* are categorized by 10 major subject divisions that are divided further into 76 specific subject categories. The subject divisions and categories are listed in the Table of Contents together with a note for each that defines its scope and provides any cross-references. For example:

16 SPACE TRANSPORTATION
Includes passenger and cargo space transportation, e.g., shuttle operations; and space rescue techniques. For related information see also *03 Air Transportation and Safety* and *18 Spacecraft Design, Testing and Performance*. For space suits see *54 Man/System Technology and Life Support*.

CROSS-REFERENCES

Individual *STAR* abstracts are not ordinarily cross-referenced, except for certain conference reports or book translations that have had separate abstracts written for their component papers or chapters. Citations and abstracts of the components follow immediately after those of the parent document. When the subject content of a component differs sufficiently from the general content of the parent, a cross-reference citation also is printed at the end of the category to which it normally would have been assigned if it were independent.

DOCUMENTS ON MICROFICHE

Documents available on microfiche are designated by a pound sign (#) following the accession number.

LIMITED REPRODUCIBILITY

A note of limited reproducibility appears in the citation, if there are factors affecting the reproducibility of more than 20% of the document. These factors include faint or broken type, color photographs, black and white photographs, foldouts, dot matrix print, or some other factor that limits the reproducibility of the document. This notation also appears on the microfiche header.

COLOR COPIES

An increasing number of NASA scientific and technical reports are being produced with color graphs, charts, illustrations, and photographs. An indication that a document has color pages follows the source and pricing (SAP) information in the *STAR* citation.

Registered users of the NASA Scientific and Technical Information Program will receive ordered documents with color at no additional cost, as long as stock copies of the document are available. Otherwise, an additional fee of $2.00 per color page will be charged. The NASA Center for AeroSpace Information staff will contact registered users to determine individual user's needs.

NASA PATENTS AND PATENT APPLICATIONS

Patents and patent applications owned by NASA are announced in *STAR* under appropriate subject categories and are referenced in the *STAR* indexes. In the Report/Accession Number Index, patents are indexed by the NASA Case Number, and the U.S. Patent Class. Patent applications are indexed by the NASA Case Number and the U.S. Patent Application Serial Number.

Printed copies of patents (which are not microfiched) are available for purchase from the U.S. Patent and Trademark Office.

When ordering patents, the U.S. Patent Number should be used, and payment must be remitted in advance, by money order or check payable to the Commissioner of Patents and Trademarks. Prepaid purchase coupons for ordering are also available from the U.S. Patent and Trademark Office.

NASA patent application specifications are sold in both paper copy and microfiche by the NASA Center for AeroSpace Information (CASI). The N accession number should be used in ordering either paper copy or microfiche from CASI.

The patents and patent applications announced in *STAR* are owned by NASA and are available for royalty-free licensing. Requests for licensing terms and further information should be addressed to:

National Aeronautics and Space Administration
Associate General Counsel for Intellectual Property
Code GP
Washington, DC 20546-0001

SOURCES FOR DOCUMENTS

One or more sources from which a document announced in *STAR* is available to the public is given in each citation. The most commonly indicated sources and their acronyms or abbreviations are listed below, and their addresses are listed on page A-6. If the publication is available from a source other than those listed, the publisher and address will be displayed on the availability line or in combination with the corporate source line.

Avail: CASI. Sold by the NASA Center for AeroSpace Information. Prices for hard copy (HC) and microfiche (MF) are indicated by a price code following the letters HC or MF in the *STAR* citation. Current values for the price codes are given in the tables on page A-7.

NOTE ON ORDERING DOCUMENTS: When ordering publications from CASI, use the N accession number or other report number. It is also advisable to cite the title and other bibliographic identification.

Avail: SOD (or GPO). Sold by the Superintendent of Documents, U.S. Government Printing Office, in hard copy.

Avail: BLL (formerly NLL): British Library Lending Division, Boston Spa, Wetherby, Yorkshire, England. Photocopies available from this organization at the price shown. (If none is given, address inquiry to the BLL.)

Avail: DOE Depository Libraries. Organizations in U.S. cities and abroad that maintain collections of Department of Energy reports, usually in microfiche form, are listed in *Energy Research Abstracts*. Services available from the DOE and its depositories are described in a booklet, *DOE Technical Information Center - Its Functions and Services* (TID-4660), which may be obtained without charge from the DOE Technical Information Center.

Avail: ESDU. Pricing information on specific data, computer programs, and details on Engineering Sciences Data Unit (ESDU) topic categories can be obtained from ESDU International Ltd. Requesters in North America should use the Virginia address while all other requesters should use the London address, both of which are on page A-6.

Avail: Fachinformationszentrum, Karlsruhe. Gesellschaft fur wissenschaftlich-technische Information mbH 7514 Eggenstein-Leopoldshafen 2, Germany.

Avail: HMSO. Publications of Her Majesty's Stationery Office are sold in the U.S. by Pendragon House, Inc. (PHI), Redwood City, CA. The U.S. price (including a service and mailing charge) is given, or a conversion table may be obtained from PHI.

Avail: Issuing Activity, or Corporate Author, or no indication of availability. Inquiries as to the availability of these documents should be addressed to the organization shown in the citation as the corporate author of the document.

Avail: NASA Public Document Rooms. Documents so indicated may be examined at or purchased from the National Aeronautics and Space Administration (JBD-4), Public Documents Room (Room 1H23), Washington, DC 20546-0001, or public document rooms located at NASA installations, and the NASA Pasadena Office at the Jet Propulsion Laboratory.

Avail: NTIS. Sold by the National Technical Information Service. Initially distributed microfiche under the NTIS SRIM (Selected Research in Microfiche) are available. For information concerning this service, consult the NTIS Subscription Section, Springfield, VA 22161.

Avail: Univ. Microfilms. Documents so indicated are dissertations selected from *Dissertation Abstracts* and are sold by University Microfilms as xerographic copy (HC) and microfilm. All requests should cite the author and the Order Number as they appear in the citation.

Avail: US Patent and Trademark Office. Sold by Commissioner of Patents and Trademarks, U.S. Patent and Trademark Office, at the standard price of $1.50 each, postage free. (See discussion of NASA patents and patent applications on page A-3.)

Avail: (US Sales Only). These foreign documents are available to users within the United States from the National Technical Information Service (NTIS). They are available to users outside the United States through the International Nuclear Information Service (INIS) representative in their country, or by applying directly to the issuing organization.

Avail: USGS. Originals of many reports from the U.S. Geological Survey, which may contain color illustrations, or otherwise may not have the quality of illustrations preserved in the microfiche or facsimile reproduction, may be examined by the public at the libraries of the USGS field offices whose addresses are listed on page A-6. The libraries may be queried concerning the availability of specific documents and the possible utilization of local copying services, such as color reproduction.

FEDERAL DEPOSITORY LIBRARIES: To provide the general public with greater access to U.S. Government publications, Congress established the Federal Depository Library Program under the Government Printing Office (GPO), with 53 regional depositories responsible for permanent retention of material, inter-library loan, and reference services. (These libraries are not sales outlets.) At least one copy of nearly every NASA and NASA-sponsored publication, either in printed or microfiche format, is received and retained by the 53 regional depositories. A list of the regional GPO libraries, appears on page A-8. A local library can contact a regional depository library to help locate specific reports, or direct contact may be made by an individual.

PUBLIC COLLECTION OF NASA DOCUMENTS

An extensive collection of NASA and NASA-sponsored publications is maintianed by the British Library Lending Divison, Boston Spa, Wetherby, Yorkshire, England, for public access. The British Library Lending Division also has available many of the non-NASA publications cited in *STAR*.

European requesters may purchase facsimile copy or microfiche of NASA and NASA-sponsored documents, those identified by both the symbols # and * from ESA—Information Retrieval Service, European Space Agency, 8-10 rue Mario-Nikis, 75738 Paris CEDEX 15, France.

SUBMITTING DOCUMENTS

All users of this abstract service are urged to forward reports to be considered for announcement in *STAR*. This will aid NASA in its efforts to provide the fullest possible coverage of all scientific and technical publications that might support aeronautics and space research and development. If you have prepared relevant reports (other than those you will transmit to NASA, DOD, or DOE through the usual contract- or grant-reporting channels), please send them for consideration to the NASA Center for AeroSpace Information, 800 Elkridge Landing Road, Linthicum Heights, MD 21090-2934.

Reprints of journal articles, book chapters, and conference papers are also welcome. These will be considered for announcement in *STAR*'s companion journal, *IAA*.

You may specify a particular source to be included in a report announcement if you wish; otherwise the report will be placed on a public sale at the NASA Center for AeroSpace Information. Copyrighted publications will be announced but not distributed or sold.

PURCHASE OF *STAR*

STAR is publicly available on annual subscription from the NASA Center for AeroSpace Information (CASI) at $114.00.

STAR is available to registered users on annual subscription from the NASA Center for AeroSpace Information, ATTN: Registration Services, 800 Elkridge Landing Road, Linthicum Heights, MD 21090-2934.

Microfiche of the abstract sections of *STAR* are available, on annual subscription, from CASI. Annual subscription rates are $216.00 North America; $432.00 foreign.

ADDRESSES OF ORGANIZATIONS

American Institute of Aeronautics and Astronautics
Technical Information Service
555 West 57th Street, 12th Floor
New York, New York 10019

British Library Lending Division,
Boston Spa, Wetherby, Yorkshire,
England

Commissioner of Patents and Trademarks
U.S. Patent and Trademark Office
Washington, DC 20231

Department of Energy
Technical Information Center
P.O. Box 62
Oak Ridge, Tennessee 37830

European Space Agency-Information Retrieval Service
ESRIN
Via Galileo Galilei
00044 Frascati (Rome) Italy

Engineering Sciences Data Unit International
P.O. Box 1633
Manassas, Virginia 22110

Engineering Sciences Data Unit International, Ltd.
251-259 Regent Street
London, W1R 7AD, England

Fachinformationszentrum Karlsruhe
Gesellschaft fur wissenschaftlich-technische
Information mbH
7514 Eggenstein-Leopoldshafen 2, Germany

Her Majesty's Stationery Office
P.O. Box 569, S.E. 1
London, England

NASA Center for AeroSpace Information
800 Elkridge Landing Road
Linthicum Heights, MD 21090-2934

National Aeronautics and Space Administration
Scientific and Technical Information Program (JTT)
Washington, DC 20546-0001

National Technical Information Service
5285 Port Royal Road
Springfield, Virginia 22161

Pendragon House, Inc.
899 Broadway Avenue
Redwood City, California 94063

Superintendent of Documents
U.S. Government Printing Office
Washington, DC 20402

University Microfilms
A Xerox Company
300 North Zeeb Road
Ann Arbor, Michigan 48106

University Microfilms, Ltd.
Tylers Green
London, England

U.S. Geological Survey Library National Center
MS 950
12201 Sunrise Valley Drive
Reston, Virginia 22092

U.S. Geological Survey Library
2255 North Gemini Drive
Flagstaff, Arizona 86001

U.S. Geological Survey
345 Middlefield Road
Menlo Park, California 94025

U.S. Geological Survey Library
Box 25046
Denver Federal Center, MS914
Denver, Colorado 80225

CASI PRICE TABLES

(Effective October 1, 1992)

STANDARD PRICE DOCUMENTS

PRICE CODE	NORTH AMERICAN PRICE	FOREIGN PRICE
A01	$ 9.00	$ 18.00
A02	12.50	25.00
A03	17.00	34.00
A04-A05	19.00	38.00
A06-A09	26.00	52.00
A10-A13	35.00	70.00
A14-A17	43.00	86.00
A18-A21	50.00	100.00
A22-A25	59.00	118.00
A99	69.00	138.00

MICROFICHE

PRICE CODE	NORTH AMERICAN PRICE	FOREIGN PRICE
A01	$ 9.00	$ 18.00
A02	12.50	25.00
A03	17.00	34.00
A04	19.00	38.00
A06	26.00	52.00
A10	35.00	70.00

IMPORTANT NOTICE

CASI Shipping and Handling Charges
U.S. — ADD $3.00 per TOTAL ORDER
Canada and Mexico — ADD $3.50 per TOTAL ORDER
All Other Countries — ADD $7.50 per TOTAL ORDER
Does NOT apply to orders
requesting CASI RUSH HANDLING.
Contact CASI for charge.

FEDERAL REGIONAL DEPOSITORY LIBRARIES

ALABAMA

AUBURN UNIV. AT MONTGOMERY LIBRARY
Documents Dept.
7300 University Drive
Montgomery, AL 36117-3596
(205) 244-3650 FAX: (205) 244-0678

UNIV. OF ALABAMA
Amelia Gayle Gorgas Library
Govt. Documents
Box 870266
Tuscaloosa, AL 35487-0266
(205) 348-6046 FAX: (205) 348-8833

ARIZONA

DEPT. OF LIBRARY, ARCHIVES, AND PUBLIC RECORDS
Federal Documents
Third Floor State Capitol
1700 West Washington
Phoenix, AZ 85007
(602) 542-4121 FAX: (602) 542-4400; 542-4500

ARKANSAS

ARKANSAS STATE LIBRARY
State Library Services
One Capitol Mall
Little Rock, AR 72201
(501) 682-2869

CALIFORNIA

CALIFORNIA STATE LIBRARY
Govt. Publications Section
914 Capitol Mall - P.O. Box 942837
Sacramento, CA 94237-0001
(916) 322-4572 FAX: (916) 324-8120

COLORADO

UNIV. OF COLORADO - BOULDER
Norlin Library
Govt. Publications
Campus Box 184
Boulder, CO 80309-0184
(303) 492-8834 FAX: (303) 492-2185

DENVER PUBLIC LIBRARY
Govt. Publications Dept. BS/GPD
1357 Broadway
Denver, CO 80203
(303) 571-2135

CONNECTICUT

CONNECTICUT STATE LIBRARY
231 Capitol Avenue
Hartford, CT 06106
(203) 566-4971 FAX: (203) 566-3322

FLORIDA

UNIV. OF FLORIDA LIBRARIES
Documents Dept.
Library West
Gainesville, FL 32611-2048
(904) 392-0366 FAX: (904) 392-7251

GEORGIA

UNIV. OF GEORGIA LIBRARIES
Govt. Documents Dept.
Jackson Street
Athens, GA 30602
(404) 542-8949 FAX: (404) 542-6522

HAWAII

UNIV. OF HAWAII
Hamilton Library
Govt. Documents Collection
2550 The Mall
Honolulu, HI 96822
(808) 948-8230 FAX: (808) 956-5968

IDAHO

UNIV. OF IDAHO LIBRARY
Documents Section
Moscow, ID 83843
(208) 885-6344 FAX: (208) 885-6817

ILLINOIS

ILLINOIS STATE LIBRARY
Reference Dept.
300 South Second
Springfield, IL 62701-1796
(217) 782-7596 FAX: (217) 524-0041

INDIANA

INDIANA STATE LIBRARY
Serials/Documents Section
140 North Senate Avenue
Indianapolis, IN 46204
(317) 232-3678 FAX: (317) 232-3728

IOWA

UNIV. OF IOWA LIBRARIES
Govt. Publications Dept.
Washington & Madison Streets
Iowa City, IA 52242
(319) 335-5926 FAX: (319) 335-5830

KANSAS

UNIV. OF KANSAS
Govt. Documents & Map Library
6001 Malott Hall
Lawrence, KS 66045-2800
(913) 864-4660 FAX: (913) 864-5380

KENTUCKY

UNIV. OF KENTUCKY LIBRARIES
Govt. Publications/Maps Dept.
Lexington, KY 40506-0039
(606) 257-3139 FAX: (606) 257-1563; 257-8379

LOUISIANA

LOUISIANA STATE UNIV.
Middleton Library
Govt. Documents Dept.
Baton Rouge, LA 70803
(504) 388-2570 FAX: (504) 388-6992

LOUISIANA TECHNICAL UNIV.
Prescott Memorial Library
Govt. Documents Dept.
305 Wisteria Street
Ruston, LA 71270-9985
(318) 257-4962 FAX: (318) 257-2447

MAINE

TRI-STATE DOCUMENTS DEPOSITORY
Raymond H. Fogler Library
Govt. Documents & Microforms Dept.
Univ. of Maine
Orono, ME 04469
(207) 581-1680

MARYLAND

UNIV. OF MARYLAND
Hornbake Library
Govt. Documents/Maps Unit
College Park, MD 20742
(301) 454-3034 FAX: (301) 454-4985

MASSACHUSETTS

BOSTON PUBLIC LIBRARY
Govt. Documents Dept.
666 Boylston Street
Boston, MA 02117
(617) 536-5400 ext. 226
FAX: (617) 267-8273; 267-8248

MICHIGAN

DETROIT PUBLIC LIBRARY
5201 Woodward Avenue
Detroit, MI 48202-4093
(313) 833-1440; 833-1409
FAX: (313) 833-5039

LIBRARY OF MICHIGAN
Govt. Documents Unit
P.O. Box 30007
Lansing, MI 48909
(517) 373-0640 FAX: (517) 373-3381

MINNESOTA

UNIV. OF MINNESOTA
Wilson Library
Govt. Publications Library
309 19th Avenue South
Minneapolis, MN 55455
(612) 624-5073 FAX: (612) 626-9353

MISSISSIPPI

UNIV. OF MISSISSIPPI
J.D. Williams Library
Federal Documents Dept.
106 Old Gym Bldg.
University, MS 38677
(601) 232-5857 FAX: (601) 232-5453

MISSOURI

UNIV. OF MISSOURI - COLUMBIA
Ellis Library
Govt. Documents
Columbia, MO 65201
(314) 882-6733 FAX: (314) 882-8044

MONTANA

UNIV. OF MONTANA
Maureen & Mike Mansfield Library
Documents Div.
Missoula, MT 59812-1195
(406) 243-6700 FAX: (406) 243-2060

NEBRASKA

UNIV. OF NEBRASKA - LINCOLN
D.L. Love Memorial Library
Documents Dept.
Lincoln, NE 68588
(402) 472-2562

NEVADA

UNIV. OF NEVADA
Reno Library
Govt. Publications Dept.
Reno, NV 89557
(702) 784-6579 FAX: (702) 784-1751

NEW JERSEY

NEWARK PUBLIC LIBRARY
U.S. Documents Div.
5 Washington Street - P.O. Box 630
Newark, NJ 07101-0630
(201) 733-7812 FAX: (201) 733-5648

NEW MEXICO

UNIV. OF NEW MEXICO
General Library
Govt. Publications Dept.
Albuquerque, NM 87131-1466
(505) 277-5441 FAX: (505) 277-6019

NEW MEXICO STATE LIBRARY
325 Don Gaspar Avenue
Santa Fe, NM 87503
(505) 827-3826 FAX: (505) 827-3820

NEW YORK

NEW YORK STATE LIBRARY
Documents/Gift & Exchange Section
Federal Depository Program
Cultural Education Center
Albany, NY 12230
(518) 474-5563 FAX: (518) 474-5786

NORTH CAROLINA

UNIV. OF NORTH CAROLINA - CHAPEL HILL
CB#3912, Davis Library
BA/SS Dept.—Documents
Chapel Hill, NC 27599
(919) 962-1151 FAX: (919) 962-0484

NORTH DAKOTA

NORTH DAKOTA STATE UNIV. LIBRARY
Documents Office
Fargo, ND 58105
(701) 237-8886 FAX: (701) 237-7138
In cooperation with Univ. of North Dakota, Chester Fritz Library
Grand Forks

OHIO

STATE LIBRARY OF OHIO
Documents Dept.
65 South Front Street
Columbus, OH 43266
(614) 644-7051 FAX: (614) 752-9178

OKLAHOMA

OKLAHOMA DEPT. OF LIBRARIES
U.S. Govt. Information Div.
200 NE 18th Street
Oklahoma City, OK 73105-3298
(405) 521-2502, ext. 252, 253
FAX: (405) 525-7804

OKLAHOMA STATE UNIV.
Edmon Low Library
Documents Dept.
Stillwater, OK 74078
(405) 744-6546 FAX: (405) 744-5183

OREGON

PORTLAND STATE UNIV.
Millar Library
934 SW Harrison - P.O. Box 1151
Portland, OR 97207
(503) 725-3673 FAX: (503) 725-4527

PENNSYLVANIA

STATE LIBRARY OF PENN.
Govt. Publications Section
Walnut St. & Commonwealth Ave. - P.O. Box 1601
Harrisburg, PA 17105
(717) 787-3752

SOUTH CAROLINA

CLEMSON UNIV.
Cooper Library
Public Documents Unit
Clemson, SC 29634-3001
(803) 656-5174 FAX: (803) 656-3025
In cooperation with Univ. of South Carolina, Thomas Cooper Library, Columbia

TENNESSEE

MEMPHIS STATE UNIV. LIBRARIES
Govt. Documents
Memphis, TN 38152
(901) 678-2586 FAX: (901) 678-2511

TEXAS

TEXAS STATE LIBRARY
United States Documents
P.O. Box 12927 - 1201 Brazos
Austin, TX 78711
(512) 463-5455 FAX: (512) 463-5436

TEXAS TECH. UNIV. LIBRARY
Documents Dept.
Lubbock, TX 79409
(806) 742-2268 FAX: (806) 742-1920

UTAH

UTAH STATE UNIV.
Merrill Library & Learning Resources Center, UMC-3000
Documents Dept.
Logan, UT 84322-3000
(801) 750-2684 FAX: (801) 750-2677

VIRGINIA

UNIV. OF VIRGINIA
Alderman Library
Govt. Documents
Charlottesville, VA 22903-2498
(804) 924-3133 FAX: (804) 924-4337

WASHINGTON

WASHINGTON STATE LIBRARY
Document Section
MS AJ-11
Olympia, WA 98504-0111
(206) 753-4027 FAX: (206) 753-3546

WEST VIRGINIA

WEST VIRGINIA UNIV. LIBRARY
Govt. Documents Section
P.O. Box 6069
Morgantown, WV 26506
(304) 293-3640

WISCONSIN

ST. HIST. SOC. OF WISCONSIN LIBRARY
Govt. Publications Section
816 State Street
Madison, WI 53706
(608) 262-2781 FAX: (608) 262-4711
In cooperation with Univ. of Wisconsin-Madison, Memorial Library

MILWAUKEE PUBLIC LIBRARY
Documents Div.
814 West Wisconsin Avenue
Milwaukee, WI 53233
(414) 278-2167 FAX: (414) 278-2137

National Aeronautics and
Space Administration
Code JTT
Washington, D.C.
20546-0001

Official Business
Penalty for Private Use, $300

SPECIAL FOURTH-CLASS RATE
POSTAGE & FEES PAID
NASA
PERMIT No. G27

NASA

POSTMASTER: If Undeliverable (Section 158
Postal Manual) Do Not Return